F 1103

R

REFERÁLVA

REVUE ROUMAINE DE CHIMIE

TOME 19

N° 1

Janvier 1974

RECHAX, **19**, *1*, 1–162 (1974)

ÉDITIONS DE L'ACADÉMIE DE LA RÉPUBLIQUE SOCIALISTE DE ROUMANIE

Rev. Roumaine Chim. **19**, *1*, p. 1–162 (1974), Bucarest

COMITÉ DE RÉDACTION

Rédacteur en chef :

I. G. MURGULESCU, membre de l'Académie de la République Socialiste de Roumanie

Rédacteurs en chef adjoints :

A.T. BALABAN et V. EM. SAHINI, membres correspondants de l'Académie de la République Socialiste de Roumanie

Collège de rédaction :

C. DRĂGULESCU, RALUCA RIPAN, CR. SIMIONESCU, membres de l'Académie de la République Socialiste de Roumanie ; EM. BRATU, ECATERINA CIORĂNESCU-NENITZESCU, P. SPACU, membres correspondants de l'Académie de la République Socialiste de Roumanie ; MARGARETA AVRAM, D. I. MARCHIDAN, G. NIAC et D. SĂNDULESCU

La Revue Roumaine de Chimie paraît 12 fois par an. Toute commande de l'étranger (fascicules ou abonnements) sera adressée à Întreprinderea Rompresfilatelia, Boîte Postale 2001, telex 011631, Bucarest, Roumanie

Les manuscrits, les livres et les revues proposés en échange, ainsi que toute correspondance seront envoyés à la rédaction

REVUE ROUMAINE DE CHIMIE

23, str. Dumbrava Roşie, Bucarest, Roumanie

ÉDITIONS DE L'ACADÉMIE DE LA RÉPUBLIQUE SOCIALISTE DE ROUMANIE
3 bis, str. Gutenberg, Bucarest

ORSZÁGOS MŰSZAKI KÖNYVTÁR ÉS DOKUMENTÁCIÓS KÖZPONT 1883

REVUE ROUMAINE DE CHIMIE

Tome 19, Nº 1 Janvier 1974

M. FLORESCU, Romanian research, a message of Romania's peaceful policy 3–8

I. G. MURGULESCU and J. PĂUN, The radiolysis of the complex oxalates in aqueous solutions. II. Kinetics and mechanism of the radiolysis of cobalt-trisoxalato-complex in neutral aqueous solution with α-Po^{210} irradiations 9–15

I. BICĂ and MONICA CĂLDĂRARU, γ-radiolysis of gaseous isobutylene. The influence of experimental conditions on the radiochemical yields of the main radiolysis products 17–23

S. STERNBERG and VALERIA PETRESCU, The galvanostatic study of the electrochemical adsorption process on the chlorine-active carbon electrode in molten salts. I. Anodic and cathodic polarization curves 25–36

RALUCA RIPAN, Z. FINTA and CS. VÁRHELYI, On α-dioximine complexes of the transition metals. XXXVIII. The $[Co(DH)_2(NO_2)(CN)]^-$ ion and its basic hydrolysis kinetics. 37–44

N. S. BIRADAR, A. L. LOCKER and V. H. KULKARNI, Addition compounds of zirconyl chloride with aromatic Schiff bases 45–48

CONST. GH. MACAROVICI, EUGENIA PERȚE, M. STRĂJESCU and MARIA BIROU, Contribution to the study of the binary system $In_2O_3-TiO_2$ . . 49–55

D. NEGOIU and LIDIA PARUTA, Complex combinations of the transition metals with tertiary stibines. II. Spectral studies Pd(II) complex combinations with tritolylstibines 57–66

ILEANA DRĂGUȚAN, C. DRĂGHICI, ANA HANEȘ, ANGELA DUMITRIU, ECATERINA CIORĂNESCU and C. D. NENITZESCU, Carbonium ion reactions. VIII. Benzobicyclooctene derivatives through π-route . . 67–78

A. M. EL-ABBADY, M. A. OMARA and N. G. KANDIL, Condensation of β-aroylpropionic acids with isatin under Perkin conditions 79–85

ALICE MARIE GLATZ, VASILE WERTHEIMER and FLORIN BADEA, Aluminium chloride catalyzed reactions of unsaturated acids with benzene. VI. Reaction of cyclopentylacrylic acid 87–98

I. IONESCU, Quelques remarques sur les propriétés des betons aux résines synthétiques sans liants minéraux. I. . . . . 99–113 R

I. NANU und C. ANDREI, Copolymere konjugierter Diene mit Monoestern der Maleinsäure. VII. Andere Aspekte der Reaktionskinetik der radikalischen Copolymerisation von Isopren mit Monoestern der Maleinsäure 115–124

Rev. Roumanie Chim. **19**, *1*, p. 1–162 (1974), Bucarest

VICTORIA DIMONIE, D. DONESCU and I. GAVĂT, Copolymerization of epichlorhydrin and propylene oxide with the $AlEt_3-H_2O$ catalytic system 125–130 R

ŞTEFANIA SPIRIDON and CARMEN GRIGORESCU-SABĂU, The influence of cross-linkage of anion exchangers on the distribution coefficient of samarium in mixed systems of organic solvent and mineral acid 131–139

GH. FACSKO und MARIA NEMEŞ, Die amperometrische Titrierung des Quecksilbers (II) in stark alkalischem Medium mit Thioacetamid 141–144

ELENA HOPÎRTEAN and C. LITEANU, Studies on the electroanalytical behaviour of membrane-electrodes under current V. The *E*-pH electrode function and the use of the PVC + tricresylphosphate membrane in the acid-base potentiometric titration at constant direct current . . . . . 145–156 R

I. FLOREA, Spektrophotometrische Dosierung des Benzidins und *o*-Tolidins mit Natriumhypochlorit 157–161

Revue Roumaine de Chimie, **19**, *1*, 3–8 (1974)

ROMANIAN RESEARCH, A MESSAGE OF ROMANIA'S PEACEFUL POLICY

MIHAIL FLORESCU

Minister of Chemical Industry

Following the tradition established by so many precedents, each voyage of comrade Nicolae Ceaușescu and of comrade Elena Ceaușescu abroad is watched by the citizens of our fatherland with that human vibration and rightful pride resulted from the belief that a proper cause to everyone is being served in far off places : the promotion of the fundamental interests of the Romanian people and implicitly the aspirations for the better, for peace and understanding between all peoples. It may be definitely stated that these attributes also characterized the visit paid by comrade Nicolae Ceaușescu together with comrade Elena Ceaușescu to the United States of America at the invitation of President Richard Nixon and of his wife, Mrs. Patricia Nixon.

This visit ranges in the context of the whole foreign policy of Romania which, while unswervingly militating for the constant strengthening of many-sided relations of friendship and alliance with socialist countries, also acts toward developing relations with all the countries in the world, regardless of their social system, in the spirit of peaceful coexistence, of requirements for détente and for a general progress in our present world. An expression of the relations of friendship and cooperation settled among our countries and peoples, the visit to the USA was concluded with particularly satisfactory results for the further development of these relations, also making an ample contribution to the general cause of peace and of international cooperation.

The profitable nature of relations of cooperation based on the rigorous observance of equality in rights is also revealed by the very evolution of Romanian-American relations which have recorded a favourable ascending course in recent years, at all levels : economic, scientific, cultural, political and in other domains.

Thus, it was again outlined that the relations of peaceful coexistence cannot and must not be considered in a static, passive way, but rather as an active, dynamic policy for strengthening the relations of cooperation, for permanently stimulating collaboration, understanding and rapprochement between peoples.

On a scientific plane, the central event of the visit was the award of the Diploma of Honorary Member of the American Institute of Chemists to Dr. Engineer Elena Ceaușescu. The ceremony of the award of this special distinction took place at the National Academy of Science of the USA.

Comrade Elena Ceaușescu was welcomed by the president of the National Academy of Science, Philip Handler. Opening the ceremony attended by a large number of well-known personalities from different states of the USA, the speaker said :

"I paid a visit to Romania last year. I got acquainted with the scientific activity developed in your country. I was left with the best impressions. The present opportunity of welcoming a remarkable scientist of this country is a joy for us all".

This appreciation is based on significant achievements all along the activity carried out as a researcher and director of ICECHIM.

Studies developed under the direct leadership of comrade Dr. Eng. Elena Ceaușescu, involving the stereospecific polymerization of isoprene, some methods for the purification of monomers and of solvents used in obtaining macromolecular compounds through various approaches of stereospecific polymerization and in emulsion through polycondensation as well as studies involving the characterization of polymers by modern analysis methods have found a wide application in industry and research.

Investigations carried out in the field of polymer synthesis are of a particular interest since a part of the studied elastomers having superior properties, natural rubber-substitutes, will be shortly developed in industry, thus enlarging the range of synthetic rubber produced in our country.

The studies and investigations in the field of the synthesis of some plastifiers involved in PVC compounds are also worth mentioning. The occurrence of macromolecular compounds determined the working out and the development of specific analysis methods capable of revealing the macro and microstructure of polymers, in view of establishing relations between their structure and properties and, hence, of anticipating the fields of utilization.

In this sense valuable work has been achieved in the field of the structural characterization of polymers and characterization methods.

The ceremony at the US Academy of Science was continued by the speech of the president of the American Institute of Chemists, Ernest Gilmont, who said :

"We award today the Diploma of Honorary Member of the American Institute of Chemists to Mrs. Elena Ceaușescu, as an acknowledgement of the remarkable manner in which she manages a research institute of high repute, for her outstanding merits in developing some important studies, for her particular contribution to the progress of scientific life and for the achievements in the field of education not only in her own country but also throughout the world. She is the first foreign scientist being awarded the Honorary Diploma. Mrs. Elena Ceaușescu's accomplishments in raising the chemical profession at higher levels on international plane is an important contribution to the international development of chemistry. Mrs. Elena Ceaușescu has worked in a highly efficient manner in the spirit of objectives also pursued by the American Institute of Chemists. Due to her activity, new prospects are being opened in the field of chemistry at present. She has done very much in order to increase the prestige and the distinction of this profession".

The president of the Branch of the district of Columbia of the A.I.C., Dr. Miloslav Rechigi Jr., presented next the statement for the award of the Diploma of Honorary Member.

"It is a privilege for us", he said, "to have the opportunity of expressing our recognition to one of the greatest chemical researchers. I say that, as we, members of our association, have come here in order to do honour to a brilliant exponent not only in Romania but also on a worldwide scale, of a profession highly thought of by all those future-oriented personalities".

"Elena Ceauşescu has graduated from the Polytechnic Institute in Bucharest obtaining the titles of chemical engineer and a doctorate in chemistry in 1957 and 1965, respectively. She is a specialist in the field of macromolecular synthesis compounds, in the chemistry of polymers and rubber and in the kinetics of polymerization. At present she holds the position of Director General at the Central Institute of Chemical Research in Bucharest. In this capacity, Dr. Elena Ceauşescu manages and coordinates multiple activities in the field of chemistry and the application of some advanced technologies in Romania's chemical industry. At the same time, Dr. Elena Ceauşescu is a member of the Executive Bureau of the National Council for Science and Technology, a governmental organization responsible for the coordination of scientific and technological development in Romania".

"As a recognition of her scientific achievements, Dr. Elena Ceauşescu has been elected a honorary member of the International Society of Chemical Engineering, an active member of the Academy of Science in New York, a honorary member of the Association of Chemists and Chemical Engineers in Costa Rica, a honorary member of the Council of the Central University in Ecuador and a honorary professor at the National Technical University of Lima".

"The results of numerous scientific investigations carried out by Dr. Elena Ceauşescu or achieved under her leadership have been inserted in various scientific publications or presented at Congresses and Symposia in Romania and abroad".

"Apart from her scientific career and her responsibilities in the management of the institute, Elena Ceauşescu plays an active part in the political life of her country and has participated in official visits abroad".

"Beside the role of first lady of her country, she is a politician and a statesman. Based on our criteria we consider her to be a politician whose activity is particularly efficient and successful. Recently, Mrs. Elena Ceauşescu has been elected in the Executive Committee of the Communist Party of her country. As far as I know she must be the most active of the first ladies throughout the world. Last but not least, I must also mention the fact that Mrs. Ceauşescu takes pride in her two sons and in her daughter".

"With such an impressive background and with such a brilliant career, Mrs. Ceauşescu certainly ranges among the most distinguished personalities".

"It certainly is a pleasure to have you among us".

"We are honoured by your presence" (the last words have been uttered in Romanian).

In answer, comrade Elena Ceauşescu addressed a cordial greeting to those present, to American chemists, on behalf of Romanian scientists and of chemical researchers and on her own part, and then thanked for the award of the Diploma of Honorary Member which she considered to be a high appreciation given to Romanian science, to the activity of Romanian chemists, as well as an expression of the friendly relations between the two countries and peoples.

In our days, comrade Elena Ceauşescu further emphasized, scientific knowledge increasingly becomes a common asset of the whole civilization, and its development places more and more imperative requirements on the expansion of contacts and of exchanges of information, on the promotion of a large cooperation among scientists and scholars all over the world.

Romania assigns a prime significance to the development of science, a major promoting factor in the multilateral progress of the economy and in raising the people's standard of living. During the last three decades since Romanian people has chosen the socialist form of development, great efforts have been made for the stimulation of scientific research, for the training of the necessary staff and the establishment of a wide network of research units. In the frame of the general activity of scientific research, a special attention has been paid to research in the field of chemistry, this being one of the decisive sectors of modern technical progress also involving the best use of our country's natural wealth.

By fulfilling the objectives regarding the development of the chemical industry and of research, Romania strongly supports the development of collaboration and of cooperation between Romanian scientists and researchers from other countries. In this sense, all the conditions have been satisfied for fruitful relations of cooperation to be developed between Romanian and American scientists, between the chemists of the two countries. In our days, cooperation and collaboration between scientists become more and more necessary not only as a basic condition of scientific progress in general, but also as a concrete contribution to the cause of understanding and rapprochement between nations, as a direct contribution to relaxation, cooperation and international peace.

In conclusion, expressing her confidence to the effect that the development of the Romanian-American scientific cooperation would mean an actual contribution to the fulfilment of desiderata of peace and progress of the two peoples, to the efforts for creating a better world, comrade Elena Ceauşescu addressed wishes of new successes to American chemists, in their activity devoted to science.

At the end of the ceremony, the president of the National Academy of Science underlined that he shared the views of the Director of the Central Institute of Chemical Research in Bucharest regarding the high responsibility incumbent upon scientists, expected to do their utmost for the understanding, cooperation and respect among peoples, as well as the considerations regarding the prospects of the Romanian-American scientific cooperation and expressed once again his warm thanks to comrade Elena Ceauşescu for her presence among American chemists.

The value of the awarded distinction is also stressed by the fact that only 64 such honorary diplomas have been granted up to the present during the 50 years which had elapsed since the foundation of this high forum of American chemists. Comrade Dr. Eng. Elena Ceauşescu is the first foreign statesman who has been awarded this high distinction. It also crowns the outstanding scientific merits of the Romanian school of chemistry, of a representative Romanian scientist.

The statement regarding the award of the diploma of honorary member of I.A.C., read in front of numerous representative scientists in the field of chemistry in USA, included the determining article concerning the award of this distinction. It states :

"Those persons are honorary members who have particularly distinguished themselves in the field of chemistry through services done to the chemical profession and to the country and also through professional achievements" (Article II, Section 3 of the document of constitution).

This high distinction has been recently granted to Dr. Philip Handler, president of the National Academy of Science and to Dr. Glenn T. Seaborg, Nobel-Prize winner for chemistry in 1951.

With regard to the American Institute of Chemists, it was founded in 1923, the president in charge being Dr. Ernest R. Gilmont. The institute numbers 8,000 members from all the 50 states and coordinates the activity of 31 governmental institutions.

A particular emphasis must be laid on the merit in organizing the research activity in the chemical industry of our country on efficient bases, an achievement attained in recent years under the direct leadership of comrade Dr. Eng. Elena Ceauşescu.

As the chemical production developed at a rapid rate, the fundamental and applicative scientific research in chemistry was expanded and the need was felt for some organizing frames expected to increase the efficiency of results obtained in the field of research, a closer bond between research and technological designing.

As a result of thorough studies developed under the direct guidance of Dr. Eng. Elena Ceauşescu, bases were set for the organization of the Central Institute of Chemical Research which controls all the central institutes and the research institutes in industry and coordinates the whole research activity in the chemical field in higher education institutes. A better coordination has been achieved in this manner, in developing research plans, in concentrating forces on the major issues in the development of the chemical industry.

The direct relation between research and technological designing will speed up the passage to industrial production. The development of technological processes which closely link research to the designing activity, the chemical engineering calculations and those relating to equipment design will permit a simplification of the entire cycle — from laboratory research to the production of industrial installations — so as to reduce it as much as possible while attaining the highest possible technical level, achieving a rational technological flow and a high economic efficiency.

It must be mentioned that the National Council of Science and Technology has introduced this system into the major industrial branches, following the model achieved at the Central Institute of Chemical Research.

The award of high scientific distinctions to a famous representative of the Romanian school of chemistry, comrade Dr. Eng. Elena Ceaușescu, also illustrates the high appreciation given by chemists from the USA and from other states to Romanian chemists, to all those who, by their activity in plants, research and designing institutes, have raised the chemical industry of our country to one of the highest levels of the world-wide chemical industry, a fact attested by the competitivness of our chemical products on the international market and also the unanimous appreciations of scientists expressed on the occasion of the presentation of some licences and inventions at various events abroad.

Revue Roumaine de Chimie, **19**, *1*, 9–15 (1974)

THE RADIOLYSIS OF THE COMPLEX OXALATES IN AQUEOUS SOLUTIONS. II[1]

KINETICS AND MECHANISM OF THE RADIOLYSIS OF COBALT-TRISOXALATO-COMPLEX IN NEUTRAL AQUEOUS SOLUTION WITH α-Po^{210} IRRADIATIONS

I. G. MURGULESCU and J. PĂUN
University of Bucharest, Department of Physical Chemistry,
Radiation Chemistry Laboratory, Bd. Republicii 13, Bucharest, Romania

Received June 13, 1973

The decomposition of the Co-trisoxalato-complex in neutral aqueous solution by irradiation with high L.E.T. ionizing radiation (α-Po^{210}) has been studied. The radiochemical decomposition reaction follows a zero order kinetic law. The $G(-[Co(C_2O_4)_3]^{3-})$ value increases with the increasing solute concentration from 0.22 to 0.52, being in accordance with the known influence of L.E.T. value on the radiochemical yield of the solute chemical transformation in radiation chemistry of aqueous solutions. The predominant process in the radiolysis of this compound is the reduction of the trisoxalato-complex ion by the hydrated electrons and hydrogen atoms:

$$[Co(C_2O_4)]^{3-} + e_{aq} \longrightarrow [Co(C_2O_4)_2]^{2-} + C_2O_4^{2-}$$

$$[Co(C_2O_4)]^{3-} + H \longrightarrow [Co\,(C_2O_4)_2]^{2-} + C_2O_4H^-$$

so that: $G\,(-[Co\,(C_2O_4)_3]^{3-}) = G_{e_{aq}^-} + G_H$

The kinetics and mechanism of the radiolysis of Co-trisoxalato-complex in neutral aqueous solution with low L.E.T. ionizing radiation has been the subject but of a few investigations.[1,2] From the puls radiolysis works, Baxendale[3,4] has shown that the Co-trisoxalato-complex ion is a very good hydrated electron scavanger and reported that in the reduction process of $[Co(C_2O_4)_3]^{3-}$ ion no short-lived transient was observed spectrophotometrically.

---

[1] I. G. Murgulescu, T. Oncescu, J. Păun and I. Mihalcea, *Rev. Roumaine Chim.*, **12**, 573 (1967).

[2] I. N. Neokladova and G. A. Shaghisultanova, *Doklady Akad. Nauk. S.S.S.R.*, **158**, 1379 (1964).

[3] J. H. Baxendale and A. J. Swallow, Nature, **201**, 4918, 468 (1964).

[4] J. H. Baxendale, E. Fielden and J. P. Keen. *Proc. Roy. Soc.*, **286**, 320 (1965).

In order to study the effect of the changing of linear energy transfer (L.E.T.) on the radiochemical decomposition yield of Co-trisoxalato-complex, $G(-[Co(C_2O_4)_3]^{3-})$, we have used α-Po^{210} particles as high L.E.T. ionizing radiations.

EXPERIMENTAL

The complex compound was prepared by the Sörensen's method.[5] For the preparation of the solutions twice distilled water was used. We have worked at three different concentrations: 10^{-3}M ; 2×10^{-3} M and 4×10^{-3} M. The decomposition of the complex in solution during the irradiation was followed spectrophotometrically by measuring the optical density of the irradiated solution at 573 nm.

For α-particles irradiation we have used 1 Curie Po^{210} type PDD source produced by the Radiochemical Center, Amersham, England. The source was made by electrodeposition of polonium on a circular area of platinum of 10 mm diameter. The metal disk was slightly recessed in an aluminium holder and covered by a very thin mica window of ~ 1 mg/cm^2 mass thickness. The source holder could be raised or lowered by means of a screw, thus enabling the distance between the source and the surface of the irradiated liquid to be varied in a controlled manner.

The irradiation cell had an irradiation zone in the form of a flat cylinder 3 cm in diameter and 1 cm deep with a very thin mica window in the center of one face. For irradiation of the solution, the cell was placed closely under the source holder so that only 1 mm gap was traversed by the α-particles in going from one to another. All mica windows were prepared by cleavage of sheets of mica which before being fitted were microscopically examined and their thicknesses determined. During irradiation, the content was agitated by a magnetically operated stirrer. The irradiation array including the source, source holder and irradiation cell is presented in figure 1.

The mean energy of α-particles on reaching the solution was calculated by using the values for the stopping power of mica given by Riezler[6] and the range-energy relationships by Jesse and Sadauskis.[7]

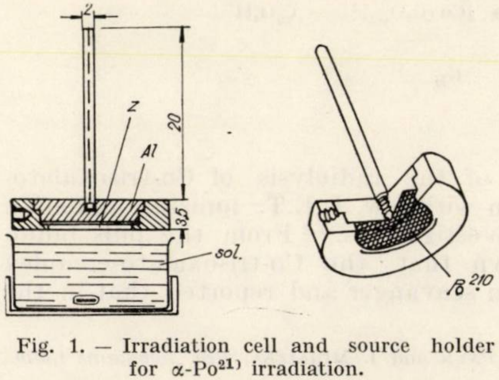

Fig. 1. — Irradiation cell and source holder for α-$Po^{21)}$ irradiation.

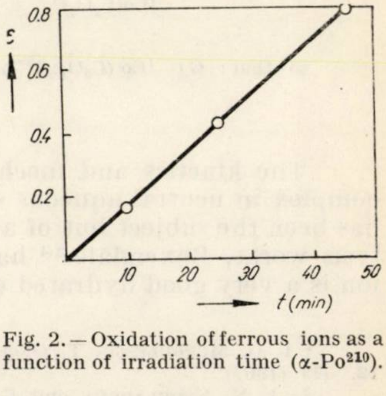

Fig. 2. — Oxidation of ferrous ions as a function of irradiation time (α-Po^{210}).

---

[5] S. P. L. Sörensen, *Z. anorg. Chem.*, **11**, 1 (1896).

[6] W. Riezler, *Ann. Phys.*, **35**, 350 (1939).

[7] W. P. Jesse and J. Sadauskis, *Phys. Rev.*, **78**, 1 (1950).

The standard Fricke ferrous sulfate dosimetric solution was used to calibrate the Po^{210} source using a value of 4.7 for $G(Fe^{3+})$. In figure 2 is given the increase of the optical density of irradiated dosimetric solution at 304 nm. The dose rate was 2.2×10^{17} eV/g min in a volume of 1.5 ml.

RESULTS

On irradiation with α-radiations, the Co-trisoxalato-complex in neutral aqueous solution decomposes slowly following a zero order kinetic law in the whole concentration range studied. In figure 3 is given the decrease of the complex concentration with the irradiation dose for three different concentrations : 10^{-3}, 2×10^{-3} and 4×10^{-3} M, in the presence of air.

The radiochemical yield $G(-[Co(C_2O_4)_3]^{3-})$ increases with the initial solute concentration from 0.22 to 0.44. In the absence of air, at a concentration of 4×10^{-3}M, we got $G(-[Co(C_2O_4)_3]^{3-}) = 0.52$.

In the presence of $C_2O_4^{2-}$ ions, at a concentration of 2×10^{-3}M, the decomposition is also linear with the irradiation dose but, the decomposition rate is lower, as can be seen from figure 4.

In the presence of the scavanger for reducing species, such as : NO_2^- and NO_3^- ions, the radiochemical decomposition rate is lower. The

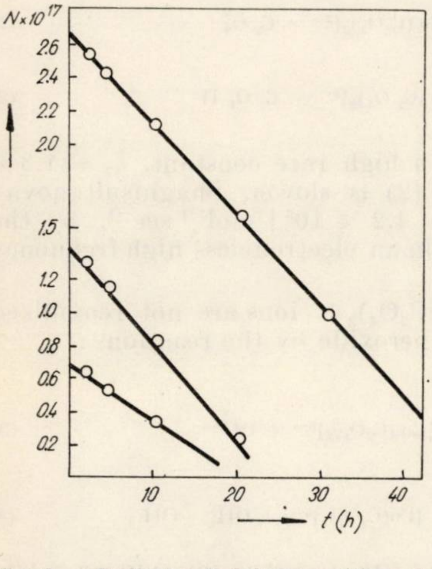

Fig. 3. — Radiochemical decomposition rate of Co-trisoxalato-complex in neutral aqueous solution at different concentrations.

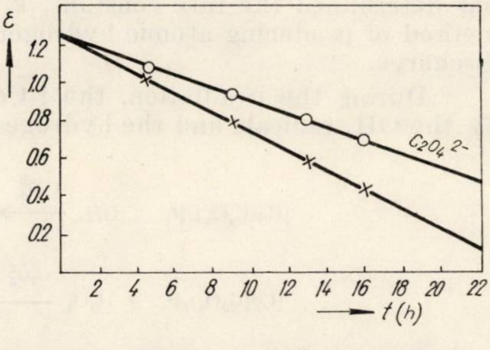

Fig. 4. — Influence of $C_2O_4^{2-}$ ions on the decomposition rate of Co-trisoxalato-complex in neutral aqueous solution, in the presence of air.

effect is greater in the presence of NO_2^- ions. In figure 5 is given the influence of NO_2^- and NO_3^- ions at a concentration of 2×10^{-3} M, on the decomposition rate of the complex in 2×10^{-3} M solution, in the presence of air.

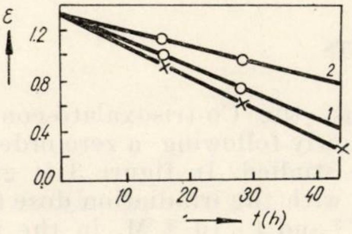

Fig. 5. — Influence of NO_2^- and NO_3^- ions on the decomposition rate of Co-trisoxalato-complex in neutral aqueous solutions, in the presence of air ($1 - NO_3^-$; 2, NO_2^-).

DISCUSSION

The decrease of the radiochemical decomposition rate of oxalato-complex in the presence of reducing species scavengers as well as the formation of CO^{2+} ions in irradiated solutions suggest that the main process taking place in the radiolysis is the reduction of $[Co(C_2O_4)_3]^{3-}$ ions, by the hydrated electrons and hydrogen atoms resulting from the radiolysis of water :

$$\bar{e}_{aq} + [Co(C_2O_4)_3]^{3-} \xrightarrow{k_1} [Co(C_2O_4)_2]^{2-} + C_2O_4^{2-} \qquad (1)$$

$$H + [Co(C_2O_4)_3]^{3-} \xrightarrow{k_2} [Co(C_2O_4)_2]^{2-} + C_2O_4H^- \qquad (2)$$

The reaction (1) is fast, having a high rate constant, $k_1 = 1.3 \times \times 10^{10}\ \text{l} \cdot \text{mol}^{-1}\,\text{sec}^{-1}$ [3,4]. The reaction (2) is slower. Shaghisultanova [8] has determined the rate constant, $k_2 = 4.2 \times 10^6\ \text{l} \cdot \text{mol}^{-1}\,\text{sec}^{-1}$, by the method of producing atomic hydrogen in an electrodeless high frequency discharge.

During the irradiation, the $[Co(C_2O_4)_2]^{2-}$ ions are not reoxidized by the OH. radicals and the hydrogen peroxide by the reactions :

$$[Co(C_2O_4)_2]^{2-} + OH. \xrightarrow{C_2O_4^{2-}} [Co(C_2O_4)_3]^{3-} + OH^- \qquad (3)$$

$$[Co(C_2O_4)_2]^{2-} + H_2O_2 \xrightarrow{C_2O_4^{2-}} [Co(C_2O_4)_3]^{3-} + OH^- + OH. \qquad (4)$$

There is so no clear evidence for the reaction (3). Allen [9] points only out that the product of reaction $Co^{2+} + OH$ may be written as $CoOH^{2+}$

---

[8] G. A. Shagisultanova, *High Energy Chemistry* (Russian edition) **5**, 187 (1971).

[9] A. Allen and D. Katakis, *J. Phys. Chem.*, **68**, 1359 (1964).

which does not immediately rearrange to the stable $Co^{3+}(aq)$ ion, remaining for a finite time in a more active form.

The reaction (4) has been studied by Wormser[10] who showed that it proceeds slowly, in a high excess of hydrogen peroxide, in the presence of high $C_2O_4^{2-}$ ions concentration ($\sim 1M$). This condition is not fulfiled in our irradiation experiments, because there were present no $C_2O_4^{2-}$ ions and the concentration of hydrogen peroxide built up during the radiolysis was not higher than the resulting $[Co(C_2O_4)_2]^{2-}$ ions concentration. As it is known, by irradiation with high L.E.T. radiations, the concentration of hydrogen peroxide is approximately 10^{-3} M.

Therefore, taking into consideration the reactions (1) and (2) only, the reaction rate becomes :

$$\frac{dx}{dt} = k_1\, C_{e^-_{aq}} \cdot (a - x) + k_2 \cdot C_H \cdot (a - x) \qquad (I)$$

where a is the initial solute concentration, $C_{e^-_{aq}}$ and C_H are the concentrations of hydrated electrons and hydrogen atoms, respectively. Assuming the well-known mechanism for the radiolysis of water[11], by applying the steady state principle to the estimation of reducing species concentrations, it results finally[1]:

$$\frac{dx}{dt} = k \cdot C_{H_2O} = k_0 \qquad (II)$$

where k_0 is the overall rate constant for a zero order process.

Experimentally, k_0 has been calculated by the equation :

$$k_0 = \frac{a_0}{\varepsilon_0} \cdot \frac{\Delta\varepsilon}{\Delta t}\ (\text{molec. cm}^{-3} \cdot \text{sec}^{-1}) \qquad (III)$$

where a_0 is the initial solute concentration, ε_0 the optical density of the solution, before irradiation at the concentration a_0, $\Delta\varepsilon$ the decrease of optical density for an irradiation time Δt. In table 1 are given the values for k_0, at three different solute concentrations, in the presence of air.

The increase of the radiochemical decomposition yield, $G(-[Co(C_2O_4)_3]^{3-})$ with the increasing complex concentration indicate that the $[Co(C_2O_4)_3]^{3-}$ ions react progressively with the hydrated electrons and the hydrogen

---

[10] Y. Wormser and G. Herve, *Comp. rend.*, **256**, 1534 (1963).

[11] A. Allen, "The Radiation Chemistry of Water and Aqueous Solutions", Van Nostrand, 1961 ; M. Anbar, "Water and Aqueous Solutions" in Fundamental Processes in Radiation Chemistry, Ed. P. Ausloss, Wiley, New York, 1968 ; I. Draganic, "Radiation Chemistry of Water", Academic Press, 1971.

Table 1

Values of k_0 and G ($-[Co(C_2O_4)_3]^{3-}$) at different concentrations in the presence of air

Concentration	t(hours)	ε	k_0(mole/ml·sec)×10^{11}	$G(-[Co(C_2O_4)_3]^{3-})$
10^{-3}M	0	0.680	—	—
	2	0.610	1.26	0.223
	4	0.570	1.20	0.213
	8	0.450	1.19	0.211
	12	0.325	1.19	0.211
	18	0.140	1.20	0.214
$2\cdot10^{-3}$M	0	1.290	—	—
	4	1.040	2.38	0.406
	9	0.810	2.29	0.390
	13	0.600	2.27	0.370
	16	0.450	2.24	0.400
	22	0.130	2.18	0.420
$4\cdot10^{-3}$M	0	1.160	—	—
	6	0.930	2.55	0.452
	11	0.830	2.46	0.437
	18	0.680	2.48	0.441
	28	0.450	2.51	0.446
	42	0.150	2.43	0.431

atoms existing freely in the bulk of solution. At higher solute concentration there are present sufficient oxalato-complex ions to scavange all the reducing species so that the radiochemical decomposition yield of the complex equals the reducing species yield $G_{e^-_{aq}} + G_H$ from the water radiolysis :

$$G(-[Co(C_2O_4)_3]^{3-}) = G_{e^-_{aq}} + G_H$$

At the concentration of 4×10^{-3} M in the absence of air we obtained $G(-[Co(C_2O_4)_3]^{3-}) = 0.52$. Taking $G_{e^-_{aq}} = 0.34$ and $G_H = 0.22$ as given from the experimental data,[12] in accordance with the theoretical values calculated by the diffusion kinetics theory, [13] we obtain the theoretical value of the yield $G(-[Co(C_2O_4)_3]^{3-}) = 0.56$ which is near to our experimental value.

The low value of the radiochemical decomposition yield $G(-[Co(C_2O_4)_3]^{3-})$ by high L.E.T. radiation is consistent with the decrease of the yield of solute chemical transformation with increasing L.E.T., as being due to the decrease of the primary radical yields from the water radiolysis with increasing L.E.T. To illustrate this, in table 2 is given the variation of the yield with the L.E.T.-value for γ-Co^{60} and α-Po^{210} radiations.

---

[12] H. Schwarz, J. Caffeny and G. Scholes, *J. Amer. Chem. Soc.*, **81**, 1801 (1959); A. Appelby and H. Schwarz, *J. Phys. Chem.*, **73**, 1937 (1969).

[13] P. Dyne and J. Kennedy, *Canad. J. Chem.*, **36**, 1518 (1958); **38**, 61 (1960); A. Kupperman, Radiation Research, "Proceedings of the Third International Congress of Radiation Research", Cortina d'Ampezzo, Italy, 1966, Northholland, Amsterdam, 1967, p. 212.

Table 2

Variation of $G(\text{-}[Co(C_2O_4)_3]^{3-})$ with L.E.T.-value in neutral aqueous solution, 4×10^{-3} M, in the absence of air

Radiation	L.E.T. (eV/Å) in water	$G_{e_{aq}^-}$	G_H	$G(-[Co(C_2O_4)_3]^{3-})$
$\gamma-Co^{60}$	0.02	2.65	0.55	3.15
$\alpha-P0^{210}$	8.80	0.34	0.22	0.52

An interesting feature of the radiolysis of aqueous solutions by high L.E.T. radiations is the small difference between the values of the primary reducing species yields $G_{e_{aq}^-}$ and G_H, where $\frac{G_{e_{aq}^-}}{G_H} = 1.54$ in comparison with the low L.E.T. radiations, where $\frac{G_{e_{aq}^-}}{G_H} = 4.81$ (see table 2). This means that the hydrogen atoms will have by α-irradiation a greater contribution to the radiolysis process. This fact is confirmed by our results concerning with the influence of the scavangers for hydrated electrons and hydrogen atoms, such as NO_2^- and NO_3^- ions. As can be seen from figure 5, NO_2^- ions reduce stronger than NO_3^- ions the rate of the decomposition of complex ions. This effect is smaller by γ-irradiation.[14] Although both ions are almost equally efficient hydrated electron scavangers, $k_{e_{aq}^- + NO_3^-} = 1.1 \times 10^{10}$ l·mol^{-1} sec^{-1}, $k_{e_{aq}^- + NO_2^-} = 8.1 \times 10^{9}$ l·mol^{-1} sec^{-1}, the NO_2^- ions are better hydrogen atoms scavangers than NO_3^- ions, $k_{H+NO_3^-} =$ $= 9.3 \times 10^{6}$ l*mol^{-1} sec^{-1}, $k_{H+NO_2^-} = 1 \times 10^{9}$ l·mol^{-1} sec^{-1}.[15]

As the yields of hydrated electrons and hydrogen atoms $G_{e_{aq}^-}$ and G_H are much smaller at high values of L.E.T., it is to be expected that the influence of oxygen on $G(\text{-}[Co\,(C_2O_4)_3]^{3-}$ will be reduced at high L.E.T., which was experimentally observed.

---

[14] T. Memetea and J. Păun, *Rev. Roumaine Chim.*, in press.

[15] M. Anbar and P. Neta, *Int. J. App. Rad. Isotopes*, **18**, 493 (1967).

Revue Roumaine de Chimie, **19**, *1*, 17–23 (1974)

γ-RADIOLYSIS OF GASEOUS ISOBUTYLENE. THE INFLUENCE OF EXPERIMENTAL CONDITIONS ON THE RADIOCHEMICAL YIELDS OF THE MAIN RADIOLYSIS PRODUCTS

I. BICĂ and MONICA CĂLDĂRARU

Institute of Physical Chemistry, str. Galaţi 31, Bucharest, Romania

Received April 27, 1973

The γ radiolysis of gaseous isobutylene on a wide range of pressures (150–760 torr) and at different irradiation doses was studied. The influence of pressure, irradiation dose and air traces on the yield of hydrogen and methane formation is discussed. Some ways which may determine the molecular hydrogen formation are also suggested.

1. INTRODUCTION

A great number of works issued lately deal with the radiolysis of gaseous alkenes. [1–6] Some important information about the irradiated gaseous isobutylene are obtained from Collin and Herman [9,10], Herman [11], Viswanathan and co-workers[7] and Volpi and co-workers'[8] works.

The effect of some experimental factors as gas density, irradiation dose and degasing procedure on the formation of radiolysis products has been studied less extensively. The aim of this work is to go thoroughly into the effects of these factors, as well as to advance an explanation of the molecular hydrogen formation, which is not well understood as yet.

---

[1] G. G. Meisels, *Adv. Chem. Ser.*, **58**, 243 (1966).

[2] G. R. Freeman, *Radiation Res. Rev.*, **1**, 1 (1968).

[3] G. G. Meisels, in "Fundamental Processes in Radiation Chemistry", P. Ausloos, (Ed.), Interscience Publ., 1968, p. 347.

[4] P. C. Kauffman, *J. Phys. Chem.*, **67**, 1671 (1963).

[5] O. Tokunaga, K. Hamanoue, J. Okamoto and K. Danno, *Bull. Chem. Soc. Japan*, **45**, 1050 (1972).

[6] J. Niedzielski and J. Gawlowski, *Radiochem. Radioanal. Letters*, **5**, 159 (1970).

[7] N. Viswanathan and L. Kevan, *J. Amer. Chem. Soc.*, **89**, 2842 (1967).

[8] V. Aquilanti, A. Galli, A. Giardini Guidoni and G. C. Volpi, *Trans. Faraday Soc.*, **63**, 926 (1967).

[9] G. J. Collin and J. A. Herman, *Canad. J. Chem.*, **45**, 3097 (1967).

[10] J. A. Herman and G. J. Collin, *Canad. J. Chem.*, **47**, 3837 (1969).

[11] J. A. Herman, *Canad. J. Chem.*, **48**, 3446 (1970).

2. EXPERIMENTAL

Isobutylene of Gerling Holtz and Co. quality was used without any purification (gas chromatographic analysis indicated a 99.7 % purity). The γ irradiations were performed in a 220 cm^3 Pyrex spherical vessel with the source placed in its center. The vessel degasing was obtained by heating (400°) and simultaneous pumping ($6 \cdot 10^{-5}$ torr) for four hours. The reaction cell was carefully washed to remove the polymer traces formed in the last experiment.

The source was a Co^{60} 480 ci with increased specific activity. Dosimetry was made with propylene as gaseous dosimeter using $G_{(H_2)} = 1.1.$[12] A 3×10^{16} eV/g dose rate was used.

The reaction products were analysed on a Pye dual collumn Gas Chromatograph, series 104, equipped with thermal conductivity detector, using Ar as carrier gas.

For C_2-C_4 hydrocarbons, a 5.4 m and 4 mm collumn filled with 20 % squalane on 60–80 mesh Chromosorb P was used, while a silica gel collumn 2.7 m and 4 mm was selected for H_2 and CH_4 analysis. The identification of the reaction products was done with suitable pure compounds. The quantitative determinations were carried out by the direct calibration method.

3. RESULTS

In this work we were particularly interested in following the H_2 and CH_4 production, as well as isobutylene conversion rate. Because of their very little importance in the analysed mixture, under our experimental conditions, the other products were determined only qualitatively.

In our work we have also observed some traces of liquid products on the wall of the reaction vessel, their amount increasing visibly with the irradiation dose.

Our work was divided into three sets of experiments. The first set dealt with the irradiation dose effect on the yields of principal products, when the internal pressure in the reaction vessel was kept constant (760 torr). Irradiation in the second series of experiments was made with a

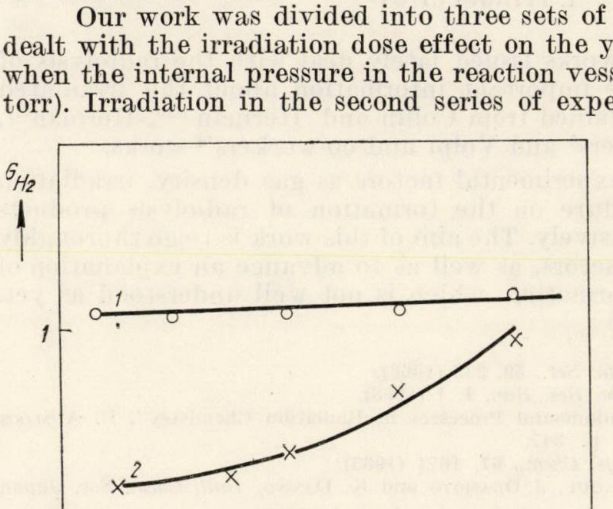

Fig. 1. — Radiochemical yield variation of molecular hydrogen *versus* irradiation dose, for the first and third set of experiments. $P = 760$ torr, *1*, First set, *2*, Third set.

---

[12] K. YANG, and P. GANT, *J. Phys. Chem.*, **65**, 1868 (1961).

Fig. 2. — Radiochemical yield variation of methane *versus* the irradiation dose, for the first and third set of experiments. $P = 760$ torr, *1*, First set, *2*, Third set.

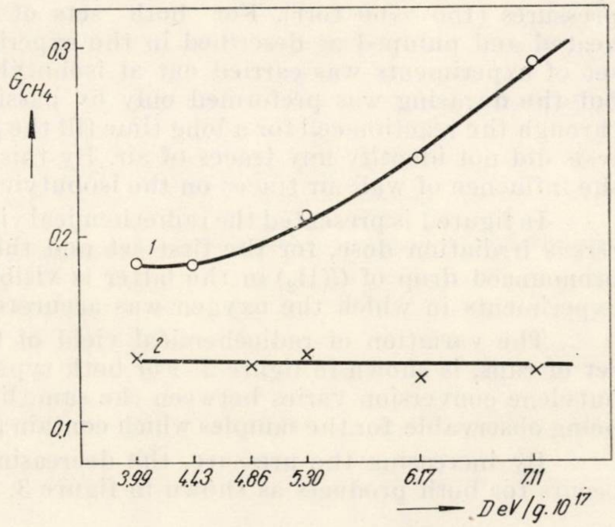

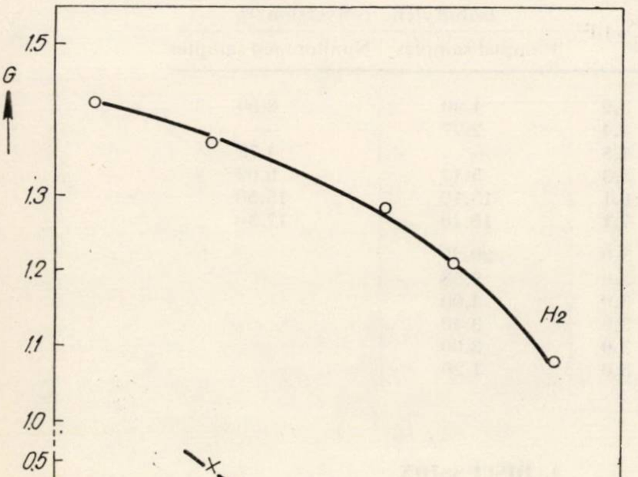

Fig. 3. — Radiochemical yields variation of H_2 and CH_4 *versus* pressure, for the second set of experiments. $D = 3.6 \cdot 10^{17}$ eV/g.

constant irradiation dose ($3.6 \cdot 10^{17}$ eV/g) but at different isobutylene pressures (150–760 torr). For both sets of experiments the cell was heated and pumped as described in the experimental section. The third set of experiments was carried out at isobutylene atmospheric pressure, but the degasing was preformed only by passing an isobutylene stream through the reaction cell for a long time till the gas chromatographic analysis did not identify any traces of air. By this procedure we determined the influence of wall air traces on the isobutylene radiolysis.

In figure 1 is presented the radiochemical yield variation of H_2, $G(H_2)$, *versus* irrdiation dose, for the first set and third set of experiments; a pronounced drop of $G(H_2)$ in the latter is visible in comparison to those experiments in which the oxygen was accurately eliminated.

The variation of radiochemical yield of CH_4, $G(CH_4)$, in the same set of runs, is shown in figure 2. For both types of experiments, the isobutylene conversion varies between the same limits, a very small increase being observable for the samples which contain air traces (table 1).

By increasing the pressure, the decreasing of radiochemical yields occurs for both products as shown in figure 3.

Table 1

Variation of isobutylene conversion in different experimental conditions

Pressure torr	Dose eV/g $\cdot 10^{17}$	Isobutylene conversion %	
		Pumped samples	Nonpumped samples
760	3.9	1.90	2.00
760	4.4	2.77	—
760	4.8	—	4.72
760	5.3	5.17	9.02
760	6.1	13.10	13.50
760	7.1	15.40	17.30
150	3.0	29.20	
310	3.0	9.08	
417	3.0	4.00	
540	3.0	3.40	
630	3.0	3.00	
760	3.0	1.20	

4. DISCUSSION

The drop of radiochemical yield of H_2 and CH_4 as well as of isobutylene conversion is an evidence that the collisional deactivation becomes more important with the increasing pressure. The pressure increase also determines a great probability of the ionic clusters formation; this process will mainly lead to condensation products.

As resulted from Magee and Funabashi's theory, [13] the formation of neutral molecules clusters around a central ion leads to a dissipation of the molecular energy over the whole assembly, which will determine its stabilization. Therefore, we can explain the decrease in yield of decomposition products (as H_2 and CH_4) with the increase of pressure, while the amount of the condensation products is higher at atmospheric pressure. This agrees with Tratchman's work,[14] which showed that the same phenomena occur in propylene radiolysis.

---

[13] J. L. Magee and K. Funabashi, *Radiation Res.*, **10**, 662 (1959).

As in figure 1, $G\ (H_2)$ varies relatively slightly with the irradiation dose; as can be seen from figure 2, $G\,(CH_4)$ is obviously increasing. In the presence of air traces, we observe a decrease of radiochemical yields of both products. This can be explained by analysing the source of product formation.

The primary radiochemical processes which occur at the isobutylene radiolysis are:

$$i-C_4H_8 \rightsquigarrow i-C_4H_8^{+*}\ (\text{or } i-C_4H_8^{+}) + \bar{e} \tag{A}$$

$$\rightsquigarrow i-C_4H_8^{*} \tag{B}$$

Related to these processes, the following reactions may be responsible for hydrogen formation as radiolysis product:

$$i-C_4H_8^{+*} \longrightarrow C_4H_6^{+} + H_2\ (\text{or } 2H) \tag{1}$$

$$i-C_4H_8^{+} \longrightarrow C_4H_6^{+} + H_2 \tag{2}$$

$$\longrightarrow C_4H_7^{+} + H \tag{3}$$

$$i-C_4H_8^{*} \longrightarrow C_4H_6 + 2H\ (\text{or } H_2) \tag{4}$$

$$\longrightarrow CH_2CCH_2 + CH_3 + H\ (\text{or } CH_4) \tag{5}$$

$$\longrightarrow CHCCH_3 + CH_3 + H\ (\text{or } CH_4) \tag{6}$$

$$\longrightarrow C_4H_7 + H \tag{7}$$

$$i-C_4H_8^{*} + i-C_4H_8 \longrightarrow C_8H_{14} + H_2 \tag{8}$$

The most probable secondary reactions of the hdyrogen atom resulting from (1), (4)—(7) are:

$$H + i-C_4H_8 \longrightarrow H_2 + C_4H_7 \tag{9}$$

$$\longrightarrow i-C_4H_9 \tag{10}$$

---

[14] M. Tratchman, *J. Phys. Chem.*, **70**, 3382 (1966).

The high ratio of the rate constants, k_{10}/k_9,[15] suggests that molecular hydrogen formation *via* a (9) type reaction could be considered as improbable. On the other hand, the works of Hatano *et al.*[16,17] evidenced that for a system containing "hot" hydrogen atoms, the alkene can be implied in a (9) type reaction; so, it can be responsible for molecular hydrogen formation. When an excited molecule produces many fragmentation products, the excitation energy is dissipated; so, it is very improbable for atomic hydrogen to be "hot", and this is the case for the reactions (5) and (6). All the other reactions may in principle generate such atoms. It follows that they may contribute to the increase of the probability of reaction (9).

The decrease of $G(H_2)$ in the presence of air traces (it means in the presence of oxygen, which is known as radical scavenger) is much higher (40%) than that obtained by Collin and Herman, [9] (10%) at low pressure and with NO as radical scavenger, but is the same with Tratchman's results in propylene radiolysis.[14] These facts can be explained by the reasons given below.

By increasing the pressure, the balance of contributions in molecular hydrogen formation changes (the molecular detachment becomes less important). On the other hand, O_2 traces also disturb a number of ionic reactions, as Niedzielski *et al.*[18] evidenced for ethylene radiolysis.

For a possible reaction as

$$i-C_4H_8^+ + i-C_4H_8 \longrightarrow C_8H_{14}^+ + H_2 \qquad (11)$$

the presence of O_2 traces will influence the molecular hydrogen formation.

As can be shown from figure 1, with increase of the irradiation dose, the influence of O_2 traces on the hydrogen yield becomes less important. The explanation of this effect is the following: by increasing the irradiation doses, the number of molecules which undergo radiolysis effect becomes more important in comparison to the constant amount of O_2 in the wall.

Concerning the methane formation, our results are in good agreement with those of Herman and Collin,[10] on the important contribution of primary molecular detachment

$$(CH_3)_2CCH_2 \longrightarrow CH_4 + CH_3CCH \qquad (12)$$

This is proved by the constance of $G(CH_4)$ in the presence of air traces, when the irradiation dose is increased. On the other hand, in our experimental conditions, other processes can become also important, and that is the reason for the steep increase of $G(CH_4)$ with increasing the irradiation dose in the absence of air traces (figure 2). Thus, "hot" hydrogen addition to isobutylene can lead to the methane formation, *via* an unstable intermediate complex

---

[15] K. R. Jennings and R. J. Cvetanovic, *J, Chem. Phys.*, **35**, 1233 (1964).

[16] Y. Hatano and S. Shida, *J. Chem. Phys.*, **46**, 4784 (1967).

[17] Y. Hatano, S. Shida and S. Sato, *Bull. Chem. Soc. Japan*, **41**, 1120 (1968).

[18] J. Niedzielski and J. Gawlowski, *Radiochem. Radioanal. Letters*, **2**, 291 (1969).

$$i - C_4H_8 + H \longrightarrow [i - C_4H_9] \longrightarrow CH_4 + C_3H_5 \qquad (13)$$

That is supported by the appearance of CD_3H and CH_3D in the radiolysis of $i\text{-}C_4H_8 - i - C_4D_8$ mixture.[10]

The methyl radical addition to isobutylene can finally lead to methane formation.

It is possible that among the secondary processes which are eliminated by oxygen traces, there are some ion-molecule reactions, which might be responsible for methane formation.

5. CONCLUSIONS

The experimental conditions have a considerable influence on the nature and amount of radiolysis products of isobutylene.

High pressure leads to formation of addition products, while at low pressure the decomposition processes are more important.

The irradiation dose has a small effect on $G(H_2)$, but is very important for $G(CH_4)$, because of the secondary processes.

Oxygen traces are important for the formation of the main products like hydrogen and methane.

Revue Roumaine de Chimie, **19**, *1*, 25–36 (1974)

THE GALVANOSTATIC STUDY OF THE ELECTROCHEMICAL ADSORPTION PROCESS ON THE CHLORINE-ACTIVE CARBON ELECTRODE IN MOLTEN SALTS. I

ANODIC AND CATHODIC POLARIZATION CURVES

S. STERNBERG and VALERIA PETRESCU
Polytechnical Institute, Str. Polizu 1, Bucharest, Romania

Received February 1, 1973

The adsorption — desorption process of the chlorine on the active carbon electrode in the AgCl—KCl system has been studied at : 400°, 500°, 600°, 700°. The existence of the thermal desorption current, that increases with increasing temperature, is evidenced. The efficiency of the charge — discharge process was determined as a function of the charge time process, t_c, and the temperature T. The existence of a remanent potential that depends on the charge and discharge current intensities I_c, I_d, on the charge time process, t_c, and the temperature T, is pointed out.

1. INTRODUCTION

The utilization of the galvanostatic charge — discharge curves method in the study of the electrochemical adsorption — desorption phenomenon of iodine on the active carbon was described in a previous paper.[1] In the present paper the same method is applied to the study of chlorine — active carbon electrode.

The scheme of the installation and the mode of obtaining the active carbon was described in previous papers.[1,2,3] A semiactive carbon electrode in the molten salt electrolyte AgCl + KCl, $x_{\mathrm{AgCl}} = 0.7$, was used at 400°, 500°, 600°, 700°.

The active carbon electrode is subjected to an anodic polarization process at a constant current intensity ($I_c = 0.1$ A) for 60 minutes obtaining the charge curve (anodic polarization curve) *oa* plotted in fig. 1. Then, the active carbon electrode was subjected to cathodic galvanostatic polarization (the intensity of current $I_d = 0.1$ A) in order to produce the electrochemical desorption of the adsorbed chlorine. In this way it was obtained the discharge curve (cathodic polarization curve) *ab* (fig. 1).

---

[1] S. Sternberg and I. Galasiu, *Rev. Roumaine Chim.*, in press.
[2] S. Sternberg and I. Galasiu, *Rev. Roumaine Chim.*, **15**, 1169 (1970).
[3] S. Sternberg and I. Galasiu, *Rev. Roumaine Chim.*, **17**, 1697 (1972).

The shape of the charge — discharge curve can be explained in the same way as the corresponding curve in the case of the active carbon-iodine electrode. On the zone *oa* of the anodic polarization curve (charge process) the discharge reaction of the chlorine ions takes place, producing the adsorbed chlorine, probably in atomic state:

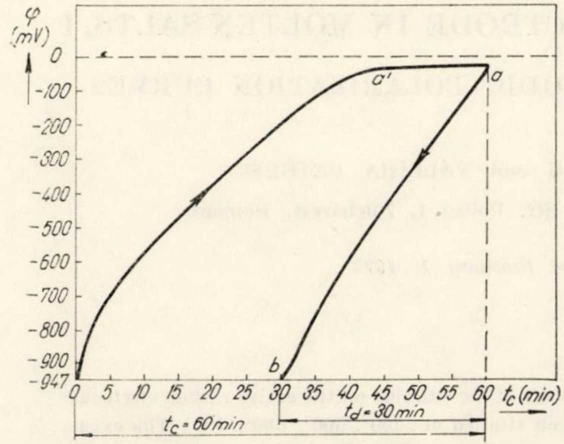

Fig. 1. — Anodic and cathodic polarization curves with $t_c = 60$ minutes; $I_c = I_d = 0.1$ A; $T = 400°$.

$$\mathrm{Cl^- = Cl\ (ads) + e^-} \qquad \text{(a)}$$

But, as it will be shown later, on this zone (*oa*) the efficiency $\eta = Q_d / Q_c$ (Q_d — quantity of electricity in the discharge process, Q_c — quantity of electricity in the charge process) is smaller than the unity. This action can be explained by the existence of a "thermal desorption" which can take place by the scheme:

$$\mathrm{2Cl\ (ads) \rightarrow Cl_2\ (ads) \rightarrow Cl_2\ (gas\ or\ dissolved\ in\ the\ salt)} \qquad \text{(b)}$$

During the discharge process *ab* (fig. 1), the process described by equation (a) occurs, but in the reversed direction. On the other hand, the thermal desorption is present too.

For a given system and a given temperature, the charge—discharge curves are different depending on the charge and discharge current intensity values (I_c and I_d) and depending also on the length of the charging process (t_c). These curves differ from each other because of the charging losses $Q_{cl} = \int_0^{t_c} dQ_{cl}$ and of the discharging losses $Q_{dl} \int_0^{t_d} dQ_{dl}$. These losses account for the hysteresis shape of the curves typically for irreversible processes.

The length of the discharge process t_d is smaller than the length of the charging process t_c, due to the mentioned losses and so the irreversibility of the process is made evident (by hysteresis curves *oa′ ab*, fig. 1).

2. ANODIC AND CATHODIC POLARIZATION CURVES

In fig. 2 (*a*, *b*) there are represented the discharge — charge curves obtained for several values of t_c, at the temperatures 400°, 500°, 600°, 700° and for different values of the current intensites $I_c = I_d = 0.05-0.15$ A.

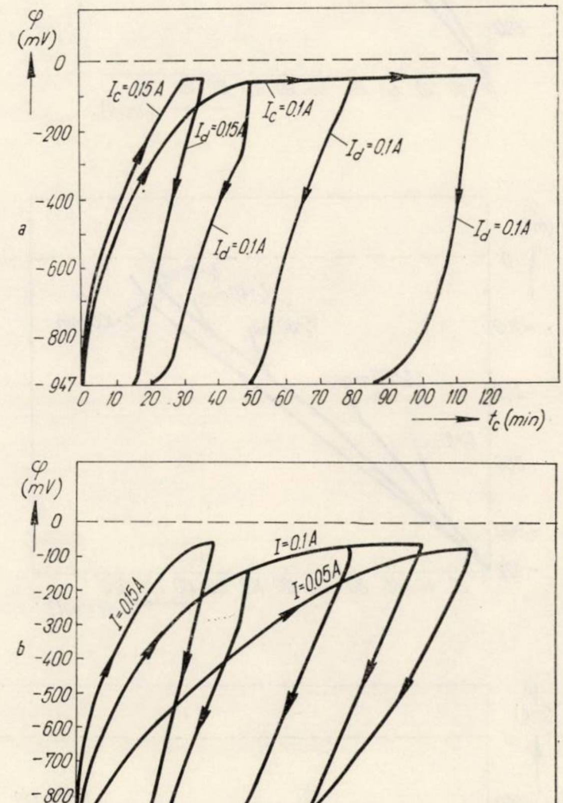

Fig. 2. — Anodic and cathodic polarization curves; *a*. $T = 400°$, $I_c = I_d = 0.15$ A and $I_c = I_d = 0.1$ A; *b*. $T = 500°$, $I_c = I_d = 0.15$ A, $I_c = I_d = 0.1$ A and $I_c = I_d = 0.05$ A.

We can see that the hysteresis curves obtained are different. After a certain length of the charge process the active carbon electrode potential tends to a plateau. The potential value at the plateau decreases and the time necessary to reach it increases with the temperature increase. At the same temperature, the value of the plateau potential decreases and the time

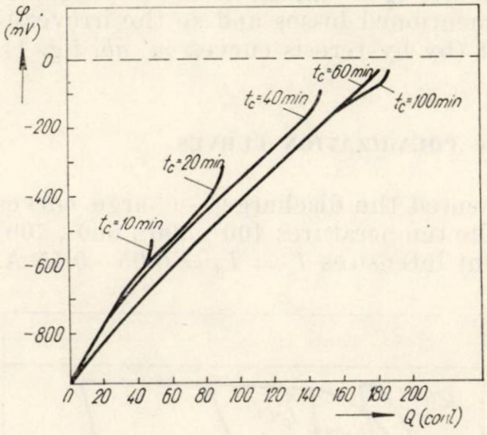

Fig. 3. — φ/Q curve for 400°, $I_c = I_d = 0.1$ A.

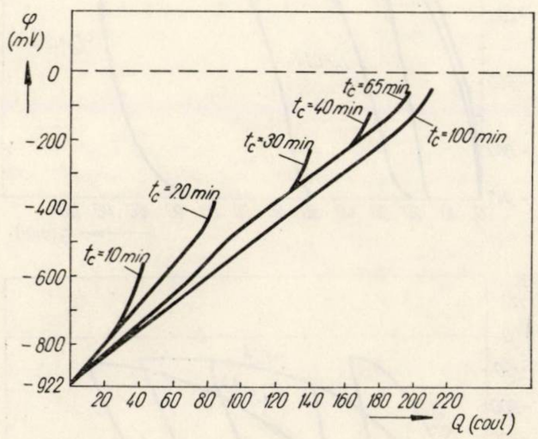

Fig. 4. — φ/Q curve for 500°, $I_c = I_d = 0.1$ A.

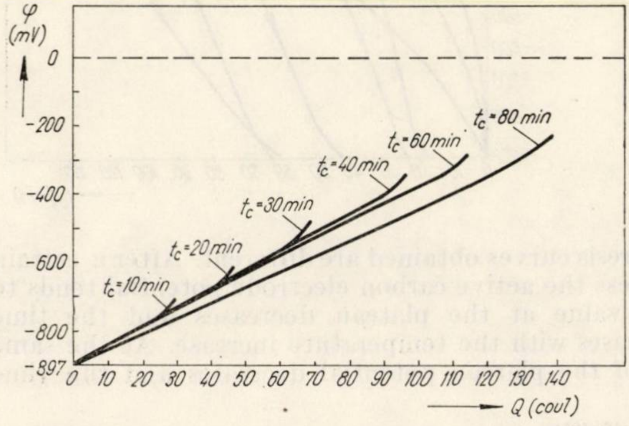

Fig. 5. — φ/Q curve for 600°, $I_c = I_d = 0.1$ A.

necessary to reach it increases with the decreasing of the intensity of the charge current.

In figs. 3−6 φ/Q curves are represented for different temperatures (400°−700°). These curves are obtained by overlapping in the origin of the discharge curves for different lengths of charging. At the beginning of every discharge curve, there is a zone with a steeper slope followed by a slower slope. When the length of the charge process increases we can notice the tendency of disappearance of the zones with the steep slope, the discharge curve having a slow slope on the whole of its length.

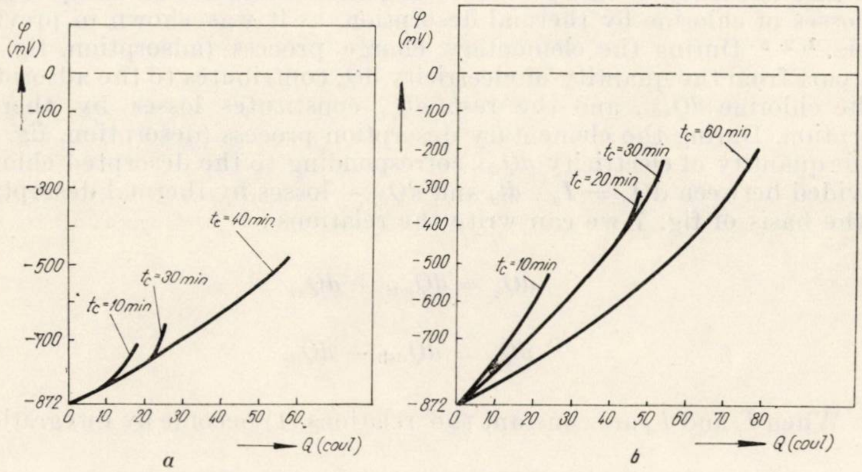

Fig. 6. — φ/Q curve for 700° ; a . $I_c = I_d = 0.1$ A ; b . $I_c = I_d = 0.2$ A.

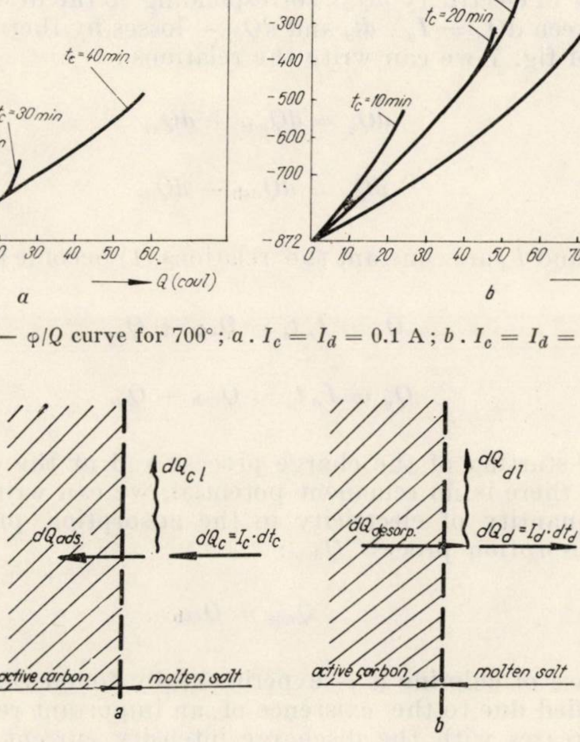

Fig. 7. — Scheme of the electrochemical adsorption — desorption process of the chlorine on the active carbon electrode (a — adsorption ; (b — desorption).

The appearance of the zones with steep slope and their tendency to decrease could be explained by a mechanism pointed out by the study of the so-called remanent potential phenomenon, which has appeared in this system more obviously.

In the following we will show how and to what degree the adsorption — desorption process is affected by the remanent potential phenomenon.

The electrochemical adsorption — desorption process of the chlorine on the active carbon electrode in molten salt is diagrammatically presented in fig. 7.

The efficiency of this process is in general smaller than unity due to the losses of chlorine by thermal desorption, as it was shown in previous papers.[1, 2, 3] During the elementary charge process (adsorption, fig. 7*a*) $\mathrm{d}t_c$ a part from the quantity of electricity $\mathrm{d}Q_c$ contributes to the adsorption of the chlorine dQ_{ads}, and the rest dQ_{cl} constitutes losses by thermal desorption. During the elementary desorption process (desorption, fig. 7*b*) $\mathrm{d}t_d$ the quantity of electricity dQ_{dsb} corresponding to the desorpted chlorine is divided between $\mathrm{d}Q_d = I_d \cdot dt_d$ and dQ_{dl} — losses by thermal desorption. On the basis of fig. 7 we can write the relations :

$$dQ_c = dQ_{\mathrm{ads}} + dQ_{cl} \tag{1}$$

$$dQ_d = dQ_{\mathrm{dsb}} - dQ_{dl}$$

When I_c and I_d are constant the relations (1) become by integration :

$$Q_c = I_c\, t_c = Q_{\mathrm{ads}} + Q_{cl} \tag{2}$$

$$Q_d = I_d\, t_d = Q_{\mathrm{dsb}} - Q_{dl} \tag{3}$$

If at the starting of the charge process and at the end of the discharge process there is no remanent potential, we can write the equality between the quantity of electricity in the adsorption process Q_{ads} and that in the desorption process Q_{dsb} :

$$Q_{\mathrm{ads}} = Q_{\mathrm{dsb}} \tag{4}$$

In the case of chlorine it is experimentally found that the equality (4) is not satisfied due to the existence of an important remanent potential which increases with the discharge intensity current. The presence of the remanent potential is explained by the fact that during the discharge process which takes place with finite intensity, a part from the adsorbed chlorine remains in the active carbon although at the surface of the active carbon electrode the potential becomes zero. After interrupting the discharge current a part of the chlorine which remains in the carbon electrode, migrate by diffusion towards the surface, generating the increase of the electrode potential up to the remanent potential value. If we denote by Q_{rem}, the quantity of electricity which could be obtained by desorption of the remained chlorine in the carbon electrode, after the potential had become zero in the discharge process, we can write the following relation :

$$Q_{\text{ads}} = Q_{\text{dsb}} + Q_{\text{rem}} \tag{5}$$

This relation is available when the remanent potential of the carbon electrode is zero at the beginning of the anodic polarization process. Substituting Q_{dsb} from (5) into (3) it is obtained :

$$Q_d = Q_{\text{ads}} - Q_{\text{rem}} - Q_{dl} \tag{6}$$

We have found that the presence of the remanent phenomenon acts like a loss which is added to the thermal desorption loss Q_{dl}, decreasing the quantity of electricity Q_d which is obtained during the discharge process.

In the experimental study of the chlorine adsorption — desorption process on active carbon electrode it is necessary in the first place to find an estimation modality of the remanent potential Q_{rem}. On the other hand, it is to be found a modality to bring the carbon electrode in the potential state zero in order to ascertain the reproductibility of the results. If this condition is not satisfied, the charge — discharge curves look like those in fig. 8.

Starting the anodic polarization process *ab* from the point *a*, in which the remanent potential is $\varphi_{\text{rem.o}}$, the anodic polarization curve will have a shape depending just on this remanent potential. Consequently, the length of the charge process up to the plateau will depend also on $\varphi_{\text{rem.o}}$ .After the discharge process (cathodic polarization process) *bc*, at interrupting the discharge current I_d we have found that the carbon electrode potential increases (the curve *cd*, fig. 8) amounting to a plateau which corresponds to a final remanent potential $\varphi_{\text{rem.f}}$. It is evident that the starting of a new anodic — cathodic polarization cycle from the point *d*, in which the final remanent potential $\varphi_{\text{rem.f}}$ becomes now the initial remanent potential, different from $\varphi_{\text{rem.o}}$, will lead to the anodic — cathodic polarization curve *db'c'*, different from the previous one *abc*.

Thus in these conditions we cannot obtain the reproducibility of the results.

Admitting the hypothesis that the remanent potential is due to the diffused chlorine in the active carbon pores, which has no time to go out totally during the cathodic polarization process (with $I_d = 0.1$ A), we have considered that it is possible to "extract" the chlorine using a relatively small discharge current (0.02 A).

In fig. 9 it is shown the process by which we can estimate Q_{rem}. After the cathodic polarization process with $I_d = 0.1$ A having the length t_d (the process *ab*) the current is interrupted and a t_{relax} time is expected, in which the carbon potential increases "by itself" (by the diffusion of the chlorine from the inner side of the pores to their outer side) up to a plateau corresponding to the remanent potential φ_{rem}. Then, the carbon electrode is discharged with a relatively small current $I_d = 0.02$ A, result-

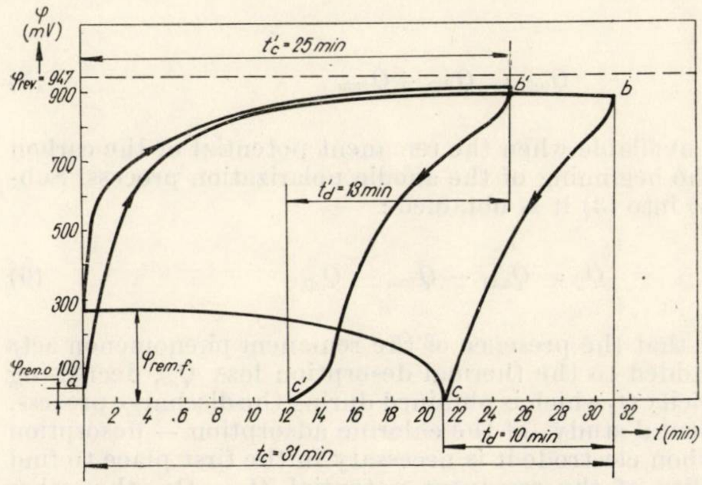

Fig. 8. — Charge — discharge curves when the carbon electrode is not in the potential state zero ; $T = 400°$.

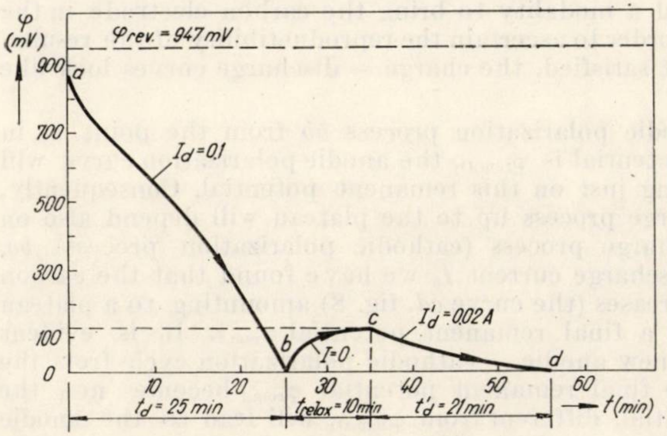

Fig. 9. — Process by which one can estimate Q_{rem} ; $T = 400°$; $I_c = 0.1$ A ; $t_c = 40$ minutes.

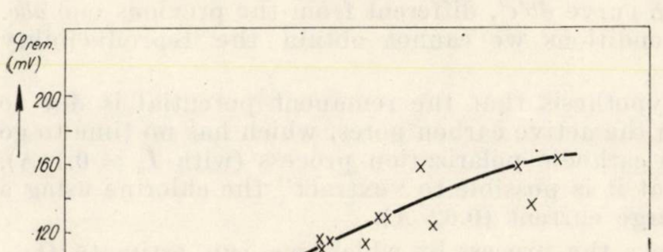

Fig. 10. — Dependence between $\Delta t_{\text{rem}}(Q_{\text{rem}})$ and φ_{rem}, $T = 400°$.

ing a t_d time. Thus, it is possible to estimate Q_{rem} by the relation :

$$Q_{\text{rem}} = I'_d \ t'_d \tag{7}$$

It is possible also to calculate the remanent correction of the t_d time, denoted by Δt_{rem}, which represents how smaller is the t_d discharge length compared to the situation in which the remanent phenomenon could not exist :

$$\Delta t_{\text{rem}} = Q_{\text{rem}}/I_d = I'_d t'_d / I_d \tag{8}$$

As is found experimentally the remanent correction increases with the discharge current intensity and has considerable values.

Using this method, besides the fact that we estimate Δt_{rem}, we can bring the carbon in the zero remanent potential state ($\varphi_{\text{rem}} = 0$) and in this way one can start a new charge—discharge cycle obtaining the reproducibility of the process by identical initial and final conditions. We have found experimentally that the remanent correction Δt_{rem} is dependent on the remanent potential φ_{rem} . It is evident that this fact is expected in the above mentioned hypothesis by which one considers the chlorine diffusion in pores as a cause of the remanent phenomenon. In fig. 10 it is shown the dependence between Δt_{rem} (Q_{rem}) and φ_{rem}.

It is expected that Δt_{rem} must depend on the discharge current intensity I_d and the quantity of electricity consumed in the charge process Q_c. This fact was observed experimentally (fig. 11).

3. CURRENT EFFICIENCY

It can be seen that Δt_{rem} increases linearly with the increase of I_d, for a Q_c constant. On the other hand, for I_d constant Δt_{rem} increases with the increase of Q_c. It is to be noted that the values of Q_{rem} are not at all negligible. Thus, for $I_d = 0.1$ A at $Q_c = 60$ coul corresponds a $Q_{\text{rem}} = 12$ coul, which represents $Q_{\text{rem}} = 20\%\ Q_c$. For $I_d = 0.1$ A and $Q_c = 24$ coul corresponds a $Q_{\text{rem}} = 8.1$ coul, which represents 33.8% from Q_c. It results that the remanent phenomenon affects considerably the efficiency of the anodic-cathodic polarization process :

$$\eta = Q_d / Q_c \tag{9}$$

This fact was observed experimentally. In the study of the dependence of the efficiency on the anodic polarization process length t_c, it is necessary to find out the variance of Δt_{rem} by t_c in order to estimate a

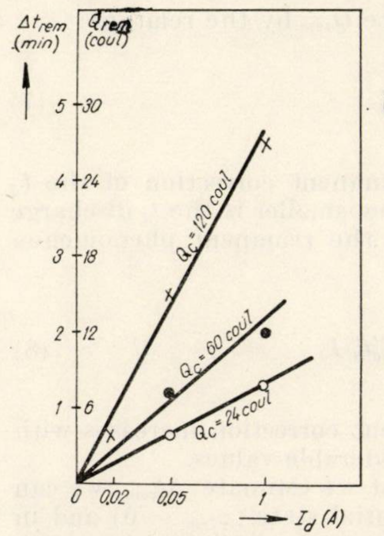

Fig. 11. — Δt_{rem} depends on the I_d and the Q_c.

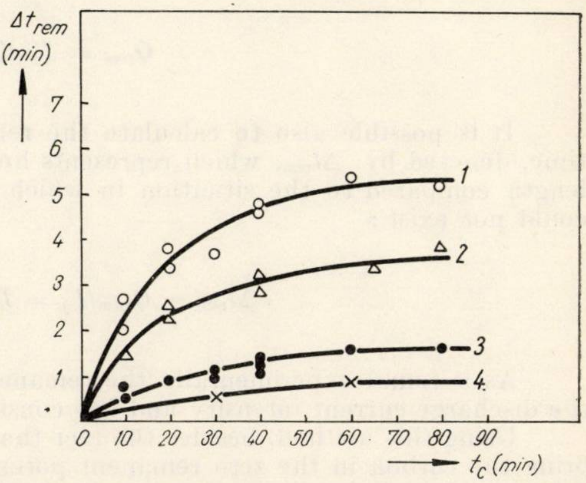

Fig. 12. — It is plotted Δt_{rem} as a function of t_c; *1*, 400°; *2*, 500°; *3*, 600°; *4*, 700°.

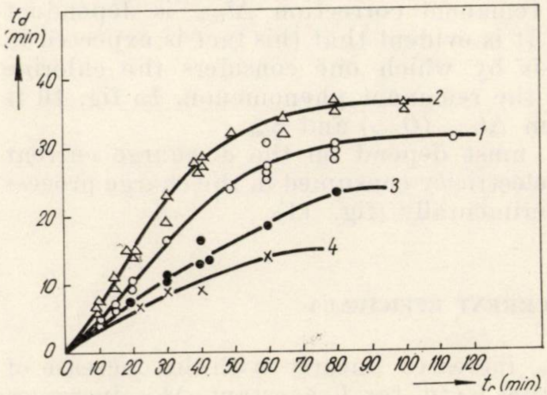

Fig. 13. — Dependence between t_d and t_c; *1*, 400°; *2* 500°; *3*, 600°; *4*, 700°.

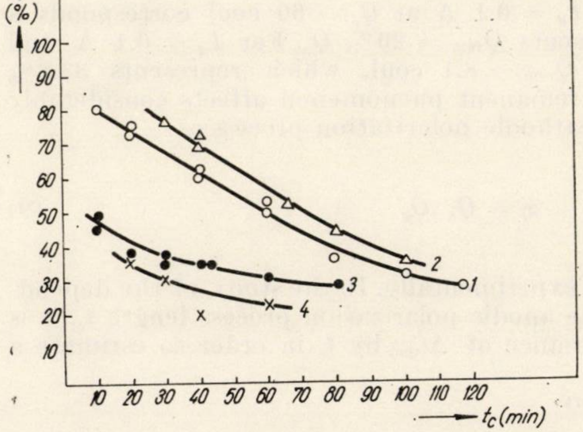

Fig. 14. — Dependence between efficiency η and t_c; *1*, 400°; *2*, 500°; *3*, 600°; *4*, 700°.

corrected efficiency :

$$\eta_{\text{cor}} = \frac{Q_d + Q_{\text{rem}}}{Q_c} = \frac{(t_d + \Delta t_{\text{rem}})\, I_d}{t_c\, I_c} \tag{10}$$

In fig. 12 is plotted Δt_{rem} as a function of t_c. We observe that Δt_{rem} increases up to the value of $t_c = 60$ minutes, and then it tends to a plateau. This can be explained by the fact that the adsorbed chlorine quantity tends to a plateau at the same time with the increase of t_c (fig. 13). Consequently, it is to be expected that Q_{rem} should not increase above a maximum value as well, whichever the t_c charge time would be. The remanent correction decreases with the increase of the temperature. At 700° it becomes practically negligible (approximately equal to one minute)

The efficiency :

$$\eta = Q_d/Q_c = t_d/t_c \tag{11}$$

was computed using the experimental data.

In fig. 14 it is plotted the efficiency as a function of charge length for different temperatures (400°, 500°, 600°, 700°). We can see that the efficiency increases from 400° to 500° and over 500° decreases very quickly. The decrease of efficiency with the increase of charge length can be explained by the increase of thermal desorption losses while the electrode potential tends to a plateau (on the plateau the thermal desorption loss in the anodic polarization process becomes equal even with the charge current).

For the same temperatures we have computed the remanent correction, using the above method and we have estimated the corrected efficiency by relation (10) ($I_c = I_d = 0.1$ A)

$$\eta_{\text{cor}} = \frac{t_d + \Delta t_{\text{rem}}}{t_c} \tag{12}$$

In order to emphasize the influence of the remanent phenomenon on the efficiency, the dependence of efficiency η and of the corrected efficiency is represented as function of the charge length at the temperature 400° (fig. 14). We observe that the influence of the remanent phenomenon is more obvious at small charge times.

In fig. 16 it is plotted the corrected efficiency (computed by relation (12)) as function of temperature for different charge lengths. For a certain charge time, a maximum of the corrected efficiency for a temperature of about 500° appears. The appearance of the above mentioned maximum can be explained by the existence of two factors with contrary influences due to the increase of the temperature. On the one hand, the increase of temperature produces the decrease of the viscosity which favoures the penetration of the salt deeper into the pores wetting in this way a larger active surface. This would correspond to an increase of the adsorbed chlorine quantity. On the other hand, the increase of the temperature favoures the increase of the thermal desorption losses, at the charge and discharge processes as well, which explains the tendency of a quick decrease of the efficiency over a certain value of the temperature.

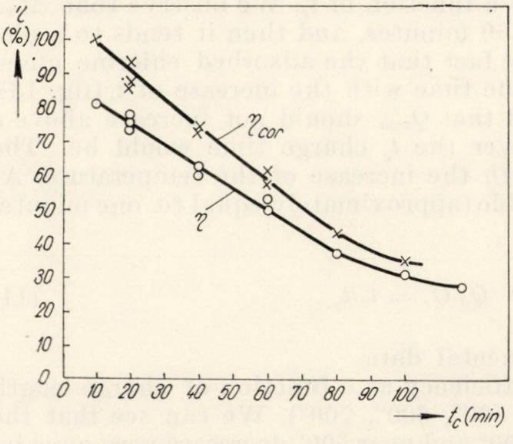

Fig. 15. — Efficiency η and corrected efficiency η_{cor} as a function of t_c ; $T = 400°$.

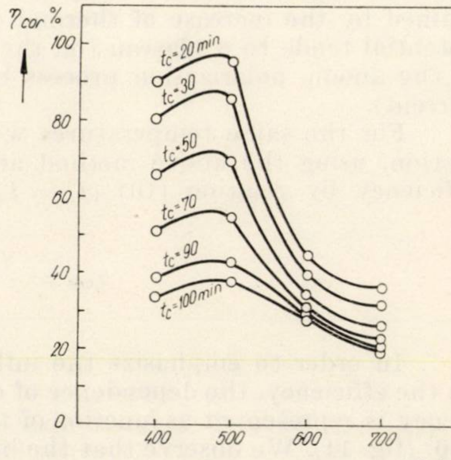

Fig. 16. — The corrected efficiency as function of the temperature for different charge lengths.

We can observe that the maximum corrected efficiency decreases and the efficiency curve tends to a flat curve while the charge time increases. The decrease of the maximum can be explained by the increase of the charge losses with the increase of the charge time. The thermal desorption losses in the anodic polarization process became at the plateau equal to the charge current intensity.

Revue Roumaine de Chimie, **19**, *1*, 37–44 (1974)

ON α-DIOXIMINE COMPLEXES OF THE TRANSITION METALS. XXXVIII*

THE $[Co(DH)_2(NO_2)(CN)]^-$ ION AND ITS BASIC HYDROLYSIS KINETICS

RALUCA RIPAN, Z. FINTA and CS. VÁRHELYI

Faculty of Chemistry, Chair of Inorganic Chemistry,
"Babeş-Bolyai" University, str. Arany János 11, Cluj, Romania

Received March 7, 1973

The $[Co(DH)_2(NO_2)(CN)]^-$ complex (where DH_2 stands for dimethylglyoxime : $C_4H_8N_2O_2$) has been obtained from the non-electrolyte $[Co(DH)_2(NO_2)(H_2O)]$ by a substitution reaction with KCN. From the aqueous solution of the resulting $K[Co(DH)_2(NO_2)(CN)]$ the complex acid and 8 new salts were separated by means of double decomposition reactions. On the basis of i.r. spectrum some structural problems are discussed. The basic hydrolysis of the $[Co(DH)_2(NO_2)(CN)]^-$ anion was colorimetrically studied and the calculated kinetic parameters were compared with those of other $[Co(DH)_2XY]^-$–type complexes.

The first dimethylglyoximin-nitro-cobalt (III)-chelate: $Na[Co(DH)_2(NO_2)_2].H_2O$ has been prepared by Chugaev [1] by a substitution reaction from $Na_3[Co(NO_2)_6]$ with dimethylglyoxime. The synthesis and characterization of some new derivatives of the $H[Co(DH)_2(NO_2)_2]$ acid were reported in our previous papers.[2–4]

The sodium salt undergoes an aquation process in acidic solutions. The aquation product, the aquo-nitro-non-electrolyte $[Co(DH)_2(NO_2)(H_2O)]$, can be used for a series of anatation reactions. The coordinated water molecule can be replaced by monovalent anions, as Cl^-, Br^-, I^-, NCS^-, N_3^-, NCO^-, $NCSe^-$ and even by SO_3^{2-} and $S_2O_3^{2-}$. Several mixed bis-dimethylglyoximine-nitro-cobalt (III) complex acids obtained in this way: $H[Co(DH)_2Cl(NO_2)]$, $H[Co(DH)_2Br(NO_2)]$ and $H[Co(DH)_2I(NO_2)]$ were described by Ablov and co-workers.[5–6]

---

* Part XXXVII. I. Gănescu, Cs. Várhelyi and A. Man, *Monatsh.* (in press).

[1] A. Chugaev, *Ber. dtsch. chem. Ges.*, **41**, 2226 (1908).

[2] R. Ripan, Cs. Várhelyi and B. Böhm, *Studii şi Cercetări Chim. Fil. Cluj*, **13** (1), 19 (1962).

[3] R. Ripan, Cs. Várhelyi and E. Kékedy, *Stud. Univ. Babeş-Bolyai, Chem.*, **5**, (2), 89 (1962).

[4] R. Ripan, Cs. Várhelyi and B. Böhm, *Stud. Univ. Babeş-Bolyai, Chem.*, **5** (1), 77 (1962).

[5] A. V. Ablov, *Doklady Akad. Nauk S.S.S.R.*, **97**, 1019 (1954).

[6] A. V. Ablov, N. M. Samus and M. S. Popov, *Doklady Akad. Nauk. S.S.S.R.*, **106**, 665 (1956).

Mixed cyano-complexes of this type have not been yet reported. Other mixed cyano-complexes of the trivalent cobalt, as $H_2[Co(CN)_5(H_2O)]$,[7] $H[Co(CN)_4(H_2O)_2]$ [8] and the halogeno-pentacyano-acids : $H_2[Co(CN)_5X]$ ($X = Cl, Br, I$) [9] are well known and the exchange of the coordinated halogens was kinetically studied.[10,11]

We observed that the anatation reaction of $[Co(DH)_2(H_2O)(NO_2)]$ with stoichiometric amount of KCN leads to the formation of the easily soluble $K[Co(DH)_2(CN)(NO_2)]$. From the aqueous solution of this potassium salt, some new derivatives have been obtained with the hydrochlorides of some heterocyclic amines and complex cations of the diacido-tetramine type. The best precipitating agents for the above cyano-nitro-complex are the $[Co(DH)_2(amine)_2]^+$ type cations, as well as for the other monobasic complex acids of the $H[Co(DH)_2X_2]$ type.

The hexamine- and monoacido-pentamine cobalt(III)- and chromium(III)-complexes are unsuitable for this precipitation reaction. Some derivatives of the $H[Co(DH)_2(CN)(NO_2)]$ acid are characterized in table 1.

Table 1

New derivatives of the complex acid $H[Co(DH)_2(CN)(NO_2)]$

Formula	Yield (%)	Aspect	Analysis		
				Calcd.	*Found*
$Ag[Co(DH)_2(CN)(NO_2)]$ ($AgC_9H_{14}N_6O_6Co$)	75	Yellow micro-crystals	Co Ag	12.56 23.00	12.40 22.65
$Tl[Co(DH)_2(CN)(NO_2)]$ ($TlC_9H_{14}N_6O_6Co$)	60	Yellow micro-crystals	Co Tl	10.42 36.14	10.20 35.80
trans-$[Co(en)_2Cl_2]$. $[Co(DH)_2(CN)(NO_2)].2H_2O$ ($Co_2Cl_2C_{13}H_{34}N_{10}O_8$)	50	Green-yellow needles	Co H_2O	18.22 5.56	18.19 5.80
trans-$[Co(en)_2Br_2]$. $[Co(DH)_2(CN)(NO_2)]$ ($Co_2Br_2C_{13}H_{30}N_{10}O_6$)	55	light green-yellow prisms	Co	16.84	16.56
$(Co(DH)_2(NH_3)_2]$. $[Co(DH)_2(CN)(NO_2)]$ $[Co_2C_{17}H_{34}N_{12}O_{10})$	50	Yellow prisms	Co N	17.23 24.56	17.10 24.30
$[Co(DH)_2(aniline)_2]$. $[Co(DH)_2(CN)(NO_2)]$ ($Co_2C_{29}H_{42}N_{12}O_{10}$)	60	Brown rhombic plates	Co N	14.09 20.10	13.90 19.80
$[Co(DH)_2(p\text{-toluidine})_2]$. $[Co(DH)_2(CN)(NO_2)]$ ($Co_2C_{31}H_{46}N_{12}O_{10}$)	70	Dark brown prisms	Co N	13.63 19.44	13.40 19.18
$[Co(DH)_2(p\text{-fenetidine})_2]$. $[Co(DH)_2(CN)(NO_2)]$ ($Co_2C_{33}H_{50}N_{12}O_{12}$)		Brown dendrites	Co	12.74	12.60

---

[7] O. Ray and N. K. Dutt, *Z. anorg. Chem.*, **234**, 65 (1937.)

[8] P. R. Ray and T. Guptachaudkuri, *Z. anorg. Chem.*, **220**, 154 (1934).

[9] A. W. Adamson, *J. Amer. Chem. Soc.*, **78**, 4260 (1956).

[10] T. Banerjea and T. P. Das Gupta, *J. Inorg. Nuclear Chem.*, **29**, 1021 (1967).

[11] R. Grassi, A. Haim and W. K. Wilmarth, *Inorg. Chem.*, **6**, 237 (1967).

The i.r. spectrum of $K[Co(DH)_2(CN)(NO_2)]$, presented in fig. 1, shows the presence of strong intramolecular O—H..O hydrogen bridges, similar to those observed in the case of the analogous dimethylglyoxime derivatives:[12] (ν_{O-H} : 2400 cm^{-1}(w) and δ_{O-H} 1720—1750 cm^{-1} (m).

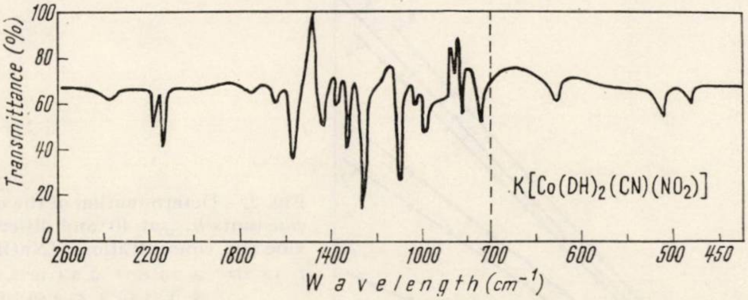

Fig. 1. — I. R. spectrum of $K[Co(DH)_2(CN)(NO_2)]$.

Valence vibrations of nitro group : ν_{as} and $\nu_s (NO_2)$ and the deformation vibrations δ_{O-N-O}, ρ_w (NO_2) appear at 1433 (v.s.), 1338 (s), 830 (s), 625 (m), cm^{-1}, respectively, as in the case of other nitro-cobalt (III)-complexes: $Na_3[Co(NO_2)_6]$,[13] $K[Co(DH)_2(NO_2)_2]$, not influenced by the coordination effect.

The strong absorption bands at 2182 and 2150 cm^{-1} are due to the valence vibrations of the coordinated cyano-group. The considerable shift of these vibrations as compared to those of the KCN (2080 cm^{-1}) can be explained by means of the resonance theory and pleads for the existence of Co—C bond.[14,15]

In aqueous solution of the cyano-nitro-complex a ligand exchange reaction occurs leading to the liberation of NO_2^-.

This process is similar to those observed in the case of other corresponding dimethylglyoxime- and alycyclic 1,2-dioxime derivatives, previously investigated.[16-18]

Aquation kinetics of the $[Co(DH)_2(CN)(NO_2)]^-$ ion in basic solutions was experimentally studied. Kinetic measurements were carried out at different temperatures in the presence of different amounts of NaOH at a constant ionic strength of $\mu = 1$ M maintained with $NaNO_3$. The concentration of the liberated NO_2^- ions was followed by colorimetric measurements.

---

[12] A. Nakahara, *Bull. Chem. Soc. Japan*, **28**, 473 (1955).

[13] K. Nakamoto, J. Fujita and H. Murata, *J. Amer. Chem. Soc.*, **80**, 4817 (1958).

[14] W. P. Griffith and G. Wilkinson, *J. Chem. Soc.*, **1959**, 2757.

[15] W. P. Griffith and G. Wilkinson, *J. Inorg. Nuclear Chem.*, **7**, 297 (1958).

[16] J. Zsakó, Z. Finta and Cs. Várhelyi, *Proceedings of the 3-rd Symposium on Coordination Chemistry* (Debrecen, Hungary), 1970, p. 333.

[17] J. Zsakó, Z. Finta and Cs. Várhelyi, *J. Inorg. Nuclear Chem.*, **34**, 2887 (1972).

[18] J. Zsakó, Cs. Várhelyi, Z. Finta and J. Kiss-Jakab, *Z. phys. Chem.* (*Leipzig*), (in press).

The graphical plot of log C_0/C *versus* time showed a good linearity up to 50–60% of the reaction, as seen in fig. 2. From the slopes of these straight lines, first order rate constants were derived. These overall rate constants k_{exp} are given in table 2.

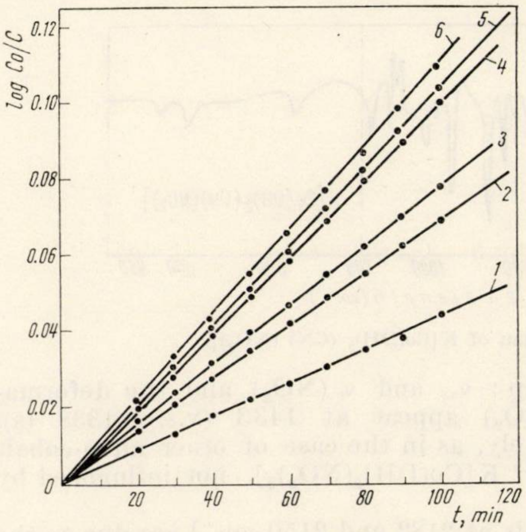

Fig. 2.—Determination of the overall rate constants k_{exp} at 40° and different hydroxide ion concentrations [NaOH] mole/l : *1*, $1.8 \cdot 10^{-3}$, *2*, $3.6 \cdot 10^{-3}$, *3*, $5.4 \cdot 10^{-3}$, *4*, $9.0 \cdot 10^{-3}$, *5*, $1.35 \cdot 10^{-2}$, *6*, $1.80 \cdot 10^{-2}$

At a given temperature, the overall rate constant k_{exp} increases with increasing hydroxide ion concentration and at higher basicities approaches a limiting value.

Table 2

Overall first order aquation rate constants for $[Co(DH)_2(CN)(NO_2)]^-$ at various hydroxide ion concentrations

$[NaOH] \cdot 10^3$ mole/l	$k_{exp} \cdot 10^5$, s^{-1}			
	29°	35°	40°	45°
1.8	—	0.94	1.67	—
3.6	0.83	1.35	2.65	
5.4	0.99	1.61	3.00	
7.2	1.04	1.81	—	5.60
9.0	1.12	1.90	3.84	6.45
13.5	1.19	2.13	3.95	7.14
18.0	1.25	—	4.20	7.41

The experimental data given in table 2 suggest the existence of a pre-equilibrium and the parallel aquation of two complex species with differing rates. In our experimental conditions there is an equilibrium between the species $[Co(DH)_2(CN)(NO_2)]^-$ and $[Co(DH)(D)(NO_2)(CN)]^{2-}$, i.e. a deprotonation of a coordinated dimethylglyoxime molecule occurs :

$$[Co\ (DH)_2\ (CN)\ (NO_2)]^- \overset{K}{\rightleftharpoons} [Co(DH)(D)(CN)(NO_2)]^{2-} + H^+ \qquad (1)$$

where K stands for the acidity constant of the $[Co(DH)_2(CN)(NO_2)]^-$ complex.

In this case the following aquation processes may take place:

$$[Co(DH)_2(CN)(NO_2)]^- + H_2O \xrightarrow{k_A} [Co(DH)_2(CN)(H_2O)] + NO_2^- \qquad (2)$$

$$[Co(DH)(D)(CN)(NO_2)]^{2-} + H_2O \xrightarrow{k_B} [Co(DH)(D)(CN)(H_2O)]^- + NO_2^- \qquad (3)$$

(k_A and k_B stand for the rate constants of the reactions (2) and (3)).

In each of these reactions, the aquation leads to the formation of an aquo-complex, but in alkaline solutions they must undergo a fast deprotonation and the final products are $[Co(DH)_2(CN)(OH)]^-$ and $[Co(DH)(D)(CN)(OH)]^{2-}$, respectively.

This scheme is to some extent similar to the S_N1 CB or S_N2 CB mechanisms proposed by Garrick[19] and extended by Basolo and Pearson.[20] It has also been suggested and discussed in our previous paper[18] in order to explain the kinetic behaviour of other nitro-complexes.

The following simple relation can be derived for the overall rate constant k_{exp} as a function of rate constants for the two species and the acidity constant of the conjugated acid:

$$k_{exp} = (k_B - k_A)\frac{[OH^-]}{K_w/K + [OH^-]} + k_A \qquad (4)$$

where K_w stands for the ionic product of water.

Since $k_A \ll k_B$, and at higher $[OH^-]$ values the equilibrium is shifted to the conjugated base, the aquation of the conjugated acid can be neglected ($k_A = 0$) and equation (4) may be written in the following form:

$$\frac{1}{k_{exp}} = \frac{K_w}{K\,k_B}\cdot\frac{1}{OH^-} + \frac{1}{k_B} \qquad (5)$$

Using the equation (5), K and k_B can be determined by a graphical method. If the above scheme is correct and the contribution of reaction (2) is very small, the plot of $\frac{1}{k_{exp}}$ *versus* $1/[OH^-]$ must give a straight line. The ordonate intercepts of these straight lines give $1/k_B$ and their slopes equal $K_w/K.\,k_B$, which allows us to derive both K and k_B from the experimental data (See fig. 3).

---

[19] F. J. GARRICK, *Nature*, **139**, 507 (1937).

[20] F. BASOLO and R. G. PEARSON, "Mechanism of Inorganic Reactions", 2nd ed., John Wiley, New York, 1967, p. 183.

These K and k_B values, derived from the data presented in table 2, are given in table 3.

The plot of log K *versus* $1/T$ showed a rather good linearity and allowed to derive enthalpy and entropy values for the reaction (1). By means of the least square method the following values have been obtained : $\Delta H^{\ddagger} = 4.8 \pm 0.8$ kcal/mole, $\Delta S^{\ddagger} = 35.8 \pm 2.5$ Cl.

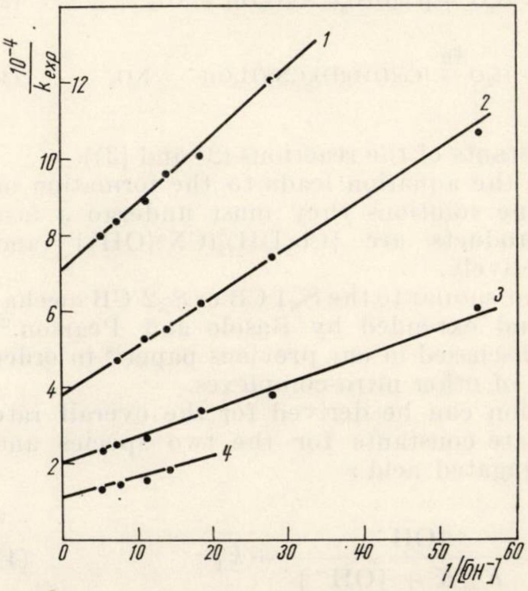

Fig. 3. — Determination of K and k_B values at different temperatures : *1*, 29° ; *2*, 35°, *3*, 40°, *4*, 45°.

Table 3

Equilibrium constants of reaction (1) and rate constants of reaction (3)

t°C	$K \times 10^{12}$	$k_B \times 10^5$, s^{-1}
29	5.52	1.42
35	6.37	2.62
40	7.76	5.21
45	8.04	9.71

By using the linear relationship between log k_B/T and $1/T$, the activation enthalpy and entropy values have been calculated for the aquation reaction of the conjugated base.

The following values have been obtained by means of the least square method :

$$\Delta H^{\ddagger} = 22.5 \pm 0.4 \text{ kcal/mole}, \quad \Delta S^{\ddagger} = -6.5 \pm 1.2 \text{ Cl}$$

In order to compare these results with those obtained for other similar nitro-complexes, the rate constants, acidity constants and kinetic parameters for the different studied species are presented in table 4.

The equilibrium constants K show $[Co(DH)_2(OH)(NO_2)]^-$ to be a weaker acid than $[Co(DH)_2(NO_2)_2]^-$ and $[Co(DH)_2(CN)(NO_2)]^-$, in agreement with the large *trans*-effect of both NO_2 and CN groups as compared to that of OH, owing to the larger electron withdrawing ability of the formers.

Table 4

Equilibrium data and kinetic parameters for the basic hydrolysis of some nitro-dimethylglyoximino-cobalt(III) complexes

Species	$K \times 10^{12}$	$k \times 10^4$, s^{-1}	$\Delta H^{\neq}$ kcal/mole	$\Delta S^{\neq}$, Cl	Reference
	at 40°C				
$[Co(DH)(D)(CN)(NO_2)]^{2-}$	7.76	0.52	22.5	−6.5	this paper
$[Co(DH)(D)(NO_2)(NO_2)]^{2-}$	7.29	2.25	22.1	−4.7	18
$[Co(DH)(D)(OH)(NO_2)]^{2-}$	1.47	1.83	27.6	12.4	18

Assuming a dissociation mechanism, the activation enthalpy values are rather easily interpreted. Each of the complex species presented in table 4 has the same electric charge, and their structure differs only by the nature of the *trans*-situated ligand.
In the case of both $[Co(DH)(D)(NO_2)_2]^{2-}$ and $[Co(DH)(D)(CN)(NO_2)]^{2-}$ a considerable decrease of the activation enthalpy occurs, as compared to the $[Co(DH)(D)(OH)(NO_2)]^{2-}$ -ion. This decrease can be explained in terms of the π-acceptor property of the NO_2 and CN groups. The formation of π-bonds between these groups and the central Co atom considerably reduces the strength of the σ-bond between the central atom and the leaving NO_2-group.

It can be observed from table 4 that aquation reactions with the lowest activation enthalpies have negative activation entropy values, whereas the activation entropy of the reaction with the highest activation enthalpy is clearly positive. This quite parallel increase of both $\Delta H^{\neq}$ and $\Delta S^{\neq}$ is an example for the kinetic compensation effect and presumably it indicates the mechanism of all these reactions to be the same, *viz.* the dissociation of the ligand to be replaced is followed by the coordination of a water molecule to the active intermediate with coordination number 5.

EXPERIMENTAL

PREPARATION OF $K[Co(DH)_2(CN)(NO_2)]\ 1/2\ H_2O$

50 mmole of $[Co(DH)_2(H_2O)(NO_2)]$ and 50 mmole of KCN in 50–60 ml water are shaken for 5–10 minutes. The brown-red crystals of the $[Co(DH)_2(H_2O)(NO_2)]$ disappear and sparkling light brown thin plates are separated from the solution.

The very easily soluble crystalline precipitate is filtered and dried on porous porcelain plate without washing.

Analysis. *Calcd.* : Co 14.40, H_2O 2.20, N 20.53
Found : Co 14.60, H_2O 2.30, N 20.40

SYNTHESIS OF $M[Co(DH)_2(CN)(NO_2)]$ AND $[M^{III}(AMINE)_4X_2]$ $[Co(DH)_2(CN)(NO_2)]$

5 mmole of MNO_3 and of the corresponding diacido-tetramine salt in 50—100 ml water are treated with 5 mmole of $K[Co(DH)_2(CN)(NO_2)]$ in 50 ml water. The crystalline precipitate is filtered after 1—2 hr, washed with a small amount of water and dried in air.

SYNTHESIS OF $[Co(DH)_2(AMINE)_2]$ $[Co(DH)_2(CN)(NO_2)]$ TYPE BINARY SALTS

To a solution of 5mmole of $Co(DH)_2$ (amine)$_2$-acetate in 60—80 ml alcohol 60—70%, a solution of 5 mmole of $K[Co(DH)_2(CN)(NO_2)]$ in 40—50 ml water is added. The characteristic crystalline precipitate is filtered after 1/2—2hr, washed with water and air dried.

Analysis. Cobalt was determined complexometrically, by using murexide as indicator in sodium acetate and dil. ammonia solution. Organic ligands were destroyed by heating with conc. sulfuric acid and several crystals of KNO_3. Nitrogen was determined by the Dumas method.

KINETIC MEASUREMENTS

Samples were dissolved in a pre-heated solution of NaOH and $NaNO_3$, containing the required amount to ensure a constant ionic strength of $\mu = 1$ M and the desired basicity, and they were kept in an ultrathermostat at working temperature maintained with an accuracy of ± 0.01°. From time to time, samples of 2 ml were taken out and added to an ice-cooled solution containing 2 ml 10^{-2} M sulphanilic acid, 2 ml of 2×10^{-2} M α-naphtylamine in 0.5% acetic acid and perchloric acid solution necessary for the neutralization of NaOH and for acidifying the solution. The mixture was kept at 0° for 5 min to allow completion of the diazotization reaction and it was diluted with 5×10^{-2} M borax solution up to 50 ml. After 2 min the absorbance of the solution was measured at 420 nm. For the determination of the NO_2^- concentrations a calibration curve has been used.

Revue Roumaine de Chimie, **19**, *1*, 45–48 (1974)

ADDITION COMPOUNDS OF ZIRCONYL CHLORIDE WITH AROMATIC SCHIFF BASES

N. S. BIRADAR, A. L. LOCKER and V. H. KULKARNI,
Department of Chemistry, Karnatak University, Dharwar-3, India

Received December 18, 1971

A few complexes of zirconyl chloride have been prepared with the Schiff bases derived from salicylaldehyde and aromatic monoamines, in acetone medium. These are yellow, amorphous substances, insoluble in common organic solvents. The elemental analysis shows that these are 1 : 2 adducts. It is shown with the aid of infrared spectra that these complexes contain Zr = O type bonds in them.

INTRODUCTION

The Schiff bases have been widely used as promising reagents for the transition metals.[1,2] During the past few years, though much information has been added to the growth of the chemical literature on zirconium (IV), [3–11] only little information has been published on zirconyl chloride Schiff base complexes.[12–14]

---

[1] R. H. Holm, G. W. Everette Jr. and A. Chakravarthy, *Progress in Inorganic Chemistry*, **7**, 83 (1966).

[2] a. L. Sacconi, *Coord. Chem., Rev.*, **1**, 192 (1966);
b. S. Yamada, E. Ohno, Y. Kuge, A. Takeuchi and K. Yamanouchi; *Coord. Chem. Rev.*, **3**, 247 (1968).
c. B. O. West, *New Pathways Inorg. Chem.*, **1968**, 303. *Chem. Abstr.*, **70**, 120604s (1969).

[3] G. Bhar and A. Thamiltz, *Z. Anorg. Chem*, **282**, 3 (1955).

[4] A. S. Kudryavestev and I. A. Savich, *Zhur. Vsesoyuz. Khim. Obshch.* im *D. I. Mendeleeva*, **7**, 591 (1962); *Chem. Abstr.*, **58**, 2121b (1963).

[5] I. A. Savich, A. K. Pikaev, I. A. Lebedev and V. I. Spytsyn, *Vistnik, Moskov, Univ II Ser. Mat. Mekh. Astron., Fiz. Chim.* **1**, 225 (1956); *Chem. Abstr.*, **53**, 1334f (1959).

[6] A. S. Kudryavestev and I. A. Savich, *Zhur, Obshchei Khim.*, **33**, 3763 (1963); *Chem. Abstr.*, **60**, 8873a (1960).

[7] D. C. Bradley, M. B. Hursthouse and I. F. Rendall, *J. Chem. Soc.* (D), **1970**, 368.

[8] L. V. Orlova, A. D. Garnovskii, O. A. Osipov, I. I. Kukushkina, *Zhur. Obshchei Khim.*, **38**, 1850 (1968), *Chem. Abstr.*, **69**, 1130559 (1969).

[9] P. Prashar, and J. P. Tandon, *J. Less-Common Metals*, **15**, 219 (1958), *Chem. Abstr.*, **69**, 7941r (1968).

[10] S. N. Poddar and D. K. Biswas, *Science and Culture* (*Calcutta*), **34**, 117 (1968).

[11] T. N. Malskvich, E. P. Trailina, and I. A. Savich, *Vistnik Moskov Univ. Khim.*, **23**, 106 (1968); *Chem. Abstr.*, **69**, 113017d (1968).

[12] A. S. Kudryavetsev and I. A. Savich, *Vestnik Moskov Univ. Ser II, Khim.*, **18**, 32 (1963);

[13] C. G. Macarovici, E. Perte and E. Motiu, *Rev. Roumaine Chim.*, **11**, 53 (1966).

[14] N. S. Biradar and V. H. Kulkarni, *J. Karn. Univ.*, (*Science*), **15**, 10 (1970).

In these recent years, a number of papers has discussed ν(M = O) vibrations in a variety of complexes.[15-17] Kharitonov *et al.*,[18] Paul *et al.*,[19] and Patel and co-workers [20] have assigned Zr = O band in spectra of zirconyl complexes, yet the information about Zr = O bond in the zirconyl chloride Schiff base complexes is lacking.

These observations tempted us to undertake a systematic investigation on zirconyl chloride Schiff base complexes.

In this communication we intend to report the preparation and spectral study of a few zirconyl chloride addends with Schiff bases.

EXPERIMENTAL

MATERIALS AND METHOD

Zirconyl chloride of Riedel grade was made anhydrous according to the standard method.[21] Salicylaldehyde, aniline, *p*-toluidine, *p*-chloroaniline and *p*-anisidine used for preparing the Schiff bases were of reagent grade.

Solvent acetone of commercial grade was purified by repeated distillation and finally made anhydrous according to the known method.[22]

The Schiff bases were prepared by refluxing equimolar proportions of salicylaldehyde and aromatic amines in alcohol medium for about an hour. The solids separated on cooling were filtered and recrystallized from alcohol. All the Schiff bases were dried in vacuum over fused calcium chloride before use.

PREPARATION OF THE COMPLEXES

Zirconyl chloride in acetone was treated with a slight excess of Schiff base in the same solvent, and refluxed for about an hour. The solid separated was filtered and washed free from the reagent with the same solvent and dried in vacuum over anhydrous calcium chloride.

ANALYSIS

Zirconium in the complexes was determined gravimetrically as ZrO_2. Chloride was estimated gravimetrically as AgCl and nitrogen by the Kjeldalh method. The results of elemental analyses are shown in table 1.

---

[15] B. C. Barraclough, J. Lewis and R. S. Nyholm, *J. Chem. Soc.*, **1954**, 3552.

[16] J. Selbin, *Chem. Rev.*, **65**, 153 (1965).

[17] S. K. Madan, and A. M. Donhue, *J. Inorg. Nuclear Chem.*, **28**, 1303 (1966).

[18] Yu. Ya. Kharitonov, L. I. Yuranova, V. E. Plyushchev, and V. G. Pervykh, *Russian J. Inorg. Chem.*, **10**, 399 (1965).

[19] R. C. Paul, A. K. Moudgil, S. L. Chandra and S. K. Vasisht, *Indian J. Chem.*, **8**, 1017 (1970).

[20] V. Krishnan and C. C. Patel, *J. Inorg. Nuclear Chem.*, **26**, 2201 (1964).

[21] T. Moeller, "Inorganic Syntheses", Vol. V, McGraw Hill Book Co., INC., New York, 1957, p. 154.

[22] A. I. Vogel, "Practical Organic Chemistry", E.L.B.S. Edn., 1968.

Table 1

Analytical data on zirconyl chloride complexes. The values in parentheses are the calculated values

Ligand	Empirical formula	% Zr	% N	% Cl
Salicylidene-aniline	$(C_{13}H_{11}NO)_2ZrOCl_2$	15.84 (15.94)	4.66 (4.89)	12.19 (12.41)
Salicylidene-*p*-toluidine	$(C_{14}H_{13}NO)_2ZrOCl_2$	15.08 (15.20)	4.96 (4.66)	12.13 (11.83)
Salicylidene-*p*-chloroaniline	$(C_{13}H_{10}NOCl)_2ZrOCl_2$	14.28 (14.22)	4.30) (4.37)	11.08 (11.08)
Salicylidene-*p*-anisidine	$(C_{14}H_{13}NO_2)_2ZrOCl_2$	14.55 (14.43)	4.00 (4.43)	11.10 (11.23)

PHYSICAL MEASUREMENTS

The infrared spectra of complexes and the ligands in nujol mull were recorded on a Perkin—Elmer Infracord Spectrometer.

RESULTS AND DISCUSSION

It is evident from the results set out in table 1 that the Schiff bases under present investigation form 1 : 2 adducts with zirconyl chloride. All these are yellow, amorphous substances and insoluble in almost all common organic solvents. The insolubility of the compounds in DMF has made it difficult to determine the molar-conductance.

The important infrared frequencies along with their assignments are given in table 2.

Table 2

Infrared frequencies (in cm^{-1}) of zirconyl chloride complexes and their assignments

$(C_{13}H_{11}NO)_2ZrOCl_2$	$(C_{14}H_{13}NO)_2ZrOCl_2$	$(C_{13}H_{10}NOCl)_2$ $ZrOCl_2$	$(C_{14}H_{13}NO_2)_2$ $ZrOCl_2$	Assignments
2941	2941	2941	2941	CH stretch
1645	1639	1639	1639	C=N stretch
1587 1550 1471	1600 1538 1471	1613 1550 1471	1600 1538 1471	C=C stretch
1282	1282	1290	1282	Phenolic C-O stretch
917	917	917	909	Zr=O stretch

The three strong intensity bands in the region 1600—1471 cm^{-1} are due to the aromatic C=C stretching vibrations.

An intense band around 1613 cm^{-1}, assigned to the C=N stretch of the free Schiff base, [23] is observed in the region 1645—1639 cm^{-1} in the complexes. The shift of the order of about 32—25 cm^{-1} towards the higher frequency suggests the possible coordination of the Schiff base through the azomethine nitrogen. These observations agree with our previous observations.[24–27]

---

[23] N. S. Biradar and V. H. Kulkarni, *J. Inorg. Nuclear Chem.*, **33**, 2451 (1971).

The broad weak band with fine structure in the region 2800—2600 cm^{-1}, due to the intramolecular hydrogen bonded —OH, and the intense band around 1280 cm^{-1}, due to the phenolic C—O stretch of the free base, [28,29] are retained in the complexes indicating that the *ortho*-hydroxy group of the base has not taken part in the complex formation.

It has been established that when a compound contains $M = O$, the infrared spectrum has a narrow band in the region 1100—800 cm^{-1} belonging to the $M = O$ stretch, whereas the broad intense band in the corresponding region shows the presence of a polymeric M—O—M chain.[18] Paul and co-workers[19] have assigned a strong band at 870 cm^{-1} to the $Zr = O$ stretch in the case of $ZrOCl_2$. They have not found this band in the complexes but they have found the bands in the regions 1000—900 cm^{-1} and 720—680 cm^{-1}. These bands have been attributed to the $Zr{\equiv}O^+$ and $Zr{=}O^-$ species in the complexes. Patel and co-workers [20,30] have assigned a narrow intense band around 980 cm^{-1} to the $Zr = O$ stretch. In view of all these observations, we have assigned a narrow intense band around 917 cm^{-1} to the $Zr{=}O$ stretch. The absence of the 720—680 cm^{-1} band in the spectra of the complexes precludes the possibility of complex being ionic in nature.

Taking into consideration all the above discussion we think that zirconium has a coordination number five in these complexes.

Acknowledgement. Research fellowship by the U.G.C. to one of us (Miss A.L.L.) is gratefully acknowledged. Authors wish to thank the Karnatak University for the facilities given to carry out this investigation.

---

[24] N. S. Biradar and V. H. Kulkarni and N. N. Sirmokadam, *Monatsh*, **101**, 551 (1970).

[25] N. S. Biradar, V. H. Kulkarni and N. N. Sirmokadam, *Indian J. Chem.*, **8**, 838 (1970).

[26] V. A. Kogan, O. A. Osipov, V. I. Minkin and V. P. Sokolov, *Zhur. Neorg. Khim*, **10**, 83 (1965); *Chem. Abstr.*, **62**, 7362a (1965).

[27] A. D. Garnovskii, V. I. Minkin, O. A. Osipov, V. T. Pyanushkin, L. I. Isaeva and M. I. Knyazhanskii, *Zhur. Neorg. Khim.*, **12**, 2443 (1967); *Chim. Abstr.*, **68**, 8894u (1968).

[28] N. S. Biradar and V. H. Kulkarni, *Rev. Roumaine Chim.*, **15**, 1993 (1970).

[29] J. E. Kovacic, *Spectrochem. Acta.*, **23** A, 183(1967).

[30] V. V. Savant and C. C. Patel, *J. Inorg. Nuclear Chem.*, **31**, 2319 (1969).

Revue Roumaine de Chimie, **19**, *1*, 49–55 (1974)

CONTRIBUTION TO THE STUDY OF THE BINARY SYSTEM $In_2O_3-TiO_2$

CONST. GH. MACAROVICI, EUGENIA PERŢE, M. STRĂJESCU and MARIA BIROU

Institute of Chemistry, Cluj, Str. Donath 65–103, Romania

Received April 21, 1973

The binary system $In_2O_3-TiO_2$ is studied by thermogravimetric, thermodifferential and roentgenographic methods. Some of the results obtained disagree with those found in the literature and the differences are tentatively explained.

The data on the interaction of In_2O_3 with TiO_2 to be found in literature are contradictory. Roth[1] shows that heating up to 1500° the mixture of indium and titanium oxides, the expected In_2TiO_5 combination is not formed because part of the indium is volatilized and does not participate in the reaction. Other authors, [2] studying the characteristic features of binary oxide type compounds with a pyrochloric structure, examine the $In_2Ti_2O_7$ compound, and in another paper [3] it is pointed out that indium titanate of the In_2TiO_5 form is obtained as a result of an interaction between the respective oxides, but the conditions of the synthesis are not given. Rozdin *et al.* [3] explain the character of the $In_2O_3-TiO_2$ system by carrying out a thermal and a roentgenographic study. All derivatograms are identical, indifferently to the molar ratio between the components and, queerely, the thermal effects corresponding to the formation of indium titanate, In_2TiO_5, are not recorded, though the authors deduce the existence of the latter by means of the X ray diffraction spectra. To conclude, they hold that no $In_2Ti_2O_7$ type compound, but only a In_2TiO_5 formula combination, is formed. The paper gives the derivatogram of the compound with a 66,7% TiO_2 mole content and the roentgenogram with a 50% TiO_2 mole content.

As the system is of some interest and wishing to find out whether an indium titanate appears in any working conditions without the process being thermally recorded, we have carried out a systematic study, by means of the same method of thermal analysis and roentgen diffraction spectra.

---

[1] R. S. Roth, *J. Res. Nat. Bur. Standards*, **56**, 17 (1956).

[2] I. K. Hulm, *Phys. Rev.*, **92**, 504 (1953).

[3] I. A. Rozdin, F. M. Spiridonov, L. N. Komissarova and V. E. Pliushchev, *Neorg. Materialy*, **10**, 1798 (1971).

1. FORMATION MECHANISM OF OXIDIC COMPOUNDS

Taking into account the fact that the individual precipitation pH of titanium and indium hydroxides has near values, as well as the fact that the respective ions do not form complex ammoniacates, made the use of ammonium hydroxide as precipitation agent possible. The precipitation reaction being total, allows to obtain some co-precipitates with an easily adjustable and well established composition, which is then found again in the double oxidic phases. The products obtained are of white colour, microcrystalline or cryptocrystalline.

Using an Erdely-Paulik type derivatograph, up to 1000°, without maintaining in isothermal conditions at maximal temperature, we have gathered information on the reaction mechanism of the studied mixtures, from the co-precipitate form to the oxidic form. The thermograms obtained are given in figures 1, 2 and 3.

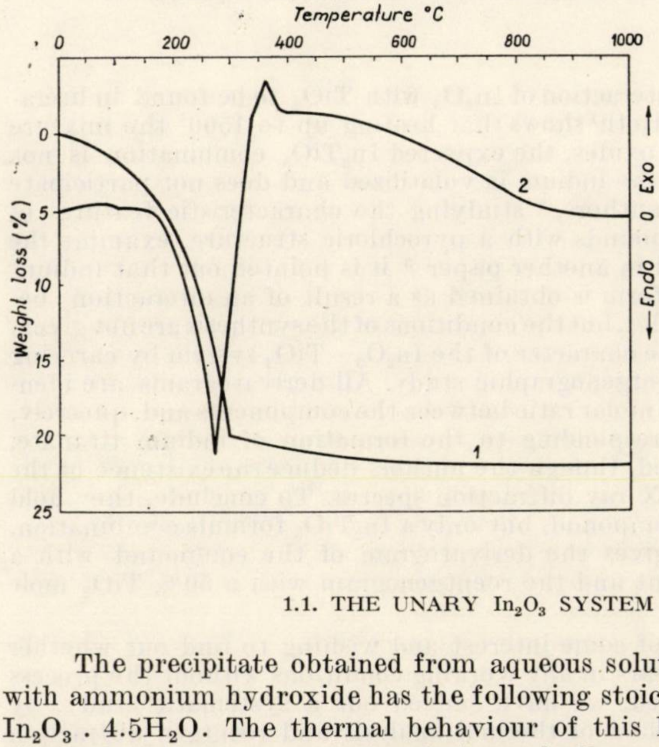

Fig. 1. — Thermogravimetric (*1*) and thermodifferential (*2*) curves of In_2O_3.x H_2O.

1.1. THE UNARY In_2O_3 SYSTEM

The precipitate obtained from aqueous solutions of indium nitrate with ammonium hydroxide has the following stoichiometric composition : $In_2O_3 . 4.5H_2O$. The thermal behaviour of this hydrated indium oxide (figure 1.2) shows a marked endothermal effect at 270°, that correlated to the loss of weight on the TGA curve, corresponds to the dehydration phenomenon. The exothermal effect, with its maximum at 360°, is brought about by the crystallization of the indium trioxide. The sequence of the reactions is given in diagram n° 1.

Diagram N⁰ 1

Formation mechanism of In_2O_3 from $In_2O_3 \cdot xH_2O$

Temperature scale (in °C)	TGA			DTA		Phenomenon
	Temp. (°C)	Calcd. %	Obtained %	Temperature (°C)		
				endo	exo	
200	50		6.50	200i		$In_2O_3 . xH_2O \rightarrow$ $In_2O_3 + x H_2O$
400		20.62	14.00	270 m 310w	360	In_2O_3 crystallization
500			0.50			
600–1000						Constant

Value calculated for x = 4.5

1.2. THE UNARY TiO_2 SYSTEM

The product obtained by precipitating the titanium ion with heated ammonium hydroxide, from an aqueous solution of titanium tetrachloride, is an amorphous gel with the $TiO_2 . H_2O$ composition. After thermal treatment up to 1000° (figure 2) TiO_2 (rutile) was obtained. The thermodifferential analysis curve shows a marked endothermal effect at 150°, corresponding to a loss of weight on the TGA curve owing to the de-

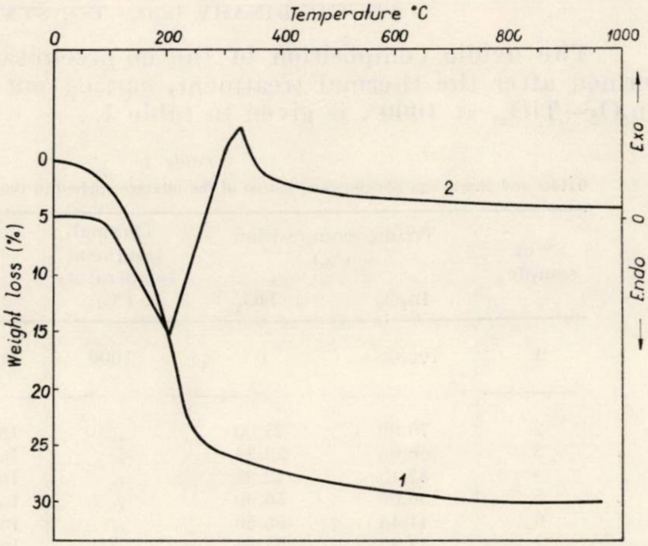

Fig. 2. — Thermogravimetric (*1*) and thermodifferential (*2*) curves of $TiO_2 . x H_2O$.

hydration of the anatase, and an exothermal effect at 325°, owing to the recrystallization of the titanium bioxide. Diagram n° 2 renders the sequence of the phenomena which are taking place.

Diagram N° 2

Formation mechanism of TiO_2 from $TiO_2 \cdot xH_2O$

Temperature scale (°C)	TGA			DTA		Phenomenon
	Temp. (°C)	Calcd. %	Obtained %	Temperature (°C)		
				endo	exo	
200	60	31.06	29.33	60 i 150 m		$TiO_2 \cdot xH_2O \rightarrow TiO_2 + xH_2O$
400			1.75	280 s	280 i 325 m 400 w	Crystallization of anatase
600 – 800					800	anatase → rutile
800 – 1000						Constant

Value calculated for x = 2.

1.3. THE BINARY $In_2O_3-TiO_2$ SYSTEM

The oxidic composition of the co-precipitates and of the phases formed after the thermal treatment, carried out on the binary system $In_2O_3-TiO_2$, at 1000°, is given in table 1.

Table 1

Oxidic and phasal equilibrium composition of the mixture studied in the In_2O_3"TiO_2" binary system

N° of sample	Oxidic composition (%)		Thermal treatment temperature (°C)	Equilibrium phase
	In_2O_3	TiO_2		
1	100.00	0	1000	In_2O_3
2	75.00	25.00	,,	$In_2TiO_5 + In_2O_3$
3	66.66	33.34	,,	In_2TiO_5
4	57.13	42.87	,,	$In_2TiO_5 + In_2O_3$
5	50.00	50.00	,,	$In_2TiO_5 + TiO_2$
6	44.44	55.56	,,	$In_2TiO_5 + TiO_2$
7	42.87	57.13	,,	$In_2TiO_5 + TiO_2$
8	40.00	60.00	,,	$In_2TiO_5 + TiO_2$
9	33.33	66.67	,,	$In_2TiO_5 + TiO_2$
10	25.00	75.00	,,	$In_2TiO_5 + TiO_2$
11	0	100.00	,,	TiO_2

By comparing the derivatograms of the synthetized samples we notice a similarity in the display of the phenomena taking place the whole way.

For the majority of the differential thermal DTA curves, the differences are insignificant for the starting and ending temperatures of the same effects so that we may treat them simultaneously. Differences are only recorded in the systems in which the quantity of indium is in excess to that of titanium (figure 4.8 and 4.9).

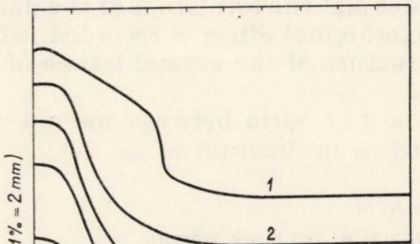

Fig. 3. — Thermogravimetric curves of indium and titanium co-precipitates:

1) 2In : 1Ti; 2) 1In : 1Ti; 3) 4In : 5Ti; 4) 3In : 4Ti; 5) 2In : 3Ti; 6) 1In : 3Ti; 7) 1In : 2Ti; 8) 4In : 3Ti; 9) 3 In : 1 Ti.

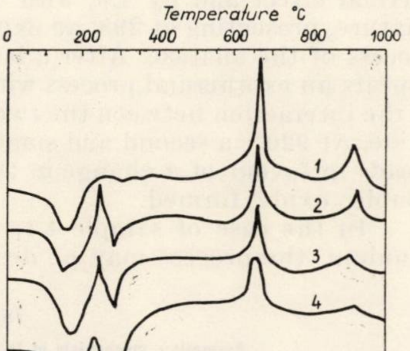

Fig. 4. — Thermodifferential curves of indium and titanium co-precipitates:

1) 2In : 1Ti; 2) 1In : 1Ti; 3) 4In : 5Ti; 4) 3In : 4Ti; 5) 2In : 3Ti; 6 1In : 3Ti; 7) 1In : 2Ti; 8) 4In : 3Ti; 9) 3 In : 1Ti.

As noticed in figure 3, the dehydration of the indium and titanium hydroxide precipitates takes place between 60° and 400°; this loss is marked by one respectively two steps on the curve, depending on the molar ratio between the components.

Two endothermal and two exothermal effects are recorded on the DTA curves (figure 4), excepting the 4.8 and 4.9 samples. The first endothermal effect, appearing between 60° and 210°, with a maximum at 140–150°, tends to go over into an exothermal effect, as a result of the crystallization process of the anatase. The dehydration phenomenon not being closed, and being a rather strong endothermal process, there appears a second endothermal effect, between 260° and 330°, with a maximum at 290°. An exception is made by the system 4.1, which has only one endothermal effect and by 4.6, with the highest quantity of titanium in the mixture, presenting at 295° an exothermal effect due to the crystallization process of the anatase. After a latent stage between 350° and 600°, there appears an exothermal process with a maximum at 665°, as a consequence of the interaction between the two oxides and the formation of the double oxide. At 920°, a second and smaller exothermal effect is recorded, which pleads in favour of a change in the structure of the crystal lattice of the double oxide formed.

In the case of sample 4.1, with a 2 : 1 ratio between indium and titanium, the process may be described as in diagram n° 3.

Diagram N° 3

Formation mechanism of In_2TiO_5 from $In_2O_3 \cdot xH_2O$ and $TiO(OH)_2$

Temperature scale (°C)	T G A			D T A		Phenomenon
	Temp. (°C)	Calcd. %	Obtained %	Temperature (°C) endo	exo	
200	60			60 i 150 m		$TiO(OH)_2 + In_2O_3 \cdot xH_2O \rightarrow TiO_2 +$ $+ In_2O_3 + (x + 1) H_2O$
400		20.14	20.00	300 w		
600 800					675	$TiO_2 + In_2O_3 \rightarrow In_2TiO_5$
800 1000					920	Change of the crystal lattice structure

Value calculated for x = 1.

For the samples 4.8 and 4.9 with the ratio between indium and titanium 1 : 2 and, respectively, 1 : 3, only the dehydration process marked by the two endothermal effects is recorded, the formation reaction of the indium titanate not being noticed.

The X-ray diffraction spectra, recorded by means of a TU-R-60 (Dresden) apparatus, are in full agreement with the results of the thermal analysis, meanwhile confirming the crystalline state of the products.

The samples heated under 400° present a diffuse roentgen diffraction spectrum. This attests their amorphous structure, determined by the processes dehydration and destruction of their crystalline lattice. Over 650°, clear spectral lines take shape, as a consequence of the appearance of the crystalline phase in the system and, as the temperature rises, the spectra are better outlined and more intense.

The individuality of the spectrum of compound 4.1 (figure 5) confirms the assumption that in the thermal decomposition process a double oxide is formed. By the plotting of the X-ray diffraction spectrum of the titanium bioxide, of the indium trioxide and of the product with a 2 In : 1Ti ratio, calcinated at 1000°, we notice the formation of a new compound to which we have assigned the formula In_2TiO_5. We have plotted only this diffraction spectrum, because the spectra of all the other samples show besides the roentgen diffraction lines belonging to the metatitanate, In_2TiO_5, characteristic lines either of the titanium bioxide, or of the indium trioxide, depending on the ratio between them.

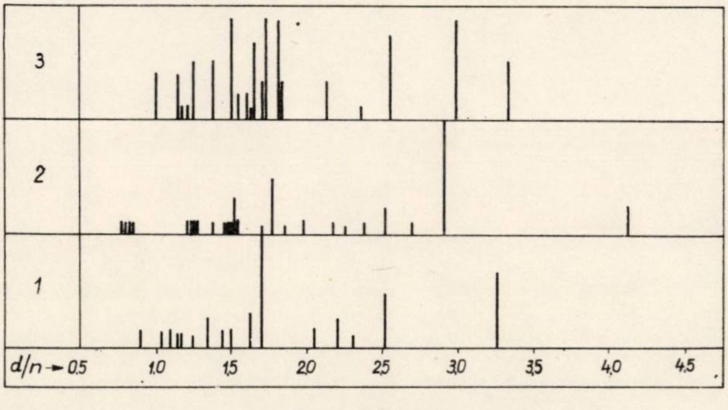

Fig 5. — Roentgen diffraction spectra of :
1) TiO_2; 2) In_2O_3; 3) In_2TiO_5.

By comparing the results obtained by us with those of Rozdin *et al.*, [3] we ascertain the following facts :

— The thermodifferential curves present two exothermal effects each pointing out, as expected, the formation process of the metatitanate.

— The curves similar to those of the sovietic scientists were obtained only for the samples with titanium excess in the mixture.

We consider that the mentioned differences may be due to the different ways of obtaining the co-precipitates, as well as to those of carrying out the thermal analysis.

Revue Roumaine de Chimie, **19**, *1*, 57–66 (1974)

COMPLEX COMBINATIONS OF THE TRANSITION METALS WITH TERTIARY STIBINES. II[1]

SPECTRAL STUDIES OF Pd(II) COMPLEX COMBINATIONS WITH TRITOLYLSTIBINES

D. NEGOIU* and LIDIA PARUTA**

* Faculty of Chemistry, University of Bucharest, Splaiul Independenţei, 89, Romania

** Centre of Physical Chemistry, Str. Dumbrava Roşie, 23, Bucharest-9, Romania

Received February 17, 1973

The paper discusses the ultraviolet visible and the IR spectra, assignments of the absorption bands in the electronic spectra being suggested. There are also made estimations about the geometric or bond isomers of some of the studied complexes.

In the electronic spectra of these compounds, bands with charge transfer and $d-d$ bands were noticed, and they were assigned by comparing them with the electronic spectra of some similar compounds.

The spectral data can be interpreted only if, besides the charge transfer $\sigma(L\rightarrow M)$, we consider its back donation through the π bond $(M\rightarrow L)$. Following the P, As, Sb series, it was to be expected that the π bond should be the strongest when the donor atom is approximately of the same size and uses the same type of d orbitals as the metal atom.

As the covalent radius assumes higher values from $P\rightarrow$Sb, it follows that the strength of the π bond also assumes higher values in the order $P<As<Sb$.

If we take into consideration the increase of the electronegative character and, therefore, the decrease of the attraction between the donor atom and the electrons of the d orbital in the metal atom we notice that the degree of the π bond assumes lower values in the reverse order $P>>As>Sb$. Therefore, along this series of donor atoms the π contribution to the strength of the donor-acceptor bond will remain approximately the same.

The appearance of such a π bond, where the central metal ion is the donor, leads to the strengthening of the M → stibine bond and contributes to the reduction of the accumulated negative charge on the central metallic ion as a result of the coordination of the stibine.

---

[1] Part I. D. Negoiu and L. Paruta-Hrehoriac, *Rev. Roumaine Chim.*, **18**, 2059 (1973).

Consequently, being a donor of strong σ bond, as well as an acceptor of π bond, the stibines will be able to stabilize both upper and lower valency states of certain elements.

The acceptor character is as important as the donor character. As a consequence of the strong field the stibines produce, there will be noticed a difference of energy between the metal *d* orbitals of low energy and those of higher energy.

The most stable compounds appear in the metal ions when the orbitals of low energy are completely occupied by electrons while those of high energy are vacant.

Cullen and Hochstrassen [2] found in the 210–340 μm domain of substituted arylphosphine and arylarsine electronic spectra two systems of bands which they characterize according to the substitution influence in the ligand and the polarity of the solvent.

The first system of bands that appears at about 270 mμ is neither influenced by the nature of the substituent nor by the solvent polarity; this system is assigned to an electronic transition similar, according to its structure, to the $\pi-\pi^*$ transition, of a high energy, that appears at about 200 mμ in the benzene monosubstituent.

The second system of bands appears at 220–250 mμ and depends on the polarity of the solvent and on the nature and position of the substituents; it may be assigned to the $n - \pi^*$ transition because one electron in the uncoupled pair of stibium atoms passes to a π. antibonding orbital in the benzene ring.

Sidman [3] points out that this transition is due to the excitation of an electron of a nonbonding orbital (n) which is placed on an atom in an antibonding orbital (the π^* orbital) antisymmetric to the reflexion in the plane of the molecule, and which is extended over several atoms in the molecule.

According to Platt,[4] this type of a transition is of little intensity, the fact being due to the difference between n and π^* orbital properties.

The n and π^* orbitals have simultaneous negative or positive high amplitudes in any region, as their lobes are orientated in different directions.

That is the reason why in solvents with a high dielectric constant the band is shifted towards higher wavelengths.

In hydroxylic solvents [5] one notices a shift of the $n-\pi^*$ transition towards blue. The phenomenon is due to the hydrogen bond formed by the hydroxylic solvent in which n electrons are implied.

It was experimentally established that for the methyl substituted arylstibines the transition $n - \pi^*$ is shifted towards red, showing an intensification of the conjugation interreaction between the vacant electronic doublet of the stibium atom and the aromatic nucleus. This shift toward red progressively appears according to the number of the substituents.

---

[2] W. R. Cullen and R. M. Hochstrasser, *J. Mol. Spectroscopy*, **5**, 118 (1960).

[3] J. W. Sidman, *Chem. Rev.*, **58**, 689 (1958).

[4] J. R. Plat, *J. Chem. Phys.*, **19**, 101 (1951).

[5] G. J. Breadly and M. Kasha, *J. Amer. Chem. Soc.*, **77**, 4462 (1955).

Our data about the tri-*p*-tolylstibine complexes also show the presence of two bands (fig. 1) : one band, which is distinct at 220 mμ, depends on the nature and on the position of the substituent and on the nature of the solvent ; it is assigned to the transition of one electron uncoupled stibium atom pair to a π antibonding orbital in the benzene nucleus ($n \to \pi^*$). The second band, which appears at 270 mμ, is less intense and is assigned to a $\pi - \pi^*$ transition similar to the higher energy at → 200 mμ in the nonsubstituted benzene nucleus.

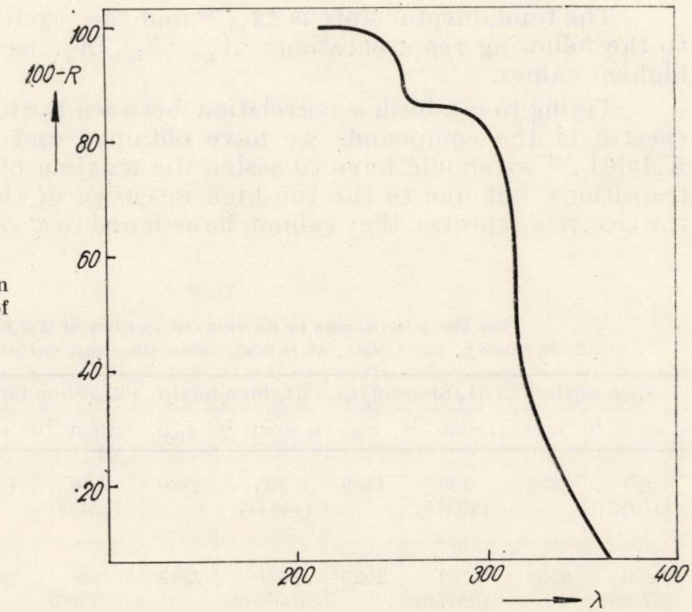

Fig. 1. — The reflection spectrum in ultraviolet of the tri-*p*-tolylstibine.

Gray and Balhausen,[6] starting from a calculation of mononuclear orbitals, show the possibility for the metal ion with a d^8 configuration to form square-planar combinations with simple ligands.

The five degenerate orbitals of the free metal ion are split into four different levels in the square-planar complex.

Several methods have been used to estimate the splitting of the *d* orbitals in the square-planar complex and to explain the spectral bands.

Fenske, Martin and Ruedenberg [7] have made a more complete calculation for the Pt (II) ion.

In the square-planar complex, starting with the splitting of the five degenerate *d* levels into four distinct levels, one asserts that the $d_{x^2-y^2}$ orbital, being placed in the direction of the bonds, is the less stable one.

We have also reached the conclusion that the d_{xz} and d_{yz} orbitals are more stable than the d_{xy} orbital and less stable than the d_{z^2} orbital.

---

[6] H. B. Gray and J. C. Balhausen, *J. Amer. Chem. Soc.*, **85**, 262 (1963).

[7] R. S. Fenske, D. S. Martin and K. Ruedenberg, *Inorg. Chem.*, **1**, 441 (1962).

The energy and, therefore, the position of the d_{z^2} orbital is not completely established.

Chatt and co-workers[8] have found the following succession of the energy levels : $d_{z^2} < d_{xy}$, $d_{yz} < d_{xy} < d_{x^2-y^2}$. According to the electrostatic calculations, Fenske and Ruedenberg[7] as well as Gray and Balhausen[9] assert that in most of the square-planar complexes this succession runs in the following way : d_{xz}, $d_{yz} < d_{z^2} < d_{xy} < d_{x^2-y^2}$. One anticipates three $d-d$ spin transitions corresponding to the transitions to three lower levels than the free orbital $d_{x^2-y^2}$.

The fundamental state is $^1A_{1g}$ [10] and the excited states correspond to the following representations $^1A_{2g}$, $^1B_{1g}$, ^1E_g, as the energy assumes higher values.

Trying to establish a correlation between the bands in the electronic spectra of the compounds we have obtained and those of K_2PtCl_4 or K_2PdCl_4,[11] we should have to assign the maxima obtained to some $d-d$ transitions, but due to the too high intensity of the bands obtained in the electronic spectra, they cannot be assigned to $d-d$ transitions (table 1).

Table 1

The absorption maxima in the electronic spectrum of $[PdI_2L_2]$ compounds

L=Sb (o-tolyl)$_3$, Sb (m-tolyl)$_3$, Sb (p-tolyl)$_3$; wavelength (mμ), maximum frequency (cm^{-1})

Sb(*p*-tolyl)$_3$		PdI_2(Sb-*p*-tolyl$_3$)$_2$		PdI_2(Sb-*o*-tolyl$_3$)$_2$		PdI_2(Sb-*m*-tolyl$_3$)$_2$		Nature of transition
λ, ν(cm^{-1})	ε_{mol}	λ, ν(cm^{-1})	ε_{mol}	λ, ν(cm^{-1})	ε_{mol}	λ, ν(cm^{-1})	ε_{mol}	
227 (44052)	3628	230 (43478)	1809	225 (44444)	1880	230 (43478)	1784	characteristic bands of aromatic ring
270 (37037)	2553	280 (35750)	2623	280 (35750)	2312	280 (37750)	2523	
		346 (28901)	2663	350 (28428)	1392	340 (29411)	1457	charge transfer bands
		490 (20408)	1399	480 (20833)	507.5	495 (20202)	703.5	

The transitions of similar intensity to $\pi-\pi^*$ transitions proper to the ligand which appear in these complexes at 320–346 mμ and 410–490 mμ, are undoubtedly due to a change transfer from the molecular orbital e_g to the molecular orbital b^*_{1g} (fig. 2). These transitions belong indeed to the complex and not to the ligand and their high intensity ($\varepsilon_{mol} \sim 10^4$) makes them easily mistaken for $d-d$ transitions.

---

[8] J. Chatt, G. A. Gamlen and L. E. Orgel, *J. Chem. Soc.*, **1958**, 487.

[9] H. B. Gray and J. C. Baelhausen, *J. Amer. Chem. Soc.*, **85**, 268 (1963).

[10] D. Martin and C. A. Lenhardt, *Inorg. Chem.*, **3**, 1368 (1964).

[11] P. Day, A. F Orchard, A. J. Thomson and J. P. Williams, *J. Phys. Chem.*, **42** (6), 1973 (1965).

From the electronic spectrum of the above mentioned compounds, one can also notice that the band at 410–490 mμ is far more intensive than the one at 320–360 mμ (fig. 3) which is in agreement with the order of the energy levels presented in fig. 2.

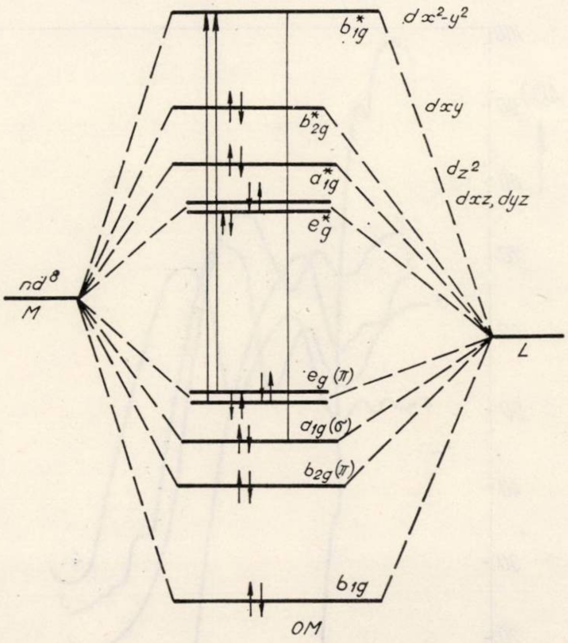

Fig. 2. – The simplified MO diagram for a square-planar complex, and the possible charge transfer transition.

The first band which is less intensive is due to two transitions with the same energy. If we refer to several halogen compounds of Pd(II) with the same ligand, of the $[PdX_2(Sb-p-tolyl_3)_2]$ type, where X = Cl^-, Br^-, I^- (table 2), one notices that the shift of the charge transfer bands is in complete agreement with the diminution of the optical electronegativities of the halide ions,[12,13] namely :

$$X_{Cl^-} = 3\,;\quad X_{Br^-} = 2.8\,;\quad X_{I^-} = 2.5$$

whereas the electronegative character of Pd(II) remains constant. In the square-planar complex, Jørgensen[14] gives for this ion the value X = = 2.2–2.4.

Jørgensen's main supposition is that the energies of the transitions with charge transfer can be directly related to the differences between

---

[12] C. K. Jørgensen and V. Gutmann, "International Review of Halogen Chemistry", Springer-Verlag, Berlin, 1966.

[13] C. K. Jørgensen, *Mol. Phys.*, **6**, 43 (1963).

[14] C. K. Jørgensen, *Solid State Phys.*, **13**, 376 (1962).

the donor orbital and the acceptor one. The energies can be evaluated from the analysis of the spectral data, and Jørgensen calls them optical electronegativities, their calculation formula being :

$$\nu_{CT} = 30{,}000\,(\lambda_{opt}\,L - \lambda_{opt}\,M)\ \mathrm{cm}^{-1}$$

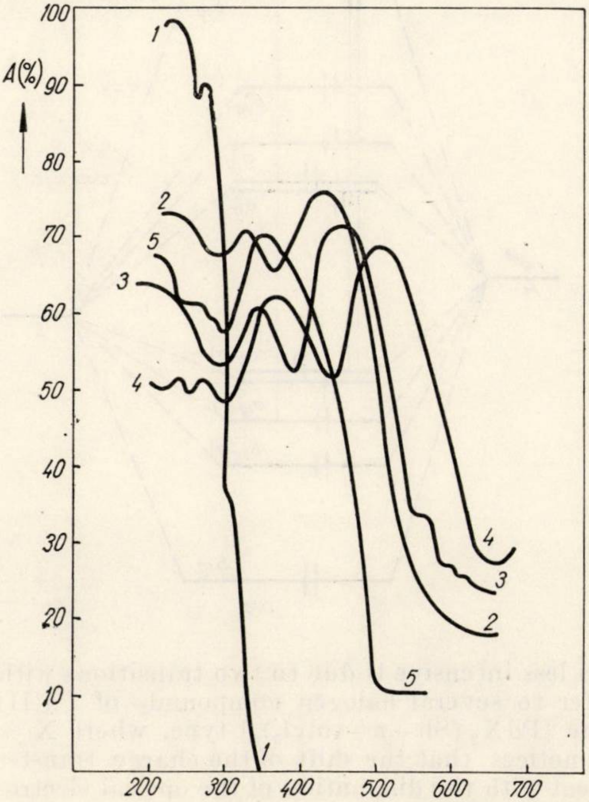

Fig. 3. — The absorption spectra in ultraviolet and visible of some complex of Pd(II) with tri-*p*-tolylstibine : *1*) Sb(*p*-tolyl)$_3$; *2*) PdCl$_2$ (Sb-*p*-tolyl$_3$)$_2$; *3*) PdBr$_2$(Sb-*p*-tolyl$_3$)$_2$; *4*) PdI$_2$(Sb-*p*-tolyl$_3$)$_2$; *5*) Pd(NO$_2$)$_2$(Sb-*p*-tolyl$_3$)$_2$.

where λ_{opt} L and λ_{opt} M are the electronegativities of donor and acceptor orbital of the ligand and respectively, of the metal. Moreover, the transition frequencies ν_{CT} are to be corrected by the variations of the interelectronic repulsions.

Table 2

λ and the maximum frequency (cm^{-1}) of the electronic spectrum of [PdX$_2$(Sb-*p*-tolyl$_3$)]$_2$ complexes

	PdCl$_2$(Sb-*p*-tolyl$_3$)$_2$		PdBr$_2$(Sb-*p*-tolyl$_3$)$_2$		PdI$_2$ (Sb-*p*-tolyl$_3$)$_2$		Pd(NO$_2$)(Sb-*p*-tolyl$_3$)$_2$	
λ	320 mμ	410 mμ	330 mμ	440 mμ	346 mμ	490mμ	345 mμ	490 mμ
ν	31.250	24.390	30.303	22.727	28.901	20.408	28.985	20.408

On the other hand, the bands being very large (fig. 3) no precise information could be found regarding the inductive effect of the methyl group on the *ortho-*, *meta-*, and *para-* positions, on the Sb—Pb bond in the respective complexes.

The differences between the absorption maxima of the three complexes are experimental errors of measuring.

THE VIBRATION SPECTRA OF Pd(II) COMPLEX COMBINATIONS WITH TRITOLYLSTIBINES

In IR spectroscopy is used to obtain information about the chemica bond type and stereochemistry of the respective compounds. Important data are obtained especially in the low frequencies domain where bands appear owing to the active vibrations metal-ligand in infrared.

The domain we have studied (300—800 cm^{-1}) is yet unsatisfactory as regards its inferior limit, because the vibration frequency $\nu(\mathrm{Pd-Br})_p$, $\nu(\mathrm{Pd-I})_t$, $\nu(\mathrm{Pd-I})_p$, $\nu(\mathrm{Sb-Pd-Sb})$, $\nu(\mathrm{Pd-Sb})$ takes values close to 200 cm^{-1} and no estimations about the geometrical configuration are possible.

Palmer[15] studied the vibration spectra of triphenylphosphine and triphenylarsine using for comparison the spectrum of the substituted benzene compounds C_6H_5X (X being a certain substituent); this spectrum has been largely studied by Whiffen[16] whose nomenclature is still used today.

Among the main vibrations this C_6H_5X molecule presents, we have chosen for the study of our complexes those below 800 cm^{-1}. Tables 3 and 4 contain the bands in the 200—800 cm^{-1} range of the triphenylphosphine and triphenylarsine spectra.

Table 3

The vibration spectrum of triphenylphosphine in the 200—800 cm^{-1} domain

λ (cm^{-1})	Intensity	Assignment
246	w	$\delta(\mathrm{P-C_6H_5})$
255	v.w	
281	w	
428	w.m.	$\nu_3(\mathrm{P-C_6H_5})$
493	sh.	$\gamma_2(\mathrm{P-C_6H_5})$
499	v.i.	
516	i	
616	w	δ_R
695	v.i.	γ_R
745	v.i.	$\gamma_5(\mathrm{C-H})$

Table 4

The vibration spectrum of triphenylarsine in the 200—800 cm^{-1} domain

λ (cm^{-1})	Intensity	Assignment
247	w	$\delta(\mathrm{As-C_6H_5})$
317	m	$\nu_3(\mathrm{As-C_6H_5})$
469	v.i.	$\gamma_2(\mathrm{As-C_6H_5})$
476	v.i.	
617	v.m.	δ_R
668	v.m.	$\nu_2(\mathrm{As-C_6H_5})$
696	v.i.	γ_R
742	v.i.	$\gamma_5(\mathrm{C-H})$

---

[15] R. S. Palmer, Thesis, Nürnberg, 1970.

[16] D. H. Whiffen, *J. Chem. Soc.*, **1956**, 1350.

In the second column, the intensities of the bands are presented using abbreviations : w — weak, i — intensive, v.i. — very intensive, m — medium, and in the third column there are the respective assignments.

The great complexity, i.e. the large number of active vibrations modes in IR, that have been noticed at the ligands we used, have limited our study on the absorption spectra of this domain, to several chloro-, bromo-, and iodo-derivatives of tritolylstibine.

The assignments of the bands due to the valency vibrations of the chemical bonds were made by comparing them with the spectra of the isostructural pairs of complexes PdX_2L_2 where : L = phosphine, arsine and stibine.

Table 5

The vibration spectrum of [Sb(p-tolyl$_3$)]

λ (cm^{-1})	Intensity	Assignment
488	m	γ_2(Sb-p-tolyl)
617	i	δ_R
670	v.i.	ν_2 (Sb-p-tolyl)
695	v.i.	γ_R
742	i.	γ_5 (C−H)

Table 6

The vibration spectrum [PdCl$_2$(Sb-p-tolyl$_3$)$_2$]

λ (cm^{-1})	Intensity	Assignment
360	m	ν (Pd−Cl)
410	i.	no assignment
450	i.	
465	m	γ_2(Sb-p-tolyl)
480	m	
620	i.	δ_R
695	i.	γ_R
710	i.	no assignment
742	v.i.	γ (C−H)

Our attributions were in agreement with the values found by other researchers.

The vibration spectra of several complex combinations prepared by us in the same frequency range are given in the following tables.

Table 7

The vibration spectrum of [PdBr$_2$(Sb-p-tolyl$_3$)$_2$]

λ (cm^{-1})	Intensity	Assignment
415	v.i.	no assignment
450	i.	
470	i	γ_2 (Sb-p-tolyl)
480	i.	
550	w	no assignment
570	m	
620	i.	δ_R
670	m	ν_2(Sb-p-tolyl)
695	i.	γ_R
745	i.	γ (C−H)

Table 8

The vibration spectrum of [PdI$_2$(Sb-p-tolyl$_3$)$_2$]

λ (cm^{-1})	Intensity	Assignment
410	w	no assignment
420	m	
465	i.	γ_2 (Sb-p-tolyl)
480	i.	
570	m	no assignment
620	i.	δ_R
670	m	ν_2 (Sb-p-tolyl)
695	i.	γ_R
750	v.i.	γ (C−H)

The related literature points out that the vibration spectra of the square-planar of Pd(II) and Pt(II) have a single band corresponding to the metal-chlorine valency vibration.[17–21]

For complexes with *trans* configuration $[PdCl_2L_2]$, L = phosphine and arsine we found that the vibration valency $\nu(Pd-Cl)$ absorbs between 350–358 cm^{-1}.

For the complexes prepared by us, the valency vibration $\nu(Pd-Cl)$ takes frequently the value of 360 cm^{-1}. Theoretically, the complexes with *cis* configuration would present two vibrations for $\nu(M-Cl)$ and $\nu(M$-ligand) which are active in IR. This is a proof of the *cis* configuration.

In the Cs_2PdCl_4 spectrum one single band has been noted at 327 cm^{-1} and is assigned to the valency vibration $\nu(Pd-Cl)$. In the $[PdCl_4]^{2-}$ ion spectrum the vibration $\nu(Pd-Cl)$ is placed at 357 cm^{-1}. As can be noticed from tables 9 and 10 in the vibration spectra of the binuclear compounds $[Pd_2Cl_4(Sb-p-tolyl_3)_2]$ and $[Pd_2I_4(Sb-p-tolyl_3)_2]$ similar positions are found for the main metal-donor and metal-halogen bands. This proves the same strength of the Sb-carbon bond.

Table 9

The vibration spectrum of $[Pd_2Cl_4(Sb$-*p*-$tolyl_3)_2]$

λ (cm^{-1})	Intensity	Assignment
362	i.	ν (Pd-Cl)
465	v.i.	γ_2(Sb-*p*-tolyl)
480	i.	
510	m.	no assignment
550	w.	
570	w.	
695	m	γ_R
748	i.	$\gamma_{(C-H)}$

Table 10

The vibration spectrum of $[Pd_2I_4(Sb$-*p*-$tolyl_3)_2]$

λ (cm^{-1})	Intensity	Assignment
467	i	γ_2 (Sb-*p*-tolyl)
475	i	
510	m.	no assignment
550	w.	
619	m	δ_R
696	m	γ_R
750	i	$\gamma_{(C-H)}$

The vibration spectra of the nitro- and dinitroderivative complexes were also studied.

As is known, the free nitro ion presents three vibration modes, all of them active in IR and belonging to the C_{2v} symmetry group : asymmetrical vibration (ν_{as}) at 1328 cm^{-1}, the N–O symmetrical vibration (ν_s) at 1261 cm^{-1} and the deformation vibration NO_2 (δ) at 828 cm^{-1}. After coordination, no matter if it is produced through nitrogen or oxygen, the number of the IR band remains constant.

The general effect of the coordination is the shift of these frequencies, given the frequencies of the free ion. It is these shifts that can be used in many cases to establish the coordination mode of the NO_2^- ion.

---

[17] G. E. Coates and C. Parkin, *J. Chem. Soc.*, **1963**, 421.
[18] D. M. Adams, J. Chatt and A. D. Westland, *J. Chem. Soc.*, **1964**, 734.
[19] J. R. Alkins and P. J. Hendra, *J. Chem. Soc.*, **1967**, 1325.
[20] R. J. Goodfellow, J. G. Evans and D. A. Duddel, *J. Chem. Soc.*, (A) **1968**, 1604.
[21] D. M. Adams and P. J. Chandler, *J. Chem. Soc.*, **1969**, 588.

Revue Roumaine de Chimie, **19**, *1*, 57–66 (1974)

Thus, the coordination through nitrogen leads to the increase of the two frequencies ν_{as} and ν_s, whereas the coordination through oxygen leads to the increase of the ν_{as} frequency and the diminution of the ν_s. The only frequency remaining almost constant in both cases is the bending frequency.

Following formation tendency and the effect of the π bond of different ligands on the nitrite ion in palladium (II) and platinum (II) complex combinations, Burmeister and Timmer [22] have shown that there is a correlation between the neutral ligands capacity to form a π bond and the valency frequencies N—O of the nitrite coordinate ion.

In the complex combinations in which the neutral ligands present a strong tendency to form a π bond, there appears the possibility to pass from the coordination through nitrogen of the ion NO_2^-, to the coordination through oxygen. [23]

Following the vibration spectra of the $[Pd(NO_2)_2(Sn\text{-}p\text{-tolyl}_3)_2]$ and $[Pd_2(NO_2)_4\ (Sb-p-\text{tolyl}_3)_2]$ compounds we may draw the conclusion that in the binuclear compounds the bond is made in both modes.

In the vibration spectrum of $[Pd(NO_2)_2\ (Sb-p-\text{tolyl}_3)_2]$ we find frequencies characteristic to the coordination through nitrogen, whereas in the vibration spectrum of $[Pd_2(NO_2)_4(Sb-p-\text{tolyl}_3)_2]$ the frequencies are characteristic both for the coordination through nitrogen and oxygen.

Therefore, in the binuclear compound the two Pd atoms are linked in a bridge bond through O—N—O groups, and the terminal groups are linked to the Pd atom through a nitrogen bond.

Table 11

The vibration spectrum of $[Pd(NO_2)_2\ (Sb\text{-}p\text{-tolyl}_3)_2]$

λ (cm^{-1})	Intensity	Assignment	Assumed structure
828—870	v. i. (breit)	δ_{NO_2}	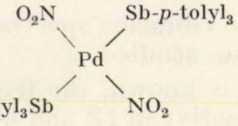
1350	i.	ν_{NO_2}	

Table 12

The vibration spectrum of $[Pd_2(NO_2)_4\ (Sb\text{-}p\text{-tolyl}_3)_2]$

λ (cm^{-1})	Intensity	Assignment	Assumed structure
820 1060 1340 1470—80	v.i. i i i	δ_{ONO} ν_s ONO ν_{NO_2} ν_{as} ONO	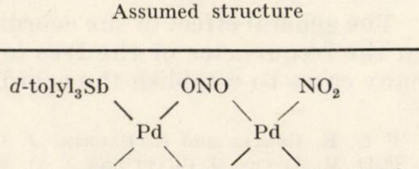 d-tolyl₃Sb ONO NO₂ Pd Pd O₂N ONO Sb-p-tolyl₃

---

[22] J. L. Burmeister and R. C. Timmer, *J. Inorg. Nuclear Chem.*, **28**, 1973 (1966).

[23] K. Nakamoto, "Infrared Spectra of Inorganic and Coordination Compounds", J. Wiley, New York, 1963, p. 151.

Revue Roumaine de Chimie, **19**, *1*, 67–78 (1974)

CARBONIUM ION REACTIONS. VIII*

BENZOBICYCLOOCTENE DERIVATIVES THROUGH π-ROUTE

ILEANA DRĂGUŢAN, C. DRĂGHICI, ANA HANEŞ, ANGELA DUMITRIU,
ECATERINA CIORĂNESCU and C. D. NENITZESCU**

Organic Chemistry Center, Bucharest, Spl. Independenţei, 202 B, Romania

Received August 4, 1973

Competition between phenonium- and π-route in the acetolysis of 1,2-benzocyclohepta-1,3-dienyl-7-methyl tosylate (**2-OTs**) is studied. Benzene ring assistance prevails over double bond assistance, giving rise to 1,2-benzocycloocta-1,3-dien-7-yl acetate (**7-OAc**) as the main product, both in the buffered and unbuffered acetolysis. Significant proportions of π-route products are formed : benzobicyclo[3.2.1]octene derivatives in the presence of NaOAc and benzobicyclo[2.2.2]octene derivatives in strongly acidic medium, in agreement with the known data about the thermodynamic stability of these systems. Assuming no cross-over between the two ionization routes, the results are rationalized by the intervention of both phenonium and bridged ions.

Solvolytic reactions involving participation of a remote carbon-carbon double bond have been extensively explored during the last decade.[1,2] Reaction rate enhancement as compared to saturated analogs indicates anchimeric assistance provided by the double bond. Formation of cyclic compounds and stereospecificity of the reaction, sometimes observed, have been explained in terms of bridged ions or nonclassical ions generated by "π-route".[1d] It is not surprising that great attention has been paid to the study of these reactions which can provide additional information about the much disputed nonclassical ions.[1,2,3]

---

* Part VII. E. Ciorănescu, A. Bucur, M. Banciu, F. Badea, M. Elian and C. D. Nenitzescu, *Rev. Roumaine Chim.*, **16**, 1555 (1971).

** Deceased July 28, 1970.

[1] a. G. Le Ny, *Compt. rend.*, **251**, 1526 (1960) ; G. Le Ny, Thèse, Université de Paris, 1964 ; b. R. G. Lawton, *J. Amer. Chem. Soc.*, **83**, 2399 (1961) ; c. P. D. Bartlett and S. Bank, *ibid.*, **83**, 2591 (1961) ; d. S. Winstein and P. Carter, *ibid.*, **83**, 4485 (1961) ; e. P. D. Bartlett, *Liebigs Ann. Chem.*, **653**, 45 (1962) ; f. P. D. Bartlett, S. Bank, R. J. Crawford and G. H. Schmid, *J. Amer. Chem. Soc.*, **87**, 1288 (1965) ; g. P. D. Bartlett, W. S. Trahanovski, D. A. Bolon and G. H. Schmid, *J. Amer. Chem. Soc.*, **87**, 1314 (1965) ; h. A. C. Cope, D. L. Nealy, P. Scheiner and G. Wood, *ibid.*, **87**, 3130 (1965) ; i. H. Felkin, G. Le Ny, C. Lion, W. D. K. Macrosson, J. Martin and W. Parker, *Tetrahedron Letters*, **1966**, 157 ; j. M. Hanack, W. Kraus, W. Rothenwöhrer, W. Kaiser and G. Wentrup, *Liebigs Ann. Chem.*, **703**, 44 (1967) ; k. P. D. Bartlett, R. M. Nicholson and R. Owyang, *Tetrahedron*, **1966**, Suppl. 8, Part II, p. 399.

[2] B. Capon, *Quart. Rev.*, **18**, 45 (1964) ; D. J. Raber, G. J. Kane and P. v. R. Schleyer, *Tetrahedron Letters*, **1970**, 4117 ; H. Felkin and C. Lion, *Tetrahedron*, **27**, 1375, 1387 (1971).

In 1960 Le Ny [1a] found that cyclohept-4-enylmethyl *p*-nitrobenzenesulphonate (**1-OBs**) underwent acetolysis 60 times faster than the corresponding saturated compound and yielded almost quantitatively bicyclo[3.2.1]oct-2-yl acetate (*endo*/*exo* = 9/1).

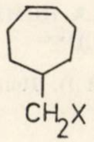

1

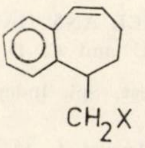

2

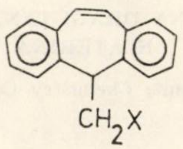

3

A different behaviour was observed in the case of the system **3** where the seven-membered ring is fused to two benzene rings. [4] The acetolysis of dibenzocycloheptatrienylmethyl tosylate (**3-OTs**), in the presence of sodium acetate, leads mainly to an acetate with dibenzocyclooctatriene skeleton, originating from a ring expansion reaction. Only a small part of the acetolysis product (6–8%) consists of bridged compounds, formed by double bond participation. [4]

In this context it seemed to us instructive to study the solvolytic behaviour of the **2** system where double bond participation could be more important than in the case of **3** and closer to that of **1**. On the other hand, the formation of compounds with benzobicyclooctene skeleton could be synthetically useful in this less studied class. In the present paper we report the results obtained from the acetolysis of **2-OTs**.

RESULTS

Benzosuberone (**4**)[5,6] was used as starting material for the synthesis of alcohol **2-OH**. Bromination of **4** with NBS and dehydrobromination with collidine afforded benzosuberenone (**5**)[7]. The purification of this unsaturated ketone was very difficult. By fractional distillation a bromine free product could be obtained, but it still contained small quantities (4–5%) of saturated ketone **4**; pure ketone **5** was separated by

---

[3] G. D. Sargent, *Quart. Rev.*, **20**, 301 (1966); P. D. Bartlett, "Nonclassical Ions", W. A. Benjamin, Inc., New York, 1965.

[4] a. E. Ciorănescu, A. Bucur, M. Elian, M. Banciu, M. Voicu and C. D. Nenitzescu, *Tetrahedron Letters*, **1964**, 3835; b. E. Ciorănescu, A. Bucur, M. Elian and C. D. Nenitzescu, *Rev. Roumaine Chim.*, **10**, 149 (1965): c. E. Ciorănescu, A. Bucur, M. Elian, M. Banciu, M. Voicu and C. D. Nenitzescu, *Rev. Roumaine Chim.*, **10**, 161 (1965); d. E. Ciorănescu, A. Bucur, F. Badea, M. Rentzea and C. D. Nenitzescu, *Tetrahedron Letters*, **1969**, 1867.

[5] R. C. Gilmore and W. J. Horton, *J. Amer. Chem . Soc.*, **73**, 1411 (1951).

[6] W. J. Horton and F. E. Walker, *ibid.*,**74**, 759 (1952).

[7] a. G. L. Buchanan and D. R. Lockhart, *J. Chem. Soc.*, **1959**, 3586; b. E. Collington and G. Jones, *J. Chem. Soc.*, (C), **1969**, 2656.

preparative v.p.c. By Darzens reaction[6,8] with chloroacetic ester the ketone **5** was converted to the aldehyde **6**; the latter was subsequently reduced with $LiAlH_4$ to the alcohol **2-OH**, from which tosylate **2-OTs** was prepared in the usual manner. IR and NMR spectra of compounds **6**, **2-OH** and **2-OTs** are in perfect agreement with the expected structures.

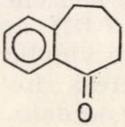

4

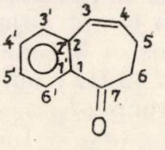

5

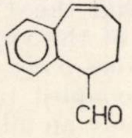

6

The acetolyses of **2-OTs** were carried out at 90° (10 hr, 12 half-lives) in the presence and in the absence of sodium acetate. The reaction product (96% and 83%, respectively, calculated on **2-OTs**) was analysed by gas-chromatography, after reduction with $LiAlH_4$ (table 1); the analysis of the acetate mixture showed the same composition.

Table 1

Acetolysis products of 2-OTs (after $LiAlH_4$ reduction)

Tosylate **2-OTs** M	NaOAc M	% Products					
		endo-**13-OH**	*exo*-**10-OH**	*endo*-**10-OH**	**7-OH**	**2-OH**	Unidentified compounds
0.04	0.08	—	20.0	2.5	65.5	4.5	7.5[a]
0.04	—	17.0	4.5	3.0	61.5	2.0	12.0[b]

[a] 4% unknown alcohol, 3.5% many unidentified hydrocarbons.
[b] 4% unknown alcohol, 8% many unidentified hydrocarbons.

The major product is the same in both cases (61.5% and 65.5%, respectively), namely the alcohol **7-OH**. Two more alcohols are found in significant amounts, *exo*-**10-OH** (20%) in the buffered acetolysis and **13-OH** (17%) in the unbuffered one. The acetates **7-OAc**, *exo*-**10-OAc**, and **13-OAc** were separated by preparative v.p.c. Two other alcohols (4%), which could not be identified or separated, are included in the figures from the last column, the remainder representing the sum of 5-6 components, probably hydrocarbons. The starting alcohol **2-OH** was identified by comparison of its retention time with that of an authentic sample.

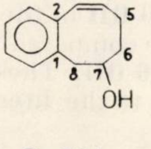

7-OH

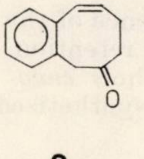

8

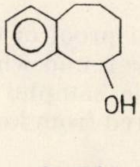

9-OH

---

[8] R. Huisgen and G. Seidl, *Chem. Ber.*, **96**, 2740 (1963).

The structure of the alcohol **7-OH** was inferred from the IR and NMR spectra of this compound, of the corresponding acetate **7-OAc** and of the ketone **8**, obtained by the oxidation of the alcohol with chromic anhydride in pyridine. Thus, the C=O stretching frequency (1715 cm^{-1}) in the IR spectrum of ketone **8** and the singlet at $\delta = 3.7$ ppm, corresponding to the benzylic protons in the NMR spectrum of the same ketone, indicate that the C=O group is not adjacent to the benzene ring. The spectrum of the vinylic protons of ketone **8**, alcohol **7-OH** and acetate **7-OAc** shows a *cis* coupling of 12 Hz; only one of the vinylic protons is vicinally coupled to a CH_2 group ($J_{45} = 5$ Hz), whereas the other one presents only an allylic coupling ($J_{35} = 1.5$ Hz). Spectral data, therefore, indicate a 1,2-benzocycloocta-1,3-diene structure for these compounds. Further support of this assignment was afforded by catalytic hydrogenation of the solvolysis mixture (after $LiAlH_4$ reduction). The main component has, after this operation, the same retention time in v.p.c. as an authentic sample of 1,2-benzocycloocten-7-ol (**9-OH**), prepared according to Huisgen and Seidl.[8] Thus, our data indicate that the major solvolysis product is 1,2-benzocycloocta-1,3-dien-7-yl acetate (**7-OAc**), formed from **2-OTs** by ring enlargement.

The starting alcohol **2-OH** from the mixture presents after hydrogenation the same retention time as the corresponding saturated alcohol[8].

The structure and configuration of alcohols **10-OH** *and* **13-OH** were established using the following data. Some components of the mixture maintained their retention times in v.p.c. after catalytic hydrogenation, showing the absence of double bonds. It seemed plausible that these components contain a benzobicyclooctene skeleton, originating from transannular participation of the double bond.

Tosylate **2-OTs** could give rise by π-route to two *exo-endo* pairs of alcohols, **10-OH** and **11-OH**, with a benzobicyclo[3.2.1]octene skeleton.

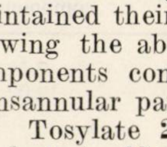

10-OH

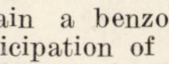

11-OH

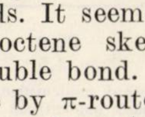

12

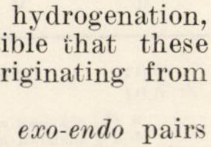

13-OH

A first proof of the presence of the alcohols **10-OH** in the acetolysis mixture was found when their retention times were compared with those of authentic samples of alcohols *endo*- and *exo*-**10-OH**. These alcohols were prepared from ketone **12** synthetized according to the literature.[9,10,11]

---

[9] W. Baker and W. G. Leeds, *J. Chem. Soc.*, **1948**, 974; A. H. Cook and R. P. Linstead, *ibid.*, **1934**, 956.

[10] H. E. Zimmerman, R. S. Givens and R. M. Pagni, *J. Amer. Chem. Soc.*, **90**, 6096 (1968).

[11] S. Julia, C. Huyhn and J. Olivie, *Bull. Soc. chim. France*, **1966**, 147.

$LiAlH_4$ reduction of ketone **12** afforded a mixture of alcohols *endo*-**10-OH** and *exo*-**10-OH** (9 : 1). The configuration of the *exo* and *endo* epimers was assigned by comparing their NMR spectra with those of alcohols *exo*- and *endo*-**10-OH** studied by Tanida *et al.* [12,13]

Acetate *exo*-**10-OAc** was subsequently isolated by preparative v.p.c. from the buffered acetolysis product and its NMR spectrum agrees with that found by the Japanese authors. [12]

As can be seen from table 1, the *exo*-2,3-benzobicyclo[3.2.1]-octen-4-ol (*exo*-**10-OH**) is formed in 20% proportion in the buffered acetolysis and only 4.5% in the unbuffered one. The *endo*-**10-OH** epimer appears in small quantities in both cases (2.5% and 3%).

In the unbuffered acetolysis another alcohol (acetate, respectively) is obtained in proportion of 17%. The NMR spectrum of the acetate **13-OAc**, isolated by preparative v.p.c., perfectly matches that of the *endo*-5,6-benzobicyclo[2.2.2]octen-2-yl acetate (**13-OAc**). [14]

The presence of a compound with a benzobicyclo[2.2.2.]octene skeleton in the unbuffered acetolysis product was to be expected. The interconversion between compounds with benzobicyclo[3.2.1]octene skeleton (**10** and **11**) and benzobicyclo[2.2.2]octene skeleton (**13**) has been studied by Tanida *et al.* [12] and Lansbury and Boggs. [15] In buffered medium sulphonic esters derived from the system **13** give rise to compounds with [3.2.1] skeleton. [12] Conversely, the latter (**10** or **11**) rearrange, in the presence of acids, to derivatives of the benzobicyclo[2.2.2]octene system. [15] Our results are in agreement with these observations : in the buffered acetolysis of **2-OTs** the kinetically controlled product (**10-OAc**), with [3.2.1] skeleton, is formed, whereas in the unbuffered one the acetate **13-OAc** with [2.2.2] skeleton arises from a thermodynamically controlled reaction.

DISCUSSION

Acetolysis of tosylate **2-OTs** in acetic acid buffered with equivalent amounts of sodium acetate shows first order kinetics. The rate constant together with those of some related compounds (at 80°) are listed in table 2.

All these tosylates, except tosylate **14-OTs** (taken as reference compound), contain in their molecule either a double bond or an aromatic ring, or both these groups able to assist ionization.

The comparison of the relative acetolysis rates of tosylates **1-OTs** and **15-OTs** shows that in this case the double bond is again superior to the fused benzene ring in assisting ionization [18].

---

[12] H. Tanida, K. Tori and K. Kitahonoki, *J. Amer. Chem. Soc.*, **89**, 3212 (1967).

[13] We thank Professor Tanida for a copy of the NMR spectra of these alcohols.

[14] K. Tori, Y. Takano and K. Kitahonoki, *Chem. Ber.*, **97**, 2798 (1964).

[15] P. T. Lansbury and N. T. Boggs, *Chem. Comm.*, **1967**, 1007.

[16] R. Huisgen, G. Seidl and J. Wimmer, *Tetrahedron*, **20**, 623 (1964).

[17] M. Voicu and F. Badea, *Rev. Roumaine Chim.*, **17**, 1551 (1972).

[18] P. D. Bartlett and W. P. Giddings, *J. Amer. Chem. Soc.*, **82**, 1240 (1960).

The position of the double bond with respect to the leaving-group, its substituents and the steric factors influence decisively the ability of the double bond to function as an internal nucleophilic agent. In tosylate **2-OTs** the double bond is located in the 5,6-position relative to the departing group, a favourable position for participation.[19] Annelation of compound **1** is expected to diminish the nucleophilic reactivity of the double bond. The rates of the acetolysis reaction decrease indeed considerably in the series of compounds **1-OTs**, **2-OTs** and **3-OTs** (table 2).

Table 2

Acetolysis rates of 2-OTs and related tosylates (at 80°)

Tosylate	$10^5 \cdot k_1$ sec^{-1}	Rate rel. to **14-OTs**
14-OTs 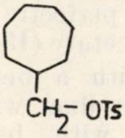	0.217[a]	1
15-OTs 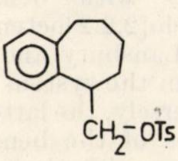	1.62[b]	7.5
16-OTs 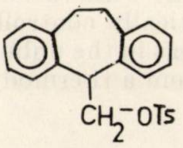	0.575[c]	2.65
1-OTs 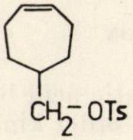	13.30[a]	61.2
2-OTs 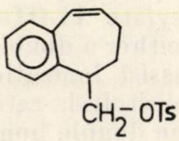	5.32	24.8
3-OTs 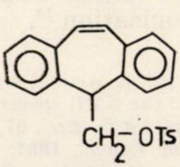	0.177[c]	0.82

[a] *Calcd.* from data for the brosylate (ref. a) with $k_{ROBs}/k_{ROTs} = 3$;

[b] The rate constant determined by Huisgen *et al.*[16] is $1.96 \cdot 10^{-5}$ sec^{-1}; c) Extrapolated value using data from ref. 17.

---

[19] P. D. Bartlett and G. D. Sargent, *ibid.*, **87**, 1297 (1965).

The k_u/k_s ratio, which is usually used for estimating the double bond participation, also decreases in the series of the three tosylate pairs (**1**/**14**, **2**/**15** and **3**/**16**) from 61.2 to 3.30 and 0.31. The failure to observe a rate acceleration cannot always be interpreted as absence of neighbouring group participation. Solvolysis product analysis showed that bridged compounds are formed both in the case of **2-OTs** (22–25%) and **3-OTs** (6–8%) (from **1-OBs** bicyclic compounds are quantitatively obtained). The smaller values (relative to **1-OTs**) found for the rate constants of tosylates **2-OTs** and **3-OTs** are a result of the various factors that operate : the rate-retarding inductive effect of β-aryl,[20] the conformational factors[17] and the additional strain associated with the fused benzene rings and ring closure, respectively.

A comparison in the series of saturated tosylates **14-OTs**, **15-OTs** and **16-OTs** shows that the relative rate increases by a factor of 7.5 for one and 2.65 for two fused benzene rings. As regards the reaction products, **14-OTs** undergoes acetolysis practically without rearrangement (only 4% cyclooctene is formed)[1a] and **15-OTs** with ring expansion, leading to benzocycloocten-4-ol. The intervention of a phenonium ion in this rearrangement has been experimentally and theoretically demonstrated by Huisgen *et al.*[8,16] Finally, the buffered acetolysis of tosylate **16-OTs** is also accompanied to a great extent (85%) by an expansion of the middle ring, proceeding probably by a similar mechanism.[4]

As pointed out in the case of **3-OTs**, acetolysis of **2-OTs** may be considered to proceed *via* two different paths : one leading to unbridged compounds (**7**, **2**) and another to bridged compounds (**13** and **10**). In order to account for them, we must admit that several intermediates are involved in these rearrangements. It is very likely that ionization of **2-OTs** is assisted by the phenyl group. The phenonium ion **17** can give rise either to acetate **7-OAc**, or to the unrearranged acetate **2-OAc**. The ring expansion **2**→**7** could also be imagined to proceed by a phenyl shift

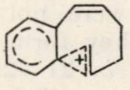

17

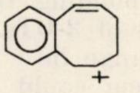

18

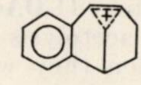

19

occurring in the primary ion (corresponding to **2-OTs**), followed by conversion into the secondary ion **18**. However, it is difficult to conceive that the vacant orbital of the developing primary ion and the aromatic ring, located in a geometrically favourable position, do not interact. (Examination of Dreiding models shows that in one of the conformers the CH_2OTs group occupies an axial position, suitable for the formation of the phenonium ion.) A similar mechanism has been suggested in the case of tosylate **15-OTs**[8] and **3-OTs**.[4]

---

[20] S. Winstein, B. K. Morse, E. Grunwald, K. C. Schreiber and J. Corse, *J. Amer. Chem. Soc.*, **74**, 1113 (1952); D. J. Cram, *ibid.*, **86**, 3767 (1964).

The formation of compounds with benzobicyclooctene skeleton (**10-AOc** and **13-OAc**) suggests the intervention of a bridged nonclassical ion **19**, generated by double bond participation. The rearrangement **17**→**19** should be energetically unfavourable and it seems likely that the two ions do not equilibrate, but arise directly from **2-OTs** by two independent ionization routes : a phenonium route and a π-route. This mechanism accounts for the constant unbridged-bridged product ratio (2.5) in the buffered and unbuffered acetolysis.

The intermediate **19** gives rise to a secondary ion **20**, stabilized by benzylic conjugation, and to a smaller extent to the secondary ion **21**. The kinetically controlled product will be that originating from **20**,[12] namely the acetates **10-OAc** with a benzobicyclo[3.2.1]octene skeleton

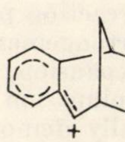

20

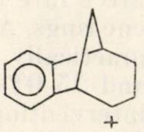

21

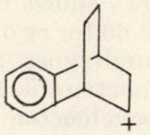

22

and indeed these acetates represent in the buffered acetolysis the main component resulted from participation. The formation of acetate **13-OAc** in the unbuffered acetolysis can be explained by the intervention of a classical ion **22** which may arise from **20** (alkyl migration) or **21** (aryl migration). The rearrangement **20**→**21** is energetically unfavourable but under thermodynamic control conditions, when repeated reionization occurs, the stable **13-OAc** can accumulate in the long run. The acetate *endo*-**13-OAc**, the most stable of the two epimers, is the major participation component (17%) in the unbuffered acetolysis.

Acetates **11-OAc**, corresponding to ion **21**, were not identified among the acetolysis products of **2-OTs**. Even if they form, in unbuffered solution they will rearrange into **13-OAc**[15] (*via* **21**→**22**). In the buffered acetolysis one of them could be the unidentified compound (4%, the last column, table 1). The behaviour and relations between compounds **10** and **13** are in agreement with those reported by the Japanese[12] and American[15] authors.

Returning now to the acetates **10-OAc**, the *exo*/*endo* ratio in which they are found (20/2.5) suggests an axial approach of AcO^- to the carbonium ion **20**, the *exo* side of which is less hindered sterically. The *exo*/*endo* ratio (1 : 9) obtained by $LiAlH_4$ reduction of ketone **12**, determined by "steric approach control"[21] (the transfer of hydride ion to the C=O group takes place from the less occupied side of the molecule) supports this idea. The *exo*-**10-OAc** isomer is a direct product of the acetolysis, as it has been reported[12] that under buffered conditions epimerization does not occur.

---

[21] W. G. Dauben, G. J. Fonken and D. S. Noyce, *J. Amer. Chem. Soc.*, **78**, 2579 (1956).

Acetolysis of tosylate **3-OTs** proceeds with middle ring expansion only in the presence of sodium acetate. In the presence of strong acids the dibenzocyclooctatrienol (formed by kinetically controlled reaction) undergoes ring contraction, leading back to **3** (the thermodynamically controlled product). In the dibenzo-derivative series, the systems with seven- and eight-membered middle rings are thus interconvertible.

Acetolysis of tosylate **2-OTs** is accompanied by ring expansion both in buffered and unbuffered solution. The formed benzocyclooctadienol (**7-OH**) remains unchanged in the presence of strong acids, behaving thus like its saturated analog **9-OH**.[22] The intervention of a dibenzohomotropylium cation in the rearrangements of the **3** system, admitted as very likely, [23] could explain its different behaviour as compared to the **2** system.

EXPERIMENTAL

Boiling points and melting points are uncorrected. IR spectra were recorded with a Carl Zeiss Jena UR 20 spectrophotometer, UV spectra with a Specord UV–VIS and NMR spectra with a Varian A–60A spectrometer, using TMS as internal standard. The v.p.c. analyses were performed on a Carlo Erba Fractovap model D using Carbowax 20 M columns (20% on Chromosorb W, 30–60 mesh), 2m × 4 mm, at 178°, with a hydrogen rate flow of 80 ml/min. Preparative v.p.c. was carried out on a Carlo Erba model GV, with columns similarly packed, 3m × 5mm, at 170°, with a hydrogen rate flow of 90 ml/min. The kinetic measurements were carried out essentially in the same way as previously described.[24]

1,2-Benzocyclohepta-1,3-dien-7-one (*Benzosuberenone*) (**5**). Ketone **5** was prepared [7] from benzosuberone (**4**) by N-bromosuccinimide bromination (molar ratio NBS/ketone **4** = 1.44, as compared to 1.17 [7a] which left 20% of the ketone **4** unchanged). In the dehydrobromination reaction [7a] a larger γ-collidine excess (10.3 mol/mol bromoderivative) and a higher temperature (145°) were used. The distilled product (75%, based on ketone **4**) had a 1.7% halogen content. Film distillation of the product on a small column (H = 200 mm; Φ = 8 mm), provided with a calibrated glass core, afforded bromine-free ketone **5** (67% yield). The removal of the halogenated compound could also be achieved by column chromatography on neutral alumina (100 g/8 g ketone), eluting with a 9 : 1 light-petroleum – ether mixture (70% yield). After this purification benzosuberenone still contained small quantities (4–5%) of ketone **4**. Pure benzosuberenone (99.2%) was obtained by preparative v.p.c. *IR spectrum* of the pure ketone **5** (CS_2 and CCl_4; cm^{-1}) : 738 ms, 786 vs, 873 s, 1196 ms, 1275 vs, 1318 s, 1348 s, 1440 vs, 1475 ms, 1598 s, 1688 vs (lit. [7a] 1680), 2838 ms, 2890 ms, 2921 s, 2966 s, 3025 s, 3068 s. *NMR spectrum* [CCl_4; δ (ppm)] : 2.20–2.65 m (2H, H_5), 2.68–3.0 m (2H, H_8), 6.15 m (2t) (1 olef. H, H_4), 6.45 m (2t) (1 olef. H, H_3), 7.0–7.6 m (3 arom. H), 7.8–8.0 q (1 arom. H, H_6).

7-Formyl-1,2-benzocyclohepta-1,3-diene (**6**). To a solution of potassium *tert*-butoxide in *tert*-butyl alcohol (obtained from potassium (4.7 g; 120 mmol) and 123 ml *tert*-butyl alcohol heated under reflux for 2 hr), cooled under dry nitrogen in a water-ice bath, a solution of ketone **5** (15 g; 95 mmol) and ethyl chloroacetate (14.1 g; 115 mmol) in 19 ml anhydrous benzene was added dropwise (over 0.3 hr), with mechanical stirring. Stirring was continued for one more hour maintaining the cooling bath and then for 3.5 hr at room temperature. Most of the solvent was removed *in vacuo* and the mixture was poured into water (50 ml) and extracted with benzene. The benzene solution was washed with water, dried on $MgSO_4$ and concentrated. 50 ml of a 15 % KOH—MeOH solution were added and the mixture was left overnight at room temperature. Methanol was distilled and the crystalline residue was dissolved in water and extracted with benzene. The alkaline aqueous solution was acidified with 89 % H_3PO_4 and the separated oil collected in ether. The water washed ethereal solution was dried on Na_2SO_4 and evaporated. The glycidic acid (13.8 g ; 67 %, based on ketone **5**) was mixed with a small amount of copper powder and decarboxylated at red. press. by careful heating on a hot water bath. When the evolution of CO_2 ceased, aldehyde **6** was distilled *in vacuo* (7.5 g ; 46 %), b.p. 132—5°/5 mm ; *IR spectrum* (CCl_4 ; cm^{-1}) : 1431 w, 1450 ms, 1498 w, 1730 vs, 2701 w, 2731 w, 2815 ms, 2862 ms, 2889 ms, 2931 ms, 3022 ms, 3068 ms. *NMR spectrum* [CCl_4 ; δ (ppm)] : 1.9—2.8 m (4 H, H_5, H_6), 3.5 m (1H, H_7), 5.6—6.05 m (2t) (1H olef., H_4), 6.4 m (2t) (1H olef., H_3), 6.9—7.3 (4H arom.), 9.55 d (1H, CHO). *DNFH* m.p. 115—120° (EtOH) (*Found* : C, 61.10 ; H, 4.87. $C_{18}H_{16}N_4O_4$ *requires* : C, 61.36 ; H, 4.54 %).

---

[22] R. Huisgen and G. Seidl, *Chem. Ber.*, **96**, 2730 (1963).

[23] M. Voicu, F. Badea and A. Bucur, *Rev. Roumaine Chim.*, **17**, 1563 (1972.)

[24] M. Voicu and F. Badea, *Rev. Roumaine Chim.*, **14**, 929 (1969).

1,2-Benzocyclohepta-1,3-dienyl-7-methanol (**2-OH**). A solution of $NaBH_4$ (2.9 g ; 76 mmol) in 22 ml water and 1.7 ml 8 % aqueous NaOH was added to a solution of freshly distilled aldehyde **6** (10 g ; 58 mmol) in 280 ml methanol. The heat evolved causes an energetic refluxing of the methanol. The mixture was left to stand overnight. Methanol was removed *in vacuo* and the residue treated with water and extracted with ether to leave on evaporation a colourless viscous liquid (9.4 g ; 93 %). (*Found* : C, 82.21 ; H, 8.27. $C_{12}H_{14}O$ *requires* : C, 82.75 ; H, 8.04 %). *IR spectrum* (CS_2 and CCl_4 ; cm^{-1}) : 752 s, 786 s, 1021 vs, 1380 ms, 1431 ms, 1450 s, 1493 ms, 2835 ms, 2880 vs, 2931 vs, 3019 s, 3061 ms, 3077 ms, 3200—3590 (assoc. OH), 3611 ms, 3635 ms. *NMR spectrum* [CCl_4 ; δ (ppm)] : 1.9—2.6 m (4H, H_5, H_6), 2.85 s (O*H*), 2.85—3.2 m (1H, H_7), 3.6 d (2H, CH_2OH), 5.55—6.01 m (2t) (1 olef. H, H_4), 6.28 m (2t) (1 olef. H, H_3), 7.06 s (4 arom. H).

The tosylate **2-OTs** was prepared from the alcohol **2-OH** with *p*-toluenesulphochloride in pyridine and anhydrous ether ; 95 % yield, m.p. 50—51° (methanol). (*Found* : C, 69.72 ; H, 6.41 ; S, 9.63. $C_{19}H_{20}O_3S$ *requires* : C, 69.51 ; H, 6.09 ; S, 9.75 %). *IR spectrum* (CS_2 and CCl_4 ; cm^{-1}) : 752 ms, 781 s, 813 s, 824 s, 963 vs, 1000 ms, 1179 vs, 1199 vs, 1371 vs, 1430 w, 1448 w, 1496 w, 1600 w, 2840 w, 2931 ms, 3021 w, 3069 w. *NMR spectrum* [CCl_4 ; δ (ppm)] : 2.0—2.7 m (4H, H_5, H_6), 2.42 s (3H, CH_3), 3.4 m (1H, H_7), 4.15 m (2H, CH_2OTs), 5.78 m (2t) (1 olef. H, H_4), 6.25 m (2t) (1 olef. H, H_3), 7.0—7.8 m (8 arom. H).

UNBUFFERED ACETOLYSIS OF 1,2-BENZOCYCLOHEPTA-1,3-DIENYL-7-METHYL TOSYLATE (2-OTs)

A solution of tosylate **2-OTs** (2 g ; 6.1 mmol) in 40 ml anhydrous acetic acid was heated at 90° for 10 hr. The mixture was poured into water (30 ml), neutralized with Na_2CO_3 and extracted with ether. The ethereal solutions were washed with water, dried on $MgSO_4$ and evaporated. The oily residue (1.1 g ; 83 %) was dissolved in 25 ml ether and the solution was added dropwise to a suspension of 0.4 g $LiAlH_4$ in 25 ml ether, with mechanical stirring. The mixture was refluxed for 5 hr and left overnight. After decomposing the mixture with 10 % H_2SO_4 and separating the ethereal layer, the aqueous layer was extracted 3 times with ether. The ethereal solution was washed with water, dried on Na_2SO_4 and then evaporated leaving an oily material (1 g ; 95 %) (v.p.c. analysis in table 1). This oil was separated into fractions by column chromatography on neutral alumina (30 g), eluting with light-petroleum (b.p. 30—40°) for the first fraction and then with a 4 : 1 light-petroleum — ether mixture. The first fraction (500 ml) contained 0.02 g unidentified hydrocarbons (IR spectrum). Mixtures of alcohols **7-OH**, **10-OH** and **13-OH** (0.65 g) were found in the next three fractions (500 ml). From the fifth fraction (100 ml) 0.2 g *1,2-benzocycloocta-1,3-dien-7-ol* (**7-OH**) was obtained. *IR spectrum* (CS_2 ; cm^{-1}) : 738 vs, 746 vs, 761 ms, 788 vs, 1031 s, 1048 s, 1062 s, 2822 ms, 2868 s, 2898 s, 2928 vs., 3015 s, 3058 ms, 3200–3450 (assoc. OH), 3578 ms, 3606 ms.

Acetate **7-OAc** was isolated by preparative v.p.c. from the acetolysis mixture. (*Found* : C, 77.31 ; H, 7.80 ; $C_{14}H_{16}O_2$ *requires* : C, 77.74 ; H, 7.46 %). *IR spectrum* (CS_2 and CCl_4 ; cm^{-1}) : 742 s, 786 ms, 1030 vs, 1240 vs, 1375 s. 1452 ms, 1737 vs, 2836 w, 2901 ms, 2941 s, 3021 s, 3070 ms. *NMR spectrum* [CCl_4 ; δ (ppm)] : 1.55–2.6 m (4H, H_5, H_6), 2.0 s (3H, CH_3), 2.98 d (2H, H_8), 4.95 m (1H, H_7), 5.78 m (2t) (1 olef. H, H_4), 6.41 m (2t) (1 olef. H, H_3), 7.15 s (4 arom. H).

Continuing the elution, two more fractions (200 ml) (mixtures of alcohols **7-OH** and **2-OH** ; 0.1 g) were separated.

1,2-Benzocycloocta-1,3-dien-7-one (**8**). A solution of alcohol **7-OH** (0.2 g, 1.1 mmol) in 5 ml pyridine was added with cooling to a complex prepared from 0.4 g CrO_3 and 6 ml pyridine. The mixture was stirred for 5 hr, left overnight, decomposed with cold water and extracted with ether. The ethereal solution was washed with water, dil. HCl, again with water and dried on $MgSO_4$. The solvent was evaporated to leave 0.15 g (76 %) ketone **8**, yellow oil. *DNFH* m.p. 70–73°. *IR spectrum* (CCl_4 ; cm^{-1}) : 1325 ms, 1451 w, 1715 vs, 2835 w, 2872 w, 2932 ms, 2910 ms, 3020 ms, 3068 w. *NMR spectrum* [CCl_4 ; δ (ppm)] : 2.0–2.4 m (4 H, H_5, H_6), 3.70 s (2H H_8), 6.0 m (2t) (1 olef. H, H_4), 6.65 m (2t) (1 olef. H, H_3), 7.1–7.5 m (4 arom. H).

endo-5,6-Benzobicyclo[2.2.2]octen-2-yl acetate (**13-OAc**). Acetate **13-OAc** was isolated by preparative v.p.c. from the unbuffered acetolysis mixture. (*Found* : C, 77.84 ; H, 7.76. $C_{14}H_{16}O_2$ *requires* : C, 77.74 ; H, 7.46 %). *IR sepectrum* (CCl_4 ; cm^{-1}) : 1030 ms, 1065 ms, 1250 vs, 1741 vs, 2871 ms, 2948 s, 3029 w, 3045 vw, 3078 vw. *UV spectrum* (EtOH) λ_{max} mμ (log ε) : 256 (2.64), 261.5 (2.72), 268 (2.72) corresponding [25,26] to a benzobicyclo[2.2.2]octene structure.

BUFFERED ACETOLYSIS OF 1,2-BENZOCYCLOHEPTA-1,3-DIENYL-7-METHYL TOSYLATE (2-OTs)

A solution of tosylate **2-OTs** (2 g ; 6.1 mmol) and anhydrous sodium acetate (0.85 g ; 10.3 mmol) in 40 ml glacial acetic acid was heated at 90° for 10 hr. The reaction mixture was worked up as described above for the unbuffered acetolysis ; 1.3 g (96 %) of a reddish oil were obtained which was subsequently reduced with $LiAlH_4$. The alcohol mixture was analysed by v.p.c. (table 1).

exo-2,3-Benzobicyclo[3.2.1]octen-4-yl acetate (**10-OAc**) [12]. Acetate *exo*-**10-OAc** was isolated by preparative v.p.c. from the buffered acetolysis mixture. *UV spectrum* (EtOH) λ_{max} mμ(log ε) : 266 (2.79), 273.9 (2.78). *IR spectrum* (CS_2 and CCl_4 ; cm^{-1}) : 757 s, 947 ms, 982 ms, 1016 s, 1208 sh., 1232 vs, 1728 vs, 2871 ms, 2960 s, 3026 w, 3071 vw. The NMR spectrum of the complex *exo*-**10-OAc**–**Eu(DPM)$_3$** allowed the determination of the geminal coupling constant $J_{8a8b} = 12$ Hz.

---

[25] K. Kitahonoki and Y. Takano, *Tetrahedron Letters*, **1963**, 1597.
[26] L. Billet and G. Descotes, *Bull. Soc. chim. France*, **1971**, 2617.

REDUCTION OF 2,3-BENZOBICYCLO[3.2.1]OCTENE-4-ONE (12)

Ketone **12** was prepared according to literature.[9,10,11]

a) A solution of $NaBH_4$ (0.25 g; 6.6 mmol) in 5 ml water and 1 ml of a 8% aqueous NaOH were added to a solution of ketone **12** (0.7 g; 4 mmol) in 15 ml methanol. The mixture was left overnight at room temperature, then worked up in the usual manner. On evaporation of the solvent a colourless liquid (0.655 g; 93.5%) was obtained. V.p.c. analysis showed the composition : 91% *endo*-alcohol (*endo*-**10-OH**) and 9% *exo*-alcohol (*exo*-**10-OH**).

b) The reduction of ketone **12** (0.7 g; 4 mmol) with $LiAlH_4$ (0.3 g; 8 mmol) in 40 ml anhydrous ether afforded, after the usual working up, a yellowish liquid (0.6 g; 86%) containing 89% *endo*-alcohol (*endo*-**10-OH**) and 11% *exo*-alcohol (*exo*-**10-OH**).

Acknowledgement. The authors thank Dr. M. Voicu for helpful discussions and Miss E. Şliam and Mrs. V. Daniel for elementary analyses.

Revue Roumaine de Chimie, **19**, *1*, 79–85 (1974)

CONDENSATION OF β-AROYLPROPIONIC ACIDS WITH ISATIN UNDER PERKIN CONDITIONS

A. M. EL-ABBADY *, M. A. OMARA and N. G. KANDIL

Department of Chemistry, University College for Women A'in Shams University, Cairo, A.R.E.

Received March 7, 1973

β-Aroylpropionic acids (I ; R = H, CH_3 and Cl) are condensed with isatin under Perkin conditions to give α-(N-acetyloxindolylidene)-γ-aryl-$\Delta^{\beta,\gamma}$-butenolides (II ; R = H, CH_3 and Cl) which on acid hydrolysis give the corresponding α-oxindolylidene-γ-aryl-$\Delta^{\beta,\gamma}$-butenolides (III ; R = H, CH_3 and Cl) respectively. Treatment of butenolides (II) with benzylamine affords the corresponding amides (IV ; R = H, CH_3 and Cl), which when heated with dilute hydrochloric acid give 1-benzyl-3-oxindolylidene-2-oxo-5-aryl-2,3-dihydropyrroles (V ; R = H, CH_3 and Cl). Furthermore, butenolides (II) react with hydrazine hydrate to give the corresponding 3-spiro-(N-acetyl-oxindol)-4-aroylmethyl-5-ketopyrazolidines (VI ; R = = H, CH_3 and Cl), which on acid hydrolysis yield 3-spiro-oxindol-4-aroylmethyl-5-ketopyrazolidines (VII ; R = H, CH_3 and Cl) respectively.

β-Aroylpropionic acids are known to condense with aldehydes [1-4] phthalic anhydride,[5] substituted phthalic anhydrides,[6] cyclohexanone and fluorenone [7] in acetic anhydride in the presence of sodium acetate [1] to give the corresponding butenolides.

In the present invetigation we report the condensation of β-benzoyl-, β-*p*-toloyl-, and β-*p*-chlorobenzoylpropionic acids (I) with isatin under the same conditions to give α-(N-acetyloxindolylidene)-γ-aryl-$\Delta^{\beta,\gamma}$-butenolides (II ; R = H, CH_3 and Cl) as dark red crystals in fairly good yields.

---

[1] "Adams Organic Reactions", vol. 1, Fourth edition, New York, John Wiley & Sons, Inc., 1947, p. 210.

[2] R. Filler and H. M. Laurdes, *J. A. Chem. Soc.*, **81**, 391 (1959).

[3] F. W. Schueler, and C. Hanna, *J. Amer. Chem. Soc.*, **73**, 3528 (1951).

[4] W. Borsche, *Univ. Cottingen, Ber.*, **47**, 2708 (1914).

[5] W. Borsche, *Univ. Cottingen, Ber.*, **47**, 1108 (1914).

[6] W. T. Smith and C. Hanna, *J. Amer. Chem. Soc.*, **73**, 2387 (1951).

[7] W. I. Awad, S.M.A. Omran and A. I. Hashem, *J. Chem. U.A.R.*, **10**, (3), 287 (1967).

* Present address : Chemistry Department, Faculty of Science, Tanta University, Tanta, Egypt.

The constitution of these products is inferred from : (i) Their analytical data. (ii) Their infrared absorption spectra [8] which show strong bands at : 1790, 1780, 1730, 1710, 1615, 1600, 1550 and 1490 cm^{-1} characteristic of the stretching frequencies of the carbonyl groups of the conjugated five-membered lactones and amides as well as the C = C aromatic skeletal in plane vibrations, respectively. (iii) Their dark red colour. (iv) Their different reactions which are investigated below :

a. Acid hidrolysis of the N-acetyloxindolylidenebutenolides (II).

Hydrolysis of the produced butenolides (II; R = H, CH_3 and Cl) using dilute hydrochloric acid give the corresponding α-oxindol-ylidene-γ-aryl-$\Delta^{\beta,\gamma}$-butenolides (III; R=H, CH_3 and Cl) as reddish black solids.

The structure of these compounds is inferred from their analytical data, and their infrared absorption spectra which show strong bands at; 3360—3100 (br.), 1790, 1780, 1730; 1705, 1670, 1620, 1555 and 1495 cm^{-1}, characteristic of the stretching frequencies of NH, C = O and C = C, respectively.

b. Action of benzylamine on the N-acetyloxindolylidenebutenolides.

Treatment of α-(N-acetyloxindolylidene)-γ-aryl-$\Delta^{\beta,\gamma}$-butenolides (II) with benzylamine gives α-(N-acetyloxindolylidene)-β-aroyl-N-benzylpropionamides (IV; R = H, CH_3 and Cl) as yellow solids.

The structure of these amides is inferred from their analytical data, and their infrared spectra which show strong absorption bands at : 3400—3100 (br.), 1705, 1685, 1615, 1585, 1550 and 1490 cm^{-1} characteristic of the stretching frequencies of the NH, ketonic C = O, amide C = O and C = C respectively.

c. Lactimization of the α-(N-acetyloxindolylidene)-β-aroyl-N-benzylpropionamides.

When propionamides (IV) are boiled with hydrochloric acid, 1-benzyl-3-oxindolylidene-2-oxo-5-aryl-2,3-dihydropyrroles (V; R = H, CH_3 and Cl) are obtained as dark violet solids in excellent yields. The structure of these dihydropyrroles is based on : their analytical data, their deep violet colour and their infrared absorption spectra which show bands at : 3400—3000 (br.), 1705, 1675, 1615, 1600, 1540 and 1500 cm^{-1} characteristic of the stretching frequencies of the NH, C = O and C = C respectively.

The two propionamides (IV; R = CH_3 and Cl) are found to undergo lactimization even on standing (in the first case) and on crystallization (in the second case). This is indicated by the change in their colour from yellow to dark violet.

d. Action of hydrazine hydrate on the N-acetyloxindolylidenebutenolides.

Hydrazine hydrate reacts with butenolides (II) in ethanol at room temperature or under reflux to give 3-spiro (N-acetyl-oxindol)-4-aroylmethyl-5-ketopyrazolidines (VI; R = H, CH_3 and Cl). It seems that cyclization occurs on the double bond in a similar manner as the hydrazides of azlactones [8] when heated.

---

[8] "The Chemistry of Penicillin", Princeton University Press, Princeton, N. J., 1949, p. 736.

The structure of these compounds is inferred from the following observations :
(i) Their analytical data. (ii) They do not form acylazides when treated with nitrous acid. (iii) Their infrared absorption spectra which show strong bands at : 3400–3000 (br.), 1720, 1665, 1655, 1610, 1540 and 1500 cm^{-1} characteristic of the stretching frequencies of the NH, the C = O of ketones and amides, and the C = C respectively.

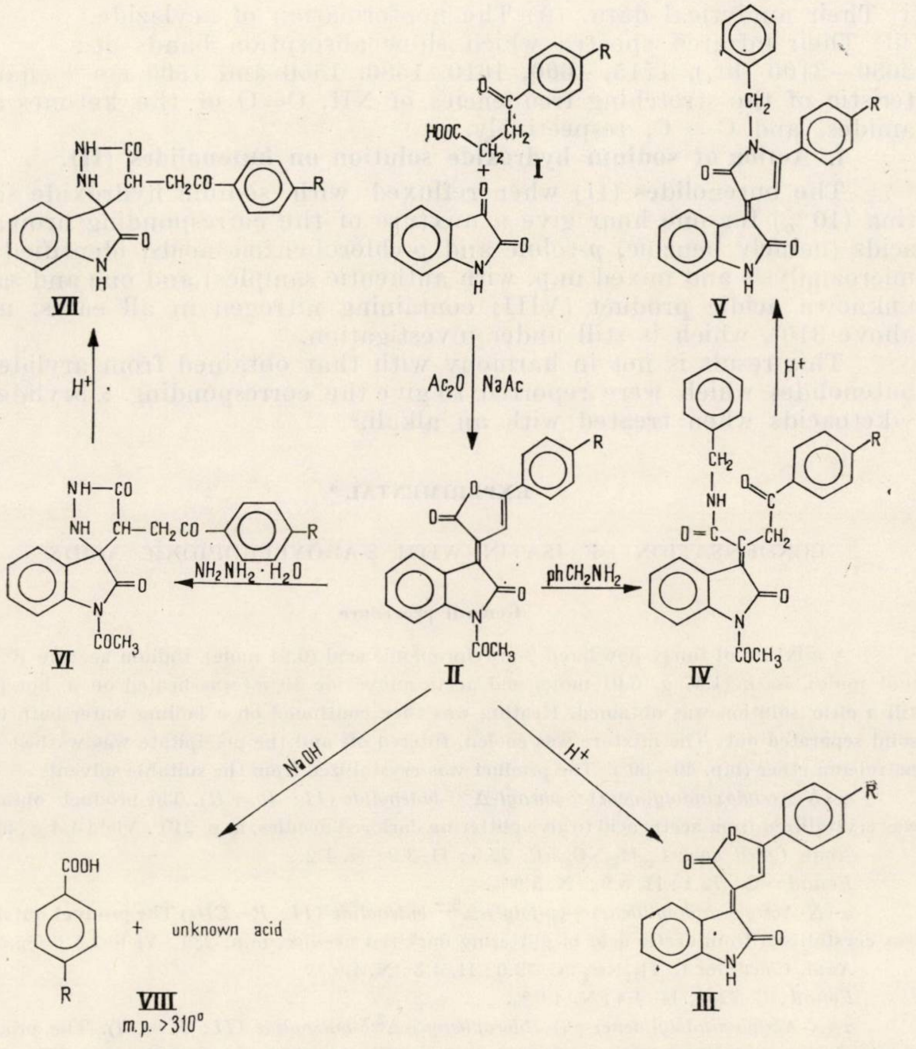
VII
I
V
H^+
Ac_2O NaAc
H^+
VI
$NH_2NH_2 \cdot H_2O$
II
$phCH_2NH_2$
IV
NaOH
H+
COOH
+ unknown acid
VIII
m.p. >310°
III

(iv) Stability of the pyrazolidine ring towards mineral acids.

e. Acid hydrolysis of 3-spiro (N-acetyloxindol)-4-aroylmethyl-5-ketopyrazolidines.

Hydrolysis of the produced 3-spiro-(N-acetyloxindol)-4-aroyl-methyl 5-ketopyrazolidines (VI) using dilute hydrochloric acid give the corresponding 3-spiro-oxindol-4-aroylmethyl-5-keto-pyrazolidines (VII; R=H, CH_3 and Cl) as yellow to brown solids. The structure of these products is inferred from the following facts:
(i) Their analytical data. (ii) The nonformation of acylazide.
(iii) Their infrared spectra which show absorption bands at: 3650–3100 (br.), 1715, 1660, 1610, 1580, 1550 and 1500 cm^{-1} characteristic of the stretching frequencies of NH, C=O of the ketones and amides, and C = C, respectively.

f. Action of sodium hydroxide solution on butenolides (II).

The butenolides (II) when refluxed with sodium hydroxide solution (10%) for one hour give a mixture of the corresponding aromatic acids (namely benzoic, *p*-toluic and *p*-chlorobenzoic acids, identified by microanalysis and mixed m.p. with authentic samples) and one and same unknown acidic product (VIII) containing nitrogen in all cases, m.p. above 310°, which is still under investigation.

This result is not in harmony with that obtained from arylidenebutenolides which were reported to give the corresponding α-arylidene-γ-ketoacids when treated with an alkali.[2]

EXPERIMENTAL [9]

CONDENSATION OF ISATIN WITH β-AROYLPROPIONIC ACIDS

General procedure

A mixture of finely powdered β-aroylpropionic acid (0.01 mole), sodium acetate (0.82 g 0.01 mole), isatin (1.47 g, 0.01 mole) and acetic anhydride 10 ml was heated on a hot plate till a clear solution was obtained. Heating was then continued on a boiling water-bath till a solid separated out. The mixture was cooled, filtered off and the precipitate was washed with petroleum ether (b.p. 40–60°). The product was crystallized from the suitable solvent.

α-(N-Acetyloxindolylidene)-γ-phenyl-$\Delta^{\beta,\gamma}$*-butenolide* (*II*; *R* = *H*). The product obtained was crystallized from acetic acid to give glittering dark red needles, m.p. 215°. Yield 1.4 g (46%).

Anal. *Calcd.* for: $C_{20}H_{13}NO_4$: C, 72.5; H, 3.9; N, 4.2.

Found: C, 72.1; H, 3.9; N, 3.9%.

α-(N-Acetyloxindolylidene)-γ-(p-tolyl)-$\Delta^{\beta,\gamma}$*-butenolide* (*II*; *R*=CH_3) The product obtained was crystallized from acetic acid in glittering dark red needles, m.p. 239°. Yield 2.1 g (65.6%).

Anal. *Calcd.* for $C_{21}H_{15}NO_4$: C, 73.0; H, 4.3; N, 4.0.

Found: C, 72.8; H, 4.4; N, 4.0%.

α-(N-Acetyloxindolylidene)-γ-(p-chlorophenyl)-$\Delta^{\beta,\gamma}$*-butenolide* (*II*; *R* = *Cl*). The product obtained was crystallized from acetic acid to give glittering dark red crystals, m.p. 226°. Yield 2.4 g (68%).

Anal. *Calcd.* for $C_{20}H_{12}NO_4Cl$: C, 65.6; H, 3.2; N, 3.8; Cl, 9.7.

Found: C, 65.1; H, 3.4; N, 3.8; Cl. 10.0%.

---

[9] a. Melting points are not corrected; b. Infrared spectra were measured on Infrared Spectrophotometer UNICAM SP 200G.

ACTION OF DILUTE HYDROCHLORIC ACID ON α-(N-ACETYLOXINDOLYLIDENE)-γ-ARYL-$\Delta^{\beta,\gamma}$-BUTENOLIDES

General procedure

The butenolide (II, 1 g) was dissolved in 50 ml acetic acid where a clear solution was obtained ; 10 ml of 6N−HCl were added and the mixture was refluxed for 1 hour. On cooling, reddish black crystals were separated. The product after filtration and washing with water was crystallized from a suitable solvent.

α-Oxindolylidene-γ-phenyl-$\Delta^{\beta,\gamma}$*-butenolide* (*III* ; *R=H*). The product obtained was crystallized from acetic acid as reddish-black needles, decomposed at 287°. Yield 0.82 g (91 %).

Anal. *Calcd.* for $C_{18}H_{11}NO_3$: C, 74.7 ; H, 3.8 ; N, 4.8.

Found : C, 74.0 ; H, 3.6 ; N, 4.8 %.

α-Oxindolylidene-γ-(p-tolyl)-$\Delta^{\beta,\gamma}$*-butenolide* (*III* ; *R=CH*$_3$). The product obtained was crystallized from toluene as reddish-black needles, decomposed at 280°. Yield 0.74 g(84 %).

Anal. *Calcd.* for $C_{19}H_{13}NO_3$: C, 75.2 ; H, 4.25 ; N, 4.6.

Found : C, 75.3 ; H, 4.25 ; N, 4.1 %.

α-Oxindolylidene-γ-(p-chlorophenyl)-$\Delta^{\beta,\gamma}$*-butenolide* (*III* ; *R = Cl*). The product obtained was crystallized from ethanol in reddish black needles, decomposed at 278°. Yield 0.88 g (88 %).

Anal. *Calcd.* for $C_{18}H_{10}NO_3Cl$: C, 66.7 ; H, 3.1 ; N, 4.3 ; Cl ; 10.9.

Found : C, 66.6 ; H, 3.6 ; N, 4.6 ; Cl, 10.6 %.

ACTION OF BENZYLAMINE ON THE BUTENOLIDES (II)

General procedure

A solution of the butenolide (II ; 0.005 mole) in dry benzene (15 ml) and benzylamine (0.6 g, 0.03 mole) was refluxed for 1 hour. On cooling a solid separated out. This was filtered off, washed with petroleum ether (b.p. 60−80°) and crystallized from the suitable solvent.

α-(N-Acetyloxindolylidene)-β-benzoyl-N-benzylpropionamide (*IV, R = H*). The product obtained was crystallized from toluene in yellow powder, m.p. 204°. Yield 2.7 g (69 %).

Anal. *Calcd.* for $C_{27}H_{22}N_2O_4$: C, 74.0 ; H, 5.0 ; N, 6.5.

Found : C, 74.8 ; H, 5.1 ; N, 6.6 %.

α-(N-Acetyloxindolylidene)-β-(p-toluyl)-N-benzylpropionamide (*IV* ; *R = CH*$_3$). The product obtained was crystallized from benzene as yellow powder, m.p. 180−81°C. Yield 1.1 g (50 %).

Satisfactory analytical data could not be obtained as the yellow product changed on standing to a dark violet powder.

α-(N-Acetyloxindolylidene)-β-(p-chlorophenyl)-N-benzylpropionamide (*IV* ; *R = Cl*). The product obtained was a yellow powder, m.p. 198−200°, which on crystallization from benzene changed to dark violet powder. Yield 1.1. g (50 %).

LACTIMIZATION OF α-(N-ACETYLOXINDOLYLIDENE)-β-AROYL-N-BENZYLPROPIONAMIDES (IV)

General procedure

The propionamide derivative (1g) was treated with 6N−HCl (50 ml) and the reaction mixture was refluxed for 1 hour. During heating the yellow colour changed gradually to violet.

The dark violet solid so obtained was washed with water and crystallized from a suitable solvent.

1-Benzyl-3-oxindolylidene-2-oxo-5-phenyl-2,3-dihydropyrrole (*V*, *R* = *H*). The product obtained was crystallized from benzene in dark violet crystals, m.p. 218°. Yield 0.57 g (71 %).

Anal. *Calcd.* for $C_{25}H_{18}N_2O_2$: C, 79.3 ; H, 4.7 ; N, 7.4.

Found : C, 79.6 ; H, 4.8 ; N, 6.7 %.

1-Benzyl-3-oxindolylidene-2-oxo-5-(p-tolyl)-2,3-dihydropyrrole (*V* ; *R* = CH_3). The product. obtained was crystallized from benzene in dark violet crystals, m.p. 250 – 51°. Yield 0.7 g (88 %).

Anal. *Calcd.* for $C_{26}H_{20}N_2O_2$: C, 79.5 ; H, 5.1 ; N, 7.1.

Found : C, 78.8 ; H, 5.1 ; N, 6.9 %.

1-Benzyl-3-oxindolylidene-2-oxo-5-(p-chlorophenyl)-2,3-dihydropyrrole (*V* ; *R* = *Cl*). The product obtained was crystallized from benzene to give dark violet crystals, m.p. 280 – 81°. Yield 0.7 g (88 %).

Anal. *Calcd.* for $C_{25}H_{17}O_2N_2Cl$: C, 72.7 ; H, 4.1 ; N, 6.7 ; Cl. 8.6.

Found : C, 71.82 ; H, 3.8 ; N, 6.8 ; Cl, 9.2 %.

ACTION OF HYDRAZINE HYDRATE ON THE BUTENOLIDES (II)

General procedure

To the butenolide (1 g) in ethanol (20 ml), hydrazine hydrate (1 g) was added. The reaction mixture was shaken at room temperature until its dark red colour changed to pale brown. The solid product obtained was separated and crystallized from a suitable solvent.

Repeating the above experiment with refluxing for 1 hour gave the same product on cooling and diluting with water.

3-Spiro-N-acetyloxindol-4-benzoylmethyl-5-keto-pyrazolidine *VI* ; *R* = *H*). The product obtained was crystallized from ethanol/benzene in a pale brown powder, m.p. 225°. Yield 0.4 g (40 %).

Anal. *Calcd.* for $C_{20}H_{17}O_4N_3$: C, 66.1 ; H, 4.7 ; N, 11.5.

Found : C, 65.3 ; H, 5.3 : N, 11.0 %.

3-Spiro-(N-acetyloxindol)-4-(p-toluylmethyl)-5-ketopyrazolidine (*VI* ; *R* = CH_3). The reaction failed by using ethanol as a solvent on cooling or heating.

Replacing the alcohol by acetic acid (20 ml) gave a solid product which was crystallized from acetic acid as a pale yellow powder, m.p. above 280°. Yield 0.35 g (35 %).

Anal. *Calcd.* for $C_{21}H_{19}O_3N_3$: C, 67.2 ; H, 4.8 ; N, 11.1.

Found : C, 66.4 ; H, 5.4 ; N, 10.4 %.

3-Spiro-(N-acetyloxindol)-4-(p-chlorobenzoylmethyl)-5-ketopyrazolidine (*VI* ; *R* = *Cl*). The product obtained was crystallized from ethanol/benzene in a pale brown powder, m.p. 235 – 6°. Yield 0.4 g (40 %).

Anal. *Calcd.* for $C_{20}H_{16}N_3ClO_4$: C, 63.2 ; H, 4.2 ; N, 10.5 ; Cl, 9.9.

Found : C, 63.0, H, 4.7 ; N, 9.9 ; Cl, 9.3 %.

ACTION OF DILUTE HYDROCHLORIC ACID ON 3-SPIRO-(N-ACETYLOXINDOL)-4-AROYLMETHYL-5-KETOPYRAZOLIDINES (VI)

The pyrazolidine derivative (VI) (1 g) was treated with 6N-HCl (30 ml) and the reaction mixture was refluxed for one hour. The solid obtained was filtered off, washed with water and crystallized from a suitable solvent.

3-Spiro-oxindol-4-benzoylmethyl-5-ketopyrazolidine (*VII*; *R* = *H*). The product obtained was crystallized from ethanol to give a yellow powder, m.p. 270° Yield 0.7 g (79 %).

Anal. *Calcd.* for $C_{18}H_{15}O_3N_3$: C, 67.4 ; H, 4.7 ; N, 13.0.

Found : C, 68.2 ; H, 4.4 ; N, 13.4 %.

3-Spiro-oxindol-4-(p-chlorobenzoylmethyl)-5-ketopyrazolidine (*VII*; *R* = *Cl*). The product obtained was crystallized from ethanol/benzene in a dark brown powder, m.p. 295°. Yield 0.7 g (77 %).

Anal. *Calcd.* for $C_{18}H_{14}N_3ClO_3$: Cl, 9.9, N, 11.8.

Found : Cl, 10.2 : N, 11.0 %.

ACTION OF NITROUS ACID ON THE PYRAZOLIDINES (VI AND VII)

A solution of sodium nitrite (2 moles) in the least amount of ice-cold water was added dropwise with stirring to an ice-cold solution of the pyrazolidines (VI ; R = Cl and H) (1 mole) in glacial acetic acid. The temperature was not allowed to rise above 5°. After the addition was completed, the reaction mixture was left at room temperature for 1/2 an hour, then diluted with water. The solid precipitate was crystallized from ethanol/benzene.

In each case the starting material was recovered unreacted.

Repeating the same experiment on the compounds (VII ; R = H, and Cl) gave back similarly the reactants unaffected.

ALKALINE HYDROLYSIS OF α-(N-ACETYLOXINDOLYLIDINE)-γ-ARYL-$\Delta^{\beta,\gamma}$-BUTENOLIDES (II)

General procedure

A mixture of the butenolide (1 g) and 20 ml of 10 % sodium hydroxide solution was refluxed for 1 hour. The solution after cooling was rendered acidic by dilute hydrochloric acid, then made just alkaline with potassium hydroxide solution and finally acidic with aqueous acetic acid. The precipitate was found to be a mixture of two acids which were separated by fractional crystallization from a suitable solvent.

Benzoic acid. The mixture produced from α-(N-acetyloxindolylidene)-γ-phenyl-$\Delta^{\beta,\gamma}$-butenolide was treated with petroleum ether (b.p. 40—60°). The soluble fraction was recrystallized from the same solvent as colourless crystals, m.p. 120°. Yield 0.3 g. This was proved to be benzoic acid by mixed m.p. experiment.

The insoluble fraction was crystallized from ethanol/benzene as light brown powder (VIII), m.p. above 310°. This compound was found to contain nitrogen (by sodium fusion test), and unaffected by hot 6N-HCl.

p-Toluic acid. The produced mixture from α-(N-acetyloxindolylidene)-γ-(*p*-tolyl)-$\Delta^{\beta,\gamma}$-butenolide was treated with petroleum ether (b.p. 40—60°). The soluble fraction was recrystallized from the same solvent as colourless crystals, m.p. 181°. Yield 0.3 g. This was found to be *p*-toluic acid by mixed m.p. experiment.

The insoluble fraction was found to be compound VIII, the same as in the case of α-(N-acetyloxindolylidene)-γ-phenyl-$\Delta^{\beta,\gamma}$-butenolide.

p-Chlorobenzoic acid. The mixture produced from α-(N-acetyloxindolylidene)-γ-(*p*-chlorophenyl)-$\Delta^{\beta,\gamma}$-butenolide was treated with benzene. The soluble fraction was crystallized from benzene as colourless crystals, m.p. 239—40°. Yield 0.3 g. This was proved to be *p*-chlorobenzoic acid by mixed m.p. experiment.

The insoluble fraction was found to be the same compound VIII.

Revue Roumaine de Chimie, **19**, *1*, 87–98 (1974)

ALUMINIUM CHLORIDE CATALYZED REACTIONS OF UNSATURATED ACIDS WITH BENZENE. VI[1]

REACTION OF CYCLOPENTYLACRYLIC ACID

ALICE MARIE GLATZ *, VASILE WERTHEIMER* and FLORIN BADEA **

* Institute of Organic Chemistry, Spl. Independenţei 202 B
** Polytechnic Institute, str. Polizu 1, Bucharest

Received September 7, 1973

Aluminium chloride catalyzed reaction of cyclopentylacrylic acid with benzene has been investigated at 40–45°, the reaction products being β-phenyl-β-cyclopentylpropionic (**5**), *trans*-2-phenyl-β-cyclopentylpropionic (**8**), *cis*-3-phenyl-β-cyclopentylpropionic (**10**) acids and the *trans*-2-phenyl-cyclohexylacetic, *cis*-3-phenyl-cyclohexylacetic and *trans*-4-phenyl-cyclohexylacetic acids (**17,19** and **21**) with rearranged skeleton. The isomerization of the reaction products has been investigated in the same conditions with the arylation reaction. Based on the distribution of reaction products and conformational analysis a reaction mechanism has been outlined.

As pointed out in earlier papers, [1–3] two ways are possible in the formation of phenylated acids during the aluminium chloride catalyzed reaction of α, β-unsaturated acids; the direct attack of benzene on the carbocations formed in the reaction and subsequent isomerizations of the finite reaction products.

The first step of the reaction, the trapping of the intermediate carbocations by benzene is a kinetically-controlled reaction and depends only on the relative stabilities of the carbocations originated from the alkylating agent.

The second step, the isomerization of phenylated acids is thermodynamically-controlled and covers to some extent the first step, modifying thus the ratio of the products.

A recent study [2] of the reaction of cyclopentylidene-acetic acid showed that only two main products are formed from the five possible isomers, namely *trans*-2-phenyl-cyclopentylacetic and *cis*-3-phenyl-cyclopentylacetic acids, the third product, *cis*-2-phenyl-cyclopentylacetic acid appearing only in a small amount (3%). The stereoselectivity of the reaction has been explained by a mechanism involving phenonium and lactoide ions, the appearance of lactoide ions in the course of Friedel-Crafts reactions of unsaturated acids being well-known in literature.[4-8]

---

[1] Part V. A. M. Glatz, F. Badea, Zs. Arvay, V. Drăguţan and F. Chiraleu, *Rev. Roumaine Chim.*, **18**, 2087 (1973).

[2] A. M. Glatz, A. C. Răzuş, F. Badea and C. D. Nenitzescu, *Rev. Roumaine Chim.*, **16**,1567 (1971).

[3] A. M. Glatz, A. C. Răzuş and C. D. Nenitzescu, *Rev. Roumaine Chim.*, **11**, 555 (1966).

It has been considered that the investigation of the reaction of cyclopentylacrylic acid (**1**) could give further details regarding the mechanism of these reactions, especially the competition between hydride shift and rearrangement of the five-membered ring.

The aluminium chloride catalyzed reaction of cyclopentylacrylic acid (**1**) with benzene at 40—45° leads with an overall yield of 60% to a mixture of acids (b.p.$_1$ 200°) having the elementary formula $C_{14}H_{18}O_2$. V.p.c.-analysis of the mixture of the corresponding methyl esters showed the presence of seven acids (table 1), which were identified by gas chromatographic comparison with authentical samples.

Table 1

Reaction products of the aluminium chloride catalyzed reaction of cyclopentylacrylic acid (1) with benzene, at 40—45°

Acids*	Moles %
β-Phenyl-β-cyclopentylpropionic (**5**)	3.8
trans-2-Phenyl-cyclohexylacetic (**17**)	10.0
trans-2-Phenyl-β-cyclopentylpropionic (**8**)	5.0
unknown	2.9
cis-3-Phenyl-cyclohexylacetic (**19**)	41.9
cis-3-Phenyl-β-cyclopentylpropionic (**10**)	5.5**
trans-4-Phenyl-cyclohexylacetic (**21**)	30.5**

* Identified as methyl esters; the herein given order corresponds to the retention times.

** Amounts determined from the NMR spectrum of the mixture of methyl esters (separated by preparative v.p.c.) using Eu (DPM)$_3$ as paramagnetic shift reagent.

As depicted in table 1, the reaction of cyclopentylacrylic acid (**1**) with benzene leads to phenylated acids with cyclopentane and cyclohexane skeleton.

Only three isomers are formed from the six phenyl-cyclopentylpropionic acids possible, these being the normal reaction products (**5**, **8** and **10**). Although the appearance of the 1-phenyl-1-(β-cyclopentyl-

---

[4] P. Four and L. Lefort, *Tetrahedron Letters*, **1968**, 6143.

[5] J. I. Brauman and A. J. Pandell, *J. Amer. Chem. Soc.*, **89**, 5421 (1967).

[6] M. F. Ansell and M. H. Palmer, *Quart. Rev.*, **1964**, 211.

[7] M. F. Ansell, B. E. Greenwood and T. M. Kafka, *J. Chem. Soc.*, (*C*), **1967**, 1802.

[8] M. F. Ansell and M. H. Palmer, *J. Chem. Soc.*, **1963**, 2640.

propionic) acid **(12)** in the course of the reaction is highly probable, this acid has not been found among the reaction products.

Unexpectedly, the main products of the reaction are the phenylcyclohexylacetic acids **17**, **19** and **21**, resulted by ring expansion and phenylation of the intermediate carbocations.

As pointed out above, the phenylation of acids takes place by the nucleophilic attack of benzene on the carbocations formed by hydride shift in the initially carbocation (in this case carbocation **2**), each ion undergoing isomerizations.[2,3,9,10]

Protonation of the double bond in acid **1** leads to carbocation **2** which may disappear in three different pathways (Chart 1) : attack of benzene on the primary formed carbocation leading to β-phenyl-β-cyclopentylpropionic acid **(5)** (path A), hydride shift which gives rise to carbocation **3** (path B) and ring enlargement of the five-membered ring to carbocation **4** (path C).

Chart 1

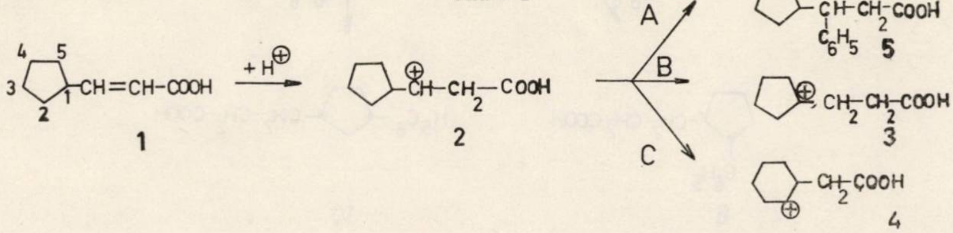

As shown in table 1, the proportion between five- and six-membered ring products is 1 : 6.

Although the data listed in table 1 should indicate an equilibrium between rings, the isomerization experiments of acids **5**, **10** and **12**, on the one hand, and of acids **17**, **19** and **21**, on the other hand, clearly showed that there is no interconversion between rings. Therefore, at least the pathways shown in Chart 1 are kinetically controlled.

Acid **5** is formed in a small amount (less than 4%) indicating that the reaction of carbocation **2** with benzene is much slower than the other two competitive transformations (paths B and C).[11] This is also supported by the failure of acid **5** to undergo isomerization and which, therefore, could be considered certainly as a primary product. The fact that acid **5** does not undergo isomerization is probably due to the imposed sterical hindrance in the formation of a phenonium ion and the vicinity of the destabilizing carboxyl group to the carbocationic center.

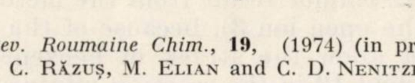

---

[9] A. M. Glatz, *Rev. Roumaine Chim.*, **19**, (1974) (in press).

[10] A. M. Glatz, A. C. Răzuş, M. Elian and C. D. Nenitzescu, *Rev. Roumaine Chim.*, **16**, 1579 (1971).

[11] G. Geiseler, P. Herrmann and G. Kürzel, *Chem. Ber.*, **98**, 1695 (1965).

Chart 2 represents the mechanism of the reaction of cyclopentylacrylic acid (**1**) leading to the acids **8** and **10**.

Chart 2

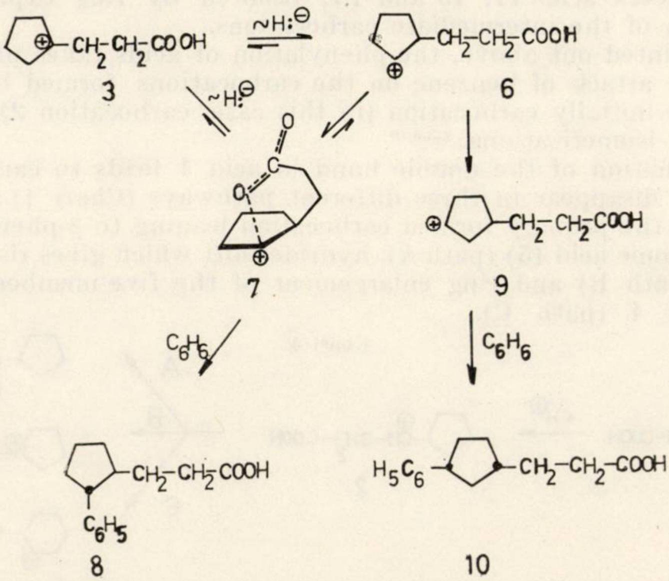

The absence of *cis*-2-phenyl-β-cyclopentylpropionic acid among the reaction products indicates a stereospecific pathway involving an ion species — the lactoide ion **7** [2,4–8] more stable than an open carbocation.

Thus, the hydride shift in **3** and participation of carboxyl group leads to the lactoide ion **7**, which reacts with benzene from the opposite side of the lactoide ring to give *trans*-2-phenyl-β-cyclopentylpropionic acid (**8**). The lactoide ion **7** may also result by carboxyl participation from ion **6**, which partly isomerizes to ion **9**. The attack of benzene on **9** yields *cis*-3-phenyl-β-cyclopentylpropionic acid (**10**).

The proportion between the acids **8** and **10** is 1 : 1.1, indicating that carboxyl participation at the cationic center and hydride shift are comparable in rates, thus confirming earlier observations.[2,9] Acid **10** undergoes isomerization in the conditions of arylation reaction yielding a mixture of acids **8** and **10**, their ratio being 1 : 1.7.

In the case of cyclopentylacrylic acid (**1**) the formation of 1-phenyl-1-(β-cyclopentylpropionic) acid (**12**) may be possible. The tertiary ion **3** is entirely different from his inferior homologue which arises in the Friedel-Crafts reaction of cyclopentylideneacetic acid,[2] the former being able to be stabilized forming the lactoide ion **11**.

However, acid **12** cannot result from the lactoide ion **11** (which is in equilibrium with the open ion **3**), because of the spiran-like structure of **11** which does not allow the attack of benzene.

The absence of acid **12** in the reaction mixture does not invalidate the possibility of his formation, since the acid **12** undergoes easily complete isomerization in the reaction conditions yielding the acids **8** and **10** in a ratio of 1 : 2.6.

Isomerization of 1-phenyl-1-(β-cyclopentylpropionic) acid **(12)** (Chart 3) involves the intermediate phenonium ion **13** resulted by hydride abstraction at carbon C-2. The subsequent attack of a hydride ion on **13** at C-1 leads to *trans*-2-phenyl-β-cyclopentylpropionic acid **(8)**.

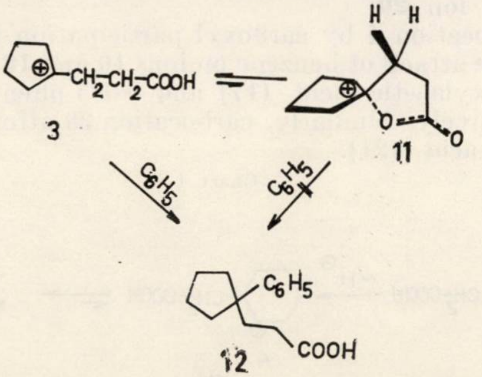
CH_2CH_2COOH
H H
3
11
C_6H_5
C_6H_5
C_6H_5
COOH
12

Similarly, from acid **8** phenonium ion **14** is formed, which is transformed by hydride shift in the stable benzylic-lactoide ion **15**. Hydride trapping by this ion yields *cis*-3-phenyl-β-cyclopentylpropionic acid **(10)**.

Chart 3

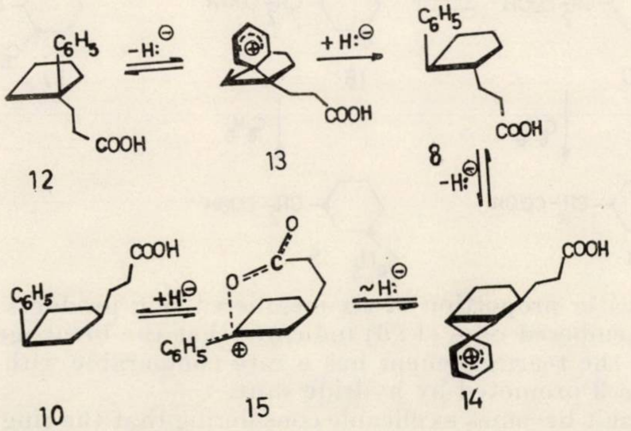
C_6H_5
$-H:^{\ominus}$
$+H:^{\ominus}$
C_6H_5
COOH
COOH
COOH
12
13
8
$-H:^{\ominus}$
COOH
C_6H_5
$+H^{\ominus}$
O
C
O
C_6H_5
$\sim H:^{\ominus}$
COOH
10
15
14

Neither in the reaction of cyclopentylacrylic acid **(1)**, nor in the isomerization of 1-phenyl-1-(β-cyclopentylpropionic) acid **(12)**, a *trans* 1,3-disubstituted acid is formed. This is due to the well-known fact that *cis*-1,3-disubstituted cyclopentane derivatives are thermodynamically more stable. [2, 12–15]

---

[12] E. Eliel "Steoreochemistry of Carbon Compounds", McGraw-Hill Comp., New York, 1962, p. 249.

[13] G. F. Nirch and R. A. Dean, *J. Chem. Soc.*, **1953**, 2477.

[14] R. C. Cookson, J. Andel, S. A. Knight and B.R.D. Whiear, *Tetrahedron*, **19**, 1955 (1963).

[15] D. Vareck, C. Ouannes and J. Jaques, *Bull. Soc. chim. France*, **1965**, 1662.

Three phenyl-cyclohexylacetic acids are present in the reaction mixture, acids **17**, **19** and **21** (table 1). These acids derive from carbocation **2** by ring enlargement which leads to carbocation **4** (Chart 1, path C). Hydride shift in **4** generates ion **18** which is then converted by another hydride shift to ion **20**.

From carbocation **4** by carboxyl participation the stable lactoide ion **16** results. The attack of benzene on ions **16** and **18** gives rise to *trans*-2-phenyl-cyclohexylacetic acid **(17)** and *cis*-3-phenyl-cyclohexylacetic acid **(19)**, respectively. Similarly, carbocation **20** affords *trans*-4-phenylcyclohexylacetic acid **(21)**.

Chart 4

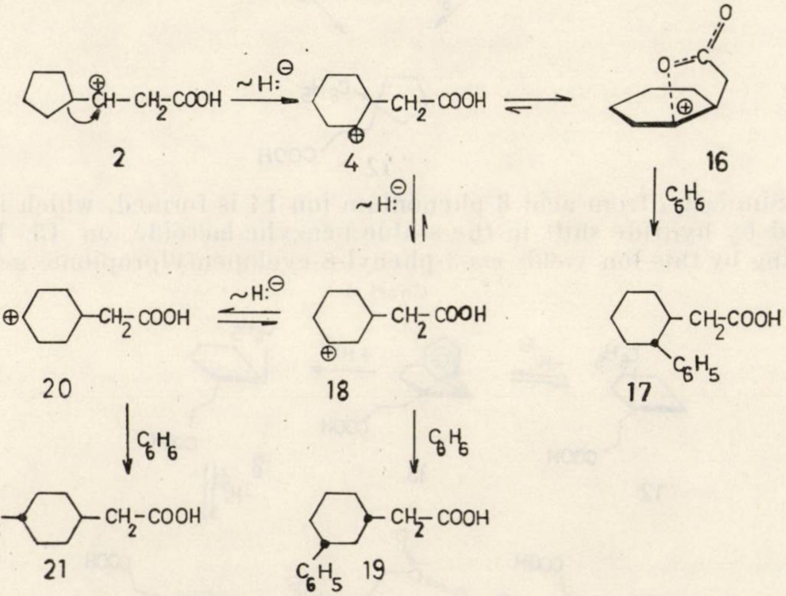

The greater proportion of six-membered ring products with respect to the five-membered ones (1 : 6) indicates that the breakage of the C—C bond during the rearrangement has a rate comparable with the isomerization of **2** in **3** promoted by hydride shift.

This result becomes explicable considering that the ring enlargement reduces not only the destabilizing effect of carboxyl group in **2**, but the eclipsing strain of the five-membered ring too.

Acid **17** results in a smaller proportion than acids **19** and **21** (1 : 7.2), it showing that the carboxyl group participates in lactoidisation to a less extent in ion **16** than in the foregoing case of ion **7**.

The stereochemistry of the formed phenyl-cyclohexylacetic acids is in agreement with the thermodynamic stabilities of dimethyl[16] — and diphenyl-cyclohexanes[17]; *trans*-1,2, *cis*-1,3 and *trans*-1,4-disubstituted derivatives are the more stable among the six diastereomers possible, the preferred conformation of the three isomers being diequatorial.[16]

---

[16] Citat 12, p. 214.

[17] A. M. GLATZ, A. C. RĂZUŞ, F. BADEA and C. D. NENITZESCU, *Rev. Roumaine Chim.*, **17**, 1735 (1972).

As shown, phenylated acids undergo isomerizations under the conditions of the arylation reaction.

Accordingly, isomerization of acid **17** yields a mixture of acids **17**, **19** and **21** in a relative proportion of 9.85 : 1.1 : 1. The mixture resulted from the isomerization of **19** contains acids **21** and **19** in a ratio of 1 : 5.25, while the same acids are formed in a ratio of 2.1 : 1 in the isomerization of acid **21**.

The results of isomerization experiments are summarized in table 2.

Table 2

Isomerization products of phenyl-cyclohexylacetic acids

Reagent	Products, moles %		
	17	**19**	**21**
17*	61.7	6.8	6.2
19	—	84	16
21	—	31.8	66.5

* In this reaction some secondary products were formed which were not identified.

A comparison of the proportions of acids **17**, **19** and **21** from tables 1 and 2 clearly shows that the equilibrium has not been attained under the employed conditions.

In the isomerization of disubstituted cyclohexane derivatives, conformational effects of the six-membered ring have to be taken into account.

Thus, *cis*-3-phenyl-cyclohexyl acetic acid **(19)** cannot result by a direct isomerization through phenonium ion from *trans*-2-phenyl-cyclohexylacetic acid **(17)**, since in this way the reaction should proceed with retention of configuration leading to *trans*-3-phenyl-cyclohexylacetic acid **(26)**. Therefore, in the isomerization of **17** to **19** a further step must be involved, which could be : a) either an isomerization 1,3-*trans* → 1,3-*cis*, subsequent to the rearrangement of the phenyl group : b) or a *trans*-1,2⇄ *cis*-1,2 isomerization prior to the formation of the phenonium ion.

The preferred *e, e* conformation of *trans*-2-phenyl-cyclohexylacetic acid **(17)** (one butane-gauche interaction) cannot give rise to a phenonium ion, because of the staggered phenyl group. Hence, the diequatorial conformer must be converted into the diaxial one, the phenyl group being now able to form the phenonium ion **25** (Chart 5). Migration of phenyl group followed by the isomerization of acid **26** should yield acid **19** (case a).

The best criterion for distinguishing between the two possibilities is the comparison of the energy differences involved in both cases.

The energy barrier imposed in the conversion of acid **17** from the *e, e* into the *a, a* conformer exceeds the enthalpy difference between *trans*- and *cis*-2-phenyl-cyclohexylacetic acid (**17** and **23**, respectively) (the energy gap between *e, e* and *a, a* dimethylcyclohexane is 2.7 kcal/

mol, whereas for converting 1,2-dimethylcyclohexane from the *trans* into the *cis* form 1.87 kcal/mol are needed[16]).

These facts show that a reaction pathway involving isomerization of **17** in *cis*-2-phenyl-cyclohexylacetic acid (**23**) and subsequent phenyl migration seems to be more probable (Chart 6, case b).

Chart 5

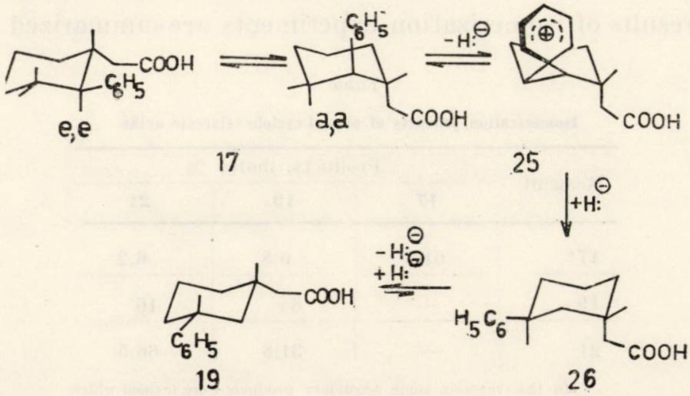
-COOH
C6H5
e,e
17
C6H5
a,a
COOH
-H:⊖
⊕
COOH
25
+H:⊖
-H:⊖
+H:⊖
COOH
C6H5
19
H5C6
COOH
26

Noteworthy is that acid **17**, compared with acids **19** and **21**, undergoes isomerization to a less extent (table 2), although the thermodynamic stabilities of disubstituted cyclohexanes decrease in the order *cis* 1.3 > *trans* 1.4 > *trans* 1.2.[16,17] This result can be explained by the fact that the isomerization of acid **17** involves the development of a cationic center, destabilized by the vicinity of carboxyl group, thus increasing the free energy of activation needed for the formation of the intermediate ion **22** (Chart 6).

Chart 6

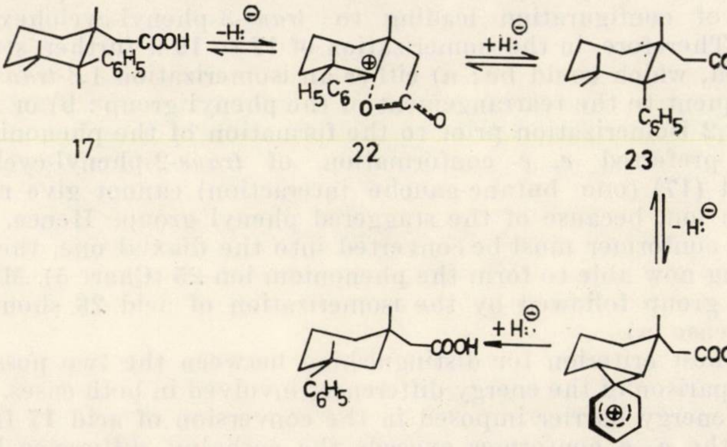
-COOH
C6H5
17
-H:⊖
⊕
H5C6
O
C
O
22
+H:⊖
-COOH
C6H5
23
-H:⊖
+H:⊖
COOH
C6H5
19
COOH
⊕
24

In a similar way, the isomerization of acid **19** in **21** takes place also through a benzylic ion (**27**), followed by the formation of phenonium ion

28 and hydride attack on this, leading to *trans*-4-phenyl-cyclohexylacetic acid (**21**) (Chart 7). In this case the energy needed for converting **19** *e*, *e* in **19** *a*, *a* exceeds also the enthalpy difference between *cis*- and *trans*-3-phenyl-cyclohexyl-acetic acid (**19** and **26**) (the corresponding values for 1,3-dimethylcyclohexane are: 5.4 kcal/mol for converting *e*, *e* into *a*, *a* and 1.8 kcal/mol for the *cis* $\rightleftharpoons$ *trans* isomerization [16]).

Chart 7

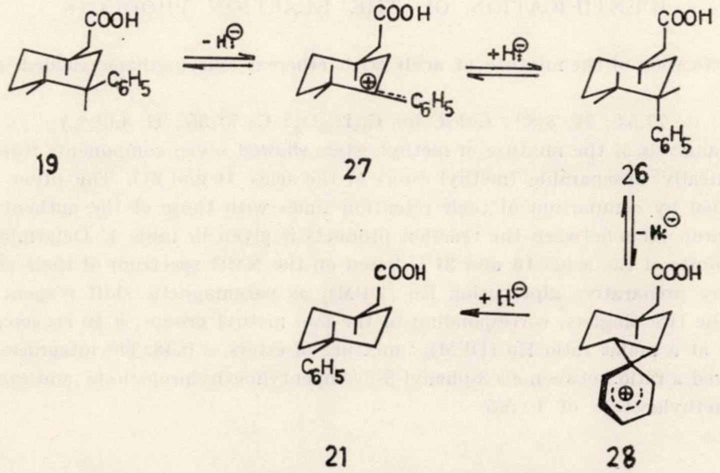

The fact that *trans*-4-phenyl-cyclohexylacetic acid (**21**) isomerizes to a larger extent than acid **19** must be due to an effect of entropy of reaction also remarked in the isomerization of the corresponding diphenylcyclohexanes.[17]

EXPERIMENTAL

All melting points are uncorrected. IR spectra were recorded on a double beam UR 20 Carl Zeiss-Jena spectrophotometer. NMR spectra were recorded on a Varian A 60-A spectrometer using TMS as internal standard. Glpc analyses were carried out on a Willy Giede model 18.3 gas chromatograph using a 3 m × 4 mm column packed with 20% ethylene-glycol-succinate on Chromosorb W (60–80 mesh); column temperature: 195°; carrier gas: hydrogen, 80 ml/min.

REACTION OF CYCLOPENTYLACRYLIC ACID (1) WITH BENZENE (ACIDS 5, 8, 10, 17, 19, 21).

A solution of 5 g (35.5 mmoles) cyclopentylacrylic acid (**1**)[18] in 45 ml anhydrous benzene was added dropwise to a stirred suspension of 6.7 g (53 mmoles) of aluminium chloride in 20 ml anhydrous benzene, at 40–45°. Stirring was continued at this temperature for 4 hrs. After quenching in ice-water and extraction of the benzene layer with 10% potassium hydroxide, the alkaline layer was acidified and extracted with ether. Drying over magnesium sulfate and removal of the solvent yielded a pale yellow oil, b.p.$_1$ 200—202°, weighing 4.6 g (60%) which rapidly solidified. (*Found* : C, 77.65 ; H, 7.93 ; *Calcd.* for $C_{14}H_{18}O_2$: C, 77.10 ; H, 8.32%)

---

[18] R. Roth and H. Erlenmeyer, *Helv. Chim. Acta*, **38**, 1278 (1955).

NMR spectrum (CCl_4, δppm) of the mixture of acids shows the following signals : 12.1 (1 carboxylic proton) ; 7.14 (5 aromatic protons, singlet) ; 2.8—0.8 (12 aliphatic protons).

IDENTIFICATION OF THE REACTION PRODUCTS

Esterification of the mixture of acids with ethereal diazomethane yielded an oil. b.p. 1 150—155°.

(*Found* : C, 77.54 ; H, 8.89 ; *Calcd.* for $C_{15}H_{20}O_2$: C, 77.55 ; H, 8.68%)

Glpc-analysis of the mixture of methyl esters showed seven components from which two were analytically unseparable (methyl esters of the acids **10** and **21**). The other components were identified by comparison of their retention times with those of the authentical samples.

The proportion between the reaction products is given in table 1. Determination of the relative amounts of the acids **10** and **21** is based on the NMR spectrum of their ester mixture (separated by preparative glpc, using Eu $(DPM)_3$ as paramagnetic shift reagent.

For the two singlets, corresponding to the two methyl groups, a 10 Hz separation could be obtained at a molar ratio Eu $(DPM)_3$: mixture of esters = 0.48. The integration of the two signals showed a ratio between *cis*-3-phenyl-β-cyclopentylmethylpropionate and *trans*-4-phenylcyclohexylmethylacetate of 1 : 5.5.

REAGENTS. CHROMATOGRAPHIC STANDARDS

β-Phenyl-β-cyclopentylpropionic acid (5) and methyl ester

The acid **5** was obtained by alkaline hydrolysis of methyl ester prepared by Arndt-Eistert synthesis from α-phenyl-α-cyclopentylacetic acid [19] ; m.p. 86—88° (aqueous ethanol).

NMR spectrum (CCl_4, δppm) of methyl ester : 7.15 (5 aromatic protons, singlet) ; 3.6 (esteric-CH_3, 3 protons, singlet) ; 3.15—2.4 (3 protons) ; 2.4—0.8 (9 protons).

trans-2-Phenyl-β-cyclopentylmethylpropionate. The methyl ester of acid **8** has been prepared by Arndt-Eistert reaction of a mixture of phenyl-cyclopentylacetic acids [2] (containing *trans*-and *cis*-2-phenyl-cyclopentylacetic acid and *cis*-3-phenyl-cyclopentylacetic acid) and concentration of the mixture in the *trans* isomer by chromatography over neutral alumina (650 × × 10 mm) eluating with petroleum ether and ethyl ether (10%). By passing repeatedly the mixtures through the column, a 70% enrichment of the mixture in *trans*-2-phenyl-β-cyclopentylpropionate could be reached, the concentration being followed by v.p.c.

cis-3-Phenyl-β-cyclopentylpropionic acid **(10)** *and methyl ester.* The acid **10** was prepared from *cis*-3-phenyl-cyclopentylacetic acid [2] by Arndt-Eistert synthesis followed by alkaline hydrolysis of *cis*-3-phenyl-β-cyclopentylmethylpropionate.

NMR spectrum (CCl_4, δppm) of methyl ester : 7.18 (5 aromatic protons, singlet) ; 3.6 (esteric-CH_3, 3 protons, singlet) ; 3.0 (1 benzylic proton, multiplet centered at δ = 3.0) ; 2.6—1.1 (11 protons).

1-Phenyl-1-(β-cyclopentylpropionic) acid **(12)** *and methyl ester.* The acid 12 has been prepared according to the method described by Arnold *et al.*[20] The methyl ester was obtained by diazomethane esterification.

---

[19] Fr. Salman-Legagneur and Y. Olivier, *Bull. Soc. chim. France*, **1965**, 640.

[20] R. T. Arnold, J. S. Buckley jr., and R. M. Dodson, *J. Amer. Chem. Soc.*, **72**, 3153. (1950).

trans-2-Phenyl-cyclohexylacetic acid (**17**) *and methyl ester*. The synthesis of the acid **17** has been described by Bachmann and Fornfeld.[21] The methyl ester was obtained by esterification with diazomethane.

cis-3-Phenyl-cyclohexylacetic acid (19) and methyl ester

2-Phenyl-6-carbethoxy-cyclohexanone was prepared by the method indicated by Baker, McOmie, *et al.*,[22] with 2-phenylcyclohexanone[23] as starting material.

cis-1-Phenyl-2-oxo-3-cyclohexylacetic acid

To a stirred suspension of 3.8 g (77 mmoles) NaH (50% mineral oil) in 100 ml anhydrous benzene, a solution of 19 g (77 mmoles) 2-phenyl-6-carbethoxy-cyclohexanone in 50 ml anhydrous benzene was added dropwise at 40—45°. Stirring was continued at 60—70° for 1.5 hrs, since no more hydrogen was evolved. A solution of 13 g (77 mmoles) of ethyl-bromoacetate in 30 ml anhydrous benzene was added slowly at 60° and stirring was continued for 45 min. The mixture was then stirred and refluxed for another 3 hrs and after cooling it was poured into ice water and slightly acidified with acetic acid. The separated benzene layer was dried over magnesium sulfate and the solvent removed *in vacuo*. The residual oil (22 g) was refluxed for 16 hrs with 200 ml concentrated hydrochloric acid and 160 ml acetic acid. After removal of solvents *in vacuo* the residual material was dissolved in ether and then extracted with aqueous KOH 7%. The alkaline layer was acidified with hydrochloric acid and deposited a highly viscous material which was crystallized two times from CCl_4 yielding 5 g of a white solid, m.p. 131.5—132.5°. (*Found* : C, 70.88 ; H, 6.78 ; *Calcd.* for $C_{14}H_{16}O_3$: C, 72. 39 ; H, 6.94%).

cis-3-Phenyl-cyclohexylacetic acid (19)

5 g of the ketoacid obtained above were reduced by the method employed by Arnold *et al.*,[20] with hydrazine and potassium hydroxide in diethylene glycol. The mixture worked up as usual yielded, after crystallization from aqueous ethanol (1 :1), 1.3 g of the acid, m.p. 83—86°.

The methyl ester was obtained by diazomethane esterification.

NMR spectrum (CCl_4, δppm) of methyl ester : 7.13 (5 aromatic protons, singlet) ; 3.6 (esteric-CH_3, 3 protons, singlet) ; 2.7 (1 benzylic proton, multiplet centered at $\delta = 2.7$) ; 2.37 (*exo*-cyclic-CH_2-, 2 protons, broadened singlet) ; 2.3—1.2 (9 protons).

trans-4-Phenyl-cyclohexylacetic acid (21) and methyl ester

Reduction of biphenyl-4-carboxylic acid,[24] according to Zimmerman,[25] yielded *trans*-4-phenyl-cyclohexyl-carboxylic acid which by Arndt-Eistert chain lengthening gave the methyl ester of **21**. Alkaline hydrolysis of the methyl ester yielded acid **21**, m.p. 71° (aqueous ethanol).

NMR spectrum (CCl_4, δ ppm) of methyl ester : 7.17 (5 aromatic protons, singlet) ; 3.67 (esteric-CH_3, 3 protons, singlet) ; 2.8—0.9 (12 protons).

---

[21] W. E. BACHMANN and E. J. FORNFELD, *J. Amer. Chem. Soc.*, **72**, 3390, 5529 (1950).

[22] W. BAKER, J. W. F. McOMIE, S. D. PARFITT and D. M. WATKINS, *J. Chem. Soc.*, **1957**, 4032.

[23] St. GOLDSCHMIDT and W. L. C. VEER, *Rec. Trav. chim.*, **67**, 489 (1948).

[24] Ch. CULL, and E. E. TURNER, *J. Chem. Soc.*, **1929**, 491.

[25] H. E. ZIMMERMAN and H. J. GIALLOMBARDO, *J. Amer. Chem. Scc.*, **78**, 5263 (1956).

ISOMERIZATIONS OF THE ACIDS 5, 10, 17, 19, 21

All isomerization experiments were carried out under identical conditions, in benzene, at 40 – 45°, 4 hrs. The molar ratio employed was : acid $AlCl_3$: benzene = 1.1.5 : 20. The reaction mixtures were worked up as pointed above, esterified with ethereal diazomethane and analysed by v.p.c.

Isomerization of β-phenyl-β-cyclopentylpropionic acid (**5**). Acid 5 failed to undergo isomerization under the conditions employed.

Isomerization of 1-phenyl-1-cyclopentylpropionic acid (**12**). The reaction mixture contained two main components corresponding to the *trans*-2-phenyl-cyclopentylpropionic (**8**) (27.1 %) and *cis*-3-phenyl-cyclopentylpropionic (**10**) (61.2 %) acids, the other components being minor. Acid **12** was completely consumed during the reaction.

Isomerization of cis-3-phenyl-β-cyclopentylpropionic.acid (**10**) yielded (a mixture of *cis*-3-phenyl-β-cyclopentylpropionic acid (**10**) (60.5 %) and *trans*-2-phenyl-β-cyclopentylpropionic acid (**8**) (35.5 %).

Isomerization of phenyl-cyclohexylacetic acids (**17, 19, 21**). The isomerization results of phenyl-cyclohexylacetic acids are summarized in table 2.

Acknowledgements. The authors wish to express their gratitude to Miss E. Şliam and Mrs. V. Daniel for microanalyses and Mr. G.M.D. Benedikt for NMR spectra.

Revue Roumaine de Chimie, 19, 1, 99–113 (1974)

QUELQUES REMARQUES SUR LES PROPRIÉTÉS DES BÉTONS AUX RÉSINES SYNTHÉTIQUES SANS LIANTS MINÉRAUX. I

ION IONESCU

Laboratoires des Bétons, Mortiers et Armatures pour Bétons — I.C.M.P.C.—Bucarest, 507, Şoseaua Giurgiului

Reçu le 18 avril 1973

On présente les résultats des recherches sur l'influence des propriétés physiques et chimiques des différents types de résines synthétiques, et des matériaux employés comme liants organiques et agrégats ou filler, ainsi que des facteurs de composition et technologique sur les principales propriétés structurales et physiques-chimiques des bétons à résines synthétiques sans liants minéraux.

1. ASPECTS GÉNÉRAUX. MATÉRIAUX UTILISÉS POUR LES RECHERCHES ET POUR LES EXPÉRIENCES. RÉSULTATS DES RECHERCHES PRÉLIMINAIRES

Les premières études sur les bétons aux résines synthétiques sans liants minéraux ont commencé, dans divers pays, après 1955. Il devenait, en effet, nécessaire de trouver des matériaux à propriétés supérieures à celles des bétons classiques, que ce soit les caractéristiques physiques et mécaniques ou, surtout, la résistance à l'action des agents chimiquement corrosifs. Dès le début, ces études se sont révélées difficiles en raison des grandes différences entre les propriétés de résines synthétiques appartenant aux mêmes groupes de produits, qui varient d'un pays à l'autre et de la nouveauté du sujet. On ignorait le comportement possible, au cours d'une exploitation prolongée, des résines synthétiques utilisées comme liants organiques, soumises à l'action des agents physiques et chimiques, ainsi qu'aux sollicitations mécaniques. Ces raisons, et les méthodologies très différentes, adoptées par les divers chercheurs en fonction du but poursuivi, expliquent la modestie des résultats obtenus jusqu'ici, en regard des perspectives expérimentales ou industrielles qu'ouvre l'étude de ces nouveaux types de bétons. Il n'existe pas encore de critères acceptés par la plupart des chercheurs et applicables à la classification des bétons de résine synthétique aux matériaux et à leurs techniques de confection.

L'une des classifications la plus souvent utilisée pour les bétons aux résines synthétiques sans liants minéraux est celle qui indique le type de la résine utilisée de la manière suivante : [1-3]

— bétons de résines époxydes, bétons de résines furanniques, bétons de résines phéno-formaldéhydes, bétons de résines polyesters, etc.

Pour l'étude des propriétés des bétons aux résines synthétiques, en tenant compte des possibilités qu'elles offrent dans diverses combinaisons avec les matériaux classiques et surtout avec les bétons de ciment, on a considéré que les bétons de résines synthétiques sans liants minéraux devraient remplir approximativement les exigences générales suivantes : aptitude à être confectionnés avec des moyens accessibles aux usines de préfabrication et aux grands chantiers, sans exiger, si possible, un personnel hautement qualifié d'exécution et de surveillance, temps de prise suffisamment prolongé pour le travail et la mise en œuvre et bonne ouvrabilité, durcissement après la mise en œuvre et performances techniques prescriptes atteintes dans un délai relativement bref, afin de permettre un décoffrage et une manutention faciles et la mise en exploitation la plus rapide possible ; ne pas nécessiter des conditions spéciales de protection immédiatement après la mise en œuvre ; faible retrait afin de permettre l'application ou le coulage en couches épaisses ; après le durcissement, bonne résistance à l'action des agents atmosphériques et aux sollicitations dues aux variations de température, au phénomène de gel-dégel, à l'action des rayons solaires et de l'eau, donc durabilité dans différentes conditions d'exploitation ; résistances supérieures à l'action de différents agents chimiquement agressifs ; résistances mécaniques supérieures, surtout résistance à la traction, module d'élasticité voisin de celui du béton de ciment (afin d'éviter de trop fortes concentrations des efforts aux joints ou dans les points de contact des différentes couches) ; fluage peu accusé par rapport à celui du béton ; bonne adhérence au béton de ciment et aux différents types d'armatures, de matériaux de construction, etc. [3] Il convient de considérer, avant même de choisir les résines, quels sont les durcisseurs, le pourcentage et les agrégats convenables, afin de pouvoir satisfaire totalement ou partiellement aux exigences énumérées ci-dessus. Remarquons que certaines des données publiées sur les bétons de résine sont contradictoires, les auteurs consultés expliquent ces contradictions par des différences sensibles entre les propriétés des résines et celles des autres matériaux utilisés. C'est pourquoi nous avons choisi, en vue des études préliminaires, les matériaux suivants, produits en Roumanie :

a) *Résines synthétiques*

1) résines époxydes : résine Dinox 040 A ;

2) résines phénol-formaldéhyde : résine LS. 1 ;

3) résines furanniques : le monomère furfurol-acétone FA ;

4) résines urée-formaldéhydes : les colles Urélit R-UR et Uréfor-U et la colle Urélit E modifiée à la mélamine URM ;

5) résines mélamine-formaldéhydes (triaziniques) : les résines M_1, M_2, M_3, M_4 et MM·

Au total 5 groupes de résines et 11 produits. Comme agrégats, on a utilisé dans cette phase du sable de rivière 0 à 7 mm, provenant de la ballastière Borleşti-Argeş dont la granulation est bonne. Les recherches ont permis de classer les bétons obtenus d'après les critères suivants :

---

[1] I. M. Elşhin, «Plastobeton», Ed. Bidvelnik, Kiev, 1957.

[2] I. Ionescu, M. Enculescu, « Întrebuinţarea maselor plastice pentru impermeabilizarea şi protecţia anticorozivă a construcţiilor hidrotehnice », Chap. IVe et V^e, I.S.C.H., Bucarest, 1964.

[3] I. Ionescu, «Contribuţii la studiul proprietăţilor betoanelor cu răşini sintetice», IIIe chap., Institutul Politehnic Timişoara, Facultatea de Construcţii, 1969.

CRITÈRE DES RÉSISTANCES MÉCANIQUES À LA TEMPÉRATURE NORMALE D'ESSAI

Les bétons étudiés sont divisés en trois groupes bien distincts :

1) bétons à fortes résistances mécaniques, $Rc_{28}=500$ à 800 daN/cm^2 et $Rt_{28} = 70$ à 240 daN/cm^2 : les bétons à résine époxyde Dinox 040 A et à résine furannique, monomère FA ;

2) bétons à résistances mécaniques moyennes, $Rc_{28} = 200$ à 350 daN/cm^2 et $Rt_{28} = 20$ à 40 daN/cm^2 : les bétons à résine phénol-formaldéhyde LS.1 ;

3) bétons à faibles résistances mécaniques, Rc_{28} au-dessous de 150 daN/cm^2 : les bétons à résines urée-formaldéhydes et mélamine-formaldéhydes.

CRITÈRE DES RÉSISTANCES MÉCANIQUES APRÈS CONSERVATION PENDANT 72 HEURES À LA TEMPÉRATURE DE 60° SUCCÉDANT À UNE CURE DE 28 JOURS À LA TEMPÉRATURE NORMALE

Les bétons étudiés peuvent être ainsi groupés :

— Comportement très bon, la résistance reste constante ou varie dans les limites de $\pm$ 5% par rapport à Rc_{28} : bétons de résine FA, LS.1, mélamine-formaldéhyde (M_3, M_4, MM) et urée-formaldéhydes modifiées à la mélamine (URM).

— Comportement bon, la résistance diminue tout au plus de 25% comparée au Rc_{28} : bétons de résine urée-formaldéhyde.

— Comportement faible, bétons de résine Dinox 040 A avec lesquels on obtient, après un traitement de 3 jours à 60°, des pertes de résistances de 50 à 80%.

CRITÈRE DE LA CONSERVATION DE LA RÉSISTANCE À L'IMMERSION DANS L'EAU, APRÈS UN DURCISSEMENT À L'AIR DE 28 JOURS, ET DE L'AUGMENTATION DE LA RÉSISTANCE APRÈS UNE CURE MIXTE DE 7 JOURS À L'AIR HUMIDE ET 21 JOURS À L'AIR À HYGROMÉTRIE ET TEMPÉRATURE NORMALES

Les bétons étudiés peuvent être ainsi groupés :

— Comportement très bon : bétons de résine urée-formaldéhydes (UR, U), urée-formaldéhyde modifiée à la mélamine (URM) et mélamine-formaldéhyde (M_3, M_4, MM), qui, conservée en régime mixte et parfois lors de l'immersion dans l'eau, enregistrent des augmentations de résistance, par rapport aux matériaux similaires conservés à l'air dans l'intervalle confection-essai.

— Comportement bon : bétons de résine furannique, monomère FA, et de résine phénol-formaldéhyde LS. 1 qui, après immersion dans l'eau, à 28 jours, ont des résistances pratiquement égales à celles des bétons conservés tout le temps à la température normale avec une humidité relative de l'air de 50 à 65%.

— Comportement assez bon : bétons de résine époxyde Dinox 040A qui, après conservation en régime mixte, enregistrent des résistances de 70 à 90% de celles des éprouvettes conservées 28 jours à l'air à température normale et humidité relative de 50 à 65%.

A partir des données des recherches préliminaires et des données techniques-économiques dont on a disposé alors, il a été possible de classer, en vue des principales applications possibles sous forme de liants organiques, les résines produites et étudiées ;

— Confection de bétons de résines synthétiques sans liants minéraux : la résine furannique, monomère FA, la résine époxyde, Dinox 040 A et la résine phénol-formaldéhyde LS. 1, priorité étant donnée à l'étude du monomère FA et de la résine LS.1.

— Stabilisation des terres : les résines urée-formaldéhydes (UR et U), la résine urée-formaldéhyde modifiée à la mélamine (URM) et les résines mélamine-formaldéhydes (M_3, M_4 et MM).

b) *Agrégats*

Les critères de qualité concernant les conditions que doivent remplir les agrégats destinés aux bétons aux résines synthétiques ont été, initialement, les suivants : les matériaux utilisés comme agrégats ne doivent pas réagir avec la résine utilisée comme liant organique et avec son durcisseur, ce qui aurait pour résultat d'affaiblir la structure du béton. Cette condition impose d'exclure, si l'on emploie des résines qui durcissent sous l'action de certains catalyseurs acides, l'utilisation des matériaux qui renferment des carbonates, car, par leur réaction avec le durcisseur acide, apparaissent à la surface des grains de carbonates, des pellicules ou une couche de matériau altéré qui affaiblit la structure du béton.[4]

Une autre cause d'affaiblissement peut être la réaction avec les carbonates d'une partie du durcisseur acide de la résine, car il est possible que le durcisseur restant ne suffise pas à assurer les réactions de polymérisation à la température ambiante et à durcir complètement la résine.

Pour obtenir une bonne adhérence, il est nécessaire d'utiliser un agrégat minéral à teneur minimale d'impuretés, car celles-ci peuvent affecter les propriétés finales du béton. Ainsi, l'argile adhérant aux agrégats empêche la formation d'une forte liaison directe entre la résine et la surface des granules par interposition d'une couche de faible résistance. De plus, quelques-uns des composants de l'argile peuvent réagir avec le durcisseur de la résine, ce qui est une autre cause de mauvais résultats. Une pellicule d'eau à la surface des agrégats rend, elle aussi, dans une certaine mesure, l'adhérence incertaine, la plupart des résines synthétiques étant insolubles dans l'eau. [1-4]

Des résistances mécaniques supérieures pour une faible consommation de résine ne peuvent être obtenues qu'aux conditions supplémentaires suivantes :

— Les agrégats proviendront de roches à résistance très élevée.

— On utilisera un agrégat à granulométrie continue et à densité maximale, avec un volume minimal de vides.

---

[4] S. Solacolu, «Chimia fizică a silicaţilor tehnici», Ed. tehnică, Bucarest, 1968.

— Le travail et le compactage du matériau frais seront effectués avec soin afin d'éviter la ségrégation des composants du mélange, la résine utilisée comme liant ayant une faible viscosité. Cette condition a été vérifiée tant par le calcul que par l'expérience et la conclusion est qu'on ne peut utiliser sans discernement les compositions d'agrégats établies et recommandées comme optimales pour la préparation des bétons de ciment. En effet, dans les bétons de ciment, le volume de vides de l'agrégat est en bonne partie compensé par le liant minéral lui-même pour lequel les normes en vigueur admettent une finesse de broyage qui inclut 85 à 90% de micro-granulats au diamètre inférieur à 0,088 mm, puisqu'on sait que les grains de ciment de diamètre supérieur à 30 μ ne sont jamais complètement hydratés et qu'ils remplissent dans le béton le rôle de micro-agrégats, raison pour laquelle le ciment durci porte encore le nom de «micro-béton». Les calculs et les expériences effectués ont prouvé la nécessité d'introduire dans le mélange d'agrégats une quantité de matériau très fin (qui doit remplir, en première approximation, les mêmes conditions de qualité que le gros agrégat) et qui, dans les bétons aux résines synthétiques, a un rôle similaire au filler calcaire utilisé dans la préparation des mélanges asphaltiques : c'est pour cette raison que, dans le présent ouvrage, le matériau fin ajouté à l'agrégat destiné aux bétons a été appelé filler. En ce qui concerne le rôle du filler dans l'agrégat destiné aux bétons de résines synthétiques, les recherches ont permis de déterminer que celui-ci répond aux considérations techniques et économiques suivantes :

— L'addition de filler en quantité optimale contribue à une bonne répartition du liant organique qui se dépose en pellicules à la surface de l'agrégat, formant avec celui-ci — qui lui donne sa rigidité — un système spatial unifié grâce aux forces d'adhésion qui se développent à la prise et au durcissement (fig. 1 *a* et *b*). On est ainsi sûr d'obtenir un matériau homogène, aux propriétés relativement uniformes au niveau de la macrostructure. Judicieusement dosé, le filler contribue à remplir les vides se trouvant entre les éléments des gros granulats et, matériau moins cher et d'obtention plus facile, il remplace partiellement la résine. Ainsi le filler contribue à la confection d'un matériau plus dense, à faible perméabilité et à résistances mécaniques élevées, avec une quantité réduite de résine (fig. 1 *a* et *b*). Il contribue encore à éviter la ségrégation des composants du mélange frais et à améliorer l'ouvrabilité du béton, lorsqu'on utilise certaines résines synthétiques à basse viscosité, tels que le monomère FA et la résine LS. 1. Un excès de filler dans le mélange d'agrégats donne des résultats négatifs, tels que : une augmentation non justifiée du dosage en résine (en raison de la grande surface spécifique du filler), une diminution du poids spécifique du béton et l'obtention d'un matériau à résistances mécaniques plus faibles (fig. 1 *c*). [1-4]

— Les conditions économiques et les possibilités de fourniture des agrégats pour les bétons de résines synthétiques exigent que ceux-ci soient les plus communs possibles. Il en résulte, en première approximation, qu'on peut utiliser les matériaux suivants : les agrégats siliceux de rivière, exempts de carbonates, les agrégats quartzeux de carrière, riches en SiO_2, les sables quartzeux fins utilisés dans la verrerie, les agrégats de concassage provenant des roches dures à caractère acide ou neutre, ainsi que le granite, l'andésite basaltique de Malnaş, etc., les agrégats spéciaux : carbure de silicium, corindon, coke de haut fourneau, etc.

— La composition granulométrique des agrégats destinés aux bétons de résines synthétiques peut être déterminée par les essais à partir des agrégats à compositions optimales pour les bétons de ciment, à granulométrie 0 à 3, 0 à 7 et 0 à 15, auxquels on ajoute la quantité nécessaire de filler (matériau finement broyé à granulométrie inférieure à 0,15 mm) jusqu'à ce qu'on obtienne le volume minimal de vides dans le mélange d'agrégat et de filler.

Afin de vérifier expérimentalement les critères de qualité établis, les recherches ont porté sur les matériaux suivants :

— A_1 : agrégat minéral siliceux de la ballastière de Borleşti, rivière d'Argeş, classes 0 à 7 et 7 à 15 mm, à 86 % de SiO_2 (environ 60 % de quartz et 30 % de feldspath) ;

— A_2 : agrégat minéral quartzeux, sable et gravier lavé de l'exploitation Glatna, Timiş, classes 0 à 1, 1 à 4, 4 à 8 et 8 à 15 mm, renfermant 98,5 % de SiO_2 (environ 95 % à 98 % de quartz), qui a été à nouveau trié au laboratoire.

— A_3 : agrégat minéral quartzeux, sable et gravier lavé de l'exploitation Făgetul Ieri — Cluj, classes 1 à 3, 3 à 7 et 7 à 15 mm à 98 % minimum de SiO_2 (environ 95 à 97 % de quartz).

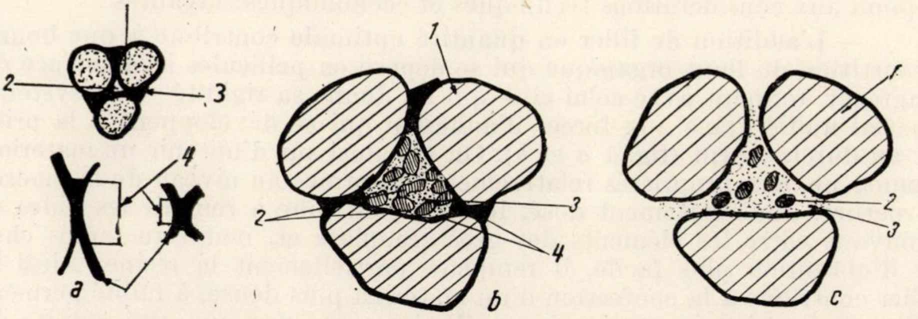

Fig. 1. — Formation de la structure du béton de résine synthétique ;

a) lorsqu'on emploie un agrégat à volume important de vides (monogranulaire). *1.* granules de gros sable ou de gravier. *2*, vide ou pore. *3* et *4*, joints de résine formés entre les particules.

b) lorsqu'il s'agit d'un agrégat à composition granulométrique judicieusement choisie, avec la quantité strictement nécessaire de matériau de remplissage. *1*, grains de gros sable ou de gravier. *2*, matériau fin de remplissage. *3*, grains de sable fin. *4*, liant organique ;

c) dans le cas d'une quantité exagérée de matériau de remplissage. *1*, grains de gros sable ou de gravier. *2* , grains de sable fin. *3*, matériau de remplissage très fin.

— A_4 : criblure d'andésité basaltique de Malnaş livrée couramment pour les travaux routiers, classes 1 à 3, 3 à 8, et 8 à 15 mm, lavée et tamisée à nouveau au laboratoire.

— A_5 : granite concassé (provenant de l'exploitation Turcoaia, Tulcea), classes 1 à 4, 4 à 8 et 8 à 15 mm, lavé et trié à nouveau au laboratoire.

— A_6 : agrégat A_1, où l'on a remplacé par du calcaire concassé (environ 93 % de CaO) les éléments de diamètre 1 à 7 dans la proportion de 15 et de 30 % de la classe correspondante de sable siliceux.

— Fc, limaille de fer (ou têtes de clou), de fuseau granulométrique 0,7—4,00 mm, déchet industriel provenant de l'industrie des Fils Métalliques, Cîmpia Turzii.

— CS, carbure de silicium, de fuseau granulométrique 0,16 à 2,00 mm.

— C, corindon, de fuseau granulométrique 0,06 à 1,6 mm.

— F_1, filler de sable quartzeux lavé, utilisé dans la verrerie, à fuseau granulométrique limite 0,04 à 0,20 mm, à 97 % de SiO_2 au minimum (environ 96 % de quartz) ;

— F_2, filler de farine de quartz, obtenu en broyant l'agrégat A_2, à granulométrie inférieure à 0,50 mm, dont environ 90 % dans le fuseau 0,04 à 0,15 mm ;

— F_3, filler d'andésite basaltique broyée (A_4) à granulométrie approximativement dans le même fuseau que F_2 ;

— F_4, filler spécial, coke de haut fourneau broyé à la même finesse que F_2.

Pour systématiser les recherches et pour mettre en ordre les nombreux paramètres étudiés, on a procédé de la manière suivante :

1) étude et sélection de l'agrégat ou des agrégats aptes à fournir les meilleurs résultats, parmi les 6 types communs — A_1—A_6 ;

2) sélection du filler ou des fillers aptes à fournir les meilleurs résultats, parmi les 4 types étudiés ;

3) détermination des taux optimaux de filler pour différentes compositions d'agrégats dans le domaine 0 à 15 mm et étude des agrégats spéciaux F_c, C_s et C, etc., pour la préparation des bétons de résine furannique — monomère FA.

Les principaux résultats des recherches à ce stade, avec les agrégats habituels A_1—A_6 et donc le filler F_1 (voir tableau 1), ont permis les conclusions suivantes : l'addition de filler influence sensiblement, de façon positive, les résistances mécaniques pour toutes les compositions d'agrégats étudiées avec conservation constante du dosage en résine, durcisseur et diluant, et procure une meilleure ouvrabilité du matériau frais, contribuant à éviter la ségrégation des composants du mélange et à fournir des résultats plus homogènes ($\pm$ 8 % au maximum par rapport à la moyenne), alors que les résultats obtenus avec les éprouvettes confectionnées sans addition de filler montrent une plus grande dispersion ($\pm$ 12 % pour les essais à 28 jours et $\pm$ 16 % pour les essais à 3 et 7 jours), ce qui confirme par voie expérimentale les critères établis.

Le rapport entre la résistance à la compression et la résistance à la traction par flexion des bétons à monomère FA étudiés varie alors entre 4,5 et 6,2. Les valeurs minimales du rapport $R_c/R_{ti} = 4{,}5-5{,}2$ sont généralement obtenues pour des compositions d'agrégats avec une addition de filler qui s'avère donc favoriser un accroissement sensible de la résistance à la traction par flexion des bétons de résine FA.

— L'agrégat A_1 = sable et gravier de la rivière d'Argeş, ballastière de Borleşti (les plus facilement disponibles) — peut être utilisé dans la préparation des bétons à monomère FA avec des résultats assez bons, s'il est bien lavé et bien séché, et si la fraction inférieure à 0,2 mm (qui contient le taux maximal d'impuretés) est complètement remplacée par du filler F_1.

— Des deux types d'agrégats quartzeux lavés étudiés, A_2 et A_3, celui qui donne les meilleurs résultats est l'agrégat A_2, le plus pur. Il est à remarquer qu'en utilisant A_2 et A_3 on obtient des résultats supérieurs à ceux obtenus avec l'agrégat de rivière A_1.

— L'agrégat de concassage A_4, andésite basaltique, donne des résultats supérieurs, comparés à ceux des agrégats de carrière A_2 et A_3 et à ceux de l'agrégat de rivière A_1, pour des dosages égaux de résine, de durcisseur et de diluant.

— Les recherches avec l'agrégat A_6 prouvent que les résistances mécaniques des éprouvettes diminuent sensiblement avec l'augmentation du taux de calcaire dans l'agrégat A_1, et confirment, toujours par voie expérimentale, les résultats théoriques.

Il résulte donc de ces études qu'il est préférable d'utiliser les agrégats suivants : A_2, agrégat quartzeux de carrière, lavé, provenant de l'exploitation Glatna-Timiş ; A_4, agrégat de concassage, criblure d'andésite basaltique provenant de la carrière de Malnaş ; A_1, agrégat de ballastière provenant de la ballastière de Borleşti de la rivière d'Argeş, comme agrégat supplémentaire et seulement pour certaines déterminations comparatives.

Les principales conclusions des recherches effectuées pour le choix du filler ou des fillers sont les suivantes : avec les bétons fins à dosage élevé (21% de résine) et approximativement dans les mêmes conditions de travail (tassement au cône normalisé = 6,2 à 7 cm), les meilleurs résultats sont obtenus en utilisant comme filler le coke de haut fourneau broyé F_4 (fig. 2*a*), ensuite, dans l'ordre, le filler d'andésite basaltique broyé F_3 et le filler de quartz broyé F_2, les résultats les plus modestes étant obtenus avec le sable fin quartzeux lavé F_1 utilisé dans les verreries. Cette constatation est confirmée par les recherches sur les bétons avec agrégats de carrière A_2 et avec agrégats de concassage A_4. Il est à remarquer que les écarts des résistances des bétons, si l'on utilise différents fillers, sont beaucoup plus faibles que ceux indiqués par l'étude des seuls fillers ; la raison en est la diminution du poids du filler dans la masse de l'agrégat (fig. 2*b* et *c*). Ainsi, par rapport au filler F_1, on obtient des différences de plus de 5 à 18% de la résistance à la compression à 28 jours des différents bétons dont la préparation comprenait des fillers F_2, F_3 et F_4. Les différences entre les résultats obtenus avec différents fillers ont incité à poursuivre les examens microscopiques afin d'élucider les points suivants : rugosité des différents fillers et agrégats utilisés et forme de leurs éléments ; adhérence dans le système filler-liant organique et agrégat-liant organique. Il en résulte que :

— Les agrégats A_2 et les 2 types de filler F_1 et F_2 ont, généralement, des éléments arrondis, rapport b/a de plus de 0,7 et rapport c/b supérieur à la valeur 0,45 à 0,50 pour la plupart des grains avec une bonne concordance en ce qui concerne la forme.

La rugosité des surfaces augmente avec la diminution du diamètre des grains. Ainsi les grains de diamètre compris entre 7 et 15 mm ont des surfaces très lisses, ceux de diamètre 3 à 7 mm également, une rugosité plus accentuée apparaissant pour les grains de diamètre 1 à 3 mm et s'accentuant de plus en plus pour les grains de diamètre inférieur à 1,00 mm. La surface la plus rugueuse a été observée pour les grains de diamètre 0,08 à 0,20 mm du filler F_1 (qui ont pu être convenablement observés au microscope (fig. 3*a*)). Dans le filler F_2 (grains de diamètre 0,08 à 0,20 mm) on observe assez aisément la rugosité accrue des surfaces (par rapport au filler F_1), les surfaces ont des striures proéminentes, des arêtes et des coins, etc., semblables à ceux qui sont observés sur l'agrégat de concassage A_4 (fig. 3*b*). Les résistances mécaniques supérieures obtenues avec le filler F_2, par rapport au filler F_1 (les deux fillers ayant la même composition minéralogique : plus de 95 % de quartz) trouvent ainsi une première explication, en ce sens que la rugosité accrue des surfaces des grains du filler F_2, obtenu par broyage, contribue à assurer une meilleure adhérence dans le système filler liant organique.

Les observations effectuées sur la forme des grains de l'agrégat A_4 et des fillers F_3 et F_4 ont montré pratiquement les mêmes rapports b/a de plus de 0,7 et c/b de plus de 0,45 à 0,50. On a remarqué que les grains de l'agrégat de concassage A_4 (andésite basaltique) et des fillers broyés F_3 et F_4 ont des formes anguleuses, à arêtes vives et des faces rugueuses, ce qui conduit à une première explication des résistances obtenues avec ces matériaux. Mais une autre question se pose : pourquoi, en utilisant le coke de haut fourneau broyé comme filler F_4, obtient-on des résistances supérieures à celles fournies par l'andésite basaltique broyée F_3 et par le quartz broyé F_2? Les observations effectuées au microscope ont prouvé qu'il y a certaines différences entre l'andésite basaltique et le quartz, dues probablement à la dureté, à la fragilité, ainsi qu'à la perfection ou à l'imperfection des plans de clivage, de sorte que lors du broyage du quartz on observe des grains présentant des arêtes vives, une cassure concoïdale à surface relativement lisse et quelques-unes peuvent même être considérées comme telles dans une certaine mesure, ce qui indique que les points d'ancrage dans la pellicule de résine seront donc moins nombreux. A la surface de plusieurs grains similaires d'andésite, on remarque des cassures à nerf à nombreuses petites proéminences qui représentent autant de points d'ancrage dans la pellicule de résine, déterminant ainsi une meilleure adhé-

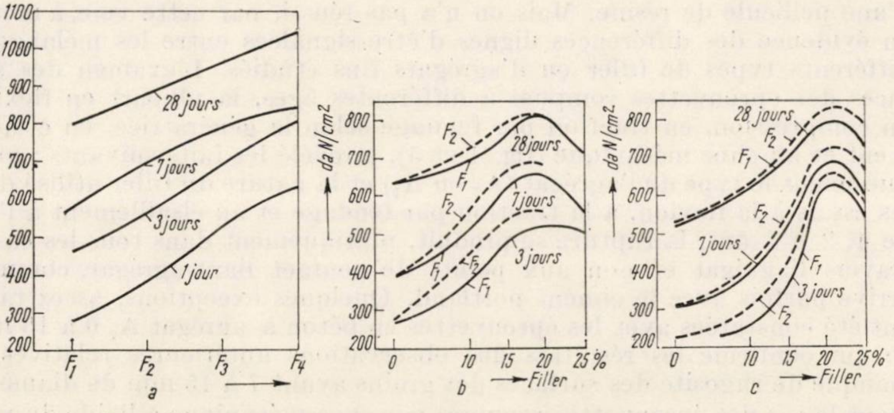

Fig. 2. — Variation de la résistance à la compression, à différents âges d'essai, en fonction du type et du pourcentage de filler.
a) pour des bétons fins FA, filler F_1, F_2, F_3 et F_4; b) pour des bétons fins FA, agrégats de carrière 0 à 7 mm ; c) pour des bétons fins FA, agrégats de carrière 0 à 15 mm.

rence dans le système filler-résine, ce qui explique, dans une certaine mesure, les différences de résistance obtenues en utilisant les fillers F_3 et F_2. Il faut mentionner qu'on n'a pas décelé au microscope de différences de ce genre, lors de l'examen parallèle des fillers F_2 et F_4 , en faveur de ce dernier, ce qui incite à limiter les conclusions relatives à l'effet de la rugosité des surfaces aux fillers de provenance minérale F_1, F_2 et F_3. Le filler F_4 (coke de haut fourneau broyé) étant un matériau qui appartient à la chimie du carbone, il est possible dans ce cas que l'augmentation de résistance du système filler-liant organique soit favorisée, tant par des phénomènes physiques que par certaines réactions chimiques de surface qui ont lieu entre le liant organique et le filler.

L'étude au microscope électronique de l'adhérence dans le système liant organique-filler et liant organique-agrégat dans un mélange frais très fluide d'agrégat fin ou de filler-liant organique (fig. 3*c*) a mis en évidence une bonne interaction dans la zone de contact filler (agrégat fin)-liant organique pour n'importe quel type d'agrégat ou de filler utilisé, la surface des grains du filler ou de l'agrégat fin étant parfaitement recouverte d'une pellicule de résine. Mais on n'a pas réussi, par cette voie, à mettre en évidence des différences dignes d'être signalées entre les mélanges à différents types de filler ou d'agrégats fins étudiés. L'examen des surfaces des éprouvettes rompues à différentes âges, la plupart en flexion, en compression, en traction par fendage selon la génératrice, en cisaillement et au choc mécanique (fig. 4 et 5), a révélé les faits suivants : quels que soient le type de l'agrégat (A_2 ou A_4) et la nature du filler utilisé dans les essais à la flexion, à la traction par fendage et au cisaillement à l'âge de 1, 2 à 3 ans, la rupture se produit, pratiquement dans tous les cas, à travers l'agrégat et non aux points de contact liant-agrégat, comme il arrive parfois avec le ciment portland. Quelques exceptions, assez rares, ont été constatées avec les éprouvettes en béton à agrégat A_2 0 à 15 mm, ce qui confirme les résultats des observations antérieures relatives au manque de rugosité des surfaces des grains ayant 7 à 15 mm de diamètre. Dans le cas des éprouvettes rompues par choc mécanique à l'aide du marteau Föpl, à l'âge de 1 à 2 ans, la rupture se produit toujours par les grains de l'agrégat et par la masse de mastic noir formée par le filler et le liant organique, pour les bétons préparés avec l'agrégat de concassage A_4, andésite basaltique, quel que soit le type du filler utilisé, ce qui procure à ce type de bétons des résistances au choc plus importantes.

Soumises de 3 à 5 fois, en compression, à des charges équivalant à 0,5—0,6 de la charge de rupture, à l'âge de 2 à 3 ans, les différentes compositions de bétons à agrégats A_2 et A_4, retenues comme objet optimal d'étude, n'ont pas montré de discontinuités ou de décollements à l'interface liant-agrégat. Le mastic de couleur noir ou marron foncé (dans le cas du liant mixte FA + LS. 1), formé d'un mélange de filler et de liant organique, se présente comme une masse compacte fortement adhérente aux éléments les plus gros de l'agrégat (fig. 5). Outre l'influence de la forme des grains, de la rugosité, de la surface du filler et des agrégats sur l'accroissement des résistances mécaniques des bétons à monomère FA, l'utilisation du filler F_2 (quartz broyé) tend à déterminer des résis-

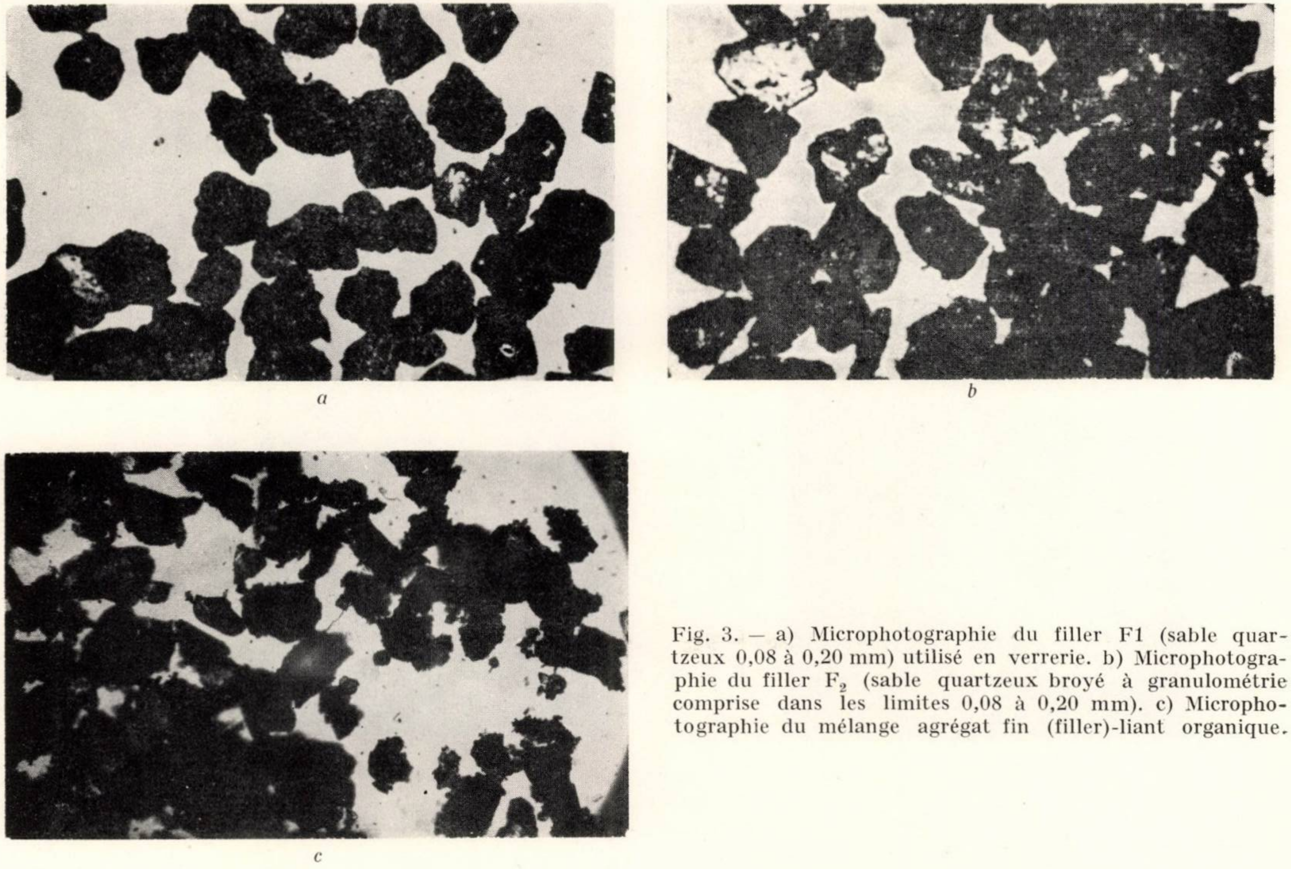

a

b

c

Fig. 3. — a) Microphotographie du filler F1 (sable quartzeux 0,08 à 0,20 mm) utilisé en verrerie. b) Microphotographie du filler F_2 (sable quartzeux broyé à granulométrie comprise dans les limites 0,08 à 0,20 mm). c) Microphotographie du mélange agrégat fin (filler)-liant organique.

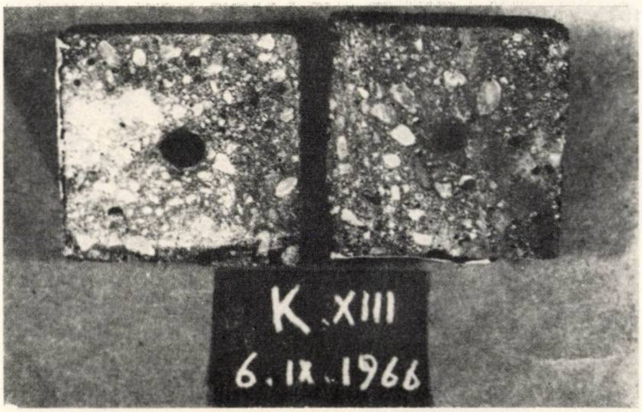

Fig. 4. — Eprouvettes en béton fin à agrégats quartzeux A2, filler Fl, monomère FA, sollicitées à 0,55 R_c rupture, permettant de vérifier l'adhérence du liant à l'agrégat après deux ans environ.

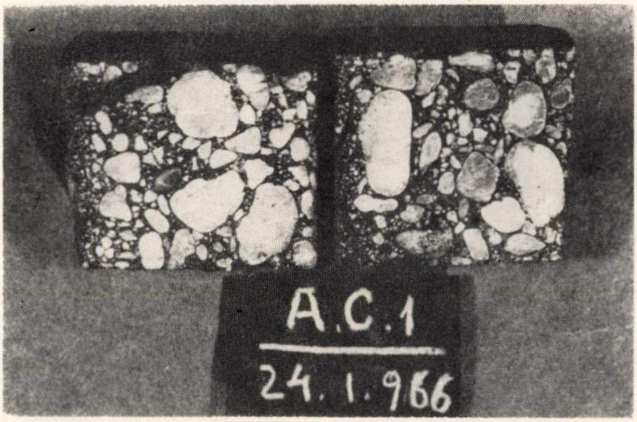

Fig. 5. — Eprouvettes sollicitées à 0,06 R_c rupture, afin de vérifier l'adhérence du liant à l'agrégat après deux ans environ (béton à agrégats quartzeux A2, filler F2 + F4, à monomère FA).

tances plus faibles, par rapport à celles obtenues avec F_3 (andésite basaltique broyée), ce qui peut être dû à l'hydrophilie plus accentuée du quartz (problème qui ne constitue pas l'objet du présent ouvrage).

Des recherches de sélection des fillers ont prouvé que les meilleurs résultats sont obtenus en utilisant des agrégats à granulométrie continue qui compactés ont un volume de vides de 20% au maximum. Avec l'agrégat utilisé les taux moyens suivants de filler ont fourni les résultats optimaux : pour l'agrégat 0 à 3 mm = 12% (10 à 15%) ; pour l'agrégat 0 à 7 mm = 15% (10 à 20 %) ; pour l'agrégat 0 à 15 mm = 20 % (15 à 25 %). Ainsi, les compositions granulométriques obtenues pour les bétons à monomère FA diffèrent de celles recommandées pour les bétons de ciment, par le fait que pour les nouveaux types de bétons un plus gros pourcentage d'agrégat fin est nécessaire, sans compter la présence du filler.

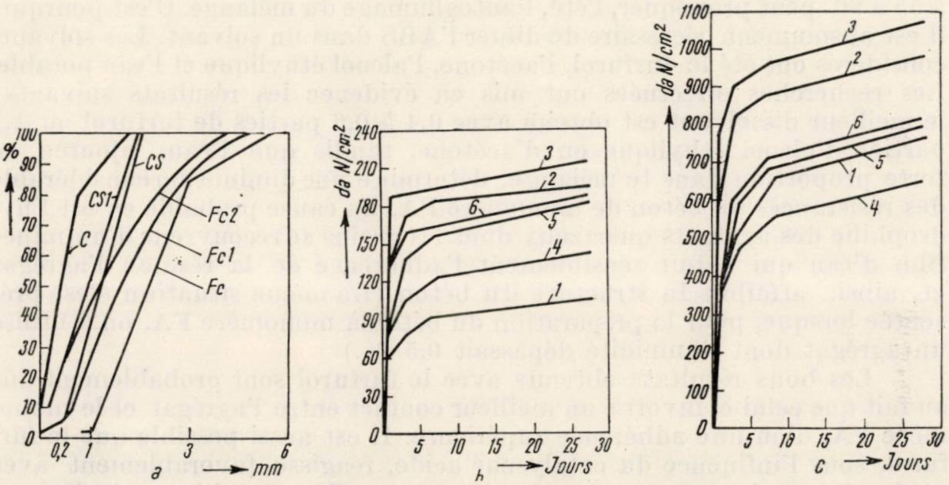

Fig. 6. — a) Compositions granulométriques pour les agrégats spéciaux utilisés dans l'étude : Fc — agrégat spécial non corrigé ; Fcl — agrégat corrigé par l'addition de 37% de sable quartzeux A2 et 16% de filler de quartz broyé F2 ; Fc2 — agrégat corrigé par l'addition de 20 % de sable quartzeux A2 et 20 % de filler de quartz broyé F2 ; Cs — agrégat spécial non corrigé ; CS1 — agrégat corrigé par l'addition de 38% de filler de quartz broyé F2 ; C — agrégat spécial non corrigé.

b) Variation de la résistance à la traction par flexion dans le temps.

c) Variation de la résistance à la compression dans le temps pour les bétons à monomère FA et agrégats spéciaux :

1, agrégat FC + 10,0% FA ; *2*, agrégat FCl + 12,0% FA ; *3*, agrégat FC2 + 9,6% FA ; *4*, agrégat CS + 16% FA ; *5*, agrégat CS + 16% FA ; *6*, agrégat C + 18% FA.

Les études sur les agrégats spéciaux Fc, Cs et C ont conduit à choisir les compositions optimales d'agrégats : Fc à correction de sable et de filler (Fc_2, Fc_1), carbure de silicium à correction (CS. 1) et corindon (C) (voir fig. 6*a*) qui ont donné les résultats maximaux (fig. 6 *b* et *c*). Il a été prouvé que les meilleurs résultats sont obtenus avec l'agrégat Fc à correction (Fc_1, Fc_2) et, dans l'ordre, les agrégats C et CS_1 (carbure de silicium à correction).

c) *Les agents durcisseurs et leurs diluants*

Le monomère FA se polymérise sous l'action de certains agents durcisseurs (catalyseurs acides) tels que les acides benzène sulfonique, toluène sulfonique, sulfurique et chlorhydrique. Des recherches comparatives ont prouvé que les meilleurs résultats sont obtenus avec l'acide benzène sulfonique et l'acide sulfurique. L'emploi de l'acide sulfurique comme durcisseur du béton à monomère FA présente toute une série de difficultés dans l'industrie et même au laboratoire et, pour cette raison, on y a renoncé ; par la suite, seul l'acide benzène sulfonique a été utilisé.

L'acide benzène sulfonique (ABS) est solide à la température de 15 à 20° et liquide à la température de 55 à 60° ; pour être utilisé comme durcisseur il doit être soit dilué dans de faibles quantités de solvant, soit réchauffé à la température de 55 à 60°. L'emploi de l'acide réchauffé à 55 à 60° peut provoquer, l'été, l'autoallumage du mélange. C'est pourquoi il est absolument nécessaire de diluer l'ABS dans un solvant. Les solvants considérés ont été le furfurol, l'acétone, l'alcool éthylique et l'eau potable. Les recherches effectuées ont mis en évidence les résultats suivants : le meilleur dissolvant est obtenu avec 0,4 à 0,6 parties de furfurol ou 1,1 parties d'alcool éthylique ou d'acétone, tandis que l'eau, ajoutée en forte proportion dans le mélange, détermine une diminution considérable des résistances du béton de monomère FA. La cause probable en est l'hydrophilie des agrégats quartzeux dont les grains se recouvrent d'un mince film d'eau qui réduit sensiblement l'adhérence de la résine à l'agrégat et, ainsi, affaiblit la structure du béton. (La même situation s'est présentée lorsque, pour la préparation du béton à monomère FA, on a utilisé un agrégat dont l'humidité dépassait 0,5 %.)

Les bons résultats obtenus avec le furfurol sont probablement dus au fait que celui-ci favorise un meilleur contact entre l'agrégat et le monomère FA, d'où une adhérence supérieure. Il est aussi possible que le furfurol, sous l'influence du catalyseur acide, réagisse favorablement avec quelques-uns des composants du monomère FA et qu'il en résulte une amélioration des propriétés du béton.

Les recherches pour établir le taux optimal de durcisseur (ABS) des bétons de monomère FA préparés par une méthode similaire et durcis à la température normale de leur conservation, avec le rapport furfurol/ABS = 0,60 et en faisant varier la quantité d'ABS utilisé, ont prouvé que lorsqu'on utilise le furfurol, ce taux optimal est de l'ordre de 20 à 25% du poids du monomère FA.

d) *Influence de certaines additions de résine phénol-formaldéhyde LS.1 sur les propriétés des bétons de monomère FA*

La recherche sur les possibilités de confectionner des bétons à base de deux résines synthétiques, furannique (monomère FA) et phénol-formaldéhyde (LS. 1), repose sur le fait que les résines de furfurol sont compatibles avec les résines phénol-formaldéhydes, et que les unes et les autres durcissent à froid ordinairement avec les mêmes durcisseurs, dans le cas présent l'acide benzène sulfonique. Quelques-uns des résultats obtenus sont représentés graphiquement par les figures 7 *a*, *b*, *c* et *d* et il en ressort que :

— Le poids apparent des bétons de monomère FA et de résine LS. 1 diminue légèrement avec le taux de LS. 1. Ceci est dû à la diminution de l'ouvrabilité du mélange en raison de la viscosité plus élevée de la résine LS. 1.

— Les résistances à la traction par flexion et à la compression, ainsi que les retraits, diminuent aussi avec l'augmentation du taux de LS. 1. La diminution des résistances est explicable, compte tenu des propriétés physico-mécaniques des résines phénolformaldéhydes et leurs plus faibles résistances mécaniques, ainsi que de leur moindre compacité (fig. 7*a*). Les retraits plus faibles sont dus eux aussi aux propriétés des résines LS.1. Il a été prouvé qu'il est possible d'utiliser les bétons de résine FA et LS.1

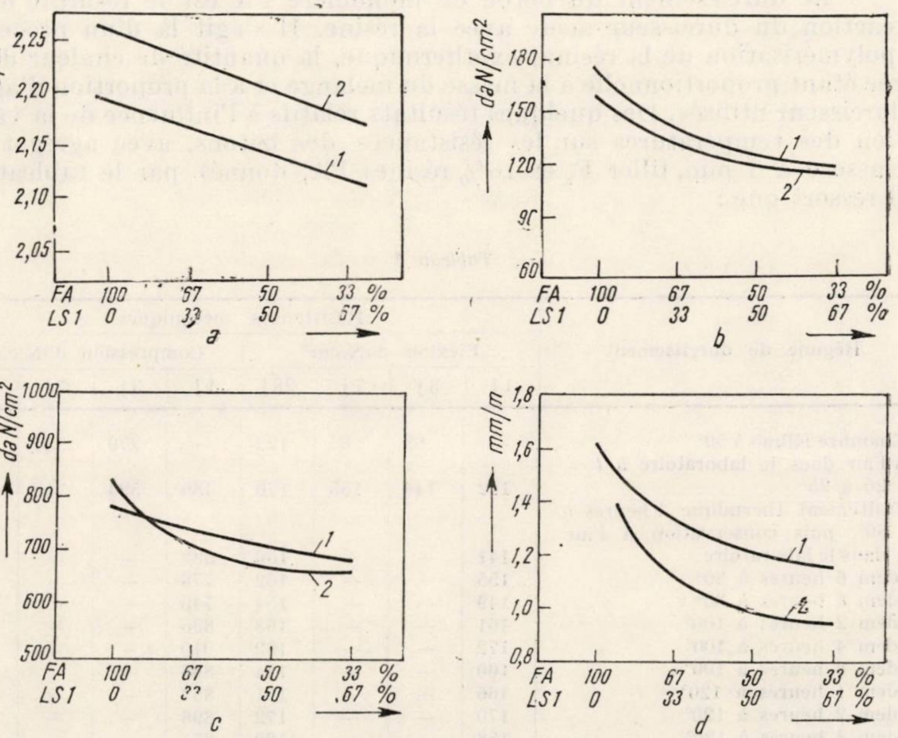

Fig. 7. — a) Variation du poids apparent des bétons à monomère FA et résine LS. 1 en fonction du pourcentage de résine LS 1. b) Variation de la résistance à la traction par flexion des bétons à monomère FA et résine LS. 1 en fonction du pourcentage de résine L.S. 1, essais effectués à 28 jours d'âge.
c) Variation des résistances à la compression des bétons à monomère FA et résine LS. 1 en fonction du pourcentage de résine LS. 1, essais effectués à 28 jours d'âge. d) Variation des contractions des bétons à monomère FA et résine LS. 1 en fonction du pourcentage de résine LS. 1, mesures effectuées à 28 jours d'âge.

1, béton à agrégats quartzeux A2 0 à 3 mm et 12% filler F2 ; *2*, béton à agrégats quartzeux A2 0 à 15 mm et 20% filler F2.

dans le rapport 1/1 lorsqu'il n'est pas nécessaire d'obtenir des résistances mécaniques supérieures à 700 daN/cm² à 28 jours et d'améliorer sensiblement les propriétés des bétons de résines phénol-formaldéhydes dont les résistances à 28 jours sont en général inférieures à 400 daN/cm².

e) *Influence de la température, de l'humidité, de la technologie de préparation et de la mise en œuvre sur les propriétés du béton de résines synthétiques sans liants minéraux*

Le durcissement du béton de monomère FA est le résultat de la réaction du durcisseur acide avec la résine. Il s'agit là d'un processus (polymérisation de la résine) exothermique, la quantité de chaleur dégagée étant proportionnelle à la masse du mélange et à la proportion d'agent durcisseur utilisée. Des quelques résultats relatifs à l'influence de la variation des températures sur les résistances des bétons, avec agrégat A_2, classe 0 à 3 mm, filler F_2 et 16% résines FA, donnés par le tableau 1 ; il ressort que :

Tableau 1

Régime de durcissement	Résistances mécaniques							
	Flexion daN/cm²				Compression daN/cm²			
	1 j	3 j	7 j	28 j	1 j	3 j	7 j	28 j
Chambre Klimo à 50°	—	68	86	122	—	279	321	518
A l'air dans le laboratoire à *t* = 20 à 25°	112	144	155	170	486	594	718	868
Traitement thermique 4 heures à 80°, puis conservation à l'air dans le laboratoire	141	—	—	166	688	—	—	842
Idem 6 heures à 80°	155	—	—	162	776	—	—	862
Idem 8 heures à 80°	149	—	—	154	746	—	—	854
Idem 2 heures à 100°	161	—	—	168	836	—	—	902
Idem 4 heures à 100°	172	—	—	162	910	—	—	880
Idem 6 heures à 100°	160	—	—	144	866	—	—	838
Idem 1 heures à 120°	166	—	—	171	854	—	—	862
Idem 2 heures à 120°	170	—	—	172	896	—	—	901
Idem 4 heures à 120°	158	—	—	160	874	—	—	831
Idem 6 heures à 120°	164	—	—	146	828	—	—	802

Remarques : Pour les éprouvettes traitées thermiquement, la température a été élevée progressivement pendant une heure ; elles ont été ensuite maintenues à la température établie durant 1 à 8 heures, conformément au programme. Le refroidissement des éprouvettes s'est effectué lentement, après arrêt de l'étuve jusqu'au lendemain matin.

— Le traitement thermique à sec des éprouvettes en béton fin de monomère FA contribue à leur durcissement rapide : en 2 heures environ à 100°, on obtient des résistances pratiquement égales aux résistances des éprouvettes durcies 28 jours dans les conditions de laboratoire. Ceci s'explique probablement par une polymérisation plus avancée du monomère FA sous l'action du traitement thermique. Des 10 régimes de traitement thermique utilisés, celui qui donne les meilleurs résultats consiste à soumettre les éprouvettes durant 2 heures à 100°, 1 à 2 heures à 120° ou à 80°.

— Les températures basses ont un effet défavorable sur les résistances du béton de monomère FA, probablement parce que les réactions entre l'agent durcisseur et la résine sont alors empêchées, et qu'il se produit une polymérisation partielle de la résine dans l'intervalle où l'on effectue les essais ;

— L'eau, en grande quantité, introduite dans le mélange de béton de monomère FA, comme solvant du durcisseur, ou l'humidité des agrégats si elle dépasse 0,5% de leur poids ont aussi un effet sensiblement défavorable sur les résistances mécaniques du béton, tant en raison de l'absorption d'eau des agrégats qui se recouvrent d'une mince pellicule d'eau, ce qui conduit à une diminution de l'adhérence dans le système agrégat minéral-liant organique, qu'en raison des pores capillaires et des vides sous les agrégats que peut causer la présence d'eau, ce qui affaiblit la structure du béton. Avec conservation des éprouvettes les 24 premières heures à l'ambiance du laboratoire, et immersion ultérieure dans l'eau jusqu'à l'âge d'essai (7, 28 jours, etc.), on obtient pour les résistances des valeurs qui représentent 35 à 60 % de celles des éprouvettes témoin conservées tout le temps à l'ambiance du laboratoire, ce qui prouve que l'eau modifie défavorablement les propriétés des bétons de monomère FA aux jeunes âges, en affectant le processus de polymérisation, et la formation de sa structure. L'humidité de l'air, dans l'intervalle décoffrage-essai, contribue aussi à réduire les résistances du béton, selon le temps qu'il se trouve exposé à l'action de l'air humide.

Les recherches effectuées ont prouvé que la technologie de préparation et de mise en œuvre influence tant la consommation de résine que les propriétés mécaniques, dans une proportion allant jusqu'à ± 30%. Ainsi, les bétons à consistance dure préparés en malaxeur forcé, mis en œuvre soigneusement et compactés par vibration, ont, pour des dosages de résine plus faibles, d'environ 10%, les mêmes propriétés physico-mécaniques. Il est à remarquer que pour les bétons à consistance dure, aussi bien que pour ceux à consistance plastique, le compactage doit être effectué très attentivement, afin d'éviter la ségrégation avec toutes les conséquences qui en découlent.

Une humidité de l'air de maximum de 65% et une température minimale de 15° sont indiquées pendant la préparation, la mise en œuvre et les 10 premiers jours après la coulée.

Revue Roumaine de Chimie, **19**, *1*, 99 – 113 (1974)

Revue Roumaine de Chimie, **19**, *1*, 115 – 124 (1974)

COPOLYMERE KONJUGIERTER DIENE MIT MONOESTERN DER MALEINSAÜRE. VII[1]

ANDERE ASPEKTE DER REAKTIONSKINETIK DER RADIKALISCHEN COPOLYMERISATION VON ISOPREN MIT MONOESTERN DER MALEINSÄURE

I. NANU* und C. ANDREI **

* Laboratorium für Makromolekulare Chemie, Polytechnisches Institut Timişoara, Romania

** Forschungslaboratorium, Ploieşti, Petrochemische Industriegruppe Brazi, Romania

Eingegangen am 3. März 1973

Im weiteren Verlauf der Untersuchung der radikalischen Copolymerisationsreaktion von Isopren mit Monoestern der Maleinsäure wird der Einfluß der Art der Monoester, der Initiatoren und der Lösungsmittel auf die Reaktion aufgezeigt. Das Anwachsen der Copolymerisationsgeschwindigkeit der Monoester der Maleinsäure mit wachsender Länge der Alkylkette erklärt sich aus der Tatsache, daß die Abbruchreaktion vom Diffusionsvorgang kontrolliert wird. Die Ergebnisse der Untersuchung des Einflußes der Verdünnung auf den Umsatz und die Zusammensetzung der Polymeren als auch der Einfluß der Art des Lösungsmittels bringt die Auffassung nahe, daß an der Copolymerisationsreaktion ein Donor-Acceptor Komplex teilnimmt, der sich zwischen den Monomeren bildet, während die Tatsache, daß die Änderung der Viskositätszahl der Copolymeren in Abhängigkeit vom Umsatz eine Konstante ist, einen typisch monoradikalischen Mechanismus anzeigt.

EINLEITUNG

In vorhergehenden Arbeiten wurden die kinetischen Aspekte der Copolymerisationsreaktion von Isopren mit verschiedenen Monoestern der Maleinsäure untersucht, besonders bei niedrigem Umsatz (unter 5%). Es wurde hervorgehoben, in welcher Weise diese Systeme den klassischen Copolymerisationsgleichungen entsprechen und welchen Einfluß die sterischen, polaren u.a. Faktoren auf die Reaktion ausüben.[1-4]

---

[1] Part VI, I. Nanu und C. Andrei, *Rev. Roumaine Chim.*, **17**, 1043 (1972).

[2] I. Nanu und C. Andrei, *Rev. Roumaine Chim.*, **15**, 1883 (1970).

[3] I. Nanu und C. Andrei, *Rev. Roumaine Chim.*, **16**, 75 (1961).

[4] I. Nanu und C. Andrei, *Rev. Roumaine Chim.*, **17**, 741 (1972).

In der vorliegenden Arbeit untersuchten wir andere Aspekte der radikalischen Copolymerisationsreaktion dieser Systeme (den Einfluß der Art der Monoester, der Initiatoren und der Lösungsmittel auf die Reaktion, die Wirkung der Verdünnung auf den Umsatz und die Zusammensetzung der Copolymeren als auch die Änderung der Viskositätszahl der Copolymeren in Abhängigkeit vom Umsatz) die ebenfalls Argumente in der Wahl und Unterstützung des Reaktionsmechanismus bilden werden.

EXPERIMENTELLER TEIL

Die verwendeten Monomeren (Isopren und Monoester der Maleinsäure) wiesen dieselben Merkmale mit denen der vorhergehenden Arbeiten auf.[2,5]

Der Lösungs-Copolymerisationsprozeß wurde in Glasampullen unter Stickstoff, in Gegenwart freier Radikale, ausgeführt.

Die Trennung und Reinigung der Copolymeren erfolgte durch Lösen des Reaktionsgemisches in Äthyläther und Aufsfällen mit Petroläther, ein Vorgang der 2—3 mal wiederholt wurde.

Die Copolymeren wurden bei einer Temperatur von 40—50° getrocknet und der Umsatz nach der erhaltenen Menge berechnet.

Die Analyse der Copolymeren erfolgte mittels der Elementarmikroanalyse.

ERGEBNISSE UND DISKUSSIONEN

DER EINFLUSS DER ART DES MONOESTERS AUF DIE REAKTION

Die Änderung des Umsatzes in Abhängigkeit von der Zeit für die radikalische Copolymerisation des Isoprens mit Monobutylmaleat, Monoheptylmaleat und Monocetylmaleat ist in Abb. 1 wiedergegeben.

Die Reaktionen wurden in homogenem Medium (Cyclohexanon) bei einem Molverhältnis Isopren : Monoester von 1 : 1 und bei gleicher Molkonzentration in allen drei untersuchten Systemen ausgeführt. Aus dieser Darstellung geht hervor, daß die Copolymerisationsgeschwindigkeit mit steigender Länge des n-Alkylradikals des Monoesters wächst, eine Tatsache, die auch für Umsätze unter 5% zutrifft. [1]

Die steigende Reaktivität des Monoesters der Maleinsäure mit wachsender Länge der Alkylkette erklärt sich aus der Tatsache, daß die Abbruchreaktion von Diffusionsvorgängen bestimmt wird, ähnlich der von Otsu und Mitarb. [6] gefundenen Beziehung für die Polymerisation der Alkylmethakrylate.

Demnach ist die Differenzierung der Geschwindigkeiten der Abbruchreaktionen nicht auf die Reaktionsfreudigkeit der Makroradikale zurückzuführen, sondern sie ergibt sich aus den Diffusionsvorgängen, durch die die Makromoleküle in eine für die Reaktion günstige Stellung

---

[5] I. Nanu und C. Andrei, *Bul, St. Tehnic I. P. Timişoara*, im Druck.

[6] T. Otsu, I. Ito und M. Imoto, *J. Polymer Sci. Part A*, **2**, 2901 (1964).

gelangen. Der Einfluß der Diffusion auf die bimolekulare Abbruchreaktion kann wie ein Dreistufenvorgang behandelt werden :

— die erste Stufe ist die Diffusion der zwei Makroradikale aus der Lösung in eine solche Nähe, daß bestimmte Segmente als in Berührung stehend angesehen werden können ;

— die zweite Stufe ist die Neuordnung der Ketten, so daß die reaktionsfreudigen Atome in eine für die chemische Reaktion günstige Stellung gelangen ;

— die letzte Stufe stellt die chemische Reaktion dar.

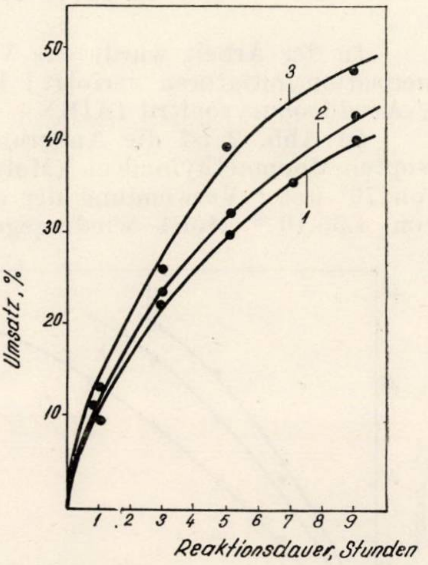

Abb. 1. — Änderung des Umsatzes mit der Copolymerisationsdauer in Cyclohexanon bei 70° ;

1, Isopren-Monobutylmaleat ; 2, Isopren-Monoheptylmaleat ; 3, Isopren-Monocetylmaleat. Molverhältnis[M_1^0] : [M_2^0]$=1 : 1$(und die gleiche Molkonzentration). Initiator : [AIBN] $\times 10^2 = 4{,}55$ Mol/l.

North und Reed [7,8] stützten sich auf die Annahme, daß die Makroradikale die statistische Konfiguration eines Knäuels aufweisen, in dessen Innerem das aktive Ende mit größerer Wahrscheinlichkeit auftritt als außerhalb und gelangten zur Schlußfolgerung, daß die die Abbruchgeschwindigkeit bestimmende Stufe die Diffusion des aktiven Endes aus dem Inneren des Knäuels in eine für die Reaktion geeignete Region ist.

In dem Maße wie die Konzentration des Polymeren wächst, hängt die Autodiffusion des aktiven Endes aus dem Molekülknäuel von der „Mikroviskosität" der dem Radikal benachbarten Regionen ab.

Die infolge des Diffusionsvorganges fallende Abbruchgeschwindigkeit führt zu einem Anwachsen der Copolymerisationsgeschwindgkeit.

Hervorzuheben ist, daß in den untersuchten Systemen dieses Anwachsen der Reaktionsgeschwindigkeit nicht von der Größe einer unter dem Namen „Geleffekt" bekannten Beschleunigung ist.

---

[7] A. M. North und G. A. Reed, *Trans. Faraday Soc.*, **57**, 859 (1961).

[8] A. M. North und G. A. Reed, *J. Polymer Sci. Part A*, **1**, 1311 (1963).

Es ist wichtig hervorzuheben, daß nicht nur die Viskosität der Monoester der Maleinsäure (mit der Anzahl der Atome aus der Alkylgruppe steigende Funktion) die Reaktionsgeschwindigkeit der Copolymerisationsreaktion beeinflußt, sondern auch die viel größere Viskosität des Diels-Alder Adduktes, das sich im System zwischen Dien und Monoester in einer Parallelreaktion bildet, von Bedeutung ist.

Aber dieser letzte Aspekt wird in einer anderen Arbeit ausführlicher behandelt werden.

DER EINFLUSS DER ART DER INITIATOREN

In der Arbeit wurde das Verhalten von drei verschiedenen Polymerisationsinitiatoren verfolgt: Benzoylperoxid, Lauroylperoxid und α, α'-Azodiizobutyronitril (AIBN).

In Abb. 2 ist die Änderung des Umsatzes der Copolymerisation Isopren-Monomethylmaleat (Molverhältnis 1 : 1) bei einer Temperatur von 70° unter Verwendung der drei Initiatoren in einer Konzentration von $4.55.10^{-2}$ Mol/l wiedergegeben.

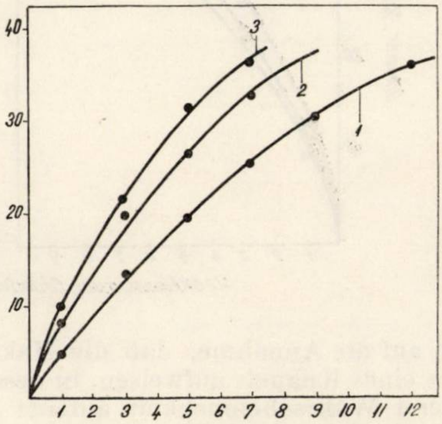

Abb. 2. – Einfluß der Art des Initiators auf die Copolymerisationsreaktion Isopren-Monomethylmaleat (Molverhältnis 1 : 1).

1, Benzoylperoxid; *2*, Lauroylperoxid; *3*, α, α'-Azodiisobutyronitril (AIBN). Initiatorkonzentration $4{,}55 \cdot 10^{-2}$ Mol/1; Temperatur 70°, Lösungsmittel: Cyclohexanon.

Die verschiedenen Ergebnisse, die mit den drei Initiatoren erhalten wurden, stimmen mit den Daten aus der Literatur überein, die die Halbwertszeit der Initiatoren betreffen, die in der Reihenfolge: Benzoylperoxid $>$ Lauroylperoxid $>$ AIBN fällt.[9]

DER EINFLUSS DER VERDÜNNUNG AUF DEN UMSATZ UND DIE ZUSAMMENSETZUNG DER COPOLYMEREN

Im Jahre 1946 schlugen Bartlett und Nozaki[10] vor, daß an der alternierenden Copolymerisation von Styrol mit Maleinsäureanhydrid ein Molekularkomplex teilnimmt, der sich zwischen den beiden Monomeren bildet. Mayo und Walling [11,12] widersetzten sich aber dieser Hypothese indem sie sich auf folgende experimentelle Beobachtungen stützten:

---

[9] * * * Polymerisation Initiators, Prospect Firma Noury Van der Lande, Olanda.
[10] P. D. Bartlett und K. Nozaki, *J. Amer. Chem. Soc.*, **68**, 1495 (1946).

— das physikalische Außerachtbleiben einer Assoziation zwischen den Monomeren in allen Fällen, die eine hohe Alternanz in der Copolymerisationsreaktion aufweisen:

— die Copolymerisationskonstanten ändern sich nicht mit der Verdünnung der Monomeren und

— die Kinetik der alternierenden Copolymerisationssysteme ist unklar.

Trotzdem hat man in den letzten Jahren mit Bestimmtheit die Bildung eines Komplexes durch Ladungsaustausch zwischen den Monomeren hervorgehoben und hat bei der Untersuchung mehrerer alternierender Systeme angenommen, daß er an der Copolymerisationsreaktion teilnimmt.[13–18]

Ebenso finden sich auch Untersuchungen über die Änderung der Copolymerisationskonstanten in radikalischen Reaktionen erwähnt,[19,20] aber die Untersuchungen über den Einfluβ der Verdünnung auf die alternierende Copolymerisation sind relativ begrenzt und wurden erst in letzter Zeit vorgelegt. [21,22]

Verfolgen wir die Copolymerisation des Isoprens mit Monomethylmaleat und Monobutylmaleat in Abhängigkeit von der Lösungsmittelmenge (für dieselbe Monomerenladung im Molverhältnis 1 : 1), so können wir ein bemerkenswertes Sinken des Umsatzes zum Polymeren feststellen (Abb. 3).

Gleichzeitig mit dem fallenden Umsatz zum Copolymeren bemerkt man auch ein Sinken des Monoestergehaltes im Copolymeren, demzufolge ein Anwachsen des Isoprengehaltes und demnach ein Entfernen von der Alternanz (Abb. 4).

Im Falle der Bildung eines Komplexes durch Ladungsaustausch zwischen den Monomeren, könnte die Änderung des Umsatzes und der Zusammensetzung des Copolymeren in Abhängigkeit von der Lösungsmittelmenge, durch das beträchtliche Zurückgehen der Konzentration des Donor-Acceptor-Komplexes mit der Verdünnung erklärt werden. Dies letztere ist für die erhöhte Reaktionsfreudigkeit und für die erhöhte Alternanz in der Copolymerisationsreaktion verantwortlich.

---

[11] C. Walling und F. R. Mayo, *J. Polymer Sci.*, **3**, 895 (1948).

[12] C. Walling, E. R. Brigs, K. B. Wolfstirn und F. R. Mayo, *J. Amer. Chem. Soc.*, **70**, 1537 (1948).

[13] S. Iwatsuki und Y. Yamashita, *Makromol. Chem.*, **89**, 205 (1965).

[14] W. Kawai, *J. Polymer Sci.*, *Part A*—1, **6**, 1945 (1968).

[15] T. Kokubo, S. Iwatsuki udd Y. Yamashita, *Makromol. Chem.*, **123**, 256 (1969).

[16] N. G. Gaylord, *J. Polymer Sci. Part C*, **31**, 247 (1970).

[17] E. Tsuchida und T. Tomono, *Makromol. Chem.*, **141**, 265 (1971).

[18] T. Ouchi und M. Oiwa, *Bull. Chem. Soc. Japan*, **43**, 2858 (1970).

[19] G. Henrici — Olivé und S. Olivé, *Makromol. Chem.*, **68**, 219 (1963).

[20] J. Drongas und R. L. Guile, *J. Polymer Sci.*, **55**, 297 (1961).

[21] S. Iwatsuki und Y. Yamashita, *J. Polymer Sci. Part. 1*, **5**, 1753 (1967).

[22] G. B. Butler, J. T. Badgett und M. Sharabash, *J. Macromol. Sci. Chem.*, **4**. 51, (1970).

Eine derartige Erklärung wurde von Iwatsuki und Yamashita[21] gegeben, die die Copolymerisation von zwei ternären Systemen untersuchten: 2-Chloräthylvinyläther-Maleinsäureanhydrid-Akrylonitril, und p-Dioxen-Maleinsäureanhydrid-Akrylonitril. Die beiden sahen diese ternären Systeme als die Copolymerisation eines bi-nären Systems (zwischen Akrylonitril und dem Donor-Acceptor Komplex, der sich zwischen den anderen beiden Monomeren bildet) an.

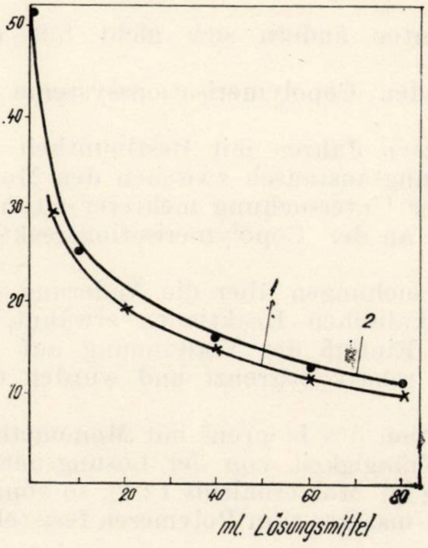

Abb.3

Abb. 3. – Änderung des Umsatzes mit der Lösungsmittelmenge (Cyclohexanon) für die gleiche Menge Monomeren (Molverhältnis 1 : 1).

1, Isopren-Monomethylmaleat; 2, Isopren-Monobutylmaleat; AIBN-Konzentration 4,55.10^{-2} Mol/l; Temperatur 70°, Copolymerisationsdauer 3 Stunden.

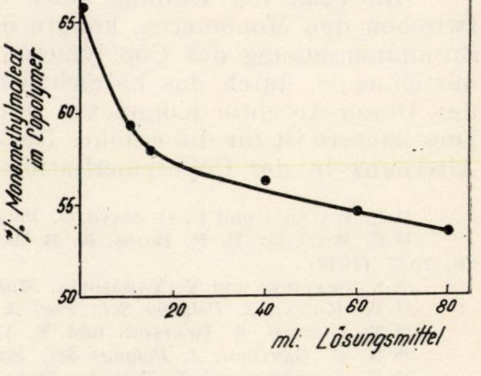

Abb. 4. – Einfluß der Verdünnung auf die Zusammensetzung der Copolymeren Isopren-Monomethylmaleat (Lösungsmittel: Cyclohexanon) Copolymerisationsbedingungen wie in Abb.3.

Wenn sich zwischen Isopren und den Monoestern der Maleinsäure kein Komplex durch Ladungsaustausch bildet, so könnte das in Abb. 3 und 4 aufgezeigte Verhalten aufgrund einer Kettenübertragungsreaktion mit dem Lösungsmittel erklärt werden (die bestätigt wird durch die viel kleinere Molekularmasse der in Lösung erhaltenen Copolymeren, im Vergleich zu denen, die in Masse erhalten werden).

Es ist klar, daβ bei diesen Copolymeren mit kleiner Molekularmasse, bei denen der Endgruppeneffekt bemerkenswert ist, auch die Zusammensetzung des Copolymeren eine andere als die alternierende ist.

Trotzdem kann man die zu groβe Änderung des Umsatzes und der Zusammensetzung der Copolymeren mit der Verdünnung eher dem Sinken der Konzentration des Komplexes durch Ladungsaustausch zwischen den Monomeren zuschreiben (gemäβ der ersten Erklärung).

DER EINFLUSS DER ART DES LÖSUNGSMITTELS

Der Gesamteffekt des Einflusses der Art des Lösungsmittels in der Copolymerisationsreaktion des Isoprens mit Monobutylmaleat (Molverhältnis 1 : 1) ist in Tab. 1 wiedergegeben.

Tabelle 1

Einfluß der Art des Lösungsmittels auf die Copolymerisation von Isopren mit Monobutylmaleat (Molverhältnis 1 : 1)

Lfd. Zahl	Lösungsmittel	Dielektrizitätskonstante [23] bei 20°	Umsatz %
1	Dioxan	2,30*	12,90
2	Tetrahydrofuran	7,70	14,35
3	Cyclohexanon	18,30	19,75
4	Methyläthylketon	18,50	19,75
5	Dimethylformamid	37,70	5,00
6	Dimethylsulfoxid	48,00	4,20
7	Benzol	2,28	32,50
8	Toluol	2,38*	32,20
9	*p*-Xylol	2,27	32,10
10	Isopropylbenzol	2,38	32,00
11	Monochlorbenzol	5,70	33,50
12	Trichloräthylen	3,42**	32,10
13	Tetrachlorkohlenstoff	2,23	32,40
14	Chloroform	4,80	32,60

* Dielektrizitätskonstante bei 25°; ** bei 16°,
– Copolymerisationstemperatur 70°;
– Reaktionszeit zwei Stunden;
– Initiatorkonzentration (AIBN) $4{,}30 \cdot 10^{-2}$ Mol/l.

Aus der Tabelle ist ersichtlich, daβ man zwischen dem Umsatz zum Copolymer und der Dielektrizitätskonstanten der Lösungsmittel keine klar umrissene Beziehung herstellen kann. Diese Tatsache ergibt sich daraus, daβ beim Untersuchen des Einflusses der Art des Lösungsmittels mehrere Faktoren berücksichtigt werden müssen:

— der Einfluβ des Lösungsmittels auf die Beschleunigung der Zersetzung des radikalischen Initiators;

— die Interaktion mit den der Copolymerisation unterworfenen Monomeren;

— die Schaffung eines homogenen oder heterogenen Mittels bei der Copolymerisation.

Infolge der Untersuchung der Copolymerisationsreaktion des Isoprens mit Monobutylmaleat in 14 Lösungsmitteln wurde festgestellt, daβ die Lösungsmittel von 1—6 bei der Copolymerisation ein homogenes System schaffen, während das gebildete Copolymer in den Lösungsmitteln 7—14 unlöslich ist (heterogenes Medium).

Unter diesen Bedingungen ist ein allgemeiner Vergleich zwischen den untersuchten Lösungsmitteln nicht möglich.

Aus Tabelle 1 geht hervor, daβ Lösungsmittel wie: Dioxan, Tetrahydrofuran und besonders Dimethylformamid und Dimethylsulfoxid die Copolymerisationsreaktion in groβem Maβe beeinflussen.

Der kleine Umsatz, der in diesen Fällen erzielt wird, beweist die Wechselwirkung zwischen Lösungsmittel und Monoester und auf diese Weise wird das Comonomere der Copolymerisationsreaktion entzogen (die Wechselwirkungen können von der Art der Wasserstoffbrücken sein). Solche Einflüsse der elektronenabgebenden Lösungsmittel sind auch in der alternierenden Copolymerisation einiger Systeme aufgezeigt worden, bei denen man die Rolle der Komplexe durch Ladungsübertragung zwischen den Monomeren in betracht gezogen hat.[21,24-27]

Novicov und Mitarb.[25] stellten bei der Untersuchung der Copolymerisation von Maleinsäureanhydrid mit Vinylbutyläther in Dimethylformamid und Dimethylsulfoxid fest, daβ man in diesen Fällen im UV-Spektrum keinen Komplex durch Ladungsübertragung zwischen den Monomeren beobachten kann, es bilden sich aber auch keine Copolymeren. Aus diesen Feststellungen schlossen die Autoren, daβ die Bildung der Komplexe zwischen den Monomeren in direktem Verhältnis zur Bildung der Copolymeren steht. In solchen Fällen wird die Abhängigkeit der Copolymerisationsgeschwindigkeit vom Charakter des Mediums durch den Einfluβ des Lösungsmittels auf die Komplexierung der Monomeren bestimmt.

Wenn wir nun diese Erwägungen in betracht ziehen, wie auch den groβen Einfluβ der erwähnten Lösungsmittel auf die Copolymerisation des Isoprens mit Monoestern der Maleinsäure, so könnten wir auch in diesem Falle voraussetzen, daβ die Reaktion unter Beteiligung eines Donor-Acceptor Komplexes zwischen den Monomeren verläuft.

Erwähnenswert ist das Verhalten der Lösungsmittel, die während der Copolymerisation ein heterogenes Medium bilden (die Lösungsmittel mit den Ordnungszahlen 7—14 aus Tab. 1). Die Verwendung dieser Lösungsmittelgruppe führt praktisch zum gleichen Umsatz an Copolymeren, der aber viel gröβer ist als im Falle der Verwendung der ersten Gruppe.

---

[23] * * * „Handbook of Chemistry and Physics", 44 th Edition, 1962, 1963, Chemical Rubber Publishing, p. 2611—2620.

[24] M. Matsuda und K. Abe, *J. Polymer Sci. Part A—1*, **6**, 144 (1968).

[25] S. N. Novicov, L. I. Danilina, A. N. Pravednikov, *Vysokomol. Soedineniya A*, **12**, 1751 (1970).

[26] B. K. Patnaik und N. G. Gaylord, *J. Macromol. Sci. Chem.*, **A5**, 1239 (1971).

[27] A. V. Ryabov, Yu D. Semchikov und N. N. Slavnitskaya, *Vysokomol. Soedineniya A*, **12**, 553 (1970).

Hervorzuheben ist die Unabhängigkeit des Umsatzes von der Dielektrizitätskonstanten des Lösungsmittels in dieser Reihe, eine Beziehung, die man auch bis jetzt in der Copolymerisation anderer Monomeren kannte.

DIE ÄNDERUNG DER VISKOSITÄTSZAHL DER COPOLYMEREN IN ABHÄNGIGKEIT VOM UMSATZ

Die Beziehung zwischen dem Molekulargewicht und dem Umsatz, bei dem die Polymeren erhalten wurden, liefert wertvolle Hinweise über den Polymerisationsmechanismus.

Es wurde festgestellt, daβ im Falle der konventionellen Polymerisation mit freiem Radikalen (monoradikalischer Mechanismus) das Molekulargewicht konstant bleibt, wenn der Umsatz mit der Zeit wächst. Im Falle eines biradikalischen Mechanismus wächst das Molekulargewicht mit dem Umsatz.[28]

Die Beziehung zwischen Viskositätszahl ($\eta_{sp/c}$) und Umsatz für das Copolymer Isopren-Monomethylmaleat, kann in Abbb. 5 verfolgt werden.

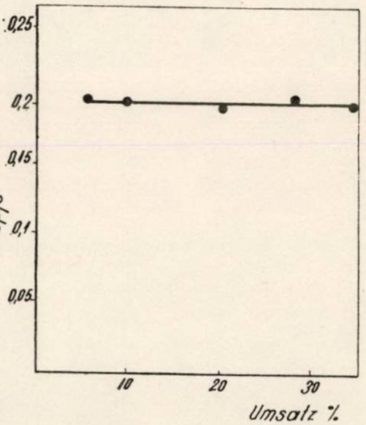

Abb. 5. — Änderung der Viskositätszahl des alternierenden Copolymeren Isopren-Monomethylmaleat mit dem Umsatz.

Die Tatsache, daβ die Viskositätszahl in Abhängigkeit vom Umsatz konstant ist, weist auf einen typisch monoradikalischen Mechanismus hin. Auch andere Arbeiten, betreffend die alternierende Copolymerisation verschiedener Systeme wie: Styrol-Maleinsäureanhydrid, [17] p-Dioxen-Maleinsäureanhydrid,[15] in denen die Beteiligung eines Komplexes durch Ladunsgsübertragung zwischen den Monomeren suggeriert wurde, haben dieselbe Unabhängigkeit der Viskositätszahl der Copolymeren vom Umsatz hervorgehoben, was eine Reaktion durch Biradikale ausschlieβt.

---

[28] N. L. Zutty, C. W. Wilson, G. H. Patter, D. C. Priest und C. J. Whitworth, *J. Polymer Sci., Part A*, **3**, 2781 (1965).

Trotzdem haben Zutty und Mitarb.[28] bei der Untersuchung der alternierenden Copolymerisation von Bicyclo-2, 2, 1-hepten-2 mit SO_2 aufgrund der steigenden Viskositätszahl mit dem Umsatz, einen Mechanismus vorgeschlagen, der anfänglich die Bildung eines Komplexes zwischen den Reaktionsteilnehmern einschließt, der eine Neuordnung dieses Komplexes zu Biradikalen und ihre Weiterreaktion zur Bildung der Copolymeren folgt.

Anders wurde die spontane alternierende Copolymerisation von 1-Methyl-Cyclopropen mit SO_2 erklärt, obwohl auch in diesem Falle das Molekulargewicht mit dem Umsatz wächst.[29] Das Verhalten in dieser letzten Reaktion wurde der Bildung eines langlebigen Radikals zugeschrieben.

---

[29] S. Iwatsuki, T. Kokubo und Y. Yamashita, *J. Polymer Sci. Part A 1*, **6**, 2441 (1968).

Revue Roumaine de Chimie, **19**, *1*, 125–130 (1974)

COPOLYMERIZATION OF EPICHLORHYDRIN AND PROPYLENE OXIDE WITH THE $AlEt_3-H_2O$ CATALYTIC SYSTEM

VICTORIA DIMONIE, D. DONESCU and I. GAVĂT

Institute of Macromolecular Chemistry "P. Poni", "Polymerization Processes" Department
Bucharest, Str. Dumbrava Roşie, 18, Romania

Received July 27, 1973

The kinetics of the epichlorhydrine (ECH) and propylene oxide (PO) copolymerization was studied with the $AlEt_3 - H_2O$ system in benzene medium. The dependence of the composition of the formed copolymers upon the composition of the initial mixture of comonomers was established, as well as the variation of the composition of the copolymer with time, the yield in copolymer after 24 hours of reaction and the evolution of the molecular weights with time. It was found that during copolymerization in the presence of $AlEt_3 - H_2O$, PO was the more active monomer.

1. INTRODUCTION

The study of the cationic copolymerization of cyclic monomers forms a much investigated problem in literature.[1]

Unlike the radical copolymerization of vinyl monomers,[2] the phenomena appearing in the ionic copolymerization of cyclic monomers are much more complex, this fact explaining the difficulty of applying the Mayo — Lewis theory to the latter case. In the cationic polymerization and copolymerization of cyclic monomers, in most cases the going on of the reactions has a non-steady character, the comonomer reactivities depend upon the nature of the catalyst and solvent used,[3-6] and even from the beginning of the monomer consumption, secondary reactions are taking place: formation of low-molecular secondary products,[7-11] depolymerization,[12] and chain transfer.[13-16]

---

[1] K. C. Frich and D. L. Reegen, "Ring-Opening Polymerization", M. Dekker, New York and London, 1969.

[2] G. Ham, "Copolymerization", Wiley-Interscience, New York, 1964.

[3] Y. Yamashita, T. Tsuda, M. Okada and S. Iwatsuki, *J. Polymer Sci. A—1*, **4**, 2121 (1966).

[4] T. Kagyia, T. Konda and K. Fukui, *Bull. Chem. Soc. Japan*, **7**, 1686 (1968).

[5] T. Higashimura, M. Matsuda and S. Okamura, *J. Polymer Sci. A-1*, **7**, 1115 (1969).

[6] K. Burg, N. Schlaf and H. Cherdron, *Makromol. Chem.*, **145**, 247 (1971).

For this reason, we consider that for the study of the copolymerization of cyclic monomers, the reactivity ratios do not represent kinetic constants significant for the characterization of the respective systems.

Since for the cationic copolymerization of cyclic monomers, the determinant factors of their reactivity are their basicity and the ring strain,[3,17] we attempted to study a system of comonomers ECH and PO, having very near ring strains, but different basicities. The copolymerization of these two monomers has already been studied with different catalytic systems: $FeCl_3-PO$,[18] $AlEt_3 - TiCl_3$,[19] $AlEt_3 - H_2O$,[20] $Al(tC_4H_9O)_3$ and $Al\ (tC_4H_9O)_3 - ZnCl_2$.[21]

The study carried out by Kropachev *et al.*[20] consists in the determination of the reactivity ratios for different comonomers using catalysts of the cationic type. In the case of the copolymerization of ECH and PO with the $AlEt_3-H_2O$ system, the following values of the constants of reactivity were found: $r_{ECH} = 0.09$ and $r_{PO} = 4.65$.

In the present work, we study the kinetics of the copolymerization of ECH and PO with the $AlEt_3-H_2O$ system, the dependence of the instantaneous composition and of the composition with time of the copolymers formed upon the composition of the comonomer mixture, as well as the evolution of the molecular weight of the copolymers with time, in order to obtain supplemental data about this system.

2. EXPERIMENTAL

2.1. MATERIALS

Epichlorhydrine — Merck A. G. product — was rectified on a column of great efficiency, deoxygenated by bubbling through purified argon, and dried on CaH_2. The monomer, fresh

---

[7] V. Jaacks, *Makromol. Chem.*, **101**, 33 (1967).

[8] T. Higoshima, A. Tanaka, T. Miki and S. Okamura, *J. Polymer Sci. A-1*, **5**, 1927 (1967).

[9] T. Higashimura, A. Tanaka, T. Miki and S. Okamura, *J. Polymer Sci. A—1*, **5**, 1937 (1967).

[10] K. Weissermel, S. Fischer, K. Gutweiler and H. D. Herman, *Kunststoffe*, **54**, 410 (1964).

[11] J. M. Mammond, J. F. Hooper and W. G. P. Robertson, *J. Polymer Sci. A—1*, **9**, 265 (1971).

[12] Y. Yamashita, H. Kasahara, K. Suyama and M. Okada, *Makromol. Chem.*, **117**, 242 (1968).

[13] St. Penczek. J. Fejgin, W. Sadowska and M. Tomasowicz, *Makromol. Chem.* **116**, 203 (1968).

[14] Y. Yamashita, T. Asachura, M. Okada and K. Ito, *Makromol. Chem.*, **129**, 1 (1969).

[15] Y. Minoura and M. Mitoch, *Makromol. Chem.*, **126**, 56 (1969).

[16] Y. Minoura and M. Mitoch, *Makromol. Chem.*, **128**, 41 (1969).

[17] S. Aoki, Y. Harita, Y. Tanaka and M. Mandai, *J. Polymer Sci. A—1*, **9**, 2585 (1968).

[18] S. Ichida, *Bull. Chem. Soc. Japan*, **33**, 727 (1960).

[19] T. Otsu, A. Akimoto and S. Aoki, *J. Appl. Polymer Sci.*, **6**, 1477 (1968).

[20] V. A. Kropacev, L. V. Alferova and N. M. Geller, "Symposium on Macromolecular Chemistry", Prague, 1965, Preprints p. 53.

[21] Sh. Sekigucki, K. Kowakami, M. Mitzutami and Y. Ishii, *J. Chem. Soc. Japan Ind. Chem. Soc.*, **65**, 979 (1968); from ref. 20.

redistilled in purified argon atmosphere, was measured in glass phials dried at 200° and vacuum of 10^{-3} mm Hg and then sealed by flame.

Propylene oxide — commercial product was conditioned in the same way as ECH.

Benzene — Reactivul, Bucharest, product — was rectified, deoxygenated and finally dried on 4 Å molecular sieves. The solvent was measured from the reservoir under argon pressure through a glass G_3 filter into a flask with magnetic cock.

Toluene — Reactivul, Bucharest, product—was conditioned as benzene. The measuring was performed with an automated microburette under argon atmosphere.

The purity of all the reagents was checked by chromatography.

Triethyl aluminium — Schering A. G. product — was used in benzene solution measured into glass bulbs with thin walls. The determination of the $AlEt_3$ solution concentration was performed by complexometry.

2.2. POLYMERIZATION

The polymerizations were carried out in purified argon medium in an apparatus previously dried for 2 hours to 10^{-2} mm Hg.

Benzene, toluene, the monomers and water (measured with the microsyringe in equimolecular amounts with $AlEt_3$), were successively introduced into the reaction flask under magnetic stirring.

The reaction mixture was homogenized, thermostated and the catalyst bulb introduced by striking. The degree of the conversion with time was followed by vapour phase chromatography determination of the unreacted monomers.

The chromatographic determination was performed on the reaction mixture precipitated at 0° in CH_3OH containing isooctane applying the internal standard method. In the present case the internal standard was toluene. A PERKIN — ELMER 452 chromatograph was used, the column being filled with 20% Carbowax 20 M on Chromosorb P 60/80 mesh support as stationary phase. The eluent gas was H_2 with a rate of flow of 100 ml/min and the column temperature 60°.

All the polymerizations have been carried out under the following conditions: overall concentration of monomers 2 moles/l, catalyst $4 \cdot 10^{-2}$ moles/l, toluene 0.524 moles/l and temperature 30°.

2.3. ANALYSIS OF THE COPOLYMERS

The copolymers composition was established by the determination of chlorine.

The composition determinations are in good concordance with the data obtained by chromatography.

The intrinsic viscosity of the copolymers has been determined in dioxan solutions at 25° with the Ubbelohde viscosimeter.

The NMR spectra have been performed in benzonitrile solutions with a JNM—C—60 HL spectrometer at 60 Mz and 70°.

3. RESULTS AND DISCUSSION

We followed the kinetics of homopolymerization of the two monomers and that of copolymerization at different molar ratios of the initial mixture of monomers.

It can be seen in figure 1 that the homopolymerization of ECH and of PO occurs in a similar manner, in two stages : a rapid stage at the beginning of the process, followed by a slow period. The initial polymerization rate (R_0) of PO is a little lower than that of ECH.

In the case of copolymerization (figure 2), the high basicity of propylene oxide ($pKb = 6.94$) as against that of ECH ($pKb = 8.84$)[3] has a determinant role, this resulting in consumption rate of PO higher than that of ECH. The consumption curves of each comonomer have the same characteristic as in the homopolymerization.

The dependence of the consumption rate of each comonomer upon its molar fraction in the feed is different (figure 3). While the consumption rate of PO substantially increases with the increase of its concentration in the initial monomer mixture, in the case of ECH only a slight increase of the reaction rate is observed. Even at high values of the ECH molar fraction, the consumption rates are with about one order of magnitude lower than the homopolymerization rate. This fact is owed to the higher basicity of PO which is preponderantly consumed. The same phenomenon is noticed in the case of co-catalytic addition of PO in the homopolymerization of ECH. [22]

The higher reaction rate of PO with respect to that of ECH causes an enrichment in PO of the copolymer formed with respect to the initial composition of the reaction mixture (figure 4).

During the process development, the molar fraction of the PO units in the copolymer is decreasing owing to the diminishing of the PO molar fraction in the mixture of unreacted comonomers. This causes the variation with time of the copolymer composition (figure 5).

The molar fraction of each monomer consumed at a certain moment is directly proportional to its instantaneous molar fraction in the mixture during the whole process, (figure 6).

The maintaining constant reactivity of the two monomers with respect to the active species, during the whole copolymerization time, shows that, regardless of the polymerization stage, the nature of the active centres is not changing. In the case of the catalytic system $AlEt_3-H_2O$, the greater reactivity of the monomer with higher basicity, PO, confirm once more the cationic character of the active species.

The yield in copolymer, after 24 hours of reaction, is strongly affected by the composition of the initial monomer mixture (figure 7). It is highest in the case of homopolymers and decreases, reaching a minimum, in the range of the PO molar fraction of 0.3 to 0.5.

In figure 7 is shown the variation of the intrinsic viscosity with conversion increase. As it occurs in many cationic polymerization of cyclic monomers, in the case of copolymerization of ECH with PO, the variation of the molecular weights with time is characterized by a curve with a maximum. The diminishing of the molecular weights is owed to the appearing of strong transfer reactions [23] with the polymer or oligomers.

We tried to settle the copolymer structures by NMR, but we had no positive result.

---

[22] M. Dimonie, C. Oprescu, Le Thi Phai, I. Orhan and O. F. Solomon, Paper presented at the IUPAC, "International Symposium on Macromolecular Chemistry", Boston, 1971.

[23] St. Penczek, *Makromol. Chem.* **134**, 299 (1970).

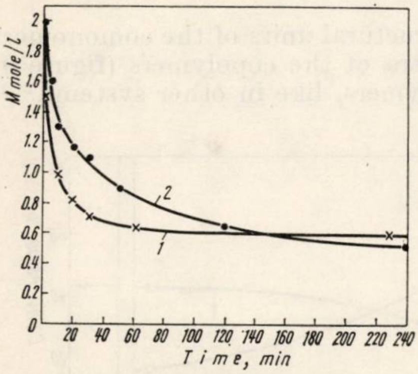

Fig. 1. — Variation of the monomer concentration in the homopolymerization of : ECH (*1*) and PO (*2*).

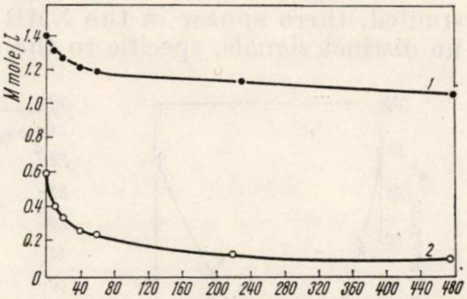

Fig. 2. — Variation of the monomers concentration in the copolymerization of PO and ECH; initial molar ratios 0.7 : 0.3 = ECH (*1*) : PO (*2*).

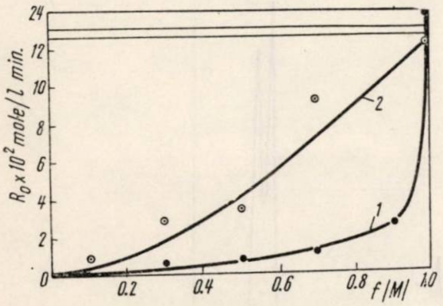

Fig. 3. — Dependence of monomer disappearance rates on the initial molar ratio of comonomers ; ECH (*1*) and PO (*2*).

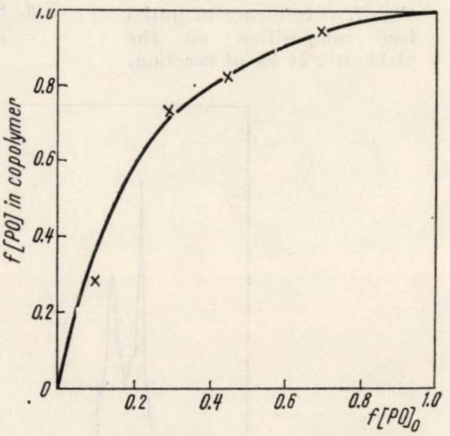

Fig. 4. — Composition diagram of copolymers as function of feed composition.

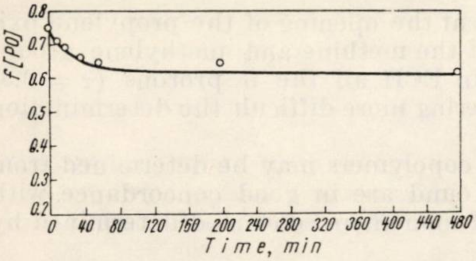

Fig. 5. — Variation of the molar fraction of PO consumed *versus* time. $|PO_0| : |ECH|_0 = 0.3 : 0.7$.

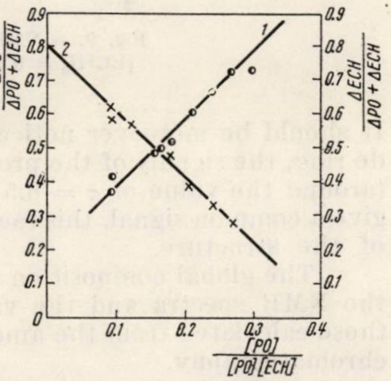

Fig. 6. — Dependence of the molar fraction of consumed monomers on the PO molar fraction in the mixture of unreacted monomers.

Owing to the resemblance of the structural units of the comonomers studied, there appear in the NMR spectra of the copolymers (figure 9) no distinct signals, specific to the copolymers, like in other systems.[24,25]

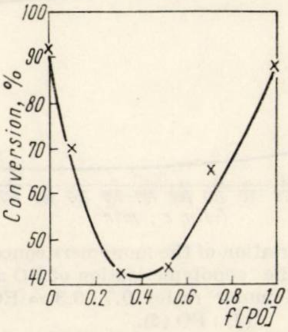

Fig. 7. — Influence of initial feed composition on the yield after 24 hs of reaction.

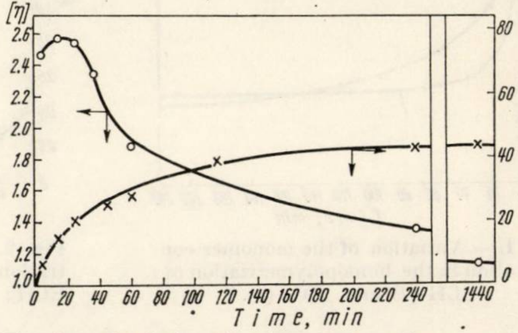

Fig. 8. — Intrinsic viscosities and copolymer conversion *versus* time; $[PO]_0 : [ECH]_0 = 1 : 1$.

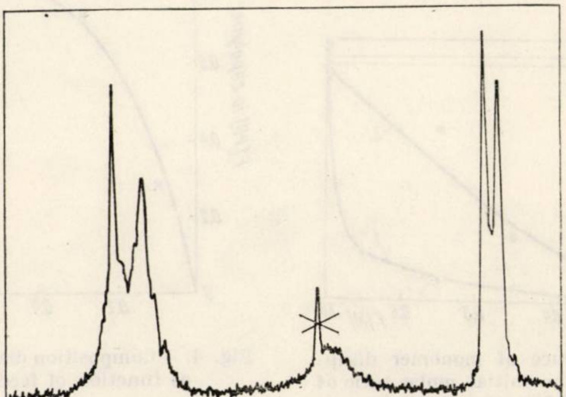

Fig. 9. — NMR spectra of copolymer; $[PO]_0$: $[ECH]_0 = 0.3 : 0.7$ time reaction : 12 min.

It should be moreover noticed that at the opening of the propylene oxide ring, the signals of the protons of the methine and methylene groups (around the value of $\tau = 6.5$) and in ECH all the 5 protons ($\tau = 6.3$) give a common signal, this fact rendering more difficult the determination of the structure.

The global composition of the copolymers may be determined from the NMR spectra and the values found are in good concordance with those calculated from the amount of monomers consumed determined by chromatography.

---

[24] Y. Yamashita, T. Inoue and K. Ito, *Makromol. Chem.*, **138** 305 (1970).

[25] Y. Yamashita, S. Konda and K. Ito, *Polymer J.*, 1, 327 (1970).

Revue Roumaine de Chimie, **19**, *1*, 131–139 (1974)

THE INFLUENCE OF CROSS-LINKAGE OF ANION EXCHANGERS ON THE DISTRIBUTION COEFFICIENT OF SAMARIUM IN MIXED SYSTEMS OF ORGANIC SOLVENT AND MINERAL ACID

ŞTEFANIA SPIRIDON and CARMEN GRIGORESCU-SABĂU

Institute of Atomic Physics, Bucharest, P.O. Box, 35, Romania

Received April 4, 1973

The distribution coefficients have been determined for Sm^{3+} ions between mixed solutions of alcohol and nitric acid and Dowex-1 resin with various cross-linkage degrees. With the aid of these values and the specific volumes determined by the picnometric method, the charge of the complex ions formed in these solutions has been calculated.

It is well known that the physical properties of the ion exchanger resins are strongly influenced by their cross-linkage, namely by the divinylbenzene content. On this content depends the size of the pores of the exchanger and its swelling capacity. Thus, the low cross-linked resins present a greater volume change in water and, inversely, the strong cross-linked resins will swell less, but they present a greater selectivity, a smaller porosity and exchange capacity.

A phenomenon connected with the changes in the water content of the resin is the dehydration of the strongly hydrated ions. It has been observed that the volume of the hydrated layer is proportional with the relative content of water in a resin. Based on this observation, the ionic radii of the hydrated and dehydrated ions can be calculated and the variations in the distribution coefficients of different ions [1–4] can be explained.

In the mixed systems of organic solvents and water with a small concentration of organic component, the content of absorbed ions differs slightly from that of water. This means that the resins in organic aqueous solutions absorb water preferentially, which leads to the supposition that the ions in the resin will become hydrated to the same degree as in water [5] and the equilibrium will be determined by variation of the properties of

---

[1] S. A. Rice and F. E. Harris *Phys. Rev.*, **8**, 314 (1956).
[2] S. Lindenbaum, C. F. Jumper and G. C. Boyd, *J. Phys. Chem.*, **63**, 1924. (1959).
[3] R. A. Horne, R. H. Hahn and M. D. Mayers, *J. Phys. Chem.*, **61**, 1661 (1957).
[4] J. Marcus and D. Maydan, *J. Phys. Chem.*, **67**, 983 (1963).
[5] Ju. J. Ignatov and J. F. Muratov, *Zhur obshchei Khim*, **37**, 521 (1967).

the solution ; consequently, the equilibrium will be displaced in the direction of intensifying the less hydrated ions.

The study of the variation of distribution coefficients in aqueous media on anion exchanger has shown that the more they increase the greater is the cross-linkage.[4, 6,7] The same is true in alcohols—nitric acid mixtures.[8-10]

The present work has studied systematically the variation of the distribution coefficients of samarium on anion exchanger of different cross-linkage in mixed media of organic solvent and nitric acid. It was also tried to establish the charge of the complexes formed.

EXPERIMENTAL

The distribution coefficients (K_d) of samarium ions have been determined as it was mentioned in a previous publication in the case of praseodymium ions.[11, 12] The Sm ions concentration was held to 2.3×10^{-5} equiv/ml and $^{153}_{62}$Sm ($T_{1/2} = 46.2$ h) was used as tracer.

The anion exchanger Dowex-1 (NO_3^-) with different cross-linkage (X2, X4, X8, X10) and the organic solvents (methyl, ethyl, *n*-propyl and isopropyl alcohol) were used in nitric acid of concentrations which varied as follows : for 70% solvent — 0.06 N, 0.15 N, 0.24 N, 0.30 N, 0.60 N, 0.90 N, 1.20 N and 1.80 N acid ; for 80% solvent : 0.04 N, 0.10 N, 0.16 N, 0.20 N, 0.40 N, 0.60 N,0.80 N and 1.20 N acid and for 90% solvent : 0.05 N, 0.08 N, 0.10 N, 0.20 N, 0.30 N, 0.40 N and 0.60 N acid.

For favouring a better separation of strong adsorbed ions in the case of great alcohol and acid concentrations, Dowex-1 (100—200 mesh) was used.

Owing to the study of the distribution coefficients of ions on ion exchange resins with different cross-linkage degree, the estimate of the charge of the adsorbed ions was possible. [13] This calculation requires the determination of the distribution coefficients of the studied ions on two kinds of resins in identical conditions.

With that end in view, the K_d-values for Sm^{3+} ions on Dowex-1X4 (NO_3^-) (20—50 mesh) for methyl alcohol (concentrations of 70%, 80%, 90%) and nitric acid (concentrations of 0.30, 0.60, 1.20 and 1.80 N) were determined. The values are given in table 1.

Table 1

The variation of K_d with the concentration of CH_3OH and HNO_3 for Dowex 1 × 4 (20—50 mesh)

Concentration of CH_3OH	Conc. HNO_3	K_d	Conc. CH_3OH	Conc. HNO_3	K_d	Conc. CH_3OH	Conc. HNO_3	K_d
70%	0.3N	3.27	80%	—	—	90%	0.3N	76.56
	0.6N	4.157		0.6N	27.83		0.6N	146.56
	1.2N	9.535		1.2N	43.52	—	—	—

---

[6] R. H. Herber, K. Tongue and J. W. Irwing jr., *J. Amer. Chem. Soc.*, **77**, 5840 (1955).

[7] J. Averston, D. A. Everest and R. A. Wells, *J. Chem. Soc.*, **231** (1958).

[8] J. Korkisch, I. Hazan and G. Arrhenius, *Talanta*, **10**, 865 (1963).

[9] J. P. Farris, *Analyt. Chem.*, **34**, 1077 (1962).

[10] J. Korkisch and I. Hazan, *Talanta*, **11**, 1157 (1964).

[11] C. Grigorescu Sabău, *J. Inorg. Nuclear Chem.*, **24**, 195 (1962).

[12] C. Grigorescu Sabău and S. Spiridon, *Talanta*, **12**, 641 (1965).

[13] A. M. Trofimov and L. N. Stepanova, *Radiokhimia*, **1**, 403 (1959).

The specific volume of the swollen resins has been determined through the picnometric method.[14] The values are given in table 2.

Table 2

$1/V$-values for the resins Dowex 1 × 4 (20–50 mesh) and Dowex 1 × 4 (100–200 mesh) determined by the picnometric method

Resin	Conc. CH_3OH	Conc. NO_3H	$1/V$	Conc. CH_3OH	Conc. HNO_3	$1/V$	Conc. CH_3OH	Conc. HNO_3	$1/V$
Dowex 1 × 4 (20–50 mesh)	70%	0.3N	1.027	80%	—	—	90%	0.3N	0.882
		0.6N	0.885		0.6N	0.878		0.6N	0.886
		1.2N	0.875		1.2N	0.881		—	—
Dowex 1 × 4 (100–200 mesh)	70%	0.3N	0.917	80%	—	—	90%	0.3N	0.919
		0.6N	0.914		0.6N	0.859		0.6N	0.927
		1.2N	0.866		1.2N	0.831		—	—

Knowing the K_d-value for Dowex-1X4 (NO_3^-) (20–50 mesh) and Dowex-1X4 (NO_3^-) (100–200 mesh), the dried resins densities and the specific volumes, the charge of the ions may be determined, with the help of the relation:

$$Z = \frac{\log K_{d_1}/K_{d_2}}{\log V_2/V_1} + 1$$

where Z = the charge of ions in the mixtures used

K_{d_1} and K_{d_2} = the distribution coefficient values for the Sm^{3+} ions on Dowex 1X4 (NO_3^-) (20–50 mesh) and Dowex 1X4 (NO_3^-) (100–200 mesh), respectively.

V_1 and V_2 = the specific volumes of the two resins determined through the picnometric method $\left(V = \frac{1}{\rho}, \text{ where } \rho \text{ is the density of dry resin} \right)$.

RESULTS AND DISCUSSION

In the present work, alcohols were preferred because they are miscible with water and are polar substances, which permit the use of metal ions as simple combinations, any addition of strange salts being unnecessary. The alcohols used have a much less dielectric constant than water, so that in mixture with it, they will diminish considerably the dielectric constant of the mixture and will increase the electrostatic forces. That means that the formation of ion pairs and their association in complex species without charge, which have less mobility because of their greater radius, will be facilitated. On the other hand, the presence of the organic solvent favours the dehydration of the metal ions, consequently the formation of complexes with negative charge, which will be preferably adsorbed by the anion exchanger, resulting the increase of K_d with the growing of organic solvent concentration (fig. 1).

---

[14] J. Inczedy, "Analytical Applications of Ion Exchangers", Akademiai Kiado Budapesta, 1966, p. 116.

The plot of log K_d as a function of the nitric acid concentration for the different cross-linkage of the resin shows an increasing distribution of the K_d values for the same solvent concentration (fig. 1). The shape of the curves is maintained for all four cross-linkage degrees used (fig. 2). In the solvent absence, the K_d values would grow with the cross-linkage. But in the presence of organic solvent these values decrease, so that the greatest distribution coefficients will be in the resin having 2% divinylbenzene and the smallest distribution coefficients in the resin having 10% divinylbenzene. Because the resins with a great content of divinylbenzene are less swelling and less sensible to the variation of the ionic strength of the solution, the diffusion processes are slower. Thus, the more convenient for work are those resins which contain 4–5% divinylbenzene and the most data in literature are given for these kinds of resins.[15,16]

Fig. 3 shows the variation of log K_d as a function of the concentration of the organic solvent. In contrast to figs. 1 and 2, the curves become concave, but keeping the same growing order of the K_d values both for the concentration of the alcohol and of the nitric acid used.

Fig. 4 represents the variation of log K_d *versus* the cross-linkage grade for different solvent concentrations. On passing from 70% to 90% solvent, the shape of the curves changes. It is interesting that in this case the curves tend to group together in pairs as follows: for 70% solvent the two similar pairs are methyl alcohol, *n*-propyl alcohol and ethyl alcohol, *iso*propyl alcohol, for 80% solvent the resemblance is made between ethyl alcohol, *n*-propyl alcohol and *iso*propyl alcohol, for 90% solvent the groups include methyl alcohol, isopropyl alcohol and ethyl alcohol, *n*-propyl alcohol.

The great similarity of physical and chemical properties of lanthanides, conferred by the electrons accomodated in the 4f shell, has made their separation very difficult. For this reason their separation was very much studied by different methods, among others also the ion exchange method.

Thus, it was shown that in nitric acid 5–6 N, the K_d of light rare earths are included between 5 and 7, while through the increasing of acidity the values become smaller.[17] Replacing a part of the aqueous phase of the acid solution by an organic solvent miscible with water, the adsorption of the lanthanides on strong basic anionites,[18-21] for example Dowex 1, increases.

The increasing of the concentration of organic solvent, as shown by Edge,[15] leads to the adsorption of rare earths. This fact was demon-

---

[15] R. A. Edge, *J. Chromatogr.*, **5**, 526 (1961).

[16] J Abstad and A. O. Brunfelt, *Analyt. Chim. Acta*, **38**, 185 (1967).

[17] J. Marcus and M. Givon, *J. Phys. Chem.*, **68**, 2230 (1964).

[18] J. Marcus and I. Abrahamer, *J. Inorg. Nuclear Chem.*, **22**, 141 (1961).

[19] J. Korkisch, "Progress in Nuclear Energy" Series IX Analyt. Chem. vol. 6, Pergamon Press 1966.

[20] J. Korkisch and F. Feik, *Analyt. Chem.*, **36**, 1793 (1964).

[21] F. Molnar, A. Horwath and V. A. Khalkhin, *J. Chromatog.*, **26**, 215, 225 (1967).

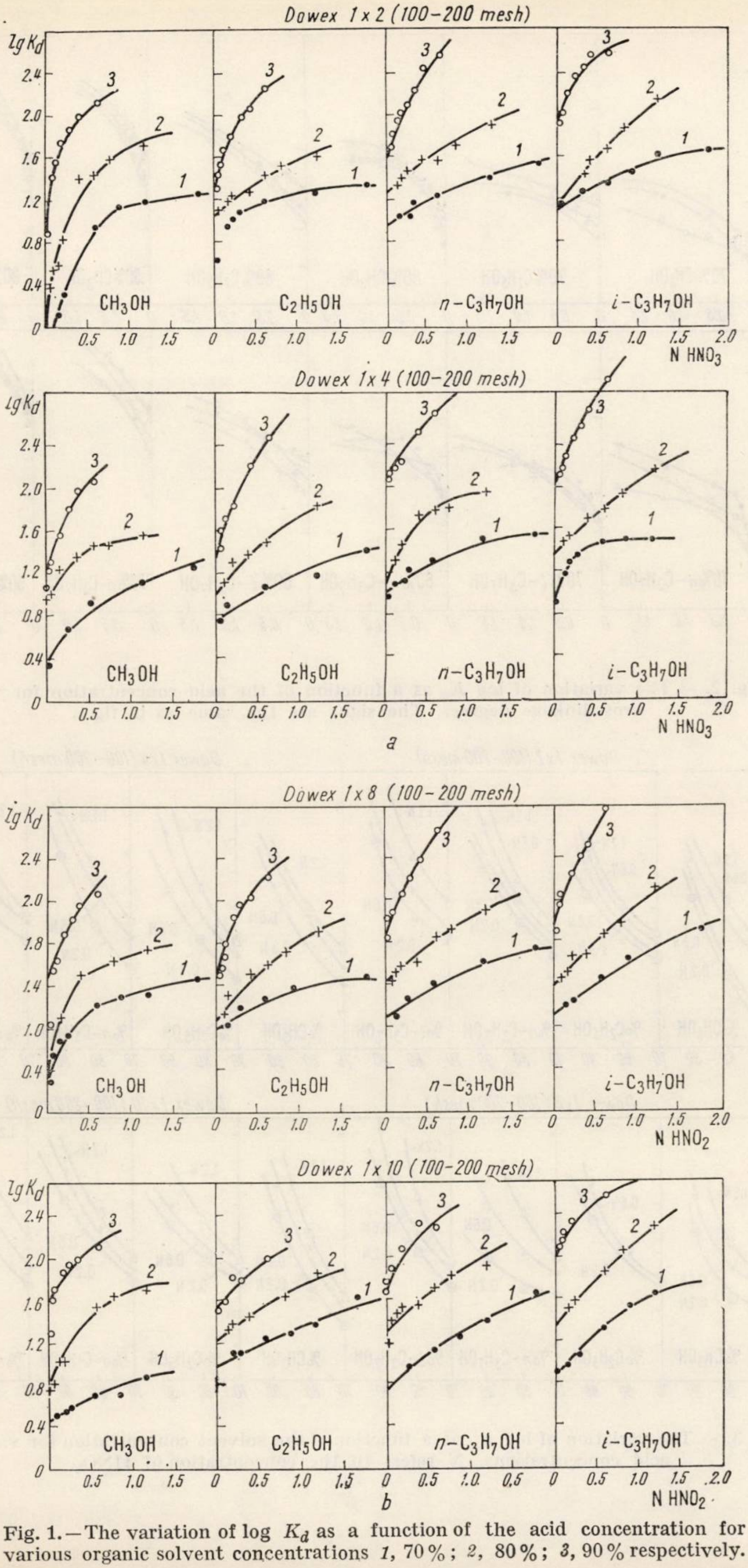

Fig. 1. — The variation of log K_d as a function of the acid concentration for various organic solvent concentrations *1*, 70 %; *2*, 80 %; *3*, 90 % respectively.

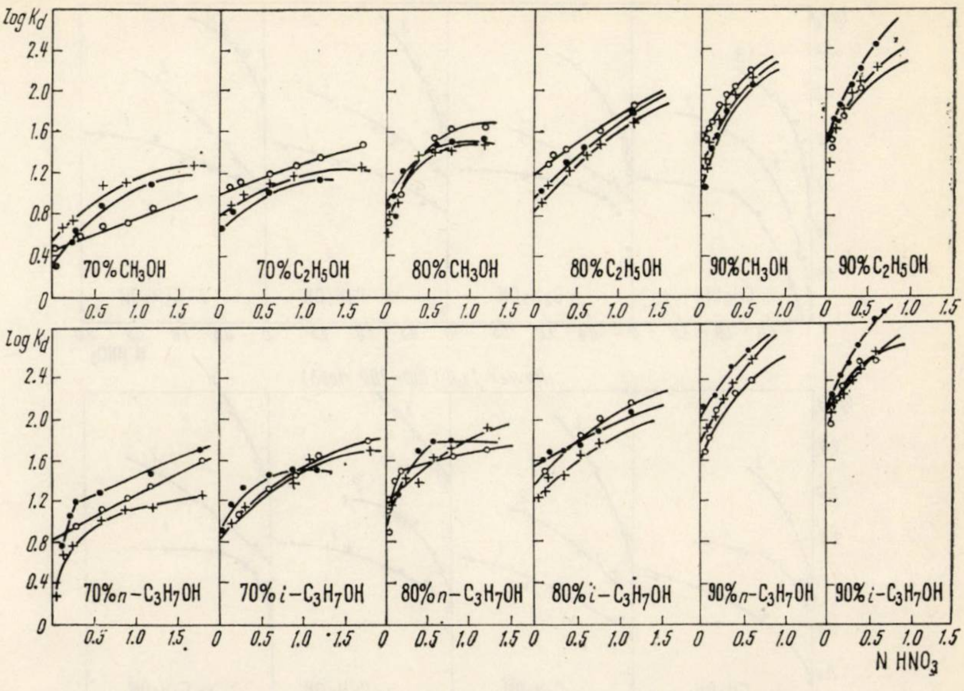

Fig. 2. — The variation of log K_d as a function of the acid concentration for various cross-linkage degrees. The signs are the same as in fig.1.

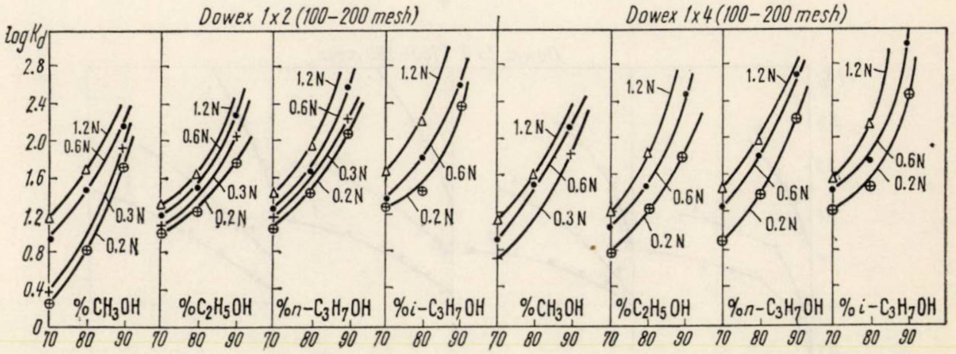

Fig. 3. — The variation of log K_d as a function of the solvent concentration for various acid concentrations. N refers to the concentration of HNO_3.

strated by Sm, where the greater values of the distribution coefficient were obtained for 90% alcohol (fig. 1). By comparing the K_d-values for the different cross-linkage degrees which were used, it was observed that these are decreasing (fig. 2) in the order 4% divinylbenzene-8% divinylbenzene; at 10% divinylbenzene they grow very little to 80% for methyl, ethyl and isopropyl alcohol and to 90% for methyl alcohol.

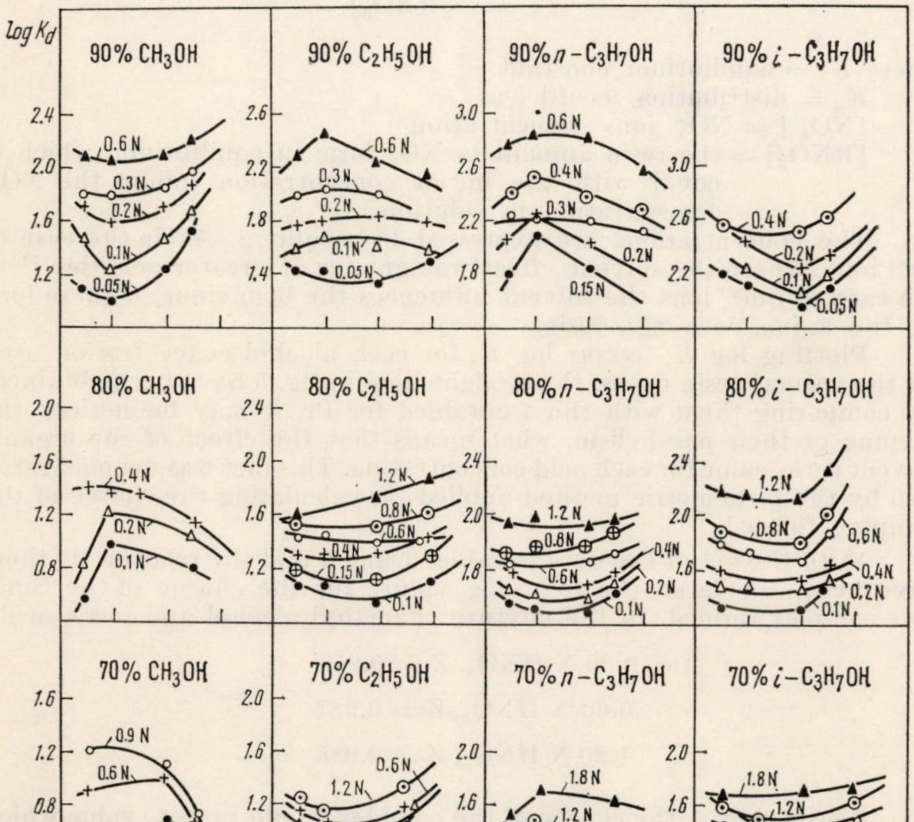

Fig. 4. — The variation of log K_d as a function of the cross-linkage degree. N is the same as in fig. 3.

The experimental data have confirmed that the reaction with Sm^{3+} ions in acid solution is influenced by the presence of an organic solvent. Assuming that in the presence of nitric acid a complexation of Sm^{3+}

ions takes place and applying the law of action in the reaction of equilibrium, the equilibrium constant may be calculated:

$$K_e = K_d \frac{[NO_3^-]}{[RNO_3]} \tag{2}$$

where K_e = equilibrium constant
K_d = distribution coefficient
$[NO_3^-]$ = NO_3^- ions concentration
$[RNO_3]$ = the resin amount in NO_3^- form in equilibrium, which is equal with the initial concentration minus the NO_3^- concentration in solution.

The concentrations are expressed in mequiv/g. As in the case of Pr^{3+} ions, where the solvent effect was greater at greater acidities, [11] in the case of Sm^{3+} ions the solvent influences the behaviour of these ions on the anion exchange resin.

Plotting log K_e *versus* log K_d for each alcohol concentration used for the various resin types, the straight lines in fig. 5 have been obtained. By comparing them with those obtained for Pr, it may be noticed the keeping of their parallelism, what means that the effect of the organic solvent is the same for each acid concentration. This fact was demonstrated also by the picnometric method applied for calculating the charge of the complex formed.

With the aid of the data in tables 1 and 2 and the relation (1) there have been calculated the following values for the charge of the Sm^{3+} ions complex-formed in the mixture of methyl alcohol and nitric acid:

for 0.30 N HNO_3, $Z = 0.959$
0.60 N HNO_3, $Z = 0.981$
1.20 N HNO_3, $Z = 0.986$

Consequently, the charge of the complex would be +1, value which explains why the K_d values are small in the mixtures used, indicating that the utilization of some great alcohol and acid concentrations could lead to negative complexes, more strongly adsorbed on the anionite.

If we use the logarithms in relation (2), we obtain:

$$\log K_e = \log K_d + \log \frac{[NO_3^-]}{[RNO_3]} \tag{3}$$

This means that for every acid concentration used, the corresponding values for the different organic solvent concentrations will give a straight line, which was on the other hand confirmed by fig. 5 and the charge determined for the complex ion.

The strength and stability of the connection metal-ligand in a complex combination depend on the nature of the central ion and of the ligand and firstly on their electronegativity. The OH^- and NH_2^-

ligands lead to the formation of a π bond,[22, 23] which decreases the charge of the central metallic ion, determining a decrease of the separation energy. As, generally, a central ion having a high valency determines the donor properties of the ligands and a small one will determine the acceptor ones, it could be shown that in the case of La^{3+} and Ce^{3+} ions the complexes obtained are stable. It might be possible that in the presence of alcohols, hence of the OH^- radical, compounds should be formed in which, by analogy with the other ions of rare earths, the complex ions of Sm^{3+} lower their valency. The present data confirm this hypothesis.

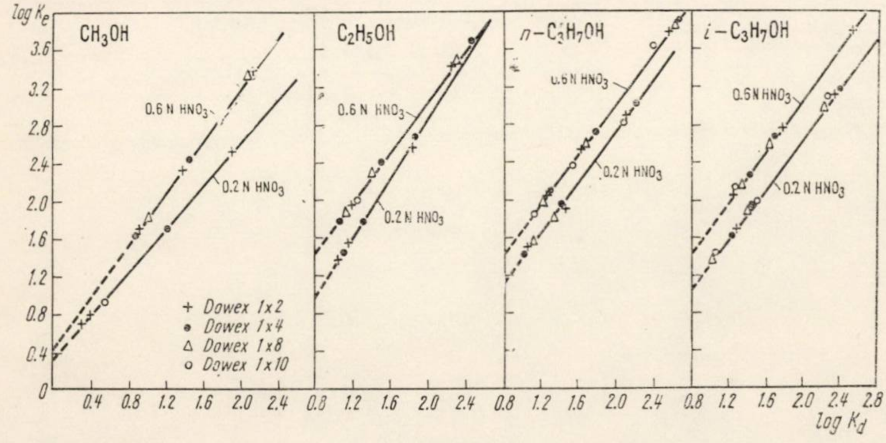

Fig. 5. — The variation of log K_d as a function of log K_e for various acid and solvent concentrations.

The results obtained in the case of the study of the behaviour of the Sm^{3+} ions on ion exchangers in mixed media of organic solvent and mineral acid are a part of a set of works carried out in view of establishing the optimum conditions for an individual separation of the elements of rare earths.

---

[22] P. Spacu and M. Brezeanu "Chimia combinaţiilor complexe", Edit. didactică şi pedagogică, Bucureşti, 1969, p. 268.

[23] E. O. Fisher and M. Werner, "Metal Complexes" vol. 1, Elsevier Amsterdam, 1966.

Revue Roumaine de Chimie, **19**, *1*, 141−144 (1974)

DIE AMPEROMETRISCHE TITRIERUNG DES QUECKSILBERS (II) IN STARK ALKALISCHEM MEDIUM MIT THIOACETAMID

GHEORGHE FACSKO und MARIA NEMEŞ
Polytechnisches Institut Timişoara, Laboratorium für Elektrochemie, Bocşa-Str. 6

Eingegangen am 26. Feb. 1973

In vorliegender Arbeit wird die amperometrische Bestimmung des Hg^{2+}-Ions in einer das Natriumsalz der 4-Sulfonamidobenzoesäure und Natriumhydroxyd enthaltenden Grundlösung untersucht. Die amperometrische Titrierung wurde bei 0,7 V (im Vergleich zur G.K.E.) vorgenommen, wobei für Hg^{2+}-Konzentrationen von $10^{-3}-10^{-4}$ Äquiv. gr/1, die Bestimmungsfehler bis zu−4 % betrugen.

Sowie wir in einer früheren Arbeit [1] zeigten, präzipitiert das Hg^{2+}-Ion in neutralem Medium mit dem Natriumsalz der 4-Sulfonamidobenzoesäure (4−Sb−Na). Der gebildete weiβ-käsige Niederschlag löst sich in Natriumhydroxyd unter Bildung einer komplexen Verbindung, anscheinend gemäβ der Gleichung:

$$H_2N - SO_2 - C_6H_4 - COO^- + Hg^{2+} + 2OH^- \rightleftarrows HgN - SO_2 - C_6H_4 - COO^- + 2H_2O \quad (1)$$

Da wir feststellen konnten,[2] daβ das Hg (II) in einer NaOH-4-SB-Na-Grundlösung eine gutausgebildete polarographische Treppe aufweist, haben wir das Unternehmen einiger Untersuchungen betreffs der amperometrischen Bestimmungsmöglichkeiten des Quecksilbers aus diesem Medium als zweckgemäβ erachtet.

Als Reagenz wählten wir Thioacetamid, das zur amperometrischen Bestimmung des Quecksilbers (II) in saurem Medium von Kalinka und Petri [3] mit entsprechenden Ergebnissen angewandt wurde.

Das von uns verwendete alkalische Medium weist aber unbestreitbare Vorteile im Vergleich zum sauren Medium auf, da das Quecksilber (II) mittels des Natriumsalzes der 4-Sulfonamidobenzoesäure in Lösung gehalten wird, während die meisten übrigen Ionen präzipitieren. Dies ermöglicht eine schnelle und bequeme Trennung des Quecksilbers von den meisten übrigen Ionen.

---

[1] GH. FACSKO und M. NEMEŞ, *Bul. St. şi Tehnic al I.P.T.* **15**, 145 (1970).

[2] GH. FACSKO und M. NEMEŞ, Vorgehende Arbeit.

[3] J. KALINKA und ST. PETRI, *Chem. Analit.*, **11**, 10.007 (1966).

ARBEITSWEISE

Die Polarogrammen wurden mittels eines Polarographen LP 60 aufgenommen. Als Anode wurde eine gesättigte Kalomelelektrode verwendet, die über eine Salzbrücke, bestehend aus einer durch Agar-Agar immobilisierten KNO_3-Lösung, mit der zu untersuchenden Lösung in Verbindung gebracht wurde.

Die amperometrischen Titrierungen wurden mittels desselben Polarographen LP 60 durchgeführt. Der Diffusionsgrenzstrom wurde an der Skala des Registrierpotentiometers abgelesen.

Die Titrationszelle bestand aus einem 100 ml — Glasbecher; die zu untersuchende Lösung wurde mittels einer Salzbrücke, bestehend aus einer durch Agar-Agar immobilisierten KNO_3-Lösung, mit einer großflächigen Kalomelelektrode in leitende Vervindung gebracht.

Die zu polarographierenden Lösungen wurden wie folgt vorbereitet: In einem 25 cm^3 -Meßkolben wurden 5 ml einer 0,5 N NaOH - 5 ml einer 0,5 M 4-SB-Na-, 1 ml einer gesättigten Na_2SO_3-Lösung, sowie aliquote Volumen einer $Hg(NO_3)_2$-Lösung bekannter Konzentration hinzugefügt. Nach der Zugabe von bidistilliertem Wasser bis zur Marke, wurde 10 Minuten zwecks Entfernung des gelösten Sauerstoffes gewartet, wonach bei einer Tropfzeit von 3 Sekunden, im Bereich 0—2 V polarographiert wurde. Zwecks Aufzeichnung der Eichkurven wurden die Lösungen bei +25° thermostatiert.

Die der amperometrischen Bestimmung unterworfenen Lösungen wurden wie folgt vorbereitet: im 100 ml-Titrierungsbecher wurde 10 ml einer 0,5 N $NaOH^-$, 10 ml einer 0,5 M 4-SB-Na-, 2 ml einer gesättigten Na_2SO_3 - Lösung sowie 4 ml einer 10^{-2}N Hg $(NO_3)_2$ - Lösung bekannter Konzentration hinzugefügt, wonach das Volumen zu 50 ml aufgefüllt wurde.

Die 4-Sulfonamidobenzoesäure wurde aus Chloramin T synthetisiert und zweimal aus Alkohol rekristallisiert. Die 0,5 N 4-SB-Na-Lösung wurde durch Abwägen der 4-Sulfonamidobenzoesäure, Hinzugabe von NaOH in stöchiometrischer Menge und darauffolgender Komplettierung mit bidistilliertem Wasser bis zum entsprechenden Volumen präpariert.

Die 10^{-2}N $Hg(NO_3)_2$-Lösung wurde durch Auflösen von genau abgewogenem Quecksilberoxyd (II) p.a. in Salpetersäure p.a. in einem Meßkolben und darauffolgender Komplettierung bis zur Marke präpariert. Das Quecksilberoxyd (II) wurde als Titrosubstanz angesehen.

Die 10^{-2}N Thioacetamid-Lösung wurde durch genaues Abwägen eines rekristalisierten Thioacetamids präpariert.

Die übrigen Reagenzen waren p.a.

EXPERIMENTELLE ERGEBNISSE

Gemäß dem in vorangehender Arbeit[2] Dargestelltem, weist das Quecksilber (II) in einer 0,1N NaOH- und 0,1 M 4-SB-Na-Grundlösung eine gutausgebildete polarographische Treppe auf, deren Höhe vom Reststrom entsprechend der Grundlösung gemessen wird. Im Konzentrationsbereich 10^{-5} bis. $2{,}4.10^{-3}$ N Hg(II) ist die polarographische Treppenhöhe der Quecksilber (II)-Konzentration genau proportional. Mit dem Anstieg der Quecksilberkonzentration verschiebt sich das Halbstufenpotential um cca 30 mV bei einer zehnfachen Vergrößerung der Hg (II)-Konzentration.

Hinsichtlich des Einflusses der Natriumhydroxyd-Konzentration im Bereich 8.10^{-3} bis 10^{-1} N wurde keine Änderung der Treppenhöhe, verzeichnet, wobei sich das Halbstufenpotential um nur 15 mV zu positiveren Werten verschob.

Im gleichen Konzentrationsbereich (8.10^{-3}—10^{-1} N) des 4SB—Na wurde eine 12%-ige Abnahme des Diffusionsgrenzstromes und keine Änderung des Halbstufenpotentials verzeichnet.

Die amperometrische Titrierungen wurden bei −0,7 V (im Vergleich zur G.K.E.) durchgeführt, da unsere Untersuchungen angaben, daß das Hg (II) in der von uns angewandten Grundlösung einen klaren Diffusionsgrenzstrom zwischen 0,3 und 1,1 V aufweist.

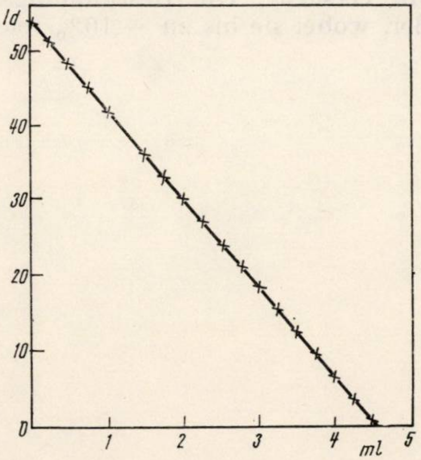

Abb. 1

Die 10^{-2} Thioacetamid-Reagenzlösung wurde aus einer geeichten 10-ml Bürette zu 0,25 ml der zu bestimmenden Lösung hinzugefügt.

Der Diffusionsgrenzstrom wurde dem Reststrom und der Volumenänderung entsprechend korrigiert.

Die graphische Darstellung des Diffusionsgrenzstromes in Abhängigkeit vom zugefügten Reagenzvolumen ergibt Titrationskurven, die jener in Abbildung 1 wiedergegebenen ähnlich sind. Der Äquivalenzpunkt erfolgt aus dem Schnittpunkt der erhaltenen Geraden mit der Abszisse.

Tabelle 1 wiedergibt einige typische Ergebnisse.

Tabelle 1

Die amperometrische Bestimmung des Hg (II) mit Thioacetamid

Nr. der Bestimmung	ml einer 10^{-2}N $Hg(NO_3)_2$—Lösung F = 0,9320	Hg in der Probe mg	Hg gefunden mg	Differenz mg	Differenz %
1	5,08	4,752	4,563	−0,189	−3,9
2	5,08	4,752	4,568	−0,184	−3,8
3	5,08	4,752	4,613	−0,139	−2,9
4	5,08	4,752	4,563	−0,189	−3,9
5	5,08	4,752	4,582	−0,170	−3,5
6	5,13	4,799	4,613	−0,186	−3,8
7	5,13	4,799	4,824	−0,025	+0,5
8	5,13	4,799	4,673	−0,126	−2,6

Wie aus der Tabelle ersichtlich, betragen die Bestimmungsfehler bis zu —4%. Trotzdem erachten wir die Ergebnisse der Methode, angesichts des bequemen Trennungsvermögens, den das genannte Medium aufweist, als zufriedenstellend.

Auch die umgekehrte Titrierung, des Thioacetamids mit dem Quecksilberkomplex, wurde versucht. Die Bestimmungsfehler sind aber für diesen Fall viel gröβer, wobei sie bis zu — 10% reichen können.

Revue Roumaine de Chimie, **19**, *1*, 145–156 (1974)

STUDIES ON THE ELECTROANALYTICAL BEHAVIOUR OF MEMBRANE-ELECTRODES UNDER CURRENT. V*

THE *E*-pH ELECTRODE FUNCTION AND THE USE OF THE PVC + TRICRESYLPHOSPHATE MEMBRANE IN THE ACID-BASE POTENTIOMETRIC TITRATION AT CONSTANT DIRECT CURRENT

ELENA HOPÎRTEAN and C. LITEANU

Chair of Analytical Chemistry, "Babeş-Bolyai" University, Str. Arany Janos 11, Cluj, Romania

Received February 12, 1973

The paper studies the electrode pH function of the PVC+ tricresylphosphate membrane in "foil" as well as in "bubble" form, under a current having an intensity between 0.1 and 0.8 μA, compared to the one obtained at zero current. We ascertain that a substantial extension of the electrode function linearity field, as well as an increase of its slope takes place under current. As a consequence of this change of the electrode function, the titrations carried out under current offer a much higher variation of the potential around the equivalence point than for zero current. The membrane-potential-current curves are also given and the behaviour mechanism under current of the PVC-tricresylphosphate membrane-electrode is discussed.

In the literature we find only two papers dealing with the analytical turning to account of membrane-electrodes under current. [1,2] The attempts to use membranes as indicator resistances in conductometric titrations on a high conductive medium [3–5] have given interesting results. Studies on the current-potential curves of the $BaSO_4$ — cellophane [6,7] or $BaSO_4$ — parchment paper [8] membrane obtained in the rectifying field, meant to bring some contributions to the understanding of the electrical transportation through the membrane, have also been published.

The present paper studies the pH electrode function of the PVC + tricresylphosphate membrane ("bubble" and "foil") under current, as

---

[*] Part IV. I. C. Popescu, C. Liteanu and L. Savici, *Rev. Roumaine Chim.*, **18**, 1983 (1973).

[1] P. Bersier, J. Bersier and F. Hügli, *Helv. Chim. Acta*, **42**, 2514 (1959).

[2] R. Geyer and P. Niklas, *Z. analyt. Chem.*, **177**, 166 (1960).

[3] C. Liteanu and E. Hopîrtean, *Rev. Roumaine Chim.*, **12**, 517 (1967).

[4] C. Liteanu and L. Ghergariu Mîrza, *Rev. Roumaine Chim.*, **15**, 1871 (1970).

[5] C. Liteanu and L. Ghergariu Mîrza, *Talanta*, **19**, 980 (1972).

[6] P. Hirsch-Ayalon, *Electrochim. Acta*, **10**, 773 (1965).

[7] E. P. Honig and J. H. Th. Hengst, *Electrochim. Acta*, **15**, 491 (1970).

[8] C. Liteanu and I. C. Popescu, *Rev. Roumaine Chim.*, **18**, 319 (1973).

compared to the one obtained at zero current. The results obtained with the PVC + tricresylphosphate membrane-electrode under current in the potentiometric titration of HCl with KOH are given. The membrane potential-current curves as well as the behaviour mechanism under current of the membrane-electrode are also given.

EXPERIMENTAL

1. *Experimental device.* The PVC + tricresylphosphate membrane-electrode [9,10] was used in "foil" as well as in "bubble" form. The draft of the working device used for the "foil" membrane, in titrations as well as to obtain the membrane-current potential curves is shown in figure 1.

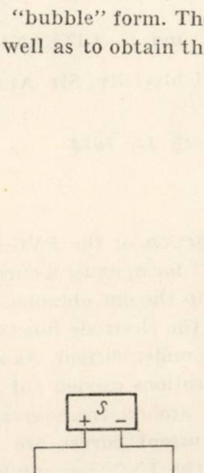

Fig. 1. — Diagram of the working device.

1, SCE with Luggin capillaries; 2, platinated Pt-electrodes; 3, membrane; *C*—cell; *S*—direct current source; *R* — resistor (330 kΩ); *P*—electronic potentiometer.

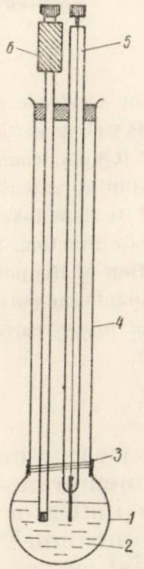

Fig. 2. — "Bubble" membrane-electrode.

1, membrane; 2, internal solution; 3, fastening system; 4, glass tube; 5, wire Pt-electrode; 6, SCE.

The working cell (*C*) [11] made of two compartments is provided with two saturated calomel electrodes with Luggin (*1*) capillaries, and with two Pt-platinized electrodes (1 cm^2 surface). The latter are used to apply a current of required intensity of the direct current source *S*, on the membrane (*3*) attached to the partition of the cell. The reference compartment contains HCl 10^{-4} N. The reference compartment can evidently be polarized anodically or cathodically. In the measurements carried out under current, the sign of the potential coincided with the polarizing sign of the reference compartment. The membrane potential was measured in stirring conditions at 25 ± 0.1° C by means of a MV-11 pH-meter (P), with a ± 1 mV precision.

In the case of the membrane used in "bubble" form (figure 2), the reference solution (10^{-4} N HCl) is inside the bubble. Lucie platinum wire electrodes were used for conduction.

[9] C. Liteanu and E. Hopîrtean, *Rev. Roumaine Chim.*, **15**, 749 (1970).

[10] C. Liteanu and E. Hopîrtean, *Talanta*, **17**, 1067 (1970).

[11] C. Liteanu, I. C. Popescu and M. Preda, *Rev. Roumaine Chim.*, **18**, 1819 (1973).

For the "foil" membrane-electrode, as well as for the "bubble" membrane-electrode, the potential was determined by measuring the e.m.f. of the following cell:

SCE ‖ 10^{-4} M HCl |Membrane| Solution to be studied ‖ SCE

2. EXPERIMENTAL RESULTS

2.1. THE pH ELECTRODE FUNCTION

The pH of the solutions used to determine the electrode functions was measured by means of a glass electrode. The pH electrode functions obtained for the "bubble" form membrane are given in figure 3.

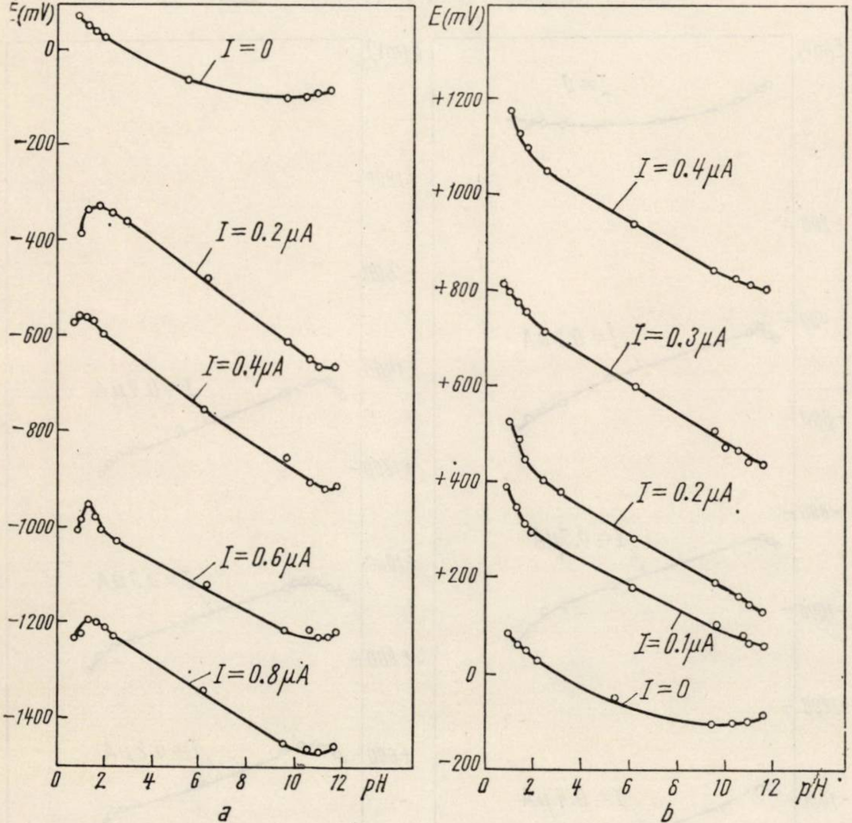

Fig. 3. — E — pH electrode function for membrane-electrode in "bubble" form. *a*, cathodic polarization; *b*, anodic polarization.

The improvement of the electrode function under current, i.e. the extending of the linearity field, as well as the increase of the average slope of the electrode function is concretized by the data in table 1.

Table 1

Influence of the applied current ("bubble" membrane) upon the slope of the electrode function

I (μA)	Polarization	pH range	Average slope (mV)
0	—	2– 9.5	17.0
0.1	anodic	2–11.5	26.0
0.2	anodic	2–11.5	32.3
0.3	anodic	2–11.5	32.3
0.4	anodic	2–11.5	30.0
0.2	cathodic	1.5–11	34.4
0.4	cathodic	1.5–11	36.3
0.6	cathodic	1.5–11	28.0
0.8	cathodic	1.5–11	28.0

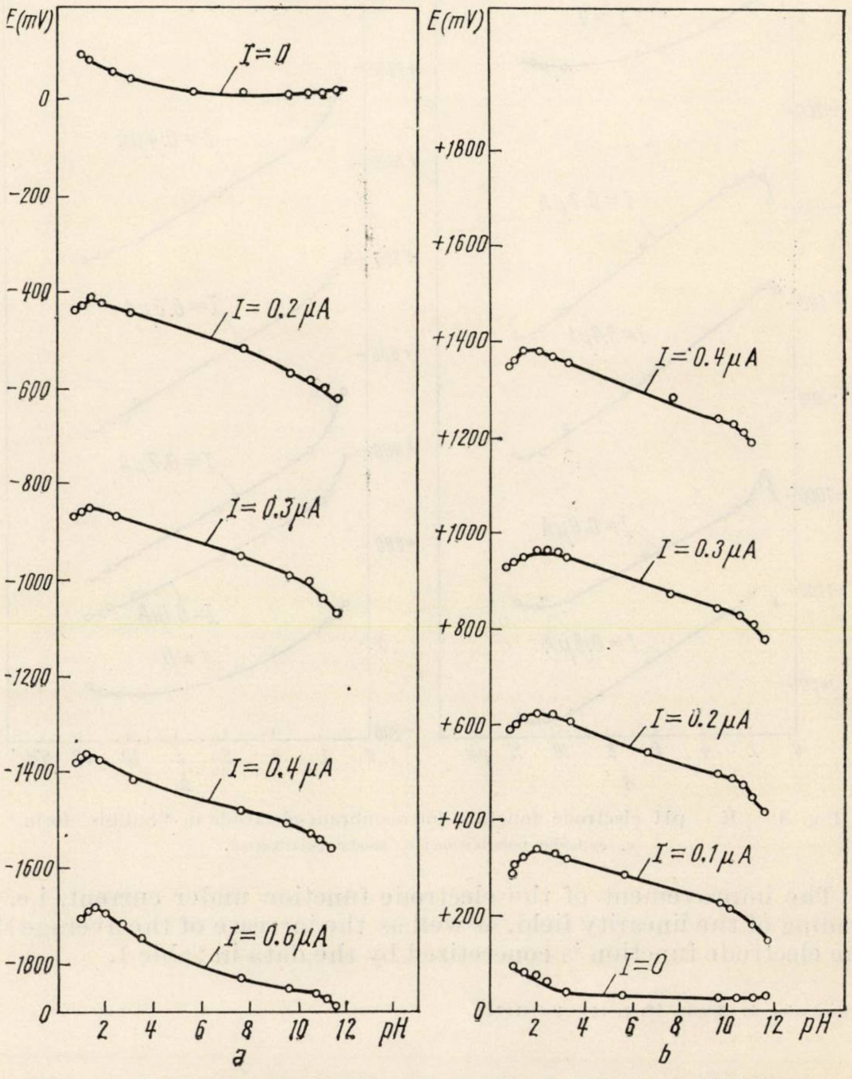

Fig. 4. — E-pH electrode function for membrane-electrode in "foil" form.
a, cathodic polarization; b, anodic polarization.

Figure 4 gives the electrode functions obtained for the "foil" membrane. It is worth pointing out that for this membrane, having initially a lower sensitivity towards the H^+ ions,[10] the turning on of the current results in a more marked improvement of the electrode function, as is seen from table 2.

Table 2

Influence of the applied current ("foil" membrane) upon the slope of the electrode function

I (μA)	Polarization	pH range	Average slope (mV)
0	—	1–3 3–11	19.0 2.7
0.1	anodic	2–11	17.0
0.2	anodic	2–11	19.6
0.3	anodic	2–11	19.0
0.4	anodic	2–11	21.3
0.2	cathodic	1.5–10.5	18.3
0.3	cathodic	1.5–10.5	18·5
0.4	cathodic	1.5–10.5	17.5
0.6	cathodic	1.5–10.5	17.2

2.2. ACID-BASE POTENTIOMETRIC TITRATIONS

We have carried out potentiometric titrations of 10^{-1} M HCl with $5 \cdot 10^{-1}$ M KOH at zero current and at net current, for anodic, as well as for cathodic polarization of the reference compartment.

Figure 5 gives the titration curves obtained with "bubble" membrane-electrode at $I = 0.2$ μA and $I = 0$, and in figure 6 are given the titration curves obtained with the "foil" membrane electrode at $I = 0.2$ μ A and $I = 0$. The titrations carried out with a membrane under current are characterized by a much higher potential variation around the equivalence point than those carried out at zero current, as it was indeed to be expected by studying the electrode functions under current. The titration curves obtained under current of other intensities have a similar form, being only placed in other potential fields. The improvement of the detection of the equivalence point was characterized by the jump index, respectively by the ratio $(\Delta E_{\pm 1\%})_{I \neq 0}/(\Delta E_{\pm 1\%})_{I=0}$. The accuracy of the titrations under current was expressed by the errors affecting the equivalence volumes calculated according to the Hahn-Weiler[12] method *versus* the equivalence volume calculated according to the same method, for the titration carried out in the presence of the glass electrode.

The data referring to the jump index and the accuracy of the 10^{-1} M HCl with $5 \cdot 10^{-1}$M KOH titration according to the intensity of the applied current and the sign of the reference compartment polarization for the "bubble" membrane-electrode are given in table 3, and for the "foil" membrane-electrode in table 4.

---

[12] F. L. HAHN and G. WEILER, *Z. analyt. Chem.*, **64**, 417 (1926).

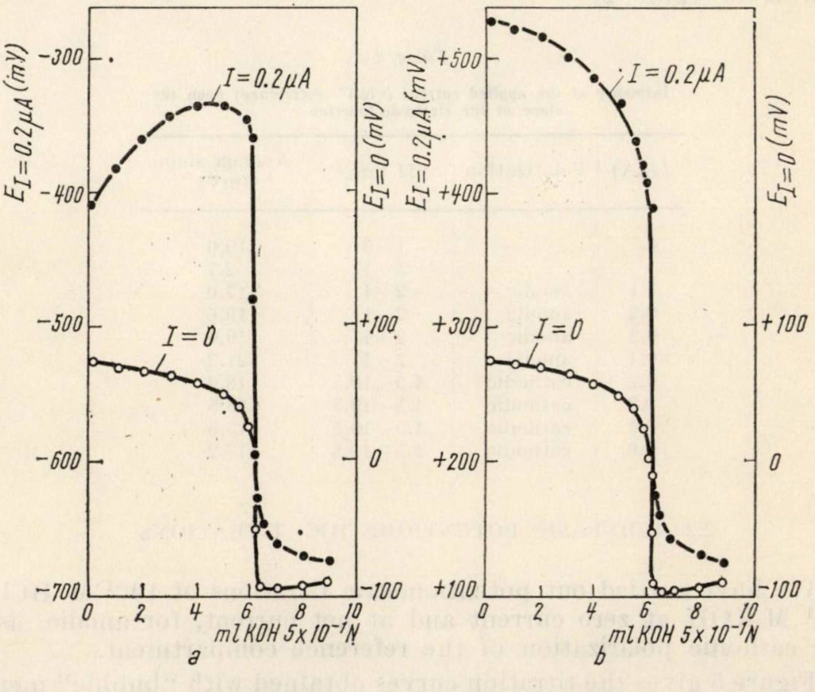

Fig. 5. — Titration of 10^{-1} M HCl with 5×10^{-1} M KOH using "bubble" membrane electrode.

a, cathodic polarization; *b*, anodic polarization.

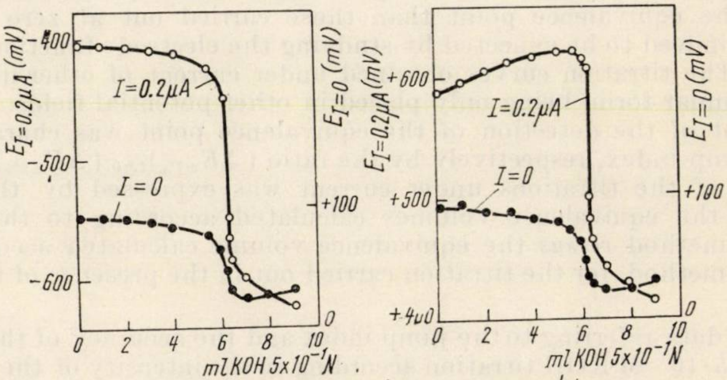

Fig. 6. — Titration of 10^{-1} HCl with 5×10^{-1} M KOH using "foil" membrane electrode.

a, cathodic polarization; *b*, anodic polarization.

The data of tables 3 and 4 show that the titrations under current have high accuracy. Excepting just one case, the recorded errors are under $\pm 0.15\%$. The variation of the potential around the equivalence point is much increased, the jump index having values between 2 and 3 for the "bubble" membrane-electrode, and between 5.4 and 6.8 for the "foil" membrane-electrode.

Table 3

Influence of current intensity upon precision and accuracy of 10^{-1} M HCl with 5×10^{-1} M KOH titration; "bubble" membrane electrode. For glass electrode $V_e = 6.22$ ml

I (μA)	Polarization	V_e(ml)	e(%)	$(\Delta E)_{\pm 1\%}$ (mV)	$\frac{(\Delta E_{\pm 1\%})_{I\neq 0}}{(\Delta E_{\pm 1\%})_{I=0}}$
0	anodic	6.23	+0.14	70	—
0.1	anodic	6.22	0.00	152	2.1
0.2	anodic	6.25	+0.46	172	2.4
0.3	anodic	6.21	−0.15	168	2.4
0.4	anodic	6.22	0.00	145	2.0
0.2	cathodic	6.22	0.00	212	3.0
0.4	cathodic	6.21	−0.15	195	2.8
0.6	cathodic	6.21	−0.15	181	2.6
0.8	cathodic	6.22	0.00	165	2.3

Table 4

Influence of current intensity upon precision and accuracy of 10^{-1} M HCl with 5×10^{-1} M KOH titration, "foil" membrane electrode. For glass electrode $V_e = 6.27$ ml

I(μA)	Polarization	V_e(ml)	e(%)	$\Delta E_{\pm 1\%}$(mV)	$\frac{(\Delta E_{\pm 1\%})_{I\neq 0}}{(\Delta E_{\pm 1\%})_{I=0}}$
0	—	6.28	+0.15	15	—
0.1	anodic	6.27	0.00	95	6.3
0.2	anodic	6.28	+0.15	102	6.8
0.3	anodic	6.28	+0.15	99	6.6
0.4	anodic	6.28	+0.15	98	6.5
0.6	anodic	6.28	+0.15	82	5.4
0.2	cathodic	6.28	+0.15	102	6.8
0.3	cathodic	6.28	+0.15	100	6.6
0.4	cathodic	6.27	0.00	95	6.3
0.6	cathodic	6.27	0.00	89	6.0

We have then studied the influence of the concentration on the magnitude of the potential jump around the equivalence point at the HCl with KOH titration under current, compared to the one at zero current. The titration curves obtained using the "foil" membrane-electrode are given in figure 7.

Table 5 gives the data of the equivalence volumes obtained at zero current and under current, as well as the data referring to the jump index for the respective titrations.

The results obtained while titrating at different concentrations using the "bubble" membrane-electrode were similar. From the titration curves in figure 7, as well as from the data in table 5, it results that by applyng

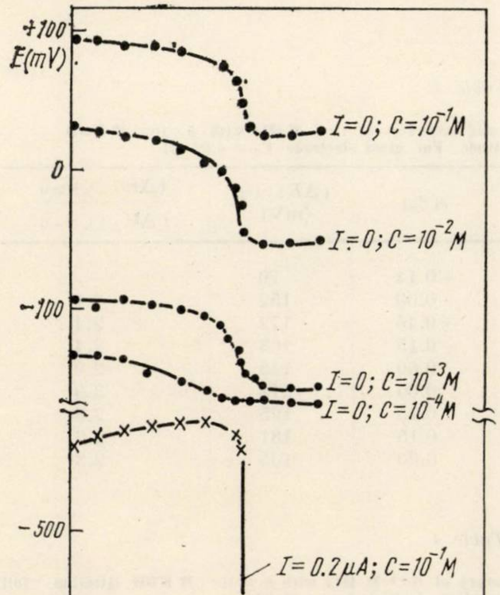

Fig. 7. — Influence of the applied current upon the HCl with KOH titration at different concentrations using "foil" membrane-electrode; cathodic polarization.

a 0.2 μA current to the membrane, the sensitivity of the latter towards the H^+ ions increases in such way as to allow a successful titration of the HCl even at a 10^{-4} M concentration.

Table 5

Results of HCl with KOH titration at different concentrations : "foil" membrane-electrode ; cathodic polarization

HCl concentration (M)	V_e(ml)		e^*(%)	$(\Delta E)_{\pm 1\%}$(mV)		$\frac{(\Delta E_{\pm 1\%})_{I \neq 0}}{(\Delta E_{\pm 1\%})_{I=0}}$
	$I = 0$	$I = 0.2\ \mu A$		$I = 0$	$I = 0.2\ \mu A$	
10^{-1}	6.28	6.28	0.00	15	102	6.8
10^{-2}	6.33	6.31	−0.31	11	51	4.6
10^{-3}	6.36	6.42	+0.95	6	29	4.8
10^{-4}	5.10	5.15	+0.98	1.5	6	4.0

* error calculated towards V_e at $I = 0$

2.3. MEMBRANE-POTENTIAL-CURRENT STATIC CURVES

The membrane-potential-current static curves obtained for the "bubble" membrane-electrode using both polarization directions are given in figure 8.

The figure shows that in this case the following relationship stands for both test solutions :

$$E_m = a + bI$$

respectively :

$$\eta = a' + bI, \text{ where}: \eta = |E_{I \neq 0} - E_{I=0}|$$

We have also proceeded in the same way for the "foil" membrane-electrode. Also making use of both polarization directions and test solutions we have obtained the curves in figure 9. When 10^{-1} M KOH was used as test solution (figure 9, curve *2*), the $E_m - I$ curve took a linear form using a semi-logarithmical rendering : $\eta - \lg I$, hence being valid a relationship of the type:

$$\eta = A + B \lg I$$

3. DISCUSSION

By examining the current-membrane potential static curves for the studied membranes (figures 8 and 9) it results that, excepting the foil-membrane system, cathodically polarized and test solution KOH, all other systems behave as ohmic resistances in the whole studied potential filed. We can thus calculate the resistance of the system from the slopes of the respective curves obtained. The obtained results are given in table 6.

We notice that while the membrane resistance, measured in alternating[9] current is of approximately 2.17 × $10^5\ \Omega$, in direct current the

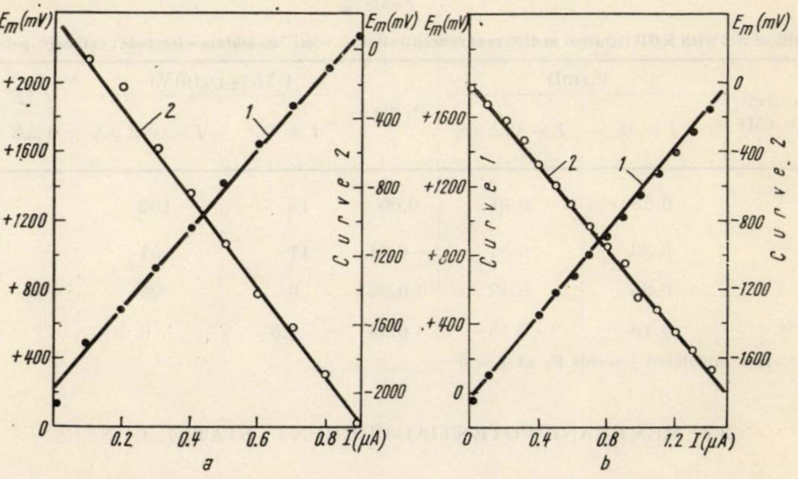

Fig. 8. — Membrane potential-current static curves for "bubble" membrane-electrode

a, test solution 10^{-1} M HCl; *1*, anodic polarization; *2*, cathodic polarization; *b*, test solution 10^{-1} M KOH; *1*, anodic polarization; *2*, cathodic polarization.

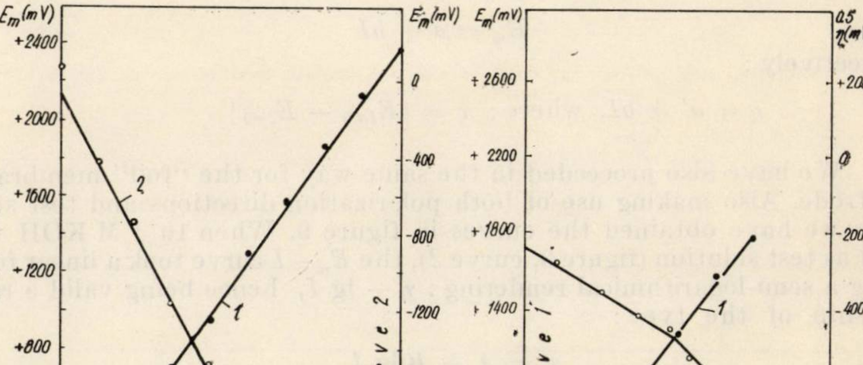

Fig. 9. — *a*) Membrane potential-current static curves for "foil" membrane-electrode. Test solution 10^{-1} M HCl.

1, anodic polarization; 2, cathodic polarization.

b) Membrane potential-current (*1*) and overvoltage — log *I*(*2*) curves for "foil" membrane-electrode. Test solution 10^{-1} M KOH.

1, anodic polarization; 2, cathodic polarization.

resistance of the system is approximately 10 times higher. The supplementary resistance appearing in these conditions is certainly due to a concentration polarization appearing in the layer of adjacent solutions on the two faces of the membrane. We meanwhile note that the resistances for the two polarization senses are not identical, as the solutions on the two faces of the membrane are not identical, either regarding the electrolyte or regarding the concentration.

Table 6

Electrical resistance of PVC + tricresylphosphate membrane calculated from the data of membrane potential-current curves

Membrane	Polarization	Test solution	Electrical resistance (Ω)
"Bubble" form	cathodic	HCl 10^{-1}M	2.64×10^6
	cathodic	KOH 10^{-1} M	1.24×10^6
	anodic	HCl 10^{-1}M	2.34×10^6
	anodic	KOH 10^{-1}M	1.21×10^6
"Foil" form	cathodic	HCl 10^{-1}M	3.60×10^6
	anodic	HCl 10^{-1}M	2.88×10^6
	anodic	KOH 10^{-1} M	2.61×10^6

For the "foil" membrane and the 10^{-1} M KOH test solution, in the case of cathodic polarization (figure 9, curve *2*), as shown, the relationship $\eta = A + B \lg I$; ($\eta > 0.1$V) is valid, which shows the installation in the working conditions of a concentration polarization.[11] In the working conditions, as $[OH^-]/[H^+] = 10^{13} = [Na^+]/[H^+]$, only a Na^+ transport through the membrane must practically take place. As in the $\eta - \lg I$ representation we obtain two curves with different slopes, we can suppose that the Na^+ ion transport takes place by two different mechanisms: directly, through the solution soaking the pores of the membrane, and by jumps, respectively by successive chelatization with the active component of the membrane (tricresylphosphate). This latter mechanism is in agreement with the fact that the membrane is also sensitive for the Na^+ ions[13] as well as with the decrease of the electrical resistance of the system with the increase of the pH (table 6).

By examining the electrode functions (figures 2 and 3) we notice that the behaviour of the membrane improves very much under current by extending its linearity field with the marked increase of the slope (tables 1 and 2). Meanwhile, a shifting of the standard potential of the electrode takes place. This is easily understood, taking into account, as shown above, that the system works as an electrical resistance, the passing of the current being meanwhile accompanied by a partial concentration polarization, which has as consequence the increase of the $(a_{H^+})_{ext}/(a_{H^+})_{int}$ ratio. Thus, for instance, in the case of a "bubble" membrane, at the anodic polarization with 10^{-1} M HCl test solution (figure 8, curve *1*), $R = 2.3$.

---

[13] C. LITEANU and E. HOPÎRTEAN, *Rev. Roumaine Chim.*, **16**, 559 (1971).

$\cdot 10^6\,\Omega$, so that for instance, for $I=0.1$ μA, there results through the ohmic effect $E = 230$ mV, respectively: $E_{I-0.1\mu\text{A}} = (E_{I=0} + 230)$ mV $= 304$ mV. Having obtained experimentally $E = 390$ mV, we assign the difference to the above mentioned concentration polarization effect, i.e.:

$$[(a_{\text{H}^+})_{\text{ext}}/(a_{\text{H}^+})_{\text{int}}]_{I\neq 0} > [(a_{\text{H}^+})_{\text{ext}}/(a_{\text{H}^+})_{\text{int}}]_{I=0}$$

The fact that electrode functions are improved under current, extending the pH field in which the slope of the electrode functions is markedly increased as compared to that at zero current (tables 1 and 2) suggests that the current has a favourable effect on the reversibility of the interface processes. Thus, the stability between the H^+ ion and tricresylphosphate being high enough, and, on the other hand, the tortuosity degree of the PVC matrix being also high, an intensitivity of the electrode towards high pH is reached by a blocking effect of the interface. The activity of the H^+ ions in the membrane thus remains superior to the one at equilibrium, so that the electrode function at zero current flattens out in an alkaline field. In the case of the membrane being under current, the H^+ ions being implied in the transport of the current through the membrane, their accumulation in the membrane phase will be prevented, having as consequence the extension of the linearity field of the electrode function.

This is confirmed by the memory effect noticed when interrupting the polarization current: the electrode potential does only slowly return to the value preceeding the polarization.

As the behaviour under current of the membrane is due to the two phenomena (ohmic effect and concentration polarization), the change of sign of the electrode function slope in the initial portion is the result of a competition between the two mentioned phenomena.

CONCLUSIONS

The application of a continuous and constant polarization current on the PVC-tricresylphosphate membrane-electrode has lead to the following important results:

— the E-pH electrode function in the case of the "bubble" electrode and especially in the case of the "foil" electrode was deeply changed by the broadening of the linearity field, the increase of the slope and the shifting of the standard potential, so that the electrode can also be used in direct potentiometry:

— the deep changes of the electrode functions under current, respectively the improvement of the electrode behaviour can be explained by the contribution of an ohmic effect as well as by the polarization concentration process at the membrane-solution interface;

— the potentiometric acid-base titrations carried out under current are characterized by a very good accuracy if compared to the glass electrode and by a substantial increase of the potential jump at the equivalence point, compared to the titration at zero current.

Revue Roumaine de Chimie, **19**, *1*, 157–161 (1974)

SPEKTROPHOTOMETRISCHE DOSIERUNG DES BENZIDINS UND *o*-TOLIDINS MIT NATRIUMHYPOCHLORIT

I. FLOREA

Technische Hochschule „Traian Vuia“, Timişoara.
Laboratorium für Allgemeine Chemie, Str. Remus 14.

Eingegangen am 31. Januar 1973

Es wird eine neue spektrophotometrische Methode für die Dosierung des Benzidins und *o*-Tolidins mit Natriumhypochlorit vorgeschlagen. Die gebildeten Verbindungen sind gelb-orange und weisen je ein Absorbtionsmaximum bei $\lambda =$ $= 429$ nm und $\lambda = 440$ nm auf. Die durchgeführten Bestimmungen zeigen, daß die Methode die Dosierung des Benzidins und des *o*-Tolidins mit Natriumhypochlorit zwischen den Grenzwerten 1—100 μg und 2—100 μg ermöglicht. Die Dosierung des Benzidins und *o*-Tolidins mit Natriumhypochlorit kann man in Gegenwart von *o, m, p*-Toluidin und β-Naphthylamin durchführen, während die Dosierung des Benzidins auch in Gegenwart von α-Naphthylamin möglich ist. Die Ergebnisse sind gut, die Empfindlichkeit der Methode ist bemerkenswert.

In zwei vorhergehenden Arbeiten [1,2] haben wir uns mit der spektrophotometrischen Dosierung des Benzidins und *o*-Tolidins mit Natriumhypochlorit beschäftigt. Die entstandenen gelb-orange Verbindungen wurden mit Chloroform extrahiert und es wurden die Extinktionen bei $\lambda = 443$ nm und $\lambda = 454$ nm gemessen. In der vorliegenden Arbeit bedienen wir und desselben Reagenzes bei der Dosierung des Benzidins und *o*-Tolidins in wäßrigem Medium.

In dieser Arbeit verfolgt man eine neue spektrophotometrische Methode für die Dosierung des Benzidins und *o*-Tolidins, wobei als Reagenz eine schwefelsaure Natriumhypochloritlösung verwendet wird. Der Methode liegt die Bildung gelb-orangefarbener Chinondiimine [3–7]

---

[1] I. FLOREA, *Rev. Roumaine Chim.*, **17**, 915 (1972).

[2] I. FLOREA, *Rev. Roumaine Chim.*, **17**, 1783 (1972).

[3] W. SCHLENK, *Liebigs Ann. Chem.*, **365**, 313 (1908); *Chem. Zentr.*, **1**, 179 (1908).

[4] J. PICCARD, *Ber. dtsch. chem. Ges.*, **44**, 956 (1911); **46**, 1843 (1913); **46**; 1860 (1913).

[5] J. M. GLASSMAN und J. W. MEIGS., *Arch. Ind. Hyg. Occupational Med.*, **4**, 519 (1951); *J. Appl. Chem.*, **6**, 525 (1956).

[6] L. T. BUTT und N. STAFFORD, *J. Appl. Chem.*, **6**, 525 (1956); *Chem. Abstr.*, **51** 7244i (1957).

[7] E. BISHOP und G. L. HARTSHORN, *Analyst.*, **96**, 1 (1971).

zugrunde, die man infolge der oxydierenden Wirkung des Natriumhypochlorits auf die Benzidin- und *o*-Tolidinlösungen erhält. Die entstandenen Verbindungen erlauben die Dosierung des Benzidins und *o*-Tolidins bei $\lambda = 429$ nm und $\lambda = 440$ nm. Die Methode empfiehlt sich für Benzidin- und *o*-Tolidinmengen zwischen 1—100 µg und 2—100 µg.

Benzidin und *o*-Tolidin können—in oben angeführten Quantitäten—mit Natriumhypochlorit in : a) Wässern, b) in Gegenwart von *o*-, *m*- und- *p*-Toluidin bis zu 40µg und c) in Gegenwart von bis zu 20 µg β-Naphthylamin dosiert werden. Benzidin kann auch in Gegenwart von bis zu 20 µg α-Naphthylamin dosiert werden. Benzidin und *o*-Tolidin können aber weder einer in Gegenwart des anderen, noch in Gegenwart von *o*-Dianisidin dosiert werden.

EXPERIMENTELLES

Gerätschaft

Besteht aus der in der vorhergehenden Arbeit verwendeten. [1,2]

Reagenzien

a) Die Benzidinlösung. — In einem 100 ml Meßkolben löst man 0,0100 g reines Benzidin in 10 ml Eisessig auf und füllt mit Wasser bis zur Marke nach. 1 ml Lösung enthält 0,1 mg Benzidin.

b) Die *o*-Tolidinlösung stellt man auf dieselbe Weise — wie die Benzidinlösung—her.

c) Die Benzidin- und *o*-Tolidinlösungen der Konzentration 0,01 mg/ml werden durch Verdünnen bis zu 200 ml von 20 ml a - bzw. b-Lösung mit 10%-ger Essigsäure zubereitet.

d) Die 0,01 %-ge *o*-, *m*- und *p*-Toluidinlösungen sowie die α- und β-Naphthylaminlösungen wurden aus abgewogenen reinen Substanzen präpariert. 1 ml Lösung enthält 0,1 mg Substanz. In den der Analyse unterworfenen Proben wurden mit Volumen zwischen 0,1—0,4 ml im Falle des *o*-, *m*- und *p*-Toluidins, und zwischen 0,1—0,2 ml im Falle des α- und β-Naphthylamin, gearbeitet. [1,2]

e) Die Natriumhypochloritlösung wird auf derselben Weise, wie in den vorhergehenden Arbeiten, hergestellt.[1,2]

ARBEITSWEISE

Mit einer Mikrobürette werden 0,1—1,0 ml a-Lösung bzw. 0,1—1,0 ml c-Lösung, welche zwischen 1—100 µg Benzidin enthalten, und 0,1—1,0 ml b-Lösung bzw., 0.2—1,0 ml c-Lösung, welche zwischen 2—100 µg *o*-Tolidin enthalten, abgemessen und in einen 25 ml Meßkolben eingeführt. Man gibt je 10 molare Schwefelsäure und 2 ml Natriumhypochloritlösung für Benzidin bzw. 2,5 ml für *o*-Tolidin dazu, schüttelt durch und ergänzt mit 10 molarer Schwefelsäure bis zu 25 ml. Nach 10 Minuten mißt man die Extinktion für Benzidin und *o*-Tolidin, bei $\lambda = 429$ nm und $\lambda = 400$ nm.Als Blindpiobe diente Wasser.

ERGEBNISSE UND DISKUSSIONEN

DAS ABSORBTIONSPEKTRUM

Die Absorbtionskurven der durch Vermengen der Benzidin bzw. *o*-Tolidinlösungen mit der Natriumhypochloritlösung entstandenen Verbindungen sind in Abb. 1 dargestellt und weisen je ein Absorbtionsmaximum für Benzidin und *o*-Tolidin auf, bei λ = 429 nm und λ = 440 nm. Die gebildeten Verbindungen eignen sich zur spektrophotometrischen Dosierung des Benzidins und *o*-Tolidins. Die Dosierung ist vorzugsweise für Dosierungen aus Amingemischen empfohlen, da Benzidin und *o*-Tolidin in Gegenwart von *o*-, *m*-, *p*-Toluidin und β-Naphthylamin und Benzidin auch in Gegenwart von α-Naphthylamin in den oben angegebenen Quantitäten- dosiert werden können.

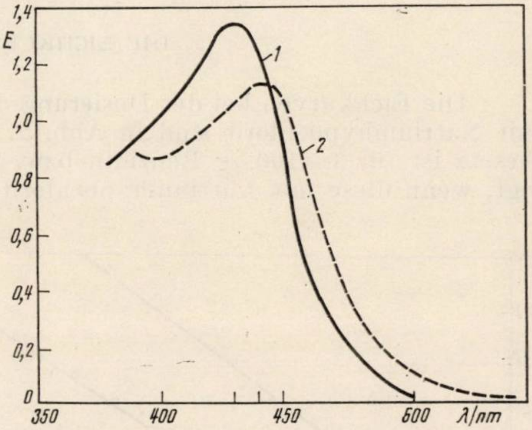

Abb. 1. — Das Absorbtionsspektrum der gebildeten Verbindungen, bei Benützung der 1 cm-Küvette.

1. 1 ml Benzidinlösung a + 10 ml molare Schwefelsäure + 2 ml Natriumhypochloritlösung e + 10 molare Schwefelsäure bis zu 25 ml Volumen. *2,* 1 ml *o*-Tolindinlösung b 10 ml 10 molare Schwefelsäure + 2,5 ml Natriumhypochloritlösung e + 10 molare Schwefelsäure bis zu 25 ml Volumen.

EINFLUSS DER ZEIT

Die Farbenbeständigkeit der sich infolge der Oxydation des Benzidins und des *o*-Tolidins durch die saure Natriumhypochloritlösung bildenden Verbindungen wurde binnen 60 Minuten verfolgt, wobei die Extinktionen bei λ = 429 nm und bei λ = 440 abgelesen wurden. Aus den erhaltenen Ergebnissen ist folgendes feststellbar: die Farbenbeständigkeit wird für beide Substanzen in 5—10 Minuten erreicht. Die aus Benzidin und Natriumhypochlorit bestehende Verbindung ist 40—50 Minuten lang beständig, während jene aus *o*-Tolidin und Natriumhypochlorit 25—30 Minuten lang beständig ist.

EINFLUSS DER REAGENZIENKONZENTRATION

Die optimalen, für die Dosierung der oben angegebenen Benzidin- und *o*-Tolidinquantitäten erforderliche Natriumhypochloritmengen sind 2—2,5 ml bzw. 2,5—3 ml. Innerhalb dieser Intervalle verhalten sich die

Extinktionswerte der entstehenden Verbindungen konstant, angenommen man geht von derselben Benzidin- bzw. *o*-Tolidinmenge aus.

EINFLUSS DER SCHWEFELSÄUREKONZENTRATION

Die Konzentration der Schwefelsäure spielt eine sehr wichtige Rolle bei der Farbenbeständigkeit der Verbindungen, die infolge der Reaktion zwischen Benzidin und *o*-Tolidin und Natriumphypochlorit entstanden sind. Aus den Extinktionsmessungen dieser Verbindungen—bei verschiedenen Molaritäten der Schwefelsäurekonzentration—geht hervor, daß die Beständigkeit der Farbe dieser Verbindungen aus Benzidin und *o*-Tolidin ihre Höchstwerte in 10 molarer Schwefelsäure erreicht.

DIE EICHKURVEN

Die Eichkurven bei der Dosierung des Benzidins und des *o*-Tolidins mit Natriumhypochlorit sind in Abb. 2. veranschaulicht. Das Beer'sche Gesetz ist für 1—100 μg Benzidin bzw. 2—100 μg *o*-Tolidin berücksichtigt, wenn diese mit Natriumhypochlorit versetzt werden.

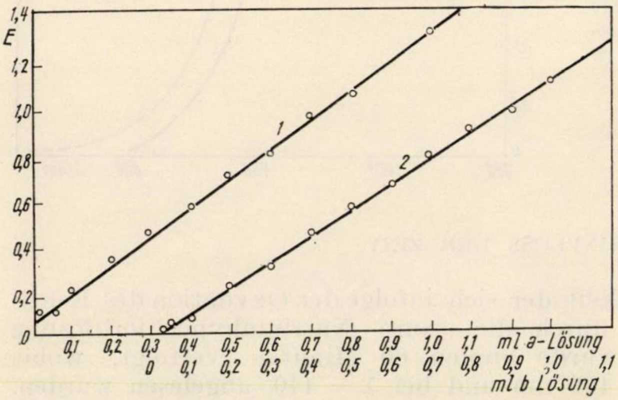

Abb. 2. — Die Absorbtionskurven.

1. Die Benzidinproben, jeweils mit 2 ml Natriumhypochlorit in 10 molarem schwefelsaurem Medium behandelt. *2.* Die *o*-Tolidinproben; jeweils mit 2,5 ml Natriumhypochlorit in 10 molarem schwefelsaurem Medium behandelt.

Die experimentellen Ergebnisse sind in den Tabellen 1 und 2 zusammengefaßt.

Die in den Tabellen 1 und 2 verzeichneten Ergebnisse bezeugen, daß Benzidin und *o*-Tolidin in Gegenwart von *o*-, *m*- und *p*-Toluidin bis zu 40 μg und β-Naphthylamin bis zu 20 μg dosiert werden können; Benzidin sogar in Gegenwart von bis zu 20 μg α-Naphthylamin.

Im Vergleich zur Chloramin T-Methode, die meist gebräuchliche Dosierungsmethode des Benzidins aus den Abwässern, welch letztere man—wegen der Farbenunbeständigkeit bei Licht— in so kurzer Zeit als nur möglich bei schwachem, diffusen Licht durchführen muß oder man vergleicht die aus Chloroform extrahierte Probe mit einer Kalium-

Tabelle 1

Die spektrophotometrsiche Dosierung des Benzidins mit Natriumhypochlorit

Lfd. Nr.	Verbrauchtes Benzidin in µg	Verbrauchtes *o*-Toluidin in µg	E d = 1 cm	Gefundenes Benzidin in µg	E %
1	4,00		0,06	3,82	−5,00
2	18,00		0,25	17,49	−2,85
3	38,00		0,52	38,94	+2,40
4	61,00		0,82	59,08	−3,15
5	84,00		1,13	84,82	+1,00
6	98,00		1,32	94,60	−3,47
7	8,00	10.00	0,12	7,69	−3,87
8	46,00	20,00	0,63	47,05	+2,30
9	71,00	30,00	0,96	72,20	+1,70
10	93,00	40,00	1,25	96,84	+4,10

Tabelle 2

Die spektrophometrsiche Dosierung des *o*-Tolidins mit Natriumhypochlorit

Lfd. Nr.	Verbrauchtes *o*-Tolidin in µg	Verbrauchtes *o*-Toluidin in µg	E d = 1 cm	Gefundenes *o*-Tolidin in µg	E %
1	6,00		0,06	5,74	−4,33
2	22.00		0,24	22,49	+2,20
3	43,00		0,43	41,62	−3,21
4	67,00		0,64	65,20	−2,69
5	81,00		0,90	83,04	+2,50
6	97,00		1,09	95,80	−1,24
7	4,00	10,00	0,04	3,83	−4,25
8	36,00	20,00	0,40	37,00	+2,80
9	74,00	30,00	0,83	74,72	+1,00
10	94,00	40,00	1,05	96,86	+3,40

bichromat-Standardlösung, bietet die neue Methode nachstehend angeführte Vorteile:

a) die bequeme, bei gewöhnlichem Licht durchgeführte Dosierung des Benzidins mit Natriumhypochlorit, dank der verhältnismäßig großen Farbenbeständigkeit der entstanden Verbindungen, ohne die oben angeführten Vorsichtsmaßnahmen berücksichtigen zu müssen:

b) Beseitigung der Chloroformextraktion der gebildeten Verbindung;

c) die in einem größeren Maßstab zu erfolgende direkte Dosierung des Benzidin, u. zw. zwischen 1—100 µg, gegenüber 1—50 µg im Falle der Chloramin T-Methode.

Zusätzlich bietet die Arbeit eine neue sehr empfindliche spektrophotometrische Dosierungsmethode des *o*-Tolidins. *o*-Dianisidin kann auf diesem Weg nicht dosiert werden.

NOTE POUR LES AUTEURS

La *Revue Roumaine de Chimie* publie des articles en anglais, français, russe, allemand ou espagnol. Les auteurs sont priés d'envoyer des articles, notes, communications et comptes rendus inédits.

Les manuscrits seront dactylographiés à deux intervalles. Les tableaux seront dactylographiés sur feuilles séparées, de même que la légende des figures. Les diagrammes seront tracés à l'encre de Chine sur papier calque. Les tableaux et les figures seront numérotés par des chiffres arabes, en nombre strictement nécessaire. Prière de ne pas inscrire les mêmes données dans les tableaux et les figures. Les formules chimiques seront incluses dans le texte ; en outre, elles seront transcrites sur des feuilles séparées. Les auteurs sont priés d'indiquer les caractères italiques (en soulignant les lettres au crayon), ainsi que tout autre caractère spécial. L'ordre des références bibliographiques sera celui de leur mention dans le texte ; le nom de l'auteur sera précédé de l'initiale du prénom ; les publications périodiques seront présentées suivant les prescriptions internationales. Les références seront ajoutées à la fin de l'article ; elles paraîtront comme des notes, au bas de la page. Le texte sera précédé d'un résumé, comprenant 15 lignes au maximum.

L'entière responsabilité du contenu des articles appartient aux auteurs. On publie des articles dus aux collaborateurs roumains ou étrangers. Les auteurs recevront 50 tirés à part.

PRINTED IN ROMANIA

TRAVAUX PARUS AUX ÉDITIONS DE L'ACADÉMIE DE LA RÉPUBLIQUE SOCIALISTE DE ROUMANIE

MARIA FIFI, **Dozimetria chimică a radiaţiilor ionizante** (La dosimétrie chimique des radiations ionisantes), 1973, 240 p., 13,60 lei.

MIHAI FLORESCU, **Eficienţa economică a cercetării ştiinţifice** (L'efficience économique de la recherche scientifique), 1972, 115 p., 15 lei.

GEORGETA LĂZĂRESCU, **Sistematizarea informaţiilor în Chimia organică** (La systématisation des informations dans la chimie organique), 1972, 252 p., 10,50 lei.

P. BALTĂ et E. BALTĂ, **Introducere în chimia fizică a stării vitroase** (Introduction à la chimie physique de l'état vitreux), 1971, 240, 15,50 lei.

LYDIA-MARIA VAICUM, **Biodegrabilitatea detergenţilor** (La biodégrabilité des détergents), 1971, 254 p., 16 lei.

TIBERIU NĂSCUŢIU, **Metode radiometrice de analiză** (Méthodes radiométriques d'analyse), 1971, 346 p., 19,50 lei.

I. ZUGRĂVESCU et L. STOICESCU-CRIVETZ, **Polimeri heterociclici** (Polymères hétérocycliques), 1971, 190 p., 9,50 lei.

CRISTOFOR SIMIONESCU et C. V. UGLEA, **Fracţionarea compuşilor macromoleculari** (Fractionnement des composés macromoléculaires), 1962, 292 p., 18,50 lei.

I. MAXIM, **Materiale nucleare** (Matériaux nucléaires), 1969, 444 p., 30 lei.

CRISTOFOR SIMIONESCU et CLEOPATRA VASILIU-OPREA, **Mecanochimia compuşilor macromoleculari** (La mécanochimie des composés macromoléculaires), 1967, 344 p., 23,50 lei.

CORNEL BODEA et collab., **Tratat de biochimie vegetală**, partea I, **Fitochimie** (Traité de biochimie végétale, Ire partie, Phytochimie), Ier vol., 1964, 747 p. + 4 annexes + 2 pl., 41 lei ; IIe vol., 1965, 1262 p., 1 pl., 56 lei ; IIIe vol., 1967, 773 p., 35 lei.

V. GHEŢIE et V. MICUŞAN, **Analiza imunochimică. Teorie şi practică** (Analyse immunochimique. Théorie et pratique), 1966, 369 p., 28 lei.

R. PORTOCALĂ et L. POPA, **Acizii ribonucleici celulari şi virali** (Les acides ribonucléiques cellulaires et viraux), 1966, 375 p., 8 pl., 26 lei.

D. PURDELEA et R. VÎLCEANU, **Chimia compuşilor organici ai fosforului şi ai acizilor lui** (La chimie des composés organiques du phosphore et de ses acides), 1965, 540 p., 37 lei.

1974 MAR 20

I.P.I. – c. 3508

43 426

Lei 25.–

F1103

R

REFERÁLVA

REVUE ROUMAINE DE CHIMIE

TOME 19
N° 2
Février 1974

RECHAX, **19**, *2*, 163–338 (1974)

ÉDITIONS DE L'ACADÉMIE DE LA RÉPUBLIQUE SOCIALISTE DE ROUMANIE

Rev. Roumaine Chim. **19**, *2*, p. 163–338 (1974), Bucarest

COMITÉ DE RÉDACTION

Rédacteur en chef:

I. G. MURGULESCU, membre de l'Académie de la République Socialiste de Roumanie

Rédacteurs en chef adjoints:

A. T. BALABAN et V. EM. SAHINI, membres correspondants de l'Académie de la République Socialiste de Roumanie

Collège de rédaction:

C. DRĂGULESCU, RALUCA RIPAN, CR. SIMIONESCU, membres de l'Académie de la République Socialiste de Roumanie; EM. BRATU, ECATERINA CIORĂNESCU-NENITZESCU, P. SPACU, membres correspondants de l'Académie de la République Socialiste de Roumanie; MARGARETA AVRAM, D. I. MARCHIDAN, G. NIAC et D. SĂNDULESCU

La Revue Roumaine de Chimie paraît 12 fois par an. Toute commande de l'étranger (fascicules ou abonnements) sera adressée à Intreprinderea Rompresfilatelia, Boîte Postale 2001, telex 011631, Bucarest, Roumanie

Les manuscrits, les livres et les revues proposés en échange, ainsi que toute correspondance seront envoyés à la rédaction:

REVUE ROUMAINE DE CHIMIE

23, str. Dumbrava Roşie, Bucarest, Roumanie

ÉDITIONS DE L'ACADÉMIE DE LA RÉPUBLIQUE SOCIALISTE DE ROUMANIE
3 bis, str. Gutenberg, Bucarest

REVUE ROUMAINE
DE
CHIMIE

Tome 19, N° 2 Février 1974

Page

V. EM. SAHINI, MARGARETA CRAIU and EUGENIA IVANA, Spectrographic determination of traces of copper, lead, chromium, nickel, molybdenum and cobalt in natural waters . . . . 165–167 R

N. BĂRBULESCU, Les tensions superficielles des fluides 169–180

ȘTEFANIA ZUCA, RODICA COSTIN and M. OLTEANU, Influence of NaCl and LiF on the density and viscosity of molten $Na_3AlF_6-BaCl_2$ system 181–186

N. PETRESCU and LUCIA GANOVICI, Diffusive atomic transport in molten antimony 187–196

S. STERNBERG and CONSTANȚA HERDLICKA, Chronopotentiometric method at high temperatures 197–206

G. BOURCEANU, GH. POPA, M. SANDULOVICIU and V. ABABI, Transformation of the toluene-water mixture in the high frequency discharge plasma. I 207–212

ANCA BANCIU, M. ELIAN, AURORA BUCUR, DOINA GEORGESCU, ECATERINA CIORĂNESCU and C. D. NENITZESCU, Carbonium ion reactions. IX. Synthesis and acetolysis of 2 : 3.5 : 6-dibenzobicyclo [5.1.0] octa-2.5-dien-4-yl-methyl tosylate and 2 : 3.5 : 6-dibenzobicyclo [5.1.0] octa-2.5-dien-4-yl-ethyl-β-tosylate 213–232

N. BĂRBULESCU and MINODORA LECA, Elimination reactions in the 8-R-tricyclo [$7.3.1.0^{2,7}$]-tridecane series. III. Dehydration of 8-R-tricyclo [$7.3.1.0^{2,7}$]tridecane-2,13-diols 233–248

M. CÂRJE, Über 1, 2, 3, 4-Tetrahydroacridin-9-Carboxyl-Säure Derivate. II. Ester und Thioester 249–253

N. RĂȘANU and O. MAIOR, Synthesis based on formyl furo (2,3-*b*) benzothiachromone 255–258

CR. SIMIONESCU, CLEOPATRA VASILIU OPREA and CLAUDIA NEGULIANU, Syntheses of new polymers by destructive methods. II. Mechanochemical complexation and complexation by irradiation using ^{60}Co γ-rays

in the system : poly(ethyleneterephthalate), ethylene-diamine and metallic salts 259–281

ВАЛЕНТИНА БОЙЕШАН и Д. ФЕЛЬДМАН, Влияние условий распылительной сушки на свойства пастообразующего поливинилхлорида. Сообщение I. Экспериментальная часть. 283–292

I. IONESCU, Quelques remarques sur les propriétés des bétons aux résines synthétiques sans liants minéraux. II 293–320

GR. TEODORESCU, Méthodes de détermination de β, β′-dichloro-diéthyl-amine. Spectre en visible et infrarouge du composé résulté entre le β, β′-dichloro-diéthyl-amine et le reineckate d'ammonium 321–327

CECILIA CONSTANTINESCU und S. FIŞEL, Spektrophotometrische Bestimmung des Thalliums mit Meta-Nitralgrün 329–335

COMPTE RENDU 337

A
francia

Revue Roumaine de Chimie, **19**, *2*, 165–167 (1974)

SPECTROGRAPHIC DETERMINATION OF TRACES OF COPPER, LEAD, CHROMIUM, NICKEL, MOLYBDENUM AND COBALT IN NATURAL WATERS

V. EM. SAHINI, MARGARETA CRAIU and EUGENIA IVANA
Centre of Physical Chemistry, str. Galaţi 31, Bucharest, Romania

Received September 28, 1973

The traces of copper, lead, chromium, nickel, molybdenum and cobalt were determined spectrographically by the carrier distillation method in natural waters. Natrium chloride, cesium chloride and a mixture of natrium chloride and silver fluoride were utilized as carriers.

The trace elements play an important role in life systems and are the constituents of natural waters that vary to a large extent. The concentration variations of trace elements reflect the interactions taking place in water. Many elements are taken in by plants or animals and after their death and decomposition they return in the water circuit.

In the selection of analysis technique[1] there are some limitations; some elements that must be quantitatively determined are very hardly examined because of their unknown distribution. The amounts of sample available are small. The elements exist in a complex matrix that varies as a function of the major and trace elements present. The sample must be accurately prepared owing to the inhomogeneous nature of the materials. These facts favour the choice of the spectral method for the determination of elements in water in a d.c. arc, by the carrier distillation method.[2]

The literature referring to spectrographic and spectrophotometric analysis of natural waters is not too rich. Thompson[3] utilized the spectrographic method for the determination of trace and major elements in ocean or sea water and in marine sediments. Most of the papers refer to the spectrographic and spectrophotometric determination in soils and extracts of soils, sediments, plants and extracts of plants.[4–9]

---

[1] G. Thompson and D. C. Bankston, *Spectrochim. Acta*, **24 B**. 335 (1969).

[2] G. Thompson, *The Spex Speaker*, **16**, 1 (1971).

[3] B. F. Scriebner and H. R. Mullin, *J. Res. Nat. Bur. Stand.*, **37**, 379 (1946).

[4] E. Lakanen, *Ann. Agr. Fenn.*, **6**, 106 (1967).

[5] K. M. Chan and J. P. Kiley, *Analyt. Chim. Acta*, **36**, 220 (1966).

[6] E. Meistas, *Okeanologiya*, **10**, 373 (1970).

[7] M. A. Kabanova, E. N. Santina, and Yu. I. Turkin, *Khim. Selskhoz.*, **8**, 148 (1970).

[8] H. H. Le Riche, *Geochim. Cosmochim. Acta*, **32**, 791 (1968).

[9] V. N. Podchainova and V. V. Patsuk, *Sbornik Nauch. Tr. Sverdlovsk, Fil. Mosk. Inst. Nar. Khoz.*, **3**, 70 (1967).

Some papers are related to the study of the influence of various carriers on trace elements evaporation from the analysed samples and to the way in which this evaporation proceeds in the arc plasma.[10] Various metal halides and combinations of these halides in various ratios were used to find the best carrier for a given matrix.

In our analyses of natural waters, three carriers were finally chosen out from several, which would be mentioned in the experimental part of the paper. These carriers have given the best results.

In this paper a method is presented for the determination of six trace elements in drinking and river water.

EXPERIMENTAL PART

STANDARDS AND CALIBRATION CURVES

The standards were prepared from high purity salts and oxides. The respective salts and oxides were diluted with SU 609 Elektrokarbon Topolcany graphite powder. First, a 1 % solution of each element in graphite powder was prepared; by successive dilutions the necessary concentration standards were obtained. To each standard the carrier was added, and to homogenized mixture of standard and carrier, the internal standard solution of $Zr(NO_3)_4 . 5H_2O$ in water was added (10 μg Zr/ml). The standards were dried at 150°. 12—13 mg of standard mixture were introduced in the anode crater of a d.c. arc and the samples were excited in the following conditions:

- d.c. arc obtained from an ABR—3 Carl Zeiss Jena generator
- graphite electrodes of high purity (SU 113 Czechoslovak — Ceramics) — anode $\Phi = 5$ mm with crater $\Phi\ 3 \times 3.5$ mm; cathode, conic shape 60°)
- analytical gap: 4 mm
- carriers: NaCl, CsCl, Ag F + NaCl (1 : 4)
- current: 9 A
- exposure time: 60 sec for copper and lead; 120—150 sec for the other metals
- spectrograph: PGS-2 Carl Zeiss Jena
- grating: 650 lines/mm; linear dispersion: 7.4 Å/mm; first order
- slit: 15 μ
- plates: ORWO, WO_3 and WU_3
- analytical lines: Cu: 3272.9 Å; Mo: 3170.3 Å; Ni: 3414.7 Å; Pb: 2833.06 Å Co: 3405.1 Å and 3453.5 Å; Cr: 4254.3 Å and 4274.8 Å
- internal standard lines: Zr: 2571.39 Å; 3391.98 Å, 3991.13 Å

The line blackening was measured photometrically and intensity corrected using calibration curves of the plates for each spectral range and type of plate.

The analytical curves were obtained by plotting log $(I_{\text{element}}/I_{\text{Zr}})$ *vs.*log C (ppm), where I_{element} is the line intensity for the element, read from the calibration curve of the plate, I_{Zr} is the intensity of the Zr line used as internal standard, and C is the concentration of the element in ppm. In table 1 the lower detection limits for the elements (in ppm) are given.

---

[10] B. Strzyzewska, *Spectrochim. Acta, Part B*, **27**, 227 (1972).

Table 1

The lower detection limits for the elements

Element	Lower detection limit (ppm)	Relative error %
Copper	0.10	10
Molybdenum	0.01	40
Nickel	0.05	40
Lead	0.05	10
Cobalt	1.00	10
Chromium	0.03	14

THE SAMPLES

The results of the determinations of trace elements were reported to the residue obtained for 1 liter of water. The residue was obtained by slow evaporation of water extended over several days, in silica glass vessels, taking care to prevent contamination of the sample during this time. After evaporation and drying at a temperature above 150°, the residue was mixed with carrier in the ratio 6 : 1, and the obtained mixture with graphite powder type SU 609 in the ratio 1 : 1. The internal standard solution was added to the sample and this was dried at 130°. In this way were obtained the samples that were excited in the same conditions as the standards.

The concentrations Z of the element per liter of water (in mg/) were obtained from the formula:

$$Z(\text{mg element/l}) = \frac{PXA}{B} \cdot 10^{-6}$$

where

B is the weight of the residue in the sample studied (in mg)

P is formed from B and an equal quantity of graphite powder

A is the weight of the residue per liter of water (mg/l)

X is the concentration of the element in mg per 100 mg sample ($X = x_{\text{ppm}} \cdot 10^4$)

x is read on the analytical curve.

The method may be extended to the determination of the other trace elements.

Acknowledgements. We wish to express our gratitude to M. Mihăilescu for help with the experimental determinations and R. Beldie and A. Butucelea for interesting discussions related with the studied problems.

Revue Roumaine de Chimie, **19**, *2*, 169–180 (1974)

LES TENSIONS SUPERFICIELLES DES FLUIDES

N. BĂRBULESCU

Faculté de Physique, Université de Bucarest

Reçu le 31 août 1973

Les phénomènes superficiels sont caractéristiques pour tous les fluides, non seulement pour les liquides ; les gaz réels et les vapeurs présentent aussi de tels phénomènes. Dans l'étude des fluides on doit introduire trois tensions superficielles, non seulement une, comme on le fait couramment. Au point critique ce n'est que la tension interfaciale liquide/vapeur qui s'annule, tandis que la tension superficielle propre du liquide présente une valeur finie. Avec ces trois tensions superficielles on obtient trois équations d'état pour les couches périphériques des fluides.

Dans la physique on considère encore pour les fluides une seule tension superficielle : la tension superficielle des liquides. Van der Waals [1] a été le premier qui a relevé l'existence d'une seconde tension superficielle des fluides : la tension superficielle des gaz. Malheureusement, cette dernière grandeur n'a pas eu la chance d'être étudiée dès le commencement, de sorte qu'elle a été complètement oubliée pour une longue période de temps.

LA TENSION SUPERFICIELLE DE GAZ (VAPEURS)

La tension superficielle est une notion parfaitement intelligible pour les membranes élastiques, de même que pour les liquides. Les gaz ayant une très grande expansibilité on a pu croire que ces fluides n'ont pas une tension superficielle. D'autre part, les physiciens ont relié toujours l'existence de la tension superficielle à la présence d'une surface libre, comme c'est le cas des liquides. Les gaz, n'ayant pas une surface libre, on a décrété qu'ils ne pouvaient avoir une tension superficielle.

Mais la surface libre n'est pas une condition *sine qua non* de l'existence d'une tension superficielle chez les fluides, car, en réalité, une telle surface n'existe même pas pour les liquides. Elle est une simple apparence, due à l'imperfection de nos sens et a, naturellement, la même réalité que la voûte céleste. Les liquides n'ont pas une surface libre, mais une « couche périphérique » (*couche de passage* de Laplace), qui fait la transition entre le liquide et sa vapeur. La propriété principale de cette couche périphérique est d'exercer la pression interne ; comme les gaz réels ont aussi une pression interne, il s'ensuit que ces fluides possèdent de même une couche périphérique.

---

[1] J. D. Van der Waals, « La continuité des états gazeux et liquides », traduit par Dommer et Pomey, Paris.

On peut donc affirmer que *la tension superficielle des fluides n'est pas conditionnée par une surface libre, mais par la couche périphérique, qui produit la pression interne.* Ce que nous appelons tension superficielle d'un fluide n'est que la tension périphérique par laquelle le volume du fluide tend à posséder une couche périphérique minimale.

L'existence de la tension superficielle des gaz peut être encore soutenue à l'aide du principe de la continuité des états (Andrews). D'après ce principe, l'état gazeux et l'état liquide sont simplement deux termes éloignés d'une série continue d'états. Il est donc possible de passer de l'état liquide à l'état gazeux d'une manière continue, le fluide restant parfaitement homogène. Par conséquent, tous les paramètres d'état, utilisés dans l'étude des liquides, doivent être valables aussi dans l'étude des gaz, ce qui signifie que la tension superficielle, définie pour l'état liquide, doit être de même un paramètre d'état pour les gaz.

D'ailleurs, van der Waals a soutenu l'existence de la tension superficielle des gaz en se basant précisément sur ce principe de la continuité des états. Dans le travail : *La continuité des états gazeux et liquides*, en discutant la tension superficielle des liquides, van der Waals écrit : « Nous rappelons seulement les surprenantes expériences, récemment exécutées par Bosscha, qui révèlent la présence de cette tension dans des cas où on ne l'avait même pas soupçonnée. Nous verrons plus tard qu'elle n'existe pas seulement dans les liquides, mais encore dans tous les gaz ». Et il dit plus loin : « Il résulte des expériences de Bosscha que la tension de la fumée de tabac, et probablement aussi celle de la vapeur d'eau à l'état de brouillard, est assez grande pour provoquer des phénomènes capillaires. Il est vrai que ce ne sont pas là de véritables vapeurs ; mais, malgré cela, il faut regarder ces expériences comme d'importants soutiens de la théorie ici développée d'après laquelle il n'y a pas de différence qualitative entre les états d'agrégation des liquides et des vapeurs ».

Cette justification phénoménologique de la tension superficielle des gaz peut être complétée par des considérations physico-mathématiques.[2] En vérité, partons de la formule de Laplace, qui exprime la relation entre la pression interne P et la tension superficielle σ d'un ménisque liquide :

$$P = K^{\pm} \sigma\left(\frac{1}{R_1} + \frac{1}{R_2}\right)$$

où R_1 et R_2 sont les rayons principaux de courbure du ménisque, K étant la pression interne de la couche périphérique plane du même liquide. Du fait que, conformément au principe de la continuité des états, il n'existe pas une différence qualitative entre le liquide et le gaz, il s'ensuit que *la formule de Laplace peut être appliquée aussi aux gaz, c'est-à-dire*

---

[2] N. Bărbulescu, *Physik. Z.*, **31**, 48 (1930).

qu'elle convient à tous les fluides, quels que soient leurs états d'agrégation. Donc, la tension superficielle σ, figurant dans cette formule, exprime une réalité physique aussi pour les gaz (vapeurs).

Passons maintenant au calcul de la tension superficielle des gaz, dans le cas spécial de vapeurs saturantes. Considérons un tube capillaire introduit dans un liquide, qui monte dans ce tube jusqu'à la hauteur h au-dessus du niveau du liquide extérieur. La pression p des vapeurs saturantes, au-dessus du ménisque concave de la colonne capillaire, est liée à la pression interne P_v de ces vapeurs par la relation :

$$p = p_i - P_v \tag{1}$$

où p_i — est la pression du gaz idéal, correspondant aux vapeurs considérées. Le ménisque concave du liquide est en contact avec le ménisque convexe de la vapeur saturante, auquel nous pouvons appliquer la formule de Laplace :

$$P_v = K_v + \frac{2\sigma_v}{R} \tag{2}$$

où σ_v — est la tension superficielle de la vapeur saturante et R — le rayon du ménisque sphérique.

Au niveau plan du liquide extérieur, la pression de la vapeur saturante est p_0 et nous avons de même :

$$p_0 = p_i - K_v \tag{3}$$

De (1) et (3) on déduit :

$$p_0 - p = P_v - K_v \tag{4}$$

D'autre part, en tenant compte de l'effet Kelvin, d'après lequel la pression p de la vapeur saturante au-dessus du ménisque capillaire est égale à la pression de la vapeur extérieure, au niveau même de ce ménisque, on a

$$p_0 = p + h\,\rho_v g \tag{5}$$

où ρ_v — est la densité de la vapeur saturante. Introduisant en (4) les expressions (2) et (5), on obtient :

$$\sigma_v = \frac{1}{2} Rh\,\rho_v g \tag{6}$$

formule qui nous permet de calculer la tension superficielle de la vapeur saturante, en déterminant l'ascension capillaire du liquide respectif, autrement dit, la position dans le tube capillaire du ménisque convexe de la vapeur saturante. A l'aide des données expérimentales de Ramsay et Shields [3] nous avons calculé la tension superficielle σ_v de quelques substances organiques, pour diverses températures, jusqu'à proximité de la température critique. Les résultats sont inscrits dans le tableau 1.

On constate que, pour les températures ordinaires, la tension superficielle σ_v est très petite, étant de l'ordre 10^{-2} dyn/cm. Elle croît avec la température pour devenir, près de la température critique, comparable à la tension interfaciale σ_i du liquide respectif. Par exemple, la tension interfaciale de l'éther éthylique liquide est de 0,16 dyn/cm à 190° ; à cette température, la vapeur saturante respective a une tension superficielle de 0,12 dyn/cm.

On constate, de même, que la tension superficielle σ_v présente un maximum au voisinage du point critique. La température réduite de ce maximum est approximativement la même 0,91 pour toutes les substances. On peut expliquer l'existence de ce maximum, sachant que la tension superficielle diminue avec l'augmentation de la température, mais elle croît avec la densité. Pour les températures moyennes, l'effet de la densité dépasse celui de la température, de sorte que la tension superficielle de la vapeur saturante croît jusqu'à une température pour laquelle ces deux effets se compensent. Ensuite, l'effet de la température dépasse celui de la densité et la tension superficielle de la vapeur saturante commence à diminuer.

Shereshefsky [4] a établi la formule :

$$\frac{\mathrm{d} \log \rho_v}{\mathrm{d}T} = \frac{0{,}4343}{T_c(1 - T_m/T_c)} \tag{7}$$

qui permet de calculer la température T_m pour laquelle la tension superficielle σ_v présente un maximum. Dans cette formule T_c représente la température critique absolue. Shereshefsky a appliqué cette formule à 19 composés, en retrouvant pour la température réduite la valeur moyenne 0,91. En mettant la relation (7) sous la forme :

$$\frac{\mathrm{d} \ln \rho_v}{\mathrm{d} \ln T} = \frac{T_m/T_c}{(1 - T_m/T_c)} = 10{,}1$$

Shereshefsky a déduit que, dans le système des coordonnées ($\ln \rho_v$, $\ln T$), la pente de la courbe au point T_m est une constante universelle.

Shereshefsky [5] a obtenu, de même, une formule qui donne la variation de la tension superficielle σ_v avec la température :

$$v = \frac{T_c \Delta}{\rho_c^{1/3} \mu^{2/3}} (1 - T/T_c)^{0 \cdot 9} \rho_v$$

---

[3] W. Ramsay et J. Shields, *Z. phys. Chem.*, **12**, 433 (1893).

[4] L. J. Shereshefsky, *J. Phys. Chem.*, **34**, 1947 (1930).

[5] L. J. Shereshefsky, *J. Phys. Chem.*, **35**, 1712 (1931).

où μ — est la masse moléculaire et Δ — une constante ayant la même valeur pour tous les liquides normaux. Cette formule donne de bons résultats pour les températures éloignées du point critique ; pour ce point, la formule indique $\sigma_c = 0$, ce qui ne correspond pas à la réalité, car, à la température critique le fluide, ayant une pression interne, doit avoir aussi une tension superficielle.

Une formule plus exacte que celle de Shereshefsky est la suivante :

$$\sigma_v = \frac{A(\tau + c)^m}{1 + K\tau^p \rho_v^{-1} \exp\left(-\frac{r}{\tau}\right)}$$

où $\tau = t_c - t$ et A, c, m, K, p, r — sont des constantes empiriques. Pour les températures éloignées du point critique, cette formule se réduit à celle de Shereshefsky. Elle permet de calculer la tension superficielle des fluides σ_c point critique, en retrouvant les valeurs obtenues par d'autres voies.

LA TENSION INTERFACIALE LIQUIDE/VAPEUR

C'est la tension superficielle σ_v de la vapeur saturante qui détermine une tension interfaciale σ_i au contact liquide/vapeur. Ce que l'on mesure par les méthodes de laboratoire ce n'est pas la tension superficielle propre (absolue) σ_l du liquide, mais cette tension interfaciale σ_i.

Par la méthode de l'ascension capillaire, Ramsay et Shields[3] ont effectué les premières déterminations rigoureuses de cette grandeur, en utilisant la formule :

$$\sigma_i = \frac{1}{2} Rhg(\rho_l - \rho_v)$$

où ρ_l — est la densité du liquide en contact avec ses vapeurs de densité ρ_v. Cette tension interfaciale diminue avec l'augmentation de la température, pour s'annuler au point critique, quand $\rho_l = \rho_v$.

Van der Waals[7] a établi la formule qui représente la variation de cette tension avec la température :

$$\sigma_i = A\left(\frac{\rho_c}{\mu}\right)^{2/3} T_c \, \varphi(t_r)$$

---

[6] N. Bărbulescu, *Anal. Univ. Buc.*, **15**, 9 (1966).

[7] D. J. Van der Waals, *Z. phys. Chem.*, **13**, 695 (1894).

où $t_r = T/T_c$, A — est une constante universelle et φ — une fonction universelle. Au voisinage du point critique, on a, d'après Van der Waals : $\varphi(t_r) = (1 - t_r)^{3/2}$: mais les valeurs expérimentales sont mieux représentées par la formule générale :

$$\sigma_i = K\tau^n \tag{8}$$

où K et n — sont des constantes empiriques, dépendant de la nature du liquide et ayant des valeurs qui ne diffèrent pas trop entre elles.

Toutefois, la dépendance de température de la tension interfaciale σ_i est plus compliquée. Elle peut être représentée par la formule :

$$\sigma_i = K\tau^n \, e^{-\frac{d}{\tau}}$$

où K, n et d — sont des constantes empiriques.[8]

LA TENSION SUPERFICIELLE ABSOLUE (PROPRE) DES LIQUIDES

Pour un système de deux phases en contact, on doit considérer trois tensions superficielles : chaque phase a sa tension superficielle propre et, au contact des deux phases, il y a une tension interfaciale.

Pour le système liquide/vapeur, les tensions superficielles propres qui interviennent sont σ_v, σ_i et de même la tension superficiale propre (absolue) du liquide. Cette dernière grandeur a été longtemps négligée, étant confondue avec la tension interfaciale. Il est vrai que, pour les températures ordinaires, la différence entre ces tensions est négligeable, mais devient notable pour les températures près du point critique (tableau 1).

Pour connaître la tension superficielle absolue σ_l d'un liquide, considérons d'abord un système composé de trois phases en équilibre superficiel. Soient σ_1 et σ_2 les tensions superficielles respectives de deux phases en contact avec la troisième. Désignons par σ_{12} la tension interfaciale entre ces deux phases. La condition d'équilibre est :

$$\sigma_1^2 = \sigma_{12}^2 + \sigma_2^2 + 2\sigma_{12}\,\sigma_2 \cos \beta$$

où β — est l'angle des vecteurs $\vec{\sigma}_{12}$ et $\vec{\sigma}_2$. Pour une surface plane de contact entre les phases, l'ongle β est nul et on a :

$$\sigma_{12} = \sigma_1 - \sigma_2$$

C'est le cas du système liquide/vapeur, pour lequel nous pouvons écrire :

$$\sigma_i = \sigma_l - \sigma_v \tag{9}$$

---

[8] N. Bărbulescu, *J. Chim. Phys.*, **29**, 418 (1932).

Tableau 1

Les tensions superficielles de quelques fluides

t °C	Éther éthylique			Formiate de méthyle			Acétate d'éthyle			Tétrachlorure de carbone			Benzène			Benzène monochloré		
	σ_l	σ_i	σ_v	σ_l	σ_i	σ_v	σ_l	σ_i	σ_v	σ_l	σ_i	σ_v	σ_l	σ_i	σ_v	σ_l	σ_i	σ_v
80	9,85	9,67	0,18	15,89	15,70	0,19	16,39	16,32	0,07	18,78	18,71	0,07	20,35	20,28	0,07			
100	7,87	7,63	0,24	13,17	12,90	0,27	14,09	13,98	0,11	16,60	16,48	0,12	18,13	18,02	0,11			
120	5,95	5,65	0,30	10,53	10,18	0,35	11,91	11,75	0,16	14,49	14,32	0,17	15,87	15,71	0,16			
140	4,11	3,77	0,34	7,97	7,54	0,43	9,79	9,57	0,22	12,44	12,22	0,22	13,68	13,45	0,23			
160	2,42	2,08	0,34	5,54	5,06	0,48	7,76	7,48	0,28	10,52	10,22	0,30	11,57	11,29	0,28	16,74	16,62	0,12
180	0,87	0,64	0,23	3,29	2,81	0,48	5,85	5,51	0,34	8,62	8,26	0,36	9,49	9,15	0,34	14,82	14,66	0,16
190	0,29	0,16	0,13	2,20	1,78	0,42	4,90	4,54	0,36	7,67	7,28	0,39	8,54	8,16	0,38	13,88	13,69	0,19
193	0,10	0,04	0,06															
200				1,20	0,87	0,33	4,01	3,64	0,37	6,76	6,34	0,42	7,58	7,17	0,41	12,94	12,72	0,22
210				0,29	0,16	0,13	3,18	2,80	0,38	5,84	5,40	0,44	6,63	6,20	0,43	12,00	11,75	0,25
220							2,33	1,96	0,37	4,93	4,47	0,46	5,71	5,25	0,46	11,09	10,81	0,28
230							1,50	1,18	0,32	4,01	3,56	0,45	4,79	4,32	0,47	10,18	9,88	0,30
240							0,71	0,49	0,22	3,18	2,74	0,44	3,88	3,41	0,47	9,27	8,94	0,33
245							0,35	0,21	0,14									
260										1,52	1,20	0,32	2,17	1,75	0,42	7,53	7,14	0,39
270										0,86	0,59	0,27	1,34	0,99	0,35	6,69	6,27	0,42
280													0,57	0,29	0,28	5,84	5,40	0,44
300																4,99	4,54	0,45
333																1,88	1,47	0,41

c'est-à-dire, *la tension interfaciale liquide/vapeur est la différence entre les tensions superficielles respectives du liquide et de sa valeur saturante.* En introduisant ici les expressions établies plus haut pour σ_i et σ_v, on obtient :

$$\sigma_l = \frac{1}{2} Rh \, \rho_l g \tag{10}$$

formule qui permet de calculer la tension superficielle absolue d'un liquide, si l'on connaît son ascension capillaire.[9] On a, de même, la formule

$$\sigma_l = \sigma_i \frac{\rho_l}{\rho_l - \rho_v}$$

à l'aide de laquelle nous avons calculé les valeurs de σ_l (tableau 1), en utilisant les données expérimentales de Ramsay-Shields.

On obtient une autre relation entre σ_l et σ_i par les considérations suivantes. [2] Pour augmenter l'aire A de la couche périphérique d'un liquide, quand on passe de la tension interfaciale σ_i à la tension superficielle absolue σ_l, on doit dépenser le travail :

$$L = -\int_{\sigma_i}^{\sigma_l} \sigma \mathrm{d}A$$

Pour une transformation isotherme, on a :

$$\sigma A = k\tau$$

où les lettres ont les significations connues. On obtient d'ici :

$$\sigma \mathrm{d}A = -k\tau \frac{\mathrm{d}\sigma}{\sigma}$$

et en intégrant :

$$\sigma_i = \sigma_l \, \mathrm{e}^{-\frac{\mathrm{d}}{\tau}} \tag{11}$$

L'expérience vérifie très bien cette formule, d étant indépendant de la température et ayant approximativement la même valeur pour tous les liquides normaux.

La variation avec la température de la tension superficielle absolue σ_l est très bien représentée par la formule :

$$\sigma_l = A\,(\tau + c)^n \tag{12}$$

---

[9] N. Bărbulescu, *J. Chim. Phys.*, **56**, 185 (1959).

où A, c et n – sont des constantes empiriques.[9] Cette formule si simple donne des résultats parfaitement corrects aux températures, pour lesquelles Ramsay et Shields ont réussi à mesurer la tension interfaciale σ_i. C'est pourquoi nous avons appliqué cette formule même au point critique, pour calculer la nouvelle constante critique σ_c, qui est de l'ordre 10^{-2} dyn/cm. Cette constante critique peut être calculée aussi par la formule :

$$P_c = 10^{-3} \frac{\sigma_c}{D} \tag{13}$$

où P_c – est la pression interne (atm) au point critique, calculée à l'aide de la constante a de van der Waals et D – est le diamètre moléculaire (cm).[9] C'est une formule analogue à celle établie pour les liquides et perfectionnée [10] sous la forme :

$$P = \pi \frac{\sigma}{D}$$

L'existence de cette constante critique infirme complètement l'affirmation que l'on trouve encore dans les publications de physique, d'après laquelle la tension superficielle des liquides s'annule au point critique. C'est seulement la tension interfaciale σ_i qui s'annule au point critique ; au contraire, la tension superficielle propre σ_l conserve une valeur finie, égale à celle des vapeurs saturantes.

LES ÉQUATIONS D'ÉTAT DE LA COUCHE PÉRIPHÉRIQUE DES FLUIDES

La physique connaît depuis un siècle l'équation d'état de la surface liquide, obtenue pour la première fois par Eötvös [11] et vérifiée expérimentalement par Ramsay-Shields [3] :

$$\sigma V_{\mu}^{2/3} = k(t_c - t - d)$$

où V_{μ} – est le volume molaire du liquide. Ostwald a donné à l'expression $\sigma V_{\mu}^{2/3}$ le nom d'*énergie superficielle moléculaire.* D'après Born et Courant [12] la formule d'Eötvös représente *l'équation d'état de la surface liquide.*

On considère aujourd'hui seulement cette équation d'état pour la surface d'un liquide. Mais les résultats précédents imposent trois équations d'état, correspondant aux trois tensions superficielles que nous avons définies plus haut.

1) La formule d'Eötvös exprime en réalité *l'équation d'état de l'interface liquide/vapeur*. Elle a été obtenue en partant du fait expérimental,

---

[10] N. Bărbulescu, *Bull. Soc. Sciences Cluj*, **8**, 462 (1936).

[11] R. Eötvös, *Wied. Ann.*, **27**, 448 (1886).

[12] M. Born et R. Courant, *Physik. Z.*, **14**, 731 (1913).

que le coefficient de température de l'expression $\sigma_i V_\mu^{2/3}$ est une constante, la même pour tous les liquides normaux :

$$\frac{\mathrm{d}}{\mathrm{d}t}(\sigma_i V_\mu^{2/3}) = -k$$

Comme l'expression $\sigma_i V_\mu^{2/3}$ s'annule au point critique, on obtient par l'intégration :

$$\sigma_i V_\mu^{2/3} = k(t_c - t) \tag{14}$$

formule qui ne contient pas la constante *d*, contrairement à celle vérifiée par l'expérience. Ce désaccord entre la théorie et l'expérience a subsisté longtemps, car il été impossible d'élucider la nature de la constante *d*.

Le problème de la constante *d* se résout d'une manière très simple [2], si nous partons de l'équation d'état de la couche périphérique du liquide, que nous avons obtenue et dans laquelle nous négligeons, dans une première approximation, la constante ω

$$\sigma_l V_\mu^{2/3} = k\tau$$

Combinant cette formule avec (11), on a :

$$\sigma_i V_\mu^{2/3} = k\tau\, \mathrm{e}^{-\frac{\mathrm{d}}{\tau}} \tag{15}$$

qui est la vraie équation d'état de l'interface liquide/vapeur. Pour des températures éloignées du point critique, on obtient :

$$\sigma_i V_\mu^{2/3} = k\tau\left(1 - \frac{d}{\tau}\right) = k(\tau - d)$$

c'est-à-dire l'équation d'Eötvös, avec la constante *d*. D'après ce que nous avons vu, *d* représente une grandeur proportionnelle au travail nécessaire pour faire passer l'air de la couche périphérique d'un liquide de la tension interfaciale σ_i à la tension superficielle σ_l.

L'équation d'état de l'interface liquide/vapeur (15) présente, en général, la même approximation que l'équation d'Eötvös-Ramsay-Shields. Mais au voisinage du point critique, l'équation (15) est supérieure à l'autre, parce qu'elle ne donne pas des valeurs négatives pour le produit $\sigma_i V_\mu^{2/3}$.[2]

2) *L'équation d'état de la surface liquide* (correctement : de la couche périphérique) s'obtient en considérant que le produit $\sigma_l V_\mu^{2/3}$ diminue linéairement avec la température jusqu'au point critique :

$$\sigma_l V_\mu^{2/3} = a - kt$$

En posant :

$$\omega = \frac{\sigma_c V_\mu^{2/3}}{k}$$

on obtient :

$$\sigma_l V_\mu^{2/3} = k(\tau + \omega) \tag{16}$$

qui est l'équation d'état cherchée.[9] C'est très surprenant le fait que cette équation, si simple, est parfaitement valable pour toutes les températures auxquelles Ramsay et Shields ont pu effectuer leurs mesures. Comme nous avons vu, ce n'est pas le cas de l'équation d'état de l'interface liquide/vapeur, qui perd complètement sa validité au voisinage du point critique.

L'équation (16) permet aussi de calculer la tension superficielle critique σ_c. Les valeurs obtenues par cette voie sont très rapprochées de celles calculées par les formules (12) et (13), comme on peut voir dans le tableau 2.

Tableau 2

La tension superficielle critique

	a_c atm. litres^2 mol^{-2}	P_c atm	10^8 D cm	σ_c dyn.cm^{-1} calculée par		
				(12)	(13)	(16)
Ether éthylique	17,40	220	4,08	0,010	0,009	0,010
Formiate de méthyle	11,39	385	3,46	0,013	0,014	0,013
Acétate d'éthyle	20,48	250	3,96	0,010	0,010	0,010
Tétrachlorure de carbone	19,56	257	4,36	0,012	0,011	0,012
Benzène	18,72	285	4,21	0,012	0,012	0,012
Benzène monochloré	25,52	269	4,35	0,012	0,012	0,013

3) *L'équation d'état périphérique de la vapeur saturante* [13] correspond au produit $\sigma_v V_\mu^{2/3}$ qu'on peut calculer à l'aide des valeurs de σ_v obtenues ci-dessus. On constate que ce produit croît avec la température, en présentant un maximum pour la température réduite 0,761. L'équation d'état périphérique, que nous avons trouvée dans ce cas est :

$$\sigma_v V_\mu^{2/3} = K\tau^{0,9} \rho_v^{1/3} \tag{17}$$

mais elle est valable seulement pour les températures éloignées du point critique.

LA TENSION SUPERFICIELLE DES LIQUIDES RARÉFIÉS

Les liquides raréfiés ont été obtenus jusqu'à présent par divers expérimentateurs, qui ont interprété leurs résultats par l'existence des pressions négatives. En réalité, il s'agit des liquides qui occupent un volume plus grand que dans les conditions normales.

---

[13] N. Bărbulescu et F. Bărbulescu, *Koll. Z.*, **101**, 161 (1942).

La plus simple méthode d'obtenir un liquide raréfié c'est de la mélanger avec un autre, en l'absence de tout solvat (mélange idéal). En occupant le volume total du mélange, les deux liquids sont raréfiés, pouvant être caractérisés par leurs *densités partielles.*[14]

Désignons par ρ la densité d'un mélange binaire idéal (où il n'existe pas des solvats) et par g la fraction massique d'un de ces composants. Les densités partielles des composants raréfiés sont :

$$\rho_1 = g\,\rho \quad \text{et} \quad \rho_2 = (1 - g)\,\rho$$

On démontre que, pour toute transformation isotherme d'un fluide on a :

$$\sigma(V - b) = \text{const.} \tag{18}$$

formule qui permet de calculer la tension superficielle d'un liquide raréfié.[15] Le tableau 3 contient les densités partielles et les tensions superficielles respectives des deux liquides raréfiés, formant un mélange idéal : benzène et acétate d'éthyle à 20°. La constante b de ces liquides raréfiés a été obtenue d'une manière empirique. Les valeurs calculées pour σ_1 et σ_2 montrent, conformément aux prévisions, que la tension superficielle des fluides diminue quand la raréfaction croît.

Tableau 3

Benzène – Acétate d'éthyle à 20°

b (benzène) = 2.1 cm³/mole b (acétate) = 2,6 cm³/mole

g	ρ_1 benzène	ρ_2 acétate	σ_1 benzène	σ_2 acétate	σ	
					exp.	calc.
1,0000	0,8783	0,0000	28,05	—	28,05	—
0,8989	0,7910	0,0890	25,20	2,22	27,51	27,42
0,7910	0,6973	0,1843	22,17	4,60	26,75	26,77
0,6004	0,5313	0,3536	16,69	8,88	25,64	25,57
0,3967	0,3526	0,5351	11,10	13,54	24,51	24,64
0,1960	0,1750	0,7180	5,48	18,22	23,74	23,70
0,1160	0,1038	0,7911	3,24	20,13	23,50	23,37
0,0000	0,0000	0,8976	—	22,92	22,92	—

On a montré, de même, que *la tension superficielle d'un mélange binaire idéal est la somme des tensions superficielles partielles des liquides raréfiés.*[15] Les valeurs numériques du tableau 3, sont calculées d'après les données expérimentales de Herzen.[16]

---

[14] N. BĂRBULESCU et F. BĂRBULESCU, *Anal. Acad. R.P.R.*, III, 8 (1949).

[15] N. BĂRBULESCU et R. MOLDOVAN, *Rev. roum. de Phys.*, **13**, 275 (1968).

[16] Ed. HERZEN, Thèse, Université de Lausanne, 1902.

Revue Roumaine de Chimie, **19**, *2*, 181 – 186 (1974)

INFLUENCE OF NaCl AND LiF ON THE DENSITY AND VISCOSITY OF MOLTEN $Na_3AlF_6-BaCl_2$ SYSTEM

ȘTEFANIA ZUCA, RODICA COSTIN and M. OLTEANU

Institute of Physical Chemistry,
Str. Galați 31, Bucharest 9, Romania

Received June 29, 1973

The density and viscosity of 40 % Na_3AlF_6 + 60 % $BaCl_2$ mixture and the influence upon them of LiF and NaCl additions are studied, over a temperature range of about 100°. The ionic interactions occurring on mixing and the most suitable composition of electrolytic bath are discussed.

The molten $NaF-AlF_3-BaCl_2$ mixtures form the basis of electrolytic bath for aluminium refining, known as Gadeau's bath. The physico-chemical properties of these mixtures have been investigated both from the theoretical viewpoint, attempting to gain structural information on ionic mixtures, and from the practical one, aiming at establishing the most suitable electrolyte for the technical process.

A special interest has been given to studying the temperature of the primary crystallization of electrolyte,[1-3] the density[4,5] and electrical conductivity.[6,7] The measurements of the viscosity of fluoride melts are rather difficult; for this reason very little is known about it in the $NaF-AlF_3-BaCl_2$ system.[8]

The viscosity as well as the density are important mainly in the separation of the metal and influence, thus, the total production, but can also provide information on the structure of the melts studied.

The present work is concerned with the binary system AlF_6Na_3 + + $BaCl_2$ and the influence of LiF and NaCl additions on the density and viscosity. These two named electrolytes have already been recommended as additives improving those physico-chemical properties of aluminium electrolyte which enhance the economics of electrolysis.[9-11]

---

[1] V. M. Guscov, "Electrolytic Refining of Aluminium", Metallurghizdat, Moscow, 1945.
[2] M. A. Kuvakin, *Zhur. neorg. Khim.*, **12**, 2744 (1961).
[3] K. Ono and K. Taniuki, *Rev. Jap. Soc. Metalls.*, **10**, 16 (1947).
[4] K. Taniuki and T. Sato, *J. Mining and Metallurgical Inst. of Japan*, **83**, 949 (1967).
[5] A. I. Beliaev, *Tvetnaia Metallurghia*, **5**, 43 (1961).
[6] M. I. Lavrentiev, *ibid*, **2**, 52 (1967).
[7] K. Taniuki, *Reports of Mining and Metallurgical Inst. of Japan*, **85**, 970, 103 (1967).
[8] I. G. Murgulescu and Ș. Zuca, *Tvetnaia Metallurghia*, **6**, 33 (1961).

Therefore, we thought of as interesting to study their influence on the density and viscosity of the refining electrolyte too.

According to Gadeau's method,[12] at the working temperature (740°), the density at the cathode and at the anode is of 2.35 g/cm^3 and 3.14 g/cm^3, respectively,[1,13,14] and, consequently, the density of the electrolyte has to be maintained within 2.6—2.8 g/cm^3 range in order to ensure a good separation of the metal. The data in literature[4,5] indicate that this requirement is accomplished in the electrolyte with 60—70% $BaCl_2$ no matter the cryolite ratio (NaF/AlF_3). Therefore, we have chosen as basic electrolyte for our experiments, the one of composition 40% AlF_6Na_3 + 60% $BaCl_2$.

EXPERIMENTAL

The density was measured by the platinum sinker method, previously described,[15] with an accuracy of 0.2—0.3%. The oscillating sphere method has been employed for viscosity measurement,[16,17] the accuracy being of ± 3%. A vertical furnace provided for working in a controlled atmosphere was used and a constant temperature within ±0.5° was mentioned during the experiments. The temperature was measured by a calibrated Pt—Pt 10% Rh thermocouple, its hot jonction being immersed into the melt.

The density and viscosity determinations were carried out on the following grade reagents : Merck *p.a.* NaF, $BaCl_2$, NaCl and LiF, Serva *p.a.* AlF_3. Cryolite was prepared by fusing the reagent grade NaF and AlF_3, previously dried at 400°, mixed in stoichiometric ratio. The $BaCl_2$, NaCl and LiF reagents were recrystallized from distilled water, dried for 24 h at 150° and melted before mixing, while a dried HCl or argon gas was bubbled through the melt. All experiments were performed in an argon atmosphere. The melts were submitted to measurement both at heating and on cooling.

The density and viscosity have been measured over a temperature range of about 100° in binary 40% Na_3AlF_6 + 60% $BaCl_2$ mixture and with 3 ; 5 ; 7% LiF or 2 ; 4 ; 6 ; 8% NaCl added.

The coefficients of equations representing the density *vs.* temperature and viscosity *vs.* temperature plots were calculated by the least squares method.

RESULTS AND DISCUSSIONS

The results obtained for the density of presently studied mixtures are summarized as linear function of temperature in tables 1 and 2. The present results for the density of 40% Na_3AlF_6 + 60% $BaCl_2$ mixture

---

[9] A. I. BELIAEV, "Electrolyte of Aluminium Bath", Metallurghizdat, Moscow, 1961.

[10] K. GRJOTHEIM, J. L. HOLM, C. KROHN and K. MATIASOVSKY, *Svensk Kem. Tidsku*, **78**, 547 (1966).

[11] K. GRJOTHEIM, K. MATIASOVSKY and M. MALINOVSKY, *Electrochim. Acta*, **15**, 259 (1970).

[12] R. G. GADEAU, D.R.P. 489869 (1930), 600585 (1934).

[13] M. YUKIO, M. WATANABE and K. ONO, "Technique of Metals Refining", Handbook, Asakura, 1963, p. 410.

[14] C. L. MANTELL, "Electrochemical Engineering", McGraw-Hill, 1960, p. 395.

[15] I. G. MURGULESCU and Ş. ZUCA, *Rev. Roumaine Chim.*, **4**, 227 (1959).

[16] I. G. MURGULESCU and Ş. ZUCA, *Z. phys. Chem. (Leipzig)*, **218**, 379 (1961).

[17] I. G. MURGULESCU and Ş. ZUCA, *Electrochim. Acta*, **14**, 519 (1969).

Table 1

Density equations in the 40% AlF_6Na_3 + 60% $BaCl_2$ mixture with NaCl additions

Content % NaCl	Density eqs.	Standard deviation	Temperature range °C
0	$d = 3.5002 - 1.0468 \cdot 10^{-3}\,t$	±0.0029	760–880
2	$d = 3.3385 - 0.8963 \cdot 10^{-3}\,t$	±0.0009	770–880
4	$d = 3.3042 - 0.8776 \cdot 10^{-3}\,t$	±0.0010	770–880
6	$d = 3.2752 - 0.8694 \cdot 10^{-3}\,t$	±0.0016	780–880
8	$d = 3{,}2248 - 0.8337 \cdot 10^{-3}\,t$	±0.0006	780–880

Table 2

Density equations in the 40% AlF_6Na_3 + 60% $BaCl_2$ mixture with LiF additions

Content % LiF	Density eqs.	Standard deviation	Temperature range °C
0	$d = 3.5002 - 1.0468 \cdot 10^{-3}\,t$	± 0.0029	760–880
1	$d = 3.3411 - 0.8832 \cdot 10^{-3}\,t$	± 0.0005	770–920
3	$d = 3.2366 - 0.7639 \cdot 10^{-3}\,t$	± 0.0024	760–890
5	$d = 3.2891 - 0.8313 \cdot 10^{-3}\,t$	± 0.0010	770–880
7	$d = 3.1894 - 0.7242 \cdot 10^{-3}\,t$	± 0.0012	780–880

Table 3

Coefficients of the temperature-viscosity relationship in the 40% AlF_6Na_3 + + 60% $BaCl_2$ mixture with NaCl additions $\log \eta^* = A + B/T(\mathrm{K})$; $\eta = A\eta\, e^{E\eta/RT}$

% NaCl	A	B	$A\eta \cdot 10^2$	$E\eta$ cal/mol	Standard deviation in $E\eta$ cal/mol	Temperature range K
0	−1.86685	2619.904	1.36	11985	117	1053–1127
2	−2.16694	2934.089	0.68	13425	152	1053–1133
4	−1.81835	2549.157	1.52	11665	94	1063–1148
6	−1.77307	2480.101	1.68	11350	90	1065–1135
8	−1.58295	2259.216	2.61	10340	260	1063–1123

* η is given in cP.

Cosma Ghe - 749

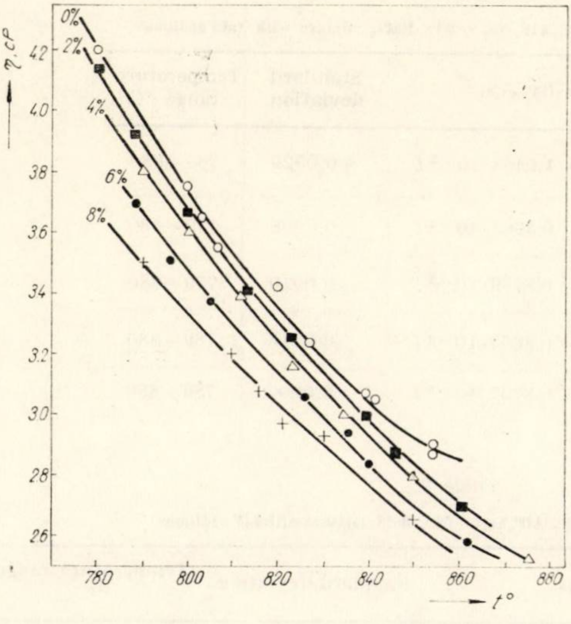

Fig. 1. — Viscosity polytherms in the 40 % AlF_6Na_3 + 60 % $BaCl_2$ system with NaCl additions.

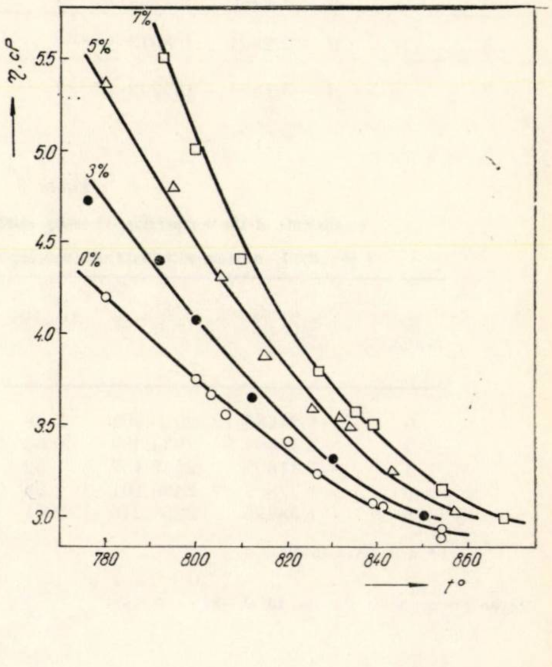

Fig. 2. — Viscosity polytherms in the 40 % AlF_6Na_3 + 60 % $BaCl_2$ system with LiF additions.

Cosma Ghe —749

differ by as much as 1.5% from the values indicated by Beliaev,[5] while a better agreement, within ±0.5% seems to exist with Taniuki's data[4] (no accurate estimation of these latter data was possible since, in the quoted paper, they are given as a graphic).

Table 4

Coefficients of the temperature-viscosity relationship in the 40% AlF_6Na_3 + 60% $BaCl_2$ mixture with LiF additions
$\log.\ \eta^* = A + B/T\ (K);\ \eta = A_\eta e^{E\eta/RT}$

% LiF	A	B	$A\eta \cdot 10^2$	$E\eta$ cal/mol	Standard deviation in $E\eta$ cal/mol	Temperature range K
0	−1.86685	2619.904	1.36	11985	117	1053−1127
3	−2.47427	3306.188	0.34	15130	340	1050−1123
5	−3.00751	3928.928	0.09	17980	385	1053−1130
7	−3.28688	4266.194	0.05	19520	640	1066−1140

* η is given in cP.

Our experimental data for viscosity are shown in figs. 1 and 2. The plot of $\log \eta$ vs $^1/T$ (K) is linear for all studied mixtures, attesting the validity of Arrhenius equation $\eta = A_\eta e^{E_\eta/RT}$. Tables 3 and 4 give numerical values of the pre-exponential constant A_η and the activation energy of viscosity E_η, as well as the equations for viscosity *vs.* temperature dependence. As can be seen in fig. 3, both NaCl and LiF additions decrease the density of the fused $Na_3AlF_6+BaCl_2$ system, the influence of NaCl being more pronounced. The corresponding values are of 0.2% per 1% LiF and of 0.5% per 1% NaCl. The relatively weak influence of LiF on the density of the basic electrolyte is probably due to the fact that the volume of the melt is mainly determined by the large complex anions AlF_6^{3-}. At NaCl addition, the larger Cl^- ions (r = 1,81 Å) compared to F^- ions (r = 1.36 Å) are expected to influence to a greater extent the volume of the melt, what is experimentally proved (fig. 3).

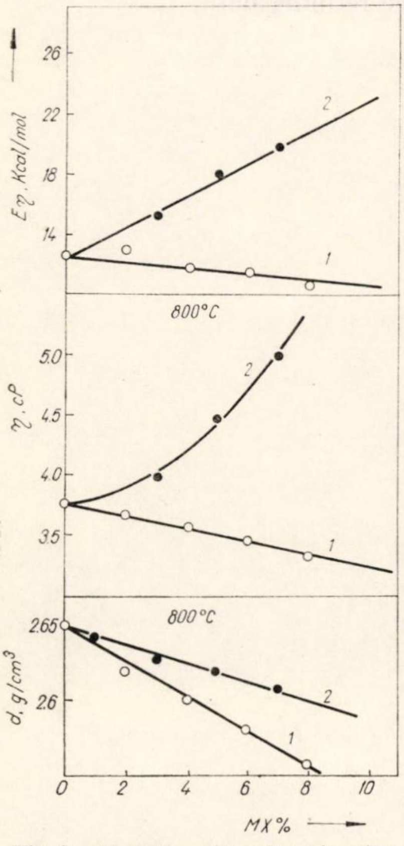

Fig. 3. — Variation of density, viscosity and E_η as a function of NaCl and LiF content in the 40% AlF_6Na_3 + + 60% $BaCl_2$ system :
1, NaCl; *2*, LiF.

Unlike the density behaviour, the viscosity is very little influenced by NaCl additions, while a substantial increase of the viscosity with increasing of LiF content in the melt takes place. Thus, an addition of 8% NaCl decreases the viscosity by 9% while, for 7% LiF added, a viscosity increase of 40% is observed. This can be explained by taking into account the small size of Li^+ ions, which allows them to occupy the free spaces existing among the large complex anions AlF_6^{3-}. Hence, the viscous flow is rended more difficult in the presence of Li^+ ions, which is also felt in the noticeable increase of the activation energy of viscosity (fig. 3). The linear dependence of both density and viscosity isotherms on composition, denote that in the concentration range studied, neither LiF nor NaCl take part in the chemical reaction on mixing and that they are, most probably, dissociated in the constituent ions. This is also supported by the linearity of E_η *vs.* composition curves.

In conclusion, we mention that from technical point of view, the NaCl addition is more advantageous, since it influences positively both density and viscosity of electrolyte. With regard to LiF, no content higher than 3% is recommended. It is certain that other parameters, as melting temperature, electrical conductivity, must be studied in order to establish the optimum composition of the refining bath.

Revue Roumaine de Chimie, 19, 2, 187–196 (1974)

DIFFUSIVE ATOMIC TRANSPORT IN MOLTEN ANTIMONY

N. PETRESCU and LUCIA GANOVICI

Centre of Physical Chemistry,
Str. Galaţi 31, Bucharest 9, Romania

Received June 11, 1973

Self-diffusion determinations in liquid antimony were carried out by the capillary-reservoir technique. The experimental results obtained in a temperature range from 640° to 800° are discussed according to several diffusion mechanisms. By statistical treatment of the data, the diffusion equations of liquid antimony are established, according to the activated mechanism of diffusion as well as for the small cooperative atomic motions mechanism based on the density fluctuations.

The observation is made that the parameters in the equation obtained for the self-diffusion in liquid antimony,

$$D = 11.48 \times 10^{-4} \exp(-5580/RT)$$

together with the parameters in the Arrhenius type diffusion equations for other elements non-closely packed in solid state, can lead to an interpretation of the diffusion phenomenon as function of the structure of the melt, expressed by the coordination number.

The self-diffusion coefficients of the molten metals represent fundamental data of great importance both for the theory of the liquid state and for numerous applications in different modern fields of technics.

Experimental determinations of the self-diffusion coefficients were performed especially for the liquid metals situated in the first four groups of the periodic table of elements. We tried in our works to enlarge the number of liquid state diffusivity determinations in metals, choosing to this purpose elements which were not studied before. So we carried out self-diffusion determinations in semimetals belonging to groups V_a and VI_a, namely in bismuth [1] and tellurium.[2] In the present paper we present the results of the self-diffusion determinations in another element of group V_a, that is in liquid antimony.

---

[1] N. Petrescu and M. Petrescu, *Rev. Roumaine Chim.*, **15**, 189 (1970).

[2] E. Nicoloiu, L. Ganovici and I. Ganovici, *Rev. Roumaine Chim.*, **15**, 1713 (1970).

EXPERIMENTAL

The experimental device we used for the determination of the self-diffusion coefficients in liquid antimony was in principle the same we devised in previous works.[3,4] Several modifications were, however, necessary because of the particular surface properties of liquid antimony.

We carried out the diffusivity determination by the capillary-reservoir technique, with radioactive labelling of the liquid antimony in the reservoir. The radioactive tracer, needed to label the molten bath in the reservoir, was obtained by the activation of antimony in a nuclear reactor. The isotopic composition of antimony and the neutron cross-sections of its natural isotopes are such that the neutron irradiation leads in fact to two radioactive isotopes, namely Sb^{122} ($T_{1/2} = 2.80$ days) and Sb^{124} ($T_{1/2} = 60$ days). To diminish the contribution of the radioactivity from the short-lived isotope Sb^{122} and, thus, to ensure a better precision to the radioactivity measurements, the tracer was used after a hundred days storage since the moment of the irradiation in the reactor. The decay of the short lived isotopes allowed the radioactivity of the long-lived isotope Sb^{124} to be taken solely into account.

In the first runs we used capillaries bored in spectrally pure graphite rods, filled with antimony by the technique we described in a previous paper.[3] Although we used for the diffusion runs only the sound capillary samples, selected by a careful radiographic control, the number of samples in which diffusion did not take place was excessively large. We ascribed this fact to the graphite that we used to contain the capillary samples, the liquid antimony having a rather bad capacity of wetting the graphite. On this account it was possible that the contact between the antimony in the capillary and the labelled antimony in the reservoir be interrupted at the diffusion interface, when introducing the capillary samples into the reservoir.

Other series of runs were performed using capillary recipients made of sintered alumina tubes (0.8 mm inner diameter and 0.3 mm uniform wall thickness). The alumina tubes were cut to about 20 mm length, sealed at one end and fixed two by two in the same specimen holder. The filling of the capillaries was carried out by immersing them in a bath of liquid antimony under vacuum, followed by argon admission under pressure.

The experimental device allowed the diffusion runs to be made continuously without solidification of the bath for changing the samples. Pure argon atmosphere was used; the temperature was kept constant within the limits $\pm 1°$.

The diffusion coefficients were derived from radioactivity measurements made on the diffusion samples and on reference samples taken from the radioactive bath. The geometry of the diffusion samples and of the reference samples was the same. The reference samples were taken from the bath by the immersion filling technique already described for the diffusion samples. The radioactivity measurements were made either on the whole sample or on sections of the sample. The radioactivity measurements on sections were performed by a screening technique, using a 1.5 mm slit width in a thick lead plate which allows the measurements on small finite portions along the sample length. Moving the sample stepwise under the slit, about 10 portions of the sample length could be exposed to measurement. From each measurement, a value of the diffusion coefficient was derived according to the relation (1):

---

[3] N. Petrescu, St. Zămîrcă, L. Ganovici and I. Ganovici, *Rev. Roumaine Chim.*, **13**, 865 (1968).

[4] M. Petrescu, *Z. Metallkde.*, **61**, 14 (1970).

$$\frac{c}{c_0} = 1 - \frac{4}{\pi} \sum_{n=0}^{\infty} \frac{1}{2n+1} \sin \frac{(2n+1)\,\pi x}{2l} \exp\left[-(2n+1)^2 \frac{\pi^2}{4} \frac{Dt}{l^2}\right] \qquad (1)$$

where c is the specific radioactivity of the sample, c_0 is the specific radioactivity of the bath in the reservoir, D is the self-diffusion coefficient (cm^2/s), t is the diffusion time (s), l is the length of the capillary column in which diffusion took place (cm) and x is the distance from the measured portion to the diffusion interface (cm).

By averaging equation (1) on the whole length of the sample, equation (2) is obtained and it was this last equation that we used for deriving the diffusion coefficients from radioactivity measurements on integral samples:

$$\frac{c}{c_0} = 1 - \frac{8}{\pi^2} \sum_{n=0}^{\infty} \frac{1}{(2n+1)^2} \exp\left[-(2n+1)^2 \frac{\pi^2}{4} \frac{Dt}{l^2}\right] \qquad (2)$$

Both equations (1) and (2) are obtained by integration of the Fick's second law for the following initial and boundary conditions: $c = 0$ for $0 < x < l$ at $t = 0$; $c = c_0$ for $\leqslant 0$ at $t \geqslant 0$ and $\partial c/\partial x = 0$ for $x = l$ at $t > 0$.

RESULTS AND DISCUSSION

The results for the self-diffusion coefficients in molten antimony as obtained from radioactivity measurements on integral samples are given in table 1. The values of the specific radioactivity in table 1 are the averages of several measurements so that the error owing to the statistical character of the decay phenomenon was less than 0.5%.

The radioactivity measurements on portions of the diffusion sample allowed more information to be gained. Penetration curves were drawn from this kind of measurements and a value of the diffusion coefficient was derived from the measurement on each portion. An experimental penetration curve is presented in fig. 1 together with the self-diffusion coefficients derived from it. The penetration curve gives an image of how the diffusion took place, but this must be taken with caution because solidification may cause perturbations in the penetration profile. A series of examples where the diffusion coefficients computed from measurements on different portions of the same sample vary very little around a mean value (as in fig. 1), attest the fact that the diffusion took place in normal conditions.

The average of the values of the diffusion coefficients derived from measurements on different portions of the same sample was generally larger than the diffusion coefficient derived from a measurement on the integral sample.

Table 1

Experimental determination of the self-diffusion in liquid antimony

Temperature °C	Time of diffusion s	Length of the capillary cm	Average specific radioactivity of the capillary counts/min g	Specific radioactivity of the bath counts/min g	$D.10^5$ cm^2/s	$\overline{D}.10^5$ cm^2/s	Relative standard deviation $\varepsilon = \Delta\overline{D}/\overline{D}$ %
640	4800	1.873	29148	90278	5.862	5.86	—
650	4845	2.124	24209	91211	5.281	5.29±0.09	1.70
		1.977	26393		5.438		
	4200	1.973	108624	408600	5.142		
683	4200	2.151	22882	89598	5.582	5.99±0.62	10.35
		2.350	21581		5.927		
	3600	2.033	93706	407297	4.739		
		2.033	119495		7.707		
725	3600	2.006	23827	91211	6.142	7.15±0.41	5.73
		2.000	25533		7.010		
		2.163	24167	90278	7.346		
		2.093	26233		8.104		
758	3000	2.040	113347	408677	8.379	7.44±0.94	12.64
		2.040	99766		6.492		
800	2100	2.043	90936	410312	7.727	8.33±0.61	7.32
	2700	2.198	22721	90278	8.940		

The temperature dependence of the diffusion coefficients of the molten metals can be interpreted according to several formalisms, corresponding to different equations, whose theoretical elaboration and taking into account of the structural characteristics of the melt are different. From the fact that several types of relations can account successfully for the temperature dependence of the diffusivity, we may infer that the diffusion in metallic melts depends firstly on other factors, the temperature being a consequential parameter of these primary factors.[5] If we adopt such a point of view, a first order importance is to be given to the interpretation of the parameters in the equations which express the temperature dependence of diffusivity. The general forms of these equations are:

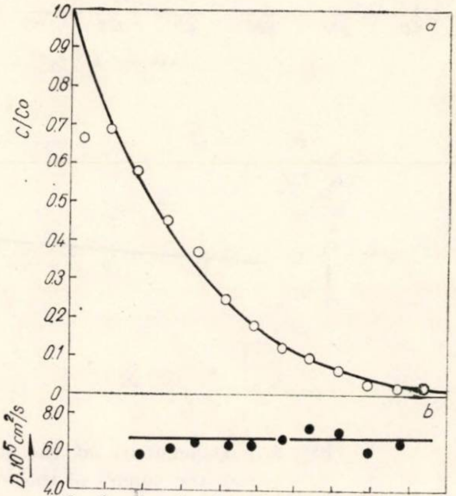

Fig. 1.— *a*) Radioactivity penetration curve along the capillary length; *b*) Values of the diffusion coefficients derived from measurements on portions along the length of the sample.

$$\ln D = AT^{-1} + B \tag{3}$$

$$D = AT^{n} + B \tag{4}$$

where n can have the values 1/2, 1, 3/2, 2.

The parameters A and B, derived from experimental sets of data for a certain type of equation, allow the diffusion phenomenon to be related to physical or structural characteristics of the melt. Among the diffusion equations whose parameters were physically interpreted it is to be noted the Arrhenius type equation, largely used to represent the variation of diffusivity with temperature. Our experimental results on the diffusivity in liquid antimony are also well rationalized by an Arrhenius type equation (fig. 2). The experimental data are to the same extent satisfactorily corroborated by a polynomial temperature function in T or T^2 (generally expressed by eq. 4) as we can see in figures 3 and 4.

---

[5] E. F. Broome and H. A. Walls, *Trans. Met. Soc. AIME*, **242**, 2177 (1968).

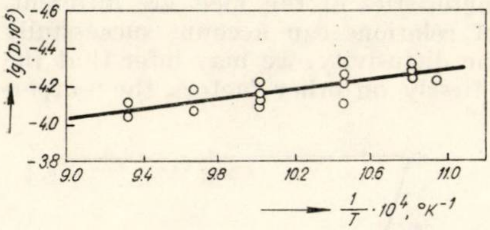

Fig. 2. — Arrhenius temperature dependence of the self-diffusion coefficients in liquid antimony.

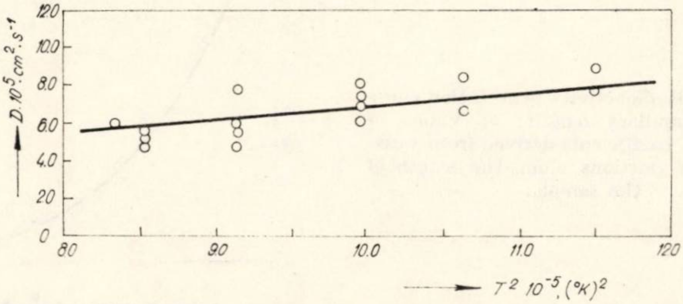

Fig. 3. — Dependence of the diffusivities in liquid antimony on the square of the absolute temperature.

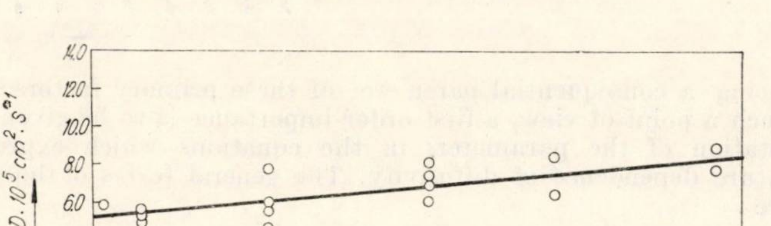

Fig. 4. — Dependence of the diffusivities in liquid antimony on the absolute temperature.

The analytical expressions of these dependences computed by a least squares statistical treatment of the experimental data are the following :

$$D = 11.48 \times 10^{-4} \exp\ (-5580/RT) \tag{5}$$

$$D = 0.684 \times 10^{-10} T^2 \tag{6}$$

$$D = -12.02 \times 10^{-5} + 0.02 \times 10^{-5}\, T \tag{7}$$

The significance of the parameters in equations (5)—(7) (plotted in figures 2—4) is worth to be discussed. The parameters in equation (5) — the preexponential factor and the activation energy — form the object of numerous attempts of correlation with several characteristics of the diffusing element or with its structural features in liquid state.

As the preexponential factor D_0 is concerned, we mention for instance that in a previous paper [1] we proposed that the dependence of D_0 on the solid state structure of the diffusing element [6] be replaced by a more adequate dependence on the coordination number in the melt. The test of this proposal that we made on the basis of the data then available can be completed successfully with the value of the preexponential factor of the diffusion equation that we obtained for molten antimony, as we can see in figure 5.

By substituting semilogarithmic coordinates in fig. 5 the dependence is linearized (fig. 6); thus, the possibility arises of expressing the coefficient D_0 by the equation:

$$D_0 = M^{-1/2} \exp\ (-Z) \tag{8}$$

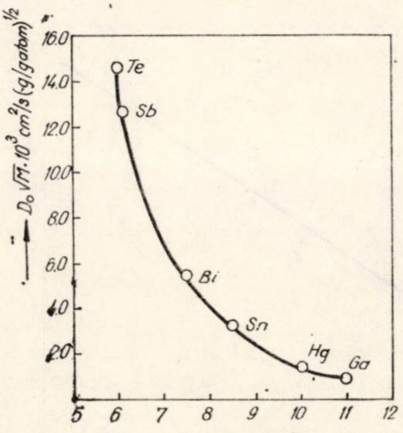

Fig. 5. — Dependence of the preexponential factor in the Arrhenius equation of several unclosely packed elements on the coordination number in liquid state.

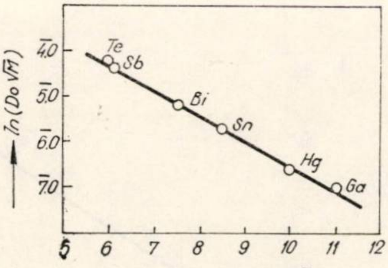

Fig. 6. — Linearization of the dependence of the preexponential factor on the coordination number in liquid state.

Further, by using the preexponential factor of eq. (8), the diffusion equation becomes:

$$D = M^{-1'2} \exp\ [-(Z + Q/RT)] \tag{9}$$

---

[6] H. J. Saxton and O. D. Sherby, *Trans. A.S M.*, **55**, 826 (1962).

and replacing the activation energy Q by the expression $Q = ART_m$, which is satisfactorily verified by most liquid metals, we obtain:

$$D = M^{-1/2} \exp\left[-(Z + AT_m/T)\right] \quad (10)$$

From eq. (10) we may infer that for the group of elements we refer to, and which was considered in previous papers [1,3] too, the self-diffusion coefficient in liquid state can be correlated with the temperature by means of two physical constants — e.g. the atomic mass M and the melting point T_m — and one structural characteristic of the melt, namely the coordination number Z.

The physical data used to check this relation (fig. 6) are the experimental self-diffusion data [1,2,7–11] and the coordination numbers in the molten elements.[12–14]

As concerning the constant A in eq. (10) we may consider the following: in figure 7 we may see that the activation energy for self-diffusion in liquid semimetals falls beneath the line $Q=3.35\ RT_m$ observed by typical metals. Saxton and Sherby [6] proposed for the semi-

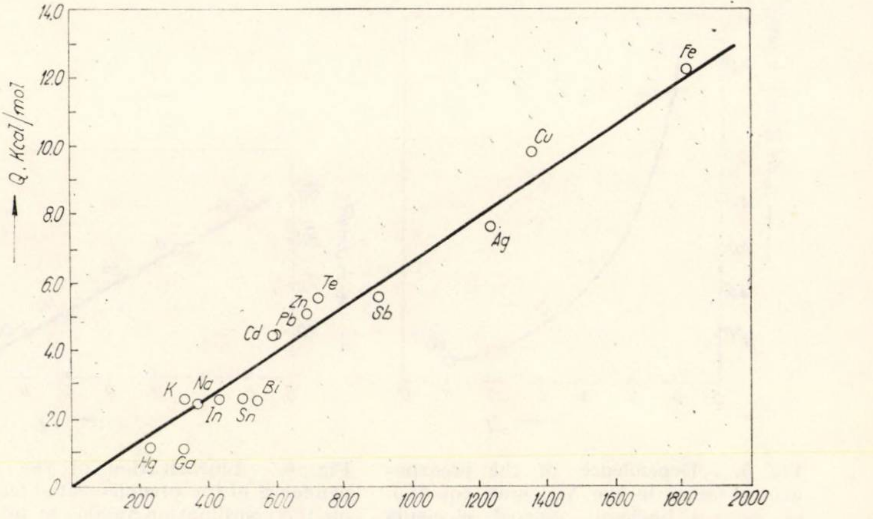

Fig. 7. — Variation of the activation energy of diffusion with the melting points of elements.

---

[7] N. H. NACHTRIEB, *Adv. Phys.*, **16**, 309 (1967).

[8] N. H. NACHTRIEB and J. PETIT, *J. Chem. Phys.*, **24**, 746 (1956).

[9] D. S. BROWN and D. G. TUCK, *Trans. Faraday Soc.*, **60**, 1230 (1964).

[10] J. PETIT and N. H. NACHTRIEB, *J. Chem. Phys.*, **24**, 1027 (1956).

[11] G. CARERI, A. PAOLETTI and M. VINCENTINI, *Nuovo Cim.*, **10**, 1088 (1958).

[12] R. M. WAGHORNE, V. G. RIVLIN and G. I. WILLIAMS, *Adv. Phys.*, **16**, 215 (1967).

[13] H. K. F. MÜLLER and H. HENDUS, *Z. Naturforsch.* (*A*), **12**, 102 (1957).

[14] G. TOURAND, B. CABANE and M. BREUIL, *J. Non-Cryst. Sollids*, **8—10**, 676 (1972).

metals the expression $Q = 2.75\ RT_m$. By substituting this latter value in eq. (10) we get :

$$D = M^{-1/2} \exp\,[-(Z + 2.75/T_r)] \tag{11}$$

where T_r is a reduced temperature T/T_m.

The interpretation of the temperature dependence of the diffusivity according to the functions in T or T^2 (eq. 4) can find a theoretical support in supposing a diffusion mechanism based on small and variable cooperative atomic movements consequential to the small density fluctuations in the liquid. According to Swalin,[15] such a mechanism results in the following expression of the self-diffusion coefficient :

$$D = 2.39 \times 10^{-7} \frac{Z}{K} T^2 \tag{12}$$

where Z is the coordination number in the liquid and K is the force constant of the interatomic bond (dyne/cm).

Further theoretical treatments within this diffusion mechanism performed by Reynik [16] and experimental testings [17] lead to a linear temperature dependence of the diffusivity according to relation :

$$D = -1.72 \times 10^{24} Z X_0^4 K + 2.08 \times 10^9 Z X_0^2 T \tag{13}$$

where X_0 is the maximum jump distance.

By identifying equations (6) and (12) a value of 2.19×10^4 dyne/cm resulted for the force constant K in antimony ; a value $K = 5.12 \times 10^4$ dyne/cm resulted from the identification of equations (7) and (13).

Equation (13) allows the maximum jump distance X_0 to be computed from diffusion data : the experimental diffusion data in liquid antimony lead to a value $X_0 = 0.386$ Å. This jump distance compared to the average interatomic distance in liquid antimony gives a ratio of 0.12 ; this figure confirming the theoretical premise of the small fluctuations mechanism of diffusion.

Another theoretical justification for the linear temperature dependence of diffusivity is given by Nachtrieb,[7] by supposing the existence of several atomic configurations with different contributions to the diffusive motion, still directly varying with temperature. By considering the cooperative atomic movement as a result of the irreversible displacement of the oscillating center of each atom on distances equal to the mean square values of the amplitudes of the thermal vibrations, the following relation is established :

---

[15] R. A. Swalin, *Acta Met.*, **7**, 736 (1959).

[16] R. J. Reynik, *Appl. Phys. Letters*, **9**, 239 (1966).

[17] M. Petrescu, *Rev. Roumaine Chim.*, **13**, 687 (1968).

$$D = \frac{k^2 \theta_D T}{hK} \tag{14}$$

where θ_D is the Debye characteristic temperature, (K).

By interpreting our experimental data on liquid antimony diffusivity, according to eq. (14), it is obtained a value of the force constant $K = 0.723 \times 10^4$ dyne/cm, considerable inferior to that obtained from equations (12) and (13). It is worth mentioning that for typical metal (K, Na, Cu, Ag) the agreement between the value of the force constant computed from diffusivity data by means of eq. (14) and the value derived from spectroscopical or compressibility data is quite good. The force constant computed for semi-metals by means of eq. (14) leads to lower values. The fair agreement obtained with eq. (14) for the typical metals and the less satisfactory corroboration observed for the semi-metals can be ascribed to the differences between the liquid structure of the metallic elements and that of the semi-metals, eq. (14), lacking the possibility to take into account such structural effects. Equations (12) and (13), in which structural characteristics of the liquid are involved, give good results both for metals and for semi-metals.

The structure of the liquid semi-metals is different from that of the liquid metals, but what is more there are marked differences from the structure of one semi-metal to another. This is why the preexponential coefficient in eq. (3) can be expressed as function of several physical characteristics including a specific structural characteristic, as we proceeded in the present paper when establishing eq. (11). The correlation expressed by eq. (11) holds well, at least for a series of semi-metals and liquid metals having an unclosely packed structure.

Revue Roumaine de Chimie, **19**, *2*, 197–206 (1974)

CHRONOPOTENTIOMETRIC METHOD AT HIGH TEMPERATURES

S. STERNBERG and CONSTANȚA HERDLICKA

Institute of Physical Chemistry,
str. Galați 31, Bucharest, Romania

Received April 9, 1973

The influence of different factors on the chronopotentiometric measurements used for interdiffusion coefficient determination in salts melting at high temperature, such as alkali chlorides, has been studied. A graphical method for transient estimation was checked up by using the method of potential-time curves analysis which allows a correct estimation of the transition time. The values of current densities and concentrations of the diffusing substance, for which both methods of the transient estimation give comparable results, have been established.

Among the electrochemical methods, the chronopotentiometric method is more frequently used to determine the interdiffusion coefficients in molten salt media.

The diffusion coefficient is calculated from the Sand's equation:

$$\tau^{1/2} = \pi^{1/2} nFD^{1/2}C_0/2i_0 \tag{1}$$

where τ (sec) is the transition time, i_0(A/cm^2) the current density, D (cm^2/sec) the diffusion coefficient of the reacting species of bulk concentration C_0 (mol/cm^3), n the number of electrons participating to the electrode reaction and F (coulombs) the Faraday constant.

The Sand's equation is applicable only when the transport of ions to the electrode surface takes place by a semi-infinite linear diffusion process. According to eq. (1), for a given concentration of the diffusing ion, the product $i_0\tau^{1/2}$ should be independent of current density and the ratio $i_0\tau^{1/2}/C_0$ has to be constant for different current densities and concentrations.

The constancy of $i_0\tau^{1/2}$ product and $i_0\tau^{1/2}/C_0$ ratio represents verification criteria for semi-infinite linear diffusion.

Laitinen and co-workers[1,2] have investigated, for the first time, the validity of the transition-time eq. (1) at molten salt systems. These

---

[1] H. A. Laitinen and W. S. Ferguson, *Analyt. Chem.*, **29**, 4 (1957).

[2] H. A. Laitinen and H. C. Gaur, *Analyt. Chim. Acta*, **18**, 1 (1958).

authors have studied the factors which influence the chronopotentiometric measurements at the diffusion of some metallic ions in LiCl + KCl at 450° and have established the ranges of current density and concentration for which Sand's equation is applicable. Laitinen and co-workers' studies have been considered as a base in chronopotentiometric measurements in molten salts made by many authors.

In our previous publications we have used the chronopotentiometric method in order to determine the diffusion coefficients of the silver ion in alkali nitrates [3,4] and chlorides [5] as well as of the lead ion in alkali chlorides.[6] The working temperatures for nitrate mixtures ranged between 260 and 480° and the working conditions were similar to those of Laitinen and co-workers.[1,2] Our measurements performed in alkali chloride media [5,6] demanding working temperatures of 400–500°, higher than in alkali nitrates, have imposed the establishing of new conditions for Sand's equation to apply. Our present work gives details about the chronopotentiometric measurements at temperatures as high as 900°.

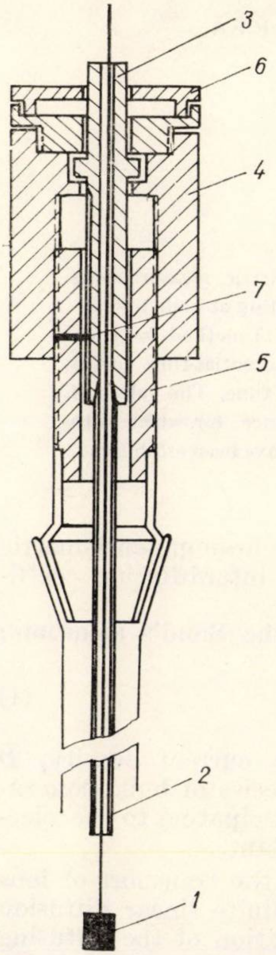

Fig. 1. – Vertical advance system for the working electrode.

1, working electrode; *2*, silica capillary; *3*, metallic holder for the electrode; *4*, movable axial advance system; *5*, fixed advance system; *6*, disk with mark; *7*, guiding peg.

EXPERIMENTAL

Chronopotentiometric equipment and experimental procedure have been described elsewere.[3–6] A quartz cell with three joint ended arms allowing the fastening of the three electrodes have been used.

The working electrode was a platinum plate hanging on a platinum wire of 0.5 mm diameter. Above 600°, which is the temperature range characteristic for alkali chlorides experiments, the delimitation of the working electrode surface area by framing it in insulators is not possible. In this temperature range any kind of glass, even quartz, cannot be used to seal the Pt wire. For this reason we have used the device in figure 1 to delimitate the working electrode surface.

The supporting wire of the plate was passed through a quartz capillary, the latter being attached to a metallic device consisting of two concentric hollow cylinders screwed in one another with a 2 cm long, M 0.5 mm thread. The electrode can be moved up and down on the desired distance, the electrical contact with the melt being signaled on a separated electrical circuit. The whole surface and 1–2 mm from the wire introduced into the melt.

---

[3] S. Sternberg and C. Herdlicka, *Rev. Roumaine Chim.*, **14**, 991 (1969).
[4] S. Sternberg and C. Herdlicka, *Rev. Roumaine Chim.*, **15**, 343 (1970).
[5] S. Sternberg and C. Herdlicka, *Rev. Roumaine Chim.*, **17**, 343 (1972).
[6] S. Sternberg and C. Herdlicka, *Rev. Roumaine Chim.*, **18**, 1689 (1973).

The counter-electrode was a greater platinum plate (~2 cm^2) placed in a separate compartment.

The reference electrode consisted of a silver wire (Ø 1 mm) introduced into a melt containing Ag Cl dissolved in the same alkali chloride with the solvent used in the diffusion experiment. The concentration of silver ion (~0.1 M) was close to that of the studied solution.

The reference electrode Ag/Ag (I) has the advantage that it is easily prepared and can be used on a large temperature range, even above 900°.[7] The thin wall of the silica tube, which contained the reference electrode, allowed the electrical contact with the studied electrolyte.

The direct contact between the studied melt and the reference electrode, through a hole in the wall of the test tube has to be eliminated since the silver wire dissolves in alkali halides changing the concentration of silver ion in solution. In this case we have observed an increase in time of the constant $i_0\tau^{1/2}$ (table 1) that may be due to an Ag^+ concentration increase in the solution studied.

Table 1

The time change of the product $i_0\ \tau^{1/2}$ when the reference electrolyte is in a direct contact with the studied electrolyte
Solvent – KCl + NaCl (1.1)
Electrochemically active substance – AgCl
$C_{Ag^+} = 33.99 \cdot 10^{-5}$ mol/cm^3. Contact time of the electrolytes – 2 hours

$i_0 . 10^3$ A.cm^{-2}	τ sec	$i_0\tau^{1/2} . 10^3$ A.cm^2.sec $^1/_2$
16.62	1.32	19.10
17.52	1.25	19.59
18.57	1.18	20.17
19.75	1.10	20.69
21.09	1.08	20.91
21.95	1.04	22.38
21.95	1.06	22.58
21.95	1.08	22.80

PURE SOLVENT STUDY

It is characteristic for the chronopotentiometric method that the concentration of the electrochemically active substance is small (10^{-5}–10^{-4} mol/cm^3) compared to that of its support, an inert electrolyte (the diffusion medium), whose concentration is much higher (about 200 times) so that to allow the transport of the electrochemically active substance only by diffusion. For this reason, the purity of the solvent is of great importance in obtaining the correct values of the transition time characterizing the diffusion of the metal ion to the electrode surface.

The chronopotentiometry allows very small quantities of impurities to be detected in the molten salts and may be used to establish the purity of a molten solvent.

---

[7] J. Hladik, Y. Pointud, M. C. Bellisent and G. Morand, *Electrochim. Acta*, **15**, 405 (1970).

Alkali halides, especially LiCl, retain easily the water which is not eliminated on heating and alkali hydroxides are formed at melting. In the literature, experimental procedures of water removing from alkali halides are described. Their efficiency can be controlled by recording the potential-time curves.

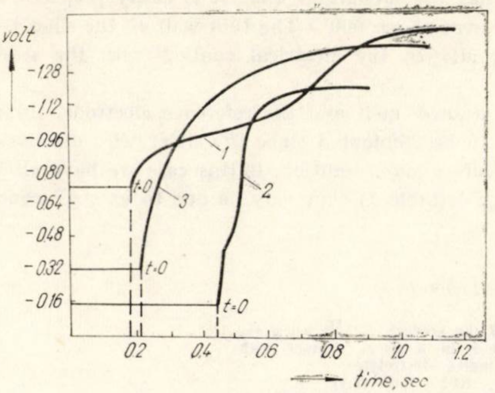

Fig. 2.—Chronopotentiograms of molten solvent.

1, untreated KCl at $i_0 = 3.55\cdot10^{-3}$ A/cm^3; *2*, KCl under vacuum and argon bubbling at $i_0 = 2.02\cdot10^{-3}$ A/cm^3; *3*, KCl untreated at $i_0 = 14.5\cdot10^{-3}$ A/cm^3.

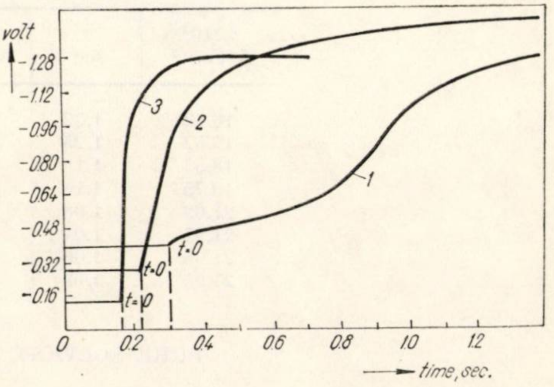

Fig. 3. — Chronopotentiograms of molten solvent.

1, KCl fused in HCl atmosphere and insufficient argon bubbling at $i_0 = 4.45\cdot10^{-3}$ A/cm^2; *2*, *3*, KCl melted in HCl atmosphere and enough argon bubbling to remove dissolved HCl traces. $i_0 = 4.45\cdot10^{-3}$ A/cm^2 (curve *2*) and $i_0 = 9.4.10^{-3}$ A/cm^2 (curve *3*).

If the potential of the working electrode is recorded *versus* time for a recrystallized, dried and melted KCl, a transition time is found which points out the traces of water (fig. 2, curve *1*). This transition time may be observed even for an electrolysis made at a current density as high as that used for a solvent containing electrochemically active substance. Removing of water may be achieved by pumping out the salt for at least 10 hours and melting it in argon atmosphere. This way, even at low current densities, ~ 2 mA/cm^2, a sudden increase of potential up to the value of the decomposition potential of the salt is recorded (fig. 2, curve *3*). A method often used for removing alkali hydroxides from the melt is HCl bubbling, but after that a great quantity of HCl remains dissolved in the melt. As can be seen from fig. 3, an incomplete removing of HCl is followed by a considerable transition time (curve *1*). This situation may be avoided by passing a big quantity of argon through the melt to remove HCl completely (fig. 3, curves *2*, *3*).

TRANSITION TIME DETERMINATION

To determine the transition time from potential-time curves, we have chosen the graphical method used for molten salts by Thalmayer and co-workers.[8]

The graphical methods for transition time determination need an extrapolation of the chronopotentiometric curve at the initial and final points, where the electrode potential suddenly changes. These points can hardly be estimated on a distorted chronopotentiogram because of the capacity current arising from electrical double layer charging. Therefore, it is very important to find out the values of concentration and current density for which the capacity current is negligible, so that τ graphically measured should represent the real transition time.

Sternberg and Vişan [9] have recently published an extensive study concerning the part played by the capacity current in the chronopotentiograms of $AgNO_3$ and alkali nitrate systems, showing that for high capacity currents the graphical method of transient estimation becomes inadequate.

To make sure that the graphical method is valid we have used the same method as Sternberg and Vişan, to get the transient and diffusion coefficient from the analyses of the potential-time curves.

The dependence of the working electrode potential, E, on the concentration according to Nernst equation is:

$$E = E_0 + \frac{RT}{nF} \ln \left(C_0 - \frac{2 i_0 t^{1/2}}{nF\, \pi^{1/2}\, D^{1/2}} \right) \tag{2}$$

where E_0 is the standard electrode potential and the paranthesis gives the concentration of the electrochemically active substance next to the electrode surface, at a time t, after the electrolysis starting. The variation of electrode potential at times t_1 and t_2 would then be:

$$\Delta E = E_2 - E_1 = - \frac{RT}{nF} \ln \left[\frac{\pi^{1/2} nFD^{1/2}\, C_0 - 2 i_0 t_2^{1/2}}{\pi^{1/2}\, nFD^{1/2} C_0 - 2 i_0 t_1^{1/2}} \right] \tag{3}$$

The equation (3) may be conveniently rearranged in an exponential form, as follows:

$$t_2^{1/2} - t_1^{1/2}\, e^{-\frac{\Delta EnF}{RT}} = \frac{\pi^{1/2}\, nFD^{1/2}}{2 i_0} \left[1 - e^{\frac{\Delta EnF}{RT}} \right] \tag{4}$$

On a graphical plot with $y = t_2^{1/2} - t_1^{1/2}\, e^{-\frac{\Delta EnF}{RT}}$ and $x = 1 - e^{-\frac{\Delta EnF}{RT}}$ as co-ordinates, a straight line is obtained whose extrapolation to $x = 1$ (for infinite potential) gives the transient $\tau^{1/2}$ from Sand's equation (1).

---

[8] C. E. Thalmayer, S. Bruckenstein and D. M. Gruen, *J. Inorg. Nuclear Chem.*, **26**, 347 (1964).

[9] S. Sternberg and T. Vişan, *Rev. Roumaine Chim.*, (under press).

We have used equation (4) to analyse a large number of potential-time curves for the AgCl – (KCl + NaCl) system under different experimental conditions (concentrations, current densities and temperatures).

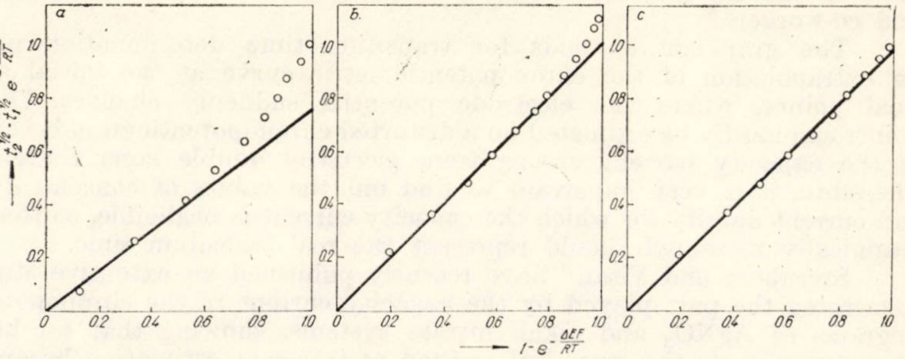

Fig. 4. – Transition time estimation by eq. (4) for Ag^+ diffusion in KCl + NaCl at. 710°.

a. $C_0 = 2.27 \cdot 10^{-5}$ mol/cm³; $i_0 = 14.23 \cdot 10^{-3}$ A/cm²; $\tau_{\text{calcd.}} = 0.60$ sec; $\tau_{\text{graph.}} = 0.77$ sec.

b. $C_0 = 5.25 \cdot 10^{-5}$ mol/cm³; $i_0 = 27.33 \cdot 10^{-3}$ A/cm²; $\tau_{\text{calcd.}} = 1.02$ sec; $\tau_{\text{graph.}} = 1.06$ sec.

c. $C_0 = 7.54 \cdot 10^{-5}$ mol/cm³; $i_0 = 41.96 \cdot 10^{-3}$ A/cm²; $\tau_{\text{calcd.}} = 0.96$ sec; $\tau_{\text{graph.}} = 0.96$ sec.

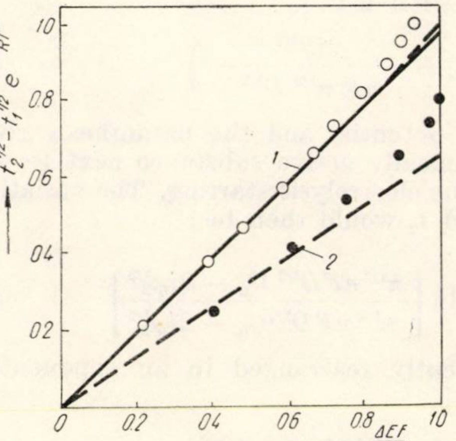

Fig. 5. – Transition time estimation by eq. (4) for Ag^+ diffusion in KCl + NaCl at 710° and $C_0 = 3.77 \cdot 10^{-5}$ mol/cm³.

1, $i_0 = 21.2 \cdot 10^{-3}$ A/cm²; $\tau_{\text{calcd.}} = 0.97$ sec.; $\tau_{\text{graph.}} = 0.98$ sec; *2*, $i_0 = 32 \cdot 10^{-3}$ A/cm²; $\tau_{\text{calcd.}} =$ = unobtainable. $\tau_{\text{graph.}} = 0.43$ sec.

In our experiments t_1 was kept constant (0.04 sec) and t_2 was varied every 0.2 sec. We supposed that i_0 is wholly a faradic current.

Appling equation (4) to curves recorded at different current densities and concentrations which give similar values of the C_0/i_0 ratio, we have obtained plots like those shown in fig. 4.

In figure 4 the values of the transition time, obtained both by eq. (4) and the graphical method, are listed.

Examination of fig. 4.*a* shows that at low concentrations some deviations from the straight line are evidently present. The chronopotentiograms recorded in the conditions indicated in figs. 4.*b*. and 4.*c*.

show a good agreement between the transition time values obtained by the graphical method and eq. (4). In the case of low concentrations (fig. 4.*a*.) the results of the two methods strongly disagree with each other.

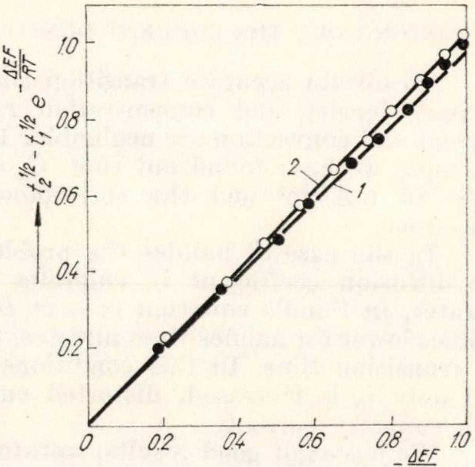

Fig. 6. — Transition time estimation by eq. (4) for Ag+ diffusion in KCl+ NaCl at 750°.

1, $C_0 = 6.91.10^{-5}$ mol/cm³; $i_0 = 57.35 \cdot 10^{-3}$ A/cm²; $\tau_{\text{calcd.}} = 0.96$ sec. and $\tau_{\text{graph.}} = 0.956$ sec.
2, $C_0 = 5.38 \cdot 10^{-5}$ mol/cm³; $i_0 = 42.04 \cdot 10^{-3}$ A/cm²; $\tau_{\text{calcd.}} = 1.025$ sec. and $\tau_{\text{graph.}} = 1.03$ sec.

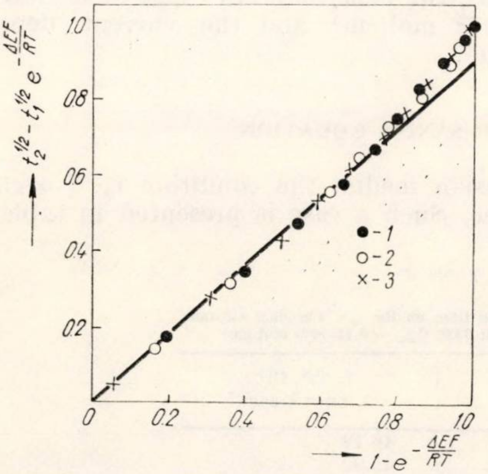

Fig. 7. — Transition time estimation by eq. (4) for Ag+ diffusion in NaCl + KCl at 808° and $C_0/i_0 \sim 1.07 \cdot 10^{-3}$.

C_0, mol/cm³	i_0, A/cm²
1, $3.40 \cdot 10^{-5}$	*1*, $31.69 \cdot 10^{-3}$
2, $5.68 \cdot 10^{-5}$	*2*, $42.57 \cdot 10^{-3}$
3, $6.74 \cdot 10^{-5}$	*3*, $62.61 \cdot 10^{-3}$

The greatest deviations from linearity are observed at high current densities and relatively small concentrations (fig. 5). At the same concentration, the higher the current density the more pronounced the deviations from linearity (figure 5, curve *2*) and τ cannot be estimated. The τ value obtained by the graphical method (dashed line in fig. 5, curve *2*) is in fact an apparent transition time.

A good agreement between the two methods (small deviations from linearity) is found in the following conditions : $C_0 > 3.10^{-5}$ mol/cm³, $i_0 < 70$ mA/cm² and transition time between 0.5 and 1.5 sec. These observations are illustrated in figures 6 and 7.

This way, we have established the conditions for obtaining slightly distorted curves so that the graphical method (which is simpler and faster) to allow a correct estimation of the transition time.

FINDING OUT THE CURRENT DENSITY AND CONCENTRATION RANGES

To obtain accurate transition times it is necessary to find out the current density and concentration ranges within which the capacity current and convection are negligible. In nitrates systems,[3,4] by successive attempts we have found out that $C_0 = 1.5 \cdot 10^{-5} - 3 \cdot 10^{-5}$ mol/cm³, $i_0 = 5 - 10$ mA/cm² and the corresponding transition time is equal to 0.5—2 sec.

In the case of halides the problem was a little more difficult. As the diffusion coefficient in chlorides is about 5 times higher than in nitrates, in Sand's equation ($\tau = ct . D(C_0/i_0)^2_2$) the ratio C_0/i_0 should be 5 times lower for halides than nitrates, to obtain the same range of values for transition time. In this conditions, if the concentration is kept low and only i_0 is increased, distorted curves are obtained because of the high capacity current.

We have got good results, working with 2—3 times greater concentrations and 4—6 times higher current densities than in nitrates.

So that, for chloride systems, the concentration range of the diffusing substance was $3 \cdot 10^{-5} - 8 \cdot 10^{-5}$ mol/cm³ and the current density range of $35 \cdot 10^{-3} - 65 \cdot 10^{-3}$ A/cm².

CHECKING UP SAND'S EQUATION

In alkali chlorides as diffusion media, the condition $i_0 \tau^{1/2} = ct.$ is fulfilled when 1 sec $\leqslant \tau < 0.5$ sec. Such a case is presented in table 2.

Table 2

The influence of the transition time on the $i_0 \tau^{1/2}$ product constant. AgCl in KCl + NaCl at 710° $C_{Ag} = 6.41 \cdot 10^{-5}$ mol/cm³

$i_0 . 10^3$ A.cm^{-3}	τ sec	$i_0 \tau^{1/2} . 10^3$ A.cm^{-2}.sec$^{1/2}$	
31.10	2.20	46.12	
34.66	1.75	45.92	
36.79	1.55	45.80	
41.37	1.23	45.87	
42.71	1.13	45.49	Average value 45.27
45.04	1.01	45.35	
47.23	0.91	45.11	
48.63	0.87	45.36	
51.09	0.78	45.15	
57.86	0.61	45.18	
69.10	0.41	44.20	

Since high temperatures facilitate convection and capacity currents enhancement, the range of transition time should be narrower in chlorides than in nitrates.

In tables 3 and 4, two examples, illustrating how the condition $i_0\tau^{1/2}/C_0 = ct$ holds in the case of chlorides mixtures, are given.

Table 3

Checking up Sand's equation in the AgCl + (KCl–NaCl) system at 710°

$C_{Ag} + .10^5$ mol.cm^{-3}	$i_0\ \tau^{1/2}.10^3$ A. sec$^{1/2}$.cm^{-2}	$i_0\ \tau^{1/2}/C_0$ A.cm.sec$^{1/2}$.mol^{-1}
3.16	22.61	715
3.67	25.38	691
4.64	33.52	722
5.43	37.68	694
6.41	45.67	711

Average value 707±11

Table 4

Checking up Sand's equation in the AgCl + KCl system at 800°

Current density number	$C_{Ag} + .10^5$ mol.cm^{-3}	$i_0^{1/2}.10^3$ A.sec$^{1/2}$.cm^{-2}	$i_0\tau^{1/2}/C_0$ A.cm.sec$^{1/2}$.mol^{-1}
4	1.61	15.30	950
6	1.90	17.10	900
4	2.13	18.76	880
6	4.40	35.80	813
6	5.72	46.00	804
7	6.29	51.10	812
5	6.57	52.68	803

From these tables it results that the ratio $i_0\tau^{1/2}/C_0$ is constant when the concentration of Ag^+ is greater than $3 \cdot 10^{-5}$ mol/cm^3.

The value $6.94.10^{-5}$ cm^2/sec we found for the diffusion coefficient of Ag^+ in the KCl – NaCl mixture at 710° is comparable to that obtained by Smirnov and co-workers,[10] using the same method, i.e. 7.06. $7.06 \cdot 10^{-5}$ cm^2/sec.

CONCLUSIONS

The chronopotentiometric measurements carried out under different conditions have shown that accurate values for transition time and interdiffusion coefficient above 500° may be obtained, provided that the current densities are 4–5 times higher and the concentrations are 2–3 times greater than those used at lower temperatures.

---

[10] A. N. Baraboshkin, M. V. Smirnov and N. A. Saltykova, "Electrockhimia Rasplavlenikh Solevikh i Tviordikh Electrolitov", Inst. Electrockhim. Akad. Nauk, U.R.S.S., Uralsk Filial nr. 2, 1961, p. 53.

Revue Roumaine de Chimie, **19**, *2*, 197–206 (1974)

To avoid the effects of convection and capacity current, the transition time should lie within a narrow range of 0.5—1 sec.

The analysis method of potential-time curves allows the determining of transition time from chronopotentiograms recorded in any conditions. It also allows to find out the concentration and current density ranges for which the graphical method of transition time estimation gives correct results.

Establishing of the limit value for these parameters is of great importance in the application of any graphical method for transition time determination. The graphical methods are convenient because they are simple, fast and they do not require accurate potential measurements, but only time measurements.

Revue Roumaine de Chimie, **19**, *2*, 207–212 (1974)

TRANSFORMATION OF THE TOLUENE-WATER MIXTURE IN THE HIGH FREQUENCY DISCHARGE PLASMA. I

G. BOURCEANU, GH. POPA, M. SANDULOVICIU and V. ABABI

Laboratory of Chemical Technology, "Al. I. Cuza" University,
Jassy, Calea 23 August 11, Romania

Received February 2, 1973

Using the high frequency discharge plasma, the transformation of the toluene-water mixture was investigated. The experiments carried out with a small power oscillator led to a slight transformation degree of toluene. On the basis of the experimental results a series of theoretical considerations on the reactions mechanism have been made.

In the recent years plasma has played an even greater role in the modern chemical technology. By means of plasma, the realization of many chemical reactions as acetylene manufacture,[1–3] hydrocyanic acid manufacture,[4] etc. that require high temperatures, has become possible.

Plasma is not only used for the realization of the chemical reactions which do not take place in usual conditions, but it is used too in the case of those reactions for which the presence of plasma leads to the increasing of their yields. Thus, Leuthner[5] succeeded in preparing dicyanogen in a nitrogen plasma jet using a consumable graphite cathode. Those reactions cited above are carried out in the arc discharge plasma, i.e. in isothermal plasma at high temperature, where the cause of the chemical reactions development is heat generation.

There are known a series of reactions which take place more intensively and selectively in those forms of discharges in which the heat generation is minimum. In this case, the influence of discharge on the chemical reactions development is the direct action of the electrons from

---

[1] H. W. Leuthner and C. S. Stokes, *Ind. Eng. Chem.*, **53**, 341 (1961).

[2] Patent U. S., 3,051,639, 1962; *Chem. Abstr.*, **58**, 7778 (1964).

[3] R. F. Baddour and J. L. Blanchet, *Ind. Eng. Chem. Process Design and Develop.*, **3**, 258 (1964).

[4] J. Scrizarc and W. Jaskovski, *Ind. Eng. Chem. Process Design and Develop.*, **4**, 371 (1965).

[5] H. W. Leuthner, *Ind. Eng. Chem. Process Design and Develop.*, **1**, 166 (1962).

the discharge plasma on the reactant molecules. Comparison of the critical velocities of the electrons with the excitation and ionization potential of the molecules shows, indeed, the formation of excited and ionized particles. Such types of reactions are met into the high frequency discharges, luminescence, microwaves, etc.[6-8] In the present paper we have studied the transformation that takes place with the toluene-water mixture in the high frequency discharge plasma.

EXPERIMENTAL

The discharge was obtained using a high frequency electromagnetic field in a Jena glass tube (3 cm in diameter) placed inside of the oscillator coil. The device sketch is presented in fig. 1.

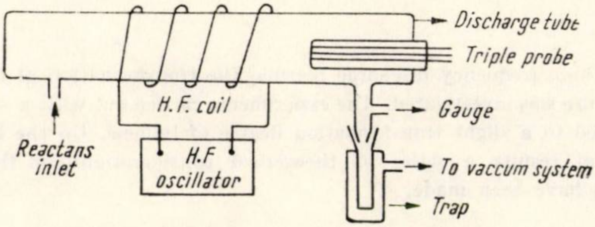

Fig. 1. — Scheme of the installation.

The oscillator power was 20 W and the frequency of the field was about 20 MHz. The reactant mixture toluene-water was fed in continuous stream. The pressure of the gaseous mixture from the discharge tube was measured by means of a differential manometer with silicone oil placed very close to the discharge zone. The condensable part of the reaction products, in given conditions of temperature and pressure, was captured by two trapes cooled with liquid nitrogen.

Analysis of products. The mixture containing the liquid and gaseous products obtained from reaction was analysed using the chromatography in gaseous phase. Carbowax-20 M and Apiezon L Grease were used as stationary phases and hydrogen was used as carrier. In order to detect all components of the mixture, a large range of flow rates and temperatures were utilized. Their identification was made by comparison of the retention distance of the components in mixture with those of the pure components. In addition to this, the NMR and IR spectra in solution of CCl_4 were carried out.

On the basis of analytical investigation, benzene, ethylbenzene, benzyl alcohol, phenol, diphenylmethane and dibenzyl were identified in the liquid phase. Ethane, ethylene and acetylene were identified in the gaseous phase.

The conditions of experiments and the composition of the obtained products, expressed in percent, are summarized in table 1.

---

[6] F. Le Goff, *J. Chim. phys.*, **65**, 883 (1968).
[7] F. Le Goff, *J. Chim. phys.*, **66**, 386 (1969).
[8] A. Streitwiser and H. R. Ward Jr., *J. Amer. Chem. Soc.*, **85**, 539 (1963).

Table 1

The experimental conditions and composition of the products obtained

Experiment run Parameters	1	2	3
Oscillator power, W	20	20	20
Flow rate of toluene, mol/h	0.015	0.018	0.036
Flow rate of water, mol/h	0.036	0.026	0.050
Pressure inside of the discharge tube, Torr	$9.8 \cdot 10^{-1}$	$9.1 \cdot 10^{-1}$	$8.4 \cdot 10^{-1}$
Toluene	80	82	86
*Benzene	40	39	38
*Ethylbenzene	30	30	28
*Benzylalcohol	5	5	6
*Phenol	3	4	4
*Diphenylmethane	8	8	10
*Dibenzyl	13	14	14
Ethane	45	46	44
Ethylene	16	15	16
Acetylene	24	23	25

* Percentages of these products are accounted in the liquid without toluene.

DISCUSSION

From theoretical point of view, it is interesting to know the transfer model of the electron energy to toluene or water molecule. Since, in plasma more complex processes take place, there are more possibilities of the energy transfer between species of the plasma, so that many types of intermediaries can occur. The primary processes that are responsible for the nature of the products obtained from reaction are of interest in these conditions.

Taking into account the obtained products as well as their proportion, two modes of the electron energy transfer are possible. One is referring to the fact that after electron-molecule collision, the molecule becomes excited and a radicalic breaking takes place. The other type of transfer should be by electron capturing.

The first hypothesis is based on the fact that the bond energy of $\gg C-CH_3$ is about 3.8 eV, whereas for the C—H bond from methyl groups, the bond energy is only 3.3 eV.[9,10] Assuming that the electrons distribution according to their energies is a Maxwellian one, it was found by means of triple probe [11] that mean energy of the electrons is 1.5 eV. Therefore, a part of these electrons of plasma, for which by means of the same method, it was found that they have a concentration of 10^8 cc^{-1}, will have an energy that ranges between 3.3—3.8 eV. In the favour of the first hypothesis pleads the fact that the maximum collision probability of the electrons with the molecule of toluene corresponds

---

[9] M. Szware, *J. Chem. Phys.*, **16**, 128 (1948).

[10] D. O. Schissler and D. P. Stevensons, *J. Chem. Phys.*, **22**, 151 (1954).

[11] Sin-Li Chen and T. Sekiguchi, *J. Appl. Phys.*, **36**, 2363 (1965).

to an electron energy of about 2 eV,[12] which is comparable with the mean energy of the plasma electrons. In this case, collisions of the electrons with the molecules of toluene lead to the following type of energy transfer :

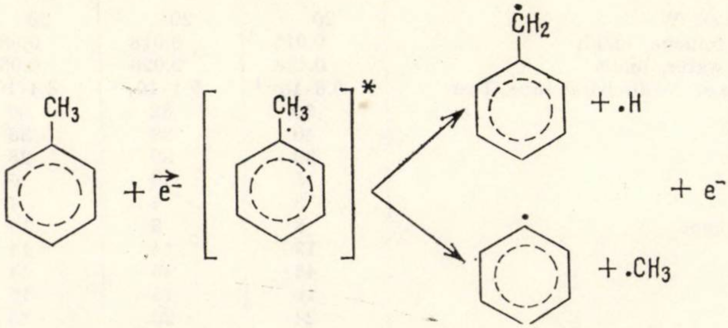

(1)

Since the energy of the C—H bond from methyl groups is weaker it is expected that benzyl radicals may occur in a larger proportion. The experimental data have confirmed this observation.

In the case of the water molecule, the maximum of the collision probability corresponds to an energy of 3.5 eV,[12] i.e. much larger than the mean energy of the electrons from plasma. Also, the energy of the H—O bond from the water molecule being 4.7 eV,[13] we consider that breaking takes place at radicals as follows :

$$\mathrm{H{-}OH} + \vec{e}^{\,-} \rightarrow \mathrm{H.} + \mathrm{.OH} + e^{-} \tag{2}$$

but in a less proportion. This fact is confirmed by the presence of small quantities of phenol and benzyl alcohol formed.

The radicals formed initially can generate the following reactions :

$$2\mathrm{C_6H_5{-}CH_2.} \rightarrow \mathrm{C_6H_5{-}CH_2{-}CH_2{-}C_6H_5} \tag{3}$$

$$\mathrm{C_6H_5{-}CH_2.} + \mathrm{.CH_3} \rightarrow \mathrm{C_6H_5{-}CH_2{-}CH_3} \tag{4}$$

$$\mathrm{C_6H_5{-}CH_2.} + \mathrm{.C_6H_5} \rightarrow \mathrm{C_6H_5{-}CH_2{-}C_6H_5} \tag{5}$$

$$\mathrm{C_6H_5{-}CH_2.} + \mathrm{.OH} \rightarrow \mathrm{C_6H_5{-}CH_2{-}OH} \tag{6}$$

$$\mathrm{C_6H_5.} + \mathrm{.H} \rightarrow \mathrm{C_6H_6} \tag{7}$$

$$\mathrm{C_6H_5.} + \mathrm{.OH} \rightarrow \mathrm{C_6H_5{-}OH} \tag{8}$$

---

[12] S. C. Brown, "Basic Data of Plasma Physics", Chap. I, M.I.T. Press, Massachusetts, 1959.

[13] L. Pauling, "The Nature of Chemical Bond" (3rd edition), Cornell, Ithaca, 1960, p. 262.

Ethane is obtained by unifying two $.CH_3$ radicals. Ethylene and acetylene form through symmetrical recombination of the $:CH_2$ and $\vdots CH$ radicals, respectively, these being formed from the decomposition of the $.CH_3$ radicals. This decomposition of $.CH_3$ was pointed out by I. A. Schneider[14] studying the decomposition of methane.

But, the $:CH_2$ radical can also be generated from the benzyl radical decomposition :

$$C_6H_5{-}CH_2. \longrightarrow C_6H_5. + :CH_2 \qquad (9)$$

The second possible transfer type of the electrons energy to the molecule of toluene, electrons capturing, is based on the fact that the affinity for electrons of the aromatic molecule, theoretically accounted, is −1.6 eV,[15] i.e. it is very close to the mean energy of the electrons from plasma for which this is 1.5 eV. In this case, the toluene molecule catches an electron and generates an anion.

The dissociative capturing should be the most possible path of the negative ions formation, when the delivered energy by the attached electron at the toluene molecule leads to such a high increase of the vibration energy of the molecule so that the excited anion molecule of toluene dissociates according to the mechanism :

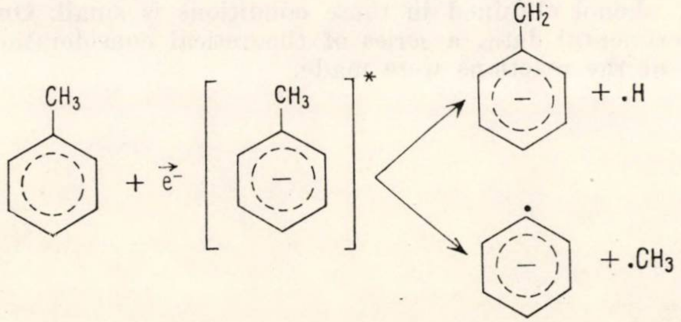

10

The following question must obviously be risen up. How can be explained that anion-radicals can generate a molecule, e.g. of dibenzyl? We have not enough data for the calculation of the energy which should be changed when, e.g., a molecule of dibenzyl is formed from two anion-benzyl radicals in order to establish if such a reaction is or not possible.

The hypothesis referring to the formation of such anion-radicals is emphasized by two arguments. The first argument is that the affinity of the aromatic molecule is −1.6 eV. The second argument starts from the observation that easier will react an anion-radical with one radical than with two radicals, because the anion-radical is more instable. The last argument is confirmed too by the larger quantity of benzene and ethylbenzene which can be generated from the following reactions:

---

[14] I. A. Schneider, *Z. phys. Chem.* (Leipzig), **220**, 199 (1962).

[15] R. S. Parr, "The Quantum Theory of Molecular Electronic Structure", W. A. Benjamin Inc., New York, 1964, p. 74.

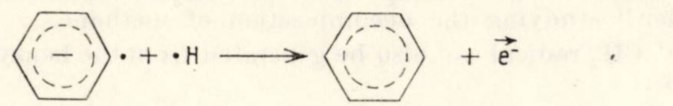

(11)

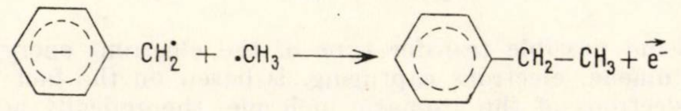

12

Dibenzyl and all others components will be generated analogously.

CONCLUSIONS

In the given conditions, it was obtained a small transformation degree of toluene, because the oscillator power was small.

Since the breaking energy of the H–O bond of water molecule is 4.7 eV and only a small portion of electrons had such energy, the quantity of phenol obtained in these conditions is small. On the basis of the experimental data, a series of theoretical considerations on the mechanism of the reactions were made.

Revue Roumaine de Chimie, **19**, *2*, 213–232 (1974)

CARBONIUM ION REACTIONS. IX*

SYNTHESIS AND ACETOLYSIS OF 2:3.5:6-DIBENZOBICYCLO[5.1.0]OCTA-2.5-DIEN-4-YL-METHYL TOSYLATE AND 2:3.5:6-DIBENZOBICYCLO[5.1.0]OCTA-2.5-DIEN-4-YL-ETHYL-β-TOSYLATE

ANCA BANCIU, M. ELIAN, AURORA BUCUR, DOINA GEORGESCU, ECATERINA CIORĂNESCU and C. D. NENITZESCU **

Centre of Organic Chemistry, Bucharest, Spl. Independenţei 202-B, Romania

Received September 15, 1973

The 2:3.5:6-dibenzobicyclo [5.1.0] octa-2.5-dien-4-yl-methyl tosylate (**14a**) and 2:3.5:6-dibenzobicyclo [5.1.0] octa-2.5-dien-4-yl-ethyl-β-tosylate (**14b**) were synthesized and solvolyzed in order to investigate the possibility of nucleophilic participation of the remote cyclopropyl ring. The main product (94.5%) of the buffered acetolysis of **14a** is the ring-enlarged alcohol *trans*-**28**; the reaction is highly stereospecific. The unbuffered acetolysis as well as the buffered formolysis yield, with shorter reaction times, the two epimers *trans*- and *cis*-**28**, which subsequently undergo elimination leading to hydrocarbon **27**. The stereospecificity of the buffered acetolysis may be accounted for by the intervention of a phenonium ion. In the unbuffered acetolysis of **14b**, besides the unrearranged alcohol **35**, two products of cyclopropyl ring opening **38** and **39** were identified. The lack of cyclopropyl participation (as shown also by kinetic measurements) is ascribed — in the case of **14a** — to the competition with the strong stabilizing influence of the aromatic ring, whereas in the case of **14b** to the unfavourable geometric conditions for interaction between the cationic center and the cyclopropane orbitals.

In the last years the solvolytic nucleophilic participation of remote cyclopropyl ring was extensively investigated.[1–8] Comparisons with double bond participation were also made on the basis of the known resemblance in some properties between double bond and cyclopropyl ring.

---

* Part VIII. I. Drăguţan, C. Drăghici, A. Haneş, A. Dumitriu, E. Ciorănescu and C. D. Nenitzescu, *Rev. Roumaine Chim.*, **19**, 67 (1974).

** Deceased, July 28, 1970.

[1] see for example in: M. T. Rogers and J. D. Roberts, *J. Amer. Chem. Soc.*, **68**, 843 (1946); R. H. Eastman and S. K. Freeman, *J. Amer. Chem. Soc.*, **77**, 6642 (1955); R. Fuchs, Ch. A. Kaplan, J. J. Bloomfield and L. F. Hatch, *J. Org. Chem.*, **27**, 733 (1962); A. Banciu, *Studii şi Cercetări Chim. Acad. Bucureşti*, **21**, 535 (1973).

Theoretical calculations[2] indicated that in some cases cyclopropyl participation could be more important than double bond participation. Such comparisons have shown in many cases a very different behaviour *e.g.*: cyclopropyl participation in compound **1**[3] is much stronger than double bond assistance in **2** (the rate ratio being 10^3), but in other systems such as **3**[4] the important participation of the cyclopropyl ring is however inferior as compared to the double bond effect in **4** (the rate ratio of the order 10^{-2}).

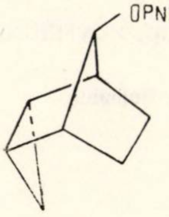

1

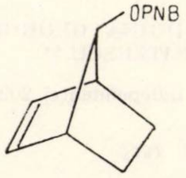

2

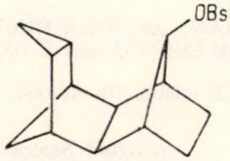

3

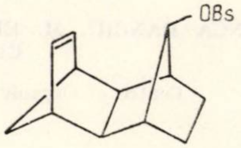

4

From the examples described in the literature some general conclusions could be drawn. The steric factors have a decisive influence on cyclopropyl participation. Due to the great difference between edge- and face-reactivity, the cyclopropane ring must be so oriented that an edge-participation be accomplished. Such a participation is greater when the interaction with the cationic *p*-orbital is symmetrical at both ends of the cyclopropyl bond (greater participation in the case of system **5** in comparison with **6**) and whenever during the ionization the distance between interacting orbitals is diminished (*e.g.* **1** in opposition to **7**[5]). The geometric requirements for overlap between cyclopropane orbitals and the vacant *p*-orbital are more strict than in the case of double bond

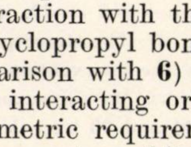

5

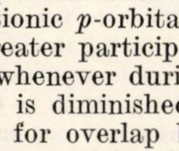

6

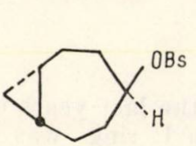

7

---

[2] R. Hoffmann, *Tetrahedron Letters*, **1965**, 3819.

[3] H. Tanida, T. Tsuji and T. Irie, *J. Amer. Chem. Soc.*, **89**, 1953 (1967); M. A. Battiste, C. L. Deyrup, R. E. Pincock and J. Haywood-Farmer, *J. Amer. Chem. Soc.*, **89**, 1954 (1967); J. S. Haywood-Farmer and R. E. Pincock, *J. Amer. Chem. Soc.*, **91**, 3020 (1969).

[4] M. A. Battiste, J. Haywood-Farmer, H. Malkus, P. Seidl, S. Winstein, *J. Amer. Chem. Soc.*, **92**, 2144 (1970).

[5] P. G. Gassman, J. Seter, F. J. Williams, *J. Amer. Chem. Soc.*, **93**, 1673 (1971).

participation. In some rigid bi- and polycyclic systems like **1**,[3] **3**,[6] **6**,[7] such favourable arrangements can be realized and maintained.

The release of the ring strain and the formation of unusually stable intermediates, *e.g.* trishomocyclopropenylium cations **8** and **9** or dibenzohomotropylium cation **10** explain the cyclopropyl participation in the solvolyses of the parent compounds **11**,[8] **1** and **12**, respectively.[9]

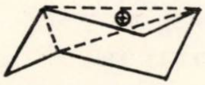

8

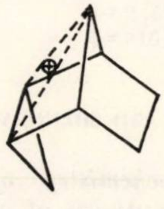

9

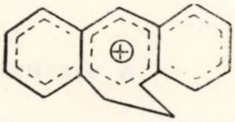

10

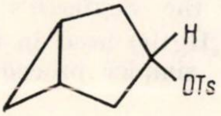

11

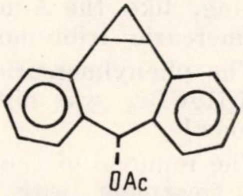

12

Previous work in this laboratory has evidenced limited transannular participation (6.5–8.5%) of the double bond in the system **13a**[10] and a considerable participation (>90%) in the solvolyses of the homologous tosylate **13b**.[11]

In the present paper we report the synthesis of tosylates **14a** and **14b** and the study of their solvolyses products.

---

[6] R. M. Coates and J. L. Kirkpatrick, *J. Amer. Chem. Soc.*, **90**, 4162 (1968); R. M. Coates and J. L. Kirkpatrick, *J. Amer. Chem. Soc.*, **92**, 4883 (1970).

[7] W. G. Dauben and C. H. Schallhorn, *J. Amer. Chem. Soc.*, **93**, 2254 (1971).

[8] S. Winstein and J. Sonnenberg, *J. Amer. Chem. Soc.*, **83**, 3244 (1961).

[9] a) R. F. Childs and S. Winstein, *J. Amer. Chem. Soc.*, **89**, 6348 (1967); b) R. F. Childs, M. A. Brown, F. A. L. Anet and S. Winstein, *J. Amer. Chem. Soc.*, **94**, 2175 (1972).

[10] a) E. Ciorănescu, A. Bucur, F. Badea, M. Rentzea and C. D. Nenitzescu, *Tetrahedron Letters*, **1969**, 1867; b) E. Ciorănescu, A. Bucur, M. Elian and C. D. Nenitzescu, *Rev. Roumaine Chim.*, **10**, 149 (1965).

[11] a) E. Ciorănescu, M. Banciu, R. Jelescu, M. Rentzea, M. Elian and C. D. Nenitzescu, *Rev. Roumaine Chim.*, **14**, 911 (1969); b) E. Ciorănescu, M. Banciu, R. Jelescu, M. Renzea, M. Elian and C. D. Nenitzescu, *Tetrahedron Letters*, **1969**, 1871.

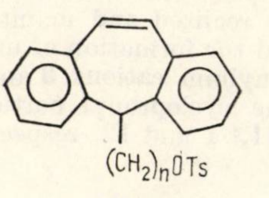

13 (a) n = 1
(b) n = 2

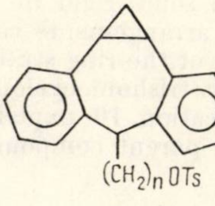

14 (a) n = 1
(b) n = 2.

A. SYNTHESIS AND SOLVOLYSIS OF TOSYLATE 14a

Synthesis and stereochemistry of the starting compounds. The starting materials in the synthesis of alcohol **15** were the dibenzocycloheptatrienyl compounds **18**[12] or **19**.[13] The cyclopropylation after usual methods (Simmons-Smith [14] or with chloroform and potassium-*t*-butoxide [15]) failed. A similar behaviour was observed by Winstein and co-workers [9] in the case of related compounds. The esters **16** and **17** were obtained * using, like the American authors, dibromocarbene generated from phenylmercuric tribromomethane after the Seyferth's procedure. [16,17]

The phenylmercuric bromide (C_6H_5HgBr) used in the preparation of $C_6H_5HgCBr_3$ was obtained after a simpler procedure [18] than the usual one.[17]

The removal of geminal bromine atoms from **16** and **17** was achieved by treatment with $LiAlH_4$ in tetrahydrofurane,[19] which leads to alcohol **15**. The subsequent treatment with tosyl chloride afforded the tosylate **14a**.

The IR, NMR spectra and elemental analyses (see Experimental) are in agreement with the structures **14a**, **15**, **16** and **17**.

The stereochemistry of the dibenzobicyclo[5.1.0]octadiene system **21**** was discussed by Winstein and co-workers [9b] in the course of their study of dibenzohomotropylium cation **10**. The American authors have shown that, from the two possible boat forms **21a** and **21b**, the one

---

* The direct addition of : CBr_2 to alcohol **20** gave unsatisfactory results.

[12] J. Rigaudy and P. Tardieu, *Compt. rend*, **248**, 1538 (1959).

[13] G. Berti, *Gaz.*, **87**, 293, 305 (1957) ; M. A. Davis, J. D. Winthrop, R. A. Thomas, T. Herr, M. P. Charest and N. Gaudry, *J. Med. Chem.*, **7**, 881 (1964).

[14] H. E. Simmons, R. D. Smith, *J. Amer. Chem. Soc.*, **81**, 4256 (1959).

[15] W. E. Doering, A. K. Hoffmann, *J. Amer. Chem. Soc.*, **76**, 6162 (1954).

[16] D. Seyferth, J. M. Burtlich, R. J. Minasz, Y. Yick-Pui Mui, H. D. Simmons Jr., A. J. H. Treiber and S. R. Dowd, *J. Amer. Chem. Soc.*, **87**, 4259 (1965).

[17] D. Seyferth and J. M. Burtlich, *Journal of Organometal. Chem.*, **4**, 127 (1965) ; D. Seyferth and R. L. Lambert Jr., *Journal of Organometal. Chem.*, **16**, 21 (1969).

[18] C. D. Nenițescu, D. Isăcescu, G. Gruiescu, *Bulet. Soc. chim. Romania*, **20**, 127 (1938).

[19] H. Yamanaka, K. Teramura and T. Ando, *Chem. Comm.*, **8**, 380 (1971).

** The *Chem. Abstr.* name of this system is : dibenzo[a,e] cyclopropa[c]cycloheptene.

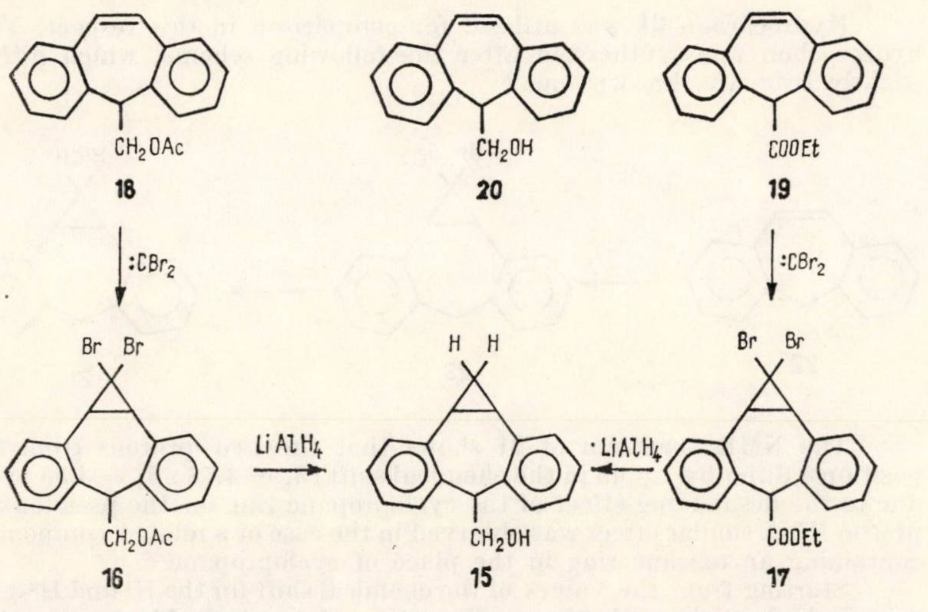
CH$_2$OAc
18
CH$_2$OH
20
COOEt
19
:CBr$_2$
:CBr$_2$
Br Br
H H
Br Br
LiAlH$_4$
LiAlH$_4$
CH$_2$OAc
16
CH$_2$OH
15
COOEt
17

in which the cyclopropane ring is pseudoequatorial (21a) is preferred.

Having in view the importance of stereochemical factors in the

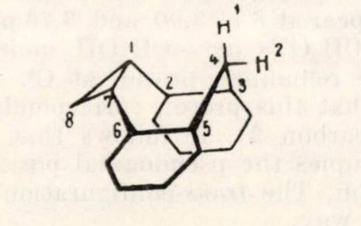
H
1
H
2
1
4
2
3
7
8
6
5

21 a

≡

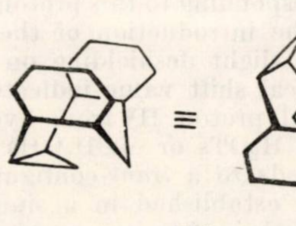

21 b

solvolytic behaviour of **14a**, a discussion of the conformation of this compound, which can exist in the form of the two *cis-trans* diastereoisomers, seems necessary.

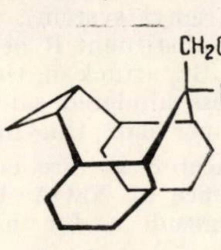

14 a (trans)

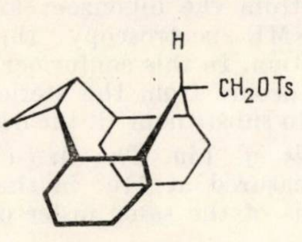

14 a (cis)

Hydrocarbon **21** was utilized for comparison in this respect. This hydrocarbon was synthesized after the following scheme, which differs slightly from the known one.[9b]

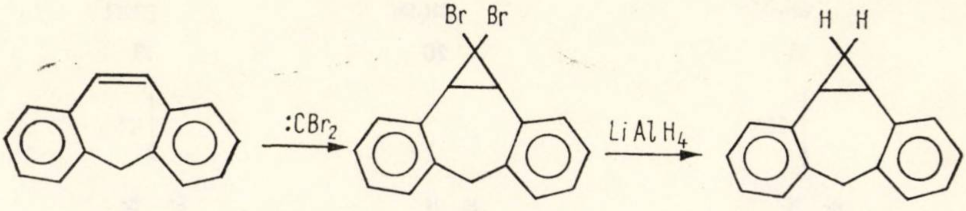

22 **23** **21**

The NMR spectrum of **21** shows that the two protons from the position 4 differ by 1 ppm in the chemical shift ($\delta_1 = 4.78$; $\delta_2 = 3.56$ ppm) due to the deshielding effect of the cyclopropane ring on the pseudoaxial proton H^1. A similar effect was observed in the case of a related compound, containing an oxirane ring in the place of cyclopropane.[20]

Starting from the values of the chemical shift for the H^1 and H^2-protons in hydrocarbon **21**, the configuration of tosylate **14a** or of other compounds resulting formally by the replacement of a proton with an R radical, may be established by taking into account the chemical shift of the remaining proton at C^4. In the tosylate **14a** and alcohol **15** the signals corresponding to this proton appear at $\delta = 3.90$ and 3.76 ppm, respectively. The introduction of the $-CH_2OTs$ or $-CH_2OH$ moieties must lead to a slight deshielding on the remaining proton at C^4. The observed chemical shift value indicates that this proton corresponds to pseudoequatorial proton H^2 from hydrocarbon **21**. It follows that the substituent ($-CH_2OTs$ or $-CH_2OH$) occupies the pseudoaxial position, which corresponds to a *trans*-configuration. The *trans*-configuration for **16** and **17** was established in a similar way.

The formation of only one of the two possible diastereoisomers, namely the *trans*-one, in the addition of :CBr$_2$ to compounds of the type **18** and **19**, could be explained by the preferred conformation of the starting compounds. Indeed, in the case of compounds **18** and **19** (and in other analogous compounds in which the substituent is separated by one C atom from the dibenzocycloheptatrienyl system), it was proved by dynamic NMR spectroscopy * that the substituent R occupies mainly the *axial* position. In this conformer the : CBr$_2$ attack on the middle-ring double bond occurs from the sterically less hindered side, namely the side opposed to substituent R, the *trans*-isomer being thus formed.

Solvolysis of **14a**. The first-order acetolysis rate constant (titrimetrically measured at 110° in the presence of NaOAc-buffer) of the tosylate **14a** is of the same order of magnitude as for the unsaturated tosylate **13a**.[21] Both rate constants are smaller than those of the saturated analog **26**, due to the rate-retarding effect of the double bond or of the cyclopropane ring, the latter exerting an inductive effect analogous to that of the double bond.

---

* Unpublished results obtained in this laboratory.

[20] R. R. FRASER and R. M. RENAUD, *Canad. J. Chem.*, **49**, 746 (1971).

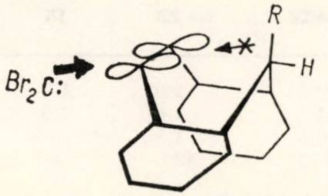

24

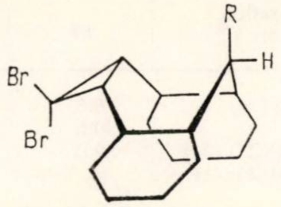

25 (trans)

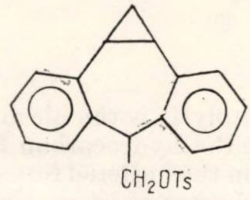

14a

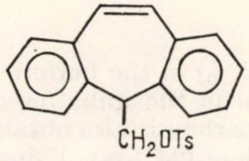

13a

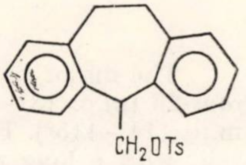

26

$k^{110°}_{AcOH+AcONa}$ $2.33 \times 10^{-5}\ s^{-1}$ $5.40 \times 10^{-5}\ s^{-1}$ $10.70 \times 10^{-5}\ s^{-1}$

In the case of tosylate **14a**, the degree of cyclopropyl participation (if any) seems to be smaller than that of double bond participation in **13a**, if one takes into account that it is solvolyzed two times slower than **13a**. (The double bond participation during the solvolyses of **13a** was proved by isolation of bridged products, 6.5–8.5% [10a]).

The acetolyses of **14a** were performed at reflux for 24 hrs with or without added NaOAc. The formolyses were carried out in the presence of sodium formate (at 100°) because in unbuffered solutions polymeric materials were soon formed (10% after 1 hr).

The solvolysis products (95% yield) were v.p.c.-analysed after $LiAlH_4$-reduction (table 1).

The results presented in table 1 show that the buffered as well as the unbuffered acetolysis of **14a** is accompanied by a middle ring

---

[21] E. Ciorănescu, A. Bucur, M. Elian, M. Banciu and C. D. Nenitzescu, *Rev. Roumaine Chim.*, **10**, 161 (1965).

Table 1

Solvolysis products of 14a (v.p.c. analysis after $LiAlH_4$ – reduction)

Conditions solvent, reflux (time, hrs.)	% Compounds				
	27	*trans*-**28**	*cis*-**28**	**15**	Other compounds
AcOH (NaOAc) (24)	0.5	94.5	2.0	1.5	1.5
AcOH (24)	90.5	4.5	4.0	1.0	—
HCOOH (NaOOCH) (24)	89.0	0.5	1.5	—	9.0
HCOOH (NaOOCH) (1)	—	54.5	43.5	—	2.0

enlargement through which the bicyclo[5.1.0]octanic system **14a** rearranges to the bicyclo[6.1.0]nonanic system.

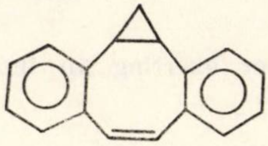

27

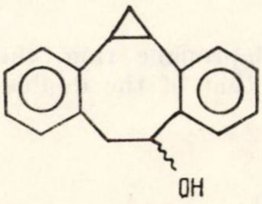

28

The major product (94.5%) in the buffered acetolysis is the alcohol *trans*-**28** (m.p. 131—133°) and in the unbuffered one the hydrocarbon **27** (m.p. 114—115°). This hydrocarbon is also obtained in the buffered formolysis, with a long reaction time (24 hrs). Using a shorter reaction time (1 hr) the product of the formolysis consists of a mixture of the two alcohols *trans*-**28** and *cis*-**28**.

The figures from the last column in table 1 represent the amount of 3—4 components with different v.p.c. retention times, which could not be identified.

The structure of the hydrocarbon **27** results from the elemental analysis, IR and NMR spectra. The catalytic hydrogenation affords the hydrocarbon **29** (m.p. 84—85°).

The alcohols **28** contain the same skeleton as the hydrocarbon **27**. The oxidation of the mixture of the two diastereoisomeric alcohols **28** (table 1, entry 4) with the Jones-reagent [22] affords the ketone **30** whose Wolff-Kishner-reduction gives rise to hydrocarbon **29**, identical with that obtained by hydrogenation of **27**.

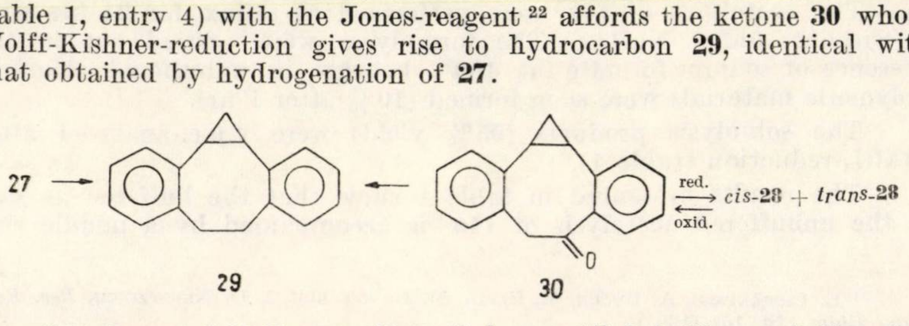

---

[22] K. Bowden, I. M. Heilbron, E. R. H. Jones and B. L. L. Weedon, *J. Chem. Soc.*, **1946**, 39; A. Bowers, T. G. Halsall, E. R. H. Jones and A. J. Lemin, *ibid.*, **1953**, 2555.

$NaBH_4$-reduction of ketone **30** affords a mixture of two epimeric alcohols **28** (*trans*/*cis* = 39/61). From this mixture the alcohol *cis*-**28** (m.p. 146–148°) was isolated by preparative v.p.c.

As in the case of the system **21** it is plausible that only one of the two boat conformations of the system **28** (pseudoequatorial cyclopropane) is stable: the substituted derivatives also present *cis*-*trans* isomerism.

The configuration of the alcohols *cis*-**28** and *trans*-**28** was established by examination of their NMR spectra recorded in the presence of tris-(dipyvaloilmethanato) europium(III), $Eu(DPM)_3$[23]. In the spectrum of one of the isomers (*cis*-**28**), one of the aromatic protons rapidly shifts on addition of europium shift reagent. In the spectrum of the other

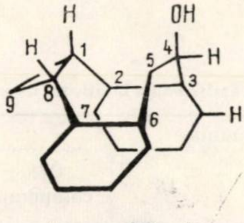

trans - **28**

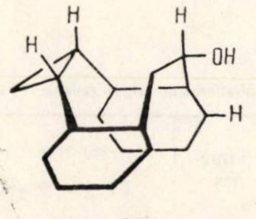

cis - **28**

somer (trans-**28**) the shift of the corresponding aromatic proton is less pronounced; however, one of the cyclopropane protons (from the position 1) is strongly influenced by $Eu(DPM)_3$ addition.

DISCUSSION

Two results from table 1 need special comment.

We shall first consider the formation of 94.5% alcohol *trans*-**28** and only 2% isomeric alcohol *cis*-**28** in the buffered acetolysis (neutralization of the resulting TsOH). For a discussion about the mechanism of the solvolysis of **14a** it would be useful to know precisely if the *trans*-isomer is the primary reaction product or if *cis*-**28** was initially formed (in addition to *trans*-**28** or as single product) and then rearranged to the *trans*-epimer.

In a control experiment, in which each alcohol (*cis* or *trans*) was heated under the conditions used for buffered acetolysis (acetic acid – NaOAc, 24 hrs, reflux), the starting compounds were recovered unchanged. The analysis of the buffered acetolysis product after a short reaction time (1–4 hrs) indicated that the *cis*-isomer was not formed in more than 1.5% yield (the remaining products were the *trans*-isomer and unreacted tosylate). We may conclude that the *trans*-isomer is the primary product in the buffered acetolysis and that no epimerization of the alcohols occurred under these conditions.

---

[23] C. C. Hinckley, *J. Amer. Chem. Soc.*, **91**, 5160 (1969); J. K. M. Sanders, D. H. Williams, *Chem. Comm.*, **1970**, 422.

Another striking result appearing in table 1 is the formation of a 54.5 : 43.5 mixture of *cis*- and *trans*-**28** alcohols in the buffered formolysis of **14a**, after a short reaction time (1 hr). It was observed [10a] that in some cases the formic acid, even in the presence of HCOONa-buffer (neutralization of the TsOH formed), is strong enough to lead to similar reaction products as in the unbuffered acetolysis. Consequently, some unbuffered acetolyses were performed at short reaction time. The results of such determinations (table 2) indicate that after 1 hr, or even after 7 hrs (reflux), the reaction product contains both *cis* and *trans*-**28** isomers, besides the alkene **27**. The latter becomes the main component of the reaction mixture after 24 hrs.

Table 2

Unbuffered acetolysis products of 14 a (118°; v.p.c. analysis after $LiAlH_4$-reduction)

Time hrs	% Compounds				
	27	*trans*-**28**	*cis*-**28**	**15**	Other compounds
1	3.5	9.0	7.5	77.0	3.0
5	14.0	8.0	36.0	38.0	4.0
7	31.5	7.5	29.5	29.0	2.5
24	90.0	3.0	6.0	—	1.0

The starting alcohol **15**, registered in table 2, results from the unreacted tosylate **14a** during $LiAlH_4$-reduction; the $-CH_2OH$ group was not found to be further reduced to $-CH_3$. A similar behaviour was also observed in the case of other tosylates.[24]

The control experiments showed an interconvertibility of *cis*- and *trans*- alcohols under unbuffered acetolysis conditions. On treatment of the *trans*- alcohol (or more correctly, an acetolysis product containing 91% *trans*-**28**) with *p*-toluenesulphonic acid in refluxing acetic acid, both isomers (*cis* and *trans*) were observed even after 1 hr (table 3). The alkene **27** occurs in steadily greater proportions, becoming the main component after 10 hrs. The figures from the last column (table 3) correspond to small amounts of starting alcohol (1–2%) besides 2–3 unidentified components. The *cis*- isomer was found te behave similarly; large amounts were recovered after short time as *trans*-isomer.

The practically quantitative formation of the alcohol *trans*-**28** during the buffered acetolysis of **14a** indicates that the reaction is highly stereospecific. An explanation of this behaviour must certainly be sought in the structure of the intermediates through which the rearrangement **14a** → *trans*-**28** occurs. The phenyl group assists from the back-side the ionization of the $-CH_2OTs-$group, situated in the favourable pseudoaxial position. The nucleophilic attack on the phenonium ion **31** which

---

[24] N. C. Gaylord, "Reduction with Complex Metal Hydrides", Interscience Publishers Inc., New York, N.Y., 1956, p. 866–872.

Table 3

Acid catalyzed * products of *trans*-28 and *cis*-28 (v.p.c.-analysis after $LiAlH_4$-reduction)

Starting alcohol	Time hrs	% Compounds			
		27	*trans*-**28**	*cis*-**28**	Other compounds
trans-**28**	—	1.0	91.0	1.0	7.0
	1	32.0	10.5	50.5	7.0
	2	45.0	9.5	40.5	5.0
	5	72.0	7.0	17.0	4.0
	10	90	2.5	5.0	2.5
cis-**28**	—	0.5	3	94	2.5
	1	12.0	29.0	54.5	4.5
	5	39.0	23.0	33.0	5.0

* *p*-TsOH in AcOH at 118°.

results could be realized only from the side originally occupied by the tosyl group.

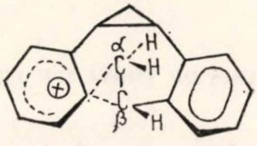

31

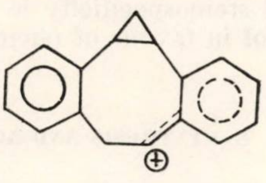

32

The examination of models indicated that the β-attack leads to a ring-enlarged product in which the substituent (—OAc) occupies a pseudoaxial position (*trans*-configuration), in agreement with the observed results.

The preferred β-attack could be due to the fact that the final eight-membered ring product is less strained than the seven-membered ring compound, which might result through α-attack.

The ring-enlargement could also occur through a benzylic ion **32**, resulted from **14a** by a simple Wagner-Meerwein rearrangement with phenyl migration. However, such an intermediate would yield a mixture of the two epimeric acetates *trans*- and *cis*-**28**-**OAc** (as the reduction of the ketone **30** gives rise to a 4 : 6 mixture of both alcohols).

The stereochemistry of the reaction product *trans*-**28** may be regarded as evidence for the intervention of phenonium ion.

The subsequent transformation of the primary solvolytic product *trans*-**28** is consistent with the intermediacy of a benzylic ion. In the presence of *p*-toluenesulphonic acid (unbuffered acetolysis) or formic acid (buffered formolysis), reionization of *trans*-**28**-**OAc** leads to the benzylic cation **32** which can subsequently yield both *trans*- and *cis*-**28** epimers.

This SN1 reaction is accompanied by an irreversible elimination reaction affording the alkene **27** which becomes, after a few hours, the main reaction product. The latter reaction makes difficult the determination of the equilibrium ratio of the two epimers.

The small amounts of *cis*-**28** alcohol and alkene **27** which appear even in the buffered acetolysis suggest also a rearrangement **31** → **32**. This rearrangement would proceed with a smaller rate than the collapse with $^{-}$OAc ion which yields **28-OAc**.

The *trans*-configuration of **14a**, having a pseudoaxial $-CH_2OTs$ group, is favourable to a cyclopropyl ring participation and the opening of this ring would diminish the ring strain in the skeleton. Nevertheless, the analysis of the solvolysis products indicates that this participation, if it occurs, is very feeble (some products of cyclopropyl participation could be found among the unidentified minor components — table 1, last column). It must be mentioned here that even in the case of the related tosylate **13a** the double bond assistance is limited.[10a]

The stabilizing influence provided by the aromatic ring is more important than that of the cyclopropane ring and the formation of the phenonium ion **31** is favoured over that of other possible intermediates. The observed stereospecificity in the buffered acetolysis could be considered as a proof in favour of phenonium ion intervention.

B. SYNTHESIS AND ACETOLYSIS OF TOSYLATE 14b

Previous work carried out in this laboratory [11] showed that in the tosylate **13b** favourable conditions for interaction between cationic center and the median double bond exist; the ionization is assisted by the double bond, the bridged products representing 85% of the reaction products. By analogy, the lengthening of the side-chain could also have a favourable effect in the case of **14**. To substantiate this hypothesis the solvolytic behaviour of tosylate **14b** was examined.

The synthesis of dibenzobicyclo[5.1.0]octadien-4-yl-ethanol(**35**) by a similar method as that applied for **15** (the addition of $:CBr_2$ to dibenzocycloheptatrien-7-yl-ethylacetate (**33**) [11a]) proceeds with a low yield (18%).

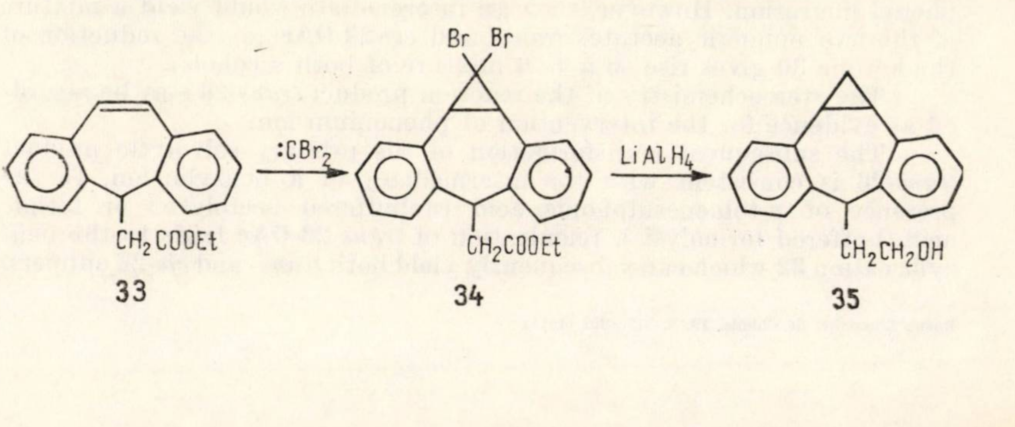

33 34 35

Better results (65%) were obtained by lengthening the side-chain of the tosylate **14a**, by usual procedures.

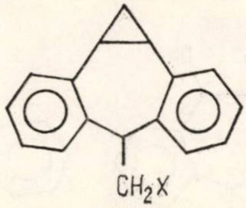

a) X = — CN
b) X = — COOH
c) X = — COOEt

36

The conversion of tosylate **14a** to the nitrile **36a** was effected on treatment with NaCN in DMSO. The hydrolysis of this compound and the subsequent esterification of **36b** and LiAlH$_4$-reduction of **36c** affords the alcohol **35**. The tosylate **14b** was obtained from **35** by a standard procedure. All the above compounds, including the tosylate **14b**, present the *trans*-configuration, as it results from the synthetic way.

The kinetic determination of the acetolyses of **14b** indicated rate constants of the order of magnitude 10^{-5}:

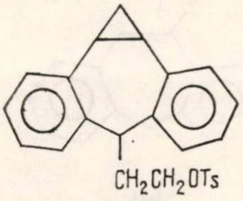

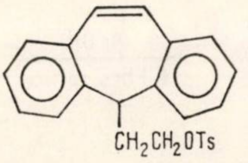

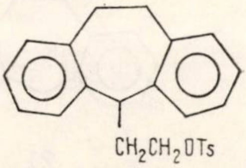

	14b	**13b**	**37**
$k^{110°}_{AcOH}$	$1.25 \times 10^{-5} s^{-1}$	$2.04 \times 10^{-4} s^{-1}$	$1.34 \times 10^{-5} s^{-1}$
$k^{110°}_{AcOH+AcONa}$	$1.87 \times 10^{-5} s^{-1}$	$2.17 \times 10^{-4} s^{-1}$	$1.47 \times 10^{-5} s^{-1}$

These rate constants are nearly equal to those of the saturated tosylate **37**, but visibly smaller than those of the unsaturated tosylate **13b**[25] or of other systems in which the double bond assistance was demonstrated.

The composition of the reaction mixture in the unbuffered acetolysis of **14b** (reflux for 60 hrs, about 10 half-lives) was v.p.c. determined after the LiAlH$_4$-reduction of the crude reaction product. Three major components were evidenced : the starting alcohol **35** (48%), the alcohol **38** (37%) and the diol **39** (12%), the remaining 3% representing unidentified components.

---

[25] M. Voicu and F. Badea, *Rev. Roumaine Chim.*, **14**, 929 (1969).

The compounds **38** and **39** were separated by preparative v.p.c. and their structures were tentatively assigned on the basis of NMR spectra in the presence of the shift reagent $Eu(DPM)_3$.

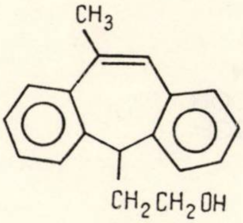

38

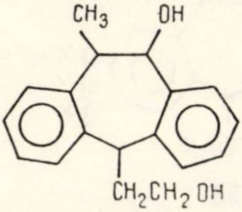

39

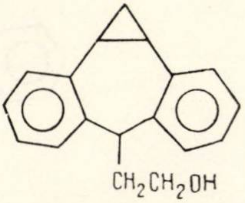

35

The compounds **38** and **39** were probably formed by the opening of the cyclopropane ring under the reaction conditions and not by cyclopropyl participation during solvolysis. Additional evidence was provided by the fact that the known [26] hydrocarbon **40** was formed on treating the hydrocarbon **21** under the same conditions as in the solvolysis of **14b**.

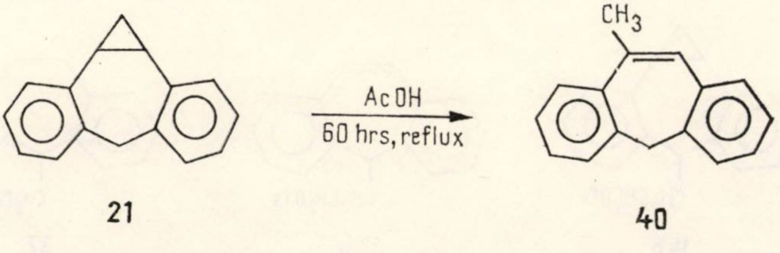

The acetolysis of **14b** using shorter reaction times (approx. 5 half-lives) yields the acetate of the unrearranged alcohol **35** in 93% yield.

In the buffered acetolysis of **14b** (5 or 10 half-lives) the same acetate of the starting alcohol was obtained in more than 90% yield.

The first question which may arise concerning the above mentioned solvolyses is why the tosylates **13b** and **14b** differ so significantly in their solvolytic behaviour; if in the first case, the double-bond assistance was proved by rate constants as well as by products, in the second case the elusive cyclopropyl participation could not be demonstrated by either of these criteria. Two explanations are available in this respect: (a) the more strict steric conditions necessary for cyclopropyl participation [4-6] as compared with double bond assistance and (b) the impossibility of the two carbon atom side-chain of tosylate **14b** to reach the conformation required for assistance. Indeed, in compound **14b** the two H-atoms dotted in the formulas are more oriented towards the median ring than the vinyl hydrogens of **13b**; it is thus plausible that the cyclopropane ring is not easily accesible to the$-CH_2OTs$ group.

---

[26] J. Rigaudy and P. Tardieu, *Compt. rend.*, **244**, 2939 (1957).

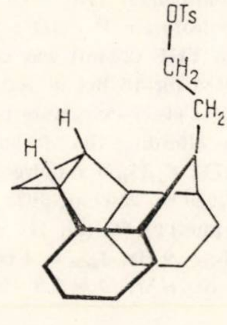

14b

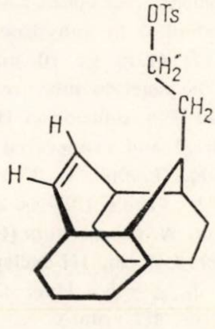

13b

EXPERIMENTAL

Melting points are uncorrected. IR spectra were recorded with a double-beam UR-20 Carl Zeiss Jena spectrophotometer. NMR spectra were obtained on a Varian A-60 A spectrometer using TMS as internal standard. The v.p.c. analyses were performed on a Carlo Erba model D gas chromatograph using Neopentylglycol succinate columns (3% on Chromosorb W), 2 m, at 205°, with a hydrogen rate-flow of 35 ml/min. The v.p.c. separations were carried out on a preparative Carlo Erba model GV chromatograph using silicone oil OV7 (20% on Chromosorb W), 1.25 m, 210°, with a hydrogen rate-flow of 100 ml/min.

The acetate of 2:3.5:6-dibenzo-8.8-dibromobicyclo[5.1.0]octa-2.5-dien-4-yl-methanol (**16**). A mixture of acetate **18** (6.6 g; 25 mmoles) and phenylmercuric tribromomethane (16 g; 30 mmoles)[16] in anhydrous benzene (30 ml) was heated with magnetic stirring at 85° for 3 hrs. The starting materials were rapidly dissolved and a precipitate of phenylmercuric bromide (m.p. 285–286°) was formed. The reaction mixture was cooled, then filtered and anhydrous ether (100 ml) was added to the filtrate. The solution was left overnight in a refrigerator and evaporated *in vacuo* after further filtration of some phenylmercuric bromide. The remaining material was easily crystallized by adding a few drops of methanol. The acetate **16** (6.5 g; 60%), m.p. 151–3° (methanol). (*Found*: C, 52.46; H, 3.80; Br, 36.71. $C_{19}H_{16}Br_2O_2$ requires C, 52.32; H, 3.69; Br, 36.64%). *IR spectrum* (CS_2; cm^{-1}): 762 vs, 784 vs, 1220 vs, 1742 vs, 3021 m, 3060 m. *NMR spectrum* ($CDCl_3$, δ ppm): 1.85 (s, 3H, $COCH_3$); 3.51 (s, 2H cyclopropyl); 3.90 (1H, Ar$CH$Ar, J = 8.15 Hz); 4.71 (m, 2H, J = 8.15 Hz); 7.1–7.6 (m, 8H arom.).

The phenylmercuric tribromomethane utilized in this reaction was prepared after Seyferth's procedure[17] and phenylmercuric bromide was obtained[18] from phenylmercuric acetate and NaBr.

2:3.5:6-Dibenzo-8.8-dibromobicyclo[5.1.0]octa-2.5-dien-4-yl-ethyl carboxylate (**17**). The addition of $:CBr_2$[16] to the ester **19** was performed in the same way as described for **16**. The ester **17** obtained in a 60% yield showed a m.p. 142–143° (ethanol). (*Found*: C, 52.59; H, 3.87; Br, 36.50. $C_{19}H_{16}Br_2O_2$ requires C, 52.32; H, 3.69; Br, 36.64. *IR spectrum* (CS_2;

cm^{-1}) : 723 s, 752 s, 1030 s, 1201 vs, 1741 vs, 2980 m, 3024 m, 3070 w. *NMR spectrum* ($CDCl_3$; δ ppm) : 1.19 (t, 3H, J = 7 Hz) ; 3.34 (s, 2H cyclopropyl) ; 4.19 (q, 2H, J = 7 Hz) ; 4.49 (s, 1H, ArC*H*Ar) ; 7.1–7.5 (m, 8H arom.).

2 :3.5 :6-Dibenzobicyclo[5.1.0]octa-2.5-dien-4-yl-methanol (**15**). To a suspension of $LiAlH_4$ (1.90 g ; 50 mmoles) in anhydrous tetrahydrofurane [19] (THF ; 15 ml) a solution of acetate **16** (or ester **17**) (4.36 g ; 10 mmoles) in THF (25 ml) was added dropwise with stirring during 1 hr. The reaction mixture was heated for 16 hrs at reflux, then cooled and decomposed with a cold 10% solution of H_2SO_4. After ether-extraction the organic layer was washed with water, dried and evaporated *in vacuo* affording the alcohol **15**, (2.2 g ; 93 %), m.p. 87–89° (*n*-hexane). (*Found* : C, 86.34 ; H, 6.74 ; $C_{17}H_{16}O$ requires C, 86.40 ; H, 6.82). *IR spectrum* (CS_2 ; cm^{-1}) : 770 vs, 1035 vs, 2890 m, 2920 m, 2960 m, 3028 m, 3070 m, 3079 m, 3200–3550 wm, 3600 m. *NMR spectrum* ($CDCl_3$; δ ppm) : 0.66 (m, 1H cyclopropyl, J_{trans} = = 5.5 Hz, J_{gem} = 4 Hz) ; 1.52 (m, 1H cyclopropyl, J_{cis}= 9 Hz, J_{gem} = 4 Hz) ; 2.4 (q, 2H cyclopropyl, J_{cis} = 9 Hz, J_{trans} = 5.5 Hz) ; 3.78 (1H, ArC*H*Ar, J = 7.9 Hz) ; 4.38 (2H, J = = 7.9 Hz) ; 6.9 –7.5 (m, 8H arom.).

The $LiAlH_4$-reduction of acetate **16** in diethyl ether (4 hrs, reflux) gave rise to the corresponding alcohol whose reaction with *n*-Bu_3SnH [27] afforded the same alcohol **15**.

2 :3.5 :6-Dibenzobicyclo[5.1.0]octa-2.5-dien-4-yl-methyl tosylate (**14a**). To a cold solution of alcohol **15** (2.36 g ; 10 mmoles) in 5 ml anhydrous ether and 1.2 ml (15 mmoles) anhydrous pyridine, tosyl chloride (2 g ; 10.5 mmoles) was added in small portions. After keeping for 24 hrs at 0° the reaction mixture was decomposed with cooled water when tosylate **14a** precipitated (3.7 g ; 94.1%), m.p. 151–3° (ethanol). (*Found* : C, 73.97 ; H, 5.78 ; S, 7.93. $C_{24}H_{22}O_3S$ requires C, 73.82 ; H, 5.68 ; S, 8.21). *IR spectrum* (CCl_4 ; cm^{-1}) : 971 s, 1180 s, 1191 s, 1379 s, 2926 w, 3028 w, 3069 w. *NMR spectrum* ($CDCl_3$; δ ppm) : 0.58 (m, 1H cyclopropyl, J_{trans} = 5.5 Hz, J_{gem} = 4 Hz) ; 1.45 (m, 1 H cyclopropyl, J_{cis} = 9 Hz, J_{gem} = 4 Hz) ; 2.18 (q, 2H cyclopropyl, J_{cis} = 9 Hz, J_{trans} = 5.5 Hz) ; 3.91 (t, 1H, ArC*H*Ar, J =7.9 Hz) ; 4.92 (d, 2H, J = 7.9 Hz) ; 6.95–7.7 (m, 12 H arom.).

The unbuffered acetolyses of tosylate **14a**. A solution of tosylate **14a** (3.9 g ; 10 mmoles) in anhydrous acetic acid (80 ml) was heated at 118° for 24 hrs (about 10 half-lives). The reaction mixture was poured into water, neutralized with Na_2CO_3 and ether-extracted. The combined ether extracts were washed with water, dried and the solvent was then removed *in vacuo*. The partially crystallized residue (2.1 g) dissolved in anhydrous ether (50 ml) was added dropwise with stirring to a suspension of $LiAlH_4$ (1 g) in 30 ml anhydrous ether. The reaction mixture was then refluxed for 6 hrs, left overnight and worked-up in the usual manner. The partially crystallized product (1.95 g ; 95.5%) was v.p.c.-analysed, (see table 1). By column-chromatography of the reaction mixture on neutral alumina *2 :3.6 :7-dibenzobicyclo[6.1.0]nona-2.4.6-triene* (**27**) was isolated (1.7 g ; 87%) on elution with petroleum ether. The alkene **27** m.p. 115° (methanol). (*Found* : C, 93.38 ; H, 6.52. $C_{17}H_{14}$ requires C, 93.53 ; H, 6.47). *IR spectrum* (CS_2 ; cm^{-1}) : 760 s, 771 vs, 1031 m, 2986 m, 3006 m, 3021 m, 3068 m. *NMR spectrum* (CCl_4 ; δ ppm) : 0.9–1.6 (m, 2H cyclopropyl) ; 2.26 (q, 2H cyclopropyl, J_{cis} = 8.2 Hz, J_{trans} = 5.5 Hz) ; 6.89 (s, 2H olef.) ; 6.9–7.5 (m, 8H arom.).

By continuing the elution of the chromatography column with diethyl ether — petroleum ether (1 : 1) mixture, a crystallized product with m.p. 131–9° was obtained (0.15 g, 7%). The v.p.c.-analysis of this product indicated the presence of three components which were identified by comparison with authentic samples (*vide infra*) as : alcohol *trans*-**28**, alcohol **15** and alcohol *cis*-**28**.

---

[27] D. Seyferth, H. Jamazaki, D. Alleston, *J. Org. Chem.*, **28**, 703 (1963).

NaOAc buffered acetolysis of tosylate **14 a**. A solution of tosylate **14 a** (3.9 g;10 mmoles) and anhydrous NaOAc (2.46 g; 30 mmoles) in 80 ml anhydrous acetic acid was hoated at 118° for 24 hrs. The reaction mixture afforded 2.8 g (97.8%) of a crystalline product which was subsequently $LiAlH_4$ reduced. The usual work-up gave rise to a white crystalline product (2.2 g; 92%) the composition of which was established by means of v.p.c. (see table 1). No pure compound could be isolated by alumina column chromatography. By recrystallization of the crude acetolysis product (after $LiAlH_4$-reduction) from *n*-hexane, the main component, *trans-2:3.6:7-dibenzobicyclo[6.1.0]nona-2.6-dien-4-ol* (**28**) was obtained. The *trans*-**28** alcohol (structure assigned from $Eu(DPM)_3$–NMR spectra), (95% purity), m.p. 131–3° (*Found*: C, 86.41; H, 7.00. $C_{17}H_{16}O$ requires C, 86.40; H, 6.82). *IR spectrum* (CS_2; cm^{-1}): 753 vs, 763 vs, 1009 m, 3602 m. *NMR spectrum* ($CDCl_3$; δ ppm): 1.1–1.7 (m, 2H cyclopropyl); 2.1 (s, 1H, OH); 2.5 (m, 2H cyclopropyl, $J_{gem} = 13.5$ Hz, $J'_{vic} = 8$ Hz); 5.04 (q, 1H, $J'_{vic} = 8$ Hz, $J_{vic} = 9.2$ Hz); 6.85–7.3 (m, 8H arom.).

Two minor components: the alkene **27** and the alcohol **15** were v.p.c. identified by comparison with authentic samples. The structure of another component, formed in a small amount (2%) during this solvolysis was chromatographically proved, its retention time being identical with that of the alcohol *cis*-**28**. This isomer could be obtained by preparative v.p.c. applied to the mixture of alcohols *trans*-**28** and *cis*-**28** formed in the $NaBH_4$-reduction of the ketone **30** (*vide infra*).

The oxidation of the mixture of alcohols trans-**28** and *cis*-**28**. To an acetone (15 ml) solution of the buffered-acetolysis product of **14a** after $LiAlH_4$ reduction (0.23 g) (which contained 94% alcohol *trans*-**28**) Jones reagent [22] (0.5 ml) was added dropwise with stirring until the yellow colour of the reaction mixture was maintained. After 5 minutes, isopropanol (0.2ml) was added to decompose the excess reagent, then 20 ml water were poured and the reaction mixture was ether-extracted. The organic solution was washed with a conc. solution of Na_2CO_3, dried and evaporated *in vacuo*. *2:3.6:7-Dibenzobicyclo[6.1.0]nona-2.6-dien-4-one* (**30**) was formed (0.2 g; 88%), m.p. 124–4,5° (methanol). *Found*: C. 87.01; H, 6.16, $C_{17}H_{15}O$ requires C, 87.14; H, 6.02). *IR spectrum* (CS_2; CCl_4; cm^{-1}): 768 vs, 775 vs, 1020 m. 1242 m, 1689 vs, 2925 w, 3028 m, 3082 m. *NMR spectrum* (CCl_4; δ ppm): 1.1–1.8 (m, 2H cyclopropyl); 2.40 (q, 2H cyclopropyl, $J_{cis} = 8.5$ Hz, $J_{trans} = 5.5$ Hz); 3.69 (d, 1H, $J_{gem} = 16.5$ Hz); 4.68 (d, 1H, $J_{gem} = 16.5$ Hz); 6.8–7.5 (m, 8H arom.).

The oxime of the ketone **30**, m.p. 235–237° (ethanol). (*Found*: C, 82.10; H, 6.2; N. 5.57.$C_{17}H_{15}NO$ requires C, 81.90; H, 6.06; N, 5.62).

$NaBH_4$ reduction of 2:3.5:6-dibenzobicyclo[6.1.0]nona-2.6-dien-4-one (**30**). To a solution of ketone (0.5 g; 2.13 mmoles) in 30 ml ethanol, a solution of $NaBH_4$ (0.05 g; 13 mmoles) in 15 ml water containing 0.06 ml 2N NaOH was added dropwise at room temperature(evolution of gases), left overnight, then most of the solvent evaporated. Water was added to the residue and the product was isolated by filtration. The v.p.c.-analysis indicated two components: the alcohol *trans*-**28** (39%) (identical with the major product of the buffered acetolysis of **14 a**) and another component (61%) which was preparatively-v.p.c. separated (93% purity), m.p. 145–8°. The NMR spectrum of this compound in the presence of $Eu(DPM)_3$ indicated the configuration of the alcohol *cis*-**28**. IR spectrum (CS_2; cm^{-1}): 756 vs, 766 vs, 1031 m, 3602 m. *NMR spectrum* ($CDCl_3$; δ ppm): 1.1–1.6 (m, 2H cyclopropyl); 2.12 (s, 1H, OH); 2.35 (q, 2H cyclopropyl, $J_{cis} = 8.5$ Hz, $J_{trans} = 5$ Hz); 2.82 (q, 1H, $J_{gem} = 15$ Hz, $J_{vic} = 6.2$ Hz); 4.10 (q, 1H, $J_{gem} = 15$ Hz, $J'_{vic} = 9$ Hz); 6.11 (q, 1H, $J_{vic} = 6.2$ Hz, $J_{vic} = 9$ Hz); 6.8–7.6 (m, 8H arom.).

HCOONa buffered formolysis of tosylate **14a**. A solution of tosylate **14 a** (3.9 g; 10 mmoles) and anhydrous HCOONa (2.04 g; 30 mmoles) in 80 ml 99% formic acid was heated at 100.5° for 24 hrs. The product analysis after 1 hr and 24 hrs was performed by v.p.c. of the reaction mixtures after $LiAlH_4$-reduction (see table 1, entries 3 and 4). The work-up was the same as in the acetolyses of **14 a** (*vide supra*). In the reaction mixture the hydrocarbon **27** and the alcohols *trans*-**28** and *cis*-**28** were identified by comparison with authentic samples.

Reaction of the buffered-acetolysis product of **14 a** *in acid medium.* A solution of the buffered-acetolysis product of **14 a** (after $LiAlH_4$-reduction) (0.23 g, containing approximately 91% *trans*-**28**) and *p*-toluenesulphonic acid (0.172 g; 1 mmole) in 25 ml anhydrous acetic acid was heated at 118°. Samples were extracted at the times registered in table 3. After the usual work-up and $LiAlH_4$-reduction, oily or partially crystallized reaction mixtures were obtained, which were subsequently v.p.c.-analysed (see table 3).

*Reaction of the alcohols trans-***28** *and cis-***28** *in NaOAc—AcOH.* A sample of alcohol *trans*-**28** (0.23 g; 1 mmole) (91% purity) (or *cis*-**28**; 94% purity) and anhydrous NaOAc (0.24 g; 3 mmoles) were heated in 25 ml anhydrous acetic acid for 24 hrs at 118°. After the work-up and $LiAlH_4$-reduction (as in the acetolysis of **14 a**) the product (0.22 g; 96%) was found to be identical with the starting material.

2:3.6:7-Dibenzobicyclo[6.1.0]nona-2.6-diene (**29**).

a) *By Wolff-Kishner procedure* applied to the ketone **30**, the saturated hydrocarbon **29** was obtained (0.15 g; 80%), m.p. 84—6° (methanol). (*Found*: C, 92.60; H, 7.40. $C_{17}H_{16}$ requires: C, 92.73; H, 7.27). *IR spectrum* (CS_2; cm^{-1}): 758 vs, 769 vs, 2891 w, 2940 m, 3021 m, 3062 m, 3074 m. *NMR spectrum* (CS_2; δ ppm): 1.1—1.6 (m, 2H cyclopropyl, J_{cis} = 8.2 Hz, J_{trans} = 5.5 Hz); 2.30 (q, 2H cyclopropyl J_{cis} = 8.2 Hz, J_{trans} = 5.5 Hz); 2.65—3.82 (m, 4H, syst. A_2B_2); 6.75—7.1 (m, 8H arom.).

b) *The reduction of hydrocarbon* **27**. The hydrocarbon **27** (0.22 g; 1 mmole) was hydrogenated in ethanol (25 ml) in the presence of PtO_2 catalyst (room temperature, atmospheric pressure). After usual work-up the saturated hydrocarbon **29** (0.2 g; 98%), m.p. 84—6° was obtained. This hydrocarbon was identical with that obtained from ketone **30**.

2:3.5:6-Dibenzobicyclo [5.1.0] octa-2.5-diene (**21**). A mixture of hydrocarbon **22** (4.75 g; 25 mmoles) and phenylmercuric tribromomethane (16 g; 30 mmoles) in 30 ml anhydrous benzene was heated with stirring at 85° for 3 hrs. After the work-up as in the case of acetate **16**, it was obtained *2:3.5:6-dibenzo-8.8-dibromobicyclo[5.1.0]octa-2.5-diene* (**23**) (3.64 g; 45%), m.p. 138—40° (methanol). (*Found*: C, 52.60; H, 3.20; Br, 43.85. $C_{16}H_{12}Br_2$ requires C, 52.75; H, 3.29; Br, 43.96. *IR spectrum* (CS_2; cm^{-1}): 752 s, 780 s, 1030 m, 2851 w, 2950 w, 3027 m, 3068 m. *NMR spectrum* ($CDCl_3$; δ ppm): 3.33 (d, 1H, ArC*H*Ar, J = 13 Hz); 3.41 (s, 2H cyclopropyl); 4.58 (d, 1H, ArC*H*Ar, J = 13 Hz); 7.10—7.70 (m, 8H arom.).

The dibromoderivative **23** (3.64 g; 10 mmoles) was reduced with $LiAlH_4$ (1.9 g; 50 mmoles) in anhydrous THF (15 ml) for 16 hrs at reflux. After the usual work-up the hydrocarbon **21** was obtained. Elemental analysis, IR and NMR spectra correspond to the literature data.[9b]

2:3.5:6-Dibenzobicyclo[5.1.0]octa-2.5-dien-4-yl-acetonitrile (**36 a**) was synthesized in 89% yield from tosylate **14 a** and NaCN after a procedure described [28] for 4-cyanocyclopentene. The nitrile **36 a** m.p. 99—100.5° (methanol). (*Found*: C, 87.98; H, 6.30; N, 5.93. $C_{18}H_{15}N$ requires C, 88.16; H, 6.13; N, 5.71). *IR spectrum* (CCl_4; cm^{-1}): 931 m, 1120 m, 1493 s, 2251 w, 2928 s, 2980 m, 3021 s, 3068 s. NMR spectrum ($CDCl_3$; δ ppm): 0.68 (m, 1H cyclopropyl, J_{gem} = 4 Hz, J_{trans} = 5.5 Hz); 1.59 (m, 1H cyclopropyl, J_{gem} = 4 Hz, J_{cis} = 8.2 Hz); 2.47 (q, 2H cyclopropyl, J_{cis} = 8.2 Hz, J_{trans} = 5.5 Hz); 3.42 (2H, J = 8.3 Hz); 3.91 (1H, J = 8.3 Hz); 6.9—7.6 (m, 8H arom.).

---

[28] C. E. Johnson, J. E. Keiser and J. C. Sharp, *J. Org. Chem.*, **34**, 860(1969).

2:3.5:6-Dibenzobicyclo[5.1.0]octa-2.5-dien-4-yl-acetic acid (**36 b**). The hydrolysis of nitrile **36a** in alkaline solution as described [29] for 5-carboxymethyl bicyclo[2.2.2]oct-2-ene affords the acid **36 b** in 95% yield, m.p. 194–5° (methanol). (*Found*: C, 81.75; H, 6.20. $C_{18}H_{16}O_2$ requires C, 81.79; H, 6.10). *IR spectrum* (CCl_4; cm^{-1}): 940 w, 1120 w, 1410 m, 1713 s, 2400–3300 associated OH absorption. *NMR spectrum* ($CDCl_3$; δ ppm): 0.66 (m, 1H cyclopropyl, $J_{trans} = 5.5$ Hz, $J_{gem} = 4$ Hz); 1.52 (m, 1H cyclopropyl, $J_{gem} = 4$ Hz, $J_{cis} = 8.5$ Hz); 2.48 (q, 2H cyclopropyl, $J_{cis} = 8.5$ Hz, $J_{trans} = 5.5$ Hz); 3.48 (2H, $J = 7.9$ Hz); 4.16 (q, 1H, $J = 7.9$ Hz); 6.85–7.5 (m, 8H arom.); 10.1 (s, 1H, COOH).

2:3.5:6-Dibenzobicyclo[5.1.0]octa-2.5-dien-4-yl-ethylacetate (**36c**) was obtained in 90% yield by direct esterification of the acid **36 b**. The ester **36 c** m.p. 60–61.5° (ethanol). (*Found*: C, 82.34; H, 7.05. $C_{20}H_{20}O_2$ requires C, 82.19; H, 6.85). *IR spectrum* (CS_2; cm^{-1}): 751 s, 761 s, 811 s, 1176 vs, 1186 vs, 1376 vs, 2922 m, 2981 m, 3046 m, 3062 m. *NMR spectrum* (CCl_4; δ ppm): 0.64 (m, 1H cyclopropyl, $J_{gem} = 3.5$ Hz, $J_{trans} = 5$ Hz); 1.03 (t, 3H, $J = 7$ Hz); 1.5 (m, 1H cyclopropyl, $J_{cis} = 8.2$ Hz, $J_{gem} = 3.5$ Hz); 2.48 (q, 2H cyclopropyl, $J_{cis} = 8.2$ Hz, $J_{trans} = 5$ Hz); 3.3 (d, 2H, $J = 7.9$ Hz); 3.91 (q, 2H, $J = 7$ Hz); 4.1 (t, 1H, $J = 7.9$ Hz); 6.7–7.5 (m, 8H arom.).

2:3.5:6-Dibenzobicyclo[5.1.0]octa-2.5-dien-4-yl-β-ethanol (**35**) was obtained (88%) by the reduction of the ester **36c** with $LiAlH_4$, m.p. 83–4.5° (methanol). (*Found*: C, 86.16; H, 7.25. $C_{18}H_{18}O$ requires C, 86.40; H, 7.20. *IR spectrum* (CCl_4; cm^{-1}): 1031 s, 1048 s, 1380 m, 1492 m, 2878 m, 2925 m, 2960 m, 3061 m, 3250–3600 s, 3639 m. *NMR spectrum* ($CDCl_3$; δ ppm): 0.68 (m, 1H, cyclopropyl, $J_{trans} = 5.2$ Hz, $J_{gem} = 3.5$ Hz); 1.56 (m, 1H cyclopropyl, $J_{cis} = 8.2$ Hz, $J_{gem} = 3.5$ Hz); 1.92 (s, 1H, OH); 2.40 (q, 2H cyclopropyl, $J_{cis} = 8.2$ Hz, $J_{trans} = 5.2$ Hz); 2.55 (q, 2H, $J = 7.5$ Hz); 3.59 (t, 2H, $J = 7.5$ Hz); 3.78 (t, 1H, $J = 7.5$ Hz); 6.9–7.5 (m, 8H, arom.).

2:3.5:6-Dibenzobicyclo[5.1.0]octa-2.5-dien-4-yl-β-ethyl tosylate (**14 b**). The treatment of the alcohol **35** with tosyl chloride led to the tosylate **14 b** (99%), m.p. 107–8° (ethanol). (*Found*: C, 74.06; H, 6.05; S, 7.64. $C_{25}H_{24}O_3S$ requires C, 74.22; H, 5.98; S, 7.93). IR spectrum (CS_2; cm^{-1}): 751 s, 761 s, 811 s, 1176 vs, 1186 vs, 1370 vs, 2922 m, 2981 m, 3046 m, 3062 m. *NMR spectrum* ($CDCl_3$; δ ppm): 0.61 (m, 1H cyclopropyl, $J_{gem} = 4$ Hz, $J_{trans} = 5.5$ Hz); 1.52 (m, 1H cyclopropyl, $J_{gem} = 4$ Hz, $J_{cis} = 8.2$ Hz); 2.36 (q, 2H cyclopropyl, $J_{cis} = 8.2$ Hz, $J_{trans} = 5.5$ Hz); 2.42 (s, 3H, CH_3); 2.71 (m, 2H); 3.68 (t, 1H, $J = 8$ Hz); 3.90 (t, 2H, $J = 6.5$ Hz); 6.85–7.9 (m, 12H arom).

Solvolysis of the tosylate **14 b** was carried out under the same conditions as those used for the tosylate **14 a**. After 5 half-lives the unbuffered as well as the buffered acetolyses afforded (after $LiAlH_4$-reduction) the starting alcohol **35** in more than 90% yield. The same result was obtained from the buffered acetolysis after 10 half-lives. The unbuffered acetolysis gave rise after 10 half-lives (and $LiAlH_4$-reduction) to a mixture (93% yield) whose v.p.c.-analysis indicated the presence of three components: the alcohols **35** (48%), **38** (37%) and **39** (12%). These components could be separated by means of v.p.c. affording the starting alcohol **35**, the alcohol **38** (92.8% purity) and the diol **39** (84.2% purity). The alcohols **38** and **39** (uncrystallized viscous oils) were identified by their NMR spectra. In the case of the compound **38** two conformers were evidenced: axial and equatorial (3 : 1 ratio). *NMR spectra* ($CDCl_3$; δ ppm): *axial conformer*: 1.5 (s, 1H, OH); 1.95 (m, 2H, $J_1 = 7.5$ Hz, $J_2 = 6-6.5$ Hz); 2.40 (d, 3H, $J_{allyl} = 1-1.5$ Hz); 3.30 (t, 2H, $J_2 = 6-6.5$ Hz); 4.13 (t, 1H, $J_1 = 7.5$ Hz); 6.90 (q, 1H olef., $J_{allyl} = 1-1.5$ Hz); 6.95–7.6 (m, 8H arom.); *equatorial conformer*:

---

[29] H. W. WHITLOCK and M. W. SIEFKEN, *J. Amer. Chem. Soc.*, **90**, 4929 (1968

2.45 (d, 3H, $J_{allyl} = 1-1.5$ Hz) ; 2.68 (2H, $J_1 = 7.5$ Hz, $J_2 = 6-6.5$ Hz) ; 3.70 (t, 2H, $J_2 = 6-6.5$ Hz) ; 3.84 (t, 1H, $J_1 = 7.5$ Hz).

The structure of the two isomers was also established using the $Eu(DPM)_3$.

The diol **39** *NMR spectrum* ($CDCl_3$; δ ppm) : 1.30 (3H, CH_3, $J^* = 6$ Hz) ; 1.98 (m, 2H, $J^*_1 = 8$ Hz, $J^*_2 = 6$ Hz) ; 2.05 (s, 2OH) ; 3.3–3.95 (m, 4H) ; 4.17 (t, 1H, $J^* = 8$ Hz) ; 7.2–7.6 (m, 8H arom.). (J^* deduced from NMR spectra with $Eu(DPM)_3$). The structure of the compound **39** was also confirmed by means of NMR spectra with $Eu(DPM)_3$.

Kinetic measurements. The acetic acid had a purity of 99.98 %. The solutions were 0.01 M in tosylate **14 a** or **14 b** and 0.03 M in AcONa. To the sample extracted from the reaction mixture (which contains an excess of AcONa) a known quantity of 0.05 M solution of $HClO_4$ was added and the mixture was titrated with a 0.05 M solution of NaOAc using p-bromophenole blue [30] as indicator.

Acknowledgement. Elemental analyses were performed by Miss E. Şliam and Mrs V. Daniel, to whom our thanks are due.

---

[30] S. WINSTEIN, E. GRÜNWALD and L. L. INGRAHAM, *J. Amer. Chem. Soc.*, **70**, 821 (1948).

Revue Roumaine de Chimie, **19**, *2*, 233–248 (1974)

ELIMINATION REACTIONS IN THE 8-R-TRICYCLO [7.3.1.$0^{2,7}$]TRIDECANE SERIES. III*

DEHYDRATION OF 8-R-TRICYCLO[7.3.1.$0^{2,7}$]TRIDECANE--2,13-DIOLS

N. BĂRBULESCU and MINODORA LECA

University of Bucharest, Chemistry Department, Organic
Chemistry Laboratory, Splaiul Independenţei 89, Romania

Received March 22, 1973

Elimination of two molecules of water from Ia leads to the linear hydrocarbons Va and VIa and to the angular hydrocarbon VIIa. The VIa : VIIa ratio, as resulted from gas-liquid chromatography, is 7 : 1. Elimination of two water molecules from Ib yields the angular hydrocarbons Vb and VIb and the linear hydrocarbon Xb. The Xb : VIb ratio, calculated from the NMR spectrum, is 1.2 : 1. The decrease of this ratio is explained by the increase of the double bond migration due to the hyperconjugation effect of the methyl group in the position 7 – 8. The formation of the reaction compounds is explained by a mechanism implying classical carbonium ions as intermediates, or by a mechanism with non-classical carbonium ions.

Chemical properties [1–3] and IR spectra [4,5] of 8-R-tricyclo-[7.3.1.$0^{2,7}$]tridecane-2,13-diols (I), where $R = H$, CH_3, C_2H_5, C_3H_7, C_6H_5, lead to the following conformation of these derivatives of bicyclo[3.3.1]nonane (figure 1) : the two fused rings have the conformation of *trans*-decalin, and the third one is situated in a plane approximately perpendicular on the medium plane of the first two rings ; the two hydroxyl groups are 1,3-*cis*, i.e. both are axial.

The tertiary hydroxyl group from C_2 is easily eliminated in acid medium. E_2 eliminations take place in the easiest way when the leaving groups are in *anti*-periplanar conformation.[6] *Anti*-periplanarity of the leaving groups in a six-membered ring system requires that they be diaxial, even if this is the conformation of higher energy. The elimination of the hydroxyl group from C_2 may occur, consequently, both with axial hydrogen atom from C_7, and with hydrogen atom from the neighbouring carbon atom of the fused ring. The formation of the 2–7 double bond is favoured by its localization at the carbon atoms without any hydrogen atoms.

---

* Part I. N. Bărbulescu, *Anal. Univ. Bucureşti*, **20**, 79 (1958).
Part II. N. Bărbulescu, M. Leca-Mînicuţă and Gr. Stănescu, *Rev. Chim. (Bucureşti)*, **16**, 76 (1965).

[1] S. Julia and D. Varech, *Compt. rend.*, **246**, 1559 (1958).

[2] N. Bărbulescu, *Anal. Univ. Bucureşti*, **13**, 101 (1957).

[3] N. Bărbulescu, *Anal. Univ. Bucureşti*, **20**, 79 (1958).

[4] S. Julia, D. Varech, Th. Bürer and Hs. H. Günthard, *Helv. Chim. Acta*, **43**, 1623 (1960).

[5] L. Ivan and N. Bărbulescu, *Anal. Univ. Bucureşti*, **41**, 155 (1963).

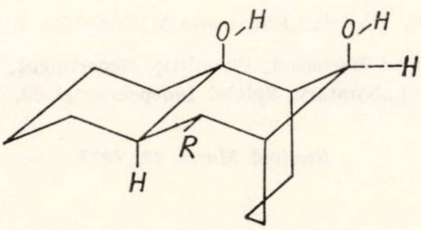

Fig. 1. – Conformation of 8-R-tricyclo-[7. 3. 1. $0^{2,7}$]tridecane-2,13-diols (I).

Arguments from orbital-overlap considerations lead to the prediction that the transition state must be coplanar not only for a dihedral angle of 180°, but also for one of 0°. Though *trans*- E_2 elimination is the prevalent one, the elimination was also observed when the leaving groups were in *sin*-periplanar conformation.[7,8] Therefore, theoretically, the elimination could also take place with the equatorial hydrogen atom from C_1. It does not occur in this way not only because the dihedral angle between the two leaving groups is different from 0°, but also because it requires the introduction of the double bond at the bridgehead of the bicyclic system, i.e. it comes into conflict with the Bredt's rule.[9]

The Bredt's rule may be stated in qualitative terms as follows: a double bond cannot be placed with one terminus at the bridgehead of a bridged ring system unless the rings are large enough to accommodate the double bond without excessive strain. The strain results from torsional forces on the double bond which tend to twist the p_z orbitals of the double bonded carbon atoms besides the parallel condition required for maximum overlap.

There were some attempts to determine the limits of the Bredt's rule. Fawcett [10] proposed that the sum of number of atoms in the bridges of a bicyclic system (S number) determines whether that system can accomodate a bridgehead double bond. He concluded from the experimental available data that the compounds with bridgehead double bonds could be isolated for $S \geqslant 9$, and that the transient intermediates with bridgehead double bonds might be possible for $S \geqslant 7$. Bicyclic $[n. 3. 1]$ system can accomodate a bridgehead double bond when $n \geqslant 5$.[11, 12]

---

[6] K. Fukui and H. Fujimoto, *Tetrahedron Letters*, **1965**, 4303.

[7] C. H. De Puy, R. D. Thurn and G. F. Morris, *J. Amer. Chem. Soc.*, **84**, 1314 (1962).

[8] C. H. De Puy, G. F. Morris, M. L. Smith and R. J. Smat, *J. Amer. Chem. Soc.*, **87**, 2421 (1965).

[9] J. Bredt, *Liebigs Ann. Chem.*, **437**, 1 (1924).

[10] F. S. Fawcett, *Chem. Rev.*, **47**, 219 (1950).

Wiseman[13] suggested another criterion to appreciate the limits of the Bredt's rule applicability. Considering the configuration of a double bond bridgehead bicyclic system, he has shown that the double bond is exocyclic to one of the rings (bc) and endocyclic in the other (ac). The double bond being at the branching point of the two rings, it must be substituted *cis* in one of the rings (ab) and *trans* in the other (ac). Wiseman suggested that the strain of the bridgehead double bonds is closely related to the strain of the corresponding *trans*-cycloalkenes. *Trans*-cyclooctene was the smallest *trans*-cycloaklene isolated ; *trans*-cycloheptene was obtained only as a transient reactive species. According to this criterion, a bicyclic birdgehead alkene can be isolated when the larger of the two rings, containing the double bond, has at least eight atoms, and a transient intermediate with bridgehead double bond is possible when the larger ring containing double bond is seven-membered. Thus, the limits of the Bredt's rule diminish to $S \geqslant 7$ for isolable compounds and to $S \geqslant 6$ for transient intermediates.

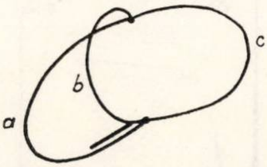

This criterion allows to determine whether a double bond can be placed at the bridgehead of a bicyclic system, as well as which branches of the system can contain a double bond.

The preparation of the following bridgehead alkenes confirmed Wiseman's hypothesis : bicyclo[4. 3. 1]dec-1(2)-ene-10-one,[14] bicyclo-[4. 2. 1]non-1(2)-ene and bicyclo[4. 2. 1]non-1(8)-ene,[15] ethyl-9-oxobicyclo.[4. 2. 1]non-6-ene-1-carboxilate,[16,17] bicyclo[3. 3. 1]non-1-ene, [13,18–20] bicyclo[3. 2. 2]non-1(2)-ene and bicyclo[3. 2. 2]non-1(7)-ene.[21] The last two, which require the introduction of the *trans*-double bond in a seven-membered ring, exist only as dimers.

RESULTS AND DISCUSSIONS

Examination of the hydroxyl group elimination products (position 2) from diols (I), where R = H and CH_3, leads to the conclusion that the elimination takes place with hydrogen atom from C_7. Thus, the

---

[11] V. Prelog, *J. Chem. Soc.*, **1950**, 420.

[12] V. Prelog, P. Barman and M. Zimmerman, *Helv. Chim. Acta*, **33**, 356 (1950).

[13] J. R. Wiseman, *J. Amer. Chem. Soc.*, **89**, 5966 (1967).

[14] B. G. Gardiner, M. R. Vegar and R. J. Wells, *Tetrahedron Letters*, **1970**, 2285.

[15] J. R. Wiseman, H.-F. Chan and C. J. Ahola, *J. Amer. Chem. Soc.*, **91**, 2812 (1969).

[16] W. Carruthers and M. I. Qureshi, *J. Chem. Soc., D*, **1969**, 832.

[17] W. Carruthers and M. I. Qureshi, *J. Chem. Soc., C*, **1970**, 2238.

[18] J. A. Marshall and H. Faubl, *J. Amer. Chem. Soc.*, **89**, 5965 (1967).

[19] J. A. Marshall and H. Faubl, *J. Amer. Chem. Soc.*, **92**, 948 (1970).

[20] J. R. Wiseman and A. Pletcher, *J. Amer. Chem. Soc.*, **92**, 956 (1970).

[21] J. R. Wiseman and J. A. Chong, *J. Amer. Chem. Soc.*, **91**, 7775 (1969).

NMR spectrum of tricyclo [7. 3. 1. $0^{2,7}$] trideca-2-ene-13-acetates (IIa), obtained by dehydration and acetylation with zinc chloride and acetic anhydride, has the following peaks (figure 2): one triplet at δ 4.74, with an area corresponding to one hydrogen atom, assigned to the hydrogen atom from C_{13}, one singlet at δ 1.96 due to the methyl of acetate

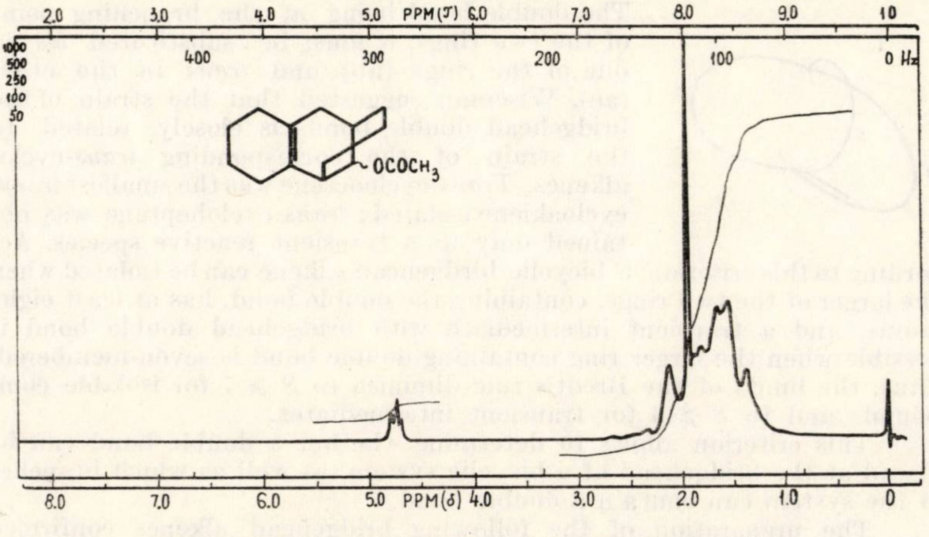

Fig. 2. — NMR spectrum of the unsaturated acetate IIa.

group and a complex absorption at δ 1.03—2.29 due to the other 18 hydrogen atoms. There is no peak for ethylene hydrogens, therefore, the double bond is in the position 2—7. This is confirmed by 2941 cm $^{-1}$ band of the IR spectrum, assigned to the bridgehead CH group. The elimination scheme is then:

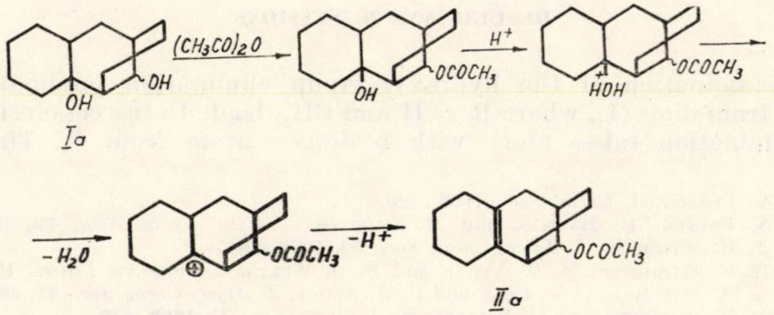

In the reaction medium it is also possible, first, the dehydration reaction followed by acetylation of the secondary hydroxyl group. The acetate group of unsaturated acetate IIa may be axial or equatorial. Their separation by gas-liquid chromatography on SE-30 and carbowax 20 M was not possible.

The NMR spectrum of 8-methyl-tricyclo[7.3.1.0^{2,7}]tridecene-13-acetates (IIb) (figure 3), which can also exist as two isomers due to the position of the acetate group, has one triplet at δ 4.88 assigned to the hydrogen from C_{13}, one singlet at δ 2.00 for methyl from acetate group, one doublet at δ 1.00 due to the methyl group from C_8, one complex absorption from δ 0.76 to 2.50, with an area corresponding to 17 hydrogen atoms, on which one singlet is superposed at δ 1.70, assigned to the methyl group attached to an ethylene carbon atom (from C_8). It follows that the acetate IIb can exist as two isomers due to the double bond position : the acetate with the double bond in the position 2–7 and the other one with double bond in the position 7–8. The formation of the first isomer is explained by the above scheme, and of the second one by the migration of the double bond in the position 7–8, due to the hyperconjugation effect of the methyl group :

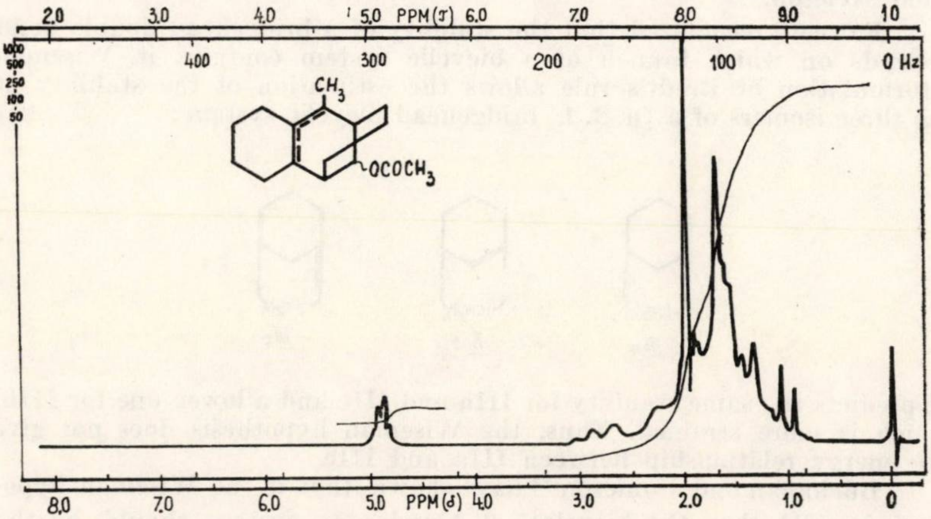

Fig. 3. – NMR spectrum of the unsaturated acetate IIb.

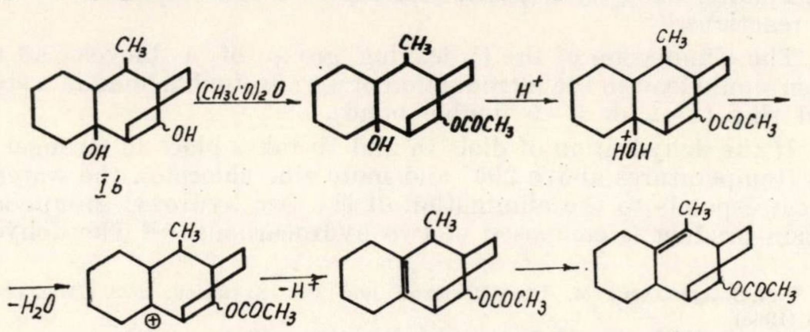

The calculation of the two isomers ratio from the integral curves of the NMR spectrum is not possible. The gas-liquid chromatograms on SE-30 and carbowax 20 M do not allow also the separation of the acetate (II b) isomers.

The elimination of the secondary hydroxyl group (from C_{13}) occurs in more energic conditions, taking place a rearrangement of the carbon atom skeleton.[3,22]

Fawcett recognized that the stability of a bridgehead double bond depends on which branch of a bicyclic system contains it. Wiseman reformulation of Bredt's rule allows the estimation of the stability of the three isomers of a [n. 3. 1] bridgehead bicyclic system :

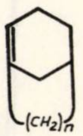

IIIa

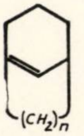

IIIb

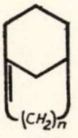

IIIc

It predicts the same stability for IIIa and IIIc and a lower one for IIIb, which is more strained. Thus, the Wiseman hypothesis does not give the energy relationship between IIIa and IIIc.

Buchanan and Jamieson [23] have shown that if the Wiseman hypothesis is valid, then the bicyclo[5. 3. 1]undecane system should be the smallest one which can tolerate bridgehead double bonds in all three possible positions. They obtained these isomers [23,24] and from NMR, IR and UV spectra and chemical properties concluded that bicyclo[5. 3. 1]-undec-7(11)-ene-8-one is really more strained than bicyclo[5. 3. 1]undec-7(8)-ene-11-one.[24]

It is a lack of information about the elimination reactions of [n. m. 1] bicyclo compounds having the leaving group in one-membered bridge. The elimination of the hydroxyl group from C_9 is studied by two papers. [22,25] It is also known a paper about the solvolysis of bicyclo-[3. 3. 1]nonyl-9-tosylate [26]; the solvolysis is accompanied by elimination reactions.

The elimination of the C_9 leaving group of a bicyclo[3.3.1]nonyl system would lead to the introduction of a *trans*-double bond in a six-membered ring (1–9 or 5–9 double bond).

If the dehydration of diols Ia and Ib takes place in stronger conditions (temperatures above 200° and more zinc chloride), the water quantity corresponds to the elimination of the two hydroxyl groups and the reaction product is composed of two hydrocarbons. [3,22] The dehydration

---

[22] N. Bărbulescu, M. Leca-Mînicuţă and Gr. Stănescu, *Rev. Chim. (Bucuresti)*, **16**, 76 (1965).

[23] G. L. Buchanan and G. Jamieson, *Tetrahedron*, **28**, 1123 (1972).

[24] G. L. Buchanan and G. Jamieson, *Tetrahedron*, **28**, 1129 (1972).

[25] N. Bărbulescu and M. Govela, *Anal. Univ. Bucuresti*, **30**, 1 (1961).

[26] C. S. Foote and R. B. Woodward, *Tetrahedron*, **20**, 687 (1964).

of unsaturated alcohols IVa and IVb zinc chloride yields the same hydrocarbons. Their formation can be explained by the reaction mechanism given above [22] :

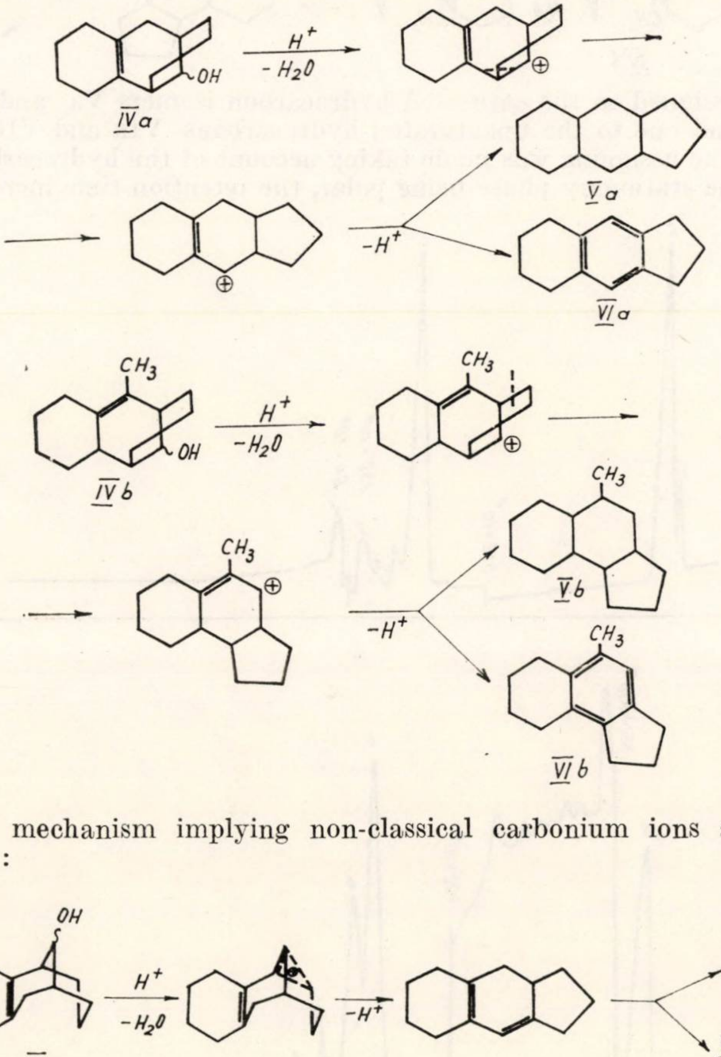

or by a mechanism implying non-classical carbonium ions as intermediates :

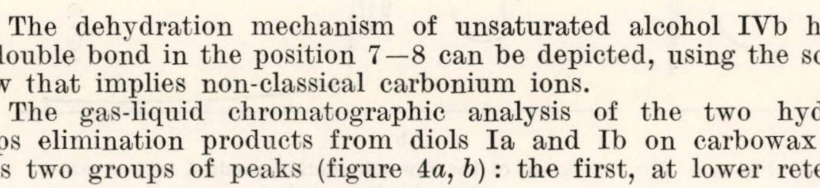

The dehydration mechanism of unsaturated alcohol IVb having the double bond in the position 7—8 can be depicted, using the scheme below that implies non-classical carbonium ions.

The gas-liquid chromatographic analysis of the two hydroxyl groups elimination products from diols Ia and Ib on carbowax 20M shows two groups of peaks (figure 4*a*, *b*) : the first, at lower retention

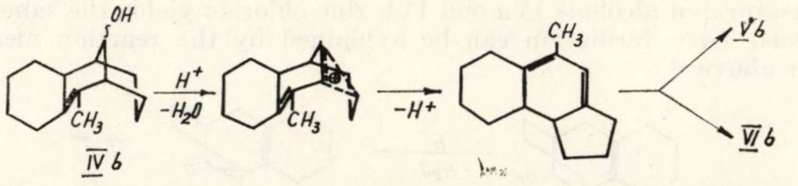

times, assigned to the saturated hydrocarbon isomers Va and Vb, and the second one to the unsaturated hydrocarbons VIa and VIb, respectively. The assigning was made taking account of the hydrocarbon structures (the stationary phase being polar, the retention time increases with

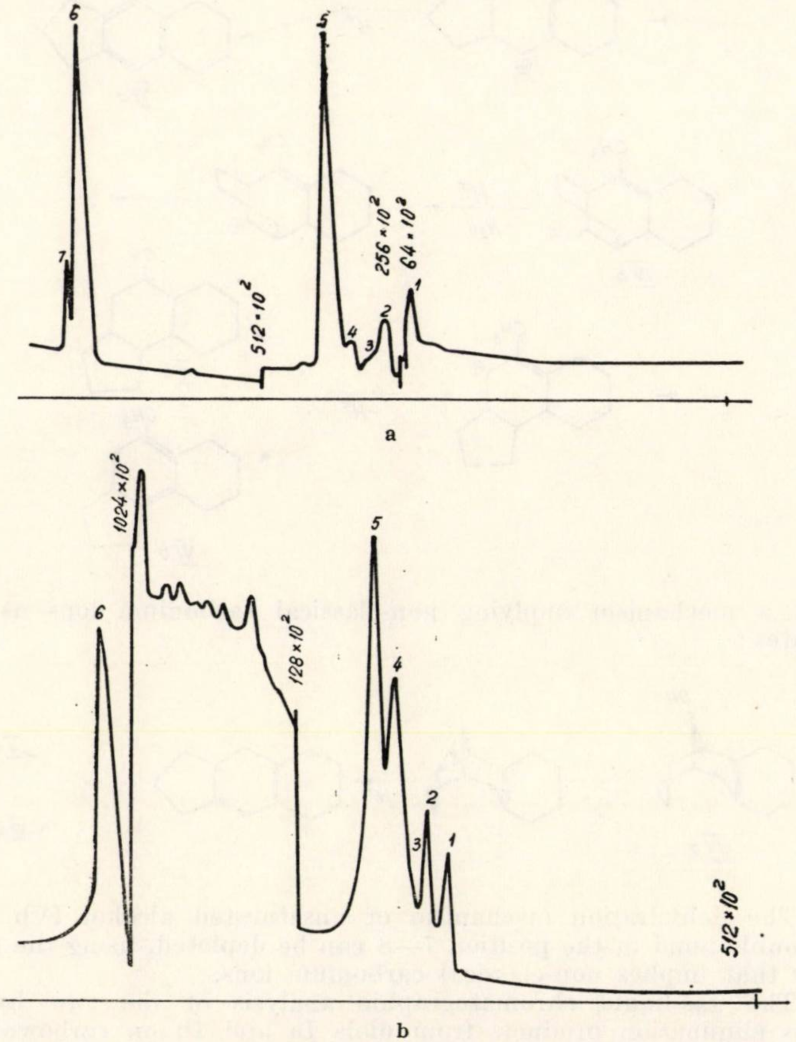

Fig. 4. — Chromatogram of the raw elimination product of two water molecules from diols :

a) Ia; *b*) Ib.

the polarity of the substance) as well as on the basis of NMR and IR spectra of the fractions separated by preparative gas-liquid chromatography on the same stationary phase.

The first group of peaks of the dehydration products of diol Ia is composed of five resolved peaks (figure 4 *a*). The hydrocarbon Va can exist as five isomers, like perhydroanthracene. The main peak is probably due to the most stable isomer *trans-anti-trans*. The second group is built up from two peaks, the first one due to the hydrocarbon VIa, and the second one due to the angular isomer VIIa. Therefore, angular isomers of the hydrocarbon Va can also exist in the first group of peaks. Percentage composition of this mixture, as calculated from the chromatogram recorded using the flame ionization detector, starting from the lowest retention times, is : 1.04, 5.02, 3.17, 27.71, 0.66, 54.53 and 7.87 per cent. The ratio between the areas of the peak 4 and 6 is 1 : 2, that corresponds to the theoretical ratio of the saturated hydrocarbon Va and unsaturated hydrocarbon VIa. The VIa : VIIa ratio is about 7 : 1.

The NMR spectrum of the main peak from the first group (peak 4) (figure 5 *a*) has a complex absorption at δ 0.60—2.65 corresponding to the saturated hydrogen atoms from the five- and six-membered rings of the compound Va. The complex absorption of the mixture of peaks 3 and 4 (figure 5 *b*) has the same limits, but different appearance.

The NMR spectrum of the peak 6 (figure 6 *a*) has the following signals : one complex absorption from δ 1.39 to 2.25, with an area corresponding to six hydrogen atoms, assigned to the two equivalent methylene groups of the six-membered ring and to the methylene group of the five-membered ring which are not attached to the benzene ring; one asymmetrical triplet at δ 2.76 ($J = 6.5$ Hz) for eight hydrogen atoms due to the four methylene groups from six- and four-membered rings attached to the benzene ring; one singlet at δ 6.77 corresponding to two hydrogens for the two equivalent aromatic hydrogen atoms. Therefore, this spectrum corresponds entirely to the structure of the compound VIa.

The peaks 6 and 7 are no longer well resolved on the carbowax 20M preparative column, so that the peak 7 could not be separated. On the other hand, the NMR spectrum of the mixture of peaks 6 and 7 were recorded, hoping that by difference the contribution of the peak 7 could be established. The spectra are completely identical, as we can see from figure 6 *a*, *b*. As a matter of fact, the two aromatic hydrogen atoms must be equivalent in practice, considering the structure of the angular isomer.

The structure of the hydrocarbon VIa was also proved by dehydrogenation with platinized asbestos. The main product was 5,6-benzindane (VIIIa), a crystalline substance — melting point 94°, picrate melting point 118° — described by McQuilin and Robinson [27] and by Sen-Gupta.[28] An oily compound was obtained in small quantity in addition to the hydrocarbon VIIIa, this being probably the angular isomer IXa

---

[27] A. McQuillin and R. Robinson, *J. Chem. Soc.*, **1941**, 586.

[28] S. C. Sen-Gupta, *J. Indian Chem. Soc.*, **16**, 89 (1939).

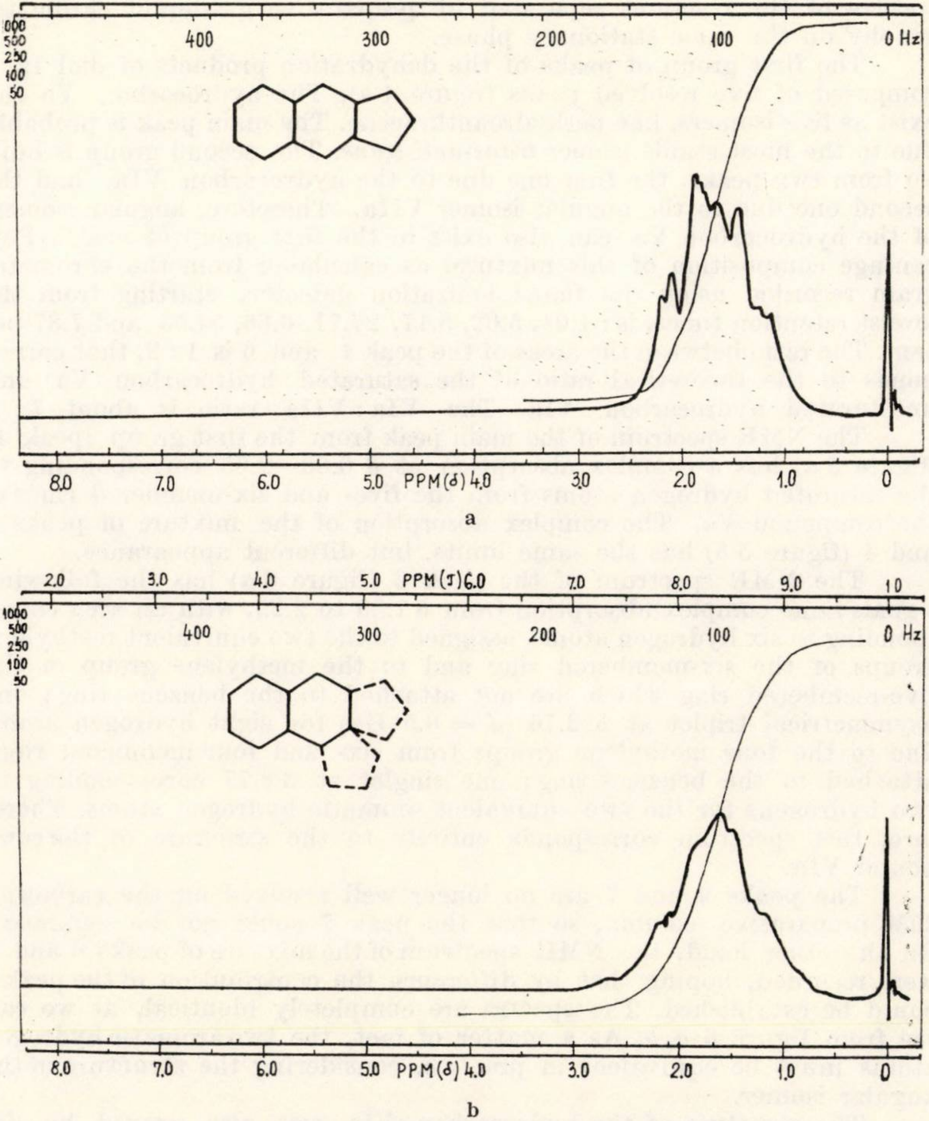

a

b

Fig. 5. — NMR spectra of the first group of peaks of the dehydration product of diol Ia : *a*) peak 4; *b*) peak 3+peak 4

which was not studied. From the literature data [29–32] it is known that this hydrocarbon is a liquid one. The hydrocarbon VIIIa was purified by column chromatography on alumina in light-petroleum solution.

---

[29] I. I. Denisenko, *Izvest. Akad. Nauk S.S.S.R., Oldel. khim. Nauk*, **1938**, 1019.

[30] I. I. Denisenko, *Zhur. obshchei Khim.* **8**, 410 (1938).

[31] R. Arnold and E. Rondestvedt, *J. Amer. Chem. Soc.*, **68**, 2176 (1946).

[32] F. Winternitz, M. Mousseron and G. Rouzier, *Bull. Soc. chim. France*, **1954**, 317.

The NMR spectrum (figure 7) is entirely consistent with the assigned structure : one quintet at δ 2.08 ($J = 7$ Hz), with an area corresponding to two hydrogen atoms, assigned to the methylene group of the five-membered ring nonattached to the naphtalene nucleus ; one asymmetrical triplet at δ 2.98 ($J = 7$ Hz) for four hydrogen atoms due to the two methylene groups of the five-membered ring attached to the naphtha-

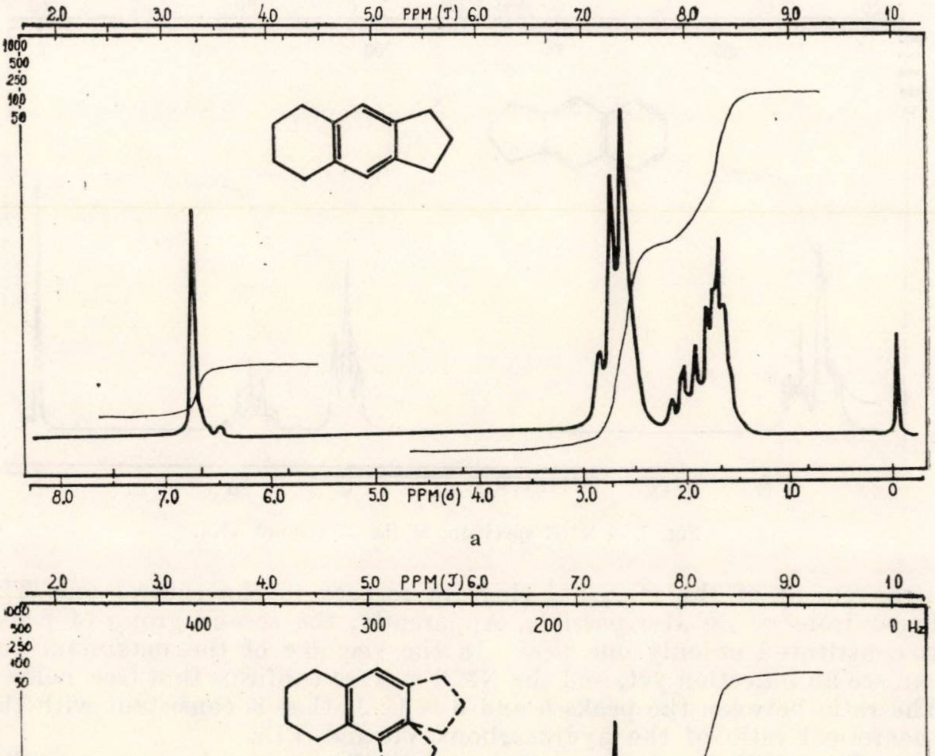

b

Fig. 6. — NMR spectra of the second group of peaks of the dehydration product of diol Ia :

a) peak 6 ; *b*) peak 6 + peak 7

lene nucleus; one complex absorption from δ 7.10 to 7.90 for the six aromatic hydrogen atoms. The gas-liquid chromatographic analysis on carbowax 20M shows only one peak.

The first group of peaks of the dehydration products of diol Ib is also composed of five peaks: four resolved and one unresolved. The hydrocarbon Vb has five isomers too, resulting from ring fusion and the arrangement of the marginal rings in respect to the central one. The linear isomers are also possible. Apparently, the second group of peaks is constituted of only one peak. In the vecinity of the maximum one can see an inflection yet, and the NMR spectra confirms that (see below). The ratio between the peaks 5 and 6 is 1 : 2, that is consistent with the theoretical ratio of the hydrocarbons Vb and VIb.

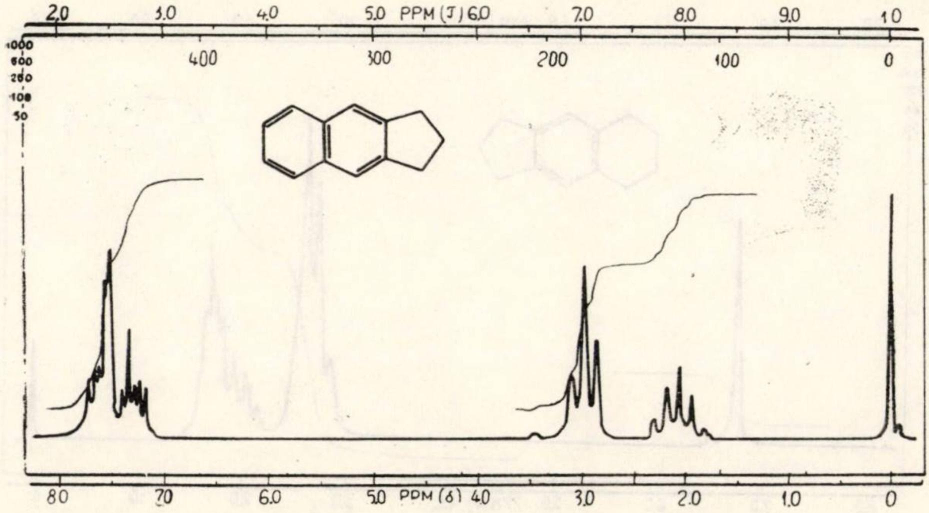

Fig. 7. – NMR spectrum of the compound IXa.

The NMR spectrum of the peak 5 (figure 8 *a*) has one complex absorption at δ 0.40–2.90 and the NMR spectrum of the peaks 2, 3, 4 and 5 (figure 8*b*) one modified complex absorption ranging the same limits.

The NMR spectrum of the peak 6 (figure 9) has a complex absorption from δ 1.37 to 2.26, with an area corresponding to 9 hydrogen atoms, assigned to the three methylene groups of the six- and five-membered rings nonattached to the benzene nucleus and to the methyl group attached to the benzene nucleus; one triplet at δ 2.58 ($J = 7$ Hz) for eight hydrogen atoms due to the four methylene groups of the five- and six-membered rings attached on the benzene ring and one apparent doublet centered at δ 6.68 for one aromatic hydrogen atom. This is not a doublet, but two closed singlets: one at δ 6.71 assigned to the aromatic hydrogen atom of the linear isomer Xb of the hydrocarbon VIb, which gives a peak at a lower field, and the other one at δ 6.64 for the aromatic hydrogen atom of VIb. The ratio VIb : Xb is about 1 : 1,2, as results from the integral curve. The splitting of the methyl group signal attached to the benzene nucleus is also observed. The methyl group of Xb gives a peak at δ 2.06, and the methyl group of VIb at δ 2.13. The integral curves are not clear enough, so that the ratio of isomers cannot be verified.

The dehydrogenation of the mixture of hydrocarbons VIb and Xb, using platinized asbestos, result in the formation of the corresponding mixture of hydrocarbons XIb and XIIb. Their NMR spectrum (figure 10)

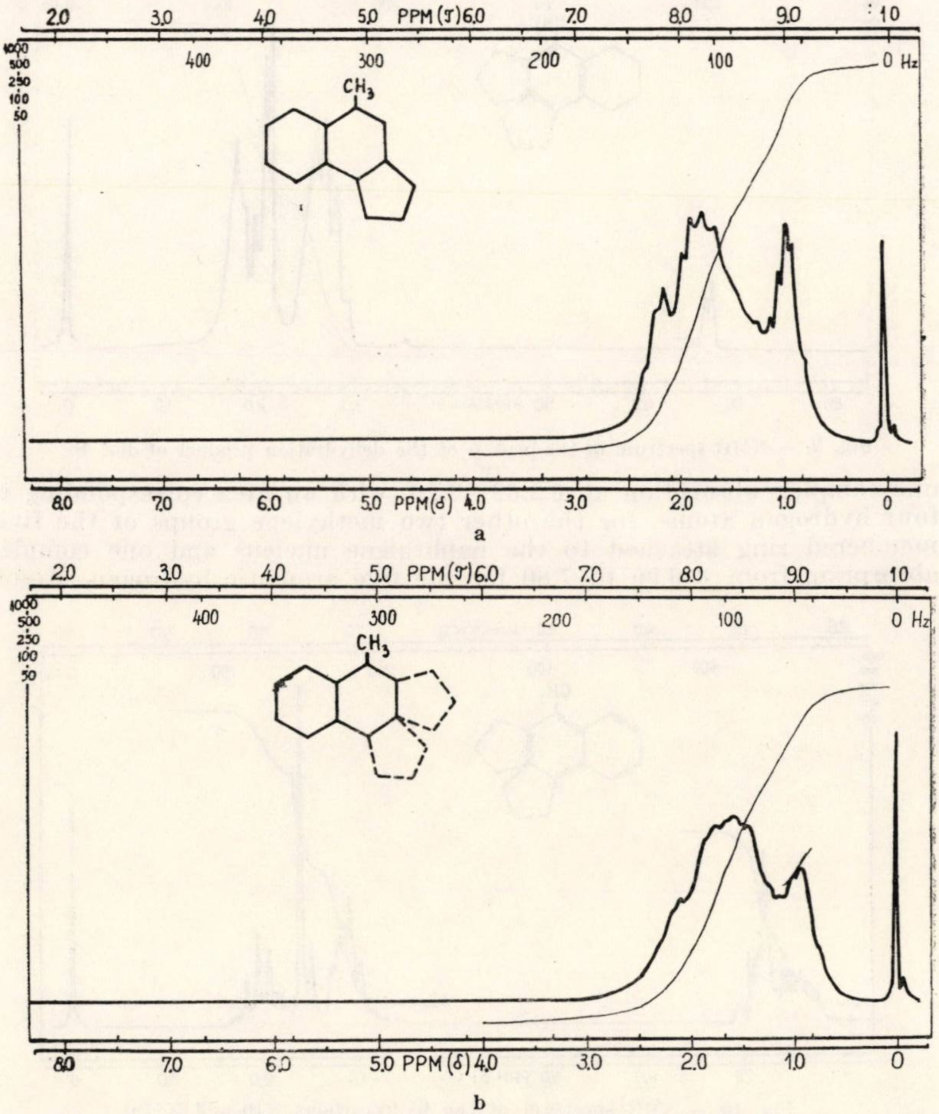

a

b

Fig. 8. — NMR spectra of the first group of peaks of the dehydration product of diol Ib :
a) peak 5; *b*) peak 2 + peak 3 + peak 4 + peak 5.

corresponds to the $C_{14}H_{14}$ formula and has one quintet at δ 1.95 ($J = 7$ Hz) assigned to the methylene group of five-membered ring nonattached on naphtalene nucleus; one doublet from δ 2.32 to 2.62 for the methyl group attached to the naphtalene nucleus (the first at δ 2.40 for the linear isomer XIIb and the second at δ 2.51 for the angular isomer XIb);

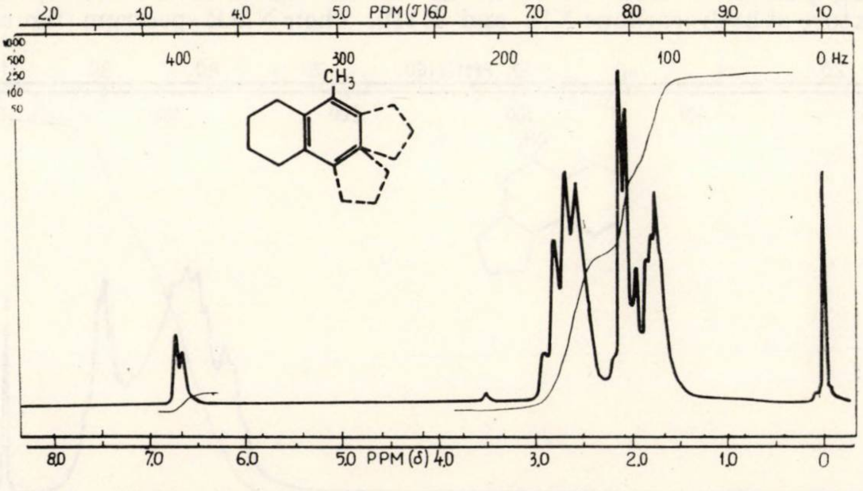

Fig. 9. — NMR spectrum of the peak 6 of the dehydration product of diol Ib.

one complex absorption at δ 2.62—3.20, with an area corresponding to four hydrogen atoms, for the other two methylene groups of the five-membered ring attached to the naphtalene nucleus and one complex absorption from δ 6.90 to 7.80 for the five aromatic hydrogen atoms.

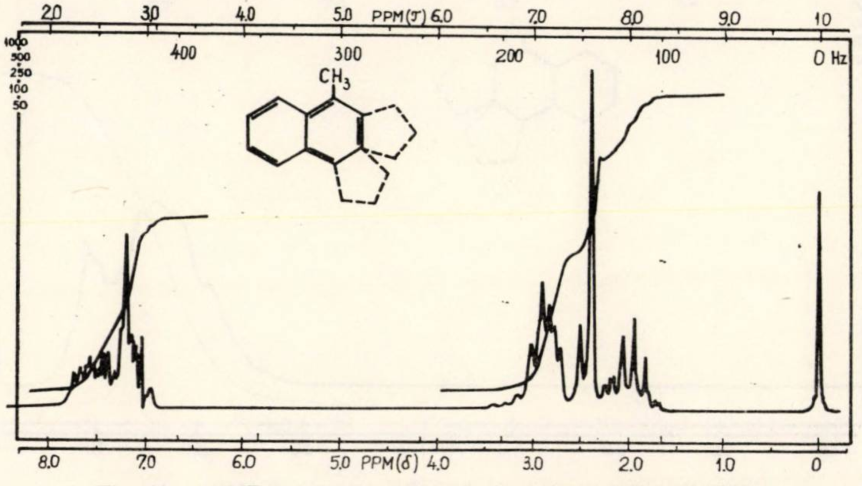

Fig. 10. — NMR spectrum of the hydrocarbons XIb and XIIb.

Therefore, the methyl groups of XIb and XIIb give characteristic signals. The XIb : XIIb ratio is about 1 : 3 as resulted from integral curve and 1 : 3.4 as resulted from gas-liquid chromatography on carbowax 20M.

CONCLUSIONS

Elimination of two water molecules from diol Ia leads to the formation of the hydrocarbons Va and VIa as main products. In addition to these linear hydrocarbons, the corresponding angular hydrocarbons may also arise. Gas-liquid chromatographic analysis on carbowax 20 M reveals the conclusion that the ratio between the linear hydrocarbon VIa and the angular one VIIa is 7 : 1, i.e. the linear isomer prevails. The existence of isomer VIIa is explained by the migration of the double bond in the position 7–8.

Elimination of the two molecules of water from diol Ib results in the formation of the hydrocarbons Vb, VIb and Xb and, probably, of the corresponding saturated linear hydrocarbons. The Xb : VIb ratio is 1,2 : 1. The decreasing of this ratio is explained by the migration of the double bond in the position 7–8 due to the hyperconjugation effect of the methyl group. The migration of the double bond is also observed in the NMR spectrum of the unsaturated acetate IIb, the methyl group giving one doublet with smaller chemical shift for the methyl attached to the saturated C_8, as well as one singlet with larger chemical shift for the methyl attached to the ethylene C_8. The spectrum does not allow the calculation of the isomers ratio.

EXPERIMENTAL PART

The preparation of diols Ia and Ib has been described in the earlier papers.[3,22]

TRICYCLO[7. 3. 1. $0^{2,7}$]TRIDECA-2-ENE-13-ACETATES IIa

98 g (0.4667 mole) of diol Ia, 241.5 g (2.367 mole) of acetic anhydride (the ratio diol Ia : acetic anhydride was 1 : 5.07) and 10 g of zinc chloride were heated gradually in an air bath in an experimental equipment consisting of a 500 ml two necks round-bottomed flask, a 80 cm Vigreux column and a distillation head leading to a graduated separating funnel for the collecting of the acetic acid resulting from the reaction. The temperature was raised after $2\frac{1}{2}$ hr of refluxing and the acetic acid began to distillate. The distillation ceased after $1\frac{3}{4}$ hr. There were collected 101 ml distillate between 116 and 124° (theoretically 80.1 ml of acetic acid). The removing of acetic anhydride was continued and another 86 ml were collected. The remaining acetic anhydride was removed using the water-jet pump. The reaction mixture was cooled and extracted with ether (4 × 200 ml). The etheric extracts were washed with water and dried with natrium bicarbonate. The solvent removal gave 104 g of raw oil, which was distilled *in vacuo* (b. p. 110–111°/2 mm Hg) to give 72.6 g (66.5%) of colourless liquid, $n_D^{20} = 1.5083$; IR (CCl_4) : 2943, 2868, 2840, 1726, 1450, 1377, 1272, 1095, 1042, 992 and 974 cm^{-1}; NMR (CCl_4) : δ 1.03–2.29 (complex absorption), δ 1.96 (singlet), δ 4.74 (triplet).

8-METHYL-TRICYCLO[7. 3. 1. $0^{2,7}$]TRIDECENE-13-ACETATES IIb

100 g (0.446 mole) of diol Ib, 228.6 g (2.241 mole) acetic anhydride and 10 g of zinc chloride were heated and worked as above. There were obtained 106.7 g raw oil, which

was distilled *in vacuo* (b.p. 112–113°/1.5 mm Hg) to give 62.9 g (56.8 %) light yellow liquid, $n_D^{20} \times 1.5118$; IR(CCl_4) : 2943, 2868, 1726, 1451, 1377, 1272, 1110, 1042 and 986 cm^{-1}; NMR (CCl_4) : δ 0.76–2.50 (complex absorption), δ 1.00 (doublet), δ 2.00 (singlet), δ 4.88 (triplet).

DEHYDRATION OF THE ALCOHOL Ia

50 g (0.238 mole) of diol Ia were heated with 25 g of zinc chloride in a Dean-Stark apparatus in an air bath. 8.6 ml of water were collected in 2 hrs (theoretically 8.6 g of water).

35.5 g of dehydration product were obtained, $n_D^{20} = 1.5521$, which were analysed by gas-liquid chromatography on carbowax 20 M.

DEHYDRATION OF THE ALCOHOL Ib

30 g (0.134 mole) of diol Ib and 6 g zinc chloride were heated in an air bath in a Dean-Stark apparatus. 4.7 ml of water were collected in 2 hrs (theoretically 4.8 g of water). 26 g of dehydration product were obtained, which were analysed by gas-liquid chromatography on carbowax 20 M.

The dehydrogenation of the hydrocarbon VI a and of the mixture of hydrocarbons VIb and Xb using platinized asbestos was made in the same conditions as the dehydration using palladium.[22]

The chromatographic analysis was performed by employing a Becker 401 type gas-liquid chromatograph, using a 6 mm o.d. copper column, 4 m in length. Packing material was 16 % carbowax 20M on 60–80 mesh celite C_{22}. The flame ionization detector was used, with nitrogen as carrier gas. The conditions were as follows :

injection temperature	210°
column temperature	100–200°, with 6°/min programing
detector temperature	240°
gas flow rate	40 ml/min
injected quantity	0.5–1µl.

The preparative gas-liquid chromatography was carried out on a Carlo Erba GT type preparative chromatograph by employing a 10 mm o.d. stainless steel column, 2 m in length, and 20 % carbowax 20M on 30–60 mesh chromosorb W as packing material. The thermal conductivity detector was used, with hydrogen as carrier gas. The conditions were :

injection temperature	280°
column temperature	195°
detector temperature	280°
gas flow rate	500 ml/min
auxiliary gas flow rate	60 ml/min
injected quantity	150µl.

The purity of fractions was verified using a 4 mm o.d. aluminium column, 2 m in length and 20 % carbowax 20M on 60–80 mesh chromosorb W as packing material, on an analytical Carlo Erba GT chromatograph in the following conditions :

injection temperature	260°
column temperature	115–170°, with 4°/min programing
detector temperature	260°
hydrogen flow rate	25 ml/min
injected quantity	0.2–0.4µl

thermal conductivity detector.

Revue Roumaine de Chimie, **19**, *2*, 249–253 (1974)

ÜBER 1,2,3,4-TETRAHYDROACRIDIN-9-CARBOXYLSÄURE DERIVATE II[1]

ESTER UND THIOESTER

M. CÂRJE

Physiologisches Institut „D. Danielopolu", Bukarest, Bd. 1 Mai, nr. 11

Eingegangen am 23. Juni 1973

Wir bemühten uns einige Ester- und Thioester - abkömmlinge der im Titel angegebenen Säure zu synthetisieren, um ihre Wirkung auf das Nervensystem studieren zu können.

Das Säurechlorid der 7-R-1,2,3,4-Tetrahydroacridin-9-Carboxyl-Säure (R = H, Cl, OCH_3) reagiert mit Äthanol, Äthylen Glykol, Athylen Chlorhydrin oder Diäthylamin-Äthanthiol, wobei die entsprechenden Ester und Thioester entstehen.

Die neusynthetisierten Ester und Thioester wurden auch durch I.R.-Spektren charakterisiert.

Von der Tatsache ausgehend, daß die Acridinstrukturen, die einen teilweise oder gänzlich gesättigten Ring besitzen, eine Wirkung auf das Nervensystem ausüben könnten, setzten wir die Synthese von Abkömmlingen der 1,2,3,4-Tetrahydroacridin-9-Carboxyl-Säure (THA-Säure) fort. Wir nahmen die Synthese einiger Ester und Thioester der Abkömmlinge der THA-Säure mit H, Cl, oder OCH_3 in Stellung 7 vor.

Die Synthese der THA-Säuren erfolgte[1], indem wir von Anilin, *p*-Chloranilin und *p*-Anisidin ausgingen, die mit Chloralhydrat und Hydroxilamin reagieren und die entsprechenden Isonitrosoacetanilide, die in Gegenwart von Schwefelsäure zu dem Isatinring führen, ergeben. Die Isatine reagieren in basischem Milieu mit Cyclohexanon, wobei die THA-Säuren entstehen. Unter Einwirkung von Phosphorpentachlorid werden die entsprechenden Säurechloride erhalten. Die Ester sind von den nachstehenden Alkoholen abgeleitet: Äthanol, Äthylenglykol und Äthylenchlorhydrin, während die Thioester von Diäthylaminäthanthiol ausgehen.

Das Säurechlorid reagiert mit den entsprechenden Alkoholen und dem Thioalkohol, wobei als Reaktionsmilieu Azeton, Dichloräthan oder auch der entsprechende Alkohol verwendet wurde. Die Thioester isolierten wir unter Form von Chlorhydraten, da die freien Basen keine Stabilität aufweisen.

---

[1] I. Mitt, M. Cârje, *Rev. Roumaine Chim.*, **18**, 1013 (1973).

Tabelle 1

Charakteristika der erhaltenen Ester und Thioester

Nr.	Benennung	R	R′	Schm. p.*	Ausbeute %	N%		Rekristallisierungsflüssigkeit
						berechnet	gefunden	
1	Äthylester der THA-Säure	H	$O-CH_2-CH_3$	54– 55	86	5,49	5,35	Petroläther
2	Äthylester der Chlor-THA-Säure	Cl	,,	88– 89	81	4,83	4,97	Petroläther
3	Äthylester der Methoxy-THA-Säure	OCH_3	,,	69– 70	90	4,91	4,78	Petroläther
4	2-Hydroxiäthylester der THA-Säure	H	$O-CH_2-CH_2-OH$	153– 54	72	5,16	5,18	Äthanol
5	2-Hydroxiäthylester der Chlor-THA-Säure	Cl	,,	171– 72	68	4,58	4,64	Äthanol
6	2-Hydroxiäthylester der Methoxy-THA-Säure	OCH_3	,,	164– 65	79	4,65	4,77	Äthanol
7	2-Chloräthylester der THA-Säure	H	$O-CH_2-CH_2-Cl$	68– 69	83	4,83	4,75	Azeton
8	2-Chloräthylester der Chlor-THA-Säure	Cl	,,	115–116	80	4,32	4,50	Benzol
9	2-Chloräthylester der Methoxy-THA-Säure	OCH_3	,,	123– 24	85	4,38	4,28	Azeton
10	Diäthylamino-2-Thioäthylester der THA-Säure	H	$S-CH_2-CH_2-$ $-NET_2.2HCl$	237– 39	55	6,75	6,59	ISO-Propanol
11	Diäthylamino-2-Thioäthylester der Chlor-THA-Säure	Cl	,,	232– 33	60	6,23	6,05	ISO-Propanol
12	Diäthylamino-2-Thioäthylester der Methoxy-THA-Säure	OCH_3	,,	225– 26	62	6,29	6,18	ISO-Propanol

* Die Schm.p. wurden nicht korrigiert.

Von den synthetisierten Ester ist ein einziges im Schrifttum [2] – und zwar das Äthylester der THA-Säure – verzeichnet, wobei sein Schmelzpunkt angegeben wird.

Die synthetisierten Ester und Thioester sind in Tab. 1 enthalten. Zur Charakterisierung der Substanzen und zur Identifizierung der verschiedenen Funktionsgruppen wurden die Infrarotspektren der neusynthetisierten Ester und Thioester bestimmt. Die Absorptionsbreite, die einer Frequenz von $\nu C = O$ entsprach, verhielt sich (siehe Tab. 2) zwischen 1714–1734 cm^{-1}, wobei sie dem in der Literatur für die Ester der aromatischen Säuren [3] angegebenen Bereich entsprach. Die Zwischenwirkung mit dem Schwefelatom in den Thioester 10–12 führte zur Minderung der Absorptionsfrequenz der Verbindung $C = O$ bis zu 1671–1678 cm^{-1} (im Schrifttum [3] 1680 $\pm$ 10 cm^{-1}). Der gesättigte Teil des dreizyklischen Systems konnte wegen Überlagerung mit dem Hydrokarbonatrest der Esterfunktion nicht nachgewiesen werden.

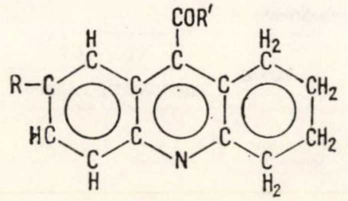

R

H,Cl, OCH_3

R'

$O-CH_2-CH_3$

$O-CH_2-CH_2-OH$

$O-CH_2-CH_2-Cl$

$S-CH_2-CH_2-N\ (C_2H_5)_2$

Die OH-Gruppe der Verbindungen 4–6 wurde durch die Frequenz $\nu O-H$ dargestellt. Es wurden breite Bänder bei cca 3200 cm^{-1} (durch Wasserstoffverbindungen) erreicht. Die Frequenzen der Auszugbreite der Verbindung $C-Cl$ ermöglicht die Identifizierung der „trans" – (700–760 cm^{-1}) und „gauche" – 650–690 cm^{-1})[4] Conformer. Die schwache Intensität dieser Bänder und die Überlagerung mit den Deformierungsbreiten der $C-H$ - Verbindungen des aromatischen Systems, lassen die Zuschreibung der dem „trans" - Conformer charakteristichen Frequenz bei den studierten Verbindungen als unsicher erscheinen.

Die Chlorhydrate der tertiären Amine 10–12 weisen ein sehr breites charakteristisches Band, um etwa 2500 cm^{-1} Frequenz auf, wie auch ein Spaltband mittlerer Intensität, bei etwa 2000 cm^{-1}, kennzeichnend für die Gruppe $C = \overset{+}{N}H$.[4] (Literatur [4]).

EXPERIMENTELLER TEIL

Äthylester der THA-Säuren. Zu 0,01 Mol. Chlorhydrat des Säurechlorids der entsprechenden THA-Säure werden 12 ml. absolutes Äthanol hinzugefügt. Es wird eine Stunde lang refluirt. Es wird anschließend mit 200 ml Wasser verdünnt, Kohle hinzugegeben und filtriert. Die entsprechenden Ester werden mit NaOH 2 N ausgefällt. Es wird filtriert und mit Wasser gewaschen.

---

[2] A. Albert, „The Acridines", E. Arnold, London, 1951, S. 207.

[3] C. N. Rao, „Chemical Applications of Infrared Spectroscopy", Academic Press, New York, 1963, S. 480, 362.

[4] M. Avram und Gh. D. Mateescu, „Spectroscopia în infraroşu", Ed.Tehnică, Bukarest, 1966.

2-Hydroxiäthylester der THA-Säuren. Zu 0,01 Mol. Chlorhydrat des Säurechlorids der entsprechenden THA-Säure werden 3,4 ml Äthylenglykol und 10 ml Azeton hinzugegeben. Es wird eine Stunde lang refluiert. Zubereitung wie oben.

Tabelle 2

Infrarot – Spektren[1])

Nr.	R.	R′	$\nu_{C=O}$	ν_{O-H}	$c_{alif}-Cl$		$C=\overset{+}{N}H$
					„gauche“	„trans“	
1	H	$O-CH_2-CH_3$	1722	—	—	—	—
2	Cl	,,	1714	—	—	—	—
3	OCH_3	,,	1725	—	—	—	—
4	H	$O-CH_2-CH_2-OH$	1722	3195[2])	—	—	—
5	Cl	,,	1726	3200[2])	—	—	—
6	OCH_3	,,	1731	3190[2])	—	—	—
7	H	$O-CH_2-CH_2-Cl$	1728	—	660	?	—
8	Cl	,,	1728	—	666	763	—
9	OCH_3	,,	1734	—	661	762	—
10	H	$S-CH_2-CH_2-NEt_2$. .2HCl	1673	—	—	1 —	1984 2006
11	Cl	,,	1679	—		—	1990 2014
12	OCH_3	,,	1671	—	—	—	1978 1996

[1]) Spektrophotometer U.R. 10, Carl Zeiss Jena, pastilliert mit K Br. Alle Frequenzen sind in cm^{-1} ausgedrückt.
[2]) Breitband.

2-Chloräthylester der THA-Säuren. Zu 0.01 Mol. Chlorhydrat des Säurechlorids der entsprechenden THA-Säure werden, 2,1 ml Athylenchlorhydrin hinzugegeben. Das Reaktionsgemisch wird eine Stunde lang auf 100–110°C über einem Ölbad erhitzt. Zubereitung wie oben.

N,N-Diäthylamino-2-Thioäthylester der THA. 2HCl.-Säuren. Zu 0,01 Mol. Chlorhydrat des Säurechlorids der entsprechenden THA-Säure in 20 ml Dichloräthan werden, 0,015 Mol. Diäthylaminoäthanthiol (aus Thioharnstoff und Diäthylamin-Chlor-2-Äthan präpariert [5]) hinzugefügt. Es wird eine Stunde lang refluiert, worauf Dichloräthan an der Wasserstrahlluftpumpe distilliert wird. Die Reaktionsmasse wird in 200 ml Wasser aufgelöst, Kohle hinzugefügt und filtriert. Die entsprechenden Thioester werden mit NaOH 2 N ausgefällt. Der Niederschlag, in Form einer schleimigen Masse, wird aus der Lösung durch Zentrifugieren abgesondert. Er wird 2—3 mal mit Wasser gewaschen und dies wieder durch Zentrifugieren entfernt. Die dickflüssige Masse wird in Azeton aufgelöst und mit wasserfreiem Na_2SO_4 ausgetrocknet. Nach Filtrieren wird dieser Lösung eine HCl Gas — in Azeton — Lösung beigefügt. Das Dichlorhydrat des Thioesters fällt aus. Es wird filtriert und mit Azeton gewaschen.

---

[5] N. F. Albertson und R. O. Clinton, *J. Amer. Chem. Soc.*, **67**, 1222 (1945).

Die erhaltenen Ester und Thioester sind in Tab. 1 aufgezeichnet.

Die elementaren Analysen wurden im Onkologischen Institut Bukarest von E. Tărnăuceanu durchgefürt, und die I. R. Spektren wurden von V. Feyns entwickelt. Wir bringen ihnen auch auf diesem Wege unseren besten Dank.

Revue Roumaine de Chimie, **19**, *2*, 255–258 (1974)

SYNTHESIS BASED ON FORMYL FURO (2,3-*b*) BENZOTHIACHROMONE

NICOLAE RĂȘANU * and OVIDIU MAIOR**

* Laboratory of Organic Chemistry, Pedagogic Institute of Constantza, Romania
** Laboratory of Organic Chemistry, University of Bucharest, Romania

Received April 24, 1973

In this work the cyclodehydration reaction has been applied to 2-carboxyphenyl-5′-formyl furylthioether in the purpose of obtaining 2-formyl furo (2,3-*b*) benzothiachromone. Chemical and IR evidences for the structure of the cyclization product are given.

One of the best methods for the synthesis of thioxantone, is orthocarboxydiphenylthioether acides cyclodehydration with different reagents such as polyphosphoric acid,[1, 2] concentrated sulphuric acid,[3] and so forth.

In order to obtain 2-formyl furo (2,3-*b*) benzothiachromone, a thioxantone analog in which one benzene ring is substituted by a furane nucleus, the cyclodehydration reaction was applied to 2-carboxyphenyl-5′-formyl furylthioether (I).

The starting material (I) was synthesized through an Ullmann reaction from thiosalicylic acid [4] and 5-iodfurfurol,[5] in the presence of potassium hydrogen carbonate and copper bronze. The yields in 2-carboxyphenyl-5′-formyl furylthioether are in the range 60–68%.

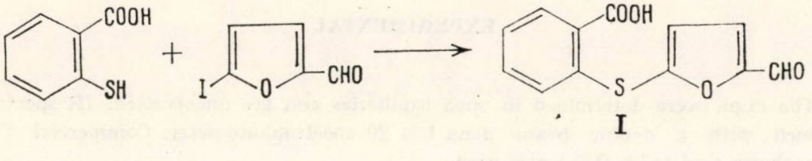

Polyphosphoric acid cyclization of (I) afforded 2-formyl furo (2,3-*b*) benzothiachromone, in 68% yield.

---

[1] M. Rajsner and M. Protiva, Pat. Ceh. 115.089, June 15 1965; *Chem. Abstr.*, **64**, 17549 g (1966).

[2] G. Vasiliu, N. Rasanu and O. Maior, *Rev. Chim.* (București), **19**, 561 (1968).

[3] K. Pelz and M. Protiva, *Coll. Czech. Chem. Comm.*, **32**, 2161 (1967).

[4] "Org. Synth." Coll. vol. II, John Wiley New York, 1943, p. 580.

[5] Z. N. Nazarova, *Zhur. obshchei. Khim.*, **25**, 539 (1955).

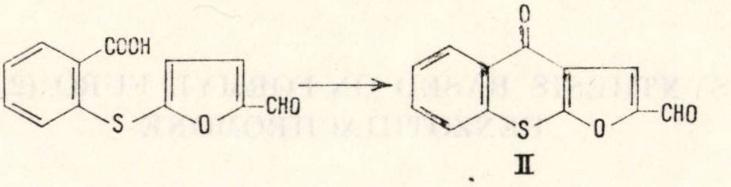

The temperature range 115—125° proved to be critical for the reaction; above this temperature non-unitary products were obtained.

The carbonyl groups in (II) have different reactivities, as evidenced by the formation of monoderivatives (IV) and (III) in the reaction with hidroxylamine and benzyl cyanide, respectively.

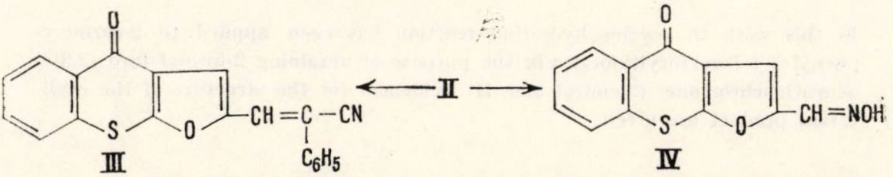

The oxime (IV) was converted into the nitrile (V) by means of acetic anhydride. Polyphosphoric acid is an excellent reagent for the hydrolysis of aromatic unhindered nitriles to amides.[6] The nitrile (V) through hydrolysis with polyphosphoric acid gave the expected amide (VI).

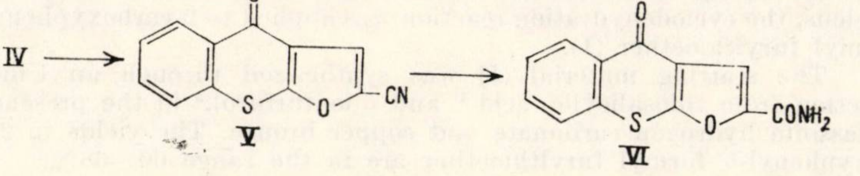

EXPERIMENTAL

The m.ps. were determined in open capillaries and are uncorrected. IR spectra were determined with a double beam Jena UR 20 spectrophotometer. Commercial "Merck" polyphosphoric acid (84 % P_2O_5) was used.

2-CARBOXYPHENYL-5-FORMYL FURYLTHIOETHER (I)

A mixture of thiosalicylic acid (5.5 g), 5-iodofurfurol (8 g), potassium hydrogen carbonate (7 g) and copper bronze (0.1 g) in 150 ml dioxan was heated under reflux for 4 hours.

---

[6] L. F. Fieser and M. Fieser, "Reagents for Organic Synthesis", John Wiley New York, 1967, p. 903.

After cooling, the mixture was diluted with 1000 ml water, filtered and the solution was acidified with dilute hydrochloric acid. The precipitate was collected by filtration. Recrystallization from methanol gave white crystals, m.p. 203--205°. 68% yield.

Found : S, 12.25 $C_{12}H_8O_4S$ requires : S, 12.51%

IR (KBr) cm^{-1} 750 (4H), 1680 (formyl), 1710 (carboxy)

2-FORMYL FURO(2,3-b) BENZOTHIACHROMONE (II)

The foregoing acid (6 g) was heated between 115–125° for 2 hours, under vigorous stirring, with polyphosphoric acid (54 g). The mixture was cooled and poured into an excess of ice-water. The resulting precipitate was collected on a Büchner funnel and washed successively with water, potassium hydrogen carbonate solution, and again with water. The crude material was recrystallized from dioxan, giving the desired product (II) 3.2 g (58%) m.p. 242–243°.

The product (II) with conc. H_2SO_4 give a brown-red colour with a slight green fluorescence.

Found : C, 62.83 ; H, 2.85 ; S, 14.16 $C_{12}H_6O_3S$ requires : C, 62.59 ; H, 2.62 ; S, 13.92

IR(KBr) cm^{-1} 740 (4H), 1225 (C–O–C), 1635 (CO), 1675 (formyl)

β-[FURO (2,3-b) BENZOTHIACHROMONE]-α-PHENYLACETONITRILE(III)

The compound (II) (0.7 g) was dissolved under slightly heating in a mixture of dioxan (20 ml) and methanol (20 ml). Benzyl cyanide (0.1 ml) and a drop of 10% NaOH was added, and the mixture was kept at room temperature for 7 hours.

Extraction of the resulting solid with dioxan, and then with glacial acetic acid for moving off impurities, gave crystalline residue (0.7 g), m.p. 265–266°. This compound with conc. H_2SO_4 give a yellow colour with green fluorescence.

Found : S, 9.90 $C_{20}H_{11}O_2SN$ requires : S, 9.73%.

IR(KBr) cm^{-1} 740 (4H), 1215 (C–O–C), 1630 (CO), 2215 (CN)

2-FORMYL FURO (2,3-b) BENZOTHIACHROMONE OXIME (IV)

A mixture of compound (II) (2 g), hidroxylaminehydrochloride (2 g) and anhydrous pyridine (30 ml) was boiled on water bath for 3 hours.

After cooling the reaction mixture was diluted with water, and the resulting precipitate after filtration and recrystallization from methanol yielded (IV) (2 g) m.p. 248–249°. This compound with conc. H_2SO_4 give a blue fluorescence.

Found : S, 13.27 $C_{12}H_7O_3SN$ requires :S, 13.07%.

IR (KBr) cm^{-1} 745 (4H), 1230 (C–O–C), 1620 (CO), 3200–3300 (OH)

2-CIANO-FURO (2,3-b) BENZOTHIACHROMONE (V)

The foregoing oxime (2 g) and acetic anhydride (20 ml) were refluxed for one hour. After cooling, the mixture was diluted with water. The resulting precipitate was filtered and recrystallized from glacial acetic acid to give (V) (1.5 g) m.p. 197–199°. With conc. H_2SO_4 blue fluorescence.

Found : S, 14.20 $C_{12}H_5O_2SN$ requires : S, 14.11 %.
IR (KBr) cm^{-1} 740 (4H), 1225 (C–O–C), 1645 (CO), 2230 (CN)

2-CARBOXAMIDO FURO (2,3-b) BENZOTHIACHROMONE (VI)

A mixture of nitrile (V) (1.5 g) and polyphosphoric acid (20 g) was stirred between 110–120° for 2 hours. The mixture was cooled and poured into an excess of ice-water.

The resulting precipitate was filtered, washed with water and recrystallized from glacial acetic acid, to give (VI) (0.3 g) m.p. > 300°. The product (VI) with conc. H_2SO_4 give a blue fluorescence.

Found : S, 13.23 $C_{12}H_7O_3SN$ requires : S, 13.07 %.
IR (KBr) cm^{-1} 740 (4H), 1220 (C–O–C), 1640 (CO), 1690 (CO), 3180 (NH)

Revue Roumaine de Chimie, **19**, *2*, 259–281 (1974)

SYNTHESES OF NEW POLYMERS BY DESTRUCTIVE METHODS. II [1]

MECHANOCHEMICAL COMPLEXATION AND COMPLEXATION BY IRRADIATION USING ^{60}Co γ-RAYS IN THE SYSTEM: POLY(ETHYLENETEREPHTHALATE), ETHYLENEDIAMINE AND METALLIC SALTS

CRISTOFOR SIMIONESCU, CLEOPATRA VASILIU OPREA and CLAUDIA NEGULIANU

Polytechnical Institute of Iassy, Department of Organic and Macromolecular Chemistry,
Str. 23 August N° 11, Romania

Received April 7, 1973

Destruction of the heterochain polymers, of the nature of poly-(ethyleneterephthalate), achieved under the action of the mechanical energy and that of γ-rays, is accompanied by the accumulation of an increasing number of functional end groups, able to react with suitable condensation agents existing in the working medium and where metallic salts are also present in system, the fragments synthesized by polycondensation act as macromolecular ligands. Processes of polycondensation and complexation activated by destructive methods are decisively influenced by some factors, as: processing time, ratio of reactants (polymer : diamine : metallic salt), temperature and atmosphere (inert, oxygen, etc.) in which the reaction occurs. The such obtained polycondensation and polycomplexation products exhibit sensibly different properties from those of the support polymers: increased thermal stability, permanent magnetic moment and chemical resistance against some aggressive media (acids, bases and solvents).

INTRODUCTION

Experimental observations registered at mechanochemical polycondensation showed the ability of such synthesized fragments to react with the building material of the apparatus in which the mechanical processing was achieved, suggesting a new sort of synthesis, namely mechanochemical complexation.[2–4] On the other hand, the achieving of polycondensation by means of a destructive factor in condition of $^{60}Co\gamma$-rays energy instead of mechanical energy, reported in the first note of this work, created complexation premises for the destruction fragments of poly (ethyleneterephthalate) in the presence of ethylenediamine and some metallic salts.

---

[1] Cr. Simionescu, Cl. Vasiliu Oprea and Cl. Negulianu, *European Polymer J.*, **10**, 61 (1974).

[2] Cr. Simionescu, Cl. Vasiliu Oprea and Cl. Negulianu, *Buletinul Institutului Politehnic Iaşi, seria nouă*, **15 (19)**, 3/4, 45–56 (1969).

[3] Cr. Simionescu, Cl. Vasiliu Oprea and Cl. Negulianu, *Makromol.* Chem., **148**, 155 (1971).

[4] Cr. Simionescu, Cl. Vasiliu Oprea and Cl. Negulianu, *Makromol. Chem.*, **163**, 75 (1973).

The aim of the present paper is to describe comparatively the complexation methods under the action of the two kinds of energy (i.e., mechanical and γ-irradiation) on the principle of satisfying the electron vacancy of some metallic elements at the expense of electrons unparticipant in the chemical bond of electronegative elements (e.g., O and N) disposed along the macromolecular backbone. The complexation reaction takes place in the presence of polycondensation fragments, simultaneously synthetized, which finally act as macromolecular ligands.

We must mention that intermediate active centres are important for process achieving, and we also suppose that the complexation reaction starts only after the accumulation of a sufficient number of $-CO-NH-$ groups by chain which will become the future ligand; the $-CO-NH-$ group has two electronegative atoms carrying free electrons which will occupy vacancies of metallic elements.

The mechanochemical complexation and that by irradiation were verified in the system: poly(ethyleneterephthalate): ethylenediamine (forming the ligand): different metallic salts (e.g., Fe^{3+}, Mn^{2+}, Co^{2+}, Ni^{2+}, etc., acetates and chlorides).

EXPERIMENTAL

1. METHODS OF INVESTIGATION

The components of the polycondensation reaction, i. e., poly(ethyleneterephthalate) and ethylenediamine, were purified as previously described [5] and metallic salts were used without purification as "pro analysis" derivatives.

The mechanochemical complexation was processed in a laboratory vibrating mill LS-60, VEB Kefama Kotzhutte/Thuringer DDR equipped with stainless-steel milling bodies and vessels, gas admission and exhaust valves and thermostating jacket. Polymer powder, metallic salt and the balls were introduced into milling vessels ensuring the desired filling ratio (i.e., $\alpha = 0.4\,\%$). After vessel sealing and their cleaning by 3 or 4 vacuum — nitrogen cycles the reaction was carried out in nitrogen atmosphere. The amount of required ethylenediamine was introduced in the last vacuum cycle through a calibrated pipette fixed at a cover valve. The reaction temperature was $18 \pm 2°$. Vibration frequency was that of motor number of revolution (i.e., 1450 r.p.m.) and vibration amplitude was of 4 mm.

The complexation reaction by irradiation was carried out in glass ampoules equipped with a sealing system and means to make vacuum or to change the inert atmosphere. After homogeneous mixing of poly-(ethyleneterephthalate), ethylenediamine and metallic salt, the ampoules were cleaned by a vacuum — nitrogen cycle and after nitrogen cycle and nitrogen filling were sealed and exposed to ^{60}Co γ-rays action of 231 rad/hour. The irradiation time was constant (i.e. 18 hours) and corresponded to a dose of 15 Mrad.

---

[5] CL. VASILIU OPREA, CL. NEGULIANU and CR. SIMIONESCU, *Makromol. Chem.*, **126**, 217 (1969).

In the case of the mechanochemical method the complexation was achieved using the following systems :

a) poly(ethyleneterephthalate) (10 g) + ethylenediamine (30 g) + $FeCl_3.6H_2O$ (6.5 g).

b) poly(ethyleneterephthalate) (10 g) + ethylenediamine (30 g) + $Mn(CH_3COO)_2.4H_2O$ (6 g).

c) poly(ethyleneterephthalate) (10 g) + ethylenediamine (30 g) + $MnCl_2.4H_2O$ (6 g).

A wide range of factors was pursued in this reaction, e.g., polymer : diamine ratio, influence of the amount of metallic salt or of its anion and reaction time.

A systematic study and the obtained data were in detail reported earlier. [3,4]

When γ-rays energy was used, the main question lay in practical verification of this possibility of synthesis. For this purpose, all the parameters considered at mechanochemical degradation and the irradiation dose were kept constant and the influence of the amount of metallic salt, which is the provider of complexing agents, was mainly followed.

The reaction products obtained under the action of these two energies, i.e. mechanical and of γ-rays, were purified by methanol extraction in a Soxhlet apparatus with a view to removing the unreacted ethylenediamine and metallic salt.

In all cases two fractions were obtained by extraction, one soluble in methanol and another insoluble in methanol. The first fraction was considered to be purified when the material from the extraction cartridge did not vary its weight and the washing liquid had not chlorine anions (at least for metallic chlorides). After separation, this part of the reaction product was dried in vacuum at 40° and analysed. The obtained extract consists in a mixture of micromolecular derivatives, i.e. ethylenediamine and metallic salt, which represent the unreacted part of the reactants taken in excess and of some complexes synthesized on the above discussed principle, but methanol soluble.

We suppose that this part of the extraction mixture results either by polycondensation of oligomers (obtained by mechanochemical destruction or by irradiation of the support — polymers) with ethylenediamine and, subsequently, complexation with metallic elements or by the reaction of polycondensate with the complexing centre.

In order to separate this part of the extract it was concentrated, precipitated with ethylether, filtered and washed with large amounts of ether up to a complete removing of micromolecular components (i.e., ethylenediamine and metallic salts). After this treatment the product was dried in vacuum at room temperature and was considered as soluble fraction. Two specifications must be made :

1 — Solubility was for the moment verified only for a limited number of solvents.

2 — The discussed fraction does not solve as a matter of fact in methanol but in a methanolic solution of ethylenediamine (after purification, this fraction becomes insoluble in ethylenediamine free methanol).

2. INFLUENCE OF SOME FACTORS ON THE COMPLEXATION REACTION IN DESTRUCTIVE CONDITIONS

2.1. Reaction time

The influence of this factor on the mechanochemically conducted reaction was followed choosing as criterion for its evolution the percentage of chemically linked nitrogen, determined by the Kjeldahl method.

The obtained results are comparatively presented together in fig. 1. We can see that metal inserting in the structural unit of the new compound obtained determines a sensible lowering of the percentage of chemically linked nitrogen by polycondensation; the more weakly linked is the metallic element in the metallic salts which provide it, the lower is this percentage.

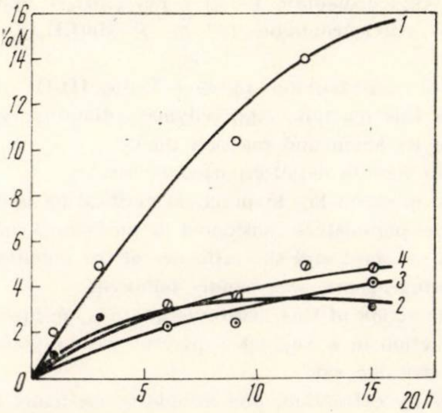

Fig. 1. – Dependence of chemically linked nitrogen on the reaction time for complexation products mechanochemically synthesized.

1, Witness polycondensation process; *2*, Complexation with $FeCl_3 . 6H_2O$; *3*, Complexation with $MnCl_2 . 4H_2O$; *4*, Complexation with $Mn(CH_3COO)_2 . 4H_2O$.

Examining curves *2* and *3* obtained using metallic chlorides salts of a strong acid – it is obvious that the content of chemically-fixed nitrogen is, for each moment of the reaction, lower than that corresponding to acetic salts (curve *4*) in which the metallic element is less bound. Owing to this fact the metallic centre is more easily attracted in the ligand sphere, the formation in the same period of several chelate centres being possible, in this last situation. At the same time, in every complexation case, the chemically linked nitrogen is lower than that corresponding to polycondensation products, proving formation of new structural units.

2.2. *Quantity of metallic salt*

The amount of ferric chloride, provider of complexing centres, is another decisive factor of reaction. In order to point out its influence, a succession of milling processes were achieved maintaining at constant values duration (3 hrs.) and diamine quantity (30 g) and varying metallic salt (i.e. ferric chloride) from 1.5 g to 15 g; the percentage of chemically linked nitrogen decreases gradually with the increase of the amount of complexing agent (fig. 2).

2.3. *Quantity of diamine*

The polycondensation process, in fact that of synthesis of the macromolecular ligand, is intimately determined by the amount of diamine introduced. The ratio between the reactants introduced represents a significative parameter of the reaction development as it regulates the proportion between the reaction of ligand synthesis and that of polycondensation.[2,5] This ratio was modified by introducing in the reaction medium variable amounts of ethylenediamine (10 – 15 ml), keeping unchanged the amounts of poly (ethylenterephthalate) and of metallic salt. The syntheses were carried out for a constant time of 9 hrs and the results are presented in fig. 3. For all investigated cases the curves are ascensive and have a flattening tendency for large diamine quantities (i.e., about 50 ml).

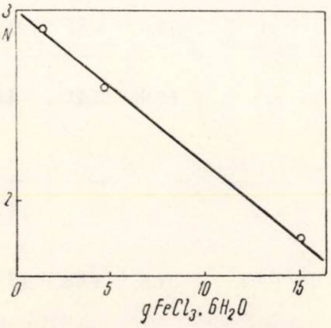

Fig. 2. Dependence of complexation reaction of poly (ethylenterephthalate) with ethylenediamine and $FeCl_3.6H_2O$ on the amount of metallic salt (iron chloride).

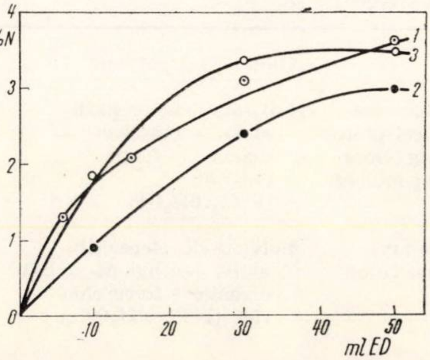

Fig. 3. Influence of amount of ethylenediamine on the process of mechanochemical complexation :
1, ferric chloride ; *2*, manganese chloride ; *3*, manganese acetate.

3. CHARACTERIZATION OF COMPLEXATION PRODUCTS SYNTHESIZED BY DESTRUCTIVE METHODS

3.1. Elementary analysis

One of the methods used for the characterization of complexes achieved by one of the two discussed routes, which allows for establishment of chemical composition, was the thermal decomposition of products in a combustion furnace at 700° and in nitrogen stream. The obtaine results are presented in tables 1 and 2.

Both at complexes based on iron and on manganese we can see a sensible modification of the elementary composition of the support polymer owing to its transformation by polycondensation and fixation of the metal as complexing centre.

Thus, it was found that the percent content of hydrogen and carbon is sensibly changed and a new element, namely nitrogen, is inserted,

Table 1

Comparative data of the chemical composition of the complexes synthesized (by mechanochemical processing and by γ-rays irradiation) from poly(ethyleneterephthalate), ethylenediamine and ferric chloride

The way in which the reaction is activated	Complex	Reaction time (hrs)	Amount of metallic salt (g)	Elementary analysis		
				%C	%H	%N
—	Unmodified polymer	0	0	63.6	4.81	0
Mechanochemical processing (vibrating milling)	Poly(ethyleneterephthalate) + ethylenediamine + ferric chloride ($FeCl_3.6H_2O$)	96	6.5	14.98	2.41	3.80
^{60}Coγ-rays irradiation	Poly(ethyleneterephthalate) + ethylenediamine + ferric chloride ($FeCl_3.6H_2O$)	18 (15 Mrads)	6.5	—	—	11.50
		18	0.02	31.9	4.63	13.10

Table 2

Comparative chemical composition of the complexes synthesized from poly(ethylenterephthalate), ethylenediamine and manganese salts

The way in which the reaction is activated	Complex	Reaction time, hrs	Amount of metallic salt, g	Elementary analysis		
				%C	%H	%N
—	Unmodified polymer	0	0	63.60	4.81	0
Mechanochemical processing (vibrating milling)	PET[a] + ED[b] + + $Mn(CH_3COO)_2H_2O$	96	6	19.84	3.35	5.98
^{60}Coγ-rays irradiation	PET + ED + + $MnCl_2.4H_2O$	18	6	—	—	6.80
		(15 Mrads)	0.02	27.5	2.85	9.40** 10.0*

[a] Poly(ethyleneterephthalate); 18 hrs irradiation = 15 Mrads. [b] Ethylenediamine;

* Determined by the Kjeldhal method;

** Determined by analysis of pyrolysis products from combustion furnace.

which increases quantitatively with the processing time or with the amount of condensation agent.

Analysis of the products obtained changing different reaction parameters showed also corresponding changes of residuum, undecomposed during pyrolysis. The amount of residuum increases with the reaction time. The attempts to establish analytically (i.e., by colorimetric, gravimetric or volumetric analysis) the chemically bonded metal failed; the obtained values were anomalously increased. Consequently, the obtained residuum cannot be identified as one of the inorganic oxidate states of the metal to be used for its percent content calculation. In our opinion, this residuum represents in fact a macromolecular compound resulted by thermal transformation of the complex synthesized by the described methods, which remains unchanged up to high temperatures (i.e. near 1000°) and is characterized by chemical resistance (solvents, acids and bases).

Analysing the elementary composition of the products obtained at the limit degree of transformation by γ-rays irradiation and mechanochemically, it has been ascertained that, in the last case, the decrease of carbon or hydrogen content is more intense but the values of chemically linked nitrogen are greater in the first case.

It can be supposed that under mechanochemical conditions for long processing time, the reaction of ligand synthesis and complexation is accompanied by pronounced decarboxylation effects, more limited under irradiation conditions.

3.2. Infrared analysis

Infrared spectroscopy was another method used in order to obtain some information regarding the ligand structure and mechanism of its synthesis eventually. This method was indeed useful since the IR spectra of products synthesized in different working conditions are also different. The characterization of polycomplexes can be realized on the basis of their chemical composition which changes with the reaction time and the amount of complexing agent in the reaction medium.

Depending on these parameters, which condition the bonding of larger or smaller amounts of diamine, the complexation products are soluble or insoluble in extraction solvents (methanol or water) with the same remark, made at polycondensation, that the solubility does not refer to pure extraction solvents but to diluted solutions of ethylenediamine used for removing of the reactant excess (i.e., ethylenediamine or metallic salt) and their IR spectra show characteristic differences. Soluble products, containing high nitrogen percentages, (about 15%) exhibit a succession of common bands comparatively with IR spectra of the witness polymers, e.g., that corresponding to the aromatic ring or to the glycolic rest $-CH_2-CH_2-O-$, but other bands are quite new, corresponding to aminic groups, at 1560 cm^{-1} or 1640 cm^{-1} or to iminic groups, at 3300 cm^{-1}, which were formed by the reaction of destruction fragments with ethylene-diamine. In addition, these spectra are void of the band from 1720 cm^{-1}, corresponding to the most peculiar group of polyesteric support, namely the esteric carboxyl (fig. 4).

The IR spectra recorded in the case of insoluble products mechanochemically obtained ascertain the same structure of the ligand and of the corresponding polycondensation products, keeping the rule that

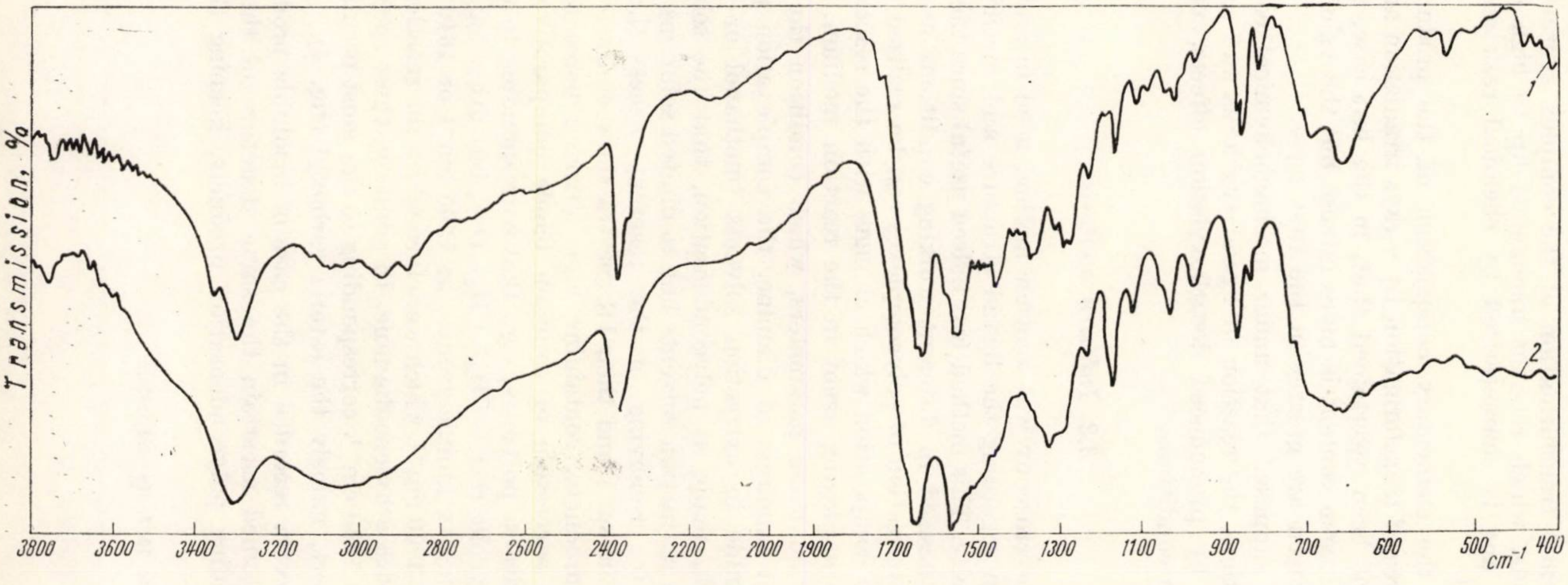

Fig. 4. — Comparative IR spectra of soluble complexes obtained by irradiation: *1*, Soluble product obtained from poly(ethyleneterephthalate), ethylenediamine and ferric **chloride**; *2*, Soluble **product** obtained from poly(ethyleneterephthalate), ethylenediamine and manganese **chloride**.

only for short reaction times the band of esteric carboxyl appears, it disappearing for long intervals of time (figs. 5, 6).

On the other hand, making a comparison between complexes characterized by limit degrees of transformation (e.g., 96 hours for mechanochemical synthesis and 18 hours for γ-rays irradiation process), we

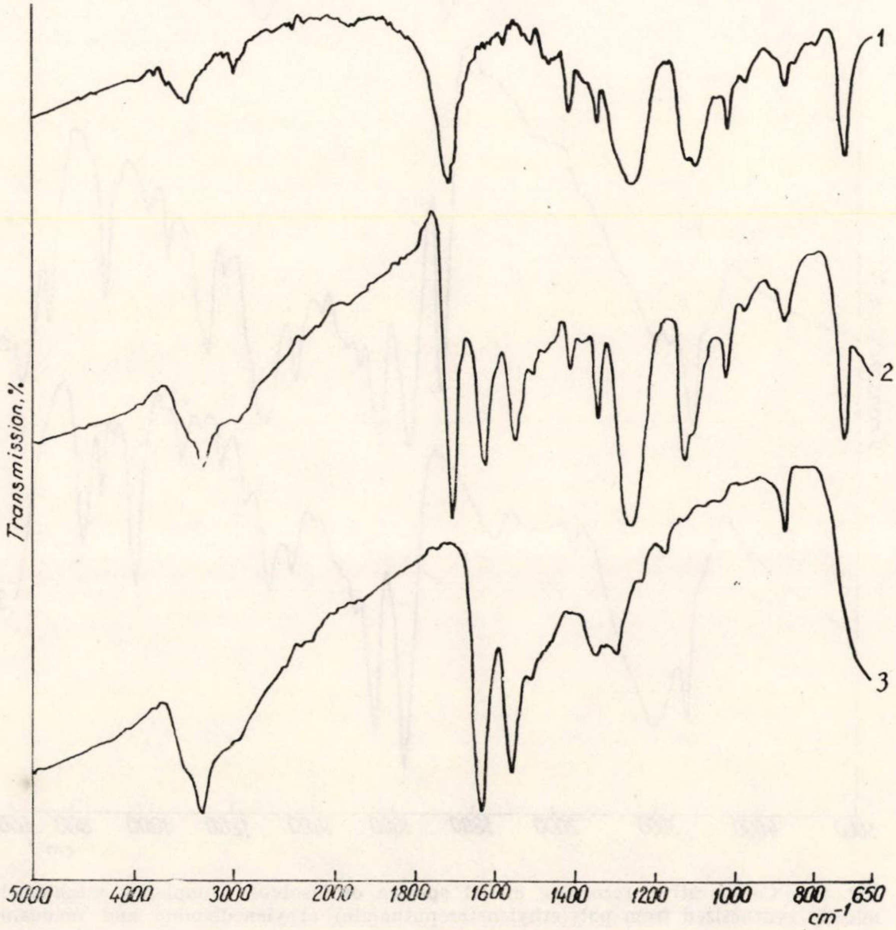

Fig. 5. — Comparative IR spectra of insoluble complexes mechanochemically obtained from poly(ethyleneterephthalate), ethylenediamine and ferric chloride:
1, Witness sample of poly(ethyleneterephthalate); *2*, Complex synthesized for a milling time of 15 hrs; *3*, Complex synthesized for a milling time of 96 hrs.

can see that, unlike the IR spectra of mechanochemical products which are void of band from 1720 cm^{-1}, the spectra of irradiation products still keep a small absorption at this wave number (fig. 7). This fact

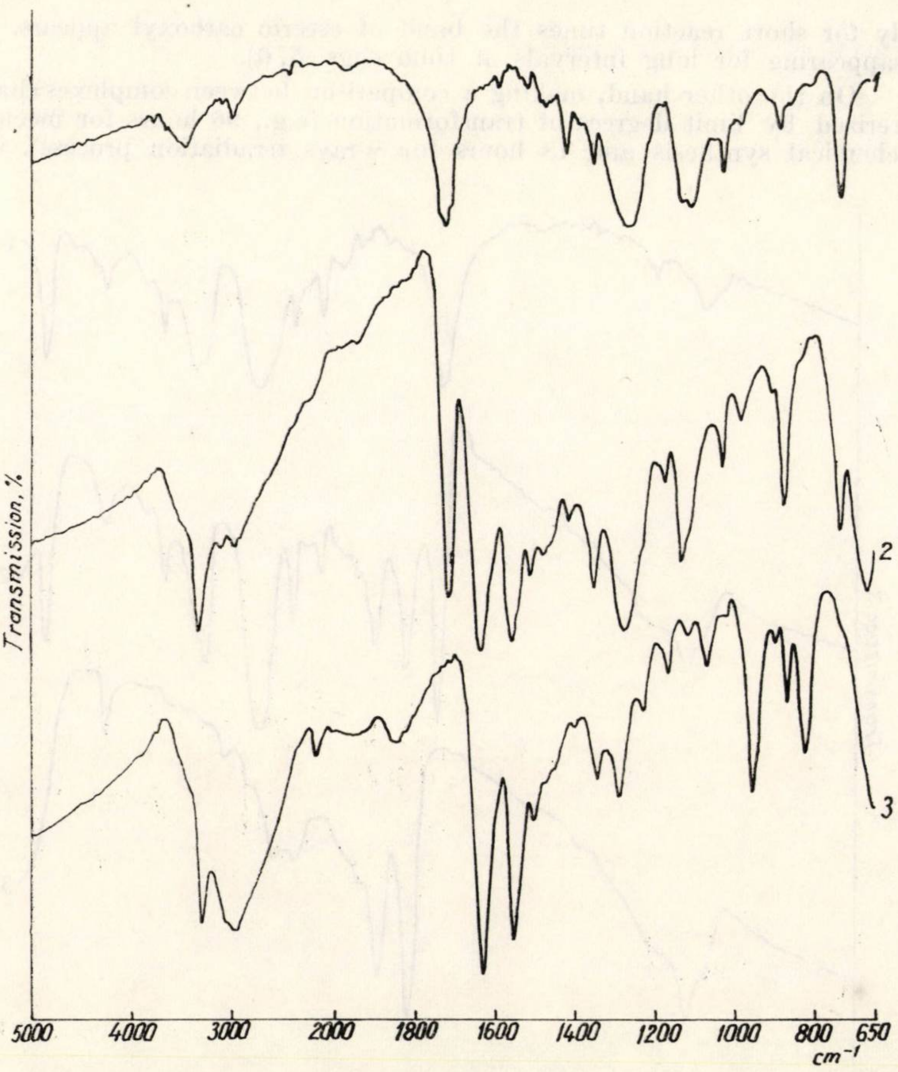

Fig. 6. — Comparative recording of IR spectra of insoluble complexes mechanochemically synthesized from poly(ethyleneterephthalate) ethylenediamine and manganese acetate;

1, witness polymer; *2*, complex synthesized for a milling time of 15 hrs.; *3*, complex synthesized for a milling time of 96 hrs.

may be explained by a more intense decarboxylation of the support for long durations of mechanochemical processing or by more intense effects of tautomer transformations $-CO-NH- \rightarrow -C=N-$, already discussed in our paper referring to polycondensation by destructive methods.

3.3. *ESR data*

The method of electron spin resonance has been used in order to point out the paramagnetic properties of the synthesized complexes.

These properties are justified on the one hand by the ligand structure (in ligands there are unparticipant electrons of electronegative elements, i.e. oxygen, nitrogen, from —CO—NH— groups formed by polycondensation) and, on the other hand, by the presence of metallic elements used as complexing centres (i.e. Fe^{3+}, Mn^{2+}). ESR spectra of samples synthesized mechanochemically or by irradiation containing variable amounts of metallic salts, were recorded using a Varian E-12 spectrometer.

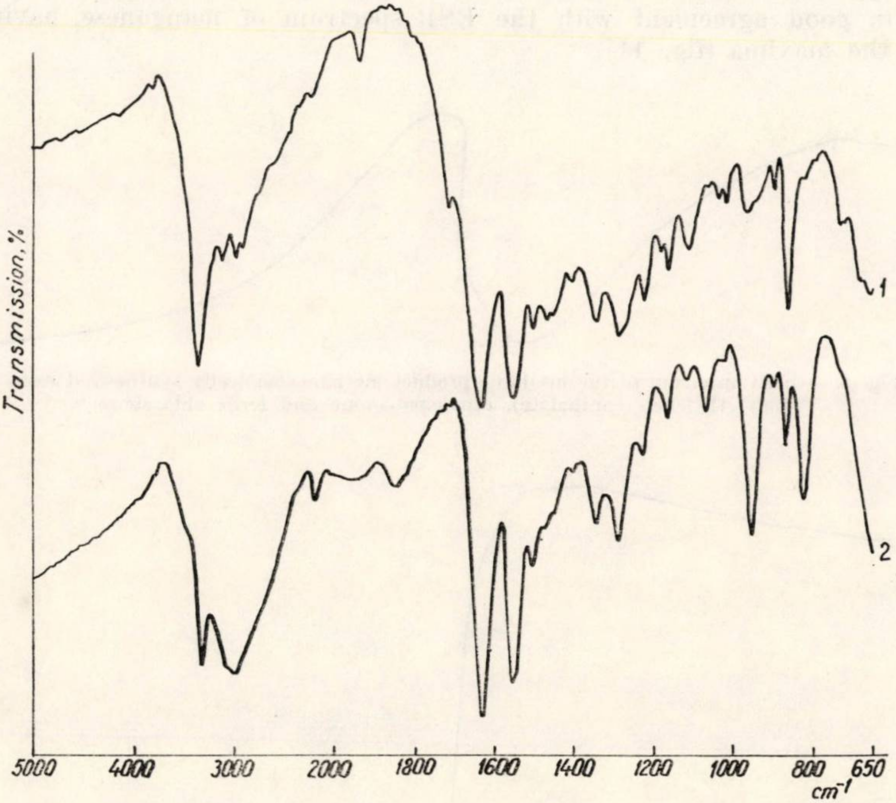

Fig. 7. — Comparative IR spectra of insoluble complexes of poly(ethyleneterephthalate), ethylenediamine and manganese acetate synthesized by irradiation (*1*) or by mechanochemical processing (*2*).

One can see that the number of complexing centres, respectively the metal amount of the polymer, has a decisive importance regarding the shape of ESR spectrum. It is well known that ESR spectra of paramagnetic metals are constituted from a number of bands which are characteristic for each element. Thus, in the case of manganese, ESR spectrum has six maxima, but,[6] in order to achieve this shape, the amount of metal has to be less than 10^{-1} g. Over this limit the bands overlap giving broader signals. In the case of the described complexes the metal amount in them exceeds almost in every case the said limit preventing the obtaining of a well-resolved spectrum. The high concentration of unpaired spins, owing to large amounts of metal, caused the overlap of the bands (figs. 8—10) both in the case of the samples mechanochemically synthesized and in the case of those obtained by irradiation. Nevertheless, in order to have a characteristic spectrum for synthesis of a complex by irradiation were used only 0.02 g of metallic salt (instead of 6.5 g, amount used in all cases). The ESR spectrum of this complex is in good agreement with the ESR spectrum of manganese, having all the maxima (fig. 11).

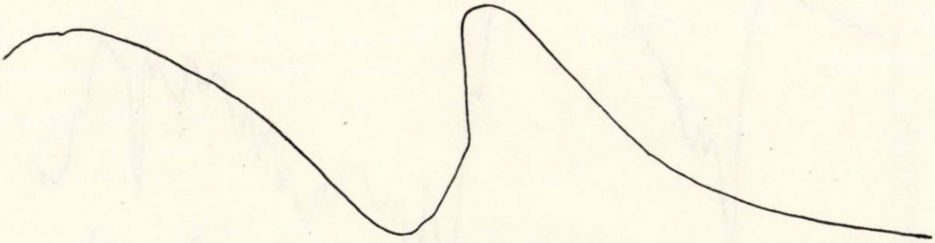

Fig. 8. — ESR spectrum of the insoluble product mechanochemically synthesized from poly(ethyleneterephthalate), ethylenediamine and ferric chloride.

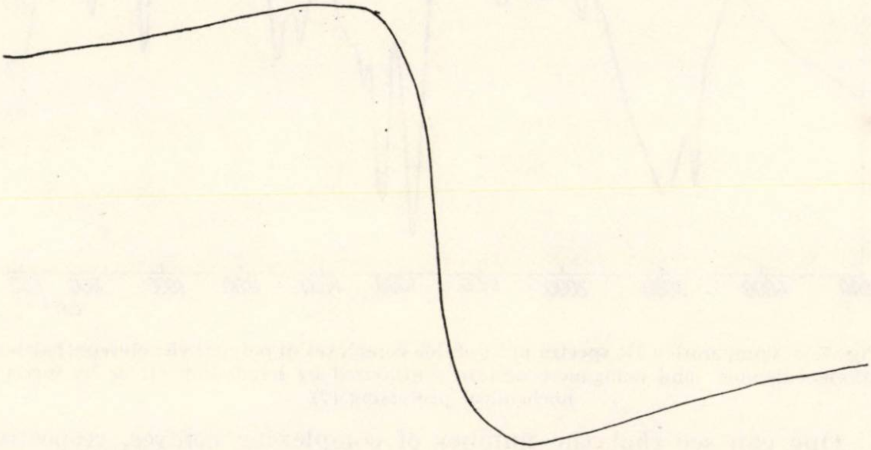

Fig. 9. — ESR spectrum of the insoluble product synthesized from poly(ethyleneterephthalate), ethylenediamine and ferric chloride by ^{60}Co γ-rays irradiation.

---

[6] I. Ursu, "Rezonanţă electronică de spin", Ed. Academiei, Bucharest, 1965, p. 198, 258.

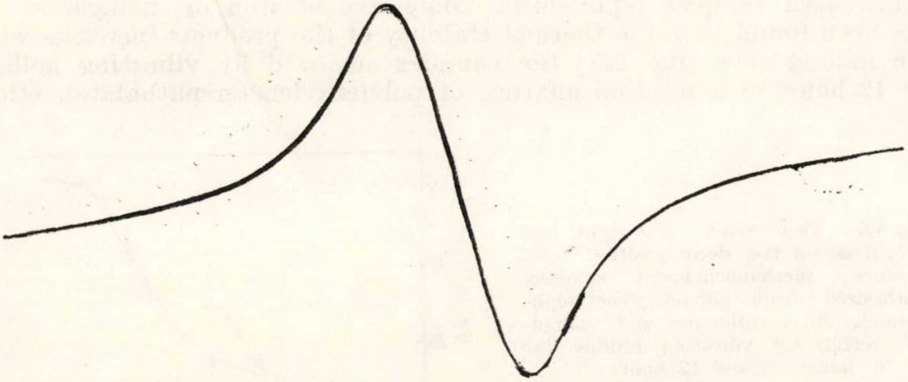

Fig. 10. — ESR spectrum of the insoluble product mechanochemically synthesized from poly(ethyleneterephthalate), ethylenediamine and manganese chloride.

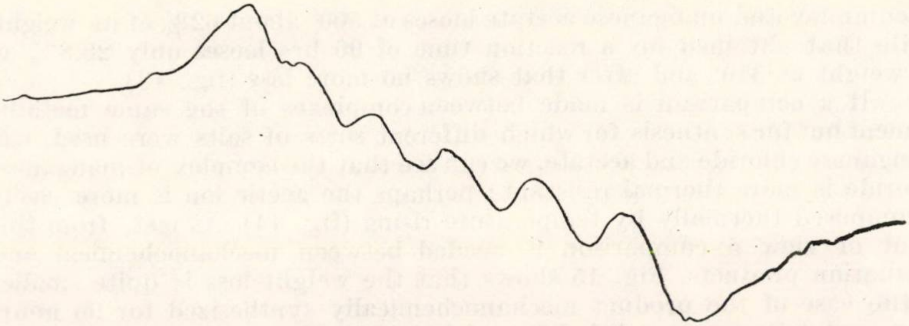

Fig. 11. — ESR spectrum of the insoluble product synthesized from poly(ethyleneterephthalate) (10 g), ethylenediamine (30 g), and manganese chloride, (0.02 g), by ^{60}Co γ-rays irradiation.

4. SOME PROPERTIES OF COMPLEXATION PRODUCTS SYNTHESIZED BY DESTRUCTIVE METHODS

4.1. Thermal stability

The thermal stability of the products synthesized in destructive conditions (i.e., by mechanochemical processing or γ-rays irradiation) was followed by thermogravimetric and thermodifferential analysis using a Paulik-Erdely thermobalance working over temperature intervals of 20—700° in inert medium and with a heating rate of 12.4°/min.

The thermal properties were studied choosing samples characterized by limit degrees of transformation obtained both by mechanochemical processing and by γ-rays irradiation using ferric and manganese acetates and chlorides as complexing agents. Some useful conclusions have been reached, as follows : making a comparison between mechanochemically synthesized samples representing complexes of iron or manganese, it has been found that the thermal stability of the products increases with the milling time (fig. 12); the complex achieved by vibrating milling for 12 hours of a reaction mixture of poly(ethyleneterephthalate), ethylenediamine and manganese acetate looses at 500° about 62 % of its weight, while that obtained for a reaction time of 96 hrs looses only 28.8 % of its weight at 310° and after that shows no more loss (fig. 13).

Fig. 12. — Dependence of weight loss percentage on the decomposition temperature; mechanochemical complex synthesized from poly(ethyleneterephthalate), ethylenediamine and manganese acetate by vibrating milling for 96 hours (*1*) and 12 hours (*2*).

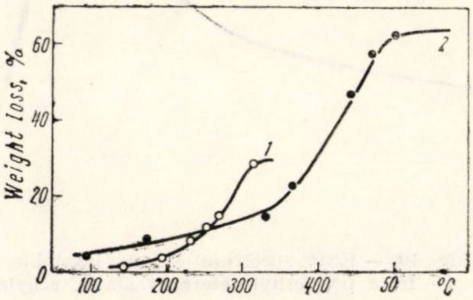

If a comparison is made between complexes of the same metallic element but for synthesis for which different sorts of salts were used, e.g. manganese chloride and acetate, we can see that the complex of manganese chloride is more thermal resistant; perhaps the acetic ion is more easily decomposed thermally by temperature rising (fig. 14). At last, from this point of view a comparison is needed between mechanochemical and irradiation products. Fig. 15 shows that the weight loss is quite smaller in the case of the product mechanochemically synthesized for 96 hours from poly(ethyleneterephthalate), ethylenediamine and ferric chloride eaching only 29 % at 440° and remaining constant up to 1000° (fig. 15, rcurve *2* and fig. 16) while the product achieved by γ-rays irradiation and characterized by a limit degree of transformation (18 hours), is totally decomposed up to 600° (fig. 15, curve *1* and fig. 16). The same conclusion arises making a comparison between manganese complexes (fig. 17).

The high thermal stability of the complexes mechanochemically synthesized as compared with that of irradiation products must be related to the reaction times required for achieving the limit degree of transformation, which are quite different: 96 hours for mechanochemical processing and only 18 hours for γ-rays irradiation. This condition has as a consequence an intense side reaction of decarboxylation in the first case which is more limited in the second case. The same conclusion was drawn analysing the IR spectra of these complexes, as it was above emphasized.

On the other hand, the high thermal resistance of some complexes is justified in addition by another structural element, namely the nature of chelate cycles which are formed between the ligand and complexing center. In the investigated case, when ethylenediamine was used as condens-

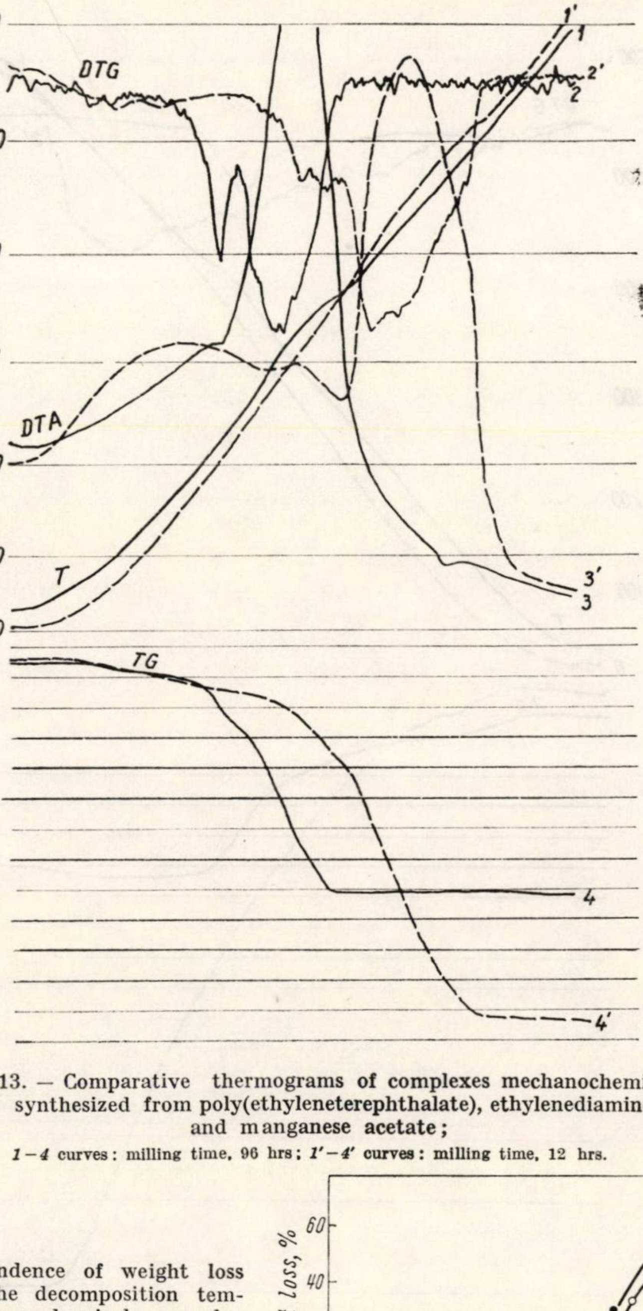

Fig. 13. — Comparative thermograms of complexes mechanochemically synthesized from poly(ethyleneterephthalate), ethylenediamine and manganese acetate;

1–4 curves: milling time, 96 hrs; *1'–4'* curves: milling time, 12 hrs.

Fig. 14. — Dependence of weight loss percentage on the decomposition temperature: mechanochemical complex synthesized from poly(ethyleneterephthalate), ethylenediamine and manganese chloride (*1*) or from manganese acetate (*2*).

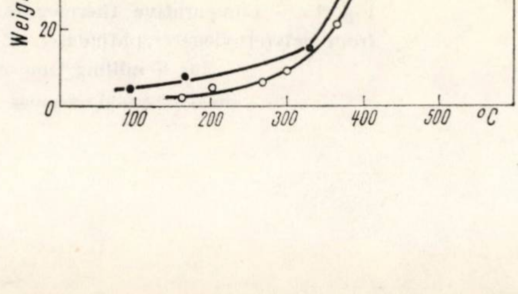

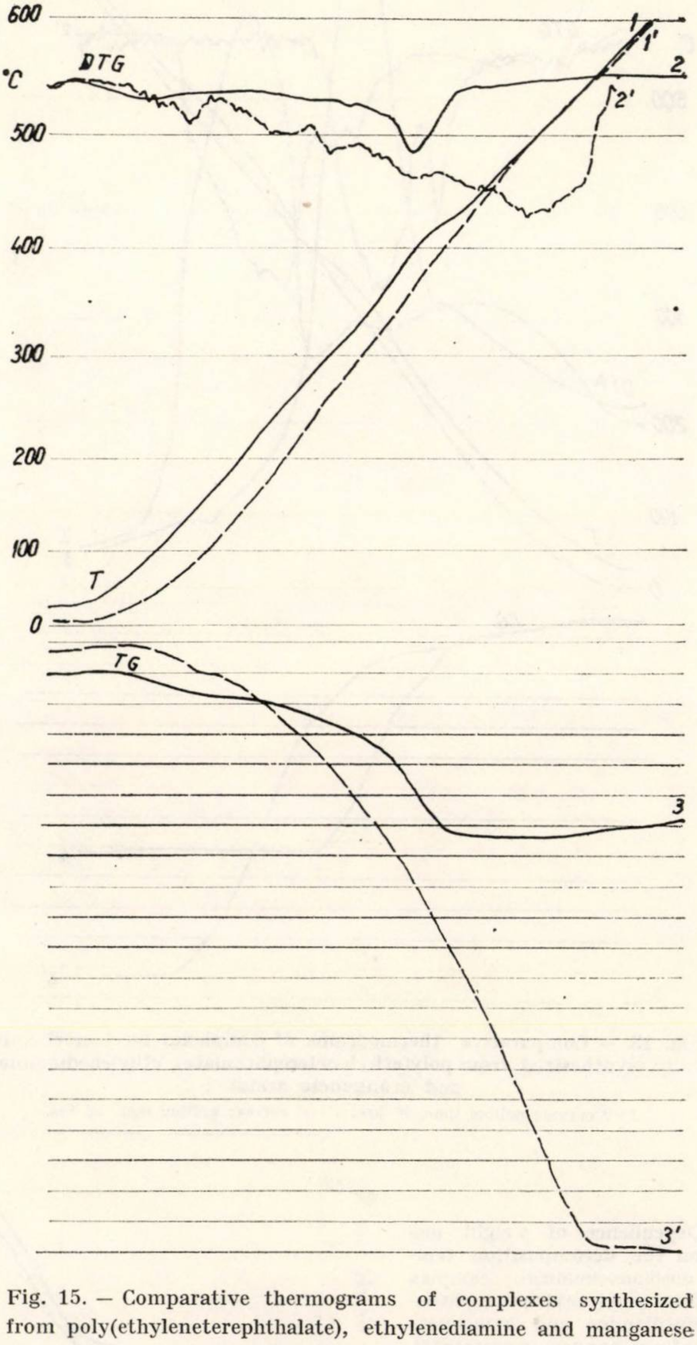

Fig. 15. – Comparative thermograms of complexes synthesized from poly(ethyleneterephthalate), ethylenediamine and manganese for a milling time of 12 hrs, by:

1–3, mechanochemical processing; *1'–3'*, γ-rays irradiation.

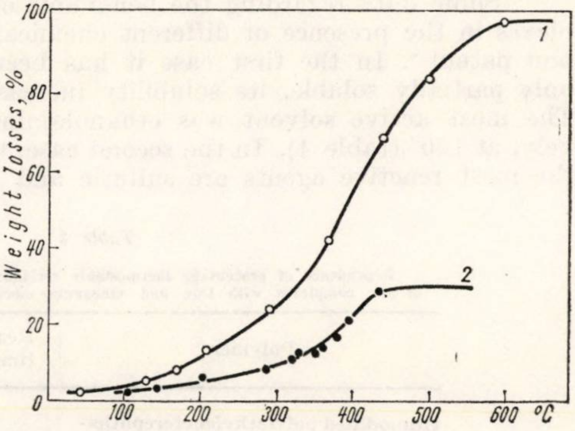

Fig. 16. — Change of weight losses as a function of decomposition temperature for complexes synthesized from poly(ethyleneterephthalate) ethylenediamine and ferric chloride, characterized by limit degrees of transformation : *1*, γ-rays irradiation ; *2*, mechanochemical processing.

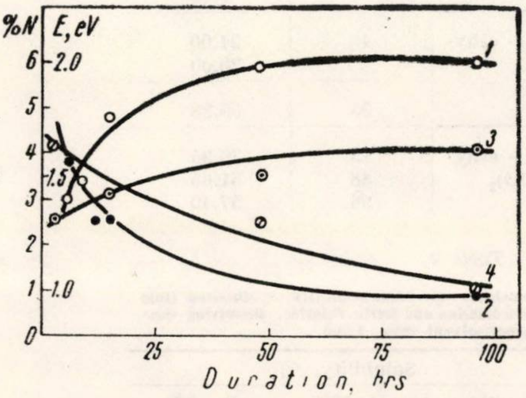

Fig. 17. — Dependence of activation energy of electric conductivity on the milling time and chemical composition of the complex :

1, Change of chemically linked nitrogen percentage with milling time for a complex based on manganese (from manganese acetate) ; *2*, Change of activation energy with milling time for a complex based on Mn^{2+}. *3*, Change of chemically linked nitrogen percentage with milling time for a complex based on Fe^{3+} ; *4*, Change of activation energy with milling time for a complex based on Fe^{3+}.

ng agent, the cycles have five terms and it is well known that these cycles are the most stable[7] as compared with the cycles constituted from six terms.

4.2. *Chemical resistance*

The complexes synthesized by the described methods are coloured powders : dark-red (ferric complexes) or yellow-brown (manganese complexes), the intensity of colour depending on the amount of complexed metal. The fractions which we call "insoluble" are infusible and thermostable ; the "soluble" ones have melting points slightly smaller than those of the corresponding supports. The fractions which are insoluble in extraction solvents used for purification, are frequently insoluble also in the solvents of the support-polymer.

---

[7] P. Spacu and M. Brezeanu, "Chimia combinaţiilor complexe", Ed. didactică, 1969, p. 246.

Some data regarding the behaviour of ferric and manganese complexes in the presence of different chemical agents are listed in table 4 and patent [8]. In the first case it has been found that the polymer is only partially soluble, its solubility increasing with temperature rising. The most active solvent was ethanolamine, used at 50° and, respectively, at 100° (table 4). In the second case, that of manganese complexes, the most reactive agents are sulfuric and hydrochloric acids.

Table 3

Dependence of procentage thermostable residuum on the reaction time of the complexes with iron and manganese mechanochemically synthesized

Polymer	Reaction time hrs	Thermostable residuum %
Unmodified poly(ethyleneterephthalate)	0	0.00
Poly(ethyleneterephthalate) + ethylenediamine + $FeCl_3 . 6H_2O$	48	21.00 20.00
	96	69.30
Poly(ethyleneterephthalate) + ethylenediamine + $Mn(CH_3COO)_2 . 4H_2O$	15	36.25
	48	51.65
	96	57.40

Table 4

Solubility of the "insoluble" complexes mechanochemically synthesized from poly (ethyleneterephthalate), ethylenediamine and ferric chloride. Dissolving time, 3 hrs; polymer/solvent ratio, 1/200

Solvent	Solubility, %		
	at 24°	at 50°	at 100°
Dimethylformamide	10.20	10.90	17.50
Aniline	0.40	5.40	5.40
Benzyl alcohol	4.40	9.30	10.10
m-cresol	2.01	4.40	10.00
Nitrobenzene	1.15	8.70	10.40
Pyridine	2.10	3.60	5.50
Ethanolamine	13.90	39.00	49.50

4.3. Electric conductivity

It is known that insertion of metallic elements in different polymeric structures by complexation confer them properties of electric conductivity, many a time more marked for trivalent than for bivalent complexing centres [9].

In the case of complexes synthesized in destructive conditions, the electric conductivity is indeed changed in this sense, and close relations between this property and the reaction conditions (i.e., reaction time and reactant ratio), or strictly speaking between electric conductivity and the chemical composition of the resulted complex, have been ascertained. Analysing for example the dependence of electric conductivity on the reaction time, we can see that it gradually rises with the reaction development (table 5).

---

[8] CR. SIMIONESCU, CL. VASILIU OPREA and CL. NEGULIANU, Patent N° 69467, 20 I 1971.

[9] V. V. RODE, "Chelate Polymers" in "Progress in Polymer Chemistry", V. V. KORSHAK, editor Izd. Nauk, Moskow, 1969.

Table 5

Dependence of electric conductivity on the parameters of the mechanochemical synthesis

Polymer	Parameter of the mechanochemical synthesis	Electric conductivity, $\sigma(\text{ohm}^{-1}\ \text{cm}^{-1})$
Complex based on Fe^{3+}	Milling time ; hrs ; 0.25 15.00 96.00	$\sigma_{30} = 2.66\times10^{-13}$; $\sigma_{106} = 1.03\times10^{-9}$ $\sigma_{30} = 2.24\times10^{-10}$ $\sigma_{108} = 5.60\times10^{-7}$ $\sigma_{30} = 3.85\times10^{-10}$ $\sigma_{106} = 1.6\ \times10^{-6}$
	Amount of diamine, ml 15 30	$\sigma_{30} = 1.59\times10^{-10}$; $\sigma_{121} = 2.60\times10^{-7}$ $\sigma_{30} = 2.24\times10^{-10}$; $\sigma_{108} = 5.60\times10^{-7}$
Polychelate based on Mn^{2+} : poly(ethyleneterephthalate) + ethylenediamine + manganese acetate	Milling time, hrs 96	$\sigma_{12} = 1.15\times10^{-10}$; $\sigma_{96} = 5.41\times10^{-8}$
Poly(ethyleneterephthalate) + manganese acetate	96	$\sigma_{34} = 1.15\times10^{-14}$; $\sigma_{119} = 1.50\times10^{-1}$

The activation energy, E_A, changes with the percentage of chemically linked nitrogen in the ranges 2.09–1.03 eV, for polychelates based on iron and manganese, respectively, mechanochemically obtained. Plotting the change of nitrogen percentage *versus* milling time (fig. 17) or the amount of diamine used in reaction (fig. 18), it is seen that besides the corresponding change of activation energy (i.e., E_A decreases with nitrogen percentage increase) the semiconductor character becomes more prominent. As a matter of fact, the importance of diamine participation in the complexation process results in addition, making a comparison between electric conductivity of a complex synthesized by one of the discussed routes and of a witness product obtained in the same reaction conditions but only from a mixture of poly(ethyleneterephthalate) and the respective metallic salt. Following the data of table 5 regarding comparatively the electric conductivity of a complex based on manganese obtained mechanochemically for a milling time of 96 hrs and that of poly (ethyleneterephthalate) sample milled for the same time and in the presence of the same amount of metallic salt but without diamine, we can see, for the second case, negligible values of the studied parameters, while in the case of complexes this change varies as a function of reaction conditions.

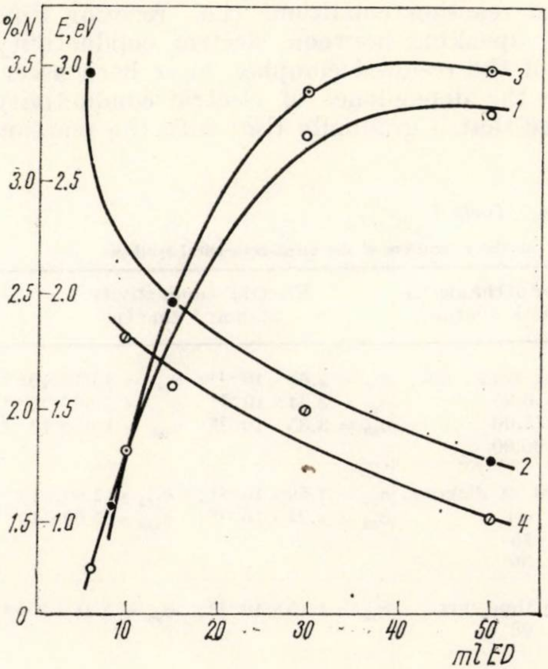

Fig. 18. — Dependence of activation energy of electric conductivity on the amount of ethylenediamine used in reaction and the chemical composition of the complex, respectively : *1*, dependence of percentage of chemically linked nitrogen on the amount of ethylenediamine for a complex with Fe^{3+} ; *2*, dependence of activation energy on the amount of ethylenediamine for a complex with Fe^{3+} ; *3*, dependence of procentage of chemically linked nitrogen on the amount of ethylenediamine for a complex based on Mn^{2+} (from manganese acetate) *4*, dependence of activation energy on the amount of ethylenediamine for a complex based on manganese.

4.4. *Dielectric constant*

Insertion of electropositive elements (i.e. Fe^{3+} and Mn^{2+}) on macromolecular backbones containing electronegative elements (i.e., oxygen and nitrogen) determines sensible changes in value of the dielectric constant and the parent polymer is transformed from an insulator into a semiconductor. Some data, referring to the dielectric constant and tangent of loss angle for different frequencies and temperatures, are given in figs. 19 and 20.

RESULTS AND DISCUSSION

The correlation of the experimental data obtained by application of different physical and chemical methods (e.g. elementary analysis, infrared spectroscopy, electron spin resonance, thermogravimetric and thermodifferential analysis, etc.), regarding the characterization of the polymers synthesized by the two already discussed destruction methods, namely mechanochemical processing and γ-rays irradiation, shows, on the one hand, that the polymers are not identical from the point of view of their structure and properties and, on the other hand, argues for the possibility of generalization of the working method used by the extension of the principle on which it is based, to other working systems: polymer — an energy source.

Polycondensation reactions carried out in systems containing poly (ethyleneterephthalate), ethylenediamine and different metallic salts con-

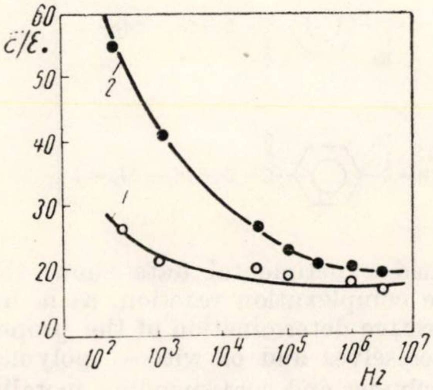

Fig. 19. — Dependence of dielectric constant on frequency for a poly(complex)based on Fe^{3+}:
1, at 20°; *2*, at 40°.

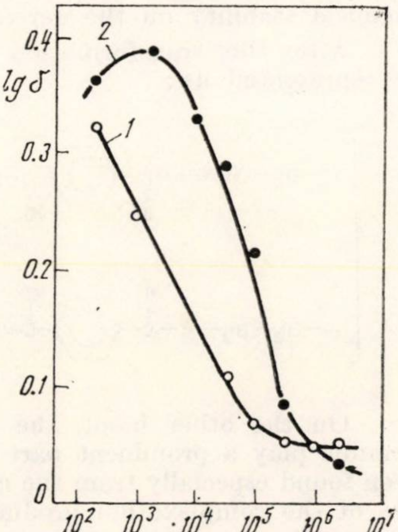

Fig. 20. — Dependence of tangent of loss angle for a complex based on Fe^{3+}
1, at 20°; *2*, at 40 °.

firm, on the other hand, the capacity of the used energies to activate the polycondensation reactions which take place between active destruction fragments of the support — polymer and ethylenediamine or other diamines. Diamines provide chains capable to complex with different metallic centres owing to the presence of the atoms having unparticipant electrons (i.e. O and N). Starting from the electronic structure of the metals as complexing centres (Fe^{3+} and Mn^{2+}) and from the chemical structure of the ligand synthesized just during the complexation reaction, the structural unit of such polymers can be depicted as follows:

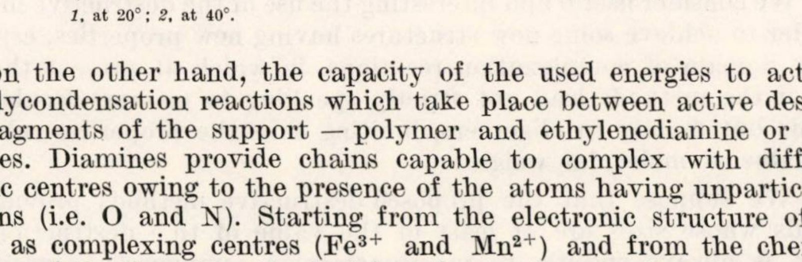

The IR data prove, especially for mechanochemical processing, that by increasing the working time the ligand undergoes a tautomeric change : 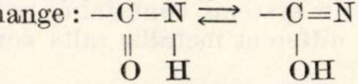 $-\underset{\underset{O}{\|}}{C}-\underset{\underset{H}{|}}{N} \rightleftarrows -\underset{\underset{OH}{|}}{C}=N-$ which confers an additional thermal and chemical stability on the derivatives formed.

After this transformation the structural unit of the complex can be represented as :

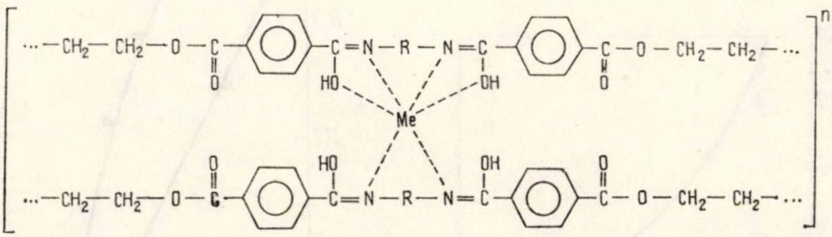

On the other hand, the obtained experimental data show that diamine play a prominent part in the complexation reaction, as it has been found especially from the comparative determination of the properties of the complexation products themselves and of witness polymers achieved by processing of support — polymer and corresponding metallic salt. The witness polymers are not sensibly different from parent polymers from the point of view of the data of structural analysis.

We consider useful and interesting the use of the destructive methods, in order to achieve some new structures having new properties, especially in the domain of complexation reactions, in which at present the great part of the methods lead not strictly speaking to macromolecular compounds but mainly to oligomers, limiting thus the properties related to the value of molecular weight.

We suppose that the proposed destructive methods provide with ligands whose sizes are at least of the value of the destruction limit which is always specific to macromolecular compounds, especially in the case of mechanochemical methods.

CONCLUSIONS

1. Mechanochemical destruction and destruction by γ-rays irradiation of some heterochain polymers, as poly(ethyleneterephthalate), achieved in the presence of diamines and metallic salts, promote complexing reactions.

2. The chemical composition of the synthesized polymers is sensibly dependent on the reaction conditions : duration, ratio of reactants and the amount of metallic salt.

3. The synthesis of the ligand takes place by destructive polycondensation occurring at the same time with complexation; the ligand undergoes simultaneously decarboxylation reactions and a tautomeric change, leading to chain stabilization.

4. Complexes synthesized by mechanochemical processing and γ-rays irradiation exhibit properties which are sensibly different from those of the support: electric conduction, increased thermal stability and increased chemical resistance at the action of acids, bases and solvents.

5. The complexation process carried out in destructive conditions represents a direct application of that of polycondensation which is activated on the same principles and occurs in the same conditions.

Revue Roumaine de Chimie, **19**, *2*, 259–281 (1974)

Revue Roumaine de Chimie, **19**, *2*, 283–292 (1974)

ВЛИЯНИЕ УСЛОВИЙ РАСПЫЛИТЕЛЬНОЙ СУШКИ НА СВОЙСТВА ПАСТООБРАЗУЮЩЕГО ПОЛИВИНИЛХЛОРИДА

СООБЩЕНИЕ I.

ЭКСПЕРИМЕНТАЛЬНАЯ ЧАСТЬ

ВАЛЕНТИНА БОЙЕШАН

Промышленный нефтехимический комплекс, Борзешть
Исследовательская лаборатория

ДОРЕЛ ФЕЛЬДМАН

Политехнический институт, Яссы

Получена 30 декабря 1972 г.

Изучалось влияние режима сушки латекса поливинилхлорида в распылительной сушилке на свойства получаемых порошков и их способность к образованию паст. Было найдено, что основным параметром сушки является температура, которая влияет на размеры частиц порошка ПВХ, седиментацию паст и их реологические свойства.

Пластизоли, или пасты, являются коллоидными дисперсиями порошкообразного поливинилхлорида в пластификаторе, которые находятся в жидком или почти жидком состоянии. Для облегчения переработки и в зависимости от назначения в них добавляется ряд вспомогательных материалов: стабилизаторы, красители, наполнители и т.п.[1,2].

Пасты готовятся смешиванием при комнатной температуре порошка ПВХ в пластификаторе. При этом заботятся о том, чтобы полученная паста обладала следующими свойствами:

— имела высокую концентрацию полимера (50—65%);
— имела хорошую текучесть (относительно низкую вязкость);
— была устойчивой при хранении.

Под этим подразумевается сохранение постоянной вязкости во времени и устойчивость коллоидная, т.е. неразделение на фазы. Способность порошка ПВХ образовывать пасты с определенными свойствами зависит от ряда факторов, из которых наиболее важными считаются следующие:

— технология полимеризации;

---

[1] O. Berger и W. Braun, *Plaste u. Kautschuk*, **14**, 663 (1967).
[2] F. Böhme и K. Müller, *Plaste u. Kautschuk*, **7**, 124 (1960).

— условия сушки;

— вид и количество эмульгатора;

— размеры частичек ПВХ, их гранулометрическое распределение и морфология.

Поскольку строение и размеры частиц ПВХ формируются во время полимеризации, сушки и, в некоторых случаях, во время размалывания, считаем, что главными и определяющими факторами являются первые три, а последний — их производное.

Авторы настоящего сообщения занимались исследованием влияний условий распылительной сушки на физические свойства порошкообразного поливинилхлорида и его способность образовывать пасты, объясняя различное поведение порошка в контакте с пластификатором через отличия в строении частиц порошка.

1. СЫРЬЕ, АППАРАТУРА И МЕТОДИКА РАБОТЫ

1.1. СЫРЬЕ

Исследования проводились используя латекс, полученный из установки непрерывной эмульсионной полимеризации хлористого винила, с применением анионно-активного эмульгатора и пероксидного инициатора.

Латекс имел содержание сухого остатка $C = 40—42$ вес %, поверхностное натяжение $\tau = 3—5$ дин/см, удельный вес $\gamma = 1{,}13$ г/см, среднюю величину латексных частиц, определенных методом электронной микроскопии — 700—1100 Å.

1.2. СУШИЛЬНАЯ УСТАНОВКА

Сушка латекса производилась в лабораторной распылительной сушилке объемом в 1 м^3, в среде нагретого воздуха. Производительность сушильной установки 5 кг воды/час. Распыление латекса осуществлялось посредством двухжидкостной форсунки воздух/латекс при помощи сжатого воздуха $P = 4$ атм.

Подвергались изменению:

— расход латекса, соответственно отношение — воздух/латекс при распылении (в пределах 3,6—9,6 л. латекса/час на форсунку, соотв. воздух/латекс = 4750—1750), сохраняя постоянным расход воздуха.

— температура сушки ($T_1 = 100—140°$ — температура воздуха на входе в сушилку; $T_2 = 60—100°$ — температура воздуха на выходе).

1.3. МЕТОДЫ АНАЛИЗА

— Средняя величина чстиц ПВХ и их гранулометрическое распределение определялись по методу седиментации в воде, описанному Шубертом и Штреллер;[3]

— Способность образовывать пасты проверялась путем смешивания в ступке в течение 15 минут порошка ПВХ с диокитилфталатом (ДОФ) в весовом отношении 60/40. У полученных таким образом паст определялась вязкость начальная, через 24 часа и через 7 дней на реовискозиметре Гепплера.

— Течение паст при различных скоростях сдвига исследовалось на реовискозиметре Ротовиско-Гааке,

---

[3] W. Schubert и H. Streller, *Plaste u. Kautschuk*, **15**, 252 (1968).

— коллоидная устойчивость паст оценивалась путем наблюдения за оседанием частиц ПВХ в пасте и измерением диаметра « пятен », образованных отделившимся из пасты пластификатором по методике, данной Рисави.[4]

2. РЕЗУЛЬТАТЫ ЭКСПЕРИМЕНТОВ

Изучая условия распыления и сушки, пришли к выводу, что только изменяя вышеуказанные параметры, из одного и того же латекса можно получить порошкообразный ПВХ с совершенно различными свойствами: порошки, которые не образуют пасты совсем или образуют пасты с различным реологическим поведением.

С точки зрения влияния, оказываемого на вязкостные свойства паст, наиболее важным фактором оказалась температура сушки; тонкость распыления имеет меньшее значение.

2.1. ВЛИЯНИЕ СТЕПЕНИ РАСПЫЛЕНИЯ

От степени распыления зависят размеры частиц сухого порошка ПВХ, поскольку в сушилке из каждой капли латекса образуется твердая частица полимера шарообразной формы. Может считаться, что капля или твердая частичка столкнутся с другой такой же и тогда, в зависимости от состояния их сухости, произойдет слияние капель или слипание зерен. Но это — случаи более редкие и в основном величина сухих зерен пропорциональна диаметру распыляемых капель.

Степень распыления зависит от конструкции форсунок и отношения воздух/жидкость при распылении. Для типа форсунки, принимаемой в этой работе, средний размер капель рассчитывался по формуле[5]

$$dm = \frac{585\sqrt{\tau_1}}{Vr\sqrt{\gamma_1}} + 597\left(\frac{\eta_1}{\gamma_1\tau_1}\right)^{0,45}(1000R_{1/2})^{1,5}, \qquad (1)$$

где

dm — средний размер капель в микронах,

τ_1 — поверхностное натяжение латекса (35 дин/см),

$Vr = V_1 - V_2$ — относительная скорость между газом (V_2) и жидкостью (латексом) (V_1), в м/сек,

η_1 — динамическая вязкость латекса (0,035 пуаз),

γ_1 — плотность латекса, $\gamma_1 = 1{,}13$ г/см^3,

$R_{1/2} = \frac{V_1}{V_2}$ — объемное отношение жидкость/газ в форсунке, рассчитанное при минимальном сечении на выходе.

---

[4] D. Ryšavy, *Kunststoffe*, **48**, 108 (1958).

[5] A. Dăscălescu, « Uscarea », Ed. tehnică, Bukarest, 1964, p. 277.

При различных отношениях $R_{1/2}$ в форсунке и различных Vr были подсчитаны средние теоретические величины диаметров капель, представленные кривой 1 на рис. 1.

Во время сушки, благодаря испарению воды из латекса, происходит сжимание капель и сближение латексных частиц в капле. В идеальном случае, если бы из каждой капли латекса образовывалась монолитная частица полимера с плотностью 1,4 г/см^3, при концентрации сухого вещества в латексе в 40% произошло бы уменьшение размеров капель в 1,46 раз, как это выходит из уравнения

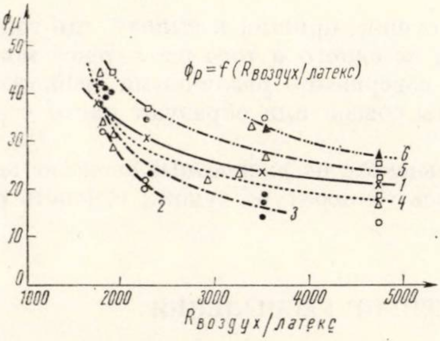

Рис. 1. — Изменения величины сухих частиц ПВХ в зависимости от соотношения воздух/латекс:
кривая *1* — средние рассчитанные размеры диаметров латексных капель (в микронах), кривые *2—6* — средние размеры (в микронах) сухих частиц ПВХ высушенных при температурах: *2* —70°, *3*—80°, *4*— 90°, *5*—10 0°, *6*—110°.

$$\frac{\pi d_1^3 \gamma_1}{6} = \frac{\pi d_2^3 \gamma_2}{6} + G, \qquad (2)$$

где

d_1 и d_2 — диаметры капель латекса и соответственно частиц ПВХ,

γ_1 и γ_2 — плотности латекса и ПВХ,

G — вес испаренной воды.

В действительности из-за быстрого испарения воды латексные частицы не успевают перегруппироваться в капле в плотную сетку и образуют пористое зерно с плотностью $< 1,4$ г/см^3. Пористость неоднородна и зависит от первоначальных размеров капли и температуры сушки.

На рис. 1 представлены практические данные изменения величины сухих частиц полимера, полученных при различных температурах сушки T на выходе из сушилки, в зависимости от степени распыления. Для сравнения тут же приведена и теоретическая кривая 1 для невысушенных капель латекса, рассчитанная по формуле (2). Видно, что:

— величина высушенных частиц изменяется пропорционально величине исходных капель;

— частицы, высушенные при более низких температурах, имеют средние размеры меньшие, чем те, что были высушены при более высоких температурах;

— при температурах сушки выше 100° вместо уменьшения размеров капель наблюдается, наоборот, увеличение средних размеров частиц.

Эти различия можно объяснить различной пористостью частиц. Ряд авторов [6-8] придают большое значение абсолютным размерам и гранулометрическому составу частиц при образовании паст из ПВХ. Считается, что вязкость паст будет тем меньше, чем шире гранулометрическое распределение частиц, или что должно существовать оптимально соотношение между большими и маленькими частицами таким образом, чтобы мелкие частици заполняли пространство между большими, оставляя минимальным объем пустот между ними. В этом случае уменьшается количество пластификатора, необходимого для заполнения пустот между частицами полимера, и при том же объеме употребляемого пластификатора оказывается свободным большее количество жидкости.

Эти соображения верны, если все частицы имеют одинакую структуру и в контакте с пластификатором не происходит разрушение частиц. На самом же деле частицы с одинаковым гранулометрическим составом, но полученные в различных условиях сушки, ведут себя неодинаково по отношению к пластификатору. Так, нами были проверены пастообразующие свойства нескольких проб поливинилхлорида со сходным гранулометрическим составом, но полученных в разных температурных условиях (см. рис. 2 a) и проб с различным гранулометрическим составом, но полученных в одинаковых условиях (см. рис. 2 b). Видно, что изменение вязкости паст во времени не зависит от размеров зерен порошков и следует за изменением температуры сушки.

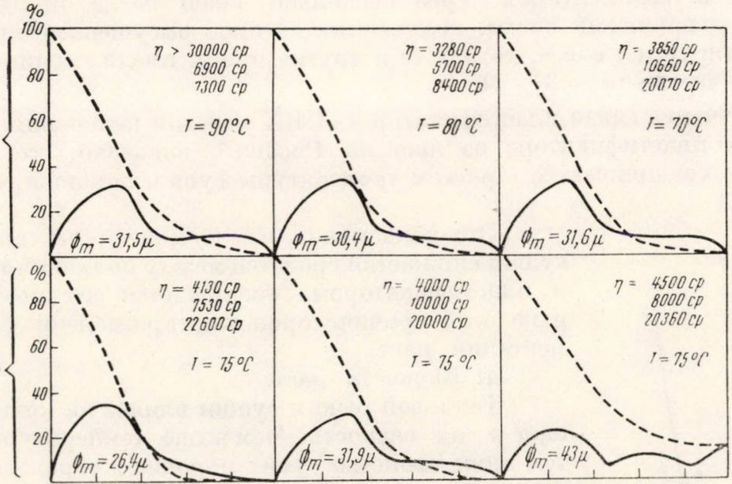

Рис. 2. — Гранулометрический состав, средний размер частиц (Ø в микронах) и изменение вязкости паст во времени (через 1 час, 24 часа и 7 дней) для проб, полученных:

а) при разных температурах сушки T_j:

б) при разных расходах латекса при распылении.

---

[6] T. Hugosson, *Kunststoffe*, **46**, 341 (1956).

[7] H. Koch и W. Sommer, *Kunststoffe*, **47**, 153 (1957).

[8] G. Wick, *Österr. Chem. Ztg.*, **62**, 5 (1961).

Выходит, что одно гранулометрическое распределение без учета условий получения порошка не может быть определяющим фактором в получении паст ПВХ определенной вязкости.

2.2. ВЛИЯНИЕ ТЕМПЕРАТУРЫ СУШКИ

Исследовалась температура воздуха на выходе из сушилки, поскольку сушилка работает в адиабатическом режиме и сразу же после входа нагретого воздуха в сушилку происходит снижение его температуры благодаря расходу тепла на испарение воды. Температура нагретого воздуха на входе в сушилку поддерживалась на необходимом уровне согласно тепловому балансу, определяемому количеством испарившейся воды.

Было замечено, что температура воздуха на выходе из сушилки (сокращенно названная температурой сушки) оказывает многочисленные влияния на свойства полихлорлвинильного порошка. От нее зависят:

а) Величина зерен сухого порошка, как показывает рис. 1.

б) Седиментация паст во времени.

С повышением температуры увеличивается склонность частиц ПВХ к седиментации в пасте, из которой начинает выделяться пластификатор даже в случае частиц небольших размеров.

Так, например, у проб, высушенных при температуре 90°, в пастах начинается седиментация через несколько часов после приготовления пасты, в то время как пасты, полученные из проб высушенные при 70°, не седиментируются вовсе, хотя и те и другие пробы имели сходные средние размеры частиц ($d = 31-80$).

Изучение связи пластификатор — ПВХ методом измерения диаметра « пятен » пластификатора из паст по Рисави[4] показало, что диаметр « пятна » увеличивается с ростом температуры сушки порошка, что видно из рис. 3.

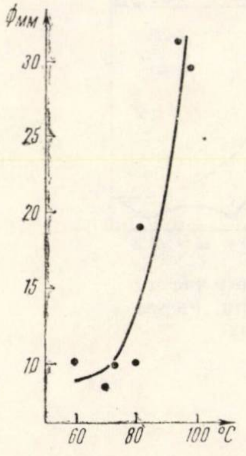

Рис. 3. — Диаметр «пятен» в зависимости от температуры сушки.

Это доказывает, что по мере роста температуры сушки снижается сродство между поливинилхлоридом и пластификатором, уменьшается его лиофильность и по этой причине происходит разделение фаз и седиментация паст.

в) Вязкость паст.

Тепловой режим сушки влияет на консистенцию паст и их вязкость. Чем выше температура сушки, тем ниже свойство сухих порошков образовывать пасты, их первоначальная вязкость растет до полного несвязывания частиц в пасты. В то же время, стабильность вязкости паст во времени улучшается с повышением температуры сушки порошка.

Эти различия видны из графиков рис. 4, где представлены изменения вязкости паст, измеренной на реовискозиметре Гепплера, во времени (начальная, через 24 часа и через 7 дней) и в зависимости от температуры сушки (T_2) порошков ПВХ.

Характер изменения вязкости во времени виден еще лучше из рис. 5—6, на которых кривые были построены на основании математических расчетов вязкости при программировании и обработке результатов по методу Бокса-Вильсона. [9–11]

Были обработаны средние данные экспериментов на 3 уровнях программирования с двумя переменными (температура и расход), получив $\eta = 3^2 = 9$ величин принятых в расчет. Были решены уравнения 2-ой степени, по которым были построены кривые.

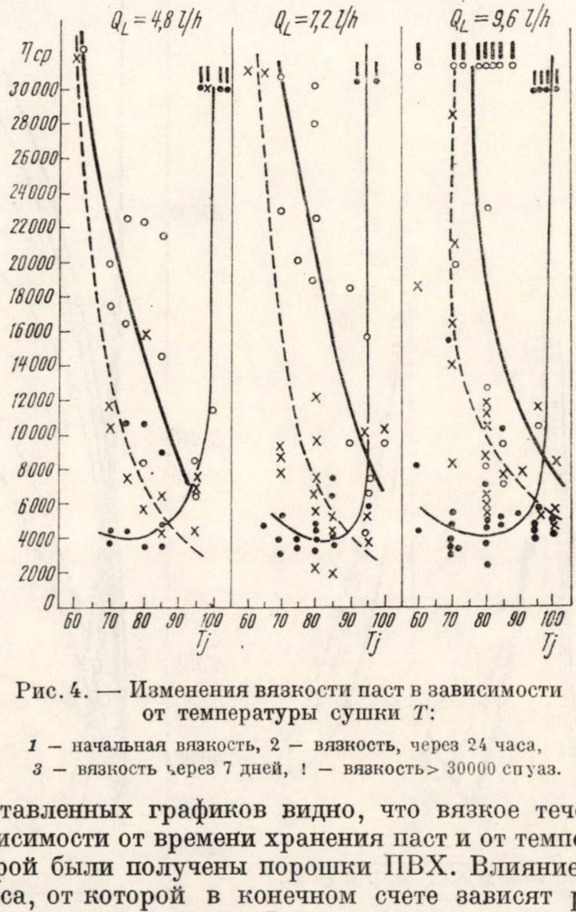

Рис. 4. — Изменения вязкости паст в зависимости от температуры сушки T:

1 — начальная вязкость, 2 — вязкость, через 24 часа,
3 — вязкость через 7 дней, ! — вязкость> 30000 спуаз.

Из представленных графиков видно, что вязкое течение паст различается в зависимости от времени хранения паст и от температуры сушки (T_j), при которой были получены порошки ПВХ. Влияние тонкости распыления латекса, от которой в конечном счете зависят размеры сухих частиц, заметно в меньшей степени. Все же, более мелкие частицы образуют более устойчивые пасты.

На рис. 7 представлены реологические кривые $\eta = f(Ds^{-1})$ (вязкость в зависимости от скорости сдвига) для паст, приготовленных из порошков, высушенных при различных температурах, но при одинаковых условиях распыления.

---

[9] G. E. P. Box и K. B. Wilson, *J. Royal Statistical Soc.* (*B*), **13**, 1 (1951).

[10] В. В. Налимов, *Усп. химии*, **29**, 1362 (1960).

[11] A. Glück, « Metode matematice în industria chimică », Ed. tehnică, Bukarest, 1971.

Видно, что снижение температуры сушки способствует псевдопластичному течению, в то время как повышение температуры ведет к дилатансии, что было замечено и другими исследователями.[1,4,12,13]

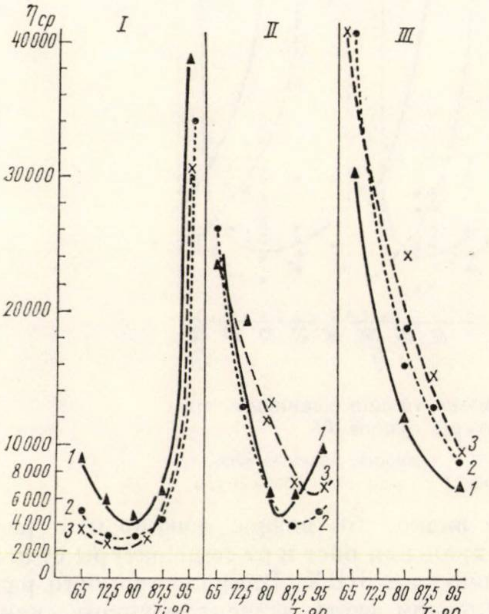

Рис. 5. — Изменения вязкости паст во времени (I — начальная, II — через 24 часа, III — через 7 дней) в зависимости от температуры T сушки ПВХ при различных расходах латекса на форсунку:

1 – 4, 8 л/час, 2 – 7, 2 л/час, 3 – 9, 6 л/час.

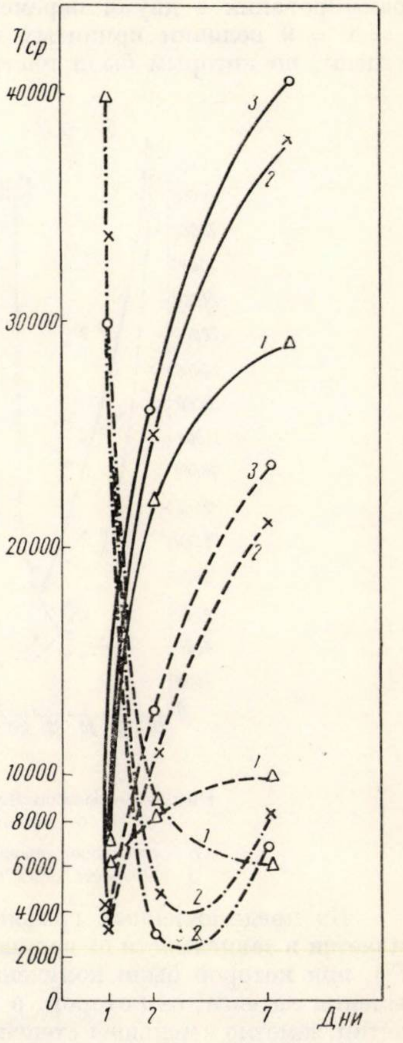

Рис. 6. — Изменение вязкости паст во времени в зависимости от температуры сушки T_j и соотношения воздух/латекс Rв/л при распылении:

——— $T_j = 65°$; 1 – R в/л = 3850;
– – – – – – $T_j = 80°$; 2 – R в/л = 23.8;
– · – · – · – $T_j = 95°$; 3 – Rв/л = 1790.

---

[12] Б. П. Штаркман и И. А. Мухина, *Пласт. массы*, **31**, 50 (1969).

[13] Б. П. Штаркман, И. А. Мухина и Л. И. Шарикова, *Коллоид. журнал*, **31**, 611 (1969).

Порошки, которые не связываются в пасты сначала, через 24 часа контакта с пластификатором образуют сильно дилатантные пасты. Влияние тонкости распыления латекса при сушке менее заметно в реологии паст. На рис. 8 представлены реологические кривые проб, полученных при 70° и различных расходах латекса при распылении, т.е. различных тонкостных распыления. Все порошки, полученные при этой температуре, образуют пасты с псевдопластичным течением, но у более крупных частиц снижения вязкости при больших скоростях сдвига выражено более ярко.

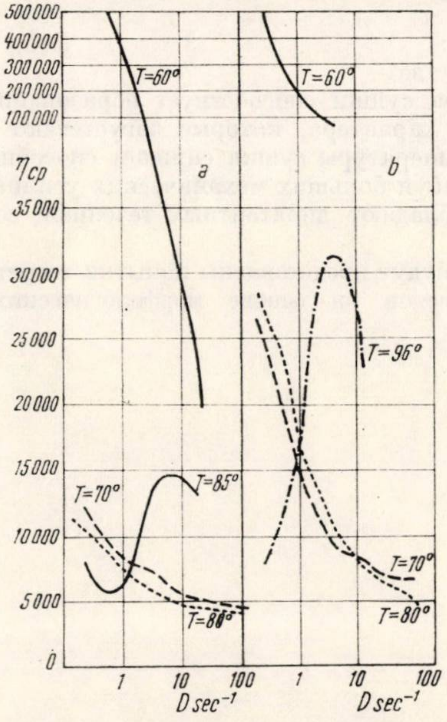

Рис. 7. — Реологические кривые паст $\eta_{cp}=f(Ds^{-1})$ в зависимости от температуры сушки ПВХ:

а) начальная вязкость; б) вязкость через 24 часа.

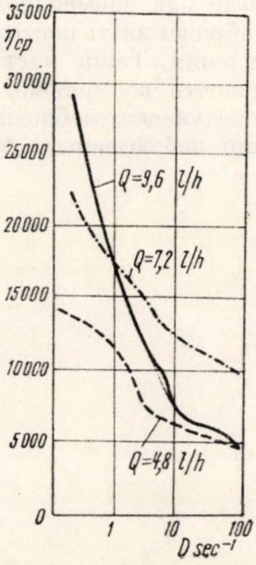

Рис. 8. — Реологические кривые паст $\eta_{cp} = f(Ds^{-1})$ в зависимости от расхода латекса форсунку, л/час. Температура сушки $T_j = 70°$.

ВЫВОДЫ

Изучалось влияние режима сушки латекса ПВХ в распылительной сушилке на свойства порошков и их способности к образованию паст.

Было найдено, что основным параметром сушки является температура; тонкость распыления можно считать вторичным фактором, который все же оказывает влияние на стабильность паст во времени.

Температура сушки оказывает следующие влияния:

— на величину частиц порошка ПВХ;
— на седиментацию паст;
— на консистенцию паст;
— на реологические свойства.

Более низкая температура сушки способствует образованию текучих паст псевдопластического характера, которые загустевают во времени, тогда как повышение температуры сушки снижает способность порошков образовывать пасты, требуя больших механических усилий для их приготовления. Такие пасты обладают дилатантным течением, со снижением вязкости во времени.

В следующем сообщении будут представлены попытки теоретических объяснений наблюдаемых феноменов на основе морфологических исследований.

Revue Roumaine de Chimie, **19**, *2*, 293–320 (1974)

QUELQUES REMARQUES SUR LES PROPRIÉTÉS DES BÉTONS AUX RÉSINES SYNTHÉTIQUES SANS LIANTS MINÉRAUX. II[1]

I. IONESCU

Laboratoires des Bétons, Mortiers et Armatures pour Bétons — I.C.M.P.C. — Bucarest

Reçu le 18 Avril 1973

On présente les résultats des recherches sur l'influence de certaines propriétés physiques-chimiques des types de résines synthétiques et des facteurs de composition sur les principales propriétés physiques-chimiques des bétons à base de résines synthétiques sans liants minéraux.

Les propriétés des bétons de résines synthétiques sans liants minéraux sont modifiées par de très nombreux facteurs, et les tentatives d'explications scientifiques sont rares encore et limitées.[1–5] En ce qui concerne les propriétés des bétons de monomère FA, nos recherches ont porté sur :

— les propriétés de la résine, du durcisseur et du solvant utilisés et leur dosage ;

— la nature, la provenance et la rugosité de l'agrégat (y compris le filler) ;

— la méthode de travail adoptée, la température et l'humidité de l'air pendant la période de préparation et dans l'intervalle préparation-essai ;

— l'âge et le milieu d'essai, etc.

1. RÉSISTANCE À LA TRACTION PAR FLEXION ET À LA COMPRESSION

Les résistances à la traction par flexion pour les bétons de monomère FA, conservés dans l'intervalle confection-essai à l'ambiance du laboratoire, ont des valeurs comprises entre 64,7 et 168 kgf/cm^2 à 1 jour et continuent à augmenter jusqu'à atteindre de 84,6 à 203 kgf/cm^2 à 7 jours, de 98,3 à 214,6 kgf/cm^2 à 28 jours de 129,8 à 256,8 kgf/cm^2 à un an, de 140,8 à 252,0 kgf/cm^2 à 3 ans. Les bétons de monomère FA et résine LS. 1 (compositions 34 à 39 tableau 1), conservés dans les mêmes conditions, ont, à un jour, des résistances de 28,5 à 29,0 kgf/cm^2, qui continuent à augmenter, de sorte qu'à 28 jours ils atteignent des valeurs de 82,4 à 126,4 kgf/cm^2 ; à un an de 122,6 à 143,1 kgf/cm^2 et de 128,9 à 149,5 kgf/cm^2 à 3 ans, augmentation sensible si on la compare à celle des bétons à résine phénol-formaldéhyde — LS.1 (composition 33, tableau 1), qui est de 42,6 kgf/cm^2 à 7 jours de 67,4 kgf/cm^2 à un an.

---

[1] I. Ionescu, *Rev. Roumaine Chim.*, **1972**, 97.

[2] I. M. Elshin, « Plastbeton », Ed. Bidvelnik, Kiev, 1967.

[3] I. Ionescu et M. Enculescu, « Întrebuinţarea maselor plastice pentru impermeabilizarea şi protecţia anticorosivă a construcţiilor hidrotehnice », chap. IV, V, I.S.C.H., Bucarest, **1964**.

[4] I. Ionescu et M. Enculescu, *Rev. Hidrotehnica*, **1964**, 352.

[5] I. Ionescu, M. Enculescu, P. Ghinescu et D. Nedelcu, *Rev. Materiale Plastice*, **1966**, 146.

Les résistances à la compression, pour les bétons de monomère FA, conservés dans les mêmes conditions, ont des valeurs comprises entre 308 et 760 kgf/cm^2 à 1 jour, qui continuent à augmenter atteignant 339 à 959 kgf/cm^2 à 7 jours, de 529 à 1042 kgf/cm^2 à 28 jours, 682 à 1249 kgf/cm^2 à un an, 706 à 1288 kgf/cm^2 à deux ans, etc. Les bétons de monomère FA et résine LS.1 (compositions 34 à 39, tableau 1) conservés dans les mêmes conditions, ont, à un jour, des résistances de 118 à 174 kgf/cm^2 qui continuent à augmenter et qui atteignent 479 à 628 kgf/cm^2 à 7 jours, 702 à 834 kgf/cm^2 à un an, 716 à 842 kgf/cm^2 à 2 ans, etc, alors qu'on obtient 207 kgf/cm^2 à 7 jours et 448 kgf/cm^2 à 2 ans pour les bétons de résine phénol-formaldéhyde — LS.1 (composition 33, tableau 1).

Les résistances à la traction par flexion et à la compression pour les bétons de monomère FA immergé dans l'eau durant l'intervalle décoffrage-essai (fig. 1 *a* et *b*) augmentent elles aussi dans le temps, mais assez lentement, de sorte qu'aux essais effectués entre 28 et 730 jours, elles représentent de 40 à 65% des résistances des éprouvettes conservées tout le temps à l'atmosphère du laboratoire, ce qui confirme les résultats des recherches préliminaires.[1,6-10] Les résistances des bétons de monomère FA conservés les 28 premiers jours depuis la coulée à l'atmosphère au laboratoire et ensuite immergés dans l'eau potable jusqu'à 365 jours, ont d'abord une légère tendance à décroître jusqu'à 90 à 180 jours, et augmentent ensuite lentement (fig. 1*c*).

Si les résistances des bétons de monomère FA augmentent jusqu'à 1 à 3 ans, leur principale augmentation est enregistrée dans les 7 premiers jours, après la coulée ; la résistance représente alors, en moyenne, 75% de la résistance à un an, puis augmente de plus en plus lentement, pour atteindre, à 28 jours, généralement plus de 90% de la résistance à un an ; celle-ci est pratiquement du même ordre de grandeur que la résistance à 3 ans. Pour les bétons de monomère FA et résine LS.1, l'augmen-

---

[6] I. Ionescu, M. Enculescu et P. Ghinescu, *Rev. Materiale Plastice*, **1965**, 91.

[7] I. Ionescu, *Rev. Materiale Plastice*, **1968**, 319.

[8] I. Ionescu et M. Enculescu, « Les résines de synthèse dans les Constructions », Ier vol., International Symposium — RILEM —, Ed. Eyrolles, Paris, 1970, p. 380.

[9] I. Ionescu, et I. Făcăoaru, « Les résines de synthèse dans les Constructions », Ier vol., International Symposium — RILEM — Ed. Eyrolles, Paris, 1970, p. 397.

[10] I. Ionescu, *Rev. Construcţiilor si a Materialelor de Construcţii*, **1968**, 640.

Tableau 1

Compositions des bétons étudiés

Numéro de la composition	Type de l'agrégat et du filler utilisés	Pourcentange de résine	Matériau frais kg/m^3	Tassement au cône cm
1	Agrégat A1 0–7 mm	14,5 FA	2180	11,5
2	Agrégat A1 0–7 mm + 15% filler F1	14,5 FA	2200	11,00
3	Agrégat A1 0–15 mm	13,0 FA	2230	11,00
4	Agrégat A1 0–15 mm + 20% filler F1	13,0 FA	2250	10,5
5	Agrégat A2 0–3 mm	16,0 FA	2040	12,0
6	Agrégat A2 0–3 mm + 12% filler F1	16,0 FA	2170	11,0
7	Agrégat A2 0–3 mm + 12% filler F2	16,0 FA	2180	11,0
8	Agrégat A2 0–7 mm	14,5 FA	2190	12,00
9	Agrégat A2 0–7 mm + 16% filler F1	14,5 FA	2310	11,0
10	Agrégat A2 0–7 mm + 16% filler F2	14,5 FA	2300	10,0
11	Agrégat A2 0–7 mm + 16% F4	14,5 FA	2200	10,0
12	Agrégat A2 0–15 mm	13,0 FA	2225	11,5
13	Agrégat A2 0–15 mm + 20% filler F1	13,0 FA	2340	10,5
14	Agrégat A2 0–15 mm + 20% filler F2	13,0 FA	2360	11,0
15	Agrégat A2 0–15 mm + 10% filler F2 + 10% filler F4	13,0 FA	2310	10,5
16	Agrégat A2 0–15 mm + 20% filler F4	13,0 FA	2290	10,0
17	Agrégat A2 0–1 mm + A5 1–15 mm	13,0 FA	2200	11,0
18	Agrégat A2 0–1 mm + A5 1–15 + 20% filler F2	13,0 FA	2340	10,0
19	Agrégat A2 0–1 mm + A4 1–15 mm	13,0 FA	2180	10,5
20	Agrégat A2 0–1 mm + A4 1–15 mm + 20% filler F2	13,0 FA	2340	9,0
21	Agrégat A2 0–1 mm + A4 1–15 mm + 10% filler F2 + 10% filler F4	13,0 FA	2300	8,5
22	Agrégat A2 0–1 mm + A4 1–15 mm + 20% filler F4	13,0 FA	2280	8,0
23	Agrégat A4 0–15 mm + 20% filler F3	13,0 FA	2240	9,0
24	Agrégat Fc$_1$ corrigé avec A2 + F2	11,50 FA	3290	10,0
25	Agrégat Fc$_2$ corrigé avec A2 + F2	9,00 FA	3780	9,0
26	Agrégat CS	15,00 FA	2400	10,0
27	Agrégat CS corrigé au F2	16,00 FA	2460	8,00
28	Agrégat C	18,60 FA	2390	8,0
29	Filler F1	24,00 FA	2120	11,5
30	Filler F2	24,00 FA	2100	10,5
31	Filler F3	24,00 FA	2100	10,0
32	Filler F4	24,00 FA	—	10,5
33	Agrégat A2 0–3 mm + 10% filler F1	20,00 LS.1	1960	8,6
34	Agrégat A2 0–3 mm + 10% filler F1	10,70 FA 5,30 LS.1	2180	11,0
35	Agrégat A2 0–3 mm + 10% filler F1	8,00 FA 8,00 LS.1	2135	10,5
36	Agrégat A2 0–3 mm + 10% filler F1	5,30 FA 10,70 LS.1	2120	9,5
37	Agrégat A2 0–15 mm + 20% filler F1	8,70 FA 4,30 LS.1	2250	11,0
38	Agrégat A2 0–15 mm + 20% filler	6,50 FA 6,50 LS.1	2200	10,0
39	Agrégat A2 0–15 mm + 20%	4,30 FA 8,70 LS.1	2180	9,0

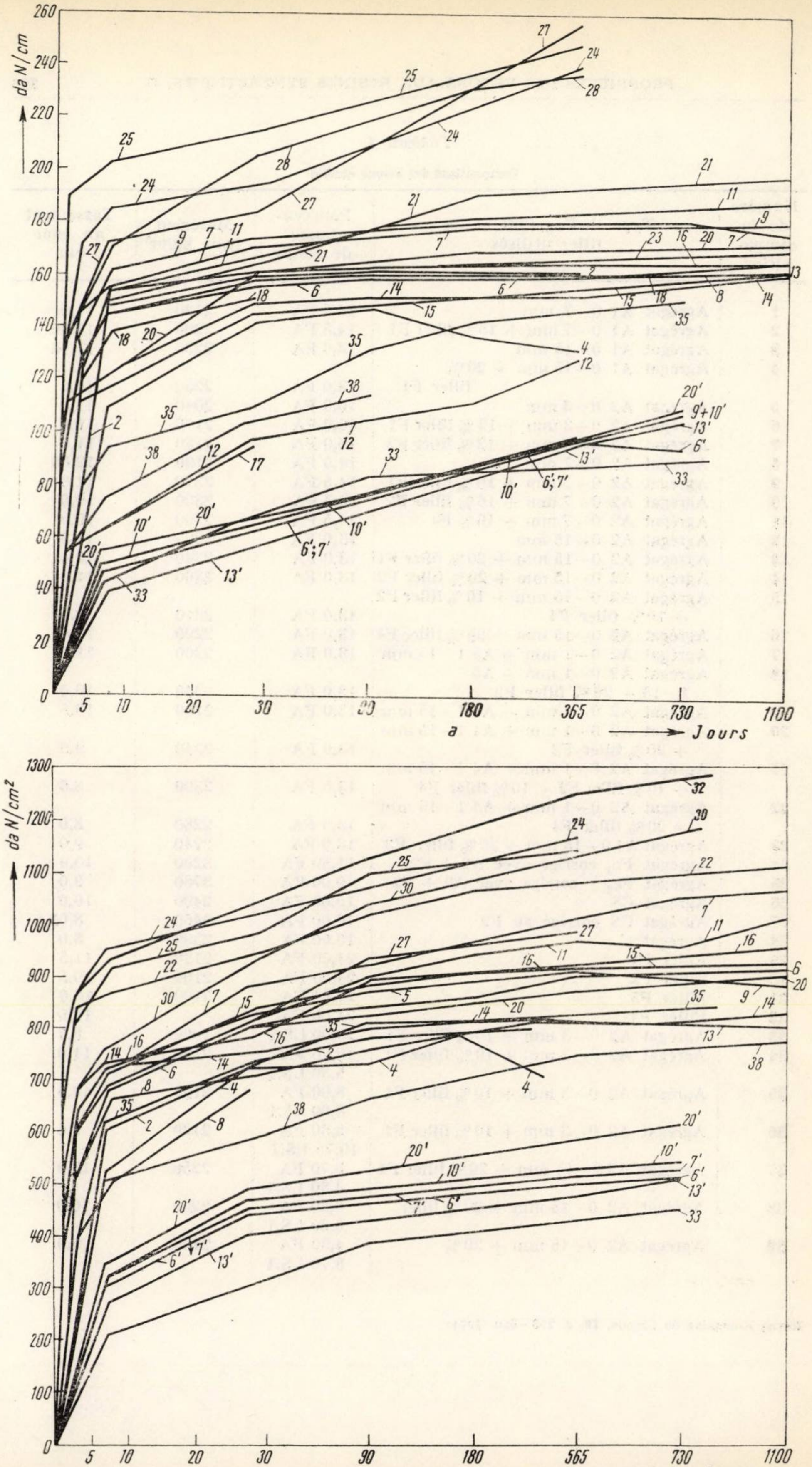
da N/cm
260
240
220
200
180
160
140
120
100
80
60
40
20
0
5
10
20
30
90
180
365
730
1100
a
Jours
25
24
27
28
21
11
9
7
7'
23
16
20
2
6
13
8
14
15
18
35
4
12
38
17
33
20'
9+10'
13'
6'
10'
6';7'
da N/cm²
1300
1200
1100
1000
900
800
700
600
500
400
300
200
100
0
5
10
20
30
90
180
365
730
1100
b
Jours
32
30
24
25
22
27
11
16
15
6
20
9
5
14
13'
38
35
4
2
8
7'
6'
10'
20'
7'
6'
13'
33

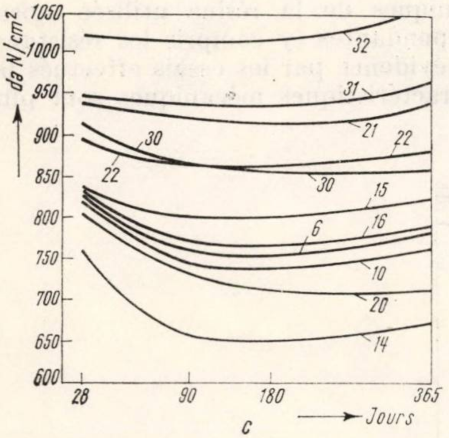

Fig. 1. — a) Variation dans le temps de la résistance à la traction par flexion pour quelques bétons à monomère FA, ou à monomère FA et résine LS.1, pour des éprouvettes conservées à l'atmosphère du laboratoire et des éprouvettes conservées dans l'eau pendant l'intervalle 24 h — âge d'essai (séries d'éprouvettes à 6′, 7′, 10′, 13′, 20′) (pour les compositions, voir tableau 1) ; b) Variation dans le temps de la résistance à la compression pour quelques bétons à monomère FA, ou à monomère FA et résine LS. 1, pour des éprouvettes conservées dans l'eau de 24 h à l'âge d'essai (séries d'éprouvettes 6′, 7′, 10′, 13′, 20′) (pour les compositions, voir tableau 1) ; c) Variation des résistances à la compression pour quelques types de béton à monomère FA lors de l'immersion dans l'eau potable, après une conservation de 28 jours à l'atmosphère du laboratoire (pour les compositions, voir tableau 1).

tation des résistances dans la période initiale est un peu plus faible. A 7 jours, on obtient des valeurs qui représentent en moyenne 55 à 65% et à 28 jours, 85 à 90% de la résistance à un an. Le rapport entre la résistance à la compression et la résistance à la traction par flexion des bétons de monomère FA se tient souvent entre 1/4,4 et 1/5,3, de sorte que pour les essais à 28 jours on peut établir avec assez de précision la relation :

$$\sigma_{ti} = 0{,}20\ \sigma_c \qquad (1)$$

Ce rapport, pour les bétons de monomère FA et résine LS.1, varie entre 1/5 et 1/7. Dans ce cas, la variation du rapport R_{ti}/R_c dans des limites plus larges est due à des modifications accusées des propriétés du liant organique utilisé (la résine LS.1 entre dans la composition du liant pour 33 à 67%).

Dans des conditions identiques de confection et d'essai, les résistances mécaniques sont sensiblement affectées, jusqu'à 180 jours, par le taux de durcisseur utilisé (fig. 2 *a* et *b*). Une petite quantité de durcisseur (ABS) dans le mélange est la cause de faibles résistances, du fait du délai prolongé de polymérisation de la résine et en même temps, d'une sensibilité beaucoup plus grande du béton à l'action prématurée de l'eau ou à d'autres actions néfastes pour la résine. Une forte quantité de durcisseur (au-delà du taux considéré comme optimal) détermine un béton de grande fragilité, cassant, de faible résistance au choc mécanique, etc. [1-10]

Les propriétés physico-mécaniques de la résine utilisée agissent elles aussi sur les propriétés correspondantes (y compris les résistances) du béton. Cet aspect a été mis en évidence par les essais effectués pour utiliser la résine LS.1 (dont les caractéristiques mécaniques sont plutôt faibles) dans différentes proportions avec le monomère FA (fig. 1 *a* et *b*). L'augmentation du dosage de la résine, entre certaines limites, pour une quantité constante d'agrégat, n'a pas pour effet un gain de résistance mécanique. Une plus forte proportion de liant peut même entraîner une diminution de résistance par l'accroissement de l'épaisseur du film de résine (matériau de faible rigidité), entre les grains de l'agrégat. Donc, pour chaque composition d'agrégat, il y a un dosage optimal de résine, qui détermine des résistances mécaniques optimales. Une modification du dosage de résine de ±5 à 7 % autour du dosage optimal affecte davantage la consistance du béton que les résistances. Des résistances mécaniques élevées pour de forts dosages peuvent être obtenues avec des agrégats adéquats, par exemple les compositions aux n°s 30 à 32 (tableau 1), préparées avec du filler de concassage (F_2 et F_3) ou avec du filler spécial (F_4) et 24 % de résine.[1-10]

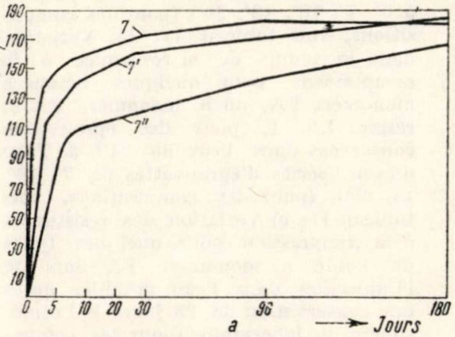

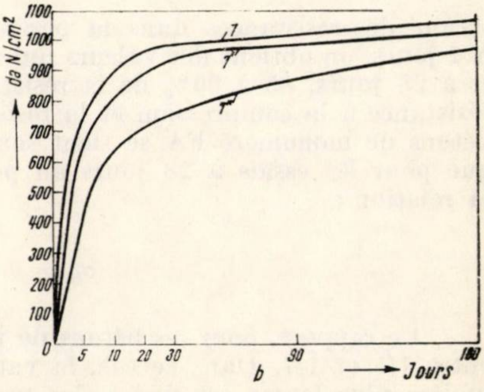

Fig. 2. a) Variation de la résistance à la traction par flexion ; b) Variation de la résistance à la compression pour la composition 7 du tableau 1, pour différents pourcentages de durcisseur (7= 100 %, 7' = 67 %, 7'' = 33 %) et pour une conservation à l'atmosphère du laboratoire à *t* = 20 à 22°.

2. RÉSISTANCE SUR PRISME

Les recherches effectuées sur différentes compositions de béton de monomère FA, à différents âges d'essai (fig. 3 *a* à *d*) indiquent que le rapport R_{pr}/R_c diminue avec l'augmentation du rapport h/b entre la hauteur du prisme et le côté de la section transversale, la diminution étant plus rapide pour h/b = 0,5 à 2,5 et devenant ensuite de plus en plus lente. Pour des compositions identiques, les valeurs du rapport R_{pr}/R_c sont différenciées selon l'âge d'essai des éprouvettes, le dosage

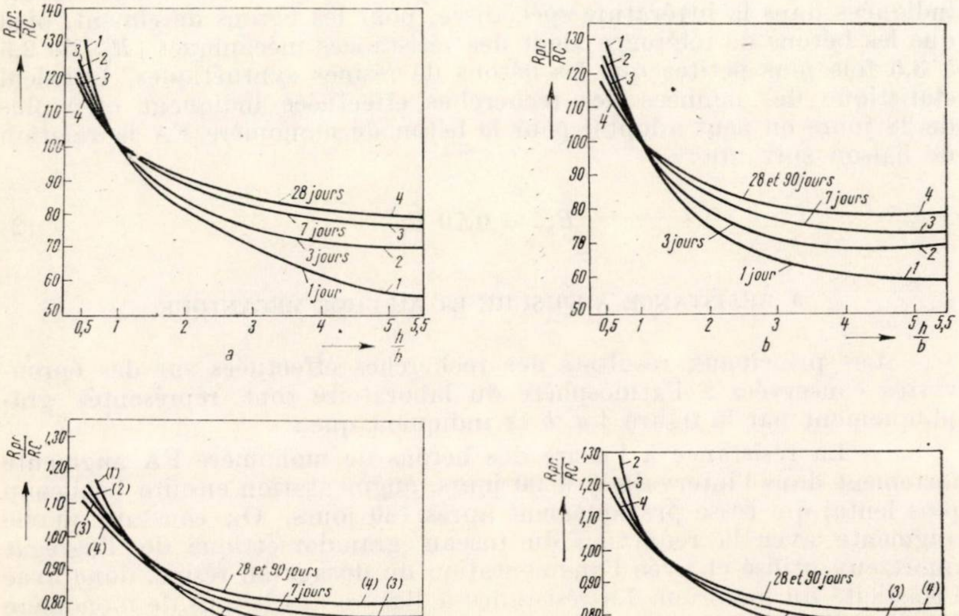

Fig. 3. — a) Variation du rapport R_{pr}/R_c dans le cas du béton fin à agrégats quartzeux broyé 0,02 à 0,30 mm additionné de 24 % de résine, essais effectués entre 1 et 28 jours. b) Variation du rapport R_{pr}/R_c dans le cas du béton fin à agrégats quartzeux 0,02 à 3 mm additionné de 16 % de résine, essais effectués entre 1 et 90 jours ; c) Variation du rapport R_{pr}/R_c dans le cas du béton à agrégats quartzeux 0,02 à 15 mm additionné de 13 % de résine, essais effectués entre 1 et 90 jours ; d) Variation du rapport R_{pr}/R_c dans le cas du béton à agrégats quartzeux 0,1 mm + agrégats basaltiques 1 à 15 mm additionné de 13 % de résine, essais effectués entre 3 et 90 jours.

en résine, la granulométrie et le type d'agrégat utilisé.[8-15] Des différences sensibles sont obtenues surtout pour les essais effectués aux jeunes âges, 1 et 3 jours (fig. 3 *a* à *d*).

A 7 jours, les différences entre les rapports R_{pr}/R_c obtenus par l'essai de bétons de différentes compositions s'atténuent sensiblement, et à 28 et 90 jours, pour la même composition, les valeurs du rapport R_{pr}/R_c sont pratiquement égales, de sorte que dans la représentation graphique les courbes sont superposées (fig. 3 *a* à *d*). Les recherches effectuées jusqu'à l'âge de 3 ans sur des bétons de monomère FA (fig. 3 *d*) ont montré que les valeurs du rapport R_{pr}/R_c sont inférieures aux valeurs indiquées dans la littérature spécialisée, pour les bétons de ciment, bien que les bétons de référence aient des résistances mécaniques (R_c) de 2,5 à 3,5 fois plus petites que les bétons de résines synthétiques. Le calcul statistique des données des recherches effectuées indiquent qu'à plus de 28 jours on peut adopter pour le béton de monomère FA la relation de liaison suivante :

$$R_{pr} = 0{,}70\ R_c \tag{2}$$

3. RÉSISTANCE À L'USURE ET AU CHOC MÉCANIQUE

Les principaux résultats des recherches effectuées sur des éprouvettes conservées à l'atmosphère du laboratoire sont représentés graphiquement par la figure 4 *a*, *b* et indiquent que :

— La résistance à l'usure des bétons de monomère FA augmente fortement dans l'intervalle 7 à 90 jours, augmentation ensuite beaucoup plus lente, qui cesse pratiquement après 180 jours. On constate qu'elle augmente avec la réduction du fuseau granulométrique de l'agrégat quartzeux utilisé et avec l'augmentation du dosage en résine, donc avec l'élasticité du matériau. La résistance à l'usure des bétons de monomère FA à agrégat quartzeux n'est pas sensiblement affectée par le type de filler utilisé (compositions 6, 7, 8, 10, 13, 14, 16, fig. 4 *a*), contrairement à ce qui se produit, dans une certaine mesure, pour les bétons à andésite basaltique, les meilleurs résultats étant dans ce cas obtenus avec les fillers F_3 et F_4. L'explication de ce fait est donnée par les résultats des recherches sur les différents fillers utilisés exposés au.[1] Avec des agrégats spéciaux tels que le carbure de silicium et le corindon, si bons que soient les résultats obtenus (compositions 27 et 28, fig. 4 a), il faut remarquer qu'ils se rapprochent de ceux obtenus pour les compositions 6 à 7 préparées avec des agrégats quartzeux 0 à 3 mm et avec un dosage en

---

[11] R. L'Hermite et J. Bresson, « Les résines de synthèse dans la construction », IIe vol., International Symposium — RILEM, Ed. Eyrolles, Paris, 1970, p. 175.

[12] L. Rechner, « Les résines de synthèse dans la construction », Ier vol., International Symposium — RILEM, Ed. Eyrolles, Paris, 1970, p. 257.

[13] S. Solacolu, « Chimia fizică a silicaţilor tehnici », Ed. tehnică, Bucarest, 1968.

[14] O. Solomon, I. Ionescu, M. Enculescu et I. Mihai, « Compuşi macromoleculari în construcţii hidrotehnice şi lucrări speciale », Ed. tehnică, Bucarest, 1966.

[15] I. Ionescu, « *Contribuţii la studiul proprietăţilor betoanelor cu răşini sintetice* », Institutul Politehnic Timişoara, Facultatea de Construcţii, 1969.

résine plus faible, d'environ 10%. Cette remarque est particulièrement importante du point de vue technique et économique, car l'utilisation de ces agrégats spéciaux, qui sont ordinairement employés comme abrasifs, ne donne de meilleurs résultats que dans certaines conditions, et le liant remplit alors un rôle tout particulier. Ainsi, le monomère FA, par ses propriétés (résistances propres très élevées, bonne adhérence à l'agrégat, etc.) garantit l'augmentation substantielle de la résistance à l'usure par abrasion mécanique du béton et on peut utiliser avec les mêmes résultats techniques les agrégats quartzeux sélectionnés au.[1] La confirmation en est donnée par le fait que les bétons à agrégats 0 à 15 mm et avec 13% de résine (compositions 13 à 23, fig. 4 *a*) ont une résistance à l'usure de 1,5 à 2,8 fois plus grande que les bétons 1 : 4 à ciment RIM 400 et à andésite basaltique 0 à 15 mm (bien que le rapport des résistances à la compression à 28 jours ait été de 1,3 à 1,5), et que les bétons à agrégat fin 0 à 3 mm (compositions 6—7, fig. 4 *a*) et avec 16% de résine ont une résistance à l'usure de 15 à 20 fois plus grande que le béton de ciment pour routes pris comme référence (le rapport des résistances à la compression à 28 jours étant de 1,3 à 1,5). Ceci permet de remarquer que la résistance à l'usure des bétons de résine synthétique dépend des propriétés du liant (résistances mécaniques, élasticité), de l'adhérence dans le système liant-agrégat et, dans une moindre mesure, des propriétés de l'agrégat. Ainsi, avec des agrégats quartzeux judicieusement choisis pour la préparation des bétons de monomère FA, on peut pratiquement obtenir des résultats comparables à ceux que donnent, dans des conditions identiques, le carbure de silicium ou le corindon. L'hypothèse sur le rapport direct entre les résistances mécaniques des bétons et leur résistance à l'usure n'est que partiellement valable et doit être complétée dans le sens suivant : « Dans le cas des bétons à monomère FA, à structure compacte et à résistance à la compression à 28 jours de plus de 700 kgf/cm^2, la résistance à l'usure augmente avec la réduction du module d'élasticité du matériau, c'est-à-dire avec la réduction du fuseau granulométrique et avec l'augmentation du dosage en résine ».[3,8-10,13-15]

La résistance au choc mécanique des bétons de monomère FA et des compositions habituelles augmente principalement dans les 7 premiers jours. Dans l'intervalle de 7 à 28 jours, l'augmentation de la résistance est très lente, puis, pour la plupart des compositions étudiées, cesse pratiquement et se maintient aux environs des valeurs obtenues de 28 jours jusqu'à 1 à 3 ans (fig. 4 *b*). Pour les bétons à agrégats très fins (filler F_2) et contenant 24% de résine (composition 30, fig. 4 *b*), la résistance au choc mécanique continue à augmenter pendant un certain temps, de sorte qu'à un an elle dépasse 200 kgf/cm^2 (résistances de la fonte de soudure); de même, d'importantes augmentations de résistance ont été enregistrées pour les éprouvettes préparées avec le carbure de silicium corrigé comme agrégat (composition 27, fig. 4 *b*), soit à un an plus de 120 kgf/cm^2. La résistance au choc mécanique des bétons préparés avec l'agrégat quartzeux A_2 augmente avec la réduction du fuseau granulométrique et aussi avec le dosage en résine (composition 6, 7, 14, fig. 4 *b*), donc avec la diminution du module d'élasticité, ce qui montre une bonne concordance entre la résistance à l'usure et au choc mécanique et les caractéristiques élastiques du matériau. Pour les mêmes dosages de résine et les mêmes fuseaux granulométriques, les meilleurs résultats sont obtenus avec le filler F2 (provenant du sable quartzeux concassé) et l'agrégat de concassage A4 (compositions 6 à 7 et 14 à 20, fig. 4 *b*).

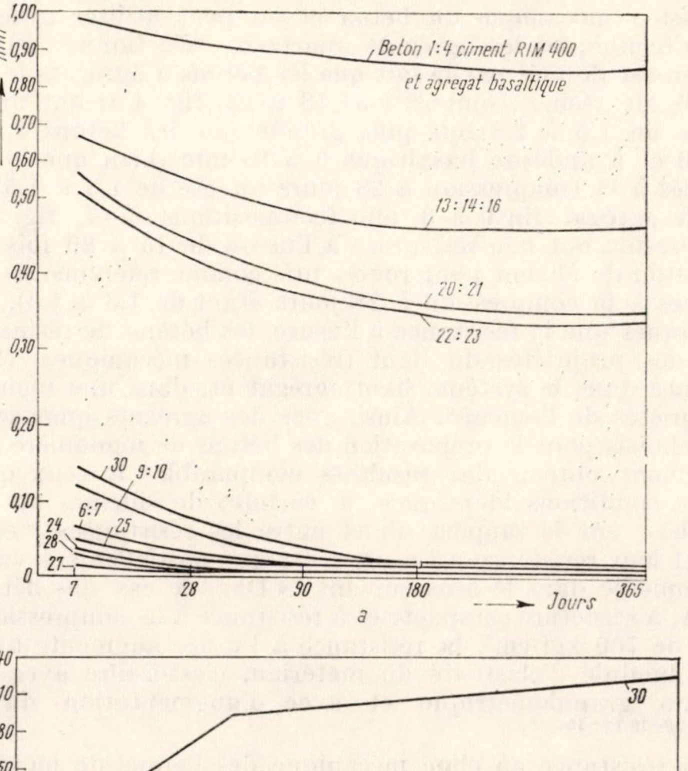

Fig. 4. — a) Variation de la résistance à l'usure dans le temps; b) Variation de la résistance au choc mécanique dans le temps pour différentes compositions de bétons aux résines synthétiques (pour les compositions voir le tableau 1).

Le gain de résistance au choc, de 40 à 50% avec le filler F2 et l'agrégat A4, s'explique par l'augmentation de l'adhérenc dans le système liant-agrégat grâce à la plus grande rugosité de la surface ou du filler de concassage, par rapport à l'agrégat et au filler de carrière.[1] C'est pourquoi il y a également une bonne concordance entre les résistances au choc mécanique et la résistance à la traction par flexion (fig. 1 *a* et 4 *b*). La résistance au choc mécanique des bétons à agrégats A2 et A4, à 28 jours, représente 30 à 55 kgf/cm², c'est-à-dire 5 à 8 fois la résistance du béton pour routes (fig. 4 *b*). L'utilisation de l'agrégat Fc corrigé augmente elle aussi la résistance au choc du béton.[8–10, 15]

4. ADHÉRENCE AU BÉTON ET À L'ARMATURE

Les faits suivants ont été mis en évidence :

— Le béton préparé au monomère FA, ou au monomère FA et à la résine LS.1, a une bonne adhérence au béton et au mortier de ciment sec : 20 kgf/cm² au minimum (*R* traction axiale) à 3 jours, qui augmente légèrement jusqu'à un an, approchant alors 35,1 à 37,6 kgf/cm². Le béton au monomère FA, ou au monomère FA à la résine LS.1, a une faible adhérence au béton et au mortier de ciment humide : 4,0 à 6,2 kgf/cm² à 28 jours, ce qu'on explique comme il suit : le processus de durcissement, dans la zone de contact, est sensiblement affecté par l'humidité du béton (aucune des deux résines ne durcit en présence d'eau, ainsi qu'on l'a déjà montré) et, de plus, il est probable que certaines solutions d'hydroxyde de calcium du béton ou du mortier de ciment, qui migrent vers la surface pendant l'immersion dans l'eau, réagissent avec le durcisseur acide de la résine, contribuant ainsi à la formation, dans la zone de contact, d'une couche de béton de résine, de faible résistance ou non durci (à structure altérée), d'où de mauvais résultats aux essais d'adhérence. De la même manière, s'explique la bonne adhérence du béton de monomère FA ou de monomère FA et de résine LS.1, aux surfaces sèches de béton ou de mortier, car, dans telles conditions, en l'absence d'humidité, la résistance mécanique du béton de résine coulé sur le béton sec augmente rapidement et, en même temps, l'adhérence au béton ou au mortier de ciment ; de même, il est probable que, sur des surfaces sèches de béton, l'action de neutralisation sur le durcisseur de la résine soit très faible ou nulle. L'application sur la surface du béton sec, ou avant l'immersion dans l'eau, d'une couche de peinture bitumineuse (durcissant à froid) semble améliorer l'adhérence du béton de résine dans une certaine mesure, tant sur une surface sèche que sur une surface humide ; dans ce dernier cas, l'adhérence atteint 6 à 12 kgf/cm² à 28 jours, ce qui atteste le rôle de l'eau dans le ralentissement du processus de durcissement du béton de résine, et la prépondérance de ce phénomène négatif.[2, 10, 11, 15]

Les recherches pour déterminer l'adhérence du béton de monomère FA aux armatures et à l'acier montrent que : l'adhérence du béton de résine aux surfaces planes en tôle est sensiblement influencée par leur rugosité : les éprouvettes coulées sur tôle polie atteignent 0,8 % au maximum de l'adhérence des éprouvettes coulées sur des surfaces de tôle brute (respectivement 28,1 et 40,6 kgf/cm² à 28 jours, par rapport à 34,7 et 59,6 kgf/cm²). L'adhérence aux surfaces de tôle brute, pour les mêmes compositions de bétons, représente 0,75 à 0,85 % de l'adhérence à des barres en acier à béton, Ø 10 mm (fig. 5 a) ce qui prouve que pour les bétons de résines synthétiques l'adhérence par collage joue un rôle beaucoup plus important que pour les bétons de ciment où elle atteint 2,7 à 19,2 kgf/cm². L'adhérence augmente, dans certaines limites, avec le dosage en résine (composition 10—14 — tableau 1) mais pour de forts pourcentages de résine, elle tend à baisser ce qui est probablement dû à l'aptitude de ces bétons à subir de fortes déformations (compositions 30).

L'étude de l'adhérence aux différents types de barres d'acier et de treillis métalliques par la méthode directe a pu être effectuée principalement sur des éprouvettes cubiques de 10 × 10 × 10 cm de côté car aux essais sur éprouvettes prismatiques longues de 21 cm et de 32 cm, l'adhérence du béton de résine aux barres d'acier (OL 38 Ø 10) dépassant la résistance à la rupture de la barre, celle-ci cassait. Les résultats des recherches pour déterminer la variation de l'adhérence (effort jusqu'au premier glissement) de certains types de bétons fins et de bétons de résine synthétique aux barres d'acier OL 38 de Ø 10 mm, placées verticalement lors de la coulée, sont représentés graphiquement par la figure 5 *a* et prouvent que l'adhérence augmente dans le temps, ses valeurs étant comprises entre 31 et 64 kgf/cm^2 à 7 jours, 45 et 67 kgf/cm^2 à 28 jours et 57 et 72 kgf/cm^2 à 365 jours. La principale augmentation de l'effort d'adhérence a été enregistrée dans les 7 premiers jours : on obtient alors 52 à 88 % de l'effort d'ahérence à 365 jours ; l'adhérence continue à augmenter légèrement jusqu'à 90 jours, et on a alors des valeurs pratiquement égales à celles obtenues à 365 jours. Si l'on continue à arracher la barre des éprouvettes de béton après le premier glissement, l'effort augmente d'abord puis baisse légèrement (après un temps qui dépend de la vitesse et de l'effort d'arrachement de la barre) pour se stabiliser autour d'une valeur qui correspond à 0,76—0,85 de l'effort exercé jusqu'au premier glissement, pour toutes les compositions de béton essayées entre 7 et 365 jours, exception faite pour les compositions de bétons fins (préparées au filler et avec 24 % de résine) où l'effort d'arrachement sous charge constante augmente de 0,40 à 7 jours, à 0,54 à 28 jours, 0,70 à 90 jours, 0,80 à 180 jours et 0,85 à 365 jours de la valeur de l'effort au premier glissement (fig. 5 *b*, *c*).

Pour des éprouvettes cubiques avec armatures placées horizontalement et verticalement (compositions n°s 7 et 10), le rapport horizontal/vertical a donné des valeurs de 0,88 et 1,10, ce qui indiquerait que pour les bétons de résine synthétique à faible viscosité, telle que le monomère FA, le fait d'avoir placé les barres d'armature parallèlement ou perpendiculairement à la direction du coulage n'exerce pas d'influence particulière. La valeur de l'effort moyen d'adhérence au premier glissement pour les barres d'acier OL de Ø 10 mm, pour les compositions 7, 10, 14, 20 aux essais à 28 et 365 jours est :

$$\tau_{\text{moyen}} = 0{,}072\, \sigma_c \tag{3}$$

et pour les compositions de béton fin (préparé avec du filler et 24 % de résine) aux essais à 28 jours :

$$\tau_{\text{moyen}} = 0{,}050\, \sigma_c \tag{4}$$

Les recherches sur l'adhérence du béton au monomère FA et à la résine LS.1 aux barres crénelées en Pc 52 de Ø 10 mm, ou au fil métallique sigma à adhérence améliorée de Ø 6 mm ont montré que l'adhérence est tellement forte qu'aux essais, d'abord à 7 jours puis à 3 et à 1 jour, la barre en Pc 52 se casse (sans déplacement de son extrémité libre) sous une force de 4 200 à 4 500 kg (c'est-à-dire un effort de 5 500 à 5 700 kgf/cm^2 à la barre), tandis que le fil métallique sigma se rompt sous un effort dans le fil de plus de 6 000 kgf/cm^2 sans déplacement de l'extrémité libre, ce qui indique que l'adhérence dépasse 140 kgf/cm^2 et que la longueur d'ancrage calculée pour de telles barres diminue pour chaque longueur de barre de 5 cm. Ceci s'explique par la grande résistance à la traction et au cisaillement de ce nouveau type de béton et par son aptitude à bien se couler sur la surface des aciers à haute adhérence. Les recherches pour déterminer l'adhérence du béton de monomère FA (compositions 7 et 10, table 1) à une barre de SBP à adhérence améliorée (fig. 5 d) ont prouvé que les barres de SBP commencent à glisser (aux essais à 28 jours) sous des efforts moyens de 180 et 206 kgf/cm², les efforts augmentent ensuite continuellement, jusqu'à ce que l'extrémité libre de la barre glisse de 5 mm (les essais ont alors été arrêtés). L'explication en est donnée par une résistance toujours plus grande grâce au moulage du béton sur la surface des barres de SBP. La détermination de l'adhérence à différents treillis de SBP a exigé des efforts importants, plus de 300 kgf/cm² jusqu'au premier glissement. Il a été constaté que, dans ce cas, l'arrachement du treillis se produit par suite des déformations qu'il subit (sous

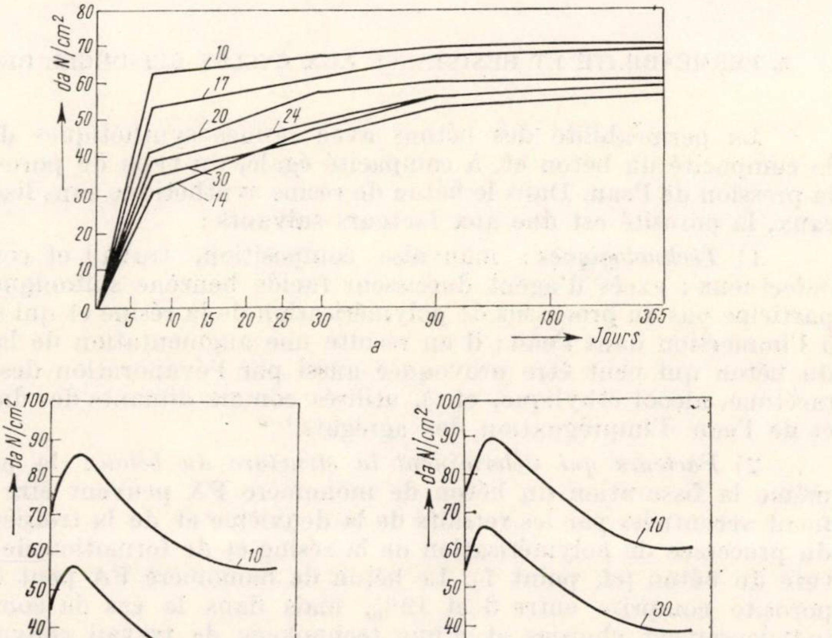

Fig. 5. — a) Variation de l'adhérence, dans le temps, déterminée par arrachement des barres en ØL 38 à profil normal pour différentes compositions de bétons aux résines synthétiques (cf. tableau 1) ; b) Variation de l'effort nécessaire pour déplacer l'extrémité libre d'une barre en OL 38 Ø 10 mm après le premier glissement, pour différentes compositions de béton (cf. tableau 1), essais à 28 jours ; c) Variation de l'effort nécessaire pour déplacer l'extrémité libre d'une barre en OL 38 Ø 10 mm après le premier glissement, pour différentes compositions de béton (cf. tableau 1), essais à 90 jours ; d) Variation de l'effort nécessaire pour déplacer l'extrémité libre de la barre Ø 5 mm en SBP enrobée dans un béton de composition 10 (cf. tableau 1), essais à 28 jours.

charge) et dues à la traction des fils métalliques, ainsi que des déformations qui se produisent sous la couche de mastic de résine autour du treillis. Les observations effectuées jusqu'à présent prouvent que les bétons de monomère FA ou de monomère FA et de résine LS.1 protègent bien l'armature, que les éprouvettes soient conservées à l'air ou dans l'eau durant l'intervalle de 28 à 365 jours ; une fois extraites, les armatures présentent une surface nette, sans aucune trace de corrosion.[10, 11, 15]

5. PERMÉABILITÉ ET RÉSISTANCE AUX CYCLES GEL-DÉGEL RÉPÉTÉS

La perméabilité des bétons avec résines synthétiques dépend de la compacité du béton et, à compacité égale, du type de porosité et de la pression de l'eau. Dans le béton de résine synthétique sans liants minéraux, la porosité est due aux facteurs suivants :

1) *Technologiques* : mauvaise composition, travail et compactage défectueux ; excès d'agent durcisseur (acide benzène sulfonique) qui ne participe pas au processus de polymérisation de la résine et qui se dissout à l'immersion dans l'eau ; il en résulte une augmentation de la porosité du béton qui peut être provoquée aussi par l'évaporation des solvants (acétone, alcool éthylique, etc.), utilisés comme diluants des durcisseurs, et de l'eau d'imprégnation des agrégats.[1–9]

2) *Facteurs qui déterminent la structure du béton* : la porosité et même la fissuration du béton de monomère FA peuvent être sensiblement accentuées par les retraits de la deuxième et de la troisième phase du processus de polymérisation de la résine et de formation de la structure du béton (cf. point 7). Le béton de monomère FA peut avoir une porosité comprise entre 3 et 12%, mais dans le cas de compositions judicieusement choisies et d'une technologie de travail convenable, la porosité ne dépasse pas 3 à 5% ; le béton est alors pratiquement imperméable, car les pores sont en général uniformément distribués dans sa masse sous forme de pores fins fermés. Ceci est confirmé par l'adsorption d'eau tout à fait insignifiante qu'ont les bétons de ce type, 0,16 à 0,36% au maximum après 360 jours d'immersion à la pression normale. Les principaux résultats des recherches, fournis par le tableau 2 entraînent les remarques suivantes : le degré d'imperméabilité est faible dans les compositions de bétons sans addition de filler, car le taux de résine de la composition n'est pas suffisant pour remplir intégralement le volume de vides des agrégats et nous obtenons ainsi une structure moins compacte (compositions 5, 8 et 12).

La résistance aux cycles gel-dégel répétés dépend des facteurs technologiques déjà indiqués pour la perméabilité et, en outre, de la résistance après conservation dans l'eau pendant une durée prolongée. Pour cette raison, et afin d'éviter des erreurs importantes — compte tenu des moyens à notre disposition — nous avons introduit trois classes de résistance (tableau 2), la dernière classe (faible) correspondant à la méthodologie indiquée par les normes pour déterminer la résistance au gel-dégel du béton de ciment. Les résultats des recherches (cf. tableau 2) présentent une très bonne concordance avec ceux relatifs à la perméabilité. On remarque aussi que toutes les compositions résistent au moins à

100 cycles de gel-dégel répétés. Le comportement très bon à 150 cycles correspond à des compositions de bétons préparées avec addition de filler (compositions optimales déduites des recherches effectuées pour déterminer d'autres propriétés) et qui ont un degré d'imperméabilité égal à P 12, les baisses de résistance y étant généralement inférieures à 5%. Ainsi, en admettant que la baisse de résistance qui apparaît à la conservation des éprouvettes dans l'eau dans l'intervalle 28 à 180 jours et celle due à l'action de 150 cycles sont annulées, il résulte que la baisse totale de résistance pour la classe très bonne est inférieure à 25% (ce que les normes pour le béton admettent) de la résistance des éprouvettes conservées uniquement à l'ambiance du laboratoire, ce que nous consi-

Tableau 2

Perméabilité et résistance au gel-dége

Numéro de la composition *	Dimensions des éprouvettes	Pression pour laquelle l'eau traverse l'éprouvette atm	Pression maximale d'essai avant que l'éprouvette ne soit pas traversée par l'eau	Résistance aux cycles gel-dégel répétés (x_{1-2})
5	20 × 20 × 5	4	—	× 1 — faible
6	20 × 20 × 5	—	12	× 2 — très bonne
8	20 × 20 × 5	5	—	× 1 — faible
9	20 × 20 × 5	—	12	× 1 — très bonne
10	20 × 20 × 5	—	12	× 2 — très bonne
11	20 × 20 × 5	—	12	× 2 — très bonne
12	20 × 20 × 10	8	—	× 1 — bonne
12	20 × 20 × 5	3		
13	20 × 20 × 5	—	12	× 2 — très bonne
14	20 × 20 × 5	—	12	× 2 — très bonne
15	20 × 20 × 5	—	12	× 2 — très bonne
16	20 × 20 × 5	—	12	× 2 — très bonne
20	20 × 20 × 5	—	12	× 2 — très bonne
22	20 × 20 × 5	—	12	× 2 — très bonne
29	20 × 20 × 2	—	12	× 2 — très bonne
30	20 × 20 × 2	—	12	× 2 — très bonne
32	20 × 20 × 2	—	12	× 2 — très bonne

* Voir tableau 1.

× 1 — éprouvettes cubiques de 10 cm de côte, ayant subi 100 cycles répétés gel-dégel (un cycle = 20 heures d'immersion dans l'eau à environ 20°, plus 4 heures dans des chambres frigorifiques à − 15 − 30°)

× 2 — idem × 1 après 150 cycles gel-dégel répétés.

L'appréciation a été effectuée de la manière suivante :

— très bonne — s'il s'agissait d'une perte de poids inférieure à 2% et d'une perte de résistance inférieure à 5% ;

— bonne — s'il s'agissait d'une perte de poids inférieure à 3% et d'une perte de résistance inférieure à 8%.

— faible — s'il s'agissait d'une perte de poids inférieure à 6% et d'une perte de résistance inférieure à 25%, en comparant aux éprouvettes témoin conservées dans l'eau pendant toute la durée des cycles gel-dégel.

Remarque

La pression maximale d'essai a été conditionnée par la puissance de l'installation disponible.

dérons comme suffisant en fonction du but poursuivi. Les mêmes observations sont valables pour la classe bonne après 100 cycles de gel-dégel répétés.[7,10,13-15]

6. DILATATION ET CONDUCTIVITÉ THERMIQUE

Les résultats des recherches et des calculs effectués à l'humidité relative de 50 % et à une température variable entre —20° et +60°, donnés dans la figure 6 entraînent les remarques suivantes :

Le coefficient de dilatation thermique des bétons de monomère FA augmente avec le dosage en résine et avec la réduction du fuseau granulométrique pour l'agrégat quartzeux utilisé. Ainsi, pour les bétons fins préparés au filler F2 et avec 24 % de résine (composition 30), le coefficient de dilatation thermique $K_t = 0{,}016$ à 0,022 mm/m°C, c'est-à-dire de 1,5 à 1,8 fois plus grand que celui de l'acier et de 1,7 à 2,2 fois plus grand que celui du béton. Pour les bétons fins à agrégats 0 à 3 mm et avec 16 % de résine (composition 7) le coefficient de dilatation thermique, $K_t = 0{,}010$ à 0,011 mm/m°C, a des valeurs assez rapprochées de celles obtenues pour OL 38 et pour le béton 1 : 4 préparé avec des agrégats quartzeux 0 à 15 mm et du ciment RIM 300 utilisés comme matériaux de comparaison. Pour les bétons à agrégats quartzeux 0 à 15 mm ou 0 à 1 et andésite basaltique, le coefficient de dilatation thermique $K_t = 0{,}005$ à 0,0058 est environ deux fois plus petit que celui de l'acier et du béton. L'influence particulière qu'exerce la résine utilisée comme liant sur la dilatation thermique du béton de la composition 25 (où 50 % de l'agrégat est représenté par les déchets d'acier utilisés) pour lequel $K_t = 0{,}062-0{,}075$ mm/m°C, donc 1,5 à 2 fois plus petit que K_t pour OL 38. La nature et la provenance de l'agrégat exercent une influence rela-

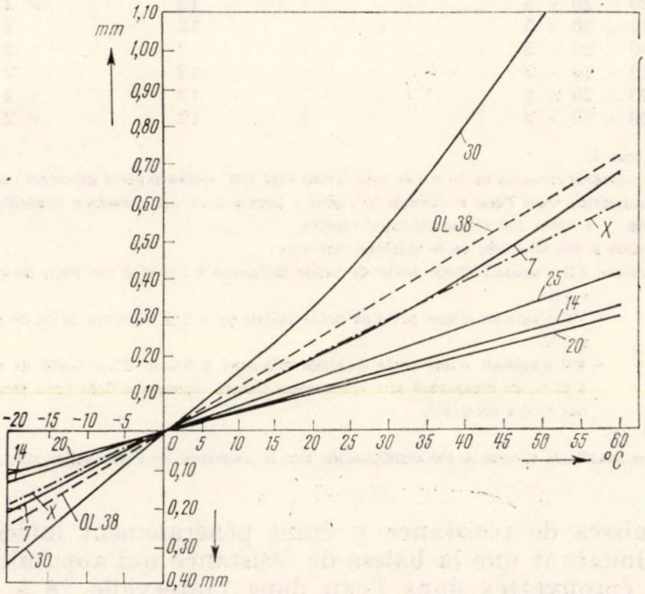

Fig. 6. — Dilatation thermique moyenne des bétons à monomère furfurol-acétone (compositions dans le tableau 1). x. bétons 1 : 4 de ciment RIM 400, agrégats quartzeux 0 à 15 mm.

tivement réduite, par rapport au dosage en résine, sur le coefficient de dilatation thermique. Les résultats obtenus démontrent la possibilité d'armer avec des aciers les bétons à agrégats 0 à 3 mm — 0 à 15 mm, contenant 13 à 16% de résine, et de les utiliser dans l'exécution des constructions mixtes ou de revêtements de protection pour les éléments de construction métalliques et en béton armé.

La conductivité thermique du béton de résine a été étudiée à l'aide de l'appareil du Dr Böke sur des plaques de 5 × 20 × 20 cm, avec différentes compositions d'agrégat quartzeux, d'andésite basaltique et d'agrégats avec addition de déchets d'acier ainsi qu'avec divers dosages en résine. Les résultats de ces recherches montrent que dans le cas des bétons aux résines synthétiques (comme dans le cas des bétons de ciment), le coefficient de conductivité thermique augmente fortement avec l'augmentation de la densité apparente du béton. Pour ce type de bétons, il semble que la nature de l'agrégat a une influence assez faible, de sorte que les bétons à andésite basaltique et ceux à agrégats quartzeux, dans des conditions identiques de préparation et à densité égale de béton, ont des coefficients de conductivité thermique pratiquement égaux (différence de ± 3 à 7%). A densités égales, les coefficients de conductivité thermique des bétons de monomère FA représentent environ 60% de la valeur des coefficients de conductivité thermique des bétons de ciment. Ceci s'explique probablement par le fait que la résine utilisée, le monomère FA, est, à des températures usuelles, un bon isolant thermique et contribue à réduire sensiblement le coefficient de conductivité thermique des bétons préparés avec des agrégats lourds.

7. RETRAITS ET GONFLEMENTS

On résume ici les principaux résultats de nos recherches et calculs, certains étant traduits graphiquement par la figure 7 *a*, et *b*. Ils montrent que le retrait des bétons de résine au monomère FA s'explique par la réduction du volume de résine utilisée comme liant pendant la période de polymérisation sous l'action de l'agent durcisseur, lorsque se produit le passage de la phase liquide à la phase solide, en même temps que la condensation des molécules et la formation d'une structure plus compacte, phénomène qui se manifeste par une légère augmentation du poids apparent du matériau durci. D'autre part, il faut tenir compte du fait que la résine utilisée contient, dans certaines proportions, des composants volatils, ou qu'on en a introduits sous forme de diluants pour le durcisseur (acétone, alcool éthylique, eau, etc.); leur perte provoque, après la coulée, un retrait du béton. Une autre cause qui contribue à accroître le retrait des bétons de résines synthétiques est le tassement et la réduction de volume consécutive du béton durant la période de durcissement du fait de la compression des pores formés par évaporation de l'eau ou des composants volatils de la masse du béton au cours de la polymérisation de la résine qui tend à prendre une structure compacte. Il en résulte que les bétons à fort dosage en résine sont ceux qui montrent les retraits les plus importants. Le retrait diminue donc avec la réduction du dosage en résine et avec l'élargissement du fuseau granulométrique de l'agrégat utilisé. Ainsi, avec des agrégats quartzeux, les bétons fins au filler et contenant 24% de résine montrent des retraits très importants (compositions 30 et 32, fig. 7 *a*), tandis que les bétons fins à agrégats 0 à 3 mm et contenant 16% de résine ont des retraits encore notables par rapport à ceux des bétons à agrégats 0 à 15 mm et contenant 13% de résine (compositions 7, 13, 14, 15 et 16, fig. 7 *a*). L'influence du type de résine, sur le retrait se manifeste différemment selon les propriétés de la résine, à savoir : sa propension à réduire de volume pendant le durcissement, sa teneur en substances volatiles, etc. Ainsi, avec le monomère FA et la résine phénol-formaldéhyde LS.1, dans différentes proportions, les retraits diminuent avec l'augmentation du taux de résine LS.1.[1] L'influence de la nature de l'agrégat utilisé se manifeste d'une manière différente, de sorte que les bétons à andésite basaltique 1 à 15 mm et contenant 13% de résine ont des retraits de 1,50 à 1,60 fois supérieurs à ceux des bétons à agrégats quartzeux 0 à 15 mm et contenant 13% de résine (compositions 13 et 20, fig. 7 *a*). Pour un même type d'agrégats et un même dosage en résine, dans les mêmes conditions de préparation, l'utilisation du filler spécial F4 (coke de haut fourneau broyé) entraîne un accroissement du retrait (compositions 13, 14, 16, 20, 23, fig. 7 *a*). Il est à remarquer que, même en remplaçant le filler F2 à un taux de 50% (quartz broyé) par du filler F4, on obtient un accroissement du retrait (compositions 13 et 15, fig. 7 *a*). De très grands retraits sont encore enregistrés pour les bétons au carbure de silicium corrigé (composition 27, fig. 7 *a*) ; par contre, les bétons aux déchets de fer (agrégats à gros module d'élasticité) montrent les retraits les plus faibles (compositions 24 et 25, fig. 7 *a*). Ceci prouve que dans le cas des bétons des résines synthétiques aussi, avec des agrégats à gros module d'élasticité on obtient de faibles retraits, exception faite pour des agrégats, tels que l'andésite basaltique et le carbure de silicium qui, bien qu'ils aient des modules d'élasticité élevés et qu'ils favorisent l'obtention de bétons de grande résistance et à hauts modules d'élasticité, les affectent de retraits importants ou même très importants (compositions 20, 22, 23, 27, fig. 7 *a*).

Pour un dosage optimal en durcisseur et avec les éprouvettes conservées à l'ambiance du laboratoire, la principale augmentation des valeurs du retrait des bétons de monomère FA a lieu dans les 24 premières heures suivant la coulée, environ de 50 à 65% de la valeur du retrait à 2 à 3 ans. Avec un taux de durcisseur réduit aux 2/3 ou à 1/3 du taux optimal, le retrait est plus faible dans la période initiale, mais continue à s'accroître rapidement, de sorte qu'il finit par atteindre pratiquement les valeurs maximales pour la composition correspondante (fig. 7 *a*, *b*). Si les éprouvettes sont conservées alternativement dans l'air et dans l'eau, on enregistre des gonflements à l'immersion (due à l'adsorption d'eau par les pores) et une tendance à revenir au retrait correspondant à la conservation dans l'air, lorsque les éprouvettes après le décoffrage sont conservées dans l'eau potable jusqu'à l'âge d'essai, le retrait est faible, probablement parce que l'eau qui a pénétré dans les pores empêche le développement normal du processus de polymérisation et, par conséquent, le retrait (compositions 7″, 10″, 13″, 20″, fig. 7 *a*).

D'après les faits exposés ci-dessus, on distingue 3 phases bien distinctes (fig. 7 *c*). Pendant la première phase, dont la durée dépend du taux de durcisseur utilisé et de la température du milieu environnant, et qui peut être de 2 à 3 heures pour le taux optimal de durcisseur et $t = 18$ à 22°, et de 12 à 30 heures pour de faibles taux de durcisseur et des températures de 12 à 18°, commence la polymérisation ; dans cette phase, le mélange ne perd pas encore complètement sa fluidité et le retrait est très faible, pratiquement négligeable. Pendant la deuxième phase, se termine probablement le processus de polymérisation, la chaleur est dégagée par exothermie, et le retrait, ainsi que les résistances mécaniques, augmentent rapidemment jusqu'à des valeurs atteignant 50 à 70% du retrait initial. Cette phase se développe approximativement pendant l'intervalle de 3 à 24 heures à la température normale et pour le taux optimal de durcisseur ; à des températures élevées, elle se développe en quelques heures, et pour de faibles taux de durcisseur elle peut même durer quelques jours (fig. 7 *a*, *b*, *c*). La troisième phase, où se développent 30 à 50% du retrait total, s'étend

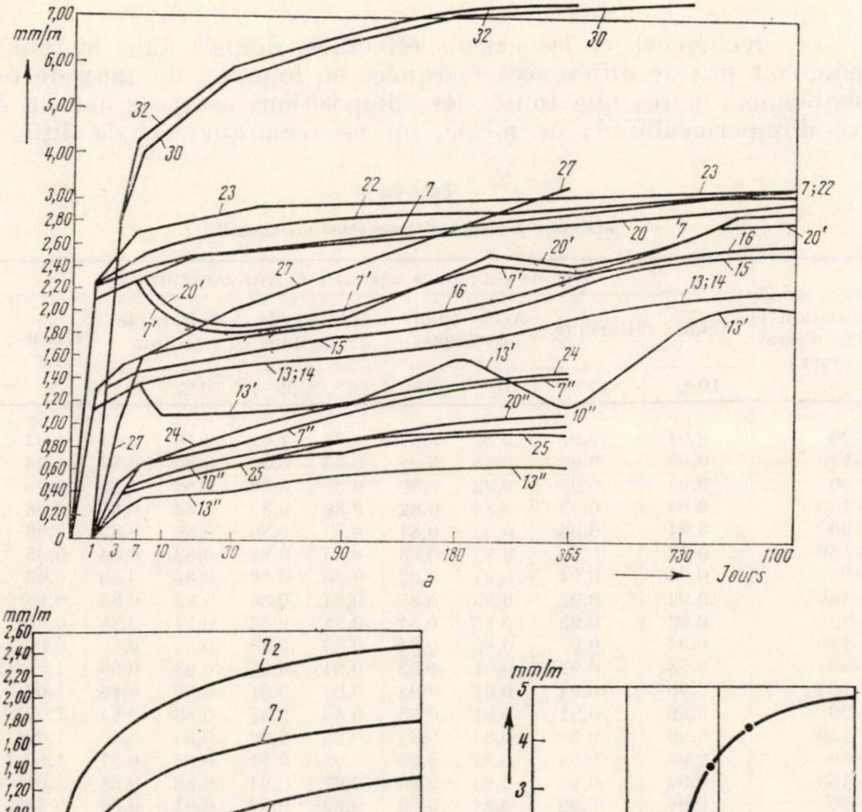

Fig. 7. — a) Retrait et gonflement de différentes compositions de bétons aux résines synthétiques (voir tableau 1) ; b) Retrait des bétons fins. Composition 7 du tableau 1 pour différents pourcentages de durcisseur (7=100%, 7'=67%, 7''=33%) et pour des éprouvettes conservées à l'atmosphère du laboratoire à $t = 20$ à 25°. c) Schéma du développement du retrait des bétons à monomère FA.

sur une période plus longue. Les retraits de la deuxième et de la troisième phase ayant des valeurs assez grandes peuvent entraîner la destruction de la structure des mortiers et des bétons aux résines synthétiques, l'apparition de fissures accentuées, des dégradations de la couche de support, etc., lorsque les déformations sont entravées. Pour cette raison, dans les travaux où l'on utilise ces matériaux, il est nécessaire de prévoir au stade du projet la neutralisation au minimum des effets négatifs qui pourraient être provoqués par la réduction des effets du retrait.[10,15]

8. RÉSISTANCE À L'ACTION DES AGENTS CHIMIQUEMENT AGRESSIFS

Les recherches et les calculs effectués, donnés dans le tableau 3 n'indiquent pas de différences marquées en fonction du taux de résine, probablement parce que toutes les compositions essayées ont un degré élevé d'imperméabilité ; de même, on ne remarque pas de différences sensibles d'après le type et la nature de l'agrégat, exception faite pour les compositions où l'on a utilisé comme filler le coke de haut fourneau broyé F4, qui ont des coefficients de résistance supérieurs pour tous les milieux agressifs où l'on a conservé les éprouvettes (compositions 16,

Tableau 3

Résistance à l'action d'agents chimiques agressifs

Numéro de la composition*) et âge d'essai jours	Agents chimiques agressifs et leur concentration									
	Acide sulfurique		Acide chlorhydrique		Hydroxyde de sodium		Sulfate de sodium		Essence	Pétrole
	10%	30%	10%	30%	10%	30%	10%	30%		
7–90	0,94	0,91	0,87	0,84	0,88	1,01	0,70	0,84	1,02	0,95
7–180	0,96	0,96	0,85	0,86	0,86	0,94	0,84	0,82	0,98	0,97
9–90	0,95	0,97	0,82	0,80	0,87	0,88	0,85	0,80	0,96	0,96
9–180	0,94	0,93	0,84	0,82	0,86	0,85	0,82	0,84	0,98	0,95
10–90	0,94	0,96	0,85	0,81	0,83	0,86	0,86	0,82	0,98	0,96
10–180	0,92	0,90	0,82	0,88	0,85	0,82	0,83	0,86	0,95	0,98
13–90	0,91	0,94	0,84	0,82	0,86	0,88	0,86	0,80	0,98	0,94
13–180	0,92	0,92	0,85	0,87	0,84	0,86	0,82	0,83	0,96	0,95
14–90	0,93	0,95	0,83	0,81	0,88	0,84	0,84	0,85	0,96	0,98
14–180	0,94	0,95	0,82	0,84	0,83	0,85	0,82	0,80	0,99	0,96
16–90	0,98	0,97	0,91	0,93	0,94	0,92	0,88	0,86	1,05	1,02
16–180	0,96	0,94	0,94	0,92	0,92	0,91	0,87	0,86	1,04	1,00
20–90	0,89	0,91	0,81	0,83	0,88	0,87	0,83	0,84	1,02	0,99
20–180	0,90	0,88	0,84	0,82	0,86	0,86	0,85	0,86	1,02	1,01
22–90	0,93	0,94	0,92	0,95	0,93	0,91	0,88	0,87	1,06	1,03
22–180	0,92	0,95	0,94	0,96	0,92	0,94	0,86	0,88	1,01	1,05
29–90	0,94	0,93	0,84	0,83	0,82	0,87	0,81	0,80	0,98	0,97
29–180	0,92	0,94	0,82	0,85	0,88	0,86	0,82	0,80	0,96	0,94
30–90	0,96	0,92	0,83	0,86	0,85	0,84	0,80	0,83	0,97	0,96
30–180	0,94	0,95	0,81	0,82	0,82	0,83	0,83	0,82	0,98	0,98
32–90	0,99	0,97	0,95	0,96	0,95	0,92	0,95	0,92	1,07	1,03
32–180	0,98	0,96	0,97	0,96	0,91	0,94	0,88	0,91	1,10	1,08

Remarque. On n'a pas remarqué de détériorations des éprouvettes après qu'elles aient été retirées de la solution d'agents chimiques agressifs.

*) Voir tableau 1.

22, 32, tableaux 1 et 3). Les bétons de monomère FA ont une très bonne résistance aux produits pétroliers (essence, pétrole lampant) ; ils ont également une bonne résistance à l'action des acides sulfurique et chlorhydrique, de l'hydroxyde et du sulfate de sodium, les coefficients de résistances obtenus aux essais étant généralement supérieurs à 0,8, ce qui prouve que les bétons essayés se sont comportés tout aussi bien sous l'action des acides que sous l'action des bases ; on peut donc envisager leur utilisation dans de très vastes domaines.

9. VARIATION DE LA VITESSE DE PROPAGATION DES ULTRASONS ET DU MODULE D'ÉLASTICITÉ DYNAMIQUE

Les résultats des recherches représentés graphiquement par les figures 8 et 9 montrent les faits principaux suivants : les courbes qui expriment la variation de la vitesse de propagation (fig. 8) et la variation du module d'élasticité dynamique dans le temps sont groupées par familles selon le dosage en résine et le fuseau granulométrique de l'agrégat. Pour un même type d'agrégats, la vitesse de propagation des ultrasons diminue avec l'augmentation du dosage en résine et avec la réduction du fuseau granulométrique pour l'agrégat utilisé.[13,15]

Les données représentées graphiquement par la figure 8 indiquent que les principales variations de la vitesse de propagation des ultrasons

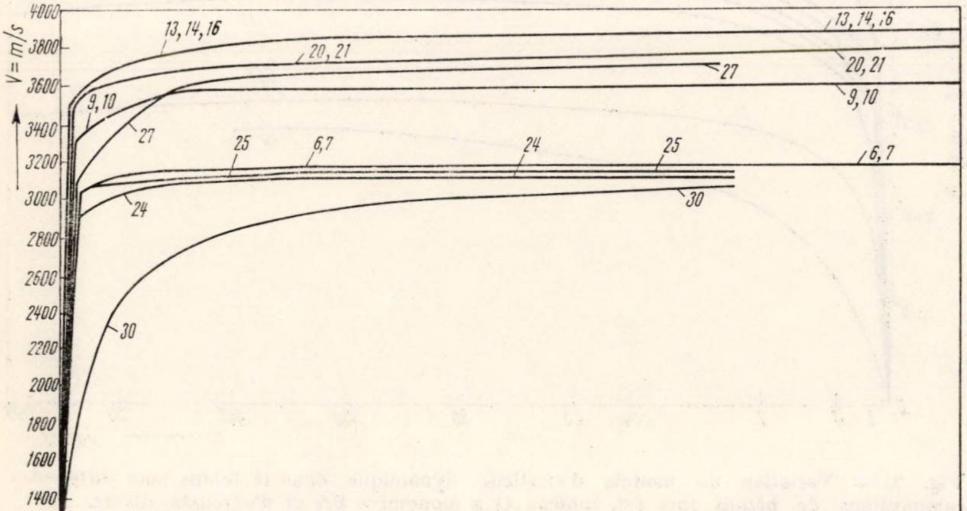

Fig. 8. — Variation de la vitesse de propagation des ultrasons dans le temps pour différentes compositions de bétons à monomère FA et d'agrégats divers (voir tableau 1)

à travers le béton de monomère FA sont enregistrées jusqu'à l'âge de 7 jours ; dans l'intervalle de 7 à 28 jours, la vitesse de propagation enregistre de faibles augmentations, et entre 28 et 1100 jours, la vitesse reste pratiquement autour des valeurs enregistrées à 28 jours.

Le module d'élasticité dynamique des bétons de résines synthétiques étudiés enregistre dans le temps des valeurs sensiblement différentes selon le dosage et le type de la résine utilisée, la nature, la composition granulométrique et la densité de l'agrégat, etc. (fig. 9). Ainsi, pour les bétons préparés avec des agrégats quartzeux, le module d'élasticité dynamique augmente de valeur avec la réduction du dosage en résine et avec l'élargissement du fuseau granulométrique pour l'agrégat utilisé. Les valeurs minimales pour le module d'élasticité ont été obtenues à tous les âges d'essai (jusqu'à un an) avec la composition n° 30 pour laquelle on a utilisé comme agrégat le filler F2 et 24 % de résine, et les valeurs maximales pour la composition 15 avec un agrégat 0 à 15 mm et 15 % de résine. La réduction du module d'élasticité avec l'augmentation du dosage en résine s'explique par la plus forte proportion d'un matériau à grande élasticité dans la masse du béton. Le module d'élasticité enregistre d'importantes augmentations dans l'intervalle de 1 à 7 jours pour toutes les compositions des bétons de monomère FA, et de très fortes augmentations avec des compositions à dosages élevés en monomère FA, phénomène explicable si nous tenons compte du fait que pendant cet intervalle la résine se polymérise en formant un réseau tridimensionnel

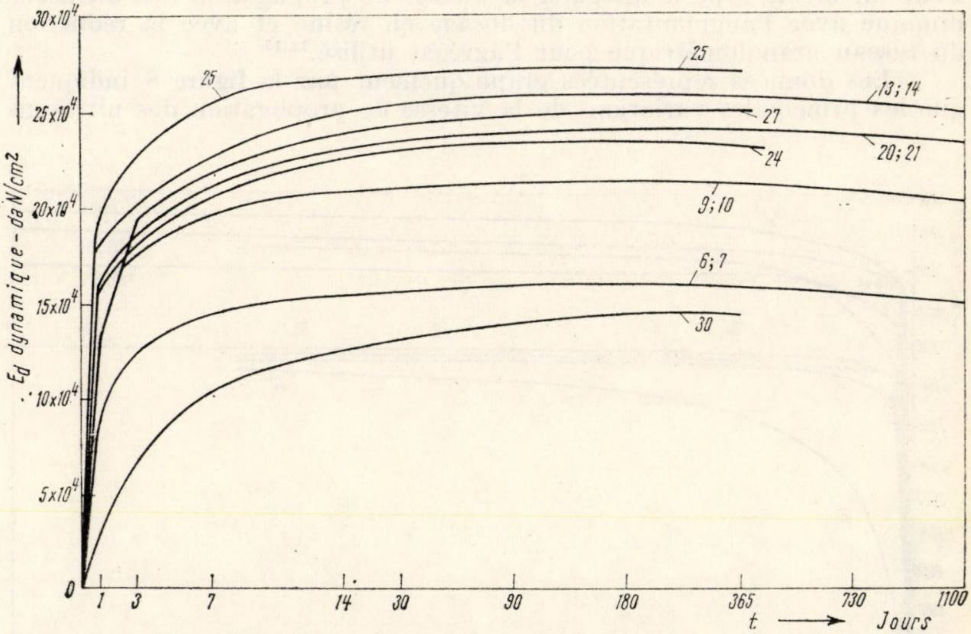

Fig. 9. — Variation du module d'élasticité dynamique dans le temps pour différentes compositions de bétons fins (cf. tableau 1) à monomère FA et d'agrégats divers.

qui devient compact et rigide à mesure que le processus de polymérisation avance. Dans l'intervalle de 7 à 28 jours, le module d'élasticité enregistre d'habitude des augmentations plus faibles. Après 28 jours, le module d'élasticité dynamique n'augmente pratiquement plus ; par contre, dans les compositions avec du monomère FA et de la résine LS.1, il augmente jusqu'à 90 jours, ce qui témoigne d'une polymérisation plus longue de la résine LS.1.

Les bétons à agrégats spéciaux Fc et Cs ont des modules d'élasticité différents selon le type et la nature de l'agrégat et selon le dosage en résine. Ainsi, les bétons au carbure de silicium (composition 27), même pour de forts dosages en résine (16 %), ont des modules d'élasticité élevés, tandis que les bétons aux déchets métalliques (Fc) ont des modules d'élasticité qui diffèrent suivant le dosage en résine et la densité de l'agrégat, le module maximal d'élasticité étant obtenu pour la composition 25 qui, pour un dosage en résine de 9 %, a atteint lors de la coulée, une densité de 3 780 kg/m^3. Mais il faut remarquer que la valeur maximale du module d'élasticité pour la composition 25 est de 270 000 kgf/cm^2, ou environ 1/8 du module d'élasticité de l'acier. Les recherches pour déterminer les relations entre le module d'élasticité statique E_{st} et le module d'élasticité dynamique E_d^* nous ont conduit à établir les relations statistiques moyennes suivantes (5) valables pour les bétons préparés avec des agrégats 0 à 3 mm et 0 à 15 mm, avec des dosages de 13 à 16 % de résine, sollicités sous des efforts $x = 0{,}16$, $0{,}33$, $0{,}50$ et $0{,}70\ \sigma_{\text{rupture}}$ et essayés à l'âge de 28 à 365 jours depuis la coulée :

$$E_{st} = E_d$$

$$E_{st} = 0{,}96\, E_d, \text{ pour } x = 0{,}16\ \sigma_{\text{rupture}} \tag{5'}$$

$$E_{st} = 0{,}84\, E_d, \text{ pour } x = 0{,}33\ \sigma_{\text{rupture}} \tag{5''}$$

$$E_{st} = 0{,}77\, E_d, \text{ pour } x = 0{,}50\ \sigma_{\text{rupture}} \tag{5'''}$$

$$E_{st} = 0{,}72\, E_d, \text{ pour } x = 0{,}70\ \sigma_{\text{rupture}} \tag{5^{iv}}$$

L'analyse des résultats des recherches pour déterminer les relations entre E_{statique} et $E_{\text{dynamique}}$ indique le module d'élasticité dynamique a des valeurs du même ordre de grandeur que le module d'élasticité statique déterminé à des stades d'essai au-dessous de $0{,}16\ \sigma_{\text{rupture}}$.

10. DÉFORMATIONS DES BÉTONS DE RÉSINES SYNTHÉTIQUES

Les résultats des recherches représentés graphiquement par la figure 10 *a* à *f* mettent en évidence les faits principaux suivants : le diagramme caractéristique (σ — ε) à la compression est semblable à celui du ciment. La valeur du coefficient de plasticité $\lambda = \varepsilon_p/\varepsilon_b$ varie selon la composition du matériau et, pour des matériaux de même composition, varie selon la température à laquelle sont conservées les éprouvettes avant l'essai et avec la vitesse d'application des charges. Le calcul statistique des résultats donne, pour les compositions avec des agrégats 0 à 3 mm jusqu'à 0 à 15 mm et 13 à 16% de résine, conservées et essayées à la température normale, $\lambda_{\text{moyen}} = 0{,}55$ avec des écarts allant jusqu'à 16% par rapport à la moyenne, et $\lambda_{\text{moyen}} = 0{,}38$ pour les bétons fins préparés avec du filler et ayant 20 à 24% de résine. Si les éprouvettes sont conservées plus longtemps à des températures élevées, de 50° à 75°, la valeur du coefficient de plasticité λ diminue beaucoup (fig. 10 *a*—*d*). Ainsi, seulement dans des conditions d'exploitation des travaux à température normale, et si l'on n'utilise que des compositions avec des agrégats 0 à 3 mm jusqu'à 0 à 15 mm, avec un dosage maximal de 16% de résine, on peut admettre pour les bétons de résine une courbe caractéristique conventionnelle du même type que celle de la figure 10 *b* et $\lambda = 0{,}50$. Les déformations du béton de résine sous l'action des charges de courte durée sont de 2 à 4 fois plus importantes que pour les bétons de ciment et augmentent avec la réduction du fuseau granulométrique de l'agrégat et avec l'augmentation du dosage en résine synthétique. Les déformations longitudinales limites à la compression peuvent atteindre 10 à 20 mm/m selon la composition du béton et le dosage en résine (fig. 10 *c* à *f*). Les différences entre les déformations pour diverses compositions de bétons (à consistance approximativement égale) augmentent avec le dosage en résine et avec le rapport $\sigma_c/\sigma_{\text{rupture}}$ ainsi, avec de dosages en résine de 13% (1/6,8), pour des efforts variant de 1/4 à 1/2 σ_{rupture}, les déformations augmentent de 0,90 % à 1,93%, tandis que pour les mêmes efforts, mais avec des dosages de 24% de résine (1/3,2) elles augmentent de 2,65% à 9% (fig. 10 *e*). A dosages égaux de résine, les bétons à andésite basaltique ont des déformations un peu plus grandes que les bétons à agrégats quartzeux. Ceci s'explique par les différences entre les caractéristiques physico-mécaniques des roches dont proviennent ces deux types d'agrégats. Il est à remarquer que les bétons à la limaille de fer, avec des taux réduits de résine, ont des déformations assez grandes par rapport aux bétons préparés avec des agrégats quartzeux.

Les déformations des bétons de monomère FA augmentent sensiblement avec la température, de sorte que, après conservation des éprouvettes pendant 72 heures dans une chambre climatisée à 50°, leurs défor-

Fig. 10. — a) Courbes caractéristiques moyennes des déformations à la compression pour des bétons à monomère FA :

1, moyenne comp. 7, 14, 20, à la température normale ; 2, idem pour la composition 30 ; 1', moyenne comp. 7, 14, 20 à 50° ; 2', idem pour la composition 30.

b) Courbe caractéristique conventionnelle pour les bétons aux résines synthétiques (agrégats 0—3 mm, 0—15 mm et addition de 13 à 16% de résine).

c) Déformations longitudinales sous charge de courte durée pour quelques bétons à monomère FA essayés à 20° (cf. tableau 1).

d) Déformations longitudinales sous effort de compression de courte durée pour quelques bétons à monomère FA essayés à 50 et 75° (compositions 7', 14', 24' et 30') (cf. tableau 1).

e) Déformations longitudinales sous charge de courte durée en fonction des pourcentages de résine et de charge à $t = 20°$.

f) Déformations longitudinales sous charge de courte durée en fonction des dosages en résine et en charge, à $t = 50°$.

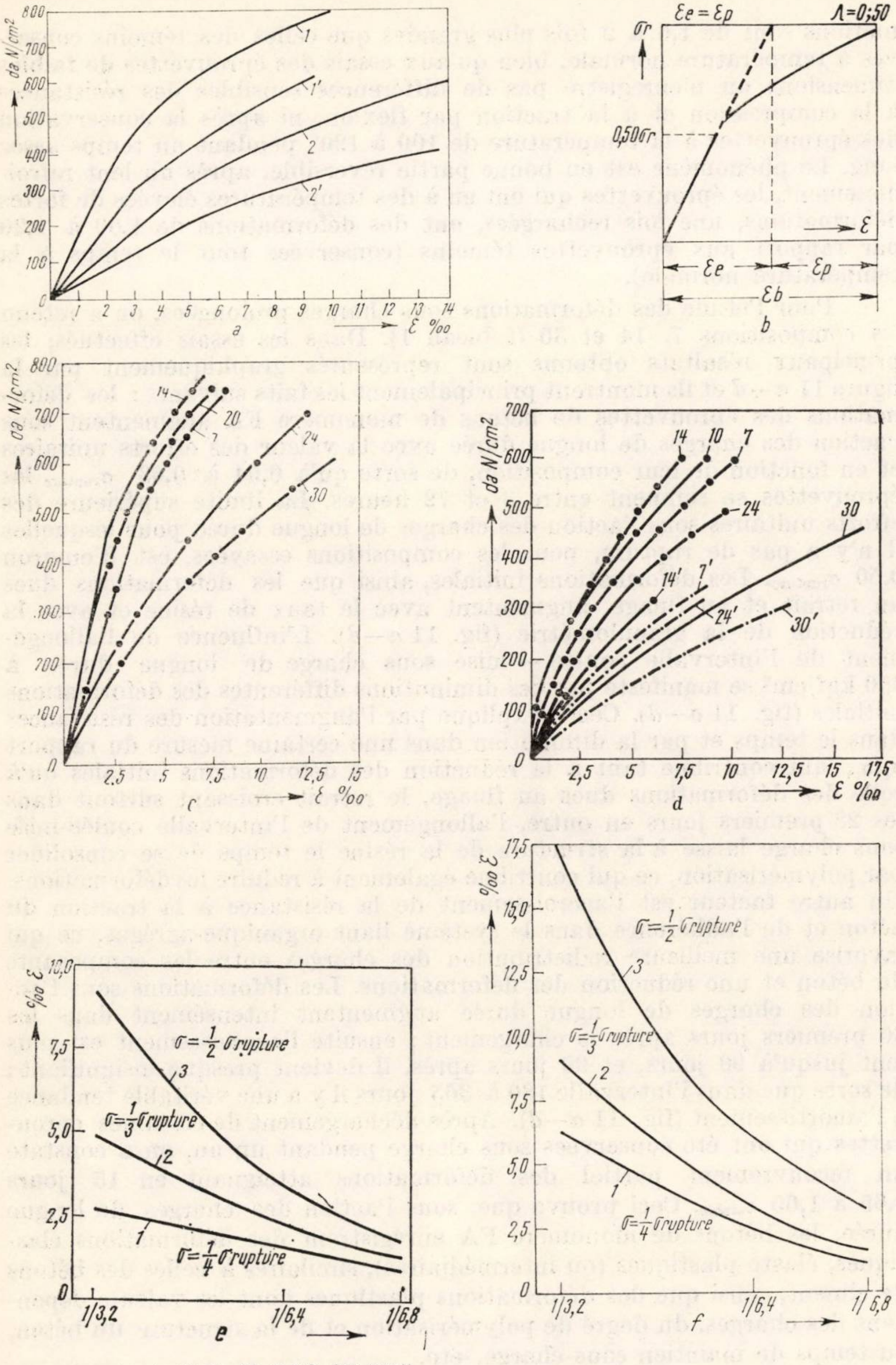
a
da N/cm²
800
700
600
500
400
300
200
100
0
1
2
3
4
5
6
7
8
9
10
11
12
13
14
ε ‰
1
1'
2
2'
b
εe = εp
Λ=0,50
σr
0,50σr
ε
εe
εp
εb
c
da N/cm²
14
20
7
24
30
0
2,5
5
7,5
10
12,5
15
ε ‰
d
da N/cm²
700
600
500
400
300
200
100
14
10
7
24
30
14'
7'
24'
30'
0
2,5
5
7,5
10
12,5
15
17,5
ε ‰
e
ε ‰
10,0
7,5
5,0
2,5
0
σ = 1/2 σrupture
σ = 1/3 σrupture
σ = 1/4 σrupture
3
2
1
1/3,2
1/6,4
1/6,8
f
ε ‰
17,5
15,0
12,5
10,0
7,5
5,0
2,5
0
σ = 1/2 σrupture
σ = 1/3 σrupture
σ = 1/4 σrupture
3
2
1
1/3,2
1/6,4
1/6,8

mations sont de 1,6 à 2 fois plus grandes que celles des témoins conservés à température normale, bien qu'aux essais des éprouvettes de faibles dimensions on n'enregistre pas de différences sensibles des résistances à la compression et à la traction par flexion, ni après la conservation des éprouvettes à la température de 100 à 120° pendant un temps assez long. Le phénomène est en bonne partie réversible, après un lent refroidissement, les éprouvettes qui ont eu à des températures élevées de fortes déformations, une fois rechargées, ont des déformations de 1,00 à 1,20 par rapport aux éprouvettes témoins (conservées tout le temps à la température normale).

Pour l'étude des déformations sous charges prolongées, on a retenu les compositions 7, 14 et 30 (tableau 1). Dans les essais effectués, les principaux résultats obtenus sont représentés graphiquement par la figure 11 *a—d* et ils montrent principalement les faits suivants : les déformations des éprouvettes de bétons de monomère FA augmentent sous l'action des charges de longue durée avec la valeur des efforts unitaires et en fonction de leur composition, de sorte qu'à 0,54 à 0,63 σ_{rupture} les éprouvettes se rompent entre 3 et 72 heures. La limite supérieure des efforts unitaires sous l'action des charges de longue durée pour lesquelles il n'y a pas de rupture, pour les compositions essayées, est d'environ 0,50 σ_{rupture}. Les déformations initiales, ainsi que les déformations dues au retrait et au fluage, augmentent avec le taux de résine et avec la réduction de la granulométrie (fig. 11 *a—d*). L'influence de l'allongement de l'intervalle coulée — mise sous charge de longue durée à 350 kgf/cm^2 se manifeste par des diminutions différentes des déformations initiales (fig. 11 *a—d*). Ceci s'explique par l'augmentation des résistances dans le temps et par la diminution dans une certaine mesure du rapport σ_c/σ_r, qui contribue tant à la réduction des déformations initiales qu'à celle des déformations dues au fluage, le retrait croissant surtout dans les 28 premiers jours en outre, l'allongement de l'intervalle coulée-mise sous charge laisse à la structure de la résine le temps de se consolider par polymérisation, ce qui contribue également à reduire les déformations. Un autre facteur est l'accroissement de la résistance à la traction du béton et de l'adhérence dans le système liant organique-agrégat, ce qui favorise une meilleure redistribution des charges entre les composants du béton et une réduction des déformations. Les déformations sous l'action des charges de longue durée augmentent intensément dans les 30 premiers jours après le chargement ; ensuite l'accroissement est plus lent jusqu'à 90 jours, et 90 jours après, il devient presque insignifiant ; de sorte que dans l'intervalle 180 à 365 jours il y a une véritable tendance à l'amortissement (fig. 11 *a—d*). Après déchargement de certaines éprouvettes qui ont été conservées sous charge pendant un an, on a constaté un recouvrement partiel des déformations atteignant en 15 jours 0,65 à 1,60 $\varepsilon_{\text{stable}}$. Ceci prouve que, sous l'action des charges de longue durée, les bétons de monomère FA enregistrent des déformations élastiques, élasto-plastiques (ou intermédiaires), similaires à celles des bétons de ciment, ainsi que des déformations plastiques dont les valeurs dépendent des charges, du degré de polymérisation et de la structure du béton, du temps de maintien sous charge, etc.

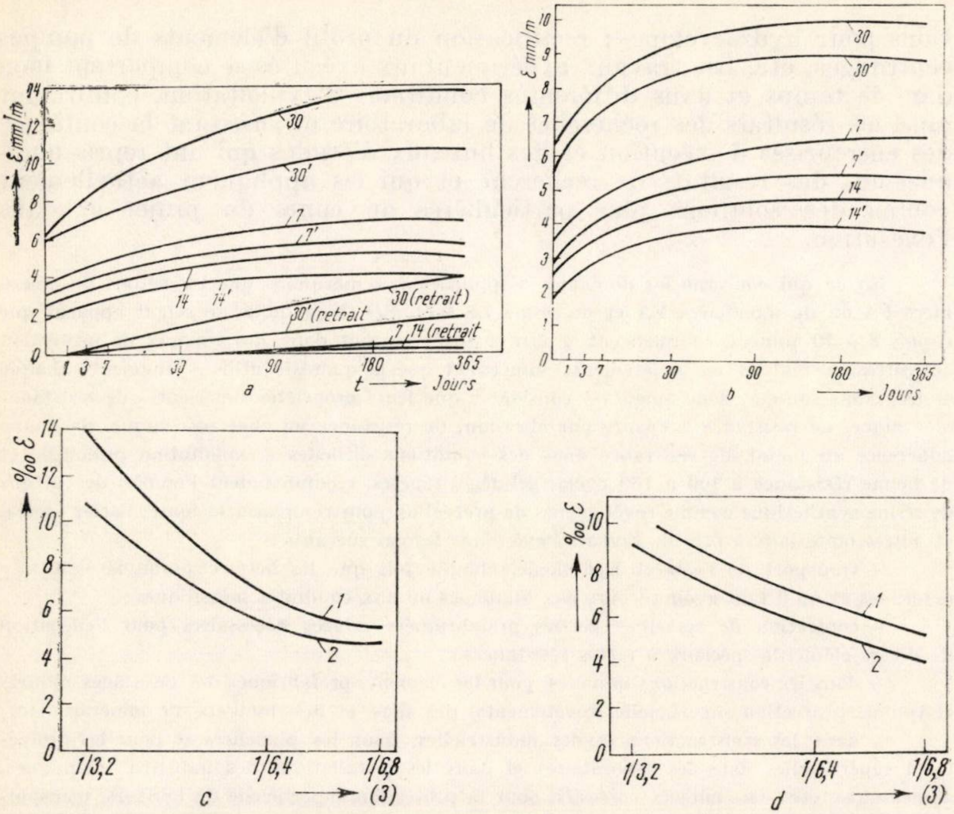

Fig. 11 — a) Déformations totales sous l'action des charges de longue durée et des retraits pour quelques bétons à monomère FA ; 7, 14, 30 — éprouvettes mises sous charge à 7 jours, 7', 14', 30' — éprouvettes mises sous charge à 28 jours depuis la coulée.

b) Déformations sous l'action des charges prolongées (sans retrait) pour quelques bétons à monomère FA. 7, 14, 30 — éprouvettes mises sous charge à 7 jours ; 7', 14', 30' éprouvettes mises sous charge à 28 jours depuis la coulée.

c) Déformations totales longitudinales sous charge de longue durée pour quelques types de bétons fins et de bétons à monomère FA à divers dosages. *1*, éprouvettes mises sous charge à 7 jours depuis la coulée ; *2*, éprouvettes mises sous charge à 28 jours depuis la coulée ; *3*, rapport résine/agrégat (en poids).

d) Déformations longitudinales (sans retrait) sous charge de longue durée pour quelques types de bétons fins et de bétons à monomère FA à divers dosages. *1*, éprouvettes mises sous charge à 7 jours depuis la coulée ; *2*, éprouvettes mises sous charge à 28 jours depuis la coulée ; *3*, rapport résine/agrégat (en poids).

11. COMPORTEMENT DANS LE TEMPS DE CERTAINS TRAVAUX EXPÉRIMENTAUX EXÉCUTÉS ET CONSIDÉRATIONS SUR LES DOMAINES D'UTILISATION PRATIQUE

Pour vérifier les résultats des recherches de laboratoire dans les conditions d'exploitation, plusieurs applications expérimentales ont été effectuées : revêtement d'usure et de protection anticorrosive ; protections pour hydrocyclones; rectification du profil d'éléments de pompes centrifuges, etc. Les travaux expérimentaux exécutés se comportent bien dans le temps et dans différentes conditions d'exploitation, confirmant ainsi les résultats des recherches de laboratoire et suscitant la confiance des entreprises d'exécution et des bureaux d'études qui ont repris quelques-uns des résultats de recherche et qui les appliquent actuellement comme des solutions plus particulières au cours du projet et dans l'exécution.

En ce qui concerne les domaines d'application, remarquons que les bétons de monomère FA ou de monomère FA et de résine LS.1 étudiés, bien qu'ils ne soient apparus que depuis 8 à 10 années, commencent à être utilisés surtout dans des travaux de protection anticorrosive réalisés en revêtements minces et que la quantité utilisée augmente chaque année. Nous sommes donc amenés à considérer que leurs propriétés supérieures de résistance mécanique, de résistance à l'usure par abrasion, de résistance au choc mécanique, de bonne adhérence au métal, de résistance dans des conditions difficiles d'exploitation prolongée et de bonne résistance à 100 à 150 cycles gel-dégel répétés, recommandent l'emploi des bétons de résine synthétique comme revêtements de protection pour remplacer la fonte, l'acier spécial et autres matériaux à prix de revient élevé, dans les cas suivants :

— transport de l'eau et hydrologie, chaque fois que les bétons communs sont vite détériorés et qu'il faut avoir recours aux blindages ou aux conduites métalliques ;

— confection de certaines parties préfabriquées minces nécessaires pour l'exécution de divers éléments spéciaux à fortes résistances ;

— dans les constructions minières, pour les éléments préfabriqués des cuvelages miniers et comme protection superficielle (revêtements) des silos et des bunkers de minérais, etc. ;

— dans les constructions civiles industrielles, pour les planchers et pour les protections superficielles dans les laboratoires et dans les installations des industries chimiques, alimentaires, etc., en milieux corrosifs, pour la protection superficielle de bunkers, transporteurs et des réservoirs, et dans tous les cas où sont nécessaires des matériaux imperméables de haute résistance à l'abrasion mécanique et à la corrosion chimique ;

— protection de différents installations et outillages technologiques contre la corrosion chimique et contre l'abrasion mécanique dans différents domaines industriels, etc.

Revue Roumaine de Chimie, **19**, *2*, 321–327 (1974)

MÉTHODES DE DÉTERMINATION DE β, β′-DICHLORO-DIÉTHYL-AMINE

SPECTRE EN VISIBLE ET INFRAROUGE DU COMPOSÉ RÉSULTÉ ENTRE LE β,β′-DICHLORO-DIÉTHYL-AMINE ET LE REINECKATE D'AMMONIUM

GRIGORE TEODORESCU

Institut Polytechnique de Bucarest, Chaire de Chimie inorganique et analytique
Bucarest, 1, str. Polizu

Reçu le 29 mars 1973

On présente des méthodes de détermination de β, β′-dichloro-diéthyl-amine (abrégé DDA) — sous forme de chlorhydrate — réalisées par la combinaison avec le reineckate d'ammonium (abrégé $NH_4^+R_c^-$), la dissolution du composé obtenu dans l'acétone, suivie de la précipitation de l'anion reineckate d'argent et le titrage de l'excès d'azotate d'argent avec du thiocyanate d'ammonium. Vu que le composé formé est soluble dans l'acétone, résultant une solution colorée, le composé a été déterminé aussi colorimétriquement. La structure du complexe obtenu a été vérifiée par la détermination de la masse moléculaire, à l'aide des spectres en visible, pour le $NH_4^+R_c^-$ et le reineckate de DDA. La structure du reineckate de DDA a été caractérisée aussi par le spectre en IR de DDA et de son composé.

Pour la détermination des amines secondaires la littérature indique plusieurs méthodes comme : titrage avec l'HCl 1 N ou avec une solution méthanolique d'acide chlorhydrique, en présence des indicateurs,[1] titrage avec l'$HClO_4$ 0,1 N en acide acétique glacial,[2] titrage des acides dithiocarbamiques qui résultent de la réaction entre l'amine et le sulfure de carbone, avec une base,[3] titrage avec une solution alcaline de l'acide chlorhydrique qui résulte de la réaction entre le tétraphénylborate de l'amine avec l'$HgCl_2$[4].

Dans cette note on présente des méthodes de détermination volumétrique et colorimétrique de DDA, matière première utilisée dans la synthèse du Lisen, médicament usité dans la thérapie de la sclérose en plaques. La méthode consiste dans la combinaison de l'amine secondaire (passée en ion *onium*) avec l'$NH_4^+R_c^-$ réactif utilisé par l'auteur aussi à la détermination d'autres produits.[5–9]

---

[1] J. Mestreit, *Chim. analyt.*, **48**, 3 (1960).

[2] P. C. Markunas et J. A. Riddick, *Analyt. Chem.*, **23**, 337 (1951).

[3] F. E. Critchfield et J. B. Johnson, *Analyt. Chem.*, **28**, 430 (1956).

[4] E. Yanson, *Ref. Zhur. Khim.*, **1958**, 43034 ; *Analyt. Abstr.*, **5**, 221 (1958).

On présente également les caractéristiques spectrales en visible et en IR du composé obtenu entre le $NH_4^+R_c^-$ et le chlorhydrate de DDA.

PRINCIPE DE LA MÉTHODE

La combinaison du chlorhydrate de DDA a lieu dans une solution aqueuse d'acide sulfurique 1 % avec du $NH_4^+R_c^-$, selon le schéma suivant :

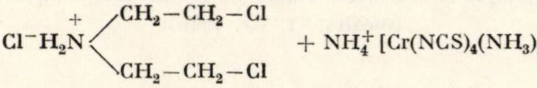

$$Cl^-\overset{+}{H_2N}\begin{matrix}\diagup CH_2-CH_2-Cl\\ \diagdown CH_2-CH_2-Cl\end{matrix} + NH_4^+[Cr(NCS)_4(NH_3)_2]^-$$

$$(ClC_2H_4)_2\overset{+}{N}H_2]\,[Cr(NCS)_4(NH_3)_2]^- + NH_4^+ + Cl^-$$

1. MÉTHODE VOLUMÉTRIQUE

On précipite la solution aqueuse de DDA par une solution de 2 % $NH_4^+R_c^-$,selon l'équation ci-dessus.

Le précipité cristallin rose obtenu est filtré, lavé et ensuite dissous en acétone.

La solution résultée est traitée par excès de solution d'azotate d'argent 0,1 N. Ainsi, le reineckate d'argent précipite conformément à la réaction :

$$[Cr(NCS)_4(NH_3)_2]^- + Ag^+ \rightarrow Ag[Cr(NCS)_4(NH_3)_2]$$

Après filtrage et lavage, l'excès d'azotate d'argent est titré avec le thiocyanate d'ammonium en présence de l'alun de fer (III) et de l'ammonium.

1.1. *Mode opératoire*

On prend 2,25 g de chlorhydrate de DDA (blanc, cristallisé) et on les entraînent quantitativement au ballon jaugé à 250 ml avec de l'acide sulfurique 1 % et on complète jusqu'à la jauge avec le même acide.

De cette solution on prend des épreuves entre 0,0360 et 0,1170 g, on ajoute 20 ml d'eau distillée et après, goutte à goutte, sous agitation continuelle, la solution fraîchement préparée de $NH_4^+R_c^-$ 3 %. Il précipite le composé cristallin nâcré rose-violet.

---

[5] GR. TEODORESCU, *Bul. Inst. Politech. București*, **32**, (2), 39 (1970).

[6] GR. TEODORESCU, *Bul. Inst. Politech. București*, **32** (4), 79 (1970).

[7] GR. TEODORESCU, *Bul. Inst. Politech. București*, **33** (1), 67 (1971).

[8] GR. TEODORESCU, *Rev. Roumaine de Chimie*, **17**, 8, 1481 (1972).

[9] GR. TEODORESCU, *Rev. Roumaine de Chimie*, **17**, 9, 1621 (1972).

Le composé formé est filtré sur un creuset à filtre G_3, entraîné par une solution de $NH_4^+R_c^-$ 0,1 %, lavé avec de l'eau distillée (4°C) jusqu'au moment, où la solution passe incolore et ensuite lavé 2 fois avec 10 à 15 ml d'éther.

On dissout directement sur le creuset le composé avec 10 à 20 ml d'acétone, jusqu'à dissolution totale. On lave finalement le creuset à 20 ml d'eau distillée et on prend la solution et les eaux de lavage dans un verre de 250 ml.

On ajoute 100 ml d'eau distillée, 10 ml d'azotate d'argent 0,1 N et 3 à 4 gouttes d'acide azotique 2 N.

Le précipité de reineckate d'argent formé est filtré et lavé par décantage à l'eau distillée. Le filtrat et les eaux de lavage sont mis dans un flacon de 750 ml. On ajoute 3 à 4 ml de solution saturée d'alun de fer (III) et d'ammonium (environ 40 %), 3 à 4 gouttes d'acide azotique 2 N et on titre l'excès d'azotate d'argent par le thiocyanate de l'ammonium 0,1 N au facteur connu (F 0,1 N = 0,9090).

Un ml d'azotate d'argent 0,1 N correspond à 0,01785 g de chlorhydrate de DDA. Les résultats obtenus sont rapportés au tableau 1.

Tableau 1

Détermination volumétrique de DDA

DDA dans l'épreuve g	DDA déterminé avec du $NH_4^+R_c^-$ g	DDA déterminé avec du $NH_4^+R_c^-$ %	DDA en produit technique par combustion * %	Données statistiques
0,0360	0,0353	98,10	98–99	$N = 10$
0,0450	0,0443	98,44	98–99	$\overline{X} = 98{,}24$
0,0540	0,0530	98,14	98–99	$S = 0{,}2435$
0,0630	0,0618	98,00	98–99	$S_m = 0{,}077$
0,0720	0,0705	97,91	98–99	variable student
0,0810	0,0796	98,27	98–99	$t^*(P = 99\,\%, \nu = 9) =$
0,0900	0,0884	98,22	98–99	$= 2{,}76$ du tableau
0,0990	0,0978	98,78	98–99	$R = 98{,}24 \pm 0{,}21$
0,1080	0,1062	98,20	98–99	
0,1170	0,1160	98,30	98–99	

*) La méthode Korshun.

2. MÉTHODE COLORIMÉTRIQUE

2.1. *Principe de la méthode colorimétrique*

On précipite le DDA avec du $NH_4^+R_c^-$ selon le même procédé dans le rapport molaire 1 : 1. Vu que le composé formé est soluble en acétone, résultant une solution colorée en rouge, le DDA peut être déterminé aussi colorimétriquement.

2.2. *La pratique*

On applique la méthode des courbes étalon. A cette fin on a employé une solution de $NH_4^+R_c^-$ avec $T = 0{,}0560$ g/ml, dont on a pris des volumes correspondants, dans des ballons jaugés de 100 ml, dilués avec 50 ml d'acétone et complétés avec de l'eau distillée, afin d'obtenir des solutions avec des concentrations $T = 0{,}00028$; 0,000560 ; 0,00840 ; 0,001120 ; 0,001680 g.

Les déterminations ont été faites à l'aide du photocolorimètre de type B. Lange, en utilisant des filtres verts ($\lambda = 533$ nm) et on a tracé la courbe étalon.

De la solution de DDA avec $T = 0,00900$ g/ml on a prélevé des épreuves entre 0,0180–0,0450 g et l'on a précipité avec du $NH_4^+R_c^-$, selon la méthode volumétrique.

Après précipitation, filtrage et lavage, les épreuves ont été quantitativement dissoutes avec de l'acétone, en prenant la solution dans des ballons jaugés à 100 ml. Après l'homogénéisation, les épreuves ont été colorimétrées, les résultats obtenus étant indiqués au tableau 2.

Tableau 2

Résultats du colorimétrage du reineckate de DDA

DDA dans l'épreuve g	DDA déterminée g	DDA déterminée g	Données statistiques
0,000180	0,000178	98,88	$N = 5$ $\overline{X} = 99,23$
0,000225	0,000221	98,22	$S = 0,2856$
0,000360	0,000354	99,44	$S_m = 0,12$
0,000405	0,000400	98,76	Variable student
0,000450	0,000454	100,88	$t^*(P = 99\,\%,\ \nu = 4) =$ $= 4,60$ du tableau Résultat $= 99,23 \pm$ $\pm\ 0,55$

3. ÉTUDE SPECTRALE

3.1. *Caractérisation du spectre en visible du reineckate de DDA*

La structure du composé obtenu peut être vérifiée par la détermination de sa masse moléculaire, à l'aide de l'absorbance (A) et de l'absorptivité (K).[10]

Les déterminations ont été faites avec le spectrophotomètre Zeiss de type VSU-1, avec une cuve de grosseur $l = 0,5$ cm et à une concentration $g_1 = 0,1\,\%$.

Les chiffres trouvés ont été pour le $NH_4^+R_c^-$:

nm	Absorbance
394	0,138
	⋮
420	0,102
	⋮
452	0,03
	⋮
482	0,093
	⋮
520	0,155
	⋮
560	0,105
	⋮

---

[10] KUM-TATT-LEE, *J. Pharm. and Pharmac.*, **12**, 666 (1960).

et pour le reineckate de DDA :

nm	Absorbance
400	0,1
420	0,07
450	0,034
480	0,062
520	0,112
553	0,083

Une caractéristique commune des spectres en visible du $NH_4^+R_c^-$ et du reineckate de DDA réside dans le fait que le maximum d'absorption (λ_{max}) est approximativement le même, $\lambda_{max} = 520$ pour le $NH_4^+R_c^-$ (dans l'éthanol 95% et $\lambda_{max} = 520$ pour le reineckate de DDA (aussi dans l'éthanol 95%).

L'absorptivité a été déterminée conformément à la relation :

$$K = A/c.l$$

sur le $NH_4^+R_c^-$, dans l'éthanol 95% à la concentration $c = 0{,}00297$ mole gramme $NH_4^+R_c^-$, à une grosseur de la cuve $l = 0{,}5$ cm et pour l'absorbance $A = 0{,}155$ correspondant à la valeur maximale $\lambda_{max} = 520$ à 525 nm.

La valeur K déterminée pour le $NH_4^+R_c^-$ est considérée, dans les limites des erreurs acceptables, comme étant valable aussi pour le reineckate de DDA, étant donné que λ_{max} pour le reineckate de DDA est égal (ou presque égal) à λ_{max} pour le reineckate.

La masse moléculaire (M_d) est déterminée selon la relation :

$$M_d = g_1/100.K/A.1.1000 \tag{1}$$

Pour le cas $g_1 = 0{,}1$ g de reineckate de DDA per 100 ml solution, la relation (1) devient :

$$M_d = (K/A).l \tag{2}$$

Pratiquement, la détermination de l'absorption en visible du reineckate est faite dans de l'éthanol 95%. L'absorbance pour $\lambda_{max} = 520$ nm à la concentration de 0,1% et à une cuve avec $l = 0{,}5$ cm (dans les mêmes conditions de travail) est de 0,112. En remplaçant dans la relation (2) on obtient :

$$M_d = (104/0{,}112) \cdot 0{,}5 = 464{,}27$$

La comparaison de cette valeur à celle de la masse moléculaire résultée du calcul $M_c = 461{,}40$ donne la possibilité de vérifier la structure du composé obtenu.

3.2. *Caractérisation en infrarouge du reineckate de DDA*

Le reineckate de DDA a été structuralement caractérisé aussi par spectre en infrarouge,[11–15] que l'on a interprété par comparaison avec le spectre du $NH_4^+R_c^-$ (tableau 3).

Tableau 3

Spectre en IR du reineckate d'ammonium

$\bar{\nu}$(cm^{-1})		T / %
472 (f)	δNCS	62
509 (f)		57
718 (i)	NH_3	39
833 (f)	νC−S	76
965	Sym	76
1265 (i)	δNH_3	34
1405 (i)	δNH_4^+	32
1605	(H_2O)	50
2059	νC−N	14
2125 (i)		1
3015 (t.f)		38
3160 (f)		30
3195 (t.f)	νNH_3	32
3238 (f)		28
3315 (f)		27

f = faible ; i = intense ; t.f. = très faible.

Le spectre en IR du composé présente des bandes pouvant être attribuées aux groupements NH_3 et NCS de l'anion reineckate du complexe, retrouvées aussi dans le spectre en IR du reineckate d'ammonium. Elles apparaissent à 965 cm^{-1} (δNCS), 1257 cm^{-1} ($\delta^{\mathrm{sym}}_{\substack{NH_3\\N-H}}$), 2100 cm^{-1} ($\nu_{C-N}$), 3168–3305 cm^{-1} ($\delta^{\mathrm{sym}}_{\substack{NH_3\\N-H}}$).

Le spectre présente aussi des bandes correspondant à la base organique (tableau 4). Ces bandes, existant à 698 cm^{-1}, 965 cm^{-1}, 1555 cm^{-1},

---

[11] Jumosuke Fujita, Kazuo Nakamoto et Moshahisa Koboyashi, *J. Amer. Chem. Soc.*, **78**, 329 (1956).

[12] B. Herzberg et C. Reid, *Discuss. Faraday Soc.*, **9**, 92 (1950).

[13] P. C. H. Mitchell et R. T. P. William, *J. Chem. Soc.*, **1961**, 4590.

[14] M. M. Chamberlain et I. C. Bailar, *J. Amer. Chem. Soc.*, **81**, 6412 (1959).

[15] M. E. Baldwin, *J. Chem. Soc.*, **1960**, (4369 ; **1961**, 471.

2965 cm^{-1} sont très peu modifiées comme position et intensité dans le spectre en IR du composé étudié (tableau 4).

Tableau 4

Spectre en IR du chlorhydrate de DDA et du reineckate de DDA

Spectre du chlorhydrate de DDA		Spectre du reineckate de DDA	
$\bar{\nu}$ (cm^{-1})	T %	$\bar{\nu}$ (cm^{-1})	T %
461 (t.f)	68	485	55
503 (t.f)	76	495	52
677 (i)	51	698 (i)	26
758 (i)	63	815 (i)	44
792	74	840 (t.f)	83
845	78	885 (t.f)	82
860	77	945	
869	74	965 (t.i)	66
890	67	1038	75
965 (i)	59	1045 (f)	74
1015	72	1055	74
1058	69	1093	74
1070	71	1195	68
1090	74	1257 (t.i)	21
1160	79	1290 (f)	69
1215	76	1330	62
1235	76	1353	64
1282	74	1430 (i)	44
1297	66	1455 (f)	57
1309 (i)	58	1555 (i)	58
1350	65	1612 (m)	60
1409	62	2100 (t.i)	1
1443 (i)	47	2340 (t.f)	77
1470	56	2380 (t.f)	77
1600 (i)	70	2587 (t.f)	69
1880 (f)	84	2710 (t.f)	62
2445 2452 } (i)	50	2800 (f)	55
2555	58	2940 (f)	49
2615	48	2965 (f)	47
2670	42	3025 (f)	41
2765	35	3060 (f)	41
2920	42	3168 (m)	34
2960 (i)	37	3210 (f)	40
2997	44	3250 (f)	38
		3305 (i)	24

t.f. = très faible ; f = faible ; i = intense ;
t.i. = très intense ; m = moyen.

Revue Roumaine de Chimie, **19**, *2*, 329–335 (1974)

SPEKTROPHOTOMETRISCHE BESTIMMUNG DES THALLIUMS MIT META-NITRALGRÜN

CECILIA CONSTANTINESCU *) und [SIMON FIŞEL **)

*) Technische Hochschule für Erdöl, Gase und Geologie Bukarest, str. Av. Traian Vuia, nr. 6
**) Al. I. Cuza-Universität Jassy, Calea 23 August, nr. 11

Eingegangen am 21. Juni 1973

In der vorliegenden Arbeit wurden die optimalen Reaktionsbedingungen zwischen dem basischen Farbstoff *meta*-Nitralgrün und den Tl(III)-Ionen studiert. Der von den Verfassern gewonnene Farbstoff wurde zuerst zum Studium der Reaktion mit Thallium (III) benützt und es wurde festgestellt, daß er mit dem Komplexanion $TlBr_4^-$ eine in Wasser unlösliche Verbindung-Tetrabromthalat von *meta*-Nitralgrün-löslich aber in Benzol, in dem extrahiert wird, bildet. Die organischen Extrakte wurden dann spektrophotometrisch untersucht. Außerdem wurde die Verbindung ausgefällt und einer Elementaranalyse unterworfen. Die durch beide Methoden erzielten Ergebnisse stimmten überein. Die studierte Reaktion ist für die Analyse des Thalliums in einem pyritischen Konzentrat mit sehr guten Ergebnissen anwendbar, und kann als spektrophotometrische Methode für die Bestimmung des Thalliums empfohlen werden.

Die Reaktionen zwischen Tl(III)-komplexionen und basischen Farbstoffen der trimethanischen Klasse sind in lezter Zeit in Vordergrund der Interessen vieler Chemiker. Manche Arbeiten beschäftigten sich mit den theoretischen Aspekten [1–3] bzw. mit der Anwendung der schon studierten Reaktionen für die Bestimmung von Thalium in verschiedenen Rohstoffen, Mineralen und Gesteinen [4]. Der Mechanismus ähnlicher Reaktionen wurde von Onishi [5] studiert und besteht in der Bildung in wäßrigen Medien der komplexen hallogeno-metallischen Säuren HMX_4 ; H_2MX_5 ; H_3MX_6, die durch die Bindung des komplexen Anions am Farbstoffskation gefolgt wird. Die in organischen Lösungsmitteln extrahierbare Verbindung ist vom Typus der ionischen Assoziation.

In dieser Arbeit werden die Synthesen des basischen Farbstoffo *meta*-Nitralgrün, die Ergebnisse der Forschungen bezüglich der Bildungsreaktion einer ionischen Assoziation zwischen dem komplexen

---

[1] C. Constantinescu, *Rev. Chim.* (*Bukarest*), **23**, 495 (1972).
[2] Gr. Popa, C. Pătroescu und C. Constantinescu, *Rev. Chim. Anal.*, **4**, 243 (1972).
[3] C. Constantinescu, *Anal. Sti. Univ. „Al. I. Cuza“ Jassy*, **19**, 47 (1973).
[4] N. T. Voscresenscaia, *Zhur. analit. Khim.*, **11**, 585 (1956).
[5] M. Onishi und E. B. Sandell, *Analyt. Chim. Acta*, **24**, 413 (1961).

Anion $TlBr_4^-$ und des Kations der Farbstoffe, die Struktur der erhaltenen Verbindung sowie auch die Anwendung der Reaktion zur Bestimmung des Thalliums in pyritischem Konzentrat dargestellt. In einer anderen Arbeit wurden die Ergebnisse des Studiums ähnlicher Reaktionen mit *ortho-* und *para*-Nitralgrün veröffentlicht [6] und gezeigt, daß die Sensibilität der Reaktion 0,04 μg Tl/cm^3 beträgt.

VERSUCHSTEIL

SYNTHESE DES FARBSTOFFS

Meta-Nitralgrün wurde durch Anwendung der geeigneten Methode zur Erhaltung des triphenylmethanischen Farbstoffs Malachitgrün synthetisiert [7], d.h. durch die Kondensierung der *meta*-Nitrobenzolaldehyd mit Dimethylanilin. Die durch Erhitzung auf dem Wasserbad erhaltene dickflüssige Masse ist mit Wasserdampf angetrieben. Der gebliebene Rückstand ist in Äthylalkohol aufgelöst, woraus die Leukobasis wiederausgefüllt wird. Durch Oxydation der Leukobasis mit Bleidioxyd erhält man das entsprechende Carbinol, welches mit Chlorwasserstoff eine Verbindung mit folgender Struktur bildet:

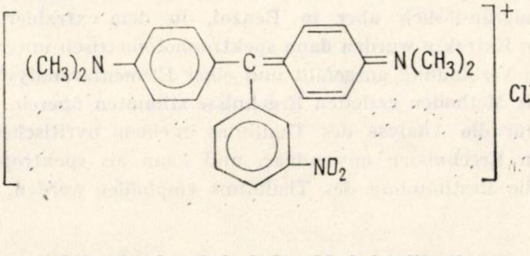

Die Reinigung erfolgte durch wiederholte Umkristallisationen, wonach die Reinheit durch die Kaliumdichromatmethode [8] bestimmt und 85,7% festgestellt wurde.

REAGENZIEN UND LÖSUNGEN

Die wäßrige Lösung des Tl(III) war durch die Auflösung des Thallium I-Nitrats, Zufügung von konzentriertem Chlorwasserstoff und Oxydierung mit Bromwasser hergestellt. Nach der Entfernung des Chlorwasserstoffs durch Verdampfen wird eine Eichlösung vorbereitet, die 204 μg Tl(III) enthält. Der Titer der Thalliumlösung wurde durch Fällung in Form von Thalliumjodid bestimmt [9]. Die in dieser Arbeit benutzten Lösungen wurden durch angemessene Verdünnungen vorbereitet.

---

[6] C. Constantinescu und S. Fişel, *Rev. Roumaine Chim.*, (unter Druck).

[7] H. Sanielevici und L. Floru, ,,Sinteza intermediarilor aromatici şi coloranţilor'', Ed. didactică şi pedagogică, Bukarest, 1971.

[8] R. P. Lestovskii und Jo. J. Vainstein, ,,Tehnicheskii analiz v proizvodstve promojutochinikh produktov i krasitelei Gosudar stvenoe nauchino tehnicheskoe izdatelistvokhimicheskoi literatury'', Moskau, 1958.

[9] N. H. Furman, ,,Standard Methods of Chemical Analysis'', Ed. VI, Van Nostrand, New York, 1962–1963, S. 1051.

– Man verwendet 0,05 %ige Lösung bezogen auf die 100 %ige Reinheit von *meta*-Nitralgrün.

– Bromwasserstoff 64 % und 40 %.

– Benzol *p.a.*

– Lösungen verschiedener Kationen unter Form von Nitraten, Sulfaten und/oder Chloriden.

EXTRAKTION DES KOMPLEXES

Die 1.10^{-5} M Lösung von Tl(III) in Volumina von 0,5–10 cm^3 wird in einen Scheidetrichter von 50 cm^3 mit 40 %-igem Bromwasserstoff (2 cm^3) und mit Reagenzlösung (0,5–2 cm^3) geführt. Man füllt destilliertes Wasser bis zum Volumina von 10 ccm, fügt 10 cm^3 Benzol hinzu und schüttelt 2 Minuten lang. Ähnlich wird auch die Blindprobe vorbereitet. Man mißt die Extinktionen der gefärbten organischen Phase bei den entsprechenden Wellenlängen in 1 cm dicken Küvette.

DIE SYNTHESE DES KOMPLEXES

Um das Kombinationsverhältnis, im festen Zustand, des thallischen Anions mit dem uvtersuchten Reagenz festzulegen, wurden 0,270 g *meta*-Nitralgrün in 30 cm^3 Wasser gelöst und mit 0,25 g in 1 cm^3 Bromwasserstoff gelöster Tl(III) gemischt. Es erscheint ein dunkelblauer Niederschlag, der durch Filtrierung unter Vakuum getrennt und mit Wasser gewaschen wurde. Die Verbindung wurde bezüglich des Gehaltes an Thallium durch die Fällungsmethode (in Form von Thalliumjodid [9]) und an Brom durch die potentiometrische Bestimmungsmethode nach Schöniger analysiert. Die erhaltenen Ergebnisse sind in Tabelle 1 eingetragen woraus hervergeht, daß das Kombinationsverhältnis metall-Ligand 1 : 1 ist

Tabelle 1

Die Elementaranalyse der Komplexverbindung

Komplex	Thallium %		Brom %		Stickstoff		Kohlenstoff		Wasserstoff	
	gerehn.	gefnd.	gerehn.	gefnd.	gerehn.	gefnd.	gerehn.	gefnd.	gerehn,	gefnd
$m-R^+TlBr_4$	22,70	22,45	35,60	35,30	4,67	4,63	37,48	37,20	2,47	2,37

DIE ABSORPTIONSSPEKTREN IM SICHTBAREN BEREICH

Die elektronischen Absorptionsspektren der wäßrigen Lösung von *meta*-Nitralgrün (Kurve C_1) mit einem Maximalwert bei $\lambda_{max} = 635$ nm und von benzolschen Lösung der Komplexverbindung mit einem Maximalwert bei $\lambda_{max} = 650$ nm wurden in der Abbildung 1 wiedergegeben. Die Benzolextrakte der Blindprobe sind farblos. Die Verschiebung der

λ_{max} von Komplexverbindungen im Vergleich zur wäßrigen Lösung ist wohl einer Bildung von Komplexen mit Ladungsübertragung vom Typus $\sigma - \pi$ zuzuschreiben.

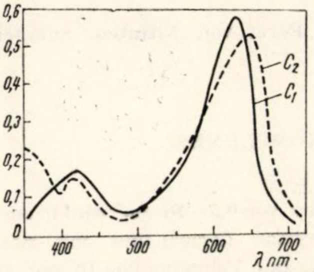

Abb. 1. — Absorptionsspektren : C_1 = Reagenz (meta-Nitralgrün), C_2 = Komplexverbindung ($TlBr_4$-meta-Nitralgrün).

DIE IR-ABSORPTIONSSPEKTREN

Diese Spektren werden in einem Bereich von 400—4000 cm^{-1} erforscht. Bei Vergleichung der IR-Spektren der freien Verbinder mit denen der entsprechenden Komplexverbindungen mit Thallium, wurde festgestellt, daß die Lagen und die Größen der Vibrationsbänder nach der Reaktion sich nicht verändert haben, ein Hinweis dafür, daß sich die Komplexe mit Ladungsübertragung bilden. Die charakteristischen Vibrationen der thallischen Verbindungen konnten nicht hervorgehoben werden, weil die betreffenden Vibrationen unter 400 cm^{-1} erscheinen und dieser Bereich nicht mit dem verwendeten Apparat erforscht wurde (Perkin-Elmer 337).

DIE AZIDITÄT DER LÖSUNG

Die Reaktion zwischen Tl (III) und der Reagenz *meta*-Nitralgrün läuft in Milieu von Bromwasserstoff ab. Bei 1,20 N HBr erhält man die maximale Absorbanz. Die Versuchsergebnisse werden in der Abbildung 2 vorgeführt. Im Medium von Chlorwasserstoff ist die Extraktionsfähigkeit klein.

DIE REAGENZKONZENTRATION

Bei Veränderung der Farbstoffsmenge von 0,2—0,3 cm^3 wurde eine Erhöhung der Absorption bis zun einer Konzentration von 1 cm^3 festgestellt, wonach sie konstant bleibt. Die optimale Konzentration liegt bei 1 cm^3 0,05%-iger wäßriger Lösung von *meta*-Nitralgrün.

DIE EICHKURVE

Das Studium der Absorptionsspektren in Abhängigkeit von der Konzentration von Tl(III) hat gezeigt, daß das Bouguer-Lambert-Beer'sche Gesetz zwischen den Grenzen 0,05—1,6 µg Metall/cm^3 Extrakt als wahr erwiesen ist, mit einem molaren Extinktionskoeffizient $\varepsilon = 69.800$ also eine kleinere Sensibilität der Reaktion im Vergleich zum *ortho*- bzw. *para*-Nitralgrün [6]. Die Beständigkeit der komplexen Kombination beträgt 48 Stunden.

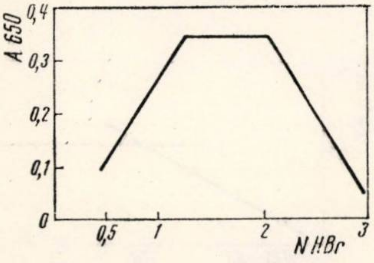

Abb. 2. — Einfluß der Lösungsazidität.

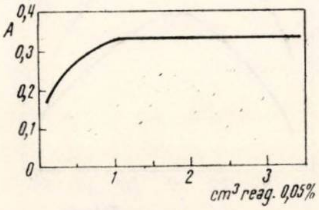

Abb. 3. — Einfluß der Farbstoffskonzentration.

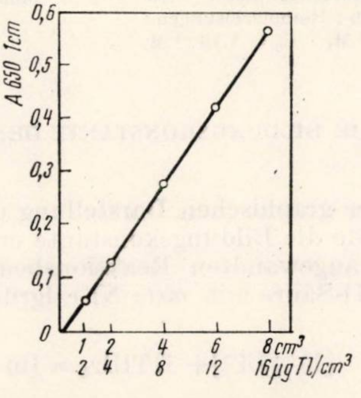

Abb. 4. — Die Eichkurve.

DAS STUDIUM DER ZUSAMMENSETZUNG GEBILDETER KOMPLEXVERBINDUNG

Für die Bestimmung des Kombinationsverhältnisses Metall/Farbstoff in der organischen Lösung kamen die Methode Job [10] und die Methode der Gefälle [11, 12] zur Anwendung. Die erhaltenen Ergebnisse bei der Durchführung der Methode Job sind in der Abbildung 5 wiedergegeben, bei der Benutzung zweier Paare von Isomolarlösungen : 1.10^{-4} M-Kurve C_1, 1.10^{-3} M-Kurve C_2. Bei der Methode des molaren Verhältnisses ist die Konzentration des Metalls konstant geblieben und die Konzentration des Farbstoffes verändert Abbildung 5. Bei der Methode des Gefälleverhältnisses verwendet man bei dem ersten Gefälle variable Mengen von Farbstoff und umgekehrt bei dem zweiten Gefälle. Die angewandten Methoden führten zum selben Ergebnis u.z. : das Kombinationsverhältnis Metall/Farbstoff für beide Verbindungen ist 1 : 1.

---

[10] P. Job, *Ann. Chim. (France)*, **9**, 113 (1928).

[11] J. H. Yoe und A. L. Jones, *Ind. Eng. Chem. Analyt.*, **16**, 111 (1944).

[12] J. H. Joe und A. F. Harvey, *J. Amer. Chem. Soc.*, **70**, 648 (1948).

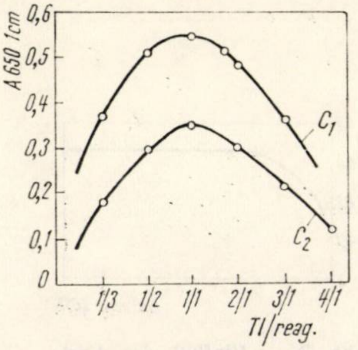

Abb. 5. – Die Bestimmung des Kombinationsverhältnisses. Die Methode Job : Isomolarlösungen : $C_1 = 1.10^{-3}$ M, $C_2 = 1.10^{-4}$ M.

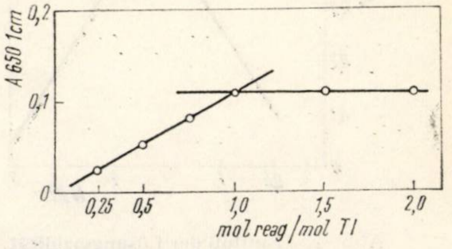

Abb. 6. – Die Bestimmung von Kombinationsverhältnis. Die Methode der Gefälle.

DIE BILDUNGSKONSTANTE DER KOMPLEXVERBINDUNG

Aus der graphischen Darstellung des molaren Verhältnisses (Abbildung 6) wurde die Bildungskonstante errechnet und $K_b = 1{,}6 . 10^5$ gefunden. Unter angewandten Reaktionsbedingungen bildet die tetrabromthallium (III)-Säure mit *meta*-Nitralgrün folgende ionische Assoziation :

$$[R^+][Cl^-] + HTlBr_4 = [m - R^+]TlBr_4^-] + HCl$$

DER EINFLUSS FREMDER IONEN

Es wurde die Interferenz jener Ionen geprüft, die gewöhnlich in verschiedenen Materialien Thallium begleiten. Die Reaktion ist vom Wachsen der Absorption in folgender Reihe gestört :

$$Au(III) > Fe(III) > In(III) > Ge(IV) > Sb(III) > Ga(III)$$

DIE BESTIMMUNG DER THALLIUMSPUREN IN ANGEREICHERTEM PYRITISCHEN KONZENTRAT

Die oben erwähnten besten Reaktionsbedingungen zwischen $HTlBr_4$ und *meta*-Nitralgrün wurden zu einer neuen Bestimmungsmethode von Thalliumspuren in einem angereicherten pyritischen Konzentrat von Baia Mare entwickelt. Die Arbeitsanweisung ist die gewöhnliche in diesen Fällen u.z. das Material wird in die Lösung gebracht, dann werden die

Einflüsse von fremden Ionen beseitigt, (SiO_2 und Fe-Ionen mit Po_4^{3-}) dann die anderen Elemente durch Zementierung mit metallischem Cadmium.

Es wurde dann der Gehalt an Thallium bestimmt. Als Vergleichsmethode kam die mit Methylviolett [4] zur Anwendung. Die Ergebnisse sind in der Tabelle wiedergegeben:

Tabelle 2

Die Ergebnisse der Analyse von angereichertem pyritischem Konzentrat

Einwaage g	Methode mit Methyl-Violett	Methode mit *meta*-Nitralgrün.
1,00	0,0131 % 131 ppm	0,0132 % 132 ppm
0,50	0,0132 % 132 ppm	0,01325 % 133 ppm

Revue Roumaine de Chimie, **19**, *2*, 329–335 (1974)

J. MIKA and **T. TÖRÖK**, "Analytical Emission Spectroscopy", Akadémiai Kiadó, Budapest, 1973, p. 529

Spectroscopic techniques are used nowadays for determining a large number of chemical elements in a wide range of both liquid and solid materials. By means of many improvements of the optical emission spectroscopy very low detection limits were obtained. This makes emission spectroscopy a very powerful technique as X-ray fluorescence spectroscopy. Recent developments, for instance the generation of emission by laser beams, have brought a new dimension which promises to find out new and interesting applications in metallurgical and geochemical sciences.

The subject of the present book is the optical emission spectroscopy analysis. The purpose of this volume is to provide an useful help for those who intend to deal with emission spectroscopy analysis in detail, and also to facilitate the work of those who devote their attention to the practical application of such techniques.

The basic theory of spectral analysis is presented in Chapter 1. Chapter 2 gives a detailed account on the various methods of excitation, including arc and spark sources, and their control. The analysis of the resulting radiations by both prism and grating devices is described in detail in Chapter 3, which also includes interference systems. The following chapter is devoted to the determination of wavelength. Measurement of the intensity of spectral lines is presented in Chapter 5. The subjects of the last two chapters are of major importance for emission spectroscopy, and, therefore, the detection of radiations and the methods of intensity measurement are largely discussed.

The limitations in the coverge have rendered it impossible to discuss all known procedures, or to provide an exhaustive literature list for them. By excluding obsolete methods from their scope the authors have aimed at a discussion of the essentials, advantages and drawbacks of the presently used methods. Also, the authors tried to cover such procedures that can only be used in special cases, or which have not found widespread applications. The list of references contains the papers that were used for writing the book; also, some monographs and general works on the topics are quoted. Numerous illustrations and tables make the book attractive and very useful for a reader.

The whole work is a very complete and competent study of various aspects of emission spectroscopy and should be of high interest for all scientists working in this domain.

T. Chirulescu

CORRIGENDA

Chemical Graphs. VIII. Graphs of degrees four or less, isomers of annulenes, and nomenclature of bridged polycyclic structures

by A.T. Balaban

Rev. Roumaine Chim., 18, 635-653 (1973).

In fig. 2, the following graph of order p=4 with degrees 4/2 (column 2, p-2) was omitted :

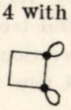

In fig. 6, the following three graphs were omitted from the line : 19 (instead of 16) (CH_2) $(CH)_2CO$:

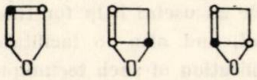

replace

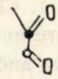

by

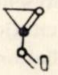

On page 646, line 14, replace 59 by 62.

On page 649, line 36, replace fig. 6 by fig. 7.

NOTE POUR LES AUTEURS

La *Revue Roumaine de Chimie* publie des articles en anglais, français, russe, allemand ou espagnol. Les auteurs sont priés d'envoyer des articles, notes, communications et comptes rendus inédits.

Les manuscrits seront dactylographiés à deux intervalles. Les tableaux seront dactylographiés sur feuilles séparées, de même que la légende des figures. Les diagrammes seront tracés à l'encre de Chine sur papier calque. Les tableaux et les figures seront numérotés par des chiffres arabes, en nombre strictement nécessaire. Prière de ne pas inscrire les mêmes données dans les tableaux et les figures. Les formules chimiques seront incluses dans le texte ; en outre, elles seront transcrites sur des feuilles séparées. Les auteurs sont priés d'indiquer les caractères italiques (en soulignant les lettres au crayon), ainsi que tout autre caractère spécial. L'ordre des références bibliographiques sera celui de leur mention dans le texte ; le nom de l'auteur sera précédé de l'initiale du prénom ; les publications périodiques seront présentées suivant les prescriptions internationales. Les références seront ajoutées à la fin de l'article ; elles paraîtront comme des notes, au bas de la page. Le texte sera précédé d'un résumé comprenant 15 lignes au maximum.

L'entière responsabilité du contenu des articles appartient aux auteurs. On publie des articles dus aux collaborateurs roumains ou étrangers. Les auteurs recevront 50 tirés à part.

PRINTED IN ROMANIA

1974 MAI 16

TRAVAUX PARUS AUX ÉDITIONS DE L'ACADÉMIE DE LA RÉPUBLIQUE SOCIALISTE DE ROUMANIE

MARIA FITI, **Dozimetria chimică a radiaţiilor ionizante** (La dosimétrie chimique des radiations ionisantes), 1973, 240 p., 13,50 lei.

MIHAI FLORESCU, **Eficienţa economică a cercetării ştiinţifice** (L'efficience économique de la recherche scientifique), 1972, 115 p., 15 lei.

GEORGETA LĂZĂRESCU, **Sistematizarea informaţiilor în chimia organică** (La systématisation des informations dans la chimie organique), 1972, 242 p., 10,50 lei.

P. BALTĂ et E. BALTĂ, **Introducere în chimia fizică a stării vitroase** (Introduction à la chimie physique de l'état vitreux), 1971, 240 p., 15,50 lei.

LYDIA-MARIA VAICUM, **Biodegrabilitatea detergenţilor** (La biodégrabilité des détergents), 1971, 346 p., 19,50 lei.

I. ZUGRĂVESCU et L. STOICESCU-CRIVETZ, **Polimeri heterociclici** (Polymères hétérocycliques), 1971, 190 p., 9,50 lei.

I. V. MAXIM, **Materiale nucleare** (Matériaux nucléaires), 1969, 444 p., 30 lei.

CORNEL BODEA et collab., **Tratat de biochimie vegetală, partea I, Fitochimie** (Traité de biochimie végétale, Ire partie, Phytochimie), Ier vol., 1964, 747 p. + 4 annexes + 2 pl., 41 lei ; IIe vol., 1965, 1962 p., 1 pl., 56 lei ; IIIe vol., 1967, 773 p., 35 lei.

CRISTOFOR SIMIONESCU et CLEOPATRA VASILIU-OPREA, **Mecanochimia compuşilor macromoleculari** (La méchanochimie des composés macromoléculaires), 1967, 344 p., 23,50 lei.

V. GHEŢIE et V. MICUŞAN, **Analiza imunochimică. Teorie şi practică** (Analyse immunochimique. Théorie et pratique), 1966, 369 p., 28 lei.

R. PORTOCALĂ et L. POPA, **Acizii ribonucleici celulari şi virali** (Les acides ribonucléiques cellulaires et viraux), 1966, 375 p., 8 pl., 26 lei.

I.P.I. – c. 3608

43 426

Lei 25.—

F 1103

R

REFERÁLVA

REVUE ROUMAINE DE CHIMIE

TOME 19
Nº 3
Mars 1974
RECHAX, **19**, *3*, 339–520 (1974)

ÉDITIONS DE L'ACADÉMIE DE LA RÉPUBLIQUE SOCIALISTE DE ROUMANIE

Rev. Roumaine Chim. **19**, *3*, p. 339–520 (1974), Bucarest

COMITÉ DE RÉDACTION

Rédacteur en chef :

I. G. MURGULESCU, membre de l'Académie de la République Socialiste de Roumanie

Rédacteurs en chef adjoints :

A.T. BALABAN et V. EM. SAHINI, membres correspondants de l'Académie de la République Socialiste de Roumanie

Collège de rédaction :

C. DRĂGULESCU, RALUCA RIPAN, CR. SIMIONESCU, membres de l'Académie de la République Socialiste de Roumanie ; EM. BRATU, ECATERINA CIORĂNESCU-NENITZESCU, P. SPACU, membres correspondants de l'Académie de la République Socialiste de Roumanie ; MARGARETA AVRAM, D. I. MARCHIDAN, G. NIAC et D. SĂNDULESCU

La Revue Roumaine de Chimie paraît 12 fois par an. Toute commande de l'étranger (fascicules ou abonnements) sera adressée à Întreprinderea Rompresfilatelia, Boîte Postale 2001, telex 011631, Bucarest, Roumanie

Les manuscrits, les livres et les revues proposés en échange, ainsi que toute correspondance seront envoyés à la rédaction

REVUE ROUMAINE DE CHIMIE

23, str. Dumbrava Roşie, Bucarest, Roumanie

EDITIONS DE L'ACADÉMIE DE LA RÉPUBLIQUE SOCIALISTE DE ROUMANIE
3 bis, str. Gutenberg, Bucarest

ORSZÁGOS MŰSZAKI KÖNYVTÁR ÉS DOKUMENTÁCIÓS KÖZPONT * * * 1983

REVUE ROUMAINE
DE
CHIMIE

Tome 19, Nº 3 MARS 1974

GH. FACSKO and MARIA PORAICU, Kinetic study of oxido-reduction reactions, by means of the vibrated electrode technique . . . . 341–351 R

LUCIA ZADOR and IUDITA MUREȘAN, Viscosimetric study of polyacrylic acid in water-ethanol mixtures . . . . 353–361 R

V. BĂRBOIU, Magnitudes and signs of ^{13}C coupling constants in several organic molecules by double resonance 363–370

I. TEOREANU and MARCELA MUNTEAN, The study of the hardening processes in tricalcium silicate-water-electrolyte system 371–379

Ș. SOLACOLU and ECATERINA RUSU, Aspects of the vitreous phase separation process in the $Fe_2O_3-BaO-B_2O_3$ system 381–385

D. NEGOIU, CONSTANȚA PÂRLOG and D. SĂNDULESCU, New coordinate compounds with molecular nitrogen. I. Synthesis and characteristic properties of some dinitrogen compounds of cobalt, nickel, iron with triarylphosphines, triaryl-arsines and triaryl-stibines 387–394

EUGENIA PERȚE and M. STRĂJESCU, Gallium metatitanate 395–398

N. VOICULESCU, A. AIRINEI et I. POPESCU, Les réactions des ligands coordinés. IV. L'étude spectroscopique et thermogravimétrique des combinaisons aluminium-organiques de diméthylglyoxime coordinée 399–405

F. MÁNOK, CS. VÁRHELYI und RODICA OPREAN, Kinetik und Mechanismus der Oxydation des Urans (IV) mit Natrium-persulfat 407–413

I. SOLACOLU, D. SĂNDULESCU et C. DRĂGULESCU, La structure cristalline et l'interaction avec la molécule de l'hydrocarbure incluse dans les clathrates du type $M(SCN)_2(4\text{-}MePy)_4.p$-xylène 415–427

FELICIA CORNEA, CORNELIA FULEA et Ș. MOLDOVEANU, Complexes moléculaires des thioamides. II. Complexes de transfert de charge du phénylthioacétamide et de la phénylthioacétopipéridide avec l'iode 429–435

MAGDA PETROVANU, ARIADNA SAUCIUC and I. ZUGRĂVESCU, Phthalazinium ylids. VI. Action of dimethylacetylenedicarboxylate on disubstituted at the exocyclic carbon phthalazinium-ylids. 437–442

N. BĂRBULESCU and MINODORA LECA, Elimination reactions in the 8-R-tricyclo[7.3.1.$0^{2,7}$]tridecane series. IV. Pyrolytic elimination of tricyclo-[7.3.1.0 ^{2,7}] trideca-2-en-13-acetate. . . . . 443–454 R

ALICE MARIE GLATZ, Aluminium chloride catalyzed condensations of un-

Revue Roumaine Chim. 19, 3, 339–520 (1974), Bucarest

saturated acids with benzene 455–484

GRIGORE TEODORESCU, Methods for the determination of 2-aminopyridine. Visible and infrared spectra of the combination with ammonium reineckate 485–492

ВАЛЕНТИНА БОЙЕШАН и Д. ФЕЛЬДМАН, Влияние условий распылительной сушки на свойства пастообразующего поливинилхлорида. II. Морфологические исследования 493–500

I. BURNEA, MARIA PLENICEANU und LUCIA BURNEA, Spektrophotometrische Untersuchung des Systems Vanadium (V)-Solochromviolett R. S. Die spektrophotometrische Bestimmung des Vanadiums 501–507

CECILIA CONSTANTINESCU und S. FIȘEL, Spektrophotometrische Bestimmung des Tl(III) mit Ortho-Nitral und Para-Nitralgrün. 509–515

COMPTES RENDUS 517–519

Revue Roumaine de Chimie, **19**, *3*, 341–351 (1974)

KINETIC STUDY OF OXIDO-REDUCTION REACTIONS, BY MEANS OF THE VIBRATED ELECTRODE TECHNIQUE

GHEORGHE FACSKO and MARIA PORAICU

Electrochemistry Laboratory,
Polytechnical Institute of Timişoara, Str. Bocşei, N° 6, Romania

Received May 29, 1973

In the following study the results of the researches, obtained at the determination of some kinetic parameters of the redox-systems Fe^{3+}/Fe^{2+} and Ce^{2+}/Ce^{4+}, are presented by means of the vibrated electrode technique. The vibration of electrode leads to a considerable increase of the limit-current density (about 10–13 times), consequently to an extension of the existence range of pure chargetransfer overvoltage and also to the possibility of determining some kinetic parameters. By means of this technique we determined the rate constants for the Fe^{3+}/Fe^{2+} system and we found : $k = 3.32 \times 10^{-3}$ cm/sec for the anodic process, and $k = 3.37 \times \times 10^{-3}$ cm/sec for the cathodic one ; the transfer coefficient was found to be $\alpha = 0.58$ and $(1 - \alpha) = 0.42$. Considering the system Ce^{4+}/Ce^{3+}, the rate constant and the transfer coefficient for the cathodic process were determined to be $k = 2.07 \times 10^{-4}$ cm/sec, respectively $(1 - \alpha) = 0.25$. The experimental results are in accordance with those described by other authors.

GENERAL CONSIDERATIONS

The redox-systems studied are represented by the following general electrode-reaction : [1,2,3]

$$\text{Red.} \rightleftarrows \text{Ox.} + e^- \tag{1}$$

There is no preceding or following chemical reaction with respect to the charge-transfer reaction, which could influence their kinetics.

The charge-transfer rate of the process could be given as current density by the following relation :

$$\begin{aligned} i = i_+ - /i_-/ &= nF\,(k_+\,C_r - k_-\,C_0) = \\ &= nF\left\{k'_+\,C_r\,\exp\left(\frac{\alpha nF}{RT}\,\varepsilon\right) - k'_-\,C_0\exp\left[-\frac{(1-\alpha)\,nF}{RT}\,\varepsilon\right]\right\} \end{aligned} \tag{2}$$

---

[1] M. Spiro, *Electrochim. Acta* **9**, 1531 (1964).

[2] R. D. Wales, *Electrochim. Acta*, **9**, 1675 (1964).

[3] Z. Gallus, and Ralph N. Adams, *J. Phys. Chem.*, **67**, 866 (1963).

where : i_+ and i_- are partial current densities, anodic and cathodic respectively, ε-the electrode potential referred to the standard hydrogen electrode, C_0 and C_r-the concentrations of the reactive kinds of ions, k'_+ and k'_--rate constants, independent of the electrode potential, the other quantities having the usual significance.

At the equilibrium, in the absence of an outer current, the two partial currents will be equal to each other, but opposite in sign and equal to the exchange-current i_0 :

$$i_0 = i_+ = /i_-/ = nF\,k'_+\,C_r\,\exp\left(\frac{\alpha nF}{RT}\,\varepsilon_{\text{ech.}}\right) = \\ = nFk'_-\,C_0\exp\left[\frac{(1-\alpha)\,nF}{RT}\,\varepsilon_{\text{ech.}}\right] \tag{3}$$

where $\varepsilon_{\text{ech.}}$ is the equilibrium potential of the electrode.

Combining relation (2) with (3) the following expression is obtained for the current density :

$$i = i_0\left\{\exp\left(\frac{\alpha nF}{RT}\,\eta\right) - \exp\left[-\frac{(1-\alpha)\,nF}{RT}\,\eta\right]\right\} \tag{4}$$

where $\eta = \varepsilon - \varepsilon_{\text{ech.}}$ is the value of charge-transfer overvoltage.

At small values of the charge-transfer overvoltage, when $/\eta/ \ll \frac{RT}{F}$, the development in series of the exponentials from equation (4) and the maintenance of each first term leads to the expression :

$$\eta = \frac{/i/}{i_0}\,\frac{RT}{F} \tag{5}$$

By graphical representation of overvoltage η dependence as a function of the current density $/i/$, we obtain a linear relation whose slope allows the calculation of the exchange current density i_0, but not of the value of the transfer-coeficient α.

For great positive overvoltages (anodic processes), the second term of equation (4) could be neglected and written as :

$$i = i_+ = i_0\exp\left(\frac{\alpha nF}{RT}\,\eta\right) \tag{6}$$

wherefrom it is obtained :

$$\eta = -\frac{RT}{\alpha nF}\ln i_0 + \frac{RT}{\alpha\,nF}\ln i \tag{7}$$

which is the well-known Tafel equation:

$$\eta = a + b \log i \tag{8}$$

For great negative overvoltages (cathodic processes) the first term of equation (4) could be neglected and written as:

$$i = |i_-| = i_0 \left\{ \exp\left[-\frac{(1-\alpha)nF}{RT}\eta \right] \right\} \tag{9}$$

from which results:

$$\eta = \frac{RT}{(1-\alpha)nF} \ln i_0 - \frac{RT}{(1-\alpha)nF} \ln |i_-| \tag{10}$$

or the Tafel equation for cathodic processes:

$$\eta = a' - b' \log |i_-| \tag{11}$$

Taking the slopes resulting from the Tafel equations (8) and (11), b respectively b', the values for αn, respectively $(1-\alpha)n$ could be calculated, where $b = 2.303\ RT/\alpha nF$ and $b' = 2.303\ RT/(1-\alpha)nF$. At 25° the calculated values are $b = 59.2/\alpha n$, respectively $b' = 59.2/(1-\alpha)\, n$ mV.

At the extrapolation of the straight line for $\eta = 0$ the logarithm of the exchange current i_0 is obtained.

If in equation (3) the value of the equilibrium potential is introduced:

$$\varepsilon_{\text{ech.}} = \varepsilon^0 + \frac{RT}{nF} \ln \frac{C_0}{C_r} \tag{12}$$

and if all the constants are included in the general constant k, it could be written as:

$$i_0 = nFkC_r^{(1-\alpha)}\, C_0^{\alpha} = i_0^0\, C_r^{(1-\alpha)}\, C_0^{\alpha} \tag{13}$$

where k is the standard rate constant, and i_0^0 — the standard exchange current, independent of concentration.

On the basis of relation (13) the value of k, or of i_0^0 could be calculated.

The considerations treated before are valid when the electrode process is controlled exclusively by charge transfer. But in reality on the charge transfer control superimposes to a greater or smaller extent the slow diffusion of ions to and from the electrode.

In this case relation (2) must be written as:

$$i = nF\left\{k'_{+}\ C_r^x \exp\left(\frac{\alpha nF}{RT}\ \varepsilon\right) - k'_{-}\ C_0^x \exp\left[-\frac{(1-\alpha)\,nF}{RT}\ \varepsilon\right]\right\} \tag{14}$$

where C_r^x and C_0^x are the concentrations of the reactive kind of ions from the immediate vicinity of the electrode, which are modified by the passing of electric current.

At equilibrium, relation (3) has its valability, the concentrations near the electrode being equal with those from the bulk of solution.

Combining relation (14) with (3) the following expression for the current density is obtained:

$$i = i_0\left\{\frac{C_r^x}{C_r} \exp\left(\frac{\alpha nF}{RT}\ \eta\right) - \frac{C_0^x}{C_0} \exp\left[-\frac{(1-\alpha)\,nF}{RT}\ \eta\right]\right. \tag{15}$$

Because the processes were studied in a great excess of indifferent electrolyte, compared with the concentrations of the reactive kind of ion, it could be written:

$$i = \frac{nFD_i}{\delta i}\,(C_i - C_i^x) \tag{16}$$

$$i_d = \frac{nFD}{\delta_i}\ C_i \tag{17}$$

where D_i is the diffusion coefficient of the kind of ion which reacts at the electrode, δ_i — the thickness of the diffusion layer, and C_i, respectively C_i^x are the concentrations of the kind of ion which reacts in the bulk of solution, respectively in the vicinity of the electrode.

Combining relations (16) and (17) it results:

$$\frac{i}{i_d} = \frac{C_i - C_i^x}{C_i} = 1 - \frac{C_i^x}{C_i} \tag{18}$$

from which:

$$\frac{C_i^x}{C_i} = 1 - \frac{i}{i_d} \tag{19}$$

If we set the values for C_i^x/C_i from relation (19) in relation (14), in the case of a combined control of charge-transfer-diffusion, we obtain the following expression for the current density:

$$i = i_0\left\{\left(1 - \frac{i}{i_{d,a}}\right) \exp\left(\frac{\alpha nF}{RT}\ \eta\right) - \left(1 - \frac{i}{i_{d,c}}\right) \exp\left[-\frac{(1-\alpha)\,nF}{RT}\ \eta\right]\right\} \tag{20}$$

Here $i_{d,a}$ and $i_{d,c}$ are anodic respectively cathodic diffusion currents. In this case relation (20) is not any more identical with relation (4), so that the dependence in the Tafel domain would not be a linear one. Thus, in the case of the superposition of the diffusion control, the method of determination of the exchange current i_0 and of the transfer coefficient α, presented before, cannot be applied any more. But it is to be seen that in the case of great diffusion currents, relation (20) approaches to and practically superposes itself with relation (4).

The diffusion-current density value increases in accordance with relation (17), with increase of concentration of the reactive kind of ion C_i, of the diffusion coefficient D_i and with decrease of the thickness of the diffusion layer δ_i.

The value of the diffusion coefficient could be increased by heating the solution. The increment of its increase with temperature has approximately the same value as that of the electrical conductibility : 2 % from its value/°.

The diffusion-layer thickness could be decreased by mixing the solution. Between all the mixing methods used to decrease the diffusion-layer thickness, the electrode-vibration is the most efficient, because it has a strong agitation effect, tearing off the adherent pelicular layer.

For this reason the electrode-vibration will bring about a considerable increase of the limit-current density, meaning an extension of the pure charge-transfer overvoltage as well as the possibility of application of the determination method of the kinetic parameters presented.

EXPERIMENTAL PART

A. THE STUDY OF THE SYSTEM Fe^{3+}/Fe^{2+}

The influence of electrode-vibration on the limit-current value was studied by drawing the polarization curves for the oxidation and also for the reduction processes of the $Fe_2(SO_4)_3/FeSO_4$ system, corresponding to the overall reaction :

$$Fe^{2+} \rightarrow Fe^{3+} + e^- \qquad (21)$$

The concentrations of the two kinds of ions (Fe^{3+} and Fe^{2+}) were equal to each other, in the limits of 2.5×10^{-2} and 10^{-2} the indifferent electrolyte being sulfuric acid of molar concentration.

The electolysis cell was constituted of a 400 ml capacity beaker-glass, separated in two compartments by a glass-cylinder, with a porous plate on its inferior part. The working electrode having a surface of 0.025 cm² was of platinum wire ; to it a Luggin tube was fixed, tied to the reference-electrode Hg/Hg_2SO_4, K_2SO_4 saturated solution. The working electrode was either stationary, or could be vibrated with a 50 Hz frequency and 3mm amplitude by means of an electromagnetic vibrator, whose construction is described in an anterior work. [4]

---

[4] G. Facsko and F. Golumbioschi, *Rev. Roumaine Chim.*, **11**, 207 (1966).

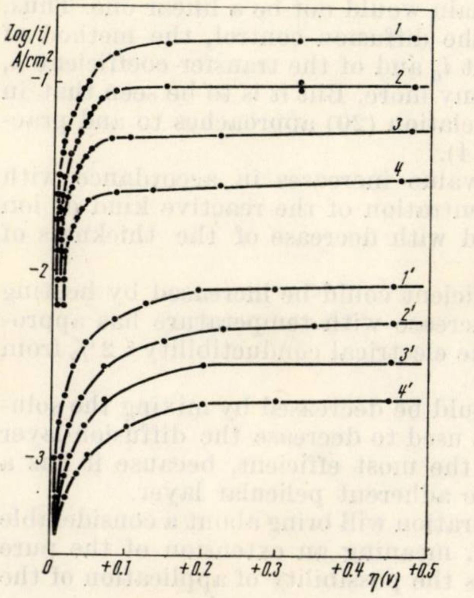

Fig. 1. — Graphic representation of the logarithm of anodic current density as a function of overvoltage for the system Fe^{3+}/Fe^{2+} in 1M H_2SO_4.
1,1′ — vibrated electrode, respectively stationary one, concentration : 1.0×10^{-1} M $Fe_2(SO_4)_3$ /1.0×10^{-1} M $FeSO_4$;
2,2′ — vibrated electrode, respectively stationary one, concentration : 7.5×10^{-2} M $Fe_2(SO_4)_3$ / 7.5×10^{-2} M $FeSO_4$;
3,3′ — vibrated electrode, respectively stationary one, concentration : 5.0×10^{-2} M $Fe_2(SO_4)_3$ /5.0×10^{-2} M $FeSO_4$;
4,4′ — vibrated electrode, respectively stationary one, concentration : 2.5×10^{-2} M $Fe_2(SO_4)_3$ /2.5×10^{-2} M $FeSO_4$.

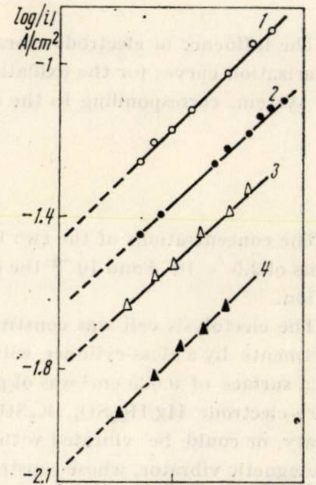

Fig. 2. — Representation of the linear portion of the logarithm of anodic current density as a function of overvoltage, for the system Fe^{3+}/Fe^{2+} in 1M H_2SO_4, on a vibrated electrode.
1, 1.0×10^{-1} M $Fe_2(SO_4)_3$ /1.0×10^{-1} M $FeSO_4$;
2, 7.5×10^{-2}M $Fe_2(SO_4)_3$/7.5×10^{-2}M $FeSO_4$;
3, 5.0×10^{-2} M $Fe_2(SO_4)_3$ /5.0×10^{-2}M $FeSO_4$;
4, 2.5×10^{-2} M $Fe_2(SO_4)_3$ /2.5×10^{-2} M $FeSO_4$;

The potential difference between the working electrode and the reference-electrode was determined using an electronic potentiometer (pH-Electrometer-ORION Type 2512).

The temperature was maintained constant at 25°, by means of a thermostat.

In figures 1 and 3, the curves of the logarithm of current densities as a function of over-voltage at the oxidation, respectively, at the reduction processes are presented, obtained on the vibrated electrode (curves *1*, *2*, *3*, and *4*) and on the stationary electrode, (curves *1'*; *2'*; *3'*; and *4'*).

There can be observed an appreciable increase of the limit-currents on the vibrated electrode, 10–13 times the corresponding values on a stationary electrode.

In figures 2 and 4 the linear portions of the curves $\log|i|$ are graphically represented as function of η for the vibrated electrode, corresponding to the equations :

$$\log i_{+} = \log i_0 + \frac{\alpha F}{2.303\,RT}\,\eta \tag{22}$$

for the oxidation process and :

$$\log |i_{-}| = \log i_0 - \frac{(1-\alpha)F}{2.303\,RT}\,\eta \tag{23}$$

for the reduction process.

From the values of ordinata at the origin $\log i_0$ and from the straight-line slopes $\alpha F/2.303\,RT$, respectively $-(1-\alpha)F/2.303\,RT$, the values for i_0, α, respectively $(1-\alpha)$ were calculated.

The calculation of the exchange-current density independent of concentration was effectuated by means of equation (13), considering that $C_r = C_0 = C$:

$$i_0^0 = \frac{i_0}{C} \tag{24}$$

whereas calculation of the rate constant, k, was done from the same expression (13) as follows :

$$k = \frac{i_0}{F}\,1\,000 \tag{25}$$

The results obtained are presented in tables 1 and 2.

Table 1

Experimental data and the calculation of the values i_0, i_0^0, k and α for the process $Fe^{2+} \rightarrow Fe^{3+} + e^-$ in 1M H_2SO_4 medium

Concentration	$\log i_0$	i_0 A/cm²	i_0^0 A·l/mol·cm²	i_0^0 med.	k cm/sec	$\frac{\alpha F}{2.3\,RT}$	α med.
1.0×10^{-1}M	−1.470	0.0338	0.338	0.32	3.32×10^{-3}	10.00	0.58
7.5×10^{-2}M	−1.655	0.0221	0.295			9.38	
5.0×10^{-2}M	−1.810	0.0155	0.314			9.55	
2.5×10^{-2}M	−2.080	0.0831	0.332			10.77	

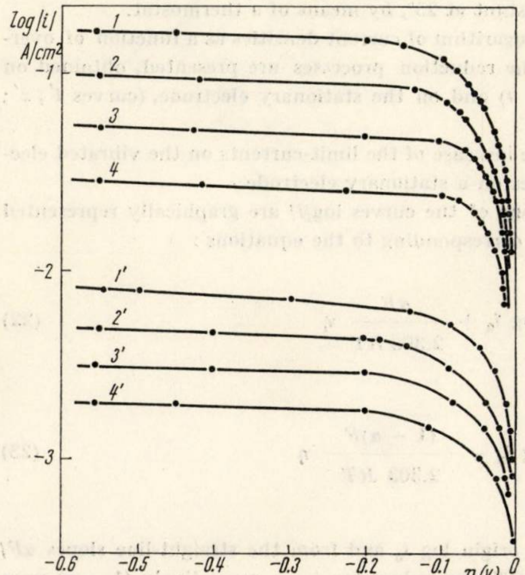

Fig. 3. — Graphic representation of the logarithm of cathodic current density as a function of overvoltage, for the system Fe^{3+}/Fe^{2+} in 1M H_2SO_4.

1,1' — vibrated electrode, respectively stationary one, concentration: 1.0×10^{-1} M $Fe_2(SO_4)_3/1.0 \times 10^{-1}$ M $FeSO_4$; *2,2'* — vibrated electrode, respectvely stationary one, concentration: 7.5×10^{-2} M $Fe_2(SO_4)_3/7.5 \times 10^{-2}$ M $FeSO_4$; *3 3'* — vibated electrode, respectively stationary one, concentration: 5.0×10^{-2} M $Fe_2(SO_4)_3/5.0 \times 10^{-2}$ M $FeSO_4$; *4,4'* — vibrated electrode, respectively stationary one, concentration: 2.5×10^{-2} M $Fe_2(SO_4)_3/2.5 \times 10^{-2}$ M $FeSO_4$.

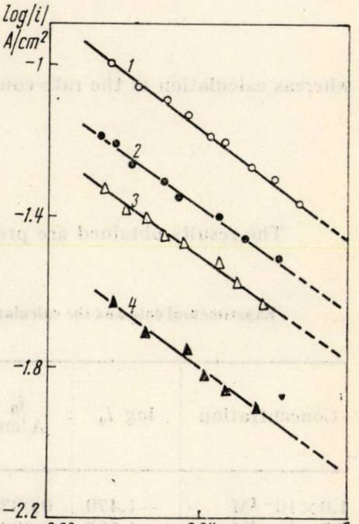

Fig. 4. — Representation of the linear portion of the logarithm of cathodic current density as a function of overvoltage for the system Fe^{3+}/Fe^{2+} in 1M H_2SO_4, on a vibrated electrode.

1, 1.0×10^{-1} M $Fe_2(SO_4)_3/1.0 \times 10^{-1}$ M $FeSO_4$;
2, 7.5×10^{-2} M $Fe_2(SO_4)_3/7.5 \times 10^{-2}$ $FeSO_4$;
3, 5.0×10^{-2} M $Fe_2(SO_4)_3/5.0 \times 10^{-2}$ M $FeSO_4$;
4, 2.5×10^{-2} M $Fe_2(SO_4)_3/2.5 \times 10^{-2}$ M $FeSO_4$.

Table 2

Experimental data and the calculation of the values i_0, i_0^0, k and $(1-\alpha)$ for the process $Fe^{3+} + e^- \rightarrow Fe^{2+}$ in 1 M H_2SO_4 medium

Concentration	log i_0	i_0 A/cm²	i_0^0 A·l/mol·cm²	i_0^0 med.	k cm/sec	$\frac{(1-\alpha)F}{2.3\,RT}$	$(1-\alpha)$ med.
1.0×10^{-1}M	−1.470	0.0338	0.338	0.326	3.37×10^{-3}	7.50	0.42
7.5×10^{-2}M	−1.650	0.0224	0.300			6.83	
5.0×10^{-2}M	−1.780	0.0166	0.332			7.16	
2.5×10^{-2}M	−2.080	0.0831	0.332			6.83	

B. THE STUDY OF THE SYSTEM Ce^{4+}/Ce^{3+}

The influence of electrode-vibration on the value of limit-current was studied only for the cathodic process :

$$Ce^{4+} + e^- \rightarrow Ce^{3+} \tag{26}$$

because at the anodic process, also at small values of the overvoltage, the oxygen-discharge curve superimposes itself.

The concentrations of the two kinds of ions (Ce^{4+} and Ce^{3+}) were equal and chosen in the range between 7.3×10^{-3} M and 3.32×10^{-2} M, the indifferent electrolyte being 1M H_2SO_4.

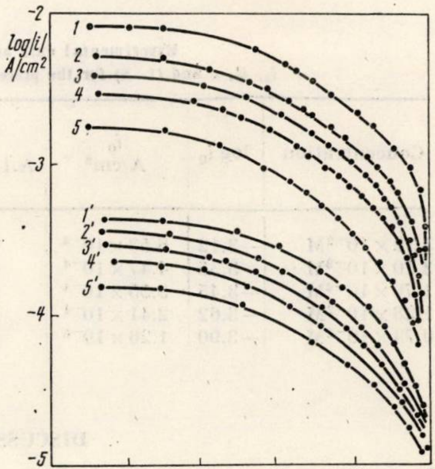

Fig. 5. — Graphic representation of the logarithm of cathodic current density as a function of overvoltage, for the system Ce^{4+}/Ce^{3+} in 1M H_2SO_4.

1,1' — vibrated electrode, respectively, stationary one, concentration : 3.32×10^{-2} M $Ce(SO_4)_2/3.32\times10^{-2}$ M $Ce_2(SO_4)_3$; *2,2'* — vibrated electrode respectively stationary one, concentration : 2.10×10^{-2}M $Ce(SO_4)_2$ 2.10×10^{-2} M $Ce_2(SO_4)_3$; *3,3'* — vibrated electrode, respectively stationary one, concentration : 1.70×10^{-2} M $Ce(SO_4)_2/1.70\times10^{-2}$ M $Ce_2(SO_4)_3$; *4,4'* — vibrated electrode, respectively stationary one, concentration : 1.28×10^{-2} M $Ce(SO_4)_2/1.28\times10^{-2}$ M $Ce_2(SO_4)_3$; *5,5'* — vibrated electrode respectively stationary one, concentration : 0.73×10^{-2} M $Ce_2(SO_4)_3/0.73\times10^{-2}$ $Ce_2(SO_4)_3$.

In figure 5 the logarithmic curves of the current density as a function of overvoltage are given, for the vibrated electrode (curves *1*, *2*, *3*, *4*, and *5*) and also for the stationary one (curves *1' 2'*, *3'*, *4'* and *5'*)

By analogy to the system Fe^{3+}/Fe^{2+}, an important increase of limit-current values by the influence of electrode-vibration was observed, namely 10 to 13 times the values obtained with the stationary electrode.

In figure 6 are represented the linear portions of the dependence of the logarithm of current densities as a function of overvoltage, obtained by electrode vibration.

The calculation were effectuated similarly to those from paragraph A, using equations (13), (23), (24) and (25), for the determination of the respective values for i_0, i_0^0, $(1 - \alpha)$ and k

The obtained results are given in table 3.

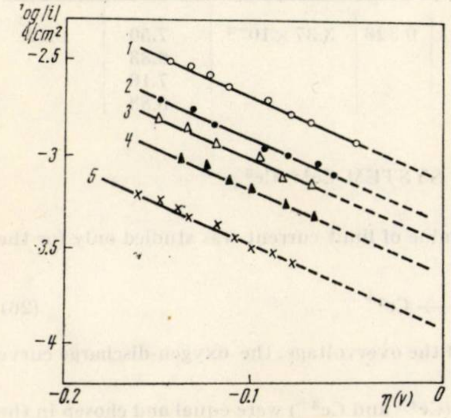

Fig. 6. — Representation of the linear portion of the logarithm of cathodic current density as function of overvoltage for the system Ce^{4+}/Ce^{3+} in 1M H_2SO_4, on a vibrated electrode

1, 3.32×10^{-2} M $Ce(SO_4)_1/3.32 \times 10^{-2}$ M $Ce_2(SO_4)_3$;
2, 2.10×10^{-2} M $Ce(SO_4)_2/2.10 \times 10^{-2}$ M $Ce_2(SO_4)_3$;
3, 1.70×10^{-2} M $Ce(SO_4)_2/2.10 \times 10^{-2}$ M $Ce_2(SO_4)_3$;
4, 1.28×10^{-2} M $Ce(SO_4)_2/1.28 \times 10^{-2}$ M $Ce_2(SO_4)_3$;
5, 0.73×10^{-2} M $Ce(SO_4)_2/0.73 \times 10^{-2}$ M $Ce_2(SO_4)_3$.

Table 3

Experimental data and the calculation of the values i_0, i_0^0, k and $(1-\alpha)$ for the process $Ce^{4+} + e^- \rightarrow Ce^{3+}$ in 1M H_2SO_4 medium

Concentration	log i_0	i_0 A/cm²	i_0^0 A.1/mol.cm²	i_0^0 med.	k cm/sec	$\frac{(1-\alpha)F}{2.3\,RT}$	$(1 - \alpha)$ med.
3.32×10^{-2}M	−3.12	6.53×10^{-4}	0.0197	0.02	2.07×10^{-4}	4.300	025
2.10×10^{-2}M	−3.35	4.47×10^{-4}	0.0213			4.250	
1.70×10^{-2}M	−3.45	3.55×10^{-4}	0.0209			4.171	
1.28×10^{-2}M	−3.62	2.41×10^{-4}	0.0190			4.171	
0.73×10^{-2}M	−3.90	1.26×10^{-4}	0.0172			4.250	

DISCUSSION OF THE RESULTS

Our experimental results show that the technique of electrode-vibration extends considerably the range of the pure charge-transfer overvoltage and thus permitted the correct calculation of the kinetic parameters in the case of systems Fe^{3+}/Fe^{2+} and Ce^{4+}/Ce^{3+}, by means of a relatively simple device. The results are comparable with those indicated in the literature, with respect to both : the values of exchange-current densities and the values of transfer coefficients.

In table 4 are given our results compared to the results given by other authors.

Table 4

Values of kinetic parameters for the systems Fe^{3+}/Fe^{2+} and Ce^{4+}/Ce^{3+} after various authors

System	Indifferent electrolyte	the technique used	Ref.	k anodic	k cathodic	$\alpha(1-\alpha)$
Fe^{3+}/Fe^{2+}	1 M H_2SO_4	Current potential curves on rotated electrode	5		3.1×10^{-3}	0.42
	1M H_2SO_4	Alternative curent	6	5.1×10^{-3}		0.61
	1M H_2SO_4	Galvanostatic method with rotated electrode	7	2.7×10^{-3}	2.7×10^{-3}	
	1 M H_2SO_4	Rotative-disc electrode	3	4.3×10^{-3}	4.3×10^{-3}	0.53 0.43
	1M H_2SO_4	Vibrated electrode		3.3×10^{-3}	3.4×10^{-3}	0.58 0.42
Ce^{4+}/Ce^{3+}	1M H_2SO_4	Current potential curves obtained with rotated electrode $i_0 = f(E)$	8		1.86×10^{-4}*	0.25
	1M H_2SO_4	Current potential curves obtained with rotated electrode $i_0 = f(C)$	8		5.18×10^{-4}*	0.25
	1M H_2SO_4	Vibrated electrode			2.07×10^{-4}	0.25

* Calculated from i_0^0

The tentative to extend the method to systems having greater values of the density of exchange-current, like the system : $K_3Fe(CN)_6/K_4Fe(CN)_6$ did not give the expected results.

We consider that the method could be applied in the described conditions, for systems having the values of the standard exchange-current densities $i_0^0 \leqslant 0.4$ A·l·/mole·cm².

---

[5] H Gerischer, *Z. Elektrochem.*, **54**, 366 (1950).

[6] M. Wijnen and W. Smit, *Rec. Trav. chim.*, **79** 203 (1960).

[7] F. C. Anson, *Analyt. Chem.*, **196**, 930 (1961).

[8] K. J. Vetter, *Z. Phys. Chem.*, (*Frankfurt*), **196**, 360 (1951).

Revue Roumaine de Chimie, **19**, *3*, 353–361 (1974)

VISCOSIMETRIC STUDY OF POLYACRYLIC ACID IN WATER-ETHANOL MIXTURES

LUCIA ZADOR and IUDITA MUREŞAN

"Babeş-Bolyai" University, Faculty of Chemistry, Cluj, Str. Arany Janos, 11, Romania

Received June 21, 1973

Experimental results are reported which, compared with the previously obtained potentiometric data, prove the occurrence of a conformational transition of polyacrylic acid (PAA) in water -ethanol mixtures containing large amounts of ethanol. This transition takes place within a critical interval of the degree of neutralization α of the polyacid. The interval is shifted towards lower α as the content of ethanol is raised. An interpretation and a scheme are given for the transition in terms of change from swollen open coils to symmetrical compact globules.

INTRODUCTION

The previous potentiometric study on polyacrylic acid (PAA) behaviour in water-ethanol mixtures [1] have shown that the well-known monotonous increase of $pK = pH + \log \frac{1-\alpha}{\alpha} + \log c_{H_2O}$ with the degree of neutralization (α) is characteristic only of the high water percentage solutions. (Even here only for α not lower than 0.1 – 0.08). In EtOH mixtures containing large amounts of EtOH, pK values pass through a very pronounced minimum with increasing α. These results have suggested a conformational transition for PAA, different from those found for polymethacrylic acid and poly-L-glutamic acid in aqueous solutions.[2-7] Since conformational transitions must be reflected on viscosimetric behaviour, the purpose of the present paper is to investigate the existence and the peculiarities of the suggested transition process by means of the viscosimetry. The effect of solvent composition and degree of neutralization on the average size of PAA chains was studied.

---

[1] I. Mureşan and L. Zador, *Stud. Univ. Babeş Bolyai, Chem,* **18** (1), 89 (1973).

[2] H. P. Gregor, D. H. Gold and M. Frederick, *J. Polymer. Sci.*, **23**, 467 (1957).

[3] M. Nagasawa and A. Holtzer, *J. Amer. Chem. Soc.*, **86**, 538 (1964).

[4] G. Barone, V. Crescenzi and F. Quadrifoglio, *Ricerca sci.*, **8**, 393 (1965); **8**, 1069 (1965); **6**, 477 (1966).

[5] T. N. Nekrasova, *Vysokomol. Soedineniya*, **11**, 1103 (1969).

[6] E. V. Anufrieva, M. V. Volkenstein, M. T. Krakoviak, and T. V. Seveleva, *Doklady Akad. Nauk S.S.S.R.*, **182**, 361 (1968).

[7] M. Mandel, J. C. Leyte and M. G. Stadhouder, *J. Phys. Chem.*, **71**, 603 (1967).

So far viscosimetric measurements in water-ethanol mixtures were performed only for PAA with $\alpha = 0$ and $\alpha = 1$ in solvent mixtures containing less than 60 v% ethanol.[8]

EXPERIMENTAL

The *PAA* was prepared by polymerization in benzene solution at 70° using benzoyl peroxide as initiating agent. The unreacted monomer was removed by extraction with benzene. Then the polymer was washed with petrol ether and dried. The average molecular weight for the Na salt of the polyacid in 2N $NaNO_3$ was determined viscosimetrically using the Mark-Houwing coefficients given by Arnold and Overbeek.[9] It was found $M_v = 977700$.

Isomolar solutions of PAA and KOH were prepared in water and 96 w% ethanol, which were mixed in the desired ratio. In order to keep the polymer concentration in volume unity unmodified (1.11×10^{-2} base mol/l $= 7.92 \times 10^{-4}$ g/ml) a calculated amount of solvent mixture was added, to compensate for the volume contraction. The calculations were based on the densities of water-ethanol mixtures given by Troy.[10]

The measurements were carried out at $25 \pm 0.1°$ in an Ubbelohde suspended level viscosimeter at constant rate of shear (capillary constant 0.1).

Since the polymer concentration was unvariable, $\eta_r = \frac{\eta}{\eta_0} = \frac{t}{t_0}$ values could be used instead of $\frac{\eta_{sp}}{c}$ (t and t_0 are the times of the flow for solutions and of the correspondent solvent mixture, respectively. The values of $\frac{\eta_{sp}}{c}$ are related to η_r by

$$\frac{\eta_{sp}}{c} = \frac{\eta_r - 1}{7.92} x 10^4$$

in order to get more direct information about the shape of *PAA* chains in different solutions, it was determined η_r also for the completely uncharged PAA at the same polymer concentration in 0.2 N HCl aqueous solution as solvent.

Using Flory's[11] relations

$$[\eta] = \frac{\Phi(\bar{h}_0^2)^{3/2}\alpha^2}{M} \quad \text{respectively} \quad \frac{[\eta]}{[\eta]_\theta} = \alpha^3$$

and accepting the completely uncharged PAA as a reference state, the following conventional measure of the expansion coefficient was used

$$A = \frac{\left(\frac{\eta_{sp}}{c}\right)^{1/3}}{\left(\frac{\eta_{sp}}{c}\right)^{1/3}_{HCl}}$$

for the polymer concentration $c = 7.92 \times 10^{-4}$ g/ml.

---

[8] J. ELIASSAF, *J. Appl. Polymer Sci*, **7**, S9 (1963).

[9] R. ARNOLD and J. Th. G. OVERBEEK, *Rec. Trav. chim.*, **69**, 192 (1950).

[10] J. TIMMERMANS, "The physico-chemical constants of binary systems in concentrated solutions", Interscience Publishers, New York, 1960, p. 188.

[11] P. FLORY, *J. Amer. Chem. Soc.* **74**, 3364 (1952).

Although the value of A is not identical with Flory's expansion coefficient on account of finite concentrations used, this ratio seemed to reflect more correctly the extent of the expansion than $[\eta]^{1/3}/[\eta]^{1/3}_{\mathrm{HCl}}$ because of the uncertainties of the extrapolation for polyelectrolyte solutions without added salts (see e.g. fig. 5).

RESULTS

THE EFFECT OF α

Fig. 1 shows the influence of the degree of neutralization on the relative viscosity in various mixtures of solvents for a given polymer concentration. While in aqueous solutions η_r increases continuously with α, in H_2O — EtOH mixtures a twofold effect of α on the shape of PAA chains is evident. The increase of α first enhances the value of η_r, but after a critical value determined by the EtOH percentage it involves a pronounced decrease of the relative viscosity which, for the content of EtOH higher than 52.2w %, may continue below the values found in the case of the completely unneutralized polyacid. A further increase of α does not modify

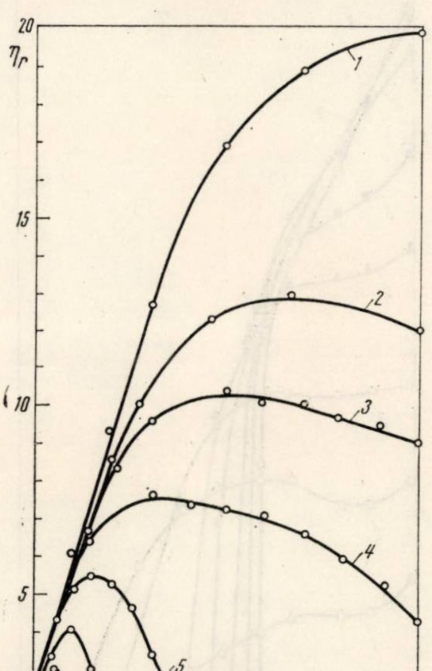

Fig. 1. — Plot of η_r against α for PAA in water-EtOH mixtures ($c = 1.11 \times 10^{-2}$ base mole/l).

1, 0 w% EtOH *2*, 19,9 w% EtOH *3*, 33.1 w% EtOH *4*, 41.3w% EtOH *5*, 52.2w% EtOH *6*. 62.2w% EtOH *7*, 72.7 w% EtOH *8*, 96. w% EtOH these low values of η_r. While the slope of the initial ascendent sections of the curves are not affected by the solvent composition (except the mixtures very rich in EtOH), as the EtOH percentage increases, the common slope is left at lower and lower α and concomitantly both coordinates of the maximum diminish. The degree of neutralization at which η_r reaches a constant minimal value also decreases with EtOH concentration.

In 96 w% EtOH only the decays and constant sections of the curves can be observed.

THE EFFECT OF EtOH CONTENT

In fig. 2 is shown the influence of solvent composition on the average size of PAA at various degrees of neutralization. The curve for $\alpha = 1$ is

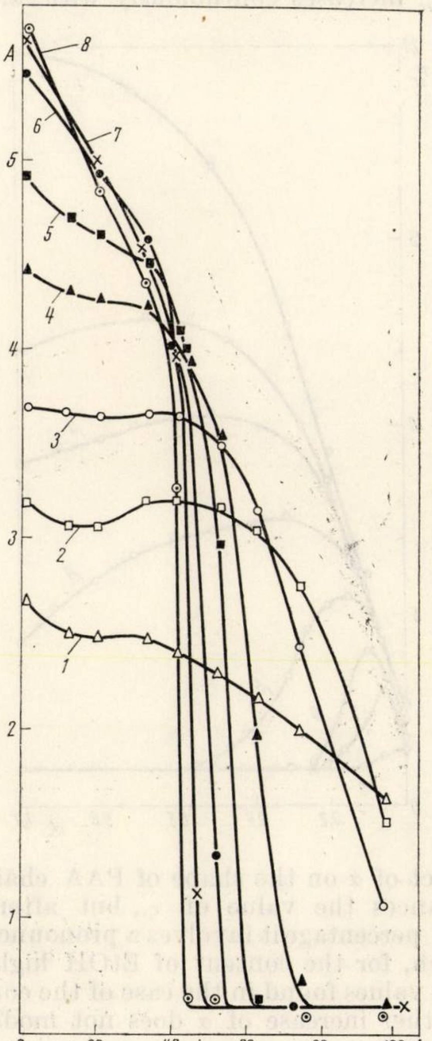

Fig. 2. — Plot of *A versus* EtOH concentration for PAA. *1*, $\alpha = 0$ *2*, $\alpha = 0.05$ *3*, $\alpha = 0.1$ *4*, $\alpha = 0.2$ *5*, $\alpha = 0.3$ *6*, $\alpha = 0.5$ *7*, $\alpha = 0.7$ *8*, $\alpha = 1$

in a good agreement with Eliassaf's [8] data for entirely neutralized PAA. Although the curves descend in each case of partially neutralized polyacid, their feature sharply depends on α.

The shape of polyions of any α does not vary significantly with the composition of solvent mixture up to about 33 w % EtOH. The further increase of EtOH percentage implies the contraction of the coils. The value of A decreases as steep as α becomes higher. For $\alpha \geqslant 0.2$ the decrease of A goes up to a value of 0.53, when the shape of the coils becomes more compact than for the completely uncharged PAA. The lowest EtOH percentage corresponding to this minimal value of A diminishes with increasing α and for $\alpha = 0.2-1$ it corresponds to 76 — 45 %.

COMPARISON WITH POTENTIOMETRIC DATA

In order to get a correct interpretation of the reported results a comparison between viscosimetric and potentiometric behaviour of the investigated solutions is given in figs.3 and 4.

The analysis of these figures permits the following facts to be pointed out :

1) For solvent mixtures containing large amounts of water the degree of neutralization at which the slope of A and pK curves suddenly diminish, has the same value. At the same time the descent of $A - \alpha$ curves corresponds to horizontal portions on the $pK - \alpha$ plots.

2) For solutions containing large amounts of ethanol a close parallelism between the two curves which is maintained up to the minimum on the $pK - \alpha$ graphs is evident. In this range the decreasing section of A curves corresponds to a sharp increase of the acidity of PAA.

3) For the intermediate solvent composition (52.2w % EtOH) the viscosimetric curve keeps the peculiarities of rich in EtOH solutions quite well, while the potentiometric one does not show any sharp increase of acidity.

These facts prove that only in solutions with higher than 52.2 % EtOH the contraction of coils is related to a decrease of the electrostatic potential. In lower content of EtOH solutions the free charge of polyions does not decrease with α. In this range only the rate of increase of pK becomes smaller and can reach the zero value.

ELECTROLYTE CHARACTER

It was worth trying to verify whether the sharp decrease of A and pK with α in solutions rich in EtOH is not due to the complete loss of electrolyte character of PAA. To this purpose the dependence of $\frac{\eta_{sp}}{c}$ on c was investigated for various α and solvent compositions. The curves obtained decrease or pass through a maximum for the whole range of EtOH % and of the α values up to the minimum of pK curves. In fig. 5 are given two examples of such curves, for solutions which correspond to the decreasing section of $A - \alpha$ and $pK - \alpha$ plots. Consequently, before the

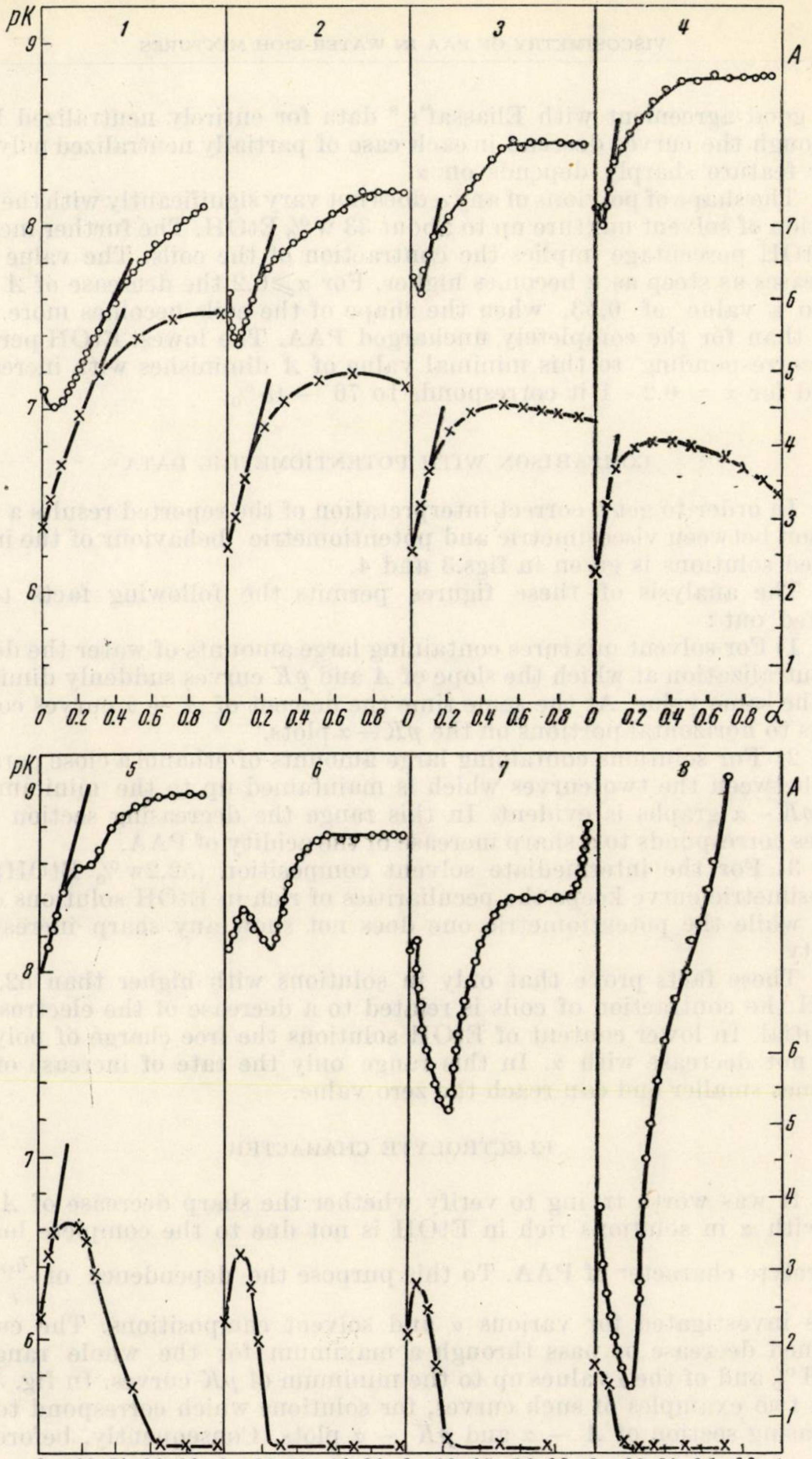

Figs. 3,4 — Plot of A (×) and pK (○) as a function of α for different compositions of the solvent mixture.

1 0w%EtOH *2*, 19.9 w% EtOH *3*, 33.1 w%EtOH *4*, 41.3 w% EtOH *5*, 52.2 w% EtOH *6*, 62.2 w% EtOH *7*, 72.7 w% EtOH *8*, 96.0 w% EtOH minimum of pK curves the PAA keeps his electrolyte character. For higher α the low values of η_r do not allow a satisfactory accuracy for such measurements.

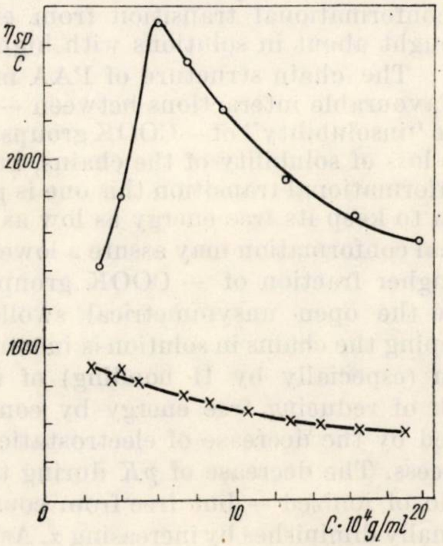

Fig. 5. — Plot of viscosity number versus c for PAA in solutions with 62.2 w% EtOH for degrees of neutralization: $\alpha = 0.15$ (.) $\alpha = 0.20$ (x).

DISCUSSION

In aqueous solution the decrease of the slope on $A - \alpha$ and $pK - \alpha$ curves above a given degree of neutralization may be attributed to the screening of the electrostatic potential in the wake of counterion binding.

The reported experimental results prove that the presence of EtOH in the solvent has besides the effect of enhancing the ion binding (by reducing the dielectric constant of the medium) another one very pronounced, to which has to be attributed the complex influence of α upon η_r, A and pK as well as the sudden decrease of A in a narrow EtOH percentage interval. This effect has to be related to the enthalpic interactions, which are responsible for the insolubility of potassium polyacrylate in absolute EtOH. The sudden decrease of η_r or A cannot be, however, the consequence of the loss of solubility of the polymer in the given solvent mixtures. Some attempts on solubility indicated that such solutions were thermodynamically stable. They were formed spontaneously if the components were put in contact in ratios corresponding to the range that follows the minimum on the $pK - \alpha$ curves. Therefore, the turbidity of such solutions has to be attributed to the more compact setting of the chain segments rather than to the loss of solubility. For the polymer concentration investigated the insolubility of the chains for a given EtOH concentration appears at α values much higher than it corresponds to the sudden contraction (for example in 72.7 % EtOH the contraction ends at $\alpha = 0.22$ while the insolubility begins at $\alpha > 0.75$).

Thus, the explanation of the observed phenomena requires to admit a conformational transition from expanded coils to compact globules, brought about in solutions with high EtOH percentage by increasing α.

The chain structure of PAA makes possible that the energetically unfavourable interactions between — COOK groups and EtOH molecules (the "insolubility" of —COOK groups in the solvent medium) do not lead to the loss of solubility of the chains, but to a change of their shape. As any conformational transition this one is predicted by the tendency of the solution to keep its free energy as low as possible. The new compact, symmetrical conformation may assure a lower interaction free energy by "hiding" a higher fraction of — COOK groups from the solvent medium than is able the open unsymmetrical swollen conformation. The function of keeping the chains in solution is incumbent in these conditions on the solvation (especially by H bonding) of unneutralized — COOH groups. The task of reducing free energy by contraction is presumably much facilitated by the decrease of electrostatic free energy, which accompanies the process. The decrease of *pK* during the transition indicates that here the ratio of ionized — but free from counterion binding — carboxylic groups actually diminishes by increasing α. As for the conformational chain entropy, it has to pass through a maximum during the transition from much more expanded conformations to those more compact than the statistical coil. Thus, the variation of the chain entropy free energy by contraction has to be negative, or if it is positive, its magnitude cannot be significant.

It can be assumed that the conformational transition is marked by the descendent sections of $pK - \alpha$ or $A - \alpha$ curves or by the sudden decrease of A — %EtOH curves. In table 1 are presented the correlated values of α and EtOH percentage where the transition is accomplished.

Table 1

The values of α marking the end of transition for different compositions of the solvent mixture

w % EtOH	α
45	1.0
50	0.7
55	0.5
61	0.3
65	0.25
70	0.21
76	0.20
96	0.19

By increasing the degree of neutralization up to higher values than are given in table 1, an aggregation process occurs, which does not imply any η_r modification (*Einstein's* rule for impermeable spheres seems to be valid) but involves the decrease of the acidity.

The independence of acidity of α, observable for 62.2 and 72.7 *w* % EtOH after the mounting sections of $pK - \alpha$ plots, between $\alpha = 0.53-0.96$ and 0.53 — 0.80 respectively, presumably corresponds to the formation of a stable secondary structure. It seems that only at higher α or EtOH percentage (f.e. $\alpha > 0.8$ for 72.7 % EtOH) the aggregation continues up to precipitation.

Fig. 6 suggests a schematic drawing of the investigated process.

It could be concluded that the observed phenomena may be attributed to a conformational transition opposed to that put in evidence for polymethacrylic acid in water solutions. [12]

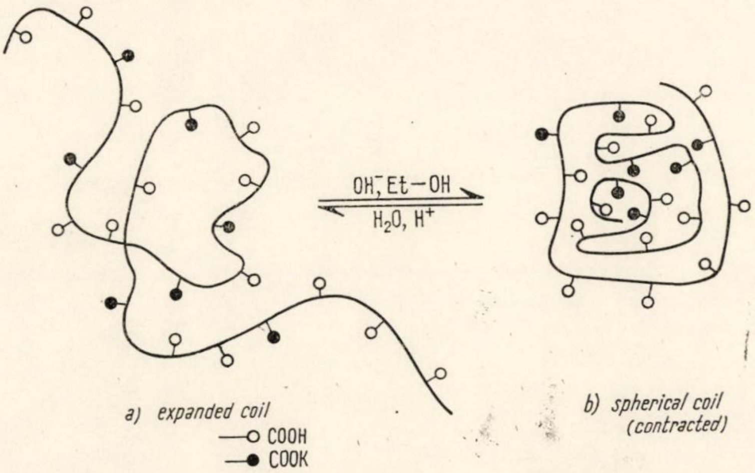

Fig. 6. — Schematic representation of PAA chains :

a) in solution containing large amounts of water or in solvent mixtures with raised EtOH content at low α b) in solution containing more than 52 w% EtOH at higher α than those given in table 1.

In the experimental measurement we acknowledge the assistance of the students I. Nistor and I. Bodea.

---

[12] A. M. LIQUORI, G. BARONE, V. CRESCENZI, F. QUADRIFOGLIO and V. VITAGLIANO, *J. Macromol. Chem.*, **1**, 291 (1966).

Revue Roumaine de Chimie, **19**, *3*, 363–370 (1974)

MAGNITUDES AND SIGNS OF ^{13}C COUPLING CONSTANTS IN SEVERAL ORGANIC MOLECULES BY DOUBLE RESONANCE

V. BĂRBOIU

The "P. Poni" Institute of Macromolecular Chemistry Aleea Gr. Ghica Vodă, nr. 41 A, Iași, Romania

Received April 14, 1973

The double resonance technique was used to determine the magnitudes and the absolute signs of the spin-spin coupling constants $^1J_{CH}$, $^2J_{CCH}$, $^1J_{CF}$, $^2J_{CCF}$, J_{HH} and J_{HF} in the following molecules: CH_3COOH, $CH_2ClCOOH$, $CHCl_2COOH$, CHF_2COOH, CH_2ClCHO, $H_3C-CH=CH-CHO$, CH_3CH_2OH and CF_3CH_2OH. The double resonance studies on $F_3^{13}C-CH_2OH$ and $H_3^{13}C-{}^{13}COOH$ are described in detail. It was found that the electronegativity and the number of substituents produce an increasing positive contribution to $^2J_{CCH}$ of halogenated acetic acids, opposite to that of halogenated acetaldehydes. Other dependences of the measured coupling constants are presented.

It is known that ^{13}C NMR studies are still difficult to be carried out Although the various PFT techniques allow to obtain ^{13}C NMR spectra of S/N ratio comparable to those of c.w. proton spectra, the following problems are not solved yet : The PFT techniques are widely used with total proton decoupling and therefore the spectra do not contain any information about J_{C-H} couplings. When the concentrations of samples are high enough these techniques can be used without the total proton decoupling, so that the ^{13}C spectra contain information about the magnitudes of hydrogen-carbon couplings but not about their signs, and the use of heteronuclear selective irradiations in PFT spectra to find the coupling signs is not yet instrumentally solved.

One way would be to use ^{13}C enriched samples but it is very expensive and even impassable for complex molecules.

However it is possible to completely study ^{13}C resonances of natural ^{13}C abundance compounds using the indirect observing methods[1-3] : the ^{13}C satellite spectra of nuclei of high sensivity, (^{1}H and ^{19}F) are observed and the parameters of their coupled carbon nuclei (chemical shifts, magnitudes and signs of coupling constants) are determined from the character-

---

[1] W. Mc. Farlane, *Ann. Rev. NMR Spectroscopy*, **1**, 135 (1968).

[2] R. A. Hoffman and S. Forsen, *Progr. NMR Spectroscopy*, **1**, 15 (1966).

[3] V. I. Kowalewski, *Progr. NMR Spectroscopy*, **5**, I (1969).

istic frequencies of double resonance spectra of types ^1H, $^{19}F - \{^{13}C\}$. The most used double resonance effects are the spin tickling and the selective decoupling. The precision of such methods is very high, (± 0.1 Hz), and it is not achieved even with PFT techniques. However, these double resonance experiments are quite difficult and require long determination times and some instrumental modifications.

All these inconveniences are the cause for the relative scarcity of data on heteronuclear couplings of ^{13}C nuclei, especially on those involving two or more bonds. This paper contains such data for a series of halogenated acetic acids, alcohols and aldehydes obtained by means of double resonance effects.

EXPERIMENTAL

We present below the double resonance experiments on the molecules $F_3^{13}C-CH_2OH$ (1,1, 1 trifluoroethanol) and $H_3^{13}C-{}^{13}COOH$ (acetic acid) to find the magnitudes and the signs of all coupling constants.

COUPLING CONSTANTS IN $F_3^{13}C-CH_2OH$

The signs of $^1J_{CF}$, $^2J_{CCH}$ and $^2J_{HF}$ and the magnitude of $^2J_{CCH}$, which is impossible to be directly observed, will be determined. Of the three spectra, (^{13}C, ^{19}F, ^1H), of this molecule, schematically shown in fig. 1 *a*, *b*, *c* assuming the same sign for all three couplings, only ^{19}F spectrum is directly observable (fig. 1 d). This single resonance spectrum allowed to determine : $|J_{HF}| = 9.1$ Hz and $|^1J_{CF}| = 277.5$ Hz. One characteristic of the double resonance experiments carried out on this molecule was that the observed spectrum (^{19}F) was obtained by field sweep mode and thus the optimum irradiating frequencies must be corrected before making a comparison between them.[1,2]

It was found that lines F_1 and F_2 are split (tickling affected) by the following two close irradiating frequencies in the ^{13}C spectrum : $\nu_2^e = 15087885.8$ Hz and $\nu_2^f = 15087892.0$ Hz, respectively (fig. 1 *e*, *f*). ν_2^e must be increased with $|J_{HF}| \cdot \gamma_{13C}/\gamma_{19F} = 2.4$ Hz (this is the difference in frequency units in ^{13}C spectrum corresponding to the field difference from F_1 to F_2) to be referred to the same magnetic field as ν_2^f. If all couplings have the same sign, the irradiating frequency which affects F_1 (of r. frequency higher than that of F_2) will be higher than that affecting F_2. As $\nu_2^{e\prime} = \nu_2^e + 2.4$ is lower than ν_2^f, it results that the couplings J_{HF} and $^2J_{CCH}$ have opposite signs and thus the ^1H spin states of ^{13}C spectrum or ^{19}F spectrum must be reversed.[1,2] The magnitude of $^2J_{CCH}$ is obviously equal to the difference $|\nu_2^{e\prime} - \nu_2^f| = 3.8$ Hz. Fig. 1 g,h shows how the two ^{19}F triplets collapse to single lines for two proton irradiating frequencies : $\nu_2^g = 59995726.0$ Hz for the high r.f. triplet (of α state for $I_z(^{13}C)$) and $\nu_2^h = 59996018.3$ Hz for the low r.f. triplet (of β state for $I_z(^{13}C)$). These selective decoupling effects happen only if the two irradiating frequencies coincide with the centres of the two proton quartets corresponding to α and β states for $I_z(^{13}C)$ and which are separated by $|^2J_{CCH}|$, ν_2^g must be increased with $|^1J_{CF}| \cdot \gamma_{1H}/\gamma_{19F} = 294.7$ Hz to be compared with ν_2^h. As $\nu_{r.f.}(F_2) > \nu_{r.f.}(F_5)$ and $\nu_2^g + 294.7 > \nu_2^h$, it results $^2J_{CCH}$ and $^1J_{CF}$ have the same sign. The difference $|\nu_2^g + 294.7 - \nu_2^h| = 2.4$ Hz does not coincide with $|^2J_{CCH}| = 3.8$ Hz, before determined, but the deviation is due to the lower precision of the decoupling experiments relative to the tickling experiments.

All three couplings and their relative signs are determined :

$$^1J_{CF} = \pm 277.5 \text{ Hz}; \; J_{HF} = \mp 9.1 \text{ Hz}; \; ^2J_{CCH} = \pm 3.8 \text{ Hz}.$$

Similar experiments, but of types $^1H - \{^{13}C, {}^{19}F\}$, on the molecule $F_3C-{}^{13}CH_2OH$ determined

$$^1J_{CH} = \pm 145.6 \text{ Hz}; \; J_{HF} = \pm 9.1 \text{ Hz}; \; ^2J_{CCF} = \pm 35.4 \text{ Hz}.$$

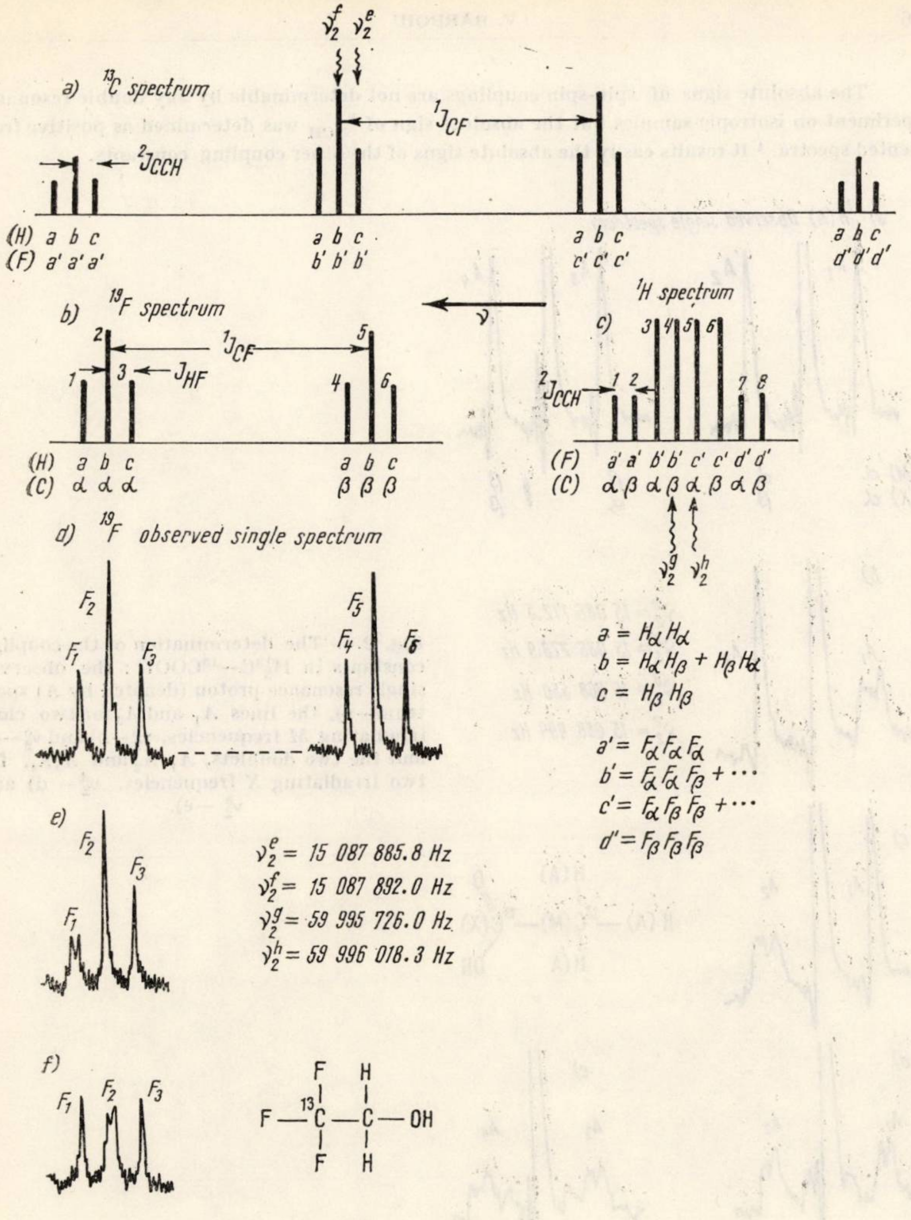

Fig. 1. — The determination of the coupling constants in $F_3^{13}C-CH_2OH$: the presumable spectra of this molecule, ^{13}C—a), ^{19}F—*b*) and ^1H—*c*), the observed single resonance ^{19}F spectrum — d), the lines F_{1-3} for two close irradiating ^{13}C frequencies, ν_2^e—e) and ν_2^f—*f*), and the collapse to single line of the two ^{19}F triplets for two irradiating ^1H frequencies, ν_2^g—*g*) and ν_2^h—*h*).

The assignment of spin states of presumable spectra is made assuming the same sign for all coupling constants.

The absolute signs of spin-spin couplings are not determinable by any double resonance experiment on isotropic samples but the absolute sign of ${}^1J_{CH}$ was determined as positive from oriented spectra. [4] It results easily the absolute signs of the other coupling constants.

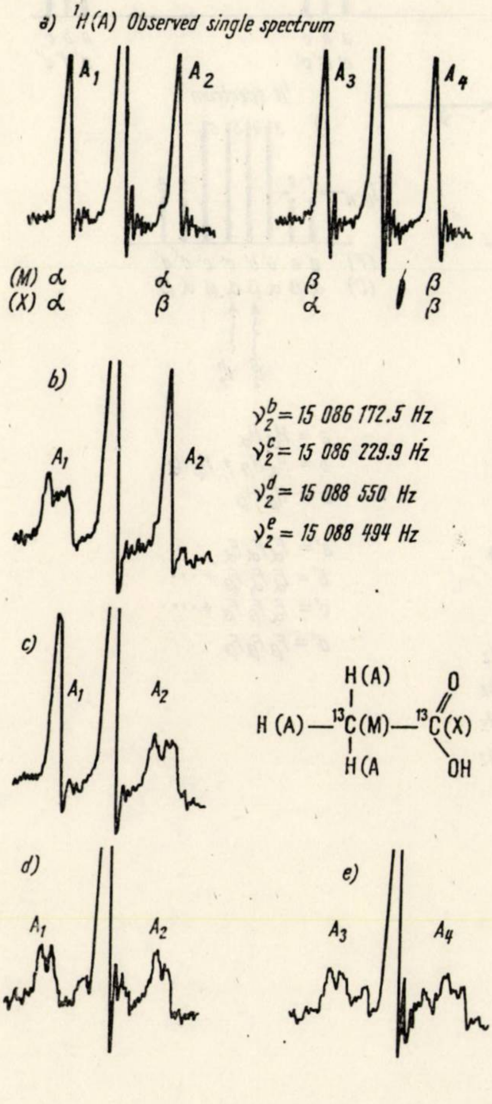

Fig. 2. — The determination of the coupling constants in $H_3^{13}C-{}^{13}COOH$: the observed single resonance proton (denoted by A) spectrum — a), the lines A_1 and A_2 for two close irradiating M frequencies, ν_2^b — b) and ν_2^c — c), and the two doublets, A_1 A_2 and A_3A_4, for two irradiating X frequencies, ν_2^d — d) and ν_2^e — e).

COUPLING CONSTANTS IN $H_3^{13}C-{}^{13}COOH$

The three coupling constants ${}^1J_{CH}$, ${}^2J_{CCH}$ and ${}^1J_{CC}$ denoted J_{AM}, J_{AX} and J_{MX} respectively (fig. 2), were obtained by $A-\{M\}$ and $A-\{X\}$ double resonance experiments. The proton spectrum A was the outer ${}^{13}C$ satellite proton spectrum of a 50 % ${}^{13}C$ enriched sample on the position — *COOH. It was recorded in frequency sweep mode, so that it is not necessary to correct the irradiating frequencies; they will correspond to the lines of ^{13}C spectra at least for the case of tickling effects. Fig. 2 *a* shows the experimental single resonance spectrum of *A* nuclei; the signals between A_1 and A_2 and A_3 and A_4 respectively arise from the molecules of type $H_3^{13}C-COOH$. This spectrum gave $|J_{AX}| = 6.5$ Hz and $|J_{AM}| = 129.5$ Hz.

---

[4] G. Englert and A. Saupe, *Mol. Cryst.*, **1**, 503 (1966).

The lines A_1 and A_2 are affected (split) by the following two close *M* irradiating frequencies : $\nu_2^b = 15086172.5$ Hz and $\nu_2^c = 15086229.9$ Hz (fig. 2 b, *c*). These frequencies must correspond to two close *M* lines of the same states for *X* spin as A_1 (α state) and A_2 (β state), and thus their difference is just $|J_{MX}|$. As $\nu_{r.f.}(A_1) > \nu_{r.f.}(A_2)$ but $\nu_2^b < \nu_2^c$ it follows J_{AX} and J_{MX} have opposite signs. The magnitude of $J_{MX} = {}^1J_{CC}$ is obviously equal to $|\nu_2^b - \nu_2^c| = 57.4$ Hz.

Two other experiments are necessary to compare the signs of J_{AM} and J_{MX}. The two doublets A_1A_2 (of α state for $I_z(M)$) and A_3A_4 (of β state for $I_z(M)$) are affected by $\nu_2^d = 15088550$ Hz and $\nu_2^e = 15088494$ Hz (fig. 2 *d,e*). The irradiating field level was kept very low to obtain a high precision. The two irradiating frequencies must correspond to the central frequencies of the two *X* quartets of the same states for $I_z(M)$ like the two A doublets. As $\nu_2^b > \nu_2^e$ it results J_{AM} and J_{MX} of the same sign. The difference $|\nu_2^d - \nu_2^e| = 56$ Hz is little different from $|J_{MX}| = 57.4$ Hz before determined by tickling effects. The absolute sign of $J_{AM} = {}^1J_{CH}$ is known as positive [4] and therefore

$$^1J_{CH} = +129.5 \text{ Hz}; \quad ^2J_{CCH} = -6.5 \text{ Hz and } ^1J_{CC} = +57.4 \text{ Hz}$$

Similar experiments were carried out to get the coupling constants of the other compounds listed in the table, except the mono and dichloroacetic acids for which $^2J_{CCH}$ was directly determined from accumulated ^{13}C spectra.

INSTRUMENTATION

All proton spectra were recorded on a JEOL JNM—C—60HL spectrometer operating in frequency sweep mode and the magnetic field was internally locked on the proton signal of a small quantity of TMS added into the samples, except the cases of acetic acids for which the lock signal was just their —OH signals. The fluorine spectra were observed in field sweep mode and the magnetic field was externally locked (the two samples method).

The irradiating fields in the experiments on compounds IV, XIV, XV were obtained using a FS—30 frequency syntesizer connected to a frequency doubler and an r. f. power amplifier, and an adjustable 15 MHz oscillator of type JNM—RH—C60A connected to a JNM—SD—HC hetero-spin-decoupler were used for the other compounds. The frequencies were measured by means of a RFT—3515 frequency counter with an error of ± 0.1 Hz.

All studied compounds were commercially available ones. The concentrations of samples were about 100 % and the work temperature was 25 ± 2 °C.

RESULTS AND DISCUSSIONS

The table below contains the coupling constants of the studied compounds. The accumulated (of 36 times) ^{13}C spectra of mono and dichloroacetic acids gave $^2J_{CCH}$ equal to 3.5 Hz and ~ 1Hz respectively. It is very plausible to consider that $^2J_{CCH}$ of monochloroacetic acid is negative because it is − 6.5 Hz in the acetic acid and + 2.2 Hz in the difluoroacetic acid. The sign cannot be deduced in the case of dichloroacetic acid. Anyway it is clear that the increasing of negativity and number of substituents at the sp^3 carbon of acetic acids has a positivation effect on the $^2J_{CCH}$ coupling constants.

Table 1

The table of the spin-spin coupling constants (magnitudes in Hz and absolute signs)

Compound	$^1J_{CH}$	$^2J_{CCH}$	$^1J_{CF}$	$^2J_{CCF}$	J_{HH}	J_{HF}	Others
I. $H_3C-COOH$	+129.5	−6.5					$^1J_{CC}=+57.4$
II. $H_2ClC-COOH$	+150	−3.5					
III. $HCl_2C-COOH$	+177	1					
IV. $HF_2C-COOH$	+193.5	+2.2	−247.9	−28.0		+52.5	
V. $F_3C-COOH$			−295.0	−44.5			
VI. $H_2ClC-{}^{13}CHO$	+182	−8.7			+1.7		
VII. $H_2Cl^{13}C-CHO$	+157	+31			+1.7		
VIII. $\overset{a}{H_3}{}^{13}C-\overset{b}{CH}=\overset{c}{CH}-\overset{d}{CHO}$	+125.2	+4.5			+6.3	(J_{ab})	$^3J_{CCH}=+6.5$
IX. $H_3C-{}^{13}CH=CH-CHO$	+153.5	−7.4	$(^2J_{CCH}{}^a)$	and	−1.9	$(^2J_{CCH}{}^c)$	
X. $H_3C-CH={}^{13}CH-CHO$	+160	+26.3	$(^2J_{CCH}{}^d)$		−1.5	(J_{ac})	
XI. $H_3C-CH=CH-{}^{13}CHO$	+172				+15.0	(J_{bc})	
XII. $^{13}CH_3-CH_2OH$	+125.4	−2.2			+7.3		
XIII. $CH_3-{}^{13}CH_2OH$	+140.4	−3.3			+7.3		
XIV. $^{13}CH_3-CH_2OH$		−3.8	−277.3			+9.1	
XV. $F_3C-{}^{13}CH_2OH$	+145.6			+35.4		+9.1	

$^1J_{CH}$ COUPLING CONSTANTS

Their magnitudes and signs agree perfectly with similar data of literature.[5] The positive signs and a proportionality dependence of the form $^1J_{CH} = A \cdot a_H^2$, where a_H^2 is the *s*-character of the C−H hybrid orbital, were well theoretically explained[6−8] and experimentally checked in detail.[9] This relationship allows to find the substituent electronegativity influence on the *s*-character of C−H bond. The values of + 177 Hz (III) and +193.5 Hz(IV) indicate an important increase of a_H^2 with the substituent electronegativity, and the values of +129.5Hz (I), +150Hz (II) and

---

[5] E. F. Mooney and P. H. Winson, *Ann Rev. NMR Spectroscopy*, **2**, 153 (1969).

[6] N. Muller and D. E. Pritchard, *J. Chem. Phys.*, **31**, 768 (1959).

[7] J. A. People and D. P. Santry, *Mol. Phys.*, **8**, 1 (1964) and **9**, 301 (1965).

[8] C. J. Jameson and H. S. Gutowsky, *J. Chem. Phys.*, **51**, 2790 (1969).

[9] T. Yonezawa, I. Morishima, M. Fujii and K. Fukui, *Bull. Chem. Soc. Japan*, **38**, 1224 (1965) ; T. Yonezawa, I. Morishima and M. Fujii, *Bull. Chem. Soc. Japan*, **39**, 2110 (1966).

+177Hz (III) are in agreement to the additivity rule of electronegative substituent effects on $^1J_{CH}$.[10,11] An empirical $a_H^2(E^x)$ dependence can be obtained using the experimental values of $^1J_{CH}$, the relation $^1J_{CH} = A \cdot a_H^2$ and the additivity rules.

$^2J_{CCH}$ COUPLING CONSTANTS

It can be observed that these coupling constants are very various, being negative and positive and having values from −10 up to +30 Hz. One distinguishes several types of such coupling constants.

— The $^2J(C_{sp3} - C_{sp3} - H)$ couplings are negative (compounds XII, XIII, XIV) being in agreement to the mechanism based on the contact interaction of Fermi and initially advanced by Ramsey[12] and then developed in the MO formalism.[7,13]

— The $^2J(C_{sp2} - C_{sp3} - H)$ couplings are also negative (compounds I, II, VI, IX) and the positive values found for the difluoroacetic acid (IV) is an exception. It may be concluded that the increase of the electronegativity and the number of substituents at the intervening carbon affects a positivation of these coupling constants for acetic acid (the table), which is opposite to the negativation evidenced for acetaldehydes (compound VI and others[5]).

— The $^2J(C_{sp3} - C_{sp2} - H)$ couplings are negative and positive.[5] Whilst the magnitudes of those negative are smaller than 3 Hz the positive couplings have uncommon large values (+ 46.3 for chloral[5]). It follows the sp^2 hybridization of intervening carbon has an important positive contribution J^π, which is larger than the negative contact contribution for most cases. Jameson and Damasco[13] calculated this π contribution by a MO method and they found a correct positive sign but too large values.

It is interesting to compare the value of this coupling in acetaldehyde (+26.6 Hz) with that in *trans*-crotonaldehyde-VIII (+4.5 Hz). The difference between them is that the intervening carbon is double bonded with an electronegative oxygen atom in the first case and with a carbon atom in the second. It seems that the positive J^π contribution increases with the polarization of π bonds; the C=0 bond is more polarized than the C = C. A semiclassical calculus[14] found that J^π is positive for values between 55° and 125° of the angle between the straight lines joining the two interacting nuclei with the most close π electron and has a maximum positive value at 90°. This angle is equal to 97° and 116° for the two cases and indicates that the positive J^π in acetaldehyde is larger than that in *trans*-crotonaldehyde-VIII.

---

[10] E. Malinowski, *J. Amer. Chem. Soc.*, **83**, 4479 (1961).

[11] C. Juan and H. S. Gutowsky, *J. Chem. Phys.*, **37** 2198 (1963).

[12] N. F. Ramsey, *Phys. Rev.*, **91**, 303 (1953).

[13] C. J. Jameson and M. C. Damasco, *Mol. Phys.*, **18**, 491 (1970).

[14] V. Bărboiu and D. Gîlea, *Rev. Roumaine Chim.* (1973), to publication.

$^1J_{CF}$ AND $^2J_{CCF}$ COUPLING CONSTANTS

The values found (compounds IV, V, XIV, XV) agree to similar data of literature.[15] The $^2J_{CF}$ couplings increase in absolute value with the number and the electronegativity of substituents at carbon atom as the $^1J_{CH}$ couplings do, but their negative sign is not well explained yet. It seems that the orbital mechanism of Gutowsky is much more important than the contact interactions because of the high polarity of C—F bonds.[16]

The author is grateful to Dr. W. McFarlane of Chem. Dept. London Polytechnics for the help and the useful discussions in the studies of compounds IV, XIV and XV.

---

[15] K. Jones and E. F. Mooney, *Ann Rev. NMR Spectroscopy*, **3**, 261 (1970).

[16] J. A. People, *Mol. Phys.*, **1**, 216 (1958).

Revue Roumaine de Chimie, **19**, *3*, 371–379 (1974)

THE STUDY OF THE HARDENING PROCESSES IN TRICALCIUM SILICATE-WATER-ELECTROLYTE SYSTEM

I. TEOREANU and MARCELA MUNTEAN

Polytechnic Institute, Str. Polizu no. 1, Bucharest,
Romania

Received June 14, 1973

Using chemical, X-ray diffraction and thermodifferential analyses the influence of alkaline chlorides added in small quantities (0.5, 2, 5 % w) upon the processes in the tricalcium silicate-water system is studied in comparison with the action of calcium chloride.

1. The control of the hardening processes of binders, especially of the portland cement, and the influence in this way, on the evolution and the value of the physico-mechanical properties of the hardened system has a particular practical importance. A way to fulfil this scope, of great practical interest, is to use electrolytes added in small quantities, usually no more than 3 % in weight, to the water-binder mixture.

The study of the action of the electrolytes upon the hardening of complex binders is a very difficult task, due to the different influences that the addings may produce, as a function of the nature of mineralogical constituents of the binder, of the nature of the electrolytes themselves, of the added quantity and the hardening conditions. For this reason, the establishment of a correct picture of the mechanism by which the admixtures act upon the hardening of binders could be much facilitated by examining the influence of the additions upon the hardening of the individual mineralogical phases of the complex binders. Thus, for a thorough understanding of the mechanism and of the processes taking place during the hardening of the portland cement, in presence of electrolytes, of a great interest is to study their influence upon the hardening of silicate phases, especially of the tricalcium silicate.

There are relatively few studies in literature concerning the tricalcium silicate-water-electrolyte system; in addition, the data for this system are disparate, sometimes contradictory, and a systematic study is still lacking.

The most elaborate studies of processes taking place during hardening of the tricalcium silicate in presence of electrolytes refer to the action of calcium chloride and gypsum.

Generally, it is accepted the point of view, sustained by experimental data, that the action of calcium chloride upon the processes taking place during the hardening of tricalcium silicate is materialized by changes in structure, morphological aspects, specific surface of the hydrated products, and at the same time, due to modifications in the ionic equilibrium of the system, changes in hydration rate. [1-7] Some investigations in tricalcium silicate-water-calcium chloride system showed that, under normal conditions and for small amounts of calcium chloride (usually less than 3 %), complex products of tricalcium silicate with calcium chloride cannot be formed and identified. [1,2,4] Under special conditions (18–20 % of added calcium chloride, temperature under 0°), it seems that calcium chloride reacts with tricalcium silicate forming a complex compound of the type $3CaO \cdot SiO_2 \cdot CaCl_2 \cdot nH_2O$ ($n = 4 \ldots 15$). [8,9]

At temperatures greater than 0°, some workers evidenced the formation of some hydroxychlorides of the type $mCaO.CaCl_2.nH_2O$ as a product of the reaction of calcium chloride with calcium hydroxyde resulting from the hydration of tricalcium silicate. [1,10-12] In accordance with some studies [10-12] the formation of calcium hydroxychlorides could be considered as the principal accelerating action of calcium chloride upon the hardening of tricalcium silicate; but, as is known, the formation and the stability of the calcium hydrochlorides are possible only at higher calcium chloride contents, [1] which is not the case for the conditions considered optimum (around 2 % of calcium chloride).

As concerns the action of gypsum upon the hardening of tricalcium silicate, the literature data show positively that this action is "physical". [13-16] It consists principally in influencing the hydration kinetics of tricalcium silicate and the crystallization capacity of hydrated phases, having as final result a modification of the structure of these products.

2. In the present paper the influence of alkaline chlorides upon the processes in the system $3CaO \cdot SiO_2$-water is studied in comparison with that

---

[1] A. Celani, M. Collepardi and A. Rio, *Ind. Ital. Cemento*, **7**, 669 (1966).

[2] V. B. Ratinov, T. I. Rosenberg and A. I. Smirnova, Colocviu RILEM, Gosstroizdat, Moskva. Aug. 1964, p. 107.

[3] G. L. Kalousek, C. Junsper and J. Tregoning, *J. Res. Nat. Bur. Stand.*, **30**, 215 (1943).

[4] N. G. Kurczyk and H. E. Schwiete, *Tonind, Zeitung*, **84** (24), 585 (1960).

[5] O. Kallauner and M. Matousek, *Silikatechnik*, **9**, 401 (1961).

[6] E. P. Andreeva and E. E. Segalova, *Doklady Akad. Nauk S.S.S.R.*, **158** (6), 1352 (1964).

[7] E. P. Andreeva and E. E. Segalova, *Kolloid. Zhur.*, (**4**), 22 (1960).

[8] N. N. Serb-Serbina and Iu. A. Savina, *Tsement*, (**1**), 3 (1955).

[9] V. E. Leirich and V. I. Vepric, "Novoe v khimii i tekhnologhii tsementa", Gosstroizdat, Moskva, 1962, p. 280.

[10] H. Gronow, *Zement Kalk Gips*, (**2**), 113 (1949).

[11] E. Candlot, *Ind. Belge*, **13**, 182 (1866), in [1].

[12] A. M. Rosenberg, *J. Amer. Concr. Inst.*, **10**, 1261 (1964).

[13] L. E. Copeland and D. L. Kantro, in "The Chemistry of Cements", H. W. Taylor, Vol. I, chap. 8, Academic Press, London — New York, 1964, p. 314.

[14] G. L. Kalousek, *Mat. Res. Stand.* (*Philadelphia*), **5** (6), 292 (1965).

[15] P. P. Budnikov, L. A. Kroichuk and B. N. Vinogradov, *Doklady Acad. Nauk S.S.SR.*, **173** (3), 630 (1967).

[16] H. Manche, *Rev. Mat. Constr.*, **541**, 277 (1960).

of calcium chloride. Pure tricalcium silicate, synthesized at 1550° (constant temperature for a period of 4—5 h, for 6 cycles) was used.[17]

The electrolytes were added in 0.5 , 2 and 5 % proportions referred to dry tricalcium silicate. The water-solid ratio (w/s) was 0.5.

At one, seven and 28 days, the content of the water bound as hydrated formation (denoted in what follows as bound water-A_1) was ascertained and roentgenographic, thermodifferential and thermogravimetric analyses were made, with a view to obtaining information regarding the nature of the processes, the compounds which have been formed and the phase changes taking place in the system.

The bound water content was determined using Butt's method.[17] The results are shown in table 1.

Table 1

The bound water content for $3CaO.SiO_2$ hydrated in the presence of electrolytes

Electrolyte	% Electrolytes	Bound water %		
		1 day	7 days	28 days
Without	—	12.40	11.98	18.02
Lithium chloride (LiCl)	0.5	17.80	18.89	19.74
	2.0	19.60	20.40	21.02
	5.0	22.00	19.21	22.17
Sodium chloride (NaCl)	0.5	15.80	17.89	19.45
	2.0	16.05	20.80	21.10
	5.0	17.90	19.50	21.31
Potassium chloride (KCl)	0.5	17.89	19.10	20.02
	2.0	16.50	19.25	21.60
	5.0	16.70	20.12	20.16
Calcium chloride ($CaCl_2$)	0.5	16.30	17.55	19.25
	2.0	19.80	20.01	22.11
	5.0	20.30	21.98	21.35

As can be seen in all cases, the presence of alkaline chlorides determines an increase in the bound water content. This increase is, as a rule, more important for the 2 % added chlorides, in comparison with the 0.5 % ones. Higher proportions, up to 5 %, do not determine, for all cases, an increase in the bound water content ; even for higher values of A_1, the increase in bound water content was not so important as compared with the pastes with 2 % chlorides, especially for the longer hardening periods used in this experiment.

As the hydration process is advancing the existence of a diminution in the bound water content calls attention. This is clearly observed for the pastes without electrolyte, as well as for some pastes with 5 % electrolyte (LiCl or $CaCl_2$). This behaviour could be explained by the composition and structure transformations of calcium hydrosilicates appearing in the system.

---

[17] IU. M. BUTT, „Praktikum po tekhnologhii viajushchih veshchestv", Gosstroizdat, Moskva, 1953.

Kantro *et al.*,[18] after an elaborate study of the tricalcium silicate and β-dicalcium silicate hydration, gave the following description of the process : in the first step at the surface of the tricalcium silicate grains an intermediate hydrosilicate is formed, with a high CaO/SiO_2 ratio, similar with that of the unhydrated support ; in the second step this product decomposes, with the liberation of calcium hydroxide, in low-lime hydrosilicates ; in the third step, the formed calcium hydrosilicate is transformed into a stable one, richer in calcium oxide, as a result of its interaction with $Ca(OH)_2$ from the solution. Yong [19] presented a similar mechanism. Taking into consideration such a picture of the mechanism the fact should be underlined that the last two steps are essential for the process development. Andreeva and Segalova, [6] Malinin and Lopatnikova, [20] Kawada and Nemoto, [21] some of them starting even from different hydration mechanisms, have also evidenced the transformation process of low-lime hydrosilicates into hydrosilicates with higher lime content. The above-mentioned transformations have to be looked at in connection with pressure, temperature and hydration medium conditions. It results that the nature and the proportion of ions from the liquid phase have a great influence upon the processes analysed above.

The changes taking place in the structure and the composition of the calcium hydrosilicates determine also changes in the bound water content. The variation in time of the bound water content appears thus as a result of the interaction of the binder with water, as well as of the transformation processes of hydrosilicates. When the latter processes are predominant, diminutions in bound water content might appear ; this is the case, as mentioned above, of the hydration of tricalcium silicate without and with 5 % LiCl or $CaCl_2$. Such discontinuities in the H_2O/SiO_2 ratio trend, specific of hydrosilicates obtained at $3CaO . SiO_2$ hydration, were also observed by Yong. [19]

The information given by X-ray diffraction and thermodifferential analyses support also the explanations given for the results regarding the bound water content.

In figs. 1–9 the thermodifferential curves for the hardened pastes with and without electrolytes after 1, 7 and 28 days are shown. Three classes of thermal effects corresponding to the removal of water from silica and calcium hydrosilicates gels (temperature range 120–165°), the dehydration of the calcium hydroxide resulting from the tricalcium silicate hydrolysis (temperature range 505–540°) and the complete dehydration of calcium hydrosilicates and their lattice transformations (at higher temperatures) are evidenced in all cases. *

---

* The latter thermal effects reflect best the chemical and morphological modifications of the hydrosilicates formed in the first stage of the hydration process.

[18] D. L. KANTRO, S. BRUNAUER and C. H. WEISE, *J. Phys. Chem.*, **66**, 1804 (1962).

[19] J. G. M. YONG, *J. Appl. Chem.*, **17** (9), 246 (1967).

[20] IU S. MALININ and L. IA LOPATNIKOVA, Colocviu RILEM, Gosstroizdat, Moskva, August 1964, p. 82.

[21]. N. KAWADA and A. NEMOTO, *Zement Kalk Gips*, **20**, 65 (1967).

Electrolyte admixtures determine the increase of the hydrosilicates quantities appearing in the system, as a result of the increase of the tricalcium silicate hydration rate; calcium chloride has a more important influence.

The hydrosilicates appeared in the first stage of the hydration process have a gelic character; in time, as a result of the developing of the crystallization processes, they lose this character; the microcrystals of which they are formed grow, developing a resistance structure typical of the hardened binder. But, during the hardening period, due to hydration of new quantities of binder, new gelic hydrosilicates phases appear; thus one establishes ratios between the gelic phases and the crystalline ones

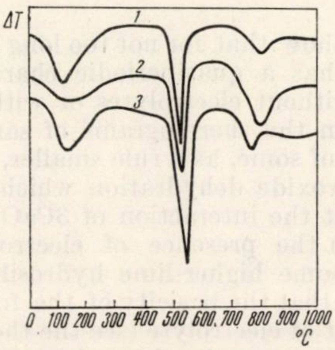

Fig. 1. — DTA for hydrated C_3S. *1* — one day; *2* — 7 days; *3* — 28 days.

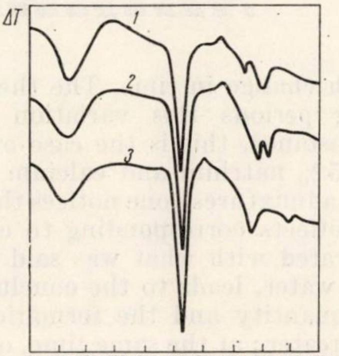

Fig. 2. — DTA for hydrated C_3S in the presence of 0.5 % $CaCl_2$. *1* — one day; *2* — 7 days; *3* — 28 days.

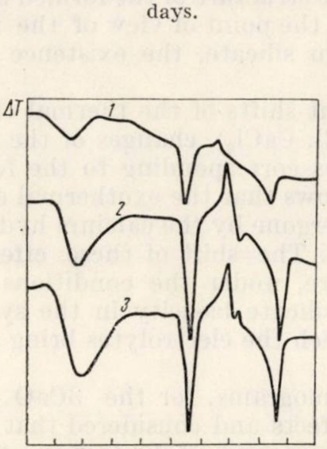

Fig. 3. — DTA for hydrated C_3S in the presence of 2 % $CaCl_2$. *1* — one day; *2* — 7 days; *3* — 28 days.

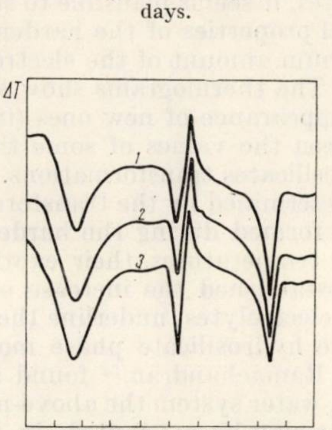

Fig. 4. — DTA for hydrated C_3S in the presence of 5 % $CaCl_2$. *1* — one day; *2* — 7 days; *3* — 28 days.

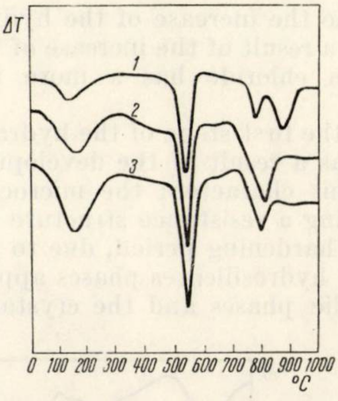

Fig. 5. — DTA for hydrated C_3S in the presence of 0.5 % NaCl. *1* — one day ; *2* — 7 days ; *3* — 28 days.

which change in time. The thermograms show that for not too long hardening periods this variation sometimes has a quasiperiodic character, for instance, this is the case of samples without electrolytes or with 2 % and 5 % natrium and calcium chloride. On the thermograms of samples with admixtures, one notices the existence of some, as a rule smaller, thermal effects corresponding to calcium hydroxide dehydration which, corroborated with what was said above about the interaction of $3CaO.SiO_2$ with water, leads to the conclusion that in the presence of electrolytes, the quantity and the formation rate of some higher-lime hydrosilicates are greater ; at the same time, one observes that the basicity of the formed hydrosilicates grows with the added amount of electrolyte (see the thermograms with calcium chloride). Taking into account the dependence on the CaO/SiO_2 ratio of the structure of the hydrosilicates, as well as the dependence of the hardened paste resistance on the structure of the formed hydrosilicates, it seems plausible to suppose, from the point of view of the mechanical properties of the hardened tricalcium silicate, the existence of an optimum amount of the electrolyte.

The thermograms show also important shifts of the thermal effects, the appearance of new ones (in case of LiCl, $CaCl_2$), changes of the ratios between the values of some thermal effects corresponding to the formed hydrosilicates transformations. This fact shows that the exothermal effects are determined by the transformations undergone by the calcium hydrosilicates formed during the hardening process. The shift of these effects to lower temperatures, their exothermic nature, under the conditions when one established the increase of the hydrosilicate basicity in the systems with electrolytes, underline the changes which the electrolytes bring about in the hydrosilicate phase morphology.

Ramachandran [22] found also on thermograms, for the $3CaO.SiO_2.CaCl_2$-water system the above-mentioned effects and considered that these effects may be attributed, in the induction period of hydration, to the formation of a complex adsorbed on the binder surface, as well as to a chemosorption of $CaCl_2$ on the hydrosilicate surface or between the layers of the hydrocompound lattice.

---

[22] V. S. Ramachandran, RILEM *Mat. Constr. Materials Struct.*, **4** (19), 3 (1971).

Without completely denying the picture presented by Ramachandran,[22] taking into account the structure peculiarities of the calcium hydrosilicates and the fact that $CaCl_2$ is a strong electrolyte it seems more probable to consider the adsorption or the inclusion of the Cl^- anion in the lattice in this latter case as a result of a partial substitution of the OH^- anion.

In the case when other chlorides are used, the nature of the cation with which Cl^- anion is bound seems to be important for the above phenomenon. From the point of view of the nature of the cation, it is to be expected that the lower the basicity of the cations, of the same group in the periodical system, the more intense the above phenomenon. The experimen-

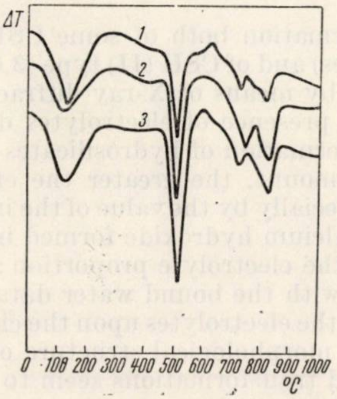

Fig. 6. — DTA for hydrated C_3S in the presence of 2 % NaCl. *1* — one day ; *2* — 7 days ; *3* — 28 days.

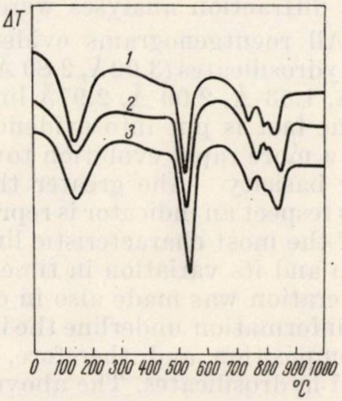

Fig. 7. — DTA for hydrated C_3S in the presence of 5 % NaCl. *1* — one day *2* — 7 days ; *3* — 28 days.

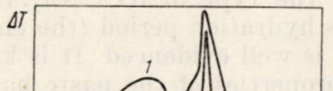

Fig. 8. — DTA for hydrated C_3S in the presence of 2 % LiCl. *1* — one day ; *2* — 7 days ; *3* — 28 days.

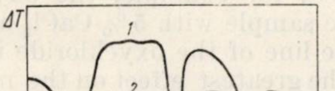

Fig. 9. — DTA for hydrated C_3S in the presence of 2 % KCl. *1* — one day ; *2* — 7 days ; *3* — 28 days.

tal data confirm this conclusion, for example in the Li—Na—K series the phenomenon is more intense for LiCl.*

The cations introduced into the system by the electrolytes may be adsorbed by the hydrosilicate complex. An exchange adsorption is possible, when Ca^{2+} ions may be replaced by more electropositive cations. In this way one should observe the relative electronegativity of the cations of the electrolytes

Cation :	Ca^{2+}	Li^+	Na^+	K^+
Electronegativity :	1.0	1.0	0.9	0.8

With a view to clarifying the nature and especially the evolution of the constituents appearing during the tricalcium silicate hydration, X-ray diffraction analyses were made.

All roentgenograms evidence the formation both of some CSH (I) type hydrosilicates (3.02Å, 2.80 Å, 1.82Å lines) and of CSH (II) type (3.07 Å, 2.80 Å, 1.83 Å, 2.00 Å, 2.97Å lines). Thus, by means of X-ray diffraction, too, the fact is put into evidence that the presence of electrolytes determines a more rapid evolution towards the formation of hydrosilicates with higher basicity — the greater the added amount, the greater the effect. In this respect an indicator is represented especially by the value of the intensity of the most characteristic line of the calcium hydroxide formed in the system and its variation in time and with the electrolyte proportion; this consideration was made also in correlation with the bound water data. All these information underline the influence of the electrolytes upon the chemical composition and therefore, upon the morphological structure of the formed hydrosilicates. The above-mentioned transformations seem to take place especially for relatively short hardening periods.

The formation of some compounds as a result of the interaction of the binder or of its hydration products with the electrolytes was observed only for longer hardening periods and especially for large amounts of electrolytes; for example, the oxychloride of the type $3CaO.CaCl_2.12H_2O$ for the sample with 5 % $CaCl_2$ after 28 days hydration period (the characteristic line of the oxychloride is 3.28 Å [23]) is well evidenced. It is known that the greatest effect on the mechanical properties of the paste hardened in presence of calcium chloride is obtained for an admixture of 2 %. Due to the fact that for this amount of chloride the formation of some chloride compounds is at least improbable, it results that the influence of this type of compounds upon the mechanical properties is of small importance and therefore it may be concluded from the above results that the main influence of the calcium chloride and of other electrolytes is of "physical" nature. This influence, due especially to the alteration of the ionic equilibrium of the system, determines changes of the hydration rate of the binder and modifications of the chemical and morphological structure of the hydrated formations.

The X-ray diffraction analysis has shown that the exothermal effects (620 — 650°) for samples with LiCl and $CaCl_2$ are due to the formation of

---

* Later works have led to the same conclusion for the Ca — Sr — Ba series, too.

[23] E. P. Andreeva and J. G. Malikova, "Fiziko-mehanika dispersnih structur", Izd. Nauka, Moskva, 1966.

$\beta - 2CaO \cdot SiO_2$. There is no evidence of any reaction between the electrolytes and the existing compounds in the system (during the thermal treatment at the above exothermal effect temperatures). Therefore, it is difficult to explain the nature of the LiCl and $CaCl_2$ influence which determines these exothermal effects. Probably this fact is, in the first place, a result of the chemical and morphological changes brought about by the electrolytes and which need further studies. A partial inclusion of the Cl^- ion in the calcium hydrosilicate network is also possible. [22]

3. From this paper we may conclude that :

— the electrolytes in amounts used in the present experiments accelerate the hydration processes ;

— the electrolytes determine the formation of some hydrosilicates with high basicity, their proportion in the hardened binder growing with the amount of the electrolyte added :

— products of interaction between the electrolytes and the system constituents appear only for large amounts of electrolytes and for longer hardening periods ($3CaO \cdot CaCl_2 \cdot 12H_2O$ for the sample with 5 % $CaCl_2$, after 28 days) ;

— the main influence of the electrolytes upon the hydration is of "physical" nature ; due to the changes in the ionic equilibrium of the system, modifications appear in the kinetics of the hydration and crystallization processes and in the chemical and morphological structure of hydrosilicates ; the existence of a certain optimum amount of the admixture results. The nature and the intensity of the effect of the admixtures upon the hardening of the calcium silicate depend on the chemical nature of the electrolytes.

Revue Roumaine de Chimie, **19**, *3*, 381–385 (1974)

ASPECTS OF THE VITREOUS PHASE SEPARATION PROCESS IN THE $Fe_2O_3-BaO-B_2O_3$ SYSTEM

ŞERBAN SOLACOLU and ECATERINA RUSU

Polytechnic Institute of Bucharest, Laboratory for Physical Chemistry of the Solid State,
Str. Polizu 1, Romania

Received June 11, 1973

The paper presents aspects of the development of the vitreous phase separation process in the $Fe_2O_3-BaO-B_2O_3$ system ; it investigates the influence of an isochronous treatment on the size of the separated particles and also on their concentration. The volume fraction of the phase with a Fe_2O_3 content is calculated for the glass having 20 % Fe_2O_3.

The separation of the vitreous phase caused by the immiscibility of two liquids occurs in most glass-forming systems. The resulting structure depends on the location of the particular composition within the limits of the immiscibility region as well as on the thermal history of the glass.

In the metastable area, decomposition takes place by nucleation and is characterized by the existence of particles from a random dispersed phase in the other phase which has the form of a continuous matrix. In the unstable area, the two phases are independently interconnected, having diffuse and irregular boundaries.

The mechanism and the kinetics of the phase separation phenomenon basically depends on a number of factors such as : the form of the gap, the cooling rate, the diffusion rate and others. The examination of these problems has both a theoretical and a practical importance in that they relate to the occurrence of some uniformly crystallized vitroceramic products.

In recent years, the advances made in various technologies involving ferromagnets and semiconductors arouse the interest in the crystallization of glasses rich in transitional metal oxides.

In this sense the masses in the $Fe_2O_3-BaO-B_2O_3$ system investigated by us have drawn attention due to their magnetic properties. [1,2] The investigations performed in the present paper deal with the liquid — liquid separations in the $Fe_2O_3 - BaO - B_2O_3$ system, a problem which has been only tangentially handled until now and only in the case of a single composition. [3]

---

[1] E. Rusu, *Ind. Uşoară*, **15**, 28 (1968).

[2] E. Rusu, *Ind. Uşoară*, **16**, 605 (1969).

[3] B. T. Shirk and W. R. Buessem, *J. Amer. Ceram. Soc.*, **53**, 192 (1970).

Although the specialty literature provides no data on thermal equilibria in this ternary system, a general consideration of the three component binary systems provides initial data concerning a clear tendency of meltings towards immiscibility. In addition, in agreement with the theory which considers the existing correlation between the immiscibility of meltings and the ionic potential (Z/r) of metal cations [4] in the case of systems containing cations $Z/r > 3$ (as in the case of iron with $Z/r = 4.5$), an intense immiscibility region is expected to exist, causing at least two distinct phases, one of which has the composition Me_xO_y.

EXPERIMENTAL METHODS

Two glass compositions were investigated : 30 % BaO ; 10 % Fe_2O_3 ; 60 % B_2O_3, and 30 %BaO ; 20% Fe_2O_3 ; 50 % B_2O_3 (% molar) termed as glass 1 and 2, respectively. The materials used and the operating procedure were described in a previous paper. [1] A preliminary assessment of the thermal treatment of phase separation was made by means of a high sensitivity differential thermal analysis.

The development of the phase separation process was observed under an electronic microscope at a 100 KV working voltage through the method of carbon and platinum replicas. Some reference samples were achieved by transparency using the chemical corrosion procedure. [5] An electronic diffraction was performed to make sure that the separated phases were vitreous and not crystalline.

The volume fraction of the separated phase was determined by direct measurement of the surfaces, considering larger areas than those presented in microphotographs.

In view of calculating the volume fraction it was assumed that the maximum thickness which may occur in the case of the replica (δ_{max}) is equal to the mean diameter (d_m) of the spheres in the dispersed phase. [6] In the case of the glasses studied preliminary experiments established that a reasonable magnification for the quantitative study is 25 000 times.

EXPERIMENTAL DATA AND DISCUSSION OF RESULTS

In accordance with the considerations postulated by Nayagawa and Izumitani [7] in the case of a third component addition to a binary system, the immiscibility region of the system increases when the difference between the immiscibility tendency between the third component (C) and the other two (A and B), in turn, is greater than the immiscibility tendency of the initial system A–B, that is, in the case in which.

$$\alpha_{AB} < |\alpha_{AC} - \alpha_{BC}|,$$

---

[4] D. BURNETT, D. CLINTON and R. P. MILLER, *J. Mat. Sci.*, **3**, 47 (1968).

[5] P. F. JAMES and P. W. MCMILLAN, *Phys. and Chem. Glasses*, **11**, 59 (1970).

[6] J. MORIJA, D. H. WARRINGTON and R. W. DOUGLAS, *Phys. and Chem. Glasses*, **8**, 14 (1967).

[7] K. NAYAGAWA and Z. IZUMITANI, *Phys. and Chem. Glasses*, **13**, 85 (1972).

where α is a factor which primarily takes into account the ionic field strength.

By applying the rule cited in the case of the $Fe_2O_3-BaO-B_2O_3$ system and coding $A = B_2O_3$; $B = BaO$ and $C = Fe_2O_3$ it results :

$$\alpha_{B_2O_3-BaO} < |\alpha_{Fe_2O_3-B_2O_3} - \alpha_{Fe_2O_3-BaO}|$$

Consequently the immiscibility volume is expected to increase in the system studied.

Indeed, all the compositions comprised in the glass formation area show a pronounced tendency towards immiscibility.[8]

The thermograms performed for the two compositions studied in the present paper reflect the existence of an additional inflection besides the normal endothermic effect due to the transformation interval (fig. 1).

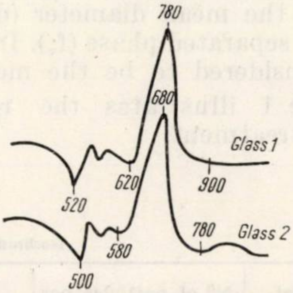

Fig. 1. – Thermograms of the studied glasses.

Since point Tg corresponds to the lower viscosity phase the inflection temperature refers to the conversion temperature of the other, the higher viscosity phase.[9] The great distance between the two conversion temperatures indicates the significant difference between the viscosities of the two phases. Figure 2 illustrates the general aspect of phase separations in glasses 1 and 2. The different morphology of the two compositions can be readily observed.

The glass containing 10 % Fe_2O_3 forms a specific interconnected structure which is maintained within the range of the studied temperatures, whereas the other composition, higher in Fe_2O_3, presents some more or less spherical distinct separations surrounded by the continuous matrix from the other phase. The dark spheres in fig. 3 present droplets from the separated phase which adhered to the replica during the detachment. This phase is more resistant to the HF action than the matrix, however it was easily attacked by HCl and this made us assume that even in this vitreous form, its composition is close to the subsequently separated magnetite which, in fact, confers to the material its magnetic properties.[10]

---

[8] E. Rusu, Teză de doctorat IPB, 1971.

[9] L. Prod'homme, *Verres Réfract.*, **25**, 71 (1971).

[10] C. De Sebata, A. Poličec and E. Rusu, *Silic. Ind.*, **37**, 139 (1972).

Appropriate measurements were made on the samples subjected to a thermal treatment at temperatures ranging between Tg_1 and Tg_2.

Figure 4 shows the curve reflecting the increase in the sizes of the separated phase relative to temperature with various thermal treatment periods. The curve is not drawn through the origin since the original glasses themselves present phase separations reaching hundreds of Angstroms. [11]

The diagram of the three processes occurring in the glass during the thermal treatment is drawn in figure 5. The optimum area of thermal treatment for the nucleation process is observed.

The dependence of the liquid phase distribution on the temperature of the thermal treatment is better seen in the value of the volume fraction of the dispersed phase. By dividing the number of particles from a selected surface by the product between this surface and the mean diameter of the particles, one obtains the concentration of the separated phase expressed by the number of particles per volume unit (N). Knowing the N value and the mean diameter (d_m) one may calculate the volume fraction of the separated phase (f_v). In the case of elliptical particles, the small axis is considered to be the mean diameter.

Table 1 illustrates the results obtained in the case of an isochronous treatment.

Table 1

Isochronous treatment data

Thermal treatment (1 hour) T(°C)	N° of particles per surface unit Xn (N°/cm²)	Mean diameter $d_m(A)$	N° of particles per volume unit N (N°/cm³)	Volume fraction f_v
initial	218×10^8	400	54×10^{14}	1.80×10^{-1}
400	118×10^8	500	24×10^{14}	1.55×10^{-1}
450	50×10^8	800	6.26×10^{14}	1.47×10^{-1}
500	11×10^8	1600	0.7×10^{14}	1.41×10^{-1}
550	4.4×10^8	2400	0.18×10^{14}	1.35×10^{-1}

An initial high concentration of the separated phase is observed which decreases as the temperature of the thermal treatment increases (fig. 4, curve *2*) and the mean diameter of the separated particles increases (fig. 4, curve *1*).

This change causes the decrease of the volume fraction particularly at the beginning of the thermal treatment, after which its value becomes almost constant.

CONCLUSIONS

The two compositions studied present a pronounced difference in the separation morphology, which is explained by the position of the two glasses

---

[11] Ş. Solacolu and E. Rusu, *Rev. Roumaine Chim.*, **16**, 265 (1971).

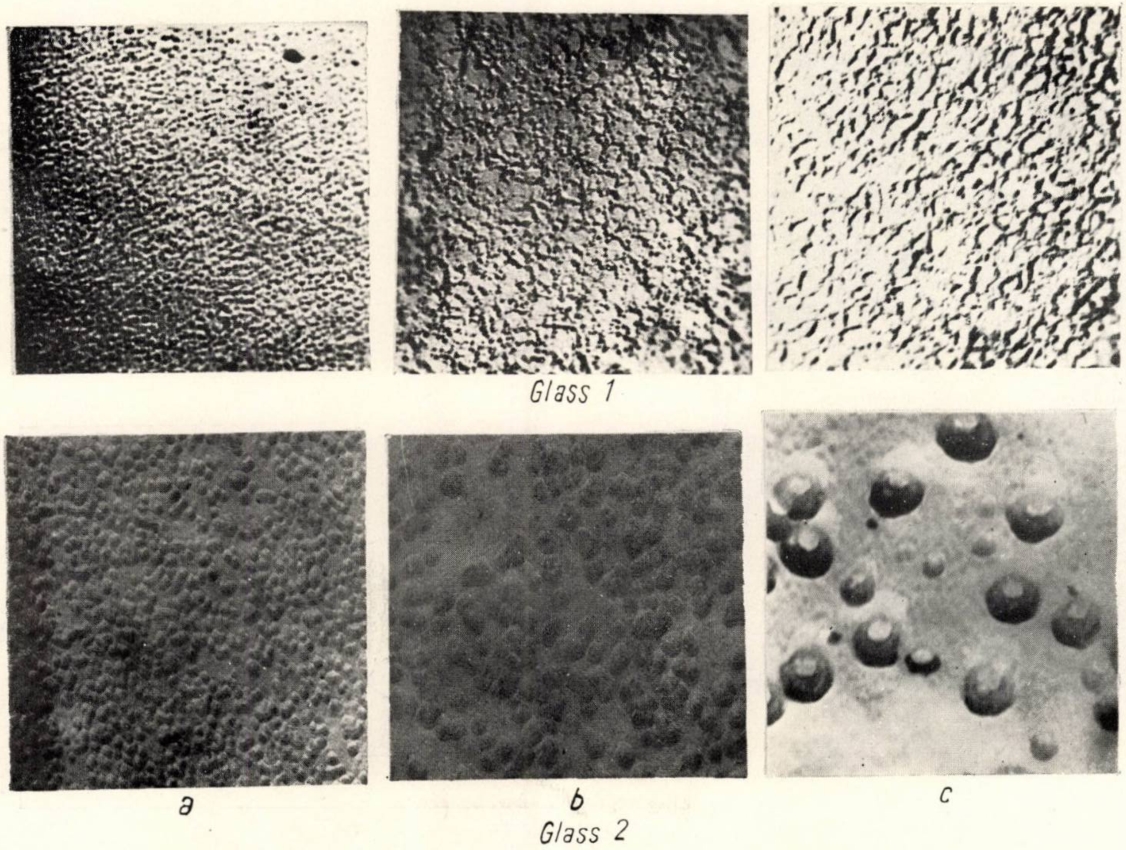

Fig. 2.—Influence of the isochronous thermal treatment on the vitreous phase separation aspect (× 25,000) : *a*, the intial glass ; *b*, the glass treated at 450°/h ; *c*, the glass treated at 550°/h.

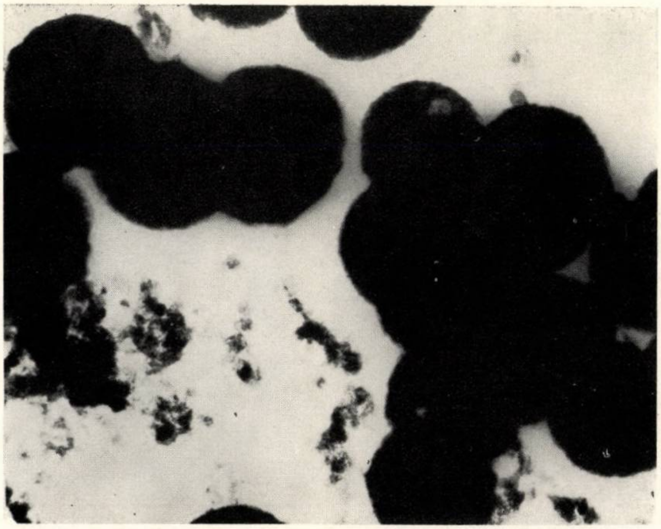

Fig. 3. — Microphotograph of glass 2 (× 50,000).

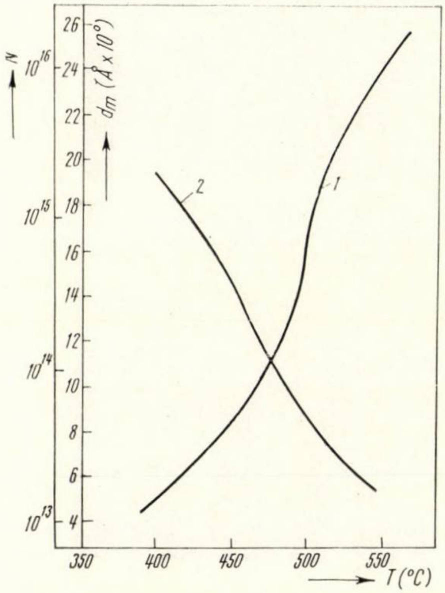

Fig. 4. — Variation in the size and concentration of particles depending on the temperature of the thermal treatment.

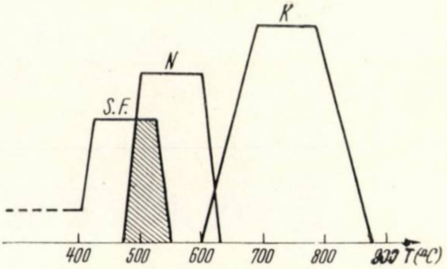
K
N
S.F.
400
500
600
700
800
900
T (°C)

Fig. 5. — Diagram of processes occurring in the glass subjected to a thermal treatment.

within the immiscibility region, in accordance with a varied Fe_2O_3 content.

It has been observed a decrease in the concentration of the separated phase with the increase of the size of the separated phase particles depending on the temperature of the thermal treatment, so that the volume fraction remains practically constant within the measurement errors which may be estimated to maximum 10%.

By making a contribution to the study of phase separations the present paper provides the possibility of controlling the glass crystallization process in the BaO $-$ Fe_2O_3 $-$ B_2O_3 system.

Revue Roumaine de Chimie, **19**, *3*, 387–394 (1974)

NEW COORDINATE COMPOUNDS WITH MOLECULAR NITROGEN. I

SYNTHESIS AND CHARACTERISTIC PROPERTIES OF SOME DINITROGEN COMPOUNDS OF COBALT, NICKEL, IRON WITH TRIARYL-PHOSPHINES, TRIARYL-ARSINES AND TRIARYL-STIBINES

D. NEGOIU *, CONSTANŢA PÂRLOG ** and D. SĂNDULESCU ***

* University of Bucharest, Faculty of Chemistry, 89, Spl. Independenţei, Bucharest
** Center of Physical Chemistry, 31, Str. Galaţi, Bucharest
*** Institute of Petroleum, Gases and Geology, 2–6, Str. Traian Vuia, Bucharest

Received July 2, 1973

A number of 16 dinitrogen compounds of cobalt, nickel and iron with triaryl-phosphines, triaryl-arsines and triaryl-stibines were synthesized. UV, visible and IR spectrophotometric studies were performed and thermal stability determinations were made. The approximate calculations of the dissociation enthalpy provided values comprised between 8,000 and 12,000 (± 1000) cal/moles.

The early attempts at fixing the molecular nitrogen in coordinate compounds of ruthenium [1] were followed by the synthesis of a large number of compounds of this type with other metals. [2] Both synthesis in itself and the physico-chemical properties of the compounds in question constitute one the most important problems of modern inorganic chemistry, from a theoretical, chemical and biochemical aspect as well as from the standpoint of possible technological applications. These dinitrogen compounds correspond to the intermediates from the reactions of chemical and biochemical "fixation" of the atmospheric nitrogen. Indeed, nitrogen, as well as other elements such as H_2 and O_2 (X_2), may intervene in coordination reactions of the type:

$$ML_n + X_2 \rightleftharpoons ML_n(X_2)$$

in which the metal is found in a reduced oxidation state; the ML_n compound must correspond to an intense nucleophilic reactivity (supernucleophilic compounds) with an important localization of the negative charge on the metallic atom, the ligands must be "soft" (tertiary phosphines, CN, molecules with π electrons delocalized like Schiff bases). In general, the coordinate compound which fixes the nitrogen must be either neutral or under an anionic form so as to ensure an intensification of the nucleophilic character.

---

[1] A. D. Allen and C. V. Senoff, *Chem. Comm.*, **1965**, 621.

[2] C. Pârlog, D. Negoiu, A. Alistar and D. Săndulescu, *Studii şi Cercetări Chimie Acad.*, (under press).

The binding manner of nitrogen in this type of compound is particularly interesting; there is a strong probability that this metal nitrogen molecule bond corresponds to the $\sigma - \pi$ type. The analogy between the compounds of a metal-carbonyl type may be considered, for instance, $Cr(CO)_6$ and the hypothetical compound $Cr(N_2)_6$, since in the case of common compounds with molecular nitrogen, the ligands (L) have a complicated structure and the molecule has a reduced symmetry.

In this case, calculations show that the π bond in the metal-carbonyl compounds is weakened to a higher extent than in the case of the metal-nitrogen, whereas the metal-carbonyl bond is strengthened, since an important fraction of the electronic density is displaced from the 5σ orbitals which acquire thus a significant character of an antibonding orbital. As these effects must be influenced by the nature of the ligands L, different from nitrogen and from the spectral characteristics and the nitrogen-metal binding energy, we undertook to synthesize a series of compounds involving various metals with molecular nitrogen with a series of ligands gradually modifiying certain structural elements in order to establish whether the introduced effects for the differentiation of ligands, respectively of the coordinate compound generating metal may be revealed and may enable a correlation with the structure of the introduced ligands.

The ligands which we used in the coordinate compounds with molecular nitrogen correspond to tertiary phosphines, to arsines, stibines and tertiary bismuthines for the metals Co, Ni, Fe ; these compounds obviously correspond to the "soft" ligand condition and provide comparative data in the series of prepared nitrogen compounds.

The stability of nitrogen compounds must be determined in the first place by the π acceptor or the σ donor character of the ligand.

Therefore the following determinations were performed : thermal stability determinations, IR absorption spectra determinations, stability thermodynamic magnitudes determinations, as well as V and UV reflectance spectra and magnetic susceptibility determinations. [3]

The syntheses took place in a pure nitrogen atmosphere which ensures an inert atmosphere and intervenes in the coordination reaction simultaneously with the reduction of the metals valence to zero. Triethylaluminium, triisobutylaluminium, aluminium ethylate, sodium borohydride hydrogen, lithium aluminhydride, sodium dispersed in toluene * were tested as reducing agents ; the most widely used reducing agents in the above-mentioned syntheses were the organo-magnesium compounds, namely *n*-butylmagnesium bromide, which offered different advantages compared to the other indicated reducing agents.

---

[3] C. PÂRLOG, Teză de doctorat, Universitatea București, 1974.

* Supplied by Mrs. C. Huch, of the Center of Organic Chemistry, whom the authors thank again hereby.

Thus, the scheme of the synthesis reaction corresponds to:

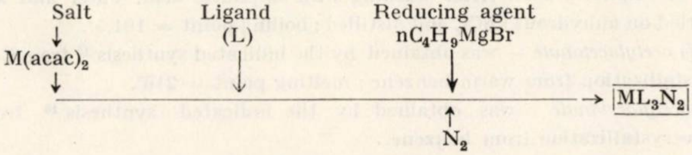

EXPERIMENTAL SECTION

The ligands were synthesized in the laboratory in agreement with indications from the literature, by means of adapted methods.[3]

Triphenlyphosphine $P\Phi_3$ — was synthesized by a known method[4] by means of the organomagnesium compound C_6H_5MgBr (prepared from $C_6H_5Br + Mg$) and of the phosphorus trichloride with yields higher than 70 %; melting point = 79.5° and the IR absorption spectrum according to data from the literature, after recrystallizing twice from absolute ethyl alcohol.

Triphenylarsine $As\Phi_3$ — was synthesized in an analogous reaction to that mentioned in the case of $P\Phi_3$ [5−7] with a 75—80 % yield, melting point = 60.5°, after recrystallization from absolute ethyl alcohol.

Triphenylbismuthine $Bi\Phi_3$ — was synthesized in an analogous reaction to the previous ones[8]; melting point = 76° and yield 35 %, after recrystallization from absolute ethyl alcohol.

*Tri-*p*-tolylphosphine* — was synthesized by an analogous method[9,10] starting from *p*-bromtoluene by means of organo-magnesium compounds; yield 60 % and melting point = 146° after recrystallization from absolute ethyl alcohol.

Tribenzylphosphine — was obtained by means of benzyl bromide which changes, with magnesium, iodine (initiator) in ethyl ether + tetrahydrofurane, in a hydrogen atmosphere, into benzylmagnesium bromide. The latter changes into raw phosphine, with phosphorus trichloride. After washing and removing the solvent, it is distilled (boiling point = 290 — 300°) and recrystallized from alcohol and ethyl ether[11]; melting point = 176°, yield = 55 %.

*Tri-*p*-xylyl phosphine* — follows the reaction scheme previously indicated, using *p*-bromxylene by means of the organo-magnesium compound, in absolute ethyl ether. Phosphine is obtained after it has been recrystallized twice from absolute ethyl alcohol, with a melting point = 155° and yield 65 %.[12]

α-Trinaphthylphosphine — is obtained by an analogous synthesis to bromnaphthaline. After recrystallization from absolute ethyl alcohol pure phosphine is obtained with the melting point = 196° and yield 45 %.[13]

α-Trinaphthylarsine — is obtained in an analogous manner from α-bromnaphthaline with magnesium and arsene chloride. After recrystallizing twice from absolute ethyl alcohol, melting point = 252°.[14]

---

[4] J. Dodonow and H. Medox, *Ber. dtsch. chem. Ges.*, **907**, 61 B (1928).
[5] W. Hamby and W. A. Waters, *J. Chem. Soc.*, **1946**, 1029.
[6] J. Michaelis. *Liebigs Ann. Chem.*, **160**, 321 (1902).
[7] J. Philips, *Ber. dtsch. chem. Ges.*, **1031**, 19 (1886).
[8] P. Pfeiffer, H. Heller and H. Pietch, *Ber. dtsch. chem. Ges.*, **4622**, 37 (1904).
[9] J. Michaelis, *Liebigs Ann. Chem.*, **315**, 79 (1901).
[10] F. G. Mann and E. J. Chaplin, *J. Chem. Soc.*, **1937**, 530.
[11] P. Pfeiffer, H. Heller and H. Pietch, *Ber. dtsch. chem. Ges.*, **37**, 4321 (1904).
[12] A. Schaenble, *Liebigs Ann. Chem.*, **315**, 99 (1901).
[13] J. Michaelis, *Liebigs Ann. Chem.*, **170**, 321 (1902).
[14] H. Büschler, *Liebigs Ann. Chem.*, **321**, 242 (1902).

n-*butyl bromide* — was obtained by the reaction between bromide and butyl alcohol in the presence of sulphuric acid. After washing with sulphuric acid, water and an alkaline solution, it is dried on anhydrous $CaCl_2$ and distilled ; boiling point = 101.5°.

Co(III) acetylacetonate — was obtained by the indicated synthesis [15] from $CoCO_3$ and purified by recrystallization from warm benzene ; melting point = 216°.

Co(II)acetylacetonate — was obtained by the indicated synthesis [16] from $CoCl_2$ *p.a.* (Merck) by recrystallization from benzene.

Ni(II)acetylacetonate — was synthesized from $Ni(NO_3)_2$ (0.12 mole) and acetylacetone (0.2 mole). After recrystallization from warm benzene, it is obtained in a pure state with a yield of 87%. [17]

The solvents — absolute ethyl ether, ethyl alcohol, tetrahydrofurane, benzene, toluene p.a. — were rendered anhydrous after the usual purifications and freshly distilled from sodium directly in the reaction vessel or in a burette directly linked to the reaction vessel through which pure nitrogen is passed.

THE INSTALLATION FOR NITROGEN PURIFICATION

Nitrogen purification was achieved by passing a nitrogen current through the solution of copper chloride I :

— absorption tube with a Deoxo BDS catalyst at 120—160° ;

— silicagel tube ;

— 4Å molecular sieves tube ;

— drying tube with P_4O_{10} ;

— diethylchloraluminium solution in benzene (5%).

Data pertaining to construction have been indicated. [3]

The obtained nitrogen contains under 0.5 ppm O_2 and 1—2 ppm H_2O. [18—20] The installation for the synthesis of compounds is well suited for handling the reactants and the initial solutions in an inert atmosphere, and for the filtering, washing and drying of the resulted precipitates.

Thermal decomposition. Samples from the synthesized nitrogen compounds were subjected to a thermal decomposition in a closed tube attached to a manometer. After degassing at 0.1 mm Hg during which the sample is frozen in liquid nitrogen, it is introduced into a thermostat and the temperature is gradually increased, reading the pressure when equilibrium has been reached (± 0.1° ; ± 0.2 mm Hg).

The resulting gas was analysed by gas chromatography on a C. Erba GV 207 device equipped with a 5 Å molecular sieve column long of 2 m, with a 4 mm inner diameter, at room temperature. The carrier gas : hydrogen, nitrogen, argon. The nitrogen determination was directly made in a V. Mayer apparatus and in a nitrometer. The presence of hydrogen was not identified.

IR absorption spectra were obtained in nujol or in tetrahydrofurane on a Zeiss UR 10 spectrophotometer.

---

[15] B. BRYANT and W. FERNELIUS, "Inorganic synthesis", vol. 1, Ed. Therald Moeller, McGraw Hall Book Company Inc., New York, 1957, p. 188.

[16] G. J. BULLEN, R. MASOU and P. PAULING, *Inorg. Chem.*, **4**, 456 (1965).

[17] L. G. UITERT, W. C. FERNELIUS and B. E. DOUGLAS, *J. Amer. Chem. Soc.*, **75**, 2739 (1953).

[18] O. PETE and D. SĂNDULESCU, *Rev. Roumaine Chim.*, **12**, 759 (1964).

[19] A. HANEŞ, D. SĂNDULESCU and C. LUPU, *Rev. Roumaine Chim.*, **1**, 412 (1961).

[20] O. PETE, P. ZUGRĂVESCU, A. POPOVICI and D. SĂNDULESCU, "Comunicările ICECHIM", vol. IV, 1965.

THE NITROGEN TRIS-TRIPHENYLPHOSPHINE COBALT SYNTHESIS

$Co[P(C_6H_5)_3]_3N_2$ (I)

2.6 g (0.01 mole) Co(II) acetylacetonate and 7.8 g (0.03 mole) triphenylphosphine are dissolved in 200 ml absolute ethyl ether in an installation with purified nitrogen which is passed through the solution for roughly 30 minutes. 40 ml reducing reagent is added to the solution dropwise and by continuous stirring (0.04 mole *n*-butylmagnesium bromide in absolute ethyl ether) ; the solution becomes more and more red and reddish-orange crystals are being formed. The mixture is stirred for 2 hours under a nitrogen current and is kept in nitrogen at 0° for 1 hour until red crystals deposit. The solution is decanted and the crystals are allowed to dry in a nitrogen atmosphere and eventually in vacuo 5.8 g are obtained ; yield 60—70 %. Elementary analysis :

calc. Co 6.26 %, N 2.94 %, C 74.22 %, H 5.15 %
found : Co 6.21 %, N 3.1 %

THE NITROGEN TRIS(TRI-*p*-TOLYLPHOSPHINE) COBALT SYNTHESIS

$Co[P(pC_7H_7)_3]_3N_2$(II)

It is obtained starting from Co(II) acetylacetonate and tri-*p*-tolylphosphine in anhydrous ethyl ether at — 5° and reduction with a solution of *n*-butylmagnesium bromide under a pure nitrogen current. The end product is analogous to compound I. 5 g are being obtained.

The following compounds were found in an analogous manner :

— $Co[P(p\text{-}CH_3)_2(C_6H_3)_3]_3N_2$III — nitrogen tris(tri-*p*-xylylphosphine)cobalt ;
— $Co[P(C_{10}H_7)_3]_3N_2$ IV — nitrogen tris(tri-α-naphthylphosphine)cobalt ;
— $Co[P(C_6H_5 - CH_2)_3]_3N_2$ V — nitrogen tris(tribenzylphosphine) cobalt ;
— $Co[As(C_6H_5)_3]_3N_2$VI—nitrogen tris(triphenylarsine)cobalt ;
— $Co[As(C_{10}H_7)_3]_3N_2$ VII — nitrogen tris(tri-α-naphthylarsine)cobalt ;
— $Co[Sb(p\text{-}(CH_3)_2C_6H_3)_3]_2N_2$ VIII — nitrogen tris(triphenylstibine)cobalt ;
— $Ni[P(C_6H_5)_3]_2N_2$ IX — nitrogen bis(triphenylphosphine)nickel
— $Ni[P(p\text{-}CH_3 - C_6H_4)_3]_2N_2$ X — nitrogen bis(tri-*p*-tolylphosphine)nickel
— $Ni[P(p\text{-}(CH_3)_2 - C_6H_3)_3]_2N_2$ XI — nitrogen bis (tri-*p*-xylylphosphine)nickel ;
— $Ni[P(C_{10}H_7)_3]_2N_2$ XII — nitrogen bis(tri-α-naphthylphosphine)nickel ;
— $Ni[P(C_6H_5 - CH_2)_3]_2N_2$ XIII — nitrogen bis(tribenzylphosphine) nickel ;
— $Ni[As(C_6H_5)_3]_2N_2$ XIV — nitrogen bis(triphenylarsine)nickel ;
— $Ni[As(C_{10}H_7)_3]_2N_2$ XV — nitrogen bis(tri-α-naphthylarsine)nickel
— $Fe[P(C_6H_5)_3]_2N_2$ XVI — nitrogen bis(triphenylphosphine)iron.

The attempts at obtaining compounds with nitrogen and with triphenylbismuthine failed to give positive results under analogous conditions, due to the bismuth reduction to the metal.

Table 1 reveals the characteristic properties of the above-mentioned compounds : colour, approximate stability in nitrogen, solubility and position of the nitrogen molecule stretching band $\nu_{N=N}$ in the coordinate compound.

DISCUSSION OF RESULTS

The formulations suggested for the dinitrogen compounds prepared in this work are based on the elementary analysis, on the absence of some detectable amounts of hydrogen by gas chromatography of gaseous products resulted from the thermal decomposition of the synthesized compounds, on the paramagnetism determined in the case of cobalt compounds, [2] since the compound of $CoH(P\Phi_3)_3$ type is diamagnetic, [21] on the appearance of an intense IR absorption band corresponding to the stretching vibration of the nitrogen molecule as a ligand. In fact, the hydrides or the hydrogen compounds of $CoH(N_2)(P\Phi_3)_3$ and $Co(H_2)(PO_3)_2$ type, respectively, are unstable in the air compared to the dinitrogen compounds of the indicated formula, as was shown by Speier and Marko. [22]

Table 1

Characteristic properties of coordinate compounds with molecular nitrogen

Compound	Colour	Approx. nitrogen stability	Solubility	$\nu_{N=N}$ cm^{-1}
$Co[P(C_6H_5)_3]_3N_2$	orange	96	THF, ethyl ether, benzene, toluene	2100
$Co[P(p\text{-}CH_3-C_6H_4)_3]_3N_2$	orange	72	THF, toluene, benzene, ethyl ether	2100
$Co[P(p\text{-}(CH_3)_2-C_6H_3)_3]_3N_2$	orange	unstable	benzene, toluene	2098
$Co[P(C_{10}H_7)_3]_3N_2$	red	48	THF, ethyl ether	1930
$Co[P(C_6H_5-CH_2)_3]_3N_2$	red	24	THF, ethyl ether, benzene, toluene	2080
$Co[As(C_6H_5)_3]_3N_2$	red	48	THF, ethyl ether	1980
$Co[As(C_{10}H_7)_3]_3N_2$	red	24	THF, ethyl ether	1980
$Co[Sb(p\text{-}(CH_3)_2C_6H_3)_3]_3N_2$	red	24	THF, ethyl ether	1905
$Ni[P(C_6H_5)_3]_2N_2$	red	48	THF, benzene, toluene	2060
$Ni[P(p\text{-}CH_3-C_6H_4)_3]_2N_2$	red	48	THF, ethyl ether, benzene, toluene	2060
$Ni[P(p\text{-}(CH_3)_2-C_oH_3)_3]_2N_2$	red	24	THF, ethyl ether	2060
$Ni[P(C_{10}H_7)_3]_2N_2$	red	unstable	—	—
$Ni[P(C_6H_5-CH_2)_3]_2N_2$	red	24	THF, benzene, toluene	2070
$Ni[As(C_6H_5)_3]_2N_2$	red	unstable	—	—
$Ni[As(C_{10}H_7)_3]_2N_2$	red	unstable	—	—
$Fe[P(C_6H_5)_3]_2N_2$	orange	24	THF, ethyl ether	1990

The relatively high stability, particularly in pure solid state compared to other dinitrogen compounds enabled the study of the reflectance spectrum in the visible domain of the compound $Co(N_2)(PO_3)_3$ which presents a maximum in the diagram $F(R\infty)-\lambda$ at 600 nm, similar to the case of dinitrogen halides pentammine, osmium and ruthenium, recognized by their high stability [1] even in an aqueous solution, permitting to be handled in the air both for spectrophotometric and for diffractometric determinations. [2]

The stability in the air largely differs in the series of synthesized compounds, compared to the stability of osmium or ruthenium compounds and particularly in solution (ethyl ether, tetrahydrofurane). This stability is markedly reduced and for this reason it is impossible to perform the common spectroscopic study, particularly in the UV and visible domain, except for cobalt combinations.

---

[21] A. Yamamoto, L. Pu, S. Kitazuma and I. Ikada, *J. Amer. Chem. Soc.*, **89**, 3071 (1969).

[22] G. Speier and L. Marko, *Inorg. Chim. Acta*, **3**, 126 (1969).

The thermal stability determined by the manometric method enables a qualitative comparison, with the observation that the determinations were repeated as the impurities and even the solvents left in the purified substance significantly influence the decomposition. The determinations were made after repeated recrystallizations and after allowing a prolonged standing in nitrogen atmosphere.

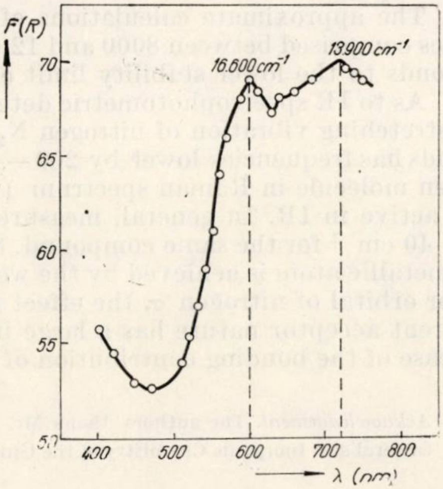

Fig. 1. — Reflexion spectra of the combination : $Co[P(C_6H_5)_3]_3N_2$.

Table 2

The temperatures of decomposition for coordination combinations with molecular nitrogen at 20 torr

Temperature °	Combination
70	$Co[P(C_6H_5)_3]_3N_2$
60	$Co[P(p\text{-}CH_3-C_6H_4)_3]_3N_2$
30	$Co[P(p\text{-}(CH_3)_2-C_6H_3)_3]_3N_2$
50	$Co[P(C_{10}H_7)_3]_3N_2$
24	$Co[P(C_6H_5-CH_2)_3]_3N_2$
40	$Co[As(C_6H_5)_3]_3N_2$
50	$Co[As(C_{10}H_7)_3]_3N_2$
32	$Co[Sb(p\text{-}(CH_3)_2C_6H_3)_3]_3N_2$
52	$Ni[P(C_6H_5)_3]_2N_2$
47	$Ni[P(p\text{-}CH_3-C_6H_4)_3]_2N_2$
35	$Ni[P(p\text{-}(CH_3)_2-C_6H_3)_3]_2N_2$
32	$Ni[P(C_{10}H_7)_3]_2N_2$
35	$Ni[P(C_6H_5-CH_2)_3]_2N_2$
32	$Ni[As(C_6H_5)_3]_2N_2$
25	$Ni[As(C_{10}H_7)_3]_2N_2$
50	$Fe[P(C_6H_5)_3]_2N_2$

Table 2 reflects the necessary temperatures for obtaining a decomposition pressure of 20 torr, a value which enables a direct comparison between the thermal stabilities of synthesized dinitrogen compounds. One clearly observes the decrease in the stability represented by this conventional temperature as a heavier aryl radical is introduced in the phosphine and arsine, respectively, found as ligands alongside with nitrogen in the molecule of the compound.

The approximate calculations of the dissociation enthalpy revealed values comprised between 8000 and 12,000 (± 1000) cal/mole, and this corresponds to the lower stability limit of the gas ligand-metal bond. [1]

As to IR spectrophotometric determinations, it has been noticed that the stretching vibration of nitrogen N_2 in the prepared dinitrogen compounds has frequencies lower by $200-400\ \mathrm{cm}^{-1}$ *vs* the frequency of the nitrogen molecule in Raman spectrum ($\nu = 2330\ \mathrm{cm}^{-1}$); this band is intensely active in IR. In general, measurements are found within a range of $20-40\ \mathrm{cm}^{-1}$ for the same compound. Since the link between nitrogen and the metallic atom is achieved by the weak acceptor orbital π and the weak donor orbital of nitrogen σ, the effect of the structure of ligands having a different acceptor nature has a large influence on the $\nu(N_2)$ band by the increase of the bonding contribution of electrons d of the metal. [23]

Acknowledgement. The authors thank Mr. A. Sacco and M. Rossi from the Institute of General and Inorganic Chemistry of the University of Bari (Italy) for the articles provided.

---

[23] J. Fergusson and J. Love, *Rev. Pure Appl. Chem.*, **20**, 33 (1970).

Revue Roumaine de Chimie, **19**, *3*, 395–398 (1974)

GALLIUM METATITANATE

EUGENIA PERŢE and M. STRĂJESCU
Institute of Chemistry, Cluj, str. Donath 65–103, Romania

Received April 21, 1973

The gallium peroxotitanate is studied by the thermogravimetric and thermodifferential method and by means of roentgenography. The results obtained show that the metatitanate is formed at a lower temperature than the hydroxide precipitates and that it has a metastable form, decomposing after a long heating at 1 000°.

Gallium and titanium hydroxides and complex oxalotitanates were studied thermally, roentgenographically and crystaloptically and the results were published by Soviet scientists.[1–3] The phase equilibrium diagrams are given in these papers and the existence of three phases, according to the different conditions, is found, namely : gallium metatitanate ($Ga_2O_3 . TiO_2$), gallium dititanate ($Ga_2O_3 . 2TiO_2$) and gallium titanate with a high titanium content.

The present paper contains the results referring to the formation of gallium metatitanate, starting exclusively from peroxotitanate.

To obtain peroxotitanates, using the method described in a former paper,[4] we have prepared several mixtures with different molar ratios of gallium and titanium, but only one product proved to be unitary. The others, according to the ratio between the components, contain, besides peroxotitanate, either a gallium, or a titanium excess.

Taking this into account, we shall further deal only with the compound resulting from the mixture with a gallium : titanium molar ratio of 2 : 1.

The obtained gallium peroxotitanate is in powder form, homogeneous, very fine-grained and of yellow colour. Submitted to chemical analysis it gives the following results (table 1).

The formula corresponding to these data is :

$$[Ga(OH)_2]_2 \cdot [O_2TiO\ (OH)_2] \cdot 3H_2O$$

---

[1] V. E. Pliushchev, I. A. Rozdin, L. I. Trenin and B. A. Jidkov, *Izvest. V.U.M.V.O. S.S.S.R. Khim. i khim. Tekhnol.*, **12**, 1472 (1969).

[2] F. M. Spiridonov, I. A. Rozdin, M. N. Sodnikova, L. N. Komissarova and V. E. Pliushchev, *Neorg. Mat.*, **5**, 817 (1971).

[3] I. A. Rozdin, F. M. Spiridonov, M. N. Sodnikova, L. N. Komissarova and V. E. Pliushchev, *Neorg., Mat.*, **10**, 1801 (1971).

[4] Const. Gh. Macarovici, E. Perţe, M. Birou and M. Străjescu, *Z. anorg. Chem.*, (under press).

Table 1

Results of the chemical analysis of gallium peroxotitanate

	Ti %	Ga %	O (peroxidic) %	H_2O %
Calculated	12.24	35.62	8.17	13.80
Found	12.22	35.78	8.08	13.64

The chemical analysis was based on :

— The reaction of Ti^{4+} with H_2O_2 in a sulphuric acid medium, with formation of the peroxi-sulphato-titanium $[TiO_2(SO_4)_2]^{2-}$ complex anion, orange-yellow coloured and colorimetrically determined.

— The determination of gallium as oxide, by the difference from the amount of oxides resulting through pyrolysis.

— The titration of peroxidic oxygen with potassium permanganate.

— The dosing of the crystallization water in vacuum (Abderhalden apparatus) at the water boiling point.

To study the thermal evolution of the formed compound we have carried through the thermogravimetric and thermodifferential analysis, by means of an Erdely-Paulik derivatograph, up to 1 000°, without maintaining it at maximal temperature under isothermal conditions.

The phasal analysis for different temperatures was achieved by the roentgenographic method, on powders (Debye-Scherrer), on a TU—R—60 (Dresden) apparatus. The experiments were carried out at 11 mA and 50 kV, making use of the CuK_α radiations ($\lambda = 1.5405$), filtered through Ni. The binding of the powdery material was achieved by means of collodium.

RESULTS AND DISCUSSIONS

Watching the thermal decomposition shown in figure 1, we notice that the loss of weight starts at 40° and takes place in two stages : till 220° the three molecules of crystallization water are lost, while between 220 — 500° the anhydrous peroxotitanate decomposes down to the oxides.

The chemical processes are recorded on the ATD curve (fig. 1. *2*), through an endothermal effect at 160°, marking the loss of the crystallization water, followed by two exothermal effects : the first one, at 295°, is due to the exothermal decomposition process of the peroxotitanate, and the second, at 560°, attests the interaction of the two oxides, with the formation of a metastable phase of gallium metatitanate, Ga_2TiO_5. At 920°, a small endothermal effect points out its polymorphous transformation.

The probable reactions taking place are :

$$[Ga(OH)_2]_2 \cdot [O_2TiO(OH)_2] \cdot 3H_2O \xrightarrow{40-220^\circ} [Ga(OH)_2]_2 \cdot [O_2TiO(OH)_2] + 3H_2O$$

$$[Ga(OH)_2]_2 \cdot [O_2TiO(OH)_2] \xrightarrow{220-300^\circ} 2Ga_2O_3 + TiO_2 + 3H_2O$$

$$2Ga_2O_3 + TiO_2 \xrightarrow{560^\circ} Ga_2TiO_5$$

The diffraction analysis of the X rays evidences the following :

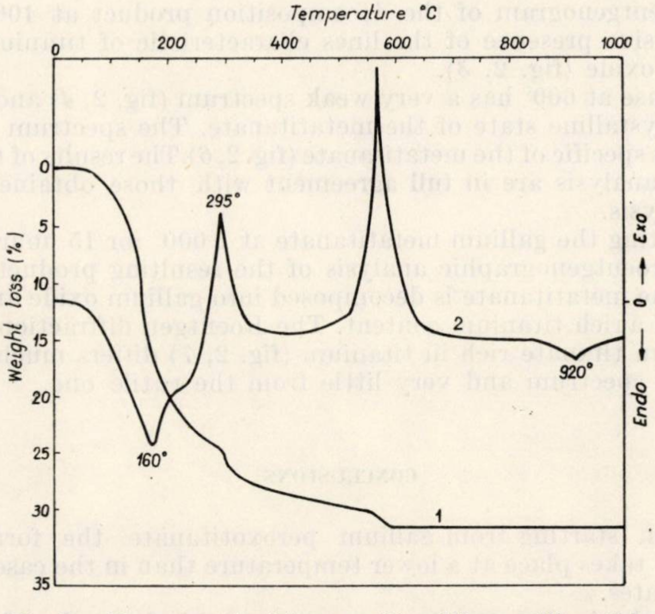

Fig. 1. — Thermogravimetric curve (*1*) and thermodifferential curve (*2*) of gallium peroxotitanate.

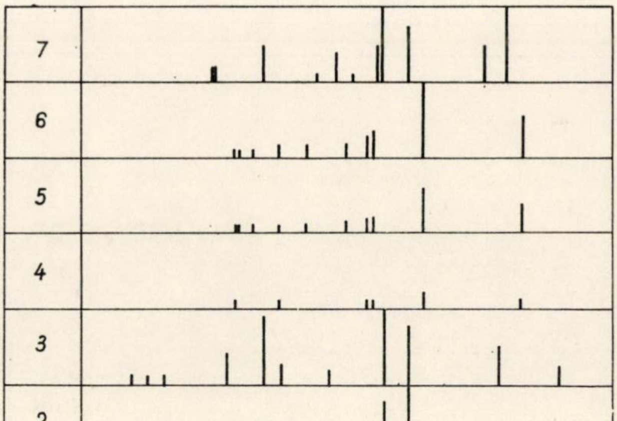

Fig. 2. — Roentgen diffraction spectra of :
1, TiO_2 ; *2*, Ga_2O_3 ; *3*, gallium peroxotitanate at 400° ; *4*, same at 600° ; *5*, at 800° ; *6* at 1 000° ; *7*, after 15 hours at 1 000°.

Revue Roumaine de Chimie, **19**, *3*, 395–398 (1974)

The roentgenogram of the decomposition product at 400° illustrates the exclusive presence of the lines characteristic of titanium bioxide and gallium oxide (fig. 2, *3*).

The phase at 600° has a very weak spectrum (fig. 2, *4*) and confirms the feebly crystalline state of the metatitanate. The spectrum at 800° of the product is specific of the metatitanate (fig. 2, *6*).The results of the reoentgenographic analysis are in full agreement with those obtained through thermal analysis.

By heating the gallium metatitanate at 1 000° for 15 hours and carrying out a roentgenographic analysis of the resulting product, we have found that the metatitanate is decomposed into gallium oxide and gallium titanate with a rich titanium content. The Roentgen diffraction spectrum of this gallium titanate rich in titanium (fig. 2, *7*) differs much from the metatitanate spectrum and very little from the rutile one.

CONCLUSIONS

— When starting from gallium peroxotitanate the formation of metatitanate takes place at a lower temperature than in the case of hydroxide precipitates.

— The obtained metatitanate is a metastable form, that decomposes into gallium oxide and gallium titanate with a rich titanium content after a fairly long heating at 1 000°.

Revue Roumaine de Chimie, **19**, *3*, 399–405 (1974)

LES RÉACTIONS DES LIGANDS COORDINÉS.[1-3] IV

L'ÉTUDE SPECTROSCOPIQUE ET THERMOGRAVIMÉTRIQUE DES COMBINAISONS ALUMINIUM-ORGANIQUES DE DIMÉTHYLGLYOXIME COORDINÉE

N. VOICULESCU, A. AIRINEI et I. POPESCU

Institut de Chimie Macromoléculaire « P. Poni », 41, Aleea Gr. Ghica Vodă, Jassy

Reçu le 22 novembre 1972

Les spectres en infrarouge et ultraviolet d'une suite de dérivés aluminium-organiques des bisdiméthylglyoximates de Ni(II), Pd(II) et Cu(II) ont été étudiés dans le but d'établir le mode de liaison et les modifications qui ont lieu dans les produits de départ par la substitution de l'hydrogène oximique par le groupe AlR_2, où $R = iC_4H_9$, C_6H_5. Ces études en corrélation avec les données thermogravimétriques ont permis à établir une suite des stabilités dépendant de la nature de l'ion métallique central du radical qui est lié à l'aluminium. Les spectres RMN des bisdiméthylglyoximates de Ni(II) et Pd(II) avec l'Al $(iC_4H_9)_2$ confirment la structure proposée par le rapport entre les intensités relatives des groupements méthyle du radical oximique et ceux du radical *iso*-butyle.

Dans les travaux antérieurs [1,2] on a présenté la synthèse de nouvelles combinaisons résultant de la réaction de $Al(iC_4H_9)_3$ et $Al(C_6H_5)_3$ avec les bisdiméthylglyoximates de quelques métaux transitionnels, qui correspondent à la formule I

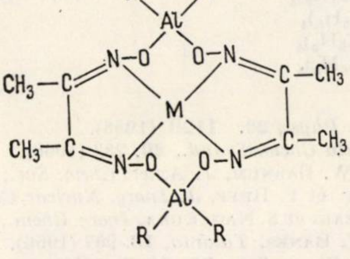

où M = Ni(II), Pd(II), Cu(II) et $R = iC_4H_9$, C_6H_5.

Pour vérifier si cette formule est plausible et aussi pour déceler les modifications survenues dans la structure intime des chélates on a effectué

---

[1] N. Voiculescu et I. Popescu, *Rev. Roumaine Chim.*, **17**, 719 (1972).

[2] N. Voiculescu et I. Popescu, *Rev. Roumaine Chim.*, sous presse.

[3] N. Voiculescu, I. Popescu et. N. Luchian, *Rev. Roumaine Chim.*, sous presse.

une étude spectrale (IR, UV, RMN) et thermogravimétrique de ces composés. Une attention à part a été accordée dans la littérature aux spectres en ultraviolet des bisdiméthylglyoximates de Ni(II), Pd(II) et Cu(II). [4–11] Au contraire, il n'y a qu'un petit nombre de données thermogravimétriques[12–14] et spectrales en infrarouge [7,15] (650 — 300 cm^{-1}) concernant ces composés. Le triphénylaluminium a été étudié [16] dans le domaine de 650 à 300 cm^{-1} et en ultraviolet [17].

PARTIE EXPÉRIMENTALE

Les composés étudiés ont été synthétisés d'après une méthode présentée dans [1,2].

Les spectres en U.V. ont été enregistrés dans une solution de *n*-heptane à l'aide d'un apparel Unicam SP — 800 B, en utilisant des cuves de 1 cm, à la température ambiante et ceux en infrarouge avec un appareil Zeiss UR—20 et Beckman IR—12 sur des pastilles à KBr.

Les spectres RMN ont été enregistrés en utilisant un spectromètre JEOL—JNM—C—6 OHL de 60 MHz à la température ordinaire.

Les thermogrammes ont éte enregistrés avec un dérivatographe MOM Budapest.

RÉSULTATS ET DISCUSSIONS

Les spectres en ultraviolet des dérivés aluminium-organiques des bisdiméthylglyoximates de Ni(II), Pd(II), Cu(II) sont discutés comparativement à ceux des composés de départ.

Les spectres des composés étudiés sont semblables à ceux des composés initiaux. Les maximums d'absorption des composés étudiés sont donnés dans le tableau 1.

Tableau 1

Les bandes d'absorption en ultraviolet des composés

Le composé	λ_{max} (nm)				
$Ni(DMG)_2Al_2(iC_4H_9)_4$	466	431	373	254	216
$Pd(DMG)_2Al_2(iC_4H_9)_4$		406	370	277	220
$Ni(DMG)_2Al_2(C_6H_5)_4$				244	208
$Pd(DMG)_2Al_2(C_6H_5)_4$				247	211
$Cu(DMG)_2Al_2(C_6H_5)_4$				248	210

[4] G. Maki, *J. Chem. Phys.*, **29**, 1129 (1958).

[5] L. L. Ingraham, *Acta Chem. Scand.*, **20**, 283 (1966).

[6] C. V. Banks et D. W. Barnum, *J. Amer. Chem. Soc.*, **80**, 4767 (1958).

[7] K. Burger, I. Ruff et F. Ruff, *J. Inorg. Nuclear Chem.*, **27**, 179 (1965).

[8] Y. Ohashi, I. Hanazaki et S. Nagakura, *Inorg. Chem.*, **9**, 2551 (1970).

[9] J. E. Caton et C. V. Banks, *Talanta*, **13**, 967 (1966).

[10] K. Sone, *J. Amer. Chem. Soc.*, **75**, 5207 (1953).

[11] M. Bosso et G. Morfurgo, *Ric. Sci.*, **37**, 1131 (1967).

[12] R. Duval et C. Duval, *Analyt. Chim. Acta*, **5**, 71 (1951).

[13] T. Tsumaki et M. Yamaguchi, *J. Chem. Soc. Japan, Pure Chem.* Sect. **70**, 10 (1949)

[14] P. Champ, P. Faurconier et C. Duval, *Analyt. Chim. Acta.*, **5**, 250 (1951).

[15] A. Bigotto, G. Costa, V. Galasso et G. DeAlti, *Spectrochim. Acta*, **26A**, 1939 (1970).

[16] H. F. Shurvell, *Spectrochim. Acta*, **23 A**, 2925 (1959).

[17] G. Sartori et G. Costa, *Z. Elektrochem.*, **63**, 105 (1959).

Faute de calculs mécaniquantiques il n'a pas été possible d'attribuer avec certitude les bandes d'absorption à certaines transitions électroniques. Les bandes d'absorption à 254 nm et à 277 nm des dérivés de Ni(II) et de Pd(II) avec le groupe $Al(iC_4H_9)_2$ peuvent être attribuées à la transition ligand-ligand [4,10] et sont observées dans le même domaine de fréquence que les bandes des produits de départ. La même transition peut être observée aux environs de 245 nm pour les composés avec le groupe $Al(C_6H_5)_2$.

Pour les deux suites de composés on constate un déplacement bathochromique de cette bande d'absorption dans l'ordre

$$Cu > Pd > Ni$$

ce qui suggère le même ordre de stabilité des composés. Les dérivés aux groupes $Al(C_6H_5)_2$ sont moins stables que ceux aux groupes $Al(iC_4H_9)_2$.

La bande intense située approximativement à 370 nm est attribuée à la structure plan quadratique avec des liaisons covalentes [18]. Cette bande est présente aussi dans les spectres de nos produits ce qui met en évidence le maintien de la structure covalente plan quadratique dsp^2 de ceux-ci.

Dans les spectres des dérivés avec de l'$Al(iC_4H_9)_2$ les bandes apparaissent à 466 nm, et 421 nm pour le composé avec du Ni(II) et à 406 nm pour le composé avec du Pd(II) qui ont été attribuées aux transitions [4] d–d. Ces transitions ont été aussi constatées par Schrauzer [19] dans les spectres en ultraviolet des composés résultés de la réaction du Ni(II) $(DMGH)_2$ avec du BR_3 ($R = F$, Cl, C_6H_5 et quelques radicaux aliphatiques). Dans les spectres des dérivées avec de l'$Al(C_6H_5)_2$ on ne constate pas l'apparition des bandes à environ 370 nm. La modification du champ des ligands des quatre atomes d'azote due à la substitution des atomes d'hydrogène oximiques par les groupes AlR_2 est réduite.

Dans le tableau 2 sont insérées les fréquences d'absorption IR observées dans le domaine de 650 à 300 cm^{-1}.

Tableau 2

Absorptions en IR caractéristiques

Produit												
$Ni(DMG)_2Al_2(C_4H_9)_4$	256					432			495	520	610	670
$Pd(DMG)_2Al_2(C_4H_9)_4$	255			373		441			490	513		
$Ni(DMG)_2Al_2(C_6H_5)_4$		325	350	360	400		437	480	492	532	615	
$Pd(DMG)_2Al_2(C_6H_5)_4$		325	345	382	395		455	480	492	527	613	671
$Cu(DMG)_2Al_2(C_6H_5)_4$		325	358		400		440		490	500	615	681

Les deux bandes intenses qui apparaissent dans ce domaine à 500 cm^{-1} et à 400 cm^{-1} sont dues probablement aux vibrations de valence M–N.

---

[18] J. B. WILLIS et D. P. MELOR, *J. Amer. Chem. Soc.*, **64**, 181 (1942) ; **69**, 1237 (1947).

[19] G. H. SCHRAUZER, *Chem. Ber.*, **95**, 1438 (1962).

L'absorption autour de 490 cm^{-1} peut être attribuée à la liaison Al—O. La liaison Al—O qui apparaît dans les dérivés aluminium-organiques des bisdiméthylglyoximates de Ni(II) et de Pd(II) est différente de la liaison Al—O des acétylacétonates [20,21].

Par comparaison avec les spectres des composés initiaux dans les spectres des dérivés aluminium-organiques-bisdiméthylglyoximates nous rencontrons un déplacement des vibrations de la liaison M—N vers des fréquences plus grandes, fait, probablement, dû à la polarisation de cette liaison.

La configuration moléculaire des composés Ni(II) $(DMG)_2Al_2(iC_4H_9)_4$ et Pd(II) $(DMG)_2Al_2(iC_4H_9)_4$ a été établie par la comparaison des spectres RMN de ces composés et de ceux des composés initiaux. Dans la figure 1 sont présentés les spectres RMN des :

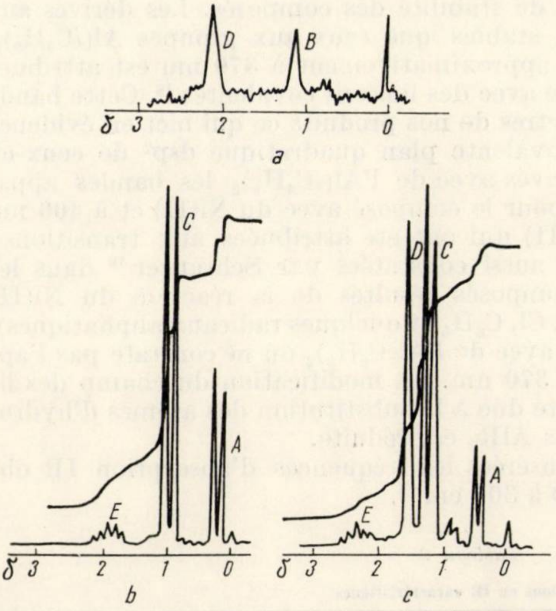

Fig. 1. — Les parts de haut champ des spectres RMN des : a) $Ni(DMGH)_2$; b) $Al(iC_4H_9)_3$; c) $Ni(DMG)_2Al_2(iC_4H_9)_4$

a) $Ni(II)(DMGH)_2$, b) $Al(iC_4H_9)_3$, c) Ni(II) $(DMG)_2Al_2(iC_4H_9)_4$

Les signaux notés avec A, C et E sont caractéristiques des protons des groupes $-CH_2$, $-CH_3$ et $-CH$ du radical iso-butyle. L'attribution est conforme aux rapports 2 : 6 : 1 des signaux intégrés, ainsi qu'à leur forme. Les signaux A et C sont des doublets dus aux couplages des protons méthyle et méthylène avec le proton méthyne, mais le signal méthyne (E) est un multiplet complexe.

---

[20] R. E. Lawson, *Spectrochim. Acta*, **17**, 248 (1961).
[21] C. Djordjevic, *Spectrochim. Acta*, **17**, 448 (1961).

Les signaux B et D sont caractéristiques des groupements méthyle du Ni(II) $(DMGH)_2$ dont les protons résonnent avec deux fréquences dû probablement à la stéricité. On remarque que le spectre (*c*) du composé Ni(II) $(DMG)_2Al_2(iC_4H_9)_4$ contient les mêmes signaux que les spectres (a) et (*b*) des composés initiaux, mais les positions de quelques-uns de signaux sont modifiées démontrant la formation du nouveau composé.

Les signaux intégrés C rapportés à la somme B + D donnent la valeur approximative 2 : 1, d'où il résulte que ce composé aurait la formule Ni(II) $(DMG)_2.2Al(iC_4H_9)_2$ qui est conforme à la structure I.

Cette structure est aussi confirmée par les déplacements observés pour quelques-unes des résonances. Ainsi les résonances B et D à 1,1 ppm et respectivement 2,1 ppm du Ni(II) $(DMGH)_2$ apparaissent à 1,60 ppm et respectivement à 0,90 ppm dans le composé avec de l'aluminium. Leur déplacement vers le haut champ (la croissance des écranages magnétiques) peut être expliqué par la formation des liaisons Al —O, c'est-à-dire par l'introduction de l'atome électropositif d'aluminium dans la molécule. La formation des liaisons Al—O expliquent aussi les désécranages (déplacements vers le bas champ) des signaux des protons du radical isobutyle. Ainsi les résonances A, C et E situées à 0,18 ppm ; 0,93 ppm et respectivement à 1,88 ppm dans l'$Al(iC_4H_9)$ apparaissent à 0.45 ppm ; 1,30 ppm et à 2,30 ppm dans Ni(II) $(DMG)_2$ $Al_2(iC_4H_9)_4$.

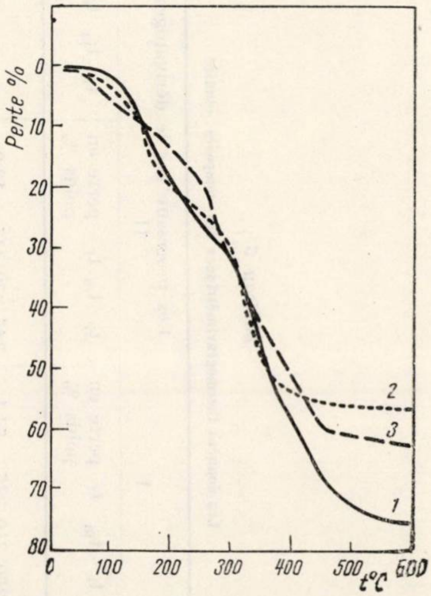

Fig. 2. — Thermogramme du composé $Ni(DMG)_2$ $Al_2(iC_4H_9)_4$; *2* — Thermogramme du composé $Pd(DMG)_2Al_2(iC_4H_9)_4$; *3*, — Thermogramme du composé $Ni(DMG)_2Al_2(C_6H_5)_4$.

La même interprétation appliquée au complexe avec du palladium conduit à une formule semblable Pd(II) $(DMG)_2Al_2(iC_4H_9)_4$.

Au point de vue spectral, la substitution de l'atome de nickel par le palladium n'affecte pas les résonances de l'isobutyle, mais seulement

Tableau 3

Les données thermogravimétriques des composés étudiés

Le composé	Nombre des processus de la décomposition	I				II				III				IV			
		t_i	t_m	t_f	perte en poids %	t_i	t_m	t_f	perte en poids %	t_i	t_m	t_f	perte en poids %	t_i	t_m	t_f	perte en poids %
$Ni(DMGH)_2$	2	260	310	345	54,1	345	370	415	13,9								
$Pd(DMGH)_2$	1	270	310	390	75,6												
$Cu(DMGH)_2$	2	150	205	240	69,4	310	340	380	6,5								
$Ni(DMG)_2Al_2(iC_4H_9)_4$	2	45	180	230	23,4	230	340	410	35,6	410	430	530	13,6				
$Pd(DMG)_2Al_2(iC_4H_9)_4$	2	40	160	230	22,2	230	325	400	32,3								
$Ni(DMG)_2Al_2(C_6H_5)_4$	4	25	70	125	8,1	125	190	210	7,3	210	270	400	32,5	400	415	480	13,8
$Pd(DMG)_2Al_2(C_6H_5)_4$	3	30	85	100	6,6	100	180	270	19,8	270	310	430	36,3				
$Cu(DMG)_2Al_2(C_6H_5)_4$	3	25	85	110	7,1	110	240	280	31,7	320	380	460	35,7				

celles de la diméthylglyoxime ; les signaux B sont situés à 0,95 ppm et respectivement à 1,80 ppm par rapport au TMS. On peut supposer aussi que les dérivés qui possèdent le groupe $Al(C_6H_5)_2$ ont le même configuration moléculaire par analogie avec les dérivés à l'$Al(iC_4H_9)_2$.

L'analyse des données thermogravimétriques (tableau 3) révèle que le mécanisme de la décomposition est d'autant plus compliqué que le volume du radical lié à l'aluminium s'accroît. Les produits du phénylaluminium sont moins stables que les produits à l'isobutylaluminium fait relevé aussi par les données spectrales en U.V. Les dérivés au palladium se décomposent plus rapidement que les dérivés aux nickel et cuivre dû probablement au volume de l'ion métallique qui a un rôle important.

Par rapport à la décomposition du M(II) ($DMGH_2$), celle des dérivés étudiés se produit à des températures de beaucoup inférieures, ceux-ci étant instables même à la température ambiante, tandis que les M(II) $(DMGH)_2$ sont stables jusqu'à des températures beaucoup plus élevées (voir tableau 3). La perte en poids totale est d'environ 70% (fig. 2).

La décomposition des dérivés M(II) $(DMG)_2 Al_2R_4$ a lieu en plusieurs étapes en comparaison des composés de type M(II) $(DMFH)_2$ qui se décomposent à une ou à deux étapes et à des températures finales plus élevées.

Les pertes en poids à différentes températures sont fonction de la nature du radical lié à l'aluminium, ainsi que de la nature du cation métallique. Le maximum de perte en poids se trouve entre les mêmes limites de température que les chélates initiaux. Nous considérons que la première décomposition peut être attribuée à la substitution des hydrogènes oximiques par le groupement AlR_2, qui conduit à l'instabilisation des molécules M(II) (DMG) $_2Al_2R_4$. Cette étape de décomposition est le résultat tant de la dégradation thermique que de l'hydrolyse des composés en présence de l'eau dans l'atmosphère.

Revue Roumaine de Chimie, **19**, *3*, 407–413 (1974)

KINETIK UND MECHANISMUS DER OXYDATION DES URANS (IV) MIT NATRIUM-PERSULFAT

F. MÁNOK, CS. VÁRHELYI und RODICA OPREAN

Lehrstuhl für Anorganische Chemie „Babeş-Bolyai“ Universität Cluj, Str. Arany János No. 11, Rumänien

Eingegangen am 25. April 1973

Es wurde die Kinetik der Oxydation der $U(SO_4)_2$-Lösungen in saurem Medium mit Natrium-persulfat untersucht. Die Änderung der U(IV)-Konzentration wurde bei 23°, 30° und 40° permanganometrisch verfolgt. Für die Aktivierungsenthalpie erhält man $\Delta H^{\ddagger} = 27{,}4$ kcal/Mol und für die Aktivierungsentropie $\Delta S^{\ddagger} = +23{,}1$ Cl. In Anwesenheit von sehr kleinen Eisen (II)-Mengen wird die Reaktion erheblich beschleunigt. Auf Grund der experimentellen Daten wurde ein wahrscheinlicher Mechanismus des Oxydationsprozesses diskutiert.

Das vierwertige Uran wird durch eine Reihe von Oxydationsmitteln in U(VI) oxydiert. Einige Oxydationsreaktionen des U(IV) verlaufen schnell, es sind aber auch Oxydationsvorgänge bekannt, welche bei Zimmertemperatur langsam stattfinden und vom kinetischem Standpunkt aus leicht zugänglich sind.

Die Kinetik des U(VI) – U(VI)-Oxydationsprozesses wurde mit Brom in Anwesenheit von Perchlorsäure von Gordon und Mitarbeiter [1,2], mit Kaliumchlorat in saurem Medium von Fedorova und Kanevski [3], mit salpetriger Säure von Koltunov [4], mit dreiwertigem Eisen von Minč und Mitarbeiter [5], mit molekularem Sauerstoff von Halpern und Smith [6], Sobkowski [7] und von Kraus und Nelson [8] untersucht. Es wurde der Mechanismus dieser Prozesse erörtert und der katalytische Einfluß von Schwermetallionen (V, Fe(II)) verfolgt.

Das Persulfation der Form $O-SO_2O - OSO_2-O$ ist ein sehr starkes Oxydationsmittel ($E_0 = \pm 2{,}0$ V), doch verlaufen im allgemeinen die

---

[1] G. Gordon und J. Kern, *Inorg. Chem.*, **2**, 367 (1963).

[2] G. Gordon und A. Andrews, *Inorg. Chem.*, **3**, 1733 (1964).

[3] L. A. Fedorova und E. A. Kanevski, *Kinetika i kataliz*, **3**, 332 (1962).

[4] V. S. Koltunov, *Khim. Transuranovykh Oskolochnykh Elem. Akad. Nauk S.S.S.R. Otd. Obshch. Tekh. Khim.*, **1967**, 3, 8, 15; *Chem. Abstr.* **70**, 23, 363e, 23, 364 f, 23, 365 g (1969).

[5] F. Minč, J. Sobkowski, and S. Miroslawa, *Nukleonika*, **10**, 747 (1965).

[6] J. Halpern und J. G. Smith, *Canad. J. Chem.*, **34**, 1419 (1957).

[7] J. Sobkowski, *Roczniki Chem.*, **40**, 271 (1966).

[8] K. A. Kraus und F. Nelson, *J. Amer. Chem. Soc.*, **77**, 1504 (1955).

Oxydationsvorgänge mit Persulfat mit meßbarer Geschwindigkeit. Es wurde beobachtet, daß diese Vorgänge von Übergangsmetallionen (Cu^{2+}, Ag^{+}) katalysiert werden. Für die Erklärung des Mechanismus der Oxydationsprozesse mit Persulfat wurde die Bildung des freien SO_4^--Radikals, welche an monoelektronischen Übergängen teilnimmt, angenommen.

Es wurde die Kinetik der Oxydation des Eisens (II) [9], des Arsens (III) [10], des Oxalats [11], des Thiosulfats [12] und des Methanols [12] mit Persulfat untersucht.

In vorliegender Arbeit wurde die Kinetik der Oxydation des Urans (IV) mit dem obenerwähnten Oxydationsmittel in verdünnter Schwefelsäure untersucht.

Für die kinetischen Messungen wurde $U(SO_4)_2 . 3\,H_2O$ in 0,25 M Schwefelsäure verwendet. Die Untersuchungen wurden bei drei Temperaturen : 23°, 30° und 40° in Anwesenheit von verschiedenen $Na_2S_2O_8$ Mengen durchgeführt. Die Änderung der Konzentration des Urans (IV) wurde permanganometrisch verfolgt. Die Oxydationsreaktion wurde mit überschüssiger Kaliumpermanganat-Lösung rasch vollendet und der Permanganat-Überschuß mit Oxalsäure rücktitriert.

Die Meßergebnisse bei verschiedenen Temperaturen sind in den Tabellen 1—3 zusammengestellt.

Tabelle 1

Kinetische Daten über die Oxydation des U(IV) mit $Na_2S_2O_8$ bei 23°

Reaktionszeit (Min).	$[Na_2S_2O_8] = 0{,}025$ M		$[Na_2S_2O_8] = 0{,}05$ M		$[Na_2S_2O_8] = 0{,}0125$ M	
	$[U] \cdot 10^2$ Mol/l	$\log \frac{[U_0]}{[U]}$	$[U] \cdot 10^2$ Mol/l	$\log \frac{[U_0]}{[U]}$	$[U] \cdot 10^2$ Mol/l	$\log \frac{[U_0]}{[U]}$
10	0,090	0,06695	0,900	0,12123	—	—
20	0,079	0,12156	0,058	0,25527	0,090	0,06221
30	0,077	0,19512	0,044	0,37603	—	—
40	0,058	0,25776	0,032	0,51108	0,079	0,12156
50	0,049	0,33089	0,024	0,63114	—	—
60	0,044	0,37774	0,018	0,76025	0,076	0,19201
70	0,037	0,45102	—	—	—	—
80	—	—	—	—	0,059	0,25624

Tabelle 2

Kinetische Daten über die Oxydation des U(IV) mit $Na_2S_2O_8$ bei 30°

Reaktionszeit (Min).	$[Na_2S_2O_8] = 0{,}0125$ M	
	$[U] \cdot 10^2$ Mol/l	$\log \frac{[U_0]}{[U]}$
20	0,077	0,13126
40	0,058	0,25310
50	0,051	0,31260
60	0,043	0,38130
80	0,033	0,49136

---

[9] P. D. BARTLETT und J. D. COTMAN, *J. Amer. Chem. Soc.*, **71**, 1419 (1949).

[10] J. W. L. FORDHAM und H. L. WILLIAMS, *J. Amer. Chem. Soc.*, **73**, 4855 (1951).

[11] R. J. ORR und H. L. WILLIAMS, *J. Amer Chem. Soc.*, **77**, 3715 (1955).

[12] E. BEN-ZVI und T.L. ALLEN, *J. Amer. Chem. Soc.*, **83**, 4352 (1961).

Tabelle 3

Kinetische Daten über die Oxydation des U(IV) mit $Na_2S_2O_8$ bei 40°

Reaktionszeit (Min.)	$[Na_2S_2O_8] = 0{,}0125$ Mol		$[Na_2S_2O_8] = 0{,}005$ Mol	
	$[U] \cdot 10^2$ Mol/l	$\log \frac{[U_0]}{[U]}$	$[U] \cdot 10^2$ Mol/l	$\log \frac{[U_0]}{[U]}$
10	0,052	0,22115	0,084	0,09307
20	0,037	0,45123	0,069	0,18186
30	0,021	0,68070	0,057	0,26221
40	0,013	0,90140	0,045	0,36305
50	—	—	0,037	0,45410
60	—	—	0,029	0,55145

Die graphische Darstellung von $\log \frac{[U_0]}{[U]}$ gegen die Zeit zeigt eine sehr gute Linearität, wie aus Abbildung 1 und 2 ersichtlich ist.

Aus diesen experimentellen Daten geht hervor, daß die globale Reaktion zweiter Ordnung ist, d.h. erster Ordnung gegen die U(IV)-Konzentration, und gegen die $S_2O_8^{2-}$-Konzentration.

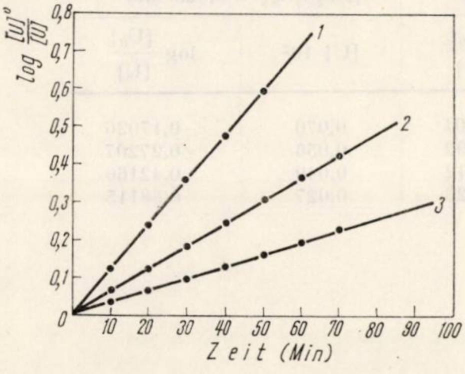

Abb. 1. — Kinetische Kurven für die Oxydation des Urans (IV) mit Persulfat bei 23°
$[H_2SO_4] = 0{,}25$ M, $[U°] = 0{,}105.10^{-2}$ M
$[Na_2S_2O_8]$: 1 – 0,05 M ; 2 – 0,025 M ; 3 – 0,0125 M

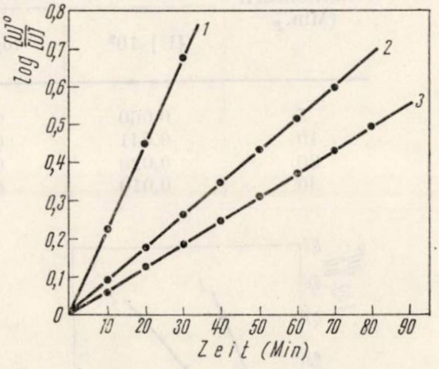

Abb. 2. — Kinetische Kurven für die Oxydation des Urans (IV) mit Persulfat bei 30° und 40°
$[H_2SO_4] = 0{,}25$ M, $[U°] = 0{,}105.10^{-2}$ M
40°: 1 – $[Na_2S_2O_8]$: 0,0125 M,
2 – $[Na_2S_2O_8]$: 0,005 M
30° : 3 – $[Na_2S_2O_8]$: 0,0125 M

Aus der Neigung der Geraden wurden die Geschwindigkeitskonstanten bei den obenerwähnten Temperaturen berechnet. Die graphische Darstellung zeigt, daß sich die Reaktionsordnung mit der Temperatur nicht ändert.

Die berechneten Geschwindigkeitskonstanten bei verschiedenen Temperaturen sind aus Tabelle 4 ersichtlich.

Es wurde auch der Einfluß des Eisens (II) auf die Oxydation des Urans (IV) in analogen Experimentierbedingungen untersucht. Die in der Tabelle 5 zusammengestellten experimentellen Daten zeigen, daß in

Tabelle 4

Geschwindigkeitskonstanten (k) der Reaktion $U(IV) + S_2O_8^{2-} \rightarrow U(VI)$

Temperatur	Experimentelle Geschwindigkeitskonstante k, sec^{-1}
23°	$9{,}9 \cdot 10^{-3}$ $9{,}81 \cdot 10^{-3}$ $9{,}50 \cdot 10^{-3}$
30°	$19{,}4 \cdot 10^{-3}$
40°	$7{,}66 \cdot 10^{-2}$ $7{,}80 \cdot 10^{-2}$

Tabelle 5

Kinetische Daten über die Oxydation des U(IV) mit $Na_2S_2O_8$ in Anwesenheit von Fe(II)

Reaktionszeit (Min.)	$[FeSO_4] = 0{,}05 \cdot 10^{-3}$ Mol $[Na_2S_2O_8] = 0{,}025$ Mol		$[FeSO_4] = 0{,}025 \cdot 10^{-3}$ Mol $[Na_2S_2O_8] = 0{,}025$ Mol	
	$[U] \cdot 10^2$	$\log \frac{[U_0]}{[U]}$	$[U] \cdot 10^2$	$\log \frac{[U_0]}{[U]}$
5	0,060	0,24204	0,070	0,17026
10	0,041	0,40192	0,056	0,27207
20	0,020	0,71012	0,040	0,42160
30	0,010	0,99123	0,027	0,58115

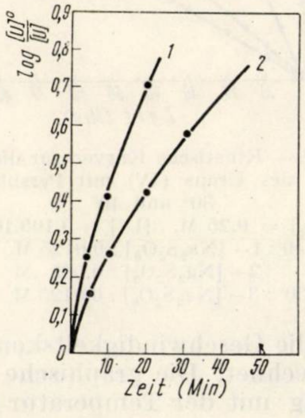

Abb. 3. — Kinetische Kurven für die Oxydation des Urans (IV) mit Persulfat bei 23° in Anwesenheit von Fe(II)-Katalysator $[H_2SO_4] = 0{,}25$ M, $[Na_2S_2O_8] = 0{,}025$ M ; 1— $[FeSO_4]$: $0{,}05 . 10^{-3}$M ; 2— $[FeSO_4]$: $0{,}025.10^{-3}$

Gegenwart von sehr kleinen Eisenmengen (U(IV) — Fe(II) Verhältnis : 20, bzw. 40) die Geschwindigkeit der Oxydation des Urans (IV) stark zunimmt.

Die graphische Darstellung von $\log \frac{[U_0]}{[U]}$ abhängig von der Zeit zeigt keine Linearität mehr und negative Abweichungen von den Geraden können beobachtet werden. (Abb. 3.)

Um den Oxydationsgrad des Urans (IV) in verschiedenen Experimentierbedingungen in An- und Abwesenheit von Fe(II) vergleichen zu können, bestimmten wir die für die Oxydation der Halbmenge des Urans (IV) nötigen Reaktionszeiten (Tabelle 6)

Tabelle 6

Die Halbzeiten der Uran (IV)-Oxydation bei verschiedenen Experimentierbedingungen

Temperatur	[Fe(II)]	$[Na_2S_2O_8]$ Mol	$t_{1/2}$ (Min)
23°	—	0,025	47
23°	$0{,}05 \cdot 10^{-3}$	0,025	6
23°	$0{,}025 \cdot 10^{-3}$	0,025	12

DISKUSSION

Aus den experimentellen Daten geht hervor, daß die Oxydation des Urans (IV) mit $Na_2S_2O_8$ in Abwesenheit des Fe(II)-Katalysators nach folgender Gleichung verläuft :

$$\frac{-\mathrm{d}[\mathrm{U(IV)}]}{\mathrm{d}t} = k[\mathrm{U(IV)}]\ [\mathrm{S_2O_8^{2-}}] \qquad (1)$$

Die globale Reaktion kann folgendermaßen ausgedückt werden

$$\mathrm{U(IV)} + \mathrm{S_2O_8^{2-}} = \mathrm{U(VI)} + 2\mathrm{SO_4^{2-}} \qquad (2)$$

Die graphische Darstellung von —log k gegen $1/\mathrm{T} \cdot 10^3$ gibt eine Gerade (siehe Abb. 4.) Aus der Neigung dieser Geraden wurde die Aktivierungsenthalpie ermittelt.

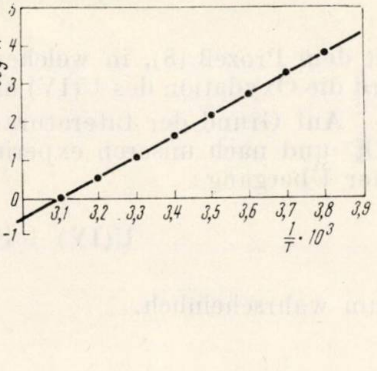

Abb. 4. — Bestimmung der Aktivierungsenthalpie der Oxydation des Urans (IV) mit Persulfat

Die Aktivierungsentropie wurde auf Grund der Gleichung:

$$\log k = \log \frac{kT}{h} + \frac{\Delta S^{\ddagger}}{2{,}3R} - \frac{\Delta H^{\ddagger}}{2{,}3\ RT} \tag{3}$$

berechnet. (k = die Boltzmann'sche Konstante, h = die Plank'sche Konstante). Die erhaltenen Aktivierungsparameter sind: $\Delta H^{\ddagger} = 27{,}4$ kcal/ /Mol; $\Delta S^{\ddagger} = +23{,}1$ Cl.

Der aktivierte Zustand ist folglich vom Standpunkt der Entropieänderung günstig, benötigt aber eine erhebliche Aktivierungsenthalpie.

Die obenerwähnte kinetische Gleichung steht mit mehreren monoelektronischen Übergangsmechanismen im Einklang.

Folgender, mit unseren Daten übereinstimmender Mechanismus, kann angenommen werden:

$$\mathrm{U(IV)} + \mathrm{S_2O_8^{2-}} = \mathrm{U(V)} + \mathrm{SO_4^{2-}} + \mathrm{SO_4^{-}}\ \text{(langsam)} \tag{4}$$

$$\mathrm{SO_4^{-}} + \mathrm{U(V)} = \mathrm{U(VI)} + \mathrm{SO_4^{2-}}\ \text{(schnell)} \tag{5}$$

Aus der Veränderung der Geschwindigkeit der Reaktion in Anwesenheit von Fe(II) geht hervor, daß wir in diesem Falle einen anderen Mechanismus des Oxydationsprozesses annehmen müssen.

Die Rolle des Katalysators und die Veränderung der Oxydationsgeschwindigkeit kann, durch folgendes Schema erklärt werden:

$$\mathrm{Fe(II)} + \mathrm{S_2O_8^{2-}} = \mathrm{Fe(III)} + \mathrm{SO_4^{2-}} + \mathrm{SO_4^{-}}\ \text{(langsam)} \tag{6}$$

$$\mathrm{U(IV)} + \mathrm{SO_4^{-}} = \mathrm{U(V)} + \mathrm{SO_4^{2-}}\ \text{(schnell)} \tag{7}$$

$$\mathrm{U(V)} + \mathrm{Fe(III)} = \mathrm{U(VI)} + \mathrm{Fe(II)}\ \text{(schnell)} \tag{8}$$

Bei Verminderung der U(V)-Konzentration konkurriert die Reaktion.

$$\mathrm{Fe(II)} + \mathrm{SO_4^{-}} = \mathrm{Fe(III)} + \mathrm{SO_4^{2-}} \tag{9}$$

mit dem Prozeß (8), in welchem das Fe(II) sich regeneriert. Demzufolge wird die Oxydation des U(IV) nachlassen.

Auf Grund der Literaturangaben über die Oxydationsprozesse mit $\mathrm{S_2O_8^{2-}}$ und nach unseren experimentellen Ergebnissen ist ein zweielektronischer Übergang:

$$\mathrm{U(IV)} + \mathrm{S_2O_8^{2-}} = \mathrm{U(VI)} + 2\mathrm{SO_4^{2-}} \tag{10}$$

kaum wahrscheinlich.

EXPERIMENTELLER TEIL

Darstellung von $U(SO_4)_2 \cdot 3H_2O$

25 g Uranylacetat werden auf einem Sandbad mit konzentrierter Schwefelsäure behandelt. Nach der Entfernung der Essigsäure wird die grüne Masse in 1 Lit. 40%igem Äthanol gelöst, mit 200 ml 50 %iger Schwefelsäure behandelt und in einem bedeckten Erlenmeyerkolben zwei Wochen lang, starkem Sonnenlicht ausgesetz. Es scheidet sich langsam eine grüne kristalline Masse aus. Nach Filtrierung wird die Substanz mit Alkohol und Äther gewaschen und an der Luft getrocknet.

Analyse : *gef.* U 49,21, SO_4 39,32, H_2O 11,10
Nach der Fomel $U(SO_4)_2\ 3H_2O$
ber. U 49,26, SO_4 39,54, H_2O 11,16

Das U(IV) wurde permanganometrisch, das SO_4^{2-} gravimetrisch, als $BaSO_4$ bestimmt.

Kinetische Messungen:

Das $U(SO_4)_2 \cdot 3\ H_2O$ wurde in vorerhitzter 1 Mol. Schwefelsäure gelöst, mit starkem Methanstrom der Sauerstoff aus der Lösung entfernt, mit luftfreier $Na_2S_2O_8$-Lösung vermischt und die Ionenstärke der Lösung mit verdünnter Schwefelsäure eingestellt. Die Konzentration des Urans (IV) war in allen Untersuchungen $0{,}105 . 10^{-2}$ Molar. Während den kinetischen Messungen wurden aliquote Teile der untersuchenden Lösung (10—20 ml) mit überschüssiger 0,1 n $KMnO_4$-Lösung versetzt und die unverbrauchte $KMnO_4$ mit 0,1 n Oxalsäure bei 60—70° volumetrisch bestimmt.

Revue Roumaine de Chimie, **19**, *3*, 415–427 (1974)

LA STRUCTURE CRISTALLINE ET L'INTERACTION AVEC LA MOLÉCULE DE L'HYDROCARBURE INCLUSE DANS LES CLATHRATES DU TYPE $M(SCN)_2$ $(4\text{-}MePy)_4 \cdot p$-xylène

I. SOLACOLU *, D. SĂNDULESCU ** et C. DRĂGULESCU ***

* Centre de Chimie Physique, Bucarest, 31, str. Galaţi
** Institut du Pétrole, des Gaz et de la Géologie, Bucarest, 2–6, str. Traian Vuia
***Institut Polytechnique « Traian Vuia », Timişoara, 2, Bd. 30 Decembrie

Reçu le 1er août 1973

L'analyse diffractométrique des cristaux de $M(SCN)_2$ $(4\text{-}MePy)_4$, (M = Co, Ni ; 4-MePy = 4-méthylpyridine), avec et sans *p*-xylène, a mis en évidence l'existence des cellules élémentaires tétragonales à 8 molécules de combinaison coordinative, caractérisées par une symétrie Laue 4/m et le groupe spatial $I_4\,1/a$, défini par les paramètres $a = b = 16{,}81$ Å ; $c = 22{,}41$ Å, respectivement, $a = b = 17{,}96$ Å ; $c = 21{,}32$ Å. Dans le cas des combinaisons $M(SCN)_2$ $(4\text{-}MePy)_2$, on a mis en évidence un réseau orthorhombique à 18 molécules dans la cellule élémentaire et le groupe spatial I222, les paramètres caractéristiques étant $a = 20{,}20$ Å ; $b = 21{,}56$ Å ; $c = 17{,}93$ Å. Les déterminations sont en concordance avec une théorie proposée auparavant sur la stabilité des combinaisons avec des hydrocarbures aromatiques par des effets d'hyperpolarisabilité d'ordre supérieur et avec le modèle établi à partir des données thermodynamiques.

Les composés d'inclusion formés entre les hydrocarbures aromatiques et les combinaisons coordinatives des métaux, du type $M(SCN)_2$ $(4\text{-}MePy)_4$, ou M = Co, Ni et 4-MePy = 4-méthylpyridine, sont très importants du point de vue de la chimie théorique. Ces combinaisons se caractérisent par le fait qu'elles sont constituées par deux composants principaux : l'un des composés — le support — forme un réseau caractérisé par des lacunes dans lesquelles est inclus, dans certaines conditions, le deuxième composant. Ces composés sont différents par rapport aux combinaisons moléculaires (du type transfert de charge ou liaison d'hydrogène) beaucoup étudiées jusqu'à présent, tels que : hydrocarbures aromatiques — nitrodérivés aromatiques (du type picrates), quinones — phénols, hydrocarbures aromatiques — halogénures métalliques, hydrocarbures oléfiniques — halogénures métalliques, cétones — dérivés halogénés. Dans ce nouveau domaine de la chimie des combinaisons moléculaires du type clathrate, le problème de la liaison qui existe entre le composant inclus et le composant d'inclusion (ou support) présente un aspect spécial, étant déterminé par le facteur géométrique. Souvent, on peut se poser la question si le composé étudié correspond à la notion habituelle de combinaison chimique, pour laquelle on admet l'existence de certaines forces de liaison, suffisamment puissantes, qui permettent de considérer ce composé comme une espèce moléculaire indépendante. Généralement, les forces van der Waals sont exclues de cette définition mais, dans le cas des combinaisons d'inclusion, les forces van der Waals sont pourtant suffisamment puissantes pour que l'on puisse considérer l'interaction moléculaire comme base de la liaison chimique.

Dans quelques travaux antérieurs [1-4] on a présenté les problèmes actuels de ce nouveau domaine de la chimie :

— la clarification de l'interaction hydrocarbure — réseau support ;

— la détermination des conditions suffisantes et nécessaires pour la formation et la stabilité de ces combinaisons, par une étude thermodynamique des équilibres de formation et par une étude cinétique des réactions de formation, respectivement, de dissociation, études associées avec la détermination des caractéristiques du réseau et de la molécule incluse ;

— l'inclusion d'un grand nombre de combinaisons coordinatives dans le domaine de la chimie des clathrates;

— l'étude de quelques nouvelles classes de clathrates, dont les caractéristiques conduisent à leur application dans des nouveaux processus de séparation.

Nous allons essayer de développer brièvement les idées présentées ci-dessus.[4] L'état de la molécule incluse dans un milieu avec une symétrie parfaitement connue ou, en tout cas, déterminable, constitue l'objet de quelques recherches actuelles liées tant à la théorie proprement dite des interactions moléculaires, qu'à la théorie des solutions. Mais, d'autre part, il faut remarquer que beaucoup de catalyseurs doivent leur activité aux combinaisons de surface du type clathrate, d'où dérive leur haute spécificité. Comme on l'a indiqué ci-dessus, la liaison entre les deux composants de la combinaison moléculaire (la molécule incluse — le réseau support) est déterminée surtout par le facteur géométrique, mais ce facteur géométrique ne doit pas être limité seulement aux dimensions longitudinales et transversales ; il doit être étendu à la symétrie et à la forme.

Dans un travail antérieur [4] on a démontré qu'une caractéristique de la molécule incluse, qui constitue un critère d'appréciation de ces combinaisons correspond aux coefficients d'hyperpolarisabilité d'ordre supérieur. En effet, à l'intérieur du réseau cristallin, le champ électrique ($\mathcal{F}$) est de l'ordre de 10^8 V/cm et la bien connue équation du moment de dipôle induit (m)

$$m = \alpha \cdot \mathcal{F} \tag{1}$$

(dans laquelle α représente la polarisabilité) est valable seulement dans les conditions expérimentales habituelles ($\mathcal{F} < 10^7$ V/cm, valeur correspondant

---

[1] V. Vântu et D. Săndulescu, *Ann. Roum. Sov., Ser. Chim.*, **3**, 99 (1960).

[2] M. Rushdy, D. Săndulescu, M. Popescu et V. Vântu, *Rev. Roumaine Chim.*, **7**, 1227 (1962).

[3] M. Rushdy, *Thèse*, 'Inst. Pétr., Gaz et Géol., Bucarest, 1962.

[4] D. Săndulescu, *Thèse*, Inst. Pétr., Gaz et Géol., Bucarest, 1968.

à la rigidité diélectrique). Dans le cas des champs électriques intenses, il faut appliquer des équations du type

$$m = \alpha \cdot \mathcal{F} + \frac{1}{2}\,\beta \cdot \mathcal{F}^2 + \frac{1}{6}\gamma\mathcal{F}^3 + \cdots \qquad (2)$$

dans lesquelles β et γ représentent les coefficients d'hyperpolarisabilité du premier et du second ordre. Dans le cas des molécules polaires, β présente des valeurs négatives, tandis que, pour les molécules avec un centre de symétrie, $\beta = 0$.[5]

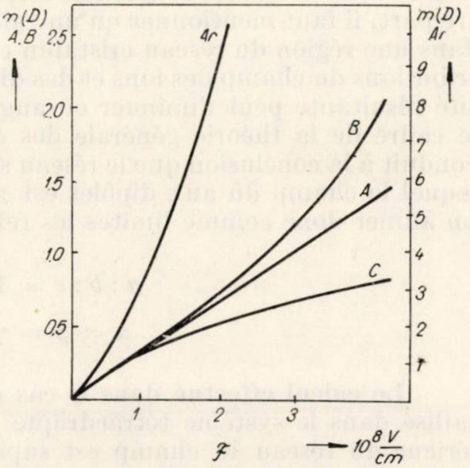

Fig. 1.— Variation du moment de dipôle induit en fonction de la valeur de champ électrique. A — champs électriques de faible intensité; *B* — champs électriques intenses, l'effet de l'hyperpolarisabilité du second ordre; *C* — champs électriques intenses, l'effet de l'hyperpolarisabilité du premier ordre; *Ar*-hydrocarbures aromatiques non disymétriques.

Dans la figure 1 on a représenté la variation du moment induit en fonction du champ électrique ; on peut observer une croissance importante du moment de dipôle induit (*m*), due au coefficient d'hyperpolarisabilité du second ordre (γ), en comparaison de la variation linéaire valable seulement pour les champs électriques de petite intensité[4] ; dans la même figure on peut aussi observer l'effet de l'hyperpolarisabilité du premier ordre (β) qui, étant négative, diminue la valeur du moment de dipôle induit (*m*). On peut aussi observer que, la croissance du moment de dipôle est très importante dans le cas de la courbe (Ar), correspondant aux hydrocarbures aromatiques non disymétriques (benzène, *p*-xylène, mésithylène). Certes, pour un calcul plus correct, il faut tenir compte de l'hyperpolarisabilité apparue dans un gradient de champ électrique (donc dans un champ électrique non uniforme), [6] qui correspond plus correctement à la situation de la cellule support. La valeur $\beta = 0$ correspond aux systèmes moléculaires non disymétriques (avec une symétrie d'inversion) [7], donc au benzène D_{6h}, au *p*-xylène

---

[5] A. Buckingham et B. Orr, *Quart. Rev.*, **21**, 195 (1967).

[6] A. Buckingham, *Quarl. Rev.*, **13**, 183 (1959).

[7] K. Mislow, « Introduction to Stereochemistry », W. Benjamin, New York, 1966, p. 33.

D_{2h}, et ne correspond pas aux autres xylènes isomères (C_3 ou C_{2v}), pour lesquels $\beta<0$. Cette interprétation a permis l'explication de l'ordre de préférence de la clathration et de l'ordre de stabilité pour la série tétra-4-méthylpyridine dithiocyanate de nickel (et de cobalt)

p-xylène > éthylbenzène > toluène > *o*- et *m*-xylène

On observe que l'ordre de stabilité ne correspond pas à l'ordre des valeurs des moments de dipôle, mais au contraire, à l'ordre inverse, parce que les moments de dipôle sont déterminés par la disparition de quelques éléments de symétrie. Il en résulte, évidemment, que la possibilité d'inclusion de la molécule d'hydrocarbure aromatique n'est pas conditionnée seulement par certaines dimensions géométriques : la molécule incluse doit remplir certaines conditions concernant la symétrie de la forme. D'autre part, il faut mentionner qu'un calcul de l'intensité du champ électrique dans une région du réseau cristallin correspond à la superposition des contributions du champ des ions et des dipôles du réseau et la valeur de l'intensité résultante peut diminuer ou augmenter. Le problème est résolu dans le cadre de la théorie générale des diélectriques et du magnétisme,[4] qui conduit à la conclusion que le réseau support ne peut pas être cubique (pour lequel le champ dû aux dipôles est nul à l'intérieur du réseau cristallin) ; on admet donc comme limites les relations cristallographiques suivantes :

$$a : b : c = 1 : 1 : y \text{ et}$$
$$\alpha = \beta = \gamma \ (= 90°) \tag{3}$$

Le calcul effectué dans le cas du clathrate $Ni(CN)_2NH_3.C_6H_6$ (cristallisé dans le système tétraédrique avec $c/a \cong 1,2$) démontre qu'à l'intérieur du réseau le champ est supérieur à la valeur calculée en tenant compte de l'effet des dipôles isolés. [4] Dans ce cas, même par un calcul approximatif, on a réussi à interpréter l'énergie de stabilisation du réseau de $Ni(CN)_2\,NH_3.C_6H_6$ ($U - U_0$), calculée à partir de la différence de l'énergie de dissociation et de l'énergie de sublimation du benzène

$$\Delta U_{\text{diss}} - \Delta U_{\text{sub}} \cong 13500 - 9200 \cong 4300 \text{ cal/mole} \tag{4}$$

qui, comparée à la valeur de l'énergie d'interaction avec le champ électrique ($E - E_0$), représentée dans la figure 2 :

$$E - E_0 = -\frac{1}{2}\alpha\mathfrak{F}^3 - \frac{1}{24}\gamma\,\mathfrak{F}^4 - \dots \tag{5}$$

démontre, dans l'hypothèse du champ uniforme, une concordance satisfaisante avec les paramètres cristallins correspondant à un champ $\mathfrak{F} \doteq 0{,}7 \ldots 0{,}8 \cdot 10^8$ V/cm.

Le diagramme présenté dans la figure 3 représente l'énergie potentielle du réseau du clathrate dans le cas de l'interaction normale de dispersion benzène — benzène (benzène pur solide) et dans le cas de la contribution de l'énergie électrique de stabilisation due à la polarisabilité .[4]

Dans le cas de l'étude de la dissociation des clathrates du type $M(SCN)_2(4\text{-}MePy)_4$. hydrocarbure aromatique [2] on a démontré que la monovariation de l'équilibre peut être interprétée par le modèle suivant : la combinaison coordinative $M(SCN)_2(4\text{-}MePy)_2$, en présence d'un excès de 4-MePy, ferme ces molécules dans des cellules du type clathrate (C_1) et, c'est le réseau de la combinaison résultante, $M(SCN)_2(4\text{-}MePy)_4$, qui contient les cellules nécessaires pour l'inclusion des molécules de l'hydrocarbure (C_2).

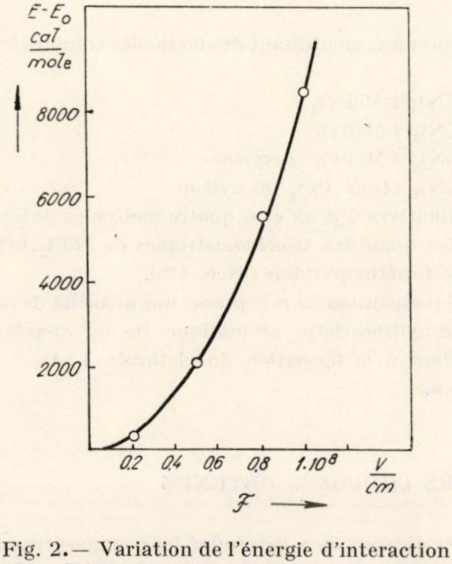

Fig. 2.— Variation de l'énergie d'interaction ($E - E_0$) en fonction du champ électrique dans le cas du composé clathrate $Ni(CN)_2 NH_3 . C_6H_6$.

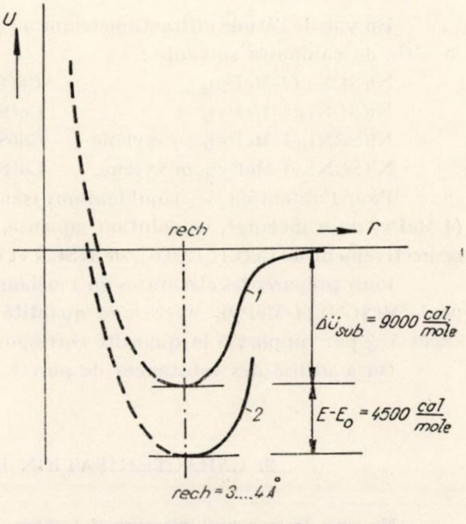

Fig. 3. — Energie potentielle du réseau du clathrate.

1, interaction normale de dispersion ; 2 – contribution de l'énergie électrique de stabilisation due à la polarisabilité.

Ce modèle qualitatif nous a permis l'interprétation de la différence qui existe entre les liaisons des quatre molécules du ligand (4-MePy) avec l'atome métallique, la dissociation de la combinaison ayant lieu en deux étapes, deux molécules de ligand par étape (déterminations manométriques, [3] gaz-chromatographiques [2] et l'analyse thermique ATD et ATG [8]). Les caractéristiques thermodynamiques de la première étape sont identiques, indépendamment de la présence de l'hydrocarbure et indépendamment du degré de remplissage, ce qui nous a conduit à la conclusion que le réseau du clathrate $M(SCN)_2(4\text{-}MePy)_4$.hydrocarbure aromatique est identique à celui du clathrate $M(SCN)_2(4\text{-}MePy)_4$: le premier a les cellules C_1 et C_2 remplies, tandis que le deuxième seulement les cellules C_1 et représente le réseau support.

Le but de ce travail est celui de vérifier ces hypothèses établies à partir des données d'équilibre de dissociation obtenues par des déterminations diffractométriques qui permettent l'appréciation des dimensions et du degré de remplissage de la cellule élémentaire des combinaisons coordinatives et des composés clathrates respectifs.

---

[8] I. Solacolu, *Thèse*, Inst. Politechnique « Traian Vuia », Timişoara, 1973.

PARTIE EXPÉRIMENTALE

1. PRÉPARATION DES COMBINAISONS COORDINATIVES ET DES CLATHRATES

En vue de l'étude diffractométrique on a préparé, en utilisant des méthodes connues [2,9,10], la série de composés suivante :

$Ni(SCN)_2(4\text{-}MePy)_2$	$Co(SCN)_2(4\text{-}MePy)_2$
$Ni(SCN)_2(4\text{-}MePy)_4$	$Co(SCN)_2(4\text{-}MePy)_4$
$Ni(SCN)_2(4\text{-}MePy)_4$. *p*-xylène	$Co(SCN)_2(4\text{-}MePy)_4$. *p*-xylène
$Ni(SCN)_2(4\text{-}MePy)_4$. *m*-xylène	$Co(SCN)_2$ (4-Me $Py)_4$. *m*-xylène

Pour l'obtention des combinaisons coordinatives à deux et à quatre molécules de ligand (4-MePy) on a mélangé, en solution aqueuse, les quantités stœchiométriques de $NiCl_2 . 6H_2O$, respectivement de $Co(CH_3COO)_2$, de KSCN et de 4-méthylpyridine (excès 4 %).

Pour préparer les clathrates on a mélangé (suspension en *n*-héptane) une quantité de composé $M(SCN)_2(4\text{-}MePy)_4$ avec une quantité d'hydrocarbure aromatique (*p*- ou *m*-xylène), excès 5 % par rapport à la quantité correspondant à la formation du clathrate 1 : 1.

On a utilisé des substances de pureté *p.a.*

2. CARACTÉRISATION DES COMPOSÉS OBTENUS

En vue de la caractérisation des composés obtenus on a déterminé leur composition chimique : le contenu en soufre, en carbone, en hydrogène (par la microméthode de Pregl), le contenu en azote (par la microméthode de Pregl-Dumas [11]) et le contenu en métal — Ni, Co — (par voie gravimétrique [12]). La composition déterminée correspond aux formules proposées. [8]

3. DÉTERMINATIONS DIFFRACTOMÉTRIQUES

Pour les déterminations diffractométriques avec des rayons X on a utilisé des cristaux obtenus par la cristallisation lente d'une solution préparée à l'aide d'un solvant organique ; dans ce but les combinaisons coordinatives et les clathrates obtenus ont été dissous dans du chloroforme, les solutions obtenues étant évaporées lentement à la température ordinaire. (Le temps de l'évaporation de la solution a varié entre 25 et 30 jours.)

La dimension moyenne des cristaux obtenus, mesurée à l'aide d'un microscope du type I.O.R., a été de 0,5 à 1 micron.

---

[9] W. D. Schaeffer, W. S. Dorsey, D. A. Skinner, et C. G. Christian, *J. Amer. Chem. Soc.*, **79**, 5870 (1957).

[10] G. Gawalek et H. G. Könnecke, *Chem. Techn.*, **15**, 609 (1963).

[11] A. Friedrich, « La pratique de la microanalyse organique quantitative », Dunod, Paris, 1939, p. 112.

[12] G. Charlot et D. Bézier, « Méthodes modernes d'analyse quantitative minérale » Masson et Cie Ed. Paris, 1949, p. 402.

Pour obtenir les Debyegrammes on a utilisé un appareil de diffraction du type TUR—M60.

Les preuves ont été préparées en utilisant, en qualité de liant, le baume de Canada (coefficient d'absorption négligeable) ; les petits bâtons obtenus (de diamètre de 0,15 à 0,20mm) ont été exposés dans la chambre Debye — Scherer (au diamètre de 114,6 mm).

La température de travail a été de $22 \pm 3°$.

Pour l'irradiation des preuves on a utilisé les tubes suivants :

— pour les composés du nickel, la radiation CuK_α filtrée avec du nickel, la longueur d'onde λ étant de 1,54177 Å ;

— pour les composés du cobalt, la radiation CoK_α filtrée avec du fer, la longueur d'onde λ étant de 1,79021 Å.

Le temps d'exposition des preuves dans la chambre Debye — Scherer a été de 10 à 12 heures.

On a utilisé des films ORWO pour la structure fine RF 44, qui, en vue de la réalisation des Debyegrammes, ont été arrangés dans la chambre d'après la méthode Straumanis.

Pour chaque film on a fait les corrections de contraction, due au processus de développement ; la correction pour la longueur du film a conduit à une valeur d'approximativement

$$1 \text{ mm film} = 1{,}0020°$$

On n'a pas fait des corrections pour l'absorption, les coefficients d'absorption des combinaisons coordinatives et des clathrates, pour les radiations utilisées étant négligeables (les corrections se placent au-dessous de la limite des erreurs expérimentales).

Les distances entre les lignes ont été mesurées à l'aide d'un microscope Karl Zeiss Jena (l'erreur de la détermination a été de 0,05 mm).

4. DÉTERMINATIONS DE DENSITÉ

En vue de la détermination du degré de remplissage de la cellule élémentaire des combinaisons coordinatives et des clathrates, on a déterminé la densité de ces composés à l'aide d'un picnomètre (immersion en *n*-héptane).

RÉSULTATS ET DISCUSSIONS

L'analyse chimique des combinaisons coordinatives et des clathrates a démontré une bonne concordance entre la composition chimique des composés obtenus et la composition théorique correspondant à un degré de remplissage maximal. [8] On n'a pas observé la formation d'un clathrate avec le *m*-xylène, ce qui a confirmé la théorie concernant l'ordre de préférence dans les réactions de clathration.

Les données diffractométriques des combinaisons coordinatives et des clathrates sont présentées dans les tableaux 1 — 6.

A partir des données obtenues par l'étude diffractométrique, on a calculé les dimensions de la cellule élémentaire des combinaisons coordinatives et des clathrates et, à l'aide des valeurs des densités, mesurées par la méthode du picnomètre, on a calculé le degré de remplissage de la cellule élémentaire (le nombre des molécules du composé par cellule élémentaire). On a utilisé la formule :

$$n = \frac{\rho V}{M} \qquad (6)$$

Tableau 1

Données diffractométriques de la combinaison coordinative $Ni(SCN)_2(4\text{-}MePy)_2$

Système orthorhombique $a = 20{,}20$ Å
Groupe spatial I 222 $b = 21{,}56$ Å
$c = 17{,}93$ Å

N⁰	Ligne Intensité	$1/d^2_{obs}$	*h k l*	$1/d^2_{calc}$
1	intense	0,0102	002	0,0098
2	moyenne intense	0,0144	121	0,0142
3	t. faible	0,0217	031	0,0218
4	t. faible	0,0350	040	0,0344
5	faible	0,0366	213	0,0366
6	faible	0,0538	233	0,0538
7	t.t. faible	0,0616	134	0,0616
8	moyenne	0,0692	314	0,0693
9	faible	0,0789	510	0,0796
10	faible diffuse	0,0995	262	0,0996
11	faible	0,1151	055	0,1150
12	t. faible diffuse	0,1305	435	0,1303
13	t. faible diffuse	0,1476	525	0,1476
14	faible	0,1690	208	0,1692
15	t. faible	0,1915	048	0,1912
16	t. faible	0,2024	185	0,2018
17	t. faible	0,2140	158	0,2136

Tableau 2

Données diffractométriques de la combinaison coordinative $Ni(SCN)_2(4\text{-}MePy)_4$

Système tétragonal $a = b = 17{,}96$ Å
Groupe spatial I_4 1/a c = 21,32 Å

N⁰	Ligne Intensité	$1/d^2_{obs}$	*h k l*	$1/d^2_{calc}$
1	intense	0,0053	101	0,0053
2	moyenne diffuse	0,0123	200	0,0124
3	moyenne diffuse	0,0142	112	0,0150
4	moyenne diffuse	0,0179	211	0,0177
5	faible diffuse	0,0208	202	0,0212
6	t. faible	0,0352	004	0,0352
7	faible	0,0425	321	0,0425
8	faible	0,0477	303	0,0477
9	t.t. faible	0,0550	411	0,0549
10	moyenne	0,0647	332	0,0646
11	t.t. faible	0,0704	215	0,0705
12	t.t. faible	0,0862	116	0,0854
13	moyenne diffuse	0,1041	226	0,1040
14	t.t. faible	0,1316	505	0,1315
15	t.t. faible	0,1485	327	0,1481
16	t.t. faible	0,1595	516	0,1598
17	t.t. faible	0,1717	318	0,1718
18	t.t. faible	0,1814	109	0,1813
19	t.t. faible	0,1910	651	0,1913

Tableau 3

Données diffractométriques du composé clathrate $Ni(SCN)_2(4\text{-}MePy)_4 \cdot p$-xylène

Système tétragonal $a = b = 16{,}81$ Å
Groupe spatial I_4 1/a $c = 22{,}41$ Å

N°	Ligne Intensité	$1/d^2_{obs}$	*h k l*	$1/d^2_{calc}$
1	moyenne intense	0,0056	101	0,0053
2	faible diffuse	0,0339	301	0,0339
3	faible diffuse	0,0356	213	0,0356
4	moyenne diffuse	0,0461	321	0,0461
5	moyenne diffuse	0,0619	411	0,0622
6	faible	0,0676	215	0,0676
7	moyenne	0,0886	404	0,0885
8	faible	0,0959	325	0,0959
9	faible	0,1008	107	0,1008
10	t.t. faible	0,1152	217	0,1152
11	t.t. faible diffuse	0,1274	600 (008)	0,1274
12	t.t. faible	0,1425	246	0,1425
13	t.t. faible	0,1680	119	0,1682
14	t.t. faible	0,1807	615	0,1807
15	t.t. faible diffuse	0,2345	802	0,2345
16	t. faible diffuse	0,2497	509	0,2497

Tableau 4

Données diffractométriques de la combinaison coordinative $Co(SCN)_2(4\text{-}MePy)_2$

Système orthorhombique $a = 20{,}20$ Å
Groupe spatial I 222 $b = 21{,}56$ Å
$c = 17{,}93$ Å

N°	Ligne Intensité	$1/d^2_{obs}$	*h k l*	$1/d^2_{calc}$
1	intense	0,0052	101	0,0052
2	intense	0,0144	211	0,0142
3	faible	0,0217	310	0,0218
4	moyenne diffuse	0,0345	400	0,0344
5	t. faible diffuse	0,0391	213 040	0,0390 0,0392
6	faible	0,0438	420	0,0442
7	moyenne	0,0538	332	0,0538
8	t. faible	0,0694	143	0,0693
9	moyenne	0,0867	343	0,0865
10	t. faible	0,1008	062	0,1006
11	t.t. faible diffuse	0,1130	154	0,1131
12	t.t. faible diffuse	0,1270	552	0,1273
13	t. faible diffuse	0,1330	703	0,1333
14	t. faible	0,1415	651	0,1417
15	t.t. faible diffuse	0,1468	255	0,1476
16	faible	0,1676	516	0,1678
17	t. faible	0,1984	190	0,1990
18	t.t. faible	0,2128	057	0,2131
19	t.t. faible	0,2263	914	0,2263

Tableau 5

Données diffractométriques de la combinaison coordinative $Co(SCN)_2(4\text{-}MePy)_4$

Système tétragonal $a = b = 17{,}96$ Å
Groupe spatial $I_4\ 1/a$ $c = 21{,}32$ Å

N°	Ligne Intensité	$1/d^2_{obs}$	*h k l*	$1/d^2_{calc}$
1	moyenne	0,0053	101	0,0053
2	moyenne faible	0,0120	200	0,0124
3	moyenne	0,0149	112	0,0150
4	faible	0,0178	211	0,0177
5	faible	0,0211	202	0,0212
6	t.t. faible	0,0252	220	0,0248
7	t.t. faible	0,0307	310	0,0310
8	t.t. faible diffuse	0,0339	222	0,0336
9	t.t. faible diffuse	0,0355	004	0,0352
10	faible	0,0427	321	0,0425
11	faible	0,0491	400	0,0496
12	moyenne	0,0548	411	0,0549
13	moyenne faible	0,0583	402	0,0581
14	t. faible	0,0625	420	0,0620
15	faible	0,0703	215	0,0705
16	moyenne	0,0856	116	0,0854
17	t.t. faible	0,0921	521	0,0921
18	t.t. faible diffuse	0,0964	244	0,0972
19	t.t. faible	0,0998	440	0,0992
20	t.t. faible	0,1541	701	0,1541
21	t.t. faible	0,1666	721	0,1665
22	t.t. faible	0,2231	617	0,2231

Tableau 6

Données diffractométriques du composé clathrate $Co(SCN)_2(4\text{-}MePy)_4 \cdot p$-xylène

Système tétragonal $a = b = 16{,}80$ Å
Groupe spatial $I_4\ 1/a$ $c = 22{,}41$ Å

N°	Ligne Intensité	$1/d^2_{obs}$	*h k l*	$1/d^2_{calc}$
1	moyenne intense	0,0055	101	0,0055
2	intense	0,0140	200	0,0141
3	faible	0,0193	211	0,0197
4	faible diffuse	0,0280	220	0,0283
5	faible diffuse	0,0338	301	0,0339
6	faible diffuse	0,0356	213	0,0356
7	moyenne	0,0461	321	0,0461
8	faible diffuse	0,0569	400	0,0566
9	faible	0,0613	411	0,0612
10	moyenne	0,0629	233	0,0629
11	moyenne faible	0,0861	206	0,0858
12	t. faible diffuse	0,0886	404	0,0885
13	moyenne	0,0958	325	0,0959
14	faible	0,1027	244	0,1026
15	t.t. faible	0,1557	228	0,1557
16	t.t .faible	0,1682	119	0,1682

dans laquelle n représente le nombre des molécules de la cellule élémentaire (le degré de remplissage), ρ la densité, mesurée par la méthode du picnomètre et exprimée en g/cm,^{3} M la masse d'une mole de substance (g), V le volume de la cellule élémentaire, exprimé en cm. ^{3}

Les caractéristiques du réseau des combinaisons coordinatives et des clathrates sont présentées dans le tableau 7.

Tableau 7

Caractéristiques du réseau des clathrates et des combinaisons support

Composé	Système de cristallisation et groupe spatial	Volume de la cellule élémentaire, Å^3	Densité, g/cm^3	N^0 molécules par cellule élémentaire
$Ni(SCN)_2(4\text{-}MePy)_2$	Orthorhombique I 222	7810	1,47	18
$Ni(SCN)_2(4\text{-}MePy)_4$	Tétragonal I_4 1/a	6880	1,17	8
$Ni(SCN)_2(4\text{-}MePy)_4\cdot$ *p*-xylène	Tétragonal I_4 1/a	6340	1,21	8
$Co(SCN)_2(4\text{-}MePy)_2$	Orthorhombique I 222	7810	1,54	18
$Co(SCN)_2(4\text{-}MePy)_4$	Tétragonal I_4 1/a	6880	1,19	8
$Co(SCN)_2(4\text{-}MePy)_4\cdot$ *p*-xylène	Tétragonal I_4 1/a	6330	1,22	8

Ainsi qu'on a démontré, le problème de l'activité catalytique de quelques matériaux (par exemple des zéolithes naturels et synthétiques) dans les réactions d'isomérisation et de craquage des hydrocarbures est très intéressant au point de vue théorique et présente des conséquences importantes pour la technologie. L'augmentation de l'activité catalytique, dans le cas des cations bivalents [13] par rapport à celle des cations monovalents, observée expérimentalement, n'a pas été interprétée de manière satisfaisante, en dépit du grand nombre de travaux publiés à ce propos ces dernières années. [14–19]

On a démontré que le système clathrate, caractérisé par un réseau support bien défini, avec une géométrie simple de la disposition des moléicules de l'hydrocarbure fermée, correspond parfaitement à un modèle déal pour l'étude de l'état de la molécule d'hydrocarbure fermée. [1,4,20].

---

[13] P. Pickert, J. Rabo, E. Dempsey et V. Schomaker, « Proc. of 3rd Int. Congr. on Catalysis », Amsterdam, 1964, North Holland Publ. Co., Amsterdam, 1965, p. 714.

[14] H. Benesi, *J. Catalysis*, **8**, 368 (1967).

[15] C. Plank, « Proc. of 3rd Int. Congr. on Catalysis », Amsterdam, 1964, North Holland Publ. Co., Amsterdam, 1965, p. 727.

[16] J. Turkevich, F. Nozacki et D. Stamires, « Proc. of 3rd Int. Congr. on Catalysis », Amsterdam, 1964, North Holland Publ. Co., Amsterdam, 1965, p. 586.

[17] P. Venuto, E. Wu et J. Cattanach, « Molecular Sieves Conf. », London, avril 1967, Publ. Soc. of Chem. Ind., London, 1968, p. 117.

[18] J. Ward, *J. Catalysis*, **10**, 34 (1968).

[19] Yun Yang Huang, J. Benson et M. Boudart, *Ind. & Eng. Chem. Fundamentals*, **8**, 346 (1969).

[20] I. Solacolu, D. Manolescu, C. Drăgulescu, A. Alistar, D. Săndulescu, et V. Vântu, *Conférence*, Sess. Jubiliaire Inst. Pétr., Gaz et Géol., Bucarest, 1969.

Dans ces travaux on a démontré qu'il est possible que la valeur du champ électrique à l'intérieur de la cellule soit très importante; en même temps, la théorie générale de la structure cristalline a conduit à l'établissement des critères géométriques de fermeture, critères qui assurent des champs électriques intenses et des énergies d'interaction puissantes.

La vérification de l'existence de ces valeurs de l'intensité du champ électrique, tellement grandes, voisines au domaine d'ionisation de la molécule d'hydrocarbure, a été faite par Benson et Boudart, [21] par l'étude de l'absorption physique de l'hydrogène sur les zéolithes Ca—Y et Na—Y et, ce dernier temps, par l'étude de l'absorption physique du krypton sur les mêmes types de zéolithes. [19]

On peut appliquer, pour le calcul du champ électrique dans les supports cristallins, les modèles suivants :

— le modèle de Barrer et Gibbons, [22,23] appliqué aux zéolithes ;

— le modèle de Pickert, [13] appliqué aux zéolithes, ou

— le modèle appliqué au clathrate du type $Ni(CN)_2NH_3.C_6H_6$ [4].

Tous ces modèles conduisent à des résultats semblables, différents par le choix de l'unité de base de l'électroneutralité, par le système de la distribution des charges électriques et par le procédé de l'addition des contributions des composants de la cellule élémentaire dans le champ électrique total. Malheureusement, dans le cas des clathrates du type $M(SCN)_2(4\text{-}MePy)_4$.hydrocarbure aromatique, les données sur la disposition exacte des ions dans le réseau support sont à présent insuffisantes pour pouvoir évaluer correctement l'intensité du champ, ainsi que dans le cas du clathrate $Ni(CN)_2NH_3.C_6H_6$; tout de même les données existantes permettent l'interprétation du diagramme approximatif représenté dans la figure 4.

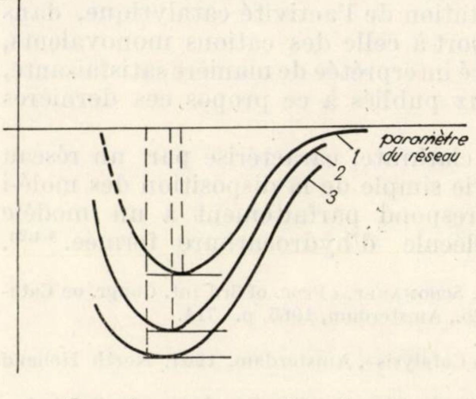

Fig. 4. — Valeur de l'énergie d'interaction avec le réseau support, pour différents xylènes isomères :

1, *m*-xylène; 2, éthylbenzène; 3, *p*-xylène.

On observe que les données diffractométriques ont vérifié l'hypothèse, démontrant une grande compacité dans le réseau du composé $M(SCN)_2(4\text{-}MePy)_2$, à 18 molécules dans la cellule élémentaire, en comparaison du réseau du composé $M(SCN)_2(4\text{-}MePy)_4$, qui comprend seulement 8 molécules.

---

[21] J. Benson et M. Boudart, *J. Catalysis*, **8**, 93 (1967).

[22] R. Barrer et R. Gibbons, *Trans. Faraday Soc.*, **59**, 2569 (1963).

[23] R. Barrer et R. Gibbons, *Trans. Faraday Soc.*, **61**, 948 (1965).

En conclusion, les déterminations diffractométriques effectuées sur les combinaisons du type $M(SCN)_2(4\text{-}MePy)_{n=2,4}$ démontrent que ces composés correspondent à des compacités différentes, ce qui explique les hypothèses antérieures sur les possibilités de clathration des combinaisons avec $n = 4$ et les hypothèses concernant la nature clathratique des nombreuses combinaisons coordinatives. De même, on peut observer la vérification des conclusions concernant le réseau support ($c/a \cong 1{,}33$), qui correspond à une intensification du champ électrique par rapport aux valeurs calculées pour les dipôles isolés.

Revue Roumaine de Chimie, 19, 3, 429–435 (1974)

COMPLEXES MOLÉCULAIRES DES THIOAMIDES. II[1]

COMPLEXES DE TRANSFERT DE CHARGE DU PHÉNYLTHIOACÉTAMIDE ET DE LA PHÉNYLTHIOACÉTOPIPÉRIDIDE AVEC L'IODE

FELICIA CORNEA*, CORNELIA FULEA* et ŞERBAN MOLDOVEANU **

* Laboratoire de Chimie organique, Faculté de Chimie, Université de Bucarest, 89, Spl. Independenţei

** Laboratoire de Chimie analytique, Faculté de Chimie, Université de Bucarest, 89, Spl. Independenţei

Reçu 31 mars 1973

En suivant les recherches antérieures on a étudié les complexes moléculaires des phénylthioacétamide et phénylthioacétopipéridide avec l'iode, en utilisant les méthodes spectroscopiques (des spectres UV, en visible et IR). A l'aide des valeurs obtenues par le calcul des paramètres thermodynamiques caractéristiques de ces complexes on a tiré la conclusion que le phénylthioacétamide et la phénylthioacétopipéridide sont des donneurs d'électrons plus faibles que le thiobenzamide et la thiobenzpipéridide. La différence entre les stabilités de ces complexes est due à la densité électronique différente à l'atome de soufre, comme une conséquence de l'effet de la nature du radical sur la densité électronique du groupement thioamidique.

Vu que les thioamides peuvent fonctionner comme donneurs d'électrons dans l'interaction avec l'iode [1], nous avons étendu l'étude concernant la formation des complexes moléculaires de type thioamide-iode soit pour obtenir de nouveaux complexes soit pour déterminer l'influence exercée par la nature du radical sur la structure électronique du groupe thioamidique afin d'expliquer la réactivité différente de quelques thioamides.

Ainsi, ont été employés comme donneurs d'électrons le phénylthioacétamide (FTA) et la phénylthioacétopipéridide (FTAP) qui forment avec l'iode comme nous avons démontré, des complexes moléculaires.

Nous avons choisi, comme donneurs, les thioamides mentionnées, pour mettre en évidence l'influence exercée par la présence du groupe méthylène intercalé entre le radical phényl et le groupement fonctionnel thioamidique.

Les complexes moléculaires formés en solution ont été étudiés par des méthodes spectrales et puis comparés avec les complexes moléculaires du thiobenzamide et de la thiobenzpipéridide.

---

[1] Ire partie : F. Cornea, C. Fulea et Ş. Moldoveanu, *Rev. Roumaine Chim.*, 15, 1415 (1970).

ÉTUDE SPECTROPHOTOMÉTRIQUE EN VISIBLE ET EN UV DES COMPLEXES FTA – I_2 ET FTAP – I_2

L'étude des solutions de FTA et FTAP dans le tétrachlorure de carbone en comparaison de celles obtenues en mélangeant quelques solutions de FTA ou FTAP et l'iode en tétrachlorure de carbone met en évidence la formation des complexes moléculaires entre les thioamides mentionnés et l'iode.

Les spectres d'absorption en visible et UV représentés dans les figures 1 et 2 indiquent des différences distinctes dans l'allure des courbes.

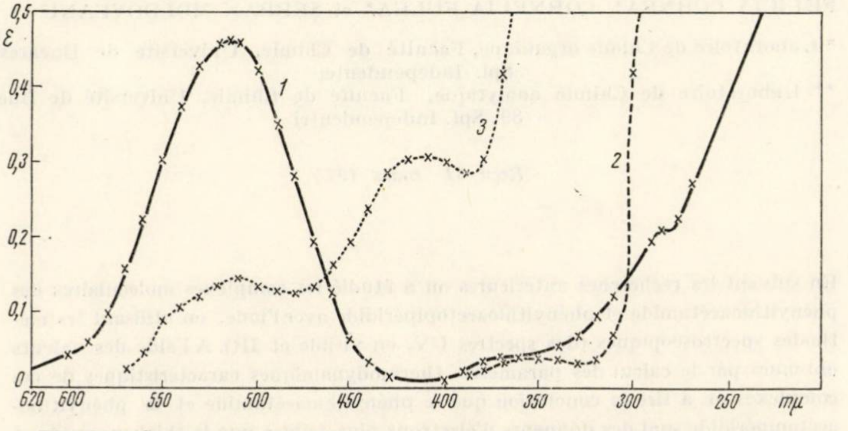

Fig. 1. — Spectres d'absorption en visible et UV des solutions de I_2, FTA et FTA – I_2 (*1*, I_2, *2*, FTA, *3*, FTA – I_2).

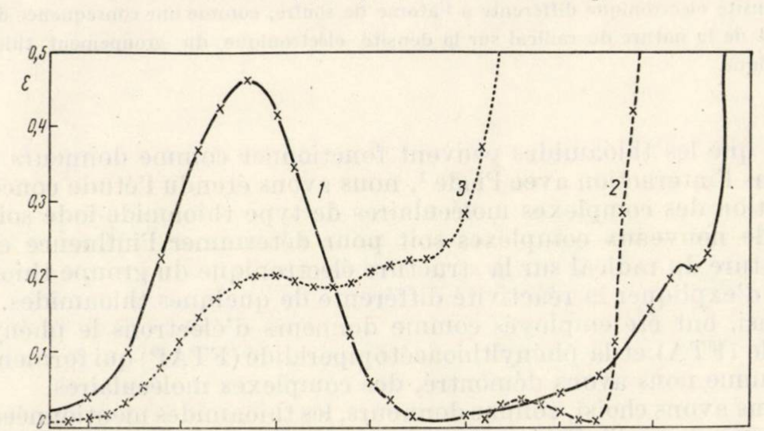

Fig. 2. — Spectres d'absorption en visible et UV des solutions de I_2, FTAP et FTAP – I_2 (*1*, I_2, *2*, FTAP, *3*, FTAP – I_2).

Le changement de couleur après le mélange des solutions du thioamide et l'iode en tétrachlorure de carbone, qui conduisent à l'apparition d'un maximum d'absorption situé à $\lambda = 410$ nm (fig. 1, courbe 3) et $\lambda = 420$ nm (fig. 2, courbe 3) sont des arguments pour la formation des complexes moléculaires thioamide-iode en solution de tétrachlorure de carbone.

Les maximums situés à 410 nm et respectivement à 420 nm peuvent être associés aux bandes de transfert de charge des complexes formés ; on remarque que la formation du complexe de transfert de charge conduit au déplacement de l'absorption avec 50 nm vers une longueur d'onde plus grande et aussi on constate une augmentation de l'intensité de l'absorption de l'ordre 10^2, en comparaison du donneur.

Le complexe FTA$-I_2$ n'a pu être séparé à l'état cristallin comme dans le cas du thiobenzamide; l'étude a été effectuée directement en solution.

Le rapport de combinaison entre les thioamides mentionnés et l'iode trouvé est 1 : 1, tel qu'il a été déterminé dans nos recherches antérieures pour le thiobenzamide et la thiobenzpipéridide.

La détermination de la variation de l'extinction des solutions dans lesquelles se forment les complexes FTA$-I_2$ et FTAP$-I_2$ à $\lambda = 410$ nm et respectivement $\lambda = 420$ nm en différentes conditions a permis la détermination des constantes de stabilité des complexes et des paramètres thermodynamiques de ceux-ci.

Ainsi on a déterminé la variation de l'extinction pour divers mélanges de solutions isomolaires d'iode et de FTA ou FTAP en tétrachlorure de carbone pris en deux concentrations, ainsi qu'à diverses températures.

Dans les tableaux 1 et 2 sont données les valeurs de l'extinction des mélanges des solutions isomolaires de FTA et I_2 et respectivement FTAP et I_2 en tétrachlorure de carbone de concentration $0{,}5 \cdot 10^{-3}$ M et $0{,}8 \cdot 10^{-3}$ M pour différentes températures.

Les constantes de stabilité des complexes étudiés ont été déterminées par une variante de la méthode Sakellaridis [2] pour les solutions isomolaires en rapport de combinaison 1 : 1.

La méthode Schwartzenbach[3] pour la détermination des constantes d'instabilité est moins précise que la variante Sakellaridis et bien que les résultats obtenus par les deux méthodes ne présentent pas de différences sensibles, nous avons considéré corrects ceux obtenus par la méthode Sakellaridis.

Dans le tableau 3 sont données les valeurs moyennes des constantes d'instabilité et de stabilité des complexes FTA$-I_2$ et FTAP$-I_2$.

LES PARAMÈTRES THERMODYNAMIQUES

Le calcul des paramètres thermodynamiques caractéristiques des complexes formés a été effectué d'une manière analogue à celle indiquée dans l'étude précédente [1].

Dans le tableau 4 on donne les valeurs obtenues pour l'énergie libre, l'enthalpie et l'entropie des complexes.

---

[2] P. Sakellaridis, *Bull. Soc. Chim. France*, **1958**, 282.

[3] G. Schwartzenbach et A. Willi, *Helv. Chim. Acta*, **39** 722 (1956).

Tableau 1

Valeurs des extinctions de quelques mélanges de solutions isomolaires de phénylthioacétamide et I_2 en CCl_4 de concentration 0,5 · 10⁻³ M et 0,8 · 10⁻³ M

Rapport FTA : I_2	Conc. 0,5 ·10^{-3} M			Conc. 0,8 ·10^{-3} M		
	20°C	30°C	40°C	20°C	30°C	40°C
1 :1	0,320	0,250	0,185	0,580	0,470	0,390
1 :2	0,290	0,225	0,165	0,530	0,430	0,335
2 :1	0,290	0,225	0,165	0,530	0,430	0,335
3 :2	0,310	0,240	0,175	0,560	0,460	0,370
2 :3	0,310	0,240	0,175	0,560	0,460	0,370
1 :3	0,230	0,185	0,140	0,420	0,355	0,275
3 :1	0,230	0,185	0,135	0,420	0,355	0,275
1 :7	0,130	0,110	0,080	0,220	0,220	0,160
7 :1	0,130	0,110	0,080	0,210	0,220	0,160
1 :9	0,105	0,090	0,065	0,170	0,150	0,130
9 :1	0,105	0,090	0,060	0,160	0,150	0,130

Tableau 2

Valeurs des extinctions de quelques mélanges de solutions isomolaires de phénylthiopipéridide et I_2 en CCl_4 de concentration 0,5 · 10⁻³ M et 0,8 · 10⁻³ M

Rapport FTAP : I_2	Conc. 0,5 ·10^{-3} M			Conc. 0,8 ·10^{-3} *M*		
	20°C	30°C	40°C	20°C	30°C	40°C
1 :1	0,210	0,165	0,115	0,330	0,260	0,230
1 :2	0,180	0,135	0,100	0,285	0,225	0,190
2 :1	0,180	0,195	0,100	0,285	0,225	0,190
3 :2	0,200	0,155	0,110	0,315	0,250	0,215
2 :3	0,200	0,155	0,110	0,315	0,250	0,215
1 :3	0,160	0,120	0,090	0,250	0,200	0,170
3 :1	0,160	0,120	0,090	0,250	0,200	0,170
1 :7	0,090	0,070	0,055	0,160	0,130	0,100
7 :1	0,090	0,070	0,055	0,160	0,130	0,100
1 :9	0,070	0,055	0,045	0,140	0,105	0,080
9 :1	0,070	0,055	0,045	0,140	0,105	0,080

La précision des déterminations est conditionnée par la méthode graphique utilisée pour trouver les constantes de stabilité. Les déviations des valeurs obtenues donnent une erreur générale d'environ 10% obtenue graphiquement pour ΔS et ΔH.

Les données indiquées dans le tableau 4 montrent le fait que le FTAP est un donneur un peu plus fort que le FTA.

Les paramètres obtenus en comparaison des paramètres thermodynamiques caractéristiques des complexes $TB-I_2$ et $TBP-I_2$ sont de beaucoup inférieurs, ce qui indique le fait que le FTA et le FTAP sont des donneurs plus faibles que les TB et TBP.

Tableau 3

Valeurs moyennes de constantes d'instabilité et stabilité du complexe $FTA-I_2$ et $FTAP-I_2$

	$FTA-I_2$			$FTAP-I_2$		
t°C	20°	30°	40°	20°	30°	40°
K instab.	$1{,}42.10^{-4}$	$2{,}27.10^{-4}$	$3{,}51.10^{-4}$	$1{,}66.10^{-4}$	$2{,}69.10^{-4}$	$4{,}20.10^{-4}$
K stab.	$0{,}704.10^{4}$	$0{,}441\cdot10^{4}$	$0{,}285.10^{4}$	$0{,}600\cdot10^{4}$	$0{,}372\cdot10^{4}$	$0{,}238\cdot10^{4}$

Tableau 4

Paramètres thermodynamiques des complexes $FTA-I_2$ et $FTAP-I_2$

	$FTA-I_2$			$FTAP-I_2$		
t°C	$-\Delta F$ cal/mole	$-\Delta H$ cal/mole	$-\Delta S$ cal/mole	$-\Delta F$ cal/mole	$-\Delta H$ cal/mole	$-\Delta S$ cal/mole
20°C	+5194	+8300	+10,6	+5100	+8500	+11,6
30°C	+5088			+4985		
40°C	+4982			+4870		

Le groupement méthylénique dans la molécule du FTA placé entre le groupement thioamidique et le radical phényle détermine la diminution de l'interaction entre ces deux parties de la molécule en comparaison du thiobenzamide.

L'augmentation de la densité électronique à l'atome de soufre est déterminée presque exclusivement par la conjugaison $p-\pi$ existant dans le groupement thioamidique.

Dans le cas de FTAP la densité électronique à l'atome de soufre sera plus grande qu'au cas de FTA comme une conséquence de l'effet + I du groupement méthylénique du noyau pipéridine.

En vue des raisons données plus haut la différence entre la capacité de donneur du FTA et celle du TB semble explicable.

LES SPECTRES EN IR

En général, les spectres en IR appartenant aux complexes de transfert de charge de type *n*, donneur-σ, accepteur[4] présentent de petites différences en comparaison des spectres de leurs composants.

Les spectres en IR des complexes $FTA-I_2$ et $FTAP-I_2$ diffèrent par rapport aux spectres de thioamide par la diminution de l'intensité des bandes caractéristiques et par un léger déplacement vers les plus petites fréquences.

Le fait que les maximums caractéristiques du groupement NH_2 ne sont pas déplacés indique que l'atome d'azote ne fonctionne pas comme donneur.

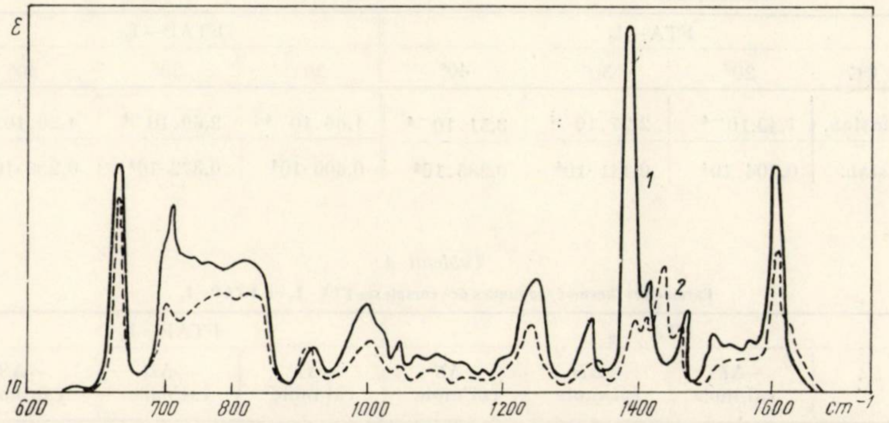

Fig. 3. — Spectres d'absorption en IR de FTA et $FTA-I_2$ (*1*, FTA 10^{-2} M en CCl_4, *2*, $FTA-I_2$, 10^{-2} M en CCl_4).

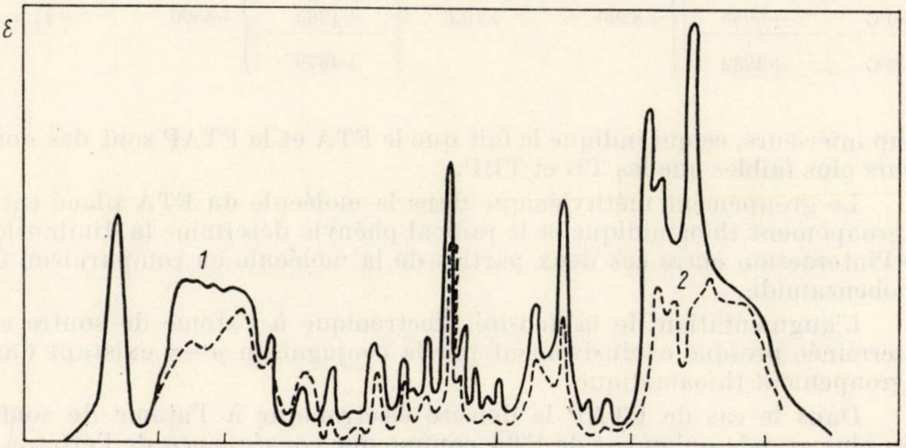

Fig. 4. — Spectres d'absorption en IR de FTAP et $FTAP-I_2$. (*1*, FTAP 10^{-2} M en CCl_4, *2*, $FTAP-I_2$ 10^{-2} M en CCl_4).

---

[4] R. FORSTER, «Organic Charge-Transfer Complexes», vol. 15, chap. 4, Academic Press, London — New York 1969.

Significatif c'est le fait que nous retrouverons les mêmes différences entre les spectres IR des complexes et des donneurs comme dans le cas des TB et TBP, ce qui indique la même manière de formation, respectivement que le donneur le plus probable c'est l'atome de soufre.

PARTIE EXPÉRIMENTALE

Le FTA a été préparé de phénylacétonitrile et de thioacétamide en milieu de chlorhydrate de diméthylformamide [5] et recristallisé de ligroïne jusqu'au P. f. = 97 – 98°.

Le FTAP a été préparé par une réaction Willgerodt-Kindler [6] et recristallisé d'éthanol jusqu'au P. f. = 79°.

Le tétrachlorure de carbone a été séché sur du $CaCl_2$ et distillé sur une colonne Vigreux de 60 cm. L'iode a été purifié par des sublimations répétées.

Les complexes moléculaires ont été obtenus en mélangeant des volumes égaux de solutions isomolaires de thioamide et d'iode.

Les complexes $FTA-I_2$ et $FTAP-I_2$ n'ont pas pu être séparés en état cristallin, étant étudiés directement en solution.

Les spectres en UV et visible ont été effectués à l'aide d'un spectrophotomètre Beckmann, de type DB muni d'un ultrathermostat U 10.

Les spectres ont été réalisés avec un appareil UR 20 dans du tétrachlorure de carbone, en utilisant des cuves de 1mm.

---

[5] E. Taylor et Z. Zolthewich, *J. Amer. Chem. Soc.*, **82**, 2656 (1960).
[6] J. A. King et C. H. Mc Millan, *J. Amer. Chem. Soc.*, **68**, 2335 (1946).

Revue Roumaine de Chimie, **19**, *3*, 429 – 435 (1974)

Revue Roumaine de Chimie, **19**, *3*, 437-442 (1974)

PHTHALAZINIUM YLIDS. VI*

ACTION OF DIMETHYLACETYLENEDICARBOXYLATE ON DISUBSTITUTED AT THE EXOCYCLIC CARBON PHTHALAZINIUM-YLIDS

MAGDA PETROVANU, ARIADNA SAUCIUC and I. ZUGRĂVESCU

Organic Chemistry Department,
"Al. I. Cuza" University,
Str. 23 August no. 11, Jassy, Romania

Received May 22, 1973

Phthalazinium-cyanocarbethoxymethylid (XI) reaction with dimethylacetylenedicarboxylate (DMAD) leads to an indolizine derivative (XII) through a mechanism which involves the appearance of the intermediate ylid XIV. By the intramolecular nucleophilic attack on the 1-position of the phthalazinic ring, the 5-membered ring is closed simultaneously with HCN elimination. Phthalazinium-dibenzoylmethylid (XV) reaction with DMAD leads to XIV by a probably analogous mechanism.

The occurrence and reactivity of some phthalazinium-ylids was studied in previous papers. [1,2] The present investigation studied the influence of electronegative groups as substituents of the exocyclic carbon on the behaviour of these ylids.

Phthalazinium-dibenzoylmethylid (I) in nonanhydrous solvents is inactivated [2] leading to dimer (IV). Since benzoic acid has been isolated and taking into account the fact that dimer (IV) is also obtained directly from phthalazinium-phenacylid (II), obtained by other means, [2] we have suggested a reaction mechanism through a carbene intermediate (III).

It has been proved experimentally that the dimerization reaction does not take place in perfectly anhydrous aprotic solvents. In this case the occurrence of the carbenic intermediate by a proton transfer seems to depend on the possibility of eliminating the benzoyl group.

---

* Part V. A. Sauciuc, I. Druță and M. Petrovanu, *Rev. Roumaine Chim*, **16**, 1789 (1971).

[1] M. Petrovanu, A. Sauciuc and I. Zugrăvescu, *Anal. Şti. Univ. „Al. I. Cuza", Iaşi*, **16**, 65 (1970).

[2] A. Sauciuc, I. Druță and M. Petrovanu, *Rev. Roumaine Chim.*, **16**, 1789 (1971).

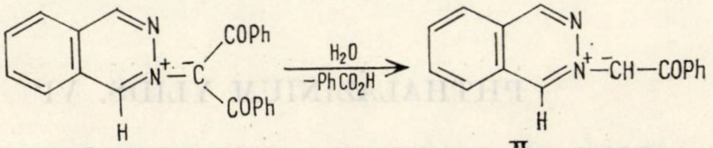

I II

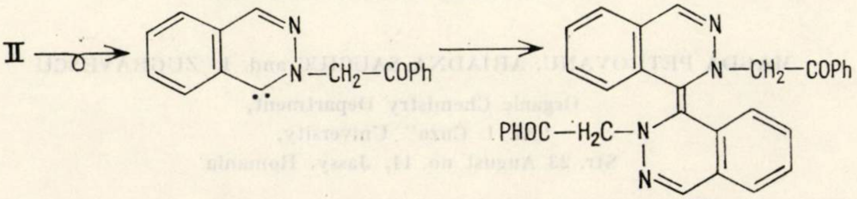

III IV

Linn and co-workers [3] have found that an indolizine derivative (VIIa) is obtained in the reaction between pyridinium-dicyanomethylid (Va) and dimethylacetylenedicarboxylate (noted DMAD) by elimination of a CN group. Henrick and co-workers [4] also show that ylid (Vb) and (Vc) lead to (VIIb) and (VIIc), by elimination of the components of ethyl formiate or benzaldehyde, respectively. A mechanism was suggested for these cases admitting the formation of the intermediate (VI) from which, by 1,4-elimination, the indolizinic derivatives (VII) are obtained.

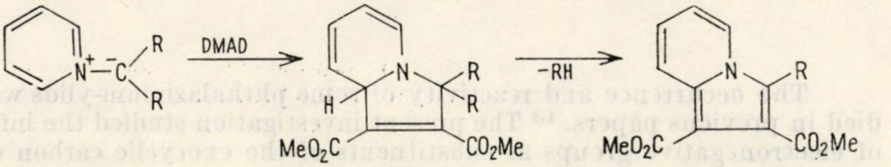

VI

Va R = CN
Vb R = CO_2Et
Vc R = COPh

VIIa R = CN
VIIb R = CO_2Et
VIIc R = COPh

As the dihydroindolizinic derivatives of structure (VI) could not be isolated, and also for steric reasons, this mechanism seems less probable for these cases. It is more convenient to admit a cyclic transition state between DMAD and the ylid, from which the formation of new covalent bonds and the RH elimination constitute a synchronous process.

We have shown [1] that the reaction between phthalazinium-dicarbethoxymethylid (VIII) and DMAD leads to an oxazepine derivative (X).

---

[3] W. J. Linn, O. W. Webster and R. E. Benson, *J. Amer. Chem. Soc.*, **87**, 3651 (1865).

[4] C. A. Henrick, E. Ritchie and W. C. Taylor, *Austral. J. Chem.*, **20**, 2467 (1967).

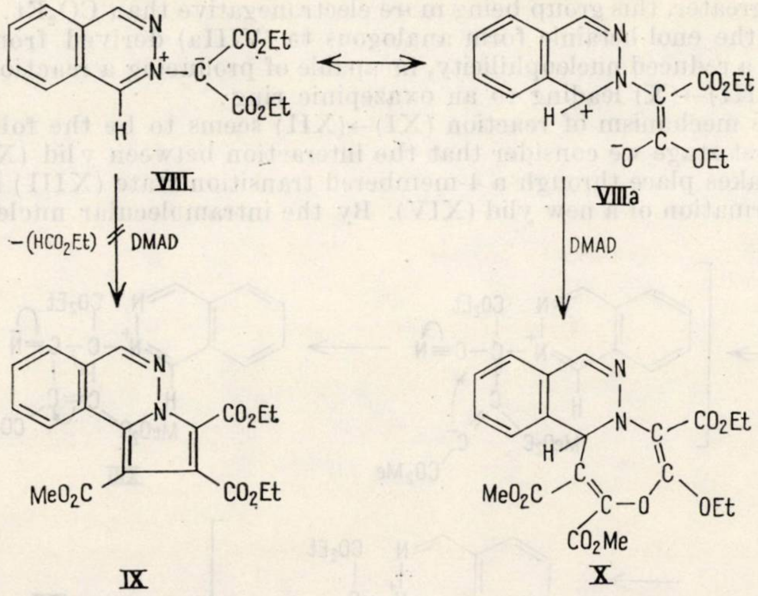

We have considered that in this reaction, the nucleophilic attack on DMAD takes place through the enol-betainic form (VIIIa) leading to a 5+2 cyclo-addition (which needs not be concerted). No elimination of a CO_2Et group, leading to structure (IX), has been noticed.

This unexpected result prompted us to study the reaction between phthalazinium-cyanocarbethoxymethylid (XI) and DMAD. In this case, by eliminating the CN group, a product (XII) analogous to indolizine (VII) is obtained.

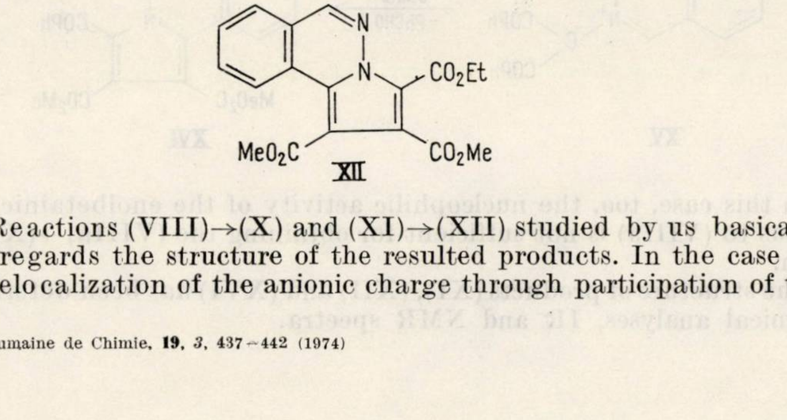

Reactions (VIII)→(X) and (XI)→(XII) studied by us basically differ as regards the structure of the resulted products. In the case of ylid (XI) delocalization of the anionic charge through participation of the CN group is greater, this group being more electronegative than CO_2Et. Consequently, the enol-betainic form analogous to (VIIIa) derived from (XI) will have a reduced nucleophilicity, incapable of producing a reaction similar to (VIII)→(X) leading to an oxazepinic ring.

The mechanism of reaction (XI)→(XII) seems to be the following. In the first stage we consider that the interaction between ylid (XI) and DMAD takes place through a 4-membered transition state (XIII) leading to the formation of a new ylid (XIV). By the intramolecular nucleophilic attack on the 1-position of the phthalazinic ring the closure of the 5-membered ring is obtained. We suppose that the HCN elimination takes place simultaneously with this process.

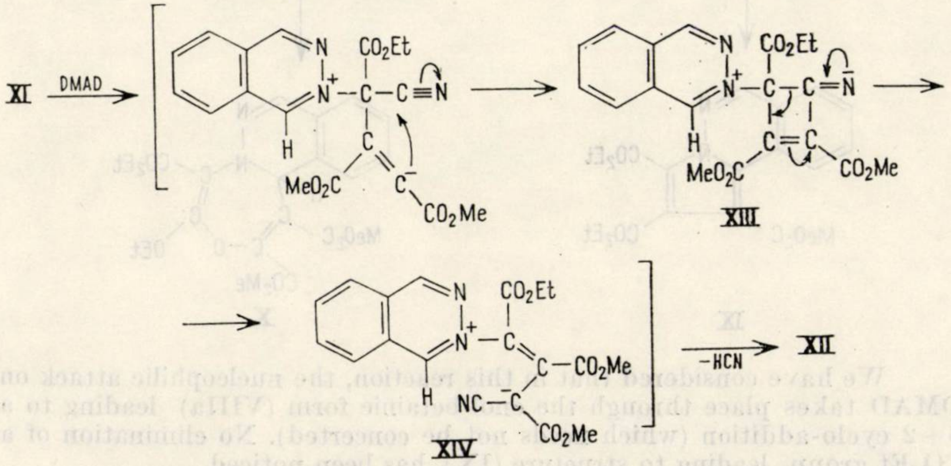

The mechanism that has been suggested is valid in the case of the phthalazinic cation whose 1-position in the ring is very sensitive to the nucleophilic attack.

We have also studied the reaction between phthalazinium-dibenzoylmethylid (XV) and DMAD which by a probably analogous mechanism leads to (XVI).

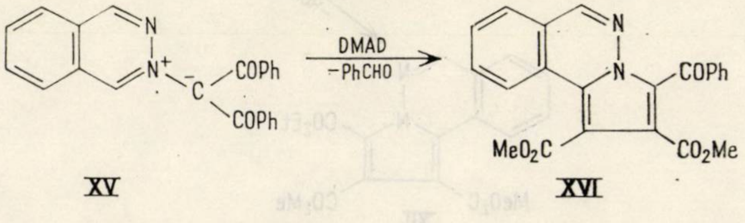

In this case, too, the nucleophilic activity of the enolbetainic form analogous to (VIIIa) is not sufficient for obtaining the (VIIIa)→(X) type reaction.

The structure of products (XI), (XII) and (XVI) has been determined by chemical analyses, IR and NMR spectra.

EXPERIMENTAL

CYANOCARBETHOXYMETHYL-PHTHALAZINIUM BROMIDE

Phthalazine, 1.3 g (0.01 mole), is dissolved in 50 ml anhydrous benzene. Ethylbromocyanoacetate, 2 ml (0.01 mole), is added. The mixture is kept at room temperature until next day. A yellow product separates, m.p. = 161–162°. Yield 75 %.

Analyses for $C_{13}H_{12}N_3O_2Br$: *Calcd.* C, 48.44 ; H, 3.72 ; N, 13,04. *Found* : C, 48.11 ; 48.07 ; H,3.90 ; 3.92 ; N, 12.55 ; 12.65 %.

PHTHALAZINIUM-CYANOCARBETHOXYMETHYLID (XI)

Cyanocarbethoxymethyl-phthalazinium bromide, 3.2 g (0.01 mole), is suspended in 100 ml water. It is cooled and a solution of 3 g (0.03 mole) K_2CO_3 in about 50 ml water is added under stirring. The ylid is extracted with chloroform, the solution is dried on Na_2SO_4 and petroleum ether is added. A yellow product separates, m.p. 204–205°. Yield 45 %.

Analyses for $C_{13}H_{11}O_2N_3$: *Calcd.* C, 64.73 ; H, 4.56 ; N, 17.42. *Found* : C, 64.78 ; 64.60 ; H, 4.95 ; 5.01 ; N, 17.63 ; 17.32 %.

IR spectra : $\nu = 3020\ cm^{-1}$ (CH aromatic) ; $2235\ cm^{-1}$ (CN) ; $1740\ cm^{-1}$ (–COOR) ; $1645\ cm^{-1}$ (C = N) ; $1620\ cm^{-1}$ (C = C) ; $1277\ cm^{-1}$ and $1220\ cm^{-1}$ (C–O–C).

1, 2-DICARBOMETHOXY-3-CARBETHOXY-PYROLO–[2.1–a]-PHTHALAZINE (XII)

Cyanocarbethoxymethyl-phthalazinium bromide, 3.22 g (0.01 mole), is suspended in 100 ml acetonitrile. DMAD, 1.42 ml (0.01 mole), and triethylamine, 2 ml (0.02 mole), is added. The mixture is kept at room temperature till next day. Meanwhile a crystalline white product is formed which is filtered ; the product recrystallizes from methanol. Light white crystals, m.p. = 125°. Yield 30 %.

Analyses for $C_{18}H_{16}O_6N_2$: *Calcd* : C, 60.67 ; H, 4.49 ; N, 7.86. *Found* : C, 60.08 ; 60, 07 ; H, 4.73 ; 4.59 ; N, 7.09 ; 8.01 %.

IR spectra : $\nu = 3025\ cm^{-1}$ (CH aromatic) ; $1637\ cm^{-1}$ and $1710\ cm^{-1}$ (3 esteric CO groups) ; $1620\ cm^{-1}$ (C = C) ; $1240\ cm^{-1}$ and $1218\ cm^{-1}$ (C–O–C) ; the characteristic band $2250\ cm^{-1}$ for CN group is missing.

NMR spectra : triplet ($3H_a$) $\delta = 1.4$ ppm, J = 7 cps ; singlet ($3H_{b\ or\ c}$)$\delta = 3.95$ ppm ; singlet ($3H_{b\ or\ c}$) $\delta = 3.98$ ppm ; quadruplet ($2H_d$) $\delta = 4.46$ ppm, J=7 cps ; centred multiplet ($3H_{1,2,3}$) $\delta = 7.8$ ppm ; singlet ($1H_4$) $\delta = 8.78$ ppm ; centred multiplet ($1H_5$) $\delta = 9.4$ ppm.

A similar spectrum is obtained through deuteration.

1.2-DICARBOMETHOXY-3-BENZOYL-PYROLO-[2.1-a]-PHTHALAZINE (XVI)

Phthalazinium-dibenzoylmethylid, 3.52 g (0.01 mole), is suspended in 50 ml anhydrous benzene. DMAD, 1.5 ml (0.01 mole), is added and the mixture is boiled for *ca* 1 hour. Meanwhile the solution is decoloured from red to orange. The hot solution is filtered to separate the white product which is formed. The orange solution evaporates and the brown resin which is separated is dissolved in benzene. Petroleum ether is added until a yellow product separates. Compound is washed with methanol, the white product is recrystallized from *o* xylene. A white crystalline product is obtained, m.p. 174–175°. Yield 30%.

Analyses for $C_{22}H_{16}O_5N_2$: *Calcd.* C, 68.04 ; H, 4.12 ; N, 7.21. *Found* : C, 67.79 ;67.93 ; H, 4.59 ; 4.32 ; N, 7.78 %.

IR spectra: $\nu = 1736\ cm^{-1}$ (esteric CO) and $1730\ cm^{-1}$ (esteric CO) ; $1656\ cm^{-1}$ (cetonic CO) ; $1265\ cm^{-1}$ (C–O–C) ; 1580 and $1606\ cm^{-1}$ (C = C).

NMR spectra : singlet $\delta = 3.57$ ppm (esteric–OCH_3) ; singlet $\delta = 3.98$ ppm (esteric –OCH_3) ; multiplet $\delta = 7.6$ ppm (aromatic 8H) ; singlet $\delta = 8.43$ ppm ($1H_4$ position of phthalazinic ring) ; supplementary coupling doublet $\delta = 8.76$ ppm apart $J = 7.5$ cps ($1H_8$ position of phthalazinic nucleus).

Revue Roumaine de Chimie, **19**, *3*, 443 – 454 (1974)

ELIMINATION REACTIONS IN THE 8-R-TRICYCLO[7.3.1.$0^{2,7}$]TRIDECANE SERIES. IV[1]

PYROLYTIC ELIMINATION OF TRICYCLO[7.3.1.$0^{2,7}$]TRIDECA-2-EN-13-ACETATE

N. BĂRBULESCU and MINODORA LECA

University of Bucharest,
Chemistry Department, Organic Chemistry Laboratory,
Splaiul Independenţei 89,
Bucharest, Romania

Received June 26,1973

The pyrolytic elimination of tricyclo[7.3.1.$0^{2,7}$]trideca-2-en-13-acetate (I) at 470° has been studied and one established that it followed the ion — pair mechanism. Due to the impossibility to introduct a double bond at the bridgeheads of the bridged bicyclic system, the reaction occurs by heterolytic breakage of the C—O bond with the formation of homoallylic carbonium ion A, which isomerizes giving as main reaction products : tetrahydronaphthalene (III), β-methyl-tetrahydronaphthalene (IV), β-propyl-tetrahydronaphthalene (VI), 2,3-tetrahydrobenzindane (VII), and 3,4-tetrahydrobenzindane (VIII). The structure of pyrolytic elimination products has been studied by IR, NMR and mass spectroscopy.

INTRODUCTION

The products formed in pyrolytic eliminations often differ appreciably in composition from those formed in other types of elimination. The pyrolytic eliminations of bicyclic [n.m.1.] acetates with the acetate group in the one-membered bridge were not studied.

The pyrolytic elimination of tricyclo [7.3.1.0 ^{2,7}] trideca-2-en-13-acetate (I) has been studied in the present work to establish the structure of the elimination products as well as the reaction mechanism, due to the theoretical importance of the elimination reactions of such class of compounds.

Acetic esters undergo elimination on heating at elevated temperatures (300 — 550°), with no other reagent present. The mechanisms of such reactions are obviously different from those of the elimination reactions in solution, which occur at low temperatures and always require a base (the solvent may be the base in some cases).

---

[1] Part III : N. Bărbulescu and M. Leca, *Rev. Roumaine Chim.*, in press.

The following mechanisms have been suggested for the pyrolytic elimination of acetates [2,3]:

a) *The six-membered ring concerted mechanism Ei.* This mechanism, suggested by Hurd and Blunck,[4] postulates a six-membered ring transition state in which a basic α atom, or one belonging to an α group, removes intramolecularly a β hydrogen; the two groups leave at the same time:

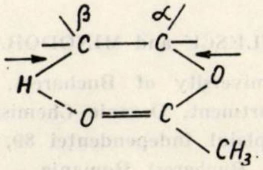

The mechanism explains the *cis* eliminations observed in most of the cases,[5] why the reactions are homogeneous and unimolecular and why the activation entropy is usually found to be negative. The model does not allow for the *trans* eliminations found in some molecules, fails to explain why the composition of the final alkene mixtures does not depend on the nature of the acid and the positive activation entropy found for tertiary acetates.[6]

b) *The ion-pair mechanism.* Maccoll[7], to eliminate some of the difficulties with the six-membered ring mechanism, postulated an intimate ion-pair as transition state:

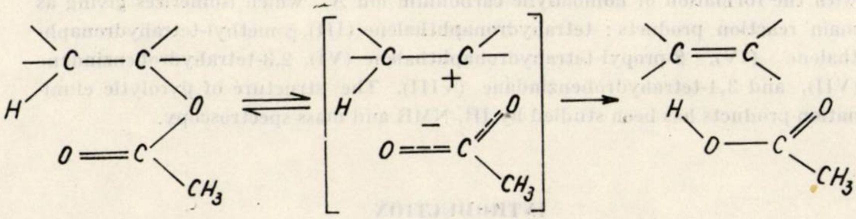

The ion-pair mechanism is very much like the E1 mechanism, except that, under the pyrolytic elimination conditions, where there is nothing available to solvate the negative ion, it remains near the carbonium ion. The ion-pair and the Ei mechanisms differ only in the timing of the steps involved.

The heterolytic dissociation of the C—O bond requires a much higher energy compared to homolytic dissociation. Part of this energy may be compensated for by the Coulombic attraction of the two ions.

---

[2] F. H. A. Rummens, *Rec. Trav. chim.*, **83**, 901 (1964).

[3] J. March, "Advanced Organic Chemistry: Reactions, Mechanisms, and Structure", McGraw-Hill Book Company, New York, St. Louis, San Francisco, Toronto, London, Sydney, 1968, p. 747—751.

[4] C. D. Hurd and F. H. Blunck, *J. Amer. Chem. Soc.*, **60**, 2419 (1938).

[5] C. H. DePuy and R. W. King, *Chem. Rev.*, **60**, 431 (1960).

[6] J. C. Scheer "Ester Pyrolysis in the Gas Phase", Thesis, Amsterdam, 1961, cf. ref. 2.

[7] A. Maccoll, *J. Chem. Soc.*, **1958**, 3398.

Some workers consider the transition state very polar, but not quite an ion-pair.[8]

The finding of the rearranged products is a strong evidence for the ion-pair mechanism.

The pyrolytic elimination of 1-arylethyl and 1,2-diarylethyl acetates follow this mechanism,[9-11] due to the carbonium-ion character of the C_1 carbon atom.

c) *The free radical mechanism* considers that by going into higher vibrational states, the molecule must reach a state where its weakest bond dissociates. The activated complex consists in the critical state where the vibrational degree of freedom of the R—OAc stretching oscillator changes into a translational degree of freedom. The formation of such a transition state being the rate determining step, the two radicals react very quickly, by a nonchain or a chain process, giving the final reaction products. This mechanism is followed by the pyrolytic elimination of the allylic acetate derivatives.[2,12]

RESULTS AND DISCUSSIONS

The pyrolytic elimination of tricyclo $[7.3.1.0^{2,7}]$ trideca-2-en-13-acetate (I) is subjected not only to the restrictions regarding the cyclic compounds (the existence of a *cis* β-hydrogen for Ei elimination), but also to Bredt's rule,[13] which applies in these reactions as in the E1—E2—E1cB mechanistic spectrum.[14] Bredt's rule, reformulated by Wiseman,[15] predicts isolable bicyclic bridgehead alkenes when the largest of the two rings containing the double bond has at least eight atoms. The elimination of the acetate group from C_{13} carbon atom of I would lead to the introduction of a *trans*-double bond in a six-membered ring. That is why the elimination of this group cannot occur without the isomerization of the bridged bicyclic system.

The unsaturated acetate I, obtained by dehydration and acetylation of tricyclo $[7.3.1.0^{2,7}]$ tridecane-2,13-diol (II) with zinc chloride and acetic anhydride,[1] has been subjected to pyrolytic elimination in flow system at temperatures ranging from 410 to 470°. The conversion has been determined by titrating the acetic acid resulted from the reaction as well as by IR spectroscopy, using the carbonyl band of the ester which appeared at 1723 cm^{-1}. The calibrating curve extinction, E, in terms of concentration — Pirlot method[16] — has been plotted for that, using the carbon tetrachloride as solvent (fig. 1). The results are in good agreement with those obtained from acetic acid titration (table 1). The highest conversions were obtained at 470°, which was selected as reaction temperature.

---

[8] S. W. Benson and A. H. Bose, *J. Chem. Phys.*, **39**, 3463 (1963).

[9] G. G. Smith, F. D. Bagley and R. Taylor, *J. Amer. Chem. Soc.*, **83**, 3647 (1961).

[10] R. Taylor, G. G. Smith and W. H. Wetzel, *J. Amer. Chem. Soc.*, **84**, 4817 (1962).

[11] G. G. Smith, D. A. K. Jones and D. F. Brown, *J. Org. Chem.*, **28**, 403 (1963).

[12] R. Low and E. C. Kooyman, *Rec. Trav. chim.*, **84**, 1511 (1965).

[13] J. Bredt, *Liebigs Ann. Chem.*, **437**, 1 (1924).

[14] G. Köbrich, *Angew. Chem.*, **85**, 494 (1973).

[15] J. R. Wiseman, *J. Amer. Chem. Soc.*, **89**, 5966 (1967).

[16] D. Bîrcă-Gălăţeanu, M. Giurgea, I. Iova, V. Sahini, A. Truţia and R. Ţiţeica, "Introducere în spectroscopia experimentală", Ed. tehnică, Bucharest, 1966, p. 224.

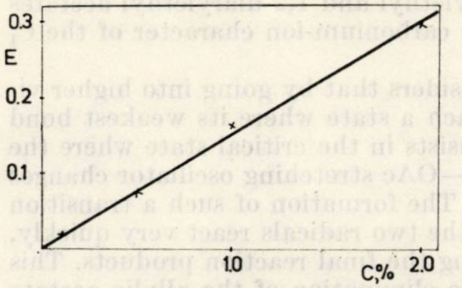

Fig. 1. — The calibrating curve extinction, *E*, in terms of concentration.

The analysis of the elimination products has been made by gas-liquid chromatography on the following columns, after removing the polymers and the unreacted acetate : SE—30 on chromosorb W, diethyleneglycol succinate on celite C_{22}, carbowax 20M on teflon and carbowax 20 M on celite C_{22}. The best resolution was obtained with the last column (fig. 2). Six (*a* - *f*) among the 26 peaks of the chromatogram, which represent 79.3 per cent of the total, were separated by preparative gas-liquid chromatography. The last two peaks, *e* and *f*, were not well resolved on the preparative column, so that they were collected together.

Table 1

Degree of conversion obtained for the pyrolytic elimination of acetate I by acetic acid titration and IR spectroscopy

n_D^{20} of the elimination products	Conversion, %	
	AcOH titration	$E = f(c)$
1.5410	71.6	73.5
1.5447	89.3	91.1
1.5549	98.2	100.0

The peaks *a* - *f* were analysed by MNR, IR, and mass spectroscopy.

The following structure were assigned for these compounds on the basis of mass, NMR, and IR spectra :

The mass spectrum of the peak *a* gives for the parent ion the value 132 and 104 for the principal ion. There are also peaks at m/e 117, 91, 65, 51, 39, and 27. The mass spectrum of this compound is represented in figure 3a, beginning from m/e = 50, and it is identical with that of tetrahydronaphthalene (III). [17,18]

Its NMR spectrum (fig. 3*b*) also presents the tetrahydronaphthalene signals : one quintet at δ 1.77 ppm, J = 2.25 Hz, one multiplet centered at

---

[17] R. H. Shapiro, J. M. Wilson and C. Djerassi, *Steroids*, **1**, 1 (1963).

[18] G. Spiteller, "Massenspektrometrische Strukturanalyse organischer Verbindungen", Verlag Chemie, GmbH, Weinheim/Bergstr., 1966, p. 149—150.

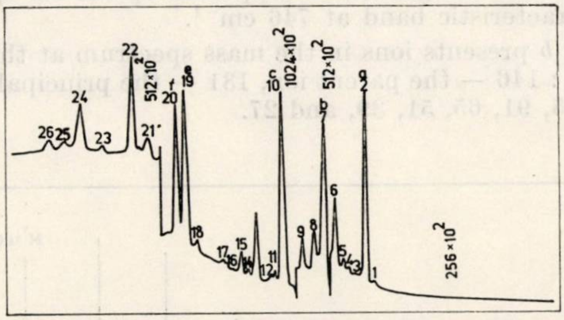

Fig. 2. — The pyrolytic elimination products chromatogram of the acetate I at 470° on carbowax 20M on celite C_{22}.

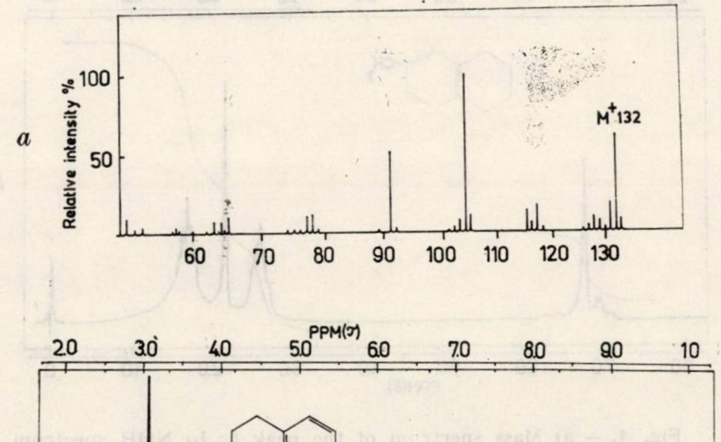

Fig. 3. — a) Mass spectrum of the peak a; b) NMR spectrum of the peak a.

δ 2.715 ppm, and one complex absorption from δ 6.62 to 7.30 ppm centered at δ 6.92 ppm. This assignment is supported by the IR spectrum, which presents a characteristic band at 746 cm^{-1}.

The peak *b* presents ions in the mass spectrum at the following m/e ratios (fig. 4a) : 146 — the parent ion, 131 — the principal ion, and other ions at 118, 105, 91, 65, 51, 39, and 27.

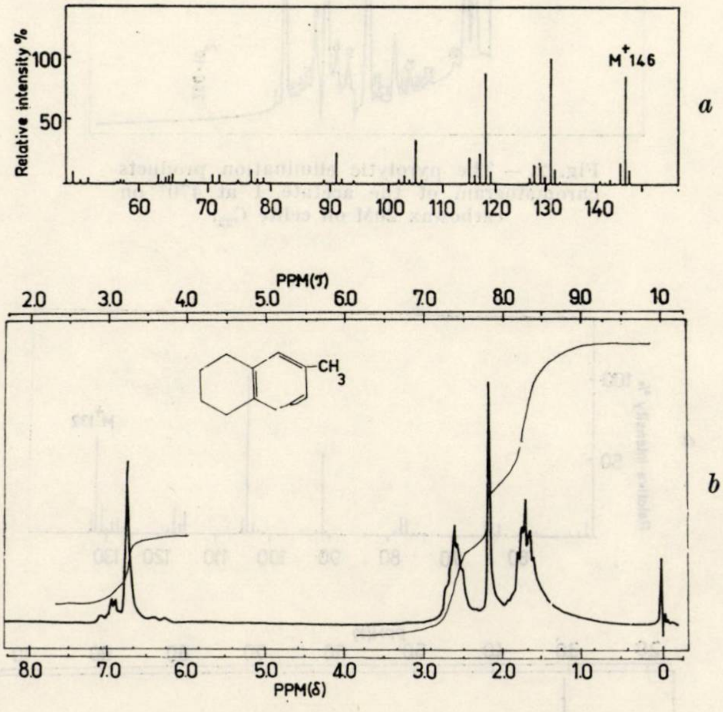

Fig. 4. — a) Mass spectrum of the peak *b* ; b) NMR spectrum of the peak *b*.

There are signals in the NMR spectrum (fig. 4b) at the following δ values : one multiplet centered at 1.72 ppm corresponding to four aliphatic protons, one singlet at 2.21 ppm specific of the CH_3-Ar system, one multiplet centered at 2.62 ppm with an area corresponding to four protons adjacent to benzene nucleus, and one complex absorption to 7.17 ppm for three aromatic protons. The β-methyl-tetrahydronaphthalene (IV) structure has been assigned to the peak *b* on the basis of the parent ion m/e value, of the way of molecule fragmentation which demonstrates the presence of the tetrahydronaphthalene skeleton, and of the NMR spectrum.

There are peaks in the mass spectrum of the compound *d* at the m/e values 174 — the parent ion, 145 — the principal ion, 131, 117, 105, 91, 65, 51, 39, 28, and 27 (fig. 5a). This demonstrates that the peak *d* is a tetrahydronaphthalene derivative.

The NMR spectrum (fig. 5b) presents one triplet at δ 0.92 ppm, J = 7 Hz, specific of the $CH_3 - CH_2 -$ system, one multiplet centered at δ 1.765 ppm corresponding to six aliphatic protons, one multiplet from δ 2.30 to 3.00 ppm with an area corresponding to six protons adjacent to benzene ring in which a triplet at δ 2.47 ppm can be distinguished, J = 7.5 Hz, which can be assigned to the $-CH_2-CH_2-$Ar system, and one multiplet from δ 6.66 to 7.00 ppm for three aromatic protons. The β-propyl-tetrahydronaphthalene (VI) structure was assigned to the peak *d* taking account of the facts presented above.

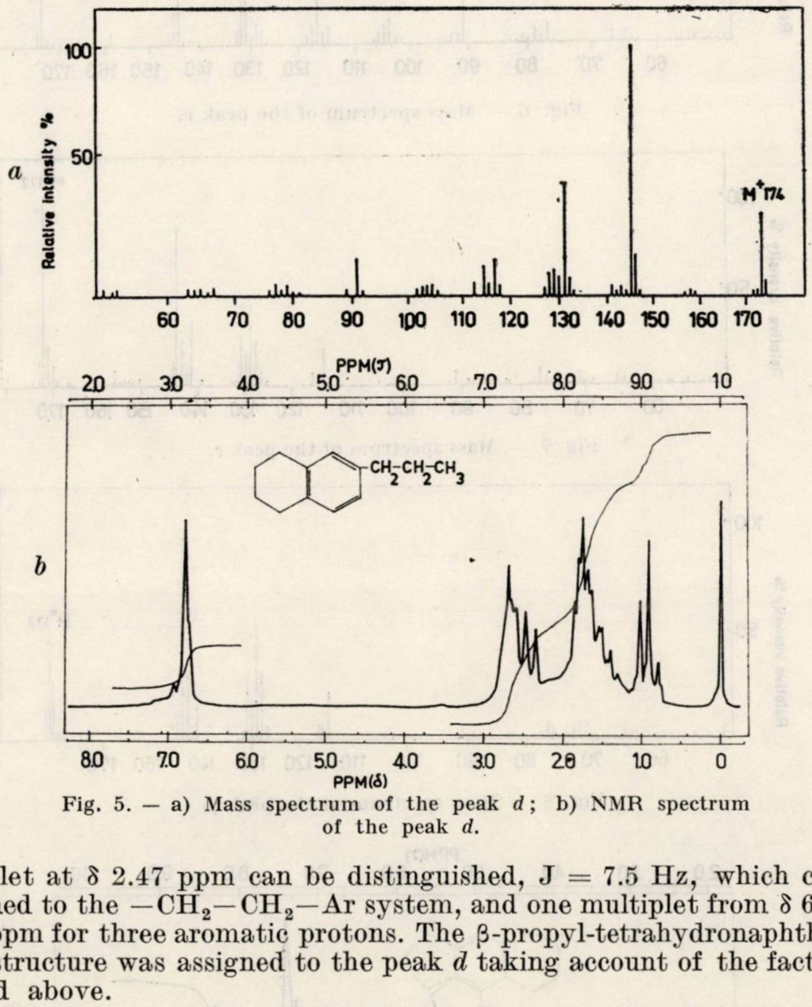

Fig. 5. — a) Mass spectrum of the peak *d*; b) NMR spectrum of the peak *d*.

The peak *c* was not well resolved on the preparative chromatographic column, and the gas-liquid chromatographic analysis shows that the collected product was not pure. The refractionation gives a very small quantity of product, which does not allow a conclusive NMR spectrum. The existence of some aliphatic protons can be seen from the spectrum, grouped in three wide signals from δ 1.30 to 1.90, 2.00 to 2.25, and 2.50 to 2.90 ppm, as well as of some aromatic protons centered at δ 6.80 ppm. The mass spectrum (fig. 6) gives a M^+ parent ion at m/e 174, showing that the peak *c* (V) and *d* are isomers.

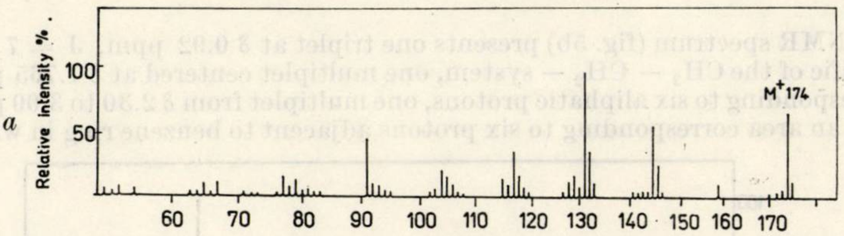

Fig. 6. — Mass spectrum of the peak *c*.

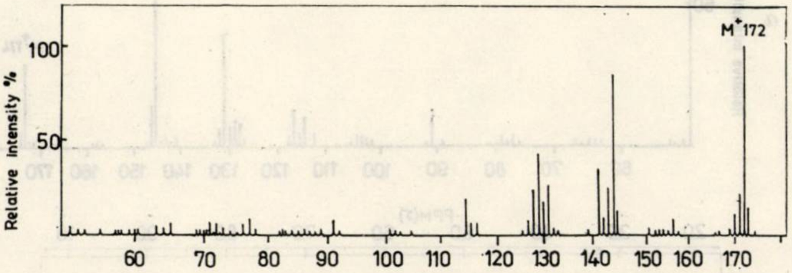

Fig. 7. — Mass spectrum of the peak *e*.

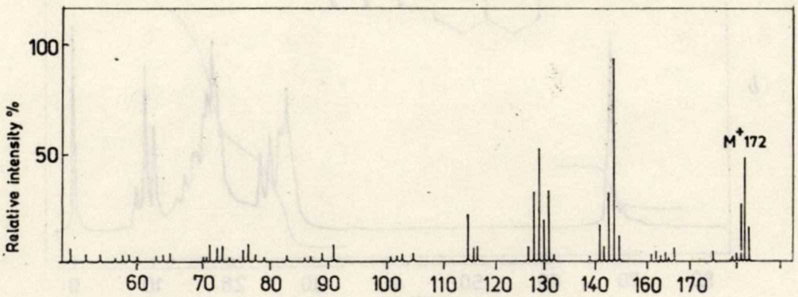

Fig. 8. — Mass spectrum of the peak *f*.

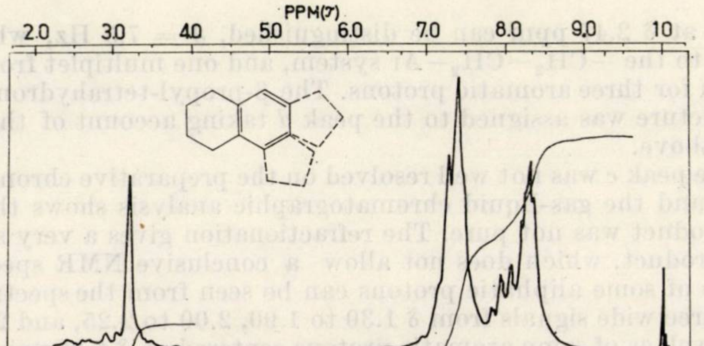

Fig. 9. — NMR spectrum of the mixture of the peaks *e* and *f*.

In contrast to the last one, the principal ion is at m/e 131, the 145 ion being not so abundant. There are also ions at m/e 117, 91, 65, 51, 39, and 28, proving that the peak *c* is also a tetrahydronaphthalene derivative.

The mass spectrum of the peak *e* (fig. 7) gives the value 172 for the parent ion, this being at the same time the principal ion. There are ions at m/e 144, 141, 131, 129, 105, 91, 65, 51, 39, and 28.

The peak *f* presents ions at the following m/e ratios (fig. 8) : 172 — the parent ion which is also the principal ion, 144 — an ion almost as intense as the preceding one, other ions at 131, 129, 105, 91, 65, 39, and 28. The NMR spectrum of the peaks *e* and *f* mixture (fig. 9) is identical with that of 2,3-tetrahydrobenzindane (VII) and 3,4-tetrahydrobenzindane (VIII) mixture. [1] The gas-liquid chromatographic analysis gives the value 1.2 : 1 for the VII : VIII ratio.

The pyrolytic elimination of tricyclo$[7.3.1.0^{2,7}]$trideca-2-en-13-acetate (I), taking account of the main reaction products, can be depicted by the ion-pair mechanism as follows :

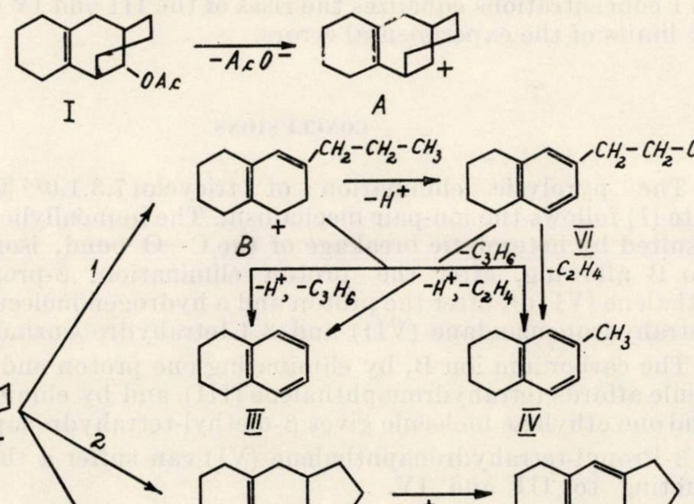

The homoallylic carbonium ion A, resulted from heterolytic dissociation of the C—O bond, isomerizes probably to B, C, and D. The carbonium ion A is transformed into carbonium ion B by homolytic breakage of the allylic C_1-C_{12} bond. The ion B can eliminate one proton giving *n*-propyl-tetrahydronaphthalene (VI) identified as

7.1 per cent in the reaction products, or affords tetrahydronaphthalene (III) and β-methyl-tetrahydronaphthalene (IV) by thermal cracking. The last two compounds form 4.4 and 8.5 per cent, respectively, of the reaction products.

The radical-ion resulted by the C_1-C_{12} bond breakage may also become stable following the ways 2 and 3, leading to VII and VIII which represent 18.7 and 15.7 per cent, respectively, of the total reaction products.

β-Propyl-tetrahydronaphthalene (VI) can suffer a thermal cracking, too, under the reaction condition (470°), allowing for the formation of III and IV. This is supported by the fact that the ratio of III and IV rises when the elimination products are reintroduced in the elimination column, and the ratio of V and VI diminishes. Reintroducing the above elimination mixture in the column, the concentration of III rises at 11.2 and that of IV at 12.7 per cent. The concentration of V decreases at the same time from 25.9 to 8.5 per cent, and of VI to 5.1 per cent. The increasing of the ratio of another unidentified compound from 1.5 to 6.5 per cent is also observed, its retention time being between that of V and VI. The decreasing of V and VI concentrations equalizes the rises of the III and IV concentrations, in the limits of the experimental errors.

CONCLUSIONS

The pyrolytic elimination of tricyclo[$7.3.1.0^{2,7}$]trideca-2-en-13-acetate (I) follows the ion-pair mechanism. The homoallylic carbonium ion A, resulted by heterolytic breakage of the C—O bond, isomerized probably to B allowing, after the proton elimination, β-propyl-tetrahydronaphthalene (VI) or, after the proton and a hydrogen molecule elimination, 2,3-tetrahydrobenzindane (VII) and 3,4-tetrahydrobenzindane (VIII).

The carbonium ion B, by eliminating one proton and one propylene molecule affords tetrahydronaphthalene (III), and by eliminating one proton and one ethylene molecule gives β-methyl-tetrahydronaphthalene (IV).

β-Propyl-tetrahydronaphthalene (VI) can suffer a thermal cracking conducting to III and IV.

EXPERIMENTAL PART

The preparation of tricyclo[$7.3.1.0^{2,7}$]*trideca-2-en-13-acetate* (I) has been described in an earlier paper. [1]

Pyrolytic elimination of tricyclo[$7.3.1.0^{2,7}$]*trideca-2-en-13-acetate* (I). The equipment for pyrolytic elimination of acetate I consisted of a 245 mm vertical Rasotherm tube, 28 mm in diameter, filled with porcelain bits 205 mm in height, equipped with a separating funnel at the upper side to introduce the compound and a two-necks round bottomed flask at the lower side to collect the reaction products. The second neck had a reflux refrigerator attached, to avoid the volatile compounds loss. The filled part of the glass column was entirely inserted into a 205 mm high electric oven, the temperature being adjusted using an autotransformer. The calibrating curve temperature was plotted in terms of voltage. The temperature was verified with the aid of a thermometer which was introduced up to the middle of the column. The asbestos fibres were used as thermal insulator.

There were introduced 0.12 ml of acetate per minute at temperatures ranging from 410 to 470°. The reaction products were collected in water, the organic portion was extracted with petroleum ether, the extract washed with water and dried with natrium bicarbonate. The resulted solution was chromatographed on aluminium oxide to remove the polymers. The row product, resulted after the petroleum ether removal, was characterized by a total refractive index, by the height of the IR absorption band from 1723 cm^{-1} using carbon tetrachloride as solvent, and by gas-liquid chromatography on carbowax 20M.

The aqueous layers were combined and the acetic acid resulted from the reaction was titrated using 1N natrium hydroxide to calculate the acetate conversion. For example, there were obtained the following results using a portion of 6.25 g acetate at 470 ± 3°: elimination products 3.8 g, $n_D^{20} = 1.5447$, after the chromatography on aluminium oxide, 23.8 ml 1N natrium hydroxide which correspond to 1.428 g acetic acid (theoretically 1.600 g, 89.3% conversion).

The unreacted acetate can be removed by careful elution with petroleum ether on aluminium oxide column.

Analytical chromatography has been performed by employing a Becker 401 type gas-liquid chromatograph, using a 6 mm o.d. copper column, 4 m in length. Packing material was 12% carbowax 20M on 60–80 mesh celite C_{22}. The flame ionization detector was used, with nitrogen as carrier gas. The conditions were as follows:

injection temperature	210°
column temperature	100–210°, with 6°/min programming
detector temperature	240°
gas flow rate	40 ml/min
injected quantity	2–2.5 µl.

The pyrolytic elimination products chromatogram of the above example, after the acetate removal, consists of 26 peaks (fig. 2).

Preparative chromatography was carried out on a Carlo Erba GT type chromatograph by employing a 10 mm o. d. stainless steel column, 2 m in length, and 20% carbowax 20 M on 30–60 mesh chromosorb W as packing material. The thermal conductivity detector was used with hydrogen as carrier gas. The conditions were:

injection temperature	300°
column temperature	195°
detector temperature	280°
hydrogen flow rate	500 ml/min
auxiliary gas flow rate	60 ml/min
injected quantity	170 µl.

The purity verification of the collected samples was made using a 4 mm o.d. stainless steel column, 2 m in length and 20% carbowax 20M on 60–80 mesh chromosorb W as packing material, on an analytic Carlo Erba GT chromatograph under the following conditions:

injection temperature	220°
column temperature	120–180°, with 4°/min programming
detector temperature	240°
nitrogen flow rate	30 ml /min
injected quantity	0.2 – 0.3 µl

The mass spectra were run using a Perkin-Elmer 900 type gas-liquid chromatograph coupled with a Perkin-Elmer RMU–6M type mass spectrometer; the coupling system is shown in figure 10.

A 2.5 m length and 3 mm i. d. stainless steel chromatographic column was used to separate the compounds, having 15 % carbowax 20M on chromosorb W 80–100 mesh as packing material.

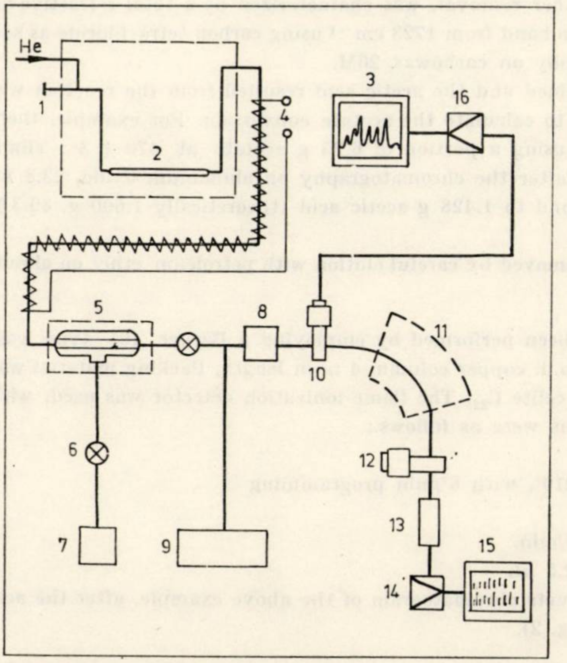

Fig. 10. – Schematic diagram of gas-chromatograph – mass spectrometer system :
1, injection point; *2*, chromatographic column; *3*, gas-chromatograph recorder; *4*, heated pipes; *5*, molecular separator; *6*, valve; *7*, diffusion pump; *8*, ionization source; *9*, diffusion pump; *10*, total ion detector; *11*, magnetic sector 60°; *12*, collector slit; *13*, multiplicator detector; *14*, amplifier; *15*, mass spectrum recorder; *16*, amplifier.

The conditions were: column temperature 100–210°, 10°/min programming, helium as carrier gas – 12 ml/min flow rate – using the total ion detector. The mass spectra were recorded under the conditions

molecular helium separator (Bicman type glass)	250°
ionization energy	70 eV
ion acceleration tension	1 500 kV
vacuum	2×10^{-7} mm Hg
mass number marking system (calibrated with perfluorobutylamine, with respect to 614 mass number)	2–900 mu
exploration speed	1 sec/decade

The following IR bands were used for the structural assignments of the collected peaks: peak *a* : 746 cm^{-1}; peak *b* : 878, 868, 860 cm^{-1}; peak *c* : 878 cm^{-1}; peak *d* : 878, 868, 860 cm^{-1}; peak *e* : 865 cm^{-1}; peak *f* : 833 cm^{-1}.

Revue Roumaine de Chimie, **19**, *3*, 455–484 (1974)

ALUMINIUM CHLORIDE CATALYZED CONDENSATIONS OF UNSATURATED ACIDS WITH BENZENE *

ALICE MARIE GLATZ

Institute of Organic Chemistry, Bucharest, Spl. Independenţei 202 B

Received September 18, 1973

The present paper reviews the aluminium chloride catalyzed condensation reactions of unsaturated acids with benzene. The behaviour of acyclic acids with one and two double bonds and of alicyclic unsaturated acids is discussed. The reaction products of these condensations are isomeric phenylated acids and cyclic ketones. The mechanism of the reactions taking place through carbocationic intermediates is presented. This paper deals largely with the occurrence of intramolecular hydride ion shifts and formation of lactoid ions in these intermediates, as well as with intermolecular hydride ion shifts. Both hydride ion acceptors and donors involved in the latter processes have proposed.

I. INTRODUCTION

The present review deals with the aluminium chloride condensation reactions of unsaturated acids with benzene, under the conditions of the Friedel-Crafts reaction.

As is well known, these reactions, largely studied in literature, due to their great theoretical interest and numerous industrial applications are the subject of excellent books [1–3] and monographs. [4–9]

---

* This paper is dedicated to the memory of Professor C. D. Nenitzescu, the promoter of the research in this field.

[1] G. Kränzlein, "Aluminiumchlorid in der organischen Chemie", Verlag Chemie, 1932, Berlin.

[2] C. A. Thomas, "Anhydrous Aluminium Chloride in Organic Chemistry", Reinhold, 1941, N. Y., p. 468–475.

[3] G. A. Olah, "Friedel-Crafts and Related Reactions", vol. 1–4, Interscience, New York, 1964.

[4] K. Le Roi Nelson and H. C. Brown, in "The Chemistry of Petroleum Hydrocarbons" vol. 3, Reinhold Publ. Co., New York, 1955, p. 465.

[5] C.C. Price, *Org. Reactions*, **3**, 1 (1948).

[6] a.G. Baddeley, *Quart Rev.*, **3**, 1 (1948); *b. idem*, **8**, 355 (1954).

[7] V. V. Lebedev, *Uspekhi Khim.*, **21**, 1399 (1952).

[8] E. S. Gould, "Mechanism and Structure in Organic Chemistry", Holt, Rinehart and Winston, New York, 1959, p. 449, writes: "The Mechanism of Friedel-Crafts Alkylations in Nonpolar Solvents is, at present, obscure".

[9] J. Hine "Physical Organic Chemistry", McGraw-Hill Book, New York, 1962, p. 353

The alkylation of aromatic hydrocarbons with alkenes is one of the most important industrial applications of the Friedel-Crafts reactions. Large quantities of ethylbenzene, cumene, dodecyl- and tridecylbenzene are thus obtained from the corresponding olefins.

Although only a small area of this immense field is discussed in this paper, the paper reviews the experimental research covering a period of more than forty years.

Considering the published works in this field, two periods may be distinguished : a pioneering period until 1960 [8,9] and a more recent one, developed as a result of the introduction of modern investigation methods in experimental research, thus permitting the formulation of new theories and perspectives for new works. In both periods, Nenitzescu and his coworkers had an important contribution in the understanding of these reactions.

The earlier works, from the first period, will be discussed herein only in order to indicate the starting point of the research, with the corresponding original discoveries, which generated more recent studies in the field, greater attention being paid to the evolution of the research in the last period, starting with 1960 until now.

The condensation of acyclic [10] and alicyclic [11,12] unsaturated acids with benzene and different aromatic compounds has been studied. There are known condensations of unsaturated esters, ethers and ketones with benzene. The present review is restricted to the condensation of different types of unsaturated acids with benzene. The condensations of functional derivatives of the unsaturated acids or other unsaturated compounds with benzene will be only incidently mentioned, if necessary, for a better understanding of the phenomena.

A survey of the results of the different works in this field enables the recognition of some general rules, governing the condensations of the different types of unsaturated acids.

II. CONDENSATIONS OF SOME ALKENOIC ACIDS WITH A SINGLE DOUBLE BOND WITH BENZENE

A. SOME GENERAL CONSIDERATIONS

All the condensation reactions of unsaturated acids, with a linear chain, longer than four carbon atoms involve intramolecular hydride ion shifts. This kind of reaction was known in litterature as early as 1907. Eijkman was the first to describe the addition of benzene and toluene to acrylic [13] and dimethylacrylic [14] acids. The formation of a single product was observed, with the aryl group situated in β position with respect to the carboxyl group. In the mentioned cases, no hydride ion shift was possible and thus no isomers of the arylated acids were formed.

---

[10] R. Konkos and B. S. Friedman, "Alkylation of Aromatics with Dienes and Substituted Alkenes", in reference 3, vol. 2, p. 318—323.

[11] Reference 2, p. 475—477.

[12] Reference 10, p. 323—328.

[13] F. J. Eijkman, *Chem. Weekblad*, **4**, 727 (1907) ; *Chem. Zentr. II*, **1907**, 2046.

[14] F. J. Eijkman, *Chem. Weekblad*, **5**, 655 (1908) ; *Chem. Zentr. II*, **1903**, 1100.

From 1935, Nenitzescu and his coworkers have observed rearrangements during the Friedel-Crafts reactions of alicyclic α,β-unsaturated acids,[15] α,β-unsaturated ketones and α-chloroethers,[16] in the condensation of 1,2-dibromocyclohexanes[17-19] as well as in the condensation of dibromoalkanes with benzene.[20]

In the condensation of either α,β-unsaturated ketones or acids with benzene, at moderate temperatures, Nenitzescu and his coworkers[21-26] have demonstrated in earlier works that the phenyl group is attached to the last but one carbon atom, related to the carbonyl, respectivly, carboxyl group, that means in the remotest possible position from the carboxyl group, and not at the atoms of the initial double bond. No substitution at the marginal primary carbon atom has ever been observed. This observation has a general character and was the starting point of other research in this field. Through modern investigations, a series of phenomena involved in the process has been observed.

B. α,β-UNSATURATED ACIDS

Condensations of 2-pentenoic,[25,27] 2-hexenoic,[22,25,28] 2-nonenoic[25,27] acids with benzene are well known in literature. The reactions were performed at 40—45 °, in 4 hours.

1. In these works, the formation of phenylated acids with the phenyl group in the last but one position, has been observed.[23,25,27-29] The oxidation with chromic acid[25] of the reaction products evinced the presence of acetophenone undoubtedly bearing out the existence of such isomers.

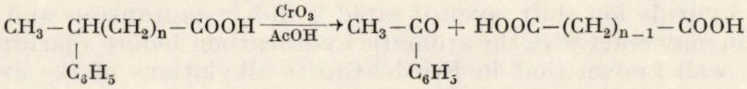

$$\underset{\substack{|\\ C_6H_5}}{CH_3-CH}(CH_2)_n-COOH \xrightarrow[AcOH]{CrO_3} \underset{\substack{|\\ C_6H_5}}{CH_3-CO} + HOOC-(CH_2)_{n-1}-COOH \qquad (1)$$

---

[15] C. D. Nenitzescu and I. Gavăt, *Ber. dtsch. chem. Ges.*, **70**, 1883 (1937).

[16] C. D. Nenitzescu and V. Przemetsky, *Ber. dtsch. chem. Ges.*, **69**, 2706 (1936).

[17] C. D. Nenitzescu and. D. Curcăneanu, *Ber. dtsch chem. Ges.*, **70**, 346 (1937).

[18] C. D. Nenitzescu and I. G. Dinulescu, *Studii și Cercetări Chim. Acad. R.S.R.*, **7**, 7 (1959).

[19] A. M. Glatz, A. C. Răzuș, F. Badea and C. D. Nenitzescu, *Rev. Roumaine Chim.*, **17**, 1735 (1972).

[20] C. D. Nenitzescu and A. M. Glatz, *Studii și Cercetări Chim. Acad. R.S.R.*, **7**, 505 (1959).

[21] C. D. Nenitzescu and I. Gavăt, *Liebigs Ann. Chem.*, **519**, 260 (1935).

[22] C. D. Nenitzescu, I. Gavăt and D. Cocora, *Ber. dtsch. chem. Ges.*, **73**, 233 (1940).

[23] C. D. Nenitzescu and A. T. Balaban, "Aliphatic acylation" in reference 3, vol. 3, p. 1066.

[24] Reference 10, p. 322.

[25] C. D. Nenitzescu and A. M. Glatz, *Bull. Soc. chim. France*, **1961**, 218.

[26] C. D. Nenitzescu and A. T. Balaban, in reference 23, vol. 3, p. 1068.

[27] M. F. Ansell and G. F. Whitfield, *Tetrahedron Letters*, **1968**, 3075.

[28] A. M. Glatz, A. C. Răzuș, and C. D. Nenitzescu, *Rev. Roumaine Chim.*, **11**, 555 (1966).

[29] P. Four and D. Lefort, *Compt. rend. C.*, **264**, 786 (1967).

2. The formation of a mixture of isomeric phenylated acids [28] has been demonstrated through vpc of the resulted methylic esters obtained from the reaction product; the structure of each component of the reaction mixture has been established through comparison with authentic samples, obtained in other ways.

In the case of 2-hexenoic acid a reaction mechanism has been formulated

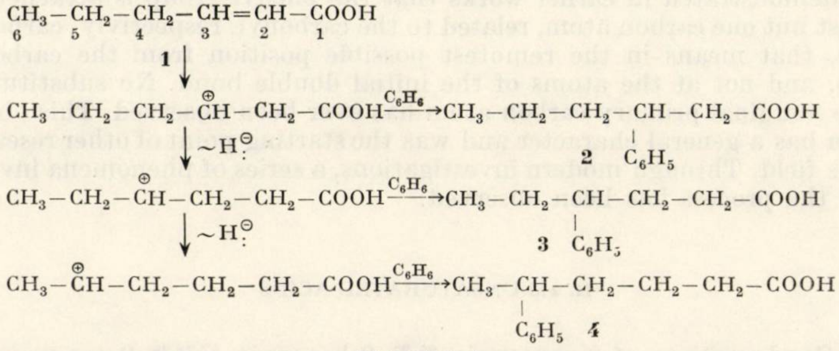

$$\begin{aligned}
&\underset{6}{CH_3}-\underset{5}{CH_2}-\underset{4}{CH_2}-\underset{3}{CH}=\underset{2}{CH}-\underset{1}{COOH}\quad \mathbf{1}\\
&\downarrow\\
&CH_3-CH_2-CH_2-\overset{\oplus}{C}H-CH_2-COOH\xrightarrow{C_6H_6}CH_3-CH_2-CH_2-\underset{C_6H_5}{CH}-CH_2-COOH\quad \mathbf{2}\\
&\downarrow\sim H^{\ominus}\\
&CH_3-CH_2-\overset{\oplus}{C}H-CH_2-CH_2-COOH\xrightarrow{C_6H_6}CH_3-CH_2-\underset{C_6H_5}{CH}-CH_2-CH_2-COOH\quad \mathbf{3}\\
&\downarrow\sim H^{\ominus}\\
&CH_3-\overset{\oplus}{C}H-CH_2-CH_2-CH_2-COOH\xrightarrow{C_6H_6}CH_3-\underset{C_6H_5}{CH}-CH_2-CH_2-CH_2-COOH\quad \mathbf{4}
\end{aligned}$$

SCHEME 1

The protonation of the double bond occurs in the first step of the reaction, leading to a carbocation * with the charge located in position 3. This carbocation suffers hydride ion shifts with the formation of two other carbocations, able to react with benzene. Each of the resulted carbocations may condense with benzene, forming thus the isomeric acids **2**, **3** and **4**.

The hydride ion shift, even if rapid is not instantaneous and thus a carbocation may react with the aromatic hydrocarbon before rearranging.[31]

It is well known that in Friedel-Crafts alkylations of the aromatic nucleus two types of isomerisations [32] may occur within the alkyl group. The isomerisation of the alkylating reagent, before the condensation with the aromatic hydrocarbon and the isomerisation within the resulted alkylation product, after the condensation.

The first types of isomerisation occur in the intermediate formed carbocation and involve 1,2-hydride ion shifts according to the well-known scheme of Whitmore.[33] These processes with low activation energies and entropies (unimolecular processes) are by far more rapid than the condensation (bimolecular reaction) and are catalysed by Friedel-Crafts catalysts (H_2SO_4, HF, BF_3, $FeCl_3$ and even $CH_3NO_2 \cdot AlCl_3$).

---

* Recently Olah [30] has proposed the generic name of *carbocation* for the organic cations with a fully or partially charge located at a carbon atom. The *classical* or tricovalent carbocations, should be named *carbenium ions*, whereas for the unclassical tetra- or pentacovalent carbocations the old nomenclature *carbonium ions* should be applied.

[30] G. A. Olah, *J. Amer. Chem. Soc.*, **94**, 808 (1972).

[31] E. Renk and J. D. Roberts, *J. Amer. Chem. Soc.*, **83**, 878 (1961).

[32] C. D. Nenitzescu, *Rev. Chim., Acad. R.P.R.*, **VII**, 394 (1962); **9**, 1 (1964); *Studii și cercetări Chim. Acad. R.S.R.*, **12**, 4 (1964).

[33] F. C. Whitmore, *Chem Eng. News*, **26**, 668 (1948).

Geiseler, Herrman and Kürzel, [34] through kinetic measurement (in the alkylation of benzene with heptene in the presence of sulfuric acid) showed that the isomerisation rates of the carbocations is about 6 times faster than the alkylation rate.

The reactions of the formed alkylated product involve three steps :

a. hydride ion abstraction (bimolecular process),
b. isomerisation of the formed carbocation,
c. hydride ion abstraction (bimolecular process).

The overall reaction rate of such reactions is much lower than the isomerisation rate in the alkylating reagent, they are favoured by increasing temperature and involve thermodynamic controlled processes. These reactions are catalyzed by the complex acid $H[AlCl_3OH]$ which abstracts a hydride ion from the saturated hydrocarbon giving raise to carbocations able to rearrange.[35] It should be remarked that the stability of the isomeric phenylalkanes is different from the stability of the alkylcarbocations involved in the Friedel-Crafts alkylations. In the latter case the isomerisations of the carbocations occur irreversibily towards the most stable ions [32]

$$R^+_{prim} \rightarrow R^+_{sec} \rightarrow R^+_{tert}$$

whereas the stability of the phenylalkanes decreases in the order [36] primary > secondary >tertiary. This fact explains why during the intramolecular rearrangements of di- and poly-alkylbenzenes the normal chain is able to migrate without branching, the alkylated benzenes with uubranched chain being thermodynamic stable isomers.

3. Studying the condensation of some acids with different length of the chain, the general character of the rearrangement has been proved.

It has been proposed [25] that the hydride ion shift is determined by the inductive effect, electron attracting of the carboxyl group. This observation seems to be true for unsaturated acids with a six or shorter carbon atom chain. It is known that the inductive effect, in longer than a six carbon atom chain, is not sufficiently strong to affect the hydride ion shift. This effect decreases rapidly with the increasing length of the chain. [37] It has been shown [38] that the inductive effect of the carboxyl group can be resented up to the 4th carbon atom of the acid chain.

4. Thus, generally, the aluminium chloride condensation of α,β-unsaturated acids with benzene occurs through intramolecular hydride ion shift, the phenyl group being attached in a single position of the aliphatic chain, but, in different positions, in all possible positions, beginning with carbon 3 and ending with the last but one carbon atom.

---

[34] G. Geiseler, P. Herrmann and G. Kürzel, *Chem. Ber.*, **98**, 1695 (1965).

[35] C. D. Nenitzescu, M. Avram and E. Sliam, *Bull. Soc. chim. France*, **1955**, 1266.

[36] Reference 3, vol. 1, p. 70.

[37] M. S. Newman, "Steric Effect in Organic Chemistry", ed. II, J. Wiley, New York, 1963, p. 592.

[38] P. Four and D. Lefort, *Tetrahedron Letters*, **1968**, 6143.

The phenyl group is never attached to the last (marginal) carbon atom (the formation of a less stable carbocation would be needed in that case) or in position 2, as the electron attracting inductive effect of the carboxyl group is opposing against to the hydride ion shift from that position.

C. FORMATION OF KETONES

1. During the condensations of α,β-unsaturated acids, Nenitzescu, Glatz, Răzuş, [28] modyfying only a little the reaction conditions (higher temperatures, longer reaction times), have observed, without isolating the products, the formation of cyclic ketones corresponding to the phenylated acids. 2-Pentenoic and 2-hexenoic acids yield in these conditions, beside a mixture of phenylated acids, a mixture of cyclic isomeric ketones.

Ansell and Whitfield [27] working in the same conditions with 2-pentenoic acid have identified two ketones ; 4-methyltetralone **(5)** and 3-ethylindanone **(6)**

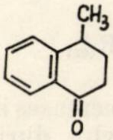

5

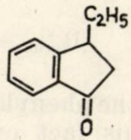

6

2. In the case of unsaturated acids with longer chain, such as 2-nonenoic acid, [39] the ketones are formed only from the phenylated acids with the phenyl group in the positions 3 and 4, substituted indanones or tetralones being thus formed. The isomeric acids with a remoter phenyl group react intermolecular with benzene yielding dihphenyl ketones (Scheme 2) *

---

* In the condensation of saturated acids with benzene [40] result aliphatic aryl ketones. A high excess of aluminium chloride [41] is used in that case. The high excess of the catalyst is necessary to decrease as much as possible the activity of the water molecules resulted in the reaction. It is difficult to decide if the reactive intermediate has the structure I or II

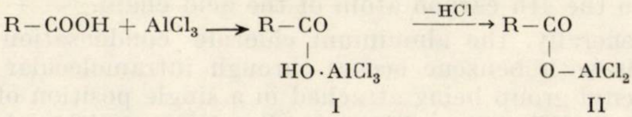

$$\mathrm{R-COOH} + \mathrm{AlCl_3} \longrightarrow \underset{\substack{|\\ \mathrm{HO\cdot AlCl_3}\\ \mathrm{I}}}{\mathrm{R-CO}} \xrightarrow{-\mathrm{HCl}} \underset{\substack{|\\ \mathrm{O-AlCl_2}\\ \mathrm{II}}}{\mathrm{R-CO}}$$

If structure I is admitted, then the reaction proceeds through ion pairs

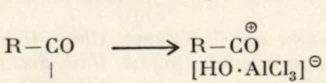

$$\underset{\substack{|\\ \mathrm{HO\cdot AlCl_3}}}{\mathrm{R-CO}} \longrightarrow \mathrm{R-C\overset{\oplus}{O}}\ [\mathrm{HO\cdot AlCl_3}]^{\ominus}$$

[39] M. F. Ansell and G. F. Whitfield, *J. Chem. Soc. C.*, **1971**, 1098.

[40] A. M. Glatz and A. C. Răzuş, *Rev. Roumaine Chim.*, **11**, 551 (1966).

[41] A. G. Peto, reference 2, vol. 3, p. 539.

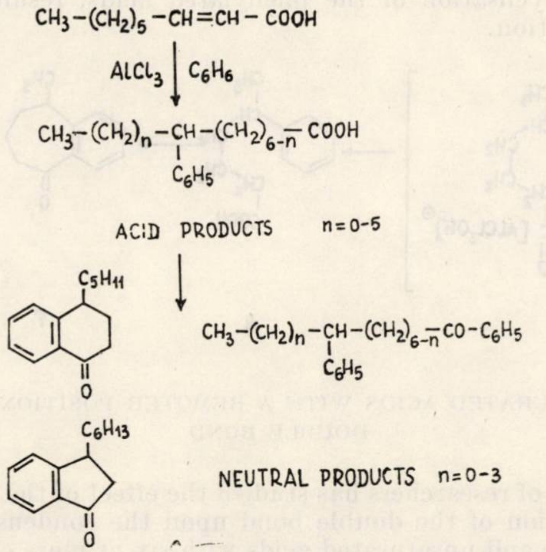
CH3-(CH2)5-CH=CH-COOH
AlCl3 C6H6
CH3-(CH2)n-CH-(CH2)6-n-COOH
C6H5
ACID PRODUCTS n=0-5
C5H11
O
CH3-(CH2)n-CH-(CH2)6-n-CO-C6H5
C6H5
C6H13
O
NEUTRAL PRODUCTS n=0-3

SCHEME 2

3. The cyclic ketones, obtained in that way do not isomerize even in very energetic conditions [28] (16 hrs in refluxing bezene with aluminium chloride). Thus, 5-phenyl-caproic acid was prepared from the lactone of 5-hydroxy-caproic acid [42] with benzene. This acid was then cyclized in the presence of aluminium chloride to 5-methylbenzosuberone (**7**), identical with that obtained by Julia and Bonnet [43] in another way. Ketone **7** does not isomerize in the above mentioned conditions.

4. Baddeley, Holt and Makar [44] have described cyclisations of aryl-vinyl-ketones (**8**; R=H or alkyl) and unsaturated acids (**8**; R = COOH) which proceed in the following manner

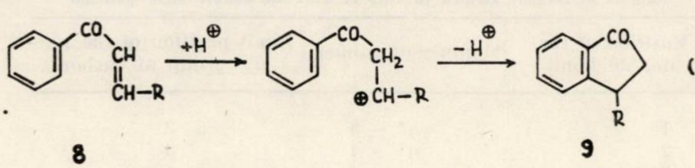
CO
CH
CH-R
+H⊕
CO
CH2
⊕CH-R
-H⊕
CO
R

(2)

8 **9**

As in the condensation of unsaturated acids, unsaturated ketones are not formed, the reaction must certainly proceed in another way, namely through cyclisation of the phenylated acids, resulted in the first step of the reaction.

---

[42] K. W. Rosenmund and H. Bach, *Chem. Ber.*, **94**, 2407 (1961).

[43] S. Julia and Y. Bonnet, *Bull. Soc. chim. France*, **1957**, 1347.

[44] G. Baddeley, G. Holt and S. M. Makar, *J. Chem. Soc.*, **1952**, 3289.

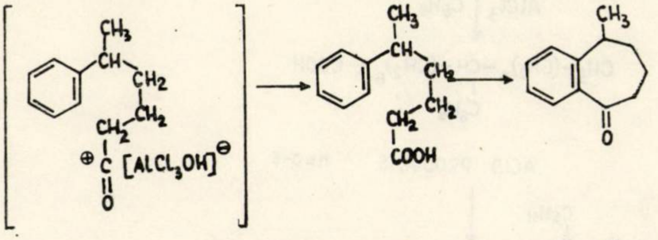

4 **7**

(3)

D. UNSATURATED ACIDS WITH A REMOTER POSITION OF THE DOUBLE BOND

1. A series of researchers has studied the effect of the carboxyl group and of the position of the double bond upon the condensation products between benzene and unsaturated acids with six or more carbon atoms in the molecule.

2. In order to establish the effect of the carboxyl group on the condensations of the unsaturated acids, Four and Lefort [29] have compared the condensation products of 4-pentenoic and 10-undecenoic acids with the condensation products of 1-decene and of 9-octadecene. They have observed that in the case of the unsaturated acids, due to the inductive effect of the carboxyl group, the number of the phenylated isomers is less than for the mentioned alkenes.

3. Based on the fact that the phenyl group is never attached to the marginal methyl group, Four and Lefort [38] have shown that the number of the resulted phenylated isomers depends also on the position of the double bond in the chain of the starting unsaturated acid (table 1) :

Table 1

Number of isomers formed in respect with the double bond position

Position of the double bond	Number of isomers	Limit position of the phenyl group at carbon
1 ,	$n^* - 3$	3
2 ,	$n - 4$	4
3 beyond	$n - 5$	5

* n = number of the carbon atoms of the chain of the unsaturated acid.

In the latter case, the limit position of the phenyl group is Cδ, the inductive effect of the carboxyl group being no further felt beyond that atom.

Thus, considering the results obtained in that field the above mentioned authors have concluded that, generally from acids with the double bond located in α, β, if n is the number of carbon atoms of the chain, n-3 isomers are formed ; from β, γ-unsaturated acids, result n-4 isomers, whereas from unsaturated acids with the double bond beyond the δ position (without respect to the distance) $n - 5$ isomers are formed.

Ansell and Whitfield [39] have studied the condensation of pentenoic acids (2-, 3- and 4-) obtaining results in agreement with those observed with the six and nine carbon atoms acids. In the case of 2-nonenoic acid they proved the formation of different phenylated acids. The same authors have completed the condensations performed by Four and Lefort, arriving at similar results with respect to the inductive effect and the effect of the position of the double bond. In table 2 are given the known results obtained until now in the condensation of alkenoic acids with benzene, at 40–45°.

Table 2

Phenyl-alkane-carboxylic acids: position of the phenyl group in the chain

Starting acid	Position of the double bond	Resulted isomers Position of the phenyl group	Ref.
Pentenoic	2,3	3 4	38,39
	3,4	4	38
	4,5	4	38,39
Hexenoic	2,3	3 4 5	28,39
	3,4	4 5	39
	5,6	5	39
Heptenoic	2,3	3 4 5 6	39
	4,5	traces 5 6	38
	6,7	5 6	39
Octenoic	2,3	3 4 5 6 7	39
	3,4	4 5 6 7	39
	7,8	5 6 7	39
Nonenoic	2,3	3 4 5 6 7 8	39
	8,9	3 4 5 6 7 8	39

4. Four, [45] studying the aluminium chloride catalyzed condensation of benzene with unsaturated acids and nitriles established that the number of phenylated isomers depends equally on the position of the double bond with respect to the functional group and on the nature of that group.

5. The acids with a remote double bond (8-nonenoic acid) [39] do not yield cyclic ketones in the conditions discussed above (chap. II, C. 1.) as no isomers, able to cyclize to indanone or tetralone, are formed. These acids give only diphenylketones (see Scheme 2).

E. OLEIC ACID

1. The aluminium chloride condensation of oleic acid with benzene was known and discussed[45-52] long since in the literature, even if the structure of the products resulted in this reaction was not established. Most of the authors considered that the reaction mixture consists of 9- and 10-phenyl-stearic acids. [53-56]

---

[45] P. Four, *Compt. rend.*, **272**, 1671 (1971).

[46] J. Marcusson, *Z. angew. Chem.*, **33**, 231 (1920).

[47] H. B. Nicolet and C. M. de Milt, *J. Amer. Chem. Soc.*, **49**, 1105 (1927).

[48] E. G. Schmidt, *J. Amer. Chem. Soc.*, **52**, 1172 (1930).

[49] R. H. McKee and H. B. Faber, U. S. Pat, 1. 972. 568, 1934 ; *Chem. Abstr.*, **28**, 6446 (1934).

[50] W. Kimura, T. Omura and H. Taniguchi, *Ber. dtsch. chem. Ges.*, **71**, 2686 (1938).

[51] H. J. Stirton and R. F. Peterson, *Ind. Eng. Chem.*, **31**, 856 (1939).

[52] N. P. Buu Hoï and P. Cagniant, *Bull. Soc. chim. France*, **10**, 477 (1943).

Nenitzescu and Glatz [23,25,57] have demonstrated that in the intermediate carbocation, generated from the unsaturated acids with a longer chain than a six carbon atoms chain, hydride ion shifts occur up to the last but one carbon atom. This has been borne out in the case of oleic acid too, when 17-phenylstearic acid was detected among the reaction products. Its existence has been proved through oxidation of the reaction mixture with chromic acid and the indentification of acetophenone and 1,14-tetradecanedicarboxylic acid.

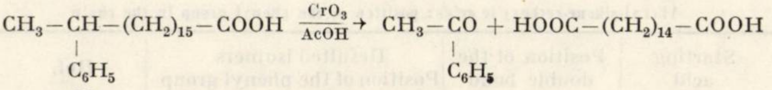

$$\mathrm{CH_3-\underset{\displaystyle C_6H_5}{\underset{|}{CH}}-(CH_2)_{15}-COOH \xrightarrow[AcOH]{CrO_3} CH_3-\underset{\displaystyle C_6H_5}{\underset{|}{CO}} + HOOC-(CH_2)_{14}-COOH} \qquad (4)$$

10

The lack of modern investigation methods has not permitted, at that time, the performance of exact quantitative measurements.

2. Later, Smith, Stirton, Kenney and Doodley [58,59] have treated oleic acid with different aromatic hydrocarbons (benzene, toluene, xylene etc.). They tried to determine, through vpc, the number of the resulted arylated isomers, after converting the reaction products in a mixture of the corresponding methyl esters. The method proved to be tedious and inconclusive, since the esters of phenylstearic acids cannot conveniently be separated. Through chromic acid oxidation of the mixture of the arylated acid obtained in the reaction, Smith, Kenney and Stirton, [58] succeeded in the identification of the arylated acids present in the reaction mixture. Using the scheme of Cason, Fesenden and Agree [60] advanced for the oxidation of some alkanoic acids, substituted with mehyl groups in the chain, the above mentioned authors have formulated a scheme of all possible products which might be obtained in the oxidation of phenylstearic acids

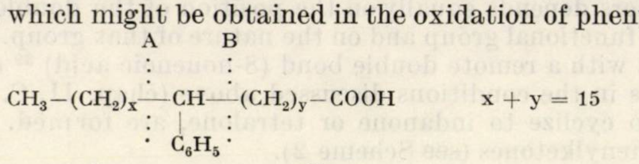

$$\mathrm{\underset{I}{CH_3-(CH_2)_x}\overset{A}{\vdots}\underset{\displaystyle C_6H_5}{\underset{|}{CH}}\overset{B}{\vdots}\underset{II}{(CH_2)_y-COOH}} \qquad x + y = 15 \qquad (5)$$

A – I $\mathrm{CH_3-(CH_2)_{x-1}-COOH}$ B – I $\mathrm{C_6H_5-CO-(CH_2)_x-CH_3}$

A – II $\mathrm{C_6H_5-CO-(CH_2)_y-COOH}$ B – II $\mathrm{HOOC-(CH_2)_{y-1}-COOH}$

---

[53] J. Harmon and C. S. Marvel, *J. Amer. Chem. Soc.*, **54**, 2515 (1932).

[54] W. Kimura and H. Taniguchi, *J. Soc. Chim. Ind. Japan*, **42**, Suppl. binding 234 (1939); *Chem. Abstr.*, **33**, 859 (1939).

[55] Reference 2, p. 472.

[56] Reference 10, p. 319.

[57] Reference 10, p. 324.

[58] F. D. Smith, H. E. Kenney and A. J. Stirton, *J. Org. Chem.*, **30**, 885 (1965).

[59] F. D. Smith, A. J. Stirton and C. J. Doodley, *J. Amer. Oil Chemists Soc.*, **45**, 747 (1968).

[60] J. Cason, J. S. Fesenden and C. L. Agree, *Tetrahedron*, **7**, 289 (1959).

From a molecule of phenylstearic acid, three types of acids might be formed, i.e. a very complex reaction, whereas only a single neutral product (B — II) accompanies the acids in the mixture (phenone). Thus, the gas-chromatographical analysis of the neutral oxidation products, might give correct information about the mixture of isomeric phenylstearic acids. The method gave the expected results : 12 ketones were found. Through vpc-comparison with authentical samples were identified : acetophenone, propiophenone, valerophenone and laurophenone ; thus, the existence of the corresponding phenylstearic acids in the mixtures has been proved.

3. According to Smith, Kenney and Stirton [58] the condensation of oleic acid proceeds similarly to the reaction of the other unsaturated acids : in the first step, the formation of a carbocation through proton addition to the double bond, then a series of hydride ion shifts follows in which 12 carbocations are formed. The limit position of the location of the position charge is at C_6 and C_{17}, each of these carbocations gives raise to phenylated acid, altogether 12 isomers. The above authors postulated that the proton is transferred from the complex acid $H^+[AlCl_4]^-$. It has been long since established [61–63] that this acid does not exist. Nenitzescu, Avram and Şiliam [35] have demonstrated that in those cases, the proton is given up by the initial acid $H^+[AlCl_3OH]^-$.

F. FORMATION OF LACTOID IONS

The number of the formed phenylated isomers, in the above discussed reaction, is limited by the formation of lactoid ions.

1. Fittig [64,65] and later other authors have shown that in strong acid medium, [60,66–68] the unsaturated acids converted in γ-and δ-lactones, respectively their stability depending on the structure of the acid and on the rection conditons. The analysis of the condensation products of oleic acid [58] indicates the absence from the reaction mixture of the phenylstearic acids with the phenyl group located in positions 5, 4, 3 or 2. In agreement with what was shown above, the absence of these isomers was ascribed to the formation of a δ-lactone which does not further allow the hydride ion shift from the neighbouring positions and implicitly the condensation with benzene

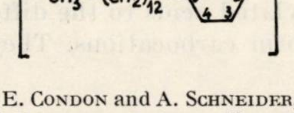

(6)

---

[61] P. D. Bartlett, F. E. Condon and A. Schneider, *J. Amer. Chem. Soc.*, **66**, 1531 (1944).

[62] H. C. Brown and H. Pearsall, *J. Amer. Chem. Soc.*, **73**, 4681 and 5096 (1951).

[63] C. D. Nenitzescu, *Uspekhi Khim.*, **26**, 399 (1957).

[64] G. Fittig, *Ber. dtsch. chem. Ges.*, **16**, 373 (1883) and **26**, 40 (1893).

[65] G. Fittig, *Liebigs Ann. Chem.*, **283**, 47 (1894).

[66] M. F. Ansell and M. H. Palmer, *J. Chem. Soc.*, **1963**, 2640.

[67] M. F. Ansell, *Quart. Rev.*, **18**, 211 (1964).

[68] M. F. Ansell, B. E. Grimwood and T. M. Kafka, *J. Chem. Soc., (C)*, **1967**, 1802.

2. Four and Lefort[38] have demonstrated the dependence of the location of the phenyl group on the position of the double bond from the unsaturated acid namely, if the double bond is placed at Cδ or further remote from the carboxyl group, the phenyl group might be attached in all possible positions between the last but one carbon atom and C_5, that is in this position the isomerisation is restricted. This restriction has been ascribed by Four and Lefort to the formation of pseudo-δ-lactonic cycle

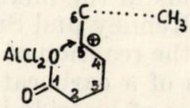

(7)

hindering the migration of a hydride ion from C_4 to C_5 and thus the formation of a carbocation with the positive charge at C_4.

The formation of only 5-phenyl-caproic acid from δ-caprolactone[28] in Friedel-Crafts condensations, pleads in its turn for the formation of a lactoid intermediate in the condensation reactions of unsaturated acids. It would have been expected that in the case of 3-octenoic acid the formation of a pseudo-δ-lactonic cycle would restrict the isomerisation at C_5 and would prevent the formation of phenylated acids with phenyl groups in positions 6 and 7. Actually these isomers do exist in the reaction mixture. Four and Lefort have explained the observed disagreement by admitting a hydride ion shift from C_6 to C_5 (nondependent on the inductive effect (7)), or less probably, through a transannular shift[69] (8) from C_7 to C_4 leading to the formation of carbocations with the positive charge at C_6 and C_7:

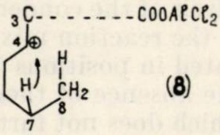

(8)

Ansell and Whitfield,[39] studying the reaction products with respect to the position of the double bond, obtained results in good agreement with Four and Lefort, but explained their results in a different manner. They do not admit the hypothesis of a transannular hydride shift ascribing the limitation of a number of phenylated acids to the different ease of the carbon atoms from the chain to form carbocations. They suggest the following sequence of this easiness

$C_\omega < C_{\omega-1}$	$C_{\omega-2} \sim C_7 \sim C_6 \sim C_5$	$> C_4 \gg C_3 \ggg C_2$
decreasing ease of formation	the same ease of formation	decreasing ease of formation
⟵	⟵⟶	⟶

---

[69] Reference 9, p. 320.

How can this sequence be explained? The carboxyl group reacts, in the first step, with aluminium chloride yielding an ion pair, as in the acylation of benzene

$$-CO_2.AlCl_2 \rightleftharpoons -\overset{\oplus}{C}O^{\ominus}OAlCl_2 \qquad (9)$$

In a similar way, the above mentioned authors consider that the intermediates involved in the rearrangements that occur in those reactions are not carbocations but light ion pairs with a certain covalent character between the carbocation center and the tetrachloro-aluminate ion. The 1,2-shifts, involved in these nucleophilic rearrangements, are stereochemically controlled, [70] since the hydride ion attacks the neighbouring carbon atom on the opposite side to that of the displaced $AlCl_4^-$ ion.

Accordingly, there will exist only a few preferential conformations in which the hydride ion shift could be possible. Using Newman's projections, Ansell and Whitfield propose two types of conformations.

The decrease of the tendency of formation of the carbocations with the positive charge located in position 4 is due to the inductive effect of the carboxyl group.

3. Another fact that pleads in the favour of the formation of lactoid ions is the difference in the observed behaviour in the condensation of some α, β-unsaturated ketones as compared with that of the α, β-unsaturated acids. Nenitzescu and Gavăt [21] observed in the condensation of hexene-3-one the formation of a phenylated ketone in the position 5, identified through the isolation of a solid compound, whereas Ansell and Mahmud [17] (with modern investigation methods) found ketones **11** and **12** in a relative ratio of respectivly 38 and 62 % that is in a different ratio (reverse order) than that determined in the condensation of unsaturated acids with the same number of carbon atoms in the chain. [28,29] This difference might have the following explanation : the inductive effect of carbonyl group is product-controlling in the condensation of unsaturated ketones, whereas in

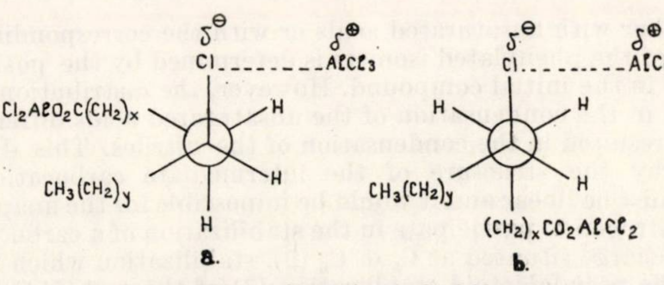

Fig. 1. *a.* Favourable conformation to hydride shift ; *b.* Unfavourable conformation to hydride shift.

---

[70] D. J. Cram and F. D. Green, *J. Amer. Chem. Soc.*, **75**, 6005 (1953) ; reference 25, p. 270.

[71] M. F. Ansell and S. A. Mahmud, *Tetrahedron Letters*, **1971**, 4129.

the similar reaction of the unsaturated acids, another factor determining the stability of the cationic intermediate is involved : the formation of a more stable ion than a carbocation, a lactoid ion.

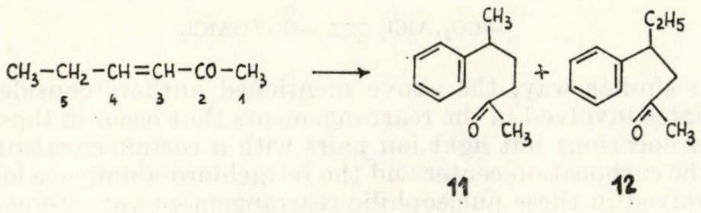

G. EFFECT OF THE FUNCTIONAL GROUP

1. Smith, Stirton and Doodley[59] observed that the distribution of the phenylated isomers is about the same either starting from the nitrile, ester, octadecylic alcohol or from oleic acid.

Comparing unsaturated acids with the corresponding nitriles Four[45] has demonstrated that the number and the relative ratio of the phenylated isomers is equelly determined by the position of the double bond and the nature of the functional group. Thus he has shown that in all the considered cases, the isomer formed in overwhelming weight is the isomer with the phenyl group situated at the last but one carbon atom, due to the stabilization through hyperconjugation of the sp^2 carbon atom with the methyl group.

2. Either with unsaturated acids or with the corresponding nitriles, the number of the phenylated isomers is determined by the position of the double bond in the initial compound. However, the distribution of the isomers formed in the condensation of the unsaturated acids differs from the distribution resulted in the condensation of the nitriles. This difference is determined by the structure of the intermediate carbocations. Thus, $C_2-C_1\equiv N$ must be linear and it would be impossible for the unapaired electrons from nitrogen to participate in the stabilization of a carbocation with the positive charge situated at C_5 or C_6 (9), stabilization which would correspond to the pseudolactoid stabilization (7) of the carbocations derived from unsaturated acids

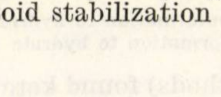

(10)

Table 3 includes comparative results of the phenylation of three unsaturated acids and their corresponding nitriles. It shows that with one exception (which hardly could be named so) the number of the formed isomers does not change from acids to nitriles. However, the remotest position of the phenyl group, is preferred in the case of the nitriles. The different isomers distribution might be explained through the more powerful in

Table 3

Comparative data between phenylated product formed from unsaturated acid and nitriles

	Ethylenic acids and nitriles	% of different phenylated isomers Phenyl bonded at carbon atom			
		C_4	C_5	C_6	C_7
1.	a $CH_3-CH_2-CH=CH-CH_2-CH_2-COOH$	4	31.8	65.0	0
	b $CH_3-CH_2-CH=CH-CH_2-CH_2-C\equiv N$	0	12.5	87.5	0
2.	a $CH_2=CH-CH_2-CH_2-CH_2-CH_2-COOH$	0	8.5	91.5	0
	b $CH_2=CH-CH_2-CH_2-CH_2-CH_2-C\equiv N$	0	2.0	98.0	0
3.	a $CH_3-CH_2-CH_2-CH=CH-CH_2-COOH$	9.0	18.0	26.5	46.5
	b $CH_3-CH_2-CH_2-CH_2-CH=CH-CH_2-C\equiv N$	6.5	8.5	30.5	54.5

ductive effect of the CN group,* or, probably, through an extra stabilization of the positive charge in one of the different conformation of the carbocation** (11)

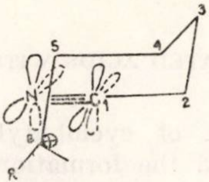

III. CONDENSATIONS OF SOME UNSATURATED ALICYCLIC ACIDS WITH BENZENE

A. GENERAL CONSIDERATIONS

In the series of alicyclic unsaturated acids will be discussed the results obtained in the condensation of alicyclic α, β-unsaturated acids containing an exocyclic double bond with a four-, five- and six-membered ring, each example being represented by a single compound. Occasionally, some related results, observed with the corresponding endocyclic double bond in the unsaturated acids, will be mentioned. Generally, these condensations have been performed in the same conditions as in the case of aliphatic α,β-unsaturated acids. Mixtures of isomeric phenyl-alicyclic acids have been obtained, in which the phenyl group is located to different cyclic carbon atoms up to the remotest carbon atom from the carboxyl group. [15,21,72]

---

* We may consider as measure of the inductive effects, the σ-values (s. for exemple J. E Leffler and E. Grunwald, "Rates and equilibria of organic reactions", John Wiley, New York 1963, p. 223). The σ_{CN} values are definitely higher than the σ_{COOH} values.

** In solution, the conformations requiring the smallest volume (such as in (11)) are preferred.

[72]. A. M. Glatz, A. C. Răzuş, F. Badea and C. D. Nenitzescu, *Rev. Roumaine Chim.*, **16**, 1567 (1971).

As in all similar reactions, the first step is the formation of a carbocation through proton addition to the alkenic double bond. This carbocation may further isomerize in a more stable lactoid ion or in another carbocation yielding different isomeric phenylated acids. Cosequently, no acid with t he phenyl group located in position 3 has ever been observed

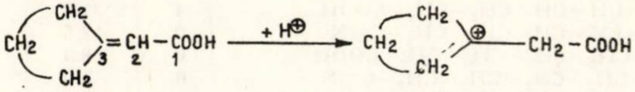

Beside the already mentioned reactions, the intramolecular hydride ion shifts, with the formation of lactoid ions, the formation of benzo-bicyclic ketones, hydrogenating ring-openings, through intermolecular hydride ion transfer (cyclobutane-derivatives) have been also observed.

B. ALICYCLIC UNSATURATED ACIDS WITH CYCLOBUTANIC RING

1. In the condensation of cyclobutylideneacetic acid [73,74] with benzene [75] has been observed the formation of a mixture of $C_{12}H_{16}O_2$ acids (branched phenyl-hexanoic acids)together with a $C_{12}H_{14}O_2$ acid (*trans*-2 phenyl-cyclobutylacetic acids), a diphenylated acid $C_{18}H_{16}O_2$ and a small proportion of ketones $C_{12}H_{14}O$ (table 4). The identification of the isomeric

Table 4

Condensation of the cyclobutylidene acetic acid (13) with benzene

Products	Acids (methylic esters)	Moles %	Yields %
A	4-Phenyl-caproic **(19)**	11.9	47.0
	3 — Methyl-4-phenyl-valeric **(20)**	11.0	
	3-Ethyl-4-phenyl-butyric **(21)**	9.8	
	trans-Phenyl-cyclobutyl-acetic **(18)**	14.8	
	3-Methyl-5-phenyl-valeric **(25)**	50.7	
	nonidentified	1.8	
B	1-Methyl-3-phenyl-indenylacetic **(27)**		10.0
Ketones	$C_{12}H_{14}O$		5.2
Polymers			37.8

---

[73] C. D. Nenitzescu, A. M. Glatz, M. Gavăt and I. Pogany, *Isvest. Akad. Nauk S.S.S.R.*, **1963**, 332.

[74] K. Wiberg, J. E. Hiatt, *J. Amer. Chem. Soc.*, **90**, 6495 (1968).

[75] A. M. Glatz, A. C. Răzuș, M. Elian and C. D. Nenitzescu, *Rev. Roumaine Chim.*, **16**, 1579 (1971).

acids in the reaction mixture has been done through gas-chromatographic comparison of the corresponding methyl esteres with authentic samples.

2. Thus, as in all similar reactions, the first step, implies the addition of a proton to the alkenic double bond of the acid **13**, forming the carbocation **14**. In this ion, hydride ion shifts are possible, with the subsequent formation of the carbocations **15** and **16**.

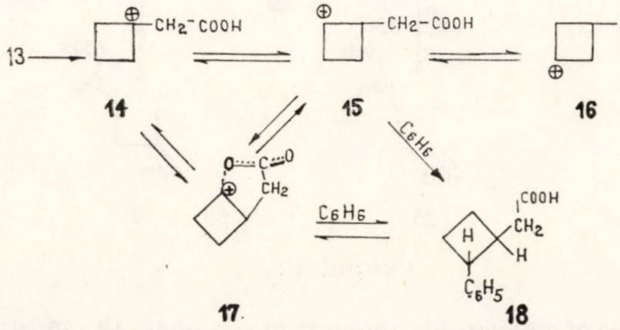

Each of these intermediate ions might suffer different transformations. Thus, the carbocation **15** rearranges in a more stable lactoid ion **17**.[61] That intermediate, through a stereospecific attack of benzene, should yield *trans*-2-phenyl-cyclobutylacetic acid (**18**).

3. *Ring openings*. The acid **18** is the single reaction product preserving the initial cyclobutane ring. The formation of $C_{12}H_{16}O_2$ acids occurs through ring opening (Schemes 3 and 4):

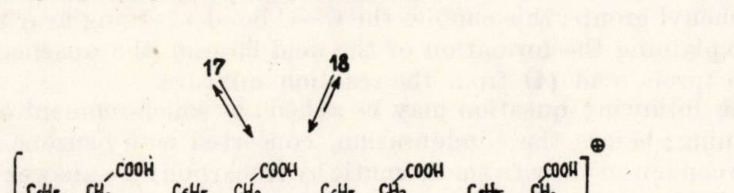

SCHEME 3

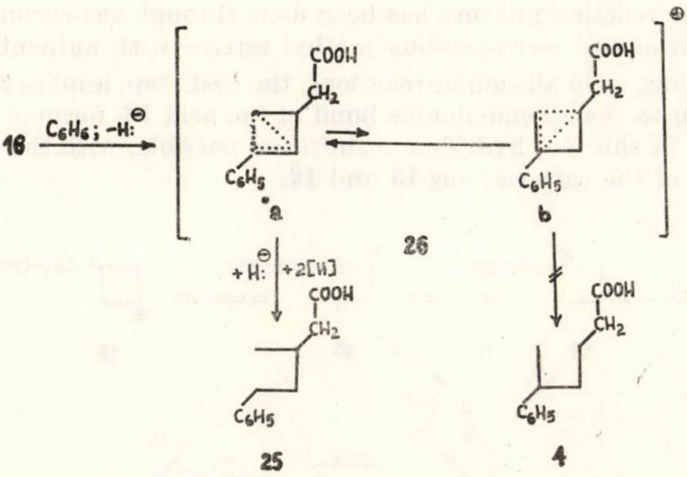

SCHEME 4

The presence of comparable amounts of the acids **19**, **20**, **21**, suggests a common intermediate, which might be the cyclobutonium ion **22**, represented in the four structure *a*, *b*, *c* and *d* (Scheme 3). These structures generate the acids **19**, **20**, **21** and, probably, the acid **23**, in small amounts.

The major component is 3-methyl-5-phenyl-valeric acid (**25**), formed from the carbocation **16**. That ion, through simultaneous benzene attack and hydride ion abstraction gives the bicyclobutonium ion **26** represented in structures *a* and *b* (Scheme 4). The equilibrium between structure *a* and *b* is favourable to structure *a*, having the maximum charge delocalization in the phenyl group ; this enables the C—C bond breaking near the pheny group explaining the formation of the acid **25** and the absence of the 5-iphenyl-caproic acid (**4**) from the reaction mixture.

The following question may be asked : at which moment occurs the ring opening : before the condensation, concerted with benzene attack or after the condensation with the aromatic hydrocarbon? To answer this question, a sample of acid **13** in carbondisulfide was refluxed in the presence of aluminium chloride several hours, without any change in its structure. This fact, together with the absence of 5-phenyl-caproic acid from the reaction mixture indicates that the ring opening does not take place before the condensation of the acid 13 with benzene. The presence of 5-phenyl-caproic acid would have confirmed the ring opening before the condensation and its formation from the bicyclobutonium ion **26** *b*.

The bicyclobutonium ions may arise either through benzene attack at the lactoid ion **17** or after the formation of the acid **18** or 3-phenyl-cyclobutylacetic acid simultaneously with the abstraction of hydride ions. To distinguish between these two alternatives, *trans*-2-phenyl-cyclobutylacetic acid (**18**) has been submitted to the same conditions described above for the acid **13**. In that case, 4-phenyl-caproic (**19**) and 3-methyl-4-phenyl-valeric (**20**) acids were identified through vpc, pleading thus for a ring opening after the formation of acid **18**.[76] The question, however, has not been completly elucidated.

4. *Intermolecular hydride ion transfers*

a. General considerations

It is well known that the intermolecular hydride ion transfers [23,77,79*] occur according to certain rules : [77,78,80]

1. In the reactions in which hydride ion changes its position, the hydride ions never become free. 2. In such reactions, in the reaction mixture, hydride donors and acceptors must exist. Compounds able to generate stable carbocations are powerful hydride donors; unstable carbocations (or their precursors) are efficient hydride acceptors. 3. intermolecular hydride ion transfers are stepwise reactions.

The theory of carbocation intermediate in the intermolecular hydride ion transfer was proposed by Bartlett, Condon and Schneider[61] and demonstrated through an intermolecular hydrogen-halogen transfer. The driving force of an intermolecular hydride ion transfer consists usually in the energy of formed acceptor-hydrogen bond and the disappearence of the carbocation.[81]

There are known a large number of intermolecular hydride ion transfer reactions occurring in condensations catalysed by aluminium chloride; these reactions were observed for the first time by Nenitzescu and Ionescu[77,82,83] in the reaction of alkyl halides with cyclohexane and aluminium chloride. Similar reactions were also observed by Nenitzescu and Isăcescu[84,85] in Anschütz type condensations of phenyl-chloro-propane and in acetylation and benzoylation of 9,10-dihydroanthracene.[86]

In the reaction of cyclohexane and acetyl chloride, catalyzed by aluminium chloride, Nenitzescu and Cantuniari[87] observed, beside the ring contraction and the formation of saturated ketones, the appearance of unsaturated cyclic ketones with a five-membered ring.

Nenitzescu and Ciorănescu,[88] in the condensation of cyclohexane with acetyl chloride in cyclohexane in the presence of aluminium chloride, have shown that the saturated hydrocarbon is able to hydrogenate the reaction products between the alkene and the acylating agent; similar results have been also obtained with other cycloalkenes.[89] These acylation reactions involve the intermolecular hydride ion transfer from the added saturated hydrocarbon to the intermediate carbocation resulted in the acylation. Such reactions are known in the literature as "Nenitzescu's reductive acylations".[90,91]

---

* According to an earlier nomenclature the hydride ion transfer is named "hydrogen transfer"; see reference 79.

[76] A. M. Glatz, unpublished results.

[77] C. D. Nenitzescu, *Studii şi Cercetări Chim. Acad. R.S.R.*, **18**, 853 (1970).

[78] C. D. Nenitzescu, "Intermolecular Hydride Transfer Reactions" in : G. A. Olah and P. von R. Schleyer, "Carbonium Ions", vol. 2, J. Willey-Interscience, New York, 1970, p. 463.

[79] "Editorial Reports on Nomenclature", *J. Chem. Soc.*, **1954**, 4714.

[80] N. C. Deno, H. J. Peterson, and G. S. Saines, *Chem. Rev.*, **60**, 7 (1960).

[81] P. D. Bartlett and J. D. McCollum, *J. Amer. Chem. Soc.*, **78**, 1441 (1956).

[82] C. D. Nenitzescu and C. N. Ionescu, *Liebigs Ann. Chem.*, **491**, 189 (1931).

[83] M. Avram, "C. D. Nenitzescu", *Studii şi Cercetări Chim. Acad. R.S.R.*, **19**, 583 (1971); idem, *Chem. Ber.*, **104**, XVII–LXV (1971).

[84] C. D. Nenitzescu and Isăcescu, *Ber. dtsch. chem. Ges.*, **66**, 1100 (1933).

[85] Reference 16, p. 1033.

[86] C. D. Nenitzescu, I. Gavăt and D. Cocora, *Ber. dtsch. chem. Ges.*, **72**, 819 (1939).

[87] C. D. Nenitzescu and I. Cantuniari, *Ber. dtsch. chem. Ges.*, **65**, 1449 (1932).

[88] C.D. Nenitzescu and E. Ciorănescu, *Ber. dtsch. chem. Ges.*, **69**, 1820 (1936).

b. The formation of the acids $C_{12}H_{16}O_2$, instead of the expected acids $C_{12}H_{14}O_2$, containing no four-membered ring products, in the condensation of cyclobutylideneacetic acid,[75] was explained by a ring opening followed by hydrogenation occurring through intermolecular hydride transfer. The presence in the reaction mixture of a crystalline acid (m.p. 140°), poor in hydrogen, $C_{18}H_{16}O_2$, indicated this acid as stabilization product of some intermediate hydride-donors. Its structure was established through IR, UV, NMR. The structure corresponds to 1-methyl-3-phenyl-indenylacetic acid **(27)**, formed from a common intermediate **(26)** with the acid **25** (Scheme 5).

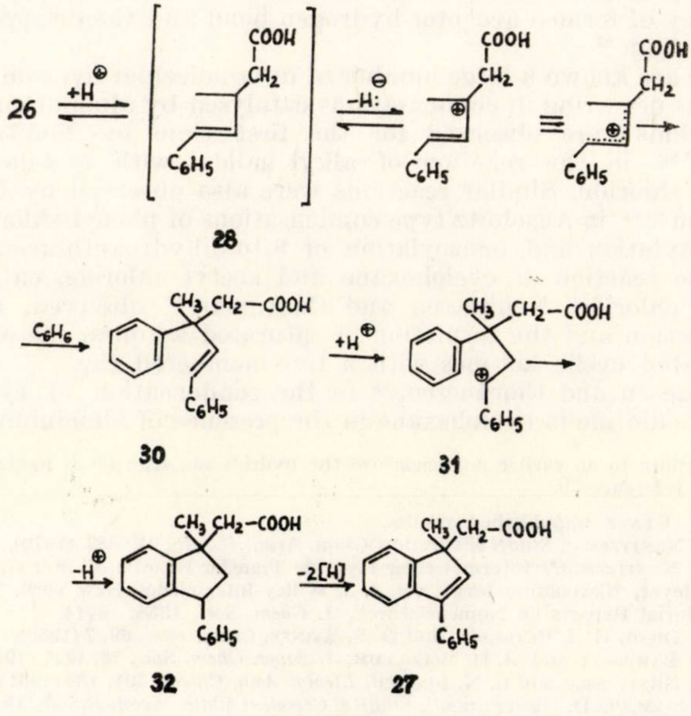

SCHEME 5

---

[89] C. D. Nenitzescu, I. Pogany and G. Mihai, *Studii şi Cercetări Chim. Acad. R.S.R.*, **6**, 375 (1958).

[90] Reference 6, b. p. 376.

[91] J. E. Gowan and T. S. Wheeler, "Name Index of Organic Reactions", Longmans, London, 1962, p. 179.

This sequence of reactions involves a series of intermolecular hydride transfers. In the Friedel-Crafts reaction conditions the hydride abstractions are much favoured. The great proton mobility in these substituded indenes is well known, it has been studied and measured.[92-94] In the case of the formation of the acid **27**, the extention of the conjugation (facilitated by a quaternary carbon atom) **(32→27)** as well as the presence of some unsaturated intermediate in the reaction medium, are the motor of hydride abstraction. These intermediates (the bicyclobutonium ions **22** and **26**) act as hydride acceptors which allow the intermolecular hydride transfer.

5. *Formation of ketones*

In the condensation of cyclobutylideneacetic acid **(13)** the formation of ketones (Table 4) $C_{12}H_{14}O$ was pointed out, a mixture of ketones similar to that obtained from the cyclisation of the isomeric phenyl-hexanoic acids, obtained in the first step of the reaction. The ketones were not identified.

C. ALICYCLIC UNSATURATED ACIDS WITH CYCLOPENTANIC RING

1. The first observation that in the condensation of 1-cyclopentenyl carboxylic acid a phenylated acid is formed in which the phenyl group is bound to the remotest carbon atom with respect to the carboxyl group (position 3) belongs to Nenitzescu and Gavăt. [21]

Later, the formation of a mixture of two isomeric phenylated acids [95] has been reported by Baker and Leeds.

Buu Hoï and Cagniant[96] have condensed the ester of 2-cyclopentenyl-acetic acid with benzene and after hydrolysis have obtained a phenylated acid which they considered to be 2-phenyl-cyclopentylacetic acid

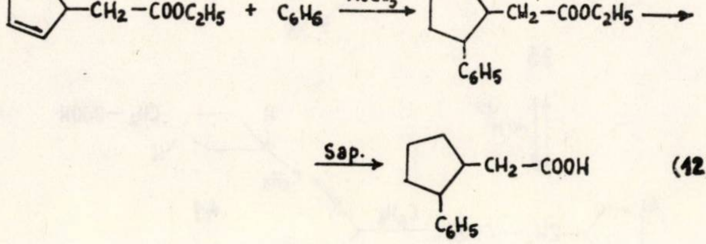

(42)

---

[92] C. D. Nenitzescu, I. Necşoiu and M. Adlersberg, in "Lucrările Consfătuirii Româno-Sovietice din 3–4 dec. 1959", Acad. R.P.R., Bucureşti, 1959, p. 213.

[93] A.M. Weidler and G. Bergson, *Acta Chem. Scand.*, **17**, 862, 1798, 2724 (1963); **18**, 1487 (1964).

[94] C. K. Ingold and R. Piggott, *J. Chem. Soc.*, **123**, 1469 (1923).

[95] W. Baker and W.G. Leeds, *J. Chem. Soc.*, **1948**, 974.

[96] N. P. Buu Hoï and P. Cagniant, *Compt. rend.* **220**. 744 (1946).

Repeating this reaction, Mousseron, Winternitz and Rouzier[97–99] have shown that the reaction product obtained by the above authors is actually a mixture of *cis* and *trans*-3-phenyl-cyclopentyl-acetic acids, together with a small amount of the 2-phenyl-cyclopentylacetic acid.

These disagreements, as well as the results obtained with acyclic α,β-unsaturated acids, [28] determined new investigations in the series of alicyclic α,β-unsaturated acids, namely cyclopentyldeneacetic acid.

2. *Formation of lactoid ions*

In the condensation of the cyclopentylideneacetic acid (**33**) with benzene, [72] in the usual conditions, [22] a mixture of three acids was obtained: *cis*-2-(**37**), *trans*-2-(**38**) and *cis*-3-phenyl-cyclopentylacetic (**39**) acids, in molar ratio **37** : **38** : **39** = 3 : 47 : 50. The absence of a phenylated acid at position 1 (**40**) must be remarked in that case too, as well as the absence of *trans*-3-phenyl-cyclopentylacetic acid (**41**) and the preferential formation of acids **37** and **38** (Scheme 6)

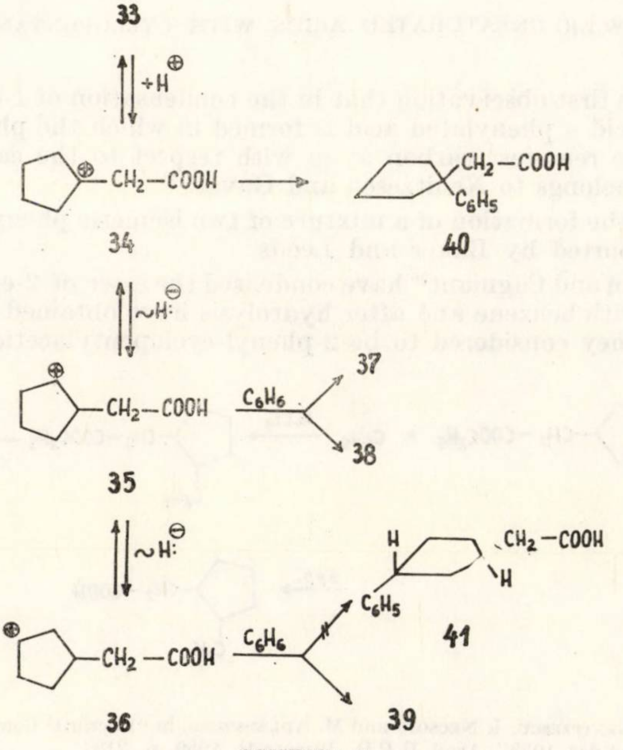

SCHEME 6

The involvement of carbocations **34**, **35** and **36**, as reaction intermediates, cannot explain the stereoselectivity of the reaction as well as the

---

[97] M. Mousseron, F. Winternitz and G. Rouzier, *Comp. rend.* **235**, 660 (1952).

[98] M. Mousseron, F. Winternitz and G. Rouzier, *Bull Soc. chim. France*, **1953**, 190.

[99] M. Mousseron, F. Winternitz and G. Rouzier, *Bull. Soc. chim. France*, **1954**, 316.

absence of some phenylated isomers. The proposed mechanism (Scheme 7 implies the involvement of other intermediates beside the cationic species of scheme 6, in order to explain the reaction products.

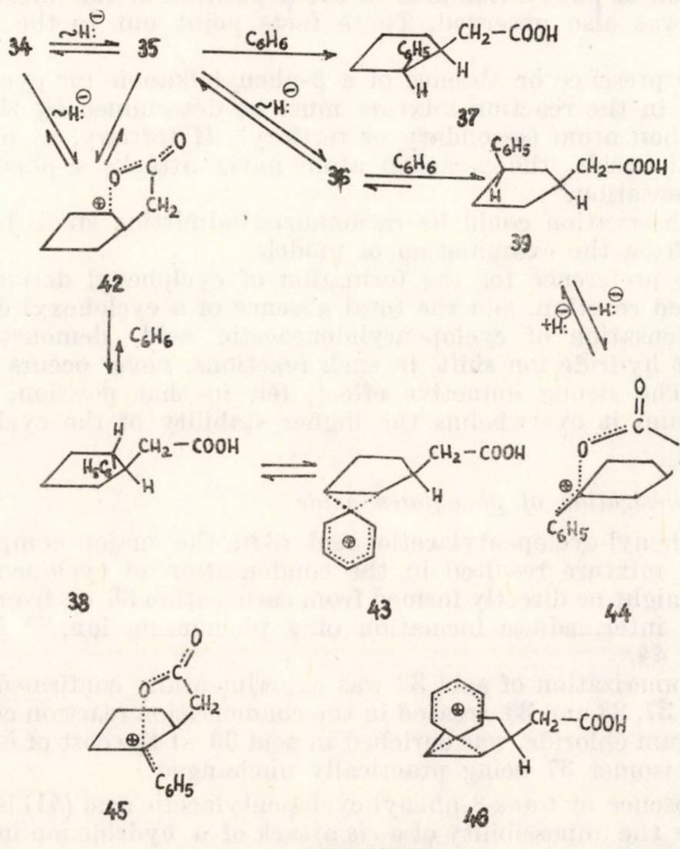
34
~H:⊖
35
C6H6
CH2–COOH
C6H5
H
~H:⊖
37
~H:⊖
C6H5
C6H6
36
CH2–COOH
H
39
CH2
42
C6H6
~H:⊖
+H:
H
CH2–COOH
H5C6
CH2–COOH
CH2
C6H5
38
43
44
CH2
CH2–COOH
C6H5
45
46

SCHEME 7

The absence of a phenylated acid in position 1 (of the cyclopentane ring) is due to the formation of a more stable lactoid ion **42**, which might yield, in stereospecific attack [100] of benzene the acid **38**. The procursor carbocation **35**, in a nonstereospecifical reaction, forms the *cis*-isomer **37** (beside **38**). The formation of a benzylic ion **45** or a phenonium ion **46**, sterically unfavourable, explains the small amount in which **37** is present in the reaction mixture.

3. *Other unsaturated acids with cyclopentane ring*

Cyclopentylacrylic acid has been condensed, in the usual manner, with benzene, [101] at 40—45°. Phenylated cyclopentyl-propionic acids, besides phenylated cyclohexylacetic acids were obtained, the cyclohexane derivatives being in overwhelming ratio in the reaction mixture (molar ratio : cyclohexane derivatives : cyclopentane derivatives = 6 : 1). The formation of phenylated acid in the β position of the initial unsaturated acid was also observed. These facts point out to the following conclusions

---

[100] J. I. Brauman and A. J. Pandell, *J. Amer. Chem. Soc.*, **89**, 5421 (1967).

[101] A. M. Glatz, V. Wertheimer and F. Badea, *Rev. Roumaine Chim.*, **19**, 87 (1974).

a. The presence or absence of a β-phenylalkanoic (or cycloalkylalkanoic) acid in the reaction mixture must be determined by the nature of the β-carbon atom (secondary or tertiary). If tertiary, as in cycloalkylideneacetic acids, the β-carbon atom never attacks a phenyl group in the condensation.*

This observation could be rationalized admitting steric hindrance, as obvious from the examination of models.

b. The preference for the formation of cyclohexyl derivatives, in the mentioned reaction, and the total absence of a cyclohexyl derivative in the condensation of cyclopentylideneacetic acid, demonstrated in its turn that hydride ion shift, in such reactions, never occurs from the α-position. The strong inductive effect, felt in that position, must be responsible and it overwhelms the higher stability of the cyclohexane-derivatives.

4. *Isomerization of phenylated acids*

cis-3-Phenyl-cyclopentylacetic acid **(39)**, the major component of the reaction mixture resulted in the condensation of cyclopentylideneacetic acid, might be directly formed from carbocation **36** or from acid **38**, through the intermediate formation of a phenonium ion,[102] **43** and a benzylic ion **44**.

The isomerization of acid **38** was experimentally confirmed. A mixture of acids **37**, **38** and **39**, treated in the condensation reaction conditions with aluminium chloride, was enriched in acid **39** at the cost of isomer **38**, the ratio of isomer **37** being practically unchanged.

The absence of *trans*-3-phenyl-cyclopentylacetic acid **(41)** is explained either by the impossibility of a *cis* attack of a hydride ion in benzylic ion **44**, or by the low stability of *trans*-1,3-disubstituted cyclopentane derivatives.[103-107]

cis-3-Phenyl-cyclopentylpropionic acid is readily isomerized into the *trans*-2-phenyl-cyclopentylpropionic acid, whereas phenyl-cyclopentylpropionic acids never isomerize into cyclohexyl derivatives.[101] The absence of the equilibration between five- and six-membered ring derivatives, in those conditions, even if equilibrium is attained in the five membered ring derivatives, must be considered as a clear demonstration of the importance of inductive effects of the carboxyl group in those reactions. As the carboxyl group, judging from the σ-values, seems not to be a very powerful electron attracting group, the result points out that the carboxyl group is transformed, in the reaction conditions, in a more efficient group, that is in anion pair in agreement with equation (9), which explains also the cyclisation reaction, which will be discussed in the following section.

---

* See reference 101.

[102] G. A. Olah, *J. Amer. Chem. Soc.*, **89**, 5259 (1967) ; idem **91**, 1450 (1969).

[103] N. F. Nirch and R. A. Dean, *J. Chem. Soc.*, **1953**, 2477.

[104] R. C. Cookson, J. Andel, S. A. Knight and B. R. D. Whear, *Tetrahedron*, **19**, 1955 (1963).

[105] E. Eliel, "Stereochemistry of Carbon Compounds", McGraw-Hill Co., New York, 1962, p. 249.

[106] D. Varek, C. Ouannes and. J. Jacques, *Bull. Soc. chim. France*, **1965**, 1662.

[107] Reference 37, p. 36.

5. *Formation of benzobicyclic ketones*

If the condensation of the unsaturated acid **33** is performed in refluxing benzene, instead of the phenylated acids **38** and **39**, the benzobicyclic ketones **47** and **48** are obtained in a similar mechanism as that described for the acyclic α, β-unsaturated acids (Chapter II C)

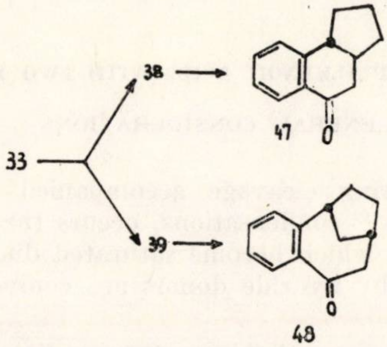

(13)

6. The condensation reaction of acid **33** with benzene might be used in preparative purposes, for the preparation of acids **38** and **39** as well as for ketones **47** and **48**. All these compounds might be obtained in that way with pure and relatively good yields.

D. ALICYCLIC UNSATURATED ACIDS WITH CYCLOHEXANE RING

The Friedel-Crafts condensations of acids of that type, although known long since (1937) were only scarcely studied.[108] Ghosh [109] has described the condensation reaction of 1-cyclohexenylacetic acid with benzene in the presence of aluminium chloride and has indicated 2-phenylcyclohexylacetic acid as the single reaction product.

Simultaneously, Cook and Goulden [110, 111] and Nenitzescu and Gavăt [15] isolated in the same reaction, 4-phenyl-cyclohexylacetic acid, whose structure was proved through an independent synthesis of the compound

---

[108] Reference 3, p. 323.

[109] R. Ghosh, *Sci. Cult. Calcutta*, **3**, 55 (1937).

[110] J. W. Cook, *Chem. and Ind.*, **56**, 290 (1937).

[111] J. W. Cook and F. Goulden, *J. Chem. Soc.*, **1937**, 1559.

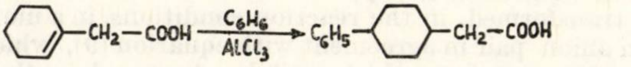

(14)

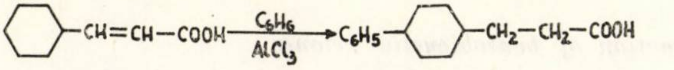

(15)

They have shown that cyclohexylacrylic acid, in the same conditions forms a phenylated product with the phenyl group situated in position 4 of the cyclohexane ring.

IV. CONDENSATIONS OF ALKENOIC ACIDS WITH TWO DOUBLE BONDS

A. GENERAL CONSIDERATIONS

The cyclobutane ring cleavage accompanied by hydrogenation during the Friedel-Crafts [75] condensations, occurs through allylic carbocations as intermediates, which become saturated due to intermolecular hydride transfers, whereby hydride donors are compounds with indane skeleton.

Based on the assumption that some intermediates of these reactions may be unsaturated acids with two double bonds containing six carbon atoms, the behaviour of sorbic acid in such kind of reactions has been studied.

B. SORBIC ACID

1. In an earlier paper, Nenitzescu and his coworkers [22] have prepared 5-phenyl-caproic acid **(4)** (as an authentical sample) with sorbic acid as starting material. The scope of this reaction was at that time a pure preparative one.

2. Later [112] it has been established that the acid 4 resulted from the condensation was one of the major reaction products, as comparable amounts of 4-phenyl-caproic **(19)** and 3,5-diphenyl-caproic **(53)** acids besides smaller quantities of *cis*- and *trans*-methylindenylacetic acid **(50** and **51)** and 5-phenyl-hex-3-ene-oic acid **(52)** (table 5). The neutral products of this reaction are hydrocarbons and not, as usually,[20,21,27,61] mixtures of ketones and hydrocarbons. Among these products two unsaturated hydrocarbons with indene skeleton (**54** and **55**) were isolated and identified.

---

[112] A. M. Glatz, F. Badea, Z. Arvay, V. Drăgutzan, F. Chiraleu and A. C. Răzuș, *Rev. Roumaine Chim.*, **18**, 2087 (1973).

Table 5

Condensation products of sorbic acid with benzene

Products	19	4	50	51	52	53	54	55
Moles %	43.0	50.4	0.8	3.8	2.0		32.5	21.5
Yield %	47.5*					2.00	20.6**	

* Calculated for $C_{12}H_{16}O_2$; ** calculated for $C_{11}H_{14}$

A convenient interpretation of the results arises from a mechanism in which protonation at two positions are considered (like butadiene) leading to two allylic carbocations **56** and **57** (Scheme 8).

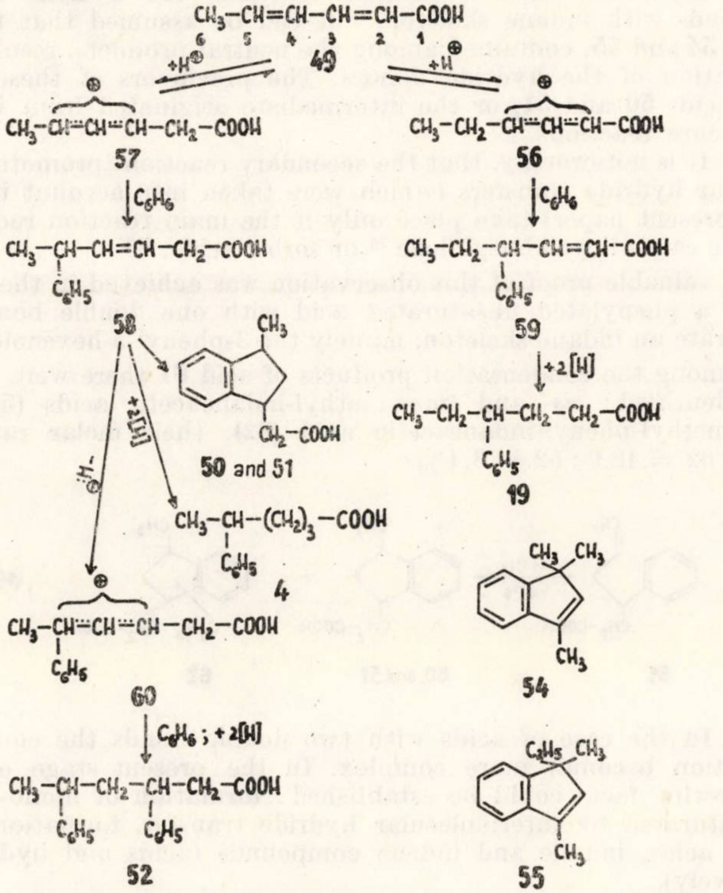
CH₃–CH=CH–CH=CH–COOH
6 5 4 3 2 1
49
+H⊕
+H⊕
⊕
CH₃–CH=CH=CH–CH₂–COOH
57
CH₃–CH₂–CH=CH=CH–COOH
56
C₆H₆
C₆H₆
CH₃–CH–CH=CH–CH₂–COOH
C₆H₅
58
CH₃–CH₂–CH–CH=CH–COOH
C₆H₅
59
+2[H]
CH₃–CH₂–CH–CH₂–CH₂–COOH
C₆H₅
19
CH₃
CH₂–COOH
50 and 51
+[H]
–H⊕
CH₃–CH–(CH₂)₃–COOH
C₆H₅
4
CH₃–CH=CH=CH–CH₂–COOH
C₆H₅
60
C₆H₆ ; +2[H]
CH₃–CH–CH₂–CH–CH₂–COOH
C₆H₅ C₆H₅
52
CH₃ CH₃
CH₃
54
C₆H₅ CH₃
CH₃
55

SCHEME 8

The relative high and comparable yields of the reaction products **4**, **15** and **53** show that in this case alkylation of benzene and hydrogenation are the main reactions.

The acids **56** and **57** react with benzene only in the 4 and 5 positions, respectively, because inductive and allylic conjugation effects act together. The resulted acids **58** and **59** are hydrogen acceptors and give rise to the acids **4** and **19**.

Another fact which points the two combined effects is the absence of a monophenylated acid in position 3, as well as the absence of 4- and 5-diphenylated acids, whose presence should have involved, in the first step, a carbocationic center at the position 3.

3. A hydride ion abstraction from the unsaturated acid **58**, favoured by the formation of an allylic benzylic carbocation **60**, leads by benzene condesation to the 3,5-diphenyl-capronic acid **(52)**.

4. The hydrogenation of the acids **58** and **59** represents an example of intermolecular hydride ion transfer, from donor compounds to unsaturated acceptors. Since in similar reactions the hydride donors are compounds with indane skeleton,[75] it can be assumed that the hydrocarbons **54** and **55**, contained among the neutral products, result from the stabilization of the hydride donors. The precursors of these could be either acids **50** and **51**, or the intermediate originated from **59** through yet obscure reactions.

5. It is noteworthy, that the secondary reactions promoted by intermolecular hydride transfers (which were taken into account in all cases of the present paper) take place only if the main reaction requires this, as in the case of cyclobutylidene [75] or sorbic acids. [112]

A valuable proof of this observation was achieved in the condensation of a phenylated unsaturated acid with one double bond, [113] able to generate an indane skeleton, namely the 3-phenyl-5-hexenoic acid **(61)**.

Among the condensation products of acid **61** there were only three acids identified: *cis*- and *trans*-methyl-indaneacetic acids **(50** and **51)** and 3-methyl-phenyl-indaneacetic acid **(62)**, their molar ratio being: 50 : 51 : 62 = 43.9 : 52.8 : 3.4 %

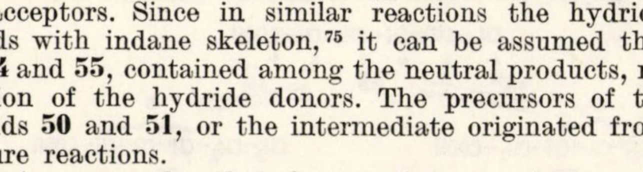

(16)

61 60 and 51 62

6. In the case of acids with two double bonds the course of the condesation becomes more complex. In the present stage of research the following facts could be established: formation of mono-plenylated acids saturated by intermolecular hydride transfer, formation of diphenylated acids, indane and indene compounds (acids and hydrocarbons, respectively).

---

[113] A. M. GLATZ, unpublished data.

Unlike the condensation of unsaturated acids with one double bond, neither intermolecular hydride transfer, nor ketone formation was observed during these condensations.

According to the observations, the rate of cyclisation to compounds with indane skeleton exceeds the rate of condensation with benzene (the case of diphenylation). Knowing that indane compounds are generally good hydride donors it can be noticed that hydride donation occurs only if is required by some unsaturated compounds present in the reaction mixture; under the same conditions they do not undergo any change if such unsaturated products are not present.

V. CONCLUSIONS

During the researches concerning aluminium chloride-catalyzed condensations of unsaturated acids with benzene, several data regarding the complex pathways of these reactions were established.

1. The condensation of alkanoic and alicyclic unsaturated acids, at 40—45°, takes place through intramolecular hydride ion transfer to the carbocation formed in the first step of the reaction.

In this way other carbocations are formed, able to generate a number of isomeric phenylated acids. This observation has a general character regarding the acids with one duble bond.

2. The phenylation of alkenoic acids takes place not only in one position of the alkanoic chain, but, with different proportions, in all possible positions (depending on the position of the double bond [27, 28, 38]). Herein the last carbon atom and the C_2 (the case of α, β- unsaturated acids) are excepted.[28]

3. The formation of pseudo-cyclic, lactoid type ions, restricts the number of isomeric phenylated acids which may arise from unsaturated acids containing six carbon atoms and where the double bond lies in a different position from α, β.[38,58]

4. In alicyclic α, β-unsaturated acids with an exocyclic double bond (between a carbon atom belonging to the ring and one to the chain), the tertiary carbon atom does not undergo phenylation, though the tertiary carbocation is the first one formed. The formation of a more stable lactoid ion also prevents the condensation at this position.[72]

5. In the case of acrylic acid substituted with a five-membered ring [101] predominantly ring enlargement (about 82%) leading to isomeric phenyl-cyclohexylacetic acids has been observed, besides the formation of phenyl-cyclopentylpropionic acids. The irreversibility of the rearrangement of the five-membered ring has been established.

6. The condensations of α, β-unsaturated acids lead to mixtures of cyclic ketones, [27, 28, 39, 72] resulted through cyclizations of the phenylated acids at higher temperature (80°).

7. The hydrogenolysis of cyclobutane ring, [75] through bicyclobutonium ions as intermediates, has been reported. In this case several other unstable unsaturated intermediates are also involved, which stabilize by intermolecular hydride transfer.[80] The unstable intermediates are thereby hydride acceptors.

8. Indane compounds are the stabilization products of the hydride donors.[75,112] Correlation between intermolecular hydride transfer and cyclization to indane compounds has been revealed.

9. A general remark is that during the condensations of unsaturated acid with benzene the formation of diphenylated acids was made evident only in the case of an advanced unsaturation (cyclobutylideneacetic[75] and sorbic[112] acids).

10. Generally, a distinction of the different rate reactions which are involved is possible. The fastest reaction is the protonation, followed by intramolecular hydride transfer (if possible), condensation with benzene, intermolecular hydride transfer (if required by the reaction pathway). The last reaction affords cyclic compounds with indene skeleton. The slowest reaction is the cyclization of phenylated acids giving rise to the cyclic ketones.

The author is deeply indebted to Professor Ecaterina Nenitzescu-Ciorănescu for helpful discussions and to Professor Florin Badea for his assistance during the last years.

Revue Roumaine de Chimie, **19**, *3*, 485 –492 (1974)

METHODS FOR THE DETERMINATION OF 2-AMINOPYRIDINE. VISIBLE AND INFRARED SPECTRA OF THE COMBINATION WITH AMMONIUM REINECKATE

GRIGORE TEODORESCU

Polytechnic Institute — Bucharest,
Department of Inorganic and Analytical Chemistry,
str. Polizu 1, Bucharest, Romania

Received May 8, 1973

The present paper presents methods for the determination of 2-aminopyridine based upon its combination with ammonium reineckate, the dissolving of the obtained compound in acetone followed by the precipitation of the reineckate anion as silver reineckate and the titration of the silver nitrate excess with ammonium thiocyanate. Since the obtained compound is also soluble in ethanol, forming a coloured solution, 2-aminopyridine has been determined spectrophotometrically as well.

The structure of the compound has been proved by the determination of the molecular weight, by means of visible spectra for ammonium reineckate and for the reineckate of 2-aminopyridine. In order to determine the structure of 2-aminopyridine reineckate, the infrared spectra of 2-aminopyridine and of its reineckate have been recorded.

1. INTRODUCTION

2-Aminopyridine is an intermediate for the manufacture of many dyes, pesticides, and pharmaceuticals.

The quantitative determination of 2-aminopyridine is therefore of interest. The well-known method for the determination of amines and of 3-aminopyridine itself cannot be used in the case of 2-aminopyridine and 4-aminopyridine. Indeed, like 2-aminobenzothiazole, 2- and 4-aminopyridine can be diazotized only in concentrated acidic media, such as concentrated sulphuric acid over 60% or nitrosylsulphuric acid.

On dilution with water, hydroxy-pyridine is formed, and no diazonium salt can be detected. The reason for its absence is probably the fact that diazonium salts of 2-and 4-aminopyridine have law electron densities in the 2- and 4-positions and are therefore more sensitive to the nucleophilic attack of water :

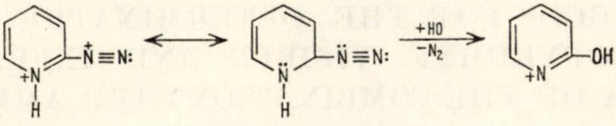

The failure of the usual method determined us to study the reaction of 2-aminopyridine (AP) in an aqueous solution in which onium ions predominate with ammonium reineckate ($NH_4^+ R_c^-$), which was also used by the author for the determination of other compounds. [1–5]

The present method may be applied to 4-aminopyridine as well as to 3-aminopyridine.

This procedure is simple and rapid and may be applied to the amine in technical mixtures.

The complex is formed from the ammonium salt (as it results in acidic media), according to the following sequence :

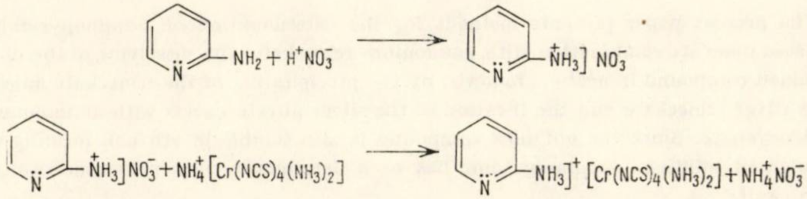
$NH_2 + H^+NO_3^-$
$\overset{+}{N}H_3] NO_3^-$
$\overset{+}{N}H_3]NO_3^- + NH_4^+[Cr(NCS)_4(NH_3)_2]$
$NH_3]^+[Cr(NCS)_4(NH_3)_2] + NH_4^+NO_3^-$

This reaction was used for the determination of AP by volumetric and spectrophotometric methods.

2. DETERMINATION METHODS

2.1. *Volumetric method.* The aqueous solution of AP was acidified with nitric acid and precipitated with 2% $NH_4^+R_c^-$.

The resulting violet-pink precipitate is filtered, washed with water and dissolved in acetone.

The acetone solution is treated with silver nitrate solution in excess. Silver reineckate precipitates according to the equation :

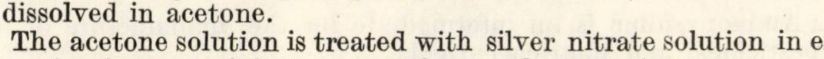
$NH_3][Cr(NCS)_4(NH_3)_2] + AgNO_3$
$NH_3]^+NO_3^- + Ag[Cr(NCS)_4(NH_3)_2]$

---

[1] Gr. Teodorescu, *Bul. Inst. Polit. București*, **32** (2), 39 (1970).

[2] Gr. Teodorescu, *Bul. Inst. Polit. București*, **32** (4), 79 (1970).

[3] Gr. Teodorescu, *Bul. Inst. Polit. București*, **33** (1), 67 (1971).

[4] Gr. Teodorescu, *Rev. Roumaine Chim.*, **17**, 1475 (1972).

[5] Gr. Teodorescu, *Rev. Roumaine Chim.*, **17**, 1621 (1972).

The precipitate is filtered and washed, then the excess of silver nitrate is titrated with thiocyanate in presence of iron (III) alumen and ammonium as an indicator.

EXPERIMENTAL PART

2-Aminopyridine, a brown crystalline compound, is easily soluble in water. 2g of technical AP are weighed, dissolved in distilled water, the solution is filtered and is taken with distilled water in a standard flask of 250 ml.

From this solution, aliquots containing between 0.0480 and 0.1200 g AP are taken out. Each aliquot is acidified with 2–3 drops of a 2 n solution of nitric acid and then treated dropwise under continuous stirring, with a freshly prepared 2% solution of $NH_4^+ R_c^-$ until the solution above the precipitate darkens to violet-red. The crystalline, nacreous violet-red precipitate is filtered on a G_4 filtrable crucible, carried along by means of 0.1 %$NH_4^+ R_c^-$ solution, washed with cold (5°C) distilled water until the solution becomes colourless, and in the end washed with two 5 ml ether portions.

The compound is dissolved with 15–20ml acetone directly on the filtrable crucible which is then washed with 10–15 ml distilled water, all filtrates being collected in a 250 ml flask. 100 ml distilled water, 20 ml 0.1 n silver nitrate and 2 drops 2 n nitric acid are then added. The silver reineckate is precipitated. The precipitate is filtered, then washed with distilled water by decanting and the filtrate is collected together with the washing water in a 750 ml titrating decanter. In the same decanter 3–4 ml saturated solution of iron (III) ammonium alumen (about 40%) and 2 ml 2 n nitric acid are added, then the excess of silver nitrate is titrated by means of 0.1 n ammonium thiocyanate of factor = 1.0152.

To 0.1 n silver nitrate corresponds 0.0094 g AP. The results are given in table 1.

Table 1

Volumetric determination of 2-aminopyridine with $NH_4^+ R_c^-$

Technical AP in aliquot	NH_4SCN[a] 0.1 n $F = 1.0152$	0.1 n Ag NO_3	AP[b]	
g	ml	ml	g	%
0.0480	15.70	4.30	0.0404	84.16
0.0560	14.90	5.10	0.0479	85.53
0.0640	14.20	5.80	0.0540	85.15
0.0720	13.50	6.50	0.0611	84.86
0.0800	12.80	7.20	0.0677	84.62
0.0880	12.00	8.00	0.0747	85.46
0.0960	11.30	8.70	0.0817	85.10
0.1040	10.50	9.50	0.0893	85.86
0.1120	9.85	10.15	0.0954	85.35
0.1200	9.15	10.85	0.1020	85.00

[a] 20 ml 0.1 n $AgNO_3$ are previously added.

[b] Mean value : 85.11 ± 0.36; by the diazotation method the purity of the technical AP was found to be 85%.

2.2. *Spectrophotometrical method.* AP is precipitated with $NH_4^+ R_c^-$ in the same way as by the volumetric method.

The compound formed is dissolved in 95% ethanol. The concentration of AP is obtained from a standard curve. In addition, the spectrophotometric method can be used to check the molecular weight.

The standard curve is obtained from different solutions with a known content of $AP^+ R_c^-$. The absorbance (A) is determined at $\lambda = 525$ nm which corresponds to the absorption maximum of $NH_4^+ R_c^-$, as in the following examples:

% $AP^+ R_c^-$	0.3	0.25	0,2	0.15	0.1
Absorbance	0.425	0.358	0.275	0.205	0.130

The standard curve is shown in figure 1.

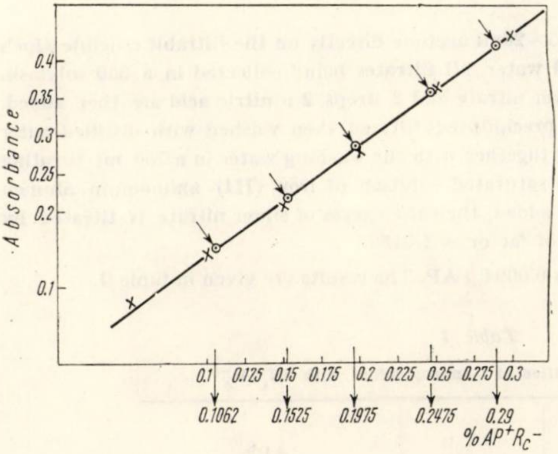

Fig. 1. — The absorbance of $NH_4^+ R_c^-$ *vs* the concentration of the corresponding ethanolic solution.

A V.S.U.-1 spectrophotometer was used with a 0.5 cm cell.

The determination of the AP in the technical product was performed as follows:

2.0475 g technical AP are dissolved in about 150 ml distilled water, filtered and washed, and the solution is collected in a 250 ml standard flask which is filled up to the mark with distilled water. One ml of this solution contains 0.0081 g technical AP. Aliquots of 3.5 ; 5 ; 6.5 ; 8 ; 9.5 ml are withdrawn (they correspond to 0.02866 ; 0.4095 ; 0.05323 ; 0.06552 and respectively 0.07780 g technical AP), acidified with 2—3 drops of 2 n nitric acid and precipitated with a freshly prepared 2% $NH_4^+ R_c^-$, added dropwise, under continuous stirring, until the solution above the precipitate is dark violet-red. The product obtained is filtered on a G_4 filtrable crucible, carried along by means of 0.1% $NH_4^+ R_c^-$, washed with two 5 ml portions of cold distilled water (about + 5°), and finally with two 5 ml portions of ether.

The compound is directly dissolved in 95% ethanol on the filtrable crucible, the crucible is washed with 95% ethanol, the filtrates being collected in a 100 ml standard flask which is filled up to the mark with solvent.

The absorbances for each solution are measured and these values plotted in fig. 1 enable the determination of the concentration in $\mathrm{AP^+ R_c^-}$. The per cent values are calculated from relation :

$$\frac{94 \cdot a}{412 \cdot b} \cdot 100 = \%\mathrm{AP}$$

where 94 is the molecular weight of AP ;

412 is the molecular weight of $\mathrm{AP}^+ R_c^-$;

a is the per cent concentration of $\mathrm{AP}^+ R_c^-$ obtained as above ;

b is the weight (g) of technical AP used in the run.

The results obtained are given in table 2.

Table 2

Per cent concentration of AP in a technical sample

Technical AP in aqueous solution		Absorbance	$\mathrm{AP^+ \overline{R_c}}$ in a 100 ml ethanolic solution	AP* in technical AP
ml	g(b)	A	g(a)	%
3.5	0.02866	0.150	0.1062	84.5
5.0	0.04095	0.215	0.1525	84.4
6.5	0.05323	0.285	0.1975	84.2
8.0	0.06552	0.355	0.2475	85.5
9.5	0.07780	0.413	0.2900	84.4

* The mean value, 84.5 ± 0.3%

3. SPECTRAL STUDY

3.1. *Checking of the molecular weight of 2-aminopyridine reineckate.* For compounds like 2-aminopyridine, containing more than one nitrogen atom, it is necessary to verify if the complex contains one or more reineckate anions.[6] For this purpose, the values of the absorbance (A) for $\mathrm{NH_4^+} R_c^-$ and $\mathrm{AP}^+ R_c^-$ and the absorptivity (K) for $\mathrm{NH_4^+} R^-$ (fig. 2) are used.

The absorptivity was calculated from the relation :

$$K = A/c \cdot l$$

---

[6] Kum-Tatt-Lee, *J. Pharm. and Pharmacol.*, **12**, 666 (1960).

With $c = 0.0297$ moles of $NH_4^+ R_c^-$ in 95% ethanol, the length of the cell, $l = 0.5$ cm, and the absorbance, $A = 0.155$ (from figure 2 at $\lambda_{max} = 520 - 525$ nm), the absorptivity is $K = 104$.

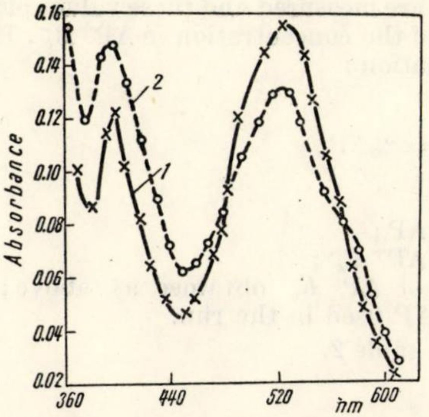

Fig. 2. – Visible spectra of $NH_4^+ R_c^-$ (1) and $AP^+ R_c^-$ (2) in 95% ethanol ($l = 0.5$ cm).

Since the two reineckates, $NH_4^+ R_c^-$ and $AP^+ R_c^-$, have nearly the same $\lambda_{max} = 525 - 530$ nm, we assume that the absorptivity, K, obtained for $NH_4^+ R_c^-$ is also valid for $AP^+ R_c^-$.

The molecular weight is calculated from the relation :

$$M_d = g_1/100 \times K/A \times l/1000$$

when $g_1 = 0.1\%$, the relation becomes :

$$M_d = K \cdot l/A$$

With $\lambda_{max} = 525 - 530$ nm for $AP^+ R_c^-$ and a concentration of 0.1%, the absorbance is $A = 0.130$ ($l = 0.5$ cm). Hence the molecular weight is :

$$M_d = \frac{104}{0.130} \cdot 0.5 = 400$$

The value for the monoreineckate is 412. The comparison of the two values allows us to assume that the compound is a monoreineckate ; it does not contain two reineckate groups.

3.2. *Infrared spectrum of 2-aminopyridine reineckate.* The infrared spectrum of AP reineckate has also been recorded for the structural characterization of the compound. [7–11]

---

[7] Junosuke Fujita, Kazuo NaKamoto, Mashahisa Kabayashi, *J. Amer. Chem. Soc.*, **78**, 3295 (1956).

[8] B. Herzberg and C. Reid, *Discuss. Faraday Soc.*, **9**, 92 (1950).

[9] P. C. H. Mitchell and R.T.P. Williams, *J. Chem. Soc.*, **1961**, 4590.

[10] M. M. Chamberlain and J. C. Bailar, *J. Amer. Chem. Soc.*, **81**, 6412 (1959).

[11] M. E. Baldwin, *J. Chem. Soc.*, **1960**, 4369 ; *ibid.*, **1961**, 471.

Table 3

IR spectrum of ammonium reineckate

$\bar{\nu}$(cm^{-1})	*T* %
472 (W) δNCS	62
509 (W)	57
718 (i) NH_3	39
833 (W) νC−S	76
1265 (i) $\delta^{Sym}_{NH_3}$	34
1405 (i) δNH_4^+	32
1605 (H_2O)	50
2059 νC−N	14
2125 (i)	1
3015 (V W)	38
3160 (W)	30
3195 (V W) νHN_3	32
3238 (W)	28
3315 (W)	27

Table 4

IR bands of 2-aminopyridine and of the product obtained with ammonium reineckate

Spectrum of AP		Spectrum of $AP^{+}R_c^{-}$	
$\bar{\nu}$(cm^{-1})	*T* %	$\bar{\nu}$(cm^{-1})	*T* %
410 (W)	58	420 (V.W)	62
440 (W)	54	493 (i)	32
530 (m)	57	514 (W)	50
568 (V.W)	72	554 (W)	72
632 (V.W)	67	632 (V.W)	69
675 (V.W)	64	712 (i)	22
743 (W)	58	750 (i)	32
775 (m)	48		
850 (V.W)	71	851 (V.W)	65
965 (V. W)	70	965 (V. W)	68
99 (m)	62	100 (W)	63
		1038 (W)	69
1150 (m)	61	1125 (W)	65
1165 (W)	64	1172 (m)	56
1283 (W)	60	1262 (i)	33
1331 (W)	57	1328 (i)	44
1450 (i)	38	1382 (m)	48
1498 (i)	41	1480 (m)	48
		1555 (m)	41
1575 (m)	51		
1610 (W)	42	1620 (i)	12
1640 (i)	37	1670 (i)	9
1840 (V.W)	78	2090 (i)	1
3080	54	3170 (W)	23
3180	50		
		3215 (W)	15
3320	52	3320 (W)	13
		3400 (W)	30
3458	48		

The IR spectrum of AP reineckate has been interpreted by comparing it with the $NH_4^+ R_c^-$ spectrum (table 3).

The IR spectrum of the complex presents bands found in the spectrum of ammonium reineckate, which can be attributed to the NH_3 and NCS groups in the reineckate anion; they appear at 493 cm^{-1} (δNCS), 1262 cm^{-1} (δ^{sym}_{N-H} NH_3), 2090 cm^{-1} (ν_{C-N}) and 3160 – 3290 ν^{sym}_{N-H} NH_3. It also shows bands corresponding to the organic base (table 4). These bands, at 750 cm^{-1}, 1172 cm^{-1}, 1480 cm^{-1}, 1620 cm^{-1}, 1670 cm^{-1}, appear also in the spectrum of the compound, where they are slightly altered in their positions and intensities.

Revue Roumaine de Chimie, 19, 3, 493–500 (1974)

ВЛИЯНИЕ УСЛОВИЙ РАСПЫЛИТЕЛЬНОЙ СУШКИ НА СВОЙСТВА ПАСТООБРАЗУЮЩЕГО ПОЛИВИНИЛХЛОРИДА. II

МОРФОЛОГИЧЕСКИЕ ИССЛЕДОВАНИЯ

ВАЛЕНТИНА БОЙЕШАН

Промышленный нефтехимический комплекс, Борзешть Исследовательская лаборатория,

ДОРЕЛ ФЕЛЬДМАН

Политехнический институт, Яссы

Получена 12 февраля 1973 г.

Путем морфологических исследований объясняется влияние режима распылительной сушки на характеристики порошков эмульсионного поливинилхлорида. В зависимости от температуры и величины капель латекса образуются сухие частицы ПВХ разного пористого строения, которые ведут себя неодинаково по отношению к пластификатору. Свойства паст определяются количественными соотношениями структур разного типа в порошке.

В предыдущем сообщении [1] были представлены экспериментальные данные относительно влияния условий распылительной сушки на свойства порошкообразного поливинилхлорида и его способность к образованию паст с пластификатором.

Было найдено, что главным фактором, с точки зрения способности образовывать пасты, является температура сушки ПВХ, которая влияет на:

— величину частиц сухого порошка (чем выше температура сушки, тем больше средняя величина частиц порошка);

— седиментацию паст (осаждаются из пасты только частицы, полученные при температуре сушки выше 80°, в то время как пасты, приготовленные из частиц той же величины, но высушенные при более низких температурах, не осаждаются);

— консистенцию паст и изменение вязкости во времени. Понижение температуры сушки благоприятствует получению паст с низкой начальной вязкостью, но которая возрастает во времени, в то время как повышение температуры сушки уменьшает способность порошков к образованию паст вплоть до совершенного несвязывания их в пасты. Напротив, вязкость таких паст снижается во времени;

---

[1] Первая часть см. в *Rev. Roumaine Chim.*, **18**, *2* (1973).

— реологические свойства паст. Повышение температуры сушки благоприятствует дилатансии, а понижение температуры—псевдопластичному течению.

Уменьшение размеров частиц порошка оказывает влияние на;

— стабильность вязкости паст во времени;

— уменьшение псевдопластичности.

С точки зрения замеченных закономерностей теряет свою важность гранулометрическое распределение порошка, из которого приготовлены пасты, т.к. при одном и том же гранулометрическом составе пасты имеют различные реологические свойства, если порошки были высушены при разных температурах (см. рис. 2 из сообщения I[1]).

В специальной научной литературе были даны различные объяснения образования паст определенной вязкости и устойчивости. Так, разница в поведении паст во времени объясняется разницей в форме частиц (ценосферы и пленосферы [2]), в их твердости [3], характере поверхности, от которой зависит адгезия и образования агрегатов в среде пластификатора [4], в образовании поверхностной труднорастворимой корки [5] и т.п.; многие авторы считают очень важным широкое гранулометрическое распределение величины частиц и их абсолютные размеры[6–9], принимая или не принимая во внимание те изменения, которые происходят в величине частиц в контакте с пластификатором. Штаркман с сотрудниками [10,11] объясняют разницу в поведении порошков ПВХ разницей в морфологии частиц, а механизм образования различных структур во время сушки латексов в распылительной сушилке был представлен в работе Ульянова и Овчинникова [12].

На основе литературных данных и собственных наблюдений относительно связи между условиями получения порошков ПВХ и свойствами самих порошков и образованных из них паст, авторы настоящей статьи дают следующее объяснение феноменов.

Считаем, что фактором, определяющим поведение порошка поливинилхлорида, полученного в различных условиях распылительной сушки, является структура зерен, или, вернее, сочетание различных структур в отношении к пластификатору.

Пасты — это дисперсии твердых частиц в жидкости. Поскольку идет речь о дисперсиях, т.е. о множестве частиц, должны действовать теории множества.

Одна частица того или другого строения отдельно не может оказать никакого влияния, в то время как сочетание различных структур дает определенный эффект, зависящий от количества различных структур и вероятного поведения каждой из них.

---

[2] J. Rowland, *Rubber Plastics Age*, **35**, 493 (1954).

[3] A. Clarkson, *Chem. and Ind.*, **67**, 751 (1949).

[4] Pryce Jones, *Kolloid. Z.*, **129**, 96 (1952).

[5] D. Ryšavy, *Kunststoffe*, **48**, 108 (1958).

[6] O. Berger и W. Braun, *Plaste u. Kautschuk*, **14**, 663 (1967).

[7] O. Berger, *Plaste u. Kautschuk*, **14**, 742 (1967).

[8] E. Bohme и K. Muller, *Plaste u. Kautschuk*, **7**, 124, (1960).

[9] Smith Ewart, *J. Chem. Phys.* **16**, 592 (1948).

[10] Б. П. Штаркман, И.А. Мухина и Л.И. Шарикова, *Коллоид. ж.* **31**, 611 (1969).

[11] Б. П. Штаркман и А. Мухина, *Пласт. массы*, № 5, 50 (1969).

[12] В.М. Ульянов и И.В. Овчинников, *Коллоид. журн.*, *33*, 757 (1971).

В ходе превращения множества латексных частичек в твердые зерна ПВХ на них действует целый ряд факторов (температура сушки, время сушки, тонкость распыления, гранулометрический состав латексных частиц в каждой капле латекса), который направляет образование частиц с тем или иным пористым строением. Может идти речь только о возможности образования какой-то определенной основной структуры, которая в наибольшей мере влияет на средние абсолютные величины при анализах порошков и паст.

Образование каких же структур является возможным при формировании частиц ПВХ в процессе распылительной сушки?

Электронно-микроскопическое изучение частиц методом реплик позволило установить следующее.

— Все частицы ПВХ полученные из латекса путём распылительной сушки представляют собой агломераты сферической или овальной формы, объединяя множество латексных глобул разных размеров (см. рис. 1).

Если эти сферические агломераты размолоть, они распадаются на индивидуальные латексные частицы или на агломераты меньших размеров (рис. 2).

Степень сближения и слипания латексных частиц в сухом зерне ПВХ зависит от природы латекса, размеров сухих зерен, расстояния изучаемого слоя от поверхности зерна и от температуры сушки. На рис. 3(а, б) представлены две частицы одной и той же пробы ПВХ, из которой половина была размолота (б). Видно, что латексные частицы из поверхностного слоя неразмолотого зерна располагаются очень близко друг к другу, как бы входят одна в другую, в то время как в размолотом зерне, в котором был снят верхний слой и представлена внутренняя часть зерна, можно видеть, что пространство более разрежено и латексные частицы менее связаны между собой.

На зернах порошка, высушенного в определенных условиях, на поверхности появляются впадины и трещины, которые ведут во внутреннюю разреженную зону частицы, что можно видеть из рис. 4—6.

Внутреннее строение зерен изучалось с помощью оптического микроскопа, применяя объектив с имерсионной жидкостью. В качестве имерсионной жидкости использовался диоктилфталат.

При рассмотрении в оптический микроскоп было обнаружено несколько видов внутреннего строения зерен ПВХ (рис. 7): зерна полные и зерна голые внутри, с каналом, ведущим во внутреннюю голую полость или без него, наконец, с внутренней полостью, заполненной более мелкими сферическими частицами, которые в определенный момент при контакте частицы с пластификатором выходят из нее через имеющийся канал.

Изучение порошков ПВХ, полученных при различных температурах, показало, что каждому температурному режиму соответствует определенная преобладающая структура частицы, но в то же время помимо нее имеются и другие типы структур.

Частицы различного строения ведут себе неодинаково по отношению к пластификатору, это можно заметить из серии фотографий, представленных на рис. 8—10.

На рис. 8 (а, в, с) показаны превращения частиц ПВХ, полученных при $T = 60^0$ в контакте с пластификатором ДОФ в течение 15 минут. Были сделаны фотографии через 1, 7 и 15 мин. после нанесения капли пластификатора на порошок ПВХ.

Очень хорошо видно, что зерна со сплошным строением и некоторыми вмятинами на поверхности через 7 мин. взаимодействия с ДОФ начинают набухать и распадаться в латексные частички, которые некоторое время еще сохраняют форму шаровых скоплений. Через 15 мин. благодаря броуновскому движению латексные частицы покидают места своего первоначального скопления и распределяются по всему видимому пространству, подобно рыбьей икре. Только два первоначальных зерна ПВХ уцелили в этом скопище латексных частиц взвешенных в пластификаторе, но и они, вероятно, не продержутся долго.

При приготовлении паст, когда используются механические силы для перемешивания, процессы разрушения зерен ПВХ происходят еще быстрее.

На рис. 9 (а, в) показаны превращения зерен порошка поливинилхлорида, высушенного при $T = 80°$. Видно, что в течение 15 мин. только несколько зерен распалось на латексные глобулы, некоторые едва набухли, а большинство не претерпело никаких изменений. Освободившиеся латексные частицы расползлись по всему свободному объему между зернами ПВХ.

На рис. 10 (а,в) представлено поведение в пластификаторе порошка ПВХ, высушенного при $T > 90°$. В течение 15 мин. ни одно зерно не распалось, и свободное пространство между ними осталось заполненным только пластификатором. Размеры частиц не имели никакого значения.

Отсюда видно, какое огромное значение при взаимодействии с пластификатором имеет внутреннее строение зерен порошка поливинилхлорида, степень спайки латексных глобул в каждом зерне. Латексные частицы, слабо связанные между собой, при воздействии пластификатора распадаются быстро, а те, что успели сплавиться во едино во время сушки при повышенной температуре, под воздействием пластификатора при комнатной температуре не изменяются.

Микроскопическое изучение поведения размолотых порошков ПВХ показало, что размол способствует более быстрому растворению осколков, полученных из сердцевины зерен, в то время как частицы, происходящие из поверхностной зоны, растворяются в пластификаторе в соответствии со степенью спекания латексных глобул во время сушки.

Чем выше температура в сушилке, тем быстрее происходит испарение воды из капель латекса, что видно из рис. 11, в которой представлены рассчитанные кривые времени испарения воды ($\tau_{\text{сек}}$) в зависимости от размеров капель и Δt процесса сушки.

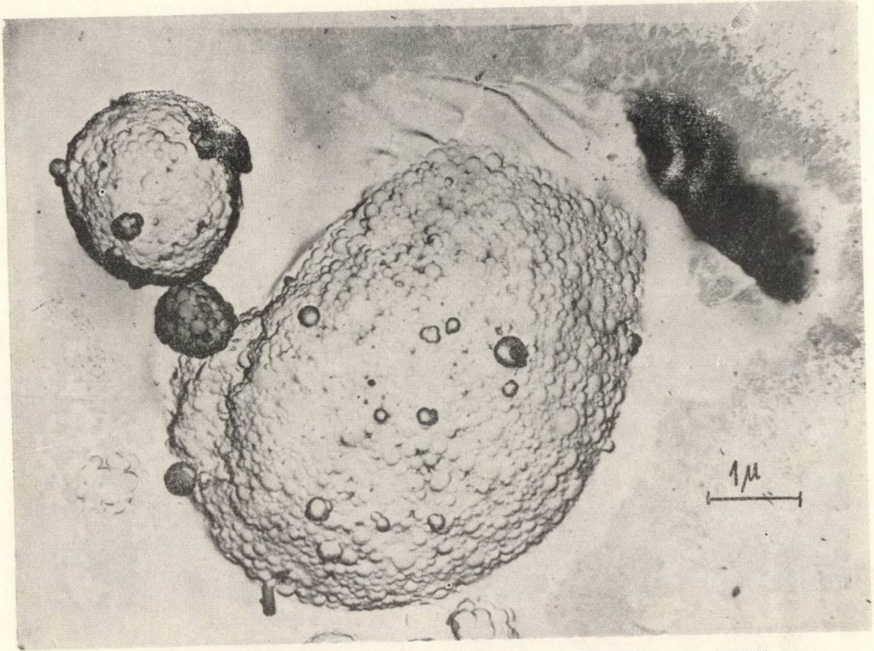

Рис. 1. — Форма частиц порошка эмульсионного ПВХ.

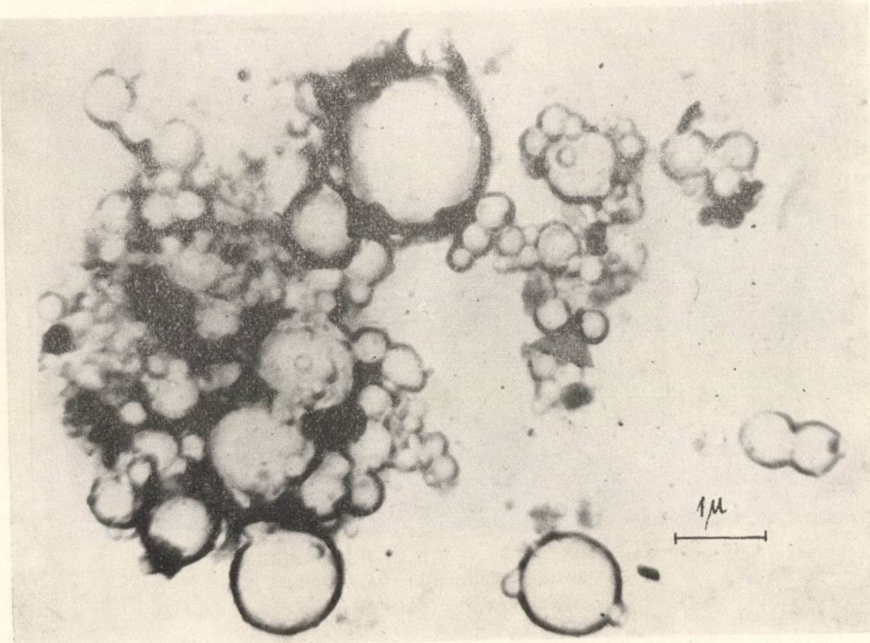

Рис. 2. — Размолотые частицы эмульсионного ПВХ.

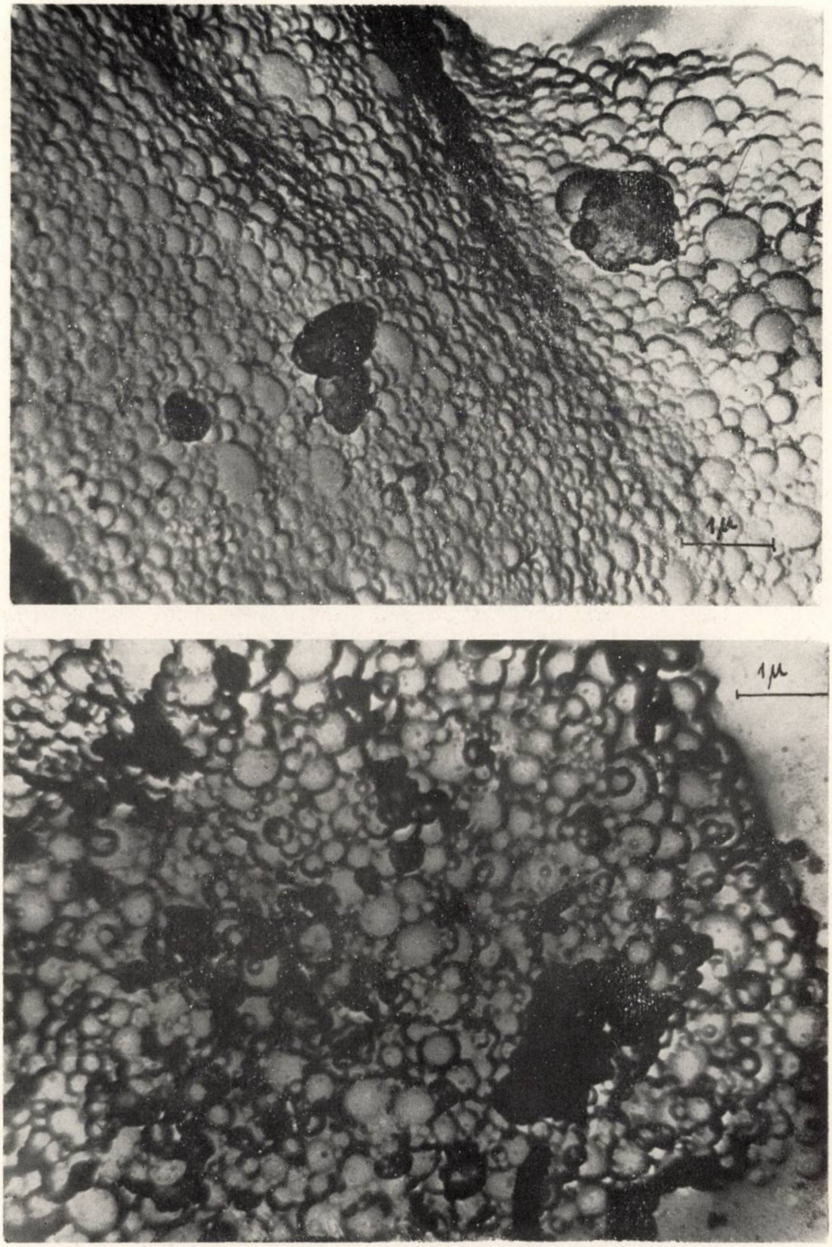

Рис. 3. — Поверхность частицы поливинилхлорида:
a) неразмолотой, b) размолотой.

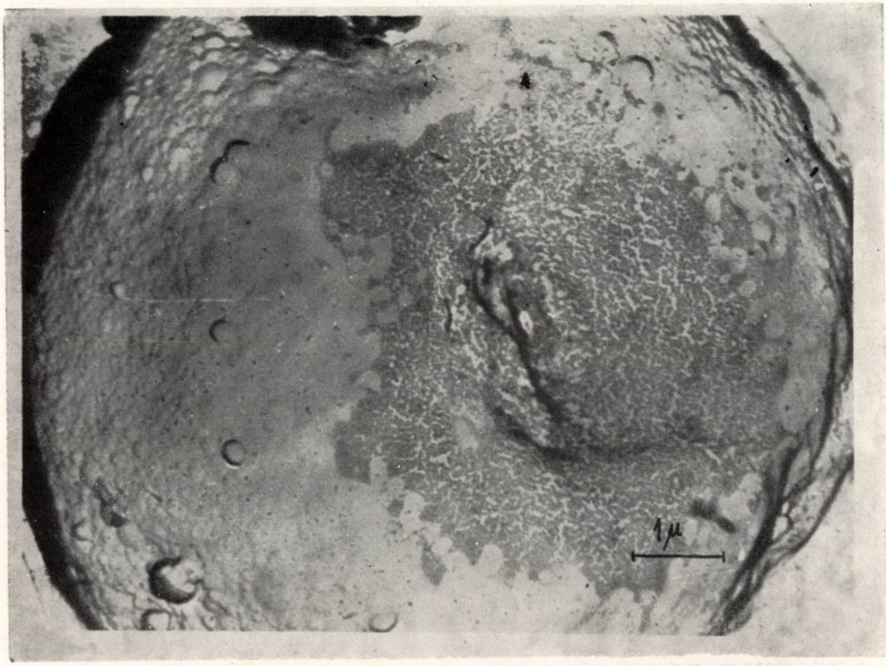

Рис. 4. — Фотография поверхности частицы ПВХ.

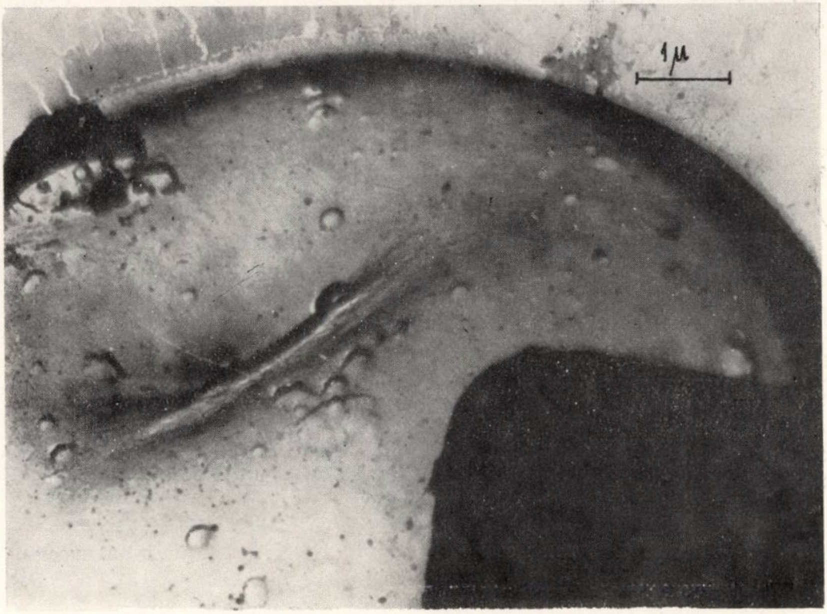

Рис. 5. — Фотография поверхности частицы ПВХ.

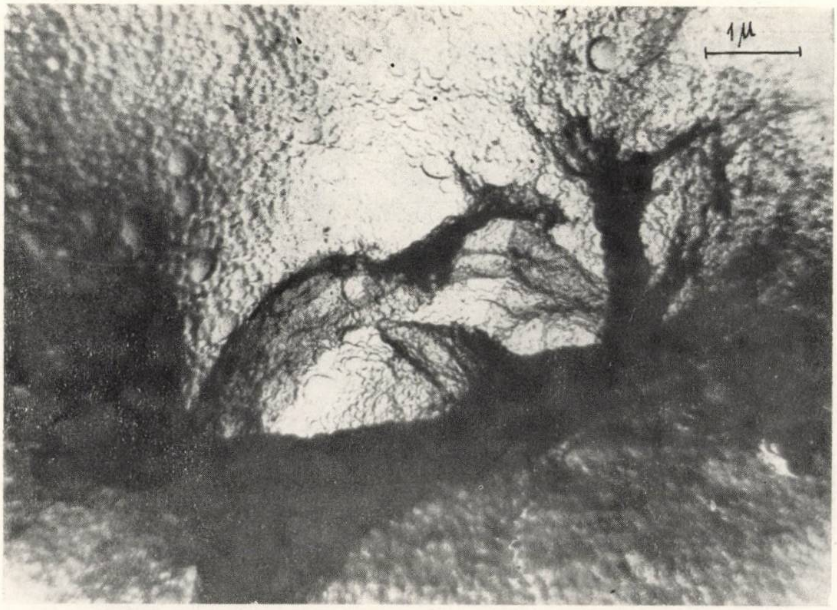

Рис. 6. — Фотография поверхности частицы ПВХ.

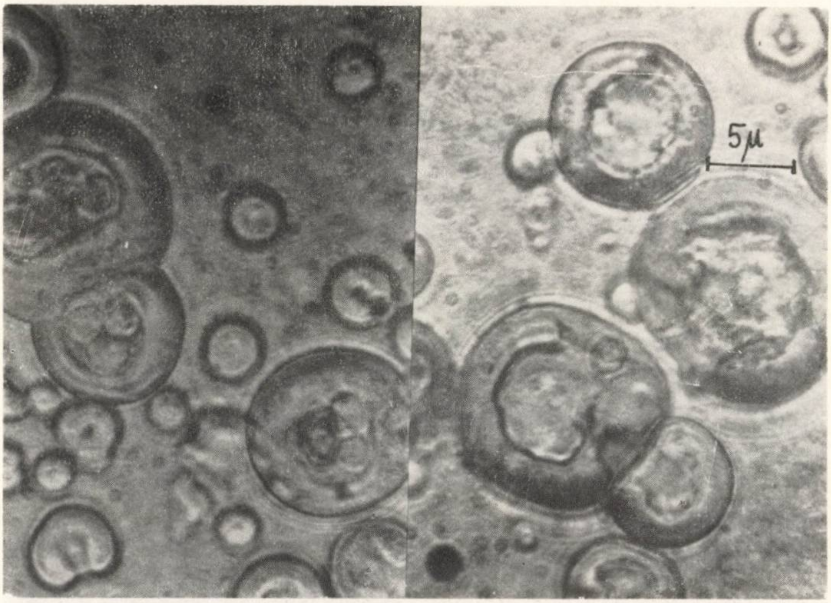

Рис. 7. — Различные типы строения частиц ПВХ, видимые в оптический микроскоп.

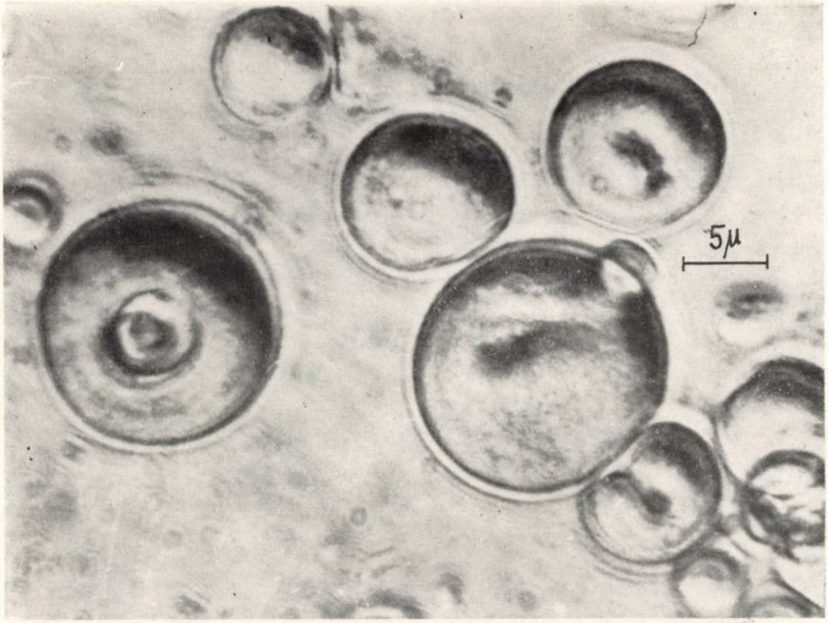

Рис. 8. — ПВХ, высушенный при температуре $T = 60°$ в контакте с пластификатором:

а) через 1 минуту; b) через 7 минут; c) через 15 минут.

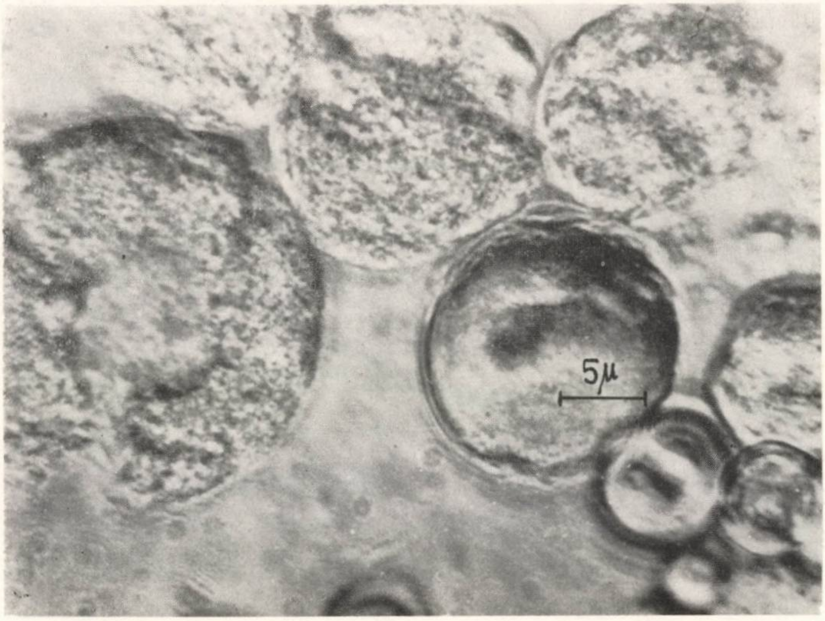

Fig. 8*b*.

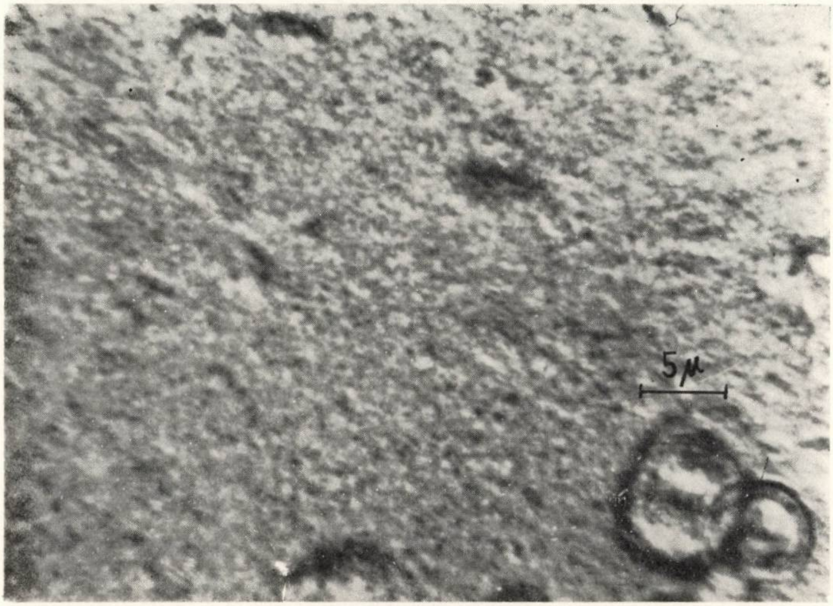

Fig. 8c.

Рис. 9. — ПВХ, высушенный при $T = 80°$ в контакте с пластификатором.

а) через 1 минуту; в) через 15 минут.

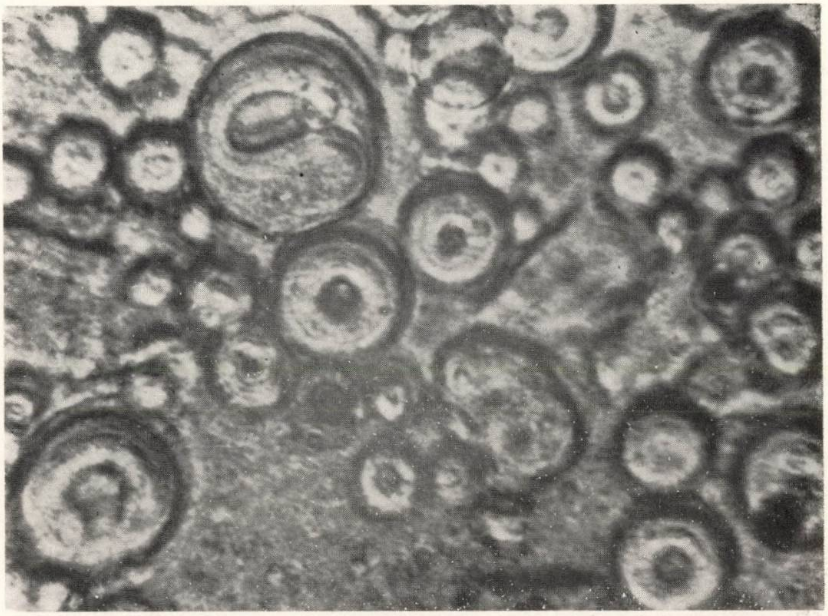

Fig. 9b.

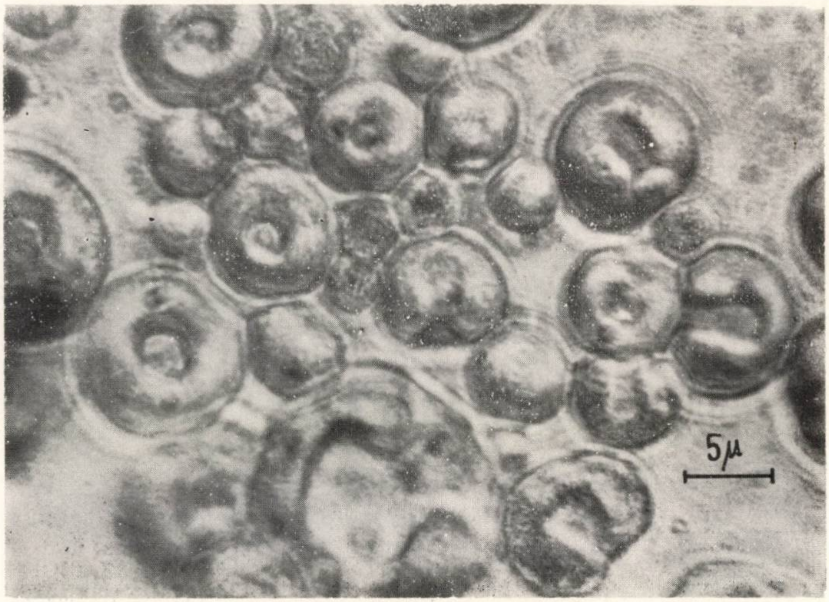

Рис. 10.—ПВХ, высушенный при $T > 90°$ в контакте с пластификатором:
a) через 1 минуту; b) через 15 минут.

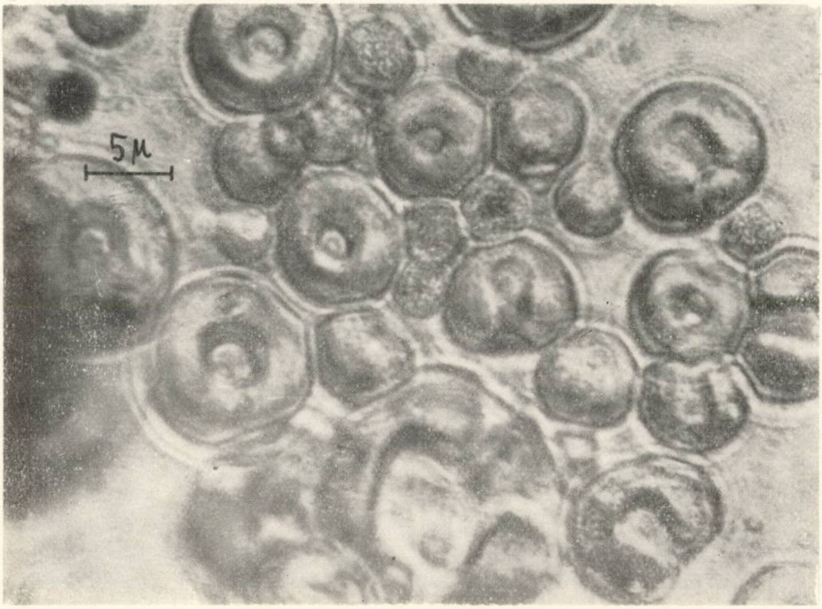

Fig. 10*b*.

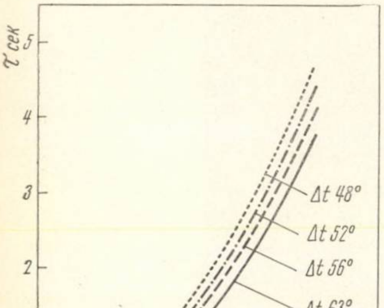

Рис. 11. — Время испарения воды из латексных капель в зависимости от диаметра капель (в микронах) и Δt процесса сушки.

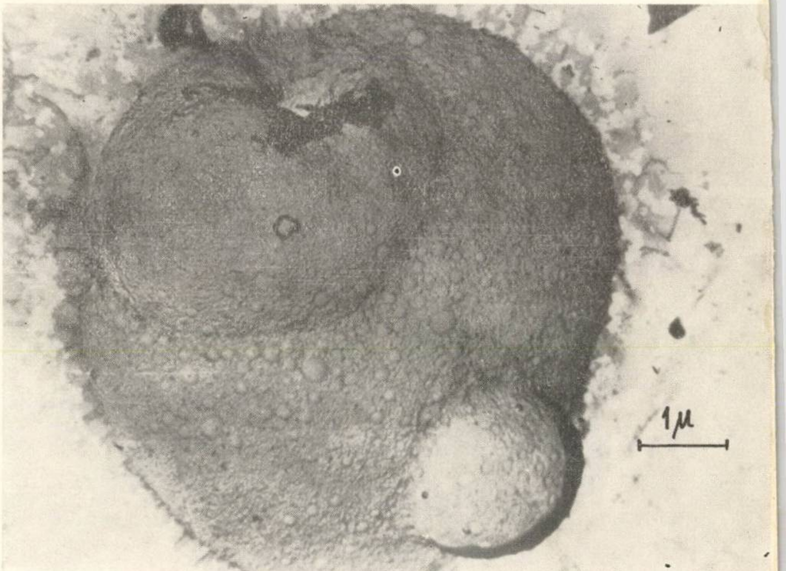

Рис. 12. — Сухая частица ПВХ, происходящая из трех первоначальных частиц.

$\tau_{\text{сек}}$ была рассчитана по формуле[13]

$$\tau_{\text{сек}} = \frac{r \cdot \gamma \cdot \Phi_m^2 \cdot 3600}{4\ \text{Nu} \cdot \lambda \cdot \Delta t},$$

где:

r — теплота испарения воды, $r = 575$ ккал/кг при $T = 42°$;
γ — плотность испаряемой жидкости, $\gamma = 1000$ кг/м^3;
Φ_m — средний диаметр разбрызгиваемых капель;
λ — теплопроводность воздуха, $\lambda = 0{,}0234 \dfrac{\text{ккал}}{\text{м. час}^0\ C}$;

Nu — критерий Нуссельта, $\text{Nu} = 2$

$$\Delta t = \frac{T_1 - T_2}{2{,}3 \lg \dfrac{T_1 - T_c}{T_2 - T_c}},$$

T_1 — температура горячего воздуха на входе в сушилку;
T_2 — то же — на выходе из сушилки;
T_c — температура влажной поверхности капли (в наших условиях

$$T_c = T \text{ мокрого термометра} = 42°.$$

Пары воды из латексных капель в первые моменты сушки направляются наружу из капли, но в следующие моменты, когда вокруг капли начинает образовываться сухая корка из латексных глобул, движение жидкости изнутри становится затруднительным и водяные пары могут задержаться внутри зерна, в полостях, образовавшихся за счет перемещения латексных частичек в верхние слои вслед за испаряющейся жидкостью. Если давление водяных паров внутри зерна велико, что может иметь место при высоких температурах сушки и при скоплении больших количеств паров в каплях относительно крупных размеров, пары прорывают стенки полусухой частицы, образуя выход-канал наружу. Эти каналы хорошо видны под микроскопом с имерсионной жидкостью.

Когда же температура сушки относительно низка, за счет более медленного испарения воды в капле происходят более равномерные процессы уплотнения латексных глобул при свободном движении воды из внутренних слоев к поверхности. В этом случае образование внутренних пустот менее вероятно, что видно из фотографии рис. 8, где частицы ПВХ предстают в виде сплошных шаров.

В порошках, полученных при более высоких температурах (рис. 9—10), напротив, велико число частиц с внутренними пустотами и связывающими их с поверхностью каналами.

Таким образом, можно сделать вывод, что по мере роста температуры сушки происходят изменения во внутреннем строении зерен ПВХ. Повы-

[1] H.G.Kessler, *Chem. Ing. Technic*, **39**, 601 (1967).

шение температуры способствует переходу от зерен, построенных из равномерно распределенных, но менее связанных между собой латексных глобул, к зернам пористым, с твердой оболочкой из спаянных глобул и наличием внутренних пустот.

Существование этих пустот, помимо микроскопических наблюдений, можно доказать и с помощью разницы в плотностях зерен ПВХ, которые будут тем ниже, чем выше температура сушки порошка.

Плотности зерен вычислялись из плотностей свежеприготовленных паст. Простым расчетом, принимая во внимание весовые соотношения между полимером и пластификатором и плотность пластификатора, была рассчитана средняя плотность зерен ПВХ по формуле:

$$\gamma_{\text{пасты}} = 0{,}6\ x + 0{,}4\ \gamma_{\text{дсф}},$$

где x — плотность зерен ПВХ в пасте.

При одинаковой скорости подачи латекса, но разных температурах сушки были получены следующие величины рассчитанных плотностей зерен ПВХ:

$T = 92°$, $x = 1{,}264$ г/см^3,

$T = 80°$, $x = 1,\ 271$ г/см^3,

$T = 70°$, $x = 1{,}302$ г/см^3.

Следует, что частицы в основном являются пористыми, имея плотность меньшую, чем плотность расплава полимера ($\gamma = 1{,}4$ г/см^3); пористость больше у частиц, полученных при более высоких температурах.

Температура сушки в большей степени влияет на строение более крупных зерен. Как было показано в первом сообщении, сжатие латексных капель во время сушки наблюдается только при температурах ниже 90° (см. рис. 1 из сообщения 1[1]), а при $T > 90°$ средние размеры зерен порошка оказываются даже крупнее первоначальных капель, что можно объяснить слипанием зерен, возможным при температурах выше точки стеклования (см. рис. 7 и 12).

Более резкое сжатие наблюдается у мелких частиц, потому что при небольших размерах зерна является менее вероятным образование внутренних пустот, латексные глобулы стремятся к сближению даже и после испарения воды благодаря равномерному прогреву всего зерна и вязкому течению латексных глобул, закрывающих все пустоты.

Внешняя оболочка более крупных зерен, как видно из рис. 4—6, покрыта трещинами и впадинами. Трещины можно объяснить неравномерным сжатием оболочки благодаря неодинаковому притяжению между собой латексных глобул. Впадины — это следы паров воды и всасывания размягченной массы полимера во внутрь. Как видно из рис. 4, и вмятины покрыты трещинами.

При соприкосновении порошка поливинилхлорида с пластификатором через трещины открывается доступ ко внутренним зонам частиц. Благодаря проникновению молекул пластификатора во внутренние пустоты порошка, объем жидкости вокруг частиц уменьшается. Если число полых частиц велико, порошок поглощает большое количество пластификатора, и паста не образуется совсем или образуется очень густая паста.

Во времени происходит растворение оболочек ПВХ в пластификаторе, как с наружной, так и внутренней стороны. Когда благодаря растворению оболочка прорывается в каком-нибудь месте, через образовавшееся отверстие выходит пластификатор, увеличивая тем самым объем свободной жидкости в пасте.

Чем быстрее идет растворение, паста становится все жиже. Механические силы перемешивания помогают разрушению стенок зерна. Этим объясняются случаи, когда некоторые порошки ПВХ образуют пасты только после длительного перетирания в ступке, смесителе или на вальцах. Жидкость, оставшаяся свободной между частицами порошка, и та, что выливается из пустот при разрушении зерен, действует как смазка при перемешивании паст. Если пасты подвергаются очень энергичному перемешиванию, частицы удаляются быстро друг от друга и между ними может не оказаться достаточно жидкости для смазки; движущиеся частицы сталкиваются друг с другом и тогда вязкость возрастает с повышением скоростей сдвига, т.е. создается дилатансия.

В случае поливинилхлоридных партий, полученных при низких температурах, число зерен со внутренними пустотами невелико и пластификатор не исчезает из пространства между частицами, благодаря чему такие порошки образуют пасты с первого момента перемешивания. По мере разрушения зерен до уровня латексных глобул пасты начинают загустевать, потому что каждая латексная частица, обладая сродством к полярному пластификатору, оказывается окруженной слоем молекул пластификатора, адсорбированного на поверхности глобул за счет проникновения молекул пластификатора между макромолекулярными цепями и частичного растворения полимера в пластификаторе.

Растворение ПВХ в пластификаторе можно доказать, измеряя показатели преломления смесей ПВХ + ДОФ во времени. Например, для смесей 10% ПВХ в ДОФ через 24 и 48 часов после приготовления были найдены следующие величины $n_{\text{д}}^{20}$ (см. табл. 1).:

Таблица 1

Величины показателей преломления для смесей ПВХ 10% + ДОФ

Пробы ПВХ	Показатель преломления $n_{\text{д}}^{20}$	
	через 24 часа	через 48 часов
ПВХ, высушенный при 90°	—	1,4881
при 80°	1,4883	1,4889
при 60°	1,4903	1,4908
диоктилфталат	1,4876	

Видно, что величины $n_{\text{д}}^{20}$ растут во времени, удаляясь от значения показателя преломления пластификатора и этот рост тем больше, чем температура сушки полимера была ниже.

Латексные глобулы, разбухшие благодаря адсорбированному на поверхности пластификатору, при высоких концентрациях полимера в пасте (C = 60% вес. или 46% об.) соприкасаются друг с другом, образуя сетчатую структуру во всей массе пасты. Но это структурирование значительно только в состоянии покоя пасты. В смесителях, когда действуют силы сдвига, образовавшиеся связи рвутся, латексные глобулы начинают движение по предпочтительным путям, и таким образом вязкость падает, появляется феномен псевдопластичности.

У проб ПВХ, высушенного при средних температурах, когда образуются несколько видов внутреннего строения зерна, вид течения — псевдопластичное или дилатантное — зависит от того, какой вид строения в порошке преобладает, а также зависит от величины приложенных сил сдвига. Таким образом может наблюдаться течение чисто дилатантное, псевдопластичное или смешанный характер течения: дилатантный + псевдопластичный.

Таким образом, анализируя различное поведение порошков ПВХ в зависимости от температуры распылительной сушки, можно сделать следующие заключительные выводы:

1. Увеличение средних размеров частиц с ростом температуры сушки объясняется быстрым испарением воды, которая затрудняет перегруппировку латексных глобул и ведет к образованию пустотелых зерен тех же или даже больших размеров, чем распыляемые капли, а также слипанием сухих частиц между собой, возможным при высоких температурах.

2. Седиментация паст, полученных из порошков ПВХ, высушенных при относительно высоких температурах, объясняется преобладанием в таких порошках зерен с застеклованной внешней оболочкой, которая трудно растворяется в пластификаторе и потому происходит выпадание зерен из общей массы и оседание их благодаря разнице в плотностях полимера и пластификатора.

Когда же пасты приготовлены из порошка, в котором преобладающими являются зерна, легко распадающиеся на латексные глобулы, адсорбирующие на своей поверхности пластификатор, в этой общей вязкой массе остаются во взвешенном состоянии и те немногие частицы, что имеют застеклованную поверхность.

3. Высокая вязкость паст или даже несвязывание в пасты порошков, высушенных при температуре на выходе из сушилки выше 90°, и падение вязкости во времени одъясняется преобладанием в таких порошках зерен со внутренними пустотами, которые через имеющиеся на поверхности трещины быстро поглощают пластификатор, а потом отдают его обратно по мере растворения стенок пустотелых зерен.

Характер прямо противоположного поведения (возрастания вязкости во времени) паст, приготовленных из ПВХ, высушенного при относительно низких температурах, объясняется преобладанием в таких порошках частиц, которые распадаются легко до уровня латексных глобул, а потом структурируются во времени.

4. Реологические свойства паст зависят также от физического состава порошка поливинилхлорида — соотношения между разными типами структур зерен. Пустотелые частицы с застеклованными оболочками дают дилатантное течение паст, а частицы, легко распадающиеся в пластификаторе до уровня латексных глобул, благоприятствуют псевдопластичному течению паст. Путем комбинирования различных типов структур можно получить желаемые кривые течения.

Revue Roumaine de Chimie, **19**, *3*, 501–507 (1974)

SPEKTROPHOTOMETRISCHE UNTERSUCHUNG DES SYSTEMS VANADIUM (V)-SOLOCHROMVIOLETT RS

DIE SPEKTROPHOTOMETRISCHE BESTIMMUNG DES VANADIUMS

IOAN BURNEA, MARIA PLENICEANU und LUCIA BURNEA
Universität Craiova, Chemische Fakultät, Calea Bucureşti, 165

Eingegangen am 8. Mai 1973

In der vorliegenden Arbeit wurde das System Vanadium(V)-Solochromviolett RS (I) spektrophotometrisch untersucht. Es wurde die Zeitbeständigkeit des gebildeten Komplexes, und der Einfluß der Konzetration des (I) und der H^+-Ionen verfolgt und das Absorbtionsspektrum des Komplexes registriert. Bei pH 3.1 bildet sich eine Komplexverbindung im Verhältnis 1 V(v) : 2(I), dessen Dissoziation durch ein $pK = 12.43 \pm 0{,}20$ charakterisiert ist. Es wurde eine Methode zur spektrophotometrischen Bestimmung des V(v) mit (I) ausgearbeitet für den Konzentrationsbereich 0.203–10.185 μg V(v)/cm^3 ($\lambda = 550$ nm).

Das Solochromviolett RS (I) ist das Natriumsalz der 2-Hydroxynaphthyl-azo-1-phenol-4-sulphonsäure :

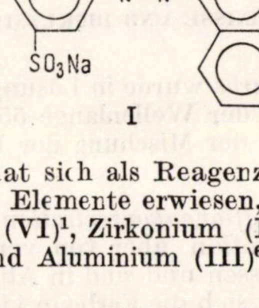

I

Diese Verbindung hat sich als Reagenz für die spektrophotometrische Bestimmung einiger Elemente erwiesen, ohne spezifisch zu sein. So konnten mit I Molybden (VI)[1], Zirkonium (IV)[2], Thorium (IV)[3], Chrom (III)[4], Gallium (III)[5], und Aluminium (III)[6] bestimmt werden.

---

[1] J. Korkisch und M. Osman, *Z. analyt. Chem.*, **171**, 107 (1959).

[2] J. Korkisch und M. Osman, *Z. analyt. Chem*, **171**, 3471 (1959).

[3] J. M. Korenman, F. R. Sheyanova und Z. M. Gurieva, *Khim. Tekhnol*, **2**, 292 (1966).

[4] R. B. Bentley und J. P. Elder, *J. Soc. Dyers and Colourists*, **72**, 332 (1956).

[5] V. Croitoru und G. Nicolae, *Chimie Analitică*, **1**, 155 (1971).

[6] Gr. Popa, M. Pleniceanu und V. Croitoru, *Anal. Univ. Bucureşti*, **1970**, 67.

In der vorliegenden Arbeit wurde die Reaktion der Bildung des dunkelroten V(v)-I-Komplexes spektrophotometrisch untersucht.

Um die besten Bedingungen der Vanadiumbestimmung mit I zu erforschen wurde die Beständigkeit der Farbe sowie der Einfluß der Konzentration der Reaktionspartner und der Wasserstoffionen untersucht. Ferner wurde die optimale Wellenlänge für die Analyse, die Zusammensetzung des Komplexes und seine Instabilitätskonstante durch die Methoden der isomolaren bzw. nichtisomolaren Mischungen von Job bestimmt sowie die Grenzen der Gültigkeit des Lambert-Beerschen Gesetzes.

Es ist noch zu bemerken, daß Vanadium (V) auch mit anderen organischen Reagentien Verbindungen bildet, die auch zu einer spektrophotometrischen Bestimmung herangezogen werden können, so z. B. Solochromschwarz RN[7].

EXPERIMENTELLER TEIL

Zur Herstellung der 10^{-3}M Stammlösungen wurde Amoniummetavanadat (Merck) und Solochromviolett RS (Serva) ohne weitere Reinigung verwendet. Die Pufferlösungen von pH 1 bis 5.6 wurden nach Walpole[8] aus 0.2 M Essigsäure und 0.2 M Natriumazetat, während die von pH 6 bis 9 nach Kolthoff und Vleeschhouwer[8] aus 0.1 Monokaliumphosphat und 0.005 M Natriumtetraborat hergestellt.

Aus den Stammlösungen wurden jeweils die angegebenen Mengen genommen und entweder im Gemisch, oder allein mit der entsprechenden Pufferlösung auf 25 cm^3 verdünnt. Die Referenzlösung für die spektrophotometrischen Messungen war – wenn nicht anders angedeutet eine I-Lösung gleicher Konzentration und vom gleichen pH wie die zu untersuchende Lösung. Das gilt auch für die Job-Kurven. Da die V(v)-Lösungen unter den gegebenen Bedingungen keine Absorption aufweisen, erhielt man auf diese Weise unmittelbar die Abweichung der gemessenen Größe von der Additivität.

Die Extinktionsmessungen wurden mit einem Zeiss VSU 1-Spektrophotometer, und die pH-Messungen mit einem Clamann-Grahnert pH-Meter mit Glaselelektrode ausgeführt.

ERGEBNISSE UND DISKUSSION

Zeitbeständigkeit der Farbe wurde in Lösungen von 8.10^{-5}M V(v) und 24.10^{-5} M I von pH 3.1 bei der Wellenlänge 550 nm verfolgt. Die Farbe erscheint augenblicklich bei der Mischung der Lösungen und ändert sich nicht mit der Zeit.

Einfluß der Wasserstoffionenkonzentration. Die Extinktionen von Lösungen obiger Konzentration aber von verschiedenem pH, wurden zwischen 1.42 und 6.1 gemessen und sind in Abb. 1 aufgetragen. Bei pH-Werten größer als 6.1 ändert sich die Farbe in violett und hat eine kleinere Extinktion als reines I. Ein ausgeprägtes Maximum wird bei pH 3.1 beobachtet, bei welchem die analytischen Messungen optimal ausgeführt werden können.

---

[7] W. Wegner, *Mikrochim. Acta*, **1961**, 599.

[8] C. Luca, „pH-ul şi aplicaţiile lui“ Ed. tehnică, Bukarest 1964, S. 57.

Einfluß der I-Konzentration. Aus Tafel 1 ist ersichtlich, daß für eine V(v)Konzentration von 4.10^{-5} M ein dreifacher Überschuß von I 12.10^{-5} M genügt um die Unabhängigkeit der Extinktion von der I-Konzentration zu erreichen.

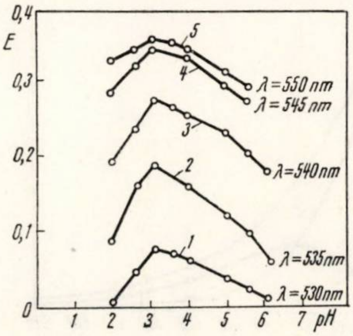

Abb. 1. — Die Abhängigkeit der Extinktion vom pH (8.10^{-5} M V (v) + + 24.10^{-5} MI).

Tafel 1

$[V(v)] = 4 \cdot 10^{-5}$ **M; pH** 3·1 λ = 550 nm

[Solochrom] × 10^{-5}M	Extinktion
2.0	0.062
4.0	0.112
6.0	0.164
8.0	0.220
10.0	0.225
12.0	0.230
14.0	0.232
16.0	0.233

Die Absorptionskurve. Um die optimale Wellenlänge für die spektrophotometrischen Messungen zu finden wurden die Absorptionskuven für a) V(v)-I gegen I, b) I gegen Wasser und c) V (v)-I, gegen Wasser registriert. Die Ergebnisse sind in Abb. 2 wiedergegeben. Die größte Extinktion der Mischung gegen reines I entspricht der Wellenlänge 550 nm.

Beim optimalen pH ist die Farbe des Reagens rosarot. In der Lösung von pH 3.1 ist das V(v) in derForm VO_2^+ vorhanden, da das stark vom pH und der Konzentration abhängende Gleichgewicht [9] :

$$[V_{10}\,O_{28}]^{6-} + 16\,H^+ \rightleftarrows 10\,VO_2^+ + 8H_2O$$

---

[9] R. Ripan und I. Ceteanu, „Chimia metalelor“, Ed. didactică și pedagogică Bukarest, 1969, S. 160.

unter den gegebenen Bedingungen praktisch vollständig nach rechts verschoben ist. Deshalb werden die Messungen durch der Absorption anderer V(v)-Formen nicht gestört.

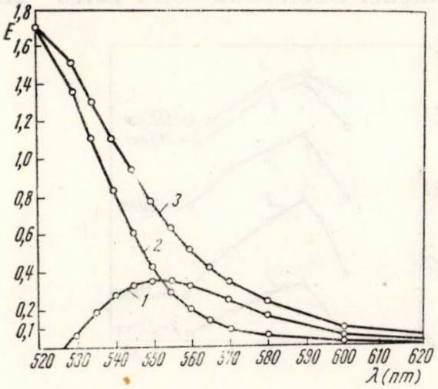

Abb. 2. — Extinktionskurven: 1.V (v) + I gegen I; 2. I gegen Wasser; 3. V(v) + I gegen Wasser (8.10^{-5} M V (v) + 24.10^{-5} MI); pH 3.1

DIE SPEKTROPHOTOMETRISCHE BESTIMMUNG DES VANADIUMS MIT SOLOCHROMVIOLETT RS

Die obigen optimalen Bedingungen der Extinktionsmessung wurden zur Bestimmung des V(v) benützt.

Die Gültigkeit des Lambert-Beerschen Gesetzes wurde unter optimalen Bedingungen für V (v)-Konzentrationen von $0.4.10^{-5}$M bis 20.1^{-5} M und der gleichen Reagenzkonzentration von 64.10^{-5} M erforscht. Wie Abb. 3 zeigt ist die Extinktion der Mischungen eine lineare Funktion der V(v)-Konzentration zwischen 0.203 — 10. 185 μg V(v)/cm³. Der relative molare Extinktionskoeffizient—gegen reines I — ist 5 000, so daß die Methode zu den empfindlichen V-Bestimmungsmethoden gezählt werden kann.

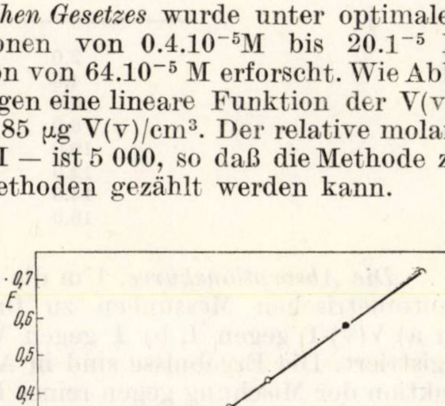

Abb. 3. — Abhängigkeit der Extinktion von der V(v)-Konzentration

Die Neigung der Lambert-Beerschen Geraden wurde durch die Methode der kleinsten Quadrate aus 16 Messungen zu m = $(69.0 \pm 1.2).10^{-3}$ berechnet, unter Berücksichtigung der Studentverteilung für eine Wahrscheinlichkeit von 95%.

DIE ZUSAMMENSETZUNG DES KOMPLEXES

Die Untersuchung der Absorptionsspektren unter verschiedenen Bedingungen führte zum Schluß dazu, daß nur eine Komplexverbindung zwischen V(v) und I gebildet wird.

Die Zusammensetzung des Komplexes wurde anhand der Extinktion isomolarer Reihen sowie anhand der Methode des molaren Verhältnisses ermittelt. Die Abb. 4 gibt die Abweichungen von der Additivität der Extinktion $\triangle E$ für die Job-schen isomolaren Reihen verschiedener Konzentrationen wieder, bei pH 3.1 und 550 nm, xR bezeichnet den Molenbruch des I im V(v) -I- Gemisch.

In Abb. 5 und 6 sind die Ergebnisse der Methode des molaren Verhältnisses wiedergegeben. Abb 5 zeigt die Änderung der Extinktion von Lösungen gleicher Konzentration von V(v) 4.10^{-5} M (Kurve 1) und 2.10^{-5} M (Kurve 2) und wachsender I-Konzentration, während Abb. 6 die Extinktionsänderung von Lösungen gleicher I—(8.10^{-5} M) aber wachsender V(v)-Konzentration enthält.

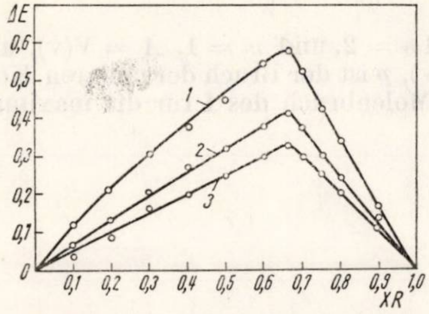

Abb. 4. — Die Bestimmung der Zusammensetzung des Komplexes durch die Methode der isomolaren Reihen: verschiedener Gesamtkonzentrationen:

1. $1.0.10^{-3}$ M; 2. $6.66.10^{-4}$; 3. $5.6.10^{-4}$ M—.

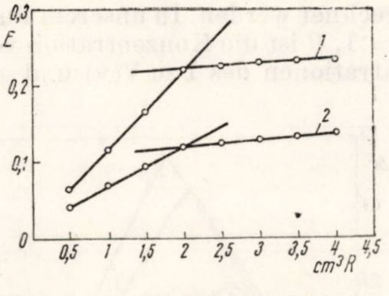

Abb. 5. — Die Bestimmung der Zusammensetzung des Komplexes durch die Methode des molaren Verhältnisses:

1. $1.0.10^{-3}$ M; 2. $5.0.10^{-4}$ M.

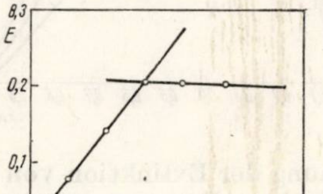

Abb. 6. — Die Bestimmung der Zusammensetzung des Komplexes durch die Methode des molaren Verhältnisses: $6.66.10^{-4}$ M.

Beide Methoden führen eindeutig zum selben Schluß : der Komplex bildet sich im Verhältnis 1 V(v) : 2 I.

DIE BESTIMMUNG DER INSTABILITÄTSKONSTANTE DES V(v)-I - KOMPLEXES

Zu der Bestimmung der Instabilitätskonstante des Komplexes wurde die Methode der nichtisomolaren Reihen von Job herangezogen.

Wird das Massenwirkungsgesetz auf das Gleichgewicht

$$\mathrm{Am\,Bn} \rightleftarrows \mathrm{mA} + \mathrm{nB}$$

angewendet, so kann für die Gleichgewichtskonstante der Ausdruck

$$K = \frac{C^{m+n-1}\, p^{n-1}\, [(pm+n)\,x - n]^{m+n}}{[m^{n-1}\, n^{m-1}\, (p-1)^{m+n-1}]\,[n - (m+n)\,x]}$$

berechnet werden. In unserem Fall sind $n = 2$, und $m = 1$, $A = \mathrm{V(v)}$, und $\mathrm{B} = 1$, C ist die Konzentration von V(v), p ist der Bruch der molaren Konzentrationen des I zu V(v) und x der Molenbruch des I für die maximale Abweichung der Extinktion von der Additivität, so daß die obige Formel eine einfachere Form annimmt :

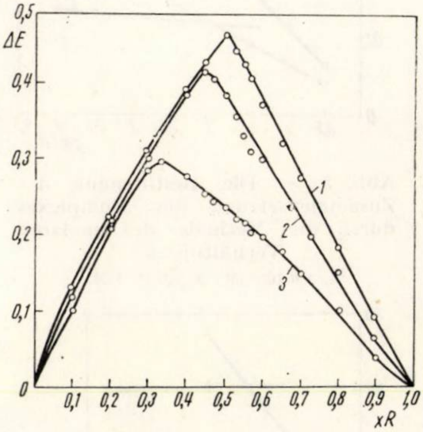

Abb. 7. — Die Bestimmung der Instabilitätskonstante des Komplexes mit Hilfe der nichtisomolaren Reihen.

$$K = \frac{C^2\, p\, [(p+2)\,x - 2]^3}{(p-1)^2\,(2 - 3x)}$$

Die Berechnung der Instabilitätskonstante erfolgte für folgende Reihen von nichtisomolaren Lösungen.

Die Kurven für die ersten drei Reihen wurden in Abb. 7 wiedergegeben, R bedeutet den Volumenbruch der I - Lösung im Gemisch.

Die berechneten pK-Werte sind in Tafel 2 enthalten. Der Sicherheitsbereich ist durch die mittlere quadratische Abweichung in der Studentverteilung für eine Wahrscheinlichkeit von 95% angegeben.

Tafel 2

Die Werte der Instabilitätskonstanten (für sechs Reihen von nichtisomolaren Lösungen berechnet)

Nichtisomolare Reihe	C	p	x	pK	$\overline{pK}$
I	$9.90 \cdot 10^{-5}$	2.0	0.505	12.50	12.43 ± 0.20
II	$8.80 \cdot 10^{-5}$	2.5	0.450	12.68	
III	$6.55 \cdot 10^{-5}$	4.0	0.345	12.18	
IV	$7.39 \cdot 10^{-5}$	5.8	0.270	12.55	
V	$7.90 \cdot 10^{-5}$	8.0	0.210	12.32	
VI	$6.60 \cdot 10^{-5}$	10.0	0.175	12.44	

Die Fehlerfortpflanzungsrechnung gibt einen Fehler der selben Größenordung an, so daß die Abweichungen vom Mittelwert als zufällig angesehen werden können und die Berechnung eines Mittelwertes berechtigt ist. Bei 25° und für die Ionenstärke $\mu = 2.0$ wurde der Mittelwert $\overline{pK}$ gleich 12.43 ± 0.20 gefunden. Dieser Wert deutet auf eine große Stabilität des Komplexes hin.

SCHLUSSFOLGERUNGEN

Die spektrophotometrische Untersuchung des Systems V (v)-I führt zu folgenden Schlußfolgerungen :

1. Vanadium (V) bildet mit Solochromviolett RS eine tiefrote Verbindung die eine leichte spektrophotometrische Bestimmung des Vanadiums gestattet.
2. Die Empfindlichkeit der Methode läßt sie zu den guten Bestimmungsmethoden des Vanadiums zählen.
3. Das große $\overline{pK}$ des gebildeten Komplexes läßt auf eine große Stabilität schließen.

Revue Roumaine de Chimie, **19**, *3*, 501–507 (1974)

Revue Roumaine de Chimie, **19**, *3*, 509–515 (1974)

SPEKTROPHOTOMETRISCHE BESTIMMUNG DES Tl(III) MIT ORTHO-NITRAL UND PARA-NITRALGRÜN

CECILIA CONSTANTINESCU* und SIMON FIŞEL **

*Technische Hochschule für Erdöl, Gase und Geologie, Bukarest, str. Av. Traian Vuia, nr. 6

** Al. I. Cuza Universität Jassy, Calea 23 August nr. 11

Eingegangen am 2. Juni 1973

In der vorliegenden Arbeit wurden die optimalen Reaktionsbedingungen zwischen den basischen Farbstoffen *ortho*-Nitralgrün bzw. *para*-Nitralgrün und dem Thallium Komplexanion $TlBr_4^-$ studiert. Die vom Verfasser gewonnenen Farbstoffe wurden zum Studium der Reaktion mit $TlBr^-$ benutzt und festgestellt, daß sie wasserunlösliche aber benzollösliche Verbindungen bilden, welche dann in Benzol extrahiert werden. Die organischen Extrakte wurden dann spektrophotometrisch untersucht. Außerdem wurden die Verbindungen ausgefällt und einer Elementaranalyse unterworfen. Die Ergebnisse stimmten überein. Die studierte Reaktion ist für die spektrophotometrische Bestimmung des Thalliums geeignet.

In einigen vorherigen Arbeiten wurden die Reaktionen zwischen den Thalliumkomplexionen und basischen Farbstoffen der trimetharischen Klasse spektrophotometrisch studiert.[1-3] Der Mechanismus ähnlicher Reaktionen wurde von Onishi[4] bestimmt und besteht in der Bildung in wäßrigen Medien der komplexen hallogenometallischen Säuren : HMX_4 ; H_2MX_5 ; H_3MX_6 ; die durch die Bindung des komplexen Anions MX_{3+n}^{n-} am Farbstoffskation gefolgt wird. Die in organischen Lösungsmitteln extrahierbare Verbindung ist vom Typus der ionischen Assoziation, dem man nachträglich die optische Dichte bestimmt.

In dieser Arbeit werden die Synthese der basischen Farbstoffe *ortho*- und *para*-Nitralgrün, die Ergebnisse der Forschungen bezüglich der Bildungsreaktion der ionischen Assoziation zwischen dem komplexen Anion $TlBr_4^-$ und der Kationen der Farbstoffe sowie auch die Struktur der erhalte nen Verbindung dargestellt.

---

[1] Gr. Popa, C. Pătroescu und C. Constantinescu, „A III-a Conferință Națională de Chimie Analitică“, 3. Bd., 1971, S. 91.

[2] C. Constantinescu, *Rev. Chim.* (*Bukarest*), **23**, 495, 1972.

[3] C. Constantinescu, *Anal. Sti. Univ. „Al. I. Cuza“, Iaşi*, **19**, 1 (1973).

[4] M. Onishi und E. B. Sandell, *Analyt. Chim. Acta*, **24**, 413 (1961).

VERSUCHSTEIL

SYNTHESE DER FARBSTOFFE

Ortho- und *para*-Nitralgrün wurden durch Anwendung der geeigneten Methode zur Erhaltung des triphenylmethanischen Farbstoffes Malachitgrüns synthetisiert[5] d.h. durch die Kondensierung der *ortho-* und *para*-Nitrobenzolaldehyde mit Dimethylanilin. Die durch Erhitzung auf dem Wasserbad erhaltene dickflüssige Masse ist mit Wasserdampf angetrieben. Der zurück gebliebene Rückstand ist in Äthylalkohol aufgelöst, woraus die Leukobasis wieder ausgefüllt wird. Durch Oxydation der Leukobasis mit Bleidioxyd erhält man das entsprechende Karbinol oder Pseudobase, welches mit Chlorowasserstoff die Kombination mit folgender Struktur bildet :

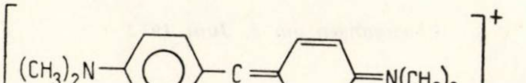

— NO_2 in *ortho-* oder *para-* Stellung

Die Farbstoffe werden weiterhin in verkürzter Form bezeichnet : $o-R^+Cl^-$; $p-R^+Cl^-$

Die Reinigung erfolgte durch wiederholte Umkristallisationen, wonach die Reinheit durch die Kaliumdichromatmethode[6] bestimmt und 82,33 % für *ortho*-Nitralgrün bzw. 96,28 % für *para*-Nitralgrün festgestellt wurde.

REAGENZIEN UND LÖSUNGEN

Die wäßrige Lösung des Tl(III) war durch die Auflösung des Thallium (I) Nitrats, Zufügung von konzentriertem Chlorwasserstoff, und Oxydierung mit Bromwasser hergestellt. Nach der Entfernung des Chlorwasserstoffs durch Verdampfen wird eine Eichlösung vorbereitet, die 204 µg Tl(III) enthält. Der Titer der Thalliumlösung wurde durch Fällung in Form von Thalliumjodid bestimmt.[7] Die in dieser Arbeit benutzten Lösungen wurden durch angemessene Verdünnungen vorbereitet.

— Man verwendet 0,05 %ige Lösungen bezogen auf die 100 %ige Reinheit von *ortho-* und *para*-Nitralgrün ;

— Bromwasserstoff 64 %ig.

— Benzol *p.a.*

— Lösungen verschiedener Kationen unter Form von Nitraten, Sulfaten und/oder Chloriden.

[5] H. Sanielevici und L. Floru, „Sinteza intermediarilor aromatici şi a colorantilor“, II. Aufl. Bukarest, 1971, S. 277.

[6] R. P. Lestonskii und Io. I. Vainstein, „Tekhnicheskii analiz b proizvodstve promjutochinykh i Kransitelei Gosundarstvenoe nauchino tekhnicheskoe izdateliestvokhimichescoi literatury“, Moskau, 1958.

[7] M. H. Furman, „Standard Methods of Chemical Analysis “ VI. Aufl. Van Nostrand, New York, 1962—1963, S. 1051.

EXTRAKTION DES KOMPLEXES

Die 1.10^{-5} M Lösung von Tl(III) in Volumina von 0,5–10 cm³ wird in einen Scheidetrichter von 50 cm³ mit 64 %igen Bromwasserstoff (1 ccm) und 0,05 %ige Reagenzlösung geführt. Man füllt destilliertes Wasser bis zum Volumen von 10 cm³, fügt 10 cm³ organisches Lösungsmittel hinzu und schüttelt 2 Minuten lang. In ähnlicher Weise wird auch die Blindprobe vorbereitet. Man mißt die Extinktionen der gefärbten organischen Phase bei den entsprechenden Wellenlängen $\lambda = 635$ nm ; $\lambda = 645$ nm.

DIE SYNTHESE DER KOMPLEXE

Um das Kombinationsverhältnis in festem Zustand des thallischen Anions mit den untersuchten Reagenzien festzulegen, wurden 0,25 *g* *ortho*- oder *para*-Nitralgrün in 25 cm³ Wasser gelöst und mit 0,25 g in 1 cm³ gelöster Tl(III) gemischt. Es erscheint ein blauer Niederschlag der durch Filtrierung unter Vakuum getrennt und mit Wasser gewaschen wurde. Die Verbindungen wurden bezüglich des Gehalts an Thallium durch die Fällungsmethode (in Form von Thalliumjodid [7]) und an Stickstoff bzw. an Brom analysiert. Die erhaltenen Ergebnisse sind in Tabelle 1 eingetragen, woraus hervorgeht, daß das Kombinationsverhältnis Metall-Ligand 1 : 1ist.

Tabelle 1

Die Analyse der Komplexe

Verbindung	Thallium %		Stickstoff %		Brom %	
	Ber.	Gef.	Ber.	Gef.	Ber.	Gef.
$[o\text{-}R^+][TlBr_4]^-$	22,7	22,1	4,67	4,62	35,6	34,9
$[p\text{-}R^+][TlBr_4]^-$	22,7	22,2	4,67	4,61	35,6	35,0

ERGEBNISSE UND DSKUSSIONEN

Die Wahl des Lösungsmittels. Es wurden folgende Lösungsmittel erprobt : Benzol, Toluol, Chloroform, Aceton, Zyklohexanol, Benzol gemischt mit Methyläthylceton und Benzol gemischt mit Äther. Man stellt fest, daß die Benzolmischung mit kleinen Mengen von Methyläthylceton zur größten Extinktion führte, gefolgt von Benzol. Da die Benzol-Methyläthylceton Mischung auch eine Menge Farbstoff mitextrahiert, wurde in unseren Forschungen nur das Benzol als Lösungsmittel für beide Komplexverbindungen verwendet.

ABSORPTIONSSPEKTREN IM SICHTBAREN BEREICH

Bei Bestimmung der elektronischen Absorptionsspektren der wäßrigen Lösungen von *ortho*-Nitralgrün (Abbildung 1) als Kurve C_1 und von *para*-Nitralgrün als Kurve C_3 wird festgestellt, daß das erste Spektrum ein Absorptionsmaximum bei $\lambda_{max} = 635$ nm und das zweite bei $\lambda_{max} =$

$=645$nm haben. Die mit Tl(III) in 10 cm^3 Benzol erhaltenen Verbindungen haben ein Absorptionsmaximum bei $\lambda_{max} = 645$ nm für das *ortho*-Nitralgrün (C_2) und bei $\lambda_{max} = 655$ nm für *para*-Nitralgrün (C_4). Wir erwähnen, daß die Benzolextrakte der Kontrollproben ohne Gehalt an Tl(III) überhaupt keine Färbung ergeben. Aus Abbildung 1 ist ersichtlich, daß die Maxima der Absorptionsbänder der Komplexe mit Tl batochrom verschoben sind, in Verhältnis zu den Farbstoffspektren, Verschiebung, die der Bildung einiger Komplexe mit Ladungsübertragung vom Typus $\sigma - \pi$ zugeschrieben werden kann.

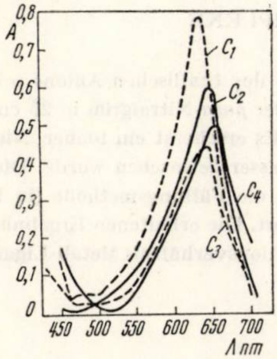

Fig. 1. — Absorptionsspektren : C_1 : Farbstoff : *ortho*-Nitralgrün ; C_2 : Komplex : Thallium-*ortho*-Nitralgrün ; C_3 : Farbstoff : *para*-Nitralgrün ; C_4 : Complex : Thallium-*para*-Nitralgrün.

DIE IR ABSORPTIONSSPEKTREN

Diese Spektren werden in einem Bereich von 400— 4 000 cm^{1-} erforscht. Bei Vergleichung der IR Spektren der freien Verbinder mit denen der entsprechenden Komplexverbindungen mit Thallium, wurde festgestellt, daß die Lagen und die Größen der Vibrationsbänder nach der Reaktion sich nicht verändert haben, ein Hinweis dafür, daß sich die Komplexe mit Ladungsübertragung bilden. Die charakteristischen Vibrationen der Verbindungen C—N (1 400 cm^{-1}), C—C (1 600 cm^{-1}), C—H (1 000 cm^{-1}) in den Spektren der Komplexe sind gewöhnlich etwas verschoben gegen kleinere Frequenzen wegen der Ausdehnung dieser Verbindungen nach der Komplexierung. Die Verbindungen mit Thallium konnten nicht hervorgehoben werden, weil die betreffenden Vibrationen unter 400 cm erscheinen und dieser Bereich nicht mit dem verwendeten Apparat erforscht wurde (Perkin-Elmer 337).

DIE AZIDITÄT DER LÖSUNG

Die Reaktionen zwischen Thallium (III) und der Reagenzien *ortho*- und *para*-Nitralgrün laufen im Milieu von Bromwasserstoff ab. Bei 1,20 N HBr für das erste Komplex (C_1) und 0,68 N HBr für den das zweite (C_2), erhält man die maximale Absorbanz. Die Versuchsergebnisse werden in der Abbildung 2 vorgeführt. Im Medium von Chlorwasserstoff ist die Extraktionsfähigkeit klein.

DIE REAGENZKONZENTRATION

Bei Veränderung der Farbstoffmenge von 0,2–2,0 cm^3 für *ortho*-Nitralgrün und von 0,2–2,5 für *para*-Nitralgrün wurde eine Erhöhung der Absorption bis zu einer bestimmten Konzentration festgestellt, nach der sie konstant bleiben. Die bestmögliche Konzentration, in Abbildung 3 ersichtlich, ist für das erste Reagens von 1,5 cm^3 0,05% wäßrige Lösung die Kurve C_1) und für das zweite von 2 cm^3 0,05%ige wäßrige Lösung (die Kurve C_2).

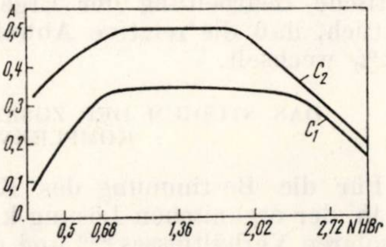

Fig. 2. — Einfluß der Lösungsazidität : C_1 : Tl-*ortho*-Nitralgrün ; C_2 : Tl-*para*-Nitralgrün.

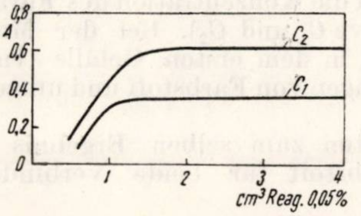

Fig. 3. — Einfluß der Farbstoffskonzentration : C_1 — *ortho*-Nitralgrün ; C_2 — *para*-Nitralgrün.

DIE EICHKURVE

Das Studium der Absorptionvariation in Abhängigkeit von der Konzentration von Thallium (III) hat gezeigt, daß das Bouguer-Lambert-Beer'sche Gesetz zwischen den Grenzen 0,05–6,1 μg Metall/cm^3 Extrakt als wahr erwiesen ist für das Komplex Tl(III)-*ortho*-Nitralgrün (C_1) Abbildung 4, mit einem molaren Extinktionskoeffizient $\varepsilon = 110\,000$ und

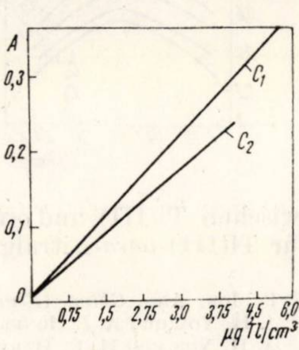

Fig. 4. — Die Eichkurve : C_1 : Tl-*ortho* Nitralgrün ; C_2 : Tl-*para*-Nitralgrün.

zwischen den Grenzen 0,04—4,0 μg Tl(III)/ccm Extrakt für das Komplex Tl(III)-*para*-Nitralgrün (C_2) mit einem molaren Extinktionskoeffizient $\varepsilon = 116\,000$. Es ist ersichtlich, daß die Reaktion zwischen Thallium und *para*-Nitralgrün empfindlicher ist. Die Beständigkeit der komplexen Kombinationen beträgt 48 Stunden.

Die Eichungsgeraden wurden durch Verbesserung der Versuchsdaten mit Hilfe der Methode der kleinsten Quadrate erhalten. Durch die statistische Bearbeitung der Ergebnisse (Wahrscheinlichkeit 0,95) wird ersichtlich, daß die relative Abweichung für beide Methoden zwischen ± 3,2% wechselt.

DAS STUDIUM DER ZUSAMMENSETZUNG GEBILDETER KOMPLEXVERBINDUNGEN

Für die Bestimmung des Kombinationsverhältnisses Metall-Farbstoff in der organischen Lösung kamen die Methode Job [8], die Methode des molaren Verhältnisses [9,10] und die Methode der Gefälle [11] zur Anwendung. Die erhaltenen Ergebnisse bei der Durchführung der Methode Job sind in der Abbildung 5 wiedergegeben, bei Benutzung zweier Paare von Isomolarlösungen : 1.10^{-4} M die Kurve C_1 und C_4 und 2.10^{-4} M die Kurven C_2 und C_3. Bei der Methode des molaren Verhältnisses ist die Konzentration des Metalls konstant geblieben und die Konzentration des Farbstoffs hat sich verändert (Zeichnung 6 die Kurve C_1 und C_2). Bei der Methode des Gefälleverhältnisses verwendet man in dem ersten Gefälle variable Mengen von Thallium und konstante Mengen von Farbstoff und umgekehrt bei dem zweiten Gefälle.

Die angewandten Methoden führten zum selben Ergebnis u.z. : das Kombinationsverhältnis Metall/Farbstoff für beide Verbindungen ist 1 : 1.

DIE BILDUNGSKONSTANTE DER KOMPLEXVERBINDUNGEN

Aus der graphischen Darstellung des molaren Verhältnisses (Abbildung 6) wurde die Bildungskonstante [9,10] K_f errechnet und es wurde für das zwischen Tl(III) und *ortho*-Nitralgrün gebildete Komplex $K = 1{,}1 . 10^5$ und für Tl(III)-*para*-Nitralgrün $K = 1{,}5 \cdot 10^5$ gefunden.

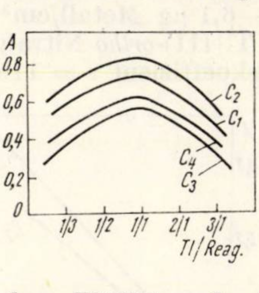

Fig. 5. — Das Kombinationsverhältnis : Die Methode Job ; C_1 : Tl-*o*-Nitralgrün 1.10^{-4} ; C_2 : Tl-*o*-Nitralgrün 2.10^{-4} ; C_3 : Tl-*p*-Nitralgrün 1.10^{-4} ; C_4 : Tl-*p*-Nitralgrün 2.10^{-4}.

---

[8] P. Job, *Ann. Chim.*, (*France*), **9**, 113 (1928).

[9] J. H. Yoe und A. L. Jones, *Ind. Eng. Chem. Analyt. Ed.*, **16**, 111 (1944).

[10] J. H. Yoe und H. E. Harvey, *J. Amer. Chem. Soc.*, **70**, 648 (1948).

[11] A. E. Harvey und D. L. Maning, *J. Amer. Chem. Soc.*, **72**, 4488 (1950).

Die erhaltenen Ergebnisse zeigen, daß durch Fällung sich Komplexe vom Typus $R^+[TlBr_4]^-$ bildeten. In Lösung wegen der Übermenge an Bromwasserstoff können folgende Gleichgewichte erscheinen :

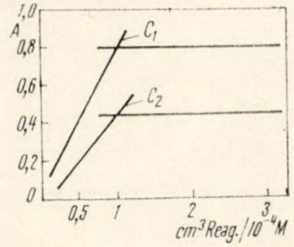

Fig. 6. — Das Kombinationsverhältnis : Die Methode des Molarverhältnisses : Tl-*o*-Nitralgrün ; C_2 : Tl-*p*-Nitralgrün.

$$TlBr_3 + HBr \rightleftarrows HTlBr_4$$

$$HTlBr_4 + HBr \rightleftarrows H_2TlBr_5$$

$$H_2TlBr_5 + HBr \rightleftarrows H_3TlBr_6$$

Unter den obenerwähneten Bedingungen herrscht das Bromkomplex $HTlBr_4$ vor, aus welchem Grund sich die ionische Assoziation bildet :

$$R^+Cl^- + HTlBr_4 \rightleftarrows R^+[TlBr_4]^- + HCl$$

Es ist aber möglich, daß in der Lösung auch andere in Gleichgewicht bleibende Arten existieren wie :

$$R_2^+[TlBr_5]^{2-} ; R_3^+[TlBr_6]^{3-}.$$

DER EINFLUSS FREMDER IONEN

Es wurden die Interferenz jener Ionen geprüft, die gewöhnlich in verschiedenen Materialien Thallium begleiten, so wie : Indium, Gallium, Eisen, Antimonium, Vanadium, Gold und Germanium . Die Reaktion ist vom Wachsen der Absorption in folgender Reihenfolge gestört :

Au(III) >Fe(III) >In(III) >Ge(III) >Ga(III)> Sb (III).

Die erhaltenen Ergebnisse zeigen, daß durch Fällung sich Komplexe vom Typus $R_x[TlBr_y]$ bildeten. In Lösung wegen der [illegible] Bromwasserstoff können folgende Gleichgewichte erscheinen:

$$TlBr_3 + HBr \rightleftharpoons HTlBr_4$$

$$HTlBr_4 + HBr \rightleftharpoons H_2TlBr_5$$

$$H_2TlBr_5 + HBr \rightleftharpoons H_3TlBr_6$$

Unter den obenerwähnten Bedingungen herrscht das Bromkomplex $HTlBr_4$ vor, aus welchem Grund sich die ionische Assoziation bildet:

$$R^+Cl^- + HTlBr_4 \rightleftharpoons R^+[TlBr_4]^- + HCl$$

Es ist aber möglich, daß in der Lösung auch andere in Gleichgewicht bleibende Arten existieren wie:

$$R_2^+[TlBr_5]^{2-} ; R_3^+[TlBr_6]^{3-}$$

DER EINFLUSS FREMDER IONEN

Es wurden die Interferenz jener Ionen geprüft, die gewöhnlich in verschiedenen Mineralien Thallium begleiten, so wie: Indium, Gallium, Eisen, Antimon, Vanadium, Gold und Germanium. Die Reaktion ist [illegible] der Absorption in folgender Reihenfolge gestört:

Au(III) > Fe(III) > In(III) > Ge(III) > Ga(III) > Sb (III)

Revue Roumaine de Chimie, 19, 3, 517–519 (1974)

H. I. ENE und S. GOGONEA ,,*Probleme în teoria filtrației*" (Probleme der Filtrationstheorie), Edit. Academiei, Bukarest 1973, 43 S.

In der vorliegenden Arbeit versuchten die Autoren die wichtigsten Probleme der Filtrationstheorie vorzubringen. Während der Darlegung fiel der Schwerpunkt auf die Entwicklung der mathematischen Modelle, ohne aber auch die konkrete, praktische Seite der Filtrationstheorie zu vernachlässigen.

Die Arbeit besteht aus drei Hauptteilen, die weiter in zehn Abschnitte untergeteilt wurden. Im ersten Abschnitt befassen sich die Autoren mit den Gleichungen der Bewegung der Fluiden in porösen Mitteln. Dieser Abschnitt hat mehr einen Einleitungscharakter. Der erste Teil des Buches beginnt erst mit dem zweiten Abschnitt der über einige Probleme der Bewegung der artesischen Gewässer in homogenen Mitteln handelt. Im nächsten Abschnitt wird dasselbe Thema erweitert und zwar wird, vom mathematischen Gesichtspunkt ausgehend, die Volterra- und Riemanngleichung gelöst. Es folgt ein Abschnitt in dem die Probleme der Bewegung der Fluiden in porösen Mitteln mit Hohlräumen behandelt werden. Es ist der größte Abschnitt des Buches und da die behandelten Probleme sehr verschieden sind, wird dieser Abschnitt in fünf Unterabschnitte geteilt. Ein Schwerpunkt wird auf die rumänischen Beiträge zur mathematischen Modellierung der Bewegung der Fluiden in dünnen Schichten gelegt. In dieser Hinsicht werden die von Prof. Gheorghiță vorgeschlagenen Lösungen besprochen.

Der zweite Teil der Arbeit besteht aus den Abschnitten fünf, sechs und sieben, und behandelt die Magnetohydrodynamik der porösen Mittel. Im fünften Abschnitt wird der Einfluß der porösen Wände auf die Bewegung der elektrizitätsleitenden Fluiden besprochen. Wie in jedem Abschnitt werden zuerst die Gleichungen des Vorgangs untersucht um dann weiter auf mehr praktische Probleme überzugehen. Der nächste Abschnitt befaßt sich mit den Gleichungen der Bewegung der elektrizitätsleitenden Fluiden durch poröse Mittel. In diesem Abschnitt wird weitgehend über den Zusammenhang zwischen den Bewegungsgleichungen und der Elektroosmose berichtet. Der letzte Abschnitt des zweiten Teils wird ,,Die Magnetohydrodynamik der porösen Körper" genannt. Das Hauptproblem in diesem Abschnitt bildet die Untersuchung der hydrodynamischen Wirkung im magnetischen Feld.

Die letzten drei Abschnitte bilden den dritten Teil der Arbeit. In diesem Teil werden die nichthomogenen porösen Mittel behandelt. Der achte Abschnitt, ,,Die Bewegung der Fluide durch nichthomogene poröse Mittel" besteht aus vier Unterabschnitten. Es werden, vom mathematischen Gesichtspunkt aus Probleme, wie z.B. die Bewegung der Fluiden in homogenen und nichthomogenen Mitteln besprochen. Im neunten Abschnitt werden die Reziprozitätsprinzipien für nichthomogene poröse Mittel behandelt. Schließlich, im letzen Abschnitt wird über den Einfluß der Temperatur auf die Bewegungen in porösen Mitteln berichtet. In diesem Abschnitt behandeln die Autoren die Gleichungen der Energie, die natürliche Konvexion in porösen Schichten und andere Probleme die mit dem Einfluß der Temperatur auf die Bewegung in verschiedenen porösen Mitteln in Zusammenhang sind.

Am Ende von jedem Abschnitt bringen die Verfasser ein reiches Literaturverzeichnis aus dem betreffenden Gebiet vor. Übrigens, am Schluß des Bandes befindet sich ein allgemeines Literaturverzeichnis das aus 15 Angaben, über Bücher die über dasselbe Gebiet handeln, besteht. Die Behandlung eines so umfangreichen Materials wird sehr systematisch und klar ausgeführt. Die Gliederung der Arbeit in 10 Abschnitte und fast 130 Unterabschnitte erleichtert wesentlich die Arbeit mit dem Buch. Das hohe wissenschaftliche Niveau der Arbeit setzt besondere mathematische Kenntnisse voraus. Sie wird daher nur einem geringen Kreis von Spezialisten empfohlen.

Al. Fruma

C. SIMIONESCU, MARGARETA GRIGORAȘ, AGATA CERNĂTESCU ASANDEI und G. ROZMARIN „*Chimia lemnului din România; Plopul și salcia*" (Die Chemie des Holzes aus Rumänien ; Pappel und Weide), Edit. Academiei, Bukarest, 1973, 293 S.

Die Ausbeutung des Holzes der Wälder ist sicher eine der ältesten Beschäftigungen der Menschen. Während der Jahrhunderte nahmen sich die Menschen das nötige Holz aus den Wäldern, denn das verfügbare Holz war immer in größerer Menge als die Nachfrage. In der letzten Zeit hat sich diese Lage grundsätzlich verändert ; die außerordentliche Entwicklung der Zellstoffindustrie und der immer größere Verbrauch von Papier und Pappe, benötigten Holzmengen die vom natürlichen Nachwuchs nicht mehr gedeckt werden konnten. Während ein Tannenwald fast 100 Jahre braucht um ausgebeutet werden zu können, vermindert sich diese Zeit im Fall der Pappel und Weide bis zu höchstens 20 Jahren. Darum gehören diese Baumarten zu denen die im höchsten Maße zur Befriedigung der Holznachfrage beitragen können.

In der vorliegenden Arbeit nahmen sich die Verfasser vor, den Fachmännern ein umfangreiches Studium der physikalisch-chemischen Eigenschaften des Pappel- und Weideholzes vorzubringen. Die Arbeit besteht aus 9 Abschnitten. Der erste Abschnitt behandelt allgemeine pedoklimatische Probleme der Wälder. In diesem Abschnitt werden, zwischen anderen, folgende Hauptthemen besprochen : Die Waldvegetation im Donautal, Waldtypen, die Züchtung der Pappel in der Donauau. Dieser Abschnitt hat mehr einen Einleitungscharakter. Erst mit dem zweiten Abschnitt beginnt das eigentliche Studium der Pappel und Weide. Es werden die Morphologie und Anatomie des Pappelholzes besprochen. Die Autoren meinen, daß ,,ein grundlegendes Kennzeichnen der anatomisch-morphologischen Struktur des Pappelholzes das Vorhandensein in größerem Maßstab, von Zugholz ist, das dieser Holzart eine Anzahl von besonderen Eigenschaften verleiht. Makroskopisch, im Stammquerschnitt ist das Zugholz weißschimmernd, glänzend und dichter als Normalholz".

Im dritten Abschnitt der Arbeit werden die chemischen Eigenschaften des Pappelholzes untersucht. Es ist die Rede über die chemische Zusammensetzung und die chemischen Eigenschaften sowohl des eigentlichen Pappelholzes, als auch der Hemizellulose und des Lignins. Dieser Abschnitt enthält auch einen sogenannten ,,experimentellen Teil" in dem über die Trennung und Reinigung des Lignins berichtet wird.

Im vierten Abschnitt werden die beim Studium des Pappelholzes benützten physikalisch-chemische Methoden besprochen. Zwischen diesen modernen Forschungsmethoden, steht an erster Stelle die Methode der Beugung der Röntgenstrahlen. Andere ebenfalls wichtige Methoden sind die I. R. Absorptionsspektroskopie des Pappelholzes, die I. R. Spektroskopie des Lignins und thermogravimetrische Studien. Dieser Abschnitt ist, vom Gesichtspunkt des Chemikers aus, der Wichtigste, da er die Möglichkeiten der Anwendung von modernen Forschungsmethoden beim Studium des Holzes behandelt.

In den zwei nächsten Abschnitten ist die Rede über die besonderen Eigenschaften des Pappelholzes bei der Papierherstellung, und über dem Pappelflaum. Angefangen mit dem siebenten Abschnitt beginnt das Studium des Weidenholzes. Die untersuchten Probleme sind fast dieselben wie beim Studium des Pappelholzes. Im Abschnitt sieben, acht, und neun wird die Morphologie und Anatomie des Weidenholzes, seine physikalischen und chemischen Eigenschaften und die Möglichkeiten der Papierherstellung aus Weidenholz besprochen.

Nach jedem Abschnitt bringen die Verfasser ein reiches Literaturverzeichnis vor. Am Ende der Arbeit befindet sich eine Zusammenfassung in rumänischer, englischer und deutscher Sprache. Die Darstellung des Materials ist äußerst systematisch unternommen, so daß die praktische Arbeit mit dem Buch sehr leicht vor sich geht. Die Arbeit setzt keine besonderen Chemie- oder Landwirtschaftskenntnisse voraus, und wird daher einem weiten Kreis von Studenten, Technikern und Spezialisten empfohlen.

Al. Fruma

NOTE POUR LES AUTEURS

La *Revue Roumaine de Chimie* publie des articles en anglais, français, russe, allemand ou espagnol. Les auteurs sont priés d'envoyer des articles, notes, communications et comptes rendus inédits.

Les manuscrits seront dactylographiés à deux intervalles. Les tableaux seront dactylographiés sur des feuilles séparées, de même que la légende des figures. Les diagrammes seront tracés à l'encre de Chine sur papier calque. Les tableaux et les figures seront numérotés par des chiffres arabes, en nombre strictement nécessaire. Prière de ne pas inscrire les mêmes données dans les tableaux et les figures. Les formules chimiques seront incluses dans le texte ; en outre, elles seront transcrites sur des feuilles séparées. Les auteurs sont priés d'indiquer les caractères italiques (en soulignant les lettres au crayon), ainsi que tout autre caractère spécial. L'ordre des références bibliographiques sera celui de leur mention dans le texte ; le nom de l'auteur sera précédé de l'initiale du prénom ; les publications périodiques seront présentées suivant les prescriptions internationales. Les références seront ajoutées à la fin de l'article ; elles paraîtront comme des notes, au bas de la page. Le texte sera précédé d'un résumé comprenant 15 lignes au maximum.

L'entière responsabilité du contenu des articles appartient aux auteurs. On publie des articles dus aux collaborateurs roumains ou étrangers. Les auteurs recevront 50 tirés à part.

PRINTED IN ROMANIA

1974 MAI 16

TRAVAUX PARUS AUX ÉDITIONS DE L'ACADÉMIE DE LA RÉPUBLIQUE SOCIALISTE DE ROUMANIE

MARIA FITI, **Dozimetria chimică a radiaţiilor ionizante** (La dosimétrie chimique des radiations ionisantes), 1973, 240 p., 13,60 lei.

MIHAI FLORESCU, **Eficienţa economică a cercetării ştiinţifice** (L'efficience économique de la recherche scientifique), 1972, 115 p., 15 lei.

GEORGETA LĂZĂRESCU, **Sistematizarea informaţiilor în Chimia organică** (La systématisation des informations dans la Chimie organique), 1972, 252 p., 10,15 lei.

P. BALTĂ et E. BALTĂ, **Introducere în chimia fizică a stării vitroase** (Introduction à la chimie physique de l'état vitreux), 1971, 240, 15,50 lei.

LYDIA-MARIA VAICUM, **Biodegrabilitatea detergenţilor** (La biodégrabilité des détergents), 1971, 254 p., 16 lei.

TIBERIU NĂSCUŢIU, **Metode radiometrice de analiză** (Méthodes radiométriques d'analyse), 1971, 346 p., 19,50 lei.

I. ZUGRĂVESCU et L. STOICESCU-CRIVETZ, **Polimeri heterociclici** (Polymères hétérocycliques), 1971, 190 p., 9,50 lei.

CRISTOFOR SIMIONESCU et C. V. UGLEA, **Fracţionarea compuşilor macromoleculari** (Fractionnement des composés macromoléculaires), 1962, 292 p., 18,50 lei.

I. MAXIM, **Materiale nucleare** (Matériaux nucléaires), 1969, 444 p., 30 lei.

CRISTOFOR SIMIONESCU et CLEOPATRA VASILIU-OPREA, **Mecanochimia compuşilor macromoleculari** (La mécanochimie des composés macromoléculaires), 1967, 344 p., 23,50 lei.

CORNEL BODEA et collab., **Tratat de biochimie vegetală**, partea I, **Fitochimie** (Traité de biochimie végetale, Ire partie, Phytochimie), Ier vol., 1964, 747 p. + 4 annexes + 2 pl., 41 lei ; IIe vol., 1965, 1262 p., 1 pl., 56 lei ; IIIe vol., 1967, 773 p., 35 lei.

V. GHEŢIE et V. MICUŞAN, **Analiza imunochimică. Teorie şi practică** (Analyse immunochimique. Théorie et pratique), 1966, 369 p., 28 lei.

R. PORTOCALĂ et L. POPA, **Acizii ribonucleici celulari şi virali** (Les acides ribonucléiques cellulaires et viraux), 1966, 375 p., 8 pl., 26 lei.

D. PURDELEA et R. VÎLCEANU, **Chimia compuşilor organici ai fosforului şi ai acizilor lui** (La chimie des composés organiques du phosphore et de ses acides), 1965, 540 p., 37 lei.

I.P.I. — c. 1001

43 426

Lei 25.—

F 1103

R

REFERÁLVA

REVUE ROUMAINE DE CHIMIE

TOME 19

N° 4

Avril 1974

RRCHAX, 19, 4, 521–736 (1974)

ÉDITIONS DE L'ACADÉMIE DE LA RÉPUBLIQUE SOCIALISTE DE ROUMANIE

Rev. Roumaine Chim. 19, 4, p. 521–736 (1974), Bucarest

COMITÉ DE RÉDACTION

Rédacteur en chef:

I. G. MURGULESCU, membre de l'Académie de la République Socialiste de Roumanie

Rédacteur en chef adjoints:

A. T. BALABAN et V. EM. SAHINI, membres correspondants de l'Académie de la République Socialiste de Roumanie

Collège de rédaction:

EM. BRATU, ELENA CEAUŞESCU, ECATERINA CIORĂNESCU-NENITZESCU, C. DRĂGULESCU, RALUCA RIPAN, CR. SIMIONESCU, membres de l'Académie de la République Socialiste de Roumanie; P. SPACU, membres correspondants de l'Académie de la République Socialiste de Roumanie; MARGARETA AVRAM, D. I. MARCHIDAN, I. MOLDOVAN, G. NIAC et D. SĂNDULESCU

La Revue Roumaine de Chimie paraît 12 fois par an. Toute commande de l'étranger (fascicules ou abonnements) sera adressée à Întreprinderea Rompresfilatelia, Boîte Postale 2001, telex 011631, Bucarest, Roumanie

Les manuscrits, les livres et les revues proposés en échange, ainsi que toute correspondance seront envoyés à la rédaction

REVUE ROUMAINE DE CHIMIE

23, str. Dumbrava Roşie, Bucarest, Roumanie

ÉDITIONS DE L'ACADÉMIE DE LA RÉPUBLIQUE SOCIALISTE DE ROUMANIE
3 bis, str. Gutenberg, Bucarest

REVUE ROUMAINE
DE
CHIMIE

Tome 19, N° 4 Avril 1974

S. STERNBERG and I. GALASIU, The galvanostatic study of the electrochemical adsorption process on the iodine-active carbon electrode in molten salts. I. The current intensity effect . . . . 523–531 R

C. LEPĂDATU and VERONICA TUFOI, On the equivalence between the crystal field and M O parametric approaches 533–541

SULTANA CIOLAC and O. RADOVICI, The corrosion of carbon steel and some austenitic stainless steels in synthetic river waters . . . . 543–551 R

ŞTEFANIA ZUCA and RODICA BORCAN, Viscosity of binary molten alkali chloride systems 553–559

I. TEOREANU, MARCELA MUNTEAN, N. CIOCEA and O. ŞANCU, Mechanism and kinetics of the dissolution in water of some hydrated binders . . 561–566

SILVIA PLOŞTINARU and P. SPACU, Mixed ligand compounds of lanthanides with neutral ligands containing donor oxygen atoms. II. Chlorosalicylates of lanthanides with triphenylarsine oxide 567–575

GH. MARCU, MARIA SUCIU und A. V. BOTAR, Papierelektrophoretische Untersuchung der Bildung von Verbindungen des Indiums mit R-Weinsäure 577–580

A. T. BALABAN and C. POMPONIU, Computer program for determining all possible E.S.R. spectra with equidistant lines 581–630

A. T. BALABAN, and F. KEREK, Chemical graphs. XX. Graphs of parallel and/or subsequent substitution reactions 631–647

I. ZUGRĂVESCU, J. HERDAN et I. DRUŢĂ, Benzimidazolium-ylures. I. L'action des acétylènes activés sur quelques benzimidazolium-ylures . . 649–658

I. ZUGRĂVESCU, J. HERDAN et I. DRUŢĂ, Benzimidazolium-ylures. II. Sur les réactions de quelques benzimidazolium-ylures avec des philodiènes . . 659–664

M. VLASSA, MARIA IONESCU and J. FABIAN, The electronic spectrum of 1, 2, 3-trimethoxyacridine-N-oxide. 665–669

D. SUCIU and Z. GYÖRFI, Electronic spectra and acid-base equilibrium of some α-acylamino-N-heterocycles 671–677

R. NUŢIU, I. SEBE and MARIA NUŢIU, 2-Thio-5-nitrobarbituric acid . . . 679–687

A. BALOG, E. VARGHA, D. BREAZU, F. GÖNCZY, and LUCIA BEU, Peptides. XV. The use of β-dicarbonyl N-protected asparagine and glutamine in peptide synthesis 689–699

Rev. Roumanie Chim. 19, 4, p. 521–736 (1974), Bucarest

V. TĂMAŞ and C. BODEA, Azlactones of carotenoids. II. Retinal azlactone and transformation products . . . . 701–707 R

M. RĂILEANU, ILEANA RADULIAN und H. KRAUSS, Säure-Basen-Indikatoren vom Phenothiazin Typ. I. Die Anwendung von 3H-Phenothiazin-3-[4-anilsulfonsäures Kalium], 3H-Phenothiazin-3-[3-Anilsufonsäures Kalium] und 3H-Phenothiazin-3-[2-anilsufonsäures Kalium] als Säure-Basen-Indikatoren 709–716

S. A. TĂTARU, An ion-exchange process for gold recovery . . . . 717–725 R

GEORGETA ANDREI, GH. ŞERBAN and CORINA FLORIŢA, Catalytic dehydrogenation kinetics of *n*-butenes to butädiene . . . . 727–734 R

COMPTE RENDU 735–736

Revue Roumaine de Chimie, **19**, *4*, 523–531 (1974)

THE GALVANOSTATIC STUDY OF THE ELECTROCHEMICAL ADSORPTION PROCESS ON THE IODINE-ACTIVE CARBON ELECTRODE IN MOLTEN SALTS. I

THE CURRENT INTENSITY EFFECT

S. STERNBERG and I. GALASIU

Centre of Physical Chemistry, Str. Galaţi 31, Bucharest

Received May 5, 1973

Anodic and cathodic polarization curves for iodine-active carbon electrode in fused AgI + KI eutectic have been determined by galvanostatic method at several intensities and 300°. The efficiency of iodine deposition on electrode has been measured *versus* intensity for different charges passed through the cell.

In previous papers the halogen-active carbon electrode has been studied by the cathodic polarization curves.$^{1-4}$ In those works the halogen-active carbon electrode has been obtained by a preliminary anodic polarization corresponding to the reversible potential. In this new series of investigations the carbon electrode is anodically polarized under galvanostatic conditions up to a stationary potential which is lower than the reversible potential. This way one can investigate the "charging" of activated carbon surface with the halogen which is electrochemically adsorbed.

EXPERIMENTAL

The deposition of iodine on the active carbon electrode has been effected by electrolysis of an eutectic mixture of AgI + KI. The anode consisted of an active carbon rod with the specific surface of 10–20 m^2/g and a weight of 2.23 g. The cathode was a silver rod of 3 mm diameter. The potential of the $Ag_{(s)}/AgI_{(l)} + KI_{(l)}/I_{2(g)}$ C cell was measured with a remanent trace oscillograph. Both for anodic and cathodic polarizations of carbon electrode a galvanostatic method has been used. The carbon electrode without iodine has been exposed to a gal-

---

[1] S. Sternberg and I. Galasiu, *Rev. Roumaine Chim.*, **13**, 991 (1968).
[2] S. Sternberg and I. Galasiu, *Rev. Roumaine Chim.*, **15**, 1169 (1970).
[3] S. Sternberg and I. Galasiu, *Rev. Roumaine Chim.*, **17**. 1697 (1972).
[4] S. Sternberg, V. Petrescu and I. Galasiu, *Rev. Roumaine Chim.*, **17**, 1689 (1972).

vanostatic anodic polarization until the desired potential was obtained, and the galvanostatic anodic polarization curve has been recorded. Then, the cell was switched on a galvanostatic cathodic polarization circuit until the iodine was completely removed from the electrode; the galvanostatic cathodic polarization curve was recorded, too.

The iodine quantities adsorbed on or desorbed from the electrode by electrolysis have been calculated with the relations:

$$Q = i \cdot t \quad \text{and} \quad a = Q/F$$

where:

Q = quantity of current in coulombs.
F = Faraday constant.
i = current intensity.
t = polarization time.
a = atom-grams of iodine.

During the experiments argon gas has been bubbled through the electrolyte, so that gaseous iodine has continuously been evolved from the cell. The apparatus and the preparation procedure of the active carbon electrodes were described in our previous works.[1-4]

The apparent surface area of the electrode was 11.33 cm². The real surface of the active carbon electrode is much greater but its value is not known since one cannot accurately determine the contact surface between electrode and electrolyte; hence no reliable value of the current densities used can be given.

RESULTS AND DISCUSSIONS

In fig. 1 the anodic polarization curves obtained at the deposition of iodine on an active carbon electrode at 300° are plotted. The anodic polarization has been effected with currents of 20, 50, 100 and 200 mA. The reversible potential of the iodine electrode in the same mixture and at the same temperature, calculated according to the equation[5]

$$E = 0.5885 - 0.225 \times 10^{-3} (T - 873)$$

has been chosen as reference potential.

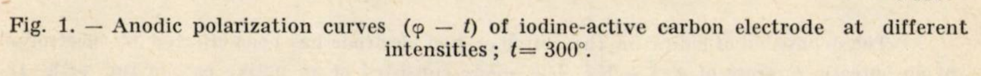

Fig. 1. — Anodic polarization curves ($\varphi - t$) of iodine-active carbon electrode at different intensities; $t = 300°$.

---

[5] S. Sternberg, I. Adorian and I. Galasiu, *Electrochim. Acta*, **11**, 385 (1966).

The general behaviour of the potential (φ)-time curves is as follows :

At a given value of the current intensity the electrode potential increases in time and reaches a stationary value which is lower than the reversible potential.

Following the galvanostatic anodic process, a galvanostatic cathodic polarization was always effected at a current equal to that used at the anodic polarization in order to measure the iodine adsorbed on the electrode. The anodic polarization has also been effected "in steps". After the anodic polarization (duration t_1) the cathodic polarization was effected, and the charging efficiency calculated according to the equation :

$$\eta = \frac{Q \text{ (cathodic polarization)}}{Q \text{ (anodic polarization)}} \cdot 100$$

After the first cathodic polarization, the anodic polarization has been resumed for a duration $t_2 > t_1$, and so on. The "in steps" anodic polarization curve was found to superimpose very well on that obtained in a single period.

This behaviour may be explained as follows :

The potential of the active carbon electrode is determined by the quantity of halogen adsorbed on carbon, that is by the degree of coverage θ. To exemplify we have studied the charging curve corresponding to $i = 100$ mA.

On the AB portion of the curve a discharging reaction of the iodine ions with formation of adsorbed iodine, probably in atomic state, takes place.

$$I^- = I_{(\text{ads})} + e^- \tag{1}$$

On this portion all the anodic polarization current is practically used for the "charging" of the electrode with adsorbed iodine. Let this current be $i_{(\text{ads})}$ adsorption current. On this portion the efficiency is practically $\eta = 100\%$. On the BC portion the efficiency begins to decrease, owing to the "thermal desorption" process :

$$2\,I_{(\text{ads})} \rightarrow I_{2_{(\text{ads})}} \rightarrow I_2 \text{ (gas or dissolved in the melt)} \tag{2}$$

We will denote as desorption current $-i_{(\text{desorption})}$ – the current used to compensate the iodine losses by "thermal desorption" according to reaction (2). Therefore, in this portion part of the iodine which is deposited on the electrode is used to compensate the "thermal desorbed" iodine. This causes the potential increase in time to become slower. The increase of the potential φ is determined by the adsorption current which is given by :

$$i_{(\text{ads})} = i - i_{(\text{desorption})} \tag{3}$$

where "i" stands for the total current used for the anodic galvanostatic polarization.

On the CD portion of the curve the φ potential becomes practically stationary and in this case the total current $i = i_{(\text{desorption})}$ while $i_{(\text{ads})} = 0$.

All these facts, in agreement with our previous works[1-3] point out a new phenomenon, namely the existence of a thermal desorption current at the polarization of active carbon electrodes in fused electrolytes. Because of high temperatures required by electrolysis processes in molten salts, the "thermal desorption current" can reach high values, *i. e.* several hundreds milliamperes. Actually, this desorption current is equal to the desorption rate of the halogen from the active carbon electrode, $v_{(\text{desorption})}$

$$i_{(\text{desorption})} = v_{(\text{desorption})}\,) = \theta \cdot K_{(\text{desorption})} \tag{4}$$

where $K_{(\text{desorption})}$ represents the desorption constant.

The degree of coverage depends on pressure and implicitly on potential

$$\theta = f(\varphi) \tag{5}$$

The more electropositive the φ potential, the higher the value of θ and consequently, according to eq. (4), the higher $i_{(\text{desorption})}$. This explains the increase of the stationary potential as a function of the charging current, taking into account that under stationary conditions $i = i_{(\text{desorption})}$ as may be seen in table 1.

Table 1

The potential dependence of Q_{charging} and $Q_{\text{discharging}}$ (reference potential: silver electrode): t = 300°

$i_{\text{charging}} = i_{\text{discharging}} = 20\text{mA}$			$i_{\text{charging}} = i_{\text{discharging}} = 50\text{ mA}$			$i_{\text{charging}} = i_{\text{discharging}} = 100\text{mA}$		
Q_{charging} coulombs	$Q_{\text{discharging}}$ coulombs	φ mV	Q_{charging} coulombs	$Q_{\text{discharging}}$ coulombs	φ mV	Q_{charging} coulombs	$Q_{\text{discharging}}$ coulombs	φ mV
12	12	100	15	15	145	30	30	305
24	24	215	30	30	270	60	60	495
36	36	315	60	60	480	120	108	560
48	48	405	90	84	530	180	138	580
60	60	465	120	102	545	240	169.5	590
72	69.6	500	150	117	555	300	181.5	595
96	82.8	525	180	128	565	360	185	595
120	93.6	540	210	138	570	420	189	595
144	100.8	545	240	145	575	480	189	595
180	106.8	550	270	150	575	540	189	595
216	108.2	550	300	151	575			
252	109	550	330	151	575			
288	109	550	360	151	575			
324	109	550						

Fig. 2 represents the dependence of the potential φ on the charge required for the anodic polarization. The Q quantities were calculated from the φ *vs.* anodic polarization time curves. Only the AB portion of the anodic polarization curves has been plotted, because in this range the efficiency is 100% for different currents. Examination of these curves shows that they do not overlap. Therefore, the same potential φ is obtained with different amounts of halogen adsorbed : the higher the current, the smaller the Q quantities at $\varphi =$ constant. The explanation could be the following : the value of the degree of coverage remains the same for a given potential, but the electrochemically active surface is larger as the charging current "i" is smaller. For smaller currents the charging time is larger and the halogen diffuses into the inner pores of the active carbon bulk. It is also possible that, in this case, the wetting of the electrode by the electrolyte is better. Under these conditions, the surface which participates in the electrochemical process is larger, and to obtain a φ potential a larger charge is necessary.

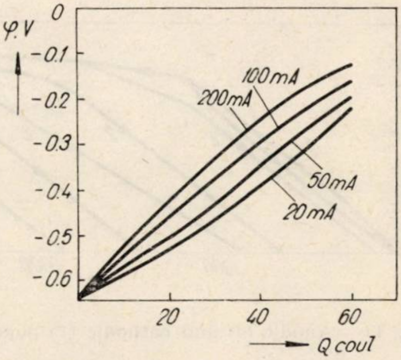

Fig. 2. — Anodic polarization curves (φ — Q) of iodine-active carbon electrode at different intensities ; $t = 300°$.

Fig. 3 shows the anodic polarization curve obtained by "steps" corresponding to $i = 100$ mA. At the end of every anodic polarization a cathodic polarization has been effected. It has been found that for short anodic polarization times the efficiency of the iodine deposition on the electrode is 100% and decreases as the anodic polarization time increases.

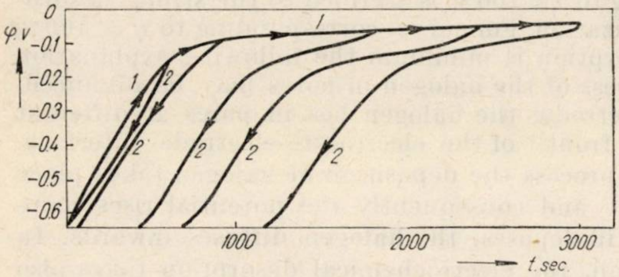

Fig. 3. — Anodic (*1*) and cathodic (*2*) polarization curves at $i = 100$ mA and $t = 300°$.

It has also been found that for higher potentials, close to the reversible potential, on both anodic and cathodic polarization curves there are characteristic plateaus which may be attributed to a capillary condensation of iodine in the active carbon pores. This is plausible because the working temperature, 300°, is below the critical point of iodine, *i. e.* 511°. The curves for anodic-cathodic polarization with $i = 50$ and $i = 20$ mA have similar shapes (figs. 4 and 5). Some hysteresis existing in case of curves corresponding to $\eta < 100\,\%$ is ascribed to the strong desorption during the anodic polarization. For curves corresponding to $\eta = 100\,\%$ for which the thermal desorption is minimum the following explanation based on the diffusion process of the halogen in pores may be advanced. On the halogen-carbon electrode, the halogen lies in pores at different distances from the "first front" of the electrolyte-electrode interface. At the anodic polarization process the deposition of halogen takes place at first on the "first front" and consequently the potential rises more rapidly in time. Then, as it deposes, the halogen diffuses inwards. In case of cathodic polarization, the electrochemical desorption takes also place at first from the "first front", and the $\varphi - t$ curve has at the beginning a higher slope.

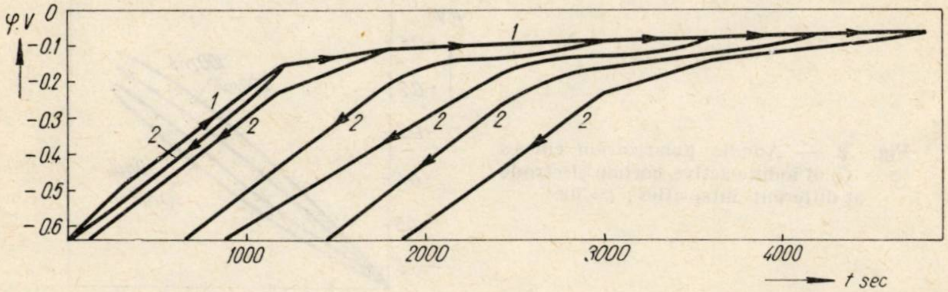

Fig. 4. — Anodic (*1*) and cathodic (*2*) polarization curves at $i = 50$ mA and $t = 300°$.

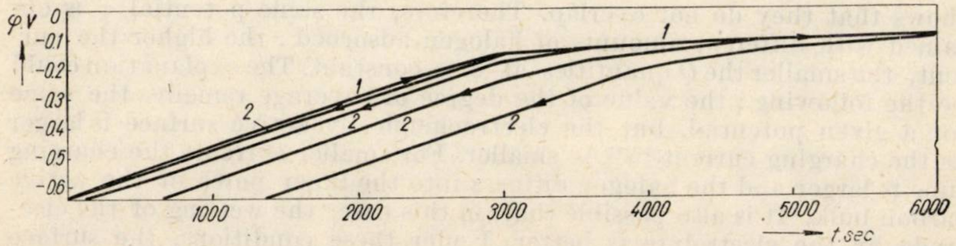

Fig. 5. — Anodic (*1*) and cathodic (*2*) polarization curves at $i = 20$ mA and $t = 300°$.

Figs. 6 and 7 represent the iodine deposition efficiency change *versus* anodic polarization time and the charge involved in anodic polarization, respectively. As expected, one observes that in the η *vs.* time coordinates (fig. 6) the lower the value of the "*i*" current, the higher the location of the curves on plots. On the other hand, if we plot the efficiency *vs.* charge used for anodic polarization (fig. 7) one observes that the positions of the three curves are reversed. In this latter case, passing through the cell some charge with a lower current requires longer times during which the thermal desorption is more important and iodine deposition efficiency lower. Fig. 7 also shows that up to a charge of 60 coulombs passed through the cell, the efficiency of iodine deposition on the electrode is 100%, no matter the current intensity used for charging. For higher charges the efficiencies are lower. Figs 8, 9 and 10 re-

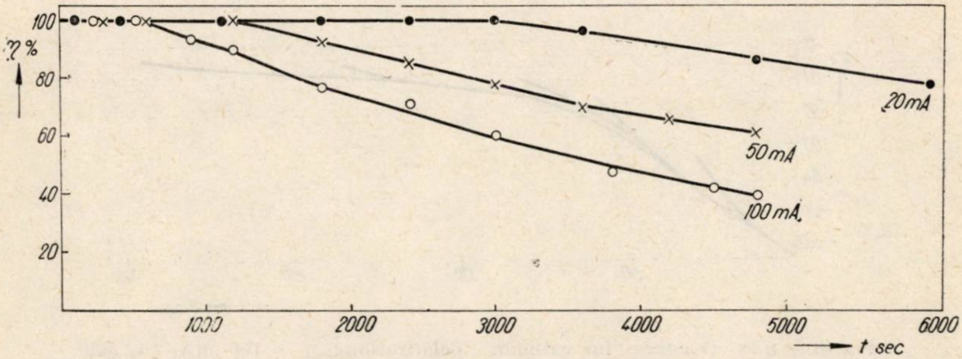

Fig. 6. — The efficiency $\eta = Q_{\text{discharging}}/Q_{\text{chargirg}}$ *versus* anodic polarization duration for several intensities; $t = 300°$.

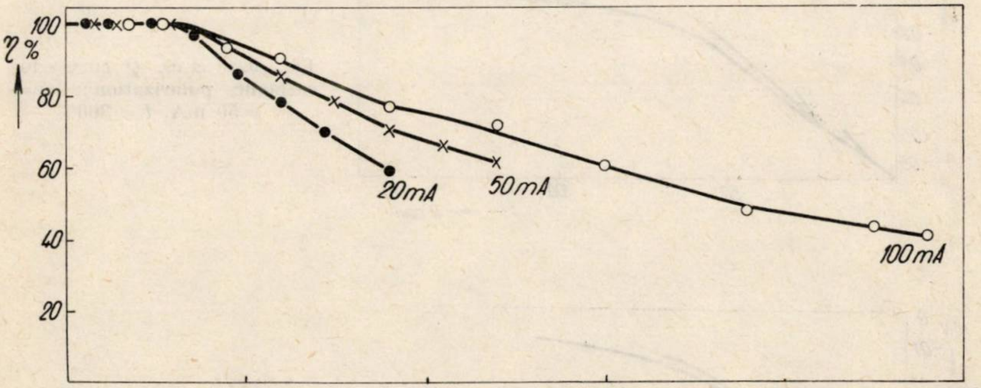

Fig. 7. — The efficiency $\eta = Q_{\text{discharging}}/Q_{\text{charging}}$ *versus* the charge used in anodic polarization at several intensitis; $t = 300°$.

present φ — Q plots based on the cathodic polarization curves. One observes that the initial portions of all the cathodic polarization curves present a faster decrease of the potential, after which all gather together in a "basic curve". The faster decrease of the potential is due either to a quantity of iodine from the electrode surface weakly bound to the carbon atoms and which leaves easier the electrode, or to an overvoltage of the iodine-active carbon electrode. We also note that the higher the cathodic polarization current, the greater the initial variation of the potential.

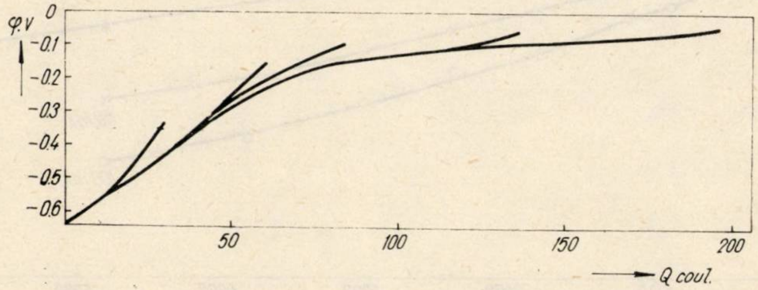

Fig. 8.— φ *vs.* Q curves for cathodic polarization; $i = 100$ mA, $t = 300°$.

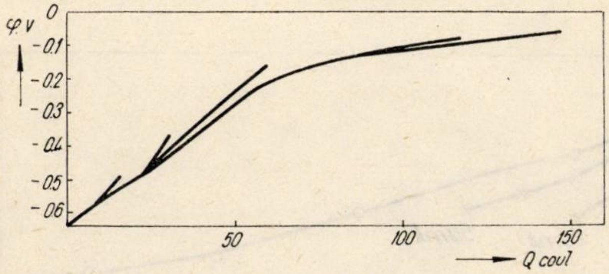

Fig. 9. — φ *vs.* Q curves for cathodic polarization; $i = 50$ mA, $t = 300°$.

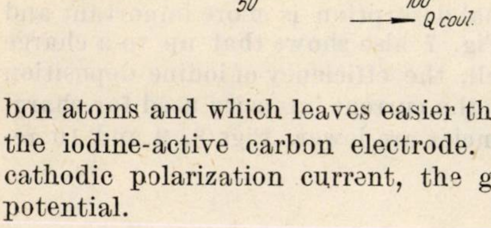

Fig. 10. — φ *vs.* Q curves for cathodic polarization; $i = 20$ mA, $t = 300°$.

The three "basic cathodic polarization curves" are shown on figure 11. Comparison of the curves plotted on fig. 11 with the anodic polarization curves from fig. 2 shows that the differences between the cathodic polarization curves are far smaller than those existing between the anodic polarization curves, while their positions are inverted. This is probably due to the self-desorption phenomena, which are more intensive during the anodic polarization.

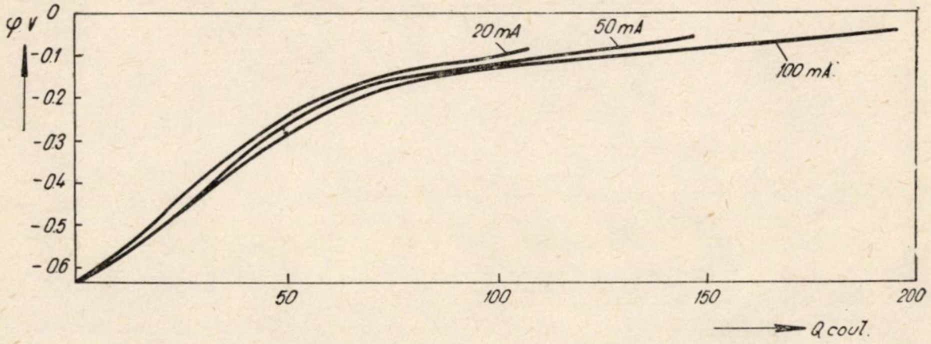

Fig. 11. — φ *vs.* Q curves for cathodic polarization at several intensities; $t = 300°$

For this reason, in the subsequent processing of the data it will be more convenient to use the cathodic polarization curves.

Revue Roumaine de Chimie, **19**, *4*, 533–541 (1974)

ON THE EQUIVALENCE BETWEEN THE CRYSTAL FIELD AND MO PARAMETRIC APPROACHES

C. LEPĂDATU and VERONICA TUFOI

Institute for Physical Chemistry Str. Dumbrava Roşie 23, Bucharest, Romania

Received May 25, 1973

It is shown that the parametric crystal field approximations are nothing else but molecular orbital alternatives with the difference that the first ones do not divide the orbital energies in the molecule according to the chemical bonding type. The quantitative equivalence between the CF and MO theories justifies the applicability and the prediction power of the crystal field approaches widely used by chemists and physicists.

It is well known that the crystal field theory in its different forms, like the operator equivalents, [1] or the strong and weak field coupling,[2] leads to good results in the interpretation of electronic and ESR spectra of the transition metal [3] and rare earth complexes,[4] when semiempirical fitting parameters for the orbital and interelectronic repulsion energies are used. The prediction power of the mentioned theory is somewhat surprising having in view the basic principles which do not take into account the chemical bond formation as the LCAOMO approximations do, the interactions between metal and ligands being reduced to a matter of electrostatic perturbations only.

It was already reported in the related literature the qualitative equivalence between the molecular orbital and crystal field energy diagrams, due to the circumstance that both theories make use of the same symmetry properties of the central atom orbitals.[5] In other words, the postulated MO and CF model hamiltonians fulfil the same invariance requirements in respect to the symmetry group to which the molecule belongs.

---

[1] W. Low, "Paramagnetic Resonance in Solids", Solid State Phys., Suppl. 2, Academic Press, 1960.

[2] J. Griffith, "The Theory of Transition Metal Ions", Cambridge Univ. Press, 1964.

[3] B. N. Figgis, "Introduction to Ligand Fields", Interscience Publ., New York, 1966.

[4] D. Y. Newman, *Adv. Physics*, **20**, 197 (1971).

[5] C. E. Schäffer and C. K. Jørgensen, *Mat. Fys. Medd. Dan. Vid. Selsk.*, **34**, 13 (1965).

Some authors [6–9] have recently suggested the possible correlation between the CF parameters and the parameters used by a contact potential approach developed by Jørgensen and Schäffer [10] under the name of Angular Overlap Model (AOM). As has been shown elsewhere,[11] the AOM may be well included into the category of semiempirical MO approximations which exploits the localizability properties of the chemical bonds.

The aim of the present note is to give a more consistent explanation to the quantitative equivalence between CF potentials and MO energies, and to show that the semiempirical CF approximations are nothing else but parametrized LCAOMO alternatives.

To this purpose, the electrostatic energies were calculated from :

$$\begin{aligned}< \varphi_n |\hat{\mathrm{H}}_{\mathrm{el}}| \varphi_n > &= < \varphi_n |\hat{\mathrm{H}}^0| \varphi_n > + < \varphi_n |\hat{\mathrm{V}}| \varphi_n > = \\ &= E^0 + R_n(0) + \sum_k \sum_m a_k P_k^m (\cos \theta_i) \cos m\varphi_i R_n(k)\end{aligned} \tag{1}$$

where φ_n's are Slater type orbitals, STO, $\hat{\mathrm{H}}_{\mathrm{el}} = \hat{\mathrm{H}}^0 + \hat{\mathrm{V}}$, is the electrostatic model hamiltonian, P_k^m – Legendre polynomials and $R_n(k)$ electrostatic potentials :

$$R_n(k) = \frac{(2\mu)^{2n+1}}{(2n)!\,\mu^{2n}} \left\{ \frac{(2n+k)!}{2^{2n+k+1}\,\alpha^{k+1}} - \alpha^{2n} \left[\underset{2n+k}{A}(2\alpha) - \underset{2n-k-1}{A}(2\alpha) \right] \right\} \tag{2}$$

where μ is the Slater exponent, $\alpha = R\mu/a_0$ (R – interatomic distance, a_0 – Bohr radius), A – incomplete gamma functions,[12] n – the principal quantum number and k, m – indices running over even numbers from 0 to 21 and all integer numbers from –1 to +1, respectively.

Master formulas for bicenter electrostatic integrals $< \varphi_n |\hat{\mathrm{V}}| \varphi_n >$ over real STO's with 1=2, 3 are given in Appendix.

The expressions for molecular orbital energies were estimated using the Generalized Angular Overlap Model,[11] where the antibonding MO energies for a cluster type molecule are of the form :

$$E_i^* = E_i^0 + \sum_k \sum_j {}^kD_{ij}^2\, \mathrm{e}_{\lambda(j)} + \sum_k \sum_{k'} \sum_j {}^kD_{ij}\, {}^{k'}D_{ij}\, \mathrm{e}_{\lambda(j)}^{k\,k'} + \ldots \tag{3}$$

where E_i^0 is the zero-order energy, the indices k, k' running over the ligand orbital set (atomic, hybrid or molecular), D_{ij} – the angular matrix

---

[6] H. H. Schmidtke. *Z. Naturforsch.*, **19a**, 1502 (1964).

[7] M. Kibler, "Travaux de Mécanique Ondulatoire Appliquée", 1967 (preprint).

[8] M. Kibler, *J. Chem. Phys.*, **55**, 1989 (1971).

[9] W. De Horrocks, Jr., *J. Amer. Chem. Soc.*, **94**, 656 (1972).

[10] C. E. Schäffer and C. K. Jørgensen, *Mol. Phys.*, **9**, 401 (1965).

[11] C. I. Lepădatu, *Z. phys. Chem.* (*Frankfurt*), **73**, 249 (1970).

[12] Yu. A. Kruglyak and D. R. Whitman, "Tables of Quantiom Chemistry Integrals", vol. 1, Computing Center Publ., Moscow, 1965.

elements necessary to bring the central atom orbital set from the proper coordinate Cartesian system to that of each ligand :

$$|i| = |{}^{k}D_{ij}||j|,$$

the indices i, j, running over the set of central atom orbitals, closed under the orbital quantum number "1". If the ligand-ligand interactions were neglected, the third term from (3) would vanish.

The quantity $e_{\lambda(j)}$ is the antibonding orbital energy, where λ is the bonding type σ, π, δ or Φ. The detailed expression for $e_{\lambda(j)}$ was given elsewhere,[11] the terms included into $e_{\lambda(j)}$ being in principle easily calculated using a monoelectronic model hamiltonian.

To prove the quantitative equivalence between the electrostatic potentials and the molecular antibonding energies consider both quantities as parameters, express $R_n(k)$ through $e_{\lambda(j)}$ from the CF splitting and differences between AOM levels, express the CF levels not used in calculations substituting $R_n(k)$ function by $e_{\lambda(j)}$ and then compare the results with those obtained directly by the AOM approximation. The calculations were performed for those coordination clusters belonging to lower symmetry groups, such that the number of energy levels be higher than that of $R_n(k)$ potentials.

We give below the energy levels for different clusters, belonging to lower symmetries calculated in both CF and AOM approximations. For the sake of simplicity, the energy expressions do not contain the zero-order energies, neither the $R_n(0)$ terms which do not contribute to the relative energy distances between levels.

I. CLUSTER WITH d-ORBITALS

$ML_4\,(D_{4h})$

$$E\,(A_{1g};\ z^2)\ \begin{cases} e_\sigma + 3e_\delta \\ -\ 0.571\ R_n\,(2) + 0.428\ R_n\ (4) \end{cases}$$

$$E\,(E_g\,;\ xz,\,yz)\ \begin{cases} 2e_\pi + 2e_\delta \\ -\ 0.285\ R_n\ (2) - 0.285\ R_n\ (4) \end{cases}$$

$$E\,(B_{1g}\,;\ x^2 - y^2)\ \begin{cases} 3e_\sigma + e_\delta \\ 0.571\ R_n\,(2) + 0.904\ R_n\ (4) \end{cases}$$

$$E\ (B_{2g}\,;\ xy)\ \begin{cases} 4e_\pi \\ 0.571\ R_n\ (2) - 0.761\ R_n\,(4) \end{cases}$$

$$E\,(A_{1g}) - E\,(B_{2g})\ \begin{cases} 0.998e_\sigma - 3.995e_\pi + 2.997\ e_\delta \\ e_\sigma - 4e_\pi + 3e_\delta \end{cases}$$

$$\mathrm{ML_5\ (C_{4v})}$$

$$E\,(A_1\,;\ z^2)\ \begin{cases} 17/16\mathrm{e}_\sigma + 9/4\mathrm{e}_\pi + 27/16\,\mathrm{e}_\delta \\ 0.142\ R_n\,(2) - 0.044\ R_n\,(4) \end{cases}$$

$$E\,(E\,;\ xz\,;\ yz)\begin{cases} 9/8\mathrm{e}_\sigma + 2\mathrm{e}_\pi + 15/8\mathrm{e}_\delta \\ 0.071\ R_n\,(2) + 0.029\ R_n\,(4) \end{cases}$$

$$E\,(B_1\,;\ x^2 - y^2)\begin{cases} 27/16\mathrm{e}_\sigma + 3/4\mathrm{e}_\pi + 41/16\mathrm{e}_\delta \\ \quad 0.142\ R_n\,(2) + 0.461\ R_n\,(4) \end{cases}$$

$$E\,(B_2\,;\ xy)\ \begin{cases} 3\mathrm{e}_\pi + 2\mathrm{e}_\delta \\ -\,0.142\ R_n\,(2) - 0.476\ R_n\,(4) \end{cases}$$

$$E\,(A_1) - E\,(B_2)\ \begin{cases} 1.06\mathrm{e}_\sigma - 0.75\mathrm{e}_\pi - 0.31\mathrm{e}_\delta \\ 1.006\mathrm{e}_\sigma - 0.675\mathrm{e}_\pi - 0.33\mathrm{e}_\delta \end{cases}$$

II. CLUSTER WITH f-ORBITALS

$$ML_3\ (D_{3h})$$

$$E_2\,(A_2''\,;\ \sigma)\ \begin{cases} 9/8\mathrm{e}_\pi + 15/8\mathrm{e}_\Phi \\ -\,0.400\ R_n\,(2) + 0.204\ R_n\,(4) - 0.218\ R_n\,(6) \end{cases}$$

$$E\,(E''\,;\ \bar{\delta},\ \delta)\ \begin{cases} 15/16\mathrm{e}_\pi + 3/2\mathrm{e}_\delta + 9/16\mathrm{e}_\Phi \\ -\,0.238\ R_n\,(4) - 0.065\ R_n\,(6) \end{cases}$$

$$E\,(E\,;\ \bar{\pi},\ \pi)\ \begin{cases} 9/16\mathrm{e}_\sigma + 3/32\mathrm{e}_\pi + 15/16\mathrm{e}_\delta + 45/32\mathrm{e}_\Phi \\ -\,0.300\ R_n(2) + 0.034\ R_n\,(4) + 0.163\ R_n\,(6) \end{cases}$$

$$E\,(A_2'\,;\ \Phi)\ \begin{cases} 45/16\mathrm{e}_\pi + 3/16\mathrm{e}_\Phi \\ 0.499\ R_n\,(2) + 0.102\ R_n(4) - 0.491\ R_n\,(6) \end{cases}$$

$$E\,(A_1'\,;\ \bar{\Phi})\begin{cases} 15/8\mathrm{e}_\sigma + 9/8\mathrm{e}_\delta \\ 0.499\ R_n\,(2) + 0.102\ R_n\,(4) + 0.513\ R_n\,(6) \end{cases}$$

$$E\,(A_2'') - E(A_1')\ \begin{cases} -\,1.87\mathrm{e}_\sigma + 1.12\mathrm{e}_\pi - 1.12\mathrm{e}_\delta + 1.87\mathrm{e}_\Phi \\ -\,1.82\mathrm{e}_\sigma + 1.01\mathrm{e}_\pi - 1.02\mathrm{e}_\delta + 1.56\mathrm{e}_\Phi \end{cases}$$

$ML_4\ (D_{4h})$

$$E(A_{2u};\ \sigma)\begin{cases}3/2e_\pi+5/2e_\Phi\\ -\ 0.533\ R_n\,(2)+0.272\ R_n\,(4)-0.290\ R_n\,(6)\end{cases}$$

$$E\ (B_{1u};\ \bar{\delta})\begin{cases}4e_\delta\\ -\ 0.848\ R_n\,(4)-0.279\ R_n\,(6)\end{cases}$$

$$E\ (B_{2u};\ \delta)\begin{cases}5/2e_\pi+3/2e_\Phi\\ 0.212\ R_n\,(4)-0.454\ R_n\,(6)\end{cases}$$

$$E\ (E_u;\ \pi,\ \bar{\pi})\begin{cases}3/4e_\sigma+1/8e_\pi+5/4e_\delta+15/8e_\Phi\\ -\ 0.400\ R_n\,(2)+0.045\ R_n\,(4)+0.218\ R_n\,(6)\end{cases}$$

$$E(E_u;\ \Phi,\bar{\Phi})\begin{cases}5/4e_\sigma+15/8e_\pi+3/4e_\delta+1/8e_\Phi\\ 0.664\ R_n\,(2)+0.136\ R_n\,(4)+0.014\ R_n\,(6)\end{cases}$$

$$E\ (A_{2u})-E\ (E_u)\begin{cases}-\ 1.25e_\sigma-0.375e_\pi+2.375e_\Phi-0.75e_\delta\\ -\ 1.25e_\sigma-0.54e_\pi+2.62e_\Phi-0.76e_\delta\end{cases}$$

$ML_5\ (D_{3h})$

$$E\ (A_2'';\ \sigma)\begin{cases}2e_\sigma+9/8e_\pi+15/18e_\Phi\\ 0.132\ R_n\,(2)+0.567\ R_n\,(4)+0.247\ R_n\,(6)\end{cases}$$

$$E\ (E'';\ \bar{\delta},\ \delta)\begin{cases}15/16e_\pi+7/2e_\delta+9/16e_\Phi\\ -\ 0.662\ R_n\,(4)+0.074\ R_n\,(6)\end{cases}$$

$$E\ (E';\ \bar{\pi},\ \pi)\begin{cases}9/16e_\sigma+67/32e_\pi+15/16e_\delta+45/32e_\Phi\\ 0.100\ R_n\,(2)+0.094\ R_n\,(4)-0.186\ R_n\,(6)\end{cases}$$

$$E\ (A_1';\ \Phi)\begin{cases}15/8e_\sigma+9/8e_\delta+2e_\Phi\\ -\ 0.168\ R_n\,(2)+0.283\ R_n\,(4)+0.490\ R_n\,(6)\end{cases}$$

$$E\ (A_2';\ \bar{\Phi})\begin{cases}45/16e_\pi+35/16e_\Phi\\ -\ 0.168\ R_n\,(2)+0.283\ R_n\,(4)-0.514\ R_n\,(6)\end{cases}$$

$$E\ (A_2'')-E\ (A_2')\begin{cases}2.04e_\sigma-1.56e_\pi-0.043e_\delta-0.44e_\Phi\\ 2e_\sigma-1.68e_\pi\qquad\qquad\qquad\ -0.31e_\Phi\end{cases}$$

$\mathrm{ML}_5\ (\mathrm{C}_{4\mathrm{v}})$

$$E\,(A_1;\ \sigma)\left\{\begin{array}{l}113/64\mathrm{e}_\sigma + 9/128\mathrm{e}_\pi + 135/64\mathrm{e}_\delta + 135/128\mathrm{e}_\Phi\\ 0.133\ R_n\,(2) - 0.028\ R_n\,(4) + 0.534\ R_n\,(6)\end{array}\right.$$

$$E\,(E;\ \pi;\ \bar{\pi})\ \left\{\begin{array}{l}9/256\mathrm{e}_\sigma + 1357/512\mathrm{e}_\pi + 510/512\mathrm{e}_\delta + 675/512\mathrm{e}_\Phi\\ 0.100\ R_n\,(2) - 0.004\ R_n\,(4) - 0.400\ R_n(6)\end{array}\right.$$

$$E\,(E;\ \Phi,\ \bar{\Phi})\left\{\begin{array}{l}135/256\mathrm{e}_\sigma + 675/512\mathrm{e}_\pi + 738/512\mathrm{e}_\delta + 877/512\mathrm{e}_\Phi\\ -\ 0.166\ R_n\,(2) - 0.014\ R_n\,(4) - 0.026\ R_n\,(6)\end{array}\right.$$

$$E\,(B_2;\ \bar{\delta})\left\{\begin{array}{l}15/8\mathrm{e}_\pi + 2\mathrm{e}_\delta + 9/8\mathrm{e}_\Phi\\ -\ 0.265\ R_n\,(4) - 0.200\ R_n\,(6)\end{array}\right.$$

$$E\,(B_1;\ \delta)\ \left\{\begin{array}{l}135/64\mathrm{e}_\sigma + 15/128\mathrm{e}_\pi + 130/128\mathrm{e}_\delta + 225/128\mathrm{e}_\Phi\\ 0.331\ R_n(4) + 0.521\ R_n\,(6)\end{array}\right.$$

$$E(A_1) - E(B_1)\left\{\begin{array}{l}-\ 0.35\mathrm{e}_\sigma - 0.037\mathrm{e}_\pi + 1.09\mathrm{e}_\delta - 0.70\mathrm{e}_\Phi\\ -\ 0.34\mathrm{e}_\sigma - 0.04\mathrm{e}_\pi + 1.09\mathrm{e}_\delta - 0.70\mathrm{e}_\Phi\end{array}\right.$$

$\mathrm{ML}_6\ (D_{3h})$

$$E\,(A_2'';\ \sigma)\left\{\begin{array}{l}3/15\mathrm{e}_\sigma + 81/32\mathrm{e}_\pi + 45/16\mathrm{e}_\delta + 15/23\mathrm{e}_\Phi\\ 0.400\ R_n\,(2) - 0.443\ R_n\,(4) - 0.207\ R_n\,(6)\end{array}\right.$$

$$E\,(E'';\ \bar{\delta},\ \delta)\ \left\{\begin{array}{l}45/32\mathrm{e}_\sigma + 135/64\mathrm{e}_\pi + 3/32\mathrm{e}_\delta + 153/64\mathrm{e}_\Phi\\ 0.517\ R_n\,(4) - 0.062\ R_n(6)\end{array}\right.$$

$$E\,(E';\ \bar{\pi},\ \pi)\left\{\begin{array}{l}81/64\mathrm{e}_\sigma + 201/128\mathrm{e}_\pi + 135/64\mathrm{e}_\delta + 135/128\mathrm{e}_\Phi\\ 0.300\ R_n\,(2) - 0.073\ R_n\,(4) - 0.155\ R_n\,(6)\end{array}\right.$$

$$E\,(A_1';\ \Phi)\ \left\{\begin{array}{l}15/32\mathrm{e}_\sigma + 45/64\mathrm{e}_\pi + 81/32\mathrm{e}_\delta + 147/64\mathrm{e}_\Phi\\ 0.499\ R_n\,(2) - 0.221\ R_n\,(4) + 0.136\ R_n\,(6)\end{array}\right.$$

$$E\,(A_2';\ \Phi')\ \left\{\begin{array}{l}45/23\mathrm{e}_\sigma + 9/4\mathrm{e}_\delta + 75/32\mathrm{e}_\Phi\\ -\ 0.499\ R_n\,(2) - 0.221\ R_n\,(4) - 0.115\ R_n\,(6)\end{array}\right.$$

$$E\,(A_2'') - E\,(A_2')\ \left\{\begin{array}{l}0.15\mathrm{e}_\sigma + 1.05\mathrm{e}_\pi + 0.52\mathrm{e}_\delta - 1.74\mathrm{e}_\Phi\\ 0.18\mathrm{e}_\sigma + 1.12\mathrm{e}_\pi + 0.56\mathrm{e}_\delta - 1.87\mathrm{e}_\Phi\end{array}\right.$$

$$\mathrm{ML}_9\,(D_{3h})$$

$$E\,(A_2''\,;\,\sigma)\begin{cases}3/16\mathrm{e}_\sigma + 117/32\mathrm{e}_\pi + 45/16\mathrm{e}_\delta + 75/32\mathrm{e}_\Phi\\ -\,0.238\ R_n\,(4) - 0.426\ R_n\,(6)\end{cases}$$

$$E\,(E''\,;\,\bar{\delta},\,\delta)\begin{cases}45/32\mathrm{e}_\sigma + 195/64\mathrm{e}_\pi + 51/32\mathrm{e}_\delta + 189/64\mathrm{e}_\Phi\\ 0.278\ R_n\,(4) - 0.127\ R_n\,(6)\end{cases}$$

$$E\,(E'\,;\,\bar{\pi},\,\pi)\begin{cases}117/64\mathrm{e}_\sigma + 213/128\mathrm{e}_\pi + 195/64\mathrm{e}_\delta + 315/128\mathrm{e}_\Phi\\ -\,0.039\ R_n\,(4) + 0.319\ R_n\,(6)\end{cases}$$

$$E\,(A_1'\,;\,\Phi)\begin{cases}75/32\mathrm{e}_\sigma + 45/64\mathrm{e}_\pi + 117/32\mathrm{e}_\delta + 147/64\mathrm{e}_\Phi\\ -\,0.119\ R_n\,(4) + 0.649\ R_n\,(6)\end{cases}$$

$$E\,(A_2'\,;\,\bar{\Phi})\begin{cases}135/32\mathrm{e}_\pi + 9/4\mathrm{e}_\delta + 81/32\mathrm{e}_\Phi\\ -\,0.119\ R_n\,(4) - 0.607\ R_n\,(6)\end{cases}$$

$$E\,(A_2'') - E\,(A_2')\begin{cases}-\,1.9\mathrm{e}_\sigma + 2.69\mathrm{e}_\pi - 0.83\mathrm{e}_\delta + 0.07\mathrm{e}_\Phi\\ -\,2.15\mathrm{e}_\sigma + 2.95\mathrm{e}_\pi - 0.84\mathrm{e}_\delta + 0.04\mathrm{e}_\Phi\end{cases}$$

The CF energies were calculated using the master formulas given in the Appendix and the Legendre polynomials tabulated in reference. [13]

The AOM energies were calculated by means of formula (3) neglecting the bond-bond interactions and using the angular matrices reported elsewhere.[6,10,14,15]

As may be seen from the cases considered above, the agreement between the predicted and calculated energy expressions for the orbital splittings (the energy differences at the end of each example, the first line indicating the predicted energy and the second one the direct AOM results) justifies the existence of a quantitative equivalence between the electrostatic potentials and the MO energies. In other words, all the crystal field approaches widely spread among the chemists and physicists are nothing else but parametric MO alternatives, with the single difference that the first ones do not take into consideration the chemical bonding types according to which the MO theory classifies the bonding and antibonding orbital energies in the molecule.

---

[13] "Tables des Fonctions de Legendre Associées", Ed. de la Revue d'Optique, Paris, 1952.

[14] C. E. Schäffer, *Struct. Bonding*, **5**, 68 (1968).

[15] P. Spacu and C. I. Lepădatu, *Rev. Roumaine Chim.*, **17**, 335 (1972).

APPENDIX

$$(nd_{z^2} \mid nd_{z^2}) = R_n\,(0) + 2/7\,[P_2^0\,(\cos\theta_i)\cdot R_n\,(2) + P_4^0\,(\cos\theta_i)\cdot R_n\,(4)]$$

$$(nd_{x^2-y^2} \mid nd_{x^2-y^2}) = R_n\,(0) - 2/7 P_2^0\,(\cos\theta_i)\cdot R_n(2) + 1/21\,[P_4^0\,(\cos\theta_i) +$$

$$+ 1/24\,P_4^4\,(\cos\theta_i)\cos 4\varphi]\,R_n\,(4)$$

$$(nd_{xy} \mid nd_{xy}) = R_n\,(0) - 2/7 P_2^0\,(\cos\theta_i)\cdot R_n\,(2) + 1/21\,[P_4^0\,(\cos\theta_i) -$$

$$- 1/24\,P_4^4\,(\cos\theta_i)\cos 4\varphi]\,R_n\,(4)$$

$$(nd_{xz} \mid nd_{xz}) = R_n\,(0) + 1/7\,[P_2^0\,(\cos\theta_i) + 1/2\,P_2^2\,(\cos\theta_i)\cos 2\varphi]\,R_n\,(2) -$$

$$- 4/21\,[P_4^0\,(\cos\theta_i) - 1/12\,P_4^2\,(\cos\theta_i)\cos 2\varphi]\,R_n\,(4).$$

$$(nd_{yz} \mid nd_{yz}) = R_n\,(0) + 1/7\,[P_2^0\,(\cos\theta_i) - 1/2\,P_2^2\,(\cos\theta_i)\cos 2\varphi]\,R_n\,(2) -$$

$$- 4/21\,[P_4^0\,(\cos\theta_i) + 1/12\,P_4^2\,(\cos\theta_i)\cos 2\varphi]\,R_n\,(4).$$

$$(nf_{y(3x^2-y^2)} \mid nf_{y(3x^2-y^2)}) = R_n\,(0) - 1/3\,P_2^0\,(\cos\theta_i)\cdot R_n(2) + 1/11\,P_4^0\,(\cos\theta_i)\cdot R_n\,(4) -$$

$$- 5/429\,[P_6^0\,(\cos\theta_i) + 1/720\,P_6^6\,(\cos\theta_i)\cos 6\varphi]\,R_n\,(6)$$

$$(nf_{x(x^2-3y^2)} \mid nf_{x(x^2-3y^2)}) = R_n\,(0) - 1/3\,P_2^0\,(\cos\theta_i)\cdot R_n\,(2) + 1/11\,P_4^0\,(\cos\theta_i)\cdot R_n(4) -$$

$$- 5/429\,[P_6^0\,(\cos\theta_i) - 1/720\,P_6^6\,(\cos\theta_i)\cos 6\varphi]\,R_n\,(6).$$

$$(nf_{xyz} \mid nf_{xyz}) = R_n\,(0) - 7/33\,[P_4^0\,(\cos\theta_i) + 1/168\,P_4^4\,(\cos\theta_i)\cos 4\varphi]\,R_n\,(4) +$$

$$+ 10/143\,[P_6^0\,(\cos\theta_i) - 1/360\,P_6^4\,(\cos\theta_i)\cos 4\varphi]\,R_n\,(6).$$

$$(nf_{z(x^2-y^2)} \mid nf_{z(x^2-y^2)}) = R_n\,(0) - 7/33[P_4^0\,(\cos\theta_i) - 1/168\,P_4^4\,(\cos\theta_i)\cos 4\varphi]\,R_n\,(4) +$$

$$+ 10/143\,[P_6^0\,(\cos\theta_i) + 1/360\,P_6^4\,(\cos\theta_i)\cos 4\varphi]\,R_n\,(6).$$

$$(nf_{y\,(5z^2-r^2)} \mid nf_{y(5z^2-r^2)}) = R_n\,(0) + 1/5\,[P_2^0\,(\cos\theta_i) - 1/3\,P_2^2\,(\cos\theta_i)\cos 2\varphi] R_n\,(2) +$$

$$+ 1/33\,[P_4^0\,(\cos\theta_i) - 1/3\,P_4^2\,(\cos\theta_i)\cos 2\varphi]\,R_n\,(4) -$$

$$- 25/143\,[P_6^0\,(\cos\theta_i) + 1/30\,P_6^2\,(\cos\theta_i)\cos 2\varphi]\,R_n\,(6).$$

APPENDIX *(continued)*

$$(\mathrm{n}f_{x(5z^2 - r^2)} \mid nf_{x(5z^2 - r^2)}) = R_n\,(0) + 1/5\,[P_2^0\,(\cos\theta_i) + 1/3\,P_2^2\,(\cos\theta_i)\cos 2\varphi]R_n\,(2) +$$

$$+ 1/33\,[P_4^0\,(\cos\theta_i) + 1/3\,P_4^2\,(\cos\theta_i)\cos 2\varphi]R_n\,(4) -$$

$$- 25/143\,[P_6^0\,(\cos\theta_i) - 1/30\,P_6^2\,(\cos\theta_i)\cos 2\varphi]\,R_n\,(6).$$

$$(nf_{z(5z^2 - 3r^2)} \mid nf_{z(5z^2 - 3r^2)}) = R_n\,(0) + 4/15\,P_2^0\,(\cos\theta_i)\cdot R_n(2) + 2/11\,P_4^0\,(\cos\theta_i)\,R_n\,(4) +$$

$$+ 100/429\,P_6^0\,(\cos\theta_i)\cdot R_n\,(6).$$

Revue Roumaine de Chimie, **19**, *4*, 533–541 (1974)

Revue Roumaine de Chimie, **19**, *4*, 543–551 (1974)

THE CORROSION OF CARBON STEEL AND SOME AUSTENITIC STAINLESS STEELS IN SYNTHETIC RIVER WATERS

SULTANA CIOLAC and O. RADOVICI

Institute of Physical Chemistry,
Str. Galaţi 31, Bucharest, Romania

Received May 14, 1973

Gravimetric and electrochemical methods have been used to determine the rate of corrosion of carbon steel and some austenitic stainless steels in synthetic river waters as function of chemical composition, temperature and stirring of corrosion media.

The obtained results have shown that the corrosion of carbon steel is controlled by the water oxygen content and that, in certain conditions, stainless steels are susceptible to pitting attack.

Even though the problem of ferrous alloys corrosion in waters has been extensively studied, the effects of several factors having a great influence on their corrosion behaviour, such as metallic composition and aggressive medium conditions, are not completely clarified today.

The object of this research was to determine the influence of a few factors on the corrosion rate of corrosive attack of carbon steel and some austenitic stainless steels.

PROCEDURE

Our observations have been made on a carbon steel and two stainless steels, having the compositions listed in table 1.

Table 1

The composition of the steels tested

Type of steel	Composition %								
	C	S	P	Mn	Si	Cr	Ni	Mo	Ti
N° 1	0.18	0.022	0.025	0.35	0.03	—	—	—	—
N° 2	$\leqslant$0.10	—	—	$\leqslant$2	$\leqslant$1	18	10	—	$\geqslant$5C
N° 3	$\leqslant$0.10	—	—	$\leqslant$2	$\leqslant$1	17.50	11.50	2.25	$\geqslant$5C

The tested steels were machined either in parallelepipedal samples (for gravimetric measurements) or in cylindric electrodes (for electrochemical measurements), having an average surface of 6 sq.cm. Before the exposure, the surfaces were mechanically polished on emery paper, then degreased in boiling benzene and chemically polished by pickling, using 5% HNO_3 for carbon steel and a mixture of HNO_3-HF-H_2O for stainless steels at 70°. After pickling, the surfaces were washed with tap water, distilled water and then acetone dried.

The synthetic river waters used in these experiments, were prepared from reagent grade chemicals and doubly distilled water. Their compositions are listed in table 2.

Table 2

The composition of synthetic river waters

Ionic content mg/l	Type of water				
	A	B	C	D	E
Ca^{2+}	52.1	89.4	89.4	89.4	89.4
Mg^{2+}	4.6	15.5	15.5	15.5	15.5
Na^{+}	20.94	68.4	79.67	228	420
K^{+}	3.58	5.43	5.43	5.43	5.43
SO_4^{2-}	49.27	67.30	67.30	67.30	67.30
Cl^{-}	31.51	163.79	250	500	800
HCO_3^{-}	134.54	159.21	159.21	159.21	159.21

The rate of corrosion of carbon steel was determined from the loss in weight of the samples exposed in stagnant conditions at room temperature, 50 and 80°, and in stirring conditions at room temperature, using a rotary stirrer of 40 r.p.m.

Independently of the exposure conditions, generally a ratio of 6 sq.cm/125 ml (exposed surface/quantity of electrolyte) was respected.

An X-ray analysis was made for the corrosion products formed by carbon steel exposure in doubly distilled water in stagnant conditions at room temperature and 80°.

For carbon steel, additional electrochemical measurements were also made.

The rates of corrosion of stainless steels were determined by electrochemical polarization.

The cylindric electrodes were assembled in a glass tub (being pressed on a Teflon gasket and threaded in a copper wire) and then placed in the centre of the electrochemical cell. A platinum gauze was used as counter electrode and an Ag/AgCl electrode, as reference.

The electrochemical measurements were made potentiostatically (step-by-step) applying 50 mV/5 min, from a Wenking potentiostate. The resulting currents were registred on a chart SEFRAM recorder.

RESULTS

CARBON STEEL

The variation in corrosion rates of carbon steel (mdd) exposed in A, B, C waters for 1–30 days, at room temperature, 50 and 80°, in stagnant conditions, is shown in figures 1, 2 and 3.

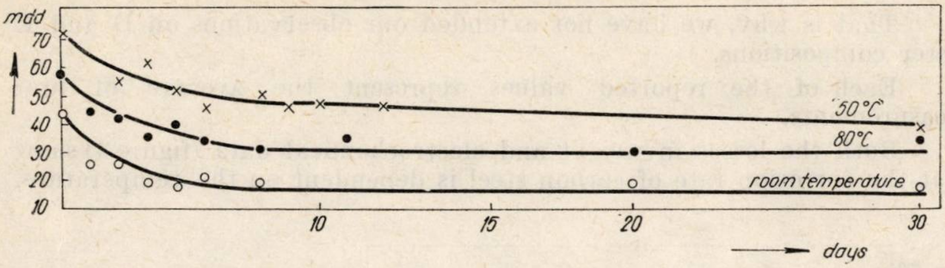

Fig. 1. — Time dependence of carbon steel corrosion rate, exposed in A composition water at different temperatures.

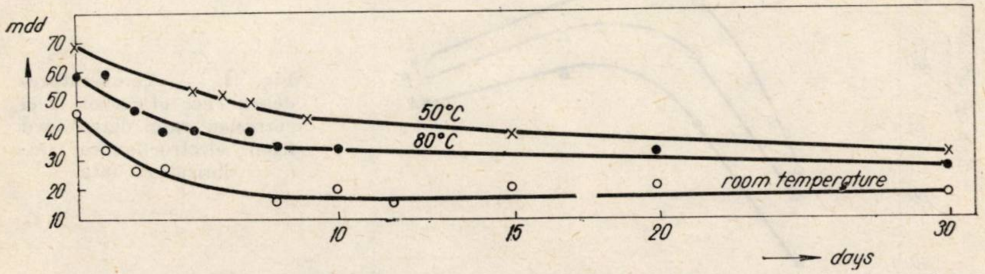

Fig. 2. — The dependence of carbon steel corrosion rate on temperature, for 1—30 days exposure in B synthetic river water and stagnant conditions.

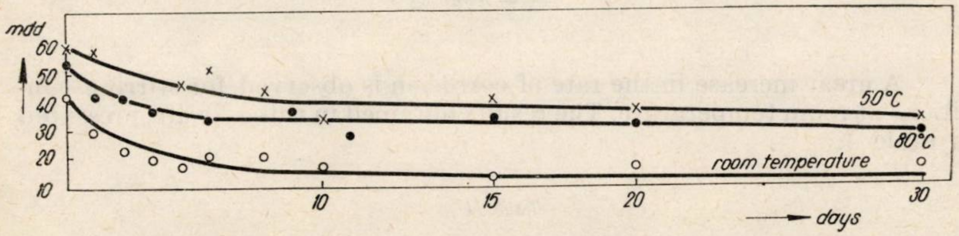

Fig. 3. — The variation in carbon steel corrosion rate as function of temperature for 1—30 days exposure in C water composition and stagnant conditions.

As can be seen from the above figures and from the amount of metal lost (mg/dm^2), only for a few exposure times (table 3), at the same temperature the rate of corrosion is nearly uninfluenced by water composition.

Table 3

The loss in weight of carbon steel (mg/dm^2), at room temperature, in stagnant conditions

Exposure time days	Type of water		
	A	B	C
1	44	46	42
3	83	86	70
6	130	130	130
8	150	140	168
15	408	300	350
30	532	560	528

That is why, we have not extended our observations on D and E water compositions.

Each of the reported values represent the average of four measurements.

Both the losses in weight and electrochemical data (figure 4) show that the corrosion rate of carbon steel is dependent on the temperature.

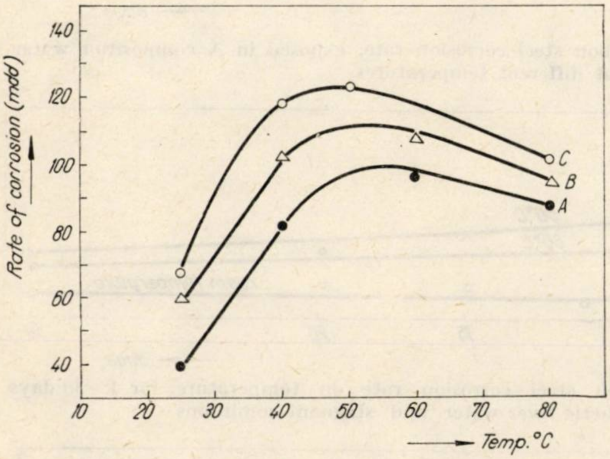

Fig. 4. — Temperature-dependence of carbon steel corrosion rate, determined from electrochemical polarization data.

A great increase in the rate of corrosion is observed for stirring conditions at room temperature. The results obtained in this case are presented in table 4.

Table 4

The loss in weight of carbon steel in stirring conditions at room temperature (mg/dm²)

Exposure time days	Type of water		
	A	B	C
1	160	200	175
3	380	350	360
6	690	630	610
10	860	870	830
30	1090	1100	1000

STAINLESS STEELS

Very well-known tendency of stainless steels to pitting in electrolytes containing halide ions, have determined us to prepare waters with high concentrations of chloride ions (D and E compositions).

In the case of stainless steel, the loss in weight technique seems inconvenient, because of the difficulty in passive film removing. Stainless steel samples, exposed for long time in synthetic water, have shown an increase in weight, proving the formation of oxide film on the surface.

Current-potential curves obtained potentiostatically (starting from −1000mV to noble potentials), were used to determine the rate of corrosion (in the absence of pitting), as well as to find out the conditions in which a localized attack occurs, as function of water composition and temperature. The results obtained are presented in tables 5 and 6.

Table 5

The corrosion rate of stainless steel No 2 and its pitting susceptibility as function of water composition and temperature (mdd)

Tempera-ture °C	Type of water				
	A	B	C	D	E
25	0.29	0.36	0.39	*	*
40	0.36	0.42	0.47	*	*
50	0.72	0.79	0.78	*	*
60	0.84	1.09	*	*	*
70	1.17	*	*	*	*

* – pitting

Table 6

The rate of corrosion of stainless steel No 3 and its pitting susceptibility as function of water composition and temperature (mdd)

Tempera-ture °C	Type of water				
	A	B	C	D	E
25	0.23	0.25	0.33	0.34	0.3
40	0.37	0.47	0.52	*	*
50	0.71	0.94	1.73	*	*
60	1.04	1.13	*	*	*
70	2.17	*	*	*	*

* – pitting

These results show the dependence of corrosion rate on both parameters.

The anodic control of the corrosion process is illustrated in figure 5.

Some differences seem to exist between the two stainless steels. For instance, in the same water and at the same temperature, stainless steel N° 3 shows a little better resistance to the pitting attack (figures 6*a* and *b*).

The increasing tendency to pitting, with an increasing content in chloride ions in waters, may be observed in figure 7.

The same effect results from the temperature increase.

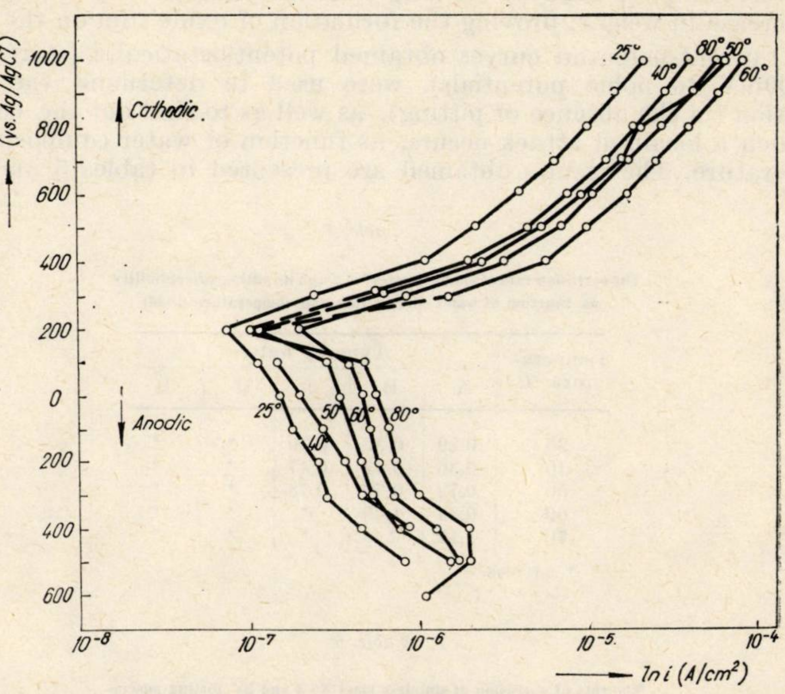

Fig. 5. — Cathodic-anodic polarisation curves of stainless steel N° 3 in B water, at different temperatures.

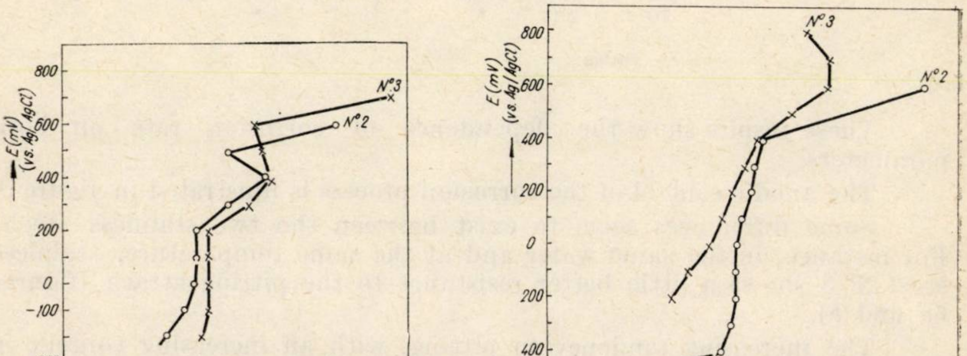

Fig. 6. — The effect of stainless steel composition on pitting susceptibility; *a*) at 80° in C water and *b*) at 25° in E water.

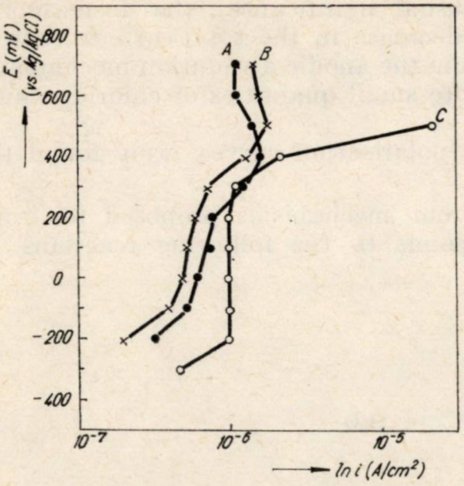

Fig. 7. — The effect of water composition on pitting susceptibility of stainless steel N° 3 at 60°.

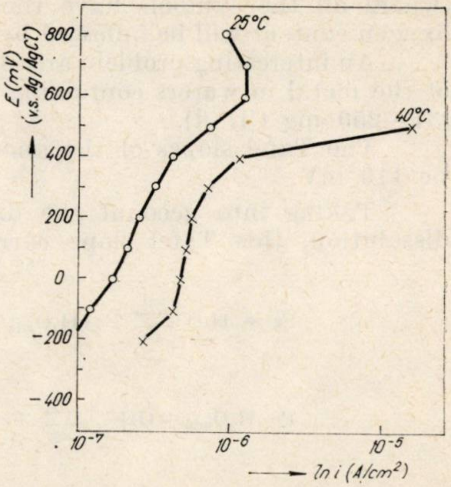

Fig. 8. — Temperature dependence of the pitting tendency of stainless steel N° 3 exposed in E water composition.

DISCUSSION

CARBON STEEL

From the results presented some conclusions may be drawn with regard to the corrosion mechanism of carbon steel in oxygen saturated water, containing small quantities of ions with high capacity of specific adsorption (chloride ions), as well as to the time evolution of the corrosion process.

The dissolution mechanism of carbon steel. As it is known, the corrosion process in neutral medium occurs under cathodic control of oxygen reduction.

Both gravimetric and electrochemical measurements show that the rate of corrosion in oxygen saturated water increases until a certain temperature is attained (~60°) and then decreases. This dependence of the corrosion rate on the temperature may be easily explained taking into account the activated character of the corrosion process, which supposes an increase in the corrosion rate as temperature increases. On the other hand, the corrosion rate is directly dependent on the content of oxygen dissolved, whose concentration decreases with temperature increase.

Thus, if the corrosion rate is determined by the cathodic current of oxygen reduction

$$i_L = zFDC_{O_2}\, 1/\delta \qquad (1)$$

(where all the symbols have their usual significance), the decrease in oxygen content will be followed by a decrease in the total corrosion rate.

An interesting problem arises from the anodic dissolution mechanism of the metal in waters containing quite small quantities of chloride ions ($31-250$ mg CL^-/l).

The Tafel slopes of the anodic polarisation curves were found to be 110 mV.

Taking into account the different mechanisms proposed for iron dissolution, this Tafel slope corresponds to the following reactions[1]:

$$Fe + H_2O \underset{-1}{\overset{-1}{\rightleftharpoons}} Fe \cdot H_2O_{ads}$$

$$Fe \cdot H_2O_{ads} + OH^- \underset{-2}{\overset{2}{\rightleftharpoons}} Fe\,OH^-_{ads} + H_2O$$

$$Fe\,OH^-_{ads} \underset{-3}{\overset{3}{\rightleftharpoons}} FeOH_{ads} + e^-$$

$$Fe\,OH_{ads} \xrightarrow{4} Fe\,OH^+ + e^- \text{ (the rate determining step)}$$

$$Fe\,OH^+ \underset{-5}{\overset{5}{\rightleftharpoons}} Fe^{2+} + OH^-$$

respecting the next kinetic equation

$$\frac{i_a}{F} = 2K_4\,\theta_{OH} - \left(\frac{K_1}{K_{-1}}\right)^{1/2} \exp\,(F\varphi/2RT) \qquad (2)$$

where : i_a is the anodic current density, θ_{OH} — is the surface coverage degree with OH^- ions, K_1, K_{-1}, K_4 are the equilibrium constants of the corresponding reactions, the other symbols having their usual meaning.

Such a mechanism supposes an absorbant-adsorbant interaction and not an adsorption-desorption one.

Thus, it may be concluded that in the dissolution process of carbon steel in electrolytes containing small concentrations of chloride ions there is no competition between chloride ions, water molecules and hydroxyl ions.

In other words, the anodic dissolution at these concentrations is controlled by H_2O and OH^- ions and not by Cl^- ions.

Time evolution of the corrosion process shows that the rate of corrosion decreases gradually in the first days and remains nearly constant after 10 days (figures 1, 2 and 3).

---

[1] MC. CAFFERTY and N. HACKERMAN, *J. Electrochem. Soc.*, **119**, 999 (1972).

This may be explained considering the possible secondary reactions due to the chemical transformation of hydrated iron oxides formed on the metallic surface under exposure conditions.

X-ray analysis of the corrosion products, covering the surface by exposure in distilled water, has shown that they are formed from quasi-amorphous hydrated oxides.

The protection conferred to the surface depends on their degree of adherence and compactness. The more adherent and compact the corrosion products layers are, the lower the corrosion rate is.

The inactivity showed by the hydrated oxides and hydroxides may be supported by the mechanism of oxolation and ollation processes. It might be appreciated that the decrease in corrosion rate of carbon steel depends on the rate of ollation and oxolation processes of the corrosion products covering the surface. These processes are accelerated by the temperature increase, in other words, the higher the temperature, the sooner the corrosion products become more compact. This fact is confirmed by our results. The great increase in the corrosion rate measured in stirring condition is due, on the one hand, to the smaller quantities of the corrosion products deposited on the surface allowing a permanent contact with the aggressive medium, and, on the other hand, to the convective transport of oxygen to the surface.[2,3]

STAINLESS STEELS

It was not our purpose to determine exactly the nucleating pitting potential values, but from the presented figures and listed data, some conclusions may be drawn about pitting susceptibility of the two stainless steels tested.

The higher the temperature and the bigger the chloride concentrations are, the stronger the tendency to pitting is. From these points of view, our results are in good agreement with some other published data.[4,5]

No conclusions in connection with the effect of metallic composition may be drawn, because the two stainless steels studied differ not only in molybdenum presence, but in nickel content, too. Both these constituents are able to give such an effect,[5,6] explaining the better resistance observed for stainless steel N° 3.

The existence, in all the cases studied, of at least 400 mV passive range, explains why no pits were formed on the metallic surface, after more than 1 year exposure, under stagnant conditions.

---

[2] C. F. Cheng, *Corrosion*, **20**, 341t (1964).

[3] H. R. Copson, *Corrosion*, **16**, 120 (1960).

[4] H. P. Heckie and H. H. Uhlig, *J. Electrochem. Soc.*, **113**, 1262 (1966).

[5] N. D. Tomashov and G. P. Chernova and O. N. Marcova, *Corrosion*, **20**, 116t (1964).

[6] J. Horvath and H. H. Uhlig, *J. Electrochem. Soc.*, **115**, 791 (1968).

This may be explained considering the possible secondary reactions due to the chemical transformation of hydrated iron oxides formed on the metallic surface under exposure conditions.

X-ray analysis of the corrosion products, covering the surface by exposure in distilled water, has shown that they are formed from quasi-amorphous hydrated oxides.

The protection conferred to the surface depends on their degree of adherence and compactness. The more adherent and compact the corrosion products layer is, the lower the corrosion rate is.

The inactivity showed by the hydrated oxides and hydroxides may be supported by the mechanism of oxidation and elution processes. It might be appreciated that the decrease in corrosion rate of carbon steel depends on the rate of elution and oxidation processes of the corrosion products covering the surface. These processes are accelerated by the temperature increase. In other words, the higher the temperature, the sooner the corrosion products become more compact. This fact is confirmed by our results. The great increase in the corrosion rate, measured in stream condition, is due, on the one hand, to the smaller quantities of the corrosion products deposited on the surface allowing a permanent contact with the aggressive medium, and, on the other hand, to the convective transport of oxygen to the surface.

STAINLESS STEELS

It was not our purpose to determine exactly the [illegible] pitting potential values, but from the presented figures and listed data, some conclusions may be drawn about pitting susceptibility of the two stainless steels tested.

The higher the temperature and the bigger the chloride concentration are, the stronger the tendency to pitting is. From these points of view, our results are in good agreement with some other published data.

No conclusions in connection with the effect of metallic components may be drawn, because the two stainless steels studied differ not only in chromium content, but in nickel content too. Both these constituents [illegible] explaining the better resistance observed for [illegible] steels.

The existence in all the cases studied of at least 100 mV passive range [illegible] the passive film formed on the metallic surface, after more than 1 year exposure, under the same conditions.

[illegible]

Revue Roumaine de Chimie, 19, 4, 553–559 (1974)

VISCOSITY OF BINARY MOLTEN ALKALI CHLORIDE SYSTEMS

ŞTEFANIA ZUCA and RODICA BORCAN

Institute of Physical Chemistry,

Str. Galaţi 31, Bucharest, Romania

Received August 3, 1973

Experimental data for the density and viscosity of (Li–K)Cl, (Li–Rb)Cl, (Li–Cs)Cl, (K–Rb)Cl, (K–Cs)Cl and (Rb–Cs)Cl systems are reported. The viscosity isotherms show the usual negative deviations from additivity. The observed $\Delta\eta$ increase with the difference between the cationic radii in the mixture and are found to obey the equation

$$\Delta\eta = a(r_1 - r_2)x_1x_2.$$

Carrying on our systematic study on the viscosity of binary mixtures of molten salts,[1–3] we presently report the results obtained in several alkali chloride mixtures: (Li–Rb)Cl; (Li–Cs)Cl; (K–Rb)Cl; (K–Cs)Cl and (Rb–Cs)Cl, for which no data are available in literature.

EXPERIMENTAL RESULTS

Both density and viscosity of pure salts and their mixtures (mole fraction $x = 0.25$; 0.50; 0.75) were determined over a temperature range of about 200°. All chemicals used in experiments were Merck or Analar (B.D.H.) *p. a.* reagent grade, twice recrystallized from water, dried for 24 h at 150° and melted while a dried HCl gas was bubbled through the melt, in order to remove any trace of humidity. LiCl melt was prepared by a special technique, successfully applied in our laboratory for very hygroscopic salts[4]. All salts were tested for neutrality with phenolphtalein, both before and after experiments.

A linear temperature dependence of density was observed over the whole temperature range covered in this work.

---

[1] I. G. Murgulescu and S. Zuca, *Electrochim. Acta*, **11**, 1383 (1966); **14**, 519 (1969).
[2] S. Zuca and R. Borcan, *ibid.*, **15**, 1817 (1970).
[3] S. Zuca and R. Borcan, *Rev. Roumaine Chim.*, **11**, 1681 (1970).
[4] S. Zuca and R. Costin, *ibid.*, **11**, 1831 (1970).

An Arrhenius plot expresses the temperature dependence of viscosity. Both density and viscosity data were fitted to the linear dependence by means of a least squares calculation. The equations for the linear fit are given in tables 1–4 along with the standard deviations and the applicable temperature range.

The present results on pure components, excepting CsCl, are in very good agreement with our earlier data.[5]

A comparison with the most recent literature data shows a satisfactory agreement for LiCl.[6,7] There is a close agreement with the literature[6,8] for KCl too, but considerably lower

Table 1

Density of single molten alkali chlorides

Salt	Density equations	Standard deviations	Temperature range °C
LiCl	$d=1.7562-0.4243\,t\times10^{-3}$	0.0003	605–800
KCl	$d=1.9564-0.5583\,t\times10^{-3}$	0.0002	780–900
RbCl	$d=2.8537-0.8514\,t\times10^{-3}$	0.0009	740–960
CsCl	$d=3.5023-1.0849t\times10^{-3}$	0.0008	660–820

Table 2

Viscosity of single molten alkali chlorides

Salt	Viscosity equation	E_{vis} cal/mol	Standard deviations for E_{vis}	Temperature range °C
LiCl	$\log\eta=-1.30016+1354.89\,1/T$	6200	64	620–810
KCl	$\log\eta=-1.26922+1403.84\,1/T$	6424	30	780–930
RbCl	$\log\eta=-1.14266+1286.42\,1/T$	5880	28	740–840
CsCl	$\log\eta=-1.07353+1177.65\,1/T$	5390	38	690–810

---

[5] I. G. Murgulescu and S. Zuca, *Z. phys. Chem.* (*Leipzig*), **222**, 300 (1963).

[6] M. V. Smirnov and B. A. Hohlov, *Akad. Nauk S.S.S.R. Uralskii Filial, Trudi Instituta Elektrokhimii*, **10**, 31 (1967).

[7] D. Dumas, B. Fjeld, K. Grojtheim and H. Øye, *Acta Chem. Scand.*, **27**, 319 (1973).

[8] N. V. Bondarenko and H. L. Streletz, "Fizicheskaia khimia i elektrokhimia rasplavlennych solei i schlakov", Izd. Khimia, Leningrad, 1968, p. 95.

Table 3

Density of (M_I-M_{II}) Cl systems

System	$x_{M_I Cl}$	Density equation	Standard deviations	Temperature range °C
(Li–Rb)Cl	0.75	$d=2.1429-0.5740\,t\times10^{-3}$	0.0006	604–810
	0.50	$d=2.4816-0.7384\,t\times10^{-3}$	0.0008	615–855
	0.25	$d=2.6642-0.7849\,t\times10^{-3}$	0.0008	611–802
(Li–Cs)Cl	0.75	$d=2.4229-0.6662\,t\times10^{-3}$	0.0005	608–807
	0.50	$d=2.9260-0.8833\,t\times10^{-3}$	0.0007	660–855
	0.25	$d=3.1820-0.9400\,t\times10^{-3}$	0.0012	611–807
(K–Rb)Cl	0.75	$d=2.2265-0.6694\,t\times10^{-3}$	0.0005	780–920
	0.50	$d=2.4348-0.7264\,t\times10^{-3}$	0.0010	780–900
	0.25	$d=2.6808-0.8249\,t\times10^{-3}$	0.0006	750–880
(K–Cs)Cl	0.75	$d=2.4491-0.7654\,t\times10^{-3}$	0.0006	750–875
	0.50	$d=2.8429-0.8840\,t\times10^{-3}$	0.0006	720–870
	0.25	$d=3.1863-0.9898\,t\times10^{-3}$	0.0007	690–870
(Rb–Cs)Cl	0.50	$d=3.2022-0.9910\,t\times10^{-3}$	0.0007	720–890

Table 4

Viscosity of (M_I-M_{II}) Cl systems

System	$x_{M_I Cl}$	Viscosity equation	$E_{vis.}$ cal/mol	Standard deviations for E_{vis}	Temperature range ° C
(Li–Rb)Cl	0.75	$\log\eta=-1.07675+1105.64\ 1/T$	5060	23	610–810
	0.50	$\log\eta=-1.20697+1265.54\ 1/T$	5791	31	610–815
	0.25	$\log\eta=-1.23806+1330.54\ 1/T$	6088	22	605–805
(Li–Cs)Cl	0.75	$\log\eta=-1.05317+1067.65\ 1/T$	4885	35	630–810
	0.50	$\log\eta=-1.16420+1212.25\ 1/T$	5550	25	640–820
	0.25	$\log\eta=-1.21303+1278.28\ 1/T$	5850	36	635–810
(K–Rb)Cl	0.75	$\log\eta=-1.15870+1281.71\ 1/T$	5865	81	775–845
	0.50	$\log\eta=-1.11520+1235.51\ 1/T$	5654	40	760–860
	0.25	$\log\eta=-1.10542+1230.34\ 1/T$	5630	42	775–840
(K–Cs)Cl	0.75	$\log\eta=-1.25879+1368.53\ 1/T$	6260	75	710–810
	0.50	$\log\eta=-1.23350+1334.99\ 1/T$	6109	57	625–830
	0.25	$\log\eta=-1.19416+1297.60\ 1/T$	5940	42	640–810
(Rb–Cs)Cl	0.50	$\log\eta=-1.20040+1316.25\ 1/T$	6023	59	670–845

(−11%) as well as higher values (+20%) are also reported by Dumas *et al.*[7] and Matsumura *et al.*[9], respectively. For RbCl, the agreement with [7] is very good but significantly higher values and a stronger temperature dependence is indicated by Janz and Reeves.[10]

A severe disagreement is found for viscosity of CsCl: the present results are by about 20% higher than our previous data[5]. With this in mind a special care was taken in purifying and melting the *p.a.* reagent grade CsCl. Samples of Merck suprapure reagent grade CsCl were also submitted to measurements. The equation for CsCl viscosity in table 2 was calculated from 56 experimental values, obtained on 1o different samples, both on heating and on cooling the melt. Only two investigations on the viscosity of CsCl have been reported in literature.[6,7] Very low values, in very good agreement with our former results [5] are reported by Smirnov and Hohlov [6]. The more recent data of Dumas *et al.*[7] are in a better agreement with our present results; the difference is of −5% at lower temperature but increases steadly with temperature to −10%.

As far as we know, a systematic investigation of viscosity in binary alkali chloride systems has not been published so far. The only data available refer to (Li−K)Cl[9] and (Li−Cs)Cl[6] systems. The results for (Li−K)Cl system were discussed elsewhere. Regarding (Li−Cs)Cl system, there is no agreement between our present data and the literature.[6] This is explained by the above mentioned discrepancies existing in the viscosity of pure CsCl melt. Moreover, even the dependence of viscosity on the composition of the mixture is different. The maximum in the CsCl rich region of viscosity isotherms reported by Smirnov and Hohlov [6] has never been observed by us.

DISCUSSION

For all presently studied systems, the plot of η *vs.* composition of the mixture, gives smooth curves which exhibit the usual negative deviations from linearity. Fig. 1 illustrates the results at 775°.

According to Rice-Alnatt theory,[11] the viscosity of an ideal binary mixture has to be additive. Since most of the ideal binary systems show systematic deviations of viscosity from linearity,[12] it was thought [7] necessary to resort to other semi-empirical theories. We believe that our previous investigations,[1−3] on the viscosity of binary molten salt systems, have proved the usefulness of additivity relationship in correlating the experimental data. Following out those results, we calculated the deviation from additivity, $\Delta\eta$, in the six presently studied alkali chloride mixtures and plotted the obtained values against mole fraction, as shown in fig. 2 for 775°. From the data in fig. 2 it is evident that the regularities established for molten binary nitrate systems [1,2] are found again:

— $\Delta\eta$ *vs.* composition curves are, within experimental errors, symmetrical, with the maximum at the value $x_1 = x_2 = 0.5$.

— $\Delta\eta$ are larger as the difference in size of the two cations in the mixture is larger.

---

[9] Y. Matsumura, M. Mizuno and K. Nishihara, Memoirs of the Faculty of Engineering, Kyoto University, vol. 29, Part. 4, 462 (1966).

[10] G. J. Janz and R. D. Reeves. *Trans. Faraday Soc.*, **61**, 2305 (1965).

[11] S. A. Rice and A. R. Alnatt, *J. Chem. Phys.*, **34**, 409 (1961).

[12] S. Bretsznajder, "Prediction of Transport and Other Physical Properties of Fluids", Pergamon Press, Oxford, 1971, p. 207.

As already stated,[1-3,13] due to the fact that transport properties depend on the energy of interaction between the ions, there is to expect that viscosity can be correlated with the length parameter. As seen in fig. 3, in all studied systems, the $\Delta\eta$ value for each composition varies linearly with the difference of the cationic radii. From fig. 3 it is obvious that, within experimental error, $\Delta\eta$ yields a straight line which passes through the origin, indicating that:

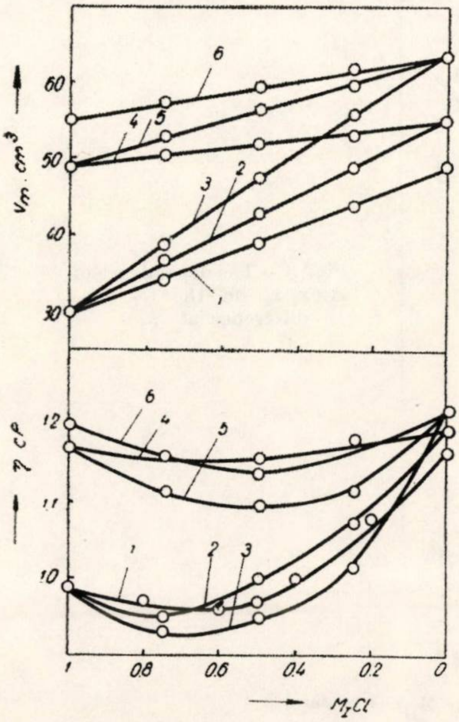

Fig. 1. — Isotherms of viscosity and molar volume at 775° in $M_I Cl - M_{II} Cl$ systems

1, (Li–K)Cl; 2, (Li–Rb)Cl; 3, (Li–Cs)Cl; 4, (K–Rb)Cl; 5, (K–Cs)Cl; 6, (Rb–Cs)Cl.

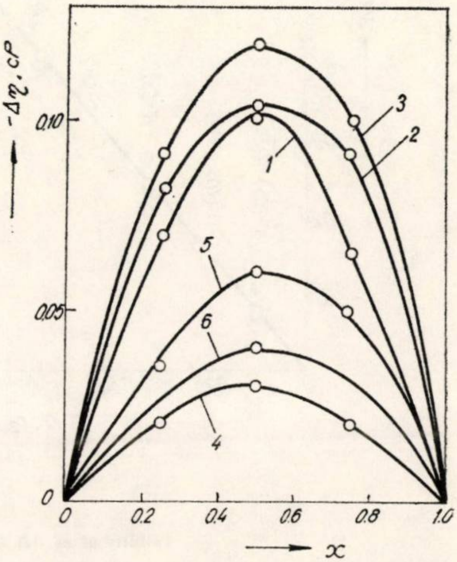

Fig. 2. — $\Delta\eta$ *vs.* molar fraction in $M_I Cl - M_{II} C$- systems at 775°.

1, (Li–K)Cl; 2, (Li–Rb)Cl; 3, (Li–Cs)Cl; 4, (K–Rb)Cl; 5, (K–Cs)Cl; 6, (Rb–Cs)Cl.

$$\Delta\eta = a(r_1 - r_2)x_1x_2 \qquad (1)$$

where *a* is a slightly temperature dependent parameter. Its kinetic molecular significance is given by Murgulescu[14] in terms of Eyring theory.

---

[13] S. Zuca and M. Olteanu, *Rev. Roumaine Chim.*, **15**, 357 (1970); **15**, 1503 (1970).

[14] I. G. Murgulescu, *J. Chim. phys. Numero special, Octobre*, **1969**, p. 43.

By subtracting from the additive value of viscosity the $\Delta\eta$ calculated with (1), it is possible to render the observed viscosity for each investigated mixture with a precision of $\pm 1\%$, as can be seen from the data in

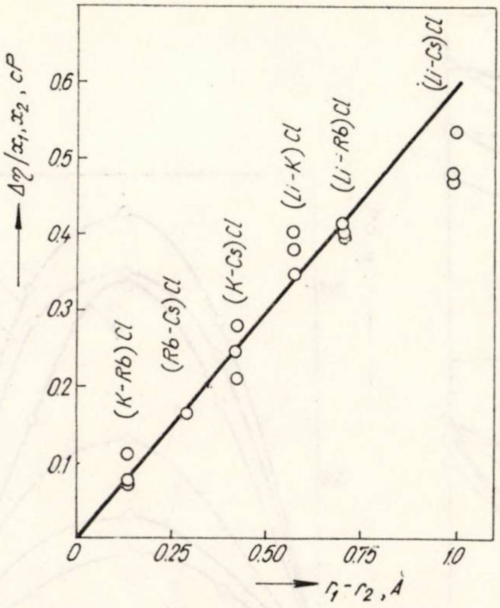

Fig. 3. — The dependence of $\Delta\eta/x_1 x_2$ on the $(r_1 - r_2)$ difference at 775°.

Table 5

Validity of eq. (1) for $(M_I - M_{II})$ Cl mixtures

System	775°		$a = 0.655$		800°	$a = 0.606$	
	$x_{M_I Cl}$	η_{exp},cP	η_c,cP	Diff. %	η_{exp},cP	η_c,cP	Diff. %
(Li−K)Cl	0.50	0.974	0.988	+1.4	0.923	0.935	+1.2
(Li−Rb)Cl	0.25	1.075	1.074	+0.1	1.004	1.011	+0.7
	0.50	1.001	0.990	−1.0	0.940	0.938	−0.2
	0.75	0.951	0.958	+0.7	0.907	0.917	+1.0
(Li−Cs)Cl	0.25	1.016	0.983	−3.2	0.950	0.928	−2.3
	0.50	0.950	0.910	−4.2	0.910	0.860	−5.4
	0.75	0.930	0.910	−2.1	0.880	0.868	−1.3
(K−Rb)Cl	0.25	1.185	1.189	+0.3	1.110	1.112	+0.1
	0.50	1.160	1.169	+0.8	1.090	1.096	+0.5
	0.75	1.160	1.159	−0.1	1.086	1.089	+0.3
(K−Cs)Cl	0.25	1.114	1.100	−1.2	1.043	1.028	−1.2
	0.50	1.097	1.090	−0.6	1.024	1.017	−0.7
	0.75	1.114	1.114	0.0	1.040	1.039	−0.1
(Rb−Cs)Cl	0.50	1.140	1.133	−0.6	1.060	1.060	0.0

table 5. The most notable exception in fig. 3 and table 5 is represented by (Li—Cs)Cl system whose $\Delta\eta$ are lower than those calculated by (1). The peculiarity of this system is also certified by its electrical conductance[13] as well as molar volume behaviour. As seen in fig. 1, the additivity of molar volume holds for the studied alkali chloride systems (ΔV are less than 0.5%), except for (Li—Cs)Cl system where ΔV values become appreciable going beyond 1%. An explanation for this behaviour may lie in the fact that the extremely large difference between the radii of the two cations (Li^+ and Cs^+) in the mixture enhances the ionic interaction to such an extent that complex ions are formed in these melts.

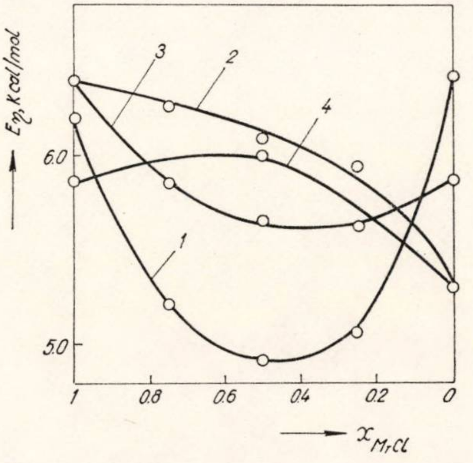

Fig. 4.—E_η *vs.* molar fraction in $(M_I - M_{II})$ Cl systems

1, (Li—K) Cl; *2*, (K—Rb) Cl; *3*, (K—Cs) Cl; *4*, (Rb—Cs)Cl.

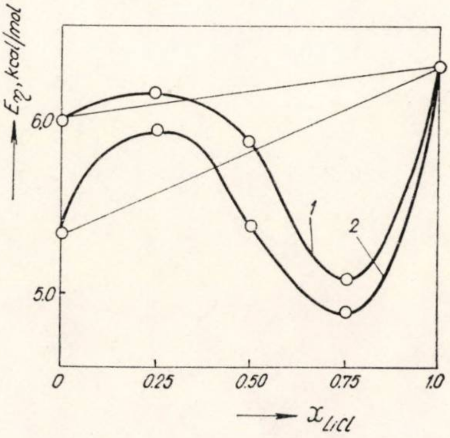

Fig. 5. — E_η *vs.* molar fraction for *1*, (Li — Rb)Cl and *2*, (Li—Cs)Cl.

As can be seen in figs. 4 and 5, for all six studied systems, the activation energy for viscous flow does not vary linearly with molar composition. These systematic deviations from additivity prove that changes in the cation-anion bonding energy take place by mixing. The larger the difference in cationic radii, the more complicated becomes the E_η *vs.* composition dependence and the larger is the deviation from additivity. The special place occupied by (Li—Cs)Cl system in the series is noticed again.

Revue Roumaine de Chimie, **19**, *4*, 561–566 (1974)

MECHANISM AND KINETICS OF THE DISSOLUTION IN WATER OF SOME HYDRATED BINDERS

I. TEOREANU, MARCELA MUNTEAN, N. CIOCEA,
and O. ŞANCU

Polytechnic Institute, Bucharest,
Str. Polizu n° 1, Romania

Received September 6, 1973

Using the "rotating disc" method, the kinetics and the mechanism of the dissolution in water of gypsum as well as of monocalcium and monobarium aluminates in hydrated state are studied.

1. INTRODUCTION

The dissolution process is considered as a result of the thermal vibrations of the particles forming the crystalline lattice and of a simultaneous action of the molecular forces exerted by the solvent. The material detached from the solid body surface passes in the solvent boundary layer and then it duffuses in the mass of the solvent. The dissolution can be congruent or incongruent; in the latter case the mechanism of the process is more intricate. When the rate of dissolution of the substance from the crystalline surface to the boundary layer is greater than the rate of diffusion into the mass of the solvent, the process is controlled by diffusion, contrarily the process is controlled by the chemical reaction.

If for the study of the mechanism and kinetics of the dissolution, the "rotating disc" method is used, according to the theory developed by Levich,[1] for the diffusion controlled domain, the following relation holds:

$$J \sim \sqrt{\omega} \tag{1}$$

where: J – is the diffusional mass flux;

ω – the disc angular velocity.

---

[1] V. G. Levicch, "Fizico-khimicheskaia ghidrodinamica", Izd. Fiz.-mat. lit., Moskva, 1959.

The J values are computed from the measurements of the quantities of material passed into solution after a period of time, by means of equation:

$$J = \frac{m}{St}, \tag{2}$$

where: m — the amount of substance passed into solution at moment t;
t — dissolution time;
S — the dissolution surface of the disc.

It results therefore that one can obtain, in a simple manner, information regarding both the mechanism of the process and its kinetics.

2. EXPERIMENTAL CONDITIONS

Gypsum ($CaSO_4 . 2H_2O$), monocalcium aluminate and monobarium aluminate hydrated for 28 days formed the hydrated binders whose behaviour was examined. The composition of monobarium and monocalcium aluminate samples has been checked before the experiment by roentgenographic analysis.

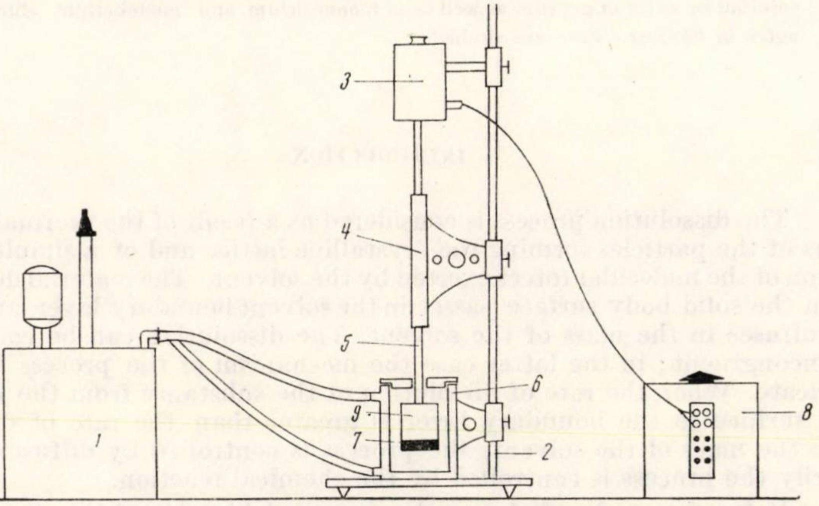

Fig. 1. — Sketch of "rotating disc" apparatus.

1, thermostat; *2*, stand; *3*, motor; *4*, guide; *5*, shaft; *6*, thermostat bath; *7*, sample (disc); *8*, autotransformer; *9*, holding head.

The experiments were carried out using the apparatus shown in fig. 1. It consists of a thermostated bath (6) filled with distilled water in which the binder disc (7), to be examined, is inserted; the binder disc is sticked to a rubber head (9) fixed on the shaft (5) driven by the variable speed motor (3). Three different speeds were used: 450 r.p.m., 850 r.p.m. and 1100 r.p.m. The dissolution time was 5, 10 and 15 minutes. At the end of the dissolution period the concentration of the solution in the bath was determined; for gypsum it was determined $CaSO_4$ concentration, for monocalcium aluminate the concentration of CaO and Al_2O_3 and for monobarium aluminate the concentration of BaO and Al_2O_3.

3. RESULTS AND DISCUSSION

The roentgenographic analysis of the hydration of the monocalcium and monobarium aluminates led to the conclusion that after 28 days of hardening both aluminates are quasitotally hydrated. Figs. 2 and 3 present the roentgenograms of the anhydrous aluminates and of the hardened samples of the same aluminates.

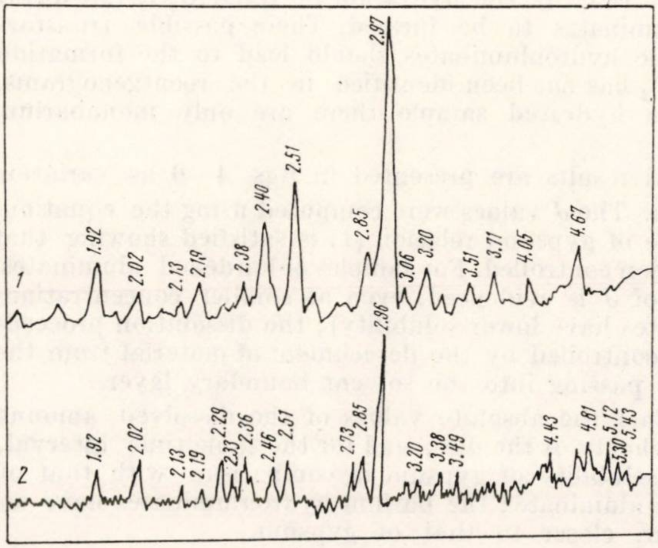

Fig. 2. — Roentgenograms for anhydrous (*a*) and hardened (28 days) (*b*) $CaO \cdot Al_2O_3$.

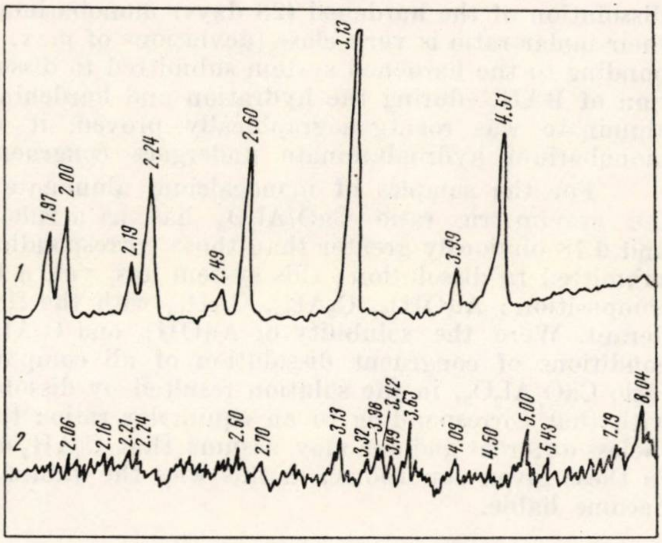

Fig. 3. — Roentgenograms for anhydrous (*a*) and hardened (28 days) (*b*) $BaO \cdot Al_2O_3$.

For the monocalcium aluminate samples hydrated and hardened for 28 days the preponderant presence of $3CaO.Al_2O_3.6H_2O$ (C_3AH_6) is ascertained; besides cubic C_3AH_6 there are smaller amounts of CAH_{10}*. Because the monocalcium decahydroaluminate formed during early hydration of $CaO.Al_2O_3$ is unstable, it passes into C_3AH_6, releasing $Al(OH)_3$; the aluminium hydroxide, initially a gel, crystallizes in time accounting for the presence of its characteristic lines in the roentgenograms of the hydrated monocalcium aluminate.

One could expect that by the hydration of $BaO.Al_2O_3$ (28 days) monobarium hydroaluminates to be formed. Their possible transformation into more basic hydroaluminates should lead to the formation of $Al(OH)_3$. As $Al(OH)_3$ has not been identified in the roentgenograms, it results that in the hydrated sample there are only monobarium hydroaluminates.

The experimental results are presented in figs. 4—6 as variation of J as function of $\sqrt{\omega}$. The J values were computed using the equations (1) and (2). In the case of gypsum, relation (1) is satisfied showing that the dissolution is diffusion controlled. For samples of hardened aluminates, the variation in time of J is evidenced, even at smaller concentrations (the hydrated aluminates have lower solubility); the dissolution proceeds in a domain which is controlled by the detachment of material from the binder surface and its passing into the solvent boundary layer.

As a matter of fact the absolute values of the dissolved amount for the same angular velocity of the disc, and for the same time interval, point out the greater solubility of gypsum in comparison with that of hardened monocalcium aluminate; the barium hydroaluminates have an intermediate behaviour, closer to that of gypsum.

The results regarding the BaO and Al_2O_3 concentration for the dissolution of the hardened (28 days) monobarium aluminate show that their molar ratio is very close (deviations of max. $+6\%$) to that corresponding to the hardened system submitted to dissolution; as the formation of BAH_x during the hydration and hardening of the monobarium aluminate was roentgenographically proved, it was assumed that the monobarium hydroaluminate undergoes congruent dissolution.

For the samples of monocalcium aluminate hardened (28 days), the gravimetric ratio CaO/Al_2O_3 has, as a rule, values between 0.6 and 0.78 obviously greater than those corresponding to the solid system submitted to dissolution; this system has, yet, a heterogeneous mineral composition: $Al(OH)_3$, C_3AH_6, CAH_{10} with the first two being preponderant. Were the solubility of $Al(OH)_3$ and C_3AH_6 comparable, in the conditions of congruent dissolution of all compounds, the gravimetric ratio CaO/Al_2O_3, in the solution resulted by dissolution, would be equal with that corresponding to an equimolar ratio; the solubility is nevertheless different and one may assume that C_3AH_6 dissolves incongruently in these given conditions; in this way the values found by experiment become liable.

---

*) Here $CaO = C$; $Al_2O_3 = A$; $BaO = B$; $H_2O = H$.

CONCLUSIONS

It results from the experimental data:

a. The solubility of hardened calcium aluminate is much lower than that of gypsum, while hydrated monobarium aluminate holds an

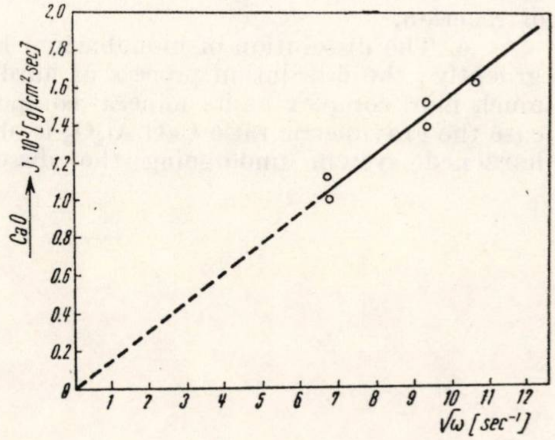

Fig. 4. — Plot of J *vs* $\sqrt{\omega}$ for gypsum.

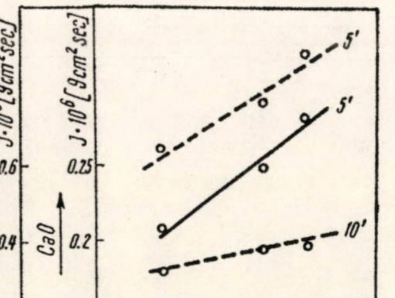

Fig. 5. — Plot of J *vs* $\sqrt{\omega}$ for hardened monocalcium aluminate; ——— Al_2O_3; --- CaO.

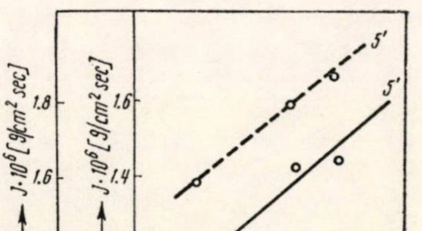

Fig. 6. — Plot of J *vs* $\sqrt{\omega}$ for hardened monobarium aluminate; ——— Al_2O_3; --- BaO.

intermediate position, closer to that of gypsum; barium-aluminous cements are, in these conditions, rather air binders.

b. The dissolution of gypsum in water, in the early stage, takes place in the diffusion domain; as the concentration of $CaSO_4$ in solution rises, the kinetics of the process becomes a mixed one, finally the dissolution becoming kinetically controlled; taking into account that the solubility in water of hardened calcium and barium aluminates is smaller, their dissolution is controlled from the very beginning by the kinetics of reaction.

c. The dissolution of monobarium hydroaluminate takes place congruently; the dissolution process of hardened monocalcium aluminate is much more complex as its mineral composition is heterogeneous; in this case the gravimetric ratio CaO/Al_2O_3 is obviously higher than that of the hardened system undergoing the dissolution.

Revue Roumaine de Chimie, **19**, *4*, 567–575 (1974)

MIXED LIGAND COMPOUNDS OF LANTHANIDES WITH NEUTRAL LIGANDS CONTAINING DONOR OXYGEN ATOMS. II

CHLOROSALICYLATES OF LANTHANIDES WITH TRIPHENYLARSINE OXIDE

SILVIA PLOŞTINARU and P. SPACU

Research Center of Physical Chemistry, Dumbrava Roşie, 23, Bucharest,
Romania

Received August 7, 1973

A new series of mixed ligand compounds of lanthanides with monodentate neutral ligands, Ln $(Ph_3AsO)_2$ $(ClSal)_3$, was synthetized. The obtained compounds have been chemically and physically characterized, by means of their UV and visible spectra which gave information concerning the nature of the chemical bonding in these complexes. The IR spectra have allowed us to establish the coordination of the ligands.

The ability of arsine and phosphine oxides to act as oxygen donors and to form complex compounds with different metal ions is well known. In this context, complex compounds of lanthanide nitrates, chlorides, thiocyanates with these ligands have been already reported.[1–3] In a previous paper,[4] the properties and the chemical behaviour of some mixed ligand compounds of lanthanides with chlorosalicylic acid and triphenylphosphine oxide were studied. The aim of the present note is to report the synthesis and the physico-chemical study of the complexes formed by lanthanide chlorosalicylates with triphenylarsine oxide (Ph_3AsO). The problem is very intricate due to the scarce coordinating ability of the lanthanide ions against monodentate ions (the entropic factor contributing to the complex stability is lower than that for bidentate ligands) and, finally, because the number of neutral ligands and their possibility to coordinate depends on the coordinating ability of the anions present in the coordination sphere. In our case, the hydroxycarboxylic acid is known as a characteristic chelating reagent for lanthanides.

---

[1] E. Parris and G. G. Long, *J. Inorg. Nuclear Chem.*, **32**, 1593 (1970).
[2] E. I. Siniavscaia and Z. A. Seca, *Zhur. neorg. Khim.*, **17**, 646 (1972).
[3] D. R. Cousins and F. A. Hart, *J. Inorg. Nuclear Chem.*, **29**, 1475 (1967).
[4] S. Ploştinaru and P. Spacu, *Rev. Roumaine Chim.*, **18**, (1973).

EXPERIMENTAL

Reagents. The following reagents were used: oxides (Ln_2O_3) of spectral purity (Matthey and Johnson); 5-chlorosalicylic acid (Fluka AG-Switzerland); triphenylarsine oxide (Fluka AG-Switzerland).

Preparation of compounds. Essential for the obtention of these compounds is the reaction medium. The compounds were prepared using the liquid — liquid extraction method with benzene as organic phase. The mixed ligand compounds of Dy(III), Ho(III) and Er(III) are difficult to be prepared. In this case, an excess amount of ligand should be necessary in order to favour the extraction which at its turn involves repeated washing and recrystallizations of the obtained compounds. Irrespective of the ligand amount used, the following compounds were allways obtained:

$Ln(Ph_3AsO)_2\ (ClSal)_3$ where Ln = Pr, Nd, Sm, Eu, Tb, Dy, Ho, Er.
Ph_3AsO = triphenylarsine oxide
ClSal = 5-chlorosalicylic acid

The chemical formulas were determined on the elemental chemical analyses. (table 1).

Table 1

Analytical data

Formula of the compound	Ln		C		H	
	Calcd.	*Found*	*Calcd.*	*Found*	*Calcd.*	*Found*
$Pr(Ph_3AsO)_2\ (ClSal)_3$	10.84	10.98	52.66	52.41	3.33	3.49
$Nd(Ph_3AsO)_2\ (ClSal)_3$	11.07	11.32	52.53	52.23	3.22	3.58
$Sm(Ph_3AsO)_2\ (ClSal)_3$	11.48	11.70	52.29	52.02	3.20	3.52
$Eu(Ph_3AsO)_2\ (ClSal)_3$	11.59	11.45	52.22	52.38	3.20	3.47
$Dy(Ph_3AsO)_2\ (ClSal)_3$	12.29	12.11	51.80	51.58	3.17	3.43
$Ho(Ph_3AsO)_2\ (ClSal)_3$	12.46	12.63	51.70	51.37	3.17	3.50
$Er(Ph_3AsO)_2\ (ClSal)_3$	12.64	12.91	51.60	51.72	3.16	3.22

Analysis and measurements. The chemical analysis was performed through micromethods; C and H were determined by microcombustion. The metal was estimated gravimetrically by ignition to oxide.

The electric conductivity measurements were made by means of a conductometer Radelkis OK-102, in alcoholic solutions, acetone and DMF of 10^{-3}M concentration. Platinum electrodes were used and the constant of the cell was determined in aqueous solutions of the KCl of different concentrations.

IR spectra within 400—3600 cm^{-1} were recorded with a UR-10 spectrophotometer using KBr pellets.

Electronic spectra in UV and visible range were recorded with a VSU-2 Zeiss-Jena spectrophotometer on the ethanolic solutions for 220—360 nm and benzenic solutions for 360—900 nm range. The reflectance spectra were recorded with a VSU-1. Zeiss-Jena spectrophotometer using MgO as standard. Thermodifferential measurements were carried out with an OD-102 derivatograph, system F. Paulik, J. Paulik and L. Erdey, in air using platinum crucible and Al_2O_3 as reference.

RESULTS AND DISCUSSION

In order to characterize the complex compounds obtained, the melting points were determined as well as the solubility in the common organic solvents. The obtained melting points being compared with those of simple lanthanide chlorosalicylates. As results from this comparison, the mixed ligand compounds are characterized by lower melting points and by a higher solubility in benzene, chloroform, acetone and DMF, but they are less soluble in alcohols (ethanol and methanol). These facts prove the increase in the covalency of the chemical bonds as a consequence of the entrance of neutral ligands into the inner coordination sphere.

To prove the chemical formula ascribed to the complex compounds studied, the molar electrical conductivity measurements were performed. The results obtained were interpreted using the data reported in the related literature concerning the limits between the molar electrical conductivities for different types of electrolytes.[5] An examination of the data reported in table 2 has lead us to the conclusion that the new synthetized mixed ligand compounds of the lanthanides behave as nonelectrolytes, all carboxylic groups being coordinated.

Table 2

Some physical properties of the compounds Ln $(Ph_3AsO)_2$ $(ClSal)_3$

Compound	Colour	m.p. (°C)	$\wedge(\Omega^{-1}\ cm^2\ mol^{-1})$		
			C_2H_5OH	acetone	DMF
$La(Ph_3AsO)_2\ (ClSal)_3$	white	120	2.09	—	32.4
$Pr(Ph_3AsO)_2\ (ClSal)_3$	green-pale	121–23	2.08	9.3	32.4
$Nd(Ph_3AsO)_2\ (ClSal)_3$	pink	124–26	2.10	9.3	32.4
$Sm(Ph_3AsO)_2\ (ClSal)_3$	white-yellow	138–40	—	—	—
$Eu(Ph_3AsO)_2\ (ClSal)_3$	yellow	141–43	2.06	9.3	32.2
$Dy(Ph_3AsO)_2\ (ClSal)_3$	white-yellow	143–45	—	9.3	—
$Tb(Ph_3AsO)_2\ (ClSal)_3$	white	143–45	—	—	32.0
$Er(Ph_3AsO)_2\ (ClSal)_3$	pink	147–51	—	9.3	31.8

The absorption spectra in UV within 220–360 nm were also studied. Their interpretation has been made by comparing the spectra obtained with those of the free ligands. The chlorosalicylic acid has two absorption maxima at 233 nm and 316 nm, corresponding to the transition $\pi-\pi^*$ and $n-\pi^*$, respectively. The spectrum of triphenylarsine oxide has three absorption maxima at 258,263 and 270 nm. The band systems, observed with the electronic spectra of different substituted arsines, were interpreted in terms of charge transfer nature [6]. The same thing happens with the corresponding arsine oxides. The absorption bands around 270 nm, unaffected by the nature of the substituents and the medium polarity, are ascribed to $\pi-\pi^*$ transitions of the aromatic ring. The second group of the bands placed at 220–266 nm strongly dependent on the substituents was assigned to one electron transition from the lone pair of arsenic to a π antibonding orbital of the benzenic ring.

---

[5] W. J. Geary, *Coord. Chem. Rev.*, **7**, 81 (1971).

[6] W. R. Cullen and R. M. Hochstrasser, *J. Mol. Spectroscopy*, **5**, 118(1960).

The absorption spectra of the mixed ligand compounds contain the absorption maxima characteristic to the free ligands. These maxima occur practically with the same wavenumbers as in the free ligands, but with higher intensities, the last observation being a testimony of the chemical bond formation (fig. 1).

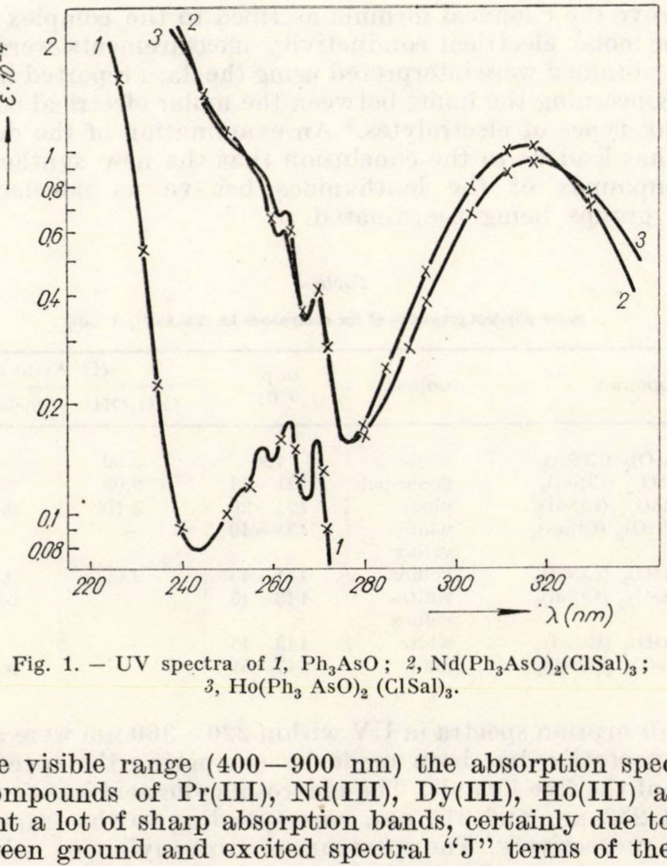

Fig. 1. – UV spectra of *1*, Ph_3AsO ; *2*, $Nd(Ph_3AsO)_2(ClSal)_3$; *3*, $Ho(Ph_3\ AsO)_2\ (ClSal)_3$.

In the visible range (400–900 nm) the absorption spectra of the complex compounds of Pr(III), Nd(III), Dy(III), Ho(III) and Er(III) ions, present a lot of sharp absorption bands, certainly due to the transition between ground and excited spectral "J" terms of the electronic configuration 4f. The spectral data obtained were used to estimate the chemical bonding in these mixed ligand complexes, and in what the lanthanide participation is concerned.

The coordination of different ligands to the central metal ion is reflected in a series of changes occurring in the absorption spectrum in the visible range of the complex, compared with the spectrum of the free metal ion. To emphasize these changes, the spectra of aquo ions were taken as reference. The spectra of Pr(f^2) and Nd(f^3) complexes show shifts of bands and an increase in their intensities. These bandshifts depend on the number of electrons in the *f*-shell, the shifts being smaller when the electron number increases. This fact should be explained by the lower ability of the "f" orbitals towards coordination, when they are filled with more electrons (table 3).

Table 3

Visible spectral data

Ln^{3+}	Transition	$\Delta\bar{\nu}$ cm^{-1}	$\Delta\varepsilon$
Pr^{3+}	$^3H_4 \longrightarrow {}^3P_2$	101	+1.04
	$\longrightarrow {}^3P_1$	137	+0.64
	$\longrightarrow {}^1D_2$	200	+1.34
Nd^{3+}	$^4I_{9/2} \longrightarrow {}^4G_{7/2}$	220	+1.33
	$\longrightarrow {}^4G_{5/2}$	297	+8.72
Er^{3+}	$^4I_{15/2} \longrightarrow {}^4F_{7/2}$	—	+1.96
	$\longrightarrow {}^2H_{11/2}$	—	+12.95
Dy^{3+}	$^6H_{15/2} \longrightarrow {}^6F_{3/2}$	—	+1.91
	$\longrightarrow {}^6F_{7/2}$	—	+1.02
Ho^{3+}	$^5I_8 \longrightarrow {}^5G_6$	—	+2.06

The nephelauxetic parameter taken as the covalency degree of the chemical metal-ligand bonds[7] has been calculated from the bandshifts observed with the absorption spectra of Pr(III) and Nd(III), taken the corresponding aquo ions as reference. In a previous paper,[8] it has been shown that the nephelauxetic ratio is due to the lowering in the interelectronic repulsion (Slater-Condon or Racah) parameters and spin-orbit constant values, caused by the increase in the radial extention of the AO's, as a consequence of MO formation. The lowering in the interelectronic repulsion energy values leads to a lowering in the transition frequencies and hence to a red shift. As it has been recently shown,[9] the covalency effects directly reflected on the lowering of the repulsion parameter and spin-orbit coupling constant values are too much small to account for the experimentally observed bandshifts at least in the case of $f-f$ transitions. The lowering of these parameters caused by central covalency suggested by Jørgensen[10] (reduction of the formal charge on the metal ion) is also too much small to explain the observed bandshifts. This is the reason why the parameter β ascribed by definition to the ratio between the interelectronic repulsion parameters or spin-orbit coupling constants may have another origins, as follows:

---

[7] S. P. Sinha and H. H. Schmidtke, *Mol. Phys.*, **10**, 7 (1965).

[8] S. P. Sinha, *Spectrochim. Acta*, **22**, 57 (1966).

[9] D. J. Newman, *J. Phys. Chem. Solids*, **34**, 541 (1973).

[10] C. K. Jørgensen, "Orbitals in Atoms and Molecules", Academic Press, London-New York, 1962.

$$\text{Let} \qquad E_f = E_f^0(F, \xi) + V_f$$

$$E = E_e^0(F, \xi) + V_e$$

the ground and excited state energies. $V_{f(e)}$ are the energetic contributions due to the chemical bonding or electrostatic perturbations caused by the chemical environment.

The transition between them will be:

$\nu = \nu_0 + \Delta V$ where ν_0 = transition in the free gaseous ion
$\Delta V = V_e - V_f$ the energetic contribution due to the chemical bond formation.

Taking the corresponding transition ν_a in aquo ion as reference, then

$$\frac{\nu_a - \nu_c}{\nu_a} = \frac{\Delta V_a - \Delta V_c}{\nu_0 + \Delta V_a}$$

Similarly to the formulas obtained in the nephelauxetic approximation one may formally obtain:

$$\frac{\Delta V_a - \Delta V_c}{\nu_0 + \Delta V_a} = 1 - \beta.$$

where $1-\beta$ also represents a measure of the covalency degree of the chemical bonds but with other signification, as mentioned above. The parameters $1-\beta$ and δ were calculated for Pr(III) and Nd(III) complexes (table 4). The positive value obtained shows that the chemical metal-ligand bonds in the studied compounds are more covalent that those in aquo ions.

Further information concerning the ligand coordination have been obtained using the IR data. For all the studied compounds, the spectra were recorded within 600–3600 cm^{-1} and for an exact assignment, the free ligand IR spectra were also recorded. The data are summarized in table 5. As may be seen from table 5, the chlorosalicylic acid has an intense band ascribed to the carbonyl group at 1670 cm^{-1}, occuring split and shifted in the complex compounds, as follows: $\nu_{as}COO^-$ (1580 cm^{-1}) and $\nu_s COO^-$(1370cm^{-1}) due to the asymmetric and symmetric vibration modes, respectively. It may be mentioned the presence in the mixed ligand compounds of absorption bands at 3050 cm^{-1} and 1620 cm^{-1} characteristic to the aromatic ring and another band at 650 cm^{-1} corresponding to the bending vibration of COO^-. In what the neutral ligand Ph_3AsO is concerned, it possesses a lot of vibrations active in IR. Some of them are perturbed by coordination, others, as an example the maxima appearing

Table 4

Values of the nephelauxetic parameter and of the covalency degree

$Nd(NO_3)_3 \cdot {}_6H_2O$ λ nm	$Nd(Ph_3AsO)_2(ClSal)_3$ λ nm	$\Delta\bar{\nu}_1$ cm^{-1}	1−β	δ%
512	514	76	0.612 10^{-2}	0.6157
520	526	220	1.144 10^{-2}	1.1572
575	585	297	1.710 10^{-2}	1.7397
755	755	—	—	—
805	815	153	0.865 10^{-2}	0.8726
$Pr(NO_3)_3 \cdot {}_6H_2O$	$Pr(Ph_3AsO)_2(ClSal)_3$			
444	446	101	0.448 10^{-2}	0.450
468	471	137	0.641 10^{-2}	0.6451
481	484	129	0.620 10^{-2}	0.6238
588	595	200	1.176 10^{-2}	1.1899

Table 5

IR spectral data

Ph_3AsO	ClSal acid	$Nd(Ph_3AsO)_2$ $(ClSal)_3$	$Er(Ph_3AsO)_2$ $(ClSal)_3$
		3050 m	3050 m
1650 m	1670 vs	1620 m	1620 m
	1605 m		
		1580 s sh.	1580 s sh.
1480 m	1470 s	1470 s	1470 s
1435 s	1440 s	1435 s	1435 s
		1370 s sh.	1370 s sh.
	1290 s	1290 w	1295 w
	1240 vs	1250 s	1250 s
1160 vw	1155 m	1150 w	1150 w
1090 s		1090 s	1090 s
1000 m		1000 w	1005 w
885 vs		897 s	906 s
	830 s	830 s	830 s
750 s		745 s	745 s
700 s		700 s	700 s
		650 m	650 m
485 m		480 s	485 s

s=strong, m=medium, w=weak, v.s.=very strong, sh=shoulder.

at frequencies higher than 1400 cm^{-1} ascribed to C=C vibrations, are overlapped with the absorption bands due to the symmetric and asymmetric frequencies of the coordinated chlorosalicyclic acid. More important changes are especially produced in the position of the absorption band corresponding to the stretching frequency of As−O bond, due to the chemical bond formation. The very intense band occurring in the spectrum of the free Ph_3AsO at 885 cm^{-1}, assigned to the stretching vibration As–O, occurs in the mixed ligand complexes shifted towards higher wavenumbers (fig. 2).

This observation should be explained, in contrast with the similar compounds of Ph_3PO,[4] by the fact that during Ph_3AsO coordination to the lanthanide ion, the strengthening of τ_{As-O} bond together with the interaction π metal-oxygen have a predominant character, while the ${}_p\pi - {}_d\pi$ oxygen-arsenic bond is very weak, which leads practically to the increase of the stretching vibration ν_{As-O}. As may be observed in figure 3, the bandshift value depends linearly on the lanthanide ionic ray.

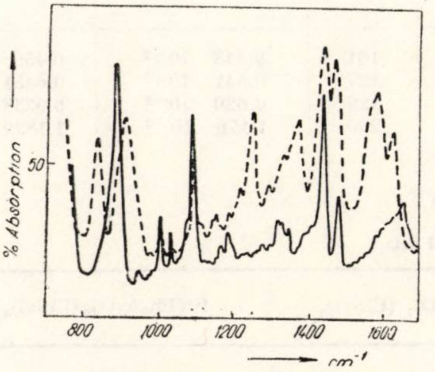

Fig. 2. – IR spectra of *1*, Ph_3AsO ; *2*, $Er(Ph_3AsO)_2$ $(ClSal)_3$.

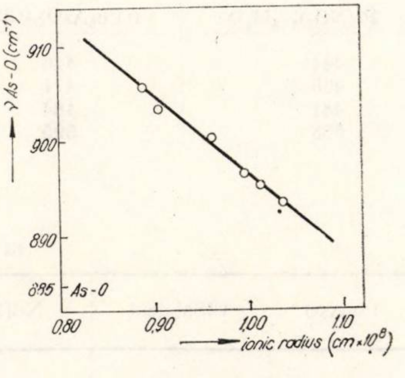

Fig. 3. – Linear dependence of ν_{As-O} on the ionic radius.

The IR data correlated with those from the physical and chemical measurements, as discussed above, have lead to the following chemical formulation :

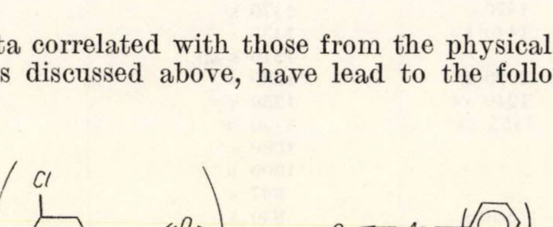

The thermodifferential analysis performed on the mixed ligand compounds herein studied gave informations on their thermal stability and their chemical behaviour function of temperature. As an example the thermal analysis results are illustrated for the $Er(Ph_3AsO)_2(ClSal)_3$. The compounds are stable until 220–240° occuring on the TG curve as a level. Over this temperature, the elimination of the neutral ligand begins, followed by the partial decomposition of Erbium chlorosalicylate which continues up to 420°. If the TG data were correlated with the initial weight of the sample, the weight loss was estimated in this temperature point. According to the theoretical calculations, the weight loss corresponds to two molecules of neutral ligand and to a third part from the organic anion. Between 460—560° the oxidation of the volatile organic products takes place, the heat being emitted in the strong exothermal effect at 510°. The initial compound is transformed after oxidation into instable intermediate compounds, most likely oxycarbonates of the form $Ln_2O_3 . nCO_2$, as indicated in the related literature.[11] At temperatures higher than 600° the decomposition of the oxycarbonates takes place, the final level obtained corresponding to the Er_2O_3 formation.

---

[11] V. P. Sevastianov and D. A. Dvornikova, *Zhur. neorg. Khim.*, **17**, 2884 (1972).

Revue Roumaine de Chimie, **19**, *4*, 577–580 (1974)

PAPIERELEKTROPHORETISCHE UNTERSUCHUNG DER BILDUNG VON VERBINDUNGEN DES INDIUMS MIT R-WEINSÄURE

GH. MARCU, MARIA SUCIU und A. V. BOTAR

vom Institut für Chemie, Donath-Str. 65, Cluj

Eingegangen am 8. Mai 1973

Die Reaktion des Ions In^{3+} mit R-Weinsäure wurde papierelektrophoretisch untersucht. Die Bildung der Ionenarten des Typus $In(C_4O_6H_3)_2^{3-}$ und $In(C_4O_6H_3)_3^{6-}$ wurde festgestellt und ihre Stabilitätskonstanten bestimmt ($\beta_1 = 4{,}78 . 10^{10}$ bzw. $\beta_2 = 8{,}71 . 10^7$). Die Werte der papierelektrophoretisch gefundenen Stabilitätskonstanten stimmen mit denjenigen nach der Bjerrum-Methode ($\beta_1 = 6{,}33 . 10^{10}$ bzw. $\beta_2 = 1{,}40 . 10^7$) gut überein.

Als Fortsetzung der Untersuchungen der Reaktionen des In^{3+}-Ions mit organischen Hydroxysäuren,[1] wurde das Verhalten dieses Ions in weinsauerem Medium in Abhängigkeit vom pH elektrophoretisch untersucht.

Es ist bekannt, daß In^{3+} mit verschiedenen organischen Hydroxysäuren in wäßrigem Medium stabile Komplexe bildet. Die Stärke der Bindung zwischen dem Ion In^{3+} und diesen Liganden wird durch den Wert der Bildungskonstante des Komplexes ausgedrückt, welche durch eine Reihe von Faktoren bedingt wird, von welchen die elektronenspendenden Eigenschaften des Anions eine wichtige Rolle spielen. In der Fachliteratur werden eine Reihe von Komplexen des In^{3+} mit organischen Hydroxysäuren angeführt.[2-9] Spektrophotometrische, konduktometrische sowie potentiometrische Studien der Stabilität der Komplexe des In^{3+} in wäßriger Lösung von R-Weinsäure ergaben das Vorhandensein folgender Ionenarten: $In(C_4O_6H_3)^0$, $In(C_4O_6H_3)_2^{3-}$ und $In(C_4O_6H_3)_3^{6-}$. Zur stufenweisen Bildung der Komplexe tragen am wahrscheinlichsten folgende chemische Reaktionen bei :

---

[1] H. Bednar, V. Bednar, L. Oprei und M. Suciu, *Z. Chem.*, **11**, 112 (1971).

[2] G. S. Savcenco und I. V. Goncearov, *Zhur. Neorg. Khim.*, **4**, 1558 (1959).

[3] D. I. Reabcicov, I. N. Marcov und Kie Min Jao, *Zhur. neorg. Khim.*, **7**, 2545, 2716 (1962).

[4] D. Cozzi und S. Vivarreli, *Z. Elektrochem.*, **57**, 408 (1953).

[5] D. Cozzi und S. Vivarreli, *Z. Elektrochem.*, **58**, 907 (1954).

[6] R. N. Srivastova und D. C. Rupainwar, *J. Indian Chem. Soc.*, **43**, 240 (1966).

[7] V. A. Timmergakl, *Zhur. neorg. Khim.*, **11**, 1016 (1966).

[8] V. Bednar und H. Bednar, *Studii şi Cercet. Chim. Acad. R.S.R.*, **15**, 719 (1967).

[9] V. Bednar, H. Bednar und F. Fătu, *Studii şi Cercet. Chim. Acad. R.P.R.*, **16**, 15 (1968).

$$C_4O_6H_6 + In^{3+} + OH^- \rightleftharpoons C_4O_6H_4^{2-} + 2H_2O$$

$$C_4O_6H_4^{2-} + In^{3+} + OH^- \rightleftharpoons In(C_4O_6H_3) + H_2O$$

$$In(C_4O_6H_3) + C_4O_6H_4^{2-} + OH^- \rightleftharpoons In(C_4O_6H_3)_2^{3-} + H_2O$$

$$In(C_4O_6H_3)_2^{3-} + C_4O_6H_4^{2-} + OH^- \rightleftharpoons In(C_4O_6H_3)_3^{6-} + H_2O$$

Die Methode der Papierelektrophorese wurde erfolgreich bei der Bestimmung der Bildungskonstanten verschiedener Komplexe angewendet.[10-12]

Da diese Methode beim Studium der Komplexverbindungen, der Radioisotopen gute Ergebnisse liefert, untersuchten wir das System In^{3+} — R-Weinsäure papierelektrophoretisch, um die Werte der Bildungskonstanten der Verbindungen des Indiums in R-Weinsäure zu bestimmen. Das Prinzip der Methode wurde in vorangegangenen Arbeiten[10-12] dargelegt.

EXPERIMENTELLER TEIL

Es wurde mit einem bereits beschriebenen[13] Papierelektrochromatographen gearbeitet. Die Versuche wurden in 0,5 m R-Weinsäure-Medium bei einem pH-Bereich von 1,08—7,92 durchgeführt. Das zu untersuchende Element wurde mittels einer Mikropipette zentral auf den chromatographischen Papierstreifen (Papier Whatman Nr. 1 der Dimensionen 32,5/1, 5 cm) aufgetragen, dessen Enden einer Potentieldifferenz von etwa 1100 V bei 15 mA ausgesetzt wurden. Die Zeit der elektrischen Wanderung war 12 Min. und die Arbeitstemperatur 15±2°.

Die Wandung der Verbindungen wurde durch Messen der Aktivität des Radioisotops ^{114}In verfolgt, und gegen die Stellung der Glukose, welche gleichzeitig auf den chromatographischen Papierstreifen aufgetragen wurde, korrigiert. Die elektrophoretischen Wanderungsgeschwindigkeiten der vorhandenen Ionenarten wurde anhand der Beziehung von Kunkel und Tiselius[14] berechnet. Die experimentell gefundenen Ergebnisse sind in Tabelle 1 angeführt unter Berücksichtigung der Absorbtion der Ionen am chromatographischen Papier ($R_f = 0{,}94$).

---

[10] Gh. Marcu und K. Samochocka, *Stud. Univ. Babeș-Bolyai, Chem.*, **10**, 71 (1965).
[11] Gh. Marcu und K. Samochocka, *Stud. Univ. Babeș-Bolyai, Chem.*, **11**, 15 (1966).
[12] Gh. Marcu und A. Botar, *Stud. Univ. Babeș-Bolyai, Chem.*, **12**, 11 (1967).
[13] Gh. Marcu und A. Botar, *Rev. Roumaine Chim.*, **12**, 645 (1967).
[14] H. G. Kunkel und A. Tiselius, *J. Gen. Physiol.*, **35**, 89 (1951).

Tabelle 1

Wanderung (d) und Werte der Summe der elektrophoretischen Wanderungsgeschwindigkeiten (*u*) des In^{3+} in 0,1 m R-Weinsäure-Medium in Abhängigkeit vom pH-Wert

pH	*T* (V)	d (cm)	$u.10^{-4}$ $cm^2.V^{-1}.S^{-1}$
1,08	1150	−4,5	−3,20
1,86	1210	−1,6	−1,08
2,46	1200	+0,5	+0,34
3,02	1200	+1,6	+1,09
3,48	1200	+2,4	+1,63
4,04	1120	+2,5	+1,83
4,56	1100	+3,0	+2,24
5,06	1150	+2,8	+2,00
5,50	1120	+2,9	+2,13
5,93	1100	+2,8	+2,09
6,50	1130	+2,8	+2,10
6,98	1200	+2,8	+1,91
7,92	1180	+2,7	+1,90

AUSWERTUNG DER ERGEBNISSE

Die graphische Darstellung der Summe der elektrophoretischen Wanderungsgeschwindigkeiten der gebildeten Ionenarten in Abhängigkeit vom pH-Wert ergibt eine Doppelkurve in „S“-Form, welche für die Bildung von Komplexverbindungen charakteristisch ist. Es wird beobachtet, daß in stark saurem Medium der In^{3+}-Ion dem Katode zuwandert. Bei $pH > 2{,}5$ wandert der In^{3+}-Ion, welcher Ionenarten des Typs $In(C_4O_6H_3)_2^{3-}$und $In(C_4O_6H_3)_3^{6-}$ gebildet hat, dem Anode zu.

Zwecks Bestimmung der Bildungskonstanten der erhaltenen Ionenarten wurde die Summe der elektrophoretischen Wanderungsgeschwindigkeiten (u) gegen die pH-Werte aufgetragen und aus der Abhängigkeit des $\lg \frac{u + u_{In^{3+}}}{u - u_{In}^{(3-3x)-} - u}$ von pH wurde der dem Nullwert dieses Verhältnisses entsprechende pH-Wert berechnet.

Zum Schluß wurden die Bildungskonstanten jeder einzelnen Ionenart berechnet, die aus Tabelle 2 ersichtlich sind.

Die erhaltenen Werte für die Bildungskonstanten sind in guter Übereinstimmung mit denen nach der Bjerrum Methode bestimmten ($\beta_1 = 6{,}33.10^{10}$ bzw. $\beta_2 = 1{,}40.10^7$).

Tabelle 2

Werte der Stabilitäts- und Instabilitätskonstanten

Untersuchte Verbindung	Stabilitätskonstante	Instabilitätskonstante
$In(C_4O_6H_4)_2^{3-}$	$4{,}78.10^{10}$	$0{,}21.10^{10}$
$In(C_4O_6H_3)_3^{6-}$	$8{,}71.10^7$	$0{,}11.10^7$

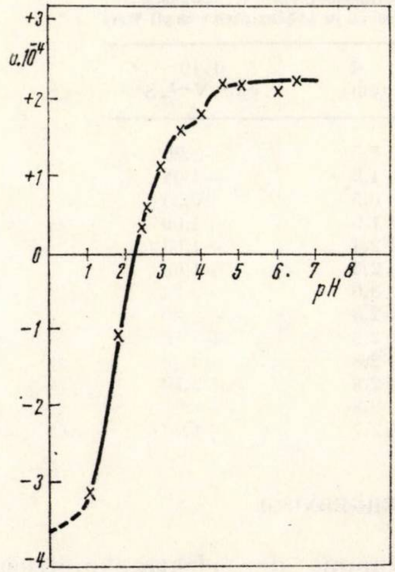

Abb. 1. — Abhängigkeit der Summe der elektrophoretischen Wanderungsgeschwindigkeit (u) von pH.

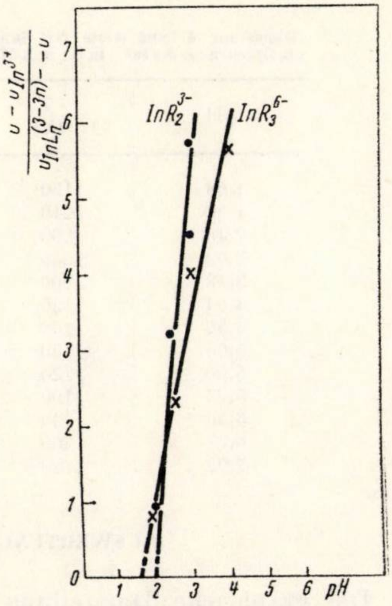

Abb. 2. — Abhängigkeit des $\dfrac{u - u_{\mathrm{In}^{3+}}}{u_{\mathrm{InL}_n}^{(3-3n)-} - u}$ von pH.

SCHLUSSFOLGERUNGEN

1. Die Bildung der Komplexe des In^{3+} mit R-Weinsäure wurde erstmals papierelektrophoretisch unter Anwendung des Radioisotops ^{114}In untersucht.

2. Es wurden die Werte der Stabilitätskonstanten der Ionenarten $In(C_4O_6H_3)_2^{3-}$ und $In\ (C_4O_6H_3)_3^{6-}$ bestimmt und gleich $\beta_1 = 4{,}78.10^{10}$ bzw. $\beta_2 = 8{,}71.10^7$ gefunden. Diese Werte sind in guter Übereinstimmung mit denen nach der Bjerrum Methode[1] bestimmten.

Revue Roumaine de Chimie, 19, 4, 581–630 (1974)

COMPUTER PROGRAM FOR DETERMINING ALL POSSIBLE E.S.R. SPECTRA WITH EQUIDISTANT LINES

A. T. BALABAN and C. POMPONIU

Institute of Atomic Physics, P. O. Box 35, Bucharest

Received September 28, 1973

A computer program was developed for displaying all possible theoretical ESR spectra of free radicals possessing nuclei with spins 1/2 and 1, and having equidistant lines (some of which may have zero intensity). A table of intensities of ESR spectra with M = 2–15 equidistant lines is presented.

INTRODUCTION

In a previous paper,[1] a method was devised for finding all possible electron spin resonance (ESR) spectra with M equidistant lines due to stable nitrogen free radicals, where the energy levels of the odd electron are split by interaction with atoms with nuclear spin 1/2 (e. g. protium) and/or 1 (e. g. nitrogen-14). This method is based on the partitions of the integer number of intervals between lines, M–1. The summands (partition numbers) in partitions must be assigned as coupling constants (in units equal to *d*, the smallest interval between lines) to ^{1}H and/or ^{14}N atoms, whereby one a_N coupling constant uses two equal summands from the partitions.[2] For instance, there are three partitions of the integer three : $3 = 2 + 1 = 1 + 1 + 1$. Therefore, there exist four and only four possible ESR spectra of free radicals with ^{1}H and /or ^{14}N atoms, with four equidistant lines, which correspond to the above three partitions namely :

Partition	$3 : 1a_H = 3d$;	intensities : 1 : 0 : 0 : 1
,,	$2 + 1 : 1a_H = 2d, \; 1a_H = 1d$;	,, 1 : 1 : 1 : 1
,,	$1 + 1 + 1 : 1a_H = 1d, \; 1a_N = 1d$;	,, 1 : 2 : 2 : 1
,,	$1 + 1 + 1 : 3a_H = 1d$;	,, 1 : 3 : 3 : 1

In the preceding paper,[1] a table was included showing all possible ESR spectra with 2–8 equidistant lines,* all having non-zero intensities (therefore, only the last three of the above ESR spectra with four lines were presented). Since inclusion of lines with zero intensity also allows the accomodation of ESR spectra with non-equidistant lines, this generalization to zero intensities will be used in the present paper.

---

[1] A. T. Balaban, *Rev. Roumaine Chim.*, **17**, 9 (1972).

[2] C. Pomponiu and A. T. Balaban, *Rev. Roumaine Chim.*, **18**, 1173 (1973).

* In the case of 8-line ESR spectra one spectrum was missing (with intensities 1 : 6 : 16 : 25 : . . .)

In practice, owing to the finite resolution of ESR spectrometers and to other factors, [3] most experimental ESR spectra can be approximated by this procedure. However, since coupling constants in fact are not multiples of a "quantum" d, this is only a first-order approximation which must be supplemented by a spectrum simulation in order to achieve an exact determination of coupling constants.[3]

For determining the complete table of all possible ESR spectra withm equidistant lines (including also lines of zero intensity*), hand calculations can be carried out up to a relatively small number of lines, around $M=10$. For interpreting ESR spectra with larger numbers of lines, two different approaches can be imagined : (i) to feed into a computer the approximate intensities of ESR lines determined from the experimental spectrum, the numbers and the types of atoms interacting with the odd electron in order to obtain the coupling constants compatible with the given ESR spectrum within adjustable error limits (this approach resulted in a computer program which can handle spectra with up to 800 equidistant lines[2]) ; (ii) to produce a table of all possible ESR spectra with the given number M of equidistant lines. This second approach is developed in the present paper.

It is, of course, tedious to handle output data with a very large number of entries. Since the number of possible ESR spectra with equidistant lines increases sharply with increasing M, as will be shown in table 1, this paper presents only the cases with $M \leqslant 15$ lines. However, the program can be used for higher M values whenever necessary. Even with this limitation, we hope that the present data will be useful because the more complex ESR spectra often contain subgroups of a relatively small number of lines, which can be deciphered by comparing them with the table of all theoretical possibilities (table 3).

ESR SPECTRA WITH EQUIDISTANT *versus* NON-EQUIDISTANT LINES

In practice, ESR spectra with more or less equidistant lines appear at low resolution of the ESR spectrometer : as the resolution of the spectrometer increases, ESR spectra with equidistant lines occur less frequently.

One can illustrate for systems with two or three spins in what cases spectra with equidistant lines appear, by planar or tridimensional diagrams, respectively. For systems with two spins we illustrate in figure 1 three cases : two hydrogens, two nitrogens, and one hydrogen plus one nitrogen. The diagram for the first case (fig. 1i) consists in a pair of points (A and B) at distance a_H ; each of these points is the apex of an isosceles triangle whose height and base are equal to a_H. The intersections of these four lines emerging from the points A and B, with a straight line parallel to line AB at distance a'_{H}, give four points which represent the ESR spectrum. In the second case (fig. 1ii), there are three collinear points A, B, and C : distances AB and BC are equal to a_{N} ; from each of these points, three lines emerge with angles of 45° between them. Again, the nine intersections of these lines with a straight line, parallel to ABC at distance a'_{N} from it, determine a model of the ESR spectrum. In the third case the diagram may start either with the hydrogen coupling constant a_{H} (fig. 1iii), or with the nitrogen coupling constant a_{N} (fig. 1iv).

---

[3] N. Negoiţă, R. Baican and A. T. Balaban, *Rev. Roumaine Chim.*, **18**, 995 (1973).

* We impose as the only condition that the first and last lines always have intensities equal to 1.

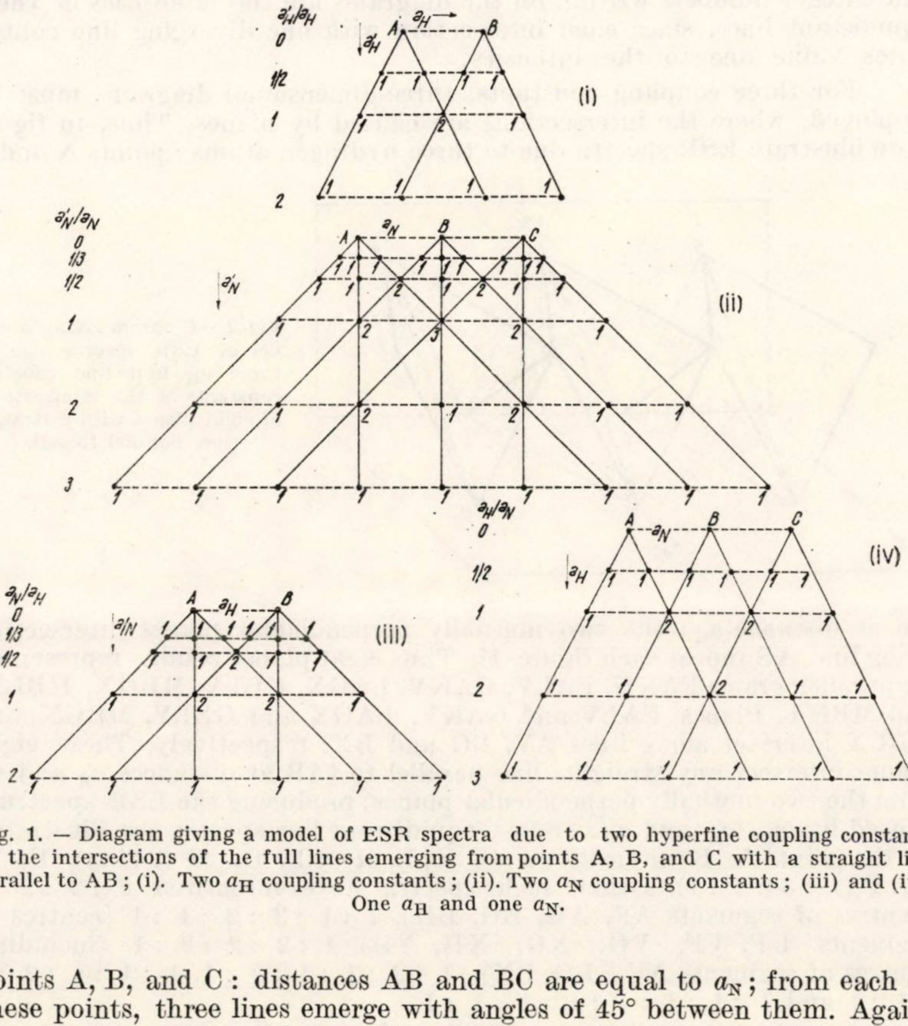

Fig. 1. — Diagram giving a model of ESR spectra due to two hyperfine coupling constants as the intersections of the full lines emerging from points A, B, and C with a straight line parallel to AB ; (i). Two a_{H} coupling constants ; (ii). Two a_{N} coupling constants ; (iii) and (iv). One a_{H} and one a_{N}.

To explore all possible ESR spectra with equidistant or non-equidistant lines due to two coupling constants for atoms with the same nuclear spin, it is sufficient in figures 1i and 1ii to sweep the ratio a/a' ranging only from zero to one. By translating the line parallel to AB through the prescribed range of a/a' values, one obtains an infinity of ESR spectra with non-equidistant lines, and a few spectra with equidistant lines corresponding to those a/a' ratios for which the divergent lines emerging from A, B(and C in appropriate cases) intersect among themselves. The integer numbers written on the diagrams are the intensities of these equidistant lines, since each intersection with one diverging line contributes value one to the intensity.

For three coupling constants, three-dimensional diagrams must be employed, where the intersections are caused by planes. Thus, in figure 2 we illustrate ESR spectra due to three hydrogen atoms : points A and B are at distance a_{H} ; the two mutually perpendicular planes intersecting along line AB repeat each figure 1i. Thus eight planes result, represented by parallelograms FAKU, FALV, GAKV, LAGX, GBLV, MBGX, HBLX, and MBHY. Planes FALV and GAKV, LAGX and GBLV, MBGX and HBLX intersect along lines AV, LG and BX, respectively. These eight planes intersect any straight line parallel to (AB at distances a'_{H} and a''_{H} from the two mutually perpendicular planes) producing the ESR spectrum caused by a_{H}, a'_{H} and a''_{H}. Some equidistant line spectra are illustrated by the points A, B (intensities 4 :4), K, L, M or F, G, H (2 :4 :2), U, V, X, Y (1 : 3 : 3 : 1). Other such spectra have intensities 2 : 2 : 2 : 2 (centres of segments AF, AG, BG, BH), 1 : 1 : 2 : 2 : 1 : 1 (centres of segments UF, VF, VG, XG, XH, YH), 1 : 2 : 2 : 2 : 1 (including centres of segments AV, LG, BX), 1 : 2 : 1 : 1 : 2 : 1, 1 : 1 : 1 : 2 : 1 : 1 : 1 and 1 : 1 : 1 : 1 : 1 : 1 : 1 : 1.

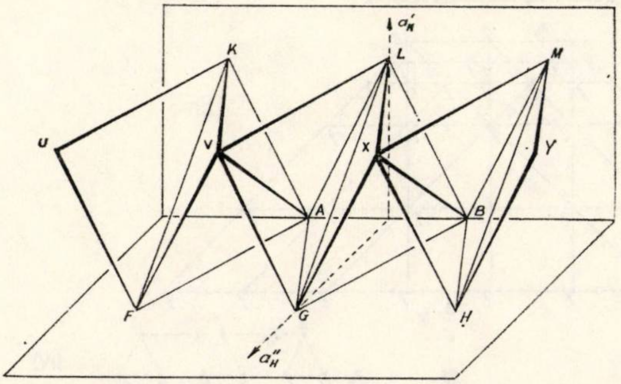

Fig. 2.—Diagram giving a model of ESR spectra due to three a_{H} hyperfine coupling constants as the intersections of eight planes with a straight line parallel to AB.

By this procedure one can easily survey the hyperfine couplings of ESR spectra due to two or three spins, but though it is possible to go beyond these numbers by a straightforward generalization to more than three dimensions, the visualization is lost.

One can see from the above diagrams that from the infinity of ESR spectra with non-equidistant lines, those spectra corresponding to certain ratios of hyperfine coupling constants approximate equidistant lines. The number of possible equidistant line spectra is quite small relatively to all possible (equidistant and non-equidistant) spectra. This serves to illustrate the usefulness of the present approach. By relating an experimental ESR spectrum to one or a few theoretical possibilities from a limited set, one can have a reasonable starting point for an exact determination of coupling constants by means of a spectrum simulator.[3]

DESCRIPTION OF THE PROGRAM

According to the performed jobs, the whole program can be split into three main parts:

I. *Generation of all spectra with a given number M of lines.* This task is accomplished by the modules:

subroutine DSPLY
subroutine MINIMA
subroutine PRDUCT
function INF
function C

As we suppose the reader to be familiar with the description of the last four modules,[2] we shall briefly comment on the first one, i. e. DSPLY. This module solves the diophantic system:

$$M-1=\sum_{i=1}^{M-1} i m_i + 2\sum_{j=1}^{M-1} j n_j$$

$$\chi_1=\sum_{i=1}^{M-1} m_i$$

$$\chi_2=\sum_{j=1}^{M-1} n_j$$

to find the values $m_1, m_2, \ldots$ for the partition numbers of atoms with spin $\frac{1}{2}$, and $n_1, n_2, \ldots$ for the partition numbers of atoms with spin 1. These partition numbers are then processed by MINIMA, PRDUCT, INF and C to yield the corresponding intensities of lines in the ESR spectrum.

II. *The arrangement of spectra in increasing order of magnitude of their intensities.* This is done by the MAINPGM itself together with the module:

subroutine COMP.

This module decides which one of the two given spectra has precedence, by successive comparison of their intensities starting from the leftmost margin. This comparison goes on as long as these intensities are equal. When a pair of unequal intensities is encountered, the spectrum with the smaller intensity is given priority. In this way the MAINPGM starts printing the smallest spectrum and proceeds along the well-known lines of sorting a set of objects (however, in this case the objects are arrays and one needs a generalized criterion for comparing them, which is just the job of COMP).

III. *Possible restrictions on the intensities of the spectra to be printed.* It may happen that one is not interested in the full output, i. e. all possible spectra with a given number of lines, M, arranged in increasing order of line intensity, but only in those spectra which exhibit a certain peculiarity. To allow for leaving out the rest of them, a module is included, called

subroutine COND

which causes the skipping of unwanted spectra.

We pass now to specific features of the above modules :

1. *Memory requirements*. To be able to perform the ordering, one must keep in the computer memory *all* spectra with a given number of lines. These are held in a matrix $V(i, j)$. Memory restriction led us to work up a table of spectra ranging from $M = 2$ to $M = 15$, because for $M \geqslant 16$, the spectra become too numerous for our computer memory. For the same reasons, we work with integers of reduced length (2 Bytes instead of 4) ; this is taken care of by appropriate INTEGER*2 statements. To further cut down the bulk of used storage, only half of a spectrum is retained and printed,* together with the corresponding values for partition numbers and coupling constants. All in all we gave a length of 28 locations (words) for every spectrum. This is quite enough for spectra with up to 20 lines. For spectra with more than 20 lines, provided one can accomodate them all at a time (as their number increases very fast, subroutine COND could be employed), one can design one's own format for printing the output. This would imply modification of the DIMENSION statements for the following arrays (see the MAINPGM) : V, PP, Q, LEAST, KMAX, LMAX, in that one assigns them the following amount of storage :

```
INTEGER*2 V, PP (MAXL), Q (MAXL), LEAST (MAXL),
KMAX, LMAX
COMMON V (MAXN, MAXL), KMAX (MAXN), LMAX (MAXN)
```

where MAXL = integer constant equal to the *estimated length* of the printing of one spectrum together with its partition numbers and coupling constants

MAXN = integer constant equal to the upper bound for the *number of spectra* with the given $M > 20$ number of lines.

2. *Arguments of the newly employed modules.*

a) subroutine DSPLY :

INTNUM = number of lines in the spectrum, i. e. M

HI1 = number of atoms with spin 1/2

HI2 = number of atoms with spin 1

ITAB = integer number used to print output in two different formats. To use the second format, set ITAB = −666666.

b) subroutine COMP :

FLAG = integer variable whose value can be +1 or −1. The value FLAG = +1 implies P bigger than Q, where

---

* Excepting the first spectrum in table 3, for M=2, which consists of only the two extreme lines.

P = integer*2 array that is to be compared
Q = integer*2 array that is to be compared
N = the largest value of index up to which comparison is made

c) subroutine COND.
I0 = integer constant equal to one, the first intensity of every spectrum
I = integer*2 array containing the next intensities of the spectrum
IT = integer constant whose value can be +1 or −1, according to whether the spectrum is to be printed or skipped.

In subroutine COND one can insert cards, specifying the particular features one is interested in. For instance, if one wishes to print only spectra whose second line has relative intensity 2, one has to insert the card :

IF (I(1). NE.2) IT = −1,
after the assignation card : IT = +1.

The listing of the new subroutines is presented in table 2 preceding the output (table 3).

DISCUSSION

Table 3 lists all possible ESR spectra with 2 through 15 equidistant lines (whose intensities may also be zero), presenting the number M of lines, the intensities of the first M/2 lines (for even M) or (M +1)/2 lines (for odd M), and the coupling constants (in *d* units, equal to the equidistance between lines). These coupling constants are formated in two groups, each one consisting of several diads : coupling constant*number of equal coupling constants/. E. g. 3*2/indicates that there are two equal coupling constants of magnitude 3*d* (three intervals). The first group includes couplings with nuclei of spin 1/2 (e. g. ^{1}H), while the second group includes couplings with nuclei of spin 1 (e. g. ^{14}N). For each spectrum the coupling constants are listed in decreasing order.

For a given number of lines the spectra are arranged in the order of increasing intensities of their lines. A special subroutine COMP was developed for ordering these spectra, considering the intensities of all their lines.

It may be seen that some ESR spectra are degenerate, i. e. the distribution of intensities can be assigned to two different sets of coupling constants.[1] Since intensities of ESR spectra due to interaction with χ_1 ^{1}H nuclei of coupling constant a_i are the binomial coefficients of $(x^{a_i} + 1)^{\chi_1}$, and those due to interaction with χ_2 ^{14}N nuclei of coupling constant a_j are [1] the trinominal coefficients of $(x^{2a_j} + x^{a_j} + 1)^{\chi_2}$, the intensities of an ESR spectrum of nitrogen free radicals (combining both types of nuclei) are the coefficients of the polynomial :

$$\prod_{i,j} (1 + x^{a_i})^{\chi_{1,i}} (1 + x^{a_j} + x^{2a_j})^{\chi_{2,j}}$$

Therefore, an ESR spectrum with six equal lines (intensities equal to 1) is degenerate, because from the equalities:

$$x^5+x^4+x^3+x^2+x+1=(x^3+1)(x^2+x+1)=(x+1)(x^4+x^2+1)$$

one sees that it can be ascribed either to a combination $a_{\mathrm{H}}=3$, $a_{\mathrm{N}}=1$, or to a combination $a_{\mathrm{H}}=1$, $a_{\mathrm{N}}=2$. These two combinations (or multiples thereof) appear in all degenerate ESR spectra. Thus, twelve equidistant lines of equal intensity (=1) constitute a triply degenerate ESR spectrum.

Table 1 was compiled on the basis of two runs of the program for up to 16 lines in the ESR spectrum: one in which the smallest number of atoms with nuclear spins 1/2 and 1 was at least one, and another in which it could be zero. The former run gave the numbers of possible ESR spectra with a_{H} *and* a_{N} presented in columns 2 and 4 of table 1, the latter run gave the remaining columns 1 and 3 with a_{H} *and/or* a_{N}. A semilogarithmic plot (fig. 3) of the data from table 1 indicates that the number of possible ESR spectra with M lines increases almost exponentially as a function of M. It can be observed that there is an alternation for even and odd N values in the number of possible ESR spectra with a_{H} and/or a_{N} (column 3) when some lines may have zero intensity and with a_{H} and a_{N} (column 2) when all lines have non-zero intensity. Maxima of column 3 occur for odd M, while maxima of column 2 occur for even M values. This alternation of column 3 values can be explained by the fact that for spectra with even N there exists the restriction that the number of hydrogen nuclei cannot be zero. When this restriction is applied to both ^{1}H

Table 1

Numbers of possibile ESR spectra of nitrogen free radicals with M equidistant lines in the spectrum (degenerate spectra are counted for each distinct set of coupling constants).

Number M of lines in the spectrum	Number of possible ESR spectra			
	All M lines have non-zero intensity		Some of the M lines may have zero intensity	
	With a_{H} and/or a_{N} (1)	With a_{H} and a_{N} (2)	With a_{H} and/or a_{N} (3)	With a_{H} and a_{N} (4)
2	1	0	1	0
3	2	0	3	0
4	3	1	4	1
5	5	2	9	2
6	9	5	12	5
7	14	7	23	9
8	21	13	31	16
9	35	22	54	27
10	53	37	73	43
11	77	52	118	69
12	118	88	159	103
13	171	128	246	158
14	244	192	329	228
15	355	276	489	339
16	495	399	649	472

and ^{14}N nuclei (number of ESR spectra with a_H and a_N, last column of table 1), the alternation disappears (fig. 3).

In conclusion, we have presented a program whose output is given in table 3 for M = 2—15 (but which table can be expanded for any desired number M of lines) giving an exhaustive list of all theoretical possible ESR spectra with M equidistant lines originating from the interaction of one odd electron with nuclei of spins 1/2 and 1. By comparing the intensities of any experimental ESR spectrum with those of the (expanded) table 3, one can pinpoint which set of coupling constants is compatible with the experimental spectrum, assisting in its interpretation. The philosophy of this approach for interpreting an ESR spectrum is best illustrated by the following quotation from A. Conan Doyle's "The Sign of the Four" and "The Beryl Coronet" : "When you have eliminated the impossible, wathever remains, however improbable, must be the truth".

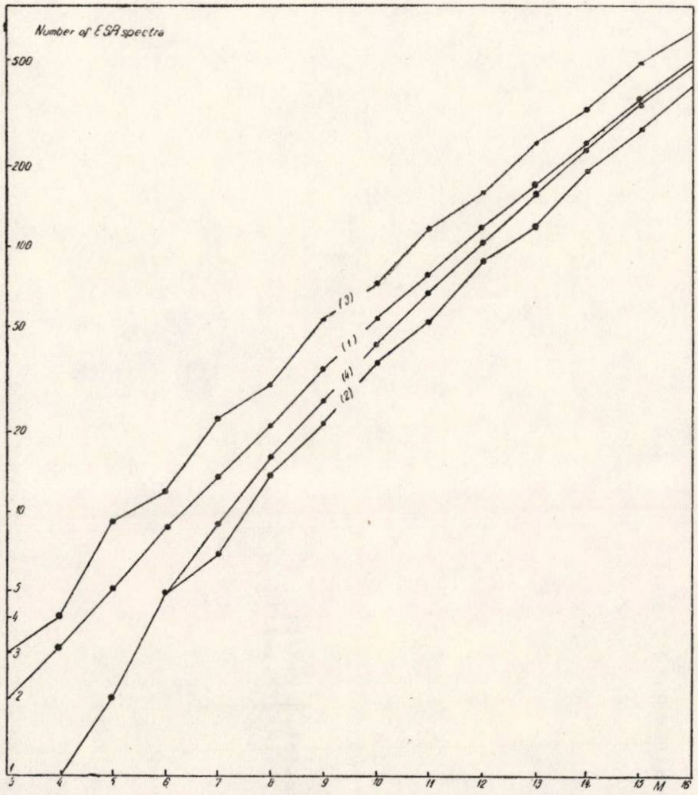

Fig. 3. — Semilogarithmic plot of the numbers of possible ESR spectra with M equidistant lines : the four curves correspond to the four columns (1)—(4) of table 1.

Table 2

Listing of subroutines which were not described previously.[2]

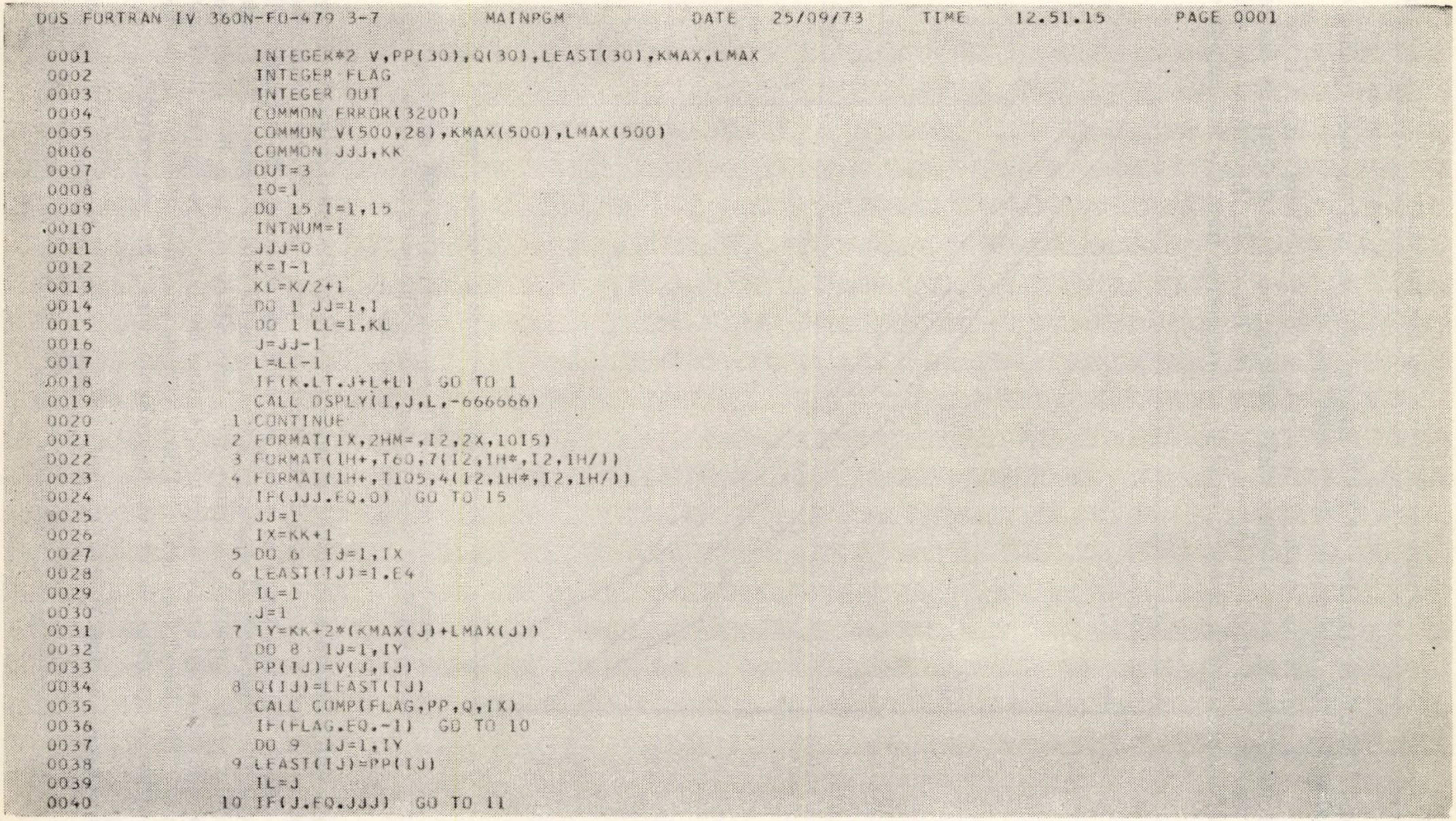

```
DOS FORTRAN IV 360N-FO-479 3-7          MAINPGM          DATE   25/09/73      TIME     12.51.15        PAGE 0001

      INTEGER*2 V,PP(30),Q(30),LEAST(30),KMAX,LMAX
      INTEGER FLAG
      INTEGER OUT
      COMMON ERROR(3200)
      COMMON V(500,28),KMAX(500),LMAX(500)
      COMMON JJJ,KK
      OUT=3
      IO=1
      DO 15 I=1,15
      INTNUM=I
      JJJ=0
      K=I-1
      KL=K/2+1
      DO 1 JJ=1,I
      DO 1 LL=1,KL
      J=JJ-1
      L=LL-1
      IF(K.LT.J+L+L)  GO TO 1
      CALL DSPLY(I,J,L,-666666)
    1 CONTINUE
    2 FORMAT(1X,2HM=,I2,2X,10I5)
    3 FORMAT(1H+,T60,7(I2,1H*,I2,1H/))
    4 FORMAT(1H+,T105,4(I2,1H*,I2,1H/))
      IF(JJJ.EQ.0)  GO TO 15
      JJ=1
      IX=KK+1
    5 DO 6  IJ=1,IX
    6 LEAST(IJ)=1.E4
      IL=1
      J=1
    7 IY=KK+2*(KMAX(J)+LMAX(J))
      DO 8  IJ=1,IY
      PP(IJ)=V(J,IJ)
    8 Q(IJ)=LEAST(IJ)
      CALL COMP(FLAG,PP,Q,IX)
      IF(FLAG.EQ.-1)  GO TO 10
      DO 9  IJ=1,IY
    9 LEAST(IJ)=PP(IJ)
      IL=J
   10 IF(J.EQ.JJJ)  GO TO 11
```

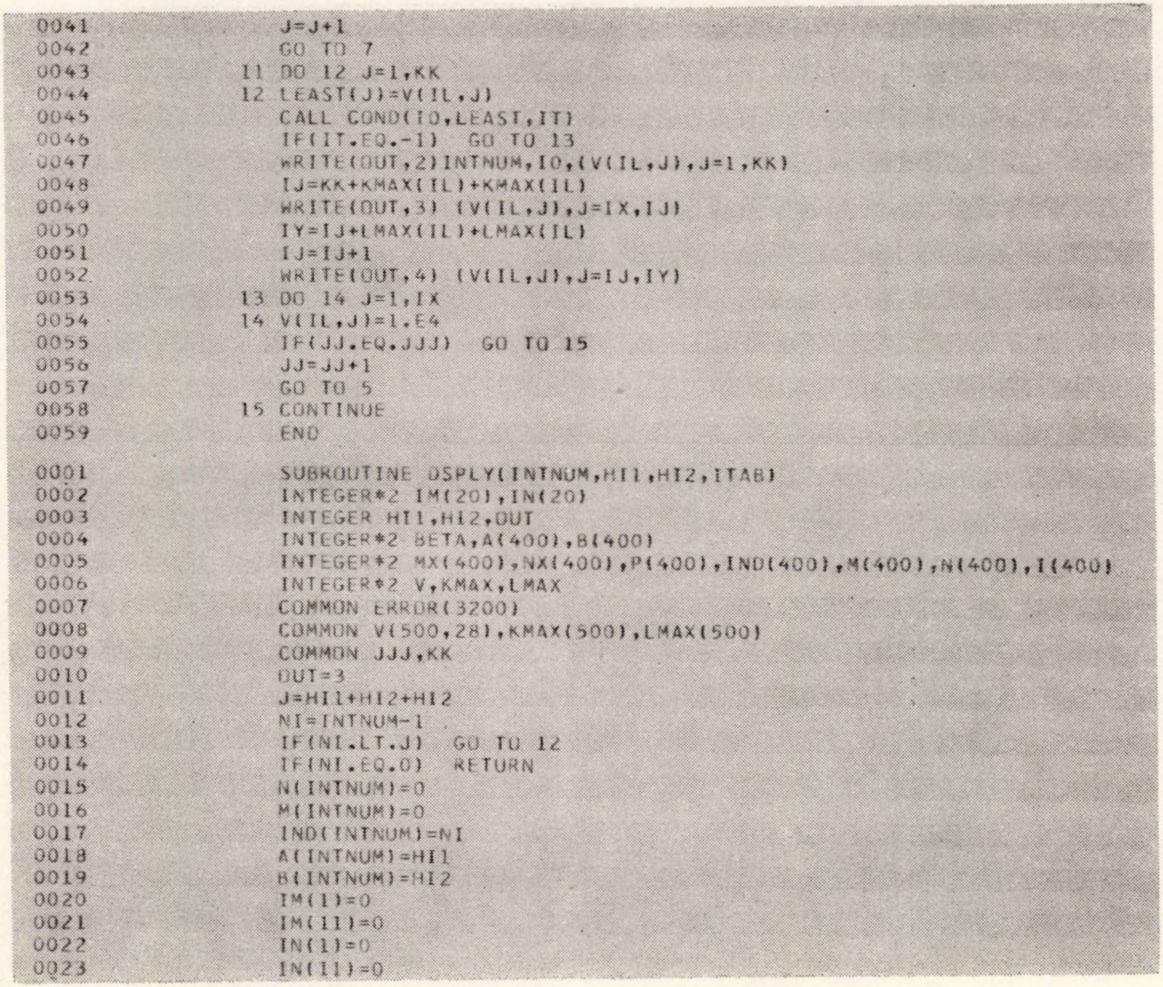

```
      J=J+1
      GO TO 7
   11 DO 12 J=1,KK
   12 LEAST(J)=V(IL,J)
      CALL COND(IO,LEAST,IT)
      IF(IT.EQ.-1)  GO TO 13
      wRITE(OUT,2)INTNUM,IO,(V(IL,J),J=1,KK)
      IJ=KK+KMAX(IL)+KMAX(IL)
      WRITE(OUT,3) (V(IL,J),J=IX,IJ)
      IY=IJ+LMAX(IL)+LMAX(IL)
      IJ=IJ+1
      WRITE(OUT,4) (V(IL,J),J=IJ,IY)
   13 DO 14 J=1,IX
   14 V(IL,J)=1.E4
      IF(JJ.EQ.JJJ)  GO TO 15
      JJ=JJ+1
      GO TO 5
   15 CONTINUE
      END

      SUBROUTINE DSPLY(INTNUM,HI1,HI2,ITAB)
      INTEGER*2 IM(20),IN(20)
      INTEGER HI1,HI2,OUT
      INTEGER*2 BETA,A(400),B(400)
      INTEGER*2 MX(400),NX(400),P(400),IND(400),M(400),N(400),I(400)
      INTEGER*2 V,KMAX,LMAX
      COMMON ERROR(3200)
      COMMON V(500,28),KMAX(500),LMAX(500)
      COMMON JJJ,KK
      OUT=3
      J=HI1+HI2+HI2
      NI=INTNUM-1
      IF(NI.LT.J)  GO TU 12
      IF(NI.EQ.0)  RETURN
      N(INTNUM)=0
      M(INTNUM)=0
      IND(INTNUM)=NI
      A(INTNUM)=HI1
      B(INTNUM)=HI2
      IM(1)=0
      IM(11)=0
      IN(1)=0
      IN(11)=0
      DO 1 J=1,NI
    1 P(J)=J
      J=1
    2 K=NI+1-J
      L=K+1
      BETA=IND(L)-L*(N(L)+N(L)+M(L))
      IF(J.EQ.INTNUM)  GO TO 4
      IND(K)=BETA
      A(K)=A(L)-M(L)
      B(K)=B(L)-N(L)
      BETA=IND(K)/(K+K)
      NX(K)=INF(B(K),BETA)
      BETA=IND(K)/K
      MX(K)=INF(A(K),BETA)
      N(K)=NX(K)
    3 BETA=IND(K)-2*K*N(K)
      BETA=BETA/K
      M(K)=INF(MX(K),BETA)
      J=J+1
      GO TO 2
    4 IF(BETA.NE.0)  GO TO 9
      IF(A(1).NE.M(1))  GO TO 9
      IF(B(1).NE.N(1))  GO TO 9
      J=NI
    5 IF(N(J)+M(J).EQ.0)  GO TO 6
      LL=J
      IF(ITAB.EQ.-666666)  GO TO 18
      GO TO 7
    6 J=J-1
      GO TO 5
    7 DO 8 J=1,NI
    8 CALL MINIMA(LL,P,N,M,J,I(J))
      IO=1
      WRITE(OUT,14) IO,(I(J),J=1,NI)
      WRITE(OUT,14)  (P(J),J=1,NI)
      WRITE(OUT,15)  (M(J),J=1,NI)
      WRITE(OUT,16)  (P(J),J=1,NI)
      WRITE(OUT,15)  (N(J),J=1,NI)
    9 J=NI-1
   10 K=NI+1-J
      IF(M(K).GT.0)  GO TO 17
      IF(N(K).GT.0)  GO TO 11
      IF(J.LE.1)  RETURN
      J=J-1
      GO TO 10
   11 N(K)=N(K)-1
      GO TO 3
   12 WRITE(OUT,13)  J,NI
   13 FORMAT(1X,'TOO SMALL NUMBER OF INTERVALS',2I20/)
   14 FORMAT(////(/20I6))
   15 FORMAT(/(20I6/))
   16 FORMAT(/(/20I6))
      RETURN
   17 J=J+1
      M(K)=M(K)-1
      GO TO 2
   18 KK=NI/2
      IF(KK.EQ.0)  KK=1
      DO 19 J=1,KK
   19  CALL MINIMA(LL,P,N,M,J,I(J))
      J=LL
      KMAX(JJJ+1)=0
      LMAX(JJJ+1)=0
   20 IF(M(J).NE.0)  GO TO 23
   21 IF(N(J).NE.0)  GO TO 24
   22 IF(J.EQ.1)  GO TO 25
      J=J-1
      GO TO 20
   23 KMAX(JJJ+1)=KMAX(JJJ+1)+1
      L=KMAX(JJJ+1)
      IM(L)=J
      IM(10+L)=M(J)
      GO TO 21
   24 LMAX(JJJ+1)=LMAX(JJJ+1)+1
      L=LMAX(JJJ+1)
      IN(L)=J
      IN(10+L)=N(J)
      GO TO 22
   25 JJJ=JJJ+1
      DO 26 J=1,KK
   26 V(JJJ,J)=I(J)
      IF(KMAX(JJJ).EQ.0)   KMAX(JJJ)=1
      L=KMAX(JJJ)
      DO 27 J=1,L
      IX=KK+J+J-1
      V(JJJ,IX)=IM(J)
```

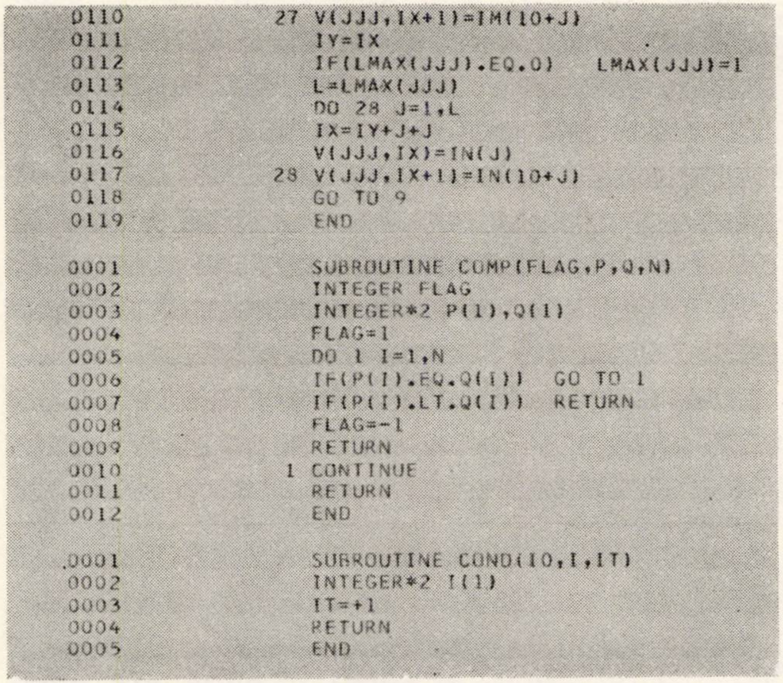

```
27 V(JJJ,IX+1)=IM(10+J)
   IY=IX
   IF(LMAX(JJJ).EQ.0)   LMAX(JJJ)=1
   L=LMAX(JJJ)
   DO 28 J=1,L
   IX=IY+J+J
   V(JJJ,IX)=IN(J)
28 V(JJJ,IX+1)=IN(10+J)
   GO TO 9
   END

   SUBROUTINE COMP(FLAG,P,Q,N)
   INTEGER FLAG
   INTEGER*2 P(1),Q(1)
   FLAG=1
   DO 1 I=1,N
   IF(P(I).EQ.Q(I))  GO TO 1
   IF(P(I).LT.Q(I))  RETURN
   FLAG=-1
   RETURN
 1 CONTINUE
   RETURN
   END

   SUBROUTINE COND(IO,I,IT)
   INTEGER*2 I(1)
   IT=+1
   RETURN
   END
```

Table 3

ESR spectra with M equidistant lines

```
M= 2     1   1                    1* 1/                      0* 0/
M= 3     1   0                    2* 1/                      0* 0/
M= 3     1   1                    0* 0/                      1* 1/
M= 3     1   2                    1* 2/                      0* 0/
M= 4     1   0                    3* 1/                      0* 0/
M= 4     1   1                    2* 1/ 1* 1/                0* 0/
M= 4     1   2                    1* 1/                      1* 1/
M= 4     1   3                    1* 3/                      0* 0/
M= 5     1   0    0               4* 1/                      0* 0/
M= 5     1   0    1               0* 0/                      2* 1/
M= 5     1   0    2               2* 2/                      0* 0/
M= 5     1   1    0               3* 1/ 1* 1/                0* 0/
M= 5     1   1    2               2* 1/                      1* 1/
M= 5     1   2    2               2* 1/ 1* 2/                0* 0/
M= 5     1   2    3               0* 0/                      1* 2/
M= 5     1   3    4               1* 2/                      1* 1/
M= 5     1   4    6               1* 4/                      0* 0/
M= 6     1   0    0               5* 1/                      0* 0/
M= 6     1   0    1               3* 1/ 2* 1/                0* 0/
M= 6     1   1    0               4* 1/ 1* 1/                0* 0/
M= 6     1   1   -1               1* 1/                      2* 1/
M= 6     1   1    1               3* 1/                      1* 1/
M= 6     1   1    2               2* 2/ 1* 1/                0* 0/
M= 6     1   2    1               3* 1/ 1* 2/                0* 0/
M= 6     1   2    3               2* 1/ 1* 1/                1* 1/
M= 6     1   3    4               2* 1/ 1* 3/                0* 0/
M= 6     1   3    5               1* 1/                      1* 2/
M= 6     1   4    7               1* 3/                      1* 1/
M= 6     1   5   10               1* 5/                      0* 0/
M= 7     1   0    0    0          6* 1/                      0* 0/
M= 7     1   0    0    1          0* 0/                      3* 1/
M= 7     1   0    0    2          3* 2/                      0* 0/
M= 7     1   0    1    0          4* 1/ 2* 1/                0* 0/
M= 7     1   0    2    0          2* 1/                      2* 1/
M= 7     1   0    3    0          2* 3/                      0* 0/
M= 7     1   1    0    0          5* 1/ 1* 1/                0* 0/
M= 7     1   1    1    0          4* 1/                      1* 1/
M= 7     1   1    1    2          3* 1/ 2* 1/ 1* 1/          0* 0/
M= 7     1   1    2    1          0* 0/                      2* 1/ 1* 1/
M= 7     1   1    3    2          2* 2/                      1* 1/
M= 7     1   2    1    0          4* 1/ 1* 2/                0* 0/
M= 7     1   2    2    2          1* 2/                      2* 1/
M= 7     1   2    2    2          3* 1/ 1* 1/                1* 1/
```

```
M= 7    1   2   3   4                  2* 2/ 1* 2/                  0* 0/
M= 7    1   2   4   4                  2* 1/                        1* 2/
M= 7    1   3   3   2                  3* 1/ 1* 3/                  0* 0/
M= 7    1   3   5   6                  2* 1/ 1* 2/                  1* 1/
M= 7    1   3   6   7                  0* 0/                        1* 3/
M= 7    1   4   7   8                  2* 1/ 1* 4/                  0* 0/
M= 7    1   4   8  10                  1* 2/                        1* 2/
M= 7    1   5  11  14                  1* 4/                        1* 1/
M= 7    1   6  15  20                  1* 6/                        0* 0/
M= 8    1   0   0   0                  7* 1/                        0* 0/
M= 8    1   0   0   1                  4* 1/ 3* 1/                  0* 0/
M= 8    1   0   1   0                  5* 1/ 2* 1/                  0* 0/
M= 8    1   0   1   1                  3* 1/                        2* 1/
M= 8    1   0   2   1                  3* 1/ 2* 2/                  0* 0/
M= 8    1   1   0   0                  6* 1/ 1* 1/                  0* 0/
M= 8    1   1   0   1                  1* 1/                        3* 1/
M= 8    1   1   0   2                  3* 2/ 1* 1/                  0* 0/
M= 8    1   1   1   0                  5* 1/                        1* 1/
M= 8    1   1   1   1                  4* 1/ 2* 1/ 1* 1/            0* 0/
M= 8    1   1   2   2                  2* 1/ 1* 1/                  2* 1/
M= 8    1   1   2   2                  3* 1/ 2* 1/                  1* 1/
M= 8    1   1   3   3                  2* 3/ 1* 1/                  0* 0/
M= 8    1   2   1   0                  5* 1/ 1* 2/                  0* 0/
M= 8    1   2   2   1                  4* 1/ 1* 1/                  1* 1/
M= 8    1   2   2   3                  3* 1/ 2* 1/ 1* 2/            0* 0/
M= 8    1   2   3   3                  1* 1/                        2* 1/ 1* 1/
M= 8    1   2   3   3                  3* 1/                        1* 2/
M= 8    1   2   4   5                  2* 2/ 1* 1/                  1* 1/
M= 8    1   3   3   1                  4* 1/ 1* 3/                  0* 0/
M= 8    1   3   4   4                  1* 3/                        2* 1/
M= 8    1   3   4   4                  3* 1/ 1* 2/                  1* 1/
M= 8    1   3   5   7                  2* 2/ 1* 3/                  0* 0/
M= 8    1   3   6   8                  2* 1/ 1* 1/                  1* 2/
M= 8    1   4   6   5                  3* 1/ 1* 4/                  0* 0/
M= 8    1   4   8  11                  2* 1/ 1* 3/                  1* 1/
M= 8    1   4   9  13                  1* 1/                        1* 3/
M= 8    1   5  11  15                  2* 1/ 1* 5/                  0* 0/
M= 8    1   5  12  18                  1* 3/                        1* 2/
M= 8    1   6  16  25                  1* 5/                        1* 1/
M= 8    1   7  21  35                  1* 7/                        0* 0/
M= 9    1   0   0   0   0              8* 1/                        0* 0/
M= 9    1   0   0   0   1              0* 0/                        4* 1/
M= 9    1   0   0   0   2              4* 2/                        0* 0/
```

```
M= 9      1    0    0    1    0                   5* 1/ 3* 1/                        0* 0/
M= 9      1    0    1    0    0                   6* 1/ 2* 1/                        0* 0/
M= 9      1    0    1    0    2                   4* 1/                              2* 1/
M= 9      1    0    1    1    0                   2* 1/                              3* 1/
M= 9      1    0    1    2    0                   3* 2/ 2* 1/                        0* 0/
M= 9      1    0    2    0    2                   4* 1/ 2* 2/                        0* 0/
M= 9      1    0    2    0    3                   0* 0/                              2* 2/
M= 9      1    0    3    0    4                   2* 2/                              2* 1/
M= 9      1    0    4    0    6                   2* 4/                              0* 0/
M= 9      1    1    0    0    0                   7* 1/ 1* 1/                        0* 0/
M= 9      1    1    0    1    2                   4* 1/ 1* 1/ 1* 1/                  0* 0/
M= 9      1    1    1    0    0                   6* 1/                              1* 1/
M= 9      1    1    1    1    0                   5* 1/ 2* 1/ 1* 1/                  0* 0/
M= 9      1    1    1    1    1                   0* 0/                              3* 1/ 1* 1/
M= 9      1    1    1    2    2                   3* 1/ 1* 1/                        2* 1/
M= 9      1    1    1    2    2                   3* 2/                              1* 1/
M= 9      1    1    2    1    2                   4* 1/ 2* 1/                        1* 1/
M= 9      1    1    2    3    2                   3* 1/ 2* 2/ 1* 1/                  0* 0/
M= 9      1    1    3    2    4                   2* 1/                              2* 1/ 1* 1/
M= 9      1    1    4    3    6                   2* 3/                              1* 1/
M= 9      1    2    1    0    0                   6* 1/ 1* 2/                        0* 0/
M= 9      1    2    1    1    2                   1* 2/                              3* 1/
M= 9      1    2    1    2    4                   3* 2/ 1* 2/                        0* 0/
M= 9      1    2    2    1    0                   5* 1/ 1* 1/                        1* 1/
M= 9      1    2    2    2    2                   4* 1/ 2* 1/ 1* 2/                  0* 0/
M= 9      1    2    3    2    2                   4* 1/                              1* 2/
M= 9      1    2    3    4    4                   2* 1/ 1* 2/                        2* 1/
M= 9      1    2    3    4    4                   3* 1/ 2* 1/ 1* 1/                  1* 1/
M= 9      1    2    4    4    5                   0* 0/                              2* 1/ 1* 2/
M= 9      1    2    4    6    6                   2* 3/ 1* 2/                        0* 0/
M= 9      1    2    5    6    8                   2* 2/                              1* 2/
M= 9      1    3    3    1    0                   5* 1/ 1* 3/                        0* 0/
M= 9      1    3    4    3    2                   4* 1/ 1* 2/                        1* 1/
M= 9      1    3    4    5    6                   3* 1/ 2* 1/ 1* 3/                  0* 0/
M= 9      1    3    5    6    6                   1* 2/                              2* 1/ 1* 1/
M= 9      1    3    5    6    6                   3* 1/ 1* 1/                        1* 2/
M= 9      1    3    6    9   10                   2* 2/ 1* 2/                        1* 1/
M= 9      1    3    7   10   12                   2* 1/                              1* 3/
M= 9      1    4    6    4    2                   4* 1/ 1* 4/                        0* 0/
M= 9      1    4    7    8    8                   1* 4/                              2* 1/
M= 9      1    4    7    8    8                   3* 1/ 1* 3/                        1* 1/
M= 9      1    4    8   12   14                   2* 2/ 1* 4/                        0* 0/
M= 9      1    4    9   14   16                   2* 1/ 1* 2/                        1* 2/
```

```
M= 9    1   4   10   16   19                    0* 0/                               1* 4/
M= 9    1   5   10   11   10                    3* 1/ 1* 5/                         0* 0/
M= 9    1   5   12   19   22                    2* 1/ 1* 4/                         1* 1/
M= 9    1   5   13   22   26                    1* 2/                               1* 3/
M= 9    1   6   16   26   30                    2* 1/ 1* 6/                         0* 0/
M= 9    1   6   17   30   36                    1* 4/                               1* 2/
M= 9    1   7   22   41   50                    1* 6/                               1* 1/
M= 9    1   8   28   56   70                    1* 8/                               0* 0/
M=10    1   0    0    0    0                    9* 1/                               0* 0/
M=10    1   0    0    0    1                    5* 1/ 4* 1/                         0* 0/
M=10    1   0    0    1    0                    6* 1/ 3* 1/                         0* 0/
M=10    1   0    0    2    0                    3* 1/                               3* 1/
M=10    1   0    0    3    0                    3* 3/                               0* 0/
M=10    1   0    1    0    0                    7* 1/ 2* 1/                         0* 0/
M=10    1   0    1    0    1                    5* 1/                               2* 1/
M=10    1   0    1    1    1                    4* 1/ 3* 1/ 2* 1/                   0* 0/
M=10    1   0    2    0    1                    5* 1/ 2* 2/                         0* 0/
M=10    1   0    2    1    2                    3* 1/ 2* 1/                         2* 1/
M=10    1   0    3    1    3                    3* 1/ 2* 3/                         0* 0/
M=10    1   1    0    0    0                    8* 1/ 1* 1/                         0* 0/
M=10    1   1    0    0    1                    1* 1/                               4* 1/
M=10    1   1    0    0    2                    4* 2/ 1* 1/                         0* 0/
M=10    1   1    0    1    1                    5* 1/ 3* 1/ 1* 1/                   0* 0/
M=10    1   1    1    0    0                    7* 1/                               1* 1/
M=10    1   1    1    1    0                    6* 1/ 2* 1/ 1* 1/                   0* 0/
M=10    1   1    1    1    2                    4* 1/ 1* 1/                         2* 1/
M=10    1   1    1    1    2                    4* 1/ 3* 1/                         1* 1/
M=10    1   1    1    2    1                    2* 1/ 1* 1/                         3* 1/
M=10    1   1    1    3    2                    3* 2/ 2* 1/ 1* 1/                   0* 0/
M=10    1   1    2    1    1                    5* 1/ 2* 1/                         1* 1/
M=10    1   1    2    2    2                    4* 1/ 2* 2/ 1* 1/                   0* 0/
M=10    1   1    2    2    3                    1* 1/                               2* 2/
M=10    1   1    2    2    3                    3* 1/                               2* 1/ 1* 1/
M=10    1   1    3    3    4                    2* 2/ 1* 1/                         2* 1/
M=10    1   1    3    3    4                    3* 1/ 2* 2/                         1* 1/
M=10    1   1    4    4    6                    2* 4/ 1* 1/                         0* 0/
M=10    1   2    1    0    0                    7* 1/ 1* 2/                         0* 0/
M=10    1   2    1    1    3                    4* 1/ 3* 1/ 1* 2/                   0* 0/
M=10    1   2    2    1    0                    6* 1/ 1* 1/                         1* 1/
M=10    1   2    2    2    1                    5* 1/ 2* 1/ 1* 2/                   0* 0/
M=10    1   2    2    2    2                    1* 1/                               3* 1/ 1* 1/
M=10    1   2    2    3    4                    3* 1/ 1* 2/                         2* 1/
M=10    1   2    2    3    4                    3* 2/ 1* 1/                         1* 1/
```

```
M=10   1   2   3   2   1                    5* 1/                             1* 2/
M=10   1   2   3   3   3                    4* 1/  2* 1/  1* 1/               1* 1/
M=10   1   2   3   5   5                    3* 1/  2* 2/  1* 2/               0* 0/
M=10   1   2   4   5   6                    2* 1/  1* 1/                      2* 1/  1* 1/
M=10   1   2   4   5   6                    3* 1/  2* 1/                      1* 2/
M=10   1   2   5   7   9                    2* 3/  1* 1/                      1* 1/
M=10   1   3   3   1   0                    6* 1/  1* 3/                      0* 0/
M=10   1   3   3   2   3                    1* 3/                             3* 1/
M=10   1   3   3   3   6                    3* 2/  1* 3/                      0* 0/
M=10   1   3   4   3   1                    5* 1/  1* 2/                      1* 1/
M=10   1   3   4   4   4                    4* 1/  2* 1/  1* 3/               0* 0/
M=10   1   3   5   5   4                    4* 1/  1* 1/                      1* 2/
M=10   1   3   5   7   8                    2* 1/  1* 3/                      2* 1/
M=10   1   3   5   7   8                    3* 1/  2* 1/  1* 2/               1* 1/
M=10   1   3   6   8   9                    1* 1/                             2* 1/  1* 2/
M=10   1   3   6   8   9                    3* 1/                             1* 3/
M=10   1   3   6  10  12                    2* 3/  1* 3/                      0* 0/
M=10   1   3   7  11  14                    2* 2/  1* 1/                      1* 2/
M=10   1   4   6   4   1                    5* 1/  1* 4/                      0* 0/
M=10   1   4   7   7   5                    4* 1/  1* 3/                      1* 1/
M=10   1   4   7   9  11                    3* 1/  2* 1/  1* 4/               0* 0/
M=10   1   4   8  11  12                    1* 3/                             2* 1/  1* 1/
M=10   1   4   8  11  12                    3* 1/  1* 2/                      1* 2/
M=10   1   4   9  15  19                    2* 2/  1* 3/                      1* 1/
M=10   1   4  10  17  22                    2* 1/  1* 1/                      1* 3/
M=10   1   5  10  10   6                    4* 1/  1* 5/                      0* 0/
M=10   1   5  11  15  16                    1* 5/                             2* 1/
M=10   1   5  11  15  16                    3* 1/  1* 4/                      1* 1/
M=10   1   5  12  20  26                    2* 2/  1* 5/                      0* 0/
M=10   1   5  13  23  30                    2* 1/  1* 3/                      1* 2/
M=10   1   5  14  26  35                    1* 1/                             1* 4/
M=10   1   6  15  21  21                    3* 1/  1* 6/                      0* 0/
M=10   1   6  17  31  41                    2* 1/  1* 5/                      1* 1/
M=10   1   6  18  35  48                    1* 3/                             1* 3/
M=10   1   7  22  42  56                    2* 1/  1* 7/                      0* 0/
M=10   1   7  23  47  66                    1* 5/                             1* 2/
M=10   1   8  29  63  91                    1* 7/                             1* 1/
M=10   1   9  36  84 126                    1* 9/                             0* 0/
M=11   1   0   0   0   0   0               10* 1/                             0* 0/
M=11   1   0   0   0   0   1                0* 0/                             5* 1/
M=11   1   0   0   0   0   2                5* 2/                             0* 0/
M=11   1   0   0   0   1   0                6* 1/  4* 1/                      0* 0/
M=11   1   0   0   1   0   0                7* 1/  3* 1/                      0* 0/
```

```
M=11   1  0  0  1   1  0        4* 1/                       3* 1/
M=11   1  0  0  2   1  0        4* 1/ 3* 2/                 0* 0/
M=11   1  0  1  0   0  0        8* 1/ 2* 1/                 0* 0/
M=11   1  0  1  0   1  0        2* 1/                       4* 1/
M=11   1  0  1  0   1  0        6* 1/                       2* 1/
M=11   1  0  1  0   2  0        4* 2/ 2* 1/                 0* 0/
M=11   1  0  1  1   0  2        5* 1/ 3* 1/ 2* 1/           0* 0/
M=11   1  0  1  1   1  1        0* 0/                       3* 1/ 2* 1/
M=11   1  0  1  2   1  2        3* 2/                       2* 1/
M=11   1  0  2  0   1  0        6* 1/ 2* 2/                 0* 0/
M=11   1  0  2  0   3  0        4* 1/ 2* 1/                 2* 1/
M=11   1  0  2  1   1  2        2* 2/                       3* 1/
M=11   1  0  2  2   1  4        3* 2/ 2* 2/                 0* 0/
M=11   1  0  3  0   4  0        4* 1/ 2* 3/                 0* 0/
M=11   1  0  3  0   5  0        2* 1/                       2* 2/
M=11   1  0  4  0   7  0        2* 3/                       2* 1/
M=11   1  0  5  0  10  0        2* 5/                       0* 0/
M=11   1  1  0  0   0  0        9* 1/ 1* 1/                 0* 0/
M=11   1  1  0  0   1  2        5* 1/ 4* 1/ 1* 1/           0* 0/
M=11   1  1  0  1   1  0        6* 1/ 3* 1/ 1* 1/           0* 0/
M=11   1  1  0  2   2  0        3* 1/ 1* 1/                 3* 1/
M=11   1  1  0  3   3  0        3* 3/ 1* 1/                 0* 0/
M=11   1  1  1  0   0  0        8* 1/                       1* 1/
M=11   1  1  1  0   1  1        0* 0/                       4* 1/ 1* 1/
M=11   1  1  1  0   2  2        4* 2/                       1* 1/
M=11   1  1  1  1   0  0        7* 1/ 2* 1/ 1* 1/           0* 0/
M=11   1  1  1  1   1  2        5* 1/ 1* 1/                 2* 1/
M=11   1  1  1  1   1  2        5* 1/ 3* 1/                 1* 1/
M=11   1  1  1  2   2  2        4* 1/ 3* 1/ 2* 1/ 1* 1/     0* 0/
M=11   1  1  2  1   1  0        6* 1/ 2* 1/                 1* 1/
M=11   1  1  2  1   3  2        4* 1/                       2* 1/ 1* 1/
M=11   1  1  2  2   1  2        5* 1/ 2* 2/ 1* 1/           0* 0/
M=11   1  1  2  2   2  2        2* 1/                       3* 1/ 1* 1/
M=11   1  1  2  3   3  4        3* 1/ 2* 1/ 1* 1/           2* 1/
M=11   1  1  2  3   3  4        3* 2/ 2* 1/                 1* 1/
M=11   1  1  3  2   4  2        4* 1/ 2* 2/                 1* 1/
M=11   1  1  3  2   5  3        0* 0/                       2* 2/ 1* 1/
M=11   1  1  3  4   4  6        3* 1/ 2* 3/ 1* 1/           0* 0/
M=11   1  1  4  3   7  4        2* 2/                       2* 1/ 1* 1/
M=11   1  1  5  4  10  6        2* 4/                       1* 1/
M=11   1  2  1  0   0  0        8* 1/ 1* 2/                 0* 0/
M=11   1  2  1  0   1  2        1* 2/                       4* 1/
M=11   1  2  1  0   2  4        4* 2/ 1* 2/                 0* 0/
```

```
M=11     1   2   1   1   2   2              5* 1/ 3* 1/ 1* 2/                 0* 0/
M=11     1   2   2   1   0   0              7* 1/ 1* 1/                       1* 1/
M=11     1   2   2   2   1   0              6* 1/ 2* 1/ 1* 2/                 0* 0/
M=11     1   2   2   2   3   4              4* 1/ 1* 2/                       2* 1/
M=11     1   2   2   2   3   4              4* 1/ 3* 1/ 1* 1/                 1* 1/
M=11     1   2   2   3   3   2              2* 1/ 1* 2/                       3* 1/
M=11     1   2   2   4   5   4              3* 2/ 2* 1/ 1* 2/                 0* 0/
M=11     1   2   3   2   1   0              6* 1/                             1* 2/
M=11     1   2   3   3   2   2              5* 1/ 2* 1/ 1* 1/                 1* 1/
M=11     1   2   3   3   3   3              0* 0/                             3* 1/ 1* 2/
M=11     1   2   3   4   4   4              4* 1/ 2* 2/ 1* 2/                 0* 0/
M=11     1   2   3   4   5   6              1* 2/                             2* 2/
M=11     1   2   3   4   5   6              3* 1/ 1* 1/                       2* 1/ 1* 1/
M=11     1   2   3   4   5   6              3* 2/                             1* 2/
M=11     1   2   4   4   5   4              4* 1/ 2* 1/                       1* 2/
M=11     1   2   4   6   7   8              2* 2/ 1* 2/                       2* 1/
M=11     1   2   4   6   7   8              3* 1/ 2* 2/ 1* 1/                 1* 1/
M=11     1   2   5   6   9   8              2* 1/                             2* 1/ 1* 2/
M=11     1   2   5   8  10  12              2* 4/ 1* 2/                       0* 0/
M=11     1   2   6   8  13  12              2* 3/                             1* 2/
M=11     1   3   3   1   0   0              7* 1/ 1* 3/                       0* 0/
M=11     1   3   3   2   4   6              4* 1/ 3* 1/ 1* 3/                 0* 0/
M=11     1   3   4   3   1   0              6* 1/ 1* 2/                       1* 1/
M=11     1   3   4   4   3   2              5* 1/ 2* 1/ 1* 3/                 0* 0/
M=11     1   3   4   4   4   4              1* 2/                             3* 1/ 1* 1/
M=11     1   3   4   5   7   8              3* 1/ 1* 3/                       2* 1/
M=11     1   3   4   5   7   8              3* 2/ 1* 2/                       1* 1/
M=11     1   3   5   5   3   2              5* 1/ 1* 1/                       1* 2/
M=11     1   3   5   6   6   6              4* 1/ 2* 1/ 1* 2/                 1* 1/
M=11     1   3   5   8  10  10              3* 1/ 2* 2/ 1* 3/                 0* 0/
M=11     1   3   6   7   7   6              4* 1/                             1* 3/
M=11     1   3   6   9  11  12              2* 1/ 1* 2/                       2* 1/ 1* 1/
M=11     1   3   6   9  11  12              3* 1/ 2* 1/ 1* 1/                 1* 2/
M=11     1   3   7  10  13  13              0* 0/                             2* 1/ 1* 3/
M=11     1   3   7  12  16  18              2* 3/ 1* 2/                       1* 1/
M=11     1   3   8  13  19  20              2* 2/                             1* 3/
M=11     1   4   6   4   1   0              6* 1/ 1* 4/                       0* 0/
M=11     1   4   6   5   5   6              1* 4/                             3* 1/
M=11     1   4   6   6   9  12              3* 2/ 1* 4/                       0* 0/
M=11     1   4   7   7   4   2              5* 1/ 1* 3/                       1* 1/
M=11     1   4   7   8   8   8              4* 1/ 2* 1/ 1* 4/                 0* 0/
M=11     1   4   8  10   9   8              4* 1/ 1* 2/                       1* 2/
M=11     1   4   8  12  15  16              2* 1/ 1* 4/                       2* 1/
```

```
M=11    1   4   8   12   15   16           3* 1/ 2* 1/ 1* 3/          1* 1/
M=11    1   4   9   14   17   18           1* 2/                      2* 1/ 1* 2/
M=11    1   4   9   14   17   18           3* 1/ 1* 1/                1* 3/
M=11    1   4   9   16   22   24           2* 3/ 1* 4/                0* 0/
M=11    1   4  10   18   25   28           2* 2/ 1* 2/                1* 2/
M=11    1   4  11   20   29   32           2* 1/                      1* 4/
M=11    1   5  10   10    5    2           5* 1/ 1* 5/                0* 0/
M=11    1   5  11   14   12   10           4* 1/ 1* 4/                1* 1/
M=11    1   5  11   16   20   22           3* 1/ 2* 1/ 1* 5/          0* 0/
M=11    1   5  12   19   23   24           1* 4/                      2* 1/ 1* 1/
M=11    1   5  12   19   23   24           3* 1/ 1* 3/                1* 2/
M=11    1   5  13   24   34   38           2* 2/ 1* 4/                1* 1/
M=11    1   5  14   27   39   44           2* 1/ 1* 2/                1* 3/
M=11    1   5  15   30   45   51           0* 0/                      1* 5/
M=11    1   6  15   20   16   12           4* 1/ 1* 6/                0* 0/
M=11    1   6  16   26   31   32           1* 6/                      2* 1/
M=11    1   6  16   26   31   32           3* 1/ 1* 5/                1* 1/
M=11    1   6  17   32   46   52           2* 2/ 1* 6/                0* 0/
M=11    1   6  18   36   53   60           2* 1/ 1* 4/                1* 2/
M=11    1   6  19   40   61   70           1* 2/                      1* 4/
M=11    1   7  21   36   42   42           3* 1/ 1* 7/                0* 0/
M=11    1   7  23   48   72   82           2* 1/ 1* 6/                1* 1/
M=11    1   7  24   53   83   96           1* 4/                      1* 3/
M=11    1   8  29   64   98  112           2* 1/ 1* 8/                0* 0/
M=11    1   8  30   70  113  132           1* 6/                      1* 2/
M=11    1   9  37   92  154  182           1* 8/                      1* 1/
M=11    1  10  45  120  210  252           1*10/                      0* 0/
M=12    1   0   0    0    0    0          11* 1/                      0* 0/
M=12    1   0   0    0    0    1           6* 1/ 5* 1/                0* 0/
M=12    1   0   0    0    1    0           7* 1/ 4* 1/                0* 0/
M=12    1   0   0    1    0    0           8* 1/ 3* 1/                0* 0/
M=12    1   0   0    1    0    1           5* 1/                      3* 1/
M=12    1   0   0    1    1    0           3* 1/                      4* 1/
M=12    1   0   0    1    2    0           4* 2/ 3* 1/                0* 0/
M=12    1   0   0    2    0    1           5* 1/ 3* 2/                0* 0/
M=12    1   0   1    0    0    0           9* 1/ 2* 1/                0* 0/
M=12    1   0   1    0    1    0           7* 1/                      2* 1/
M=12    1   0   1    0    1    1           5* 1/ 4* 1/ 2* 1/          0* 0/
M=12    1   0   1    1    0    1           6* 1/ 3* 1/ 2* 1/          0* 0/
M=12    1   0   1    1    2    1           4* 1/ 3* 1/                2* 1/
M=12    1   0   1    2    0    2           3* 1/ 2* 1/                3* 1/
M=12    1   0   1    3    0    3           3* 3/ 2* 1/                0* 0/
M=12    1   0   2    0    1    0           7* 1/ 2* 2/                0* 0/
```

```
M=12    1   0   2   0   2   1            5* 1/ 2* 1/                      2* 1/
M=12    1   0   2   1   2   2            4* 1/ 3* 1/ 2* 2/                0* 0/
M=12    1   0   2   1   3   2            3* 1/                            2* 2/
M=12    1   0   3   0   3   1            5* 1/ 2* 3/                      0* 0/
M=12    1   0   3   1   4   3            3* 1/ 2* 2/                      2* 1/
M=12    1   0   4   1   6   4            3* 1/ 2* 4/                      0* 0/
M=12    1   1   0   0   0   0           10* 1/ 1* 1/                      0* 0/
M=12    1   1   0   0   0   1            1* 1/                            5* 1/
M=12    1   1   0   0   0   2            5* 2/ 1* 1/                      0* 0/
M=12    1   1   0   0   1   1            6* 1/ 4* 1/ 1* 1/                0* 0/
M=12    1   1   0   1   1   0            7* 1/ 3* 1/ 1* 1/                0* 0/
M=12    1   1   0   1   2   1            4* 1/ 1* 1/                      3* 1/
M=12    1   1   0   2   3   1            4* 1/ 3* 2/ 1* 1/                0* 0/
M=12    1   1   1   0   0   0            9* 1/                            1* 1/
M=12    1   1   1   0   1   2            5* 1/ 4* 1/                      1* 1/
M=12    1   1   1   1   0   0            8* 1/ 2* 1/ 1* 1/                0* 0/
M=12    1   1   1   1   1   1            2* 1/ 1* 1/                      4* 1/
M=12    1   1   1   1   1   1            6* 1/ 1* 1/                      2* 1/
M=12    1   1   1   1   1   1            6* 1/ 3* 1/                      1* 1/
M=12    1   1   1   1   2   2            4* 2/ 2* 1/ 1* 1/                0* 0/
M=12    1   1   1   2   1   2            5* 1/ 3* 1/ 2* 1/ 1* 1/          0* 0/
M=12    1   1   1   2   2   2            1* 1/                            3* 1/ 2* 1/
M=12    1   1   1   2   2   2            3* 1/                            3* 1/ 1* 1/
M=12    1   1   1   3   3   3            3* 2/ 1* 1/                      2* 1/
M=12    1   1   1   3   3   3            3* 3/                            1* 1/
M=12    1   1   2   1   1   0            7* 1/ 2* 1/                      1* 1/
M=12    1   1   2   1   2   2            5* 1/                            2* 1/ 1* 1/
M=12    1   1   2   2   1   1            6* 1/ 2* 2/ 1* 1/                0* 0/
M=12    1   1   2   2   3   3            4* 1/ 2* 1/ 1* 1/                2* 1/
M=12    1   1   2   2   3   3            4* 1/ 3* 1/ 2* 1/                1* 1/
M=12    1   1   2   3   2   3            2* 2/ 1* 1/                      3* 1/
M=12    1   1   2   4   3   5            3* 2/ 2* 2/ 1* 1/                0* 0/
M=12    1   1   3   2   3   2            5* 1/ 2* 2/                      1* 1/
M=12    1   1   3   3   4   4            4* 1/ 2* 3/ 1* 1/                0* 0/
M=12    1   1   3   3   5   5            2* 1/ 1* 1/                      2* 2/
M=12    1   1   3   3   5   5            3* 1/ 2* 1/                      2* 1/ 1* 1/
M=12    1   1   4   4   7   7            2* 3/ 1* 1/                      2* 1/
M=12    1   1   4   4   7   7            3* 1/ 2* 3/                      1* 1/
M=12    1   1   5   5  10  10            2* 5/ 1* 1/                      0* 0/
M=12    1   2   1   0   0   0            9* 1/ 1* 2/                      0* 0/
M=12    1   2   1   0   1   3            5* 1/ 4* 1/ 1* 2/                0* 0/
M=12    1   2   1   1   2   1            6* 1/ 3* 1/ 1* 2/                0* 0/
M=12    1   2   1   2   4   2            3* 1/ 1* 2/                      3* 1/
```

```
M=12   1   2   1   3   6   3           3* 3/ 1* 2/                    0* 0/
M=12   1   2   2   1   0   0           8* 1/ 1* 1/                    1* 1/
M=12   1   2   2   1   1   2           1* 1/                          4* 1/ 1* 1/
M=12   1   2   2   1   2   4           4* 2/ 1* 1/                    1* 1/
M=12   1   2   2   2   1   0           7* 1/ 2* 1/ 1* 2/              0* 0/
M=12   1   2   2   2   2   3           5* 1/ 1* 2/                    2* 1/
M=12   1   2   2   2   2   3           5* 1/ 3* 1/ 1* 1/              1* 1/
M=12   1   2   2   3   4   4           4* 1/ 3* 1/ 2* 1/ 1* 2/        0* 0/
M=12   1   2   3   2   1   0           7* 1/                          1* 2/
M=12   1   2   3   3   2   1           6* 1/ 2* 1/ 1* 1/              1* 1/
M=12   1   2   3   3   4   5           4* 1/ 1* 1/                    2* 1/ 1* 1/
M=12   1   2   3   3   4   5           4* 1/ 3* 1/                    1* 2/
M=12   1   2   3   4   3   3           5* 1/ 2* 2/ 1* 2/              0* 0/
M=12   1   2   3   4   4   4           2* 1/ 1* 1/                    3* 1/ 1* 1/
M=12   1   2   3   5   6   7           3* 1/ 2* 1/ 1* 2/              2* 1/
M=12   1   2   3   5   6   7           3* 2/ 2* 1/ 1* 1/              1* 1/
M=12   1   2   4   4   4   3           5* 1/ 2* 1/                    1* 2/
M=12   1   2   4   5   6   6           4* 1/ 2* 2/ 1* 1/              1* 1/
M=12   1   2   4   5   7   8           1* 1/                          2* 2/ 1* 1/
M=12   1   2   4   5   7   8           3* 1/                          2* 1/ 1* 2/
M=12   1   2   4   7   8  10           3* 1/ 2* 3/ 1* 2/              0* 0/
M=12   1   2   5   7  10  11           2* 2/ 1* 1/                    2* 1/ 1* 1/
M=12   1   2   5   7  10  11           3* 1/ 2* 2/                    1* 2/
M=12   1   2   6   9  14  16           2* 4/ 1* 1/                    1* 1/
M=12   1   3   3   1   0   0           8* 1/ 1* 3/                    0* 0/
M=12   1   3   3   1   1   3           1* 3/                          4* 1/
M=12   1   3   3   1   2   6           4* 2/ 1* 3/                    0* 0/
M=12   1   3   3   2   3   4           5* 1/ 3* 1/ 1* 3/              0* 0/
M=12   1   3   4   3   1   0           7* 1/ 1* 2/                    1* 1/
M=12   1   3   4   4   3   1           6* 1/ 2* 1/ 1* 3/              0* 0/
M=12   1   3   4   4   5   7           4* 1/ 1* 3/                    2* 1/
M=12   1   3   4   4   5   7           4* 1/ 3* 1/ 1* 2/              1* 1/
M=12   1   3   4   5   6   5           2* 1/ 1* 3/                    3* 1/
M=12   1   3   4   6   9   9           3* 2/ 2* 1/ 1* 3/              0* 0/
M=12   1   3   5   5   3   1           6* 1/ 1* 1/                    1* 2/
M=12   1   3   5   6   5   4           5* 1/ 2* 1/ 1* 2/              1* 1/
M=12   1   3   5   6   6   6           1* 1/                          3* 1/ 1* 2/
M=12   1   3   5   7   8   8           4* 1/ 2* 2/ 1* 3/              0* 0/
M=12   1   3   5   7   9  11           1* 3/                          2* 2/
M=12   1   3   5   7   9  11           3* 1/ 1* 2/                    2* 1/ 1* 1/
M=12   1   3   5   7   9  11           3* 2/ 1* 1/                    1* 2/
M=12   1   3   6   7   6   4           5* 1/                          1* 3/
M=12   1   3   6   8   9   9           4* 1/ 2* 1/ 1* 1/              1* 2/
```

```
M=12   1   3   6  10  13  15                 2* 2/ 1* 3/                        2* 1/
M=12   1   3   6  10  13  15                 3* 1/ 2* 2/ 1* 2/                  1* 1/
M=12   1   3   7  11  15  17                 2* 1/ 1* 1/                        2* 1/ 1* 2/
M=12   1   3   7  11  15  17                 3* 1/ 2* 1/                        1* 3/
M=12   1   3   7  13  18  22                 2* 4/ 1* 3/                        0* 0/
M=12   1   3   8  14  21  25                 2* 3/ 1* 1/                        1* 2/
M=12   1   4   6   4   1   0                 7* 1/ 1* 4/                        0* 0/
M=12   1   4   6   5   6  10                 4* 1/ 3* 1/ 1* 4/                  0* 0/
M=12   1   4   7   7   4   1                 6* 1/ 1* 3/                        1* 1/
M=12   1   4   7   8   7   5                 5* 1/ 2* 1/ 1* 4/                  0* 0/
M=12   1   4   7   8   8   8                 1* 3/                              3* 1/ 1* 1/
M=12   1   4   7   9  12  15                 3* 1/ 1* 4/                        2* 1/
M=12   1   4   7   9  12  15                 3* 2/ 1* 3/                        1* 1/
M=12   1   4   8  10   8   5                 5* 1/ 1* 2/                        1* 2/
M=12   1   4   8  11  12  12                 4* 1/ 2* 1/ 1* 3/                  1* 1/
M=12   1   4   8  13  18  20                 3* 1/ 2* 2/ 1* 4/                  0* 0/
M=12   1   4   9  13  14  13                 4* 1/ 1* 1/                        1* 3/
M=12   1   4   9  15  20  23                 2* 1/ 1* 3/                        2* 1/ 1* 1/
M=12   1   4   9  15  20  23                 3* 1/ 2* 1/ 1* 2/                  1* 2/
M=12   1   4  10  17  23  26                 1* 1/                              2* 1/ 1* 3/
M=12   1   4  10  17  23  26                 3* 1/                              1* 4/
M=12   1   4  10  19  28  34                 2* 3/ 1* 3/                        1* 1/
M=12   1   4  11  21  32  39                 2* 2/ 1* 1/                        1* 3/
M=12   1   5  10  10   5   1                 6* 1/ 1* 5/                        0* 0/
M=12   1   5  10  11  10  11                 1* 5/                              3* 1/
M=12   1   5  10  12  15  21                 3* 2/ 1* 5/                        0* 0/
M=12   1   5  11  14  11   6                 5* 1/ 1* 4/                        1* 1/
M=12   1   5  11  15  16  16                 4* 1/ 2* 1/ 1* 5/                  0* 0/
M=12   1   5  12  18  19  17                 4* 1/ 1* 3/                        1* 2/
M=12   1   5  12  20  27  31                 2* 1/ 1* 5/                        2* 1/
M=12   1   5  12  20  27  31                 3* 1/ 2* 1/ 1* 4/                  1* 1/
M=12   1   5  13  23  31  35                 1* 3/                              2* 1/ 1* 2/
M=12   1   5  13  23  31  35                 3* 1/ 1* 2/                        1* 3/
M=12   1   5  13  25  38  46                 2* 3/ 1* 5/                        0* 0/
M=12   1   5  14  28  43  53                 2* 2/ 1* 3/                        1* 2/
M=12   1   5  15  31  49  61                 2* 1/ 1* 1/                        1* 4/
M=12   1   6  15  20  15   7                 5* 1/ 1* 6/                        0* 0/
M=12   1   6  16  25  26  22                 4* 1/ 1* 5/                        1* 1/
M=12   1   6  16  27  36  42                 3* 1/ 2* 1/ 1* 6/                  0* 0/
M=12   1   6  17  31  42  47                 1* 5/                              2* 1/ 1* 1/
M=12   1   6  17  31  42  47                 3* 1/ 1* 4/                        1* 2/
M=12   1   6  18  37  58  72                 2* 2/ 1* 5/                        1* 1/
M=12   1   6  19  41  66  83                 2* 1/ 1* 3/                        1* 3/
```

```
M=12     1    6   20   45   75   96                  1* 1/                              1* 5/
M=12     1    7   21   35   36   28                  4* 1/ 1* 7/                        0* 0/
M=12     1    7   22   42   57   63                  1* 7/                              2* 1/
M=12     1    7   22   42   57   63                  3* 1/ 1* 6/                        1* 1/
M=12     1    7   23   49   78   98                  2* 2/ 1* 7/                        0* 0/
M=12     1    7   24   54   89  113                  2* 1/ 1* 5/                        1* 2/
M=12     1    7   25   59  101  131                  1* 3/                              1* 4/
M=12     1    8   28   57   78   84                  3* 1/ 1* 8/                        0* 0/
M=12     1    8   30   71  120  154                  2* 1/ 1* 7/                        1* 1/
M=12     1    8   31   77  136  179                  1* 5/                              1* 3/
M=12     1    9   37   93  162  210                  2* 1/ 1* 9/                        0* 0/
M=12     1    9   38  100  183  245                  1* 7/                              1* 2/
M=12     1   10   46  129  246  336                  1* 9/                              1* 1/
M=12     1   11   55  165  330  462                  1*11/                              0* 0/
M=13     1    0    0    0    0    0    0            12* 1/                              0* 0/
M=13     1    0    0    0    0    0    1             0* 0/                              6* 1/
M=13     1    0    0    0    0    0    2             6* 2/                              0* 0/
M=13     1    0    0    0    0    1    0             7* 1/ 5* 1/                        0* 0/
M=13     1    0    0    0    1    0    0             8* 1/ 4* 1/                        0* 0/
M=13     1    0    0    0    2    0    0             4* 1/                              4* 1/
M=13     1    0    0    0    3    0    0             4* 3/                              0* 0/
M=13     1    0    0    1    0    0    0             9* 1/ 3* 1/                        0* 0/
M=13     1    0    0    1    0    0    2             6* 1/                              3* 1/
M=13     1    0    0    1    1    1    0             5* 1/ 4* 1/ 3* 1/                  0* 0/
M=13     1    0    0    2    0    0    2             6* 1/ 3* 2/                        0* 0/
M=13     1    0    0    2    0    0    3             0* 0/                              3* 2/
M=13     1    0    0    3    0    0    4             3* 2/                              3* 1/
M=13     1    0    0    4    0    0    6             3* 4/                              0* 0/
M=13     1    0    1    0    0    0    0            10* 1/ 2* 1/                        0* 0/
M=13     1    0    1    0    0    1    0             2* 1/                              5* 1/
M=13     1    0    1    0    0    2    0             5* 2/ 2* 1/                        0* 0/
M=13     1    0    1    0    1    0    0             8* 1/                              2* 1/
M=13     1    0    1    0    1    0    2             6* 1/ 4* 1/ 2* 1/                  0* 0/
M=13     1    0    1    0    2    0    1             0* 0/                              4* 1/ 2* 1/
M=13     1    0    1    0    3    0    2             4* 2/                              2* 1/
M=13     1    0    1    1    0    1    0             7* 1/ 3* 1/ 2* 1/                  0* 0/
M=13     1    0    1    1    1    1    2             4* 1/ 2* 1/                        3* 1/
M=13     1    0    1    1    1    2    0             5* 1/ 3* 1/                        2* 1/
M=13     1    0    1    2    1    2    2             4* 1/ 3* 2/ 2* 1/                  0* 0/
M=13     1    0    2    0    1    0    0             8* 1/ 2* 2/                        0* 0/
M=13     1    0    2    0    2    0    2             2* 2/                              4* 1/
M=13     1    0    2    0    2    0    2             6* 1/ 2* 1/                        2* 1/
M=13     1    0    2    0    3    0    4             4* 2/ 2* 2/                        0* 0/
```

```
M=13     1   0   2   0   4   0   4              4* 1/                               2* 2/
M=13     1   0   2   1   1   3   0              5* 1/ 3* 1/ 2* 2/                   0* 0/
M=13     1   0   2   1   2   2   2              2* 1/                               3* 1/ 2* 1/
M=13     1   0   2   2   2   4   2              3* 2/ 2* 1/                         2* 1/
M=13     1   0   3   0   3   0   2              6* 1/ 2* 3/                         0* 0/
M=13     1   0   3   0   5   0   6              4* 1/ 2* 2/                         2* 1/
M=13     1   0   3   0   6   0   7              0* 0/                               2* 3/
M=13     1   0   3   1   3   3   2              2* 3/                               3* 1/
M=13     1   0   3   2   3   6   2              3* 2/ 2* 3/                         0* 0/
M=13     1   0   4   0   7   0   8              4* 1/ 2* 4/                         0* 0/
M=13     1   0   4   0   8   0  10              2* 2/                               2* 2/
M=13     1   0   5   0  11   0  14              2* 4/                               2* 1/
M=13     1   0   6   0  15   0  20              2* 6/                               0* 0/
M=13     1   1   0   0   0   0   0             11* 1/ 1* 1/                         0* 0/
M=13     1   1   0   0   0   1   2              6* 1/ 5* 1/ 1* 1/                   0* 0/
M=13     1   1   0   0   1   1   0              7* 1/ 4* 1/ 1* 1/                   0* 0/
M=13     1   1   0   1   1   0   0              8* 1/ 3* 1/ 1* 1/                   0* 0/
M=13     1   1   0   1   1   1   2              5* 1/ 1* 1/                         3* 1/
M=13     1   1   0   1   2   1   0              3* 1/ 1* 1/                         4* 1/
M=13     1   1   0   1   3   2   0              4* 2/ 3* 1/ 1* 1/                   0* 0/
M=13     1   1   0   2   2   1   2              5* 1/ 3* 2/ 1* 1/                   0* 0/
M=13     1   1   1   0   0   0   0             10* 1/                               1* 1/
M=13     1   1   1   0   0   1   1              0* 0/                               5* 1/ 1* 1/
M=13     1   1   1   0   0   2   2              5* 2/                               1* 1/
M=13     1   1   1   0   1   1   2              6* 1/ 4* 1/                         1* 1/
M=13     1   1   1   1   0   0   0              9* 1/ 2* 1/ 1* 1/                   0* 0/
M=13     1   1   1   1   1   1   0              7* 1/ 1* 1/                         2* 1/
M=13     1   1   1   1   1   1   0              7* 1/ 3* 1/                         1* 1/
M=13     1   1   1   1   1   2   2              5* 1/ 4* 1/ 2* 1/ 1* 1/             0* 0/
M=13     1   1   1   1   2   2   2              4* 1/                               3* 1/ 1* 1/
M=13     1   1   1   2   1   1   2              6* 1/ 3* 1/ 2* 1/ 1* 1/             0* 0/
M=13     1   1   1   2   3   3   2              4* 1/ 3* 1/ 1* 1/                   2* 1/
M=13     1   1   1   2   3   3   2              4* 1/ 3* 2/                         1* 1/
M=13     1   1   1   3   2   2   4              3* 1/ 2* 1/ 1* 1/                   3* 1/
M=13     1   1   1   4   3   3   6              3* 3/ 2* 1/ 1* 1/                   0* 0/
M=13     1   1   2   1   1   0   0              8* 1/ 2* 1/                         1* 1/
M=13     1   1   2   1   2   1   2              2* 1/                               4* 1/ 1* 1/
M=13     1   1   2   1   2   1   2              6* 1/                               2* 1/ 1* 1/
M=13     1   1   2   1   3   2   4              4* 2/ 2* 1/                         1* 1/
M=13     1   1   2   2   1   1   0              7* 1/ 2* 2/ 1* 1/                   0* 0/
M=13     1   1   2   2   2   3   2              5* 1/ 2* 1/ 1* 1/                   2* 1/
M=13     1   1   2   2   2   3   2              5* 1/ 3* 1/ 2* 1/                   1* 1/
M=13     1   1   2   2   3   3   3              0* 0/                               3* 1/ 2* 1/ 1* 1/
```

```
M=13   1   1   2   3   3   4   4      4* 1/ 3* 1/ 2* 2/ 1* 1/      0* 0/
M=13   1   1   2   3   4   5   4      3* 1/ 1* 1/                  2* 2/
M=13   1   1   2   3   4   5   4      3* 2/                        2* 1/ 1* 1/
M=13   1   1   3   2   3   1   2      6* 1/ 2* 2/                  1* 1/
M=13   1   1   3   2   5   3   6      4* 1/ 2* 1/                  2* 1/ 1* 1/
M=13   1   1   3   3   3   4   2      5* 1/ 2* 3/ 1* 1/            0* 0/
M=13   1   1   3   3   4   4   4      2* 2/                        3* 1/ 1* 1/
M=13   1   1   3   4   5   7   6      3* 1/ 2* 2/ 1* 1/            2* 1/
M=13   1   1   3   4   5   7   6      3* 2/ 2* 2/                  1* 1/
M=13   1   1   4   3   7   4   8      4* 1/ 2* 3/                  1* 1/
M=13   1   1   4   3   8   5  10      2* 1/                        2* 2/ 1* 1/
M=13   1   1   4   5   7  10   8      3* 1/ 2* 4/ 1* 1/            0* 0/
M=13   1   1   5   4  11   7  14      2* 3/                        2* 1/ 1* 1/
M=13   1   1   6   5  15  10  20      2* 5/                        1* 1/
M=13   1   2   1   0   0   0   0     10* 1/ 1* 2/                  0* 0/
M=13   1   2   1   0   0   1   2      1* 2/                        5* 1/
M=13   1   2   1   0   0   2   4      5* 2/ 1* 2/                  0* 0/
M=13   1   2   1   0   1   2   2      6* 1/ 4* 1/ 1* 2/            0* 0/
M=13   1   2   1   1   2   1   0      7* 1/ 3* 1/ 1* 2/            0* 0/
M=13   1   2   1   1   3   3   2      4* 1/ 1* 2/                  3* 1/
M=13   1   2   1   2   5   4   2      4* 1/ 3* 2/ 1* 2/            0* 0/
M=13   1   2   2   1   0   0   0      9* 1/ 1* 1/                  1* 1/
M=13   1   2   2   1   1   3   4      5* 1/ 4* 1/ 1* 1/            1* 1/
M=13   1   2   2   2   1   0   0      8* 1/ 2* 1/ 1* 2/            0* 0/
M=13   1   2   2   2   2   2   2      2* 1/ 1* 2/                  4* 1/
M=13   1   2   2   2   2   2   2      6* 1/ 1* 2/                  2* 1/
M=13   1   2   2   2   2   2   2      6* 1/ 3* 1/ 1* 1/            1* 1/
M=13   1   2   2   2   3   4   4      4* 2/ 2* 1/ 1* 2/            0* 0/
M=13   1   2   2   3   3   3   4      5* 1/ 3* 1/ 2* 1/ 1* 2/      0* 0/
M=13   1   2   2   3   4   4   4      1* 2/                        3* 1/ 2* 1/
M=13   1   2   2   3   4   4   4      3* 1/ 1* 1/                  3* 1/ 1* 1/
M=13   1   2   2   4   6   6   6      3* 2/ 1* 2/                  2* 1/
M=13   1   2   2   4   6   6   6      3* 3/ 1* 1/                  1* 1/
M=13   1   2   3   2   1   0   0      8* 1/                        1* 2/
M=13   1   2   3   2   2   3   3      0* 0/                        4* 1/ 1* 2/
M=13   1   2   3   2   3   4   6      4* 2/                        1* 2/
M=13   1   2   3   3   2   1   0      7* 1/ 2* 1/ 1* 1/            1* 1/
M=13   1   2   3   3   3   4   4      5* 1/ 1* 1/                  2* 1/ 1* 1/
M=13   1   2   3   3   3   4   4      5* 1/ 3* 1/                  1* 2/
M=13   1   2   3   4   3   2   2      6* 1/ 2* 2/ 1* 2/            0* 0/
M=13   1   2   3   4   5   6   6      4* 1/ 2* 1/ 1* 2/            2* 1/
M=13   1   2   3   4   5   6   6      4* 1/ 3* 1/ 2* 1/ 1* 1/      1* 1/
M=13   1   2   3   5   5   5   6      2* 2/ 1* 2/                  3* 1/
```

```
M=13   1   2   3   6   7   8  10       3* 2/ 2* 2/ 1* 2/            0* 0/
M=13   1   2   4   4   4   2   2       6* 1/ 2* 1/                  1* 2/
M=13   1   2   4   4   6   6   8       4* 1/                        2* 1/ 1* 2/
M=13   1   2   4   5   5   5   4       5* 1/ 2* 2/ 1* 1/            1* 1/
M=13   1   2   4   5   6   6   6       2* 1/                        3* 1/ 1* 2/
M=13   1   2   4   6   7   8   8       4* 1/ 2* 3/ 1* 2/            0* 0/
M=13   1   2   4   6   8  10  10       2* 1/ 1* 2/                  2* 2/
M=13   1   2   4   6   8  10  10       3* 1/ 2* 1/ 1* 1/            2* 1/ 1* 1/
M=13   1   2   4   6   8  10  10       3* 2/ 2* 1/                  1* 2/
M=13   1   2   5   6   9   8  10       4* 1/ 2* 2/                  1* 2/
M=13   1   2   5   6  10  10  13       0* 0/                        2* 2/ 1* 2/
M=13   1   2   5   8  11  14  14       2* 3/ 1* 2/                  2* 1/
M=13   1   2   5   8  11  14  14       3* 1/ 2* 3/ 1* 1/            1* 1/
M=13   1   2   6   8  14  14  18       2* 2/                        2* 1/ 1* 2/
M=13   1   2   6  10  15  20  20       2* 5/ 1* 2/                  0* 0/
M=13   1   2   7  10  19  20  26       2* 4/                        1* 2/
M=13   1   3   3   1   0   0   0       9* 1/ 1* 3/                  0* 0/
M=13   1   3   3   1   1   4   6       5* 1/ 4* 1/ 1* 3/            0* 0/
M=13   1   3   3   2   3   3   2       6* 1/ 3* 1/ 1* 3/            0* 0/
M=13   1   3   3   3   6   6   4       3* 1/ 1* 3/                  3* 1/
M=13   1   3   3   4   9   9   6       3* 3/ 1* 3/                  0* 0/
M=13   1   3   4   3   1   0   0       8* 1/ 1* 2/                  1* 1/
M=13   1   3   4   3   2   3   4       1* 2/                        4* 1/ 1* 1/
M=13   1   3   4   3   3   6   8       4* 2/ 1* 2/                  1* 1/
M=13   1   3   4   4   3   1   0       7* 1/ 2* 1/ 1* 3/            0* 0/
M=13   1   3   4   4   4   5   6       5* 1/ 1* 3/                  2* 1/
M=13   1   3   4   4   4   5   6       5* 1/ 3* 1/ 1* 2/            1* 1/
M=13   1   3   4   5   7   8   8       4* 1/ 3* 1/ 2* 1/ 1* 3/      0* 0/
M=13   1   3   5   5   3   1   0       7* 1/ 1* 1/                  1* 2/
M=13   1   3   5   6   5   3   2       6* 1/ 2* 1/ 1* 2/            1* 1/
M=13   1   3   5   6   7   9  10       4* 1/ 1* 2/                  2* 1/ 1* 1/
M=13   1   3   5   6   7   9  10       4* 1/ 3* 1/ 1* 1/            1* 2/
M=13   1   3   5   7   7   6   6       5* 1/ 2* 2/ 1* 3/            0* 0/
M=13   1   3   5   7   8   8   8       2* 1/ 1* 2/                  3* 1/ 1* 1/
M=13   1   3   5   8  11  13  14       3* 1/ 2* 1/ 1* 3/            2* 1/
M=13   1   3   5   8  11  13  14       3* 2/ 2* 1/ 1* 2/            1* 1/
M=13   1   3   6   7   6   3   2       6* 1/                        1* 3/
M=13   1   3   6   8   8   7   6       5* 1/ 2* 1/ 1* 1/            1* 2/
M=13   1   3   6   8   9   9   9       0* 0/                        3* 1/ 1* 3/
M=13   1   3   6   9  11  12  12       4* 1/ 2* 2/ 1* 2/            1* 1/
M=13   1   3   6   9  12  15  16       1* 2/                        2* 2/ 1* 1/
M=13   1   3   6   9  12  15  16       3* 1/ 1* 1/                  2* 1/ 1* 2/
M=13   1   3   6   9  12  15  16       3* 2/                        1* 3/
```

```
M=13     1   3   6  11  15  18  20              3* 1/ 2* 3/ 1* 3/                 0* 0/
M=13     1   3   7  10  13  13  14              4* 1/ 2* 1/                       1* 3/
M=13     1   3   7  12  17  21  22              2* 2/ 1* 2/                       2* 1/ 1* 1/
M=13     1   3   7  12  17  21  22              3* 1/ 2* 2/ 1* 1/                 1* 2/
M=13     1   3   8  13  20  23  26              2* 1/                             2* 1/ 1* 3/
M=13     1   3   8  15  23  30  32              2* 4/ 1* 2/                       1* 1/
M=13     1   3   9  16  27  33  38              2* 3/                             1* 3/
M=13     1   4   6   4   1   0   0              8* 1/ 1* 4/                       0* 0/
M=13     1   4   6   4   2   4   6              1* 4/                             4* 1/
M=13     1   4   6   4   3   8  12              4* 2/ 1* 4/                       0* 0/
M=13     1   4   6   5   5   7   8              5* 1/ 3* 1/ 1* 4/                 0* 0/
M=13     1   4   7   7   4   1   0              7* 1/ 1* 3/                       1* 1/
M=13     1   4   7   8   7   4   2              6* 1/ 2* 1/ 1* 4/                 0* 0/
M=13     1   4   7   8   9  12  14              4* 1/ 1* 4/                       2* 1/
M=13     1   4   7   8   9  12  14              4* 1/ 3* 1/ 1* 3/                 1* 1/
M=13     1   4   7   9  11  11  10              2* 1/ 1* 4/                       3* 1/
M=13     1   4   7  10  15  18  18              3* 2/ 2* 1/ 1* 4/                 0* 0/
M=13     1   4   8  10   8   4   2              6* 1/ 1* 2/                       1* 2/
M=13     1   4   8  11  11   9   8              5* 1/ 2* 1/ 1* 3/                 1* 1/
M=13     1   4   8  11  12  12  12              1* 2/                             3* 1/ 1* 2/
M=13     1   4   8  12  15  16  16              4* 1/ 2* 2/ 1* 4/                 0* 0/
M=13     1   4   8  12  16  20  22              1* 4/                             2* 2/
M=13     1   4   8  12  16  20  22              3* 1/ 1* 3/                       2* 1/ 1* 1/
M=13     1   4   8  12  16  20  22              3* 2/ 1* 2/                       1* 2/
M=13     1   4   9  13  13  10   8              5* 1/ 1* 1/                       1* 3/
M=13     1   4   9  14  17  18  18              4* 1/ 2* 1/ 1* 2/                 1* 2/
M=13     1   4   9  16  23  28  30              2* 2/ 1* 4/                       2* 1/
M=13     1   4   9  16  23  28  30              3* 1/ 2* 2/ 1* 3/                 1* 1/
M=13     1   4  10  16  20  20  20              4* 1/                             1* 4/
M=13     1   4  10  18  26  32  34              2* 1/ 1* 2/                       2* 1/ 1* 2/
M=13     1   4  10  18  26  32  34              3* 1/ 2* 1/ 1* 1/                 1* 3/
M=13     1   4  10  20  31  40  44              2* 4/ 1* 4/                       0* 0/
M=13     1   4  11  20  30  36  39              0* 0/                             2* 1/ 1* 4/
M=13     1   4  11  22  35  46  50              2* 3/ 1* 2/                       1* 2/
M=13     1   4  12  24  40  52  58              2* 2/                             1* 4/
M=13     1   5  10  10   5   1   0              7* 1/ 1* 5/                       0* 0/
M=13     1   5  10  11  11  16  20              4* 1/ 3* 1/ 1* 5/                 0* 0/
M=13     1   5  11  14  11   5   2              6* 1/ 1* 4/                       1* 1/
M=13     1   5  11  15  15  12  10              5* 1/ 2* 1/ 1* 5/                 0* 0/
M=13     1   5  11  15  16  16  16              1* 4/                             3* 1/ 1* 1/
M=13     1   5  11  16  21  27  30              3* 1/ 1* 5/                       2* 1/
M=13     1   5  11  16  21  27  30              3* 2/ 1* 4/                       1* 1/
M=13     1   5  12  18  18  13  10              5* 1/ 1* 3/                       1* 2/
```

```
M=13    1   5  12   19   23   24   24          4* 1/ 2* 1/ 1* 4/                          1* 1/
M=13    1   5  12   21   31   38   40          3* 1/ 2* 2/ 1* 5/                          0* 0/
M=13    1   5  13   22   27   27   26          4* 1/ 1* 2/                                1* 3/
M=13    1   5  13   24   35   43   46          2* 1/ 1* 4/                                2* 1/ 1* 1/
M=13    1   5  13   24   35   43   46          3* 1/ 2* 1/ 1* 3/                          1* 2/
M=13    1   5  14   27   40   49   52          1* 2/                                      2* 1/ 1* 3/
M=13    1   5  14   27   40   49   52          3* 1/ 1* 1/                                1* 4/
M=13    1   5  14   29   47   62   68          2* 3/ 1* 4/                                1* 1/
M=13    1   5  15   32   53   71   78          2* 2/ 1* 2/                                1* 3/
M=13    1   5  16   35   60   81   90          2* 1/                                      1* 5/
M=13    1   6  15   20   15    6    2          6* 1/ 1* 6/                                0* 0/
M=13    1   6  15   21   21   21   22          1* 6/                                      3* 1/
M=13    1   6  15   22   27   36   42          3* 2/ 1* 6/                                0* 0/
M=13    1   6  16   25   25   17   12          5* 1/ 1* 5/                                1* 1/
M=13    1   6  16   26   31   32   32          4* 1/ 2* 1/ 1* 6/                          0* 0/
M=13    1   6  17   30   37   36   34          4* 1/ 1* 4/                                1* 2/
M=13    1   6  17   32   47   58   62          2* 1/ 1* 6/                                2* 1/
M=13    1   6  17   32   47   58   62          3* 1/ 2* 1/ 1* 5/                          1* 1/
M=13    1   6  18   36   54   66   70          1* 4/                                      2* 1/ 1* 2/
M=13    1   6  18   36   54   66   70          3* 1/ 1* 3/                                1* 3/
M=13    1   6  18   38   63   84   92          2* 3/ 1* 6/                                0* 0/
M=13    1   6  19   42   71   96  106          2* 2/ 1* 4/                                1* 2/
M=13    1   6  20   46   80  110  122          2* 1/ 1* 2/                                1* 4/
M=13    1   6  21   50   90  126  141          0* 0/                                      1* 6/
M=13    1   7  21   35   35   22   14          5* 1/ 1* 7/                                0* 0/
M=13    1   7  22   41   51   48   44          4* 1/ 1* 6/                                1* 1/
M=13    1   7  22   43   63   78   84          3* 1/ 2* 1/ 1* 7/                          0* 0/
M=13    1   7  23   48   73   89   94          1* 6/                                      2* 1/ 1* 1/
M=13    1   7  23   48   73   89   94          3* 1/ 1* 5/                                1* 2/
M=13    1   7  24   55   95  130  144          2* 2/ 1* 6/                                1* 1/
M=13    1   7  25   60  107  149  166          2* 1/ 1* 4/                                1* 3/
M=13    1   7  26   65  120  171  192          1* 2/                                      1* 5/
M=13    1   8  28   56   71   64   56          4* 1/ 1* 8/                                0* 0/
M=13    1   8  29   64   99  120  126          1* 8/                                      2* 1/
M=13    1   8  29   64   99  120  126          3* 1/ 1* 7/                                1* 1/
M=13    1   8  30   72  127  176  196          2* 2/ 1* 8/                                0* 0/
M=13    1   8  31   78  143  202  226          2* 1/ 1* 6/                                1* 2/
M=13    1   8  32   84  160  232  262          1* 4/                                      1* 4/
M=13    1   9  36   85  135  162  168          3* 1/ 1* 9/                                0* 0/
M=13    1   9  38  101  191  274  308          2* 1/ 1* 8/                                1* 1/
M=13    1   9  39  108  213  315  358          1* 6/                                      1* 3/
M=13    1  10  46  130  255  372  420          2* 1/ 1*10/                                0* 0/
M=13    1  10  47  138  283  428  490          1* 8/                                      1* 2/
```

```
M=13   1  11  56 175 375 582 672          1*10/                        1* 1/
M=13   1  12  66 220 495 792 924          1*12/                        0* 0/
M=14   1   0   0   0   0   0   0         13* 1/                        0* 0/
M=14   1   0   0   0   0   0   1          7* 1/ 6* 1/                  0* 0/
M=14   1   0   0   0   0   1   0          8* 1/ 5* 1/                  0* 0/
M=14   1   0   0   0   1   0   0          9* 1/ 4* 1/                  0* 0/
M=14   1   0   0   0   1   1   0          5* 1/                        4* 1/
M=14   1   0   0   0   2   1   0          5* 1/ 4* 2/                  0* 0/
M=14   1   0   0   1   0   0   0         10* 1/ 3* 1/                  0* 0/
M=14   1   0   0   1   0   0   1          7* 1/                        3* 1/
M=14   1   0   0   1   0   1   0          3* 1/                        5* 1/
M=14   1   0   0   1   0   2   0          5* 2/ 3* 1/                  0* 0/
M=14   1   0   0   1   1   0   1          6* 1/ 4* 1/ 3* 1/            0* 0/
M=14   1   0   0   2   0   0   1          7* 1/ 3* 2/                  0* 0/
M=14   1   0   0   2   1   0   2          4* 1/ 3* 1/                  3* 1/
M=14   1   0   0   3   1   0   3          4* 1/ 3* 3/                  0* 0/
M=14   1   0   1   0   0   0   0         11* 1/ 2* 1/                  0* 0/
M=14   1   0   1   0   0   1   1          6* 1/ 5* 1/ 2* 1/            0* 0/
M=14   1   0   1   0   1   0   0          9* 1/                        2* 1/
M=14   1   0   1   0   1   0   1          7* 1/ 4* 1/ 2* 1/            0* 0/
M=14   1   0   1   0   2   1   1          5* 1/ 4* 1/                  2* 1/
M=14   1   0   1   1   0   1   0          8* 1/ 3* 1/ 2* 1/            0* 0/
M=14   1   0   1   1   0   2   1          5* 1/ 2* 1/                  3* 1/
M=14   1   0   1   1   1   1   1          3* 1/ 2* 1/                  4* 1/
M=14   1   0   1   1   1   1   1          6* 1/ 3* 1/                  2* 1/
M=14   1   0   1   1   2   1   2          4* 2/ 3* 1/ 2* 1/            0* 0/
M=14   1   0   1   2   0   3   1          5* 1/ 3* 2/ 2* 1/            0* 0/
M=14   1   0   1   2   1   2   2          3* 1/                        3* 1/ 2* 1/
M=14   1   0   1   3   1   3   3          3* 3/                        2* 1/
M=14   1   0   2   0   1   0   0          9* 1/ 2* 2/                  0* 0/
M=14   1   0   2   0   2   0   1          7* 1/ 2* 1/                  2* 1/
M=14   1   0   2   0   2   1   2          5* 1/ 4* 1/ 2* 2/            0* 0/
M=14   1   0   2   0   3   1   2          5* 1/                        2* 2/
M=14   1   0   2   1   1   2   1          6* 1/ 3* 1/ 2* 2/            0* 0/
M=14   1   0   2   1   3   2   3          4* 1/ 3* 1/ 2* 1/            2* 1/
M=14   1   0   2   2   1   4   2          3* 1/ 2* 2/                  3* 1/
M=14   1   0   2   3   1   6   3          3* 3/ 2* 2/                  0* 0/
M=14   1   0   3   0   3   0   1          7* 1/ 2* 3/                  0* 0/
M=14   1   0   3   0   4   1   3          5* 1/ 2* 2/                  2* 1/
M=14   1   0   3   1   4   3   4          4* 1/ 3* 1/ 2* 3/            0* 0/
M=14   1   0   3   1   5   3   5          3* 1/ 2* 1/                  2* 2/
M=14   1   0   4   0   6   1   4          5* 1/ 2* 4/                  0* 0/
M=14   1   0   4   1   7   4   7          3* 1/ 2* 3/                  2* 1/
```

```
M=14   1   0   5   1  10   5  10          3* 1/ 2* 5/                       0* 0/
M=14   1   1   0   0   0   0   0         12* 1/ 1* 1/                       0* 0/
M=14   1   1   0   0   0   0   1          1* 1/                             6* 1/
M=14   1   1   0   0   0   0   2          6* 2/ 1* 1/                       0* 0/
M=14   1   1   0   0   0   1   1          7* 1/ 5* 1/ 1* 1/                 0* 0/
M=14   1   1   0   0   1   1   0          8* 1/ 4* 1/ 1* 1/                 0* 0/
M=14   1   1   0   0   2   2   0          4* 1/ 1* 1/                       4* 1/
M=14   1   1   0   0   3   3   0          4* 3/ 1* 1/                       0* 0/
M=14   1   1   0   1   1   0   0          9* 1/ 3* 1/ 1* 1/                 0* 0/
M=14   1   1   0   1   1   0   2          6* 1/ 1* 1/                       3* 1/
M=14   1   1   0   1   2   2   1          5* 1/ 4* 1/ 3* 1/ 1* 1/           0* 0/
M=14   1   1   0   2   2   0   2          6* 1/ 3* 2/ 1* 1/                 0* 0/
M=14   1   1   0   2   2   0   3          1* 1/                             3* 2/
M=14   1   1   0   3   3   0   4          3* 2/ 1* 1/                       3* 1/
M=14   1   1   0   4   4   0   6          3* 4/ 1* 1/                       0* 0/
M=14   1   1   1   0   0   0   0         11* 1/                             1* 1/
M=14   1   1   1   0   0   1   2          6* 1/ 5* 1/                       1* 1/
M=14   1   1   1   0   1   1   1          7* 1/ 4* 1/                       1* 1/
M=14   1   1   1   1   0   0   0         10* 1/ 2* 1/ 1* 1/                 0* 0/
M=14   1   1   1   1   0   1   1          2* 1/ 1* 1/                       5* 1/
M=14   1   1   1   1   0   2   2          5* 2/ 2* 1/ 1* 1/                 0* 0/
M=14   1   1   1   1   1   1   0          8* 1/ 1* 1/                       2* 1/
M=14   1   1   1   1   1   1   0          8* 1/ 3* 1/                       1* 1/
M=14   1   1   1   1   1   1   2          6* 1/ 4* 1/ 2* 1/ 1* 1/           0* 0/
M=14   1   1   1   1   1   2   2          5* 1/                             3* 1/ 1* 1/
M=14   1   1   1   1   2   2   1          1* 1/                             4* 1/ 2* 1/
M=14   1   1   1   1   2   2   1          3* 1/                             4* 1/ 1* 1/
M=14   1   1   1   1   3   3   2          4* 2/ 1* 1/                       2* 1/
M=14   1   1   1   1   3   3   2          4* 2/ 3* 1/                       1* 1/
M=14   1   1   1   2   1   1   1          7* 1/ 3* 1/ 2* 1/ 1* 1/           0* 0/
M=14   1   1   1   2   2   2   3          4* 1/ 2* 1/ 1* 1/                 3* 1/
M=14   1   1   1   2   2   3   2          5* 1/ 3* 1/ 1* 1/                 2* 1/
M=14   1   1   1   2   2   3   2          5* 1/ 3* 2/                       1* 1/
M=14   1   1   1   3   3   3   4          4* 1/ 3* 2/ 2* 1/ 1* 1/           0* 0/
M=14   1   1   2   1   1   0   0          9* 1/ 2* 1/                       1* 1/
M=14   1   1   2   1   2   1   1          7* 1/                             2* 1/ 1* 1/
M=14   1   1   2   1   2   2   3          5* 1/ 4* 1/ 2* 1/                 1* 1/
M=14   1   1   2   2   1   1   0          8* 1/ 2* 2/ 1* 1/                 0* 0/
M=14   1   1   2   2   2   2   2          2* 2/ 1* 1/                       4* 1/
M=14   1   1   2   2   2   2   2          6* 1/ 2* 1/ 1* 1/                 2* 1/
M=14   1   1   2   2   2   2   2          6* 1/ 3* 1/ 2* 1/                 1* 1/
M=14   1   1   2   2   3   3   4          4* 2/ 2* 2/ 1* 1/                 0* 0/
M=14   1   1   2   2   4   4   4          4* 1/ 1* 1/                       2* 2/
```

```
M=14   1   1   2   2   4   4   4        4* 1/ 3* 1/                      2* 1/ 1* 1/
M=14   1   1   2   3   2   4   3        5* 1/ 3* 1/ 2* 2/ 1* 1/          0* 0/
M=14   1   1   2   3   3   4   4        2* 1/ 1* 1/                      3* 1/ 2* 1/
M=14   1   1   2   3   3   4   4        3* 1/ 2* 1/                      3* 1/ 1* 1/
M=14   1   1   2   4   4   6   6        3* 2/ 2* 1/ 1* 1/                2* 1/
M=14   1   1   2   4   4   6   6        3* 3/ 2* 1/                      1* 1/
M=14   1   1   3   2   3   1   1        7* 1/ 2* 2/                      1* 1/
M=14   1   1   3   2   4   3   4        5* 1/ 2* 1/                      2* 1/ 1* 1/
M=14   1   1   3   3   3   3   2        6* 1/ 2* 3/ 1* 1/                0* 0/
M=14   1   1   3   3   5   5   6        4* 1/ 2* 2/ 1* 1/                2* 1/
M=14   1   1   3   3   5   5   6        4* 1/ 3* 1/ 2* 2/                1* 1/
M=14   1   1   3   3   6   6   7        1* 1/                            2* 3/
M=14   1   1   3   3   6   6   7        3* 1/                            2* 2/ 1* 1/
M=14   1   1   3   4   4   6   5        2* 3/ 1* 1/                      3* 1/
M=14   1   1   3   5   5   9   8        3* 2/ 2* 3/ 1* 1/                0* 0/
M=14   1   1   4   3   6   4   5        5* 1/ 2* 3/                      1* 1/
M=14   1   1   4   4   7   7   8        4* 1/ 2* 4/ 1* 1/                0* 0/
M=14   1   1   4   4   8   8  10        2* 2/ 1* 1/                      2* 2/
M=14   1   1   4   4   8   8  10        3* 1/ 2* 2/                      2* 1/ 1* 1/
M=14   1   1   5   5  11  11  14        2* 4/ 1* 1/                      2* 1/
M=14   1   1   5   5  11  11  14        3* 1/ 2* 4/                      1* 1/
M=14   1   1   6   6  15  15  20        2* 6/ 1* 1/                      0* 0/
M=14   1   2   1   0   0   0   0       11* 1/ 1* 2/                      0* 0/
M=14   1   2   1   0   0   1   3        6* 1/ 5* 1/ 1* 2/                0* 0/
M=14   1   2   1   0   1   2   1        7* 1/ 4* 1/ 1* 2/                0* 0/
M=14   1   2   1   1   2   1   0        8* 1/ 3* 1/ 1* 2/                0* 0/
M=14   1   2   1   1   2   2   3        5* 1/ 1* 2/                      3* 1/
M=14   1   2   1   1   3   3   1        3* 1/ 1* 2/                      4* 1/
M=14   1   2   1   1   4   5   2        4* 2/ 3* 1/ 1* 2/                0* 0/
M=14   1   2   1   2   4   3   3        5* 1/ 3* 2/ 1* 2/                0* 0/
M=14   1   2   2   1   0   0   0       10* 1/ 1* 1/                      1* 1/
M=14   1   2   2   1   0   1   2        1* 1/                            5* 1/ 1* 1/
M=14   1   2   2   1   0   2   4        5* 2/ 1* 1/                      1* 1/
M=14   1   2   2   1   1   2   3        6* 1/ 4* 1/ 1* 1/                1* 1/
M=14   1   2   2   2   1   0   0        9* 1/ 2* 1/ 1* 2/                0* 0/
M=14   1   2   2   2   2   2   1        7* 1/ 1* 2/                      2* 1/
M=14   1   2   2   2   2   2   1        7* 1/ 3* 1/ 1* 1/                1* 1/
M=14   1   2   2   2   2   3   4        5* 1/ 4* 1/ 2* 1/ 1* 2/          0* 0/
M=14   1   2   2   2   3   4   4        4* 1/ 1* 1/                      3* 1/ 1* 1/
M=14   1   2   2   3   3   2   3        6* 1/ 3* 1/ 2* 1/ 1* 2/          0* 0/
M=14   1   2   2   3   5   6   5        4* 1/ 3* 1/ 1* 2/                2* 1/
M=14   1   2   2   3   5   6   5        4* 1/ 3* 2/ 1* 1/                1* 1/
M=14   1   2   2   4   5   4   6        3* 1/ 2* 1/ 1* 2/                3* 1/
```

```
M=14    1   2   2   5   7   6   9            3* 3/ 2* 1/ 1* 2/                0* 0/
M=14    1   2   3   2   1   0   0            9* 1/                            1* 2/
M=14    1   2   3   2   2   3   5            5* 1/ 4* 1/                      1* 2/
M=14    1   2   3   3   2   1   0            8* 1/ 2* 1/ 1* 1/                1* 1/
M=14    1   2   3   3   3   3   3            2* 1/ 1* 1/                      4* 1/ 1* 1/
M=14    1   2   3   3   3   3   3            6* 1/ 1* 1/                      2* 1/ 1* 1/
M=14    1   2   3   3   3   3   3            6* 1/ 3* 1/                      1* 2/
M=14    1   2   3   3   4   5   6            4* 2/ 2* 1/ 1* 1/                1* 1/
M=14    1   2   3   4   3   2   1            7* 1/ 2* 2/ 1* 2/                0* 0/
M=14    1   2   3   4   4   5   5            5* 1/ 2* 1/ 1* 2/                2* 1/
M=14    1   2   3   4   4   5   5            5* 1/ 3* 1/ 2* 1/ 1* 1/          1* 1/
M=14    1   2   3   4   5   6   6            1* 1/                            3* 1/ 2* 1/ 1* 1/
M=14    1   2   3   4   5   6   6            3* 1/                            3* 1/ 1* 2/
M=14    1   2   3   5   6   7   8            4* 1/ 3* 1/ 2* 2/ 1* 2/          0* 0/
M=14    1   2   3   5   7   9   9            3* 1/ 1* 2/                      2* 2/
M=14    1   2   3   5   7   9   9            3* 2/ 1* 1/                      2* 1/ 1* 1/
M=14    1   2   3   5   7   9   9            3* 3/                            1* 2/
M=14    1   2   4   4   4   2   1            7* 1/ 2* 1/                      1* 2/
M=14    1   2   4   4   5   5   6            5* 1/                            2* 1/ 1* 2/
M=14    1   2   4   5   5   4   3            6* 1/ 2* 2/ 1* 1/                1* 1/
M=14    1   2   4   5   7   8   9            4* 1/ 2* 1/ 1* 1/                2* 1/ 1* 1/
M=14    1   2   4   5   7   8   9            4* 1/ 3* 1/ 2* 1/                1* 2/
M=14    1   2   4   6   6   7   6            5* 1/ 2* 3/ 1* 2/                0* 0/
M=14    1   2   4   6   7   8   8            2* 2/ 1* 1/                      3* 1/ 1* 1/
M=14    1   2   4   7   9  12  13            3* 1/ 2* 2/ 1* 2/                2* 1/
M=14    1   2   4   7   9  12  13            3* 2/ 2* 2/ 1* 1/                1* 1/
M=14    1   2   5   6   8   7   7            5* 1/ 2* 2/                      1* 2/
M=14    1   2   5   7  10  11  12            4* 1/ 2* 3/ 1* 1/                1* 1/
M=14    1   2   5   7  11  13  15            2* 1/ 1* 1/                      2* 2/ 1* 1/
M=14    1   2   5   7  11  13  15            3* 1/ 2* 1/                      2* 1/ 1* 2/
M=14    1   2   5   9  12  17  18            3* 1/ 2* 4/ 1* 2/                0* 0/
M=14    1   2   6   9  15  18  21            2* 3/ 1* 1/                      2* 1/ 1* 1/
M=14    1   2   6   9  15  18  21            3* 1/ 2* 3/                      1* 2/
M=14    1   2   7  11  20  25  30            2* 5/ 1* 1/                      1* 1/
M=14    1   3   3   1   0   0   0           10* 1/ 1* 3/                      0* 0/
M=14    1   3   3   1   0   1   3            1* 3/                            5* 1/
M=14    1   3   3   1   0   2   6            5* 2/ 1* 3/                      0* 0/
M=14    1   3   3   1   1   3   4            6* 1/ 4* 1/ 1* 3/                0* 0/
M=14    1   3   3   2   3   3   1            7* 1/ 3* 1/ 1* 3/                0* 0/
M=14    1   3   3   2   4   6   5            4* 1/ 1* 3/                      3* 1/
M=14    1   3   3   3   7   9   6            4* 1/ 3* 2/ 1* 3/                0* 0/
M=14    1   3   4   3   1   0   0            9* 1/ 1* 2/                      1* 1/
M=14    1   3   4   3   2   4   7            5* 1/ 4* 1/ 1* 2/                1* 1/
```

```
M=14    1    3    4    4    3    1    0          8* 1/ 2* 1/ 1* 3/               0* 0/
M=14    1    3    4    4    4    4    4          2* 1/ 1* 3/                     4* 1/
M=14    1    3    4    4    4    4    4          6* 1/ 1* 3/                     2* 1/
M=14    1    3    4    4    4    4    4          6* 1/ 3* 1/ 1* 2/               1* 1/
M=14    1    3    4    4    5    7    8          4* 2/ 2* 1/ 1* 3/               0* 0/
M=14    1    3    4    5    6    6    7          5* 1/ 3* 1/ 2* 1/ 1* 3/         0* 0/
M=14    1    3    4    5    7    8    8          1* 3/                           3* 1/ 2* 1/
M=14    1    3    4    5    7    8    8          3* 1/ 1* 2/                     3* 1/ 1* 1/
M=14    1    3    4    6   10   12   12          3* 2/ 1* 3/                     2* 1/
M=14    1    3    4    6   10   12   12          3* 3/ 1* 2/                     1* 1/
M=14    1    3    5    5    3    1    0          8* 1/ 1* 1/                     1* 2/
M=14    1    3    5    5    4    4    5          1* 1/                           4* 1/ 1* 2/
M=14    1    3    5    5    5    7   10          4* 2/ 1* 1/                     1* 2/
M=14    1    3    5    6    5    3    1          7* 1/ 2* 1/ 1* 2/               1* 1/
M=14    1    3    5    6    6    7    8          5* 1/ 1* 2/                     2* 1/ 1* 1/
M=14    1    3    5    6    6    7    8          5* 1/ 3* 1/ 1* 1/               1* 2/
M=14    1    3    5    7    7    5    4          6* 1/ 2* 2/ 1* 3/               0* 0/
M=14    1    3    5    7    9   11   12          4* 1/ 2* 1/ 1* 3/               2* 1/
M=14    1    3    5    7    9   11   12          4* 1/ 3* 1/ 2* 1/ 1* 2/         1* 1/
M=14    1    3    5    8   10   10   11          2* 2/ 1* 3/                     3* 1/
M=14    1    3    5    9   13   15   18          3* 2/ 2* 2/ 1* 3/               0* 0/
M=14    1    3    6    7    6    3    1          7* 1/                           1* 3/
M=14    1    3    6    8    8    6    4          6* 1/ 2* 1/ 1* 1/               1* 2/
M=14    1    3    6    8   10   12   14          4* 1/ 1* 1/                     2* 1/ 1* 2/
M=14    1    3    6    8   10   12   14          4* 1/ 3* 1/                     1* 3/
M=14    1    3    6    9   10   10    9          5* 1/ 2* 2/ 1* 2/               1* 1/
M=14    1    3    6    9   11   12   12          2* 1/ 1* 1/                     3* 1/ 1* 2/
M=14    1    3    6   10   13   15   16          4* 1/ 2* 3/ 1* 3/               0* 0/
M=14    1    3    6   10   14   18   20          2* 1/ 1* 3/                     2* 2/
M=14    1    3    6   10   14   18   20          3* 1/ 2* 1/ 1* 2/               2* 1/ 1* 1/
M=14    1    3    6   10   14   18   20          3* 2/ 2* 1/ 1* 1/               1* 2/
M=14    1    3    7   10   12   11   10          5* 1/ 2* 1/                     1* 3/
M=14    1    3    7   11   15   17   18          4* 1/ 2* 2/ 1* 1/               1* 2/
M=14    1    3    7   11   16   20   23          1* 1/                           2* 2/ 1* 2/
M=14    1    3    7   11   16   20   23          3* 1/                           2* 1/ 1* 3/
M=14    1    3    7   13   19   25   28          2* 3/ 1* 3/                     2* 1/
M=14    1    3    7   13   19   25   28          3* 1/ 2* 3/ 1* 2/               1* 1/
M=14    1    3    8   14   22   28   32          2* 2/ 1* 1/                     2* 1/ 1* 2/
M=14    1    3    8   14   22   28   32          3* 1/ 2* 2/                     1* 3/
M=14    1    3    8   16   25   35   40          2* 5/ 1* 3/                     0* 0/
M=14    1    3    9   17   29   39   46          2* 4/ 1* 1/                     1* 2/
M=14    1    4    6    4    1    0    0          9* 1/ 1* 4/                     0* 0/
M=14    1    4    6    4    2    5   10          5* 1/ 4* 1/ 1* 4/               0* 0/
```

```
M=14   1   4   6   5   5   6   5           6* 1/ 3* 1/ 1* 4/                    0* 0/
M=14   1   4   6   6   9  12  10           3* 1/ 1* 4/                          3* 1/
M=14   1   4   6   7  13  18  15           3* 3/ 1* 4/                          0* 0/
M=14   1   4   7   7   4   1   0           8* 1/ 1* 3/                          1* 1/
M=14   1   4   7   7   5   5   7           1* 3/                                4* 1/ 1* 1/
M=14   1   4   7   7   6   9  14           4* 2/ 1* 3/                          1* 1/
M=14   1   4   7   8   7   4   1           7* 1/ 2* 1/ 1* 4/                    0* 0/
M=14   1   4   7   8   8   9  11           5* 1/ 1* 4/                          2* 1/
M=14   1   4   7   8   8   9  11           5* 1/ 3* 1/ 1* 3/                    1* 1/
M=14   1   4   7   9  12  15  16           4* 1/ 3* 1/ 2* 1/ 1* 4/              0* 0/
M=14   1   4   8  10   8   4   1           7* 1/ 1* 2/                          1* 2/
M=14   1   4   8  11  11   8   5           6* 1/ 2* 1/ 1* 3/                    1* 1/
M=14   1   4   8  11  13  16  19           4* 1/ 1* 3/                          2* 1/ 1* 1/
M=14   1   4   8  11  13  16  19           4* 1/ 3* 1/ 1* 2/                    1* 2/
M=14   1   4   8  12  14  13  12           5* 1/ 2* 2/ 1* 4/                    0* 0/
M=14   1   4   8  12  15  16  16           2* 1/ 1* 3/                          3* 1/ 1* 1/
M=14   1   4   8  13  19  24  27           3* 1/ 2* 1/ 1* 4/                    2* 1/
M=14   1   4   8  13  19  24  27           3* 2/ 2* 1/ 1* 3/                    1* 1/
M=14   1   4   9  13  13   9   5           6* 1/ 1* 1/                          1* 3/
M=14   1   4   9  14  16  15  13           5* 1/ 2* 1/ 1* 2/                    1* 2/
M=14   1   4   9  14  17  18  18           1* 1/                                3* 1/ 1* 3/
M=14   1   4   9  15  20  23  24           4* 1/ 2* 2/ 1* 3/                    1* 1/
M=14   1   4   9  15  21  27  31           1* 3/                                2* 2/ 1* 1/
M=14   1   4   9  15  21  27  31           3* 1/ 1* 2/                          2* 1/ 1* 2/
M=14   1   4   9  15  21  27  31           3* 2/ 1* 1/                          1* 3/
M=14   1   4   9  17  26  33  38           3* 1/ 2* 3/ 1* 4/                    0* 0/
M=14   1   4  10  16  19  17  14           5* 1/                                1* 4/
M=14   1   4  10  17  23  26  27           4* 1/ 2* 1/ 1* 1/                    1* 3/
M=14   1   4  10  19  29  38  43           2* 2/ 1* 3/                          2* 1/ 1* 1/
M=14   1   4  10  19  29  38  43           3* 1/ 2* 2/ 1* 2/                    1* 2/
M=14   1   4  11  21  33  43  49           2* 1/ 1* 1/                          2* 1/ 1* 3/
M=14   1   4  11  21  33  43  49           3* 1/ 2* 1/                          1* 4/
M=14   1   4  11  23  38  53  62           2* 4/ 1* 3/                          1* 1/
M=14   1   4  12  25  43  60  71           2* 3/ 1* 1/                          1* 3/
M=14   1   5  10  10   5   1   0           8* 1/ 1* 5/                          0* 0/
M=14   1   5  10  10   6   6  10           1* 5/                                4* 1/
M=14   1   5  10  10   7  11  20           4* 2/ 1* 5/                          0* 0/
M=14   1   5  10  11  10  12  15           5* 1/ 3* 1/ 1* 5/                    0* 0/
M=14   1   5  11  14  11   5   1           7* 1/ 1* 4/                          1* 1/
M=14   1   5  11  15  15  11   6           6* 1/ 2* 1/ 1* 5/                    0* 0/
M=14   1   5  11  15  17  21  26           4* 1/ 1* 5/                          2* 1/
M=14   1   5  11  15  17  21  26           4* 1/ 3* 1/ 1* 4/                    1* 1/
M=14   1   5  11  16  20  22  21           2* 1/ 1* 5/                          3* 1/
```

```
M=14   1   5   11   17   25   33   36          3* 2/ 2* 1/ 1* 5/          0* 0/
M=14   1   5   12   18   18   12    6          6* 1/ 1* 3/                1* 2/
M=14   1   5   12   19   22   20   17          5* 1/ 2* 1/ 1* 4/          1* 1/
M=14   1   5   12   19   23   24   24          1* 3/                      3* 1/ 1* 2/
M=14   1   5   12   20   27   31   32          4* 1/ 2* 2/ 1* 5/          0* 0/
M=14   1   5   12   20   28   36   42          1* 5/                      2* 2/
M=14   1   5   12   20   28   36   42          3* 1/ 1* 4/                2* 1/ 1* 1/
M=14   1   5   12   20   28   36   42          3* 2/ 1* 3/                1* 2/
M=14   1   5   13   22   26   23   18          5* 1/ 1* 2/                1* 3/
M=14   1   5   13   23   31   35   36          4* 1/ 2* 1/ 1* 3/          1* 2/
M=14   1   5   13   25   39   51   58          2* 2/ 1* 5/                2* 1/
M=14   1   5   13   25   39   51   58          3* 1/ 2* 2/ 1* 4/          1* 1/
M=14   1   5   14   26   36   40   40          4* 1/ 1* 1/                1* 4/
M=14   1   5   14   28   44   58   66          2* 1/ 1* 3/                2* 1/ 1* 2/
M=14   1   5   14   28   44   58   66          3* 1/ 2* 1/ 1* 2/          1* 3/
M=14   1   5   14   30   51   71   84          2* 4/ 1* 5/                0* 0/
M=14   1   5   15   31   50   66   75          1* 1/                      2* 1/ 1* 4/
M=14   1   5   15   31   50   66   75          3* 1/                      1* 5/
M=14   1   5   15   33   57   81   96          2* 3/ 1* 3/                1* 2/
M=14   1   5   16   36   64   92  110          2* 2/ 1* 1/                1* 4/
M=14   1   6   15   20   15    6    1          7* 1/ 1* 6/                0* 0/
M=14   1   6   15   21   22   27   36          4* 1/ 3* 1/ 1* 6/          0* 0/
M=14   1   6   16   25   25   16    7          6* 1/ 1* 5/                1* 1/
M=14   1   6   16   26   30   27   22          5* 1/ 2* 1/ 1* 6/          0* 0/
M=14   1   6   16   26   31   32   32          1* 5/                      3* 1/ 1* 1/
M=14   1   6   16   27   37   48   57          3* 1/ 1* 6/                2* 1/
M=14   1   6   16   27   37   48   57          3* 2/ 1* 5/                1* 1/
M=14   1   6   17   30   36   31   23          5* 1/ 1* 4/                1* 2/
M=14   1   6   17   31   42   47   48          4* 1/ 2* 1/ 1* 5/          1* 1/
M=14   1   6   17   33   52   69   78          3* 1/ 2* 2/ 1* 6/          0* 0/
M=14   1   6   18   35   49   54   53          4* 1/ 1* 3/                1* 3/
M=14   1   6   18   37   59   78   89          2* 1/ 1* 5/                2* 1/ 1* 1/
M=14   1   6   18   37   59   78   89          3* 1/ 2* 1/ 1* 4/          1* 2/
M=14   1   6   19   41   67   89  101          1* 3/                      2* 1/ 1* 3/
M=14   1   6   19   41   67   89  101          3* 1/ 1* 2/                1* 4/
M=14   1   6   19   43   76  109  130          2* 3/ 1* 5/                1* 1/
M=14   1   6   20   47   85  124  149          2* 2/ 1* 3/                1* 3/
M=14   1   6   21   51   95  141  171          2* 1/ 1* 1/                1* 5/
M=14   1   7   21   35   35   21    8          6* 1/ 1* 7/                0* 0/
M=14   1   7   21   36   42   42   43          1* 7/                      3* 1/
M=14   1   7   21   37   49   63   78          3* 2/ 1* 7/                0* 0/
M=14   1   7   22   41   50   42   29          5* 1/ 1* 6/                1* 1/
M=14   1   7   22   42   57   63   64          4* 1/ 2* 1/ 1* 7/          0* 0/
```

```
M=14     1    7   23   47   67   73   70          4* 1/ 1* 5/                1* 2/
M=14     1    7   23   49   79  105  120          2* 1/ 1* 7/                2* 1/
M=14     1    7   23   49   79  105  120          3* 1/ 2* 1/ 1* 6/          1* 1/
M=14     1    7   24   54   90  120  136          1* 5/                      2* 1/ 1* 2/
M=14     1    7   24   54   90  120  136          3* 1/ 1* 4/                1* 3/
M=14     1    7   24   56  101  147  176          2* 3/ 1* 7/                0* 0/
M=14     1    7   25   61  113  167  202          2* 2/ 1* 5/                1* 2/
M=14     1    7   26   66  126  190  232          2* 1/ 1* 3/                1* 4/
M=14     1    7   27   71  140  216  267          1* 1/                      1* 6/
M=14     1    8   28   56   70   57   36          5* 1/ 1* 8/                0* 0/
M=14     1    8   29   63   92   99   92          4* 1/ 1* 7/                1* 1/
M=14     1    8   29   65  106  141  162          3* 1/ 2* 1/ 1* 8/          0* 0/
M=14     1    8   30   71  121  162  183          1* 7/                      2* 1/ 1* 1/
M=14     1    8   30   71  121  162  183          3* 1/ 1* 6/                1* 2/
M=14     1    8   31   79  150  225  274          2* 2/ 1* 7/                1* 1/
M=14     1    8   32   85  167  256  315          2* 1/ 1* 5/                1* 3/
M=14     1    8   33   91  186  291  363          1* 3/                      1* 5/
M=14     1    9   36   84  127  135  120          4* 1/ 1* 9/                0* 0/
M=14     1    9   37   93  163  219  246          1* 9/                      2* 1/
M=14     1    9   37   93  163  219  246          3* 1/ 1* 8/                1* 1/
M=14     1    9   38  102  199  303  372          2* 2/ 1* 9/                0* 0/
M=14     1    9   39  109  221  345  428          2* 1/ 1* 7/                1* 2/
M=14     1    9   40  116  244  392  494          1* 5/                      1* 4/
M=14     1   10   45  121  220  297  330          3* 1/ 1*10/                0* 0/
M=14     1   10   47  139  292  465  582          2* 1/ 1* 9/                1* 1/
M=14     1   10   48  147  321  528  673          1* 7/                      1* 3/
M=14     1   11   56  176  385  627  792          2* 1/ 1*11/                0* 0/
M=14     1   11   57  185  421  711  918          1* 9/                      1* 2/
M=14     1   12   67  231  550  957 1254          1*11/                      1* 1/
M=14     1   13   78  286  715 1287 1716          1*13/                      0* 0/
M=15     1    0    0    0    0    0    0    0    14* 1/                      0* 0/
M=15     1    0    0    0    0    0    0    1     0* 0/                      7* 1/
M=15     1    0    0    0    0    0    0    2     7* 2/                      0* 0/
M=15     1    0    0    0    0    0    1    0     8* 1/ 6* 1/                0* 0/
M=15     1    0    0    0    0    1    0    0     9* 1/ 5* 1/                0* 0/
M=15     1    0    0    0    1    0    0    0    10* 1/ 4* 1/                0* 0/
M=15     1    0    0    0    1    0    1    0     6* 1/                      4* 1/
M=15     1    0    0    0    1    1    0    0     4* 1/                      5* 1/
M=15     1    0    0    0    1    2    0    0     5* 2/ 4* 1/                0* 0/
M=15     1    0    0    0    2    0    1    0     6* 1/ 4* 2/                0* 0/
M=15     1    0    0    1    0    0    0    0    11* 1/ 3* 1/                0* 0/
M=15     1    0    0    1    0    0    1    0     8* 1/                      3* 1/
M=15     1    0    0    1    0    1    1    0     6* 1/ 5* 1/ 3* 1/          0* 0/
```

```
M=15     1    0    0    1    1    0    0    2            7* 1/ 4* 1/ 3* 1/                         0* 0/
M=15     1    0    0    1    1    0    1    1            0* 0/                                     4* 1/ 3* 1/
M=15     1    0    0    1    2    0    1    2            4* 2/                                     3* 1/
M=15     1    0    0    2    0    0    1    0            8* 1/ 3* 2/                               0* 0/
M=15     1    0    0    2    0    1    2    0            5* 1/ 3* 1/                               3* 1/
M=15     1    0    0    2    1    0    1    2            3* 2/                                     4* 1/
M=15     1    0    0    2    2    0    1    4            4* 2/ 3* 2/                               0* 0/
M=15     1    0    0    3    0    1    3    0            5* 1/ 3* 3/                               0* 0/
M=15     1    0    1    0    0    0    0    0           12* 1/ 2* 1/                               0* 0/
M=15     1    0    1    0    0    0    1    0            2* 1/                                     6* 1/
M=15     1    0    1    0    0    0    2    0            6* 2/ 2* 1/                               0* 0/
M=15     1    0    1    0    0    1    0    2            7* 1/ 5* 1/ 2* 1/                         0* 0/
M=15     1    0    1    0    1    0    0    0           10* 1/                                     2* 1/
M=15     1    0    1    0    1    0    1    0            8* 1/ 4* 1/ 2* 1/                         0* 0/
M=15     1    0    1    0    1    1    0    1            0* 0/                                     5* 1/ 2* 1/
M=15     1    0    1    0    1    2    0    2            5* 2/                                     2* 1/
M=15     1    0    1    0    2    0    2    0            4* 1/ 2* 1/                               4* 1/
M=15     1    0    1    0    2    0    2    0            6* 1/ 4* 1/                               2* 1/
M=15     1    0    1    0    3    0    3    0            4* 3/ 2* 1/                               0* 0/
M=15     1    0    1    1    0    1    0    0            9* 1/ 3* 1/ 2* 1/                         0* 0/
M=15     1    0    1    1    0    1    2    0            6* 1/ 2* 1/                               3* 1/
M=15     1    0    1    1    1    1    0    2            7* 1/ 3* 1/                               2* 1/
M=15     1    0    1    1    1    2    1    2            5* 1/ 4* 1/ 3* 1/ 2* 1/                   0* 0/
M=15     1    0    1    1    2    1    2    2            4* 1/                                     3* 1/ 2* 1/
M=15     1    0    1    2    0    2    2    0            6* 1/ 3* 2/ 2* 1/                         0* 0/
M=15     1    0    1    2    0    2    3    0            2* 1/                                     3* 2/
M=15     1    0    1    2    2    2    2    4            4* 1/ 3* 2/                               2* 1/
M=15     1    0    1    3    0    3    4    0            3* 2/ 2* 1/                               3* 1/
M=15     1    0    1    4    0    4    6    0            3* 4/ 2* 1/                               0* 0/
M=15     1    0    2    0    1    0    0    0           10* 1/ 2* 2/                               0* 0/
M=15     1    0    2    0    1    1    0    2            2* 2/                                     5* 1/
M=15     1    0    2    0    1    2    0    4            5* 2/ 2* 2/                               0* 0/
M=15     1    0    2    0    2    0    1    0            8* 1/ 2* 1/                               2* 1/
M=15     1    0    2    0    2    0    3    0            6* 1/ 4* 1/ 2* 2/                         0* 0/
M=15     1    0    2    0    3    0    3    0            2* 1/                                     4* 1/ 2* 1/
M=15     1    0    2    0    3    0    3    0            6* 1/                                     2* 2/
M=15     1    0    2    0    4    0    5    0            4* 2/ 2* 1/                               2* 1/
M=15     1    0    2    1    1    2    0    2            7* 1/ 3* 1/ 2* 2/                         0* 0/
M=15     1    0    2    1    2    2    3    2            4* 1/ 2* 2/                               3* 1/
M=15     1    0    2    1    2    3    1    4            5* 1/ 3* 1/ 2* 1/                         2* 1/
M=15     1    0    2    1    3    2    3    3            0* 0/                                     3* 1/ 2* 2/
M=15     1    0    2    2    2    4    3    4            4* 1/ 3* 2/ 2* 2/                         0* 0/
M=15     1    0    2    2    3    4    3    6            3* 2/                                     2* 2/
```

```
M=15    1   0   3   0   3   0   1   0            8* 1/ 2* 3/                      0* 0/
M=15    1   0   3   0   4   0   4   0            2* 3/                            4* 1/
M=15    1   0   3   0   4   0   4   0            6* 1/ 2* 2/                      2* 1/
M=15    1   0   3   0   5   0   7   0            4* 2/ 2* 3/                      0* 0/
M=15    1   0   3   0   6   0   8   0            4* 1/ 2* 1/                      2* 2/
M=15    1   0   3   1   3   4   1   6            5* 1/ 3* 1/ 2* 3/                0* 0/
M=15    1   0   3   1   4   3   4   4            2* 2/                            3* 1/ 2* 1/
M=15    1   0   3   2   4   6   4   8            3* 2/ 2* 2/                      2* 1/
M=15    1   0   4   0   6   0   5   0            6* 1/ 2* 4/                      0* 0/
M=15    1   0   4   0   8   0  11   0            4* 1/ 2* 3/                      2* 1/
M=15    1   0   4   0   9   0  13   0            2* 1/                            2* 3/
M=15    1   0   4   1   6   4   5   6            2* 4/                            3* 1/
M=15    1   0   4   2   6   8   5  12            3* 2/ 2* 4/                      0* 0/
M=15    1   0   5   0  11   0  15   0            4* 1/ 2* 5/                      0* 0/
M=15    1   0   5   0  12   0  18   0            2* 3/                            2* 2/
M=15    1   0   6   0  16   0  25   0            2* 5/                            2* 1/
M=15    1   0   7   0  21   0  35   0            2* 7/                            0* 0/
M=15    1   1   0   0   0   0   0   0           13* 1/ 1* 1/                      0* 0/
M=15    1   1   0   0   0   0   1   2            7* 1/ 6* 1/ 1* 1/                0* 0/
M=15    1   1   0   0   0   1   1   0            8* 1/ 5* 1/ 1* 1/                0* 0/
M=15    1   1   0   0   1   1   0   0            9* 1/ 4* 1/ 1* 1/                0* 0/
M=15    1   1   0   0   1   2   1   0            5* 1/ 1* 1/                      4* 1/
M=15    1   1   0   0   2   3   1   0            5* 1/ 4* 2/ 1* 1/                0* 0/
M=15    1   1   0   1   1   0   0   0           10* 1/ 3* 1/ 1* 1/                0* 0/
M=15    1   1   0   1   1   0   1   2            7* 1/ 1* 1/                      3* 1/
M=15    1   1   0   1   1   1   1   0            3* 1/ 1* 1/                      5* 1/
M=15    1   1   0   1   1   2   2   0            5* 2/ 3* 1/ 1* 1/                0* 0/
M=15    1   1   0   1   2   1   1   2            6* 1/ 4* 1/ 3* 1/ 1* 1/          0* 0/
M=15    1   1   0   2   2   0   1   2            7* 1/ 3* 2/ 1* 1/                0* 0/
M=15    1   1   0   2   3   1   2   4            4* 1/ 3* 1/ 1* 1/                3* 1/
M=15    1   1   0   3   4   1   3   6            4* 1/ 3* 3/ 1* 1/                0* 0/
M=15    1   1   1   0   0   0   0   0           12* 1/                            1* 1/
M=15    1   1   1   0   0   0   1   1            0* 0/                            6* 1/ 1* 1/
M=15    1   1   1   0   0   0   2   2            6* 2/                            1* 1/
M=15    1   1   1   0   0   1   1   2            7* 1/ 5* 1/                      1* 1/
M=15    1   1   1   0   1   1   1   0            8* 1/ 4* 1/                      1* 1/
M=15    1   1   1   0   2   2   2   0            4* 1/                            4* 1/ 1* 1/
M=15    1   1   1   0   3   3   3   0            4* 3/                            1* 1/
M=15    1   1   1   1   0   0   0   0           11* 1/ 2* 1/ 1* 1/                0* 0/
M=15    1   1   1   1   0   1   2   2            6* 1/ 5* 1/ 2* 1/ 1* 1/          0* 0/
M=15    1   1   1   1   1   1   0   0            9* 1/ 1* 1/                      2* 1/
M=15    1   1   1   1   1   1   0   0            9* 1/ 3* 1/                      1* 1/
M=15    1   1   1   1   1   1   1   2            7* 1/ 4* 1/ 2* 1/ 1* 1/          0* 0/
```

```
M=15   1  1  1  1  1  1  2  2     6* 1/                                3* 1/ 1* 1/
M=15   1  1  1  1  2  3  2  2     5* 1/ 4* 1/ 1* 1/                    2* 1/
M=15   1  1  1  1  2  3  2  2     5* 1/ 4* 1/ 3* 1/                    1* 1/
M=15   1  1  1  2  1  1  1  0     8* 1/ 3* 1/ 2* 1/ 1* 1/              0* 0/
M=15   1  1  1  2  1  2  3  2     5* 1/ 2* 1/ 1* 1/                    3* 1/
M=15   1  1  1  2  2  2  2  2     3* 1/ 2* 1/ 1* 1/                    4* 1/
M=15   1  1  1  2  2  2  2  2     6* 1/ 3* 1/ 1* 1/                    2* 1/
M=15   1  1  1  2  2  2  2  2     6* 1/ 3* 2/                          1* 1/
M=15   1  1  1  2  2  2  3  3     0* 0/                                3* 2/ 1* 1/
M=15   1  1  1  2  3  3  3  4     4* 2/ 3* 1/ 2* 1/ 1* 1/              0* 0/
M=15   1  1  1  3  2  3  4  2     5* 1/ 3* 2/ 2* 1/ 1* 1/              0* 0/
M=15   1  1  1  3  3  3  4  4     3* 1/ 1* 1/                          3* 1/ 2* 1/
M=15   1  1  1  3  3  3  4  4     3* 2/                                3* 1/ 1* 1/
M=15   1  1  1  4  4  4  6  6     3* 3/ 1* 1/                          2* 1/
M=15   1  1  1  4  4  4  6  6     3* 4/                                1* 1/
M=15   1  1  2  1  1  0  0  0    10* 1/ 2* 1/                          1* 1/
M=15   1  1  2  1  1  1  1  2     2* 1/                                5* 1/ 1* 1/
M=15   1  1  2  1  1  2  2  4     5* 2/ 2* 1/                          1* 1/
M=15   1  1  2  1  2  1  1  0     8* 1/                                2* 1/ 1* 1/
M=15   1  1  2  1  2  1  3  2     6* 1/ 4* 1/ 2* 1/                    1* 1/
M=15   1  1  2  1  3  2  3  1     0* 0/                                4* 1/ 2* 1/ 1* 1/
M=15   1  1  2  1  4  3  5  2     4* 2/                                2* 1/ 1* 1/
M=15   1  1  2  2  1  1  0  0     9* 1/ 2* 2/ 1* 1/                    0* 0/
M=15   1  1  2  2  2  2  1  2     7* 1/ 2* 1/ 1* 1/                    2* 1/
M=15   1  1  2  2  2  2  1  2     7* 1/ 3* 1/ 2* 1/                    1* 1/
M=15   1  1  2  2  2  3  3  4     5* 1/ 4* 1/ 2* 2/ 1* 1/              0* 0/
M=15   1  1  2  2  3  3  4  4     4* 1/ 2* 1/                          3* 1/ 1* 1/
M=15   1  1  2  2  3  4  3  4     5* 1/ 1* 1/                          2* 2/
M=15   1  1  2  2  3  4  3  4     5* 1/ 3* 1/                          2* 1/ 1* 1/
M=15   1  1  2  3  2  3  3  2     6* 1/ 3* 1/ 2* 2/ 1* 1/              0* 0/
M=15   1  1  2  3  4  5  5  6     4* 1/ 3* 1/ 2* 1/ 1* 1/              2* 1/
M=15   1  1  2  3  4  5  5  6     4* 1/ 3* 2/ 2* 1/                    1* 1/
M=15   1  1  2  4  3  5  6  4     3* 1/ 2* 2/ 1* 1/                    3* 1/
M=15   1  1  2  5  4  7  9  6     3* 3/ 2* 2/ 1* 1/                    0* 0/
M=15   1  1  3  2  3  1  1  0     8* 1/ 2* 2/                          1* 1/
M=15   1  1  3  2  4  2  4  2     2* 2/                                4* 1/ 1* 1/
M=15   1  1  3  2  4  2  4  2     6* 1/ 2* 1/                          2* 1/ 1* 1/
M=15   1  1  3  2  5  3  7  4     4* 2/ 2* 2/                          1* 1/
M=15   1  1  3  2  6  4  8  4     4* 1/                                2* 2/ 1* 1/
M=15   1  1  3  3  3  3  1  2     7* 1/ 2* 3/ 1* 1/                    0* 0/
M=15   1  1  3  3  4  5  4  6     5* 1/ 2* 2/ 1* 1/                    2* 1/
M=15   1  1  3  3  4  5  4  6     5* 1/ 3* 1/ 2* 2/                    1* 1/
M=15   1  1  3  3  5  5  6  6     2* 1/                                3* 1/ 2* 1/ 1* 1/
```

```
M=15    1   1   3   4   5   7   7   8      4* 1/ 3* 1/ 2* 3/ 1* 1/         0* 0/
M=15    1   1   3   4   6   8   8  10      3* 1/ 2* 1/ 1* 1/               2* 2/
M=15    1   1   3   4   6   8   8  10      3* 2/ 2* 1/                     2* 1/ 1* 1/
M=15    1   1   4   3   6   3   5   2      6* 1/ 2* 3/                     1* 1/
M=15    1   1   4   3   8   5  11   6      4* 1/ 2* 2/                     2* 1/ 1* 1/
M=15    1   1   4   3   9   6  13   7      0* 0/                           2* 3/ 1* 1/
M=15    1   1   4   4   6   7   5   8      5* 1/ 2* 4/ 1* 1/               0* 0/
M=15    1   1   4   4   7   7   8   8      2* 3/                           3* 1/ 1* 1/
M=15    1   1   4   5   8  11  11  14      3* 1/ 2* 3/ 1* 1/               2* 1/
M=15    1   1   4   5   8  11  11  14      3* 2/ 2* 3/                     1* 1/
M=15    1   1   5   4  11   7  15   8      4* 1/ 2* 4/                     1* 1/
M=15    1   1   5   4  12   8  18  10      2* 2/                           2* 2/ 1* 1/
M=15    1   1   5   6  11  15  15  20      3* 1/ 2* 5/ 1* 1/               0* 0/
M=15    1   1   6   5  16  11  25  14      2* 4/                           2* 1/ 1* 1/
M=15    1   1   7   6  21  15  35  20      2* 6/                           1* 1/
M=15    1   2   1   0   0   0   0   0     12* 1/ 1* 2/                     0* 0/
M=15    1   2   1   0   0   0   1   2      1* 2/                           6* 1/
M=15    1   2   1   0   0   0   2   4      6* 2/ 1* 2/                     0* 0/
M=15    1   2   1   0   0   1   2   2      7* 1/ 5* 1/ 1* 2/               0* 0/
M=15    1   2   1   0   1   2   1   0      8* 1/ 4* 1/ 1* 2/               0* 0/
M=15    1   2   1   0   2   4   2   0      4* 1/ 1* 2/                     4* 1/
M=15    1   2   1   0   3   6   3   0      4* 3/ 1* 2/                     0* 0/
M=15    1   2   1   1   2   1   0   0      9* 1/ 3* 1/ 1* 2/               0* 0/
M=15    1   2   1   1   2   1   2   4      6* 1/ 1* 2/                     3* 1/
M=15    1   2   1   1   3   4   3   2      5* 1/ 4* 1/ 3* 1/ 1* 2/         0* 0/
M=15    1   2   1   2   4   2   2   4      6* 1/ 3* 2/ 1* 2/               0* 0/
M=15    1   2   1   2   4   2   3   6      1* 2/                           3* 2/
M=15    1   2   1   3   6   3   4   8      3* 2/ 1* 2/                     3* 1/
M=15    1   2   1   4   8   4   6  12      3* 4/ 1* 2/                     0* 0/
M=15    1   2   2   1   0   0   0   0     11* 1/ 1* 1/                     1* 1/
M=15    1   2   2   1   0   1   3   4      6* 1/ 5* 1/ 1* 1/               1* 1/
M=15    1   2   2   1   1   2   2   2      7* 1/ 4* 1/ 1* 1/               1* 1/
M=15    1   2   2   2   1   0   0   0     10* 1/ 2* 1/ 1* 2/               0* 0/
M=15    1   2   2   2   1   1   2   2      2* 1/ 1* 2/                     5* 1/
M=15    1   2   2   2   1   2   4   4      5* 2/ 2* 1/ 1* 2/               0* 0/
M=15    1   2   2   2   2   2   1   0      8* 1/ 1* 2/                     2* 1/
M=15    1   2   2   2   2   2   1   0      8* 1/ 3* 1/ 1* 1/               1* 1/
M=15    1   2   2   2   2   2   3   4      6* 1/ 4* 1/ 2* 1/ 1* 2/         0* 0/
M=15    1   2   2   2   2   3   4   4      5* 1/ 1* 1/                     3* 1/ 1* 1/
M=15    1   2   2   2   3   4   3   2      1* 2/                           4* 1/ 2* 1/
M=15    1   2   2   2   3   4   3   2      3* 1/ 1* 1/                     4* 1/ 1* 1/
M=15    1   2   2   2   4   6   5   4      4* 2/ 1* 2/                     2* 1/
M=15    1   2   2   2   4   6   5   4      4* 2/ 3* 1/ 1* 1/               1* 1/
```

```
M=15   1  2  2  3  3  2  2  2      7* 1/ 3* 1/ 2* 1/ 1* 2/      0* 0/
M=15   1  2  2  3  4  4  5  6      4* 1/ 2* 1/ 1* 2/            3* 1/
M=15   1  2  2  3  4  5  5  4      5* 1/ 3* 1/ 1* 2/            2* 1/
M=15   1  2  2  3  4  5  5  4      5* 4/ 3* 2/ 1* 1/            1* 1/
M=15   1  2  2  4  6  6  7  8      4* 1/ 3* 2/ 2* 1/ 1* 2/      0* 0/
M=15   1  2  3  2  1  0  0  0     10* 1/                        1* 2/
M=15   1  2  3  2  1  1  2  3      0* 0/                        5* 1/ 1* 2/
M=15   1  2  3  2  1  2  4  6      5* 2/                        1* 2/
M=15   1  2  3  2  2  2  4  4      6* 1/ 4* 1/                  1* 2/
M=15   1  2  3  3  2  1  0  0      9* 1/ 2* 1/ 1* 1/            1* 1/
M=15   1  2  3  3  3  3  2  2      7* 1/ 1* 1/                  2* 1/ 1* 1/
M=15   1  2  3  3  3  3  2  2      7* 1/ 3* 1/                  1* 2/
M=15   1  2  3  3  3  4  5  6      5* 1/ 4* 1/ 2* 1/ 1* 1/      1* 1/
M=15   1  2  3  3  4  5  6  6      4* 1/                        3* 1/ 1* 2/
M=15   1  2  3  4  3  2  1  0      8* 1/ 2* 2/ 1* 2/            0* 0/
M=15   1  2  3  4  4  4  4  4      2* 2/ 1* 2/ .                4* 1/
M=15   1  2  3  4  4  4  4  4      6* 1/ 2* 1/ 1* 2/            2* 1/
M=15   1  2  3  4  4  4  4  4      6* 1/ 3* 1/ 2* 1/ 1* 1/      1* 1/
M=15   1  2  3  4  5  6  7  8      4* 2/ 2* 2/ 1* 2/            0* 0/
M=15   1  2  3  4  6  8  8  8      4* 1/ 1* 2/                  2* 2/
M=15   1  2  3  4  6  8  8  8      4* 1/ 3* 1/ 1* 1/            2* 1/ 1* 1/
M=15   1  2  3  4  6  8  8  8      4* 1/ 3* 2/                  1* 2/
M=15   1  2  3  5  5  6  7  6      5* 1/ 3* 1/ 2* 2/ 1* 2/      0* 0/
M=15   1  2  3  5  6  7  8  8      2* 1/ 1* 2/                  3* 1/ 2* 1/
M=15   1  2  3  5  6  7  8  8      3* 1/ 2* 1/ 1* 1/            3* 1/ 1* 1/
M=15   1  2  3  6  8 10 12 12      3* 2/ 2* 1/ 1* 2/            2* 1/
M=15   1  2  3  6  8 10 12 12      3* 3/ 2* 1/ 1* 1/            1* 1/
M=15   1  2  4  4  4  2  1  0      8* 1/ 2* 1/                  1* 2/
M=15   1  2  4  4  5  4  5  4      2* 1/                        4* 1/ 1* 2/
M=15   1  2  4  4  5  4  5  4      6* 1/                        2* 1/ 1* 2/
M=15   1  2  4  4  6  6  9  8      4* 2/ 2* 1/                  1* 2/
M=15   1  2  4  5  5  4  2  2      7* 1/ 2* 2/ 1* 1/            1* 1/
M=15   1  2  4  5  6  7  7  8      5* 1/ 2* 1/ 1* 1/            2* 1/ 1* 1/
M=15   1  2  4  5  6  7  7  8      5* 1/ 3* 1/ 2* 1/            1* 2/
M=15   1  2  4  5  7  8  9  9      0* 0/                        3* 1/ 2* 1/ 1* 2/
M=15   1  2  4  6  6  6  5  4      6* 1/ 2* 3/ 1* 2/            0* 0/
M=15   1  2  4  6  8 10 11 12      4* 1/ 2* 2/ 1* 2/            2* 1/
M=15   1  2  4  6  8 10 11 12      4* 1/ 3* 1/ 2* 2/ 1* 1/      1* 1/
M=15   1  2  4  6  9 12 13 14      1* 2/                        2* 3/
M=15   1  2  4  6  9 12 13 14      3* 1/ 1* 1/                  2* 2/ 1* 1/
M=15   1  2  4  6  9 12 13 14      3* 2/                        2* 1/ 1* 2/
M=15   1  2  4  7  8 10 11 10      2* 3/ 1* 2/                  3* 1/
M=15   1  2  4  8 10 14 17 16      3* 2/ 2* 3/ 1* 2/            0* 0/
```

```
M=15    1    2    5    6    8    6    6    4         6* 1/ 2* 2/                   1* 2/
M=15    1    2    5    6   10   10   14   12         4* 1/ 2* 1/                   2* 1/ 1* 2/
M=15    1    2    5    7    9   10    9   10         5* 1/ 2* 3/ 1* 1/             1* 1/
M=15    1    2    5    7   10   11   12   12         2* 2/                         3* 1/ 1* 2/
M=15    1    2    5    8   11   14   15   16         4* 1/ 2* 4/ 1* 2/             0* 0/
M=15    1    2    5    8   12   16   18   20         2* 2/ 1* 2/                   2* 2/
M=15    1    2    5    8   12   16   18   20         3* 1/ 2* 2/ 1* 1/             2* 1/ 1* 1/
M=15    1    2    5    8   12   16   18   20         3* 2/ 2* 2/                   1* 2/
M=15    1    2    6    8   14   14   19   16         4* 1/ 2* 3/                   1* 2/
M=15    1    2    6    8   15   16   23   20         2* 1/                         2* 2/ 1* 2/
M=15    1    2    6   10   16   22   25   28         2* 4/ 1* 2/                   2* 1/
M=15    1    2    6   10   16   22   25   28         3* 1/ 2* 4/ 1* 1/             1* 1/
M=15    1    2    7   10   20   22   32   28         2* 3/                         2* 1/ 1* 2/
M=15    1    2    7   12   21   30   35   40         2* 6/ 1* 2/                   0* 0/
M=15    1    2    8   12   26   30   45   40         2* 5/                         1* 2/
M=15    1    3    3    1    0    0    0    0        11* 1/ 1* 3/                   0* 0/
M=15    1    3    3    1    0    1    4    6         6* 1/ 5* 1/ 1* 3/             0* 0/
M=15    1    3    3    1    1    3    3    2         7* 1/ 4* 1/ 1* 3/             0* 0/
M=15    1    3    3    2    3    3    1    0         8* 1/ 3* 1/ 1* 3/             0* 0/
M=15    1    3    3    2    3    4    5    6         5* 1/ 1* 3/                   3* 1/
M=15    1    3    3    2    4    6    4    2         3* 1/ 1* 3/                   4* 1/
M=15    1    3    3    2    5    9    7    4         4* 2/ 3* 1/ 1* 3/             0* 0/
M=15    1    3    3    3    6    7    6    6         5* 1/ 3* 2/ 1* 3/             0* 0/
M=15    1    3    4    3    1    0    0    0        10* 1/ 1* 2/                   1* 1/
M=15    1    3    4    3    1    1    3    4         1* 2/                         5* 1/ 1* 1/
M=15    1    3    4    3    1    2    6    8         5* 2/ 1* 2/                   1* 1/
M=15    1    3    4    3    2    3    5    6         6* 1/ 4* 1/ 1* 2/             1* 1/
M=15    1    3    4    4    3    1    0    0         9* 1/ 2* 1/ 1* 3/             0* 0/
M=15    1    3    4    4    4    4    3    2         7* 1/ 1* 3/                   2* 1/
M=15    1    3    4    4    4    4    3    2         7* 1/ 3* 1/ 1* 2/             1* 1/
M=15    1    3    4    4    4    5    7    8         5* 1/ 4* 1/ 2* 1/ 1* 3/       0* 0/
M=15    1    3    4    4    5    7    8    8         4* 1/ 1* 2/                   3* 1/ 1* 1/
M=15    1    3    4    5    6    5    5    6         6* 1/ 3* 1/ 2* 1/ 1* 3/       0* 0/
M=15    1    3    4    5    8   11   11   10         4* 1/ 3* 1/ 1* 3/             2* 1/
M=15    1    3    4    5    8   11   11   10         4* 1/ 3* 2/ 1* 2/             1* 1/
M=15    1    3    4    6    9    9   10   12         3* 1/ 2* 1/ 1* 3/             3* 1/
M=15    1    3    4    7   12   13   15   18         3* 3/ 2* 1/ 1* 3/             0* 0/
M=15    1    3    5    5    3    1    0    0         9* 1/ 1* 1/                   1* 2/
M=15    1    3    5    5    4    5    8   10         5* 1/ 4* 1/ 1* 1/             1* 2/
M=15    1    3    5    6    5    3    1    0         8* 1/ 2* 1/ 1* 2/             1* 1/
M=15    1    3    5    6    6    6    6    6         2* 1/ 1* 2/                   4* 1/ 1* 1/
M=15    1    3    5    6    6    6    6    6         6* 1/ 1* 2/                   2* 1/ 1* 1/
M=15    1    3    5    6    6    6    6    6         6* 1/ 3* 1/ 1* 1/             1* 2/
```

```
M=15    1    3    5    6    7    9   11   12        4* 2/ 2* 1/ 1* 2/                   1* 1/
M=15    1    3    5    7    7    5    3    2        7* 1/ 2* 2/ 1* 3/                   0* 0/
M=15    1    3    5    7    8    9   10   10        5* 1/ 2* 1/ 1* 3/                   2* 1/
M=15    1    3    5    7    8    9   10   10        5* 1/ 3* 1/ 2* 1/ 1* 2/             1* 1/
M=15    1    3    5    7    9   11   12   12        1* 2/                               3* 1/ 2* 1/ 1* 1/
M=15    1    3    5    7    9   11   12   12        3* 1/ 1* 1/                         3* 1/ 1* 2/
M=15    1    3    5    8   11   13   15   16        4* 1/ 3* 1/ 2* 2/ 1* 3/             0* 0/
M=15    1    3    5    8   12   16   18   18        3* 1/ 1* 3/                         2* 2/
M=15    1    3    5    8   12   16   18   18        3* 2/ 1* 2/                         2* 1/ 1* 1/
M=15    1    3    5    8   12   16   18   18        3* 3/ 1* 1/                         1* 2/
M=15    1    3    6    7    6    3    1    0        8* 1/                               1* 3/
M=15    1    3    6    7    7    6    7    7        0* 0/                               4* 1/ 1* 3/
M=15    1    3    6    7    8    9   13   14        4* 2/                               1* 3/
M=15    1    3    6    8    8    6    3    2        7* 1/ 2* 1/ 1* 1/                   1* 2/
M=15    1    3    6    8    9   10   11   12        5* 1/ 1* 1/                         2* 1/ 1* 2/
M=15    1    3    6    8    9   10   11   12        5* 1/ 3* 1/                         1* 3/
M=15    1    3    6    9   10    9    7    6        6* 1/ 2* 2/ 1* 2/                   1* 1/
M=15    1    3    6    9   12   15   17   18        4* 1/ 2* 1/ 1* 2/                   2* 1/ 1* 1/
M=15    1    3    6    9   12   15   17   18        4* 1/ 3* 1/ 2* 1/ 1* 1/             1* 2/
M=15    1    3    6   10   12   13   13   12        5* 1/ 2* 3/ 1* 3/                   0* 0/
M=15    1    3    6   10   13   15   16   16        2* 2/ 1* 2/                         3* 1/ 1* 1/
M=15    1    3    6   11   16   21   25   26        3* 1/ 2* 2/ 1* 3/                   2* 1/
M=15    1    3    6   11   16   21   25   26        3* 2/ 2* 2/ 1* 2/                   1* 1/
M=15    1    3    7   10   12   10    8    6        6* 1/ 2* 1/                         1* 3/
M=15    1    3    7   10   14   16   20   20        4* 1/                               2* 1/ 1* 3/
M=15    1    3    7   11   14   15   14   14        5* 1/ 2* 2/ 1* 1/                   1* 2/
M=15    1    3    7   11   15   17   18   18        2* 1/                               3* 1/ 1* 3/
M=15    1    3    7   12   17   21   23   24        4* 1/ 2* 3/ 1* 2/                   1* 1/
M=15    1    3    7   12   18   24   28   30        2* 1/ 1* 2/                         2* 2/ 1* 1/
M=15    1    3    7   12   18   24   28   30        3* 1/ 2* 1/ 1* 1/                   2* 1/ 1* 2/
M=15    1    3    7   12   18   24   28   30        3* 2/ 2* 1/                         1* 3/
M=15    1    3    7   14   21   29   35   36        3* 1/ 2* 4/ 1* 3/                   0* 0/
M=15    1    3    8   13   20   23   27   26        4* 1/ 2* 2/                         1* 3/
M=15    1    3    8   13   21   26   33   33        0* 0/                               2* 2/ 1* 3/
M=15    1    3    8   15   24   33   39   42        2* 3/ 1* 2/                         2* 1/ 1* 1/
M=15    1    3    8   15   24   33   39   42        3* 1/ 2* 3/ 1* 1/                   1* 2/
M=15    1    3    9   16   28   36   46   46        2* 2/                               2* 1/ 1* 3/
M=15    1    3    9   18   31   45   55   60        2* 5/ 1* 2/                         1* 1/
M=15    1    3   10   19   36   49   65   66        2* 4/                               1* 3/
M=15    1    4    6    4    1    0    0    0       10* 1/ 1* 4/                         0* 0/
M=15    1    4    6    4    1    1    4    6        1* 4/                               5* 1/
M=15    1    4    6    4    1    2    8   12        5* 2/ 1* 4/                         0* 0/
M=15    1    4    6    4    2    4    7    8        6* 1/ 4* 1/ 1* 4/                   0* 0/
```

```
M=15   1   4   6   5   5   6   4   2        7* 1/ 3* 1/ 1* 4/                 0* 0/
M=15   1   4   6   5   6  10  11  10        4* 1/ 1* 4/                       3* 1/
M=15   1   4   6   6  10  16  15  12        4* 1/ 3* 2/ 1* 4/                 0* 0/
M=15   1   4   7   7   4   1   0   0        9* 1/ 1* 3/                       1* 1/
M=15   1   4   7   7   5   6  11  14        5* 1/ 4* 1/ 1* 3/                 1* 1/
M=15   1   4   7   8   7   4   1   0        8* 1/ 2* 1/ 1* 4/                 0* 0/
M=15   1   4   7   8   8   8   8   8        2* 1/ 1* 4/                       4* 1/
M=15   1   4   7   8   8   8   8   8        6* 1/ 1* 4/                       2* 1/
M=15   1   4   7   8   8   8   8   8        6* 1/ 3* 1/ 1* 3/                 1* 1/
M=15   1   4   7   8   9  12  15  16        4* 2/ 2* 1/ 1* 4/                 0* 0/
M=15   1   4   7   9  11  12  13  14        5* 1/ 3* 1/ 2* 1/ 1* 4/           0* 0/
M=15   1   4   7   9  12  15  16  16        1* 4/                             3* 1/ 2* 1/
M=15   1   4   7   9  12  15  16  16        3* 1/ 1* 3/                       3* 1/ 1* 1/
M=15   1   4   7  10  16  22  24  24        3* 2/ 1* 4/                       2* 1/
M=15   1   4   7  10  16  22  24  24        3* 3/ 1* 3/                       1* 1/
M=15   1   4   8  10   8   4   1   0        8* 1/ 1* 2/                       1* 2/
M=15   1   4   8  10   9   8   9  10        1* 2/                             4* 1/ 1* 2/
M=15   1   4   8  10  10  12  17  20        4* 2/ 1* 2/                       1* 2/
M=15   1   4   8  11  11   8   4   2        7* 1/ 2* 1/ 1* 3/                 1* 1/
M=15   1   4   8  11  12  13  15  16        5* 1/ 1* 3/                       2* 1/ 1* 1/
M=15   1   4   8  11  12  13  15  16        5* 1/ 3* 1/ 1* 2/                 1* 2/
M=15   1   4   8  12  14  12   9   8        6* 1/ 2* 2/ 1* 4/                 0* 0/
M=15   1   4   8  12  16  20  23  24        4* 1/ 2* 1/ 1* 4/                 2* 1/
M=15   1   4   8  12  16  20  23  24        4* 1/ 3* 1/ 2* 1/ 1* 3/           1* 1/
M=15   1   4   8  13  18  20  21  22        2* 2/ 1* 4/                       3* 1/
M=15   1   4   8  14  22  28  33  36        3* 2/ 2* 2/ 1* 4/                 0* 0/
M=15   1   4   9  13  13   9   4   2        7* 1/ 1* 1/                       1* 3/
M=15   1   4   9  14  16  14  10   8        6* 1/ 2* 1/ 1* 2/                 1* 2/
M=15   1   4   9  14  18  22  26  28        4* 1/ 1* 2/                       2* 1/ 1* 2/
M=15   1   4   9  14  18  22  26  28        4* 1/ 3* 1/ 1* 1/                 1* 3/
M=15   1   4   9  15  19  20  19  18        5* 1/ 2* 2/ 1* 3/                 1* 1/
M=15   1   4   9  15  20  23  24  24        2* 1/ 1* 2/                       3* 1/ 1* 2/
M=15   1   4   9  16  23  28  31  32        4* 1/ 2* 3/ 1* 4/                 0* 0/
M=15   1   4   9  16  24  32  38  40        2* 1/ 1* 4/                       2* 2/
M=15   1   4   9  16  24  32  38  40        3* 1/ 2* 1/ 1* 3/                 2* 1/ 1* 1/
M=15   1   4   9  16  24  32  38  40        3* 2/ 2* 1/ 1* 2/                 1* 2/
M=15   1   4  10  16  19  16  11   8        6* 1/                             1* 4/
M=15   1   4  10  17  22  23  21  20        5* 1/ 2* 1/ 1* 1/                 1* 3/
M=15   1   4  10  17  23  26  27  27        0* 0/                             3* 1/ 1* 4/
M=15   1   4  10  18  26  32  35  36        4* 1/ 2* 2/ 1* 2/                 1* 2/
M=15   1   4  10  18  27  36  43  46        1* 2/                             2* 2/ 1* 2/
M=15   1   4  10  18  27  36  43  46        3* 1/ 1* 1/                       2* 1/ 1* 3/
M=15   1   4  10  18  27  36  43  46        3* 2/                             1* 4/
```

```
M=15    1   4   10   20   32   44   53   56       2* 3/ 1* 4/                    2* 1/
M=15    1   4   10   20   32   44   53   56       3* 1/ 2* 3/ 1* 3/              1* 1/
M=15    1   4   11   20   30   36   40   40       4* 1/ 2* 1/                    1* 4/
M=15    1   4   11   22   36   50   60   64       2* 2/ 1* 2/                    2* 1/ 1* 2/
M=15    1   4   11   22   36   50   60   64       3* 1/ 2* 2/ 1* 1/              1* 3/
M=15    1   4   11   24   41   60   75   80       2* 5/ 1* 4/                    0* 0/
M=15    1   4   12   24   41   56   69   72       2* 1/                          2* 1/ 1* 4/
M=15    1   4   12   26   46   68   85   92       2* 4/ 1* 2/                    1* 2/
M=15    1   4   13   28   52   76   98  104       2* 3/                          1* 4/
M=15    1   5   10   10    5    1    0    0       9* 1/ 1* 5/                    0* 0/
M=15    1   5   10   10    6    7   15   20       5* 1/ 4* 1/ 1* 5/              0* 0/
M=15    1   5   10   11   10   11   11   10       6* 1/ 3* 1/ 1* 5/              0* 0/
M=15    1   5   10   12   15   21   22   20       3* 1/ 1* 5/                    3* 1/
M=15    1   5   10   13   20   31   33   30       3* 3/ 1* 5/                    0* 0/
M=15    1   5   11   14   11    5    1    0       8* 1/ 1* 4/                    1* 1/
M=15    1   5   11   14   12   10   12   14       1* 4/                          4* 1/ 1* 1/
M=15    1   5   11   14   13   15   23   28       4* 2/ 1* 4/                    1* 1/
M=15    1   5   11   15   15   11    5    2       7* 1/ 2* 1/ 1* 5/              0* 0/
M=15    1   5   11   15   16   17   20   22       5* 1/ 1* 5/                    2* 1/
M=15    1   5   11   15   16   17   20   22       5* 1/ 3* 1/ 1* 4/              1* 1/
M=15    1   5   11   16   21   27   31   32       4* 1/ 3* 1/ 2* 1/ 1* 5/        0* 0/
M=15    1   5   12   18   18   12    5    2       7* 1/ 1* 3/                    1* 2/
M=15    1   5   12   19   22   19   13   10       6* 1/ 2* 1/ 1* 4/              1* 1/
M=15    1   5   12   19   24   29   35   38       4* 1/ 1* 4/                    2* 1/ 1* 1/
M=15    1   5   12   19   24   29   35   38       4* 1/ 3* 1/ 1* 3/              1* 2/
M=15    1   5   12   20   26   27   25   24       5* 1/ 2* 2/ 1* 5/              0* 0/
M=15    1   5   12   20   27   31   32   32       2* 1/ 1* 4/                    3* 1/ 1* 1/
M=15    1   5   12   21   32   43   51   54       3* 1/ 2* 1/ 1* 5/              2* 1/
M=15    1   5   12   21   32   43   51   54       3* 2/ 2* 1/ 1* 4/              1* 1/
M=15    1   5   13   22   26   22   14   10       6* 1/ 1* 2/                    1* 3/
M=15    1   5   13   23   30   31   28   26       5* 1/ 2* 1/ 1* 3/              1* 2/
M=15    1   5   13   23   31   35   36   36       1* 2/                          3* 1/ 1* 3/
M=15    1   5   13   24   35   43   47   48       4* 1/ 2* 2/ 1* 4/              1* 1/
M=15    1   5   13   24   36   48   58   62       1* 4/                          2* 2/ 1* 1/
M=15    1   5   13   24   36   48   58   62       3* 1/ 1* 3/                    2* 1/ 1* 2/
M=15    1   5   13   24   36   48   58   62       3* 2/ 1* 2/                    1* 3/
M=15    1   5   13   26   43   59   71   76       3* 1/ 2* 3/ 1* 5/              0* 0/
M=15    1   5   14   26   35   36   31   28       5* 1/ 1* 1/                    1* 4/
M=15    1   5   14   27   40   49   53   54       4* 1/ 2* 1/ 1* 2/              1* 3/
M=15    1   5   14   29   48   67   81   86       2* 2/ 1* 4/                    2* 1/ 1* 1/
M=15    1   5   14   29   48   67   81   86       3* 1/ 2* 2/ 1* 3/              1* 2/
M=15    1   5   15   30   46   56   60   60       4* 1/                          1* 5/
M=15    1   5   15   32   54   76   92   98       2* 1/ 1* 2/                    2* 1/ 1* 3/
```

```
M=15    1   5  15  32  54  76  92  98       3* 1/ 2* 1/ 1* 1/              1* 4/
M=15    1   5  15  34  61  91 115 124       2* 4/ 1* 4/                    1* 1/
M=15    1   5  16  35  61  86 105 111       0* 0/                          2* 1/ 1* 5/
M=15    1   5  16  37  68 103 131 142       2* 3/ 1* 2/                    1* 3/
M=15    1   5  17  40  76 116 150 162       2* 2/                          1* 5/
M=15    1   6  15  20  15   6   1   0       8* 1/ 1* 6/                    0* 0/
M=15    1   6  15  20  16  12  16  20       1* 6/                          4* 1/
M=15    1   6  15  20  17  18  31  40       4* 2/ 1* 6/                    0* 0/
M=15    1   6  15  21  21  22  27  30       5* 1/ 3* 1/ 1* 6/              0* 0/
M=15    1   6  16  25  25  16   6   2       7* 1/ 1* 5/                    1* 1/
M=15    1   6  16  26  30  26  17  12       6* 1/ 2* 1/ 1* 6/              0* 0/
M=15    1   6  16  26  32  38  47  52       4* 1/ 1* 6/                    2* 1/
M=15    1   6  16  26  32  38  47  52       4* 1/ 3* 1/ 1* 5/              1* 1/
M=15    1   6  16  27  36  42  43  42       2* 1/ 1* 6/                    3* 1/
M=15    1   6  16  28  42  58  69  72       3* 2/ 2* 1/ 1* 6/              0* 0/
M=15    1   6  17  30  36  30  18  12       6* 1/ 1* 4/                    1* 2/
M=15    1   6  17  31  41  42  37  34       5* 1/ 2* 1/ 1* 5/              1* 1/
M=15    1   6  17  31  42  47  48  48       1* 4/                          3* 1/ 1* 2/
M=15    1   6  17  32  47  58  63  64       4* 1/ 2* 2/ 1* 6/              0* 0/
M=15    1   6  17  32  48  64  78  84       1* 6/                          2* 2/
M=15    1   6  17  32  48  64  78  84       3* 1/ 1* 5/                    2* 1/ 1* 1/
M=15    1   6  17  32  48  64  78  84       3* 2/ 1* 4/                    1* 2/
M=15    1   6  18  35  48  49  41  36       5* 1/ 1* 3/                    1* 3/
M=15    1   6  18  36  54  66  71  72       4* 1/ 2* 1/ 1* 4/              1* 2/
M=15    1   6  18  38  64  90 109 116       2* 2/ 1* 6/                    2* 1/
M=15    1   6  18  38  64  90 109 116       3* 1/ 2* 2/ 1* 5/              1* 1/
M=15    1   6  19  40  62  76  80  80       4* 1/ 1* 2/                    1* 4/
M=15    1   6  19  42  72 102 124 132       2* 1/ 1* 4/                    2* 1/ 1* 2/
M=15    1   6  19  42  72 102 124 132       3* 1/ 2* 1/ 1* 3/              1* 3/
M=15    1   6  19  44  81 122 155 168       2* 4/ 1* 6/                    0* 0/
M=15    1   6  20  46  81 116 141 150       1* 2/                          2* 1/ 1* 4/
M=15    1   6  20  46  81 116 141 150       3* 1/ 1* 1/                    1* 5/
M=15    1   6  20  48  90 138 177 192       2* 3/ 1* 4/                    1* 2/
M=15    1   6  21  52 100 156 202 220       2* 2/ 1* 2/                    1* 4/
M=15    1   6  22  56 111 176 231 252       2* 1/                          1* 6/
M=15    1   7  21  35  35  21   7   2       7* 1/ 1* 7/                    0* 0/
M=15    1   7  21  36  43  49  63  72       4* 1/ 3* 1/ 1* 7/              0* 0/
M=15    1   7  22  41  50  41  23  14       6* 1/ 1* 6/                    1* 1/
M=15    1   7  22  42  56  57  49  44       5* 1/ 2* 1/ 1* 7/              0* 0/
M=15    1   7  22  42  57  63  64  64       1* 6/                          3* 1/ 1* 1/
M=15    1   7  22  43  64  85 105 114       3* 1/ 1* 7/                    2* 1/
M=15    1   7  22  43  64  85 105 114       3* 2/ 1* 6/                    1* 1/
M=15    1   7  23  47  66  67  54  46       5* 1/ 1* 5/                    1* 2/
```

```
M=15     1    7   23   48   73   89   95   96          4* 1/ 2* 1/ 1* 6/                      1* 1/
M=15     1    7   23   50   85  121  147  156          3* 1/ 2* 2/ 1* 7/                      0* 0/
M=15     1    7   24   53   84  103  107  106          4* 1/ 1* 4/                            1* 3/
M=15     1    7   24   55   96  137  167  178          2* 1/ 1* 6/                            2* 1/ 1* 1/
M=15     1    7   24   55   96  137  167  178          3* 1/ 2* 1/ 1* 5/                      1* 2/
M=15     1    7   25   60  108  156  190  202          1* 4/                                  2* 1/ 1* 3/
M=15     1    7   25   60  108  156  190  202          3* 1/ 1* 3/                            1* 4/
M=15     1    7   25   62  119  185  239  260          2* 3/ 1* 6/                            1* 1/
M=15     1    7   26   67  132  209  273  298          2* 2/ 1* 4/                            1* 3/
M=15     1    7   27   72  146  236  312  342          2* 1/ 1* 2/                            1* 5/
M=15     1    7   28   77  161  266  357  393          0* 0/                                  1* 7/
M=15     1    8   28   56   70   56   29   16          6* 1/ 1* 8/                            0* 0/
M=15     1    8   28   57   78   84   85   86          1* 8/                                  3* 1/
M=15     1    8   28   58   86  112  141  156          3* 2/ 1* 8/                            0* 0/
M=15     1    8   29   63   91   92   71   58          5* 1/ 1* 7/                            1* 1/
M=15     1    8   29   64   99  120  127  128          4* 1/ 2* 1/ 1* 8/                      0* 0/
M=15     1    8   30   70  114  140  143  140          4* 1/ 1* 6/                            1* 2/
M=15     1    8   30   72  128  184  225  240          2* 1/ 1* 8/                            2* 1/
M=15     1    8   30   72  128  184  225  240          3* 1/ 2* 1/ 1* 7/                      1* 1/
M=15     1    8   31   78  144  210  256  272          1* 6/                                  2* 1/ 1* 2/
M=15     1    8   31   78  144  210  256  272          3* 1/ 1* 5/                            1* 3/
M=15     1    8   31   80  157  248  323  352          2* 3/ 1* 8/                            0* 0/
M=15     1    8   32   86  174  280  369  404          2* 2/ 1* 6/                            1* 2/
M=15     1    8   33   92  192  316  422  464          2* 1/ 1* 4/                            1* 4/
M=15     1    8   34   98  211  356  483  534          1* 2/                                  1* 6/
M=15     1    9   36   84  126  127   93   72          5* 1/ 1* 9/                            0* 0/
M=15     1    9   37   92  155  191  191  184          4* 1/ 1* 8/                            1* 1/
M=15     1    9   37   94  171  247  303  324          3* 1/ 2* 1/ 1* 9/                      0* 0/
M=15     1    9   38  101  192  283  345  366          1* 8/                                  2* 1/ 1* 1/
M=15     1    9   38  101  192  283  345  366          3* 1/ 1* 7/                            1* 2/
M=15     1    9   39  110  229  375  499  548          2* 2/ 1* 8/                            1* 1/
M=15     1    9   40  117  252  423  571  630          2* 1/ 1* 6/                            1* 3/
M=15     1    9   41  124  276  476  654  726          1* 4/                                  1* 5/
M=15     1   10   45  120  211  262  255  240          4* 1/ 1*10/                            0* 0/
M=15     1   10   46  130  256  382  465  492          1*10/                                  2* 1/
M=15     1   10   46  130  256  382  465  492          3* 1/ 1* 9/                            1* 1/
M=15     1   10   47  140  301  502  675  744          2* 2/ 1*10/                            0* 0/
M=15     1   10   48  148  330  566  773  856          2* 1/ 1* 8/                            1* 2/
M=15     1   10   49  156  360  636  886  988          1* 6/                                  1* 4/
M=15     1   11   55  166  341  517  627  660          3* 1/ 1*11/                            0* 0/
M=15     1   11   57  186  431  757 1047 1164          2* 1/ 1*10/                            1* 1/
M=15     1   11   58  195  468  849 1201 1346          1* 8/                                  1* 3/
M=15     1   12   67  232  561 1012 1419 1584          2* 1/ 1*12/                            0* 0/
M=15     1   12   68  242  606 1132 1629 1836          1*10/                                  1* 2/
M=15     1   13   79  298  781 1507 2211 2508          1*12/                                  1* 1/
M=15     1   14   91  364 1001 2002 3003 3432          1*14/                                  0* 0/
```

Revue Roumaine de Chimie, **19**, *4*, 631–647 (1974)

CHEMICAL GRAPHS. XX.[1]

GRAPHS OF PARALLEL AND/OR SUBSEQUENT SUBSTITUTION REACTIONS

A. T. BALABAN [a] and F. KEREK [b]

[a] Institute of Atomic Physics, P. O. Box 35, Bucharest
[b] Organic Chemical Laboratory, The Timişoara Polytechnic

Received September 28, 1973

A graph-theoretical model is given for parallel and/or successive substitution reactions of chemical species with *s* substitution sites, the total number of reagents which may become attached to one site being *r*. Three cases are discussed : the equivalent case giving rise to "involution graphs" $H(r^s)$, when all *s* sites are equivalent during all stages of the substitution ; the non-equivalent case, the only one which leads to regular graphs denoted by $G(r^s)$ and called "power graphs" ; and the mixed case, when no general treatment can be given because the graphs $L(r^s, M)$ depend also on the cycle index of the molecule M undergoing substitution. For the equivalent case, a computer program was devised to prepare the table giving the number of vertices with various degrees.

INTRODUCTION

Graph theory [2] was applied in chemistry in two major ways : either the points (vertices) of graphs symbolize atoms, and the lines (edges) symbolize covalent bonds in structural applications, or the points represent chemical species, and the lines represent interconversions of these species. Several recent reviews of both aspects are available.[3–8] Directed graphs (digraphs) found some applications in kinetics, [8] but most applications concern non-directed graphs. In the present paper, only non-directed graphs without loops or multiple edges will be considered; since reactions are assumed to be reversible, non-directed graphs must be employed. Among the second type of applications, the main emphasis so far was on stereoisomerizations of penta- and hexa-coordinated complexes. In the following, a different application of the second type will be developed.

---

* To whom correspondence should be addressed.

[1] A. T. Balaban, *Rev. Roumaine Chim.*, **18**, 855 (1973), part XIX.

[2] F. Harary, "Graph Theory", Addison-Wesley, Reading, Mass., 1969.

[3] A. T. Balaban (editor), "Chemical Applications of Graph Theory", Academic Press (in print).

[4] A. T. Balaban, in "Cercetările multidisciplinare şi interdisciplinare. Originea, dezvoltarea şi perspectivele lor", Edit. Academiei, Bucharest, 1972, p. 203.

[5] D. H. Rouvray, *R. I. C. Revs.*, **4**, 173 (1971).

[6] J. Gutman and N. Trinajstić, *Fortschr. Chem. Forsch.*, **42**, 49 (1973).

[7] M. Gielen, "Stéréochimie dynamique" (in press).

[8] K. B. Yacimirski, *Z. Chem.*, **13**, 201 (1973).

Using the DARC topological system for codification of molecular structure[9] to describe chemical interconversions, Dubois and Panaye first mentioned the graph of reaction paths in the polyalkylation of aliphatic ketones.[10] We examine in the present paper the generalization of this idea for various substitution reactions.

NOTATIONS AND CLASSIFICATION

If in a molecule there are s reaction *sites* able to be substituted by $r-1$ types of *reagents*,* several chemical species will result in this substitution by parallel and/or subsequent processes. Each of these p species (including the initial, unsubstituted, one) will be represented by a vertex of the graph. The case when $r=1$ is to be excluded since it leads to the trivial graph consisting of only one point. Two points will be joined by an edge (line), i. e. will be adjacent, whenever they represent species resulting from one another by an elementary substitution (one displacement at one reaction site). The total number of elementary reactions will be denoted by q, i. e. the number of edges of the graph. The number of edges d_i incident with vertex i is called its *degree*. The total number of chemical species, p, i. e. of vertices of the graph, will be called the *order* of the graph.

Depending on the chemical structure of the initial species undergoing substitution, there are three cases to be discussed:

1. All s reaction sites are non-equivalent, e. g. in the halogenation of $R_2CH-CHR'-CHR_2''$ with $R \neq R' \neq R''$ assuming that the substitution involves only the displacement of the three hydrogens by halogens without affecting the other substituents (the non-equivalent case).

2. All reaction sites are equivalent at all stages of the substitution, e. g. in the deuteration or halogenation of methane, or in the hydrolysis of boron halides (the equivalent case). Enantiomerism will be ignored in this paper.

3. The mixed case, when either (i) the reaction sites become non-equivalent at some stage of the substitution though they are equivalent in the unsubstituted molecule, e. g. in the halogenation of benzene, ethane, or cycloalkanes, or in substitutions at square planar or octahedral complexes, or when (ii) the initial molecule has some equivalent and some non-equivalent sites as in the halogenation of alkylbenzenes or of alkanes higher than ethane, or in substitutions at trigonal-bipyramidal complexes.

---

* Yielding a total of r groups which can be bonded to one site.

[9] J. E. Dubois, *Entropie*, **27**, 1 (1969).

[10] J. E. Dubois and A. Panaye, *Tetrahedron Letters*, **1969**, 1501, 3275.

1. THE NON-EQUIVALENT CASE

A previous paper [11] described combination graphs whose order (number of vertices) was expressible either as a combination: $\binom{a}{(a-1)/2}$ for regular halved combination graphs, or as a sum of combinations: $2\binom{a}{(a-1)/2}$ for regular combination graphs; $\binom{a}{b}+\binom{a}{b+1}$ for semiregular combination graphs; and $\sum_{i=0}^{(a-1)/2}\binom{a}{i} = 2^{a-1}$ for the halved hypercubes (regular chequered graphs); a and b were integers subject to the condition $1 \leqslant b \leqslant (a-1)/2$.

The present section describes a new class of graphs whose order p is expressible as a power r^s with both r and s being positive integers. Such graphs are therefore called "power graphs" and are denoted by $G(r^s)$.

Each vertex is labelled with s symbols from the set of the first r positive integers. The order of these symbols is important. No two vertices may have the same label. It results that the total number of vertices is[12a] the s-permutation with unrestricted repetition of r objects, i. e. $p = r^s$.

Two vertices are adjacent *iff* they differ by one and only one digit in the same position of the label. The resulting graph is therefore regular of degree $d = (r-1)s$. From the formula $2q = pd$ one obtains: $2q = s(r-1)r^s$.

According to this definition, all graphs $G(r^1)$ are the complete graphs K_r. They represent the set of chemical species which can be formed by substitution at one site with $r-1$ reagents, e. g. the interconversions of alkyl halides when there are r different halide anions present (including the one from the initial alkyl halide).

Whenever possible, graphs in the following enumerations will be presented so as to evidence Hamiltonian circuits.

1.1. Power graphs with $r=2$

These graphs with 2^s vertices, labelled with r symbols from a binary set (in our case, digits 1 and 2) are the well-known s-cubes.[2] Their degree is s. In combinatorics, such graphs are also encountered as the set of binary words of length s. Such graphs are presented in the first column of table 1, and in figure 1. They can be formed by a recurrence relationship: from a pair of graphs $G(2^{s-1})$ one obtains a graph $G(2^s)$ by linking pairwise corresponding vertices, i. e. each graph $G(2^s)$ has two identical vertex-disjoint subgraphs $G(2^{s-1})$.

---

[11] A. T. Balaban, *Rev. Roum. Math. Pures Appl.*, **17**, 3 (1972).

[12] J. Riordan, a) "An Introduction to Combinatorial Analysis", Wiley, New York, 1958, p. 4; b) ibid, p. 7; c) "Combinatorial Identities", Wiley, New York, 1968, p. 8.

Table 1

Orders r^s and degrees in brackets $(rs-s)$ of power graphs $G(r^s)$

s \ r	2	3	4	5
1	2^1 (1)	3^1 (2)	4^1 (3)	5^1 (4)
2	2^2 (2)	3^2 (4)	4^2 (6)	5^2 (8)
3	2^3 (3)	3^3 (6)	4^3 (9)	5^3 (12)
4	2^4 (4)	3^4 (8)	4^4 (12)	5^4 (16)
5	2^5 (5)	3^5 (10)	4^5 (15)	5^5 (20)

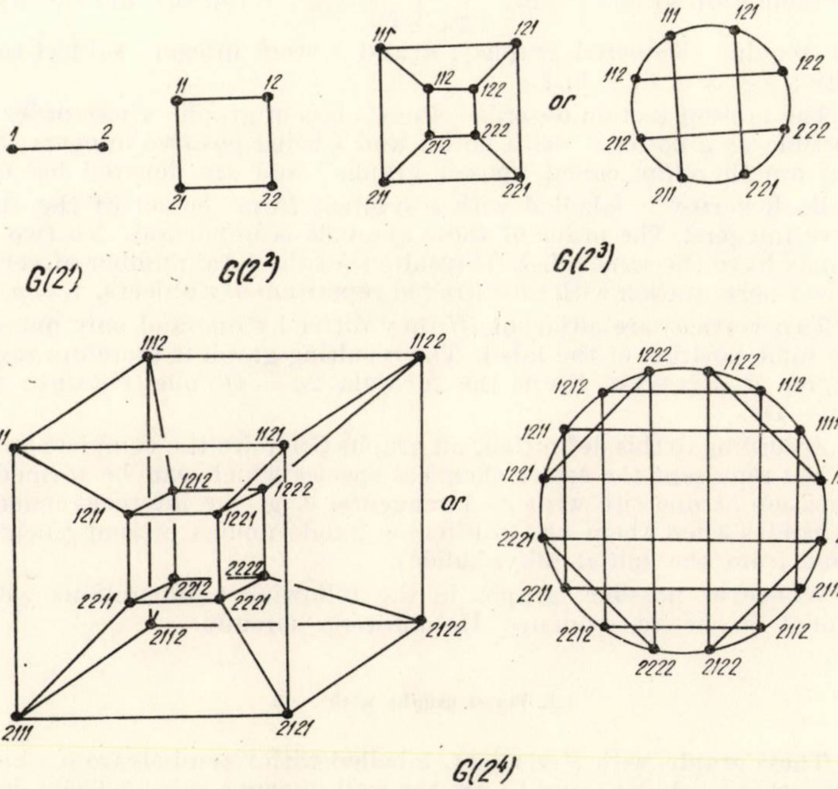
1
2
11
12
21
22
111
121
112
122
222
212
211
221
or
G(2¹)
G(2²)
G(2³)
1112
1122
1111
1121
1212
1222
1211
1221
2222
2212
2211
2221
2112
2122
2111
2121
G(2⁴)

Fig. 1. — Regular power graphs G (2^s), i. e. s-cubes with $s = 1-4$.

Such graphs represent substitution at s non-equivalent sites by $r-1 = 1$ reagent, e. g. the chlorination of $R_2CH-CHR'-CHR''_2$ is represented by the 3-cube $G(2^3)$: there are $s=3$ reaction sites, and $r = 2$ reagents (H and Cl).

1.2. Power graphs with $r=3$

Such graphs have not been discussed previously. Their orders and degrees are presented in the second column of table 1. They have 3^s vertices and even degrees $d = 2s$. Also in this case a recurrent procedure for the construction of these graphs is apparent : each graph $G(3^s)$ consists of three $G(3^{s-1})$ subgraphs (figure 2).

Graph $G(3^2)$ is 1-unitransitive [2] and the order of its symmetry group is 72. Each of its nine vertices is common to two edge-disjoint three-circuits ; this property can be generalized to all $G(3^s)$ graphs by stating that each of their vertices is common to s edge-disjoint three-circuits. The topological representation of intramolecular rearrangements of octahedral complexes *via* digonal twists, disregarding enantiomerism,[13] con-

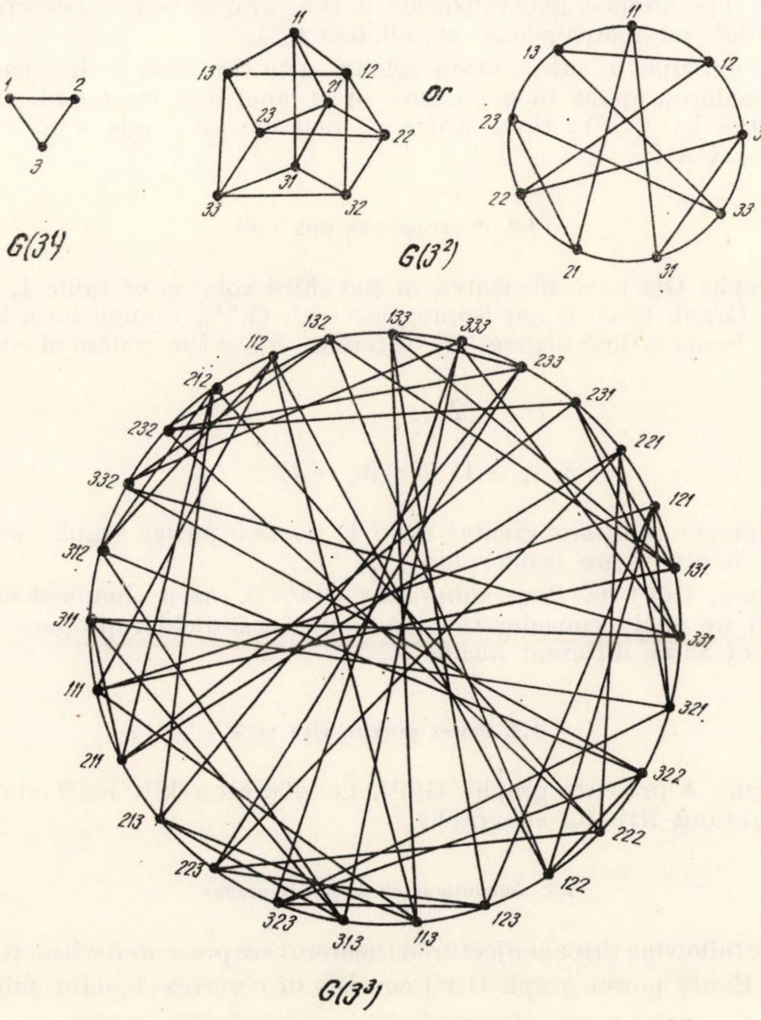
1
2
3
$G(3^1)$
11
13
12
21
23
22
31
33
32
or
11
13
12
23
32
22
33
21
31
$G(3^2)$
132
133
333
112
233
212
231
232
221
332
121
312
131
311
331
111
321
211
322
213
222
223
122
323
313
113
123
$G(3^3)$

Fig. 2. – Regular power graphs G (3^s) with $s = 1$, 2, and 3.

---

[13] A. T. Balaban, *Rev. Roumaine Chim.*, **18**, 841 (1973).

sisted in a graph $G(3^2) + K_{3,3}$. The same graph $G(3^2)$ describes conformational interconversions of the nine possible conformers of propane :[13a] the notation of vertices in this case results by assigning digits 1, 2, and 3 to the three torsion energy minima of the $C_1 - C_2$ and $C_2 - C_3$ bonds of propane. The obvious generalization is that graphs $G(3^{n-1})$ describe conformational interconversions of alkanes C_nH_{2n+2}.

An example of substitution belonging to this case is the alcoholysis of 1,2-dichloropropane in a mixture of ethanol and methanol, which is represented by $G(3^2)$: there are $s=2$ reaction sites and $r=3$ reagents (Cl, OMe, OEt).

1.3. Power graphs with $r=4$

Graphs $G(4^s)$ are presented in the third column of table 1, and in figure 3. Graph $G(4^2)$ is not isomorphic with $G(2^4)$, though both have 16 vertices, because their degrees are different. Since the system of equations

$$r_1^{s_1} = r_2^{s_2}$$

$$s_1(r_1 - 1) = s_2(r_2 - 1)$$

has no integer solutions greater than 1, no two power graphs with different r (hence s) are isomorphic.

Again, $G(4^s)$ has four subgraphs $G(4^{s-1})$. As a chemical example for $G(4^2)$ we could consider the reaction of 1,2-dichloropropane with a mixture of three different alcohols.

1.4. Power graphs with $r=5$

Figure 4 presents graphs $G(5^1)$, i.e. Kuratowski's K_5,[14] and $G(5^2)$ which contains five K_5 subgraphs.

1.5. Conclusions about power graphs

The following three conjectured theorems are presented without proof :

(i) Every power graph $G(r^s)$ consists of r vertex-disjoint subgraphs $G(r^{s-1})$.

(ii) Power graphs $G(r^s)$ are Hamiltonian. In all figures 1—4, Hamiltonian circuits were presented for power graphs.

(iii) The order of the symmetry group of power graphs $G(r^s)$ is $s!\,(r!)^s$.*

---

* This formula was found by Dr. R. W. Robinson from the Department of Mathematics of the University of Michigan, Ann Arbor, in April 1973.

[13a] J. Dugundji, P. Gillespie, I. Ugi and D. Marquarding, in "Chemical Applications of Graph Theory" (A. T. Balaban, editor), Academic Press, London (to appear).

[14] C. Kuratowski, *Fundamenta Math.*, **15**, 271 (1930).

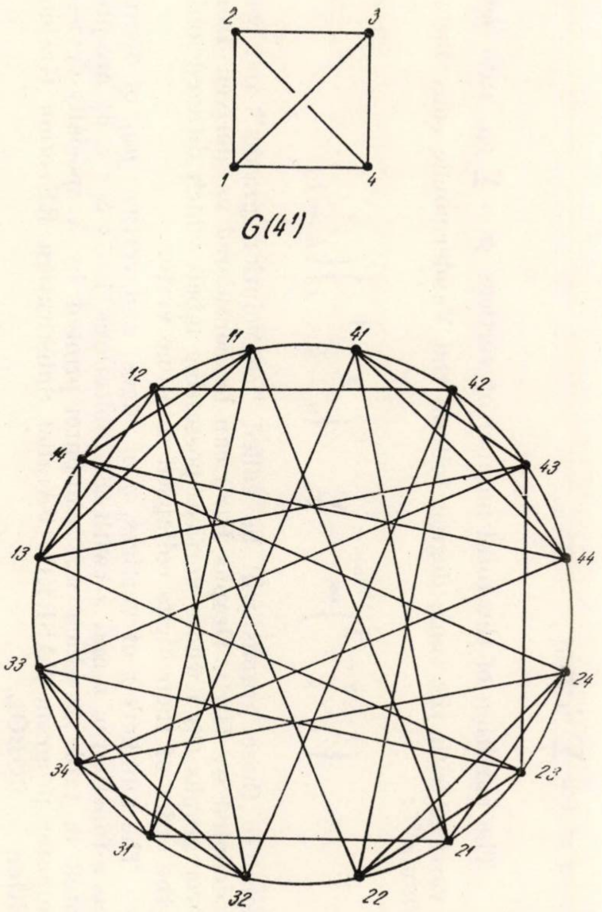
2
3
1
4
G(4¹)
11
41
12
42
14
43
13
44
33
24
34
23
31
21
32
22

Fig. 3. – Regular power graphs G (4^s), with $s=1$, and 2.

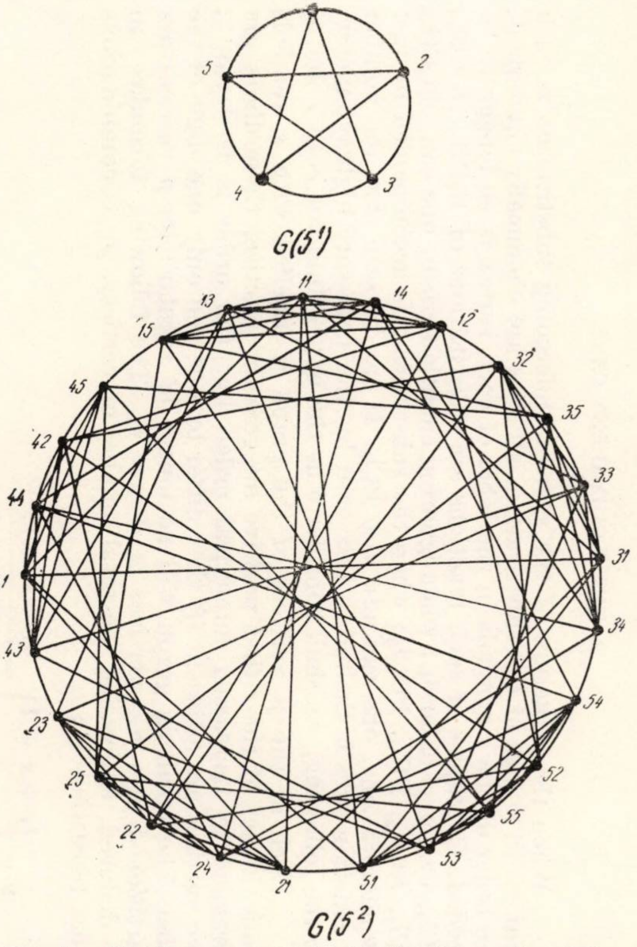
5
2
4
3
G(5¹)
11
13
14
12
15
32
45
35
42
33
44
31
41
34
43
54
23
52
25
55
22
53
24
21
51
G(5²)

Fig. 4. – Regular power graphs G (5^s) with $s = 1$ and 2.

2. THE EQUIVALENT CASE

When the structure of the species undergoing substitution is such that at all stages of the substitution, all sites are chemically equivalent, the order of the r symbols in the label of each vertex is no longer to be heeded. Examples of such reactions are substitutions of R_2CH_2, R_2CCl_2, BCl_3, cyanuryl chloride; when ignoring enantiomerism, one can add CH_4, CCl_4, RCH_3, PCl_3, $POCl_3$; when the substitution is accompanied by fast pseudorotations, one can add also PCl_5. It can be seen that the number of reaction sites is limited in this case by the necessary high symmetry. In the following, we shall consider 6 as the upper limit for both r and s.

Each of the p vertices of the graph is labelled with s symbols from the set of the r first positive integers (in practice, these digits are arranged in increasing numerical order, but the order is irrelevant); two vertices are adjacent *iff* they differ by one and only one digit of the label. The resulting graph will no longer be regular: its p vertices are partitioned into $p_{(d_i)}$ vertices of degree d_i. The following formulas can be deduced, expressing the total number of vertices, p, as combinations with repetition[12b]:

$$p = \binom{r+s-1}{s} = \frac{(r+s-1)!}{s!\,(r-1)!}$$

$d_i = (r-1)\,l_i$, l_i being the number of different symbols in the label of vertex i, with the limitations $1 \leqslant l_i \leqslant \min(r, s)$.

$$q = 1/2 \sum_i d_i \cdot p_{(d_i)}$$

The partition of the total number of vertices $p = \sum_i p_{(d_i)}$ into sets of vertices with the same degree follows the Vandermonde convolution formula[12c]:

$$\binom{r+s-1}{s} = \sum_{k=0}^{\min(r-1,\, s-1)} \binom{s-1}{s-k-1}\binom{r}{k+1}$$

Therefore these graphs will be called "convolution graphs" and will be denoted by $H(r^s)$. Graphs $H(r^s)$ can be considered as derived from power graphs $G(r^s)$ whose vertices possessing labels which differed only in the order of their digits collapsed into one vertex.

The numbers p of vertices, q of edges, and vertices $p_{(d_i)}$ of degree d_i as a function of r and s (with the limitations $1 \leqslant r \,\&\, s \leqslant 6$) are presented in table 2 which was computer-printed by a specially-devised computer program PASREG (PArallel Substitution REaction Graphs) written in COBOL.

It is easily seen that for $s = 1$, $G(r^1) = H(r^1) = K_r$, i. e. the complete graphs of order r, because there is no ordering when there is just one symbol.

Table 2

Number of vertices, edges and partition of vertices, according to their degrees for graphs H(r^s)

SITES	REAGENTS	VERTICES	EDGES	VERTICES OF DEGREE P(D)					
S = 6	R = 6	462	3780	K*05= 6	K*10= 75	K*15= 200	K*20= 150	K*25= 30	K*30= 1
S = 6	R = 5	210	1260	K*04= 5	K*08= 50	K*12= 100	K*16= 50	K*20= 5	
S = 6	R = 4	84	336	K*03= 4	K*06= 30	K*09= 40	K*12= 10		
S = 6	R = 3	28	63	K*02= 3	K*04= 15	K*06= 10			
S = 6	R = 2	7	6	K*01= 2	K*02= 5				
S = 5	R = 6	252	1890	K*05= 6	K*10= 60	K*15= 120	K*20= 60	K*25= 6	
S = 5	R = 5	126	700	K*04= 5	K*08= 40	K*12= 60	K*16= 20	K*20= 1	
S = 5	R = 4	56	210	K*03= 4	K*06= 24	K*09= 24	K*12= 4		
S = 5	R = 3	21	45	K*02= 3	K*04= 12	K*06= 6			
S = 5	R = 2	6	5	K*01= 2	K*02= 4				
S = 4	R = 6	126	840	K*05= 6	K*10= 45	K*15= 60	K*20= 15		
S = 4	R = 5	70	350	K*04= 5	K*08= 30	K*12= 30	K*16= 5		
S = 4	R = 4	35	120	K*03= 4	K*06= 16	K*09= 12	K*12= 1		
S = 4	R = 3	15	30	K*02= 3	K*04= 9	K*06= 3	1		

S = 4	R = 2	5	4	K.01= 2	K.02= 3				
S = 3	R = 6	56	315	K.05= 6	K.10= 30	K.15= 20			
S = 3	R = 5	35	150	K.04= 5	K.08= 20	K.12= 10			
S = 3	R = 4	20	60	K.03= 4	K.06= 12	K.09= 4			
S = 3	R = 3	10	18	K.02= 3	K.04= 6	K.06= 1			
S = 3	R = 2	4	3	K.01= 2	K.02= 2				
S = 2	R = 6	21	90	K.05= 6	K.10= 15				
S = 2	R = 5	15	50	K.04= 5	K.08= 10				
S = 2	R = 4	10	24	K.03= 4	K.06= 6				
S = 2	R = 3	6	9	K.02= 3	K.04= 3				
S = 2	R = 2	3	2	K.01= 2	K.02= 1				
S = 1	R = 6	6	15	K.05= 6					
S = 1	R = 5	5	10	K.04= 5					
S = 1	R = 4	4	6	K.03= 4					
S = 1	R = 3	3	3	K.02= 3					
S = 1	R = 2	2	1	K.01= 2					

2.1. Convolution graphs with $r=2$

These graphs $H(2^s)$ are simple paths with two end-points of degree one, and $s-1$ points of degree two. For instance, the graph describing the chlorination of methane has five points, with methane and carbon tetrachloride as the endpoints, and with methyl chloride, dichloromethane and chloroform as the points of degree two.

2.2. Convolution graphs with $r=3$ and 4

Figure 5 represents graphs $H(3^s)$ for $s = 2$, 3, and 4. As it may be seen, all these graphs are planar [2] triangulated graphs which possess Hamiltonian circuits. Graph $H(3^3)$ has ten vertices and can represent the reaction of boron trichloride with a mixture of ethanol and methanol, or the reaction of cyanuryl chloride with a mixture of two aromatics or primary amines.

Graphs $H(4^2)$ and $H(4^3)$ are presented in figure 6.

3. THE MIXED CASE

No general treatment of the mixed case can be indicated, therefore no general notation of the vertices is available : the notation must indicate both the number and the position of the substituents, therefore the usual chemical nomenclature will be applied. Most graphs corresponding to this case will be irregular.

Employing Pólya's theorem,[2] the numbers of isomers resulting from various substitution reactions can be calculated, e. g. those formed in the halogenation or hydrogen isotopic exchange of ethane, propane, benzene or toluene, resulting in a configuration-counting series.[15, 16] The cycle index of the molecule M determines these numbers of isomers.

To construct the graph of the substitution of such molecules, we shall join by edges those vertices which correspond to species derived from one another by an elementary substitution act (displacement by one reagent at one site). Such graphs will be denoted by $L(r^s, M)$, indicating by M which molecule (hence, cycle index) is involved.

3.1. Systems with initially equivalent sites

Thus, though in both ethane and benzene there are six hydrogens which can be gradually substituted by deuterium, the resulting graphs are different : $L(2^6, \text{benzene}) \neq L(2^6, \text{ethane})$. These two graphs are illustrated in figure 7, where the vertices without a label represent the hydrocarbons, and the other vertices in the usual chemical nomenclature the structure of the substitution (e. g. deuteration, chlorination) products.

---

[15] A. T. Balaban and H. Harary, *Rev. Roumaine Chim.*, **12**, 154 (1967).

[16] A. T. Balaban, D. Fărcaşiu and F. Harary, *J. Labelled Comp.*, **6**, 211 (1970).

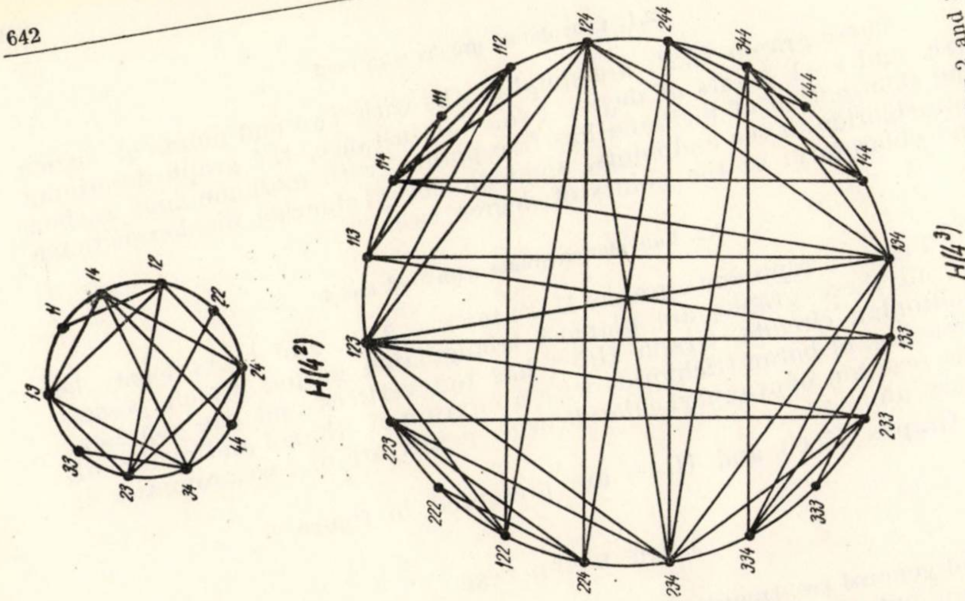
11
14
12
22
24
44
34
23
33
13
H(4²)
111
112
124
244
344
444
144
134
133
233
333
334
234
224
122
222
223
123
113
114
H(4³)

Fig. 6. — Convolution graphs H(4^s) for s = 2 and 3.

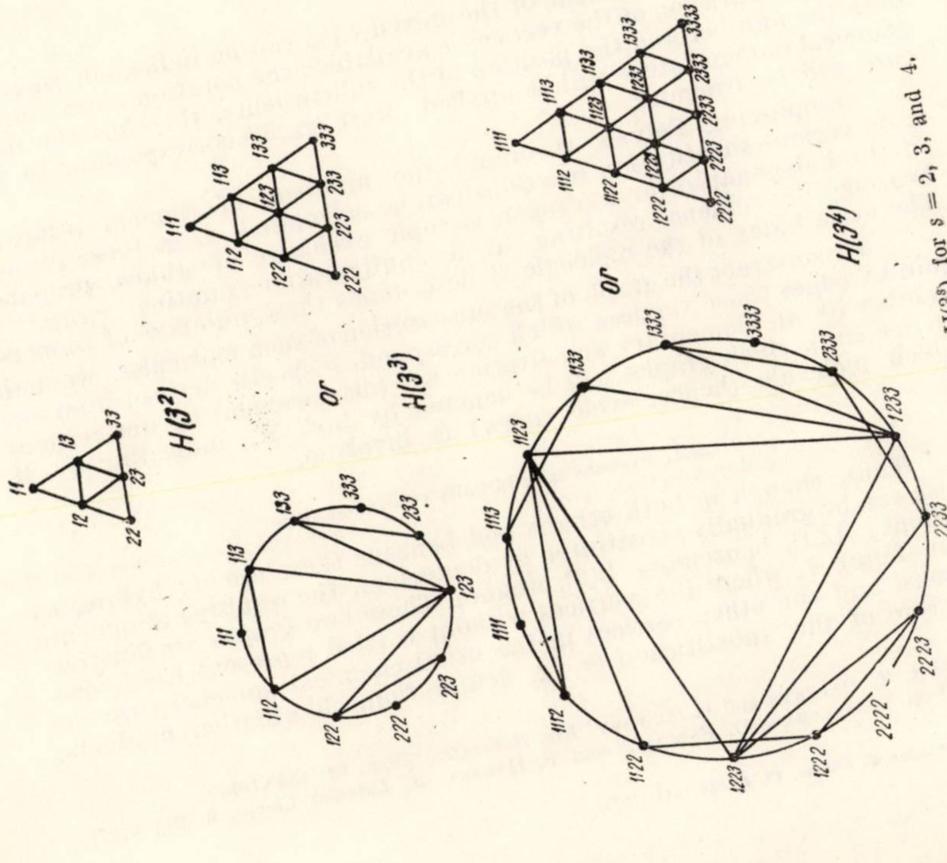
11
13
33
12
23
22
H(3²)
or
H(3³)
111
113
133
333
233
123
223
222
122
112
or
H(3⁴)
1111
1113
1123
1133
1333
3333
2333
1233
2233
2223
2222
1222
1223
1122
1112

Fig. 5. — Convolution graphs H(3^s) for s = 2, 3, and 4.

For $s = 3$, the numbers increase markedly, e. g. L(3^6, benzene) has 92 vertices, and L(3^6, ethane) has 55 vertices. These numbers of vertices result from the summation of appropriate terms in the coefficients of configuration counting series. Thus, the last figure for benzene results by summing all coefficients of $Z(D_{6h}, 1 + x_1 + x_2)$ exemplifying[16] the isomerism of benzene labelled with ^{13}C and ^{14}C.

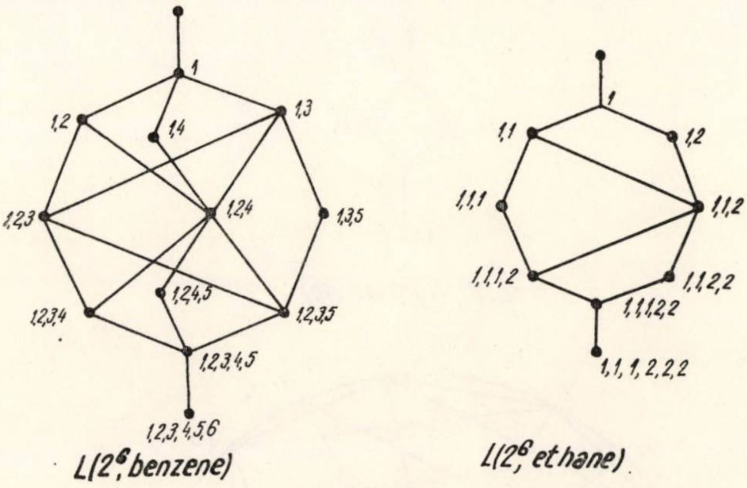
1
1,2
1,3
1,4
1,2,4
1,2,3
1,3,5
1,2,4,5
1,2,3,4
1,2,3,5
1,2,3,4,5
1,2,3,4,5,6
L(2⁶, benzene)
1
1,1
1,2
1,1,1
1,1,2
1,1,1,2
1,1,2,2
1,1,1,2,2
1,1,1,2,2,2
L(2⁶, ethane)

Fig. 7. — Graphs for deuteration of ethane and benzene.

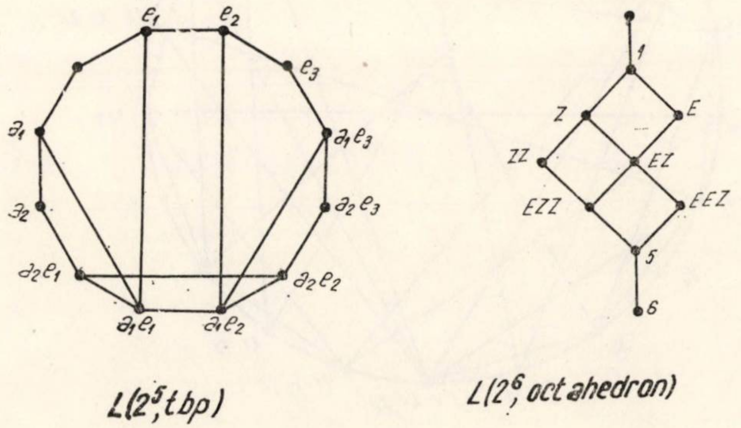
e1
e2
e3
a1
a1e3
a2
a2e3
a2e1
a2e2
a1e1
a1e2
L(2⁵, tbp)
1
Z
E
ZZ
EZ
EZZ
EEZ
5
6
L(2⁶, octahedron)

Fig. 8. — Graphs for substitution with one added reagent of trigonal-bipyramidal and of octahedral complexes.

Figure 8 represents the graphs of substitution by one added reagent (i. e. $r = 2$) of trigonal-bipyramidal and octahedral complexes, ignoring enantiomerism: in both cases, stereochemical rigidity is, however, assumed by forbidding pseudorotations. Notations in the former case indicate how many axial (a) and equatorial (e) sites were substituted; in the latter case, figures indicate how many octahedral sites are substituted when only one isomer is possible; when two isomers are possible, they are indicated by letters E and Z relatively to a first substituent (the total number of substituents being greater by 1 than the number of letters E and/or Z).

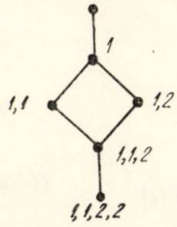
1
1,1
1,2
1,1,2
1,1,2,2

L(2^4, hydrazine)

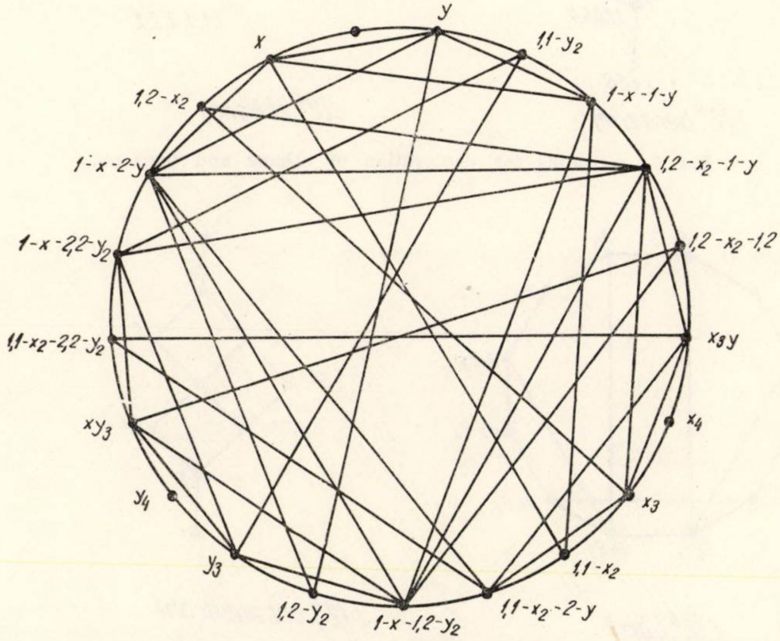
y
x
1,1-y_2
1,2-x_2
1-x-1-y
1-x-2-y
1,2-x_2-1-y
1-x-2,2-y_2
1,2-x_2-1,2-y_2
1,1-x_2-2,2-y_2
x_3y
xy_3
x_4
y_4
x_3
y_3
1,1-x_2
1,2-y_2
1-x-1,2-y_2
1,1-x_2-2-y

L(3^4, hydrazine)

Fig. 9. — Graphs for substitution of hydrazine with one or two types of added reagents.

Figure 9 represents two graphs for hydrazine, namely L(2^4, hydrazine) with a self-explanatory notation indicating the number and location of the substituents of one type, and L(3^4, hydrazine) where two different types of substituents, x and y, are considered.

3.2. Systems with initially partly equivalent sites

As a last example we shall discuss systems whose initial molecules have some equivalent and some non-equivalent reaction sites. We shall confine ourselves to systems $H_mX - YH_n$ with $s = m + n$ sites. The m hydrogens are equivalent, and so are the n hydrogens, but X is different from Y, therefore substituents bonded to X are not equivalent to those bonded to Y.

Notations employed in figure 10 have digits 1, 2, ..., r for the reagents (including the substituent in the initial molecule). The s sites are partitioned by a fraction line into two groups, namely the m sites of atom X as the numerator, and the n sites of atom Y as the denominator of the fraction. Arbitrarily, whenever $m \neq n$, the larger number of sites was placed in the numerator. The notation for graphs $L(r^s, H_mX - YH_n)$ will be simplified for this case to $L(r^{m+n})$.

For substitution by one added reagent, e. g. deuteration of H_mX-YH_n, we obtain graphs $L(2^{m+n})$ which are "chequered $(m+1)(n+1)$ rectangles" identical to the Cartesian products [2] of two simple paths $H(2^m)$ and $H(2^n)$ with $m+1$ and $n+1$ vertices, respectively. Dubois and Panaye's graph [10] is $L(2^{3+2})$, presented in fig. 10A.

In general, graphs $L(r^{m+n})$ have $\dfrac{(m+r-1)!}{m!\,(r-1)!}\cdot\dfrac{(n+r-1)!}{n!\,(r-1)!}$ vertices and are Cartesian products of two convolution graphs : $L(r^{m+n}) = H(r^m) \times H(r^n)$. The orders of graphs $L(r^{m+n})$ according to the above formulas are presented in table 3.

Table 3

Orders of graphs $L(r^{m+n})$

s	r m n	2	3	4
2	1 1	4	9	16
3	2 1	6	18	40
4	3 1	8	30	80
	2 2	9	36	100
5	4 1	10	45	140
	3 2	12	60	200
6	5 1	12	63	224
	4 2	15	90	350
	3 3	16	100	400

For instance, $L(3^{1+1}) = H(3^1) \times H(3^1) = G(3^2)$; the isomorphism of $L(3^{1+1})$ and $G(3^2)$, or of $L(2^{1+1})$ and $G(2^2)$, originates in the non-equivalence of the two hydrogens in HX−YH with $m = n = 1$. This is general

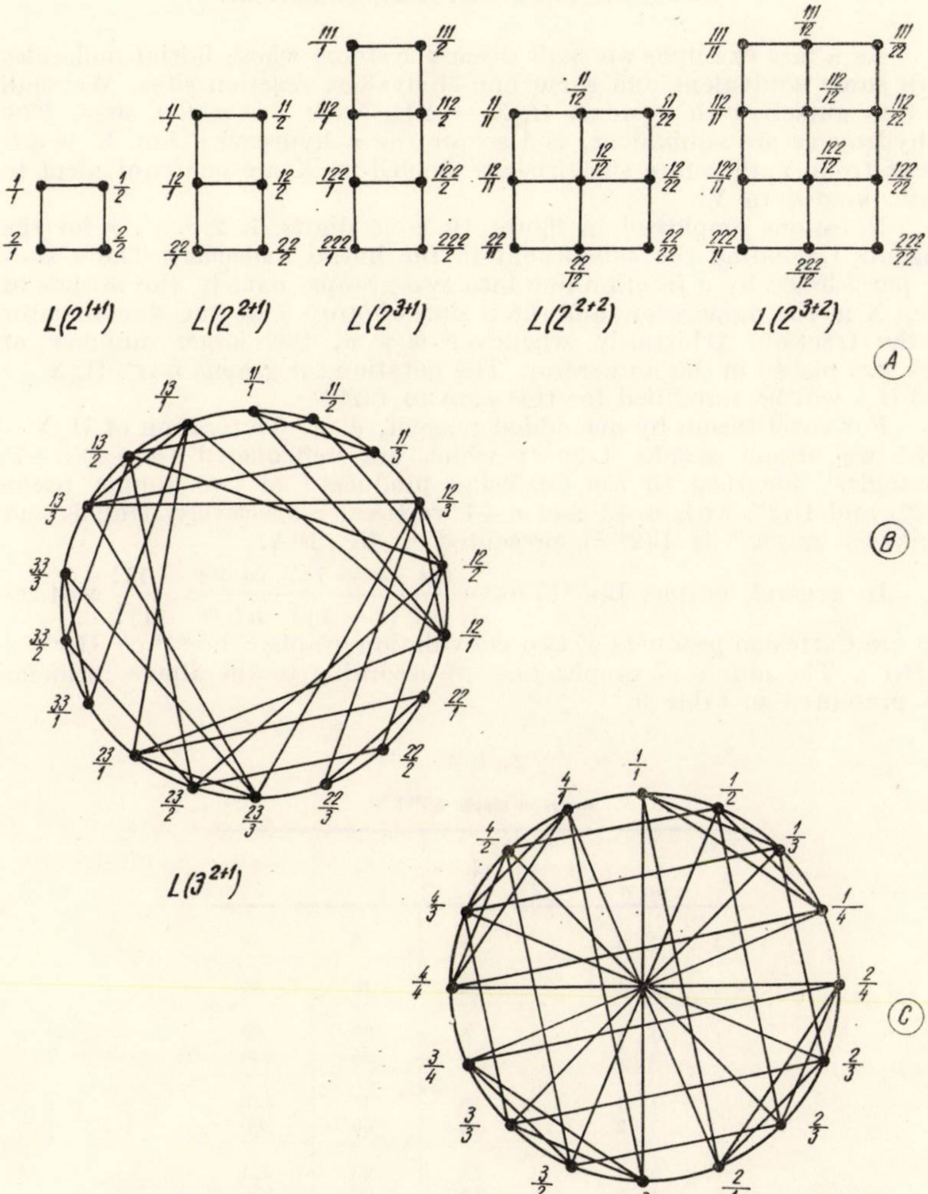
$L(2^{1+1})$
$L(2^{2+1})$
$L(2^{3+1})$
$L(2^{2+2})$
$L(2^{3+2})$
A
B
$L(3^{2+1})$
C
$L(4^{1+1})$

Fig. 10. — Graphs $L(r^{m+n})$ for substitution of H_mX-YH_n with $r=2$, 3, or 4.

for all graphs $L(r^{1+1}) = G(r^2)$ and is illustrated by a presentation of $L(4^{1+1})$, isomorphic to $G(4^2)$ (notwithstanding the apparent difference between fig. 3 and fig. 10C).

The partition of degrees $p = \sum_i p_{(d_i)}$ for graphs $L(r^{m+n})$ is described by the product of two Vandermonde convolution formulas for the two graphs $H(r^m)$ and $H(r^n)$:

$$\frac{(m+r-1)!}{m!\,(r-1)!}\cdot\frac{(n+r-1)!}{n!\,(r-1)!} =$$

$$= \sum_{j=0}^{r-1}\binom{m-1}{m-j-1}\binom{r}{j+1}\cdot\sum_{k=0}^{r-1}\binom{n-1}{n-k-1}\binom{r}{k+1}$$

Thus, in general the properties of graphs representing substitutions depend on r, s, and on the cycle index of the molecule undergoing substitution : with particular forms of the cycle index we discussed separately the totally equivalent and non-equivalent cases.

Acknowledgement. Thanks are expressed to Mr. Cs. Ferencz, Regional Computing Centre, Timişoara, for assistance with FASREG computing program.

Revue Roumaine de Chimie, **19**, *4*, 649–658 (1974)

BENZIMIDAZOLIUM-YLURES. I

L'ACTION DES ACÉTYLÈNES ACTIVÉS SUR QUELQUES BENZIMIDAZOLIUM-YLURES

ION ZUGRĂVESCU, JEAN HERDAN et ION DRUȚĂ

Laboratoire de Chimie organique,
Université «Al. I. Cuza», Jassy, 11, str. 23 August

Reçu le 31 juillet 1973

On a étudié les réactions des benzimidazolium-ylures obtenus « in situ » par élimination d'acide bromhydrique, à partir des sels respectifs, avec des philodiènes acétyléniques. La réaction des benzimidazolium-carbétoxyméthylures avec le diméthylacétylènedicarboxylate conduit à un produit à caractère d'ylure (IX), très stable, et avec le propyolate d'éthyle à 1-oxo-pyrido [1,2-a] benzimidazole (XV). Les benzimidazolium-phénacylures réagissent avec les acétylènes activés en formant les produits de cycloaddition 2+3 dipolaires (XIV) et (XVII).

Reuschling et Kröhnke[1] ont établi que le bromure de 1-méthyl-3-(4-bromophénacyl) benzimidazolium réagit avec le chlorure de pycrile, en milieu alcalin, pour conduire à 1,3-dinitro-3-méthyl-11-(4-bromobenzoyl)-5H-benzimidazo[2,1-a]isoindole, par l'intermédiaire du 1-méthylbenzimidazolium-*p*. broophénacylure.

Des benzimidazolium-ylures ont été récemment mis en évidence par Ogura et Kikuchi,[2] en traitant les bromures correspondants par le carbonate de potassium en diméthylformamide. Les ylures obtenus « in situ » réagissent avec le propyolate d'éthyle conduisant au pyrrolo [1,2-a] benzimidazole. La réaction du 1-méthylbenzimidazolium-carbéthoxyméthylure avec le diméthylacéthylènedicarboxylate (DMAD) conduit[2] à un mélange de deux produits : le cycloadduct normal (I) et le 1-oxo-pyrido[1,2-a]benzimidazole (II)

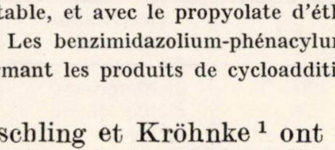

I

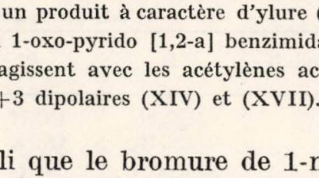

II

D. B. Reuschling et F. Kröhnke, *Chem. Ber.*, **104**, 2103 (1971).
[2] H. Ogura et K. Kikuchi, *J. Org. Chem.*, **37**, 2679 (1972).

Pour expliquer la formation du produit (II) les auteurs proposent un mécanisme réactionnel, qui admet l'apparition d'un intermédiaire non isolable, qui par décyclisation et élimination d'alcool conduit à (II).

Ces résultats nous ont déterminé à étudier le comportement d'autres benzimidazolium-ylures vis-à-vis des acétylènes activés.

Les benzimidazolium-ylures, que nous avons étudiés ont été préparés par la méthode « du sel ». Les benzimidazoles 1-alcoyl substitués réagissent avec les esters de l'acide bromoacétique et avec le bromure de phénacyle, en solution benzénique et il en résulte les bromures correspondants (IV) (tableau 1)

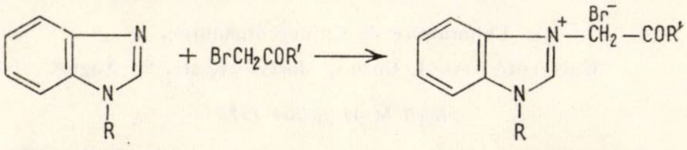

III a ; $R=CH_2C_6H_5$
b ; $R=CH_3$

IV a ; $R=CH_2C_6H_5$; $R'=OC_2H_5$
b ; $R=CH_2C_6H_5$; $R'=OCH_3$
c ; $R=CH_2C_6H_5$; $R'=C_6H_5$
d ; $R=CH_3$; $R'=OC_2H_5$

Tableau 1

Sels quaternaires de benzimidazolium (IV)

Produit	*R*	*R'*	P.f.	Recristallisé dans du :	Rend.
IVa	$CH_2C_6H_5$	OC_2H_5	170–2°	dichloréthane	77 %
IVb	$CH_2C_6H_5$	OCH_3	152–4°	dichloréthane	86 %
IVc	$CH_2C_6H_5$	C_6H_5	211–2°	méthanol	80 %
IVd	CH_3	OC_2H_5	85–7°	dichloréthane	83 %

Leur structure a été confirmée par les analyses chimiques et par les spectres IR et RMN (tableau 2).

Le spectre RMN du produit (IVc) révèle, à part l'existence du bromure, celle de l'ylure correspondant et d'un dimère à double liaison éthylénique. L'ylure (V) se formerait par élimination spontanée d'acide bromhydrique, tandis que le dimère (VII) prendrait naissance à partir du carbène (VI), formé de l'ylure par suite de transfert de proton

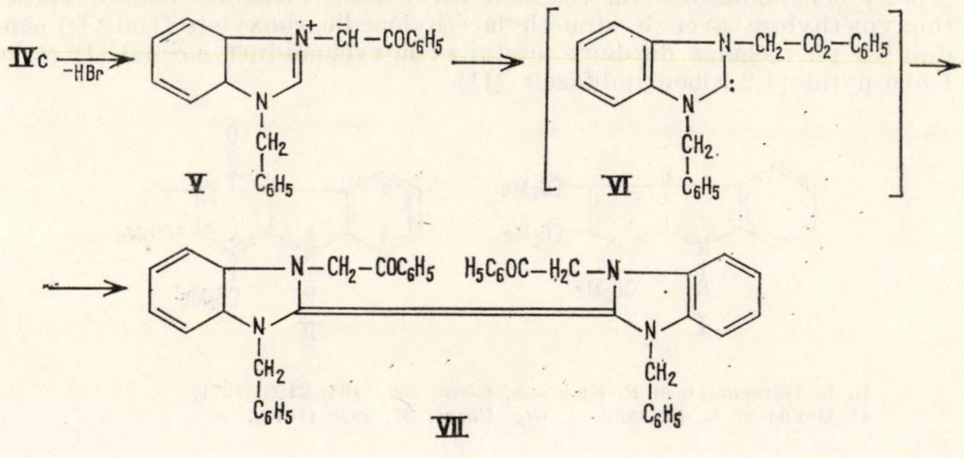

Cette supposition est suggérée par la présence des 3 singulets dans la région de résonance du groupement méthylène benzylique, qui pourraient être attribués aux 3 produits existants dans le mélange.

En comparaison d'autres carbalcoxy-méthylures,[3-5] les benzimidazolium-carbalcoxyméthylures (VIII) sont beaucoup moins stables, ce qui nous a déterminé à effectuer les réactions de cycloaddition « in situ ».

Tableau 2

Analyses chimiques et spectres IR et RMN des produits (IV)

Produit	Analyses chimiques		$\nu_{C=O}$ cm^{-1}	RMN
	Calculé	Trouvé		
IVa	C 57,55 % H 5,07 % N 7,46 %	57,64 4,92 7,81	1760	($CDCl_3$) : triplet $\delta = 1,31$ (3H) CH_3 du groupement éthyle estérique ; quartet $\delta = 5,82$ (2H) CH_2 du groupement éthyle estérique ; singulet $\delta = 5,91$ (2H) CH_2 benzylique ; multiplet $\delta = 7,30-7,92$ (9H) protons aromatiques ; singulet $\delta = 11,71$ (1H) H de la position 2
IVb	C 56,50 % H 4,71 % N 7,55 %	56,82 4,57 8,21	1760	
IVc	C 64,90 % H 4,67 % N 6,89 %	65,61 5,03 7,26	1680	(DMSO) : singulet $\delta = 5,18$ (2H) CH_2 lié de N^+ ; singulet $\delta = 5,82$; 5,94 ; 6,05 (2H) CH_2 benzylique ; multiplet $\delta = 7,22 - 8,45$ (14H) protons aromatiques ; singulet $\delta = 10,27$ (1H) H de la position 2
IVd	C 48,20 % H 5,01 % N 9,36 %	48,36 5,16 9,50	1755	($CDCl_3$) : singulet $\delta = 4,36$ (3H) CH_3 de la position 1 ; triplet $\delta = 1,34$ (3H) CH_3 du groupement éthyle estérique ; quartet $\delta = 4,15-4,53$ (2H) CH_2 du groupement éthyle estérique ; singulet $\delta = 5,82$ (2H) CH_2 lié de N^+ ; multiplet $\delta = 7,50-8,20$ (4H) protons aromatiques ; singulet $\delta = 11,24$ (1H) H de la position 2

Ainsi, les bromures de méthylcarbalcoxy-benzimidazolium (IVa, b, d), dans du benzène ou de l'acétonitrile anhydre, en présence de triéthylamine, réagissent avec le DMAD en formant un seul produit de réaction.

Dans le spectre RMN du composé résulté (IX) on observe l'absence des signaux correspondant aux groupements éthyle et respectivement méthyle estériques. Ces données, et aussi le fait que, indifféremment de l'ylure intermédiaire (VIIIa) ou (VIIIb), on obtient le même produit, montrent que pendant la réaction a lieu l'élimination d'une molécule d'alcool éthylique, respectivement méthylique. On peut supposer pour

---

[3] M. Petrovanu, A. Sauciuc et I. Zugrăvescu, *Anal. Şti., Univ. «Al. I. Cuza» Iaşi, Secl. I*, **16**, 65 (1970).

[4] I. Zugrăvescu, E. Rucinschi et G. Surpăţeanu, *Anal. Sti., Univ. «Al. I. Cuza» Iaşi, Sect., I*, **16**, 41 (1970).

[5] I. Zugrăvescu, M. Petrovanu, M. Caproşu et I. Druţă, *Rev. Roumaine. Chim.*, **17**, 397 (1972).

les produits de réaction deux structures : une structure similaire à (II) ou une structure à caractère d'ylure (IX)

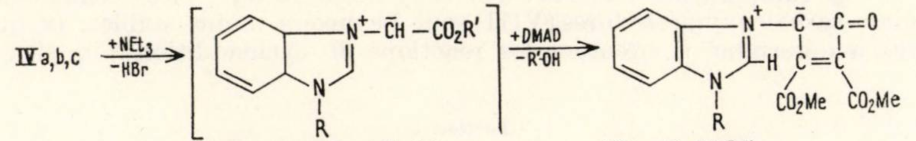

VIII a; $R=CH_2C_6H_5$; $R'=C_2H_5$
b; $R=CH_2C_6H_5$; $R'=CH_3$ c; $R=CH_3$; $R'=C_2H_5$

IX a; $R=CH_2C_6H_5$
b; $R=CH_3$

Le composé (II), obtenu par Ogura et Kikuchi [2] a le même point de fusion et le même spectre IR que le composé (IXb) isolé par nous. Dans le spectre RMN à $\delta = 8{,}21$ ppm les auteurs cités [2] trouvent un doublet, pendant que nous avons trouvé un singulet. Ce doublet est attribué par eux au proton aromatique de la position 6 dans la structure (II). En tenant compte que les autres protons aromatiques apparaissent à $\delta = 7{,}50$ ppm, la structure (II) ne peut pas expliquer un déplacement de 0,71 ppm du signal de ce proton. Il est toujours difficile à expliquer la différence de 30 cm^{-1} entre les deux maxima IR correspondant aux vibrations des groupements carbonyles estériques. Le singulet trouvé par nous à $\delta = 8{,}21$ a été attribué au proton de la position 2 du cycle benzimidazolique.

Pour prouver que le produit de réaction entre l'ylure (VIIIa) et le DMAD correspond à la structure (IX), proposée par nous, on a substitué l'hydrogène de la position 2 du cycle benzimidazolique par le deutérium. Le 1-benzyl-2D-benzimidazole (X) traité par le bromoacétate d'éthyle conduit au sel de benzimidazolium deutéré (XI). Le même produit (XI) peut être obtenu par deutération directe du sel (IVa)

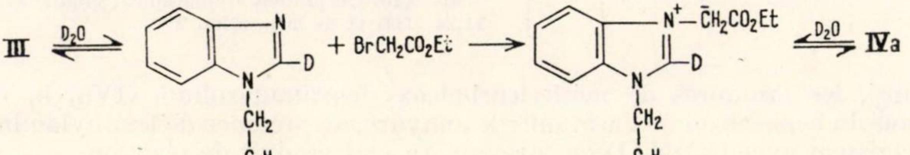

X XI

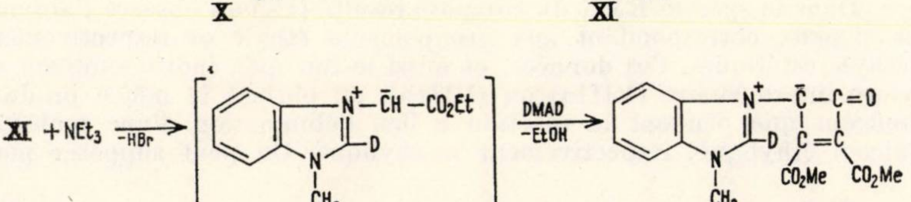

XII

Les spectres RMN du benzimidazole (X) et du bromure (XI) présentent un amoindrissement d'environ 50% des signaux correspondant aux protons de la position 2, pendant que tous les autres signaux restent non modifiés. Ces faits nous indiquent que, dans les conditions expérimentales utilisées par nous, seulement le proton de la position 2 subit l'échange partiel avec le deutérium.

Le bromure de benzimidazolium (XI), dans de l'acétonitrile, en présence de triéthylamine, réagit avec le DMAD conduisant au composé (XII). Dans le spectra RMN de ce produit (XII) le singulet de 8,21 ppm, que nous avons attribué, par différence des auteurs cités, [2] au proton de la position 2 du cycle benzimidazolique présente, conformément à l'intégrale, un amoindrissement de 50%. Cela prouve que ce proton ne s'élimine pas, comme on le prétend dans le travail cité. [2] En conséquence l'élimination d'alcool implique un autre proton, fait qui infirme la structure proposée (II). En outre, la bande de 1200 cm^{-1}, qui appartient à la vibration de déformation C—H et qu'on trouve dans les spectres IR des benzimidazoles (III) et aussi dans le spectre IR du composé (IX) est déplacée dans le spectre IR du produit (XII) à 875 cm^{-1}. Le rapport 1200/875 correspond à la valeur 1,35 trouvée dans d'autres cas [6] pour le rapport ν_{C-H}/ν_{C-D}.

En tenant compte des faits expérimentaux mentionnés plus haut on peut supposer pour la formation du produit de structure (IX) le mécanisme réactionnel suivant:

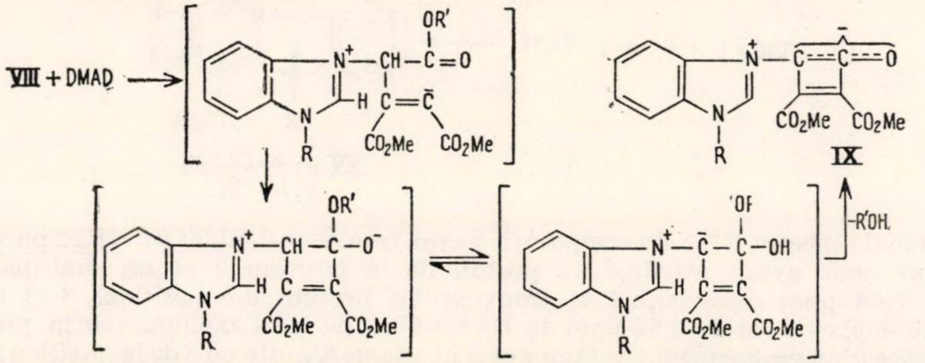

Par différence de (VIIIa, b, c) le 1-benzylbenzimidazolium-phénacylure (V) réagit avec le DMAD d'après le schéma d'une cycloaddition 2+3 dipolaire, conduisant au pyrrolo[1, 2-a]benzimidazole (XIV)

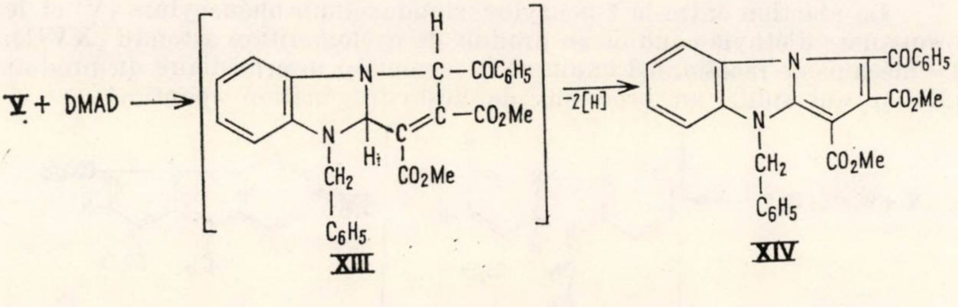

---

[6] L. A. Kazitzyna et N. B. Koupletskaya, «Primenenie UF—, IK— i YaMR spektroskopij v organicheskoj khimij», Vyschaya Shchola, Moskwa, 1971, p. 214—234.

Dans une première phase se forme le composé non isolable (XIII), qui subit un processus de déshydrogénation sous l'influence de l'oxygène atmosphérique ou d'une partie de DMAD. Dans le spectre RMN apparaissent seulement les deux signaux des groupements CH_3 estériques à 3,30 et à 3,72 ppm, le groupement méthylène benzylique à 5,72 ppm et les signaux des protons aromatiques.

La différence de comportement de ces deux ylures (V) et (VIII) dans la réaction avec le DMAD s'explique par la difficulté d'élimination d'une molécule de benzène dans le cas de l'ylure (V), qui réagit donc d'après le schéma habituel.

La réaction entre le 1-benzylbenzimidazolium-carbéthoxy-méthylure (VIIIa) et le propyolate d'éthyle prend un cours différent de celui indiqué dans la littérature. [2] Ainsi, on obtient le même produit (XV) dans la réaction du propyolate d'éthyle, soit avec du 1-benzylbenzimidazolium-carbéthoxyméthylure (VIIIa), soit avec du 1-benzylbenzimidazolium-carbométhoxyméthylure (VIIIb). L'analyse des spectres IR et RMN indique pour (XV) une structure de 1-oxo-pyrido[1, 2-a]benzimidazole

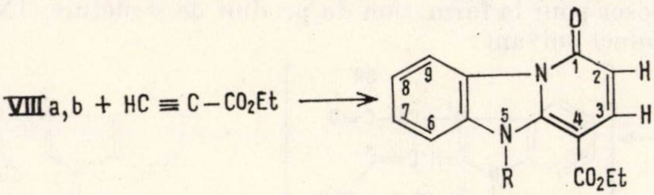

XV a; $R=CH_2C_6H_5$
b; $R=CH_3$

Dans le spectre RMN du composé (XVa) on trouve un doublet à $\delta=8,22$ ppm, que nous avons attribué au proton de la position 2 et un multiplet à 7,68 ppm dans lequel se trouvent les protons des positions 3 et 6. Le déplacement de 0,54 ppm du H^2 vis-à-vis de H^3 s'explique par la présence d'un groupement C=O en α et d'un atome d'azote en β de la position 2.

Comme dans d'autres cas, [7] on observe aussi pour les benzimidazolium-ylures une différence de comportement entre le propyolate d'éthyle et le DMAD, qui peut être attribuée à la différence de réactivité et de symétrie structurelle entre ces deux philodiènes.

La réaction entre le 1-benzylbenzimidazolium-phénacylure (V) et le propyolate d'éthyle conduit au produit de cycloaddition attendu (XVII). Le mécanisme réactionnel implique la formation intermédiaire du produit (XVI), qui subit un processus de déshydrogénation spontané

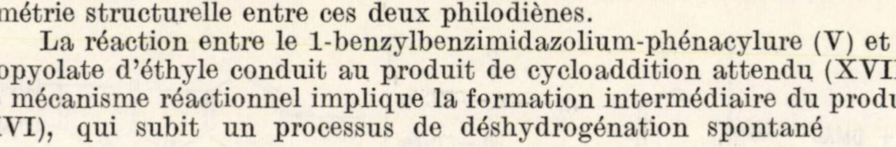

XVI XVII

---

[7] C. Leonte, *Thèse de doctorat*, Univ. «Al. I. Cuza », Iaşi, 1972.

La structure (XVII) est soutenue par les spectres IR et RMN. Le proton de la position 2 apparaît à 8,95 ppm et dans le spectre IR on trouve le groupement carbonyle estérique à 1702 cm^{-1} et le groupement carbonyle cétonique à 1630 cm^{-1}.

PARTIE EXPÉRIMENTALE

Le 1-benzylbenzimidazole a été préparé par l'alcoylation du benzimidazole avec du chlorure de benzyle selon la méthode de Reddy et Rao [8] et le 1-méthylbenzimidazole selon la méthode de Pojarskii et Simonov. [9]

Modé opératoire général de la préparation des sels quaternaires de benzimidazolium (IV)

On dissout 0,05 moles de benzimidazole dans 100 cm^3 de benzène anhydre et on ajoute 0,05 moles de dérivé halogéné. Le mélange est maintenu pendant 5 jours à la température ambiante. On filtre le sel formé, on lave sur le filtre avec un peu de benzène et on le recristallise dans un solvant approprié (tableau 1). Les analyses chimiques et les spectres IR et RMN des produits se trouvent dans le tableau 2.

Réaction du DMAD avec le 1-benzylbenzimidazolium-carbéthoxy-méthylure et avec le 1-benzylbenzimidazolium--carbométhoxyméthylure (IXa)

a) 0,005 moles de bromure de 1-benzyl-3-méthylcarbéthoxy-benzimidazolium (IVa) ou de bromure de 1-benzyl-3-méthylcarbométhoxy-benzimidazolium (IVb) suspendus dans 30 cm^3 de benzène anhydre sont traités par 1,4 cm^3 de triéthylamine et 0,615 cm^3 (0,005 moles) de DMAD. Le mélange est maintenu pendant la nuit à la température ambiante et après on porte à reflux pendant 5 heures. On filtre la solution benzénique, le benzène est distillé sous pression réduite et le résidu est recristallisé dans n-héxane et dans du dichloréthane. Cristaux blancs fusibles à 258–9°. Rend. 12%.

b) On dissout 1,9 g (0,005 moles) du produit (IVa) ou (IVb) dans 20 cm^3 d'acétonitrile anhydre et on ajoute 1,4 cm^3 de triéthylamine et 0,615 cm^3 de DMAD. On porte la solution à reflux pendant 3 heures. Après le refroidissement de la solution, le produit insoluble dans l'acétonitrile est recristallisé dans du dichloréthane. On obtient (IXa) en rendement de 14%.

Analyses $C_{22}H_{18}N_2O_5$:

Calculé : C 67,60 ; H 4,61 ; N 7,18%

Trouvé : C 67,81 ; H 4,58 ; N 7,47%

Spectre IR : 1720 cm^{-1}, 1760 cm^{-1} $\nu_{C=O}$ estérique ; 1670 cm^{-1} $\nu_{C=O}$ cétonique.

Spectre RMN ($CDCl_3$) : singulet $\delta = 3{,}82$ (3H) CH_3 estérique ; singulet $\delta = 3{,}97$ (3H) CH_3 estérique ; singulet $\delta = 5{,}39$ (2H) CH_2 benzylique ; multiplet central $\delta = 7{,}29$ (8H) protons aromatiques ; multiplet $\delta = 7{,}50-7{,}75$ (1H) H de la position 7 ; singulet $\delta = 8{,}175$ (1H) H de la position 2.

Réaction du DMAD avec le 1-méthylbenzimidazolium-carbéthoxyméthylure (IXb).

On suspend 1,09 g (0,005 moles) de bromure de 1-méthyl-3-méthylcarbéthoxy-benzimidazolium (IVd) dans 30 cm^3 de benzène anhydre et on ajoute 1,4 cm^3 de triéthylamine et

---

[8] K. K. Reddy et N. V. S. Rao, *Proc. Indian Acad. Sci.*, *Sect. A*, **70**, 81 (1969).

[9] A. F. Pojarskij et A. M. Simonov, *Zhur. obshchei Khim.* **33**, 179 (1953).

0,615 cm^3 de DMAD. Du mélange réactionnel on obtient le produit (IXb) de la manière décrite plus haut. P. f. 255—7°. Rend. 10%.

Analyses $C_{16}H_{14}N_2O_5$:

Calculé: C 61,10 ; H 4,46 ; N 8,92%

Trouvé: C 61,24 ; H 4,28 ; N 9,15%

Spectre IR : 1725 cm^{-1}, 1752 cm^{-1} $\nu_{C=O}$ estérique ; 1658 cm^{-1} $\nu_{C=O}$ cétonique.

Spectre RMN ($CDCl_3$) : singulet $\delta = 3,68$ (3H) CH_3 de la position 1 ; singulet $\delta = 3,96$ (3H) CH_3 estérique ; singulet $\delta = 4,12$ (3H) CH_3 estérique ; multiplet $\delta = 7,30-8,02$ (4H) protons aromatiques ; singulet $\delta = 8,21$ (1H) H de la position 2.

1-Benzyl-2D-benzimidazole (X)

On dissout 5,02 g (0,025 moles) de 1-benzylbenzimidazole dans 40 cm^3 de dioxanne. On ajoute 3 cm^3 (0,15 moles) d'eau deutérée et on chauffe le mélange à 80°, pendant 12 heures. Après le refroidissement de la solution on distille sous vide le solvant et l'excès d'eau deutéré. Le produit obtenu est deutéré en proportion d'environ 50%.

Spectre RMN ($CDCl_3$) : singulet $\delta = 5,34$ (2H) CH_2 benzylique ; multiplet $\delta = 7,34-7,42$ (8H) protons aromatiques ; multiplet $\delta = 7,86-8,04$ (1,5H) H^6 et H^2.

Bromure de 1-benzyl-2D-3-méthylcarbéthoxy-benzimidazolium (XI)

a) Le produit (XI) résulte de la réaction entre le 1-benzyl-2D-benzimidazole et le bromoacétate d'éthyle d'après le mode opératoire général de la préparation des sels quaternaires de benzimidazolium décrit plus haut.

b) 1,9 g (0,005 moles) de bromure de 1-benzyl-3-méthylcarbéthoxy-benzimidazolium sont dissous dans 100 cm^3 de dioxanne et on ajoute 1 cm^3 (0,05 moles) d'eau deutérée. La solution est chauffée à 80° pendant 12 heures. On distille sous vide le solvant et l'excès d'eau deutéré.

Spectre RMN ($CDCl_3$) : singulet $\delta = 11,71$ (0,5H) H de la position 2 ; le reste du spectre est identique à celui du composé (IVa).

Réaction du DMAD avec le bromure de 1-benzyl-2D-méthylcarbéthoxy-benzimidazolium (XII)

On dissout 1,9g (0,005 moles) de bromure de benzimidazolium (XI) dans 20 cm^3 d'acétonitrile. On ajoute 1,4 cm^3 de triéthylamine et 0,615 cm^3 de DMAD. On procède comme pour la préparation du produit (IXa).

Spectre IR : 1760 cm^{-1}, 1719 cm^{-1} $\nu_{C=O}$ estérique ; 1667 cm^{-1} $\nu_{C=O}$ cétonique ; 875 $cm^{-1}\nu_{C=D}$.

Spectre RMN ($CDCl_3$) : singulet $\delta = 8,21$ (0,5H) H de la position 2 ; le reste du spectre est identique à celui du composé (IXa).

Réaction du DMAD avec le 1-benzylbenzimidazolium-phénacylure (XIV)

2,035 g (0,005 moles) de bromure de 1-benzyl-3-phénacyl-benzimidazolium (IVc) dans 30 cm^3 de benzène anhydre sont traités par 1,4 cm^3 de triéthylamine et 0,615 cm^3 de DMAD. Après 24 heures de repos à la température ambiante le mélange est porté à reflux pendant 3—4 heures. Après le refroidissement on filtre la solution benzénique et on chasse le solvant sous pression réduite. Le résidu est recristallisé dans du dichloréthane (XIV). Cristaux blancs, fusibles à 212–3°. Rend. 8%.

Analyses $C_{28}H_{22}N_2O_5$:

Calculé: C 72,05 ; H 4,72 ; N 6,01%

Trouvé: C 71,84 ; H 4,96 ; N 6,63%

Spectre IR : 1722 cm^{-1}, 1695 cm^{-1} $\nu_{C=O}$ estérique ; 1618 cm^{-1} $\nu_{C=O}$ cétonique.

Spectre RMN ($CDCl_3$) : singulet $\delta = 3,30$ (3H) CH_3 estérique ; singulet $\delta = 3,72$ (3H) CH_3 estérique ; singulet $\delta = 5,72$ (2H) CH_2 benzylique ; multiplet $\delta = 6,86-7,63$ (13H) protons aromatiques ; multiplet $\delta = 8,08-8,36$ (1H) H de la position 5.

Réaction du propyolate d'ethyle avec le 1-benzylbenzimidazolium-carbéthoxyméthylure ou avec le 1-benzylbenzimidazolium-carbométhoxyméthylure (XVa)

On introduit 0,005 moles de sels (IVa) ou (IVb) dans 30 cm^3 de benzène anhydre. On ajoute 1,4 cm^3 de triéthylamine et 0,49 g (0,005 moles) de propyolate d'éthyle. Le mélange est maintenu 24 heures à la température ambiante et après on porte à reflux pendant 3 heures. On filtre la solution benzénique, on distille le benzène sous pression réduite et on recristallise le résidu dans du méthanol. On obtient (XVa). Produit blanc fusible à 178–9°. Rend. 10,3%.

Analyses : $C_{21}H_{18}N_2O_3$:

Calculé: C 72,80 ; H 5,20 ; N 8,09%

Trouvé: C 73,24 ; H 4,95 ; N 8,60%

Spectre IR : 1721 cm^{-1} $\nu_{C=O}$ estérique ; 1622 cm^{-1} $\nu_{C=O}$ cétonique.

Spectre RMN ($CDCl_3$) : triplet central $\delta = 1,43$ (3H) CH_3 du groupement éthyle estérique : quartet $\delta = 4,23-4,58$ (2H) CH_2 du groupement éthyle estérique ; singulet $\delta = 5,52$ (2H) CH_2 benzylique ; multiplet central $\delta = 7,29$ (8H) protons aromatiques ; multiplet central $\delta = 7,68$ (2H) H^3 et H^6 ; doublet $\delta = 8,22$ (1H) H^2.

Réaction du propyolate d'éthyle avec le 1-méthylbenzimidazolium-carbéthoxyméthylure (XVb)

1,09 g (0,005 moles) du produit (IVd) dans 30 cm^3 de benzène anhydre sont traités par 1,4 cm^3 de triéthylamine et 0,49 g de propyolate d'éthyle. Le mélange est chauffé à reflux pendant 4–5 heures. Après le refroidissement on filtre la solution benzénique, on chasse le solvant sous vide et on recristallise le résidu dans du méthanol. On obtient des cristaux aciculaires, blancs, fusibles à 196–7° (XVb). Rend. 9%.

Analyses $C_{15}H_{14}N_2O_3$:

Calculé: C 66,66 ; H 5,19 ; N 10,04%

Trouvé: C 66,84 ; H 5,07 ; N 10,42%

Spectre IR : 1720 cm^{-1} $\nu_{C=O}$ estérique ; 1668 cm^{-1} $\nu_{C=O}$ cétonique.

Spectre RMN ($CDCl_3$) : triplet central $\delta = 1,41$ (3H) CH_3 du groupement éthyle estérique ; singulet $\delta = 3,56$ (3H) CH_3 de la position 5 ; quartet $\delta = 4,11-4,48$(2H) CH_2 du groupement éthyle estérique ; multiplet central $\delta = 7,52$ (3H) protons aromatiques ; multiplet $\delta = 7,47-7,73$ (2H) H^3 et H^6 ; doublet $\delta = 8,07$ (1H) H^2.

Réaction du propyolate d'éthyle avec le 1-benzylbenzimidazolium-phénacylure (XVII)

Un mélange formé de 2,035 g de bromure de 1-benzyl-3-phénacyl-benzimidazolium (IVc), 1,4 cm^3 de triéthylamine et 0,49 g de propyolate d'éthyle dans 30 cm^3 de benzène anhydre est porté à reflux pendant 3 heures. On filtre la solution benzénique et le résidu, obtenu après la distillation du benzène sous vide, est recristallisé dans du méthanol. Cristaux blancs, aciculaires, fusibles à 175–8° (XVII). Rend. 17%.

Analyses $C_{27}H_{22}N_2O_3$:

Calculé: C 76,75 ; H 5,21 ; N 6,64%

Trouvé: C 76,54 ; H 5,09 ; N 6,98%

Spectre IR : 1702 cm^{-1} $\nu_{C=O}$ estérique ; 1630 cm^{-1} $\nu_{C=O}$ cétonique.

Spectre RMN ($CDCl_3$) : triplet central $\delta = 1,27$ (3H) CH_3 du groupement éthyle estérique ; quartet $\delta = 4,09-4,45$ (2H) CH_2 du groupement éthyle estérique ; singulet $\delta = 6,10$ (2H) CH_2 benzylique ; multiplet $\delta = 7,22-8,00$ (14H) protons aromatiques ; multiplet $\delta = 8,95$ (1H) H de la position 2.

Les spectres RMN ont été enregistrés avec des appareils Jeol 60 Mhz et Varian 60 Mhz et les spectres obtenus ont été identiques.

Revue Roumaine de Chimie, **19**, *4*, 659–664 (1974)

BENZIMIDAZOLIUM-YLURES. II[1]

SUR LES RÉACTIONS DE QUELQUES BENZIMIDAZOLIUM-YLURES AVEC DES PHILODIÈNES

ION ZUGRĂVESCU, JEAN HERDAN et ION DRUȚĂ

Laboratoire de Chimie organique
Université « Al. I. Cuza », Jassy, 11, str. 23 August

Reçu le 13 octobre 1973

Le 1-benzylbenzimidazolium-carbéthoxyméthylure (Ib) réagit avec l'acrylonitrile en formant le produit (V) de cycloaddition 2+3 dipolaire. Avec l'isocyanate de phényle les ylures (Ia) et (Ib) conduisent aux ylures carbanion-disubstitués (VIa) et respectivement (VIb), très stables. La réaction entre le 1-benzyl-2-méthylbenzimidazolium-carbéthoxyméthylure (IX) et l'isocyanate de phényle conduit au produit (XI), par suite d'un transfert 1,6 de proton.

Dans un travail précédent [1] on a présenté les réactions de cycloaddition du 1-benzylbenzimidazolium-phénacylure (Ia) et du 1-benzylbenzimidazolium-carbéthoxyméthylure (Ib) sur des acétylènes activés. L'ylure (Ia) réagit avec le propyolate d'éthyle et avec le diméthylacétylènedicarboxylate (DMAD) donnant naissance aux produits attendus (II)

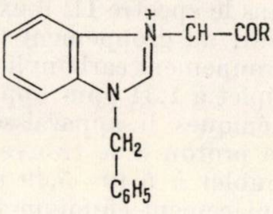

I a ; $R=C_6H_5$
b ; $R=OC_2H_5$

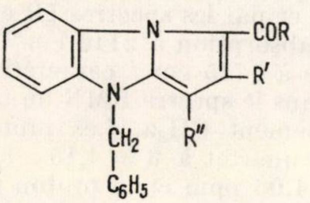

II a ; $R=C_6H_5$, $R'=R''=CO_2Me$.
b ; $R=C_6H_5$, $R'=H$, $R''=CO_2Et$

Le 1-benzylbenzimidazolium-carbéthoxyméthylure (Ib) réagit d'une autre manière conduisant à des produits différents de ceux connus dans la littérature [2]. Dans la réaction de l'ylure (Ib) avec le DMAD on obtient un nouvel ylure stable (III) et avec le propyolate d'éthyle on obtient le 1-oxo-pyrido [1, 2-a] benzimidazole (IV)

---

[1] I. Zugrăvescu, J. Herdan et I. Druță, *Rev. Roumaine Chim.* (sous presse).

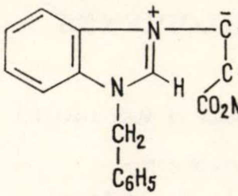

III

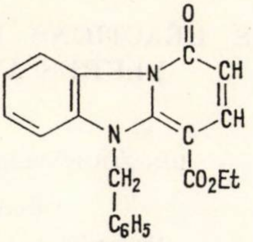

IV

Continuant ces recherches nous avons étudié les réactions des benzimidazolium-ylures (I) avec des philodiènes à doubles liaisons. L'ylure (Ib), obtenu « in situ » par le traitement du bromure correspondant avec de la triéthylamine, réagit en milieu de benzène anhydre avec de l'acrylonitrile, conduisant au tétrahydropyrrolo[1, 2-a]benzimidazole (V)

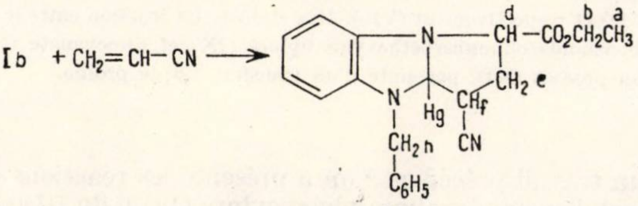

V

Une structure similaire a été obtenue par Froelich et Kröhnke [3] dans la série des pyridinium-ylures. La structure (V) est confirmée par l'analyse chimique et par les spectres IR et RMN. Dans le spectre IR il existe une bande d'absorption à 2140 cm^{-1} correspondant au groupement C≡N, et une autre à 1745 cm^{-1} caractéristique du groupement carbonylique estérique. Dans le spectre RMN on trouve un triplet à 1,34 ppm appartenant au groupement CH_3a. Les protons méthyléniques b apparaissent sous forme de quartet à $\delta = 4{,}15-4{,}45$ ppm. Le proton d se trouve comme triplet à 4,06 ppm et le proton f comme doublet à 5,40–5,49 ppm. Le groupement méthylène benzylique h a un déplacement chimique différent des autres cas ($\delta = 4{,}61$ ppm), fait qui indique une interaction stérique entre le groupement C≡N et le noyau benzénique qui affecte l'anisotropie de la molécule.

L'ylure (Ia) avec le même réactant conduit à un produit huileux à structure indéfinie.

[2] H. Ogura et K. Kikuchi, *J. Org. Chem.*, **37**, 2679 (1972).

[3] J. Froelich et F. Kröhnke, *Chem. Ber.*, **104**, 1621 (1971).

On a étudié aussi les réactions des ylures (I) avec une philodiène à double liaison carbone-azote. L'isocyanate de phényle donne avec les ylures deux types de produits de réaction. Dans certains cas [4] on a isolé les produits de cycloaddition de l'isocyanate de phényle sur l'ylure et dans d'autres cas on a obtenu un nouvel ylure carbanion-disubstitué [5].

Les 1-benzylbenzimidazolium-ylures (Ia) et (Ib) réagissent avec l'isocyanate de phényle, en milieu de benzène ou d'acétonitrile anhydre, conduisant, par transfert 1,3 de proton aux ylures (VI), très stables. On n'observe pas, dans ce cas, la réaction de cycloaddition 2+3 dipolaire et on ne peut pas isoler un produit de structure (VII)

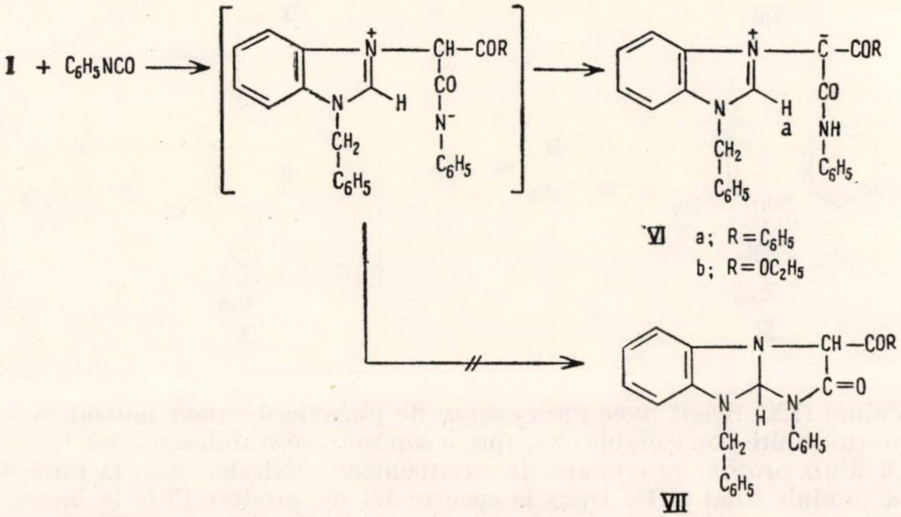

Dans le spectre IR du produit (VIa) on trouve une bande à 2950 cm^{-1} correspondant au groupement NH amidique et deux bandes à 1625 et à 1690 cm^{-1}, correspondant aux vibrations des groupements C=O cétoniques et respectivement amidiques. L'une des bandes amidiques est superposée à la bande du groupement cétonique. Le déplacement de ces bandes vers des longueurs d'onde plus élevées que leur valeur normale nous indique un amoindrissement de la constante de force de la liaison, due au voisinage de la charge anionique. Le spectre de RMN a deux signaux à $\delta = 9{,}98$ et 12,82 ppm qui disparaissent après la deutération. Ces signaux ont été attribués au NH et respectivement au proton de la position du cycle benzimidazolique. Les spectres IR et RMN du composé (VIb) sont tout à fait semblables.

---

[4] R. Huisgen, M. Morikawa, K. Herbig et E. Brunn, *Chem. Ber.*, **100**, 1094 (1967).

[5] I. Zugrăvescu, E. Rucinschi et G. Surpăţeanu, *Tetrahedron Lett.*, **12**, 941(1970).

Si dans la position 2 du cycle benzimidazolique on substitue un groupement méthyle, la réaction des ylures avec l'isocyanate de phényle prend un cours différent et il se forme le produit (XI)

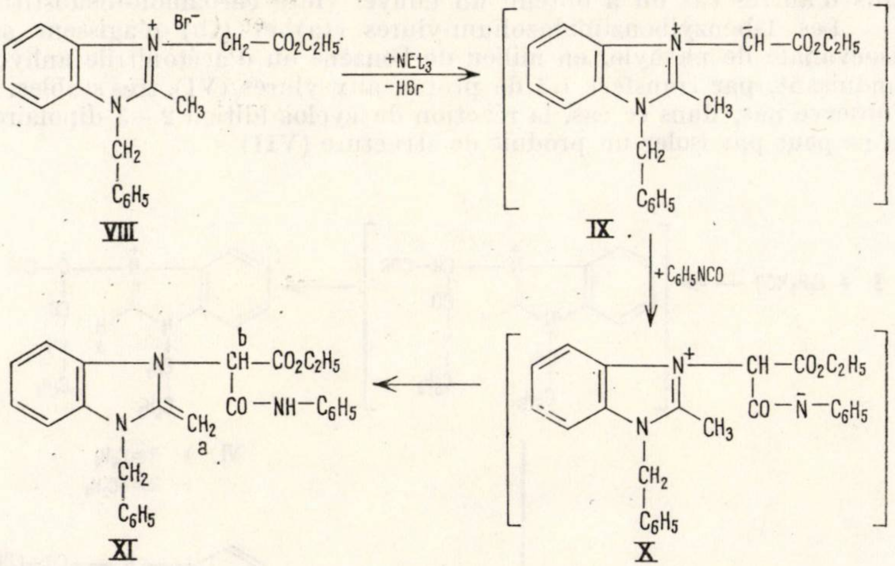

L'ylure (IX) réagit avec l'isocyanate de phényle donnant naissance à un intermédiaire non isolable (X), qui, à son tour, se stabilise par un transfert 1,6 d'un proton, provenant du groupement méthyle, avec la formation du produit final (XI). Dans le spectre IR du produit (XI) la bande de 1735 cm^{-1} a été attribuée au groupement carbonylique estérique et les bandes de 1630 cm^{-1}et 1590 cm^{-1} aux deux vibrations amidiques. Les valeurs normales trouvées pour ces vibrations prouvent l'absence de la charge anionique sur l'atome de carbone. Les deplacements chimiques observés dans le spectre RMN correspondent à la structure (XI), formulée plus haut.

PARTIE EXPÉRIMENTALE

Les ylures ont été préparés « in situ », en traitant les bromures correspondant par la triéthylamine.

Réaction du 1-benzylbenzimidazolium-carbéthoxyméthylure avec l'acrylonitrile (V)

On suspend 1,9 g (0,005 moles) de bromure de 1-benzyl-3-méthylcarbéthoxybenzimidazolium dans 30 cm^3 de benzène anhydre et on ajoute 1,4 cm^3 (0,01 moles) de triéthylamine et 0,106 cm^3 d'acrylonitrile (0,005 moles). On maintient le mélange 24 heures à la température ambiante et ensuite on porte à reflux pendant 3 heures. On filtre la solution benzénique et on chasse le solvant sous pression réduite. Le résidu est recristallisé dans du *n*-hexane et puis dans de l'alcool éthylique. Le produit obtenu (V) est fusible à 108°. Rend. 18%.

Analyses $C_{21}H_{21}N_3O_2$:

Calculé : C 72,60 ; H 6,05 ; N 12,10%

Trouvé : C 72,71 ; H 6,09 ; N 12,36%

Spectre IR : 2140 cm^{-1} $\nu_{C\equiv N}$; 1745 cm^{-1} $\nu_{C=O}$.

Spectre RMN ($CDCl_3$) : triplet central $\delta = 1,34$ (3H) CH_3 a ; multiplet $\delta = 2,20-2,42$ (2H) CH_2 e ; quartet $\delta = 2,91-3,20$ (1H) CH f ; triplet central $\delta = 4,30$ (2H) CH_2 b ; singulet $\delta = 4,61$ (2H) CH_2 h ; doublet $\delta = 5,40-5,49$ (1H) H g ; multiplet central $\delta = 6,86$ (4H) protons aromatiques multiplet central $\delta = 7,52$ (5H) protons aromatiques.

Réaction du 1-benzylbenzimidazolium-phénacylure avec l'isocyanate de phényle (VIa)

2,035 g (0,005 moles) de bromure de 1-benzyl-3-phénacylbenzimidazolium dans 30 cm^3 de benzène anhydre sont traités par 1,4 cm^3 de triéthylamine et 0,6 cm^3 (0,005 moles) d'isocyanate de phényle. Le mélange est chauffé à reflux pendant 5 heures, après quoi on filtre la solution benzénique. Par évaporation partielle du benzène on obtient un produit blanc, qui recristallisé dans du méthanol est fusible à 235–8°. Les analyses chimiques et le point de fusion nous ont indiqué qu'il s'agit du N, N'-diphénylurée. Le mélange avec un échantillon original de N, N'-diphénylurée présente le même point de fusion.

On recristallise le produit insoluble dans du benzène dans du méthanol, en obtenant le produit (VIa). Cristaux blancs, fusibles à 218–9°. Rend. 12%.

Analyses $C_{29}H_{23}N_3O_2$:

Calculé : C 78,21 ; H 5,17 ; N 9,44%

Trouvé : C 78,84 ; H 5,36 ; N 9,22%

Spectre IR : 2950 cm^{-1} ν_{N-H} amidique ; 1625 cm^{-1} $\nu_{C=O}$; 1590 cm^{-1} $\nu_{C=O}$.

Spectre RMN (DMSO-D_6) : singulet $\delta = 5,67$ (2H) CH_2 benzylique ; multiplet $\delta = 6,58-8,18$ (19H) protons aromatiques ; singulet $\delta = 9,98$ (1H) deutérable NH ; singulet $\delta = 12,8$ (1H) deutérable CHa.

Réaction du 1-benzylbenzimidazolium-carbéthoxyméthylure avec l'isocyanate de phényle (VIb)

On dissout 1,9 g de bromure de 1-benzyl-3-méthylcarbéthoxybenzimidazolium dans 20 cm^3 d'acétonitrile. On ajoute 1,4 cm^3 de triéthylamine et 0,6 cm^3 d'isocyanate de phényle. On porte à reflux pendant 5 heures. On chasse sous pression réduite la moitié du solvant et on recristallise le produit obtenu dans du dichloréthane. Cristaux blancs fusibles à 210–1° (VIb). Rend. 16%.

Analyses $C_{25}H_{23}N_3O_3$:

Calculé : C 72,25 ; H 6,02 ; N 10,12%

Trouvé : C 71,54 ; H 6,21 ; N 10,50%

Spectre IR : 2980 cm^{-1} ν_{N-H} amidique ; 1625 cm^{-1} $\nu_{C=O}$ estérique ; 1600 et 1580 cm^{-1} $\nu_{C=O}$ amidique.

Spectre RMN (DMSO-D_6) ; triplet central $\delta = 0,92$ (3H) CH_3 du groupement éthyle estérique ; quartet $\delta = 3,79-4,15$ (2H) CH_2 du groupement éthyle estérique ; singulet $\delta = 5,8$ (2H) CH_2 benzylique ; multiplet $\delta = 6,84-8,04$ (14H) protons aromatiques ; singulet $\delta = 9,93$ (1H) deutérable NH ; singulet $\delta = 10,96$ (1H) deutérable CH *a*.

Bromure de 1-benzyl-2-méthyl-3-méthylcarbéthoxy-benzimidazolium (VIII)

Le produit (VIII) est obtenu à partir du 1-benzyl-2-méthyl-benzimidazole et le bromoacétate d'éthyle, d'après le mode opératoire général pour la préparation des sels quaternaires de benzimidazolium.[1] Recristallisé dans du méthanol ; P. f. 245—8°. Rend. 68 %.

Analyses $C_{19}H_{21}BrN_2O_2$:

Calculé : C 57,12 ; H 5,26 ; N 7,02 %

Trouvé : C 56,78 ; H 5,31 ; N 7,25 %

Spectre IR : 1760 cm^{-1} $\nu_{C=O}$ estérique.

Spectre RMN (DMSO-D_6) : triplet central $\delta = 1,22$ (3H) CH_3 du groupement éthyle estérique ; singulet $\delta = 2,93$ (3H) CH_3 de la position 2 ; quartet $\delta = 4,01-4,37$ (2H) CH_2 du groupement éthyle estérique ; singulet $\delta = 5,60$ (2H) CH_2 lié de N^+ ; singulet $\delta = 5,82$ (2H) CH_2 benzylique ; multiplet $\delta = 7,27-8,05$ (9H) protons aromatiques.

Réaction du 1-benzyl-2-méthylbenzimidazolium-carbéthoxyméthylure avec l'isocyanate de phényle (XI)

On introduit 1,9 g (0,005 moles) de bromure de 1-benzyl-2-méthyl-3-méthylcarbéthoxy-benzimidazolium dans 30 cm^3 de benzène anhydre. On ajoute 1,4 cm^3 de triéthylamine et 0,6 cm^3 d'isocyanate de phényle. Le mélange est maintenu pendant 5 jours à la température ambiante. On filtre la solution benzénique et on chasse le solvant sous vide. Le produit huileux obtenu est maintenu pendant 2 jours à +4° et il devient cristallin. On recristallise ce produit dans de l'éthanol (XI). Produit blanc, fusible à 181—4°. Rend. 21 %.

Analyses $C_{26}H_{25}N_3O_3$:

Calculé : C 73,37 ; H 5,85 ; N 9,83 %

Trouvé : C 73,12 ; H 6,04 ; N 10,21 %

Spectre IR : 3000 cm^{-1} ν_{N-H} ; 1735 cm^{-1} $\nu_{C=O}$ estérique ; 1630 et 1590 cm^{-1} $\nu_{C=O}$ amidiques.

Spectre RMN ($CDCl_3$) : triplet central $\delta = 1,22$ (3H) CH_3 du groupement éthyle estérique ; quartet $\delta = 3,90-4,25$ (2H) CH_2 du groupement éthyle estérique ; singulet $\delta = 5,08$ (1H) CH b ; singulet $\delta = 5,32$ (2H) CH_2 a ; singulet $\delta = 5,49$ (2H) CH_2 c ; multiplet δ 6,88—7,42 (14H) protons aromatiques ; singulet $\delta = 9,4$ (1H) deutérable NH.

Revue Roumaine de Chimie, **19**, *4*, 665–669 (1974)

THE ELECTRONIC SPECTRUM OF 1, 2, 3-TRIMETHOXYACRIDINE-N-OXIDE

M. VLASSA, MARIA IONESCU and J. FABIAN *

Institute of Chemistry, Cluj, Str. Donath 65–103, Romania
*Department of Chemistry, Technical University of Dresden,
The Democratic Republic of Germany

Received May 8, 1973

The π-electronic transitions of 1,2,3-trimethoxyacridine-N-oxide and those of the 9-chloro-substituted derivative were computed by the SCF-MO-CI (PPP) method. The calculated electronic transitions are in satisfactory agreement with the experimental data. The influence on the π-electronic transitions of acridine of three methoxy groups in vicinal position 1, 2 and 3 is compared with that of the N–O group.

1. INTRODUCTION

In connection with our current investigations on chemical and physico-chemical properties of 1,2,3-trimethoxyacridine derivatives[1,2,3] we have calculated the π-electronic transitions of 1,2,3-trimethoxyacridine N-oxide (**1**). The success of the PPP method, in spite of the rather drastic approximations involved, in computing the π-electronic structure and transitions of 1,2,3-trimethoxyacridine and acridine [3] encouraged us to extend the calculations to the N-oxide derivative.

2. METHOD AND PARAMETERS EVALUATION

The SCF-MO-CI variant of the PPP method was utilized. The SCF calculations were performed by using the Mataga-Nishimoto procedure,[4] for the two center repulsion integrals.

---

[1] M. Ionescu and M. Vlassa, *Rev. Roumaine Chim.*, **16**, 743 (1971).
[2] M. Ionescu, M. Vlassa and I. Goia, *J. prakt. Chem.*, **314**, 441 (1972).
[3] M. Vlassa, M. Ionescu and J. Fabian, *Rev. Roumaine Chim.*, **18**, 99 (1973).
[4] K. Nishimoto and L. Forster, *Theor. Chim. Acta*, **4**, 155 (1966).

The π-electronic system of the 1,2,3-trimethoxyacridine-N-oxide (**1**) molecule consists of a number of 22 π-electrons delocalized over 17 centers. The molecule is assumed to be planar (C_s symmetry group) with an idealized overall bond distance $r_{\mu\nu}$ of 1.40 Å.

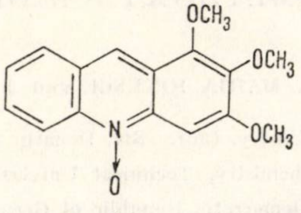

1

The parameters used are listed in table 1 and the determination of these parameters is described below.

Table 1

Parameter summary

Resonance integrals eV	One-center repulsion integrals eV	Ionization potential eV	$a_{\mu\nu}$
$\beta_{CC} = -2.38$	$\gamma_{\dot{C}\dot{C}} = 8.25$	$I_{\dot{C}} = 8.72$	1.745
$\beta_{CN} = -2.636$	$\gamma_{\dot{O}\dot{O}} = 10.60$	$I_{\dot{O}} = 13.72$	1.358
$\beta_{NO} = -2.241$	$\gamma_{\dot{N}\dot{N}} = 12.00$	$I_{\ddot{N}} = 19.22$	1.999
$\beta_{CCl} = -1.534$	$\gamma_{\ddot{O}\ddot{O}} = \gamma_{\ddot{N}\ddot{N}} = \gamma_{\ddot{Cl}\ddot{Cl}}$	$I_{\ddot{O}} = 20.72$	1.999
$\beta_{CO} = \beta_{CC}$		$I_{\ddot{Cl}} = 21.50$	1.999

For the two center repulsion integrals $\gamma_{\mu\nu}$, the Nishimoto and Mataga procedure [4] was used, as in our previous work [3] ($\gamma_{\mu\nu} = 14.397\text{eV}/a_{\mu\nu} + r_{\mu\nu}$).

The one-center repulsion integrals $\gamma_{\mu\nu}$ and ionization potentials I_μ were taken identical with those used in the calculation of the π-electronic structure of unsubstituted acridine-N-oxide. [5]

The resonance integrals $\beta_{\mu\nu}$, were derived from the π-bond order of acridine-N-oxide given by Mantsch and co-workers [5] using the following β/p relations [4]:

$$\beta_{CC} = -0.51p - 2.04 \text{ eV}$$

$$\beta_{CN} = -0.53p - 2.34 \text{ eV}$$

$$\beta_{NO} = -0.56p - 2.00 \text{ eV}$$

---

[5] H. H. Mantsch, W. Seiffert and V. Zanker, *Rev. Roumaine Chim.*, **14**, 125 (1969).

The calculations were carried out on a Elliot 503 b computer using an autocode program.

3. RESULTS AND DISCUSSION

Table 2 shows the results of our calculations in comparison to 1,2,3-trimethoxyacridine, reported in a previous paper.[3] The electronic transitions calculated for 1,2,3-trimethoxyacridine-N-oxide (**1**) are in satisfactory agreement with the experimental data.

The ultraviolet spectra of azanaphtalene N-oxides and their benzenoid homologs can be interpreted by considering the N-oxide group as a simple substituent because the larger the conjugated system in the parent heterocycles, the smaller the charge transfer character pertinent to the N-oxide group.

Table 2

The experimental and calculated singlet-singlet transition energies for 1,2,3-trimethoxyacridine (TMA), 1,2,3-trimethoxyacridine-N-oxide (TMANO) and 1,2,3-trimethoxy-9-caloroacridine-N-oxide (TMAClNO)

Band [6]	TMA[3] eV		TMANO eV		TMACINO eV		TMANO nm	TMACINO nm
	Calcd.	*Exp.*	*Calcd.*	*Exp.*	*Calcd.*	*Exp.*	*Exp.*	*Exp.*
I(^1L_a)*	2.93	3.17	2.48	2.70	2.58	2.63	459 434 412	471 446 423
II(^1L_b)	3.56	3.43	3.26	3.20	3.34	3.13	387 367 349	396 374 354
			3.41		3.50			
III(^1B_b)	4.66	4.76	4.55	4.37	4.56	4.27	283,8	290
			4.77		4.77			
			5.12		5.09			
			5.41		5.40			
			5.42		5.41			
			5.79		5.79			
			6.00		5.99			

* Only (0 – 0′) transmisions are considered.

N-oxidation stabilizes considerably the transitions along the short axis of the parent heterocycle and the red shift of the ^1L_a band is larger than the one of the ^1L_b band.[7]

This bathochromic shift becomes evident also by comparing the experimental and calculated data of acridine and 1,2,3-trimethoxyacridine with those of acridine-N-oxide and **1** (see tables 2 and 3).

It is interesting to note (see table 4) that the bathochromic shift, of all three bands, due to the presence of vicinal methoxy groups in the acridine molecule is smaller than that produced by the N-oxide group. In a nonpolar solvent (e. g. heptane) the smaller the polarity of the molecule, the higher the degree of solvation. The polarity of these molecules increases in the following order: acridine $<$ 1,2,3-trimethoxyacridine $<$ acridine-N-oxides.[3] The excited states of acridine-N-oxides are less polar than the ground states. Consequently, there is a higher bathochromic shift in nonpolar solvents due to the N-oxide group as compared to three vicinal methoxy groups. This interpretation is also supported by the bathochromic shift of acridine derivatives compared to the hypsochromic shift of acridine-N-oxide derivatives with increasing solvent polarity.[7]

---

[6] V. Zanker and W. Fluegel, *Z. Naturforsch.*, **19**, 376 (1964); *Acta Chim.*, **40**, 45 (1964).

[7] E. Ochiai, "Aromatic Amine Oxides" Elsevier, Publishing Company, Amsterdam, New York, 1967, p. 126.

Table 3

Experimental and calculated singlet-singlet transition energies for acridine and acridine-N-oxide (ANO), eV

Band[6]	Acridine [3]		ANO	
	Calcd.	*Exp.*	*Calcd.*	*Exp.*
I(^1L_a)*	3.10	3.31	3.03	2.74
II(^1L_b)	3.66	3.49	3.48	3.22
III(^1B_b)	4.84	4.96	4.72	4.50

* Idem table 2.

Table 4

The bathochromic shift (Δ) due to methoxy and N-oxide groups (experimental values), eV

	ΔI (^1L_a)	ΔII(^1L_b)	ΔIII (^1B_b)
Δ Acridine-TMA	0.14	0.06	0.20
Δ ANO-TMANO	0.04	0.02	0.13
Δ Acridine-ANO	0.57	0.27	0.47
Δ TMA-TMANO	0.47	0.23	0.39

The extension of the conjugation in the 1,2,3-trimethoxy-9-chloroacridine-N-oxide reduces the transition energy in comparison with the compound without such a substituent[8] (see experimental values in tables 2 and 3).

---

[8] I. Goia and M. Ionescu, *Studia Univ. Babeş-Bolyai (Cluj), Ser. Chem.*, **2**, 65 (1971).

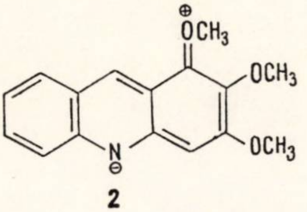

2

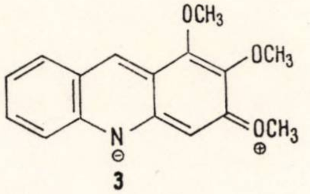

3

In contrast to N-oxidation, which stabilizes the transitions along the short axis of the parent heterocycle, the introduction of 3 vicinal methoxy groups stabilizes the transitions along both axes, since the structures **2** and **3** are energetically equivalent.

EXPERIMENTAL

The U.V. spectra were recorded in heptane, on a Carl Zeiss Specord spectrometer.

The 1,2,3-trimethoxyacridine, 1,2,3-trimethoxyacridine-N-oxide and 1,2,3-trimethoxy-9-chloroacridine were obtained by the methods previously reported.[1 2]

Revue Roumaine de Chimie, **19**, *4*, 665–669 (1974)

Revue Roumaine de Chimie, **19**, *4*, 671–677 (1974)

ELECTRONIC SPECTRA AND ACID-BASE EQUILIBRIUM OF SOME α-ACYLAMINO-N-HETEROCYCLES

D. SUCIU and Z. GYÖRFI

Oncological Institute, Cluj, Str. Republicii 34–36, Romania

Received April 24, 1973

The formation of the sodium salts derived from α-acylamino-N-heterocycles is associated with a strong bathochromic shift of the near ultraviolet absorption band. The ionization constants indicate that the stability of the sodium salts is determined by both the electron attracting properties of the acyl group and the resonance stabilization of the exocyclic N=C bond. The later effect increases in the series: pyridines < pyrimidines < thiazoles < thiadiazoles.

α-Acylamino-N-heterocycles are capable of a vinylogous amidine type of tautomerism. On the basis of the ultraviolet spectra recorded in neutral solvents of different polarities as well as of the infrared spectra, Sheinker *et al.*[1] have shown that the imido form is stable only from the derivatives which contain acyl groups with strong electron attracting properties ($CO-CCl_3$, $CO-CF_3$ etc.). The ultraviolet absorptions of the imido tautomeric form are generally shifted to longer wavelengths as compared with those of the amido form.

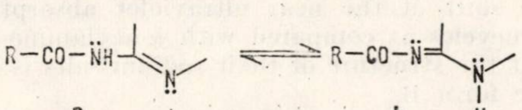

In the present work we report some ultraviolet data on the formation of the sodium salts and the protonation of α-acylamino-N-heterocycles. The spectra of 2-acylamino-thiazoles, 2-acylamino-1,3,4-thiadiazoles and 2-acylamino-pyrimidines in alkaline solution show bathochromic shifts of the near ultraviolet absorption bands as compared with the spectra recorded in neutral medium (tables 1–3). This effect could be explained if we assume the formation of the corresponding sodium salts of α-acylamino-N-heterocycles. As it was elsewhere described by Brzozowski[2] such a sodium salt derived from 2-acetylamino-thiazole has been isolated from a concentrated sodium hydroxide solution. Taking into account

---

[1] Y. N. Sheinker, E. M. Peresleni, N. P. Zosimova and Y. I. Pomerantsev, *Zhur. fiz. Khim.*, **33**, 2096 (1959).

[2] Z. Brzozowski, *Roczniki Chem.*, **41**, 391 (1967).

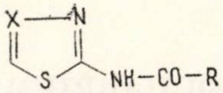

Table 1

Ultraviolet mxima and *pKb* values of some 2-acylamino-thiazoles and 2-acylamino-1,3,4-thiadiazoles

Compound	X	R	Phosphate buffer pH = 6.98		0.1 N−NaOH		0.1 N−HCl		*pKb*
			λmax (nm)	log ε	λmax (nm)	log ε	λmax (nm)	log ε	
Ia	CH	CH_3	267	3.97	287	3.99	272	4.04	11.02
Ib	CH	C_6H_5	283	4.02	317	4.13	285	4.06	9.60
Ic	CH	CH_2Cl	272	3.86	292	3.98	275	3.75	9.38
Id	CH	$CHCl_2$	286	3.90	298	4.06	280	3.91	8.09
Ie	CH	CCl_3	304	3.92	298	3.88	a)		
IIa	N	CH_3	247	3.90	230 275	3.35 4.04	247	3.88	9.22
IIb	N	C_6H_5	265	4.13	230 300	3.77 4.02	263	4.15	7.99
IIc	N	CH_2Cl	250	3.84	278	3.96	249	3.88	7.20
IId	N	$CHCl_2$	282	4.04	282	4.06	280	4.04	
IIe	N	CCl_3	a)		a)		a)		

a) **IIe** is hydrolyzed during the recording of the spectrum.

the bathochromic shift of the near ultraviolet absorption band of α-acylimino-N-heterocycles as compared with α-acylamino-N-heterocycles,[1] it is probably that the structure of their sodium salts is better described by the mesomeric form B.

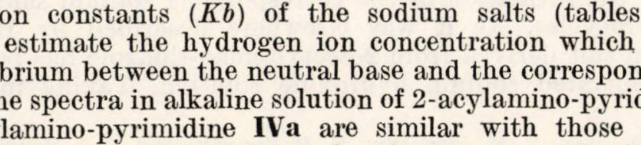

The spectral properties of α-acylamino-N-heterocycles in alkaline solutions permit us the determination by spectrophotometric titration of the ionization constants (*Kb*) of the sodium salts (tables 1—3). The *pKb* values estimate the hydrogen ion concentration which corresponds to the equilibrium between the neutral base and the corresponding sodium salt. Since the spectra in alkaline solution of 2-acylamino-pyridines (**IIIa-e**) and 2-acetylamino-pyrimidine **IVa** are similar with those recorded in neutral medium, it is probably that for these compounds the formation of the corresponding sodium salts is prevented.

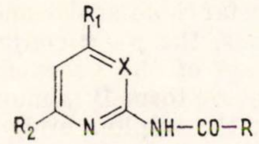

Table 2

Ultraviolet maxima, *pKa* and *pKb* values of some 2-acylaminopyridines and 2-acylaminopyrimidines

Compound	X	R	R_1	R_2	Phosphate buffer pH=6.98		0.1N−NaOH		0.1N−HCl		*pKa*	*pKb*
					λ_{max} (nm)	log ε	λ_{max} (nm)	log ε	λ_{max} (nm)	log ε		
IIIa	CH	CH_3	H	H	232 274	3.92 3.74	234 274	4.03 3.75	230 291	3.93 4.03	4.17	
IIIb	CH	C_6H_5	H	H	277	3.90	278	3.93	243 297	4.07 4.27	3.93	
IIIc	CH	CH_2Cl	H	H	234 274	3.93 3.83	225 275	3.91 3.68	230 291	3.96 4.05	3.22	
IIId	CH	$CHCl_2$	H	H	235 275	3.98 3.96	225 275	3.86 3.79	230 292	3.99 4.08	2.68	
IIIe	CH	CCl_3	H	H	235 274	3.88 3.88	227 275	3.90 3.78	230 292	3.94 4.03	2.20	
IVa	N	CH_3	CH_3	CH_3	234	4.14	234	3.92	232 280	4.18 3.91	2.74	
IVb	N	C_6H_5	CH_3	CH_3	250	4.23	258	4.02	250 283	4.22 4.19	2.56	11.74
IVc	N	CH_2Cl	CH_3	CH_3	239	4.03	255	3.71	230 280	3.98 3.71	2.21	10.72
IVd	N	$CHCl_2$	CH_3	CH_3	242	4.04	261	3.78	230 280	3.97 3.76	1.82	9.06
IVe	N	CCl_3	CH_3	CH_3	243	3.99	262	3.83	a)			7.54

a) The compound is hydrolyzed during the recording of the spectrum

The results (tables 1 and 2) indicate that the stability of the sodium salts of α-acylamino-N-heterocycles is determined not only by the presence of an acyl group with strong electron attracting properties, but also by the nature of the heterocycle. From this point of view, the stability of the mesomeric form B decreases in the order thiadiazoles, thiazoles and pyrimidines. It appears that, the shift from the neutral base to the corresponding sodium salt should be the result of both the electron withdrawing effect of the acyl group which decreases the strength of the amidic N−H bond and the $p-\pi$ conjugation effect which allows the resonance stabilization of the exocyclic N=C bond. As the charge density of the ring decreases by the presence of the second nitrogen atom for thiadiazoles and pyrimidines as compared with thiazoles and pyridines, the $p-\pi$ conjugation effect is increased and allows the stabilization of the exocyclic N=C bond. The results also indicate that the mesomeric form B is more stable for the five-membered heterocycles containing the sulphur bridge, which probably enhances the resonance stabilization of the exocyclic N=C bond.

With the purpose to establish a correlation between the basicity of α-acylamino-N-heterocycles and their ability to form the corresponding sodium salts an attempt was made to determine the *pKa* values. It can be seen from table 2 that the *pKa* values of 2-acylamino-pyrimidines decrease with the increasing of electron attracting properties of the acyl group, and the ability of these compounds to form the corresponding sodium salts (*pKb*) increases in the same order. On the other hand, the protonation of 2-acyl-amino-pyridines takes place at lower hydrogen ion concentrations than the protonation of the corresponding 2-acylamino-pyrimidines. Since 2-acylamino-thiazoles and 2-acylamino-thiadiazoles present similar ultraviolet spectra in neutral and acid media, the spectrophotometric determination of their *pKa* values failed (table 1). As it appears from the above mentioned data the stability of sodium salts of α-acylamino-N-heterocycles increases as the charge deficit of the heteroaromatic ring is increased. Therefore, it was regarded as a matter of interest to test the influence of some ring substituents on the formation of the sodium salts. It can be seen from tables 1 and 3 that 2-acylamino-5-acetylthiazoles (**Va**—**h**) have lower pKb values than the corresponding 2-acylamino-5-(α-hydroxy)ethylthiazoles (**VIa**—**e**) and 2-acylamino-thiazoles (**Ia**—**e**). Therefore, the sodium salts of the derivatives which contain a ring substituent with strong electron attracting properties are more stable. By plotting on logarithmic co-ordinates the *Kb* values of 2-acylamino-thiazoles or 2-acylamino-5-(α-hydroxy)-ethylthiazoles *versus* the corresponding values of 2-acylamino-5-acetylthiazoles, parallel straight lines were obtained (fig. 1).

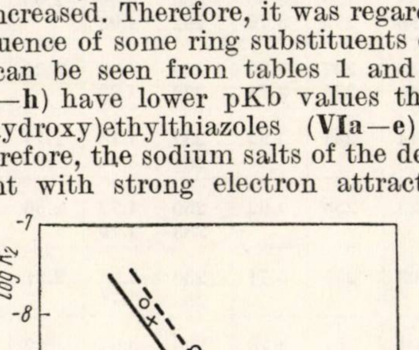

Fig. 1. — Logarithmic plot of the basic dissociation constants of 2-acylamino-thiazoles (table 1) and 2-acylamino-5-(α-hydroxy)ethylthiazoles (broken line) *versus* the corresponding values of 2-acylamino-5-acetylthiazoles (table 3).

If the free-energy change of the 2-acylamino-thiazole system is calculated for the derivatives containing an additional 5-acetyl group, the $|\Delta F|$ values (table 3) decrease in accordance with the strength of

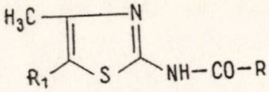

Table 3

Ultraviolet maxima and *pKb* values of some 2-acylamino-5-acetyl and 5-(α-hydroxy)ethylthiazoles h-a

Compound	R	R_1	Phosphate buffer pH=6.98 λmax (nm)	Phosphate buffer pH=6.98 log ε	0.1N−NaOH λmax (nm)	0.1N−NaOH log ε	*pKb*	$|\Delta F|$ (kcal/mole)
Va	CH_3	$CO-CH_3$	229 309	3.90 4.10	242 344	3.92 4.29	9.37	2.17
Vb	CH_2Cl	$CO-CH_3$	230 308	4.02 4.21	243 342	4.00 4.33	7.98	1.62
Vc	$CHCl_2$	$CO-CH_3$	230 314	3.93 4.21	242 342	3.95 4.44	7.26	1.26
Vd	CCl_3	$CO-CH_3$	235 328	3.81 4.18	b)			
Ve	C_6H_5	$CO-CH_3$	242 319	4.16 4.28	243 362	4.17 4.46	8.19	1.85
Vf	$C_6H_4-NO_2(m)$	$CO-CH_3$	241 319	4.22 4.28	235 362	4.17 4.43	7.71	1.40 c)
Vg	$C_6H_4-NO_2(p)$	$CO-CH_3$	259^a 328	3.93 4.21	248 376	4.18 4.39	7.16	1.15 c)
Vh	$C_6H_4-OCH_3(p)$	$CO-CH_3$	243^a 320	3.99 4.39	255 366	4.08 4.53	8.41	2.08 c)
VIa	CH_3	$CHOH-CH_3$	278	3.99	297	4.04	10.86	
VIb	C_6H_5	$CHOH-CH_3$	228 306	4.02 4.04	230 329	3.99 4.14	9.13	
VIc	$C_6H_4-NO_2(m)$	$CHOH-CH_3$	228 303	4.09 4.12	229 330	4.13 4.19	8.49	
VId	$C_6H_4-NO_2(p)$	$CHOH-CH_3$	262 320	4.06 3.98	271 368	4.05 3.97	7.91	
VIe	$C_6H_4-OCH_3(p)$	$CHOH-CH_3$	302	4.28	252 328	4.13 4.42	9.30	

a) Determined in ethanol; b) The compound is hydrolyzed during the recording of the spectrum; c) Calculated by interpolation following the data recorded in fig. 1.

the electron attracting effect exercised by the 2-acylamino group. That means that the contribution of the electron withdrawing effect of the 5-acetyl group to the

$$\Delta F = - RT \ln \frac{K_1}{K_2}$$

K_1 — ionization constants (Kb) of 2-acylamino-5-acetyl-thiazoles (**Va—c, e**)

K_2 — ionization constants of 2-acylamino-thiazoles (**Ia—d**)

stabilization of the mesomeric form B decreases as the electron attracting properties of the 2-acylamino group are increased.

In conclusion, the position of the tautomeric equilibrium of 2-acylamino-thiazoles, 2-acylamino-thiadiazoles and 2-acylamino-pyrimidines is largely dependent on the hydrogen ion concentration. Generally, in neutral and acid media the amido form a dominates. On the contrary, in alkaline medium, as a result of the formation of the sodium salts, the resonance stabilization of the imido mesomeric form B is preferred. However, the ultraviolet spectra indicate that 2-acylamino-pyridines did not form the corresponding sodium salts. The results support the assumption that the stability of the sodium salts of α-acylamino-N-heterocycles is determined not only by the presence of an acyl group with strong electron attracting properties, which enhances the elimination of the amidic proton, but also by a reasonable resonance stabilization of the exocyclic N=C bond. The intensity of the later effect increases in the order pyridines, pyrimidines, thiazoles and thiadiazoles. On the other hand, for the same heterocycle the resonance stabilization of the exocyclic N=C bond is enhanced for the derivatives which contain ring substituents with strong electron attracting properties.

EXPERIMENTAL

The compounds employed were partially synthesized as it has been previously described: **Ia**,[3] **Ib**[4], **Ic**,[5] **Id**, **e**, **IIa,d,e**[1], **IIIa**,[6] **IIIb**[7], **IIIc—e**,[1] **IVa,b**,[8] **Va**,[9] **Vb,c,e**,[10] **Vf**,[11] **Vg—h**, **VIa—e**.[12]

---

[3] V. Traumann, *Liebigs Ann. Chem.*, **249**, 36 (1888).

[4] K. A. Jensen and T. Thorsteisson, *Dansk Tiddsskr. Farm.*, **15**, 41 (1941).

[5] K. C. Kauer, (to Dow Chemical Co.), U. S. Pat. 2780631, 5 Feb. 1957; *Chem. Abstr.*, **51**, 10587e (1957).

[6] R. Camps, *Arch. Pharm.*, **240**, 349 (1902).

[7] A. E. Tschitschibabin and J. G. Bylinkin, *Ber. dtsch. chem. Ges.*, **55**, 998 (1922).

[8] F. D. Asplin, E. Boyland, S. Sargent and G. Wolf, *Proc. Roy. Soc.*, **B 139**, 358 (1952).

[9] P. M. Kocergin, *Zhur. obshchei. Khim.*, 26, 2897 (1956).

[10] D. Suciu, *Stud. Univ. Babeş-Bolyai, Chem.*, **15**, 123 (1970).

[11] D. Suciu, *J. prakt. Chem.*, **313**, 193 (1971).

[12] D. Suciu, *J. prakt. Chem.*, **314**, 961 (1972).

Compounds **IIb,c** and **Vd** were prepared by the treatment of the corresponding amines (0.01 mole) with the appropriate acylchloride (0.01 mole) in benzene (20 ml). The mixture was refluxed for 5–7 hours, then evaporated to dryness and the residue was triturated with a $NaHCO_3$ solution. The suspended material was filtered, dried and recrystallized from the suitable solvent. The analytical data of compounds **IIb,c** and **Vd** are found in table 4.

Table 4

Physical and analytical data of compounds IIb, c, IVc-e and Vd

Compound	Molecular formula	m.p°. (solvent)	Yield %	Nitrogen %	
				Calcd.	*Found*
IIb	$C_9H_7N_3OS$	208–209 Ethanol	65	20.46	20.32
IIc	$C_4H_4ClN_3OS$	178–180 Ethanol	47	28.18	27.95
IVc	$C_8H_{10}ClN_3O$	106 Ethanol	74	21.05	20.80
IVd	$C_8H_9Cl_2N_3O$	130 Acetone	81	17.94	18.11
IVe	$C_8H_8Cl_3N_3O$	86 Acetone	67	15.63	15.52
Vd	$C_8H_7Cl_3N_2O_2S$	179–181 Ethanol	83	9.29	9.44

The preparation of compounds **IVc–e** was achieved by the treatment of 2-amino-4,6-dimethylpyrimidine (0.01 mole) with the appropriate acylchloride (0.01 mole) and pyridine (0.01 mole) in chloroform (20 ml). The reaction mixture was heated for 5–10 min, then cooled and extracted 3 times with water. The chloroform layer was dried over Na_2SO_4, then evaporated to dryness and the residue was recrystallized from the suitable solvent. Table 4 includes the physical and analytical data of compounds **IVc–e**.

The ultraviolet spectra were recorded with a VSU-2P (Carl Zeiss-Jena) spectrophotometer.

The *pKa* values were determined with standard spectrophotometric technique in glycine–HCl and Na citrate-HCl buffer solutions and the ionization constants of the sodium salts of α-acylamino-N-heterocycles in glycine–NaOH, Na borate–HCl and phosphate buffer solutions. The *pKa* and *pKb* data represent mean values of 4 determinations carried out near the pH of equivalence (25°).

Revue Roumaine de Chimie, **19**, *4*, 679 – 687 (1974)

2-THIO-5-NITROBARBITURIC ACID

R. NUŢIU, I. SEBE and MARIA NUŢIU *

University of Timişoara, Department of Chemistry, Bd. V. Pîrvan 4, Romania

* The "Traian Vuia" Polytechnic Institute, Department of Organic Chemistry, Timişoara, Romania

Received March 20, 1973

The synthesis of a new compound, 2-thio-5-nitrobarbituric acid, and its characterization by infrared and ultraviolet spectroscopy as well as by thermogravimetric analysis are presented. The structure of the anhydrous acid is established as corresponding to 2-thio-6-keto-4-hydroxy-5-nitro-1,2,3,6-tetrahydropirimidine, while the trihydrate is 2-mercapto-4,6-diketo-hexahydropyrimidine-5-nitronic acid. The second ionization constant as determined by spectrophotometry is $pK_2 = 8.95$. The molecular formulae, thermal behaviour and solubility in water at 25° were established for the compounds of this acid, obtained by precipitation with the ions of alkaline and alkaline-earth metals. A method for potassium determination is given, consisting in the spectrophotometry of the solution obtained by dissolution of the potassium salt of this acid in alkaline medium.

In a previous work [1] we reported the synthesis of 2-thio-5-nitrobarbituric acid (ATNB) by condensation of diethylnitromalonate with thiourea, ATNB gives scarcely soluble compounds with the ions of alkaline and alkaline-earth metals, similarly to dilituric acid [2] (5-nitrobarbituric acid). ATNB, as well as its compounds with alkaline and alkaline earth metals, give an intense yellow colour in alkaline medium, enabling the spectrophotometric determination of these ions.

The aim of this note is to characterize ATNB and its compounds with the alkaline and alkaline-earth metal ions, as well as to elaborate a spectrophotometric method for the determination of potassium, as its ATNB compound has the lowest solubility among those of ATNB with alkaline metal ions.

[1] R. Nuţiu and I. Sebe, *Rev. Roumaine Chim.*, **16**, 919 (1971).

[2] a) H. Biltz and K. Sedlatscheek, *Chem. Ber.*, **57**, 339 (1924).
b) A. Berlin and R. Robinson, *Analyt. Chim. Acta*, **24**, 319 (1961).
c) I. G. Ishak, *Zavodskaya Lab.*, **29**, 1060 (1963).

EXPERIMENTAL

SYNTHESIS OF ATNB

In 100 ml flask with round bottom, provided with an ascending condenser, to which a tube containing calcium chloride is attached at the top, sodium ethoxide is prepared by gradually introducing 1.84 g (0.08 moles) metallic sodium through the condenser into 40–50 ml absolute ethyl alcohol. After the reaction of the metallic sodium is completed and the solution cooled to room temperature, 6.8 ml (0.04 moles) diethyl-nitromalonate and afterwards 3–3.2 g (0.05 moles) anhydrous thiourea are introduced with precaution, in small portions and under cooling. The mixture is then vigorously stirred and refluxed for 3.5–4 hours at 105–110°. After cooling, a gelatinous dirty-brown product results, to which drops of (1 :1) hydrochloric acid are added until a pH 6–6.5 is attained. The monosodium salt of ATNB precipitates at intense cooling (on ice) and is filtered in vacuum. ATNB sodium salt falls out as intensely yellow crystals from a water-alcohol (50 % vol) solution, after recrystallization and decolouration with charcoal.

The elementary analysis of the anhydrous sodium salt gave the following results :

Found : C, 22.88 ; H, 1.06 ; N, 20.22%

Calcd. : C, 22.75 ; H, 0.95 ; N, 19.90 %

Determination of crystallization water was performed by thermogravimetry. The thermogram (compound II) is given in figure 3.

The free acid, crystallized with three molecules of water, is obtained through the passing of an aqueous solution of the sodium salt, of about 1 %, over an ion exchanger (Amberlite IR–120) and concentration in vacuum of the solution obtained. The ATNB ($C_4H_3O_4N_3S.3H_2O$) thus obtained has the colour of sulphur, is soluble in water and alcohol and insoluble in the usual organic solvents. The anhydrous product ($C_4H_3O_4N_3S$) is obtained by dehydration of the crystalline acid in an Abderhalden apparatus, at 100° and is lemon-yellow with the same transformation (189–190°) and decomposition (193°) temperatures as the trihydrate.

While ATNB trihydrate undergoes a slow decomposition – it smells like hydrogen sulphyde – anhydrous ATNB is stable and can be stored for a long time.

The following results were obtained by the elementary analysis of anhydrous ATNB :

Found : S, 16.79 ; C, 25.70 ; H, 1.84 ; N, 22.26%

Calcd. : S, 16.93 ; C, 25.40 ; H, 1.60 ; N, 22.21 %

Determination of crystallization water was performed by thermogravimetric analysis ; the derivatogram of this compound, recorded on a "OD 102 – Paulik-Paulik-Erdely" type derivatograph, is given in fig. 1.

SPECTROPHOTOMETRIC DETERMINATIONS

Infrared spectrophotometry was performed on a Perkin-Elmer, type 457 Spectrophotometer. The samples were studied [3] as tablets in KBr (concentration 1–5 mg per 100 mg KBr) and in a nujol suspension, because anhydrous ATNB reacts with KBr during pastillation.

Ultraviolet spectrophotometric determinations [4] were performed on a Unicam SP-8000 Spectrophotometer, with a 5 mm quartz vat. The concentrations used were always 10^{-4} M in the solvents listed in table 2. The buffers used to determine the ionization constant were aqueous borax solutions the pH being also checked with an LPY-ol, USSR, model 1968, type pH-meter.

---

[3] H. Hoyer and E. Muller, "Infrarot spektroskopie", in "Methoden der Organischen Chemie. Physikalische Methoden", III. Bd., II. Teil, Thieme Verlag, Stuttgart, 1955, p. 820.

[4] C. N. R. Rao, "Ultraviolet and Visible Spectroscopy", London, Butterwoths, 1961.

Preparation and characterization of the alkaline and alkaline earth salts. For the precipitation of the alkaline and alkaline-earth salts, aqueous-alcoholic (50% vol) solutions of 2% ATNB were used, obtained by dissolution in warm water and dilution with alcohol. Chlorides or sulphates of the respective metals were employed. The molar precipitation ratio was 1.2 moles ATNB for one metal equivalent. After cooling the solution with the sediment to about 10°, the precipitate is filtered, washed with a 5–6 times diluted ATNB solution and then with alcohol and ether. The products are dried by prolonged aspiration at a water-jet pump.

The solubilities of the studied compounds were determined at 25°±0.1° by the method used of Berlin and Robinson,[5] which we also used in previous works.[6]

The thermograms were performed by means of a manufactured thermobalance with reading on a calibrated milivoltmeter, at a temperature increase rate of 5° per minute.

GRAVIMETRIC AND SPECTROPHOTOMETRIC DETERMINATION OF THE POTASSIUM ION

Gravimetric determination of the potassium ion by precipitation with ATNB was performed under the precipitation conditions described above. The spectrophotometric determinations were performed with a Spekol ZV type Cakl Zeiss Jena spectrophotometer, of the solutions obtained as described below:

In 5 centrifuge test tubes of about 10 ml, 0.5; 1.0; 2.0; 3.0 and 4.0 ml aqueous n/100 KCl solution were pipetted and 4 ml alcoholic-aqueous (about 75% vol) 0.5% ATNB solution were added to each test tube.

In another test tube the sample to be analysed is introduced with about the same molar potassium ion concentration and 4 ml ATNB solution are added. The walls of the test tube are rubbed with a suitable glass rod.

The test tubes are kept for 5–6 hours, or better overnight, in order to assure the completion of the precipitation. A temperature difference of ±3° does not influence the result. The test tubes are centrifugated at 5–6000 rotations per minute. The supernatant is decanted, the precipitate is washed two or three times with alcohol, stirred with the rod, and the interior walls of the test, on which crystal rests are observed, are washed.

After a last washing, centrifugation and separation of the alcohol used for washing, 5 ml KOH 10% is added to each test tube and the dissolution of the precipitate is ascertained by vigorous stirring with the rod. The solutions thus obtained, of intense yellow colour, are passed quantitatively, by washing with distilled water, into 100 ml marked flasks.

In another marked flask, 5 ml KOH 10% are added and completed with water up to the sign; this solution is used for comparison, respectively compensation.

The solutions thus obtained are spectrophotometrated by reading the extinctions at 410 or 420 nm, using 5 mm vats. The results are recorded as a plot of extinction (E) or extinction module (E_d) *vs.* the potassium ion concentration. The spectrophotometration of the solutions can be performed within two hours, during which the extinction remains constant.

---

[5] A. Berlin and R. Robinson, *Analyt. Chim. Acta*, **24**, 319 (1961).

[6] Fr. Mihai and R. Nuţiu, *Rev. Roumaine Chim.*, **15**, 573 (1970).

EXPERIMENTAL RESULTS AND DISCUSSIONS

STRUCTURE AND PROPERTIES OF ATNB

The derivatogram of ATNB (figure 1), indicates that the three water molecules are eliminated in two steps ; the first two molecules in the 25°—70° interval and the third in the 75°—98° interval. We conclude from these facts that the first two water molecules are network water, while the third seems to be included in the structure of the ATNB, the activation energy for the second step being of 23 kcal/mol (as determined according to the mehod of Freeman and Caroll [7]). Following the derivatogram at higher temperatures, it results that ATNB is stable until 150°, when decomposition begins, and becomes explosive at 175° ; the exothermicity of this process is apparent also on the DTA curve. The decomposition is completed at about 500°.

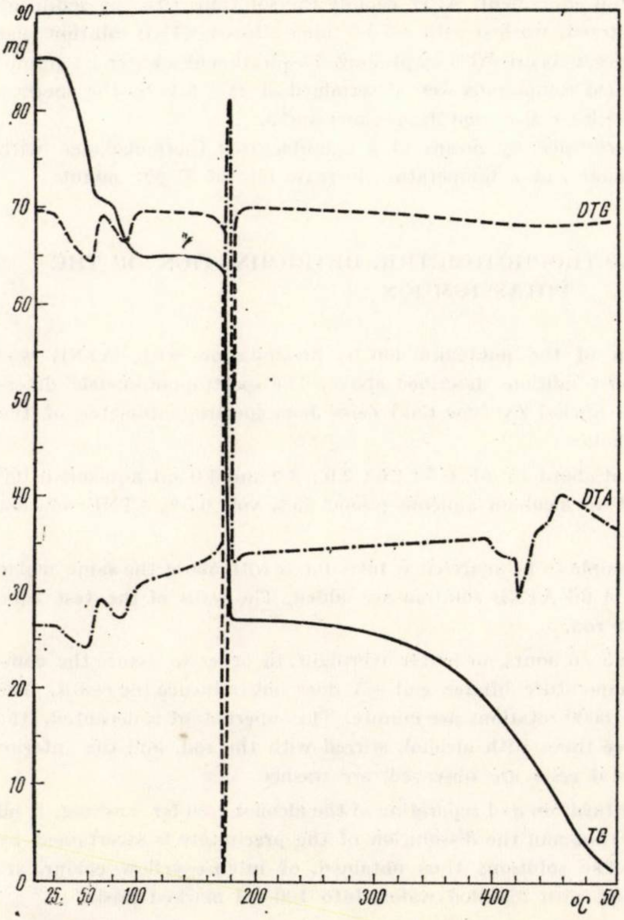

Fig. 1. —ATNB-derivatogram.

---

[7] E. S. Freeman and B. Carrol, *J. Phys. Chem.*, **62**, 394 (1958).

Table 1 gives the infrared absorption maxima recorded in the spectra of anhydrous ATNB, of the monohydrate and the sodium salt respectively. The spectrum of the trihydrate differs from that of the monohydrate only by a broad absorption of mean intensity at 3400–3550 cm^{-1}.

Table 1

Absorption maxima recorded in infrared spectra, in cm^{-1}

ATNB anhydrous (in nujol mulls)	ATNB. H_2O (in KBr pellet)	ATNBNa.H_2O (in KBr pellet)
	3420–40 m, b	3450–70 m, b
3115–25 m, b	3100–10 i, b	3110–20 i, b
	3060 i, s	3065–80 i, s
2960 i, s		
2930 i	2920 i	2920 i
2860 i		
	2595 w, sh	2590 w
1560–85 m, b,	1645–80 i, b	1640–80 i, b
	1560 m	1570 m
1460–70 i	1430 m	1480 m
		1435 m
1380 m	1378 i	1380–90 i, b
1345 m		
1295 w	1292–98 i	1290–1310 i, b
1270 w	1260 m, sh	1270 m, s
1160–70 i	1190 i	1195 i
	1110 w	1100 w
	1095 w	
	1020 w	1020 w
800–10 m, s	820 m	870 m
		820 m
788–90 i	790 m	
720 m	740 w	740 w

i = intense; m = medium; w = weak; b = broad; s = shoulder; sh = sharp.

Comparing the absorption maxima given in table 1 with the infrared spectrum and its interpretation for dilituric acid, [8] we conclude that anhydrous ATNB exists as 2-thio-6-keto-4-hydroxy-5-nitro-1,2,3,6-tetrahydropyrimidine. This conclusion is based on the absorption at 1600 cm^{-1}, characteristic for the double carbon-carbon bond [9] and at 1345 cm^{-1} and respectively 1560–85 cm^{-1}, characteristic for the symmetric and respectively asymmetric valence vibration of the nitro group. [10] The strong absorption at 1670–80 cm^{-1} which does not appear in the IR-spectrum of 5-nitro-5-ethyl-barbituric acid is attributed to the thio group, respectively to the α,β-unsaturated carbonyl.[11] The thioamidic group may be responsible [12, 13] also for the absorption at 1295 cm^{-1}. The absorption for the hydroxylic group appears at very low values, as for the dilituric acid, because of the probably intramolecular association of the hydroxyl group, with the nitro group. The intense band at 1292–98 cm^{-1}, accompanied by a medium band at 1260 cm^{-1}, which appears for hydrate ATNB, suggests that this compound is in the aci-nitro form, as these bands are characteristic for the aci-nitro ion [14] ($=NOO^-$).

---

[8] a) FR. MIHAI and R. NUȚIU, *Rev. Roumaine Chim.*, **13**, 39 (1968).
b) R. NUȚIU and Z. SIMON, *Rev. Roumaine Chim.*, **14**, 311 (1969).

[9] a) S. F. MASSON, *J. Chem. Soc.*, **1957**, 4874.
b) E. SPINNER, *J. Chem. Soc.*, **1960**, 1232.

[10] a) M. AVRAM and GH. D. MATEESCU, "Spectroscopia în infraroșu-Aplicații în chimia organică", Ed. tehnică, Bucharest, 1966, p. 369.
b) L. N. SHORT and H. W. THOMPSON, *J. Chem. Soc.*, **1952**, 168.

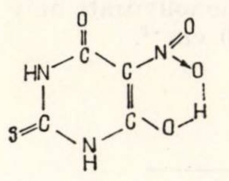

Absorption recorded at 1560 cm^{-1} is attributed to vibrations of the pyrimidinic cycle,[8] as well as the one at 1378 cm^{-1}; both are found also for other pyrimidines (for ethylbarbituric acid, as an example). A weak and narrow band is recorded at 2595 cm^{-1} for the hydrated compound which can be attributed only to the mercapto group (–SH).[13] The broad absorption at 1645–80 cm^{-1} may include the carbonyl valencevibration and also the one for the carbon-nitrogen double bond ($C=N$)[15] of the aci-nitro form. We conclude, thus, that the hydrated ATNB exists as 2-mercapto-4,6-diketo-1,4,5,6-tetrahydropyrimidine-5-nitronic acid, probably the anion associated with a hydroxonium cation. The high activation energy (23 kcal/mol) for the elimination of the last water molecule also favours this interpretation.

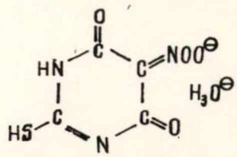

The sodium compound of ATNB has a similar spectrum with that of ATNB trihydrate and might thus be a salt of this nitronic acid.

The ultraviolet spectra of ATNB are given in table 2. They contain bands characteristic for π-π* transitions. The K bands at 208 and 217 nm may be attributed to the NO_2 chromophor in the monoanion and the B bands at 337 and 357 nm to the dianion corresponding, assumedly, to the dissociation of the mercapto group (–SH). The isosbestic point at 348.5 nm ($\varepsilon = 14000$) is recorded in this region and used for the determination of the second ionization constant. The value of this constant, $K_2 = 1.12 \times 10^{-9}$, established from spectrophotometric titration, is much higher than that for dilituric acid [16] ($K_2 = 5.6 \times 10^{-11}$).

According to our potentiometric and colorimetric evaluations, the first ionization constant is similar to that of hydrochloric acid.

---

[11] L. J. BELLAMY, "Infrared Spectra of Complex Molecules", London, Methuen Co., 1959, p. 136.

[12] M. AVRAM and Gh. D. MATEESCU, "Spectroscopia în infraroşu-Aplicaţii în chimia organică", Ed. tehnică, Bucharest, 1966, p. 356.

[13] K. NAKANISHI, "Infrared Absorption Spectroscopy", Nankodo Company Limited, Tokyo, 1962, p. 54.

[14] N. JONATHAN, *J. Mol. Spectroscopy*, **7**, 105 (1961).

[15] a) J. F. BROWN, *J. Amer. Chem. Soc.*, **77**, 6341 (1955).
b) Z. BUCKOWSKY and T. URBANSKI, *Spectrochim. Acta*, **18**, 1187 (1962).

[16] M. E. TAYLOR and R. J. ROBINSON, *Talanta*, **8**, 518 (1961).

Table 2

Absorption maxima recorded in ultraviolet spectra

Solvent	Absorption					
	λ_{max}	ε_{max}	λ_{max}	ε_{max}	λ_{max}	ε_{max}
H_2O	208	19200	271	7600	337	16800
HCl N/10	208	19000	271	7500	337	16750
NaOH N/10	217	19900	243– 248 288	8100– 8000 5440	354	14200

These spectra demonstrate also a bathochromic effect, when ATNB is solved in alkaline solutions, a fact which we used for quantitative spectrophotometric evaluations.

SALTS WITH ALKALINE AND ALKALINE-EARTH IONS

Table 3 gives the combinations of ATNB with the ions of the alkaline and alkaline-earth ions, while figures 2 and 3 the thermograms of these ions. The solubilities of these compounds decrease from lithium to potassium and from magnesium to barium. The thermal stabilities of these salts are higher than that of ATNB, except for the calcium salt. A gravimetric determination of potassium, rubidium and cesium with ATNB is possible (in the conditions described in a previous paragraph) with errors below ± 2.5%.

Table 3

Results of nitrogen elementary analysis, water solubility at 25° and decomposition temperatures for the salts of ATNB with alkaline and alkaline-earth ions

N°	Compound Molec. form.	Nitrogen %		Solubility 25°±0.1° mmol/l	Temp. of decomposition (from thermogravimetric data)
		Calcd.	*Found*		
I	$C_4H_2O_4N_3SLi.4H_2O$	15.70	15.48	highly soluble	170°
II	$C_4H_2O_4N_3SNa.H_2O$	18.40	18.25	51.70	265°
III	$C_4H_2O_4N_3SK$	18.45	18.67	3.12	285°
IV	$C_4H_2O_4N_3SRb$	15.40	15.35	4.72	275°
V	$C_4H_2O_4N_3SCs$	13.08	13.00	7.20	285°
VI	$(C_4H_2O_4N_3S)_2Mg.4H_2O$	17.79	17.68	21.70	230°
VII	$(C_4H_2O_4N_3S)_2Ca.3.5\,H_2O$	17.52	17.30	14.73	120°; 210°
VIII	$(C_4H_2O_4N_3S)_2Sr.3H_2O$	16.23	15.95	8.95	175°; 250°
IX	$(C_4H_2O_4N_3S)_2Ba.H_2O$	15.75	15.89	2.49	265°

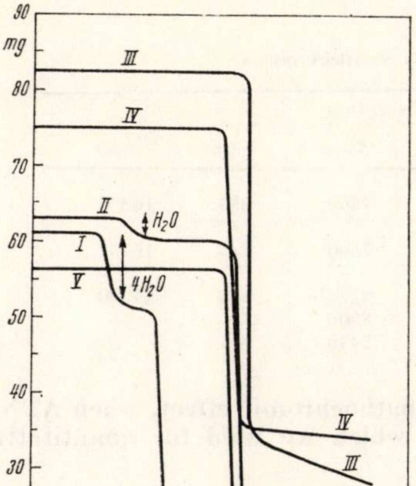

Fig. 2. — Thermogravimetric curves of compounds (I)–(V).

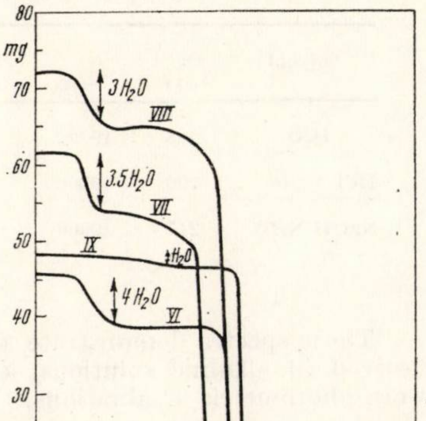

Fig. 3. — Thermogravimetric curves of compounds (VI)–(IX).

ATNB and its metal salts studied are solved in strongly basic solutions, with an intense yellow colour which respects the Lambert-Beer law up to a concentration of $4 \cdot 10^{-5}$ M. A spectrophotometric dosage of these ions is thus possible.

SPECTROPHOTOMETRIC DETERMINATION OF THE POTASSIUM ION

The determination of potassium with ATNB, under the conditions described in this paper, has the advantage of a spectrophotometry in the visible range of a solution obtained by solving the precipitated potassium salt of ATNB in basic solutions which have an intense yellow colour. The determination of potassium with ATNB is disturbed by the other ions of alkaline metals, within the solubility limits given in table 3.

Figure 4 gives the calibration curve at 410 and 420 nm for our method. The errors for the determinations performed by us were below ±0.8%.

We would like to specify that all compounds of ATNB with a solubility below 10 mmol/l can be determined by this spectrophotometric method.

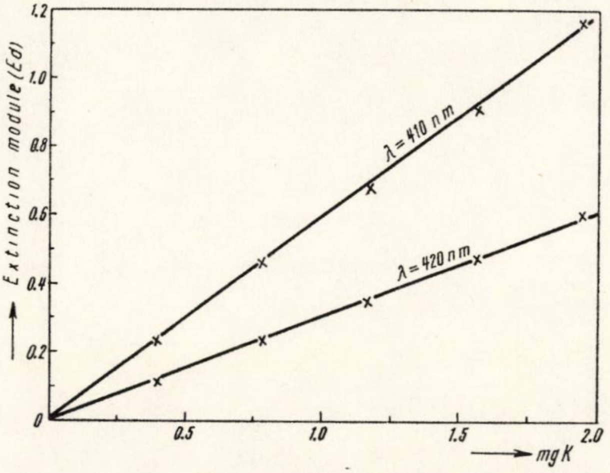

Fig. 4. – Calibration spectrophotometric curves for the determination of potassium ion with ATNB.

Revue Roumaine de Chimie, **19**, *4*, 689–699 (1974)

PEPTIDES. XV [1]

THE USE OF β-DICARBONYL N-PROTECTED ASPARAGINE AND GLUTAMINE IN PEPTIDE SYNTHESIS

A. BALOG*, E. VARGHA**, D. BREAZU*, F. GÖNCZY*, and LUCIA BEU*

* Institute for Chemical and Pharmaceutical Research, str. Fabricii 126, Cluj, Romania

** The Department of Organic Chemistry, Babeş-Bolyai University, Str. Arany J. 11, Cluj, Romania

Received May 8, 1973

The potassium and dicyclohexylammonium salts I—VIII of asparagine and glutamine were prepared using for α-amino protection the AE, CP, AC and BA*** groups. These salts were converted readily into the corresponding phenacyl and *p*-nitrobenzyl esters (IX—XIX). After removal of the amino protecting groups in acidic medium, the asparagine and glutamine ester hydrochlorides or hydrobromides (XX—XXIII) were obtained in good yields. The dipeptide esters involving N-terminal or C-terminal asparagine and glutamine respectively (XXIV—XXX), were synthesized *via* the mixed anhydride method.

The investigations which have been developed in peptide synthesis, involving asparagine or glutamine, showed that the peptide-bond formation is accompanied by several side reactions.[2] Thus, dehydration or hydrolysis of the ω-amidic group, appearance of isoasparagine and isoglutamine derivatives [2] as well as formation of N-substituted α-glutarimides [3,4] and pyroglutamic acid derivatives, [5] respectively, were observed.

*** The abbreviations used in this paper are the followings : AE = 1-ethoxycarbonyl propen-2-yl ; CP = 2-ethoxycarbonyl-cyclopenten-1-yl ; AC = 1-acetyl-propen-2-yl ; BA = = 1-benzoyl-propen-2-yl ; DCHA = dicyclohexylamine ; THF = tetrahydrofuran ; AcOEt = = ethyl acetate ; DMF = dimethylformamide ; EtOH = ethanol ; MeOH = methanol ; TEA = = triethylamine.

The symbols used for amino acid derivatives correspond to the recommendations of IUPAC-IUB Commission on Biochemical Nomenclature (1971), *J. Biol. Chem.*, **247**, 977 (1972).

[1] Previous paper : E. Vargha, A. Balog, F. Gönczy, D. Breazu and L. Beu, *Rev. Roumaine Chim.*, 18, 1627 (1973).

[2] E. Schröder and K. Lübke, "The Peptides", vol. 1, Academic Press, New York — London, 1965, p. 110, 191, 202—204.

[3] E. Zahn and Th. J. Fölsche, *Chem. Ber.*, **102**, 2158 (1969).

[4] Ch. Meyers, R. T. Hauran, J. L. Schwartz and L. Walter, *Chem. and Ind.*, **1969**, 136.

[5] E. Schnabel, H. Kostermeyer, J. Dahlmans and H. Zahn, *Liebigs Ann. Chem.*, **707**, 232 (1967).

To avoid these undesired reactions new N-protecting groups were introduced in the ω-amide residue.[6] Of course this procedure increased the steps of synthesis and at the same time decreased the solubility of N-substituted derivatives of the amides in the usually employed solvents for peptide synthesis.

Owing to the promising results obtained by us in the peptide synthesis involving bifunctional amino acids [7,8] as well as several trifunctional amino acids,[9,10] using for the protection of the α-amino group β-dicarbonyl compounds, we have also extended this method to the asparagine and glutamine series.

A. *The protection of α-amino group*. Among the β-dicarbonyl compounds the benzoylacetone was used at first for the α-N-protection of asparagine and glutamine (Southard and co-workers, 1971).[11] The N-protected derivatives IVb and VIII, respectively, were isolated as dicyclohexylammonium salts only without using them for peptide synthesis. Before the publication of Southard's paper, we embarked our investigation on the α-amino protection of asparagine and glutamine, using for this purpose ethyl acetoacetate, 2-ethoxycarbonyl cyclopentanone, acetylacetone and benzoylacetone.

According to the earlier elaborated method,[7] about 8–10% excess of the amino acid and about 30% excess of the β-dicarbonyl compound were added to a solution of methanolic potassium hydroxide or dicyclohexylamine, respectively. The mixture is then refluxed until the most part of the amino acid is dissolved. Working up as usual, the potassium and dicyclohexylammonium salts were obtained with over 70% yields. The scheme below shows, that only one potassium salt was isolated in the glutamine series (Va). It is to be remarked that, by treating the potassium salt Va with dicyclohexylammonium bromide, the corresponding dicyclohexylammonium salt Vb was obtained in a higher purity than by direct synthesis.

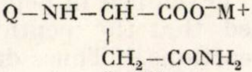

$$Q-NH-\underset{\displaystyle CH_2-CONH_2}{\underset{|}{CH}}-COO^-M^+$$

I–IV

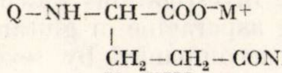

$$Q-NH-\underset{\displaystyle CH_2-CH_2-CONH_2}{\underset{|}{CH}}-COO^-M^+$$

V–VIII

	Q	M		Q	M
I	AE	K	Va	AE	K
II	CP	DCHA·H	Vb	AE	DCHA·H
IIIa	AC	K	VI	CP	DCHA·H
IIIb	AC	DCHA·H	VII	AC	DCHA·H
IVa	BA	K	VIII	BA	DCHA·H
IVb	BA	DCHA·H			

---

[6] W. König and R. Geiger, *Chem. Ber.*, **103**, 2034 (1970).

[7] A. Balog, D. Breazu, E. Vargha, F. Gönczy and L. Beu *Rev. Roumaine Chim.*, **15**, 1375 (1970).

[8] A. Balog, E. Vargha, D. Breazu, L. Beu and F. Gönczy, *Rev. Roumaine Chim.*, **15**, 1391 (1970).

[9] C. Daicoviciu, A. Balog, D. Breazu, L. Beu and F. Gönczy, *Rev. Roumaine Chim.*, **16**, 751 (1971).

[10] A. Balog, D. Breazu, C. Daicoviciu, E. Vargha, L. Beu and F. Gönczy, *Rev. Roumaine Chim.*, **16**, 1601 (1971).

[11] G. L. Southard, G S. Brooke and J. M. Pettee, *Tetrahedron*, **27**, 1359 (1971).

Our attempts to obtain from asparagine the potassium salt, using 2-ethoxycarbonyl cyclopentanone for N-protection, or dicyclohexylammonium salt by protecting with ethyl acetoacetate, failed.

The dicyclohexylammonium salt of the β-dicarbonyl N-protected asparagine and glutamine are in general fairly soluble in organic solvents used for peptide syntheses (THF, AcOEt, DMF, dioxan). These salts (I—VIII) are suitable starting materials both for the protection as well as for the activation of the α-carboxyl group.

B. *Preparation of phenacyl and p-nitro-benzyl esters.* The phenacyl and *p*-nitrobenzyl group, frequently used for the protection of amino acid carboxyl, can be easily introduced into N-protected asparagine and glutamine. Thus, the potassium or dicyclohexylammonium salts I—VIII were treated in acetone and dimethylformamide solution with phenacyl bromide or *p*-nitrobenzyl bromide. The reaction takes place according to equation (1), either at room temperature, or at the boiling point of the solvent mixture (about 80°).

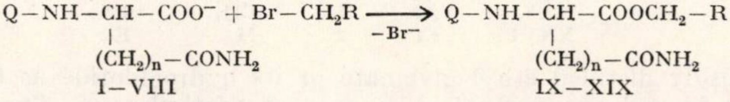

$$\underset{\text{I}-\text{VIII}}{Q-NH-\underset{\underset{\displaystyle (CH_2)_n-CONH_2}{|}}{CH}-COO^-} + Br-CH_2R \xrightarrow[-Br^-]{} \underset{\text{IX}-\text{XIX}}{Q-NH-\underset{\underset{\displaystyle (CH_2)_n-CONH_2}{|}}{CH}-COOCH_2-R} \qquad (1)$$

	Q	R	n		Q	R	n
IX	AE	COC_6H_5	1	XIV	AE	$C_6H_4NO_2(p)$	1
X	CP	,,	1	XV	CP		1
XI	BA	,,	1	XVI	AC	,,	1
XII	AE	,,	2	XVII	BA		1
XIII	CP	,,	2	XVIII	AE	,,	2
				XIX	CP	,,	2

The removal of the N-protecting groups was carried out conveniently in an adequate solvent at room temperature, by acidification to pH 2.5—2 with hydrogen chloride in ethanol, or hydrogen bromide in water or anhydrous acetic acid :

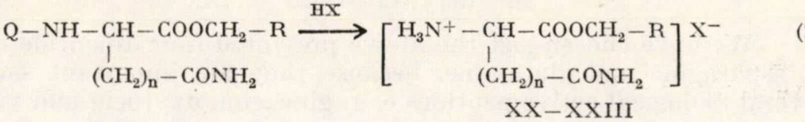

$$Q-NH-\underset{\underset{\displaystyle (CH_2)_n-CONH_2}{|}}{CH}-COOCH_2-R \xrightarrow{HX} \underset{\text{XX}-\text{XXIII}}{\left[H_3N^+-\underset{\underset{\displaystyle (CH_2)_n-CONH_2}{|}}{CH}-COOCH_2-R\right]X^-} \qquad (2)$$

	X	R	n		X	R	n
XXa	Cl	COC_6H_5	1	XXIIa	Cl	$C_6H_4NO_2(p)$	1
XXb	Br	,,	1	XXIIb	Br	,,	1
XXI	Br	,,	2	XXIII	Br	,,	2

The phenacyl esters XX—XXI and *p*-nitrobenzyl esters XXII—XXIII were isolated as hydrochlorides (a) or hydrobromides (b) and, as usual, crystallized relatively easily from anhydrous ethanol-ether.

C. *Peptide bond formation.* For the preparation of asparaginyl and glutaminyl peptides only those methods are promising, which avoid the undesired side reactions due to the ω-carbonyl group. Thus, satisfactory results were obtained by applying the mixed anhydride [2] and *p*-nitrophenyl ester method,[2] or more recently the N-carboxy anhydride one.[12]

We have found, that the potassium and dicyclohexylammonium salts I–VIII are adequate starting materials for the synthesis of both asparaginyl and glutaminyl peptides by using for mixed anhydride formation ethyl chloroformate, pivaloyl or benzoyl chloride and a catalytical amount of N-methyl morpholine. Starting from the dicyclohexylammonium salts, the mixed anhydride solution was filtered to eliminate the insoluble dicyclohexylammonium chloride. The coupling was carried out

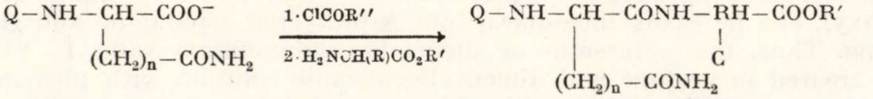

$$\underset{\substack{|\\(CH_2)_n-CONH_2}}{Q-NH-CH-COO^-}\xrightarrow[2\cdot H_2NCH(R)CO_2R']{1\cdot ClCOR''}Q-NH-\underset{\substack{|\\(CH_2)_n-CONH_2}}{CH}-CONH-\underset{\substack{|\\C}}{RH}-COOR' \quad (3)$$

XXIV–XXVI

	Q	n	R	R′
XXIV	CP	1	H	Et
XXV	AE	1	CH_3	PAc
XXVI	CP	2	H	Et

with freshly distilled ethyl glycinate or its hydrochloride as C-terminal amino acid and one equivalent amount of triethylamine. The dipeptide esters were isolated according to the general method proposed by us,[7, 8, 10] treating the reaction mixture with saturated sodium hydrogen carbonate solution and evaporating the organic solvents under reduced pressure.

For the synthesis of peptides with C-terminal asparagine and glutamine, their phenacyl or *p*-nitrobenzyl esters were used. Thus, the N-protected dipeptide esters XXVII–XXX were obtained in good yields (over 80%) by means of the mixed anhydride method :

AE–ALa–Asn–ONBzl	(XXVII)
AE–Ala–Gln–ONBzl	(XXVIII)
CP–Gln–Asn–OPAc	(XXIX)
CP–Gln–Asn–ONBzl	(XXX)

We have chosen just the above presented four dipeptide derivatives of asparagine and glutamine, because they are important sequences in several biological active peptides e. g. glucagon, oxytocin and vasopressin.

EXPERIMENTAL

Melting points were taken in capillary tubes and are uncorrected. The analyticasamples were dried *in vacuo* over P_2O_5 for 3–4 hours at 64° and 16–30 torr. Optical rotations were measured with a Metra 400/a Prague polarimeter. Infrared spectra were determined on a Carl Zeiss UR–10 spectrophotometer and the UV-spectra on a Zeiss VSU–1 model in methanol. Yields were calculated on the weight of vacuum dried (over P_2O_5 and KOH) substances.

---

[12] R. Hirschmann, H. Schwam, R. G. Strachan, E. F. Schoenewaldt, H. Barkemeyer, S. M. Miller, J. B. Conn, V. Garsky, D. F. Veber and R. G. Denkewaltel, *J. Amer. Chem. Soc.*, **93**, 2746 (1971).

A. SALT FORMATION *

N-(1-Ethoxycarbonyl-propen-2-yl)-L-asparagine potassium salt (*AE-Asn-O$^-$K$^+$, I*). 15 g (0.1 mol) L-asparagine monohydrate in 68 ml of methanolic potassium hydroxide of 7.84 g/100 ml concentration (0.095 mol) was treated with a solution of 14 ml ethyl acetoacetate in 30 ml methanol. The reaction mixture was heated on the steam bath for 1 hr and filtered off (0.9 g unreacted amino acid). The clear solution was concentrated *in vacuo* and dried by addition of benzene (4 × 50 ml) and distilled azeotropically. The remaining solid was treated with petroleum ether, filtered and washed with light petroleum, dried in desiccator. Yield 25 g (94%); mp. 175–176° (decomp.); $[\alpha]_D^{21}$: +45.2° (c = 0.97, methanol).

Found: N, 9.72; K, 13.70

Calcd. for $C_{10}H_{15}KN_2O_5$: N, 9.92; K, 13.85

N-(2-Ethoxycarbonyl-cyclopenten-1-yl)-L-asparagine dicyclohexylammonium salt (*CP-Asn-O$^-$DCHA.H$^+$, II*). A mixture of 3 g (20 mmoles) L-asparagine, 4 ml (25 mmoles) of 2-ethoxycarbonyl-cyclopentanone in 50 ml methanol was treated with freshly distilled dicyclohexylamine (4.4 ml, 22 mmoles) on a steam bath for 5 hr and filtered while hot, to remove any unreacted amino acid (0.8 g). The filtrate was concentrated *in vacuo* and the residue evaporated three times to dryness *in vacuo* by adding three portions of benzene (50 ml). The remaining yellow oil was treated with 100 ml anhydrous ether. After standing for 24 hours the crystals were collected. Yield 6.4 g (71%); mp. 148–150°; $[\alpha]_D^{22}$: +11.2° (c = 1.02, methanol).

UV : λ_{max} 295 nm ($\log \varepsilon = 4.25$)
IR : ν_{NH} 3050; ν_{CO} 1710, 1690; ν_{COO^-} 1570; δ_{NH} 1650, 1370 cm^{-1}
Found: C, 63.80; H, 9.68; N, 9.12;
Calcd. for $C_{24}H_{41}N_3O_5$: C, 63.83; H, 9.15; N, 9.30)

N-(1-Acetylpropen-2-yl)-L-asparagine potassium salt (*AC-Asn-O$^-$K$^+$, IIIa*). 10.4 ml (0.1 mol) acetylacetone and 78 ml methanolic potassium hydroxide of 7.2 g/100 ml concentration (0.1 mol) was added to 16.5 g (0.11 mol) of asparagine suspended in 10 ml methanol and refluxed for one hour, filtered while hot (0.8 g unreacted asparagine) and the filtrate was concentrated *in vacuo*. The solid residue was dried by the addition of benzene (3×50 ml) followed by evaporation *in vacuo*. After trituration with petroleum ether and recrystallization from anhydrous ethanol, it yielded 11.5 g (45%); m.p. 185° (decomp.); $[\alpha]_D^{21}$: +82.3° (c = 1.02, methanol).

UV : λ_{max} 315 nm ($\log \varepsilon = 4.24$)
IR : ν_{NH} 3275; ν_{CO} 1670; ν_{COO^-} 1570; δ_{NH} 1684, 1395 cm^{-1}
Found: N, 10.60; K, 14.90
Calcd. for $C_9H_{13}KN_2O_4$: N, 11.10; K, 15.53

N-(1-Acetylpropen-2-yl)-L-asparagine dicyclohexylammonium salt (*AC-Asn-O$^-$DCHA·H$^+$ IIIb*). To 14.5 g (96.5 mmoles) of L-asparagine monohydrate suspended in 10 ml water was added a solution of 18.9 ml (96 mmoles) of dicyclohexylamine in 80 ml methanol, followed by the addition of a hot solution of 10 ml (96 mmoles) acetylacetone in 80 ml ethanol. The mixture was refluxed for 3 hours and filtered while hot, to remove any unreacted L-asparagine. The filtrate was concentrated *in vacuo* and the residue was dried by azeotropic distillations with two 100 ml portions of propanol-2 and 100 ml of benzene, respectively. The isolated crystalline product was recrystallized from methylene chloride (75 ml) and ether (125 ml). Yield 24 g (63.5%) ;mp. 148–149°; $[\alpha]_D^{27}$: +35° ($c = 1.32$, methanol).

---

* Yields calculated on the reacted asparagine and glutamine, respectively.

Found: C, 63.22; H, 9.82; N, 10.82

Calcd. for $C_{21}H_{37}N_3O_4$: C, 63.77; H, 9.43; N, 10.62

N-(1-Benzoylpropen-2-yl)-L-asparagine potassium salt (*BA-Asn-O⁻K⁺, IV*). 8.5 g (56.5 mmoles) L-asparagine monohydrate and 8.1 g (50 mmoles) benzoylacetone in 15 ml methanol was refluxed on the steam bath for 3 hours after treating with 35 ml methanolic potassium hydroxide solution of 8 g/100 ml concentration (50 mmoles). Filtered while hot (0.9 g unreacted amino acid), the filtrate was concentrated *in vacuo* and the residue was dried by azeotropic distillations with three 50 ml portions of benzene. The solid residue was suspended in anhydrous ether with stirring, filtrated and washed three times with ether. Yield 15.5 g (85%); m.p. 212°. Recrystallization from ethanol (120 ml) gave 9.8 g (62%) needles of m.p. 222° (decomp.); $[\alpha]_D^{22}$: +73.9° ($c = 1$, methanol).

UV: λ_{max} 346 nm ($\log \varepsilon = 4.22$), 235 nm ($\log \varepsilon = 3.86$)
IR: ν_{NH} 3200; ν_{CO} 1680; ν_{COO^-} 1540; δ_{NH} 1635, 1380 cm^{-1}
Found: N, 8.81; K, 12.75
Calcd. for $C_{14}H_{15}KN_2O_4$: N, 8.91; K, 12.43

N-(1-Ethoxycarbonyl-propen-2-yl)-L-glutamine potassium salt (*AE-Gln-O⁻K⁺, Va*). 40 mmoles of L-glutamine were worked up in the usual manner as described by AE-Asn- O⁻K⁺ (I). Yield 8.9 g (75%); m.p. 145–147°; $[\alpha]_D^{22}$: +13.5° ($c = 1$, methanol).

Found: N, 9.28; K, 13.70
Calcd. for $C_{11}H_{17}KN_2O_5$: N, 9.45; K, 13.26

N-(1-Ethoxycarbonyl-propen-2-yl)-L-glutamine dicyclohexylammonium salt (*AE-Gln-O⁻ DCHA·H⁺, Vb*). To a mixture of 8.8 g (60 mmoles)finely powdered L-glutamine and 9 ml (71 mmoles) ethyl acetoacetate in 100 ml methanol heated to reflux, 12 ml (60 mmoles) freshly distilled dicyclohexylamine in 20 ml methanol were added from a dropping funnel during a period of 25 minutes. Heating was continued for 5 hours and the unreacted glutamine (1.7 g) was removed by filtration and the filtrate worked up in the usual manner as described by the CP-Asn-O⁻DCHA·H⁺ (II). Yield 21 g (79.6%); mp. 154–155° (methanol-ether); $[\alpha]_D^{23}$: +11.5° ($c = 1$, methanol).

Found: C, 62.86; H, 9.88; N, 9.54
Calcd. for $C_{23}H_{41}N_3O_5$: C, 62.84 ;H, 9.40; N, 9.55

N-(2-Ethoxycarbonyl-cyclopenten-1-yl)-L-glutamine dicyclohexylammonium salt (*CP-Gln O⁻DCHA·H⁺, VI*). It was prepared as described before from 5 g (34 mmoles) L-glutamine, 6.2 ml (42 mmoles) 2-ethoxycarbonyl-cyclopentanone and 7 ml (35 mmoles) dicyclohexylamine in 100 ml methanol, after refluxing for 15 hours. Yield 12.5 g (79%); m.p. 143–154°. After recrystallization from ethyl acetate, 2 g yielded 1.05 g salt of m.p. 155–156°; $[\alpha]_D^{23}$: +6.4° ($c = 1$, methanol).

UV: λ_{max} 300 nm ($\log \varepsilon = 4.14$)
IR: ν_{NH} 3156; ν_{CO} 1665; ν_{COO^-} 1575; δ_{NH} 1635, 1380 cm^{-1}
Found: C, 64.30; H, 9.43; N, 9.08
Calcd. for $C_{25}H_{43}N_3O_5$: C, 64.48; H, 9.23; N, 9.03

N-(1-Acetylpropen-2-yl)-L-glutamine dicyclohexylammonium salt (*AC-Gln-O⁻DCHA·H⁺, VII*). 1.1 g (7.5 mmoles) L-glutamine, 1 ml (10 mmoles) acetylacetone and 1.5 ml (7.5 mmoles) dicyclohexylamine in 40 ml of methanol were refluxed for 5 hours and filtered. The filtrate was worked up in the usual manner as decribed before. Yield 2.5 g (81 %); m.p. 144–146°; $[\alpha]_D^{23}$: +32.3° (c = 1, methanol). Recrystallized from acetone, m.p. 147–148°; $[\alpha]_D^{23}$ +35.4° (c = = 1, methanol).

Found: C, 64.28; H, 9.83; N, 10.35
Calcd. for $C_{22}H_{39}N_3O_4$: C, 64.51; H, 9.59; N, 10.25

N-(1-Benzoylpropen-2-yl)-L-glutamine dicyclohexylammonium salt (*BA-Gln-O$^-$DCHA·H$^+$, VIII*). 1.5 g (10 mmoles) L-glutamine, 1.7 g (11 mmoles) benzocylacetone and 2 ml (10 mmoles) dicyclohexylamine in 50 ml ethanol were refluxed for 11 hours and filtered off (0.3 g unreacted glutamine). The filtrate was concentrated in the usual manner yielding 4.1 g crystals (87.2 %). After recrystallization from anhydrous ethanol m.p. 157–158°; $[\alpha]_D^{25}$: 35.0° (c = = 0.97, methanol), +48.6° (c = 2, ethanol). Lit[11]. m.p. 163–165°; $[\alpha]_D^{25}$: +48.05° (c = 2, ethanol).

Found: C, 68.35; H, 9.06; N, 8.80
Calcd. for $C_{27}H_{41}N_3O_4$: C, 68,75; H, 8.76; N, 8.90)

B. PHENACYL AND *p*-NITROBENZYL ESTERS

N-(1-Ethoxycarbonyl-propen-2-yl)-L-asparagine phenacyl ester (*AE-Asn-OPAc, IX*). A mixture of 2.8 g (10 mmoles) AE-Asn-O$^-$K$^+$ (I) and 2 g (10 mmoles, ω-bromacetophenone in 40 ml acetone and 10 ml dimethylformamide was refluxed on the steam bath for 2 hours and diluted with 500 ml water. The filtered and washed crystalline precipitate was dried in desiccator over $CaCl_2$ and P_2O_5. Yield 3 g (83 %); m.p. 158–160°; recrystallized from ethanol m.p. 165–166°; $[\alpha]_D^{23}$: +98.8° (c = 1, dioxan).

UV: λ_{max} 242 nm (log ε = 4.20), 282 nm (log ε = 4.37)
IR: ν_{NH} 3350; ν_{CO} 1732, 1710; 1670; δ_{NH} 1645, 1395 cm^{-1}
Found: C, 59.82; H, 6.48; N, 7.96
Calcd. for $C_{18}H_{22}N_2O_6$: C, 59.67; H, 6.12; N, 7.73

N-(2-Ethoxycarbonyl-cyclopenten-1-yl)-L-asparagine phenacyl ester (*CP-Asn-OPAc, X*). 2.25 g (5 mmoles) CP-Asn-O$^-$DCHA·H$^+$ (II), 1 g (5 mmoles) ω-bromoacetophenone in 25 ml acetone and 10 ml dimethylformamide were heated to reflux on a water bath for 15 minutes. The reaction mixture was filtered while hot to remove the dicyclohexylammonium bromide and the filtrate was diluted with 300 ml water. The isolated and dried precipitate weighed 1.2 g (60 %) and was recrystallized from ethanol (20 ml); m.p. 175–176° $[\alpha]_D^{23}$: +93.5° (c = 1, methanol).

Found: C, 62.13; H, 6.50; N, 7.54
Calcd. for $C_{20}H_{24}N_2O_6$: C, 61.85; H, 6.22; N, 7.21

N-(1-Benzoylpropen-2-yl)-L-asparagine phenacyl ester (*BA-Asn-OPAc, XI*). 3.5 g (11 mmoles) of BA-Asn-O$^-$K$^+$ (IV) and 2 g (mmoles) (10 mmoles) ω-bromoacetophenone in 10 ml acetone and 10 ml dimethylformamide was allowed to stand at room temperature for 24 hours, refluxed the next day for 2 hours and poured into 300 ml water. Yield 3.2 g (81 %); m.p. 174–175°. Recrystallized from methanol, m.p. 176–177°, from acetone 179–180°; $[\alpha]_D^{23}$: +152.8° (c = 1, dimethylformamide).

Found: C, 67.14; H, 5.94; N, 7.36
Calcd. for $C_{22}H_{22}N_2O_5$: C, 67.00; H, 5.62; N, 7.10

L-Asparagine phenacyl ester hydrochloride ($^{+}H_2$*-Asn-OPAc.Cl*$^{-}$, *XXa*). 2.4 g (6 mmoles) AE-Asn-OPAc (IX) dissolved in 25 ml hot methanol were acidified with an ethanolic solution of hydrochloric acid (13 %) to pH 2.5–2. After 15–20 minutes the crystals of the asparagine phenacyl ester hydrochloride are deposited. Isolated and washed with ethyl acetate-ether yielded 1.8 g (90 %); m.p. 162–163°; $[\alpha]_D^{23}$: +29.9° ($c = 1$, methanol). 0.3 g BA-Asn-OPAc (XI), respectively 0.6 g CP-Asn-OPAC (X) deprotected in the above described manner yielded 0.2 g respectively 0.31 g hydrochlorides; m.p. 157–159°, respectively 158–159°. Recrystallized from ethanol-ether, m.p. 157–158°; $[\alpha]_D^{28}$: +32.4° ($c = 1$, methanol).

Found: C, 50.83; H, 5.80; N, 9.31; Cl, 12.07

Calcd. for $C_{12}H_{15}ClN_2O_4$: C, 50.27; H, 5.26; N, 9.77; Cl, 12.36

L-Asparagine phenacyl ester hydrobromide ($^{+}H_2$*-Asn-OPAc. Br*$^{-}$, *XXb*). The deprotection of AE-Asn-OPAc (IX) was carried out with aqueous hydrobromic acid solution 60 % up to pH value of 2.5–2, m.p. 148–149° (decomp.); $[\alpha]_D^{25}$: +25.8° ($c = 1$, methanol)

Found: C, 43.70; H, 4.95; N, 8.56

Calcd. for $C_{12}H_{15}BrN_2O_4$: C, 43.52; H, 4.56; N, 8.46

N-(1-Ethoxycarbonyl-propen-2-yl)-L-glutamine phenacyl ester (*AE-Gln-OPAc, XII*). It was prepared from 5.9 g (20 mmoles) of AE-Gln-O^{-}K^{+} and 4 g of ω-bromoacetophenone in dimethylformamide solution as described for IX. Yield 6 g (79 %); m.p. 121–123°; $[\alpha]_D^{23}$: +118.1° ($c = 1$, methanol) and +110.6° ($c = 1$, dioxan), respectively.

Found: C, 60.83; H, 6.80; N, 7.50

Calcd. for $C_{19}H_{24}N_2O_6$: C, 60.60; H, 6.43; N, 7.44

N-(2-Ethoxycarbonyl-cyclopenten-1-yl)-L-glutamine phenacyl ester (*CP-Gln-OPAc, XIII*). 4.7 g (10 mmoles) CP-Gln-0^{-}DCHA·H^{+} (VI) in 30 ml acetone and 10 ml dimethylformamide were heated on the water bath with 2 g (10 mmoles) ω-bromoacetophenone for 1 hour. After filtration and dilution of the filtrate with 400 ml water, 3.5 g (87 %) phenacyl ester was obtained, m.p. 150–151°. Recrystallized from ethanol m.p. 150–151°, from ethyl acetate 148–150°; $[\alpha]_D^{28}$: +68.6° ($c = 1$, methanol).

Found: C, 62.70; H, 6.83; N, 7.27

Calcd. for $C_{21}H_{22}N_2O_6$: C, 62.68; H, 6.50; N, 6.96

L-Glutamine phenacyl ester hydrobromide ($^{+}H_2$*-Gln-OPAc·Br*$^{-}$, *XXI*). To a suspension of 6 g (16 mmoles) of AE-Gln-OPAc (XII) in 25 ml of anhydrous acetone, a solution of hydrogen bromide in acetic acid (30 %) was added until a constant pH value of 2.5–2 was reached. After 45–50 minutes the separated ester hydrobromide crystals were collected and recrystallized from methanol-ether; yield 5.5 g (78 %); m.p. 146–147°; $[\alpha]_D^{23}$: +26.8° ($c = 1$, methanol).

Found: C, 45.80; H, 5.68; N, 7.92; Br, 22.80

Calcd. for $C_{31}H_{17}BrN_2O_4$: C, 45.23; H, 4.96; N, 8.11; Br, 23.15

N-(1-Ethoxycarbonyl-propen-2-yl)-L-asparagine p-nitrobenzyl ester (*AE-L-Asn-ONB, XIV*). 2 g (7 mmoles) AE-Asn-O^{-} K^{+} (I) suspended in 20 ml anhydrous acetone and 10 ml dimethylformamide were treated with 1.5 g (7 mmoles) *p*-nitrobenzyl bromide and refluxed for 4 hours. Diluting with 500 ml water, 1.7 g (64 %) ester was separated, m.p. 180–181° (ethanol); $[\alpha]_D^{23}$: +76.7° ($c = 1$, dioxan).

UV: λ_{max} 280 nm (log $\varepsilon = 4.45$)
IR: $_{\nu NH}3450$; ν_{CO} 1745, 1670; ν_{NO_2} 1520, 1350; δ_{NH} 1650, 1390 cm^{-1}
Found: C, 53.46; H, 5.89; N, 11.24
Calcd. for $C_{17}H_{21}N_3O_7$: C, 53.82; H, 5.58; N, 11.07

N-(2-Ethoxycarbonyl-cyclopenten-1-yl)-L-asparagine p-nitrobenzyl ester (CP-Asn-ONB, XV). 5 g (11 mmoles) CP-Asn-O^-DCHA·H^+ (II) was dissolved in 40 ml acetone and 10 ml dimethylformamide and 2.16 g (10 mmoles) *p*-nitrobenzyl bromide was added. Next day the separated dicyclohexylamine hydrobromide (2.5 g, theoretically 2.62 g) was eliminated by filtration and the filtrate diluted with 300 ml water. The isolated precipitate dried over P_2O_5 in desiccator, weighed 3.3 g (81.5%), m.p. 165—167°. Recrystallized from ethanol m.p. 173—174°; $[\alpha]_D^{28}$: +72.6° (c = 1, methanol).

Found: C, 56.30; H, 6.02; N, 10.70

Calcd. for $C_{19}H_{23}N_3O_7$: C, 56.29; H, 5.71; N, 10.36

N-(1-Acetylpropen-2-yl)-L-asparagine p-nitrobenzyl ester (AC-Asn-ONB, XVI). This compound was prepared in a similar manner as described before (by ester XV) from AC-Asn-O^-DCHA·H^+ (IIIb). Yield 63%, m.p. 153—155° (ethyl acetate); $[\alpha]_D^{23}$: +118.6° (c = 0.45, methanol).

Found: C, 55.15; H, 5.75; N, 12.00

Calcd. for $C_{16}H_{19}N_3O_6$: C, 55.01; H, 5.48; N, 12.03

N-(1-Benzoylpropen-2-yl)-L-asparagine p-nitrobenzyl ester (BA-Asn-ONB, XVII). 3.5 g (10 mmoles) BA-Asn-O^-K^+ (IV) in 40 ml acetone and 10 ml dimethylformamide was treated with 2.15 g (10 mmoles) *p*-nitrobenzyl bromide and worked up as described by CP-Asn-ONB (XV). Yield 4 g (97%); m.p. 171—172° (ethanol); $[\alpha]_D^{25}$: +113.8° (c=1, methanol).

Found: C, 61.36; H, 5.90; N, 10.40

Calcd. for $C_{21}N_{21}N_3O_6$: C, 61.31; H, 5.15; N, 10.21

L-Asparagine p-nitrobenzyl ester hydrobromide ($^+H_2$-Asn-ONB.Br$^-$, XXIIb). 1 g AE-Asn-ONB (XIV) suspended in 15 ml anhydrous ethanol was treated with hydrogen bromide in acetic acid (30%) to a pH value of 2.5—2 and heated to 55—60° under stirring. The formed solution was then filtered and treated with 20 ml anhydrous ether. Yield 0.7 g (76%). Recrystallized from ethanol-ether, m.p. 171—172°; $[\alpha]_D^{24}$; +10.4° (c = 1, methanol). Lit.[13] 170—171°.

L-Asparagine p-nitrobenzyl ester hydrochloride ($^+H_2$-Asn-ONB.Cl$^-$, XXIIa). 1 g AE-Asn-ONB (XIV) was deprotected with ethanolic hydrochloric acid (13%) as described before. Yield 80%; m.p. 184—185° (ethanol-ether); $[\alpha]_D^{24}$: +7.0° (c = 0.75, methanol).

Found: C, 43.59; H, 5.21; N, 13.43; Cl, 11,56;

Calcd. for $C_{18}H_{14}ClN_3O_5$: C, 43.50; H, 4.65; N, 13.83; Cl. 11.67

N-(1-Ethoxycarbonyl-propen-2-yl)-L-glutamine-p-nitrobenzyl ester (AE-Gln-ONB, XVIII). 3 g (10 mmoles) AE-Gln-O^-K^+ and 2 g *p*-nitrobenzyl bromide in 40 ml acetone and 10 ml dimethylformamide were refluxed for 2 hours and diluted with 400 ml water. The filtered and dried precipitate (2.4 g, 62%) was recrystallized from ethyl acetate — ether; m.p.120—121°; $[\alpha]_D^{23}$: +41.3° (c = 0.7, dioxan).

Found: C, 54.56; H, 6.00; N, 10.60

Calcd. for $C_{18}H_{23}N_3O_7$: C, 54.95; H, 5.89; N, 10.68)

N-(2-Ethoxycarbonyl-cyclopenten-1-yl)-L-glutamine p-nitrobenzyl ester (CP-Gln-ONB, XIX). The synthesis was executed according to the model described by CP-Gln-OPAc (XIII). Yield 2.3 g (52.5%); m.p. 120—122°, recrystallized from ethanol-water 118—120°; $[\alpha]_D^{28}$: +67° (c = 1, methanol).

Found: C, 57.60; H, 6.24; N, 10.28

Calcd. for $C_{20}H_{25}N_3O_7$: C, 57.27; H, 6.01; N, 10.01)

---

[13] E. SONDHEIMER and R. J. SEMERARO, *J. Org. Chem.*, **26**, 1847 (1961).

L-Glutamine p-nitrobenzyl ester hydrobromide (*$^+H_2$-Gln-ONB·Br$^-$, XXIII*). 1.7 g (4 mmoles) CP-Gln-ONB (XIX) suspended in 10 ml anhydrous acetone was treated with hydrogen bromide in acetic acid (30%) to pH value of 2.5–2. The substance entered into solution and after 1 hour the separated crystals (1 g, 68%) were isolated. Recrystallized from ethanol-ether m.p. 173–174°; $[\alpha]_D^{21}$: +15.6° (c = 1, methanol). Lit.[13] m.p. 175°.

C. DIPEPTIDES

N-(2-Ethoxycarbonyl-cyclopenten-1-yl)-L-asparaginylglycine ethyl ester (*CP-Asn-Gly-OEt, XXIV*). A solution of 2.5 g (5 mmoles) CP-Asn-O$^-$DCHA·H$^+$ (II) in 25 ml of methylene chloride was treated with 1–2 drops of N-methylmorpholine[14] and under vigorous stirring at 8–10°, 0.5 ml (5 mmoles) of ethyl chloroformate were added. After 25 minutes stirring the separated dicyclohexylamine hydrochloride was filtered off and the mixed anhydride solution was treated with 0.5 ml (5 mmoles) of freshly distilled ethyl glycinate. Stirring was continued with cooling for one hour and for three hours at room temperature. A solution of 25 ml saturated sodium hydrogen carbonate was added and the organic layer removed by distillation *in vacuo*. The separated crystalls were colllected (1.2 g, 66.6%); recrystallized from dimethylformamide-ether m.p. 189–190°; $[\alpha]_D^{28}$: +107.3° (c = 0.75, dimethylformamide).

Found: C, 53.88; H, 7.30; N, 11.86
Calcd. for $C_{16}H_{25}N_3O_6$: C, 54.07; H, 7.09; N, 11.82

N-(1-Ethoxycarbonyl-propen-2-yl)-L-asparaginyl-L-alanine phenacyl ester (*AE-Asn-Ala-OPAc, XXV*). The mixed anhydride was prepared from 15 mmoles AE-Asn-O$^-$K$^+$ (I) and 15 mmoles benzoyl chloride in methylene chloride in the usual manner and treated with 15 mmoles alanine phenacyl ester obtained from its hydrochloride[8] with triethylamine in methylene chloride. Yield 89%; m.p. 159–161°. Recrystallized from methanol, 170–171°; $[\alpha]_D^{23}$: +19.0° (c = 1, methanol).

Found: C, 57.72; H, 6.59; N. 9.58
Calcd. for $C_{21}H_{27}N_3O_7$: C, 58.20; H, 6.27; N, 9.70

N-(2-Ethoxycarbonyl-cyclopenten-1-yl)-L-glutaminylglycine ethyl ester (*CP-Gln-Gly-OEt, XXVI*). It was prepared from 4.7 g (10 mmoles) CP-Gln-O$^-$DCHA·H$^+$ (VI) as described by XXIV. Yield 2.2 g (59.5%); m.p. 162–164°. Recrystallized from aqueous ethanol, m.p. 171–172°; $[\alpha]_D^{28}$: +67.2° (c = 1, methanol).

Found: C, 55.50; H, 7.80; N, 11.43
Calcd. for $C_{17}H_{27}N_3O_6$: C, 55.28; H, 7.37; N, 11.37

N-(1-Ethoxycarbonyl-propen-2-yl)-L-alanyl-L-asparagine p-nitrobenzyl ester (*AE-Ala-Asn-ONB, XXVII*). The mixed anhydride prepared from 10 mmoles of AE-Ala-O$^-$DCHA.H$^+$ and 10 mmoles of pivaloyl chloride as described before,[7] was treated with L-asparagine *p*-nitrobenzyl ester liberated from its hydrochloride (XXIIa). Working up in the usual manner yielded 1.8 g (81.8%) ester m.p. 172–175° (recrystallized from 250 ml ethanol); $[\alpha]_D^{27}$: 114.4° (c = 1, dimethylformamide).

Found: C, 53.75; H 5.96; N, 12.60
Calcd. for $C_{20}H_{26}N_4O_8$: C, 53.33; H, 5.82; N, 12.44

---

[14] G. R. Fosker, J. H. Ch. Nayler and J. A. Wilcox, *Brit. Pat.*, 991, 586, Beecham Research Laboratories Ltd., Brentford, 1962; *Chem., Zentr.*, **1967**, 33–1856.

N-(1-Ethoxycarbonyl-propen-2-yl)-L-alanyl-L-glutamine phenacyl ester (*AE-Ala-Gln-OPAc, XXVIII*). Prepared according to the general method as described for XXIV. Yield 76.7%; m.p. 174—175° (propanol); $[\alpha]_D^{24}$: +139.6° ($c = 1$, methanol).

Found: C, 59.00; H, 6.80; N, 9.13

Calcd. for $C_{22}H_{29}N_3O_7$: C, 59.05; H, 6.53; N, 9.39)

N-(2-Ethoxycarbonyl-cyclopenten-1-yl)-L-glutaminyl-L-asparagine phenacyl ester (*CP-Gln-Asn-OPAc, XXIX*). The mixed anhydride was prepared in 50 ml tetrahydrofuran from 2.4 g (5 mmoles) of CP-Gln-O^-DCHA·H^+ (VI) and 0.5 ml ethyl chloroformate in the usual manner and treated with L-asparagine phenacyl ester set free from 1.45 g (5 mmoles) hydrochloride in 30 ml tetrahydrofuran. Yield 2.7 g (84.5%); m.p.209—211°. Recrystallized from dimethylformamide-acetone, m.p. 207—209°; $[\alpha]_D^{28}$: +29.8° ($c = 1$, dimethylformamide).

Found: C, 58.58; H, 6.60; N, 10.97

Calcd. for $C_{25}H_{32}N_4O_8$: C, 58.12; H, 6.24; N, 10.84

N-(2-Ethoxycarbonyl-cyclopenten-1-yl)-L-glutaminyl-L-asparagine p-nitrobenzyl ester (*CP-Gln-Asn-ONB, XXX*). It was prepared as described for XXIV. Yield 42%; .m.p. 188—191°. Recrystallized from ethanol, m.p. 201—203°; $[\alpha]_D^{23}$: +39.0° ($c = 1$, dimethylformamide).

Found: C, 54.19; H, 6.20; N, 13.45

Calcd. for $C_{24}H_{31}N_5O_9$: C, 54.02; H, 5.85; N, 13.12

evue Roumaine de Chimie, **19**, *4*, 701–707 (1974)

AZLACTONES OF CAROTENOIDS. II[1]

RETINAL AZLACTONE AND TRANSFORMATION PRODUCTS

V. TĂMAŞ and C. BODEA

Department of Biochemistry, Institute of Agronomy, Str. Mănăştur 3, Cluj, Romania

Received June 23, 1973

By condensation of retinal (I) with hippuric acid the oxazolonic compound III was obtained with high yield. Opening of the oxazolonic ring by action of nucleophilic reagents such as water, hydrazine hydrate or phenylhydrazine on III resulted in the formation of the benzylamide-carotenoic acid IV and the hydrazides V and VI. The properties of these compounds are described.

Retinal (vitamin A_1 aldehyde) is a metabolite of some carotenoids and a usual component of human and animal organisms.[2,3,4] Various physical[5,6] and chemical[7,8,9] methods for the identification and determination of retinal in natural products have been described. Among the chemical methods, condensation with rhodanine is commonly used to identify retinal.[9] The efficiency of this method is rather low because of the formation of numerous *cis-trans* condensation products.

These last years researches have been carried out on condensation of retinal with indene, to obtain fulvenes,[10] with dicarboxylic acids[11] and with several other compounds having an active methylene group.[12]

In a previous paper[1] we have reported on the condensation of some aldehyde-carotenoids (β-apo-carotenals and diapo-carotenodials) with hippuric acid leading to carotenoid-azlactones. These compounds are obtained with good yields and can give valuable indications about the structure of aldehyde-carotenoids.

---

[1] V. Tămaş, V. Ciurdaru and C. Bodea, *Rev. Roumaine Chim.*, **18**, 1409 (1973).

[2] J. Kahan, *J. Chromatog.*, **30**, 506 (1967).

[3] S. R. Targan, S. Merril and A. D. Schwabe, *Clin. Chem.*, **15**, 479 (1969).

[4] O. Isler, "Carotenoids", Birkäuser Verlag Basel-Stuttgard, 1971, p. 717–738.

[5] D. E. Duggan, S. Udenfriend, R. L. Bowman and B. B. Brodie, *Arch. Biochem. Biophys.*, **68**, 1 (1957).

[6] B. D. Drujan, R. Castillon and E. Guerrero, *Analyt. Biochem.*, **23**, 44 (1968).

[7] R. Kuhn and H. Roth, *Ber. dtsch. chem. Ges.*, **66**, 1274 (1933).

[8] A. J. Aasen and S. Liaaen-Jensen, *Acta Chem. Scand.*, **21**, 2185 (1967).

[9] A. Winterstein and B. Hegedus, *Chimia (Basel)*, **14**, 18 (1960).

[10] H. H. Haeck and T. Kralt, *Rec. Trav. chim.*, **85**, 339 (1966).

[11] H. H. Haeck and T. Kralt, *Rec. Trav. chim.*, **87**, 709 (1968).

[12] H. H. Haeck, T. Kralt and P. H. Van Leeuwen, *Rec. Trav. chim.*, **85**, 334 (1966).

Continuing these investigations we have submitted retinal (retinaldehyde) to the condensation with hippuric acid in acetic anhydride. Carrying out the reaction for two hours at 85°, we obtained as principal product the azlactone of all-*trans*-retinal (III), accompanied by smaller quantities of a *cis-trans* isomer (II).

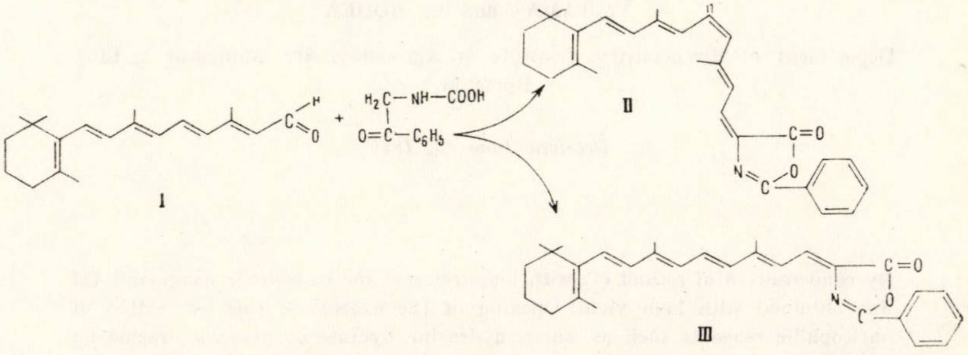

Fig. 1

It is known that among the *cis-trans* isomers of retinal formed under the action of various reagents the 11-*cis*-retinal is predominant. This isomer occurs also in the natural visual pigments. Acting only with acetic anhydride upon all-*trans*-retinal under the conditions leading to the formation of azlactones, part of the all-*trans* form proved by its characteristic absorption spectrum[13] to be converted into the 11-*cis* isomer. The difference between λ_{max} of all-*trans*- and 11-*cis*-retinal is about 4 nm, identic with the difference between the azlactone III and its isomer II. We therefore believe that isomer II should be the azlactone of 11-*cis*-retinal.

Azlactone III being the principal reaction product in the condensation with hippuric acid we have studied its chemical behaviour.

It has been demonstrated that the C=N group in azlactones is an acceptor of electrons, thus preventing the adjacent oxygen atom to interact with the carbonyl group of C-5. Therefore, exposing this carbonyl group to the action of nucleophylic reagents the azlactonic ring opens in the way shown in fig. 2.[14,15,16,17,18]

According to this mechanism the hydrolysis of azlactone III in dimethylformamide at room temperature resulted in the formation of 15′-N-benzylamide-β-apo-14′-carotenoic acid, IV. Through hydrazinolysis and phenylhydrazinolysis the azlactone III has been transformed with high yields into hydrazide V and phenylhydrazide VI, respectively (see fig. 3 and table 1).

---

[13] H. M. Rauen and R. Kuhn, "Biochemisches Taschenbuch", Springer-Verlag, Berlin-Göttingen-Heidelberg, vol. I, 1964, p. 384–385.

[14] A. E. Carter, "Organic Reactions", vol. 3, Pergamon Press, 1947, New York, p. 206.

[15] P. H. Stodola, *J. Org. Chem.*, **13**, 757 (1948).

[16] K. Nápela and J. Slouka, *Monatsh.*, **98**, 412 (1967).

[17] K. Nápela and V. Bekarek, *Monatsh.*, **100**, 2004 (1969).

[18] C. Bodea, V. Fărcăşan and I. Oprean, *Rev. Roumaine Chim.*, **10**, 11 (1965).

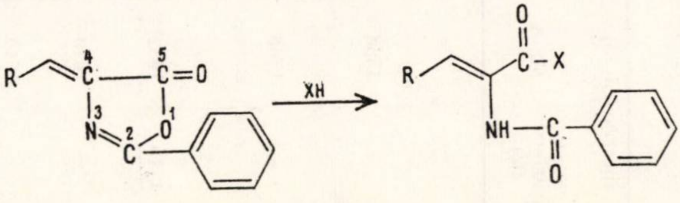

Fig. 2

The absorption spectra in ultraviolet and visible light of compounds III, IV, V and VI in benzene shows no fine structure (see fig. 4).

Comparing the position of λ_{max} of III with those of IV, V and VI there is to be noticed a hypsochromic shift of 100 nm in the case of λ_{max} III. This can serve as a valuable criterion for their differentiation and identification.

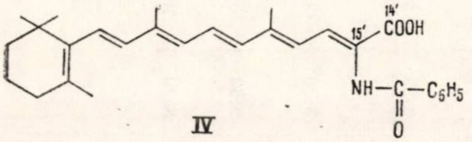

IV

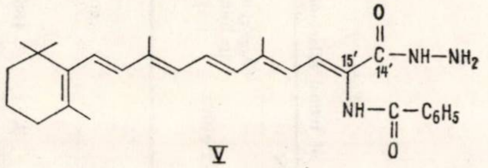

V

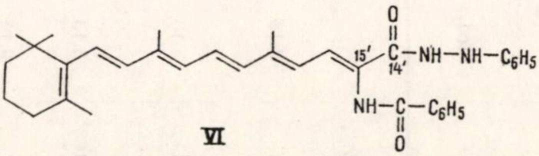

VI

Fig. 3

As compared to retinal, compounds IV, V and VI have an additional C=C group, which explains the bathochromic shift of about 10—16 nm in the absorption spectra of these compounds.

The I.R. spectra recorded in CCl_4 show the presence of the characteristic peaks for the C=O and C=N groups (see table 1). It is worth mentioning that some of the bands are very strong, i. e. in the spectrum of III the band at 1638 cm^{-1}, of V and VI at 1615 cm^{-1} characteristic for the an C=N group and in the spectrum of IV the band at 1715 cm^{-1} assigned to the C=O group.

Compounds IV, V and VI are structurally related both to vitamin A_1 and to carotenoids, enriching the chemistry of carotenoids with new

Table 1

Characteristics of retinal azlactones and derivatives

Compound	Yield %	m.p.	% N		λ_{max}, nm (in benzene)	I.R. spectra (cm^{-1})					
			Calcd.	Found		ν_{C-O}	$\nu_{C=O}$	$\nu_{C=O}$ (carboxylic)	$\nu_{C=N}$	ν_{NH}	ν_{O-H}
all-*trans*-Retinal (I) ; $C_{20}H_{28}O$	—	55–56°	—		380	—	1590 1666	—	—	—	—
11-*cis*-Retinal azlactone (II) ; $C_{29}H_{33}O_2N$	15	95–97°	3.13	3.15	486	1070 1085	1750 1778	—	1368	—	—
all-*trans*-Retinal azlactone (III) ; $C_{29}H_{33}O_2N$	75	110–112°	3.13	3.25	490	1070 1085	1750 1778	—	1368	—	—
15′-N-benzylamide-β-14′-carotenoic acid (IV) ; $C_{29}H_{35}O_3N$	98	162–163°	3.13	3.20	390(350	1120	1760	1715	1632	—	3450
Hydrazide of IV(V) ; $C_{29}H_{37}O_2N_3$	98	195°	9.15	9.33	393	—	1666	—	1613	3320	—
Phenylhydrazide of IV (VI) ; $C_{35}H_{42}O_2N_3$	99	186°	7.83	8.29	396	—	1665	—	1615	3325	—

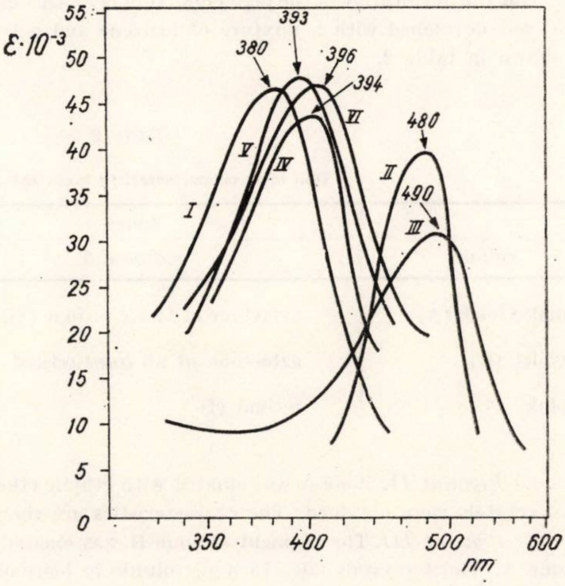

Fig. 4. – Absorption spectra in ultraviolet and visible light of compounds III, IV, V and VI in benzene.

synthetical nitrogen containing derivatives. Eventually biological activities of these compounds are under investigation.

EXPERIMENTAL

MATERIALS AND METHODS

The retinal used in the condensation reaction with hippuric acid was a synthetical product from Badische Anilin-Soda Fabrik A.G., Ludwigshafen/Rh, West Germany.

The reaction products were separated by means of thin layer chromatography, using as absorbent silica gel G. All the absorbent and solvents used had analytical and proanalysis purity.

Electronic spectra were recorded on a Spectrophotometer Zeiss VSU-1 and IR spectra on a – Unicam SP. 200 G.

Melting points uncorrected were determined on a Boëtius apparatus.

Azlactone of Retinal. Retinal (100 mg), hippuric acid (85 mg) and anhydride sodium acetate (80 mg) were thoroughly mixed in a test tube and acetic anhydride (0.75 ml) was added. The test tube was introduced in a drying oven and kept for 2 hours at 85°. After about 15 minutes, the mixture started to darken. After 2 hours, the mixture was cooled down at the room temperature, placed in a G_3 filtrant crucible and washed 5–6 times with water. From the residue the pigments were extracted till colourless with a mixture of benzene and ethylic ether (1 : 1). The solution of the pigments was concentrated to a small volume (1–2 ml).

The pigments were precipitated by adding 50 ml petroleum ether. The precipitate was filtered and washed with 30 ml petroleum ether. Yield about 90 %.

For the purification of the pigments, thin layer chromatography was used. The chromatoplate was developed with a mixture of benzene and petroleum ether (1 : 1). The R_f values are shown in table 2.

Table 2

Thin layer chromatography; zones and R_f values

Zones		R_f
colour	compound	
pink-violet (A)	azlactone of 11-*cis*-retinal (II)	0.85
violet (B)	azlactone of all-*trans*-retinal (III)	0.80
pink	retinal (I)	0.65

— *Pigment II.* Zone A was eluated with ethylic ether; after evaporation of the solvent, violet crystals were obtained. The characteristics are shown in table 1.

— *Pigment III.* The pigment of zone B was eluated in the same manner as the pigment of zone A. Violet crystals (70—75 mg), soluble in benzene, $CHCl_3$, CCl_4, ethylic ether, ethanol, insoluble in water.

Transformation of pigment III.—Hydrolysis. III (100 mg) was solved in dimethylformamide (20 ml) and 5% NaOH (10 ml) was added. The mixture was homogenized and kept for 15 minutes at room temperature. The solution was poured into ether and washed with water containing 2% acetic acid. The ether solution was dried with Na_2SO_4 sicc. and the ether evaporated. Compound IV was obtained with an almost quantitative yield.

Compound IV is soluble in $CHCl_3$, ethylic ether, benzene, CCl_4, ethanol and NaOH solution. Characteristics are shown in tables 1 and 3.

Table 3

R_f values of compounds IV, V and VI (thin layer chromatogram with silica gel G)

Compound	R_f	The developing mixture
IV	0.45	benzene-ether-ethanol (10 : 0.5 : 0.1)
V	0.30	benzene-ethanol (10 : 0.5)
VI	0.50	benzene

— *Hydrazinolysis.* Solving III (100 mg) in dimethylformamide (3 ml) or better in absolute ethanol (10 ml) and adding hidrazine hidrate (2 ml), a yellow precipitate appears immediately. The precipitate was filtered and washed with petroleum ether (5—10 ml). The transformation of III into V is almost quantitative.

Compound V is easily soluble in $CHCl_3$ and ethanol, but less in CCl_4 and insoluble in water. Characteristics are shown in tables 1 and 3.

— *Phenylhydrazinolysis.* A solution of III (100 mg) in dimethylformamide (3 ml) was treated with phenylhydrazine (2 ml). The formed precipitate was filtered off and washed with some ml of petroleum ether. The transformation III into VI was quantitative. Characteristics of hydrazide VI are shown in tables 1 and 3.

Acknowledgements. The authors are indebted to Dr. Horst Schumacher from Badische Anilin-Soda Fabrik AG, Ludwigshafen, West Germany, for providing a sample of retinal.

Revue Roumaine de Chimie, **19**, *4*, 709–716 (1974)

SÄURE-BASEN-INDIKATOREN VOM PHENOTHIAZIN TYP. I

DIE ANWENDUNG VON 3H-PHENOTHIAZIN-3-[4-ANILSULFONSAURES KALIUM], 3H-PHENOTHIAZIN-3-[3-ANILSULFONSAURES KALIUM] UND 3H-PHENOTHIAZIN-3-[2-ANILSULFONSAURES KALIUM] ALS SÄURE-BASENINDIKATOREN

M. RĂILEANU [*], ILEANA RADULIAN [*] und H. KRAUSS [**]

[*] Lehrstuhl der organischen Chemie, Universität Craiova, Str. A. I. Cuza 13, S. R. Rumänien

[**] Kraftwerk Craiova

Eingegangen am 20. März 1973

3H-Phenothiazin-3-[4-anilsulfonsaures Kalium] (Ia), 3H-Phenothiazin-3-[3-anilsulfonsaures Kalium] (Ib) und 3H-Phenothiazin-3-[2-anilsulfonsaures Kalium] (Ic) können als Säure-Basen-Indikatoren zur Titration einer starken Säure mit einer starken Base und umgekehrt, sowie zur Titration einer schwachen Säure mit einer starken Base benützt werden. Diese drei Verbindungen, entsprechend Chamäleonblau I(Ia), II(Ib) und III(Ic) genannt, sind in Wasser löslich und haben zwei Protonierungsstufen. Der pK_s-Wert der monoprotonierten Form ist bei 21° gleich 7,7 für die Indikatoren Ia und Ic und 7,93 für den Indikator Ib.

EINFÜHRUNG

In einer vorhergehenden Arbeit[1] synthetisierten wir 3H-Phenothiazin-3-[4-anilsulfonsaures Kalium] (Ia), 3H-Phenothiazin-3-[3-anilsulfonsaures Kalium] (Ib) und 3H-Phenothiazin-3-[2-anilsulfonsaures Kalium] (Ic) über die Oxydation des Phenothiazins mit Eisen-3-chlorid in Anwesenheit der Kaliumsalze der Sulfanil-, Metanil- und Ortanilsäure. 3-Anil-3H-Phenothiazin, von welchem die Salze Ia, Ib und Ic abkommen, wurde von Kehrmann und Vesely noch im Jahre 1902 erhalten[2].

Die Synthese und Reinigung dieser drei Substanzen ist äußerst einfach; sie bilden mit Wasser blaue Lösungen und bieten in Abhängigkeit vom pH-Wert zwei Protonierungsstufen, welche durch eine zweifache Farbänderung bemerkbar sind.

---

[1] M. Răileanu und I. Radulian, *Rev. Roumaine Chim.*, **18**, 1005 (1973).
[2] F. Kehrmann und O. Vesely, *Liebigs Ann. Chem.*, **322**, 41 (1902).

Die Verbindungen Ia, Ib und Ic sind in Lösung in der basischen Form violett-rosa, in der monoprotonierten Form (IH$^+$) blau und in der diprotonierten Form (IH$_2^{2+}$) grün gefärbt. Wegen diesem Verhalten wurde sie der Reihe nach Chamäleonblau I(Ia), II(Ib) und III(Ic) genannt.

Die in der Lösung vorhandenen Gleichgewichte zwischen den basischen und monoprotonierten Formen, sowie zwischen den protonierten Formen sind leicht auf spektrophotometrischem Wege wahrnehmbar [1].

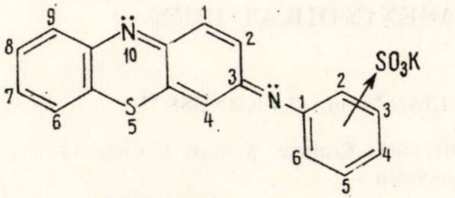

Violett-rosa
Ia : –SO$_3$K (4)
Ib : –SO$_3$K (3)
Ic : –SO$_3$K (2)

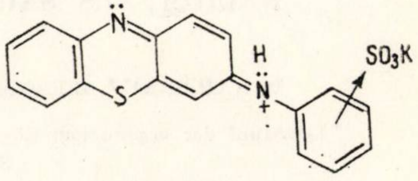

Blau
IaH$^+$: –SO$_3$K (4)
IbH$^+$: –SO$_3$K (3)
IcH$^+$: –SO$_3$K (2)

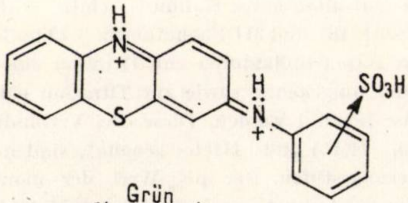

Grün
IaH$_2^{2+}$: –SO$_3$K (4)
IbH$_2^{2+}$: –SO$_3$K (3)
IcH$_2^{2+}$: –SO$_3$K (2)

DER MONOPROTONIERUNGSGRAD α UND DER FARBUMSCHLAGSBEREICH

Die Absorptionsmaxima und die entsprechenden Extinktionsmolarkoeffizienten des Chamäleonblau I, II und III in der basischen und monoprotonierten Form sind in der Tabelle 1 wiedergegeben.

Der Monoprotonierungsgrad α wurde auf spektrophotometrischem Wege in Abhängigkeit vom pH-Wert bestimmt. Zu diesem Zwecke wurden die Absorptionen der Farbstoffe bei den Wellenlängen von 660 nm für Ia, 640 nm für Ib und 620 nm für Ic, in Betracht gezogen. Der Protonierungsgrad des Chamäleonblau I, II und III als Funktion des pH ist in Tab. 2 – 4 illustriert.

Tabelle 1

Die Absorptionsmaxima und die entsprechende Extinktionsmolarkoeffizienten des Chamäleonblau I, II und III in der basischen und monoprotonierten Form

	Chamäleonblau I	Chamäleonblau II	Chamäleonblau III
pH = 11 basische Form	$\lambda_{max(1)} = 560$ nm $\varepsilon_{560} = 27.370$	$\lambda_{max\,(1)} = 560$ nm $\varepsilon_{560} = 23.050$	$\lambda_{max\,(1)} = 546$ nm $\varepsilon_{546} = 22.900$
	$\lambda_{max\,(2)} = 294$ nm $\varepsilon_{294} = 37.620$	$\lambda_{max\,(2)} = 290$ nm $\varepsilon_{290} = 27.740$	$\lambda_{max\,(2)} = 290$ nm $\varepsilon_{290} = 29.310$
pH = 5,80 säure Form	$\lambda_{max\,(1)} = 660$ nm $\varepsilon_{660} = 50.620$	$\lambda_{max\,(1)} = 648$ nm $\varepsilon_{648} = 36.000$	$\lambda_{max\,(1)} = 640$ nm $\varepsilon_{640} = 49.750$
	$\lambda_{max\,(2)} = 308$ nm $\varepsilon_{308} = 42.370$	$\lambda_{max\,(2)} = 304$ nm $\varepsilon_{304} = 28.920$	$\lambda_{max\,(2)} = 304$ nm $\varepsilon_{304} = 33.620$

Tabelle 2

Der Protonierungsgrad α des Chamäleonblau I in Verhältnis zum pH (im Falle einer $1{,}6 \times 10^{-5}$ M Lösung bei 21°)

pH	E_{660}	α
2,20	0,8100	1,0000
5,90	0,8100	1,0000
6,10	0,7960	0,9802
6,55	0,7700	0,9434
7,00	0,6680	0,7993
7,40	0,5690	0,6594
7,70	0,4560	0,4997
7,80	0,4260	0,4573
8,00	0,3716	0,3804
8,30	0,2366	0,1895
8,40	0,2007	0,1389
8,60	0,1549	0,0742
8,95	0,1308	0,0401
9,95	0,1024	0,0000
11,00	0,1024	0,0000

Der Protonierungsgrad α wurde über folgenden Ausdruck berechnet :

$$\alpha = \frac{E_a - E_2}{E_1 - E_2}$$

in welchem :

E_a — die Extinktion des Gemisches beider Formen, basisch und monoprotoniert, darstellt ;

E_1 — die Extinktion der monoprotonierten Form (für Ia bei pH = = 2,2, für Ib bei pH = 6 und für Ic bei pH = 3) ist;

E_2 — die Extinktion der basischen Form (für Ia, Ib, Ic bei pH = = 11) ist.

Tabelle 3

Der Protonierungsgrad α des Chamäleonblau II im Verhältnis zum pH (im Falle einer 1,25 × 10^{-5} M Lösung bei 21°)

pH	E_{640}	α
6,60	0,4440	1,0000
6,55	0,4440	1,0000
6,75	0,4320	0,9670
7,00	0,4180	0,9284
7,20	0,3925	0,8565
7,38	0,3665	0,7865
7,60	0,3325	0,6929
7,80	0,2840	0,5593
7,95	0,2596	0,4921
8,00	0,2480	0,4602
8,40	0,1871	0,2925
8,72	0,1487	0,1867
8,95	0,1249	0,1212
9,15	0,1135	0,0897
9,80	0,0915	0,0292
10,60	0,0809	0,0000
11,00	0,0809	0,0000

Tabelle 4

Der Protonierungsgrad α des Chamleonblau III, im Verhältnis zum pH (im Falle einer 1,6 × 10^{-5} M Lösung bei 21°)

pH	E_{620}	α
6,00	0,6680	1,0000
6,40	0,6680	1,0000
6,80	0,6540	0,9756
7,00	0,6278	0,9300
7,25	0,5610	0,8135
7,50	0,4906	0,6908
7,65	0,4260	0,5782
7,70	0,3872	0,5105
7,80	0,3645	0,4711
8,05	0,2549	0,2801
8,25	0,2135	0,2080
8,40	0,1818	0,1527
8,65	0,1379	0,0761
8,80	0,1238	0,0515
9,55	0,0942	0,0000
11,00	0,0942	0,0000

In den Abbildungen 1–3 sind die charakteristischen Kurven des Chamäleonblau I, II und III wiedergegeben. Aus diesen ersieht man die Farbumschlagsintervalle (für $0{,}10 \leqslant \alpha \leqslant 0{,}90$) der drei Indikatoren

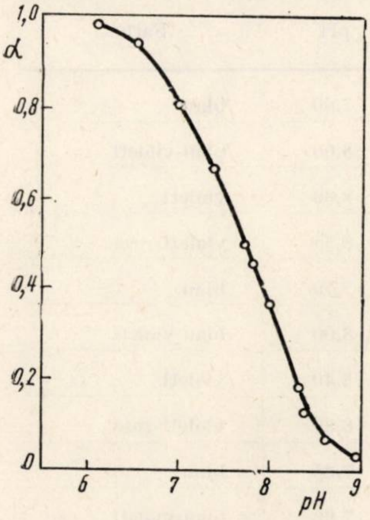

Abb. 1.—Die charakteristische Kurve des Chamäleonblau I.

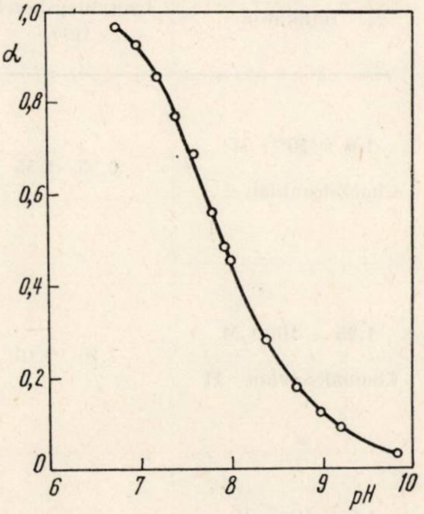

Abb. 2.—Die charakteristische Kurve des Chamäleonblau II.

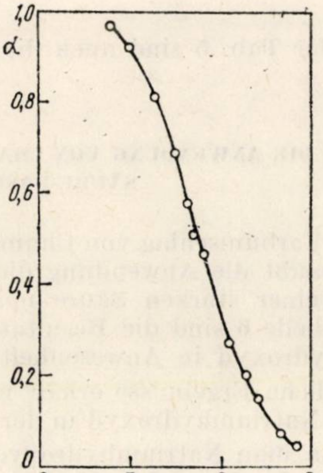

Abb. 3.—Die charakteristische Kurve des Chamäleonblau III.

(Tab. 5), sowie den pK_s-Wert der monoprotonierten Form, der für das Chamäleonblau I und III gleich 7,7, und für das Chamäleonblau II gleich 7,93 ist.

Tabelle 5

Die Farbumschlagsintervalle des Chamäleonblau I, II und III für $0{,}10 \leqslant \alpha \leqslant 0{,}90$

Indikator	Umschlagsbereich (pH)	Farbänderung im Umschlagsbereich	
		pH	Farbe
$1{,}6 \times 10^{-5}$ M Chamäleonblau I	6,75–8,55	7,60	blau
		8,00	blau-violett
		8,30	violett
		8,55	violett-rosa
$1{,}25 \times 10^{-5}$ M Chamäleonblau II	7,10–9,10	7,70	blau
		8,00	blau-violett
		8,40	violett
		8,80	violett-rosa
$1{,}6 \times 10^{-5}$ M Chamäleonblau III	7,05–8,50	7,25	blau
		7,80	blau-violett
		8,05	violett-rosa
		8,40	rosa-violett

In der Tab. 5 sind auch die Farbänderungen der Indikatoren angegeben.

DIE ANWENDUNG VON CHAMÄLEONBLAU I, II UND III ALS SÄURE-BASEN-INDIKATOREN

Der Farbumschlag von Chamäleonblau I, II und III von blau nach violett erlaubt die Anwendung dieser Indikatoren mit gutem Erfolg zur Titration einer starken Säure mit einer starken Base und umgekehrt. In der Tabelle 6 sind die Resultate der Titration von Schwefelsäure mit Natriumhydroxyd in Anwesenheit von Chamäleonblau I wiedergegeben.

Ähnliche Ergebnisse erhält man auch beim Titrieren der Schwefelsäure mit Natriumhydroxyd in der Gegenwart der Indikatoren Ib und Ic.

Wenn man Natriumhydroxyd mit Schwefelsäure in Anwesenheit der Indikatoren Ia, Ib und Ic titriert, ist der Äquivalenzpunkt durch einen umgekehrten Farbumschlag, von violett nach blau angezeigt, während die Titrationsfehler von der gleichen Größenordnung sind wie jene die in der Tabelle 6 angegeben sind.

Der gut sichtbare Farbumschlag des Chamäleonblau I und II von blau nach violett-rosa erlaubt auch die Bestimmung des Äquivalenzpunktes im Falle der Titration einer schwachen Säure mit einer starken Base (Tabelle 7).

Tabelle 6

Die Titration von Schwefelsäure mit Natriumhydroxyd in Anwesenheit von Chamäleonblau I (Farbumschlag von blau nach violett)

H_2SO_4 N/10 zur Titration (in ml)	Verbrauch an NaOH N/10 (in ml)	Abweichung in ml	Abweichung in %
10	9,98	−0,02	−0,20
10	9,99	−0,01	−0,10
10	10,01	+0,01	+0,10
10	10,01	+0,01	+0,10
10	10,00	0,00	0,00
10	10,01	+0,01	+0,10
10	10,00	0,00	0,00
10	10,01	+0,01	+0,10

$\overline{X} = 10{,}00125$

$s_{\overline{x}} = 0{,}00375$

$\varepsilon = t_{95}\, s_{\overline{x}} = 2{,}37 . 0{,}00375 = 0{,}00889$

$\overline{X} \pm \varepsilon = 10{,}00125 \pm 0{,}00889$

Tabelle 7

Titration von Essigsäure mit Natriumhydroxyd in Anwesenheit von Chamäleon blau I (Farbumschlag von blau nach violett-rosa)

CH_3COOH N/10 zur Titration (in ml)	Verbrauch an NaOH N/10 (in ml)	Abweichung in ml	Abweichung in %
10	9,99	−0,01	−0,10
10	9,98	−0,02	−0,20
10	10,00	0,00	0,00
10	9,99	−0,01	−0,10
10	9,99	−0,01	−0,10
10	9,98	−0,02	−0,20
10	10,01	+0,01	+0,10
10	9,99	−0,01	−0,10

$\overline{X} = 9{,}99125$

$s_{\overline{x}} = 0{,}0048$

$\varepsilon = t_{95} . s_{\overline{x}} = 2{,}77 . 0{,}0048 = 0{,}0114$

$\overline{X} \pm \varepsilon = 9{,}99125 \pm 0{,}0114$

Tatsächlich erhält man beim Titrieren der Essigsäure mit Natriumhydroxyd in der Gegenwart der Indikatoren Ia und Ib Fehler der gleichen Größenordnung wie in der Tabelle 6.

Zwecks einer guten Wahrnehmung des Äquivalenzpunktes, setzt man zu 10 ml Probe 1 ml wäßrige 1×10^{-4} M Lösung Chamäleonblau I oder III, oder 1 ml $1{,}25 \times 10^{-5}$ M Lösung Chamäleonblau II.

Wir stellten fest, daß die neuen Indikatoren zeitlich stabil sind, so im sauren als auch im basischen Medium. Im sauren Medium werden sie aber von manchen starken Reduzierungsmitteln entfärbt (z. B. Ascorbinsäure, Schwefelwasserstoff, Merkaptane, u.s.w.) und gehen in ihre Leukoderivate über. Schwefeldioxyd entfärbt aber diese Indikatoren viel schwerer.

ZUSAMMENFASSUNG

Zur Titration einer starken Säure mit einer starken Base und umgekehrt können die Indikatoren Ia, Ib und Ic ohne Vorzug mit den gleichen Ergebnissen verwendet werden, weil der Äquivalenzpunkt sehr leicht zu bemerken ist.

Im Falle der Titration einer schwachen Säure mit einer starken Base wird empfohlen als Indikator nur das Chamäleonblau I und II zu verwenden, weil in Anwesenheit von Chamäleonblau III der Äquivalenzpunkt schwer zu bemerken ist, bzw. das Übergehen von violett-rosa nach rosa-violett.

REGISTRIERUNGSBEDINGUNGEN DER ABSORBTIONSSPEKTREN

Die Pufferlösungen mit verschiedenen pH-Werten wurden nach Sörensen und Mc.Ilvain hergestellt. Der pH-Wert wurde ständig mit einem pH-meter geprüft.

Zur spektralen Absorptionsprüfung wurden 1,6 $\times 10^{-5}$ M Lösungen von Chamäleonblau I und III und 1,25 $\times 10^{-5}$ M Lösungen von Chamäleonblau II verwendet. Die Extinktionen wurden mit einem Beckman DB Spektrophotometer bei 21° bestimmt.

Revue Roumaine de Chimie, **19**, *4*, 717–725 (1974)

AN ION-EXCHANGE PROCESS FOR GOLD RECOVERY

SEVER A. TĂTARU

Department of Technological Research for Radioactive Metals, Bucharest —
Măgurele, P. O. Box 35, Romania

Received October 27, 1972

An ion-exchange process has been developed for gold recovery from cyanide solutions. It is shown that strongly basic ion-exchange resins, having a high adsorption capacity but a low selectivity for gold, offer the possibility to recover besides precious metals also the alkaline cyanide, which can finally be recycled to leaching. By using a mixture of hydrochloric acid and thiourea, a total elution of the precious metals and cyanide was obtained. The hydrocyanic acid resulting from the elution and the decomposition of the cyanides was wholly converted into sodium cyanide by contacting it with a sodium hydroxide solution. Lead cementation and electrolytic precipitation of hold have been tested for gold recovery from thiourea eluates. Two possible procedures using the resin-in-pulp process for gold recovery are described.

1. INTRODUCTION

The only known hydrometallurgical procedure for the recovery of gold and silver from ore, cyanidation, followed by reduction with zinc and refining, has several disadvantages and this has led to the use of combined and diversified processing technologies and also to research work aiming at improving the process.

One possible recovery technique is by use of ion-exchange resins. The first attempts to adsorb gold on ion exchange resins are very probably due to Gans,[1-2] but later the preparation of better quality resins offered the possibility of obtaining better results,[3-5] and of applying the procedure in practical industrial purposes.[6-9] The lack of selectivity of strongly basic

---

[1] R. Gans, German Patent, N° 174095 (1905).

[2] R. Gans, *Jahrb. Kgl. Preuss. Geol. Ladensanstalt*, **29**, 179 (1905).

[3] H. Burell, USA Patent N° 21611936 (1939).

[4] E. Bauer, *Helv. Chim. Acta*, **25**, 1202 (1942).

[5] F. Nachod, USA Patent, N° 2371119 (1945).

[6] F. N. Burstell, P. Y. Forrest, N. F. Kember and R. A. Wells, *Ind. Eng. Chem.*, (1953), 8, LV, 1948.

[7] I. N. Plaksin and M. S. Guirdasov, Brevet URSS N°. 108076 (1957).

[8] M. S. Guirdasov and I. N. Plaksin, *Izvest. VUZ Tvetnaia Metallurgia*, **1**, 74 (1959).

[9] J. Davison, F. O. Read, F. D. L. Noakes and T. V. Arden, *Bull. Min. and Met.*, **651**, 217 (1961).

ion-exchange resins for precious metals, noted in all papers, has hindered their use in gold hydrometallurgy, although in some cases, this lack of selectivity leads to the possibility of using ion exchange resins in cyanidation, because, after complete adsorption of all the complex cyanides and of the free cyanide, not only the precious metals can be recovered but also the alkaline cyanide,[10-12] which then can be recycled to leaching.

The aim of this work is to show how can ion exchange non-selective resins be used for gold recovery, in conjunction with cyanidation.

2. EXPERIMENTAL

2.1. RAW MATERIALS

The gold bearing raw material, on which the present research work was carried out, was the residue coming from an industrial plant in which the major part of the chalkophile elements, of gold and silver contained in the ore has been separated by flotation. These residues are commonly processed on an industrial scale by cyanidation to extract the remaining gold and silver. In the present investigation the feed material ground to 0.1 mm has cyanided for 6 hours with solutions containing 0.06% NaCN and 0.05% CaO, and the leach solutions after filtration had the following composition (in g/l):

Cu – 0.033
Fe – 0.0178
Zn – traces
SiO_2 – 0.007
NaCN – 0.34
CaO – 0.154
Au – 6 g/m^3
Ag – 0.8 g/m^3

The study of the adsorption was undertaken on different ion-exchange resins, chosen between those which, as the result of previous trials, had been shown to have the best adsorption characteristics and the best kinetics for gold and silver. All the resins used in the experiments were initially in the chloride form.

2.2. GOLD ADSORPTION BY ION EXCHANGE RESINS

The relatively simple composition of the solution obtained by cyaniding has allowed us to examine the use of highly basic resins. Previous research work has shown that these have a high adsorption capacity, but exhibit a law selectivity for gold. A typical highly basic resin AV–17 is the copolymerization product of chloromethylated styrene, having divinylbenzene as cross-linking substance. This resin was contacted with the gold-bearing solution under both staic and dynamic conditions, to determine the adsorption capacity and the saturation isotherms.

In the static conditions the resin was stirred with clarified solution or with pulp directly after cyaniding. From the chemical point of view the results were almost identical but the rate of adsorption from pulp solutions was lower. This, however, was due to the fact that resin size of the resin beads was larger in the RIP tests. The results obtained have made it possible to conclude that the main technological parameters are actually the same for the adsorption of the gold from clear and from pulp solutions.

---

[10] S. TĂTARU, "Primenenie ionnoobmennoi tekhnologii v usloviakh flotatsionno-tsianistogo portsessa" Disertatsia (1962), Moskva.

[11] I. BAIMAKOV and A. ZHURINE, "Elektroliz v khidrometallurghii", Metallurgizdat, Moskva, 1962, p. 254.

[12] I. N. PLAKSIN and S. TĂTARU, "Gidrometalurgia c primeniem ionitov", Ed. Metallurgia, Moskva, 1964, p. 74–169.

2.2.1. Influence of the accompanying elements on gold adsorption

The tests in which the ion-exchange resin and the industrial gold-bearing solution were contacted under dynamic conditions, passing the solution through a fixed resin bed at a constant rate of 1 l solution/1 l resin per minute, have shown that copper and iron saturate the resin rapidly, their concentrations in the effluent being equal to their concentration in the initial solution after passing about 600 volumes of solution through a single volume of resin. Once the saturation is reached, one notices a partial elution of the adsorbed copper and iron, their place being very probably taken by the free cyanide. The saturation of the resin by CN ions was observed after having passed about 1800 volumes of the solution. At this point some cyanide is present in the exit solution. The maximum dynamic capacity for gold was reached after having passed about 3 000 volumes of the solution for each volume of resin, and it was equal to 5.54 kg Au/m^3 resin. Under these conditions the resin contained the following quantities of other adsorbed components :

— silver	1.2 kg/m^3
— cooper	80 ,,
— iron	34 ,,
— NaCN	100 ,,

Because of the low selectivity of the resin regarding gold and silver, the proportion of precious metals on the resin is low.

2.2.2. Influence of the flotation reagents

As the majority of the flotation reagents pass into the pulp submitted to ion exchange, they can influence the adsorption of the gold by ion-exchange resins. To study this influence, controlled quantities of reagent were added, after cyanidation, to the industrial solution and adsorption tests then carried out under dynamic conditions.

The results obtained (figure 1) show that the collecting reagents have a negative influence on the adsorption of gold, by reducing the adsorption capacity for gold. This is very probably due to the adsorption of the reagents themselves by the resin.[13]

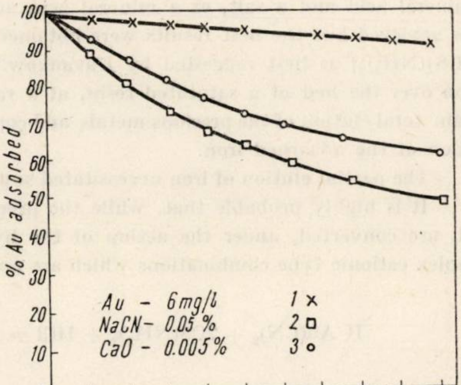

Fig. 1. — Influence of the flotation reagents on gold adsorption by the ion exchange resin AV—17

1, pine oil; *2*, butyl xanthate; *3*,aerofloat N 15.

---

[13] S. TĂTARU, *Studii și Cercetări de Metalurgie*, **2**, 139 (1965).

2.3. THE ELUTION

2.3.1. Elution by means of hydrochloric acid

With HCl solution (0.5 N) as the elution reagent it is possible to recover the cyanide after its decomposition in the resin phase, by the action of the acid. In the present work the equipment was operated at 600 mmHg pressure and the released hydrocyanic acid was entirely captured by the solution of the first flask.

The quantity of sodium cyanide determined in the Tishtchenko absorber exceeded by 36% the whole quantity of free cyanide adsorbed by the ionite resin, which infers that partial destruction of the adsorbed complex cyanides has taken place. The hydrochloric effluent, however, contained only 2% of the adsorbed copper and only traces of iron and the gold and silver were not eluated at all. It is, therefore, highly probable that the cyanide excess in the eluent is due to the formation, in the resin phase, of the iron and copper cyanides, poorer in CN.

By further adsorption into resin, partially eluated by HCl, it was possible, after 3 adsorption-eluation cycles, to obtain a higher degree of adsorption of gold and silver, and a more favourable proportion of precious metals in the resin phase, namely:

— gold . . . . . 8.8 kg/m^3 — cooper 112 kg/m^3
— silver . . . . . 2.7 ,, — iron . . . . 57 ,,
— NaCN . . . 41 ,,

This saturation procedure is however inconvenient, as it requires very strict measures to avoid release of hydrocyanic acid, and, having a fairly low efficiency, has been considered as lacking in practical importance.

2.3.2. Elution with a mixture of hydrochloric acid and thiocarbamide

Attempts have been made to eluate the resin by means of different mixtures containing a mineral acid and a salt, or a mineral acid and an organic solvent. Total elution has not been achieved but the best results were obtained by using a mixture containing 2% HCl and 6% $CS[(NH_2)_2]$ as first suggested by Davankow.[14] By passing a solution having this composition over the bed of a saturated resin, at a rate of 0.3 l/l resin-minute, it was possible to obtain total elution of the precious metals and copper, a recuperation of the cyanide and 93.2% elution of the adsorbed iron.

The partial elution of iron necessitated supplementary research work.

It is highly probable that, while the precious metals and the copper adsorbed on the resin are converted, under the action of the hydrochloric and thiocarbamide solution, into complex cationic type combinations which are not retained by the anionic resin:

$$R\,Au(CN)_2 + 2CS(NH_2)_2 + HCl = RCl + Au[CS(NH_2)_2]Cl + HCN \qquad (1)$$

the complex cyanides of iron are not totally decomposed by the mixture and remain in the resin phase.

Increasing the hydrochloric acid concentration in the elution mixture did not increase the quantity of eluated iron, but stimulated the formation of molecular sulphur.

[14] A. B. Davankov and V. M. Laufer, *Zhur. priklad. Khim.*, **32**, 117 (1959).

2.3.3. Elution by means of sodium cyanide

The total elution of the iron retained by the resin has been achieved by means of 2N NaCN solutions. By working in conditions identical to those mentioned above using concentrated cyanide solutions, a total elution of the iron that remained in the resin was possible. Though elution by means of concentrated sodium cyanide solutions, before or after elution by hydrochloric thiocarbamide solutions, is not very desirable, it has the advantage of being periodical, according to the accumulation of iron in the resin phase, and to imply only a consumption of hydrochloric acid and sodium hydroxide. The relevant elution curves are shown in figure 2.

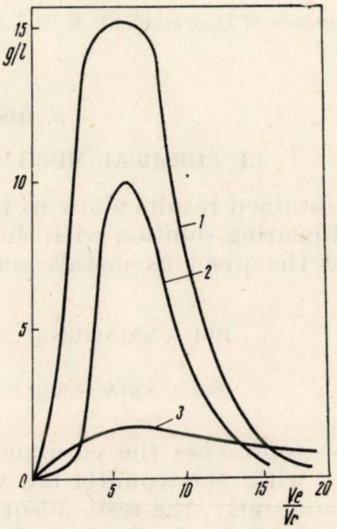

Fig. 2. — Elution of the ion exchange resin AV−17

1, Fe, by means of NaCN; *2*, Au, by means of HCl + CS(NH$_2$)$_2$; *3*, Fe, by means of HCl+CS(NH$_2$)$_2$: V_e/V_r is the ratio: volume of exit solution/volume of resin.

2.4. RECOVERY OF GOLD

The recovery of gold from hydrochloric thiocarbamide solutions after elution is possible by displacement with any less noble metal. Iron and copper were tested and have shown positive results but the precipitates obtained could not be conveniently treated by the existing technology.

2.4.1. Cementation with lead

The precipitation of gold by cementation with lead was tested both by passing an eluate solution containing 8.34 g Au/l over a granular lead bed and by stirring the solution thoroughly with lead powder. These experiments have shown that the lead surface has a preponderant role and that cementation by stirring is more advantageous since a finer powder can be used with no difficulties of a hydrodynamic nature.

The minimal lead consumption was 7.5 g Pb/g Au. This was obtained by contacting the eluate with lead particles having a 43 micron diameter.

Under these conditions the cementation by stirring had the advantage that the eluate was fully stripped and that of securing the depolarization of the cathodes of the system microelements through a continuous flow of solved oxygen fixing the released hydrogen.

The precipitate obtained by lead cementation was treated by cupellation and a "Dore" alloy was obtained which could be turned into good use.

2.4.2. Electrolytic precipitation of gold

The electrolytic precipitation of gold has proved more advantageous than other procedures. It has been achieved in several ways under different technological conditions. The use of pure gold cathodes has proved valuable for practical use but other materials are also suited for cathodes.[15]

The presence of thiocarbamide in the electrolyte has favoured the production of dense precipitates.[16]

3. DISCUSSION

3.1. CHEMICAL MECHANISM OF THE PROCESS

The obtained results allow us to conclude that during the contacting of the gold-bearing solution with the ion-exchange resins these adsorb the cyanides of the precious metals according to reactions of the following type :

$$\mathrm{RCl} + \mathrm{Na[Au(CN)_2]} \rightleftarrows \mathrm{RAu(CN)_2} + \mathrm{NaCl} \tag{2}$$

$$\mathrm{RCl} + \mathrm{Na[Ag(CN)_2]} \rightleftarrows \mathrm{RAg(CN)_2} + \mathrm{NaCl} \tag{3}$$

where : R — represents the cationic frame of the resin initially charged with the counter-ion Cl.

Concomitantly, the resin adsorbs the complex cyanides of the heavy metals contained in the feed to the ion exchange step :

$$\mathrm{RCl} + \mathrm{Na[Cu(CN)_2]} \rightleftarrows \mathrm{R[Cu(CN)_2]} + \mathrm{NaCl} \tag{4}$$

$$\mathrm{RCl} + \mathrm{Na[Cu(CN)_3]} \rightleftarrows \mathrm{R[Cu(CN)_3]} + \mathrm{NaC} \tag{5}$$

$$\mathrm{2RCl} + \mathrm{Na_2[Cu(CN)_3]} \rightleftarrows \mathrm{R_2[Cu(CN)_3]} + \mathrm{2NaCl} \tag{6}$$

$$\mathrm{2RCl} + \mathrm{Na_2[Zn(CN)_4]} \rightleftarrows \mathrm{R_2[Zn(CN)_4]} + \mathrm{2NaCl} \tag{7}$$

$$\mathrm{4RCl} + \mathrm{Na_4[Fe(CN)_6]} \rightleftarrows \mathrm{R_4[(Fe(CN)_6]} + \mathrm{4NaCl} \tag{8}$$

Taking into account the possible presence in the cyaniding solution of other complex cyanides and the different forms these may adopt, the above relationships can be synthetized in a more general form according to the equation :

$$\mathrm{nRCl} + \mathrm{Me(CN)}_i^{n-} \rightleftarrows \mathrm{R_nMe(CN)_i} + \mathrm{nCl^-} \tag{9}$$

---

[15] S. Tătaru, I. N. Plaksine and S. I. Sinelnikova, Brevet URSS N° 186707 (1966).

[16] S. Tătaru, Brevet R.S.R. N° 48367 (1963).

where :

Me — is the dissolved metal ;

n — is the valence of the complex anion ;

i — is the coordinative number.

It is worth mentioning that ion-exchange resin also adsorbs, concomitantly with the complex cyanides, the free cyanide in the solution :

$$RCl + NaCN \rightleftarrows RCN + NaCl \quad (10)$$

The lack of selectivity of the strongly basic ion-exchange resins for precious metals is not in this case, a disadvantage, as the acid thiocarbamide elution allows the recovery and recirculation of cyanide which occupied the major part of the active groups of the resin.

The contacting of the acid eluent with the saturated resin has permitted the replacement of the hydrocyanic ions by Cl^- ions :

$$RCN + HCl = RCl + HCN \quad (11)$$

The hydrocyanic acid thus released was absorbed in sodium hydroxide solution and transformed into an alkaline cyanide, which could then be recycled :

$$HCN + NaOH = NaCN + H_2O \quad (12)$$

The experiments undertaken have shown that the hydrocyanic acid resulting through the elution and the decomposition of the complex cyanides was totally converted into sodium cyanide.

The complex combinations of the copper adsorbed by the resin are eluted by the mixture of hydrochloric acid and thiocarbamide, and a complex cationic combination $Cu[CS(NH)_2]_2$ is formed. This is not held by the anionic resins. This elution of copper enables us to obtain a supplementary quantity of hydrocyanic acid, which, reacting with sodium hydroxide, forms the alkaline cyanide according to reaction (12).

The pecipitation of gold by means of lead powder takes place very probably according to a reaction [17,18] :

$$2Au[CS(NH_2)_2]_2Cl + Pb \longrightarrow Pb[CS(NH_2)_2]_4Cl_2 + 2Au \quad (13)$$

3.2. POSSIBILITIES OF CARRYING OUT THE PROCESS

There are several ways in which ion-exchange resins can be used in cyanidation, and the best way is determined by local conditions.

It is to be expected that the most difficulties will arise when the process is applied to the cyanidation of auriferous concentrates obtained

---

[17] I. E. Reynolds, *Ann. Chem. Pharm.*, **150**, 235 (1868).

[18] N. S. Kurnakov, *Zhur. rusk. fiz. Khim. Obschch*, 1891, 559.

by flotation. Indeed these have a high content of sulphur and of chalcophile elements, which form complex cyanides that can be adsorbed by the resin.

Conversely, one of the most favourable cases is very probably to be found when the process is applied to the cyanidation of auriferous tailings, as the tenor of sulphur and accompanying metalls is then at its lowest.

The results obtained enable us to suggest several possible variants for the use of ion-exchange resins in cyanidation ; two of these variants are presented below :

A — Cyanidation of auriferous raw material followed by separation of the phases and adsorption of the gold by ion-exchange resins from clarified solutions. This process is illustrated in figure 3.

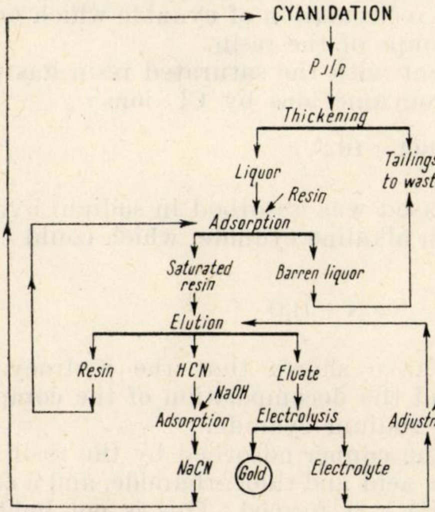
CYANIDATION
Pulp
Thickening
Liquor
Tailings to waste
Resin
Adsorption
Saturated resin
Barren liquor
Elution
Resin
HCN
Eluate
NaOH
HCL+CS(NH2)2
Adsorption
Electrolysis
Adjustment
NaCN
Gold
Electrolyte

Fig. 3. — Flowsheet for gold recovery from clarified cyanhydride solutions.

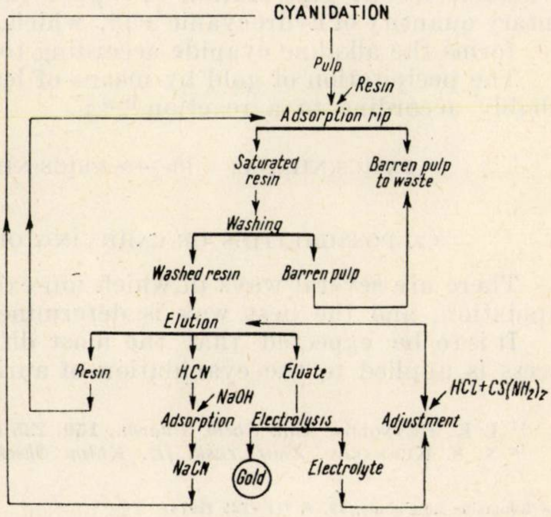
CYANIDATION
Pulp
Resin
Adsorption rip
Saturated resin
Barren pulp to waste
Washing
Washed resin
Barren pulp
Elution
Resin
HCN
Eluate
NaOH
HCL+CS(NH2)2
Adsorption
Electrolysis
Adjustment
NaCN
Gold
Electrolyte

Fig. 4. — Flowsheet for gold recovery from pulps.

In this case the adsorption is not selective, the ionite resin adsorbs, besides the gold cyanide, the complex cyanides of common metals and the free cyanide. The barren liquor can be sent to the waste-dump, together with the tailings from the last stage of the phase separation.

The saturated resin is submitted to elution by means of a 2 % HCl + +6% $CS(NH_2)_2$ solution. The hydrocyanic acid released in gaseous form is absorbed by a 20% NaOH solution, and the resulting sodium cyanide is recycled to leaching. The liquid eluate is submitted to electrolysis.

B. A second technological variation (figure 4) differs from the preceding one by the fact that the adsorption on the ion exchange resin does not take place from the clarified solution, but directly from the pulp, by the RIP (resin in pulp) procedure.

A technology without phase separation has positive repercussions on the economy of the procedure but its practical use is conditioned by the existence of ion exchange resins with high granulation and mechanical resistance, comparable, for instance, to those used in uranium hydrometallurgy ("RIP" procedure).

The efficiency of the procedure and exhaustion degree of the liquid phase depend on the number of devices in the adsorption chain, on the quality of the proportioning of the substances, and on the maintaining of the ratio resin/pulp.[19,20]

The economy of the process is influenced by the fact that a certain loss of resin in unavoidable after contacting it with a rather dense pulp, but the loss of gold with the macerated resin is immaterial, as it comes out of the apparatus with the poorest solution (the last contacting of the pulp before draining into the waste-dump).

The "Resin in Pulp" variant allows the use of the "counter-current" principle for the saturation of the resin, and a different retention time in each stage for the resin and for the pulp has proved favourable. The elution may also be carried out in counter-current (after a previous washing to remove the dirt) with a good-enough ruling of the gold content in the eluent.

We must point out that variant B offers obvious advantages compared to variant A as the resin totally adsorbs the gold of the liquid phase and ensures a better exhaustion of it, without requiring rather costly and difficult operations, such as tickening or washing on filters.

---

[19] S. TĂTARU, Romanian Brevet N° 54308 (1963).

[20] S. TĂTARU, Romanian Brevet N° 45311 (1963).

In the case the adsorption B, not selective, the entire resin adsorbs, besides the gold cyanide, the complex cyanides of common metals and the free cyanide. The barren liquor can be sent to the waste dump, together with the tailings from the last stage of the phase separation.

The saturated resin is submitted to elution by means of a $2\,N$ HCl + 6% NH_4Cl solution. The hydrocyanic acid released in gaseous form is adsorbed by a 20% NaOH solution, and the resulting sodium cyanide is recycled to leaching. The liquid eluate is submitted to electrolysis.

D. A severe technological variation (Figure 4) differs from the preceding one by the fact that the adsorption on the ion exchange resin does not take place from the clarified solution, but directly from the pulp by the "RIP" (resin in pulp) procedure.

A technology without phase separation has positive repercussions on the economy of the procedure but its practical use is conditioned by the existence of ion exchange resins with high granulation and mechanical resistance, comparable, for instance, to those used in uranium hydrometallurgy ("RIP" procedure).

The efficiency of the procedure and exhaustion degree of the liquid phase depend on the number of devices in the adsorption chain, on the quality of the proportioning of the substances, and on the maintaining of the ratio resin-pulp.[27,28]

The economy of the process is influenced by the fact that a certain loss of resin is unavoidable after contacting it with a rather dense pulp, but the loss of gold with the uncaptured resin is immaterial, as it comes out of the equipments with the poorest solution (the last contacting of the pulp before draining into the waste dump).

The "Resin in Pulp" variant allows the use of the "counter-current" principle for the saturation of the resin, and a different retention time in each stage for the resin and for the pulp has proved favourable. The elution may also be carried out in counter-current (after a previous washing to remove the dirt) with a good enough raising of the gold content in the eluent.

We must point out that variant B offers obvious advantages compared to variant A as the resin totally adsorbs the gold of the liquid phase and ensures a better exhaustion of it, without requiring rather costly and difficult operations, such as thickening or washing on filters.

---

[27] S. Tătaru, Roumanian Brevet Nº 51498 (1968).
[28] S. Tătaru, Roumanian Brevet Nº 49311 (1968).

Revue Roumaine de Chimie, **19**, *4*, 727–734 (1974)

CATALYTIC DEHYDROGENATION KINETICS OF *n*-BUTENES TO BUTADIENE

GEORGETA ANDREI, GHEORGHE ŞERBAN, CORINA FLORIŢA

Petrochim Research Institute, B-dul Republicii N° 291, Ploieşti, Romania

Received March 24, 1973

The present paper investigates the kinetics of dehydrogenation reaction of *n*-butenes to butadiene at temperatures ranging between 440–480°, at *n*-butenes partial pressures of 0.03 to 0.12 atm in the presence of water vapour, over a $Cr_2O_3-Fe_2O_3-ZnO$ catalyst. From the reaction rate data determined experimentally by the technique of a continuous differential reactor, it was found that the rate determining step is the surface reaction which is taking place on dual sites based on a Langmuir – Hinshelwood mechanism. The reaction rate constants, the adsorption equilibrium constants of *n*-butenes and hydrogen as well as the apparent activation energy for the transformation reaction on the catalyst, were calculated.

INTRODUCTION

Butadiene, one of the basic monomers used to obtain synthetic rubber is manufactured in industry by *n*-butenes catalytic dehydrogenation.

The practical and scientific importance of *n*-butenes catalytic dehydrogenation to butadiene is illustrated among others by a great number of papers referring to this item.

Thus, even since 1948, Beckberger and Watson have carried out a kinetic study on *n*-butenes dehydrogenation in the presence of water vapour and of a catalyst made of an oxides mixture.[1]

Using an integral reactor and a corresponding technique the authors have discovered experimentally that the rate-determining step is the surface reaction on dual active sites.

Another remarkable contribution to the elucidation of this reaction was brought by Balandin's papers.[2,3]

---

[1] L. H. Beckberger and K. M. Watson, *Chem. Eng. Progr.*, **44**, 229 (1948).

[2] A. A. Balandin, O. K. Bogdanova and A. P. Scheglova, *Izvest. Akad. Nauk S. S. S. R., Otdel khim. Nauk*, **1946**, 497.

[3] O. K. Bogdanova, A. P. Scheglova and A. A. Balandin, *Doklady Akad. Nauk S. S. S. R.*, **129**, 1293 (1959).

Important contributions to the study of the kinetics of *n*-butenes dehydrogenation to butadiene in the presence of water vapour and catalysts of oxide mixture type were brought by Liubarskii, Pşejetskii[4] and Tiuriaev.[5]

In all the above papers, the kinetic studies were performed on continuous integral reactors at high temperature.

Quite recently the researchers have started to use more and more frequently for the study of the kinetics of organic compounds dehydrogenation the technique of the continuous differential reactor at low conversions.

The authors of the present paper intend to apply this technique to the study of the kinetics of *n*-butenes dehydrogenation in the presence of water vapours on a catalyst made of a mixture of chromium, iron and zinc oxides.

The experimental data were read using the Langmuir-Hinshelwood mechanism, admitting that the *n*-butenes dehydrogenation rate is determined by the surface reaction which takes place on dual active sites.

EXPERIMENTAL

EQUIPMENT AND PROCEDURE

Chemical kinetics experiments were performed in a continuous type unit (fig. 1), in a microreactor with an inside diameter of 22 cm, equipped with a serpentine for preheating the gas mixture and heated with a bronze block furnace.

The reaction temperature was measured at the middle of the catalytic bed using a Philips microthermocouple and was kept constant with a precision of ±1°.

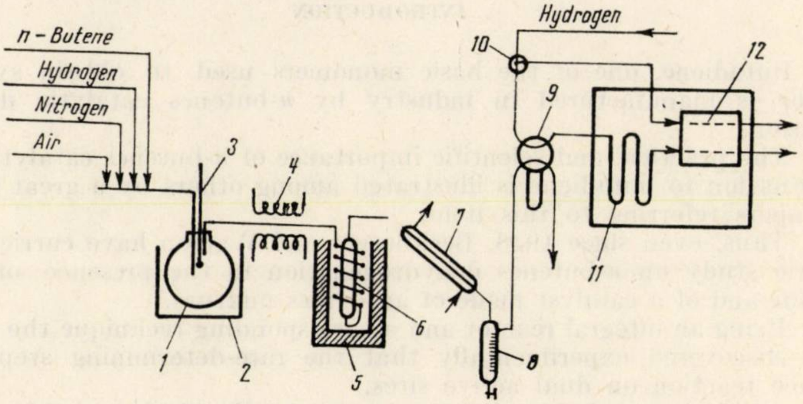

Fig. 1. — Installation scheme.

1, water saturator; 2, thermostat; 3, thermometer; 4, electric resistance; 5, bronze block furnace; 6, quartz reactor; 7, refrigerent; 8, collecting funnel; 9, chromatographic valve; 10, three-way stopcock; 11, chromatographic column; 12, conductivity detector.

---

[4] N. A. Scheglova and S. Ia. Pshejetskii, *Zhur. fiz. Khim.*, **28**, 1280 (1954).

[5] I. Ia. Tiuriaev and V. A. Kolobihin, *Kinetika i Kataliz.*, **2**, 429 (1961).

The mixture between *n*-butenes and water vapour, corresponding to the different partial pressure of the hydrocarbon, was achieved in an evaporator (1) heated by a thermostat (2).

At the reactor outlet, after condensing the water vapour, the reaction products were analysed using a Willy-Giede chromatograph equipped with a cell for thermal conductivity.

The chromatographic column had a length of 6 m, an inside diameter of 5 mm and was stuffed with celit of 100 – 200 mesh, impregnated with 20 % dimethylsulfolane.

Hydrogen was used as the carrier.

In all kinetic determinations 2 g were used of an industrial catalyst of the type Cr_2O_3, Fe_2O_3 and ZnO mixture, at a granulosity of 0.3 – 0.6 mm brought at the same activation conditions. The catalyst has BET surface area of 25 m^2/g and pores bulk volume of 0.342 cm^3/g. To avoid temperature gradients in the catalytic bed the catalyst was diluted with 10 cc quartz of the same granulosity.

The catalyst was heated up to the working temperature in a stream of inert gases (nitrogen or argon). After introducing the mixture of *n*-butene and water vapour in the reaction area, at a certain partial pressure for the *n*-butenes, gas samples were withdrawn from time to time in order to be analysed by chromatography up to the moment when a constant activity of the catalyst was reached. In order to check the kinetic data reproducibility the gas sampling was repeated several times. After finishing the kinetic experiments, at a certain temperature the regeneration of the catalyst with air and water vapour was performed up to the total disappearance of the carbon dioxide from the gaseous effluent at the reactor outlet.

The reaction rate was calculated from the value of *n*-butenes conversion to butadiene and the time factor using the following formula

$$r = x/w/F \tag{1}$$

where

r — reaction rate, mole/h g

x — butene conversion to butadiene, % moles

w — catalyst weight, g

F — *n*-butene feed rate, mole/h

The results of an analysis obtained at the dehydrogenation of a mixture of *n*-butene having a concentration of 98.8 % mole on $Cr_2O_3 - Fe_2O_3 - ZnO$ catalyst are given in table 1.

Table 1

An example for a typical analysis

Reaction temperature, °C	440
n-butenes partial pressure, at	0.05
n-butenes feed rate, l/h	1.8
n-butene/water, molar ratio	1 : 19
Catalyst weight, g	2
Chromatographic analyses for reaction products, % mole :	
Ethane + ethylene	—
Propane	—
Propylene	0.0014
1-butene	38.364
trans-2-butene	22.365
cis-2-butene	38.047
Butadiene	0.505
n-butene conversion to butadiene, % mole	0.511
Selectivity, % mole	99.730
Reaction rate, mole/h g catalyst	0.000205

EXPERIMENTAL RESULTS

PRELIMINARY RUNS

In order to establish the reaction conditions, in which the catalyst keeps its activity constant, preliminary studies were made on the variation of *n*-butenes conversion as function of the reaction temperature and *n*-butenes partial pressure.

Thus, maximum conversions of 3% moles were determined by experiment at temperatures ranging between 440 to 480° and *n*-butenes partial pressures of 0.03–0.12 at, corresponding to some dilution ratios of 1 : 32.3 – 1 : 7.3 mole of *n*-butene/water vapour.

The preliminary runs also included those which aimed at checking the catalyst stability in the most favourable conditions for cracking reactions. In this case it was found experimentally that after a reaction time of 280 min, the conversion for transforming *n*-butenes into butadiene remained practically constant.

By passing *n*-butenes over quartz, under favourable conditions for the cracking reaction, it was found by experiment that *n*-butenes conversion is negligible in comparison with that obtained in *n*-butenes catalytic dehydrogenation.

Thus, at *n*-butenes dehydrogenation at the maximum reaction temperature of 480° and *n*-butene feed rate of 1.08 l/h, the *n*-butenes total conversion under 0.02% mole was achieved.

INFLUENCE OF EXTERNAL DIFFUSION

To evaluate the effect of external diffusion on *n*-butenes dehydrogenation rate to butadiene, the value of the $\Delta P_B/P_B$ ratio was calculated in the reaction conditions, where ΔP_B represents the difference between *n*-butenes partial pressure in the gas stream and the partial pressure of the same gas at the surface of the catalytic particles.[6]

The $\Delta P_B/P_B$ ratio was calculated employing the following relation

$$\Delta P_B/P_B = r/a_m\, k_g P_B \tag{2}$$

where

P_B — *n*-butenes partial pressure, atm,

r — *n*-butenes transforming rate into butadiene, mole/h g, catalyst,

a_m — catalytic particles external surface, cm^2/g catalyst,

k_g — *n*-butenes mass transfer coefficient, mole/sec cm^2 atm.

The *n*-butenes mass transfer coefficient (k_g) was determined using the mass transfer factor J_D[7]. The value $\Delta P_B/P_B$ thus calculated of 0.000335 for the experimental determinations, performed on the catalyst studied, shows that the partial pressure decrease on catalyst is so small that the external diffusion effect can be neglected.

---

[6] S. Carra, L. Forni and C. Vintani, *J. Catalysis*, **9**, 154, (1967).

[7] J. De Acetis and G. Thodos, *Ind. Eng. Chem.*, **52**, 1003 (1960).

INFLUENCE OF INTERNAL DIFFUSION

The influence of *n*-butenes internal diffusion inside the catalyst particles was studied on Thiele modulus [8] calculated with the following formula

$$\O = r_p^2\ \rho_p r/\mathrm{Deff}\ C_B \tag{3}$$

in which

r_p — catalyst particle mean radius, cm,
ρ_p — catalyst density, g/cm³,
r — reaction rate, mole/h g catalyst,
Deff — the effective diffusion coefficient, cm²/sec,
C_B — the surface concentration of *n*-butenes.

For an effective diffusion coefficient of 0.0985 cm²/sec, at a temperature of 480°, the following values for Thiele modulus were found which correspond to different partial pressures

$$\begin{aligned} \O &= 0.00113, \text{ at } P_{C_4H_8} = 0.03 \text{ atm.} \\ \O &= 0.000467, \text{ at } P_{C_4H_8} = 0.12 \text{ atm.} \end{aligned} \tag{4}$$

The practical effectiveness factor is equal to unity for such small values of the Thiele modulus and thus it can be asserted that the internal diffusion does not influence the reaction rate.

REACTION KINETICS

The kinetics of *n*-butenes dehydrogenation to butadiene was studied by following the influence of *n*-butenes partial pressure upon the reaction rate at temperatures of 440°, 460°, 480° and $P_{C_4H_8} = 0.03-0.12$ atm.

From the values obtained for the reaction rates plotted in fig. 2 it can be noticed that the determining step for the reaction rate is the surface reaction which involves two active centres in compliance with the Langmuir — Hinshelwood mechanism.

The reaction rate equation corresponding to this mechanism in the case of *n*-butenes dehydrogenation reaction is

$$r = \frac{k_r b_B\ (P_B - P_D P_H/K)}{(1 + b_B P_B + b_D P_D + b_H P_H + b_A P_A)^2} \tag{5}$$

---

[8] C. N. Satterfield, "Mass Transfer in Heterogeneous Catalysis" M.I.T. Press, Cambridge, Mass, 1970, Chap. 4, p. 164–207.

where

k_r — reaction rate constant (mol/h g catalyst),

P_B, P_D, P_H, P_A — n-butenes, butadiene, hydrogen and water partial pressures, atm,

b_B, b_D, b_H, b_A — adsorption equilibrium constants for n-butenes, butadiene, hydrogen and water, atm^{-1},

K — equilibrium constant in gas phase, atm.

As by this technique low conversions (up to 3% vol) were obtained, working in conditions which were far from being in equilibrium (n-butenes conversions to butadiene were of 60—80% as compared with the equilibrium values) the influence of the reverse reaction and of the reaction products was neglected.

Equation (1) in a simplified form becomes

$$r = \frac{k_r\, b_B\, P_B}{(1+b_B P_B)^2} \tag{6}$$

From the plot of equation 6, under linearized form, both the reaction rate constants and the adsorption equilibrium constant of n-butenes for each reaction temperature (fig. 3) may be calculated.

Table 2 gives the values of n-butenes rate constants and adsorption equilibrium constants for the temperatures studied.

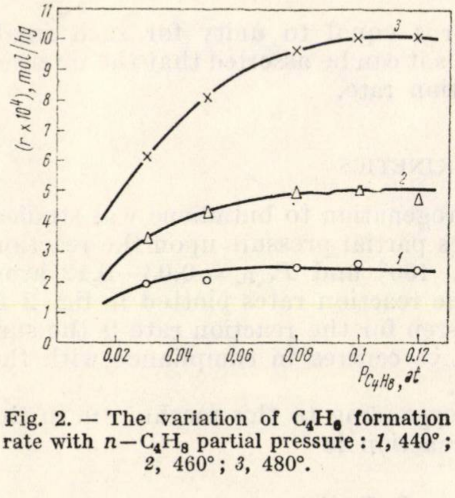

Fig. 2. — The variation of C_4H_6 formation rate with $n-C_4H_8$ partial pressure : *1*, 440° ; *2*, 460° ; *3*, 480°.

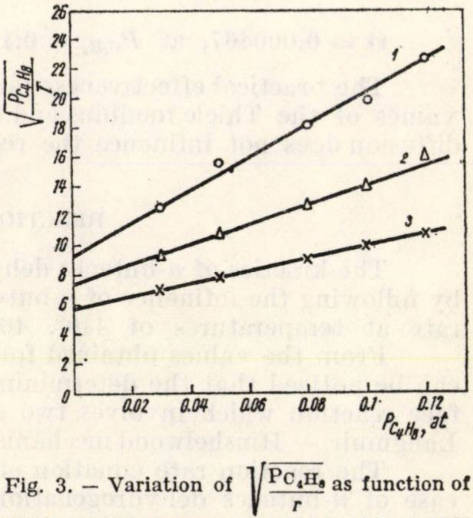

Fig. 3. — Variation of $\sqrt{\frac{P_{C_4H_8}}{r}}$ as function of n-C_4H_8 partial pressure : *1*, 440° ; *2*, 460° ; *3*, 480°.

To follow how the rates achieved by equation (6) verify the experimental results, the reaction rates were calculated using the values established for k_r and b_B (table 2).

From fig. 2 a good agreement can be noticed between the reaction rate values experimentally determined and the calculated values (solid-lines).

Using the Arrhenius plot, made in the well-known way (fig. 4), the activation energy of 36.840 cal/mol was obtained for *n*-butenes transformation reaction, on the studied catalyst, as well as the equation for $\log k_r$ determined by the absolute reaction temperature (T).

Table 2

Reaction rate and adsorption equilibrium constants

Temperature (°C)	$k_r \times 10^4$ (mol/h g catalyst)	b_B (atm^{-1})	b_{H_2} (atm^{-1})	$\frac{b_{H_2}}{b_B}$
440	10.00	12.345	10.646	0.86
460	20.20	9.279	8.556	0.92
480	40.48	7.782	6.656	0.85

$$\log k_r = 8.3 - \frac{36.840}{2.303\,R} \cdot \frac{1}{T} \tag{7}$$

In view of calculating the adsorption equilibrium constant for hydrogen, the reaction was performed at a constant partial pressure for *n*-butenes of 0.08 atm and hydrogen was introduced into the reaction zone at H_2/C_4H_8 molar ratios of 1 : 10 : 1 : 30.

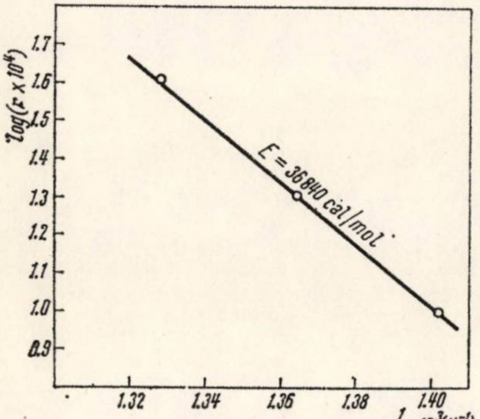

Fig. 4. — Variation of $\log (k_r \times 10^4)$ as function of $1/T$.

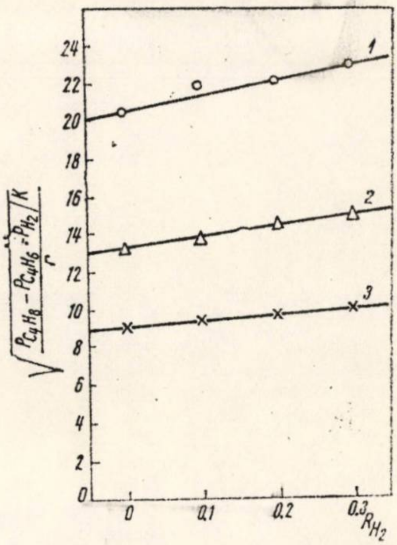

Fig. 5. — $\sqrt{\frac{P_{C_4H_8} - P_{C_4H_6}\ P_{H_2}/K}{r}}$ as function of R_{H_2}. (hydrogen/*n*-butenes molar ratio in the feed mixture) *1*, 440°; *2*, 460°; *3*, 480°.

Revue Roumaine de Chimie, **19**, *4*, 727–734 (1974)

In such a case equation (5) can be written

$$r = \frac{k_r b_B (P_B - P_D P_H / K)}{(1 + b_B P_B + b_H P_B R_H)^2} \tag{8}$$

in which R_H is the molar ratio for hydrogen and *n*-butene.

From the graphical representation of equation (8) under linearized form, the hydrogen adsorption equilibrium constants were calculated for the temperatures at which the reaction was performed (fig. 5).

Table 2 shows the hydrogen to *n*-butenes equilibrium constants ratios which are of 0.86 ; 0.92 ; 0.85 for the temperatures of 440°, 460°, 480°, these values being comparable with those from literature.[9]

CONCLUSIONS

From the present paper it may be seen that it is possible to use a continuous differential microreactor technique to study the kinetics of *n*-butenes catalytic dehydrogenation, a reaction frequently studied on an integral continuous reactor.

The kinetic data were read using the Langmuir-Hinshelwood mechanism.

---

[9] A. A. Balandin, O. K. Bogdanova and A. P. Scheglova, *Izvest. Akad. Nauk S.S.S.R., Otdel khim Nauk*, **1955**, 723.

Revue Roumaine de Chimie, **19**, *4*, 735–736 (1974)

COMPTE RENDU

ZENO SIMON, *Quantum Biochemistry and Specific Interactions*, Editura ştiinţifică, Bucharest, 1973, 270 p.

The book of Simon Zeno from the University of Timişoara fills a gap in the rather scarcely available literature in this field of interest. The particular concern manifested in recent years for the application of quantum chemistry to applied biochemistry studies proves the usefulness of a theoretical discipline in the development of applicative sciences. Only a quantitative handling of interactions occurring between highly complicated molecules found in living organisms can explain some of the experimentally obtained effects. The quantitative evaluation of interaction energies and also of spatial configurations of biologic macromolecules largely accounts for the properties of biomolecules. The extremely high specificity of living biomolecules still sets particularly difficult problems in front of biochemists who want to influence processes occurring within organisms.

The seven chapters of the book provide a balanced coverage of the proposed thematic field and the relevant bibliography is richly illustrated for those wishing to get an in-depth insight into the field.

1. *Introduction*. The reader is introduced to the problem area of biochemistry and of quantum chemistry, basic concepts of kinetics and chemical thermodynamics and also notions regarding the structural organization of biomolecules are presented.

2. *Molecular orbitals*. As shown by its title, the chapter deals with the theory of molecular orbitals and the types of chemical bond. Theories advanced by Hückel, Hoffman, Del Re, Pariser-Parr-Pople are presented alongside with some more up-to-date approaches. A particular emphasis is laid on molecular reactivity.

3. *Intermolecular forces*. The semi-empirical handling of intermolecular forces is presented through various approximations and their perturbational handling is mentioned in relation to electronic structure indices. Various types of possible interactions in biomolecules are treated, insisting on amino acids and nucleic acids.

4. *Electronic structure and biomolecular reactivity*. The author elaborates on the close relationship between the two factors, for proteins and amino acids, nitrate bases and nucleic acids, various active biological substances (cancerigenous, medicines). Enzymatic reactions and coenzymes (cofactors) are explained with reference to the electronic aspects of the enzymatic activity.

5. *Spatial structure of biomolecules*. A geometrical characterization of the spatial structure of biopolymers is made and energetic calculations related to the structure are performed. In conclusion the chapter deals with spatial structure of nucleic acids and with structural transitions.

6. *Specific interactions*. The chapter deals with the quantitative characterization of interaction specificity and with the role of spatial structure and of intermolecular forces. It is completed by 5 appendices explaining some calculations of relations being used and of the method of multiple correlation applied by the author.

7. *Analysis of some processes of recognition*. The last chapter reviews some enzymatic reactions, the precision in ADN replication and in the synthesis processes of proteins as well as hybridization — a competition between nucleic acids. The chapter ends with repressor-operator interactions, the specificity in immunity phenomena and with some ideas on cancer therapy.

The book leads to the conclusion that in our days quantum chemistry may be of use to biochemistry in explaining the magnitude of rate constants of various elementary reactions and their variation determined by molecular changes, and in sometimes predicting semiquantitatively the variations in question. Quantum chemistry may provide data on elementary reaction processes and on associative interactions between biomolecules.

Received December 7, 1973

D. I. Marzhidan

CORRIGENDUM

Im Artikel *Über die Synthese einiger Quartaren Pyridiniumsalze,* der in Nr. 8/1973 dieser Publikation erschienen ist, soll folgendes beachtet werden:

K (Kalium) — wird im Schema von Seite 1361 und in den Gleichungen I—VI von Seite 1362—1363, als zum Zyklus gehörend betrachtet.

NOTE POUR LES AUTEURS

La *Revue Roumaine de Chimie* publie des articles en anglais, français, russe, allemand ou espagnol. Les auteurs sont priés d'envoyer des articles, notes, communications et comptes rendus inédits.

Les manuscrits seront dactylographiés à deux intervalles. Les tableaux seront dactylographiés sur feuilles séparées, de même que la légende des figures. Les diagrammes seront tracés à l'encre de Chine sur papier calque. Les tableaux et les figures seront numérotés par des chiffres arabes, en nombre strictement nécessaire. Prière de ne pas inscrire les mêmes données dans les tableaux et les figures. Les formules chimiques seront incluses dans le texte ; en outre, elles seront transcrites sur des feuilles séparées. Les auteurs sont priés d'indiquer les caractères italiques (en soulignant les lettres au crayon), ainsi que tout autre caractère spécial. L'ordre des références bibliographiques sera celui de leur mention dans le texte ; le nom de l'auteur sera précédé de l'initiale du prénom ; les publications périodiques seront présentées suivant les prescriptions internationales. Les références seront ajoutées à la fin de l'article ; elles paraîtront comme des notes, au bas de la page. Le texte sera précédé d'un résumé, comprenant 15 lignes au maximum.

L'entière responsabilité du contenu des articles appartient aux auteurs. On publie des articles dus aux collaborateurs roumains ou étrangers. Les auteurs recevront 50 tirés à part.

PRINTED IN ROMANIA

1974 AUG 21

TRAVAUX PARUS AUX ÉDITIONS DE L'ACADÉMIE DE LA RÉPUBLIQUE SOCIALISTE DE ROUMANIE

- TIBERIU NĂSCUŢIU, **Metode radiochimice de analiză** (Methodes radiochimiques d'analyse) 1973, 384 p., 23 lei.
- MARIA FITI, **Dozimetria chimică a radiaţiilor ionizante** (La dosimétrie chimique des radiations ionisantes), 1973, 240 p., 13,50 lei.
- MIHAI FLORESCU, **Eficienţa economică a cercetării ştiinţifice** (L'efficience économique de la recherche scientifique), 1972, 115 p., 15 lei.
- GEORGETA LĂZĂRESCU, **Sistematizarea informaţiilor în Chimia organică** (La systématisation des informations dans la chimie organique), 1972, 252 p., 10,50 lei.
- P. BALTĂ et E. BALTĂ, **Introducere în chimia fizică a stării vitroase** (Introduction à la chimie physique de l'état vitreux), 1971, 240, 15,50 lei.
- LYDIA-MARIA VAICUM, **Biodegrabilitatea detergenţilor** (La biodégrabilité des détergents), 1971, 254 p., 16 lei.
- TIBERIU NĂSCUŢIU, **Metode radiometrice de analiză** (Méthodes radiométriques d'analyse), 1971, 346 p., 19,50 lei.
- I. ZUGRĂVESCU et L. STOICESCU-GRIVETZ, **Polimeri heterociclici** (Polymères hétérocycliques), 1971, 190 p., 9,50 lei.
- CRISTOFOR SIMIONESCU et C. V. UGLEA, **Fracţionarea compuşilor macromoleculari** (Fractionnement des composés macromoléculaires), 1962, 292 p., 18,50 lei.
- I. MAXIM, **Materiale nucleare** (Matériaux nucléaires), 1969, 444 p., 30 lei.
- CRISTOFOR SIMIONESCU et CLEOPATRA VASILIU-OPREA, **Mecanochimia compuşilor macromoleculari** (La mécanochimie des composés macromoléculaires), 1967, 344 p., 23,50 lei.
- CORNEL BODEA et collab., **Tratat de biochimie vegetală**, partea I, **Fitochimie** (Traité de biochimie végétale, Ire partie, Phytochimie), Ier vol., 1964, 747 p. + 4 annexes + 2 pl., 31 lei ; IIe vol., 1965, 1262 p., 1 pl., 56 lei ; IIIe vol., 1967, 773 p., 35 lei.
- V. GHEŢIE et V. MICUŞAN, **Analiza imunochimică. Teorie şi practică** (Analyse immunochimique. Théorie et pratique), 1966, 369 p., 28 lei.
- R. PORTOCALĂ et L. POPA, **Acizii ribonucleici celulari şi virali** (Les acides ribonucléiques cellulaires et viraux), 1966, 375 p., 8 pl., 26 lei.

I.P.I. – c. 1133

43 426

Lei 25.—

F 1103

R

REVUE ROUMAINE DE CHIMIE

REFERÁLVA

TOME 19
Nº 5
Mai 1974

RECHAX, **19**, *5*, 737–928 (1974)

ÉDITIONS DE L'ACADÉMIE DE LA RÉPUBLIQUE SOCIALISTE DE ROUMANIE

Rev. Roumaine Chim. **19**, *5*, p. 737–928 (1974), Bucarest

COMITÉ DE RÉDACTION

Rédacteur en chef:

I. G. MURGULESCU, membre de l'Académie de la République Socialiste de Roumanie

Rédacteurs en chef adjoints:

A.T. BALABAN et V. EM. SAHINI, membres correspondants de l'Académie de la République Socialiste de Roumanie

Collège de rédaction:

EM. BRATU, ELENA CEAUŞESCU, ECATERINA CIORĂNESCU - NENITZESCU, C. DRĂGULESCU, RALUCA RIPAN, CR. SIMIONESCU, membres de l'Académie de la République Socialiste de Roumanie; P. SPACU, membre correspondant de l'Académie de la République Socialiste de Roumanie; MARGARETA AVRAM, D. I. MARCHIDAN, G. NIAC, I. MOLDOVAN et D. SĂNDULESCU

La Revue Roumaine de Chimie paraît 12 fois par an. Toute commande de l'étranger (fascicules ou abonnements) sera adressée à Întreprinderea Rompresfilatelia, Boîte Postale 2001, telex 011631, Bucarest, Romania

Les manuscrits, les livres et les revues proposés en échange, ainsi que toute correspondance seront envoyés à la rédaction

REVUE ROUMAINE DE CHIMIE

23, str. Dumbrava Roşie, Bucarest, Roumanie

ÉDITIONS DE L'ACADÉMIE DE LA RÉPUBLIQUE SOCIALISTE DE ROUMANIE
3 bis, str. Gutenberg, Bucarest

The 4th National Conference of Pure and Applied Physical Chemistry will be held in Bucharest, Romania, between 2 and 5 Septembre, 1974.

TOPICS

The Conference will be organized in Sessions, covering the topics listed below :

1. Quantum chemistry ; theory of chemical bond ; molecular structure ; reactivity.

2. States of matter ; transport phenomena ; colloids ; chemical kinetics ; photochemistry ; radiochemistry.

3. Chemisorption ; homogeneous and heterogeneous catalysis ; catalytic reactions.

4. Chemical thermodynamics ; thermochemistry ; statistical thermodynamics ; thermodynamics of metallurgical processes ; thermodynamics of irreversible processes.

5. Electrochemistry ; solutions of electrolytes ; ionic liquids (molten salts) ; electrode processes ; electrometallurgy ; corrosion and anticorrosion protection.

6. Chemical engineering ; mass and heat transfer ; effect of surface phenomena ; kinetics of unit processes ; modelling, optimization and automation of processes in chemical industry.

7. Physico-chemical analysis ; automation of physicochemical analysis and control.

The official language of the Conference is Romanian ; foreign authors may deliver their papers in English, Russian, French, Spanish or German. No arrangements will be made for simultaneous translation.

The papers presented by Romanian authors will have their abstracts published in one of the above mentioned languages.

The Organizing Committee invites applications from prospective participants who wish to attend the Conference.

We hope that the Fourth National Conference of Pure and Applied Physical Chemistry will be of most interest to you and/or your colleagues, and would be happy to welcome you at our Conference.

Prof. dr. docent I. G. MURGULESCU
Chairman

ADDRESS :

CONFERINȚA DE CHIMIE FIZICĂ
Bucharest, Romania
Cable : **CHIMFIZ BUCUREȘTI ROMÂNIA**

REVUE ROUMAINE DE CHIMIE

ORSZÁGOS MŰSZAKI KÖNYVTÁR ÉS DOKUMENTÁCIÓS KÖZPONT 1883

Tome 19, N° 5 Mai 1974

I. G. MURGULESCU and A. LEIBOVICI, An equation of state for metallic liquids 739–745

D. R. ARMSTRONG, P. G. PERKINS and K. S. SORBIE, The electronic structures of BH_3 and BH_4^- 747–753

ELENA VOLANSCHI, C. VLĂDESCU and C. VOLANSCHI, ESR spectra of some anion-radicals from dibenzo-[b,e]-thiepinone and related compounds 755–761

S. STERNBERG and CONSTANȚA HERDLICKA, Interdiffusion and self-diffusion of monovalent cations in fused alkali nitrates and chlorides . . 763–778 Bef

R. L. BHATIA and H. C. GAUR, Chronopotentiometric study of Ag(I) in molten mixtures of alkali-alkaline earth metal nitrates 779–784

RODICA VÎLCU and I. CIOCĂZANU, Calorimetric kinetics. IV. The reaction of benzoyl chloride with sodium methoxide and ethoxide . . . . . 785–790 Bef

RODICA VÎLCU and ELENA LUCINESCU, Enthalpies of mixing of the carboxylic acid-water systems 791–799

C. DRĂGULESCU, S. POLICEC and T. SIMONESCU, Complexes of anthranil-N,N-diacetic acid with trivalent metals. III. Entropy change calculation 801–804

CONST. GH. MACAROVICI, MARIA BIROU, EUGENIA PERȚE and M. STRĂJESCU, Cobalt and germanium double oxides. 805–810

C. I. LEPĂDATU and CRISTINA RUSU, On the redox potentials in the transition - metal complexes 811–816

A. C. BANCIU and P. SPACU, Ni(II) chelates synthetized with 1-methyl-2-carbetoxy-glyoxalanil-(1)-tolylhydrazones-(2) 817–825

GH. MARCU, MARIANA RUSU and A. V. BOTAR, Heteropolytungstates with U(IV) as central atom. Synthesis and physico-chemical study of the UL_2 complex where $L = P_2W_{17}O_{61}^{10-}$ 827–831

A. BĂRBULESCU, Synthesis and thermal analysis of titanium oxyhydrate ultrafine powders 833–838

HAROLD KREHM and GEORGE F. WRIGHT, The hydroxymercuration of nor-bornene 839–845

S. M. ISMAIL, M. A. ALEEM and ASHRAF ALI, The activation of palladium catalysts by rare earth and other oxides for the hydrogenation of cyclohexene . . . . . 847–857 Bef

Revue Roumaine de Chimie 19, 5, 737–928 (1974) Bucarest

M. D. GHEORGHIU and P. FILIP, Electronic structure of cyclobutadiene fused with heterocyclic ring. I. Heterobenzocyclobutadienes 859–867

N. BĂRBULESCU et ANCA NICOLAE, Recherches dans la série des tricyclo [7.3.1.$0^{2,7}$] tridécanes. III. Hydrazones de la 2-hydroxy-8-R-tricyclo [7.3.1.$0^{2,7}$] tridécan-one-13 869–876

M. MORARU and G. M. BENEDIKT, On the conformational mobility of bicyclo [3.3.1] nonane-2-ones and bicyclo [3.2.1] octane-2-ones. 877–880

M. IOVU, G. CÎMPEANU et N. MICLOVICI, Tris-éthers. II. Condensation du bis(chlorométhyl)éther avec des cyclohexylphénoxydes, méthylcyclohexylphénoxydes et chlorocyclohexylphénoxydes de sodium 881–885

C. HÖLSZKY, COSTELA SUCIU, D. SĂNDULESCU, Über den Einfluss der Elektrolyten auf die Zähigkeit der Polyvinyl-Alkohol-Lösungen 887–901

VICTORIA DIMONIE, D. DONESCU, MARIANA MUNTEANU, C. HAGIOPOL and I. GAVĂT, Kinetics of emulsion polymerization of vinyl acetate in the presence of polyvinyl alcohol 903–910

ADELAIDA LIGA, I. NEGULESCU and CR. SIMIONESCU, Researches in the terpolymerization field. IV. Preliminary theoretical structural studies of some binary copolymers 911–919

ELENA HOPÎRTEAN, C. LITEANU and ANA MAŞA, Studies on the polymer+plasticizer membrane-electrode. XI. Influence of the plasticizer of the PVC on its electrode behaviour 921–927

Revue Roumaine de Chimie, 19, 5, 739–745 (1974)

AN EQUATION OF STATE FOR METALLIC LIQUIDS

I. G. MURGULESCU and A. LEIBOVICI

Center of Physical Chemistry,
str. Galaţi 31, Bucharest, Romania

Received December 7, 1973

It is shown that, assuming the validity of the Haber-Thomson model, the Buehler-Hirschfelder-Curtis equation of state leads to satisfactory results for liquid metals near their melting points.

It was shown in a previous paper[1] that, for liquids whose energy can be expressed by a relationship of the form:

$$a_M \frac{e^2}{V}, \tag{1}$$

the Lennard-Jones and Devonshire approximation:

$$\Psi(\rho) - \Psi(0) = \sum_n m_n \frac{1}{2}\int_0^\pi [\varphi(\sqrt{a_n^2 + \rho^2 - 2\rho a_n \cos\theta}) - \varphi(a_n)] \sin\theta \, d\theta, \tag{2}$$

in which the various symbols have well-known meaning[2], becomes equal to zero. Under these circumstances, the free volume v_f, generally defined by:

$$v_f = \int e^{-\frac{\Psi(\boldsymbol{r}_i) - \Psi(0)}{kT}} \, d\boldsymbol{r}_i,$$

takes a simple form:

$$v_f = \frac{4\pi}{3}(a - \sigma)^3, \tag{3}$$

---

[1] I. G. Murgulescu and E. Sălăgeanu, *Rev. Roumaine Chim.*, **17**, 603 (1972).

[2] J. A. Barker, "Lattice Theories of the Liquid State", Macmillan, New York, 1966, p. 50.

where σ is the diameter of the particles and a is a distance defined by :

$$a = \gamma^{1/3}\left(\frac{V}{N}\right)^{1/3} \tag{4}$$

In this expression V is the molar volume and N is the Avogadro number. γ can be 1, $3\sqrt{3}/4$, or $\sqrt{2}$ for simple cubic, body-centered cubic, face-centered cubic structure of the liquid, respectively.

The method of the partition functions leads to the following equation of state :

$$PV\left(1 - \frac{\sigma}{a}\right) = RT$$

This is the Buehler-Hirschfelder-Curtis equation [3], which was successfully applied to ionic liquids (molten salts) [4]. If we introduce eq. (4) in the previous one, we obtain :

$$PV\left(1 - \frac{2N^{1/3}}{\gamma^{1/3}\,V^{1/3}}\,r\right) = RT, \tag{5}$$

where r is the radius of particles in the liquid.

Therefore, we know that in the Haber-Thomson [5] model, the lattice energy of metals can also be expressed by an equation of the form (1), with r representing the distance between ions and electrons, unlike its meaning in eq. (1) where it denoted ion-ion distance. Extending the validity of the cell model to metallic liquids, we find out that eq. (5) can approximate the behaviour of these liquids as well.

In order to check up the validity of eq. (5) for metallic liquids, the expansion coefficients α_P and the compressibility coefficients β_T of some metallic liquids are calculated in the present paper and they are compared with the corresponding experimental data. We obtain from eq. (5):

$$\alpha_P = \frac{1}{V}\left(\frac{\partial V}{\partial T}\right)_P = \frac{1}{T}\cdot\frac{1 - \dfrac{2N^{1/3}}{\gamma^{1/3}V^{1/3}}\,r}{1 - \dfrac{2}{3}\,\dfrac{2N^{1/3}}{\gamma^{1/3}\,V^{1/3}}\,r}, \tag{6}$$

$$\beta_T = -\frac{1}{V}\left(\frac{\partial V}{\partial P}\right)_T = \frac{V}{RT}\cdot\frac{\left(1 - \dfrac{2N^{1/3}}{\gamma^{1/3}\,V^{1/3}}\,r\right)^2}{1 - \dfrac{2}{3}\cdot\dfrac{2N^{1/3}}{\gamma^{1/3}V^{1/3}}\,r} = \frac{V}{R}\,\alpha_P\left(1 - \frac{2N^{1/3}}{\gamma^{1/3}\,V^{1/3}}\,r\right) \tag{7}$$

---

[3] J. O. Hirschfelder, C. F. Curtis and R. Byron Bird, "Molecular Theory of Gases and Liquids", John Wiley & Sons, New York, London, 1954, p. 286.

[4] I. G. Murgulescu, *Rev. Roumaine Chim.*, **11**, 965 (1969); **15**, 1463 (1970).

[5] F. Haber, *Berl. Akad. Ber.*, **506**, 990 (1919); J. J. Thomson, *Phil. Mag.*, **43**, 721 (1922).

The experimental values for the expansion coefficients can be derived from the densities ρ by means of:

$$\alpha_P = \frac{1}{\rho}\left(\frac{\partial \rho}{\partial T}\right)_P \tag{8}$$

Within intervals of temperature of several hundred degrees, the densities can be expressed by linear equations of the form:

$$\rho = a - bT \tag{9}$$

where a and b are constant for the same metal. In table 1 these constants are given for the metals we shall refer to in the following;

Table 1

The constant a and b from eq. (9)

	a, g/cm^3	$b \cdot 10^4$ g/cm^{3}K	T, K
Li[6]	0.5541	0.9318	$T_m - 600$
Na[7]	1.0202	2.4310	$T_m - 900$
K[7]	0.9456	3.5000	$T_m - 700$
Rb[6]	1.6265	4.9500	$T_m - 450$
Cs[6]	2.0202	5.9742	$T_m - 500$
Cu[8]	9.9900	14.7500	$T_m - 1600$
Ag[9]	10.5310	9.7830	$T_m - 1500$
Au[9]	18.8600	11.8100	$T_m - 1600$
Mg[10]	1.8077	2.4166	$T_m - 1200$
Zn[10]	7.2990	10.6800	$T_m - 900$
Cd[11]	8.4390	8.6800	$T_m - 750$
Hg[12]	14.2600	24.4200	$T_m - 400$
Al[13]	2.6600	3.1100	$T_m - 1200$
Ga[14]	6.3200	7.2500	$T_m - 700$
Sn[15]	7.2390	6.9470	$T_m - 800$
Pb[10]	11.8700	16.3000	$T_m - 1000$
Bi[15]	10.8260	13.0790	$T_m - 700$
Fe[16]	9.8270	15.4500	$T_m - 1900$
Co[16]	9.9110	12.6800	$T_m - 1900$
Ni[16]	9.7360	11.4500	$T_m - 1900$

---

[6] E. N. C. ANDRADE and E. R. DOBBS, *Proc. Roy. Soc.*, **211A**, 12 (1952).

[7] C. T. ERWING, J. A. GRAND and R. R. MILLER, *J. Amer. Chem. Soc.*, **73**, 1168 (1951); *J. Phys. Chem.*, **58**, 1086 (1954).

[8] E. GEBHARDT, M. BECKER and S. SHÄFER, *Z. Metallk.*, **43**, 292 (1952).

[9] E. GEBHARDT and G. WÖRWAG, *ibid.*, **42**, 358 (1951); **43**, 106 (1951).

[10] E. GEBHARDT, M. BECKER and E. TRËGNER, *ibid.*, **46**, 90 (1955); **44**, 379 (1953).

[11] C. J. SMITHELLS, "Metals References Book", vol. 2, 2nd ed., Butterworth Sci. Pub., London, 1955, p. 639.

[12] "Handbook of Chemistry and Physics", 41 ed., Chemical Rubber Pub. Co., Cleveland, Ohio, 1959–1960, p. 2185.

[13] E. GEBHARDT, M. BECKER and S. DARNER, *Z. Metallk.*, **44**, 510(1953).

[14] K. E. SPELLS, *Proc. Phys. Soc.*, **48**, 299 (1936).

[15] E. GEBHARDT, M. BECKER, H. SEBASTIAN, *Z. Metallk*, **46**, 684 (1956) **48**, 601 (1957).

[16] L. D. LUCAS, *Compt. rend.*, **250**, 1850 (1966).

they have been evaluated from the existing data concerning metal densities. The temperature interval, starting from the melting point, within which the constants a and b are valid, is given in the last column of the table.

Table 2 allows us to compare the expansion coefficients of several metallic liquids, calculated by eq. (6), with the experimental values, derived from the densities by means of eq. (8) and eq. (9), for the melting temperature. We chose this value of the temperature for comparison since under these circumstances the liquids respond best for the demands of the cell model, which is the basis for eq. (5).

Table 2

Expansion coefficients of metallic liquids, at the melting temperature

	T_m K	ρ_m g/cm^3	V_m cm^3	r A	$\alpha_m \cdot 10^4$ degree^{-1} exp., eq. (8)	$\alpha_m \cdot 10^4$ degree^{-1} calcd., eq. (6)
Li	453.15	0.512	13.56	1.519	1.82	2.53
Na	370.95	0.930	24.73	1.858	2.61	2.99
K	336.75	0.828	47.12	2.272	4.23	4.29
Rb	311.95	1.472	58.08	2.475	3.37	3.41
Cs	311.65	1.840	72.29	2.654	3.25	3.78
Cu	1356.15	7.990	7.95	1.278	1.89	0.75
Ag	1239.95	9.138	11.82	1.444	1.07	1.02
Au	1336.15	17.280	11.40	1.442	0.68	0.74
Mg	932.15	1.585	15.33	1.598	1.53	0.97
Zn	692.65	6.560	9.97	1.332	1.63	2.61
Cd	594.15	7.923	14.19	1.489	1.10	2.98
Hg	234.25	13.691	14.65	1.502	1.78	8.24
Al	933.15	2.370	11.39	1.432	1.31	1.25
Ga	302.95	6.100	11.43	1.221	1.19	13.32
Sn	505.05	6.946	17.09	1.405	0.83	7.83
Pb	600.55	10.895	19.02	1.750	1.50	0.64
Bi	544.15	10.079	20.74	1.547	1.36	6.44
Fe	1810.15	7.030	7.93	1.241	2.20	0.94
Co	1765.15	7.673	7.677	1.253	1.65	0.69
Ni	1726.15	7.760	7.565	1.246	1.48	0.71

The value $\sqrt{2}$ was adopted for γ, which agrees with what is likely to come out from the X ray analysis of the molten metals. The significance of various columns of table 2 needs no explanation.

As one can see in table 2, the expansion coefficients of the alkaline metals, silver and aluminium, calculated according to eq. (6), are in good agreement with those derived from the densities using eq. (8). A good agreement is found in the case of many metals as Cu, Au, Zn, Cd, Pb, and Fe, Co, Ni too. Hg, Ga, Sn, and Bi present very high theoretical values compared with the experimental ones. As it is known, these elements form complex lattices, which suggests they are far from ideal metallic state. These are the metals, the limit molecular volumes of which, found from the viscosity equation of Bacinski, display striking anomalies, as it was shown in a previous paper[17].

---

[17] I. G. Murgulescu and M. Şerban, *Rev. Roumaine Chim.*, **17**, 431 (1972).

The compressibility coefficients were evaluated from the propagation speed of ultrasound v_l. The adiabatic compressibility β_S is given directly by eq.:

$$\beta_S = \frac{1}{\rho v_l^2}, \tag{10}$$

where ρ is the fluid density. The value of the isothermal compressibility, which is to be the object of the following considerations, is given by eq.:

$$\beta_T = \gamma \beta_S = \frac{\gamma}{\rho v_l^2}$$

where γ is the ratio of the heat capacities C_P/C_V. Taking into account the Lewis equation:

$$C_P - C_V = \frac{\alpha_P^2 V}{\beta_T} T,$$

the previous relation becomes:

$$\beta_T = \frac{1}{\rho v_l^2} + \frac{\alpha_P^2 V}{C_P} T \tag{11}$$

We shall use this relation within our computations.

In table 3 the compressibility coefficients of several metallic liquids derived from eq. (7), are given together with those obtained from the speed of ultrasound, according to eq. (11).

The expansion coefficients and the other magnitudes needed (T_m, ρ_m, etc.) in eq. (11) were taken from table 2.

Examination of table 3 shows that the agreement of theoretical and experimental values of the compressibility coefficients is hardly satisfactory. For real metals, the calculated values are generally much lower than the experimental ones. But for elements whose behaviour is far from that of the metallic state, such as Hg, Sn, Bi, the theoretical values of the liquid state compressibility coefficients are largely higher than the corresponding experimental values.

Such a behaviour is contrary to what we found when studying the respective expansion coefficients.

The behaviour of Zn and Cd is to be placed between the two indicated extreme behaviours; in this case, the agreement between the calculated and experimental values is satisfactory.

All these results are in full agreement with those derived from the study of the metallic liquid viscosity [17].

Table 3

Compressibilities of metallic liquids at the melting points

	T_m K	ρ_m g/cm^3	V_m cm^3/mol	r A	v_l [18] m/s	C_p [19] cal/mol K	$\beta_T \cdot 10^{11}$ cm^2 dyne^{-1}	
							calcd. eq. (7)	exp. eq. (11)
Na	370.95	0.930	24.73	1.858	2526	7.61	0.36	1.87
K	336.75	0.828	47.12	2.272	1890	7.68	1.30	4.27
Rb	311.95	1.472	58.08	2.475	1260	7.50	0.91	4.93
Cs	301.65	1.840	72.29	2.654	967	7.62	1.35	6.53
Cu	1356.15	7.990	7.95	1.278	3460	7.50	0.026	0.224
Ag	1239.95	9.138	11.82	1.444	2710	7.50	0.066	0.203
Zn	692.65	6.560	9.97	1.332	2712	7.50	0.31	0.27
Cd	594.15	7.923	14.19	1.489	2166	7.10	0.38	0.30
Hg	234.25	13.691	14.65	1.502	1478	6.81	1.11	0.37
Al	933.15	3.370	11.39	1.432	4670	7.00	0.072	0.256
Ga	302.95	6.100	11.43	1.221	2873	6.62	3.38	0.22
Sn	505.05	6.947	17.09	1.405	2464	7.10	2.88	0.26
Pb	600.55	10.895	19.02	1.750	1776	7.32	0.019	0.374
Bi	744.15	10.079	20.74	1.547	1649	7.60	2.45	0.43

In order to extend the validity of Buehler-Hirschfelder-Curtis equation to metallic liquids, let us observe that the ratio of experimental compressibility over the respective calculated value stays, for ideal metallic liquids of constant valence, within the 4—5 interval and, for those of variable valence, within 4—5 times their maximum valence. Then eq. (5) becomes:

$$PV\left(1-\frac{2N^{1/3}}{\gamma^{1/3}V^{1/3}}r\right)=\frac{RT}{5n_v}, \tag{12}$$

where n_v is, for the liquids of the elements of variable valence, equal to the maximum valence (the number of unpaired electrons).

The expression for the compressibility coefficient takes the form:

$$\beta_T=\frac{5n_v V}{R}\cdot\frac{\left(1-\frac{2N^{1/3}}{\gamma^{1/3}V^{1/3}}r\right)^2}{1-\frac{2}{3}\,\frac{2N^{1/3}}{\gamma^{1/3}V^{1/3}}r}=\frac{5n_v V}{R}\,\alpha_P\left(1-\frac{2N^{1/3}}{\gamma^{1/3}V^{1/3}}r\right) \tag{7'}$$

The values in table 4 were calculated by using this equation. The data needed were taken out of the preceeding table 3.

The accordance between the values derived from eq. (7′) and the experimental ones is satisfactory and prove the validity of eq. (12). It

---

[18] R. T. Smith, G. M. B. Webber, F. R. Young and R. W. B. Stephens, *Adv. Phys.*, **16**, 515 (1967).

[19] J. R. Wilson, *Metallurgical Reviews*, **10**, *40*, 1965.

Table 4

Compressibility coefficients at the melting temperature

	n_v	$\beta\ 10^{11}$ cm^2 dyne^{-1}	
		calcd. eq. (7)	exper. eq. (11)
Na	1	1.80	1.87
K	1	6.50	4.27
Rb	1	4.55	4.93
Cs	1	6.75	6.53
Ag	1	0.33	0.20
Al	1	0.36	0.26
Cu	2	0.26	0.22
Pb	4	0.38	0.37

is not likely that eq. (7′) should be verified in the case of the elements far from the ideal metallic state (especially in the case of Ga, Sn, Bi).

Until a theoretical justification for introducing the corrective term $5n_v$ is found, eq. (12) should be considered as partially empirical.

Revue Roumaine de Chimie, **19**, 5, 747–753 (1974)

THE ELECTRONIC STRUCTURES OF BH_3 and BH_4

D. R. ARMSTRONG, P. G. PERKINS and K. S. SORBIE

Department of Pure and Applied Chemistry, University of Strathclyde,
Glasgow Gl 1XI, Scotland

Received August 27, 1973

The electronic structures and energies of the species BH_3 and BH_4^- have been examined by *ab initio* calculations. The effect of surrounding the anion by four cationic point charges ont its electronic properties is reported. Vibrational frequencies calculated from the data are in good agreement with experiment. The thermodynamics of the reaction $BH_3 + H^- \rightarrow BH_4^-$ was also studied and heat of formation ΔH_f in the gas-phase was calculated to be -278.6 kJ mol^{-1}.

BH_3 and BH_4^- are the simplest boron-hydrogen species although the former exists only as the dimer B_2H_6 in the laboratory. Nevertheless BH_3 has been postulated to occur as an intermediate in a number of boron hydride degradation reactions [1], and low-temperature matrix isolation may yet detect this unstable species. Hence, it is of some interest to study its electronic structure particularly in relation to its coordination complexes. The simplest of these is the borohydride anion : borohydrides (*e.g.* $NaBH_4$) are frequently good, mild, selective, reducing agents and, as such, find common use in organic synthesis. Determination of the crystal structure of $NaBH_4$ shows that it possesses a face-centred cubic lattice [2]. However, it is also observed that the BH_4^- ion is sterically free to rotate in its environment. Hence, the ion experiences a symmetrical distribution of positive cationic charges.

The purpose of this paper is to present results of *ab initio* calculations on the electronic structures of the two species BH_3 and BH_4^- and on the thermodynamics of the reaction.

$$BH_{3(g)} + H^-_{(g)} \rightarrow BH^-_{4(g)}$$

The calculations were performed within the standard LCAO-MO-SCF formalism [3] in which all atomic orbitals are represented by Gaussian functions [4]. In the case of the boron atomic orbitals, nine *s* and five *p* Gaussian primitive orbitals [5] were contracted to four *s* and two *p* orbitals respectively, whilst two contracted orbitals were formed from four primitive *s* Gaussian orbitals simulated the hydrogen 1*s* orbital.

---

[1] L. H. Long, *J. Inorg. Nuclear Chem.*, **32**, 1097 (1970).

[2] A. M. Soldate, *J. Amer. Chem. Soc.*, **69**, 987 (1947).

[3] C. C. J. Roothaan, *Revs. Mod. Phys.*, **23**, 69 (1951).

RESULTS AND DISCUSSION

a. BOND LENGTH OPTIMISATION AND CALCULATION OF SELECTED VIBRATION FREQUENCIES

The optimum bond lengths for both species were obtained by minimising the total energy with respect to the B—H bond distances. For obvious reasons all of these were simultaneously varied in phase. When this is carried out for BH_3 the calculated bond length is 0.119 nm a value very similar to that found for terminal B—H bonds in the higher boron hydrides. [6] The computed bond length in the borohydride ion spans 0.124 nm, in good agreement with that in sodium borohydride [2] (0.125nm). The longer bond length in the tetrahedral case is rationalised on the basis that the higher coordination number in the ion introduces powerful interelectronic repulsions which are relieved mainly by the expansion of the electron cloud and hence the whole anion.

Changes in bond length for optimisation purposes simulate the bond stretching vibrations of the system, in this case the totally symmetric breathing frequencies. For small atomic displacements Δx, the change in energy is given by,

$$\Delta E = \frac{1}{2} k (\Delta x)^2$$

The force constant, k, also interconnects the vibrational frequency, ν, and the reduced mass m^* of the system thus

$$\nu = \frac{1}{2\pi} \sqrt{\frac{k}{m^*}}$$

Hence, the vibrational frequency of the symmetrical stretching mode should be obtainable from the energy *vs* bond length calculations. It is of course the whole normal coordinate for ν_1 we should deal with here but it is possible to introduce a reasonable simplification *i.e.* as it is the force constant of one bond that is involved, we use the approximation that the energy required to stretch one bond in BH_3 and BH_4^- is one-third and one-quarter of the energy needed to stretch all the bonds in BH_3

---

[4] S. F. Boys, *Proc. Roy. Soc.* (A) **200**, 542 (1950).

[5] S. Huzinaga, *J. Chem. Phys.*, **42**, 1292 (1965).

[6] W. N. Lipscomb, "Boron Hydrides", W. A. Benjamin, New York, 1963.

and BH_4^-, respectively. The calculated vibrational frequencies are then 2405 cm^{-1} and 2100 cm^{-1} for the borohydride and borane entities, respectively. Considering the approximations involved, the agreement with the experimental values (2264 cm^{-1} for BH_4^- [7] observed in the Raman, and 2400 cm^{-1} for BH_3[8]) is very satisfactory.

A further calculation of the E; ν_2 deformation mode of BH_4^- was next attempted. In a similar way to the calculation of the ν_1 mode the force constant is again defined by the equation cited. In this case, however, the change in energy ΔE is caused by small angle displacements $\Delta\theta$ and hence Δx can be equated to $R_0 \sin \Delta\theta$. It is assumed that, during this mode of vibration, the bond length R_0 remains constant at the optimal value. Hence, the energy of the BH_4^- anion was computed in a number of cases incorporating small variations in the $H\hat{B}H$ bond angle (for example, 2° contraction and 3° expansion) in a manner consistent with the motion of the hydrogen atoms in the ν_2 vibrational mode. We again made the assumption that there was a simple relation between the deformation energy of one bond and that of the whole molecule. For the ν_2 mode of BH_4^- we obtained the values 1308 cm^{-1} and 1300 cm^{-1} for the 2° contraction and 3° expansion, respectively. These values are in reasonable agreement with experiment (1205 cm^{-1} [7]).

We can reasonably project that this approach to calculating vibrational modes of molecules will give good agreement with experiment in other cases. This is of particular value when the computation involved in a more accurate model for a certain molecule is very heavy. For BH_3 and BH_4^- we expect that employment of a larger basis set could yield very accurate values for the energies of these vibrational modes.

b. BH_4^- IN A CRYSTAL LATTICE

In the crystal lattice the BH_4^- ion is associated with a gegenion. A natural question is how the crystal lattice influences the electronic properties of the borohydride ion. In an attempt to obtain a picture of BH_4^- surrounded by cationic species, as in the crystal, four positive charges of magnitude 0.25 were placed at a distance of 0.307 nm from the boron atom each along a line projected from the B—H bonds. This model was chosen as it is simple yet presents a fairly accurate picture of the sodium borohydride lattice. Although the lattice has a face-centred cubic structure, the borohydride ion is free to rotate and so an essentially spherically symmetrical distribution of positive charge is experienced by the anion.

The optimum B—H bond length was redetermined from a number of calculations and a value of 0.125 nm was obtained. The length is in better agreement with the experimental value than the distance calculated in section (*a*). Utilising these results the symmetric stretch vibrational mode ν_1 was recalculated and a value of 2240 cm^{-1} was obtained. This is closer to experiment than the non-ionic model. Thus, we can conclude that our simple model is a reasonable representation of the ionic borohydride ion.

---

[7] R. C. Taylor, D. R. Shultz and A. R. Emery, *J. Amer. Chem. Soc.* **80**, 27 (1958).

[8] J. R. Morrey, A. B. Johnson, Y. Fu, and G. R. Mill, *Advances in Chemistry Ser.*, **32**, 157 (1961).

Imposition of a tetrahedral array of positive charges about BH_4^- lowers the total energy of the system by 357.4 kJ mol^{-1}. This stabilisation energy is related to the lattice energy although clearly not equal to it since our model only simulates the immediate environment of BH_4^- and does not attempt to describe an infinite lattice. Nevertheless, it clearly illustrates the order of energy gain by an anion due to the introduction of positive charges.

The eigenvalues of BH_4^- are also dramatically lowered in value by the surrounding cations. Figure 1 shows the increase in stability of each molecular orbital due to superimposition of the point charges. At the optimum bond length the $1t_2$ and $2a_1$ levels become more stable to the extent of 5.21 eV whilst the $1a_1$ orbital loses 3.90 eV. This is to be expected as the higher energy molecular orbitals are more diffuse and interact more strongly with the positive charges. A chemical effect which may well arise from this anion stabilisation occurs in reactions which proceed readily with $M^+ X^-$ but much less well with M'^+X^- although X^- is known to be the important reacting species. For instance, the chemistry of the

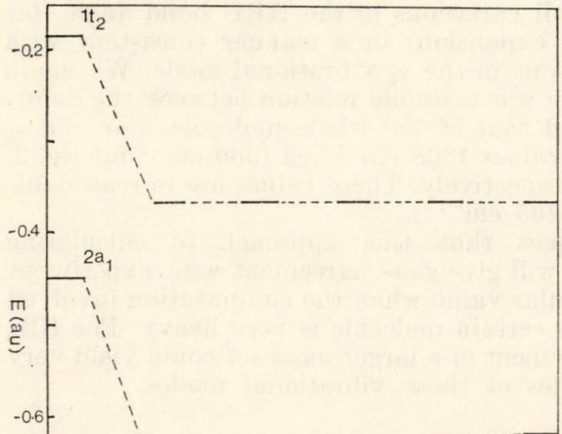

Fig. 1. — Effect on energy levels of BH_4^- of change in r(B — H) in a lattice.

borohydride salts[9] depends largely upon the cation present. Addition of certain metal ions to sodium borohydride enhances the reducing power and produces a more selective reagent. We expect that these different spheres of positive charge will exert a different influence on the eigenvalues for BH_4^- and hence alter the reduction potential of the hydrogen atoms.

A survey of the change in energy of the two occupied a_1 orbitals with the B–H bond length (figure 1) reveals that the lowest filled orbital becomes stabilised whilst the $2a_1$ level gains energy when the B–H bond length is increased. The $1a_1$ orbital, which is largely composed of boron $1s$, must become more stable due to smaller interelectronic repulsion energy as the hydrogen atoms move away from the central atom. The $2a_1$ orbital is a bonding orbital involving the boron $2s$ orbital and the hydrogen s orbital and so becomes destabilised as the overlaps of the boron-hydrogen orbitals diminish. The $1t_2$ level remains constant while the bond length is varied and so the change in the various energy terms must effectively be neutralized.

c. MULLIKEN POPULATION ANALYSIS [10]

The overlap and gross atomic populations of BH_3, BH_4^- and BH_4^- in a lattice are presented in table 1. In BH_3 there is no polarisation of electronic charge whereas on the addition of the hydride ion, the excess electronic charge builds up mainly on the boron atom. On surrounding the BH_4^- ion by positive charges an appreciable electron flow from the boron to the hydrogen atoms is caused with a resulting weakening in the bonding framework.

Table 1

Electronic populations of BH_3, and BH_4^-

	Atomic populations		B–H overlap population
	boron	hydrogen	
BH_3	−0.078	+0.026	0.408
BH_4^-	−0.307	−0.173	0.401
BH_4^- [a]	−0.038	−0.241	0.382

[a] in this calculation the ion was enclosed in a lattice of positive charges.

---

[9] R. M. Adams and A. R. Siedle "Boron, Metallo-Boron Compounds and Boranes", Interscience, New York, 1964, p. 429.

[10] R. S. Mulliken, *J. Chem. Phys.* **23**, 1833 (1955).

d. THERMODYNAMICS OF COMPLEX ION FORMATION

The heat of the reaction

$$H^-_{(g)} + BH_{3(g)} \rightarrow BH^-_{4(g)}$$

at $T°$ K is given by

$$\Delta H_T = \Delta E_T - RT$$

where ΔE_T is the difference in total energy between BH_4^- and the combined total energies of BH_3 and H^-. The total energy of a species is made up of the following terms

$$E_T = E_{HF} + E_{vib} + E_{trans} + E_{rot} + E_{corr} + E_{rel}$$

where E_{HF} is the computed Hartree-Fock energy, E_{vib} is the zero-point vibrational energy, E_{rot} is the rotational energy, E_{trans} is the translational energy, E_{corr} is the correlation energy, and E_{rel} is the relativistic energy.

At 0° K the rotational and translational energies are zero. The vibrational energy is of course not zero and was calculated from

$$E_{vib} = \frac{1}{2} h \sum_i \nu_i$$

where the ν_i are the fundamental vibration frequencies. These are known for BH_4^-[7,11]: for BH_3 the vibration species were obtained from ref. 8. The correlation energy was obtained by using the pair population method of Hollister and Sinanoglu[12]. In this procedure the energy is evaluated in terms of the gross atomic populations ρ_i and the atomic orbital correlation energies,[13] e_{ij}

$$E_{corr} = \frac{1}{2} \sum_i e_{ii} \rho_i + \sum_{i>j} \sum e_{ij} \rho_i \rho_j$$

The relativistic energy was not evaluated as it has been shown[14] that it is an atomic constant independent of the chemical environment and so ΔE_{rel} will be zero.

The calculated energies refer to the absolute zero and we must adjust them to a more convenient reference temperature. This can be

---

[11] G. Herzberg, "Infrared and Raman Spectra", Ván Nostrand Inc., N. Y., 1945.

[12] G. Hollister and O. Sinanoglu, *J. Amer. Chem. Soc.*, **88**, 13 (1966).

[13] R. K. Nesbet, *Phys. Rev.*, **155**, 56 (1967).

[14] E. Clementi and A. D. McLean, *Phys. Rev.*, **133**, 4419 (1964).

accomplished *via* the integrated form of Kirchoffs equation

$$\partial(\Delta H)/\partial T = \Delta C_P$$

The necessary specific heats for BH_3, H^- and BH_4^- can readily by estimated [15]: the correction term is then similar to those calculated for BF_3 complexes [16]. The resulting energy terms (in kJ mol^{-1}) for the reaction at 298 K are given below

ΔE_{HF}	ΔE_{vib}	ΔE_{corr}	$\Delta C_P \Delta T - RT$	ΔH_{calcd} (298 K)
−269.0	+19.3	−20.2	−8.7	−278.6

The results show that the reaction is exothermic and illustrate the strong affinity of BH_3 for the H^- ion. In order to estimate the experimental energy for this process we need a Born-Haber cycle (figure 2). With regard to the terms in the cycle the heat of formation of KBH_4 from solid KH and gaseous BH_3 is not known but, by analogy with other complexes of BF_3 and BH_3, one would expect it to be little different from that of KBF_4 (121 kJ mol^{-1} [17]). The lattice energy of KBH_4 is also unknown but we may reasonably employ a value scaled from those of KBF_4 [18], KF [19], and KH [19]. This yields a value of 568 kJ mol^{-1}. If these figures are now combined in the cycle we arrive at a value of −267 kJ mol^{-1} for the heat of the reaction

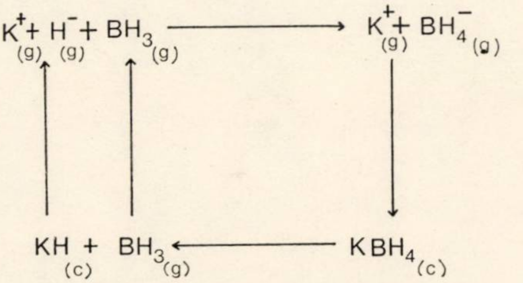
$K^+_{(g)} + H^-_{(g)} + BH_{3(g)}$
$K^+_{(g)} + BH^-_{4(g)}$
$KH_{(c)} + BH_{3(g)}$
$KBH_{4(c)}$

Fig. 2. — Thermodynamic cycle for the energy of $BH_3 + H^- \rightarrow BH_4^-$.

$$H^-_{(g)} + BH_{3(g)} \rightarrow BH^-_{4(g)}$$

The agreement with the calculated value is very satisfactory.

One of us (K.S.S.) thanks the Scottish Education Department for a Maintenance Grant.

[15] JANAF Thermochemical Tables, Dow Chemical Coy, Midland, Michigan, 1961.

[16] R. M. Archibald, D. R. Armstrong and P. G. Perkins, *J. Chem. Soc. Faraday*, in press.

[17] J. H. De Boer and J. A. M. Van Liempt, *Rec. Trav. Chim.*, **46**, 124 (1927).

[18] A. P. Altschuller, *J. Amer. Chem. Soc.*, **77**, 6187 (1955).

[19] T. C. Waddington, "Progress in Inorganic Chemistry and Radiochemistry, **1**, 157 (1959).

Revue Roumaine de Chimie, **19**, *5*, 747–753 (1974)

Revue Roumaine de Chimie, **19**, *5*, 755–761 (1974)

ESR SPECTRA OF SOME ANION-RADICALS FROM DIBENZO-[b, e]-THIEPINONE AND RELATED COMPOUNDS

ELENA VOLANSCHI*, C. VLĂDESCU** and C. VOLANSCHI*

Department of Physical Chemistry, Bd. Republicii 13,
University of Bucharest, Romania
**Institute of Internal Medicine of the Academy for Medical Sciences,
Şos. Şt. cel Mare, 19, Bucharest, Romania

Received July 3, 1973

Chemical and electrochemical reduction in DMF and DMSO of seven derivatives in the dibenzo-[b,e]-thiepinone series was performed. It was found that in these conditions a cleavage of the molecule occurs, leading to the anthraquinone anion-radical. This process is dependent on time, method of reduction and sulphur- or ring-substitution.

Dibenzo-[b, e]-thiepin-11-one, DBTP [b, e], (fig. 1) is known for its antialergical activity, but there is no information about its structural and spectral properties.

The single paper of which we are aware is concerned with the ESR spectrum of a related compound, dibenzo-[b, f]-thiepinone [1]. Since the sulphur atom is out of the plane of the aromatic rings, we thought that the study of its anion-radicals, if at all, will provide information about the sulphur conjugation in nonplanar systems.

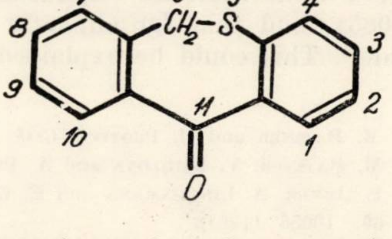

Fig. 1.— Dibenzo-[b, e]-thiepinone and the numbering used in this paper.

In this paper, we present the experimental results concerning the behaviour of dibenzo-[b, e]-thiepinone and some related compounds by the chemical or electrochemical reduction.

---

[1] M. M. Urberg and E. T. Kaiser, *J. Amer. Chem. Soc.*, **89**, 5931 (1967).

EXPERIMENTAL PART

The thiepinone derivatives were synthetized by literature methods, as follows: (numbering as in fig. 1)

- dibenzo-[b, e]-thiepin-11-one [2], m.p. = 86°
- dibenzo-[b, e]-thiepin-11-one-5-oxide [2], m.p. = 98°
- 2-chloro-dibenzo-[b, e]-thiepin-11-one [3] m.p. = 136°—37°
- 2-methyl-dibenzo-[b, e]-thiepin-11-one [4] m.p. = 121°
- 8-chloro-dibenzo-[b, e]-thiepin-11-one [5] m.p. = 152°—3°
- 9-chloro-dibenzo-[b, e]-thiepin-11-one [3] m.p. = 88°—90°
- dibenzo-[b, e]-oxepin-11-one [6] m.p. = 69°—71°

The anion-radicals were prepared by reduction with metallic sodium in anhydrous dimethyl-formamide (DMF), or by simple dissolution in strongly alkaline dimethylsulphoxide (DMSO + KOH).

The electrochemical reduction was performed directly in the ESR cavity, in a cell with two platinum electrodes. The potential was controlled with an Ag-wire, passed through a glass capillary and dipped into the solution till above the cathode [7].

Anhydrous DMF was used as solvent, and tetrabutylammonium-iodide (TBAI) 0.1 M as supporting electrolyte.

The ESR spectra were recorded on a JES-3 B Spectrometer in the X-band frequency, and the optical ones on a Beckmann DK-2 spectrophotometer.

RESULTS AND DISCUSSION

The parent compounds and the parameters of the ESR spectra of the thiepinone derivatives are collected in table 1.

By the chemical reduction of DBTP-(b, e) two radicalic species with different g-values are obtained; the first one, having a g-factor of 2.0096 points out a sulphur-containing radical. This value is in the range indicated in literature for sulphur aromatic systems like thianthrene ($g = 2.0085$), and that for aliphatic sulphides ($g = 2.0263$) for dimethylsulphide [8]. This could be explained by the localization of the unpaired

---

[2] M. Rajsner and M. Protiva, *Cesk. Farm.*, **11**, 404 (1962).

[3] M. Rajsner, V. Seidlova and A. Protiva, *Cesk. Farm.*, **11**, 451 (1962).

[4] E. Juker, A. Lindenmann and E. Gadient, Belgian Patent, 626, 301 (1963), *Chem. Abstr.*, **60**, 10658 (1964).

[5] C. Vlădescu and O. Maior (in press).

[6] K. Tach and H. Spingler, *Monatsh.*, **93**, 889 (1962).

[7] I. B. Goldberg and A. J. Bard, *J. Phys. Chem.*, **75**, 3281 (1971).

[8] Y. Sato, M. Kinoshita, M. Sano and H. Akamatu, *Bull. Chem. Soc. Japan*, **40**, 2539 (1967).

Table 1

Parent compounds and parameters of the best resolved ESR spectra

Parent compound	Method of reduction and solvent	I-radicalic species		II-radicalic species
		a_H (G)	g-factor	g-factor
Dibenzo-[b, e]-thiepin-11-one	KOH + DMSO	1.39 (4H)	2.0096	2.0043*
Dibenzo-[b, e]-thiepin-11-one-5-oxide	KOH + DMSO	1.39 (4H)	2.0097	2.0043*
	electrochemical reduction (DMF)	1.39 (4H)	2.0097	the second radical is not obtained
2-Chloro-dibenzo [b, e] thiepin-11-one	,,	1.24 (3H)	2.0102	2.0043
2-Methyl-dibenzo [b, e] thiepin-11-one	KOH + DMSO	1.50 (6H)	2.0095	2.0042
8-Chloro-dibenzo [b, e] thiepin-11-one	,,	1.30 (4H)	2.0100	2.0043
9-Chloro-dibenzo [b, e] thiepin-11-one	,,	1.20 (3H)	2.0102	2.0043
Dibenzo-[b, e]-oxepin-11-one	electrochemical reduction (DMF)	first radical is not obtained		2.0043*

* The same his constants were found for these radicals ($a_H = 1.01$ G (4H)).
($a_H = 0.33$ G (4H)).

electron on the sulphur atom, as it is implied by a resonating formula of type (b), that is :

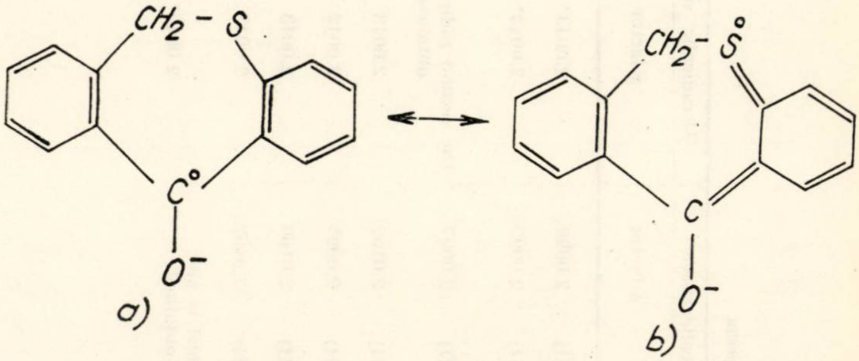

A splitting of 1.39 G due to 4 equivalent protons was evidenced Further splitting is apparent in strongly alkaline DMSO solutions, but at this poor resolution the hyperfine constant could not be determined.

From the 4 protons observed we can assign only two, to positions 2 and 9, respectively, since in the spectra of the 2-or 9-chloro-DBTP only three quasiequivalent protons are apparent (4 lines in the intensity ratio 1 : 3 : 3 : 1).

The 7-lines spectrum of the 2-methyl-thiepinone supports the same idea. As the spectrum of the 8-chloro derivative is nearly the same as that of the parent compound, (table 1) it is probably that the proton 8 is not one of the four equivalent protons in the molecule ; however, we do not possess sufficient experimental data to assign the other hfs constants.

The second radical with a g-value of 2.0043 evidences a splitting of 8 protons, with the a_{H} given in table 1.

The general pattern of the spectrum and the values of the hfs constants point out the identity of this spectrum to that obtained in aprevious work starting from anthrone [9].

In a recent paper [10], Tabner and Zdysiewicz proved that the chemical or electrochemical reduction of anthrone at room temperature leads to the anion-radical of anthraquinone. It seems probable therefore that dibenzo-[b, e]-thiepinone undergoes a desulphuration leading, *via* anthrone, to the 9,10-anthrasemiquinone anion.

The desulphuration of [b, e]-DBTP was observed to occur in other reactions too, as it was proved byVlădescu and Maior [11], who obtained 9,10-dichloroanthracene from DBTP and thyonil chloride, and not 11,11-dichlorodibenzo-[b, e]-thiepine as it was expected.

In order to check the mechanism proposed here, we started from anthrone and anthraquinone in strongly alkaline DMSO solutions and in both cases ESR spectra identical to those of the DBTP — second radicalic species were obtained.

---

[9] V. Em. Sahini, L. Ciurea and E. Volanschi, *Rev. Roumaine. Chim.*, **12**, 355 (1967).

[10] B. J. Tabner, and J. R. Zdysiewicz, *J. Chem. Soc.*, **1971 B**, 1659.

[11] C. Vlădescu and O. Maior, *Rev. Chim.* (*Bucuresti*), **22**, 197 (1971).

It was also observed that starting from three different compounds, that is 2-chloro, 8-chloro and 9-chloro-DBTP, the same spectrum of the second radicalic species is obtained. This fact supports also the idea that 9,10-anthraquinone is the second anion-radical formed, because only in such symmetrical molecule, positions 2,8 and 9 are equivalent.

It was proved by chemical methods too that anthraquinone is the main final product of the reduction of [b, e]-DBTP, by performing its synthesis from DBTP in DMSO + KOH and analysing the reaction mixture by thin layer chromatography *.

We observed also that the desulfuration process of thiepinone is influenced by the reduction method, time and ring — or sulphur-substitution. Thus, the electrochemical reduction in DMF leads to a low percent of anthraquinone — *vs.* thiepinone radical, while in the KOH + DMSO mixture the ratio is reversed. In every case the quotient of the 9,10-anthrasemiquinone-*vs.* the thiepinone — radical is increased the day following the preparation.

The 2- or 9-chloro or methyl-substitution leads to higher amounts of anthraquinone-anion relatively to the first radicalic species.

The substitution at the sulphur atom in dibenzo-[b, e]-thiepinone-sulphoxide does not affect much the ESR spectrum leading to the both radicalic species observed for the sulphur-unsubstituted analogue, the ratio being clearly favourable to the first one. It was however remarked

---

* In a flask fitted with a condenser 1 g of dibenzo-[b, e]-thiepin-11-one was dissolved in 5 ml of dimethylsulphoxide and 0.5 g of solid potassium hidroxide were added. The mixture was warmed on a steam bath for 4 hrs; it was then decomposed with water, acidulated with concentrated HCl and extracted with benzene. The extract was washed with water and dried over calcium chloride (on acidulation, H_2S was identified, proving that sulphur is leaving as suphide).

The benzenic extract was analysed by thin layer chromatography on silicagel G (eluant benzene : petroleum ether 3 : 1). The chromatogram was studied in u.v. or after development in concentrated H_2SO_4.

The u.v. study evidences the following compounds in the order of their migration *versus* marking substances :

— not reactioned dibenzo-[b, e]-thiepinone (green fluorescence)

— a dark spot of anthraquinone (not fluorescent)

— two fluorescent compounds near the start.

The study of the developed chromatogram evidences the [b, e]-DBTP as a red spot and behind it anthraquinone as a yellow spot. The remaining two compounds are not coloured in concentrated H_2SO_4.

After chromatography, the benzenic solution was evaporated and recrystallized several times from benzene, alchool and acetic acid (1 : 1) alternatively, and anthraquinone crystals with m.p. 285—86° were obtained.

The melting point of a mixture with authentic anthraquinone does not give depression. The yield after the first recrystallization is 0.8 g and the m.p. becomes 268—75° *vs.* 86° for the initial compound.

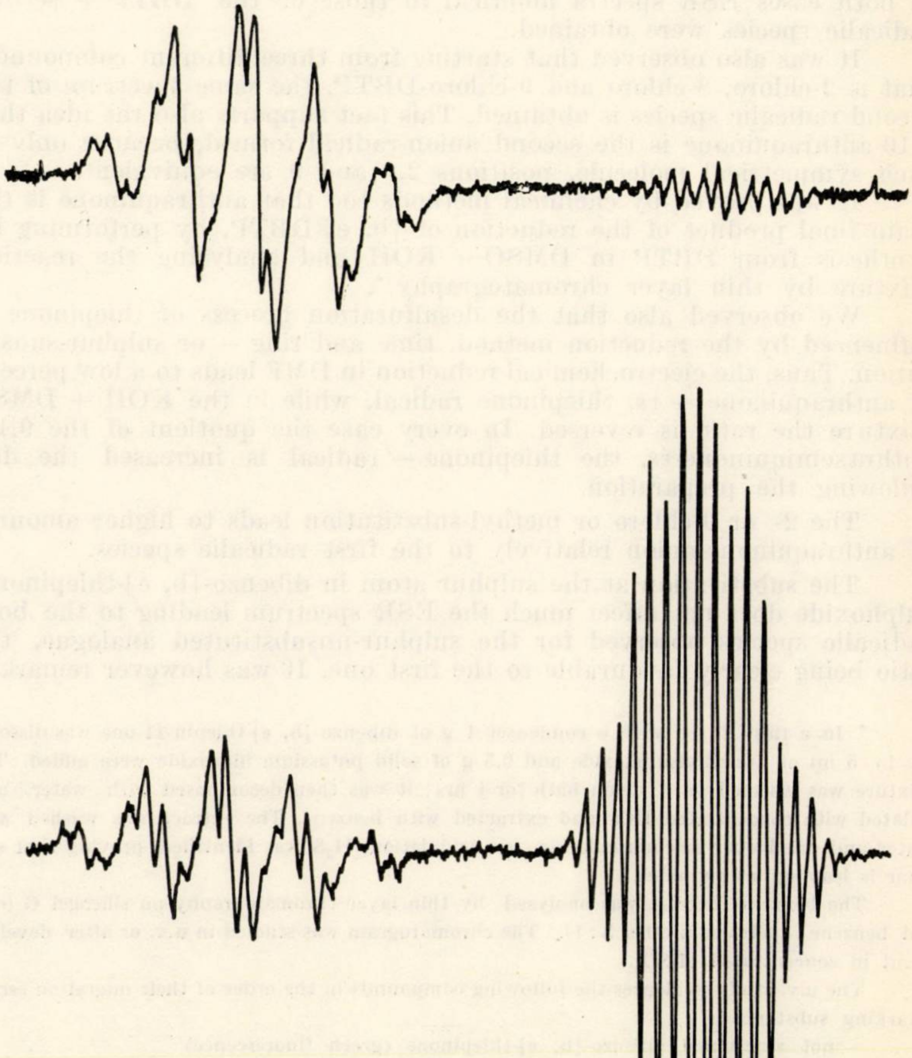

Fig. 2. — The two radicalic species obtained from [b, e]-DBTP : *a*) on electrochemical reduction in DMF. *b*) in the KOH + DMSO mixture.

that in the electrochemical reduction, the second radical could not be detected in our conditions.

The replacement of sulphur by oxygen in dibenzo-[b, e]-oxepinone leads to an ESR spectrum identical to that obtained from anthrone at room temperature [10] not depending on the reduction agent employed.

To obtain more data about the radicalic species provided by thiepinone, optical spectra were also recorded. All the radicals studied present two absorption bands in the visible range (one at about 500 nm and another at *ca.* 530 nm). Since anthrone and anthraquinone recorded in similar conditions present maxima in the same range, no assignment of the peaks to the different radicalic species was possible.

In conclusion, it was found that by chemical or electrochemical reduction-[b, e]-DBTP undergoes a desulphuration process leading to the anthrasemiquinone ion. The mechanism was not yet elucidated step by step, but, as it was observed that the sulphur is leaving as sulphide, it seems probable that the desulphuration occurs *via* anthrone, which, under the influence of traces of dissolved oxygen leads to anthraquinone.

Revue Roumaine de Chimie, **19**, *5*, 763–778 (1974)

INTERDIFFUSION AND SELF-DIFFUSION OF MONOVALENT CATIONS IN FUSED ALKALI NITRATES AND CHLORIDES

S. STERNBERG and CONSTANȚA HERDLICKA
Institute of Physical Chemistry, str. Galați 31, Bucharest, Romania

Received May 17, 1973

A corrected form of Stokes-Einstein equation applicable to inter- and self-diffusion of monovalent cations in fused alkali nitrates and chlorides is suggested. The correction term increases exponentially with the volume change on melting (ΔV) of the diffusion medium. A critical discussion of several diffusion theories on the basis of which the preexponential factor and activation energy for cationic diffusion in alkali nitrates and chlorides have been calculated is also given.

Some experimental data regarding silver ion interdiffusion in alkali nitrates [1–5] and alkali chlorides, [6] as well as alkali cations self-diffusion in these solvents, [7–10] have already been published.

These data allow us to make an extensive discussion on the diffusion mobility in molten salts.

A first generalization of these data may be done by using Stokes-Einstein equation:

$$D_i = \frac{KT}{a \pi \eta r_i} \tag{1}$$

---

[1] C. E. Thalmayer, S. Bruckenstein and D. M. Gruen, *J. Inorg. Nuclear Chem.*, **26**, 347 (1964).

[2] C. A. Sjöblom and A. Behn, *Z. Naturforsch.*, **23a**, 1774 (1968).

[3] S. Sternberg and C. Herdlicka, *Rev. Roumaine Chim.*, **14**, 991 (1969).

[4] S. Sternberg and C. Herdlicka, *Rev. Roumaine Chim.*, **15**, 343 (1970).

[5] G. A. Mazzochin and G. Schiavon, *J. Electroanalyt. Chim.*, **38**, 229 (1972).

[6] S. Sternberg and C. Herdlicka, *Rev. Roumaine Chim.*, **17**, 343 (1972).

[7] A. S. Dworkin, R. B. Escue and E. R. Van Arstdalen, *J. Phys. Chem.*, **64**, 872 (1960).

[8] S. Zuca and M. Constantinescu, *Rev. Roumaine Chim.*, **17**, 385 (1972).

[9] J. O'M Bockris and G. W. Hooper, *Discuss. Faraday Soc.*, **32**, 218 (1961).

[10] J. O'M Bockris, S. R. Richards and L. Nanis, *J. Phys. Chem.*, **69**, 1627 (1965).

where D_i is the diffusion coefficient of a r_i radius particle moving in a medium having the viscosity η, a is a constant and the other magnitudes have known significances. In the classical formulation the constant a has the value 6 and corresponds to cases for which the diffusing species are much larger than those of the medium. For smaller diffusing particles, Li and Chang[11] have reported a modificated S–E equation with $a=4$.

In the following, we shall try to analyse the applicability of the S–E equation for cationic self-diffusion and Ag^+ interdiffusion in alkali nitrates and chlorides, over a large temperature range of at least 100° above the solvent melting point.

The experimental data of self-diffusion coefficients for alkali cations in alkali nitrates and chlorides are plotted in figure 1 together with the values resulting from S–E equation.

The experimental self-diffusion coefficients were obtained by using Arrhenius equations indicated by Dworkin and co-workers[7] for alkali nitrates and Bockris and co-workers[9,10] for alkali chlorides.

To calculate the viscosity values use has been made of experimental Arrhenius equations for alkali nitrates[12] and chlorides[13] available in literature.

The alkali ionic radii were assimilated to the crystallographic radii given by Pauling[14].

As can be seen from figure 1, the experimental data for nitrates are in fairly good agreement with the calculated ones, but large deviations occur in alkali chlorides. These deviations seem to be systematic and to depend on the volume change on melting.

In the alkali nitrates series except for $LiNO_3$, all the other nitrates give small volume changes[15], ΔV, being even negative in $RbNO_3$. The deviations of experimental self-diffusion coefficients from S–E equation are also small. They become important for D_{Cs^+} in $CsNO_3$ which has the second largest ΔV (12%) after $LiNO_3$.

In the alkali chlorides series the deviations increase from CsCl to LiCl, as ΔV[16] does.

The proportionality between the diffusion coefficient D and the $T/\eta r$ ratio holds for alkali chlorides but the straigth lines which result present two sorts of deviations : a) each straight line intersects the ordinate at distances from the origin having considerable values for NaCl, KCl and smaller for RbCl and CsCl, b) the slopes of experimental straight lines differ from the theoretical one in the case of RbCl and CsCl, but they are almost equal for NaCl and KCl.

---

[11] J. C. U. Li and P. Chang, *J. Chem. Phys.*, **23**, 518 (1955).

[12] S. Zuca and R. Borcan, *Electrochim. Acta*, **15**, 1817 (1970).

[13] I. G. Murgulescu and S. Zuca, *Z. Phys. Chem.*, **220**, 300 (1963).

[14] L. Pauling, "The Nature of Chemical Bond", Cornell University Press, New York, 1960, p. 547.

[15] G. J. Janz, "Molten Salt Handbook", Academic Press, New York (1967).

[16] H. Spindler and F. Sauerwald, *Z. anorg. Chem.*, **335**, 267 (1965).

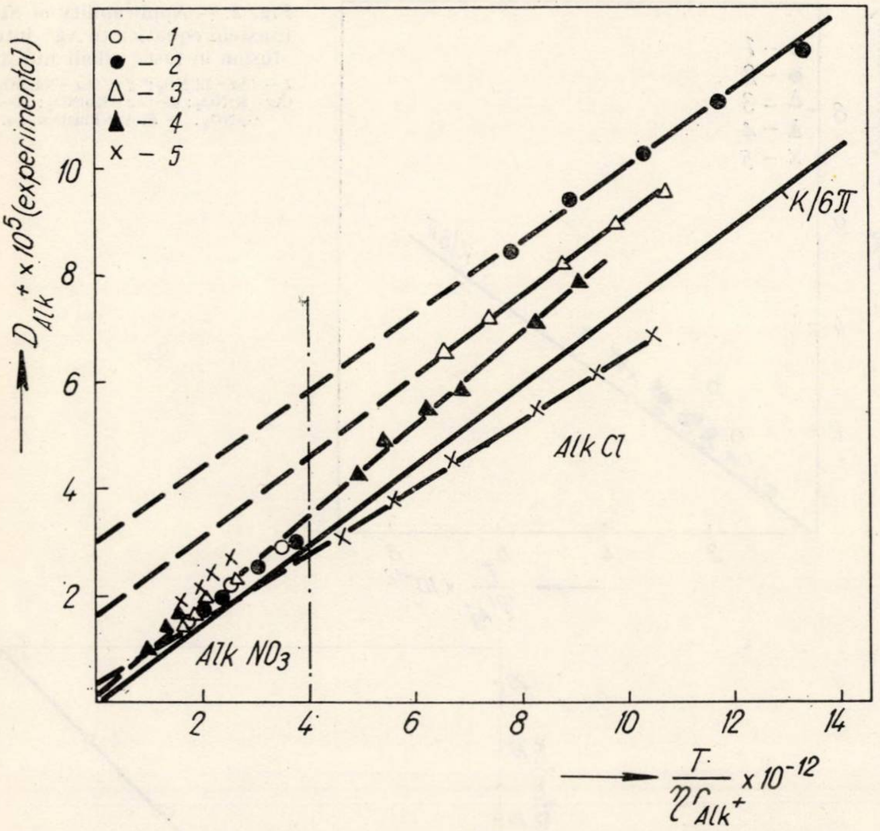

Fig. 1. — Applicability of Stokes-Einstein equation to cationic self-diffusion in fused alkali nitrates and chlorides:
1 – Li+; 2 – Na+; 3 – K+; 4 – Rb+; 5 – Cs+; — Stokes-Einstein eq.

In figures 2 and 3 the interdiffusion coefficient of Ag^+ in alkali nitrates and chlorides resulted both from S—E equation and experimental measurements are plotted.

Interdiffusion coefficients of Ag^+ ion were obtained by us from chronopotentiometric measurements [3,4,6,17]. The concentration of silver ion being very small (10^{-5}—10^{-4} mol/cm^3) the viscosity of the system was considered as equal to that of the diffusion medium. The silver ion radius published by other authors [12,18,19] is smaller than 1.26 Å (given by Pauling [14]) and 1.13 Å (according to Ketelaar [20]) and very close to that of sodium ion. In our calculations we have taken an average value of 0.98 Å.

---

[17] C. Herdlicka, Thesis, Bucharest, 1972.

[18] I. G. Murgulescu and S. Sternberg, *Z. phys. Chem.* (*Leipzig*), **219**, 114, (1962).

[19] M. Blander, *J. Chem. Phys.*, **36**, 1092 (1962).

[20] J. A. A. Ketelaer, "Chemical Constitution", Amsterdam, 1957.

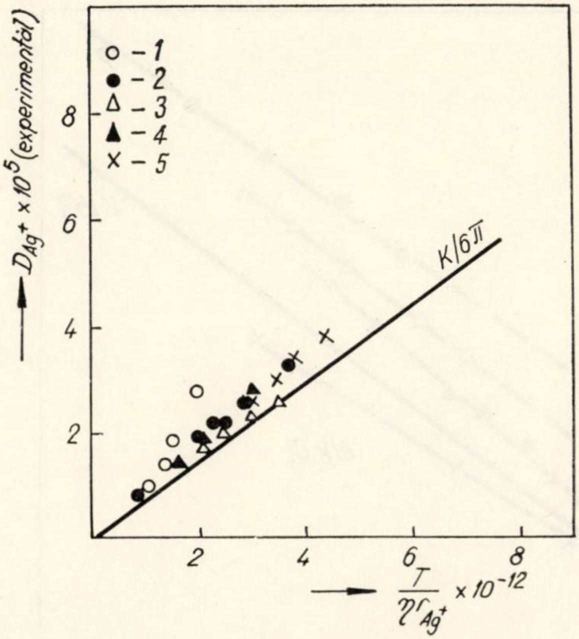

Fig. 2. — Applicability of Stokes-Einstein equation to Ag^+ interdiffusion in fused alkali nitrates:

1 – $(Ag-Li)NO_3$; 2 – $(Ag-Na)NO_3$; 3 – $(Ag-K)NO_3$; 4 – $(Ag-Rb)NO_3$; 5 – $(Ag-Cs)NO_3$; — Stokes-Einstein eq.

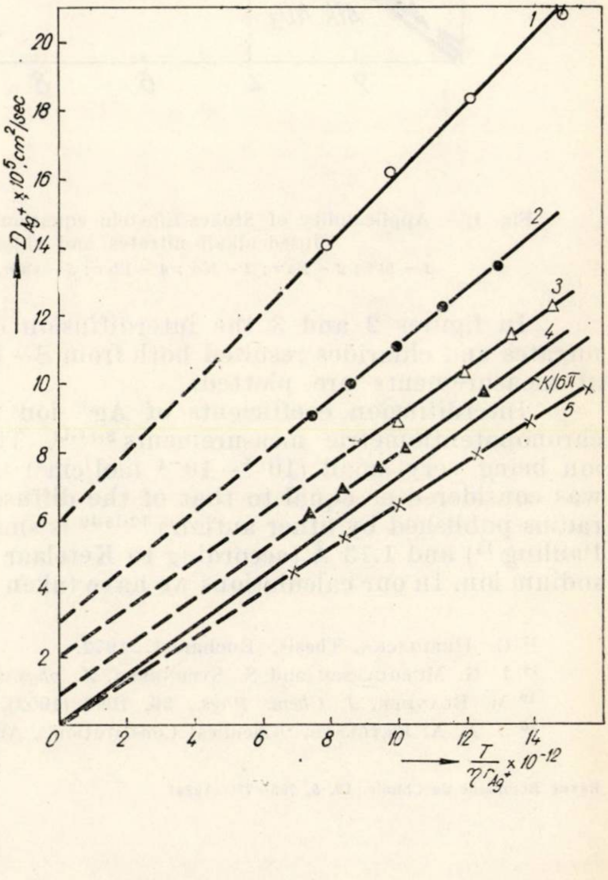

Fig. 3. — Applicability of Stokes-Einstein equation to Ag^+ interdiffusion in fused alkali chlorides:

1, $(Ag-Li)Cl$; 2, $(Ag-Na)Cl$; 3, $(Ag-K)Cl$; 4, $(Ag-Rb)Cl$; 5, $(Ag-Cs)Cl$; — Stokes-Einstein eq.

The experimental Arrhenius equations for Ag^+ diffusion in alkali nitrates, we have already referred to (references [3] and [4]), have subsequently been processed [17] by I.M.B. 360/30 computer so that the data show the standard deviations too.

Therefore, the complete equations we have used in this study are :

$AgNO_3 + LiNO_3$

$$D_{\mathrm{Ag}^+} = (8.36 \pm 4)10^{-3}\ \exp\left(\frac{7166 \pm 493}{RT}\right)$$

$AgNO_3 + NaNO_3$

$$D_{\mathrm{Ag}^+} = (0.96 \pm 0.18)10^{-3}\ \exp\left(\frac{4520 \pm 238}{RT}\right)$$

$AgNO_3 + KNO_3$

$$D_{\mathrm{Ag}^+} = (0.65 \pm 0.04)10^{-3}\ \exp\left(\frac{4340 \pm 93}{RT}\right)$$

$AgNO_3 + RbNO_3$

$$D_{\mathrm{Ag}^+} = (1.67 \pm 0.4)10^{-3}\ \exp\left(\frac{5620 \pm 306}{RT}\right)$$

$AgNO_3 + CsNO_3$

$$D_{\mathrm{Ag}^+} = (2.04 \pm 0.32)10^{-3}\ \exp\left(\frac{5920 \pm 228}{RT}\right)$$

As can be seen from figures 2 and 3 the experimental interdiffusion coefficients show deviations from S–E equation, behaviour which is similar to self-diffusion (fig. 1). The ordinates at origin given by the representative lines are larger than those for self-diffusion and depend both on volume change at melting and on the $r_{\mathrm{Alk}^+}/r_{\mathrm{Ag}^+}$ ratio.

It may be concluded from figures 1–3 that S–E equation is unsatisfactory for the explanation of experimental data and that besides $D_{\mathrm{S-E}}$ a supplimentary diffusion coefficient denoted by D_h, exists. The above figures suggest the existence of two contributions to D_h : the first and most important comes from the ordinate at origin of the straight lines, the second comes from the difference between experimental and theoretical slopes. The corresponding diffusion coefficients will be referred to as D_h' and D_h''.

Plotting of self-diffusion and interdiffusion coefficients, D_h', *versus* relative volume change on melting, ΔV, ($\Delta V = (V_l - V_s)/V_s$ with s and l subscripts indicating solid and liquid states of salt at melting point) leads to the representation in fig. 4.

From this figure it comes out quite clearly that D_h' is negligible for ΔV lower than 10% and increases exponentially with increasing ΔV.

The equation corresponding to the curve in fig. 4, is :

$$\log\,(D'_h - C) = A + B\,\Delta V \tag{2}$$

where A, B and C are constants.

The self-diffusion coefficients curve D'_h (fig. 4a) is described by the equation :

$$\log\,(D'_h - 0.15 \times 10^{-5}) = 7.37\ \ \Delta V - 6.17 \tag{3}$$

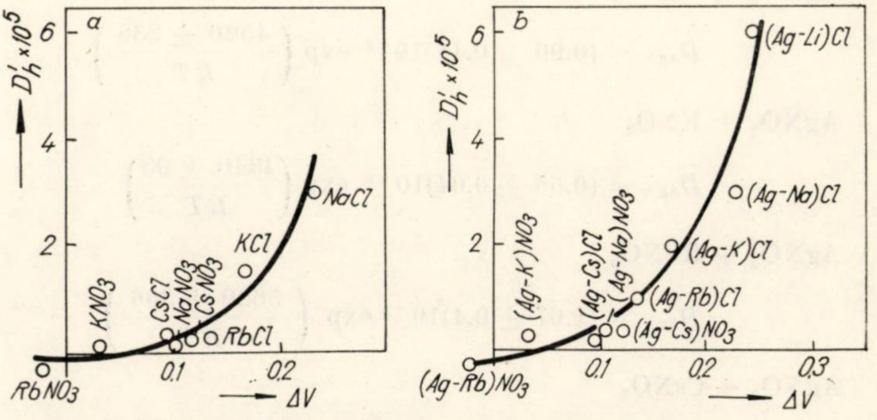

Fig. 4. — The variation of D'_h coefficient with volume change on melting for fused nitrates and chlorides :

a – Alk^+. self-diffusion ; b – Ag^+ interdiffusion.

The values D'_h (self) obtained by means of eq. (3) were used for correcting the D_{Alk^+} (self) experimental values.

A new plot of corrected experimental values shows a good agreement between the $(D_{\mathrm{Alk}^+} - D'_h)_{\mathrm{self}}$ experimental and D_{Alk^+} (self) calculated by S–E equation (fig. 5).

D'_h (inter) for Ag^+ interdiffusion has the same dependence on volume change ΔV as D'_h (self), and the higher its value, the bigger the ratio $r_{\mathrm{Alk}^+}/r_{\mathrm{Ag}^+}$ (fig. 4b).

In this case the following equation is valid :

$$D'_h\ (\mathrm{inter}) = D'_h\ (\mathrm{self})\,\frac{r_{\mathrm{Alk}^+}}{r_{\mathrm{Ag}^+}} \tag{4}$$

where D'_h (self) is given by equation (3).

Comparable results with those predicted by S–E eq. are obtained by making the correction $(D_{\mathrm{Ag}^+} - D'_h)_{\mathrm{inter}}$ (fig. 6) for interdiffusion.

The experimental data correction may be further improved by taking into account D''_h contribution arising from experimental and theoretical slope differences. This may be done by using the cubic cell model developed by Houghton [21] for self-diffusion in molecular liquids.

According to this theory :

$$D = \frac{\lambda^2 K T}{24\, m\eta} \tag{5}$$

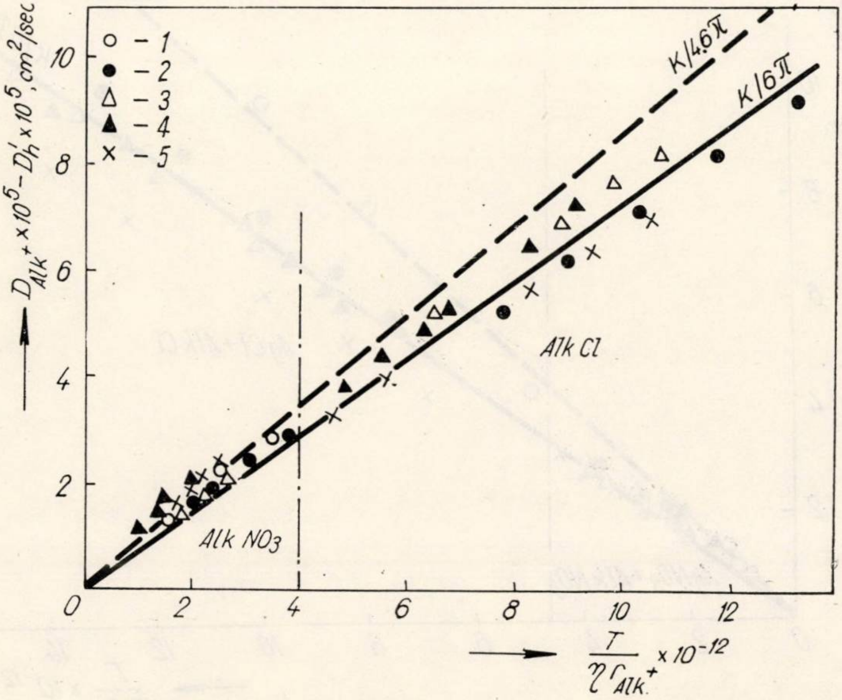

Fig. 5. — Corrected self-diffusion coefficients ($D_{\mathrm{Alk}^+} - D_h'$) for fused alkali nitrates and chlorides :

1 – Li$^+$; *2* – Na$^+$; *3* – K$^+$; *4* – Rb$^+$; *5* – Cs$^+$; ---- Stokes-Einstein eq.

where ρ is the liquid density, η the viscosity, *m* the diffusing particle mass and λ the linear dimension of a cubic cell in which the diffusing particle should accomodate. The theory approximates $\lambda = 2v^{1/3}$ where *v* represents the volume occupied by a single molecule. Equation (5) is equivalent to S—E equation when ρ and *m* refer to the same substance, in other words in the case of self-diffusion in a molecular liquid. Its employment for interdiffusion processes in molten salts involves some difficulties which we are not going to treat in this paper.

---

[21] G. Houghton, *J. Chem. Phys.*, **40**, 1628 (1964).

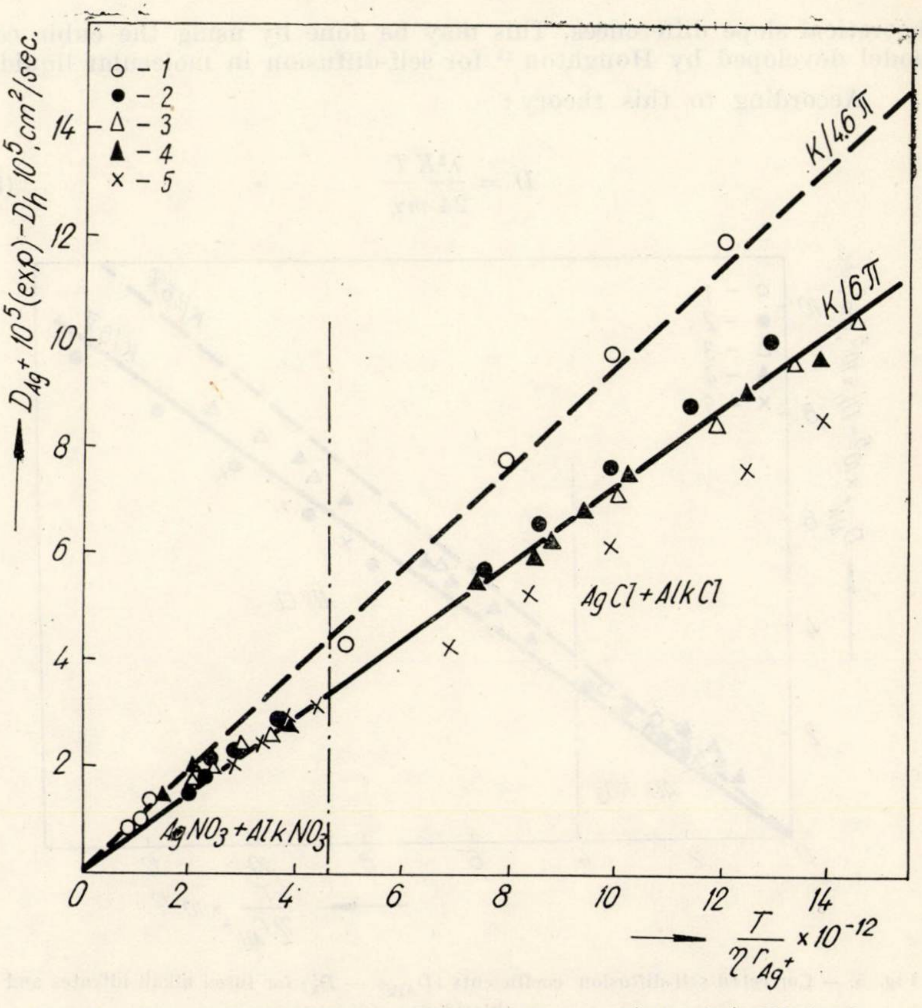

Fig. 6. – Corrected interdiffusion coefficients ($D_{Ag^+} - D'_h$) for Ag^+ diffusion in fused alkali nitrates and chlorides:
1 – Li^+ ; 2 – Na^+ ; 3 – K^+ ; 4 – Rb^+ ; 5 – Cs^+ ; ---- Stokes-Einstein eq.

However, we have tried a semiempirical equation similar to eq. (5):

$$D = \frac{(1.6+\alpha)^2\, KT}{48\eta r} = \frac{2.56\, KT}{48\eta r} + \frac{(3.2\,\alpha + \alpha^2) KT}{48\eta r} \tag{6}$$

where $\lambda = 1.6 + \alpha$ and has the same significance as above, namely the linear dimension of a cubic cell within which the diffusing ion is accomodated. In equation (6) λ is not a constant but is corrected by a value α depending on $\Delta V \cdot \lambda$ was considered equal to 1.6 in order to get Stokes-Einstein eq. (the first term of eq. 6). Therefore, the constant a from S–E eq. (1) appears in eq. (6) as a variable which depends on the structure of the diffusion medium. Assuming that the second term of eq. (6) is equal to D_h'' it was possible to calculate α values for each of the diffusion media (table 1).

From table 1 it results that the value of α parameter is a function of volume change ΔV, which may be considered as holes volume. For small values of ΔV, α becomes very small, even negative. If D_h'' were taken into account, better results would have been found for Cs^+ and Rb^+ self-diffusion and for Ag^+ interdiffusion is CsCl and RbCl which show deviations, even after the first correction has been applied (figs. 5, 6). In these cases D_h'' has negative values and making this second correction in addition to the first (D_h'), would result in a good agreement between corrected $D_{\text{exp.}}$ and $D_{\text{S-E}}$.

Table 1

Parameter α *versus* relative volume change on melting for cationic self-diffusion and Ag^+ interdiffusion in alkali nitrates and chlorides

Diffusion medium	α Alk^+ (self)	α Ag^+ (inter)	$\frac{V_l - V_s}{V_s}$
$LiNO_3$	0.15	0.75	0.21
$NaNO_3$	0.08	0.06	0.107
KNO_3	0.10	−0.11	0.033
$RbNO_3$	0.06	−0.3	−0.002
$CsNO_3$	0.01	0.04	0.121
LiCl	—	0.22	0.25
NaCl	0.06	0.079	0.23
KCl	0.009	0.01	0.168
RbCl	−0.05	−0.065	0.134
CsCl	−0.06	−0.17	0.098

The above observations show that adding up the S—E theory and cubic cell model, the experimental self-diffusion coefficient is defined by the sum of three terms, as follows:

$$D_{\text{self}} = D_{\text{S-E}} + D_h' + D_h''$$

where

$$D_{\text{S-E}} = \frac{KT}{6\pi\eta r} = \frac{2.56\,KT}{48\,\eta r}$$

$$D_h' = e^{-6.17 + 7.37\,\Delta V} - 0.15 \times 10^{-5} \tag{7}$$

$$D_h'' = \frac{(3.2\alpha + \alpha^2)\,KT}{48\,\eta r}$$

and for the diffusion of a foreign ion:

$$D_{\text{inter}} = (D_{\text{S-E}} + D_h' + D_h'')\,\frac{r^*_{\text{Me}^+}\,(\text{self})}{r_{\text{Me}^+}\,(\text{inter})} \tag{8}$$

The above equations allow the quantitative explanation of the deviations from S—E equation. The appearance of the additional term D_h, besides the diffusion coefficient $D_{\text{S-E}}$, might be explained by the fact that the volume of holes within the melt facilitates the ionic movements in the diffusion process more than in viscous flow.

Stokes-Einstein equation seems to be quite satisfactory for those salts having small ΔV (less than 10%). Salts with high volume changes on melting (LiCl, NaCl, KCl, RbCl, $CsNO_3$) have appreciable D_h values.

Further on we are going to show how different diffusion theories for liquids based on models might be applied to molten salts. These theories give the expression for self-diffusion coefficient and in order to extend them at the interdiffusion process we have considered as valid the next equation:

$$D_+\,(\text{inter}) = D_+\,(\text{self})\,\frac{r^*_{\text{Me}^+}\,(\text{inter})}{r_{\text{Me}^+}\,(\text{self})} \tag{9}$$

where D_+ (self) is given by every model.

In the free volume theory of Cohen and Turnbull [22] the self-diffusion coefficient in molecular liquides is expressed as:

$$D_i = ga^*\,(3\,K\,T/m)^{1/2}\exp\left[-\frac{\gamma v^*}{\bar{v}_m\,\alpha(T-T_0)}\right] \tag{10}$$

We have used this equation for self-diffusion in molten salts assuming that: the critical volume v^* needed by a hole to produce the diffusion of an ion is equal to the volume of diffusing ion itself considered as spherical. The average volume of an ionic hole $\bar{v}_m$ was $v_i - (V_1 - V_s)/2N$ where $v_i = 4\pi r_i^3/3$ (r_i is the diffusing ion radius and V_1 and V_s are the molar volumes of salts in solid and liquid states at melting point, respectively). The parameter a^* representing the jump distance was taken, according to the theory premises, as equal to the diameter of diffusing ion, g is a geometrical factor equal to 1/6 and γ a correction factor which was taken equal to 1/2. For the glass transition temperature T_0 we have used the values listed by Sjöblom [23] for some inorganic salts.

D_{Alk^+} (self) and D_{Ag^+} (inter) values, calculated by using eq. (10) for a few molten salts are listed in table 2.

As can be observed from this table, D_{Alk^+} (self) values calculated for alkali nitrates, except $LiNO_3$ are in good agreement with experimental data. This theory is unapplicable to alkali chlorides. A similar situation occurs in Ag^+ interdiffusion in the same solvents.

---

[22] M. H. Cohen and D. Turnbull, *J. Chem. Phys.*, **31**, 1164 (1959).

[23] C. A. Sjöblom, *Z. Naturforsch.*, **23a**, 933 (1968).

Quasi-lattice model (Eyring)[24] gives the kinetic-molecular significance of the pre-exponential coefficient D_0 and may thus be used as a verification criterion of D_0 coefficient from Arrhenius experimental equations.

Table 2

Applicability of the free volume model on the cationic self-diffusion and Ag+ interdiffusion in some molten salts

Solvent (nitrate or chloride)	Temp. K	Cationic self-diffusion		Interdiffusion	
		D (calcd.) cm²/sec	D (exp.) cm²/sec	D_{Ag^+} (calcd.) cm²/sec	D_{Ag^+} (exp.) cm²/sec
$LiNO_3$	623	$14.2 \cdot 10^{-5}$	$2.93 \cdot 10^{-5}$	$7.52 \cdot 10^{-5}$	$2.7 \cdot 10^{-5}$
$NaNO_3$	623	$2.74 \cdot 10^{-5}$	$2.35 \cdot 10^{-5}$	$2.65 \cdot 10^{-5}$	$2.5 \cdot 10^{-5}$
KNO_3	623	$1.63 \cdot 10^{-5}$	$1.54 \cdot 10^{-5}$	$2.21 \cdot 10^{-5}$	$1.95 \cdot 10^{-5}$
$CsNO_3$	623	$2.07 \cdot 10^{-5}$	$1.20 \cdot 10^{-5}$	$3.1 \cdot 10^{-5}$	$1.7 \cdot 10^{-5}$
NaCl	1093	$17.9 \cdot 10^{-5}$	$7.8 \cdot 10^{-5}$	$17.35 \cdot 10^{-5}$	$9.7 \cdot 10^{-5}$
RbCl	1018	$8.58 \cdot 10^{-5}$	$4.7 \cdot 10^{-5}$	$11.2 \cdot 10^{-5}$	$6.8 \cdot 10^{-5}$
CaCl	973	$19.8 \cdot 10^{-5}$	$4.0 \cdot 10^{-5}$	$29.5 \cdot 10^{-5}$	$5.5 \cdot 10^{-5}$

According to this model:

$$D = \frac{\lambda^2}{v_f^{1/3}} \left[\frac{KT}{2\pi m} \right]^{1/2} \exp\left(- \frac{E}{RT} \right) \tag{11}$$

where v_f is the free volume of liquid, m the mass of diffusing particle, λ the jump distance of the particle, the other symbols having the usual meanings. For the calculation of the pre-exponential coefficient D_0 (self) we have considered $\lambda = (V/N)^{1/3}$, where V is the molar volume of the melt[15] and the free volume $v_f = V_f/N$ values were those obtained from ultrasonic velocity measurements[25,26]. The calculations were carried out at 350° for nitrates and 850° for chlorides. The magnitudes in the expressions of D_0 (inter) and D_0(self) are identical except for the mass.

The quasi-lattice model gives the same order of magnitude for experimental and calculated D_0 (table 3). A very good agreement in the absolute values is observed for self-diffusion in alkali chlorides.

Another way to verify the above models is to control how the theoretical ratio D_+(self)/D_+(inter) corresponds to the experimental value. The ratio D_+(self)/D_+(inter) is, according to S−E eq., equal to $r^*_{Me^+}$ (self)/ /r_{Me^+} (inter) while, according to the free volume and quasi-lattice models, it is equal to $(m^*_{Me^+}\text{(self)}/m_{Me^+}\text{ (inter)})^{1/2}$. The first equality was confirmed

---

[24] S. Glasstone, K. J. Laidler and H. Eyring, "The Theory of Rate Processes" McGraw-Hill, New York, 1941, p. 47.

[25] J. O'M Bockris and N. E. Richards, *Proc. Roy. Soc.*, **A241**, 44 (1957).

[26] S. Sternberg and V. Vasilescu, *Rev. Roumaine Chim.*, **13**, 265 (1968).

Table 3

Comparison between the experimental and calculated pre-exponential coefficient, according to quasi-lattice model for cationic self-diffusion and Ag+ interdiffusion in some molten salts

Salt	Cationic self-diffusion		Ag+ interdiffusion	
	D_0 (calcd.) cm²/sec.	D_0 (exp) cm²/sec	D_0 (calcd) cm²/sec	D_0 (exp) cm²/sec
$NaNO_3$	$5.63 \cdot 10^{-3}$	$1.13 \cdot 10^{-3}$	$2.58 \cdot 10^{-3}$	$1.07 \cdot 10^{-3}$
KNO_3	$4.89 \cdot 10^{-3}$	$1.48 \cdot 10^{-3}$	$2.93 \cdot 10^{-3}$	$0.65 \cdot 10^{-3}$
NaCl	$4.52 \cdot 10^{-3}$	$3.36 \cdot 10^{-3}$	$2.07 \cdot 10^{-3}$	$4.66 \cdot 10^{-3}$
RbCl	$2.47 \cdot 10^{-3}$	$2.51 \cdot 10^{-3}$	$2.17 \cdot 10^{-3}$	$1.86 \cdot 10^{-3}$
CsCl	$1.65 \cdot 10^{-3}$	$1.73 \cdot 10^{-3}$	$1.83 \cdot 10^{-3}$	$2.6 \cdot 10^{-3}$

by our results (table 4) for nitrates and chlorides having the same alkali cation, i.e. D_{Ag^+} (inter)/D_{Alk^+}(self) is nearly equal to r_{Alk^+}/r_{Ag^+}. From table 4 it results that a better agreement is obtained by making the D'_h correction to experimental diffusion coefficients. The ratio of diffusing ion masses in no case predict the experimental value of the ratio of diffusion coefficients.

Table 4

Relationships between Ag+ interdiffusion and cationic self-diffusion coefficients, ionic radii and masses in several diffusion media

Solvent (nitrate or chloride)	Nitrates		Chlorides		$\frac{r_{Alk^+}}{r_{Ag^+}}$	$\left(\frac{m_{Alk^+}}{m_{Ag^+}}\right)^{1/2}$
	D_{Ag^+}/D_{Alk^+} (exp)	$\frac{(D_{exp}-D'_h)\text{ inter}}{(D_{exp}-D'_h)\text{ self}}$	D_{Ag^+}/D_{Alk} (exp)	$\frac{(D_{exp}-D'_h)\text{ inter}}{(D_{exp}-D'_h)\text{ self}}$		
Li^+	0.66	0.61	—	—	0.61	0.24
Na^+	1.08	1.13	1.08	0.95	0.97	0.46
K^+	1.27	1.30	1.27	1.39	1.35	0.60
Rb^+	1.30	1.34	1.38	1.44	1.51	0.88
Cs^+	1.40	1.67	1.44	1.38	1.72	1.11

As for the diffusion activation energy, E_D, a comparison of the experimental values obtained from the Arrhenius equations with those for other transport processes shows that the interdiffusion activation energies are close to the self-diffusion and viscous flow activation energies and that they are quite different from those of the electrical conductivity (table 5).

According to the cubic cell model, the temperature dependence of the diffusion coefficient follows the equation:

$$D = CT \exp\,(-E_\eta/RT) \tag{12}$$

where C is a constant.

From eq. (12) it results that the activation energies of the diffusion process and viscous flow are equal. The experimental values E_η and E_D

Table 5

Comparison between activation energies (cal/mol) for cationic self-diffusion, Ag^+ interdiffusion, viscous flowing and electrical conductivity in molten alkali nitrates and chlorides

Salt	$LiNO_3$	$NaNO_3$	KNO_3	$RbNO_3$	$CsNO_3$	References
E_D(self Alk^+)	5490	4800	5670	5480	5810	7,8
E_D(inter. Ag^+)	7167	4645	4340	5600	5800	17
E_η	4440	3886	4430	3790	5300	12
E_λ	3589	3215	3577	3496	3685	27
E_D(inter)/E_D(self)	1.44	0.94	0.78	0.99	1.00	
E_D(inter)/E_η	1.80	1.19	0.98	1.47	1.09	
E_D(inter)/E_λ	2	1.44	1.21	1.60	1.57	
Salt	LiCl	NaCl	KCl	RbCl	CsCl	
E_D(self Alk^+)	—	7860	6880	8010	7320	9,10
E_D(inter. Ag^+)	5516	8404	7709	6712	7428	6
E_η	7070	8690	6520	6080	5800	13
E_λ	1895	2530	3440	3750	4000	28
E_D(inter)/E_D(self)	—	1.06	1.12	0.83	1.01	
E_D(inter)/E_η	0.78	0.90	1.17	1.1	1.3	
E_D(inter)/E_λ	2.9	3.3	2.2	1.78	1.85	

from table 5 are in agreement with the cubic cell model predictions, in most cases the ratio E_D/E_η being almost equal to unity.

Quasi-lattice theory does not give a rigorous theoretical expression for the diffusion activation energy, E_D (eq. 11). According to Eyring [29] the activation energy may be considered as a fraction $1/n$ of the vaporization energy, the empirical factor n having values between 2 and 4. For molten salts the following empirical equation was proposed:

$$E_D = \Delta E_{\text{vap}}/n\nu \tag{13}$$

where ν is the number of ions per molecule resulting on melting. Expressions similar to eq. (13) were suggested by other authors by considering variants of the quasi-lattice model. Thus, McLaughlin [30] established the following expression for the activation energy:

$$E_D = E_{\text{vap}}(1/2 + 1/n\nu) \tag{14}$$

---

[27] G. J. Janz in "Molten Salts: Electrical Conductance, Density and Viscosity Data", Nat. Bur. Stand., 1968.

[28] S. Zuca and M. Olteanu, *Rev. Roumaine Chim.*, **15**, 357 (1970).

[29] H. Eyring and J. Hirschfelder, *J. Phys. Chem.*, **41**, 249 (1937).

[30] Mc. Laughlin, *Trans. Faraday Soc.*, **55**, 28 (1959).

[31] H. A. Walls and W. R. Upthergrave, *Acta Met.*, **12**, 481 (1964).

Walls and Upthergrove[31] found an empirical relation between the activation energy and the viscous flow energy:

$$E_D = E_\eta + RT + \alpha RT^2 \tag{15}$$

where α is the thermal expansion coefficient.

From the above empirical equations it follows that, for the same diffusion medium, the activation energies for self-and interdiffusion processes are equal.

In figure 7 the E_D experimental values are compared with those resulting from eqs. (13)—(15). In our calculations we used the values of vaporization energies obtained by Topor[32] and the viscosity activation energies found by Murgulescu and Zuca[13]: n was taken as equal to 2.

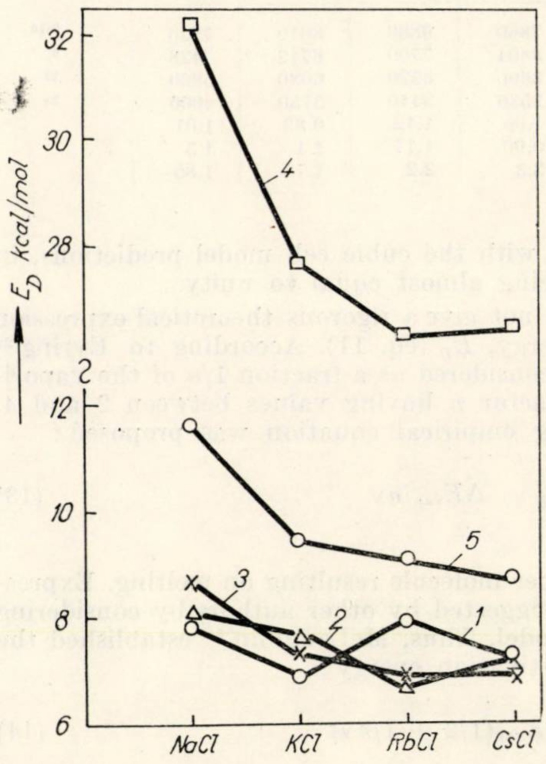

Fig. 7. — Activation energies for diffusion according to the quasi-lattice model: 1, E_D (exp.) for Alk$^+$ self-diffusion; 2, E_D (exp.) for Ag$^+$ interdiffusion; 3, eq. (13); 4, eq. (14); 5, eq. (15).

As can be observed from figure 7 our experimental data are in agreement with the predictions of the equation (13) only.

---

[32] L. Topor, Thesis, Bucharest, 1970.

The experimental data of self- and interdiffusion activation energies seem to be the best explained by the hole model [33]. Starting from the hole theory for liquids, Bockris and co-workers [34] found for the hole formation energy the equation :

$$E_D = 3.74\ RT_m \tag{16}$$

where T_m is the melting point of the solvent. The applicability of eq. (16) is illustrated in fig. 8.

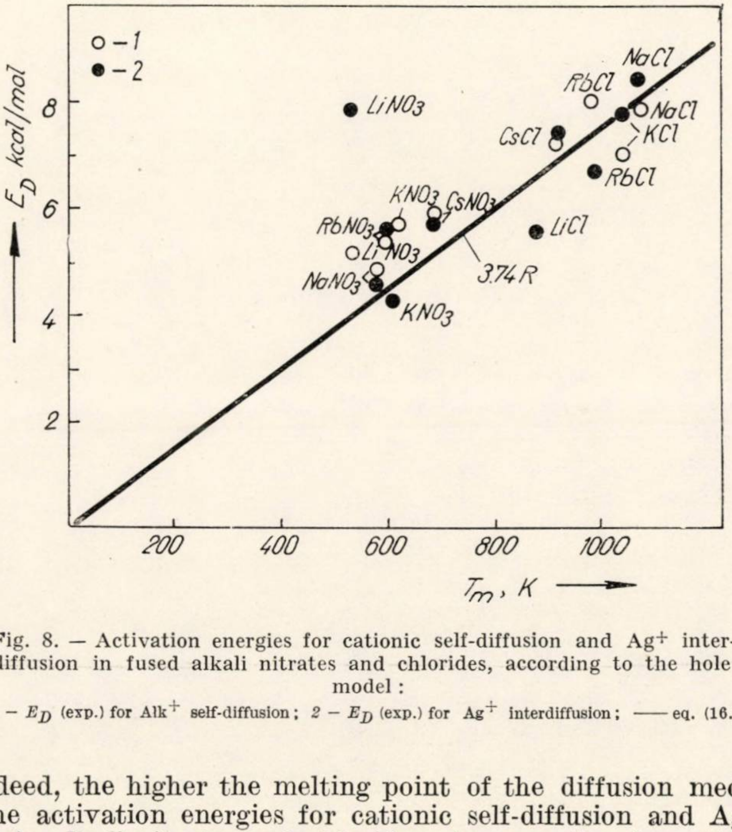

Fig. 8. — Activation energies for cationic self-diffusion and Ag^+ interdiffusion in fused alkali nitrates and chlorides, according to the hole model :

1 – E_D (exp.) for Alk^+ self-diffusion; 2 – E_D (exp.) for Ag^+ interdiffusion; —— eq. (16.)

Indeed, the higher the melting point of the diffusion medium the larger the activation energies for cationic self-diffusion and Ag^+ interdiffusion in alkali nitrates and chlorides. An exception from this rule is found for lithium salts.

It may be concluded that the diffusional mobility of monovalent ions in alkali nitrates and chlorides is mainly determined by the viscosity of the solvent, the diffusing ion and solvent cation radii and by the volume of the holes in the melt.

---

[33] R. Fürtz, *Proc. Cambridge Phil, Soc.*, **37**, 252 (1941).

[34] J. O'M Bockris, S. R. Richards and L. Nanis, *J. Phys. Chem.*, **69**, 1627 (1965).

The experimental activation energies for cationic self-diffusion and Ag^+ interdiffusion in nitrates and chlorides are in a satisfactory agreement with the hole model predictions, suggesting that the main part of the activation energy is formed from the holes formation energy.

At the same time, our results suggest that a correction factor D_h, correlated with the volume of holes from the diffusion medium, should be added to the diffusion coefficient obtained from the Stokes-Einstein equation.

Revue Roumaine de Chimie, 19, 5, p. 779–784 (1974)

CHRONOPOTENTIOMETRIC STUDY OF Ag(I) IN MOLTEN MIXTURES OF ALKALI-ALKALINE EARTH METAL NITRATES

R. L. BHATIA and H. C. GAUR*

Department of Chemistry, University of Delhi, Delhi—110007, India

Received June 30, 1973

Interdiffusion coefficients of Ag^+ (D_{Ag^+}) in molten mixtures of alkali and alkaline earth metal nitrates have been studied by chronopotentiometry over a wide temperature range. The applicability of Sand's equation was examined. Temperature dependence of D_{Ag^+} was represented by Arrhenius type equations :

$D_{Ag^+} = 0.90 \times 10^{-3} \exp(-5015/RT)$ in (K, Sr)NO_3 90 : 10 mole %

$D_{Ag^+} = 0.41 \times 10^{-3} \exp(-4348/RT)$ in (K, Sr)NO_3 80 : 20 mole %

$D_{Ag^+} = 1.9 \times 10^{-3} \exp(-5998/RT)$ in (K, Ba)NO_3 90 : 10 mole %

$D_{Ag^+} = 1.43 \times 10^{-3} \exp(-5856/RT)$ in (K, Ba)NO_3 80 : 20 mole %

in the temperature range 310–418°, 331–402°, 309–409° and 356–416°, respectively.

The need for an insight into the transport phenomenon in ionic melts has led to the applicability of several electro-analytical techniques. Out of these, chronopotentiometry offers a convenient method of determining the interdiffusion coefficients in molten salt solutions.

A study on the interdiffusion coefficients of Ag^+ (D_{Ag^+}) in molten mixtures of $NaNO_3$ with alkaline earth metal nitrates was carried out previously in this laboratory. [1] In the present paper, this technique has been applied to study the effect of varying divalent ion concentration (10 and 20 mole %) on D_{Ag^+} in the molten mixtures of potassium nitrate with alkaline earth metal nitrates *viz.* strontium and barium nitrates. Data have been obtained over a sufficiently wide temperature range to enable calculation of the activation energy for the diffusion process. Changes in D_{Ag^+} with the melt composition have been examined.

---

* To whom all correspondence should be addressed.

[1] H. C. Gaur, N. P. Bansal and S. K. Jain, *Indian J. Chem.*, (in press).

EXPERIMENTAL

Potassium, strontium and barium nitrates were AnalaR (BDH) grade chemicals used without further purification. These were dried at 150–170° for several days before use. Silver nitrate also AnalaR (BDH) grade chemical was powdered and desiccated under vacuum. 150 to 200 g of the binary mixture $KNO_3-xM(NO_3)_2$ (M = Sr, Ba and $x = 10$, 20 mole%) was taken in a pyrex cylindrical vessel (*c.* 380 mm long, 68 mm o.d.) which was vertically held in an electrical furnace (750 W) and fused under an inert atmosphere. Melt temperature could be controlled within ± 1° of the set value and measured with a calibrated Chromel-Alumel thermocouple held in a glass sheath dipping into the melt. Melt densities were used from data of Petersen *et al.* [2] The melt was divided into several compartments by glass tubes with fritted bottom (porosity G–4).

A three electrode system was used. Ag/Ag^+ (*c.* 0.011 m) in melt was the reference system. A platinum foil (area *c.* 2.5 cm^2.) dipping into another compartment was the auxiliary electrode. The microelectrode was also a platinum foil (area *c.* 0.5035 cm^2) spot welded to a 26 gauge platinum wire which was sealed in soda-lead (Corning 0120) glass tubing. Electrode area was determined using an optical micrometer.

An oscilloscopic method of measuring transition time [3] was employed. The instrumentation and technique used have been described elsewhere. [4] The chronopotentiograms were observed on Hewlett & Packard (model 122 A) oscilloscope and photographed with a Fairchild Dumont (Type 450 A) 35 mm camera on an ORWO NP-7 panchromatic film. The time-base was provided by *z*-modulation of the electron beam with a square wave from an H & P function generator (3300 A). Measurements were made with enlarged traces (× 100) using a Nikon Profile Projector.

Blank runs showed that decomposition potential of melt was *c.* 0.5 volt *versus* Ag/Ag^+ (*c.* 0.010 m) reference. Weighed increments of $AgNO_3$ were added to the indicator half-cell with a small platinum scoop provided with a long glass handle. The current density was so adjusted that the transition time was within the range 0.5 to 1.5 sec.

RESULTS AND DISCUSSION

D_{Ag^+}'s were determined in molten mixtures of $KNO_3-Sr(NO_3)_2$ (90 : 10 mole %), $KNO_3-Sr(NO_3)_2$ (80 : 20 mole%), $KNO_3-Ba(NO_3)_2$ (90 : 10 mole %) and $KNO_3-Ba(NO_3)_2$ (80 : 20 mole%) in the temperature range 310–418°, 331–402°, 309–409° and 356–416°, respectively.

Diffusion coefficients (D_{Ag^+}) were computed using Sand's equation [5]

$$\tau^{\frac{1}{2}} = \pi^{\frac{1}{2}} nFD^{\frac{1}{2}}_{Ag^+} C/2i_0 \tag{1}$$

where τ is the transition time (sec); C, the depolarizer concentration (moles cm^{-3}); i_0, the current density ($A \cdot cm^{-2}$) and π, n, F are well-known constants. This equation holds good when the mass transfer towards the electrode is governed solely by linear diffusion.

[2] G. F. Petersen, W. M. Ewing and G. P. Smith, *J. Chem. Eng. Data*, **6**, 540 (1961).

[3] H. A. Laitinen and H. C. Gaur, *Analyt. Chim. Acta*, **18**, 1 (1958).

[4] H. C. Gaur, *D. Sc. Thesis*, Agra University, Agra, India (1960).

[5] J. H. S. Sand, *Phil. Mag.*, **1**, 45 (1901).

Figure 1 shows a typical chronopotentiogram for the reduction of Ag^+ ion on PME in which the method of evaluating the transition time (cf. Thalmayer *et al.* [6]) has also been indicated. Table 1 gives the variation of $i_0\tau^{\frac{1}{2}}$ as a function of i_0 for a fixed depolarizer concentration ($0.873 \times \times 10^{-5}$ mole cm^{-3}). Variation of $i_0\tau^{\frac{1}{2}}$ with C in different molten mixtures is shown in figure 2 (A, B). All the plots are rectilinear and pass through the origin, indicating the applicability of Sand's equation. Each point in figure 2 denotes the average of $i_0\tau^{\frac{1}{2}}$ at 4 to 5 current densities.

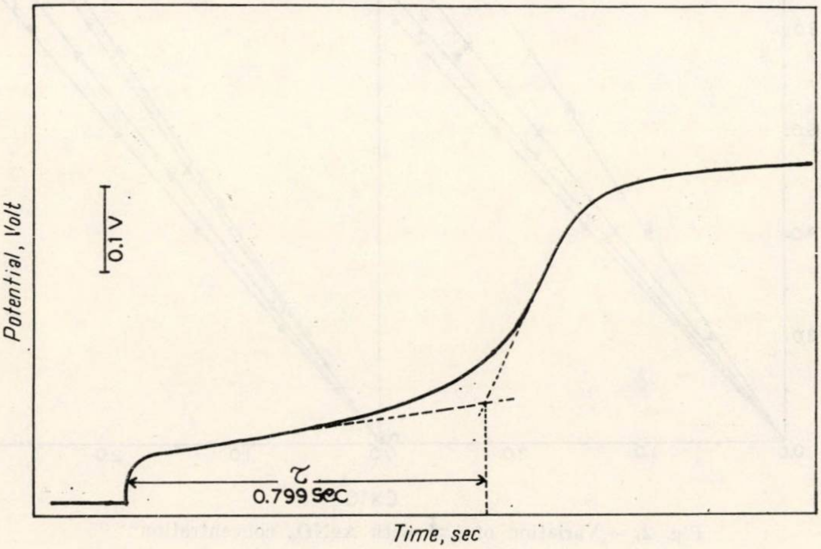

Fig. 1. — Potential-time curve for the reduction of silver ion in molten $KNO_3-Ba(NO_3)_2$ (90 : 10 mole %) at 333°.
$C = 0.873 \times 10^{-5}$ mole cm^{-3}; $i_0 = 3.20 \times 10^{-3}$ amp. cm^{-2}.

Table 1

Chronopotentiometric data for the reduction of Ag^+ ion in $KNO_3-Ba(NO_3)_2$ at 333°, $C = 0.873 \times 10^{-5}$ mole cm^{-3}

$i_0 \times 10^3$ A·cm^{-2}	3.00	3.21	3.50	3.85	3.92	4.00	3.20
$i_0\tau^{\frac{1}{2}} \cdot 10^3$ A·sec$^{\frac{1}{2}}$ cm^{-2}	2.90	2.88	2.89	2.91	2.86	2.92	2.86

AV $(i_0\tau^{\frac{1}{2}}) = 2.89 \pm 0.03$

---

[6] C. E. Thalmayer, S. Bruckenstein and G. M. Gruen, *J. Inorg. Nucl. Chem.*, **26** 347 (1964).

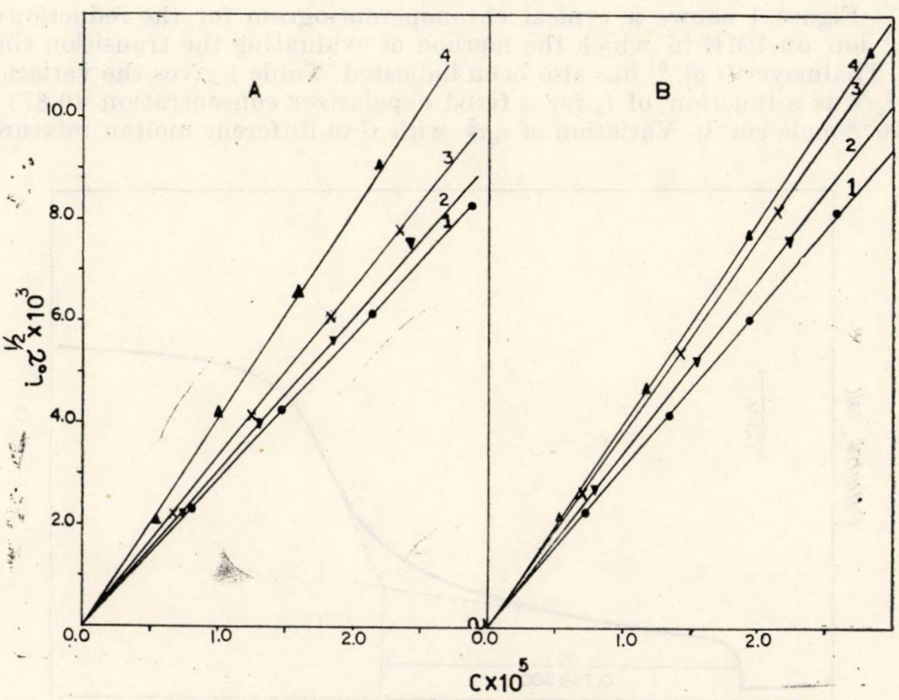

Fig. 2. — Variation of $i_0\tau^{\frac{1}{2}}$ with $AgNO_3$ concentration:

(A) in molten $KNO_3-Sr(NO_3)_2$ mixtures:
90 : 10 mole %; *2* (at 322°) and *4* (at 415°).
80 : 20 mole %; *1* (at 340°) and *3* (at 392°).

(B) in molten $KNO_3-Ba(NO_3)_2$ mixtures:
90 : 10 mole %; *2* (at 351°) and *4* (at 401°).
80 : 20 mole %; *1* (at 361°) and *3* (at 418°).

The temperature dependence of D_{Ag^+} (figure 3 (A, B)) could be represented by an Arrhenius type equation

$$D_{Ag^+} = D_0 \exp(-E_D/RT) \qquad (2)$$

where E_D is the activation energy for diffusion and D_0 the preexponential factor. The values of these parameters were determined by least square fitting of the data.

In table 2 the interdiffusion coefficients of Ag^+ at 384.7° as well as the values of Arrhenius parameters in various compositions of molten mixtures are given. For comparison, results of Sternberg and Herdlicka[7] in molten KNO_3 are also included. It is seen that there is a decrease in the magnitude of D_{Ag^+} with the increase in divalent ion concentration in the melt composition. This can be explained due to the change in cation field strength, $\sum \frac{n_i Z_i}{r_i}$ where n_i is the mole fraction, Z_i the ionic charge

---

[7] S. Sternberg and C. Herdlicka, *Rev. Roumaine Chim.*, **14**, 991 (1969).

Table 2

Interdiffusion coefficients of Ag+ at 384.7° and Arrhenius parameters for diffusion of Ag+ in molten nitrate melts

Solvent	D_{Ag^+} cm² sec⁻¹	$\Sigma \frac{n_i z_i^*}{r_i}$ of solvent	D_0 cm² sec⁻¹	E_D cal·mole⁻¹	Std. Dev.	Range of temperature °C
KNO_3**	2.36	0.752	0.65×10^{-3}	4340	—	340–423°
$KNO_3-Sr(NO_3)_2$ (90 : 10 mole %)	1.90	0.854	0.90×10^{-3}	5015	0.011	310–418°
$KNO_3-Sr(NO_3)_2$ (80 : 20 mole %)	1.46	0.956	0.41×10^{-3}	4348	0.005	331–402°
$KNO_3-Ba(NO_3)_2$ (90 : 10 mole %)	1.98	0.825	1.97×10^{-3}	5998	0.019	309–409°
$KNO_3-Ba(NO_3)_2$ (80 : 20 mole %)	1.59	0.898	1.43×10^{-3}	5856	0.009	356–416°

* $r_{K^+} = 1.33$ Å, $r_{Sr^{++}} = 1.13$ Å, $r_{Ba^{++}} = 1.35$ Å (Ref. [8])

** S. STERNBERG & C. HERDLICKA (Ref.[7]).

---

[8] L. PAULING, "Nature of Chemical Bond", Cornell Univ. Press, Ithaca, New York, 1948.

and r_i the radius of ith ion, of the solvent. It is seen that with an increase in cation field strength, a decrease in D_{Ag^+} is observed.

It may be pointed out that in crystalline nitrates and chlorides the extent of ion migration is enhanced by the incorporation of divalent ions into their lattices [9] whereas melts being more compressible than the corresponding crystals, the increasing cation field strength due to the presence of the divalent ion in the molten mixtures causes a shrinkage of the free volume in them which probably hinders the diffusion of Ag^+ ion towards the electrode. Our observations are supported by the conductance measurements in halide [10] and nitrate, [11-13] which also show a decrease in ionic conductance, when a divalent cation replaces a univalent cation in the melt.

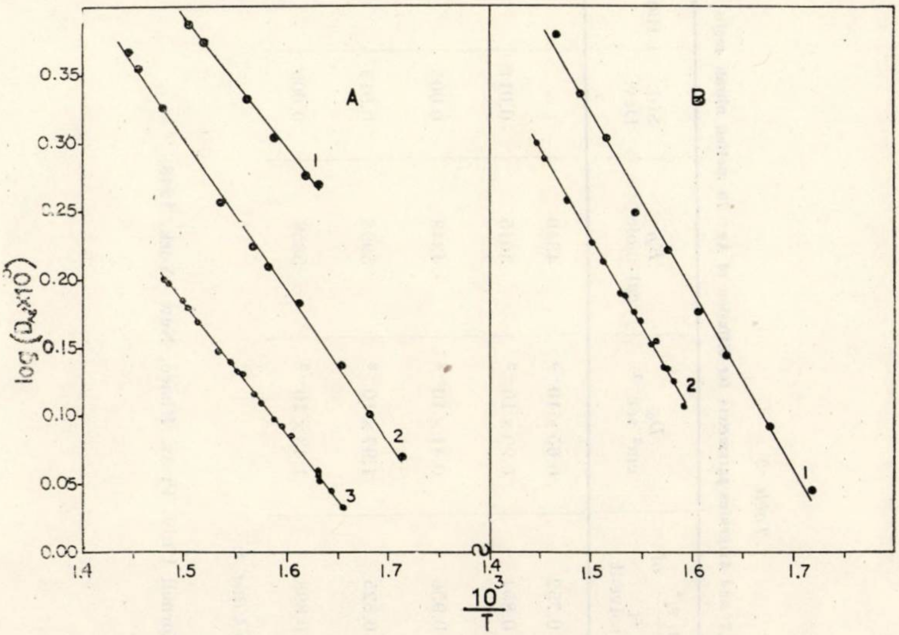

Fig. 3. — Arrhenius plots for the interdiffusion coefficients of Ag(I): (A) *1*, KNO_3[7]; *2*, $(K, Sr)NO_3$ (90 : 10 mole %); *3*, $(K, Sr)NO_3$ (80 : 20 mole %) and (B) *1*, $(K, Ba)NO_3$ (90 : 10 mole %); *2*, $(K, Ba)NO_3$ (80 : 20 mole %).

One of the authors (RLB) thanks the Council of Scientific and Industrial Research, New Delhi for the award of a research fellowship during the progress of this work.

---

[9] S. Forcheri and V. Wagner, *Z. Naturforsch*, **22a**. 1171 (1967).

[10] K. Grjotheim, R. Nikolic and H. A. Øye, *Acta Chem., Scand.*, **24**, 489 (1970).

[11] E. P. Honig and J. A. A. Katelaar, *Trans. Faraday Soc.*, **62**, 190 (1966).

[12] J. O'M. Bockris, J. A. Kitchener, S. Ingnatowicz and J. W. Tomlinson, *Trans. Faraday Soc.*, **48**, 75 (1952).

[13] B. Cleaver, E. Rhodes and A. R. Ubbelohde, *Discuss. Faraday Soc.*, **32**, 210 (1962).

Revue Roumaine de Chimie, **19**, *5*, p. 785–790 (1974)

CALORIMETRIC KINETICS. IV[1]

THE REACTION OF BENZOYL CHLORIDE WITH SODIUM METHOXIDE AND ETHOXIDE

RODICA VÎLCU and I. CIOCĂZANU

Chair of Chemical Thermodynamics and Electrochemistry,
University of Bucharest, Bdul Republicii N° 13, Romania

Received June 14, 1973

The kinetic parameters of the reaction between benzoyl chloride and sodium methoxide and ethoxide were derived through an anisothermal calorimetric method. The reactions have been investigated within the 15–35° temperature range as pseudomonomolecular reactions and bimolecular reactions of equal initial concentrations.

INTRODUCTION

The reactions of the benzoyl chloride with certain sodium alkoxides have been studied by a thermal maximum method version. [2] The thermal maximum method consists in observing, in nonadiabatic conditions, the maximum (or minimum) temperature reached during the reaction, comparative to the environmental constant temperature.

Benzoyl chloride reactions with sodium alkoxides:

$$C_6H_5COCl + R - ONa \rightleftarrows C_6H_5COOR + NaCl$$

have been investigated as bimolecular reactions with equal initial concentrations. The rate constants and activation energy were computed.

These reactions were also studied as pseudomonomolecular reactions. In this case, the rate constants, the activation energy and other activation thermodynamic functions ($\Delta H^{\neq}$, $\Delta G^{\neq}$, and $\Delta S^{\neq}$) were calculated.

---

[1] Part III. R. Vîlcu and I. Ciocăzanu, *Rev. Roumaine Chim.*, **5**, 643 (1971).

[2] R. P. Bell and J. C. Clunie, *Proc. Roy. Soc. A*, **16**, 212 (1952).

THEORY

The rate constant of bimolecular reactions with equal initial concentration is given by the relation :

$$k_2 = \frac{1}{t}\left(\frac{1}{a - x} - \frac{1}{a}\right) \tag{1}$$

where a is the reactant concentration at the initial moment and x the decrease of concentration at the t moment of the reaction.

Correlating the reactants concentration at the various moments by the corresponding temperature variations, the following relation is obtained :

$$T = \frac{k_2\, t T_0^2}{1 + k_2 t T_0} \tag{2}$$

where T is the temperature at the moment t and T_0 is the changed temperature, in the adiabatic conditions and it is a measure of reactions of a moles of reactants.

Differentiating the equation (2) with respect to time and taking into account the thermal losses through the calorimetric vessel walls, the thermal equation of such a process is obtained :

$$\frac{\mathrm{d}T}{\mathrm{d}t} = \frac{k_2 T_0^2}{(1 + k_2 t T_0)^2} - k_2' T \tag{3}$$

where k'_2 is the cooling rate constant of the calorimeter.

The general solution of differential equation (3) well take the form :

$$T = A_0\, \mathrm{e}^{-k_2' t} + k_2 T_0^2\, \mathrm{e}^{-k_2' t} \int_{t_0}^{t} \frac{\mathrm{e}^{k_2' t}}{(1 + k_2 T_0 t)^2}\, \mathrm{d}t \tag{4}$$

The purpose of this relation is the computation of rate constant k_2 as function of the magnitudes that can be experimentally determined. Thus, by solving this relation for the lower limit it is obtained :

$$k_2 = \frac{k_2'}{2\, T_0(\mathrm{e}^{k_2' T_m} - 1)} \tag{5}$$

and for the upper limit :

$$k_2 = \frac{k_2'}{2\, T_0\left(\mathrm{e}^{k_2' T_m} - 1 - \dfrac{T_m k_2'}{2}\right)} \tag{5'}$$

In the relations (5) and (5′) T_m represents the maximum recorded temperature in nonadiabatic conditions during this process, and T_0 is the thermal effect recorded in adiabatic conditions by consumption of *a* moles of reactant.

The computation of the rate constants of pseudomonomolecular reactions was presented in a previous paper.[1]

The activation energy of reactions as well as the frequency factors were calculated by an Arrhenius type relation :

$$\ln k = \ln A - \frac{E}{RT} \tag{6}$$

The activation thermodynamic functions of reactions ($\Delta H^{\neq}$, $\Delta G^{\neq}$ and $\Delta S^{\neq}$) have been computed by the theory of the absolute reaction rate from the kinetic parameters of reactions.

Thus, in the activated complex theory it is shown that the activated complex entropy is correlated with the other parameters by the relation[3] :

$$k = x\frac{\mathbf{k}T}{h}\,\mathrm{e}^{\frac{\Delta s^{\neq}}{R}}\cdot \mathrm{e}\cdot \mathrm{e}^{-E/RT} \tag{7}$$

where **k** is the Boltzmann's constant, *h* is the Planck's constant and *x* is a corrective term (close to the unity).

By identification with Arrhenius' equation, the value of frequency factor is obtained :

$$A = x\frac{\mathbf{k}T}{h}\,\mathrm{e}\cdot \mathrm{e}^{\Delta S^{\neq}/R} \tag{8}$$

The other activation thermodynamic functions are computed by the well-known relations.

THE EXPERIMENTAL DEVICE AND REACTANTS

An anisothermal calorimeter formerly described was employed.[4] The calorimeter is immersed in a U 10 ultra-thermostat which maintains the water temperature within $\pm 2\cdot 10^{-2}$. Due to the calorimeter construction, a constant temperature within $\pm 1\cdot 10^{-3}$ in the calorimeter vessel was obtained. A platinum thermal resistance of 100 Ω ± 0.1 Ω at 0°C with a thermal coefficient of $3.8\cdot 10^{-3}$ Ω/degree was employed as thermal transductor.

---

[3] G. NIAC and E. SCHÖNBERGER, "Chimie fizică", vol. 3, Editura tehnică, Bucureşti, 1970, p. 382.

[4] R. VÎLCU and I. CIOCĂZANU, *Rev. Roumaine Chim.*, **14**, 429 (1969).

This thermal resistance was mounted in a D.C. Wheatstone bridge. The other three arms of the Wheatstone bridge are manganin resistances of 100 Ω each.

The temperature variation inside the calorimeter was observed by a Sefram recording galvanometer Type VAM (of $4 \cdot 10^{-9}$ A/mm sensitivity).

The benzoyl chloride employed was chemically pure (Analar). The purity of substance was checked by the refractive index.

Amounts of 0.1 – 0.15 g of benzoyl chloride have been sealed in ampouls. The alkoxides used were obtained in laboratory from metallic sodium and the respective alcohols. The alkoxides concentration has been determined by titration with salicylic acid 0.1 N in the presence of bromine-thymol blue.

EXPERIMENTAL RESULTS AND DISCUSSION

The temperature-time curves plotted for the studied reactions have the shape illustrated in fig. 1

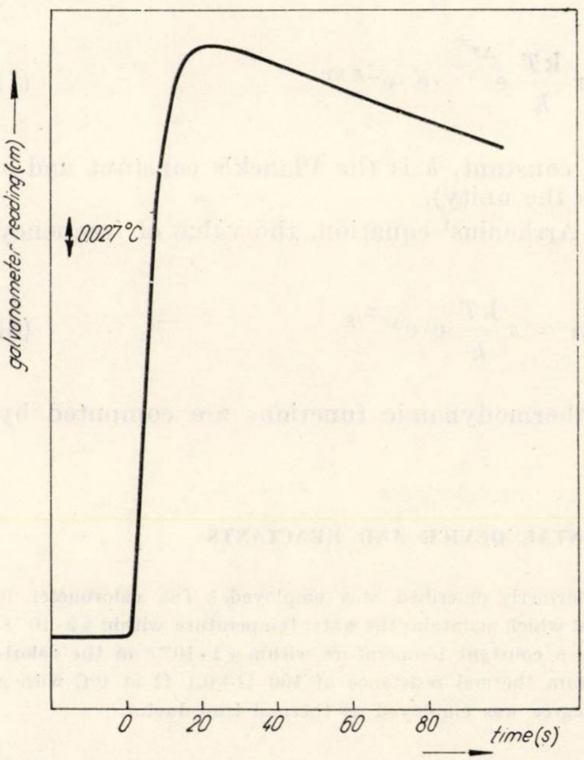

Fig. 1. – Temperature-time curve.

If the reactions have been treated as pseudomonomolecular reactions, the rate constants and the activation energy ($cal \cdot mol^{-1}$) are those given in table 1.

Besides these data, this table include also the working temperatures (°C), the time values for which the maximal temperatures (s) were recorded. These values are the mean of 4 or 5 determinations of each working temperature. The frequency factors computed according to Arrhenius' equation are $5.3\cdot10^{6}$ and $3.59\cdot10^{9}$ (s^{-1}) respectively.

Table 1

Rate constants, activation energies and the frequency factors corresponding to the reactions $C_6H_5COCl + RONa$

RONa	T°C	t_m(s)	$k_1(s^{-1})$	E cal·mol^{-1}	A_{exp} (s^{-1})
CH_3ONa	16 25 35	20 13 9	0.324 0.537 0.897	9540	$5.3\cdot10^{6}$
C_2H_5ONa	20 25 35	32 23 12	0.185 0.274 0.590	13820	$3.59\cdot10^{9}$

The representation in semi-logarithmical coordinates $\left(\log k = f\left(\frac{1}{T}\right)\right)$ leads to lines (fig. 2) from the slopes of which the activation energies of the reactions have been computed.

The activation thermodynamic functions of the two reactions, computed by relations (6) and (7) and the Gibbs-Helmholtz relations are given in table 2.

From the negative activation entropy values it may be concluded than an arrangement of the molecules is taking place during the reaction.

When reactions were studied in conditions of equal initial concentrations, the rate constants obtained are indicated in table 3 and presented as $\log k_2$ vs $\frac{1}{T}$ coordinates in figure 3.

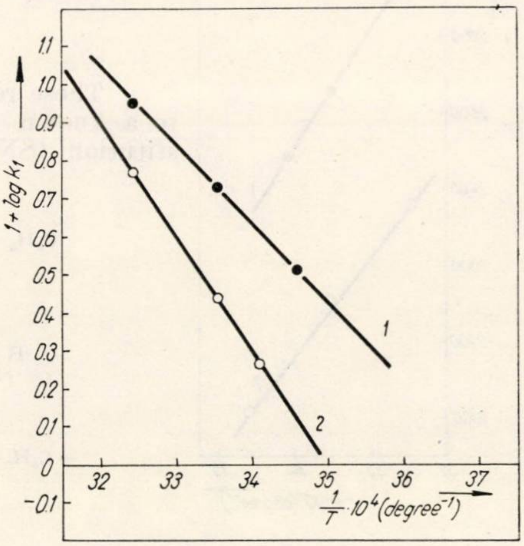

Fig. 2. — $\log k_1$ *versus* $1/T$:
1, $C_6H_5COCl + CH_3ONa$;
2, $C_6H_5COCl + C_2H_5ONa$.

From these rate constants the following values for the activation energies are calculated : 6300±800 and 7250±800 cal·mol^{-1}, respectively.

Table 2

Activation parameters of the reactions $C_6H_5COCl + RONa$

RONa	$\Delta H^{\neq}$ cal·mol^{-1}	$\Delta S^{\neq}$ cal·deg^{-1}·mol^{-1}	$\Delta G^{\neq}$ cal·mol^{-1}
CH_3ONa	8,950	−24.2	16,160
C_2H_5ONa	13,220	−21.20	19,540

Table 3

Rate constants of the reactions $C_6H_5COCl + RONa$ in conditions of equal initial concentrations

RONa	$a.10^3$ mol·l^{-1}	t°C	$10^{-1}\, k_2$ l·mol^{-1} min^{-1}	E cal·mol^{-1}
CH_3ONa	10.18	16	12.770	6300
	12.29	25	17.940	
	12.81	35	23.898	
C_2H_5ONa	10.04	20	27.667	7250
	12.35	25	34.118	
	13.64	35	50.119	

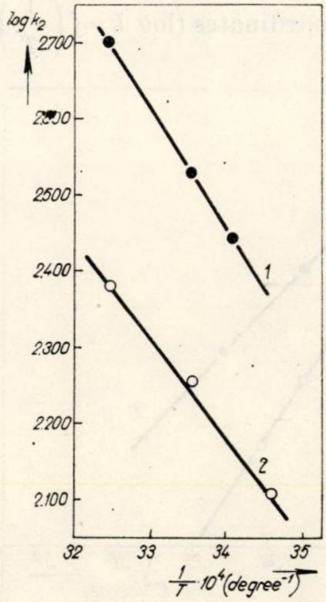

Fig. 3. — log k_2 *versus* $1/T$:

1, $C_6H_5COCl + C_2H_5ONa$; *2*, $C_6H_5COCl + CH_3ONa$.

These reactions are taking place according to a known mechanism of nucleophilic substitution (SN). [5]

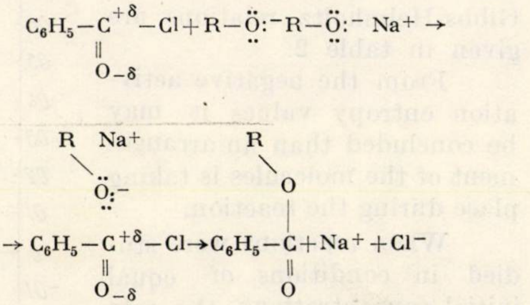

$$C_6H_5-\underset{\underset{O_{-\delta}}{\|}}{C^{+\delta}}-Cl + R-\ddot{\underset{..}{O}}:^- R-\ddot{\underset{..}{O}}:^- Na^+ \rightarrow$$

$$\rightarrow C_6H_5-\underset{\underset{O_{-\delta}}{\|}}{\overset{\overset{R\diagdown\ddot{\underset{..}{O}}:^-\quad Na^+}{}}{C^{+\delta}}}-Cl \rightarrow C_6H_5-\underset{\underset{O}{\|}}{\overset{\overset{R\diagdown O}{|}}{C}} + Na^+ + Cl^-$$

It can be assumed, in conclusion, that the thermal method employed in studying these reactions is an easy and rapid procedure, allowing at the same time the determination of kinetic and thermodynamic magnitudes of great practical importance.

---

[5] R. F. Hudson and J. E. Wardill, *J. Chem. Soc.*, **1950**, 1729.

Revue Roumaine de Chimie, 19, 5, p. 791–799 (1974)

ENTHALPIES OF MIXING OF THE CARBOXYLIC ACID-WATER SYSTEMS

RODICA VÎLCU and ELENA LUCINESCU

University of Bucharest, Chair of Thermodynamic Chemistry,
Electrochemistry and Macromolecules, Bd. Republicii 13, Romania

Received June 14, 1973

The enthalpies of mixtures of the binary systems : formic acid-water, acetic acid-water and propionic acid-water were determined, at standard temperature, directly by the calorimetric methods. Variation with the composition was expressed by equations of the Redlich-Kister form and the corresponding curves were interpreted by means of structural data. It was pointed out that the behaviour of the formic acid differs from that of the other acids under consideration.

INTRODUCTION

In contrast with alcohols, which constituted the basic experimental and theoretical material in the study of the thermodynamic properties of associated systems, the carboxylic acids offer but a scanty information from this standpoint, because of the complexity of the association process both in a pure state and in some mixtures, in the case of mixed associated molecules.

In this paper, we deal with the behaviour of the first three acids in the aliphatic series, when mixed with water, by measuring their enthalpies of mixing. These effects will result from opposite contributions — — the breaking of the hydrogen bond from the pure components and the exothermal formation of bonds in the mixed acid-water associates, the magnitude and contribution of which vary widely with the mixture composition.

For these reasons, from the thermal data supplied by experiments, we can only suggest a few standpoints permitting to understand this behaviour on the basis of the available structural data about these aqueous solutions.

It is known for a long time that the association of acids is expressed by the equilibrium between monomer and dimer, but some researches propose equally, by virtue of experimental data, the formation of higher polymers-linear [1,5] or cyclic [6], the polymerization degree diminishing with increasing the chain length. But generally, the quantitative interpretations amount to the consideration of the dimer, or at most of the trimer.

The formic acid offers more probable proofs as to the association in linear polymers, [7,8] rather than in dimers, which would only characterize the vapour phase. The linking to the carboxyl of a hydrocarbon radical renders the dimerization more probable. The strength of the hydrogen bond increase in the order $HCOOH < CH_3COOH < CH_3-CH_2-COOH$. [9] Applying the LCAO-MO computation method, Schuster [10] found the same energy hydrogen bond in the cyclic as in the linear dimer, which can constitute the link in a chain.

For the aqueous mixtures where mixed associated molecules also appear, whose structure changes with the concentration, the most abundant data in the literature refer to the system acetic acid-water and are chiefly based on the study of the Raman spectrum. For the other acids, the literature presents many gaps. In the concentrated acetic acid solutions the cyclic dimeric form is predominant and by dilution this form tends to change in linear dimers [11,14], or to polymers. This change is taking place predominantly at the concentration under 60% moles acid. [15,16] For these solutions, the data supplied by the Raman spectra, infrared, as well as the dielectric properties, indicate the formation of hydrates. [12,13,17-23] In the case of equimolecular solutions and those with moderate

---

[1] P. Koteswaran, *Indian J. Phys.*, **14**, 340 (1941).

[2] M. Davies and D. M. L. Griffiths, *Z. Phys. Chem.* (*Frankfurt*), **2**, 353 (1954).

[3] J. Lascombe, M. Haurie and M. L. Josien, *J. Chim. phys.*, **59**, 1233 (1962).

[4] P. Simova, *Izvest. Bulgar. Akad. Nauk. Ser. Fiz.*, **2**, 107 (1951).

[5] M. Haurie, *J. Chim. phys.*, **62**, 137 (1965).

[6] G. Allen and E. F. Caldin, *Quart. Rev.*, **7**, 255 (1953).

[7] A. E. Lutskii and S. A. Mikhailenko, *Zhur. strukt. Khim.*, **4**, 14 (1963).

[8] G. C. Pimentel and A. L. M. C. Clellan, "The Hydrogen Bond", W. H. Freeman and Company, San Francisco and London, 1960.

[9] M. D. Taylor and J. Burton, *J. Amer. Chem. Soc.*, **74**, 4151 (1952).

[10] P. Schuster, *Chem. Phys. Letters*, **2**, 587 (1967).

[11] M. I. Batuev, *Izvest. Akad. Nauk. S.S.S.R. Ser Fiz.*, **12**, 611 (1948).

[12] S. Fénéant, *Compt. rend.*, **235**, 240 (1952). *Ibid.* 1292 ; *J. Ph. et Radium*, 4, 325 (1954).

[13] I. Cucurezeanu, *Studii și Cercetări Fiz.*, *Acad. R.P.R.*, **9**, 269 (1958).

[14] M. I. Shakhparanov and L. V. Lanshina, *Vestn. Mosk. Univ. Khim.*, **23**, 5 (1968).

[15] K. P. Miscenko and A. Ponomareva, "Trudy Soveschiania op Termodinamiki", 27–30 January, 1958, Moscow.

[16] P. Waldstein and L. A. Blatz, *J. Phys. Chem.*, **71**, 2271 (1967).

[17] Fh. Traynard, *Bull. Soc. Chim. France.*, **1947**, 316.

[18] A. A. Glagoleva and A. A. Ferkhim, *Zhur. obshchei Khim.*, **28**, 289 (1958).

[19] P. Krisnamurthy- *Nature*, **128**, 639 (1931).

[20] A. I. Shakaline, *Ref. Zhur. Khim.*, **1967**, Pt. I. Abstr. N° 9 B. 970 (CA. 68–6868 m).

[21] R. Rao, *Indian J. Pure Appl. Phys.*, **6**, 430 (1968).

[22] R. B. Stumpf and L. A. Crum, *J. Acoust. Soc. Am.*, **39**, 170 (1966).

[23] A. N. Campbell and J.M.T.M. Gieskes, *Canad. J. Chem.*, **42**, 1379 (1964).

concentrations, the most probable structure seems to be[12,13]

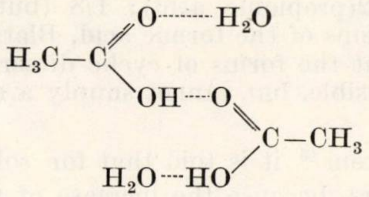

while for more dilute solutions the dihydrated monomer

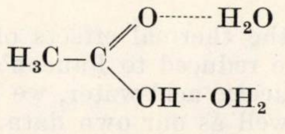

can equally appear. Campbell[23] and Shakaline[20] propose the formation first of the monohydrated dimer and then of dihydrated dimer. In the case of advanced dilutions ($x < 0.002$), there also appears an electrolytic dissociation, followed by the ion solvation of $>COO^-$ with coordination number 6 and the strength of the bond of 22 kcal/mol[24].

The following diagram supplied by Misčenko[15] summarizes the composition complexity of the aqueous mixtures of acetic acid.

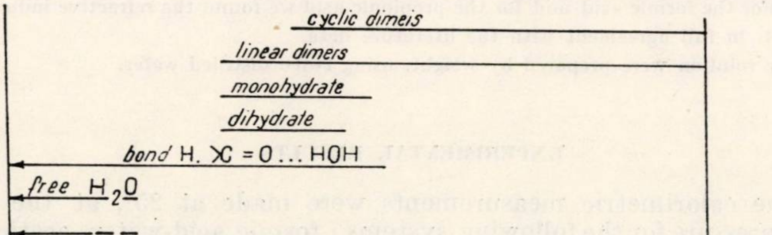
cyclic dimeis
linear dimers
monohydrate
dihydrate
bond H. >C = O ... HOH
free H2O
CH3COOH → H3O+ + CH3COO−
mol % acetic acid
20
40
60
80
100

For the aqueous solutions of the other acids, very few data are available and even those are rather uncertain.

From R.M.N. data[25] and dielectric properties[21] with anomalous values for the 50% acid volume composition, we deduce that this is the best composition for the formation of the propionic acid-water complex.

---

[24] G. H. Haggis, *J. Chem. Phys.*, **20**, 1465 (1952).

[25] B. N. Bahr and G. Lindström, *J. Chem. Phys.*, **23**, 1958 (1955).

From ultrasonic researches,[22] we have the following values for the ratio number of acid molecules/number of water molecules : 3(formic acid); 1(acetic acid); 2(propionic acid); 1/8 (butyric acid).

For aqueous solutions of the formic acid, Blatz,[16] based on Raman researches, supposes that the forms of cyclic dimers, which are as open as the hydrâtes, are possible, but cannot supply a reliable attribution of the frequencies.

For the same system[26] it is told that for solutions with $x < 0.1$, there are only monomers, because the increase of the concentration involves the decrease of the hydration degree; two water molecules for an acid molecule, for about $x < 0.2$, and afterwards a water molecule for an acid molecule.

The information about the thermal effects of the mixture in the case of acid-water systems, are reduced to Faucon's data[27] for the first four acids at 7°, while for the acetic acid-water, we have the more recent data of Gieskes,[28] at 25°, as well as our own data,[29] at three temperatures (17.4°, 25.4° and 34.2°).

APPARATUS

The calorimeter was described in a previous paper[29].

REAGENTS

The purity of the reagents was verified for the acetic acid by titration with a hydroxide solution. For the formic acid and for the propionic acid we found the refractive indices 1.3714 and 1.3871, in full agreement with the literature data.

The solution were prepared by weight, using twice distilled water.

EXPERIMENTAL RESULTS

The calorimetric measurements were made at 25°, at the atmospheric pressure for the following systems : formic acid-water, acetic acid-water, propionic acid-water. The solutions were obtained by successively mixing of the components, by concentrating in acid the solutions with a molar fraction lower than 0.4 or by adding water to the other solutions. The thermal effects observed during the successive mixings, appear equally in the case of the direct mixing of the components for a given composition. The right branch of the curve fitted perfectly with the left one.

For each system, we effected two series of measurements and the data intercalated perfectly in the graphical representations.

[26] L. V. Lanșina and L. G. Sergeeva, *Vest. Mosk. Univ. Khim.*, **23**, 12 (1968).

[27] M. A. Faucon. *Ann. Chim. Phys.*, 19, 70 (1910).

[28] J.M.T.M. Gieskes, *Canad. J. Chem.*, **43**, 2448 (1965).

[29] R. Vîlcu and E. Lucinescu, *Bul. Inst. Politeh. Iași.* (*Serie Nouă*) Secția II, Tom. XVI (XX) fasc. 1–2, 29 (1970).

The enthalpies of mixing, accompanying the formation of a mole of solutions of various compositions, were computed with the help of the calorimetric data, by equation

$$H_r^M = \left\{\frac{(H^M)_{r-1}}{(n_2)_{r-1}}\,[(n_2)_{r-1} - x] + C_r\theta_r\right\}\frac{1}{(n_1)_r + [(n_2)_{r-1} - x + y]}$$

n — number of moles
1,2 — indices of components
r — the determination number
x — concentration diminution of component 2 (moles)
y — concentration increase of component 2 (moles)
C — heat capacity of the system
θ — temperature variation during mixing.

The successive mixtures were obtained by withdrawing a volume of mixture and by adding an equal volume of component 2.

The evaporation of the liquids, during their 8 hours in the thermostat, was avoided by maintaining a very small dead space. By weighing the solutions after the experiment, we have found that the liquid losses were quite small, owing probably also to their careful operating.

Since in the whole domain of heat capacities, the literature gives only the values concerning the acid acetic-water system, [30] we were compelled to proceed to the measurement of these quantities; we made them at about 25°.

The results of the calorimetric measurements were expressed as a function of the acid concentration, by equations of the Redlich-Kister form. The values of the empirical constants were determined by the method of least squares:

formic acid-water: $$H^M = x(1 - x)[-374.853 - 157.331\ (2x - 1) + 187.323\ (2x - 1)^2 + 49.072\ (2x - 1)^3]$$

acetic acid-water: $$H^M = x(1 - x)\ [315.740 + 152.870\ (2x - 1) - 28.417\ (2x - 1)^2 + 434.109\ (2x - 1)^3]$$

propionic acid-water: $$H^M = x(1 - x)[943.462 + 375.797\ (2x - 1) - 27.120\ (2x - 1)^2 + 529.878\ (2x - 1)^3]$$

The first table contains the values of the molar enthalpies of mixing both experimental and computed by one of the above equations, while in figure 1, these values are represented as a function of the acid molar fraction.

The continuous curve represents the computed values, while the spots supply the experimental data. The best concordance appears in the case of the formic acid-water system and the largest deviation is found in the case of the diluted solutions of propionic acid, when experimental data are negative while the respective equation supply positive values. A good concordance appears in the case of the compositions with

---

[30] M. B. Neumann, *Z. Phys. Chem.*, A 158, 258 (1932).

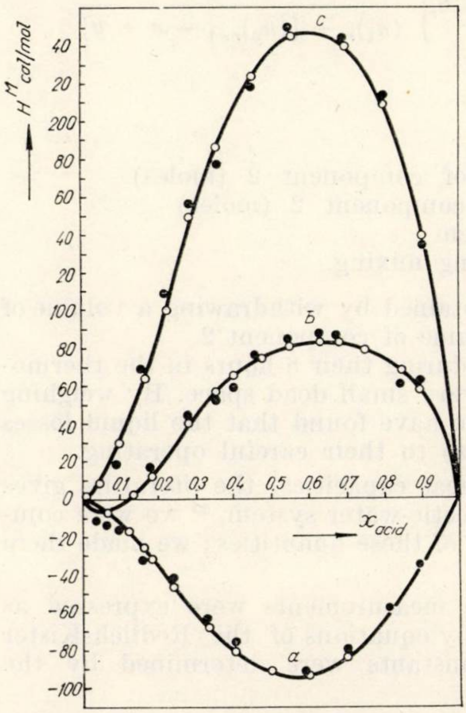

Fig. 1. — Enthalpies of mixing for the systems : *a*) $HCOOH-H_2O$; *b*) $CH_3COOH-H_2O$; *c*) $CH_3.CH_2.COOH-H_2O$; ● experimental data ; o calculated data.

$x > 0.22$. It should probably be added that, in the equation of this system, there is a term that vanishes when $x > 0.2$. However, for the sake of unitary treatment, we made use of an equation of the same form for all three systems.

For comparison, the literature supply data only for the acetic acid-water system. [28] The agreement is satisfying and the largest differences, reaching about 5%, appear in the range of the highest enthalpies.

DISCUSSION OF THE RESULTS

Our results represented by figure 1, just like those supplied by Faucon, [27] emphasize the exceptional behaviour of the formic acid as compared with the other acids of the series and also from the standpoint of the thermal mixing effects. Along the whole range of concentrations, the aqueous solutions of the formic acid are always formed with heat release, while the binding of a hydrocarbon radical to the carboxyl leads to endothermal water mixtures, except the very diluted solutions, where the exothermal effects reappear. Curves $H^M - x$ of the acetic and propionic acids are therefore of an S-form, the negative branch diminishing noticeably from the acetic to the propionic acid, while the positive branch offers an increase of about 3 times in the maximum region.

To establish that this behaviour is the rule, we must moreover make the measurements in the *n*-butyric-water system. According to Faucon's data, this system would deviate from the above rule and intercalate between the curves of the acetic and propionic acids. The extreme values of the enthalpies of mixing, in the case of these 3 systems, are however in the neighbourhood of a 0.6 molar fraction of the acid. Faucon made this study hoping to be able to deduce from the curves of the thermal effects, what hydrates should be formed corresponding to a maximum exothermal effect.

From the behaviour of these systems, it would be deduced that HCOOH alone could form a hydrate. Now, the enthalpy of mixing is a global value of thermal effects due to the breaking of the hydrogen bonds from the pure components and the formation of acid-water bonds either through the carboxyl or through the carboxylic oxhydryl. Therefore, this quantity can on no account constitute for these systems the criteria to decide whether or not hydrates of the carboxylic acids are formed. And that is why Faucon drew the erroneous conclusion that acids do not form associate molecules with water, a fact that cannot be called in question any more, nowadays. This was proved by the most adequate structural methods of the I.R. or Raman spectroscopy that lead to the direct study of the molecule, and reflect all the vibrations modifications due to changes in molecular bonds.

A quantitative interpretation of these thermal effects of the mixtures is impossible with the available data. All we can do, is to suggest a few qualitative aspects related to the known structural data. As a matter of fact, the acetic acid-water system is the only one that allows a qualitative discussion, the other two systems being insufficiently studied.

The endothermal effects, yielded by adding water to acids, indicate rather the prevalence of the processes of bond breaking, than the creation of new bonds.

On the basis of the explanation given by Joerges and Nikuradze, [31] we can admit that the energy necessary ot break an acid is at all events higher than that required by the depolymerization of the water, while the number of mixed associate molecules is in any case smaller than the total number of the dissociated molecules.

On the other hand, the endothermal contribution in the case of concentrated solutions can be due to the breaking of cyclic dimers into open ones, as it appears in the increase of the excess entropy [29] that indicates a loss of the system order when water is added. The exothermal contribution of the formation of hydrates seems to begin of being felt at concentrations lower than $x = 0.6$. According to Misčenko, [15] in this

---

[31] N. Joerges and A. Nikuradze, *Z. Naturforsch*, **5 a**, 259 (1950).

Table 1

The molar enthalpies of mixing for carboxylic acid – water systems

$HCOOH + H_2O$ (25°)			$CH_3COOH + H_2O$ (25.4°)			$CH_3.CH_2.COOH + H_2O$ (25°)		
x_{acid}	$H^M_{exp.}$	$H^M_{calcd.}$	x_{acid}	$H^M_{exp.}$	$H^M_{calcd.}$	x_{acid}	$H^M_{exp.}$	$H^M_{calcd.}$
0.028	−4.126	−2.74	0.04	−8.72	−7.17	0.0135	−3.80	+0.85
0.052	−7.084	−5.856	0.05	−9.06	−7.69	0.0299	−3.55	+3.64
0.058	−7.99	−6.79	0.06	−9.10	−7.70	0.0425	−0.08	+6.95
0.076	−10.27	−9.59	0.085	−6.59	−6.13	0.062	+9.42	+13.79
0.100	−14.025	−13.88	0.129	+1.50	+1.05	0.097	+32.40	+30.26
0.116	−16.97	−16.998	0.170	+12.16	+10.96	0.154	+71.59	+64.46
0.132	−19.53	−20.297	0.277	+41.85	+40.68	0.220	+113.82	+108.35
0.164	−26.019	−27.342	0.342	+55.68	+56.45	0.286	+150.41	+150.31
0.180	−30.652	−31.039	0.401	+64.57	+67.49	0.355	+181.72	+187.59
0.237	−43.65	−44.739	0.475	+76.61	+76.80	0.366	+191.97	+192.73
0.388	−68.92	−68.442	0.537	+83.40	+81.20	0.454	+223.14	+225.14
0.404	−82.42	−81.406	0.616	+85.60	+83.99	0.570	+245.72	+244.36
0.493	−93.73	−93.135	0.651	+85.40	+84.35	0.684	+241.69	+239.36
0.584	−96.13	−96.148	0.721	+83.00	+83.70	0.790	+208.24	+208.31
0.695	−84.61	−85.809	0.847	+66.50	+70.8	0.898	+134.15	+136.72
0.824	−55.48	−55.804	0.905	+56.70	+57.78			
0.905	−31.607	−30.375						

domain the hydrated forms are prevalent, the formation of which is accompanied by effects comparable with those of dissociation of the associated molecules ; when dissociating, the dimer absorbs *ca.* 13.8 kcal/mol, while the monomer releases 12.4 kcal/mol, [32] when the dihydrate is formed. Besides, in the case of very diluted solutions, the hydration of the acid radical yields the high enough energy of 22 kcal/mol.

In spite of very high positive values in the case of the propionic acid, according to the curve aspect, similar to that of the acetic acid, it seems that the propionic acid-water system would present a similar mechanism of the formation mixtures, to that of the acetic acid-water system, though much more pronounced. The same conclusion is arrived by Ramakrishna Rao [21] : discussing the dielectric behaviour of these two systems, he supposed the formation of hydrogen acid-water bonds.

As to the formic acid-water system, the exothermal effects along the entire domain of concentrations, suggest the predominance of formation effects of new associate molecules, probably hydrates, with regard to the dissociation effects. Indded, if we admit a chain structure of the acid, with the free oxhydryl and carbonyl groups, able to bond water molecules, the formation of mixed asssociated molecules is more probable than the breaking of the existent ones with loss of energy, than can occur, but in a much smaller measure.

---

[32] S. A. TAYLOR, *Diss. Abstr.*, **26**, 4276 (1966).

Revue Roumaine de Chimie, **19**, *5*, p. 801–804 (1974)

COMPLEXES OF ANTHRANIL-N,N-DIACETIC ACID WITH TRIVALENT METALS. III[1]

ENTROPY CHANGE CALCULATION

C. DRĂGULESCU, S. POLICEC and T. SIMIONESCU

Center of Chemistry, Bd. Mihai Viteazul, 24, Timişoara, Romania

Received October 18, 1973

The entropy change during chelating reactions performed between each of the following Ga^{3+}, In^{3+}, Sc^{3+}, Y^{3+} and La^{3+} as central metal ion and the anthranil-N,N-diacetic acid (ANDA) as ligand, has been computed by means of the expression $\Delta S^\circ = \Delta H^\circ + 2.303\ RT \log K/T$ and the corresponding, previously determined ΔH° and K values have been used. As ΔS° values showed there is a big entropy increase during the reaction, accounting for the formation and stability of the metal chelates in spite of unfavourable reaction enthalpy. The complex stability was thus attributed to entropy factors only, particularly to the chelate effect. An interpretation of the entropy effect as well as of the chelate effect was next attempted for the investigated Me^{III}-ANDA complexes.

INTRODUCTION

In previous works concerning chelating equilibria in liquid phase of the anthranil-N,N-diacetic acid with Ga^{3+}, In^{3+}, Sc^{3+}, Y^{3+} and La^{3+} metal ions, the composition and stability of the chelate complexes formed in certain conditions as well as the amount of heat change during the reaction [2] were determined. [1]

The composition and stability study performed spectrophotometrically showed the formation in aqueous solution of mononuclear, equimolar complexes with a medium stability. The reaction enthalpy, determined thermometrically, has previously shown that the chelation process is endothermic, thus energetically unlikely to proceed.

As in a given system the sense of spontaneous transformations is indicated by the balance of the reaction enthalpy and the entropy change, an unfavourable enthalpy factor may be compensated by a favourable entropy one. In order to explain, in these conditions, the formation and stability of the investigated Me-ANDA complexes it was assumed that the reactions are accompanied by a positive entropy change, large enough to determine the sense of reaction towards the chelate complex formation. This had to be proved by the entropy change calculation, which has been performed in the present work and is next presented.

---

[1] C. Drăgulescu, S. Policec and T. Simonescu, *Talanta,* **13,** 1451 (1966); **13,** 1543 (1966).

[2] S. Policec, T. Simonescu and C. Drăgulescu, "III-rd National Conference on Analytical Chemistry", Braşov, Romania, vol. IV, 1971, p. 354.

RESULTS AND DISCUSSION

COMPUTATION OF ENTROPY AND FREE ENERGY VARIATION

From the expression

$$\ln K = \frac{T\Delta S^\circ - \Delta K^\circ}{RT}$$

it follows that the stability constant K is thermodynamically a measure of the entropy change and reaction enthalpy.

The entropy change of the investigated chelating reactions was computed by introducing in the following expression

$$\Delta S^\circ = \frac{\Delta H^\circ + 2.303\ RT\ \log\ K}{T},$$

the ΔH° and K values, which were previously determined [1,2] (see table 1). The calculated ΔS° values, together with the temperature of the reaction medium are given in the same table.

Table 1

Thermodynamic functions of the $\mathrm{Me}^{\mathrm{III}}$-ANDA chelate formation reaction

Me^{3+}	T K	ΔH° joule/mol	K	ΔS° joule/mol·K	$-\Delta F^\circ$ joule/mol
Ga^{3+}	297	35,700	1.4×10^6	237.8	34.933
In^{3+}	299	28,600	1.8×10^6	215.3	35,792
Sc^{3+}	298	33,200	6.6×10^5	222.7	33.186
Y^{3+}	298	28,000	3.0×10^5	198.7	31,235
La^{3+}	299	20,600	3.4×10^5	174.7	31,649

$-\Delta F^\circ$ values (last column in the table) computed by means of the

$$-\Delta F^\circ = RT\ \ln K$$

relation, indicate an increase of the equilibrium constant, i.e. of the chelate formation.

As ΔS° values show, there is a remarkable entropy increase during the reaction which proves the formation of new species with an increased stability compared to the initial ones. In this large entropy increase resides the explanation of the formation and stability of the investigated Me-ANDA chelate compounds. It follows, therefore, that the stability cannot be attributed to the Metal-Ligand bonding energy but it may be attributed to entropy factors only and particularly to the chelate effect.

An interpretation of the large entropy effect exhibited by the investigated compounds is next attempted.

In a chemical reaction a favourable entropy effect is a measure of the amount of disorder of that particular system. In the chelating reactions of Ga^{3+}, In^{3+}, Sc^{3+}, Y^{3+} and La^{3+} with ANDA (a 3-charged anionic ligand) equimolar, chargeless chelate compounds are formed. In aqueous medium, prior to reaction, the Me^{3+} metal ions are causing a significant ordering of the solvent molecules in the hydration sphere. The chargeless reaction products will have a considerable lower solvent ordering effect, leading to a greater disorder, thus to an entropy increase of the system.

Bulky ions or molecules exert upon this same ordering process of solvent molecules a less important effect than small particles. Chelate compounds, usually having a larger size than the reactants, will determine by their formation a smaller ordering effect upon the solvent, thus a disorder increase, i.e. a positive entropy change.

An important contribution to the entropy growth of the investigated systems is brought by the chelate effect. Its value may be interpreted in two ways.

— The anthranil-N,N-diacetic acid as quadridentate ligand, having a suitable structure for strainless ring closure, is probably going — — after coordinating one position of the metal ion — to successively coordinate, all the remaining coordination sites of the same ion. According to the coordination number of the metal ion, 1 : 1 = Me : ANDA compounds are formed (the remainder coordination positions being probably occupied by solvent molecules).

— The investigated metal ions will coordinate, in the absence of the ligand, a certain number of solvent molecules. In the presence of the quadridentate ligand, one ligand molecule will determine by chelation the release of four solvent molecules.

One independent ligand molecule disappears thus and four solvent ones are liberated. This process should and does proceed with an entropy increase.

The chelate effect is dependent on a series of factors.

The nature of metal ions is one of them. Spike and Parry [3] showed that for chelate compounds of nontransition metals the heat content change being negligible, the chelate effects has to be essentially an entropy effect. Research concerning the reaction enthalpy of the investigated systems has shown [2] that the enthalpy has no contribution to the driving force leading to the chelation reaction. Consequently, the chelate effect, primarily responsible for the large entropy change, is in the case a pure entropy effect.

---

[3] Spike C. G. and Parry R. W., *J. Amer. Chem. Soc.*, **75**, 2726, 3770 (1953).

The number of chelate rings, as well as that of the atoms in a ring, is another factor having direct influence upon the complex stability. ANDA being able to act as a quadridentate ligand may close with the tervalent Ga^{3+}, In^{3+}, Sc^{3+}, Y^{3+} and La^{3+} metal ions as many as three chelate rings, two five-membered, with saturated bonds and a six-membered one with unsaturated, aromatic bonding. The stability of a six-membered ring with aromatic contribution — comparable with a five-membered one — may be attributed to some steric characteristics of the benzene ring.[4] The last is orienting the chelate ring into the benzene plane, thus providing a better approach of the donor atoms. Resonance of the aromatic carboxylic group and tertiary nitrogen with the benzene ring leads to a bond shortening and thus to an increase of ring stability.

Ligand structure is another factor the chelate effect is depending upon. Connected with the preferred stereochemistry of the metal ion it may or may not lead to a strained arrangement. The stability constant values of the investigated metal chelates prove that strainless steric arrangements are formed.

---

[4] A. E. Martell and M. Calvin, "Die Chemie der Metallchelat-Verbindungen", Verlag-Chemie, Berlin, 1958.

Revue Roumaine de Chimie, **19**, *5*, 805–810 (1974)

COBALT AND GERMANIUM DOUBLE OXIDES

CONST. GH. MACAROVICI, MARIA BIROU, EUGENIA PERȚE and M. STRĂJESCU
Institute of Chemistry, Cluj, Str. Donath 65–103, Romania

Received July 25, 1973

The paper covers the formation of cobalt and germanium double oxides starting from complex compounds, and their study by the following methods : the thermogravimetric, thermodifferential analysis, Roentgen and IR spectra.

It is known [1] that double oxides may be obtained through several approaches : starting from complexes, from metallic ion coprecipitates and through the reaction between various metallic oxides intimately mixed and subjected to high temperature.

In the present paper cobalt and germanium double oxides are prepared considering their properties as catalysts, semiconductors, etc.

Two complex compounds were synthesized, i.e. :

1. Starting from the ammonium germanium-oxalate, the ammonium was replaced by Co(III) hexamine. This type of complex was also investigated by Kurnevici and Saghisultanova. [2]

The above complex was obtained in crystalline form by mixing a concentrated aqueous solutions of both components, in various proportions. Regardless of the mixing order, a fine precipitate is separated and the analysis reveals in all the cases the formation of one single compound with a 1 Co : 1 Ge ratio.

The precipitate after filtration is washed with water alcohol and ether, and dried in a desiccator. The data obtained from the chemical analysis (table 1) permit the formulation of the complex as follows :

$$[Co(NH_3)_6]\,Cl.[Ge(C_2O_4)_3] \qquad (1)$$

The sum of the oxides was determined by calcining the product at 1100° ; after dissolving, the cobalt was determined as phosphate [3] while the germanium content was determined by the difference. Water was determined by an Abderhalden apparatus, at the boiling temperature of water, while chlorine, carbon, hydrogen and nitrogen were determined by classical approaches.

---

[1] J. Paris and R. Paris, *Bull. Soc. chim. France*, **4**, 1138 (1965).

[2] G. I. Kurnevici and Saghisultanova, *Zhur. nerog. Khim.*, **9**, 2559 (1964).

[3] Const. Gh. Macarovici, "Chimie analitică cantitativă", Ed. tehnică, Bucharest, 1959, p. 151.

Table 1

Chemical analysis of the complexes

Substance	C_2O_4 %	Cl %	$CoO + GeO_2$ %	Co %	Ge %	N %	H_2O %
I $[Co(NH_3)_6]Cl.[Ge(C_2O_4)_3]$	*Calcd.* 49.52	6.65	33.67	11.05	13.60	15.76	—
P.M. = 533.2	*Found* 49.28	6.67	33.48	11.76	12.86	15.73	—
II $[Co(NH_3)_6]_4[Ge(C_6H_6O_8)_2]_3.4H_2O$	C %	H %	$CoO+GeO_2$ %	Co %	Ge %	N %	H_2O %
P.M. = 2171.07	*Calcd.* 19.92	5.38	28.26	13.81	14.46	15.49	3.31
	Found. 19.72	5.56	28.31	14.00	14.31	15.28	3.60

The calcination of the complex yielded the double oxide $CaO.GeO_2$ known in the literature.

2. Starting with the germanium saccharate :

$$Na_4[Ge(C_6H_6O_8)_2]\cdot 4H_2O$$

described by us in a previous paper, [4] we focused on the substitution of sodium by Co(III) hexamine.

To do this, the components were separately dissolved in water and then mixed in a 4/3 molar ratio

$$[Co(NH_3)_6]^{3+} : [Ge(C_6H_6O_8)_2]^{4-}$$

A yellow precipitate was separated immediately thereafter. It was filtered, washed with water, alcohol and ether and dried in a desiccator. The analysis was performed as in the case of the preceding complex (table 1).

The results provided by the analysis enable the following formulation of the complex :

$$[Co(NH_3)_6]_4\ [Ge(C_6H_6O_8)_2]_3\cdot 4H_2O \qquad \text{II}$$

By calcining the above complex we obtained the double oxide $4CoO.3GeO_2$ which has not been reported in the literature.

Both complexes were subjected to thermogravimetric and thermodifferential analysis, using an apparatus without automatic recording. The heating rate was 5°/min throughout the procedure (figs. 1 and 2).

Samples were subjected to IR spectral analysis and to Roentgen analysis. The IR absorption spectra were measured with an UR-10 Carl-Zeiss Jena instrument as potassium bromide pellets (figs. 3, 4).

The X-ray diffraction spectra were taken by a TUR-60 apparatus, applying the Debye-Scherrer powder method (fig. 5).

RESULTS AND DISCUSSION

Considering the similar behaviour of both complexes studied during thermal decomposition, we will study them together.

As seen in figs. 1 and 2, the gradual rise in the temperature leads to the loss of water, a phenomenon occurring concomitantly with hexamine decomposition and ending around 200°. The organic substance is then burnt with the elimination of CO_2 and H_2O and the formation of the corresponding oxides.

---

[4] Const. Gh. Macarovici, and M. Voloșniuc-Birou, *Rev. Roumaine Chim.* **12**, 163 (1967).

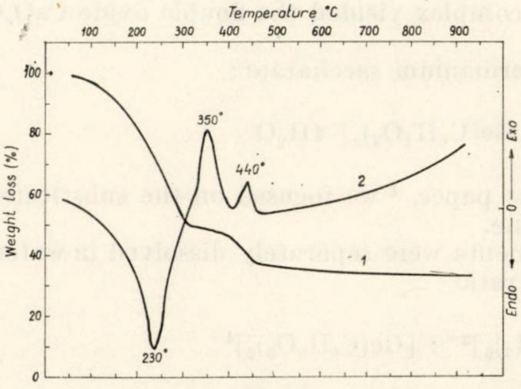

Fig. 1. — Thermogravimetric (1) and thermodifferential (2) curve of the complex $[Co(NH_3)_6]Cl[Ge(C_2O_4)_3]$.

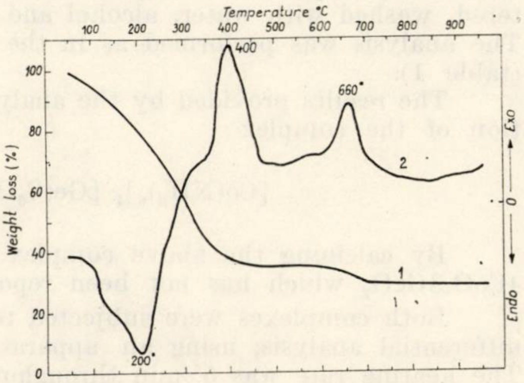

Fig. 2. — Thermogravimetric (*1*) and thermodifferential (*2*) curve of the complex $[Co(NH_3)_6]_4 \cdot [Ge(C_6H_6O_8)_2]_3 \cdot 4H_2O$.

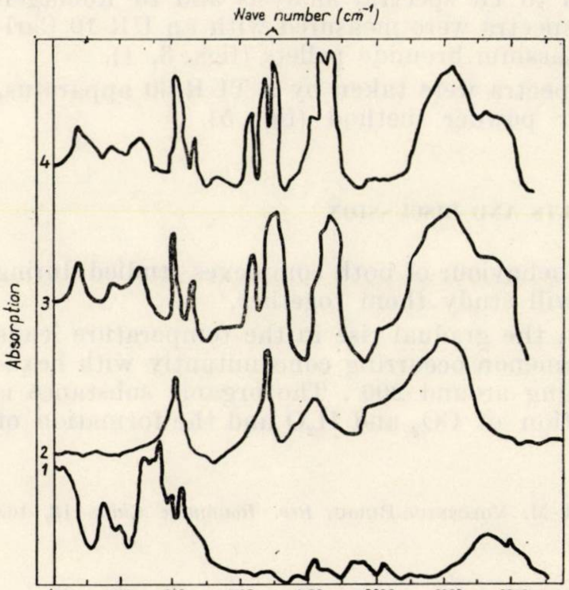

Fig. 3. — IR spectra of :1) $CoO \cdot GeO_2$; 2) $[Co(NH_3)_6]Cl_3$; 3) $[Ge(C_2O_4)_2](NH_4)_2 \cdot 4H_2O$; 4) complex I.

Fig. 4. — IR spectra of : 1) GeO_2 ; 2) CoO ; 3) Co_3O_4 ; 4) $4CoO \cdot 3GeO_2$; 5) complex II at 650° ; complex II at 450° ; 7) complex II.

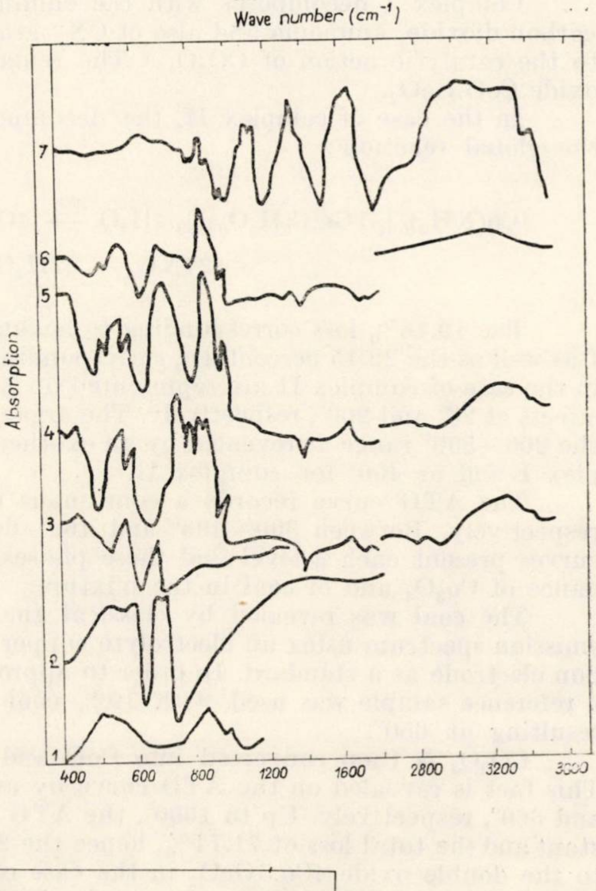

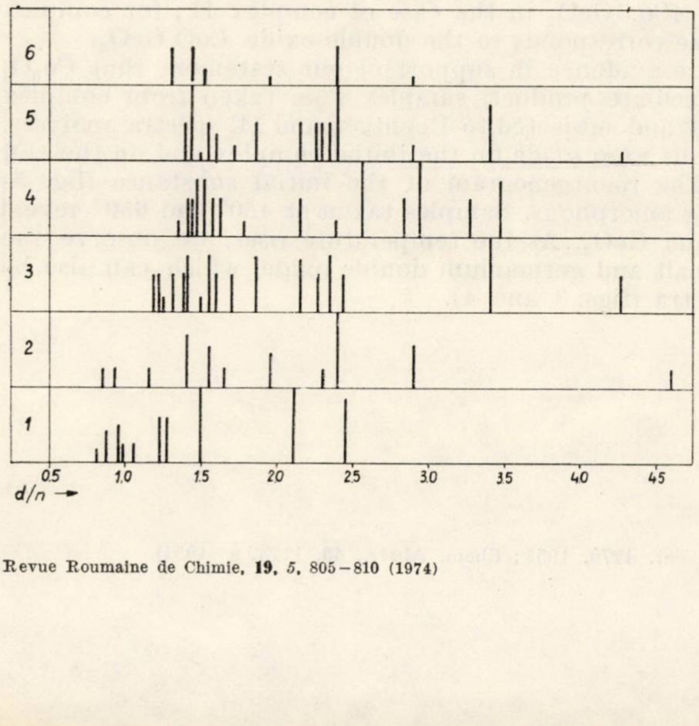

Fig. 5. — Roentgen diffraction spectra of : 1) CoO ; 2) Co_3O_4 ; 3) GeO_2 ; 4) $4CoO_3 \cdot$ $\cdot 3GeO_2$; 5) complex II at 650° ; 6) complex II at 450°.

Complex I decomposes with the elimination of hydrochloric acid, carbon dioxide, ammonia and also of CN^- groups which were formed due to the catalytic action of CO_3O_4.[5] The remaining residue is the double oxide $CoO.GeO_2$.

In the case of complex II, the decomposition occurs according to the global reaction:

$$[Co(NH_3)_6]_4.[Ge(C_6H_6O_8)_2]_3.4H_2O \xrightarrow{26O_2} 4CoO.3GeO_2 + 36CO_2 + \\ + 24NH_3 + 22H_2O$$

The 19.16% loss corresponding to hexamine in the case of complex I as well as the 22.15 percentage, corresponding to hexamine and to water in the case of complex II are represented on ATD curves by endothermic effects at 23° and 200°, respectively. The organic substance is burnt within the 200—500° range as revealed by an exothermic effect, at 350° for complex I and at 400° for complex II.

The ATG curve records a continuous decrease to 300° and 460°, respectively. Between 300—400° and 460—600°, respectively, the ATG curves present each a level and these phases correspond to the maintenance of Co_3O_4 and of coal in the mixture.

The coal was revealed by classical analysis and by means of the emission spectrum using an electrolyte copper electrode and a 100% carbon electrode as a standard. In order to approximate the coal percentage a reference sample was used with 10% coal in the mixture of oxides resulting at 650°.

CO_3O_4 is then converted into CoO and the coal is totally burnt. This fact is revealed on the ATD curve by an exothermic effect at 440° and 660°, respectively. Up to 1000°, the ATG curve remains almost constant and the total loss of 71.74%, hence the 28.31% residue, corresponds to the double oxide $4Co.3GeO_2$ in the case of complex II; for complex I, the 33.48% residue corresponds to the double oxide $CoO.GeO_2$.

To supply more evidence in support of our statement that Co_3O_4 results as an intermediate product, samples were taken from complex II at 450° and at 650° and subjected to Roentgen and IR spectra analyses. Similar determinations were made on the initial complex and on the end product at 1000°. The roentgenogram of the initial substance (fig. 5) shows no lines, being amorphous. Samples taken at 450° and 650° reveal the lines of Co_3O_4 and GeO_2. As the temperature rises, we observe the formation of the cobalt and germanium double oxide, which can also be seen in the IR spectra (figs. 3 and 4).

---

[5] K. Sasaki, Jap. Pat. 4770, 1953; Chem. Abstr., **48**, 11739 g (1954).

Revue Roumaine de Chimie, **19**, *5*, 811–816 (1974)

ON THE REDOX POTENTIALS IN THE TRANSITION-METAL COMPLEXES

C. I. LEPĂDATU and CRISTINA RUSU

Centre of Chemical Physics, Dumbrava Roşie 23, Bucharest, Romania

Received June 11, 1973

A molecular orbital treatment of the chemical bonding contribution to the redox potentials in the transition-metal complexes is presented. It has been shown that the ligand field interpretation of these contributions must be reformulated, because of the inconsistency of the baricenter conservation rule of the split *d*-levels. A correlation between the chemical bonding contribution to the redox potentials and the spectral behaviour of the complexes is also given.

It has been suggested that among other main factors determining the values of the redox potentials in the transition-metal complexes, [1] an important role would play the so-called ligand field stabilization energies (LFSE) of the two M^{+z}/M^{+z+1} ions in the field produced by the ligands directly bound to the central metal.

As has been recently shown,[2,3] the stabilization problem of the coordination clusters must be reformulated in terms of the MO theory which leads to a more realistic basic concept on the spatial stabilization of the complexes, quite different of that offered by the ligand field theory, exclusively based on the baricenter conservation rule of the split energy levels, valid only in the elctrostatic approach of the interactions in molecule.

This is the reason why the mentioned factor contributing to the redox potentials must be reconsidered in the framework of the LCAO MO theory. The aim of the present note is to give a MO treatment of the contribution due to the chemical bonds to the redox potentials in the *d*-complexes, and to see the possible correlation with the spectral and magnetic behaviour of the complexes. As may be seen in the following, the chemical bonding effects included into the redox potential values have nothing to do with the ligand field stabilization energy, and may be put, on the contrary, in connection with the destabilization of the

---

[1] D. P. Perrin, "Organic Complexing Reagents", chap. 4, Intersc. Publ., New York, 1964.

[2] C. I. Lepădatu, *J. Cryst. Mol. Structure (London)*, **1**, 397 (1971).

[3] C. I. Lepădatu, *Rev. Roumaine Chimie*, **17**, 863 (1972).

d-state, going from the d-levels to the antiboding molecular levels in which the d-states are involved.

Let us consider the following oxidation-reduction mechanism for the gaseous metal ion

$$d^n \rightleftarrows d^{n-1} + e^- \tag{1}$$

whose energy balance

$$\varepsilon(d^{n-1}) - \varepsilon(d^n) = V(d^n/d^{n-1}) \tag{2}$$

is the oxidation-reduction potential, equal to the difference with changed sign between the energies of the ground spectral terms of the metal having the electronic configurations d^{n-1} and d^n.

Because we are dealing with coordinate metal ions, the energies of their ground states in complexes will differ from those in the free metal ion, difference mainly produced by the chemical bond formation and by the possible rearrangements occurring in the electron population (high spin and low spin states).

If (1) and (2) are considered not for gaseous metal ions but for the free ions before coordination in their proper valence states in complexes, the differences

$$\begin{aligned} \varepsilon_c(d^{n-1}) - \varepsilon(d^{n-1}) &= \Sigma(d^{n-1}) \\ \varepsilon_c(d^n) - \varepsilon(d^n) &= \Sigma(d^n) \end{aligned} \tag{3}$$

will give the chemical bonding effects, where ε_c's are the ground state molecular energies in the complex molecules. Like (2), the oxidation-reduction potentials of the coordinate metal ion will be

$$V_c(d^n/d^{n-1}) = \varepsilon_c(d^{n-1}) - \varepsilon_c(d^n) = V(d^n/d^{n-1}) + [\Sigma(d^{n-1}) - \Sigma(d^n)] \tag{4}$$

where $V(d^n/d^{n-1})$ is the redox potential of the free metal ion before coordination but for its proper valence states in complexes, Σ's being the chemical bonding effects taken with changed sign. Expression (4) gives us a way to estimate the contribution of the chemical bond formation to the redox potential values (the last right-hand term).

We give below the energy expressions for the ground states in the free and coordinate metal ion in its two possible spin distributions (high spin and low spin states, the last one marked by an asterisk) for orthoaxial complexes, that is cluster molecules having six identical ligands located along the Cartesian axes of the central ion

$$\varepsilon(d^0) = \varepsilon_c(d^0) = \varepsilon^{\text{core}}(0)$$

$$\begin{cases} \varepsilon(d^1) = \varepsilon^{\text{core}}(1) \\ \varepsilon_c(t_2^1,\ {}^2T_{2g}) = \varepsilon^{\text{core}}(1) + 4e_\pi(1) \end{cases}$$

$$\begin{cases} \varepsilon(d^2) = \varepsilon^{\text{core}}(2) - 8B(2) \\ \varepsilon_c(t_2^2,\ {}^3T_{1g}) = \varepsilon^{\text{core}}(2) + 8e_\pi(2) - 5\alpha_\pi^4 B(2) \end{cases}$$

$$\begin{cases} \varepsilon(d^3) = \varepsilon^{\text{core}}(3) - 15B(3) \\ \varepsilon_c(t_2^3,\ {}^4A_{2g}) = \varepsilon^{\text{core}}(3) + 12e_\pi(3) - 15\alpha_\pi^4 B(3) \end{cases}$$

$$\begin{cases} \varepsilon(d^4) = \varepsilon^{\text{core}}(4) - 21B(4) \\ \varepsilon_c(t_2^3e^1,\ {}^5E_g) = \varepsilon^{\text{core}}(4) + 3e_\sigma(4) + 12e_\pi(4) - [15\alpha_\pi^4 + \\ \qquad + 6\alpha_\sigma^2\alpha_\pi^2]\,B(4) \\ \varepsilon_c^*(t_2^4,\ {}^3T_{1g}) = \varepsilon_c(t_2^3e^1) - [\,\Delta(4) - \Pi(d^4)] \end{cases}$$

$$\begin{cases} \varepsilon(d^5) = \varepsilon^{\text{core}}(5) - 35B(5) \\ \varepsilon_c(t_2^3e^2, {}^6A_{1g}) = \varepsilon^{\text{core}}(5) + 6e_\sigma(5) + 12e_\pi(5) - [15\alpha_\pi^4 + 12\alpha_\sigma^2\alpha_\pi^2 + \\ \qquad + 8\alpha_\sigma^4]B(5) \\ \varepsilon_c^*(t_2^5,\ {}^2T_{2g}) = \varepsilon_c(t_2^3e^2) - 2[\,\Delta(5) - \Pi(d^5)] \end{cases}$$

$$\begin{cases} \varepsilon(d^6) = \varepsilon^{\text{core}}(6) - 35B(6) + 7C(6) \\ \varepsilon_c(t_2^4e^2,\ {}^5T_{2g}) = \varepsilon^{\text{core}}(6) + 6e_\sigma(6) + 16_\pi(6) - [15\alpha_\pi^4 + 12\alpha_\sigma^2\alpha_\pi^2 + \\ \qquad + 8\alpha_\sigma^4]B(6) + [5\alpha_\pi^4 + 2\alpha_\sigma^2\alpha_\pi^2]\,C(6) \\ \varepsilon_c^*(t_2^6,\ {}^1A_{1g}) = \varepsilon_c(t_2^4e^2) - 2[\,\Delta(6) - \Pi(d^6)] \end{cases}$$

$$\begin{cases} \varepsilon(d^7) = \varepsilon^{\text{core}}(7) - 43B(7) + 14C(7) \\ \varepsilon_c(t_2^5e^2,\ {}^4T_{1g}) = \varepsilon^{\text{core}}(7) + 6e_\sigma(7) + 20e_\pi(7) - [20\alpha_\pi^4 + 12\alpha_\sigma^2\alpha_\pi^2 + 8\alpha_\sigma^4]B(7) + \\ \qquad + [10\alpha_\pi^4 + 4\alpha_\sigma^2\alpha_\pi^2]\ C(7) \\ \varepsilon_c^*(t_2^6e^1,\ {}^2E_g) = \varepsilon_c(t_5^5e^2) - [\Delta(7) - \Pi(d^7)] \end{cases}$$

$$\begin{cases} \varepsilon(d^8) = \varepsilon^{\text{core}}(8) - 50B(8) + 21C(8) \\ \varepsilon_c(t_2^6e^2,\ {}^3A_{2g}) = \varepsilon^{\text{core}}(8) + 24e_\pi(8) + 6e_\sigma(8) - [38\alpha_\pi^4 + 12\alpha_\sigma^2\alpha_\pi^2]B(8) + \\ \qquad + [15\alpha_\pi^4 + 6\alpha_\sigma^2\alpha_\pi^2]C(8) \end{cases}$$

$$\begin{cases} \varepsilon(d^9) = \varepsilon^{\text{core}}(9) - 56B(9) + 28C(9) \\ \varepsilon_c(t_2^6e^3,\ {}^2E_g) = \varepsilon^{\text{core}}(9) + 24e_\pi(9) + 9e_\sigma(9) - [30\alpha_\pi^4 + 18\alpha_\sigma^2\alpha_\pi^2 + \\ \qquad + 8\alpha_\sigma^4]B(9) + [15\alpha_\pi^4 + 9\alpha_\sigma^2\alpha_\pi^2 + 4\alpha_\pi^4]C(9) \end{cases}$$

$$\varepsilon(d^{10}) = \varepsilon_c(d^{10}) = \varepsilon^{\text{core}}(10) - 70B(10) + 35C(10)$$

where $\varepsilon^{\text{core}}(n)$ is the core energy

$$\varepsilon^{\text{core}}(n) = nU + \frac{n(n-1)}{2}A \tag{5}$$

U being the one-electron energy summing up the kinetic and potential electron-SCF metal core energies, A, B, C the Racah interelectronic repulsion energies, $e_{\sigma(\pi)}$ the antibonding orbital energies, $\Delta(n) = 3e_\sigma(n) - 4e_\pi(n)$ the orbital parameter, $\Pi(d^n)$ the spin-pairing energies and $\alpha_{\sigma(\pi)}$ the mixing coefficients of the d-orbitals in the $\sigma(\pi)$ MO's (usually antibonding) practically located on the central metal ion. The above master formulas were obtained using truncated MO's in a strong-coupling scheme,[4] which reproduce in general lines the three parametric (Δ, B, C) ligand field energies in the strong field-coupling, [5] except the LFSE's coming from the baricenter rule which cannot be accepted in a MO approach. Concerning the spin-pairing energies, their master formulas expressed in terms of Racah energies and mixing coefficients may be found elsewhere. [4]

According to (3)—(4), the redox potentials of the coordinate transition-metal ions could be calculated if the ground state energies as written above, were known. These energies may be in principle estimated using *ab initio* or semiempirical MO approximations in order to find $e_{\sigma(\pi)}$ and $\alpha_{\sigma(\pi)}$ values. Unfortunately, this problem represents a difficult task, because there are not as yet reliable quantum-mechanical methods suitable to this purpose. For this reason, we shall try in the following to get different quantities involved in (3)—(4) from the spectral and the magnetic behaviour of the transition-metal complexes. We can obtain in this way all necessary Σ's, which according to (3)—(4), do contribute to the redox potentials.

The quantity

$$V(d^n/d^{n-1}) = \varepsilon^{\text{core}}(n-1) - \varepsilon^{\text{core}}(n) \tag{6}$$

which would represent the redox potential of the free metal ion in its proper valence state before coordination, remains thereby undetermined. Since the core energies are dependent on the formal charge on the SCF metal core, according to the electroneutrality principle generally valid for the majority of the transition-metal complexes, it results that $V(d^n/d^{n-1})$ may be roughly considered as being practically unchanged in the complexes of the pair $M(d^n)/M(d^{n-1})$ with different ligands.

If the electroneutrality principle holds, it follows that the dependence of the redox potential values on the ligand nature should be straightforwardly linked with the chemical bonding effects. One may therefore conclude that the changes occurring in the electrochemical redox potentials of the systems $M(d^n/)/M(d^{n-1})L_6$ and $M(d^n)/M(d^{n-1})L'_6$ will be, according to (4), equal to

$$V_{L,L}(d^n/d^{n-1}) = V_L(d^n/d^{n-1}) - V_L'(d^n/d^{n-1}) = \delta_L(n-1, n) - \delta_{L'}(n-1, n) \tag{7}$$

where

$$\delta(n-1,\ n) = \Sigma(d^{n-1}) - \Sigma(d^n)$$

---

[4] P. Spacu and C. I. Lepădatu, *Z. phys. Chem.* (*Frankfurt*), **63**, 15 (1969).

[5] J. S. Griffith, "The Theory of Transition-Metal Ions", University Press, Cambridge, 1964.

Σ's being the chemical bonding effects taken with changed sign. We give below some of the known systems for which the spectral and the magnetic behaviour are well studied. Since it was not possible in each case, to have a collection of spectrally determined mixing coefficients, we adopted in the following the approximation of the isotropic covalency, in order to make use of ligand field data, at least as the mean energies Δ and B are concerned. Since the B values are less dependent on the oxidation state than the orbital energies, one may consider $B(d^{n-1}) \approx B(d^n)$. With these approximations in mind, the following $\delta(n-1, n)$ expressions may be obtained for $n = 3-7$:

d^3/d^4

$$\delta(3,\ 4) = 12e_\pi(3) - 16e_\pi(4) - \Delta(4)$$

$$\delta(3,\ 4^*) = 12e_\pi(3) - 16e_\pi(4) - \Pi(d^4)$$

where the asterisk shows the low spin ground state $d^4(t_2^4)$.

For the system $Cr^{3+/2+}(H_2O)_6$, both complexes have high spin ground states, [5,6] for which $\Delta(3) = 17.4$ kK, $\Delta(4) = 14$ kK, and $e_\pi(3) = 1.25$ kK independently calculated by Lever [7] and by one of us [8] With

$$\frac{e_\pi(n-1)}{e_\pi(n)} \approx \frac{\Delta(n-1)}{\Delta(n)} \text{ (see ref. }^{9}\text{)} \tag{8}$$

one obtains $\delta_{H_2O}(3, 4) \approx +1.85$ eV.

For the system $Cr^{2+/3+}(CN)_6$, the orbital energies e_π, arisen from the π ligand $\leftarrow$ metal bonds, may be ignored due to the fact that for strongly heteropolar chemical bonds the bonding effects are much smaller than the antibonding ones.

Considering the spin-pairing energy $\Pi(d^4, M^{2+}) \approx 17.5$ kK, as it results from magnetic and spectral studies, [10] and taking into account that $Cr(d^4)(CN)_6$ has a low spin electron distribution [6] we find $\delta(3, 4^*) \approx$ $\approx +2.169$ eV. According to (7), we have $V_{H_2O,\ CN}(Cr^{3+}/Cr^{2+}) \approx -$ -0.32 eV which may be compared with -0.87 eV experimentally found [1] ($\pi_{H_2O} = +0.41$ eV ; $\pi_{CN} = +1.28$ eV).

d^4/d^5

We find in the same way

$$\delta(4,\ 5) = \Delta(4) - 2\,\Delta(5) + 16e_\pi(4) - 20e_\pi(5)$$

$$\delta(4^*,\ 5^*) = \Pi(d^4) - 2\Pi(d^5) + 16e_\pi(4) - 20e_\pi(5)$$

---

[6] C. J. BALLHAUSEN, "Introduction to Ligand Field Theory", chap. 10, McGraw-Hill Book, Comp., Inc., New York, 1962.

[7] A. B. P. LEVER, *Coord. Chem. Rev.*, **3**, 119 (1968).

[8] C. I. LEPĂDATU, *Z. phys. Chem. (Frankfurt)*, **60**, 205 (1968).

[9] C. I. LEPĂDATU, *Z. phys. Chem. (Frankfurt)*, **57**, 28 (1968).

[10] E. KÖNIG and S. KREMER, *Theor. Chim. Acta*, **23**, 12 (1971).

For the system $Mn^{3+/2+}(H_2O)_6$ we have the following spectral data [5,6] $\Delta(4) = 20$ kK (in oxalate), $\Delta(5) = 8.3$ kK, $e_\pi(5) = \chi_{Mn^{2+}} \times 1.25$ kK where $\chi_{Mn^{2+}} = 0.517$ is the spectrochemical ratio taking Cr(III)-ligand bonds as standard, [9] $e_\pi(4) = 1.53$ kK (eq.(8)). Hence, $\delta(4, 5) = -1.819$ eV.

For the system $Mn^{3+/2+}(CN)_6$, both complexes are low spin [6], $e_\pi \approx \approx 0$, $\Pi(d^4, M^{3+}) = 20.1$ kK and $\Pi(d^5, M^{2+}) = 10.1$ kK (see ref. [10]). Hence, $\delta(4^*, 5^*) = +0.26$ eV, and therefore $V_{H_2O,\,CN}(Mn^{3+}/Mn^{2+}) = -2.079$ eV which may be compared with -1.73 eV experimentally found [1]

d^5/d^6

$$\delta(5,\ 6) = 2[\Delta(5) - \Delta(6)] + 20e_\pi(5) - 24e_\pi(6)$$

$$\delta(5^*,\ 6^*) = 2[\Pi(d^5) - \Pi(d^6)] + 20e_\pi(5) - 24e_\pi(6)$$

System $Fe^{3+/2+}(H_2O)_6$; $\Delta(5) = 14.2$ kK, $\Delta(6) = 10.4$ kK (see ref [5]) and $e_\pi(6) = \chi_{Fe^{2+}} \times 1.25$, where [9] $\chi_{Fe^{2+}} = 0.597$, $e_\pi(5) = 1.01$ kK (eq.(8)). Therefore, $\delta(5, 6) = -1.15$ eV.

System $Fe^{3+/2+}(CN)_6$: $e_\pi \approx 0$, $\Pi(d^5, M^{3+}) = 19$ kK, $\Pi(d^6, M^{2+}) = = 12$ kK.

Both complexes are low spin [6] and, therefore, $\delta(5^*, 6^*) = -1.73$ eV, and hence $V_{H_2O,\,CN}(Fe^{3+}/Fe^{2+}) = +0.58$ eV (exp.[1] -0.42 eV).

As may be seen, there is an obvious disagreement between the predicted value and that experimentally found. One of the sources of errors could be found in the dependence of $V(d^n/d^{n-1})$ of the formal charge on the SCF metal core. It may happen that the formal charge on the metal core be very different going from high spin complexes to low spin complexes and this is undoubtedly the case in the systems $Fe^{3+/2+}L_6$, where $L = H_2O, CN^-$. A confirmation of this statement is supplied by the next systems whose $\delta(n-1, n)$ are evaluated using the same master formula.

d^6/d^7

$$\delta(6^*,\ 7) = 2[\Pi(d^6) - \Delta(7)] + 24e_\pi(6) - 28e_\pi(7) - 3B$$

System $Co^{3+/2+}(H_2O)_6$: $\Delta(6) = 18.5$ kK, $\Delta(7) = 9.3$ kK, $B = = 0.800$ kK (ref. [5]), $e_\pi(6) = \chi_{Co^{3+}} \times 1.25$, where $\chi_{Co^{3+}} = 1.051$ (ref, [9]), $e_\pi(7) = 0.66$ kK (eq. [8]), $\pi(d^6, M^{3+}) = 13.1$ kK (ref.[10]). Therefore $\delta(6^*, 7) = -2.12$ eV.

System $Co^{3+/2+}(NH_3)_6$: $\Delta(7) = 10.1$ kK, $B = 0.680$ kK (ref.[5]), $e_\pi = 0$ (ref. [8]), $\pi(d^6, M^{3+}) = 13.1$ kK (ref.[10]). Therefore, $\delta(6^*, 7) = - - 0.49$ eV.

Consequently, $V_{H_2O,\,NH_3}(Co^{3+}/Co^{2+}) = -1.63$ eV, which agrees with the experimentally found change in the electrochemical redox potentials [10], equal to -1.70 eV.

Revue Roumaine de Chimie, **19**, *5*, 817–825 (1974)

Ni(II) CHELATES SYNTHETIZED WITH 1-METHYL-2-CARBETHOXY-GLYOXALANIL-(1)-TOLYLHYDRAZONES-(2)

A. C. BANCIU and P. SPACU

Center of Physical Chemistry, Str. Dumbrava Roşie, 23, Bucharest, Romania

Received November 21, 1973

Using the three 1-methyl-2-carbethoxy-glyoxalanil-(1)-tolylhydrazones-(2) as ligands, depending on the preparation conditions, two types of Ni(II) complexes were obtained, some of them containing the mentioned ligands and other having the anil group in the molecule substituted by an imino group. The elemental analysis data, IR and electronic spectra as well as the magnetic measurements show that all the prepared complexes are tetracoordinate chelates with a low-spin square-planar arrangement of the coordination Ni-(II)-N bonds. The intense colour of the chelates is due to the CT metal → ligand bands, occurring in the visible range.

In a previous paper, [1] two complexes formed by the Ni(II) ion with 1-methyl-2-carbethoxy-glyoxalanil-(1)-phenylhydrazone-(2), the simplest ligand from the class of these substituted aryl-hydrazones, were described. In a subsequent paper, [2] there were studied the ligands, the complexing way and the coordination compounds of Co(II) with the 1-methyl-2-carbethoxy-glyoxalanil-(1)-tolylhydrazones-(2), (Ia-c).

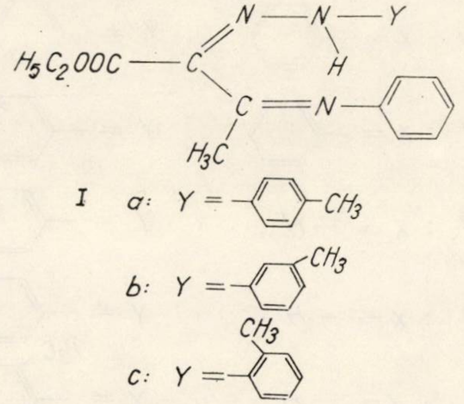

---

[1] P. Spacu, A. C. Banciu and C. I. Lepădatu, *Rev. Roumaine Chim.*, **18**, 7, 1143 (1973).

[2] A. C. Banciu and P. Spacu, *Rev. Roumaine Chim.*, under press.

The present note deals with five Ni(II) complexes prepared with the organic compounds Ia-c, the preparation of the last ones being already described elsewhere. [2]

EXPERIMENTAL

Reagents. Acetylacetic ester (Merck, reagent for synthesis, minimal content 98 %), aniline (tri-distilled), *p*-toluidine (Carlo Erba, minimal content 99 %), *m*-toluidine (Schuchardt, p.*a.*), *o*-toluidine (Loba-Chemie, *p.a.*), anhydrous $NaCH_3COO$ (Austranal, *p.a.*), $NiCl_2 \cdot 6H_2O$ (Reactivul, Bucharest, *p.a.*), NH_3 25 % solution (Reactivul, Bucharest, *p.a.*).

Preparation of the Ni(II) chelates. The Ni(II) chelates were synthetized using a known method, [3] refluxing alcoholic solutions, containing amounts of 1/100 m ligand and 1/200 m $NiCl_2 \cdot 6H_2O$, plus a slight excess of 15 % from this theoretical quantity in the case of the last reagent, in order to assure the completeness of the reaction. The chelates IIa-1 and IIb-1 were obtained in the presence of a small amount of triethylamine (*ca.* 1 cc). The attempts to prepare the corresponding Ni(II) chelate with the compound Ic have invariably failed as the previous attempts to get the corresponding Co(II) chelate. [2] Using the same conditions and amounts of reagents as shown above, in the absence of triethylamine, but in the presence of a quantity of about 20 cc of 25 % solution NH_3, the chelates IIa-2, IIb-2 and IIc were obtained using the compounds Ia-c. Under the catalytic influence of the Ni(II) salt, NH_3

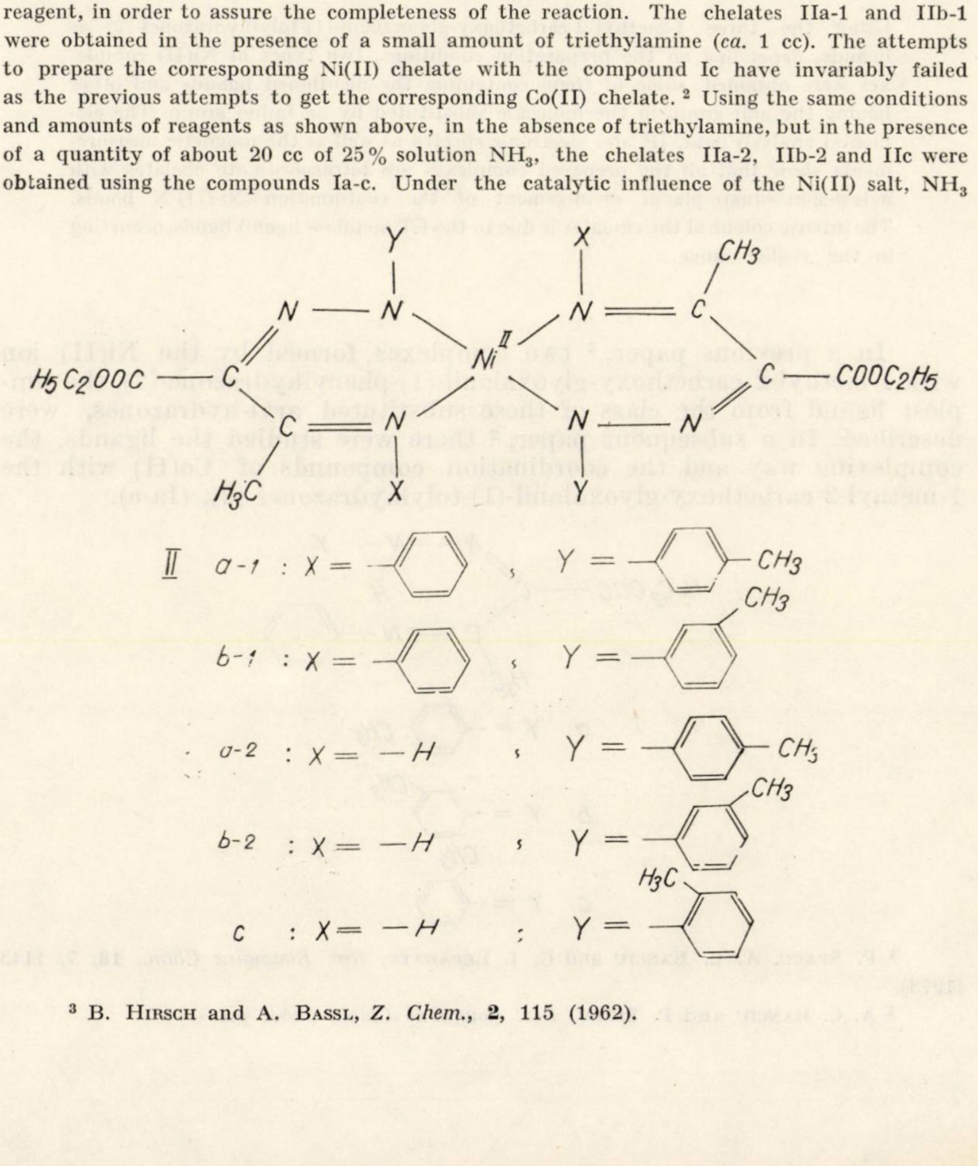

---

[3] B. HIRSCH and A. BASSL, *Z. Chem.*, **2**, 115 (1962).

generates the anil group splitting and its substitution by the imino group, NH, in the ligand molecule. [4]

The obtained products were repeatedly washed with 3% acetic acid, warmed at 40°, until the washing solutions did not contain Ni(II) ions. The chelates IIa-2, IIb-2 and IIc, which are less soluble, were afterwards repeatedly washed with warmed absolute ethanol, and the chelates IIa-1, IIb-1, which are more soluble, were recrystallized from absolute ethanol in the presence of active charcoal. After washings and recrystallizations, respectively, the compounds were dried under vacuum on di-P_2O_5.

The elemental analyses of C, H and N were made by microcombustion. For the Ni(II) dosing the chelates were disintegrated with H_2SO_4 and H_2O_2 and the Ni(II) ions dosed with dimethylglyoxime.

The absorption spectra of compounds were recorded with a VSU-2 Carl Zeiss (Jena) spectrophotometer on acetonic solutions of $0.25\times10^{-4}-2.5\times10^{-4}$ m/l (complexes IIa-2, IIb-2 and IIc) and $0.5\times10^{-4}-5\times10^{-4}$ m/l (complexes IIa-1 and IIb-1) concentrations.

The reflectance spectra of the chelates were recorded with a VSU-1 Carl Zeiss (Jena) spectrophotometer, using MgO as standard.

The IR spectra of the compounds were recorded within 400–4000 cm^{-1} range by means of a UR-10 Carl Zeiss (Jena) spectrophotometer, using KBr pellets.

The magnetic susceptibilities were measured at the room temperature, according to the Faraday method, using $Hg[Co(NCS)_4]$ as standard.

RESULTS AND DISCUSSIONS

The analytical data of all Ni(II) chelates are summarized in table 1. On these results and IR data, the chelatic structural fromulas of IIa-c complexes have been thereby established.

The IR spectra of one of the ligands used, namely the 1-methyl-2-carbethoxy-glyoxalanil-(1)-*p*-tolylhydrazone-(2), (Ia), and of the chelates IIa-1 and IIa-2, synthetized with this ligand, are systematized in table 2.

Table 1

Analytical data of the Ni(II) chelates

Chelate	Ni %		C %		H %		N %		m.p. °C
	Calcd.	*Found*	*Calcd.*	*Found*	*Calcd.*	*Found*	*Calcd.*	*Found*	
IIa–1	8.34	8.07	64.88	65.03	5.73	5.90	11.95	12.12	158–160.5
IIb–1	8.34	8.12	64.88	64.32	5.73	6.04	11.95	12.32	138–141
IIa–2	10.65	10.20	56.65	56.89	5.85	6.12	15.24	16.00	200
IIb–2	10.65	10.51	56.65	56.54	5.85	6.21	15.24	15.91	179–181
IIc	10.65	10.15	56.65	56.16	5.85	6.28	15.24	15.87	198–199.5

One may observes that the spectra of both Ni(II) chelates are in general lines similar but they markedly differ in what the very intense band at 3305 cm^{-1} is concerned, this band occurring only in the spectrum

---

[4] B. Hirsch and A. Bassl, *Z. Chem.*, **2**, 340 (1962).

Table 2

The IR spectra of the ligand Ia and of the cnelates IIa-1 and IIa-2 (cm^{-1})

Ligand Ia	Chelate IIa−1	Chelate IIa−2
470 w	460 w	470 w
	475 w	
490 w		
505 m	510 w	520 w
515 sh		
	535 w	
	565 w	
		585 w
605 w	600 m	
620 w	630 w	
640 w	640 w	
660 w	675 w	675 w
700 m	700 m	
720 m	725 m	730 m
750 m	760 m	765 s
	775 w	
790 sh	795 w	795 m
810 s	810 m	820 m
	815 m	
	830 m	830 m
850 w		855 m
930 sh	920 m	920 w
		960 m
1000 w	1020 m	1025 m
1040 sh	1040 w	
1070 vs	1085 vs	1090 vs
1115 w		
1180 s	1180 vs	1190 vs
1200 vs	1210 vs	
1230 s	1225 vs	
1280 m	1290 sh	
1310 m		1300 vs
1330 m	1330 vs	1320 vs
	1350 vs	
1370 m		1370 vs
		1380 vs
1400 w		1405 vs
1450 w	1440 s	1440 vs
1490 m		1480 w
	1505 sh	1510 m
1530 m	1530 s	
1580 m	1590 w	1560 m
1620 sh		
		1690 vs
1710 vs	1710 vs	
		2980 w
2980 w		
		3305 vs

vs = very strong; s = strong; m = medium; w = weak; sh = shoulder.

of the chelate IIa-2 being due to a vibration frequency proper to the imino group, NH, in agreement with the analytical data and the structural formula ascribed by us to the chelate IIa-2.

The strongest differences in the IR spectra of the ligand and chelates are those within 1270—1360 cm^{-1}. For the free ligand there is a band of mean intensity within 1270—1340 cm^{-1}, with maxima at 1280, 1310 and 1330 cm^{-1}. In the case of the chelate IIa-1, as a consequence of the coordination, the above band occurs as broadened and very intense within 1290—1360 cm^{-1}, with a shoulder at 1290 cm^{-1} and maxima, at 1330 and 1350 cm^{-1}, and in the case of the chelate IIa-2 the same band appears as very intense within 1280—1340 cm^{-1}, with two maxima at 1300 and 1320 cm^{-1}. It is known that in the case of the secondary aromatic amines (C_6H_5-NH-) an absorption band occurs in the region between 1280—1350 cm^{-1} and in almost the same range (1310—1360 cm^{-1}) there is an intense band for the tertiary aromatic amines (C_6H_5-N=), both bands being due to the C-N stretching vibration inside of this group.[5] As a consequence of the coordination of the nitrogen atom from the hydrazonic group directly bound to the aryl radical, structural modifications will be therefore expected to occur, reflected in the IR spectra as shown above. It may be, therefore, concluded that the changes observed with the IR spectra of the compounds going from the free ligand to irrespective of the two chelates, and namely the slight shifts and the strong enhancements of the vibration bands in the 1270—1360 cm^{-1} range tell us that the coordination *via* nitrogen atom took place.

It should be important to mention that in the 1690—1710 cm^{-1} range no changes have taken place, compared with the free ligand spectrum. The intense band with a maximum in this domain, occurring in the spectra of all mentioned compounds, has been assigned [5] to the esteric group ($COOC_2H_5$). Its appearance in the spectra of the two chelates (for the chelate IIa-2 slightly moved, at 1690 cm^{-1}) would indicate that this group does not participate to coordination, a possibility which could not be *a priori* avoided. If the esteric group participated to coordination, a strong shift of its band [5] was expected to occur at approximately 1635—1665 cm^{-1}, which is not, obviously, the case.

It may be, therefore, concluded that the strong modifications in the 1280 — 1360 cm^{-1} range and the lack of any modification in the 1690—1720 cm^{-1} domain in the spectra of the chelates compared with that of the free ligand, show that the coordination has taken place only *via* the nitrogen atoms, the esteric group being not involved into coordination, in agreement with the structural formulas IIa-c of all the chelates.

ELECTRONIC SPECTRA AND MAGNETIC PROPERTIES

The magnetic susceptibility measurements performed on the chelates IIa-1 and IIa-2 have shown that both the compounds are diamagnetic.

---

[5] L. J. Bellamy, "The Infrared Spectra of Complex Molecules", Methuen, London, 1962.

The absorption spectra in the visible range of all five Ni(II) complexes, recorded on acetonic solutions, are plotted in figure 1.

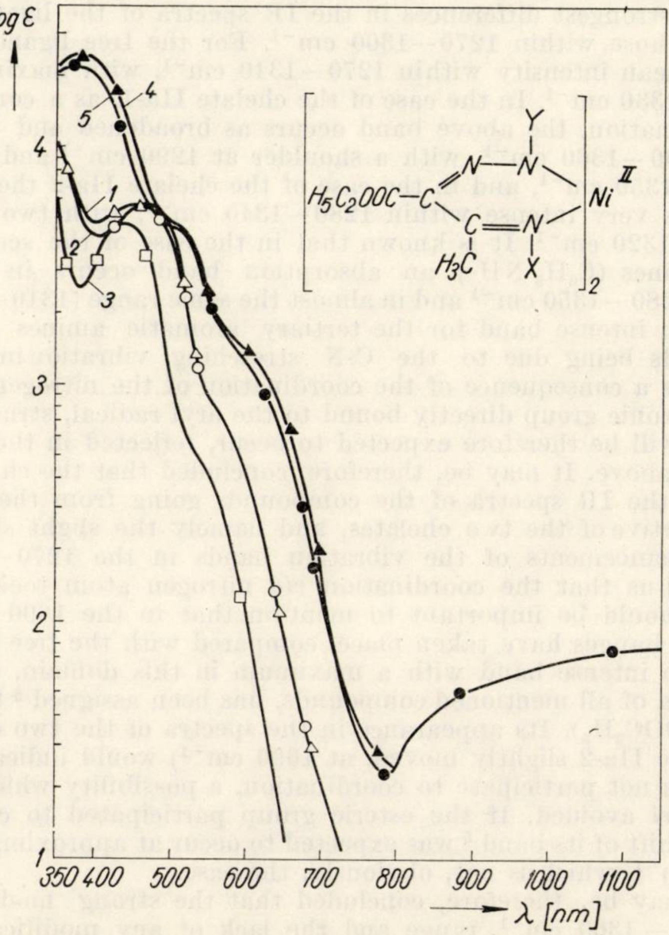

Fig. 1. – The electronic spectra of the Ni(II) chelates.

1, Chelate IIa-2: X=H, Y=$p-CH_3-C_6H_4$; *2*, Chelate IIb-2: X=H, Y=$m-CH_3-C_6H_4$: *3*, Cnelate IIc: X=H, Y=$o-CH_3-C_6H_4$; *4*, Chelate IIa-1: X=C_6H_5; Y=$p-CH_3-C_6H_4$; *5*, Chelate IIb-1: X=C_6H_5, Y=$m-CH_3-C_6H_4$.

One may observe that the spectra of the chelates IIa-1, IIb-1 and IIa-2, IIb-2 and IIc are strikely similar respectively, which allow us to ascribe the diamagnetic properties to the other chelates for which the magnetic susceptibilities were not determined. It may be, therefore, concluded that the diamagnetism is a general feature of the five synthetized chelates, indicating the low spin $Ni^{2+}(3\ d^8)$ electronic configuration in a square-planar coordination geometry.

The spectra of the chelates IIa-2, IIb-2 and IIc. As may be seen in figure 1, the spectra of the chelates IIa-2 and IIb-2 are very similar in the 350–500 nm range, being practically the same at wavelengths higher than 500 nm. The spectrum of the chelate IIc, though similar to the spectrum of the first two chelates is hypsochromically moved with about 40 nm on the whole visible range. The very high intensity ($\varepsilon \approx$ ≈ 6000) of the bands occurring approximately at 470 nm, for the chelates IIa-2 and IIb-2, and at 430 nm for the chelate IIc, shows the fact that these bands are of CT nature.

Taking into account the Jørgensen's formula [6,7]

$$\nu_{\mathrm{CT}} = 30{,}000\ (x_{\mathrm{N}} - x_{\mathrm{Ni}})\ \mathrm{cm}^{-1}$$

where [6] $x_{\mathrm{Ni(square\text{-}planar)}} = 2.2$ and [7] $x_{\mathrm{N}} = 3.2$ are the corresponding optical electronegativities, it results that the CT bands ligand → metal should occur at approximately 330 nm (30,000 cm^{-1}) which, of course, is not the case. The single remained alternative is to assign the absorption band to a CT metal → ligand transition, namely, from the filled MO placed on the metal to the empty antibonding MO's of the organic ligand.

The other less intense bands ($\varepsilon \approx 650$ for the IIa-2 and IIb-2 chelates and $\varepsilon \approx 400$ for the IIc chelate) occurring at higher wavelengths, as shoulders of the previously mentioned CT bands, may indoubtedly be ascribed to the spin-allowed $d-d$ transition.

The energetical expressions for the spin-allowed $d-d$ transitions for the low spin square-planar d^8 configuration obtained in the strong field are

$$^1A_{1g}(e_g^4\ b_{2g}^2\ a_{1g}^2) \rightarrow {}^1B_{1g}(e_g^4\ b_{2g}^2\ a_{1g}^1\ b_{1g}^1);\ \Delta_1 - C$$

$$^1A_{1g}(e_g^4\ b_{2g}^2\ a_{1g}^2) \rightarrow {}^1E_g(e_g^3\ b_{2g}^2\ a_{1g}^2\ b_{1g}^1);\ \Delta_1 + \Delta_2 + \Delta_3 - 3B - C$$

$$^1A_{1g}(e_g^4\ b_{2g}^2\ a_{1g}^2) \rightarrow {}^1A_{2g}(e_g^4\ b_{2g}^1\ a_{1g}^2\ b_{1g}^1);\ \Delta_1 + \Delta_2 - C$$

where B and C are the Racah parameters for the interelectronic repulsion energies, and Δ_1, Δ_2 and Δ_3 the orbital energies in the most probable MO energy diagram for the mentioned chelates. If one takes into account that the "π" metal-nitrogen bonds, if they occur, are too much weak to bring down the d_{z^2} orbital under d_{xy} one, such that the D_{4h}-strong distortion orbital scheme to be valid, it remains as the most probable energy diagram for the studied chelates that of D_{4h}-weak distortion with the following orbital sequence: $e_g(d_{xz},\ d_{yz}) < b_{2g}(d_{xy}) < a_{1g}(d_{z^2}) < b_{1g}(d_{x^2-y^2})$. In this diagram, the orbital energies Δ_3, Δ_2 and Δ_1 from the above expressions, would represent the energy distances between e_g and b_{2g}; b_{2g} and a_{1g}; and a_{1g} and b_{1g}, respectively.

The most like assignment of these d-d bands would correspond to a transition up to the double degenerate excited spectral term ^1E_g, i.e.

$$^1A_{1g}(e_g^4\ b_{2g}^2\ a_{1g}^2) \rightarrow {}^1E_g(e_g^3\ b_{2g}^2\ a_{1g}^2\ b_{1g}^1)$$

---

[6] A. B. P. Lever, "Inorganic Electronic Spectroscopy", Chap. 8–9, Elsevier Publishing Company, Amsterdam-London-New York, 1968.

[7] C. K. Jorgensen, "Electron Transfer Spectra", in "Progress in Inorganic Chemistry", vol. 12, Interscience Publishers, New York–London–Sydney–Toronto, 1970, p. 101–158.

This assignment which involves a transition from the most stable "π" antibonding e_g level to the highest "σ" antibonding level is in agreement with the relative high intensity of these bands ($\varepsilon \approx 400-650$) for a centrosymmetric arrangement. It should be, however, emphasized that the above assignment represents only an attempt. If one takes into consideration the fact that the shoulders in the spectra of the chelates IIa-2, IIb-2 and IIc are broad enough, these absorption bands could be constituted from many (at least two) unresolved *d-d* transitions. In this way similar absorption bands (extinctions, positions and their widths) were interpreted by Coussmaker, Venanzi *et al.*[8] for diamagnetic Ni(II)phosphine chelates.

The hypsochromic shift of about 40 nm of the *d-d* band occurring as a shoulder at approximately 530 nm in the spectrum of the chelate IIc, compared with the corresponding bands of the chelates IIa-2 and IIb-2, is difficult to be interpreted only through the inductive, electron repeller effect, of the CH_3 substituent, stronger if it is attached on the *ortho* position of the hydrazonic phenyl, than the same CH_3 group placed on the *meta* or *para* positions. Most probably, the hypsochromic shift of this band of the chelate IIc should be caused by the shift in the same direction and with the same amount of the very intense CT metal → ligand band, to the shoulder of which it belongs. In any way, the hypsochromic shift of the whole visible spectrum of the chelate IIc shows that in this case the steric hindrances due to the aromatic groups (*o*-tolyl) directly attached to the two donor nitrogen atoms involved in the Ni(II) coordination cannot overpass the inductive, electron repeller effect of the CH_3 group attached to the phenyl radical, which is very relevant for the *ortho* position[9] (*o*-tolyl group).

The electronic spectra of the chelates IIa-1 and IIb-1 are very similar and practically coincide in some domains of wavelengths. Even though they are similar to the already discussed spectra of the chelates IIa-2 and IIb-2, some differences nevertheless appear. For instance, the intense bands ($\varepsilon \approx 5000$) which may be in the same manner, as above, regarded as CT metal → ligand transitions, occurring as shoulders of the more intense bands ($\varepsilon \approx 23{,}000$), placed in the UV range.

The position of these shoulders, approximately at 500 nm, shows a bathochromic shift of about 30 nm of these CT bands compared with those of the former chelates. The other very broad shoulders at 600 nm show a bathochromic shift of about 40 nm compared with those assigned as $d-d$ transitions in the aforementioned chelates. More relevant than their widths is the enhancement in the intensity of the bands occurring as shoulders at approximately 600 nm. It may be mentioned that their molar extinction coefficient values $\varepsilon > 1200$ unobserved even for the $d-d$ transitions in the majority of the tetrahedral chelates, make the assignment as *d-d* bands for a centrosymmetric arrangement less probable.

---

[8] C.R.C. Coussmaker, M. H. Hutchinson, J. R. Mellor, L. E. Sutton and L. M. Venanzi, *J. Chem. Soc.*, **1961**, 2705.

[9] H. Becker, "Einführung in die Elektronen-theorie organish-chemischer Reaktionen", Deutscher Verlag der Wissenschaften Berlin, 1965, p. 362.

For this reason, the best assignment of these bands should be of CT metal → ligand nature, occurring, as has been earlier emphasized, in the visible range. These bands obscure the possible less intense *d-d* transitions, which may be expected to appear in this region, taking into consideration the bathochromic shift of the whole visible spectra of the chelates IIa-1 and IIb-1, compared with the already discussed complexes, where the *d-d* transitions were placed at approximately 560 nm.

The authors thank the lecturer V. Mincu of University of Bucharest for the magnetic susceptibility measurements and Mrs. M. Popa for the C, H and N elemental analyses.

Revue Roumaine de Chimie, 19, 5, 827–831 (1974)

HETEROPOLYTUNGSTATES WITH U(IV) AS CENTRAL ATOM

SYNTHESIS AND PHYSICO-CHEMICAL STUDY OF THE UL_2 COMPLEX WHERE $L=P_2W_{17}O_{61}^{10-}$

GH. MARCU*, MARIANA RUSU** and A. V. BOTAR**

* Chemistry Laboratory of Radioactive Elements,
University of Cluj, Str. Arany János 11, Romania
**Institute of Chemistry of the Ministry of Education,
str. Donath 65, Cluj, Romania

Received May 21, 1973

The U(IV) ion has a rapid reaction with the unsaturated heteropolyanions, forming UL_2 complexes where $L = PW_{11}O_{39}^{7-}$ and $P_2W_{17}O_{61}^{10-}$. The potassium salt of the $U(P_2W_{17}O_{61})_2^{16-}$ heteropolyanion has been isolated. The chemical analysis, the photocolorimetric study of the reaction between U(IV) and $P_2W_{17}O_{61}^{10-}$, as well as the basicity determinations of the heteropolyacid show that the U/W combination is 1/17.

GENERAL CONSIDERATIONS

The heteropolyanions of $X_2'ZW_{17}O_{62}^{x-}$ type are obtained from the $X_2'W_{18}O_{62}^{p-}$ anion by substituting a tungsten atom with a Z metalic atom. [1] These heteropolyanions are obtained after the partial degradation of the $X_2'W_{18}O_{62}^{p-}$ type anions under the influence of the potassium acetate up to pH 6–7, in the presence of the Z metalic atom in different oxidation states.[2–6] In every 18-tungsten heteropolyanion the Z atom substitutes a single tungsten atom octahedronically coordinated. It is well known that these "unsaturated" heteropolyanions react with a whole series of bi-, tri- and tetravalent atoms, forming a series of heteropolyanions.[3-11]

---

[1] P. Souchay, *Ann. Chim. (France)*, **20**, 73 (1967).

[2] S. A. Malik and T. J. R. Weakley, *Chem. Comm.*, **1049** (1967).

[3] S. A. Malik and T. J. R. Weakley, *J. Chem. Soc. (A)*, **1968**, 2647.

[4] C. M. Tourne and G. T. Tourne, *Compt. rend.*, **266**, 1363 (1968).

[5] C. M. Tourne and G. F. Tourne, *Bull. Soc. chim. France*, **1969**, 1124.

[6] C. M. Tourne, *Compt. rend.*, **266**, 702 (1968).

It has been found that the U(IV) ion forms UL_2 type complexes where $L = PW_{11}O_{39}^{7-}$ and $P_2W_{17}O_{61}^{10-}$.

In the present paper we study only the type complex where $L = P_2W_{17}O_{61}^{10-}$

EXPERIMENTAL

The potassium salt of the $U(P_2W_{17}O_{61})_2^{16-}$ type heteropolyanion has been obtained by applying a largely used procedure for the synthesis of this kind of heteropolyanions, with small differences. To a $K_{10}P_2W_{17}O_{61}.22\ H_2O$ solution heated at 70–80° a U(IV) solution was added, stepwise and stirring continuously.

The U(IV) salt has been obtained from a U(IV) salt by reduction through a Zn-amalgamated column. [12]

After cooling at 5°, 1,4-dioxan was added in order to extract the synthesized heteropolycombination which was separated under the form of an oily mass.

The purification of the synthesized heteropolycombination has been made by dissolving it in water and repeated extractions with 1,4-dioxan. The product was reduced to dryness at 40–50° and ground.

WORKING METHOD AND CHEMICAL ANALYSIS

The chemical analysis of the synthesized U(IV) heteropolytungstate has been made using the general method. [13] The uranium was photocolorimetrically recognized with Arsenazo III. [14] The tungsten was recognized by precipitation with cinchonine and calcination at WO_3.[15] The phosphorus was recognized by precipitation as magnesium and ammonium

Table 1

Analytical data for $K_{16}U(P_2W_{17}O_{61})_2.39\ H_2O$

%	K	U	P	W	Water
Calcd.	6.32	2.40	1.25	63.18	7.19
Found.	6.36	2.38	1.32	63.30	7.17

[7] C. M. Tourne, G. F. Tourne, S. M. Malik and T. J. R. Weakley, *J. Inorg. Nuclear Chem.*, **32**, 3875 (1970).

[8] T. J. R. Weakley and S. A. Malik, *J. Inorg. Nuclear Chem.*, **29**, 2935 (1967).

[9] L. C. W. Baker and J. S. Figgis, *J. Amer. Chem. Soc.*, **92**, 3794 (1970).

[10] R. D. Peacock and T. J. R. Weakley, *J. Chem. Soc. (A)*. **1971**, 1836.

[11] A. V. Botar and T. J. R. Wealkey, *Rev. Roumaine Chim.*, **18**, 1155 (1973).

[12] J. H. Kenedy, *Analyt. Chem.*, **32**, 150 (1960).

[13] V. E. Simmons, Ph. D. Thesis, Boston University, 1963.

[14] B. S. Savvin, *Talanta*, **8**, 673 (1961).

[15] A. I. Vogel, "A Text Book of Quantitative Inorganic Analysis", 2nd ed. London, 1951, p. 418.

phosphate and calcination at $Mg_2P_2O_7$.[16] Potassium was recognized with tetraphenylborate.[17] The results of the chemical analysis are presented in table 1.

The water content of the complex has been determinated by thermogravimetric analysis. The temperature increase was 5°/min. The experimental results obtained are presented in figure 1.

The basicity has been determined by conductometric titration of a $K_{16}U(P_2W_{17}O_{61})_2$ 39 H_2O solution ($T_W = 0.00743$) with a thalium acetate solution ($T_{\mathrm{Tl}} = 0.0448$), as shown in figure 2. Measurements have been carried out by means of a Radelkis OK−102 type conductometer.

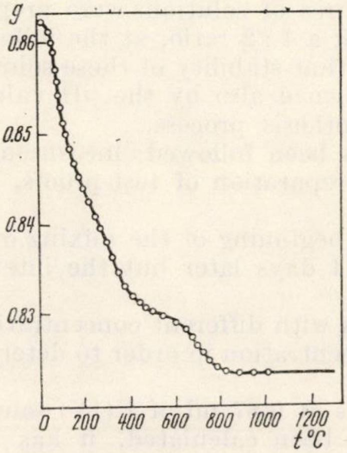

Fig. 1. — A.G.T. curve for $K_{16}U \cdot (P_2W_{17}O_{61})_2 \cdot 39\ H_2O$.

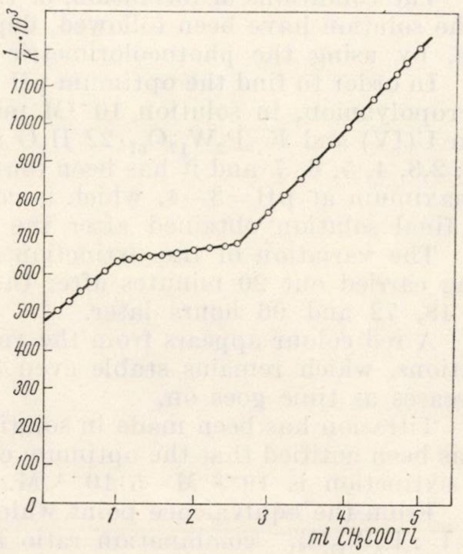

Fig. 2. — Conductometric titration curve for 30 ml $K_{16}U(P_2W_{17}O_{61})_2 \cdot 39H_2O$ solution with $T_W = 0.00743$ with a $TlCH_3COO$ solution with $T_{\mathrm{Tl}} = 0.0448$.

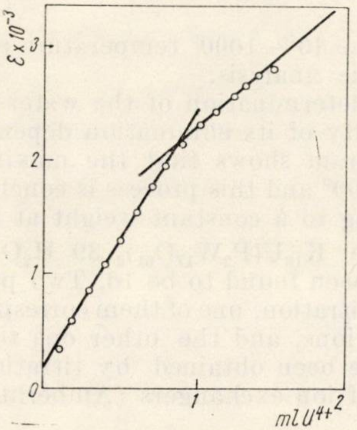

Fig. 3. — Photocolorimetric titration curve for 20 ml $K_{10}P_2W_{17}O_{61} \cdot 22\ H_2O$ solution with $T_W = 0.00307$ with a U^{4+} solution with $T_U = 0.00267$.

---

[16] A. I. Vogel, "Quantitative Inorganic Analysis", 3rd ed., London, 1961, p. 575.
[17] G. H. Glass, *Chemist Analyst*, 42, 50 (1953).

The photocolorimetric study of the reaction between the $P_2W_{17}O_{61}{}^{10-}$ heteropolyanion and the U(IV) ion has been performed by measuring the extinction of the solution containing the $K_{16}U(P_2W_{17}O_{61})_2 \cdot 39\ H_2O$ compound by means of a FEK-M type photocolorimeter. Titration curve is in figure 3.

RESULTS AND DISCUSSION

The conditions of formation, of the $U(P_2W_{17}O_{61})_2^{16-}$ heteropolyanion in the solution have been followed, depending on concentration, pH and time, by using the photocolorimetric titration method.

In order to find the optimum pH for the formation of the respective heteropolyanion, in solution 10^{-2}M mixtures of solutions were prepared from U(IV) and $K_{10}P_2W_{17}O_{61} \cdot 22\ H_2O$ with a 1 : 2 ratio, at the following pH : 2,3, 4, 5, 6, 7 and it has been found that stability of these solutions is maximum at pH=3—4, which is confirmed also by the pH value of the final solution obtained after the synthesis process.

The variation of the extinction has been followed, measurements being carried out 20 minutes after the preparation of test-proofs, 1, 6, 24, 48, 72 and 96 hours later.

A red colour appears from the very beginning of the mixing of the solutions, which remains stable even 3—4 days later but the intensity decreases as time goes on.

Titration has been made in solutions with different concentrations; it has been notified that the optimum concentration in order to determine the extinction is 10^{-2} M—$5 \cdot 10^{-3}$ M.

From the equivalence point which is at 0.87 ml of U(IV) solution, the $U : P_2W_{17}O_{61}^{10-}$ combination ratio has been calculated, it has been found that the ratio is 1 : 2, a value which has been also found by chemical analysis of the $K_{16}U(P_2W_{17}O_{61})_2 \cdot 39\ H_2O$ salt.

These results are in good agreement with the calculated data for the respective salt, as seen in table 1.

The transformations of the salt in the 40°—1000° temperature range have been studied by thermogravimetric analysis.

The thermogram permits a direct determination of the water contained in the complex and of the modality of its elimination depending on temperature. The aspect of thermogram shows that the maximum speed of water removal is between 80°—200° and this process is concluded between 500°—600°, the substance coming to a constant weight at 800°.

By conductometric titration of the $K_{16}U(P_2W_{17}O_{61})_2 \cdot 39\ H_2O$ salt with thalium acetate, total basicity has been found to be 16. Two points of inflexion have been obtained for this titration, one of them corresponding to the substitution of 6 potassium ions, and the other one to the substitution of 16. The same results have been obtained by titration of the acid in aqueous solution by means of ion exchangers (Amberlite IR 120 H^+ form).

The basicity of the $U(P_2W_{17}O_{61})_2^{16-}$ anion, very easily to be predicted theoretically (the degree of oxidation of the complex generator being precisely known), is in good agreement with that one determined by conductometric titration.

CONCLUSIONS

1. The $U(P_2W_{17}O_{61})_2^{16-}$ type heteropolyanion was synthesized for the first time, extending the class of the heteropolycombinations that have a U(IV) central atom. The $K_{10}U(PW_{11}O_{39})_2 \cdot x\ H_2O$ compound was isolated, the results being the subject of another scientific paper.

2. The photocolorimetric study of the reaction between $P_2W_{17}O_{61}^{10-}$ and the U(IV) ion, as well as the analysis of the isolated potassium salt $K_{16}U(P_2W_{17}O_{61})_2 \cdot 39\ H_2O$ show that the U/W combination ratio is 1/17.

3. The study by paper electrophoresis, the obtaining of the corresponding acid using the ion exchangers, as well as the photocolorimetric study of the formation and stability of the $U(P_2W_{17}O_{61})_2^{16-}$ heteropolyanion show that it is not a mixture of combinations we deal with, but a unitary product which is stable.

4. Magnetic measurements being carried out on the $K_{16}U(P_2W_{17}O_{61})_2 \cdot 39\ H_2O$ complex show that uranium is in a 4+ oxidation state.

Revue Roumaine de Chimie, **19**, *5*, p. 833–838 (1974)

SYNTHESIS AND THERMAL ANALYSIS OF TITANIUM OXYHYDRATE ULTRAFINE POWDERS

A. BĂRBULESCU

Polytechnic Institute of Bucharest, Str. Polizu N⁰ 1, Bucharest, Romania

Received March 24, 1973

Ultrafine non-crystalline titanium oxyhydrate separated by freezing from hydrogel was examined by various thermal methods of analysis. The thermal behaviour of the powdering product was pointed out. A large dehydration process up to 400°, coalescence phenomena at 305° and anatase to rutile polymorphic transformation at the range of 680° have been found out. High purity active TiO_2 powder may be obtained, for calcination temperatures ranging between 300 and 600°.

1. INTRODUCTION

Obtainment of oxydic products by the sol-gel procedure [1] or by ion coprecipitation [2] is of great interest today in connection with the development of certain materials for electronics, the nuclear technique or the catalyst industry. In this way, ultrafine powdery products, solid phases homogenized at ionic scale, as well as synthesis at low temperatures of refractory compounds, etc., may be obtained. The features of the products thus obtained depend to a large extent on the synthesis and thermal treatment conditions, and a control of these factors is decisive for obtaining the desired quality.[3] Thus, the synthesis and thermal behaviour of non-crystalline titanium oxyhydrate ultrafine powders were studied, when obtained by the sol-gel procedure. The results are discussed by the present paper.

2. EXPERIMENTAL

2.1. SYNTHESIS OF TITANIUM OXYHYDRATE POWDERS

Titanium tetrachloride was turned into aqueous solution without its hydrolysis, after the method described by Clabaugh and collaborators.[4] Titanium hydrogel was obtained through ammonia neutralization by spraying the aqueous solution in a precipitation bath heated up to 80°, at pH $\simeq 7$ maintained as a result of continually adding NH_4OH. The precipitate was washed through decantation and separated in a Buchner funnel. In this state, titanium hydrogel is consistent and has an about 95 p.c. water content. The separation of water from hydrogel was achieved by the freezing procedure .[5] In this way a powdery product was directly obtained and it was further decanted and dried at 50°.

---

[1] J. L. Woodhead, *Silicates Industriels*, **1973**, 191.

[2] K. S. Mazdiyasni, R. T. Dollof and J. S. Smith II, *J. Amer. Ceram. Soc.*, **52**, 523 (1969).

[3] I. Yida and S. Ozaki, *J. Amer. Ceram. Soc.*, **44**, 120 (1961).

[4] W. S. Clabaugh, E. M. Swiggard and R. Gilchrist, *J. Res. Nat. Bur. Stand.*, **56**, 289 (1956).

2.2. CHARACTERIZATION METHOD

The powder obtained was examined from a morphological and structural point of view, then it was subjected to thermal analysis. The thermal behaviour was studied through differential thermal analysis (DTA), thermogravimetric analysis (TGA), dilatometric analysis (DA) and thermal analysis of the electric resistance (TAER). The thermal analysis was completed with structure, specific area and colour determinations.

The JEM 7 A electronic microscope was used in the microscopic examination and electronic diffraction, the TUR M 61 equipment in X-ray analysis, and a STRÖHLEIN apparatus in measuring the specific area after the BET method. In the thermal analysis the NETZSCH installation with electronic recorder was used, as well as Stanton thermobalance and an absolute dilatometer of own design. In TAER the working technique is described in a published paper .[6]

3. RESULTS

3.1. *The morphology of the powder.* The powdery products are made up of agglomerated granules, each consisting of particles of about 10 nm or smaller. The specific area of the powder is of 300 sq.m/g and it confirms the microscope examination. Under the influence of the electronic beam, agglomeration phenomena of the powder were noticed with each intensity growth.

When the product was checked up by means of X-rays and electronic difraction, non diffraction lines were visible, hence the powder obtained was practically amorphous.

3.2. *The differential thermal analysis* evidenced a large endothermal effect within the interval up to 400°, which was interupted at 305° by a strong sharp exothermic peak. At over 400° a range of exothermic effects appear, which are manifest up to about 850°. The DTA curve rising up to 1300° at a speed of 10°/min was recorded to have the sensitivity of ± 0.5 mV up to 400° and of ± 0.1 mV at over 400° (fig. 1).

3.3 *The thermogravimetric analysis* showed a total mass loss of about 34 p.c. manifest up to about 400°. The mass loss curve function of temperature (fig. 2) is drawn for a heating speed of 5°/min.

3.4. *The dilatometric analysis* of a sample obtained by isostatic compacting at 1500 at evidenced the anomaly of contraction when the temperature reaches about 700° (fig. 3). At this temperature the process

---

[5] A. Bărbulescu, Doctorial Thesis, Bucharest, 1971.

[6] S. Solacolu and A. Bărbulescu, *Rev. Roumaine Chim.*, **15**, 1851 (1970).

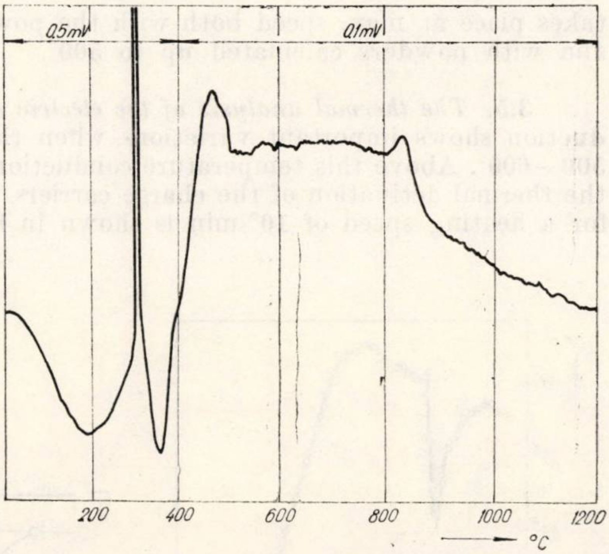

Fig. 1. – The DTA curve of titanium oxyhydrate ultrafine powder. Sensitivity ±0.5 mV up to 400° and ± 0.1 mV over 400°.

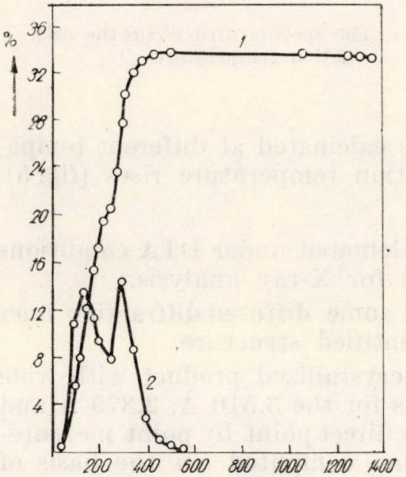

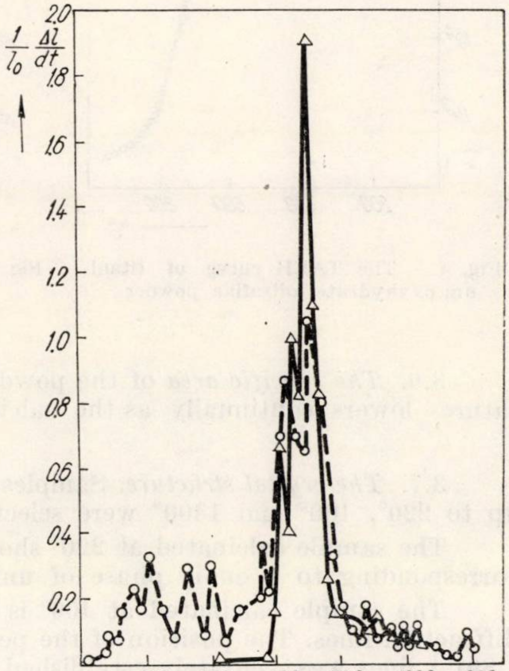

Fig. 2. – The mass loss (*1*) and its derivative (*2*) as a function of temperature for titanium oxyhydrate ultrafine powder.

Fig. 3. – The contraction derivative relative to temperature.

Revue Roumaine de Chimie, **19**, *5*, 833–838 (1974)

takes place at max. speed both with the powders calcinated under 200° and with powders calcinated up to 500°.

3.5. *The thermal analysis of the electric resistance.* The electric conduction shows important variations when the powder is heated up to 500—600°. Above this temperature conduction rises as a consequence of the thermal activation of the charge carriers. The TAER curve obtained for a heating speed of 10°/min is shown in fig. 4.

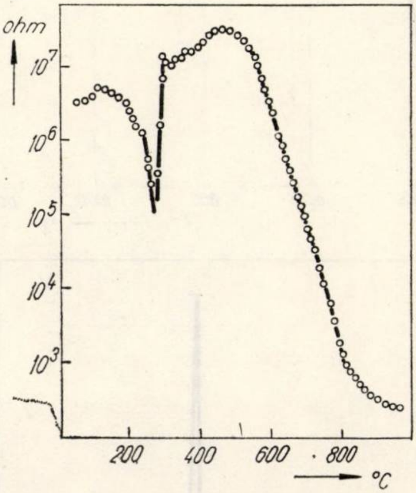

Fig. 4. — The TAER curve of titanium oxyhydrate ultrafine powder.

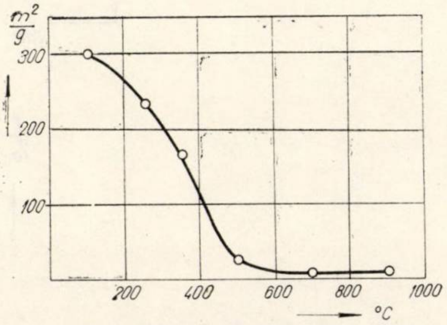

Fig. 5. — The specific area *versus* the calcination temperature.

3.6. *The specific area* of the powders calcinated at different temperatures lowers continually as the calcination temperature rises (fig. 5).

3.7. *The crystal structure.* Samples calcinated under DTA conditions up to 220°, 400° and 1300° were selected for X-ray analysis.

The sample calcinated at 220° shows some diffused diffraction lines corresponding to a cubic phase of unidentified structure.

The sample calcinated at 400° is a crystallized product with wide diffraction lines. The position of the peaks for the 3.510 Å, 2.379 Å and 1.891 Å lines was accurately established by direct point by point measurements. The following lattice parameters computed on the basis of the data obtained:

$$a = 3.783 \pm 0.05 \text{ p.c. and } b = 9.51 \pm 0.05 \text{ p.c.}$$

correspond to TiO_2 under the form of anatase.

The sample calcinated at 1300° is TiO_2 under the form of rutile. The following lattice parameters were computed on the basis of the value of the 18.03 Å and 27.15 Å lines :

$$a = 4.594 \pm 0.01 \text{ p.c. and } b = 2.958 \pm 0.01 \text{ p.c.}$$

4. DISCUSSION

Titanium hydrogel is liable to contain solid phase in both max. dispersion and min. crystalline ordering stages.[7,8]

The morphology of the powdery product obtained, its specific area and the state of the structure reveal the formation of an ultrafine non-crystalline powder as a consequence of the freezing procedure which brought about the destruction of the gel structure and the separation of water. The avoidance of heating allows for the conservation of the advanced dispersion and of the low structural ordering level, corresponding to the solid phase within hydrogel. At the same time, direct formation of the powder, i.e. with no physical mechanical loosening or grinding, eliminates any chance of contamination.

Thus, it is possible to obtain high purity active TiO_2 powders depending on the heat treatment conditions.

When titanium oxyhydrate is heated, dehydration processes as well as the formation of titanium dioxide under the form of anatase and the turning of anatase into rutile [9] take place.

The endothermal effect shown by the DTA curve and the mass loss recorded by the TGA curve are caused by the dehydration process. The mass loss becomes insignificant at over 360° and it ceases completely at about 500°. TiO_2 and the total water quantity released are in a ratio corresponding to a titanium oxyhydrate of the $TiO_2.2H_2O$ form. The dehydration can be shown by the following reactions :

$$TiO_2 \cdot 2H_2O \xrightarrow{150} TiO_2 \cdot H_2O \xrightarrow{300} TiO_2$$

The attempts to evidence the way in which water is connected into the structure, through nuclear magnetic resonance and infrared absorption, did not yield conclusive results.

The exothermal effect at 305° is caused by a process similar to that noticed when zirconia [10] gels are calcinated. The process is due to a coalescence phenomenon[11] whose physical significance is not yet clarified. The

---

[7] CH. de ROHDEN, *Chimie et Industrie*, **75**, 287 (1958).

[8] J. E. LATTY, *J. Appl. Chem.*, **8**, 96 (1958).

[9] W. F. SULLIVAN and S. S. COLE, *J. Amer. Ceram. Soc.*, **42**, 127 (1959).

[10] R. CYPRÈS, R. WALLAST and J. RAUCY, *Ber. dtsch. keram. Ges.*, **40**, 527 (1963).

[11] R. C. MACKENZIE, "Differential Thermal Analysis", vol. I, Academic Press, London, 1970, p. 277.

TAER curve contains an important discontinuity at the coalescence temperature. Up to this temperature a significant temperature growth of the charge carriers is perceptible, then their sudden reduction and the growth of the electric resistance by a number of largeness levels.

In accordance with Towe and Bradley [12] who consider that the continuous release of water leads to the formation of a residue which nucleates in oxydic phase, the TAER result is explainable if we admit that water is released according to reaction:

$$2OH^- \rightarrow H_2O + O^{2-}$$

and that the negative charges of the oxygen ions participate in the mechanism of the electric conduction, up to the moment in which the ions are rearranged and the bonds are re-established.

By releasing water from titanium oxyhydrate, TiO_2 under the form of anatase is obtained. The dimensions of the lattice parameters for the anatase obtained through calcination at 400°, greater than the usual ones, are the consequence of the presence of the hydroxyl ions, as well as of the conservation of an extraquantity of energy within the recently formed lattice. The crystalo-chemical features and the high ratio between area and mass confer to the anatase thus formed a great reactivity. The growth of the temperature causes a rapid diminution of the specific surface and of reactivity up to about 600°.

At a temperature above 600° anatase turns into rutile. This process, shown by the contraction-temperature curve, takes place between 600° and 800° and reaches its peak at about 680°.

5. CONCLUSIONS

Freshly prepared titanium hydrogel can be directly turned into a ultrafine, non-crystalline powdery product through the freezing procedure.

The powdery product is titanium oxyhydrate under the form of $TiO_2.2H_2O$ which is dehydrated through heating according to the following reactions:

$$TiO_2 \cdot 2H_2O \xrightarrow{150^\circ} TiO_2 \cdot H_2O \xrightarrow{300^\circ} TiO_2$$

When ultrafine non-crystalline powders of titanium oxyhydrate are heated a coalescence phenomenon appears at 305°, accompanied by an important modification in the electric conduction.

The release of water from the oxyhydrate leads to the formation of TiO_2 under the form of anatase. Anatase turns into rutile through heating between 600° and 800°, the turning speed being maximum at about 680°.

The suitable conditions for the obtaining of TiO_2 powders of increased reactivity correspond to the calcination temperatures ranging between 300 and 600°.

---

[12] K. M. Towe and W. F. Bradley, *J. Colloid. Sci.*, **24**, 384 (1967).

Revue Roumaine de Chimie, **19**, *5*, p. 839–845 (1974)

THE HYDROXYMERCURATION OF NOR-BORNENE

HAROLD KREHM and GEORGE F. WRIGHT
Lash Miller Chemical Laboratories, 80 St. George St., Toronto, Canada

Received July 23, 1973

We have found that treatment of [2,2,1]-bicycloheptene with mercuric perchlorate or mercuric nitrate forms two *exo*-hydroxymercurials and two *bis*-(2-chloromercuri-bicycloheptyl-3) ethers.

INTRODUCTION

The question of configuration of the oxymercurials formed by addition of mercuric salts to the carbon-carbon double bond seems now to have been decided by several workers.[1] Therefore, this report does not involve configuration, but instead involves the formation of two isomeric hydroxymercurials and at least two isomeric bis-ethers when [2, 2, 1]-bicycloheptene-2 is hydroxymercurated by means of aqueous mercuric perchlorate or mercuric nitrate.

We have found that this hydroxymercuration, by contrast with the more complex reaction involving mercuric acetate ,[2] results not only in the predominant yield of the diastereomer previously reported, the structure of which has been designated[1] as 2-*exo*-chloromercuri-3-exo-hydroxy [2, 2, 1]bicycloheptane but also in a small yield of a second diastereomer. We shall designate this second diastereomer as α in conformity with earlier nomenclature [3] and the more prevalent isomer as β because it is the one with the higher dipole moment. The dipole moment of the α-3-hydroxy-2-chloromercuri-bicyclo-heptane in benzene at 20° is found to be 3.63 D in contrast to the more prevalent β diastereomer of moment 4.9 D in benzene at 20°.

Earlier observations have shown that when cyclopentene, cyclohexene or other alkenes have been oxymercurated only one diastereomer is formed ; it has always been the one more rapidly deoxymercurated by use of strong (molecular) hydrochloric acid than the other diastereomer derived by radical-induced isomerization. The single products of these oxymercurations (not acid catalyzed) have lower dipole moments than the β diastereomers derived from them by radical-induced isomerization. By contrast the preponderant product from the present (acid catalyzed) oxymercuration of [2, 2, 1]-bicycloheptene has a higher dipole moment than the other diastereomer formed concomitantly in smaller amounts. But the diastereomer of higher dipole moment (by our convention the β isomer) is in the present instance more readily deoxymercurated than is the α isomer of lower dipole moment. In short the ease of deoxymercuration is now shown not to be directly related to the dipole moment.

---

[1] a. H. J. Lucas, F. R. Hepner and S. Winstein, *J. Amer. Chem. Soc.*, **61**, 3102 (1939) ; b. T. G. Traylor and A. W. Baker, *Tetrahedron Letters*, **19**, 14 (1959) ; c. M. M. Anderson and P. M. Henry, *Chemistry and Industry*, **1961**, 2053.

[2] M. G. Abercrombie, Alan Rodgman, K. R. Bharucha and G. F. Wright, *Canad. J. Chem.*, **37**, 1328 (1959).

[3] G. F. Wright, *Ann. New York Acad. Sci.*, **65**, 436 (1957).

Both these α and β diastereomers upon reduction with sodium borohydride yield *exo*-2-hydroxy-[2, 2, 1]-bicycloheptane. Therefore, according to present configurational designation[1] the α-isomer must be 2-*endo*-chloromercuri-2-*exo*-hydroxy [2, 2, 1]bicycloheptane.

Hydroxymercuration of [2, 2, 1]-bicycloheptene yields, besides the hydroxy diastereomers, also a mixture of *bis*-(3-chloromercuri-[2, 2, 1]-bicycloheptyl-2) ethers. Formation of *bis*-ethers concomitant with hydroxymercurials is not unprecedented[4] but some of the conditions for their formation are now discernible. In aqueous solution with 3.4 equivalents of free acid per equivalent of mercury salt the yield of ethers is about 3–4%. But this can be increased to about 20% (at the expense of the hydroxy compound) by carrying out the reaction in *tert*-butyl alcohol. It may be observed that in this medium precipitation of products by addition of sodium chloride is slower than in water.

Clearly if the ethers were derived from two diastereomeric alcohols then 6 ethers could be expected — two *meso* isomers and two chiral pairs. In point of fact when the ether mixture, of wide melting point range, is reduced by sodium borohydride a single *bis*-[2, 2, 1]-bicycloheptyl ether is obtained. This latter compound has the same melting point as one obtained, along with *exo*-hydroxy-[2, 2, 1]-bicycloheptane, by Bruson[5] and Schmerling.[6]

By laborious crystallization we have been able to isolate two isomeric ethers but have not established their configurations. It is of interest that these two ethers can be obtained in small (10%) yield if β-*exo*-3-hydroxy-[2, 2, 1]-bicycloheptyl-2-mercuric chloride is converted to the analogous organomercuric nitrate and then is treated with [2, 2, 1]-bicycloheptene.

The authors are grateful to the National Research Council of Canada from whom a grant in-aid made this investigation possible.

EXPERIMENTAL

Physical constants. Melting points have been corrected against reliable standards.[7] Electrical polarization measurements in benzene solution at 20° for the β-3-exo-hydroxy-

---

[4] K. A. Hoffmann and J. Sand, *Ber. dtsch. chem. Ges.*, **33**, 1340 (1900).

[5] H. A. Bruson, U. S. Patent 2, 345, 573 (1944); *Chem. Abstr.*, **38**, 4274 (1943).

[6] C. Schmerling, U. S. Patent, 2, 448, 156 (1948); *Chem. Abstr.*, **43**, 689 (1949).

[7] G. F. Wright, *Canad. J. Technol.*, **34**, 89 (1956).

[2,2,1]-bicycloheptyl-2-mercuric chloride showed $\Delta E/\Delta\omega$, 8.22, and $\Delta V/\Delta\omega$, -0.744 which may be calculated to $\mu = 4.94$ D from an electronic polarization of 48 cc based on atom, or bond refraction values. On the same basis the α-3-*exo*-hydroxy-[2,2,1]-bicycloheptylmercuric chloride showed $\Delta E/\Delta\omega$ of 4.76 and $\Delta V/\Delta\omega$ of -0.77 which may be calculated to $\mu = 3.63$ D. From the determinations of dielectric constant of the solid substances [8] the distortion polarization of the β-form is found to be 61 cc and that of the α-form to be 63 cc, which would alter the dipole moments only slightly from those calculated according to electronic alone.

Reagents. The [2,2,1]-bicycloheptene (100 g) was skaken twice at 50° with 200 ml of 5% aqueous ferrous sulphate under nitrogen, then twice with 50 ml of water. It was dried under nitrogen with magnesium sulphate and distilled under nitrogen, b.p. 94—96°. The distillate, m.p. 46.3—46.8, was peroxide-free by test with potassium iodide.

The *tert*-butyl alcohol was partially frozen and the remainder was decanted. The melted residue was twice treated with sodium and once with lithium aluminum hydride under nitrogen, b.p. 82—82.5°, peroxide-free.

Both Merck and Fisher Reagent grade mercuric nitrate or its monohydrate were used as received. The yellow mercuric oxide was used as received from Mallinckrodt.

β-3-*EXO*-HYDROXY-[2,2,1]-BICYCLOHEPTYL-2-MERCURIC CHLORIDE

To 3.06 g (0.009 mole) of mercuric nitrate monohydrate in 18 ml water plus 2 ml *conc* nitric acid was added a solution of 0.9 g (0.01 mole) of [2,2,1]-bicycloheptene in 8 ml of tert-butyl alcohol. After 7 hours the system was decanted (from 0.037 g (2%) of metallic mercury) into 6 ml of 10% aqueous sodium chloride chilled 50 —10°. The precipitate was filtered (filtrate being reserved) after 6 hours at 20°, wt 2.9 g m.p. 95—102°. Extraction with ethanol gave a 70% yield of crude β-isomer (m.p. 123—126°) leaving a residue extractable with hot benzene to separate the *bis* ethers, in 5% yield, from mercurous chloride (10% of total mercury). Three crystallizations from 85% ethanol (2.5 ml per gram) raised the mp of the β-isomer to 130—131.5°.

The long reaction time mentioned above is not necessary for initial consumption of the inorganic mercury. This is evident because treatment of an aliquot with aqueous sodium hydroxide after a reaction time of 1 minute does not cause any precipitate of mercuric oxide. Also when the reaction is worked up after one minute of reaction time any oxidation is avoided, with a consequent higher crude yield (90%) of the β-isomer with m.p. 126—8°. However, only traces of the ethers are formed and none of the α isomer can be found. Essentially the same results are obtained when the reaction system is made up with mercuric oxide and perchloric acid instead of mercuric nitrate and nitric acid, but the extent of mercurous salt formation is greater with perchloric acid.

The infrared spectrum of the β-isomer, m.p. 131°, in chloroform, (2%) showed absorptions in cm^{-1} with extinctions (E) as follows: 3600 (133), 3450 (7), 2950 (22), 2450 (62), 1750 (77), 1460 (120), 1370 (115), 1335 (185), 1170 (172), 1145 (161), 1115 (142), 1030 (244), 945 (134), 920 (142), 888 (107), 878 (107), 860 (125).

α-3-*EXO*-HYDROXY-[2,2,1]-BICYCLOHEPTYL-2-MERCURIC CHLORIDE

The reserved filtrate from which the crude product was filtered in the previous experiment was extracted 4 times with a total of 100 ml of chloroform. The combined extracts, vacuum-evaporated to a volume of 5 ml precipitated 0.199 g (6%) of crude α-isomer upon dilution with 5 ml of petroleum ether. This material, m.p. 118−19°, may be crystallized from chloroform, m.p. 119−20°. Anal. *Calcd.* for $C_7H_{11}ClHgO$: C, 24.2 ; Hg, 3.20. *Found*: C, 24.0 ; 3.39. The infrared spectrum of a 1.6% solution in chloroform in cm^{-1} with extinction (E) is as follows: 3600 (130), 3450 (86), 2950 (246), 2450 (76), 1490 (123), 1460 (153), 1400 (130), 1340 (155), 1308 (191), 1170 (191), 1120 (189), 1114 (191), 1050 (216), 1000 (408), 950 (153), 940 (147), 925 (143), 845 (155).

---

[8] M. Bedard, H. Huber, J. L. Myers and G. F. Wright, *Canad. J. Chem.*, **40**, 2278 (1962).

3-*EXO*-HYDROXY-[2,2,1]-BICYCLOHEPTANE

To a stirred solution at 0° of 3.5 g (0.01 mole) of the α-isomer described above with 0.40 g (0.01 mole) of sodium hydroxide in 45 ml of methanol and 3 ml of water was added 0.46 g (0.012 mole) of sodium borohydride during 25 minutes. After 8 hours subsequently at 20° metallic mercury (2.05 g, 102%) was filtered off. The filtrate was diluted with 300 ml of water and brought to pH 7.2−7.5 by cautious addition of diluted hydrochloric acid. This solution was extracted 5 times with 50 ml portions of diethyl ether. Evaporation of the combined extracts left 0.74 g (66%) of the exo-alcohol m.p. 124−6.5°. A mixture melting point with an authentic sample was not depressed.

To 0.10 g (9×10^{-4} mole) of this product in 3 ml of dry petroleum ether (b.p. 60−70°) was added 0.1 ml of phenylisocyanate. After 8 hours 0.16 g (62%) of the urethane m.p. 143−6° was obtained. After crystallization from benzene the melting point was 145−6° and it was not depressed by admixture with the authentic phenylurethane.

An identical experiment with the β−isomer gave identical results. Admixture of products and derivatives gave no depression in melting point.

BIS-(EXO-3-HYDROXY-[2,2,1]-BICYCLOHEPTYL-2)-MERCURY

A solution of 1.4 g (0.0004) of the β-isomer and 0.32 (0.008 mole) of sodium hydroxide in 1 ml of water and 18 ml of methanol was treated with 0.4 ml (0.0008 mole) of 100% hydrazine hydrate and the whole was refluxed for 6 hours. The hot system was then filtered to remove 0.55 g (69%) of metallic mercury. When the filtrate was cooled it yielded 0.25 g (60%) of colourless needles, m.p. 162−3°. Anal : *Calcd.* for $C_{14}H_{22}O_2Hg$: C, 39.8 ; H, 5.20. *Found* : C), 40.1 ; H, 5.32.

A solution of 100 mg of the *bis*-organomercury and 75.6 mg of mercuric acetate in 3 ml methanol was heated to 50° for 15 minutes. Dilution with 6 ml of water and 0.2 ml of 10% aqueous sodium hydroxide was followed by addition of 0.3 ml of 5% aqueous sodium chloride and then carbon dioxide. The product, 100 mg, m.p. 129 − 29.5 was shown to be the β-diastereomer by mixture melting point.

3-*EXO*-HYDROXY-[2,2,1]-BICYCLOHEPTYL-2-MERCURIC CHLORIDE HYDRAZINATE

To a solution of 1.75 g (0.005 mole) of the β-isomer m.p. 131°, in 7 ml of absolute ethanol was added 0.25 ml (0.005 mole) of 100% hydrazine hydrate with stirring. The white precipitate, which formed at once, weighed 1.60 g (90% m.p. 143−6°, decomp.). Five crystallizations from acetonitrile raised this m.p. to 154.5 − 6° (decomp.). The compound releases gas and deposits mercury upon treatment with mercuric acetate in methanol. It slowly decomposes spontaneously. Anal. *Calcd.* for $C_7H_{15}ON_2HgCl$: C, 22.2 ; H, 3.97 ; N, 7.4. *Found* : C, 22.5 ; H, 3.99 ; N, 6.6.

ACID HYDROLYSIS OF THE α AND β ISOMER MIXTURE

To a solution of 0.19 g each of the β and α isomer in 3 ml of 95 % ethanol was added 1 ml of *conc.* hydrochloric acid. After one minute the system was poured into 2 ml of 20 % aqueous sodium hydroxide. Filtration removed 0.10 g (80 %) of mercuric oxide which was washed with ether. The ether washings and extract of the filtrate yielded [2,2,1]-bicycloheptene in 30 % yield. The aqueous phase was treated with 0.5 ml of 10 % aqueous sodium chloride and gaseous carbon dioxide. Vacuum evaporation of the ethanol left 42 mg (20 %) of the α-isomer, m.p. 119 – 120°, authenticated by mixture melting point.

CIS-CYCLOPENTANE-1,3-DICARBOXYLIC ACID

To a solution of 3.47 g (0.01 mole) of the β chloromercurial in 16 ml of 10 % aqueous sodium hydroxide and 75 ml of water was added during 150 minutes 4.74 g (0. 03 mole) of potassium permanganate with stirring. After addition of a few ml of methanol the system was stirred for 27 hours longer then was filtered and the filtrate was evaporated to a small volume. After acidification the hydrated manganic oxide was filtered off. Further evaporation of the filtrate and three-fold extraction of the residue with 60 ml portions of absolute ethanol left 1.33 g, m.p. 110 – 120° (83 %) after evaporation of the solvent. This product, containing no mercury, was crystallized from 2.5 ml of hot water, m.p. 118 – 19°. [9]

A repetition of the experiment except for use of the α instead of the β-isomer gave a 70 % crude yield mp 100–109°. Crystallization from water raised this m.p. to 118–9° and it was not depressed by admixture with the product of the previous reaction. A 4 mg sample in 400 mg of potassium bromide gave the following infrared spectrum (cm^{-1}) : 3600–2300 (s), 1725–1600 (s), 1470 (m), 1410 (s), 1340 (m), 1320–1220 (s), 1210 (s), 1170 (s), 1090 (m), 1065 (w), 100–880 (s), 740 (m), 720–690 (m), 665 (m).

BIS-(2-CHLOROMERCURI-[2,2,1]-BICYCLOHEPTYL-3)ETHERS

Formation. To a solution of 94 g (1 mole) of [2,2,1]-bicycloheptene in 900 ml of tert-butyl alcohol was added a solution of 304 g (0.89 mole) of mercuric nitrate monohydrate and 144 ml (2.27 mole) of *conc* nitric acid (d 1.42) in 2320 ml of water. After 7 hours the clear solution did not test positively for presence of mercurous salt. To the stirred system was added during 2 hours 1052 ml of 5 % aqueous sodium chloride. The system was chilled and filtered, 283 g m.p. 118–28°. The aqueous filtrate was exhaustively extracted with chloroform. Evaporation of the extract left a residue which was crystallized from absolute ethanol to yield 8.0 g, m.p. 119–120°, of the α-isomeric hydroxymercuric chloride, authenticated by mixture melting point.

---

[9] J. F. Birch, W. H. Oldman and E. A. Johnson, *J. Chem. Soc.*, **1947**, 818.

The crude yield of 283 g was extracted with 1200 ml of hot 95% ethanol to leave an insoluble residue of 93.5 g of crude ethers, m.p. 145—56°. The cooled ethanol solution yielded 173 g (50%) of the β-isomer, m.p. 131°. Crystallization of the crude ethers from hot 3 : 2 chloroform-absolute ethanol yielded 68 g m.p. 200—203. This amount may be considered to comprise the actual yield of the mixture of ethers (20%) because of the elemental analysis (% C, 25.0; % H, 3.31) and because the infrared spectrum in potassium chloride shows no hydroxyl absorption.

Benzene (35 ml per g) may be used instead of chloroform-ethanol to raise the melting point of the crude ethers from 140° to 200°. Another useful method, especially when small amounts are involved, is dependent upon the marked difference in stability between the β-isomer and the ethers toward molecular hydrogen chloride. When 2 g crude product (m.p. 145—50°) was shaken with a solution of 5 ml *conc.* hydrochloric and 5 ml of methanol for one minute and then filtered the melting point of the solid which survived was 190—200°. About 5% of the ethers originally present are deoxymercurated together with all of the β-isomer. When 2.4 g (0.026 mole) of [2,2,1]-bicycloheptene, in 16 ml of *tert*-butyl alcohol was treated with a solution of 4.32 g of mercuric oxide in 6.5 ml (0.075 mole) of perchloric acid and 36 ml of water during 7 hours followed by subsequent treatment with aqueous sodium chloride the crystalline product contained mercurous salt (5% of total mercury), a 14% yield of the ethers, 200—203°, 60% of the β and 4% of the α-isomer, all calculated on the mole percent yield basis.

The mixtures of ethers (m.p. 200—203°, approximately in equal amounts according to rough thermal analysis) may be obtained also from the β-isomer and bicycloheptene in acid. To a warm solution of 1.3 g (3.76 mmole) of the β-isomer, m.p. 131°, in 5 ml of *tert*-butyl alcohol was added 3.6 ml of a molar solution of silver nitrate in water. After 30 minutes on the steam bath the system was filtered. The precipitate, washed with 7 ml of hot water and dried, weighed 0.69 (110% as silver chloride). To the filtrate was added 0.15 g (1.6 mmole) of [2,2,1]-bicycloheptene and 0.8 ml (13 mmole) of *conc.* nitric acid (d, 1.42). After 7 hours the system was then shaken with 2.3 ml (0.5 equiv.) of 5% aqueous sodium chloride. When the precipitated oil had coagulated another 2.3 ml of the aqueous sodium chloride was added and the thoroughly mixed system was chilled at 4° for 5 hours. The crude product, 1.0 g m.p. 115—135°, was then filtered off. This crude material was extracted with 10 ml of hot 85% ethanol to remove the β-isomer (m.p. 128—9, 60% recovery upon cooling) and to leave 0.21 g m.p. 164—176°. Multiple crystallization from benzene raised this m.p. to 200—203°, 0.18 g (10%). No attempt was made to isolate the α-isomer from the system.

The high melting ether. The mixture of ethers was fractionally crystallized from nitrobenzene (33 ml per gram) to give half the original weight m.p. 232°. Sometimes this m.p. was 242° but it reverted to 232° on subsequent crystallization and both melting points were definite, indicating polymorphism. Anal. *Calcd.* for $C_{14}H_{20}Cl_2Hg_2O$: C, 24.9; H, 3.00. *Found*: C, 24.9; H, 3.33. The infrared spectrum of 3 mg in 400 mg of potassium chloride (cm^{-1}) is 2950 (s), 2700 (s), 1450 (shoulder, m) 1380 (w), 1345 (m), 1315 (shoulder, m), 1927 (w), 1880 (w), 1220 (s), 1200 (w), 1178 (m), 1165 (m), 1140 (m), 1110 (m), 1050 (s), 1030 (s), 1015 (s), 955 (w), 940 (w), 925 (m), 890 (m), 860 (m), 780 (w), 765 (m).

The low melting ether. The mother liqours from the fractional crystallization out of nitrobenzene were vacuum-evaporated to dryness. Four or five crystallizations from benzene (35 ml per g) yielded the other ether, m.p. 215—16° in quantity about half of the original weight. Anal. *Found* for $C_{14}H_{20}Cl_2Hg_2O$: C, 24.9; H, 3.33. The infrared spectrum of 3 mg in 400 mg of potassium chloride (cm^{-1}) is 2950 (s), 2865 (s), 1460 (m), 1360 (m), 1325 (s), 1314 (s), 1297 (d), 1250 (s), 1218 (w), 1210 (w), 1185 (w), 1155 (shoulder, s) 1140 (m), 1025 (very broad, s), 988 (s), 955 (w), 926 (shoulder, m), 878 (w), 858 (m), 800 (w), 776 (s), 758 (w), where intensities are indicated as strong, medium and weak.

BIS-[2,2,1]-BICYCLOHEPTYL-3-ETHER

To a shaken slurry of 2.89 (4.1 mole) of high-melting ether in 60 ml of tetrahydrofuran with 0.22 g (8 mole) of sodium hydroxide in 3 ml of water was added 8.2 mole of sodium borohydride at 0° during 30 minutes. After 6 hours subsequently at 20° the system was filtered to remove 1.75 g (105 % of metallic mercury). The clear filtrate was diluted with 150 ml of water, neutralized with 1.3 ml of *conc.* hydrochloric acid and extracted three times with a total of 100 ml of petroleum ether (b.p. 35–56°). Evaporation of the extracts left 0.64 g (77 %) m.p. 60–62°. Crystallization from 1.5 ml of hot methanol raised this m.p. to 65–66°. Anal. *Calcd.* for $C_{14}H_{22}O$: C, 81.4 ; H, 10.75. *Found* : C, 80.6 ; H, 10.71. The infrared spectrum (cm^{-1}) of a 10 % solution in carbon tetrachloride was 2950 (v.s.), 1484 (m), 1450 (s), 1315 (m), 1285 (w), 1250 (w), 1215 (w), 1170 (s), 1148 (s), 1113 (s), 1089 (v.s.), 1036 (s), 1022 (v.s.), 980 (m), 945 (s), 917 (w), 880 (w), 855 (w), 833 (w).

The exepriment was repeated except that low-melting ether was reduced. The yield of mercury was 93 % and that of the ether, m.p. 62–64, was 67 %. After crystallization from methanol (m.p. 65–66°) the product was shown by mixture melting point and infrared spectra to be identical with the ether obtained from the high-melting diastereomer.

Revue Roumaine de Chimie, **19**, *5*, p. 847–857 (1974)

THE ACTIVATION OF PALLADIUM CATALYSTS BY RARE EARTH AND OTHER OXIDES FOR THE HYDROGENATION OF CYCLOHEXENE

S. M. ISMAIL, M. A. ALEEM and ASHRAF ALI

Pakistan Council of Scientific and Industrial Research, Karachi, Pakistan

Received May 14, 1973

It has been found that small quantities of metallic oxides, mainly of the rare earth type and including, thoria, zirconia, chromia, titania, vanadium pentoxide, ceria, lanthanum oxide, praseodymium oxide, thallium oxide and samarium oxide, act as strong promoters in the hydrogenation of cyclohexene by reduced palladium at 30° and at normal atmospheric pressure. In general the activity of a constant amount of palladium on varying amounts of promoters first rises to a peak (true promoter action) and subsequently falls as the ratio of promoters to palladium is further increased. The order of activities of these promoters follows the sequence : $\mathrm{ThO_2} > \mathrm{ZrO_2} > \mathrm{Cr_2O_3}$ $\mathrm{CeO_2} > \mathrm{TiO_2} > \mathrm{V_2O_5} > \mathrm{La_2O_3} > \mathrm{Pr_2O_{11}} > \mathrm{Tl_2O_3} > \mathrm{Sm_2O_3}$. The degree of activation is considerable being almost five times the unpromoted value for thoria and zirconia at the peak point in the activity curves. The apparent activation energies of hydrogenation of cyclohexene in alcoholic solution have been determined at 30°. Hydrogen adsorbed by these promoted catalysts have been determined by a chemical dehydrogenation method. Activation energies observed were higher for the promoted catalysts than for reduced palladium. A variation in the palladium : promoter ratio affected both the apparent activation energy and the total volume of hydrogen adsorbed per gram of palladium. A strict logarithmic dependence of the activation energy results in the disappearence of the promoter action of the supports at low temperatures. There was no dependence of catalytic activity on the hydrogen content of these catalysts, as has been found in the case of Raney nickel [1] except that the adsorbed hydrogen per gram of supported palladium was more than that on reduced palladium.

The only approach to a complete understanding of catalytic process is through an analysis of all factors involved, investigating each variable as completely separated from all other variables as possible. In molecular reactions the reactants must often be adsorbed to yield the product. The rate determining steps in such reactions may be the rate of adsorption or desorption of the reactants on the surface. By definition, catalysts reduce the energy of activation of a reaction and thus an equilibrium is achieved through the formation of an activated adsorption complex with the catalyst. For supported catalysts in particular, it is of interest to determine the separate contributions of the temperature independent factor and of the activation energy to the total activity, to know whether a support increases the activity by virtue of a decrease in the activation energy, by an increase in the frequency factor, or by both. Supported catalysts have been used to hydrogenate cyclohexene in alcoholic solutions at temperatures considerably below the inversion, in the region in which the reaction is strictly of the first order with respect to the concentration. The classical methods of rate determining steps have shown that the catalysts were employed under conditions in which mass transfer did not control the reaction rates. The first order reaction having, $k = (1/t)\ [1\mathrm{n}a/(a - x)]$, giving a linear graph on plotting $\log\ [a/(a - x)]$ against time t, and a slope of 0.0648 per min was obtained. The value of the constant k obtained was 1.492×10^{-1} per min. The measure of activity taken was the volume in ml of hydrogen adsorbed in the first four minutes of the reaction which does not affect the concentrations, and can thus be regarded as preliminary rates.

---

[1] H. Gautt and G. Mason, *Compt. rend.*, **1947**, 224, 281.

The independence of the hydrogenation rates on the concentrations can be attributed to a saturation of the catalyst surface with the olefin, and the first order dependence on near atmospheric pressures suggest that the reaction occurs through a Rideal-Eley type of mechanism. [2] There are many variations of this mechanism, the simplest of which involves adsorption of the olefin and its collision with free hydrogen. Various reaction mechanisms can, however, result in a first order dependence on the hydrogen pressure. The capacity of the catalyst to adsorb hydrogen under conditions similar to those prevailing during the reaction is of interest. A correlation between the hydrogen content of Raney nickel and its activity has been reported by many authors. [3] The adsorption of hydrogen from the liquid phase on to the supported palladium has been measured by Sokolskii, [4] but its catalytic activity has not been determined.

EXPERIMENTAL

All the reagents used were of ordinary laboratory grade and were used as purchased Ceric ammonium sulphate, being a primary standard, analytical reagent grade was used Cyclohexene and ethyl alcohol were distilled twice under vacuum.

Preparation of the catalyst. The catalysts were deposited on the supports by precipitation in situ. This method has been used with excellent results by Maxted *et al.* Finely divided palladium were prepared by the reduction of palladous chloride with aqueous formaldehyde. By this method, the tendency of the palladium to form a colloid was avoided, and the catalysts could then be readily separated by centrifuging.

---

[2] J. H. de Boer, *Adv. Catalysis*, **8**, 91 (1954).

[3] O. Beeck, A. W. Ritchie and A. Wheeler, *J. Colloid Sci.*, **3**, 505 (1948).

[4] D. V. Sokolskii and L. P. Dunina, *Doklady Akad. Nauk. S.S.S.R.*, **132**, 1111 (1960).

[5] E. B. Maxted and S. Akhtar, *J. Chem. Soc.*, **1960** 405, 1995; E. B. Maxted and S. I. Ali, *Ibid.*, **1961**, 4137; E. B. Maxted and S. M. Ismail, *Ibid.*, **1962**, 447.

Amount of catalysts. 9.976 mg of reduced palladium was deposited on a varying amount, 0.1 g to 2.0 g of the oxide supports. The charge in the reaction pipette consisted of 0.1 mole of cyclohexene and 9 ml of absolute alcohol. The rate of hydrogenation was taken as the ml of hydrogen adsorbed in the first four minutes. Hydrogenation data are shown in figures 1 and 2, having been separated in two figures to avoid excessive overcrowding.

Weight of the catalyst. With all considerations standardized at a constant, the dependence of the rate of hydrogenation upon the weight of the catalyst used was determined. Typical data are shown in figure 3.

The nature of the catalyst. Under the same experimental conditions and with the same amount of catalyst, the rate of hydrogenation of palladium over various metallic oxides follow the sequence: $ThO_2 > ZrO_2 > Cr_2O_3 > CeO_2 > TiO_2 > V_2O_5 > La_2O_3 > Pr_6O_{11} > Tl_2O_3 >$ Sm_2O_3. The results indicate that the solvent composition does not affect the reaction-order in any way.

Occlusion of hydrogen. A small amount of hydrogen occluded by palladium in the presence of 9 ml of alcohol at 30° was also measured by the same method as that for hydrogenation. It was found that 9.976 mg of unsupported palladium occluded 0.2 ml of hydrogen in 4 min and that supported palladium occluded 1.4 ml of hydrogen in the same period of time. Any correction for occlusion was however not made, as in a comparative study such as this, the amount occluded was the same for all the catalysts and this in any case being a very small percentage of the total volume of hydrogen adsorbed.

Agitation frequency. In a static system such as the present work, in which the mixing of hydrogen and the liquid is carried out by shaking, it is important to ensure that the reaction rate is independent of the rate of shaking. The influence of the mode of frequency of agitation upon the rate of hydrogenation was determined for several different lots of catalysts using a magnetic stirrer at 920 RPM in comparison with the mechanical shaker operating at a frequency of 200 oscillations/min. The resulting data showed that the use of a mechanical shaker gave increased rates of hydrogenation for all weights of catalysts, and that this effect is more pronounced for some supports than for others. However, it was established after repeated experiments that the activity of 9.976 mg of palladium on 1.0 g thoria at 30° became independent of the shaking speed when this exceeded 450 oscillations per minute. As such, the shaking rates for all subsequent activity measurements were adopted at 550 oscillations per minute, to take account of any variations due for instance to the belt slip.

Carriers and promoters. When a carrier increases the rate of a reaction, it is no longer a carrier, but becomes a promoter. It is often hard to make a distinction between the promoter, the active catalyst component and the carrier, in that definitions are somewhat arbitrary, synonyms such as support and activator are also cited in the literature. For our purposes, a promoter can be defined as a substance, added in small amounts to the catalyst, which in itself has little activity but which imparts a higher activity, stability or selectivity. Its amount is just economic, but optimal amounts show sharp maxima. Whereas carriers give quantitative mechanical extension to the catalyst, the function of a promoter is a specific one, in that it interacts with the adsorption complex fo form intermediate compounds

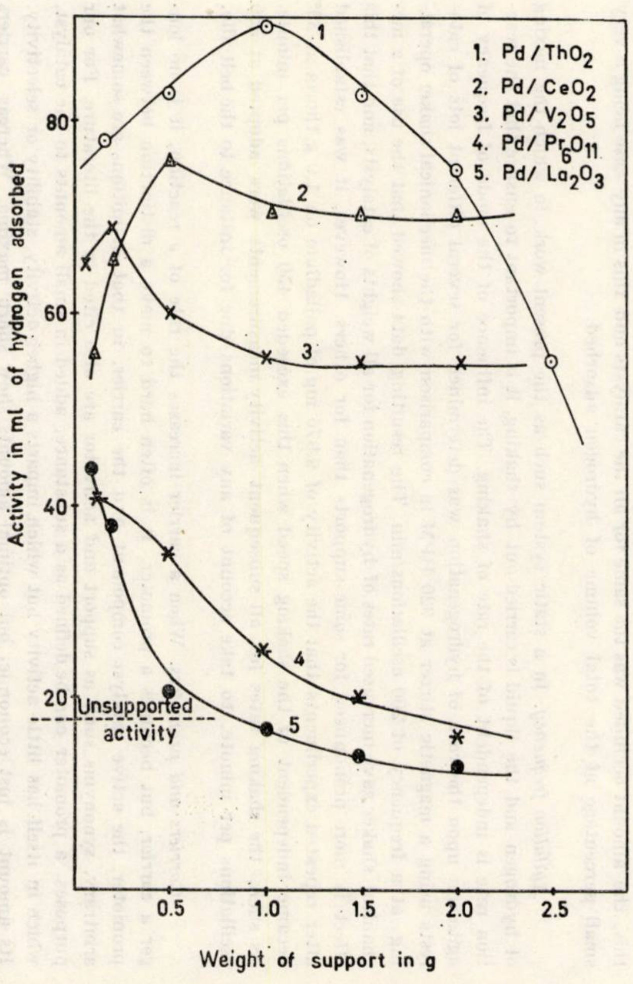

Fig. 1. — Activity/Support isotherm.

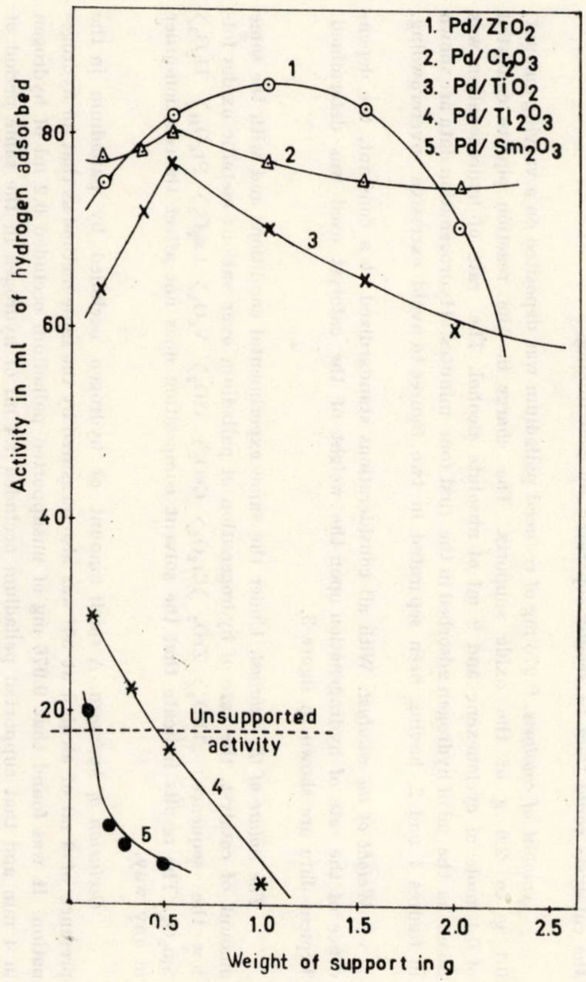

Fig. 2. — Activity/Support isotherm.

between the catalyst and the components of the reaction. Since there is no *a priori* difference between structural promotion and pure carrier action, ambiguity can be avoided by confining the term promoter action to cases in which the specific activity of a two or more component catalyst is greater than the sum of the specific activities of the separate components.

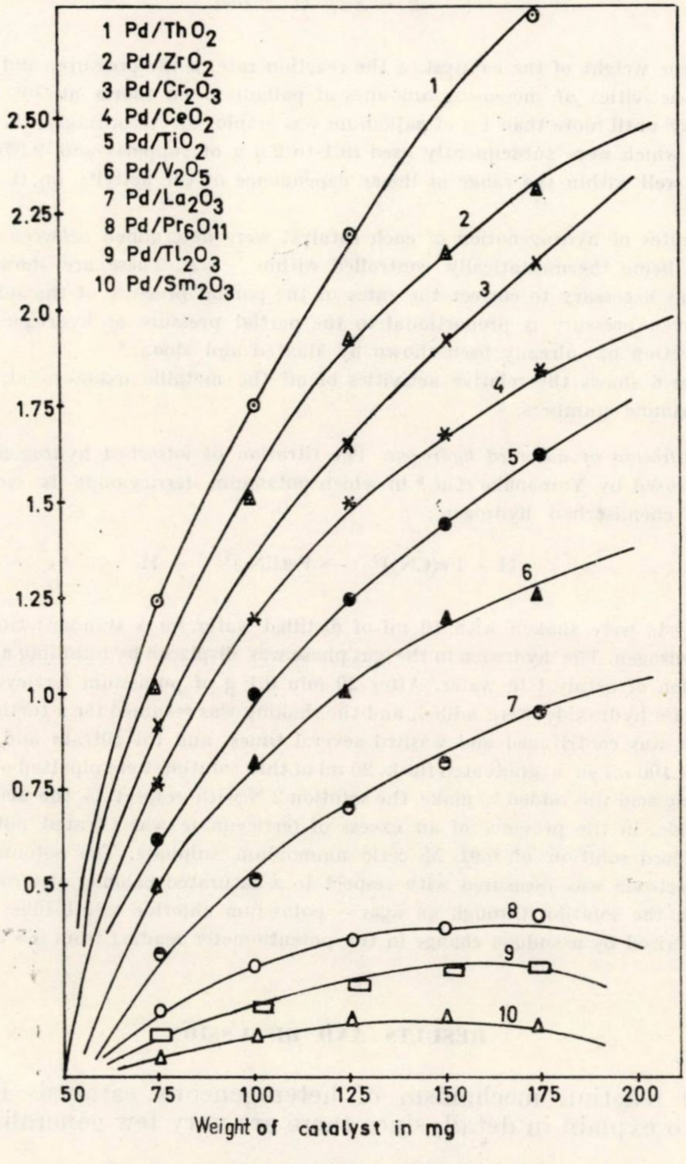

Fig. 3. — Activity/Weight of the catalysts.

Kinetic factors of the reaction. The first order dependence of the reaction rate on the weight of the catalyst is a necessary condition for the absence of mass transfer effects. As the amount of the catalyst is increased, the reaction rate increases linearly at first, but subsequently becomes independent of the weight of the catalyst. Watt and Walling [6] represented this limiting value by an empirical formula :

$$k = Awp \ (1 + Bw)$$

where w is the weight of the catalyst, k the reaction rate, p the pressure, and A, B are constants. The activities of increasing amounts of palladium on thoria at 30° do not deviate from linearity until more than 1 g of palladium was employed. Accordingly, the small amounts of catalysts which were subsequently used (0.1 to 2.0 g of supports and 9.976 mg of palladium) were well within the range of linear dependence of the activity on the weight of the catalyst.

The rates of hydrogenation of each catalyst were determined between 0° and 40°, the temperature being thermostatically controlled within $\pm 0.2°$. These are shown in figures 4 and 5. It was necessary to correct the rates of the partial pressure of the solvent, since the rate at a given pressure is proportional to the partial pressure of hydrogen. [7] The validity of this correction has already been shown by Maxted and Moon. [8]

Figure 6 shows the relative activities of all the metallic oxides used, arranged with increasing atomic numbers.

The titration of adsorbed hydrogen. The titration of adsorbed hydrogen was based on the method used by Yamanaka *et al.* [9] in which potassium ferricyanide is reduced to ferrocyanide by chemisorbed hydrogen :

$$\mathrm{H} + \mathrm{Fe(CN_6)^{3-}} \rightarrow \mathrm{Fe(CN_6)^{4-}} + \mathrm{H^+}$$

Catalysts were shaken with 10 ml of distilled water for a standard time in an atmosphere of hydrogen. The hydrogen in the gas phase was displaced by bubbling nitrogen through the suspension of catalyst in water. After 20 min 0.1 g of potassium ferricyanide and 2 ml of N – sodium hydroxide were added, and the shaking was resumed for a further known time. The catalyst was centrifuged and washed several times, and the filtrate and washings were made up to 100 ml in a graduated flask. 20 ml of this solution were pipetted out in a beaker, and sulphuric acid was added to make the solution 2 N with respect to the acid. This solution of ferricyanide, in the presence of an excess of ferricyanide was titrated potentiometrically with a standard solution of 0.01 M ceric ammonium sulphate. The potential of a bright platinum electrode was measured with respect to a saturated calomel electrode which made contact with the solution through an agar – potassium chloride salt bridge. The end point was characterized by a sudden change in the potentiometer reading from 0.5 to 1 volt.

RESULTS AND DISCUSSION

The reaction mechanism of heterogeneous catalysis is extremely difficult to explain in detail, since there are very few generalizations. One

---

[6] A. W. Watt and M. T. Walling, *J. Phys. Chem.*, **59**, 7 (1955).

[7] E. B. Maxted, *J. Soc. Chem. Ind.*, **40**, 169 (1921).

[8] E. B. Maxted and C. H. Moon, *J. Chem. Soc.*, **1935**, 1190.

[9] T. Yamanaka, K. Taya and Y. Takagi, *Sci. Papers Inst. Phys. Chem. Res.*, **52** 224 (1959).

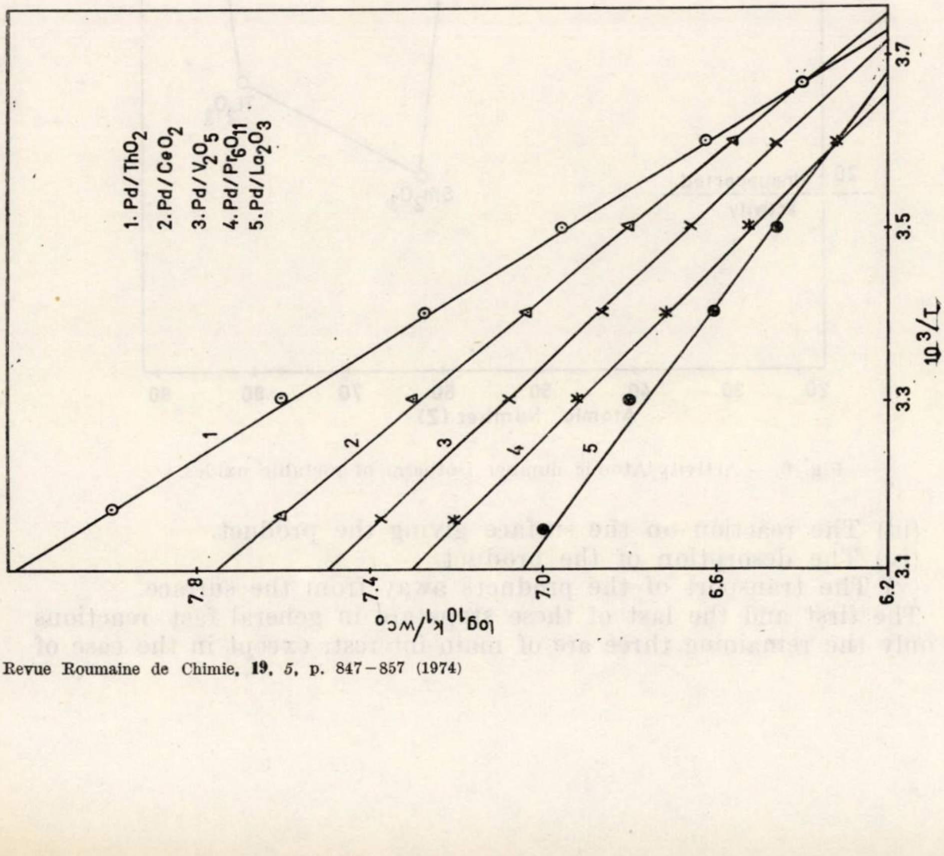

Fig. 4. — Activity as a function of temperature.

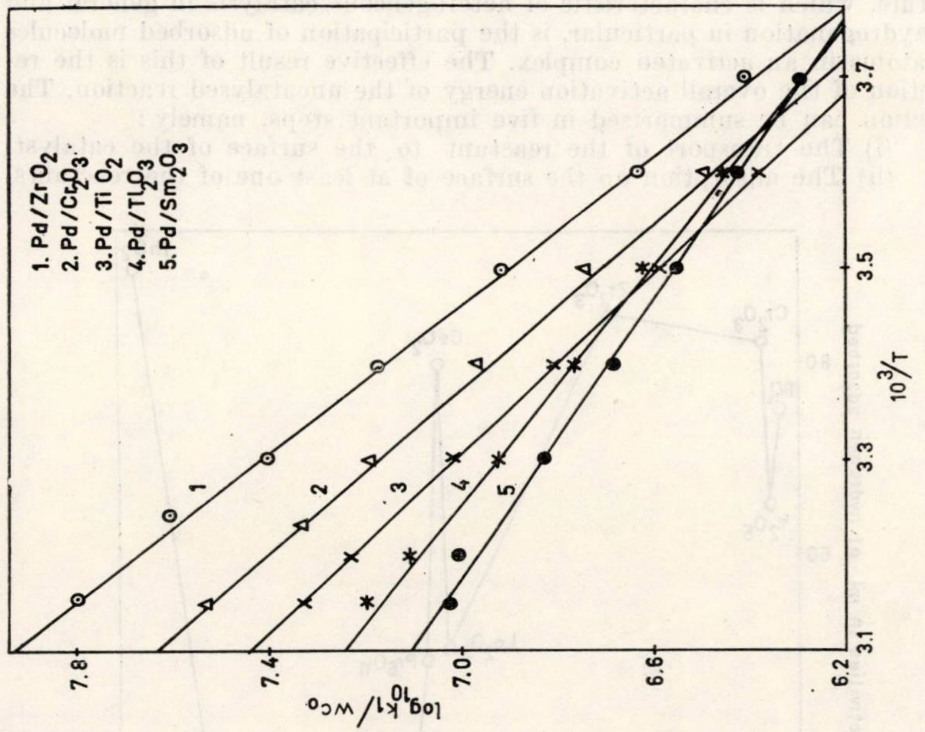

Fig. 5. — Activity as a function of temperature.

feature, which is characteristic of heterogeneous catalysis in general and of hydrogenation in particular, is the participation of adsorbed molecules or atoms in an activated complex. The effective result of this is the reduction of the overall activation energy of the uncatalysed reaction. The reaction can be summarized in five important steps, namely :

(i) The transport of the reactant to the surface of the catalyst.
(ii) The adsorption on the surface of at least one of the reactants.

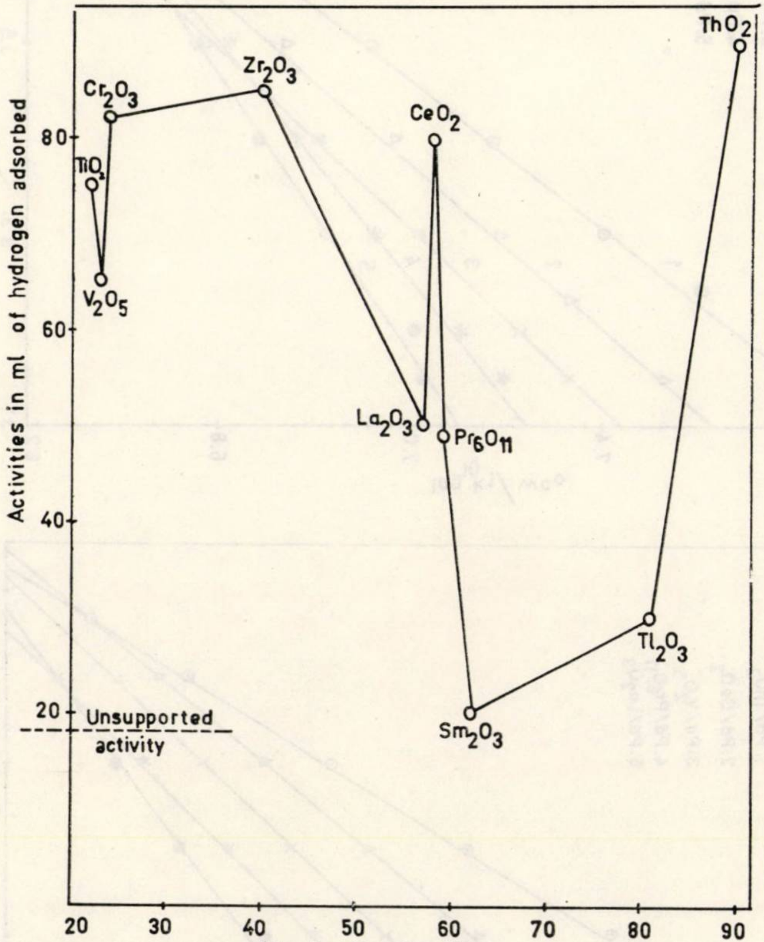

Fig. 6. — Activity/Atomic number isotherm of metallic oxides.

(iii) The reaction on the surface giving the product.
(iv) The desorption of the product.
(v) The transport of the products away from the surface.

The first and the last of these steps are in general fast reactions and only the remaining three are of main interest, except in the case of reactions involving highly porous catalysts such as kieselguhr or diatomaceous earth.

In hydrogenations two molecular species are involved in the reaction in that the second of the above steps will have either one or both reactants chemisorbed on the catalytic surface. These two possibilities will lead to two different reaction mechanisms, namely :

(i)

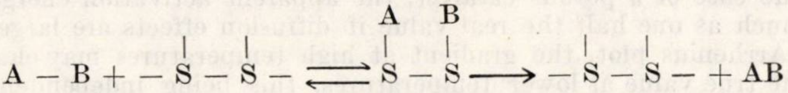

$$A - B + -\overset{|}{S} - \overset{|}{S} - \rightleftharpoons \overset{A}{\overset{|}{S}} - \overset{B}{\overset{|}{S}} \longrightarrow -\overset{|}{S} - \overset{|}{S} - + AB$$

Let A and B represent the two molecules involved in the reaction and S represent the surface atoms. The rate of reaction in this mechanism will be dependent on the probability of A and B being adsorbed on neighbouring sites. If θ_A and θ_B are the fractions of surface covered by reactants A and B respectively, the following expression can be deduced from the Langmuir[10] adsorption isotherm :

$$\frac{Kp}{1 + Kp}$$

where K is the ratio of the rate of adsorption and desorption and p the pressure of the gas in equilibrium with the surface.

(ii)

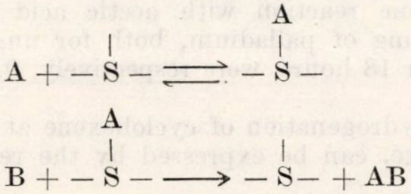

$$A + -\overset{|}{S} - \rightleftharpoons -\overset{A}{\overset{|}{S}} -$$

$$B + -\overset{A}{\overset{|}{S}} - \longrightarrow -\overset{|}{S} - + AB$$

This mechanism involves an adsorbed reactant A and a non-adsorbed reactant B. The effect of adsorbed but non-reacting molecules of B should also be considered.

These kinetic mechanisms have been derived on the assumption that the adsorption is localized, that each adsorption site is occupied by only one atom or molecule and that the heat of adsorption is independent of the coverage.

The influence of temperature on the observed activity is a useful guide in the determination of the rate controlling step, since the activation energies of diffusion processes are generally much smaller than those of adsorption or reaction. The activation energy of the transfer of hydrogen into water has been calculated to be 2.7 kcal mole^{-1} on the basis of diffusion coefficients. Since activation energies as low as this were not obtained, the activities were of the first order with respect to the weight of the catalyst and were independent of the rate of shaking. The transfer of hydrogen across the gas liquid boundary, or of products from the catalyst surface, cannot control the overall reaction rates.

---

[10] I. Langmuir, *J. Amer. Chem. Soc.*, **38**, 2221 (1916) ; **40**, 1361 (1918).

The quantitative effect of diffusion in lowering the true activation energy of gas reaction on solids has been described by Weiss and Prater .[11] The same would apply in principle to the liquid phase catalytic reactions. In the case of a porous catalyst, the apparent activation energy can be as much as one half the real value if diffusion effects are large; and in the Arrhenius plot, the gradient at high temperatures may change over to the true value at lower temperatures, this being independent of the relative rates of the chemical and diffusion processes.

The standard time allowed for the saturation of the catalysts with hydrogen was 30 min, although preliminary experiments showed that the adsorption of hydrogen was virtually complete after only 15 min. The reduction of ferricyanide took longer. Titres obtained with reduced palladium, after 10,45 and 960 min were, respectively, 9.15, 10.55 and 10.53 mls of hydrogen per gram. A similar variation of the hydrogen titre with time was found for supported catalysts.

If a decrease in the amounts of catalyst did not alter the apparent activation energies, it can be assumed that diffusion effects did not control the activities. Quantitative transference of reduced palladium to the reaction vessel was found to be inaccurate with amounts less than 0.02 g, so the hydrogenation rate was substantially reduced by sintering. The activation energy did not change on sintering, as has been previously reported for the same reaction with acetic acid as the solvent. [8] The activities of 9.976 mg of palladium, both for unsintered and sintered at 300° and at 400° for 18 hours, were respectively, 9.6, 4.8 and 0.9 ml. per min at 30°.

The rate of hydrogenation of cyclohexene at unit pressure, i.e. the specific reaction rate, can be expressed by the relationship;

$$k_1 = wSk_s$$

Where w is the weight of palladium, S its specific surface area, and k_s the activity per unit area. The activity is related to a frequency factor A, and the apparent energy of activation, E_A, by the usual Arrhenius expression $k_s = A_{\text{exp}}(-E_A/RT)$. Although absolute values of S are not known, they can be assumed to be proportional to the reciprocals of the poisoning coefficients per gram of palladium. The appropriate values of $C_0/0.00625$ are given by Maxted. [7] The value of C_0 for reduced palladium used in this work is 7.2×10^{-5} mole g^{-1}. Plots of $\log (k_1/wc_0)$ against $1/T$ are given in figures 4 and 5 for different ratios of palladium on the supports containing the optimum ratio of platinum to support activity at maximum.

If k is the true velocity constant, K_H the adsorption coefficient of hydrogen in the Langmuir adsorption isotherm, and p_H the partial pressure of hydrogen, the reaction rate is given by $v = kK_H p_H$ and the true first order velocity constant $k_1 = k K_H$. It can readily be shown that, whenever the apparent first order constant is given by the product of an adsorption equilibrium constant and the true velocity constant, the apparent activation energy is lower than the true activation energy by the value of the heat of adsorption of hydrogen, irrespective of the reaction mechanism. The apparent activation energies should therefore be corrected by the addition of 16—18 kcal $mole^{-1}$ in order to obtain the true values.

---

[11] P. W. Weiss and C. D. Prater, *Adv. Catalysis*, **6**, 143 (1954).

Another factor which can affect the activation energy observed, for a series of related catalysts, is a compensation effect between the activation energy and the frequency factor. The absence of a strict logarithmic relation between E_A and A is apparent in figures 4 and 5, since a necessary condition for this is that the Arrhenius plots should intersect at a common point, i.e. a temperature exists at which all the reaction rates are equal. Nevertheless, it is evident that the relative activities at a given temperature also depend on the activation energy.

At room temperatures, promoter action of the supports become active, since the specific activities of the supported catalysts are greater than the corresponding activity of unsupported palladium. Owing to a compensation effect, the degree of this promoter action becomes smaller as the temperature decreases. At sufficiently low temperatures, the increase in the temperature independence factor for the supported catalysts becomes inadequate to overcome the effect of a larger activation energy, and promotion does not occur. For supported palladium catalysts, these temperatures lie in the experimental region from 3° to 15°.

The temperature coefficient of hydrogenation processes is also of considerable importance. By virtue of the dependence of the reaction velocity on the adsorbed concentration, a decrease in the hydrogenation velocity as the temperature is increased, may occur at high temperatures. A change in the kinetic form with increasing temperature has been observed in liquid-phase hydrogenation by Maxted and Moon. [8] For this reason, the hydrogenation temperature was kept as low as possible, an optimum value being found to be at 30°.

Revue Roumaine de Chimie, **19**, *5*, 859–867 (1974)

ELECTRONIC STRUCTURE OF CYCLOBUTADIENE FUSED WITH HETEROCYCLIC RING. I. HETEROBENZOCYCLOBUTADIENES

M. D. GHEORGHIU and P. FILIP

Institute of Organic Chemistry, Spl. Independenţei 202–B, Bucharest 15, Romania

Received August 3, 1973

The electronic structure of nine unknown heterobenzocyclobutadiene (HBCB) is discussed in comparison with benzocyclobutadiene (BCB). The investigated HBCB are, according to our findings, more reactive than BCB.

Cyclobutadiene is an elusive compound, [1] challenging a large number of experimental efforts. Partly, these efforts were directed towards the synthesis of more stable derivatives of cyclobutadiene classified as using (i) electronic, (ii) steric and (iii) stereoelectronic factors. While (ii) would leave the electronic π system of cyclobutadiene unchanged, (iii) and especially (i) could alter the π system substantially, making some examples hardly recognizable as cyclobutadienes.

Among the numerous reported works on cyclobutadiene and derivatives, few have succeeded to isolate stable compounds; to our best knowledge, nowadays there are known: push-pull cyclobutadienes (**1**) [2] e.g. electronic stabilized cyclobutadiene, having a symmetric structure with C–C average bond distances equal to 1.455 Å [3] and a second example as a sterically hindered cyclobutadiene (**2**). [4] Recently, the isolation of cyclobutadienes (substituted and unsubstituted in solid matrix) was reported. [5]

---

[1] For excellent compilations see (a) M. P. Cava and M. J. Mitchell, "Cyclobutadiene and Related Compounds", Academic Press, New York, 1967; (b) D. Seebach, S. Beckmann and H. Geiger in "Methoden der Organischen Chemie (Houben-Vely)", Ed. E. Müller, Band IV/4, G. Thieme Verlag, Stuttgart, 1971, p. 231.

[2] R. Gommper and G. Seybold, *Angew. Chem.*, **80**, 804 (1968); *ibid.*, **83**, 44 (1971); M. Neuenschwander and Niederhause, *Helv. Chim. Acta*, **53**, 519 (1970).

[3] H. J. Linder and R. von Gross, *Angew. Chem.*, **83**, 489 (1971).

[4] H. Kimling and A. Krebs, *Angew. Chem.*, **84**, 952 (1972).

[5] A. Kratz, C. Y. Lin and M. D. Newton, *J. Amer. Chem. Soc.*, **95**, 2744 (1973) and the references cited therein.

The interest in this field, from a theoretical point of view is focused on the electronic structure. As the system is very unstable, one must search models in which the π system becomes more stable. As we already mentioned above, one way to stabilize the π system of the cyclobutadiene is to add on the ring donor (s) and accepter (s) substituents in such a way, that they can exert their push-pull effects.[6] Another way would be to fuse aromatic ring[7] on one side of the cyclobutadiene leading to compounds such as BCB (**3**), naphto [b] cyclobutadiene (**4**), anthra [b] cyclobutadiene (**5**), phenanthro [l]cyclobutadiene (**6**), etc.

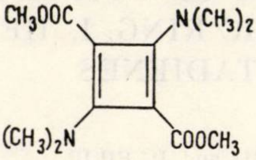

1

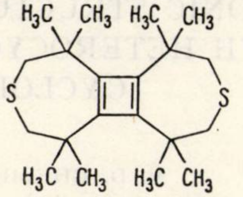

2

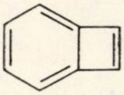

3

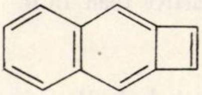

4

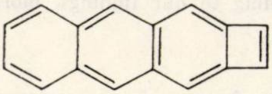

5

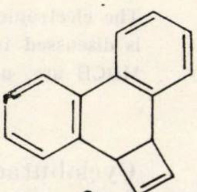

6

However, **4** and **5** were reported as transient reaction intermediates; the fusion of an aromatic ring seems to confer probably only a relative stability of the above mentioned systems with respect to the parent cyclobutadiene. Substituents such as Br— and C_6H_5— on the side of the double bond to the cyclobutadiene ring in **4**, were reported to confer stability to these compounds.[8]

We would like to confine our theoretical interest to the area of BCB and some heterobenzocyclobutadienes (HBCB), the latter being formally considered as obtained by fusing to the double bond of the cyclobutadiene either a six-membered heteroaromatic ring or a five-membered heteroaromatic ring.

The present paper deals only with the six-membered heteroaromatic cyclobutadienes while in a forthcoming paper we would like to present our results regarding the five-membered heteroaromatic cyclobutadienes.

No heterobenzocyclobutadiene (HBCB) was reported until now. Benzocyclobutadiene (BCB) is a highly reactive species, never isolated, but inferred from trapping experiments, especially with dienes.[9] One

[6] R. Hoffmann, *J.C.S. Chem. Comm.*, **1969**, 241.

[7] see reference la, chap. 6 and 9.

[8] M. P. Cava, B. Y. Hwang and J. P. van Meter, *J. Amer. Chem. Soc.*, **85**, 4032 (1963); M. P. Cava and B. Y. Hwang, *Tetrahedron Letters*, **1965**, 2297; trapping experiments for **6** are disclosed in: T. Mujamoto, S. Tanaka and Y. Odaira, *J.C.S. Perkin* I, **1973**, 138.

[9] see reference la, chap. 6, 1b p. 231.

of the most important questions to be answered is whether HBCB systems are more or less stable than BCB.

METHODS OF COMPUTATION

The calculations were carried out within the framework of a standard ω-Hückel Molecular Orbital (HMO) method.[10,11] The diagonal matrix element H_{ii} is calculated according to the following expression:

$$H_{ii} = H^0_{ii} + \omega \times (N - Q_{ii}) \qquad (1)$$

where H^0_{ii} is the initial coulomb integral (see table 1); $\omega = 1.4$; N is the number of electrons contributing to the π-system, Q_{ii} is the computed atomic charge density.

The off-diagonal matrix elements, H^0_{ij} were not modified during the iterative step calculation. The heteroatoms were treated in the usual manner[12]:

$$\alpha_X = \alpha_C + k_X \cdot \beta_{C-C} \qquad (2)$$

$$\beta_{X-Y} = r_{X-Y} \cdot \beta_{C-C} \qquad (3)$$

Values chosen for k_X and r_{X-Y} are presented in table 1.

Table 1

Parameters of heteroatoms

Atom	k_X	Bond	X−Y
N	0.5	C−N	1.0
		N−N	1.0

To speed up the convergence, a procedure for averaging consecutive iterated values of charge densities was used[13], especially in the first stages of calculations (av-average, iter-represents an iterative index):

$$Q^{av}_{ii} = 0.5 \times (Q^{iter-1}_{ii} + Q^{iter}_{ii}) \qquad (4)$$

---

[10] The program was kindly supplied by QCPE (registered under number 110) Chemistry Department, Indiana University, Indiana 47401, USA. It was written by P. Grund, University of Massachusetts, Amherst, Mass. USA, and was adpoted on a IBM 1130 computer of Polytechnic Institute, Bucharest.

[11] A. Streitwieser, "Molecular Orbital Theory for Organic Chemists", J. Wiley, New York, 1963, chap. 4.

[12] reference 8, chap. 5.

[13] R. Ettinger, *Tetrahedron*, **20**, 1579 (1964).

DISCUSSION OF THE RESULTS

Let us summarize briefly the main features of the cyclobutadiene π system. One can visualize this molecule as resulting from two ethylene units approaching each other in parallel planes :

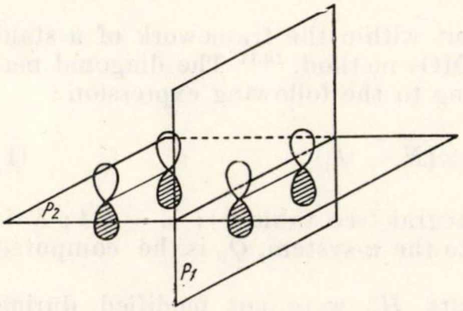

Fig. 1. — Definition of symmetry planes for two ethylenic units side-approach.

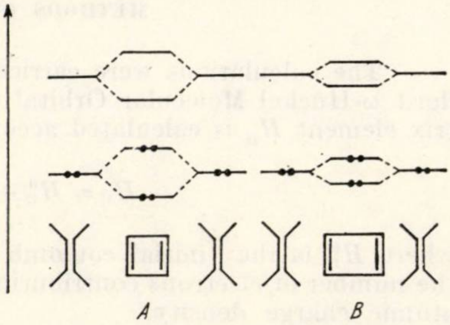

Fig. 2. — Perturbation diagram for two ethylene-side approach. (A) strong interaction, (B) weak interaction.

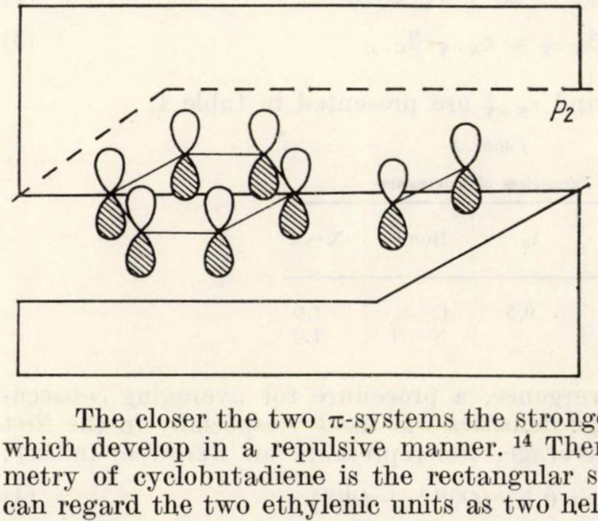

Fig. 3. — Definition of symmetry planes for the ethylene + + benzene system.

The closer the two π-systems the stronger their mutual interactions, which develop in a repulsive manner.[14] Therefore, the most stable geometry of cyclobutadiene is the rectangular structure. Alternatively, one can regard the two ethylenic units as two helium atoms, which approach each other without presenting any again in stabilization, on the contrary the system becomes less stable.[15] Indeed elaborate calculations predict for cyclobutadiene a rectangular structure which keeps the two double bonds further appart having single C—C bonds equal to 1.51 Å, and double bonds equal to 1.338 Å.[16]

---

[14] M. D. Gheorghiu and R. Hoffmann, *Rev. Roumaine Chim.*, **14**, 781 (1969).

[15] For an excelent discussion of the above arguments based upon interaction diagrams see : M. J. Goldstein and R. Hoffmann, *J. Amer. Chem. Soc.*, **93**, 6193 (1971).

[16] M. J. S. Dewar and G. J. Gleicher, *J. Amer. Chem. Soc.*, 87 (1965) ; M. J. S. Dewar, M. C. Kohn and N. Trinajstic, *ibid.*, **93**, 3437 (1971).

The BCB-π system could be conceived, in a similar manner, as resulting from the benzene π system perturbated by an ethylene unit. The approach is achieved so that the whole system preserves continuously the plane of symmetry P_1.

In respect to this plane the wave functions of benzene, ethylene and benzocyclobutadiene are either S (symmetric) or A (antisymmetric). The levels with like symmetry will interact. The consequences are that half of them become stabilized while the other half are destabilized. The interaction diagram of pertinent levels is depicted in fig. 4, where index B means benzene, while E is related to the ethylene unit.

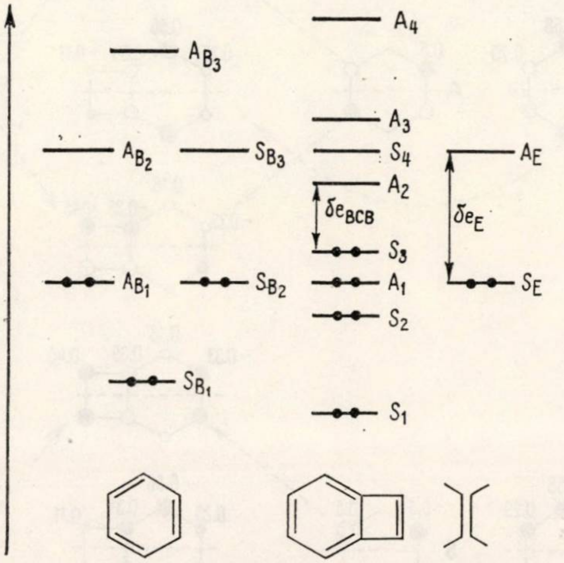

Fig. 4. — Energetic scheme for the benzene — ethylene interaction.

An inspection of wave function diagram (fig. 5) reveals for the highest occupied molecular orbital (HOMO), S_3, as being mainly a double bond located in the outer part of the four-membered ring of BCB, so is the next level, the lowest unoccupied molecular orbital (LUMO), A_2. Both levels are, therefore, in fact a very reactive double bond, not only due to their high energy content, but also to the very low value of the splitting. Thus, S_3 is higher than S_E with 0.5 β, while $\Delta e_{BDB} \simeq 0.5\ \Delta e_E$.

The very reactive nature of BCB is therefore the consequence of the fact that it has a destabilized double bond in respect to an isolated ethylene system. The available experimental[17] and theoretical[18] data support these conclusions.

Continuing our examination beyond the topmost occupied orbitals, one should note the position of S_1 level as being lower than the S_{BI} level

---

[17] see reference la, page 201.

[18] M. D. Gheorghiu and M. Avram, *Rev. Roumaine Chim.*, **12**, 1063 (1967).

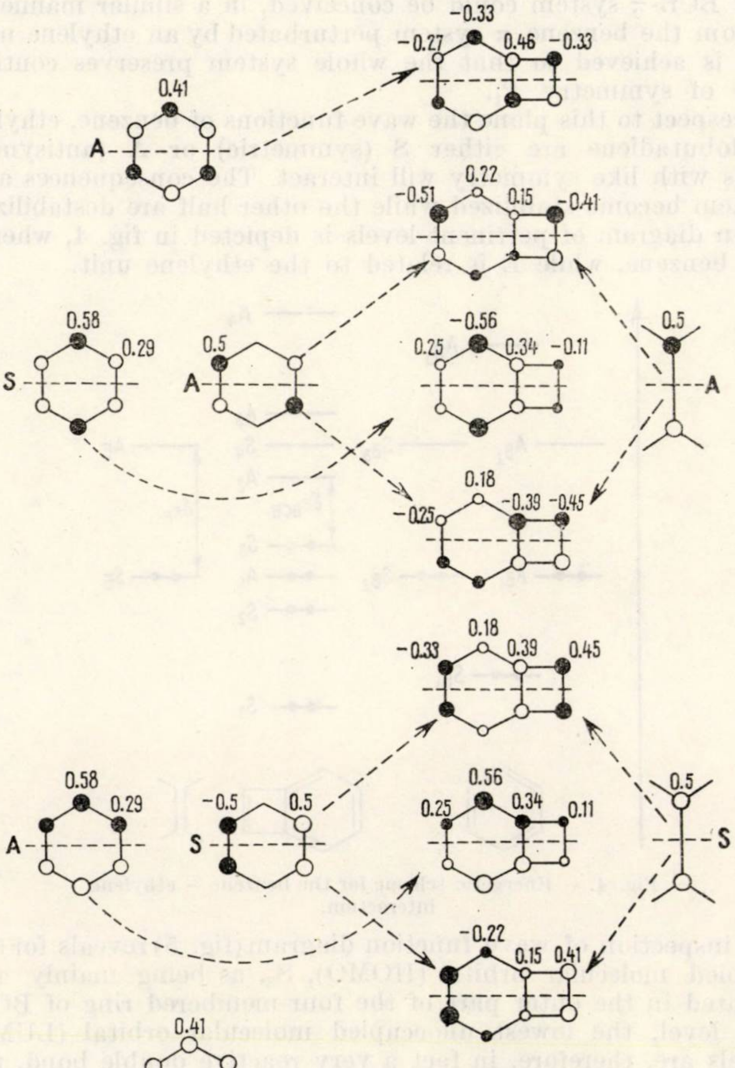
0.33
-0.27
0.46
-0.33
0.41
A
0.22
-0.51
0.15
-0.41
0.58
0.29
S
0.5
A
-0.56
0.25
0.34
-0.11
0.5
A
0.18
-0.25
-0.39
-0.45
0.18
-0.33
0.39
0.45
0.58
0.29
A
-0.5
0.5
S
0.56
0.25
0.34
0.11
0.5
S
-0.22
0.15
0.41
0.41
S
0.33
0.27
0.46
0.33

Fig. 5. — Molecular π-wave functions of benzene (left), benzocyclobutadiene (middle) and ethylene (right).

of benzene, as a result of secondary interactions, especially with the S_2 level of BCB, which is pushed upwards.

Next, we turn our attention on the molecular wave functions corresponding to the energetic scheme of BCB presented in fig. 5. Here the figures represent the coefficients of the atomic orbitals belonging to the atom above which they are written. The shaded circles represent an atomic orbital participating with a minus sign in the wave function. The horizontal dotted line corresponds to the plane of symmetry according to which the molecular wave functions are classified.

Since benzocyclobutadinee is a highly reactive olefin, one can ask whether a bicyclo [4.2.0] octatetraene system can be stabilized in some way. Therefore, we decided to examine derivatives of BCB in which the benzene ring is replaced by a heteroaromatic ring such as pyridine, 1,2-diazine, 1,2,3-triazine, 1,2,4-triazine and 1,2,3,4-tetrazine. Unfortunately, none of these compounds are known, to our knowledge there were never mentioned any synthetic or trapping attempts. We would like to provide, however, some prognosis concerning their reactivity relatively to that of BCB. Two criteria are used to indicate the stability.

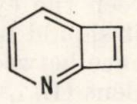

7

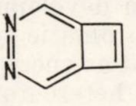

10

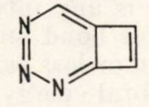

13

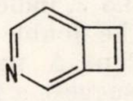

8

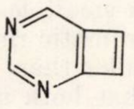

11

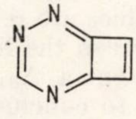

14

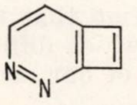

9

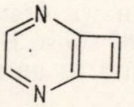

12

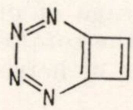

15

(1) There are many reasons to believe that both HOMO and LUMO play a crucial role in determining the chemical stability of a molecule. [19] The energy gap δe between HOMO and LUMO is related to the chemical reactivity. Examining the energy of all HBCB's, it is interesting to note that they are more destabilized relatively to BCB.

Table 2

Significant energetic figures of HBCB (in beta units)

Compound	Total energy of HBCB E_{HBCB}	Total energy of the Aromatic + ethylene (2β) E	$\Delta = E_{HBCB} - E$	Energy of HMO	$\delta e = E_{HOMO} - E_{LUMO}$
3	10.54	10	0.54	0.554	1.102
7	10.90	10.52	0.48	0.30	0.52
8	10.90	10.52	0.48	0.30	0.51
9	11.41	11.03	0.38	0.35	0.53
10	11.41	11.03	0.38	0.35	0.50
11	11.41	11.03	0.38	0.35	0.52
12	11.41	11.03	0.38	0.32	0.525
13	11.92	11.53	0.39	0.39	0.51
14	11.92	11.53	0.39	0.40	0.535
15	12.42	12.03	0.39	0.44	0.525

---

[19] K. Fukui, *Accounts Chem. Res.*, **4**, 57, (1971).

Additionaly, we note also that δe, the splitting of HOMO-LUMO, is approximately half of the corresponding value of BCB. We mentioned above that the high reactivity of BCB is related to the low value of its δe; but now we figure that our HBCB models have even lower values, which are situated approximatively at $0.5\,\delta e_{BCB}$, in other words one fourth from the δe value of an isolated olefine bond. Based on this result, we tentatively consider that the HBCB's studied will display an even higher reactivity than BCB, due to the presence in the four-membered ring of a very reactive double bond.

(2) Our second criterium of stability relies on the energetic scheme related to the perturbation diagram discussed for cyclobutadiene and BCB. If there is any interaction developing between the cyclobutadiene unshared double bond and the aromatic system, it should be reflected in the energy gain or loss calculated as energy difference between the HBCB and the sum total energy of the heteroatomic nucleus (E_{HAr}) plus an isolated double bond (2β). This difference is presented as Δ in table 2. As expected, Δ values are relatively small, less than $0.5\ \beta$, indicating a slight interaction between the heteroaromatic ring and the double bond. Again, our models present a Δ_{HBCB} smaller than Δ_{BCB}. Thus Δ parallels the δ values, leading to conclusions that both indexes suggest a relative instability of HBCB compared to an already unstable BCB.

At this stage of discussion we draw attention that the accidental coincidence of the total energy of those HBCB's which differ only by the relative position of heteroatom (s), is an artifact of our method of computation.

BOND ORDER DIAGRAMS

BCB is a hybrid of three neutral resonating structures **3A**, **3B** and **3C**:

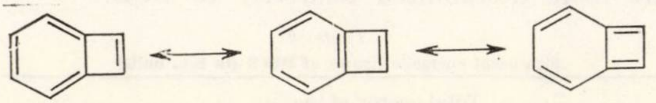

3A **3B** **3C**

while structure **3C** could be neglected, since it is in fact an orthoquinodimethane, the remaining structures **3A** and **3B**, which should have a significant contribution to the structure of BCB, posses antagonistic features. In **3A**, the cyclobutadiene system is "avoided", the system consisting of a dimethylenecyclobutene; this is an example of what we called in the introduction of this paper as a hardly recognizable cyclobutadiene. Structure **3B** contains a cyclobutadiene unit. Double bond diagram shows for BCB a preference for structure **3A**, in which the cyclobutadiene structure does not in fact exist. Moreover this is true also for all our HBCB models. In table 3 the bond orders for the pertinent bonds are presented.

The original bond order of the same bond is also presented for comparison. As a general feature, it has a lower value in the HBCB than in

Table 3

Bond order diagram*)

Compound	1–2	2–3	3–4	Same bond in the isolated aromatic compounds	3–5	1–4	4–6
3	0.949	0.151	0.544	0.667	0.75	0.151	0.75
7	0.896	0.214	0.551	0.668	0.728	0.216	0.723
8	0.896	0.216	0.549	0.666	0.726	0.215	0.729
9	0.893	0.220	0.545	0.662	0.727	0.220	0.728
10	0.898	0.212	0.555	0.669	0.722	0.212	0.722
11	0.895	0.215	0.549	0.667	0.729	0.219	0.721
12	0.893	0.219	0.547	0.664	0.724	0.219	0.724
13	0.871	0.246	0.521	0.664	0.721	0.218	0.722
14	0.889	0.226	0.541	0.658	0.730	0.223	0.729
15	0.887	0.226	0.541	0.655	0.722	0.226	0.722

*) The numbering scheme for the entries of the first column of table 3 results from the superposition of the corresponding formula on the skeleton

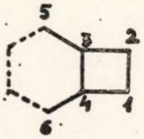

parent aromatic systems, since in the former an electronic density shift occurs, favoured by a **3A** type resonance structure.

CONCLUDING REMARKS

Our analysis suggests that a heteroaromatic system does not improve the stability of HBCB's derived from it. They are destabilized in respect of the already very reactive BCB.

This work was inspired from the experimental chemistry started and directed in our laboratory by the late Prof. C. D. Nenitzescu in collaboration with Prof. M. Avram.

A generous allotment of computer time made available by Computer Center of the Polytechnic Institute is gratefully acknowledged.

Revue Roumaine de Chimie, **19**, 5, 869–876 (1974)

RECHERCHES DANS LA SÉRIE DES TRICYCLO [7.3.1.$0^{2,7}$] TRIDÉCANES. III*

HYDRAZONES DE LA 2-HYDROXY-8-R-TRICYCLO[7.3.1.$0^{2,7}$]TRIDÉCAN-ONE-13

N. BĂRBULESCU et ANCA NICOLAE
Université de Bucarest, Faculté de Chimie, Splaiul Independenţei

Reçu 18 juillet 1973

Dans le présent mémoire on a étudié la réaction de l'hydrazine avec des dérivés de 2-hydroxy-8-R-tricyclo[7.3.1.0 ^{2,7}]tridécan-one-13 où R=H et CH_3. Suivant les conditions, la réaction fournit les hydrazones ou les azines symétriques respectives. On a établi que le cours de la réaction est déterminé par le rapport molaire cétol : hydrate d'hydrazine et aussi par la présence des quantités catalytiques d'acide. Les hydrazones ont été caractérisées par voie chimique (formation de dérivés acétylés). Les hydrazones et les azines obtenues ont été également analysées par des méthodes physico-chimiques.

Dans le présent mémoire on a abordé l'étude de la réaction de l'hydrazine avec la 2-hydroxy-8-R-tricyclo [7.3.1.$0^{2,7}$]tridécan-one-13 où R=H et CH_3. Suivant les conditions de réaction on a obtenu les hydrazones ou les azines correspondantes.

Vu les réactions secondaires qui l'accompagne, la synthèse des hydrazones non substituées à l'atome d'azote est généralement assez difficile. Les hydrazones obtenues lors de la réaction de condensation des composés carbonyliques avec l'hydrazine peuvent réagir par la suite avec le composé carbonylique en obtenant les azines symétriques respectives [1-5]

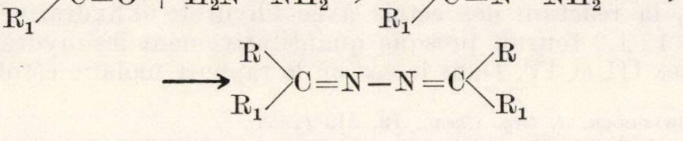

$$\overset{R}{\underset{R_1}{>}}C=O + H_2N-NH_2 \rightarrow \overset{R}{\underset{R_1}{>}}C=N-NH_2 \xrightarrow{\overset{R}{\underset{R_1}{>}}C=O} \overset{R}{\underset{R_1}{>}}C=N-N=C\overset{R}{\underset{R_1}{<}}$$

---

[*] Ire partie : N. Bărbulescu, A. Nicolae, *Rev. Chim.* (*Bucureşti*) (à paraître)
IIe partie : N. Bărbulescu, A. Nicolae, *Anal. Univ. Buc.*, *Chimie* (à paraître)

[1] D. Kolbah et D. Koruncev, «Methoden der organischen Chemie», Band X/2, Georg Thieme Verlag, Stuttgart, 1965, p. 89.

[2] H. Wolf et H. Westphal, *Liebigs Ann. Chem.*, **657**, 39 (1962).

[3] H. H. Szmant et C. McGinnis, *J. Amer. Chem. Soc.*, **72**, 2890 (1950).

[4] A. N. Kost et I. I. Grandberg, *Zhur. obshchei Khim.*, **25**, 2064 (1955).

[5] R. M. Dupeyre, H. Lemaire et A. Rassart, *J. Amer. Chem. Soc.*, **87**, 3771 (1965).

La formation des azines avec les aldehydes est plus facile qu'avec les cétones. La tendance de formation des azines diminue dans l'ordre suivant :

aldehyde > dialkylcétone > alkylarylcétone > diarylcétone.

L'emploi de l'hydrazine en excès permet d'éviter la formation des azines. Parfois sont utilisés des agents de condensation tels la triéthylamine, l'oxyde de baryum ou l'hydroxyde de sodium. [6,7]

D'autres produits secondaires formés lors de la synthèse des hydrazones non substituées proviennent des réactions de cyclisation, d'élimination, etc.. [8-11]

La séparation de l'hydrazone n'a plus lieu dans le cas de certains composés carbonyliques. [12,13]

En fonction du rapport molaire cétol : hydrazine, les cétols de la série de 2-hydroxy-8-R-tricyclo[$7.3.1.0^{2,7}$]tridécan-one-13 (I $R=H$; II $R=CH_3$) fournissent des paires d'hydrazone (III_α, III_β $R = H$; IV_α, IV_β $R=CH_3$) ou bien les azines correspondantes (V_α, V_β $R=H$; VI_α, VI_β $R=CH_3$) conformément au schéma 1 :

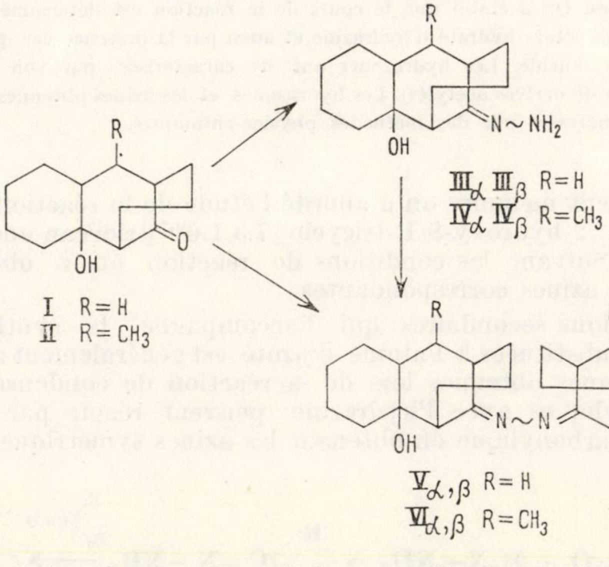

Ainsi, la réaction des cétols avec l'hydrate d'hydrazine de 100% en rapport 1 : 1,2 fournit presque quantitativement les hydrazones correspondantes III et IV. Dans le cas où le rapport molaire cétol : hydrate

---

[6] L. Braddock, *J. Org. Chem.*, **18**, 313 (1953).

[7] Weygand-Hilgetag, «Organisch-chemische Experimentierkunst », Johann Ambrosius Barth / Verlag, Leipzig, 1964, p. 575.

[8] B. Eistert et W. Schade, *Chem. Ber.*, **91**, 1411 (1958).

[9] R. Metze, *Angew. Chem.*, **68**, 580 (1956).

[10] A. N. Kost et R. S. Sagitullin, *Uspekhi Khim.*, **33**, 361 (1964).

[11] R. Bacon et W. Lintsay, *J. Chem. Soc.*, **1958**, 1375, 1382.

[12] C. Overberger et I. Hall, *J. Org. Chem.*, **26**, 4359 (1961).

[13] T. Kauffmann, G. Ruckelshauss et T. Schulz, *Angew. Chem.*, **75**, 1204 (1963).

d'hydrazine est 2 : 1 en présence de quantités catalytiques d'acide acétique la réaction conduit à la formation des azines symétriques correspondantes V et VI. On admet [3] que la présence de l'acide chlorhydrique ou de l'acide acétique favorise la formation de l'azine. En effet, si l'on conduit la réaction dans le même rapport molaire, mais en l'absence de l'acide acétique, les rendements en azine symétrique V ou VI sont très faibles. Les azines symétriques des cétols mentionnés peuvent être obtenues également à partir des hydrazones correspondantes en présence d'acide. Dans le tableau 1 sont présentées les hydrazones III, IV et les azines V et VI.

Tableau 1

Les constantes caractéristiques des hydrazones et des azines

Cétol	Hydrazone III, IV				Azine V, VI		
	η%	p.f^o·brut	Solvant	p.f^o·isomère	η%	Solvant	p.f^o·isomère
I	99	95–98	$CHCl_3$-éther de pétrole	77–81 90–92	96	MeOH	133–134 174–176
II	99	105–107	Et_2O	63–65 109–110	91	MeOH	112–113 173–174

Étant donné l'asymétrie de ces systèmes et l'existence de la liaison C=N–, les hydrazones III et IV peuvent présenter deux isomères notés conventionnellement par α et β et qui peuvent avoir les configurations suivantes :

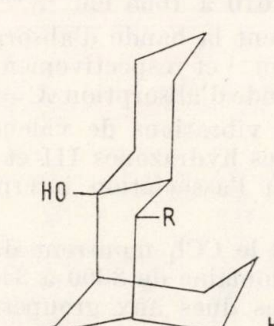

III$_\alpha$ R=H
IV$_\alpha$ R=CH$_3$

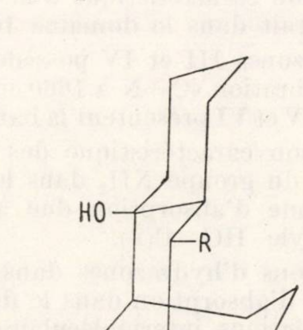

III$_\beta$ R=H
IV$_\beta$ R=CH$_3$

Dans les deux configurations on n'observe pas de liaison hydrogène intramoléculaire, car la distance des atomes qui pourraient être impliqués est trop grande. La séparation des hydrazones et aussi des azines isomères est difficile due à la facilité de transformation d'un isomère dans l'autre.

La séparation complète des hydrazones isomères III et IV par cristallisation fractionnée n'a pas été possible ; on a réussi seulement à obtenir une fraction enrichie d'un des isomères.

L'instabilité des hydrazones III et IV et leur tendance de transformation en azine pendant les opérations de recristallisation rendent encore plus difficile la séparation des isomères.

La présence de l'azine a été vérifiée par chromatographie sur couche mince. L'hydrazone de départ ne présente pas le spot caractéristique pour l'azine ; cependant il apparaît après la recristallisation. Par la suite on a essayé la séparation des isomères de l'azine. Ainsi, l'azine V par cristallisation fractionnée dans le méthanol fournit deux isomères de p.f. 133 – 134° et respectivement p.f. 174–176°. La plupart de l'azine V fournit par cristallisation fractionnée un produit de p.f. 152 – 153°.

Par cristallisation fractionnée dans le méthanol l'azine VI conduit à deux isomères de p.f. 173–174° et respectivement p.f. 112–113°.

Les isomères de bas point de fusion sont instables en se convertissant en isomères de haut point de fusion.

Dans les spectres I.R. des hydrazones et des azines de 2-hydroxy-8-R-tricyclo$[7.3.1.0^{2,7}]$tridécane-one-13 on peut observer l'apparition des vibrations caractéristiques du groupement hydrazone, respectivement azine. Ainsi, les spectres des hydrazones présentent la vibration $\nu C{=}N$ dans le domaine 1570 à 1650 cm^{-1} [14,15] et les vibrations symétrique et asymétrique du groupe NH_2 dans le domaine 3200 à 3400 cm^{-1}. [15–19]

L'absorption caractéristique à la vibration de valence $\nu C{=}N$ dans les azines apparaît dans le domaine 1610 à 1665 cm^{-1}. [15,20,21]

Les hydrazones III et IV possèdent la bande d'absorption caractéristique de la vibration $\nu C{=}N$ à 1660 cm^{-1} et respectivement à 1665 cm^{-1}. Les deux azines V et VI présentent la bande d'absorption $\nu C{=}N$ à 1655 cm^{-1}.

L'absorption caractéristique des vibrations de valence symétrique et asymétrique du groupe NH_2 dans les hydrazones III et IV est superposée à la bande d'absorption due à l'association intermoléculaire du groupe hydroxyle HO–C(2).

Les solutions d'hydrazones dans le CCl_4 montrent dans le spectre I.R. une bande d'absorption dans le domaine de 3300 à 3400 cm^{-1} attribuée aux associations intermoléculaires dues aux groupes NH_2 et OH. Dans les spectres I.R. des solutions diluées ($< 10^{-1}$M) des hydrazones dans le CCl_4 apparaissent les bandes caractéristiques aux vibrations

---

[14] B. V. Ioffe et L. M. Gerstein, *Zhur. org. Khim.*, **5**, 268 (1969).

[15] J. P. Chapelle, J. Elguero, R. Jacquier et G. Tarrago, *Bull. Soc. chim. France*, **1971**, 285.

[16] D. W. Scott, G. D. Oliver, M. E. Gross, W. N. Hubbard et H. M. Huffman, *J. Amer. Chem. Soc.*, **71**, 2293 (1949).

[17] J. W. ApSimon, P. V. Demarco et D. W. Mathieson, *Tetrahedron*, **26**, 119 (1970).

[18] B. V. Ioffe, V. S. Stopski et Z. V. Sergheva, *Zhur. org. Khim.*, **6**, 986 (1968).

[19] A. Krebs et H. Kimling, *Tetrahedron Letters*, **1970**, 761.

[20] L. D. Frederickson, *Analyt. Chem.*, **36**, 1349 (1964).

[21] J. Elguero, R. Jacquier et C. Marzin, *Bull. Soc. chim. France*, **1968**, 713.

ν NH_2 non associées à 3350 à 3400 cm^{-1} et ν OH non associé à 3600 à 3610 cm^{-1}.

La présence de l'hydrazone a été mise en évidence également par l'étude des spectres de R.M.N.

Ainsi, les spectres R.M.N. des hydrazones en solution dans le DMSO-d_6 montrent le signal des protons du groupe $=N-NH_2$ dans le domaine $\delta = 5{,}3-5{,}4$ ppm.

Les données de la littérature indiquent pour ces protons le domaine $\delta = 4{,}3-5{,}8$ ppm [18,22].

En solution dans le DMSO-d_6 en présence de T.F.A.-d_1, la résonance des protons du groupe $=N-NH_2$ est déplacée à $\delta = 6{,}2$ à 7,1 ppm (voir fig. 1) en accord avec la mobilité des deux protons.

La comparaison des spectres R.M.N. des hydrazones en solution dans le DMSO-d_6 et dans le DMSO-d_3 + T.F.A-d_1 permet de constater le déplacement de la résonance du proton HO—C(2).

Ainsi, son signal apparaît à $\delta = 3{,}6-3{,}64$ ppm en solution dans le DMSO-d_6 et se déplace à $\delta = 6{,}1-7{,}1$ ppm en solution dans le DMSO-d_6 + T.F.A-d_1 (voir fig. 1).

Les spectres R.M.N. des azines ne présentent plus le signal caractéristique des protons $=N-NH_2$ (voir fig. 2).

Les hydrazones III et IV ont été caractérisées également par leurs dérivés acétylés VII et VIII :

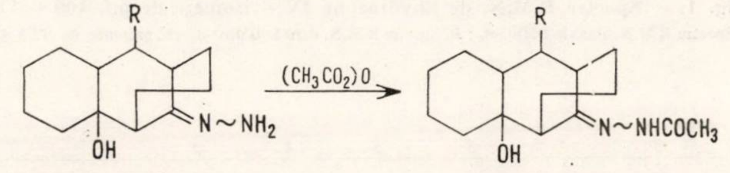

III_β R=H
IV_β $R=CH_3$

VII_β R=H
VIII_β $R=CH_3$

Après l'acétylation, les isomères III_β et IV_β fournissent les dérivés monoacétylés VII_β et VIII_β dont les caractéristiques sont présentées dans le tableau 2.

Tableau 2

Les constantes caractéristiques des dérivés acétylés

Hydrazone	Dérivé acétylé					
	M	p.f.°	ν $NHCOCH_3$ cm^{-1}			
III	264	213—214	1558	1680	3065	3250
IV	278	203—204,5	1562	1670	3058	3230

---

[22] B. A. Arbuzov, Yu. Yu. Samitov et P. Yu. Kitaev, *Izvest. Akad. Nauk S.S.S.R., Otdel. khim. Nauk.*, 1, 55 (1966).

Comparés aux spectres I.R. des hydrazones les spectres I.R. des dérivés acétylés montrent l'apparition de quelques bandes supplémentaires dues aux vibrations du groupement $NHCOCH_3$. Leurs valeurs sont présentées dans le tableau 2.

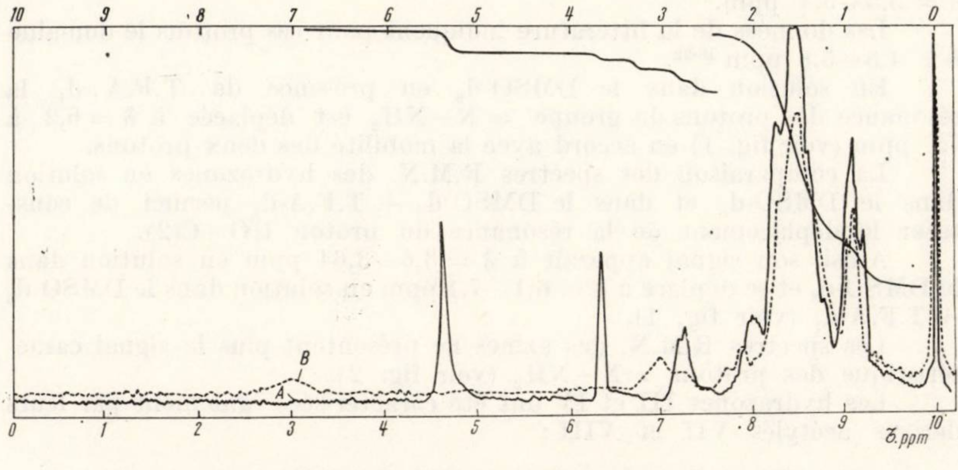

Fig. 1. — Spectre R.M.N. de l'hydrazone IV — isomère de p.f. 109 — 110°.
A, Spectre R.M.N. dans le DMSO-d_6 ; *B*, Spectre R.M.N. dans le DMSO-d_6 en présence de TFA-d_1

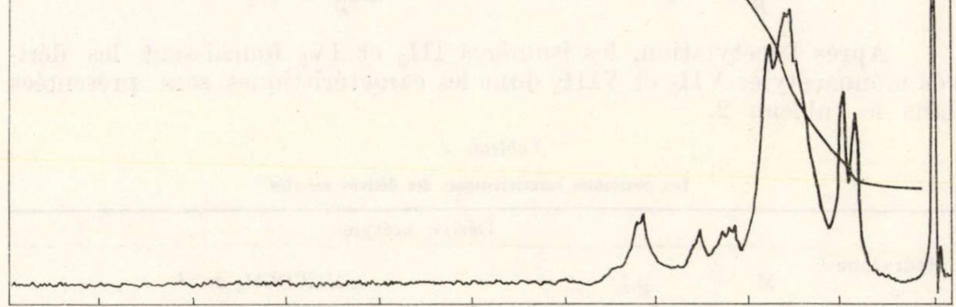

Fig. 2. — Spectre R.M.N. de l'azine VI dans le $CDCl_3$.

La réaction d'acétylation des hydrazones présente un intérêt particulier car elle permet la séparation de l'hydrazone à partir d'un mélange hydrazone-azine.

PARTIE EXPÉRIMENTAL

Les spectres I.R. ont été enregistrés avec un appareil U.R.—20 en utilisant la méthode en pastille de KBr ou les solutions dans le CCl_4.

Les spectres de R.M.N. ont été enregistrés avec un appareil Perkin-Elmer R—12 à 60 MHz avec le tétraméthylsilane comme étalon interne.

SYNTHÈSE DES HYDRAZONES III ET IV

Une solution de 0,022 moles de cétol (I ou II) dans 8 ml d'éthanol est traitée graduellement à une solution de 0,025 moles d'hydrate d'hydrazine de 100% dans 12 ml d'éthanol. Le mélange réactionnel est porté à l'ébullition au reflux pendant une heure et ensuite le solvant est distillé sous vide. On reprend le résidu par de l'éther de pétrole et après 24h de séjour à la température ambiante l'hydrazone cristallisée est filtrée.

On obtient avec un rendement de 99% des cristaux d'hydrazone III de p.f. 90—94°. Le produit est purifié par dissolution dans du chloroforme à froid et précipitation avec de l'éther de pétrole, en obtenant les hydrazones de p.f. 77—81°, et respectivement p.f. 90—92°.

$C_{13}H_{22}ON_2$ p.f. 77—81° *Calculé* N = 12,61% *Trouvé* N = 12,33%

$C_{13}H_{22}ON_2$ p.f. 90—92° *Calculé* N = 12,61% *Trouvé* N = 12,40%

L'hydrazone IV a été obtenue selon la méthode décrite plus haut. Le produit brut (Rd. 99%) de p.f. 105—107° fournit par cristallisation fractionnée dans l'éther les deux hydrazones de p.f. 63—65° et respectivement p.f. 109—110°.

$C_{14}H_{24}ON_2$ p.f. 63—65° *Calculé* N = 11,86% *Trouvé* N = 11,94%

$C_{14}H_{24}ON_2$ p.f. 109—110° *Calculé* N = 11,86% *Trouvé* N = 11,98%

SYNTHÈSE DES AZINES V ET VI

0,022 moles de cétol (I ou II) dans 8 ml d'éthanol sont traités par une solution de 0,011 moles d'hydrate d'hydrazine de 100% dans 20 ml d'éthanol. On introduit ensuite 1—2 gouttes d'acide acétique et le mélange réactionnel est porté à l'ébullition au reflux pendant 2h. Après l'élimination du solvant sous vide le résidu est repris à l'éther de pétrole. Les cristaux formés au bout de quelques heures sont filtrés. Dans le cas de l'azine V on a obtenu un produit brut de p.f. 124—128° (Rd. 96%). Par cristallisation fractionnée dans le méthanol on a réussi la séparation des deux isomères de p.f. 133—134° et respectivement p.f. 174—176°, mais en petites quantités. La plupart de l'azine est retrouvée sous forme d'un produit de p.f. 152—153°.

$C_{26}H_{40}O_2N_2$ p.f. 133—134° *Calculé* N = 6,79% *Trouvé* N = 7,17%

$C_{26}H_{40}O_2N_2$ p.f. 174—176° *Calculé* N = 6,79% *Trouvé* N = 7,10%

L'azine VI a été obtenue selon la même méthode (Rd. 91%). Par cristallisation fractionnée dans le méthanol il en résulte deux isomères de p.f. 112 — 113° et respectivement p.f. 173 — 174°.

$C_{28}H_{44}O_2N_2$ p.f. 112—113°; *Calculé* N = 6,36% *Trouvé* N = 6,59%

$C_{28}H_{44}O_2N_2$ p.f. 173—174°; *Calculé* N = 6,36% *Trouvé* N = 6,63%

SYNTHÈSE DES DÉRIVÉS ACÉTYLÉS VII ET VIII

Une solution de 0,009 moles d'hydrazone (III ou IV) dans 15 ml d'éthanol à chaud est traitée par 0,01 moles d'anhydride acétique. Le mélange réactionnel est chauffé à 80° pendant 15 mn et ensuite laissé pendant une heure à la température ambiante. Les cristaux du dérivé acétylé sont filtrés et lavés à l'eau. La synthèse donne des rendements quantitatifs dans le cas des deux hydrazones. L'hydrazone III donne un dérivé acétylé brut de p.f. 198—204° dont la recristallisation dans l'éthanol fournit des cristaux de p.f. 213—214°

$C_{15}H_{24}O_2N_2$ *Calculé* N = 10,60 % *Trouvé* N = 10,84 %

Le dérivé acétylé VIII brut de p.f. 198 à 199°, par recristallisation dans l'éthanol, fournit des cristaux de p.f. 203—204°.

$C_{16}H_{26}O_2N_2$ *Calculé* N = 10,07 % *Trouvé* N = 10,30 %

Revue Roumaine de Chimie, **19**, *5*, 877–880 (1974)

ON THE CONFORMATIONAL MOBILITY OF BICYCLO[3.3.1]NONANE-2-ONES AND BICYCLO[3.2.1]OCTANE-2-ONES

M. MORARU* and G. M. BENEDIKT**

*Department of Organic Chemistry of University, Splaiul Independenţei 89, Bucharest, Romania

**Institute of Organic Chemistry, Splaiul Independenţei 202B, Bucharest, Romania

Received June 15, 1973

The NMR study of the title ketones substituted with phenyl groups, using $Eu(DPM)_3$* as paramagnetic shift reagent is reported. Marked differences between the conformational mobilities of the two skeletons are revealed.**

Studies concerning the conformation of byciclo[3.3.1] nonanes have dealt either with qualitative correlations between conformation and spectral properties, [1] or with the evaluation of the position of equilibrium between chair-chair and chair-boat forms of substituted derivatives. [2,3] Much less attention has been given to bicyclo[3.2.1] octanes, except some considerations related to the reflex effect. [4] Presently, no comparison between the conformational mobilities of these systems is available, although recent "force field" calculations seem to indicate marked differences. [4,5] Thus, in agreement with the experimental values, the potential energy difference between chair-chair and chair-boat forms of bicyclo [3.3.1] nonane is 3.5–3.7 kcal/mole, much less than the calculated chair-boat difference of 5.8–6.2 kcal/mole for bicyclo [3.2.1] octane.

*** Europium(III)-tris(dipivaloylmethanato)

[1] M. Fisch, S. Smallcombe, J. C. Gramain, M. A. McKervey and J. E. Anderson, *J. Org. Chem.*, **35**, 1886 (1970) and the literature cited therein.

[2] E. N. Marvell and R. S. Knutson, *J. Org. Chem.*, **35**, 388 (1970).

[3] J. A. Peters, J. E. Remijnse, A. Van Der Wiele and H. Van Bekkum, *Tetrahedron Letters*, **1971**, 3065.

[4] J. Fournier and B. Waegell, *Tetrahedron*, **28**, 3407 (1972).

[5] E. N. Marvell, G. J. Gleicher, D. Sturmer and K. Salisbury, *J. Org. Chem.*, **33**, 3393 (1968).

In the present paper we wish to report an experimental evidence supporting the above considerations, the NMR study of bicyclic ketones I—IV.

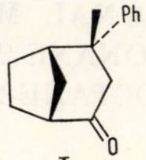

I

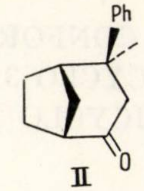

II

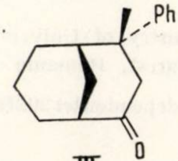

III

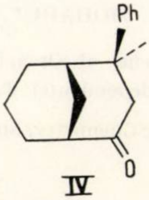

IV

The synthesis of these ketones is described in literature [6,7] and their configuration at C_4 is undoubtedly.

EXPERIMENTAL

The NMR study consisted in the gradual addition of weighed amounts of freshly sublimed $Eu(DPM)_3$ complex in the NMR tube containing a weighed amount (40—60 mg) of ketone, in CCl_4, each time waiting till the complex solved or helping it by gentle warming the tube in a water bath, and recording the spectrum (on a 60 Mc. VARIAN A 60-A NMR Spectrometer).

At the molar ratio (r_m), shift reagent per substrate, of 0.6 the main coupling constants and chemical shifts became readable.

RESULTS AND DISCUSSION

The vicinal coupling constants for compounds I and II show the normal trend for an essentially chair conformation of the six-membered ring (see table 1).

On the other side, $J_{3\alpha,4}$ and $J_{3\beta,4}$ for compounds III and IV are not consistent with a double chair conformation.

In the case of compound IV with an exo-phenyl group, the vicinal coupling constants are abnormally high for a chair conformation and they could be explained only by assuming a boat conformation or an equilibrium in which the boat is preferred. The epimeric ketone III exhibits vicinal coupling constants whose magnitudes do not correspond to axial-axial and axial-equatorial normal couplings. In this case it must be assumed either a distorted chair, in which the C_3 and C_7 atoms are spread apart more than in the parent hydrocarbon, or a conformational equilibrium in which the double chair form predominates.

---

[6] N. Bărbulescu and M. Moraru, *Rev. Chim. (Bucharest)*, **43**, 447 (1972).

[7] W. Dressler and K. Bodendorf, *Liebigs Ann. Chem.*, **720**, 71 (1968).

Table 1

Coupling constants: a) estimated from the normal spectrum, b) from the Eu(DPM)$_3$ shifted spectrum (at r_m = 0.6) (Hz.)

	$J_{3\alpha 4}$		$J_{3\beta,4}$		$J_{3\alpha,3\beta}$		$J_{4,5}$	
	a	b	a	b	a	b	a	b
I	11.7	12.4	6.6	6.0	15.2	16.0	2.4	—
II	6.0	8.8	3.4	1.3	16.0	16.8	—	4
III	10.3	—	9.1	—	16.8	—	3.3	—
IV	6.8	6.9	9.0	8.8	16.0	16.1	9.5	—

Further data on the conformation are given by the study of Eu (DPM)$_3$ induced shifts. The dependence of pseudocontact shifts with the lanthanide-proton distance and the proton-lanthanide-complexating heteroatom angle is well established, but any attempt to calculate molecular geometries from experimental data fails without a precise positioning of the lanthanide. [8] Attempts to optimize this position in some particular cases, using computer programs, have been made. [9] The above mentioned difficulty can be avoided by comparing the relative induced shifts of a given proton in structurally similar compounds such as I—IV.

The plots of δ (induced shift, in ppm) *versus* r_m were linear in the range of r_m 0—0.6 for all the compounds, that meaning that the conformation is not changed by complexation [10,11] (there is in fact a little change of the coupling constants as shown in table 1). The slopes of these plots (table 2) show some interesting points :

Table 2

Slopes $\Delta\delta/r_m$ in ppm

	I	II	III	IV	V
H_1	14.7	14.5	14.4	14.3	14.9
$H_{3\alpha}$	12.4	12.8	12.5	13.4	12.2
$H_{3\beta}$	13.1	14.7	12.5	12.2	—
H_4	6.0	4.6	5.3	5.5	—
H_0	2.1	5.9	2.7	2.7	6.6
$H_{m,p}$	0.7	0.7	0.5	0.8	0.4

a) All the compounds exhibit comparable values for the protons α as to carbonyl.

b) The slopes of *ortho*-aromatic protons in compounds I and II are in agreement with a chair conformation in both compounds, showing a marked difference between the axial and equatorial phenyl group.

---

[8] C. C. Hinckley, *J. Amer. Chem. Soc.*, **91**, 5160 (1969); J. K. Sanders and D. H Williams, *Chem. Comm.*, **1970**, 422; R. Von Ammon and D. Fischer *Angew. Chem.*, **84**, 737 (1972).

[9] F. A. Hart, J. Briggs, G. H. Frost, G. P. Moss, M. L. Staniforth, *Chem. Comm.*, **1970**, 1506; S. Farid, A. Ateya and M. Maggio, *Chem. Comm.*, **1971**, 1285; M. R. Willcot III, R. E. Lenkinski and R. E. Davis, *J. Amer. Chem. Soc.*, **94**, 1742 (1972).

[10] I. Fleming, S. W. Hanson and J. K. M. Sanders, *Tetrahedron Letters*, **1971**, 3733.

[11] M. R. Vegar and R. J. Wells, *Tetrahedron Letters*, **1971**, 2847.

Moreover, the values for II compare well with those reported for ketone V,[12] with an axial phenyl group.

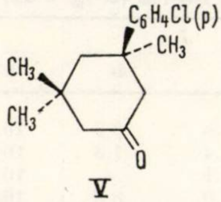

V

c) The compounds III and IV have identical slopes for ortho-aromatic protons, comparable with that of compound I and very different of that of compound II. This is in agreement only with a boat conformation of the substituted six-membered ring of compound IV, the keto and the phenyl group having a similar relative position as in compounds I and III.

d) The slopes for H_4 protons also indicate that the substituted ring adopts a chair conformation in compounds I, II, III and a boat conformation in compound IV, but the differences are not so marked as shown above.

All the above considerations lead to the following conformations of compounds I–IV (denoted by I'–IV'):

Concluding, all the data presented above suggest that the bicyclo [3.2.1] octane-2-one skeleton remains unaffected by bulky substituents (such as phenyl group) having a chair conformation of the six-membered ring, while the same substituents change dramatically the chair-boat equilibrium of the corresponding six-membered ring of bicyclo [3.3.1] nonane-2-one (some of its derivatives preferring a boat conformation). One can consider that the latter system has a greater conformational mobility than the former.

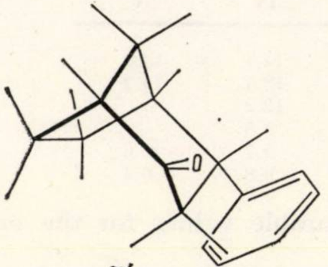

I'

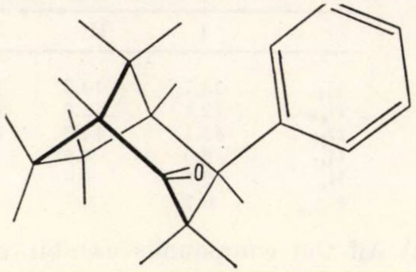

II'

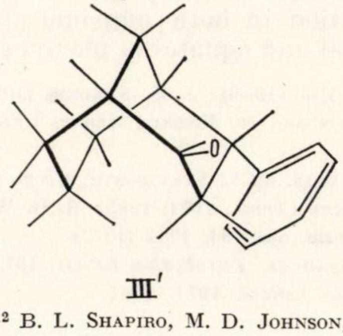

III'

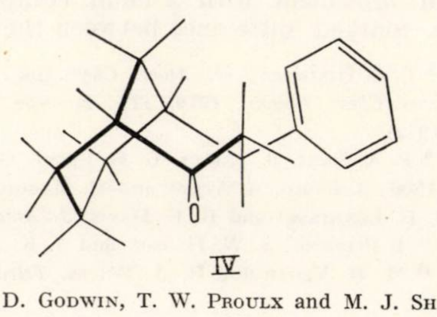

IV'

---

[12] B. L. Shapiro, M. D. Johnson, A. D. Godwin, T. W. Proulx and M. J. Shapiro, *Tetrahedron Letters*, **1972**, 3233.

Revue Roumaine de Chimie, **19**, *5*, 881–885 (1974)

TRIS-ÉTHERS. II[1]

CONDENSATION DU BIS(CHLOROMÉTHYL)ÉTHER AVEC DES CYCLOHEXYLPHÉNOXYDES, MÉTHYLCYCLOHEXYLPHÉNOXYDES ET CHLOROCYCLOHEXYLPHÉNOXYDES DE SODIUM

M. IOVU, G. CÎMPEANU et N. MICLOVICI

Faculté de Chimie, Université de Bucarest
89, Splaiul Independenţei, Bucarest

Reçu le 7 decembre 1972

Dans un article précédent on a montré la possibilité de condensation du bis(chlorométhyl) éther avec les phénoxydes alcalins anhydres dans les conditions dans lesquelles on a obtenu antérieurement une série de biséthers par la condensation des dérivés dichlorométhylés aromatiques avec des phénoxydes alcalins. La condensation du bis(chlorométhyl)éther avec du phénoxyde, des crésoxydes et xylénoxydes de sodium ayant lieu aisément en milieu anhydre d'alcool et benzène, on a passé à la condensation de certains cyclohexylphénoxydes des sodium avec du bis(chlorométhyl)éther. Il en résulte, travaillant dans les mêmes conditions, des tris-éthers dont la formule générale est $Ar-O-CH_2-O-CH_2-O-Ar$ où le noyau Ar est substitué par un radical cyclohexyle et en certains cas aussi par un radical méthyle ou chlore.

La méthode qui permet d'obtenir les phénoxydes alcalins anhydres par distillation azéotropique de l'eau résultée de la réaction des phénols avec les hydroxydes alcalins, utilisée pour obtenir des phénoxydes alcalins nécessaires à la condensation avec des dérivés dichlorométhylés aromatiques [2-5] a servi aussi à l'obtention de tris-éthers par la condensation des phénoxydes alcalins avec le bis(chlorométhyl)éther. [1]

Comme nous venons de démontrer dans un article antérieur [1] les phénoxydes alcalins anhydres résultent par la réaction du phénol avec les hydroxydes alcalins en milieu d'alcool et de benzène (proportion 1 : 1

---

[1] Ire partie : M. Iovu et G. Cimpeanu, *Rev. Roumaine Chim.*, **18**, 883 (1973).

[2] M. Iovu, *Rev. Roumaine Chim.*, **16**, 1223 (1971).

[3] M. Iovu et N. Nicolau, *Rev. Roumaine Chim.*, **16**, 1919 (1971).

[4] M. Iovu, *Rev. Roumaine Chim.*, **17**, 1261 (1972).

[5] M. Iovu, N. Miclovici et S. Creţu, *Rev. Roumaine Chim.*, **17** 1417, (1972).

en volumes) et l'élimination de l'eau par distillation azéotropique d'un mélange eau-alcool-benzène. Par exemple :

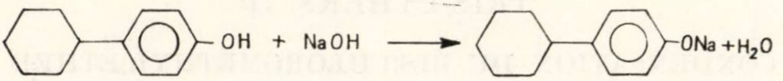

Au phénoxyde de sodium se trouvant dans le mélange benzène-alcool pas encore distillé, on ajoute du bis(chlorométhyl)éther

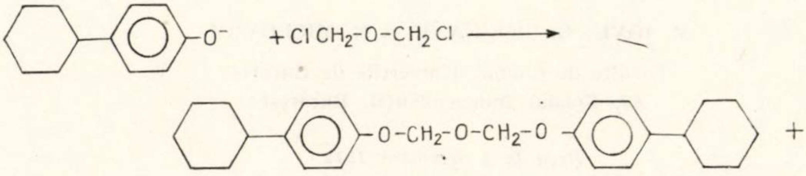

Le tris-éther et le chlorure de sodium qui en résultent précipitent. Le précipité est séparé du solvant, qui contient aussi de petites quantités de matières premières et de produits intermédiaires, par filtrage sous vide.

Le chlorure de sodium est éliminé du mélange de précipités par lavage à l'eau sur un filtre. Le tris-éther resté sur le filtre est séché et recristallisé toujours du mélange d'alcool et de benzène.

Dans les conditions mentionnées, le bis(chlorométhyl) éther a été condensé avec les sels de sodium du 2-cyclohexylphénol, 4-cyclohexylphénol, 2-cyclohexyl-4-méthylphénol, 4-cyclohexyl-2-méthylphénol, 2-cyclohexyl-4-chlorophénol et 2-chloro-4-cyclohexylphénol en obtenant 6 nouveaux tris-éthers ayant la formule générale : $Ar-O-CH_2-O-CH_2-O-Ar$ où le noyau Ar est substitué par un radical cyclohexyle ou par un radical cyclohexyle et un radical méthyle ou chlore.

RÉSULTATS ET DISCUSSIONS

Le tableau 1 comprend les formules des tris-éthers synthétisés, les résultats de l'analyse élémentaire de carbone, d'hydrogène et de chlore, les températures de fusion, les valeurs des longueurs d'onde et des coefficients molaires d'extinction obtenus lors de l'analyse en UV (en cyclohexane) aussi bien que les rendements.

Tous les tris-éthers sont solides et cristallins. Les températures de fusion des produits ayant le radical cyclohexyle en position *para* sont inférieures à leurs isomères correspondants ayant le radical cyclohexyle en position *ortho*.

Les spectres électroniques sont ressemblants à ceux des tris-éthers synthétisés antérieurement.[5] La substitution d'un radical méthyl par un radical cyclohexyle sur le noyau aromatique ne favorise pas des déplacements importants des maximums d'absorption. Mais la présence en même temps d'un radical cyclohexyle et d'un radical méthyle sur le même

Tableau 1

Tris-éthers

Formule		C % Calculé / Trouvé	H % Calculé / Trouvé	Point de fusion °C	λ_{max} mμ	ε_{max}	Rdt %
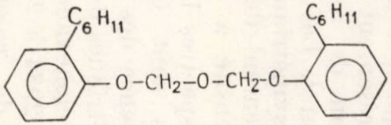	$C_{26}H_{34}O_3$	78,89 78,58	10,97 10,77	125	263 267 274	2200 2850 2650	79,45
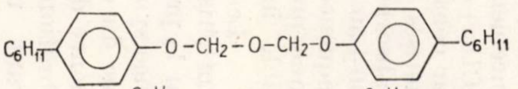	$C_{26}H_{34}O_3$	78,89 79,14	10,97 10,56	113–114	265,2 270,5 272 280,5	1850 2350 2700 2400	85,12
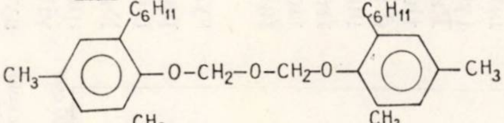	$C_{28}H_{38}O_3$	79,57 79,59	9,08 8,88	128	265 270 274 280	2900 2370 3300 2900	65,71
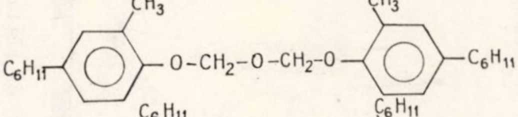	$C_{28}H_{38}O_3$	79,57 79,77	9,08 8,87	80–81	266,5 272 274,5 280	2400 3100 3200 2900	63,08
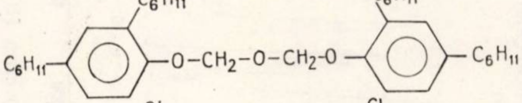	$C_{26}H_{32}O_3Cl_2$*	67,38 67,84	6,96 6,92	115	271,5 277 285	2900 3300 2800	66,46
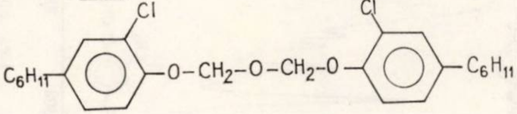	$C_{26}H_{32}Cl_2O_3$**	67,38 67,69	6,96 6,74	77	271,5 275 277 284	2700 3400 3450 3100	59,58

* Cl: *Calculé* 15,20% *trouvé* 5,30%
** Cl: *Calculé* 15,20% *trouvé* 4,81%

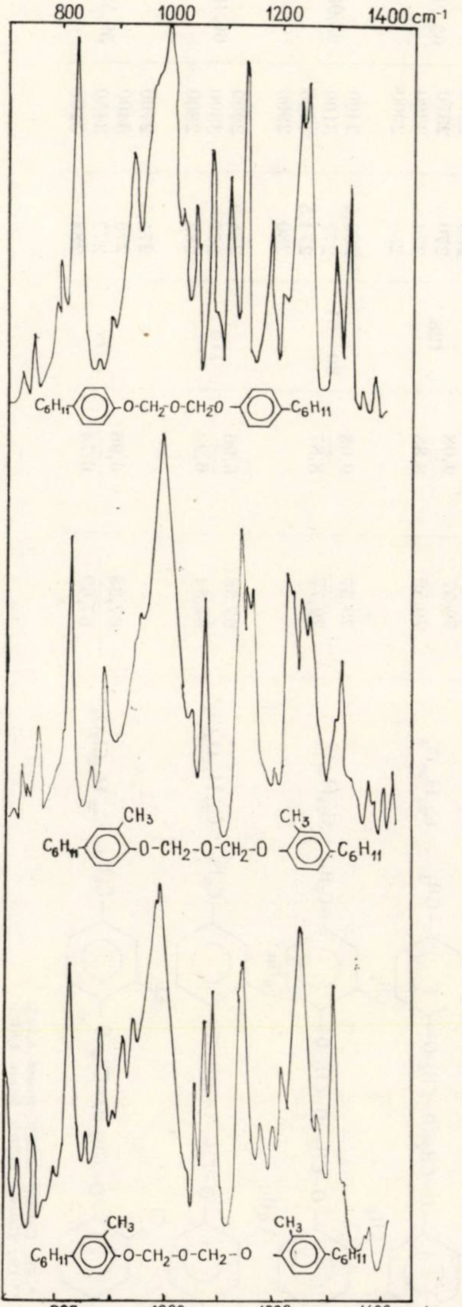

Fig. 1. — Les spectres IR du bis(4-cyclohexylphénoxyméthyl)éther, bis(2-méthyl, 4-cyclohexylphénoxyméthyl)éther et du bis (2-chloro, 4-cyclohexylphénoxyméthyl)éther.

noyau aromatique détermine un déplacement des maximums d'absorption vers des longueurs d'onde de 2 à 4 mμ plus grandes. La substitution du noyau aromatique par un atome de chlore cause un déplacement des maximums d'absorption vers des longueurs d'onde de 7,5 à 8 mμ plus grandes.

Les spectres IR mettent en évidence la présence des fonctions éther aliphatique $-CH_2-O-CH_2-$ et mixte $Ar-O-CH_2-$. Sur la figure 1 on peut suivre les spectres de certains composés synthétisés. Les bandes dues au ν_{asym} $C-O-C$ se trouvent entre 1240 et 1215 cm^{-1}. Tous les éthers synthétisés présentent une absorption très intense de 1240 à 1220 cm^{-1} due à la fréquence asymétrique de $C-O-C$ correspondant à l'éther mixte. De même, une absorption intense se manifeste de 1140 à 1130 cm^{-1}, due à la fréquence asymétrique d'éther aliphatique. Les bandes dues à la fréquence symétrique ν_{sym} $C-O-C$ d'éther mixte sont plus difficiles à identifier car dans cette région d'absorption a lieu aussi l'absorption due à la vibration de balancement en plan du groupe $-CH_2-$ (γCH_2r) de l'anneau cyclohexanique. Par conséquent tous les éthers synthétisés présentent une large bande d'absorption de haute intensité à 990 ± 30 cm^{-1}. Les bandes dues à la fréquence symétrique d'éther aliphatique présentent des absorptions de faible intensité à 940 à 920 cm^{-1}.

Les spectres IR des tris-éthers synthétisés sont bien caractérisés par la présence des vibrations de valence symétriques des groupes méthylène du cyclohexane ayant une fréquence de 2934 à 2853 cm^{-1} et de la vibration de valence asymétrique ayant une fréquence de 2930 à 2926 cm^{-1} (des bandes qui ne sont pas présentées sur la figure 1).

L'analyse thermogravimétrique indique une bonne stabilité des tris-éthers étudiés jusqu'à leur température d'ébullition. Dans le cas des produits sans chlore la perte de poids commence à 250 à 260° et se produit à grande vitesse au-dessus de 300°. Dans le cas des produits contenant du chlore, la perte commence à 300° et se produit rapidement au-dessus de 350°.

PARTIE EXPÉRIMENTALE

Le bis(chlorométhyl)éther a été obtenu en passant un courant d'acide chlorhydrique à travers une suspension de paraformaldéhyde en acide sulfurique concentré .[6]

Le 2-cyclohexylphénol, le 4-cyclohéxylphénol, le 4-méthyl-2-cyclohexylphénol et le 2-méthyl 4-cyclohexylphénol ont été obtenus par la cyclohexylation du phénol respectif, des crésols avec le cyclohexène en présence de $ZnCl_2$ anhydre et de l'HCl comme catalyseurs. [7]

Le 2-chloro 4-cyclohexylphénol a été obtenu par chloruration du 4-cyclohexylphénol avec le chlorure de sulfuryle .[7]

Le 4-chloro 2-cyclohexylphénol a été obtenu par la cyclohexylation du 4-chlorophénol avec le cyclohexène en présence de $ZnCl_2$ et HCl. [7]

Le cyclohexène a été obtenu par déshydratation du cyclohexanole en présence du H_3PO_4, la pureté étant contrôlée par chromatographie.

Le phénol, les crésols et le 4-chlorophénol ont été des produits commerciaux.

Les spectres IR ont été obtenus en tablettes de KBr en utilisant un appareil Karl Zeiss-Jéna.

Les spectres UV ont été obtenus en cyclohexane en utilisant un appareil CF-Optica Milano.

L'analyse thermogravimétrique a été effectuée à l'acide d'un dérivatographe de type Pauli.

LA SYNTHÈSE DU BIS(2-CYCLOHEXYL-PHÉNOXYMÉTHYL) ÉTHER

Dans un ballon de 50 ml, ayant deux cols et muni d'un réfrigérant ascendant et d'un thermomètre, on a introduit 3,524 g de 2-cyclohexyl-phénol (1/50 moles), 0,808 g NaOH (1/50 moles) avec un excès de 1/5000 moles et 30 ml de mélange d'alcool-benzène (1 : 1 en volumes) et on a chauffé jusqu'à l'ébullition et à la totale réaction du cychlohexyl-phénol avec l'hydroxyde de sodium (2 heures). On a remplacé ensuite le réfrigérant ascendant par un réfrigérant descendant et on a distillé 15 ml de mélange d'alcool-benzène-eau afin d'éliminer l'eau. On a ajouté 1,650 g (1/100 moles) de bis(chlorométhyl)éther et on a monté un réfrigérant ascendant. On a chauffé à reflux pendant 3 heures afin d'assurer la formation complète du tris-éther. (Tout d'abord la réaction a été violente). Ensuite on a laissé refroidir le contenu du ballon à la température ambiante, on l'a filtré sur un filtre G—2 et on a lavé le précipité constitué par le tris-éther et le NaCl avec 1 ml éthanol, puis plusieurs fois par de l'eau, pour éliminer le NaCl. Pour le séchage on a lavé le précipité sur le filtre avec 2 à 3 ml d'éthanol. Après le séchage ont résulté 2,800 g de bis(2-cyclohexylphénoxyméthyle) éther. Le rendement est de 79,45%. Après deux recristallisations du mélange d'alcool-benzène (50% en volumes) le produit a eu la température de fusion de 125°.

Les autres éthers, mentionnés dans le tableau 1, ont été synthétisés de façon identique.

---

[6] H. Schneider, *Z. anorg. Chem.*, **51**, 274 (1938).

[7] M. Iovu, M. Manolescu et N. Miclovici, *Bull. Soc. chim., France.*, **11**, 4004 (1970).

L'analyse thermogravimétrique indique une bonne stabilité des [illegible] jusqu'à leur température d'ébullition. Dans le cas des [illegible] la perte de poids commence à 150 à 200 °C et se produit à grande vitesse au-dessus de [illegible]. Dans le cas des produits contenant du chlore, la perte commence à 200° et se produit rapidement au-dessus de 250°.

PARTIE EXPÉRIMENTALE

[illegible]

Le [illegible] a été obtenu par la cycloalkylation du [illegible] en présence de $ZnCl_2$ [illegible]

[illegible] a été obtenu par la cycloalkylation du [illegible] avec le cyclohexène en présence de $ZnCl_2$ et HCl [illegible].

Le cyclohexène a été obtenu par déshydratation du cyclohexanol en présence de H_3PO_4, la pureté étant contrôlée par chromatographie.

Le phénol, les crésols et le p-chlorophénol ont été des produits commerciaux.

Les spectres IR ont été obtenus en tablettes de KBr en utilisant un appareil Karl Zeiss Iena.

Les spectres UV ont été obtenus en cyclohexane en utilisant un appareil [illegible]

L'analyse thermogravimétrique a été effectuée à l'aide d'un [illegible]

LA SYNTHÈSE DE [illegible]

[illegible]

[illegible]

[illegible]

Revue Roumaine de Chimie, **19**, 5, 887–901 (1974)

ÜBER DEN EINFLUSS DER ELEKTROLYTEN AUF DIE ZÄHIGKEIT DER POLYVINYL-ALKOHOL-LÖSUNGEN

C. HÖLSZKY*, COSTELA SUCIU**, D. SĂNDULESCU***

* Institut für Erdöl, Ploieşti
** D. Bolintineanu-Schule, Bukarest
*** Institut für Erdöl, Gas und Geologie, Bukarest, str. T. Vuia nr. 6

Eingegangen am 23. Juni 1973

Es wurden Löslichkeitsmessungen von Polyvinylalkohol (PVA) in elektrolytischen Lösungen von LiCl, NaCl, KCl, NH_4Cl, $MgCl_2$ $CaCl_2$ durchgeführt und die negativen Setchenow-Aussalzungskoeffizienten bei 20° bestimmt. Die Viskositätsbestimmungen dieser Lösungen führten zur B-Koeffizientbestimmung der Jones-Dole Gleichung und gleichsam zur Bestimmung der Veränderung dieser Größe in Abhängigkeit der PVA-Konzentration. Die bemerkte Senkung durch die Struktur der Elektrolytlösungen und der PVA-Elektrolytlösungen im Wasser ist erläutert. Die Grenzviskositätsberechnung $[\eta]$ zeigt eine anionische Ausdehnung der PVA-Ketten in $CaCl_2$-Lösungen, im Verhältnis von NaCl-Lösung an.

In letzter Zeit wurden zahlreiche experimentale und theoretische Studien betreffend den „Verflüssigungseffekt“ („drag reduction“) bekannt. Diese Studien befassen sich demnach mit dem hervorgerufenen Wachsen der volumetrischen Durchflußmenge einer wässerigen Lösung bei gleichem Druckunterschied, die durch Zugabe von kleinen Mengen von makromolekularen Verbindungem mit großem Molekulargewicht wie Polyäthylenglykol, Carboximethylzellulose, Separan (teilweise hydrolisiertes Polyakrylamid) verursacht wird.[1–3]

Die eventuelle Verwendung des Polyvinylalkohols (P.V.A.) zur Verbesserung der rheologischen Eigenschaften der Bohrschlämme hat uns zu einem Studium betreffend den Einfluß der Elektrolyten auf die Zähigkeit der P.V.A.-Lösungen sowie auf den Aussalzungseffekt angeleitet.

Die Angaben betreffend den Einfluß der Elektrolyten auf die Zähigkeit der wässerigen P.V.A.-Lösungen sind sehr beschränkt, obwohl diese Effekte allgemein ein bedeutendes Forschungsgebiet in der Flüssigkeitslehre darstellen; diese Effekte entsprechen den in wässerigen Lösungen eintretenden Strukturveränderungen sowohl der aufgelösten Stoffe als auch des Wassers, und kann somit über das Wesen und die

---

[1] J. Rodriguez, J. Zakin und G. Patterson, *Soc. Petroleum Eng. J.*, **7**, 325 (1967).

[2] G. Patterson, J. Zakin und J. Rodriguez, *Ind. Eng. Chem.* **61**, 22 (1969).

[3] N. Sylvester und J. Tayler, *Ind. Eng. Chem. Prod. Res. Develop.* **9**, 548 (1970).

gegenseitige Wirkungsstärke Lösungsmittel-aufgelöster Stoff Auskunft geben.

Von diesem Standpunkt ist das Wasser eine einzigartige Flüssigkeit da es die Fähigkeit besitzt mittels Wasserstoffbindungen quasikristallartige Raumgitter zu bilden. Obwohl über das Wasser und die wässerigen Lösungen sehr viel geschrieben wurde, bildet die sichere Struktur des reinen flüssigen Wassers und der wässerigen Lösungen den Gegenstand vieler Widersprüche.[4-6]

Im allgemeinen sind die wässerigen Lösungen von Nichtelektrolyten durch Bildung von Klatraten oder durch die Verstärkung der Struktur des normalen Wassers[7,8] dem Effekt der hydrofoben Hydratation zu Folge, zu erklären.[9]

Sicherlich ist das Erscheinen rings um die Kettenteile der Makromoleküle von in einer anderen als die bei reinem Wasser normalen lokalen Anordnung geliederten Wassermolekülschichten möglich, mittels einer vielleicht vollkommen unbekannten Strukturinduktion[10,11] unter fortdauerndem Zerreissen, Entformung und Wiederherstellung.[12,13]

Es is bekannt, daß der P.V.A. sowohl im festen Zustand als auch in wässerigen Lösungen eine Gitterstruktur aus Inter- und intramolekulären Bindungen bestehend, aufweist.[14-17] Demzufolge ist es umso interessanter den Einfluß der Elektrolyte auf die Zähigkeit der wässerigen Lösungen und im Vergleich mit polymerlosen wässerigen Lösungen welche niedrige Alkohole, Dioxan, Dimethylsulphoxyd, Harnstoff u.s.w. enthalten, festzustellen.

EXPERIMENTALTEIL

Polyvnylalkohol (P.V.A.) durch K-Wert (Fikentscher) $=75$ gekennzeichnet (mittlere Molmasse $\overline{M}_\eta \approx 85000$)

Destilliertes Wasser.

Elektrolyten : $LiCl.2H_2O$, $NaCl$, KCl, NH_4Cl, $MgCl_2.6H_2O$, $CaCl_2$ anh., Erzeugnisse p.a. von ,,Reactivul" oder ,,Merck". Die Konzentration der Lösungen der stark hygroskopischen Li, Mg und Ca-Salze wurde auch durch Titration des Cl-Ions geprüft.

---

[4] F. Franks und D. Ives, *Quart. Rev.* **20**, 1 (1966).

[5] F. Franks und W. Wen, *Discuss. Faraday Soc.* **24**, 133 (1957).

[6] G. Némethy und H. Scheraga, *J. Chem. Phys.*, **36**, 3401 (1967).

[7] D. Glew, *J. Phys. hem.* **66**, 605 (1962).

[8] W. Wen und S. Saito, *J. Phys. Chem.* **68**, 2639 (1964).

[9] F. Franks, Ann. New York *Acad. Sci.*, **125**, 277 (1965).

[10] R. Horne, *Nature* **200**, 418 (1963).

[11] R. Horne und J. Birkett, *Electrochim. Acta* **12**, 1153 (1967).

[12] A. Narten, M. Dandord und A. Levy, *Discuss. Faraday Scc.* **43**, 97 (1967).

[13] J. Pople, *Proc. Roy. Soc. A* **205**, 163 (1951).

[14] E. Nagai und N. Sagane, ,,Annual Meeting of High Polymers" Tokyo June 1957, p. 27.

[15] S. Matsumoto und K. Insi, *Chem. High Polymers* (Japan) **15**, 160 (1958).

[16] S. Nohara, *Chem. High Polymers* (Japan) **15**, 105 (1958).

[17] H. Moeda, T. Kawai und M. Sekii, *J. Polymer Sci.* **35**, 288 (1959).

Bestimmung der Löslichkeit der Polymeren. Zu gleichen Volumen der obigen verschieden konzentrierten Elektrolytlösungen wurde tropfenweise eine 2%-ige P.V.A.-Lösung bis zum Erscheinen des Polymerniederschlages zugefügt. Die Löslichkeitsschwelle des sich in Lösung befindenden Polymers wird durch Wiedererrechnung der Kozentration des Elektrolytes festgestellt.

Die Zähigkeitsbestimmungen wurden bei 25° ± 0,05° in einem Ostwald-Kapilarviskosimeter durchgeführt. Die Ergebnisse wurden auf Grund von(H_2O bei 25°) $\eta = 0{,}8903$ cP berechnet. Die Korrekturen der kynetischen Energie wurden vernachlässigt (Fließdauer des Wassers 60,0 Sek.). Die Wiederholbarkeit der Ergebnisse der Zähligkeitsbestimmungen war besser als ± 0,2%.

ERGEBNISSE

Die Tabelle Nr. 1 enthält die Ergebnisse der Aussalzung des P.V.A. bei 25° mit NaCl, KCl und NH_4Cl. Im Falle $MgCl_2$ und $CaCl_2$ wurde kein P.V.A.-Niederschlag bemerkt.

Tabelle 1

Konzentration des Elektrolytes dem Polyvinylalkohol-Ausfällungspunkt entsprechend

Na Cl		KCl		NH_4 Cl	
Gew. % Salz	Gew. % Polymer	Gew. % Salz	Gew. % Polymer	Gew. % Salz	Gew. % Polymer
14,40	0,068	16,50	0,058	25,0	0,214
12,80	0,095	14,51	0,077	21,70	0,276
10,91	0,181	12,83	0,113	18,60	0,333
9,13	0,260	10,82	0,181	15,07	0,461
6,26	0,610	7,86	0,470		

Tabelle Nr. 2 enthält die Ergebnisse der Zähigkeitsbestimmungen der P.V.A.-Lösungen in Gegenwart von folgenden Elektrolyten: NaCl, KCl, NH_4Cl, LiCl, MgCl, $MgCl_2$, $CaCl_2$ — bei 25°.

DISKUSSIONEN

Der Aussalzungseffekt kann durch Übereinanderlegen der Hydrationsprozesse der Ionen und der unterschiedlichen Polarisation des Wassers und der Nichtelektrolytmoleküle, folglich größtenteils rein elektrostatische Effekte, aber auch durch spezifische Lösungseffekte und Dispersionseffekte erfolgen. [18–21]

---

[18] B. Conway, J. Desnoyers und A. Smith, *Phil. Trans.* A **256**, 389 (1964).

[19] J. Desnoyers und F. Ichaperia, *Canad. J. Chem.* **47**, 4639 (1969).

[20] J. O'M. Bockris, J. Bowler-Reed und J. Kitchener, *Trans. Faraday Soc.* **47**, 184 (1951) .

[21] F. Long und W. Mc Devitt, *Chem. Rev.* **51**, 119 (1952).

Tabelle 2

Dynamische Viskosität bei 25° (cP) der P.V.A.-Lösungen in Gegenwart von Elektrolyten

Molalität der Elektrolytlösung. / Konzentration der Polymerlösung, %	Ohne Elektrolyt.	NaCl			KCl	NH_4Cl	LiCl	$MgCl_2$		$CaCl_2$			
		0,4	0,8	2,1	1,2	1,2	1,2	1,2	3,5	0,6	1,2	3,5	6,0
2	4,155	4,048	—	—	—	3,683	4,598	—	—	4,667	5,610	11,040	25,929
1	1,946	1,932	1,698*	—	1,773	1,816	2,233	2,900	4,803	2,263	2,670	5,848	14,051
0,5	1,310	1,337	1,359	1,370	1,248	1,274	1,535	1,969	3,069	1,537	1,826	3,835	10,516
0,25	1,078	1,107	1,128	1,162	1,055	1,060	1,271	1,589	2,685	1,256	1,509	3,210	9,159
0,125	0,976	1,008	1,039	1,078	0,955	0,986	1,147	1,490	2,514	1,151	1,374	2,916	8,577
0	0,890	0,929	0,958	0,995	0,907	0,885	1,049	1,344	2,148	1,045	1,259	2,706	0,873

* bei einer Konzentration der Polymerlösung von 0,8%,

Die für die Löslichkeit des P.V.A. erhaltenen Werte entsprechen dem Setchenow Gesetz

$$\lg \frac{s}{s_0} = km$$

wo $k < 0$ für die Aussalzung (salting out) mit der im allgemeinen anerkannten Regel übereinstimmend, s und s_0 die Löslichkeit des Polymers in der Elektrolytlösung von Molalität m, beziehungwseise $m = 0$.

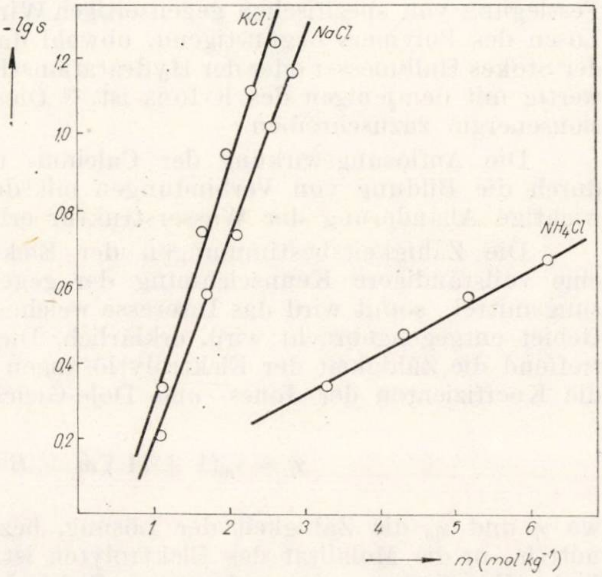

Abb. 1. – Prüfung der Setchenow'schen Gleichung.

Abb. 1 stellt die lineare Variation des lg s abhängend von der Molalität der Elektrolyten NaCl, KCl und NH_4Cl dar, die Gültigkeit des Setchenow-Gesetzes bestärkend und ergibt für die Aussalzungskonstanten bei 25°C die Werte :

für KCl $k = -0{,}65(\pm 0{,}02)\mathrm{Kg\,Mol^{-1}}$;
für NaCl $k = -0{,}55\,(\pm 0{,}02)\mathrm{Kg\,Mol^{-1}}$;
für NH_4Cl $k = -0{,}11\,(\pm 0{,}01)\mathrm{Kg\,Mol^{-1}}$

(für den entsprechenden Konzentrationsbereich).

Im Falle der Elektrolyten $MgCl_2$ und $CaCl_2$ konnte keine Aussalzungsschwelle festgestellt werden bis $c = 2\%$ Polymer.

Diese Werte ermöglichen die beiläufige Berechnung der freien Überführungs-Enthalpie aus dem Wasser in die Elektrolytlösung des Polymers :

$$\Delta G = -\mathrm{RT}\ln\frac{\gamma_0}{\gamma} = -\mathrm{RT}\ln\frac{s}{s_0} = -2{,}3\,\mathrm{RT}\,km$$

wo γ_0 und γ die Aktivitäts-Koeffizienten des Polymers in Wasser bezw. in der Elektrolytlösung darstellen.

Für m = 1 Mol Kg^{-1} Elektrolyt ergibt sich bei 25°

ΔG (1m KCL Lösung) = +3700 ± 100 $J.mol^{-1}$

ΔG (1m NaCl Lösung) = + 3100 ± 100 $J.mol^{-1}$

ΔG (1m NH_4Cl Lösung) = + 650 ± 50 $J.mol^{-1}$ (extrapoliert).

Die berechneten Werte stimmen nicht genau mit den freien Überführungs-Enthalpien überein, sie ermöglichen jedoch die unmittelbare Festlegung von spezifischen gegenseitigen Wirkungen des NH_4^+-Ions, das Lösen des Polymers begünstigend, obwohl das ionische Potential, bezw. der Stokes Halbmesser oder der Hydratations-Halbmesser praktisch gleichwertig mit demjenigen des K-Ions ist.[22] Diese Effekte sind der Dispersionsenergie zuzuschreiben.

Die Auflösungswirkung der Calcium- und Magnesium-Ione kann durch die Bildung von Verbindungen mit den P.V.A. oder durch eine wichtige Abänderung der Wasserstruktur erläutert werden.

Die Zähigkeitsbestimmungen der Elektrolytlösungen ermöglichen eine vollständigere Kennzeichnung der gegenseitigen Wirkung Ion-Lösungsmittel, somit wird das Interesse welches in der letzten Zeit diesem Gebiet entgegengebracht wird, erklärlich. Die theoretischen Studien betreffend die Zähigkeit der Elektrolytlösungen versuchen im wesentlichen die Koeffizienten der Jones- und Dole-Gleichung[23] zu deuten

$$\eta = \eta_0(1 + A \sqrt{m} + B\, m)$$

wo η und η_0 die Zähigkeit der Lösung, beziehungsweise des Lösungsmittels, m die Molalität des Elektrolyten ist, während A und B spezifische Koeffizienten des aufgelösten Elektrolyten sind. Diese Gleichung wurde sehr gut studiert, besonders um eine Beziehung zwischen den Werten von A oder B und den Eigenschaften der Ionen festzustellen.

In zahlreichen Studien[24–26] wurde bewiesen, daß das Glied $A\sqrt{m}$ von der ionischen Wechselwirkung bestimmt ist und mittels der Debye-Hückel-Theorie berechnet werden kann.[27] Ohne eine präzise theoretische Erklärung ist man zu dem Schluß gekommen, daß B das Resultat der Wechselwirkung Ion-Lösungsmittel bezeichnet.

Im allgemeinen ist $\frac{A}{B} \ll 1$,[28] so daß das Glied welches A enthält bei Konzentrationen über 2.10^{-3} m vernachlässigt werden kann, während die Gleichung linearen Charakter bekommt:

---

[22] E. Nightingale Jr., *J. Phys. Chem.* **63**, 1381 (1959).

[23] G. Jones und M. Dole, *J. Amer. Chem. Soc.* **51**, 2950 (1929).

[24] H. Falkenhagen und M. Dole, *Phys. Z.* **30**, 611 (1929).

[25] H. Falkenhagen und E. Vernon, *Phil. Mag.* **14**, 537 (1932).

[26] H. Falkenhagen, *Phys. Z.* **32**, 745 (1931).

[27] L. Onsager und R. Fuoss, *J. Phys. Chem.* **36**, 2689 (1932).

[28] R. Kay, T. Vituccio, C. Zawoyski, und D. Evans, *J. Phys. Chem.* **70**, 2336 (1966).

$$\frac{\eta - \eta_0}{\eta_0} = Bm$$

Somit ist die unmittelbare Berechnung des Wertes des Koeffizienten B möglich. Abb. 2 ist die graphische Darstellung der Gleichung für LiCl, NaCl, KCl, NH_4Cl bei verschiedenen Konzentrationen *c* des P.V.A. Es muß beobachtet werden, daß im Falle von Lösungen in reinem Wasser ($c = 0$) die Werte der Koeffizienten *B* mit den bekannten Werten übereinstimmen,[29-31] während unter dem Einfluß des Polymers der Wert von B sinkt, in Übereinstimmung mit Abb. 3.

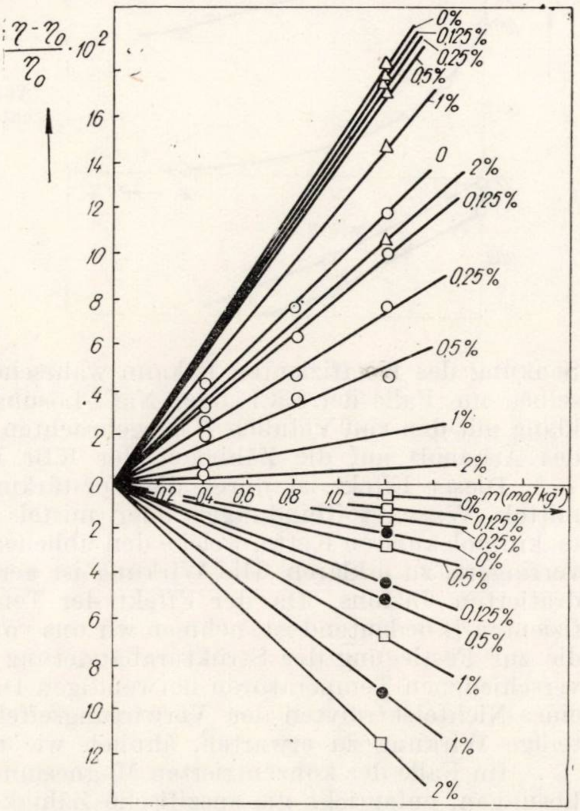

Abb. 2. — Graphische Darstellung der Gleichung $\frac{\eta - \eta_0}{\eta_0} = Bm$ für Elektrolytlösungen bei 20°: Δ — LiCl; ○ — NaCl; ● — KCl; □ — NH_4Cl.

Die Anzahl der Studien betreffend die Wirkung der Nichtelektrolyten auf die Zähigkeit der wässerigen Elektrolytlösungen ist gering.[32]

---

[29] W. Cox und J. Wolfenden, *Proc. Roy. Soc.* A **145**, 475 (1934).

[30] M. Kaminsky, *Discuss Faraday Soc.* **24**, 171 (1957).

[31] V. Asmus, *Z. Naturforsch.* **49**, 589 (1949).

[32] B. Oliver und A. Campbell, *Canad. J. Chem.*, **47**, 4207 (1969).

Es ist der bedeutende Effekt des Polymers auf die Struktur der Lösung im Falle NaCl zu bemerken und mit dem Falle der anderen Elektrolytlösungen in welchen die Wirkung ähnlich ist, zu vergleichen. Die Senkung des Koeffizienten B kann wahrscheinlich zu negativen Werten, selbst im Falle der LiCl- oder NaCl-Lösungen führen. Dies ist im Einklang mit den von Vidulich [33] dargebrachten Daten im Falle der Wirkung des Äthanols auf die Zähigkeit der KBr Lösungen.

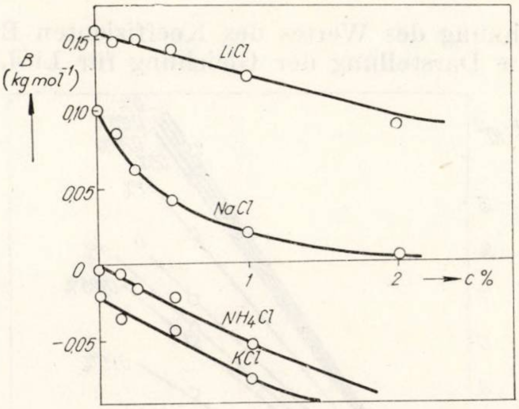

Abb. 3. — Abhängigkeit des Koeffizienten B der Elektrolytlösungen von der Konzentration des P.V.A.

Dieser Effekt ist durch die Verstärkung der Struktur von P.V.A. mittels Wasserstoffbindungen oder mittels hydrofoben Bindungen der makromolekularen Kette, welche den üblichen Effekt der Ionen im Wasser verringert, zu erklären. Die Wirkung ist geringer im Falle des stark hydratierten Li-Ions. Da der Effekt der Temperatur im Falle des Koeffizienten B bedeutend ist, nehmen wir uns vor in einem weiteren Studium die zur Festlegung der Strukturabänderung der geprüften Lösungen bei verschiedenen Temperaturen notwendigen Daten festzulegen. Bei Zugabe eines Nichtelektrolyten der Verwirrungseffekte ausübt, ist eine gegenteilige Wirkung zu erwarten, ähnlich wie beim Dioxan. [32]

Im Falle der konzentrierten Magnesiumchlorid- und Calciumchlorid-Lösungen, entspricht die spezifische Zähigkeit einer polinomialen Gleichung der From:

$$\frac{\eta - \eta_0}{\eta_0} = Bm + Cm^2 + Dm^3 + \dots$$

welche auch der Wechselwirkung der in der Lösung befindlichen Ionen entspricht (Abb .4).

Auch in diesen Fällen ist eine Senkung der Koeffizienten B im Zwischenraum $m = 0 \dots 2$ Mol.Kg^{-1} zu beobachten, doch ist diese Senkung bei der Polymerzugabe viel geringer als im Falle der Li^+, Na^+, K^+, NH_4^+-Ionen, wegen dem kräftigen Feld der Mg^{2+} und Ca^{2+}-Ionen.

---

[33] G. VIDULICH, G. ANDRADE, P. BLANCHETTE und T. GILLIGAN, *J. Phys. Chem.* **73**, 1621 (1969).

Wie schon früher bemerkt wurde, entspricht der Wert des Koeffizienten B der Wechselwirkung Lösungsmittel-Ion und kann eine Bewertung des durch das Ion hervorgerufenen Ordnungs- bezw. Unordnungsgrades der Lösungsmittelstruktur ermöglichen.[5,34] So haben die Li^+, Na^+, Ca^{2+}, Mg^{2+}-Ionen in polymerlosem Wasser positive B-Koeffizienten, was einem ordnungshervorrufenden Effekt entspricht, während NH_4^+, K^+, Cl^--Ionen negative (verhältnismäßig kleine) Koeffizienten haben, folglich wirken sie Verwirrung-hervorrufend auf die Struktur des Wassers. In einigen Veröffentlichungen wurden sogar die Ausdrücke „positive oder negative Hydratation“ eingeführt, um diese Effekte zu bezeichnen.

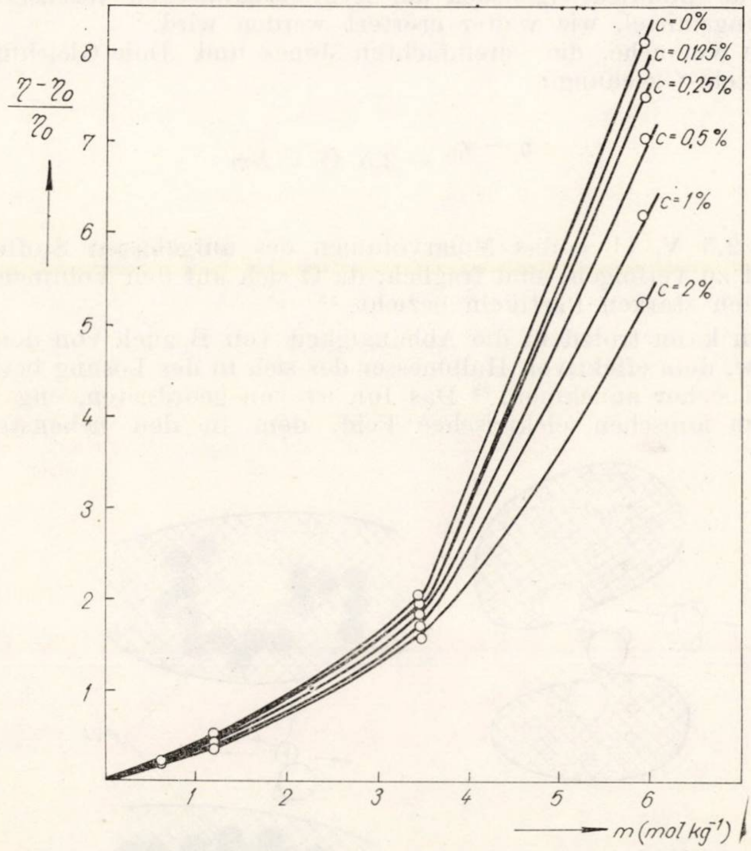

Abb. 4. — Abänderung der spezifischen Viskosität der $CaCl_2$-Lösungen bei 20°.

Eigentlich muß in diesem Falle der Begriff „Ordnung-hervorrufend“ und „Verwirrung-hervorrufend“ oder „Strukturierung“ und „Entstruk-

---

[34] H. Rüterjans, F. Schreiner, V. Sage und T. Ackerman *J. Phys. Chem.* **73**, 986 (1969).

turierung“ mehr als ein dem Sinken bezw. Wachsen der freien Translationsmöglichkeiten der Wasserstoffmoleküle entsprechender Begriff angesehen werden, also als ein sich in der Zeit abspielender Durchschnittseffekt. Das entspricht eigentlich der hydrodynamischen Wechselwirkung Ion-Lösungsmittel, wie weiter erörtert werden wird.

Die Versuche, die vereinfachten Jones und Dole-Gleichung mit der Einstein-Gleichung :

$$\frac{\eta - \eta_0}{\eta_0} = 2{,}5\ \emptyset = Bm$$

wo $B = 2{,}5$ V, (V = das Molarvolumen des aufgelösten Stoffes) vergleichend zu verfolgen, sind fraglich, da $\emptyset$ sich auf den Volumenteil der sphärischen starken Partikeln bezieht. [35]

Man kann trotzdem die Abhängigkeit von B auch von dem Volumen bezw. dem effektiven Halbmesser des sich in der Lösung befindenen Iones als sicher annehmen. [22] Das Ion ist von geordneten, eng verbundenen, im ionischen, elektrischen Feld, dem in den nebenstehenden Schemen (Abb. 5) angegebenen Möglichkeiten gemäß orientierten Wassermolekülen, umgeben. Diese Schemen ermöglichen die Deutung der Strukturverstärkung durch die relative Verminderung der Translationsmöglichkeit der Wassermoleküle in der Elektrolytlösung und der in P.V.A. enthaltenden Elektrolytlösung.

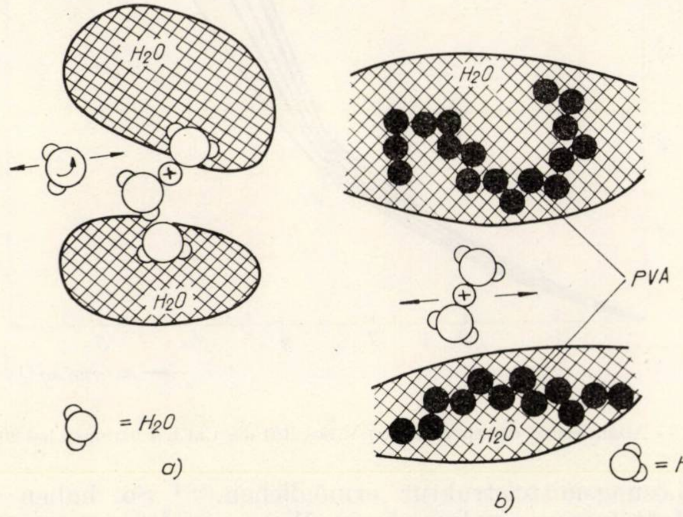

Abb. 5. — Strukturmodell der Elektrolytlösungen in Wasser (a) und in P.V.A.-Lösungen (b).

Die erste von orientierten Molekülen gebildete Schicht, deren Dicke von der Intensität des elektrischen Feldes abhängt, folglich von dem

---

[35] B. Breslau und J. Miller, *J. Phys., Chem.* **74**, 5, 1057 (1970).

Halbmesser des Kristalls und von der Ladung, ist von einer Schicht von strukturlosen Molekülen umgeben und dann folgen in der bei flüssigem Wasser üblichen Struktur gebundene Wassermoleküle.

Man kann annehmen, daß im Falle der positiven Werte des Koeffizienten B der Hydratationsdurchmesser des Ions der ersten im elektrischen ionischen Feld geordneten Schicht entspricht, während die zweite Schicht unterschiedlich ist im Vergleich zu dem Falle der negativ-wirkenden Ione ($B < 0$), wo diese zweite Schicht in zerstreuter Form bis in die Nähe des Ions eingedrungen ist, was selbstverständlich den verhältnismäßig kleineren Halbmessern des in der Lösung hydratierten-Ions (K^+, Rb^+, Cs^+, NH_4^+, Cl^-, Br^-), [22] oder im Falle der großen polyatomischen Ione einer kleinen oberflächlichen elektrischen Dichte entspricht. Sicherlich werden die Wassermoleküle der ersten Schicht nur von Ionen mit starken elektrischen Feldern, folglich mit kleinen Kristallhalbmessern gerodnet, was zu hydratierten Ionen mit großen Halbmessern führt, den Werten von $B > 0$ entsprechend.

Die Ionen welche in der Lösung kleine Halbmesser besitzen mit einer kleinen Hydratation, üben bedeutende elektrische Wirkungen aus, indem sie das pseudo-tetraedrische Gitter des Wassers zerreißen oder schwächen und somit ein Sinken der Zähigkeit der Lösung hervorrufen.

Der Einfluß des Nichtelektrolyten P.V.A. äußert sich in allen Fällen (sowohl für die Elektrolyten mit $B > 0$ sowie für $B < 0$) wie schon erwähnt, im Sinken der B-Werte, im Bereich der beobachteten Konzentrationen und zeigt somit eine Veränderung der Hydratationsfähigkeit durch Verminderung der Dimensionen des hydratierten Ions an, folglich eine Verbreiterung der zerstreuten, ungeordneten Schicht, da die Struktur des Wassers durch die Erweiterung des Volumens oder der Anzahl der Inseln mit pseudotetraedrischer Struktur des Wassers, sowohl durch den hydrophoben Effekt der Polymerkette als auch dem Effekt der polaren OH-Gruppen zufolge, welche direkt mit dem Wasserstoffbindungengitter verbunden sind, verstärkt wird. Diese Effekte lösen den Einfluß des elektronischen, ionischen Feldes, welches die molekulären Dipole des Wassers in der ersten ionischen Hydratationsschicht ordnet, auf; gleichfalls können diese Wirkungen den verhältnismäßig kleineren, bei $MgCl_2$ und $CaCl_2$ (Abb. 4) beobachteten Einfluß erläutern, wo das kationische elektrische Feld hohe Werte erreicht.

Andererseits stimmt diese Erläuterung mit der linearen Variation des Koeffizienten B in Abhängigkeit von der partiell molaren, auf den Gaszustand bezogenen Hydratationsentropie der Ionen S_g^0 überein:

$$S_h^0 = S_{aq}^0 - S_g^0 < 0$$

was auf ein Zunehmen der Hydratationsentropie S_g^0 mit dem Abnehmen des B-Wertes hindeutet. [22] Tatsächlich entspricht die Regelung in der ersten Schicht dem Sinken der Hydratationsentropie der Ione.

Es muß andererseits erwähnt werden, daß im allgemeinen eine gewisse Ungewißheit bezüglich des Ausdruckes „Reißen der Wasserstoff-bindung“ herrscht, gleichwertig mit dem Verwirrungs- bezw. Ordnungs-Effekt. Im reinen, flüssigen Wasser kann man bei 0°, 10—15% bewegliche Wasserstoffbindungen schätzen (Reißen und Wiederbildung) im Vergleich zu 0% im Eis bei derselben Temperatur.[36]

Das flüssige reine Wasser besteht somit aus regelmäßigen (quasikristallinen) Zonen, wo die Wasserstoffbindungen andauernd reißen und sich wieder bilden. Das elektrisch ionische Feld hat einerseits die Orientierung der Dipole der einfachen oder der verbundenen Moleküle im Kontaktgebiet der geordneten „Inseln“ zur Folge und andererseits bewirkt es das Zerreißen des Gitters auf größeren oder kleineren Strecken, bezw. das Ansteigen des Prozentsatzes an einfachen Molekülen, was ein Wachsen der Translationsmöglichkeit (in Übereinstimmung mit der obigen Darstellung) zur Folge hat. Dieser Effekt herrscht im Falle der Ione welche in der Lösung ein starkes Feld aufweisen, folglich ähnlich den oben angedeuteten Ionen, eine kleine relative Hydratation besitzen, vor; dieser letztere Effekt kann mit Zerfallwirkung bezeichnet werden und ist der Wirkung des Anstiegs der Temperatur ähnlich (z.B. bei 300° erhält dieser Prozentsatz den beiläufigen Wert von 60%, während bei 370° der Wert 100% erreicht).[36]

Im Falle des polaren Nichtelektrolyten vom P.V.A.-Typus wächst die Anzahl oder die Fläche der quasi-kristallinen „Inseln“ zum Nachteil der Verwirrungszonen, wodurch die Möglichkeiten des allgemeinen Ordnungseffektes des elektrischen ionischen Feldes verringert werden. Abbildung 5 stellt ein annäherndes Schema des Falles Elektrolytlösung und Elektrolytlösung mit Nichtelektrolytzugabe, als Strukturerzeuger, vom Typus P.V.A., dar. Gewiß kann das Sinken des B-Koeffizienten, bezw. das Steigen der Hydratationsentropie oder des effektiven Hydratationshalbmessers der hydrodynamischen Wechselwirkung, nicht einer linearen Variation entsprechen, außer im Falle eines bestimmten Konzentrationsbereiches (siehe Abb. 3 und).[37] Die obigen Werte hängen von der Intensität des effektiven ionischen elektrischen Feldes ab, z.B. im Falle NaCl (Abb. 4) und streben asymptotisch nach einem Grenzwert des hydrodynamischen Wechselwirkungseffektes Elektrolyt-Wasser-Nichtelektrolyt.

Es kann noch erwähnt werden, daß im Falle der Ione mit kleinem Kristall-Halbmesser, z.B. Li^+, Na^+, die Leerräume in dem „offenen“ Quasi-Kristallgitter des Wassers ihr Eindringen in diese Hohlräume ermöglichen. Das Ergebnis ist ein Wachsen des Gleitwiderstandes, da die Kontaktflächen der Verwirrungszonen sich durch die Bildung von Keilen verkleinern (Abb. 5).

Andere Gesichtspunkte der Wechselwirkung in Lösungen Elektrolyt-Wasser-P.V.A. können festgestellt werden mittels der Werte der grundmolaren Viskositätszahl, oder Grenzviskosität welche mit Hilfe der Gleichung:

$$[\eta] = \lim_{c \to 0} \frac{\eta - \eta_0}{\eta_0} = \lim_{c \to 0} \frac{\eta_{sp}}{c}$$

---

[36] G. Haggis, J. Hasted und T. Buchanan, *J. Chem. Phys.* **20**, 1452 (1962).

[37] H. Frank und M. Evans, *J. Chem. Phys.* **13**, 507 (1945).

bestimmt wird, wo c die Konzentration des Polymers darstellt η_0 und η sind die Zähigkeiten des den Elektrolyt bezw. Polymer enthaltenden Lösungsmittels. Die Huggins'sche Gleichung stellt die reduzierte Zähigkeit dar:

$$\eta_r = \frac{\eta_{sp}}{c} = [\eta] + k[\eta]^2 c + \ldots$$

wo die Konstante k die hydrodynamische Wechselwirkung in der Lösung darstellt.

Unsere experimentalen Bestimmungen ermöglichen die Feststellung der grundmolaren Viskositätszahl im Falle der Lösungen NaCl—P.V.A. in Wasser bei 20° mittels der Diagramme Abb. 6 und 7.

Man kann somit den Wert der grundmolaren Viskositätszahl der P.V.A.-Lösung im Wasser bestimmen, $[\eta] = (0{,}68 \pm 0{,}02)$ (100 g/g). Im Falle der NaCl-Lösungen ($m = 0{,}4-1{,}2$ Mol/Kg), sinkt $[\eta]$, doch bleibt sie praktisch in diesem Konzentrationsbereich identisch mit $[\eta] = 0{,}62 \pm 0{,}2$ (100 g/g). Im Falle der P.V.A.-Lösungen in $CaCl_2$ schwankt die grundmolare Viskositätszahl bedeutend: nach einem Anstieg von 0,68 auf 0,74 im Falle $m = 0{,}6$, bemerkt man ein bedeutendes Sinken bis auf $(0{,}46 \pm 0{,}02)$ 100 g/g bei $m = 6$ Mol. Kg^{-1}, folglich in konzentrierten Elektrolytlösungen. Die Variationen der grundmolaren Viskositätszahl mit der Konzentration des Elektrolyten in der Lösung ist mittels der Kurven in Abbildung 8 dargestellt.

Die Kurven der P.V.A.-Lösungen in anderen Elektrolyten wurden nicht dargestellt; es ist leicht ersichtlich, daß im Falle der LiCl-Lösungen ($m = 1{,}2$ Mol. Kg^{-1}) die Verminderung der grundmolaren Viskositätszahl unwesentlich ist $[\eta] = (0{,}68-0{,}67)$ 100 g/g; Im Falle de NH_4Cl-Lösungen ($m = 1{,}2$ Mol. Kg^{-1}) entspricht die grundmolare Viskositätszahl beiläufig $[\eta] = (0{,}66)$ 100 g/g aber bei KCl-Lösungen ($m = 1{,}2$ Mol. Kg^{-1}) bestimmt man annähernd $[\eta] = (0{,}58 \pm 0{,}04)$ 100 g/g. Im Falle der MgCl-Lösungen $m = 1{,}2$ bezw. 3,5 Mol.Kg^{-1}) ist im Bereich der P.V.A.-Konzentration von 0—0,5% eine bedeutende Verminderung der reduzierten Zähigkeit $\eta sp/c$ bemerkbar, was zu wichtigen Werten für $[\eta]$ führen könnte.

Im allgemeinen kann der Effekt den die Elektrolyten auf den Wert $[\eta]$ ausüben durch die Verringerung des hydrodynamischen Halbmessers $\sqrt{\overline{r^2}}$ des in der Lösung befindenden Makromoleküls dessen Molekularmasse M ist, gedeutet werden, der bekannten Theorie entsprechend. [38]

$$[\eta] = \Phi \frac{(\overline{r^2})^{\frac{3}{2}}}{M}$$

---

[38] P. Flory und T. Fox, *J. Amer. Chem. Soc.* **73**, 1904 (1951).

wo $\varnothing$ eine allgemeine Konstante Flory des Lösungsmittels ist. Die obige Gleichung weist auf das in größerem Maße möglich Zusammenballen der makromolekularen Kette in Gegenwart von Elektrolyten, und zwar weniger im Falle der Li^+, Na^+-Ionen, wo die Hydratation die Intensität des elektrischen ionischen Feldes verkleinert, und mehr im Falle der K^+-Ionen wegen der reduzierten Hydratation sowie bei konzentrierten Ca^{2+}-Lösungen. Im Falle des $CaCl_2$-Elektrolyten kann das Ansteigen der grundmolaren Viskositätszahl im Bereich von $m = 0-0{,}6$ Mol.Kg^{-1} (Abb. 8) durch das von dem Erscheinen von negativen Ladungen an gewissen Stellen der Kette hervorgerufene Ausdehnung der makromolekularen Kette gedeutet werden, folglich durch Entstehung von Verbindungen Ca^{2+} – Makromolekularkette oder Ca^{2+} – verschiedene Makromolekular ketten. Diese „anionische" Ausdehnung der Kette kann von der von Takahashi und Nagasawa [39] hingewiesenen Art sein. Diese Erläuterung

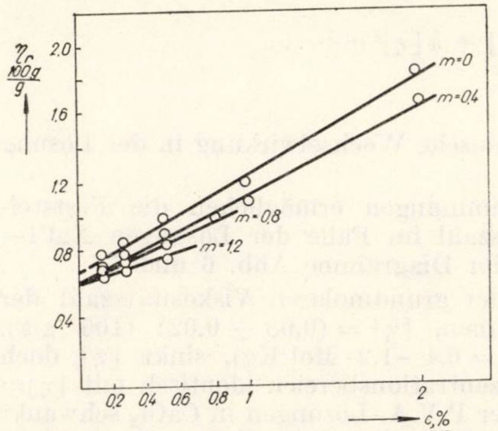

Abb. 6. — Bestimmung der Grenzviskosität $[\eta]$ von NaCl-P.V.A.-Lösungen in Wasser bei 20°.

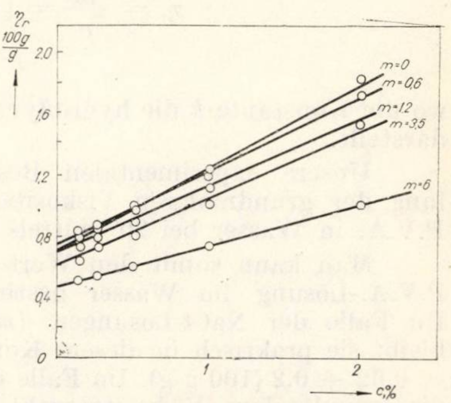

Abb. 7. — Bestimmung der Grenzviskosität $[\eta]$ von $CaCl_2$-P.V.A.-Lösungen in Wasser bei 20°.

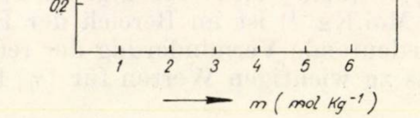

Abb. 8. — Abhängigkeit der $[\eta]$ von der Konzentration der CaNl und $CaCl_2$ Elektrolyten bei 20°.

---

[39] A. TAKAHASAHI und M. NAGASAWA, *J. Amer. Chem. Soc.* **86**, 543, (1964).

ist auch mit den annähernden Werten der Konstante k (hydrodynamische Wechselwirkungskonstante) der Huggins'schen Gleichung in Übereinstimmung; k steigt von 0,85 im Falle NaCl ($m = 1{,}2$ Mol.Kg^{-1}) bis zu 0,96 (100 g/g) im Falle $CaCl_2$ ($m = 1{,}2$ Mol.Kg^{-1}). Dieser Anstieg zeigt das Vorhandensein von elektrostatischen abstoßenden Wechselwirkungen zwischen den Ketten oder im Inneren einer Polymerkette.

Abschließend kann bemekrt werde, daß unserer Meinung nach das Ansteigen der grundmolaren Viskositätszahl allen Ionen gemeinsam ist, in einem gewissen Bereich von kleinen Konzentrationen. Dieser Bereich ist für jedes Ion spezifisch, abhängig von den elektrostatischen Effekten (Ladung, Kristallhalbmesser und Hydratation) und von den Dispersionseffekten (Polarisierbarkeit). Dieser von der „anionischen" Ausdehnung hervorgerufene Anstieg der grundmolaren Viskositätszahl bei kleinen Konzentrationen des Polymers kann auch den oben angegebenen Effekt der Reibungsverminderung erklären.

Revue Roumaine de Chimie, **19**, *5*, 903–910 (1974)

KINETICS OF EMULSION POLYMERIZATION OF VINYL ACETATE IN THE PRESENCE OF POLYVINYL ALCOHOL

VICTORIA DIMONIE, D. DONESCU, MARIANA MUNTEANU, C. HAGIOPOL and I. GAVĂT
Institute of Macromolecular Chemistry "P. Poni",
Section "Polymerization Processes", Bucharest, Str. Dumbrava Roşie N^0 18, Romania

Received November 12, 1973

The kinetics of emulsion polymerization of vinyl acetate (VAc) was studied in the presence of polyvinyl alcohol (PVA) and of hydrogen peroxide, in the redox system. The dependence of the maximum rate of polymerization on the initial concentrations of VAc and hydrogen peroxide is of the form $R_{\max} \sim [\mathrm{VAc}]_0^1$, $R_{\max} \sim [\mathrm{H_2O_2}]_0^{1/2}$. Under these conditions, the existence of some intensive chain-transfer reactions with PVA, noticed through the decrease of the polymerization rate and formation of an important amount of gel as the emulsifier concentration increases, has been emphasized. The effect of reaction conditions on composition and Fikentscher constant (*K* value) of the obtained polymers was determined.

1. INTRODUCTION

Relatively few studies have been published with regard to the kinetics and mechanism of emulsion polymerization of vinyl acetate in the presence of high-molecular emulsifiers [1].

Emulsion polymerization of VAc shows some deviations from the quantitative theory of Smith and Ewart,[1,2] owing essentially to the greater solubility in water of this monomer than that of other monomers. At the same time, the polyvinyl acetate macroradical shows a high reactivity towards chain transfer agents [3].

When using macromolecular compounds as emulsifiers for the polymerization of VAc, an unexpected kinetic effect has been noticed: the rate of reaction decreases with the increase of the initial concentration of emulsifier [2].

---

[1] C. Hagiopol, D. Donescu and V. Dimonie, *Studii şi Cercetări Chim. Acad. R.S.R.*, **21**, 929 (1973).

[2] S. Okamura and T. Motoyama, *J. Polymer Sci.*, **58**, 221 (1962).

[3] J. D. Jenkins, "Kinetics and Mechanism of Polyreactions", IUPAC. International Symposium of Macromolecular Chemistry. Plenary and main lectures, Budapest, 1969, p. 417.

In the case of using PVA as emulsifier, literature data show apparent disagreements due to the choice by the respective authors of extreme ranges of parameter variation: low molecular weights of PVA, [4] monomer concentrations below the limit of solubility of VAc in water, small PVA concentrations [5].

In the present work, the kinetic effects of monomer, emulsifier and initiator concentrations were studied, working in the range of high monomer concentration under conditions similar to those of industrial processes, and with a high molecular weight PVA. The effect of these parameters on the structure of the polymers obtained was also studied.

2. EXPERIMENTAL

2.1. MATERIALS

Vinyl acetate, commercial reagent, was purified on a high efficiency column. No traces of aldehydes could be identified after reactification.

Polyvinyl alcohol of the "Rodoviol" type was utilized as aqueous solution of 8 to 10% concentration, from which suspensions remaining undissolved were removed by centrifuging. The polyvinyl alcohol contains 9% acetate groups and has a molecular weight of 151,000, determined by the viscometric method.[6]

The polyvinyl alcohol solutions were also characterized from the point of view of surface tension, the dependence of which on concentration was established by using a torsion balance and is given in figure 1.

The resulting dependence is characteristic to the formation of a highly ordered arrangement without the appearance of micelles.

Hydrogen peroxide, a "Chemapol" product, was used in a solution of 30% concentration.

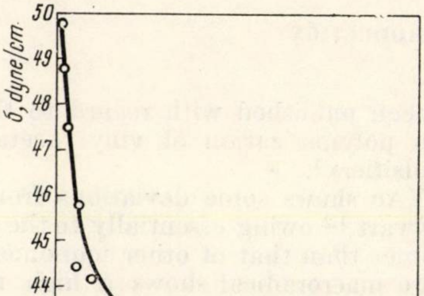

Fig. 1. — Variation of the surface tension of PVA aqueous solutions with concentration at 63°C.

Iron (II) sulfate, a "Reactivul" product, was used in aqueous freshly prepared solution.

---

[4] J. T. O'Donnell, *J. Polymer Sci.*, **28**, 171 (1958).

[5] S. Hayashi, K. Iwase and N. Hoyo, *Polymer Journal*, **3**, 226 (1972).

[6] A. Bereswiewicz, *J. Polymer Sci.*, **39**, 63 (1969).

2.2. POLYMERIZATION CONDITIONS

Polymerizations were performed at 63±0.5°, in a four-necked flask equipped with thermometer, dropping funnel, reflux cooler and mechanical stirrer.

The procedure was the following; the polyvinyl alcohol solution was introduced into the polymerization flask, distilled water was then added to adjust to the desired concentration. It was heated on the water bath to the polymerization temperature. After thermostating, formic acid was added up to pH = 3, then the iron (II) sulfate solution and, subsequently, the vinyl acetate drop by drop for 10 minutes. The moment when hydrogen peroxide was introduced was considered the zero moment of the reaction. In all the polymerizations, the overall reaction volume, the stirring speed and the rate of addition of reactants were maintained constant.

During polymerization, samples were withdrawn to determine gravimetrically the conversion and to analyse the polymer obtained.

2.3. POLYMER ANALYSIS

From the samples taken in the course of polymerization, films were obtained by drying at room temperature and were subjected to successive extractions in water and in benzene at boiling for 5 to 6 hours each, obtaining finally 3 fractions. The amounts of polymer soluble in water, soluble in benzene and insoluble in benzene were determined gravimetrically.

The water soluble fraction was analysed from the point of view of chemical composition by determining the acetate groups.

The *K* value of the polymer separated from the fraction soluble in benzene was determined according to the Fikentscher equation [7] by means of the viscometric measurements of 0.5% solutions in benzene:

$$\frac{1}{c}\log \eta_{\text{rel}} = k + \frac{75\,k^2}{1 + 1.5\,kc}\,; \qquad K = k.10^3$$

3. RESULTS AND DISCUSSION

The emulsion polymerization of VAc in the presence of PVA has a characteristic course, in three stages.

In figure 2 a kinetic curve is represented, and the existence of an accelaration period of the polymerization rate of 15 to 30 minutes can be noticed, followed by an interval of linear variation of the conversion with time, up to values in the range of 70 to 90%, the rate of polymerization decreasing subsequently.

During the second stage of the reaction, the polymerization rate ($R_{\max}$) depends linearly on the initial monomer concentration (figure 3).

$$R_{\max} \sim [M]_0^{\,1.0}$$

This evolution in time, typical of other emulsion polymerization processes too, may be interpreted in the following way: in the first stage, monomer — polymer particles are formed in which the polymerization takes place, and the number of which in the volume unit is proportional to the initial concentration of monomer. In the second stage the concentration of these polymerization loci remains constant [8], the polymerization rate being determined by the processes of the monomer diffusion to the growing macroradicals.

---

[7] A. Smith, "Addition Polymers. Formation and Characterization", London, 1968, p. 200.

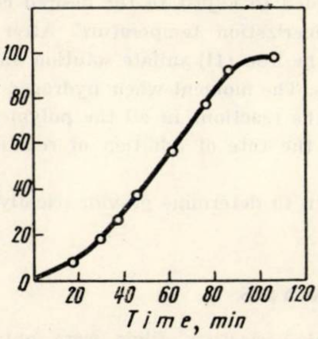

Fig. 2. — Time-conversion curve for the polymerization of VAc at 63°C.

$[VAc]_0 = 3.44$ mole/l; $[PVA]_0 = 35.4$ g/l; $[H_2O_2]_0 = 3 \times 10^{-3}$ mole/l; $[FeSO_4]_0 = 5.85 \times 10^{-5}$ mole/l

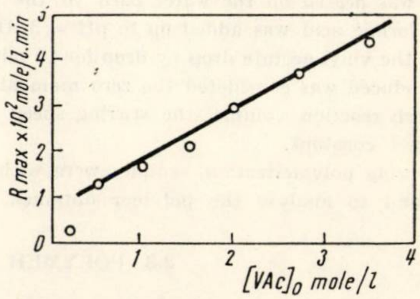

Fig. 3. — Dependence of the maximum polymerization rate on the monomer initial concentration at 63°C.

$[PVA]_0 = 35.4$ g/l; $[H_2O_2]_0 = 3 \times 10^{-4}$ mole/l; $[FeSO_4]_0 = 5.85 \times 10^{-5}$ mole/l.

For VAc concentrations below its limit of solubility in water, the polymerization does not take place by the same mechanism, the polymerization rate being smaller than the rates at higher monomer concentrations, and comparable to those found for aqueous solution polymerization [9a].

Along with the increase of the polymerization rate, due to a greater initial concentration of monomer, an increase of the molecular weight of the formed polymer was also noticed (figure 4).

It is already known that in the emulsion polymerization of VAc in the presence of PVA there exists the possibility of formation of graft copolymers owing to the transfer reactions of the polyvinyl acetate macroradical to the emulsifier [9b,10]

Some information about the grafting process were obtained by investigating the variation in time of the weight of polymer fractions resulting from the extractions in water and in benzene.

If graft reactions had not occurred, the weight of the fraction soluble in water would have had to correspond to the amount of PVA introduced into the reaction.

Actually, by following the variation of the water-soluble fraction in the course of the conversion of monomer to polymer, an increase of this fraction by 35 to 55% of the amount of PVA initially introduced into the system, was observed (figure 5).

---

[8] D. N. French, *J. Polymer Sci.*, **32**, 395 (1958).

[9] a G. E. Ham, "Vinyl Polymerization", vol. 1 (part II), Marcel Dekker, New York, 1969, p. 89;

b ibid, vol 1 (part I) 1967, p. 288.

[10] F. D. Hartley, *J. Polymer Sci.*, **34**, 397 (1959).

As can be seen in figure 5, the dependence of the water-soluble fraction on conversion is always represented by a curve having a maximum, the position of the maximum depending upon the experimental conditions.

From the determination of the acetate groups, carried out on the polymer extracted in aqueous phase, it resulted that with the advancing of the process, the content of PVA in this fraction is continuously diminishing (figure 5, dotted line).

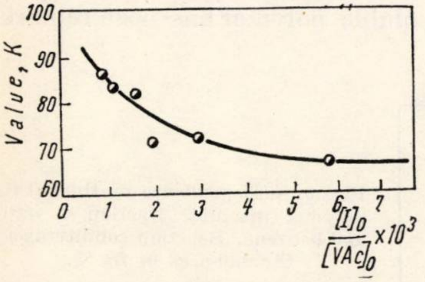

Fig. 4. — Variation of the *K* value of the polymer fraction soluble in benzene with the molar ratio initiator/monomer. Reaction conditions are the same as in fig. 3.

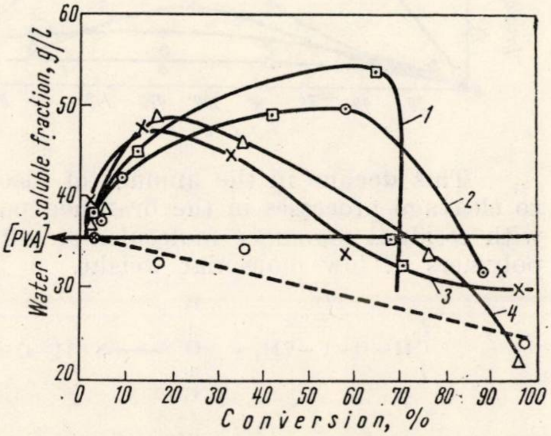

Fig. 5. — Variation of the water soluble fraction with conversion. Reaction conditions are the same as in fig. 3.
$[VAc]_0$ = *1* – 1.0; *2* – 1.5; *3* – 2.72; *4* – 3.44 mole/l. – – – : the weight of PVA extracted in water soluble fraction.

That means that the PVA part on which grafting has occurred very intensively is contained in the fraction insoluble in water.

In the same way the variation in time of the fraction soluble in water may also be interpreted, this fraction increasing at the beginning due to the formation of graft polymers of VAc on PVA which still contain a sufficient number of OH groups to ensure its solubility in water. The decrease of the fraction soluble in water, in a later stage, is due to the progress of the grafting process, this leading to the formation of the polymer insoluble in water and benzene.

The change in position of the maximum depending on the experimental conditions may be explained in a similar way. At great initial concentrations of monomer, i.e. small PVA/VAc ratios, a strongly grafted polymer is formed right from the start and in consequence the maximum is shifted towards lower conversions. The situation is different for small initial concentrations of monomer, when grafting occurs with lower rate, the insolubilization of PVA appearing at substantially higher conversions, of 60 to 70%.

It has been observed that, during synthesis, the insoluble fraction increases in all the cases, the increase being more marked in the experiments wherein the $[PVA]_0/[VAc]_0$ ratio is low (figure 6). In these experiments, a decrease of the amount of insoluble polymer has been remarked, during the last reaction stage.

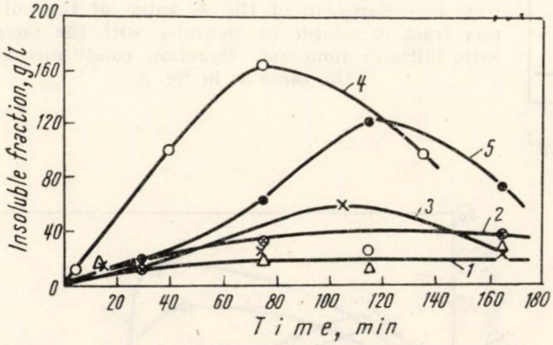

Fig. 6. — Dependence on time of the polymer insoluble fraction in water and benzene. Reaction conditions are the same as in fig. 3.

$[VAc]_0$: *1* – 0.5; *2* – 1.0; *3* – 2.0; *4* – 2.72; *5* – 3.44 mole/l.

This decline in the amount of insoluble polymer may be ascribed to cleavage processes in the branched polymer due to transesterification with residual monomer molecules or with acetate groups of the homopolymers of low molecular weight.

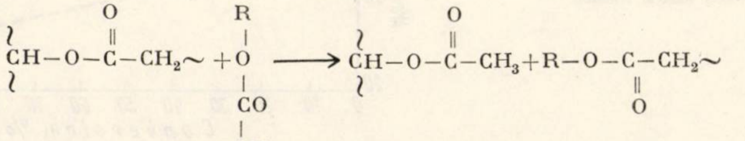

$$\underset{\wr}{\overset{\wr}{\mathrm{CH}}}-\mathrm{O}-\overset{\mathrm{O}}{\overset{\|}{\mathrm{C}}}-\mathrm{CH_2}\sim+\underset{\substack{|\\ \mathrm{CO}\\ |\\ \mathrm{CH_3}}}{\overset{\substack{\mathrm{R}\\ |}}{\mathrm{O}}}\longrightarrow\underset{\wr}{\overset{\wr}{\mathrm{CH}}}-\mathrm{O}-\overset{\mathrm{O}}{\overset{\|}{\mathrm{C}}}-\mathrm{CH_3}+\mathrm{R}-\mathrm{O}-\underset{\substack{\|\\ \mathrm{O}}}{\mathrm{C}}-\mathrm{CH_2}\sim$$

To verify the assumption stated, the loss of weight of the insoluble fraction treated with benzene and formic acid (blank-assay) or with benzene, formic acid and ethyl acetate was followed. The same sample was twice treated with ethyl acetate. These results are shown in table 1.

Table 1

Treatment of polymer fraction insoluble in water and benzene with ethyl acetate
Reaction conditions: 0.6 g polymer, 70 g benzene solution of ethyl acetate and 0.5 % HCOOH: 3 hours at 65°C

	Concentration of ethyl acetate %	Loss of weight %
Blank assay	—	0
First treatment	2.5	6.8
Second treatment	2.5	4.2

A determining influence on the development of the polymerization reaction is exerted by the concentration of polyvinyl alcohol. It is a peculiarity of this process, that in the ranges of reactant concentrations studied, the rate of polymerization diminished with the increase of polyvinyl alcohol concentration. This diminishing is the more marked, the lower the monomer concentration.

The data obtained, which are in apparent disagreement with the general theory of emulsion polymerization, according to which the rate of polymerization increases with the raise in emulsifier concentration, can be explained in the following way : the decrease of the rate of reaction with the increase of emulsifier concentration is due to the lower reactivity of the radical being formed as a result of the transfer reaction to PVA. The ratio between the concentrations of the two radical types usually appearing in the reaction medium, i.e. the active VAc radical and the less active PVA radical, will depend upon the relative concentrations of the two reactants PVA and the monomer, the overall number of radicals in the volume unit remaining constant.

In this way, at low monomer concentrations, this ratio will change in favour of inactive radicals and, in consequence, the decrease in the rate of reaction at the same time with the increase of PVA concentration will be the most marked ($R_{\max} \sim [\mathrm{PVA}]_0^{-2.4}$). With the increase of monomer concentration, the concentration of active radicals will proportionally increase, the negative effect of the increase of PVA concentration on the polymerization rate being less marked ($R_{\max} \sim [\mathrm{PVA}]_0^{-0.4}$).

In all cases, the effect of the increase of the polymerization rate with the increase of PVA concentration is marked by these transfer processes which lead to the diminishing of the rate of polymerization.

In order to check this hypothesis, in a separate series of experiments a strong chain — transfer agent (diallyl-ether [11]) was introduced in view of diminishing the importance of the chain-transfer reactions to the emulsifier. Under these conditions, the dependence of the polymerization rate upon PVA concentration is represented by a curve with a maximum (figure 7). Within the range of low PVA concentrations, on the ascending part of the curve, the emulsifier effect of PVA prevails. As the PVA concentration increases above a certain value, the weight of the chain transfer reactions to PVA increases, this having as effect the diminishing of the polymerization rate.

In a paper to be published, the authors found that diallyl ether also shows a retardation effect in the emulsion polymerisation of vinyl acetate in the presence of PVA [12].

When the two variations of the rate of polymerization for the same initial concentration of monomer (2 moles/l) in the absence and in the presence of a chain transfer agent are compared in the latter case the cumulative effect of the two transfer processes is noticed.

The existence of the chain transfer to the emulsifier (PVA) has also been proved by measurements made on the *K* value of the polymer fraction soluble in benzene. The molecular weight of polyvinyl acetate is noticeably influenced by the polyvinyl alcohol concentration (figure 8).

---

[11] J. P. J. Higgins and K. E. Weale, *J. Polymer Sci.*, *A—1*, **6**, 3007 (1968).

[12] V. Dimonie, D. Donescu, C. Hagiopol, M. Munteanu and I. Gavăt, *Rev. Roumaine Chim.* (in press).

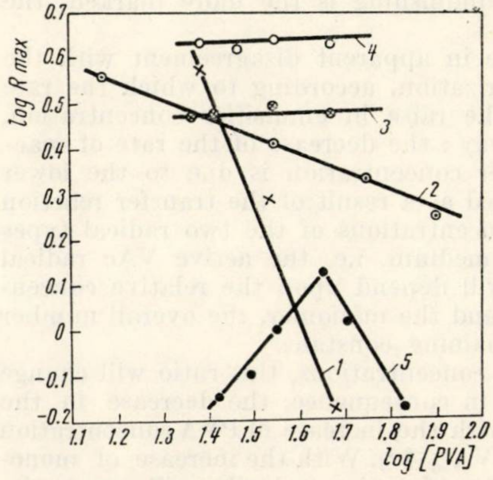

Fig. 7. — Relationship between log R_{max} and log (PVA) for the polymerization of VAc at 63°C.

$[H_2O_2]_0 = 3 \times 10^{-3}$ mole/l; $[FeSO_4]_0 = 5.85 \times 10^{-5}$ mole/l. $[VAc]_0$: *1* – 1.5; *2* – 2.0; *3* – 2.7; *4* – 3.5 mole/l. *5* – – $[VAc]_0$ = 2.0 mole/l and $[\text{diallylether}]_0 = 6 \times 10^{-3}$ mole/l.

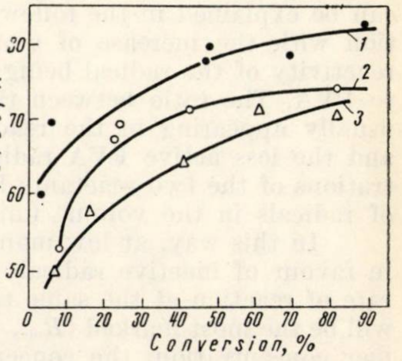

Fig. 8.— Dependence of the *K* value of the polymer fraction soluble in benzene on conversion.

$[VAc]_0$ = 2.0 mole/l; $[H_2O_2]_0 = 3 \times 10^{-3}$ mole/l $[FeSO_4]_0 = 5.85 \times 10^{-5}$ mole/l; temp. 63°C. $[PVA]_0$; *1* – 35.4 g/l; *2* – 56.1 g/l; *3* – 80 g/l.

The reaction order with respect to the initiator (hydrogen peroxide) concentration has a value of 0.5 over the entire range of concentrations investigated. The results are shown in figure 9 and are in good agreement with those found in literature [5,13].

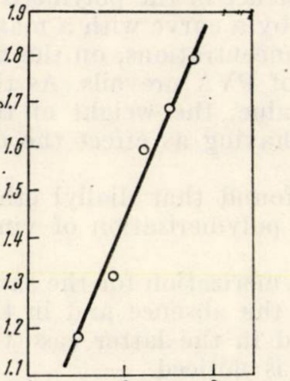

Fig. 9. — Relationship between log R_{max} and log [initiator]

$[VAc]_0$ = 1.5 mole/l; $[APV]_0$ = 35.4 g/l, temp. 63°C. $[H_2O_2]_0$ / $[FeSO_4]_0$ = ct.

As it results from the above mentioned data, in the case of the vinyl acetate polymerization, in the presence of a high molecular weight emulsifier, clear differences are appearing compared to the polymerization with low molecular weight emulsifiers, concerning both the process kinetics and the structure of the polymers formed. These particularities are due both to the frequent transfer reactions to the macromolecular emulsifier and especially to the specific character of the macromolecular aggregates formed in PVA solution [14]. These aggregates, which contain one or more emulsifier molecules, allow the penetration of the monomer into their interior constituting thus the main locus of polymerization.

---

[13] S. S. MEDVEDEEV, "Kinetics and Mechanism of Polyreaction", IUPAC International Symposium of Macromolecular Chemistry. Plenary and main lectures, Budapest, 1969, p. 39.

[14] J. G. PRITCHARD, "Poly(vinyl alcohol)", Mac Donald & Co., London, 1970.

Revue Roumaine de Chimie, **19**, *5*, 911–919 (1974)

RESEARCHES IN THE TERPOLYMERIZATION FIELD. IV*.

PRELIMINARY THEORETICAL STRUCTURAL STUDIES OF SOME BINARY COPOLYMERS

ADELAIDA LIGA, I. NEGULESCU and CR. SIMIONESCU
Institute of Macromolecular Chemistry "P. Poni",
Aleea Gr. Ghica Vodă 41 A, Jassy, Romania

Received May 19, 1973

Based on kinetical and probability relationships, the main structural features of some binary vinyl copolymers are presented : distribution of different length sequences, sequence mean length, alternation degree etc.

The copolymerization theory of vinyl monomers was elaborated many years ago [1], being strongly supported by a lot of experimental findings. The majority of these studies referred to the composition of copolymers. Only few papers on the microstructure of macromolecular chains were published, owing to some technical difficulties.

Since the equations predicting the distribution of the sequence length are based on the same supposition as that of the copolymer composition, without any supplementary hypothesis, it is reasonable to consider the computed structural details as correct. The kinetic and statistic studies on the copolymerization led to the already known relationships concerning the existence probability of different kinds of sequences. [1-11]

---

* Part III : Paper presented at the 39-th International Congress of Industrial Chemistry, Bucharest, Sept., 1970.

[1] T. Alfrey Jr., J. J. Bohrer and H. F. Mark, "Copolymerization", Interscience Publ., New York, London, 1952.

[2] G. E. Ham, "Copolymerization" ed. G. E. Ham, Interscience Publ., New York, London, Sydney, 1964.

[3] F. A. Bovey, *J. Polymer Sci.*, **62**, 197 (1962).

[4] A. Miyake and R. Chujo, *J. Polymer Sci.*, **46**, 160 (1960).

[5] R. L. Miller and L. E. Nielsen, *J. Polymer Sci.*, **46**, 303 (1960).

[6] G. Natta, G. Mazzanti, A. Valvassori, G. Sartori and D. Morero, *Chimica e Industria*, **42**, 125 (1960).

[7] F. P. Price, *J. Chem. Phys.*, **36**, 209 (1962).

[8] W. Ring, *J. Polymer Sci.*, B, **1**, 323 (1963).

[9] B. D. Coleman and T. G. Fox, *J. Polymer Sci.*, A **1**, 3183 (1963).

[10] J. Harwood and W. Ritchey, *J. Polymer Sci.*, B **3**, 419 (1965).

[11] K. Ito and Y. Yamashita, *J. Polymer Sci.*, A **3**, 2165 (1965).

In this work the results obtained by applying the classical copolymerization theory on some structural parameters of low conversion copolymers such as : acrylonitrile (M_1) — methacrylic acid (M_2), acrylonitrile (M_1) — methyl methacrylate (M_3) and methacrylic acid (M_2) — methyl methacrylate (M_3)[12] are presented.

1. PROBABILITIES OF THE ADDITION TYPES IN THE PROPAGATION STEP

1.1. EXPRESSIONS DERIVED FROM THE CLASSICAL THEORY OF COPOLYMERIZATION

According to the simplest scheme for copolymerization of two monomers M_i and M_j and admitting that the propagation step is a simple Markov process and the macromolecular chain is long enough (without taking into account the effects of initiation and termination steps), the four rates of the chain growth reactions are :

$$\begin{aligned} v_{ii} &= k_{ii}\,[m_i^{\cdot}]\,[M_i] \\ v_{ij} &= k_{ij}\,[m_i^{\cdot}]\,[M_j] \\ v_{jj} &= k_{jj}\,[m_j^{\cdot}]\,[M_j] \\ v_{ji} &= k_{ji}\,[m_j^{\cdot}]\,[M_i] \end{aligned} \tag{1}$$

where $[m_i^{\cdot}]$ and $[m_j^{\cdot}]$ represent concentrations of the growing chain ends of the type M_i and M_j respectively, $[M_i]$ and $[M_j]$ are the initial monomer concentrations.

In terms of these amounts, the probabilities of the four addition types ("conditional" or "transition" probabilities) may be expressed as follows[13] :

$$\begin{aligned} P_{ii} &= \frac{k_{ii}\,[m_i^{\cdot}][M_i]}{k_{ii}\,[m_i^{\cdot}]\,[M_i] + k_{ij}[m_i^{\cdot}]\,[M_j]} = \frac{r_{ij}[M_i]}{r_{ij}\,[M_i] + [M_j]} = \frac{r_{ij}F}{r_{ij}\,F+1} \\ P_{ij} &= \frac{k_{ij}\,[m_i^{\cdot}][M_j]}{k_{ii}\,[m_i^{\cdot}]\,[M_i] + k_{ij}\,[m_i^{\cdot}]\,[M_j]} = \frac{[M_j]}{r_{ij}\,[M_i] + [M_j]} = \frac{1}{r_{ij}\,F+1} \\ P_{ji} &= \frac{k_{ji}\,[m_j^{\cdot}]\,[M_j]}{k_{jj}\,[m_j^{\cdot}]\,[M_j] + k_{ji}\,[m_j^{\cdot}]\,[M_i]} = \frac{[M_j]}{r_{ji}\,[M_j] + [M_i]} = \frac{1}{1+\frac{r_{ji}}{F}} \\ P_{jj} &= \frac{k_{jj}\,[m_j^{\cdot}][M_j]}{k_{jj}\,[m_j^{\cdot}][M_j] + k_{ji}\,[m_j^{\cdot}]\,[M_i]} = \frac{r_{jj}\,[M_j]}{r_{ji}\,[M_j] + [M_i]} = \frac{r_{ji}}{r_{ji}+F} \end{aligned} \tag{2}$$

---

[12] CR. I. SIMIONESCU, N. ASANDEI and A. LIGA, *Makromol. Chem.*, **110**, 278 (1967).

[13] G. GOLDFINGER and T. KANE, *J. Polymer Sci.*, **3**, 462 (1948).

where r_{ij} and r_{ji} are the reactivity ratios of the monomers and F represents initial monomer ratio $[M_i]/[M_j]$.

1.2. THE ADDITION PROBABILITIES BASED ON THE CONVENTIONAL PARAMETER *R*

The run number[10] R is the average number of closed monomer sequences of both types per 100 consecutive monomer units and it may be expressed by :

$$R = \frac{200}{2 + r_{ij}F + \frac{r_{ji}}{F}} \tag{3}$$

Using this parameter, the probabilities of the addition types are as follows :

$$\begin{aligned} P_{ii} &= \frac{[m_i] - R/2}{[m_i]} \\ P_{ij} &= \frac{R}{2\,[m_i]} \\ P_{ji} &= \frac{R}{2\,[m_j]} \\ P_{jj} &= \frac{[m_j] - R/2}{[m_j]} \end{aligned} \tag{4}$$

where $[m_i]$ and $[m_j]$ represent the monomer concentrations in the copolymer.

In tables 1–3 the results concerning the values of the probabilities obtained for the three copolymers by using eqs. (2) and (4) are summarized. The reactivity ratios were[12] :

$$r_{12} = 0.093 \qquad r_{13} = 0.15 \qquad r_{23} = 0.92$$

$$r_{21} = 2.5 \qquad r_{31} = 1.09 \qquad r_{32} = 0.6$$

One can see that by using both eq. (2) and eq. (4) the results are almost identical.

Table 1

Addition probabilities in the acrylonitrile (1)-methacrylic acid(2) copolymer

F	R	Appl. eq.	P_{11}	P_{12}	P_{22}	P_{21}
33	39	(2)	0.75	0.25	0.07	0.93
		(4)	0.75	0.25	0.06	0.94
5.3	67	(2)	0.32	0.68	0.32	0.68
		(4)	0.34	0.66	0.34	0.66
0.7	35	(2)	0.06	0.94	0.22	0.78
		(4)	0.07	0.93	0.23	0.77

Table 2

Addition probabilities in the acrylonitrile(1)-methyl methacrylate(3) copolymer

F	R	Appl. eq.	P_{11}	P_{13}	P_{33}	P_{31}
21	38	(2)	0.75	0.25	0.04	0.96
		(4)	0.75	0.25	0.05	0.95
2.6	72	(2)	0.28	0.72	0.71	0.29
		(4)	0.28	0.72	0.71	0.29
0.3	36	(2)	0.04	0.96	0.22	0.78
		(4)	0.10	0.90	0.22	0.78

Table 3

Addition probabilities in the methacrylic acid(2)-methyl methacrylate (3) copolymer

F	R	Appl. eq.	P_{22}	P_{23}	P_{33}	P_{32}
3.96	34	(2)	0.78	0.22	0.13	0.87
		(4)	0.78	0.22	0.15	0.85
0.8	57	(2)	0.42	0.58	0.42	0.57
		(4)	0.43	0.57	0.43	0.57
0.16	34	(2)	0.13	0.87	0.78	0.22
		(4)	0.15	0.85	0.78	0.22

2. THEORETICAL DISTRIBUTION OF DIFFERENT LENGTH SEQUENCES

In order to determine the distribution function of different length sequences, one has to mind that for the appearance of a sequence of -n- "m_i" units, the addition reaction of M_i to the growing chain C

$$C - m_i^{\cdot} + M_i \tag{5}$$

(the probability of which is P_{ii}) must be repeated for $(n - 1)$ times. The probability of these $(n - 1)$ successive additions is P_{ii}^{n-1}. This sequence is interrupted by the addition of a M_j unit, with P_{ij} probability, or $(1 - P_{ii})$ respectively. The probability that a sequence of m_i should contain -n- terms (or the fraction of all the sequences constituted from -n- terms) is[14] then:

$$P(m_i)_n = P_{ii}^{n-1} \cdot (1 - P_{ii})$$

and (6)

$$P(m_j)_n = P_{jj}^{n-1} \cdot (1 - P_{jj})$$

The distribution functions of different length sequences, evaluated by eq. (6) for the three copolymers, are recorded in tables 4–6.

Table 4

Sequence distribution in the acrylonitrile(1)-methacrylic acid(2) copolymer

$[m_x]$ molar fr.	F	$\% P(m_x)$									
		$n = 1$	$n = 2$	$n = 3$	$n = 4$	$n = 5$	$n = 6$	$n = 7$	$n = 8$	$n = 9$	$n \geqslant 10$
80	33	25.0	18.8	14.0	10.0	7.8	5.8	4.4	3.3	2.5	8.4
60	10	52.0	25.0	12.0	5.7	2.7	1.2	0.6	0.3	0.1	0.4
50	5.3	67.0	22.0	7.0	2.3	0.8	0.25		1.3		
40	2.8	78.0	17.0	4.0	0.8	0.2					
20	0.7	93.0	6.0	0.4	0.05	0.05					

$x = 1$ or 2; $F = [M_1]/[M_2]$

Table 5

Sequence distribution in the acrylonitrile(1)-methyl methacrylate(3) copolymer

$[m_y]$ molar fr.	F	$\% P(m_y)$									
		$n = 1$	$n = 2$	$n = 3$	$n = 4$	$n = 5$	$n = 6$	$n = 7$	$n = 8$	$n = 9$	$n \geqslant 10$
80	21	24.0	18.0	13.7	10.0	7.6	5.7	4.3	3.2	2.4	11.5
60	5.3	56.0	24.0	10.5	5.5	2.0	0.5	0.1			
50	2.6	72.0	20.0	5.6	2.0	0.5	0.1				
40	1.3	84.0	13.0	2.0	0.3	0.5					
20	0.3	96.0	4.0								

$y = 1$ or 3; $F = [M_1]/[M_3]$

Table 6

Sequence distribution in the methacrylic acid(2)-methyl methacrylate(3) copolymer

$[m_z]$ molar fr.	F	$\% P(m_z)$									
		$n = 1$	$n = 2$	$n = 3$	$n = 4$	$n = 5$	$n = 6$	$n = 7$	$n = 8$	$n = 9$	$n \geqslant 10$
80	3.96	22.0	17.0	13.0	10.0	7.8	6.0	4.4	3.6	2.8	13.0
60	1.3	45.0	24.0	13.0	7.0	4.0	2.0	1.0	0.5	0.3	3.1
50	0.8	58.0	24.0	10.0	4.0	2.0	0.6	0.3	0.1	0.05	2.1
40	0.49	69.0	21.0	6.0	2.0	0.6	0.2	0.07	0.02	0.001	1.0
20	0.16	88.0	10.5	1.2	0.2						

$z = 2$ or 3; $F = [M_2]/[M_3]$

---

[14] T. Alfrey and G. Goldfinger, *J. Chem. Phys.*, **12**, 322 (1944).

One can point out, as a general remark, that the existence probability of long m_i sequences increases with the content of M_i monomer in the copolymer composition.

3. DISTRIBUTION OF MONOMER UNITS IN DIFFERENT LENGTH SEQUENCES

From all units of a certain type (m_i) in a very long chain, the molar fraction of "n" length sequences is [6]:

$$\varphi(m_i, n) = \frac{nP(m_i)_n}{\sum_{n=1}^{\infty} nP(m_i)_n} = \frac{nP_{ii}^{n-1} \cdot P_{ij}}{\sum_{n=1}^{\infty} nP_{ii}^{n-1} \cdot P_{ij}} \tag{7}$$

which finally becomes

$$\varphi(m_i, n) = \frac{nP_{ii}^{n-1} \cdot (1 - P_{ii})}{1/P_{ij}} = nP_{ii}^{n-1}(1 - P_{ii})^2 \tag{8}$$

and respectively

$$\varphi(m_j, n) = nP_{jj}^{n-1}(1 - P_{jj})^2 \tag{9}$$

One can also see from the above tables that at a high content of a certain monomer in copolymers (i.e., over 50%), the most part of that monomer units appears in superunitary sequences

$$(n > 1).$$

3.1. DISTRIBUTION OF MONOMER UNITS IN COMPOSITIONAL TRIADS

In a binary copolymer with M_i and M_j units, each monomer may be the center of some triads of the type $M_iM_iM_i$, $M_jM_iM_i$ ($M_iM_iM_j$) or $M_jM_iM_j$ in the case of M_i and $M_jM_jM_j$, $M_jM_jM_i$ ($M_iM_jM_j$) or $M_iM_jM_i$ in the case of M_j, respectively. The molar fractions of these monomer units from the center of the triads are given by [3]:

$$\begin{aligned} F_{iii} &= P_{ii}^2 \\ F_{jjj} &= P_{jj}^2 \end{aligned} \tag{10}$$

$$\begin{aligned} F_{jii}(F_{iij}) &= 2P_{ii}(1 - P_{ii}) \\ F_{ijj}(F_{jji}) &= 2P_{jj}(1 - P_{jj}) \end{aligned} \tag{11}$$

$$\begin{aligned} F_{jij} &= (1 - P_{ii})^2 \\ F_{iji} &= (1 - P_{jj})^2 \end{aligned} \tag{12}$$

The F_{iii}, F_{jii} and F_{jij} functions of the above binary copolymers are plotted in figure 1 for different initial compositions.

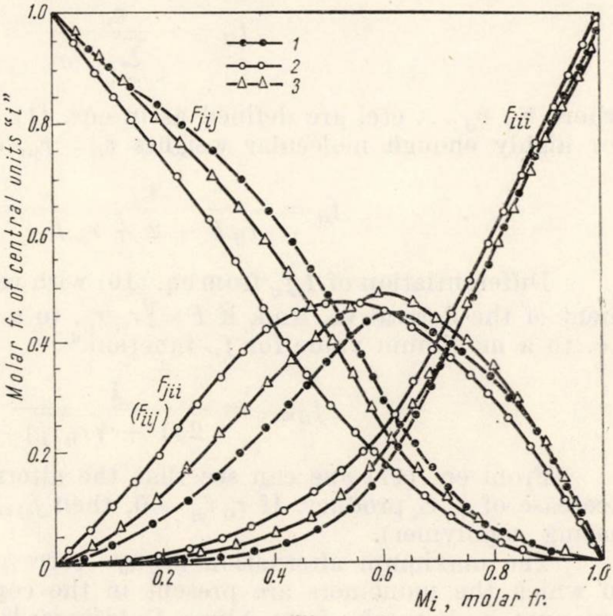

Fig. 1.— Molar fraction of central -*i*- units in compositional triads *versus* the monomer content in the feed ($i \neq j$; i, $j = 1, 2, 3$).
1 – acrylonitrile (1)-methacrylic acid (2) copolymer *2* – acrylonitrile (1)methyl methacrylate (3) copolymer *3* – methacrylic acid (2)-methyl methacrylate (3) copolymer.

4. MEAN SEQUENCE LENGTH

The number-average length of sequences can be defined as [9]:

$$\mu_i = \sum_{n=1}^{\infty} nP(m_j\, m_i^n\, m_j) / \sum_{n=1}^{\infty} P(m_j\, m_i^n\, m_j) \tag{13}$$

where $P(m_j m_i^n m_j)$ is the appearance probability of a sequence composed of $(n + 2)$ units, i.e., of a sequence composed of -n- units of m_i having one m_j unit at each extremity. Finally, for any statistical chain of m_i and m_j units, eq. 13 takes the forms:

$$\begin{aligned} \mu_i &= 1/P_{ij} \\ \mu_j &= 1/P_{ji} \end{aligned} \tag{14}$$

According to eqs. (14), the shortest average length of a sequence is 1 (one monomer unit), a case which characterizes the copolymers with a reduced content of the monomer concerned (tables 4–6).

5. ALTERNATION DEGREE OF THE COPOLYMERS

As measure of the alternation of the monomer units in a given copolymer, the fraction of bonds between nonidentical monomer units can be taken (f_{ij}). The alternation is highest when this fraction is maximum. The f_{ij} function can be expressed by:

$$f_{ij} = \frac{v_{ij}}{\sum\limits_{i,\, j=1,\, 2} v_{ij}} \tag{15}$$

where v_{ii}, v_{ij} ... etc. are defined as in eqs. (1). Finally, considering that for highly enough molecular weights $v_{ij} = v_{ji}$, eq. (15) becomes:

$$f_{ij} = \frac{1}{r_{ij}F + 2 + r_{ji}/F} = f_{ji} \tag{16}$$

Differentiation of $1/f_{ij}$ from eq. (16) with respect to F and the annulment of the derivative, lead, if $F = \sqrt{r_{ji}/r_{ij}}$, to a minimum value for $1/f_{ij}$, i.e. to a maximum value for f_{ij} function[6]:

$$f_{ij\,\text{max.}} = \frac{1}{2\,(1 + \sqrt{r_{ij}\,r_{ji}})} \tag{17}$$

From eq. (17) one can see that the alternation increases with the decrease of $r_{ij}\,r_{ji}$ product. If $r_{ij}\,r_{ji} \to 0$, then $f_{ij\,\text{max.}} = 0.5$ (perfectly alternating copolymer).

The maximum alternation always corresponds to the composition in which the monomers are present in the copolymer in equimolecular amounts, as it results from Alfrey-Goldfinger[15] and Mayo-Lewis's equation[16].

The corresponding alternation degrees of our copolymers are presented in fig. 2.

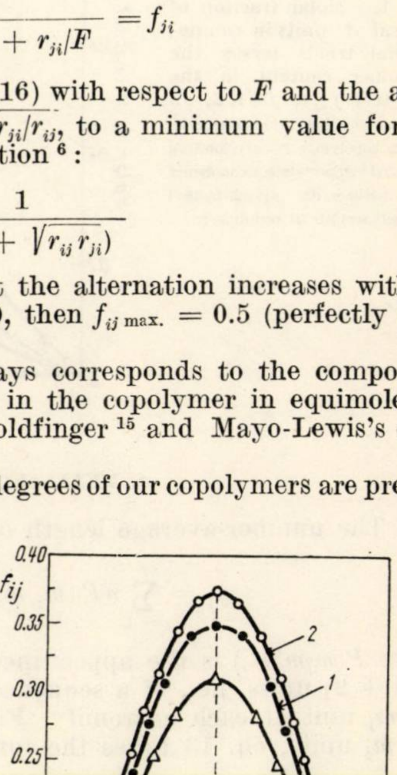

Fig. 2. — Alternation degrees (f_{ij}) — composition (M_i) dependence in the copolymers

1 – acrylonitrile(1)-methacrylic acid(2) copolymer
2 – acrylonitrile(1)-methyl methacrylate(3) copolymer
3 – methacrylic acid(2)-methyl methacrylate(3) copolymer.

---

[15] T. Alfrey and G. Goldfinger, *J. Chem. Phys.*, **12**, 205 (1944).

[16] F. R. Mayo and F. M. Lewis, *J. Amer. Chem. Soc.*, **66**, 1594 (1944).

The values of $f_{12\max.}$ and $f_{13\max.}$ (0.33 and 0.35, respectively) show that in equimolar acrylonitrile (1) — methacrylic acid (2) and acrylonitrile (1) — methyl methacrylate (3) copolymers, the four types of bonds do not appear with equal percentage (the addition of the other monomer being preferred in the case of acrylonitrile radical). The values of $f_{23} = 0.29$ for methacrylic acid (2) — methyl methacrylate (3) copolymer suggests somewhat equal rates for the four addition types of the propagation step.

The experimental check of a part of these calculations, by the NMR spectroscopy data, will be presented in a subsequent work.

Revue Roumaine de Chimie, **19**, *5*, 921–927 (1974)

STUDIES ON THE POLYMER + PLASTICIZER MEMBRANE-ELECTRODE. XI*.

INFLUENCE OF THE PLASTICIZER OF THE PVC ON ITS ELECTRODE BEHAVIOUR

ELENA HOPÎRTEAN, C. LITEANU and ANA MAŞA
"Babeş-Bolyai" University, Chair of Analytical Chemistry,
str. Arany János 11, Cluj, Romania

Received June 15, 1973

The paper deals with E-pH electrode functions as well as the results obtained at the acid-base potentiometric titration, using for indicating electrode the PVC-membrane plastified by a series of plasticizers : dibutylphthalate, dioctylphthalate, diisooctylphthalate, C_7-C_9 phthalate, $C_{10}-C_{11}$ phthalate, dibutylsebacate, diisooctylsebacate, benzylbutylphthalate and bis (2-ethylhexyl) phthalate. The accuracy of the titrations is expressed in comparison with the results obtained with the glass electrode.

A series of former papers have dealt with the obtention, [1] the analytical evaluation [2-8] and the working mechanism [9] of the PVC-tricresylphosphate membrane-electrode. We have shown that the plasticizer is the active electrode component of this type of membranes. [9,10] The paper aims to extend this study to the electrode behaviour of the PVC-membrane according to the plasticizer used. The $E-$pH electrode functions were established for different plasticizers (dibutylphthalate, dioctylphthalate, dibutylsebacate, etc.) and the membrane-electrodes obtained in the acid-base potentiometric titration were turned to account.

---

[*] Part X: E. Hopîrtean, M. Radu and O. Gabor, *Stud. Univ. Babeş-Bolyai, Chem.*, **13**, (1), 111(1973).

[1] C. Liteanu and E. Hopîrtean, *Rev. Roumaine Chem.*, **15**, 749 (1970).

[2] C. Liteanu and E. Hopîrtean, *Talanta*, **17**, 1067 (1970).

[3] C. Liteanu and E. Hopîrtean, *Rev. Roumaine Chim.*, **15**, 1331 (1970).

[4] C. Liteanu and E. Hopîrtean, *Stud. Univ. Babeş-Bolyai, Chem.*, **15** (2), 41 (1970).

[5] C. Liteanu and E. Hopîrtean, *Rev. Roumaine Chim.*, **16**, 55 (1971).

[6] C. Liteanu and E. Hopîrtean, *Stud. Univ. Babeş-Bolyai, Chem.*, **16** (1), 83 (1971).

[7] C. Liteanu and E. Hopîrtean, *Rev. Roumaine Chim.*, **16**, 559 (1971).

[8] C. Liteanu and E. Hopîrtean, *Talanta* **19**, 971 (1972).

[9] C. Liteanu and E. Hopîrtean, *Chem. Analit.*, **17**, 859 (1972).

[10] T. Higuchi, C. R. Illian and J. L. Tossounian, *Analyt. Chem.*, **42**, 1674 (1970).

EXPERIMENTAL

1. OBTENTION OF MEMBRANE-ELECTRODES

The PVC-membranes plastified with : dibutylphthalate, dioctylphthalate, diisooctylphthalate, C_7-C_9 phthalate, $C_{10}-C_{11}$ phthalate, dibutylsebacate, diisooctylsebacate, benzylbutylphthalate and bis (2-ethylhexyl) phthalate, were obtained according to the procedure described in a former paper [1]. The membrane-electrodes were obtained by attaching the membranes in bubble form at the end of a glass tube using 10^{-3} N HCl for inner solution and a saturated calomel electrode (SCE) as inner reference electrode.

2. *E*-pH ELECTRODE FUNCTION.

Using the MV–11 pH-meter, we have measured the e.m.f. of the following electrolytic chain :

SCE | inner solution | membrane | test solution | SCE

We have made use, as standard test solutions, of solutions with different pH, of HCl–KC and KOH–KCl, of a constant ionic strength ($J = 0.1$ M). The pH of the test solutions was meaured with the glass electrode. The *E*-pH dependence, i.e. the electrode function, was provedl or each membrane-electrode. Figure 1 gives the electrode functions obtained for the membranes with C_7-C_9 phthalate and $C_{10}-C_{11}$ phthalate for plasticizers, as well as the electrode function of the tricresylphosphate membrane. [2]

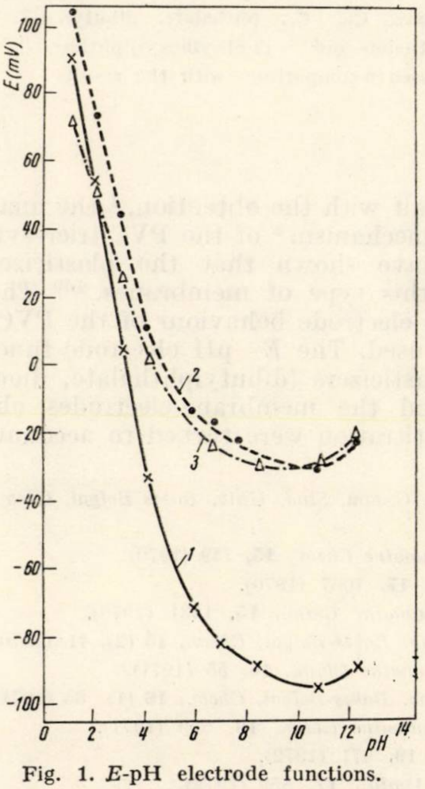

Fig. 1. *E*-pH electrode functions.
1, PVC-tricresylphosphate ; *2*, PVC – C_7-C_9 phthalate ; *3*, PVC – $C_{10}-C_{11}$ phthalate.

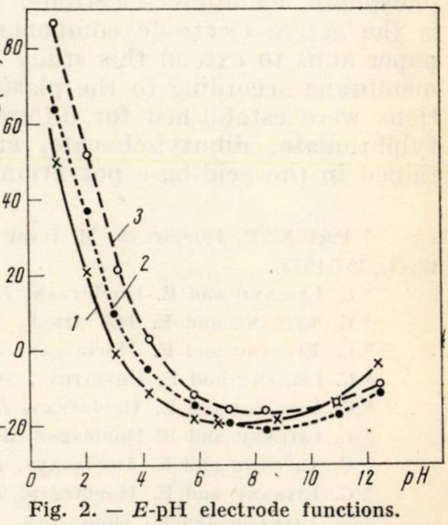

Fig. 2. — *E*-pH electrode functions.
1, PVC-dibutylphthalate ; *2*, PVC-dioctylphthalate ; *3*, PVC-diisooctylphthalate.

In the 1–4.5 and 6.5–12.5 pH intervals, the sensitivity of the two phthalates towards the H^+ ions is comparable to that of tricresylphosphate, and lower than this in the 4.5–6.5 pH interval. Figure 2 gives the electrode functions of the membranes obtained with the following plasticizers: dibutylphthalate, dioctylphthalate and diisooctylphthalate. The slope of these electrode functions has noticeable values (20–22 mV/pH) in the 1–4.5 pH interval. We must meanwhile point out, as in the case of the electrode functions in figure 1, the sign change of the electrode function slope in the alkaline domain. The electrode obtained with diisooctylsebacate has shown a similar electrode behaviour. The PVC-membrane plasticized with benzylbutylphthalate, bis (2-ethylhexyl) phthalate and dibutylsebacate have shown a less pronounced electrode behaviour.

3. ACID-BASE POTENTIOMETRIC TITRATIONS

3.1. *HCl titration with KOH.* The titration curves obtained are given in figures 3 and 4. In every case, the equivalence points are marked by a clear potential jump, the behaviour of membranes with C_7-C_9 phthalate and $C_{10}-C_{11}$ phthalate being outstanding.

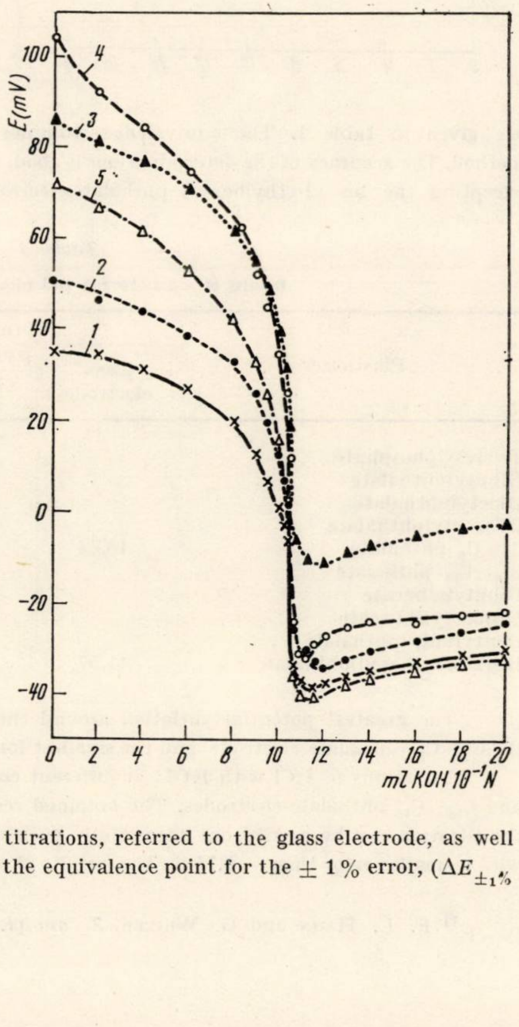

Fig. 3. — Titration of $\sim 3.3 \times 10^{-2}$N HCl with 10^{-1}N KOH.
1, **PVC-dibutylphthalate**; *2*, **PVC-dioctylphthalate**; *3*, **PVC-diisooctylphthalate**; *4*, **PVC – C_7 – C_9 phthalate**; *5*, **PVC-C_{10}–C_{11} phthalate.**

The data about the accuracy of the titrations, referred to the glass electrode, as well as the size of the potential variation around the equivalence point for the ± 1% error, ($\Delta E_{\pm 1\%}$

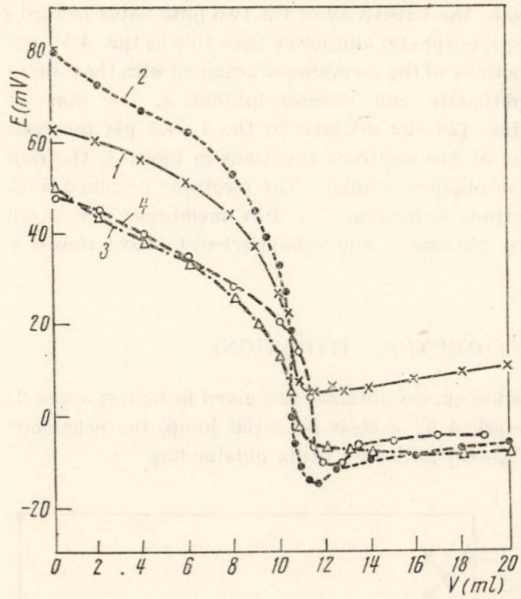

Fig. 4. — Titration of $\sim 3.3 \times 10^{-2}$N HCl with 10^{-1}N KOH.

1, PVC-dibutylsebacate; *2*, PVC-diisooctylsebacate; *3*, PVC-benzylbutylphthalate; *4*, PVC-bis(2-ethylhexyl)phthalate.

are given in table 1. The equivalence volumes were calculated by the Hahn-Weiler[11] method. The accuracy of the determinations is good, the recorded errors being less than − 0.5 %, excepting the bis (2-ethylhexyl) phthalate-electrode.

Table 1

Results of $\sim 3.3 \times 10^{-2}$ N HCl with 10^{-1} N KOH titration

Plasticizer	V_e (ml) glass electrode	V_e (ml) PVC + plasticizer membrane-electrode	Error (%)	$\Delta E_{\pm 1\%}$ (mV)
Tricresylphosphate	10.64	10.62	−0.19	79
Dibutylphthalate		10.61	−0.28	23
Dioctylphthalate		10.62	−0.19	27
Diisooctylphthalate		10.59	−0.45	28
C_7-C_9 phthalate		10.61	−0.28	50
$C_{10}-C_{11}$ phthalate		10.61	−0.28	30
Dibutylsebacate		10.61	−0.28	13
Diisooctylsebacate		10.61	−0.28	25
Benzylbutylphthalate		10.59	−0.45	8
Bis(2-ethylhexyl)phthalate	11.57	11.34	−1.10	11

The greatest potential variation around the equivalence point (50 mV) was recorded for the C_7-C_9 phthalate-electrode and the smallest for the benzylbutylphthalate-electrode (8 mV).

Titrations of HCl with KOH at different concentrations were carried out using C_7-C_9 and $C_{10}-C_{11}$ phthalate-electrodes. The obtained results are given in table 2. It is found that the titration can be carried out successfully even at an acid concentration of $\sim 3.3 \times 10^{-4}$ N, with a smaller error than − 0.75 %. The results of a HCl with KOH titration carried out in the

---

[11] F. L. Hahn and G. Weiler, *Z. analyt. Chem.*, **69**, 417 (1926).

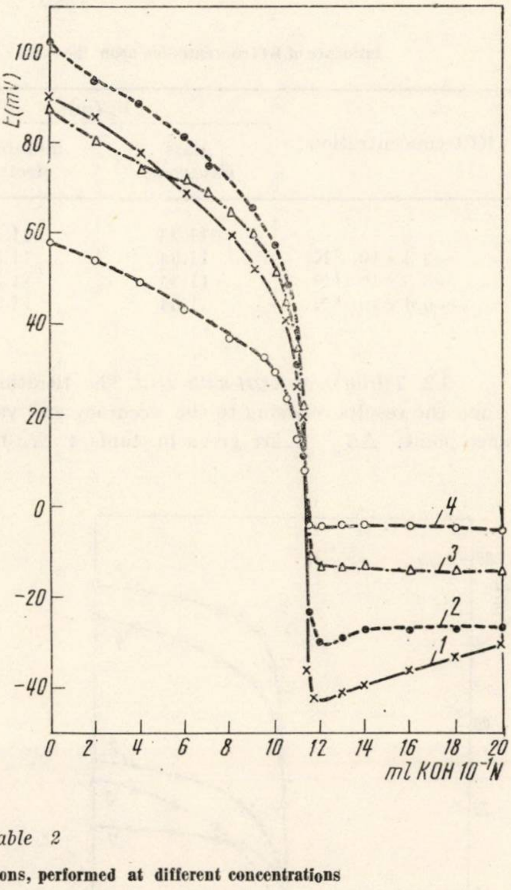

Fig. 5.— Influence of KCl concentration on the titration curve of ~ 3.3×10^{-2} NHCl with 10^{-1} N KOH. Membrane-electrode PVC—C_7—C_9 phthalate.
1, without KCl initially; 2, ~ 3.3×10^{-2}N KCl; 3, ~ 3.3×10^{-1}N KCl; 4, ~ 6.6×10^{-1}N KCl

Table 2

Results of HCl with KOH titrations, performed at different concentrations

Plasticizer	Acid concentration	Base concentration	V_e (ml)		Error (%)	$\Delta E_{\pm 1\%}$ (mV)
			glass electrode	membrane electrode		
C_7—C_9 phthalate	~3.3×10^{-2}N	10^{-1}N	10.64	10.61	−0.28	50
	~3.3×10^{-3}N	10^{-2}N	11.38	11.29	−0.79	35
	~3.3×10^{-4}N	10^{-3}N	11.38	11.35	−0.26	8
C_{10}—C_{11} phthalate	~3.3×10^{-2}N	10^{-1}N	10.64	10.61	−0.28	30
	~3.3×10^{-3}N	10^{-2}N	11.38	11.30	−0.70	27
	~3.3×10^{-4}N	10^{-3}N	11.38	11.31	−0.62	7

presence of a saline medium of KCl of different concentrations, using the PVC —C_7 — C_9 phthalate-electrode, are given in figure 5 and table 3.

A decrease of the value of $\Delta E_{\pm 1\%}$ is noticed with the increase of the electrolyte concentration in the solution, as in the case of the membrane-electrode with tricresylphosphate, [2] but the accuracy of the determinations is not altered, the error being less than ± 0.2%.

Table 3

Influence of KCl concentration upon the $\sim 3.3\times10^{-2}$N HCl with 10^{-1} N KOH titration

KCl concentration	V_e (ml) glass electrode	 membrane electrode	Error (%)	$\Delta E_{\pm 1\%}$ (mV)
—	11.34	11.38	+0.35	50
$\sim 3.3\times10^{-2}$N	11.34	11.36	+0.18	39
$\sim 3.3\times10^{-1}$N	11.34	11.35	+0.08	33
$\sim 6.6\times10^{-1}$N	11.34	11.32	−0.18	12

3.2. *Titration of KOH with HCl.* The titration curves obtained are given in figures 6 and 7, and the results referring to the accuracy and variation of the potential around the equivalence point, $\Delta E_{\pm 1\%}$, are given in table 4. We notice that, excepting the electrodes with dibutylsebacate and benzylbutylphthalate, all the others may be successfully used to show the end of the titration of KOH with HCl, the recorded errors being less than ± 0.69 %.

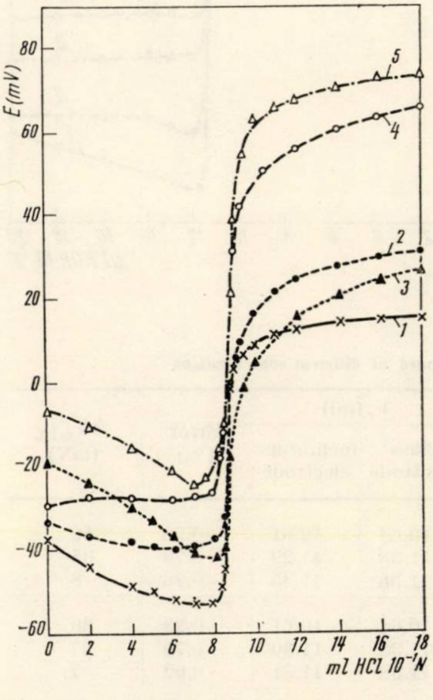

Fig. 6. — Titration of $\sim 3.3\times10^{-2}$N KOH with 10^{-1}N HCl.

1, PVC-dibutylphthalate; *2*, PVC-dioctylphthalate; *3*, PVC-diisooctylphthalate; *4*, PVC$-C_7-C_9$ phthalate; *5*, PVC$-C_{10}-C_{11}$ phthalate

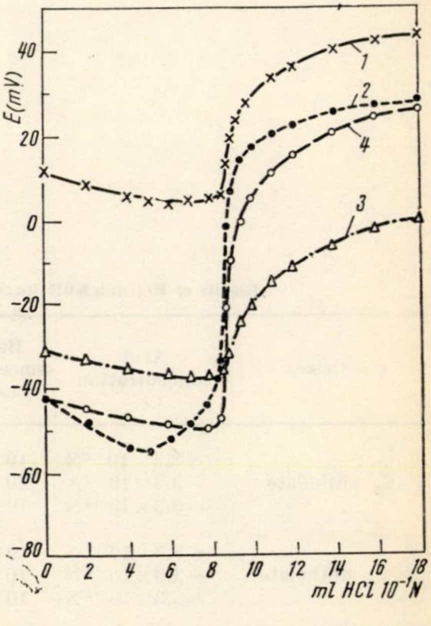

Fig. 7. — Titration of $\sim 3.3\times10^{-2}$N KOH with 10^{-1}N HCl.

1, PVC-benzylbutylphthalate; *2*, PVC- bis(2-ethylhexyl) phthalate; *3*, PVC-dibutylsebacate; *4*, PVC-diisooctylsebacate.

Table 4

Results of $\sim 3.3\times 10^{-2}$N KOH with 10^{-1} N HCl titration

Plasticizer	V_e (ml)		Error (%)	$\Delta E_{\pm 1\%}$ (mV)
	glass electrode	membrane-electrode PVC + plasticizer		
Tricresylphosphate	8.60	8.63	+0.34	81
Dibutylphthalate		8.62	+0.23	43
Dioctylphthalate		8.63	+0.34	30
Diisooctylphthalate		8.63	+0.34	22
C_7-C_9 phthalate		8.64	+0.46	49
$C_{10}-C_{11}$ phthalate		8.64	+0.46	33
Dibutylsebacate		8.71	+1.16	5
Diisooctylsebacate		8.66	+0.69	26
Benzylbutylphthalate		8.70	+1.16	8
Bis(2-ethylhexyl)-phthalate		8.63	+0.34	31

We have also carried out KOH with HCl titrations at different concentrations using C_7-C_9 phthalate and $C_{10}-C_{11}$ phthalate electrodes. The results obtained, included in table 5 point out in this case too the possibility of using the above mentioned membrane-electrodes for the KOH with HCl titration, even at $\sim 3.3\times 10^{-4}$ N concentration.

Table 5

Results of KOH with HCl titrations, performed at different concentrations

Plasticizer	Base concentration	Acid concentration	V_e (ml)		Error (%)	$\Delta E_{\pm 1\%}$ (mV)
			glass electrode	membrane electrode		
C_7-C_9 phthalate	$\sim 3.3\times 10^{-2}$N	10^{-1}N	8.60	8.64	+0.46	27
	$\sim 3.3\times 10^{-3}$N	10^{-2}N	8.62	8.57	−0.58	25
	$\sim 3.3\times 10^{-4}$N	10^{-3}N	8.35	8.38	+0.34	5
$C_{10}-C_{11}$ phthalate	$\sim 3.3\times 10^{-2}$N	10^{-1}N	8.60	8.64	+0.46	27
	$\sim 3.3\times 10^{-3}$N	10^{-2}N	8.62	8.55	+0.46	22
	$\sim 3.3\times 10^{-4}$N	10^{-3}N	8.35	8.33	−0.24	6

CONCLUSIONS

The study carried out shows that the following plasticizers have a good electrode behaviour : dibutylphthalate, dioctylphthalate, diisooctylphthalate, C_7-C_9 phthalate, $C_{10}-C_{11}$ phthalate, and diisooctylsebacate, while the membranes plasticized with dibutylsebacate, benzylbutylphthalate and bis(2-ethylhexyl)phthalate have less pronounced electrode properties. We have found that the nature of the ester acid, as well as that of the alcohol, influences the electrode behaviour.

The response speed of all the electrodes is very good(3—4 seconds), a fact allowing their use in automatic acid-base potentiometric titrations.

NOTE POUR LES AUTEURS

La *Revue Roumaine de Chimie* publie des articles en anglais, français, russe, allemand ou espagnol. Les auteurs sont priés d'envoyer des articles, notes, communications et comptes rendus inédits.

Les manuscrits seront dactylographiés à deux intervalles. Les tableaux seront dactylographiés sur feuilles séparées, de même que la légende des figures. Les diagrammes seront tracés à l'encre de Chine sur papier calque. Les tableaux et les figures seront numérotés par des chiffres arabes, en nombre strictement nécessaire. Prière de ne pas inscrire les mêmes données dans les tableaux et les figures. Les formules chimiques seront incluses dans le texte ; en outre, elles seront transcrites sur des feuilles séparés. Les auteurs sont priés d'indiquer les caractères italiques (en soulignant les lettres au crayon), ainsi que tout autre caractère spécial. L'ordre des références bibliographiques sera celui de leur mention dans le texte ; le nom de l'auteur sera précédé de l'initiale du prénom ; les publications périodiques seront présentées suivant les prescriptions internationales. Les références seront ajoutées à la fin de l'article ; elles paraîtront comme des notes, au bas de la page. Le texte sera précédé d'un résumé comprenant 15 lignes au maximum.

L'entière responsabilité du contenu des articles appartient aux auteurs. On publie des articles dus aux collaborateurs roumains ou étrangers. Les auteurs recevront 50 tirés à part.

PRINTED IN ROMANIA

1974 SEP 25

TRAVAUX PARUS AUX ÉDITIONS DE L'ACADÉMIE DE LA RÉPUBLIQUE SOCIALISTE DE ROUMANIE

TIBERIU NĂȘCUȚIU, **Metode radiochimice de analiză** (Méthodes radiochimiques d'analyse), 1973, 384 p., 23 lei.

MARIA FITI, **Dozimetria chimică a radiaţilor ionizante** (La dosimétrie chimique des radiations ionisantes), 1973, 240 p., 13,50 lei.

MIHAI FLORESCU, **Eficienţa economică a cercetării ştiinţifice** (L'efficience économique de la recherche scientifique), 1972, 115 p., 15 lei.

GEORGETA LĂZĂRESCU, **Sistematizarea informaţiilor în chimia organică** (La systématisation des informations dans la chimie organique), 1972, 242 p., 10,50 lei.

P. BALTĂ et E. BALTĂ, **Introducere în chimia fizică a stării vitroase** (Introduction à la chimie physique de l'état vitreux), 1971, 240, 15,50 lei.

LYDIA-MARIA VAICUM, **Biodegrabilitatea detergenţilor** (La biodégrabilité des détergents), 1971, 254 p., 16 lei.

TIBERIU NĂŞCUŢIU, **Metode radiometrice de analiză** (Méthodes radiométriques d'analyse), 1971, 346 p., 19,50 lei.

I. ZUGRĂVESCU et L. STOICESCU-CRIVETZ, **Polimeri heterociclici** (Polymères hétérocycliques), 1971, 190 p., 9,50 lei.

I. V. MAXIM, **Materiale nucleare** (Matériaux nucléaires), 1969, 444 p., 30 lei.

CRISTOFOR SIMIONESCU et C. V. UGLEA, **Fracţionarea compuşilor macromoleculari** (Fractionnement des composés macromoléculaires), 1969, 292 p., 18,50 lei.

CORNEL BODEA et collab., **Tratat de biochimie vegetală**, partea I, **Fitochimie** (Traité de biochimie végétale, Ire partie, Phytochimie), Ier vol., 1964, 747 p. + 4 annexes + 2 pl., 41 lei ; IIe vol., 1965, 1962 p., 1 pl., 56 lei ; IIIe vol., 1967, 773 p., 35 lei.

CRISTOFOR SIMIONESCU et CLEOPATRA VASILIU-OPREA, **Mecanochimia compuşilor macromoleculari** (La mécanochimie des composés macromoléculaires), 1967, 344 p., 23,50 lei.

V. GHEŢIE et V. MICUŞAN, **Analiza imunochimică. Teorie şi practică** (Analyse immunochimique. Théorie et pratique), 1966, 369 p., 28 lei.

R. PORTOCALĂ et L. POPA, **Acizi ribonucleici celulari şi virali** (Les acides ribonucléiques cellulaires et viraux), 1966, 375 p., 8 pl., 26 lei.

I.P.I. — c. 1229

43 426

Lei 25.—

F 1103

REFERÁLVA

REVUE ROUMAINE DE CHIMIE

TOME 19

N° 6

Juin 1974

RECHAX, **19**, *6*, 929–1120 (1974)

ÉDITIONS DE L'ACADÉMIE DE LA RÉPUBLIQUE SOCIALISTE DE ROUMANIE

Rev. Roumaine Chim. **19**, *6*, p. 929–1120 (1974), Bucarest

COMITÉ DE RÉDACTION

Rédacteur en chef:

I. G. MURGULESCU, membre de l'Académie de la République Socialiste de Roumanie

Rédacteurs en chef adjoints:

A. T. BALABAN et V. EM. SAHINI, membres correspondants de l'Académie de la République Socialiste de Roumanie

Collège de rédaction:

EM. BRATU, ELENA CEAUŞESCU, ECATERINA CIORĂNESCU-NENITZESCU, C. DRĂGULESCU, RALUCA RIPAN, CR. SIMIONESCU, membres de l'Académie de la République Socialiste de Roumanie; P. SPACU, membre correspondant de l'Académie de la République Socialiste de Roumanie; MARGARETA AVRAM, D. I. MARCHIDAN, I. MOLDOVAN, G. NIAC et D. SĂNDULESCU

Toute commande de l'étranger (fascicules ou abonnements) sera adressée à Întreprinderea Rompresfilatelia, Boîte Postale 2001, telex 011631, Bucarest, Roumanie

Les manuscrits, les livres et les revues proposés en échange, ainsi que toute correspondance seront envoyés à la rédaction

REVUE ROUMAINE DE CHIMIE

23, str. Dumbrava Roşie, Bucarest, Roumanie

ÉDITIONS DE L'ACADÉMIE DE LA RÉPUBLIQUE SOCIALISTE DE ROUMANIE
3 bis, str. Gutenberg, Bucarest

REVUE ROUMAINE DE CHIME

ORSZÁGOS MŰSZAKI KÖNYVTÁR ÉS DOKUMENTÁCIÓS KÖZPONT

Tome 19, N° 6 Juin 1974

TATIANA ONCESCU and M. CONTINEANU, Kinetics and mechanism of diphenyldiazomethane radiolysis in benzene solution 931–939

J. PĂUN and TATIANA MEMETEA, Radiolysis of the complex oxalates in aqueous solutions. III. The influence of some OH scavengers on the radiolysis of potassium trisoxalatocobaltate in neutral aqueous solution . . . 941–946

R. HUBIN, Etude du spectre vibrationnel, infrarouge et Raman, du pyrophosphate de plomb (IV) – PbP_2O_7. 947–954

S. STERNBERG, S. PETRESCU and VALERIA PETRESCU, The galvanostatic study of the electrochemical adsorption process on the chlorine-active carbon electrode in molten salts. III. Anodic polarization (charging) equation 955–965

S. STERNBERG et I. GALASIU, L'étude galvanostatique du processus de l'adsorption électrochimique sur l'électrode d'iode-charbon actif dans les sels fondus. II. Influence de la température 967–976

RODICA VÎLCU and ALEXANDRINA SIMION, Thermodynamic excess magnitudes of binary systems of organic liquids 977–984

LETIȚIA TOPOR and IVONA MOLDOVEANU, Vapor pressures of molten $CdBr_2$, CdI_2, $MgBr_2$ and molecular association in gaseous phase 985–990

SIMONA BĂDILESCU, Molecular interactions in solutions. Calculations of the interaction potential energy in the carbon disulphide – chloroform system 991–996

D. RIMER, Généralisations du triangle de Gibbs pour les systèmes quaternaires et quinaires 997–1008

CONST. GH. MACAROVICI and MARIA ZAHARESCU, Contributions to the study of the $NiO-SiO_2-TiO_2$ ternary system 1009–1018

A. C. BANCIU and P. SPACU, Co(II) chelates with 1-methyl-2-carbethoxyglyoxalanil-(1)-tolylhydrazones-(2) 1019–1030

D. NEGOIU and VASILICA MUREȘAN, Contributions to the chemistry of thiocomplexes. V. Complex compounds of Pt(II) with thioamides . . . 1031–1038

D. NEGOIU, ANGELA KRIZA et MARTHA NASTA, Sur les composés d'addition du tétrachlorure de thorium avec des azométhynes 1039–1044

I. ANGHELACHE, D. SĂNDULESCU and V. VÂNTU, Hydrogen transfer reactions between hydrocarbons and free radicals. II. The study of molecular combinations between aromatic hydrocarbons and the 1,1-diphenyl-2-picrylhydrazyl free radical (DPPH) 1045–1051

Rev. Roumaine Chim. **19**, *6*, p. 929–1120 (1974), Bucarest

SCHELY AVRAMOVICI, IOANA CIOCOIU and G. I. RUSU, Electrical conductivity of some salicylidenanils 1053–1059

M. IOVU and ANCA ANGELESCU, Bis-thioethers. I. Condensation of sodium thiophenolates with dichloromethylated derivatives 1061–1065

I. SIMITI, DOINA GHIRAN, I. SCHWARTZ and R. D. POP, Study of some heterocycles. XXVI. Nitration of 2-anilino-5-phenyl-1,3,4-oxadiazole . . . 1067–1072

A. POP and POMPILIA DUMITRESCU, Study of cyclohexane dehydrogenation equilibrium and kinetics in pulsed reactor 1073–1082

A MARIA FITI, Some aspects of radiolytic oxidation of phenol in aqueous solution 1083–1091

ARJUN D. TANEJA and N. U. M. RAO, Potentiometric determination of dissociation constants of some aromatic acetoacetamides 1093–1097

B S. W. BISHARA, M. E. ATTIA and H. N. A. HASSAN, Microdetermination of organic sulphur or inorganic sulphate 1099–1105

A. CONSTANTINESCU and C. LITEANU, Separation of creatinine from leucine in a proteic hydrolysate by paper chromatography with a combined temperature and stationary phase section gradient 1107–1111

COMPTES RENDUS 1113–1119

Revue Roumaine de Chimie, 19, 6, 931–939 (1974)

KINETICS AND MECHANISM OF DIPHENYLDIAZOMETHANE RADIOLYSIS IN BENZENE SOLUTION

TATIANA ONCESCU and MIHAI CONTINEANU

Department of Physical Chemistry, University of Bucharest,
Bd. Republicii 13, Bucharest, Romania

Received October 3, 1973

The kinetics of diphenyldiazomethane radiolysis in benzene solution shows that the reaction order varies with the concentration of the solution. It was thus established that the mechanism involving energy transfer from excited benzene molecules to diphenyldiazomethane molecules is predominant in dilute solutions while a direct interaction of radiations with the substance occurs in concentrated solutions.

In his radiochemical studies, Dainton[1] reported in 1965 the fact that excited solvent molecules, capable of activating the molecules of the dissolved substances by energy transfer, also participate in some solutions irradiated, besides the radicalar and ionic mechanism, which is typical of radiochemical reactions. The present paper deals with a system which confirms such a behaviour.

EXPERIMENTAL

Diphenyldiazomethane benzene solutions of various concentrations (10^{-3}, 4.12×10^{-3} 2×10^{-2}, 0.1 and 1 moles/l were irradiated, using a 15 Ci (Co^{60}) radiation source. A 15 Ci and a 10,000 Ci Co^{60} source was used for the concentration of 3 moles/l respectively for the solid samples. Dosimetry was performed by means of a Fricke dosimeter [2-4] and the energies obtained are presented in table 1.

A UNICAM SP 800 spectrophotometer was used for measuring the absorbance of the irradiated solutions at $\lambda = 540$ nm (in the diphenyldiazomethane absorption band) which permitted the determination of the solution concentration after each irradiation time, knowing the absorption molar coefficient ($k_{540} = 94$). Diphenyldiazomethane was prepared by oxidizing the appropriate hydrazone according to the method indicated in the literature.[5]

---

[1] F. S. Dainton, *Pure Appl. Chem.*, **10**, 395 (1965).

[2] H. Fricke and S. Morse, *Am. J. Roentgenol*, **18**, 430 (1927).

[3] H. Fricke and S. Morse, *Phil. Mag.*, **7**, 129 (1929).

[4] H. Fricke and E. J. Hart, *J. Chem. Phys.*, 3 60 (1935).

[5] J. B. Miller, *J. Org. Chem.*, **24**, 560 (1964).

Table 1

The dose calculation by the Fricke dosimeter method

Initial concentration moles/l	10^{-3}	4.12×10^{-3}	2×10^{-2}	0.1	1	3
Volume of the irradiated solution (cm^3)	12	6	2.5	1	1	0.5
Dose eV/g.min	1.0×10^{17}	1.77×10^{17}	2.03×10^{17}	2.5×10^{17}	2.5×10^{17}	5.5×10^{17}

RESULTS AND DISCUSSION

No significant differences were found by irradiating solid diphenyldiazomethane at a 15 Ci source (a temperature of 20°) for a long period of time (96 hours), dissolving subsequently the sample in benzene and measuring its absorption in both visible and ultraviolet, compared to the nonirradiated reference sample. This shows that the solid phase radiolysis occurs at a very reduced, almost negligible rate on irradiation at this dose.

However, diphenyldiazomethane in benzene solution, irradiated at a temperature of 20°, decomposes more rapidly as the solution becomes more dilute, as follows below.

Solutions having concentrations of 10^{-3} and 4.12×10^{-3} moles/l that is, the most dilute ones within the range of concentrations being prepared, verify a first-order kinetics. As an example, table 2 reflects the values of the rate constants obtained for solutions having a concentration of 10^{-3} moles/l.

Table 2

Unimolecular rate constant and radiochemical yield for the radiolysis of dilute solutions

t min	ε	$C \times 10^3$ moles/l	$k_1 \times 10^5$ s^{-1}	G
0	0.40	1.06	—	—
60	0.35	0.93	3.71	1.29
120	0.31	0.82	3.54	1.01
240	0.24	0.64	3.54	1.03
300	0.21	0.56	3.57	0.93
360	0.17	0.45	3.96	0.99
480	0.14	0.37	3.64	0.84
710	0.09	0.24	3.50	0.68
900	0.05	0.132	3.85	0.60

$(k_1)_a = 3.66 \times 10^{-5}$

$A^{\frac{1}{2}}$ order-kinetics is verified on irradiation of more concentrated solutions : 2×10^{-2}, 10^{-1} and 1 moles/l. A solution with a concentration of 10^{-1} moles/l is presented in table 3.

Table 3

Fractionary rate constant and radiochemical yield characteristic for the radiolysis of the moderate concentration solutions

t min	ε	$C \times 10^3$ moles/l	$k_{\frac{1}{2}} \times 10^7$ moles$^{\frac{1}{2}}$/l$^{\frac{1}{2}}$s^{-1}	G
0	1.90	101.0	—	—
900	1.44	76.6	1.52	6.4
1470	1.19	63.3	1.49	6.05
1770	1.05	55.9	1.53	6.02
2880	0.69	36.7	1.46	5.26
4320	0.28	14.9	1.51	4.72

$(k_{\frac{1}{2}})_a = 1.49 \times 10^{-7}$

In order to study the radiolysis both in highly concentrated solutions 3 moles/l and in the solid substance, we used a stronger source, namely a 10,000 Ci one. In this case, decomposition occurs according to a first-order kinetics.

Table 4 shows the rate constant radiolysis in the case of a 3.12 moles/l diphenyldiazomethane solution and table 5 refers to the solid state.

Table 4

Unimolecular rate constant for the radiolysis of concentrated solutions

t hours	C moles/l	$k_1 \times 10^6$ s^{-1}
0	3.08	—
48	2.25	1.80
72	1.94	1.78
76	1.83	1.90
97	1.65	1.78
123	1.54	1.57
146	1.36	1.55
148	1.34	1.56
169.5	1.27	1.45
220	0.95	1.48

$(k_1)_a = 1.65 \times 10^{-6}$ s^{-1}

Table 5

Unimolecular rate constant of the radiolysis in the solid state

t hours	$C \times 10^2$ moles/l	$k_1 \times 10^6$ s^{-1}
0	5.0	
71.5	3.3	1.64
95	2.77	1.73
121	2.2	1.89
144	1.7	2.12
162	1.62	1.93
168	1.59	1.88
189.5	1.38	1.88
191.5	1.14	2.13

$(k_1)_a = 1.85 \times 10^{-6}$

The last column in tables 2, 3 and 4 refers to the values of the chemical yields calculated by the relation:

$$G = \frac{\Delta C}{I} 100$$

where ΔC is the concentration diminution (the number of converted moles/cm³) and I is the dose in eV/cm³.

The reaction final products resulting from the radiolysis of the concentrated solutions were identified by IR spectra as being benzophenone and benzophenonazine.

Benzophenone, revealed by the presence of $\rangle C = O$ frequency at 1665 cm^{-1}, forms in small amounts by benzophenonazine, the predominant final product, for reasons shown in a previous paper [6].

The same reaction products, benzophenonazine and benzophenone, were also isolated by irradiating a 3.12 moles/l concentrated solution. The melting point (164°) determined for benzophenonazine, was identical to that indicated in the literature. Thus, in accordance with these final products obtained by irradiation, the total reaction may be the following :

$$(C_6H_5)_2 - CN_2 \overset{\gamma}{\rightsquigarrow} (C_6H_5)_2 - C = N - N = C - (C_6H_5)_2 + (C_6H_5)_2CO + N_2$$

Three reaction mechanisms were developed in respect of the concentration of the irradiated solution.

a) DILUTE SOLUTIONS

In this case it is assumed that the reaction takes place by means of the excited benzene molecules formed by interaction with radiations. It is therefore an indirect mechanism.

---

[6] T. Oncescu, M. Contineanu and G. Bălăceanu, *Rev. Roumaine Chim.*, **17**, 213 (1972).

Let us denote the benzene molecules by B ; the interaction between γ radiations and benzene may be illustrated as follows :

$$B \overset{\gamma}{\rightsquigarrow} B^{+} + e^{*}.$$

The resulting electron loses its energy on the way causing at the same time the triplet-state excitation of the encountered benzene molecules[7-10] so that, at a certain distance of B^{+} the electron becomes thermalized (e_t)

$$B + e \rightarrow B^{T} + e_t$$

The coulombian interaction between the parent ion and the thermalized electron is sizeable due to the small dielectric constant (non-polar) so that this electron will very likely be recaptured by the positive ion, leading again to triplet-state excited benzene molecules

$$B^{+} + e_t \rightarrow B^{T}$$

The latter either transfer their energy to the dissolved diphenyldiazomethane molecules which decompose, or become extinct through collision with similar molecules. Under these conditions, the following processes are very probable :

$$4B \overset{k_0 I}{\rightsquigarrow} 4B^{T} \tag{a}$$

$$4D \overset{k_0' I}{\rightsquigarrow} 4D^{T} \tag{b}$$

$$D \overset{k_0'' I}{\rightsquigarrow} R + N_2 \tag{c}$$

$$2B^{T} \xrightarrow{k_1} 2B \tag{d}$$

$$B^{T} + B \xrightarrow{k_2} 2B \tag{e}$$

$$B^{T} + D \xrightarrow{k_3} B + D^{T} \tag{f}$$

$$2D^{T} \xrightarrow{k_4} 2D \tag{g}$$

$$D^{T} + D \xrightarrow{k_5} 2D \tag{h}$$

---

[7] S. Gordon, A. R. van Dyken and T. F. Doumani *J. Phys. Chem.*, **62**, 20 (1958).

[8] W. G. Burns and C. R. Reed, *Trans. Faraday Soc.*, **59**, 101 (1963).

[9] M. Inokuti, *Isotopes and Radiation*, **1**, 82 (1958).

[10] W. G. Burns, R. B. Cundall, P. A. Griffiths and W. R. Marsh, *Trans. Faraday Soc.*, **64**, 129 (1968).

$$D^T + B \xrightarrow{k_6} D + B \tag{i}$$

$$D^T \xrightarrow{k_7} R + N_2 \tag{j}$$

$$R + D \xrightarrow{k_8} C \tag{k}$$

$$R + O_2 \xrightarrow{k_9} RO_2 \tag{l}$$

$$RO_2 + D \xrightarrow{k_{10}} B_z \tag{m}$$

where D, C, B_z represent the diphenyldiazomethane, benzophenonazine and benzophenone molecules, respectively, and R and CO_2 are the radicals $(C_6H_5)_2\dot{\underset{\cdot}{C}}$ and $(C_6H_5)_2CO_2$.

The reaction rate of the diphenyldiazomethane radiolysis is written :

$$\frac{dC_D}{dt} = -4k_0' I C_D - k_0'' I C_D - k_3 C_{B^T} C_D + 2k_4 C_{D^T} + k_5 C_{D^T} C_D + \\ + k_6 C_{D^T} C_B - k_8 C_R C_D - k_{10} C_{RO_2} C_D \tag{1}$$

By applying the approximation according to which the intermediate concentrations of D^T, B^T, R, RO_2 are stationary, we obtain :

$$\frac{dC_{D^T}}{dt} = 4k_0' I C_D + k_3 C_{B^T} C_D - 2k_4 C_{D^T} - k_5 C_{D^T} C_D - k_6 C_{D^T} C_B - k_7 C_{D^T} = 0 \tag{2}$$

$$\frac{dC_{B^T}}{dt} = 4k_0 I C_B - 2k_1 C_{B^T} - k_2 C_{B^T} C_B - k_3 C_{B^T} C_D = 0 \tag{3}$$

$$\frac{dC_R}{dt} = k_0'' I C_D + k_7 C_{D^T} - k_8 C_R C_D - k_9 C_R C_{O_2} = 0 \tag{4}$$

$$\frac{dC_{RO_2}}{dt} = k_9 C_R C_{O_2} - k_{10} C_{RO_2} C_D = 0 \tag{5}$$

By adding up (1) with (2) and subtracting (4), it results :

$$\frac{dC_D}{dt} = -2k_0'' I C_D - 2k_7 C_{D^T} \tag{6}$$

From (3) we obtain:

$$C_{B^T} = \frac{4k_0 IC_B}{2k_1 + k_2C_B + k_3 C_D} \tag{7}$$

which, introduced in (2), leads to:

$$C_{D^T} = \frac{4k_0' IC_D (2k_1 + k_2C_B + k_3C_D) + 4k_0k_3IC_B C_D}{(2k_1 + k_2 C_B + k_3 C_D)(2k_4 + k_5 C_D + k_6 C_B + k_7)} \tag{8}$$

By introducing relations (7) and (8) in (1), we obtain:

$$\frac{\mathrm{d}C_D}{\mathrm{d}t} = -2k_0 IC_D - 2k_7 \frac{4k_0' I C_D (2k_1 + k_2C_B + k_3C_D) + 4k_0 k_3 IC_B C_D}{(2k_1 + k_2C_B + k_3C_D)(2k_4 + k_5 C_D + k_6C_B + k_7)} \tag{9}$$

In the case of dilute solutions, processes (b) and (c), which refer to the direct interaction of diphenyldiazomethane molecules with the radiation are negligible and (g) and (h), concerning the deactivation of excited diphenyldiazomethane molecules, are also highly improbable compared to the other processes in the considered sequence, that is:

$$k_3C_D \ll 2k_1 + k_2C_B$$

$$k_5 C_D + 2k_4 \ll k_6 C_B + k_7$$

Under these conditions, equation (9) becomes:

$$-\frac{\mathrm{d}C_D}{\mathrm{d}t} = 2k_7 \frac{4k_0 k_3 IC_B C_D}{(2k_1 + k_2 C_B)(k_6 C_B + k_7)} = K C_D \tag{10}$$

that is the differential equation of a first-order reaction.

Our experimental results, as reflected in table 2, confirm such a kinetics. Also, equation (10) accounts for the fact that the radiolysis in a dilute solution depends on the excitation of solvent molecules (a) and on its energy transfer on diphenyldiazomethane molecules which become decomposed (f) and (j).

b) CONCENTRATED SOLUTIONS AND SOLIDS

This case rules out the processes involving the solvent molecule, namely: (a), (d), (e), (f) and (i) which simplify equation (9), where, if condition

$$2k_5 C_D \ll 2k_4 + k_7$$

is formed, we obtain:

$$-\frac{\mathrm{d}C_D}{\mathrm{d}t} = \left(2k_0'' I + 2k_7 \frac{4k_0' I}{2k_4 + k_7}\right) C_D \tag{11}$$

It results from this equation that the reaction rate is proportional to the concentration of diphenyldiazomethane as required by the first-order kinetic equation, verified by the rate constant presented in table 4.

This equation also shows that the reaction depends primarily on the direct interaction of radiations with diphenyldiazomethane molecules. The same behaviour is obtained by studying the radiolysis of the solid substance (table 5). It must be pointed out that a dependence of C_D concentration on t was found when irradiating a very concentrated solution (3.12 moles/l) or the solid state, as it results from figure 1.

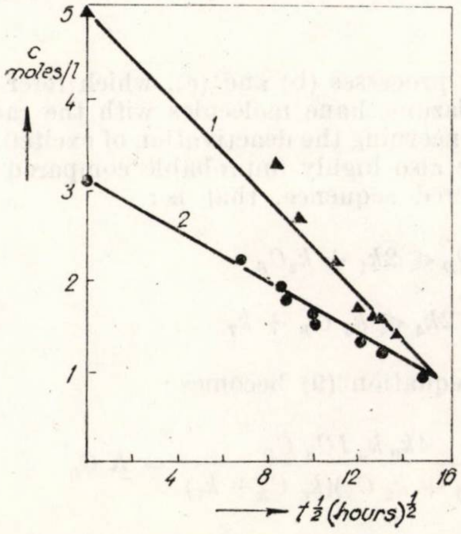

Fig. 1. — Plotting of the diphenyldiazomethane concentration versus $t^{1/2}$: *1*, for a 3.42 moles/l solution; *2*, for a solid sample.

Such a dependence suggests also the concomitant existence in kinetic handling, of a diffusion process which we have not implied. This may account for the larger error factors found in determining the rate constant in these situations (25–30%) compared to those determined in more dilute solutions (5–12%).

c) INTERMEDIATE CONCENTRATION SOLUTIONS

The results of the study performed for solution with an intermediate concentration which verify a 1/2 order kinetics (table 2) are presented in table 6.

The second column gives the times corresponding to a 65% conversion, which increase with the diphenyldiazomethane concentration.

Table 6

The constancy of the $k_{1/2}$ rate constant for the range of moderate concentrations solutions

t hours	C moles/l	$k_{\frac{1}{2}} \times 10^6$ $\text{moles}^{\frac{1}{2}}\ \text{l}^{\frac{1}{2}}\ \text{s}^{-1}$
163	1	1.25
58	10^{-1}	1.49
24	2×10^{-2}	1.44

In column 3, which presents the mean values of k rate constants, the rate constant is noticed as remaining practically constant although the concentration varied 50 times. This may be explained by the fact that the number of excited molecules increases correspondingly with the increase in the concentration of diphenyldiazomethane. At the same time the deactivation of the excited molecules clustered along the trajectories of the secondary electrons is favoured. As a result of the action of these two antagonistic processes, the rate constant does not vary with the initial concentration, which forces us to admit that processes (b) and (g) are in equilibrium :

$$2\text{D} \underset{k_4}{\overset{k_0' I}{\rightleftarrows}} 2\text{D}^{\text{T}}$$

where from results the equality :

$$2k_0' I C_D = k_4 C_{D^T}^2$$

whence :

$$C_{D^T} = \left(\frac{2k_0' I}{k_4}\right)^{1/2} C_D^{1/2} \tag{12}$$

If (12) is introduced in (6), it results :

$$\frac{dC_D}{dt} = -\,2\,k_0''\,IC_D - 2k_7\left(\frac{2k_0' I}{k_4}\right)^{1/2} C_D^{1/2} \tag{13}$$

This equation justifies the $\frac{1}{2}$ reaction order verified by our experimental data, if the first term, which refers to the formation of radicals by direct interaction between molecules and the radiation (process c) is neglected. This result shows that the radiolysis of a benzene solution of diphenyldiazomethane in this range of concentration 2×10^{-2}—1 moles/l occurs mainly owing to the excited diphenyldiazomethane molecules resulted both from direct interaction (b) and from the process involving energy transfer (f).

Revue Roumaine de Chimie, **19**, *6*, 941–946 (1974)

RADIOLYSIS OF THE COMPLEX OXALATES IN AQUEOUS SOLUTIONS. III [1,2]

THE INFLUENCE OF SOME OH SCAVENGERS ON THE RADIOLYSIS OF POTASSIUM TRISOXALATOCOBALTATE IN NEUTRAL AQUEOUS SOLUTION

J. PĂUN and TATIANA MEMETEA

University of Bucharest, Radiation Chemistry Laboratory, Bd. Republicii 13, Bucharest

Received October 10, 1973

The influence of some OH free radical scavengers such as Br^- and SCN^- ions and aliphatic alcohols on the radiochemical decomposition yield $G(-[Co(C_2O_4)_3]^{3-})$ in neutral aqueous solution has been studied. The presence of *t*-butyl alcohol in a concentration up to 0.1 M does not change the $G(-[Co(C_2O_4)_3]^{3-})$ value, suggesting that OH free radical does not take part in the radiolytic process of $[Co(C_2O_4)_3]^{3-}$ ion. The Br^- and SCN^- ions added to the solution strongly decrease the $G(-[Co(C_2O_4)_3]^{3-})$ yield due to the oxidation of cobaltous complex ion formed from the radiolysis of cobaltic complex, by the Br and SCN radicals : $X^- + OH \rightarrow$ $\rightarrow X + OH^- (X^- = Br^-, SCN^-)$; $[Co(C_2O_4)_2]^{2-} + X\cdot \xrightarrow{C_2O_2^{4-}} [Co(C_2O_4)_3]^{3-} + X^-$.

In previous papers [1,2] we investigated the radiolysis of potassium trisoxalatocobaltate in aqueous solutions in various conditions. The predominant process in the decomposition of the complex ion was suggested to be the reduction of this ion by the reactions with hydrated electron and hydrogen atom.

In order to complete the understanding of the radiolytic mechanism we studied the influence of some selective OH scavengers such as : Br^- and SCN^- ions, isopropyl and t — butyl alcohol on the decomposition kinetics.

EXPERIMENTAL

Potassium trisoxalatocobaltate was synthesized by the method described in the literature.[3] The solutions were prepared with triply distilled water. All the reagents being of ana-

---

[1] I. G. Murgulescu, T. Oncescu, J. Păun and I. Mihalcea, *Rev. Roumaine Chim.*, **12**, 573 (1967).

[2] I. G. Murgulescu and J. Păun, *Rev. Roumaine Chim.*, 19, 1 (1974).

[3] S. P. L. Sörensen, *Z. anorg. Chem.*, **11**, 1 (1896).

lytical purity, were used as such. In all the runs we used a constant concentration of the complex of 2×10^{-3}M.

The radiolysis was performed in the presence as well as in the absence of the air. The deaeration was carried out by bubbling purified argon for 30 minutes or by freezing-pumping cycles whenever needed.

The irradiation was carried out in a $\gamma - Co^{60}$ facility of the mobile source type with telemanipulation, of 500 Ci initial activity and 20 Ci/g specific activity. The dosimetry was carried out by chemical method using Fricke dosimeter.

The kinetics of the decomposition of the complex was followed by spectrophotometrical method, recording the decrease of the optical density at 595 nm during irradiation.

The overall zero order rate constant was calculated by relation :

$$k_0 = \frac{a}{E_0} \, \frac{\Delta E}{\Delta t} \tag{I}$$

where :

a is the initial solute concentration,

E_0 the optical density of the unirradiated solution,

ΔE the change in the optical density for irradiation time Δt.

RESULTS

The rate of the radiochemical decomposition of the complex ion in neutral aqueous solution in the presence of Br^- and SCN^- ions as selective OH scavengers is decreasing, the zero order kinetic law being maintained, in the presence of air as well as in its absence. The higher the concentration of the added scavenger, the slower the decomposition rate of the complex ion.

Figures 1 and 2 show the decrease of the optical density of the deaerated solution containing Br^- and SCN^- ions, during irradiation.

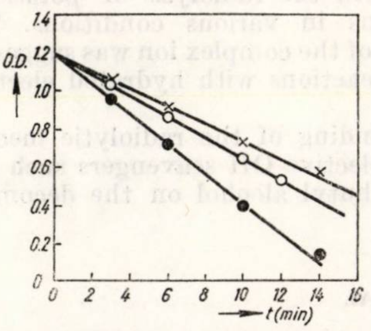

Fig. 1. — The influence of Br^- ions on the decomposition rate of $K_3[Co(C_2O_4)_3]$ in the absence of air. $K_3[Co(C_2O_4)_3]$ 2×10^{-3} M without scavenger ; O KBr 2×10^{-3} M added ; × KBr 10^{-2}M added. Dose rate 9.12×10^{19} eV/hg

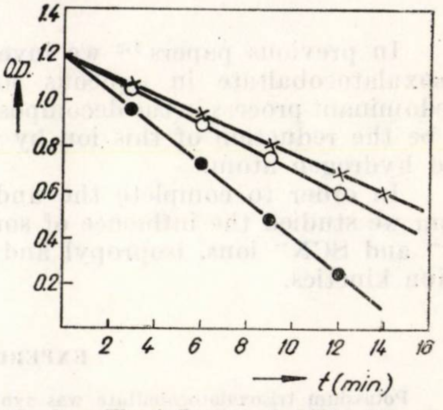

Fig. 2. — The influence of SCN^- ions on the decomposition rate cf $K_3[Co(C_2O_4)_3]$ in the absence of air. $K_3[Co(C_2O_4)_3]$ 2×10^{-3}M without scavenger ; O KSCN 2×10^{-3} M added ; X KSCN 10^{-2} added. Dose rate 9.12×10^{19} eV/hg.

The diminution of the radiochemical yield $G(-[(CoC_2O_4)_3]^{-3})$ and of the overall zero order constant (k_0) as a function of the scavenger concentration in the presence and the absence of the air is listed in table 1.

Table 1

The influence of Br^- and SCN^- ion on the G and k_0 values in the radiolysis of aqueous aerated and deaerated $K_3[Co(C_2O_4)_3]$ solutions of 2×10^{-3} M complex concentration

Scavenger conc (M)	KBr				KSCN			
	Argon		Air		Argon		Air	
	G	$k_0 \times 10^9$ (mol/cm³ s)	G	$k_0 \times 10^9$ (mol/cm³ s)	G	$k_0 \times 10^9$ (mol/cm³ s)	G	$k_0 \times 10^9$ (mol/cm³ s)
0	4.95	2.41	3.19	1.30	4.90	2.41	3.19	1.30
2×10^{-3}	3.60	1.51	2.64	1.12	3.27	1.38	2.42	1.02
10^{-2}	3.13	1.31	2.20	0.92	2.85	1.20	2.02	0.85

As can be seen from table 1, the SCN^- ion is more effective in reducing the $G(-[Co(C_2O_4)_3]^{3-})$ and k_0, both in the presence and the absence of the air. If the radiolysis is performed at a lower dose rate namely 6.73×10^{18} eV/h/g, a change of the slope will take place after 6% decomposition as is shown in figure 3.

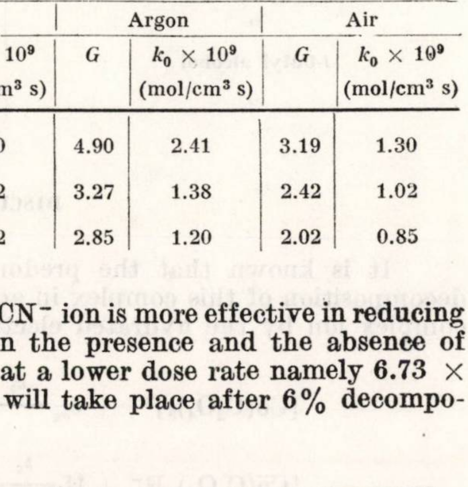

Fig. 3. — The influence of Br^- ions on the decomposition of $K_3[Co(C_2O_4)_3]$ deaerated solutions; ● $K_3Co(C_2O_4)_3$ without scavenger; O KBr 10^{-3} M added; X KBr 10^{-2} M added. Dose rate 6.73×10^{18} eV/hg

The radiochemical yield of the decomposition of the complex does not change in the presence of isopropyl alcohol concentrations up to 10^{-2}M and is slightly enhanced if the concentration of the alcohol is 10^{-1} M, as can be seen from table 2. *T*-butyl alcohol has no influence on $G(-[Co(C_2O_4)_3]^{3-})$ value even at concentration as high as 2×10^{-1} M.

Table 2

The influence of some aliphatic alcohols on the decomposition yield of the complex ion in aqueous 2×10^{-3} M solution

Scavenger	Scavenger concn.	$G(-[Co(C_2O_4)_3]^{3-})$
—		4.95 ± 0.05
isopropyl alcohol	10^{-2}	5.68
,,	10^{-1}	6.42
t-butyl alcohol	2×10^{-2}	4.90
,,	2×10^{-1}	5.00

DISCUSSION

It is known that the predominant process in the radiochemical decomposition of this complex in aqueous solution is the reduction of the complex ion by the hydrated electron and hydrogen atom:

$$[Co(C_2O_4)_3]^{3-} + e_{aq} \xrightarrow{k_1} [Co(C_2O_4)_2]^{2-} + C_2O_4^{2-} \quad (1)$$

$$[Co(C_2O_4)_3]^{3-} + H \xrightarrow{k_2} [Co(C_2O_4)_2]^{2-} + C_2O_4^{2-} + H^+ \quad (2)$$

From the pulse radiolysis data[4] it is known that $k_1 = 1.3 \times \times 10^{10} M^{-1}s^{-1}$, which indicates that $[Co(C_2O_4)_3]^{3-}$ ion is a good e_{aq} scavenger.

Recently, Shagisultanova[5] found for k_2 a value of $4.6\times10^6 M^{-1}s^{-1}$ by the method of introducing into the solution hydrogen atoms produced by electrodeless high frequency discharge in molecular hydrogen.

The above mentioned behaviour of the complex decomposition in the presence of *t*-butyl alcohol supports the fact that the free OH radicals do not take part in the complex decomposition. This assumption is also supported by our previous experiments[2] showing that the accumulation of hydrogen peroxide in the solution of the complex is linear with dose, $G(H_2O_2)$ being the same as in pure water.[6]

The slight increase in the decomposition yield of the complex in the presence of isopropylalcohol (table 2) is due to the reduction of the complex ion by the free radical $CH_3\dot{C}(OH)CH_3$, coming from reaction (3), between isopropylalcohol and the OH radical:

$$CH_3CH(OH)CH_3 + OH \longrightarrow CH_3\dot{C}(OH)CH_3 + H_2O \quad (3)$$

---

[4] J. Baxendale and A. Swallow, *Nature*, **201**, 468 (1964).

[5] G. Shagisultanova, *Khimia Vysokii Energhii* (russian edition), **5**, 187 (1971).

[6] A. Allen, *Radiation Res. Suppl.*, **4**, 54 (1964).

When the complex is irradiated in the presence of Br^- and SCN^- ions, these are quantitatively scavenging the free OH radicals by reactions (4) and (5):

$$Br^- + OH \xrightarrow{k_5} Br + OH^- \tag{4}$$

$$SCN^- + OH \xrightarrow{k_6} SCN + OH^- \tag{5}$$

From the data given in literature $k_4 = 10^9 M^{-1} s^{-1}$ [7] and $k_5 = 1.08 \times \times 10^9 M^{-1} s^{-1}$.[8] Recent works [9] have reported the identification of Br and SCN radical by E.S.R. method.

The decrease of the decomposition yield is due in this situation to the oxidation of $[Co(C_2O_4)]^{2-}$ ion resulted from the reaction (1) and (2), by the entities Br and SCN:

$$[Co(C_2O_4)_2]^{2-} + Br. \xrightarrow{C_2O_4^{2-}} [Co(C_2O_4)_3]^{3-} + Br^- \tag{6}$$

$$[Co(C_2O_4)_2]^{2-} + SCN. \xrightarrow{C_2O_4^{2-}} [Co(C_2O_4)]^{3-} + SCN^- \tag{7}$$

The stronger diminution of the decomposition yield in the presence of SCN^- scavenger (table 1) suggests that this ion has an ability of oxidation higher than that of Br^- ions. If the scavenger is Br^- ion, at both dose rate mentioned, in the presence of air as well as at the lower dose rate in the absence of air, a decrease of the slope (fig. 3) will be noticeable after a certain dose. This phenomenon support also the idea of a lower oxidation ability of Br^- ions expressed by the higher amount of $[Co(C_2O_4)_2]^{-2}$ ions required for reaction (6) to become more effective.

The lower extent of complex decomposition in aerated solution in the presence of Br^- or SCN^- ions is due to the fact that hydrogen peroxide builds up in a resonable concentration which results in a competition between reactions (6), (7) and (8), (9).

$$Br + H_2O_2 \rightarrow Br^- + H^+ + HO_2. \tag{8}$$

$$SCN + H_2O_2 \rightarrow SCN^- + H^+ + HO_2. \tag{9}$$

---

[7] "Pulse Radiolysis", Ed. M. Ebert and J. P. Keene, Academic Press, London and New York, 1965 61 p.

[8] "Pulse Radiolysis" Ed. M. Ebert and J. P. Keene, Academic Press, N. Y. London, p. 133.

[9] D. Behar and R. Fessenden, *J. Phys. Chem.*, **76**, 1706 (1972).

The decrease of the $G(-[Co(C_2O_4)_3]^{3-})$ yield may also be due to the capture of hydrogen atom by the Br^- and SCN^- ion, but these reactions are less probable than those involving OH free radicals. On the other hand, Draganič showed recently that the reaction $Br^- + H$ is relatively slow having a rate constant of $3.3 \times 10^7\ M^{-1}s^{-1}$.[10]

These qualitative remarks will constitute the starting point for a quantitative treatment of the process in order to get a better understanding of the contribution of reactions (6) and (7).

---

[10] Z. D. Draganič and I. G. Draganič, *J. Phys. Chem.*, **76**, 2733 (1972).

Revue Roumaine de Chimie, **19**, *6*, 947–954 (1974)

ÉTUDE DU SPECTRE VIBRATIONNEL, INFRAROUGE ET RAMAN, DU PYROPHOSPHATE DE PLOMB (IV) — PbP_2O_7

R. HUBIN

Université de Liège, Institut de Chimie. Sart Tilman par B-4000, Liège 1, Belgique

Reçu le 10 octobre 1973

Le spectre vibrationnel, infrarouge et Raman, du pyrophosphate de plomb (IV) est interprété en considérant une symétrie D_{3d} pour le groupement P_2O_7 (pont P—O—P linéaire). Dans une approche simplifiée du problème, le groupement P_2O_7 est décomposé en trois entités indépendantes au point de vue vibrationnel (deux pyramides PO_3 de symétrie C_{3v} et un pont central P—O—P linéaire), ce qui constitue une approximation due à Bues et Gehrke. Ensuite, le groupement P_2O_7 est considéré lui-même comme une entité au point de vue vibrationnel, ce qui permet de montrer qu'il est justifié de recourir à la dite approximation, comme cela a été fait dans de précédents articles consacrés à l'étude du spectre vibrationnel de pyrophosphates, pyroarséniates et pyrovanadates.

INTRODUCTION

Le pyrophosphate de plomb IV — PbP_2O_7 — est isotype [1] des composés cubiques $M^{IV}P_2O_7$ (M^{IV} = Si, Sn, Ti, Zr...) dont la structure a été déterminée par Lévi et Peyronel [2]; l'étude du radiogramme X de poudre de ces composés a permis à ces auteurs de les rattacher au système cubique à faces centrées : ils ont proposé un modèle de structure de groupe spatial T_h^6 avec une maille unitaire comportant 40 « atomes » (28 oxygène, 8 phosphore et 4 ions métalliques). De cette étude de Lévi et Peyronel découlent deux conclusions importantes : l'hexacoordinence de l'élément tétravalent par rapport à l'oxygène et l'existence d'un groupement P_2O_7 de symétrie D_{3d} (avec un angle $\widehat{P—O—P}$ de 180°).

Cependant, Wittmann et coll.[3] ont été amenés à envisager, pour les pyrophosphates d'éléments tétravalents, l'existence d'une maille élémentaire cubique plus grande, ayant un paramètre triple de celui de la maille élémentaire de Lévi et Peyronel. En effet, le diagramme X de poudre de ces composés révèle, à côté des raies intenses observées par Lévi et Peyronel et caractéristiques de la petite maille, la présence de raies d'intensité beaucoup plus faible, qu'il est impossible de justifier par la maille de Lévi et Peyronel. L'interprétation de ces raies exige l'adoption d'une maille triple de cette maille élémentaire.

---

[1] G. Peyronel, *Gazz. chim. Ital.*, **69**, 254 (1939).

[2] G. R. Lévi et G. Peyronel, *Z. Krist.*, **92**, 190 (1935).

[3] A. Wittmann, H. Völlenkle et H. Nowotny, *Monatsh.*, **94**, 956 (1963).

L'existence d'une grande maille cubique repose la question de la valeur de l'angle $\widehat{P-O-P}$ dans le groupement P_2O_7. En effet, les raisons de symétrie imposant le caractère rectiligne de la liaison $P-O-P$ dans la petite maille n'existent plus dans la maille triple. Ainsi, il est nécessaire d'envisager un angle $\widehat{P-O-P}$ différent de 180° dans le cas du pyrophosphate cubique de thorium pour pouvoir interpréter le spectre infrarouge de ce composé[4] dont l'isotypie avec les autres pyrophosphates cubiques d'éléments tétravalents est pourtant établie par la diffraction des rayons X.

Nous avons cependant pu montrer[5] que, dans le cas de PbP_2O_7, le spectre infrarouge témoignait d'une symétrie D_{3d} pour le groupement P_2O_7.

Le but de cet article est de proposer, tout d'abord, une interprétation du spectre Raman de PbP_2O_7 en utilisant l'approximation de Bues et Gehrke,[6] comme nous l'avons fait en ce qui concerne son spectre infrarouge[5]; ensuite, nous renoncerons à cette approximation, afin de proposer une interprétation plus rigoureuse des spectres infrarouge et Raman de ce composé.

PARTIE EXPÉRIMENTALE

Le spectre infrarouge a été enregistré dans le domaine 200 à 1300 cm^{-1} à l'aide d'un appareil Beckman IR 12 à double faisceau et, dans le domaine 70 à 200 cm^{-1} à l'aide d'un appareil Cameca à simple faisceau. La méthode des pastilles d'iodure de potassium a été utilisée (6 mgrs de substance sont dispersés dans 0,9 gr de KI). Un appareil Coderg PH 1 a été utilisé pour l'enregistrement du spectre Raman. La raie excitatrice est la 6328 Å produite par un laser He—Ne de marque «Spectra Physics».

MODES NORMAUX DE VIBRATION DU GROUPEMENT P_2O_7

L'APPROXIMATION DE BUES ET GEHRKE [6]

Bues et Gehrke ont montré par le calcul et la mesure de distances phosphore — oxygène que les liaisons $P-O$ dans le pont central étaient 33% plus faibles que les liaisons $P-O$ dans les groupes PO_3 latéraux (dans le cas de pyrophosphates, dans le cadre d'une étude d'ensemble de phosphates condensés); en première approximation, ces ensembles peuvent, dès lors, être considérés comme indépendants au point de vue vibrationnel : cette approximation permet de décomposer le schéma $O_3P-O-PO_3$ en deux parties indépendantes :

---

[4] R. HUBIN, *Spectrochim. Acta*, **27A**, 311 (1971).

[5] R. HUBIN et P. TARTE, *Spectrochim. Acta*, **23A**, 1815 (1967).

[6] W. BUES et H. W. GEHRKE, *Z. anorg. Chem.*, **288**, 291 (1956).

— le pont central P—O—P présentant les modes normaux de vibration d'un groupe XO_2 linéaire (dans le cas d'une symétrie D_{3d} du groupement P_2O_7);

— les pyramides latérales PO_3 présentant les modes normaux de vibrations d'ensembles XO_3 dont la symétrie est C_{3v} dans le cas d'une symétrie D_{3d} du groupement P_2O_7.

Le dénombrement des vibrations de ces ensembles permet de déterminer les vibrations d'un groupement P_2O_7 ; le couplage des vibrations des deux groupes PO_3 de chaque groupe P_2O_7 occasionne, en outre, le dédoublement de chacune des fréquences de vibration des groupes PO_3 : les unes pour lesquelles les deux groupes PO_3 vibrent en opposition de phase (affectées d'un indice ′), les autres pour lesquelles les deux groupes PO_3 vibrent en phase (non affectées d'un indice particulier).

Les représentations de symétrie désignent parmi ces vibrations celles qui sont actives en infrarouge et en Raman (tableau 1).

Tableau 1

Modes normaux de vibration d'un groupement P_2O_7 de symétrie D_{3d}

Classe de symétrie	A_{1g}	A_{2u}	E_g	F_u
Eléments de symétrie conservés	toute la symétrie	axe ternaire 3 plans axe binaire	un plan centre	aucun élément
Activité en infrarouge activité en Raman	inactif *actif*	*actif* inactif	inactif *actif*	*actif* inactif
Mouvements s'y rattachant	ν_s POP ν_s PO_3 δ_s PO_3	ν_{as} POP ν'_s PO_3 δ'_s PO_3	ν'_{as} PO_3 δ'_{as} PO_3	δ_s POP ν_{as} PO_3 δ_{as} PO_3

En renonçant à cette approximation, le groupe P_2O_7 est considéré comme une entité indécomposable au point de vue vibrationnel ; la théorie des groupes permet un classement des modes normaux de cette entité :

$$\Gamma_{(D_{3d})} = 3\,A_{1g} + 1\,A_{1u} + 3\,A_{2u} + 3\,E_g + 4\,E_u$$

Cependant, lorsque le groupe P_2O_7 est considéré dans le réseau cristallin de PbP_2O_7,[7] la symétrie réelle, due à l'entourage, devient C_{3i} ; la répartition des modes normaux de vibration devient alors :

$$\Gamma_{(C_{3i})} = 3\,A_g + 4\,A_u + 3\,E_g + 4\,E_u$$

---

[7] R. S. Halford, *J. Chem. Phys.*, **14**, 8 (1946).

La différence entre les symétries D_{3d} et C_{3i} est donc très faible : toutes deux présentent un centre de symétrie (ce qui signifie que toute vibration active en infrarouge sera inactive en Raman et vice-versa) et, en fait, le passage de l'une à l'autre n'entraîne que les légères variations suivantes dans la répartition des modes normaux de vibration dans les classes de symétrie :

$$\begin{array}{lcl} \underline{D_{3d}} & & \underline{C_{3i}} \\ 3\,A_{1g} & \longrightarrow & 3\,A_g \\ 1\,A_{1u} & \searrow & \\ & & 4\,A_u \\ 3\,A_{2u} & \nearrow & \\ 3\,E_g & \longrightarrow & 3\,E_g \\ 4\,E_u & \longrightarrow & 4\,E_u \end{array}$$

Ce schéma montre qu'il est possible de continuer à travailler en ne considérant que la symétrie locale (D_{3d}) du groupe P_2O_7.

Sur la base d'une symétrie D_{3d}, Mooney et coll.[8] ont calculé les valeurs des différentes fréquences de vibration. Ce calcul, assez complexe, ne peut être basé que sur des constantes de force estimées de façon assez grossière. Nous comparerons ces valeurs aux valeurs des fréquences des vibrations observées dans les spectres infrarouge et Raman.

INTERPRÉTATION DU SPECTRE RAMAN DE PbP_2O_7 (en utilisant l'approximation de B. et G.)

La connaissance des diverses vibrations actives en Raman (tableau 1) et du domaine d'absorption des vibrations actives en infrarouge[5] permet de proposer une attribution quasi directe du spectre Raman de PbP_2O_7 (ainsi, ν_{as} PO_3 est la fréquence la plus élevée observée dans le spectre infrarouge, tandis que ν'_{as} PO_3 est la plus élevée du spectre Raman ; de même, la fréquence d'absorption de la vibration ν'_s PO_3 dans le spectre infrarouge sera assez proche de celle de ν_s PO_3 dans le spectre Raman). Le résultat de ces attributions est repris dans le tableau 2.

Ces attributions attirent cependant deux remarques très importantes :

1) La vibration ν_{as} du pont central $P-O-P$ active en infrarouge devrait normalement être inactive en Raman : cependant, cette vibration, de faible intensité dans le spectre infrarouge, apparaît dans le spectre Raman avec une intensité encore beaucoup plus faible : nous reviendrons sur ce point.

2) Il est tentant d'attribuer la raie de faible intensité observée à 522 cm^{-1} dans le spectre Raman à la vibration δ'_{as} PO_3 (puisque la vibration δ_{as} PO_3 se marque à 536 cm^{-1} dans le spectre infrarouge) ; cependant, une autre attribution peut être proposée : à partir de la fréquence de la vibration ν_{as} $P-O-P$ (à 732 cm^{-1} dans le spectre infrarouge), on peut

---

[8] R. W. Mooney, S. Z. Toma et J. Brunvoll, *Spectrochim. Acta*, **23A**, 1541 (1967)

Tableau 2

Fréquences, en cm^{-1}, du pyrophosphate de plomb IV et attributions

Attributions	Infrarouge	Raman
ν_{as} PO_3	1117ff	
ν'_{as} PO_3		1050f
ν_s PO_3		1014m
ν'_s PO_3	972m	
ν_{as} P—O—P	732f	736ff
δ_{as} PO_3	536m	
δ'_{as} PO_3		522f[a]
δ'_s PO_3	376f	
δ_s PO_3		336ff
ν_{as} PbO_6	224m	
ν_s PbO_6		192f
		95ff[b]

a) Plus vraisemblablement, cette fréquence sera attribuée à ν_s P—O—P (tableau 4).

b) Intensités : FF très forte, m moyenne, f faible, ff très faible.

estimer la fréquence de la vibration ν_s P—O—P entre 500 et 525 cm^{-1} en utilisant les formules simplifiées suivantes [9] :

$$\nu_{sym} \simeq \frac{1}{2\pi C}\sqrt{k\left(\frac{1}{m_P} + \frac{1 + \cos\alpha}{m_0}\right)}$$

$$\nu_{asym} \simeq \frac{1}{2\pi C}\sqrt{k\left(\frac{1}{m_P} + \frac{1 - \cos\alpha}{m_0}\right)}$$

avec α désignant l'angle $\widehat{P-O-P}$ (180° dans ce cas) et $k = 6{,}4 . 10^5$ dyn/cm.[8]

Dès lors, il apparaît plus logique d'attribuer la raie 522 cm^{-1} à la vibration ν_s P—O—P ; nous reviendrons également sur cette question.

INTERPRÉTATION DES SPECTRES INFRAROUGE ET RAMAN DE PbP_2O_7

(en considérant le groupe P_2O_7 comme une entité au point de vue vibrationnel)

Renoncer à l'approximation de Bues et Gehrke devrait, en principe, permettre une attribution plus rigoureuse des vibrations observées dans les spectres : dans le tableau 3, les fréquences observées dans le spectre infrarouge sont comparées aux fréquences calculées par Mooney et coll. : en découlent des attributions qui sont comparées aux attributions proposées dans le cadre de l'approximation de Bues et Gehrke. Cette comparaison entre fréquences calculées et observées provoque certaines ambiguïtés :

---

[9] N. B. Colthup, L. H. Daly et S. E. Wiberley, « Introduction to Infrared and Raman Spectroscopy », Academic Press, New York, 1964.

Tableau 3

Fréquences calculées (8) et fréquences observées, en cm^{-1}, dans le spectre infrarouge de PbP_2O_7

Vibrations actives en infrarouge	Description de la vibration	Fréquence calculée	Fréquence observée	Attributions proposées dans le cadre de l'approximation de B.G.
$\nu_4\ (A_{1u})$	τ (OPPO)	69		
$\nu_5\ (A_{2u})$	ν (PO)	1012	972	$\nu'_s\ PO_3\ (A_{2u})$
$\nu_6\ (A_{2u})$	ν (PO*)	1260[a]	732	$\nu_{as}\ P-O-P\ (A_{2u})$
$\nu_7\ (A_{2u})$	δ (OPO*)	510 →	→ 376	$\delta'_s\ PO_3\ (A_{2u})$
	δ (OPO)			
$\nu_{11}\ (E_u)$	ν (PO)	1138	1117	$\nu_{as}\ PO_3\ (E_u)$
$\nu_{12}\ (E_u)$	δ (OPO)	537	536	$\delta_{as}\ PO_3\ (E_u)$
$\nu_{13}\ (E_u)$	δ (OPO*)	384 ↗		
$\nu_{14}\ (E_u)$	τ (OPPO)	19		

a) Voir à ce sujet la discussion dans le texte.

— Alors que la liaison centrale P—O * (nous désignerons par O* l'oxygène central du groupe P_2O_7 : $O_3P-O^*-PO_3$) est fortement affaiblie par rapport aux liaisons latérales P—O, il apparaît assez étonnant que le calcul de Mooney et coll. conduise à une valeur plus élevée ($1260\ cm^{-1}$) pour $\nu_6(A_{2u})$ [νPO*] que pour $\nu_5\ (A_{2u})$ ($1012\ cm^{-1}$) et $\nu_{11}\ (E_u)$ (à $1138\ cm^{-1}$), alors que ces dernières sont des vibrations [νPO]. En fait, nous avions attribué une fréquence beaucoup plus basse à $\nu_6(A_{2u})$: $732\ cm^{-1}$, ce qui paraît plus logique.

— Deux vibrations $\delta(O-P-O^*)$: $\nu_7(A_{2u})$ à $510\ cm^{-1}$ et $\nu_{13}\ (E_u)$ à $384\ cm^{-1}$ sont calculées, alors qu'une seule est observée dans le spectre infrarouge à $376\ cm^{-1}$: on est tenté de l'attribuer à $\nu_{13}\ (E_u)$, calculée à une fréquence très proche et constater ainsi l'absence de $\nu_7\ (A_{2u})$ dans le spectre. Cependant, il n'en demeure pas moins une incertitude renforcée par les arguments suivants :

— à plusieurs reprises, des divergences importantes apparaissent entre fréquences calculées et observées.

Tableau 4

Fréquences calculées (8) et fréquences observées, en cm^{-1}, dans le spectre Raman de PbP_2O_7

Vibrations actives en Raman	Description de la vibration	Fréquence calculée	Fréquence observée	Attributions dans le cadre de l'approximation de B.G.
$\nu_1\ (A_{1g})$	ν (PO)	1047	1014	$\nu_s\ PO_3\ (A_{1g})$
$\nu_2\ (A_{1g})$	ν (PO*)	713	522	$\nu_s\ P-O-P\ (A_{1g})$
$\nu_3\ (A_{1g})$	$\left\{\begin{array}{l}\delta\ (OPO^*)\\ \delta\ (OPO)\end{array}\right.$	288	336	$\delta_s\ PO_3\ (A_{1g})$
$\nu_8\ (E_g)$	ν (PO)	1133	1050	$\nu'_{as}\ PO_3\ (E_g)$
$\nu_9\ (E_g)$	δ (OPO)	445		
$\nu_{10}\ (E_g)$	δ (OPO*)	283		
$\nu_6\ (A_{2u})$	ν (PO*)		736	$\nu_{as}\ P-O-P$[a]

a) Vibration normalement inactive Raman.

— Dans le cadre de l'approximation de Bues et Gehrke, une seule vibration de ce type apparaît parmi les vibrations actives en infrarouge : δ'_s PO_3 (A_{2u}).

Dans le cas des autres vibrations, on peut observer une meilleure concordance entre fréquences calculées et observées ; il subsiste cependant des écarts de 20 à 40 cm^{-1}, ce qui est peu étant données les approximations réalisées lors du calcul des fréquences. Une autre cause d'écarts, réside dans le fait que les fréquences ont été calculées pour un groupe P_2O_7 « isolé », sans tenir compte des influences de la nature du cation sur les différentes vibrations ; nous avons pu montrer [5] que ces influences étaient particulièrement importantes.

Le tableau 4 reprend les fréquences observées dans le spectre Raman, comparées aux valeurs calculées et mises en parallèle avec les attributions réalisées en utilisant l'approximation de Bues et Gehrke. Sauf dans le cas de deux fréquences que nous discuterons ci-dessous, les fréquences calculées correspondent assez bien aux fréquences observées, avec parfois des écarts de 30 à 80 cm^{-1}, comme dans le cas du spectre infrarouge. Nous ferons cependant les remarques suivantes à propos des raies observées à 522 et 736 cm^{-1} :

— La bande observée à 732 cm^{-1} dans le spectre infrarouge a été attribuée à la vibration antisymétrique ν_6 (A_{2u}) [ν_{as} P—O—P] ; la fréquence calculée pour la vibration symétrique correspondante, ν_2(A_{1g})[ν_s P—O—P], est beaucoup trop élevée (nous l'estimions entre 500 et 525 cm^{-1}, voir plus haut). Dès lors, dans ce cas, on a observé un décalage trop important entre fréquence calculée et fréquence observée.

— Le problème de l'apparition dans le spectre Raman de la vibration ν_6 (A_{2u}) [ν_{as} P—O—P] provoque également une difficulté d'interprétation. Cependant, que l'on utilise ou non l'approximation de Bues et Gehrke, on ne peut expliquer la présence de cette vibration dans le spectre Raman sans envisager une déformation du groupe P_2O_7 : cette observation montre en effet qu'il y a rupture des règles de sélection valables pour les « molécules » centrosymétriques et indique que l'angle P—O—P s'écarte légèrement de 180°, supprimant ainsi le centre de symétrie caractéristique de la configuration D_{3d}.

Les calculs de Mooney et coll. amènent ces auteurs à attribuer la bande 747 cm^{-1} du spectre infrarouge de ZrP_2O_7 à la vibration ν_2 (A_{1g}) normalement active en Raman et inactive en infrarouge : considérant la faible intensité de cette bande dans le spectre infrarouge (dont elle devrait être absente d'après leurs calculs) et son absence dans le spectre Raman (où ils l'attendaient), ils envisagent que la déformation est si faible qu'il serait encore possible de considérer une symétrie D_{3d} pour le groupe P_2O_7 de ce composé !

CONCLUSIONS

Les calculs de Mooney et coll., s'ils confirment dans les grandes lignes les attributions proposées dans le cadre de l'approximation de Bues et

Gehrke, n'apportent pas de solution plus satisfaisante aux difficultés rencontrées lors de l'utilisation de cette approximation (par exemple, la présence de ν_{as} P—O—P dans le spectre Raman) ; en outre, certaines ambiguïtés sont apportées aux attributions (par exemple, dans le cas de la bande observée à 376 cm^{-1} dans le spectre infrarouge).

Ces éléments, ajoutés au fait qu'il n'est possible d'utiliser que des fréquences calculées de manière très approximative, ne correspondant que d'assez loin aux fréquences observées, montrent qu'il est justifié de continuer à utiliser l'approximation de Bues et Gehrke qui présente l'avantage de caractériser beaucoup plus concrètement les différentes vibrations et permet un dépouillement plus aisé des spectres vibrationnels des composés de ce type.

Revue Roumaine de Chimie, **19**, *6*, 955–965 (1974)

THE GALVANOSTATIC STUDY OF THE ELECTROCHEMICAL ADSORPTION PROCESS ON THE CHLORINE-ACTIVE CARBON ELECTRODE IN MOLTEN SALTS. III[1]

ANODIC POLARIZATION (CHARGING) EQUATION

S. STERNBERG, S. PETRESCU and VALERIA PETRESCU

Polytechnic Institute, Str. Polizu 1, Bucharest, Romania

Received July 4, 1973

An equation is given which correlates the active carbon potential φ with the anodic polarization time, *t*, of a process of anodic polarization in a molten salt system. The obtained equation was verified and found to agree with the experimental data for the AgCl – KCl system within a temperature range of 400° – 600°.

In this paper we intend to find an equation which correlates the active carbon potential φ with the anodic polarization time *t*, of an anodic polarization process, in a molten salt system. We have started with the following equation (fig. 1):

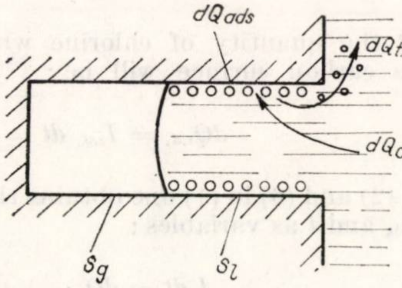

Fig. 1. — Model of the charging (anodic polarization) process.

$$dQ_c = dQ_{\text{ads}} + dQ_{t.d.} \tag{1}$$

in which:

dQ_c – quantity of chlorine deposited on the active carbon surface during the elementary charging time *dt*, with the current intensity I_c

$$dQ_c = I_c \, dt \tag{2}$$

---

[1] Part II: S. Petrescu, S. Sternberg and V. Petrescu, *Rev. Roumaine Chim.*, **18**, 1715 (1973).

dQ_{ads} – quantity of chlorine adsorbed on the active carbon electrode which remained on it in dt

$dQ_{t.d.}$ – quantity of chlorine which is "lost" from the active carbon electrode by thermal desorption, in dt.

1. THE HYPOTHESIS OF QUASIEQUILIBRIUM CHARGING (SMALL I_c)

The hypothesis is advanced that the thermal desorption "losses" in time unit (the thermal desorption current $I_{t.d.}$) increase with increasing surface concentration of chlorine adsorbed on electrode, c_s :

$$I_{t.d.} = K\, c_s \tag{3}$$

If the anodic polarization (charging) process takes place sufficiently slowly (low I_c), the surface concentration c_s can be expressed in terms of the amount of adsorbed chlorine, Q_{ads} (at the instant t) and the active surface, S, of the carbon electrode ; assuming the system is in equilibrium (uniform distribution of chlorine on active carbon surface outside as well as inside the carbon electrode) one obtains :

$$c_s = Q_{\mathrm{ads}}/S \tag{4}$$

Consequently :

$$I_{t.d.} = K\, Q_{\mathrm{ads}}/S \tag{5}$$

During dt the quantity of chlorine which is thermally desorbed from the active carbon surface will be :

$$dQ_{t.d.} = I_{t.d.}\, dt = (K/S)\, Q_{\mathrm{ads}}\, dt \tag{6}$$

Replacing (2) and (6) in (1) one obtains the following differential equation, having Q_{ads} and t as variables :

$$I_c dt = dQ_{\mathrm{ads}} + (K/S)\, Q_{\mathrm{ads}}\, dt \tag{7}$$

Separating the variables it results :

$$dt = dQ_{\mathrm{ads}}/(I_c - K\, Q_{\mathrm{ads}}/S) \tag{8}$$

By integrating this equation, it is obtained :

$$t = -\,(S/K) \ln{(I_c - KQ_{\mathrm{ads}}/S)} + \mathrm{const} \tag{9}$$

To determine the integration constant we impose the following condition :

$$t = 0 \rightarrow Q_{\mathrm{ads}} = 0 \tag{10}$$

Thus, with this condition, it results from (9):

$$\text{const} = (S/K)\ln I_c \tag{11}$$

Replacing (11) in (9):

$$t = (S/K)\ln I_c/(I_c - KQ_{\text{ads}}/S) \tag{12}$$

or in an exponential form:

$$I_c/(I_c - K\,Q_{\text{ads}}/S) = \text{Exp}\,(K\,t/S) \tag{13}$$

It results for Q_{ads} the following equation:

$$Q_{\text{ads}} = (I_c S/K)\,(1 - e^{-Kt/S}) \tag{14}$$

This equation perfectly satisfies from the qualitative point of view. Thus it was expected to obtain Q_{ads} proportional to the active carbon surface S and to the charging current I_c. Also, one can observe that as t increases, Q_{ads} increases, reaching a plateau as t tends to infinity (fig. 2). At the plateau the thermal discharge "losses" become equal to charging current $I_c = I_{t.d.}$. In this case Q_{ads} becomes limiting Q_{ads}:

$$Q_{\text{ads. limit}} = I_c\,S/K \tag{15}$$

From this relation we can find constant K:

$$K = I_c\,S/Q_{\text{ads. limit}} \tag{16}$$

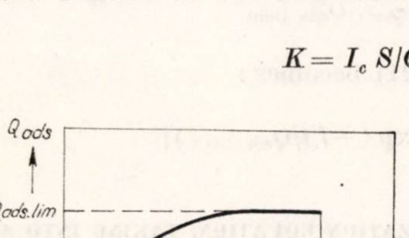

Fig. 2. — Qualitative variation of Q_{ads} against the time.

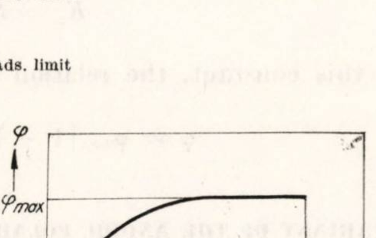

Fig. 3. — Qualitative variation of φ against the time.

Replacing (16) in (14) it results:

$$Q_{\text{ads}} = Q_{\text{ads. limit}}\,[1 - \text{Exp}\,(-I_c\,t/Q_{\text{ads. limit}})] \tag{17}$$

We can also calculate the thermal desorption current $I_{t.d.}$, replacing (14) in (5):

$$I_{t.d.} = I_c[1 - \mathrm{Exp}\,(-I_ct/Q_{\mathrm{ads.\,limit}})] \tag{18}$$

This relation, like (14) and (17), suits perfectly from the qualitative point of view, namely we observe that the thermal desorption current increases asymptotically from zero (for $t = 0$) up to a maximum value equal to I_c (fig. 3).

Admitting the hypothesis that the potential φ is proportional to the adsorbed chlorine concentration on the active surface, we can write:

$$\varphi = K_\varphi c_s \tag{19}$$

But, in agreement with (4),

$$\varphi = K_\varphi Q_{\mathrm{ads}}/S \tag{20}$$

Replacing Q_{ads} from (17) in (20) it results:

$$\varphi = (K_\varphi Q_{\mathrm{ads.\,limit}}/S)\,[1 - \mathrm{Exp}(-I_ct/Q_{\mathrm{ads.\,limit}})] \tag{21}$$

The constant K_φ can be obtained by placing the time to the infinity $t \to \infty$; then $\varphi \to \varphi_{\max}$ (corresponding to a given charging current I_c).

From (22) it results:

$$\varphi_{\max} = K_\varphi\, Q_{\mathrm{ads.\,limit}}/S \tag{22}$$

From this:

$$K_\varphi = S\ \varphi_{\max}/Q_{\mathrm{ads.\,limit}} \tag{23}$$

With this constant, the relation (21) becomes:

$$\varphi = \varphi_{\max}[1 - \mathrm{Exp}\,(-I_ct/Q_{\mathrm{ads.\,limit}})] \tag{24}$$

2. A VARIANT OF THE ANODIC POLARIZATION EQUATION, TAKING INTO ACCOUNT THE VARIATION OF THE ACTIVE SURFACE DURING THE CHARGING PROCESS

We admit, also in this case, as the starting point, the equation (1):

$$I_cdt = dQ_{\mathrm{ads}} + dQ_{t.d.} \tag{25}$$

Since, during the anodic polarization, the active surface of the carbon increases, at a given instant there coexist different zones of the electrode surface having different concentrations. Those zones which have worked from the beginning of the process as active surfaces will have a maximum concentration; and those zones which started to work as active surfaces later, will have a smaller concentration.

We admit that the active carbon electrode potential φ is proportional to the chlorine concentration on those zones which are the most active (that is, those zones which are active from the beginning of the anodic polarization process). On these zones the concentration will be maximum at the instant t, comparatively with the other zones. We will denote this instant maximum concentration $c_{\max,t}$. In this case, we can write :

$$\varphi = K\, c_{\max,t} \tag{26}$$

The "losses" by thermal desorption can be expressed aggregately in a manner similar to the equation (6) :

$$dQ_{t.d.} = I_{t.d.}\, dt \tag{27}$$

but in this case (in the presence of the concentration gradient on the active surface of the carbon electrode) we admit that $I_{t.d.}$ is proportional to the maximum concentration at the considered instant t:

$$I_{t.d.} = K_1 c_{\max,t} \tag{28}$$

Taking into account the relation (26), $I_{t.d.}$ becomes :

$$I_{t.d.} = K_1 \varphi / K \tag{29}$$

Q_{ads} can be expressed by means of the average concentration at the instant t, $c_{\text{med},t}$, on the total adsorption surface of the active carbon $S_{\max}$:

$$Q_{\text{ads}} = c_{\text{med},t}\; S_{\max} \tag{30}$$

or :

$$Q_{\text{ads}} = c_{\max,t}\, S_{\max}\;\; c_{\text{med},t}/c_{\max,t} = S_{\max}(\varphi/K)c_{\text{med},t}/c_{\max,t} \tag{31}$$

From this relation :

$$dQ_{\text{ads}} = (c_{\text{med},t}/c_{\max,t})\,(S_{\max}/K)d\varphi = (1/\alpha)\,(S_{\max}/K)d\varphi \tag{32}$$

where we have denoted (see fig. 4)

$$\alpha = c_{\max,t}/c_{\text{med},t} \geqslant 1 \tag{33}$$

With (27) and (32) in (25):

$$I_c dt = (1/\alpha)\,(S_{\max}/K)d\varphi + (K_1\varphi/K)dt \tag{34}$$

By separating variables :

$$\alpha dt = (S_{\max} d\varphi/K)\;/\;(I_c - K_1\varphi/K) \tag{35}$$

Integrating, we obtain:

$$\alpha t = -(S_{\max}/K_1)\ln(I_c - K_1\varphi/K) + \text{const} \tag{36}$$

The integration constant can be found by imposing the following condition: at the moment $t = 0$, the potential φ must be equal to the remanent potential ($\varphi = \varphi_{\text{rem}}$). It results for the constant the expression:

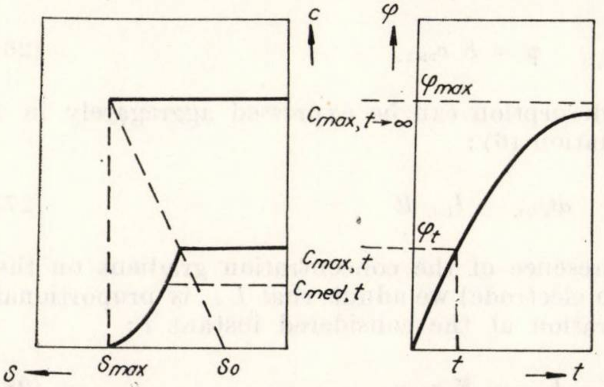

Fig. 4. – Chlorine concentration distribution against the active surface S at different instants during the charging process.

$$\text{const} = (S_{\max}/K_1)\ln(I_c - K_1\varphi_{\text{rem}}/K) \tag{37}$$

With (37) in (36) we obtain:

$$\varphi = (K/K_1)\,I_c[1 - \text{Exp}\,(-K_1\alpha t/S_{\max})] + \\ + \varphi_{\text{rem}}\,\text{Exp}\,(-K_1\alpha t/S_{\max}) \tag{38}$$

for $t \to \infty$, $\varphi \to \varphi_{\max}$

$$\varphi_{\max} = K\,I_c/K_1 \tag{39}$$

Consequently:

$$K_1 = K\,I_c/\varphi_{\max} \tag{40}$$

In order to find K we can use the equation (26) in that point where φ becomes maximum and Q_{ads} becomes $Q_{\text{ads. limit}}$:

$$\varphi_{\max} = K\,Q_{\text{ads. limit}}/S_{\max} \tag{41}$$

Therefore:

$$K = \varphi_{\max}\,S_{\max}/Q_{\text{ads. limit}} \tag{42}$$

With (42) in (40):

$$K_1 = S_{\max}I_c/Q_{\text{ads. limit}} \tag{43}$$

With (39) and (43) in (38) it results:

$$\varphi = \varphi_{\max}\,[1 - \text{Exp}\,(-\alpha I_c\,t/Q_{\text{ads. limit}})] + \\ + \varphi_{\text{rem}}\,\text{Exp}\,(-\alpha I_c\,t/Q_{\text{ads. limit}}) \tag{44}$$

We have tried to check up in what measure the equation of anodic polarization curve (44) is in agreement with experimental data at the following temperatures: 400°, 500°, 600°, in the system $AgCl + KCl$ for different values of charging current I_c : 0.02 A, 0.05 A, 0.1 A, 0.15 A, 0.2 A. For all the anodic polarization curves obtained experimentally, the remanent potential has been done zero by a cathodic polarization (previous to the anodic polarization) with a small current intensity [2] (I_d — discharging intensity $= 0.01$ A). Consequently, for $\varphi_{\text{rem}} = 0$, the equation (44) becomes:

$$\varphi = \varphi_{\max} \left[1 - \operatorname{Exp}\left(-\alpha I_c t / Q_{\text{ads. limit}}\right)\right] \tag{45}$$

In this equation we will denote:

$$\beta = \alpha I_c / Q_{\text{ads. limit}} \tag{46}$$

with which (45) becomes:

$$\varphi = \varphi_{\max} \left[1 - \operatorname{Exp}\left(-\beta t\right)\right] \tag{47}$$

If $\varphi_{\max}$ and one couple of the values φ_1, t_1 are known from the experimental data, it results from the equation (47) the value of K:

$$\beta = (1/t_1) \ln \left[\varphi_{\max} / (\varphi_{\max} - \varphi_1)\right] \tag{48}$$

With this value, using now equation (47), we can compute the values of φ, for any instant t. Because we have found that the β values for different values of the couple φ, t have a certain variation (generally a small decrease with the increase of time t), in the data processing we have computed several values of β corresponding to several pairs φ, t. Then, with these values of β we have found the average value of β, presented in table 1, for the temperatures, 400°, 500°, 600° and for different current

Table 1

Variation of potential φ as a function of time

T	I_c [A]	equation	β
400	0.1	$\varphi = 890\ (1 - e^{-0.07081\ t})$	0.07081
400	0.15	$\varphi = 885\ (1 - e^{-0.08613\ t})$	0.08613
400	0.2	$\varphi = 980\ (1 - e^{-0.14485\ t})$	0.14485
500	0.02	$\varphi = 780\ (1 - e^{-0.00871\ t})$	0.00871
500	0.05	$\varphi = 845\ (1 - e^{-0.02261\ t})$	0.02261
500	0.1	$\varphi = 875\ (1 - e^{-0.04639\ t})$	0.04639
500	0.15	$\varphi = 865\ (1 - e^{-0.09569\ t})$	0.09569
600	0.02	$\varphi = 745\ (1 - e^{-0.06512\ t})$	0.006512
600	0.1	$\varphi = 810\ (1 - e^{-0.02331\ t})$	0.02331
600	0.15	$\varphi = 845\ (1 - e^{-0.19571\ t})$	0.19571

---

[2] S. Sternberg and V. Petrescu, *Rev. Roumaine Chim.*, **19** (1974).

intensities. In the same table there are presented the corresponding equations of the anodic polarization curves.

With these equations we have found the theoretical values of φ from minute to minute, using an electronic computer. In figures 5, 6, 7, 8 are shown the anodic polarization curves drawn by the computer, for the

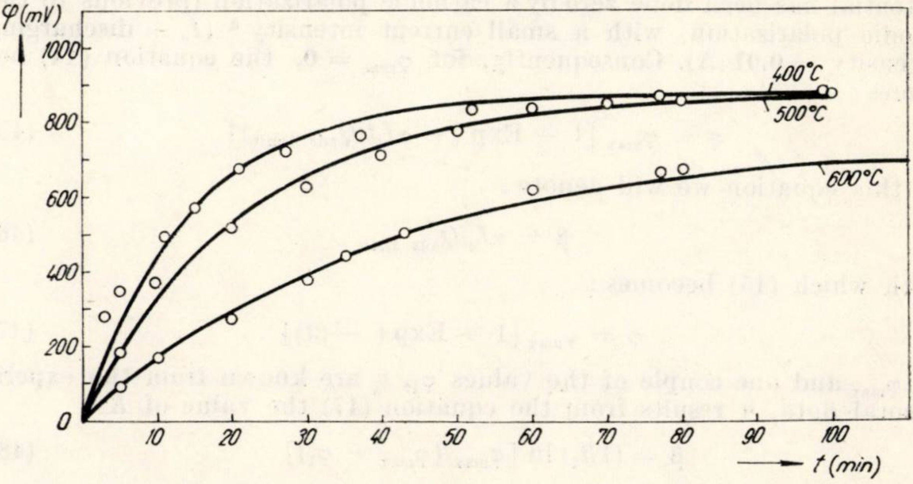

Fig. 5. — Anodic polarization curves drawn by the computer (full lines) and the experimental points (small circles) for $I_e = 0.1$ A at 400°, 500°, 600°.

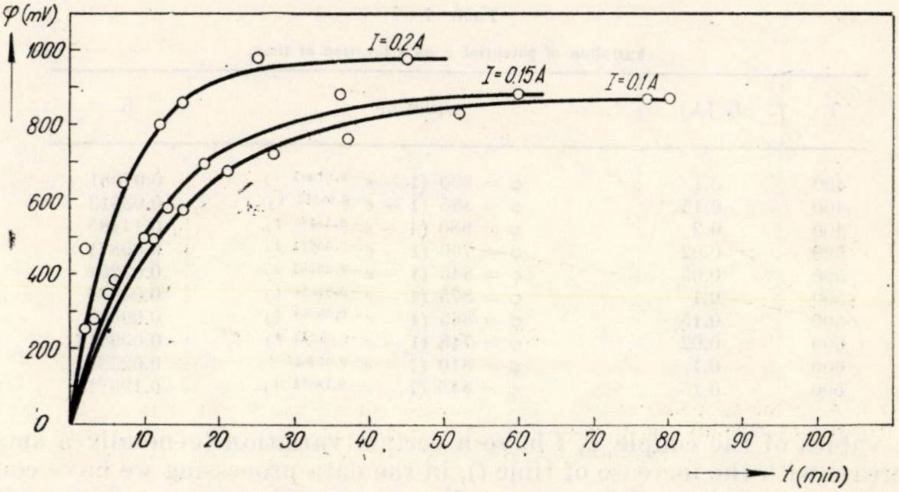

Fig. 6. — Anodic polarization curves drawn by the computer (full lines) and the experimental points (small circles) at the temperature 400°, for the current intensities : 0.2 A, 0.15 A, 0.1A.

equations from table 1. The points marked by small circles correspond to the experimental data. One ascertains that the mathematical from of the anodic polarization curve (47) is in good agreement with the experi-

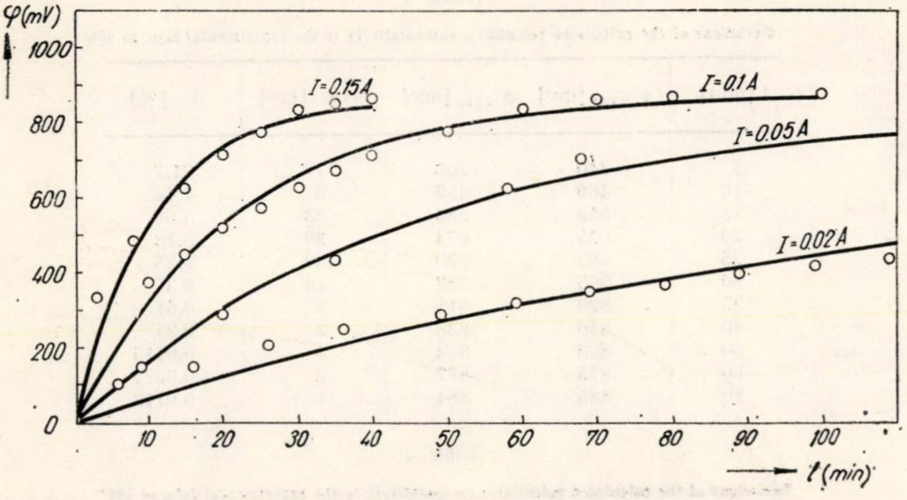

Fig. 7. — Anodic polarization curves drawn by the computer (full lines) and the experimental points (small circles) at the temperature 500°, for the current intensities: 0.15 A, 0.1 A, 0.05 A, 0.02 A.

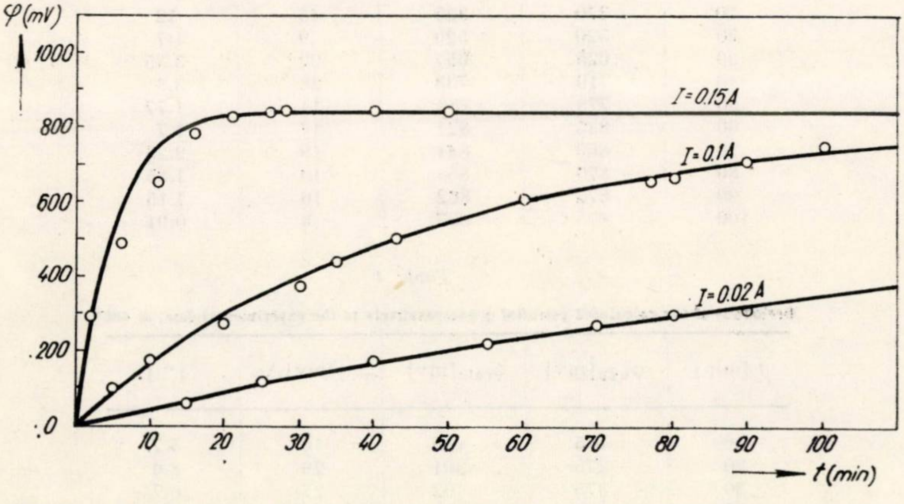

Fig. 8. — Anodic polarization curves drawn by the computer (full lines) and the experimental points (small circles) at the temperature 600°, for the current intensities: 0.15 A, 0.1 A, 0.02 A.

mental data. In order to estimate the deviations from the experimental data, there are presented in tables 2, 3 and 4 the computed values and experimental values of φ, at different times t, together with the absolute and relative errors (for $I_c = I_d = 0.1$ A; for the mentioned temperatures 400°, 500°, 600°).

Table 2

Deviations of the calculated potential φ comparatively to the experimental data, at 400°

t [min]	$\varphi_{exp.}$ [mv]	φ_{calc} [mv]	error [mv]	$\Delta\varphi$ [%]
5	340	266	74	21.7
10	460	452	8	1.74
15	550	583	33	5.66
20	635	674	39	5.78
25	700	739	39	5.28
30	765	783	18	2.3
35	820	815	5	0.61
40	840	838	2	0.24
50	863	864	1	0.0115
60	875	877	2	0.0227
70	885	884	1	0.0113

Table 3

Deviations of the calculated potential φ comparatively to the experimental data, at 500°

t [min]	φ_{exp} [mv]	φ_{calc} [mv]	error [mv] $\Delta\varphi$	[%]
10	370	325	45	12
20	520	529	9	1.7
30	625	657	22	3.35
40	710	738	28	3.8
50	775	789	14	1.77
60	835	821	14	1.7
70	860	841	19	2.25
80	870	854	16	1.85
90	872	862	10	1.15
100	875	867	8	0.91

Table 4

Deviations of the calculated potential φ comparatively to the experimental data, at 600°

t [min]	φ_{exp} [mv]	φ_{calc} [mv]	error [mv] $\Delta\varphi$	[%]
10	175	165	10	5.7
20	275	301	26	8.6
30	375	402	27	6.7
35	442	452	10	2.2
43	502	512	10	1.9
60	610	610	0	0
80	670	685	15	2.2
90	710	708	2	0.28
100	745	730	15	2

We observe that for charging times greater than 10—20 minutes, the deviations become equal to some per cents. The greater deviations which appear at the small charging times can be explained by the fact that α — defined by the relation (33) — is greater than α_{medium} (corresponding to β_{medium}) at the small times. This fact is in agreement with the hypotheses admitted when we have defined the coefficient α (33). A better proof of these hypotheses consists in estimating the magnitude order of the coefficient α. In order to do that we can use the relation (46):

$$\alpha = \beta Q_{\mathrm{ads.\,limit}} / I_c \qquad (49)$$

We observe that $Q_{\mathrm{ads.\,lim}}$ can be estimated approximately (neglecting the thermal desorption losses during the cathodic polarization process) by using the following formula:

$$Q_{\mathrm{ads.\,limit}} \cong I_d(t_d + \Delta t_{\mathrm{rem}}) \qquad (50)$$

Table 5

Values of the coefficient α as a function of temperature

T [°C]	I_c[A]	t_c[min]	$\varphi_{\max}$ [mv]	I_d[A]	t_d[min]	Δt_{rem}	β	α
400	0.1	80	890	0.1	29	8.2	0.07081	2.64
500	0.1	100	875	0.1	35	5	0.04639	1.85
600	0.1	175	810	0.1	50	1.6	0.02331	1.20

With the values presented in table 5, for three charge — discharge processes (anodic and cathodic polarization) at 400°, 500° and 600°, with $I_c = I_d = 0.1$ A we obtain for α the values corresponding to α_{approx} (in the approximation specified in relation (50)):

$$\alpha_{\mathrm{approx}} = \beta I_d(t_d + \Delta t_{\mathrm{rem}})/I_c \qquad (51)$$

First of all we observe that α_{approx} is greater than the unit, as it was expected in agreement with the hypotheses we admitted (33), and is closer to the unit when the temperature increases. This behaviour is explained by the fact that the molten salts wet better and better the carbon surface during the increase of the temperature, so that greater surfaces become efficient for the adsorption process right from the beginning of the anodic polarization peocess. That is, S_0 is closer to $S_{\max}$ with the increase of the temperature (see fig. 4).

We remark that the α_{approx} values from table 5 are a little smaller than the effective values of α, because of the fact that $Q_{\mathrm{ads.\,lim}}$ was estimated approximately (50). If we knew the efficiency of the cathodic polarization:

$$\eta_d = Q_d / Q_{\mathrm{ads.\,limit}} \qquad (52)$$

we could calculate the α value corresponding to its definition (33) with the relation:

$$\alpha = \beta\,(t_d + \Delta t_{\mathrm{rem}})\, I_d / \eta_d I_c \qquad (53)$$

The development of this possibility and the attempt to improve the anodic polarization curve taking into account the dependence of α on time will be presented in a subsequent paper.

Revue Roumaine de Chimie, **19**, *6*, 955–965 (1974)

Revue Roumaine de Chimie, 19, 6, 967–976 (1974)

L'ÉTUDE GALVANOSTATIQUE DU PROCESSUS DE L'ADSORPTION ÉLECTROCHIMIQUE SUR L'ÉLECTRODE D'IODE-CHARBON ACTIF DANS LES SELS FONDUS. II[1]

INFLUENCE DE LA TEMPÉRATURE

S. STERNBERG et I. GALASIU

Centre de chimie Physique, 31, str. Galaţi, Bucarest

Reçu le 5 juillet 1973

On a déterminé les courbes potentiel — temps pendant la polarisation anodique et cathodique galvanostatique de l'électrode d'iode-charbon actif dans les sels fondus aux températures de 300°, 400°, 500°, 600° et 700°. A basses températures, sur les courbes de polarisation cathodique galvanostatique existent des paliers caractéristiques qu'on peut attribuer à une condensation capillaire de l'iode dans les pores du charbon actif et qui diminuent quand la température augmente. A basses températures et aux potentiels éloignés du potentiel réversible le rendement du dépôt de l'iode sur l'électrode est de 100 % et il diminue quand la température augmente ou à mesure que le potentiel s'approche du potentiel réversible.

Dans un travail antérieur [1] on a déterminé les courbes de polarisation anodique et cathodique de l'électrode d'iode-charbon actif dans les sels fondus dans des conditions galvanostatiques à la température de 300° en fonction de l'intensité de courant. Le présent travail continue cette étude pour l'intervalle de températures de 300° à 700°.

PARTIE EXPÉRIMENTALE

Pour le dépôt de l'iode sur l'électrode de charbon actif on a fait l'électrolyse d'un mélange eutectique $AgI + KI$. L'anode est une barre de charbon actif à surface spécifique de 10 à 20 m^2/g et dont le poids est de 2,23 g (ayant les dimensions 12 × 12,5 × 17 mm), la cathode une barre en argent de 3 mm de diamètre. Le potentiel de la cellule a été mesuré à l'aide d'un oscilographe cathodique à trace rémanente. Pour la polarisation anodique, ainsi que pour la polarisation cathodique de l'électrode de charbon on a utilisé une méthode galvanostatique.

---

[1] Ire partie : S. Sternberg et I. Galasiu, *Rev. Roumaine Chim.*, 19, 523 (1974).

L'électrode de charbon dépourvue totalement d'iode a été soumise à une polarisation anodique galvanostatique jusqu'au potentiel désiré tout en enregistrant entre temps la courbe de polarisation anodique galvanostatique. Puis, on a commuté la cellule sur un circuit de polarisation cathodique galvanostatique jusqu'à l'éloignement total de l'iode de l'électrode, enregistrant aussi la courbe de polarisation cathodique galvanostatique.

Les quantités d'iode déposées sur l'électrode par l'électrolyse ou désorbées de l'électrode ont été calculées des relations :

$$Q = i.t \text{ et } a = \frac{Q}{F}$$

où :

Q = quantité de courant exprimée en coulombs ;
F = constante de Faraday ;
i = intensité du courant ;
t = temps de la polarisation ;
a = atomes — grammes d'iode.

Durant les expériences on a barboté dans l'électrolyte un puissant courant d'argon de sorte que l'iode gazeux soit éliminé continuellement de la cellule d'électrolyse.

Le schéma de l'installation et la manière de préparer les électrodes de charbon actif ont été donnés dans nos travaux antérieurs [2–5].

La surface apparente de l'électrode est de 11,33 cm^2. La surface réelle de l'électrode de charbon actif est beaucoup plus grande, mais inconnue à cause du fait qu'on ne connaît pas exactement la surface de contact entre l'électrode et l'électrolyte et par conséquent on ne peut pas accorder une valeur sûre aux densités de courant employées.

RÉSULTATS ET DISCUSSIONS

Dans la figure 1 on donne les courbes de polarisation anodique obtenues au dépôt de l'iode sur une électrode de charbon actif à la température de 700°. La polarisation anodique a été faite avec des courants de 20 mA, 50 mA, 100 mA et 200 mA. Comme potentiel de référence (zéro) nous avons choisi le potentiel réversible de l'électrode d'iode dans le même mélange et à la même température, calculé d'après l'équation [6] :

$$E = 0{,}5885 - 0{,}225 . 10^{-3} \, (T - 873) \tag{1}$$

Ainsi que nous l'avons déjà montré dans un travail antérieur[1] pour la température de 300° l'allure générale des courbes potentiel (φ) — temps est la suivante. A une intensité de courant donnée, le potentiel de l'électrode augmente en temps, après quoi il arrive à une valeur stationnaire, inférieure à celle du potentiel réversible. A basses températures la valeur du

[2] S. Sternberg et I. Galasiu, *Rev. Roumaine Chim.*, **13**, 991 (1968).
[3] S. Sternberg et I. Galasiu, *Rev. Roumaine Chim.*, **15**, 1169 (1970).
[4] S. Sternberg et I. Galasiu, *Rev. Roumaine Chim.*, **17**, 1697 (1972).
[5] S. Sternberg, V. Petrescu et I. Galasiu, *Rev. Roumaine Chim.*, **17**, 1689 (1972).
[6] S. Sternberg, J. Adorian et I. Galasiu, *Electrochim. Acta*, **11**, 385 (1966).

potentiel stationnaire est rapprochée de la valeur du potentiel réversible mais quand la température augmente, la différence entre ces deux valeurs augmente elle aussi pour toutes les intensités de courant employées.

Après l'achèvement de la polarisation anodique galvanostatique, on a toujours fait une polarisation cathodique à une intensité de courant égale à celle utilisée dans la polarisation anodique pour mesurer la quantité d'iode absorbée sur l'électrode. La polarisation anodique a été aussi faite « par portions »[1].

Dans les figures 2—6 on a représenté les courbes de polarisation anodique « par portions » pour $i = 100$ mA à diverses températures. Chaque polarisation anodique a été suivie d'une polarisation cathodique ayant la même intensité de courant. Après la première polarisation cathodique on a repris la polarisation anodique jusqu'à $t_2 > t_1$, etc. On a constaté que la courbe de polarisation anodique « par portions » se superpose très bien à celle obtenue dans un seul temps (voir fig. 2—6).

Le rendement de charge-décharge (fig. 7—8) a été calculé d'après la relation :

$$\eta = \frac{Q_{(\text{polarisation cathodique})}}{Q_{(\text{polarisation anodique})}} \, 100$$

où :

$Q_{(\text{polarisation cathodique})}$ est la quantité d'électricité utilisée à la polarisation cathodique ;

$Q_{(\text{polarisation anodique})}$ est la quantité d'électricité employée à la polarisation anodique.

Ainsi que nous l'avons déjà montré dans un travail antérieur,[1] sur la première portion de la courbe de polarisation anodique (fig. 1), tout le courant est employé pour « charger » l'électrode avec de l'iode adsorbé. Le courant employé pour charger de l'iode sur l'électrode a été dénommé courant d'adsorption, $i_{(\text{adsorption})}$. C'est ensuite que le rendement du dépôt de l'iode sur l'électrode a commencé à diminuer à cause de la « désorption thermique », ce qui fait que l'augmentation du potentiel en temps devienne plus lente. On a dénommé ce courant qui correspond à la désorption thermique, courant de désorption, $i_{(\text{desorption})}$. Sur la dernière partie de la courbe de polarisation anodique, où le potentiel reste constant, le courant de désorption devient égal au courant total de polarisation et $i_{(\text{adsorption})} = 0$.

Pour chaque température on, a continué la polarisation anodique jusqu'à ce que $Q_{(\text{polarisation cathodique})}$ reste constant[1] (c'est-à-dire jusqu'à ce que $i_{(\text{adsorption})} = 0$). A une polarisation anodique plus prolongée, la courbe de polarisation cathodique se superpose à la précédente.

A cause des hautes températures auxquelles on effectue l'électrolyse des sels fondus, le courant de désorption arrive à de grandes valeurs, à de centaines de milliampères. Ce courant de désorption est en réalité égal à la vitesse de désorption de l'halogène de l'électrode de charbon.

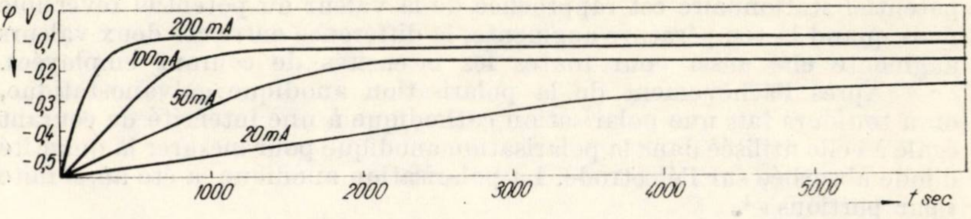

Fig. 1. — Courbes de polarisation anodique (φ — t) de l'électrode d'iode-charbon actif à différentes intensités de courant ; t = 700°.

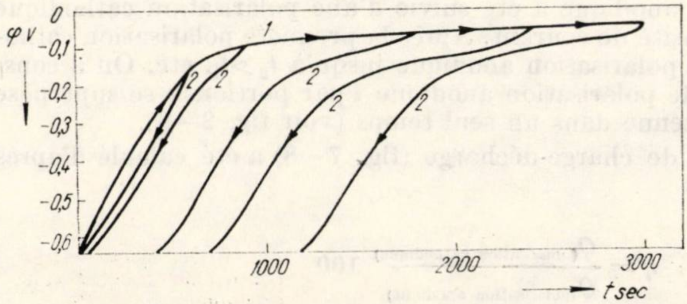

Fig. 2. — Courbes de polarisation anodique (*1*) et cathodique (*2*) où i = 100 mA ; t = 300°.

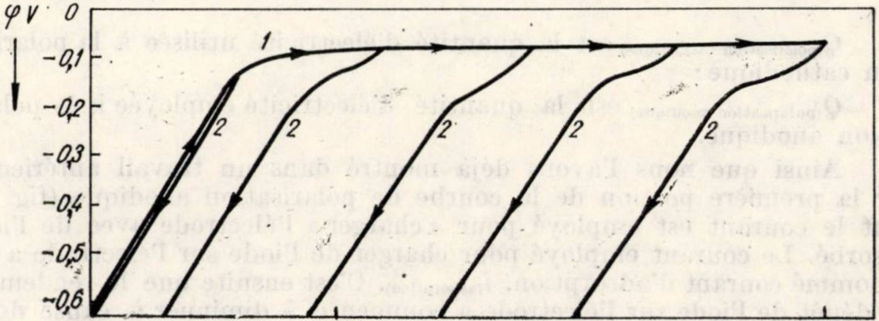

Fig. 3. — Courbes de polarisation anodique (*1*) et cathodique (*2*) où i = 100 mA ; t = 400°

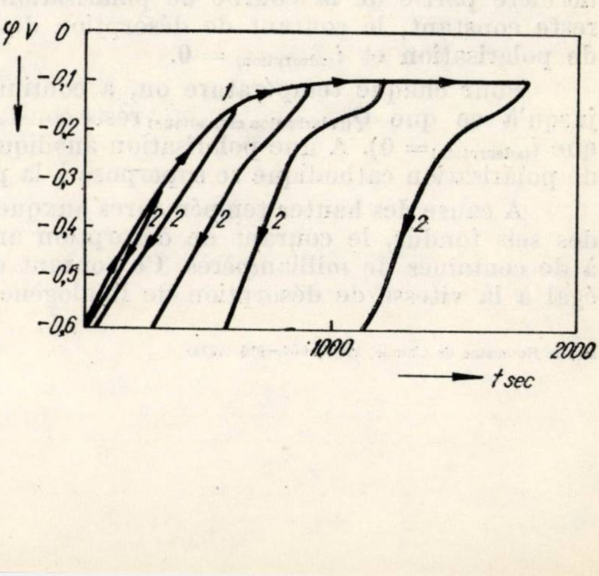

Fig. 4. — Courbes de polarisation anodique (*1*) et cathodique (*2*) où i = 100 mA ; t = 500°.

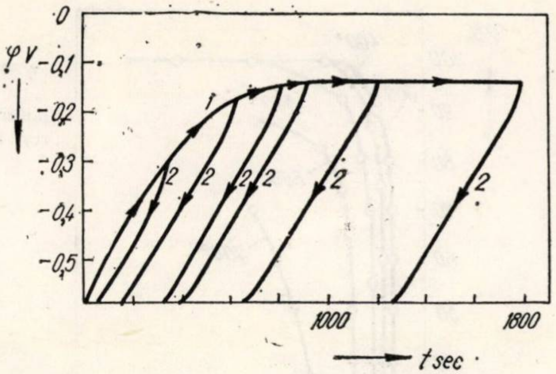

Fig. 5. — Courbes de polarisation anodique (*1*) et cathodique (*2*) où $i = 100$ mA ; $t = 600°$.

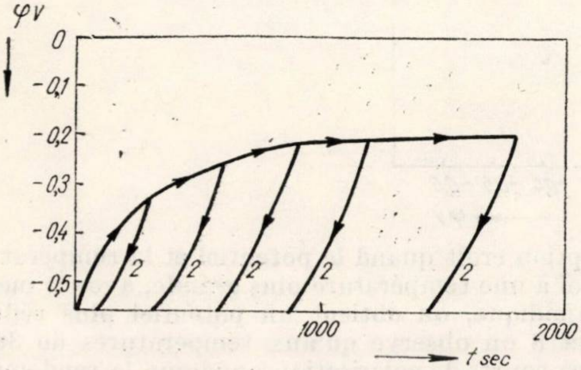

Fig. 6. — Courbes de polarisation anodique (*1*) et cathodique (*2*) cú $i=100$ mA ; $t = 700°$.

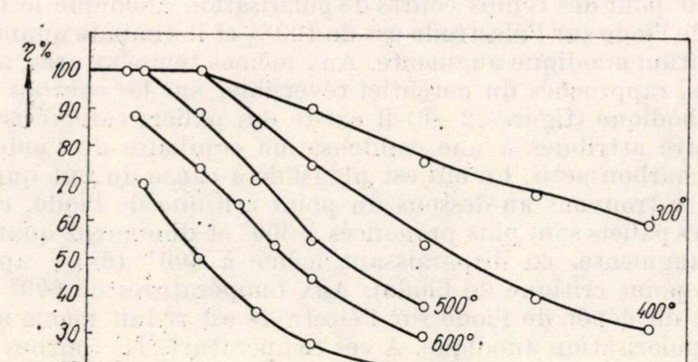

Fig. 7. — Le rendement $\eta = \frac{Q_{\text{décharge}}}{Q_{\text{charge}}}$ en fonction de la quantité d'électricité employée à la polraisation anodique à diverses températures : $i_{\text{charge}} = i_{\text{décharge}} = 100$ mA.

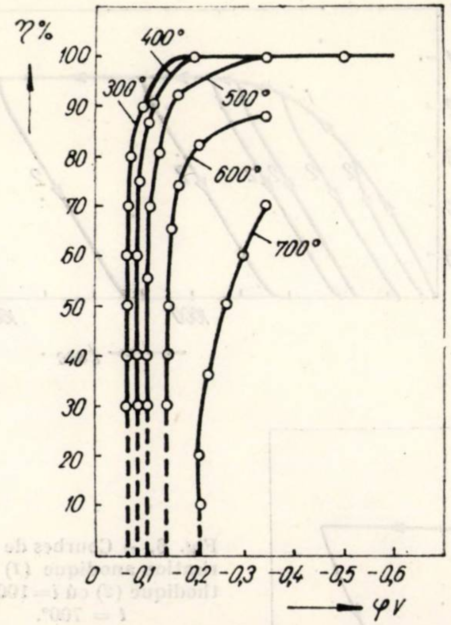

Fig. 8. – Le rendement $\eta = \frac{Q_{\text{décharge}}}{Q_{\text{charge}}}$ en fonction du potentiel à diverses températures : $i_{\text{charge}} = i_{\text{décharge}} = 100$ mA.

Le courant de désorption croît quand le potentiel et la température augmentent. C'est pourquoi à une température plus grande, avec le même courant de polarisation anodique, on obtient un potentiel plus réduit.

Dans les figures 7 et 8 on observe qu'aux températures de 300°, 400° et 500° pour des temps courts de polarisation anodique le rendement du dépôt de l'iode sur l'électrode est de 100 % et il diminue quand le temps de polarisation anodique augmente. Aux mêmes températures, aux potentiels élevés, rapprochés du potentiel réversible, sur les courbes de polarisation cathodique (figures 2–6) il existe des paliers caractéristiques qui peuvent être attribués à une condensation capillaire de l'iode dans les pores du charbon actif. Ce qui est plausible à cause du fait que ces températures se trouvent au-dessous du point critique de l'iode, celui-ci est de 511°. Ces paliers sont plus prononcés à 300° et diminuent quand la température augmente, en disparaissant même à 600° (donc après avoir dépassé le point critique de l'iode). Aux températures de 600° et 700° le rendement du dépôt de l'iode sur l'électrode est réduit même aux temps courts de polarisation anodique. A ces temperatures les courbes de polarisation cathodique changent leur concavité, ce que nous avons déjà montré dans un travail antérieur [3].

Dans la figure 9 on a représenté la dépendance du potentiel φ de la quantité d'électricité consommée à la polarisation anodique pour la température de 600°. Les quantités Q ont été calculées des courbes φ — temps de polarisation anodique. On a représenté seulement les portions des courbes qui se trouvent avant le palier, pour lesquelles le rendement est maximum. On constate que ces courbes ne se superposent pas entre elles. Donc, on peut obtenir le même potentiel φ avec différentes quantités d'halogène adsorbé. Ou, pour la même quantité d'électricité Q passée par l'électrode

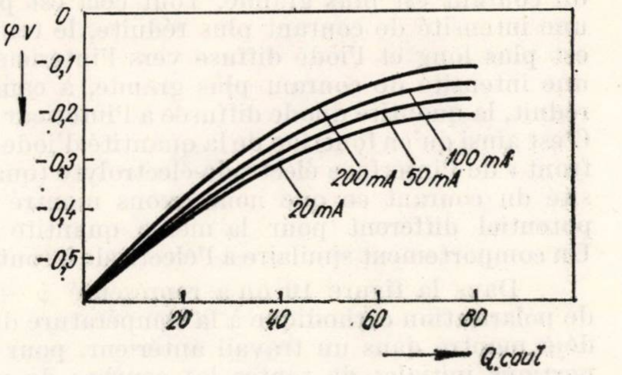

Fig. 9. — Courbes de polarisation anodique (φ — Q) de l'électrode d'iode-charbon actif à diverses intensités de courant ; t = 600°.

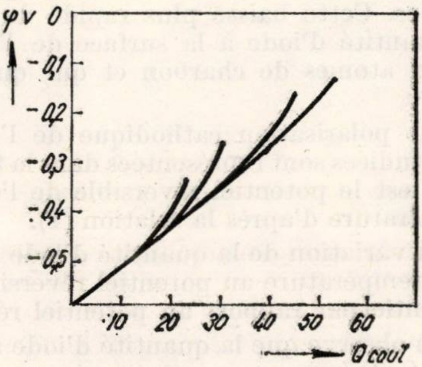

Fig. 10. — Courbes φ — Q de polarisation cathodique t = 600° ; i = 100 mA.

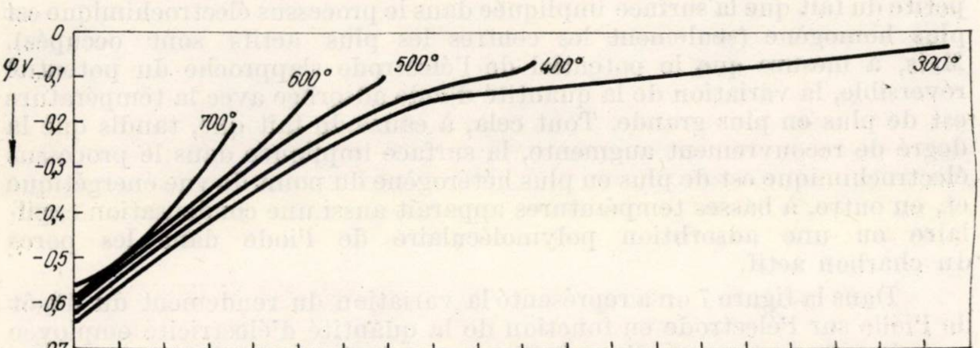

Fig. 11. — Courbes φ — Q de polarisation cathodique à diverses températures ; i = 100mA.

on obtient un potentiel φ qui sera d'autant plus élevé que l'intensité du courant est plus grande. Tout cela est probablement dû au fait qu'à une intensité de courant plus réduite, le temps de polarisation anodique est plus long et l'iode diffuse vers l'intérieur de l'électrode, tandis qu'à une intensité de courant plus grande, à cause du temps de polarisation réduit, la quantité d'iode diffusée à l'intérieur de l'électrode est plus petite. C'est ainsi qu'en fonction de la quantité d'iode qui se trouve sur le « premier front » de l'interface électrode-électrolyte (quantité qui dépend de l'intensité du courant ce que nous avons montré plus haut) on obtient un potentiel différent pour la même quantité totale d'iode sur l'électrode. Un comportement similaire a l'électrode à toutes les températures étudiées.

Dans la figure 10 on a représenté $\varphi - Q$ sur la base des courbes. de polarisation cathodique à la température de 600°. Ainsi que nous avons déjà montré dans un travail antérieur, pour la température de 300°, les portions initiales de toutes les courbes de polarisation cathodique présentent une baisse plus rapide du potentiel, après quoi toutes se joignent dans « une courbe de base ». L'électrode a aussi le même comportement aux autres températures étudiées. Cette baisse plus rapide du potentiel est probablement due à une quantité d'iode à la surface de l'électrode qui est plus faiblement liée aux atomes de charbon et qui quitte plus facilement l'électrode.

« Les courbes de base » de polarisation cathodique de l'électrode d'iode à toutes les températures étudiées sont représentées dans la figure 11. Le potentiel de référence (zéro) est le potentiel réversible de l'électrode d'iode calculé pour chaque température d'après la relation (1).

Dans la figure 12 on voit la variation de la quantité d'iode adsorbée sur l'électrode en fonction de la température au potentiel réversible (OV) et à plusieurs différences de potentiel par rapport au potentiel réversible.

Dans les figures 11 et 12 on observe que la quantité d'iode adsorbée sur l'électrode diminue quand la température augmente. Aux potentiels éloignés du potentiel réversible cette variation avec la température est très petite du fait que la surface impliquée dans le processus électrochimique est plus homogène (seulement les centres les plus actifs sont occupés). Mais, à mesure que le potentiel de l'électrode s'approche du potentiel réversible, la variation de la quantité d'iode adsorbée avec la température est de plus en plus grande. Tout cela, à cause du fait que, tandis que la degré de recouvrement augmente, la surface impliquée dans le processus électrochimique est de plus en plus hétérogène du point de vue énergétique et, en outre, à basses températures apparaît aussi une condensation capillaire ou une adsorbtion polymoléculaire de l'iode dans les pores du charbon actif.

Dans la figure 7 on a représenté la variation du rendement du dépôt de l'iode sur l'électrode en fonction de la quantité d'électricité employée pour la polarisation anodique à diverses températures. On observe qu'à 300°, 400° et 500° pour de petites quantités d'électricité passées par la cellule, le rendement du dépôt de l'iode sur l'électrode est de 100% et ensuite il diminue. Pour les températures de 600° et 700° les rendements sont beaucoup plus réduits.

Ce qui est très intéressant, c'est la dépendance du rendement du dépôt d'iode sur l'électrode de potentiel. D'après la figure 8, à basses températures, pour un grand intervalle de potentiel, le rendement est de 100%, ensuite il diminue rapidement à zéro. Pour des températures plus élevées (au-dessus du point critique de l'iode), même aux potentiels réduits le rendement est au-dessous de 100%. De plus, la diminution du rendement quand le potentiel augmente est beaucoup plus lente si la température est plus élevée.

La figure 8 montre encore qu'à un courant d'électrolyse donné et à une température donnée, après avoir obtenu un certain potentiel (le potentiel stationnaire), donc après avoir obtenu un certain degré de recouvrement, cesse pratiquement l'adsorption d'iode sur l'électrode.

Dans la figure 13 on observe l'influence du barbotage d'argon dans l'électrolyte sur la forme des courbes de polarisation anodique et cathodique. On voit aussi dans cette figure que sur une grande partie de la courbe de polarisation anodique le barbotage d'argon n'a aucune influence parce que tout l'iode déposé par électrolyse est adsorbé par l'électrode. Du moment où une partie de l'iode se désorbe thermiquement en se dissolvant dans l'électrolyte qui entoure l'électrode, les courbes de polarisation anodique obtenues avec ou sans barbotage d'argon ne se superposent plus, à la polarisation anodique obtenue sans barbotage d'argon étant enregistré un potentiel plus élevé. De même, sur la courbe de polarisation cathodique obtenue sans barbotage d'argon il existe un palier plus prononcé, le temps de polarisation cathodique étant plus long. Une influence similaire sur le comportement de l'électrode a aussi le barbotage d'argon aux autres températures étudiées.

En conclusion on peut faire les observations suivantes :

A basses températures sur les courbes de polarisation cathodique (voir fig. 2–6)

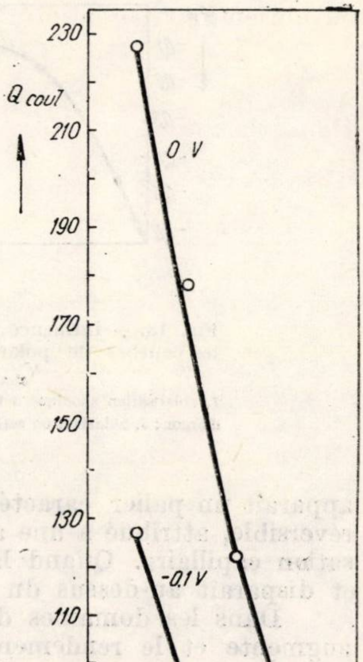

Fig. 12. – Variation de la quantité d'iode adsorbée par l'électrode en fonction de la température au potentiel réversible (O V) et à plusieurs différences de potentiel par rapport au potentiel réversible.

Revue Roumaine de Chimie, 19, 6, 967–976 (1974)

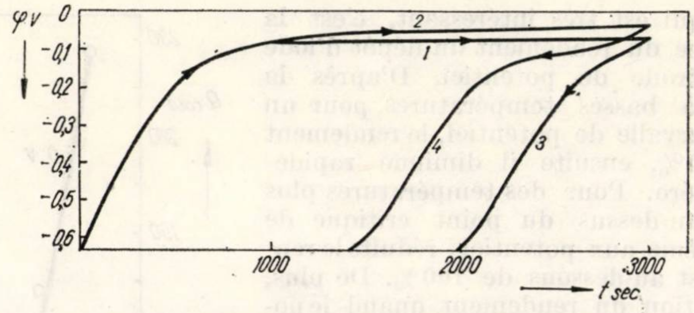

Fig. 13. — Influence du barbotage d'argon dans l'électrolyte sur les courbes de polarisation anodique et cathodique ; $t = 400°$
$i_{\text{charge}} = i_{\text{décharge}} = 100$ mA :
1, polarisation anodique à barbotage d'argon ; *2*, polarisation anodique sans barbotage d'argon ; *3*, polarisation cathodique à barbotage d'argon ; *4*, polarisation cathodique sans barbotage d'argon.

apparaît un palier caractéristique aux potentiels rapprochés de celui réversible, attribué à une adsorption polymoléculaire, ou à une condensation capillaire. Quand la température augmente ce palier diminue et disparaît au-dessus du point critique de l'iode.

Dans les domaines de potentiel étudiés, le courant de désorption augmente et le rendement diminue quand la température augmente.

Revue Roumaine de Chimie, **19**, *6*, 977–984 (1974)

THERMODYNAMIC EXCESS MAGNITUDES OF BINARY SYSTEMS OF ORGANIC LIQUIDS

RODICA VÎLCU and ALEXANDRINA SIMION

Bucharest University, Chair of Chemical Thermodynamics and Electrochemistry, Bd. Republicii 13

Received February 22, 1973

The densities and the ultrasonic velocities were measured in acetic acid+benzene and acetic acid+ethylmethylketone systems, at 25°, 35° and 45°. The densities were determined by the pycnometer method and the velocities with a two quartz crystal interferometer built up by the authors. The excess volumes and the excess adiabatic compressibilities of these solutions at various concentrations were calculated.

INTRODUCTION

Ultrasonic methods find more and more applications owing to their ability of characterizing the physico-chemical behaviour of liquid systems, from the absorption and propagation velocity data.

The measurement of the ultrasonic velocity in solutions formed by liquid components allows to establish : their degree of deviation from ideality, eventual molecular associations in solutions, as well as important correlations with various magnitudes such, as compressibility (adiabatic and isothermal), ratio of heat capacities [1], free volume and internal pressure [2] corrective constants *a* and *b* of Van der Waals equation of state [3,4].

In the case of electrolyte solutions ionic associations [5] and hydration numbers [6] may be evidenced.

The equilibrium sonic velocity is correlated with the adiabatic compressibility β_s of the medium by the relation :

$$c^2 = \frac{1}{\rho\beta s} \qquad (1)$$

where ρ is the density.

---

[1] A. Weissler, *J. Amer. Chem. Soc.*, **70**, 1634 (1948).

[2] C. Collins, W. Brandt and M. H. Navidi, *J. Chem. Phys.*, **25**, 581 (1956).

[3] W. Schaafs, *Z. Physik*, **1939**, 114, 110, 251 **1940** 69.

[4] B.B. Kudryavtev, *Zhur. fiz. Khim.*, **28**, 930 (1945).

[5] S. Prachash Srivastava, Sheo Prachasi and Satya Praclish, *Z. phys. Chem.*, **201**, 91 (1952).

[6] T. Jasunaga, J. Surata, J. Kawano and M. Miura, *Bull. Chem. Soc. Japan*, **37**, 867 (1964).

The measurement of the adiabatic compressibility of liquids at various pressures constitutes a method of establishing certain equations of state.[7]

Important correlations[8] can equally be established between ultrasonic velocities, compressibilities and the derivatives of the thermodynamic functions.

For the measurement of the ultrasonic velocity in liquids various experimental techniques have been used; they make use of either continuous waves or pulses. The first ones, interferometric, determine the wavelength of vibrations of known frequency, generally, by either optical or electronic determinations, with progressing or standing waves. The latter ones may be of the time of flight, ,,sing around'' or interferometric type.

For our measurements we have chosen o two crystal continuous wave interferometric technique[9] with variable path.

EXPERIMENTAL

The variable path interferometer consisted of an emitting crystal (lower) connected to a signal generator and a receiving crystal (upper) whose signal was displayed on the y axis of an oscilloscope.

Both crystals were χ-cut quartz. The upper crystal was movable; its displacements were made by help of a micrometric screw. Both the screw and a dial indicator were used for displacement measurements (measurements of changes in optical path). The sweeping of the oscilloscope was triggered by the signal generator (fig. 1) and so Lissajou's ellipses were displayed on the screen; a change in acoustical path of one wavelength (λ) corresponds to a 360° rotation of the figure on the screen. If for a Δl displacement of the upper crystal one counts n full rotations of the Lissajou figure, c is:

$$c = \lambda\nu = \frac{\Delta l}{n}\,\nu \tag{2}$$

where ν is the frequency of ultrasounds.

Experiments were carried out at 1 MHz which was the resonance frequency of the two crystals (40 mm in diameter and 4 mm thick).

The interferometer (fig. 2) consists of a stainless steel vessel (A) (80 mm diameter, 150 mm height). The flange E supports the micrometric screw system C and serves as lid of the vessel; it is sealed on collar B. The two crystal holders H are identical but the upper one is attached to the micrometric screw while the lower one is mounted on the bottom of the vessel; special alignment precautions were taken with them.

Mounting of crystals in holders was made so as to ensure electrical contact and prevent leaks. Both crystals G were mounted in special profile polyethylene rings I and their sides facing the liquid were covered with polyethylene films; a small pressure was applied upon them by the mounting metal rings through teflon seals. The liquid was introduced either in the steel vessel or in a smaller flat bottom glass vessel whose acoustical contact with

---

[7] LANCE A. DAVIS, ROBERT B. GORDON, *J. Chem. phys.*, **46** 2650 (1967).

[8] S. PRACHASH and JATA DHARY PANDEY, *Rev. Sci. Ind. Research*, **213**, 593 (1962).

[9] W. J. FRY, *J. Acoust. Soc. Amer.*, **21**, 17 (1948).

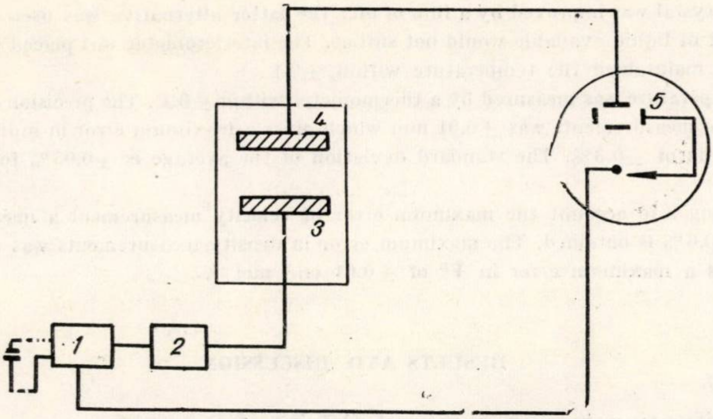

Fig. 1. — Block diagram of the interferometer.
1. Oscillator. *2,* Power stage, *3,* Emitting crystal, *4,* Receiving crystal. *5,* Oscillograph.

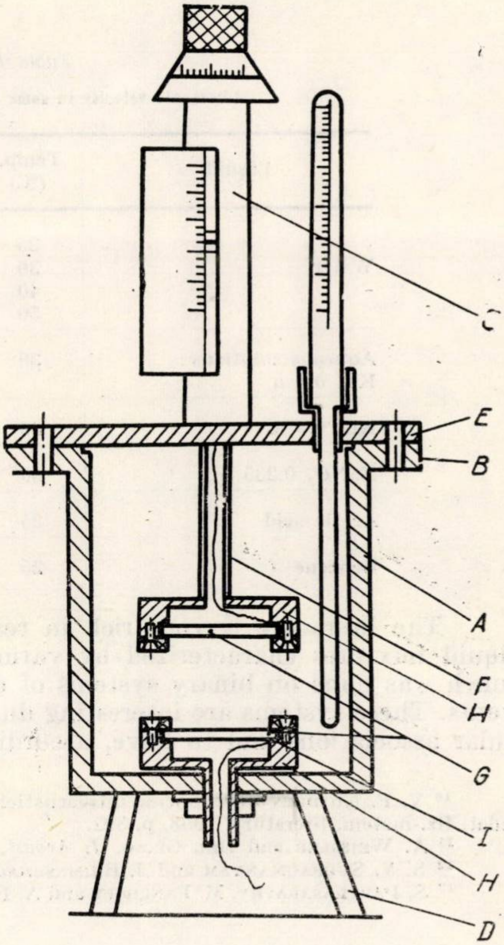

Fig. 2. — General diagram of the interferometer.

A—Stainless steel cell. *B*—Stainless steel flange. *C*— Micrometric screw. *D*—Supports. *E* — Flange *F*—Hollow rod. *G*—Crystals. *H*—Crystal holder. *I* — Polyethylene ring.

the lower crystal was improved by a film of oil; the latter alternative was used in the cases the amount of liquid available would not suffice. The interferometer was placed in a thermostat which maintained the temperature within ±0.1°.

Temperature was measured by a thermometer within ±0.1°. The precision of acoustical path change measurements was ±0.01 mm which gives a maximum error in individual speed measurements of ±0.3%. The standard deviation of the average is ±0.05% for 20 measurements.

Taking into account the maximum error of velocity measurement a maximum error in β_S of ±0.6% is obtained. The maximum error in density measurements was of ±0.004% which gives a maximum error in V^E of ±0.01 $cm^3\ mol^{-1}$.

RESULTS AND DISCUSSION

Verification measurements of the interferometer on several liquids were carried out before each series of runs.

Some of the results are listed in table 1.

Table 1

Ultrasonic velocity in some liquids and solutions

Liquid	Temp. (°C)	Velocity (ms^{-1})	Comparison data
Water	25	1495	1495
	30	1508	1510[10]
	40	1530	1533[10]
	50	1544	1548[10]
Aqueous solutions: KCl 0.4 n	30	1531	1530.9[11]
KCl 0.8 n	30	1553	1550.2[11]
$NaNO_3$ 0.235 n	30	1523	1523[12]
Acetic acid	25	1132	1126[13] 30°
Benzene	25	1297	1275[10] 30°

The literature is very rich in results of measurements on binary liquid mixtures characterized by various types of interactions. Not so much was done on binary systems of carboxylic acids with organic solvents. These systems are interesting due to their tendency to form molecular associations and to have, accordingly, non-ideal behaviour.

[10] V. F. Nozdrev "Primenenie ultraacustichi v moleculiarnoi fiziche", Gosudarstvenoe zdat. fiz.-matem. literatury, 1958, p. 392.

[11] A. Weissler and Del Groso, *J. Acoust. Soc. Amer.*, **219**, 23 (1951).

[12] S. V. Subrahmanyam and J. Bhimasenachar, *J. Acoust. Soc. Amer.*, **32**, 835 (1960).

[13] S. Parthasarathy, M. Pancholy and A. F. Chhapgar, *Nuovo Cimento*, **10**, 111 (1958).

In the present work the study of binary systems of acetic acid with benzene (non-polar) and ethylmethylketone (polar) as solvents was carried out.

The densities (pycnometric method) and ultrasound velocities were determined at 25°, 35° and 45° for mole fractions between 0 and 1 acetic acid ; n from equation (2) was usually equal to 5. The densities and molar excess volumes V^E for the two systems are given in tabels 2 and 3.

Table 2

Densities and excess volumes in the acetic acid+benzene system

Mole fraction of the acid	ρ (g cm^{3})			V^E (cm^3 mol^{-1})
	25°	35°	45°	25°
0	0.8727	0.8636	0.8537	
0.1999	0.8913	0.8811	0.8697	0.56
0.3975	0.9190	0.9080	0.8915	0.57
0.5999	0.9465	0.9349	0.9239	0.81
0.7998	0.9928	0.9808	0.9697	0.26
1	1.0449	1.0341	1.0221	

Table 3

Densities and excess volumes in the acetic acid+ ethylmethylketone system

Mole fraction of the acid	ρ (g cm^{-3})			V^E (cm^3 mol)$^{-1}$
	25°	35°	45°	25
0	0.8002	0.7903	0.7810	
0.1998	0.8381	0.8274	0.8180	−0.43
0.3137	0.8606	0.8500	0.8396	−0.48
0.3806	0.8739	0.8636	0.8534	−0.43
0.5995	0.9250	0.9131	0.9020	−0.40
0.7617	0.9687	0.9578	0.9468	−0.29
1	1.0449	1.0341	1.0221	

V^E is given by the equation :

$$V^E = V^{sol} - V^{vid} = \frac{\widetilde{M}}{\rho} - x_1 V_1 + x_2 V_2)$$

where :

$\widetilde{M} = x_1 M_1 + x_2 M_2$ is the average molecular mass ;

x_1, x_2 are the mole fractions ;

M_1, M_2 are the molar masser of components ;

V_1, V_2 are the molar volumes of components ;

ρ is the solution density.

For the acetic acid + benzene system the excess volumes are positive; the molecules of the components are not similar either as to their form or to their size; that is why they mix with a volume growth. The variation of the excess volumes with the mole fraction is not symmetrical.

In the acetic acid + ethylmethylketone system the excess volumes are negative. This effect is the consequence of the strong interactions between the two polar components, the mixing of which takes place with a volume contraction. In figures 3 and 4, the ultrasonic velocities of the two systems are plotted. From these values, we deduced by means of eq. 1, the adiabatic compressibilities β_S, that are listed in table 4.

As can be seen from fig. 3 and table 4 the ultrasonic velocity decreases with increasing acid concentration while the adiabatic compressibility increases and reaches its maximum for the mole fraction 0.6. According to the Rao's results[14] these data could be accounted for by the planar

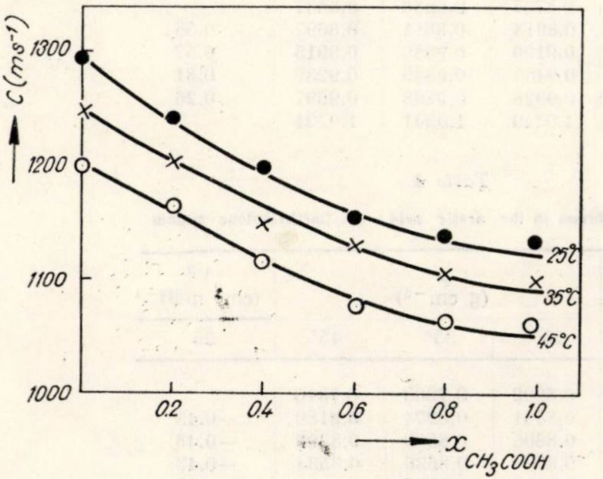

Fig. 3. — Ultrasonic velocity *vs* mole fraction of acetic acid, for the acetic acid + benzene system.

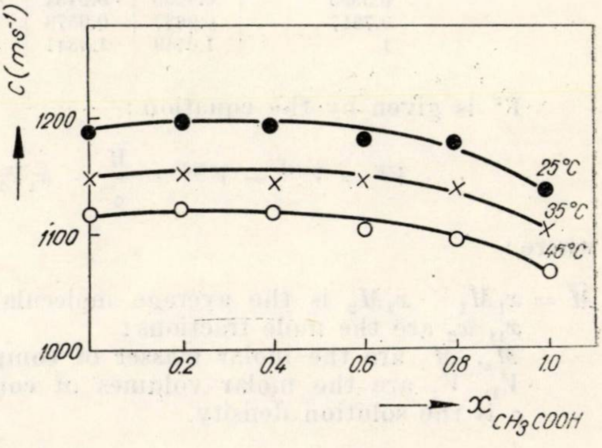

Fig. 4. — Ultrasonic velocity *vs* mole fraction of acetic acid, for the acetic acid + ethylmethylketone system.

---

[14] M. G. Seshagiri Rao and B. Ramachandra Rao, *Ind. J. Pure Appl. Phys.*, 3, 207 1965).

Table 4

Adiabatic compressibilities in the acetic acid + benzene and acetic acid + ethylmethylketone systems

acetic acid + benzene				acetic acid + ethylmethylketone			
Mole fraction of the acid	$10^{12}\beta_s$ (cm^2 dyne^{-1})			Mole fraction of the acid	$10^{12}\beta_s$ (cm^2 dyne^{-1})		
	25°	35°	45°		25°	35°	45°
0	67.9	74.2	80.9	0	78.5	95.6	101.5
0.1999	72.7	78.5	84.4	0.1998	83.6	89.9	97.6
0.3975	76.6	83.5	90.0	0.3806	86.5	88.0	90.0
0.5999	79.5	83.3	93.1	0.5995	78.2	82.9	88.0
0.7998	77.9	93.1	90.9	0.7617	74.3	80.2	87.5
1	74.4	79.8	86.2	1	74.4	79.8	86.2

structure and by the high polarizability of benzene. Taking into consideration the polarizing effect, it is possible that the induction forces occurring between the benzene and acetic acid molecules increase the cohesive force between these molecule and meanwhile diminish the cohesive forces between the molecules of acid. The effect could be equally accounted for by the acetic acid molecules being accomodated into the volume occupied by benzene molecules.

The velocity curve for the system acetic acid + ethylmethylketone (fig. 4) differs from that of acetic acid + benzene (fig. 3) its convexity being directed upwards. The variation of the adiabatic compresibility β_s is also different.

In table 5, the excess adiabatic compressibilities are listed.

Table 5

Excess adiabatic compressibilities 10^{12} β_S^E (cm^2 dyne)

acetic acid + benzene				acetic acid + ethylmethylketone		
XCH^{3}COOH	25°	35°	45°	25°	35°	45°
0.2	4.7	3.8	2.8	6.1	−3.4	−1.7
0.4	7.5	7.5	7.5	9.6	−3.1	
0.6	9.1	6.4	9.6	9.8	−5.0	−6.1
0.8	8.7	1.4	7.4	0.0	−4.7	−4.9

The excess adiabatic compressibilities were calculated by equation

$$\beta_S^E = \beta_S^{sol} - \beta_S^{id}$$

where

$$\beta_S^{id} = \Phi_1\beta_{S1} + \Phi_2\beta_{S2}$$

Φ_1, Φ_2 are the volume fractions of components β_{S1}, β_{S2} the adiabatic compressibilities of components.

For the acetic acid + benzene system, the excess compressibilities are positive and seem to reach a maximum for mole fraction 0.6 of acetic acid. The β_S^E behaviour parallels the behaviour of V^E In the other system (acetic acid + ethylmethylketone), at 25°, β_S^E is positive while V^E is negative; at 35 and 45°. β_S^E is positive.

CONCLUSIONS

The non-ideal behaviour of the two above mentioned systems is observed both in the non-linear variation of ultrasonic velocities *vs* mole fraction and in deviations from ideality of compressibilities as well as of molar volumes.

The interactions, different in the two studied systems are revealed both by the aspect of the velocity *vs* concentration curves and by the excess volumes. The excess compressibilities have generally the same sign as the excess volumes and vary, approximately, in the same manner.

Revue Roumaine de Chimie, **19**, *6*, 985–990 (1974)

VAPOUR PRESSURES OF MOLTEN $CdBr_2$, CdI_2, $MgBr_2$ AND MOLECULAR ASSOCIATION IN GASEOUS PHASE

LETIȚIA TOPOR and IVONA MOLDOVEANU

Center of Physical Chemistry,
Str. Galați 31, Bucharest, Romania

Received October 19, 1973

The vapour pressures and molecular association in the gaseous phase of molten $CdBr_2$ and CdI_2 have been determined by the transpiration method and of molten $MgBr_2$ by Rodebush-Dixon and transpiration methods. A low percentage of gaseous polymers was found in the $CdBr_2$ and CdI_2 saturated vapours and a higher one in $MgBr_2$ saturated ones. The heat of vaporization of $MgBr_2$ monomers and dimers was deduced.

The study on the vapour pressures of molten halides from the second group [1,2] and the association of their vapours is being continued with measurements carried out on molten $CdBr_2$, CdI_2 and $MgBr_2$.

The vapour pressure of molten $CdBr_2$ and CdI_2 has been previously determined by the boiling point and Rodebush-Dixon methods.[1,3–5] In view of obtaining indications on the existence of polymers in gaseous phase in equilibrium with liquid $CdBr_2$ and CdI_2, a combination of absolute pressure measurements and transpiration data is necessary. The available transpiration data cannot be used for this purpose since Greiner and Jellinek [6] obtained only one value of the vapour pressure for $CdBr_2$ at 752°, Schmidt and Walter [7] examined CdI_2 around the melting point (390°–450°) and Tolmacheva and Andrinovskaya's data [8] are lower than the absolute vapour pressure measurements. We have determined the vapour pressure of molten $CdBr_2$ and CdI_2 by the transpiration method.

---

[1] L. Topor and Y. Wypartowicz, *Rev. Roumaine Chim.*, **17**, 831 (1972).

[2] L. Topor and I. Moldoveanu, *Rev. Roumaine Chim.*, **17**, 1705 (1972).

[3] H. Bloom, J. O'M. Bockris, N. E. Richards and A. Taylor, *J. Amer. Chem. Soc.*, **80**, 2044 (1958).

[4] I. N. Beliaev and V. V. Kesarev, *Zhur. neorg. Khim.*, **15**, 1418 (1970).)

[5] I. N. Beliaev and V. V. Kesarev, *Zhur. neorg. Khim.*, **15**, 1434 (1970).

[6] B. Greiner and C. Jellinek, *Z. Phys. Chem.*, **A165**, 97 (1933).

[7] G. C. Schmidt and R. Walter, *Ann. Physik.*, **72**, 565 (1923).

[8] A. T. Tolmacheva and T. L. Andrianovskaya, *Vestnik Leningrad Univ., Ser. Fiz. Khim.*, **15(10)**, 131 (1960).

Information concerning the vapours composition have been obtained by using the transpiration data and the previous absolute vapour pressure values [1]. The vapour pressure of molten $MgBr_2$ has not been determined experimentally as yet. We have used the Rodebush-Dixon and transpiration methods to determine the vapour pressure of molten $MgBr_2$ and the mean molecular mass of the vapours.

EXPERIMENTAL

The transpiration and Rodebush-Dixon setups, their operation and the method used for purifying and dehydration of $CdBr_2$ and CdI_2 have been previously described. [19,10] However, anhydrous $MgBr_2$ was more difficult to obtain. Firstly we have tried the dehydration by the procedure recently presented by Østvold.[11] As the results were not satisfactory we have prepared anhydrous $MgBr_2$ directly from Br_2 and Mg in freshly distilled anhydrous diethyl ether.[12,13] We have dropped the freshly distilled liquid bromine in anhydrous ether containing pure metallic Mg turnings. The flask was cooled below room temperature. The unreacted metallic Mg was removed by filtering through G 2 – frit and the crystallization of the $MgBr_2$ trietherate was initiated by cooling the solution below 0°. The white crystals formed were rapidly filtered off by a water jet aspirator and introduced directly in the cell. To obtain anhydrous $MgBr_2$, the trietherate was decomposed in vacuum by rising its temperature from room temperature to 150°–175° (in two hours); it was then kept at 175° for 30 minutes, after which it was melted in dry pure argon.

RESULTS AND DISCUSSION

The vapour pressures of molten $CdBr_2$ and CdI_2 have been determined by the transpiration technique. From the experimental data the following equations were obtained by the least squares method, using an IBM computer:

$CdBr_2$ (607.5°–703.8°)

$$\log p = -\frac{(6106.2 \pm 22.1)}{T} + (8.312 \pm 0.024) \quad (1)$$

CdI_2 (528.3° – 628.5°)

$$\log p = -\frac{(5600.7 \pm 23.7)}{T} + (8.333 \pm 0.028) \quad (2)$$

The vapour pressure values obtained by the transpiration method are greater than the absolute pressures measured by Rodebush-Dixon

---

[9] I. G. Murgulescu and L. Topor, *Rev. Roumaine Chim.*, **11**, 1353 (1966).

[10] I. G. Murgulescu and L. Topor, *Rev. Roumaine Chim.*, **13**, 1109 (1968).

[11] T. Østvold, *J. Phys. Chem.*, **76**, 1619 (1972).

[12] G. Brauer "Handbook of Preparation Inorganic Chemistry" Vol. I, Academic Press, New York, London, 1963, p. 909.

[13] H. H. Rowley, *J. Amer. Chem. Soc.*, **72**, 3305 (1950).

method.[1] Since the differences are too large to be attributed to experimental errors, they suggest that some associations occur in the vapours. If we assume the existence of the monomers and dimers in the gaseous phase, like in $CdCl_2$ vapours[2,14] from absolute vapour pressures and transpiration data we can calculate the mean molecular mass of the vapours.

The vapour pressure values of molten $CdBr_2$ and CdI_2 obtained at different temperatures by transpiration (p_{trans}) and Rodebush-Dixon (p) methods, the mean molecular mass of vapcurs ($\overline{M}$), the mole fractions of dimer x_2 and their mean $\overline{x_2}$ are presented in tables 1 and 2.

Table 1

Transpiration and absolute vapour pressures of molten $CdBr_2$ the mean molecular mass of vapours and the mole fractions of dimer*

T (K)	p_{trans} (mm Hg)	p (mm Hg)	$\overline{M}$	x_2	$\overline{x_2}$
880.5	23.90	22.50	286.93	0.054	0.064
880.8	24.03	22.62	292.35	0.074	
894.3	30.58	28.72	293.4	0.078	
892.9	29.83	28.03	289.47	0.063	
897.5	32.34	30.36	291.53	0.071	0.067
897.0	32.06	30.10	289.27	0.063	
898.1	32.68	30.68	288.61	0.060	
922	49.03	45.88	295.94	0.087	
921.5	48.63	45.51	290.98	0.069	0.078
946.7	72.98	68.09	292.10	0.073	
944.7	70.72	65.99	300.40	0.104	
947.6	72.02	69.05	297.46	0.093	0.081
946.4	72.54	67.77	290.66	0.068	
945.7	71.84	67.22	290.09	0.066	
960	89.65	83.50	291.41	0.100	0.077
959.3	88.70	82.62	294.53	0.082	
970.6	105.19	97.85	293.36	0.085	
972.7	108.53	101.23	297.55	0.080	0.085
974.4	111.31	103.49	289.60	0.081	
976.8	115.32	107.20	293.51	0.095	

* The $CdBr_2$ molecular mass is 272,25.

The concentration of dimers in the vapours vary between 6.4%–8.5% for $CdBr_2$ and 2.3%–3.7% for CdI_2. The percentage of dimers in $CdBr_2$ vapours is close to that in $CdCl_2$ vapours, while in CdI_2 vapours the concentration is lower.

---

[14] F. J. Keneshea and D. D. Cubicciotti; *J. Chem. Phys.*, **40**, 1778 (1964).

Table 2

Transpiration and absolute vapour pressures of the molten CdI_2, the mean molecular mass of vapours and the mole fractions of dimer *

T (K)	p_{trans} (mm Hg)	p (mm Hg)	$\overline{M}$	x_2	$\bar{x}_2$
801.3	22.11	21.54	374.35	0.022	0.023
801.1	22.02	21.45	374.95	0.024	
822.4	33.40	32.50	376.85	0.029	0.036
822.1	33.21	32.32	384.69	0.050	
824.2	34.57	33.63	377.23	0.030	
839.7	46.14	44.85	371.81	0.015	0.027
840.7	46.99	45.67	380.93	0.040	
849.3	54.88	53.32	375.67	0.026	0.034
848.4	54.00	52.47	385.33	0.052	
846.4	52.10	50.62	375.56	0.025	
858.8	64.91	63.03	379.94	0.037	0.026
864.5	71.67	69.58	378.45	0.033	
862.9	69.71	67.68	371.55	0.014	
863.4	70.32	68.25	373.27	0.019	
869.0	77.42	75.14	379.07	0.035	0.035
869.9	78.62	76.30	379.6	0.036	
901.5	132.17	128.08	380.31	0.038	0.037
899.8	128.65	124.68	379.83	0.037	
900.0	129.06	125.07	379.53	0.036	

* The CdI_2 molecular mass is 366.23.

The only existent vapour pressure values for molten $MgBr_2$ have been calculated by Brewer.[15,16] The vaporization entropy and boiling point values have been established by comparison with the neighbouring halides, particulary MgF_2 and MgI_2.

The $MgCl_2$, $MgBr_2$ and MgI_2 vapours in equilibrium with the solid have been examined in the mass spectrometer.[17] The results have indicated the presence of a small amount of dimers in these conditions (~1%).

We have determined the vapour pressure of molten $MgBr_2$ from 846° to 994° by the Rodebush-Dixon method. The experimental vapour pressure values were fitted by the Σ plot method [18] and the equation for vapour pressure variation as a temperature function has been deduced by the least squares method at an IBM computer. The difference between the heat capacities for the gas and the liquid phase, ΔC_p, was assumed

---

[15] L. BREWER, Paper N° 7 "Chemistry of Miscellaneous Materials", McGraw-Hill Book Co. Inc., New York, 1950, p. 193.

[16] L. BREWER, G. R. SOMAYAJULU and E. BRACKETT, *Chem. Rev.*, **63**, 111 (1963).

[17] J. BERKOWITZ and J. R. MARQUART, *J. Chem. Phys.*, **37**, 1853 (1962).

[18] K. K. KELLEY, *U.S. Bur. Mines. Bull.*, **601**, 3 (1962).

-9.3 cal mole^{-1} deg^{-1}. We have obtained :

$$\log p = -\frac{(10504.9 \pm 57.3)}{T} - 4.682 \log T + (24.736 \pm 0.048) \quad (3)$$

The standard deviation of vapour pressure values is 2.26%. The heat of vaporization at temperature T, ΔH_T, calculated from equation (3) is :

$$\Delta H_T = (48.1 \pm 0.3) - 9.3 \times 10^{-3} T \quad (4)$$

We have utilized the transpiration method too. From absolute vapour pressures and transpiration data we have calculated the mean molecular mass of the vapours by using the relations previously reported.[2,10] The temperatures, the mean molecular mass $\overline{M}$, the mole fractions and partial pressures of monomers and dimers x_1, x_2, p_1, p_2 are listed in table 3.

Table 3

The mean molecular mass, mole fractions and partial pressures of monomers and dimers in the vapours of molten $MgBr_2$ *

T (*K*)	$\overline{M}$	x_1	x_2	p_1 (mm Hg)	p_2 (mm Hg)
1101.0	243.51	0.678	0.322	6.09	2.89
1123.0	257.18	0.604	0.396	7.62	4.96
1145.7	254.15	0.620	0.380	10.80	6.62
1164.7	260.33	0.587	0.413	13.35	9.39
1182.7	271.56	0.525	0.475	15.24	13.79
1205.7	272.08	0.521	0.477	20.43	18.79

* The $MgBr_2$ molecular mass is 184.16.

The presented values are averaged over 3–6 experiments.

From these data an important amount of dimers in $MgBr_2$ vapours results (between 32 mole % and 47 mole %). This percentage is higher than in $MgCl_2$ vapours [2] (29–33 mole %).

The temperature variation of partial vapour pressures is given by the equations :

$$\log p_1 = -\frac{(6681.2 \pm 247.2)}{T} + (6.649 \pm 0.214) \quad (5)$$

$$\log p_2 = -\frac{(10201.6 \pm 393.9)}{T} + (9.743 \pm 0.342) \quad (6)$$

The heats of vaporization of the liquid $MgBr_2$ into monomers and dimers are from equations (5) and (6): $\Delta H_{1v} = 30.6$ kcal.mole^{-1} and $\Delta H_{2v} = 46.7$ kcal.mole^{-1}.

The only existing value of the heat of vaporization for $MgBr_2$ obtained by Brewer[15] from calculation is $\Delta H_v = 35$ kcal.mole^{-1}. From equation (4) the heat of vaporization at 1000 K is 38.8 kcal. mole^{-1}. For monomers and dimers the heat of sublimation has been determined previously by mass spectrometry technique ($\Delta H_{1s} = 50.3$ kcal.mole^{-1} and $\Delta H_{2s} = 63.2$ kcal.mole^{-1}).[17] We have calculated the heat of sublimation of monomers and dimers from the heat of vaporization and the heat of fusion (8.3 kcal.mole^{-1}) and we have obtained, $\Delta H_{1s} = 38.6$ kcal.mole^{-1} and $\Delta H_{2s} = 62.9$ kcal.mole^{-1}, respectively. The value obtained for the monomers is very different from the previous one, but the one for dimer is very similar.

Revue Roumaine de Chimie, **19**, *6*, 991–996 (1974)

MOLECULAR INTERACTIONS IN SOLUTIONS
CALCULATIONS OF THE INTERACTION POTENTIAL ENERGY IN THE CARBON DISULPHIDE – CHLOROFORM SYSTEM *

SIMONA BĂDILESCU

Petrochemical Works, Pitești, Romania

Received August 22, 1973

The interaction potential energy was calculated in the carbon disulphide – chloroform system based on a reticular model. The vibration frequency ν_3 of the carbon disulphide molecule in a chloroform environment was calculated and compared to the experimentally determined frequency.

In a recent work, Devaure et al.[1] reported that the shape of some CO, HCl, CH_4 bands at 1500 atm. or at −23° in the plastic phase of carbon tetrachloride is identical to the shape of those bands in dilute solutions of the same solvent. The results obtained by Devaure et al. show that the utilization of some solid-state models to describe the perturbations suffered by a vibrator under the influence of molecular interactions in solution may be very fruitful.

In the present paper, we calculated the frequency shift $\Delta\nu$ of the band corresponding to the anti-symmetric stretching vibration ν_{as} of the carbon disulphide molecule in chloroform solution (a shift with respect to the value of the frequency corresponding to the isolated molecule).

Calculations were made based on a reticular model suggested by Galatry et al.[2-4] and the results obtained were compared to our experimental data.[5] The expression of "sphericalized"[6] potential energy was used to describe the interactions dissolved substance – solvent, permitting a numerical estimation of the influence of the perturbating molecules aggregate.

---

* Paper presented at the 3rd Republican Conference of General and Applied Physical Chemistry, Bucharest, September 4–7, 1972.

[1] J. Devaure, J. J. Martin, M. Perrot, P. V. Huong and J. Lascombe, *Spectrochim. Acta*, **27A**, 2283 (1971).

[2] D. Pierre, L. Galatry and J. F. Lemen, *J. Phys. (Paris)*, **27**, 269 (1966).

[3] L. Bonamy, D. Robert and L. Galatry, *J. Mol. Struct.*, **1**, 91 (1967).

[4] L. Bonamy, D. Robert and L. Galatry, *J. Mol. Struct.*, **1**, 139 (1967).

[5] S. Bădilescu, *Rev. Roumaine Chim.*, **16**, 9 (1971).

[6] L. Saighi and D. Robert, *Spectrochim. Acta*, **26A**, 1731 (1970).

When estimating the potential energy, the interactions are considered binary and additive, considering the dispersion and repulsion energy.

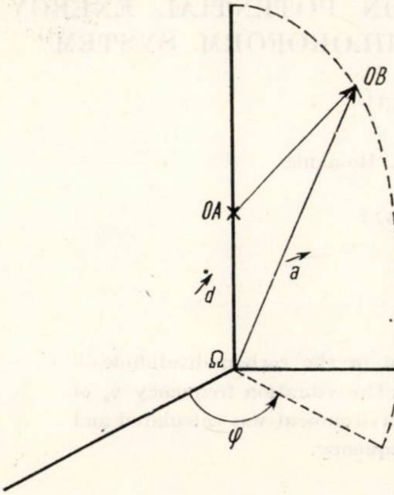

Fig. 1. — Reduced coordinates in reticular model.

The potential energy is expressed in the reduced coordinates τ $\left(\text{which represent a reduced shift compared to the center } \Omega \text{ of the cell, } \tau = \frac{\vec{d}}{a}\right)$ and φ (fig. 1), and the expression of the potential energy is :

$$\overline{V}^0(\tau, \varphi) = \overline{V}_1^0(\tau) + \overline{V}_2^0(\tau)\cos^2\varphi \qquad (1)$$

The terms $\overline{V}_1^0(\tau)$ and $\overline{V}_2^0(\tau)$ in equation (1) are of the form;

$$\overline{V}_1^0(\tau) = -\left[12\,\Delta^{Ab}\alpha_A\alpha_b a^{-6} + 24\,\Delta^{Bb}\alpha_B\alpha_b a^{-6}\right]\frac{1-\tau^2}{(1-\tau^2)^4} - $$

$$- \frac{24\,\Delta^{Bb}\alpha_B\alpha_b s^2 a^{-8}}{(1-\tau^2)^8}(5 - 16\tau^2 + 2\tau^4 + 4\tau^6 + 3\,\tau^8) +$$

$$+ \frac{12}{5}\,\varepsilon_{a-b}\left(\frac{R_{a-b}}{a}\right)^{12}\frac{20 + 240\,\tau^2 + 504\,\tau^4 + 240\,\tau^6 + 20\,\tau^8}{(1-\tau^2)^{10}} \qquad (2)$$

and

$$\overline{V}_0^2(\tau) = -\frac{\Delta^{Bb}\alpha_b s^2 a^{-8}}{(1-\tau^2)^8}(1344\tau^2 - 1824\tau^4 + 48\tau^6 + 576\tau^8) \qquad (3)$$

The significances of the terms in equations (2) and (3) are:

$$\Delta^{Ab} = \Delta^{\mathrm{C-CHCl_3}} = \frac{3\,U^{\mathrm{C}}\,U^{\mathrm{CHCl_3}}}{2\,(U^{\mathrm{C}} + U^{\mathrm{CHCl_3}})}$$

and

$$\Delta^{Bb} = \Delta^{\mathrm{S-CHCl_3}} = \frac{3\,U^{\mathrm{S}}\,U^{\mathrm{CHCl_3}}}{2(U^{\mathrm{S}} + U^{\mathrm{CHCl_3}})}$$

in which U^{C} and U^{S} represent the ionization potentials of carbon and sulphur atoms, and $U^{\mathrm{CHCl_3}}$, the ionization potential of the chloroform molecule; $\alpha_B = \alpha_{\mathrm{S}}$ and $\alpha_A = \alpha_{\mathrm{C}}$ are the atomic polarizabilities, $\alpha_b = \alpha_{\mathrm{CHCl_3}}$ the solvent polarizability, s – the carbon – sulphur interatomic distance, a – the cell parameter and ε and R are the Lennard-Jones parameters of the molecular couple.

The numerical values of the terms used in the calculation of the potential energy are given in table 1 and the values of Lennard-Jones constants, calculated according to the known combinational rules,[9] are:

$$\varepsilon_{\mathrm{CHCl_3-CS_2}} = 308\ \mathrm{cm^{-1}} \text{ and } \sigma_{\mathrm{CHCl_3-CS_2}} = 4.93\ \text{Å}$$

Table 1

Numerical values used in the calculation of potential energy

Term	Value	Ref.
U^{C}	11.256 eV	7
U^{S}	10.357 eV	7
$U^{\mathrm{CHCl_3}}$	11.42 eV	8
α_{C}	$1.35.10^{-25}$ cm^3	6
α_{S}	$71.3.10^{-25}$ cm^3	6
α_{CHCl3}	$82.3.10^{-25}$ cm^3	9
s	$1.56.10^{-8}$ cm	6
$\varepsilon_{\mathrm{CS_2}}$	340 cm^{-1}	9
$\varepsilon_{\mathrm{CHCl3}}$	279 cm^{-1}	9
$\sigma_{\mathrm{CS_2}}$	$4.438.10^{-8}$ cm	9
σ_{CHCl3}	$5.43.10^{-8}$ cm	9

---

[7] V. I. Vedeneev, L. V. Gurvich, V. N. Kondratiev, V. A. Medvedev, and E. L. Frankevich, "Energii razryva khimicheskikh svyazei. Potentsialy ionizatsii i srodstvo k elektronu", Spravochnik, Izdatel'stvo Akad. Nauk SSSR, Moscow, 1962, p. 164.

[8] K. Watanabe, *J. Chem. Phys.*, **26**, 542 (1957).

[9] J. O. Hirschfelder, Ch. F. Curtiss and R. B. Bird, "Molecular Theory of Gases and Liquids", Wiley, New York, 1954, Russian Edition, Izdatel'stvo Innostranoi Literatury, Moscow, 1961.

The cell parameter a is :

$$a = \left(\frac{M\sqrt{2}}{Nd} \right)^{1/3} \tag{4}$$

in which d is the solvent density, M — the molecular weight and N the Avogadro number.

The $\Delta\nu_3$ shift of the ν_3 vibration frequency of the chloroform molecule was calculated using expression [6]:

$$\Delta\nu_3 = \frac{\nu_3}{K_3} \left(\frac{\partial^2 \overline{V}}{\partial z^2} \right)_0 \tag{5}$$

in which ν_3 is the frequency value of the anti-symmetric vibration mode of the C — S bond in gaseous carbon disulphide molecule [10] (1536.5 cm^{-1}), k_3 is the corresponding force constant and $\left(\frac{\partial^2 \overline{V}}{\partial z^2} \right)_0$ denotes the "sphericalized" expression of the second derivative of the potential energy in relation to the vibration coordinate z.

The term $\left(\frac{\partial^2 \overline{V}}{\partial z^2} \right)_0$ takes the form :

$$\left(\frac{\partial^2 \overline{V}}{\partial z^2} \right)_0 = k_1(\tau) + k_2(\tau) \tag{6}$$

in which

$$k_1 = \left(\Delta^{Ab} \alpha_A \alpha_b a^{-8} + \frac{2M}{m} \Delta^{Bb} \alpha_B \alpha_b a^{-8} \right) \left[\frac{-240 + 96\tau^2 + 144\tau^4}{(1 - \tau^2)^6} \right] \tag{7}$$

and

$$k_2 = -\left(144\, \Delta^{Ab} \alpha_A \alpha_b a^{-8} + \frac{2M}{m} \cdot 288\, \Delta^{Bb} \alpha_B \alpha_b a^{-8} s \right) \times$$

$$\times \frac{18\tau^2 + 2213\tau^4 + 2\tau^6 + 2\tau^8}{(1 - \tau^2)^8} \tag{8}$$

RESULTS AND DISCUSSION

The variation curves of the potentials $\overline{V}_1^0(\tau)$ and $\overline{V}_2^0(\tau)$ calculated for the reduced shift values τ comprised between 0 and 0.3 are plotted in figures 2 and 3. Table 2 records the values of $\left(\frac{\partial^2 \overline{V}}{\partial z^2}\right)_0$ calculated by eqn. (5) for some values of τ, and the $\Delta\nu$ shifts of the ν_3 vibration frequency of CS_2 molecule in chloroform solution.

---

[10] J. Jacob and J. P. Benaisch, *J. Chim. phys.*, **64**, 1282 (1967).

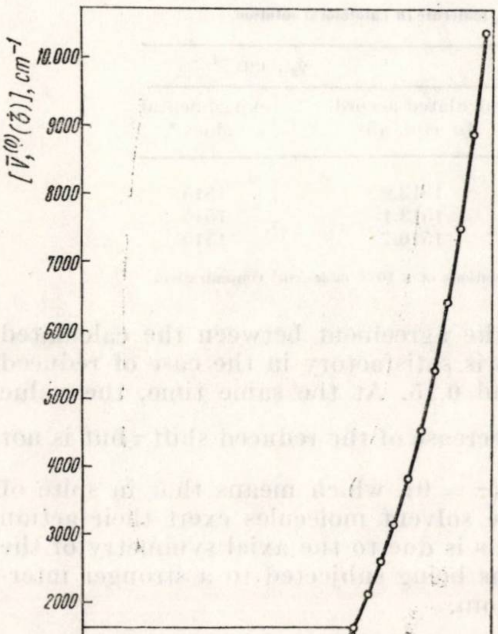

Fig. 2. — Variation of potential energy $\overline{V}_1^0(\tau)$ along with reduced shift τ.

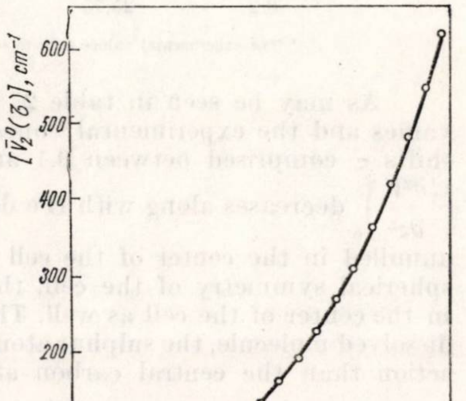

Fig. 3. — Variation of potential energy $\overline{V}_2^0(\tau)$ along with reduced shift τ.

Figures 2 and 3 illustrate that $\overline{V}_2^0(\tau)$ has an important weight in the expression of the total potential energy at low values of the reduced shift ($\tau < 0.15$), whereas at $\tau > 0.15$, $\overline{V}_1^0(\tau)$ becomes preponderant and it rapidly increases. This manner of variation can be explained by the specific nature of the two energies, $\overline{V}_2^0(\tau)$ representing the orientation energy and $\overline{V}_1^0(\tau)$ the translation energy. Around the value $\tau = 0.15$ both energies reach the value of the thermal motion energy (313 cm^{-1} at 300°K).

The probability density that the gravity center of the dissolved substance may be found at a distance τ from the center of the cell (determined by expression $\tau^2 e - \frac{\overline{V}^0(\tau)}{kT}\Big)$ attains a maximum at $\tau = 0.15$.

At any value of the reduced shift, the potential energy $\overline{V}_2^0(\tau)$ is much higher than the rotation constant B of the dissolved molecule, which means that the rotation levels are strongly perturbated.

Table 2

Vibration frequency ν_3 of CS_2 molecule in chloroform solution

τ	$\Delta\nu$ cm^{-1}	ν_3, cm^{-1}	
		calculated accord. to eqn. (5)	experimental values *
0.1	-22.6	1513.9	1515
0.15	-23.4	1513.1	1515
0.2	-25.75	1510.7	1515

* The experimental values refer to solutions of a 10^{-5} moles/cm^3 concentration.

As may be seen in table 2, the agreement between the calculated values and the experimental [5] ones is satisfactory in the case of reduced shifts τ comprised between 0.1 and 0.15. At the same time, the value $\left(\frac{\partial^2 \overline{V}}{\partial z^2}\right)_0$ decreases along with the decrease of the reduced shift τ but is not annulled in the center of the cell ($\tau = 0$), which means that in spite of spherical symmetry of the cell, the solvent molecules exert their action in the center of the cell as well. This is due to the axial symmetry of the dissolved molecule, the sulphur atoms being subjected to a stronger interaction than the central carbon atom.

Revue Roumaine de Chimie, **19**, *6*, 997–1008 (1974)

GÉNÉRALISATIONS DU TRIANGLE DE GIBBS POUR LES SYSTÈMES QUATERNAIRES ET QUINAIRES

D. RIMER
Séminaire Mathématique « A. Myller »,
Université « Al. I. Cuza », 11, str. 23 August, Jassy, Roumanie

Reçu le 3 septembre 1973

On construit dans le plan, un modèle géométrique des systèmes quaternaires et l'un des systèmes quinaires, en réalisant une représentation plane suffisamment exacte de tels systèmes. Dans ces modèles on résout graphiquement les mêmes types de problèmes qui sont résolus dans le triangle de Gibbs pour les systèmes ternaires.

I. INTRODUCTION

On connaît les multiples utilisations du triangle de Gibbs dans la chimie physique et la technologie chimique, pour la représentation géométrique des systèmes ternaires, ainsi que pour la solution graphique de divers problèmes concernant ces systèmes.[1-3]

On connaît aussi les difficultés qui surviennent en passant aux systèmes quaternaires, parce qu'il faut utiliser le tétraèdre.

En effet, c'est beaucoup moins commode et c'est peut-être pourquoi on n'a étudié qu'un nombre restreint de systèmes quaternaires.[4]

Le problème de l'étude des systèmes quinaires à l'aide d'un pentatôpe, — le correspondant du triangle, dans un espace à quatre dimensions — n'est pas considéré, habituellement, à cause de la difficulté de matérialiser les figures de l'espace euclidien à quatre dimensions.

Nous estimons avoir vaincu ces difficultés en réalisant, *dans un plan*, une représentation biunivoque et continue (les points distincts sont représentés par des points distincts et les points voisins sont représentés par des points voisins) d'un tétraèdre [5,6] ou d'un pentatôpe,[7] dont nous

---

[1] L. Alders, « Liquid-liquid Extraction », Princeton, New York, 1959.

[2] Em. Bratu, « Operaţii şi utilaje în industria chimică », Ier vol., Ed. tehnică, Bucarest, 1970, p. 116, IIe vol., Ed. tehnică, Bucarest, 1970, p. 565.

[3] R. E. Kirk et D. F. Othmer, « Encyclopedia of Chemical Technology », VIe vol., Interscience, New York, 1951.

[4] S. Soare, I. Precup et C. Taran, « Extracţia lichid-lichid », Ed. tehnică, Bucarest, 1963.

[5] D. Rimer, *Bull. math. Bucureşti*, **14** (62), 75 (1970).

[6] D. Rimer, *Anal. Şti. Univ. « Al. I. Cuza » Iaşi, sect. I, mat.*, **18**, *2*, 427 (1972).

[7] D. Rimer, *Anal. Şti. Univ. Timişoara, sect. mat.* (sous presse).

avons ôté seulement les points à deux, respectivement à trois coordonnées, nombres irationnels.

Ces figures ont été dénommées par nous *pseudo-tétraèdre*, respectivement *pseudo-pentatôpe*.

Nous avons élaboré la base mathématique de cette représentation en étudiant ses divers aspects ; tout de même nous avons considéré aussi certaines applications.[8,9]

Mentionnons que *dans le pseudo-tétraèdre et dans le pseudo-pentatôpe on peut résoudre graphiquement tous les types de problèmes que l'on résout dans le triangle de Gibbs.*

II. LE PSEUDO-TÉTRAÈDRE QUI GÉNÉRALISE LE TRIANGLE DE GIBBS

A. Soit, dans un plan (fig. 1) un repère $(0\,;\,\bar{e}_1, \bar{e}_2)$ et un vecteur $\bar{u}$, donné par la relation

$$\bar{u} = a\bar{e}_1 = b\bar{e}_2 \ (a \in R-Q,\ b \in R), \quad (1)$$

où R est l'ensemble des nombres réels, Q celui des nombres rationnels et, donc, $R-Q$ est l'ensemble des nombres irationnels.

Dans la figure 1 nous avons considéré :

$$\bar{u} = (-\,6/\sqrt{75}\,)\,\bar{e}_1 - (\sqrt{13}\,/5)\,\bar{e}_2 \approx -\,0{,}69\,\bar{e}_1 - 0{,}72\bar{e}_2.$$

Nous renotons ces vecteurs par

$$\bar{v}_1 = \bar{u}, \quad \bar{v}_2 = \bar{e}_1, \quad \bar{v}_3 = \bar{e}_2 \quad (2)$$

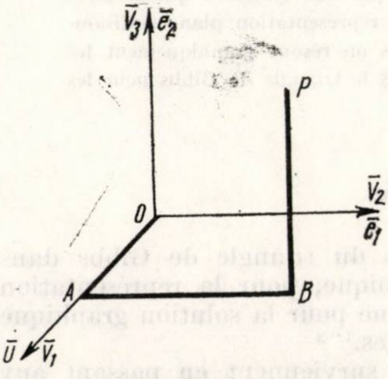

Fig. 1. — Repère d'un espace pseudo-affine à trois dimensions, construit dans un plan.

Considérons maintenant $(0\,;\,\bar{v}_1, \bar{v}_2)$ comme un repère du plan et imaginons-nous tous les points du plan qui ont, par rapport à ce repère, toutes les deux coordonnées, des nombres rationnels. Par chacun de ces points, nous considérons la droite, parallèle à $\bar{v}_3$.

Nous avons démontre,[7] que ces droites sont distinctes, c'est-à-dire qu'il n'y a pas, parmi elles, deux droites confondues ou — c'est la même chose — aucune d'entre elles ne passe par deux tels points. L'ensemble des points de ces droites nous l'appelons *espace pseudo-affine à trois dimensions construit dans un plan* et $(0\,;\,\bar{v}_1, \bar{v}_2, \bar{v}_3)$ est le *repère* de cet espace.

Puisqu'on ne peut pas tracer l'ensemble de toutes ces droites, nous nous contenterons à représenter les points par rapport à ce repère, en gardant le contour de coordonnées respectif. Ainsi, étant donné un triplet ordonné de nombres (x_1, x_2, x_3), dont $x_1, x_2 \in Q$, $x_3 \in R$, nous construisons

---

[8] D. Rimer, *Bull. Soc. Franc. Minéral. Cristallogr., Paris,* **91**, 513 (1968).
[9] D. Rimer, *Bull. Soc. Franc. Minéral. Cristallogr., Paris,* **92**, 508 (1969).

ainsi le point correspondant : nous prenons (fig. 1) le point A sur Ov_1 tel que $OA = x_1$, puis $AB = x_2$, parallèlement à $\bar{v}_2$ et enfin $BP = x_3$, parallèlement à $\bar{v}_3$. Réciproquement, étant donné le point P avec le contour de coordonnées OABP, nous mesurons, sur le dessin, les coordonnées $x_1 = OA$, $x_2 = AB$, $x_3 = BP$.

Les nombres x_1, x_2, x_3 ($x_1 \in Q$, $x_2 \in Q$, $x_3 \in R$) sont denommés les *coordonnées pseudo-affines* du point P par rapport au repère $(0, \bar{v}_1, \bar{v}_2, \bar{v}_3)$. Le point P peut être écrit : $P = x_1\bar{v}_1 + x_2\bar{v}_2 + x_3\bar{v}_3$.

Si l'on considère, dans cet espace pseudo-affine, rapporté à ce repère, tous les points P, donnés par :

$$P = x_1\bar{v}_1 + x_2\bar{v}_2 + x_3\bar{v}_3, \; (x_1, x_2 \in Q, \; x_3 \in R, \; x_1, x_2, x_3 \geqslant 0, \qquad (3)$$
$$x_1 + x_2 + x_3 \leqslant 100),$$

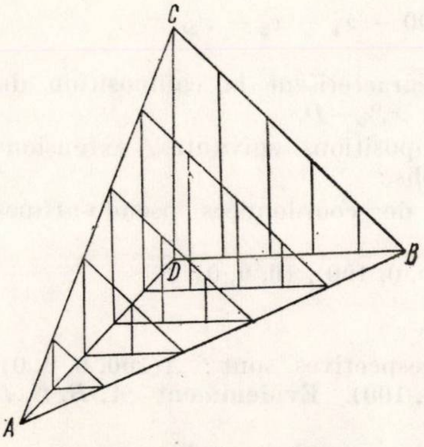

Fig. 2. – Pseudo-tétraèdre.

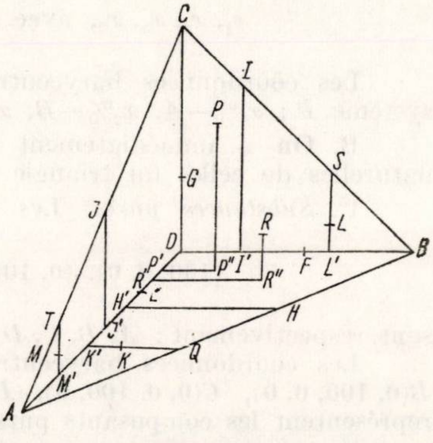

Fig. 3. – Représentation des systèmes binaires, ternaires et quaternaires dans un pseudo-tétraèdre.

on obtient une figure plane que nous avons dénommée *pseudo-tétraèdre*. Dans la figure 2, nous avons matérialisé seulement les points du pseudo-tétraèdre pour lesquels on a : $x_1 = 20\,k$, $x_2 = 20k'$ ($k, k' = 0, 1, 2, 3, 4, 5$), $0 \leqslant x_3 \leqslant 100 - x_1 - x_2$.

Les autres points du pseudo-tetraèdre qui nous intéresseraient peuvent être construits selon les nécessités, par interpolation. Evidemment, il est utile de construire aussi des pseudo-tétraèdres plus grands, où l'on puisse matérialiser tous les points ayant, par exemple $x_1 = 10k$, $x_2 = 10k'$ ($k, k' = 0, 1, 2, \ldots, 10$), $x_1 = 5k$, $x_2 = 5k'$ ($k, k' = 1, 2, \ldots \ldots, 20$), etc.

Dans tout ce qui suit nous considérerons un repère pseudo-affine ayant l'origine D, les axes DA, DB, DC et les unités : $\frac{1}{100}\,DA$, $\frac{1}{100}\,DB$, $\frac{1}{100}\,DC$. Un point arbitraire du pseudo-tétraèdre (fig. 3) sera construit vu ses coordonnées pseudo-affines par rapport à ce repère, en traçant effectivement le contour de coordonnées, ainsi que nous l'avons fait dans la figure 1.

Naturellement, il faut considérer aussi, à côté des coordonnées pseudo-affines, les coordonnées barycentriques classiques : si un point P du pseudo-tétraèdre a les coordonnées pseudo-affines :

$$x_1,\ x_2,\ x_3\ (\text{avec } x_1, x_2 \in Q,\ x_3 \in R,\ x_1, x_2, x_3 \geqslant 0,\ x_1 + x_2 + x_3 \leqslant 100)$$

alors il a les coordonnées barycentriques

$$x_1,\ x_2,\ x_3,\ x_0,\ \text{avec } x_0 = 100 - x_1 - x_2 - x_3.$$

Les coordonnées barycentriques caractérisent la composition du système P : $x_1\%-A$, $x_2\%-B$, $x_3\%-C$, $x_0\%-D$.

B. On a immédiatement les propositions suivantes, extensions naturelles de celles du triangle de Gibbs :

1°. *Substances pures.* Les points de coordonnées pseudo-affines

$$(100, 0, 0),\ (0, 100, 0),\ (0, 0, 100),\ (0, 0, 0)$$

sont, respectivement : A, B, C, D (fig. 3).

Les coordonnées barycentriques respectives sont : $A(100, 0, 0, 0)$, $B(0, 100, 0, 0)$, $C(0, 0, 100, 0)$, $D(0, 0, 0, 100)$. Evidemment A, B, C, D représentent les composants purs.

2°. *Systèmes binaires*

α) Les points de coordonnées pseudo-affines

$$(a, 0, 0),\ (0, b, 0),\ (0, 0, c),\ 0 < a, b,\ c < 100,$$

sont illustrés, respectivement, par E, F, G (fig. 3). Ils ont, respectivement les coordonnées barycentriques

$$E(a, 0, 0\ , d,)\ F(0, b, 0, d')\ G(0, 0, c, d''),$$

$$d = 100-a,\ d' = 100-b,\ d'' = 100-c$$

et représentent des systèmes binaires, comme il suit :

$$E(a\%-A,\ d\%-D),\ F(b\%-B,\ d'\%-D),\ G(c\%-C,\ d''\%-D).$$

β) Les points de coordonnées pseudo-affines

$$(a_1, b_1, 0), (0, b_2, c_2), (a_3, 0, c_3)\ a_1 + b_1 = 100, b_2 + c_2 = 100, a_3 + c_3 = 100$$

sont illustrés dans la figure 3, par H, I, J, avec les contours de coordonnées respectifs : $DH'H$, $DI'I$, $DJ'J$.

Voici l'explication du fait que H est situé sur l'arrête AB du pseudotétraèdre. De la relation $a_1 + b_1 = 100$, il résulte $b_1 = 100 - a_1$ et, en prenant : $DH' = a_1$ on a : $H'A = 100 - a_1 = b_1$. Le triangle DAB étant isoscèle, on a : $H'H = H'A = b_1$; il résulte que le point H est situé sur AB. De la même manière on démontre que I et J sont situés sur BC, respectivement AC.

Les coordonnées barycentriques des points H, I, J sont, respectivement :

$$H(a_1, b_1, 0, 0),\quad I(0, b_2, c_2, 0),\quad J(a_3, 0, c_3, 0).$$

Ces points représentent des systèmes binaires

$$H(a_1\%-A, b_1\%-B), I(b_2\%-B, c_2\%-C), J(a_3\%-A, c_3\%-C).$$

3°. *Systèmes ternaires.* α) Les points de coordonnées pseudo-affines

$$(a', b', 0),\quad (0, b'', c''),\quad (a''', 0, c'''),\quad a' + b' < 100,\ b'' + c'' < 100,$$
$$a''' + c''' < 100$$

sont illustrés, dans la figure 3, par K, L, M avec les contours de coordonnées respectifs : $DK'K$, $DL'L$, $DM'M$. En notant : $d' = 100 - a' - b'$, $d'' = 100 - b'' - c''$, $d''' = 100 - a''' - c'''$, les points K, L, M ont les coordonnées barycentriques

$$K(a', b', 0, d'), L(0, b'', c'', d''), M(a''', 0, c''', d''')$$

et représentent les systèmes ternaires

$$K(a'\%-A, b'\%-B, d'\%-D), L(b''\%-B, c''\%-C, d''\%-D),$$
$$M(a'''\%-A, c'''\%-C, d'''\%-D).$$

Les nombres d', d'', d''' sont représentés dans la figure 3 par les segments : $KQ = d'$, $LS = d''$, $MT = d'''$.

β) Un point de coordonnées pseudo-affines

$$(a, b, c),\ a + b + c = 100$$

est illustré, dans la figure 3 par P, avec le contour de coordonnées $DP'P''P$. Evidemment, ici $d = 0$ et les coordonnées barycentriques du point P sont :

$$P(a, b, c, 0)$$

Il représente un système ternaire

$$P(a\%-A,\ b\%-B,\ c\%-C)$$

Les points K, L, M, P sont situés sur les « faces » du pseudo-tétraèdre :

$$K - \text{sur } ABD,\ L - \text{sur } BCD,\ M - \text{sur } ACD,\ P - \text{sur } ABC$$

4°. *Systèmes quaternaires.* Le point de coordonnées pseudo-affines

$$(a, b, c),\ a + b + c < 100$$

est illustré dans la figure 3 par R, avec le contour de coordonnées $DR'R''R$. En notant $d = 100 - a - b - c$, ses coordonnées barycentriques sont (a, b, c, d). R représente un système quaternaire, avec la composition

$$R(a\%-A,\ b\%-B,\ c\%-C,\ d\%-D)$$

C. Tel qu'il résulte, le pseudo-tétraèdre constitue un *modèle géométrique* des divers systèmes binaires, ternaires et quaternaires, qu'on peut réaliser avec quatre substances.

Nous passons maintenant à la résolution de quelques problèmes typiques, extensions naturelles obtenues en partant du triangle de Gibbs.

1°. Etant donné un système ternaire, par exemple, $E(a\%-A, b\%-B, d\%-D)$ et la substance pure restée C, (fig. 4), les systèmes

$$R = E + C, \text{ avec } e\%-E,\ c\%-C,\ e + c = 100$$

sont des systèmes quaternaires avec la composition

$$R(a'\%-A,\ b'\%-B,\ c'\%-C,\ d'\%-D), \text{ tel que}$$

$$a'/a = b'/b = d'/d = e/100 \tag{4}$$

Les points R sont situés naturellement sur le segment CE, et

$$RC/RE = e/c,\ e + c = 100.$$

Les relations (4) résultent des couples de triangles semblables : CDE et RFE, DHE et DGF et les propriétés des suites de rapports égaux. Cette propriété est analogue à celle connue dans le triangle de Gibbs.[4]

Dans la figure 4 nous avons considéré les données suivantes : $E(40, 48, 0, 12)$, $e/c = RC/RE = 62{,}5/37{,}5$. Il a résulté, suivant les relations (4) : $a' = 40 . 62{,}5/100 = 25$, $b' = 30$, $d' = 7{,}5$ et ensuite $c' = 37{,}5$; les mêmes résultats peuvent être lis sur la figure 4 : $DG = 25$, $GF = 30$, $FR = 37{,}5$.

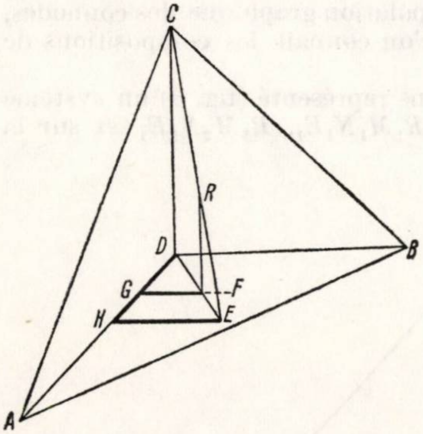

Fig. 4. — Système quaternaire obtenu d'un système ternaire et un composant pur.

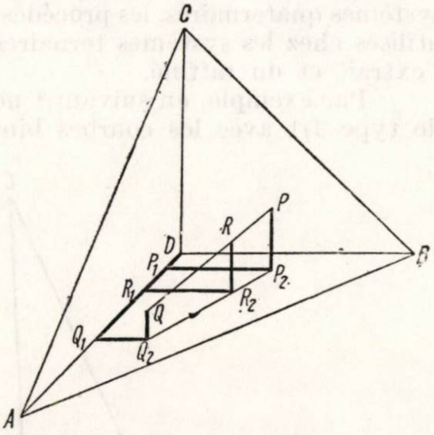

Fig. 5. — Système quaternaire obtenu de deux systèmes quaternaires.

2°. Etant donné deux systèmes (binaires, ternaires ou quaternaires) P et Q (fig. 5), un système R, obtenu de P et Q, pris dans le rapport $p/q (p + q = 100)$, est représenté dans le pseudo-tétraèdre, par un point du segment PQ, tel que l'on ait :

$$RQ/RP = p/q$$

propriété analogue à celle du triangle de Gibbs.[4]

Etant connu les compositions (a_1, b_1, c_1, d_1) et (a_2, b_2, c_2, d_2) de P et Q, et le rapport p/q, $(p + q = 100)$, on construit (fig. 5) les points P et Q avec les contours de coordonnées $D\,P_1P_2P$, $D\,Q_1Q_2Q$ et le point R sur le segment PQ ; afin de trouver graphiquement les coordonnées du point R, on mène $RR_2 \| DC$, $R_2 \in P_2Q_2$, $R_2R_1 \| DB$, $R_1 \in P_1Q_1$. Alors DR_1R_2R définit les coordonnées pseudo-affines du point R : $a = DR_1$, $b = R_1R_2$, $c = R_2R$; en prenant $d = 100 - a - b - c$, on a la composition (a, b, c, d) du système R.

Réciproquement, étant donné les systèmes P et Q dont les compositions sont connues et afin de réaliser avec P et Q un système R ayant une certaine composition $(a\% - A,\ b\% - B,\ c\% - C,\ d\% - D)$, il faut déterminer graphiquement les nombres p et q, tels que $R = (p\% - P) + (q\% - Q)$, $(p + q = 100)$. Dans ce but, on construit — de la manière décrite plus haut — les points P, Q, R en utilisant les coordonnées pseudo-affines respectives et, si le problème est possible du point de vue chimique, le point *R* sera situé sur le segment *PQ* et l'on aura : $p/q = RQ/RP$.

3°. Tout de même, dans les problèmes d'extraction liquide-liquide, on peut représenter assez exactement dans un pseudo-tétraèdre, les courbes binodales, la surface binodale et les courbes d'intersection de la surface binodale avec certains plans, ce qui permet de prolonger, aux systèmes quaternaires, les procédés d'interpolation graphique des connodes, utilisés chez les systèmes ternaires lorsqu'on connaît les compositions de l'extrait et du raffiné.

Par exemple, en suivant,[4] nous avons représenté (fig. 6) un système de type 4/1 avec les courbes binodales $R_1M_1N_1E_1$, $R_1M_2N_2E_1$ et sur la

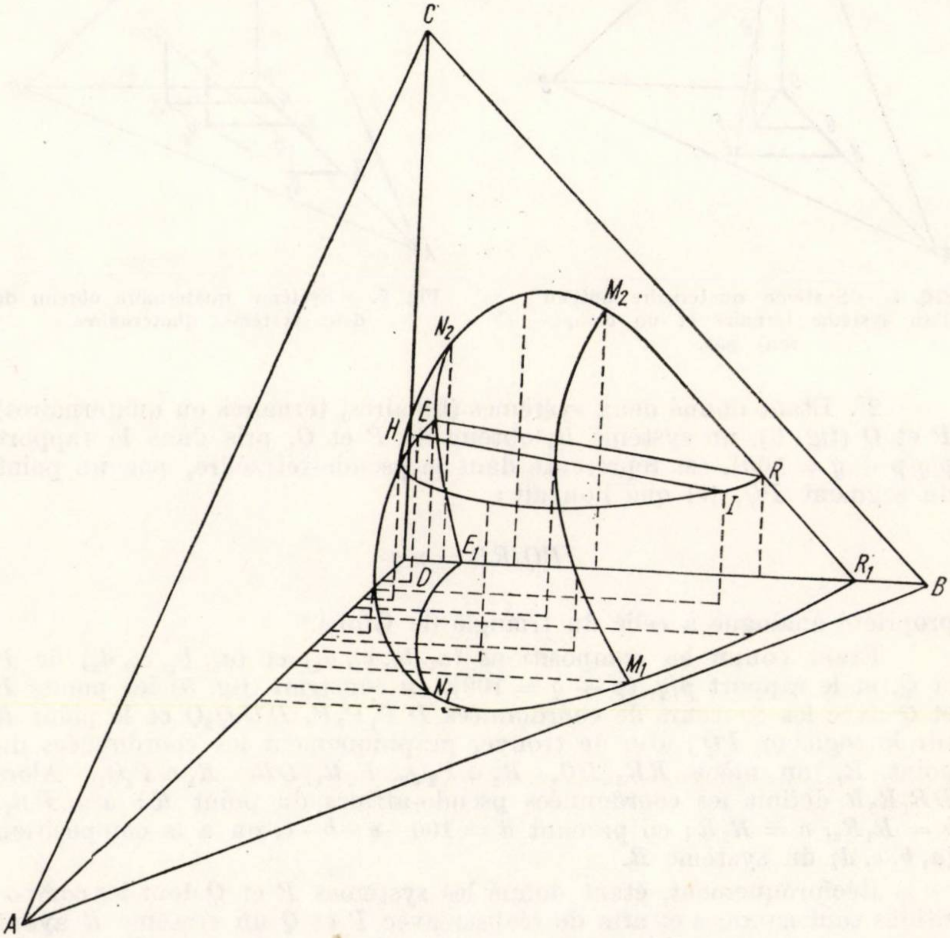

Fig. 6. — Courbes tracées sur une surface binodale.

surface binodale déterminée par elles — les courbes M_1M_2, N_1N_2, la section RIHE de cette surface par un plan et la connode *IH*. Mais tandis qu'un dessin habituel peut nous donner seulement une idée qualitative sur cette configuration, ici nous avons une représentation presque exacte, parce qu'on peut mesurer, sur le dessin, les coordonnées des divers points et faire des interpolations graphiques, on peut donc déterminer du dessin les points appartenant au domaine d'hétérogénéité, ainsi que les points appartenant au domaine d'homogénéité, ce qui nous peut dispenser d'un grand nombre d'expériences.

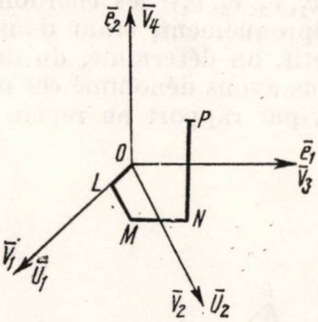

Fig. 7. – Repère d'un espace pseudo-affine à quatre dimensions construit dans un plan

D'ailleurs, ce que nous avons présenté plus haut contient les éléments suffisants pour la résolution graphique de tout problème concernant les systèmes quaternaires.

III. LE PSEUDO-PENTATÔPE QUI GÉNÉRALISE LE TRIANGLE DE GIBBS

Dans un plan rapporté à un repère $(0\,;\bar{e}_1, \bar{e}_2)$ (fig. 7) on considère les vecteurs $\bar{u}_1$, $\bar{u}_2$ donnés par :

$$\bar{u}_1 = a_1\bar{e}_1 + b_1\bar{e}_2,\ \bar{u}_2 = a_2\bar{e}_1 + b_2\bar{e}_2\,;\ \ a_1, a_2 \in R-Q, (a_1/a_2) \in R-Q$$

$$b_1, b_2 \in R \tag{5}$$

Dans la figure 7 nous avons pris : $\bar{u}_1 = (-6/\sqrt{75})\bar{e}_1 - (\sqrt{13/5})\,\bar{e}_2 \approx$ $\approx -\,0{,}69\ \bar{e}_1 - 0{,}72\ \bar{e}_2\,;\ \bar{u}_2 = (1/\sqrt{5})\ \bar{e}_1 - (2/\sqrt{5})\ \bar{e}_2 \approx 0{,}45\ \bar{e}_1 - 0{,}9\ \bar{e}_2$, c'est-à-dire $a_1 = -\ 6/\sqrt{75}$, $a_2 = 1/\sqrt{5}$, $a_1/a_2 = -\ 6/\sqrt{15}$ et donc : a_1, a_2, $(a_1/a_2) \in R-Q$.

Nous renotons ces vecteurs :

$$\bar{v}_1 = \bar{u}_1,\ \bar{v}_2 = \bar{u}_2,\ \bar{v}_3 = \bar{e}_1,\ \bar{v}_4 = \bar{e}_2 \tag{6}$$

Nous faisons une construction analogue à celle de l'espace pseudo-affine à trois dimensions et nous obtenons *l'espace pseudo-affine à quatre dimen-*

sions construit dans un plan ; $(0\,;\,\bar{v}_1, \bar{v}_2, \bar{v}_3, \bar{v}_4)$ est un repère de cet espace.* Etant donné un système ordonné de quatre nombres (x_1, x_2, x_3, x_4), $(x_1, x_2, x_3 \in Q,\ x_4 \in R)$, nous faisons le contour de coordonnées $OLMNP$ (fig. 7) : $OL = x_1$, $LM \| \bar{v}_2$, $LM = x_2$; $MN \| \bar{v}_3$; $MN = x_3$; $NP \| \bar{v}_4$; $NP = x_4$. Nous avons ainsi obtenu le point P, qui a, par rapport au repère $(0\,;\,\bar{v}_1, \bar{v}_2, \bar{v}_3, \bar{v}_4)$, les coordonnées x_1, x_2, x_3, x_4 avec $x_1, x_2, x_3 \in Q$, $x_4 \in R$. Réciproquement, étant donné le point P, avec le contour polygonal respectif, on détermine, du dessin, les nombres x_1, x_2, x_3, x_4. C'est pourquoi nous avons dénommé ces nombres les *coordonnées pseudo-affines* du point P, par rapport au repère $(0\,;\,\bar{v}_1, \bar{v}_2, \bar{v}_3, \bar{v}_4)$.[7]

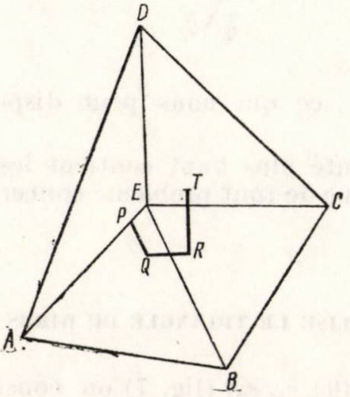

Fig. 8. – Représentation d'un système quinaire dans un pseudo-pentatôpe.

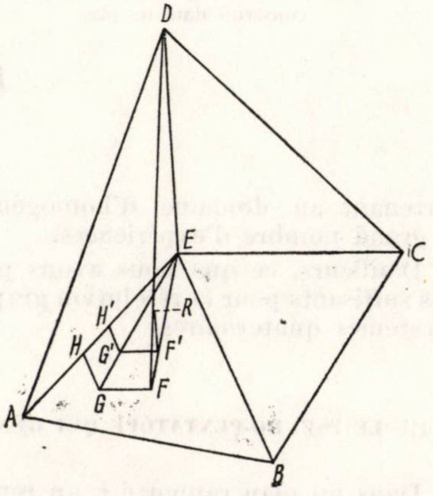

Fig. 9. – Système quinaire obtenu d'un système quaternaire et un composant pur.

Soit l'espace pseudo-affine à quatre dimensions construit dans un plan, rapporté à un repère (fig. 8) ayant E pour origine et $\bar{v}_1 = \dfrac{1}{100}\overrightarrow{EA}$, $\bar{v}_2 = \dfrac{1}{100}\overrightarrow{EB}$, $\bar{v}_3 = \dfrac{1}{100}\overrightarrow{EC}$, $\bar{v}_4 = \dfrac{1}{100}\overrightarrow{ED}$ pour vecteurs unité.

---

* Voici cette construction :

Nous considérons (fig. 7) $(0\,;\,\bar{v}_1, \bar{v}_2)$ comme un repère du plan et l'ensemble des points M du plan, $M = x_1\bar{v}_1 + x_2\bar{v}_2$, ayant, par rapport à ce repère, les coordonnées x_1, x_2, nombres rationnels. Par chacun de ces points M, on considère la droite parallèle à $\bar{v}_3$ (selon que nous avons déjà montré, ces droites sont distinctes) ; sur ces droites nous considérons les points N, donnés par : $N = x_1\bar{v}_1 + x_2\bar{v}_2 + x_3\bar{v}_3$, avec x_1, x_2, $x_3 \in Q$. Par chacun des points N on considère la droite parallèle à $\bar{v}_4$. Nous avons démontré que ces droites sont aussi distinctes. On considère sur ces droites tous les points P donnés par : $P = x_1\bar{v}_1 + x_2\bar{v}_2 + x_3\bar{v}_3 + x_4\bar{v}_4$ $(x_1, x_2, x_3 \in Q,\ x_4 \in R)$. L'ensemble des points P est un espace pseudo-affine à quatre dimensions construit dans un plan.

Considérons l'ensemble des points P donnés par

$$P = x_1\bar{v}_1 + x_2\bar{v}_2 + x_3\bar{v}_3 + x_4\bar{v}_4,\ x_1, x_2, x_3 \in Q,\ x_4 \in R,\ x_i \geqslant 0, \qquad i = 1, 2, 3, 4\ ;\ \sum_{i=1}^{4} x_i \leqslant 100. \tag{7}$$

Cette figure a été dénommée par nous *pseudo-pentatôpe*[7] ; elle constitue un *modèle géométrique* de divers systèmes qu'on peut réaliser avec cinq substances.

Précisons que la position d'un point dans le pseudo-pentatôpe est fixée par les quatre coordonnées pseudo-affines x_1, x_2, x_3, x_4 qui satisfont aux conditions (7) et que, afin de passer aux coordonnées barycentriques, on introduit une cinquième coordonnée, $x_0 = 100 - x_1 - x_2 - x_3 - x_4$. En notant les cinq coordonnées barycentriques par *(a, b, c, d, e), ces nombres expriment la composition du système,* $a\%-A$, $b\%-B$, $c\%-C$, $d\%-D$, $e\%-E$.

Le procédé de représentation d'un système par un point unique est le même que dans le pseudo-tétraèdre, c'est pourquoi nous allons nous résumer seulement au cas d'un système quinaire. Soit, donc, un système T ayant la composition : $a\%-A$, $b\%-B$, $c\%-C$, $d\%-D$, $e\%-E$, $a, b, c, d, e > 0$, $a + b + c + d + e = 100$. Alors on construit le contour de coordonnées $EPQRT$ (fig. 8) avec : $EP = a$, $PQ \| EB$, $PQ = b$; $QR \| EC$, $QR = c$; $RT \| ED$, $RT = d$. Réciproquement, étant donné dans le pseudo-pentatôpe le point T avec son contour de coordonnées, on détermine directement dans la figure les coordonnées et l'on a, ainsi, la composition du système T. En particulier, les points P, Q, R représentent respectivement : P — un système binaire ; $a\%-A$, $e'\%-E$ $(a + e' = 100)$, Q — un système ternaire : $a\%-A$, $b\%-B$, $e''\%-E$ $(a + b + e'' = 100)$, R — un système quaternaire : $a\%-A$, $b\%-B$, $c\%-C$, $e'''\%-E$ $(a + b + c + e''' = 100)$.

Reprenons certains types de problèmes analogues aux problèmes usuels chez les systèmes ternaires :

1°. Étant donné un système quaternaire, $F(a\%-A,\ b\%-B,\ c\%-C,\ e\%-E)$ et la substance pure D, (fig. 9) un système $R = F + D(f\%-F,\ d\%-D,\ f + d = 100)$ est un système quinaire de composition $R(a'\%-A,\ b'\%-B,\ c'\%-C,\ d'\%-D,\ e'\%-E)$, avec $a'/a = b'/b = c'/c = e'/e = f/100$ et le point R est situé sur le segment DF, tel que : $RF/FD = d/f$.

Réciproquement, étant donné un point R sur DF, il représente un système quinaire dont la composition s'obtient graphiquement en traçant le contour de coordonnées : la parallèle par R à DE coupe EF en F' ; la parallèle par F' à GF coupe EG en G' et la parallèle par G' à HG coupe EH en H'. Alors $a = EH'$, $b = H'G'$, $c = G'F'$, $d = F'R$ donnent la composition de R en ce qui concerne A, B, C, D ; le reste jusqu'à 100 est le nombre e, qui indique la composante E.

2°. Etant donné deux systèmes quinaires, représentés par les points

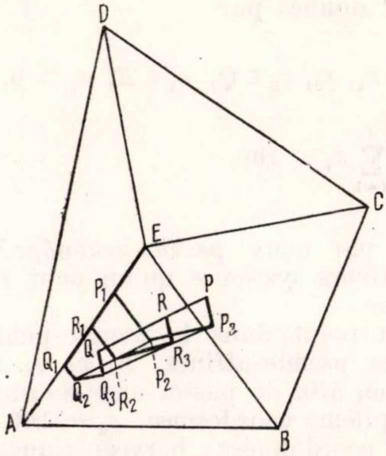

Fig. 10. — Système quinaire obtenu de deux systèmes quinaires.

P et Q (fig. 10), alors le segment PQ est le lieu géométrique des points R qui représentent les systèmes obtenus de P et Q, dans les proportions $p\%-P$, $q\%-Q$ $(p+q=100)$ où $p/q = RQ/RP$. Si $E\,P_1P_2P_3P$ et $EQ_1Q_2Q_3Q$ sont les contours de coordonnées des points P et Q, alors le contour de coordonnées de R est $ER_1R_2R_3R$, tel que l'on ait $R_1P_1/R_1Q_1 = R_2P_2/R_2Q_2 = R_3P_3/R_3Q_3 = RP/RQ = q/p$.

Il résulte que, si l'on connaît les compositions de P et Q et le rapport p/q on a directement, du diagramme, la composition de R et réciproquement, les compositions des systèmes P, Q et R étant connues, on détermine du diagramme, directement, le rapport p/q.

Revue Roumaine de Chimie, **19**, *6*, 1009–1018 (1974)

CONTRIBUTIONS TO THE STUDY OF THE $NiO-SiO_2-TiO_2$ TERNARY SYSTEM

CONST. GH. MACAROVICI * and MARIA ZAHARESCU **

* Institute of Chemistry, str. Donath 65–103, Cluj
** Centre of Physical Chemistry, str. Dumbrava Roșie 23, Bucharest

Received September 6, 1973

Studies were carried out on the reaction mechanisms and phase equilibrium relations in the $NiO-SiO_2-TiO_2$ system in the subsolidus field, starting from reactive mixtures obtained by quantitative coprecipitation.

The $MO-SiO_2-TiO_2$ type oxide systems (where M = transitional metal) have been investigated in a very reduced number of papers,[1,2] although their properties proved to be very interesting both from a theoretical and an applicative standpoint.[3-5]

Taking into account this fact, the present paper deals with the study of the $NiO-SiO_2-TiO_2$ ternary system, which, according to bibliographical data, has not been studied until now. However, there are numerous pieces of information referring to the component binary systems SiO_2-TiO_2, $NiO-SiO_2$, and $NiO-TiO_2$.

We shall present below the results of investigations made into the $NiO-SiO_2-TiO_2$ system, with regard to reaction mechanisms and phase equilibrium relations in the subsolidus field, starting from reactive mixtures obtained by quantitative coprecipitation.

Attempts to obtain reactive mixtures in systems containing NiO by precipitation from solution were previously reported.[6-10] However, some of these methods are not quantitative [6,7] and others make use of sodium hydroxide or carbonate[8-10] as a precipitation reagent, which is difficultly washed and disturbs the subsequent determinations.

---

[1] E. M. Levin, H. F. McMurdie and E. P. Hall, "Phase Diagrams for Ceramists" Ed. The American Ceramic Society, Inc., Ohio, 1964.

[2] E. M. Levin, C. R. Robbins and H. F. McMurdie, "Phase Diagrams for Ceramists. 1969 Supplement", Ed. The American Ceramic Society, Inc., Ohio, 1969.

[3] S. Smolensky, *Z. anorg. Chem.*, **73**, 299 (1912).

[4] J. B. MacChesney and A. Muan, *J. Amer. Ceram. Soc.*, **43**, 588 (1960).

[5] M. S. R. Heynes and H. Rawson, *Phys. and Chem. Glasses*, **2**, **1** (1961).

[6] B. Phillips, J. J. Hutta and I. Warshaw, *J. Amer. Ceram. Soc.*, **46**, 579 (1963).

[7] N. A. Toropov and S. A. Babaian, *Zhur. neorgan. Khim.*, **11**, 28 (1966).

[8] T. Shirasahi, M. Okada and K. Morikawa, *Kagoya Hogaku Zasshi*, 68, 593 (1965); *Chem. Abstr.*, **63**, 10737 (1965).

[9] N. S. Rassudova, A. I. Terekova and G. N. Lilo, *Lakokrasochnye Materialy i ikh Primenenie*, **1963**, 25.

[10] N. S. Rassudova, I. S. Striltsov and N. A. Aleksandrova, *Lakokrasochnye Materialy i ikh Primenenie*, **1963**, 27.

The choice of quantitative coprecipitation in view of obtaining reactive mixtures in the system under consideration was due, in the first place, to the difficulties in obtaining a mixed complexation of Si^{4+} ion. On the other hand, by comparison to the method for obtaining mixed complex combinations,[11] which performed a homogenization at a molecular scale, but which are quantitative only for certain stoichiometric, well determined relations of the components, oxide mixtures in any proportion may be obtained through coprecipitation.

1. EXPERIMENTAL METHODS

1.1. QUANTITATIVE COPRECIPITATION

$Ni(NO_3)_2$, $TiCl_4$ and $SiCl_4$ solutions were used, having 0.5 m concentration and the precipitation reagent consisted of a 1 % dimethyl glyoxime alcoholic solution in ammoniacal medium.

The precipitation reagent for masses in the $NiO-TiO_2$, $NiO-SiO_2$ binary systems and in the $NiO-SiO_2-TiO_2$ ternary system had to be dimethylglyoxime since the common reagents, such as ammonia, ammonium carbonate, tetramine-hexamethylene, etc. do not precipitate Ni^{2+} quantitatively. Ammonia addition was necessary for establishing a weakly ammoniacal medium, indispensable for the formation of the $Ni-(C_4H_7N_2O_2)_2$ complex and also for the quantitative precipitation of Ti^{4+} as $TiO_2 . xH_2O$ and of Si^{4+} as $SiO_2 . xH_2O$.

$Ni(NO_3)_2$, $TiCl_4$ and $SiCl_4$ solutions were mixed in predetermined proportions and heated allowing to boil while continuously stirring. Dimethylglyoxime solution was then added and finally ammonia was added dropwise. Conditions were thus established for the concomitant precipitation of the three ions.

The completed precipitation was tested in the filtrate, using H_2O_2 in sulphuric acid medium for the identification of Ti^{4+} ion, dimethylglyoxime reaction for the Ni^{2+} ion, and for Si^{4+} ion, its reaction with $SnCl_2$ ammoniacal solution.[12]

It was found that under the above conditions, precipitation is quantitative for any ratio of the three components of the mixture.

The reddish-pink precipitate obtained was filtered, washed with distilled water until the Cl^- was freed and then dried at approx. 100°.

1.2. THERMOGRAVIMETRIC AND THERMODIFFERENTIAL ANALYSIS

The thermogravimetric and thermodifferential analysis of each separate coprecipitated sample was performed in order to observe the reaction mechanism of the studied mixtures from the precipitate to the oxide form. An OD-102 type Erdey-Paulik derivatograph was used, with a 5°/minute heating rate up to a temperature of 1000°.

1.3. CHEMICAL ANALYSIS

The chemical analysis of oxide masses resulting from the thermal treatment was based on the following reactions :

— SiO_2 insolubilisation, applying the classical HCl method[13];

---

[11] J. Paris and R. Paris, *Bull. Soc. chim. France*, **1965**, 1138.

[12] R. Ripan, E. Popper and C. Liteanu, "Chimie analitică calitativă", IVth ed., Ed. didactică şi pedagogică, Bucharest, 1963, p. 262.

[13] A. Lassieur, *Z. analyt. Chem.*, **72**, 160 (1927).

— Ti^{4+} reaction with H_2O_2 in sulphuric oxide medium and formation of peroxi-sulphate-titanium $TiO_2(SO_4)_2^{2-}$-complex anion, having a yellow-orange-brown colour, according to the concentration ;

— complexometric titration of Ni^{2+} with 10^{-2} m complexon III in presence of the murexide as indicator.[14]

1.4. DETERMINATION OF PHASE COMPOSITION

The phase analysis of unheated and thermally treated coprecipitated mixtures was carried out by applying the röntgenographic and IR-spectroscopic methods, the optical microscopy and electron microprobe analysis.

1.4.1. *The röntgenographic analysis* was performed on powders by the Debye-Scherrer method, using Cu_{K_α} radiation on a TUR M-60 apparatus.

1.4.2. *The microscopic analysis* was performed on powders and thin sections using the MC-1-type IOR research microscope and the MIN-5 polarizing microscope.

1.4.3. *The IR-spectroscopic analysis* was performed on a UR-10-type Zeiss apparatus in an 1800—400 cm^{-1} interval, applying the pelleting technique in KBr.

1.4.4. *The electron microprobe analysis* was carried out on cylindrical samples, having the size of approx. 8 × 8 mm and a polished surface similar to samples for metallographic studies, which was carbon metallized in view of preventing overheating and local overchanging. A JXA 3A Jeol apparatus was used at 16 kV electron acceleration voltage.

2. EXPERIMENTAL RESULTS

The oxide and equilibrium phase composition of the mixtures studied in the $NiO-SiO_2-TiO_2$ ternary system is presented in table 1.

2.1. COMPOSITION OF THE COPRECIPITATED MIXTURES

The röntgenographic and IR-spectroscopic analysis of the coprecipitated mixtures in the studied ternary system revealed that the quantitative coprecipitation of components takes place both in the case of binary and ternary mixtures.

The röntgenographic analysis permits the positive identification of the $Ni-(C_4H_7N_2O_2)_2$ complex in the mixture and also of the hydrated microcrystalline anatase by the presence of the principal characteristic diffraction lines of $Ni-(C_4H_7N_2O_2)_2$ and of the most pronounced line of the anatase (d = 3.520).

The occurrence of the hydrated microcrystalline anatase by precipitating Ti^{4+} ion with ammonia from a $TiCl_4$ solution by allowing to boil was reported in a previous work.[15]

The third component in precipitates, $SiO_2.H_2O$, is not crystallized and cannot be röntgenographically detected. Its presence in mixtures

---

[14] C. Liteanu, "Chimie analitică cantitativă. Volumetria", Vth ed. Ed. didactică şi pedagogică, Bucharest, 1969, p. 607.

[15] C. Gh. Macarovici and M. Zaharescu, *Rev. Roumaine Chim.*, **16**, 577 (1971).

Table 1

Oxide composition and phases resulting from calcination at 1000°, for the masses studied in the $NiO-SiO_2-TiO_2$ telnary system

N°	Symbol	Oxide composition (%)			Phases identified owing to thermal analysis at 1000°	(Equilibrium) phases identified in samples calcinated for 6 hours at 1000°
		NiO	TiO_2	SiO_2		
1	$STN_{4.77}$	4.77	9.54	85.68	$NiO.TiO_2 + \alpha$-cristobalite	$NiO.TiO_2 + \alpha$-cristobalite
2	$STN_{9.56}$	9.65	9.04	81.39	$NiO.TiO_2 + \alpha$-cristobalite	$NiO.TiO_2 + \alpha$-cristobalite
3	$STN_{11.62}$	11.62	23.25	65.10	$NiO.TiO_2 + \alpha$-cristobalite	$NiO.TiO_2 + \alpha$-cristobalite
4	$STN_{10.00}$	10.00	80.00	10.00	$NiO.TiO_2 + \alpha$-crist. + rutile	$NiO.TiO_2 + \alpha$-crist. + rutile
5	$STN_{14.38}$	14.38	8.55	77.05	$NiO.TiO_2 + \alpha$-cristobalite	$NiO.TiO_2 + 2NiO.SiO_2 + \alpha$-crist.
6	$STN_{21.76}$	21.76	20.56	57.65	$NiO.TiO_2 + \alpha$-cristobalite	$NiO.TiO_2 + \alpha$-cristobalite
7	$STN_{20.00}$	20.00	50.00	30.00	$NiO.TiO_2 + \alpha$-crist. + rutile	$NiO.TiO_2 + \alpha$-crist. + rutile
8	$STN_{30.66}$	30.66	18.23	51.10	$NiO.TiO_2 + \alpha$-crist. + NiO	$NiO.TiO_2 + 2NiO.SiO_2 + \alpha$-crist.
9	$STN_{30.00}$	30.00	30.00	40.00	$NiO.TiO_2 + \alpha$-cristobalite	$NiO.TiO_2 + \alpha$-cristobalite
10	$STN_{31.00}$	31.00	59.00	10.00	$NiO.TiO_2 + \alpha$-crist. + rutile	$NiO.TiO_2 + \alpha$-crist. + rutile
11	$STN_{50.00}$	50.00	20.00	30.00	$NiO.TiO_2 + \alpha$-crist. + rutile	$NiO.TiO_2 + 2NiO.SiO_2 + \alpha$-crist.
12	$STN_{41.70}$	41.70	44.70	14.23	$NiO.TiO_2 + \alpha$-cristobalite	$NiO.TiO_2 + \alpha$-cristobalite
13	$STN_{62.70}$	62.70	10.44	26.86	$NiO.TiO_2 + \alpha$-crist. + NiO	$NiO.TiO_2 + 2NiO.SiO_2 + \alpha$-crist.
14	$STN_{60.05}$	60.05	18.75	21.17	$NiO.TiO_2 + \alpha$-crist. + NiO	$NiO.TiO_2 + 2NiO.SiO_2 + \alpha$-crist.
15	$STN_{60.00}$	60.00	30.00	10.00	$NiO.TiO_2 + \alpha$-crist. + NiO	$NiO.TiO_2 + 2NiO.SiO_2$
16	$STN_{80.00}$	80.00	10.00	10.00	$NiO.TiO_2 + \alpha$-crist. + NiO	$NiO.TiO_2 + 2NiO.SiO_2 + NiO$

Table 2

Röntgen diffraction lines of coprecipitated mixtures corresponding to NiO.TiO$_2$, 2NiO.SiO$_2$ formation and of STN$_{21\cdot76}$, STN$_{41\cdot7}$^{0} and STN$_{60\cdot05}$ ternary samples

NiO.TiO$_2$			2NiO.SiO$_2$			STN$_{21\cdot76}$			STN$_{41\cdot70}$			STN$_{60\cdot05}$		
I	d	belong	I	d	belong	I	d	belong	I	d	belong	I	d	belong
s	5.66	Ni(Dm)	s(d)	5.66	Ni(Dm)	s(d)	5.661	Ni(Dm)	s	5.666	Ni(Dm)	s	5.664	Ni(Dm)
w	4.505	Ni(Dm)	w	4.50	Ni(Dm)	w	4.51	Ni(Dm)	w	4.503	Ni(Dm)	w	4.505	Ni(Dm)
w	3.515	anatase	vw	3.510	anatase	vw	3.522	anatase	w	3.520	anatase	vw	3.518	anatase
s	3.317	Ni(Dm)	s	3.32	anatase	ms	3.315	Ni(Dm)	s	3.32	Ni(Dm)	s	3.317	Ni(Dm)
vs	3.135	Ni(Dm)	vs	3.133	Ni(Dm)	vs	3.133	Ni(Dm)	vs	3.134	Ni(Dm)	vs	3.134	Ni(Dm)
s	2.980	Ni(Dm)	s	2.97	Ni(Dm)	ms	2.970	Ni(Dm)	s	2.970	Ni(Dm)	s	2.970	Ni(Dm)
s(d)	2.569	Ni(Dm)	s(d)	2.470	Ni(Dm)	ms	2.470	Ni(Dm)	s(d)	2.470	Ni(Dm)	s	2.469	Ni(Dm)
w(d)	2.275	Ni(Dm)	w(d)	2.277	Ni(Dm)	vw	2.273	Ni(Dm)	w(d)	2.274	Ni(Dm)	w	2.274	Ni(Dm)
vw	2.199	Ni(Dm)	vw	2.196	Ni(Dm)	sv	2.195	Ni(Dm)	vw	2.196	Ni(Dm)	vw	2.194	Ni(Dm)
s(d)	1.940	Ni(Dm)	s(d)	1.950	Ni(Dm)									
vw	1.888	anatase	sv	1.885	anatase	sv	1.888	anatase	vw	1.880	anatase	sv	1.885	anatase
vw	1.850	Ni(Dm)	vw	1.850	Ni(Dm)	sv	1.851	Ni(Dm)	sv	1.850	Ni(Dm)	sv	1.850	Ni(Dm)
vw	1.681	Ni(Dm)	vw	1.690	Ni(Dm)									
w	1.599	Ni(Dm)	w	1.595	Ni(Dm)	vw	1.595	Ni(Dm)	vw	1.596	Ni(Dm)	vw	1.596	Ni(Dm)

Ni(Dm) = Ni – $(C_4H_7N_2O_2)_2$

vs = very strong
s = strong
ms = moderately strong
w = weak
vw = very weak
sv = slightly visible

may however be obviously outlined by IR spectroscopy owing to the presence in IR spectra of mixtures of intense absorption bands, specific of $SiO_2 . xH_2O$,[16] at approx. 1100, 800, and 475 cm^{-1}.

To illustrate, table 2 presents Röntgen diffraction lines and figure 1, IR spectra for mixtures corresponding to $NiO . TiO_2$ and $2NiO . SiO_2$ formation and also for three ternary mixtures situated in different areas of the ternary system and noted : $STN_{21.76}$, $STN_{41.70}$, and $STN_{60.05}$.

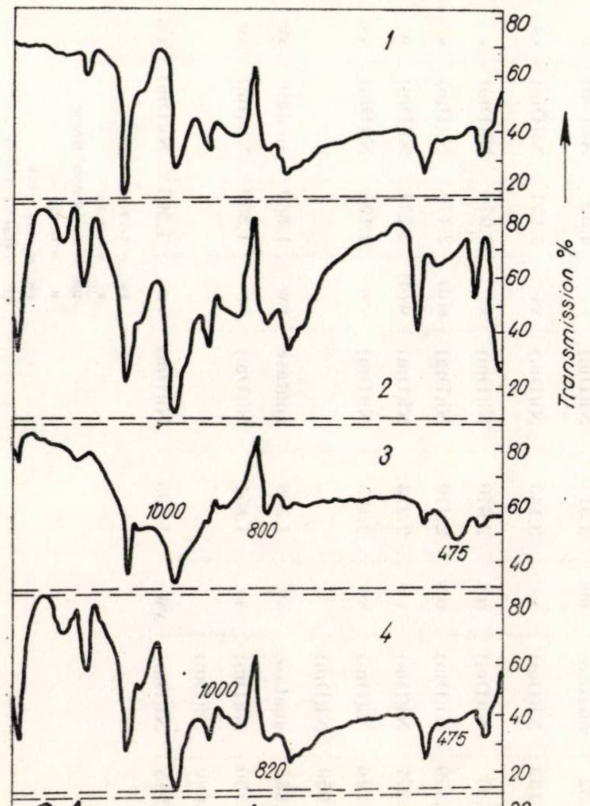

Fig. 1. — IR spectra for coprecipitated mixtures corresponding to $NiO . TiO_2$ and $2NiO . SiO_2$ formation and for three ternary mixtures : $STN_{21.76}$, $STN_{41.70}$, and $STN_{60.05}$. *1*, $Ni-(C_4H_7N_2O_2)_2 + TiO_2 . xH_2O$ (1 : 1); *2*, $Ni-(C_4H_7N_2O_2)_2 + SiO_2 . xH_2O$ (2 : 1); *3*, $STN_{21.76}$; *4*, $STN_{41.70}$; *5*, $STN_{60.05}$.

---

[16] H. Moenke, „Mineralspektren", Berlin, 1962.

2.2. REACTION MECHANISMS IN THE FORMATION OF DEFINED COMPOUNDS AND OF TERNARY OXIDE MIXTURES

2.2.1. NiO . TiO$_2$ formation

The mechanism of NiO . TiO$_2$ formation from coprecipitated mixtures was established in a previous work,[15] which highlighted the particularly important effect of coprecipitation on the reactivity of oxide mixtures in the NiO . TiO$_2$ system, manifested by a decrease of the temperature of the NiO . TiO$_2$ formation from over 1000° to 410°.

2.2.2. 2NiO . SiO$_2$ formation

The thermodifferential and thermogravimetric analysis curves of the coprecipitated mixture corresponding to the formation of 2NiO . SiO$_2$ are presented in figure 2.

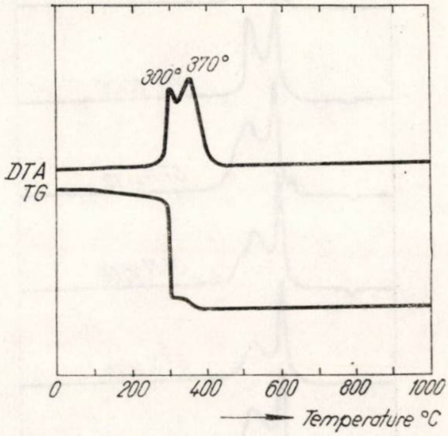

Fig. 2. — Thermogravimetric and thermodifferential analysis curves of the coprecipitated mixture corresponding to the 2NiO . SiO$_2$ formation.

The occurrence of two exothermic effects on the DTA curve is observed at 300 and 370° ; they are identical to those reported in the case of the decomposition of the Ni$-$(C$_4$H$_7$N$_2$O$_2$)$_2$ complex.[15] The appearance of other thermic effects up to 1000°, which would indicate a reaction between the two resulting oxides, has not been observed. This was also tested by röntgenographic approach.

In view of achieving the reaction between SiO$_2$ and NiO, the samples resulted after the thermogravimetric and thermodifferential analysis were compressed and maintained at a temperature of 1000° for prolonged time intervals. It was found that at this temperature 2NiO . SiO$_2$ formation was not completed even after a 96-hour thermal treatment, the presence of NiO and SiO$_2$ in significant amounts being röntgenographycally identified, alongside with 2NiO . SiO$_2$.

The result obtained is in agreement with the data from the literature which point to the low reactivity of NiO against SiO_2. [6, 17, 18]

At a temperature of 1400° a $2NiO.SiO_2$ formation was detected only after an hour of thermal treatment and was completed after 5 hours, while at a temperature of 1450° the complete reaction was already reached after one hour of thermal treatment.

The results presented indicate that in the case of the $NiO-SiO_2$ system, the effect of coprecipitation on oxides' reactivity is less obvious.

2.2.3. Formation of thernary oxide mixtures

The thermodifferential analysis curves of the principal ternary mixtures studied are presented in figure 3.

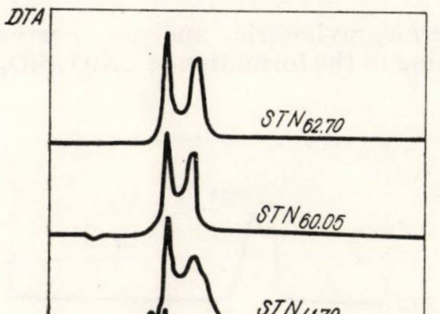

Fig. 3. — Thermodifferential analysis curves of the principal ternary mixtures coprecipitated in the $NiO-SiO_2-TiO_2$ system.

The review of these curves shows that they do not contain additional thermic effects, compared to those recorded for the formation of defined compounds in the case of binary mixtures.

---

[17] P. Tarte, *Spectrochim. Acta*, **19**, 25 (1963).

[18] H. Hayashi and S. Naka, *Nagoya Kogyo Shikensho Hohokoku*, **9**, 196 (1960); *Chem. Abstr.*, **54**, 10620 (1960).

A first conclusion, which has been röntgenographycally confirmed (table 1), is that no ternary compounds are formed under the conditions of the mentioned thermal treatment.

However, considering the very slow formation rate of $2NiO.SiO_2$ at a temperature of 1000°, it was estimated that the phases resulting from the thermal analysis are not equilibrium phases. Due to this fact, the same samples were compactly compressed and burnt again at 1000° for 24 hours. Neither in this case was the formation of ternary compounds revealed.

Results obtained by observing the formation of defined compounds in the $NiO-SiO_2-TiO_2$ ternary system at higher temperatures (1400°) were identical to those found after calcination at 1000°.

The absence of ternary compounds was verified by analysing the $STN_{21.76}$ mixture by means of electron microprobe.

By applying the semiquantitative method of the linear scanning of the electron fascicle after a direction, the variation of the TiO_2 concentration was found to be inverse to the variation of the SiO_2 concentration, which is indicative of the fact that no chemical bond was achieved between the two oxides through NiO, therefore the formation of a ternary compound is excluded (figure 4).

2.3. PHASE EQUILIBRIUM RELATIONS IN THE $NiO-SiO_2-TiO_2$ SYSTEM

In order to establish the phase equilibrium relations, the division of $NiO-TiO_2-SiO_2$ into coordination subsystems was studied, supposing that no ternary compounds exist.

The results of the röntgenographic analysis, indicated in table 1, confirmed the hypothesis that the two binary compounds coordinate as follows :

1. $NiO.TiO_2-SiO_2$
2. $NiO.TiO_2-2\,NiO.SiO_2$

dividing the $NiO-SiO_2-TiO_2$ ternary system into three subsystems :

I. $TiO_2-SiO_2-NiO.TiO_2$
II. $SiO_2-NiO.TiO_2-2NiO.SiO_2$
III. $NiO.TiO_2-2NiO.SiO_2-NiO$

The results concerning the phase equilibrium relations and the division of the system in paragenesis subsystems are presented in figure 5.

The conditions under which the ternary masses belong to these three paragenesis subsystems are defined by the equations presented in table 3.

Table 3

Belonging conditions of the ternary masses in the component subsystems of the $NiO-SiO_2-TiO_2$ system

Subsystem	Belonging conditions
I. $TiO_2-SiO_2-NiO.TiO_2$	$N - 0.946\,T < 0$
II. $SiO_2-NiO.TiO_2-2NiO.SiO_2$	$S - 1.3N + 63.22 > 0$
III. $NiO.TiO_2-2NiO.SiO_2-NiO$	$S - 1.3N + 63.22 < 0$

3. CONCLUSIONS

— A unique method was developed for quantitative coprecipitation with dimethylglyoxime and ammonia in view of obtaining initial oxide mixtures with a high reactive capacity in both the component binary systems and the $NiO-SiO_2-TiO_2$ ternary system.

— The formation of defined compounds was followed starting from the coprecipitate mixtures, establishing that no ternary defined compounds are formed in the $NiO-SiO_2-TiO_2$.

— Phase equilibrium relations were established in the ternary system in the subsolidus field by determining the coordination of the binary compounds and the division of the system into paragenesis subsystems.

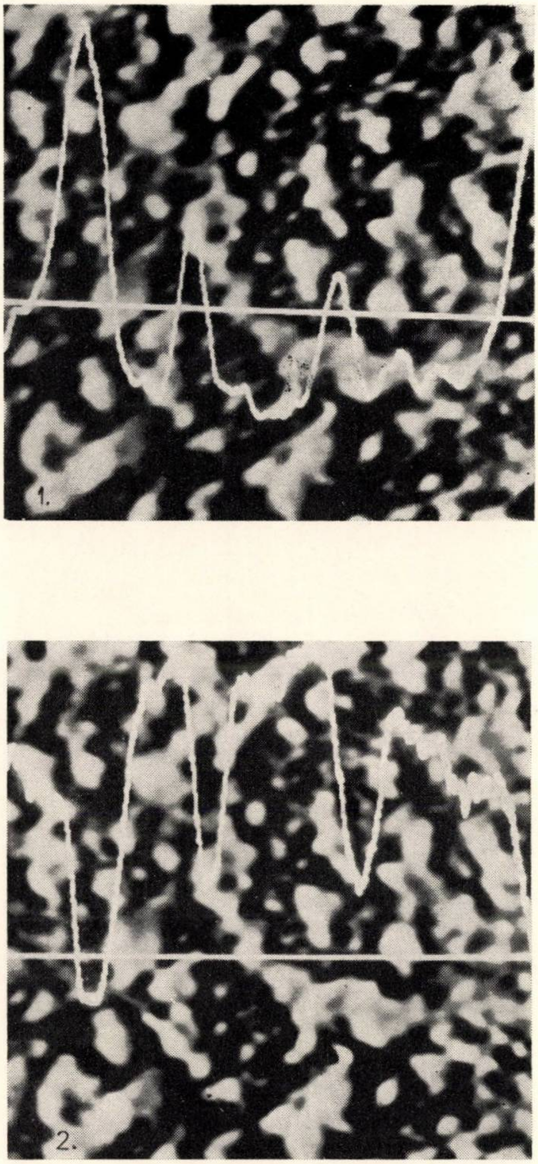

Fig. 4. — Electron micrograph and the variation of the SiO_2 and TiO_2 concentration in the $STN_{21.76}$ sample. *1*, SiO_2 ; *2*, TiO_2.

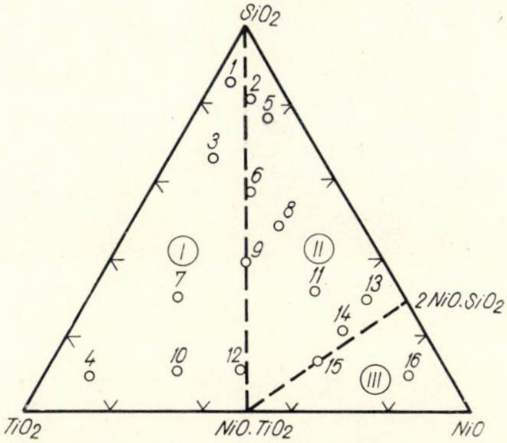
SiO2
TiO2
NiO.TiO2
NiO
2NiO.SiO2
I
II
III
1
2
3
4
5
6
7
8
9
10
11
12
13
14
15
16

Fig. 5. — Phase equilibrium relations in the $NiO-SiO_2-TiO_2$ system.

Revue Roumaine de Chimie, **19**, *6*, 1019–1030 (1974)

Co(II) CHELATES WITH 1-METHYL-2-CARBETHOXY--GLYOXALANIL-(1)-TOLYLHYDRAZONES-(2)

A. C. BANCIU and P. SPACU

Centre of Chemical Physics, str. Dumbrava Roșie 23, Bucharest, Romania

Received October 26, 1973

Among the three new compounds, derivatives of the 1-methyl-2-carbethoxy-glyoxalanil-(1)-phenylhydrazone-(2), which are methyl-substituted to the phenyl radical of the hydrazone group, the derivatives having methyl groups on *para* or *meta* position form coordination compounds, while the *ortho*-derivative does not coordinate the Co(II) ion. The elemental analysis data, IR and electronic spectra as well as magnetic measurement show that both obtained compounds are tetracoordinated chelates with tetrahedral structure, high spin ground state and a significant covalency degree of the metal-ligand bonds (nephelauxetic ratio $\beta \approx 0.75$).

In a previous paper [1] we have already described some new compounds from the class of the 1-methyl-2-carbethoxy-glyoxalanil-(1)-ariylhydrazones-(2), substituted on the *para*-position to the phenyl radical of the hydrazone group. It has been shown in that paper that all these compounds behave as bidentate chelate ligands, the Co(II) and Ni(II) complexes formed with the simplest compound in this class, namely the 1-methyl-2-carbethoxy-glyoxalanil-(1)-phenylhydrazone-(2) being studied there. It seems worthwhile to follow our investigations on the complexes formed by the substituted arylhydrazones having the same group attached in different positions of the phenyl radical, this kind of study being at least equally interesting as the discussions made on the complexes formed by *para*-substituted arylhydrazones with different substituents at the hydrazone phenyl (in the previous note [1] CH_3, OCH_3, NO_2, Cl and Br). It should be expected that besides the electronic effects, dependent on the substituent positions, the different steric hindrances produced by one and the same substituent attached to the phenyl radical gradually closer to the coordinating centres, should play a significant role.

---

[1] P. Spacu, A. C. Banciu and C. I. Lepădatu, *Rev. Roumaine Chim.*, **18**, *7*, 1143 (1973).

Besides the already described compound Ia,[1] this note presents, for this reason, the syntheses of the compound Ib and Ic :

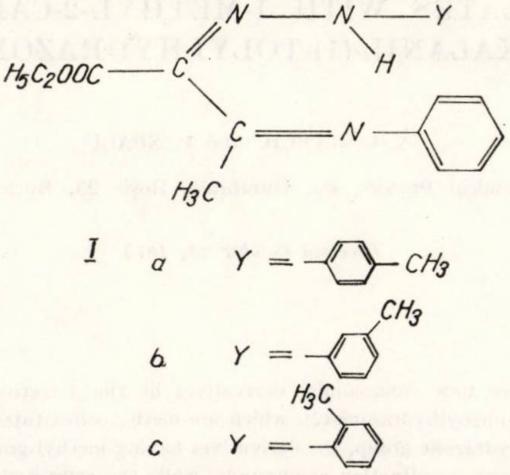

and the preparation methods of the Co(II) complexes with all these three mentioned possible ligands.

EXPERIMENTAL

Reagents. Ethyl acetoacetate (Merck, reagent for synthesis, min. content 98 %), *p*-toluidine (Carlo Erba, min. content 99 %), *m*-toluidine (Schuchardt, *p.a.*), *o*-toluidine (Loba-Chemie, *p.a.*), anhydrous $NaCH_3COO$ (Austranal, *p.a.*), $CoCl_2 . 6H_2O$ (Reactivul, Bucharest, *p.a.*), $NaNO_2$ (Reactivul, Bucharest, *p.a.*).

Synthesis of the compounds Ia – c has been similar to that already described,[1] starting from acetylacetic ester, by condensation with aniline. The compounds Ia – c were finally obtained from the resulting anil,[2] through azoic coupling reactions with solutions of the diazonium salts of toluidines, freshly prepared and instantly buffered with an addition of solid $NaCH_3COO$, brought up to pH = 3. All these products were separated as solidificated oils and after their drying on a porous plate, followed by repeated washings with small amounts of cooled methanol, they could be brought into the dried form, able to be recrystallized. After recrystallizations, performed from ethanol in the presence of charcoal, the pure compounds Ia – c were obtained, with scarce yields, of 12 %, 27 % and 20 % from the theoretical ones, respectively. The complexes were synthesized using the compounds thus obtained, but for their chemical analyses and the recording of their spectra, they were repeatedly recrystallized, the product being dried under vacuum on di-P_2O_5.

Preparation of chelates. Similar attempts were made to prepare the Co(II) chelates, as earlier emphasized,[1] under the conditions of refluxing alcoholic solutions of the reagents in the presence of small amounts of triethylamine (cca 1 ccm), using 1/100 m amounts of ligand and 1/200 m $CoCl_2 . 6H_2O$ plus an excess of 15 % from this theoretical value of the last reagent, in order to ensure the completeness of the reaction. After the reaction mixture cooling and the partial evaporation of the solvent, if the complexation has taken place dark blue, almost black-coloured crystals of complex were separated, impurified by products resulted from the ligand degradation (which are obviously of a lighter colour than the used ligand, i.e. yellowish instead of bright orange-yellow). This heterogeneous mass was repeatedly washed with 3 % acetic acid, warmed at 40°, in order to remove completely the unreacted Co(II) ions, two further recrystallizations being afterwards performed from alcoholic solutions in the presence of charcoal. If, after drying under vacuum on di-P_2O_5, the elemental analysis data showed a carbon content which surpassed the theoretical one with more than the experimental errors of the microcombustion, the recrystallization, drying and analyses were once more repeated.

---

[2] L. KNORR, *Ber. dtsch. chem. Ges.*, **20**, 1397 (1887).

When the compounds Ia and Ib were used as ligands, the complexes IIa and IIb were obtained :

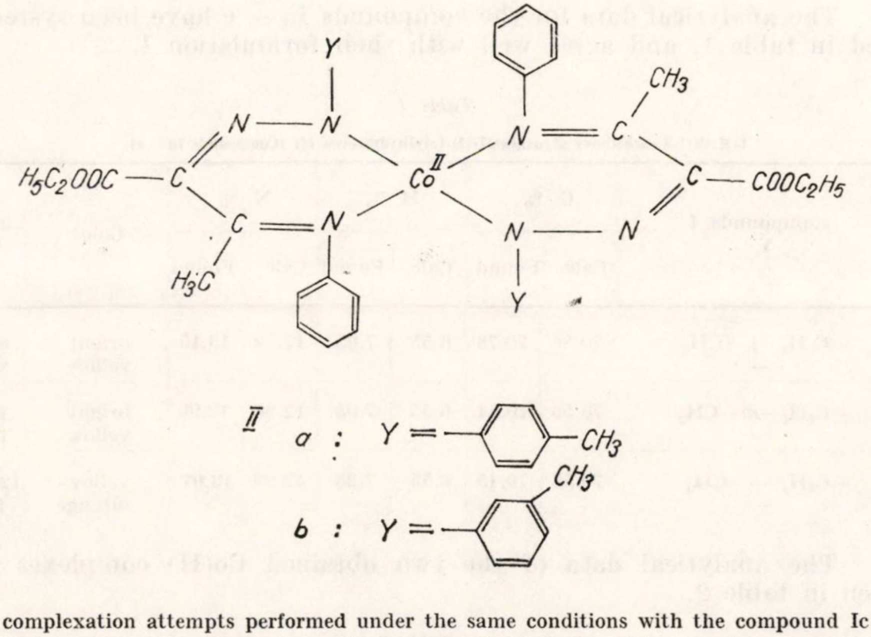

The complexation attempts performed under the same conditions with the compound Ic did not lead to any result, since on cooling the reaction mixture this organic compound was entirely separated and therefore practically unreacted.

The elemental analyses of C, H and N were made by microcombustion. The Co amount was measured by disintegration with H_2SO_4 and H_2O_2 followed by precipitation as $Co(C_5H_5N)_4(SCN)_2$, according to G. Spacu.[3]

The absorption spectra of compounds were recorded on a VSU-2 Carl Zeiss (Jena) spectrophotometer on $0.5 \times 10^{-4} - 0.5 \times 10^{-3}$ mol/l solutions in absolute ethanol and acetone.

[3] G. SPACU and I. DICK, *Z. analyt. Chem.*, **71**, 97 (1927).

The reflectance spectra of the chelates were recorded on a VSU-1 Carl Zeiss (Jena) spectrophotometer using MgO as standard.

The IR spectra of the compounds were recorded within the 400–4000 cm^{-1} range by means of a UR-10 Carl Zeiss (Jena) spectrophotometer, using KBr pellets.

The magnetic susceptibilities were measured at the room temperature, according to the Faraday method, using $Hg[Co(NCS)_4]$ as standard. The magnetic moments were calculated from $\mu = 2.828\ (\chi'_M \cdot T)^{1/2}$, where : $\chi'_M = \chi_M - \chi_{dia}$ is the corrected molar susceptibility. In the case of both isomer chelates the diamagnetic correction was $\chi_{dia} = -366 \times 10^{-6}$ (c.g.s.u.).

RESULTS AND DISCUSSIONS

The analytical data for the compounds Ia – c have been systematized in table 1, and agree well with their formulation I.

Table 1

1-Methyl-2-carbethoxy-glyoxalanil-(1)-tolylhydrazones-(2) (Compounds Ia – c)

Compounds I Y	C %		H %		N %		Color	m.p. °C
	Calc.	Found	Calc.	Found	Calc.	Found		
$-C_6H_4-p-CH_3$ —	70.56	70.76	6.55	7.05	12.99	13.15	bright yellow	87–89
$-C_6H_4-m-CH_3$ —	70.56	70.54	6.55	7.08	12.96	12.96	bright yellow	100–103.5
$-C_6H_4-o-CH_3$ —	70.56	70.43	6.55	7.28	12.99	13.01	yellow-orange	128.5–131.5

The analytical data of the two obtained Co(II) complexes are given in table 2.

Table 2

Co(II) chelates. Analytical data

Chelate	Co %		C %		H %		N %		m.p. °C
	Calc.	Found	Calc.	Found	Calc.	Found	Calc.	Found	
IIa	8.37	8.09	64.86	64.45	5.73	6.03	11.94	12.38	169–171
IIb	8.37	8.12	64.86	64.59	5.73	6.14	11.94	12.23	160–162

Based on these results and on the IR spectral data, the chelatic structural formulas IIa – b for these complexes have been ascribed.

The fact that these virtual ligands behave strikingly different, the compounds Ia and Ib being real chelatic bidentate ligands, while the compound Ic is deprived of the specific properties of such a ligand, shows us how much different may be the influence of the same substituent exerted on the complexation, as a function of its different position on the phenyl radical of the hydrazone group of the ligands, as earlier described. The fact that the CH_3 substituent in the *para* and *meta* positions does not markedly influence the Co(II) chelation, while the same substituent in the *ortho* position does brake it, may be explained only through steric hindrances induced in this last position. This is not surprising, if one takes into account the fact that in the *ortho* position the substituent is placed in the immediate neighbourhood of one the two donor nitrogen atoms in the molecule, as well as the fact that the CH_3 group, although much smaller than other substituents, is however relatively bulky, having (as a measure of its spatial extent) the van der Waals radius of cca 2 Å, greater than that of Cl (1.8 Å) and Br (1.95 Å) and only a little smaller than that of I (2.15Å).[4]

The IR spectra of one of the ligands, namely the 1- methyl-2-carbe ethoxy-glyoxalanil-(1)-*p*-tolylhydrazone-(2) (Ia), and of the corresponding Co(II) chelate (IIa) are systematized in table 3.

Obvious changes may be observed in the IR spectra of the ligand and the Co(II) chelate within 1280 – 1370 cm^{-1}. In this range of frequencies two bands of medium intensity, namely the first comprised between 1270 and 1340 cm^{-1}, with maxima at 1280, 1310 and 1330 cm^{-1}, and the second between 1365 and 1385 cm^{-1}, with a maximum at 1370 cm^{-1}, occur in the free ligand IR spectrum. Due to the perturbations caused by coordination, a single broadened band comprised between 1270 and 1390 cm^{-1}, with maxima at 1290, 1315, 1340 and 1360 cm^{-1} occurs in the Co(II) chelate IR spectrum, which is the most intense in the whole IR range of the chelate. It is well known that in the case of secondary aromatic amines ($C_6H_5 - NH -$) an absorption band appears in the region 1280 – 1350 cm^{-1} and in almost the same range (1310 – 1360 cm^{-1}) a strong band occurs in the case of tertiary aromatic amines ($C_6H_5 - N =$), both frequencies being produced by the C – N stretching vibration inside the amine groups.[5] Because of the coordination of the nitrogen atom from the hydrazone group, diretly attached to the phenyl radical, changes should be expected in the IR spectra of those absorption maxima ascribed to the vibration modes where the nitrogen atom was involved. It should be important to mention that in the range 1690 – 1720 cm^{-1} no other changes take place in the IR spectrum of the chelate compared with that of the free ligand. The intense band with a maximum at 1705—1710 cm^{-1} occurring in the IR spectra of both compounds is ascribed [5] to the ester group ($COOC_2H_5$). Its unmodified presence in the spectrum of the chelate shows this that group does not participate to coordination, even though this possibility could not be *a priori* excluded. If that group had played a certain role in coordination, its band would have been obviously shifted[5] to 1635 – 1665

---

[4] C. D. Nenițescu, "Chimie organică", Bucharest, 1966, vol. 1, p. 80.

[5] L. J. Bellamy, "The Infrared Spectra of Complex Molecules", Methuen, London, 1962.

cm^{-1}, but this is obviously not the case here. One may therefore conclude that the strong changes taking place in the region 1280 – 1370 cm^{-1} and the lack of any modifications within 1690 – 1720 cm^{-1} in the spectrum of the chelate, compared with that of the free ligand, show that the chelation takes place exclusively *via* nitrogen atoms, the esteric group playing no role, in agreement with the chemical formulations IIa and IIb for the Co(II) chelates.

Table 3

The IR spectra of the 1-methyl-2-carbethoxy-glyoxalanil-(p)-tolylhydrazone-(2)(ligand Ia), and its Co(II)chelate (chelate IIa)

Ligand Ia	Chelate IIa
470 w	
490 w	490 sh
505 m	505 m
515 sh	525 m
	580 m
605 w	615 sh
620 w	635 w
640 w	640 w
660 w	675 sh
700 m	695 m
720 m	725 m
750 m	755 w
	780 w
790 sh	795 w
815 s	825 m
850 w	860 w
930 sh	915 w
	960 w
1000 w	1000 m
	1010 m
1040 sh	1030 m
1070 vs	1080 vs
1115 w	1115 m
1180 s	1175 vs
1200 vs	1205 vs
1230 s	1240 w
1280 m	1290 vs
1310 m	1315 vs
1330 m	1340 vs
1370 m	1360 vs
1400 w	
1450 w	1440 s
1490 m	1490 w
	1510 sh
1530 m	1525 s
1580 m	1595 w
1620 sh	
1710 vs	1705 vs
2980 w	2950 w

vs – very strong;
s – strong;
m – medium;
w – weak.

The small differences between the bands in the absorption spectra of the chelates recorded on solutions (absolute ethanol and acetone) and in the reflectance spectra recorded on the solid state of the compounds, show that the chelate dissolution in the mentioned solvents is not accompanied by important structural changes (dissociations, etc.), the same molecular species being present either in solution or in solid state.

ELECTRONIC SPECTRA AND MAGNETIC PROPERTIES

The electronic spectra of the two chelates were recorded on acetonic solutions of $0.5 \times 10^{-4} - 0.5 \times 10^{-3}$ mol/l and they are plotted in figure 1.

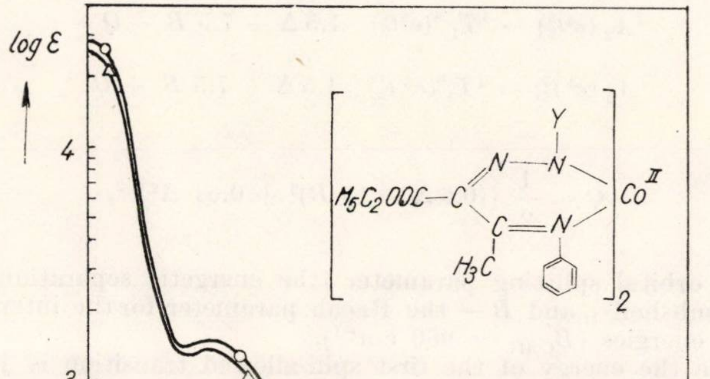

Fig. 1. — The visible and near IR spectra of the Co(II) chelates.

1, $Y = p-CH_3-C_6H_4$
2, $Y = m-CH_3-C_6H_4$

At the first sight one may observe that the differences between them are obvious but nevertheless small enough, and this fact shows that the CH_3 substituent placed at the phenyl radical of the hydrazone group exerts an influence only through its inductive effect, electron repellent, and only to a small extent on the spectral properties of the chelates. The absorption bands at 560 nm (17,860 cm^{-1}) and $\sim$ 1000 nm (10,000 cm^{-1}), which can be assigned to the d — d transitions proper to a d^7 tetrahedral configuration, are of chemical interest for the characterization of the metal-ligand bond.

The energetic expressions for the spin-allowed transitions for the d^7 (T_d) configuration obtained in a weak field coupling are as follows[6-8]:

$$^4A_2\,(e^4t_2^3) \rightarrow {}^4T_2\,(e^3t_2^4) \quad \Delta$$

$$^4A_2\,(e^4t_2^3) \rightarrow {}^4T_1{}^{a}(e^3t_2^4) \quad 1.5\,\Delta + 7.5\,B - Q$$

$$^4A_2\,(e^4\,t_2^3) \rightarrow {}^4T_1{}^{b}(e^3\,t_2^4) \quad 1.5\,\Delta + 7.5\,B + Q$$

where :

$$Q = \frac{1}{2}\,[(0.6\,\Delta - 15\,B)^2 + 0.64\,\Delta^2]^{1/2},$$

Δ is the orbital splitting parameter (the energetic separation between t_2 and e subshells), and B — the Racah parameter for the interelectronic repulsion energies ($B_{Co(II)} = 980\ cm^{-1}$).

Since the energy of the first spin-allowed transition is just equal to Δ, taking into account that $\Delta_{T_d} = 4/9\ \Delta_{O_h}$ and $\Delta_{O_h} = 10{,}000 - 15{,}000$ cm^{-1} (a relationship also valid in the framework of LCAOMO theory[9]) it results that this transition must occur in infrared, beyond the measuring possibility of the used instrument.

The two absorption bands appearing in spectrum may therefore be attributed to the other spin-allowed transition, as follows :

$$\nu_2\ ({}^4A_2 \rightarrow {}^4T_1{}^{a}) = 9{,}800\ cm^{-1}\ \text{for both chelates}$$

$$\nu_3\ ({}^4A_2 \rightarrow {}^4T_1{}^{b}) = 17{,}700\ cm^{-1}\ \text{for chelate IIa}$$

$$= 17{,}860\ cm^{-1}\ \text{for chelate IIb.}$$

Solving the energetic expressions for these transitions, one obtains the values :

$$\Delta = 5{,}550\ cm^{-1}\ \text{for chelate IIa,}$$

$$= 5{,}540\ cm^{-1}\ \text{for chelate IIb}$$

---

[6] A. B. P. LEVER, "Inorganic Electronic Spectroscopy", Elsevier Publishing Company, Amsterdam — London — New York, **1968**, chap. 8—9.

[7] Y. TANABE and S. SUGANO, *J. Phys. Soc. Japan*, **9**, 753 (1954).

[8] E. KÖNIG, *Struct. and Bonding*, **9**, 175 (1971).

[9] H. H. SCHMIDTKE, *Z. Naturforsch.*, **19a**, 1502 (1964).

and with these quantities,

$$B = 720\ \text{cm}^{-1} \text{ for chelate IIa}$$

$$= 740\ \text{cm}^{-1} \text{ for chelate IIb}$$

and

$$\beta = \frac{B}{B_0} = 0.74 \text{ for chelate IIa}$$

$$= 0.75 \text{ for chelate IIb.}$$

The Δ and *B* values thus obtained reproduce the absolute values of the absorption maxima and the differences between them.

One observes that a small, hardly detectable spectral shift, of 5 nm, of the ν_3 transition, i.e. from 565 to 560 nm going from the chelate IIa to the IIb one, reflected in a shift of 160 cm^{-1} of the wavenumbers, does not practically lead to any modification of the Δ value, but to a 20 cm^{-1} change in the *B* value (740 cm^{-1} instead of 720 cm^{-1}) which affects the β value with one centesimal digit (0.75 instead of 7.44). This fact may be directly seen in the formula according to which the *B* parameter was estimated :

$$B = \frac{(\nu_2 + \nu_3)/2 - 1.5\,\Delta}{7.5}$$

where, besides the value — in our case practically constant — of the Δ parameter, there is the half sum of ν_2 and ν_3 wavenumbers.

It is important to see whether these slight differences in the *B* and β values have any significance, or whether they are included with in the limit of the experimental errors. For this reason, the electronic spectra of both chelates were recorded on solutions of absolute ethanol and the spectrum of the unsubstituted chelate of type I ($Y = C_6H_5$), earlier described,[1] was also recorded on acetonic solutions. The band positions, their intensities as well as the Δ, *B* and β values calculated for these bands are summarized in table 4.

One may observe that, due to a scarce solvent effect, the ν_3 band is sometimes moved with 5 nm (cca 160 cm^{-1}), even for the same complex, when its spectrum is recorded on solutions of different solvents. Because of the high width of the ν_2 band, the estimation of its maximum position implies an error of 20 nm, i.e. cca 200 cm^{-1} for this band. For these reasons, differences of about 20 cm^{-1} in the B values appearing even for the same complex lead to an estimation error of the nephelauxetic ratio β of one figure in the second decimal. One may therefore conclude that the small differences found in the *B* and β values do not overpass the limit of the experimental errors and therefore, the influence of the CH_3 substituent attached in *pata* and *meta* positions to the phenyl radical bound to the

Table 4

Electronic spectra recorded on solutions of acetone and ethanol ($c = 0.5 \times 10^{-4} - 0.5 \times 10^{-3}$ mol/l) and the Δ, B and β values of the Co(II) chelates

Chelate type II	Solvent	ν_3		$\varepsilon_3$max $\times 10^3$	ν_2		ε_2 max $\times 10^2$	Δ cm^{-1}	B cm^{-1}	β
		nm	cm^{-1}		nm	cm^{-1}				
$Y = C_6H_5$	acetone	555	18,020	1.376	1,020...	9,800...	1.166	5,520	750	0.76
					1,040	9,620		5,400	760	0.77
	ethanol	560	17,860	1.180	1,040	9,620	1.053	5,400	750	0.76
$Y = p-CH_3-C_6H_4$	acetone	565	17,700	1.490	1,020	9,800	1.160	5,550	720	0.74
	ethanol	565	17,700	1.340	1,020	9,800	1.053	5,550	720	0.74
$Y = m-CH_3-C_6H_4$	acetone	560	17,860	1.360	1,020	9,800	1.206	5,540	740	0.75
	ethanol				1,000...	10,000..	1.160	5,680	720	0.74
		560	17,860	1.248	1,020	9,800		5,540	740	0.75

nitrogen donor atom may be practically ignored, at least as far as the increasing of the covalency degree of the complexes is concerned. In our opinion this fact is worth being mentioned, having in view other reported papers and monographs where the nephelauxetic ratio β values are sometimes given with three exact figures (see, for instance, reference 6, p. 324, where for the tetrahedral $CoBr_4^{2-}$ ion β is given to be equal to 0.714).

Mention should also be made (see table 4) of the obvious hyperchromic shift of the two bands ν_2 and ν_3 in the spectra of the same compounds when the solvent is changed from ethanol to acetone. This fact shows, in our opinion, that the tempting proposal advanced by Cotton and Soderberg,[10,11] to plot in two dimensions the covalency degree of the tetrahedral Co(II) complexes, must be carefully regarded. According to these authors, taking on the ordinate axis the quantity $\Delta B(= B_{\text{free}}$ ion$- B_{\text{complex}}$ ion) and on the abscissa axis the oscillator strength of the ν_3 band, all tetrahedral Co(II) complexes may be represented by points, those placed up to the right corner being the strongest covalent. The hyperchromic shifts of the absorption bands, due to the solvent effects mentioned above, show how different the calculated value as well as the graphical representation of the oscillator strength of the ν_3 transition can be and therefore how inexact is its position on the abscissa, even for the same complex. An eventual comparison should be made only for absorption spectra recorded on solutions using the same solvent. More exact is therefore the β value as covalency measure, the solvent effects acting insignificantly on its value, as only one unit to the second decimal, in our case.

The Δ quantity, spectrally determined, may be used to estimate the orbital contribution term of the magnetic moment value. For the d^7 tetrahedral high spin configuration, the magnetic moment may be evaluated from the formula [12,13]:

$$\mu = \left(\mu_s - 15.59\frac{\lambda}{\Delta}\right) \text{BM}$$

where: $\lambda = -178$ cm^{-1} is the spin-orbit constant, Δ is the orbital splitting parameter and $\mu = 3.89$ BM is the spin only contribution to the value of the magnetic moment. Using the value $\Delta = 5{,}550$ cm^{-1}, practically found for both complexes, one finds that the $(-15.59\lambda / \Delta)$

---

[10] F. A. Cotton and R. H. Soderberg, *J. Amer. Chem. Soc.*, **84**, 872 (1962).

[11] R. L. Carlin, "Electronic Structure and Stereochemistry of Cobalt (II)", in "Transition Metal Chemistry", Marcel Dekker, New York, 1965, vol. 1, p. 1–33.

[12] R. Stahl-Broda and W. Low, *Phys. Rev.*, **113**, 775 (1959).

[13] F. A. Cotton and M. Goodgame, *J. Amer. Chem. Soc.*, **83**, 1777 (1961).

quantity is of about 0.5 BM, and therefore the magnetic moment calculated for both complexes is 4.39 BM.

It has been experimentally found:

$$\mu = 4.31 \pm 0.08 \text{ BM for the chelate IIa}$$
and
$$\mu = 4.37 \pm 0.08 \text{ BM for the chelate IIb},$$

which are in good agreement with that spectrally evaluated. The agreement between the spectral and magnetic properties allow us to assign to the Co(II) — nitrogen bonds a preponderant tetrahedral arrangement in the case of both Co(II) chelates herein studied.

Acknowledgement. We express our thanks to Mr. V. Mincu from the University of Bucharest for the magnetic susceptibility measurements.

Revue Roumaine de Chimie, **19**, *6*, 1031 – 1038 (1974)

CONTRIBUTIONS TO THE CHEMISTRY OF THIOCOMPLEXES. V[1]

COMPLEX COMPOUNDS OF Pt(II) WITH THIOAMIDES

DUMITRU NEGOIU * and VASILICA MUREŞAN **

* Faculty of Chemistry, University of Bucharest, Splaiul Independenţei 89
** Faculty of Chemistry, University of Craiova, Calea Bucureşti 165

Received September 11, 1973

The paper presents new complex compounds of Pt(II) with thioamides of the phenylthioacetamide series and with unsaturated aromatic thioamides. These are of a Pt L_2Cl_2 type (L = phenylthioacetamide, *o*-tolylthioacetamide, 2,5-dimethylphenylthioacetamide, cynamthioamide and *p*-methoxycynamthioamide) and of a Pt L Cl_2 type (L = diphenylthioacetamide). The substances are characterized based on the results of the chemical analysis and also of UV, visible and IR spectra. Assignments of absorption bands are made on the basis of electronic reflexion spectra which show that they have a plane-square disposition belonging to the symmetry group D_{4h}.

Recent studies [2-7] have investigated the capability of thioamides to function as ligands to central metal ions with a pronounced class character (b), such as Cu(I), Hg(II), Pd(II), Pt(II), as well as in the case of certain metal ions with a less pronounced class character (b), such as Co(II), Ni(II), Cu(II). Ray and Sathyanarayana [2] have studied N,N-dimethylthioacetamide as a ligand, illustrating by IR spectral analysis that in complex compounds with Co(II), Cu(I) and Hg(II) both C : S and C — N groups are involved in the bond.

A similar conclusion was reached in the previous papers [1,8-10] which reported the results of the study performed on ion complex compounds of class (b) : Hg(II) and Pd(II) with thioamides.

---

[1] Part IV : D. NEGOIU, V. MUREŞAN and S. FLOREA, *Rev. Roumaine Chim.*, **18**, 1875 (1973).

[2] A. RAY and D. N. SATHYANARAYANA, *Bull. Chem. Soc. Japan*, **45**, 2712 (1972).

[3] R. R. IYENGAR, D. N. SATHYANARAYANA and C. C. PATEL, *J. Inorg. Nuclear Chem.*, **34**, 1088 (1972).

[4] K. K. CHATERJEE, *Inorg. Chim. Acta*, **6**, 8 (1972).

[5] T. BIRCHALL and M. F. MORRIS, *Canad. J. Chem.*, **50**, 211 (1972).

[6] Y. N. KUKURSHKIN, S. A. SIMANOVA and N. N. KNYAZERVA, *Zhur. neorg. Khim.*, **16**, 2488 (1971).

[7] Y. N. KUKURSHKIN, S. A. SIMANOVA and V. P. ALASHKEVICH, *Zhur. priklad. Khim.*, **44**, 1640 (1971).

[8] D. NEGOIU and V. MUREŞAN, *Anal. Univ. Bucureşti, Chim.*, **1971**, 121.

[9] D. NEGOIU, V. MUREŞAN and C. FULEA, *Anal. Univ. Bucureşti, Chim.*, **1973**, . . .

[10] D. NEGOIU, V. MUREŞAN and C. FULEA, *Rev. Roumaine Chim.*, **18**, 1749 (1973).

In this paper, we present the results of chemical and physico-chemical investigations into the complex compounds of a different metal ion, a typical representative of class (b), Pt(II) with thioamides belonging to phenylthioacetamide series : phenylthioacetamide (FTAA), *o*-tolylthioacetamide (OTTAA), 2,5-dimethylpenylthioacetamide (DMFTAA), diphenylthioacetamide (DFTAA), and with two unsaturated thioamides : cynamthioamide (CTA) and *p*-methoxycynamthioamide (MCTA). [10,11]

RESULTS AND DISCUSSION

Platinum (II) complex compounds with these thioamides are microcrystalline, stable powders coloured in various yellowish-orange shades, difficultly or partially soluble in inorganic and organic solvents, having higher melting points than the corresponding ligands. They were prepared by adding a thioamide ethanol solution to the solution of platinum dichloride in a weakly acidic medium.

The elementary chemical analysis of complexes presented in table 1 leads us to the following formulations :

$Pt\ L_2Cl_2$ (L = FTAA, OTTAA, DMFTAA, CTA, MCTA)

$Pt\ L\ Cl_2$ (L = DFTAA)

Table 1

Chemical analysis of Pt(II) complexes with thioamides

Compound	S %		C %		H %		Formula *	Colour
	Calc.	Exp.	Calc.	Exp.	Calc.	Exp.		
Pt(II)–FTAA	11.33	12.14	34.03	35.82	3.18	3.63	$Pt\ L_2\ Cl_2$	yellow
Pt(II)–OTTAA	10.76	11.35	36.32	37.95	3.69	4.12	$Pt\ L_2\ Cl_2$	yellowish-orange
Pt(II)–DMFTAA	10.24	9.87	38.41	39.55	4.16	4.73	$Pt\ L_2\ Cl_2$	yellowish-orange
Pt(II)–DFTAA	6.48	7.29	34.06	35.28	2.64	3.64	$Pt\ L\ Cl_2$	yellowish-orange
Pt(II)–CTA	10.80	9.93	36.47	38.11	3.03	4.10	$Pt\ L_2\ Cl_2$	orange
Pt(II)–MCTA	9.80	10.24	36.77	38.42	3.67	3.60	$Pt\ L_2\ Cl_2$	orange

*L = ligand

A good agreement is observed with the results presented in the case of complex compounds of Pd(II) with the same thioamides.[10]

In order to be able to refer to the nature of the chemical bond achieved in these complex compounds we systematized in specific domains the results of the IR spectral analysis both for ligands [11,12] (table 2) and for the corresponding complexes with Pt(II) (table 3).

---

[11] F. Cornea and C. Fulea, *Anal. Univ. Bucureşti, Chim.*, **1969**, 85.

[12] K. A. Jensen and P. H. Nielsen, *Acta Chem. Scand.*, **20**, 597 (1966).

Table 2

Characteristic frequencies in IR spectra of thioamides (cm^{-1})

Substance	3500 – 3100 ν NH$_2$	1650 – 1600 δ NH$_2$	1600 – 1350		1350 – 900		900 – 600	
			1600 – 1450 ν C – N coupling C – C	1450 – 1350 ν C – N coupling NH$_2$	1350 – 900 ν CS, δNH$_2$	1000 – 900 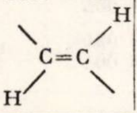	900 – 700 NCS	700 – 600 C = S
FTAA	3160 i 3385 i 3290 i	1640 i	1420 sh 1460	1330 i	1230 m 960 m 1255 m 975 m	—	795 m	490 i 585 i 620 sh
OTTAA	3150 i 3390 i 3275 sh	1622 i	1412 i	1331 m	1220 m 962 i	—	755 i 785 m	632 m
DMFTAA	3145 m 3390 i 3260 w	1615 i	1405 m	1330 w	1220 m 962 m	—	755 w 780 m	637 m
DFTAA	3180 i 3355 i	1652 m	1440 i	1300 w	1000 w 1035 w 1085 w	—	730 i	615 m 640 sh
CTA	3160 i 3320 i	1640 m	1428 i	1330 m	1210 w 1260 m	980 m	785 i	620 m
MCTA	3160 i 3390 m 3300 m	1615 m 1645 m	1432 m	1330 m	1265 i	985 m	745 m 775 w	612 m

i = intense, m = medium, w = weak, sh = shoulder

Table 3

Characteristic frequencies in IR spectra of Pt(II) complexes with thioamides (cm^{-1})

Substance	3500 – 3000	1650 – 1600	1600 – 1350		1350 – 900		900 – 600	
			1600 – 1450	1450 – 1350	1350 – 900	1000 – 900	900 – 700	700 – 600
	ν NH_2	δ NH_2	ν C – N Coupling C – C	ν C – N Coupling NH_2	ν CS, δ NH_2	$\mathrm{H{>}C{=}C{<}H}$	NCS	C = S
$Pt(FTAA)_2Cl_2$	3180 m 3230 m 3320 w	1620 m	1490 m	1409 sh	1210w 970w	—	700 m	—
$Pt(OTTAA)_2Cl_2$	3180 m 3240 sh 3350 sh	1620 m	1490 sh 1460 sh	1409 w	1210m 980sh	—	725 w 784 m	—
$Pt(DMFTAA)_2Cl_2$	3050 sh 3425 sh	1620 m	1500 w	1380 w	1180sh 1050m	—	855 m	—
$Pt(DFTAA)Cl_2$	3050 sh 3250 sh 3300 sh	1620 w	1490 m	1390 sh	1180sh 1050m	—	755 w	—
$Pt(CTA)_2Cl_2$	3050 sh 3250 sh	1620 sh	1450 m	1300 sh	1180sh	970 m	700 m 760 m	—
$Pt(MCTA)_2$	3050 sh 3230 sh	1600 sh	1460 m	1420 m	1250sh 1180sh	970 w	720 sh 855 m	

i = intense, m = medium, w = weak, sh = shoulder

The arguments concerning the achievement of the bond by the sulphur atom of the thioketo group are materialized by:

a) the modification of the band at 1220 cm^{-1}, which expresses a significant contribution of the C : S bond, appearing pronouncedly less intense or even levelled off in complexes;

b) the disappearance, in complexes, of the intense band in the 550 – 680 cm^{-1} region of the thioamide spectrum, this being generally attributed to vibration C : S.

The evidence concerning the participation of nitrogen of the thioamide group in the achievement of the bond is materialized by the following:

a) in the 3500 – 3000 cm^{-1} region, the bands characteristic of ν NH$_2$ sym. and ν NH asym. appear in complexes at modified frequencies compared to the respective thioamides, and much weaker;

b) the characteristic band of the stretching vibration of group NH$_2$ in the 1650 – 1600 cm^{-1} range appears to be situated at slightly higher frequencies in complexes, but with a variable intensity;

c) the band at $\sim$960 cm^{-1} attributed to the stretching vibration of group NH$_2$, in complexes, is reduced or totally disappears, except for complexes with CTA and MCTA in which the band at 970 cm^{-1}, typical of the unsaturated group 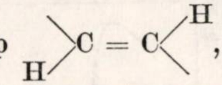 $\underset{\mathrm{H}}{>}\mathrm{C}=\mathrm{C}\overset{\mathrm{H}}{<}$, is maintained.

It has thus been concluded that the chemical bond implies in these complex combinations the participation of both a sulphur atom and a nitrogen atom of the thioamide group.

In view of completing our study on these complexes we achieved electronic reflexion spectra in solid powder in the UV and visible domain (figures 1, 2, 3).

We made the assignments of bands in the electronic spectra of the studied complexes on the basis of Gray and Ballhausen's article[13]; they applied the method of molecular orbitals to explain the spectra of plane-square metal complexes of the elements belonging to configuration d^8. In this case, the authors[13] proposed the following succession of orbitals 5 d : (d_{xz}, d_{yz}), d_{z^2}, d_{xy} and $d_{x^2-y^2}$, in contrast to Chatt et al.[14] and, lately, Martin et al.[15] who suggested the succession: d_{z^2}, (d_{xz}, d_{yz}), d_{xy}, $d_{x^2-y^2}$.

The correlation of bands observed in the electronic spectra of platinum (II) complexes with those of Pt Cl$_4^{2-}$ prompts us to assume the following assignments:

a) the band at 30,303 cm^{-1} (330 nm), appearing in complexes, is attributed to transition $^1A_{1g} \rightarrow {}^1E_g$;

b) the band at 25,640 cm^{-1} (390 nm), appearing in complexes, is attributed to transition $^1A_{1g} \rightarrow {}^1B_{1g}$;

[13] H. B. Gray and C. J. Ballhausen, *J. Amer. Chem. Soc.*, **85**, 260 (1963).

[14] J. Chatt, G. A. Gamlen and L. E. Orgel, *J. Chem. Soc.*, **1958**, 487.

[15] D. S. Martin, M. A. Tucker and A. J. Kassman, *Inorg. Chem.*, **1965**, 1682.

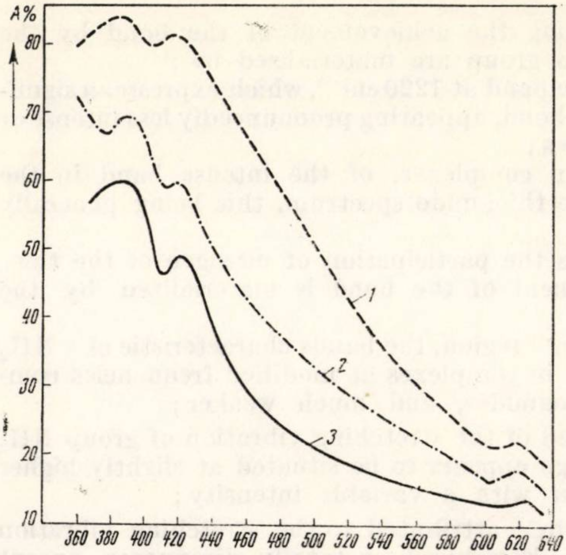

Fig. 1. — Visible electronic reflexion spectra of Pt(II) complexes with CTA (1), DMFTAA (2), and DFTAA (3).

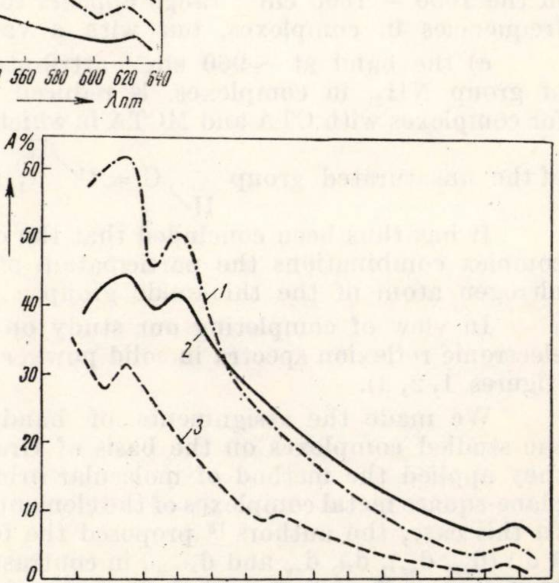

Fig. 2. — Visible electronic reflexion spectra of Pt(II) complexes with OTTAA (1), MCTA (2), and FTAA (3).

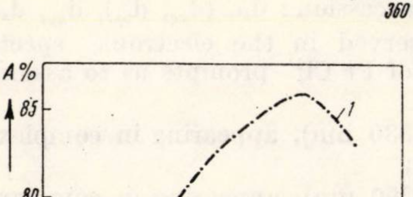

Fig. 3. — U.V. electronic reflexion spectra of Pt(II) complexes with CTA (1) and MCTA (2).

c) the band at 23,800 cm^{-1} (420 nm) or 20,830 cm^{-1} (480 nm) in complexes is attributed to transition $^1A_{1g} \rightarrow {}^1A_{2g}$;

d) the shoulder at 16,129 cm^{-1} (620 nm) in complexes is attributed to transition $^1A_{1g} \rightarrow {}^3A_{2g}$.

The correspondence of these four bands observed in the prepared complexes, with the bands described for $Pt\,Cl_4^{2-}$ makes us conclude that these have an analogous symmetry with $Pt\,Cl_4^{2-}$ and hence they are plane-square, belonging to the symmetry group D_{4h}.

EXPERIMENTAL

Reagents: an aqueous solution, acidulated with HCl of platinum dichloride and thioamide ethanol solutions.

IR spectra were recorded on a 157 Perkin Elmer device in an anhydrous KBr pellet.

The electronic spectra in the UV and visible domain were taken on a VSU_1 Zeiss-Jena spectrophotometer, in a MgO pellet.

PREPARATION OF COMPLEXES

Dichlorobisphenylthioacetamide-Pt(II) The phenylthioacetamide ethanol solution is added to the platinum dichloride hydrochloric solution while continually stirring so as to have a 1 : 2 molar ratio. A yellowish-orange precipitate is observed to appear immediately thereafter, which is allowed to stand for an hour. It is then filtered through a porosity filter G_4, washed with alcohol and ether and dried under vacuum.

The aspect of complexes is that of a microcrystalline powder of a yellowish-orang colour in various shades, which is stable over time and presents a reduced solubility in inorgani and organic solvents.

The other complexes have been prepared in a similar manner.

CONCLUSIONS

Pt(II) complex compounds with aromatic thioamides described in this paper are of the type:

$Pt\,L_2\,Cl_2$ (L = FTAA, OTTAA, DMFTAA, CTA, MCTA)

$Pt\,L\,Cl_2$ (L = DFTAA)

By correlating the data of the chemical analysis with the study of IR spectra which provide arguments on the achievement of the chemical bond both by a sulphur and by a nitrogen atom of the thioamide group, it results that the following structural formulations are possible:

PtL_2Cl_2

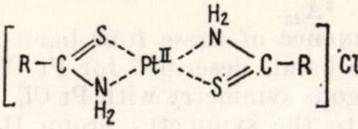

$PtLCl_2$

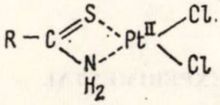

It has been observed that thioamides participate in all these complexes under the form of "thioketo".

Diphenylthioacetamide is the only ligand in this series which generates complexes of the type $M^{II} L Cl_2$, in which M^{II} may be Hg[9], Pd[10] and Pt. The binding of only one single thioamide molecule is explained by its high volume which would produce steric hindrances.

The UV and visible electronic reflexion spectra of the studied complexes prompt us to conclude that they have a plane-square disposition belonging to the symmetry group D_{4h}.

Revue Roumaine de Chimie, 19, 6, 1039–1044 (1974)

SUR LES COMPOSÉS D'ADDITION DU TÉTRACHLORURE DE THORIUM AVEC DES AZOMÉTHYNES

D. NEGOIU, ANGELA KRIZA et MARTHA NASTA

Université de Bucarest, Faculté de Chimie, Chaire de Chimie inorganique, 89, Splaiul Independenţei

Reçu le 2 octobre 1973

On a obtenu et étudié six nouveaux composés du tétrachlorure de thorium et des bases Schiff aromatiques. Les données de l'analyse élémentaire, ainsi que l'étude des spectres IR et électroniques nous permettent de conclure que les composés obtenus sont des complexes moléculaires du type $ThCl_4.2SBH$.

Dans la littérature on trouve peu de données sur la synthèse et l'étude des composés du thorium avec des bases Schiff. En 1964, Kogan, Osipov et Garnovski [1] ont obtenu quelques dérivés du tétranitrate de thorium et de la salicylal-aniline et de ses dérivés. Quoique les bases Schiff soient des ligands capables de former des complexes internes, les composés obtenus sont du type complexes moléculaires.

En 1957, Garnovski et collaborateurs ont publié une étude plus détaillée [2] sur quelques composés du titane (IV), de l'étain (IV) et du thorium avec des azométhynes dont la molécule comprend, à part l'azote azométhynique, d'autres atomes d'azote : —aminique, pyridinique, etc., comme centres donneurs.

Un travail plus récent [3] s'occupe de la synthèse des composés complexes internes du thorium avec des salicylaldimines. Les études par spectres IR, électroniques et RMN plaident dans un certain sens pour la formation des composés Chelates.

Tenant compte de ces données sur la chimie coordinative du thorium nous nous sommes intéressés au problème de la synthèse des complexes moléculaires de ce métal avec une variété plus large de bases Schiff dont la molécule contient le groupement hydroxyle.

RÉSULTATS ET DISCUSSIONS

La synthèse des composés a été faite par la réaction directe du tétrachlorure de thorium et de la base Schiff par rapport molaire 1 : 2.

---

[1] V. A. Kogan, O. A. Osipov et A. D. Garnovski, *Zhur. obshchei Khim.*, **9**, 494 (1964).

[2] A. D. Garnovski, V. I. Minkin, O. A. Osipov, V. T. Paniushkin, L. K. Isaeva et M. I. Kniazhanski, *Zhur. neorg. Khim.*, **12**, 2443 (1967).

[3] N. S. Biradar et V. H. Kulkarni, *Z. anorg. Chem.*, **387**, 275 (1972).

Tenant compte de la sensibilité à l' humidité du tétrachlorure de thorium et des composés obtenus, surtout en solution, toutes les opérations de synthèse, de séparation et de purification de ces composés ont été accomplies dans des conditions d'élimination totale de l'humidité atmosphérique, dans des solvants rigoureusement anhydrisés.

En employant l'éthanol comme solvant par rapport à la séparation des composés nous avons rencontré certaines difficultés, les composés étant solubles.

Les composés obtenus, ainsi que les résultats de l'analyse élémentaire sont indiqués dans le tableau 1.

Tableau 1

Données analytiques des composés du thorium et des bases Schiff aromatiques

Composé	Couleur	Th %		Cl %		N %	
		calc.	exp.	calc.	exp.	calc.	exp.
$ThCl_4$. 2SOT	vert	29,14	29,04	17,83	—	3,52	3,46
$ThCl_4$. 2SMT	orange	29,14	28,98	17,83	17,01	3,52	3,57
$ThCl_4$. 2SPT	jaune	29,14	29,10	17,83	17,65	3,52	3,54
$ThCl_4$. 2SOA	vert	28,02	28,20	15,26	—	3,28	3,26
$ThCl_4$. 2SPA	jaune	28,02	27,97	15,26	14,71	3,28	3,10
$ThCl_4$. 2BPT	beige	30,37	30,71	18,58	18,52	3,66	3,62

En ce qui concerne les composés obtenus à partir de la salicylal-*o*-toluidine et de la salicylal-*o*-anisidine, le produit solide s'est formé seulement après l'élimination, par distillation, de l'éthanol et l'addition d'une petite quantité de benzène anhydre.

Les composés se présentent sous forme de cristaux, colorés, stables à l'air, insolubles dans le tétrachlorure de carbone, l'éther, mais présentant une certaine solubilité dans les alcools ; le point de fusion des complexes est au-dessus de 200°, avec décomposition. Le composé obtenu à partir de la benzal-*p*-toluidine présente une stabilité moindre que ceux provenant des salicylal-arylamines.

Les composés du thorium sont beaucoup plus stables que ceux du titane et même de l'étain.

Les résultats des analyses prouvent que les composés du tétrachlorure de thorium avec des bases Schiff aromatiques sont du type : $ThCl_4.2SBH$. On a aussi essayé de détecter l'acide chlorhydrique qui pourraît être mis en liberté par suite de la réaction. Par suite de l'absence des traces d'acide chlorhydrique dans les gaz de réaction et dans le filtrat on a conclu qu'au cours des synthèses il ne se dégage pas de l'acide chlorhydrique.

Par conséquent, on peut conclure que dans les conditions de synthèse rigoureusement établies les composés obtenus sont des complexes moléculaires du type donneur-accepteur. Donc, les composés obtenus à partir des salicylal-arylamines et du tétrachlorure de thorium ne contiennent pas une liaison Th — O. Le simple fait qu'on a pu obtenir le composé avec de la benzal-*p*-toluidine, ligand qui ne contient pas le groupement hydroxyle, prouve que, pour ce type de ligands la formation des complexes peut avoir lieu sans la participation du groupement —OH.

Pour établir le type de liaison des complexes on a étudié les déplacements de certaines bandes d'absorption dans les spectres IR des composés par rapport à ceux des ligands.

Par exemple, la figure 1 présente les spectres IR des composés avec de la salicylal-*o*-toluidine et de la salicylal-*p*-anisidine, ainsi que les spectres IR des ligands respectifs.

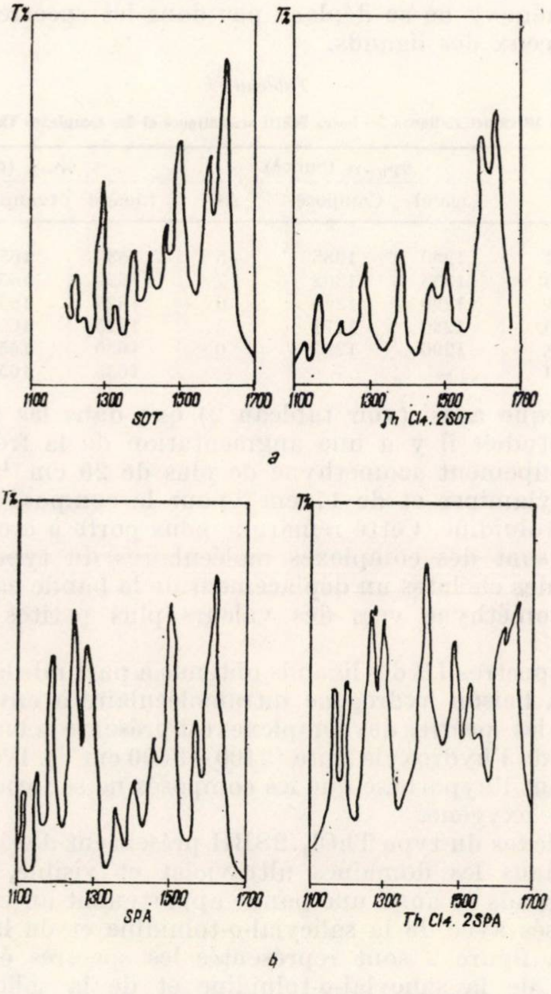

Fig. 1 a) — Spectres IR de la salicylal-*o*-toluidine et du composé $ThCl_4$. 2SOT.
b) — Spectres IR de la salicylal-*p*-anisidine et du composé $ThCl_4$.2SPA.

Dans la littérature on indique pour le groupement phénoxy-une bande caractéristique à 1285 cm^{-1}. Dans les spectres des ligands qui contiennent ce groupement on trouve une bande caractéristique à 1290 ± ± 5 cm^{-1} (tableau 2). Si les complexes étaient formés par l'intermédiaire de la liaison Th — O la bande de 1290 cm^{-1} devrait être déplacée avec environ 50 cm^{-1} vers des fréquences plus hautes, pour les composés avec des salicylalarylamines. Dans le cas des composés obtenus les variations de la fréquence caractéristique du groupement phénoxy sont très petites : ± 5 cm^{-1}. On peut donc conclure, que, pratiquement, la fréquence du groupement phénoxy ne se déplace pas dans les spectres des complexes par rapport à ceux des ligands.

Tableau 2

Bandes IR caractéristiques des bases Schiff aromatiques et des complexes $ThCl_4.2SBH$

Composé	ν_{Ph-O} (cm^{-1})			$\nu_{C=N}$ (cm^{-1})		
	Ligand	Composé	$\Delta\nu$	Ligand	Composé	$\Delta\nu$
$ThCl_4$. 2SOT	1290	1285	−5	1630	1650	+20
$ThCl_4$. 2SMT	1295	1302	+7	1629	1650	+21
$ThCl_4$. 2SPT	1290	1290	0	1625	1650	+25
$ThCl_4$. 2SOA	1280	1275	−5	1625	1650	+25
$ThCl_4$. 2SPA	1290	1290	0	1630	1650	+20
$ThCl_4$. 2BPT	—	—	—	1635	1652	+17

On remarque aussi (voir tableau 2) que dans les spectres de tous les composés étudiés il y a une augmentation de la fréquence caractéristique du groupement azométhyne de plus de 20 cm^{-1} pour les dérivés des salicylal-arylamines et de 17 cm^{-1} pour le composé obtenu à partir de la benzal-*p*-toluidine. Cette remarque nous porte à croire que les composés obtenus sont des complexes moléculaires du type : $ThCl_4.2SBH$, car dans le cas des chélates un déplacement de la bande caractéristique du groupement azométhyne vers des valeurs plus petites aurait dû être observé.

Dans les spectres IR des ligands obtenus à partir de la salicylaldéhyde on remarque la liaison hydrogène intramoléculaire à environ 2850 cm^{-1}, tandis que dans les spectres des complexes est présente la bande de vibration caractéristique de l'hydroxyle libre (3400—3600 cm^{-1}). C'est un argument de plus soutenant l'hypothèse que les composés ne se forment pas par une liaison métal — oxygène.

Les complexes du type $ThCl_4.2SBH$ présentent des bandes d'absorption intenses dans les domaines ultraviolet et visible, bandes caractéristiques des ligands et aussi une bande appartenant au complexe dans le cas des composés avec de la salicylal-*o*-toluidine et de la salicylal-*o*-anisidine. Dans la figure 2 sont représentés les spectres électroniques des composés avec de la salicylal-*o*-toluidine et de la salicylal-*p*-anisidine, ainsi que les spectres des ligands respectifs, dans le domaine 240 à 660 nm.

Les maximums d'absorption de 265 nm et de 360 à 370 nm sont des bandes propres aux ligands, caractéristiques du cycle benzénique et de la liaison du groupement azométhynique conjuguée au cycle benzénique. Par coordination de l'azote les niveaux énergétiques moléculaires π, qui sont impliqués dans les transitions électroniques, sont perturbés et conduisent aux déplacements vers des longueurs d'onde plus grandes. On remarque, par exemple, dans le cas du composé dérivé de la salicylal-

p-anisidine un déplacement très petit de 360 nm, dans le spectre du ligand, à 365 nm dans le spectre du composé.

La bande caractéristique du complexe qui apparaît à 605 nm dans le spectre du composé obtenu à partir de la salicylal-*o*-toluidine et à 640 nm dans le spectre du composé obtenu à partir de la salicylal-*o*-anisidine est probablement due à un transfert de charge L — M.

L'ion central Th(IV), à configuration d^0, ne peut pas générer des transitions électroniques *d — d* et non plus des bandes de transfert de charge *M — L*.

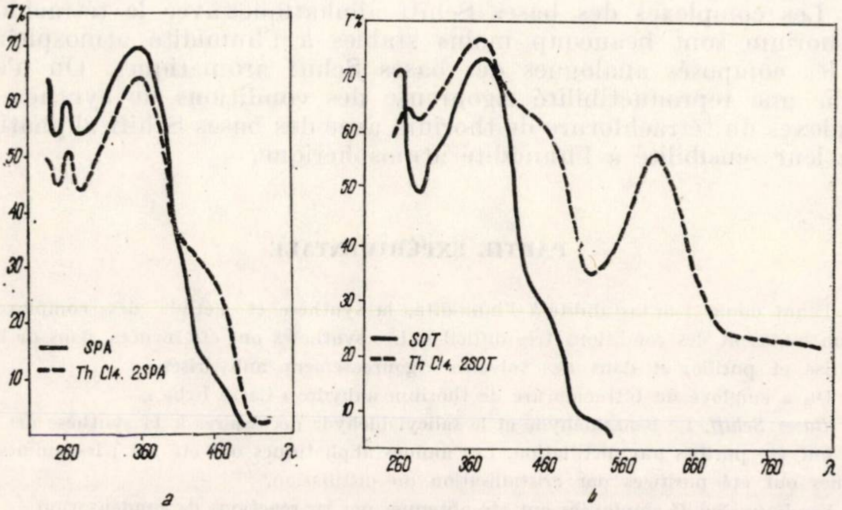

Fig. 2 a) — Spectres électroniques de la salicylal-*o*-toluidine et du composé $ThCl_4 . 2SOT$
b) — Spectres électroniques de la salicylal-*p*-anisidine et du composé $ThCl_4 . 2SPA$

Les données de l'analyse élémentaire portée sur les composés obtenus, ainsi que les études spectrales permettent de conclure que les complexes du tétrachlorure de thorium avec des bases Schiff aromatiques sont des complexes moléculaires du type donneur-accepteur, entre l'atome de thorium et la base Schiff par l'intermédiaire du doublet électronique libre de l'azote azométhynique.

Pour les complexes obtenus on peut imaginer la structure suivante :

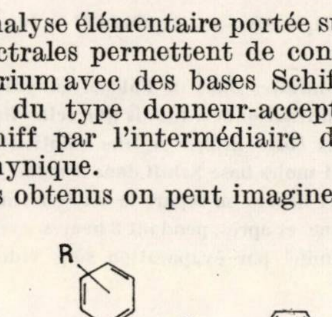

Si on fait réagir le tétrachlorure de thorium sur des bases Schif aliphatiques par rapport molaire 1 : 2 dans l'éthanol anhydre on obtient des produits solides. On a obtenu ainsi les composés du tétrachlorure de thorium avec les bases Schiff suivantes : Salicylal-éthyl-, propyl- et butylamine et benzal-butyl-amine.

Les composés obtenus sont des poudres jaunes excepté le composé de la benzal-butylamine qui est blanc. Les composés sont insolubles dans des solvants organiques ordinaires et présentent une faible solubilité dans l'éthanol.

Les complexes des bases Schiff aliphatiques avec le tétrachlorure de thorium sont beaucoup moins stables à l'humidité atmosphérique que les composés analogues des bases Schiff aromatiques. On n'a pu établir une reproductibilité rigoureuse des conditions de synthèse des complexes du tétrachlorure de thorium avec des bases Schiff aliphatiques dû à leur sensibilité à l'humidité atmosphérique.

PARTIE EXPÉRIMENTALE

Etant donné leur instabilité à l'humidité, la synthèse et l'étude des complexes du thorium imposent des conditions très difficiles. Les synthèses ont été menées dans de l'azote anhydrisé et purifié, et dans des solvants rigoureusement anhydrisés.

On a employé du tétrachlorure de thorium anhydre « Carlo Erba ».

Bases Schiff. Le benzaldéhyde et le salicylaldéhyde nécessaires à la synthèse des bases Schiff ont été purifiés par distillation. Les amines aliphatiques ont été *p.a.*; les amines aromatiques ont été purifiées par cristallisation ou distillation.

Les bases Schiff employées ont été obtenues par les réactions de condensation :

$$C_6H_4(OH)CHO + H_2N-C_6H_4R \rightarrow C_6H_4(OH)CH{=}N-C_6H_4R + H_2O$$

$$C_6H_4(OH)CHO + H_2N-R \rightarrow C_6H_4(OH)CH = N-R + H_2O$$

Les synthèses ont été conduites dans de l'alcool anhydre. Les bases Schiff solides ont été purifiées par cristallisation fractionnée, tandis que celles liquides ont été distillées.

Composés du $ThCl_4$ *et des bases Schiff.* A une solution de 0,005 moles $ThCl_4$ dissous dans de l'éthanol on ajoute 0,01 moles base Schiff dans le même solvant. On porte à l'ébullition pendant 2 à 3 heures. Après 24 heures on sépare le solide formé. Le solide a été lavé d'abord avec du tétrachlorure de carbone et après, pendant 8 heures, avec de l'éther dans un extracteur Soxhlet. Le solvant a été éliminé par évaporation sous vide.

Revue Roumaine de Chimie, 19, 6, 1045 – 1051 (1974)

HYDROGEN TRANSFER REACTIONS BETWEEN HYDROCARBONS AND FREE RADICALS. II[1]

THE STUDY OF MOLECULAR COMBINATIONS BETWEEN AROMATIC HYDROCARBONS AND THE 1,1-DIPHENYL-2-PICRYLHYDRAZYL FREE RADICAL (DPPH)

I. ANGHELACHE, D. SĂNDULESCU and V. VÂNTU

Department of Organic and Physical Chemistry, Institute of Petroleum, Gas and Geology,
Str. Tr. Vuia 6, Bucharest, Romania

Received December 17, 1973

The existence of a molecular combination, in solid state, between DPPH and benzene was evidenced. The molar ratio of components and thermal dissociation enthalpy of benzene from the molecular combination DPPH-benzene were determined by gas chromatography. The molar ratio of components was found to be 1 : 1. The calculation of benzene dissociation enthalpy on the basis of equilibrium compositions at various temperatures gave the value 10 ± 0.5 kcal/mole which corresponds to an apparent bonding energy of 1.5 – 2 kcal/mole characteristic of a charge transfer molecular combination. Electronic absorption spectra (visible) have evidenced molecular combinations in solution between DPPH and benzene toluene and *o*-xylene. The possibility that molecular combinations with charge transfer occur in aromatic hydrocarbons explains the existing differences between apparent activation energies of hydrogen transfer in DPPH reaction with aromatic and olefinic hydrocarbons previously studied.

In previous papers[1-3] the reaction kinetics of hydrogen transfer from several alkyl aromatic or olefinic hydrocarbons to the stable free radical 1,1-diphenyl-2- picrylhydrazyl (DPPH) was studied. Comparison of apparent activation energies calculated for alkyl aromatic hydrocarbons with those determined in olefines showed that the former (20 – 26 kcal/mole) are considerably higher than the latter (13 – 16 kcal/mole).

To explain the difference, the hypothesis of molecular combinations between DPPH and aromatic hydrocarbons has been considered. The existence of molecular combinations of DPPH in solution has been mentioned in literature for compounds with phenols, alcohols, acids.[4,5] Likewise, in either newer or older works[6-8] the possibility of forming molecular combinations with a series of aromatic hydrocarbons or functional derivates has been evidenced. In this latter case the existing data support the idea of complex combinations with charge transfer but of low stability. Evidence has been gathered for a series of molecular combinations of DPPH with benzene in solid state of molar ratio 1 : 1[6,9] or according to other authors of 1 : 0.8,[10] with chloroform[11,12] and even with oxygen.[13,14] In this respect X ray studies on DPPH-benze molecular combinations have reached the conclusion that solvation benzene molecule is accommodated into the holes characteristic of DPPH crystal lattice and benzene-free radical interaction forces are weak.[15]

---

[1] I. Anghelache, D. Săndulescu and V. Vântu, *Rev. Roumaine Chim.*, Part I, **16** 1901 (1971).

[2] I. Anghelache, D. Săndulescu and V. Vântu, "Republican Conference of Chemistry", Timişoara, 1966.

[3] I. Anghelache, "Doctorate thesis", 1971.

In the present experiment we aimed at investigating these solid molecular combinations between DPPH and aromatic hydrocarbons by gas chromatography.[16]

Determination of dissociation enthalpies of the new formed molecular combinations might provide indications on the nature and strength of bonds between the aromatic component and DPPH. We have also attemped to study to what extend and in which solution one may evidence molecular combinations of DPPH and alkyl aromatic hydrocarbons employed in kinetic studies.

MOLECULAR COMBINATIONS BETWEEN DPPH FREE RADICAL AND AROMATIC HYDROCARBONS IN SOLID STATE.

MOLAR RATIOS FOR THE MOLECULAR COMBINATIONS DPPH-BENZENE AND DPPH-TOLUENE

Gas chromatography[16] has been applied to determine molar ratios in molecular combinations formed in solid state between DPPH free radical on one side and benzene and toluene on the other; use has been made of a Carlo Erba chromatograph to which a microreactor has been attached (Fig. 1). Molecular DPPH-benzene combination has been obtained by solving DPPH in benzene followed by evaporation of benzene, drying at low pressure and 40° for about 5 hours, up to constant weight.

For quantitative determination of benzene included into molecular combination, the weighed complex samples have been heated in a microreactor (previously pumped out) at 170° for 60 minutes, under which conditions the crystal lattice is broken down.

---

[4] C. J. Mc.Gowan and T. Powell, *J. Chem. Soc.*, **1961**, 2161.

[5] S. Singh, R. K. Bhaskar and R. N. Rao, *Canad. J. Chem.*, **44**, 2657 (1966).

[6] J. Lyons and W. Watson, *J. Polymer Sci.*, **18**, 147 (1955).

[7] H. Gutowski, *J. Chem. Phys.*, **39**, 208 (1963).

[8] R. Sagdeev and I. O. Molin, *Zhur. struct. Khim.*, **7**, 38 (1966).

[9] J. Zanchetta, A. Marchand and A. Pacault, *Compt. rend.*, **258**, 1496 (1964).

[10] J. Lothe and G. Eia, *Acta Chem. Scand.*, **12**, 1533 (1958).

[11] J. Bevington, *Nature*, **175**, 477 (1955).

[12] M. B. Krishnafi, *J. Chem. Phys.*, **41**, 1027 (1964).

[13] J. Kyraly, P. Feyes, F. Tudös and M. Azori, *Acta Chim. Acad. Sci. Hung.*, **29**, 409 (1961).

[14] A. Revina and N. A. Bach, *Doklady Akad. Nauk S.S.S.R.*, **141**, 409 (1961).

[15] D. E. Williams, *J. Amer. Chem. Soc.*, **89**, 4280 (1967).

[16] M. Rushdy, D. Săndulescu, M. Popescu and V. Vântu, *Rev. Chim. Acad. București*, **7**, 1227 (1962).

The benzene dissociated from the molecular combination has been quantitatively determined against a standard diagram previously plotted for known benzene amounts. The molar ratio calculated in this case for the solid molecular DPPH-benzene combination was 1 : 1 ; it was figured out on the basis of data which will be presented in the experimental section of the present article.

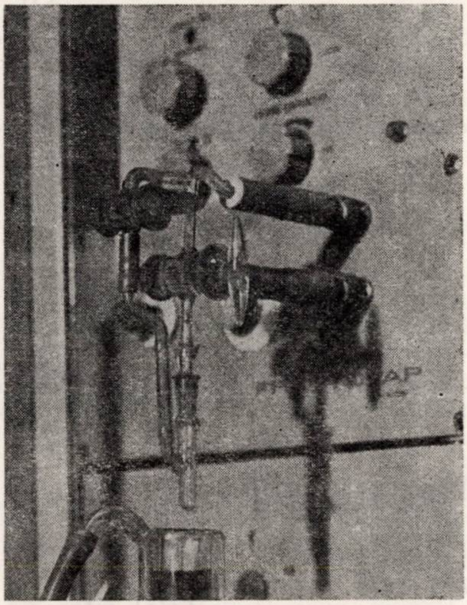

Fig. 1.—Microreactor adapted to the gas chromatograph for the study of solid complexes DPPH — benzene.

A similar procedure extended to DPPH-toluene system has been reiterated and has proved the existence of a solid molecular combination whose stability was not enough for the measurements which are being presented.

DETERMINATION OF DISSOCIATION ENTHALPIES

Gas cromatographic technique has been used for measurement of dissociation enthalpy of solid DPPH-benzene molecular combinations.

The amounts of benzene of equilibrium and several temperatures in static system have been determined in a thermoset microreactor at constant volume ; the gas phase has been evacuated into the analysis circuit of the chromatograph fast enough to prevent errors occurring from changes in solid-gas equilibrium.

The equilibrium is a monovariant one and corresponds to the heterogeneous dissociation equilibrium of the type :

$$\text{molecular combinations } (S) \rightarrow \underset{\substack{\text{support}\\\text{component}\\\text{(DPPH)}}}{C_m(S)} + \underset{\text{hydrocarbon}}{\mathrm{RH}(g)}$$

which is similar to some clathrates of coordinative combinations of aromatic hydrocarbons.[11]

This dissociation equilibrium allows calculation of dissociation enthalpy by equation

$$\lg K_p = -\frac{\Delta H}{2{,}3\, RT} + \mathrm{ct}$$

As $K_p \simeq p_{\mathrm{RH}}$, surfaces areas ($S$) of recorded gas chromatograms were measured, they are proportional to the amount of benzene delivered by the molecular combination and the partial pressures at working temperatures.

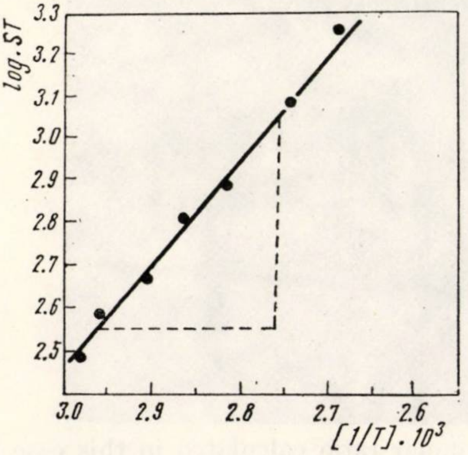

Fig. 2. — The plot of log. ST versus l/T which has been used in determining dissociation enthalpy of benzene from the DPPH-benzene complex; S = surface area under elution curve of benzene; T = absolute temperature.

One can apply the simple equations :

$$pV = \mathrm{nRT}\,;\; S = \frac{PV}{RT}\,;\; \lg S \cdot T \simeq \lg PV \simeq \lg K_p$$

The dissociation enthalpy was calculated from the slope of $\lg ST \simeq \simeq \frac{1}{T}$ plot (fig. 2).

In case of DPPH-benzene molecular combination the dissociation enthalpy of benzene was found to be 10 ± 0.5 kcal/mole resulting in a bonding energy of 1.5 — 2 kcal/mole which corresponds to charge transfer combinations.

MOLECULAR COMBINATIONS BETWEEN DPPH FREE RADICAL AND AROMATIC HYDROCARBONS IN SOLUTION

The present determinations evidenced the formation of charge transfer molecular combinations in solution between DPPH and aromatic hydrocarbons (benzene, toluene, xylene).

To obtain indications on stability and also to determine wavelengths of absorption maxima and values of molar extinction the UV and visible spectral behaviour of solutions has been studied.

At the present stage of experimental technique it is possible to obtain only qualitative appreciations on molecular combinations occurring in the systems :

— DPPH — benzene (in CCl_4)
— DPPH — toluene (in CCl_4)
— DPPH — *o*-xylene (in CCl_4)

Results are shown in fig. 3

Examination of fig. 3 shows that the spectra within 340—390 nm at DPPH concentrations of 6.39 10^{-5}M in CCl_4 (in absence and presence of small benzene concentrations — curves 1—3-do not allow evidencing new absorption maxima in addition to those mentioned in literature for pure DPPA.

However if DPPH spectra have been drawn in presence of higher aromatic hydrocarbon concentration (benzene, toluene, *o*-xylene — curves 4—7) fig. 3) and are compared to those of similar concentration of DPPH in CCl_4 solutions, new absorption maxima bathochromically shifted, to wavelength of 740—750 nm of low extinction have been found which may be ascribed to the formation of charge transfer molecular combinations. The measured absorption increases with the concentration of aromatic hydrocarbon e.g. from 0.75% at 5.62 M. benzene in CCl_4 to 1.75% at 11.21 M. The above investigation has been carried out with a Jobin Yvon spectrorecording photometer point by point. The same absorption maximum (at 750 nm) has been found with a UNICAM SP-800-automatic recording spectrometer.

The forming of such molecular combinations between DPPH and aromatic hydrocarbons could explain the difference in values of apparent activation energy of hydrogen transfer reactions under study[1-3]; values for monoalkyl aromatic hydrocarbons are considerably higher than those for olefines. The observed differences may be interpreted, in our oppinion, by non-specific physical interactions and specific chemical interactions between the stability of either a molecular combination

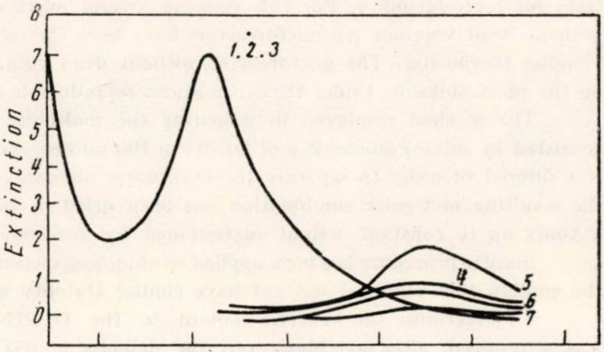

Fig. 3. — Spectra of DPPH — aromatic hydrocarbon solutions.

1, DPPH (6.39 10^{-5} M) in CCl_4; *2*, DPPH (6.39 10^{-5} M) — benzene (0.082 10^{-2} M) in CCl_4; *3*, DPPH (6.39 10^{-5} M) benzene (2.2 10^{-2} M) in CCl_4; *4*, DPPH (7.85 10^{-4} M) — benzene (5.62 M) in CCl_4; *5*, DPPH (7.85 10^{-4} M) — benzene (11.21 M); *6* DPPH (7.85 10^{-4}M) — toluene (4.71 M) in CCl_4; *7*, DPPH (7.85 10^{-4} M)-*o*-xylene (4.07 M) in CCl_4.

formed in solution or a transition complex, according to the potential energy diagram shown in fig. 8 reference.[1]

The low bonding energy of benzene with DPPH (obtained by substracting sublimation enthalpy from dissociation energy of pure benzene) agrees with the interpretation of the bond formed.

In this instance a sequence of reactions is accepted :

$$\begin{tikzcd} \mathrm{DPPH} + \mathrm{ArH} \arrow[r, shift left, "\text{fast}"] & \mathrm{DPPH} \ldots \mathrm{ArH} \arrow[l, shift left] \arrow[r, shift left] & {[\mathrm{DPPH} \ldots \mathrm{ArH}]} \arrow[l, shift left] \arrow[d, "\text{hidrogen extraction}"] \\ & & \text{DPP Hydrazine} + \mathrm{Ar}^{\cdot} \end{tikzcd}$$

Since these molecular combinations are very likely to be formed in solution at a concentration which is practically constant, following reversible rapid reactions, their formation does not influence the formal kinetics of hydrogen transfer reactions previously studied.

EXPERIMENTAL

THE TECHNIQUE APPLIED TO DETERMINATION OF MOLAR RATIOS IN MOLECULAR COMBINATIONS OF DPPH WITH BENZENE AND TOLUENE IN SOLID STATE

A type C Carlo-Erba-Fractovap gas chromatograph with ionization detector and thermistors to which a micro-reactor was added has been used.

Finding out the method has required test runs which had to establish optimal conditions for reproducibility. For this purpose several microreactors have been tried (with and without dead volume). All microreactors have been thermoset by help of a paraffin bath and Höppler thermostat. The microreactor without dead volume shown on fig. 1 has proved to be the most suitable. Under these conditions reproducible results have been obtained.

The method employed in preparing the molecular DPPH-benzene solid combination consisted in solving about 2 g of DPPH in 100 ml benzene (distilled on sodium). The solution was filtered in order to separate the eventually undissolved product. After benzene removal the resulting molecular combination has been dried in vacuo (5 mm Hg) at 40° for about 5 hours up to constant weight (determined by successive weighing).

Similar procedure has been applied to obtaining molecular combination of DPPH-toluene ; the combination obtained did not have similar stability with the benzene one.

To determine the benzene content in the DPPH-benzene combination the sample was introduced, after weighing, into the detachable test tube of the microreactor. After checking up the tightness by a pressure test the whole device was heated up to working temperature.

The chromatograph working conditions :

- Column length 1 m (15% dibutyl phtalate/celite)
- Column temperature : 55°
- Vaporizer temperature : 100°
- Eluant : nitrogen 40 ml/min.

TECHNIQUE APPLIED IN DETERMINING THE DISSOCIATION ENTHALPIES OF BENZENE FROM DPPH-BENZENE MOLECULAR COMBINATIONS

Experiments have been carried out at temperatures ranging between 60 and 100°C : within this range no DPPH degrading occurs. Above 100° appreciable thermal decomposing of DPPH takes place. Tests carried out have shown that within 1.5 hours 12% DPPH decomposes at 120° and 100% at 150°.

Procedure : 0.01 – 0.03 g of molecular combination weighed on an analytic scale is introduced into the microreactor.

The tightness is checked by a pressure test and the microreactor is cut off the chromatograph circuit by a three way tapper. The microreactor is then brought to the desired temperature which is maintained long enough for gas-solid equilibrium to take place (this is done by the thermostat). The time required for reaching equilibrium has been determined by attempts ; for the molecular combination under study it was of 30 – 60 minutes.

After this time has elapsed the reaction is connected to the analysis circuit of the chromatograph and the eluant (nitrogen) is flown through in order to evaluate the gas phase.

This operation must take a short time so that the possible changes in solid-gas equilibrium may not represent important errors.

THE EXPERIMENTAL TECHNIQUE APPLIED TO EVIDENCING MOLECULAR COMBINATIONS OF DPPH WITH ALKYL AROMATIC HYDROCARBONS IN SOLUTION

Carbon tetrachloride (Serva spectral reagent grade) was used as solvent in preparation of complex solutions. Benzene, toluene, *o*-xylene have been spectral reagent grade too.

DPPH has been synthetized and purified in our laboratory according to the method previously described.[2,3]

Recording spectra. U.V. and visible spectra have been recorded with a silica-optics Jobin Yvon spectrophotometer. Ordinary and silica glass cuvettes 1-cm thick have been used. Extinction was read on a galvanometer within ± 0.002. Use has also been made of an automatic UNICAM SP.800 spectrophotometer.

The absorption of the solvent has been looked for by using reference cuvettes filled up with CCl_4 and solution of DPPH in CCl_4 of the same concentration as mixtures under consideration.

Spectra of solutions of both pure DPPH and DPPH in aromatic hydrocarbons (benzene, toluene, *o*-xylene) at different concentrations are shown on fig. 3.

[illegible] IN [illegible] DISSOCIATION [illegible] OF BENZENE FROM [illegible] COMPLEXES

Experiments [illegible] DPPH [illegible]

[illegible]

[illegible]

[illegible]

[illegible] MOLECULE [illegible] CONFORMATIONS [illegible] IN SOLUTION

[illegible] DPPH [illegible]

[illegible]

[illegible]

[illegible]

Revue Roumaine de Chimie, **19**, *6*, 1053–1059 (1974)

ELECTRICAL CONDUCTIVITY OF SOME SALICYLIDENANILS

SCHELY AVRAMOVICI, IOANA CIOCOIU and G. I. RUSU *

Department of Organic Chemistry, "Al.I. Cuza" University, 23 August, 11, Jassy, Romania

* Physics Department, "Al. I. Cuza" University, Jassy

Received August 21, 1973

In the present paper the electrical properties of some salicylidenanils have been investigated. Thin film samples with polycrystalline structure were used. The experiments showed that the heat treatment determined a reversible change of electrical conductivity as a function of temperature and a stable film structure. For the studied compounds, a correlation between thermal activation energies and their chemical structure was established.

1. INTRODUCTION

In recent years, numerous experimental and theoretical investigations have had the object to establish a correlation between the semiconductor properties of organic compounds and their chemical structure.[1-6]

The present paper studies the electrical conductivity for some Schiff bases, prepared from condensation of the salicyl, 5-nitrosalicyl, 5-bromsalicyl, 3-nitrosalicyl and 3-nitro-5-bromsalicylaldehydes with 2-amino-6-methylbenzthiazole, 2-amino-6-methoxybenzthiazole, 2-amino-β-naphthothiazole and *p*-aminodimethylaniline.

It is the aim of this paper to establish a dependence between chemical structure of substances and their electrical properties.

---

[1] F. Gutman and L. N. Lyons, "Organic Semiconductors", John Wiley, New York, 1967.

[2] * * * "Organische Halbleiter", Akademie Verlag, Berlin, 1966.

[3] R. E. Burgess, *J. Polymer Sci.*, *C*, **1967**, 51.

[4] D. D. Eley, *J. Polymer Sci.*, *C*, **1967**, 73.

[5] M. Strul, G. I. Rusu and I. Zugrăvescu, *Phys. Status Solidi*, **9**, 129 (1872).

[6] S. Avramovici, A. Airinei, M. Rusu and A. Pollak, *Anal. Şti. Univ. "Al. I. Cuza" Iaşi, Sect. I*, **13/2**, 167 (1970).

The general chemical formula of investigated compounds is :

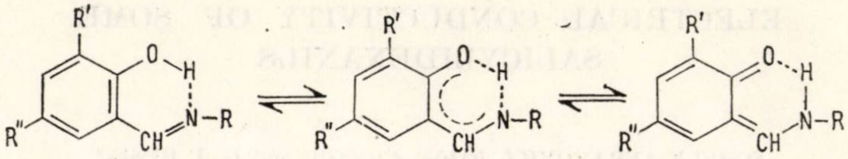

Ia Ib Ic

where the substituents R, R′ and R″ are given in table 1.

The technique of preparation, some chemical and physical properties of substances were described in detail.[7,8] The purity of substances has been controlled by using chemical and spectral analyses.

2. EXPERIMENTAL PROCEDURE

The thin films were deposited on glass substrates from benzene solutions and thermal evaporation.

For electrical resistivity measurements, aluminium electrodes were used.

The experimental arrangement and measurement technique have been reported.[9,10] The film temperature has been measured with a Fe-constantan thermocouple. In all cases temperature rate was 2°/min. The interferometrically determined sample thickness ranged from 0.10 to 2.00 μm. The investigations showed that the electrical properties of films prepared by thermal evaporation are not essentially different from those of films obtained from benzene solutions.

We shall present the experimental results obtained by using the films prepared by the second method.

3. EXPERIMENTAL RESULTS AND DISCUSSION

The metallographic investigations showed that all films have a polycrystalline structure. The size of the film granules depends on the film thickness *d*. A structure with bigger granules was observed for high values of *d*.

For compounds I_9 and I_{12} (Table 1), the curves which give the electrical resistivity ρ depending on the film thickness *d* are presented in fig. 1.

A similar behaviour was also found for all investigated substances. The resistivity ρ decreases with film thickness and tends to a constant value.

---

[7] S. Avramovici, A. Airinei and I. Ciocoiu, *Rev. Roumaine Chim.*, **18**, (1973).

[8] S. Avramovici, I. Ciocoiu, A. Airinei and I. Soifer, *Anal. Şti. Univ. "Al. I. Cuza" Iaşi, Sect.* 1, **18/1**, 61 (1972).

[9] G. I. Rusu, Kandidatskaya Dissertatsia, Leningrad, 1969.

[10] G. I. Rusu, *Anal. Şti. Univ. "Al. I. Cuza" Iaşi*, **15/2**, 149 (1969).

An analogous behaviour was remarked on other inorganic and organic semiconductors in thin films.[1,2,10,11]

We may suppose that the growth mechanism of films is identical for the respective substances.

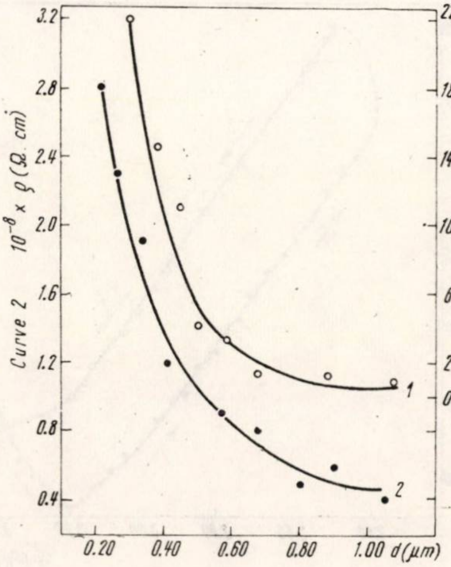

Fig. 1. — The dependence of the specific resistivity ρ as a function of film thickness d (curve 1 – compound I_9, curve 2 – compound I_{12}).

In order to obtain a structure stability and reproducibility of the electrical properties, all the investigated samples were subjected to subsequent heatings and coolings in ΔT temperature ranges indicated in table 1.

The temperature dependence of the electrical conductivity σ during this heat treatment has been studied. The curves $\ln \sigma = f\left(\frac{1}{T}\right)$ have the following aspect : at the first heating, with increasing temperature, the electrical conductivity σ decreases at the beginning ($T < 350 - 370$ K). This decrease in conductivity is probably due to the elimination of the absorbed gas as well as of the humidity. As it is known these factors have a strong influence on electrical conductivity of organic semiconducting compounds.[1,2]

For higher temperatures, the conductivity increases with temperature, obeying the usual exponential law [1,2,12]

$$\sigma = \sigma_{0e} - \frac{\Delta E}{2KT}$$

---

[11] V. V. Slutkaja, "Tonkie plionki v tekhnike sverkhvjsokijkh thastot", Izd. Sov. Radio, Moskva, 1967.

[12] P. Smith, "Poluprovodniki", Izd. inostr. lit., Moskva, 1962.

On cooling, electric conductivity decreases but no longer reaches original values, gases and humidity having been eliminated from the film.

Experiments have shown that by following the heat treatment curves are obtained which, within limit of errors, overlap the curve

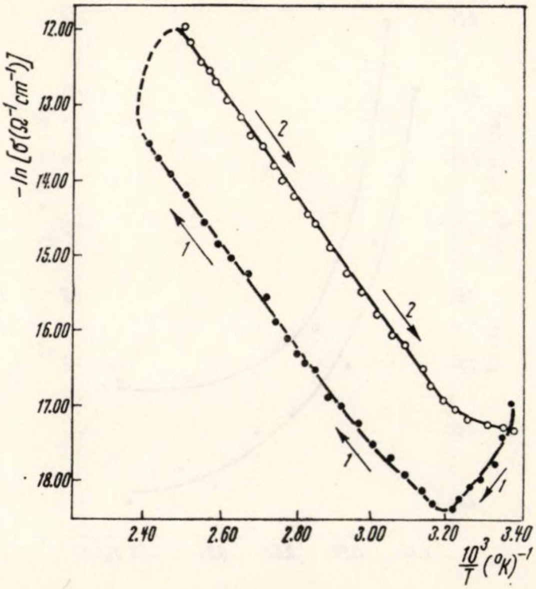

Fig. 2. — The curves $\ln\sigma = f\left(\frac{10^3}{T}\right)$ for the compound I_5 at the first heating and cooling (*1* = heating, *2* = cooling).

obtained at the first cooling. We conclude that heat treatment determined a reversible change of the electrical conductivity as a function of temperature and a stability of film structure.

In fig. 2 we represent the curves $\ln\sigma = f\left(\frac{10^3}{T}\right)$ for the compound I_5. For all studied samples there was found a similar behaviour.

For heat-treated specimens, starting with a temperature T_i, characteristic of each compound, a linear dependence of the $\ln\sigma = f\left(\frac{1}{T}\right)$ curves was observed. The values of T_i for investigated substances are given in table 1. The table also shows the specific conductivities at room temperature σ 20° C, studied temperature range ΔT, and film thickness d.

According to the sign of Seebeck coefficient the conductivity of the compounds is of p-type. For $T > T_i$ the compounds have an intrinsic conductivity. For heat-treated samples, the temperature dependence of the electrical conductivity in the intrinsic domain is represented in figs 3 and 4.

The calculated values of the thermal activation energy ΔE are given in table 1.

It can be observed that these values strongly depend on the chemical structure of compounds.

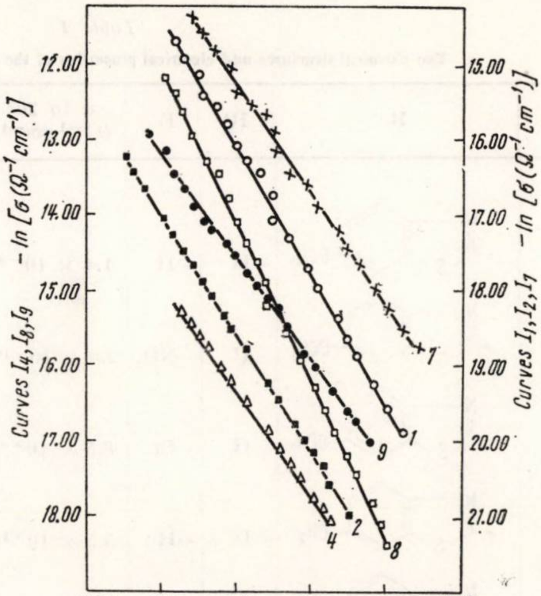

Fig. 3. — The temperature dependence of the conductivity of compounds I_1, I_2, I_4, I_7, I_8, I_9 (the numbers represent the products corresponding to those in table 1).

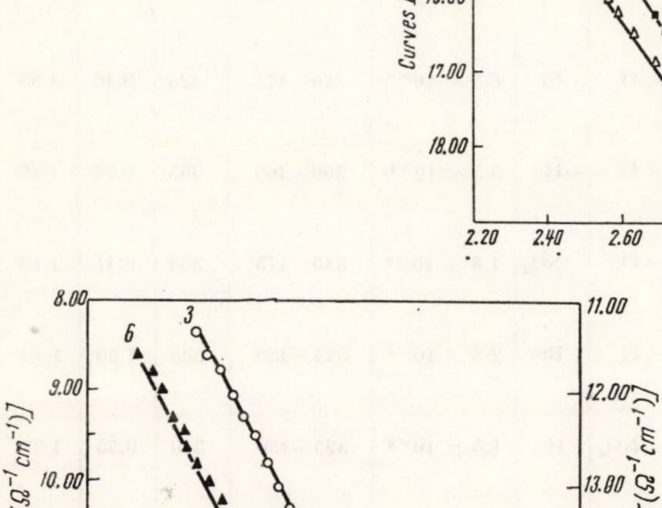

Fig. 4. — The temperature dependence of the conductivity of compounds I_3, I_5, I_6, I_{10}, I_{11}, I_{12} (the numbers represent the products corresponding to those in table 1).

Table 1

The chemical structures and electrical properties of the investigated salicylidenanils

Nº	R	R′	R″	σ to 20° (Ω^{-1} cm^{-1})	ΔT (K)	T_i (K)	d (μm)	ΔE (eV)
I_1	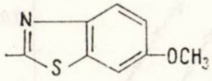	$-H$	$-H$	1.4×10^{-9}	300–400	330	0.40	1.50
I_2	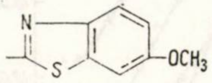	$-H$	$-NO_2$	2.0×10^{-10}	310–480	345	0.35	1.40
I_3	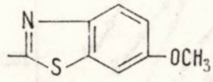	$-H$	$-Br$	8.5×10^{-9}	310–475	325	0.40	1.65
I_4	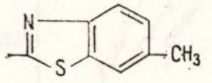	$-H$	$-H$	5.5×10^{-10}	300–400	355	0.55	1.25
I_5	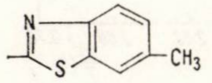	$-H$	$-NO_2$	1.8×10^{-9}	340–475	365	0.41	1.10
I_6	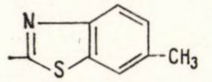	$-H$	$-Br$	2.8×10^{-9}	325–450	335	1.50	1.70
I_7	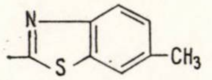	$-NO_2$	$-H$	1.5×10^{-9}	325–450	360	0.75	1.30
I_8	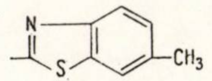	$-NO_2$	$-Br$	1.0×10^{-10}	320–470	335	0.70	1.80
I_9	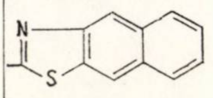	$-H$	$-NO_2$	1.0×10^{-9}	300–420	340	0.50	1.25
I_{10}	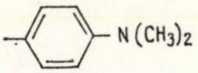	$-H$	$-H$	1.6×10^{-9}	310–440	365	0.33	1.80
I_{11}	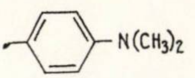	$-H$	$-NO_2$	5.0×10^{-9}	300–430	330	0.50	1.70
I_{12}	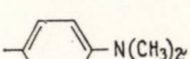	$-H$	$-Br$	6.6×10^{-9}	330–440	365	0.50	1.40

As a first remark we must mention that the benzthiazolic nucleus in the aminic rest of the anils determines a different behaviour as against the *p*-dimethylaminobenzoic rest in the same position. The activation energy value is much greater in the latter case.

The substituent nature in the benzthiazolic nucleus [(6)$-OCH_3$, (6)$-CH_3$, (5)$-CH=CH-CH=CH-$(6)] has not a marked influence on the activation energy value. In exchange, a greater influence is due to the substituent from the salicylaldehydic ring. Thus, if the aminic rest is unchanged by comparing the activation energy from a series of products it is found that the NO_2-group in the 5-position of the salicylaldehyde ring (prod. I_2, I_5) determines a decrease of the activation energy value, whereas the Br in the same position (prod. I_3, I_6) has an opposite effect.

Similar results were found when calculating the optical energy values from the same compounds,[7-8] especially those in polar solvents.

From the experimental results we must suppose that the NO_2-grouping in the 5-position determines a spreading conjugation, with an increase in the amount of quinoid structure (I_c), while the Br in the same position has the effect of decreasing conjugation.

The NO_2-grouping in the 3-position of the salicylaldehydic nucleus (prod. I_7) has the same effect as the Br in 5-position, but less intense.[1,13]

The existence of both substituents, NO_2 in the 3-position and Br in the 5-position, leads to the expected result, i.e. the adding up of the effects, the respective product (I_8) showing the greatest activation energy. These results agree with the data of electronic spectra by which it was established that the NO_2 grouping from the 3-position of salicylaldehydic nucleus causes a disturbance of quasiquinoidic structure, reorienting the hydrogen bridge[7].

The variation of the activation energy in relation to the nature of substituents in the salicylidenanils with *p*-dimethylaminobenzenic rest no longer follows the same course, the presence of a substituent in the salicylaldehyde nucleus leading, irrespective of its nature, to a depression of the activation energy value.

---

[13] I. Pogany and M. Banciu, „Metode fizice în chimia organică", Ed. ştiinţifică, Bucharest, 1972.

Revue Roumaine de Chimie, **19**, *6*, 1061–1065 (1974)

BIS-THIOETHERS. I

CONDENSATION OF SODIUM THIOPHENOLATE WITH DICHLOROMETHYLATED DERIVATIVES

M. IOVU and ANCA ANGELESCU

University of Bucharest, Faculty of Chemistry
Splaiul Independenţei 89, Bucharest, Romania

Received June 23, 1973

Using the method previously described by us in the synthesis of phenyl benzyl sulphides, which was also applied, for the first time, to the synthesis of aromatic bis-ethers, we prepared a new class of bis-thioethers with the general formula : $Ar-S-CH_2-Ar-CH_2-S-Ar$, in which Ar is a substituted or unsubstituted aromatic nucleus with methyl radical. Bis-thioethers were obtained by the condensation of the anhydrous sodium thiophenolates – which were obtained through azeotropic distillation of the water resulted from the reaction between thiophenol or *p*-methylthiophenol with sodium hydroxide – with dichloromethylated derivatives.

In the previous paper[1] we presented the results of the synthesis of some phenyl benzyl sulphides using a similar method to that also applied by us for the first time, in the synthesis of some polyethers[2] or aromatic bis-ethers.[3]

According to our method, the phenol or the thiophenol is converted into its anhydrous sodium or potasium salt, by treating it with alkali hydroxides in a solvent or in a mixture of solvents (preferably ethanol-benzene).

The resulting water is removed by azeotropic distillation as follow :

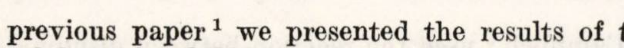

The thiophenolate thus obtained is then treated with chloromethylated derivative, which may be monochloromethylated as in the previous note,[1] or dichloromethylated as in other papers [2-4] or as in the present paper.

---

[1] M. Iovu and A. Angelescu, *Rev. Roumaine Chim.*, **18**, 263 (1973).
[2] M. Iovu and M. Manolescu, Romanian Patent, 61.805, 1969.
[3] M. Iovu, *Rev. Roumaine Chim.*, **16**, 1223 (1971).

The nucleophilic attack of the phenoxide or thiophenolate ion on the halogenated derivative takes place, as shown below:

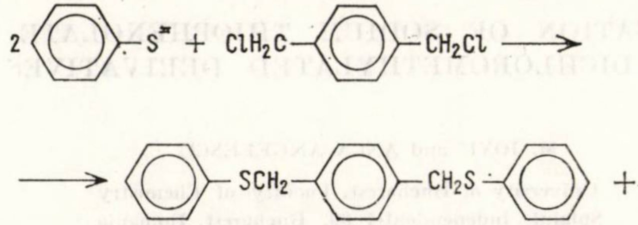

After three or four hours the reaction will be considered total.

The bis-thioether precipitates and after a suitable treatment it could be purified by recrystallization.

Based upon this method we wish to report in this paper the synthesis of ten bis-thioethers, belonging to a new class, with the general formula $Ar-SCH_2-Ar-CH_2S-Ar$ in which Ar is a substituted or unsubstituted aromatic nucleus with methyl radical.

Using this new method we condensed the sodium thiophenolate and the sodium *p*-methyl thiophenolate with the: 1,4-dichloromethyl benzene; 1,4-dichloromethyl-2,5-dimethyl benzene; 1,3-dichloromethyl-4,6-dimethyl benzene; 1,3-dichloromethyl-2,4,6-trimethyl benzene and 1,4-dichloromethyl-2,3,5,6-tetramethylbenzene, obtaining ten new products.

The bis-thioethers having the general formula: $Ar-S-CH_2-Ar-CH_2-S-Ar$ have not been prepared up to now; but their isomers with the general formula $Ar-CH_2-S-Ar-S-CH_2Ar$ have been synthesized.

Thus, Campbell [5] used the reaction between disulphides and dihaloaromatic compounds, which were condensed in the presence of copper powder at 160–170° in dimethylacetamide as solvent:

$$C_6H_5-CH_2-S-S-CH_2-C_6H_5 + BrC_6H_4Br \xrightarrow{Cu}$$

$$\longrightarrow C_6H_5-CH_2-S-C_6H_4-S-CH_2-C_6H_4$$

RESULTS AND DISCUSSION

Table 1 gives the structural formulas of the synthesized sulphides, their melting points, the microanalytical results of sulphur determination, λ_{max} and ε_{max}, from UV spectrometry and the yields.

All the synthesized bis-thioethers are in a solid state. Their melting points depend on the number and the positions of the methyl substituted radicals, especially on the aromatic central nucleus.

---

[4] M. Iovu, *Rev. Roumaine Chim.*, **17**, 1261 (1972).

[5] J. R. Campbell, *J. Org. Chem.*, **27**, 2207 (1962).

Table 1

Bis - thioethers

	Thioethers	Formula	S % calc. found	Melting point °C	λ_{max} nm	$\varepsilon_{max}\cdot 10^{-4}$	Yield %
1.	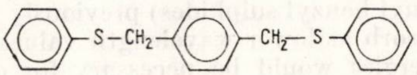	$C_{20}H_{18}S_2$	19.88 19.55	141.5 – 143	251.5	1.6	84.1
2.	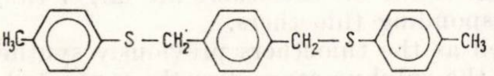	$C_{22}H_{22}S_2$	18.29 18.11	159 – 161	252	3.1	78.7
3.	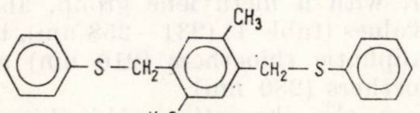	$C_{22}H_{22}S_2$	18.29 18.30	138 – 139	241	2.4	85.7
4.	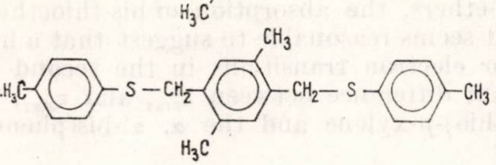	$C_{24}H_{26}S_2$	16.94 16.73	110.5 – 111	236	2.4	76.1
5.	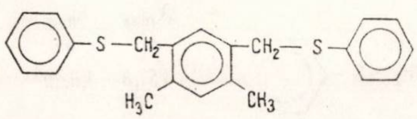	$C_{22}H_{22}S_2$	18.29 18.09	74.5 – 75	254	1.5	63.4
6.	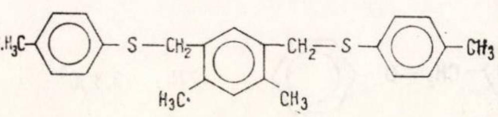	$C_{24}H_{26}S_2$	16.94 16.66	82.5 – 83.5	255	1.3	62.4
7.	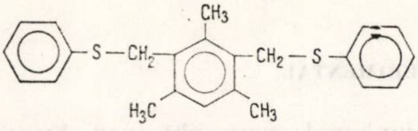	$C_{23}H_{24}S_2$	17.60 17.11	82 – 83	255	1.9	93.20
8.	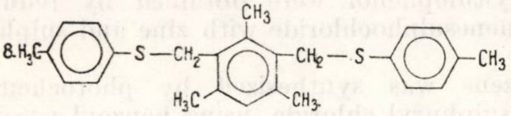	$C_{25}H_{28}S_2$	16.32 16.20	85 – 86.5	253	1.9	96.6
9.	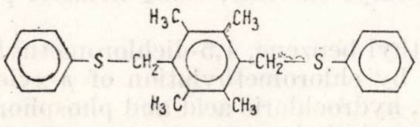	$C_{24}H_{26}S_2$	16.94 16.64	235	247	2.5	85.7
10.	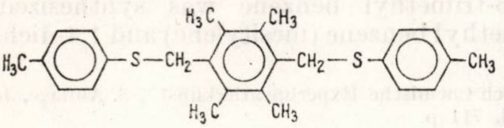	$C_{26}H_{30}S_2$	15.77 15.57	194	245	2.8	87.6

The bis-thioethers present lower melting points, up to 30°, comparatively to the corresponding bis-ethers.[3]

A slight difference exists only between α, α′-bis-(phenylthio)-*p*-xylene (m.p. 141.5 – 143°) and α, α′-bis(phenoxy) *p*-xylene (m.p. 143.5 – 144°).

Compared to thioethers (phenyl benzyl sulphides) previously synthesized by us,[1] the bis-thioethers absorb at lower wavelength values. These results point out that higher energies would be necessary for electron transitions in the case of bis-thioethers.

Also, the absorption bands of the bis-thioethers are larger than the absorption bands of the corresponding thioethers.

The bis-thioethers, as well as the thioethers previously synthesized by us,[1] having one valence of the sulphur atom directly connected with an aromatic nucleus and another, with a methylene group, absorb in U.V. at intermediary wavelength values (table 1) (231–258 nm), between the characteristic value of the aliphatic thioethers (210 nm) and the typical value of the aromatic thioethers (280 nm).

By comparison with bis-ethers, the absorption of bis-thioethers is shifted to lower wavelengths. It seems reasonable to suggest that a higher energy would be necessary for electron transitions in the second case.

Thus we find an important difference between λ_{max} and ε_{max}, if we compare the α, α′-bis(phenylthio)-*p*-xylene and the α, α′-bis(phenoxy)-*p*-xylene [3]:

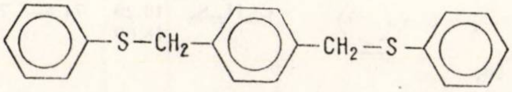

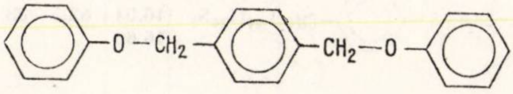

λ_{max} nm	ε_{max} nm
251,5	$1{,}6.10^4$
271.	$3{,}8.10^3$

EXPERIMENTAL

Thiophenol and 4-methylthiophenol were obtained by reducing benzenesulphochloride and toluenesulphochloride with zinc and sulphuric acid (33%).[6]

1,4-Dichloromethyl benzene was synthesized by photochemical chlorination of *p*-xylene with sulphuryl chloride, using benzoyl peroxide as activator.

1,4-Dichloromethyl 2,5-dimethyl benzene, 1,5-dichloromethyl 2,4-dimethyl benzene were synthesized by chloromethylation of *p*-xylene and *m*-xylene, using paraformaldehyde, hydrochloric acid and phosphoric acid.

1,5-Dichloromethyl 2,4,6-trimethyl benzene was synthesized by chloromethylation of 1,3,5-trimethyl benzene (mesitylene) and 1,4-dichloromethyl 2,4,5,6-tetramethyl benzene was synthesized by chloromethylation of 1,2,4,5-tetramethyl benzene (durene) in a similar way.

---

[6] Weygand-Hilgetag, "Organisch-Chemische Experimentierkunst", 3. Auflage, Johann Ambrosius Barth-Verlag, Leipzig, 1964, 711 p.

The determination of sulphur was made by the oxidation of bis-thioethers with oxygen in the presence of platinum catalyst, and with hydrogen peroxide, followed by the volumetric determination of sulphuric acid.

UV spectra were obtained on a Hitachi Recording spectrophotometer.

SYNTHESIS OF α, α'–BIS (PHENYLTHIO)–*p*–XYLENE

In a double-necked, 50 ml flask, equipped with a reflux refrigerator and a thermometer, we insert 2.2035 g thiophenol (1/50 mol), 0.805 g NaOH (1/50 mol plus an excess of 1/5000 mol) and 30 ml of an ethanol-benzene mixture (in a 1 : 1 ratio by volume). The mixture is heated to the boiling point for 3 hours, till sodium thiophenolate has formed. The reflux refrigerator is then changed with a distillation refrigerator and 15 ml azeotropic mixtures are distilled to remove the water resulting from the reaction.

After cooling the flask, 1.7497 g, 1,4-dichloromethyl benzene (1/100 mol) are added, the distillation refrigerator is again changed with the refluxing one, to which a tube with calcium chloride has been connected and it is heated for 3 hours at 65–67°. Sodium chloride is formed, which precipitates together with the bis-thioether.

After cooling the flask to 5°, the reaction mixture is filtered, so as to separate the solid sodium chloride and the solid sulphide from the solvent and the liquid unreacted raw materials. The solid mixture is then washed with water to remove sodium chloride. The precipitate is dried in vacuum; 2.7136 g α, α'-bis(phenyl-thio)-*p*-xylene results after two recrystalizations from an ethanol benzene mixture (in a 1 : 3 ratio by volume); its melting point will be 141,5–143°.

Other compounds were obtained in a similar way, with the mention that mixtures of ethanol – benzene in different ratios were used for recrystallization.

Thus, compounds no. 2, 3, 4 (table 1) were recrystallized from the mixture of ethanol-benzene in a 1 : 3 ratio by volume.

Compounds no. 5, 6, 7, 8 (table 1) were recrystallized from the mixture of ethanol-benzene in a 3 : 1 ratio by volume.

Compounds 9, 10 (table 1) were recrystallized from benzene.

Revue Roumaine de Chimie, 19, 6, 1067–1072 (1974)

STUDY OF SOME HETEROCYCLES. XXVI*

NITRATION OF 2-ANILINO-5-PHENYL-1,3,4-OXADIAZOLE

I. SIMITI, DOINA GHIRAN, I. SCHWARTZ and R. D. POP

Institute of Medicine and Pharmacy, Laboratory of Organic Chemistry, str. V. Babeş 41,
Cluj, Romania

Received July 6, 1973

The present paper investigates the nitration of 2-anilino-5-phenyl-1,3,4-oxadiazole under various conditions. The structure of the resulted compounds was established by chemical and physico-chemical studies.

In an earlier paper we dealt with the bromination of some 2-anilino-5-(*p*-X-phenyl)-1,3,4-oxadiazoles and found that the substitution takes place in the *para* position of the aniline rest.[1]

Further studies on the nitration of 2-anilino-5-phenyl-1,3,4-oxadiazole (I) under various reaction conditions showed that this cannot be accomplished with HNO_3 ($d = 1.40$) in a glacial acetic acid medium, 50% sulphuric acid, while small amounts of nitration compounds occur in 85% H_2SO_4, the non-nitrated initial compound prevailing in the mixture. When the reaction takes place in an acetic anhydride medium, a mixture of various nitration compounds is obtained.

A systematic study led us to the conclusion that the best results can be obtained by the nitration of a 2-anilino-5-phenyl-1,3,4-oxadiazole suspension in nitrobenzene with a sulphonitric mixture at a temperature ranging between 0 and 10°, when a mixture of three nitration products (II, III, IV) is formed and a small amount of non-nitrated 2-anilino-5-phenyl-1,3,4-oxadiazole (I) also remains. These were identified by thin-layer chromatography.

Similar results are also constantly obtained if the reaction is carried out in a concentrated sulphuric acid medium. However, the separation of compounds (II, III, IV) is more difficult in this case.

In order to establish the position in which nitration took place, the following reference compounds were prepared : 2-(*p*-nitro-anilino)-5-phenyl-1,3,4-oxadiazole (II) and the *meta*-nitro-substituted derivative (IV) ; 2-anilino-5-(*p*-nitro-phenyl)-1,3,4-oxadiazole (V) ; 2-(*p*-nitro-anilino)-

---

* Note XXV. I. Simiti, E. Chindriş and I. Schwartz, *Rev. Chim.* (*Bucureşti*), **23**, 460 (1972).

[1] I. Simiti, D. Ghiran and I. Schwartz, *Arch. Pharm.*, **304**, 230 (1971).

-5-(*p*-nitro-phenyl)-1,3,4-oxadiazole (III) as well as their N-acetyl derivatives.

By separating the compounds from the nitration mixture we found that the largest amount consisted of 2-(*p*-nitro-anilino)-5-phenyl-1,3,4-oxadiazole (II), a very small amount was identical with (III) and a somehow larger amount of a dinitro-derivative (IV) was not identical with either of the reference compounds prepared by us.

This last compound (IV) is also obtained by nitration of 2-(*p*-nitro-anilino)-1,3,4-oxadiazole (II) alongside with a small amount of (III) and a part of the unreacted compound (II).

As expected, a large amount of compound (III) is obtained by nitration of 2-anilino-5-(*p*-nitro-phenyl)-1,3,4-oxadiazole (V).

Physico-chemical studies were performed on the above-mentioned mono- and dinitro-derivatives in view of establishing the structure of compound (IV).

By performing IR spectra in KBr pellets * of all these compounds we found a good agreement with the respective formulations except for compound III which displays, surprisingly, a band at 1680 cm^{-1} and another at 2800 cm^{-1}, which do not appear in the spectrum of other derivatives.

Table 1

Characteristic absorption bands in IR spectra

	ν NH		δ NH	$\nu C=N$	νNO_2		$\nu C-NO_2^2$
	ν a	ν s			ν a	ν s	
I	3250	3050	1615	1603	—	—	—
II	3270	3060	1625	1600	1515	1335	855
III	3300	3100 2850	1672	1625	1510 1525	1325	845 850 doublet
IV	3230	3060	1625	1605	1510 1520	1330	845 860 doublet
N-acetyl * deriv. III	—	—	—	1600	1520 1525	1335	850 865
2,4-dinitro-aniline	—	—	—	—	1510 1520	1320	830 835

* $C=0=1720\ cm^{-1}$

In the case of the acetyl-derivative of compound III, these bands disappear, which makes us believe that they are due to the —NH— grouping. This would plead for the fact that not only the band at 1672 cm^{-1} belongs to the —NH— grouping but also that at 2850 cm^{-1}, considering the fact that spectra of all derivatives constantly reflect an absorption at 1180 cm^{-1}, the band at 2850 cm^{-1} may be considered as a combination band.

---

* IR spectra were recorded on a Shimadzu 27 G spectrophotometer in KBr pellets, in the 4000 — 400 cm^{-1} spectral range.

[2] B. Franck, H. Hörmann and S. Scheibe, *Chem. Ber.*, **90**, 330 (1957).

It is worth mentioning that these bands fail to appear in the case of dinitro-derivative (IV), which proves that its structure must be different.

In order to elucidate the structure of compound IV we further made a polarographic study of the mentioned compounds.* On this occasion we found a normal behaviour,[3] all mononitro-derivatives having one single reduction wave whereas in the case of dinitro-derivatives a different

Table 2

Polarographic waves of nitroderivatives

E 1/2(V)	pH	Compounds				
		V	II	III	IV	2,4-dinitro-aniline
Waves	A a	−0.09	−0.172	−0.02	−0.02	−0.22
	b	−0.30	−0.56	−0.26	−0.142	−0.55
	c	−0.42	−0.65	−0.33	−0.220	−0.63
	d	−0.50	−0.71	−0.40	−0.34	−0.69
	e	−0.52	−0.76	−0.48	−0.420	−0.705
	B a	—	—	−0.19	−0.22	−0.455
	b	—	—	−0.63	−0.585	−0.72
	c	—	—	−0.71	−0.69	−0.84
	d	—	—	−0.765	−0.81	−0.915
	e	−0.75	—	−0.785	−0.750	−0.935
	C a	—	—	—	—	—
	b	—	—	—	—	—
	c	—	—	—	—	—
	d	—	−1.015	−1.06	−1.01	—
	e	—	−1.015	−1.05	−0.960	−1.245
Diffusion current (μA)	A a	—	4.46	—	—	4.7
	b	2.76	4.06	1.90	3.94	4.84
	c	3.16	3.94	2.44	3.9	4.46
	d	3.3	2.86	2.6	3.98	4.14
	e	1.56	1.96	2.26	4.22	4.52
	B a	—	—	2.99	5.1	5.3
	b	—	—	2.9	4.1	3.96
	c	—	—	2.64	3.74	3.88
	d	—	—	1.52	2.6	3.44
	e	2.1	—	0.78	0.4	2.16
	C a	—	—	—	—	—
	b	—	—	—	—	—
	c	—	—	—	—	—
	d	—	0.5	0.82	1.4	—
	e	—	1.36	0.86	3.64	2

* Polarographic determinations were made on a L.P. 7 polarograph Laboratorny pristroje in an aqueous DMF solution. 2.5% LiCl was used as a basic electrolyte and maxima were recorded by means of a 1% gelatine solution. The pH levels involved were 1.2; 3.6; 5.2; 8.5; and 10.

[3] K. Kemula, *Roczniki Chem.*, **33**, 1485 (1958).

behaviour of the two waves can be observed relative to the pH. Thus, the height of polarographic waves of compound III varies relative to the pH (table 2) whereas in the case of dinitro-derivative (IV) the height of waves is independent of pH variations. The polarogram of the latter is highly similar to that of 2,4-dinitroaniline.

The structure of these compounds was also confirmed by mass spectra,* the molecular peaks being in keeping with their molecular weight.

Thus all mononitro-derivatives (II, V, IV) display molecular peaks at $M^+ = 282$ whereas dinitro-derivatives (III, IV) show them at $M^+ = 327$, proving once again that compound (IV) is certainly a dinitro-derivative. Mass spectra of nonsubstituted compounds on phenyl (I, II, IV) reveal a peak at 145, characteristic of a peak also found in the spectrum of

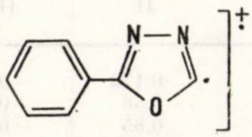

Schema 1

compound (IV). This proves that phenyl is nonsubstituted and the two $-NO_2$ groupings are situated on the aniline rest.

In the case of compounds (III and V) with the NO_2 group on phenyl, the peak at 145 is missing, yet a large peak appears at 190 specific of :

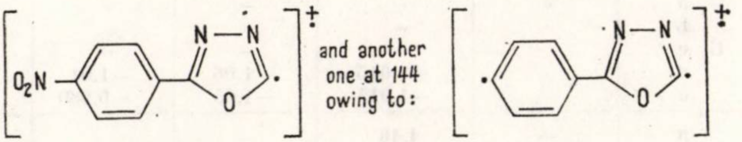

Schema 2

which is missing with derivatives I, II, IV and VI.

Based on the polarographic study, on IR and mass spectra we may conclude that dinitro-derivative (IV), whose structure could not be elucidated by synthesis, is 2-(2′, 4′-dinitro-anilino)-5-phenyl-1,3,4-oxadiazole.

In conclusion, comparing the bromination and nitration reactions of 2-anilino-5-phenyl-1,3,4-oxadiazole it resulted that in the bromination reaction one single bromine atom is introduced in the *para* position of the aniline rest regardless of the amount of bromine, phenyl-oxadiazole behaving as a deactivator. In the case of nitration even if we use equimolecular amounts of NO_3H, we constantly obtain the mixture of the three mentioned nitro-derivatives, the prevailing amount being 2-(*p*-nitro-anilino)-5-phenyl-1,3,4-oxadiazole.

---

* Mass spectra were recorded by a M.A.T. 311 (M.A.T. Bremen-Varian) device with double focalization.

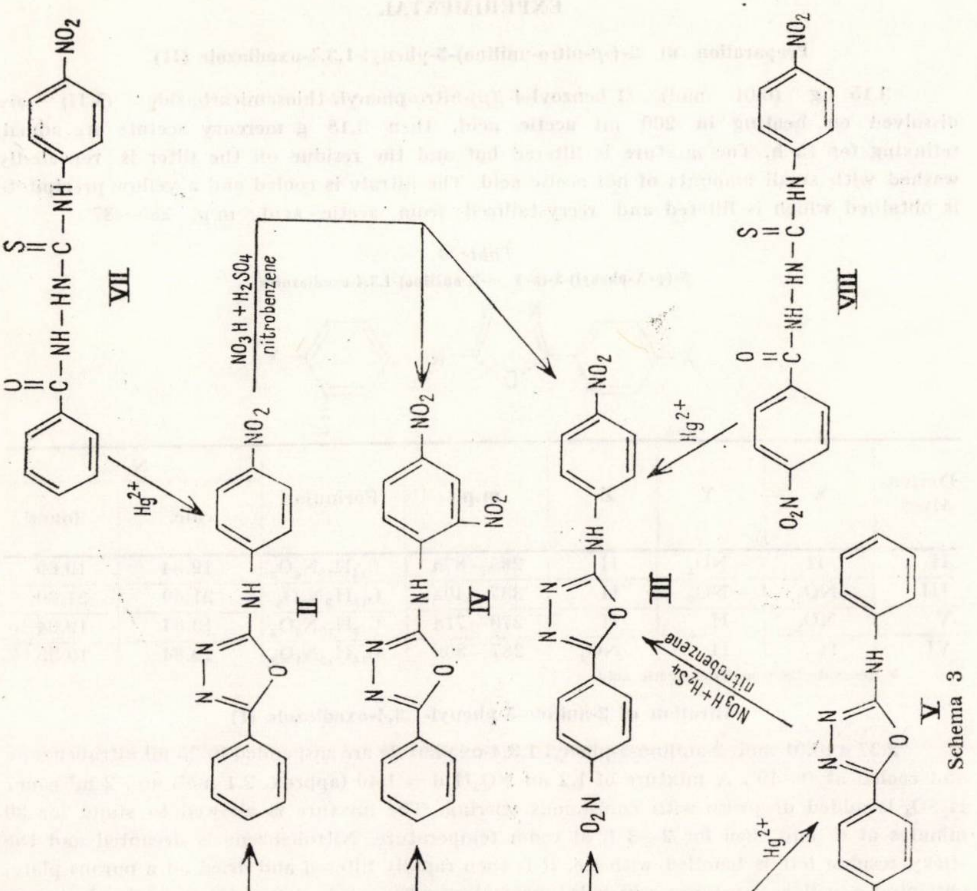
VII
VIII
I
II
III
IV
V
IX
Hg^{2+}
Hg^{2+}
Hg^{2+}
$NO_3H + H_2SO_4$ nitrobenzene
$NO_3H + H_2SO_4$ nitrobenzene
$NO_3H + H_2SO_4$ nitrobenzene

Schema 3

EXPERIMENTAL

Preparation of 2-(-*p*-nitro-anilino)-5-phenyl-1,3,4-oxadiazole (II)

3.15 g (0.01 mol) 1-benzoyl-4-/(*p*)-nitro-phenyl/-thiosemicarbazide (VII) are dissolved on heating in 200 ml acetic acid, then 3.18 g mercury acetate are added, refluxing for 15 h. The mixture is filtered hot and the residue on the filter is repeatedly washed with small amounts of hot acetic acid. The filtrate is cooled and a yellow precipitate is obtained which is filtered and recrystallized from acetic acid, m.p. 285–87°.

Table 3

5-(*p*-X-phenyl)-2-(*p*-Y, *m*-Z-anilino)-1,3,4-oxadiazoles

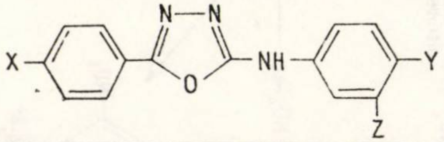

Derivatives	X	Y	Z	m.p.°	Formulae	N %	
						calc.	found
II	H	$-NO_2$	H	285–87a	$C_{14}H_{10}N_4O_3$	19.84	19.69
III	$-NO_2$	$-NO_2$	H	337–40a	$C_{14}H_9N_5O_5$	21.40	21.30
V	$-NO_2$	H	H	270–71a	$C_{14}H_{10}N_4O_3$	19.84	19.94
VI	H	H	$-NO_2$	287–80a	$C_{14}H_{10}N_4O_3$	19.84	19.55

[a] Recrystallization from acetic acid

Nitration of 2-anilino-5-phenyl-1,3,4-oxadiazole (I)

2.37 g (0.01 mol) 2-anilino-5-phenyl-1,3,4-oxadiazole are suspended in 25 ml nitrobenzene and cooled at 0–10°. A mixture of 1.2 ml NO_3H d = 1.40 (approx. 2.1 mol) and 2 ml conc. H_2SO_4 is added dropwise with continuous stirring. The mixture is allowed to stand for 30 minutes at 0° and then for 2–3 h at room temperature. Nitrobenzene is decanted and the sticky residue left is handled with ice. It is then rapidly filtered and dried on a porous plate, obtaining a yellow substance which is chromatographed and shows three spots characteristic of nitro-derivatives and a weak R.f. spot identical with that of the initial compound (I). Repeated recrystallizations from acetic acid and then dioxane lead to a pure chromatographic compound with m.p. 285°, identical with 2-(*p*-nitro-anilino)-5-phenyl-1,3,4-oxadiazole (II) $C_{14}H_{10}N_4O_3$ – N% calc. 19.84, found 19.94.

The remaining portions after separation of this compound (m.p. 190–200°) also show 3 spots. By fractionated recrystallizations from ethanol, acetone, dioxane acetic acid we separated a chromatographically pure compound with m.p. 240°, $C_{14}H_9N_5O_5$ – N% calc. 21.40, found 21.79 (IV) and trace amounts of a compound with m.p. 340°, identical with 2-(*p*-nitro--anilino)-5-(*p*-nitro-phenyl)-1,3,4-oxidiazole (III) $C_{14}H_9N_5O_5$ – N%, calc. 21.40, found 21.29.

OBSERVATIONS

The reaction was carried out under similar conditions with an equimolecular amount of HNO_3 and the same results were obtained by varying the time from 1 to 24 hours. Identical results were also obtained by conducting the reaction in a medium of concentrated sulphuric acid.

Nitration of 2-(*p*-nitro-anilino)-5-phenyl-1,3,4-oxadiazole (II) was identically carried out, resulting in a mixture of II, III and IV.

Nitration of 2-anilino-5-(*p*-nitro-phenyl)-1,3,4-oxadiazole (V) results exclusively in compound III.

Revue Roumaine de Chimie, 19, 6, 1073–1082 (1974)

STUDY OF CYCLOHEXANE DEHYDROGENATION EQUILIBRIUM AND KINETICS IN PULSED REACTOR

A. POP and POMPILIA DUMITRESCU
Faculty of Chemistry, Str. Arany Ianoş 11, Cluj, România

Received August 4, 1973

The authors study the activity of a chlorinated Pt/Al_2O_3 catalyst in a reaction of cyclohexane dehydrogenation. The reaction is monitored in a pulsed reactor operating according to the gas – solid chromatography process under the conditions of the reaction reversibility and in a current of hydrogen as eluent. On this occasion the chemical equilibrium of the dehydrogenation – hydrogenation reaction was studied, establishing the following relation for the equilibrium constant in the sense of dehydrogenation : $\log K_p = 19.413 - 10751/T$ which is verified in comparison with the values obtained from the thermal data and with those obtained from the Jarkov-Frost equation, within a temperature range of 513–633 K, good results being recorded. Thus, emphasis is laid on the use of the pulsed reactor in the study of chemical equilibria. At the same time the kinetics of the reaction is studied under conditions of reversibility, in the same pulsed reactor, in the range of 547.5–584 K. An apparent activation energy of 13.0 Kcal/mole is calculated.

The pulsed reactor or the reactor operating according to the gas chromatographic technique has been used quite frequently since 1955 in the study of some heterogeneous reactions to determine the activity of the catalysts. The technique initiated by Kokes et al.[1] was followed with great interest by many other researchers and it basically consists in the following:

The reactor is a catalyst column maintained under reaction conditions; through it flows a constant current of carrier gas which can be inert to the reactant system or to one of the reactants. According to the gas chromatographic technique the reactants are introduced as pulses in this column.

The reaction resultants, leaving the reactor, pass directly into an analytical chromatographic column and are subjected to an analysis similar to that performed by Kokes et al. or they are first wholly condensed and the condensate is analysed by the same technique as that applied by several researchers.

---

[1] R. J. Kokes, H. Tobin Jr. and P. H. Emett, *J. Amer. Chem. Soc.*, **77**, 5870 (1955).

By using this technique, Bassettand Habgood [2] studied the kinetics of a first order reaction, i.e. the isomerism of trimethylene, and established the relations between the adsorption equilibrium, the reaction rate constant and the chromatographic retention values, showing that the corrected chromatographic retention time, or a proportional value of it, such as the corrected retention volume, may be considered as reaction time in kinetic calculations.

These values, correlated to the molar conversions obtained in the reaction and related to the catalyst mass unit, are used in the known kinetic equations and allow the calculation of rate constants (catalyst activity) and the corresponding activation energy.

Considering the complex phenomenon in the pulsed reactor from the point of view of contact effect and of the separation effect that occur simultaneously in the catalyst column, Roginskii et al.[3,4] established the mathematical relations of this process, based upon the mass balance for pulsation passage through a catalyst zone. Magee,[5] Hattori and Murakami,[6] Langer and Yurchak,[7] Blanton et al.[8] and other investigators have also subjected these processes to mathematical analysis. The effect of the pulse shape is studied in particular by Gaziev et al.[9]

All of them postulate that the technique of the pulsed reactor is rigorously applicable to first order reactions in which the slowest stage is represented by the surface reaction.

On the other hand, it is inferred that in the column of the pulsed reactor the reaction products being separated during their passage through the catalyst layer, the counter-reaction may be avoided for any reversible reaction of the type $A \rightleftarrows R + S$ in which equilibrium has been slowly established. Thus, in a sufficiently long catalyst column the reaction may occur until the final transformation has taken place.

A much studied reaction in the pulsed reactor is the dehydrogenation of cyclohexane. Most investigations carried out to this end employed conditions under which the counter-reaction takes place only in an insignificant proportion. Roginskii et al.[4] study the reaction with Pt/Al_2O_3 catalyst with argon as carrier gas within a temperature range of 145°–280°. Although equilibrium conversions should be obtained within this range, in fact higher conversions are obtained due to the above-mentioned separation of hydrogen from benzene when the pulse passes through the catalyst column. Gaziev et al.[9] treat the same reaction as a first order irreversible reaction on Pt/Al_2O_3 catalyst and on aluminium-silica catalyst within a temperature range of 130–200°. The same school[10] also studies the reaction on some carbides, silicides, borides in argon current at the temperature of about 500° as a first order reaction; the counter-reaction does not occur. Mathsen et al.[11] experiment the reaction in the 183°—225° range of temperatures where equilibrium conversions are reduced, in a reactor with Pt/Al_2O_3 in a helium current. They also confirm the *a priori* obvious fact that higher conversions are obtained than the equilibrium ones. Berezkin et al.[12] study the reaction at lower temperatures (90—145°), in helium or argon current. They reach the same conclusions as to the separation of reaction resultants and to the reaction order and propose the calculation of the reaction kinetics on the basis of the outlet peaks of the reactor resultants, particularly that of hydrogen. Recently Barbul et al.[13] have studied the kinetics of this reaction in a pulsed reactor and in the straight through reactor in a hydrogen current. They did not take into account the counter-reaction which undoubtedly takes place in the studied range of temperatures.

---

[2] D. V. Bassett and H. B. Habgood, *J. Phys. Chem.*, **64**, 769 (1960).

[3] S. Z. Roginskii, M. I. Ianovskii and G. A. Gaziev, *Doklady Akad. Nauk S.S.S.R.*, **140**, 1125 (1961).

[4] S. Z. Roginskii, M. I. Ianovskii and G. A. Gaziev, *Kinetika i Kataliz*, **3**, 529 (1962).

[5] E. M. Magee, *Ind. and Eng. Chem. (fundamentals)*, **2**, 32 (1963).

[6] T. Hattori and Y. Murakami, *J. Catalysis*, **10**, 114 (1968).

[7] S. H. Langer and J. Y. Yurchak, *Ind. and Eng. Chem.*, **61**, 11 (1969).

[8] W. A. Blanton Jr., Ch. H. Byers and H. P. Merrill, *Ind. and Eng. Chem. (fundamentals)*, **7**, 611 (1968).

[9] G. A. Gaziev, V. Ju. Filinovskii and M. I. Ianovskii, *Kinetika i Kataliz*, **4**, 688 (1963).

The authors of this work, concerned with the obtaining of some active alumina, tested their behaviour after impregnating them with finely dispersed platinum, in the same reaction of cyclohexane dehydrogenation. The testings were carried out in a pulsed reactor employing hydrogen as carrier gas, as reactant and also as reaction medium. The testing range of temperatures was 274.5 — 311°, and the pressure range was 1.2 — 1.8 atm. Under these conditions no secondary reaction occurs. The adsorption and desorption rates both of the reactants and the resultants are high and the surface reaction is the slowing down stage.

Since this reaction is of zero order in relation to hydrogen, it means that from the point of view of kinetics it may be interpreted in both ways following the first order equation.

The known equation of such reactions at a given temperature value is:

$$\frac{k\,a}{x_e} = \frac{1}{t} \ln \frac{x_e}{x_e - x} \tag{1}$$

where a = initial molar concentration;

x_e = modification of the initial concentration, under conditions of equilibrium;

x = modification of initial concentration after reaction time t, before reaching equilibrium.

Noting by $\alpha_e = x_e / a$ the equilibrium conversion, in moles/mole, and by $\alpha = x/a$ the conversion at time t, in moles/mole, equation (1) becomes

$$\frac{k}{\alpha_e} = \frac{1}{t} \ln \frac{\alpha_e}{\alpha_e - \alpha} = \frac{2{,}303}{t} \log \frac{\alpha_e}{\alpha_e - \alpha} \tag{2}$$

---

[10] G. A. Gaziev, O. B. Krylov, C. Z. Roginskii, G. M. Samsonov, E. A. Fokina and M. I. Ianovskii, *Doklady Akad. Nauk S.S.S.R.*, **140**, 863 (1961).

[11] J. M. Mathsen, J. W. Harding and E. M. Magee, *J. Phys. Chem.*, **69**, 522 (1965).

[12] V. G. Berezkin, V. S. Kruglikova and F. V. Belikova, *Doklady Akad. Nauk S.S.S.R.*, **158**, 182 (1964).

[13] M. Barbul, Gh. Şerban, I. Ghejan and T. Filotti, *Petrol şi Gaze Bucureşti*, **19**, 181 (1968).

At a determined temperature and at constant pressure, α_e is constant and may be easily and readily determined in the pulsed reactor. It results that an $\alpha_e/(\alpha_e - \alpha)/-t$ diagram allows the calculation of the specific rate k and then of the apparent activation energy of the reaction.

The equilibrium conversions for various temperatures may be calculated using the values of the equilibrium constants, which in turn are calculated according to empirical equations such as:

$$\log K_p = f(T)$$

Such equations were established on the basis of the thermal data of the reaction.

The need for knowing such an equation prompted us to establish it, in the case of this reaction, by achieving the following equilibrium in the pulsed reactor:

$$C_2H_{12} \rightleftharpoons C_6H_6 + 3\,H_2 \tag{3}$$

According to reaction (3), and considering that this system behaves perfectly, the known expression of the equilibrium constant is:

$$K_p = \frac{p_2 \cdot p_3^3}{p_1} = \frac{p_2 \cdot p_3^3}{p_1} \tag{4}$$

where:

p_1 = partial pressure of cyclohexane vapors
p_2 = partial pressure of benzene vapors
p_3 = partial pressure of hydrogen in the system.

In the absence of an inert gas, the total pressure in the system will be:

$$P = p_1 + p_2 + p_3 \tag{5}$$

If we identify by p_{1i} the partial pressure of cyclohexane vapors in the initial pulse, prior to the reaction, we get

$$p_{1i} = p_1 + p_2 \text{ and}$$

$$P = p_{1i} + p_3 \text{ while}$$

$$p_3 = P - p_{1i}$$

so that

$$K_p = \frac{p_2(P - p_{1i})^3}{p_{1i} - p_2} \tag{6}$$

Simplifying the right hand side of (6) by p_{1i} and marking with $p_2/p_{1i} = \alpha_e$ the equilibrium conversion, it results:

$$K_p = \frac{\alpha_e}{1 - \alpha_e}\,(p - p_{1i})^3 \tag{7}$$

In general, within a not very broad range of temperatures and with quite a good approximation the equilibrium constant of a reaction is:

$$\log K_p = \frac{a}{T} + b \tag{8}$$

Writing equation (7) in log form and then comparing it with (8) we obtain:

$$\log \frac{\alpha_e}{1 - \alpha_e} = \frac{a}{T} + b - \log (P - p_{1i})^3 \tag{9}$$

It results that if α_e' is measured for various temperatures while maintaining the $P - p_{1i}$ difference constant, a plot

$$\log \alpha_e / (1 - \alpha_e) + 3 \log (P - p_{1i}) = f(1/T)$$

will allow the calculation of constants a and b.

Value P is measured experimentally, and value p_{1i} is calculated based on the pulse quantity.

As mentioned before, this work was carried out in hydrogen as reaction medium and the pulse quantity did not exceed 1% of P; therefore the $P - p_{1i}$ difference may be considered equal to P in a first approximation. For more accurate calculations it will be corrected with the p_{1i} value, calculated as shown in the experimental section below.

EXPERIMENTAL

1. INSTRUMENTATION AND WORKING PROCEDURE

The apparatus used is similar to the apparatus described by Kokes et al.[1] The detection in chromatographic flux was made by thermal conduction cell. The reactant (cyclohexane or benzene) sample is introduced with a microsyringe in a 1.5–2 μl amount. The chromatographic spectrum of the reaction resultant is shown in fig. 1.

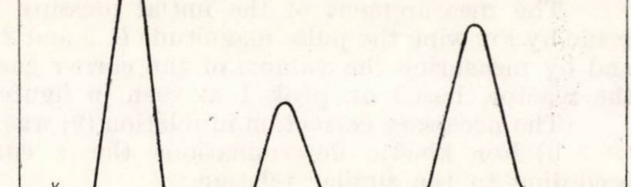

Fig. 1. — Chromatogram of the reaction resultant: *1*, reactant+reaction resultant; *2*, cyclohexane; *3*, benzene.

The temperature in the catalytic layer was maintained constant with a ± 1° error. The carrier gas flow was kept constant at the value of 53 ± 0.5 ml/min.

In fig. 1 peak 1 represents the zone composed of the reactant and the reaction resultant, at the outlet of the reactor. No separation of components is found.

Peaks 2 and 3 are the peaks of cyclohexane and respectively of benzene separated in the analytical column.

In case of equilibrium measurements, cyclohexane and benzene pulses were alternately introduced in the reactor to verify the attainment of the equilibrium. The differences of the respective conversions, measured by comparison with cyclohexane, were maintained within the limits of ± 0.1 per cent.

The analytical column: l = 1.5 m, Ø = 44.0 mm, brick C_{22} 60–80 mesh, ethylene benzoate impregnation,[14] 10% by weight.

2. THE CATALYST

A Pt/Al_2O_3 type catalyst of own manufacture was used. Its features are :

- composition : 0.4 per cent Pt
- specific surface 220–240 sqm/g
- total acidity (after calcination at 500°) 2.1 milliequiv. pyridine/g.

Amount of catalyst

- For equilibrium measurements, 1 g, i.e. a 1.2 cm high column
- For kinetic measurements, 0.0773 g in a ca. 1 mm high column

The catalyst was activated by heating the reactor in a hydrogen current for 6–12 hours at a temperature of 500°.

3. CALCULATIONS

a) In equilibrium measurements, the α_e conversion was calculated according to relation :

$$\alpha_e = \frac{A_{3e}}{A_{2e} + A_{3e}} \tag{10}$$

where A_{2e} and A_{3e} are the areas of the peaks 2 and 3 corresponding respectively to the non-reacted cyclohexane and to the obtained benzene, under equilibrium conditions. It is obvious that the areas were corrected relative to a standard mixture.

The measurement of the initial pressure of the reactant p_{1i} was made by knowing the pulse magnitude (1.5 and 2 microliters, respectively) and by measuring the volume of the carrier gas in which this pulse left the reactor, based on peak 1 as seen in figure 1.

The necessary correction in relation (9) was made with a mean value.

b) For kinetic determinations the α conversion was calculated according to the similar relation :

$$\alpha = \frac{A_3}{A_2 + A_3} \tag{11}$$

---

[14] A. Pop and P. Dumitrescu, *Rev. Roumaine Chim.* "Omagiu Raluca Ripan", 1966, p. 449.

One considered as reaction time t (relation (2)), a conventional time, the spatial time t_s, as defined by relation

$$t_s = \frac{m\, p_r\, T_r}{D_v\, p_a\, T_a} \tag{12}$$

where

m = the mass of catalyst in the reactor
D_v = the volumetric flow (ml/s) measured at air pressure and room temperature
p_a, p_r = the mean pressure in the catalytic layer and the air pressure, respectively
T_r, T_a = the reactor and the room temperatures, respectively, measured in Kelvin degrees.

The operating conditions were achieved so as to have no pressure drop in the catalytic layer, hence the pressure p_a was identical to the pressure measured at the reactor inlet and equal to P in relations (5) (6).

For our kinetic measurements we considered the chromatographic retention time as reaction time, because the length of the catalyst column was too reduced and so no difference could be made between the retention time of a reactant and that of an inert gas. On the other hand, for first order reactions, where conversions are not dependent on either the pulse concentration or on the shape of the peak, we considered as reaction time the spatial time as in the case of a continuously operated reactor.

RESULTS AND DISCUSSION

a) ESTABLISHMENT OF THE EQUILIBRIUM EQUATION

Table 1 includes the equilibrium conversions measured for a series of seven temperatures (546 – 609.5 K) and six total pressures (P = = 1.32 – 1.8).

Table 1

Equilibrium conversions (α_e) at various temperatures and pressures

Temp. K	Pressure (atm.)					
	1.32	1.40	1.50	1.60	1.70	1.80
546.0	—	0.203	0.180	0.143	0.130	0.104
558.5	0.381	0.361	0.256	0.223	0.207	0.184
567.5	0.570	0.561	0.525	0.520	0.455	0.427
576.0	0.620	0.635	0.603	0.587	0.518	0.484
583.5	0.812	0.790	0.773	0.715	0.697	—
596.0	0.950	0.903	0.874	0.842	0.839	0.825
609.5	0.972	0.974	0.950	0.948	0.938	0.913

Using the data from table 1, the $\log \frac{\alpha_e}{1 - \alpha_e} + 3 \log (P - p_{1i})$ values were calculated. Further, these values permitted to determine the constants *a* and *b* of equation (8), by employing the method of least squares.

Thus, the following equation is established for the equilibrium constant of the cyclohexane dehydrogenation reaction at a $P = 1$ atm.

$$\log K_p = 19.413 - \frac{10.751}{T} \tag{13}$$

The *a* and *b* constants were determined with a medium error of ± 3 per cent.

The resulting equation was verified by means of the thermal data found in the literature,[15 16] and of the equation established by Jarkov and Frost[4] for benzene hydrogenation:

$$\log K_p = \frac{9590}{T} - 9.9194 \log T + 0.002285\, T + 8.565 \pm 0.084 \tag{14}$$

by calculating several comparative values of the respective quantities. Thus:

The temperatures for which K_p is 1 ($\log K_p = 0$) are:

— According to equation (13) established by us 553.84
— According to the thermal data 555.13
— According to the Jarkov and Frost equation 552.02

We also calculated the log K_p values for seven temperatures of the studied range, which are listed in table 2.

Table 2

Values of the equilibrium constant (log K_p) of the cyclohexane dehydrogenation reaction calculated based on various equations

Temp. K	log. K_p		
	Based on thermal data[15,16]	Based on equation (13)	Based on the Jarkov and Frost eq. (14)
513.16	−1.6715	−1.6270	−1.5416
533.16	−0.8421	−0.7520	−0.7203
553.16	−0.0708	−0.0203	+0.0434
573.16	+0.6457	+0.6550	+0.7541
593.16	+1.3136	+1.2880	+1.4206
613.16	+1.9428	+1.8790	+2.0440
633.16	+2.5346	+2.4330	+2.6311

As illustrated, the results obtained from the relation established by us are close to the thermal data and this entitles us to deduce that our approach is suitable for the study of chemical equilibria in all the cases in which the reactant stage is gaseous and the heterogeneously catalysed reaction is rapid enough. The procedure is adequate both for

---

[15] A. P. I. National Bureau of Standards, edited by F. D. Rossini, "Selected Values of Properties of Hydrocarbons", Washington, 1947, p. 552.

its efficiency and for the satisfactory accuracy of results. We consider that the accuracy of results would be significantly improved if the instrumentation employed for the temperature control and for the measurement of the pressure in the reactor yielded better performances than the instrumentation employed by us.

The errors altering the measurement of these characteristics may bring about most significant errors in all the measurements of this kind. Analytical errors are much reduced (below 1%) if the analysis is carried out in a column that totally separates the compounds involved and under conditions in which the areas of chromatographic peaks are large enough (i.e. a high detection sensitivity and also a high rolling speed of the recording paper).

b) CALCULATION OF KINETICS OF THE STUDIED REACTION UNDER REVERSIBILITY CONDITIONS

To calculate the reaction rate and the activation energy the cyclohexane conversion to benzene was determined for three temperature values under the shown experimental conditions.

The values of α_e corresponding to the respective temperature and reaction pressures were calculated according to equation (13).

The results are shown in table 3.

Table 3

Conversions of cyclohexane to benzene (α), under conditions of reversibility

Temp. K 547.5		558.5		584.0	
t_s (sec)	α	t_s (sec)	α	t_s (sec)	α
0.184	0.1546	0.101	0.4834	0.085	0.8233
0.220	0.1736	0.124	0.5312	0.091	0.8311
0.241	0.1899	0.178	0.5759	0.111	0.8831
0.300	0.3399	0.184	0.6067	0.137	0.8913
—	—	0.210	0.6240	0.199	0.9093
—	—	0.344	0.6410	0.240	0.9213
—	—	—	—	0.271	0.9285

t_s – spatial time calculated based on equation (12).

The kinetic isotherms in fig. 2 were obtained by using equation (2) and the data above, establishing the apparent overall rate constants which are shown in table 4.

Table 4

Values of apparent rate constant (k)

Temperature k	k (cm^3 g^{-1})
547.5	0.809
558.5	0.942
584.0	1.692

Finally, using an Arrhenius plot $\log k - 10^3/T$, the activation energy was determined for reaction $E_a = 13.0$ kcal/mol which is in agreement with a large number of data in the literature.[13,17]

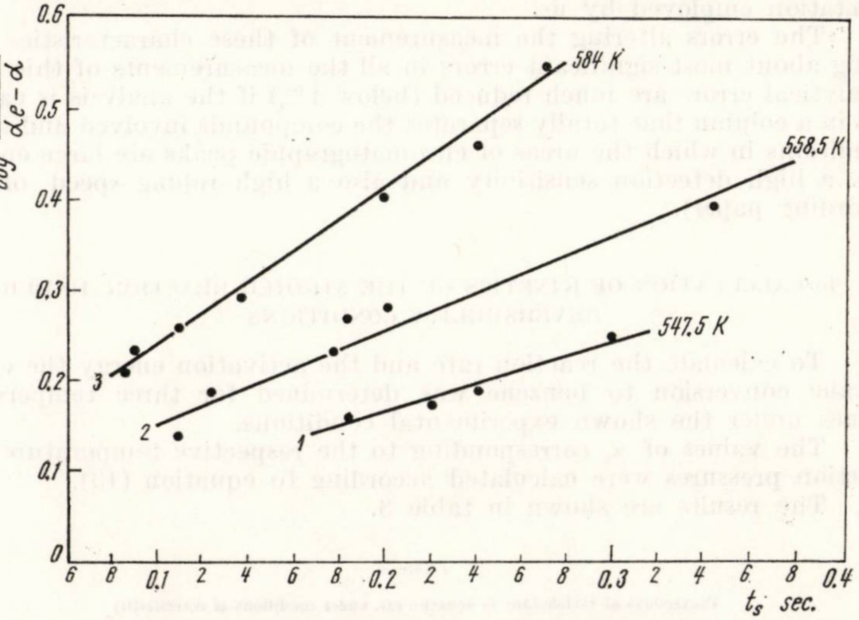

Fig. 2. — Kinetic isotherms based on equation (2):
1, dependence $\log \alpha_e/\alpha_e - \alpha$, — t_s, at 547.5 K;
2, dependence $\log \alpha_e/\alpha_e - \alpha$, — t_s, at 558.5 K;
3, dependence $\log \alpha_e/\alpha_e - \alpha$, — t_s, at 584.0 K.

---

[16] "Girdler Cadalyst, Physical and Thermodynamic Properties of Elements and Compounds,", Gesamtherstellung, Freisinger Druck, Werbung K. G., München, 1960, p. 562.

[17] H. Katsuzawa, J. Koboyashi, and J. Higuchi, *Kogyo Kagaku Zasshi*, **72**, 8238 (1969); *Chem. Abstr.*, **71**, 74621 (1969).

Revue Roumaine de Chimie, **19**, *6*, 1083–1091 (1974)

SOME ASPECTS OF RADIOLYTIC OXIDATION OF PHENOL IN AQUEOUS SOLUTION

MARIA FITI

Institute of Atomic Physics, P.O. Box 35,
Bucharest — Romania

Received July 27, 1973

in the megarad range radiolysis of aqueous solution of phenol in appropriate conditions, a final solid product P_A is formed corresponding to the G (-phenol) = = 1–2 mol/100 eV. In acid solution (pH < 3) P_A is formed during irradiation and can be separated as an amorphous white yellow powder. This material is readily soluble in ethanol, acetone and water at an alkaline pH and is insoluble in water and in other nonpolar solvents at an acid pH. The dry product P_A is unstable, it gradually turns into a dark material. In neutral solution (pH = 6–8) P_A is formed as a colloid solution from which P_A can be separated by acidifying the solution, after irradiation. The alkaline solution (pH > 8) develops a brown-red colour by irradiation and does not give any solid P_A-like products. The present results showed that P_A is probably a "so-called" polymer formed by intermolecular association between phenol and its radiolytic oxidation products.

INTRODUCTION

The literature[1-3] concerning the radiolysis of aqueous phenol solution has shown that free OH radicals can hydroxylate phenol and only *ortho* and *para* dihydroxy-derivatives (catechol and quinol) and *ortho* and *para*-benzoquinone are formed.

More recent papers,[1-10] using pulse radiolysis technique reported data concerning the transient species primarily formed in the reactions of e^-_{aq}, H and OH radicals with phenol and the rate constants of these reactions.

[1] G. Stein and J. Weiss, *J. Chem. Soc.*, **1951**, 3265.

[2] K. C. Kurien, P. V. Phung and M. Burton, *Radiation Res.*, **11**, 283 (1959).

[3] S. Kerteş, M. Lederer and M. Lefort, *J. Chim. phys.*, **53**, 959 (1956).

[4] L. M. Dorfman, J. A. Taub and R. E. Buhler, *J. Chem. Phys.*, **36**, 3051 (1962).

[5] Anbar and E. J. Hart, *J. Amer. Chem. Soc.*, **86**, 5633 (1964).

[6] J. H. Baxendale in "Pulse Radiolysis", Ed. M. Ebert et al., Academic Press., London 1965, p. 15.

[7] G. E. Adams, J. W. Brag, J. Currant and B. D. Michael, in „Pulse Radiolysis" Ed. M. Ebert et al., Academic Press., London 1965, p. 140.

[8] M. Anbar, D. Meyerstein and P. Neta, *J. Phys. Chem.*, **70**, 2660 (1966).

[9] G. E. Adams, B. D. Michael and E. J. Land, *Nature*, **211**, 293 (1966).

[10] E. J. Land and M. Ebert, *Trans. Faraday Soc.*, **63**, 1181 (1966).

In spite of this progress there are no results, in the literature on the radiolytic oxidative association of phenol in aqueous solution.

The present work was concerned to investigate particularly this process apparently leading to a polymeric material.

EXPERIMENTAL

Materials. All materials used for preparation of solutions and for analysis were of analytical grade purity without further purification and water was triple distilled. Deaeration of solutions, before irradiation, was carried out either in vacuum or by bubbling pure argon, through the solution of interest, for at least 30 minutes.

Iradiations were carried out in 10–20 ml solution samples contained in pirex ficels of 16 mm diameter.

As radiation source we used a 2 MeV electrons beam from a linear accelerator which gives a dose-rate of 1,5 Mrad/min and a Cobalt-60 γ-rays source at a dose-rate of 3 Krad/min. The total dose used was within 0,2 to 10 Mrad range.

Analysis of the main radiolytic products was carried out by different methods as follows.

Ultra violet spectrophotometry [1,11] was used to determine the oxidation products of phenol, as dihydroxybenzene which absorbs at λ of 288 nm ($\varepsilon = 2700\ M^{-1}\ cm^{-1}$) and benzoquinone absorbing at of 245 nm ($\varepsilon = 21500\ M^{-1}\ cm^{-1}$).

Visible spectrophotometry has been used to measure the optical absorption of coloured products in irradiated phenol solutions. This colour is attributed [12] to benzoquinone formation which has a maximum absorption at λ of 430 nm.

For phenol analysis we used the colorimetric method with *p*-nitroaniline.[13] We calculated *G*(-phenol) value corresponding to the solid product P_A formation by measuring the remaining phenol in the irradiated solution after P_A product separation.

RESULTS AND DISCUSSION

By irradiation under certain conditions, the aqueous phenol solution led to the formation of a polymer product P_A ignored in the previous work concerning the radiolysis of this system.

The results of the present work show that P_A product formation seems to be a process of both theoretical and practical importance.

Dose-effect. The solid radiolysis product of phenol is apparently formed only by irradiation of its acid aqueous solution at dose values higher than 0,1 Mrad. Even so it seems to be dose-independent because it does not require any induction period.

Dose-rate effect is also insignificant in the range of 3 Krad/min to 1,5 Mrad/min.

There is no apparent change in the nature and yield of P_A product between two samples irradiated at the same total dose but at

---

[11] C. Vermeil and L. Saloman, *Compt. rend.*, **249**, 268 (1959).

[12] G. E. Adams and B. D. Michael, *Trans. Faraday Soc.*, **63**, 1171 (1967).

[13] T. D. Ionescu, S. Constantinescu, G. Marcoci, M. Moţoc and T. Petre, "Analiza Apelor", Ed. tehnică, Bucharest, 1968, p. 147.

the extreme above values of dose-rate range. In other words the P_A product does not result from a long chain process.

Concentration effect of phenol within 10^{-4} to 5.10^{-2} M range is not significant but at concentrations higher than 5.10^{-2} M the product formed changes gradually into a brown, yellow, sticky oil-like product.

Oxygen and additives effect

The aqueous phenol solution saturated by oxygen does not give any solid product P_A, while by deaerating the solution, G(-phenol) has its maximum value of 1–2 molecules/100 eV. In normal aerated solution P_A is formed only at high dose irradiation when all oxygen is consumed. This means that the process of P_A formation does not take place in the presence of oxygen.

On the other hand, the presence of OH radicals scavengers such as ethanol leads to the decrease of P_A formation as well. This result shows that P_A precursor is mainly the intermediate entity formed by phenol reaction with OH radical.

The role of pH.

Amongst other parameters the effect of pH solution on P_A-like product formation is most important, as one can see below.

1) Acid solution (pH < 3) irradiation at doses higher than 0,2 Mrad gives during irradiation a solid product P_A which can separate as an amorphous white-yellow powder. Using NaOH aqueous solution the P_A product is readily dissolved and a yellow brownish solution is obtained. Acidifying gradually P_A alkaline solution the solid P_A product is reversibly formed.

The dry P_A powder shows a relatively poor stability turning into a dark material, but its suspension in water at an acid pH is stable. It is also easily soluble in polar solvents such as alcohols and acetone and insoluble in nonpolar solvents such as carbon tetrachloride, chloroform, benzene.

2) *Neutral solution* (pH $= 5-8$) irradiated under the same conditions turns into a yellow colloid solution which yields the solid P_A-like product at acid pH values.

The solid product formed in this case is somewhat different from that obtained in the above acid solution; it appears as a dark yellow coloured gel.

3) *Alkaline solution* (pH > 8) gets a brown-red colour by irradiation and when acidified, it turns gradually into yellow reversible colour without formation of any P_A -like solid products. This colour is attributed to the benzoquinone formed as a results of phenol oxidation.

Nature of P_A product

In order to understand the radiolytic mechanism of P_A. formation we must know the structure and the properties of this new product. As we shall see later this seems to be a "so called polymer of phenol" formed by intermolecular complex association of radiolytic oxidation products of phenol.

Infra-red spectrum of solid P_A product separated from both irradiated acid and neutral solution shows some new characteristics compared to the infra red spectrum of solid phenol.

The absorption due to the OH phenol group is considerably wider in P_A spectrum and shifted to lower frequencies. In literature[14] this fact is attributed to the OH group intermolecular association. The maximum of OH appears at 3425 cm^{-1} for pure solid phenol whereas for P_A product it appears shifted at 3390 cm^{-1} with an appreciable shoulder at 2930 cm^{-1}.

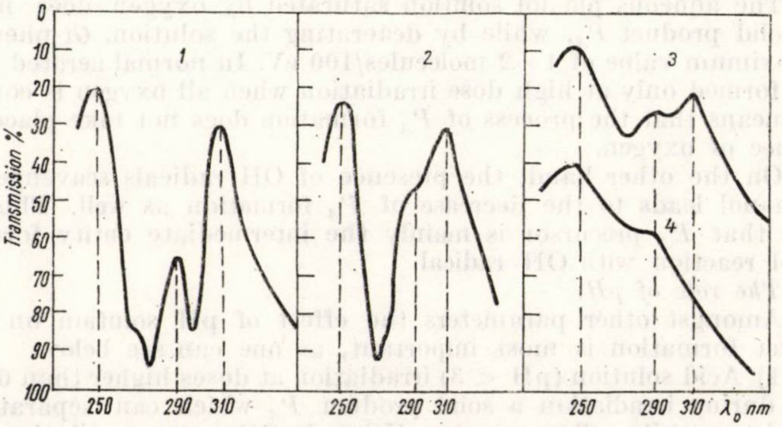

Fig. 1. — Ultra-violet spectra of 5.10^{-3}M aqueous phenol solution irradiated with 1,5 Mrad dose at different pH values but recorded at pH = 9.
1) pH ≃ 2; 2) pH ≃ 6; 3) pH ≃ 9; 4) quinhydrone aqueous solution at pH = 9.

On the other hand, the P_A product spectrum shows a new absorption at frequencies from 1650 to 1720 cm^{-1} which covers the characteristic band of benzoquinone carbonyl group.

It is known[14] that *o*-benzoquinone absorbs at 1667 cm^{-1} and *p*-benzoquinone at 1669 cm^{-1}.

This result shows that the P_A product is a complex polymer containing both phenolic and quinonoid products of phenol radiolytic oxidation. This product is probably formed by association bonds between OH group and C=O quinonoid group.

The ultra-violet spectrum of the alkaline aqueous solution of P_A essentially shows the characteristic absorptions of quinol and benzoquinone. The spectra of irradiated phenol solution at different pH values are shown in figure 1 (curves *1*, *2*, *3*). Spectrum 4 corresponds to the aqueous solution of quinhydrone. All these spectra were recorded at pH = 9.

As we can see, in spite of apparently big differences between the irradiated phenol solution 1, 2, 3, the spectra are rather similar in all cases, the maximum absorptions are at the same wavelengths of about 250, 290 and 310 nm.

---

[14] « Infrared Structural Correlation Tables », Ed. Hyden & Son. Ltd. London, 1962, table 3.

It is known from previous papers [1,11] that the 288 nm absorption is due to quionol and catechol and that of 245 nm is due to benzoquinone. The three spectra 1,2,3, differ from one another only by the absorption intensities and the relationship between them.

Using as a reference the spectrum of aqueous solution of quinhydrone, as a typical association complex of hydroquinone with benzoquinone, we can see that only the 310 nm maximum is characteristic of irradiated phenol solution but it cannot be attributed to the P_A because it appears even in the case of alkaline phenol solution (spectrum 3) where P_A is not at all formed.

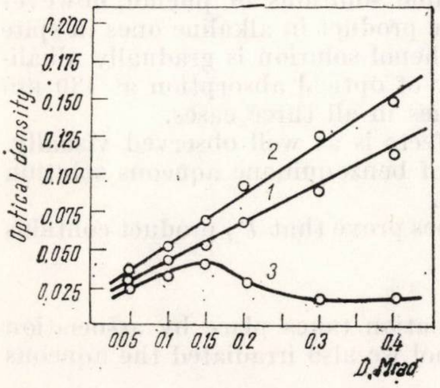

Fig. 2. — Optical absorption of 5.10^{-3}M aqueous phenol solution at $\lambda = 290$ nm as a function of irradiation dose.

1) neutral solution irradiated and measured at pH $\simeq 6$; 2) acid solution pH $\simeq 2$, measured at pH $\simeq 9$; 3) filtrate of acid solution after P_A removal, measured at pH $\simeq 9$.

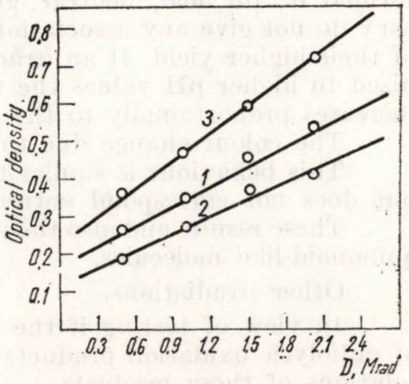

Fig. 3. — Optical absorption of 5.10^{-3} M aqueous phenol solution at $\lambda = 430$ nm recorded at pH = 9, as a function of irradiation dose.

1) acid solution pH = 2; 2) neutral solution pH = 6; 3) alkaline solution pH = 9.

Measuring optical density as a function of irradiation dose at 290 nm we obtained the results shown in figure 2.

In neutral solution we measured the optical density directly in irradiated solution (curve 1), but in acid solution we adjusted in advance the pH at about 9 in order to dissolve P_A product (curve 2). At the same time we measured the filtrate of irradiated acid solution after P_A removal and after adjusting pH to the same value (curve 3).

These results show clearly that optical absorption of 290 nm is due to the P_A product. This behaves similarly to the known radiolysis products of phenol studies before[1-10] and this fact suggests that P_A is formed from these compounds by weak intermolecular association bonds.

The visible absorption spectra of irradiated phenol solutions as above (cases 1,2,3) and of quinhydrone aqueous solution recorded at an alkaline pH are also very similar to each other. They show a broad unstructured absorption band within 360 and 640 nm which decreases gradually after 430 nm. The spectra recorded at an acid pH, in the case 3 and 4, show a maximum at 430 nm, attributed to the quinonoid like products.[1] In the case 1 and 2, because of $P_A^{\cdot}$ formation as an insoluble product at acid pH, we could measure the 430 nm optical absorption only at an alkaline pH to ensure the dissolution of the product.

Figure 3 shows the optical absorption at 430 nm as a function of irradiation dose in the three cases 1,2,3. (The measuring pH = 9). As we see from these results the quinonoid products absorbing at 430 nm are formed in all, acid, neutral and alkaline solutions of phenol, however they do not give any association P_A like product in alkaline ones in spite of their higher yield. If an irradiated phenol solution is gradually alkalinized to higher pH values the intensity of optical absorption at 430 nm increases proportionally to the pH values in all three cases.

The colour change due to this effects is as well observed visually.

This behaviour is similar to that of benzoquinone aqueous solution but does not correspond entirely to it.

These results and also the above ones prove that P_A product contains quinonoid-like molecules.

Other irradiations.

In view of testing if the P_A formation takes place by association of radiolytic oxidation products of phenol we also irradiated the aqueous solutions of these products.

The mixtures of hydroquinone, catechol with *o* and *p*-benzoquinone in aqueous solution with or without phenol, were irradiated in the same conditions as phenol solutions discussed above but no solid $P_A^{\cdot}$-like product has been obtained. This means that $P_A^{\cdot}$ is formed during radiolytic oxidation of phenol rather than from phenol radiolysis final products.

The mechanism of radiolytic association of phenol in aqueous solution.

All the results obtained in this work show that a complex radicalic association process takes place in this case. It leads to a polymer-like product of poor stability containing phenol and quinonoid molecules. The properties of P_A product show that it is not a true polymer but rather a complex association product.

The spectral data show both the similarities and differences between P_A and quinhydrone (a reference, well-known, association complex of hydroquinone and *p*-benzoquinone).

The structure of the P_A product is also more complex probably due to the fact that *o* and *p* isomers of dihidroxybenzene and benzoquinone and perhaps phenol molecules are contributing to the process.

Our analytical methods fail to establish the exact contribution of each component molecule.

By colorimetric method of *p*-nitroaniline we proved qualitatively that P_A product contains phenols with free para position (phenol and/or catechol).

In the case of high phenol concentration solutions, the phenol molecule will very likely also participate in the association because the product formed is essentially different from P_A; it is a dark yellow oil-like product.

In spite of the uncertainities connected with the real composition and structure of P_A product, our results may reveal some interesting features of this radiolytic association process.

First of all the P_A association product does not result directly by association of phenolic and quinonoid products issuing from radiolytic oxidation of phenol molecule.

As mentioned above, P_A like products do not appear by irradiating the mixtures of these compounds in their aqueous solutions.

It is very likely that P_A formation depends on some radicalic entity which appears as an intermediate of phenol radiolysis and which is subject to a pH dependent equilibrium.

It has been shown that the final radiolytic products are essentially the same at all pH values but nevertheless the process does not occur at alkaline pH.

This fact leads to the idea that radicalic entity involved in association process at an alkaline pH takes an anionic form which does not allow the formation of association bonds.

The P_A^{-} formation appears in appropriate conditions even at small irradiation doses but it could be observed only at high dose irradiation when its concentration becomes high enough to give a precipitate.

The linear dose dependence which we obtained in both acid and alkaline solution (figure 3) supports this idea because there is no induction period for the formation of radiolytic products.

All these facts lead to the conclusion that the homolytic oxidation mechanism of phenol by radicals as studied in the previous paper [1,11,15-17] should be essentially the same for P_A product because the latter one contains the phenol oxidation product.

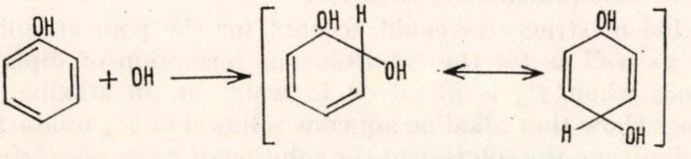

(1)

Hydroxylation of phenol starts with OH adduct formation in *ortho* and *para* position of aromatic ring (see scheme 1)

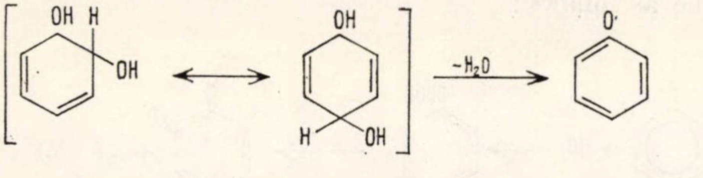

(2)

---

[15] K. Omura and T. Matsuura, *Tetrahedron*, **24**, 3475 (1968).

[16] "The Chemistry of Hydroxyl Group", Ed. S. Patai, Interscience, London, 1971, p. 327, 506, 915.

[17] N. A. Waters., « Mechanism of Oxidation of Organic Compounds », Cap. 9, Methuen Co. Ltd., London, 1964, p. 132.

OH adduct of phenol by water elimination changes into a relatively more resonance stabilized radical, fenoxyl radical (see scheme 2)

This water elimination reaction is fully reported in a pulse radiolysis work [10] as an acid-base catalysis process which could proceed, via separate OH^- and H^+ removal as follows (see scheme 3)

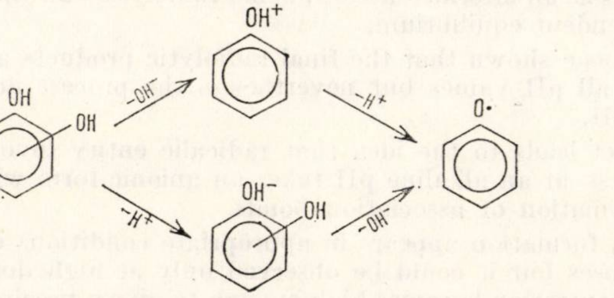

(3)

This reaction appears to be a general one for OH adducts of phenols and probably other types of aromatic compounds.[12] The issuing phenoxyl radical seems to be the radical species involved in the association process leading to the P_A-like product.

It is very difficult to know exactly what is the role of phenoxyl radical in the association process but in the absence of oxygen it is likely that phenoxyl radical reacts with the environment radicals and molecules yielding some semiquinonoid structures.

This kind of structures could account for the poor stability of the P_A product as well as for the simultaneous formation of diphenols and benzoquinones when P_A is dissolved in water at an alkaline pH. Our above findings show that alkaline aqueous solution of P_A product behaves practically similar to the solution of the solution of its unassociate phenolic and quinonoid component.

In the presence of oxygen an ozonide like structure is formed by the O_2 or HO_2 addition to the phenoxyl radical and yields directly benzoquinone as follows :

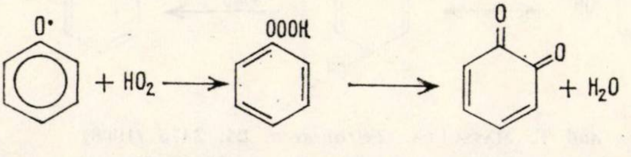

(4)

In our conditions the HO_2 radical cannot be involved in radiolytic formation of P_A product and of benzoquinone molecule which it contains. On the other hand the G(-phenol) value is too high to be explained only on the basis of OH radicals reaction. It is well known that $G_{OH} = 2{,}8$

and the phenol oxidation to benzoquinone via dihydrobenzene needs four oxidation equivalents.

This fact leads to the idea that the radiolytic formation of P_A product probably involves also another species, such as H atom radicals, H^+ ions and water molecules. The P_A^{-} product structure might result as a compromise of phenol OH group participation to both charge transfer and H bond association with $C = O$ quinonoid group.[18]

In a subsequent work we intend to make some further studies on the structure of P_A^{-}-like products because this radiolytic process seems to be of practical and theoretical importance.

---

[18] R. Foster „Organic Charge-Transfer Complexes", Organic Chemistry", vol. 15, Academic Press, London, 1969, p. 235.

Revue Roumaine de Chimie, 19, 6, 1093–1097 (1974)

POTENTIOMETRIC DETERMINATION OF DISSOCIATION CONSTANTS OF SOME AROMATIC ACETOACETAMIDES

ARJUN D. TANEJA and N. U. M. RAO

Department of Chemistry, Birla Institute of Technology and Science, PILANI (Rajasthan), India

Received July 7, 1973

Acid dissociation constants of acetoacetanilide (AAAH); acetoacet-*ortho*-toluidide (AATH); 2,4-acetoacet-xylidide (AAXH); acetoacet-*ortho*-chloroanilide (CAAAH); acetoacet-*ortho*-anisidide (OAAAH); benzoylacet-anilide (BAAH) and benzoyl-*meta*-nitroacetanilide (NBAAH) have been determined potentiometrically in 50% ethanol and at various ionic strengths. Thermodynamic dissociation constants were obtained by extrapolating to zero ionic strength. The difference in thermodynamic dissociation constants of the studied 1,3-dicarbonyl compounds has been discussed on the basis of substituent effect.

INTRODUCTION

During the last few years, studies on the complex compounds of acetoacetanilide, benzoylacetanilide and their derivatives with bivalent and trivalent metal ions have received major attention.[1–5] Harries et al. have reported the determination of ionisation constants of some acetoacetarylamides[6,7]. The present work was undertaken with a view to study the dissociation constants of acetoacetanilide (AAAH), acetoacet-*ortho*-toluidide (AATH); acetoacet-*ortho*-chloroanilide (CAAAH); 2,4-acetoacetxylidide (AAXH); acetoacet-*ortho*-anisidide (OAAAH); benzoylacetanilide (BAAH) and benzoyl-*meta*-nitroacetanilide (NBAAH) by using the Bjerrum-Calvin titration technique.[8–9]

---

[1] R. L. Dutta and A. Syamal, *J. Indian Chem. Soc.*, **44**, 381 (1967).

[2] A. Syamal and R. L. Dutta, *Indian J. Chem.*, **6**, 520 (1968).

[3] D. N. Sen and P. Umapathy, *J. Indian Chem. Soc.*, **45**, 810 (1968).

[4] A. D. Taneja and K. P. Srivastava, *J. Inorg. Nuclear Chem.*, **35**, 1397 (1973).

[5] A. D. Taneja and K. P. Srivastava, *J. Indian Chem. Soc.*, **49**, 889 (1972).

[6] H. J. Harries, S. Savage, G. Wright and N. Logan, *J. Inorg. Nuclear Chem.*, **31**, 2477 (1969).

[7] H. J. Harries and G. Wright, *J. Inorg. Nuclear Chem.*, **31**, 3149 (1969).

[8] J. Bjerrum, "Metal Amine Formation in Aqueous Solutions", P. Haase, Copenhagen, 1941.

[9] M. Calvin and K. W. Wilson, *J. Amer. Chem. Soc.*, **67**, 2003 (1945).

EXPERIMENTAL

Analytical grade acetoacetanilide, benzoylacetanilide (Aldrich Chemicals, U.S.A.), acetoacet-*ortho*-toluidide, 2,4-acetoacetxylidide, acetoacet-*ortho*-chloroanilide, and benzoyl-*meta*-nitroacetanilide (Eastman Kodak, U.S.A.) and acetoacet-*ortho*-anisidide (BDH, England) were used for experiments. All compounds were recrystallized before use. All other chemicals used were of analytical or reagent grade quality. Sodium hydroxide and perchloric acid solutions were standardised by usual methods. Beckman pH meter (model H2) with a glass calomel electrode assembly was used to determine the charge in hydrogen ion concentration. Solutions of 1,3-dicarbonyl compounds were prepared in ethanol.

Method: The dissociation constants were determined by using the Bjerrum-Calvin titration technique [8,9] as adapted by Irving and Rossotti.[10,11] For reasons of solubility, dissociation constants were determined in 50% ethanol-water mixture (by volume) and sufficient amount of $NaClO_4$ was added to give a definite overall ionic strength. A number of titration were carried out at different ionic strengths viz. 0.02, 0.05, 0.10, 0.15 and 0.20. The following mixtures were titrated in small increments, with standard 1.0M NaOH and the corresponding change in pH was noted. Necessary corrections in pH for alcoholic media were applied.

Mixture 'A': 5.0 ml of 0.20M perchloric acid + 50 ml ethanol + × ml of 1.0M $NaClO_4$ (x = = volume of $NaClO_4$ required for desired ionic strength) + required volume of water to make up the volume of the mixture to 100 ml.

Mixture 'B': 5.0 ml of 0.20M perchloric acid + 40 ml of M/100 1,3-dicarbonyl compound solution in ethanol + 10 ml of ethanol + × ml of 1.0M $NaClO_4$ + required volume of water to make up the volume of the mixture to 100 ml.

All the experiments were carried out at 22.0 ± 0.1°C.

Calculations of dissociation constants: Irving and Rossotti's method was used to calculate the dissociation constants.[10] The average number of dissociable protons attached per molecule ($\bar{n}_A$) can be determined by using the following equation

$$\bar{n}_A = Y + \frac{(v' - v'')(N^\circ + E^\circ)}{(V^\circ + v')\,T_L}$$

Y = total number of dissociable protons present in the compound
T_L = total concentration of the compound
N° = NaOH concentration
E° = initial concentration of the free acid
V° = total volume of the mixture
v' = volume of alkali used for mixture 'A'
v'' = volume of alkali used for mixture 'B'

The dissociation constants were calculated by plotting $\bar{n}_A$ against pH and using the following computational methods: [10]

(i) interpolation at half $\bar{n}_A$ values (*H*)
(ii) interpolation at various $\bar{n}_A$ values (*V*)
(iii) Least square method (*L*)

The values of thermodynamic dissociation constants were obtained by determining the dissociation constants at various ionic strengths and extrapolating to zero ionic strength. The results are recorded in Table 1.

---

[10] H. Irving and H. S. Rossotti, *J. Chem. Soc.*, **1953**, 3397.
[11] H. Irving and H. S. Rossotti, *J. Chem. Soc.*, **1954**, 2904.

Table 1

Ionisation constants of some 1,3-dicarbonyl compounds at various ionic strengths and at 22.0 ± 0.1°C

Compound	Ionic strength	Ionisation constants				Thermodynamic ionisation pK^T constants
		Interpolation at half $\bar{n}_A$ values (H)	Interpolation at various $\bar{n}_A$ values (V)	Least square method (L)	Average pK$_a$	
AAAH	0.02	10.44	10.42	10.42	10.43	10.46
	0.05	10.33	10.32	10.34	10.33	
	0.10	10.24	10.25	10.23	10.24	
	0.15	10.19	10.18	10.18	10.18	
	0.20	10.05	10.07	10.06	10.06	
AATH	0.02	10.13	10.14	10.15	10.14	10.16
	0.05	10.08	10.08	10.06	10.07	
	0.10	10.00	10.01	10.00	10.00	
	0.15	9.93	9.96	9.94	9.94	
	0.20	9.87	9.88	9.88	9.87	
AAXH	0.02	10.03	10.02	10.02	10.02	10.05
	0.05	9.98	9.97	9.99	9.98	
	0.10	9.94	9.93	9.95	9.94	
	0.15	9.90	9.88	9.98	9.89	
	0.20	9.83	9.81	9.82	9.82	
CAAAH	0.02	9.46	9.45	9.46	9.46	9.49
	0.05	9.40	9.42	9.41	9.41	
	0.10	9.36	9.35	9.34	9.35	
	0.15	9.26	9.27	9.26	9.26	
	0.20	9.17	9.18	9.16	9.17	
OAAAH	0.02	10.06	10.05	10.04	10.05	10.07
	0.05	10.02	10.03	10.02	10.02	
	0.10	9.98	9.97	9.98	9.98	
	0.15	9.95	9.95	9.94	9.95	
	0.20	9.90	9.89	9.91	9.90	
BAAH	0.02	9.44	9.43	9.42	9.43	9.46
	0.05	9.36	9.36	9.35	9.36	
	0.10	9.24	9.26	9.25	9.25	
	0.15	9.19	9.18	9.18	9.18	
	0.20	9.10	9.09	9.11	9.10	
NBAAH	0.02	9.38	9.37	9.36	9.37	9.41
	0.05	9.29	9.27	9.26	9.28	
	0.10	9.18	9.17	9.18	9.18	
	0.15	9.09	9.08	9.08	9.08	
	0.20	8.98	8.99	8.98	8.98	

RESULTS AND DISCUSSION

It can be seen from Table-I that the thermodynamic dissociation constants (pK_a^T) values of 1,3-dicarbonyl compounds studied decrease in the order AAAH $>$ AATH $>$ OAAAH $>$ AAXH $>$ CAAAH $>$ $>$ BAAH $>$ NBAAH. This trend can be traced to the presence ofdifferent substituents in the 1,3-dicarbonyl compounds under discussion. The enol form of these 1,3-dicarbonyl compounds may be represented by structure II.

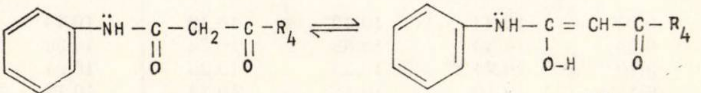

I II

$R_n = \mathrm{H}$ except $R_4 = -\mathrm{CH_3}$ (AAAH);
R_1 and $R_4 = -\mathrm{CH_3}$ (AATH);
R_1, R_3 and $R_4 = -\mathrm{CH_3}$ (AAXH);
$R_1 = -\mathrm{Cl}$ (CAAAH) and $R_4 = -\mathrm{CH_3}$ (CAAAH);
$R_1 = -\mathrm{OCH_3}$ (OAAAH) and $R_4 = -\mathrm{CH_3}$ (OAAAH)
$R_4 = -\mathrm{C_6H_5}$ (BAAH); $R_2 = -\mathrm{NO_2}$ (NBAAH), and
$R_4 = -\mathrm{C_6H_5}$ (NBAAH)

Then the dissociation processes may be denoted as.

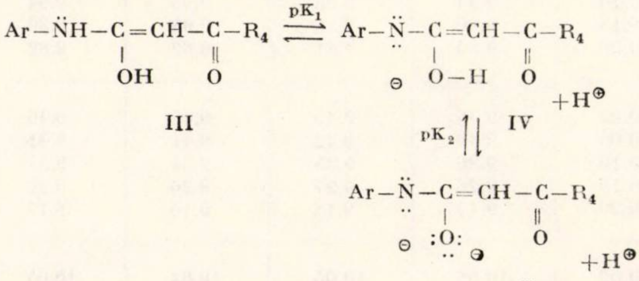

$$\underset{\mathrm{III}}{\mathrm{Ar{-}\ddot{N}H{-}C(OH){=}CH{-}C({=}O){-}R_4}} \xrightleftharpoons{pK_1} \underset{\mathrm{IV}}{\mathrm{Ar{-}\ddot{N}^{\ominus}{-}C(O{-}H){=}CH{-}C({=}O){-}R_4}} + \mathrm{H}^{\oplus} \xrightleftharpoons{pK_2} \underset{\mathrm{V}}{\mathrm{Ar{-}\ddot{N}^{\ominus}{-}C(\ddot{O}{:}^{\ominus}){=}CH{-}C({=}O){-}R_4}} + \mathrm{H}^{\oplus}$$

III IV V

Thus the first dissociation constant is due to the liberation of the proton from the $-\mathrm{NH}-$ group; in which case the value of pK_a should be sensitive to the nature of Ar (aryl). This is not in agreement with the results reported by Harries et al.[6,7] According to them,[6,7] the first dissociation step involves the proton of the enolic $-\mathrm{OH}$ group. If we assume this to be true, we cannot account for the large substituent effects (Table-I). They can only be accounted for if the liberation of the first proton from the $-\mathrm{NH}-$ groups is considered. It is well known that the phenyl group can act as both an electron donor and acceptor. If we assume that it acts as an acceptor in the cases of 1,3-dicarbonyl compounds studied, we see that it can accommodate the negative charge on nitrogen in the acid anion by delocalisation, thus facilitating the removal of proton from the $-\mathrm{NH}-$ group. The lower values of pK_a^T in the cases of AAXH, OAAAH and AATH are surprising as the substituents in these cases are quite strong electron donors; but here it is quite reasonable to attribute their low pK_a^T to steric factors being more significant than electronic factors. It is a common observation that substituent groups *ortho* to the acidic function in a phenyl ring have large and unexplained effects, always leading to an increase in acidity. This has been termed the '*Ortho Effect*'. Within these three compounds, however, the order of pK_a^T values is AATH > OAAAH > AAXH, which is the same as the order for the electron donor properties of the substituents in these cases. The lower pK_a^T values of CAAAH is explained on the basis of the electronic effects due to the ortho-substituted chlorine. In this case the steric effect is of little consequence. The presence of chlorine in the ortho-position makes the phenyl ring a stronger acceptor leading to the easier release of the proton from —NH—. This enhancement of acceptor properties of chlorine (in general halogen) substituted phenyl ring is supported by the fact that electrophilic substitution is faster in benzene than in halo-substituted benzene.

The low values of pK_a^T in the cases of BAAH and NBAAH are mainly due to the nature of R_4 (structure III) substituent viz. the phenyl group. The presence of this group permits extended conjugation in the whole molecule which stabilises the acid anion. The nitro-substituent in NBAAH at meta position is not expected to contribute significantly towards the raising or lowering of pK_a^T which is amply borne out by our results.

From these results it can be concluded that pK_a values depend mainly on the nature of the substituents attached to the aryl amido phenyl ring. A coarse linear correlation could be detected between experimental pK_a values and Hammett (σ) constant.[12] For the *ortho*-substituents (R_1 in formula I—II), σ values obtained for *ortho*-substituted benzoic acids.[13] This relationship is illustrated in Fig. 1.

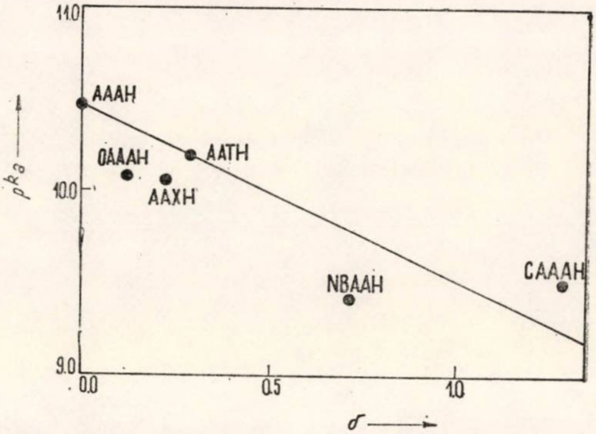

Fig. 1. — Relationship between acidity (pK_a) and Hammet substitution constants (σ) for AAAH, AATH, AAXH, CAAAH, OAAAH and NBAAH.

Acknowledgements. The authors are thankful to the authorities of B.I.T.S. for providing necessary facilities and to Dr. H. P. Tiwari, Dr. B. C. Pant and Dr. C.S.G. Prasad for helpful discussion. The help rendered by Dr. A.N. Pant is gratefully acknowledged.

---

[12] L. P. Hammett, "Physical Organic Chemistry", Chapter 7, McGraw-Hill, New York, 1940.

[13] G. B. Barlin and D. D. Perrin, *Quart. Rev.*, **20**, 75 (1966).

Revue Roumaine de Chimie, **19**, *6*, 1099–1105 (1974)

MICRODETERMINATION OF ORGANIC SULPHUR OR INORGANIC SULPHATE

S. W. BISHARA, M. E. ATTIA, and H. N. A. HASSAN

Microanalytical research Laboratories, National Research Center, Dokki, Cairo, Egypt

Received September 19, 1973

The use of methylthymol blue as a metallochromic indicator for barium has been applied for the indirect microdetermination of sulphate. Inorganic sulphate or sulphate produced from oxidative combustion of organic sulphur is precipitated using an excessive volume of Ba^{2+}. Without separation of the precipitate, excess of Ba^{2+} is titrated, in alkaline medium, against EDTA using methylthymol blue. A colour change from bright blue to light grey denotes the end point. A slight modification allows elimination of interference due to phosphorus or metals; halides (including fluoride) and nitrate do not interfere. For 56 determinations, whether in absence or in presence of one of the interfereing elements, the average percent error amounts to ±0.14; the standard deviation ranges between ±0.02 and ±0.28.

Trace amounts (0.01–0.20 %) of sulphur can be determined through reduction into hydrogen sulphide followed by absorption in sodium hydroxide or zinc acetate or in a mixture of both; the S^{2-} is then determined polarographically,[1] potentiometrically,[1] or titrimetrically.[2] On the other hand, determination of sulphur in amounts usually arising from combustion of sulphur-containing organic compounds depends mainly on oxidation to sulphate [3] followed by a gravimetric,[4,5] titrimetric,[6–11] spectrophotometric,[12] or polarographic [13] method of finish. Usually, an inorganic barium salt solution is reacted with the sulphate formed although salts of other metals, e.g., lead[14,15] have been proposed. This is not unexpected, however, since barium sulphate has the least solubility among sulphates of other metals (0.222 mg/100 ml of cold water).

---

[1] B. Philipp and H. Dautzenberg, *Analyt. Chim. Acta*, **30**, 384 (1964).

[2] M. Jaworski and E. Chromniak, *Chem. Analit.*, **11**, 705 (1966); *Analyt. Abstr.*, **14** 6862 (1967).

[3] W. Schöniger, *Mikrochim. Acta*, **1955**, 123; **1956**, 869.

[4] C. L. Ogg, *J. Assoc. Offic. Agr. Chem.*, **38**, 377 (1955).

[5] I. Lysyj and J. E. Zarembo, *Analyt. Chem.*, **30**, 428 (1958).

[6] H. Wagner, *Mikrochim. Acta*, **1957**, 19.

[7] A. Steyermark, E. A. Bass, C. C. Johnston and J. C. Dell, *Microchem. J.*, **4**, 55 (1960).

[8] K. F. Novikova, N. N. Basargin and M. P. Tayganova, *Zhur. analit. Khim.*, **16**, 348 (1961).

[9] D. C. White, *Mikrochim. Acta*, **1962**, 807.

[10] A. F. Colson, *Analyst*, **88**, 26 (1963).

[11] B. Budesinsky, *Analyt. Chem.*, **37**, 1159 (1965).

[12] I. Lysyj and J. E. Zarembo, *Microchem. J.*, **3**, 173 (1959).

[13] S. W. Bishara, *Microchem. J.*, **15**, 211 (1970).

Since evolution of the O-filled flask method of combustion,[3] the technique has been extensively used for decomposition of organosulphur compounds as evidenced from the large number of publications reported in this connection.[3,5-17] The accuracy and simplicity of the method enabled analysis of solid and liquid organic compounds of sulphur content of up, to 70%.[17] The majority of methods reported for estimation of organic sulphur depends on the fact that the sulphate formed, after fusion or absorption in an oxidising medium, can be determined gravimetrically as barium sulphate[4,5] or titrimetrically against barium ion solution.[6-11,18-21] Thorin,[6,9,10] tetrahydroxyquinone,[7] carboxyarsenazo,[8] sulphonazo III,[11,18] arsenazo III,[19] nitchromazo,[20] and chlorphosphonaze III[21] are suggested as visual indicators for barium but there seems to be some difficulty in detecting the equivalence point with most of these indicators.[11,22] Alternatively, the sulphate formed can be precipitated with Ba^{2+} and excess of the latter determined complexometrically using EDTA. Titrimetric,[3,16,17,23-25] potentiometric,[26] and amperometric[27] methods have been applied for location of the equivalence point. However, the titrimetric finish attracts much attention due to its simplicity and accuracy. Eriochrome Blact T (Erio T)[3,16,23,24] and metaphthalein[25] were applied for the microdetermination of organic sulphur after oxidation to sulphate and precipitation using an excessive volume of Ba^{2+}. However, direct chelatometric estimation of Ba^{2+} using Erio T has been criticized by Pribil[28]; even in the presence of magnesium chelatonate the method is still unsatisfactory since barium forms a somewhat weaker complex than magnesium ($\log_{MgY} K = 8.69$; $\log_{BaY} K = 7.76$).[29] Belcher, Gibbons, and West[24] determined the barium content indirectly through addition of excess of chelaton followed by back titration against magnesium chloride solution using Erio T as indicator.

In the present method, excess of barium is determined, without separation of the precipitated barium sulphate, complexometrically using methylthymol blue as the indicator. A distinct colour change, from

---

[14] H. Soep and P. Demoen, *Microchem. J.*, **4**, 77 (1960).

[15] W. Selig, *Mikrochim. Acta*, **1970**, 168.

[16] U. Bartlls and H. Höyme, *Chem. Tech.* (*Berlin*), **11**, 600 (1959).

[17] G. Vetter, *Chem. Techn* (*Leipzig*), **15**, 43 (1963).

[18] V. Nuti and P. L. Ferrarini, *Farmaco Ed. Scient.*, **24**, 930 (1969).

[19] K. Hozumi and K. Umemoto, *Microchem. J.*, **12**, 46 (1967).

[20] V. V. Mikhailoy and T. I. Tarasenko, *Zavodskaya Lab.*, **33**, 1380 (1967).

[21] A. M. Lukin and T. V. Chernysheva, *Zavodoskaya Lab.*, **34**, 1054 (1968).

[22] A. M. G. Macdonald, *Analyst*, **86**, 3 (1961).

[23] K. Yoshikawa and T. Mitsui, *Japan Analyst.*, **10**, 723 (1961).

[24] R. Belcher, D. Gibbons and T. S. West, *Chem. and Ind.* (*London*), **80**, 127 (1954).

[25] K. Hozumi and K. Mizuno, *Japan Analyst*, **10**, 383 (1961).

[26] R. N. Boos, *Analyst*, **84**, 633 (1959).

[27] E. A. Terenteva and H. V. Bernatskaya, *Zhur analit. Khim.*, **19**, 876 (1964); **21** 870 (1966).

[28] R. Pribil, "Chelometry", Chemapol Co., Praha, 1961.

[29] W. Biedermann and G. Schwarzenbach, *Chimia* (*Zürich*), **2**, 56 (1948).

bright blue to light grey, denotes the end point. Nitrogen oxides and halogens (including fluoride) has no effect on the method while interferences due to phosphorus or metals could be overcome.

EXPERIMENTAL

Reagents and materials

Amberlite IR-120 (H^+) cation exchange resin.

Ammonia, aqueous conc solution.

Barium perchlorate, exactly about 0.01 M solution prepared from the A.R. grade quality and standardised against standard EDTA solution using methylthymol blue as the indicator.[28]

Ethylenediaminetetraacetic acid, 0.02 M solution standardised against standard zinc chloride solution.[30]

Hydrogen peroxide, A.R., 35% solution.

Methylthymol blue, mixed in the ratio of 1 : 100 with solid potassium nitrate.

Potassium sulphate, standard about 0.01 M solution prepared from the M.A.R. grade quality (1 ml = 0.960 mg of sulphate).

Thorium nitrate, about 0.01 M solution.

Procedures

Burn an exactly weighed amount (3–8 mg) of the organic sample as usual [3] using 250-ml conical flask charged with 5 ml of bidistilled water plus three drops of 35% hydrogen peroxide. After combustion shake for 5 minutes. Rinse the platinum gauze out and boil to remove excess of oxidant. Continue boiling till the reaction medium is 4–5 ml in volume. While the solution is still hot, introduce, dropwise with stirring, 7 ml of 0.01 M barium perchlorate solution (total volume should not exceed 11 ml).[4] After precipitation, dilute with bidistilled water till the volume is about 40 ml then add 10 ml of conc aqueous ammonia. Before titrating against 0.02 M EDTA solution, add few milligrams of methylthymol blue and continue titration till the blue colour changes to light grey.

Carry out a blank determination.

Determination of sulphur in presence of a metal. After combustion and withdrawal of the sample holder, pass the absorption solution through a 20-cm long column of Amberlite IR-120 (H^+) cation exchange resin at a rate of 2 ml/minute. Wash the resin 5 times with 10-ml portions of bidistilled water. Receive the percolate, and washings, in a conical flask. Boil to remove excess of the peroxide and continue boiling till volume is less than 5 ml. Add barium perchlorate solution and proceed as described before.

Determination of sulphur in presence of phosphorus. After combustion, boil to remove excess of hydrogen peroxide. Cool and then add 1 ml of 1 N nitric acid to attain a pH value of about 3. Introduce 2 ml of 0.01 M thorium nitrate solution. Filter to separate the precipitated thorium phosphate. Pass the filtrate through the cation exchange resin to remove excess of thorium. Wash the resin with 10-ml portions of bidistilled water (5 times). Boil the percolate, and washings, till the total volume is less than 5 ml then continue as already described.

---

[30] H. A. Flaschka and A. J. Barnard, Jr., in "Comprehensive Analytical Chemistry", vol. 18, C. L. Wilson and D. W. Wilson (ed), Elsevier, Amsterdam, 1960, p. 336.

RESULTS AND DISCUSSION

The presence of sulphur even as a minor constituent (down to 0.001% or less) in many products whether organic, e.g., petroleum, or inorganic, e.g., metals such as copper, causes some undesirable phenomenae during the different industrial processes. It is always, therefore, preferable to have alternative procedures for its accurate determination. This implies well both when sulphur constitutes a minor or a major part of the substance. The majority of synthetic organo-sulphur compounds, on the other hand, contain 5–50% by weight as sulphur. The present method has been successfully applied for determination of 0.3–2.0 mg of sulphur present in 3–8 mg samples. Nineteen compounds (aliphatic and aromatic) containing 4–42% sulphur as sulphide, disulphide, thiol, sulphoxide, sulphonic, thiourea, dithiocarbamate, or heterocyclic were analysed (Table I). Correct results were obtained with all types of sulphur linkages. For 38 determinations, the average percent error amounts to ±0.14 with a standard deviation ranging from ±0.02 to ±0.25. The method is simple and expeditive : one determination consumes less than 25 minutes including the weighing step.

Organic sulphur is transformed quantitatively into sulphate anion by combustion in an O-filled flask charged with an oxidising absorbent (aqueous hydrogen peroxide). After removal of the excess of oxidant, a measured excess of barium is used to precipitate the sulphate. The development of conditions most suitable for complete removal of sulphate as the barium salt is undoubtedly the first limiting step for any analytical method based on the interaction between sulphate and barium. Ogg,[4] after an extensive and detailed study on the gravimetric microdetermination of sulphur, recommended a reaction medium not more than 10–11 ml in volume to ensure quantitative precipitation of barium sulphate. Since the author has been interested in a gravimetric determination, he advocated digestion for 15 minutes to coagulate the precipitate. Obviously, this is no longer important when a titrimetric finish, without separation of the precipitate, is to follow.

The excess of Ba^{2+} is titrated complexometrically against EDTA solution using methylthymol blue as the indicator.[31,32] The blue-coloured barium-methylthymol blue complex changes to light grey at the end point. The change in colour is more distinct and much easier to be detected than that noticed with some other indicators, e.g., thorin. Barium (like Ca^{2+}, Sr^{2+}, and Mg^{2+}) forms with EDTA a complex of moderate stability (Log_{BaY} K = 7.76). From Bingbombs curve,[33] describing the relation between the pH value and stability constant, it is clear that the minimum pH value at which the titration of Ba^{2+} against EDTA can be conducted is slightly above 10. Aqueous ammonia or sodium hydroxide have been first proposed [31] to attain the required alkalinity but ammonia proved more advantageous.[32] The only shortcoming underlying the use of such

---

[31] J. Körbl and R. Pribil, *Chem. Listy*, **51** 1061 (1957); *Analyt. Abstr.*, **5**, 10 (1958).

[32] J. Körbl and R. Pribil, *Coll. Czech. Chem. Comm.*, **23**, 873 (1958).

[33] R. Pribil, *Analyst*, **83**, 188 (1958).

Table 1

Microdetermination of sulphur in some organo-sulphurcompounds

Compound	Sample wt (mg)	S, %			SD σ
		Calc.	Found	Error	
Sulphanilic acid	5.210	18.52	18,65	+0.13	±0.16
	5.307		18.43	−0.09	
Cystine	2.964	26.68	26.63	−0.05	±0.05
	2.548		26.70	+0.02	
Dibenzothiophene	3.567	17.40	17.31	−0.09	±0.10
	3.275		17.45	+0.05	
α-Dinitrodiphenylamine sulphoxide	5.479	10.54	10.68	+0.14	±0.25
	5.393		10.32	−0.22	
p-Tosylphenyl-alanine	5.411	10.04	10.05	+0.01	±0.02
	5.002		10.07	+0.03	
7-Iodo-8-hydroxyquinoline-5-sulphonic acid	7.571	9.13	9.35	+0.22	±0.08
	5.664		9.24	+0.11	
Toluene-*p*-sulphonic acid	3.805	17.38	17.17	−0.21	±0.08
	4.054		17.28	−0.10	
Thiourea	4.314	42.12	42.11	−0.01	±0.16
	4.274		42.34	+0.22	
Bromophenol blue (Tetrabromophenolsulphonphthalein)	6.896	4.79	4.64	−0.15	±0.06
	6.704		4.55	−0.24	
6-Chloro-5-nitrotoluene-3-sulphonic acid	5.421	11.72	11.87	+0.15	±0.19
	4.186		12.14	+0.42	
2-Nitroso-1-naphthol-4-sulphonic acid (sodium salt)	5.298	11.65	11.54	−0.11	±0.08
	4.785		11.43	−0.22	
Sodium diethyldithiocarbamate	3.677	28.47	28.69	+0.22	±0.02
	3.630		28.71	+0.24	
Cysteine hydrochloride	5.987	19.13	19.25	+0.12	±0.16
	6.222		19.03	−0.10	
Thymol blue $C_{17}H_{30}O_5S$	6.176	6.87	6.67	−0.20	±0.12
	6.020		6.84	−0.03	
Methyl orange $C_{14}H_{14}O_3N_2SNa$	4.340	9.79	9.78	−0.01	±0.11
	5.444		9.93	+0.14	
Nitroso-R-salt	5.256	16.99	16.65	−0.34	±0.22
	3.072		16.96	−0.03	
Dithizone (Diphenylthiocarbazone)	5.346	12.51	12.76	+0.25	±0.24
	5.802		12.42	−0.09	
Methionine	4.623	21.49	21.57	+0.08	±0.08
	4.860		21.45	−0.04	
Research compound $C_{29}H_{23}O_5N_3S_2$	5.118	11.50	11.78	+0.28	±0.05
	6.370		11.72	+0.22	

Table 2

Microdetermination of sulphur in some organic compounds containing phosphorus or a metal

Compound	Sample wt (mg)	S, %			SD σ
		Calc.	Found	Error	
Triphenylphosphine sulphide	5.309	10.89	10.63	−0.26	±0.15
	5.239		10.85	−0.04	
	5.622		10.95	+0.06	
	5.497		10.95	+0.06	
Cystine + Triphenylphosphine	5.246	26.68	26.67	−0.01	±0.02
	5.362		26.64	−0.04	
p-Tosylphenylalanine Triphenylphosphine	5.042	10.04	10.09	+0.05	±0.02
	5.256		10.06	+0.02	
Methionine + Triphenylphosphine	3.180	21.49	21.45	−0.04	±0.08
	4.003		21.56	+0.07	
Cadmium pyridine thiocyanate $C_{12}H_{10}N_4S_2Cd$	3.649	16.59	16.81	+0.22	±0.28
	5.926		16.51	−0.08	
	5.799		16.20	−0.39	
	5.838		16.75	+0.16	
Zinc dibenzyldithiocarbamate	3.675	21.02	20.66	−0.36	±0.12
	3.426		20.83	−0.19	
Zinc-*p*-phenolsulphonate	6.269	11.56	11.73	+0.17	±0.24
	5.660		11.39	−0.17	

Different weights ranging from 3 to 10 mg of triphenylphosphine (P, % = 11.81) are mixed with the organo-sulphur compound before combustion.

a high pH value is that phosphate ion, if present, interferes leading to high results for sulphur. This could be overcome through a preliminary treatment with thorium nitrate solution. Addition of the latter to the acidified absorption solution (pH 3) precipitates the thorium phosphate quantitatively.[28] After separation of the precipitate, excess of Th^{4+} is removed by passage through a cation exchange resin. To the percolate, the known excess of Ba^{2+} is added, the solution made alkaline and then titrated normally for the sulphur figure. Correct results were obtained for sulphur in triphenylphosphine sulphide (4 determinations; Table 2). Owing to the lack of organo-sulphur compounds containing phosphorus, synthetic mixtures of triphenylphosphine with different sulphur compounds were analysed. In all cases correct sulphur figures were obtained. Up to 1.2 mg of phosphorus (found in about 10 mg of triphenylphosphine; cf. Table 2) did not interfere. It is expected that higher amounts of phosphorus can be tolerated provided the required excess of Th^{4+} is added.

Methylthymol blue forms blue-coloured chelates with a wide variety of metal cations whether in acidic (Bi, Pb, Th, Sc, La, Hg, Cd, Zn, Al, Fe, Ni, Co, In, Ga, U, V, Cr, rare-earth metals, Sn^{4+}, and Pd^{2+}) or in alkaline (Mn, Mg, Ca, Sr, and Ba) medium.[28] Consequently, many metals would interfere. However, passing the reaction solution, prior to precipitation, through a cation exchange resin eliminates the risk of possible interference by any of the metals mentioned above. As representative examples, three organo-sulphur compounds containing cadmium or zinc were analysed following this procedure. Correct results and sharp end points were obtained for sulphur with the three compounds (Table II). Sodium or potassium did not interfere even without treatment with the resin (Tables 1 and 3). This can be explained in view of the very low stability constants of these metal complexes with EDTA, e.g., $\log_{NaY} K = 1.66$.[28]

Table 3

Estimation of the sulphate ion

Ml 0.01 M K_2SO_4	Titre, ml EDTA	SO_4, mg		mg
		Calc.	Found	
—	⊙ 1.40	—	—	—
0.5	1.15	0.480	0.482	+0.002
1.0	0.91	0.960	0.944	−0.016
1.5	0.65	1.440	1.446	+0.006
2.0	0.40	1.920	1.927	+0.007
2.5	0.15	2.400	2.409	+0.009

⊙ Equivalent to 3 ml of barium perchlorate solution; a blank value of 0.04 ml is subtracted from the original titre of 1.44 ml.

Perchlorate, chloride, bromide, and iodide have no effect on the method; addition of up to 40 mg of chloride ion were found harmless. Since the H^+ increases the solubility of barium sulphate,[34] Cl^- was introduced as sodium chloride. Fluoride, also, did not interfere. Mixing cystine with about 8 mg of fluorobenzoic acid (1.25 mg F^-) gave accurate results for sulphur. This is not unexpected, however, since the solubility of barium fluoride is 120 mg/100 ml of cold water. Some of the compounds analysed in Table I contain nitrogen whether in the partially or fully oxidised form. However, the amount of nitrogen oxides produced after oxidative combustion of such class of compounds did not affect the sulphur figure. Furthermore, addition of as much as 50 mg of NO_3^-, added as potassium nitrate, still proved tolerable. That such high nitrate concentrations exert no influence on the result for sulphur suggests suitability of the proposed method for estimation of sulphur in nitrate explosives.

The present method hasbeen successfully applied for determination of inorganic sulphate. Obviously, the same procedure is adequate after elimination of the oxidative combustion step. Results obtained using standard potassium sulphate solution are given in Table 3.

---

[34] V. H. ALEXEYEV, "Quantitative Analysis", Mir, Moscow, p. 157 (English Translation).

Revue Roumaine de Chimie, **19**, 6, 1107 – 1111 (1974)

SEPARATION OF CREATININE FROM LEUCINE IN A PROTEIC HYDROLYSATE BY PAPER CHROMATOGRAPHY WITH A COMBINED TEMPERATURE AND STATIONARY PHASE SECTION GRADIENT*

A. CONSTANTINESCU and C. LITEANU

"Babeş-Bolyai" University, str. Arany Ianoş 11, Cluj, Romania

Received October 12, 1973

The chromatographic resolution has been largely increased by associating a temperature gradient with a complex gradient of stationary phase section, enabling thus the separation of a creatinine and a leucine mixture. The possibility of an interaction between creatinine chromatographic spots and some amino acids having close R_f values is discussed. In order to reveal the effect of the change in the stationary phase section (baffles) in the separation process, the growth effect of the chromatographic column length was calculated for the creatinine + leucine mixture.

In addition to essential amino acids, proteic hydrolysates may also include unessential amino acids, such as creatine and its internal anhydride, creatinine. Although these do not play a major part with regard to the quality of the proteic hydrolysate, their separation from complex mixtures with other amino acids of the hydrolysate raises a series of analytical difficulties, particularly due to the presence of other amino acids in significant proportions, such as leucine and isoleucine. The aim of this paper has been to solve this difficulty in the case in which leucine is present in the creatine and creatinine mixture.

WORKING PROCEDURE

The technique of isothermal ascending chromatography on Whatman No. 1 paper was first used with an *n*-butanol + acetic acid + water 4 : 1 : 5 v/v mixture as an eluent.

Samples were also chromatographed in a temperature gradient, making use of a suitable chromatographic chamber for this purpose.[1]

---

* Paper presented at the Symposium "Gradient chromatography", Cluj, September 1972

[1] C. LITEANU and S. GOCAN, *Bull. Soc. chim. France*, **1969**, 1416.

Creatine and creatinine, their mixture, a leucine + isoleucine + creatine + creatinine mixture were chromatographed in parallel, as well as the proteic hydrolysate, both on baffle-free columns and on baffled chromatograms, first isothermally and then in a temperature gradient, with similar chromatographic times. As a support of chromatographic migration, we used, under the same conditions, in addition to continuous strips (the classical form of chromatogram), also baffle-punched paper chromatograms employed in a previous work.[2]

Data obtained for samples containing only creatinine and only leucine and creatine, respectively, are listed in table 1.

Table 1

Separation of creatinine from leucine

Time (h)	t_1	t_2	t. grad (°/cm)	R_f					
				Creatinine		Leucine		Creatine	
				with baffles	baffle-free	with baffles	baffle-free	with baffles	baffle-free
1.5	25	25	0	0.80	0.66	0.78	0.62	0.54	0.48
1.5	25	55	4.3	0.91	0.80	0.83	0.67	0.62	0.56

RESULTS AND DISCUSSION

R_f 0.48 and 0.60, respectively, resulted in the case of creatine and creatinine separated and identified from proteic hydrolysate under isothermal conditions and on a baffle-free band.

The deviation of the R_f value reported in the case of creatinine ($R_f = 0.60$) versus that found in the reference sample ($R_f = 0.66$) may be explained on the basis of the interaction between the creatinine spot and amino acid spots having close R_f values, concomitantly separated from proteic hydrolysate on the same chromatographic support, filter paper. Similar interactions are in fact reported in other papers as well.[3,4]

The amino acids leucine and isoleucine, phenyl alanine, methionine and valine are present in the proteic hydrolysate with R_f values which are close to creatine and creatinine. Consequently, the interaction between creatine and creatinine spots may be discussed only in relation to these amino acids.

Although the creatine spot ($R_f = 0.48$) is located on the chromatogram between the phenyl alanine spot ($R_f = 0.52$) and the valine-methionine spot ($R_f = 0.40$), it fails to interact with the latter ones, keeping its R_f value unchanged.

We explain this finding by means of data obtained by us on the chemical composition of proteic hydrolysate.[5] Measurements of areas delimiting the chromatographic spots of essential amino acids separated from hydrolysate result in a 1.9% composition of phenyl alanine. This reduced phenyl alanine content as well as the value $\Delta R_f = 0.04$ (phenylalanine-creatine) rules out the possibility of an interaction between creatine and phenyl alanine spots.

---

[2] C. Liteanu and A. Constantinescu, *Rev. Roumaine Chim.*, **18**, 156 (1973).

[3] C. Liteanu and D. Dulămiță, *Rev. Roumaine Chim.*, **13**, 437 (1968).

[4] A. Constantinescu, Doctorate thesis, Cluj, 1971.

[5] D. Ştefănescu, A. Constantinescu, Fl. Coman and I. Ionescu, *Farmacia*, **9**, 528 (1970).

Although valine content is higher (6.2%), an interaction of the creatine spot with valine spot is unlikely in this case too, due to a difference $\Delta R_f = 0.08$, sufficient for a good delimitation of the two spots on the chromatogram.

Although $\bar{\Delta} R_f > 0.05$ (creatinine-leucine (isoleucine)), the interaction of the leucine-isoleucine spot with the creatinine one becomes possible considering the higher leucine + isoleucine content (16.8%) in the hydrolysate.

The assumed interaction was verified by further cromatographing, under the same working conditions, 0.01 ml of an aqueous solution of an artificial mixture containing 0.1% leucine + 0.1% isoleucine and 0.1% creatine + 0.1% creatinine in equal volumes, compared to the same pure reference amino acids. It has been found that while the R_f value of creatine in the mixture practically remains the same as in the case of pure creatine, the R_f of the creatinine in the mixture decreases to 0.60 against 0.66 obtained for the pure reference substance. These data may contribute to the verifying of the above-mentioned hypothesis on the spot interaction.

In view of reducing this effect which hinders separation, all the samples were also chromatographed in a temperature gradient. For $\Delta t = 30°$ ($t_1 = 25°$; $t_2 = 55°$) the distance between the site of the chromatographic spot corresponding to creatinine and that corresponding to leucine exceeds 3 cm, so that the separation of creatinine from leucine in an artificial mixture becomes evident in the temperature gradient. The chromatogram of the proteic hydrolysate also reflected two clearly delimited spots at the migration distances of pure creatinine and leucine. The chromatographic separation of creatine from leucine, hindered by the big difference of their concentrations in the composition of the proteic hydrolysate, is therefore possible in a temperature gradient.

The R_f values obtained in a temperature gradient for creatinine (0.80), leucine (0.67) and creatine (0.56), both in the case of hydrolysate and of the artificial mixture containing leucine + isoleucine + creatine + + creatinine, were similar.

To reveal the effect of the modification of the stationary phase section (baffles) on the separation process, we may calculate the growth effect of the chromatographic column length, for instance for a creatinine + leucine mixture.

The separating effect of the temperature gradient may be calculated by means of Liteanu and Gocan relations[6] :

$$\Delta(R_f)_{\text{t.grad}} = \Delta(R_f)_{\text{isot.}} \cdot \frac{V + \Delta V}{V} \tag{1}$$

---

[6] C. Liteanu and S. Gocan, *Bull. Soc. chim. France*, **1969**, 1416.

where V is the volume of the mobile phase and ΔV is the additional eluent volume leaving the chromatographic column through evaporation due to atmospheric nonsaturation and to its condensation on the surface of the eluent in the vessel.

By replacing the data from table 1 in relation (1), we obtain for the baffled paper chromatogram:

$$0.91-0.83 = 0.02\,\frac{V + \Delta V}{V}$$

respectively $V = 3\ V$.

Since $V = lA_M$ for $l = 7$ cm (after 1.5 h) (l is the height reached by the solvent front) and A_M^- is the mobile phase section, we obtain:

$$\Delta V = \Delta l A_M$$

that is:

$$3lA_M = \Delta l A_M$$

$$\Delta l = \frac{3l\,A_M}{A_M} = 3 \times 7 = 21\text{cm}$$

Similarly, we may also calculate the "chromatographic column stretching" in a temperature gradient for the continuous strip chromatogram:

$$0.80 - 0.67 = 0.04 \times \frac{V + \Delta V}{V}$$

$$0.13 = 0.04 \times \frac{V + \Delta V}{V}$$

$$0.13\ V = 0.04\ V - 0.04\,\Delta V$$

$$0.09\ V = 0.04\,\Delta V$$

$$\Delta V = 2.25\ V$$

$$0.25\ V = \Delta l A_M$$

$$\Delta l = 2.25\ \times 7 = 15.75\ \text{cm}.$$

Therefore, the baffle-punched paper chromatogram increases even more the separating effect of the temperature gradient, favouring separation which does not actually take place under the conditions of an isothermal chromatography. As the size of the stationary phase surface A_s changes due to the new form of the chromatogram, an increase in the flow rate of the stationary phase will occur in the area of baffles.

Fig. 1 illustrates the complex gradient of the stationary phase section associated with a complex gradient of the eluent flow rate.

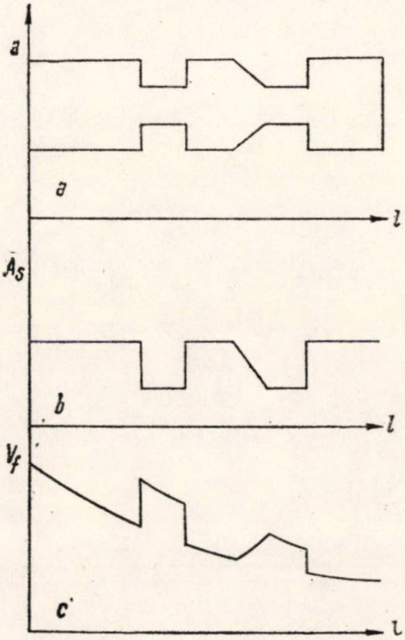

Fig. 1. Combined temperature and stationary phase section gradient: *a*, shape of chromatographic paper; *b*, variation of he support section; *c*, variation of the eluent flow rate.

CONCLUSIONS

The association of a temperature gradient with a complex gradient of the stationary phase section largely increases the chromatographic resolution, enabling thus the separation of the creatinine and leucine mixture.

Revue Roumaine de Chimie, **19**, *6*, 1113–1119 (1974)

COMPTES RENDUS

MARIA FITI, "Dozimetria chimică a radiaţiilor ionizante" (Chemical dosimetry of ionizing radiations), Ed. Academiei, Bucharest, 1973, 240 p.

The past half century has witnessed an explosive growth of interest in the radiation sources field and a significant increase of the number of physical and chemical methods of radiation dosimetry. This is due, in part, to the development of radiation physics and chemistry and, in part, to the imperative necessity of determining the radiation dose in various cases of radiation sources applications.

A monograph dealing almost exclusively with dosimetry may be justified because today the progress of nuclear techniques is closely related to the methods of measuring the radiative energy and its physical, chemical and biological effects. In this field chemical dosimetry is a preferable method because of its simplicity and this monograph intends to provide an outline of the main methods available for it. The material is organized to cover both aspects of chemical dosimetry : the fundamental principles of radiation chemistry, dosimetry and the practical applications. The first two chapters deal with general problems in radiation dosimetry and with fundamental principles of radiation chemistry. The subsequent four chapters treat the gas-phase, aqueous solution, organic liquids and solid-state chemical dosimeters with details on their preparation and on the chemical analysis methods involved. The last one gives some applications of chemical dosimetry for special problems, such as high dose-rate electron beams dosimetry, mixed radiation field dosimetry, and medical and biological dosimetry.

The monograph is distinguished by the following features :

I) it indicates the main directions towards which the subject is now moving,

2) it gives an insight into the recent literature in this field and makes references mainly to recent papers,

3) the book will be particularly suitable for chemists, physicists, radiobiologists, and physicians.

Popa Gabriela

MARIUS PROTOPOPESCU. "Teoria electronică a metalelor" (Electronic theory of metals) Ed. Academiei, Bucharest, 1973, 365 p.

The book undertakes to present a coherent way of explaining a series of physico-chemical properties of solids, with a particular emphasis on metals.

To approach this work some knowledge of classical theoretical mechanics is necessary, but to approach the quantum mechanics concepts, sufficient data are included in the book.

It begins defining, from a quantic viewpoint, the laws of electrons behaviour as microparticles in potential fields, after the notions of oprator in quantum mechanics and Schrödinger equation have been presented. The movement of free electrons, the movement of electrons in a constant potential field, the tunnel effect, potential barrier and the electron in a potential hole are treated. Then, we pass to the treatment of the hydrogen atom, analysing the problem of the electrons in a spherical symmetry potential field. Parameters *M* and *L* whose important physical significance is further explained are introduced in resolving Schrödinger equation.

Further on an approximation is presented for obtaining Schrödinger equation solutions, in the case of multielectron atoms : some physico-mathematical models of electrons behaviour in atoms are briefly presented, such as : the self-consistent field method (Hartree-Fock), variational calculus (Hylleraas), models based on perturbation theory, matricial model (Slater) and statistical model (Fermi-Dirac) and also some periodical atomic properties, among which most important are the paragraphs dealing with the electronic stucture of the atoms in relation with the Mendeleyeff's system, electronegativity (special attention is paid to Pauling's way of defining this concept) and atomic and ionic radii.

The nature of interatomic bonds is presented by a discussion of Stark effect and Zeeman effect ; then Van der Waals type bonds, quantic forces (Heitler— London method, molecular orbitals method and types of hybridization included), ionic bonds (cohesive energy of the lattice is calculated and comparison is made between theoretically and experimentally determined values) and metallic bond are presented.

The work includes an important chapter dealing with the crystalline state, providing the reader with a modern and complete description of the crystal symmetry question, using the group theory and representation theory.

The state of electrons in crystals is described according to the perfect electronic gas model (Drude-Lorentz) on grounds of the Boltzmann statistics, whose inconsistency is shown, then the quantum statistics, theory (Fermi) is described.

Zone theory comes next : plane wave functions modulated by the periodic field of the lattice are defined (Bloch functions) and zonal structure of energetic spectrum of electrons moving in periodic fields is deduced. Bidimensional and tridimensional model of zones are described and examples are given : determination of Brillouin zones for cubic and hexagonal compact networks. The interrelation between Brillouin zones shape and X-ray diffraction patterns is shown.

The connexion between metals, semiconductors and dielectrics is also briefly described, then quasifree electron theory and quasibound electron theory are described and Fermi surface is defined.

The last chapter of this work is devoted to the calculus of energetical zones structure ; the calculus methods described are cellular method (Wigner-Seitz), LCAO method (Linear Combination of Atomic Orbitals) (Bloch 1928) and OPW method (Orthogonalized Plane Wawe (Herring 1940) developed by pseudopotentials method (Harrison 1966). The physical essence of electric resistivity of metals is shown, as being the scattering of electronic waves in metals because of thermal vibrations and lattice defects.

The work is concluded by an exposition of some methods for determining Ferm surfaces ; the relative weight of the chapter, important enough, is explained by the fact that actually all electronic properties of metals are determined by the density of energetical states at the Fermi surface.

Remarkable is the very concise and clear exposition, covering a wide range of subjects in a resctricted volume.

Throughout the whole book the effort for assigning a physical meaning to mathematical concepts used is obvious ; in important cases, the calculated data are correlated with the experimentally determined ones, and the inconsistencies of the theory are shown.

The book would have been more profitable for those who need further information about the subject, if more precise references had been made.

The work does not contain a discussion of superconductivity.

V. Stancovski

"Topics in Current Chemistry" (Fortschritte der chemischen Forschung), **41**, New Concepts I, Springer-Verlag, Berlin, Heidelberg, New York, 1973

B. M. TROST, "Sulfuranes in Organic Reactions and Synthesis", p. 1—29. Trost's review covers the most recent area on sulfurane chemistry. The two classes of sulfuranes, π- and σ-sulfuranes, are today widely applied in the new organic synthesis.

After an introductory chapter, two chapters refer to π-sulfurane addition and elimination reactions and another one to σ-sulfuranes. Many examples are given in which the sulfuranes are intermediates.

The use of diphenylsulfoniumallilyde and diphenylsulfoniumcyclopropyilide in addition reactions is largely illustrated. The new synthesis of oxaspiropentanes and the subsequent one step cyclobutanone synthesis using diphenylsulfoniumcyclopropylide are exemplified. The ready availability of butyrolactones as well as of 5-mono and 5,5-disubstituted-γ-butyrolactones from the parent carbonyl compounds is described.

The paper illustrates the role σ-sulfuranes play in the reactions generating new carbon-carbon bonds such as formation of biaryls or allylaryls. The reaction of phenyllithium and vinyllithium with S-phenyldibenzothiophenium fluoroborate is a significant example. The only mechanism that is consistent with the reaction products is that by a sulfurane intermediate. Other types of reactions which find an interesting interpretation in the new concept of sulfurane chemistry are stereospecific desulfurizations and fragmentations of alicyclic three-, four-, and fivemembered ring sulfuranes.

The organic chemist will find in Trost's review a fascinating domain and an attractive tool for manipulating organic synthesis.

W. KUTZELNIGG, "Electron Correlation and Electron Pair Theories", p. 31—73. Kutzelnigg's original paper surveys the role of electron correlation energy in quantum chemical processes and develops some outstanding methods for calculating correlation energy related to electron pair theories. 70 references are cited therein.

The correlation energy is defined as the difference between the "true" Hartree-Fock energy and the "true" non-relativistic energy. Considerations are made mainly upon closed-shell states. Methods for estimating the correlation energy are discussed. The author emphasizes in particular the comparison between "experimental" and "computed" correlation energies for known molecules in order to check the reliability of the correlation energies predicted for unknown molecules. An example is given where the importance of correlation energy for quantum chemical predictions is outlined. The relationship between correlation energy and some physical quantities is shown. Correlation energy is analysed in terms of electron density and pair density. The concept of probability theory is applied to electron correlation considering statistically independent and correlated distributions. The main causes of electron correlation in space are discussed : the Pauli principle, spin and spatial symmetry requirement of the electron state and the Coulomb repulsion between the electrons. The correlation of the electrons in space for the ground state of the H_2 molecule is further examined. The method for calculating the electron correlation energy by independent electron-pair approximation (IEPA) is developed. The advantages of both pseudo-natural-orbital configuration-interaction (PNO—CI) method and coupled-electron-pair approximation (CEPA) method are demonstrated. The author also mentions some other methods for calculating electron correlation energy based on the idea of electron pairs, for instance those using antisymmetrized geminal power (AGP) or n-projected BCS function or pure perturbation theoretical methods. The use of calculated electron correlation energy values in the general methods of quantum chemistry as well as in the modern interpretation of chemical structure is outlined.

The theoretical chemist finds in Kutzelnigg's paper an excellent treatment of the most recent advances in electron correlation energy calculation.

R. G. PEARSON, "Orbital Symmetry Rules for Inorganic Reactions from Perturbation Theory", p. 75—112. Pearson's paper on symmetry rules is a new interesting treatment of this subject in which the author is responsible for a great number of achievements. The paper deals with some of the most up to date aspects of modern chemistry viewed by orbital molecular theory.

After an introductory description of basic principles of symmetry the author develops widely the concept of bond symmetry rule. Using the orbital symmetry properties of the bonds to be broken and the bonds to be made the bond symmetry rule defines an allowed reaction as a reaction in which the symmetry of the bonds that are made is the same as the symmetry of the bonds that are broken. The rule is applied to reactions of any molecularity.

Examples of the symmetry rule are given in the paper. Possible reactions of diatomic molecules with each other are first considered. This concept is extended to addition reactions to carbon-carbon double bond and to some other addition reactions.

The symmetry of possible reaction coordinates is analysed for a wide range of reactions : the unimolecular decomposition of water, the ring opening reactions of organic molecules in disrotatory and conrotatory ways and the olefin disproportionation (metathesis) reaction catalysed by transition metal complexes. The case when no elements of symmetry exist in molecules or no elements of symmetry are conserved during the reaction is analogous to forbidden transitions in electronic spectroscopy. In this case a reduction in symmetry can make a forbbiden reaction partly allowed but it still has a high activation energy. The phenomenon of partial forbiddness or allowness is explained by means of wave function properties. The allowness and forbiddness of a reaction is generalized beyond the symmetry properties. The mechanism of some important reactions of transition metal organometallic compounds (ligand migration or insertion reaction, oxidative-addition reaction and oxidative-cyclization reaction) are detailed in the terms of the general concept of the reaction path.

Pearson's paper is very useful for both theoretical and experimental chemists interested in the recent progress on symmetry subject.

H. GELERNTER, N. S. SRIDHARAN, A. J. HART, S.-C. YEN, F. W. FOWLER, H.-J. SHUE "The Discovery of Organic Synthetic Routes by Computer", p. 113—150. This paper deals with one of the most fascinating problems of up to date chemistry, the discovery of multistep organic syntheses for relatively complex structures with the aid of computer. The paper describes a computer programme written for the IBM System 360/67 called Synchem. The algorithm that governs Synchem is then discussed. Using a limited library containing information about organic reactions and reaction mechanisms, provided initially in a tabular form to the computer, a correct synthesis for some dozens structures was developed without the chemist's intervention. The particularly interesting synthesis of the polycyclic molecule of twistanone was chosen by these authors as an illustration of the way the programme works. Another example discussed is the synthesis of Vitamin A. The results obtained by means of computer are vizualized as a promising future in discovering novel and useful synthetic routes in organic chemistry.

Valerian Drăguțan

Structure and bonding. 13. Springer Verlag, Heidelberg, New York, 1973, 273 p.

The term rare earths is commonly assigned to the 14 lanthanides, representing the 4 f transition elements. The present compendium includes under the name rare earths also the 5 f transition elements (the actinides). Both series 4 f and 5 f are object of growing interest from theoretical as well as from practical point of view.

The first article deals with structural systematics in actinide fluoride complexes. R.A. Penneman and R.R. Ryan show in this survey that the 5 f electrons have little directional effects in determining actinide fluoride complex structures. Radius and charge play a predominant role in the determination of structure and coordination type. The authors note amongst the principal trends, the multiplicity of valences displayed by these elements, as well as fixed valences for upwards a dozen of consecutive elements, the large cation size and its reduction with increasing atomic number, for the tri- and tetravalent ions. Comparing actinide and lanthanide fluorides, it can be seen that these obviously large ions of both series, preclude lower than six coordination with F^- and make six coordination a rarity. But as the size diminishes with atomic number, changes are apparent (diminution of coordination number and recurrence of structures previously observed for the smaller d-transition elements).

The article is a survey of the structural characteristics displayed by the actinide fluoride complexes. The data based on powder X ray diffraction and neutron diffraction by single crystal technique were reported on coordination numbers from 6 to 9.

The next 3 articles concern the lanthanides. The shrinkage of the atomic volume as the 4 f subshell is filled, commonly referred to as "the lanthanide contraction" is due to an especially imperfect shielding from the nuclear charge of one f electron by another f electron. Unlike the d transition elements, the lanthanides show a gradual, monotonic variation in the ionic radius amounting to 20% from La^{3+} (1.06 Å) to Lu^{3+} (0.85 Å) for sixfold coordination. The influence of this varying ionic size on coordination number and coordination geometry is a unifying concept in chemistry.

In the 2nd article concerning the spectra and energy transfer of rare earths in inorganic glasses, Renata Reisfeld shows a remarkable similarity between the above mentioned phenomena in glasses and in crystals. Despite the absence of both long range and cellular disorder, the author considers that the immediate vicinity of all rare earth ions does not significantly vary from one site to another and all sites have a definite microsymmetry. Hence the optical properties of rare earths in glasses are analysed in a manner similar to that of impurities in crystals, the principal difference being that the disorder will introduce perturbative effects of these properties. The conclusions are drawn, based on a large number of experimental data.

The 3rd article, written by J. Felsche, is devoted to the crystal chemistry of the rare earths silicates. The above mentioned compounds form a chapter in the chemistry of large-cation silicates. The RE^{3+} ionic radii are ranging from 0.85 to 1.28 Å, the crystal structures consist of isolated (SiO_4) tetrahedra or groups of (Si_2O_7) or $(Si_3O_{10})$and oxygen-coordination reaches six to tenfold values.

A detailed structural description of rare-earth silicates no more complex than ternary compounds, is presented; compounds containing OH groups or molecular H_2O are not included. The data are correlated in order to show periodicity or discontinuities along the rare-earth series.

In the last article, C. K. Jørgensen discusses the inner mechanism of rare earths elucidated by photo-electron spectra. According to the arguments drawn from the refined spin-pairing energy theory, applied to the spectra of solutions and crystals and the data of photo-electron spectrometry, the writer concludes that the value $1 = 3$ certainly contributes to the specific properties (ionization energy, average radius contributing to the relatively strong photo-electron signals and to the almost monoatomic character of the $4f^9$ J-levels in compounds) of the 4 f group.

The compendium is written with the cooperation of outstanding specialists, each article ending with a minute bibliography, making the whole work very useful to specialists in the matter.

Florica Popea

Structure and bonding. 14. Springer Verlag, Berlin, Heidelberg, New York, 1973, 170 p.

This volume of the series is intended to offer informations on main topics of general interest in inorganic chemistry.

The first article is a survey of the studies concerning the structural chemistry of polynuclear transition metals. The deep colors of some members of this class of compounds has always been an attraction for the chemists. These inorganic polymers display a rich variation in their stoichiometrics and therefore in their properties. The broad range of compounds having the general composition $M_K^A\,[M^B(CN)m]_1 \times H_2O$ is due to the large number of possible combinations of transition metals M^A and M^B and particularly by considering the possible oxidation states.

The authors, Andreas Ludi and Hans Ulrich Güdel, restrict the discussion only to structural properties of crystalline cyano compounds containing $M^B(CN)_6$ groups, with the characteristic construction element, the four atomic sequence $M^A - N - C - M^B$. M^B is a transition metal, M^A a transition metal, or a metal of class B or hydrogen.

The first recorded synthetic coordination compound, Prussian blue, $Fe_4[Fe(CN)_6]_3 \times \times H_2O$ is the prototype of the polymeric cyanides. Altough a wide variety of physical methods has been used to elucidate its structure and its analogs, the characterization of their crystal structure has been accomplished only recently when suitable single crystals could be prepared.

The electronic spectra drawn from diffuse reflectance measurements of fine powders, represent in many cases a simple superposition of two isolated chromophores. The further improvement of growth of single crystals is expected to permit precise spectroscopic studies leading to a more detailed picture of the electronic structure of these compounds.

In the second article, the authors, A. Müller, E. Dieman and C. K. Jørgensen discuss the electronic spectra of tetrahedral oxo, thio and seleno complexes formed by elements of the beginning of the transition groups. The topics enclosed are : a comparison with halide complexes, molecular orbitals in tetrahedral complexes, mixed complexes with three oxide and a fourth ligand, spectra of complexes with four chalkogenide ligands, chalkogen binding ligands and photo-electron spectra.

The third article, written by B. J. Hathaway deals with the evidence for "out-of-the-plane" bonding in axial complexes of the copper (II) ion. With the continuous increasing number of axial copper (II) complexes of known crystal structure, the "effective" coordination number of the local copper (II) ion environment is becoming less certain. The stereochemistry of the copper(II) ion is commonly described as being dominated by the four coordinate square coplanar stereochemistry, involving four relatively short in plane bonds of ca. 0.2 Å. The presence of further ligands along the axial directions, at appreciably longer bond-lenghts is recognized and described by such expressions as 4+2 coordination (elongated tetragonal octahedral) or 4+1 coordination (square piramidal). However, it is not clearly expressed whether or not these fifth and sixth axial ligands are actually involved in coordination along these axial directions or simply present due to the packing of the complex in the crystal lattice. The author, B. J. Hathaway, collects together the different types of evidence for out-of-the-plane bonding in axial copper (II) complexes and assesses the different methods available for satisfying the out-of-the-plane bonding potential of a strilcty square coplanar CuL_4 chromophore.

The fourth article concerns two symmetry parametrization of the angular-overlap model of the ligand-field. Relation to the crystal-field model.

Ligand-field models have been successfully applied for parametrizing experimental results. In this paper, C. E. Schäffer treats the reparametrization of the angular-overlap model (AOM) for the case when the central ion to ligand bonds have a linear symmetry and makes a comparison with the conventional perturbation model. The author shows that an electrostatic contribution to the semiempirical parameters can never be evaluated from experiments determining parameters and discusses some of the problems associated with the zero points for the energy.

The fifth article is devoted to saltebullioscopy. B. Magyar presents the theory and some experimental results obtained with the method. He underlines its usefulness in cases when the usual ebullioscopy and cryoscopy fail to give reliable results.

The last article treats the structural chemistry and bonding in azides. Ulrich Müller considers the interatomic distances between the nitrogen atoms and other atoms of the compound, as the main criteria for the assignement of an azide to one of the three groups : ionic, coordinative or molecular azides. In this article, the author presents the structure data for the principal members of the three classes of azides mentioned above.

Each article ends with an up-to-date bibliography so that the whole work presents attraction for the specialists in the domain.

Florica Popea

of the location of the [illegible] groups. The [illegible] are [illegible] molecular orbitals in [illegible] complexes [illegible] and a basis [illegible], species of complexes [illegible] and [illegible].

The third article, [illegible] deals with [illegible] [illegible] of the [illegible] between [illegible] [illegible] [illegible] [illegible] [illegible] [illegible] [illegible] of the [illegible] [illegible] [illegible] [illegible] the [illegible] [illegible] [illegible] [illegible] [illegible] [illegible] [illegible] whether [illegible] [illegible] [illegible] [illegible] directions of [illegible] [illegible] [illegible] [illegible] [illegible] [illegible] [illegible] [illegible] [illegible].

The [illegible] [illegible] [illegible] [illegible] [illegible] [illegible] [illegible] [illegible].

[illegible] [illegible] have been [illegible] [illegible] [illegible] [illegible] [illegible] [illegible] [illegible] [illegible] [illegible] [illegible] [illegible] [illegible] [illegible] [illegible] [illegible].

The fifth article [illegible] [illegible] [illegible] [illegible] [illegible] [illegible] [illegible] [illegible] [illegible].

The last article [illegible] [illegible] [illegible] [illegible] [illegible] [illegible] in the same [illegible] [illegible] [illegible] [illegible] [illegible] [illegible].

[illegible] [illegible] [illegible] [illegible] [illegible] [illegible].

[illegible]

NOTE POUR LES AUTEURS

La *Revue Roumaine de Chimie* publie des articles en anglais, français, russe, allemand ou espagnol. Les auteurs sont priés d'envoyer des articles, notes, communications et comptes rendus inédits.

Les manuscrits seront dactylographiés à deux intervalles. Les tableaux seront dactylographiés sur feuilles séparées, de même que la légende des figures. Les diagrammes seront tracés à l'encre de Chine sur papier calque. Les tableaux et les figures seront numérotés par des chiffres arabes, en nombre strictement nécessaire. Prière de ne pas inscrire les mêmes données dans les tableaux et les figures. Les formules chimiques seront incluses dans le texte; en outre, elles seront transcrites sur des feuilles séparées. Les auteurs sont priés d'indiquer les caractères italiques (en soulignant les lettres au crayon), ainsi que tout autre caractère spécial. L'ordre des références bibliographiques sera celui de leur mention dans le texte; le nom de l'auteur sera précédé de l'initiale du prénom; les publications périodiques seront présentées suivant les prescriptions internationales. Les références seront ajoutées à la fin de l'article; elles paraîtront comme des notes, au bas de la page. Le texte sera précédé d'un résumé, comprenant 15 lignes au maximum.

L'entière responsabilité du contenu des articles appartient aux auteurs. On publie des articles dus aux collaborateurs roumains ou étrangers. Les auteurs recevront 50 tirés à part.

PRINTED IN ROMANIA

1974 OKT 1

TRAVAUX PARUS AUX ÉDITIONS DE L'ACADÉMIE DE LA RÉPUBLIQUE SOCIALISTE DE ROUMANIE

CRISTOFOR SIMIONESCU, MARGARETA GRIGORAȘ, AGATA CERNĂTESCU-ASANDEI et GHEORGHE ROZMARIN, **Chimia lemnului din România — plopul și salcia** (La chimie du bois en Roumanie — le peuplier et le saule), 1973, 228 p., 28 lei.

TIBERIU NĂȘCUȚIU, **Metode radiochimice de analiză** (Méthodes radiochimiques d'analyse), 1973, 384 p., 23 lei.

MARIA FITI, **Dozimetria chimică a radiațiilor ionizante** (La dosimétrie chimique des radiations ionisantes), 1973, 240 p., 13,50 lei.

MIHAI FLORESCU, **Eficiența economică a cercetării științifice** (L'efficience économique de la recherche scientifique), 1972, 115 p., 15 lei.

GEORGETA LĂZĂRESCU, **Sistematizarea informațiilor în chimia organică** (La systématisation des informations dans la chimie organique), 1972, 242 p., 10,50 lei.

P. BALTĂ și E. BALTĂ, **Introducere în chimia fizică a stării vitroase** (Introduction à la chimie physique de l'état vitreux), 1971, 240 p., 15,50 lei.

LYDIA-MARIA VAICUM, **Biodegrabilitatea detergenților** (La biodégrabilité des détergents), 1971, 346 p., 19,50 lei.

I. ZUGRĂVESCU et L. STOICESCU-CRIVETZ, **Polimeri heterociclici** (Polymères hétérocycliques), 1971, 190 p., 9,50 lei.

I. V. MAXIM, **Materiale nucleare** (Matériaux nucléaires), 1969, 444 p., 30 lei.

CORNEL BODEA et collab., **Tratat de biochimie vegetală**, partea I, **Fitochimie** (Traité de biochimie végétale, Ire partie, Phytochimie), Ier vol., 1964, 747 p. + 4 annexes + 2 pl., 41 lei ; IIe vol., 1965, 1962 p., 1 pl., 56 lei ; IIIe vol., 1967, 773 p., 35 lei.

CRISTOFOR SIMIONESCU et CLEOPATRA VASILIU-OPREA, **Mecanochimia compușilor macromoleculari** (La méchanochimie des composés macromoléculaires), 1967, 344 p., 23,50 lei.

V. GHEȚIE et V. MICUȘAN, **Analiza imunochimică. Teorie și practică** (Analyse immunochimique. Théorie et pratique), 1966, 369 p., 28 lei.

R. PORTOCALĂ et L. POPA, **Acizii ribonucleici celulari și virali** (Les acides ribonucléiques cellulaires et viraux), 1966, 375 p., 8 pl., 26 lei.

I.P.I. — c. 1306

43 426

Lei 25.—

F1103

REVUE ROUMAINE DE CHIMIE

REFERÁLVA

TOME 19
Nº 7
Juillet 1974

RRCHAX, 19, 7, 1121–1284 (1974)

ÉDITIONS DE L'ACADÉMIE DE LA RÉPUBLIQUE SOCIALISTE DE ROUMANIE

Rev. Roumaine Chim. 19, 7, p. 1121–1284 (1974), Bucarest

COMITÉ DE RÉDACTION

Rédacteur en chef :

I. G. MURGULESCU, membre de l'Académie de la République Socialiste de Roumanie

Rédacteurs en chef adjoints :

A. T. BALABAN et V. EM. SAHINI, membres correspondants de l'Académie de la République Socialiste de Roumanie

Collège de rédaction :

EM. BRATU, ELENA CEAUŞESCU, ECATERINA CIORĂNESCU-NENITZESCU, C. DRĂGULESCU, RALUCA RIPAN, CR. SIMIONESCU, membres de l'Académie de la République Socialiste de Roumanie; P. SPACU, membre correspondant de l'Académie de la République Socialiste de Roumanie; MARGARETA AVRAM, D. I. MARCHIDAN, I. MOLDOVAN, G. NIAC et D. SĂNDULESCU

Toute commande de l'étranger (fascicules ou abonnements) sera adressée à Întreprinderea Rompresfilatelia, Boîte Postale 2001, telex 011631, Bucarest, Romania

Les manuscrits, les livres et les revues proposés en échange, ainsi que toute correspondance seront envoyés à la rédaction

REVUE ROUMAINE DE CHIMIE
23, str. Dumbrava Roşie, Bucarest, Roumanie

ÉDITIONS DE L'ACADÉMIE DE LA RÉPUBLIQUE SOCIALISTE DE ROUMANIE
3 bis, str. Gutenberg, Bucarest

ORSZÁGOS MŰSZAKI KÖNYVTÁR ÉS DOKUMENTÁCIÓS KÖZPONT
1883

REVUE ROUMAINE
DE
CHIMIE

Tome 19, N° 7 Juillet 1974

RODICA VÎLCU and I. GĂINAR, The interaction second virial coefficient of gas mixtures. I. The nitrogen + hydrogen mixture 1123–1138

SIMONA BĂDILESCU, Simultaneous vibrational transitions. III. Collision complexes of chloroform in nonpolar solvents 1139–1143

SIMONA BĂDILESCU, Simultaneous vibrational transitions. IV. Shape of some bands of carbon disulphide and chloroform, and relaxation mechanisms in solutions 1145–1152

P. BUDRUGEAC and M. I. VASS, Some considerations concerning Gibbs free energy of gas-solid interface 1153–1155

RODICA MICU-SEMENIUC, C. GH. MACAROVICI and MAGDALENA BOSSANYI, Investigation of complex compounds with diaminobiphenyl derivatives. XXVIII. Cobalt (II) complex pseudohalides 1157–1167

A. C. BANCIU and P. SPACU, Co(II) chelates with 1-methyl-2-carbethoxy-glyoxalanil-(1)-methoxy-phenylhydrazones-(2) 1169–1178

M. BANCIU, M. ELIAN, C. DRĂGHICI and ECATERINA CIORĂNESCU, The $PdCl_2$-induced rearrangement of dibenzobullvalene into dibenzo [*g*, *h*] bicyclo [4.2.2.] deca-2,4,7,9-tetraene 1179–1184

A. T. BALABAN, Chemical graphs. XXI. Valence isomers of benzoannulenes . . . 1185–1196

I. G. DINULESCU, M. POP, F. CHIRALEU, MARGARETA AVRAM and C. D. NENITZESCU, Investigations in the cyclobutane series. XXXIII. Synthesis of *syn*-dibenzo [*c*, *g*]tricyclo [$4.2.2.0^{2,5}$] deca-3,7,9-triene. A new dibenzo $(CH)_{10}$ hydrocarbon 1197–1202

DOINA OȘIANU, ELENA NICOARĂ and C. BODEA, Inchain-epoxides of Carotenoids. IV. Metal-chloride complexes of canthaxanthin inchain-epoxides 1203–1206

M. IOVU et ECATERINA TUDOR, Formation d'isomères dans les réactions de cyclohexylation catalytique de benzène 1207–1219

P. BUCHWALD and F. DOMNARIU, The synthesis of 2,2-dichlorobenzaldoxime from 4-nitrotoluene 1221–1225

MIHAELA HILLEBRAND and M. RĂILEANU, Radical-ions. II. Nitrophenothiazine radical-ions 1227–1232

I. MOȚOC, Mathematische Darstellung der Homologie und der homologen Serien. I. Über die Beschreibung der chemischen Systeme mit Hilfe der be-Matrizen 1233–1237

I. MOȚOC, Mathematische Darstellung der Homologie und der homologen Serien. II. Behandlung in Kategorien 1239–1242

R D. DONESCU, C. HAGIOPOL, MARIANA MUNTEANU, VICTORIA DIMONIE and I. GAVĂT, Chain transfer in emulsion polymerization of vinyl acetate 1243–1250

N. COBIANU, C. BOGHINĂ, B. MĂRCULESCU, C. CINCU and I. AMĂLINEI, Copolymerization of N-vinylcaprolactam with vinylpyridines 1251–1264

ELENA HOPÎRTEAN and EUGENIA ȘTEFĂNIGĂ, Liquid membrane-electrodes. V. Electrodic behaviour of sodium tetraphenylborate in cyclohexanone to certain monovalent cations 1265–1269

R VL. MOCEAROV, GEORGETA CSOMONTANYI, CORNELIA CORICIUC and A. PANOVICI, Correlation of the porous structure to the activity and selectivity of some dehydrogenation catalysts 1271–1277

R P. ONU and V. ABABI, Rare earth ion exchange of synthetic faujasite substituted isomorphously by boron 1279–1282

COMPTES RENDUS 1283

Revue Roumaine de Chimie, **19**, *7*, 1123–1138 (1974)

THE SECOND INTERACTION VIRIAL COEFFICIENT OF GAS MIXTURES. I

THE NITROGEN + HYDROGEN MIXTURE

RODICA VÎLCU and I. GĂINAR
University of Bucharest, Laboratory of Chemical Thermodynamics

Received June 14, 1973

The construction and operation of an original installation for the measurement of pressure variations when mixing two real gases, are described. The apparatus is used for estimating the excess volumes and the second interaction virial coefficient of the $N_2 + H_2$ mixture at the standard temperature and at pressures ranging from 10 to 80 atm. Experimental data are compared with values calculated by the authors using the equations of state as well as other experimental data from the literature.

INTRODUCTION

Large number of equations of state have been proposed in order to correlate the variables $P-V-T$ for real gases. However, most of them have a purely phenomenological nature and their parameters can hardly be correlated to the molecular parameters of the systems. The only equation with a sound theoretical foundation is the equation with virial coefficients set forth by Kamerlingh Onnes,[1] that may be written as a sequence of powers, after the gas density ρ, as follows

$$\frac{PV}{RT} = 1 + B\rho + C\rho^2 + D\rho^3 + \cdots \qquad (1)$$

where B, C, D, etc. are the 2nd, 3rd, 4th, etc. ... virial coefficients.

The convergence of the series is very good for low pressure; the higher terms may be omitted since they are negligible. However, at higher pressures one should include a large number of terms in order to obtain a satisfactory agreement with the virial coefficients to be determined from experiment.

Only the second virial coefficient, B, may be obtained with fairly good accuracy; the values of C, from $P-V-T$ data, are less accurate, and the coefficient D cannot be experimentally [2] determined. Even the sign of D is uncertain, although theoretical considerations favour a positive value, except for low temperatures.

---

[1] H. Kamerlingh Onnes, *Comm. Phys. Lab. Leiden*, **71**, 74 (1901).

In the case of a gas mixture, the virial coefficients of that mixture have to be defined. For a binary system, the second virial coefficient of the mixture, B_m, is written as :

$$B_m = x_1^2 B_{11} + 2x_1 x_2 B_{12} + x_2^2 B_{22} \tag{2}$$

where B_{11} and B_{22} represent the second virial coefficient of the pure components, while B_{12} is the interaction virial coefficient, defined by the relation

$$B_{12} = 2\pi N \int_0^\infty [1 - e^{-\varphi(r_{12})/kT}]\, r_{12}^2 \, dr_{12} \tag{3}$$

where $\varphi(r_{12})$ is the interaction potential and the universal constants N, k have the well-known physical significance.

We see therefore that the second interaction virial coefficient is expressed in terms of the interaction potential $\varphi_{12}(r)$, between two neighbouring molecules belonging to different chemical species.

The interaction virial coefficient B_{12} may be theoretically calculated from rel. (3), if we know the potential $\varphi_{12}(r)$ describing the interaction between the molecules 1 and 2.

To this purpose, we make use of the empirical potentials (Lennard-Jones 6 — 12, Buckingham, Kihara, Stockmayer).

The choice of the potential function depends, of course, on the specific properties (geometrical shape, electrical magnetical properties, etc.) of the interacting molecules.

To obtain the potential parameters of the mixture, combinational rules are used, which enable us to calculate these parameters from the corresponding values of the pure components (provided that both the pure components and the mixture involve a potential of identical form).

Except for some very simple cases, these combinational rules have no theoretical foundations.

A very precise determination of the second interaction virial coefficient might serve for establishing some criteria allowing to remove the empirical character of the choice of potential functions.

In order to obtain thermodynamical excess functions and interaction virial coefficients in binary systems, we have initiated a systematic study of the thermodynamical properties of gas mixtures at high pressures.

In our experiments, we used the method advanced by Edwards and Roseveare, [3] i.e. the variant used by a group of physicists of the Kamerlingh Onnes laboratory in Leyden. [4]

---

[2] E. A. MASON and T. H. SPURLING, "The Virial Equation of State", Pergamon Press Ltd., 1969.

[3] A. E. EDWARDS and W. E. ROSEVEARE, *J. Amer. Chem. Soc.*, **64**, 2816 (1942).

[4] P. ZANDBERGEN and J. J. M. BEENAKKER, *Physica*, **33**, 343 (1967).

The method has extensively been applied at low pressures, [5-8] while for high pressures there was only one experiment, [4] where measurements have been extended up to about 100 atm.

Generally, the technique of low pressure measurements has been very much refined in the last years, with the aid of modern electronics. Nevertheless, at high pressures there are still only few contributions which describe particularly accurate techniques for estimating pressures, because of the difficulties in the operation of working devices.

If such difficulties are however overcome, the results can provide particularly rich information on the deviations of the real gases from the ideal behaviour.

PRINCIPLE OF THE METHOD

If two molecular gaseous species 1 and 2, in two containers A and B, connected to a third one C, which serves as reference vessel (with identical input pressures), are mixed under isothermal conditions, we always note the appearance of a pressure variation whose value depends, for a given pressure and temperature, on the gas nature.

Within the variant used by Edwards and Roseveare, [3] the volume variation accompanying the mixing phenomenon is measured while keeping constant the working pressure.

At high pressures the isochore conditions are preferred since it is much more convenient to measure the pressure variation by a suitable pressure gauge (manometer). To this end one may successfully use U-shaped, differential manometers, simple and highly sensitive to small pressure variations. [4] To reach the particularly high pressure required by the method (minimum $1/10^4$ from the value of the static pressure) we have used a manometer of own design, operating as a baroresistive transducer, described in this paper.

Since the dead space of the gauge is a pressure function, a small amount of gas has to be removed from the mixture so that the pressure should recover the gas filling value of the apparatus. The number of gas moles removed from the system may be found by letting the gas into a container of known volume, previously emptied, perfectly thermostated and sufficiently large to enable the application of the law of ideal gases on calculating.

CALCULATION OF THE EXCESS VOLUME WITHIN THE PROPOSED METHOD [4]

To obtain the excess volume we shall proceed as follows : consider that, prior to mixing, in container A there are n_1 moles of gas 1, and in container B, n_2 moles of gas 2, at the same pressure P and temperature T.

---

[5] A. Michels and J. H. Boerboom, *Bull. Soc. chim. belges*, **62**, 119 (1953).

[6] C. M. Knobler, *Rev. Sci. Instr.*, **38**, 184 (1967).

[7] E. M. Dantzler, C. M. Knobler and M. L. Windsor, *J. Phys. Chem.*, **72**, 676 (1968).

[8] C. M. Knobler, J. J. M. Beenakker and H. F. P. Knaap, *Physica*, **25**, 909 (1959).

If we denote the volumes of both vessels by V_A and V_B, we may write

$$V_A + V_B = n_1 V_1^0 + n_2 V_2^0 \tag{4}$$

where V_1^0 and V_2^0 are the molar volumes of pure components. Subsequent to mixing and the recovery of the initial pressure, by removing Δn moles from the system, we get

$$V_A + V_B = (n_1 + n_2 - \Delta n) \cdot V^M = n_1 V_1^0 + n_2 V_2^0 \tag{5}$$

where V^M is the molar volume of the mixture. By introducing the molar fractions x_1 and x_2, we obtain

$$\frac{\Delta n}{n_1 + n_2} = \frac{V^M - (x_1 V_1^0 + x_2 V_2^0)}{V^M} = \frac{V^E}{V^M} \tag{6}$$

where V^E is the excess volume defined by the well-known rel.

$$V^E = V^M - V^{M,id}\ ; \quad V^E = V^M - (x_1 V_1^0 + x_2 V_2^0) \tag{7}$$

The combination of the last two relations allows to remove V^M so that

$$V^E = \frac{\Delta n}{(n_1 + n_2) - \Delta n} (x_1 V_1^0 + x_2 V_2^0) \tag{8}$$

To obtain the excess volume by eq. (8), one should determine the molar volumes of pure components V_1^0 and V_2^0, the numbers of moles n_1 and n_2 contained in the two vessels A and B under certain pressure and temperature conditions, the corresponding molar fractions x_1, x_2 as well as magnitude Δn. The first six magnitudes may be obtained by equations of state chosen so that they should describe most accurately the behaviour of gases at high pressures. In our calculations we used the Beattie-Bridgemann equation. The estimation of Δn resulted from intricate and tedious experimental measurements, as described in the next section.

If we admit the effect of high order virial coefficients as being negligible, then the virial equations for gas 1, gas 2 and the mixture assume the simple form of

$$\frac{PV_1}{n_1} = RT + B_{11}P\ ; \quad \frac{PV_2}{n_2} = RT + B_{22}P\ ; \quad \frac{PV^M}{n_1 + n_2} = RT + BmP \tag{9}$$

If we consider the reference rel. (7), we get

$$V^E = B_m - x_1 B_{11} - x_2 B_{22} \tag{10}$$

Combining this equation with eq. (2) deduced by Lennard-Jones and Cook, for molecules obeying a potential with spherical symmetry, we get

$$\frac{V^E}{x_1x_2} = 2B_{12} - (B_{11} + B_{22}) \tag{11}$$

If one assumes that the real gas mixture has an ideal behaviour, then

$$B_{12} = \frac{1}{2}(B_{11} + B_{22})$$

which is similar with the lack of volume and pressure variations on mixing.

For the real gas mixtures this relation does not work and therefore the magnitude of the deviation is expressed by the excess virial coefficient E:

$$E = B_{12} - \frac{1}{2}(B_{11} + B_{22}) \tag{12}$$

The measurements have shown that for low pressures, the excess virial coefficient, E, is always positive and does not depend on the mixture composition.

Relations (11) and (12) lead to a very simple expression that stands for the dependence of the excess virial coefficient E on the excess volume V^E :

$$V^E = 2x_1x_2E \tag{13}$$

Thus, the interaction virial coefficient B_{12} is obtained due to an indirect calculation involving many stages. Assuming that x_1 and x_2 are determined with negligible error as compared to the error affecting the magnitudes B_{11}, B_{22} and V^E, the value of B_{12} is obtained with an uncertainty degree increased after each calculation stage.

We shall present our results concerning the $N_2 + H_2$ system. The choice of this system has been made from practical considerations :

1. Pure gases are easily available and cheap. The thermodynamical behaviour of the $N_2 + H_2$ mixture has also applicative significance, related to the manufacturing process of ammonia.

2. This mixture ranges among the few systems investigated at high pressures, a fact allowing to draw some conclusions referring to the operation and the accuracy of data provided by our experimental, wholly original apparatus.

The experimental apparatus (figure 1) is made up of the following parts :

1. Filling system with compressed gas
2. Gauging system for pressure inspection and measurement
3. Working device
4. Mixing system
5. Thermostating system

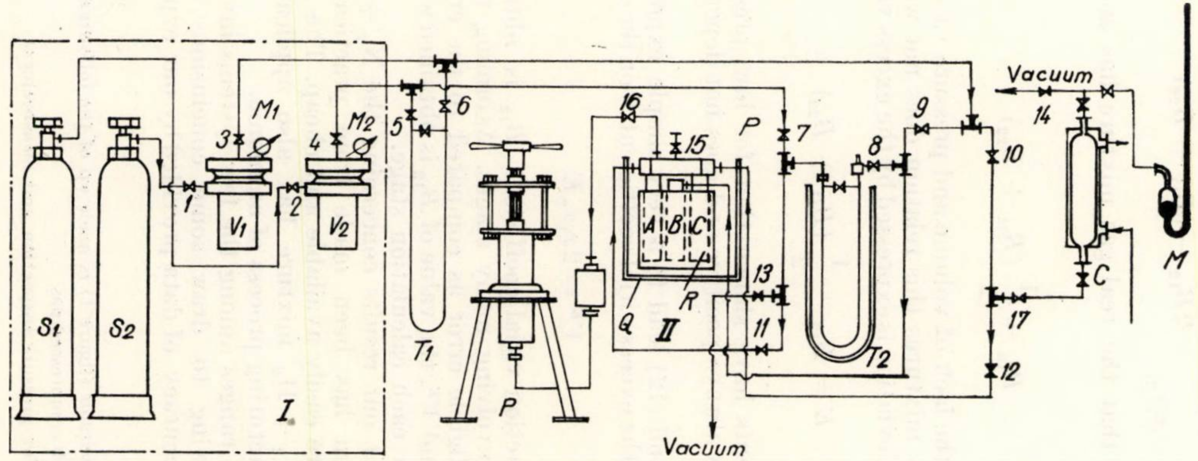
S1
S2
I
M1
3
1
V1
M2
4
2
V2
5
6
T1
P
16
15
A
B
C
Q
R
II
P
7
13
11
9
8
T2
10
17
12
Vacuum
14
C
M
Vacuum

Fig. 1. — General scheme of the installation for the measurement of pressure variations on mixing two gases.
I, Charging system; T_1, T_2, pressure trasducers; II, Mixing vessel; *M*, Hg manometer; *P*, Hg pump; *C*, thermostatic glass reservoir.

1. *The filling system* (see fig. 1) has two autoclaves, V_1 and V_2, of approximately 2 liters each, made of stainless steel with metal disc packing ; the autoclaves have inspection manometers and special input and output pressure valves.

The connection with the gas source — either compressed gas pipes, S_1 and S_2, or a compressor delivered by the firm "Andreas Hoffer" — is performed with pipes of $\varnothing_{\text{int}} = 1$ mm and $\varnothing_{\text{ext}} = 2$ mm.

Since gases are of high purity (beyond 99.8 %) no additional purification has been necessary . Gases have been, however, passed, prior to their admission into V_1 and V_2, through a cylindrical container each, of about 1 liter in volume and charged with heat-activated molecular sieves, in view of removing any water traces.

2. *The gauging system* is made up of usual manometers, with Bourdon tubes, M_1 and M_2, and of special manometers, T_1, T_2 and M. The use of the latter is required by the fact that even the finest classical manometer, with elastical element, does not allow the filling with gas pressure, with an accuracy that should go beyond a few cm Hg, at some tens of atm.

This shortcoming is removed by using special manometers, which increase the filling accuracy of two enclosures, in a differential system, up to a limit located below 0.1 mm Hg for statical pressures over 100 atm.

The fine adjustment of pressure occurs in two stages :

In a first stage we used a manometer, T_1, with a dislevelment capacity of 1.5 atm. Construction and operation : a U-shaped stainless-steel pipe is filled with a known amount of Hg, purified by successive distillations. At one of its tips a piece is axially connected with the body, where a glass rod, approximately of 1.5 m in length , is mounted. On this Hg-immersed rod is widely coiled a thin wolfram wire ($\varnothing = 0.02$ mm) with a total resistance of some hundreds ohms. The Hg level in equilibrium determines a fixed and constant value of the resistance ; the shift of the Hg level is accompanied by a decrease or an increase in the ohmic resistance.

The change in the intensity of the signal generated by a multivibrator which is applied to a resistance bridge made up of a wolfram resistance, is due to the shift of the mercury level with respect to the pressure variations.

The moment a pressure variation is recorded by the manometer, the bridge loses its balance and a signal appears that is amplified and reproduced by a loud speaker.

To cancel the signal — a situation corresponding to pressure leveling at the two arms of the manometer — one operates the input valves by introducing or removing from one of the vessels a certain amount of gas. This system allows the supply in a differential system, irrespective of the value of the static pressure, with an accuracy of ± 10 mm Hg.

The second stage which ensures the adjustment of the supply in a differential system with a ± 0.02 mm Hg accuracy is required by the characters of the method : the pressure variations, a result of the gas mixing , show values ranging from $1/10^5$ to $1/10^4$ from the static filling pressure.

The achievement of such a high accuracy is based on the use of the resistive transducer T_2 already mentioned, of original construction, where the very small pressure variations are read by means of a galvanometer with a 1×10^{-9} A/mm sensitivity.

This manometer is based on the variation of the ohmic resistance of a thin-film, metallic deposition on glass, immersed in Hg, owing to the pressure variations. The device plays the part of a null instrument in terms of pressure. Construction details and operation may be found in a distinct work. [9]

3. *The proper working apparatus* is made up of a massive stainless steel cylinder (see details in fig. 2) where three holes were applied which by their closing resulted in the two working vessels A and B and the reference vessel C. According to their construction all the

---

[9] R. Vîlcu and I. Găinar, *Rev. Roumaine Chim.* (in press).

three enclosures have the same volume (477.26 ccm). A stainless steel piece of special construction, D, with a built-in valve, E, with needle closing, ensures the sealing-off of containers A and B, enabling at the same time—due to the furrow grooves — the discharging, filing, mixing and emptying.

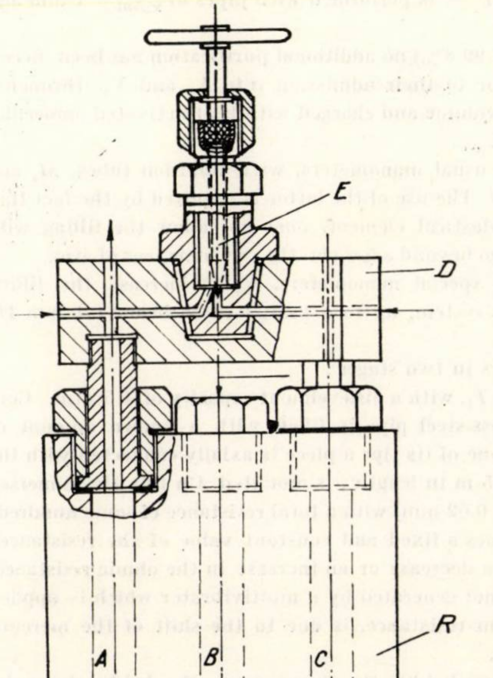

Fig. 2. — Mixing vessel (details).

A, B, Mixing cells; C, Reference cell; D, Coupling piece between the mixing vessel and charging system; E, stainless steel valve; R, massive stainless steel cylinder.

In order to obtain variations with the composition of the thermodynamical magnitudes of the mixture, use has been made of two additional pressure vessels (both with a 400 ccm volume) which may be in series connected with the main vessels by means of a metallic capillary.

The great number of connecting pipes as well as the existing valves, denoted by figures, have been a source of difficulties until we obtained a high degree of tightness. To this end we have used needle closing systems and original valves with steel ball tightening.

4. *Mixing system.* The gas mixing is carried out with a mercury pump P of own design. The electro-mechanically operated piston has an efficient volume of about 300 ccm that is enough to obtain perfect mixing after 80—100 expansions and compressions.

5. *Thermostating system.* The accuracy of the measurements depends to a considerable extent on the achievement of a best possible thermostating. To this end, the working vessel R and the additional containers (not represented in our design) are immersed in a thermostating 40 — 1 bath, Q, with paraffin oil and provided with a mighty stirrer.

Since at the measurement transducer, T_2, the dislevelment is followed on a single arm, its thermostating is required so that no fluctuations greater than ± 0.01° should be allowed. This is achieved by means of an electronic thermoregulating device with proportional action that uses, as temperature transducer, a 150-ohm Philips thermistor.

The mercury manometer, M, serves for the control of vacuum in the installation to be operated and of the small pressures in vessel C, determined by the procedure that has been chosen, as it will be seen in the next section.

PROCEDURE

The thermostating systems are actuated; on reaching the desired working temperature we start the gas filling. While all the valves are open we proceed to the connection with the vacuum installation and the vacuum is followed at the Hg manometer. After reaching a vacuum of the order of 10^{-2} mm Hg, valves 13, 15, 16 and 17 are closed; the valves at the containers with compressed gas are opened and the gas is let in carefully under permanent control by means of manometers M_1 and M_2, mounted on autoclaves.

When both manometers show the same pressure, valves 1 and 2 are shut and the fine adjustment occurs by means of baroresistive transducers T_1 and T_2. When the differential control system points out a pressure difference between the two containers of at most 0.1 mm Hg, valves 3, 4, 5, 6, 7, 8, 9 ,10, 11 and 12 are closed and valves 15 and 16 are opened.

The determination of accurate pressure variation on mixing is related particularly to a best possible mixing of the two gases. This requirement is carried out performing a great number of expansions and compressions with the mercury pump, *P*. If Zandbergen and Beenakker [4] considered only a number of 10—20 mixings, in our experiments, when the volume of the vessels is 10—15 times greater, a number of 80—100 mixings are required so that two consecutive measurements should not lead to pressure variations beyond 0.01—0.02 mm Hg.

The pressure variation is measured after completion of the mixing process. To this end we open valve 11 and the deviation from balance, prior to mixing, is read at the galvanometer mounted in the circuit of transducer T_2 and it is converted into pressure units (mm Hg) with the help of the calibration graph. The previously thermostated vessel *C* is emptied; then valves 12 and 17 are consecutively opened. Valve 17 with micrometric screw allows the finest possible removal of the gas excess into vessel *C* until the light spot of the galvanometer recovers the balance prior to mixing. With a precision cathetometer (± 0.005 mm Hg) we read on manometer *M*, the pressure in vessel *C*.

Knowing the volume ($\sim$ 2 000 cm^3) and the temperature, we calculate the number of gas moles Δn, which must be removed from the system, so that the pressure should come back to the original value.

RESULTS AND DISCUSSIONS

Besides the use of the experimental data for the evaluation of excess volumes, the calculation of the excess volumes was reconsidered for a great number of compositions and pressures, performed according to the procedure, as described in an earlier paper. [10] To this purpose a programme for a digital computer IBM 360 was used.

A set of calculated values for V^E which integrate within the pressure domain experimentally studied, are shown in table 1. These data are worth being plotted (see figure 3) in order to emphasize the perfect symmetry of the parabolas representing the V^E dependence — composition and the almost insignificant change of the excess volume with pressure. The experimental values for the excess volume given in table 2, differing somewhat from the calculated ones, show the same behaviour against pressure. Table 3 gives comparatively the values of excess volume, as obtained by us at 25°, at pressures comprised between 10 and 80 atm and variable

---

[10] R. Vîlcu and I. Găinar, *Rev. Roumaine Chim.*, **14**, 695 (1969).

Table 1

Excess volumes of the mixture $N_2 + H_2$ for various pressures and compositions at the standard temperature (l/mol)

x_{N_2} P(atm)	10	20	30	40	50	60	70	80	90	100
0.1	0.001876	0.001865	0.001851	0.001835	0.001818	0.001799	0.001777	0.001754	0.001730	0.001705
0.2	0.003333	0.003314	0.003291	0.003263	0.003231	0.003195	0.003155	0.003112	0.003067	0.003020
0.3	0.004375	0.004352	0.004321	0.004284	0.004241	0.004192	0.004139	0.004081	0.004020	0.003956
0.4	0.005002	0.004976	0.004942	0.004900	0.004851	0.004793	0.004732	0.004665	0.004593	0.004517
0.5	0.005213	0.005189	0.005155	0.005115	0.005061	0.005009	0.004937	0.004865	0.004788	0.004707
0.6	0.005009	0.004988	0.004958	0.004919	0.004872	0.004815	0.004751	0.0044681	0.004606	0.004526
0.7	0.004387	0.004372	0.004348	0.004316	0.004275	0.004227	0.004171	0.004110	0.004043	0.003971
0.8	0.003347	0.003338	0.003322	0.003300	0.003270	0.003254	0.003192	0.003145	0.003093	0.003038
0.9	0.001884	0.001883	0.001975	0.001864	0.001849	0.001929	0.001806	0.001779	0.001750	0.001718

Table 2

Excess volumes of the mixture $N_2 + H_2$ from experimental data

P(atm)	x_{H_2}	n_{H_2}	$n_{H_2}+n_{N_2}$	$\Delta n \times 10^3$ mole	ΔP mmHg	P^E mmHg	$V^{M \cdot id}$ cm^3/mole	V^E cm^3/mole
	0.423	0.202	0.477	0.644	9.65	6.34	2449.17	3.31
10	0.337	0.202	0.599	0.709	9.35	7.87	2447.56	2.89
	0.556	0.358	0.634	0.607	5,67	5.97	2451.50	2.59
	0.462	0.388	0.840	2.260	37.02	22.23	1226.06	3.30
20	0.346	0.388	1.125	2.540	28.94	25.07	1224.96	2.77
	0.611	0.408	1.160	2.468	27.35	24.28	1229.76	2.62
	0.477	0.574	1.203	4.800	77.14	47.22	820.09	3.29
30	0.348	0.574	1.650	5.150	59.70	50.71	817.79	2.55
	0.628	1.058	1.687	5.040	79.42	49.58	822.78	2.47
40	0.486	0.760	1.566	8.280	120.71	81.50	616.81	3.27
50	0.491	0.946	1.929	12.480	177.85	122.17	495.098	3.21
60	0.494	1.133	2.292	17.240	229.90	169.00	414.05	3.14
70	0,497	1.132	2.655	23.100	289.37	222.53	356.30	3.12
80	0.499	1.505	3.018	28.420	358.85	276.20	313.08	2.98

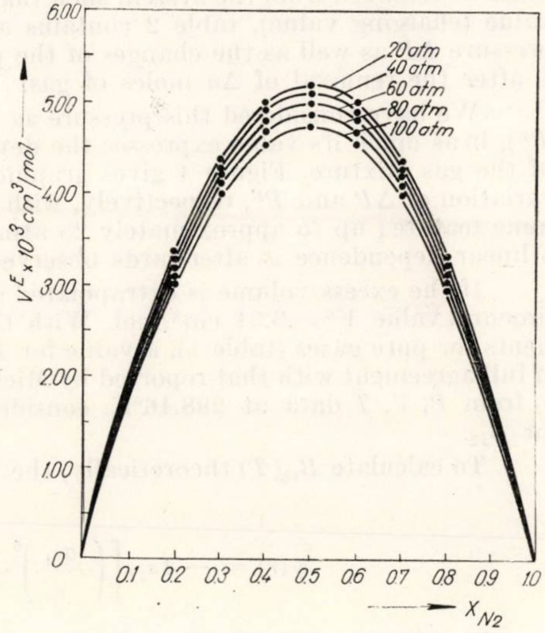

Fig. 3. — Variation of excess volume of the mixture $N_2 + H_2$ with the composition and the pressure at the standard temperature.

compositions, and the Zandbergen and Beenakker's [4] values in the same pressure interval but extrapolated to the molar ratio 0.5.

A brief examination of the presented values leads to an excellent agreement between our values and the values of the mentioned authors, [4] with the single observation that, in full concordance with the theory, our values are somewhat smaller, due to the difference of about 6° between our working temperature and that of the mentioned authors.

Table 3

Excess volumes of the mixture $N_2 + H_2$ from experimental and from comparative data

$T = 298.16$			$T = 292.16$		
P(atm)	x_{H_2}	$V^E(\mathrm{cm^3 \cdot mol^{-1}})$	(P(atm)	x_{H_2}	$V^E(\mathrm{cm^3 \cdot mol^{-1}})$
10	0.423	3.31	10	0.5	3.30
20	0.462	3.30	20	0.5	3.27
30	0.477	3.29	30	0.5	3.28
40	0.486	3.27	40	0.5	3.26
50	0.491	3.21_4	50	0.5	3.24
60	0.494	3.13_8	60	0.5	3.17
70	0.497	3.12_3	70	0.5	3.15
80	0.499	2.98	80	0.5	3.04

Besides the values of excess volumes V^E and the mole number which must be removed from the system such that the pressure reach the original value (charging value), table 2 contains also the changes of the mixing pressure ΔP as well as the changes of the pressure attained in the vessel C after the removal of Δn moles of gas.

We have considered this pressure as an excess quantity (denoted by P^E), in as much its value expresses the deviation degree from the ideality of the gas mixture. Figure 4 gives graphically the curves expressing the variation of ΔP and P^E, respectively, with pressure. Both curves have the same feature ; up to approximately 25 atm ΔP and P^E obey a curve, but a linear dependence is afterwards observed for both quantities.

If the excess volume is extrapolated at $P = 0$, one obtains an experimental value $V^E = 3.31$ cm³/mol. With this value and the virial coefficients for pure gases (table 4), a value for B_{12} of 11.1 cm³/mol is obtained, in full agreement with that reported by Michels and Wassenaar [11] (see table 5) from P, V, T data at 298.16°K, considered as the best available value for B_{12}.

To calculate $B_{12}(T)$ theoretically, the Lennard-Jones potential (6, 12)

$$\varphi(r) = -4\,\varepsilon_{12}\left[\left(\frac{\sigma_{12}}{r}\right)^{6} - \left(\frac{\sigma_{12}}{r}\right)^{12}\right] \tag{14}$$

as well as the mixing rules

$$\varepsilon_{12} = (\varepsilon_{11} \cdot \varepsilon_{22})^{1/2} \tag{15}$$

$$\sigma_{12} = (\sigma_1 + \sigma_2)/2$$

were used.

[11] A. MICHELS and T. WASSENAAR, *Appl. Sci. Res.*, A_1, 258 (1949).

Table 4

Second virial coefficients of H_2 and N_2, at the standard temperature

	$B_{298.1}(cm^3.mol^{-1})$
H_2	13.81^a
N_2	-4.71^b

[a] A. Michels, M. Goudeket, *Physica's Grav.*, 8, 347 (1941).

[b] A. Michels, H. Wouters J. de Boer, *Physica's Grav.*, 1, 587 (1934).

Table 5

Second interaction virial coefficient of the mixture $N_2 + H_2$

Mixture	T(K)	$B_{12}(cm^3.\ mol^{-1})$			
		Experim.			Calc.
$N_2 + H_2$	298.16	12.0 [a]	11.1 [b]	11.1 [c]	11.5

[a] R. Lunbeck, *Physica*, 17, 76 (1951).

[b] A. Michels and T. Wassenaar. [11]

[c] This paper.

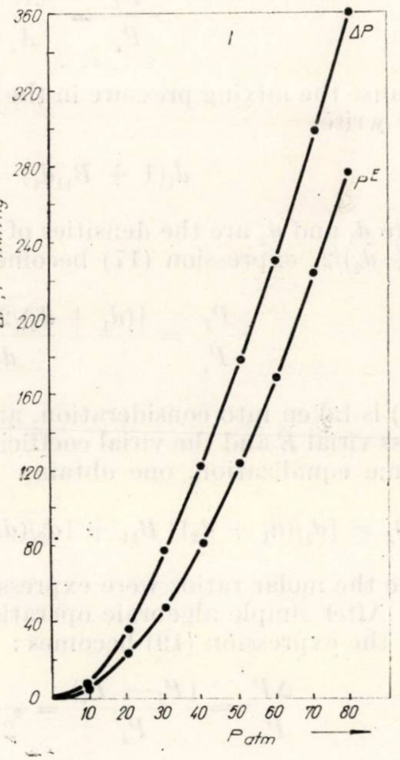

Fig. 4. — Variation of ΔP and PE with the pressure of the mixture $N_2 + H_2$, at the standard temperature.

Since the equation (3) cannot be exactly integrated, the values given in the Tables I – B from "Molecular Theory of Gases and Liquids" [12] were used.

If the values of potential parameters for hydrogen and nitrogen are used, as reported in the above-mentioned paper, [12] a theoretical value for B_{12} at 298,16° K equal to 11.5 $\mathrm{cm^3/mol}$ is obtained, in good agreement with that experimentally found.

In order to get information concerning the pressure influence on the excess virial coefficient – and hence implicitly on the interaction virial coefficient B_{12} – the experimental measurements concerning the pressure changes ΔP which occurred during the mixing of the two gases were taken into account (see table 2).

The calculation scheme (reported in ref. 8) is the following : the gas pressure at constant temperature may be expressed as a function of density and the second virial coefficient, according to the expression

$$P = A \cdot d\,(1 + Bd) \tag{16}$$

The ratio between the initial and final (after mixing) pressures could be in this case written as follows :

$$\frac{P_f}{P_i} = \frac{A_f \cdot d_f\,(1 + B_f \cdot d_f)}{A_i \cdot d_i\,(1 + B_i \cdot d_i)} \tag{17}$$

Because the mixing pressure in the two working reservoirs is the same, we may write

$$d_1(1 + B_{11}d_1) = d_2(1 + B_{22} \cdot d_2) \tag{18}$$

where d_1 and d_2 are the densities of the two gases before mixing ; if $d_f = (d_1 + d_2)/2$, expression (17) becomes

$$\frac{P_f}{P_i} = \frac{[(d_1 + d_2)/2]\ [1 + B_f\,(d_1 + d_2)/2]}{d_1\,[1 + B_{11}d_1]} \tag{19}$$

If (2) is taken into consideration, and B_{12} is expressed by means of the excess virial E and the virial coefficients for the pure gases, according to the volume equalization, one obtains

$$B_f = [d_1/(d_1 + d_2)]\,B_{11} + [d_2/(d_1 + d_2)]\,B_{22} + 2d_1\,d_2E/(d_1 + d_2)^2 \quad (2\,0$$

where the molar ratios were expressed in terms of density.

After simple algebraic operations and taking into account the result (2 0), the expression (19) becomes :

$$\frac{\Delta P}{P_i} = \frac{(P_f - P_i)}{P_i} = \frac{d_2E}{2\,(1 + B_{11}\,d_1)} + \frac{(d_2 - d_1)^2}{4\,d_1\,d_2} \tag{21}$$

---

[12] J. O. Hirschfelder, C. F. Curtiss and R. B. Bird, "Molecular Theory of Gases and Liquids", J. Wiley & Sons, Inc., N Y., 1967, p. 1114.

which may be well extended by introducing the third virial coefficients C_{111} and C_{222} as well as the third excess virial coefficient

$$E = 2\left[\frac{\Delta P}{P} - \frac{(d_1 + d_2)^2}{4\, d_1 d_2}\right]\frac{P}{RT\, d_1 d_2} + \frac{(d_1^2 - d_2^2)(C_{111} - C_{222}\, d_2)}{4\, d_1 d_2} -$$

$$- 3/4\ (d_1 F_1 + d_2 F_2) \tag{22}$$

where F_1 and F_2 represent the 3rd excess virial coefficient defined according to the following expression :

$$F_i = C_{iij} - \frac{1}{3}(2C_{iii} + C_{jjj}) \tag{23}$$

Equation (22) may be written in a more suitable form as a result of the substitution

$$d_i = P/RT - B_{ii}\left(\frac{P}{RT}\right)^2 + (2B_{ii} - C_{iii})\left(\frac{P}{RT}\right)^3 + \dots \tag{24}$$

performed for both components.
One finally obtains

$$E = \frac{2\ RT\Delta P}{P^2} - 2[(B_{11} - B_{22})^2/4 - E(B_{11} + B_{22})/2 + 3\ (F_1 +$$

$$+ F_2)/8]\frac{P}{RT} - 2\Big\{3/4\ (B_{11} - B_{22}) \times [(C_{111} - B_{11})^2 - (C_{222} - B_{22})^2] +$$

$$+ \frac{E}{2}(2B_{11} + B_{11}B_{22} + 2B_{22} - C_{111} - C_{222}) - 3[F_1(2B_{11} + B_{22}) +$$

$$+ F_2(B_{11} + 2B_{22})]\Big\} \times \left(\frac{P}{RT}\right)^2 + \cdots \tag{25}$$

If only the first two terms in the expansion are retained and neglecting the upper terms (of negligible values), after all the necessary substitutions, the following relationship is obtained for the system $N_2 + H_2$ at $T = 298.16°K$:

$$E = 0.6438 \cdot \frac{\Delta P}{n^2} - 2\left[84.732 - \frac{9E}{2}\right] . 4.08 \cdot 10^{-4}\, n \tag{26}$$

where $n = P \cdot 10^{-1}$ atm.

Table 6 summarizes the results obtained. As may be seen in this table a marked increase takes place with pressure values of the inter-reactions in pure gases compared with the mixture, such that the virial coefficients of the interaction diminish with the pressure increase.

Table 6

The dependence of the excess virial coefficient on pressure

P	10	20	30	40	50	60	70	80
E	6.21	5.96	5.52	4.86	4.58	4.11	3.80	3.61

As a final remark, one may state that only few studies have been hitherto devoted to the domain of intermolecular interactions in the binary mixtures of real gases at high pressures.

The present paper may be quoted in the line of the most recent existing researches in this field and the authors hope that the importance of the mentioned subject justifies the effort to design an original experimental equipment able to fulfil the exigency required by the exact measurements accomplished under the conditions of moderate or high pressures.

Revue Roumaine de Chimie, **19**, 7, 1139–1143 (1974)

SIMULTANEOUS VIBRATIONAL TRANSITIONS. III*

COLLISION COMPLEXES OF CHLOROFORM IN NONPOLAR SOLVENTS

SIMONA BĂDILESCU

Petrochemical Works Pitești, Romania

Received June 26, 1973

The frequencies and half-widths of the (C–H)-stretching band of chloroform in mixtures of carbon disulphide and carbon tetrachloride were determined. The formation of short-lived aggregates — collision complexes — was demonstrated and the spectral parameters of the complexes were studied.

INTRODUCTION

The conditions for the applicability of solvent shift theories based on the reaction field model have been considered, and the mechanisms of the various types of the solvation processes have been discussed by Horák et al. [1–6] The simple Kirkwood – Bauer – Magat (KBM) relation has been experimentally extensively tested and it was found to agree statisfactorily with the observed shifts in some nonpolar solvents and solvent mixtures.

In this work we wish to report the results of the study on the behaviour of C–H stretching vibration of chloroform in mixtures of two nonpolar solvents and to correlate the data thus obtained, with the general picture of the simultaneous vibrational transitions (ST) in these mixtures. [7,8]

The ability of the chloroform proton to form hydrogen bonding with various solvents is well established [9–12] and, as already known, in nonpolar

---

[*] Previous part in the series in ref. [8]

[1] R. L. Williams, *Annu. Reports Progr. Chem.*, **58**, 34 (1961).

[2] M. Horák and J. Plíva, *Spectrochim. Acta*, **21**, 911 (1965).

[3] M. Horák J. Moravec and J. Plíva, *Spectrochim. Acta*, **21**, 919 (1965).

[4] M. Horák, J. Polacova, M. Jakoubkova, J. Moravec and J. Plíva, *Coll. Czech. Chem. Comm.*, **31**, 622 (1966).

[5] M. Horák and J. Moravec, *Coll. Czech. Chem. Comm.*, **36**, 544 (1971).

[6] M. Horák and J. Moravec, *Coll. Czech. Chem. Comm.*, **36**, 2757 (1971).

[7] S. Bădilescu, *Rev. Roumaine Chim.*, **13**, 1297 (1968).

[8] S. Bădilescu, *Rev. Roumaine Chim.*, **15**, 1931 (1970).

[9] M. D. Magee and A. Walker, *J. Chem. Phys.*, **50**, 1019 (1969).

[10] C. M. Huggins and G. C. Pimentel, *J. Chem. Phys.*, **23**, 1244 (1955).

[11] W. Lis and S. Tsay, *J. Phys. Chem.*, **74**, 1037 (1970).

[12] K. Sato and A. Nishioka, *Bull. Chem. Soc. Japan*, **44**, 1506 (1971).

solvents chloroform exhibits a single, sharp (C—H)-stretching band, in the 3 000 cm^{-1} region, which is assigned to the ν_{C-H} stretching vibration. However, we ascribe this band to the primary collision complex "chloroform — nonpolar solvent", which is solvated by further molecules of the nonpolar solvent in the secondary solvation shell. When the solvent is a mixture of two nonpolar compounds, chloroform might afford collision complexes with both solvents and thus the ν_{C-H} band is in fact a double unresolved band which appears near 3 000 cm^{-1} as a broad band, owing to the presence of two kinds of complexes.

EXPERIMENTAL

The materials used were of adequate purity and were dried on molecular sieves, before use.

The infrared spectral measurements were accomplished on a Perkin — Elmer (Model 621) spectrophotometer, in the 3 000 cm^{-1} region and with a Carl Zeiss — Jena (Model UR—10) spectrophotometer (LiF optics), in the 4500 cm^{-1} region.

The wavenumber scale was rechecked before and after each measurement, by scanning the (C—H)-band of chloroform in carbon tetrachloride, at 3015 cm^{-1}. The wavenumber reproducibility was about ± 1 cm^{-1} for the sharp bands and about ± 2 cm^{-1} in the case of the broad bands.

The cells used were of 1 mm thickness (KBr windows) and the concentration of the chloroform was kept at about 0.2 mole$\cdot$l^{-1} in each mixture. The ST-bands in carbon disulphide — chloroform mixtures were measured as reported, [7,8] using a 10 mm special cell.

The binary solvent mixtures were obtained by mixing appropriate volumes of solvent, measured with a precision of $\pm$ 0.01 ml at the same temperature as in measurements.

The ε values of the solvent mixtures were calculated by means of the procedure used by Horák et al.[4] It was assumed that v_1 and v_2 are the concentrations of the two components (in volumes) and ε_1 and ε_2 — the dielectric constants of the pure components.

The relative concentrations of the collision complexes in binary solvent mixtures were estimated from the absorptivities measured in each nonpolar solvent.

RESULTS AND DISCUSSIONS

The frequency values and the half-widths of (C—H)-stretching band of chloroform, in eleven mixtures with various CS_2 — CCl_4 ratios, were measured and the results are listed in table 1. The ν_{C-H} dependence on the dielectric constant factor is approximately linear, thus confirming the validity of the KBM relation for the secondary solvation shell in which the collision complexes are clustered (fig. 1). The extrapolation to "zero field effects" ($f(\varepsilon)=0$) would bring an evidence about the properties of the complex molecule not affected by external forces. However, such an extrapolation failed, the determination of ν_0 involving a fairly long extrapolation which limits the accuracy of the values thus obtained; the case is similar with the one encountered by Horák et al. [4] in one instance.

The ST-band frequency of CS_2 — $CHCl_3$ collision complex in mixture of CS_2 and CCl_4 correlates also well with the dielectric constant of the solvent mixture (fig. 1).

It is seen that the difference between the ST-band frequency of collision complex and the value of the ν_{C-H} band in solvated complex is roughly of the same magnitude and the value is the same as that of the

Table 1

Wavenumbers and half-widths of ν_{C-H} bands of collision complexes of chloroform in solvent mixtures CS_2 – CCl_4

Mixture No.	CS_2 content of mixture, moles %	ν_{C-H} (cm^{-1})	$\Delta\nu\ ^1/_2$ (cm^{-1})	$f(\varepsilon)$
1	100.0	3003.8	16.2	0.2603
2	93.5	3005.1	17.9	0.255
3	86.1	3005.4	19.6	0.252
4	78.3	3006.4	20.8	0.249
5	70.0	3007.2	21.6	0.245
6	60.7	3009.3	24.1	0.242
7	50.8	3011.0	23.3	0.239
8	39.0	3011.8	23.3	0.235
9	26.1	3013.4	22.5	0.231
10	12.0	3014.3	21.6	0.226
11	0.0	3015.3	22.9	0.2251

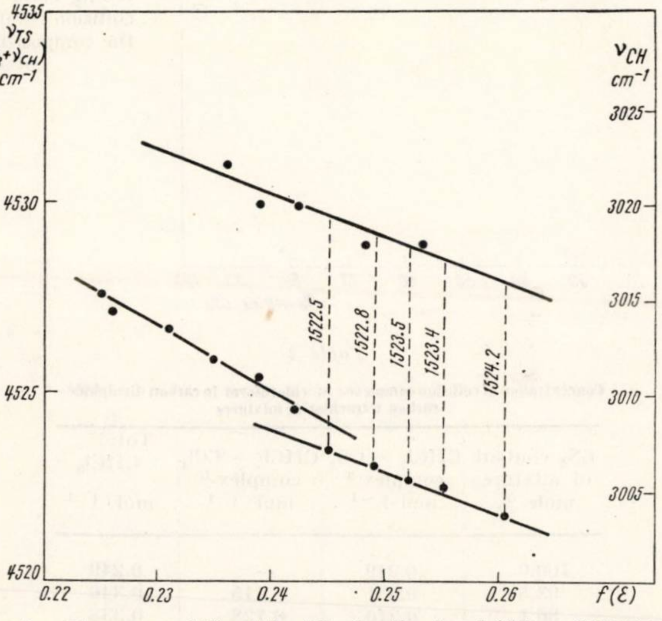

Fig. 1. —Frequency shifts of the ST-vibration band (CS_2 — $CHCl_3$) in CS_2 — CCl_4 mixtures.

asymmetrical frequency of CS_2 molecule — the partner in ST-band. This is a strong evidence for the existence of a distinct primary collision complex which is solvated by the solvent molecules in the secondary shell. The ν_{C-H} band of the individual collision complexes, and also the ST-band, shift along with the change of the composition of the secondary solvation shell according to the simple KBM relation.

Horák reported that the existence of collision complexes is in line with the lattice theories of the liquid states. [2] It is obvious that for an effective collision, the solvent molecule should reach the near vicinity of the active group in solute molecule. The distance of approach will be larger than that in case of a stable, donor—acceptor type complex. In the preceding paper of this series,[13] it was shown that the $CS_2 - CHCl_3$ collision complex possesses a certain degree of geometric orientation.

The curve in figure 2 shows that the greatest value of the chloroform ν_{C-H} half band-width, in the collision complex, was found in case of a solvent mixture containing 50—60% moles carbon disulphide.

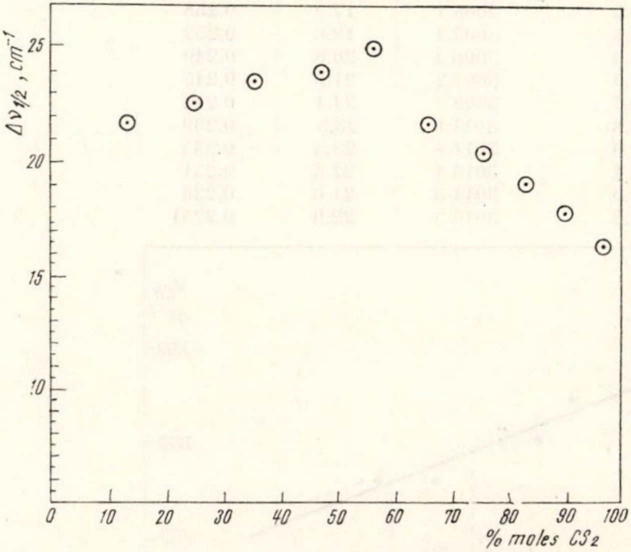

Fig. 2. — The half-width of the unresolved (C—H)-stretching band of chloroform collision complexes against the composition of solvent mixture.

Table 2

Concentration of collision complexes of chloroform in carbon disulphide—carbon tetrachloride mixtures

CS_2 content of mixture, mole %	$CHCl_3 - CS_2$ complex[a] mol·l^{-1}	$CHCl_3 - CCl_4$ complex[b] mol·l^{-1}	Total[c] $CHCl_3$ mol·l^{-1}
100.0	0.249	—	0.249
93.5	0.231	0.115	0.346
86.1	0.210	0.128	0.338
78.3	0.181	0.136	0.317
70.0	0.163	0.152	0.315
60.7	0.134	0.165	0.299
50.8	0.104	0.177	0.281
39.0	0.089	0.200	0.289
26.1	0.068	0.214	0.282
12.2	0.064	0.237	0.301
0.0	—	0.249	0.249

[a] Concentration of $CHCl_3 - CS_2$ complex calculated from experimental absorbance values of the corresponding ν_{C-H} band.

[b] Concentration of $CHCl_3 - CCl_4$ complex calculated from experimental absorbance values of the corresponding ν_{C-H} band.

[c] Analytical concentration of chloroform.

---

[13] S. Bădilescu, *Rev. Roumaine Chim.*, **16**, 9 (1971).

An estimation of the relative concentration of the chloroform in CS_2-CHCl_3 and CCl_4-CHCl_3 collision complexes in the solvent mixtures has been made assuming that both absorptivities and half-widths of the component bands are approximately constant (table 2). The results show that the assumption of a constant half-width may be only a first approximation, valid in a rather narrow range of solvent properties (mixtures 8 $\div$ 11, table 2). Nevertheless, the average deviation of the sum of the estimated concentration from the total quantity of chloroform used is 10–15%.

CONCLUSIONS

The behaviour of the chloroform ν_{C-H} spectral parameters in mixtures of nonpolar solvents afforded strong evidence for the existence of short-lived aggregates, formed by collisions between one molecule of a solute and, probably, one molecule of a nonpolar solvent. The aggregates of this kind — collision complexes — are distinct spectroscopic species, with characteristic ST-band frequencies, which are solvated in the secondary shell by a mixture of the molecules of the two solvents.

Revue Roumaine de Chimie, **19**, 7, 1131–1143 (1974)

Revue Roumaine de Chimie, 19, 7, 1145-1152 (1974)

SIMULTANEOUS VIBRATIONAL TRANSITIONS. IV[1]

SHAPE OF SOME BANDS OF CARBON DISULPHIDE AND CHLOROFORM, AND RELAXATION MECHANISMS IN SOLUTIONS

SIMONA BĂDILESCU

Petrochemical Works Pitești, Romania

Received August 9, 1973

The half band-width of ν_1 vibration of chloroform molecule in a carbon disulphide environment and also of carbon disulphide ν_3 vibration in a chloroform environment have been experimentally determined and various vibrational relaxation mechanisms have been discussed. The half band-width of the simultaneous vibrational transition (ST) corresponding to the collision complexes have been determined and the relationship between the lifetime of the complex and the relaxation times of the concurrent vibrations have been discussed.

INTRODUCTION

It is well known that apart from the vibration frequency of the IR absorption bands, the molecular interactions in liquids and in solutions are also identified by their width. [2-9] Rossi et al. [10] reported the results of the frequency and half band-width determinations of the ν_{C-H} vibration mode of haloforms in carbon disulphide and carbon tetrachloride solutions and pointed out the perturbing influence of carbon disulphide in the reorientation movements of haloforms. This influence is attributed to the shape of the carbon disulphide molecule, but the results differ from Rakov's theory. [11] Indeed, according to the latter theory, molecular reorientations should take place much easier in carbon disulphide than in carbon tetrachloride, since the reorientation barrier in carbon disulphide is much smaller ($U_{or} =$

---

[1] Part. III : S. Bădilescu, *Rev. Roumaine Chim.*, **19**, 1139 (1974).

[2] J. Vincent-Geisse and J. Jacob, *Compt. rend.*, **264**, 864 (1967).

[3] C. Alliot, M. Cameo and J. Vincent-Geisse, *Compt. rend.*, **266**, 391 (1968).

[4] J. Jacob, J. Leclerc and J. Vincent-Geisse, *Compt. rend.*, **265**, 976 (1967).

[5] Pham Van Huong, J. Jacob and J. Vincent-Geisse, *Compt. rend.*, **266**, 1117 (1968).

[6] J. Vincent-Geisse and D. Plumejfaud, *Compt. rend.*, **264**, 1404 (1967).

[7] M. O. Bulanin and M. V. Tonkov, *Optika i Spektroskopiya*, **16**, 429 (1964).

[8] J. Jacob, *Compt. rend.*, **253**, 425 (1961).

[9] J. Jacob and H. Symvoulidou, *J. Chim. phys.*, **62**, 829 (1965).

[10] I. Rossi, A. Levy and C. Haeusler, *Canad. J. Chem.*, **46**, 2103 (1968).

[11] A. V. Rakov, *Optica i Spektroskopiya*, **13**, 203 (1962).

$=1.2$ kcal/mole, *versus* 2.6 kcal/mole for carbon tetrachloride). Rossi's et al. experimental data might be interpreted as a result of the inhibition of reorientation movements of haloforms subsequently to the formation of their collision complexes with solvent molecules.[12,13]

The results of the study of half band-widths ν_{C-H}(ν_{C-D}) of haloforms ($CHCl_3$, $CHBr_3$, CHI_3 and $CDCl_3$) in carbon disulphide solutions and of the corresponding simultaneous vibrational transition (ST) bands, $\nu_{TS} = \nu_3 + \nu_1(CHX_3)$ are presented below.

EXPERIMENTAL

The half band-widths of fundamental and TS vibration bands were determined using a Carl Zeiss – Jena spectrophotometer (Model UR – 10). Accurate measurements of the geometric slit were performed at all wave numbers and the spectral slit was calculated by the following relation :

$$s = \overline{A}s' + F(s)\overline{B}$$

where $\overline{A}$ and $\overline{B}$ are constants of the spectrophotometer, $F(s) = 0.5$, and s' is the value of the geometric slit. The results of the slit measurements at the wave numbers corresponding to the fundamental bands and to ST bands are presented in table 1.

Table 1

Values of spectral slits on a Carl Zeiss – Jena (UR – 10) spectrophotometer

$\overline{\nu}$, cm^{-1}	$\overline{A}$(cm^{-1}/mm)	$\overline{B}$ (cm^{-1})	s' (mm)	s, cm^{-1}
1515	23.5	2.21	0.261	7.23
1730	35.5	2.96	0.206	8.79
1827	41.5	3.30	0.178	9.04
1970	51.0	3.80	0.128	8.43
3020	19.6	0.945	0.1562	3.53
4530	63.0	2.09	0.0954	7.00

The ν_{C-H} half band-width of chloroform in carbon disulphide was also determined by means of a Perkin-Elmer (Model 621) spectrophotometer with an automatic slit programme (1.22 cm^{-1} at 3 000 cm^{-1}), the spectral slit being determined by the relation :

$$s(cm^{-1}) = C + BW$$

in which the constants have the following values : $C = 0.141$, $B = 0.00794$ and $W = 136$.

The fundamental half band-widths were determined by the Vincent-Geisse[14] procedure, suitable for intense bands. Determinations were performed within $0.1-3.10^{-3}$ moles/cm^3 concentration ranges (thicknesses comprised between 1 and $10 \cdot 10^{-2}$ cm). The $s/\Delta\nu$ ratios varied between 0.1 and 0.15 and the half band-widths were corrected according to Ramsay tables.[15]

---

[12] S. Bădilescu, *Rev. Roumaine Chim.*, **13**, 1297 (1968).
[13] S. Bădilescu, *Rev. Roumaine Chim.*, **15**, 1931 (1970).
[14] J. Vincent-Geisse and E. Cohen de Lara-Benzaquen, *Compt. rend.*, **260**, 6319 (1965).
[15] D. A. Ramsay, *J. Amer. Chem. Soc*, **74**, 72 (1952).

The dependence of the ν_1 half band-width ($CHCl_3$) on chloroform concentration in carbon disulphide was tested by making determinations in solutions containing between 20 and 80% chloroform.

Since the spectral slit in the 1500 cm^{-1} region is 7cm^{-1}, the half band-width ν_3 (CS_2) at 1515cm^{-1} may present extremely large errors and therefore these values were not taken into consideration.

The ST half band-widths were determined by the method of extrapolation using cells with thicknesses between 6 and 30 mm. The ST half band-widths were determined in mixtures with various proportions of carbon disulphide and chloroform and the values obtained did not require corrections. The half band-widths were also determined in the presence of variable amounts of carbon tetrachloride.

RESULTS AND DISCUSSION

The results of measurements of the half band-width of ν_1 vibration are given in table 2, and those of the ST bands are listed in table 3. Fig.1 illustrates (*a*) the variation of the ST half band-width (CS_2 + $CHCl_3$) with the mixing ratio $\left(\text{m.r.} = \dfrac{\text{ml.}CHCl_3}{\text{ml.}CHCl_3 + \text{ml. }CS_2}\right)$, and curve *b* represents the same value in the presence of carbon tetrachloride ($CS_2 + CHCl_3 + CCl_4$).

Table 2

Half band-width of $\nu_1(CHCl_3)$ and $\nu_3(CS_2)$ vibrations in various molecular environments

Compound	Vibration	Solvent	Frequency cm^{-1}	$\Delta\nu_{1/2}$ cm^{-1}
Chloroform	$\nu_1(C-H)$	CCl_4	3015	16.5
Chloroform	$\nu_1(C-H)$	CS_2	3003	12*, 14
Bromoform	$\nu_1(C-H)$	CS_2	3022	12.4
Iodoform	$\nu_1(C-H)$	CS_2	3003	12.7
Carbon disulphide	$\nu_3(CS_2)$	$CHCl_3$	1515	13.4

* The value has been determined on a Perkin-Elmer (Model 621) spectrophotometer.

The results show that $\Delta\nu_{1/2}$ is practically independent of the concentration of the solution, which proves that the relaxation of this vibration in a carbon disulphide medium is of a reorientational type. The results are quite close to other experimental data[10,16,17] and also to the results of the determination of the vibrational relaxation time from dielectric relaxation measurements.[18]

---

[16] M. T. Forel, J. P. Leicknam and M. L. Josien, *J. Chim. phys.*, **57**, 1103 (1960).
[17] R. B. Bernstein and M. Tamres, *J. Chem. Phys.*, **23**, 2201 (1955).
[18] A. Spernol and K. Wirtz, *Z. Naturforsch.*, **8A**, 522 (1953).

Table 3

Half band-width of ST vibration

Collision complex	ν_{ST} cm^{-1}	$\Delta\nu_{1/2\,ST}$ cm^{-1}
$\nu_3(CS_2) + \nu_1(CHCl_3)$	4533	56
$\nu_3(CS_2) + \nu_1(CHBr_3)$	4538	40
$\nu_3(CS_2) + \nu_1(CHI_3)$	4517	38
$\nu_3(CS_2) + \nu_1(CDCl_3)$	3760	33
$\nu_3(CS_2) + \nu_2(CCl_4)$	1734	32
$\nu_3(CS_2) + \nu_4(CCl_4)$	1828	38
$\nu_3(CS_2) + \nu_1(CCl_4)$	1927	43

According to Rakov's theory, [11] the relaxation time gives the time during which the molecule maintains a given orientation and is related to the half band-width value by the relation :

$$\Delta\nu_{1/2} = \frac{1}{c\pi\tau} \qquad (1)$$

By calculating the relaxation times of ν_1 vibration of the chloroform we find $\tau = 0.64 \cdot 10^{-12}$ sec. in carbon tetrachloride and $\tau = 0.88 \cdot 10^{-12}$ sec. in carbon disulphide ; these values attest a hindrance of the reorientation in carbon disulphide. The relaxation time (the hindrance) is longer in CS_2 than in CCl_4 (inert solvent) but it is significantly more reduced than in the case in which complexes are formed by hydrogen bonds (for instance in benzene) where the relaxation times range within 1.5 and $2 \cdot 10^{-12}$ sec. [19]

With regard to vibration ν_3 (CS_2) in a chloroform environment some authors interpreted this half band-width in terms of a reorientational relaxation. [3] However, some recent data [20] provided evidence in support of a relaxation mechanism in which the major weight is represented by the vibrational relaxation of the "resonance between identical vibrators" type, a relaxation which is dependent on the solution concentration. Kakimoto and Fujiyama [20] calculated the band-width resulted from this type of relaxation, applying Valiev's formula [21]

$$\Delta\nu_{1/2} = \frac{c}{\pi}\sqrt{\rho\,\frac{c_m}{3W_m}\cdot S\cdot\Gamma} \qquad (2)$$

in which ρ is the density of the dissolved substance, c_m — the molar concentration in solution, W_m is the molecular weight and Γ the absolute intensity of the absorption band (expressed in cm^2 · mol^{-1}).

---

[19] O. F. Bezrukov, M. F. Vuks and V. A. Suchkov, *Optica i Spektroskopiya, Sbornik Statei*, **II**, *Izdat. Akad. Nauk. S.S.S.R., Leningrad*, **1963**, 234.

[20] Masao Kakimoto and Tsunetake Fujiyama, *Bull. Chem. Soc. Japan*, **45**, 2970 (1972).

[21] K. A. Valiev, *Optika i Spektroskopiya*, **11**, 253 (1961).

Vincent-Geisse [22] developed a formula for the calculation of a band-width when passing from the solution in an inert solvent to the state of pure liquid and explained this width by a coupling between identical vibrators:

$$\delta(\Delta\nu_{1/2}) = 0.04 \cdot 10^3 \, \frac{d}{M} \cdot \frac{A}{g\,\nu_0} \qquad (3)$$

In formula (3), A is the intensity of the band corresponding to the isolated (gaseous) molecule, expressed in *darks*, ν_0 — the wavenumber of the band of the molecule in an inert solvent, g is the vibrational degenerescence degree and 0.04 is a coupling coefficient (calculated by the author by using a large number of data from the literature). Thus, for carbon disulphide—pure liquid — , the author found [22] a broadening by 24 cm^{-1} of the band ν_3 (the total width of the band being 30 cm^{-1}, as compared to 6 cm^{-1} in carbon tetrachloride solution).

We considered of interest to apply formula (3) in order to calculate the ν_3 band-width of carbon disulphide in liquid mixtures with chloroform, introducing in the formula the molar fraction of the carbon disulphide from the respective solution (which expresses in fact the percentage of identical oscillators which may be coupled and which relax through resonance). The results obtained in this manner are compared with Kakimoto and Fujiyama's[20] experimental data in table 4, and a very good agreement is observed in the concentration range from 0.6 to 50%. In the case of a relaxation of this type, the relaxation time would depend only on the number of the identical oscillators and on the absolute intensity of the vibration corresponding to the isolated molecule rather than on the molecular environment and on its characteristics. For this reason, for the calculation of the relaxation time it is more appropriate to use the intensity of the vibration of the isolated molecule than that of the value of the intensity in the respective solvent, as postulated by Valiev. [21] Although some data in the literature referring to the ν_3 half band-width of CS_2 in various molecular environment support this idea, [23] the extreme scarcity of data in this field does not allow a generalization.

Table 4

Half band-width values of ν_3 (CS_2) band

CS_2 moles %	$\Delta\nu_{1/2}$ calculated accord. to (3)	$\Delta\nu_{1/2}$ from data [20]
100	30.0	20.6
80	25.2	19.3
60	20.4	17.5
40	15.6	15.0
20	10.8	11.5
0.6	7.4	6.4

[22] J. Vincent-Geisse, *Spectrochim. Acta*, **24A**, 1 (1968).

[23] J. Jacob and J. P. Benaich, *J. Chim. phys.*, **64**, 1282 (1967).

Additional data with regard to the relaxation of these vibrations may be obtained from the study of ST half band-width corresponding to the collision complexes occurring in solutions. The half band-width is maximum at a 0.5 mixing ratio (fig. 1, curve *a*) which indicates the existence of bimolecular collision complexes. In the process of simultaneous vibrational transition a modification of the charge distribution takes place along the carbon — sulphur and carbon — hydrogen bonds aligned in the complex, as a result of the simultaneous interaction of vibration ν_3 (CS_2) and ν_1 ($CHCl_3$) with the exciting radiation. The absorption process occurs practically instantaneously and the molecules surrounding the complex do not manage to reorient so as to "adjust" to the new charge distribution in the complex. The deactivation of the complex occurs by molecular interactions which modify the reciprocal orientations of molecules in such a way as to reduce the interaction energy.

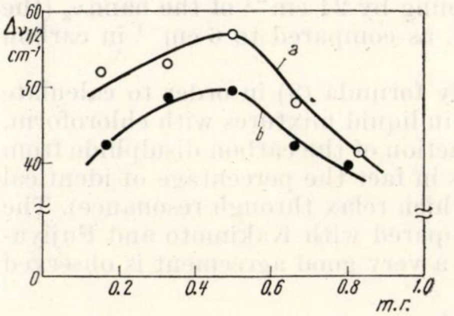

Fig. 1. — Dependence of the half band-width of $ST_{(CS_3+CHCl_2)}$ band on the mixing ratio $\left(\text{m.r.} = \dfrac{\text{ml. } CHCl_3}{\text{ml.} CHCl_3 + \text{ml. } CS_2}\right)$: *a*, $ST_{(CS_2+CHCl_3)}$ half band-width; *b*, $ST_{(CS_2+CHCl_3)}$ half band-width, in the presence of CCl_4.

The half band-width of the ST band reflects the relaxation time of the molecular interactions τ_{ST} and the lifetime of the collision complex, respectively. The variation manner of $\Delta\nu_{1/2\,ST}$ with the mixing ratio provides indications concerning the process of equilibration in the system "collision complex — surrounding solvent molecules". Thus, it seems that the intermolecular relaxation (the deactivation of the complex) does not take place continuously but rather in jumps, the passage from $U_{\max}$ to $U_{\min}$ being made over a potential barrier owing to the local interactions between the two bonds of the molecules participating in the simultaneous transition process.

The lifetime of the complex is also dependent on the relaxation times of the fundamental vibrations involved in the simultaneous transition as they constitute a measure of the reorientation rates of the molecules. The vibrational relaxation leads to the modification of the reciprocal orientation of the dipoles of the respective bonds and hence to the deactivation of the collision complex. Thus, if the relaxation times are increased it means that the orientation of dipoles is maintained longer and the lifetime of the complex is longer. On the contrary, the short relaxation times indicate rapid change of the reciprocal orientation and therefore a rapid deactivation of the complex.

By calculating the lifetime of the collision complex (τ_{ST}) from the experimental value of the corresponding simultaneous transition half band-width, it results $\tau_{ST} = 1.9 \cdot 10^{-12}$ sec. This value roughly corresponds to the difference of the relaxation times of the two fundamental vibrations $\nu_3(CS_2)$ and $\nu_1(CHCl_3)$:

$$\tau_{ST} = \tau_3(CS_2) - \tau_1(CHCl_3) \tag{4}$$

The experimental data of the investigated systems (table 3) seem to obey this empirical relation. From equation (4) we may write :

$$\Delta\nu_{1/2\,(ST)} = \frac{\Delta\nu_{1/2}(\nu_3) \cdot \Delta\nu_{1/2}(\nu_1)}{\Delta\nu_{1/2}(\nu_1) - \Delta\nu_{1/2}(\nu_3)} \tag{5}$$

and, by means of this relation, we may calculate the half band-width of the vibration, knowing the ST half band-width and that of one of the vibrations participating in the simultaneous transition. Table 5 shows the values of ν_1 half band-width ($CHCl_3$) calculated in this manner and it can be seen that they are quite equal with the values obtained experimentally. Similarly, table 6 presents the results of the calculation of ν_3 (CS_2) half band-width in iodoform and deuteriochloroform, respectively, from $\Delta\nu_{1/2\,ST}$ and the half band-width ν_{C-H} (ν_{C-D}).

Table 5

Half band-width of the ν_{C-H} calculated from τ_{ST}

	CS_2 moles %	$\Delta\nu_{1/2}$ (cm^{-1})			
		$\nu_3(CS_2)$	ν_{ST}	$\nu_1(CHCl_3)$ calculated	$\nu_1(CHCl_3)$ found
$CHCl_3$	0.6	6.4	40	7.5	10.6 [10]
		7.4		9.0	
$CHCl_3$	20.0	11.4 [6]		14.3	
			56		12, (13)*
		10.8		13.1	
$CHCl_3$	0.1	9.4	40	12.2	11.8
$CHBr_3$	0.1	9.2	40	11.8	10.4 [10]
					12.4

* The value has been determined on a Carl Zeiss – Jena (UR – 10) spectrophotometer.

Table 6

Half band-width of the $\nu_3(CS_2)$ calculated from τ_{ST}

	$\Delta\nu_{1/2}$ (cm^{-1})		
	$\nu_1(CXCl_3)$	ν_{ST}	$\nu_3(CS_2)$
$CHCl_3$	12.7	38	9.5
$CDCl_3$	10.0		7.7
	12.0 [24–26]	33	8.8

---

[24] M.-L. Josien, J. P. Leicknam and N. Fuson, *Bull. Soc. chim. France*, 1958, 188.

[25] C. M. Huggins and G. C. Pimentel, *J. Chem. Phys.*, **23**, 896 (1955).

[26] J. Lascombe, J. Devaure and M.-L. Josien, *J. Chim. phys.*, **61**, 1271 (1964).

The half band-width of some Raman bands of carbon tetrachloride involved in simultaneous transition with the ν_3 band of carbon disulphide were calculated in the same manner and the results are given in table 7.

Table 7

Some Raman half band-width of CCl_4 from τ_{ST}

ν, cm^{-1} (CCl_4)	ν_{ST}, cm^{-1} ($CCl_4 + CS_2$)	$\Delta\nu_{1/2}$ (cm^{-1})		
		ν_{ST}	Raman width	
			calculated*	found
219	1734	32	5	
313	1828	38	5.1	
455	1927	43	5.2	5.4[27]

* Half band-width $\nu_3(CS_2)$ in carbon tetrachloride was taken[2] equal to 6 cm^{-1}

In a previous paper[1] we reported that the carbon tetrachloride added to chloroform solutions in carbon disulphide determines an increase of the ν_{C-H} half band-width which reaches a maximum for about 40% CCl_4, after which the half band-width decreases again. In the mixture of the two solvents ($CS_2 + CCl_4$) the chloroform molecules may reorient easier than in CS_2 (as has been shown, ν_{C-H} of chloroform in CCl_4 is smaller than in CS_2). However, when the CCl_4 concentration in mixture is high, the interactions between CS_2 and CCl_4 molecules are more effective and the ν_{C-H} vibrational relaxation in the environment of these complexes occurs difficultly and consequently the half band-width decreases (Fig. 1*b*).

The results obtained in this work are in accordance with the existing experimental data and prove the dependence of the lifetime of the complex on the relaxation times of the vibrations participating in a simultaneous transition. Similarly, the half band-widths in the haloform series in an environment of carbon disulphide reveal close values, which indicate similar relaxation mechanism. On the other hand, the reorientation movements are inhibited (to a certain extent) by the formation of collision complexes and the bands appear to be narrower than in totally inert solvents but larger than in solvents in which stable complexes (of the donor-acceptor type) are formed.

As an additional observation we note the fact that the ST half band-width in the $CS_2 - CDCl_3$ system is much smaller than that corresponding to the $CS_2 - CHCl_3$ system. This may be explained to be due to a slower relaxation of ν_{C-D} vibration as compared to the ν_{C-H}, which agrees with the data from literature concerning the relaxation of deuterated molecules.[28]

The above data constitute experimental proofs of some weak interactions of a peripheral type in which only certain parts of the molecule are involved by the corresponding vibrations. In general, our results favour the idea of some binary interactions in solutions in view of expressing the shape of bands, in agreement with works of Vincent-Geisse et al.[6]

[27] H. S. GABELNICK and H. STRAUSS, *J. Chem. Phys.*, **49**, 2334 (1968).

[28] T. .L. COTTRELL and A. J. MATHESON, *Trans. Faraday Soc.*, **58**, 2336 (1962).

Revue Roumaine de Chimie, 19, 7, 1153–1155 (1974)

SOME CONSIDERATIONS CONCERNING GIBBS FREE ENERGY OF GAS-SOLID INTERFACE

P. BUDRUGEAC and M. I. VASS

Institute of Physical Chemistry, str. Dumbrava Roşie 23,
Bucharest, Romania

Received December 25, 1973

Starting with several hypotheses, a more general expression for the infinitesimal variation of internal energy of gas-solid interface is given. A new way of expressing the Gibbs free energy of gas-solid interface is advanced.

In the thermodynamic treatments of gas adsorption on solid adsorbents, developed by different authors, [1–5] the surface area is an important variable which characterizes the adsorption equilibrium. By making an analogy between disperse and porous solids, Dubinin [6] has shown that the above assumption is valid only for the non -porous and wide-pore adsorbents. From the thermodynamic viewpoint, the process of adsorption in micropores is similar to the formation of a sort of solution, resulting in a change of the chemical potentials of both components of the system. [6,7]

In order to find a more general expression for the variation of internal energy of gas-solid interface, the following hypotheses about the adsorption system and the adsorption phenomenon are made:

(a) The thermodynamic system consists of: the adsorbent with an energetic homogeneous surface, the interface and the gas.

(b) The chemical nature of the adsorbent is not changed by adsorption.

(c) The adsorption is reversible.

(d) The number of molecules of the adsorbed gas is negligible as compared to the number of molecules from the gaseous phase.

For all the extensive thermodynamic quantities, X, an excess surface quantity, X^s, can be defined as:

$$X^s = X - X^0 \tag{I}$$

---

[1] T. L. Hill, *Adv. Catalysis*, **4**, 211 (1952).

[2] D. M. Young and A. D. Crowell, "Physical Adsorption of Gases", Butterworths London, 1962, p. 66.

[3] E. A. Guggenheim, *Trans. Faraday Soc.*, **36**, 397 (1940).

[4] E. A. Flood, "The Solid-Gas Interface", vol. 1, Edward Arnold (Publishers) LTD., London, Marcel Dekker, Inc., New York, 1967, p. 11.

[5] G. Schay, *J. Colloid Interface Sci.*, **35**, 254 (1971).

[6] M. M. Dubinin, "Adsorption-Desorption Phenomena", (Ed. F. Ricca), Academic Press, London and New York, 1972, p. 3.

[7] B. P. Bering, A. L. Myers and V. V. Serpinsky, *Doklady Akad. Nauk S.S.S.R.*, **193** (1970).

where : X^0 is the extensive thermodynamic quantity of the hypothetical gas-solid system in which adsorption does not occur and X is the same quantity in case adsorption occurs.

The symbols used below stand : E for internal energy, G for Gibbs free energy, S for entropy, V for volume, n for number of molecules, A for surface area, T for temperature, P for pressure, μ for chemical potential. Subscript a denotes the adsorbent while subscript g stands for gas ; uper indexes 0 and s refer to the gas-solid system in which the adsorption does not occur, and to the interface, respectively.

The expression of the infinitesimal change of internal energy of the system defined in (a) is usually given by the relation :

$$dE = TdS - PdV + \mu_a dn_a + \mu^s dn^s - \gamma dA \tag{II}$$

where :

$$\gamma = -\left(\frac{\partial E}{\partial A}\right)_{S,V,n_a,n^s} \tag{III}$$

The expression of the infinitesimal change of internal energy of the system in which the adsorption does not occur is given by the relation :

$$dE^0 = TdS^0 - PdV^0 + \mu_a^0 dn_a - \gamma^0 dA \tag{IV}$$

Subtracting, member by member (IV) from (II) we obtain :

$$dE^s = TdS^s - PdV^s + (\mu_a - \mu_a^0)dn_a + \mu^s dn^s - (\gamma - \gamma^0)\, dA \tag{V}$$

Relation (V) may be applied to all types of adsorbents described in reference [6] and to adsorbents with mixed structures. This relation includes the cases for which $\mu_a = \mu_a^0$ (the adsorbent is not microporous) as well as the case for which $\mu_a \neq \mu_a^0$ (the adsorbent is microporous). The same as for the treatments given by Hill [1] and Guggenheim, [3] in the eq. (V) V^s is taken as different from zero, while Gibbs, [1,4] Schay [5] and Bering and co-workers [7] consider V^s zero.

In the above-mentioned papers two expressions for G^s are given :

$$G^s = E^s + PV^s - TS^s \tag{VI}$$

$$G^s = E^s + PV^s + (\gamma - \gamma^0)\, A - (\mu_a - \mu_a^0)\, n_a - TS^s \tag{VII}$$

Expression (VI) was given by Schay [5] and expression (VII) by Hill, [1] Gibbs, [1,4] Guggenheim [3] and Bering and co-workers. [7]

Starting with hypotheses (a—d), we aim at finding the expression of G^s.

Let the system defined as in (a) be in equilibrium with the environment with which our system does not exchange any substance.

The subscript t refers to the environment.

In accordance with the second law of thermodynamics, we can write :

$$dS + dS_t = 0 \tag{VIII}$$

We make the following assumption :

$$\begin{aligned} dE + dE_t &= 0 \\ dV + dV_t &= 0 \end{aligned} \tag{IX}$$

Obviously :

$$dS_t = \frac{dE_t + PdV_t}{T} \qquad (X)$$

Relations (II), (VIII), (IX) and (X) lead to :

$$-\gamma dA + \mu_a dn_a + \mu^s dn^s = 0 \qquad (XI)$$

At equilibrium, from (II) and (XI), it results that :

$$dE - TdS + PdV = -\gamma dA + \mu_a dn_a + \mu^s dn^s = 0 \qquad (XII)$$

For $dT = dP = 0$, we have :

$$dG = d(E + PV - TS) = 0 \qquad (XIII)$$

For the above given system, without adsorption, dG^0 is given by :

$$dG^0 = d(E^0 + PV^0 - TS^0) \qquad (XIV)$$

Subtracting, member by member, (XIV) from (XIII), it results that :

$$dG^s = d(E^s + PV^s - TS^s) \qquad (XV)$$

and by integration one gets :

$$G^s = E^s + PV^s - TS^s \qquad (XVI)$$

Eq. (XVI) is identical to (VI).

Since there are two different expressions for G^s((VI) and (VII)) we expect to have also different expressions for $d\mu^s$. However, in papers [1-5,7] similar expressions are given for $d\mu^s$. This could be explained by the fact that an expression of $d\mu^s$ is obtained from (V) for which the following Gibbs-Duhem equation is written :

$$S^s dT - V^s dP + n_a d\mu_a^0 + n^s d\mu^s - Ad(\gamma - \gamma^0) = 0 \qquad (XVII)$$

which leads to :

$$d\mu^s = -\frac{S^s}{n^s} dT + \frac{A}{n^s} d(\gamma - \gamma^0) - \frac{n_a}{n^s} d\mu_a + \frac{V^s}{n^s} dP \qquad (XVIII)$$

Hence it is possible to obtain an expression of $d\mu^s$ which does not depend on the expression of G^s.

Acknowledgments. The authors wish to acknowledge many clarifying discussions with Dr. V. Vasilescu, A. Ivanov and I. Sitaru.

obtained:

$$[illegible] \qquad (X)$$

Equations (II), (VIII), (IX) and (X) lead to:

$$s_a dT + \rho_a d\sigma - v_a dp' = 0 \qquad (XI)$$

By combining equations, from (II) and (XI), it results that:

$$dG = [illegible] \qquad (XII)$$

For $dT = dp = 0$, we have:

$$dG = [illegible] \qquad (XIII)$$

For the adsorptive system, without adsorption, dG^0 is given by:

$$dG^0 = [illegible] \qquad (XIV)$$

Subtracting equation (XIV) from (XIII), it results that:

$$[illegible] \qquad (XV)$$

and by integration one gets:

$$[illegible] \qquad (XVI)$$

Eq. (XVI) is identical to (VI).

Since there are two different expressions for G (VI) and (XVI) we expect to have also different expressions for dσ. However, in papers [illegible] similar expressions are given for dσ. This could be explained by the fact that an expression of dσ is obtained from (I) for which the following Gibbs-Duhem equation is written:

$$[illegible] \qquad (XVII)$$

which leads to:

$$[illegible] \qquad (XVIII)$$

Hence it is possible to obtain an expression of dσ which does not depend on the expression of G.

Acknowledgement. The authors wish to acknowledge some clarifying discussions with Dr. V. Vasilescu, A. Ionescu and L. Stern.

Revue Roumaine de Chimie, **19**, 7, 1157–1167 1974

INVESTIGATION OF COMPLEX COMPOUNDS WITH DIAMINOBIPHENYL DERIVATIVES. XXVIII[*]

COBALT(II) COMPLEX PSEUDOHALIDES

RODICA MICU-SEMENIUC, C. GH. MACAROVICI and MAGDALENA BOSSANYI

"Babeş-Bolyai" University, Chemistry Department, str. Arány Janoş 11, Cluj, Romania
and Chemistry Institute, str. Donath 65–103, Cluj

Received September 26, 1973

The authors report the results obtained in the synthesis and structural investigation of complex cobalt (II) thio- and selenocyanates with diamino derivatives. Compounds of the following type were obtained : $Co(NCX)_2.nL$, where X = S, Se, and L = *o,o'*-DABF (n = 2) ; L = *m,m'*-DABF (n = 1) ; L = *p,p'*-DABF ((n = = 1 and 3) ; L = *p,p'*-DADFM (n = 3) and 2,7-DAF (n = 2.5). The compounds obtained are high spin complexes, having magnetic moments characteristic of a cobalt (II) ion in a six-coordinate configuration, with ${}^4T_{1g}$ ground term. Electronic spectra were recorded, either as diffuse reflection spectra or solution spectra (in DMF), as well as infrared spectra. The data show that all the compounds reported are six-coordinate, with a various degree of tetragonal distortion. Some of the compounds are monomeric, others are polymeric ; both the inorganic and organic ligands used coordinate in two ways : monodentate and/or bidentate, forming – in the last case – bridges between two metallic ions.

INTRODUCTION

In a broad program of investigating the coordinative ability of some divalent metals and organic (diamino derivatives) and inorganic (pseudohalide) ligands, we have undertaken the study of complex pseudohalides of Mn(II), [1] Co(II), [2] Ni(II), [2,3] and Cu(II) [4–6] with diamino compounds, particularly diaminobiphenyl derivatives. These metals are known to form several complex compounds derived from benzidine [7,8] and some from *o,o'*-DABF [8-11] and *m, m'*-DABF. [8]

---

[*] Preceding part is ref. 6.

[1] C. Gh. Macarovici and R. Micu-Semeniuc, *Rev. Roumaine Chim.*, **16**, 1367 (1971).

[2] R. Micu-Semeniuc and C. Gh. Macarovici, *Rev. Roumaine Chim.*, **17**, 981 (1972).

[3] R. Micu-Semeniuc, to be published.

[4] A. Nicula, R. Micu-Semeniuc and C. Gh. Macarovici, *Rev. Roumaine Chim.*, **13**, 1329 (1968).

[5] C. Gh. Macarovici and R. Micu-Semeniuc, *Rev. Roumaine Chim.*, **14**, 357 (1969).

[6] R. Micu-Semeniuc, C. Gh. Macarovici and D. Lupu, *Rev. Roumaine Chim.*, **17**, 993 (1972).

In this paper we report the results obtained with *o,o'*-, *m,m'*- and *p,p'*-diaminobiphenyl (DABF), *p,p'*-diaminodiphenylmethane (*p,p'*-DADFM) and 2,7-diaminofluorene (2,7-DAF). These ligands are known to form metal complexes with the following combination ratios: 1 M : 1L for L = *m,m'*- and *p,p'*-DABF; 1M : 2L for L = *o,o'*- and *p,p'*-DABF; and 1 M : 3 L for L = *o,o'*- and *p,p'*-DABF, and *p,p'*-DADFM; the local symmetry of the complexed metal ion is D_{2h} or D_{4h}. The highest symmetry is exhibited by the compounds of $M(o,o'\text{-DABF})_3X_2$ type. [11] The existence of some Co(II),[12] Co(III) [13] and Pt(II) [14] complexes with *o,o'*-DABF as ligand is also worth mentioning; these complexes exhibit optical activity and some of them have been resolved into the corresponding optical isomers. The investigation of the optical properties of complexes containing *o,o'*-DABF showed, surprisingly, that the diamine is a good ligand, in spite of the known modest coordinating ability of aromatic amines. The chelate ring with this ligand is a seven-membered ring. The coordination of *o,o'*-DABF becomes possible through a reciprocal rotation of the aromatic rings, and the readiness of this rotation confers stability on the chelate ring. [13] It was demonstrated that *o,o'*-DABF is the source of asymmetry in its complexes. [14]

The two other isomers, namely *m,m'*- and *p,p'*-DABF were found unable to form chelates; these diamines coordinate with one or/and both amine functions, in the last case forming polymers, or at least dimers. [1,5,8,15]

In this paper we report and discuss the results obtained in the investigation of cobalt (II) thio- and selenocyanate complexes containing the diamines mentioned above.

EXPERIMENTAL PART

Preparation of complexes. The synthesis of the compounds under discussion was generally simple, and it was described for other similar compounds. [1,2,6,16] The experimental data concerning combination ratios, elemental analyses and some properties were listed in table 1. The yields were in the range 60 – 80 %. It should be noted that some of these compounds have been also synthesized by other authors: $Co(NCS)_2(p,p'\text{-DABF})$ [17] and $Co(NCSe)_2(p,p'\text{-DABF})_3$, [18] but no detailed investigation upon them was done; the compound $Co(NCS)_2(o,o'\text{-DABF})_2$ has been prepared [9] and investigated [11] only recently.

[7] C. Gh. Macarovici, *Anal. Şti. Univ. "Al. I. Cuza" Iaşi, Sect. I*, **6**, 883 (1960).

[8] G. Schmidt, Ph. D. Thesis, "Babeş-Bolyai" University, 1963.

[9] F. Hein and W. Jehn, *Z. anorg. Chem.*, **341**, 244 (1965).

[10] S. Onaka, T. Iwamoto, I. Sasaku and S. Fujiwara, *Bull. Chem. Soc. Japan*, **40**, 1298 (1967).

[11] B. J. A. Kakazai and G. A. Melson, *Inorg. Chim. Acta*, **2**, 186 (1968); **4**, 360 (1970).

[12] F. Mc Cullough and J. C. Bailar, *J. Amer. Chem. Soc.*, **78**, 714 (1956).

[13] J. C. Bailar and L. F. Dempsey. *Rev. Chim. Mineral*, **3**, 1029 (1966).

[14] I. Habu and J. C. Bailar, *J. Amer. Chem. Soc.*, **88**, 1128 (1966).

[15] C. Gh. Macarovici and G. Schmidt, *Rev. Roumaine Chim.*, **9**, 51 (1964).

[16] C. Gh. Macarovici and R. Micu-Semeniuc, *Stud. Univ. Babeş-Bolyai Chem.*, **I**, 151 (1963).

[17] G. Spacu, *Bull. Soc. Sci. Cluj*, **III**, 285 (1927).

[18] G. Spacu and C. Gh. Macarovici, *Bull. Soc. Sci. Cluj*, VI, 95 (1931).

Table 1

Analasis and some properties of the complex compounds

Compounds	% Metal		% Anion (Se)		% N		Colour	M. p. (Dc) °C
	calc.	found	calc.	found	calc.	found		
Co(NCS)$_2$(*o,o'* – DABF)$_2$	10.83	10.47	21.35	21.08	15.43	15.08	pink	260
Co(NCSe)$_2$(*o,o'*-DABF)$_2$	9.25	8.89	24.52	24.18	13.18	13.05	pink	(183)
Co(NCS)$_2$ (*m,m'*-DABF)	16.41	16.18	32.30	32.58	15.59	15.64	violet-brown	250
Co(NCSe)$_2$ (*m,m'*-DABF)	13.01	12.65	34.58	34.06	12.36	12.42	brown	(220)
Co(NCS)$_2$(*p,p'*-DABF) [17]	16.41	16.34					brown	240
Co(NCSe)$_2$ (*p, p'*-DABF)	13.01	12.68	34.58	34.65	12.36	12.53	brown	(270)
Co(NCS)$_2$(*p, p'*-DABF)$_3$	8.10	8.13	15.94	15.70	11.54	11.44	pink	120
Co(NCSe)$_2$(*p,p'*-DABF)$_3$[18]	7.17	7.36					pink-brick	122
Co(NCS)$_2$(*p,p'*-DADFM)$_3$	7.66	8.23	15.06	15.28	14.56	14.23	pink	140
Co(NCSe)$_2$ (*p, p'*-DADFM)$_3$	6.83	7.24	18.08	18.30	12.97	13.20	light brown	(188)
Co(NCS)$_2$(2,7-DAF)$_{2.5}$	8.17	8.53	16.10	16.53	13.60	13.85	brown	140
Co(NCSe)$_2$ (2,7-DAF)$_{2.5}$	7.70	7.86	20.65	20.70	12.84	12.52	brown	160

Physical measurements. Magnetic susceptibility measurements were carried out at room temperature, with a Faraday balance, calibrated with CoHg(SCN)$_4$. The magnetic moments have been calculated with the relation : $\mu_{eff} = 2.84\sqrt{\chi_{Mc} \cdot T}$. The results are given in table 2.

The electronic spectra were obtained with the aid of a VSU–1 Carl Zeiss–Jena type spectrophotometer, equipped with a reflexion device, by using pressed pellets of the compounds investigated and MgO as reference. The absorption bands are listed in table 3.

Infrared spectra were recorded with a UR–20 Carl Zeiss–Jena instrument, in the range 3 600 – 400 cm^{-1}, in KBr pellets. The bands and their assignments are listed in table 4.

RESULTS AND DISCUSSION

Along with the synthesis of the new coordination compounds the combination ratios were established, as well as some of their properties. It was found that the combination ratios M : DABF are similar to those obtained for metals other than cobalt ; thus, for L = *p*, *p'*-DADFM the ratio is 1M : 3L and for L = 2,7-DAF, a compound with the combination ratio 1M : 2.5 L is obtained.

The solubility of the compounds obtained is lower than that of similar Mn(II) complexes, but sensibly higher than that of the related Ni(II) compounds.[3] They are partially soluble in ethanol and acetone, forming blue or dark-green solutions, probably, in a manner similar to the complex cyanates of the same type. [2] Dimethylformamide (DMF) dissolves well the compounds investigated, and forms blue solutions (the thiocyanates) and beige-brown solutions (the selenocyanates). This behaviour suggests, from the very beginning, essential changes in the coordination sphere of the metallic ion. Pyridine also dissolves these compounds, and gives solutions coloured in pink, beige or brown.

The solubility of compounds containing only one diamine molecule per metal (*m,m'*- or *p,p'*-DABF) is lower than the solubility of the other ones, whereas their thermal stability is higher (table 1). It was also noted a higher thermal stability of the thiocyanates, as compared with the selenocyanates. The complex compounds, containing three molecules of *p,p′*-DABF per metal, exhibit a behaviour similar to that of the related Mn (II) derivatives. [1] This makes us believe that the three ligand molecules do not occupy identical positions in the coordination sphere and probably one of them is weakly bonded and can be easily split off on heating.

The *magnetic properties* of the cobalt (II) ion are strongly dependent on the symmetry of the crystal field around the metal. The magnetic moments for a six-coordinate configuration exhibit values in the range 1.8 to 5.6 BM, depending on the strength of the crystal field. [19-21] In a field of tetrahedral symmetry, the magnetic moments show values in the range 4.30 to 4.8 BM. [19,22]

The values obtained by us for the diaminobiphenyl and related derivatives indicate high-spin metal ions and are in the range characteristic of six-coordinate complexes (table 2). In some cases the μ values are somewhat higher for selenocyanates than for thiocyanates, but are smaller than those for the corresponding cyanates. [2] They remain, however, in the range specific for an octahedral coordination of the ligands around the metal ion.

The *electronic spectra* were recorded only for the compounds containing diaminobiphenyl derivatives, both in solution (dimethylformamide, DMF as solvent) (fig. 1) and in solid state (diffuse reflection electronic spectra) (figs 2 and 3). The magnetic moments suggest that the ground state of the cobalt (II) ion in these compounds is a $^4\Gamma_{1g}$ triplet. From the succession of the following terms in a six-coordinate configurations, one can expect the occurrence of three bands in the electronic spectrum, corresponding

Table 2

Magnetic properties

Compound	χ /g · 10^6	$\chi_{\mathrm{Mcorr.}} \cdot 10^6$	μ_{BM}	T°K
$Co(NCS)_2$(*po,o′*-DABF)$_2$	18.43	10,339	4.96	295
$Co(NCSe)_2$(*o,o′*-DABF)$_2$	15.55	10,252	4.94	298
$Co(NCS)_2$(*m, m′*-DABF)	29.30	10,728	5.05	295
$Co(NCSe)_2$(*m,m′*-DABF)	22.97	10,631	5.05	298
$Co(NCS)_2$(*p,p′*-DABF)	26.86	9,854	4.87	298
$Co(NCSe)_2$(*p,p′*-DABF)	22.86	10,574	5.02	298
$Co(NCS)_2$(*p,p′*-DABF)$_3$	13.11	9,987	4.90	298
$Co(NCSe)_2$(*p,p′*-DABF)$_3$	12.66	10,863	5.11	298
$Co(NCS)_2$(*p,p′*-DADFM)$_3$	12.53	10.120	4.90	298
$Co(NCSe)_2$(*p,p′*-DADFM)$_3$	12.62	11,399	5.20	298
$Co(NCS)_2$(2,7-DAF)$_{2.5}$	14.57	10,090	4.92	298
$Co(NCSe)_2$(2,7-DAF)$_{2\cdot5}$	12.14	9,629	4.81	298

---

[19] B. N. Figgis and R. S. Nyholm, *J. Chem. Soc.*, **1954**, 12 ; **1959**, 338.

[20] E. K. Barefield, D. H. Busch and S. M. Nelson, *Quart. Rev.*, **22**, 457 (1968).

[21] M. Gerloh, P. N. Quested and R. C. Slade, *J. Chem. Soc., A*, **1971**, 3741.

[22] F A. Cotton and M. Goodgame, *J. Amer. Chem. Soc.*, **83**, 1777 (1961).

to the following transitions: ${}^4T_{1g} \rightarrow {}^4T_{2g}(\nu_1)$; ${}^4T_{1g} \rightarrow {}^4A_{2g}(\nu_2)$; ${}^4T_{1g} \rightarrow {}^4T_{1g}(P)(\nu_3)$. The shapes of spectra (figs 2 and 3) and the values of the absorption bands (table 3) indicate indeed the six-coordinate configuration of the compounds investigated. The ν_1 transition occurs as a single band for most of the compounds and it is found in the range 8800–9500 cm^{-1}. The ν_2 band occurs as shoulders [11,23-25] or less well resolved bands, in the range 16,600 to 18,200 cm^{-1} usually higher for selenocyanates. Generally, the assignment of this band is difficult, due to the nature of the transition. It was stated [25] that the ν_2/ν_1 ratio should be between the limits 2.1—2.2. for six-coordinate cobalt compounds; anyway, a band or a shoulder located at more than 2.2 ν_1 cannot be due to a transition to ${}^4A_{2g}$. The values of the ν_2/ν_1 ratio obtained for our compounds are somewhat lower than 2.00 (being in the range 1.79 to 1.95), as in the case of the $Co(H_2O)_6{}^{2+}$ complex; therefore, we conclude that the assignment of the ν_2 band to a shoulder located on the lower value branch of the ν_3 band is not incorrect.

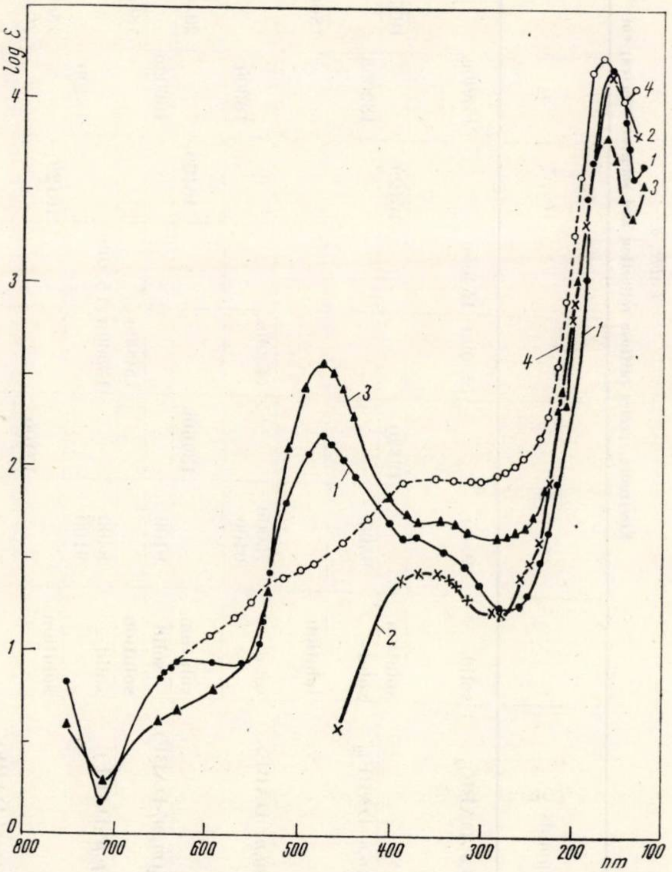

Fig. 1. — Electronic spectra in solution (DMF): *1*, $Co(NCS)_2 - (o,o'\text{-}DABF)_2$; *2*, $Co(NCSe)_2(o\,o'\text{-}DABF)_2$; *3*, $Co(NCS)_2(m,\ m'\text{-}DABF)$; *4*, $Co(NCSe)_2(m, m'\text{-}DABF)$.

---

[23] M. Goodgame, *J. Chem. Soc., A*, **1966**, 63.

[24] C. K. Jörgensen, *Acta Chem. Scand.*, **9**, 116 (1955).

[25] A. B. P. Lever and D. Ogden, *J. Chem. Soc., A*, **1967**, 2041.

Table 3

Electronic spectra (diffuse reflection and solution spectra) cm^{-1})

Componds		ν_1				$(\nu_3)^\star$	ν_2		ν_3	other bands	$10D_q$	$\Delta\nu_3$	Probable local symmetry
$Co(NCS)_2(o,o'\text{-}DABF)_2$	solid	9500		14300u	15400u		17800u		19600u 20100 21300u		8300	1700	D_{4h}
	solution		12820			16129		19230u		33333			
$Co(NCSe)_2(o,o'\text{-}DABF)_2$	solid	9500					18200u		20000 21500u		8700	1500	D_{4h}
	solution							1800		25000u 33333			
$Co(NCS)_2(m,m'\text{-}DABF)$	solid	7500u 9100		14300u			16300		18000	22400	8900	—	D_{2h}
	solution		13460u			16129		20400u		27770u 32077			
$Co(NCSe)_2(m,m'\text{-}DABF)$	solid	9100					16600u		18300		9200		D_{2h}
	solution			15000u				18800u		32077			
$Co(NCS)_2(p,p'\text{-}DABF)$	solid	8400 9100		13800u	15100u		17200		18500 22000	24600	9300	3700	D_{2h}
	solution		13100			16129		18800u 20409		33333			
$Co(NCSe)_2(p,p'\text{-}DABF)$	solid	8800		12300u	14900u		17200		18200u 18000 21800		9700	3600	D_{2h}
	solution		13400			16000 16700		18800 20409		33333			
$Co(NCS)_2(p,p'\text{-}DABF)_3$	solid	9100					17200u		19600 21200		8100	600	D_{4h}
	solution		13100			16600u		21700		27400 33333			
$Co(NCSe)_2(p,p'\text{--}DABF)_3$	solid	8900					16900u		19200	23300	8200	—	D_{4h}
	solution					16129		18800 22222		33333			

$\star$ υ_3 (tetrahedron)

The ν_3 band is split into 2–3 components (sometimes it appears as a single band but then it is much broadened) in the range 21,400 – 18,200 cm^{-1}. The lifting of the degeneracy may be due to the spin-orbit coupling or to low symmetry ligand field efects. It is known that the degree of distortion can be correlated with the energy difference between components of higher and lower energy of the ν_3 band. Accordingly, it is observed that the thiocyanates are more distorted than selenocyanates (table 3), and the compounds with only one molecule of amine (*m,m'*- and *p,p'*-DABF) (figs 2 and 3, *b* and *c*) are of a lower symmetry than those with two molecules of ligand (*o,o'*-DABF) (table 3 ; figs 2 and 3, *a*). This can be understood if one accepts that for achieving six-coordination, one of the ligands has to coordinate by forming a bridge, which imposes some steric restrictions.

From the difference between ν_2 and ν_1 the magnitude of the crystal field (10D$_q$) can be estimated.[11] It is found that this value is higher for selenocyanates, in accordance with the sense of the crystal field increase.

The spectra also show some shoulders in the ranges 15,000 – 14,000 cm^{-1}, which can be due either to some spin-forbidden transitions (to the

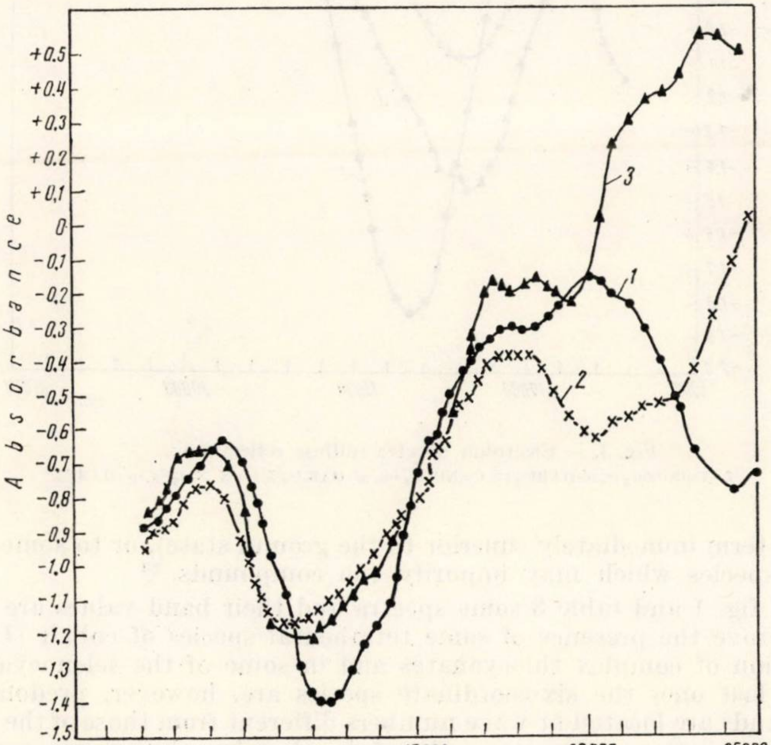

Fig. 2. — Electronic spectra (diffuse reflection) :

1, Co(NCS)$_2$ (*o*, *o'*-DABF)$_2$; *2*, Co(NCS)$_2$ (*m*, *m'*-DABF) ; *3*, Co(NCS)$_2$ (*p*, *p'*-DABF).

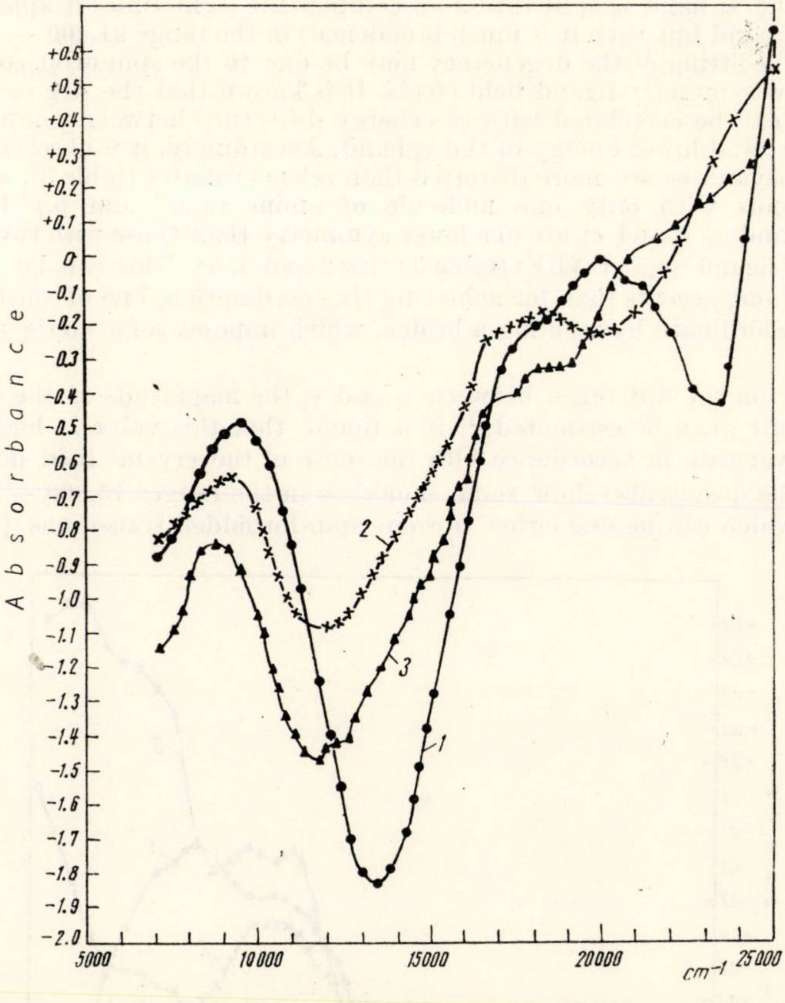

Fig. 3. — Electronic spectra (diffuse reflection) :
1, $Co(NCSe)_2$ (o, o'-DABF)$_2$; 2, $Co(NCSe)_2$ (m, m'-DABF) ; 3, $Co(NCSe)_2$-(p,-p'-DABF).

doublet term immediately superior to the ground state), or to some tetrahedral species which may impurify the compounds. [23]

In fig. 1 and table 3 some spectra and their band values are given, which prove the presence of some tetrahedral species of cobalt (II) ions in solution of complex thiocyanates and in some of the selenocyanates; for the last ones the six-coordinate species are, however, predominant. Their bands are located at wave numbers different from those of the diffuse reflection spectra; we suppose, therefore, that in solution, six-coordination is achieved by coordinating two solvent molecules.

With the aid of *infrared spectra* we followed the occurrence and the shift of the bands characteristic of the anions, on the one side, and on the other side the bands of the diamines, as compared with the uncoordinated ligands.

The difunctional coordinative capacity of pseudohalides and/or their ability to form bridges between two metal atoms are well known [26,27]; both anions have characteristic frequencies, which occur in three regions of the three infrared active vibrations, and which exhibit different values, depending on the types of bonds which they form. [28-31]

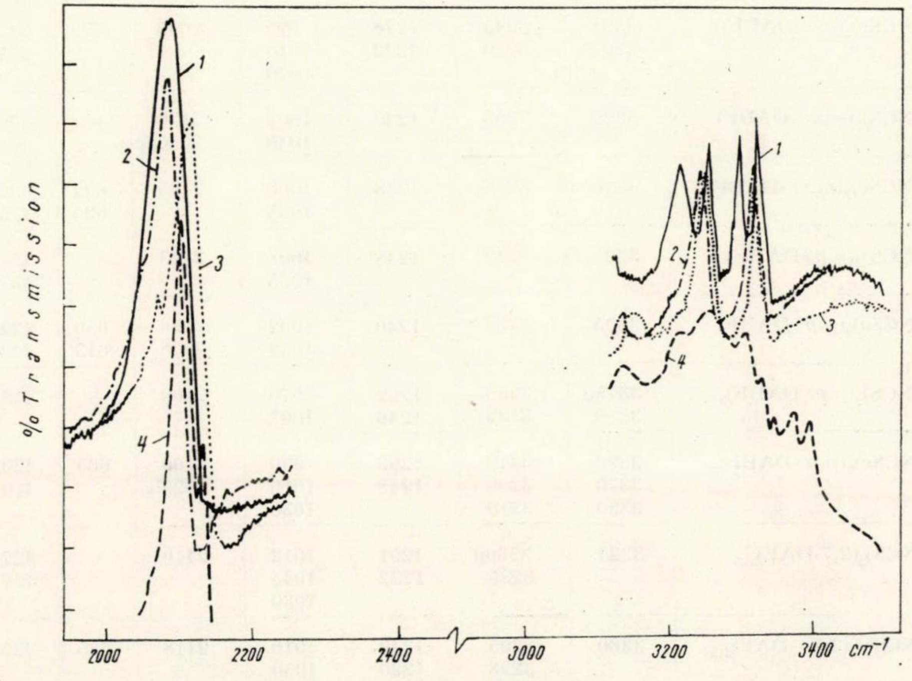

Fig. 4. — Infrared spectra of :

1 $Co(NCS)_2$ (*o,o'*-DABF)$_2$; 2, $Co(NCSe)_2$ (*m,m'*-DABF); 3 $Co(NCS)_2$ (*p,p'*-DABF); 4, $Co(NCSe)_2$ (*p p'*-DABF)$_3$.

The anion bands in our spectra (table 4) are found in the expected regions. Thus, ν_{CN} exhibits higher values for the compounds containing only one amine molecule (*m,m'*- and *p,p'*-DABF), then, in decreasing sequence, for the compounds with three molecules of amine, with 2.5 molecules of 2,7-DAF and, finally, the lowest values are obtained for compounds with *o,o'*-DABF (fig. 4). It is obvious that in the first case the pseudohalide group forms bridge (weak), whereas in the last case, a bond through the nitrogen atom. In the compounds containing several amine molecules per metal, the ν_{CN} values suggest the occurrence of a coordinated anion, in spite of the

---

[26] A. Tramer, *J. Chim. phys.*, **59**, 232 (1962).

[27] F. A. Cotton, D. M. L. Goodgame and T. E. Haas, *Inorg. Chem.*, **1**, 565 (1962).

[28] L. H. Jones, *J. Chem. Phys.*, **25**, 1069 (1956).

[29] H. W. Morgan, *J. Inorg, Nuclear Chem.*, **16**, 367 (1961).

[30] Yu. Ya. Kharitonov and G. V. Tsintsadze, *Zhur. neorg. Khim.*, **10**, 1191, (1965).

[31] Yu Ya. Kharitonov and V. V. Skopenko, *Zhur. neorg. Khim.*, **10**, 1803. (1965).

Table 4

Infrared spectra (cm^{-1})

Compound	ν_a NH$_2$	ν_s NH$_2$	νCN	δ_s	νCN(X)	νCX	δ NCX
$Co(NCS)_2(o,o'\text{-}DABF)_2$	3328 3301	3258 3220	1280 1227	990 1010 1035	2090	—	470
$Co(NCSe)_2(o,o'\text{-}DABF)_2$	3321 3297	3245 3210	1278 1222	995 1010 1040	2095	635	417 407
$Co(NCS)_2(m,m'\text{-}DABF)$	3329	3255	1240	1002 1040	2120 2080 ic	—	470 460
$Co(NCSe)_2(m,m'\text{-}DABF)$	3320	3248	1238	1000 1035	2125	627 620	420 415
$Co(NCS)_2(p,p'\text{-}DABF)$	3320	3239	1248	1008 1035	2123	—	471 457
$Co(NCSe)_2(p,p'\text{-}DABF)$	3305	3237	1240	1002 1032	2126 2078	650 613	422 408
$Co(NCS)_2(p,p'\text{-}DABF)_3$	3375u 3359	3265 3122	1262 1246	970 1007	2100	—	415
$Co(NCSe)_2(p,p'\text{-}DABF)_3$	3390 3370 3330	3310 3260 3210	1268 1248	990 1010 1030	2100 2125ic	665	420 410
$Co(NCS)_2(2,7\text{-}DAF)_{2.5}$	3327	3260u 3235	1251 1222	1012 1045 1080	2110	—	427 407
$Co(NCSe)_2(2,7-DAF)_{2.5}$	3380	3305 3228	1240 1220	1010 1050	2118	635	420

possibility to achieve six-coordination without its coordinative participation; this is in agreement with our previous observations[1] concerning the thermal behaviour of the benzidine complexes, which suggests that not all of the amine molecules occupy equivalent positions in the complex.

Regarding the vibrations ν_{CX} it is not possible to make correct assignments for thiocyanates, because of the superposing of their bands in the range 800 — 700 cm^{-1} with the rocking vibrations of the amines, but ν_{CSe} can be identified in certain cobalt compounds, being in accordance with the bonding suggested above.

The frequency of the δ_{NCX} vibrations can be localized in all compounds investigated, but the information they provide concerning the bonding of the anion is insignificant; the δ_{NCSe} bands occur, as expected, at lower wave numbers than those of the thiocyanate.

Concerning the spectroscopic behaviour of the coordinated amines, it is observed that some of their characteristic bands are shifted, generally towards lower wave numbers, as compared with the free (uncoordinated) amines (table 4; fig. 4). Thus, in the range of ν_{NH_2} frequencies, only two bands occur in the spectra of the complexes containing only one amine molecule per metal; this is the case with the complexes of *m,m'*- and *p,p'*- DABF and the bands are due to ν_{as} and ν_s (NH_2). This suggests that the amine functions are equivalent and coordinated, without the formation of a chelate ring.[15,16] Therefore, *m,m'*- and *p,p'*-DABF from bridges between two cobalt atoms. The occurrence of several bands (four) in the compounds containing *o,o'*-diaminobiphenyl is due to the existing distortions, first in the molecule of the amine, all the amino groups being coordinated; in other compounds this number of bands can be correlated with the presence of both coordinated amine groups and non-bonded (free) amine groups. The frequency of the stretching vibration $C_{aromatic} - N_{amin}$ in the range 1300 — 1200 cm^{-1} follows exactly the behaviour of the frequencies ν_{NH_2} in the range 3 400 — 3 200 cm^{-1}.

In other regions of the infrared spectra, characteristic of the amines, the occurrence of a remarkably strong band in the range 1 100 — 1 000cm^{-1} is observed. This band is absent in the infrared spectrum of the free (uncoordinated) amine and can be assigned to a skeleton vibration[32,33] or to a deformation band δ_{NH_2}, infrared inactive for the free amine, which becomes infrared active by coordination.

A somewhat higher value is generally noticed for the ν and δ bands in the spectra of cobalt compounds, as compared with the spectra of manganese compounds.[1] If we take into account that the bands in the range 1010 — 990 cm^{-1} belong to δ_s NH_2 vibrations, we find that their value is somewhat lower than in manganese compounds, which is in accordance with the shift of the symmetrical deformation bands by coordination.[34,35]

With the aid of electronic and infrared spectra and magnetic properties we proved that the complex thio- and selenocyanates of cobalt (II) with diamine derivatives, investigated in the present work, are monomeric compounds with the pseudohalide group coordinated in *trans* via the nitrogen atom (the compounds with *o,o'*-DABF) or polymeric compounds, with the anion and amine bonded as bridges (the compounds with *m,m'*- and *p,p'*-DABF, 2,7-DAF and *p,p'*-DADFN). In the compounds containing a larger number of organic ligands per metal atom, we established the coordination of the pseudohalide — probably in *trans* — and the nonequivalent bonding of the amines.

---

[32] M. Kobayashi and J. Fujita, *J. Chem. Phys.*, **23**, 354, (1955).

[33] M. E. Baldwin, *Spectrochim. Acta*, **18**, 1455 (1962).

[34] A. V. Babaeva and O. N. Evstafieva, *Zhur. neorg. Khim.*, **6**, 61 (1961).

[35] A.A.Grinberg and Yu. S. Varshavskii, *Doklady Akad. Nauk S.S.S.R.*, **159**, 1072(1964).

Revue Roumaine de Chimie, **19**, 7, 1169–1178 (1974)

Co(II) CHELATES WITH 1-METHYL-2-CARBETHOXY-GLYOXALANIL-(1)-METHOXY-PHENYLHYDRAZONES-(2)

A. C. BANCIU and P. SPACU

Centre of Physical Chemistry, str. Dumbrava Roșie 23, Bucharest 9, Romania

Received November 28, 1973

From the three new compounds, derivatives of 1-methyl-2-carbethoxy-glyoxalanil-(1)-phenylhydrazone-(2), methoxy-substituted at the phenyl radical of the hydrazone group, the derivatives *para-* and *meta*-substituted are able to form chelates with the Co(II) ion, while the *ortho*-derivative cannot complex the metal ion. The elemental analysis data, IR and electronic spectra as well as the magnetic measurements show that both obtained complexes are tetracoordinate chelates, with high spin tetrahedral d^7 electronic configuration and with a noticeable but in each case different covalency degree of the metal-ligand bonds. The chelate with the *meta*-derivative has the mean nephelauxetic ratio $\beta \approx 0.76$, whereas the chelate with the *para*-derivative has $\beta \approx 0.71$, that is lower than in the well-known $CoCl_4^{2-}$ ion ($\beta \approx 0.73$).

The present paper carries further our research presented in notes [1,2] concerning the Co(II) complexes with ligands from the class of 1-methyl-2-carbethoxy-glyoxalanil-(1)-arylhydrazones-(2), dealing with the preparation of the three possible ligands from the group of 1-methyl-2-carbethoxy-glyoxalanil-(1)-methoxy-phenylhydrazones-(2), the synthesis of the two Co(II) complexes which can be obtained by means of these potentate ligands, and with the main chemical and physical properties (spectral and magnetic) of both chelates prepared . For this reason, besides the already mentioned [1] compound Ia, the present note describes the synthesis of the new compounds Ib and Ic

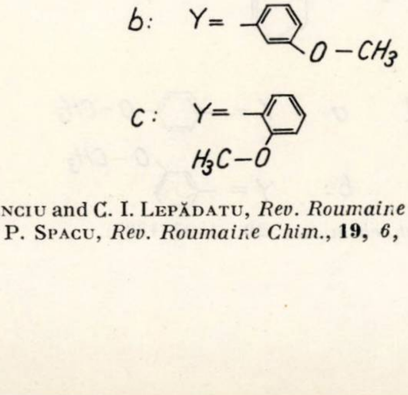

---

[1] P. Spacu, A. C. Banciu and C. I. Lepădatu, *Rev. Roumaine Chim.*, **18**, *7*, 1143 (1973).
[2] A. C. Banciu and P. Spacu, *Rev. Roumaine Chim.*, **19**, *6*, 1019 (1974).

as well as the preparation attempts of the Co(II) complexes formed with these possible ligands.

EXPERIMENTAL

Reagents. Acetylacetic ester (Merck, reagent for synthesis, min. content 98%), aniline (tridistilled), *p*-anisidine (VEB-Berlin-Chemie, p.a.), *m*-anisidine (B.D.H., reagent for laboratory, boiling interval 243–248°), *o*-anisidine (B.D.H., reagent for laboratory, boiling interval 222–226°), anhydrous $NaCH_3COO$ (Austranal, p.a.), $CoCl_2 \cdot 6H_2O$ (Reactivul, Bucharest, p.a.), $NaNO_2$ (Reactivul, Bucharest, p.a.).

The preparation of the compounds Ia–c was similarly made with that already reported,[1,2] starting from acetylacetic ester. By its condensation with aniline the corresponding anil [3] was obtained, from which, through azoic coupling reactions with freshly prepared solutions of diazonium salts of the anisidines, instantly buffered with solid amounts of $NaCH_3COO$, until pH = 3, the compounds Ia–c were thereby obtained. The compounds Ia and Ib were separated as a solidified oil, which, dried on a porous plate and repeatedly washed with cooled methanol, could be brought to a dry form able to be recrystallized. After recrystallizations done from ethanol in the presence of active charcoal, the pure compounds Ia–c were obtained, but with scarce yields, of 18%, 14% and 38% from the theoretical ones, respectively. The syntheses of the complexes were made using these compounds but for their chemical analyses they were once more recrystallized and the products dried under vacuum on di-P_2O_5.

The preparation of the chelates. The attempts at obtaining the Co(II) chelates were performed in the same manner as earlier described, [1,2] under the refluxing conditions of the alcoholic solutions of the reagents, in the presence of small amounts of triethylamine (about 1 ccm), working with amounts of 1/100 m ligand and 1/200 m $CoCl_2 \cdot 6H_2O$ plus a little excess of 15% from this theoretical value of the last reagent, in order to ensure the completeness of the reaction. After cooling of the reaction mixture and the partial evaporation of the solvent, if the complexation took place, dark blue till black crystals of complex were separated, impurified with degradation products of the ligands, of obviously lighter colour than that of the used ligands. This heterogeneous mass was repeatedly washed with 3% acetic acid warmed at 40°, to remove completely the unreacted Co(II) ions, and then two recrystallizations were made from alcoholic solutions in the presence of active charcoal, followed by the drying of the purified complexes, under vacuum on di-P_2O_5. Using the compounds Ia and Ib, the following complexes IIa and IIb have been synthesized:

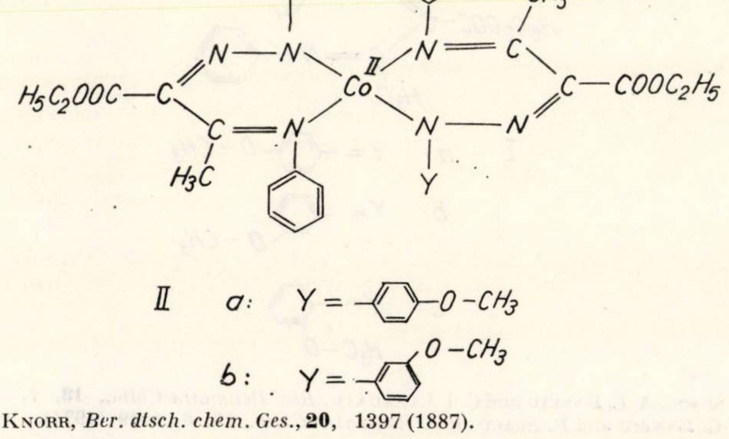

---

[3] L. Knorr, *Ber. dtsch. chem. Ges.*, **20**, 1397 (1887).

The attempts made under the same conditions in order to obtain the compound Ic have failed, after the cooling of the reaction mass, the ligand being separated practically as unreacted.

The elemental analyses of C, H and N were made by microcombustion. The Co amount was determined by disintegration with H_2SO_4 and H_2O_2 followed by precipitation as $Co(C_5H_5N)(SCN)_2$, according to. [4]

The adsorption spectra of the compounds were recorded with a VSU–2 Carl Zeiss (Jena) spectrophotometer on $0.5 \times 10^{-4} - 0.5 \times 10^{-3}$ m/l solutions in absolute ethanol and acetone.

The reflectance spectra of the chelates were recorded on a VSU-1 Carl Zeiss (Jena) spectrophotometer using MgO as standard.

The IR spectra of the compounds were recorded within 400–4 000 cm^{-1} range by means of a UR-10 Carl Zeiss (Jena) spectrophotometer, using KBr pellets.

The magnetic susceptibilities were measured at the room temperature, according to the Faraday method, using $Hg[Co(NCS)_4]$ as standard. The magnetic moments were calculated from $\mu = 2.828(\chi'_M \cdot T)^{1/2}$, where $\chi'_M = \chi_M - \chi_{dia}$ is the corrected molar susceptibility. In the case of both isomer chelates the diamagnetic correction was $\chi_{dia} = -375 \times 10^{-6}$ (c.g.s.u.).

RESULTS AND DISCUSSIONS

The analytical data for the compounds Ia–c have been systematized in table 1 and agree well with their formulation I.

Table 1

1-Methyl-2-carbethoxy-glyoxalanil-(1)-methoxy-phenylhydrazones-(2) (Compounds Ia – c)

Compounds I Y	C%		H%		N%		Colour	m.p. °C
	Calc.	Found	Calc.	Found	Calc.	Found		
$C_6H_4-p-OCH_3$	67.24	67.62	6.24	7.00	12.38	12.79	orange	88–90.5
$C_6H_4-m-OCH_3$	67.24	67.13	6.24	6.80	12.38	12.65	yellow-orange	86.5–89
$C_6H_4-o-OCH_3$	67.24	67.89	6.24	6.53	12.38	12.71	yellow	89–91.5

The analytical data for the two obtained Co(II) complexes are given in table 2. These data and the IR spectral results allow us to ascribe the chelatic structural formulas IIa–b for these complexes.

The fact that the compound Ic behaves differently than the compound Ia–b, being deprived of the specific properties of a ligand, could be explained by the relevant steric hindrances due to the OCH_3 substituent when attached in the *ortho* position to the phenyl radical of the hydrazonic group. A strong steric hindrance which hampered the chelation has been also observed with the CH_3 substituent attached in the *ortho* position to the phenyl radical of the hydrazonic group. [2]

The IR spectra of both compounds having ligand properties, Ia and Ib, as well as of their corresponding Co(II) chelates are summarized in table 3.

---

[4] G. Spacu and I. Dick, *Z. analyt. Chem.*, **71**, 97 (1927).

Table 2

Co(II) chelates. Analytical data

Chelate	Co%		C%		H%		N%		m.p. °C
	Calc.	Found	Calc.	Found	Calc.	Found	Calc.	Found	
IIa	8.01	7.52	62.04	62.11	5.48	5.88	11.42	11.64	149–152
IIb	8.01	7.73	62.04	62.27	5.48	5.90	11.42	11.83	134–136

One may observe obvious differences between the IR spectra of the free ligands and of the corresponding chelates in the range comprised within 1290 –1370 cm^{-1}. For the two free ligands there appear bands of mean intensity. In the case of the chelates, one may observe the appearance of a very broad band with maxima placed at 1290, 1310, 1340, and 1370 cm^{-1}, which are the most intense bands from the whole spectrum of the chelates. One knows that in the domain between 1280 and 1360 cm^{-1} there is an intense band in the case of the secondary aromatic amines (C_6H_5-NH-) and almost in the same region (1310–1360 cm^{-1}) an intense band in the case of the tertiary aromatic amines ($C_6H_5-N=$), both bands being due to the C–N stretching vibration inside these groups.[5] According to the structural formulations assumed for the Co(II) chelates, changes should be expected in the IR spectra in this region, caused by the coordination of the donor nitrogen atom from the hydrazonic group, which is straightforwardly attached to the phenyl radical. The fact that the intense band at 1700 cm^{-1}, which may be undoubtedly ascribed[5] to the esteric group ($COOC_2H_5$), appears as unshifted in the spectra of the two chelates shows that this group does not participate in coordination, an alternative which could not be *a priori* excluded. If the esteric group coordination took place, its proper band would have been strongly moved,[5] at approximately 1635 –1665 cm^{-1}, which obviously is not the case. One may conclude that the IR data are in a good agreement with the structural formulas IIa and IIb for the Co(II) chelates.

Electronic spectra and magnetic properties

The only small shifts of the bands in the reflectance spectra recorded in the solid state of the compounds compared with those in the absorption spectra of the chelates recorded in solutions (absolute ethanol and acetone) show that the chelates dissolved in the above-mentioned solvents did not lead to important structural modifications (dissociation, etc.) the same molecular species being therefore present in both solution and solid state.

The electronic spectra of the two chelates recorded on acetonic solutions of $0.5 \times 10^{-4} - 0.5 \times 10^{-3}$ m/l are plotted in figure 1. The vertical lines in this figure show the position of the absorption maximum of the bands

---

[5] L. J. Bellamy, "The Infrared Spectra of Complex Molecules", Methuen, London, 1962

Table 3

IR spectra of the ligands Ia and Ib and of the corresponding Co(II) chelates (IIa and IIb) (cm − 1)

Ligand Ia	Ligand Ib	Chelate IIa	Chelate IIb
			430 w
470 sh	460 w	465 w	460 sh
480 w	490 w		485 w
525 w		500 w	515 w
		535 w	530 w
545 w	545 w	545 w	
560 w	560 w		
	575 w	585 w	570 w
605 w	610 w	615 w	595 m
620 w	625 w	630 w	625 sh
635 w		640 w	640 w
665 w	665 w	675 w	675 m
700 m	690 m	700 m	690 m
	720 m	725 m	725 m
755 m	775 m	765 m	760 m
	765 m		775 m
		780 w	
	790 w	795 w	
805 m	810 w		800 w
840 m	850 m	830 m	830 m
			845 w
		860 w	860 m
	875 w		885 w
		900 w	
	915 w	920 w	920 w
			940 w
		960 w	965 m
	990 w	1000 m	1000 m
		1010 m	1015 m
1030 m	1030 sh	1030 s	1040 m
	1045 m		
1075 s	1085 m	1080 v.s.	1080 v.s.
1110 w		1110 w	
	1145 m		1140 v.s.
1175 m	1185 m	1180 v.s.	1180 s
			1195 s
1200 m	1215 w	1200 v.s.	1210 v.s.
1220 m			
1245 m	1250 m	1250 v.s.	1255 s
	1285 m	1295 s	1285 s
1300 m		1310 sh	1300 s
1330 m	1320 m	1345 v.s.	1335 v.s.
1370 m	1370 m	1370 v.s.	1370 v.s.
1400 w	1400 w		
1430 sh	1435 m		1435 s
1440 w		1440 m	
1450 w			
1470 m	1465 m	1460 sh	1455 sh
1490 m	1490 m		1490 s
1515 s	1520 m	1510 v.s.	1525 s
1580 m	1590 m		
1590 sh		1600 m	1600 s
1620 sh	1610 m		
1700 s	1705 m	1710 v.s.	1710 v.s.

Table 3 (continued)

Ligand Ia	Ligand Ib	Chelate IIa	Chelate IIb
2835 w	2840 w	2830 w	2835 m
	2900 w	2900 w	
2940 w	2940 w	2945 m	2950 m
	2960 w		
2980 w	2985 w	2990 m	
3000 sh	3010 sh		3000 m
3060 w	3050 w	3050 w	3070 w

v.s. = very strong; s = strong; m = medium;
w = weak; sh = shoulder

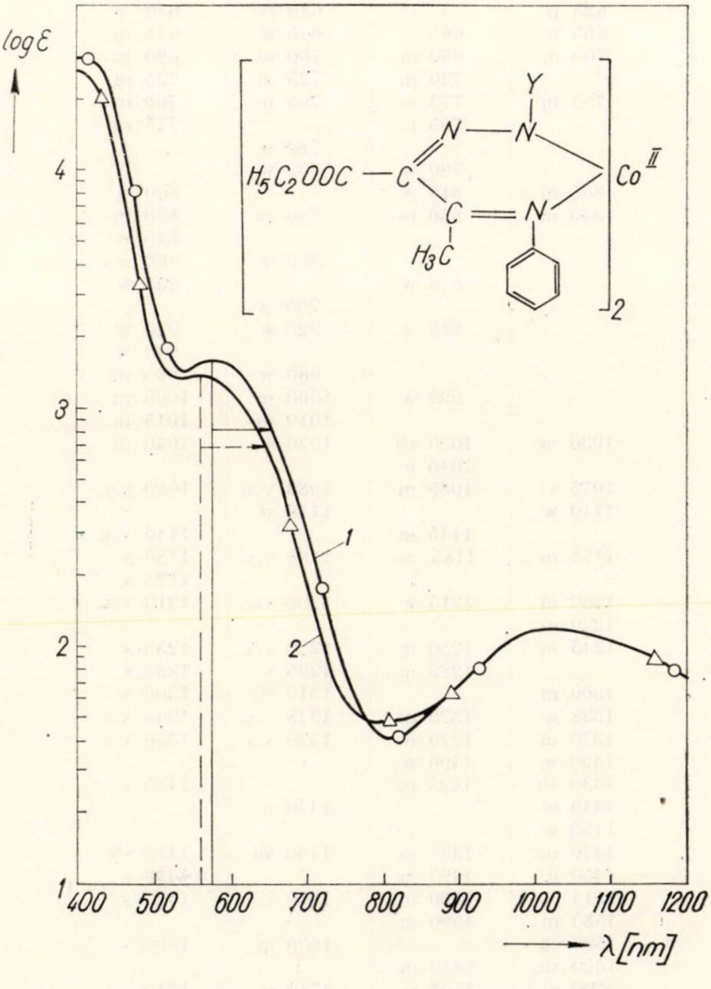

Fig. 1. – The electronic spectra of the Co(II) chelates. *1*, chelate IIa : $Y = p-CH_3O-C_6H_4$; *2*, chelate IIb : $Y = m-CH_3O-C_6H_4$.

occurring approximately at 570 nm, and the horizontal arrows show the half of the half-widths of these bands. One may observe that even though the spectra are almost similar and practically coincide in the near IR region, there are obvious differences in the visible range, especially the bathocromic shift of about 20 nm in the spectrum of the chelate IIa (with the OCH_3 substituent placed in the *para* position at the phenyl radical of the hydrazonic group) compared with that of the chelate IIb (with the same substituent but in the *meta* position). These differences occurring in the spectra of the chelates are much more obvious than those yet detectable but very small, observed with chelates of type II, in the case of the CH_3 substituent.[2]

The bands placed approximately at 560 and 1020 nm could be ascribed to the *d*–*d* transitions proper to a high spin tetrahedral d^7 electronic configuration. The energetic expressions for the spin-allowed d–d transitions for d^7 (T_d) obtained in a weak field coupling are as follows[6–8]:

$$ {}^4A_2(e^4\,t_2^3) \rightarrow {}^4T_2(e^3\,t_2^4) \qquad \Delta $$

$$ {}^4A_2(e^4\,t_2^3) \rightarrow {}^4T_1^{a}(e^3\,t_2^4) \quad 1.5\,\Delta + 7.5\,B - Q $$

$$ {}^4A_2(e^4\,t_2^3) \rightarrow {}^4T_1^{b}(e^3\,t_2^4) \quad 1.5\,\Delta + 7.5\,B + Q $$

where :

$$ Q = \frac{1}{2}\,[(0.6\,\Delta - 15\,\mathrm{B})^2 + 0.64\,\Delta^2]^{1/2}, $$

Δ is the orbital splitting parameter (the energetic separation between t_2 and e subshells), and *B* is the Racah parameter for the interelectronic repulsion energies ($B_{\mathrm{Co(II)}} = 980\ \mathrm{cm}^{-1}$). The energy of the first transition is just equal to the parameter Δ, and taking into account that $\Delta_{T_d} = 4/9\ \Delta_{O_h}$ and $\Delta_{O_h} = 10{,}000 - 15{,}000\ \mathrm{cm}^{-1}$ (relationship also valid in the framework of LCAOMO theory[9]), it results that this transition must occur in infrared, beyond the measuring possibility of the used instrument.

The two absorption bands occurring in the electronic spectra should be assigned to the other remaining d–d transitions, as follows :

$$ \nu_2\,({}^4A_2 \rightarrow {}^4T_1^{a}) = 9{,}800\ \mathrm{cm}^{-1} \text{ for both chelates II a–b} $$

$$ \nu_3\,({}^4A_2 \rightarrow {}^4T_1^{b}) = 17{,}390\ \mathrm{cm}^{-1} \text{ for the chelate IIa} $$

$$ = 17{,}860\ \mathrm{cm}^{-1} \text{ for the chelate IIb} $$

---

[6] A. B. P. Lever, "Inorganic Electronic Spectroscopy", Elsevier Publishing Company, Amsterdam–London–New York, 1968, chap. 8–9.

[7] Y. Tanabe and S. Sugano, *J. Phys. Soc. Japan*, **9**, 753 (1954).

[8] E. König, *Struct. and Bonding*, **9**, 175 (1971).

[9] H. H. Schmidtke, *Z. Naturforsch.*, **19a**, 1502 (1964).

Solving the energetic expressions for these transitions, the following values are obtained:

$$\Delta = 5{,}580\ \mathrm{cm}^{-1} \text{ for the chelate IIa}$$

$$= 5{,}540\ \mathrm{cm}^{-1} \text{ for the chelate IIb}$$

and with these values

$$B = 698\ \mathrm{cm}^{-1} \text{ for the chelate IIa}$$

$$= 736\ \mathrm{cm}^{-1} \text{ for the chelate IIb}$$

and finally

$$\beta = \frac{B}{B_0} = 0.71 \text{ for the chelate IIa}$$

$$= 0.75 \text{ for the chelate IIb.}$$

The Δ and *B* values thus obtained reproduce the absolute values of the absorption maxima as well as the difference between their wavenumbers.

In order to check how much reproducible are the spectra of the chelates as well as the spectrally estimated parameters, the electronic spectra have been also recorded on solutions of absolute ethanol. The band positions, their intensities and the Δ, *B* and β values calculated for these bands are collected in table 4.

Table 4

Electronic spectra recorded on solutions of acetone and abs. ethanol ($c = 0.5 \times 10^{-4} - 0.5 \times 10^{-3}$ m/l) and the Δ, B and β values of the Co(II) chelates

Chelate type II	Solvent	ν_3 nm	ν_3 cm^{-1}	ε_3 max $\times 10^3$	ν_2 nm	ν_2 cm^{-1}	ε_2 max $\times 10^2$	Δ cm^{-1}	B cm^{-1}	β
$Y = C_6H_5$	acetone	555	18,020	1.376	1,020...	9,800...	1.166	5,520	750	0.76
					1,040	9,620		5,400	760	0.77
	ethanol	560	17,860	1.180	1,040	9,620	1.053	5,400	750	0.76
$Y = p-CH_3O-C_6H_4$	acetone	575	17,390	1.620	1,020	9,800	1.173	5,580	698	0.71
	ethanol	575	17,390	1.432	1,020	9,800	1.066	5,580	698	0.71
$Y = m-CH_3O-C_6H_4$	acetone	560	17,860	1.380	1,020	9,800	1.160	5,540	736	0.75
	ethanol	560	17,860	1.268	1,030	9,710	1.080	5,480	743	0.76

One observes that in the case of the chelate IIa the solvent effect is reduced to a hyperchromic shift of both absorption maxima ν_3 and ν_2, when the solvent is changed, i.e. absolute ethanol instead of acetone. The positions of the absorption maxima remain practically unchanged, and so do the Δ, *B* and β values.

In the case of the chelate IIb, besides the above-mentioned hyperchromic shift when the used solvent is changed, acetone being replaced by absolute ethanol, a shift of about 10 nm (cca 100 cm^{-1}) of the maximum position of the band ν_2 takes place, which causes a slight modification, of about

10 cm^{-1}, in the B value and finally modifies with a figure of the second decimal the nephelauxetic ratio β (from 0.76 to 0.75). In an earlier paper [2] we have already shown that such a change in the β ratio constitutes the expected recording error which may appear not only when the used solvent is changed, but even for the same solvent, due to the lack of precision in the establishing of the assumed exact positions of the absorption maxima (determination error up to ± 200 cm^{-1}).

The change in the nephelauxetic ratio β value with 5 centesimal units (from 0.76 for the chelate IIb to 0.71 for the chelate IIa) clearly overpasses the experimental errors of measurements and shows a real increasing in the covalency degree of the metal-ligand bonds for the chelate IIa, when compared with IIb.

This result is not surprising. The fact that the OCH_3 substituent placed in the *meta* position at the phenyl radical of the hydrazonic group does not practically change the covalency degree of the complex against that of the chelate having only unsubstituted phenyl radicals attached to the donor nitrogen atoms is explained by that the OCH_3 substituent placed in the *meta* position does influence only through a feeble inductive effect [10] the electronic density of the substituted benzenic ring, as well as that of the donor nitrogen atoms directly bound to the aryl group. For these reasons the nephelauxetic ratio β rests practically unchanged (0.75 — 0.77).

In the *para* position the OCH_3 substituent exerts, however, a strong mesomeric effect, [10] leading to a marked increase in the electronic density values of the nitrogen donor atoms directly bound to the aryl group, and thence to the increase in the covalency degree value (lowering of the β ratio from 0.76 to 0.71).

The β ratio value in the case of the chelate IIa shows that its covalency degree is higher than that of the well-known $CoCl_4^{2-}$ion ($\beta = 0.73$) and practically equal to that of the $CoBr_4^{2-}$ ion ($\beta \approx 0.71$).

For a high spin tetrahedral d^7 configuration the magnetic moment may be calculated from [11,12]

$$\mu = \left(\mu_s - 15.59\frac{\lambda}{\Delta}\right) BM$$

where $\lambda = - 178$ cm^{-1} is the spin-orbit coupling constant, Δ the orbital splitting parameter, which in the case of both Co(II) chelates has been spectrally determined (see table 4), and $\mu_s = 3.89$ *BM* is the spin-only contribution to the magnetic moment value. Using the found Δ values (table 4) one finds that the quantity $(-15.59\lambda/\Delta)$, which is the orbital contribution to the magnetic moment value, is for both chelates of about 0.50 BM, so that their calculated magnetic moments are of 4.39 BM.

---

[10] H. Becker, "Einführung in die Elektronentheorie organisch-chemischer Reaktionen", Deutscher Verlag der Wissenschaften, Berlin, 1965, p. 362.

[11] R. Stahl-Broda and W. Low, *Phys. Rev.*, **113**, 775 (1959).

[12] F. A. Cotton and M. Goodgame, *J. Amer. Chem. Soc.*, **83**, 1777 (1961).

Experimentally, one finds:

$$\lambda = 4.35 \pm 0.05 \ BM \text{ for the chelate IIa}$$

$$\mu = 4.41 \pm 0.05 \ BM \text{ for the chelate IIb}$$

which are in good agreement with those spectrally determined.

The agreement between the spectral and magnetic properties allows us to assign a preponderant tetrahedral symmetry for the Co(II)–nitrogen bonds and a high spin electron distribution of the central metal ion in the case of both studied Co(II) chelates.

Acknowledgement. The authors thank the lecturer V. Mincu of the University of Bucharest for the magnetic susceptibility measurements.

Revue Roumaine de Chimie, **19**, 7, 1179 – 1184 (1974)

THE $PdCl_2$-INDUCED REARRANGEMENT OF DIBENZOBULLVALENE INTO DIBENZO [*g,h*] BICYCLO [4.3.2.] DECA-2,4,7,9-TETRAENE

M. BANCIU, M. ELIAN, C. DRĂGHICI and ECATERINA CIORĂNESCU

Organic Chemistry Research Center, Spl. Independenţei 202-B, Bucharest 15, Romania

Received February 4, 1974

By treating dibenzobullvalene (**1**) or dibenzo [*g, h*] bicyclo [4.2.2] deca-2,4,7,9-tetraene (**2**) with $PdCl_2 \cdot (C_6H_5CN)_2$, the same complex **3** of the $(C_{18}H_{14})_2 \cdot (PdCl_2)_3$-type was obtained; the decomposition with aqueous pyridine led to the diene **2**. Similar results were obtained working with deuterated hydrocarbons (10-*d*-**1** and 3-*d*-**2**). A mechanism for this valence isomerization is proposed which is also consistent with the behaviour of *d*-compounds.

In a previous paper [1] the synthesis, the thermal and photochemical rearrangements of dibenzobullvalene and of some other dibenzo $(CH)_{10}$-hydrocarbons have been reported.

The metal-induced skeletal rearrangements of bullvalene were extensively investigated in the last years.[2] The recent report of Vedejs and co-workers[3] about homotropylidene-palladium dichloride complexes prompted us to report our results with dibenzobullvalene.

RESULTS AND DISCUSSIONS

By treating dibenzobullvalene (**1**)[1] with bis (benzonitrile)palladium dichloride in anhydrous benzene at 70° for 3 hrs, a reddish-brown complex (m.p. $>350°$) precipitates in good yield, with the expected displacement of benzonitrile. The elemental analysis of the complex indicates the composition $(C_{18}H_{14})_2. (PdCl_2)_3$. The same complex was invariably obtained with different molar ratios of reactants, between 1-2 moles $PdCl_2 (C_6H_5CN)_2$ per mole of **1**.

---

[1] M. Banciu, M. Elian, E. Ciorănescu and C. D. Nenitzescu, *Tetrahedron Letters*, **1972**, 2573.

[2] G. N. Schrauzer, P. Glockner and R. Merenyi, *Angew. Chem.*, **76**, 498 (1964); E. Vedejs, *J. Amer. Chem. Soc.*, **90**, 4751 (1968); H. P. Loffler and G. Schröder, *Angew. Chem.*, **80**, 758 (1968); R. Aumann, *Angew. Chem.*, **82**, 810 (1970); G.N. Schrauzer, P. Glockner, K. I. G. Reid and I. C. Paul, *J. Amer. Chem. Soc.*, **92**, 4479 (1970).

[3] E. Vedejs, M. F. Salomon and P. D. Weeks, *J. Amer. Chem. Soc.*, **95**, 6770 (1973).

On decomposition of this complex with pyridine-water solution at room temperature, dibenzo[*g, h*]bicyclo[4.2.2]deca-2,4,7,9-tetraene (**2**) was isolated in 75% yield and more than 92% purity.

The same complex (IR spectrum, elemental analysis) precipitates in nearly quantitative yield by treatment of the diene **2** with bis(benzonitrile)palladium dichloride at room temperature for 24 hrs.

Unfortunately, the insolubility of the complex renders impossible its characterization through NMR spectrum or by borohydride reduction. Nevertheless, taking into account the composition and the easier formation of the complex when **2** was used as starting material (as compared to **1**), the structure **3** is suggested :

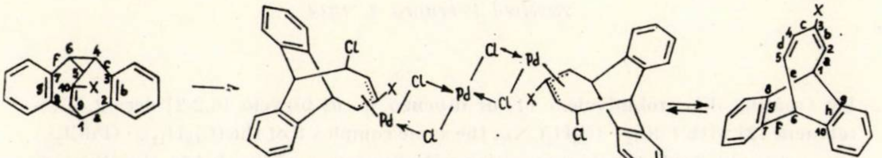

1 (X=H)
d-1 (X=D)

3 (X=H)
d-3 (X=D)

2 (X=D)
d-2 (X=D)

Attempts to obtain a complex having dibenzobullvalene as ligand failed. From **1** with $PdCl_2 \cdot (C_6H_5CN)_2$ *at 50°* only the complex **3** was isolated in good yield after 24 hrs. *At room temperature* no sign of complexation could be evidenced by following the reaction by NMR for 48 hrs ; however, the complex 3 precipitates in small yield even under these conditions after a week.

In order to obtain additional information concerning the valence isomerization, the same reactions were performed with deuterated compounds. The synthesis of *d*-compounds was realized by reduction of the ketone **4**[1] with $LiAlD_4$:

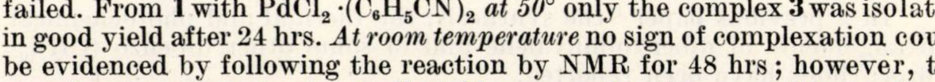

4

5

d-2

d-1.

The *d*-alcohol **5** (m.p. 115 — 116°) obtained in a good yield was dehydrated, affording a mixture of alkenes. From this mixture the pure *d*-**2** (m.p. 177—179°) was separated through recrystallization from methanol, while *d* - **1** (m.p. 109—115°) was isolated in 85% purity (the only impurity being *d* - **2**) through column chromatography on neutral alumina.

The NMR spectra (see Experimental) of the compounds 10-*d*-**5**, 10-*d*-**1** and 3-*d*-**2** are in agreement with the position of deuterium label.

By treating the *d*-**1** or *d*-**2** hydrocarbon with $PdCl_2 \cdot (C_6H_5CN)_2$ under the same conditions as described for **1** and for **2** respectively, a complex with the same composition $(d\text{-alkene})_2 \cdot (PdCl_2)_3$ was obtained. After pyridine-water decomposition of this complex only the deuterated hydrocarbon *d*-**2** was isolated.*

As in other cases,[4] it is difficult to know exactly the stepwise process by which the rearranged structure is attained. Nevertheless the following scheme, which is in agreement with the results of experiments using deuterated compounds, could be suggested :

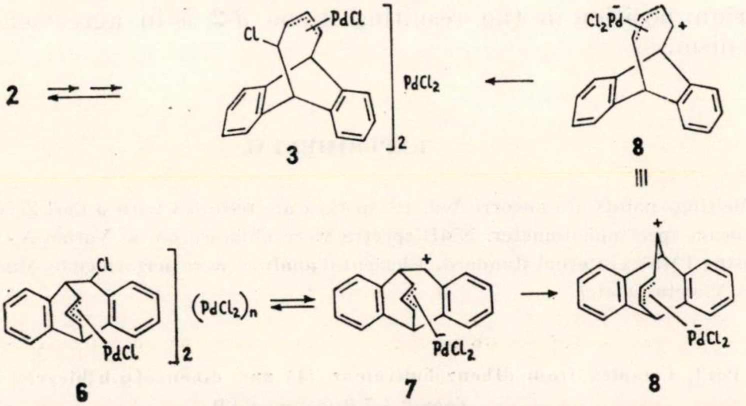

The complex **3**, obtained from the diene **2** and $PdCl_2 \cdot (C_6H_5CN)_2$ is very probably of the π-allylic type. The formation of π-allylic complexes from 1,3-dienes is generally accepted and supported by many examples.[5] However, the same complex **3** resulted also from dibenzobullvalene (**1**), evidently after skeletal rearrangement.

For the first intermediate which occurs on treatment of dibenzobullvalene with $PdCl_2 \cdot (C_6H_5CN)_2$, the structure **6** could be admitted. Formation of π-allylic complexes of this type from vinylcyclopropanes is also known.[4,5,6] An analogous structure has been proposed by Vedejs[3] for the complexes of bullvalene and benzobullvalene (by analogy with the more soluble complex of dihydrobullvalene which could be characterized spectrally and by usual reactions).

---

* The converse valence isomerization **2**→**1** reported to occur photochemically[1] was also performed with d-**2** under the same conditions ; in the resulted dibenzobullvalene the label was equally distributed in 5- and 10-positions.

[4] R. M. Moriarty, C. L. Yeh, K. N. Chen, E. L. Yeh, K. C. Ramey and C. W. Jefford, *J. Amer. Chem. Soc.*, **95**, 4756 (1973).

[5] P. M. Maitlis, "The Organic Chemistry of Palladium", Academic Press, New York, 1971, vol. I, p. 145, 192.

[6] D. T. Shono, T. Yoshimura, Y. Matsumura and R. Oda, *J. Org. Chem.*, **33**, 876 (1968) ; R. Aumann, *Angew. Chem.*, **83**, 175, 176, 177 (1971) ; A. Eisenstadt, *Tetrahedron Letters*, **1972**, 2005 ; R. M. Moriarty, C. L. Yeh and R. Srinivasan, *Tetrahedron Letters*, **1972**, 5325.

In dibenzobicyclic systems, having a benzylic leaving group, rearrangements accompanied by ring contraction occur very easily[7]; this could account for the failure to isolate a complex of the **6**-type which could regenerate dibenzobullvalene on decomposition. The skeletal rearrangement leading to the complex **3** fits pretty well with an ionic mechanism. The conversion of **6** to **8** could occur through a benzylic intermediate **7** which undergoes a phenyl migration or by displacement of the chlorine group assisted by the aromatic ring from the β-position. The homobenzylic intermediate **8** leads then to the complex **3** (much more stable than **6**). The deuterium position in the resulting diene *d*-**2** is in agreement with this mechanism.

EXPERIMENTAL

Melting points are uncorrected. IR spectra are recorded with a Carl Zeiss-Jena UR 20 double beam spectrophotometer. NMR spectra were obtained on a Varian A - 60 A spectrometer using TMS as internal standard. Elemental analyses were performed by Miss Elvira Sliam and Mrs Violeta Daniel.

$PdCl_2$ Complex from dibenzobullvalene (1) and dibenzo[g,h]bicyclo[4.2.2]-deca-2,4,7,9-tetraene (2)

A filtered solution of bis (benzonitrile) palladium dichloride[8] (175 mg; 0.45 mmole) in anhydrous benzene (8 ml) was dropped during 30 min over a solution of dibenzobullvalene (**1**)[1] (70 mg; 0.3 mmole) in anhydrous benzene (3 ml). The solution was heated to 70° for 3 hrs; then the precipitated reddish-brown complex was filtered from the cooled reaction mixture. The complex was triturated with petroleum ether (removal of benzonitrile traces), filtered and dried. The complex **3**, m.p.$>$350°, was obtained, 92 mg (62% yield). Found: C, 43.28; H, 3.22; Pd, 33.54; Cl, 20.04. $(C_{18}H_{14})_2 \cdot (PdCl_2)_3$ requires: C, 43.54; H, 2.84; Pd, 32.21 and Cl, 21.41%.

IR spectrum (Nujol, cm^{-1}): 434 m, 448 m, 569 m, 588 m, 620 m, 669 s, 698 s, 728 vs, 751 s, 779 m, 951 m and 1119 w.

The same complex was obtained working at 50° for 24 hrs (precipitation begins in less than 1 hr). At room temperature the NMR spectrum of this reaction mixture remained unchanged for 48 hrs; after a week the complex **3** precipitates in about 10% yield. When different molar ratios of dibenzobullvalene to bis(benzonitrile)palladium dichloride were used (1 : 1 or 1 : 2) the same complex as above was always obtained.

---

[7] See for example: S. J. Cristol, F. P. Parungo, D. E. Plorde and K. Schwarzenbach, *J. Amer. Chem. Soc.*, **87**, 2879 (1965); E. Ciorănescu, A. Mihai, G. Mihai, M. Elian and C. D. Nenitzescu, *Rev. Roumaine Chim.*, **10**, 175 (1965); S. J. Cristol, R. M. Sequeira and G. O. Mayo, *J. Amer. Chem. Soc.*, **90**, 5564 (1968); E. Ciorănescu, M. Banciu, R. Jelescu, M. Rentzea, M. Elian and C. D. Nenitzescu, *Tetrahedron Letters*, **1969**, 1871; *Rev. Roumaine Chim.*, **14**, 911 (1968); M. Banciu, *Stud. Cerc. Chim.*, **21**, 773 (1973).

[8] M. S. Kharasch, R. C. Seyler and F. R. Mayo, *J. Amer. Chem. Soc.*, **60**, 882 (1938).

By treating a solution of dibenzo [*g*, *h*] bicyclo [4.2.2] deca-2, 4, 7, 9-tetraene (**2**)[1] (45 mg ; 0.195 mmole) in anhydrous benzene (3 ml) with a filtered solution of bis (benzonitrile) paladium dichloride (76 mg ; 0.198 mmole) in anhydrous benzene (7 ml) *at room temperature*, a reddish-brown precipitate sedimentates in 24 hrs, after which time the supernatant solution becomes practically colourless. Filtration and washing of the precipitate with petroleum ether afforded the complex **3**, 55 mg (85 % yield, calculated on bis(benzonitrille)palladium dichloride). This complex was found to be identical (by elemental analysis and IR spectrum) with that obtained from dibenzobullvalene. The combined filtrates afforded on evaporation about 10 mg of unreacted diene **2**. The same complex **3** was obtained using 2 — 3 equivalents of bis (benzonitrile)palladium dichloride for 1 equivalent of **2** ; in this case from the evaporated filtrates a solid was formed (on petroleum ether addition) whose IR spectrum was identical with that of authentic bis-(benzonitrile)palladium dichloride.

From reaction of **2** and Na_2PdCl_4 in methanol an isoluble complex resulted which was not characterized.

$PdCl_2$ Complex from 3-d-dibenzo[g, h]bicyclo[4.2.2]deca -2,4,7,9-tetraene (d-2) and 10-d-dibenzobullvalene (d-1)

From *d* - **2** (see later) and bis(benzonitrile)palladium dichloride (in 2 : 3 molar ratio) as described above for **2**, the deuterated $PdCl_2$-complex precipitated and could be separated in 85 % yield, by working at room temperature. Found : C, 43.96 ; H, 3.21 ; Pd, 33.04 ; Cl, 19.84. $(C_{18}H_{13}D)_2 \cdot (PdCl_2)_3$ requires : C, 43.44 ; H, 3.03 ; Pd, 32,16 and Cl, 21.37 %.

IR spectrum (Nujol, cm^{-1}) : 441 m, 531 w, 546 m, 575 m, 589 m, 621 m, 671 s, 685 s, 731 vs, 751 s, 778 m, 940 w and 1114 w.

In the case of deuterated dibenzobullvalene (*d* - **1**) (see later) the reaction mixture (the same quantities as described above for **1** being used) was initially maintained for 24 hrs at room temperature, when a little amount (10 mg) of complex from the *d* - **2** (existing as contaminant of *d* - **1** ; see later) precipitates. The clear supernatant liquid was then heated for 3 hrs at 70°, when the same complex (elemental analysis, IR spectrum) as from *d* - **2** was obtained (86mg ; 58 %).

Experiments using alkene (*d* - **1** or *d* - **2**) : $PdCl_2 \cdot (C_6H_5CN)_2$ molar rations of 1 : 1 or 1 : 2 afforded always the same complex ; the unreacted component (alkene or bis (benzonitrile)-palladium dichloride) was recovered.

Decomposition of the $PdCl_2$ complexes 3 and d - 3

A pyridine : water 1 : 2 solution (7.5 ml) was added with stirring at room temperature over the $PdCl_2$ complex **3** (or *d* - **3**) 60 mg. In a few minutes the complex was decomposed (decoloration) and a white microcrystalline product was formed. The reaction mixture was ether extracted, the extract was washed with water, dil. HCl, again with water, then dried and evaporated. The crystalline product obtained (19.2 mg ; 70 %) was (as indicated by its NMR spectrum) *dibenzo* [*g*, *h*] *bicyclo* [*4.2.2*] *deca-2, 4, 7, 9-tetraene* (**2**)[1] (or *d* - **2**, respectively). The purity of these products checked on v.p.c. (20 % Silicone OV7 on Chromosorb P columns, 220°) was more than 92 %.

10-d-Dibenzo [b,g] tricyclo [3.3.2.0.^{4,6}] deca-2,7-dien-10-ol 5

Over a cooled stirred suspension of $LiAlD_4$ (0.3 g ; 7.15 mmoles) in anhydrous ether (25ml), a suspension of dibenzo *[b, g]* tricyclo [3.3.2.0 ^{4,6}] deca-2,7-dien-10-one (**4**)^1 (2.2 g ; 9 mmoles) in anhydrous ether (200 ml) was dropped during 1 hr. The reaction mixture was then refluxed for 7 hrs and left overnight. The usual work-up afforded 2.1 g (94 %) *10-d-dibenzo[b, g]tricyclo-[3.3.2.0.^{4,6}] deca-2,7-dien-10-ol* (**5**) m.p. 115–116° (methanol).

IR spectrum (KBr ; cm^{-1}) : 756 vs, 1065 s, 1075 s, 1493 m, 2105 w, 2155 w, 2863 w, 2926 m, 3013 m, 3058 m and 3100–3450 ms.

NMR spectrum ($CDCl_3$; δppm) : 6.95–7.50 (m ; 8H ; H_{arom}) ; 3.71 (t ; 1H ; J = 5.5Hz ; H_1) ; 1.9–2.7 (m ; 6H ; $H_{4,5,6,9,OH}$).

3-d-Dibenzo[g, h] bicyclo[4. 2.2] deca 2, 4, 7, 9-tetraene (d-2) and 10-d-dibenzobullvalene (d-1) from the d-alcohol 5

An intimate mixture of *d*-alcohol **5** (**2**g ; 8 mmoles) and H_3BO_3 (1.6 g ; 25.7 mmoles) was sublimated in 4 equal portions at 180°/1 mm Hg (every portion required approximately 1 hr for sublimation). The partially crystallized products were combined (0.6 g ; 33 %) then recrystallized from methanol affording 0.17 g of crude *d*-**2** (m.p. 165 – 172°). After a new recrystallization from ethanol 0.12 g pure *3-d-dibenzo[g, h]bicyclo [4.2.2.]deca-2,4,7,9-tetraene* (*d*-**2**) was obtained, m.p. 177–179°.

IR spectrum (CS_2 ; CCl_4 ; cm^{-1}) : 550 ms, 570 ms, 648 s, 744 vs, 880 m, 1369 s, 1480 m, 2234 vw, 2924 m, 3024 s and 3070 m.

NMR spectrum ($CDCl_3$, δ ppm) : 7.0–7.3 (m ; 8H ; H_{arom}) ; 6.1–6.7 (m ; 2H ; $H_{2;5}$) ; 5.45 (d ; *J* = 12.5 Hz ; 1H ; H_4) ; 4.47 (d ; J = 9.5 Hz ; 2H ; $H_{1;6}$).

The combined filtrates from the above recrystallizations were evaporated *in vacuo,* and the partially crystallized residue (0.4 g) was chromatographed on a short neutral alumina column which was eluted with petroleum ether (b.p. 30–40°). The first eluates (75 ml) afforded on evaporation an uncrystallizable oil (0.2 g), a mixture of *d*-**2** and *d*-**1**. The following eluates (200 ml) afforded on evaporation white crystals (0.17)g) of crude *10-d-dibenzobullvalene* (*d*-**1**) which, after washing with cold ethanol, showed a m.p. of 109–115°. The v.p.c. analysis (20 % Silicone OV 7 on Chromosorb P columns, 220°) of this product indicated a purity of 85 % *d*-**1**, the single contaminant being *d*-**2**.

IR spectrum (CS_2 ; CCl_4 ; cm^{-1}) : 754 vs, 773 s, 905 m, 1370 s, 1494 m, 2252 vw, 2850 vw, 2926 m, 3026 s and 3066 m.

NMR spectrum (CCl_4, δ ppm) : 6.9–7.2 (m ; 8H ; H_{arom}) ; 5.95 (d, J = 9.2 Hz ; 1H ; H_9) ; 3.68 (d ; J = 9.2 Hz ; 1H ; H_1) ; 2.1–2.95 (A_2B-type spectrum ; 3H ; $H_{4,5,6}$).

Revue Roumaine de Chimie, **19**, 7, 1185–1196 (1974)

CHEMICAL GRAPHS. XXI[1]

VALENCE ISOMERS OF BENZOANNULENES

A. T. BALABAN
Institute of Atomic Physics, P.O.B. 35, Bucharest, Romania

Received February 28, 1974

Starting from tables of cubic multigraphs corresponding to the formulas of valence isomers of annulenes, two procedures are presented for obtaining the formulas of valence isomers of monobenzoannulenes (or polybenzoannulenes, noted by [b] benzo-[n]annulenes): (i) the trivial one, selecting from the table of cubic multigraphs with n + 4b points those graphs which have b 1,3-cyclohexadienic rings, and (ii) a direct procedure based on the table of cubic multigraphs with n points and at least b double bonds, replacing b double bonds by condensed benzenoid rings.

INTRODUCTION

The enumeration of valence isomers * of [n]annulenes [3,4] was possible starting from the observation that their formulas are cubic (trivalent) multigraphs with n points, where a point corresponds to a CH group and a line to a covalent band. Hence the enumeration of all such graphs was at the same time the enumeration of valence isomers of annulenes. However, this was an unsolved problem of graph theory, [5] so that an algorithm based on general graphs had to be found,[6] enabling the construction of complete tables for cubic multigraphs with 4 — 10 points, [3] and later with 12 points. [4] Since chemically only molecules corresponding to planar graphs can be synthesized, the table for cubic multigraphs with 12 points was restricted to planar ones in order to reduce the number of formulas and to provide a table of significant isomers.

In the meantime, a mathematical procedure for counting graphs and multigraphs has been found, [7,8] but it is not amenable to numerical computation and even less to providing the pictures of the graphs.

---

* The definiton of valence isomeric formulas is : these formulas correspond to connected graphs having the same partition of degrees of their vertices. [2]

[1] Preceding part : A. T. Balaban, *Rev. Roumaine Chim.*, **19**, 000 (1974).

[2] A. T. Balaban, *Rev. Roumaine Chim.*, **18**, 635 (1973).

[3] A. T. Balaban, *Rev. Roumaine Chim.*, **11**, 1097 (1966) ; Erratum, *ibid.*, **12**, Nr. 1, 103 (1967).

[4] A. T. Balaban, *Rev. Roumaine Chim.*, **17**, 865 (1972).

[5] F. Harary, *Publ. Math. Inst. Hungar. Acad. Sci.*, **5**, 63 (1960).

[6] A. T. Balaban, *Rev. Roumaine Chim.*, **15**, 463 (1970)

[7] R. W. Robinson, unpublished.

[8] F. Harary and A. R. Palmer, "Graphical Enumeration", Academic Press, New York, 1973.

Benzoderivatives of annulenes are hydrocarbons possessing an *ortho*-fused benzenoid ring condensed with the annulene, and can be theoretically derived by replacing a double bond with such a benzenoid ring. If b benzenoid rings are thus condensed to an [n]annulene, we obtain a polybenzo-[n]annulene which will be denoted by [b]benzo-[n]annulene.

Thus, a valence isomer of an [n]annulene is $(CH)_n$, but its [b]benzoderivative has b pairs of adjacent CH group replaced by b *ortho*-phenylene groups C_6H_4. Therefore the molecular formula of a [b]benzo-[n]annulene or of any of its valence isomers is $C_{n+4b}H_{n+2b}$; these compounds possess 2b quaternary carbon atoms and n + 2b CH groups.

In [b]benzo-[n]annulenes, we have necessarily $1 \leqslant b \leqslant n/2$. Starting from a valence isomer of an [n]annulene $(CH)_n$ and conserving the number of carbon atoms, one can obtain by theoretical stepwise abstractions of two hydrogen atoms, valence isomers of mono-benzo-[n — 4] annulene C_nH_{2n-2}, then of dibenzo-[n — 8] annulene C_nH_{2n-4}, etc., arriving in the end to valence isomers of $\left[\left\langle \frac{n}{6} \right\rangle\right]$ benzo-$\left[n - 4\left\langle \frac{n}{6} \right\rangle\right]$ annulene $C_nH_{n-2}\left\langle \frac{n}{6} \right\rangle$, where $\left\langle \frac{n}{6} \right\rangle$ is the integer part of n/6. The ratio of carbon *versus* hydrogen atoms in a [b]benzo-[n]annulene valence isomer being denoted by x, $\left(\frac{n+4b}{n+2b} = x\right)$, we have $1 < x \leqslant 1.5$. The highest value of x, i.e. 1.5, is attained in polyphenylenes $(C_6H_4)_{n/2}$, i.e. in $\left[\frac{n}{2}\right]$ benzo-[n] annulenes.

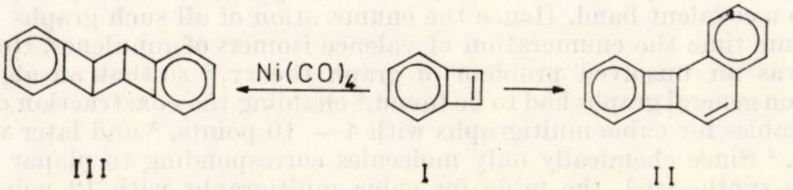

III I II

The simplest example of a monobenzoannulene* is benzocyclobutadiene I [9,**] an elusive compound which dimerizes spontan-

---

[*] The smallest annulene is considered to be [4] annulene. Theoretically, one could consider acetylene to be the smallest annulene, as in ref. 6, but for the present discussion this would be too far-stretched, since one would have to devise a convention as to how many "double bonds" there are in acetylene.

[**] The nomenclature in this paper follows the traditional usage and is at variance with the *Chemical Abstracts* nomenclature, adopted also by Beilstein's Dritter Ergänzungswerk. According to *Chem. Abstr.* Index Guide Introduction **76**, § 151 (1972), "cyclooctene as part of a fused system is not meant to imply the presence of a *single* bond; instead, saturated carbon atoms are indicated by 'hydro' prefixes". We shall, however, use [b]benzocyclooctatetraene instead of [b]benzocyclooctene, benzocyclobutadiene instead of benzocyclobutene, and dibenzocyclobutadiene instead of dibenzocyclobutene, in such names.

[9] M. P. Cava and M. J. Mitchell, "Cyclobutadiene and Related Compounds", Academic Press, New York, 1967; W. Baker and J. F. W. McOmie, in "Progress in Organic Chemistry" (ed. J. W. Cook), Butterworths, London, **3**, 44 (1955); "Non-Benzenoid Aromatic Compounds" (ed. D. Ginsburg), Interscience, New York, 1959; J. W. Barton, in "Nonbenzenoid Aromatics" (ed. J. P. Snyder), Academic Press, New York, 1969.

eously to give II,[10] or in the presence of $Ni(CO)_4$ catalyst to give III.[11]

Naphthalene IV is a monobenzo-[6]annulene, phenanthrene V and anthracene VI are dibenzo-[6] annulenes, and triphenylene VII is tribenzo-[6]annulene. It is apparent that all polybenzoannulenes are *cata*-condensed systems.[12]

Whereas naphthalene, phenanthrene and triphenylene can be obtained from the Kekulé formula of benzene by replacing one or more double bonds with condensed benzenoid rings, anthracene cannot, hence it is somewhat different from the other ones; we will call it an *o*-quinonoid benzoderivative.*

We shall inscribe in benzenoid rings a circle according to the usual convention when the structure is not *o*-quinonoid, but shall write double bond structures in *o*-quinonoid derivatives, as exemplified by formulas IV – VI, throughout the present paper.

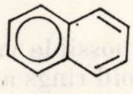
IV

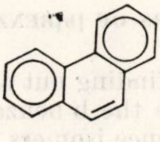
V

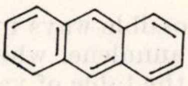
VI

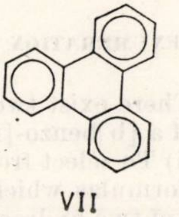
VII

No special significance of the type proposed by Clar[13] will be attached to the presence or absence of inscribed circles, this being only a convention to discriminate *o*-quinonoid formulas (as will be shown below, an asterisk will serve the same purpose in notations). The structural condition for the existence of *o*-quinonoid benzoderivatives is to have an initial structure VIII with at least two conjugated double bonds. Then, in addition to the normal mono- and polybenzoderivatives IX and X, *o*-quinonoid benzoderivatives XI are possible.

---

* The name *o*-xylylenoid would be more correct, but is less convenient.

[10] M. P. Cava and D. R. Napier, *J. Amer. Chem. Soc.*, **78**, 500 (1956); **79**, 1701 (1957); **80**, 2255 (1958); M. P. Cava, *Bull. Soc. Chim. France*, **1959**, 1744; M. P. Cava and M. J. Mitchell, *J. Amer. Chem. Soc.*, **81**, 5409 (1959); C. D. Nenitzescu, M. Avram and D. Dinu, *Chem. Ber.*, **90**, 2541 (1957).

[11] M. Avram, D. Dinu and C. D. Nenitzescu, *Chem. and Ind.*, **1959**, 257; M. Avram, D. Dinu, G. Mateescu and C. D. Nenitzescu, *Chem. Ber.*, **93**, 1789 (1960); M. Avram, I. G. Dinulescu, D. Dinu, G. Mateescu and C. D. Nenitzescu, *Tetrahedron*, **19**, 309 (1963); M. P. Cava and R. Pohlke, *J. Org. Chem.*, **28**, 1012 (1963).

[12] A. T. Balaban and F. Harary, *Tetrahedron*, **24**, 2505 (1968).

[13] E. Clar, "The Aromatic Sextet", Wiley, London, 1972; "Polycyclic Hydrocarbons", Academic Press, New York, 1964.

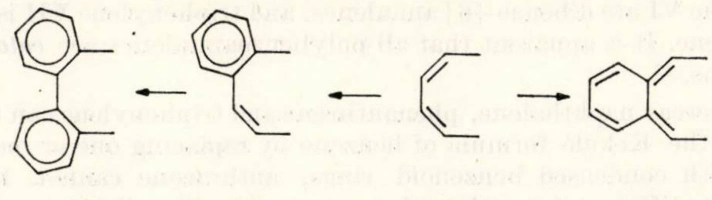

X IX VIII XI

In the following discussion only constitutional (topological) isomerism will be considered, ignoring stereoisomerism. The formulas are drawn so as to avoid crossing lines, emphasizing that all graphs are planar, rather than so as to mimic the geometry of the molecules.

ENUMERATION OF VALENCE ISOMERS OF [b]BENZO-[n]ANNULENES

There exist two possible ways in finding out all possible valence isomers of a [b]benzo-[n] annulene, where the b benzenoid rings are intact :

(i) To select from the table of valence isomers of [n + 4b] annulenes those formulas which have b condensed 1,3-cyclohexadienic rings, which by loss of two hydrogen atoms can be converted into b annelated benzenoid rings.

This is the trivial, crude approach. Since tables for valence isomers of [4]- through [12] annulene are available, only valence isomers of monobenzoderivatives of [4]- to [8]annulene and the dibenzoderivative of [4]annulene (biphenylene) can thus be found. We are interested, however, especially in valence isomers of polybenzo-[10]annulene.

(ii) To start from the table of valence isomers of [n]annulenes and replace b double bonds by benzenoid rings. We shall follow this latter approach, which is called annelation.

Tables 1 and 2 present the number of valence isomers of [n] annulenes having exactly β double bonds : planar and non-planar graphs in table 1, only planar graphs in table 2. They were compiled on the basis of data provided in references 3, 4 and 6.

Starting from the data in table 2, we can construct table 3 giving the number of planar valence isomers of [n]annulenes having *at least* β double bonds. Each entry (n, β) from table 3 is the sum of entries $\sum_i (n, \beta_i)$ from table 2 with $\beta_i = \beta, \beta + 1, \ldots, n/2$.

For obtaining the valence isomers of a [b]benzo-[n]annulene we have to replace b double bonds in each valence isomer having at least b double bonds (cf. table 3) by b benzenoid rings. We have to find out whether the double bonds are equivalent or not, i.e. whether there exists an automorphism of the multigraph mapping the double bonds on one another.

Table 1

Number of ***planar and non planar*** **valence isomers of [n]annulenes having** ***exactly*** **β double bonds**

β \ n	4	6	8	10
0	1	2	5	19
1	0	1	5	23
2	1	2	5	25
3	—	1	4	16
4	—	—	1	7
5	—	—	—	1
Total	2	6	20	91

Table 2

Number of ***planar*** **valence isomers of [n]annulenes having** ***exactly*** **β double bonds**

β \ n	4	6	8	10	12
0	1	1	3	9	32
1	0	1	4	16	75
2	1	2	5	22	112
3	—	1	4	16	86
4	—	—	1	7	41
5	—	—	—	1	10
6	—	—	—	—	1
Total	2	5	17	71	537

Table 3

Number of ***planar*** **valence isomers of [n] annulenes having** ***at least*** **β double bonds**

β \ n	4	6	8	10	12
0	2	5	17	71	357
1	1	4	14	62	325
2	1	3	10	46	250
3	—	1	5	24	138
4	—		1	8	52
5	—	—	—	1	11
6	—	—	—	—	1

All multigraphs with 2 or 3 double bonds and n = 4 or 6 points have equivalent double bonds. However, for n ⩾ 8 there exist multigraphs with two or more non-equivalent double bonds, so that in these cases one cubic multigraph gives rise to more than one mono- or poly-benzoderivative.

As notation for the benzoderivatives we shall use the notation of the valence isomers of annulenes * preceded by the symbol bB_i (or $bB_i{}^*$ for *o*-quinonoid structures), where b indicates the number of annelated benzenoid rings, B stands for benzo, and i is absent when there exists only one polybenzoderivative (i. e. when all double bonds to be annelated are equivalent), but is a serial index starting with 1 when one cubic multigraph gives rise to more than one polybenzoderivative. The order in which the polybenzoderivatives, resulted by annelation at non-equivalent bonds, are assigned serial indices i = 1, 2, ... is given by the following rules :

(i) *o*-Quinonoid structures follow all structures which are not *o*-quinonoid but are derived by annelation of the same valence isomer of an annulene.

(ii) When the annelated double bond is not involved in a ring, the serial index is lower than when it is involved in a ring.

(iii) The smaller is the smallest ring in which the annelated double bond is involved, the smaller is the serial index.

(iv) When all previous rules fail to provide a precedence criterion for mono- or polybenzoderivatives derived from annulene valence isomers with several double bonds in larger rings, then double bonds to be annelated with precedence are those closer to a smaller ring.

(v) When all previous rules fail to provide a precedence criterion for polybenzoderivatives this is done on the basis of the shortest path between the double bonds to be annelated : the longer this path (or sum of paths), the smaller is the serial index.

Thus, according to the above rules, acyclic double bonds to be annelated take precedence over cyclic ones, double bonds in smaller rings take precedence over those in larger rings, non-*o*-quinonoid structures take precedence over *o*-quinonoid ones, and annelation of clustered double bonds takes precedence over annelation of remote double bonds.

The application of all above ideas can be seen in table 4 (presenting all possible valence isomers of polybenzo-[n]annulenes with n = 4, 6 and 8) and in table 5 (for n = 10).

---

* This notation consists of a string of five numbers separated by hyphens indicating in turn the numbers of :

— points (CH groups), i.e. the order of the graph, n

— double bonds, i.e. circuits with two points, β

— circuits with three points, t

— circuits with four points, q

— a serial number s which starts with 1 and is larger only when n, β, t and q have the same values for more than one graph ; the order in which graphs are assigned s = 1, 2, ... is that of increasing number of circuits with 5,6 ... points. Thus, a wholly convention-free notation can be designed. Notations of ref. 3, 4 and 6 did not observe this last criterion for s, but in the present paper this has been done.

Table 5C

Valence isomers of [b] benzo-[10] annulenes with b = 3, 4, and 5.

b = 3

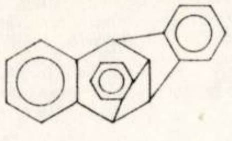
3B-10-3-0-0-1

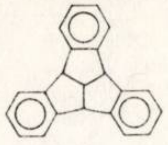
3B-10-3-0-0-2

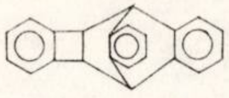
3B-10-3-0-1-1

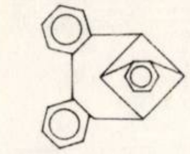
3B-10-3-0-1-2

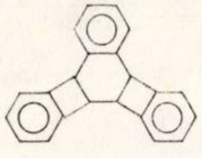
3B-10-3-0-2-1

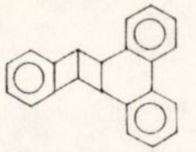
3B-10-3-0-2-2

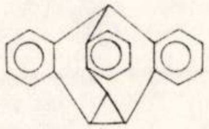
3B-10-3-1-0-1

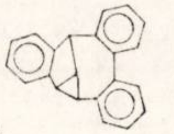
3B-10-3-1-0-2

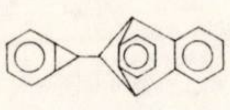
3B-10-3-1-0-3

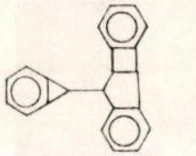
3B-10-3-1-1-1

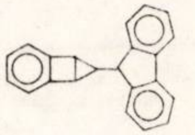
3B-10-3-1-1-2

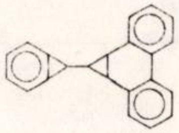
3B-10-3-2-0-1

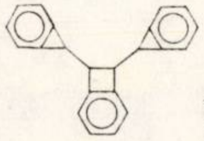
3B-10-3-2-1-1

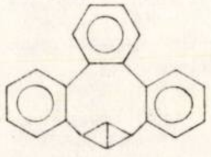
3B-10-3-2-1-2

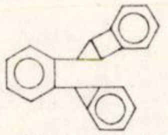
3B-10-3-2-1-3

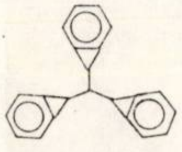
3B-10-3-3-0-1

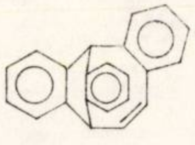
$3B_1$-10-4-0-0-1

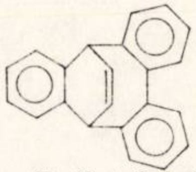
$3B_2$-10-4-0-0-1

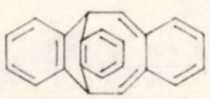
$3B_3^*$-10-4-0-0-1

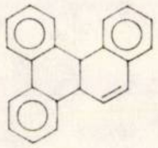
$3B_1$-10-4-0-0-2

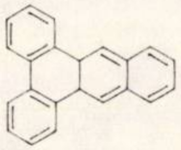
$3B_2^*$-10-4-0-0-2

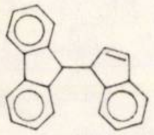
$3B_1$-10-4-0-0-3

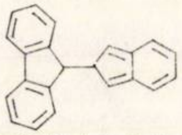
$3B_2^*$-10-4-0-0-3

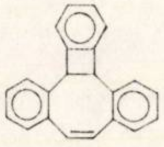
$3B_1$-10-4-0-1-1

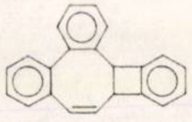
$3B_2$-10-4-0-1-1

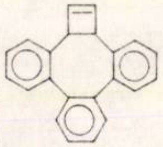
$3B_3$-10-4-0-1-1

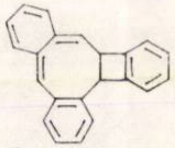
$3B_4^*$-10-4-0-1-1

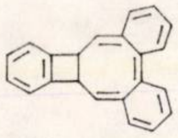
$3B_5^*$-10-4-0-1-1

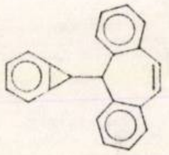
$3B_1$-10-4-1-0-1

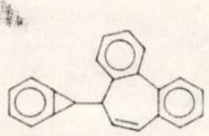
$3B_2$-10-4-1-0-1

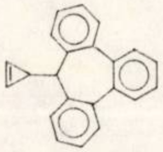
$3B_3$-10-4-1-0-1

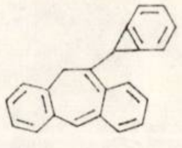
$3B_4^*$-10-4-1-0-1

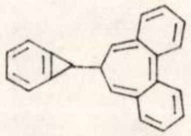
$3B_5^*$-10-4-1-0-1

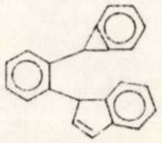
$3B_1$-10-4-1-0-2

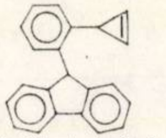
$3B_2$-10-4-1-0-2

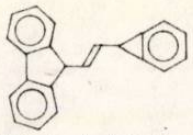
$3B_3$-10-4-1-0-2

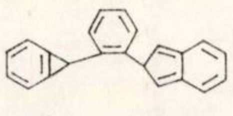
$3B_4^*$-10-4-1-0-2

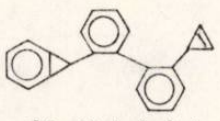
$3B_1$-10-4-2-0-1

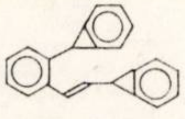
$3B_2$-10-4-2-0-1

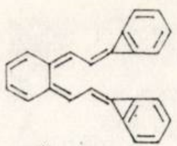
$3B_3^*$-10-4-2-0-1

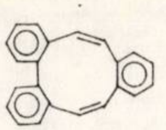
$3B_1$-10-5-0-0-1

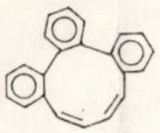
$3B_2$-10-5-0-0-1

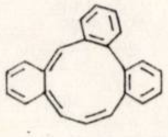
$3B_3^*$-10-5-0-0-1

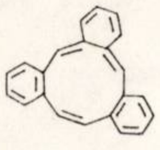
$3B_4^*$-10-5-0-0-1

b = 4

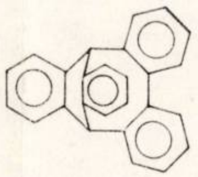
4B-10-4-0-0-1

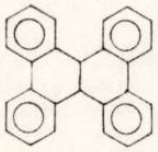
4B-10-4-0-0-2

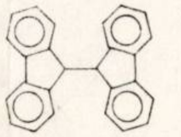
4B-10-4-0-0-3

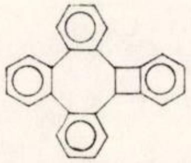
4B-10-4-0-1-1

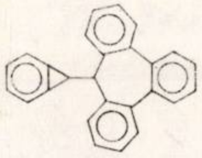
4B-10-4-1-0-1

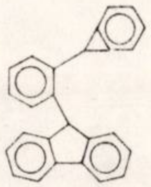
4B-10-4-1-0-2

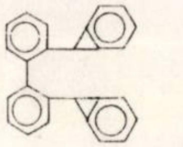
4B-10-4-2-0-1

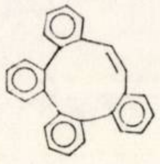
$4B_1$-10-5-0-0-1

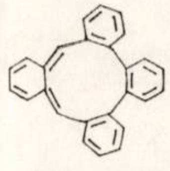
$4B_2^*$-10-5-0-0-1

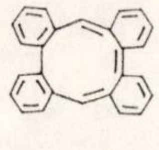
$4B_3^*$-10-5-0-0-1

b = 5

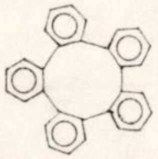
5B-10-5-0-0-1

Table 5B

Valence isomers of dibenzo-[10] annulenes

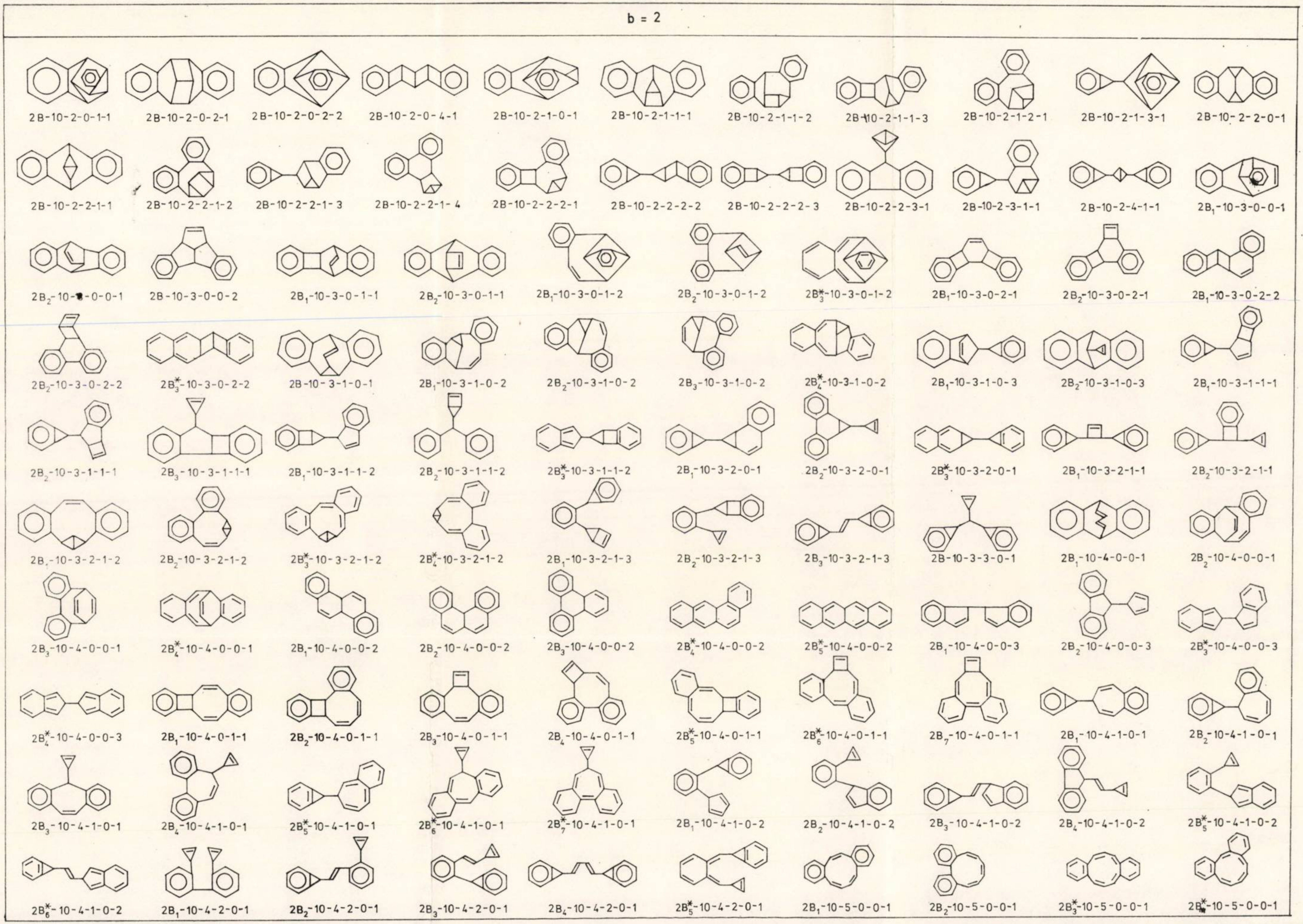
b = 2
2B-10-2-0-1-1
2B-10-2-0-2-1
2B-10-2-0-2-2
2B-10-2-0-4-1
2B-10-2-1-0-1
2B-10-2-1-1-1
2B-10-2-1-1-2
2B-10-2-1-1-3
2B-10-2-1-2-1
2B-10-2-1-3-1
2B-10-2-2-0-1
2B-10-2-2-1-1
2B-10-2-2-1-2
2B-10-2-2-1-3
2B-10-2-2-1-4
2B-10-2-2-2-1
2B-10-2-2-2-2
2B-10-2-2-2-3
2B-10-2-2-3-1
2B-10-2-3-1-1
2B-10-2-4-1-1
$2B_1$-10-3-0-0-1
$2B_2$-10-3-0-0-1
2B-10-3-0-0-2
$2B_1$-10-3-0-1-1
$2B_2$-10-3-0-1-1
$2B_1$-10-3-0-1-2
$2B_2$-10-3-0-1-2
$2B^*_3$-10-3-0-1-2
$2B_1$-10-3-0-2-1
$2B_2$-10-3-0-2-1
$2B_1$-10-3-0-2-2
$2B_2$-10-3-0-2-2
$2B^*_3$-10-3-0-2-2
2B-10-3-1-0-1
$2B_1$-10-3-1-0-2
$2B_2$-10-3-1-0-2
$2B_3$-10-3-1-0-2
$2B^*_4$-10-3-1-0-2
$2B_1$-10-3-1-0-3
$2B_2$-10-3-1-0-3
$2B_1$-10-3-1-1-1
$2B_2$-10-3-1-1-1
$2B_3$-10-3-1-1-1
$2B_1$-10-3-1-1-2
$2B_2$-10-3-1-1-2
$2B^*_3$-10-3-1-1-2
$2B_1$-10-3-2-0-1
$2B_2$-10-3-2-0-1
$2B^*_3$-10-3-2-0-1
$2B_1$-10-3-2-1-1
$2B_2$-10-3-2-1-1
$2B_1$-10-3-2-1-2
$2B_2$-10-3-2-1-2
$2B^*_3$-10-3-2-1-2
$2B^*_4$-10-3-2-1-2
$2B_1$-10-3-2-1-3
$2B_2$-10-3-2-1-3
$2B_3$-10-3-2-1-3
2B-10-3-3-0-1
$2B_1$-10-4-0-0-1
$2B_2$-10-4-0-0-1
$2B_3$-10-4-0-0-1
$2B^*_4$-10-4-0-0-1
$2B_1$-10-4-0-0-2
$2B_2$-10-4-0-0-2
$2B_3$-10-4-0-0-2
$2B^*_4$-10-4-0-0-2
$2B^*_5$-10-4-0-0-2
$2B_1$-10-4-0-0-3
$2B_2$-10-4-0-0-3
$2B^*_3$-10-4-0-0-3
$2B^*_4$-10-4-0-0-3
$2B_1$-10-4-0-1-1
$2B_2$-10-4-0-1-1
$2B_3$-10-4-0-1-1
$2B_4$-10-4-0-1-1
$2B^*_5$-10-4-0-1-1
$2B^*_6$-10-4-0-1-1
$2B_7$-10-4-0-1-1
$2B_1$-10-4-1-0-1
$2B_2$-10-4-1-0-1
$2B_3$-10-4-1-0-1
$2B_4$-10-4-1-0-1
$2B^*_5$-10-4-1-0-1
$2B^*_6$-10-4-1-0-1
$2B^*_7$-10-4-1-0-1
$2B_1$-10-4-1-0-2
$2B_2$-10-4-1-0-2
$2B_3$-10-4-1-0-2
$2B_4$-10-4-1-0-2
$2B^*_5$-10-4-1-0-2
$2B^*_6$-10-4-1-0-2
$2B_1$-10-4-2-0-1
$2B_2$-10-4-2-0-1
$2B_3$-10-4-2-0-1
$2B_4$-10-4-2-0-1
$2B^*_5$-10-4-2-0-1
$2B_1$-10-5-0-0-1
$2B_2$-10-5-0-0-1
$2B^*_3$-10-5-0-0-1
$2B^*_4$-10-5-0-0-1

Table 5A

Valence isomers of monobenzo-[10]annulenes

b = 1

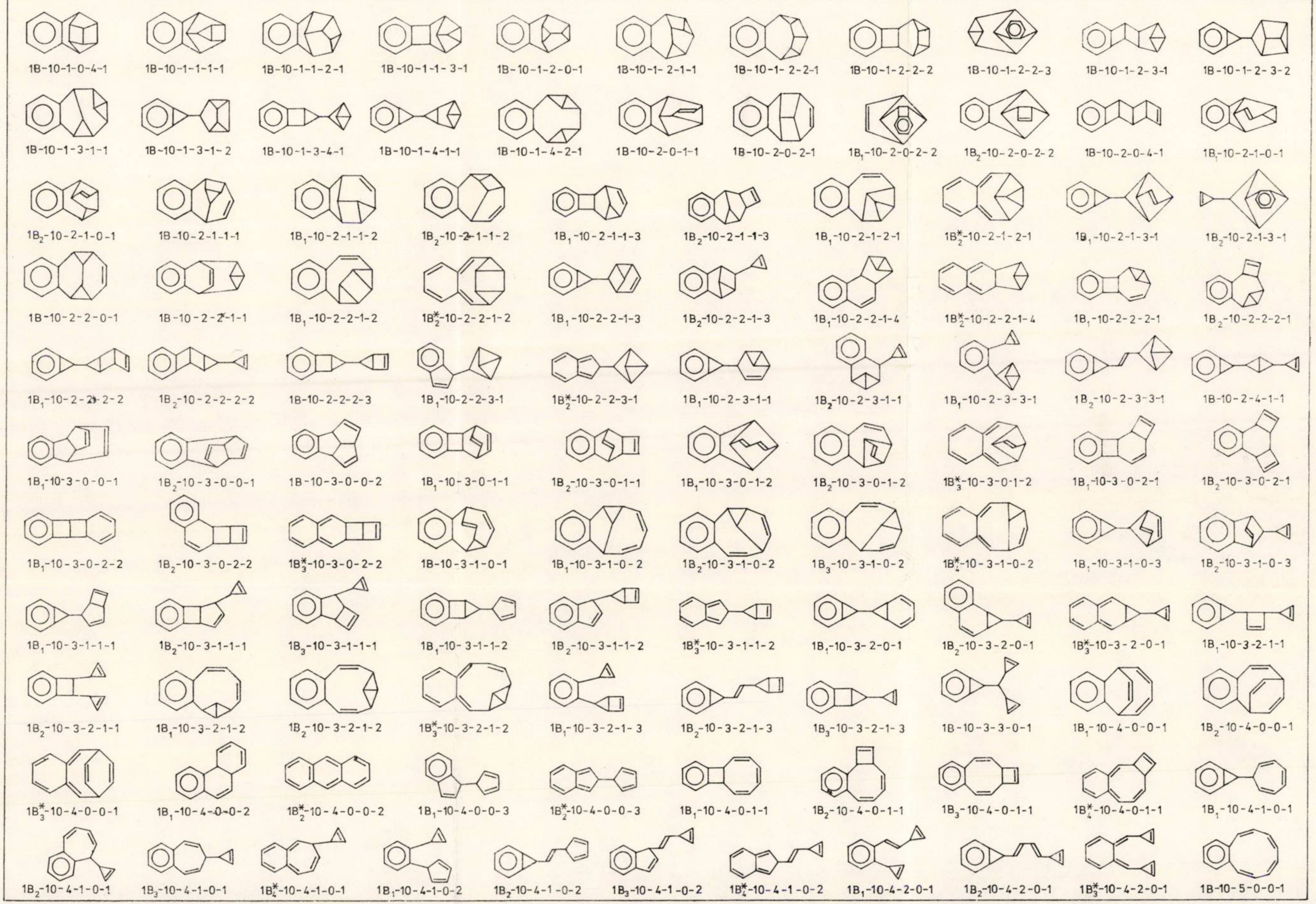

1B-10-1-0-4-1 · 1B-10-1-1-1-1 · 1B-10-1-1-2-1 · 1B-10-1-1-3-1 · 1B-10-1-2-0-1 · 1B-10-1-2-1-1 · 1B-10-1-2-2-1 · 1B-10-1-2-2-2 · 1B-10-1-2-2-3 · 1B-10-1-2-3-1 · 1B-10-1-2-3-2

1B-10-1-3-1-1 · 1B-10-1-3-1-2 · 1B-10-1-3-4-1 · 1B-10-1-4-1-1 · 1B-10-1-4-2-1 · 1B-10-2-0-1-1 · 1B-10-2-0-2-1 · $1B_1$-10-2-0-2-2 · $1B_2$-10-2-0-2-2 · 1B-10-2-0-4-1 · $1B_1$-10-2-1-0-1

$1B_2$-10-2-1-0-1 · 1B-10-2-1-1-1 · $1B_1$-10-2-1-1-2 · $1B_2$-10-2-1-1-2 · $1B_1$-10-2-1-1-3 · $1B_2$-10-2-1-1-3 · $1B_1$-10-2-1-2-1 · $1B^*_2$-10-2-1-2-1 · $1B_1$-10-2-1-3-1 · $1B_2$-10-2-1-3-1

1B-10-2-2-0-1 · 1B-10-2-2-1-1 · $1B_1$-10-2-2-1-2 · $1B^*_2$-10-2-2-1-2 · $1B_1$-10-2-2-1-3 · $1B_2$-10-2-2-1-3 · $1B_1$-10-2-2-1-4 · $1B^*_2$-10-2-2-1-4 · $1B_1$-10-2-2-2-1 · $1B_2$-10-2-2-2-1

$1B_1$-10-2-2-2-2 · $1B_2$-10-2-2-2-2 · 1B-10-2-2-2-3 · $1B_1$-10-2-2-3-1 · $1B^*_2$-10-2-2-3-1 · $1B_1$-10-2-3-1-1 · $1B_2$-10-2-3-1-1 · $1B_1$-10-2-3-3-1 · $1B_2$-10-2-3-3-1 · 1B-10-2-4-1-1

$1B_1$-10-3-0-0-1 · $1B_2$-10-3-0-0-1 · 1B-10-3-0-0-2 · $1B_1$-10-3-0-1-1 · $1B_2$-10-3-0-1-1 · $1B_1$-10-3-0-1-2 · $1B_2$-10-3-0-1-2 · $1B^*_3$-10-3-0-1-2 · $1B_1$-10-3-0-2-1 · $1B_2$-10-3-0-2-1

$1B_1$-10-3-0-2-2 · $1B_2$-10-3-0-2-2 · $1B^*_3$-10-3-0-2-2 · 1B-10-3-1-0-1 · $1B_1$-10-3-1-0-2 · $1B_2$-10-3-1-0-2 · $1B_3$-10-3-1-0-2 · $1B^*_4$-10-3-1-0-2 · $1B_1$-10-3-1-0-3 · $1B_2$-10-3-1-0-3

$1B_1$-10-3-1-1-1 · $1B_2$-10-3-1-1-1 · $1B_3$-10-3-1-1-1 · $1B_1$-10-3-1-1-2 · $1B_2$-10-3-1-1-2 · $1B^*_3$-10-3-1-1-2 · $1B_1$-10-3-2-0-1 · $1B_2$-10-3-2-0-1 · $1B^*_3$-10-3-2-0-1 · $1B_1$-10-3-2-1-1

$1B_2$-10-3-2-1-1 · $1B_1$-10-3-2-1-2 · $1B_2$-10-3-2-1-2 · $1B^*_3$-10-3-2-1-2 · $1B_1$-10-3-2-1-3 · $1B_2$-10-3-2-1-3 · $1B_3$-10-3-2-1-3 · 1B-10-3-3-0-1 · $1B_1$-10-4-0-0-1 · $1B_2$-10-4-0-0-1

$1B^*_3$-10-4-0-0-1 · $1B_1$-10-4-0-0-2 · $1B^*_2$-10-4-0-0-2 · $1B_1$-10-4-0-0-3 · $1B^*_2$-10-4-0-0-3 · $1B_1$-10-4-0-1-1 · $1B_2$-10-4-0-1-1 · $1B_3$-10-4-0-1-1 · $1B^*_4$-10-4-0-1-1 · $1B_1$-10-4-1-0-1

$1B_2$-10-4-1-0-1 · $1B_3$-10-4-1-0-1 · $1B^*_4$-10-4-1-0-1 · $1B_1$-10-4-1-0-2 · $1B_2$-10-4-1-0-2 · $1B_3$-10-4-1-0-2 · $1B^*_4$-10-4-1-0-2 · $1B_1$-10-4-2-0-1 · $1B_2$-10-4-2-0-1 · $1B^*_3$-10-4-2-0-1 · 1B-10-5-0-0-1

Table 4

Valence isomers of [b] benzo- [n] annulenes with n = 4, 6, and 8.

n \ b	1	2	3	4
4	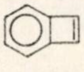 1B-4-2-0-1-1	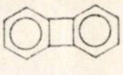 2B-4-2-0-1-1		
6	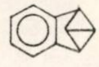 1B-6-1-2-1-1 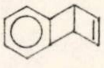 1B-6-2-0-2-1 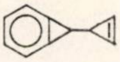 1B-6-2-2-0-1 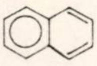 1B-6-3-0-1-1	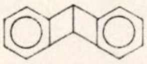 2B-6-2-0-2-1 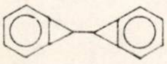 2B-6-2-2-0-1 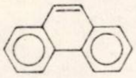 2B$_1$-6-3-0-1-1 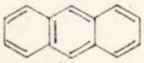 2B$_2^*$-6-3-0-1-1	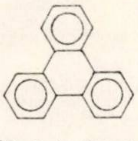 3B-6-3-0-1-1	
8	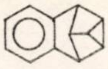 1B-8-1-1-2-1 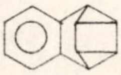 1B-8-1-2-1-1 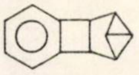 1B-8-1-2-2-1 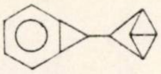 1B-8-1-3-3-1 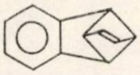 1B-8-2-0-1-1 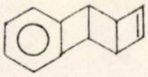 1B-8-2-0-3-1 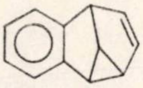 1B-8-2-1-0-1 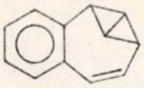 1B$_1$-8-2-2-1-1 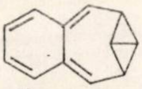 1B$_2^*$-8-2-2-1-1 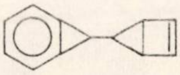 1B$_1$-8-2-2-1-2 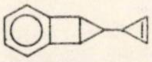 1B$_2$-8-2-2-1-2 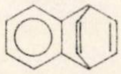 1B-8-3-0-0-1 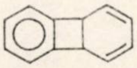 1B$_1$-8-3-0-1-1 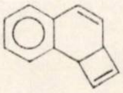 1B$_2$-8-3-0-1-1 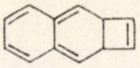 1B$_3^*$-8-3-0-1-1 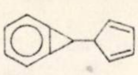 1B$_1$-8-3-1-0-1 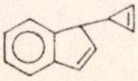 1B$_2$-8-3-1-0-1 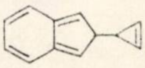 1B$_3^*$-8-3-1-0-1 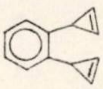 1B$_1$-8-3-2-0-1 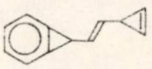 1B$_2$-8-3-2-0-1 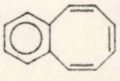 1B-8-4-0-0-1	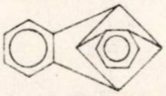 2B-8-2-0-1-1 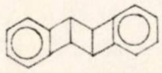 2B-8-2-0-3-1 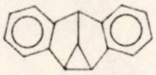 2B-8-2-1-0-1 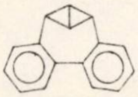 2B-8-2-2-1-1 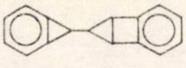 2B-8-2-2-1-2 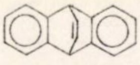 2B-8-3-0-0-1 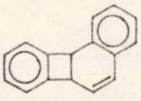 2B$_1$-8-3-0-1-1 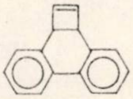 2B$_2$-8-3-0-1-1 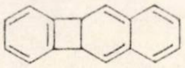 2B$_3^*$-8-3-0-1-1 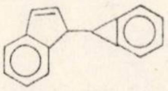 2B$_1$-8-3-1-0-1 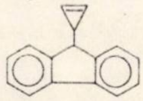 2B$_2$-8-3-1-0-1 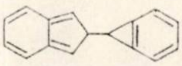 2B$_3^*$-8-3-1-0-1 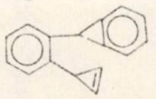 2B$_1$-8-3-2-0-1 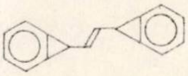 2B$_2$-8-3-2-0-1 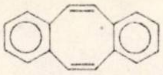 2B$_1$-8-4-0-0-1 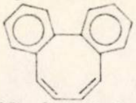 2B$_2$-8-4-0-0-1 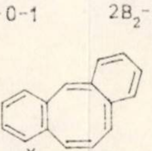 2B$_3^*$-8-4-0-0-1	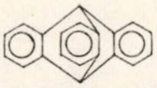 3B-8-3-0-0-1 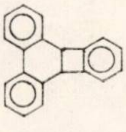 3B-8-3-0-1-1 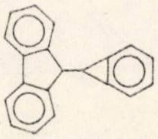 3B-8-3-1-0-1 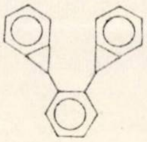 3B-8-3-2-0-1 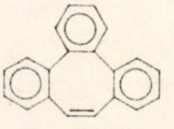 3B$_1$-8-4-0-0-1 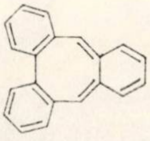 3B$_2^*$-8-4-0-0-1	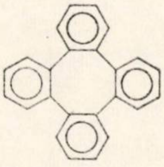 4B-8-4-0-0-1

It can be seen that in table 4 biphenylene appears as dibenzocyclobutadiene (2B—4—2—0—1—1) and dihydrobiphenylene as a monobenzoderivative of a valence isomer of cyclooctatetraene ($1B_1$—8—3—0——1—1). This is a general feature of tables 4 and 5, where phenanthrene $2B_1$—6—3—0—1—1 and anthracene $2B_2^*$—6—3—0—1—1 appear as dibenzo-[6]annulenes, and their dihydroderivatives as monobenzo-[10] annulene valence isomers $1B_1$—10—4—0—0—2 and $1B_2^*$—10—4—0—0—2, respectively.

The numbers of possible valence isomers of benzoannulenes are given in table 6.

At first sight it seems rather queer to treat structures like XII as valence isomers of benzoannulenes, because chemically they differ little from their *para*-isomers XIII which are not included in tables 4 — 6. However, this is in keeping with the definitions of valence isomerism and of annelation to benzoderivatives.

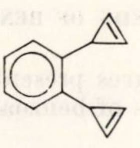
XII

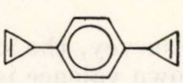
XIII

Table 6

The number of planar valence isomers of [b]benzo[n]annulenes[a,b]

n / b	4	6	8	10
1	1(0)	4(0)	21(3)	113(17)
2	1(0)	4(1)	17(3)	102(23)
3	—	1(0)	6(1)	44(11)
4	—	—	1(0)	10(2)
5	—	—	—	1(0)
Total	2(0)	9(1)	45(7)	270(53)

[a] The figures for b = 0 can be found in table 2 in the line "total".

[b] The number of *o*-quinonoid structures is given in brackets; the number of non-*o*-quinonoid structures results by difference.

Of course, in appropriate cases, when the geometry is favourable, a dibenzoderivative can be further bridged, leading to interesting structures. Thus, taking dibenzoderivatives of cyclooctatetraene as examples, they

can lead to such structures as XIV (x = 1 or 2), XV or XVI (x = 3 or 4)* which can be built strain-free from molecular models.

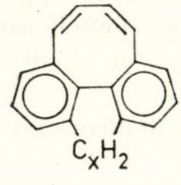

XIV

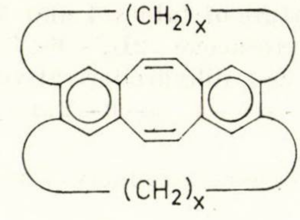

XV

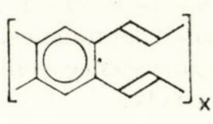

XVI

SURVEY OF KNOWN VALENCE ISOMERS OF BENZOANNULENES

In the following survey, the structures presented in tables 4 and 5 are correlated with known valence isomers of benzoannulenes. The survey is illustrative rather than exhaustive.

Both valence isomers of [b]benzo-[4]annulene are known. Benzocyclobutadiene 1B—4—2—0—1—1 (I) is a short-lived species which dimerizes [10] rapidly to $2B_1$—8—3—0—1—1 (II); in the presence of nickel tetracarbonyl catalyst, however, [11] another dimer is formed, namely 2B—8—2—0—3—1, which goes easily into dibenzo[*a*, *e*]cyclooctatetraene $2B_1$—8—4—0—0—1; in the presence of silver ions, a third dimer results, [14] namely 2B—8—2—1—0—1; this was explained by a different ring-opening of the Diels-Alder adduct from two molecules of benzocyclobutadiene leading, in the presence of silver ions, to the intermediate formation of the elusive dibenzo[*a*, *e*]cyclooctatetraene $2B_3^*$ 8—4—0—0—1. Dibenzocyclobutadiene (biphenylene)[9,15] is a stable hydrocarbon.

From the nine possible [b]benzo-[6] annulenes, six are known; naphthalene 1B—6—3—0—1—1, phenanthrene $2B_1$—6—3—0—1—1, anthracene $2B_2^*$—6—3—0—1—1 and triphenylene 3B—6—3—0—1—1 are too well-known benzenoid aromatic hydrocarbons [13] to warrant more than a cursory mention. It is noteworthy that anthracene is the only stable *o*-quinonoid valence isomer of a benzoannulene known so far: in other cases the presence of such a structural feature gives too unstable *o*-xylylenic structures. Substituted [16] and unsubstituted [17] hemi-Dewar-naphthalenes (benzobicyclo[2.2.0] hexa-2,5-diene, 1B—6—2—0—2—1) were prepared recently and are appreciably more stable than Dewar-benzene. A derivative of Dewar-anthracene (dibenzo-Dewar-benzene 2B—6—2—0—2—

---

* The originator of structure XVI is professor H. J. Bestmann (Erlangen, the Federal Republic of Germany).

[14] W. Merk and R. Pettit, *J. Amer. Chem. Soc.*, **89**, 4787 (1967).

[15] W. C. Lothrop, *J. Amer. Chem. Soc.*, **63**, 1187 (1941).

[16] D. T. Carty, *Tetrahedron Letters*, **1969**, 4753.

[17] R. N. McDonald and D. G. Frickey, *J. Amer. Chem. Soc.*, **90**, 5315 (1968); R. N. McDonald, D. G. Frickey and G. M. Muschik, *J. Org. Chem.*, **37**, 1304 (1972).

—1) is also known,[18] in 9,10-dehydro-dianthracene, and like the previous monobenzo-Dewar-benzene, it is a stable substance.

From the 45 possible constitutionally different valence isomers of [*b*]benzo-[8]annulene, 15 are known as stable compounds (chart 1*). The reaction of cyclobutadiene with benzocyclobutadiene[14] affords 1B—8—2—0—3—1, which can ring-open to benzocyclooctatetraene slowly by a thermal, symmetry-forbidden reaction, and rapidly in the presence of silver ions,[19] passing through an unstable *o*-quinonoid valence isomer 1B$_3^*$— — 8 — 3 — 0 — 1 — 1 which could be trapped by dienophiles. Benzosemibullvalene 1B—8—2—1—0—1 (benzo[*c*] tricyclo-[3.3.0.0.^{2,8}] octa-3,6-diene) was prepared photochemically from benzobarrelene 1B—8—3—0—0—1, along with benzocyclooctatetraene.[20] Benzosemibullvalene or its substituted derivatives,[21] unlike semibullvalene which gives a degenerate rearrangement evidenced by its NMR spectrum, does not fluctuate. A substituted benzo[b]-bicyclo [4.2.0]octa-2,4, 7-triene, 1B$_2$ — 8 — 3— 0— 1 — — 1, isomerizes to the corresponding benzocyclooctatetraene but much more slowly than the non-annelated compound.[21] Benzobarrelene is, along with benzocyclooctatetraene, one of the reaction products from benzene and benzyne. Benzocyclooctatetraene 1B—8—4—0—0—1 was mentioned repeatedly above.[14,20–24] The three dibenzo-$(CH)_8$ structures obtained by the dimerization of benzocyclobutadiene under different conditions were mentioned above : 2B — 8 — 2— 0 — 3 — 1,[11,19] 2B$_1$ — 8 — 3 — 0 — 1— — 1,[10] and 2B — 8 — 2 — 1 — 0 — 1.[14] In the opening of the first transannular bond of 2B — 8 — 2 — 0 — 3 — 1, the *o*-quinonoid valence isomer 2B$_3^*$ — 8 — 3— 0— 1— 1 appears as an unstable intermediate which can be trapped by dienophiles and which rapidly valence isomerizes to dibenzo [*a*, *e*] cyclooctatraene.[19] Dibenzosemibullvalene[25] 2B — 8 — 2 — 1 — — 0 — 1 or its substituted derivatives[26] can be also obtained photochemically from dibenzobarrelene 2B — 8 — 3 — 0 — 0 — 1. The preparation of the latter hydrocarbon and its derivatives was described earlier.[27–33]

---

* In charts 1 and 2 the geometry of molecules is also taken into account.

[18] D. E. Applequist and R. Searle, *J. Amer. Chem. Soc.*, **86**, 1389 (1964).

[19] W. Merk and R. Pettit, *J. Amer. Chem. Soc.* **89**, 4788 (1967).

[20] H. E. Zimmerman, R. S. Givens and R. M. Pagni, *J. Amer. Chem Soc.*, **90**, 6096 (1968); S.S. Hixson, P.S. Mariano and H.E. Zimmerman, *Chem. Revs*, **73**, 531 (1973).

[21] J. A. Elix, M. V. Sargent and F. Sondheimer, *J. Amer. Chem. Soc*, **89**, 5081 (1967).

[22] G. Wittig, H. Eggers and P. Duffner, *Liebigs Ann. Chem*, **619**, 10 (1958).

[23] L. Friedman, *J, Amer. Chem. Soc.*, **89**, 3071 (1967); L. Friedman and D. F. Lindow, *Ibid*, **90**, 2329 (1968).

[24] L. B. Anderson and L. A. Paquette, *J Amer. Chem. Soc.*, **94**, 4915 (1972).

[25] E. Ciganek, *J. Amer. Chem Soc.*, **88**, 2882 (1966).

[26] L. A. Paquette and. G. V. Meehan, *J. Amer. Chem, Soc.*, **92**, 3039 (1970).

[27] S. J. Cristol and N. L. Hause, *J. Amer. Chem. Soc*, **74**, 2193 (1952); S. J. Cristol and R. K. Bly, *ibid*; **82**, 6155 (1960)

[28] W. R. Vaughan and A. C. Schoenthaler, *J. Amer. Chem. Soc.*, **80**, 1956 (1958).

[29] R. G. Miller and M. Stiles, *J. Amer. Chem. Soc.*, **85**, 1798 (1963).

[30] J. C. Muller and J. Vergne, *Compt. rend.* (C), **263**, 1452 (1966).

[31] P. W. Rabideau, J. B. Hamilton and L. Friedman, *J. Amer. Chem. Soc.*, **90**, 4465 (1968).

[32] E. Zbiral and A. Stutz, *Tetrahedron*, **27**, 4953 (1971).

[33] H. P. Figeys and A. Dralants, *Tetrahedron*, **28**, 3031 (1972).

From the three possible dibenzocyclooctatetraenes, only the non-*o*-quinonoid are stable, whereas the *o*-quinonoid dibenzo[*a*, *d*]cyclooctatetraene $2B_3^* - 8 - 4 - 0 - 0 - 1$ was discussed as an unstable intermediate in the $Ag^{\oplus}$-catalyzed formation of dibenzosemibullvalene from benzocyclobutadiene.[14] Dibenzo[*a*, *c*]cyclooctatetraene $2B_2 - 8 - 4 - 0 - 0 - 1$ valence isomerizes to dibenzo[*b*, *d*]bicyclo[4.2.0]octa-2,4,7-triene $2B_2 - 8 - 3 - 0 - 1 - 1$ photochemically, whereas the reverse thermal reaction requires very high temperatures (350°)[34]; this evidences how drastic the effect of the annelation is on the tautomeric equilibrium between cyclooctatetraene and bicyclo [4.2.0] octa-2,4,7-triene.[35] Dibenzo-[*a*, *e*]cyclooctatetraene $2B_1 - 8 - 4 - 0 - 0 - 1$ was mentioned above.[11,19,24,31] Its preparation is of earlier date.[36-42] Tribenzobarrelene is the well-known triptycene[43] $3B - 8 - 3 - 0 - 0 - 1$. Tribenzocyclooctatetraene $3B - 8 - 4 - 0 - 0 - 1$ is known.[44] Tetrabenzocyclooctatetraene or tetraphenylene[41,44-46] $4B - 8 - 4 - 0 - 0 - 1$ can be obtained from *o,o'*-dilithiobiphenyl by oxidation with transition metal halides[47] along with bi- and hexaphenylene.

From the 270 possible constitutionally different valence isomers of [b]benzo-[10]annulene (disregarding stereoisomerism which gives a larger number of possible structures), 21 are known as stable compounds (chart 2).

Benzobasketene[48,49] $1B - 10 - 1 - 0 - 4 - 1$ is obtained photochemically, along with $1B_2 - 10 - 2 - 1 - 1 - 3$,[48,49] from the *anti*-benzo-Nenitzescu hydrocarbon $1B_2 - 10 - 3 - 0 - 1 - 1$ which is available by cycloaddition of benzene to 7,8-dichlorobicyclo [4. 2. 0] octa-2,4-diene[48] or to cyclooctatetraene.[50] The *syn*-isomer of $1B_2 - 10 - 3 - 0 - 1 - 1$ is also known.[51] The *anti*-benzo[*g*] tricyclo [4.2.2.0 ^{2,5}] deca-3,7,9-

---

[34] E. VOGEL, W. FRASS and J. WOLPERS, *Angew. Chem.*, **75**, 979 (1963).

[35] G. SCHRÖDER, "Cyclooctatetraen", Verlag Chemie, Weinhein, 1965 ; L. E. CRAIG, *Chem. Rev.*, **49**, 103 (1951).

[36] L. F. FIESER and M. PECHET, *J. Amer. Chem. Soc.*, **68**, 2557 (1946).

[37] A. C. COPE and S. W. FENTON, *J. Amer. Chem. Soc.*, **73**, 1668 (1951).

[38] G. WITTIG, G. KÖNIG and K. CLAUSS, *Liebigs Ann. Chem.*, **593**, 127 (1955).

[39] C. E. GRIFFIN and J. A. PETERS, *J. Org. Chem.*, **28**, 1715 (1963).

[40] G. SCHRÖDER, W. MARTIN and J. F. M. OTH, *Angew. Chem. Internat. Edit.*, **6**, 870 (1967).

[41] P. W. RABIDEAU, *Diss. Abstr.*, **30 B**, 4059 (1970).

[42] T. W. CUTSHALL and P. W. RABIDEAU, *Canad. J. Chem.*, **50**, 2364 (1972).

[43] A. STEITWISER JR., *Tetrahedron Letters*, **1971**, 3927.

[44] W. S. RAPSON, R. G. SHUTTLEWORTH and J. N. VAN NIEKERK, *J. Chem. Soc.*, **1943**, 326 ; W. S. RAPSON, H. M. SCHWARTZ and E. T. STEWART, *ibid.*, **1944**, 73 ; W. S. RAPSON and R. G. SHUTTLEWORTH, *ibid.*, **1941**, 847 ; R. G. SHUTTLEWORTH, W. S. RAPSON and E. T. STEWART, *ibid.*, **1944**, 71.

[45] H. A. STAAB and V. WÜNSCHE, *Chem. Ber.*, **101**, 887 (1968).

[46] H. P. FIGEYS and A. DRALANTS, *Tetrahedron Letters*, **1971**, 3901.

[47] G. WITTIG and G. KLAR, *Liebigs Ann. Chem.*, **704**, 91 (1967).

[48] L. A. PAQUETTE, M. J. KUKLA and J. C. STOWELL, *J. Amer. Chem. Soc.*, **94**, 4920 (1972).

[49] J. MURATA and Y. SUGIHARA, *Tetrahedron Letters*, **1972**, 3785.

[50] E. VEDEJS and R. A. SHEPHERD, *Tetrahedron Letters*, **1970**, 1863.

[51] I. MURATA, Y. SUGIHARA and N. UEDA , *Tetrahedron Letters*, **1973**, 1183,

Chart 2. — Known valence isomers of [b]benzo-[10]annulenes and their interconversions.

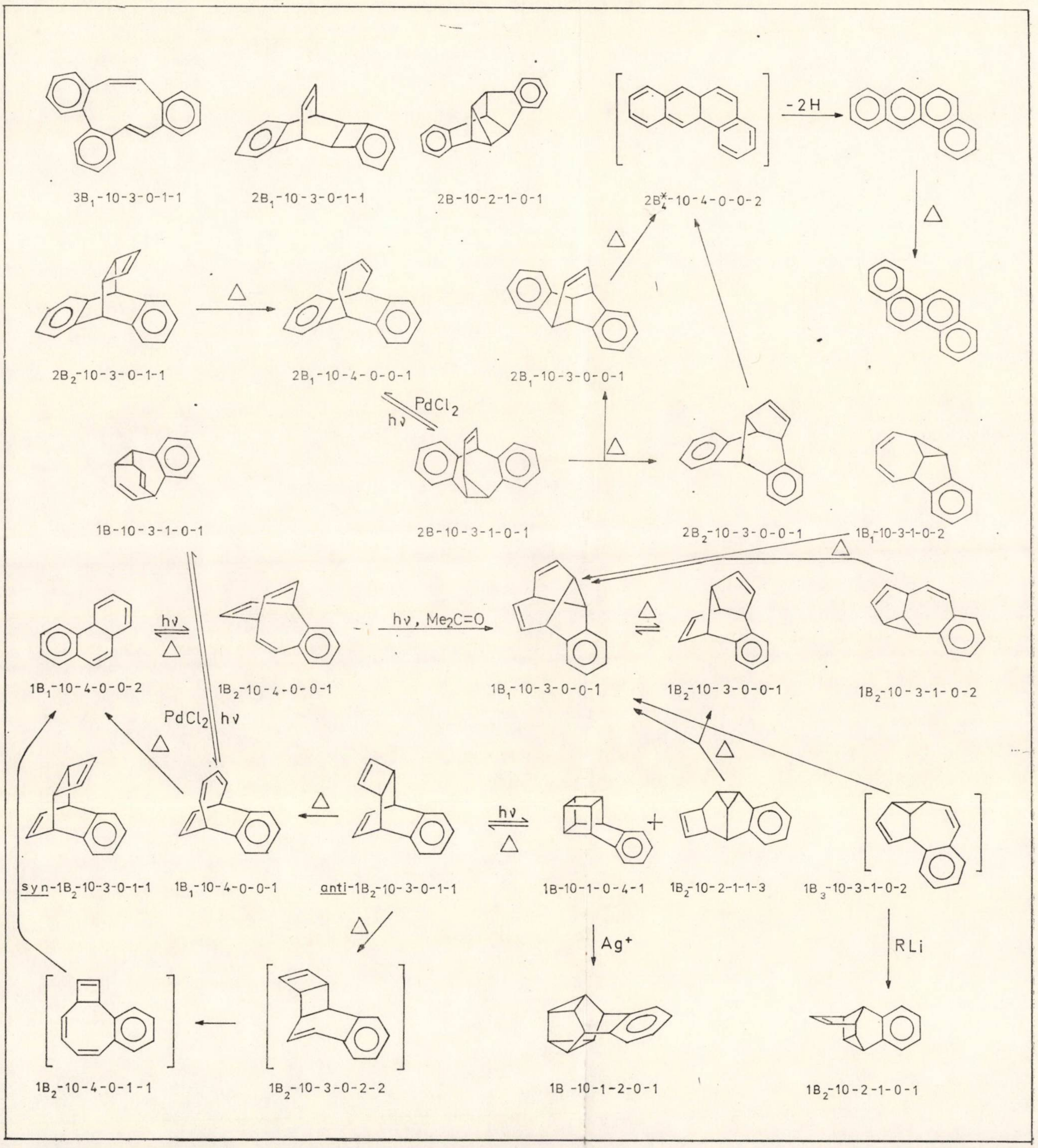
3B$_1$-10-3-0-1-1
2B$_1$-10-3-0-1-1
2B-10-2-1-0-1
-2H
2B$^*_4$-10-4-0-0-2
Δ
Δ
2B$_2$-10-3-0-1-1
Δ
2B$_1$-10-4-0-0-1
Δ
2B$_1$-10-3-0-0-1
PdCl$_2$
hν
Δ
1B-10-3-1-0-1
2B-10-3-1-0-1
2B$_2$-10-3-0-0-1
1B$_1$-10-3-1-0-2
Δ
hν
Δ
hν, Me$_2$C=O
Δ
1B$_1$-10-4-0-0-2
1B$_2$-10-4-0-0-1
1B$_1$-10-3-0-0-1
1B$_2$-10-3-0-0-1
1B$_2$-10-3-1-0-2
PdCl$_2$ hν
Δ
Δ
Δ
hν
Δ
syn-1B$_2$-10-3-0-1-1
1B$_1$-10-4-0-0-1
anti-1B$_2$-10-3-0-1-1
1B-10-1-0-4-1
1B$_2$-10-2-1-1-3
1B$_3$-10-3-1-0-2
Δ
Ag$^+$
RLi
1B$_2$-10-4-0-1-1
1B$_2$-10-3-0-2-2
1B -10-1-2-0-1
1B$_2$-10-2-1-0-1

Chart 1. — Known valence isomers of [b]benzo-[8]annulenes and their interconversions.

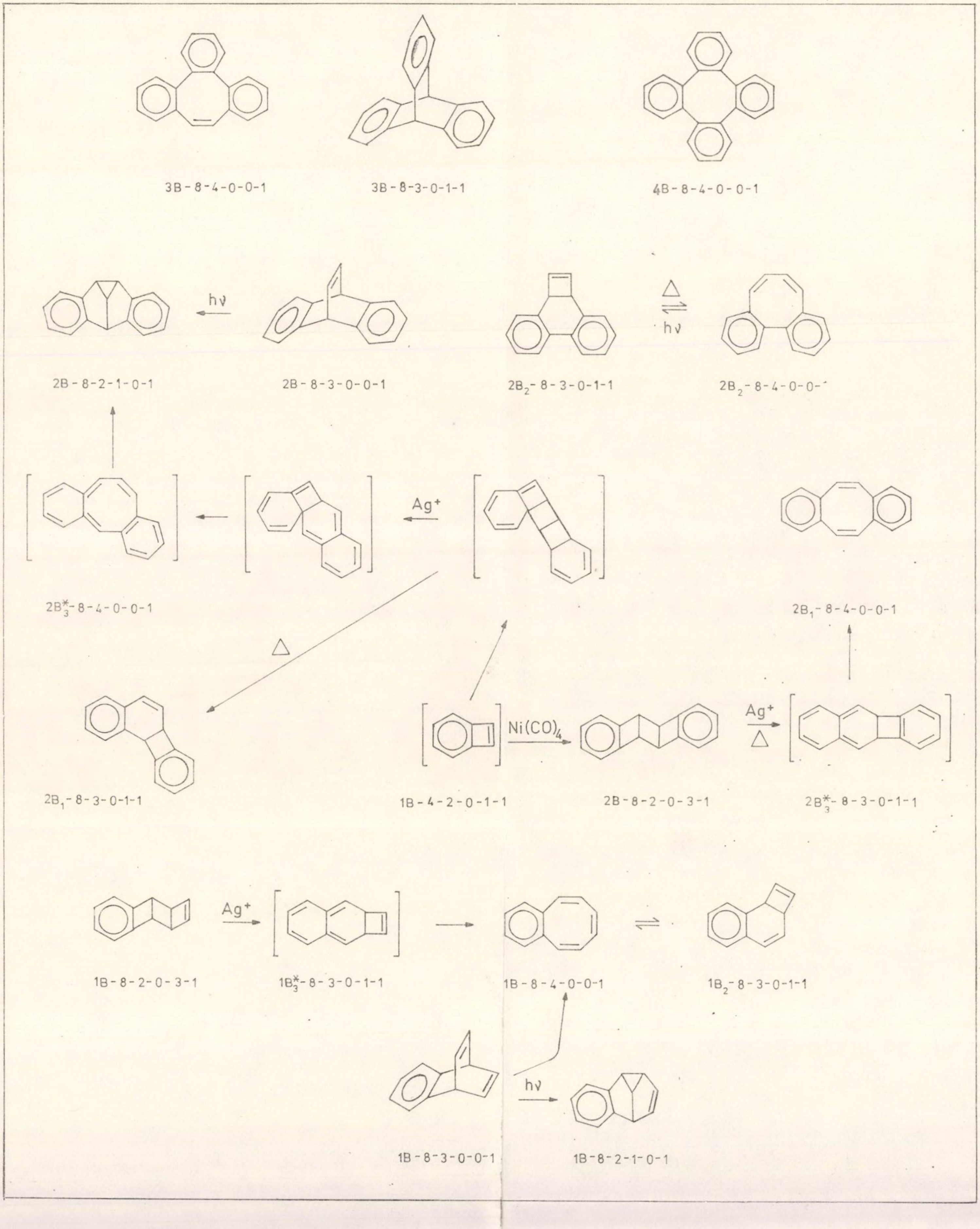
3B-8-4-0-0-1
3B-8-3-0-1-1
4B-8-4-0-0-1
hν
2B-8-2-1-0-1
2B-8-3-0-0-1
Δ
hν
$2B_2$-8-3-0-1-1
$2B_2$-8-4-0-0-
Ag^+
$2B_3^*$-8-4-0-0-1
$2B_1$-8-4-0-0-1
Δ
$Ni(CO)_4$
Ag^+
Δ
$2B_1$-8-3-0-1-1
1B-4-2-0-1-1
2B-8-2-0-3-1
$2B_3^*$-8-3-0-1-1
Ag^+
1B-8-2-0-3-1
$1B_3^*$-8-3-0-1-1
1B-8-4-0-0-1
$1B_2$-8-3-0-1-1
hν
1B-8-3-0-0-1
1B-8-2-1-0-1

triene $1B_2 - 10 - 3 - 0 - 1 - 1$ [52-54] rearranges thermally to *cis*-4*b*, 8*a*-dihydrophenanthrene $1B_1 - 10 - 4 - 0 - 0 - 2$ [48, 53, 54]; in this reaction, $1B_1 - 10 - 4 - 0 - 0 - 1$ is an isolable intermediate. [53]

Benzobasketene rearranges under the influence of silver ions to benzosnoutene $1B - 10 - 1 - 2 - 0 - 1$. [48] In the addition of benzyne to cyclooctatetraene, [50] silver ions influence the proportion of reaction products: absence of metal favours $1B_2 - 10 - 3 - 0 - 1 - 1$, whereas $Ag^{\oplus}$ causes the predominant formation of $1B_1 - 10 - 3 - 1 - 0 - 2$; a third product is $1B_1 - 10 - 4 - 0 - 0 - 1$.[52] From the three non-*o*-quinonoid benzo-lumibullvalenes, $1B_3 - 10 - 3 - 1 - 0 - 2$ is unstable because of a Cope rearrangement which converts it into $1B_1 - 10 - 3 - 0 - 0 - 1$, [55] which also results by thermal rearrangements from the other two benzo-lumibullvalenes, $1B_1 - 1 - 0 - 3 - 10 - 2$ and $1B_2 - 10 - 3 - 1 - 0 - 2$ [55]; both these isomers result together by thermolysis of $1B_2 - 10 - 2 - 1 - 1 - 3$. [48] An anionic rearrangement under the influence of organolithium reagents converts $1B_2 - 10 - 3 - 1 - 0 - 2$ into $1B_2 - 10 - 2 - 1 - 0 - 1$. [56] Photolysis of the dihydrophenanthrene $1B_1 - 10 - 4 - 0 - 0 - 2$ gives benzo[*g*]-bicyclo[4.2.2]deca-2,4,7,9-tetraene $1B_2 - 10 - 4 - 0 - 0 - 1$, [48] which on irradiation in acetone gives $1B_1 - 10 - 3 - 0 - 0 - 1$. [48]

A recent paper[57] reports the preparation of benzobullvalene $1B - 10 - 3 - 1 - 0 - 1$, whose topomerization only involves the homotropylidene moiety. A substituted benzobullvalene had been known for several years. [58]

Monobenzo-$(CH)_{10}$ valence isomers which were discussed as unstable reaction intermediates or alternative structures are $1B_2 - 10 - 3 - 0 - 2 - 2$, [53] $1B_2 - 10 - 4 - 0 - 1 - 1$, [48,53] $1B_2 - 10 - 3 - 0 - 1 - 2$,[55] $1B_1 - 10 - 3 - 0 - 1 - 2$, [48] $1B - 10 - 3 - 0 - 0 - 2$, [48] and $1B_3 - 10 - 3 - 1 - 0 - 2$. [48,55]

From the dibenzo-$(CH)_{10}$ valence isomers, dibenzo[*g, h*]tricyclo-[4.2.2.0 ^{2,5}] deca-3,7,9-triene $2B_2 - 10 - 3 - 0 - 1 - 1$, [51,59] and *syn*-dibenzo[*c, g*]-tricyclo[4.2.2.0 ^{2,5}] deca-3,7,9-triene $2B_1 - 10 - 3 - 0 - 1 - 1$, [60] are both annelated derivatives of the Nenitzescu hydrocarbon $(CH)_{10}$. Dibenzobullvalene $2B - 10 - 3 - 1 - 0 - 1$ was obtained together with $2B_1 - 10 - 4 - 0 - 0 - 1$; the latter is thermally stable (and is formed by pyrolysis of $2B_2 - 10 - 3 - 0 - 1 - 1$), but is converted on photolysis into dibenzobullvalene, [61a] Pyrolysis of dibenzobullvalene affords dibenzo[*b*, *i*]-tricyclo [5.3.0.0 ^{4,8}] deca-2,5,9-triene $2B_2 - 10 - 3 - 0 - 0 - 1$,[61] together with $2B_1 - 10 - 3 - 0 - 0 - 1$.[61b] At higher temperatures, tetraphene and chrysene are formed, presumably *via* the dihydrotetraphene $2B_4^* - 10 - 4 - 0 - 0 - 2$.[61b]

---

[52] E. Vedejs, *Tetrahedron Letters, 1968*, 2633.

[53] E. Vedejs, *Tetrahedron Letters, 1970*, 4963.

[54] L. A. Paquette and J. C. Stowell, *Tetrahedron Letters*, **1970**, 2259.

[55] E. Vedejs, R. A. Shepherd and R. P. Steiner, *J. Amer. Chem. Soc.*, **92**, 2158 (1970).

[56] E. Vedejs and R. P. Steiner, *Chem. Comm.*, **1973**, 599,

[57] E. Vedejs, M. F. Salomon and P. D. Weeks, *J. Amer. Chem. Soc.*, **95**, 6770 (1973).

[58] G. Schröder, H. Röttele, R. Merenyi and J. F. M. Oth, *Chem. Ber.*, **100**, 3527 (1967).

[59] M. Avram, I. G. Dinulescu, and. C. D. Nenitzescu, *Liebigs Ann Chem.*, **691**, 9 (1966).

[60] I. G. Dinulescu, M. Pop, F. Chiraleu, M. Avram and C. D. Nenitzescu, *Rev. Roumaine Chim.*, **19**, (1974).

[61] a. M. Banciu, M. Elian, E. Ciorănescu and C. D. Nenitzescu, *Tetrahedron Letters*, **1972**, 2573; b. *Idem.* to be published.

Another dibenzo-$(CH)_{10}$ valence isomer, $2B - 10 - 2 - 1 - 0 - 1$, was obtained from benzene and benzyne,[23] and its structure was established by electron diffraction.

trans-[*a*, *c*, *g*] Tribenzo-[10]annulene, $3B_1 - 10 - 5 - 0 - 1 - 1$, is a stable hydrocarbon, unlike the non-annelated [10] annulene, since it cannot give an intramolecular ring closure to a 9,10-dihydronaphthalene derivative.[62]

From this survey of known valence isomers of [*b*]benzo-[n]annulenes with n = 4, 6, 8 and 10, one can conclude that with the exception of anthracene, *o*-quinonoid valence isomers of benzoannulenes tend to be unstable, and that so far no molecule with a benzocyclopropene moiety is known. This reduces somewhat the numbers of possible valence isomers in table 6.

For benzoderivatives of [*n*] annulenes with n >10, the numbers of possible isomers increase sharply whereas the number of known compounds is at present small. For instance hexaphenylene is hexabenzo-[12]-annulene (two isomers are known); [*a*, *e*, *i*] tribenzo-[12]annulene has also been prepared[63,64]; a dibenzo-[14]annulene valence isomer (XVII) is also known.[65] Photodimerization of 2-methoxynaphthalene yields several dibenzo-$(CH)_{12}$ valence isomers.[66]

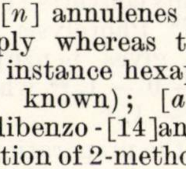

XVII

Owing to these reasons, the tables of valence isomers of [b] benzo-[n]annulenes were restricted to n = 4 – 10, but they can be expanded to n >10 when need arises.

---

[62] K. Grohmann and F. Sondheimer, *J. Amer. Chem. Soc.*, **89**, 7119 (1967).

[63] H. A. Staab, F. Graf and B. Junge, *Tetrahedron Letters*, **1966**, 743 ; H. Brunner, K. H. Hausser, R. Rewitscher and H. A. Staab, *ibid.*, **1966**, 2775.

[64] J. Castells and M. Moreno-Manas, *An. Quim.*, **68**, 193 (1972).

[65] T. Knittel-Wismonsky, G. Fischer and E. Fischer, *Tetrahedron Letters*, **1972**, 2853.

[66] T. Teitei, D. Wells and W. H. F. Sasse, *Tetrahedron Letters*, **1974**, 367.

Revue Roumaine de Chimie, 19, 7, 1197–1202 (1974

INVESTIGATIONS IN THE CYCLOBUTANE SERIES. XXXIII.[1]

SYNTHESIS OF *syn*-DIBENZO [*c*, *g*] TRICYCLO [4.2.2.0 ^{2,5}] DECA-3, 7, 9-TRIENE. A NEW DIBENZO $(CH)_{10}$ HYDROCARBON

ILIE G. DINULESCU, MIRCEA POP, FILIP CHIRALEU, MARGARETA AVRAM and COSTIN D. NENITZESCU *

Institute of Organic Chemistry, Spl. Independenţei 202 B, Bucharest, Romania

Received February 6, 1974

The synthesis of the dibenzo $(CH)_{10}$ hydrocarbon **3** is described.

Considering the particular interest raised by the chemistry of $(CH)_0$ hydrocarbons, [2] the investigation of the dibenzo-derivatives of $(CH)_{10}$ Nenitzescu hydrocarbon (**1**) [3] seemed appropriate.

In the course of previous studies, the synthesis [4] and the thermal behaviour [5] of isomer **2** were described.

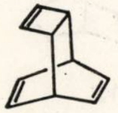

1

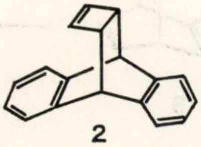

2

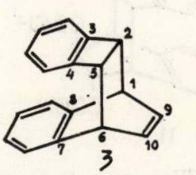

3

In this work we report the synthesis of a new isomer in the same series : *syn*-dibenzo[*c*, *g*] tricyclo[4.2.2.0 ^{2,5}]deca-3,7,9-triene (**3**).

---

* Deceased Jully 28, 1970.

[1] Part XXXII : M. Avram, I. G. Dinulescu, F. Chiraleu and C. D. Nenitzescu, *Rev. Roumaine Chim.*, **18**, 863 (1973).

[2] Reviews for rearrangements and interconversions of compounds with formula $(CH)_n$: L.T. Scott and M. Jones, Jr., *Chem. Rev.*, **72**, 181 (1972) ; S. Masamune and N. Darby, *Accounts Chem. Res.*, **5**, 272 (1972).

[3] C. D. Nenitzescu, M. Avram, I. Pogany, G. D. Mateescu and M. Fărcaşiu, *Studii şi Cercetări Chim. Acad. R.P.R.*, **11**, 7 (1963).

[4] M. Avram, I. G. Dinulescu and C. D. Nenitzescu, *Liebigs Ann. Chem.*, **691**, 9 (1966).

[5] M. Banciu, M. Elian, E. Ciorănescu and C. D. Nenitzescu, *Tetrahedron Letters*, **1972**, 2573.

By gradual heating (1°/min) to 120° of stoechiometrical amounts of dibenzo [*c*, *g*] tricyclo [4.2.0.0 ^{2,5}] octa-3,7-diene (**4**)[6] and fumaryl chloride (**5**) in xylene, the adduct **7** results by a Diels-Alder reaction of the *ortho*-quinonoid hydrocarbon **6** generated *in situ* from the hydrocarbon **4**.

Refluxing of **7** in methanol afforded (69% yield calcd. on **4**) the *trans*-ester **8**, colourless crystals with m.p. 180° (from methanol).

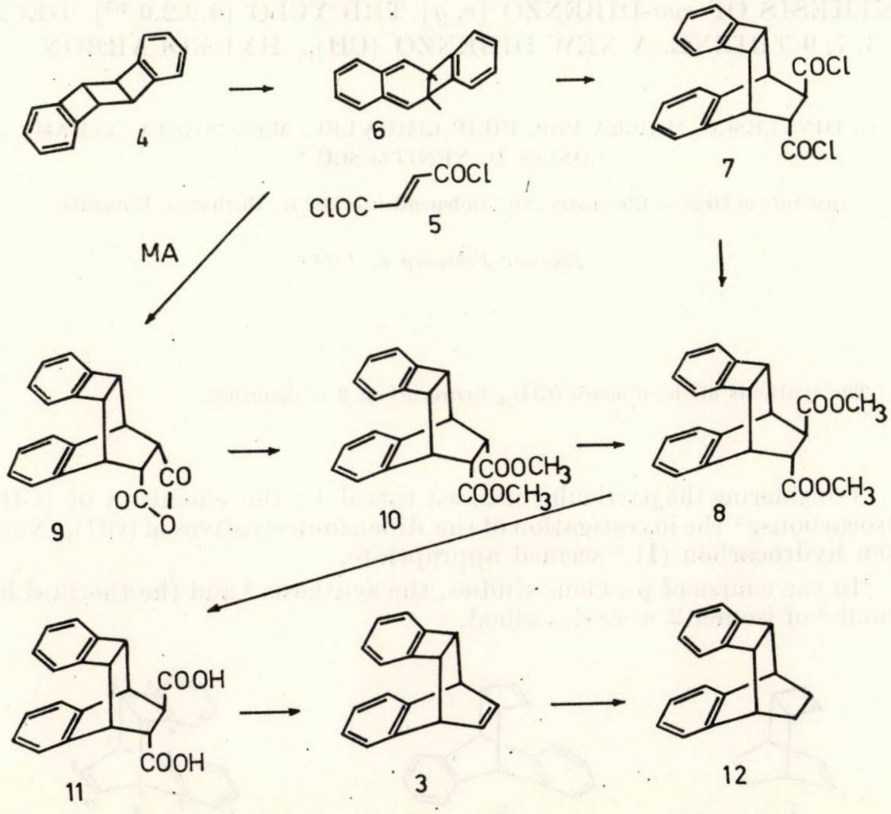

The structure and stereochemistry of compounds **7** and **8** are evident from their method of synthesis and examination of their NMR spectra.

The NMR spectrum of **8** ($CDCl_3$, δ, ppm) exhibits the following signals: 6.65 — 7.00 (m, 8H, aromatics), 3.65 — 3.95 (m, 4H, H-1, H-2, H-5, H-6), 3.26 and 3.53 (splitted AB system, J = 6 and 2.5 Hz, H-9, H-10), 3.85 (s, 3H from *exo*-carbomethoxy group), 3.60 (s, 3H from *endo*-carbomethoxy group); IR (CCl_4) : ν_{CO} 1734 cm^{-1}.

The same *trans*-ester **8** was obtained also from the earlier described[7,8]. anhydride **9**. Hydrolysis of the latter and treatment of the resulted *cis*-acid with an ethereal solution of diazomethane afforded the *cis*-ester **10**, m.p. 155° (from methanol) ; NMR ($CDCl_3$, δ, ppm) : 6.60 – 7.00 (m, 8H, aromatics), 3.65 (s, 4H, H-1, H-2, H-5, H-6), 3.40 (s, 6H from carbomethoxy groups), 3.15 (s, 2H, H-9, H-10) ; IR (CCl_4) : ν_{co} 1751 cm^{-1}.

---

[6] M. Avram, D. Dinu and C. D. Nenitzescu, *Chem. and Ind.*, **1959**, 257; M. Avram, D. Dinu, G. Mateescu and C. D. Nenitzescu, *Chem. Ber.*, **93**, 1789 (1960).

[7] M. Avram, I. G. Dinulescu, D. Dinu, G. Mateescu and C. D. Nenizescu, *Tetrahedron*, **19**, 309 (1963).

[8] M. P. Cava and R. Pohlke, *J. Org. Chem.*, **28**, 1012 (1963); W. Merk and R. Pettit, *J. Amer. Chem. Soc.*, **89**, 4788 (1967).

Heating of the *cis*-ester **10** in methanol with catalytic quantities of sodium methoxide gave rise to the *trans*-ester **8** in 84 % yield.

Alkaline hydrolysis of ester **8** led to the *trans*-acid **11**, m.p. 264° (from 50 % aqueous methanol), NMR ($CDCl_3$+$(CD_3)_2SO$, δ, ppm) : 6.60 - 7.00 (m, 8H, aromatics), 3.65-3.85 (m, 4H, H-1, H-2, H-5, H-6), 3.11 and 3.41 (splitted AB system, J = 6 and 2.5 Hz, H - 9, H-10).

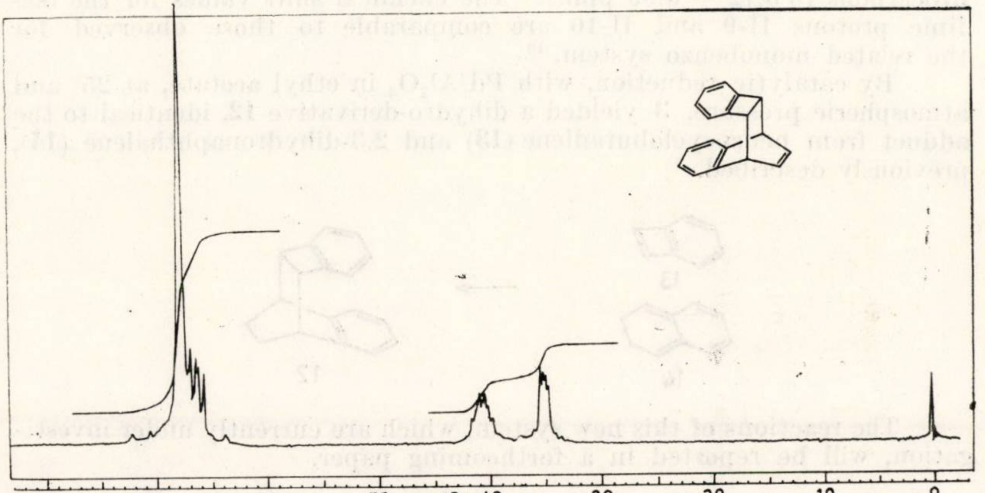

Fig. 1. — NMR spectra of the olefins **2** and **3**.

The acid **11**, on treatment with 3 moles lead tetraacetate, in pyridine solution, after extraction with petroleum ether, afforded olefin **3** in 47% yield, as colourless crystals with m.p. 132°. The NMR spectrum of olefin **3** in $CDCl_3$ shows the following signals (δ, ppm) : 6.75 (broad s, 8H, aromatics), 6.64 (m, 2 olefinic H, H-9, H-10, a part of an A_2X_2 system), 4.04 (m, 2H, H-1, H-6), 3.48 (m, 2H, H-2, H-5). UV (ethanol) : λ_{max} (log ε) : 262.8 nm (3.328), 268.4 (3.436), 275.1 (3.410).

The *syn* orientation of both aromatic rings is reflected in the value of aromatic protons which is shifted toward higher field, namely with 0.25 ppm, as compared with **2** (δ arom. 6.95 – 7.30 ppm) ; this value is also in good agreement with the chemical shift of some tribenzo $(CH)_{10}$ hydrocarbons (δ 6.12 – 6.90 ppm). [9] The chemical shift values for the olefinic protons H-9 and H-10 are comparable to those observed for the related monobenzo system. [10]

By catalytic reduction, with Pd/Al_2O_3 in ethyl acetate, at 25° and atmospheric pressure, **3** yielded a dihydro-derivative **12**, identical to the adduct from benzocyclobutadiene (**13**) and 2.3-dihydronaphthalene (**14**), previously described. [7]

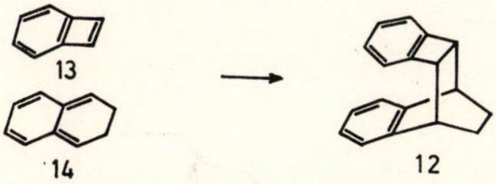

The reactions of this new system, which are currently under investigation, will be reported in a forthcoming paper.

EXPERIMENTAL

Microanalyses were performed by Miss Elvira Sliam and Mrs. Violeta Daniel. IR and NMR spectra were recorded using a Jena UR-20 spectrophotometer and a Varian A-60A spectrometer, respectively.

Dimethyl dibenzo [c, g] tricyclo [4.2.2.0^{2,5}] deca-3, 7-dien-*trans*-9, 10-dicarboxylate (8)

A well stirred mixture of 1.02 g (5 mmoles) *anti*-dibenzo[*c*, *g*] tricyclo [4.2.0.0^{2,5}] octa-3,7-diene (**4**), 0.80 g (0.57 ml ; 5 mmoles) fumaryl chloride (**5**) and 2.5 ml xylene was gradually heated (1°/min) until the temperature reached 120° ; this temperature was maintained for 1 hour. After evaporation *in vacuo* of the solvent and unreacted **5**, the oily residue (crude dichloride **7**) was treated with 25 ml methanol and was boiled for 5 hours. After cooling, the crystals which separated were filtered, yielding 1.2 g (69%) **8**, m.p. 185° (from methanol).

$C_{22}H_{20}O_4$	*Calcd.* :	C, 75.84 ; H, 5.79
	Found :	C, 75.67 ; H, 6.01

---

[9] D. M. Willand and C. G. McCarty, *J. Org. Chem.*, **37**, 4285 (1972).

[10] I. Murata, Y. Sugihara and N. Ueda, *Tetrahedron Letters*, **1973**, 1183.

Dimetyl dibenzo [e, g] tricyclo [4.2.2.0^{2,5}] deca -3,7- dien-*cis*-9,10-dicarboxylate (10)

Into a solution of 1.0 g potassium hydroxide in 20 ml water, 1.6 (2 mmoles) anhydride **9** were added and the mixture was heated at 60 — 70° for 15 min. After cooling at approx. 40°, the undissolved impurities were filtered and the clear solution was acidified with hydrochloric acid. The precipitate was filtered, washed with water and dried, yielding 0.4 g (66%) *cis*-acid, m.p. 243° (with anhydrization), which was utilized further without purification.

A suspension of 0.4 g crude *cis*-acid in 5 ml methanol and 25 ml ether was treated with an ethereal solution of diazomethane in excess, and the mixture was left ar room temperature for 4 hours until the evolution of nitrogen ceased. After evaporation of the solvent, a crystalline residue was obtained, which was purified by recrystallization from methanol, yielding 0.3 g (69%) ester **10**, m.p. 155°.

$C_{22}H_{20}O_4$	*Calcd.* :	C, 75.84 ; H, 5.79
	Found :	C, 76.10 ; H, 5.99

Isomerization of *cis* ester 10 to *trans* ester 8

A solution of 0.1 g (43.5 mmoles) sodium in 30 ml anhydrous methanol was treated with 0.30 g (0.86 mmoles) *cis*-ester **10**, and the mixture was boiled for 7 hours. After evaporation of the solvent, 20 ml water were added and the crystals were filtered, yielding 0.25 g (84%) *trans*-ester **8**, identical (m. p., mixed m.p., IR and NMR spectra) with the above described product.

Dibenzo [e, g] tricyclo [4.2.2.0^{2,5}] deca- 3, 7-dien- *trans*-9, 10- dicarboxilic acid (11)

a. *By hydrolysis of the trans-ester* **8**. A solution of 0.50 g (9 mmoles) potassium hydroxide in 10 ml methanol was heated with 0.50 g (1.44 mmoles) *trans*-ester **8** and the mixture was boiled for 6 hours. The solvent was then distilled, the residue was dissolved in 12 ml hot water, the solution was filtered and acidified, yielding 0.30 g (60%) *trans*-acid **11**, m.p. 264° (from 50% aqueous methanol).

$C_{20}H_{14}O_4$	*Calcd.* :	C, 74.98 ; H, 5.04
	Found :	C, 74.24 ; H, 5.30

b. *Preparative method for the trans-acid* **11** *starting from* **4**. A well stirred mixture of 6.12 g (30 mmoles) **4**, 5.6 g (35 mmoles ; 4.0 ml) fumaryl chloride (**5**) and 15 ml xylene was gradually heated (1°/min) until the temperature reached 120°, and this temperature was maintained for 1 hour. After evaporation *in vacuo* of the solvent and the unreacted **5** the oily residue was boiled with 110 ml methanol for 4 hours. The solvent was removed by distillation and the oily residue was treated with a solution of 7.5 g potassium hydroxide in 120 ml methanol and refluxed for 6 hours. After evaporation of the solvent, the residue was stirred for 15 min with 185 ml hot water, the coled solution was filtered and acidified under cooling with concentrated hydrochloric acid. By filtration, 5.25 g (55%) practically pure *trans*-acid **11** were obtained, which can be used further without purification.

syn- Dibenzo [e, g] tricyclo [4.2.2.0^{2,5}] deca- 3, 7, 9 - triene (3)

A solution of 5.0 g (15.6 mmoles) *trans*-acid **11** in 92 ml anydrous pyridine was treated, at 30—i35°, with 20.2 g (45 mmoles) lead tetraacetate, and the mixture was vigorously stirred until the evolution of carbon dioxide aceased. The reaction mixture was extracted with petroleum ether (b. p. 28–32°) and the resulted solution was washed several times with 2% hydrochloric acid, until all pyridine was removed. After washing with water and drying, the petroleum ether was removed by distillation and the crude crystalline residue was purified by chromatography on aluminium oxide with petroleum ether, yielding 1.7 g (47%) **3**, mp. 132°.

$C_{18}H_{14}$ *Calcd.*: C, 93.87; H, 6.13
Found: C, 93.59; H, 6.37

syn-Dibenzo [e, g] tricyclo [4.2.2.0^{2,5}] deca-3,7-diene (12)

A solution of 0.3 g olefin **3** in 15 ml ethyl acetate was stirred in hydrogen atmosphere with a small quantity of Pd/C, until the absorption ceased. The catalyst was filtered, the solvent was evaporated *in vacuo* and the residue was recrystalized from methanol yielding 0.25 g (13%) **12**, identical (m.p., IR and NMR spectra) with the previously described [7] adduct of benzocyclobutadiene with 2.3-dihydronaphthalene.

Revue Roumaine de Chimie, **19**, 7, 1203–1206 (1974)

INCHAIN-EPOXIDES OF CAROTENOIDS. IV[1]

METAL-CHLORIDE COMPLEXES OF CANTHAXANTHIN INCHAIN-EPOXIDES

DOINA OŞIANU, ELENA NICOARĂ and C. BODEA

Institute of Agronomy "Dr. Petru Groza", Department of Chemistry and Biochemistry,
str. Mănăştur 3, Cluj, Romania

Received November 13, 1973

Canthaxanthin mono and di-inchain-epoxides form coloured complexes with $AlCl_3$ and $FeCl_3$. These complexes have characteristic electronic spectra which can be used for the identification of inchain-epoxides. The complexes are instable in the presence of acetone, being converted into a mixture of canthaxanthin and initial epoxide.

Acting with perbenzoic acid on canthaxanthin we have obtained so far two mono-inchain-epoxides, 9,10- and 13,-14-epoxy-canthaxanthin [2] and a diepoxide, 9, 10, 9′, 10′-diepoxy-canthaxanthin.[3]

As we have shown in a previous paper, [1] canthaxanthin inchain-epoxides form green complexes with $HgCl_2$ differing by their weak stability from the $HgCl_2$ complexes of 5,6- and 5, 8-epoxy-carotenoids obtained by Yamamoto et al. [4] The $HgCl_2$ complexes of the inchain-epoxides are sufficiently stable in benzene to allow the electronic spectra to be recorded. The electronic spectra of these mercury-chloride complexes show a sharp maximum at 700–750 nm.

Monties and Costes [5] have mentioned a colour reaction for 5,6- and 5,8-epoxy-carotenoids with aluminium chloride.

We have obtained colour reactions for inchain-epoxides of canthaxanthin by using ferric chloride and aluminium chloride.

The ferric-chloride complexes were obtained by treating the benzenic solution of the inchain-epoxides with a benzenic solution of the anhydrous $FeCl_3$.

The complexes of inchain-epoxides of canthaxantin with aluminium chloride can be obtained in benzenic as well as in ethereal solution. The ethereal solutions being however more stable, they were prefered for the recording of the electronic spectra.

---

[1] D. Oşianu, E. Nicoară and C. Bodea, *Rev. Roumaine Chim.*, **16**, 765 (1971).

[2] E. Nicoară, D. Oşianu and C. Bodea, *Rev. Roumaine Chim.*, **15**, 1965 (1970).

[3] D. Oşianu, E. Nicoară and C. Bodea, *Rev. Roumaine Chim.*, **16**, 925 (1971).

[4] H. I. Yamamoto, C. O. Chichester and T.O.M. Nakayama, *Analyt. Chem.*, **33**, 1792 (1961).

[5] B. Monties and C. Costes, *Compt. rend. Ser. C.*, **266**, 481 (1968).

The colour of the metal-chloride complexes of inchain-epoxides is blue-green for $FeCl_3$ and violet for $AlCl_3$.

The attempt to separate from solution the pure $FeCl_3$ and $AlCl_3$ complexes, respectively, failed.

The electronic spectra of the complexes are shown in figures 1 and 2.

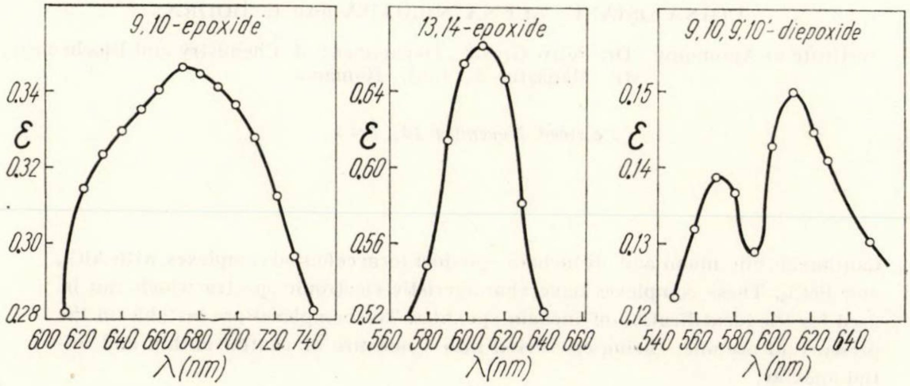

Fig. 1.—Visible light absorption spectra of $FeCl_3$ complexes of canthaxanthin inchain-epoxides.

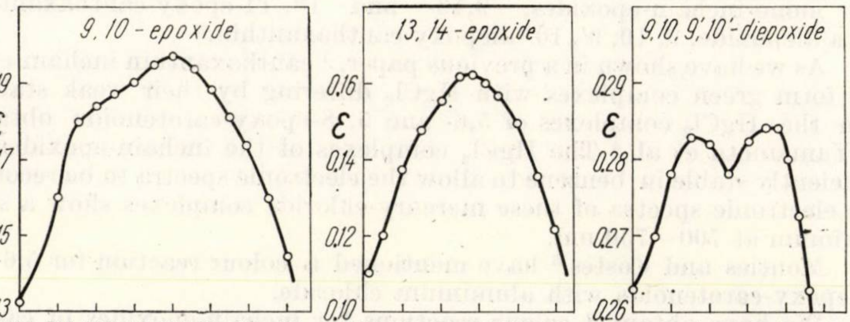

Fig. 2.—Visible light absorption spectra of $AlCl_3$ complexes of canthaxanthin inchain-epoxides.

As the inchain-epoxides have the chromophoric system shortened and show the electronic spectra at low wave lengths, the complexation reaction with metal chlorides is useful for their identification.

The absorption maxima of the inchain-epoxides and their complexes with $FeCl_3$ and $AlCl_3$, as well as with $HgCl_2$, are shown in table 1. As it is seen, the mercury-chloride complexes present the highest and the aluminium-chloride complexes the lowest absorption.

For the identification of the inchain-epoxides the complexation reaction with ferric chloride and aluminium chloride is recommended because it can be carried out in the solution without any difficulty.

Table 1

Visible light absorption maxima of metal-chloride complexes of canthaxanthin inchain epoxides

	Solvent	λ_{max} (nm)		
		9,10-epoxide	13,14-epoxide	9,10,9′, 10′-diepoxide
Initial epoxide	benzene	434	376	344
$HgCl_2$-complexes	benzene	754	700	754
$FeCl_3$-complexes	benzene	670	610	600 ;570
$AlCl_3$-complexes	diethyl ether	555	515	470 ;430

Under the action of acetone the $FeCl_3$ and $AlCl_3$ complexes are split into a mixture of canthaxanthin, initial epoxide and metal chloride. This behaviour is similar to that shown by the HCl[2,3] and $HgCl_2$ [1] complexes.

Thus, the decomposition reaction followed by partial deepoxidation is characteristic of the metal-chloride complexes of inchain-epoxides. Under the same conditions the decomposition of the 5,6-epoxy-complexes is associated with the isomerization in the corresponding 5,8-epoxide.

EXPERIMENTAL

Materials and apparatus

All the reagents and solvents were of analytical grade. Diethyl ether and benzene were dried over Na prior to use.

Electronic spectra were recorded with a Zeiss-Jena V.S.U.1 Universal spectrophotometer.

Methods

The canthaxanthin inchain-epoxides were prepared as described in previous papers, [2,3] by acting with perbenzoic acid upon canthaxanthin.

The $FeCl_3$ and $AlCl_3$ contents of the solutions were established by the chloride ion contents determined according to Morhr's method commonly used.

Canthaxanthin inchain-epoxy-$FeCl_3$ complexes

A ferric chloride solution in benzene was obtained by shaking a few minutes the anhydrous salt (in excess) with the solvent. The concentration of the solution determined according to the content of chloride ions was 10^{-3} M.

The $FeCl_3$ reagent was added dropwise to the epoxide solution until the formation of a soluble complex showing an intense green colour in the case of 9,10 epoxide ($\lambda_{max}=670$ nm), a blue colour for the 13,14-epoxide($\lambda_{max}=610$nm)and a green colour for 9.10,9',10'-diepoxide(λ_{max} = 600 and 570 nm). The absorption maxima were performed 15—30 minutes after the formation of the complex, using the initial solution diluted beforehand with the same solvent. The molar ratio inchain-epoxide : $FeCl_3$ of the complexes in solution was 2 :1. The attempt to isolate the complexes by thin layer chromatography on MgO or silicagel and by paper chromatography failed.

Through acetonolysis the complexes result in the formation of canthaxanthin and the initial epoxide. Compounds formed through acetonolysis were identified by cochromatography using authentic samples.

Canthaxanthin inchain-epoxy-$AlCl_3$ complexes

An aluminium chloride solution 10^{-2}M in diethyl ether was obtained by shaking a few minutes anhydrous salt (in excess) with the solvent.

The inchain-epoxide solutions, obtained as above with diethyl ether, were treated with the $AlCl_3$ reagent, dropwise, until the formation of a soluble complex showing an intense violet colour for 9,10 -epoxide ($\lambda_{max}=555$ nm), a violet colour for 13,14-epoxide($\lambda_{max}=515$ nm), and a red colour for 9,10,9', 10'-diepoxide ($\lambda_{max}=470$ and 430 nm). The absorption maxima were recorded not later than 20 minutes after preparation.

The molar ratio inchain-epoxide : $AlCl_3$ of the complexes in the ethereal solution was 1 : 1.

The $AlCl_3$ reagent as well as the complexes can be prepared also in benzene, but the obtained complexes are less stable than in the ethereal solution.

The $AlCl_3$ complexes of canthaxanthin epoxides show on acetonolysis and chromatography the same behaviour as the $FeCl_3$ complexes.

Revue Roumaine de Chimie, 19, 7, 1207–1219 (1974)

FORMATION D'ISOMÈRES DANS LES RÉACTIONS DE CYCLOHEXYLATION CATALYTIQUE DE BENZÈNE*

M. IOVU et ECATERINA TUDOR

Faculté de chimie, Université de Bucarest, Splaiul Independenţei 89, Bucarest

Reçu le 4 avril 1973

Dans les nombreux travaux effectués jusqu'à présent, concernant la cyclohexylation du benzène avec chlorure de cyclohexyle, cyclohexène ou cyclohexanol, en présence d'acides Lewis ou Brönsted, les auteurs considèrent le cyclohexylbenzène comme unique produit de réaction avec C_{12}. Compte tenu que le cyclohexène subit la polymérisation en présence des acides Lewis ou Brönsted et que le cyclohexane peut subir un rétrécissement du noyau, en présence des acides Lewis, nous avons estimé que telles réactions conduiraient aussi à la formation d'autres hydrocarbures avec du C_{12}, outre le cyclohexylbenzène, en pourcentages fonction de la méthode de synthèse du cyclohexylbenzène. Par l'application des voies de synthèse employées de plus couramment, et en respectant les conditions de réaction mentionnées par leurs auteurs, nous avons constaté que, sauf le cas où l'on utilise du chlorure de cyclohexyle comme agent de cyclohexylation, en présence de chlorure d'aluminium comme catalyseur, quand le cyclohexylbenzène résulté dépasse 99,5 %, dans les autres cas, outre le cyclohexylbenzène apparaissent également des bicycloalkyls, (méthylcyclopentyle) cyclohexane, hydrocarbures non saturés, isomères du (méthylcyclopentyl) benzène et cyclopentyl-phénylméthane. Les produits secondaires de réaction ont été mis en évidence par chromatographie.

INTRODUCTION

Les hydrocarbures cycloalkyl-aromatiques, intéressants comme « hydrocarbures modèles » du pétrole, sont employés à l'obtention d'initiateurs de polymérisation, comme matières premières pour la préparation de certains combustibles spéciaux et dernièrement on a étudié l'oxydation du cyclohexylbenzène au phénol et au cyclohexanone, matières premières importantes pour la préparation du caprolactame.

Les auteurs qui ont effectué les réactions de cycloalkylation des hydrocarbures aromatiques ne se sont pas posé le problème d'un rétrécissement de cycle avant ou après alkylation, notamment dans les conditions de réaction de type Friedel-Crafts.

---

* Travail présenté à la IIIe Conférence de Chimie Physique Générale et Appliquée — Bucarest, 4 — 7 septembre 1972.

Il est bien connu le fait que le cyclohexane en présence d'$AlCl_3$ humide passe en methylcyclopentane [1,2]. A 80° il atteint un équilibre[3] où méthylcyclopentane se trouve en proportion de 25%. Le méthylcyclohexane, de même, subit l'isomérisation, mais dans une moindre mesure (à l'équilibre existent 3% d'éthylcyclopentane et des diméthylcyclopentanes seulement[4]).

D'autre part, en cherchant d'obtenir du 1,4-dicyclohexylbenzène par cyclohexylation du benzène, ou a constaté que celui-ci résulte dans des proportions différentes par rapport à 1,2-et 1,3-dicyclohexylbenzène, en fonction du catalyseur et de l'agent de cyclohexylation utilisé. Ce fait pourrait être dû à certains rétrécissements du noyau saturé de 6 atomes de carbone, ce qui conduirait à la perte de la symétrie, dont la conséquence est la baisse de la température de fusion et la diminution du rendement en 1,4-dicyclohexylbenzène.

Pour vérifier si l'on peut obtenir du cyclohexylbenzène pur par cyclohexylation du benzène, on a passé à la cyclohexylation de celui-ci selon les conditions mentionnées dans la littérature, en selectionnant les catalyseurs et les procédés les plus indiqués. Les procédés de cyclohexylation peuvent être répartis selon les agents de cyclohexylation employés, notamment: chlorure de cyclohexyle, cyclohexène et cyclohexanol. Les catalyseurs sont soit des acides Lewis, tels que l'$AlCl_3$ et le $TiCl_4$ qui peuvent être employés

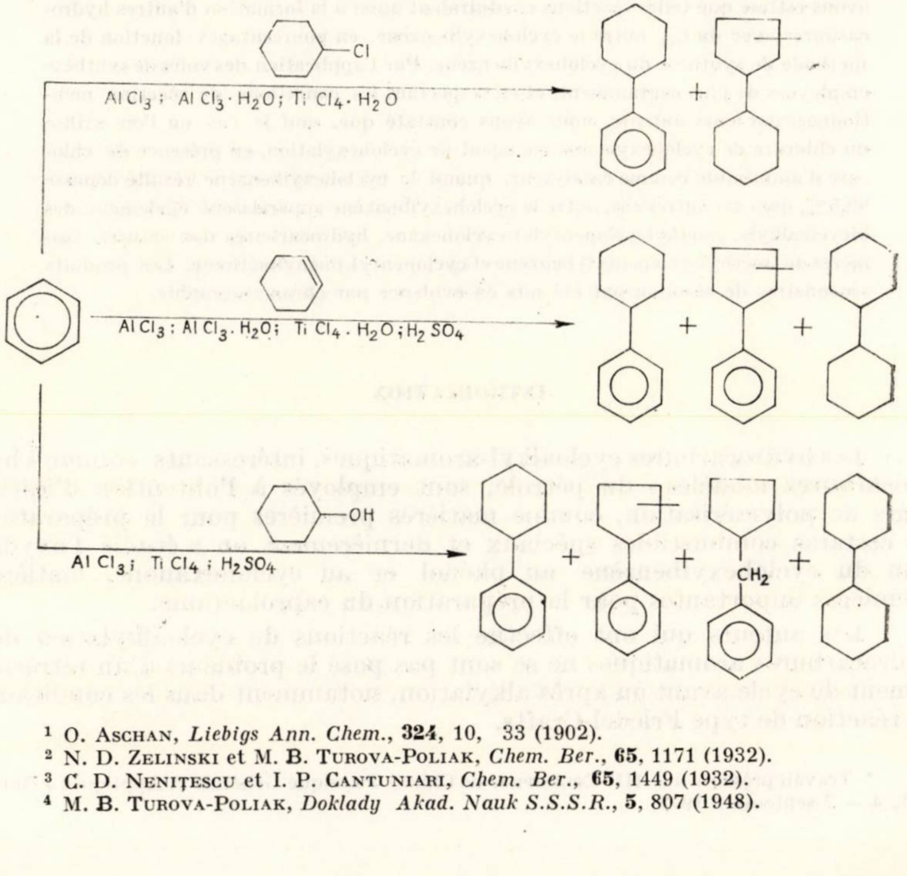
Cl
AlCl3 ; AlCl3 · H2O ; TiCl4 · H2O
+
AlCl3 ; AlCl3 · H2O ; TiCl4 · H2O ; H2SO4
+
+
OH
AlCl3 ; TiCl4 ; H2SO4
+
+
+
CH2

---

[1] O. Aschan, *Liebigs Ann. Chem.*, **324**, 10, 33 (1902).

[2] N. D. Zelinski et M. B. Turova-Poliak, *Chem. Ber.*, **65**, 1171 (1932).

[3] C. D. Nenițescu et I. P. Cantuniari, *Chem. Ber.*, **65**, 1449 (1932).

[4] M. B. Turova-Poliak, *Doklady Akad. Nauk S.S.S.R.*, **5**, 807 (1948).

pour tous les agents de cyclohexylation, soit des acides Brönsted, tels que le H_2SO_4 utilisés pour le cyclohexène et le cyclohexanol seulement.

Dans les synthèses effectuées par nous on a maintenu les différents rapports moléculaires : benzène : agent de cyclohexylation : catalyseur (tableaux 1, 2, 3) indiqués par la littérature, puisque le rapport benzène : agent de cyclohexylation influence seulement le rapport entre monoalkylat et polyalkylats, ce qui ne présente pas d'intérêt dans le présent ouvrage. Nous avons maintenu cependant la température constante, 25°, qui pourrait influencer l'équilibre entre les molécules au cycle de 6 et de 5 atomes de carbone.

Bien que la cyclohexylation du benzène avec du chlorure de cyclohexyle en présence de $AlCl_3$[5] et de $TiCl_4$[6] a été récemment effectuée, ses auteurs n'ont pas posé le problème d'une éventuelle obtention d'un mélange d'isomères.

La cyclohexylation du benzène avec du cyclohexène[7–10], en présence de $AlCl_3$ anhydre, a été effectuée à un moment où les moyens techniques de mise en évidence des isomères résultés de la réaction n'étaient pas encore connus. Plus tard, au lieu de $AlCl_3$, nous avons utilisé comme catalyseur le sesquichlorure d'éthylaluminium l'$AlEt_2Cl$. $AlEtCl_2$[11], mais nous n'avons pas étudié la formation des isomères.

Dans cet ouvrage nous consignons également les résultats de la cyclohexylation du benzène avec du cyclohexène en présence de $AlCl_3$ hydraté (cas qui n'est pas encore mentionné par la littérature), afin de voir si celui-ci a une action différente du chlorure d'aluminium anhydre.

Pojeau [6] utilise le $TiCl_4$, partiellement décomposé dans l'eau, à la cyclohexylation du benzène avec du cyclohexène.

Tous les auteurs, [9,12–16] qui effectuent la cyclohexylation du benzène avec du cyclohexène, en présence d'acide sulfurique considèrent le cyclohexylbenzène comme unique produit de 12 atomes de carbone, quoiqu'on puisse s'attendre à l'apparition d'un nombre plus grand de produits, compte tenu que l'acide sulfurique catalyse la réaction de polymérisation du cyclohexène.

La cyclohexylation avec du cyclohexanol en présence de $AlCl_3$ est attribuée à Tsukervanic [17] qui, plus tard, relève la commodité de cette méthode [18] par rapport aux cyclohexylations avec du chlorure de cyclohexyle et cyclohexène, matières premières que l'on doit synthétiser en partant du cyclohexanol. L'auteur cité ne met pas en évidence l'existence de certains isomères. De même, Lipovich [19], en répétant cette synthèse et en utilisant le cyclohexanol à carbone marqué, souligne que les bons rendements obtenus s'expliquent par l'absence de l'isomérisation du cycle de 6 atomes de carbone.

---

[5] S. D. Mehtiev et E. T. Subermanova, *Azerb. Khim. Zhur.*, **1964**, 49.

[6] R. Pojeau, *Compt. rend.*, **252**, 3060 (1961).

[7] T. M. Beery et E. R. Keid., *J. Amer. Chem. Soc.*, **49**, 3142 (1927).

[8] D. Bodroux, *Ann. Chim.*, (*France*), **11**, 511 (1939).

[9] B. B. Corson et V. N. Ipatieff, J. Amer. Chem. Soc., **59**, 645 (1937)-

[10] S. S. Nametkin et E. S. Pokrovskaia, *Zhur. obshchei Khim.*, **7**, Chem. Abstr., **31**, 5332 (1937).

[11] I. V. Nicolescu, M. Iovu J. Blackwell, K. M. Davies et W.J. Hickimbottom, *Chemistry and Industry*, **1962**, 1329.

[12] R. Truffault, *Compt. rend.*, **202**, 1286 (1936).

[13] T. A. Paşaev, S. D. Mehtiev et A. F. Aliev, *Azerb. Khim. Zhur.*, **2**, 39 (1959).

[14] S. D. Mehtiev, T. A. Paşaev et F. A. Useeva, *Azerb. Khim. Zhur.*, **5**, 41 (1962).

[15] S. D. Mehtiev, T. A. Paşaev et F. A. Useeva., « Sin.Prevasch. Monomernich Soedin ». Izd. Akad. Nauk,Azerb. SSR, Baku, 1967 ; *Chem. Abstr.*, **70**, 36783 (1969).

[16] E. Vizsoley, *Mágyar Tudomanyos*, **4**, 98 (1956) (; *Chem. Abstr.*, **53** 4200 (1959).

[17] I. P. Tsukervanik et N. G. Sidorova, *Zhur obshchei Khim.*, **7**, 641 (1937) ; *Chem. Abstr.*, vol 5780 (1930).

Pojeau [6] effectue la cyclohexylation du benzène avec du cyclohexanol aussi en présence de $TiCl_4$ et mentionne également que l'emploi du cyclohexanol est avantageux en comparaison d'autres agents de cyclohexylation, synthétisés en partant du cyclohexanol.

La cyclohexylation du benzène avec du cyclohexanol en présence de H_2SO_4 a été réalisée plus tard par Zavgorodnyi et ses collaborateurs [20] qui, bien qu'employant la chromatographie des produits obtenus, ne mettent pas en évidence la formation simultanée du cyclohexylbenzène et des méthylcyclopentylbenzènes ou des hydrocarbures cycliques saturés.

Comme agent de cyclohexylation on a utilisé le plus couramment le cyclohexène.

Corson et Ipatieff[21] par le traitement de grandes quantités de cyclohexylbenzène (825 g) à l'$AlCl_3$, à 80°, mettent en évidence la formation des dicyclohexylbenzène, diphénylcyclohexane, benzène, cyclohexane et methylcyclopentane, mais sans observer la formation de (méthyl-cyclopentyle) benzènes.

De même, en 1944, Nenitzescu [22] montrait qu'à la distillation du cyclohexylbenzène en présence d'$AlCl_3$ humide, une décomposition a lieu avec formation de benzène, de cyclohexane et de méthylcyclopentane. Aucune isomérisation du phénylcyclohexane n'est enregistrée.

RÉSULTATS ET DISCUSSIONS

Dans les tableaux 1—3 on a reporté, en pour cent, les différents produits à C_{12}, résultés de la cyclohexylation du benzène analysés par chromatographie, après une séparation préalable, par distillation en atmosphère et sous vide, du benzène pris à l'excès et des produits plus lourds de cyclohexylation ou de polymérisation.

Les données des tableaux révèlent que, dans la majorité des cas, outre le produit principal — le cyclohexylbenzène — des produits secondaires apparaissent aussi à la cyclohexylation du benzène, notamment :

Bicycloalkyls, tels que : *bi* (*méthyl-cyclopentyle*), *bicyclohexyle* et (*methyl-cyclopentyle*) *cyclohexane*. L'apparition de ces produits est plus facile à comprende lorsqu'on utilise comme agent de cyclohexylation le cyclohexène qui peut aussi subir des réactions de dimérisation, trimerisation,

---

[18] I. P Tsukervanik „Isledovanie v Oblasti aromaticeskih iader", Izdatelstvo Erevansk i Universitet, Erevan, 1955.

[19] V. D. Lipovichi et V. V. Cernets, *Zhur. org. Khim.*, **1**, 2151 (1965).

[20] S. V. Zavgorodnyi, I. A. Iasyr, J. N. Novikov et E. V. Alisova, *Ukrainskii Khim Zhur.*, **35**, 374 (1969).

[21] B. B. Corson et V. N. Ipatieff, *J. Amer. Chem. Soc.*, **60**, 747 (1938).

[22] C. D. Nenițescu, *Bull. Académie Roumaine de la section scientifique*, **27**, 681 (1944).

Table 1

Les produits de réaction du benzène avec du chlorure de cyclohexyle

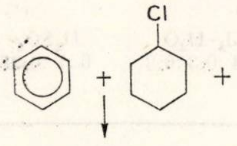	$AlCl_3$ 4 :1: 0,025	$AlCl_3 \cdot H_2O$ 4 : 1 : 0,05 : 0,05	$TiCl_4 : H_2O$ 1 : 0,4 : 0,3
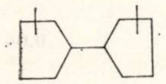	0,03	—	0,03
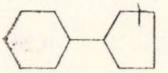		—	0,01
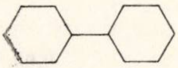	traces	traces	0,006
hydrocarbures non saturés	—	—	0,01
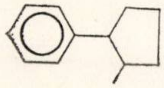 *cis*	0,08	0,03	0,34
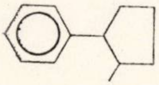 *trans*	0,32	0,25	0,38
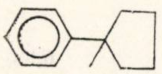			
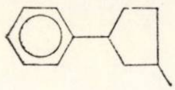			
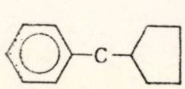	0,01	—	1,05
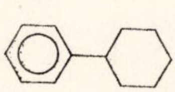	99,56	99,72	98,18

Table 2

Les produits de réaction du benzène avec du cyclohexène

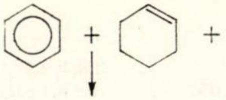	$AlCl_3$ 4 :1 :0,05	$AlCl_3 \cdot H_2O$ 2 :1 :0,05 :0,05	$TiCl_4 \cdot H_2O$ 1 :0,4 :0,3 :0,3	H_2SO_4 6 :1 :0,25
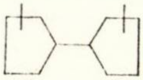	0,02	0,06	—	0,08
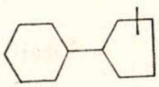	0,08	0,13	0,16	0,20
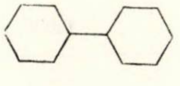	0,45	0,51	1,73	0,63
hydrocarbures non saturés	—	—	—	0,95
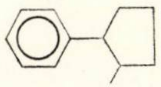 *cis*	0,03	0,11	0,20	0,06
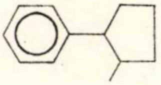 *trans*	0,14	0,29	0,21	0,33
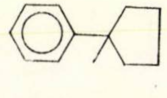				
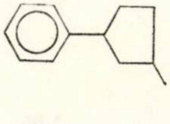				
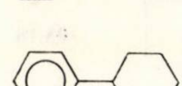	—	0,04	0,03	0,06
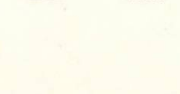	99,38	98,86	97,67	97,69

Table 3

Les produits de réaction du benzène avec du cyclohexanol

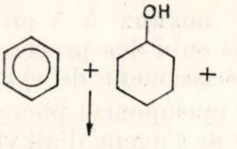		$AlCl_3$ 1 : 0,5 : 0,5	$TiCl_4$ 1 : 0,4 : 0,3	H_2SO_4 3 : 1 : 3
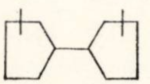		0,05	—	0,24
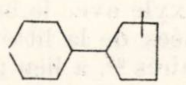		0,07	—	0,65
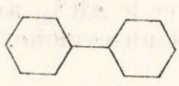		0,03	traces	0,28
hydrocarbures non saturés		0,50	—	0,29
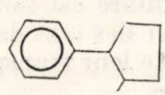	*cis*	1,13	0,32	0,10
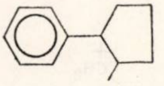	*trans*	2,25	0,38	0,76
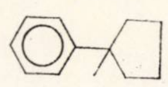				
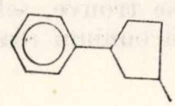				
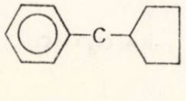		0,14	1,12	—
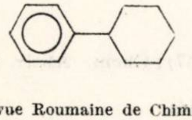		95,87	98,18	97,95

etc.[23]. Le dimère qui doit être non saturé et qui se trouve en quantité appréciable au cas du catalyseur H_2SO_4 peut être transformé en produit saturé après les processus de transfert d'hydrogène [24].

Hydrocarbures non saturés constitués de deux noyaux à 5 ou 6 atomes de carbone dont l'un non saturé, qui n'ont pas subi des processus de disproportionnation, mais qui ont pu subir un rétrécissement de cycle.

Isomères du (méthylcyclopentyl) benzène et le cyclopentyl-phenylmethane, résultés soit par un rétrécissement de cycle de l'agent d'alkylation soit par une isomérisation ultérieure du cyclohexylbenzène.

Cyclohexylation du benzène avec du chlorocyclohexane

On suppose que la réaction du chlorure de cyclohexyle avec le benzène, en présence d'acides Lewis, compte tenu des données de la littérature concernant la cinétique de certaines réactions similaires [25], a lieu par l'attaque électrophile du benzène par l'ion de carbone qui apparaît à la complexation du chlorure de cyclohexyle, par exemple avec le $AlCl_3$, avec la formation d'un complexe qui se décompose conduisant au cyclohexylbenzène

$$C_6H_{11}Cl + AlCl_3 \rightleftharpoons C_6H_{11}^+ + AlCl_4^-$$

La formation des ions de carbonium, même si l'équilibre est fortement déplacé à gauche, dû à l'impossibilité de la solvatation des ions dans le solvant non polaire (benzène), pourrait aussi être suivie de leur transposition par le transfert intramoléculaire d'un ion d'hydrure

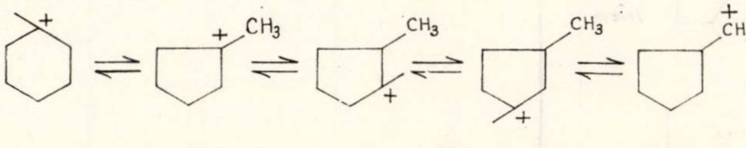

Les deux ions $C_6H_{11}^+$ et $AlCl_4^-$ restent cependant réunis par une attraction électrostatique sous forme d'une paire d'ions qui se trouve, selon Nenitzescu, [25] dans une « Cage de dissolvant ». L'ion de carbonium réagit avec le benzène sans se détacher de l'anion

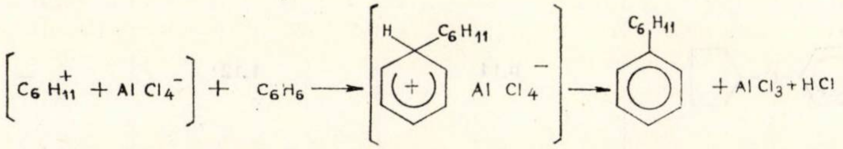

---

[23] R. Sperlyng, *J. Chem. Soc.*, **1949**, 1928.

[24] S. S. Nametkin et M. G. Rudenko, *Zhur org. Khim.*, **7**, 763 (1937) ; Chem. Abstr. **31**, 5750 (1937).

[25] C. D. Nenițescu, *Studii și Cercetări Chimice. București*. **12**, 5 (1964).

La formation du cyclohexylbenzène qui dépasse 99,5% (tableau 1) est en accord avec l'hypothèse de l'existence des paires d'ions ; l'apparition de certains ions de carbonium libres aurait mené à leur transposition et ensuite à l'attaque électrophile du benzène par les nouveaux ions de carbonium, avec formation de (méthylcyclopentyle) benzènes et cyclopentylphénylméthane en proportions fonction de la stabilité des différents ions de carbonium. Le pourcentage réduit d'isomères du cyclohexylbenzène, 0,41%, (0,08 + 0,32 + 0,01), atteste que dans les conditions de travail utilisées (25°), ce processus est très réduit, et cela sans tenir compte qu'une partie des isomères du cyclohexylbenzène serait due aux impuretés du chlorure de cyclohexyle utilisé (1,81% cyclohexanol).

L'addition d'eau au chlorure d'aluminium n'influence pratiquement pas les résultats (tabl. 1), ce qui montre que la cyclohexylation avec du chlorure de cyclohexyle ne subit pas de catalyse par l'acide $H^+(AlCl_3OH)^-$.

De même, le fait que le pourcentage d'isomères du cyclohexylbenzène ne s'élève pas (il est par contre moindre), par l'emploi du chlorure d'aluminium hydraté, en comparaison du cas où l'on utilise du chlorure d'aluminium anhydre, démontre que, au moins à 25°, le $H^+ (AlCl_3OH)^-$ ne réussit pas à arracher un ion d'hydrure du cyclohexylbenzène une fois formé pour le transformer ensuite en un ion de carbonium qui subisse par la suite la transposition.

En présence du tétrachlorure de titane (catalyseur plus faible que l'$AlCl_3$) la cyclohexylation du benzène avec du chlorure de cyclohexyle conduit à des quantités appréciables de cyclopentylphenylmethane(1,05%) en comparaison des cas où l'on utilise le chlorure d'aluminium. Le cyclopentylphénylméthane est probablement l'isomère thermodynamiquement le plus stable. La formation de l'isomère le plus escompté issu d'un ion de carbonium secondaire a été aussi rencontrée au cas d'autres hydrocarbures alkylaromatiques [25].

Cyclohexylation du benzène avec du cyclohexène

Un grand groupe d'impuretés dans le produit principal le cyclohexylbenzène, est formé de bicycloalkyls et cycloalkylcyclènes, qui sont présents si l'on utilise comme matières premières le cyclohexène et le cyclohexanol et sont pratiquement absents au cas du chlorure de cyclohexyle.

L'acide sulfurique (acide Brönsted) comme le chlorure d'aluminium et le chlorure de titane (acides Lewis) en présence de l'eau catalyseur, lorsqu'on forme par exemple le $H^+AlCl_3OH^-$, peuvent protonner le cyclohexène en créant un ion de carbonium : ensuite les réactants nucléophiles du milieu de réaction, le cyclohexène et le benzène, subissent l'attaque électrophile de l'ion de carbonium

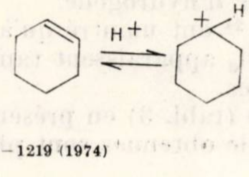

Le pourcentage très élevé de cyclohexylbenzène est dû d'une part au caractère nucléophile plus accusé du benzène par rapport au cyclohexène, et d'autre part à sa quantité à l'excès.

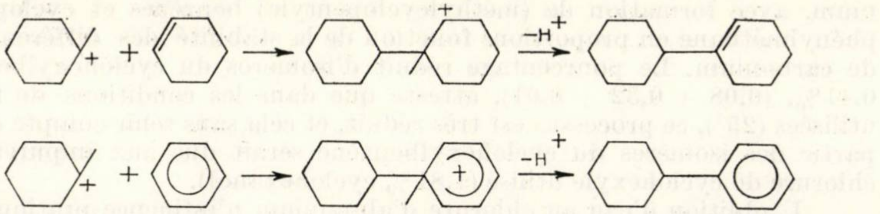

Du fait que l'ion de carbonium subit la transposition à l'attaque électrophile du cyclohexène par l'un des nouveaux ions de carbonium, il résulte un nouvel ion de carbonium qui peut expulser un proton ou peut subir une transposition suivie de l'expulsion du proton, comme par exemple :

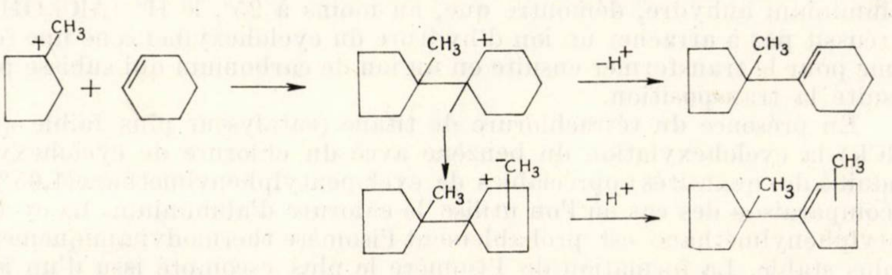

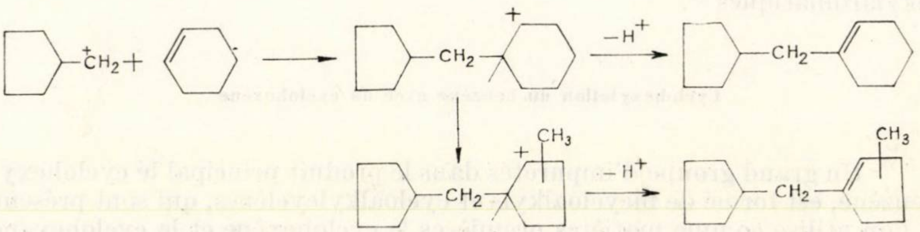

Conformément à ce mécanisme il faudrait q'il résulte des hydrocarbures dicycliques non saturés. Ces hydrocarbures sont présents en quantité accrue surtout lorsqu'on travaille en présence d'acide sulfurique (tabl. 2,3), mais de plus, on a mis en évidence également des hydrocarbures dicycliques saturés comme résultat de l'hydrogénation des dicyclènes simultanément avec la déshydrogénation de certains noyaux jusqu'au benzène par un processus de transfer d'hydrogène.

Nametkin et Rudenko [24] ont montré qu'à la polymérisation du cyclohexène en présence d'$AlCl_3$ apparaissent tant d'hydrocarbures saturés que de cycloalkyl-aromatiques.

Au cas du cyclohexène (tabl. 3) en présence des catalyseurs Lewis, les quantités de bicyclohexyle obtenues sont plus élevées, tandis que, en présence de l'acide sulfurique, les hydrocarbures non saturés sont prédominants.

A l'attaque électrophile du benzène par les ions de carbonium, il résulte les isomères suivants, sans tenir compte des isomères de conformation.

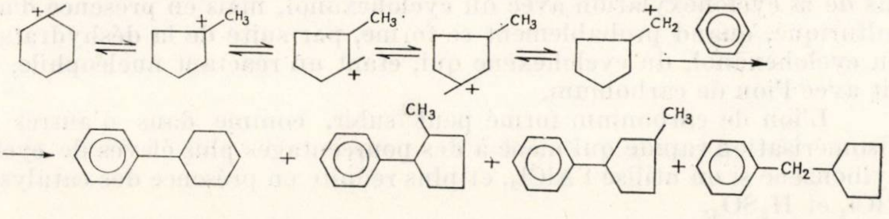

Le chlorure d'aluminium humide conduit à la formation d'une quantité double d'isomères cycloalkylbenzéniques par rapport au chlorure d'aluminium anhydre. Le fait s'explique par la production de l'acide $H^{+}(AlCl_3OH^{-})$ qui protonne le cyclohexène et qui détermine la formation de produits secondaires en proportions plus proches de celles obtenues par l'emploi de H_2SO_4 que par l'$AlCl_3$ anhydre (tableau 2).

Le tétrachlorure de titane, étant utilisé à l'état d'hydrat seulement, exerce, lui aussi, une action similaire à celle de l'acide sulfurique.

Lebedev [26] étudiant la cinétique de la réaction de cyclohexylation du benzène avec du cyclohexène en présence de $AlCl_3$ montre que l'agent d'alkylation est le chlorure de cyclohexyle formé par l'addition d'acide chlorhydrique (provenu de l'hydrolyse d'$AlCl_3$ avec les traces inhérentes d'eau) au cyclohexène. Ce fait concorde avec le rapprochement des résultats obtenus à la cycloalkylation du benzène avec cyclohexylchlorure et cyclohexène, en présence d'$AlCl_3$ anhydre (tabl. 1,2).

Cyclohexylation du benzène avec du cyclohexanol

A la cycloalkylation du benzène avec du chlorure de cyclohexyle et cyclohexène, l'$AlCl_3$ est nécessaire en quantités catalytiques seulement, tandis qu'à la cyclohexylation avec du cyclohexanol la quantité d'$AlCl_3$ est considérablement plus élevée (tableau 3), dû à la réaction.

$$C_6H_{11}OH + AlCl_3 \longrightarrow C_6H_{11}^{+}\ OHCl_3^{-} \longrightarrow$$

$$\begin{tikzcd}[column sep=small] \longrightarrow C_6H_{11}^{+} + & {[HOAlCl_3]^{-}} \arrow[dl] \arrow[dr] & \\ HO^{-} + AlCl_3 & & Al(OH)Cl_2 + Cl^{-} \end{tikzcd}$$

L'ion de carbonium attaque de façon électrophile l'unique réactant nucléophile présent, le benzène, formant le cycloalkylbenzène, ce qui explique le pour cent réduit de dicycloalkyls (0,03 %) au cas des catalyseurs $AlCl_3$ et $TiCl_4$ (tabl. 3), en comparaison de la cycloalkylation avec du cyclohexène (tabl. 2), en présence des mêmes catalyseurs où, par exemple, le bicyclohexyle se trouve en proportion de 0,45 %.

---

[26] N. N. Lebedev, *Zhur. obshchei Khim.*, **10**, 1782 (1954).

La quantité de bicycloalkyl est de même plus grande aussi dans le cas de la cyclohexylation avec du cyclohexanol, mais en présence d'acide sulfurique, quand probablement se forme, par suite de la déshydratation du cyclohexanol, du cyclohexène qui, étant un réactant nucléophile, réagit avec l'ion de carbonium.

L'ion de carbonium formé peut subir, comme dans d'autres cas, l'isomérisation rapide qui mène à des pourcentages plus élevés de cycloalkylbenzène si on utilise l'$AlCl_3$, et plus réduite en présence des catalyseurs $TiCl_4$ et H_2SO_4.

De même, les ions de carbonium peuvent réagir avec les ions de chlore résultés de la décomposition de l'ion complexe $(HOAlCl_3)^-$, avec la formation de chlorure de cyclohexyle, dont la présence a été d'ailleurs mise en évidence par chromatographie.

Les isomères formés à la cyclohexylation du benzène avec du cyclohexanol en présence de H_2SO_4 comme catalyseur (tableau 3) sont également dus, aussi dans ce cas, à la formation de l'ion de carbonium qui est isomérisé.

$$C_6H_{11}OH + H_2SO_4 \longrightarrow C_6H_{11}OSO_2 + H_2O$$

$$C_6H_{11}OSO_2OH \rightleftharpoons C_6H_{11}^+ + HSO_4^-$$

PARTIE EXPÉRIMENTALE

Le benzène utilisé a été un produit commercial Reactivul séché sur au sodium et dont la pureté a été vérifiée par chromatographie.

Le chlorure de cyclohexyle a été obtenu du cyclohexanol et de l'acide chlorhydrique et purifié par rectification, à la chromatographie le produit purifié contenait 97,65 % chlorure de cyclohexyle, 1,81 % cyclohexanol, 0,16 % cyclohexanone et 0,25 % benzène, la reste constituant des impuretés indéterminées.

Le cyclohexène a été obtenu par déshydratation du cyclohexanol, avec de l'acide phosphorique comme cataylseur [28], son analyse chromatographique révèlent une pureté de 99,8 %.

Le cyclohexanol, produit Reactivul, analysé par chromathographie, avait une pureté de 97,6 % les impuretés principales étant le cyclohexanone 0,7 % et l'eau 1 %.

L'$AlCl_3$ a été un produit commercial Merck (sublimiert zur synthese).

Le $TiCl_4$ — un produit commercial Fluka.

Le H_2SO_4 — un produit commercial *p.a.*

La cyclohexylation du benzène a été realisée dans un ballon de 250 ml, à quatre cols muni d'un agitateur, réfrigérant ascendant, d'un tube de $CaCl_2$, d'un thermomètre et d'un entonnoir compte gouttes. Dans le ballon est d'abord introduit le benzène et le catalyseur, et ensuite graduellement l'agent d'alkylation, de façon que la température ne dépasse pas 20° (le ballon était refroidi dans un bain d'eau). Au cas de la cyclohexylation de benzène avec du cyclohexène et du

---

[27] H. Pines, W. D. Huntsman et V. N. Ipatieff, *J. Amer. Chem. Soc.*, **73**, 4343 (1951).

[28] W. M. Dehn et K. E. Jackson, *J. Amer. Chem. Soc.*, **55**, 4285 (1933).

chlorure de cyclohexyle en présence de $TiCl_4$, sur les réactants et le catalyseur on a ajouté de l'eau en portions réduits, tenant compte que la réaction du $TiCl_4$ avec l'eau est violente.

Les produits de réaction ont été traités, au cas où l'on utilise les acides Lewis, comme catalyseurs, avec une solution de HCl pour la solubilisation du catalyseur et au cas de H_2SO_4 on a éliminé le goudron formé. Les produits de réaction sont ensuite lavés à l'eau à une solution de $NaHCO_3$ 10% et de nouveau à l'eau. On sèche sur chlorure de calcium et, ensuite, par distillation à pression normale, le benzène à l'excès est écarté ; le reste est distillé *in vacuum* (12mm Hg). On a séparé la fraction correspondant aux hydrocarbures à C_{12}.

L'analyse chromatographique a été effectuée à l'aide d'un chromatographe Carlo Erba modèle G.T. —200 à double détecteur de conductibilité thermique et à gaz porteur hydrogène, à savoir.

Pour les matières premières — sur une colonne à carbowax 20 M, 20% sur chromosorb W 60/80 msh, $l = 2{,}5$ m, $\varnothing = 2$ mm, respectivement à 50° pour le cyclohexène et à 110° pour le chlorure de cyclohexyle et cyclohexanol ; la pureté du cyclohexanol a été aussi vérifiée a une température plus élevée de la colonne (150°).

Pour la composition de la fraction C_{12}, l'identification, et la séparation ont été effectuées conformément aux procédés décrits dans un travail précédent.[29]

Les résultats quantitatifs sont exprimés en % aires.

CONCLUSIONS

On a analysé pour la première fois, par la méthode chromatographique des gaz les produits de cyclohexylation à C_{12} du benzène.

La cyclohexylation du benzène avec du chlorure de cyclohexyle en présence d'$AlCl_3$ anhydre ou hydraté conduit au produit le plus pur, du cyclohexylbenzène au-dessus de 99,5%. Des dimères du cyclohexène n'apparaissent pas, l'ion de carbonium intermédiaire ne trouvant pas autre réactant nucléophile dans le milieu de réaction en dehors du benzène. Le rétrécissement du noyau de 6 atomes de carbone du radical cyclohexyle se produit en petite mesure.

La cyclohexylation du benzène avec du cyclohexène mène à la formation de bicycloalkyls par suite des réactions de dimérisation et de transfert d'hydrogène, en présence de $AlCl_3$ (anhydre et hydraté), de $TiCl_1$(hydraté) et de H_2SO_4, catalyseurs, ainsi qu'à la formation d'hydrocarbures non saturés en présence de H_2SO_4, ce qui est possible dû à l'attaque électrophile des ions de carbonium intermédiaires non seulement contre le benzène, mais aussi contre le cyclohexène.

La cyclohexylation du benzène du cyclohexanol, recommandée par certains auteurs comme la voie la plus commode d'obtention du cyclohexylbenzène (vu que le chlorure de cyclohexyle et le cyclohexène sont préparés en partant du cyclohexanol) n'est pas indiquée, celle-ci menant à des produits secondaires toujours avec du C_{12}, impossibles à séparer par les méthodes courantes, en proportion de 2 à 4%.

---

[29] E. Tudor et M. Iovu, Résultats présentés à la IIIe Conférence de Chimie Physique Générale et Appliquée — Bucarest, 4—7 septembre 1972.

Revue Roumaine de Chimie, 19, 7, 1207—1219 (1974)

Revue Roumaine de Chimie, **19**, 7, 1221–1225 (1974)

THE SYNTHESIS OF 2,6-DICHLOROBENZALDOXIME FROM 4-NITROTOLUENE

P. BUCHWALD and F. DOMNARIU

Chemical-Pharmaceutical Research Institute, str. Fabricii 126, Cluj, Romania

Received July 17, 1971

Revised text received October 5, 1973

The synthesis of 2,6-dichlorobenzaldehyde and the respective 2,6-dichlorobenzaldoxime from 4-nitrotoluene by successive nucleus and side-chain chlorination is described. It is shown that by nucleus chlorination, besides 2-chloro-4-nitrotoluene and 2,6-dichloro-4-nitrotoluene, the derivative chlorinated in 2, 3, 6 positions is also produced. In side-chain chlorination of 2,6-dichlorotoluene under free radical conditions, the products containing one, two and three chlorine atoms in their side chain are also resulting. A convenient chemical method for their separation is described.

According to the literature the 3(2,6-dichlorophenyl)-5-methylisoxazole-4-carboxylic acid—the principal intermediate in dicloxacilline synthesis — usually is obtained from 2,6-dichlorobenzaldehyde.

Our principal aim being the synthesis of this semisynthetic penicilline, as a first step in our investigation we proposed to find a method for the preparation of the 2,6-dichlorobenzaldehyde and the respective 2,6-dichlorobenzaldoxime from a convenient starting material.

It was shown [1] that the 2,6-dichlorobenzaldehyde has been obtained by the hydrolysis of the 2,6-dichlorobenzal chloride. The latter has been prepared by the chlorination of the 2-nitro-6-chlorotoluene, when besides the side-chain chlorination, the nitro group was also substituted with chlorine atom. [2]

We have considered as a first step for the synthesis of 2,6-dichlorobenzaldehyde the preparation of 2,6-dichlorotoluene because of its easy conversion into 2,6-dichlorobenzal chloride, under the side-chain chlorination conditions.

It is well known [3] that the direct nucleus chlorination of the toluene is not selective, for it leads to a complex mixture of the positional isomers of the chlorotoluenes. From this the isolation of 2,6-dichlorotoluene is very difficult.

Since the separation of the positional isomers of dichlorotoluene is more difficult than the isolation of mono-, di-, and trichlorotoluenes, we intended to chlorinate in nucleus a toluene derivative in which the 3, 4 and 5 positions were protected by a convenient group which was easy to eliminate after chlorination.

Although it seemed that 4-aminotoluene was a convenient starting material in this direction, the method which involved the treatment of the acetyl derivative of *p*-toluidine was not really satisfactory, for it led to a very crude amine, with a low yield.[4]

---

[1] G. Stork and W. N. White, *J. Amer. Chem. Soc.*, **78** 4609 (1956).

[2] "Shell" Research Ltd. Belg. Pat. 610, 998, May 1962; *Chem. Abstr.*, **58**, 3358 (1963).

[3] E. Seelig, *Liebigs Ann. Chem.*, **237**, 129 (1886).

Thus, to obtain 2,6-dichlorobenzaldoxime we used as starting material the 4-nitrotoluene, the synthesis involving the following steps (see scheme):

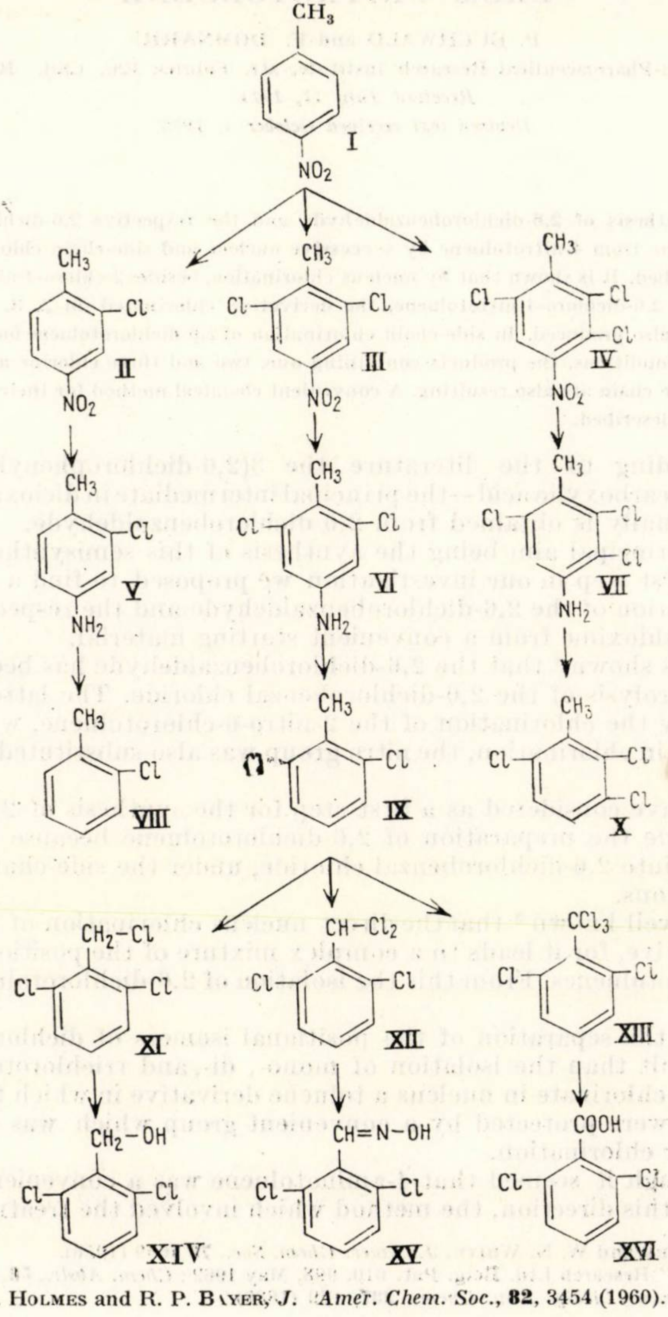

---

[4] R. R. Holmes and R. P. Bayer, *J. Amer. Chem. Soc.*, **82**, 3454 (1960).

Naturally, we supposed that in this case the nitro group would protect the 3, 4, and 5 positions from chlorination.

However, when the chlorination of 4-nitrotoluene (I) was effected by Davies' method [5] at 65 – 75° with chlorine in the presence of antimony pentachloride, until the reaction mixture increased in weight corresponding to two chlorine atoms, besides 2-chloro-4-nitrotoluene (II) and 2,6-dichloro-4-nitrotoluene (III) the 2, 3, 6-trichloro-4-nitro-compound (IV) was also produced. This was confirmed by the isolation of 2-chloro-4-aminotoluene (V), 2,6-dichloro-4-aminotoluene (VI), and 2,3,6-trichloro-4-aminotoluene (VII) from the reaction mixture obtained by reduction of the corresponding nitro compounds by Béchamp's method (iron filings, acetic acid in aqueous solution). These were separated by fractionated distillation under reduced pressure and were characterized by their acetyl derivatives' melting points.

The replacement of the amino group by hydrogen was carried out by a modification of Coleman and Talbot's method [6] for the preparation of sym.-tribrombenzene from 2, 4, 6-tribromoaniline. In this way, working at 70 – 80° in benzene-ethanol (1 : 3) solution in the presence of concentrated sulphuric acid, and using crystalline sodium nitrite we succeeded to synthesize 2,6-dichlorotoluene (IX) with an 80 % yield as referred to (III).

By the side-chain chlorination of 2,6-dichlorotoluene (IX) under free radical conditions (at 180° with UV source, or at 90 – 110° in the presence of 2,2′-azo-bis-isobutyronitrile [7]) there resulted also the entrance of one, two and three chlorine atoms in the side chain. Although their isolation is possible by fractionated distillation, the boiling points being very close an efficient fractionating column must be used. In order to avoid these inconveniences and the inevitable loss of compounds owing to the fractionated distillation, we proposed to use for the separation a chemical method. Thus, by hydrolysing together the side-chain chlorinated derivatives of 2,6-dichlorotoluene (XI – XIII) with concentrated sulphuric acid (90 – 94 %) in the presence of hydroxylamine hydrochloride, followed by transfer of the reaction mixture in water-ice, in the hydrolysate there will be obtained : 2,6-dichlorobenzylic alcohol (XIV) (formed by hydrolysis of (XI)), 2,6-dichlorobenzaldoxime (XV) (from (XII)), and 2,6-dichlorobenzoic acid (XVI) (from (XIII)). When the hydrolysate is extracted with an organic solvent (it has been proved that the most convenient is the butyl acetate) the products of hydrolysis pass into the organic phase. After washing the organic layer with water (to eliminate the inorganic acid traces) the butyl acetate solution is treated with saturated sodium bicarbonate solution. Thus, the 2,6-dichlorobenzoic acid passes into the aqueous phase as sodium salt. From this, after treatment with dilute hydrochloric acid, the pure (XVI) is obtained. Melting point : 143 – 145° (141 – 142° [1]).

By repeated extractions with diluted sodium hydroxide (10 %) from the organic layer the 2,6-dichlorobenzaldoxime, as sodium salt, passes into the aqueous alkaline phase, from which the almost pure (XV) is precipitated by acidulation. Melting point : 149° (133–137°[2]; 147 – 148°[8]).

---

[5] W. Davies, *J. Chem. Soc.*, **121**, 812 (1922).

[6] G. H. Coleman and W. F. Talbot, "Organic Syntheses", Coll. Vol. 2, New York, 1948, p. 592.

[7] "Shell" Research Ltd. Fr. Pat. 1, 343, 178 Dec. 12, 1962 ; *Chem. Abstr.*, **60**, 9208 (1964).

The 2,6-dichlorobenzylic alcohol (XIV) and other by-products without an acid character remain in the organic layer. Thus, the quantitative isolation of the side-chain chlorinated compounds, respectively their hydrolysis products, is possible.

By hydrolysis of 2,6-dichlorobenzaldoxime, followed by steam distillation, the 2,6-dichlorobenzaldehyde may be obtained in a good yield. Since the first step in the 3 (2,6-dichlorophenyl)-5-methyl-isoxazole-4-carboxylic acid synthesis is just the preparation of dichlorobenzaldoxime from 2,6-dichlorobenzaldehyde, it was not necessary to accomplish the hydrolysis of (XV).

EXPERIMENTAL

Melting points are uncorrected.

1. The nucleus chlorination of 4-nitrotoluene

548 g (4 moles) of 4-nitrotoluene were chlorinated by barbotage of chlorine at 70–80° in the presence of antimony pentachloride (20 g) in about 5 hours, until the reaction mixture increased in weight 270–280 g. The reaction mixture was poured into about 4 l cold water, the lower oil layer was separated and washed with dilute sodium hydroxide and water successively.

The resulted crude chlorinated 4-nitrotoluene (containing (II), (III), and (IV) weighed 768 g and was used as such for the preparation of the chlorinated 4-aminotoluene.

2. The reduction of nitro group

A mixture of the above obtained crude chlorinated 4-nitrotoluene (768 g), grease-free iron filings (500 g) — previously activated by washing with dilute hydrochloric acid, - ammonium chloride (17 g), acetic acid (15 ml), and water (about 1 l), was heated gently at 80–90° and maintained at this temperature under vigorous stirring, by alternate heating and cooling, for two –three hours. When the exotherm reaction was finished, the reaction mixture was heated on a water bath under stirring for another 10 hours, in order to complete the reaction. After cooling, the amine separated as an oil, the iron residues were filtered off and washed with benzene. The filtrate was separated, the solvent was removed and then distilled at reduced pressure. The mixture of mono-, di-, and trichloro-4-aminotoluene (V – VII) distils at 105–141° /4–5 mm.

529 g (400 ml) chlorinated 4-aminotoluene derivatives were obtained.

3. The replacement of the amino group by hydrogen

The chlorinated 4-aminotoluene (529 g) was dissolved in an ethanol (4 l)–benzene (1.5 l) mixture, and was treated under stirring with concentrated sulphuric acid (300 ml). To the hot solution at 70–72° the powdered sodium nitrite was added in three portions (3 × 100 g).

---

[8] "Bristol-Myers Co." U.S.A.Pat. 6, 603, 496, Sept. 19, 1966 ; *Chem. Abstr.*, **63**, 15390 (1965).

The reaction heat and nitrogen evolution led to a vigorous boiling of the solution. After the boiling slowed down, the reaction mixture was heated on a boiling water bath as long as gas was evolved (about 2–3 hours), and then was distilled in steam until no more oil passed over (about 5 l distillate). The distillate was separated , washed successively with sodium hydroxide solution (10%) and water, the solvent was removed and the halogenated toluene derivatives were fractionated at reduced pressure. At 5 mm :

between 43–45° there were distilled 113 g of 2-chlorotoluene (VIII)
61–64° ,, 117 g of 2,6-dichlorotoluene (IX)
87–100° ,, 90 g of 2, 3, 6 – trichlorotoluene (X)

4. The side-chain chlorination of 2,6-dichlorotoluene

Dry chlorine gas was bubbled in 2,6-dichlorotoluene (117 g) at 90–100° in the presence of 2,2′-azo-bis-isobutyronitrile (5g), until the reaction mixture increased in weight with 51–52 g (corresponding to the obtaining of 2,6-dichlorobenzal chloride). The cooled reaction mixture was poured into water, the lower oil layer was extracted with benzene (500 ml) and after separation dried on calcium chloride. After this, the solvent was removed and the obtained crude mixture of 2,6-dichlorobenzyl chloride (XI), 2,6-dichlorobenzal chloride (XII) and 2,6-dichlorobenzenyl chloride (XIII) was hydrolysed as such.

5. The obtaining and isolation of 2,6-dichlorobenzaldoxime

The crude mixture of chlorinated 2,6-dichlorotoluene was mixed with concentrated sulphuric acid (200 ml) and then treated under stirring with hydroxylamine hydrochloride (50 g) in portions (vigorous hydrogen and azote gas evolution !). After the hydroxylamine hydrochloride was introduced, the mixture was stirred for three hours at 55–60°, then poured into an ice-water mixture. The separated crystals were extracted with butyl acetate (500 ml). The organic layer was washed with water and then extracted three times with saturated sodium bicarbonate solution (3 × 200 ml). From the acidulated aqueous solution the crystalline 2,6-dichlorobenzoic acid (XVI) (6.5 g) with m.p. 143 – 145° was obtained. After recrystallization from ethanol-water (1 :1), the melting point rised at 149–150° (141–142° [1]).

The 2,6-dichlorobenzaldoxime (XV) was extracted from butyl acetate solution with dilute sodium hydroxide (10%) solution (6 × 100 ml). When the aqueous alkaline solution was acidulated to pH = 1, the crystalline (XV) separated and was filtered off. After washing with water and drying, 80 g 2,6-dichlorobenzaldoxime (XV) with m.p. 139–143° resulted. After recrystallization from ethanol-water (1 : 1), the melting point rised at 149° (147° [8]).

The yield of 2,6-dichlorobenzaldoxime calculated on 4-nitrotoluene is 12.5%.

The reaction heat and nitrogen evolution led to a vigorous boiling of the solution. After the boiling slowed down, the reaction mixture was heated on a boiling water bath as long as gas was evolved (about 2 - 3 hours), and then was distilled in steam until no more oil passed over (about 5 l distillate). The distillate was separated, washed successively with sodium hydroxide solution (15%) and water, the solvent was removed and the halogenated toluene derivatives were fractionated at reduced pressure. At 5 mm:

between 50 - 60° there were distilled 113 g of 2-chlorotoluene (VIII)
61 - 84° 117 g of 2,6-dichlorotoluene (IX)
87 - 110° 90 g of 2,3,6 - trichlorotoluene (X)

4. The side-chain chlorination of 2,6-dichlorotoluene

Dry chlorine gas was bubbled in 2,6-dichlorotoluene (117 g) at 160 - 180° in the presence of 2,2'-azodi-isobutyronitrile (1g), until the reaction mixture increased in weight with 51 - 52 g corresponding to the obtaining of 2,6-dichlorobenzal chloride. The cooled reaction mixture was poured into water. The lower oil layer was extracted with benzene (500 ml) and after separation dried on calcium chloride. After this, the solvent was removed and the obtained crude mixture of 2,6-dichlorobenzyl chloride (XI), 2,6-dichlorobenzal chloride (XII) and 2,6-dichlorobenzotrichloride (XIII) was hydrolysed as such.

5. The hydrolysing and oximation of 2,6-dichlorobenzalchlorides

The crude mixture of chlorinated 2,6-dichlorotoluene was mixed with concentrated sulphuric acid (200 ml) and then heated under stirring with hydroxylamine hydrochloride (41 g) in portions. Vigorous hydrogen chloride gas evolution. After the hydroxylamine hydrochloride was introduced, the mixture was stirred for three hours at 55 - 60°, then poured into an ice-water mixture. The separated crystals were extracted with butyl acetate (500 ml). The organic layer was washed with water and then extracted three times with saturated sodium bicarbonate solution (3 x 200 ml). From the acidulated aqueous solution the crystalline 2,6-dichlorobenzoic acid (XIV) (5.5 g) with m.p. 140 - 142° was obtained. After recrystallization from diluted ethanol (1:1), the melting point rose to 148 - 150° (141 - 142° [1]).

The 2,6-dichlorobenzaldoxime (XV) was extracted from butyl acetate solution with diluted sodium hydroxide (10%) solution (3 x 150 ml). When the aqueous alkaline solution was acidulated to pH = 1, the crystalline (XV) separated and was filtered off. After washing with water and drying, 50 g 2,6-dichlorobenzaldoxime (XV) with m.p. 139 - 141° resulted. After recrystallization from ethanol-water (1 : 1), the melting point fixed at 149 (149° [2]).

The yield of 2,6-dichlorobenzaldoxime calculated on 4-nitrotoluene is 12.7%.

[illegible]

Revue Roumaine de Chimie, **19**, 7, 1227–1232 (1974)

RADICAL-IONS. II[1]

NITROPHENOTHIAZINE RADICAL-IONS

MIHAELA HILLEBRAND[a] and M. RĂILEANU[b]

[a] University of Bucharest, Department of Physical Chemistry, B-dul Republicii 13

[b] University of Craiova, Department of Organic Chemistry, Str. Alex. I. Cuza 13

Received October 31, 1973

ESR spectra of the positive and negative radical-ions of some nitrophenothiazines are presented and discussed. The hyperfine splitting constants point out an essential change of the spin density pattern for the two radical species.

Three radical species, the radical-cation, the neutral free radical and the nitroxide radical, were previously described for phenothiazine and some of its N-substituted derivatives, [1–11] but no data on the negative radical-ions are available. * As nitrophenothiazines connect the donor character of the phenothiazinic cycle with the electronegative property of the nitro group it was expected to obtain from them both positive and negative radical-ions. It is the aim of this paper to report the ESR spectra of both kinds of radicals prepared from some nitro-substituted pheno-

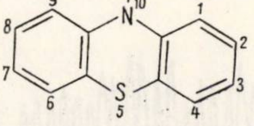

---

* The paper of Bruin et al.[12] claiming the formation of negative ions from some phenothiazine derivatives is not very conclusive, as the hyperfine splittings reported are more consistent with the neutral free radicals in spite of the experimental technique used.

[1] M. Răileanu, I. Radulian, O. Duliu and S. Radu, *Coll. Czech. Chem. Comm.*, **37**, 478 (1972)

[2] J. P. Billon, G. Cauquis and J. Combrisson, *Compt. rend.*, **253**, 1593 (1961).

[3] C. Bodea and J. Silberg, *Rev. Roumaine Chim.*, **9**, 505 (1964).

[4] H. J. Shine and E. E. Mach, *J. Org. Chem.*, **30**, 2130 (1965).

[5] H. J. Lhoste and F. Tonnard, *J. Chim. phys.*, **63**, 678 (1966).

[6] B. C. Gilbert, P. Hanson, R. O. C. Norman and B. T. Sutcliffe, *Chem, Commun.*, **1966**, 161.

[7] Y. Tsujino, *Tetrahedron Letters*, **1968**, 4111.

[8] P. D. Sullivan and J. R. Bolton, *J. Magnetic Res.*, **1**, 356 (1968).

[9] M. F. Chiu, B. C. Gilbert and P. Hanson, *J. Chem. Soc., B*, **1970**, 1700.

[10] L. L. Kamenov, D. Simov and B. V. Golubev, *Teoret. i experim. himia*, **1971**, 129.

[11] P. Hanson and R. O. C. Norman, *J.C.S. Perkin II*, **1973**, 264.

[12] M. Bruin, F. Bruin and F. W. Heinecken, *J. Org. Chem.*, **29**, 507 (1964).

thiazines and phenothiazine-5-oxides, and to reveal their completely different spin density pattern.

EXPERIMENTAL

The 3-nitro- and 3,7-dinitrophenothiazine radical-cations were obtained by solving the parent compound[13] or the correspondent sulphoxides [14] in concentrated sulphuric and perchloric acids .[4] Due to the strong effect of the four nitro groups on the donor properties of phenothiazine, the preparation of the radical-cation from 1, 3, 7, 9-tetranitrophenothiazine [15] failed.

The negative radical-ions from the same compounds were electrolytically generated in dimethylformamide (DMF). In order to verify some assumptions on the nautre of the negative species obtained, the radical-ion of the sodium salt of 1,3,7,9-tetranitrophenothiazine-5-oxide was also prepared.

The ESR spectra were registered on a JES—3B spectrometer in the X band frequency at room temperature. The spectra were interpreted following the technique described by Balaban[16] and simulated using the QCPE—83 simulation program adapted for an IMB—360 computer.

RESULTS AND DISCUSSION

The low resolution spectra of 3-nitro- and 3,7-dinitro-phenothiazine radical-cations exhibit the general pattern of the phenothiazinic radical-cation, that is four lines with the intensities 1 : 2 : 2 : 1, due to the quasi-equivalent coupling of the heterocyclic nitrogen and the iminic proton. At higher resolution the hyperfine interaction with the other nuclei was also evidenced (figs. 1 and 2), but only the spectrum of the 3,7-dinitrophenothiazine cation-radical was completely interpreted. Owing to the high viscosity of the solvents and to the *g* factor anisotropy,[17] the spectra present important line-width effects, that render their analysis more difficult and intro-

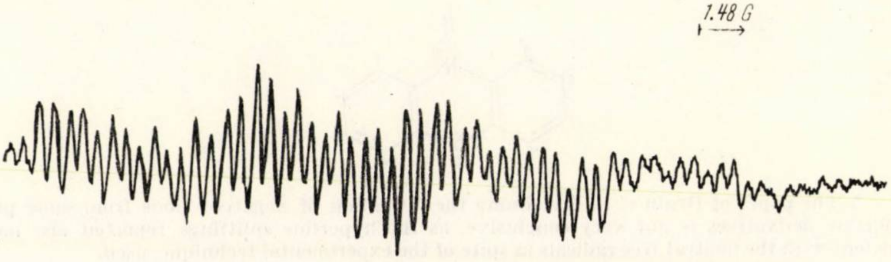

Fig. 1. — ESR spectrum of the 3-nitrophenothiazine radical-cation in perchloric acid.

---

[13] C BODEA and M. RĂILEANU, *Studii și Cercetări Chim. Fil. Cluj*, **8**, 303 (1957).

[14] M. RĂILEANU and A. TURCU, *Rev. Roumaine Chim*, **11**, 1423 (1966).

[15] A. TURCU and M. RĂILEANU, *Rev. Roumaine Chim.*, **14**, 1579 (1969).

[16] A. BALABAN, *Rev. Roumaine Chim.*, **17**, 9 (1972).

[17] Y. SATO, M. KINOSHITA, M. SANO and H. AKAMATU, *Bull. Chem. Soc. Japan*, **40**, 2539 (1967).

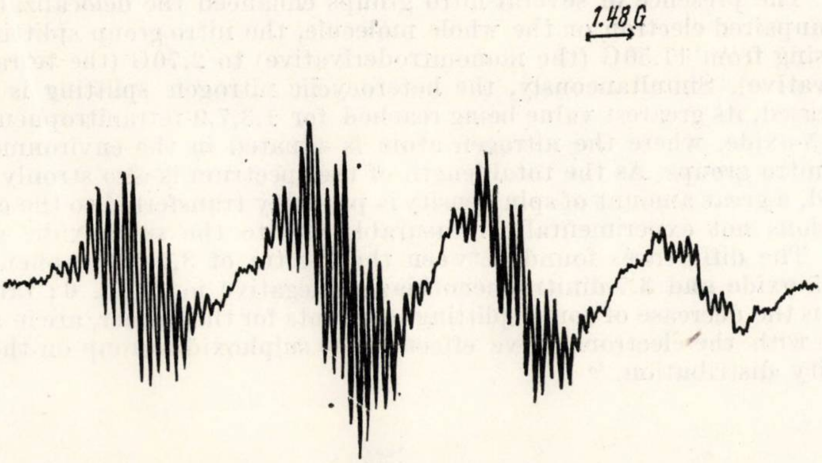

Fig. 2. — ESR spectrum of the 3,7-dinitrophenothiazine radical-cation in perchloric acid.

duce some uncertainty in the estimation of the a_N, a_H splittings. The hyperfine splitting constants are listed in table 1.

Table 1

Hyperfine splittings of nitrophenothiazine radical-ions

Parent compound	Radical species	Hyperfine splittings (Gauss)			
		a_N	a_H^{NH}	a_{NO_2}	Ring proton splittings
3-Nitrophenothiazine	Positive ion	6.30	7.03		
3,7-Dinitrophenothiazine	Positive ion	6.22	6.95	0.59	0.30(2) ; 1.18(2)
3-Nitrophenothiazine-5-oxide	Negative ion	—	—	11.50	1.11 ; 2.22 ; 4.74
3,7-Dinitrophenothiazine-5-oxide	Negative ion	1.18	—	4.59	0.78(2) ;1.96(4)
1,3,7,9-Tetranitrophenothiazine-5-oxide	Negative ion	1.48	—	1.48 2.70	—
3,7-Dinitrophenothiazine	Negative ion	1.92	—	4.22	0.96(2) ; 1.92(2) ; 4.22(2)

The unpaired electron is mainly localized on the heterocyclic nitrogen, the nitro group splitting being unsignificant, although the 3,7 positions are characterized by a high spin density in the unsubstituted phenothiazine radical-cation.

The spectra of the negative species obtained for the nitrophenothiazine-5-oxides are presented in figs. 3—5, the constants being also listed in table 1.

The presence of several nitro groups enhanced the delocalization of the unpaired electron on the whole molecule, the nitro group splitting decreasing from 11.50G (the mononitroderivative) to 2.70G (the tetranitroderivative). Simultaneously, the heterocyclic nitrogen splitting is fairly increased, its greatest value being reached for 1,3,7,9-tetranitrophenothiazine-5-oxide, where the nitrogen atom is situated in the environment of two nitro groups. As the total length of the spectrum is also stronly diminuted, a great amount of spin density is probably transferred to the carbon positions not experimentally measurable and to the sulphoxidic group.

The differences found between the spectra of 3,7-dinitrophenothiazine-5-oxide and 3,7-dinitrophenothiazine negative ions (fig. 6 ; table 1), that is the decrease of some splitting constants for the former, are in agreement with the electronegative effect of the sulphoxidic group on the spin density distribution.[18]

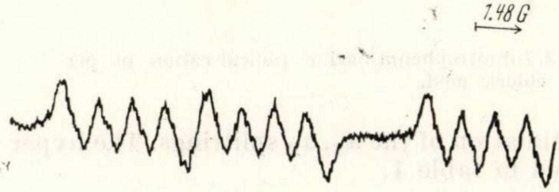

Fig. 3. — Low field half of the ESR spectrum of the 3-nitrophenothiazine-5-oxide negative ion.

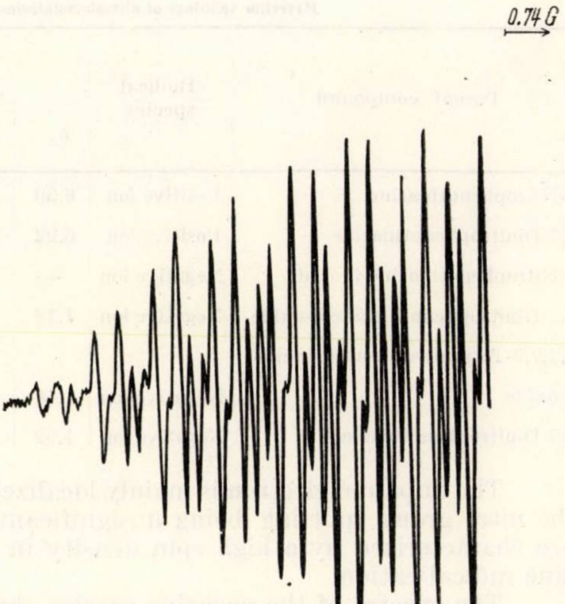

Fig. 4. — Low field half of the ESR spectrum of the 3,7-dinitrophenothiazine-5-oxide negative ion.

---

[18] E. T. Kaiser and D. H. Eargle, *Proc. Chem. Soc.*, **1964**, 22.

Fig. 5. — High field half of the ESR spectrum of the 1, 3, 7, 9-tetranitrophenothiazine-5-oxide negative ion.

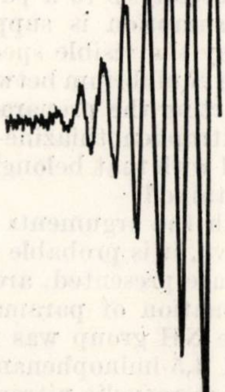

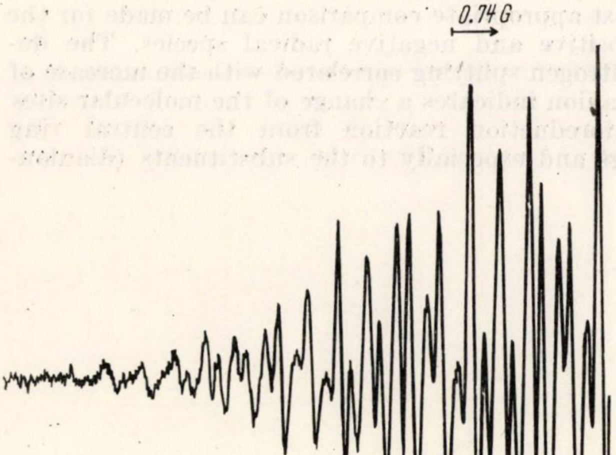

Fig. 6. — Low field half of the ESR spectrum of the 3,7-dinitrophenothiazine negative ion.

In none of the ESR spectra of the negative ions the iminic proton splitting was observed. Although for 3-nitrophenothiazine-5-oxide this could be due to the lack of a total resolution, in the other cases it is unlikely, as the heterocyclic nitrogen has a measurable splitting. The absence of the iminic proton could be explained by a previous dissociation of the parent compound, the nitrophenothiazinic anion being further reduced during the electrolysis to a paramagnetic dianion-radical.

This assumption is supported for the 1,3,7,9-tetranitrophenothiazine-5-oxide by the visible spectrum in the same solvent (DMF), [19] which agrees with an equilibrium between the dissociated and undissociated forms. Secondly, starting the preparation of the radical from the sodium salt of 1,3,7,9-tetranitrophenothiazine-5-oxide, completely dissociated, a spectrum identical with that belonging to the 1,3,7,9-tetranitrophenothiazine-5-oxide was obtained.

Although the arguments hitherto presented refer only to the tetranitro derivative, it is probable that in all cases the negative species whose ESR spectra are presented, are paramagnetic dianion-radicals.

The formation of paramagnetic dianion-radicals from heterocycles containing the NH group was previously reported by Janzen et al. [20] for carbazole and 4,5-iminophenanthrene. Their result concerning the small value of the heterocyclic nitrogen splitting is consistent with ours and it is probably characteristic of this kind of radicals.

The hyperfine splitting constants from table 1 reveal the important differences in the spin density distribution between the positive and negative radicals-ion. The most appropriate comparison can be made for the 3,7-dinitrophenothiazine positive and negative radical species. The decrease of the heterocyclic nitrogen splitting correlated with the increase of the NO_2 splitting for the dianion indicates a change of the molecular sites mainly implied in the oxidoreduction reaction from the central ring (cations) to the lateral rings and especially to the substituents (dianion-radicals).

---

[19] M. Răileanu, M. Olteneanu, I. Radulian, C. Volanschi, A. Turcu and H. Căldăraru, *Rev. Roumaine Chim.*, **16**, 1269 (1971).

[20] E. G. Janzen, J. G. Pacifici and J. L. Gerlock, *J. Phys. Chem.*, **70**, 3021 (1966).

Revue Roumaine de Chimie, 19, 7, 1233–1237 (1974)

MATHEMATISCHE DARSTELLUNG DER HOMOLOGIE UND DER HOMOLOGEN SERIEN. I

ÜBER DIE BESCHREIBUG DER CHEMISCHEN SYSTEME MIT HILFE DER be-MATRIZEN

IOAN MOŢOC

Fakultät für Industriechemie, Polytechnisches Institut „Traian Vuia“ Timişoara

Eingegangen am 8. Mai 1973

Diese Arbeit versucht zu dem Bergriff der von I.Ugi und P. P. Gillespie vorgeschlagenen be-Matrizen, durch ein konstruktives Verfahren, das auf Operationen in einem Ring fußt, zu gelangen. Gleichfalls werden einige Zusätze zu obengenannter Arbeit gebracht. Es wird eine neue Erläuterung des Begriffs der chemischen Reaktion vorgeschlagen.

1. EINLEITUNG

In ihrer Arbeit „Beschreibung chemischer Systeme und ihrer Umwandlungen durch be-Matrizen und ihre Transformationseigenschaften“ [1] schlagen die Autoren die Verwendung der be-Matrizen vor, als vorteilhafte Möglichkeit der Beschreibung chemischer Systeme.

Eine Familie isomerer Ensembles von Molekülen (FIEM) wird als Menge der Ensembles von Molekülen, die aus demselben Satz (A) abgeleitet werden, definiert. Also:

$$\mathrm{FIEM} = \{\mathrm{EM}_0, \mathrm{EM}_1, \ldots, \mathrm{EM}_f\} \tag{1}$$

Im allgemeinen kann man beweisen, daß der Rang der Menge (1) gleich ist mit:

$$|\mathrm{FIEM}| \leqslant (2N)!/2^T \cdot (2N - T)! \tag{2}$$

wobei N die Gesamtanzahl der im Grundzustand besetzten AO und der ICAO-MO darstellt. T stellt die Anzahl der Valenzelektronen in A dar.

Wenn der Rang der Menge A gleich $|A| = n$ ist, dann wird die M_j zugeordnete Matrix vom Typ $n \times n$ sein, für jedwelches $\mathrm{EM}_j \in \mathrm{FIEM}$, $j = 1 \div f$.

---

[1] I. Ugi u. P. Gillespie, *Angew. Chem.*, **23**, 980 (1971).

Dies ist im Grunde genommen der wichtigste Vorteil, den man durch die Einführung des Begriffes FIEM erzielt : Alle Matrizen, mit welchen man im Rahmen eines FIEM operiert, werden dieselben Dimensionen besitzen.

Die be-Matrizen werden als $Mn \times n$ Matrizen wie folgt definiert :

$$M = [m_{ij}], \quad i = 1 \div n \,; \; j = 1 \div n \,; \tag{3}$$

wobei die Elemente :

m_{jj} für $i > j$ als $m_{ij} = b_{ij}$ bezeichnet werden. Die Menge der Elemente b_{ij} bilden die b-Zone der Matrix.

m_{ij} für $i < j$, werden mit $m_{ij} = i_{ij}$ bezeichnet. Die Menge der Elemente i_{ij} bilden die i-Zone der Matrix.

m_{ij}, für $i = j$ bezeichnet man mit $m_{ij} = \mathrm{e}_{\lambda = ii = jj}$.

2. ÜBER DIE M-MATRIZEN

Was diese Arbeit Neues gegenüber der angeführten Arbeit bringt, ist die Eingliederung dieses Formalismus in die Theorie der Kategorien, was zu einem höheren Abstraktisierungsgrad führt.

Gegeben sei die Kategorie $C \in U - A$, so daß :

$$\mathrm{Ob\,C} = M \tag{4}$$

M definiert man :

$M : R \in U$-Ens, wobei R die Menge der reellen Zahlen darstellt M stellen die der FIEM zugeordneten b-Matrizen dar, wobei $|A| = n$, mit F wurde die Menge $\{M_0, M_1, \ldots, M_f\}$ bezeichnet.

Die Menge $\mathscr{F}$ der Matrizen $n \times n$ kann mit der Addition $(+)$ und dem direkten Produkt $(\times)$ als Verknüpfungsgesetz ausgestattet werden. Also erhält man in Wirklichkeit ein Objekt aus $U - A$. Selbstverständlich $F \subset \mathscr{F}$.

Ein EM$\in$FIEM kam durch ein symmetrisches Graph $G = (X, \Gamma)$ dargestellt werden, was die Gleichheit $g_{ij} = g_{ji}$ in der Einfallsmatrix $\mathscr{G}$ bestimmt. G wird im allgemeinen mehrere konexe Komponenten (selbstverständlich nicht stark konexe) besitzen. Die Anzahl dieser konexen Komponenten ist gleich mit der Anzahl der Moleküle, die das EM bilden.

Das Vorhandensein mehrerer konexer Komponenten führt zur Tatsache, daß wenigstens eine Indexierung der Eckpunkte des Graphes existenzfähig ist, für welchen die Einfallsmatrix in blockierter Form erscheint.

Die Einfallsmatrix baut man auf, indem man als Element g_{ij} die formale Ordnung der Bindung zwischen den Atomen i und j setzt. Es ist offensichtlich, daß man so eine Matrix $[b_{ij}]$ erhält.

Um eine be-Matrix zu erhalten, kann man wie folgt vorgehn :

$$[b_{ij}] \times [\lambda_{ij}] \tag{5}$$

wobei :

$$\lambda_{ij} = \begin{cases} 0, & i < j \\ 1, & i > j \end{cases}$$

Die Matrix (5) enthält die b-Zone, der Rest der Elemente ist gleich mit Null.
Weiterhin :

$$[b_{ij}] \times [\lambda_{ij}] + [\delta_{ij} \cdot e_{ij}] \tag{6}$$

Wobei :

$$\delta_{ij} = \begin{cases} 0, & i \neq j \\ 1, & i = j \end{cases}$$

Die Matrix (6) enthält auch die Elemente $e_{\lambda=ii=ji}$.

Die Matrix (7) ist eine be-Matrix :

$$[b_{ij}] \times [\lambda_{ij}] + [\delta_{ij} \cdot e_{ij}] + [i_{ij} \cdot \lambda'_{ij}] \tag{7}$$

wobei :

$$\lambda'_{ij} = \begin{cases} 0, & i > j \\ 1, & i < j \end{cases}$$

Die Beziehung (7) zeigt an,daß die Informationen bezüglich der Eigenschaften $L_1 \ldots, L_l$ der Paare A_i, A_j nur so angeordnet sein müssen, wie es die Regeln $\mathfrak{L}_1, \ldots, \mathfrak{L}_l$ erfordern.

$\mathfrak{L}_j$ können matriziell dargestellt werden. Z. B. : Wenn L_1 sich auf die Valenzelektronen bezieht, so hat $\mathfrak{L}_1$ die Form :

$$\mathfrak{L}_1 \sim [\delta_{ij}]$$

BEMERKUNGEN

In der gewöhnlichen Schreibweise :

$$A_1 + A_2 + \ldots \rightleftharpoons B_1 + B_2 + \ldots \tag{8}$$

hat das Zeichen ,, + “nicht den Sinn eines Verknüpfungsgesetzes in der additiven Notierung. Man könnte ein solches Verknüpfungsgesetz nicht einmal definieren, ,, + “ besitzt den Sinn einer Vereinigung.

Heute ist die Schreibweise :

$$A_1UA_2U \ldots \rightleftharpoons B_1UB_2U \ldots \tag{9}$$

nicht mehr üblich, obzwar sie dem von der Beziehung (8) ausgedrückten Sinn näher ist. Die be-Matrizen führen zu einer der Beziehung (9) analogen Darstellung der Reaktion.

Eine be-Matrix enthält mehrere Informationen als eine gewöhnliche chemische Formel. Die in den chemischen Formeln enthaltenen Informationen befinden sich in der b-Zone der Matrix. Nach Durchführung der Operation (5) stehen $n^2 - n(n+1)/2$ Stellungen der Einfallsmatrizen zur

Verfügung, in welchen die in den *i*- und *e*-Zonen der be-Matrizen enthaltenen Informationen verstanden werden.

3. ÜBER DEN R_ρ OPERATOR

In der Arbeit[1] wird der R_ρ Operator im Rahmen einer FIEM wie folgt definiert :

$$\mathrm{EM}_\Phi \rightarrow R_\rho \cdot \mathrm{EM}_\psi \tag{10}$$

wobei EM_Φ, $\mathrm{EM}_\psi \in \mathrm{FIEM}$.

R_ρ stellt den chemischen Prozeß dar, der die Umwandlung der Reaktanten EM_Φ in die Produkte EM_ψ bewirkt. Die Definitionsbeziehung (10) verfügt über den Vorteil, daß der Operator R eine matrizielle From annehmen kann.

Es sei nun : $M_\Phi = [\Phi_{ij}]$ die EM_Φ zugeordnete Matrix, $M_\psi = [\psi_{ij}]$ die EM_ψ zugeordnete Matrix und $R = [r_{ij}]$ die R zugeordnete Matrix.

Die Beziehung (10) wird nun zu :

$$[\Phi_{ij}] = [r_{ij}] \times [\psi_{ij}] \tag{11}$$

Aus (11) folgt unmittelbar, daß :

$$\Phi_{ij}/\psi_{ij} = r_{ij} \tag{12}$$

Selbstverständlich wird $\psi_{ij} \neq 0$ vorausgesetzt. Wenn $\psi_{ij} = 0$, kann man $\psi_{ij} = \varepsilon$ setzen, wobei ε willkürlich klein ist. So hat die Beziehnung (12) immer einen Sinn und also auch die folgende Interpretierung für R : R mißt die Veränderung der Eigenschaften (die im gegebenen Fall interessieren) bei der der Umwandlung $\mathrm{EM}_\Phi \xrightarrow{R_\rho} \mathrm{EM}_\psi$.
Aber R kann auch (und im allgemeinen ist es auch natürlich so) durch folgende Beziehung definiert werden :

$$R = [r_{ij}(t)] \tag{13}$$

Also sind die Elemente der Matrix von der Zeit abhänging.

DISKUSSIONEN

Wir glauben, daß es noch eine Möglichkeit der Interpretierung für eine chemische Umwandlung (chemische Reaktion) gibt, und zwar, eine chemische Reaktion ist ein Funktor. Diese Interpretierung könnte sich nützlicher als jene von I. Ugi und P. P. Gillespie mit Hilfe von R_ρ erweisen, aber die Entwicklung eines, für alle von der Chemie studierten Beziehungen, allgemeinen und abstrakten funktoriellen Formalismus setzt unbedingt eine feste Basis für die Chemie in der Mengenlehre voraus.

Man kann voraussehen, daß eine Anpassung der organischen Chemie an den Formalismus der Mengenlehre leichter sein wird, als im Falle der anorganischen Chemie.

Umso mehr könnte ein Formalismus in der Mengenlehre für die organische Chemie zu einem einheitlichen Standpunkt in bezug auf die wichtigen, mit Hilfe der Graphen [2] und der algebraischen Methoden [3] erzielten Ergebnisse führen.

---

[2] Für eine komplette Bibliographie : A. T. BALABAN, „Cercetările multidisciplinare şi interdisciplinare. Originea, dezvoltarea şi perspectivele lor." Ed. Academiei, Bukarest, S. 1972, 203 L.

[3] Als Zusammenfassung einiger erzielten Resultate : E. RUCH, *Accounts Chem. Res.*, **5**, 49 (1972).

Revue Roumaine de Chimie, 19, 7, 1239–1242 (1974)

MATHEMATISCHE DARSTELLUNG DER HOMOLOGIE UND DER HOMOLOGEN SERIEN. II[1]

BEHANDLUNG IN KATEGORIEN

IOAN MOŢOC
Fakultät für Industriechemie
Polytechnisches Institut „Traian Vuia“
Timişoara

Eingegangen am 8. Mai 1973

Diese Arbeit versucht eine neue Festlegung im Zusammenhang mit dem Begriff der Homologie und der homologen Serien. Der Unterschied zwischen diesen beiden Begriffen wird gleichfalls hervorgehoben. Einige unmittelbare Folgen unserer in der vorhergehenden Arbeit[1] ausgesagten Standpunkte werden ebenfalls behandelt.

1. EINLEITUNG

Für jedwelches $j = 1 \div \ldots$, hat S_j folgende Eigenschaften :

i) wenn $s_{ji} \in S_j$, dann ist $\{s_{ij}\} \in S_j$

ii) wenn $s_{ji} \in X$, $X \in S_j$, dann gehört $s_{ij} \in S_j$

iii) wenn $X \in S_j$, dann gehört die Menge der Teile $P(X) \in S_j$

iv) wenn $(X_i)_{i \in I}$ eine Mengenfamilie $X_i \in S_j$ ist und wenn $I \in S_j$, dann ist $\bigcup\limits_{i \in I} X_i \in S_j$

v) die Dublette $(s_{jp}, s_{jq}) \in S_j$, wenn und nur wenn s_{jp} und $s_{jq} \in S_j$, also ist die Menge S_j eine Univers-Menge.

Die Gesamtheit der homologen Serien $(S_j)_{j \in J}$ ist eine Familie von Universen.

$\bigcap\limits_{i \in J} S_j$ wird als leeres Universum bezeichnet.

Folgendes Axiom wird als erfüllt vorausgesetzt :

Für jedwelche Menge A gibt es ein Universum $\mathcal{U}$, welches A als Element enthält. In dieser Arbeit ist es vorteilhaft $S_j, j \in J$ anstelle von A und $\bigcup\limits_{j \in J} S_j$ als Menge $\mathcal{U}$ zu betrachten. Laut Definition wird die Beziehung angenommen :

$$\bigcap_{j \in J} S_j \in \mathcal{U} \tag{1}$$

---

[1] I. Moţoc, *Rev. Roumaine Chim.*, **18**, 1419 (1973).

2. KATEGORIEN

Man kann zeigen, daß die Menge $\mathcal{U} = \bigcup_{j \in J} S_j$ eine Kategorie $\mathcal{C}$ ist [2]. Dadurch erzielt man die Möglichkeit einer eleganten und kurzgefaßten Behandlung des Homologie- und homologen-Problems. Man kan feststellen, daß sich in Wirklichkeit folgende Eigenschaften als richtig erweisen:

i) es gibt eine Menge Ob$\mathcal{C}$, deren Elemente Objekte von $\mathcal{C}$ genannt werden, u. zw.: Ob$\mathcal{C}$ ist $S_j, j \in J$

ii) für jedwelches S_p, S_q $\in$ Ob $\mathcal{C}$ existiert eine Menge HOM$_{\mathcal{C}}$ (S_p, S_q), deren Elemente Morphismen genannt werden.

iii) für S_x, S_y $S_z \in$ Ob$\mathcal{C}$ existiert:

$$\text{HOM}_{\mathcal{C}}\ (S_x, S_y) \times \text{HOM}_{\mathcal{C}}\ (S_y, S_z) \rightarrow \text{HOM}_{\mathcal{C}}\ (S_x, S_z)$$

Die Morphismen erfüllen folgende Axiome:

1. Für jedwelches $S_j \in$ Ob $\mathcal{C}$, existiert ein Morphismus 1 $S_j \in \text{HOM}_{\mathcal{C}}(S_j, S_j)$, der als Identität von S_j bezeichnet wird.
2. Die Zusammensetzung der Morphismen ist assoziativ.
3. Die Mengen HOM$_{\mathcal{C}}$ (S_p, S_q) sind jede mit jeder disjunkt.

Daraus ist ersichtlich, daß $P(\mathcal{U})$, d.h. die Menge der Teile von $\mathcal{U}$, zusammen mit den Einschlußbeziehungen, eine Kategorie bilden.

Man kann feststellen daß, falls S_p, S_q $P(\quad)$:

$$\text{HOM}\ (S_p, S_q) = \Phi \tag{2}$$

da:

$$S_p \not\subset S_q,\ \forall\ p, q \in J \tag{3}$$

Mit den Beziehungen (1) und (2) kann man leicht die Wahrheit des folgenden Satzes beweisen:

Satz 1: Die Kategorie $\mathcal{C}$ ist eine $\mathcal{U}$-Kategorie.

Folgende Beziehung:

$$\text{Ob}\ \mathcal{C} \in \mathcal{U} \tag{4}$$

beweist den

Satz 2: Die Kategorie $\mathcal{C}$ ist eine kleine $\mathcal{U}$-Kategorie.

Diese erzielten Ergebnisse ermöglichen die in der früheren Arbeit [1] gegebene Definition 2 wie folgt zu vervollständigen:

Definition 1: Die unäre Beziehung $S_j \in S\ (= \mathcal{U})$ besitzt die Eigenschaft: $S_j \in$ Ob ($\mathcal{U}$-Ens)

Eine homologe Serie ist also eine amorphe Menge, laut Definition.

Die Homologiebeziehung ($\wedge$) ist eine Abbildung der Menge:

$$\wedge\ :\{s_{ji}\}\ U\ S_0 \rightarrow \mathrm{S}_j$$

Die in der Arbeit [1] angeführte Definition 3 wird wie folgt vervollständigt:

Definition 2. Die binäre Beziehung $\wedge$ besitzt folgende Eigenschaft: $\wedge \in$ Ob($\mathcal{U}$-Ens)

---

[2] C. A. CAZACU, A. DELEANU, M. JURCHESCU, „Topologie, categorii, suprafeţe riemanniene", Ed. Academiei, Bukarest, 1966.

Der Begriff der Homologie und der homologen Serien (nur als Sammlung von Homologen betrachtet) sind Objekte in $\mathcal{U}$-Ens.

Es ist leicht ersichtlich, daß obige Betrachtungen ohne Schwierigkeit auch auf polymerhomologe Serien ausgedehnt werden können.

Die Kardinalzahlen der Menge N der natürlichen Zahlen wird mit $\# N = \aleph$ bezeichnet.

Die Beziehung (12) aus der Arbeit [1] führt unmittelbar zum Beweis folgenden Satzes :

Satz 3 : Für jedwelches $p, q \in J$ besteht die Beziehung :

$$\# S_p = \# S_q = \aleph \tag{5}$$

Tatsächlich können für $p, q \in$ J, folgende eineindeutige Beziehungen festgelegt werden :

$$\begin{gathered} s_{p1} \in S_p \to 1 \in N \\ s_{p\lambda} \in S_p \to \lambda \in N, \quad \lambda \geqslant 2 \\ s_{q1} \in S_q \to 1 \in N \\ s_{q\lambda} \in S_q \to \lambda \in N, \quad \lambda \geqslant 2 \end{gathered} \tag{6}$$

Die Beziehungen (6) beweisen die Behauptung (5).

Stellt man der Beziehung (7) aus der Arbeit [1] die Bedingung $p - n \leqslant -1$, gelangt man zu folgendem Ergebnis : Man baut schrittweise eine neue Menge auf :

$$\{s_{p0}, s_{j,-1}, s_{j,-2}, \ldots, s_{j,-n}, \ldots\} = S_j^- \tag{7}$$

die den gleichen Sinn wie Menge S_j hat, aber einer anderen formellen Situation entspricht, u. zw. :

$$s_{jp} \wedge ns_1 \to s_{j,p+n} \quad \text{für } S_j \tag{8}$$

$$s_{j,p+n} \leftarrow s_{jp} \wedge ns_j \quad \text{für } S_j \tag{8a}$$

Man bemerkt, daß in den Beziehungen (8) und (8a) die Richtung der Pfeile entgegengesetzt ist. Die Situationen (8) und (8a) können auf Grund ihres Vergleichens unterschieden werden. Diese Tatsache wird in folgenden Beziehungen widerspiegelt :

$$\{-1\} \cdot S_j = S_j^- \tag{9}$$

$$\{-1\} \cdot S_j^- = S_j \tag{9a}$$

Die Beziehungen (9) und (9a) können schrittweise abgeleitet werden. Das Ergebnis des schrittweisen Aufbauverfahrens wurde als direktes Produkt zwischen den Mengen (9) bezeichnet. Die Menge der pseudoskalaren Eigenschaften, die dem Element s_{ji} zugeordnet werden, bezeichnet man mit $\bar{s}_{ji}$. Mit $\bar{S}_j$ bezeichnet man die Menge $\{\bar{s}_{j0}, \bar{s}_{j1}, \ldots\}$

Die Beziehung (10) ist offensichtlich :

$$\# S_j = \# S_j^- = \delta \tag{10}$$

S_j^- kann also S_j in den Beziehungen (9) ersetzen :

$$\{-1\}\ S_j = S_j^- \tag{11}$$

$$\{-1\}\ S^- = S_j \tag{11a}$$

Mit den Beziehungen (11) wurde ein interessantes Ergebnis wiederentdeckt, u. zw. das in der physikalischen Chemie verwendete Verfahren zum Berechnen einiger pseudoskalaren Eigenschaften der Moleküle (z. B. die Berechnung der Reaktionsentalpien).

Es ist bemerkenswert, daß eine Grundlage aus der Mengenlehre für die organische Chemie äußerst nützlich wäre. Die Mengenlehre stellt einen ausreichlich abstrakten Formalismus dar und es hat sich erwiesen, daß dieser Formalismus sich einer Anwendung in der organischen Chemie nicht widersetzt.

Herzlichen Dank schulde ich Herrn Professor A.T. BALABAN für die mir zuteil gewordenen Ratschläge, die zur vorliegenden Arbeit führten.

Revue Roumaine de Chimie, **19**, 7, 1243–1250 (1974)

CHAIN TRANSFER IN EMULSION POLYMERIZATION OF VINYL ACETATE

D. DONESCU, C. HAGIOPOL, MARIANA MUNTEANU, VICTORIA DIMONIE
and I. GAVĂT

"P. Poni" Institute of Macromolecular Chemistry, Section of Polymerization Processes,
str. Dumbrava Roșie 18, Bucharest

Received January 10, 1974

Studies have been made on the influence of aromatic hydrocarbons and allyl derivatives as chain transfer agents, on the emulsion polymerization of vinyl acetate (VAc) in the presence of polyvinyl alcohol (PVA). The dependence of the polymerization rate and of the polymer structure on the concentration of the above-mentioned substances was determined. The activity as transfer agents increases for aromatic hydrocarbons in the order: toluene, ethyl benzene, isopropyl benzene, tetraline, while for allyl derivatives: allyl alcohol, allyl acetate, diallyl ether, allyl bromide.

1. INTRODUCTION

Vinyl acetate polymerization is characterized by a high reactivity of the increasing macroradical. This reactivity is revealed by its sensitivity to substances capable of releasing a hydrogen atom by chain transfer. [1] A comparative study both of propagation rate constants (k_p) in homopolymerization and of chain transfer constants (C) for VA and for styrene [2] shows an increased reactivity of poly(vinyl acetate) macroradical (PVAc) ($k_{p\,\mathrm{VAc}} \approx 1500\ k_{p\,\mathrm{St}},\ C_{\mathrm{VAc}} \approx 100\ C_{\mathrm{St}}$).

The previous study [3] regarding VAc emulsion polymerization in the presence of polyvinyl alcohol as an emulsifier focussed on the effects of transfer reactions on the polymerization kinetics and also on the structure of the formed polymer. Strong transfer reactions occur in the mentioned system to emulsifier (PVA), polymer (PVAc) and to other substances additionally introduced and capable of participating in such reactions (diallyl ether).

---

[1] A. D. Jenkins, "Kinetics and Mechanism of Polyreactions", IUPAC International Symposium of Macromolecular Chemistry, Plenary and Main Lectures, Budapest, 1969, 417 p.

[2] J. T. Clarke, R. O. Howard and W. H. Stockmayer, *Makromol. Chem.*, **44–46**, 427(1961).

[3] V. Dimonie, D. Donescu, M. Munteanu, C. Hagiopol and I. Gavăt, *Rev. Roumaine Chim.*, (in press).

This transfer reaction causes the occurrence of PVAc graft copolymers on PVA and PVAc branched polymers.

To eliminate the appearance of PVAc branched polymers, it is necessary to find some more active compounds in chain transfer processes than the above-mentioned homopolymer and emulgator. Data provided by the literature show that aromatic hydrocarbons [1,2,4-6] and allyl derivatives[7-9] were chosen as transfer agents, being known as active factors in vinyl polymerizations with free radicals.

The above-mentioned substances are known as active agents also in other homolytic reactions of the same type : autooxidation [10-13] and hydrogen atom extraction by the free radicals of a small molecular mass. [14-21]

The present paper is concerned with the influence of these substances on the reaction rate and on the structure of polymers obtained by emulsion polymerization of VAc in the presence of PVA.

2. EXPERIMENTAL

Materials. Conditions for the purification of materials and for the preparation of the emulgator solution are similar to those reported in the previous paper.[3]

The transfer agents, p.a. products, were subjected to an extra purification on a highly efficient column.

Polymerization procedure. The apparatus involved and the working procedure were reported to be identical with those presented in the previous paper. [3] The concentrations of reactants (except for transfer agents) were kept constant : $[\mathrm{VAc}]_0 = 2.72$ mole/l, $[\mathrm{PVA}]_0 = 25.4$ g/l, $[\text{peroxide of hydrogen}]_0 = 3.10^{-3}$ mole/l, $[\mathrm{FeSO_4}]_0 = 3.85.10^{-5}$ mole/l. Transfer agents were added to the monomer before placing it in the reactor.

Analyses of polymer. The succession of operations for the determination of solubilities and of K values of polymers was identical with that previously mentioned.

---

[4] I. Gavăt, D. Donescu, V. Dimonie, M. Munteanu, I. Rogoz, E. Dan and I. Obogeanu, Patent Appl. 67095(1971).

[5] W. A. Pryor and Tzu Lee Huong, *Macromolecules*, **2**, 70(1969).

[6] Farwerke Hoechst A. G., Patent Neth Appl. 6507983, 1966 ; *Chem. Abstr.*, **64**, 17810 (1966).

[7] J. A. Meyer, V. Stannett and M. Szwarc, *J. Amer. Chem. Soc.*, **83**, 25(1961).

[8] A. P. Titov and V. V. Kotov, *Vysokomol. Soedineniya, B*, **10**, 495(1968).

[9] J. P. J. Higgins and K. E. Weale, *J. Polymer Sci. A — 1*, **6**, 3007(1968).

[10] E. Niki, Y. Kamiya and N. Ohta, *Kogyo Kagaku Zasshi*, **71**, 859 (1968) ; *Chem. Abstr.*, **70**, 2983(1969).

[11] E. Niki, Y. Kamiya and N. Ohta, *Bull. Chem. Soc. Japan*, **42**, 512(1969).

[12] C. Gadelle and G. Clement, *Bull. Soc. chim. France*, **41**, 1175(1967).

[13] E. Niki, Y. Kamiya and N. Ohta, *Bull. Chem. Soc. Japan*, **42**, 2312(1969).

[14] K. Makuyama, K. Ono and J. Osugi, *Bull. Chem. Soc. Japan*, **42**, 3357(1969).

[15] D. H. Hey, B. W. Pengilly and G. H. Williams, *J. Chem. Soc.*, **1**, 9(1955).

[16] N. B. Neiman, *Doklady Akad. Nauk S.S.S.R.*, **144**, 392(1962).

[17] W. R. Foster and G. H. Williams, *J. Chem. Soc.*, **8**, 2862(1962).

[18] W. A. Pryor, D. L. Fuller and J. P. Stanley, *J. Amer. Chem. Soc.*, **94**, 1632(1972).

[19] I. B. Burkley, *J. Phys. Chem.*, **67**, 168(1963).

[20] G. P. Curran, *Amer. Chem. Soc. Div. Fuel Chem. Preprints*, **10**, 130 (1966) ; *Chem. Abstr.*, **66**, 30829(1967).

[21] J. A. Haward and K. V. Ingold, *Can. J. Chem.*, **46**, 2661(1968).

3. RESULTS AND DISCUSSION

3.1. Effects of aromatic hydrocarbons on VAc emulsion polymerization

A systematic study of the relationship between the structure of the aromatic hydrocarbon and its reactivity to free radicals shows the following order : toluene< ethyl benzene< isopropyl benzene. At the same time 1,2,3,4-tetrahydronaphthaline, tetraline, was found to display a surprisingly high reactivity in the above-mentioned reactions. [21–23]

The use of the above-mentioned aromatic hydrocarbons as chain transfer agents results in a decrease of the polymerization rate (R) of VAc relative to the polymerization rate in their absence (R_0).

Fig. 1 illustrates the influence of the concentration of various transfer agents on the polymerization rate of VAc.

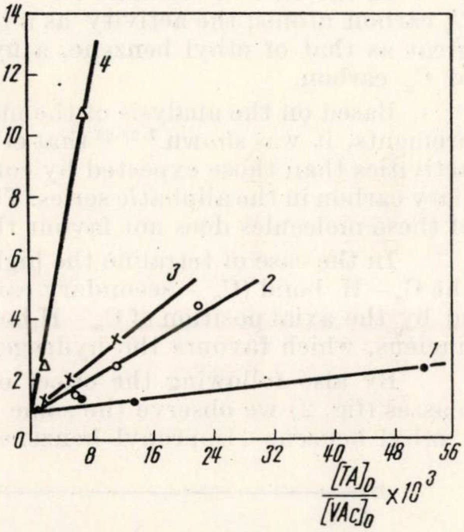

Fig. 1. — Influence of the transfer agent/ monomer ratio on the polymerization rate : *1*, toluene; *2*, ethyl benzene; *3*, isopropyl benzene; *4*, tetraline.

A dependence has been found in the case of all used aromatic hydrocarbons between the polymerization rate R and the concentration of the respective transfer agent, similar to that established by Allen et al. [24] for VAc polymerization in solution

$$\frac{R_0}{R} = 1 + A\,\frac{[TA]_0}{[\mathrm{VAc}]_0}$$

where

$[TA]_0$ = initial concentration of the transfer agent
A = characteristic constant for each transfer agent.

[22] E. C. KOOYMAN, *Tetrahedron*, **19**, 415(1963).

[23] A. E. EACHUS, J. A. MEYER, J. PEARSON and M. SZWARC, *J. Amer. Chem. Soc.*, **90**, 3646(1968).

[24] P. W. ALLEN, F. M. MERRETT and J. SCANLEN, *Trans. Faraday Soc.*, **51**, 95(1955).

The values of constant A characterize the capability of the aromatic hydrocarbon in question to slow down the polymerization rate of VAc in emulsion. A comparison of these values shows a similar succession of the activity (toluene $<$ ethyl benzene $<$ isopropyl benzene $<$ tetraline) to that reported in papers dealing with homolytic reactions. [5,7,12–16,18,19,21–23]

This reactivity order is due to the different capacity of extracting a hydrogen atom from the position relative to benzene nucleus (C_α carbon).

The lability of the C—H bond depends on a multitude of factors: degree of substitution of C_α carbon (primary carbon $<$ secondary carbon $<$ tertiary carbon), mobility of $C_\alpha—C_\beta$ bond, position of hydrogen atoms in C_α carbon with respect to the plane of benzene nucleus, interaction of hydrogen atoms in C_β carbon with the hydrogen atom in the *ortho* position of the nucleus. [7,21–23]

In the case of tetraline ($A = 1480$), a hydrocarbon with secondary C_α carbon atoms, the activity as a transfer agent is roughly nine times as great as that of ethyl benzene, a hydrocarbon with similar substitution of C_α carbon.

Based on the analysis of the molecular structure and of kinetic measurements, it was shown [7,22,23] that ethyl benzene and cumene have smaller activities than those expected by comparison with the secondary and tertiary carbon in the aliphatic series. This is due to the fact that the structure of these molecules does not favour the extraction of the hydrogen atom. [7]

In the case of tetraline the higher reactivity similar to that found for the $C_\alpha—H$ bond (C_α — secondary carbon) of the aliphatic series is explained by the axial position of $C_\alpha—H$ bond relative to the plane of the benzene nucleus, which favours the hydrogen extraction by a free radical.

By also following the effect of these substances on the molecular masses (fig. 2) we observe the same succession of the efficiency toluene $<$ $<$ ethyl benzene $<$ isopropyl benzene $<$ tetraline.

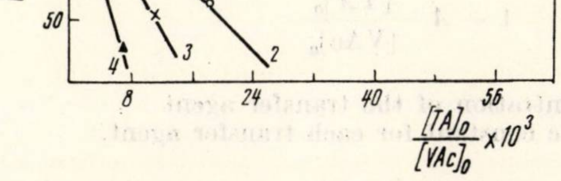

Fig. 2. — Modification of the K value of the benzene-soluble fraction as a function of the transfer agent/monomer ratio: *1*, toluene; *2*, ethyl benzene; *3*, isopropyl benzene; *4*, tetraline.

The increase of the molar ratio $\frac{[TA]_0}{[VAc]_0}$ determines a decrease of K value for the fraction of benzene-soluble polymer.

The presence of transfer agents of the aromatic series diminishes the chain transfer to PVA, VAc and PVAc which corresponds to a decrease in the weight of the water- and benzene gel-insoluble polymer and to an increase in the weight of the benzene-soluble polymer (table 1).

Table 1

Decrease of the amount of benzene-insoluble polymer and increase of the amount of benzene-soluble polymer as a function of the molar ratio $\frac{[TA]_0}{[VAc]_0}$ ($[VAc]_0$ = 2.72 mole/l, $[PVA]_0$ = 25.4 g/l, $[H_2O_2]_0 = 3.10^{-3}$ mole/l, $[FeSO_4]_0 = 3.85.10^{-5}$ mole/l, t = 63°)

Chain transfer agent	$\frac{[TA_c]_0}{[VA_c]_0} \cdot 10^3$ mole/mole	Benzene-insoluble polymer mass %	Benzene-soluble polymer mass %
—	0	38.5	50
Toluene	3.3	25.5	61.2
	6.6	24.6	63.5
	13.2	21.4	65.8
	53.5	15.25	68.5
Ethyl benzene	5.36	16.5	62.0
	10.72	16.2	66.8
	21.44	11.55	68.5
Isopropyl benzene	1.1	39.2	60.3
	2.2	23	62.8
	5.5	14.5	71.3
	11.0	11.3	72.2
Tetraline	1.37	15.9	67.3
	6.85	4.95	32.6

3.2. Effect of allyl compounds on VAc emulsion polymerization

Compared to aromatic hydrocarbons analyzed above, allyl compounds display a higher reactivity as to the transfer of a hydrogen atom to a free radical. [7,25]

Allyl derivatives studied in the present work are allyl acetate, allyl alcohol, diallyl ether and allyl bromide. The ratio between allyl compounds and VAc was chosen so as to practically eliminate the possibility of copolymerization. [26]

In fig. 3 and table 2 we may observe the decrease of K value of the benzene-soluble fraction and of water- and benzene-insoluble fraction, respectively, with the increase in the amount of transfer agent.

The activity as a transfer agent presents a gradual increase in the order allyl acetate < allyl alcohol < diallyl ether < allyl bromide.

[25] G. M. Bristow, *Trans. Faraday Soc.*, **54**, 1239(1958).

[26] E. Y. C. Chang and C. C. Price, *J. Amer. Chem. Soc.*, **83**, 4650(1961).

Table 2

Decrease of the amount of benzene- and water-insoluble polymer as a function of the nature and the concentration of the molar ratio $[TA]_0$ $[VAc]_0 = 2.72$ mole/l, $[PVA]_0 = 25.4$g/l $[H_2O_2]_0 = 3.10^{-3}$ mole/l, $[FeSO_4]_0 = 3.85.10^{-5}$ mole/l, t = 63°)

Chain transfer agent	$\frac{[TA]_0}{[VAc]_0} . 10^3$ mole/mole	Benzene- and water-insoluble polymer mass %
—	0	38.5
Ethyl acetate	18.9	37
Allyl bromide	2.5	7
	5.0	4.46
Allyl alcohol	3.42	19.5
	17.1	4.4
Allyl acetate	3.42	34.6
	11.3	15.5
	18.9	7.6
Diallyl ether	2.3	11.2
	3.45	19.6
	4.93	12.6

The transfer of the radicalic species may take place at the allyl group[27,28] or at the acetate group [29] in the case of allyl acetate :

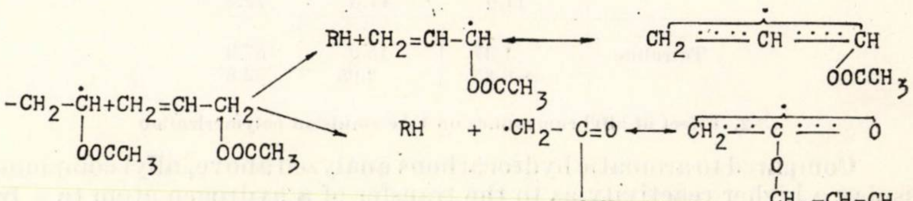

The abstraction of hydrogen atom from the allyl group has a much greater role. [27-31] Our experimental results with ethyl acetate confirm this fact (fig. 3, fig. 4 and table 2). The higher reactivity of allyl acetate was explained by the existence of an axial configuration [7] of the C—H bond of the carbon in α relative position to the carbon—carbon double bond.

---

[27] P. D. Bartlett and R. Altschul, *J. Amer. Chem. Soc.*, **67**, 812(1945).

[28] P. D. Bartlett and F. A. Tati, *J. Amer. Chem. Soc.*, **75**, 91(1953).

[29] N. G. Gaylord, *J. Polymer Sci.*, **22**, 71 (1956).

[30] M. Litt and F. R. Eirich, *J. Polymer Sci.*, **45**, 379(1960).

[31] N. G. Gaylord and F. R. Eirich, *J. Amer. Chem. Soc.*, **74**, 337(1952).

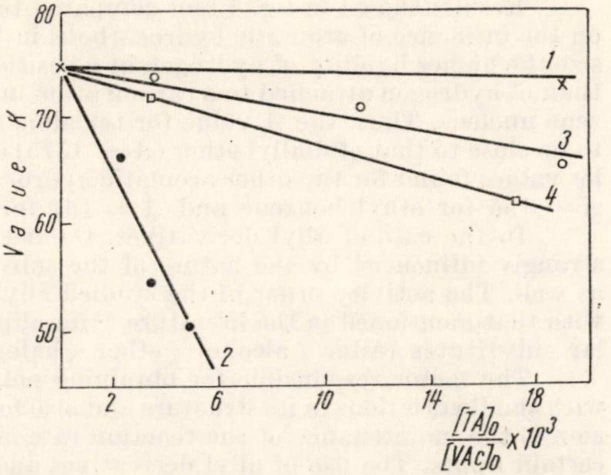

Fig. 3. — Influence of the transfer agent/monomer molar ratio on the K value of the benzene-soluble polymer fraction :

1, ethyl acetate; 2, diallyl ether; 3, allyl acetate; 4, allyl alcohol.

The freshly formed allyl radical has a lower reactivity but it may participate in a new initiation reaction.[28] This lower reactivity due to the interaction of the odd electron orbital with the π electrons of the double bond, determines the decrease of the all polymerization rate.

The behaviour of these allyl compounds is controlled by the same laws as those applying for aromatic hydrocarbons (fig. 4).

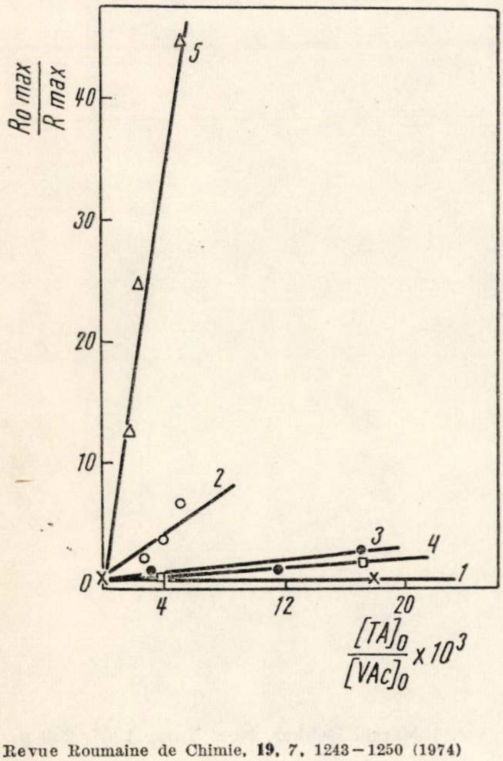

Fig. 4. — Dependence of the polymerization rate on the transfer agent/monomer molar ratio :

1, ethyl acetate; 2, diallyl ether; [3, allyl acetate; 4, allyl alcohol; 5, 'allyl bromide.

Results shown in fig. 4 and compared to the kinetic determinations on the influence of aromatic hydrocarbons in VAc polymerization emphasize the higher liability of hydrogen in α position relative to a double bond than of hydrogen attached to a carbon atom in position α relative to a benzene nucleus. Thus, the A value for tetraline ($A = 1430$) is also observed to be close to that of diallyl ether ($A = 1575$) compared to the much smaller values found for the other aromatic hydrocarbons ($A = 29$ for toluene, $A = 156$ for ethyl benzene and $A = 187$ for isopropyl benzene).

In the case of allyl derivatives, the activity as a transfer agent is strongly influenced by the nature of the substitute in the allyl grouping as well. The activity order of the studied allyl compounds compares well with that mentioned in the literature [32] for aliphatic derivatives with similar substitutes (ester $<$ alcohol $<$ ether $<$ halogenated derivative).

The factor responsible for obtaining poly(vinyl acetate) in emulsion with small variations in its structure and also for the properties of the emulsion is the maintenance of the reaction rate and of gel proportion within certain limits. The use of allyl derivatives and of aromatic hydrocarbons provides the possibility of controlling the mentioned factors, an essential condition for the completion of the emulsion polymerization of vinyl acetate without a strong exothermal reaction.

---

[32] G. E. Ham, "Vinyl Polymerization", vol. 1, Marcel Dekker, New York, 1967, 239 p.

Revue Roumaine de Chimie, **19**, 7, 1251–1264 (1974)

COPOLYMERIZATION OF N-VINYLCAPROLACTAM WITH VINYLPYRIDINES

N. COBIANU *, C. BOGHINĂ *, B. MĂRCULESCU *, C. CINCU *, I. AMĂLINEI **
* Labora tory of Macromolecular Chemistry, Polytechnic Institute, Bucharest, Romania.
**Research Department of the Synthetic Fiber Plant Săvineşti, Romania.

Received September 13/1973

The binary copolymerizations of N-vinylcaprolactam (I) with 2-vinylpyridine (II), 4-vinylpyridine (III) and 2-methyl-5-vinylpyridine (IV) were studied in solution at 70°. The reactivity ratios of these pairs of monomers were determined, the following values being obtained:

$$r_1^{\mathrm{I}} = 0.123 \qquad r_1^{\mathrm{I}} = 0.096 \qquad r_1^{\mathrm{I}} = 0.037$$

$$r_2^{\mathrm{II}} = 4.35 \qquad r_2^{\mathrm{III}} = 4.43 \qquad r_2^{\mathrm{IV}} = 11.58$$

The average values of the Q and e parameters are the following:

$$Q_{\mathrm{I}} = 0.169 \qquad e_{\mathrm{I}} = -1.26$$

1. INTRODUCTION

Data concerning free radical copolymerization of N-vinylcaprolactam (NVC) are still scarce. The reactivity ratios for the binary copolymerization of NVC with phenyl vinyl ether (PVE), [1] butylmethacrylate, [2] vinyl acetate (AV), [3] acrylonitrile (AN), methylmethacrylate (MMA) and styrene (ST)[4] have been determined.

The average values of the Q_{NVC} and e_{NVC} parameters (0.116 and −1.1, respectively) determined from the binary copolymerization with AN, MMA, and ST[4] are in good agreement with the parameters Q and e of the N-vinylpyrolidone, obtained by Alfrey.[5] These parameters anticipate the fact that the radical reactivity of NVC is higher than that of AV($Q_{AV} = 0.02$; $e_{AV} = -0.56$[6]).

---

[1] F. P. Sidelkovskaya, M. I. Askarov and F. Ibragimov, *Vysokomol. Soedinenya*, **A 3**, 976 (1961).

[2] F. Ibragimov, D. Mukhamadaliev and T. G. Gafurov, *Vysokomol. Soedinenya*, **A 12**, 1475 (1970).

[3] El Sabban, M. Zaki, S. I. Dimitrieva and A. I. Meos, *Vysokomol. Soedinenya*, **B 12**, 243 (1970).

[4] N. Cobianu, C. Boghină, B. Mărculescu and I. Amălinei, *Rev. Roumaine Chim.*, **18**, 305 (1973).

The average value $e_{NVC} = -1.1$ shows a lower donor effect of the substituent of this vinylic monomer than that assumed in the copolymerization with PVE,[1] AV[3] and ST[4] and anticipates a relatively weak tendency of NVC toward cationic polymerization.

The observed values Q_{NVC} and e_{NVC} largely depend upon the nature of the comonomer in copolymerization. They increase with the increase in the acceptor effect of the comonomer.[4]

In order to obtain more accurate information regarding this latter aspect, this paper has studied the binary copolymerization of NVC with vinylpyridines (VPy).

2. EXPERIMENTAL

a. *Materials.* NVC was obtained and purified according to indications given in the literature.[7] The product, purified and encapsulated in an argon atmosphere, was redistilled under vacuum prior to use. The fraction used in the experiments had a refractive index, $n_D^{20} = 1.5135$.

2-Vinylpyridine (2VPy) was purified by distillation under vacuum (17 torr) at 60°. The product used in the experiments had a refractive index, $n_D^{20} = 1.5510$, according to the literature data.[8]

4-Vinylpyridine (4VPy) was purified by distillation under vacuum (15 torr) at 65°. The fraction used had a refractive index, $n_D^{20} = 1.5499$.[8]

2-Methyl-5-vinylpyridine (2M5VPy) was purfied by distillation under vacuum (15 torr) at 76°. The freshly distilled fraction used in the experiments had a refractive index, $n_D^{20} = 1.5454$.[9]

The commercial α,α'-azobisisobutyronitrile (AIBN) was twice recrystallized from ethanol ($B_P = 102.5°$).

Dioxan as a pure solvent ($n_D^{20} = 1.4224$) was obtained by refluxing it on metallic sodium; it was then rectified using a twenty theoretical plates column.

b. *Polymerization procedure.* Copolymerization reactions for the determination of reactivity ratios and the calculation of parameters Q_{NVC} and e_{NVC} were carried out in two-arm glass ampoules.[10] The two monomers of the binary system under study were determined in the two arms of the ampoule. The initiator solution in dioxan was added in the arm containing NVC.

---

[5] J. F. Bork and L. E. Coleman, *J. Polymer Sci.*, **43**, 413 (1960).

[6] L. J. Young and C. C. Kenedy, in "Copolymerization", edited by G. E. Ham, Interscience Publishers, New York, 1964, p. 862.

[7] F. M. Shostakovskii, *Izvest. Akad. Nauk S.S.S.R., Otdel. khim. Nauk*, **1953**, 108; F. M. Shostakovskii, F. P. Sidelkovskaya and M. G. Zelenskaya, *Doklady Akad. Nauk S.S.S.R., Otdel. khim. Nauk*, **1952**, 643; F. M. Shostakovskii, N. A. Medzikovskaya and M. G. Zelenskaya, *Izvest. Akad. Nauk S.S.S.R., Otdel. khim. Nauk*, **1952**, 682; F. M. Shostakovskii and M. G. Zelenskaya, *Izvest. Akad. Nauk S.S.S.R., Otdel. khim. Nauk*, **1952**, 690.

[8] Y. Iwakura, T. Tamikado, M. Yamaguchi and K. Takei, *J. Polymer Sci.*, **39**, 203 (1959).

[9] R. L. Frank, *Ind. Eng. Chem.*, **40**, 879 (1948).

[10] T. Otsu and H. Inoue, *Makromol. Chem.*, **128**, 31 (1969).

After filling, one of the arms was stoppered, the content was frozen in liquid nitrogen, with air removal at 1...2.10^{-2} torr, introducing thereafter argon purified by water and oxygen and warming at 20°. This cycle (freezing , removal of gas, filling with argon and warming at 20°) was run three times. Finally, the ampoules, brought at normal pressure by introducing argon, were closed and the solution in the two arms of the ampoules were rapidly mixed at the reaction temperature.

After the established reaction time, the copolymerization reaction was stopped by abrupt freezing, and the polymers were isolated from solution by precipitating them with a nonsolvent, filtering, washing with the nonsolvent and drying under vacuum at 50 ... 60°. The nonsolvent used for the copolymer NVC—2M5VPy was ethyl ether and the nonsolvent used for the other copolymers was petroleum ether.

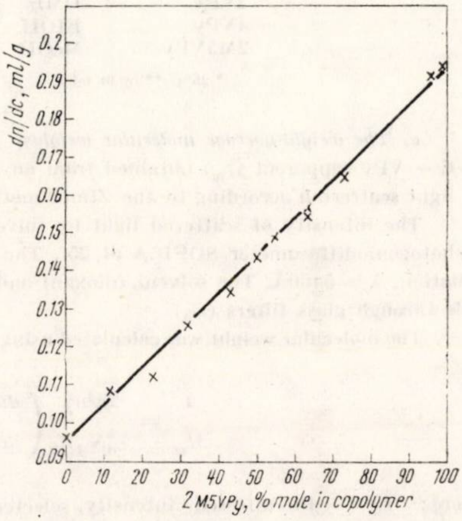

Fig. 1. — The calibrated curve $\frac{dn}{dc}$ upon the composition of homopolymer mixtures.

c. *Analyses of the copolymers.* For the composition determination of the copolymers NVC — 2M5VPy two methods were used, the analysis of carbon content and interferometry, the latter being based on the assumption of the additivity of refractive index increments of the components of the copolymer in a single solvent :

$$\left(\frac{dn}{dc}\right)_{12} = X_1 \left(\frac{dn}{dc}\right)_1 + (1 - X_1) \left(\frac{dn}{dc}\right)_2 \qquad (1)$$

The calibrated curve $\frac{dn}{dc} = f_{(X_1)}$ of mixtures of homopolymers (NVC and 2M5VPy) is presented in figure 1.

The measurements were made with a Zeiss — Jena interferometer at 25° and $\lambda = 5460$Å.

The composition of the copolymers NVC — 2VPy and NVC — 4VPy was determined by the Dumas classical micromethod.

d. *Viscosity measurements.* Intrinsic viscosities of copolymers were calculated by means of the following relationship [11]:

$$[\eta] = \eta^{sp}/C\ (1 + 0.333\ \eta sp),\ \text{ml/g} \qquad (2)$$

---

[11] O. F. Solomon and B. Gottesman, *Makromol. Chem.*, **104**, 177 (1967).

Viscometric determinations for diluted solutions (copolymer concentration less than 0.2 g/dl) were made with an Ubbelohde viscometer at 25° ± 0.05°. The molecular weights of homopolymers of 2VPy, 4VPy and 2M5VPy were estimated with the equation of table 1.

Table 1

The equations used for the calculation of molecular weights of homopolymers 2VPy, 4VPy and 2M5VPy [12,13]

Homopolymer of	Solvent *	Equation **
2VPy	DMF	$/\eta/ = 1.47 \cdot 10^{-2}\, M^{0.67}$
4VPy	EtOH	$/\eta/ = 2.5 \cdot 10^{-2}\, M^{0.68}$
2M5VPy	MeOH	$/\eta/ = 0.8 \cdot 10^{-2}\, M^{0.76}$

* 25°; ** $/\eta/$ in ml/g.

e. *The weight-average molecular weights*, $\overline{M_w}$, for homopolymer of NVC and copolymer NVC – VPy (apparent $\overline{M_W}$) obtained from an approximate equimolar feed were determined by light scattering according to the Zimm method. [14]

The intensity of scattered light by solvent and polymer particles was measured with a photogoniodiffusometer SOFICA at 25°. The light source was a mercury lamp of selected radiation, λ = 5460Å. The solvent (dioxan) and the polymer solutions were filtered into the cells through glass filters (G_5).

The molecular weight was calculated using the following relationship :

$$\frac{1}{M_w} = \frac{2\pi^2 n_B^2}{\lambda_0^4 N_A R_\theta}\left(\frac{dn}{dc}\right)^2 I_B \left(\frac{c}{I_{\mathrm{cor}}}\right)_{\theta=0}^{c=0} \tag{3}$$

where: I_β — the diffused intensity, selected for the standard benzene;

$$I_{\mathrm{cor}} - (I - I_0)\sin\theta/(1+\cos^2\theta) \tag{3a}$$

I — the scattered light intensity of the solution;

I_0 — the scattered light intensity of the solvent.

3. RESULTS AND DISCUSSION

3.1. The establishment of the optimum parameters for the copolymerization of NVC with VPy

Taking into account the activity of NVC as chain transfer agent,[4,15-17] and the fact that Mayo's differential equation [18]:

$$d[M_1]/d[M_2] = [M_1]\,(r_1[M_1] + [M_2])/[M_2]\,(r_2[M_2] + [M_1]) \tag{4}$$

---

[12] J. Brandrup and E. H. Immergut, "Polymer Handbook", Interscience Publishers New York, 1966.

[13] R. M. Fuoss *et al.*, *J. Polymer Sci.*, **28**, 69 (1958).

[14] G. Oster, P. M. Doty and B. H. Zimm, *J. Amer. Chem. Soc.*, **69**, 1193 (1947).

[15] O. F. Solomon, M. Corciovei and C. Boghină, *J. Appl. Polymer Sci.*, **12**, 1843 (1968).

[16] O. F. Solomon, D.S. Vasilescu and V. Tărărăscu, *J. Appl. Polymer Sci.*, **13**,1 (1969).

[17] F. M. Shostakovskii, F. P. Sidelkovskaya and A. N. Homutov, *Izvest. Akad. Nauk S.S.S.R., Otdel. khim. Nauk*, **1955**, 919.

[18] F. R. Mayo, F. N. Lewis and W. F. Hulse, *J. Amer. Chem. Soc.*, **70**, 1523 (1942).

is applied only to the copolymerization processes which give high polymers, preliminary tests were made to establish the monomer and initiator concentration so that the reaction product at 70° should have a molecular weight of scores and even hundreds of thousands.

The 70° temperature was chosen to compare Q_{NVC} and e_{NVC} constants with previously obtained[4] average values for Q and e.

The copolymerization process was carried out in the presence of small concentrations of dioxan, this solvent allowing a more precise and rapid dosing of the initiator.

In order to have a representation of the feed composition influence on the reaction kinetics, the AIBN was used as initiator (the substance whose splitting rate does not depend on the nature of the reaction medium[19]) in all the processes of the binary copolymerization NVC — VPy.

Anticipating a more pronounced chain transfer of 2M5VPy than that of the other VPy's, the copolymerizations of NVC with 2M5VPy were carried out with a lower concentration of AIBN than that used in the copolymerization processes of NVC — 2VPy and NVC — 4VPy, that is 0.873 mmole/l and respectively 1.17 mmole/l.

A homopolymer of NVC with an intrinsic viscosity similar to that of the copolymers obtained from the equimolecular feed of the two monomers (86 ml/g) was obtained in bulk at 50° with $[AIBN]_0 = 1.10^{-4}$ mole/l.

The Zimm plots were drawn with the values of light scattering intensity at different angles and polymer concentrations in dioxan.

Two of these plots are presented in Figs. 2 and 3.

As a result of double extrapolation the characteristic values $\left(\frac{c}{I_{cor}}\right)_{\theta=0}^{c=0}$, necessary to the calculation of the weight-average molecular weight, were obtained by means of the relationship (3). The obtained values are summarized in table 2.

Table 2

The data of average molecular weights of polymers and copolymers obtained from NVC (M_1) and VPy (M_2) at 70°

Polymer	$[AIBN]_0$ mmole/l°	Feed composition (mole fr.)		$[M_1]_0 + [M_2]_0$ mole/l	Yield (%)	$[\eta]$ ml/g	$\overline{M}$	$\frac{dn}{dc}$ ml/g at 25° in dioxan	Ref.
		x_1	x_2						
Poly 2VPy	1.17	—	1.000	6.42	22.2	88.6	438,500	—	[12]
Poly 4VPy	1.17	—	1.000	6.42	24.0	146.8	348,600	—	[13]
Poly 2M5VPy	0.873	—	1.000	7.23	9.10	163.9	471,000	—	[12]
Poly NVC*	0.10	1.000	—	bulk	35.2	86	1,570,000	0.096	—
Copolymer NVC—2VPy($X_2 = 0.90$)	1.17	0.506	0.494	7.14	9.24	78.7	347,000	0.159	—
Copolymer NVC—4VPy ($X_2 = 0.90$)	1.17	0.506	0.494	7.14	9.85	82.2	532, 000	0.132	—
Copolymer NVC — 2M5VPy ($X_2=0.907$)	0.873	0.535	0.465	6.91	7.35	—	516,000	0.135	—

* The reaction temperature 50°.

---

[19] P. S. Bartlett and N. Nozaki, *J. Amer. Chem. Soc.*, **69**, 2299 (1947); P. S. Bartlett and W. Wanger, *J. Phys. Col. Chem.*, **51**, 926 (1947); H. Boiley and G. Godin, *Trans. Faraday Soc.*, **52**, 68 (1956).

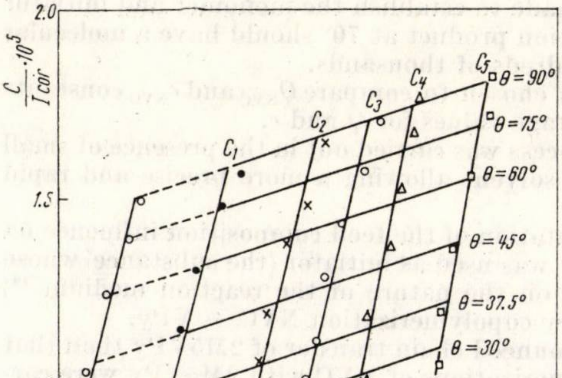

Fig. 2. — **Zimm plot for poly-NVC in dioxan at 25° :** $C_1 = 47.9.10^{-5}$; $C_2 = 95.8.10^{-5}$; $C_3 = 124.5\ 10^{-5}$; $C_4 = 153.3.10^{-5}$; $C_5 = 191.6.10^{-5}$.

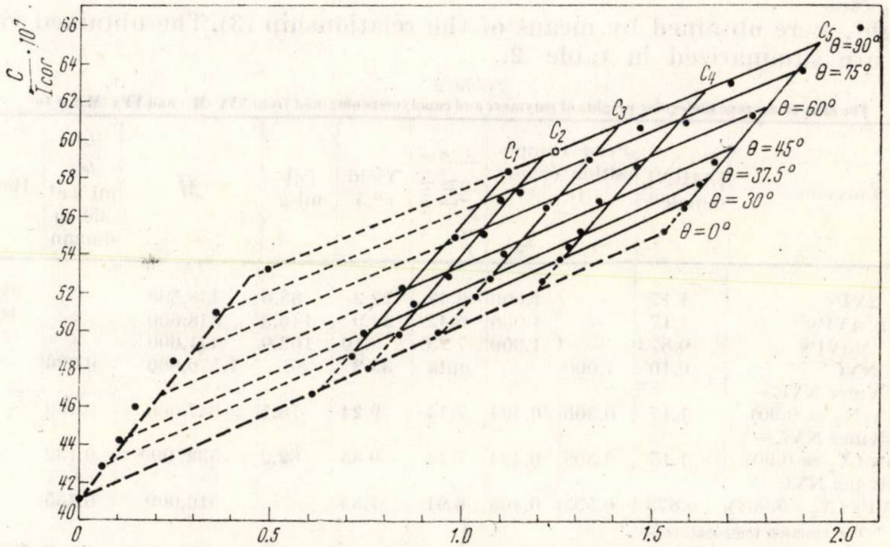

Fig. 3. — **Zimm plot for the copolymer NVC — 2M5VPy in dioxan at 25° :** $C_1 = 60.92.10^{-5}$; $C_2 = 79.62.10^{-5}$; $C_3 = 97.47.10^{-5}$; $C_4 = 121.84.10^{-5}$; $C_5 = 154.3.10^{-5}$.

It may be seen that in all these cases the weight-average molecular weights of polymers are high enough.

When comparing the molecular weights of the homopolymers of VPy with those of the copolymers obtained under the same conditions, it may be observed that the latter are higher.

The apparent molecular weight results from the light scattering data concerning the copolymer solutions with structural polydispersity (statistical, graft, bloc-copolymers :

$$M_{\text{ap}} = M_{\text{real}} + P\alpha + Q\alpha^2 \qquad (5)$$

where P and Q are constants,

$$\alpha = \left[\left(\frac{dn}{dc}\right)_1 - \left(\frac{dn}{dc}\right)_2\right] \Big/ \left(\frac{dn}{dc}\right)_{\text{cop}} \qquad (6)$$

and indexes 1 and 2 in equation (6) refer to the two homopolymers.

The theoretical basis of equation (5) was established by Stockmayer et al.,[20] Bushuk and Benoit,[21] Leng and Benoit[22] and others. The experimental test of this equation was made for many copolymers with structural polydispersity.[21-24] From the dependence of $\bar{M}_{\text{ap}}$ on the parameter α it may be observed that to establish $\bar{M}_{\text{real}}$ it is necessary to determine $\bar{M}_{\text{ap}}$ in different solvents or in the solvent in which α is very small so that $\bar{M}_{\text{ap}} \simeq \bar{M}_{\text{real}}$.

There are substantial differences between $\bar{M}_{\text{ap}}$ and $\bar{M}_{\text{real}}$ in the case of the copolymers NVC — VPy, because the parameter α is higher than 0.3 (table 2).

All the copolymerizations were carried out at the reaction times established, so that the copolymer yields did not exceed 3 %, except the copolymers for the average molecular weight establishment.

3.2. Some particular kinetic aspects

The binary copolymerization of NVC — VPy was in fact carried out in bulk, at different feed compositions. The determination of the copolymer composition led to the calculation of the reduced copolymerization rates. Some kinetic data regarding the dependence of the initial copolymerization rate on the feed composition are given in table 3 for a copolymerization process of NVC — 2M5VPy at 70°.

The values of the reduced copolymerization rates calculated from the copolymers composition determination by differential refractometry, correspond to those calculated from carbon analyses of the copolymers.

Figure 4 presents the dependence of the reduced copolymerization rate on the feed composition in the copolymerization of NVC with VPy.

---

[20] H. W. Stockmayer et al., *J. Polymer Sci.*, **16**, 517 (1955).

[21] W. Bushuk and H. Benoit, *Canad. J. Chem.*, **36**, 1616 (1958).

[22] M. Leng and H. Benoit, *J. Polymer Sci.*, **57**, 263 (1962).

[23] Y. Shimura, Y. Mito and H. Kombe, *J. Polymer Sci.*, **B 2**, 403 (1964).

[24] J. Mita, *J. Chem. Phys.*, **58**, 480 (1961).

Table 3

The copolymerization of NVC (I) with 2M5VPy (II)in dioxan with AIBN at 70° $[AIBN]_0 = 0.873\ 10^{-3}$ mole/l

$[M_2]$ in the feed (mole %)	Reaction time (min)	Initial total monom. conc. $[M_1]_0 + [M_2]_0$ (mole/l)	Conv. (%)	Elem. analysis (C %)	$[M_2]$ in copolymer (mol. fraction)		Reduced * copolym. rate $R_{po} \cdot 10^6$	$[\eta]$ ** (ml/g)
					C %	$\frac{dn}{dc}$	$[M_1]_0 + [M_2]_0\ (s^{-1})$	
4.2	58	5.004	0.062	73.52	0.426	—	1.894	—
8.3	171	4.827	1.88	75.28	0.579	0.555	1.968	51.42
12.0	150	6.713	2.19	76.17	0.647	0.645	2.635	—
15.1	130	4.782	1.83	76.98	0.720	—	2.562	—
18.0	120	6.470	1.88	77.40	0.754	0.728	2.847	101.4
21.4	100	6.770	1.76	78.04	0.805	0.820	3.212	—
36.3	105	6.320	2.60	79.30	0.902	—	4.441**	100.3
46.6	65	6.906	2.17	79.36	0.907	0.910	5.973	128.2
66.2	60	7.099	2.17	79.65	0.931	—	6.303	—
94.6	21	6.474	2.51	80.22	0.972	0.990	19.95***	137.0

* Calculated from the composition data of the copolymer established by carbon analysis, C%.

** Solvent $CHCl_3$, 25°.

*** $[AIBN]_0 = 1.591.10^{-3}$ mole/l.

It may be observed that, in all the cases, the copolymerization rate increases with the VPy molar fraction in the feed. The copolymerization rates of NVC with 2VPy and 4VPy are similar, which suggests the similarity in the two VPy reactivities.

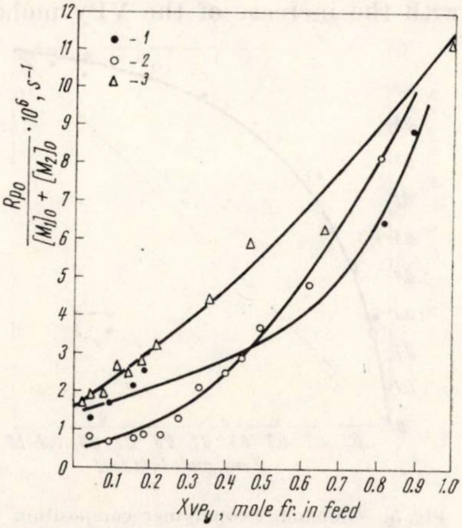

Fig. 4. — Copolymerization rate against composition feed for the NVC — VPy systems at 70°.
1, ●, 4VPy $[AIBN]_0 = 1.16.10^{-3}$ mole/l.
2, ○, 2VPy
3, Δ, 2M5VPy $[AIBN]_0 = 0.873.10^{-3}$ mole/l.

In the copolymerization reaction of NVC with 2VPy and 4VPy the reduced copolymerization rate shows a parabolic dependence on the molar feed composition. A quasi-parabolic dependence was found in the copolymerization reaction of NVC with 2M5VPy.

Although the AIBN concentration was lower in this process, the reduced copolymerization rate for the same composition of the feed was higher than that of the binary copolymerization of NVC with 2VPy and 4VPy respectively.

It is evident that, in all these copolymerization processes, the most reactive comonomer is the VPy.

In the reaction with NVC the reactivity series of the studied VPy is : 2M5VPy >2VPy ≃ 4VPy. This fact is also confirmed by the the monomer/copolymer composition curves representing the three binary systems, presented in figs 5 and 6.

The shape of these monomer/copolymer composition curves is particular for binary systems with $r_1 < 1$ and $r_2 > 1$, proving a higher reactivity of VPy in the reactions with both macroradicals of the system.

Another interesting kinetic aspect in these copolymerization processes is the dependence of the molecular weight on the feed composition.

It is rather difficult to establish this dependence. The chemical nature and the feed composition affect directly the average molecular weight by the chain transfer reactions and the kind of termination reaction.

Fig. 7 presents the dependence of the intrinsic viscosity on the composition of the copolymer.

Because the viscosity of the statistical copolymers depends on certain factors (the molecular weight, the chemical composition and the distribution of the structural unities in the copolymer), the influence of the feed composition on the molecular weight, established in this way, has only a qualitative value.

It may be seen that the intrinsic viscosity increases parabolically with the increase of the VPy molar fraction in the copolymer. This dependence points out a more pronounced chain transfer of NVC as compared with VPy. This fact corresponds to literature data.[4,15-17, 25-28]

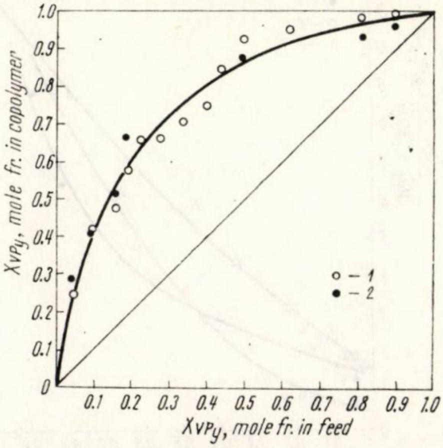

Fig. 5. — Monomer/copolymer composition curves for radical copolymerization of the NVC — 2VPy and NVC — 4VPy systems, temperature 70° :
1, ○, 2 VPy; 20, ●, 4VPy.

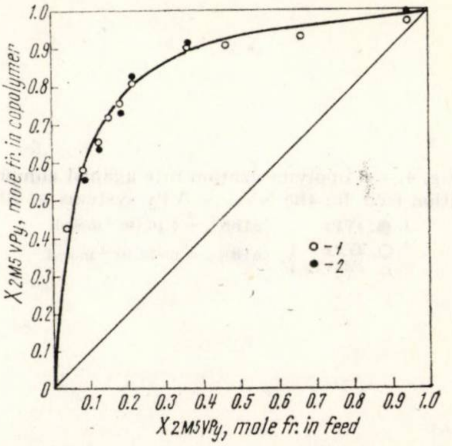

Fig. 6. — Monomer/copolymer composition curve for radical copolymerization of the NVC — 2M 5VPy system, temperature 70° :
1, ○, from $\frac{dn}{dc}$; 2, ●, from carbon analyses.

3.3. Calculation of the reactivity ratios

The available literature mentions neither the reactivity ratios for these binary systems, nor the experimental data which can be used to calculate these reactivity ratios.

Two possibilities were used for the determination of the reactivity ratios r_1 and r_2 for these binary systems (in all the cases NVC was noted M_1) : the linearization of the differential composition equation of the copolymerization using Fineman-Ross' method[29] in both variants :

$$\frac{Ri}{\rho_i}(\rho_i - 1) = r_1 \cdot \frac{Ri^2}{\rho_i} - r_2 \tag{7}$$

and

$$\frac{\rho_i - 1}{R_i} = r_1 - r_2 \frac{\rho_i}{Ri^2} \tag{7'}$$

---

[25] R. L. Dannley et al., *J. Polymer Sci.*, **19**, 285 (1956).

[26] M. M. Koton, *J. Polymer Sci.*, **30**, 331 (1958).

[27] A. Kacialski et al., *J. Polymer Sci.*, **23**, 455 (1957).

[28] P. F. Onyon, *Trans. Faraday Soc.*, **51**, 400 (1955).

[29] M. Fineman and S. D. Ross, *J. Polymer Sci.*, **5**, 259 (1950).

and the least square method.[30]

For the latter case, the normal equations were :

$$\sum \frac{R_i}{\rho_i}(\rho i - 1) = r_1 \sum \frac{R_i^2}{\rho_i} - n r_2$$

$$\sum \frac{R_i^3}{\rho_i^2}(\rho i - 1) = r_1 \sum \frac{R_i^4}{\rho_i^2} - r_2 \sum \frac{R_i^2}{\rho_i} \qquad (8)$$

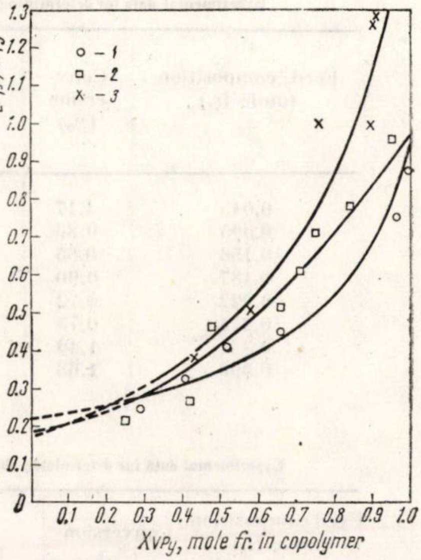

Fig. 7. — Dependence of the intrinsic viscosity upon the composition of copolymers : *1*, ○, 4 VPy; *2*, □, 2VPy; *3*, X, 2M5VPy.

where n = the number of feeds for which the copolymerization was made ; $R_i = \frac{x_{1i}}{x_{2i}}$ and $\rho_i = \frac{X_{1i}}{X_{2i}}$; x_i and X_i being the molar fraction of the monomer in the feed and respectively in the copolymer.

The necessary data for the determination of the reactivity ratios for the systems NVC — 2VPy and NVC — 4VPy are presented in tables 4 and 5, respectively. The experimental data necessary to the determination of the reactivity rations for the system NVC — 2M5VPy were presented in table 3.

As shown in the monomer/copolymer composition curves (figures 5 and 6), the variation of the composition of the copolymer obtained by the feed rich in M_2 takes place within very narrow ranges of the feed composition, while the variation at the feed poor in M_2 takes place within very wide ranges (the ascending slope of the monomer/copolymer curve).

The compositions of the copolymers affected by the highest errors correspond to the cases $x_2 > 0.6$.

Therefore, the contribution of the samples of copolymers obtained at the values of highest x_2 was diminished in the calculation of the reactivity ratios.

[30] L. M. Batuner and M. E. Pozin, "Mathematical Methods in Chemistry", translated into Romanian from Russian, 2nd edition, Bucharest, 1956, p. 480.

Some graphs regarding the linearization of the differential equation of the binary copolymers NVC − VPy by Fineman-Ross' method are presented in fig. 8, 9 and 10.

The values of the reactivity ratios for the three binary systems are summarized in table 6.

Table 4

Experimental data for determining the NVC (M_1) −2 VPy (M_2) system constants at 70°

Feed composition (mole fr.) x_2	Conversion (%)	N % Dumas	2VPy in copolymer (mole fr.) X_2	R_i	ρ_i
0.045	1.17	10.71	0.247	21.22	3.049
0.095	0.86	11.20	0.415	9.526	1.410
0.156	0.85	11.40	0.479	5.410	1.088
0.187	0.90	11.73	0.580	4.348	0.724
0.222	0.72	11.98	0.653	3.504	0.531
0.274	0.73	12.0	0.658	2.650	0.520
0.331	1.49	12.16	0.704	2.021	0.420
0.398	1.68	12.32	0.748	1.512	0.337

Table 5

Experimental data for determining the NVC (M_1) −4 VPy (M_2) system constants at 70°

Feed composition (mole fr.) x_2	Conversion (%)	N % Dumas	4VPy in copolymer (mole fr.) X_2	R_i	ρ_i
0.045	2.03	10.80	0.284	21.22	2.521
0.095	2.27	11.18	0.408	9.526	1.451
0.156	2.51	11.51	0.514	5.410	0.945
0.187	2.51	12.02	0.665	4.348	0.504
0.493	1.08	12.79	0.870	1.028	0.149
0.808	2.26	13.02	0.927	0.238	0.079
0.896	2.61	13.18	0.965	0.116	0.036

Table 6

Values of the copolymerization constants for the binary systems NVC (M_1) − VPy (M_2)

M_2	r_1		r_2	
	Least square method	Fineman-Ross method	Least square method	Fineman-Ross method
2VPy	0.123	0.10	4.35	3.7
4VPy	0.096±0.024	0.094	4.43±1.37	3.9
2M5VPy	0.037	0.04	11.58	10.70

As shown in this table, the values of the reactivity ratios obtained by Fineman-Ross' method and the least square method correspond to each other.

According to the kinetic determinations, the values of the reactivity ratios show that the best reactive monomers in these processes are the VPy.

It may be seen that the 2M5VPy reactivity and polarity are similar to those of ST ; this is based both on the values of the reactivity ratios of these monomers in their reactions with NVC[4] and on the binary copolymerization of ST with 2M5VPy.[31]

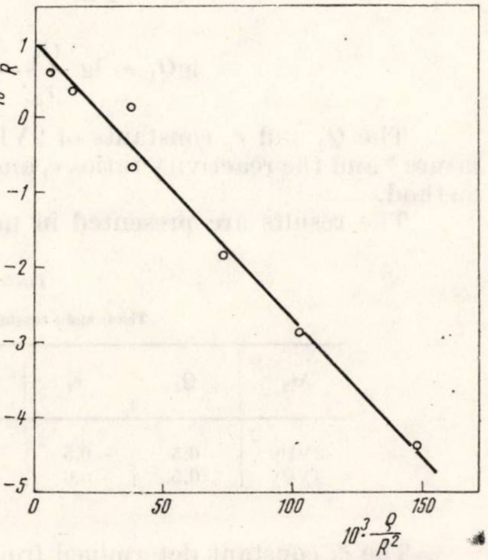

Fig. 8. — Graphic determination of the NVC — 2VPy system constants after Fineman-Ross.

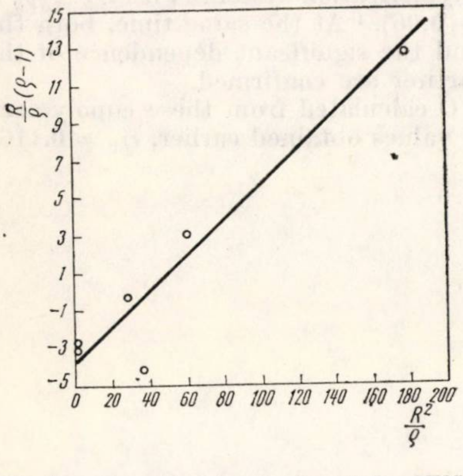

Fig. 9. — Graphic determination of the NVC —4VPy system constants after Fineman-Ross.

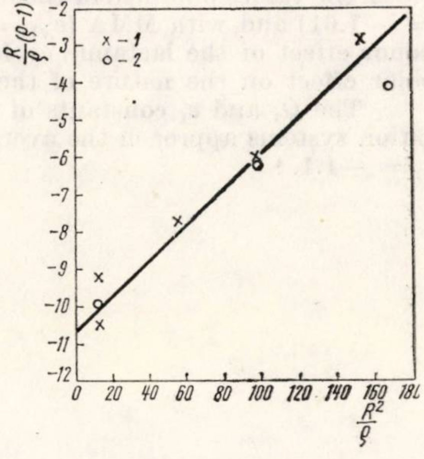

Fig.10. — Graphic determination of the NVC — 2M5VPy system constants after Fineman-Ross.

Calculated data from : *1*, × $\frac{dn}{dc}$; *2*, ○. C %.

---

[31] Y. Sakurada, *Chem. High Polymers, Japan*, **18**, 496 (1961).

3.4. Calculation of the Q and e constants

The Q_1 and e_1 constants for NVC were calculated by means of the equation derived from the Alfrey and Price's scheme [32] :

$$e_1 = e_2 \pm (-2.303 \ \lg \ r_1 r_2)^{1/2} \tag{9}$$

$$\lg Q_1 = \lg \frac{Q_2}{r_2} - \frac{e_2}{2.303}(e_2 - e_1) \tag{10}$$

The Q_2 and e_2 constants of 2VPy and 4VPy were found in the literature [8] and the reactivity ratios r_1 and r_2 were obtained by the least square method.

The results are presented in table 7.

Table 7

The Q and e constants for NVC (M_1)

M_2	Q_2	e_2	r_1	r_2	Q_1	e_1
2VPy	0.5	−0.5	0.123	4.35	0.171	−1.29
4VPy	0.5	−0.6	0.096	4.43	0.167	−1.22

The e_1 constant determined from these systems is intermediary between the values obtained in the copolymerization systems with ST ($e_{NVC} = -1.61$) and with MMA ($e_{NVC} = -0.96$). [4] At the same time, both the donor effect of the lactamic cycle and the significant dependence of the polar effect on the nature of the partner are confirmed.

The Q_1 and e_1 constants of NVC calculated from these copolymerization systems approach the average values obtained earlier, $\bar{Q}_1 = 0.116$; $\bar{e}_1 = -1.1$. [4]

---

[32] T. Alfrey and C. C. Price, *J. Polymer Sci.*, **2**, 101 (1947).

Revue Roumaine de Chimie, **19**, 7, 1265 – 1269 (1974)

LIQUID MEMBRANE-ELECTRODES. V*

ELECTRODIC BEHAVIOUR OF SODIUM TETRAPHENYLBORATE IN CYCLOHEXANONE TO CERTAIN MONOVALENT CATIONS

ELENA HOPÎRTEAN and EUGENIA ŞTEFĂNIGĂ

"Babeş-Bolyai" University, Department of Analytical Chemistry, Cluj, str. Arany Janos 11
Romania

Received October 29, 1973

The paper is concerned with obtaining and establishing the electrodic behaviour of a sodium tetraphenylborate liquid membrane dissolved in cyclohexanone. The electrodic behaviour to the following cations was studied : K^+, Cs^+, NH_4^+ and Ag^+. A good electrodic behaviour has particularly been observed to K^+ and Ag^+ both in the absence and in the presence of some interfering ions (Na^+, Ca^{2+}, Mg^{2+}).

1. INTRODUCTION

One of the liquid membrane-electrodes described in the speciality literature is that whose active electrodic component is sodium tetraphenylborate. The electrode accomplished by Scholer and Simon [1] has been obtained by evaporating tetrahydrofurane from the solution containing sodium tetraphenylborate, tenoyltrifluoracetone in *p*-nitrocymole and PVC in tetrahydrofurane. The resulting electrode was employed by the authors in the direct potentiometric determination of certain organic cations (ammonium quaternary salts) as well as of Cs^+ and K^+.

The present paper deals with a simpler approach for obtaining a liquid membrane-electrode with sodium tetraphenylborate as an active component and also tries to establish its behaviour to some monovalent cations : K^+, Cs^+, NH_4^+ and Ag^+.

2. EXPERIMENTAL SECTION

2.1. *Manner of obtaining the membrane-electrode.* The electrode body was achieved according to the chart in fig. 1. The active electrodic component (2) (sodium tetraphenylborate dissolved in cyclohexanone) is introduced into the space between the walls of the two concentric glass tubes having a glass frit G_4(1) fixed at their end. The central tube contains the internal solution (3) into which the internal reference electrode (5) (calomel saturated electrode) will be introduced by means of an electrolytic trap (4) (10^{-1}M $NaNO_3$+1 % agar-agar). The internal solutions used was the tested ion salt solution of a 10^{-4} M concentration.

---

* Part IV : E. Hopîrtean, M. Mioşcu and C. Liteanu, *Stud. Univ. Babeş-Bolyai, Chem.*, **18** (1), 133 (1973).

[1] R. Scholer and W. Simon, *Helv. Chim. Acta*, **55**, 1801 (1972).

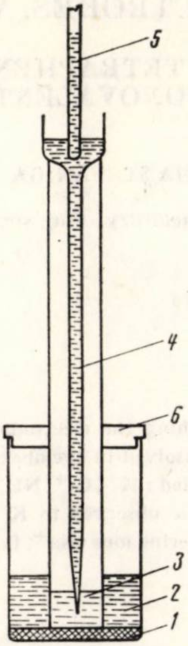

Fig. 1. — Liquid membrane-electrode: *1*, glass frit G_4; *2*, active electrodic component; *3*, internal solution; 4, electrolytic trap; *5*, internal reference electrode (SCE) *6*, lid.

2.2. *E-pM electrodic functions.* A MV—11 pH-meter was used for measuring the f.e.m. of the following electrolytic chain:

SCE | electrolytic trap | internal solution | membrane | external solution | electrolytic trap | SCE

Measurements were performed at room temperature under non-stirring conditions. A preliminary determination was made on the electrodic behaviour to K^+ of the liquid membrane with various proportions of sodium tetraphenylborate : 0.1 %, 0.25 %, 0.5 % and 1%, in view of establishing its optimum composition. A good electrodic behaviour was found in the case of the membrane having a 0.25 % $Na[B(C_6H_5)_4]$ content in cyclohexanone. All the results reported in this paper have been obtained with a membrane of this composition. The electrodic functions have been established both in the absence and in the presence of some interfering ions.

Fig. 2 presents the electrodic functions obtained for K^+ in presence of Na^+ having various concentrations, compared to the electrodic function obtained in the absence of the interfering ion. The electrodic functions shown in fig. 3 were obtained for K^+ in the presence of Mg^{2+}. Investigations were also made on the membrane electrodic behaviour to K^+ in the presence of ion Ca^{2+}. The results concerning the membrane electrodic behaviour to K^+ in the presence of interfering ions Na^+, Mg^{2+} and Ca^{2+} are presented in table. 1. Data in table 1 clearly illustrate that the concentration range in

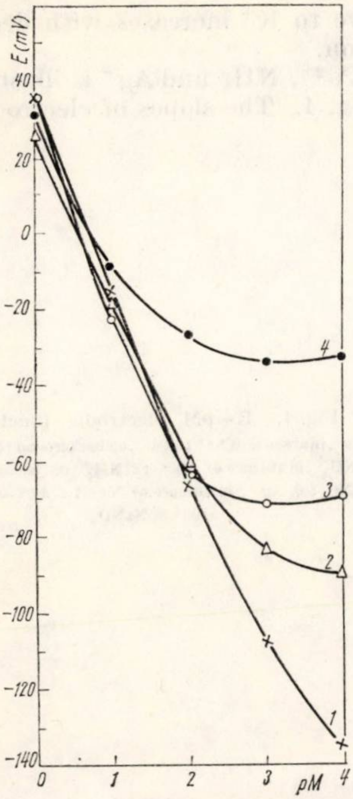

Fig. 2. — Electrodic functions for K$^+$:
1, in absence of Na$^+$; *2*, background 10^{-3} M NaCl ; *3*, background 10^{-2} M NaCl ; 4, background 10^{-1} M NaCl.

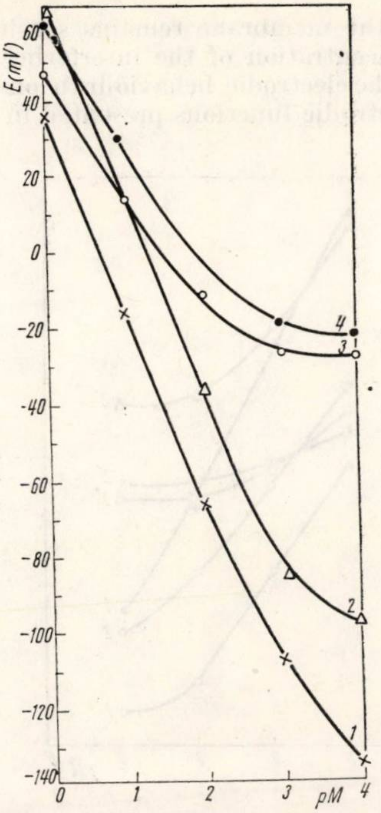

Fig. 3. — Electrodic functions for K$^+$:
1, in absence of Mg^{2+}; *2*, background 10^{-3}M $MgCl_2$; *3*, background 10^{-2} M $MgCl_2$; 4, background 10^{-1}M $MgCl_2$.

Table 1

Electrode behaviour of the membrane to K$^+$

Interfering ion	Concentration of interfering ion	pK interval	Slope (mV)
—	—	0−3	48.0
Na$^+$	10^{-3} M	0−3	42.0
	10^{-2} M	0−2	41.0
	10^{-1} M	0−1.5	35.0
Ca^{2+}	10^{-2} M	0−2	44.0
	10^{-1} M	0−1.5	30.0
Mg^{2+}	10^{-3} M	0−3	48.0
	10^{-2} M	0−2	30.0
	10^{-1} M	0−2	30.0

which the membrane remains sensitive to K^+ increases with decrease in the concentration of the interfering ion.

The electrodic behaviour to ions Ca^{2+}, NH_4^+ and Ag^+ is illustrated by the electrodic functions presented in fig. 4. The slopes of electrodic functions obtained for these ions both in the absence and in the presence of ion Na^+ are plotted in table 2. The presence of ion Na^+ in solution hinders in particular the electrodic behaviour to NH_4^+. Emphasis is also laid on the super-Nernstian value of the electrodic function slope obtained for ion Ag^+ in the absence of the interfering ion.

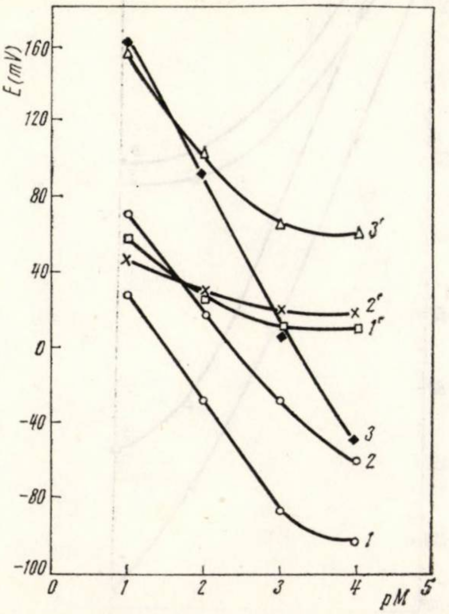

Fig. 4. — E — pM electrodic functions: 1, Cs^+, in absence of Na^+; 1, Cs^+, on background 10^{-1} M $NaNO_3$; 2, NH_4^+, in absence of Na^+; 2′ NH_4^+, on background 10^{-1} M $NaNO_3$; 3, Ag^+, in absence of Na^+; 3′ Ag^+ on background 10^{-1} M $NaNO_3$.

Table 2

Electrode behaviour of the membrane to Cs^+, NH_4^+ and Ag^+

Ion	In the absence of background		On background 10^{-1} M $NaNO_3$	
	pM interval	Slope (mV)	pM interval	Slope (mV)
Cs^+	1 – 3	49.5	1. – 2.5	24.0
NH_4^+	1 – 3	59.0	1 – 2.5	12.0
Ag^+	1 – 4	72.6	1 – 2.5	36.1

2.3. *Potentiometric titrations.* The membrane-electrode was used in the determination, by potentiometric titration, of tetraphenylborate with $AgNO_3$ and KCl, respectively, and also of KCl with sodium tetraphenylborate. The resulting titration curves are shown in fig. 5. As it was expected, a larger potential variation at equivalence has been found when using $AgNO_3$ as a titrant.

In conclusion, the liquid membrane-electrode obtained by impregnating the glass frit G_4 with a sodium tetraphenylborate solution in cyclohexanone revealed a good electrodic behaviour, particularly to K^+ and Ag^+. The electrode may be used both in direct determinations for Ag^+, K^+, Cs^+ and NH_4^+ and in the potentiometric titration of sodium tetraphenylborate (titrant $AgNO_3$ or KCl) and of KCl (titrant Na $[B(C_6H_5)_4]$.

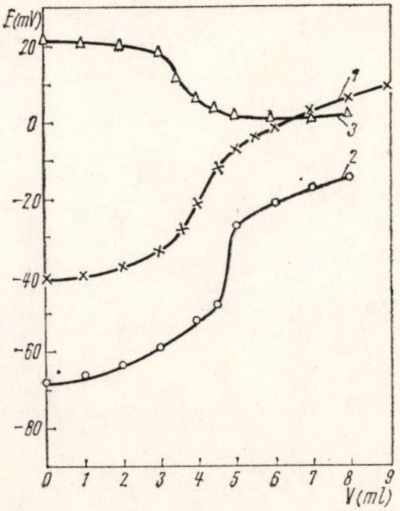

Fig. 5. – Potentiometric titrations : *1*, 2×10^{-2} M Na $[(B(C_6H_5)_4]$ with ~ 10^{-1} M $AgNO_3$; *2*, 2×10^{-2} M Na $[B(C_6H_5)_4]$ with ~ 10^{-1} M KCl ; *3*, 10^{-2} M KCl with ~ 5×10^{-2} M Na $[B(C_6H_5)_4]$.

Revue Roumaine de Chimie, 19, 7, 1271–1277 (1974)

CORRELATION OF THE POROUS STRUCTURE TO THE ACTIVITY AND SELECTIVITY OF SOME DEHYDROGENATION CATALYSTS

VLADIMIR MOCEAROV, GEORGETA CSOMONTANYI, CORNELIA CORICIUC
and ALEXANDRU PANOVICI

"I.C.P.R.P." Petroleum Refining and Petrochemistry Research and Design Institute, Ploieşti,
Bd. Republicii 291, Romania

Received November 7, 1972
Revised March 18, 1974

The possibilities of performing increased conversions in catalytic dehydrogenation of ethylbenzene, in an adiabatic reactor are analysed, based on theoretical considerations. A suitable catalyst is chosen for this purpose, according to its kinetic characteristics. Its porous structure is correlated to its activity and selectivity in the reaction studied. In order to eliminate the inner diffusional influences on the reaction rate, the porous structure of the catalyst was changed and the effect of this transformation on the catalyst performances was examined.

It is a well-known fact that the dehydrogenation of ethylbenzene to styrene is an equilibrium endothermal reaction which takes place with a volume increase.

Thermodynamic calculations enable us to establish the conditions favouring the progress of the reaction in the desired direction, namely towards :

a) temperatures over 550°, the upper limit being a function of kinetic features of the used catalysts, and of their selectivity at high temperatures ;

b) high dilutions of the reactant to lower its partial pressure. Generally, the dilution of hydrocarbon is achieved by steam, which, besides lowering the partial pressure of the hydrocarbon, plays also the role of heat carrier, and of regenerating agent of coke deposited on the surface of the catalyst.

The favourable effect of temperature and dilution on the dehydrogenation equilibrium of ethylbenzene is shown in figure 1.

Isobars 1 and 2 represent the variation of the conversion at equilibrium with the temperature, without dilution, and with molal dilution of 20 : I, respectively. Adiabatics 3, 4, 5, and 6, illustrate the decrease of temperature with the conversion, owing to the endothermic character of the reaction. For different values of the initial temperature – To, that is for 650°, 640°, 620°, and 580°C, under the conditions of the same conversion of about 65 mole per cent, effluent will leave the reaction zone with different temperatures, i. e. : 580°, 570°, 550° and 510°. An increase from 550° to 575° of the effluent temperature, at the outlet, displaces the equilibrium by approximately eight mole percent in favour of the formation of styrene (curve 2) so that, by reaching a 575° temperature at the bottom of an adiabatic styrene reactor, it becomes possible to perform conversions above 60 mole percent.

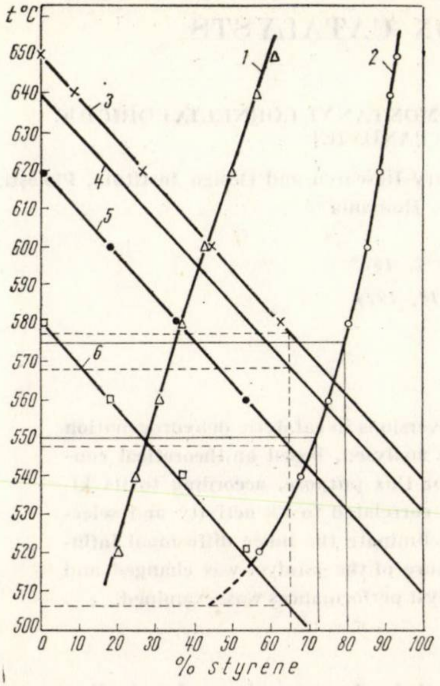

Fig. 1.— Conversion at equilibrium dependence on temperature, during dehydrogenation of ethylbenzene without dilution (1) and with dilution of 20 moles H_2O to one mole hydrocarbon (2). The adiabatics $\Delta T/\Delta x$ for different values T^0 (3, 4, 5, 6) dilution molal ratio 20 : I.

In modern styrene processes, such performances are obtained either in tubular polytropic reactors with outer heating or in a succession of several adiabatic reactors set in a series, with supplementary heating of the effluents from each reactor.[1-4]

The basic problem for achieving high conversions, on a single adiabatic reactor, consists in operating the latter in such a way as to have the effluent leaving the reactor at a temperature of about 575°. To achieve this, there are two possibilities namely :

— to obtain very high steam/hydrocarbon dilutions

---

[1] Kirk and Othmer, "Encyclopedia of chemical Technology", vol. 19, Second Edition, Interscience Publishers, New York, 1969, p.55.

[2] H. Ohlinger and S. Stadelmann, *Chem. Ing. Tech.*, **37**, 4 (1965).

[3] Hülls Chem. Werke, Brit. pat. 765025, 2 January, 1957;

[4] Monsanto, Chem. Co., Brit. pat. 966704, 12 August, 1964;

— to raise the temperature of the feed at the entrance of the reaction zone.

The reaction carried out at high dilutions in order to obtain the minimal values of the ratio $\Delta T/\Delta x$ (where T = the temperature in the reaction zone and x = conversion), may lead, theoretically, to the reduction of the temperature gradient on the catalytic layer at 45° for an approximate 65 mole per cent conversion.

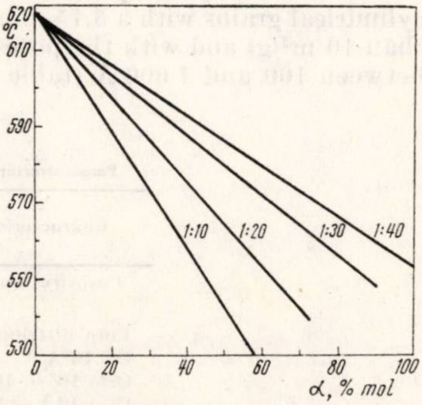

Fig. 2. — Decrease of the temperature with the degree of conversion in an adiabatic reactor, during dehydrogenation of ethylbenzene for different molal dilutions (T^o = 620°C).

As it results from figure 2, which shows the adiabatics of the temperature variation of different conversions for different dilutions, the above mentioned performances will be achieved, for instance, at a molal dilution of 40 : I if the entrance temperature of the stream on the catalytic layer is 620°. It is not profitable to obtain such high dilutions because this requires higher investments, owing to the large dimensions of the reactor, and to a supplementary energy consumption needed for the transport, evaporation and condensation of the diluent in excess.

The solution recommended to achieve higher conversions in the adiabatic styrene reactor, is to raise the temperature of the feed entering the reaction zone to approximately 640°, maintaining the molal dilution ratio at a value of 20 :1. At this temperature, the majority of catalysts involved in styrene process present low selectivities, either owing to their kinetic characteristics, or due to the shifting of the reaction into the diffusion rate controlled area.

EXPERIMENTAL

To obtain higher conversions in the adiabatic dehydrogenation reactor of ethylbenzene, we have recommended, as a result of our studies, the use of a catalyst based on iron oxides and additives differing from the variants of conventional catalysts by kinetic characteristics, namely : ability to work at high thermal level, possesing close values for the apparent activation energy of the main reaction and of the secondary reactions, i. e. the selectivity of the process is not significantly affected in the interval of 600 – 650°. This catalyst has been termed "catalyst *A*" in the present paper.

The kinetic characterization of "catalyst *A*" was carried out in a dynamic laboratory isothermal system, under kinetic conditions, the diffusional influences on the reaction rate being negligible.

The test reaction was the dehydrogenation of ethylbenzene in dilution with steam.

From a physical point of view, "catalyst *A*" occurs in the shape of cylindrical grains with a 3.75 mm diameter with a low specific surface (less than 10 m^2/g) and with the pores radia spread mainly in the field ranging between 100 and 1 000 Å (table 1).

Table 1

Porous structure of catalyst "A" and "B"

Characteristics	Catalysts "*A*"	Catalysts "*B*"
Porosity, $cm^3/100$ g	40.0	57.0
Pore distribution, %		
$Ø < 10^2$ Å	3.0	2.6
$Ø = 10^2 - 10^3$ Å	70.0	39.4
$Ø = 10^3 - 10^4$ Å	22.0	10.0
$Ø > 10^4$ Å	5.0	48.0

The study was further continued to establish the amount of inner and outer diffusion resistences. We have taken the partial pressure gradient of the reactant in the bulk gas phase and at the surface of the catalyst grain, as a measure of the external diffusion resistance.

Making use of the calculation relationship for the pressure gradient of the reactant, in the bulk gas phase and on the surface of the grain :

$(p_g - p_i) = \dfrac{N}{K_g}$, where : N = mass flow, moles/cm^2. sec.

K_g = mass transfer coefficient in the gaseous phase, moles/cm^2. atm. sec.

p_g = partial pressure of the reactant in the bulk gas phase, atm.

p_i = partial pressure of the reactant at the grain surface, atm.

Under hydrodynamic conditions favourable to the normal run of the process the values determined for $(p_g - p_i)$ were of the 10^{-2} atm order, a fact which entitled us to consider that outer diffusion does not control the process studied.

To evaluate the contribution of the inner diffusion on the dehydrogenation reaction rate in the presence of "catalyst *A*" we calculated the values of the dimensionless parameters γ and β determined by relationships :

$\gamma = \dfrac{E}{R \cdot T}$, where : E = activation energy, kcal/mol.

R = gas constant, kcal/mol. degree Kelvin

T = temperature, degree Kelvin

$\beta = \frac{\text{Co.H.Deff}}{K_{\min} \cdot T}$, where : C_0 = concentration of the reactant at the outside of the grain, mol/cm^3

H = reaction heat, kcal/mol.

Deff = effective diffusion coefficient, cm^2/sec.

K = thermal conductivity of the catalyst, kcal/cm. sec. degree Kelvin.

Using the values given in table 2, we calculated $\gamma = 19$ and, $\beta = 0.0038$ respectively. The very low value of parameter β leads us to the conclusion that no notable temperature decrease takes place inside the grain throughout reaction.

Table 2

Values for the calculation of parameters γ and β

Magnitude	Value
Apparent activation energy, E, kcal/mol	34,7
Gas constant, R, kcal/mol Kelvin degree	0,002
Temperature, T, Kelvin degree	913
Initial hydrocarbon concentration, C_0 mol/cc.	$6.75 \cdot 10^{-7}$
Reaction heat, H, kcal/mol	29.0
Grain thermal conductivity, kcal/ /cm.s°.K	$9 \cdot 10^{-8}$
Effective diffusion coefficient, cm^2/sec.	$1.59 \cdot 10^{-2}$
Dimensionless parameter γ	19
Dimensionless parameter β	0.0038

The calculus of the value of Thiele's modulus, by means of relations :

$\text{Ø} = R\sqrt{\frac{K}{\text{Deff}}}$, where : R = the effective grain radius, cm.

k = apparent rate constant, sec^{-1}.

Deff = effective diffusion coefficient, cm^2/sec.

in the case of "catalyst A" for a temperature of 640°C, based on the data of table 3, the module value of 6.04 was calculated.

Making use of the diagram representing the utilization factor η as a function of Thiele's modulus Ø, according to Weisz and Hicks[5] for $\gamma = 20$ (figure 3), we note that with "catalyst *A*", the utilization factor $\eta = 0,4$, what shows that the inner diffusion slows down the reaction rate.

---

[5] P. B. Weisz and J. S. Hicks, *Chem. Eng. Sci.*, **17** , 265 (1962).

Table 3

Values of Thiele's modulus for catalysts "A" and "B"

Catalyst	Rate constant k, $\sec^{-1}$	Effective grain radius cm	Ø
"*A*"	$2.95 \cdot 10^9 \exp\left(-\frac{34{,}700}{R.T}\right)$	0.187	6.04
"*B*"	$1.05 \cdot 10^9 \exp\left(-\frac{31{,}650}{R.T}\right)$	0.02	0.67

There are two means for eliminating this deficiency, namely : either to reduce the diameter of the catalyst grain, or to create, inside the grain, cavities in which the diffusion should take place, approximately according to the same laws as in the free intergranular space. Since the first solution implies an important pressure drop on the catalytic layer, we have chosen the second solution. Thus, acting on the porous structure of "catalyst *A*", by means of an original patented technique we created the catalyst, termed "catalyst *B*" in this paper.

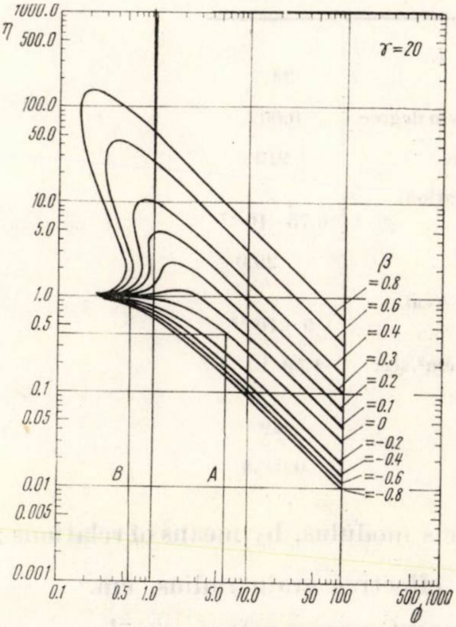

Fig. 3 — Utilization factor dependence on Thiele's modulus Ø, for the value $\gamma = 20$, in the case of catalysts "*A*" and "*B*".

From the texture point of view, "catalyst *B*" is characterized by a prevailing area of macropores, approximately 50 % of the pores having radia over 10.000 Å, the porosity being also higher than that of the "catalyst *A*" (table 1).

The kinetic characteristics of "catalyst *B*" are only slightly different from those of "catalyst *A*", and the differences between the values of dimensionless parameters γ and β are also very slight. According to the data presented in table 3, the marked differences in the value of the effective radii of the grains, as well as those of the effective diffusion coefficient, for "catalyst *B*", compared to "catalyst *A*", resulted in a 10 time smaller value of Thiele's modulus for "catalyst *B*", respectively 0.67 (table 3).

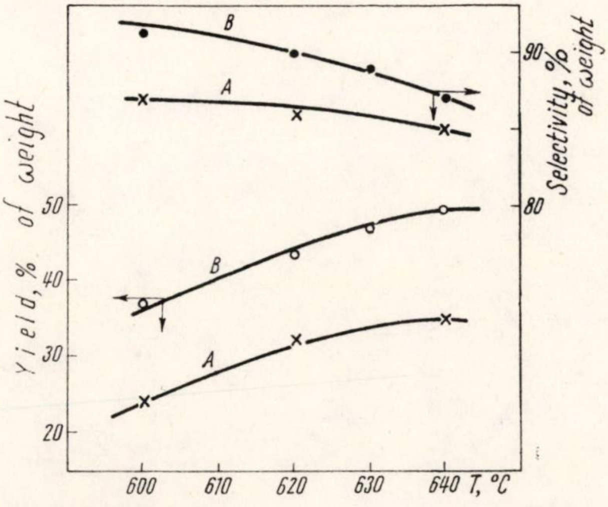

Fig. 4. — Yield (*R*) and selectivity (*S*) dependence on temperature, during dehydrogenation of ethylbenzene on catalysts "*A*" and "*B*".

According to the Weisz and Hicks diagram, for $\gamma = 20$, an utilization factor practically equal to I corresponds to a value 0.67 of Thiele's modulus, which means that the inner diffusion no longer bear any influence on the dehydrogenation rate (figure 3).

The effects of the change in the catalyst porous structure on its activity and selectivity in the dehydrogenation reaction of ethylbenzene are emphasized in the example given in figure 4.

By representing the variation of the yield and selectivity during the dehydrogenation of a steam diluted ethylbenzene (molal ratio water/ethylbenzene, 18 :I) one notices the superiority of the catalyst with modified porosity, "*B*", over "catalyst *A*" in yield as well as in selectivity.

To conclude, by combining harmoniously the kinetic properties and those of porous structure, we have obtained a catalyst with the desired qualities : high yields and selectivity at a high thermal working regime, without increasing the pressure drop on catalytic layer. The above performances were confirmed by a commercial practice.

Revue Roumaine de Chimie, **19**, 7, 1279–1282 (1974)

RARE EARTH ION EXCHANGE OF SYNTHETIC FAUJASITE SUBSTITUTED ISOMORPHOUSLY BY BORON

PETRU ONU and VASILE ABABI

Department of Chemical Technology, "Al. I. Cuza" University, Iași, Str. 23 August, nr. 11,
Romania.

Received May 25, 1973.

We studied the ion exchange capacity for europium and uranyl of synthetic faujasite zeolites, substituted isomorphously by boron. The ion exchange process is comparatively analysed relative to that involving X or Y type zeolites but without boron in their composition. Also, a few data about the thermal stability of the investigated samples are presented.

Faujasite zeolites have pores with a cross section of about 8 – 9 Å, which allow a great number of saturated and aromatic hydrocarbons to diffuse to the inside of the cavities. For this reason, these zeolites have important practical applications, among which their use in the different catalysis process is of great interest.

From the point of view of the catalytic activity, and their thermal stability, most important are faujasite zeolites in the alkaline earth metals form and especially those in the rare earth form.[1-3]

The latest investigations showed that besides zeolites with molecular sieve properties in the $Na_2O - Al_2O_3 - SiO_2 - H_2O$ system, it is also possible to form zeolites with aluminium and silicon, or only with one of these to be substituted isomorphously by other elements.[4]

This paper presents data concerning the ion exchange study with europium and uranyl on faujasite zeolites, substituted isomorphously by boron. This type of zeolites has been prepared hydrothermally by us, and the practical data with respect to their synthesis and structural adsorptive characterization was reported in a previous paper. [4]

From the cited literature it has resulted that no detailed study was reported up to now with regard to ion exchange with europium and uranyl on molecular sieves and especially on those substituted isomorphously by boron.

---

[1] D. H. Hickson and S. M. Csicsery, *J. Catalysis*, **10**, 27 (1968).

[2] P. E. Pickert, A. P. Bolton and M. A. Lanewala, *Chem. Eng. Progr., Symp.*, **63**, 50 (1967).

[3] P. B. Venuto and P. S. Landis, *Adv. Catalysis*, **1968**, p. 259.

[4] P. Onu and V. Ababi, *Materiale de construcție*, **2**, 1973. Under press.

EXPERIMENTAL SECTION

For the determination of ion exchange capacity of the zeolites substituted by boron, we have chosen the samples number 43, 44 and 46,[4] comparatively with two reference samples without boron; one of Y type and the other of 13X type. The composition of these samples, expressed by the mole ratio between SiO_2, Al_2O_3 and B_2O_3 is presented in table 1.

Table 1

The chemical composition of the investigated zeolites

Sample	SiO_2/Al_2O_3	$SiO_2/Al_2O_3 + B_2O_3$
43	2.77	2.77
44	2.90	2.88
46	3.42	3.00
Y	4.40	
13X	2.70	—

For all determinations carried out by us, the reagents used were 0.3 N $EuCl_3.6H_2O$ and $(CH_3 - COO)_2UO_2$ solutions and the contact time and the ion exchange temperature were varied so as to obtain different degrees of exchange.

The variation of the exchange capacity for the UO_2^{2-} and Eu^{3+} ions, for all above mentioned samples is represented in figures 1 and 2.

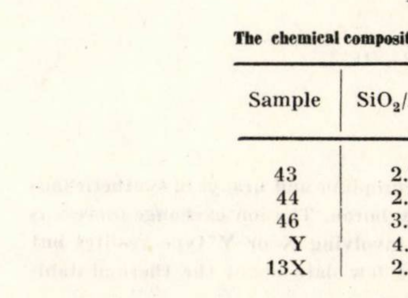

Fig. 1. — The exchange capacity variation for europium vs. time and for 25° temperature: 1 — Y; 2 — 46; 3 — 44; 4 — 13X; 4 — 43.

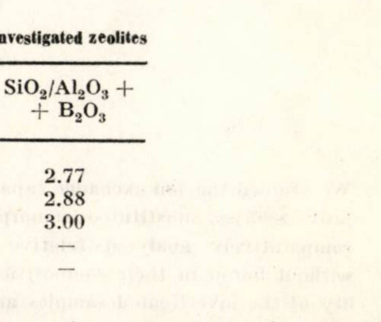

Fig. 2. — The exchange capacity variation for uranyl ion vs. time and contact time sample 46.

The contact time was varied from 10 minutes to 28 hours and the temperature between 25 and 85°. On the basis of the practical data it was found that the ion exchange process can be conducted in such a manner as to substitute either only the sodium ions from S_{III} positions, or also those from S_{II} positions.

RESULTS AND DISCUSSION

Kinetics of the ion exchange process shows that the ion exchange capacity for a certain contact time is greater for samples number 43,44 and 46, compared to that of Y sample. It is explicable because the $SiO_2/Al_2O_3 + B_2O_3$ ratio in our synthesis samples is lower than that of the Y sample. At the same contact time these data prompt us to consider that the windows of the cavities of the samples obtained by us are large enough and they allow a rapid diffusion of the ions from the inside to the outside and vice versa. As a result of the fact that the openings of the pores which link the cavities to each other have a sufficiently large diameter, both in our samples and in the reference samples, the rate of the ion exchange process at the first contact with europium solutions is high enough and after 10 minutes about 14% of the total sodium ions are exchanged. This value is about similar to the percentage of the sodium ions which are placed inside of the faujasite cavities, in the S_{III} positions. After an almost total substitution of sodium ions by those of europium, the rate of the exchange process slowly decreases, so that for 10 hours contact time, only 47% of the total number of sodium ions of sample 46 are exchanged by europium. As regards the rate of the europium exchange process for a given temperature and a certain contact time, the investigated samples are situated in the following order : $43 > 13X > 44 > 46 > Y$.

The temperature influence on the ion exchange process with europium is insignificant. This may be illustrated by the fact that at a temperature of 25° and 24 hours contact time, the degree of exchange on the Y sample is 56.68% and at 85°, for the same contact time, it is only 64.98%. It also results from these data that for a 24 hours contact time and at 85° the ion exchange process involved only 91% of the total sodium ions, placed in the S_{II} positions. This demonstrates that not all S_{II} positions are identical and as accessible for ion exchange process, the influence of diffusion being more marked. The same observations may be reported for samples number 43, 44, 46 and 13X.

The sodium ions exchange from the S_I positions, placed inside the hexagonal prisms, is difficult to obtain with europium or uranyl ions and we consider that in our experiments, this did not take place. It is estimated that this drawback is due to the hydrated europium or uranyl radius, which has a higher value than that of the opening window of the hexagonal prism [2]. On the basis of the experiments the ion exchange of sodium ions by europium was found to have positive influence on the thermal stability of all the investigated samples.

Using the derivatographic method is was found that there is a great difference between the thermal stability of the Y sample in sodium form and that of the Y sample with 63.27% exchanged by europium. In this way it was found that the temperature at which the destruction of the crystalline structure takes place at maximum rate is 898° for the sample in the sodium form and 967° for the sample in the sodium-europium form. The same effect was also found for samples with boron in the network. It results from the analysis of the experimental data that the crystalline

---

[5] H. S. Sherry, *J. Colloid Inter. Science*, **28**, 288 (1968).

structure of the sample number 46, with 60.25% sodium exchanged, resists up to 858° temperature. This temperature is by 78° higher than the destruction temperature of the sample 46, but only in the sodium form. As regards the ion exchange with uranyl ion compared to europium, this takes place at a lower rate and is more dependent on the temperature. Thus, it was found that for an exchange only of the sodium ions placed in the S_{III} positions it is necessary to have a contact time of four hours at 25° or one hour for a temperature of 40°. This may be explained by the fact that the uranyl ion has a bigger radius than that of the europium and as a result, the diffusion to the exchange positions is lower.

Analysing the ion exchange capacity value we can find that in the case of the uranyl ion exchange, the sodium ions placed in the S I positions did not participate in the exchange process.

From the point of view of the thermal stability the samples in the uranyl form are inferior to those with europium. This is due to the uranium tendency to form high oxides more stable in the presence of oxygen and high temperatures.

CONCLUSIONS

The investigations of the ion exchange with rare earth by zeolites faujasite type substituted isomorphously or unsubstituted by boron led to the following conclusions :

— By the ion exchange method we have obtained zeolites of faujasite type substituted isomorphously by boron, in which sodium was replaced in different proportions by europium and uranyl.

— To exchange about the same quantity of sodium ions only from the S_{III} positions of a faujasite zeolite structure it is necessary to have a contact time of 10 minutes for europium and 4 hours for uranyl ions, at a temperature of 25°.

— According to the rate of the exchange process with europium for a given temperature and for a certain contact time, the investigated samples range in the order $43 > 13X > 44 > 46 > Y$.

— Replacement of sodium ions by those of europium for a faujasite structure substituted isomorphously or unsubstituted by boron, induces the increase of the network thermal stability, yet this remins lower than in the case of the same type of structure without boron. The thermal stability of zeolites with europium is higher than that of zeolites with uranyl.

COMPTES RENDUS

R. DAUDEL, ,,*Quantum theory of chemical reactivity*'', D. Reidel Publishing Company, Dodrecht. Holland, 1973, 158 p.

The aim of Professor Daudel's book is to point out how the application of quantum mechanics to the chemical phenomena may contribute to make clear a vital aspect of today chemistry, namely the chemical reactivity. As the author writes in the preface, it is intended for students as well as for physical-chemists and chemists, research workers and engineers taking an interest in quantum chemistry for its own sake or for its application in industry, pharmacology and the life sciences.

Divided into four chapters, the book is based on the transition state method used in order to expose the main factors which determine chemical equilibrium and rate constants.

The introduction of the first part presents the importance of the walls, the part played by the impurities and the intervention of the solvent, as factors determining the course of a reaction. After this brief introduction, the theory of Eyring and Polanyi is examined and equations are established for equilibrium constants in the gaseous phase as well as for rate constants of bimolecular, monomolecular and termolecular processes in the gaseous phase.

The second chapter contains an analysis of both intermolecular forces and methods of calculation of intermolecular interactions, being mainly devoted to the interactions between unbonded atoms.

As a conclusion of this part it is discussed the possibility to make conformational analysis based on these types of calculations and the limits of such theoretical calculations of molecular conformation energy. The possibility to predict conformational equilibrium constants is also discussed.

In the third chapter, equilibrium constants of reversible reactions are treated, presenting the actual state of the quantum theory of balanced reactions in solution. There is a survey of the role played by different factors which determine oxido-reduction potentials, particularly the polarographic half-wave potentials, strength of acids and bases as well as the tautomeric equilibria. The solvent effect is underlined and some applications in biochemistry and in the analysis of the mechanism of mutations are presented.

The last part contains the examination of the methods which make it possible to estimate theoretically the rate constants of a few reactions of organic chemistry. This capter is an application of quantum chemistry methods to the study of nucleophilic, electrophilic and radical substitutions, addition and polymerization reactions and of some reactions in radiation chemistry and photochemistry.

The book contains, in a particularly clear and condensed style, the most significant information in this field. A large and meaningful list of papers is quoted and critical surveys of various aspects of the topics are presented.

In conclusion this book represents an excellent tool for chemists which are interested in the application of the most modern methods in the interpretation and prediction of the chemical reactivity of molecules.

Marina Olteneanu

NOTE POUR LES AUTEURS

La *Revue Roumaine de Chimie* publie des articles en anglais, français, russe, allemand ou espagnol. Les auteurs sont priés d'envoyer des articles, notes, communications et comptes rendus inédits.

Les manuscrits seront dactylographiés à deux intervalles. Les tableaux seront dactylographiés sur feuilles séparées, de même que la légende des figures. Les diagrammes seront tracés à l'encre de Chine sur papier calque. Les tableaux et les figures seront numérotés par des chiffres arabes, en nombre strictement nécessaire. Prière de ne pas inscrire les mêmes données dans les tableaux et les figures. Les formules chimiques seront incluses dans le texte ; en outre, elles seront transcrites sur des feuilles séparées. Les auteurs sont priés d'indiquer les caractères italiques (en soulignant les lettres au crayon), ainsi que tout autre caractère spécial. L'ordre des références bibliographiques sera celui de leur mention dans le texte ; le nom de l'auteur sera précédé de l'initiale du prénom ; les publications périodiques seront présentées suivant les prescriptions internationales. Les références seront ajoutées à la fin de l'article ; elles paraîtront comme des notes, au bas de la page. Le texte sera précédé d'un résumé, comprenant 15 lignes au maximum.

L'entière responsabilité du contenu des articles appartient aux auteurs. On publie des articles dus aux collaborateurs roumains ou étrangers. Les auteurs recevront 50 tirés à part.

PRINTED IN ROMANIA

TRAVAUX PARUS AUX ÉDITIONS DE L'ACADÉMIE DE LA RÉPUBLIQUE SOCIALISTE DE ROUMANIE

MARIA FITI, **Dozimetria chimică a radiațiilor ionizante** (La dosimétrie chimique des radiations ionisantes), 1973, 240 p., 13,50 lei.

MIHAI FLORESCU, **Eficiența economică a cercetării științifice** (L'efficience économique de la recherche scientifique), 1972, 115 p., 15 lei.

GEORGETA LĂZĂRESCU, **Sistematizarea informațiilor în Chimia organică** (La systématisation des informations dans la chimie organique), 1972, 252 p., 10,50 lei.

P. BALTĂ et E. BALTĂ, **Introducere în chimia fizică a stării vitroase** (Introduction à la chimie physique de l'état vitreux), 1971, 240, 15,50 lei.

LYDIA-MARIA VAICUM, **Biodegrabilitatea detergenților** (La biodégrabilité des détergents), 1971, 254 p., 16 lei.

TIBERIU NĂȘCUȚIU, **Metode radiometrice de analiză** (Méthodes radiométriques d'analyse), 1971, 346 p., 19,50 lei.

I. ZUGRĂVESCU et L. STOICESCU-GRIVETZ, **Polimeri heterociclici** (Polymères hétérocycliques), 1971, 190 p., 9,50 lei.

CRISTOFOR SIMIONESCU et C. V. UGLEA, **Fracționarea compușilor macromoleculari** (Fractionnement des composés macromoléculaires), 1962, 292 p., 18,50 lei.

I. MAXIM, **Materiale nucleare** (Matériaux nucléaires), 1969, 444 p., 30 lei.

CRISTOFOR SIMIONESCU et CLEOPATRA VASILIU-OPREA, **Mecanochimia compușilor macromoleculari** (La mécanochimie des composés macromoléculaires), 1967, 344 p., 23,50 lei.

CORNEL BODEA et collab., **Tratat de biochimie vegetală**, partea I, **Fitochimie** (Traité de biochimie végétale, Ire partie, Phytochimie), Ier vol., 1964, 747 p. + 4 annexes + 2 pl., 31 lei ; IIe vol., 1965, 1262 p., 1 pl., 56 lei ; IIIe vol., 1967, 773 p., 35 lei.

V. GHEȚIE et V. MICUȘAN, **Analiza imunochimică. Teorie și practică** (Analyse immunochimique. Théorie et pratique), 1966, 369 p., 28 lei.

R. PORTOCALĂ et L. POPA, **Acizii ribonucleici celulari și virali** (Les acides ribonucléiques cellulaires et viraux), 1966, 375 p., 8 pl., 26 lei.

TIBERIU NĂȘCUȚIU, **Metode radiochimice de analiză** (Méthodes radiochimiques d'analyse), 1973, 384 p., 23 lei.

1974 DEC 17

I.P.I. – c. 1359

43 426

Lei 25.—

F 1103

ACADÉMIE DE LA RÉPUBLIQUE SOCIALISTE DE ROUMANIE

R

REVUE ROUMAINE DE CHIMIE

REFERÁLVA

TOME 19
N° 8
Août 1974

RECHAX, 19, *8*, 1285–1414 (1974)

ÉDITIONS DE L'ACADÉMIE DE LA RÉPUBLIQUE SOCIALISTE DE ROUMANIE

Rev. Roumaine Chim. 19, *8*, p. 1285–1414 (1974), Bucarest

ACADÉMIE DE LA RÈPUBLIQUE SOCIALISTE DE ROUMANIE

COMITÉ DE RÉDACTION

Rédacteur en chef :

I. G. MURGULESCU, membre de l'Académie de la République Socialiste de Roumanie

Rédacteurs en chef adjoints :

A. T. BALABAN et V. EM. SAHINI, membres correspondants de l'Académie de la République Socialiste de Roumanie

Collège de rédaction :

EM. BRATU, ELENA CEAUŞESCU, ECATERINA CIORĂNESCU-NENITZESCU, C. DRĂGULESCU, RALUCA RIPAN, CR. SIMIONESCU, membres de l'Académie de la République Socialiste de Roumanie; P. SPACU, membres correspondant de l'Académie de la République Socialiste de Roumanie; MARGARETA AVRAM, D. I. MARCHIDAN, I. MOLDOVAN, G. NIAC et. D. SĂNDULESCU

Toute commande de l'ètranger (fascicules ou abonnements) sera adressée à Intreprinderea Rompresfilatelia, Boîte Postale 2001, telex 011631, Bucarest, Roumanie

Les manuscrits, les livres et les revue proposés en èchange, ainsi que toute correspondance seront envoyés à la rédaction

REVUE ROUMAINE DE CHIMIE

23, str. Dumbrava Roşie, Bucarest, Roumanie, téléphone 12 41 60

ÉDITIONS DE L'ACADÉMIE DE LA RÉPUBLIQUE SOCIALISTE DE ROUMANIE
3 bis, str. Gutenberg, Bucarest, Roumanie, téléphone 164079

REVUE ROUMAINE
DE
CHIMIE

ORSZÁGOS MŰSZAKI KÖNYVTÁR ÉS DOKUMENTÁCIÓS KÖZPONT

Tome 19, N° 8 Août 1974

NAROTTAM P. BANSAL, Interdiffusion coefficients of silver (I) in molten sodium nitrate — alkaline earth nitrates mixtures 1287–1295

D. FĂTU and ALEXANDRA SCHIOPESCU, Thermal decomposition of potassium ferrate. VI 1297–1302

CONSTANȚA PÂRLOG, D. CIOMÂRTAN, D. SĂNDULESCU and D. NEGOIU, The crystal structure of ammonium hexahalogenoosmiate and its dinitrogen compounds 1303–1306

A. C. BANCIU and P. SPACU, Ni(II) chelates synthetized with 1-methyl-2-carbethoxy-glyoxalanil-(1)-methoxy-phenylhydrazones-(2) 1307–1315

R P. MARKOV, S. CHORBADJIEV and V. TARPANOV, On the reactivity of some metal-sulphur combinations in liquid ammonia 1317–1321

A. T. BALABAN, Chemical graphs. XXII. Valence isomers of heteroannulenes or of substituted annulenes. Coisomeric cubic multigraphs 1323–1342

M. BANCIU, ECATERINA DRAGU, DOINA GEORGESCU and ECATERINA CIORĂNESCU, Carbonium ion reactions. X. Nitrous acid deamination of 5-aminomethyl-5H-6,7-dihydro-dibenzo[*a*, *c*]cycloheptene 1343–1349

R ALI ALI KHALAF and ROYSTON M. ROBERTS, Modern Friedel-Crafts chemistry. V. The fragmentation and dealkylation of straight-chained diphenylbutanes under the influence of water-activated aluminium chloride at 100°C 1351–1360

ALI ALI KHALAF, Modern Friedel-Crafts chemistry. VII. On the question of group participation in the rate-determining ionization step during inter- and intramolecular Friedel-Crafts alkylations and the mechanism of formation of 1-methyltetralin during the $AlCl_3$-catalyzed reaction of 1-chloro-2-methyl-4-phenylbutane 1361–1372

ALI ALI KHALAF, Modern Friedel-Crafts Chemistry. VIII. Cyclialkylations of some aryl- and diarylalkanols in the presence of the mild $AlCl_3/CH_3NO_2$ catalyst 1373–1380

N. S. BĂRBULESCU and MINODORA LECA, Elimination reactions in the 8-substituted-tricyclo[$7.3.1.0^{2,7}$]tridecane series. V. Configuration of 8-substituted-tricyclo-[$7.3.1.0^{2,7}$]tridecen-13-ols 1381–1391

R D. S. VASILESCU, Alternating tendency in copolymerization. I. Copolymerization of butyl vinyl ethers with acrylic monomers. 1393–1405

H. NAȘCU and C. LITEANU, The effect of S-chamber shape on the separation of ethanolamines by thin layer chromatography 1407–1411

COMPTES RENDUS 1413

Rev. Roumaine Chim. **19**, *8*, p. 1285–1414 (1974), Bucarest

Revue Roumaine de Chimie, 19, 8, 1287–1295 (1974)

INTERDIFFUSION COEFFICIENTS OF SILVER (I) IN MOLTEN SODIUM NITRATE – ALKALINE EARTH NITRATES MIXTURES

NAROTTAM P. BANSAL

Department of Chemistry, Ramjas College, University of Delhi,
Delhi – 110007, India

Received November 13, 1973

The interdiffusion coefficients D, of silver (I) in molten binary eutectic $NaNO_3-M(NO_3)_2$ (M = Ba, Sr, Ca) mixtures have been determined in the temperature range 572–692 K using a chronopotentiometric method. The temperature variation of D in the three melts in the range studied could be expressed, respectively, by the equations

$$D = 0.633 \times 10^{-3} \exp\left(-\frac{4070}{RT}\right),$$

$$D = 1.159 \times 10^{-3} \exp\left(-\frac{4704}{RT}\right),$$

$$D = 0.648 \times 10^{-3} \exp\left(-\frac{4175}{RT}\right).$$

Values of D in these solvents have been compared with those available in other nitrate melts and the effect of the presence of divalent alkaline earth metal cations in the solvent on the diffusion process has been discussed. Applicability of Stokes-Einstein equation to $NaNO_3-Ca(NO_3)_2$ system has also been described.

INTRODUCTION

The diffusion coefficients in molten melts are important for relating thermodynamic and transport properties,[1] evaluation of structural models for transport processes [2] and the theoretical equations of electroanalytical chemistry.[3,4] Of the several techniques employed for the determination of diffusion coefficients in molten salts, mention may be made of the constant mass diffusion cell (Laity and Miller[5]), the gravimetric method using a porous frit (Sjoblom[6,7]), polarography[8,9] and oscillographic polarography.[10,11] More recently chronopotentiometry has also been applied for the determination of diffusion coefficients of various metal ions in different molten salts[12–15] and their mixtures.[15–18] Laity and McIntyre[19] have shown, via irreversible thermodynamics, that at low solute concentrations the chronopotentiometric diffusion coefficient of an ion may be equated to both its interdiffusion and self-diffusion coefficients.

---

[1] C. A. Angell, *J. Phys. Chem.*, **70**, 2793 (1966).
[2] C. T. Moynihan, *J. Phys. Chem.*, **70**, 3399 (1966).
[3] J. H. Wang, *J. Amer. Chem. Soc.*, **76**, 1528 (1954).
[4] C. A. Angell and J. W. Tomlinson, "Electrochemistry", 1st Australian Conf., Sydney, Feb. 13–15 and Hobart, Feb. 18–20, Pergamon Press, Oxford, 1964, p. 557.

In chronopotentiometry, the solution of a depolarizer in the presence of a large excess of an indifferent electrolyte is electrolysed at constant current and variations of the potential of the microelectrode with time are recorded *versus* a suitable reference. The diffusion coefficient (D) of the electroactive species is computed from the equation

$$D^{\star} = \frac{4 i_0^2 \, \tau}{\pi F^2 \, n^2 \, c^{02}} \tag{1}$$

where i_0 is the current density (amp cm^{-2}), τ the transition time (sec), F the Faraday constant, n the number of electrons required in the reduction process and C° the bulk concentration (mole cm^{-3}) of the depolarizer. In the derivation of eq. (1) it has been assumed that the whole electrolysis current is used in the Faradaic process, but actually a part of it is always consumed in charging the electrode double layer capacitance. However, it has been shown that eq. (1) may still be employed provided that τ is much larger than the time used in charging the double layer.

---

[5] R. W. Laity and M. P. Miller, *J. Phys. Chem.*, **68**, 2145 (1964).

[6] C. A. Sjöblom, *Z. Naturforsch.*, **20a**, 1572 (1965).

[7] C. A. Sjöblom and A. Behn, *Z. Naturforsch*, **23A**, 1774 (1968).

[8] J. Braunstein, L. Orr, A. R. Alvarez-Funes and H. Braunstein, *J. Electroanal. Chem.*, **15**, 337 (1967).

[9] D. Inman, D. G. Lovering and R. Narayan, *Trans. Faraday Soc.*, **63**, 3017 (1967).

[10] W. K. Behl and H. C. Gaur, *J. Electroanal. Chem.*, **32**, 293 (1971).

[11] K. Kawamura, *Electrochim. Acta*, **12**, 1233 (1967).

[12] C. T. Moynihan and C. A. Angell, *J. Phys. Chem.*, **74**, 736 (1970).

[13] S. Sternberg and C. Herdlicka, *Rev. Roumaine Chim.*, **14**, 991 (1969).

[14] S. Sternberg and C. Herdlicka, *Rev. Roumaine Chim.*, **15**, 343 (1970).

[15] C. E. Thalmayer, S. Bruckenstein and D. M. Gruen, *J. Inorg. Nuclear Chem.*, **26**, 347 (1964).

[16] H. A. Laitinen and H. C. Gaur, *Analyt. Chim. Acta*, **18**, 1 (1958).

[17] Yu. K. Delimarskii, A. B. Gorodyskii and V. V. Kuzmovich *Coll. Czech. Chem. Comm.*, **25**, 3056 (1960).

[18] F. Caligara, L. Martinot and G. Duyckaerts, *Bull. Soc. chim. belges*, **76**, 15 (1967).

[19] R. W. Laity and J. D. E. McIntyre, *J. Amer. Chem. Soc.*, **87**, 3806 (1965).

* The thermodynamic diffusion coefficient, D', is related to the ordinary diffusion coefficient D as

$$D' = D / \left[1 + \frac{d \ln \gamma}{d \ln X} \right]$$

where γ and X are the activity coefficient and mole fraction of the solute. In the present investigation, the concentration of Ag(I) is very low so that $d \ln\gamma / d \ln X$ may be taken as zero.

The present communication reports the interdiffusion coefficients of Ag(I) in molten binary eutectic $NaNO_3-M(NO_3)_2$ (M = Ba, Sr, Ca) mixtures in the temperature range 572–692 K using the chronopotentiometric method with a view to examine the influence of the presence of doubly charged alkaline earth cations on the diffusion process of Ag(I) in the mixed solvents. The Arrhenius activation energies for the diffusion process have also been computed.

MATERIALS AND EXPERIMENTAL METHOD

Sodium nitrate, barium nitrate and silver nitrate were AnalaR(BDH) chemicals and were used without further purification except for drying. Strontium nitrate, laboratory reagent (BDH), was twice recrystallized from demineralized water and dried at 523–573 K for several days. Anhydrous calcium nitrate was prepared from the tetrahydrate by melting under reduced pressure when most of the water was expelled, finely powdering the solid mass and vacuum drying at 573 K for 6–8 hrs.

The method of solvent preparation was essentially the same in all cases and has been described elsewhere.[20,21] About 2 moles of the eutectic mixture was used for each run. A slow stream of dry and oxygen free nitrogen was always kept flowing over the melt surface during the period of measurements. The temperature was measured with a calibrated chromel-alumel thermocouple and controlled within $\pm 1°$ of the set value.

The micro-electrode was a small platinum foil, welded to a small length of platinum wire emerging from a platinum-soda lead glass seal in a piece of glass tubing. The surface area of the microelectrode, as determined from optical micrometry, was 0.398 cm^2. The counter electrode was a large platinum foil of area *circ.* 2 cm^2. The reference electrode was Ag^2/Ag in the melt as solvent. Both the reference and the counter electrodes were separated from the main solution by glass tubes having fritted discs of porosity G-4 at the bottoms.

An oscilloscope method of recording the chronopotentiograms was employed and details of the set up have already been described earlier.[20,22] The potential-time traces were displayed on the long persistence screen of a Hewlett-Packard (model 122-A) oscilloscope, the time base being provided by Z-modulation of the electron beam with a square wave from a Hewlett-Packard function generator (model 3300-A). The traces were photographed with a Fairchild-Dumont (type 450A) camera attachment on 35 mm Indu IP-200 panchromatic film. The analysis was made from enlargements made with a Nikon Profile Projector.

At the same temperature 4–5 chronopotentiograms were recorded using different current densities. After recording a chronopotentiogram, the metal deposited on the microelectrode surface was anodically stripped off, the electrode wiggled for a few seconds and the solution allowed to attain equilibrium for a few minutes before taking the next observation.

RESULTS AND DISCUSSION

The method described by Thalmayer *et al.*[15] was used for determining the transition time from the chronopotentiograms. The uncertainty in τ was less than 2%. τ was kept in the range 0.4–1.5 sec; for smaller τ, the time used in charging the electrical double layer becomes significant and for larger τ the diffusion layer extends sufficiently farther from the electrode surface into the solution such that convection interferes.

---

[20] N. P. BANSAL, *Ph. D. Thesis*, University of Delhi, 1972.

[21] H. C. GAUR and N*. P. BANSAL, *Indian J. Chem.*, **9**, 1273 (1971). *J.C.S. Faraday I*, **68**, 1368 (1972).

[22] H. C. GAUR, N. P. BANSAL and S. K. JAIN, *Indian J. Chem.* (in press).

The concentration of the depolarizer and the quantity of the melt were such that 40–50 chronopotentiograms could be run on a sample without affecting the initial depolarizer concentration. Densities of the solvent at different temperatures were taken from the work of McAuley *et al.*[23]

Verification of Sand's Equation

Typical data of τ measurements for the reduction of Ag(I) in molten $NaNO_3-Sr(NO_3)_2$ at 611 K using different current densities for various $C^\circ_{Ag}+$'s are presented in Table 1. Figures 1 and 2 represent the plots

Table 1

Typical chronopotentiometric data for the diffusion of silver (I) in molten $NaNO_3-Sr(NO_3)_2$ at 611 K

$C^\circ_{Ag^+} \cdot 10^5$ (mol cm^{-3})	$i_0 \cdot 10^3$ (amp cm^{-2})	τ (sec)	$i_0\tau^{\frac{1}{2}} \cdot 10^2$ (cmp cm^{-2} sec$^{\frac{1}{2}}$)	$\frac{i_0\tau^{\frac{1}{2}}}{C^\circ_{Ag^+}} \cdot 10^{-3}$ (amp cm sec$^{\frac{1}{2}}$ mol^{-1})
0.528	2.019	0.94	0.196	
	3.031	0.46	0.206	
	2.808	0.47	0.192	
	2.298	0.68	0.189	
			av. 0.196	0.371
1.504	5.470	1.19	0.597	
	5.997	0.98	0.597	
	6.249	0.92	0.600	
	6.728	0.82	0.609	
			av. 0.600	0.399
2.454	8.957	1.17	0.969	
	9.434	1.09	0.987	
	10.392	0.91	0.989	
	10.909	0.83	0.993	
	9.882	1.00	0.985	
			av. 0.986	0.401
3.195	12.767	0.98	1.267	
	13.379	0.91	1.279	
	11.879	1.17	1.285	
	13.770	0.89	1.299	
			av. 1.283	0.401
4.115	16.429	1.02	1.663	
	15.765	1.13	1.671	
	16.813	1.00	1.681	
	18.414	0.85	1.699	
	18.996	0.82	1.720	
			av. 1.687	0.410
4.977	19.206	1.05	1.965	
	18.776	1.14	2.005	
	18.210	1.22	2.010	
	19.845	1.03	2.014	
	21.520	0.89	2.031	
			av. 2.006	0.403

---

[23] W. J. McAuley, E. Rhodes and A. R. Ubbelohde. *Proc. Roy. Soc.*, **289A**, 151 (1966).

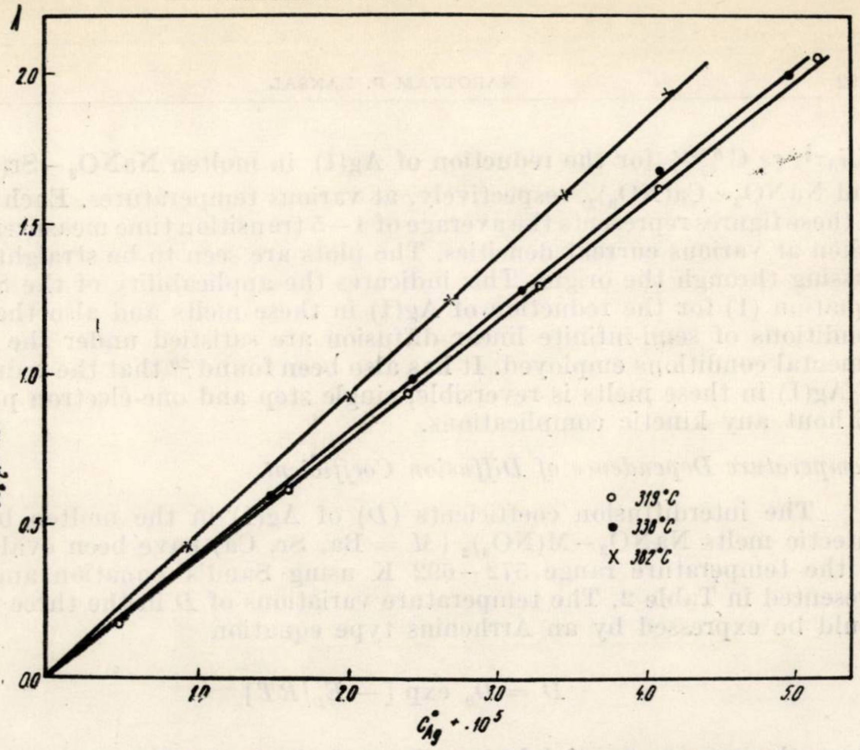

Fig. 1. — Plots of $i_0\tau^{\frac{1}{2}}$ vs. $C^0_{Ag}+$ in molten $NaNO_3 - Sr(NO_3)_2$ at various temperatures.

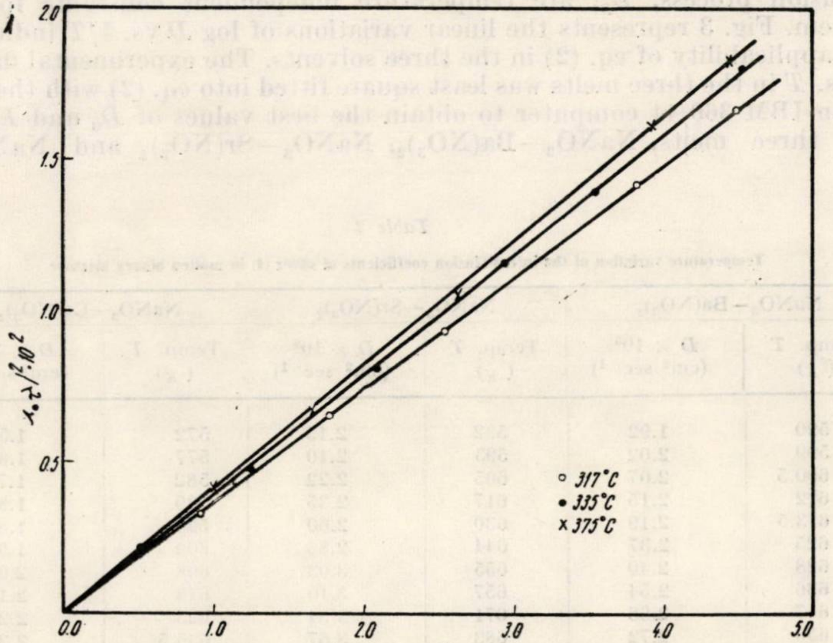

Fig. 2. — Variations of $i_0\tau^{\frac{1}{2}}$ with $C^0_{Ag}+$ in molten $NaNO_3 - Ca(NO_3)_2$ at various temperatures.

of $i_0\tau^{\frac{1}{2}}$ *vs* $C^{0}_{Ag^+}$ for the reduction of Ag(I) in molten $NaNO_3-Sr(NO_3)_2$ and $NaNO_3-Ca(NO_3)_2$, respectively, at various temperatures. Each point in these figures represents the average of 4—5 transition time measurements taken at various current densities. The plots are seen to be straight lines passing through the origin. This indicates the applicability of the Sand's equation (1) for the reduction of Ag(I) in these melts and also that the conditions of semi-infinite linear diffusion are satisfied under the experimental conditions employed. It has also been found [20] that the reduction of Ag(I) in these melts is reversible, single step and one-electron process without any kinetic complications.

Temperature Dependence of Diffusion Coefficient

The interdiffusion coefficients (D) of Ag(I) in the molten binary eutectic melts $NaNO_3-M(NO_3)_2$ (M = Ba, Sr, Ca) have been evaluated in the temperature range 572—692 K using Sand's equation and are presented in Table 2. The temperature variations of D in the three melts could be expressed by an Arrhenius type equation

$$D = D_0 \exp\left[-E_D/RT\right] \qquad (2)$$

where the pre-exponential factor, D_0, and the activation energy for the diffusion process, E_D, are temperature independent constants for the system. Fig. 3 represents the linear variations of log D vs. $1/T$ indicating the applicability of eq. (2) in the three solvents. The experimental data of D vs. T in the three melts was least square fitted into eq. (2) with the help of an IBM 360/44 computer to obtain the best values of D_0 and E_D. In the three melts, $NaNO_3-Ba(NO_3)_2$, $NaNO_3-Sr(NO_3)_2$ and $NaNO_3-$

Table 2

Temperature variation of the interdiffusion coefficients of silver (I) in molten binary mixture

$NaNO_3-Ba(NO_3)_2$		$NaNO_3-Sr(NO_3)_2$		$NaNO_3-Ca(NO_3)_2$	
Temp. T ($^\circ K$)	$D \times 10^5$ ($cm^2\ sec^{-1}$)	Temp. T ($^\circ K$)	$D \times 10^5$ ($cm^2\ sec^{-1}$)	Temp. T ($^\circ K$)	$D \times 10^5$ ($cm^2\ sec^{-1}$)
590	1.92	592	2.15	572	1.58
599	2.02	593	2.10	577	1.60
600.5	2.07	605	2.22	582	1.71
612	2.15	617	2.35	589	1.80
613.5	2.19	630	2.60	590	1.88
625	2.37	644	2.86	600	1.96
628	2.40	655	3.03	608	2.04
636	2.54	657	3.10	613	2.10
647	2.68	671	3.34	625	2.22
656	2.72	683	3.67	636.5	2.31
667	2.88			650	2.34
675	3.01			662	2.73
684	3.11			674	2.89
$C^{\circ}_{Ag^+}$ at 623° K = 1.215×10^{-5} mole cm^{-3}		$C^{\circ}_{Ag^+}$ at 623°K = 2.588×10^{-5} mole cm^{-3}		$C^{\circ}_{Ag^+}$ at 623°K = 1.786×10^{-5} mole cm^{-3}	

$-Ca(NO_3)_2$, the temperature variations of D could be represented, respectively, by the following expressions

$$D = 0.633 \times 10^{-3} \exp\left(-\frac{4070}{RT}\right), \tag{3}$$

$$D = 1.159 \times 10^{-3} \exp\left(-\frac{4704}{RT}\right), \tag{4}$$

$$D = 0.648 \times 10^{-3} \exp\left(-\frac{4175}{RT}\right). \tag{5}$$

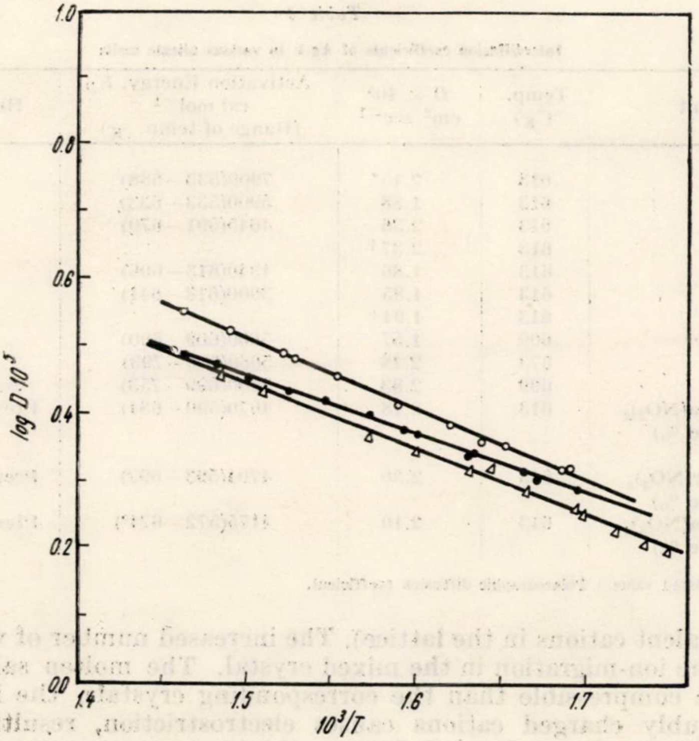

Fig. 3. — Arrhenius plots for the temperature variations of the diffusion coefficients of silver (I) in molten $NaNO_3-Ba(NO_3)_2$, ●, $NaNO_3-Sr(NO_3)_2$, ○, and $NaNO_3-Ca(NO_3)_2$, Δ.

Effect of the Presence of Divalent Cations on the Diffusion of Silver (I)

The data have also been analysed to study the influence of the introduction of divalent alkaline earth metal cations (Ba^{2+}, Sr^{2+}, Ca^{2+}) into the solvent on the diffusion of Ag(I) in the mixed melt. The values of the diffusion coefficients of Ag(I) along with the activation energies for diffusion process in various nitrate melts have been summarized in Table 3. The value of D is seen to be less in the three mixed melts studied as compared to that in pure $NaNO_3$. The specific conductance of these binary mixtures have also been reported [24-26] to be lower than of molten $NaNO_3$. On the other hand, incorporation of the divalent cations into crystals of uni-univalent halides and nitrates increases the extent of ionic migration (Wagner effect [27]). It has been pointed out that the extent of ion migration depends on the number of vacancies in a system. Incorporation of small concentrations of divalent cations in the solid solutions in uni-univalent crystals of halides and nitrates is considered merely to create an equivalent number of cation vacancies in the lattice to keep the whole assembly electrically neutral (one divalent cation will replace two monovalent cations in the lattice). The increased number of vacancies enhances the ion-migration in the mixed crystal. The molten salts being much more compressible than the corresponding crystals, the introduction of doubly charged cations causes electrostriction, resulting in a shrinkage of the free volume.[28] This would hinder ionic migration and consequently a decrease in ionic conductance and in the diffusion coefficient also, is observed. Since the sizes of Na^+ (0.95Å) and Ca^{2+} (0.99 Å) ions are virtually the same, a smaller value of D in $NaNO_3-Ca(NO_3)_2$ as compared to that in pure $NaNO_3$ can be considered to arise due to

Table 3

Interdiffusion coefficients of Ag(I) in various nitrate melts

Solvent	Temp. (°K)	$D \times 10^5$ $cm^2\ sec^{-1}$	Activation Energy, E_D cal mol^{-1} (Range of temp, °K)	Reference
$LiNO_3$	613	2.45*	7900(533–588)	13
	613	1.88	5900(533–633)	23
$NaNO_3$	613	2.36	4645(591–670)	14
	613	2.37+	—	11
KNO_3	613	1.86	4340(613–696)	13
	613	1.85	3900(613–641)	28
	613	1.94+	—	11
$RbNO_3$	609	1.57	5600(609–690)	14
$CsNO_3$	673	2.48	5060(683–793)	15
	699	2.83	5800(699–753)	14
$NaNO_3-Ba(NO_3)_2$ (94 : 6 mole %)	613	2.18	4070(590–684)	Present work
$NaNO_3-Sr(NO_3)_2$ (94 : 6 mole %)	613	2.30	4704(593–692)	Present work
$NaNO_3-Ca(NO_3)_2$ (94 : 6 mole %)	613	2.10	4175(572–674°)	Present work

* Interpolated value. + Polarographic diffusion coefficient.

---

[24] B. Cleaver, E. Rhodes and A. R. Ubbelohde, *Disscuss. Faraday Soc.*, **32**, 210 (1962).

[25] H. C. Gaur and S. K. Jain, *Indiana J. Chem.*, **10**, 624 (1972).

[26] H. C. Gaur, O. P. Mehta and S. K. Jain, *Indian J. Chem.*, **9**, 570 (1971).

[27] E. Koch and C. Wagner, *Z. phys. Chem.*, **38B**, 295 (1937).

charge differences on two ions. However, the trend in the values of D in other mixed melts is not explicable from the consideration of the differences in the charge densities alone.

Applicability of Stokes-Einstein Equation

The viscosity and the diffusion coefficient are correlated by the Stokes-Einstein equation

$$D_i = \frac{k\,T}{a\pi\eta r_i}\,, \tag{6}$$

where r_i is the radius of the diffusing ion (cm), η the viscosity of the solvent (g cm^{-1} sec^{-1}) and k the Boltzmann constant. In the classical formulation, the value of the constant a is 6 for the diffusion of a big particle. Li and Chang [29] have modified the S—E equation for the diffusion of a small particle and obtained a value of 4 for the constant a. Forcheri [30] has reported a value 4.6 for the self-diffusion coefficient of Tl in $TlNO_3$ and other diffusion coefficients in alkali nitrates. Sternberg and Herdlicka[13,14,31] have also found a value of 4.6 for the constant a for the chronopotentiometric diffusion coefficients of Ag(I) in molten alkali nitrates and chlorides. The radius of silver ion found in literature is $r_{Ag^+} = 1.13$ Å. The study of thermodynamic properties of silver halide-alkali halide systems [32] indicates that the radius of silver ion is smaller than 1.13 Å. The average kinetic radius of silver ion in molten alkali nitrates has been calculated [14] to be 1.00 Å. Using $r_{Ag^+} = 1.00$ Å, $a = 4.6$ and $\eta = 26.5 \times 10^{-3}$ poise for the viscosity [33] of molten $NaNO_3-Ca(NO_3)_2$ (94.0 : 6.0 mole %) at 623 K, the value of D as computed from equation (6) comes to be 2.24×10^{-5} cm^2 sec^{-1}. The experimental value of D in this melt at 623 K is 2.2×10^{-5} cm^2 sec^{-1}. This shows the applicability of the Stokes-Einstein equation indicating that the diffusion of Ag(I) ions is controlled by the viscous forces according to the Stokes mechanism. Similar comparison in the other melts could not be made due to the non-availability of the viscosity data.

The author is grateful to the Council of Scientific and Industrial Research, New Delhi, India, for the award of a research fellowship. Thanks are also due to Professor H. C. Gaur, Department of Chemistry, University of Delhi, for providing necessary facilities to carry out these investigations.

---

[28] K. Kawamura, *Denki Kagaku*, **38**, 12 (1970).

[29] J. C. U. Li and P. Chang, *J. Chem. Phys.*, **23**, 518 (1955).

[30] S. Forcheri and V. Wagner, *Z. Naturforsch*, **22a**, 1171 (1967).

[31] S. Sternberg and C. Herdlicka, *Rev. Roumaine Chim.*, **17**, 343 (1972).

[32] I. G. Murgulescu and S. Sternberg, *Z. phys. Chem.* (Leipzig), **219**, 114 (1962).

[33] E. Rhodes, W. E. Smith and A. R. Ubbelohde, *Trans. Faraday Soc.*, **63**, 1943 (1967).

Revue Roumaine de Chimie, **19**, *8*, 1287—1295 (1974)

Revue Roumaine de Chimie, 19, 8, 1297 – 1302 (1974)

THERMAL DECOMPOSITION OF POTASSIUM FERRATE. VI

D. FĂTU * and ALEXANDRA SCHIOPESCU**

* Department of Physical Chemistry, Faculty of Chemistry, University of Bucharest, Romania — Bd. Republicii nr. 64

** Department of Chemistry and Physics, Institute of Petroleum, Gas and Geology, Str. Traian Vuia nr. 6 — Bucharest, Romania

Received June 23, 1973

The thermal decomposition of potassium ferrate (VI) has been studied by means of the thermo-gravimetric analysis (T.G.A.), derivative thermogravimetric analysis (D.T.G.A.) and differential thermal analysis (D.T.A.). The thermal stability of this compound is discussed based on experimental results and some conclusions are presented regarding the kinetics of the decomposition process.

1. INTRODUCTION

The potassium ferrate (VI) has formed the subject of a number of studies which resulted in the development of some methods for its preparation in pure state.

Scholder *et al.*[1] studied the thermal decomposition of potassium ferrate (VI) in an oxygen atmosphere. It was shown that the process may be described by means of the following equations :

$$\text{I. } 2K_2FeO_4 \rightarrow K_3FeO_4 + KFeO_2 + 0_2 \qquad (T < 700)$$

$$\text{II. } K_3FeO_4 \rightarrow KFeO_2 + K_2O + 1/20_2 \qquad (T > 700)$$

The recent investigations carried out by Ichida [2] on the decomposition products of K_2FeO_4 failed to reveal through the Mössbauer effect the valence (V) state of iron. Since the X rays analysis indicates the presence of the compound $KFeO_2$ and the Mössbauer spectrum leads to the conclusion that the valence state is Fe (III) in the decomposition products, the author[2] proposes for the thermal decomposition the following equation:

---

[1] V. R. Scholder and K. Kraus, *Z. anorg. Chem.*, **268**, 279 (1952).

[2] Toshio Ichida, *Bull. Chem. Soc. Japan*, **46**, 71 (1973).

$$\text{III. } K_2FeO_4 \rightarrow KFeO_2 + KO_x + (2 - x/2)\, O_2$$

The present paper is an attempt to obtain additional information on the decomposition process of potassium ferrate (VI) by means of thermoanalytical approaches.

2. EXPERIMENTAL

The potassium ferrate (VI) was prepared according to the method postulated by Schreyer *et al.*[3] The T.G., D.T.G., D.T.A., and T. analysis curves were simultaneously plotted by means of a Paulik, Paulik, Erdey type M.O.M. Budapest – derivatograph. The samples were heated in the air at a 10°/min. rate. The reference substance used for obtaining D.T.A. curve was Al_2O_3 calcined at 1200°.

The reactant grains were studied during the decomposition by means of a Karl Zeiss Jena optical microscope.

3. RESULTS AND DISCUSSION

The inspection of the thermoanalytical curves (Fig. 1) shows that the air thermal decomposition of the freshly prepared potassium ferrate (VI) will begin at a temperature of 50° if the heating rate is 10°/min.

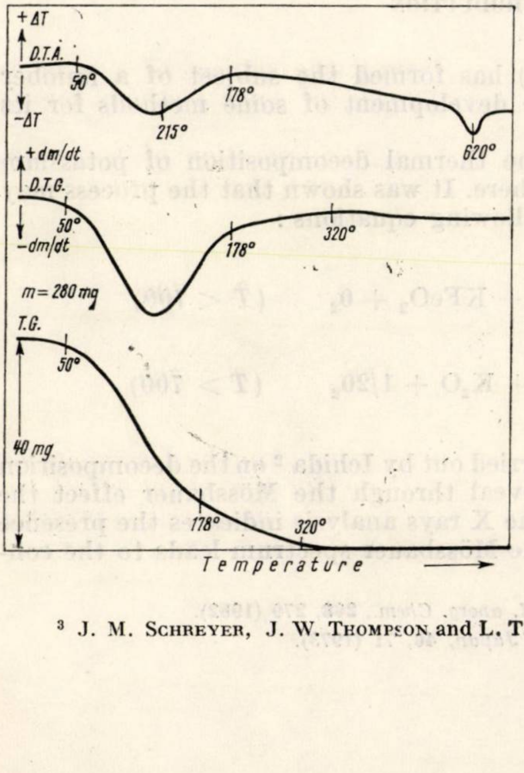

Fig. 1. – Aspect of thermoanalytical curves corresponding to the thermal decomposition of K_2FeO_4.

---

[3] J. M. Schreyer, J. W. Thompson and L. T. Ockerman, *Analyt. Chem.*, 22, 691 (1950).

The mass variation — determined from the data of the T.G. curve — corresponds to the release of 3/4 moles O_2 for each mole of decomposed K_2FeO_4. Since the solid decomposition products are ($K_2O.Fe_2O_3$) and the potassium oxide (K_2O), the overall stoichiometric equation of the process can be formulated as follows :

$$\text{IV. } 2\ K_2FeO_4 \rightarrow K_2O.Fe_2O_3 + K_2O + 3/2\ O_2$$

The reactant decomposition is total at a temperature of 320°. At temperatures ranging within 178°—380° the decomposition rate has a reduced value and as the thermal effect corresponding to this step is equally reduced, it cannot be observed on the D.T.A. curve.

At a temperature of 620° (see the D.T.A. curve) a second endothermic effects is recorded which is not accompanied by a mass variation this time. This endothermic effect may be assigned to the phase transition presented by ferric oxide (III).

The observations made on the microscope reveal some green — yellowish nuclei constitued of $K_2O.Fe_2O_3$ mixed with K_2O which arise and grow in the reactant mass in the course of the thermal decomposition.

Consequently the thermal decomposition process of potassium ferrate (VI) may be considered to be the result of the occurrence and growth of the nuclei.

The kinetics of such a process may be expressed by means of equation [4] :

$$\alpha = Kt^{(\lambda+\beta)}, \tag{1}$$

where α represents the decomposition degree

K — global rate constant

t — time

λ — number of dimensions according to which the growth of nuclei takes place

β — number of nucleation steps.

The formation of some bulky tridimensional nuclei is observed during the decomposition of potassium ferrate (VI). Therefore $\lambda = 3$. Considering that the nucleation takes place during one single step ($\beta = 1$) and that the temperature dependence of parameter K may be expressed by the Arrhenius' relation,

$$K = Z\,e^{-E/RT}, \tag{2}$$

in which

Z — represents the preexponential factor

E — the overall activation energy

R — the gas constant

T — the absolute temperature.

---

[4] P. W. M. Jacobs and F. C. Tompkins, "Chemistry of the Solid State", W. E. Garner, Butterworth Scientific Publications, London, 1955, p. 191.

Equation (1) may be thus transcribed :

$$\alpha = Z\, e^{-E/RT}\, t^{(\lambda+\beta)}\,. \tag{3}$$

Hence, in a log form, it results :

$$-\lg\frac{\alpha}{t^4} = -\lg Z + \frac{E(\text{cal/mol})}{4.575}\cdot\frac{1}{T}. \tag{4}$$

The above equation can be graphically verified by plotting the diagram $-\lg(\alpha/t^4) \div 1/T$.

The value $E = 9.2$ kcal/mole was determined for the activation energy from the angular coefficient of the straight line obtained in this manner (Fig. 2). From the ordinate at the origin it results that $Z = 0.76\ \text{mn}^{-4}$.

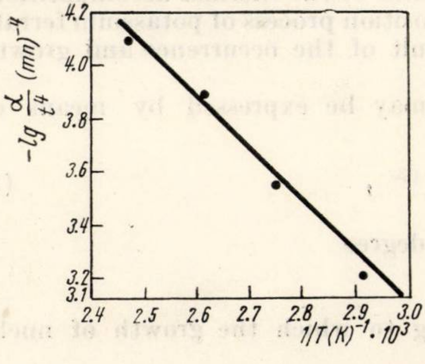

Fig. 2. — Graphical verification of equation (4).

The equation (4) describes satisfactorily the kinetics of the decomposition of potassium ferrate (IV) in the $0.05 \leqslant \alpha \leqslant 0.7$ range. The elimination of the volatile component and the formation of the new solid phase results in the division of crystals, so that by the end of the process the non-decomposed reactant grains are disseminated in the mass of the reaction product.

Assuming that the decomposition probability in the time unit is similar for any reactant grain, it results that the rate of the process $(d\alpha/dt)$ is proportional to the reactant fraction $(1-\alpha)$ existing at the moment t. Based on these hypotheses, [5] the rate of the final decomposition is formulated as follows :

$$\frac{d\alpha}{dt} = K(1-\alpha). \tag{5}$$

---

[5] A. K. Galwey, "Chemistry of Solids", Chapman and Hall, London, 1967, 139.

The temperature dependence of the K constant is described by Arrhenius' law, so that the preceding equation may be transcribed again under the form:

$$\frac{d\alpha}{dt} = Z'e^{-E/RT} \cdot (1 - \alpha), \tag{6}$$

where Z' and E' represent the preexponential factor and the activation energy of the final decomposition stage, respectively.

Finally in a log form, one obtains the equivalent expression

$$\lg \frac{d\alpha/dt}{1 - \alpha} = \lg Z' - \frac{E'}{4.575} \cdot \frac{1}{T} \cdot \tag{7}$$

The reaction rate (expressed in arbitrary units), the non-decomposed reactant fraction and the temperature are determined from the data of the D.T.G., T.G. and temperature (t) curves and this enables us to plot the diagram $\lg [(d\alpha/dt)/(1 - \alpha)] \div 1/T$ — (Fig. 3) and to calculate the values of the parameters Z and E. The equation (7) describes satisfactorily the kinetics of the process in the $0.6 \leqslant \alpha \leqslant 0.95$ range.

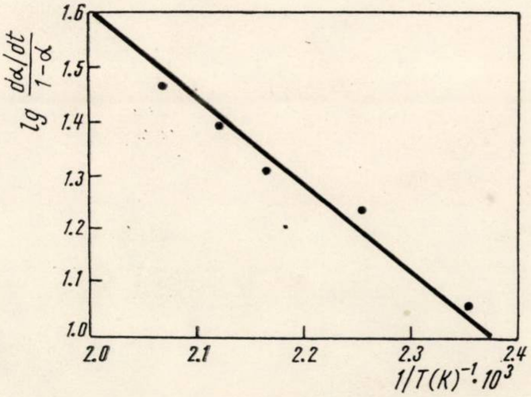

Fig. 3. — Graphical verification of equation (7).

The calculation leads to the results $E = 8.1$ kcal/mole, $Z = 3.1\ 10^3\ (\text{mn})^{-1}$.

The reaction heat is about 10.4 kcal/mole. This value has been determined from the area of D.T.A. peak.

To accomplish this, potassium ferrate (VI) was mixed in ≈ a 2/1 mass proportion with cadmium carbonate which was used as a standard substance. A thermal effect[6] $Q = 26.02$ kcal/mole was considered for the decomposition process of cadmium carbonate.

---

[6] A. G. Berg, "Vvedenie v Termografiyu" Izd. Akad. Nauk S.S.S.R. Moscow, 1961, 231.

4. CONCLUSIONS

When using a 10°/mn heating rate, the decomposition of the freshly prepared potassium ferrate (VI) begins at a temperature of 50°.

Taking into account the nature of the reaction products and the reaction of the sample mass, the decomposition process may be expressed by the stoichiometric equation:

$$2K_2FeO_4 \rightarrow K_2O.Fe_2O_3 + K_2O + 3/2\, O_2.$$

Within the $0.05 \leqslant \alpha \leqslant 0.7$ range the kinetics of the process is described by the equation $\alpha = kt^4$.

The final period of the process corresponds to a first order kinetics.

From the data provided by the D.T.A. curve the reaction heat was estimated at 10.4 kcal/mole value.

Revue Roumaine de Chimie, **19**, *8*, 1303–1306 (1974)

THE CRYSTAL STRUCTURE OF AMMONIUM HEXAHALOGENOOSMIATE AND ITS DINITROGEN COMPOUNDS

CONSTANȚA PÂRLOG, D. CIOMÂRTAN,* D. SĂNDULESCU,** D. NEGOIU ***

* Centre of Physical Chemistry, 31 Galaţi, Bucharest

** Institute of Petroleum, Gases and Geology, 2–6 Traian Vuia, Bucharest

*** University of Bucharest, Faculty of Chemistry, 89 Spl. Independenţei, Bucharest

Received January 17, 1971

The crystalline systems were determined and the parameters of the elementary cells were calculated for $(NH_4)_2[OsX_6]$ and $[Os(NH_3)_5N_2]X_2$ (X = Cl, Br). Compounds $(NH_4)_2[OsCl_6]$ and $(NH_4)_2[OsBr_6]$ crystallize in the cubic system and the parameters of the elementary cells are : a = 8.94 Å and a = 9.86 Å, respectively. Compounds $[Os(NH_6)_5N_2]Cl_2$ and $[Os(NH_3)_5N_2]Br_2$ belong to the tetragonal system having the parameters of the elementary cells : a = 17.50 Å, c = 16.73 Å and a = 20.74 Å, c = 18.63 Å, respectively.

Structural determinations based on the X-ray studies were made for compounds $K_2[OsCl_6]$ and $K_2[OsBr_6]$.[1] These compounds are isomorphic with those prepared by us. Early attempts at determining the structure of coordinative compounds with molecular nitrogen were made by Bottomely and Nyburg [2] for compound $[Ru(NH_3)_5N_2]Cl_2$ and were carried on with similar types of compounds of metals Cu, Ni, Re.[3–9]

The present paper aims at determining the parameters of the elementary cells and at establishing the spatial groups for compounds $(NH_4)_2[OsX_6]$ and $[Os(NH_3)_5N_2]X_2$ (X = Cl, Br).

[1] R. W. G. Wyckoff, "Crystal Structures", 3, 411, Wiley, New York, p. 341.

[2] F. Bottomley and S. C. Nyburg, *Acta Cryst.*, Sect. B, **24**, 1289 (1968).

[3] J. H. Enemark, B. R. Davis, J. A. McGiunety and J. A. Ibers, *Chem. Comm.*, 96 (1968).

[4] B. R. Davis, H. C. Payne and J. A. Ibers, *J. Am. Chem. Soc.*, **91**, 1240 (1969).

[5] B. R. Davis, H. C. Payne and J. A. Ibers, *Inorg. Chem.*, **12**, 2719 (1968).

[6] B. R. Davis, and J. A. Ibers, *Inorg. Chem.*, **9**, 2768 (1970).

[7] B. R. Davis, and J. A. Ibers, *Inorg. Chem.*, **10**, 578 (1971).

[8] P. W. Jally, K. Jonas, C. Kruger and Y. H. Tsay, *J. Organometal, Chem.*, **33**, 109 (1971).

[9] T. Uchida, Y. Uchida, M. Kidai and T. Kodama, *Bull. Chem. Soc. Japan*, **44**, 2883 (1971).

EXPERIMENTAL

The compounds were synthesized according to methods mentioned in the literature.[10,11] Diffraction diagrams on powders of the studied compounds $(NH_4)_2[OsCl_6]$, $(NH_4)_2[OsBr_6]$, $[Os(NH_3)_5N_2]Cl_2$ and $[Os(NH_3)_5N_2]Br_2$ were recorded on a HZG 1 type diffractometer (German DR) using radiation CuK_α (λ = 1.5405 Å) filtered through Ni.

RESULTS AND DISCUSSION

The results of the studies carried out are listed in the tables below. These exhibit, besides the experimental and calculated $1/d^2 Å^{-2}$, the indices (hkl) and I/I_0.

Table 1

Roentgenographic data for compound $(NH_4)_2[OsBr_6]$

$1/d^2$calc $[Å^{-2}]$	$1/d^2$exp. $[Å^{-2}]$	hkl	I/I_0
0.02427	0.0250	110	50
0.037516	0.0377500	111	100
0.100003	0.100000	220	48
0.11247	0.112500	221	57
0.14989	0.150000	222	96
0.17505	0.17500	321	13
0.20003	0.20000	400	63
0.24997	0.25000	420	25
0.29994	0.30000	422	54
0.337001	0.33700	511	34
		333	
0.41250	0.41250	522	15
		441	
0.45005	0.45000	600	17
		442	
0.47975	0.47975	611	16
		532	
0.49759	0.50000	620	16
0.60020	0.60000	444	10

Table 2

Roentgenographic data for compound $(NH_4)_2[OsCl_6]$

$1/d^2$calc. $[Å^{-2}]$	$1/d^2$exp. $[Å^{-2}]$	hkl	I/I_0
0.03043	0.03087	111	100
0.04134	0.04116	200	73
0.0821	0.08232	220	28
0.1131	0.1132	311	47
0.1647	0.1646	400	58
0.1958	0.1955	331	29
0.2029	0.2058	420	47
0.2470	0.2469	422	19
0.2779	0.2778	511	46
0.3299	0.3293	440	31
0.3607	0.3602	531	34
0.4120	0.4116	620	7
0.4433	0.4425	533	18
0.4945	0.4939	444	15
0.5243	0.5248	711	17
0.5336	0.5354	640	15
0.5762	0.5762	642	10
0.6075	0.6071	731	11

It results from table 1 that the crystalline system for compounds $(NH_4)_2[OsBr_6]$ is cubic, having the parameter of the elementary cell a = 8.94 Å. From the extinction conditions of the indices (khl) it results that :

hko ; h + k = 2n
hoo ; h = 2n
hkl ; no conditions.

---

[10] F. P. Dwyer and J. W. Hogarth, "Inorganic Synthesis", V, McGraw-Hill, New York, 204, 1957.

[11] A. D. Allen and J. R. Stevens, *Chem. Comm.*, 1147 (1967).

Based on these conditions, Pn3 and Pn3m are suggested as probable spatial groups.

The compound $(NH_4)_2[OsCl_6]$ also crystallizes in the cubic system having the parameter of the elementary cell a = 9.86 Å.

By following the extinction conditions of indices (hkl) :

hkl; h + k = 2n
h + l = 2n
k + l = 2n
hko; h + k = 2n
h, k = 2n
hkl; h + l = 2n

the following spatial groups were proposed for this compound : Fm3m, Fn32, $F\bar{4}3m$ and F23.

In the series of compounds of a $M_2^I[OsX_6]$ type, where $M_2^I = NH_4^+$, Na^+ and K^+ (X=Cl or Br), all compounds crystallize in the cubic system. However, the value of the parameter of the elementary cell decreases as the ionic radius of the alkaline metal decreases.

Table 3

The variation of the parameter of the elementary cell of the compounds $M_2[OsX_6]$ as a function of the ionic radius

Compound	M_I^+	Ionic radius [Å]	a [Å]
$K_2[OsCl_6]$	K^+	1.33	9.73
$(NH_4)_2[OsCl_6]$	NH_4^+	0.99 – 1.113	8.94
$Na_2[OsCl_6]$	Na^+	0.95	8.86
$K_2[OsBr_6]$	K^+	1.33	10.30
$(NH_4)_2[OsBr_6]$	NH_4^+	0.99 – 1.113	9.86
$Na_2[OsBr_6]$	Na^+	0.95	—

The results obtained in the case of the compounds with molecular nitrogen $[Os(NH_3)_5N_2]Cl_2$ and $[Os(NH_3)_5N_2]Br_2$ are further discussed. Both compounds crystallize in the tetragonal system.

The coordinative compound $[Os(NH_3)_5N_2]Br_2$ has the parameters of the elementary cell : a = 17.45 Å and c = 16.73 Å. The following extinction conditions of indices (hkl) result from table 4 :

hkl; no condition
hko; h + k = 2n
okl; no condition
hhl; l = 2n
ool; no condition

Based on the above, the spatial group $P4_2/nmc$ was proposed for this compound.

The results obtained for the similar substance $[Os(NH_3)_5N_2]Cl_2$ are listed in table 5, the parameters of the elementary cell being : $a = 20.74$ Å and $c = 18.63$ Å. The extinction conditions of indices (hkl) are :

hkl ; no condition
hko ; $h + k = 2n$
hhl ; no condition
okl ; $k + 1 = 2n$
ool ; no condition

and this leads to the following probable spatial group : $P4_2/nnm$.

Table 4

Roentgenographic data for compound $[Os(NH_3)_5N_2]Br_2$

$1/d^2$calc. [$Å^{-2}$]	$1/d^2$exp. [$Å^{-2}$]	hkl	I/I_0
0.0293	0.0293	003	100
0.0553	0.0555	014	3
0.0713	0.0720	240	24
0.0756	0.0755	233	29
0.0814	0.0814	005	55
0.0806		224	
0.0957	0.0947	025	6
0.1005	0.1002	243	26
0.1127	0.1122	144	10
0.1212	0.1212	350	11
0.1271	0.1274	442	4
0.1342	0.1348	352	4
0.1350		126	
0.1426	0.1422	260	18
0.1576	0.1576	063	3
0.1732		055	4
0.1733		354	
0.1736	0.1735	362	
0.1814	0.1826	336	6
0.1916	0.1914	037	8
0.2410		274	13
0.2412	0.2415	280	
0.2418		256	
0.2226	0.2217	028	22

Table 5

Roentgenographic data for compound $[Os(NH_3)_5N_2]Cl_2$

$1/d^2$calc. [$Å^{-2}$]	$1/d^2$exp. [$Å^{-2}$]	hkl	I/I_0
0.0313	0.03113	003	100
0.0378	0.0375	221	18
0.0430	0.04331	130	15
0.0528	0.0530	123	3
0.0640	0.0646	114	6
0.0808	0.0802	331	32
0.0872	0.0870	233	19
0.0867		005	
0.0909	0.0904	015	10
0.1081	0.1084	125	17
0.1173	0.1177	333	13
0.1285	0.1287	144	3
0.1334	0.1351	116	11
0.1376		440	
0.1462	0.1471	126	12
0.1463		350	
0.1548	0.1534	060	3
0.1560	0.1572	153	3
0.1739	0.1738	162	8
0.1904	0.1907	163	9
0.2073	0.2076	362	5
0.2085		037	
0.2076		453	
0.2150	0.2155	170	4
0.2257	0.2263	237	12
0.2366	0.2345	156	13
0.2546	0.2538	463	4
0.2629	0.2627	455	5
0.2808	0.2808	009	7
0.3062	0.3063	182	3
0.3183	0.3188	366	5

These coordination compounds have been observed to present a slight deviation from the cubic system, as the ratio $a/c = 1.04$, respectively 1.11. This fact compares well with the results obtained by Bottomely and Nyburg [2] who determined the crystalline systems for similar compounds with molecular nitrogen of Ru(II), compounds which crystallize in the cubic system.

Revue Roumaine de Chimie, 19, 8, 1307–1315 (1974)

Ni(II) CHELATES SYNTHETIZED WITH 1-METHYL-2-CARBETHOXY-GLYOXALANIL-(1)-METHOXY-PHENYLHYDRAZONES-(2)

A. C. BANCIU and P. SPACU

Center of Chemical Physics, Dumbrava Roşie, 23
Bucharest, Romania

Received December 21, 1973

Using the three 1-methyl-2-carbethoxy-glyoxalanil-(1)-methoxy-phenylhydrazones-(2) as ligands, depending on the preparation conditions, two different types of Ni(II) complexes were obtained, some of them containing the mentioned ligands and others having the anil group from the ligand molecule substituted by an imino group. The elemental analysis data, IR and electronic spectra as well as the magnetic measurements show that all prepared complexes are tetracoordinate chelates with a low spin square-planar arrangement of the Ni(II)-nitrogen bonds. The intense colour of the chelates is due to the charge transfer metal → ligand bands occurring in the visible range.

In the previous papers [1,2] Ni(II) complexes with different 1-methyl-2-carbethoxy-glyoxalanil-(1)-arylhydrazones-(2) have been already reported. In a very recent paper [3] the ligands and the complexes formed by the Co(II) ion with the three 1-methyl-2-carbethoxy-glyoxalanil-(1)-methoxy-phenylhydrazones-(2), (Ia—c) have also been studied.

The aim of the present note is to study the five Ni(II) complexes prepared with the compounds Ia—c. The preparation of these organic compounds has been described elsewhere.[3]

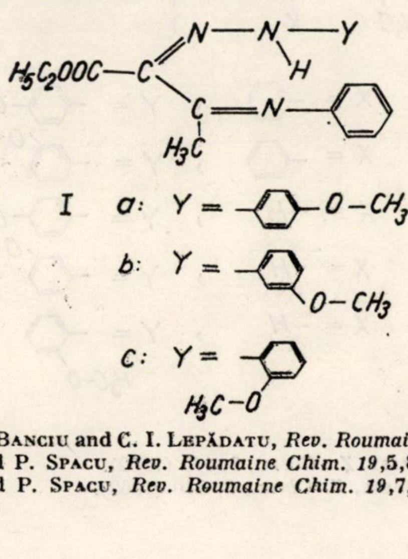

---

[1] P. Spacu, A. C. Banciu and C. I. Lepădatu, *Rev. Roumaine Chim.*, **18**, 7, 1143 (1973).

[2] A. C. Banciu and P. Spacu, *Rev. Roumaine Chim.* *19*,5,817(1974).

[3] A. C. Banciu and P. Spacu, *Rev. Roumaine Chim.* *19*,7,1177(1974).

EXPERIMENTAL

Reagents. Acetoacetic ester (Merck, reagent for synthesis, min. content 98%), aniline (tridistilled), *p*-anisidine (VEB Berlin – Chemie, *p.a.*), *m*-anisidine (B.D.H., laboratory reagent, boiling interval 243–248°), *o*-anisidine (B.D.H., laboratory reagent, boiling interval 222–226°), anhydrous $NaCH_3COO$ (Austranal, p.a.), $NaNO_2$ (Reactivul, Bucharest, p.a.), $NiCl_2.6H_2O$ (Reactivul, Bucharest, *p.a.*), 25% solution NH_3 (Reactivul, Bucharest, p.a.).

Preparation of the Ni(II) chelates. The Ni(II) chelates were synthetized using a known method,[4] under the refluxing conditions of alcoholic solutions of the reagents, working with 1/100 m amounts of ligand and 1/200 m $NiCl_2.6H_2O$ plus a slight excess of 15% from the theoretical quantity of the last mentioned reagent, in order to complete the reaction.

In the presence of a small quantity of triethylamine (circ. 1 ml), using the ligands Ia and Ib, the chelates IIa–1 and IIb–1 were obtained. The attempts to prepare the corresponding Ni(II) chelate using the compound Ic have invariably failed, as well as the earlier attempts [2] to obtain the Ni(II) chelate with the *o*-tolylhydrazone-(2) corresponding to the compound Ic.

Using the same reagent quantities and the same reaction conditions as indicated above, but in the presence of about 20 ccm of 25% NH_3 solution, using the three compounds Ia–c the chelates IIa–2, IIb–2 and IIc, were obtained. Under the cathalytical action of the Ni(II) salt, the NH_3 induces the splitting of the anil group and its substitution by the imino group, NH, in the ligand molecule.[5] For this reason, the complexes IIa –2, IIb–2 and IIc are formed with each from the three ligands which could not be isolated during the reaction and arised from the degradation of each from the compound Ia–c. The obtained compounds were washed with 3% acetic acid, warmed at 40°, till the washing solutions did not contain Ni(II) ions. The hardly soluble chelates IIa–2, IIb–2 and IIc were repeatedly washed with warmed abs. ethanol, and the more soluble chelates IIa–1 and IIb–1 have been recrystallized from abs. ethanol in the presence of active charcoal. After washings and recrystallizations respectively, the compounds have been dried under vacuum on ai$-P_2O_5$.

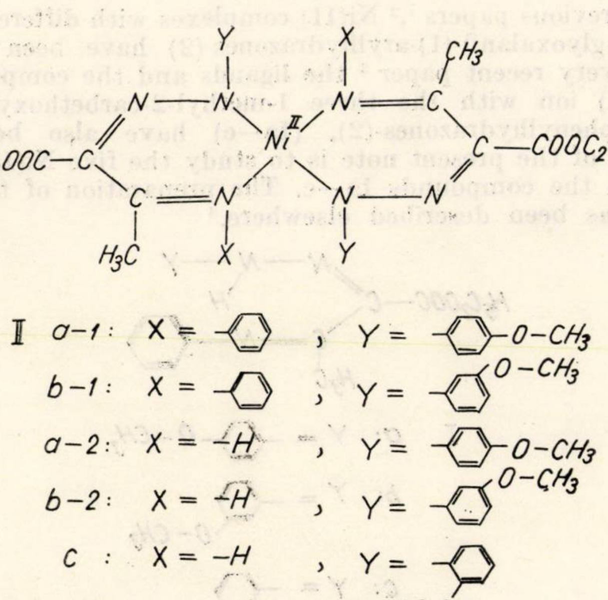

---

[4] B. Hirsch and A. Bassl, *Z. Chem.*, 2, 115 (1962).

[5] B. Hirsch and A. Bassl, *Z. Chem.*, 2, 340 (1962).

The elemental analyses of C, H and N have been carried out through microcombustion. For the Ni(II) dosing, the chelates were disintegrated with H_2SO_4 and H_2O_2 and the Ni(II) ion then dosed with dimethylglyoxime.

The absorption spectra of the chelates were recorded by means of a VSU−2 Carl Zeiss (Jena) spectrophotometer, on acetonic solutions of $0.25 \times 10^{-4} - 2.5 \times 10^{-4}$ mol/l concentration (complexes IIa−2, IIb−2 and IIc) and $0.5 \times 10^{-4} - 5 \times 10^{-4}$ mol/l (complexes IIa−1 and IIb−1).

The reflectance spectra of the chelates were recorded with a VSU−1 Carl Zeiss (Jena) spectrophotometer, using MgO as standard.

The IR spectra of the compounds were recorded within 400−4000 cm^{-1}, with a UR−10 Carl Zeiss (Jena) spectrophotometer, using pellets of KBr.

The magnetic susceptibility were determined at room temperature according to Faraday method, using $Hg[Co(NCS)_4]$ as reference.

RESULTS AND DISCUSSION

The analytical data for all Ni(II) complexes are given in table 1. These data together with the IR spectral results have allowed to establish the chelatic structural formulas IIa-c for all complexes.

Table 1

Analytical data of the Ni(II) chelates

Chelate	Ni %		C %		H %		N %		m.p. °C
	Calc.	Found	Calc.	Found	Calc.	Found	Calc.	Found	
IIa−1	7.98	7.39	62.06	61.89	5.48	5.93	11.43	11.80	168 −170.5
IIb−1	7.98	7.48	62.06	62.62	5.48	5.88	11.43	11.72	133 −136
IIa−2	10.06	9.82	53.54	52.89	5.53	5.99	14.41	14.52	218 −220.5
IIb−2	10.06	9.58	53.54	53.97	5.53	5.92	14.41	14.83	190.5−193
IIc	10.06	9.66	53.54	52.94	5.53	5.70	14.41	14.79	215 −218.

The IR spectra of one from the used ligands, and namely the 1-methyl-2-carbethoxy-glyoxalanil-(1)-*p*-methoxy-phenylhydrazone-(2), (Ia), and of the chelates IIa−1 and IIa−2, obtained with this ligand, are systematized in table 2.

The most striking differences in the IR spectra between the free ligand and the chelates are observed within the 1290−1370 cm^{-1} range. An absorption band of mean intensity occurs in this range for the free ligand, with maxima at 1300 and 1330 cm^{-1}. In the case of the corresponding chelates, the appearance of a very intense band has been, on the contrary, observed, for the chelate IIa−1 as a shoulder at 1300 and with maxima at 1325 and 1360 cm^{-1}, and for the chelate IIa−2 with maxima placed at 1295 and 1320 cm^{-1}, which are the most intense bands from the whole IR domain of the chelates. One knows[6] that in the range 1280−1360 cm^{-1} must appear a band characteristic to the secondary aromatic amines (C_6H_5-NH-) and almost in the same region (1310−1370 cm^{-1}) must occur an intense band characteristic to the tertiary aromatic amines ($C_6H_5-\bar{N}=$), both representing the C−N stretching

---

[6] L. J. BELLAMY, "The Infrared Spectra of Complex Molecules", Methuen, London, 1962.

Table 2

IR spectra of the ligand Ia and of the chelates IIa-1 and IIa-2 (cm^{-1})

Ligand Ia	Chelate IIa–1	Chelate IIa–2	Ligand Ia	Chelate IIa–1	Chelate IIa–2
	420 vw	415 w	1200 m	1197 vs	1200 vs
470 sh	470 sh	460 vw	1220 m	1220 s	
480 w	485 w–m	490 w	1245 m	1250 vs	1250 vs
525 w	525 w–m	525 m	1300 m	1300 sh	1295 vs
	535 w–m		1330 m	1325 vs	1320 vs
545 w	550 m	555 m	1370 m	1360 vs	1375 vs
560 w	565 m	585 w	1400 w		1390 vs
605 w	600 w		1430	1435 s	
620 w	630 w		1440 w		
635 w	645 w	650 vw	1450 w	1460 m	1450 w–m
665 w	685 sh	680 m	1470 m		1470 w–m
700 m	700 m–s		1490 m	1503 vs	
	710 s		1515 s	1535 m–s	1510 vs
755 m	765 m	765 vs	1580 m		1560 m
	780 w–m		1590 sh	1590 m	
	797 w–m	795 m	1620 sh	1610 m	1610 m
805 m		805 m	1	1645 sh	
840 m	830 s	830 m	1700 s	1680 vs	1695 vs
	920 m	920 w	2835 w	2830 vw	2840 vw
	960 sh	965 w		2910 w	2910 vw
	1000 m		2940 w	2950 w	2950 vw
1030 m	1040 s	1025 vs	2980 w	2980 w	2970 vw
1075 s	1080 vs	1085 vs			2990 vw
1110 w	1110 vw		3000 sh	3010 w	
1175 m	1180 vs	1170 vs			3320 vs

vs = very strong; s = strong; m = medium; w = weak; sh = shoulder.

vibration inside these groups. The expected structural modifications due to the coordination of the nitrogen atom of the hydrazone group to which the aryl radical is directly bound must be naturally reflected in the IR spectra, as has been shown above. The strong enhancement of the absorption bands in the chelate spectra in this domain, compared with the band of the free ligand, shows that the coordination took place to the nitrogen atom of the hydrazone group. The intense band occurring at 1700 cm^{-1} could be undoubtedly assigned[6] to the esteric group ($COOC_2H_5$) and it remains unshifted in the spectra of both chelates, showing that this group does not participate into coordination, a possibility which could not be a priori ignored. It should be expected, in the contrary case, that this absorption band to be strongly shifted, at approximately 1635–1665 cm^{-1}, which obviously is not the case.

The most striking difference between the IR spectra of the two chelates consists in the fact that in the spectrum of the chelate IIa–2 occurs a very intense band at 3320 cm^{-1}. This band is ascribed [6] as being proper to the imino group, NH, frequency. Its appearance agrees with the chemical analysis data, indicating the fact that in the chelate IIa–2 the coordinated ligand does no more contain the anil group, but the imino one, in agreement with the structural formula suggested by the chemical analysis.

The appearance of absorption bands with maxima at 1075 and 1110 cm^{-1} in the free ligand, at 1040 and 1080 cm^{-1} in the chelate IIa$-$1 and at 1085 cm^{-1} in the chelate IIa$-$2 is also important. The above absorption bands are ascribed to the etheric aliphatic group (CH_3-O-). In the case of the chelate IIa$-$2 there is a very intense band at 1250 cm^{-1} (while for the free ligand and the chelate IIa$-$1 the domain 1230$-$1270 cm^{-1} is overlapped by maxima of more broad bands, comprised between 1170 and 1260 cm^{-1}), which could be assigned to the alkyl-aryl-etheric group ($CH_3-O-C_6H_4-$). The appearance of these bands (1085 and 1250 cm^{-1}) in the IR spectrum of the chelate IIa$-$2 shows that the *p*-anisidyl group ($p-CH_3O-C_6H_4-$) has been maintained in the molecule, i.e. under the reaction conditions for the synthesis of the chelate from the original ligand molecule, Ia, the anil group ($C_6H_5-N=$) and not the hydrazonic group ($p-CH_3O-C_6H_4-NH-N=$) is splitted, in agreement with the formulation IIa$-$2 of the chelate.

ELECTRONIC SPECTRA AND MAGNETIC PROPERTIES

The only small differences between the absorption bands in the electronic spectra of the chelates and those in the reflectance spectra recorded for the compounds in the solid state, show that the chelate dissolution was not accompanied by important structural modifications (dissociations, etc.), the same molecular species being existent both in solution and solid state.

The magnetic susceptibility measurements performed on the chelates IIa$-$1, IIa$-$2 and IIc have shown that all compounds are diamagnetic.

The spectra of the chelates IIa$-$2, IIb$-$2 and IIc

The absorption spectra in the visible range for the complexes IIa$-$2, IIb$-$2 and IIc are plotted in figure 1.

One strikely observes that the spectra of IIa$-$2 and IIb$-$2 are very similar both in their shape and position of the maxima which practically coincide on the whole visible domain. The above observation allows us to ascribe likely the diamagnetic properties to the chelate IIb$-$2 for which the magnetic behaviour was not studied. The intense absorption maxima of $\varepsilon \approx 6500$ coincide for both mentioned chelates, appearing exactly at 475 nm. The shoulders occurring at higher wavelengths represent bands with maxima placed approximately at 560 nm, but with low intensity, of $\varepsilon \approx 700$, i.e. of a order size lower than that of the first mentioned bands.

The spectrum of the chelate IIc differs very much when compared with those of the chelates IIa$-$2 and IIb$-$2. Much more, this spectrum is different from those of the corresponding chelate IIc, already described,[2] where instead of $Y = o-CH_3O-C_6H_4-$ as in the present case, the substituent attached to the two of the four nitrogen donor atoms, was

$Y = o-CH_3-C_6H_4-$. In the case of the last mentioned complex, its electronic spectrum shows a hypsochromic shift only, of 40 nm, in the whole visible range against the spectra which practically coincide between them, of the corresponding chelates IIa—2 ($Y = p-CH_3-C_6H_4-$) and IIb—2 ($Y = m-CH_3-C_6H_4-$). The maximum of the intense band

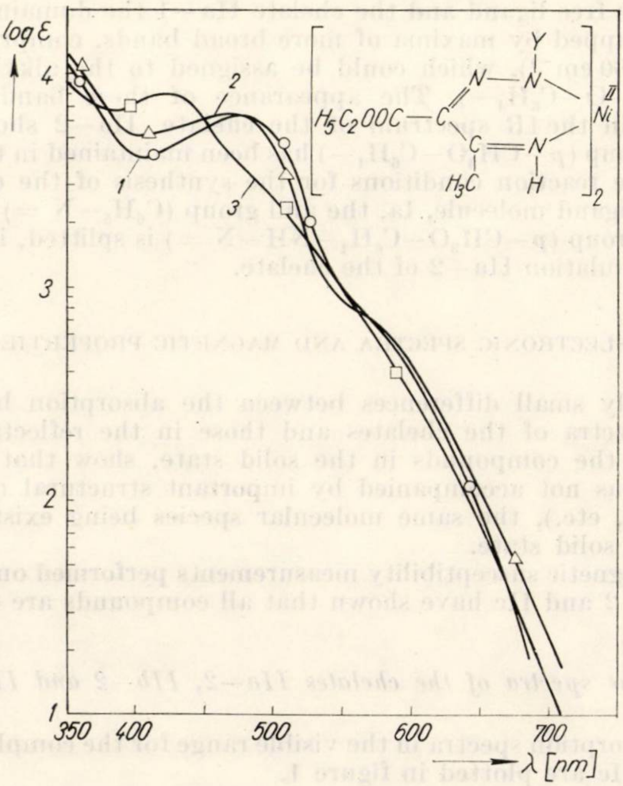

Fig. 1. — Electronic spectra of the Ni(II) chelates. *1.* Chelate IIb—2; $X = H$, $Y = m-CH_3O-C_6H_4$; *2.* Chelate IIa—2 $X = -H$, $Y = p-CH_3O-C_6H_4$; *3.* Chelate IIc; $X = -H$, $Y = o-CH_3O-C_6H_4$;

occurring at 430 nm, takes $\varepsilon = 4800$, that is a lower value than in the corresponding complexes of type IIa—2 and IIb—2 ($\varepsilon \approx 6000$), and the shoulder observed at 530 nm is less intense, with $\varepsilon \approx 400$. In the present case the single analogy between the electronic spectrum of the chelate IIc ($Y = o-CH_3OC_6H_4-$) and that of the type IIc already mentioned ($Y = p-CH_3-C_6H_4$) consists in the obvious hypsochromic shift of the first intense band from the visible range. This band has a maximum placed at 420 nm, compared with 475 nm in the case of the chelates IIa—2 and IIb—2. This maximum shows however, in this case $\varepsilon \approx 8000$, higher than that for the chelates IIa—2 and IIb—2 ($\varepsilon = 6500$). Near to 460 nm ($\varepsilon = 4500$) there is a very broad shoulder extented at the end of the visible range (at about 700 nm). The gaussian analysis of the spectrum shows that this shoulder must include an intense band with $\varepsilon \approx 2500$, with the maximun placed approximately at 480 nm. The high intensity of this band ($\varepsilon > 2000$) makes it comparable with the first bands only from the visible domain of the chelates ($\varepsilon = 6500...8000$) and not with the bands occurring as shoulders for the complexes IIa—2 and IIb—2 at approximately 560 nm ($\varepsilon \approx 700$). This situation is strikingly similar with the case of the square-planar Ni(II) mixed ligand complexes, containing alkyl-aryl-phosphines, studied by Coussmaker et al,[7] where a band occurring approximately at 460 nm with $\varepsilon \approx 2700$ was included into the disscusion of the "high intensity and freqency bands".

The diamagnetism of the complexes shows that Ni(II) ($3d^8$) has a square-planar arrangement of the metal-ligand bonds with low spin electron distribution.

The high intensity of the bands appearing at 475 nm in the case of the chelates IIa—2 and IIb—2 ($\varepsilon = 6500$) and that of the two bands (at 420 nm with $\varepsilon = 8000$ and the shoulder at 480 nm with $\varepsilon \sim 2500$) of the chelate IIc shows these bands as being of a charge transfer (CT) nature. Taking into account the Jørgensen's formula [8,9]:

$$\nu_{CT} = 30{,}000\,(x_N - x_{Ni})\ \mathrm{cm}^{-1}$$

where[8] $x_{Ni(\text{square-planar})} = 2.2$ and [9]$x_N = 3.2$ are the corresponding optical electronegativities, one may conclude that a ligand → metal CT transition must occur at approximately 330 nm (30,000 cm^{-1}) which, obviously, is not the case. The only remained alternative is to ascribe these bands to a CT metal → ligand mechanism, i.e. from the filled MO's practically localized on the central metal ion, to the free antibonding MO's mainly placed on the organic ligand.

The absorption bands of almost an order of lower intensity ($\varepsilon \approx 700$) occurring for the chelates IIa—2 and IIb—2 as shoulders to the intense CT bands, could be undoubtedly ascribed to spin-allowed d—d transitions.

If one uses the most probable MO energy pattern for the studied chelates, i.e. an orbital scheme for weak D_{4h}-distortion, corresponding to the orbital sequence $e_g\,(d_{xz}, d_{yz}) < b_{2g}(d_{xy}) < a_{1g}\,(d_{z^2}) < b_{1g}\,(d_{x^2-y^2})$, the most like assignement of the d—d bands may correspond to a transition up to the double degenerate excited spectral term ${}^1E_g$, i.e.

$${}^1A_{1g}\,(e_g^4\, b_{2g}^2\, a_{1g}^2) \rightarrow {}^2E_g\,(e_g^3\, b_{2g}^2\, a_{1g}^2\, b_{1g}^1).$$

This assignement implies a transition from the most stable "π" antibonding orbital (e_g) : to the highest "σ" antibonding orbital (b_{1g}) arisen from the d orbitals of the Ni(II) ion. Having in view the relative high intensity of these bands ($\varepsilon \approx 700$) for a centrosymmetric environment, this assignement constitutes, of course, only an attempt.

---

[7] C. R. C. COUSSMAKER, M. H. HUTCHINSON, J. R. MELLOR, L. E. SUTTON and L. M. VENANZI, *J. Chem. Soc.*, **1961**, 2705.

[8] A. B. P. LEVER, "Inorganic Electronic Spectroscopy", chapt. 8—9, Elsevier, Amsterdam, 1968.

[9] C. K. JØRGENSEN, "Electron Transfer Spectra", in "Progress in Inorganic Chemistry", vol. 12, Interscience, New York, 1970, p. 101—158.

The very broad shoulder at 460–700 nm of the chelate IIc includes, certainly a very weak d–d band, overlapped by the more intense CT band. The appearance of an intense CT band at approximately 480 nm in the spectrum of the chelate IIc cannot be explained through different electronic effects but through more strong steric hindrances caused by the methoxy group, CH_3O, attached to the ortho position of the phenyl radical of the hydrazonic group. In the case of a less bulky substituent, as an example the methyl group, CH_3, (the case of the chelate IIc already described by us,[2] where $Y = o-CH_3-C_6H_4-$) only a shoulder at 500 nm representing a weak d–d band is observed in the spectrum of the chelate ($\varepsilon \approx 400$). The steric repulsions caused by the *p*-anisidyl group ($Y = o-CH_3O-C_6H_4-$) bound to the nitrogen donor atoms, even though much stronger than those produced by other substituents, are not able to impose a tetrahedral configuration for the complex, which remains square-planar, diamagnetic. The same important conclusion, that is the maintaining of a preponderant square-planar symmetry for the metal-nitrogen bonds, is valid for the chelates IIa–1 and IIb–1. In these complexes to each coordination point (the nitrogen donor atoms of the ligands) bulky groups are attached : to two of the four nitrogen donor atoms there are *p*- or *m*-anisidyl groups ($Y = CH_3O-C_6H_4-$) and phenyl radicals ($X = -C_6H_5$) to the other two nitrogen atoms.

The spectra of the chelates IIa–1 and IIb–1 are plotted in figure 2.

The spectra are very similar between them in the whole visible range, except an insignificative shift of 10–15 nm. This similitude allows also to ascribe diamagnetic properties to the chelate IIb–1, for which the magnetic susceptibility measurements were not carried out.

Even though the electronic spectra of these complexes are similar with those of the chelates IIa–2 and IIb–2, there are nevertheless some differences. Thus, the intense bands ($\varepsilon \approx 4600$), which can be regarded as charge-transfer metal → ligand, occur as shoulders of the more intense bands placed in the UV range. The positions of these shoulders, approximately at 500 nm, shows a slight bathochromic shift only, of about 20 nm, of these CT bands, compared with those of the chelates IIa–2 and IIb–2. The very broad shoulders at 600 nm shows, on the contrary, a marked bathochromic shift, of about 60 nm, against the corresponding shoulders, ascribed as d–d transitions, in the chelates IIa–2 and IIb–2. The intensity of these shoulders is unusually high, $\varepsilon > 1100$, for the majority of tetrahedral complexes. For this reason more likely is the assignement of these bands as charge transfer metal → ligand transitions, taking also into consideration that for centrosymmetric environments as that square-planar, the d–d transitions are weak, even for the d^8 electronic configuration for which the intensity of this kind of transitions takes unusual high values, $\varepsilon \approx 10^2$. Thus, for the square-planar Ni(II) complexes these kinds of bands were reported in different papers as being d–d transitions having invariably $\varepsilon < 700$.

The high width of these shoulders occurring approximately at 600 nm in the spectra of these complexes, comparable with that of the broad shoulder appearing in the spectra of the already discussed chelate IIc, shows more probably the fact that they include more than a single band, which could not be resolved. If the intense band ($\varepsilon > 1100$) is a CT metal → ligand transition, it overlaps the more weak bands corresponding to d—d transitions.

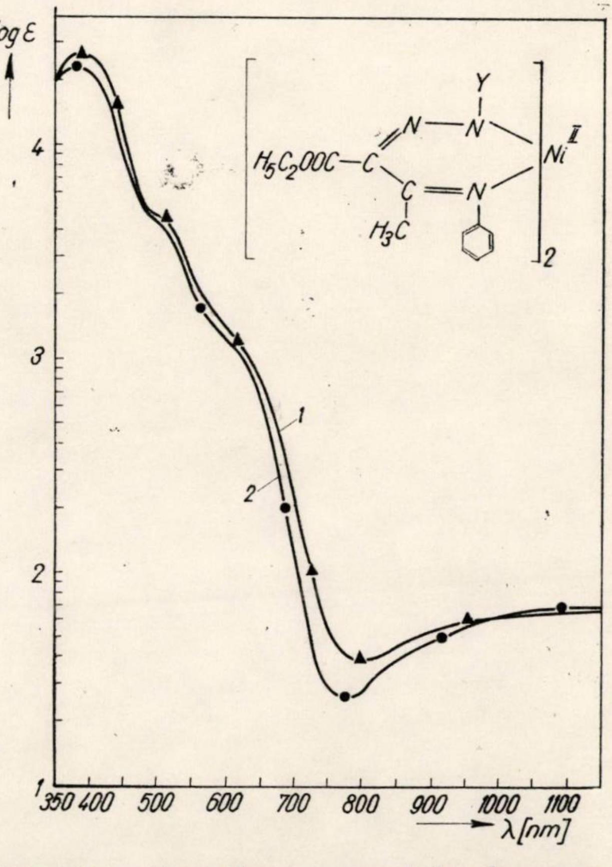

Fig. 2. — Electronic spectra of the Ni(II) chelates. *1.* Chelate IIa—1 : $X = C_6H_5$, $Y = p-CH_3O-C_6H_4$; *2.* Chelate IIb—1 : $X = C_6H_5$, $Y = m-CH_3O-C_6H_4$.

It should be expected that these bands to occur even in this range, in view of the bathochromic shift of the whole visible range of the chelate IIa—1 and IIb—1, compared with that of the already discussed chelates IIa—2 and IIb—2, where the d—d bands appeared as shoulders at approximately 540 nm. On the other hand, it should be not excluded the possibility that the absorption bands with $\varepsilon > 1100$, occurring as shoulders at about 600 nm, to be of d—d nature, their intensity being enhanced by the proximity of the more intense bands, at 500 nm, undoubtedly due to a charge transfer mechanism.

The authors thank lecturer V. Mincu of the University of Bucharest for the magnetic susceptibility measurements.

Revue Roumaine de Chimie, **19**, *8*, 1307—1315 (1974).

Revue Roumaine de Chimie, **19**, *8*, 1317–1321 (1974)

ON THE REACTIVITY OF SOME METAL-SULPHUR COMBINATIONS IN LIQUID AMMONIA

P. MARKOV, S. CHORBADJIEV and V. TARPANOV

Department of Organic Chemistry, University of Sofia, Bulgaria

Received November 6, 1973

It was established that magnesium and sulphur react in liquid ammonia while calcium practically does not interact with sulphur under the same conditions. Considerable differences were found in the character of the interaction of benzyl chloride and benzhydryl chloride with the combinations magnesium-sulphur and sodium-sulphur in liquid ammonia.

The reactivity of alkali metals with sulphur in liquid ammonia was well studied.[1–3] Depending on the ratio metal-sulphur different alkali sulphides were obtained. In one of our previous papers [4] we reported the interaction between different halogen organic compounds and the sodium-sulphur combination in liquid ammonia using the ratio RX : Na : S 2 : 2 : 1 and 1 : 1 : 1. In all the cases the corresponding organic mono- and disulphides were isolated. Only in the case of benzyl chloride the corresponding disulphide was not obtained. In some cases besides these reaction products higher sulphides were found.

The present work continues the investigation in this field aiming to elucidate the influence of the nature of the metal used and the ratio metal-sulphur on the course of the interaction with halogen organic compounds. The interaction of benzyl chloride and benzhydryl chloride with the combinations sodium-sulphur, magnesium-sulphur and calcium-sulphur in liquid ammonia was studied.

The reaction of magnesium with sulphur had been studied in detail.[5] It is established that the elements combine to form magnesium sulphide, MgS. There are several different methods of preparing magnesium sulphide, in all the cases the reaction being carried out at high temperatures. There are no data regarding the existence of other magnesium sulphides.[6] The

---

[1] F. Fehér and H. J. Berthold, *Z. anorg. Chem.*, **273**, 144 (1953).

[2] W. Klemm, H. Sodomann and P. Langmesser, *ibid.*, **241**, 281 (1939).

[3] F. Fehér and H. J. Berthold, *ibid.*, **274**, 223 (1953).

[4] S. Chorbadjiev and P. Markov, *Compt. rend. Acad. bulg. Sci.*, **25**, 763 (1972).

[5] J. W. Mellor, "A Comprehensive Treatise on Inorganic and Theoretical Chemistry", vol. 4, Longmans, Green and Co., London, 1957, p. 318.

[6] "Inorganic Sulphur Chemistry", edited by G. Nickless, Elsevier Publishing Company, Amsterdam, 1968, p. 689–690.

interaction of sulphur with magnesium suspended in liquid ammonia has not been studied so far.

Our study showed that magnesium and sulphur react in liquid ammonia forming a yellow-orange precipitate which when exposed to air changed quickly and, on adding water, it evolved hydrogen sulphide forming magnesium hydroxide. The product of the interaction between magnesium and sulphur in 1 : 1 ratio was isolated under inert solvent (ether-benzene). On decomposing it with dilute hydrochloric acid it was found that 45% of the sulphur had been combined.

An analogous experiment showed that calcium and sulphur did not interact in liquid ammonia, the sulphur being recovered almost completely. This result is to a certain extent in contradiction with the fact that calcium possesses a higher affinity for sulphur than magnesium itself.[7] On the other hand it is well known that calcium dissolves in liquid ammonia forming calcium-ammonium [8] while magnesium is practically insoluble in this medium. The observed difference in the reactivity of the two alkali-earth metals towards sulphur in liquid ammonia could be explained with the formation of a ligand sphere of ammonia molecules round the calcium atoms.

The interaction of benzyl chloride and benzhydryl chloride with the combinations magnesium-sulphur and calcium-sulphur was studied in detail. Only the reaction between benzyl chloride and magnesium-sulphur combination gave organic sulphide. The interaction of calcium-sulphur combination with benzyl chloride and benzhydryl chloride led to the formation of *trans*-stilbene (8%) and tetraphenyl ethane (27%), respectively. These hydrocarbons were due to a Wurtz type reaction.

The results of the reaction between benzyl chloride and magnesium-sulphur combination are presented in table 1. They show that regardless of the chosen magnesium + sulphur ratio high yields of dibenzyl disulphide were obtained. Other organic sulphides were not isolated from the reaction mixture. This fact could be of preparative significance. The obtained results mean that magnesium and sulphur in liquid ammonia form a product containing a chain of two sulphur atoms.

Table 1

Interaction of benzyl chloride with magnesium-sulphur combination

Halogencontaining compound	Ratio RX : Mg : S	Reaction product	Yield of purified product, %	M.p. °C
Benzyl chloride	1 : 1 : 1	Dibenzyl disulphide	66.7	70
Benzyl chloride	2 : 2 : 3	Dibenzyl disulphide	71.6	69
Benzyl chloride	1 : 1 : 2	Dibenzyl disulphide	82.3	69
Benzyl chloride	1 : 1 : 4	Dibenzyl disulphide	77.7	69

As it was mentioned benzhydryl chloride does not react with magnesium-sulphur combination. A series of experiments was carried out using the same reaction ratios as in the case of benzyl chloride. In all the cases the benzhydryl chloride was recovered completely. It should be remarked that when the ratio benzhydryl chloride : magnesium : sulphur was 1 : 1 : 2 and 1 : 1 : 4 a small amount (less than 1%) of tetraphenyl ethylene was isolated from the reaction mixture.

---

[7] J. W. MELLOR, "A Comprehensive Treatise on Inorganic and Theoretical Chemistry", vol. **10**, Longmans, Green and Co., London, 1957, p. 87.

[8] J. W. MELLOR, *ibid.*, vol. **3**, p. 639.

The question about the lack of reactivity of benzhydryl chloride with magnesium-sulphur combination cannot be solved entirely as the detailed mechanism of the reaction is not known. Whereas it is sure that this is a nucleophilic substitution it must be assumed that in this case the nucleophilic attack is hindered in comparison with the case of benzyl chloride. On the other hand it is well known that the reactivity of the chlorine atom in benzhydryl chloride is much greater which is due to additional delocalization possibility of the positive charge in the intermediate carbonium ion. That is why it is reasonable to accept that the steric factors are of primary importance for the examined interaction.

On the other hand it could be expected that, because of the coordinating ability of magnesium in liquid ammonia, the reactive particles are very bulky. This decreases the possibility of the access to the reaction centre of benzhydryl chloride. Aiming to verify this assumption, the reactivity of benzhydryl chloride with sodium-sulphur combination was studied.

It is well known that sodium possesses insignificant coordinating ability towards electron-donor molecules. Also, it should not be ignored the difference in the polarities of sodium-sulphur and magnesium-sulphur bonds. Moreover, up to now there are no data on obtaining different benzhydryl sulphides by means of the interaction between benzhydryl chloride and alkali sulphides.

The results of the experiments carried out with benzhydryl chloride and sodium-sulphur combination are given in table 2. The ratio of reaction components 1 : 1 : 1 gave the highest yield of dibenzhydryl disulphide. An increase in the amount of sulphur led to a certain decreasing in the yields of organic disulphide. Other sulphides were not obtained. No reaction was observed when 2 : 1 ratio of sodium : sulphur was used. Only small amount (less than 4%) of tetraphenyl ethylene was isolated from the reaction mixture. Whereas in this case sodium monosulphide, Na_2S, is formed [2] it could be concluded that benzhydryl chloride is not reactive towards this sulphide. On the other hand, as it was shown earlier,[4]

Table 2

Interaction of benzhydryl chloride with sodium-sulphur combination

Halogencontaining compound	Ratio RX :Na :S	Reaction product	Yield of purified product, %	M.p. °C
Benzhydryl chloride	2 : 2 : 1	Tetraphenyl ethylene	3.8	222 – 223
Benzhydryl chloride	1 : 1 : 1	Dibenzhydryl disulphide	77.2	153
Benzhydryl chloride	2 : 2 : 3	Dibenzhydryl disulphide	52.9	153
Benzhydryl chloride	1 :1 : 2	Dibenzhydryl disulphide	52.3	153

benzyl chloride reacts with sodium sulphide in liquid ammonia with the formation of the corresponding monosulphide. In this sense the observed difference is very unexpected.

The obtained results show that the course of the reaction depends on the nature of the metal used as well as on the structural characteristics of the halogen-organic compounds. More detailed investigation is necessary for elucidation of the nature of the products that are formed during the interaction between alkali and alkali-earth metals with sulphur in liquid ammonia. The character of the interaction of these products with halogen organic compounds is a matter of additional study.

EXPERIMENTAL

The melting points of the obtained products were determined on a Koffler apparatus and were not corrected. The experiments were carried out with commercially dry liquid ammonia in a threeneck flask fitted with a dropping funnel and a tube for releasing the evaporating ammonia.

Interaction between magnesium and sulphur. A 1 : 1 ratio was used. Powdered sulphur (0.8 g, 0.025 gA) and magnesium (0.6 g, 0.025 gA) were added to about 750 ml liquid ammonia. The mixture was left to stay for 48 hours during which the solution became orange-brown and an orange-brown precipitate was formed. After adding 100 ml of dry ether the liquid ammonia was evaporated by means of an alcohol bath and then 100 ml of dry benzene was added. The mixture was heated and a hydrochloric acid (1 : 1) was dropped into it. The evolved hydrogen sulphide was passed through a washing bottle containing a solution of zinc sulphate, ammonium chloride and ammonia. The precipitate of zinc sulphide was filtered off and decomposed with hot hydrochloric acid (1 : 1). The zinc containing solution was titrated with complexon II. The determined amount of zinc corresponded to 45.0% of the sulphur used in the reaction.

Interaction of calcium with sulphur. This interaction in liquid ammonia was carried out analogously to that of magnesium and sulphur. When the reaction mixture was decomposed with hydrochloric acid no hydrogen sulphide evolved and 91.5% of the sulphur was recovered.

Interaction of magnesium-sulphur combination with benzyl chloride and benzhydryl chloride. To about 800 ml of liquid ammonia 0.025 gA (0.6g) of magnesium and the corresponding amount of sulphur according to the ratio used was added (See table 1). Three hours later 0.05 gM of the halogen derivative dissolved in 50 ml of dry ether was added. After staying for 48 hours 150 ml of dry ether was added and the liquid ammonia was removed by means of an alcohol bath. 150 ml of water was added and the mixture was extracted with ether. The extracts were washed with water, dried with sodium sulphate and the ether was distilled. The remaining dibenzyl disulphide was recrystallized from ethyl alcohol and identified by its m.p. and quantitative analysis (found : % C 68.43, H 5.85 ; calculated : % C 68.29, H 5.64). The yields of crude dibenzyl disulphide were very high and for the different ratios benzyl chloride : magnesium : sulphur they were : ratio 1 : 1 : 1 — 85.9% ; ratio 2 : 2 : 3 — 89.1% ; ratio 1 : 1 : 2—97.2% and ratio 1 : 1 : 4—97.2%.

In the experiments with benzhydryl chloride after removing of the ether from the extract the residue was distilled in vacuum (161—162°/16 mm Hg; refractive index n_D^{20} 1.5952). In all the cases the initially added benzhydryl chloride was recovered almost completely. When the ratio magnesium : sulphur was 1 : 2 and 1 : 4 after distilling of the unreacted benzhydryl chloride a small residue (less than 1%) was obtained which after recrystallization from petroleum ether was identified as tetraphenyl ethylene (m.p. 223—224°).

Interaction of benzyl chloride and benzhydryl chloride with calcium-sulphur combination. The reaction was carried out analogously to the case of magnesium-sulphur combination. The ratio RX : Ca : S was 1 : 1 : 1. The halogen derivatives were recovered from the reaction mixtures. In the case of benzyl chloride some amount of trans-stilbene was isolated (yield 8%, m.p. 123—124°, quantitative analysis : found % C 92.80, H 7.08, calculated % C 93.20, H 6.78). In the experiment with benzhydryl chloride tetraphenyl ethane was found in the distillation residue (yield 27%, m.p. 210—211°, quantitative analysis : found % C 93.18, H 6.49, calculated % C 93.40, H 6.58).

Interaction of sodium-sulphur combination with benzhydryl chloride. This interaction was carried out in the same way as described in our previous paper.[4] The amounts of sodium and benzhydryl chloride were 0.05 gA and 0.05 gM respectively, and the quantity of sulphur depended on the chosen ratio metal : sulphur (See table 2). The obtained dibenzhydryl disulphide was recrystallized from ethyl alcohol (m.p. 153°, quantitative analysis : found % C 78. 28, H 5.51, calculated % C 78.64, H 5.52). The yields of crude product for the different ratios benzhydryl chloride : sodium : sulphur were as follows : ratio 1 : 1 : 1 — 97.2%; ratio 2 : 2 : 3 — 72.2%; ratio 1 : 1 : 2 — 63.5%.

When the sodium : sulphur ratio was 2 : 1 after distilling of the unreacted benzhydryl chloride 3.8% of tetraphenyl ethylene was isolated and recrystallized from petroleum ether (m.p. 222—223°; quantitative analysis: found % C 94.29, H 6.06, calculated % C 93.97, H 6.03; TLC upon silicagel G and silicagel G impregnated with 10% of silver nitrate, mobile phase petroleum etherbenzene 9 : 1, Rf values 0.49 and 0.29, resp.).

Revue Roumaine de Chimie, **19**, *8*, 1323–1342 (1974)

CHEMICAL GRAPHS. XXII [1]

VALENCE ISOMERS OF HETEROANNULENES OR OF SUBSTITUTED ANNULENES. COISOMERIC CUBIC MULTIGRAPHS

ALEXANDRU T. BALABAN

Institute of Atomic Physics, P.O. Box 35, Bucharest

Received 27 March, 1974

By applying Pólya's counting theorem to the cycle indices of valence isomers of [n]annulenes (cubic multigraphs with n points), the numbers of constitutional isomers for heteroannulenes or substituted annulenes are presented (all multigraphs with $n = 4$ and 6, and a few with $n = 8$ and 10). Cases of coisomeric graphs (i.e. those like benzene and benzprismane yielding the same numbers of constitutional isomers because they possess the same cycle indices) are reviewed. Examples of known heteroannulene valence isomers are presented. Reaction graphs $L(2^n, M)$ for some of the above molecules M are discussed.

1. INTRODUCTION

Valence isomers were defined as molecules whose reduced structural graphs have the same partition of their vertex degrees.[2,3a] By *reduced* structural graphs, we mean graphs whose points (vertices) represent atoms with valence *higher than one*, and whose lines (edges) represent covalent bonds. It is necessary to specify that these are *structural graphs*, because reduced *reaction graphs* [3b] also exist (in the latter graphs, points represent chemical species, and lines represent elementary reactions).

Valence isomers of annulenes yield reduced structural graphs which are cubic (trivalent) multigraphs, i.e. regular multigraphs [4] of degree three. By an algorithm based on general cubic graphs, a systematic approach was devised for the construction of all possible cubic multigraphs with n points, i.e. of order n. This enabled us to enumerate these graphs for $n = 4$, 6, 8, and 10,[5] and more recently for $n = 12$.[6] A mathematical approach for the corresponding numerical problem was discovered by R. W. Robinson,[7–8] but it is not yet amenable for numerical computation, and still less for constructing the various graphs.

---

[1] Part XXI, A. T. Balaban, *Rev. Roumaine Chim.*, **19**, 1185 (1974).

[2] A. T. Balaban, *Rev. Roumaine Chim.*, **18**, 635 (1973).

[3] A. T. Balaban (editor), "Chemical Applications of Graph Theory", Academic Press, London, 1974; a) Chapter 5, by A. T. Balaban; b) Chapter 6, by J. Dugundji, P. Gillespie, I. Ugi and D. Marquarding; c) Chapter 3, by F. Harary, E. M. Palmer, R. C. Read and R. Robinson.

[4] F. Harary, "Graph Theory", Addison-Wesley, Reading, Mass., 1969.

[5] A. T. Balaban, *Rev. Roumaine Chim.*, **11**, 1097 (1966), erratum *ibid.*, **12**, Nr. 1, 103 (1967); A. T. Balaban, *ibid.*, **15**, 463 (1970).

[6] A. T. Balaban, *Rev. Roumaine Chim.*, **17**, 865 (1972).

Taking account of the chemical counterparts of cubic multigraphs, it was natural to discuss in more detail *planar* cubic multigraphs,* since no molecule is yet known whose reduced structural graph is non-planar. The smallest cubic graph which is non-planar is I, which corresponds to the reduced structural graph of the diagonal benzene formula proposed by Claus [10] before it was modified into the centric formula.[11]

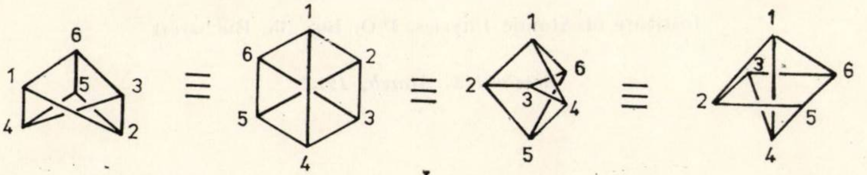

I

Formula I results from that of benzprismane by inverting two bonds so as to convert the closed strip of three condensed four-membered rings into a Möbius strip. We will call accordingly graph I "benz-möbius-stripane". This should not be misinterpreted as involving a Möbius strip of six atomic orbitals in a simple ring of six carbon atoms, as discussed in the literature.[12]

The five other valence isomers of benzene [5] are all planar graphs, since they can be written in a plane without crossing lines, and are all known as chemical species.

VALENCE ISOMERS OF HETEROANNULENES OR OF SUBSTITUTED ANNULENES

To find out the numbers of valence isomers of heteroannulenes such as pyridine, or of substituted annulenes such as chlorobenzene, we start from the valence isomers of annulenes and examine how many isomers result from each by introducing heteroatoms or substituents. The most powerful and elegant procedure consists in applying Pólya's counting theorem.[3c, 13–16]

---

* It should be emphasized that "planarity" is here meant as a topological,[4] not a geometrical, concept. Planar multigraphs can exist in various geometries, including tridimensional ones. Chemical texts [9] occasionally mention "non-planar valence isomers" meaning tridimensional molecules whose reduced structural graphs are planar multigraphs.

[7] R. W. Robinson, unpublished.

[8] F. Harary and E. M. Palmer, "Graphical Enumeration", Academic Press, New York, 1973.

[9] M. G. Barlow, R. N. Haszeldine and J. G. Dingwall, *J. C. S. Perkin I*, **1973**, 1542.

[10] A. Claus, "Theoretische Betrachtungen und deren Anwendungen zur Systematik der organischen Chemie", Freiburg, 1867, p. 207 (cited after C. K. Ingold, ,,Structure and Mechanism in Organic Chemistry", G. Bell and Sons, London, 1953, p. 159).

[11] A. Claus, *Ber. dtsch. chem. Ges.*, **15**, 1407 (1882); **20**, 1423 (1887); E. Bamberger, *ibid.*, **24**, 1758 (1891); **26**, 1946 (1893); H. E. Armstrong, *J. Chem. Soc.*, **51**, 254 (1887); A. von Baeyer, *Liebigs Ann. Chem.*, **245**, 118 (1887)

[12] E. Heilbronner, *Tetrahedron Letters*, **1964**, 1923.

Pólya showed that the number of such isomers results by substituting a figure counting series y_k into the cycle index $Z(A)$ of the reduced structural graph of the respective molecule. The cycle index is the expression of symmetry operations around proper or improper axes of rotation (disregarding symmetry operations involving centres or planes of symmetry). Expressed as operations on permutation groups A, the cycle index $Z(A)$ is a sum of terms Πy_k^j, where $j + k = n$, n being the order of the graph.

$$Z(A) = \frac{1}{|A|} \sum_{\alpha \in A} \prod_{k=1} y_k^{j_k(\alpha)}$$

where $|A|$ is the order of the group A, and $j_k(\alpha)$ is the number of cycles of length k in the disjoint-cycle representation of the permutation α.

The figure counting series to be substituted for y_k is

$$y_k = \sum_{i=1}^{m} x_i^k$$

where m is the number of different kinds of substituents ($m \leqslant n$).

The result of this substitution is a configuration counting series, or a counting polynomial. In it, the coefficient of any term $\prod_i x_i^{k_i}$ gives the number of isomers with k_i substituents (heteroatoms) of type i.

Table 1 presents in detail the derivation of cycle indices for valence isomers of [4]- and [6]annulene. Unless otherwise stated, the cycle indices are topological rather than geometrical, expressing constitutional isomerism rather than stereoisomerism. The symmetry operations are represented as cyclic permutations of vertices, according to their numbering given in the formulas. Each symmetry operation corresponds to a term y_k^j in the cycle index. For completeness, with the graphs of order 6 we included the non-planar graph I representing the chemically impossible benz-möbius-stripane; it has the highest symmetry from all cubic multigraphs of order 6, being the "6-cage".[4,17] It is the graph of the

---

[13] G. Pólya, *Acta Math.*, **68**, 145 (1937).

[14] F. Harary (editor), "A Seminar on Graph Theory", Holt, Rinehart and Winston, New York, 1967, p 25; "Graph Theory and Theoretical Physics", Academic Press, London, 1967, p. 5.

[15] N. G de Bruijn, in "Applied Combinatorial Mathematics" (E. F. Beckenbach, editor), Wiley, New York, 1964, p. 144; W. G. Klemperer, *Inorg. Chem.*, **11**, 2669 (1972); D. H. McDaniel, *ibid.*, 2678; J. E. Leonard, *Diss. Abstr.*, **32**, B, 5659 (1972).

[16] A. T. Balaban and F. Harary, *Rev. Roumaine Chim.*, **12**, 1511 (1967); A. T. Balaban, D. Fărcaşiu and F. Harary, *J. Labelled Comp.*, **6**, 211 (1970).

[17] W. T. Tutte, "Connectivity in Graphs", University of Toronto Press, 1966, p. 71.

Table 1

Symmetry operations and corresponding cycle index terms for valence isomers of [4]- and [6] annulene

Valence isomer	Permutation	Cycle index term
Cyclobutadiene (square)	(1) (2) (3) (4)	y_1^4
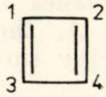	(1) (3) (2, 4) ; (2) (4) (1, 3)	$2y_1^2y_2$
	(1, 2) (3, 4) ; (1, 4) (2, 3) ; (1, 3) (2, 4)	$3y_2^2$
	(1, 2, 3, 4) ; (1, 4, 3, 2)	$2y_4$
Cyclobutadiene (rectangular)	(1) (2) (3) (4)	y_1^4
	(1 ,2) (3, 4) ; (1, 4) (2, 3) ; (1, 3) (2, 4)	$3y_2^2$
Tetrahedrane (including stereoisomerism)	(1) (2) (3) (4)	y_1^4
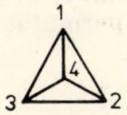	(1) (2, 3, 4) ; (1) (2, 4, 3) ; (2) (1, 3, 4) ; (2) (1, 4, 3) ; (3) (1, 4, 2) ; (3) (1, 2, 4) ; (4) (1, 2, 3) ; (4) (1, 3, 2)	$8y_1y_3$
	(1, 2) (3, 4) ; (1, 4) (2, 3) ; (1, 3) (2, 4)	$3y_2^2$
Benzvalene	(1) (2) (3) (4) (5) (6)	y_1^6
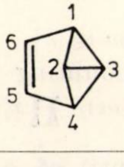	(1) (4) (5) (6) (2, 3)	$y_1^4y_2$
	(2) (3) (1, 4) (5, 6)	$y_1^2y_2^2$
	(1, 4) (2, 3) (5, 6)	y_2^3
Dewar-benzene	(1) (2) (3) (4) (5) (6)	y_1^6
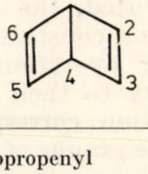	(1) (4) (2, 6) (3, 5)	$y_1^2y_2^2$
	(1, 4) (2, 5) (3, 6) ; (1, 4) (2, 3) (5, 6)	$2y_2^3$
Bicyclopropenyl	(1) (2) (3) (4) (5) (6)	y_1^6
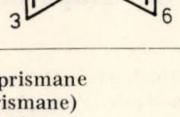	(1) (2) (3) (4) (5, 6) ; (1) (4) (5) (6) (2, 3)	$2y_1^4y_2$
	(1, 4) (2, 6) (3, 5) ; (1, 4) (2, 5) (3, 6)	$2y_2^3$
	(1) (4) (2, 3) (5, 6)	$y_1^2y_2^2$
	(1, 4) (2, 6, 3, 5) ; (1, 4) (2, 5, 3, 6)	$2y_2y_4$
Benzprismane (triprismane) (excluding stereoisomerism)	(1) (2) (3) (4) (5) (6)	y_1^6
	(1, 2, 3) (4, 5, 6) ; (1, 3, 2) (4, 6, 5)	$2y_3^2$
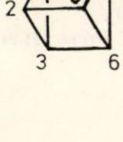	(1, 4) (2, 5) (3, 6) ; (1, 5) (2, 4) (3, 6) ; (1, 4) (2, 6) (3, 5) ; (1, 6) (2, 5) (3, 4)	$4y_2^3$
	(1, 5, 3, 4, 2, 6) ; (1, 6, 2, 4, 3, 5)	$2y_6$
	(2) (5) (1, 3) (4, 6) ; (3) (6) (1, 2) (4, 5) ; (1) (4) (2, 3) (5, 6)	$3y_1^2y_2^2$

Table 1 (continued)

Valence isomer	Permutation	Cycle index term
Benzprismane (including stereoisomerism)	(1) (2) (3) (4) (5) (6)	y_1^6
	(1, 2, 3) (4, 5, 6) ; (1, 3, 2) (4, 6, 5)	$2y_3^2$
	(1, 5) (2, 4) (3, 6) ; (1, 4) (2, 6) (3, 5) ; (1, 6) (2, 5) (3, 4)	$3y_2^3$
Benzene	(1) (2) (3) (4) (5) (6)	y_1^6
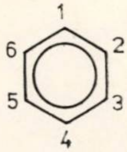	(1, 3, 5) (2, 4, 6) ; (1, 5, 3) (2, 6, 4)	$2y_3^2$
	(1, 4) (2, 5) (3, 6) ; (1, 6) (2, 5) (3, 4) ; (1, 2) (3, 6) (4, 5) ; (1, 4) (2, 3) (5, 6)	$4y_2^3$
	(1, 2, 3, 4, 5, 6) ; (1, 6, 5, 4, 3, 2)	$2y_6$
	(2) (5) (1, 3) (4, 6) ; (3) (6) (1, 5) (2, 4) ; (1) (4) (2, 6) (3, 5)	$3y_1^2y_2^2$
Benz-möbius-stripane	(1) (2) (3) (4) (5) (6)	y_1^6
	(1) (2) (3, 5) (4, 6) ; (1) (4) (3, 5) (2, 6) ; (1) (6) (3, 5) (2, 4) ; (3) (6) (1, 5) (2, 4) ; (2) (3) (1, 5) (4, 6) : (3) (4) (1, 5) (2, 6) ; (2) (5) (1, 3) (4, 6) ; (4) (5) (1, 3) (2, 6) ; (5) (6) (1, 3) (2, 4)	$9y_1^2y_2^2$
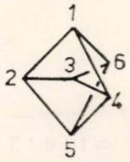	(1, 2) (3, 6) (4, 5) ; (1, 2) (3, 4) (5, 6) ; (1, 4) (2, 5) (3, 6) ; (1, 4) (2, 3) (5, 6) ; (1, 6) (2, 3) (4, 5) ; (1, 6) (2, 5) (3, 4) ; (1, 3, 5) (2, 4, 6) ; (1, 5, 3) (2, 6, 4) ;	$6y_2^3$
	(1, 3, 5) (2, 6, 4) ; (1, 5, 3) (2, 4, 6)	$4y_3^2$
	(1) (3) (5) (2, 4, 6) ; (1) (3) (5) (2, 6, 4) ; (2) (4) (6) (1, 3, 5) ; (2) (4) (6) (1, 5, 3)	$4y_1^3y_3$
	(1, 2, 3, 4, 5, 6) ; (1, 6, 5, 4, 3, 2) ; (1, 2, 3, 6, 5, 4) ; (1, 4, 5, 6, 3, 2) ; (1, 2, 5, 6, 3, 4) ; (1, 4, 3, 6, 5, 2) ; (1, 2, 5, 4, 3, 6) ; (1, 6, 3, 4, 5, 2) ; (1, 6, 3, 2, 5, 4) ; (1, 4, 5, 2, 3, 6) ; (1, 6, 5, 2, 3, 4) ; (1, 4, 3, 2, 5, 6)	$12y_6$

"three houses – three utilities problem", therefore it also has a trigonal axis.

For the two valence isomers of [4]annulene (cyclobutadiene and tetrahedrane), four cycle indices are presented in table 3, since cyclobutadiene could exist in a triplet D_{4h} square geometry, or in a singlet D_{2h} rectangular geometry with localized double bonds; for tetrahedrane one may consider topological (constitutional) isomerism when all 4! permutations between the vertices of the complete graph K_4 are possible (cf. next paragraph), or geometrical isomerism when only half of these permutations, corresponding to the symmetry axes of a tetrahedron, are allowed. In other words, when the symmetry operations are performed on a geometrical object we obtain numbers of isomers including stereoisomerism, and when they are performed on a topological object (graph which may assume all possible geometries), we obtain numbers of isomers excluding stereoisomerism, i.e. constitutional isomers.

In the case of the complete graph K_n with n points, let

$$n = 1.k_1 + 2.k_2 + 3.k_3 + \ldots$$

be one of the partitions of n. Then, according to the Cauchy identity[18] extended over all partitions of n, denoted by $p(n)$

$$n! = \sum \frac{n!}{1^{k_1}\cdot k_1!2^{k_2}\cdot k_2!3^{k_3}\cdot k_3!\ldots}$$

the n! permutations can be grouped, according to their cyclic representations, as a sum of $p(n)$ terms. Thus for the complete graph K_4 (tetrahedrane excluding stereoisomerism), the $4! = 24$ permutations are grouped into $p(4) = 5$ terms (according to the respective cycle index formula in table 3). Accordingly the Cauchy identity becomes

$$\begin{array}{ccccccccccc} \text{Partition:} & & 1+1+1+1 & & 2+1+1 & & 2+2 & & 3+1 & & 4 \\ 24 & = & \dfrac{4!}{1^4\cdot 4!} & + & \dfrac{4!}{1^2\cdot 2!2^1\cdot 1!} & + & \dfrac{4!}{2^2\cdot 2!} & + & \dfrac{4!}{3^1\cdot 1!1^1\cdot 1!} & + & \dfrac{4!}{4!\cdot 1!} = 1+6+3+8+6. \end{array}$$

These are the coefficients of the cycle index for tetrahedrane excluding stereoisomerism presented in table 3. Since all permutations are allowed, this case was not included in table 1.

On the other hand, for benzene, only the delocalized D_{6h} structure was considered; thus [6]annulene is represented by the cyclic graph C_6 which is regular of degree 2, rather than 3.

Table 2 presents the coefficients of the terms $\prod_{i=1}^{n} x_i^j$ resulted from the figure counting series $y_k = \sum_{i=1}^{n} x_i^k$, grouped according to the partition of exponents j. Only those partitions are considered which will be encountered in the next tables. By operating with the coefficients presented in table 2 according to the cycle indices from tables 3 and 4, the numbers of isomers shown in the right-hand side of tables 3 and 4 were found: to convert the figure counting series into numbers of isomers, we have

---

[18] J. Riordan, "An Introduction to Combinatorial Analysis", Wiley, New York, 1958, p. 69.

Table 2

Coefficients of terms $\prod_{i=1}^{n} x_i^j$ resulted from figure-counting series $y_k = \sum_{i=1}^{n} x_i^k$, grouped according to the partition of exponents j

Term \ Partition	4	3, 1	2, 2	2, 1, 1	1, 1, 1, 1
y_1^4	1	4	6	12	24
y_2^2	1	0	2	0	0
y_1y_3	1	1	0	0	0
$y_1^2y_2$	1	2	2	2	0
y_4	1	0	0	0	0

Term \ Partition	6	5, 1	4, 2	3, 3	4, 1, 1	3, 2, 1	2, 2, 2	3, 1, 1, 1	2, 2, 1, 1	2, 1, 1, 1, 1	1, 1, 1, 1, 1, 1
y_1^6	1	6	15	20	30	60	90	120	180	360	720
$y_1^4y_2$	1	4	7	8	12	16	18	24	24	24	0
$y_1^3y_3$	1	3	3	2	6	3	0	6	0	0	0
$y_1^2y_2^2$	1	2	3	4	2	4	2	0	4	0	0
y_2^3	1	0	3	0	0	0	6	0	0	0	0
y_2y_4	1	0	1	0	0	0	0	0	0	0	0
y_3^2	1	0	0	2	0	0	0	0	0	0	0
y_6	1	0	0	0	0	0	0	0	0	0	0

Term \ Partition	8	7, 1	6, 2	5, 3	4, 4	etc.
y_1^8	1	8	28	56	70	
$y_1^6y_2$	1	6	16	26	30	
$y_1^4y_2^2$	1	4	8	12	14	
$y_1^2y_2^3$	1	2	4	6	6	
y_2^4	1	0	4	0	6	
$y_2^2y_4$	1	0	2	0	2	
y_4^2	1	0	0	0	2	
y_8	1	0	0	0	0	

Term \ Partition	10	9, 1	8, 2	7, 3	6, 4	5, 5	etc.
y_1^{10}	1	10	45	120	210	252	
$y_1^8y_2$	1	8	29	64	98	112	
$y_1^6y_2^2$	1	6	17	32	46	52	
$y_1^4y_2^3$	1	4	9	16	22	24	
$y_1y_3^3$	1	1	0	3	3	0	
y_2^5	1	0	5	0	10	0	
$y_2^3y_4$	1	0	3	0	4	0	
$y_2y_4^2$	1	0	1	0	2	0	
y_5^2	1	0	0	0	0	2	
y_{10}	1	0	0	0	0	0	

Table 3

Valence isomers of substituted [4]annulene

$n = 4$	Cycle index	Partitions of substituents 4	 3, 1	 2, 2	 2, 1, 1	 1,1,1,1
		Number of isomers				
Cyclobutadiene (square)	$\frac{1}{8}(y_1^4 + 2y_1^2y_2 + 3y_2^2 + 2y_4)$	1	1	2	2	3
Idem (rectangular)	$\frac{1}{4}(y_1^4 + 3y_2^2)$	1	1	3	3	6
Tetrahedrane (including stereoisomerism)	$\frac{1}{12}(y_1^4 + 3y_2^2 + 8y_1y_3)$	1	1	1	1	2
Idem (excluding stereoisomerism)	$\frac{1}{24}(y_1^4 + 6y_1^2y_2 + 3y_2^2 + 8y_1y_3 + 6y_4)$	1	1	1	1	1

Table

Valence isomers of

$n = 6$	Cycle index[a]
Benzvalene	$\frac{1}{4}(y_1^6 + y_1^4y_2 + y_2^3 + y_1^2y_2^2)$
Dewar-benzene	$\frac{1}{4}(y_1^6 + 2y_2^3 + y_1^2y_2^2)$
Bicyclopropenyl	$\frac{1}{8}(y_1^6 + 2y_1^4y_2 + 2y_2^3 + y_1^2y_2^2 + 2y_2y_4)$
Benzprismane (including stereoisomerism)	$\frac{1}{6}(y_1^6 + 3y_2^3 + 2y_3^2)$
Benzprismane (excluding stereoisomerism)	$\frac{1}{12}(y_1^6 + 4y_2^3 + 3y_1^2y_2^2 + 2y_3^2 + 2y_6)$
Benzene	$\frac{1}{12}(y_1^6 + 4y_2^3 + 3y_1^2y_2^2 + 2y_3^2 + 2y_6)$
Benz-möbius-stripane	$\frac{1}{36}(y_1^6 + 6y_2^3 + 9y_1^2y_2^2 + 4y_3^2 + 12y_6 + 4y_1^3y_3)$

[a] Cycle indices were calculated to express only constitutional isomerism, unless otherwise stated.

to apply Pólya's theorem. These numbers are grouped according to the partition of substituents.*

Thus, valence isomers of [4]annulene can have one of the four CH groups substituted (partition 3, 1), or two of them substituted by one type (partition 2,2) or by two types of substituents (partition 2, 1, 1). There exist [18,19] five partitions of 4 as indicated above by $p(4) = 5$, and eleven partitions of 6, as seen in the headings of tables 3 and 4, respectively.

---

* Since heteroatoms give the same numbers of constitutional isomers as do substituents, one may replace "substituent" by "heteroatom" in this and subsequent phrases. However, when stereoisomerism is not ignored the numbers of valence isomers for aza-annulenes and substituted annulenes may be different because of the easy nitrogen inversion e.g. in the case of

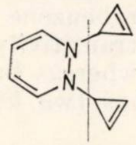

and

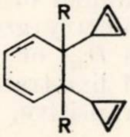

[19] A. T. Balaban, *Rev. Roumaine Chim.*, **16**, 9 (1972).

4

substituted [6] annulene

Partitions of substituents										
6	5, 1	4, 2	3, 3	4, 1, 1	3, 2, 1	2, 2, 2	3, 1, 1, 1	2, 2, 1, 1	2, 1, 1, 1, 1	1, 1, 1, 1, 1, 1
Numbers of isomers										
1	3	7	8	11	20	29	36	52	96	180
1	2	6	6	8	16	26	30	46	90	180
1	2	5	5	7	12	20	21	29	51	90
1	1	4	4	5	10	18	20	30	60	120
1	1	3	3	3	6	11	10	16	30	60
1	1	3	3	3	6	11	10	16	30	60
1	1	2	2	3	3	4	4	6	10	20

It is apparent from table 4 that benzene and benzprismane (triprismane) have the same cycle index and hence afford the same numbers of substituted isomers, if stereoisomerism is ignored. This is a general property of [n]annulenes and their $\left(\frac{n}{2}\right)$-prismane valence isomers with $n = 6$ and $n \geqslant 10$, as will be shown further below in the case of delocalized cyclodecapentaene and pentaprismane. The presence of an improper axis of rotation S_6 in triprismane explains the occurrence of the cyclic permutations involving all six vertices, which in benzene are derived from the proper axis C_6.

It shoul be emphasized that the number of isomers depends only on the cycle index, and not on the symmetry group (for benzene the point group is D_{6h}, for benzprismane it is D_{3h}) or on the transitivity of lines in the graph (benzene is point- and line-transitive, whereas benzprismane is point-transitive but line- intransitive, i.e. it has two kinds of lines or C—C bonds).

We will call such molecules (or graphs, respectively) having identical cycle indices, "coisomeric". Coisomeric graphs must have the same symmetry operations and the same vertex transitivity, i. e. the same partition of different types of vertices.

Historically, the coincidence of cycle indices for benzene and benzprismane formulas caused much confusion and debate during the years when the benzene formula was under discussion. Ladenburg [20] had advocated the triprismane formula for benzene against Kekulé's, since the former formula explained the numbers of isomers without having recourse to Kekulé's additional hypothesis of "oscillating valencies" (refined into today's delocalized bonds). The correspondence between *ortho*, *meta*, and *para*-disubstituted isomers in both cases is seen from table 5 on the basis of numbers of isomers on going from partition 4, 2 to parition 3, 2, 1.* In agreement with tables 4 and 5, there are 3 and 4 isomers, respectively, for triprismane with two identical substituents (partition 2, 4) when ignoring, respectively including, stereoisomerism, but 6 and 10 isomers, respectively, for partition 3, 2, 1. The *para*-substituted derivatives have two orthogonal axes C_2, and afford therefore the smallest number of isomers. The *ortho*- and *meta*-substituted derivatives have only one C_2 axis : in the *ortho*-derivatives (point group C_{2h} for the triprismane derivative), this axis does not pass through two points, therefore an intermediate number of isomers is obtained. In *meta*-derivatives, this axis passes through two atoms (point group C_{2v} for the triprismane derivative) and leads to the highest number of isomers. This may be generalized to all [n]annulenes and $\left(\frac{n}{2}\right)$-prismanes (which are coisomeric, with the exception of $n = 8$ since the cube has a higher symmetry than the octogon).

---

* The presence or absence of a bond between *ortho*, *meta* or *para* positions is opposite in benzene and benzprismane.

[20] A. Ladenburg, *Ber. dtsch. chem. Ges.*, **12**, 141, 272 (1879).

Table 5

***ortho*-Disubstituted derivatives $C_6H_4A_2$ afford two constitutional isomers $C_6H_3A_2B$, *meta*-substituted ones afford three, and *para*-substituted ones afford one isomer in benzene and triprismane (benzprismane), ignoring the possible stereoisomerism of the latter (indicated by asterisks)**

Partition	Benzene			Benzprismane		
4+2	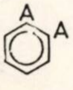 ortho	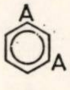 meta	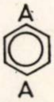 para	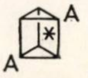 "ortho"	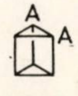 "meta"	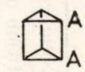 "para"
3+2+1	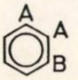 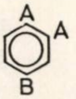	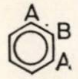 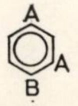 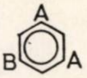	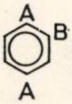	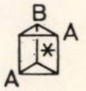 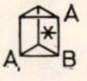	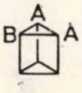 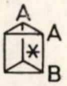 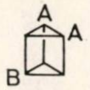	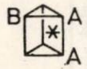

The polemic around the benzene formula gradually favoured the Kekulé formula when *ortho*-fused systems like naphthalene were discovered, since their prismane formulas were extremely awkward, and was ended when Baeyer [21] showed that *o*-disubstituted benzenes afford on hydrogenation only one isomer of a cyclohexane derivative, a fact which could not be rationalized by Ladenburg's formula. Also, no optical activity could be demonstrated in substituted benzenes, as required by the triprismane formula (in table 5, enantiomeric structures are indicated by asterisks).

A complete search was made for cycle indices of all possible planar valence isomers of [8]annulene, and three pairs of coisomeric graphs were found, which are presented in table 6. It should be mentioned that two other pairs of cubic planar multigraphs of order 8 afford the same numbers of mono- and disubstituted isomers, but since they have different cycle indices, this is only a coincidence: indeed, the numbers of tri- and tetrasubstituted isomers are different, as seen from table 7. Similar cases exist for $n = 10$.

Table 6 also presents examples of coisomeric valence isomers of [10]annulene, namely pairs, triplets, quadruplets, and quintets. For $n = 10$, table 6 may not be exhaustive, but it is so for $n = 6$ and 8.

---

[21] A. von Baeyer, *Ber. dtsch. chem. Ges.*, **19**, 1797 (1888); **23**, 1272 (1890); *Liebigs Ann. Chem.*, **245**, 103 (1887); **251**, 257 (1889); **256**, 1 (1890); **258**, 145 (1890); **266**, 169 (1892); **276**, 259 (1893).

Table 6

Coisomeric cubic graphs of order n (valence isomers of substituted [n]annulenes)

n	Formulas	Cycle index	Number of isomers Partition of substituents: $n-1, 1$	$n-2, 2$	$n-3, 3$	$n-4, 4$	$n-5, 5$
6	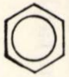 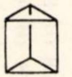	$\frac{1}{12}(y_1^6 + 3y_1^2y_2^2 + 4y_2^3 + 2y_3^2 + 2y_6)$	1	3	3	3	1
8	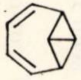 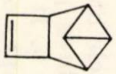	$\frac{1}{4}(y_1^8 + y_1^6y_2 + y_1^2y_2^3 + y_2^4)$	4	13	22	28	22
	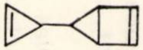 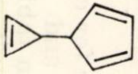	$\frac{1}{4}(y_1^8 + y_1^6y_2 + y_1^4y_2^2 + y_1^2y_2^3)$	5	14	25	30	25
	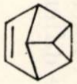 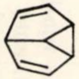	$\frac{1}{2}(y_1^8 + y_1^2y_2^3)$	5	16	31	38	31
10	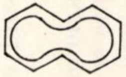 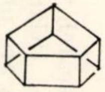	$\frac{1}{20}(y_1^{10} + 5y_1^2y_2^4 + 6y_2^5 + 4y_5^2 + 4y_{10})$	1	5	8	16	16
	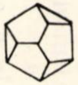 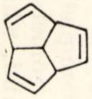	$\frac{1}{6}(y_1^{10} + 3y_1^2y_2^4 + 2y_1y_3^3)$	3	10	25	41	48
	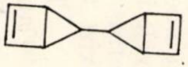 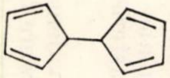	$\frac{1}{8}(y_1^{10} + 2y_2^6y_2^2 + y_1^2y_2^4 + 2y_2^5 + 2y_2y_4^2)$	3	12	24	42	46

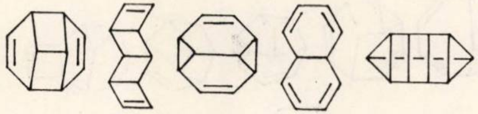	$\frac{1}{4}(y_1^{10} + y_1^2y_2^4 + 2y_2^5)$	3	15	32	60	66
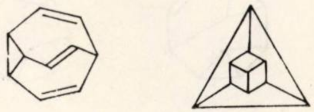	$\frac{1}{6}(y_1^{10} + 3y_1^4y_2^3 + 2y_1y_3^3)$	4	12	29	47	54
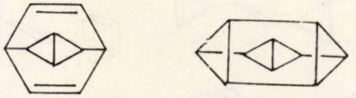	$\frac{1}{8}(y_1^{10}+y_1^8y_2+y_1^6y_2^2+y_1^4y_2^3+2y_1^2y_2^4+2y_2^5)$	4	15	31	52	58
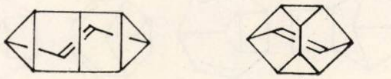	$\frac{1}{4}(y_1^{10} + y_1^4y_2^3 + y_1^2y_2^4 + y_2^5)$	4	16	36	63	72
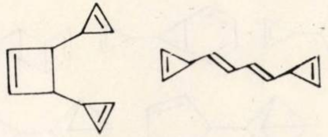	$\frac{1}{8}(y_1^{10} + 2y_1^8y_2 + y_1^6y_2^2 + 2y_2^5 + 2y_2^3y_4$	4	17	35	60	66
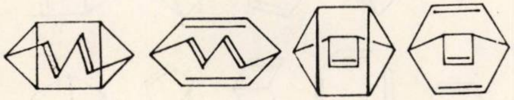	$\frac{1}{4}(y_1^{10} + y_1^6y_2^2 + 2y_2^5)$	4	18	38	69	76
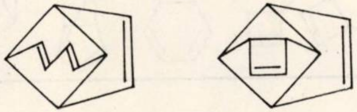	$\frac{1}{4}(y_1^{10} + y_1^6y_2^2 + y_1^4y_2^3 + y_2^5)$	5	19	42	72	82
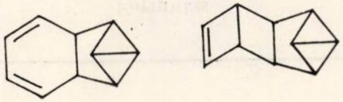	$\frac{1}{4}(y_1^{10} + y_1^8y_2 + y_1^2y_2^4 + y_2^5)$	5	21	48	82	94

Table 6 (continued)

n	Formulas	Cycle index	Number of isomers				
			Partition of substituents:				
			$n-1,1$	$n-2,2$	$n-3,3$	$n-4,4$	$n-5,5$
10	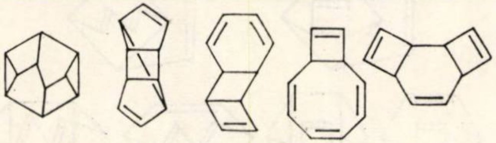	$\frac{1}{2}(y_1^{10}+y_2^5)$	5	25	60	110	126
	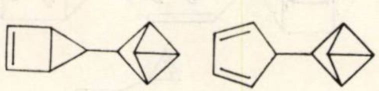	$\frac{1}{8}(y_1^{10}+2y_1^8y_2+2y_1^6y_2^2+2y_1^4y_2^3+y_1^2y_2^4)$	6	20	44	69	80
	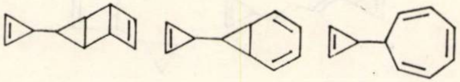	$\frac{1}{4}(y_1^{10}+y_1^8y_2+y_1^4y_2^3+y_1^2y_2^4)$	6	22	52	85	100
	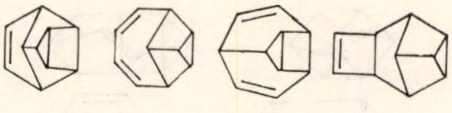	$\frac{1}{2}(y_1^{10}+y_1^2y_2^4)$	6	25	64	110	132
	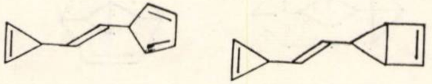	$\frac{1}{4}(y_1^{10}+y_1^8y_2+y_1^6y_2^2+y_1^4y_2^3)$	7	25	58	94	110
	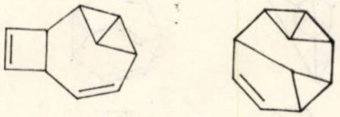	$\frac{1}{2}(y_1^{10}+y_1^8y_2)$	9	37	92	154	182
	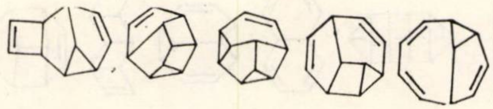	y_1^{10}	10	45	120	210	252

Table 7

Pairs of cubic graphs of order 8 which are not coisomeric

Formula	Cycle index	Number of isomers			
		7, 1	6, 2	5, 3	4, 4
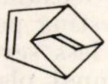	$\frac{1}{8}(y_1^8 + 2y_1^4y_2^2 + 2y_4^2 + 3y_2^4)$	2	7	10	15
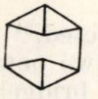	$\frac{1}{16}(y_1^8 + 2y_1^6y_2 + 3y_1^4y_2^2 + 4y_2^4 + 6y_2^2y_4)$	2	7	9	13
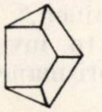	$\frac{1}{4}(y_1^8 + 2y_1^2y_2^3 + y_2^4)$	3	10	17	22
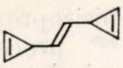	$\frac{1}{8}(y_1^8 + 2y_1^6y_2 + y_1^4y_2^2 + 2y_2^4 + 2y_2^2y_4)$	3	10	15	20

As noted above, pentaprismane is coisomeric with delocalized [10]annulene. Pentaprismane is not yet known, and [10]annulene is much less stable than benzene. It is interesting to note that bullvalene is coisomeric with a saturated valence isomer of [10]annulene. Another observation concerning table 6 is provided by the five coisomeric valence isomers of [10]annulene with cycle index $(y_1^{10} + y_2^5)/2$: two of these have point group C_{2h} (including a symmetry centre and one plane of symmetry), the remaining three have point group C_{2v} (including two symmetry planes). The number of isomers does not depend on reflections, but only on symmetry axes.

EXAMPLES

1. *Valence isomers of substituted annulenes.* The first valence isomers of [4]- and [6]annulene to be prepared were substituted ones (tetramethylcyclobutadiene,[22] t-butyl-substituted Dewar-benzene [23] and benzprismane,[24] phenyl-substituted bicyclopropenyl [25]). Since the literature

---

[22] R. Criegee, *Angew. Chem.*, **74**, 703 (1962); *Bull. Soc. Chim. France*, **1965**, 1; R. Criegee and W. Funke, *Chem. Ber.*, **87**, 2934 (1964).

[23] E. E. van Tamelen and S. P. Pappas, *J. Amer. Chem. Soc.*, **85**, 3297 (1963).

[24] K. E. Wilzbach and L. Kaplan, *J. Amer. Chem. Soc.*, **87**, 4004 (1965); L. Kaplan, J. S. Ritscher and K. E. Wilzbach, *ibid.*, **88**, 2066, 2881 (1966).

[25] R. Breslow and P. Gal, *J. Amer. Chem. Soc.*, **81**, 4747 (1959); R. Breslow, W. Bahary and W. Reinmuth, *ibid.*, **83**, 1763 (1961); R. Breslow, P. Gal, H. W. Chang and L. J. Altman, *ibid.*, **87**, 5139 (1965).

was summerized in recently published reviews for valence isomers of $[n]$annulenes with or without substituents, we will only quote these reviews: $n = 4$,[26] $n = 4 - 10$,[5,6,27] $n = 6, 10$,[28a] $n = 10$,[28b] $n = 12$,[6] and $n > 12$.[29]

2. *Valence isomers of heteroannulenes.* Two reviews have so far been published on this topic.[27] In the following, a few non-exhaustive examples will show the huge non-explored area offered by these interesting possibilities, especially for larger n values where steric strain is less severe. According to table 4, there should exist 9 constitutional planar valence isomers of pyridine, 24 of diazine and 25 of triazine.

Valence isomers of pyridine were claimed,[30] then retracted,[31] and finally first prepared by a photochemical reaction: one of the two possible Dewar-pyridines, namely that with the heteroatom at a bridgehead position.[32] Pentakis-pentafluoropyridine valence isomers, namely a similar Dewar-pyridine and an azabenzprismane, were recently obtained.[9] The photochemical conversions of pyrylium salts are believed to involve oxonia-analogues of benzvalene, or, less probably, of benzprismane or Dewar-benzene.[33]

The photochemical rearrangement of perfluoro-(4,5-bisisopropylpyridazine) into the corresponding pyrazine derivative [34a] proceeds *via* diaza-Dewar-benzene intermediates, one of which could be isolated.[34b]

Valence isomers of mono- and diazacyclooctatetraene are known. The heteroatom exerts a strong influence on the valence tautomerism between [8]annulene and bicyclo[4.2.0]octa-2,4,7-triene. Monoazacyclooctatetraene or azocine (with a 2-alkoxy substituent) evidences by spectroscopic methods only the existence of the monocyclic tautomer, II, but the mobile equilibrium with the bicyclic tautomer III in minute amounts allows diene reactions leading to products IV derived from the latter, namely with the heteroatom in position 7 (the other three possible bicyclic isomers are absent).[35] By contrast, hydrolysis of the alkoxy

[26] G. MAIER, *Angew. Chem.*, **86**, 491 (1974); *Angew. Chem. Internat. Ed.*, **13**, 425 (1974).

[27] a) L. T. SCOTT and M. JONES, Jr., *Chem. Rev.*, **72**, 181 (1972); b) G. MAIER, "Valenzisomerisierungen", Verlag Chemie, Weinheim, 1972.

[28] a) E. E. VAN TAMELEN, *Accounts Chem. Res.*, **5**, 186 (1972); b) S. MASAMUNE and N. DARBY, *Accounts Chem. Res.*, **5**, 272 (1972).

[29] A. T. BALABAN and V. CIORBA, to be published.

[30] E. C. TAYLOR, W. W. PAUDLER and J. KUNTZ, *J. Amer. Chem. Soc.*, **83**, 2967 (1961).

[31] E. C. TAYLOR and R. O. KAN, *J. Amer. Chem. Soc.*, **85**, 776 (1963); E. C. TAYLOR, R. O. KAN and W. W. PAUDLER, *ibid.*, **83**, 4484 (1961).

[32] K. E. WILZBACH and D. J. RAUSCH, *J. Amer. Chem. Soc.*, **92**, 2178 (1970); S. CAPLAIN and A. LABLACHE-COMBIER, *J.C.S. Chem. Comm.*, **1970**, 1247.

[33] J. A. BARLTROP, K. DAWES, A. C. DAY and A. J. H. SUMMERS, *J.C.S. Chem. Comm.*, **1972**, 1240; J. A. BARLTROP, K. DAWES, A. C. DAY, S. J. NUTTALL and A. J. H. SUMMERS, *ibid.*, **1973**, 410; J. A. BARLTROP, K. DAWES, A. C. DAY and A. J. H. SUMMERS, *J. Amer. Chem. Soc.*, **95**, 1967 (1973).

[34] a) C. G. ALLISON, R. D. CHAMBERS, YU. A. CHERBUKOV, J. A. H. MACBRIDE and W. K. R. MUSGRAVE, *J.C.S. Chem. Comm.*, **1969**, 1200; b) R. D. CHAMBERS, W. K. R. MUSGRAVE and K. S. SRIVASTAVA, *ibid.*, **1971**, 264.

[35] L. A. PAQUETTE and T. KAKIHANA, *J. Amer. Chem. Soc.*, **90**, 3897 (1968); L. A. PAQUETTE and J. C. PHILIPS, *ibid.*, **90**, 3898 (1968); L. A. PAQUETTE, T. KAKIHANA, J. F. HANSENAND and J. C. PHILIPS, *ibid.*, **93**, 152 (1971).

group affords the amide which exists entirely as the bicyclic valence isomer V [36]

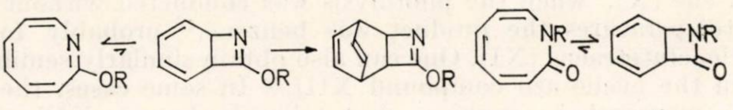

II III IV V

1,2-Diazacyclooctatetraene with phenyl and methyl substituents also exists as the bicyclic tautomer VI. On heating, it splits off nitrogen, affording a benzene derivative, presumably *via* the monocyclic valence isomer, VII [37]

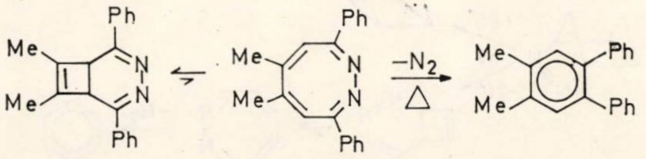

VI VII

It was predicted by M. J. S. Dewar [38a] and by R. Hoffmann [38b] that the low-barrier degenerate rearrangement of semibullvalene could become even easier with appropriate donor (Do) or acceptor (Acc) substituents (VIIIa) or with heteroatoms (VIIIb), so that such structures would be good candidates for mesovalent molecules.[38a] By contrast, hexamethyl-2-methoxy-azasemibullvalene (IX) presents no degenerate rearrangement in the temperature range −40° to 150°.[39]

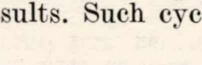

VIIIa

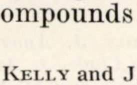

VIIIb

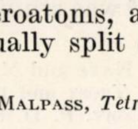

IX

If two carbon atoms joined by a double bond in a valence isomer of an [*n*]annulene are replaced by nitrogen heteroatoms, a cyclic azo compound results. Such cyclic azo compounds usually split off nitrogen thermally or photolytically affording valence isomers of [n-2]annulenes: thus was synthesized benzprismane[40] from 7,8-diazatetracyclo[3.3.0.0^{2,4}.0^{3,6}]oct-7-ene (X), when the photolysis was conducted without cooling; at low temperatures the product was benzene,[41] probably formed *via* diazacyclooctatetraene (XI). One can also obtain similarly semibullvalene XII from the cyclic azo compound XIII.[42] In some cases, the reaction takes an unexpected course, e. g. 1,2-diazabasketene XIV (7,8-diazapentacyclo[4.2.2.0^{2,5}.0^{3,9}.0^{4,10}]dec-7-ene) yields the unsubstituted azocine XVI by loss of hydrogen cyanide from a diazaderivative XV of the Nenitzescu hydrocarbon, formed intermediately.[43] Cyclic bis-azo derivatives are also known[44]

---

[36] L. A. Paquette, T. Kakihana, J. F. Kelly and J. R. Malpass, *Tetrahedron Letters*, **1969**, 1455.

[37] G. Maier, *Chem. Ber.*, **99**, 1232 (1966); G. Maier, U. Heep, M. Wiessler and M. Strasser, *ibid.*, **102**, 1928 (1969).

[38] a) M. J. S. Dewar and W. W. Schoeller, *J. Amer. Chem. Soc.*, **93**, 1481 (1971); M. J. S. Dewar and D. H. Lo, *ibid.*, **93**, 7201 (1971); M. J. S. Dewar, Z. Náhlovská and B. D. Náhlovský, *J.C.S. Chem. Comm.*, **1971**, 1377. b) R. Hoffmann and W. D. Stohrer, *J. Amer. Chem. Soc.*, **93**, 6941 (1971).

[39] L. A. Paquette, *Tetrahedron Letters*, **1968**, 2133; L. A. Paquette and G. R. Krow, *J. Amer. Chem. Soc.*, **91**, 6107 (1969).

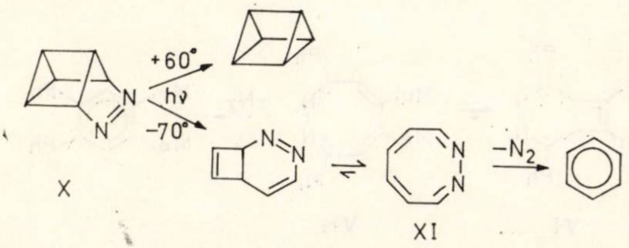

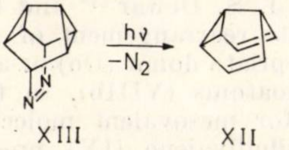

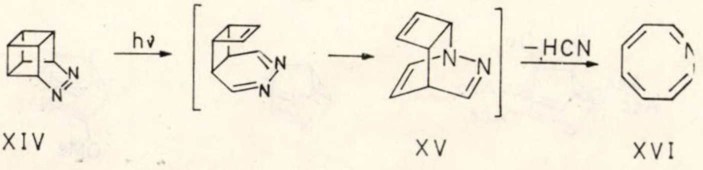

In the valence isomers of hetero-[10]annulenes, 1,6-dimethyl-2,5-diphenyl-3,4-azabicyclo[4.4.0]deca-2,4,7,9-tetraene, XVII, undergoes a facile 1,5-carbon migration.[45] The degenerate rearrangement of azabullvalene[46] was studied by Paquette[47] using NMR techniques at variable temperatures. 2-Methoxyazabullvalene (3-methoxy-4-azatricyclo[3.3.2.$0^{2,8}$]deca-3,6,9-triene, XVIII) can be obtained photochemically from 8-methoxy-7-azabicyclo[4.2.2]deca-2,4,7,9-tetraene, XIX.[48] Pyrolysis of either of these two valence isomers affords the same mixture of substituted quinoline and isoquinoline isomers, XXIV, and this was interpreted as involving the transient formation of four common valence isomeric intermediates XX – XXIII[48]

---

[40] T. J. Katz and N. Acton, *J. Amer. Chem. Soc.*, **95**, 2738 (1973).

[41] B. M. Trost and R. M. Cory, *J. Amer. Chem. Soc.*, **93**, 5572, 5573 (1971); B. M. Trost, R. M. Cory, P. H. Scudder and H. B. Neubold, *ibid.*, **75**, 7813 (1973).

[42] R. M. Moriarty, C. L. Yeh and N. Ishibi, *J. Amer. Chem. Soc.*, **92**, 5766 (1970); L. A. Paquette, *ibid.*, **92**, 5766 (1970); R. Askani, *Tetrahedron Letters*, **1970**, 3349.

[43] D. W. McNeil, M. E. Kent, E. Hedaya, P. F. D'Angelo and P. O. Schissel, *J. Amer. Chem. Soc.*, **93**, 3817 (1971).

[44] K.-W. Shen, *J. Amer. Chem. Soc.*, **93**, 3064 (1971).

[45] G. Maier, I. Fuss, and M. Schneider, *Tetrahedron Letters*, **1970**, 1057.

[46] P. Wegener, *Tetrahedron Letters*, **1967**, 4985.

[47] L. A. Paquette, J. R. Malpass, G. R. Krow and T. J. Barton, *J. Amer. Chem. Soc.*, **91**, 5296 (1969); L. A. Paquette and G. R. Krow, **90**, 7149 (1968); L. A. Paquette and T. J. Barton, *ibid.*, **89**, 5840 (1967); L..A. Paquette, T. J. Barton and E. B. Whipple, *ibid.*, **89**, 5841 (1967).

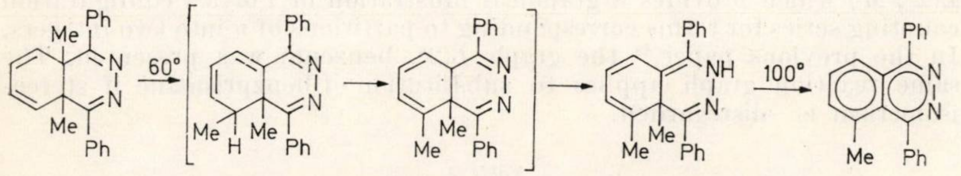

XVII

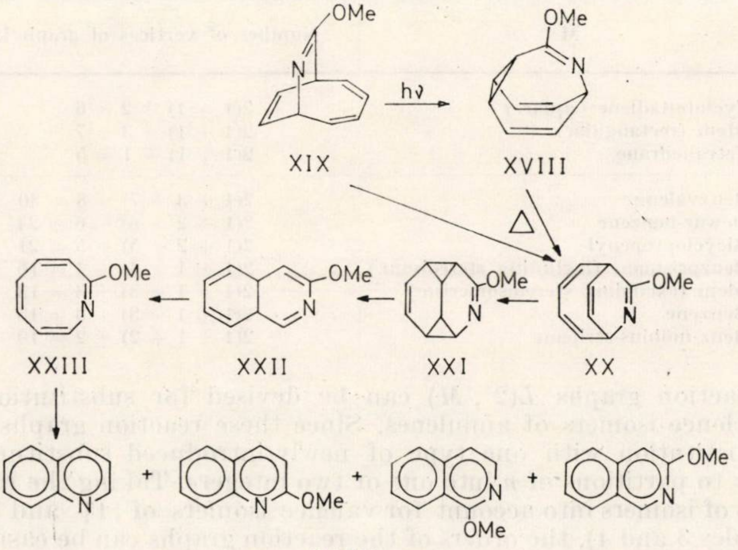

REACTION GRAPHS FOR SUBSTITUTING VALENCE ISOMERS OF [n]ANNULENES

In a previous paper,[49] reaction graphs corresponding to substitution reactions were defined and discussed. When the *s* substitution sites are non-equivalent, or when they become so at a certain step of the substitution, the reaction graphs are denoted by $L(r^s, M)$, where M is the reduced structural graph of the molecule undergoing substitution, and r is the number of types of substituents (thus, in the case of one type of substituent, e. g. in progressive halogenations, deuterations, or alkylations, $r = 2$, i. e. the preexisting hydrogens, and the newly introduced Hal, D or Alk groups).

---

[48] L. A. Paquette, G. R. Krow and J. R. Malpass, *J. Amer. Chem. Soc.*, **91**, 5522 (1969); L. A. Paquette, C. R. Krow, J. R. Malpass and T. J. Barton, *ibid.*, **90**, 3600 (1968).

[49] A. T. Balaban, and F. Kerek, *Rev. Roumaine Chim.*, **19**, 631 (1974).

Thus the progressive substitution (with one type of substituent) of a valence isomer of an [n]annulene gives rise to a reaction graph $L(2^n, M)$ which provides a graphical illustration of Pólya's configuration counting series for terms corresponding to partitions of n into two integers. In the previous paper,[49] the graph $L(2^6$, benzene) was presented. The same reaction graph applies to substitution of benzprismane if stereoisomerism is disregarded.

Table 8

Order of reaction graphs $L(2^n, M)$ for substitution of valence isomers of [4]- and [6]annulene

n	M	Number of vertices of graph $L(2^n, M)$
4	Cyclobutadiene (square)	$2(1 + 1) + 2 = 6$
	Idem (rectangular)	$2(1 + 1) + 3 = 7$
	Tetrahedrane	$2(1 + 1) + 1 = 5$
6	Benzvalene	$2(1 + 3 + 7) + 8 = 30$
	Dewar-benzene	$2(1 + 2 + 6) + 6 = 24$
	Bicyclopropenyl	$2(1 + 2 + 5) + 5 = 21$
	Benzprismane (including stereoisom.)	$2(1 + 1 + 4) + 4 = 16$
	Idem (excluding stereoisomerism)	$2(1 + 1 + 3) + 3 = 13$
	Benzene	$2(1 + 1 + 3) + 3 = 13$
	Benz-möbius-stripane	$2(1 + 1 + 2) + 2 = 10$

Reaction graphs $L(2^n, M)$ can be devised for substitution of all other valence isomers of annulenes. Since these reaction graphs concern only substitution with one type of newly-introduced substituent, they all apply to partitions of n into one or two integers. Taking the respective numbers of isomers into account for valence isomers of [4]- and [6]annulene (tables 3 and 4), the orders of the reaction graphs can be easily calculated as follows : since the numbers of isomers for partitions $n, 0$; $n - 1, 1$; $n - 2, 2$; ... ; $n/2 + 1, n/2 - 1$ are equal to those for partitions $0, n$; $1, n - 1$; $2, n - 2$; ... ; $n/2 - 1, n/2 + 1$, respectively, one has to add twice these numbers to the number of isomers for partition $n/2, n/2$. The results are presented in table 8 which gives the orders (numbers of vertices) of these graphs.

Revue Roumaine de Chimie, **19**, *8*, 1343–1349 (1974)

CARBONIUM ION REACTIONS. X*

NITROUS ACID DEAMINATION OF 5-AMINOMETHYL-5H-6,7-DIHYDRO-DIBENZO[*a,c*]CYCLOHEPTENE

M. BANCIU, ECATERINA DRAGU, DOINA GEORGESCU and
ECATERINA CIORĂNESCU
Laboratory of Organic Chemistry, Polytechnic Institute, str. Polizu nr. 1, Bucharest,
Romania

Received February 4, 1974

The title compound, **1-NH$_2$**, was synthesized and subjected to nitrous acid deamination. The major reaction products were: the ring enlarged alcohol **5**, the tertiary alcohol **10** and the unrearranged alcohol **1-OH**. Two olefins, **2** and **3**, are also formed in small quantities. The reaction mechanism and a comparison with the known solvolysis of the tosylate with the same skeleton are presented.

INTRODUCTION

As previously described,[1] the acetolysis of 5-tosyloxymethyl-5H-6,7-dihydro-dibenzo[*a,c*]cycloheptene **(1-OTs)** proceeds with extensive ring enlargement, giving rise (after LiAlH$_4$-reduction) to compounds **1-OH** – **5** (see Table 1).

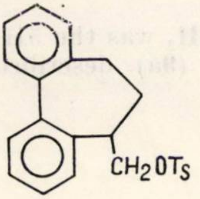

1-OTs

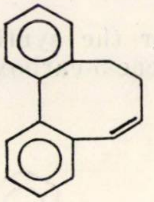

2

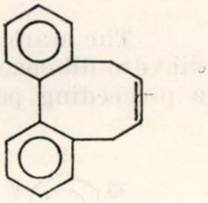

3

---

* Part IX. A. Banciu, M. Elian, A. Bucur, D. Georgescu, E. Ciorănescu and C. D. Nenitzescu, *Rev. Roumaine Chim.*, **19**, 213 (1974).

[1] E. Ciorănescu, M. Banciu, M. Elian, A. Bucur and C. D. Nenitzescu, *Liebigs Ann. Chem.*, **739**, 121 (1970).

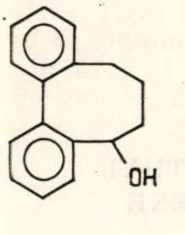

4

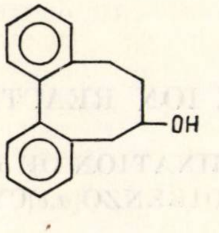

5

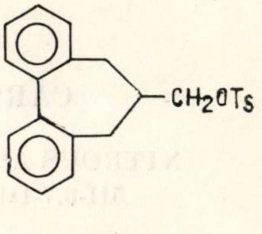

6-OTs

The reaction rate of **1-OTs**, 20 times greater than that of the isomeric tosylate **6-OTs** (at 110°), indicated [1] the assistance of a neighbouring phenyl group and the intermediate appearance of a phenonium ion **7**. The product distribution suggested the intervention of a benzylic ion **8** (generating **2** and **4**) beside the phenonium ion (giving rise to **3**, **5** and **1-OH**).

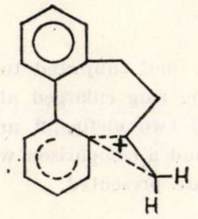

7

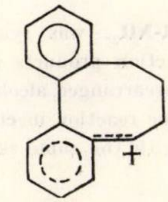

8

In the present paper the results obtained on nitrous acid deamination of the amine **1-NH$_2$**, possessing the same skeleton as the above tosylate, are described.

RESULTS AND DISCUSSION

The starting material for the synthesis of **1-NH$_2$** was the 5H-6,7-dihydro-dibenzo[*a,c*]cycloheptene-5-carboxylic acid (**9a**) described in a preceeding paper [1]:

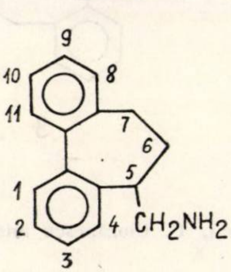

1-NH$_2$

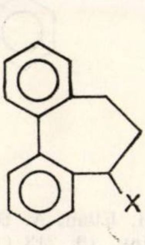

a: X = COOH
b: X = COCl
c: X = CONH$_2$
d: X = CN

9

The acid chloride **9b** afforded, on treatment with NH_3 solution, the crystalline amide **9c** (m.p. 204°). Due to the poor solubility of **9c** in ether, the $LiAlH_4$-reduction of the amide was performed in THF, giving rise to amine **1-NH$_2$** in 38% yield. This yield could be augmented up to 75% by conversion of **9c** to the corresponding nitrile **9d** (m.p. 81−3°) and subsequent $LiAlH_4$-reduction carried out in ether.

The amine **1-NH$_2$**, a viscous oil, was characterised through its crystalline hydrochloride (m.p. 219−220°) and acetoxy-derivative (m.p. 162°) (for IR- and NMR-spectra see Experimental part).

The nitrous acid deaminations were performed with the free amine **1-NH$_2$** as well as with hydrochloride **1-NH$_2$·HCl** in the presence of sodium nitrite in anhydrous acetic acid. The temperature was maintained at 2−5° during the nitrite addition, then the reaction mixture was kept at room temperature for 24 hrs.

In Table 1 the product composition in the deamination of **1-NH$_2$** is presented (v.p.c. analyses after $LiAlH_4$-reduction) and for comparative purposes the results obtained [1] in the solvolysis of **1-OTs** are also registered.

Table 1

Product distribution in the nitrous acid deamination of 1-NH$_2$ and acetolysis of 1-OTs (after LiAlH$_4$-reduction)

Products % (v.p.c. analysis) / Starting compound (reaction conditions) (Solvent : AcOH)	2, 3	Unidentified olefins (2 components)	10	5	4	1-OH	Unidentified components
1-NH$_2$ + $NaNO_2$ (1 mole : 1 mole ; 5°)	5.0 + 3.0	0.8	20.0	52.0	—	15.5	3.7 (1 comp.)
1-NH$_2$·HCl + $NaNO_2$ (1 mole : 1−2.5 moles ; 5°)	1.5 + 0.5	10.0	17.5	53.5	—	10.0	7.0 (5 comp.)
1-OTs + NaOAc[a] (1 mole ; 3 moles ; 110°)	6.0 + 2.0	14	—	25.0	38.0	15.0	—

(a) data from ref.[1]

The v.p.c. analysis indicated the presence of 4 olefinic components in the deamination reaction mixture of the amine **1-NH$_2$** (as well as in the acetolysis products of **1-OTs**). It was proved that two of these olefins were identical (retention times and mixed samples in the v.p.c.) with olefins **2** and **3** obtained (as a mixture) after the method of Cope and Smith.[2] The remaining two alkenes have not been investigated.

The major component of the reaction mixture ($> 50\%$) was identical with the authentic alcohol **5** prepared also after Cope and Smith.[2] The minor alcoholic component was found to be the unrearranged alcohol **1-OH**, described in our previous paper[1].

---

[2] A. C. Cope and R. D. Smith, *J. Amer. Chem. Soc.*, **78**, 1012 (1956).

A third alcohol, **10**, which does not appear in the solvolyses of **1-OTs**, was separated by preparative v.p.c. (of an enriched fraction containing **5** and **10**, obtained by column chromatography). The structure of 5-methyl-5H-6,7-dihydro-dibenzo[*a,c*]cycloheptene-5-ol was attributed to **10** on the basis of its IR- and NMR-spectra (see Experimental part).

By comparison (v.p.c. and spectral characteristics) with an authentic material obtained from the reaction of 5H-6,7-dihydro-dibenzo[*a,c*]cycloheptene-5-one (**11**)[3] with methyl magnesium iodide, the structure of **10** was confirmed.

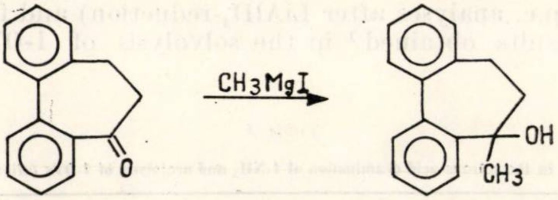

11 **10**

The data from Table 1 show that the results obtained in the deamination of **1-NH$_2$** differ in two respects from those of the solvolysis of **1-OTs**. In the deamination of **1-NH$_2$** the tertiary alcohol **10** was formed, while the benzylic alcohol **4** was found to be absent. In the solvolysis of **1-OTs** this situation was reversed.

Differences in product distribution indicates specific intermediates for each case.

Comparisons between deamination and solvolyses of the same systems have frequently been made.[4] A general mechanism which could explain all the characteristic features of nitrous acid deaminations has not yet been advanced. It is generally assumed that the first intermediate formed from the diazonium ion, by N_2 elimination, is an open "hot" ion, highly reactive toward nucleophiles.

Inspection of Dreiding stereomodels reveals the existence, in the case of **1-NH$_2$**, of two conformations interconvertible by rotation of the aromatic rings around the C_2—C_3 bond, the —CH_2—NH_2 group being either in the pseudo-axial or in the pseudo-equatorial position.

---

[3] J. W. Cook, G. T. Dickson and J. D. London, *J. Chem. Soc.*, **1947**, 746.

[4] J. H. Ridd, *Quart. Rev.*, **15**, 418 (1961); H. Zollinger, "Azo and Diazo Chemistry", Interscience, New-York, 1961, p. 123; R. Huisgen and C. Rückhardt, *Liebigs Ann. Chem.*, **601**, 1, 21 (1961); E. H. White in "The Chemistry of Amino Group", S. Patai (Editor), Interscience, London, 1968, p. 407.

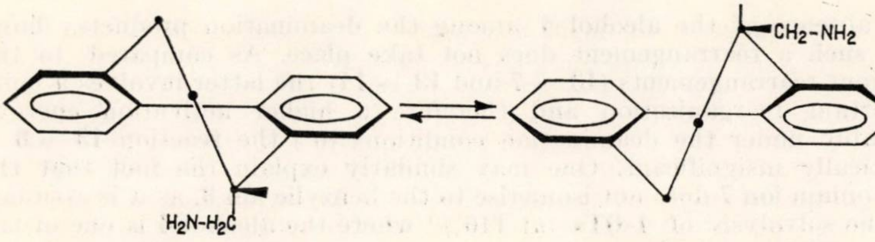

1-NH$_2$ (axial) **1-NH$_2$** (equatorial)

It seems that the axial conformation is favoured over the more hindered equatorial one in which the repulsions between the $-CH_2NH_2$ group and neighbouring atoms are more important.

If it is assumed [5] that the "hot" carbonium ion produced by decomposition of the diazonium ion retains the conformation of the initial amine, then the intermediates **12** and **13** would be formed successively from **1-NH$_2$**.

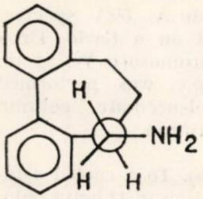

1-NH$_2$

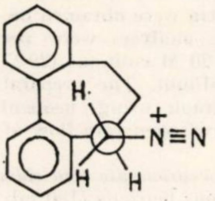

12

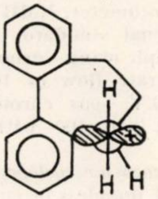

13

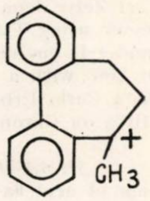

14

The highly reactive open carbonium ion **13** rearranges rapidly into other more stable intermediates. There are several ways by which this stabilization could occur.

The assistance of the phenyl group from the β-position may lead to the phenonium ion **7**. This can further give rise to the acetates of the ring-enlarged alcohol **5** and of the unrearranged alcohol **1-OH** as well as to the olefin **3** (may be also to the olefin **2**). The predominant population of the axial conformation of the starting material, the only one which can lead to a phenonium ion, is in agreement with the formation of the alcohol **5** as the major product ($>50\%$).

A hydride shift in the "hot" carbonium ion **13** (irrespective of the axial or equatorial precursor) leads to the stable tertiary benzylic ion **14** from which the alcohol **10** (20%) is formed (the latter alcohol does not appear in the solvolysis of **1-OTs**).

A third possibility for the stabilization of ion **13** is an alkyl migration which would lead to the benzylic ion **8** (Demyanov ring expansion).

---

[5] F. A. Abd Elhafez and J. D. Cram, *J. Amer. Chem. Soc.*, **74**, 5846 (1952); J. D. Cram and J. E. McCarthy, *ibid.*, **79**, 2866 (1957).

The absence of the alcohol **4** among the deamination products shows that such a rearrangement does not take place. As compared to the previous rearrangements (**13** → **7** and **13** → **14**) the latter involves a more important reorganization and therefore a higher activation energy; probably under the deamination conditions (0°) the reaction **13** → **8** is kinetically insignificant. One may similarly explain the fact that the phenonium ion **7** does not isomerise to the benzylic ion **8**, as it is assumed for the solvolysis of **1-OTs** (at 110°)[1] where the alcohol **4** is one of the major products.

Finally, one may suppose that at least part of the alcohol **1-OH** (of its acetate respectively) arises from the reaction of ion **13** with the solvent or even from a direct displacement on the diazonium ion as was suggested in other cases.[6]

EXPERIMENTAL

Melting points are uncorrected. IR spectra were recorded with a double-beam UR−20 Carl Zeiss Jena spectrophotometer. NMR spectra were obtained on a Varian A−60A spectrometer using TMS as internal standard. V.p.c. analyses were performed on a Carlo Erba model D gas chromatograph using Carbowax 20 M columns (20% on Chromosorb W), 1 m, at 200° with a hydrogen rate flow of 100 ml/min. The preparative v.p.c. was performed on a Carlo Erba model G.V. gas chromatograph using neopentylglycolsuccinate column (10% on Chromosorb W), 2 m, 190° with a hydrogen rate flow of 120 ml/min.

5H-6,7-Dihydro-dibenzo[a,c]cycloheptene-5-carboxylic acid chloride (**9b**). To a cooled solution of acid **9a**[1] (20 g; 84 mmoles) in anhydrous benzene (180 ml) a solution of thionyl chloride (14 g; 12.2 ml; 118 mmoles) in 75 ml anhydrous benzene was added dropwise with stirring for 1 hr. The solution was then refluxed for 4 hrs. The solvent and excess $SOCl_2$ were evaporated *in vacuo*. The residue was then treated with ether (2 × 50 ml) which was subsequently evaporated, affording the *acid chloride* **9b** 20.3 g (95%) as a pale-yellow oil. *IR spectrum* (CCl_4, cm^{-1}): 1073 m, 1460 m, 1494 m, 1780 s (shoulder), 1815 vs, 2865 m, 2934 vs, 2960 s, 3036 m and 3073 m. The acid chloride was utilized in the next step without further purification.

5H-6,7-Dihydro-dibenzo[a,c]cycloheptene-5-carboxamide (**9c**). A solution of acid chloride **9b** (20.3 g; 79 mmoles) in 200 ml anhydrous benzene was added dropwise with vigorous stirring to an ice-cooled solution of 28% ammonia (300 ml). Instantaneously a white precipitate of amide **9c** was formed. The reaction mixture was stirred for 1 hr., then diluted with 500 ml water and filtered. The precipitate was washed on the funnel with a little ether, leading to 17 g (90% yield) of the crude amide **9c**, m.p. 202−3°. After two recrystallizations from methanol the *amide* **9c** melts at 204°. (*Found*: C, 80.95; H, 6.56; N, 5.95. $C_{16}H_{15}NO$ requires C, 80.97; H, 6.38; N, 5.91%). *IR spectrum* (CH_2Cl_2, cm^{-1}): 1036 w, 1481 m, 1589 m, 1691 s, 2862 vw, 2953 w, 3045−3085 m, 3401 m, 3516 m.

The nitrile of 5H-6,7-dihydro-dibenzo[a,c]cycloheptene-5-carboxylic acid (**9d**). $POCl_3$ (12.5 g; 7.5 ml; 84 mmoles) was poured over solid amide **9c** (2.5 g; 10.5 mmoles) and the reaction mixture was maintained at 85° for 1 hr. After cooling, the reaction mixture was poured in ice-cooled water and ether-extracted. The organic layer was washed with $NaHCO_3$, with water and then evaporated *in vacuo* affording a viscous oil (2.2 g; 95%) which crystallizes rapidly. The *nitrile* **9d** has a m.p. 81−3° (ethanol). (*Found*: C, 87.54; H, 6.25; N, 6.32. $C_{16}H_{13}N$ requires: C, 87.63; H, 5.98; N, 6.39%. *IR spectrum* (CS_2, CCl_4, cm^{-1}): 760 vs, 1465 m, 1490 m, 2250 w, 2882 w, 2931 w, 2952 m, 3028 w, 3082 w.

5-Aminomethyl-5H-6,7-dihydro-dibenzo[a,c]cycloheptene (**1-NH$_2$**). (a) *By $LiAlH_4$-reduction of the amide* **9c**. To a suspension of $LiAlH_4$ (1 g; 26.3 mmoles) in anhydrous tetrahydrofuran (30 ml) a solution of amide **9c** (4.8 g; 20.3 mmoles) in tetrahydrofuran (150 ml) was added dropwise during 2 hrs. The reaction mixture was refluxed for 8 hrs and left overnight. After decomposition with cold water (50 ml) the organic layer was separated and the aqueous one was ether-extracted. The combined organic layers were washed with water, dried and evaporated under inert atmosphere, affording 4.0 g (88%) crude **1-NH$_2$**, a viscous oil which could not be crystallized.

---

[6] E. F. Cox, M. C. Caserio, M. S. Silver and J. D. Roberts, *J. Amer. Chem. Soc.*, **83**, 2719 (1961).

The hydrochloride of the amine **1-NH$_2$** was precipitated from the crude oily amine by treating with HCl-saturated ether. After dissolving in 5 ml anhydrous ethanol, filtration and reprecipitation with anhydrous ether the *hydrochloride of the amine* (**1-NH$_2$·HCl**) was obtained (2 g; 38%) m.p. 219–220° (*Found* : C, 73.79 ; H, 7.22 ; Cl, 14.43 ; N, 5.62. $C_{16}H_{18}NCl$ requires : C, 73.96 ; H, 6.99 ; Cl, 13.65 ; N, 5.39%). *IR spectrum* (KBr, cm^{-1}) : 733 w (shoulder), 751 s, 757 s, 771 m (shoulder), 1443 m, 1481 m, 1517 m, 1590 m, 1611 m, 2500–3200 m, 2900 s.

1-NH$_2$-Acetate, from the oily amine **1-NH$_2$** (liberated on neutralization of **1-NH$_2$·HCl**) with Ac_2O, 0.5 hr at 100° ; m.p. 162° (methanol) (*Found* : C, 81.73 ; H, 7.42. $C_{18}H_{19}NO$ requires : C, 81.46 ; H, 7.22%). *IR spectrum* (KBr, cm^{-1}) : 751 vs, 1372 m, 1449 s, 1487 s, 1575 vs, 1650 vs, 1655 s (shoulder), 2848 m, 2875 m, 2920 m, 2930 m, 3021 m, 3070 m, 3276 vs. *NMR spectrum* ($CDCl_3$, δ ppm) : 1.79 s (3H) ; 1.8–3.0 m (5H) ; 3.53 t (2H ; $J_{CH} \approx J_{NH} \approx 7.8$ cps) ; 5.52 m (1H) ; 7.2–7.5 m (8H, arom).

(b) *By LiAlH$_4$-reduction of the nitrile* **9d**. The reduction was carried out in anhydrous ether after the procedure described for (a). From 4.4 g nitrile **9d**, 4.1 g (79%) *1-NH$_2$-hydrochloride* with m.p. 219° were obtained (75% yield calculated from the amide **9c**).

Deamination reactions of 5-aminomethyl-5H-6,7-dihydro-dibenzo[a,c] cycloheptene (**1-NH$_2$**). To an ice-cooled solution of **1-NH$_2$** hydrochloride (2.0 g; 7.7 mmoles) in anhydrous acetic acid (110 ml), $NaNO_2$ (0.55 g, 8 mmoles) was added in small portions, then the reaction mixture was left overnight. After pouring in cold water (100 ml) and neutralization with solid Na_2CO_3 the mixture was ether-extracted. The ethereal layer was washed with water, dried and evaporated *in vacuo*, affording an oily mixture (2 g ; 97%) of acetates which was subsequently reduced with $LiAlH_4$ (0.3 g ; 7.9 mmoles) in 100 ml anhydrous ether. After the usual work-up a partially crystallized reaction mixture was obtained (1.35 g ; 80%) whose composition was determined by v.p.c. analysis (Table 1). For the components **2** + **3** and **5**, authentic samples were synthesized (in view of a v.p.c. comparison) after Cope and Smith.[1] The alcohol **1–OH** was obtained as in reference[1].

The structure of *5-methyl-5H-6,7-dihydro-dibenzo[a,c]cycloheptene-5-ol* for the component **10** was proved in two ways :

(a) The reaction mixture from the deamination of the amine **1-NH$_2$** was chromatographied on a neutral Al_2O_3 column, eluting with a mixture of petroleum ether and dietyl ether (70 : 30), yielding a mixture of **10** and **5**. (V.p.c. analysis indicates 36% **10** and 64% **5**.) Preparative v.p.c. of this mixture affords the alcohol **10** (uncrystallizable oil).

IR spectrum (CCl_4 ; cm^{-1}) : 950 m, 1064 m, 1447 s, 1481 m, 2855 m, 2938 s, 3023 m, 3065 s, 3100 w, 3200–3550 w, 3608 m.

NMR spectrum ($CDCl_3$; δ ppm) : 1.28 s (3H) ; 1.94 s (OH) ; 2.1–3.8 m (4H) ; 7.1–7.85 m (8H, arom.).

(b) *The treatment of 5H-6,7-dihydro-dibenzo[a,c]cycloheptene-5-one* (**11**)[3] with a slight excess of methyl magnesium iodide in anhydrous ether affords, after usual work-up, the alcohol **10** whose IR and NMR spectra were identical with those of the preparatively v.p.c.-separated *5-methyl-5H-6,7-dihydro-dibenzo[a,c]cycloheptene-5-ol*.

Other deaminations, using different molar ratios of reactants as well as the free amine **1-NH$_2$** (obtained on neutralization of **1-NH$_2$·HCl**) were performed using the same procedure ; the results are also given in Table 1.

was added [illegible] during [illegible] and the mixture was refluxed for 5 hr [illegible] overnight. After [illegible] water [illegible] the [illegible] layer was separated and [illegible] ether [illegible]. The [illegible] with water, dried and [illegible] under reduced pressure [illegible] 1-NH [illegible] of which could not be [illegible].

The [illegible] from the [illegible] (1-NH [illegible]) [illegible]

[illegible] 1-NH [illegible]

[illegible] 1-NH [illegible] water [illegible]

The structure of [illegible] the compound 10 was proved in two ways:

(a) The reaction mixture from the [illegible] of the [illegible] 1-NH was chromatographed on a neutral Al_2O_3 column, eluting with a mixture of petroleum ether and diethyl ether [illegible], yielding a mixture of 10 and 3. [illegible] indicates 30% 10 and [illegible] 3. [illegible] 10 [illegible]

UV spectrum [illegible]

[illegible]

(b) The treatment of 13 [illegible] with a slight excess of [illegible]. The IR and NMR spectra were identical with those of the [illegible] separated [illegible]

Other determinations, using different [illegible] as well as the free base 1-NH, obtained on neutralization of 1-NH, HCl, were performed using the same procedure; the results are also given in Table I.

Revue Roumaine de Chimie, **19**, *8*, 1351–1360 (1974)

MODERN FRIEDEL-CRAFTS CHEMISTRY. V[1]

THE FRAGMENTATION AND DEALKYLATION OF STRAIGHT-CHAINED DIPHENYLBUTANES UNDER THE INFLUENCE OF WATER-ACTIVATED ALUMINIUM CHLORIDE AT 100°C

ALI ALI KHALAF

Chemistry Department, Assiut University, Assiut, Arab Republic of Egypt
and
ROYSTON M. ROBERTS
Chemistry Department, University of Texas at Austin, Austin, Texas 78712, U.S.A.

Received November 13, 1973

The action of water-activated aluminium chloride on 2,2-, 1,1-, 1,2- and 1,3-diphenylbutane at 100° was investigated using different reaction periods. Both gaseous and nongaseous products were separated, identified and estimated by modern analytical techniques. In all cases, the gaseous products were shown to be mixtures consisting chiefly of isobutane in addition to smaller amounts of lower and higher components. On the other hand, the nongaseous products were shown to consist of varying proportions of methyl-, ethyl-, propyl- and butylbenzenes in fractions boiling below 184° and of starting and rearranged diphenylbutanes in higher fractions.

In a preceding part of this series [1] we reported the results of treatment of 1,1- and 1,2-diphenylbutane with $AlCl_3$ in benzene both at room temperature and at 68–70°. Under such conditions we observed two main types of reactions : First, dephenylation of both isomers to *n*-butylbenzene and, second : isomerisation in accordance with the sequence : 1,1-diphenylbutane → 1,2-diphenylbutane → 1,3-diphenylbutane. Fragmentation reactions were inappreciable, however.

In the present article we wish to report the results of further experiments in which 2,2-, 1,1-, 1,2- and 1,3-diphenylbutane were subjected to the action of water-activated $AlCl_3$ at 100° for various periods. Using such conditions, we hoped, to induce some dealkylation and fragmentation reactions and to obtain some information regarding the patterns of these reactions with such straight-chained diphenylbutanes.

RESULTS AND DISCUSSION

The conditions and results of treatment of 2,2-, 1,1-, 1,2- and 1,3-diphenylbutane with water-activated $AlCl_3$ are summarized in Tables 1–6 in this section and Tables 7–9 in the experimental section.

---

[1] R. M. Roberts and A. A. Khalaf, Part IV of this series, *Rev. Roumaine Chim.*, **18**, 1937 (1973).

It can be seen from the results of Tables 1, 3 and 5 that, similar to branched diphenylbutanes, the fragmentation products from non-branched diphenylbutanes contained varying amounts of methyl-, ethyl-, dimethyl- and propylbenzenes. Again butylbenzenes resulting mainly from direct dephenylation of the starting diphenylbutanes constituted the major part of the liquid mixtures boiling in the range extending from 85 to 184°. Significantly, however, the relative yields of the produced alkylbenzenes revealed an obvious dependence upon both the positions

Table 1

Liquid dealkylation and fragmentation products from 2,2-diphenylbutane[a]

Experiment N°	Time, min	Liquid Mixture, R—C_6H_5, Boiling Range 85—176°								
		Total, wt. % of original	Me, %[b]	Et, %[b]	*o*-Xylene	Pr, %[b]		Butylbenzenes		
						i-	*n*-	*t*- %[b]	*i*- %[c]	*s*- %[c]
1C[d]	5	15[e]	0.1	7.3	Tr.	1.1	0.2	1.3	5	85
2C	10	13	0.2	13.2	Tr.	1.3	0.3	Tr.	8	76
3C	15	15	0.7	20.3	Tr.	1.6	0.2	—	8	69
4C	30	18	0.6	17.3	Tr.	1.6	0.5	—	20	60
5C	60	21	0.6	17.2	Tr.	1.6	0.6	—	18	62
6C	120	24	4.2	21.0	3	2.7	2.1	Tr.	20	42
7C	180	22	5.6	23.0	4	2.7	2.7	Tr.	20	42
8C[f]	180	16	10.7	26.0	3	4.0	1.3	Tr.	25	28

[a] Reactions at 100°; reactants: hydrocarbon, 0.05 mole; $AlCl_3$, 0.0166 mole; H_2O, 0.0008 mole. The amounts of $AlCl_3$ and H_2O were doubled in experiment 8C.

[b] Percentage of each alkylbenzene in the liquid mixture as found by v.p.c.

[c] The total percentages were found by v.p.c. and individual percentages by infrared analysis.

[d] Since this work is a continuation of our study of the reactions of diphenylalkanes,[3] we decided to start here with the designation C as the previous results were designated by A and B.

[e] Contained traces of an unidentified octane.

[f] Double catalyst was added as one batch.

Table 2

Gaseous dealkylation and fragmentation products from 2,2-diphenylbutane[a]

Experiment N°	Time, min	Gaseous Mixture					
		Volume,[b] ml	Total, %[c]	C_2H_6, %[d]	C_4H_{10}, %[d]		C_5H_{12}, %[d]
					i-	*n*-	*i*-
1C	5	50	4.5	1	97	—	2
2C	10	65	5.8	2	95	—	3
3C	15	80	7.1	18	79	—	3
4C	30	82	7.3	1	95	Tr.	4
5C	60	100	8.9	10	80	Tr.	10
6C	120	138	12.3	Tr.	86	1	13
7C	180	180	16	Tr.	84	2	14
8C[e]	180	180	16	Tr.	83	4	13

[a] Reactions at 100°; reactants: hydrocarbon, 0.05 mole; $AlCl_3$, 0.0166 mole; H_2O, 0.008 mole. In experiment 8C double catalyst ($AlCl_3$ and H_2O) was used.

[b] At S.T.P.

[c] Mole % conversion to alkane based on hydrocarbon, calcd. from the volume of gas collected.

[d] Percentage of each alkane in the mixture as found by v.p.c.

[e] Double catalyst was added as one batch.

Table 3

Liquid dealkylation and fragmentation products from 1.1-diphenylbutane[a]

Experiment N°	Time, min	Liquid mixture, $R-C_6H_5$, Boiling range 85–184°						
		Total, Wt. % of Original compound	Me, %[b]	Et, %[b]	Pr, %[b]		Bu, %[b]	
					i-	*n-*	*s-/i-*	*n-*
1D	5	11[c,d]	0.1	0.2	0.2	1.2	0.2	98.0
2D	10	12[c,d]	0.1	0.3	0.1	1.2	0.2	98.0
3D	15	13[c,d]	0.1	0.6	0.3	1.2	0.3	97.0
4D	30	14[d]	Tr.	1.5	0.6	0.5	0.4	97.0
5D	60	15[d]	Tr.	2.7	1.1	0.7	0.5	95.0
6D	120	18	Tr.	5.0	1.6	1.0	0.4	92.0
7D	180	19	0.1	9.1	3.0	2.4	0.4	85.0
8D[e]	120[f] 180[g]	—	4.8	16.8	4.2	3.6	0.6	70.0

[a] Reactions at 100°; reactants (in experiments 1D–7D): hydrocarbon, 0.075 mole; $AlCl_3$, 0.025 mole; H_2O, 0.0125 mole. In experiment 8D, the reactants were: hydrocarbon, 0.025 mole; $AlCl_3$, 0.0166 mole; H_2O, 0.0083 mole. In the latter experiment the speed of the magnetic stirring apparatus also was doubled.

[b] Percentage of each alkylbenzene in the liquid mixture as found by v.p.c.

[c] Contained traces of *o*-xylene.

[d] In experiments 1D–5D, this contained *ca*, 0.1%, 0.2%, 0.4% and traces, respectively, of what is believed to be an octane.

[e] Double catalyst added in two steps.

[f] With first batch of catalyst.

[g] With second batch of catalyst.

Table 4

Gaseous dealkylation and fragmentation products from 1,1-diphenylbutane[a]

Experiment N°	Time, min	Gaseous Mixture						
		Volume,[b] ml	Total, %[c]	C_2H_6, %[c]	C_3H_8, %[d]	C_4H_{10}, %[d]		C_5H_{12}, %[d] *i-*
						i-	*n-*	
1D	5	29[h]	1.7	—	—	97	2	1
2D	10	33[h]	2.0	—	1	97	1	1
3D	15	32[h]	1.9	—	1	96	2	1
4D	30	31[h]	1.8	—	1	95	2	2
5D	60	33[h]	2.0	—	—	95	3	2
6D	120	30[h]	1.8	—	—	95	3	3
7D	180	55[h]	3.3	4	1	90	2	3
8D[e]	120[f]	180	10.7	Tr.	Tr.	26	70	4
	180[g]	285	17.0	Tr.	Tr.	33	63	4

[a] Reactions at 100°; reactions: hydrocarbon, 0.075 mole; $AlCl_3$, 0.025 mole; H_2O, 0.0125 mole. In experiment 8D the catalyst ($AlCl_3$ and H_2O) and the speed of the stirring apparatus were doubled.

[b] Measured at S.T.P.

[c] Mole % conversion to alkane based on hydrocarbon, calcd. from the volume of gas collected.

[d] Percentage of each alkane in the gaseous mixture as found by v.p.c.

[e] Double catalyst added in two steps.

[f] With first batch of catalyst.

[g] With second batch of catalyst.

[h] This represents the composition of the gas produced immediately after dropping the hydrocarbon onto the hot catalyst since after that the evolution of gas had practically stopped.

Table 5

Liquid dealkylation and fragmentation products from 1,2- and 1,3-diphenylbutane, and the indan mixture[a]

Compound	Liquid mixture, $R-C_6H_5$, b.p. 85–184°									
	Time, min	Total, %[b]	Me, %[c]	Et, %[c]	Pr, %c		Butylbenzenes			
					i-	*n*-	*t*-, %[c]	*i*-, %[c]	*s*-, %[c]	*n*-, %[c]
1,2-Diphenylbutane	10	6.0	Tr.	2.6	—	2.4	—	Tr.		95.0
1,2-Diphenylbutane	120	11.0	1.0	7.0	2.0	1.3	—	—		88.7
1,3-Diphenylbutane	10	3.4	0.2	3.2	1.4	—	Tr.	0.2		95.0
1,3-Diphenylbutane	120	7.0	0.2	3.4	1.8	—	—	0.4		94.2
Indan mixture	120	9.6	3.0	18.0	3.0	2.0	2.0		70.0	—

a Temperature 100°; reactants: hydrocarbon, 0.05 mole; $AlCl_3$, 0.0166 mole; H_2O, 0.008 mole. In case of 1,3-diphenylbutane (10 minutes exp.) reactants were: 0.025 mole of hydrocarbon, 0.008 mole of $AlCl_3$ and 0.004 mole of H_2O.

b Weight % of original hydrocarbon.

c Percentage of each alkylbenzene as found by v.p.c.

Table 6

Gaseous dealkylation and fragmentation products from 1,2- and 1,3-diphenylbutane and the indan mixture[a]

Compound	Time, min	Volume[b] ml	Total, %[c]	C_2H_6, %[d]	C_3H_8, %[d]	C_4H_8, %[d]		C_4H_{10}, %[d]		C_5H_{12}, %[d] *i*-
						cis-	*trans*-	*i*-	*n*-	
1,2-Diphenylbutane	10	50	4.5	3	—	—	—	83	—	14
1,2-Diphenylbutane	120	110	9.8	3	—	—	—	85	—	12
1,3-Diphenylbutane	10	15	2.7	23	—	11	4	48	Tr.	14
1,3-Diphenylbutane	120	162	14.4	7	—	15	8	43	3	24
Indan mixture	120	163	14.5	—	—	—	—	75	—	25

a Temperature 100°; reactants: hydrocarbon, 0.05 mole; $AlCl_3$, 0.0166 mole; H_2O, 0.008 mole. In case of 1,3-diphenylbutane (10 minutes exp.) the reactants were: 0.025 mole hydrocarbon, 0.008 mole of $AlCl_3$ and 0.004 mole of H_2O.

b Measured at S.T.P.

c Mole % conversion to alkane based on hydrocarbon, calcd. from volume of gas collected.

d Percentage of each alkane in the gaseous mixture as found by v.p.c.

of the two phenyl groups in the chain and the reaction conditions. These facts will become apparent as we proceed with our discussion.

Regarding the fragmentation of 2,2-diphenylbutane, the data given in Table 1, show that ethylbenzene remained to be the major fragmentation product given by this isomer under all conditions employed. This is supposed to arise from isomerisation of 2,2-diphenylbutane to 2,3-diphenylbutane,[2] followed by the cleavage of the latter to ethylbenzene as suggested before.[2,3] Besides ethylbenzene, smaller amounts of the fragments toluene, *o*-xylene and *n*- and isopropylbenzene were also formed. These can result from the fragmentation of other isomeric diphenylbutanes produced by the rearrangement of the starting 2,2-diphenylbutane isomer. In fact, it has been previously shown that aluminum chloride, catalyzes the rearrangement of 2,2-diphenylbutane to 2,3-diphenylbutane and of the latter to 1,1-diphenyl-2-methylpropane, 1,2-diphenyl-2-methylpropane and 1,3-diphenylbutane.[2]

---

[2] R. M. Roberts, A. A. Khalaf and R. N. Greene, *J. Amer. Chem. Soc.*, **86**, 2846 (1964).

[3] R. M. Roberts, E. R. Baylis and G. R. Fonken, *J. Amer. Chem. Soc.*, **85**, 3454 (1963).

From the results of Table 3, it is noted that *n*-propylbenzene was the chief fragmentation product obtained from 1,1-diphenylbutane during the early stages of reaction (up to 15 min.). After longer reaction times, however, ethylbenzene and isopropylbenzene became more abundant. This observation is explicable in terms of the expected stepwise isomerisation of 1,1-diphenylbutane to 1,2- and 1,3-diphenylbutane[1]; the former can be considered as a precursor for *n*-propylbenzene formation and the latter as a precursor for ethylbenzene formation. The fragmentation results from 1,2- and 1,3-diphenylbutane given in Table 5 provide the experimental support for this suggestion. Thus if we compare the percentage yields of ethylbenzene and propylbenzene from 1,1-, 1,2- and 1,3-diphenylbutane after 10 min. of reaction, we find that the 1,2-isomer gave the highest percent of *n*-propylbenzene (2.4%) compared to 1.2% from the 1,1-isomer and 0% from the 1,3-isomer) and that the 1,3-isomer gave the highest percent of ethylbenzene (3.2% compared to 0,2% from the 1,1-isomer and 2.6% from the 1,2-isomer). The carbonium ion processes outlined in paths (a) to (e) of Scheme 1, illustrate diagramatically how toluene, ethylbenzene, isopropylbenzene and *n*-propylbenzene can be produced from 1,1-, 1,2- and 1,3-diphenylbutane through a series of various rearrangement and fragmentation reactions.

On the basis of path (b) of Scheme 1, one would expect 1,2-diphenylbutane to yield equal amounts of toluene and *n*-propylbenzene if not more of the former. The fact that toluene was obtained in much smaller amounts from the fragmentation of 1,1- and 1,2-diphenylbutane leads one to believe that path (a) could be the operable one. The detection of small amounts of diphenylmethane can be attributed to either path (e) or path (a) since in the latter the benzyl carbonium ion produced can alkylate benzene giving rise to diphenylmethane.[4]

In the fragmentation of 1,3-diphenylbutane according to paths (c) and (d), one would predict the rate of production of ethylbenzene to be roughly twice that of isopropylbenzene because the two primary carbonium ions involved are expected to be equally stable. This is in accordance with the experimental results obtained since the results of Table 5 show that the ratio of ethylbenzene to isopropylbenzene roughly amounts to 2 : 1.

Considering the significant differences in the fragmentation products obtained from the various diphenylbutanes, one can offer three generalizations that are helpful in explaining the distribution of fragmentation products in all of the compounds studied. First, cleavages which produce the most stable carbonium ions are always favoured. Secondly, under the conditions used, cleavages of the alkyl moieties may occur

---

[4] G. A. OLAH, S. J. KUHN, and S. H. FLOOD, *J. Amer.Chem. Soc.*, **84**, 1688, 1695 (1962).

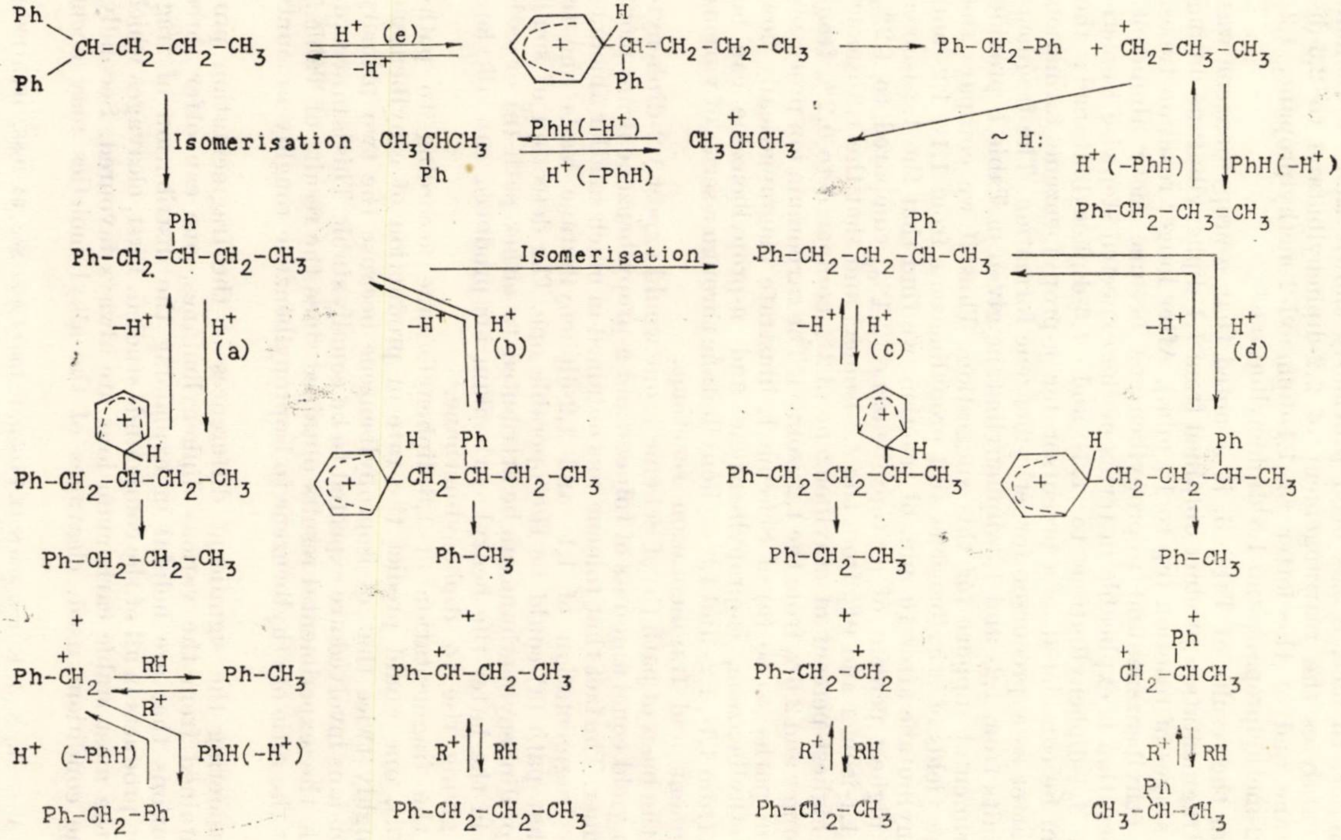

Scheme

Scheme 1

before isomerisations of diphenylbutanes, but rates of cleavages and isomerisations are of the same order. Thirdly, whereas diphenylbutanes are the major source of the fragmentation products, two other minor sources are worthy of note: (i) Cleavage of the butylbenzenes resulting from dephenylation of the starting diphenylbutanes as is exemplified by fragmentation of isobutylbenzene to toluene and isopropyl carbonium ion, the latter giving propane or isopropylbenzene as shown in Scheme 2

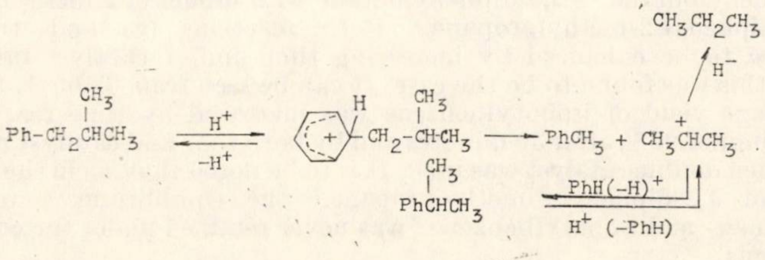

Scheme 2

(ii) Some of the fragmentation products could arise from the cleavage of the bimolecular reaction products. For example, the mechanism previously proposed [3] to account for the occurrence of isopentane in the gaseous products can also account for the presence of the fragmentation product, isopropylbenzene. Again, the bimolecular products, 1,2,3-trimethyl-1-ethylindan which is known [5,6] to result from the dimerisation of $Ph\overset{+}{C}(CH_3)C_2H_5$ and whose presence in the reaction mixture is highly likely can also contribute to the fragmentation process. In fact, as can be seen from Table 5, when a mixture consisting chiefly of the latter indan [5,6] was subjected to the fragmentation procedure it gave results quite similar to those obtained from 2,2-diphenylbutane under identical conditions.

So far in our discussion we have been primarily concerned with the fragmentation behaviour of the diphenylbutanes under consideration. As to the dealkylation behaviour, it can be seen from the results that, similar to other diphenylalkanes [2,3] both liquid and gaseous dealkylation products were produced. While 1,1-, 1,2- and 1,3-diphenylbutane, which contain one benzene ring in the 1-position, yielded almost exclusively *n*-butilbenzene mixed with negligible amounts of *sec*- and/or isobutylbenzene, 2,2-diphenylbutane with the two phenyl groups attached to the 2-position gave *sec*-butylbenzene mixed with varying amounts of *i*-butylbenzene depending upon the conditions employed. The formation of *n*-butylbenzene can be attributed to dephenylations at the 1-, 2- and 3-positions in the cases of 1,1-, 1,2- and 1,3-diphenylbutane, respectively.

---

[5] A. A. Khalaf and R. M. Roberts, *J. Org. Chem.*, **31**, 926 (1966).

[6] This was obtained by treating 2-chloro-2-phenylbutane with $AlCl_3$ in benzene. Also obtained by the reaction of 2-phenyl-2-butene with concentrated sulphuric acid in benzene.[5]

Similarly, the formation of *sec*-butylbenzene from 2,2-diphenylbutane can be attributed to direct dephenylation at the 2-position of the starting 2,2-isomer as well as to dephenylation of the 2,3-diphenylbutane produced by rearrangement therefrom.[2] The formation of considerable amounts of isobutylbenzene in the case of the 2,2-isomer can be attributed to two types of reactions : (a) rearrangement of the primarily formed *sec*-butylbenzene [7] and (b) dephenylation of 1,1- and 1,2-diphenyl-2-methylpropane produced by rearrangement through the previously established sequence : 2,2-diphenylbutane → 2,3-diphenylbutane→1,2-diphenyl-2-methylpropane → 1,1-diphenyl-2-methylpropane.[2] Both reactions (a) and (b) were expected to be enhanced by increasing time and/or catalyst ratio, and indeed this was found to be the case. It can be seen from Table 1, that the percentage yield of isobutylbenzene was increased by time reaching an upper limit of 20 % after 30 minutes and by both time and catalyst reaching 25 % when double catalyst was used. It is to be noted that, as in the cases of 1,1- and 1,2-diphenyl-2-methylpropane,[3] the equilibrium composition between *sec*- and isobutylbenzene [7] was never retained under the employed conditions.

In regard to the gaseous products, it is evident from Tables 2, 4 and 6 that :

(a) Except for one experiment (i.e. 8 D), the major alkane from all of the diphenylbutane isomers was isobutane. Its formation can be attributed to rapid rearrangement of *n*- and *sec*-butylbenzene to *t*-butylbenzene followed by immediate dealkylation as suggested before to give isobutane and benzene.[1-3]

(b) Small amounts of the lower alkanes, ethane, propane and *n*-butane were produced in most cases. The only exception to this was the formation of *n*-butane as the major alkane when 1,1-diphenylbutane was treated with double catalyst (exp. 8 D, Table 4). The reason for this abnormal behaviour is not clear.

(c) Isopentane was produced in all cases and its amount was usually larger than that of *n*-butane.

As suggested before,[8] the formation of isopentane can be explained in terms of unsymmetrical cleavage of an octane isomer formed from addition of *t*-butylcarbonium ion to isobutylene followed by hydride exchange.

EXPERIMENTAL

Analytical Procedures : These were similar to those described before.[3]

Starting Diphenylbutanes : These were prepared by the methods outlined in our previous publications.[1, 5]

Treatments of Diphenylbutanes with Water-activated $AlCl_3$ at 100° : These were carried out using the apparatus and the general procedure described before.[3]

2,2-Diphenylbutane :

Experiments 1C — 7C : 2,2-Diphenylbutane, 10.5 g (0.05 mole), was treated with 2.2 g (0.017 mole) of aluminium chloride and 0.15 ml (0.008 mole) of water at 100° for 5, 10, 15, 30, 60, 120 and 180 min in experiments 1C — 7C, respectively.

---

[7] R. M. Roberts, Y. W. Han, C. H. Schmid and D. A. Davis, *J. Amer. Chem. Soc.*, **81**, 640 (1959).

[8] R. M. Roberts and A. A. Khalaf, Part III of this series, *Rev. Roumaine Chim.*, **18**, 1929 (1973).

Experiment 8C : 2,2-Diphenylbutane, 10.5 g. (0.050 mole), was treated with 4.4 g (0.033 mole) of aluminum chloride and 0.3 ml (0.017 mole) of water at 100° for three hours.

The results for experiments 1C–8C are given in Tables 1 and 2 in the discussion section and Table 7 in this section.

Table 7

Distillation of the liquid products obtained from 2,2-diphenylbutane by treatment with $AlCl_3$ at 100°

Experiment N°	Distillation data, Weight, g.			
	Benzene	b.p. 81–168°	b.p. 168–176°	Residue[a]
1C	2.60	0.20	1.35	4.80
2C	2.83	0.30	1.36	4.95
3C	2.41	0.33	1.34	5.00
4C	2.40	0.40	1.47	5.00
5C	1.99	0.46	1.74	5.30
6C	1.89	0.76	1.80	5.00
7C	1.90	1.00	1.30	4.90
8C	2.82	0.72	1.00	5.30

[a] Contained *dl*- and *meso*-2,3-diphenylbutane and 1,2-diphenyl-2-methylpropane.

1,1-Diphenylbutane :

Experiments 1D–7D : 1,1-Diphenylbutane, 15.75 g (0.075 mole), was treated with 3.3 g (0.025 mole) of aluminum chloride and 0.225 ml (0.0125 mole) of water at 100° for 5, 10, 15, 30, 60, 120 and 180 min in experiments 1D–7D, respectively.

Experiment 8D : 1,1-Diphenylbutane, 5.25 g (0.025 mole), was treated with 1.1 g (0.008 mole) of aluminum chloride and 0.075 ml (0.004 mole) of water for two hours at 100°. In this experiment the speed of the magnetic stirring apparatus was double that used in experiments 1D–7D. At this point, the gaseous products were collected and analysed. The reaction flask was cooled and contents were treated with 1.1 g (0.008 mole) of aluminum chloride and 0.075 ml (0.004 mole) of water at 100° for three hours.

The results obtained for experiments 1D–8D are given in Tables 3 and 4 in the discussion section and Table 8 in this section.

Table 8

Distillation of the liquid products obtained from 1,1-diphenylbutane by treatment with $AlCl_3$ at 100°

Experiment N°	Distillation data, Weight, g.		
	Benzene	b.p., 85–184°	Residue[a]
1D	2.57	1.68	8.38
2D	2.67	1.79	6.90
3D	2.62	2.01	8.16
4D	3.50	2.18	7.10
5D	3.81	2.40	7.70
6D	3.82	2.79	7.51
7D	3.95	2.92	8.50
8D	Crude mixture weighed 3.9 g.		

[a] Contained some 1,2- and 1,3-diphenylbutane as well as trace amounts of diphenylmethane.

1,2-Diphenylbutane :

1,2-Diphenylbutane, 10.5 g (0.05 mole) ,was treated with 2.2 g (0.017 mole) of aluminum chloride and 0.15 ml (0.008 mole) of water at 100° for 10 and 120 min. The results of these two experiments are given in Tables 5 and 6 in the discussion section and Table 9 in this section.

Table 9

Distillation of liquid products obtained from 1,2-diphenylbutane, 1,3-diphenylbutane and 1,2,3-trimethyl-1-ethyl-3-phenylindan by treatment with $AlCl_3$ at 100°

Compound	Distillation data, Weight, g				
	Benzene	b.p., 85−176°		b.p., 176−184°	Residue
1,2-Diphenylbutane	0.50		0.60		6.90
1,2-Diphenylbutane	0.70	0.20		1.00	5.60
1,3-Diphenylbutane	0.15		0.30		3.50
1,3-Diphenylbutane	1.30		2.40		3.30
Indan mixture	0.40	1.27			8.76

1,3-Diphenylbutane :

This was treated with aluminum chloride at 100° for 10 and 120 min. In the ten-minute experiment, the amounts of reactants were 5.2 g (0.025 mole) of the hydrocarbon, 1.1 g (0.008 mole) of aluminum chloride and 0.075 ml (0.004 mole) of water. In the two-hour experiment the amounts were 10.5 g (0.05 mole) of 1,3-diphenylbutane, 2.2 g (0.017 mole) of aluminum chloride and 0.15 ml (0.008 mole) of water. The results are given in Tables 5, 6 and 9.

1,2,3-Trimethyl-1-ethyl-3-phenylindan [6] :

The mixture containing this indan, 13.2 g (0.05 mole), was treated with 2.2 g (0.017 mole) of aluminum chloride and 0.15 ml and 0.15 ml (0.008 mole) of water at 100° for two hours. The results of this treatment are given in Tables 5, 6 and 9.

Revue Roumaine de Chimie, **19**, *8*, 1361–1372 (1974)

MODERN FRIEDEL-CRAFTS CHEMISTRY. VII [1]

ON THE QUESTION OF GROUP PARTICIPATION IN THE RATE-DETERMINING IONIZATION STEP DURING INTER- AND INTRAMOLECULAR FRIEDEL-CRAFTS ALKYLATIONS AND THE MECHANISM OF FORMATION OF 1-METHYLTETRALIN DURING THE $AlCl_3$-CATALYZED REACTION OF 1-CHLORO-2-METHYL-4-PHENYLBUTANE*

ALI ALI KHALAF
Chemistry Department, Assiut University, Assiut, Arab Republic of Egypt

Received November 13, 1973

The following halo and dihalo-compounds were prepared by unequivocal methods: 1,2-dibromo-2-methylpropane (isobutylene dibromide, 8 : X = Br), 1-chloro-2-methyl-2-phenylpropane (neophyl chloride, 9, X = Cl), 1-chloro-4-phenylbutane (12), 1-chloro-2-methyl-4-phenylbutane (13) and 1-chloro-2-methyl-4-p-tolybutane (14). The intramolecular alkylations of the last three chlorides (12, 13, and 14) and the intermolecular alkylations of benzene with the first two halides (8 and 9) as well as with *n*-propyl and *n*-butyl chlorides were investigated in the presence of the mild $AlCl_3/CH_3NO_2$ catalyst. The relative rates of these inter- and intramolecular reactions clearly demonstrated the occurrence of varying degrees of group participation during the rate determining ionization step in which the halide ion is removed. As regards variation in the extent of participation with the location of the aryl group relative to the halogen atom, the relative rates observed indicate that the sequence in β-aryl > δ-aryl > γ-aryl. This sequence correlates nicely with that observed previously for similar solvolytic reactions. Apart from the forthgoing findings, the results of this work also led to a new mechanism for the formation of 1-methyltetralin during the $AlCl_3$-catalyzed reaction of 1-chloro-2-methyl-4-phenyl-butane.

INTRODUCTION

It is very well established that many carbonium ion reactions are acclerated by neighbouring group participation. Such reactions are sometimes said to be anchimerically[2] assisted [3,4] as they proceed through an "internally attached form" of the involved substrate.[2,3,4] The results of many studies have shown that anchimeric assistance may involve participation by different groups such as aryl, alkyl, alkoxyl, aryloxyl, carboxyl, carbo-alkyoxyl, amino, alkylamino, dialkylamino, mercapto, thioalkyl, thioaryl and carboxylate anion or by single atoms such as hydrogen and the halogens.[5]

---

* Presented at the 7th Scientific Arab Congress, Cairo, Egypt (A.R.E.), Sept. 22–26, 1973.

[1] For preceding parts of this series, see *Rev. Roumaine Chim.*, **18**, 297, 478, 1929, 1937 (1973); *ibid*, in press (1974).

[2] S. Winstein, C. R. Lindegren, H. Marshall and L. L. Ingraham, *J. Amer. Chem. Soc.*, **75**, 147 (1953).

[3] S. Winstein, B. K. Morse, E. Gaunwald, K. C. Schreiber and J. Corse, *J. Amer. Chem. Soc.*, **74**, 1113 (1952).

[4] S. Winstein and K. C. Schreiber, *J. Amer. Chem. Soc.*, **74**, 2171 (1952).

For many years it has been proposed that aryl participation plays a determining role during the solvolysis of β-arylalkyl systems.[6] Moreover, participation by aryl groups located at positions more distant than *beta* has also been shown to occur.[7] Examples of such participation are Ar_1-5 and Ar_2-6, illustrated schematically in Scheme 1, by the conversion of 1 to 2 and 3 ($n = 2$), respectively.[8]

Scheme 1

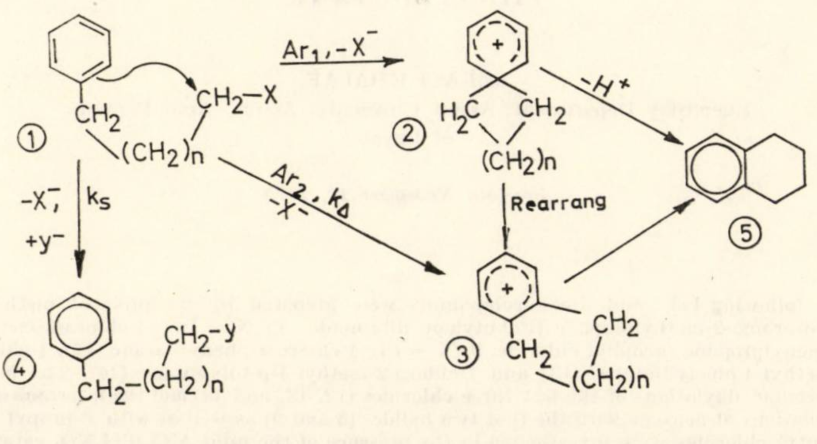

In systems of the type shown in Scheme 1, analysis of solvolytic reactions led to two important conclusions: First,[6a] there are two competing paths for displacement of the leaving group, which are designated as k_Δ and k_s. These paths are simultaneous reactions, each with its own characteristics, and there is no cross-over between them. The k_Δ path involves aryl participation as the leaving group leaves giving a nonclassical ion and this accounts for scrambling of the two carbons of the ethyl side chain in β-arylethyl systems [9] and for the formation of tetralin derivatives in δ-arylbutyl systems.[7] The k_s path involves direct S_N2 displacement of the leaving group by nucleophiles. Secondly, as regards variation of K_Δ in Ar_1-n participation with the size of the ring being formed in the intermediate spiro-carbonium ion, 2, the observed rate sequence is 3 (i.e. $n = 0) \gg 4$ (i.e. $n = 1) \ll 5$ (i.e. $n = 3) \gg 6$ (i.e. $n = 2$).[7]

---

[5] For reviews of this subject, see (a) S. WINSTEIN, *Bull. Soc. chim. France*, **18**, C-55 (1951); (b) A. STREITWIESER, JR., *Chem. Revs.*, **56**, 675 (1956); (c) A. STREITWIESER, JR., "Solvolytic Displacement Reactions", McGraw-Hill Book Co., Inc., Nes York, N. Y., 1962.

[6] For example see the following recent references and the older references listed therein: a) M. G. JONES and J. L. COKE, *J. Amer. Chem. Soc.*, **91**, 4284 (1969); b) C. J. KIM and H. C. BROWN, *J. Amer. Chem. Soc.*, **91**, 4289 (1969); c) P. VON R. SCHLEYER, *J. Amer. Chem. Soc.*, **91**, 4297 (1969); d) A. F. DIAZ and S. WINSTEIN, *J. Amer. Chem. Soc.*, **91**, 4300 (1969), e) R. J. JABLONSKI and E. I. SNYDER, *J. Amer. Chem. Soc.*, **91**, 4445 (1969).

[7] a) R. HECK and S. WINSTEIN, *J. Amer. Chem. Soc.*, **79**, 3105 (1957); b) R. HECK and S. WINSTEIN, *J. Amer. Chem. Soc.*, **79**, 3114 (1957).

[8] S. WINSTEIN and his collaborators[7] has adopted a notation in which participation of a β-phenyl group is symbolized Ar_1-3. According to these authors, the general notation is Ar_a-n, where Ar denotes aryl and the subscript a refers to the position in the participating aryl group involved in the creation of the ring in the transition state for anchimerically assisted ionization. The size of the ring being made is indicated by the number n.

Gould [10] has pointed out that there are three principal types of evidence that point to neighbouring group participation. These are based on stereochemical changes, molecular rearrangements and relative rates. According to the latter evidence, if aryl participation occurs during the rate-determining step in a given reaction, the reaction is almost certain to be significantly more rapid than other reactions that are similar but do not involve such participation. It may then be asked whether the last criterion for neighbouring group participation, namely, the enhancement of reaction rate, is also applicable to cases involving inter- and intramolecular Friedel-Crafts alkylations. For this reason, the relative rates of intramolecular alkylations (cyclialkylations) of chlorides 12, 13 and 14, and of intermolecular alkylations of benzene with 1-chloro-2-methyl-2-phenylpropane (neophyl chloride, 9), n-propyl chloride and n-butyl chloride were investigated in the presence of the mild $AlCl_3/CH_3NO_2$ catalyst and the results obtained were correlated with anticipated participations

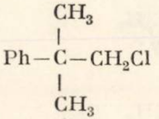

$$Ph-\underset{CH_3}{\overset{CH_3}{C}}-CH_2Cl$$

9

$Ph-CH_2CH_2CH_2CH_2Cl$

12

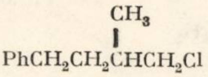

$$PhCH_2CH_2\overset{CH_3}{C}HCH_2Cl$$

13

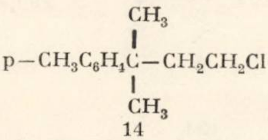

$$p-CH_3C_6H_4\underset{CH_3}{\overset{CH_3}{C}}-CH_2CH_2Cl$$

14

Understandably, arylalkyl chlorides, 9, 12, 13 and 14 were specifically chosen because they offer good models wherein there exists the possibility for the following : a) a combination of β-phenyl and β-dimethyl participations in the reaction of chloride 9, (b) δ-phenyl participation in the reaction of chloride 12, (c) a combination of δ-phenyl and β-methyl participations in the reaction of chloride 13, (d) a combination of γ-p-tolyl and γ-dimethyl participations in the reaction of chloride 14.

---

[9] a) D. J. Cram and L. A. Singer, *J. Amer. Chem. Soc.*, **85**, 1075 (1963); b) J. L. Coke, F. E. McFarlane, M. C. Mourning and M. G. J. Jones, *J. Amer. Chem. Soc.*, **91**, 1154 (1969).

[10] E. S. Gould, "Mechanism and Structure in Organic Chemistry", Holt, Rinehart and Winston", New York, N. Y., 1960, Chapter 14, pp. 561–617.

RESULTS AND DISCUSSION

As Friedel-Crafts alkylations with the strong $AlCl_3$ catalyst are known to be rapid,[11] it seemed advisable to attempt the study of the relative rates of the concerned inter- and intramolecular alkylations in the presence of the moderated $AlCl_3/CH_3NO_2$ catalyst. This catalyst which is known to induce both inter-[12,13] and intramolecular[14] Friedel-Crafts alkylations with tertiary,[12] secondary[12c,13a] and benzylic[13b] type halides, can induce the reactions of ordinary primary halides only if they involve participation by aryl and/or alkyl groups.[12c,15,16] Illustration of these facts about the catalytic abilities of $AlCl_3/CH_3NO_2$ can be found in the finding that reaction of 1,3-dichloro-3-methylbutane (6) with benzene in the presence of $AlCl_3/CH_3NO_2$ gave 1-chloro-3-methyl-3-phenylbutane (7) and no diphenyl[15] while treatment of either 1,2-dibromo-2-methylpropane (8, $X = Br$) or 1-chloro-2-methyl-2-phenylpropane (neophyl chloride, 9, $X = Cl$) under the same conditions yielded a mixture of the two isomeric diphenyl propanes 10 and 11 (see Scheme 2).[15,16]

Scheme 2

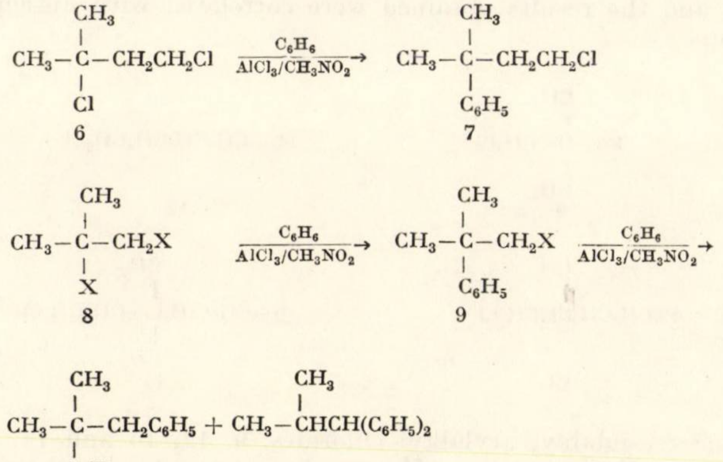

---

[11] a) A. A. Khalaf and R. M. Roberts, *J. Org. Chem.*, **31**, 89 (1966); b) G. Baddeley and R. Williamson, *J. Chem. Soc.*, **1956**, 4647.

[12] a) A. A. Khalaf and R. M. Roberts, *J. Org. Chem.*, **35**, 3717 (1970); b) M. Inatome, K. W. Greenlee, J. M. Derfer and C. E. Boord, *J. Amer. Chem. Soc.*, **74**, 292 (1952); c) R. M. Roberts and S. E. McGuire, *J. Org. Chem.*, **35**, 102 (1970); d) B. S. Friedman, F. L. Morritz, C. J. Morrissey and R. Koncos, *J. Amer. Chem. Soc.*, **80**, 5867 (1958).

[13] a) G. A. Olah *et al.*, *J. Amer. Chem. Soc.*, **86**, 1046 (1964). b) G. A. Olah, S. J. Kuhn and S. H. Flood, *J. Amer. Chem. Soc.*, **84**, 1688 (1962).

[14] A. A. Khalaf and R. M. Roberts, *J. Org. Chem.*, **37**, 4227 (1972). b) A. A. Khalaf, *Rev. Roumaine, Chim.*, **18**, 297 (1973).

[15] L. Schmerling, R. W. Welch and J. P. West, *J. Amer. Chem. Soc.*, **78**, 5406 (1956).

[16] A. A. Khalaf and R. M. Roberts, *J. Org. Chem.*, **31**, 926 (1966).

The failure of alkylation to occur at the primary carbon atom in 7, whereas it occurred readily in the reaction of 9 under the same experimental conditions, has strongly suggested phenyl participation as a deriving force in the case of halide 9.[15,16]

It appears from the previous discussion that the use of $AlCl_3/CH_3NO_2$ as catalyst is advantageous for the present purpose not only because it is milder and in general effects isomerizations to a lesser extent than does aluminum chloride alone,[17] but also because it offers a simple test for the occurrence and extent of group participation.

With the above essential background in mind, it is now suitable to look at the results of treatment of the chlorides : 1-chloro-2-methyl-2-phenylpropane (neophyl chloride, 9, X = Cl), 1-chloro-4-phenylbutane (12), 1-chloro-2-methyl-4-phenylbutane (13) and 1-chloro-3-methyl-3-p-tolybutane (14) with $AlCl_3/CH_3NO_2$ catalyst. In this work, chlorides 12, 13 and 14 were treated with the mild $AlCl_3/CH_3NO_2$ catalyst and the samples taken from the reaction mixtures after varying time intervals were decomposed and analysed by vapour-phase chromatography. The results obtained from 1-chloro-4-phenylbutane (12) and 1-chloro-2-methyl-4-phenyl-butane (13) are summarized in Tables 1 and 2, respectively. These are also shown graphically in Figure 1. Treatment of 1-chloro-3-methyl-3-p-tolylbutane (14) with $AlCl_3/CH_3NO_2$ under similar conditions resulted in inappreciable reaction, however.

Table 1

The action of $AlCl_3/CH_3NO_2$ on 1-Chloro-4-phenylbutane (12)

Time (hour)	Relative %	
	Starting Chloride	Tetralin
4	98	2
17	93	7
24	92	8
48	86	14
72	69	31

Table 2

The Action of $AlCl_3/CH_3NO_2$ on 1-chloro-2-methyl-2-phenylbutane (13)

Time (hour)	Relative %		
	Chloride	1,1-Dimethylindan	2-Methyltetralin
1	91	6	4
4	67	17	16
8	54	27	19
24	6	44	40
48	Trace	56	44

---

[17] L. Schmerling, *Ind. Eng. Chem.*, **40**, 2072 (1948).

Examination of the results given in Tables 1 and 2 and the slopes of the curves drawn in Fig. 1 indicates clearly that the reaction of 1-chloro-2-methyl-4-phenylbutane (13) is much faster than that of 1-chloro-4-phenylbutane (14). The simplest and most ominous explanation for this result lies in the fact that the removal of the chloride ion from 1-chloro-2-methyl-4-phenylbutane (13) is assisted by both β-methyl and δ-phenyl participations while the removal of the chloride ion from 1-chloro-4-phenylbutane (12) is assisted solely by δ-phenyl participation. The failure of 1-chloro-3-methyl-3-p-tolylbutane (14) to undergo any significant reaction in the presence of the weak catalyst $AlCl_3/CH_3NO_2$ under conditions similar to those effecting intramolecular alkylations of chlorides 12 and 13 reveals that no appreciable incursion of γ-phenyl participation in the rate-determining ionization step is indicated for the γ-phenyl chloride examined. Apart from that, the behaviour of chloride 14 is in line with the known fact that primary closure to a five-membered ring is highly unfavourable.[11a,18–21]

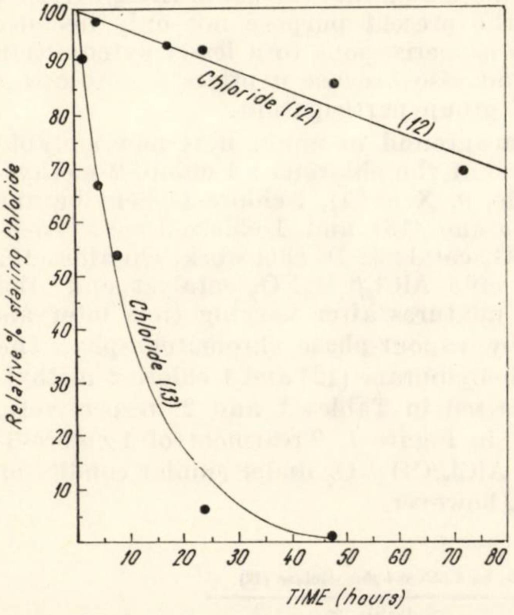

Fig. 1. — Rates of reaction of 1-chloro-4-phenylbutane (12) and 1-chloro-2-methyl-4-phenylbutane (13) with $AlCl_3/CH_3NO_2$ at room temperature; data are taken from Tables 1 and 2.

It may be of interest to indicate at this point that the difficulty of reaction of chloride 14 with the weak catalyst $AlCl_3/CH_3NO_2$ is parallel to that previously observed[17] in the reaction of *n*-propyl chloride with benzene and $AlCl_3/i{-}C_3H_7NO_2$. In the latter case a 4% yield of isopropylbenzene was only isolated after conducting the reaction for 18 hours at room temperature and for an additional hour at 60° to 70°C. This analogy in the behaviour of the primary arylalkyl chloride 14 and the primary *n*-propyl chloride again signifies that similar to the latter, the ionization of the former chloride is also unchimerically unassisted. Further support for this view was also obtained in this work when preliminary attempted alkylations of benzene with either *n*-propyl chloride or *n*-butyl

---

[18] A. A. Khalaf and R. M. Roberts, *J. Org. Chem.*, **34**, 3571 (1969).

[19] A. A. Khalaf and R. M. Roberts, *J. Org. Chem.*, **36**, 1040 (1971).

[20] R. M. Roberts, G. P. Anderson, Jr., A. A. Khalaf and Chow-Eng Low, *J. Org. Chem.*, **36**, 3342 (1971).

[21] A. A. Khalaf and R. M. Roberts, *J. Org. Chem.*, **38**, 1388 (1973).

chloride in the presence of the weak $AlCl_3/CH_3NO_2$ catalyst at room temperature failed to yield any alkylation products. These results indicate that, similar to intramolecular γ-participations, intermolecular participations are also inappreciable in the course of Friedel-Crafts alkylations.

To compare the relative rates of reactions of primary halides involving γ-aryl or δ-aryl participation with those involving neighbouring β-aryl participation, it seemed desirable to investigate the relative rate of reaction of a compound such as 1-chloro-2-methyl-2-phenylpropane (neophyl chloride) under the influence of the moderated $AlCl_3/CH_3NO_2$ catalyst. Since this chloride cannot undergo intramolecular alkylation, its reaction with benzene was rather studied. To carry this intermolecular reaction under conditions resembling those used for the other chlorides, a solution of neophyl chloride in benzene was added at once to a stirred solution of the catalyst in carbon disulfide. In contrast to the cases of chlorides 12, 13 and 14 a relatively rapid evolution of hydrogen chloride was noted and the reaction was shown to be completed in about an hour. Analysis of the product mixture obtained from this reaction after one hour using various methods of identification showed it to be a mixture of 1,2-diphenyl-2-methyl-propane (10) and 1,1-diphenyl-2-methyl-propane (11) in a ratio of about 2 : 1 with none of the starting material remaining. A similar result was also obtained when 1,2-dibromo-2-methylpropane was allowed to react with benzene under comparable conditions. Notably, the products from benzene alkylation with both neophyl chloride and isobutylene dibromide in the presence of $AlCl_3/CH_3NO_2$ are similar to those reported before [16] and expressed structurally in Scheme 2.

The above observations of the enhanced alkylation of benzene with both neophyl chloride and isobutylene dibromide, coupled with the finding that Friedel-Crafts alkylation of aromatics with 2-phenylethyl-1-C^{14} chloride not only occurs rapidly but also results in products which show isotope position rearrangement corresponding to an essentially 50% rearrangement of the C^{14} labeled atom from the C−1 to the C−2 position in the original chloride [22] demonstrate clearly that the ionization of the halogen atom in β-arylalkyl halides is easier and comparatively faster than in γ- and in δ-arylalkyl halides.

In conclusion, it appears from the forthgoing results of this work that, similar to solvolytic reactions, the ionization of arylalkyl halides under Friedel-Crafts conditions is assisted, to a varying degree, by aryl participation depending upon the location of the aryl group relative to the halogen atom. As regards variation in the extent of participation with the distance of the aryl group from the reaction site, the observed relative rates for chlorides 9, 12, 13 and 14 shows that the sequence is β-aryl $>$ $>$ δ-aryl $>$ γ-aryl. It cannot be concluded on the basis of this work, however, whether the types of participation involved in the ionization of the δ-arylalkyl halides is of the Ar_1—5 (Structure 22) or the Ar_2—6 (Structure 23) type or a combination of both types. Nevertheless, it has been pointed out by Heck and Winstein [7b] that Ar_1-5- and Ar_2-6- assisted

---

[22] a) C. C. Lee, A. G. Forman and A. Rosenthal, *Canad. J. Chem.*, **35**, 220 (1957); b) M. A. McMahon and S. C. Bunce, *J. Org. Chem.*, **29**, 1515 (1964); c) E. H. Adena and F. L. J. Sixma, *Rec. Trav. chim.*, **81**, 323 (1962); d) E. H. Adema and F. L. J. Sixma, *ibid*, **81**, 336 (1962).

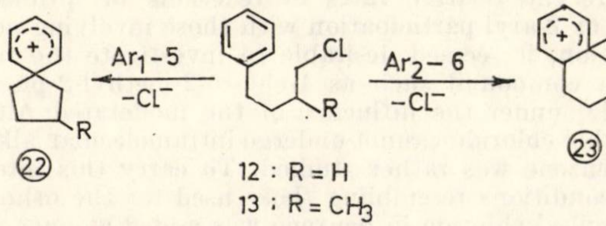

ionizations have nearly equal rates for equivalent degrees of activation of the benzene ring. In this laboratory, further work is being conducted to cast some light on the type or types of participation that may be involved under Friedel-Crafts conditions.

Mechanism of Formation of 1-Methyltetralin During the $AlCl_3$-Catalyzed Reaction of 1-Chloro-2-methyl-4-phenylbutane (13)

Apart from its main objectives in this study, the $AlCl_3/CH_3NO_2$-catalyzed Friedel-Crafts intramolecular alkylation (cyclialkylation) of 1-chloro-2-methyl-4-phenylbutane (13) has also provided a very interesting piece of information which is worthy of mention. In this work, treatment of chloride 13 with the mild $AlCl_3/CH_3NO_2$ catalyst gave a mixture of 2-methyltetralin and 1,1-dimethylindan. Previously, however, the treatment of chloride 13 with the strong $AlCl_3$ catalyst was shown by Khalaf and Roberts [11a] to give a more complex mixture consisting of the cyclization product 1,1-dimethylindan (15), 1-methyltetralin (16) and 2-methyltetralin and of the hydride exchange product isopentylbenzene (17). While the cyclization product, 2-methyltetralin was the major component from reactions conducted in carbon disulfide solvent, the hydride exchange product, isopentylbenzene, was the major product in the hydrocarbon solvent, petroleum ether. The results from the $AlCl_3$-catalyzed reaction of chloride 13 was explained by the authors in terms of Scheme 3.

The fact that 1-methyltetralin (16) was produced in the reaction of 1-chloro-2-methyl-4-phenylbutane (13) in the presence of $AlCl_3$ but not in the presence of $AlCl_3/CH_3NO_2$ is significant as it has some bearing on the mode of formation of 16. The formation of 16 from 13 in the presence of $AlCl_3$ was suggested by Khalaf and Roberts [11a] to follow the route 19 → 20 → 21 → 16 as shown in Scheme 3. On the basis of the present results, this route can be disqualified as if it is the operable one, it should be possible to obtain 1-methyltetralin regardless of the type of catalyst initiating the reaction. This is because carbonium ion 19 (or its equivalent) would always be present whether the catalysts is $AlCl_3$ or $AlCl_3/CH_3NO_2$. An alternative plausible mechanism for the formation of 1-methyltetralin during the $AlCl_3$-catalyzed reaction of chloride 13 is offered in Scheme 4.

Scheme 3

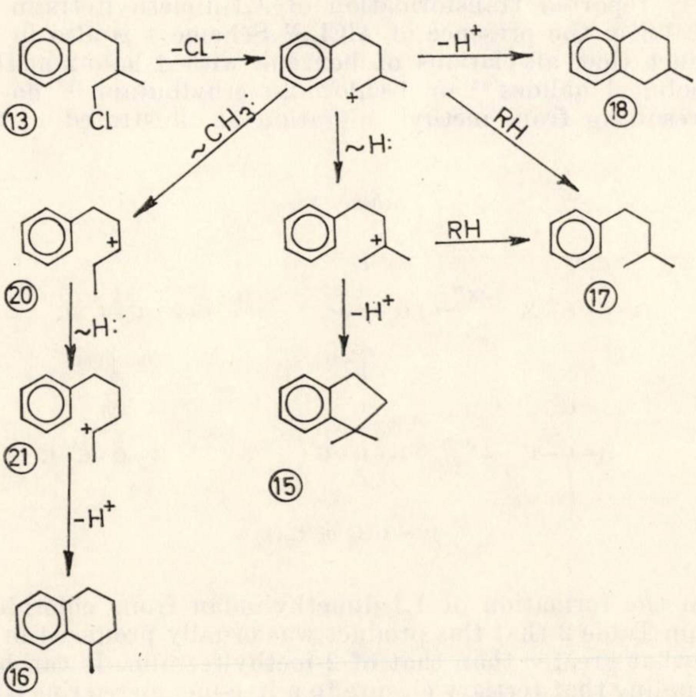
-Cl
-H+
13
Cl
18
~CH3:
~H:
RH
RH
20
17
~H:
-H+
21
15
-H+
16

Scheme 4

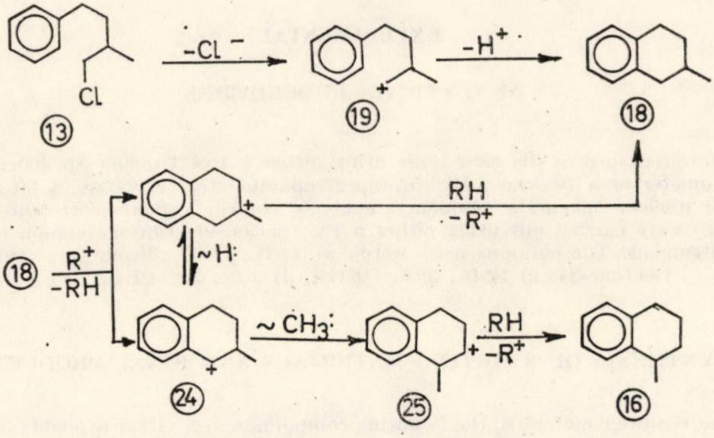
-Cl-
-H+
Cl
13
19
18
RH
-R+
18
R+
-RH
~H:
~CH3:
RH
-R+
24
25
16

According to the above mechanism, the primarily formed 2-methyltetralin is subsequently isomerized to 1-methyltetralin via the route 18 → → 24 → 25 → 16. The abstraction of a hydride ion from 18 to produce 24 can only occur in the presence of the strong $AlCl_3$ catalyst.[12,14,16–19,21]

Experimental credence to the mechanism of Scheme 4 can be found in the recently reported transformation of 1,1-dimethyltetralin to 2,2-dimethyltetralin in the presence of $AlCl_3$.[21] Scheme 4 is also in agreement with the fact that alkylations of benzene with 1-halo-2-methylalkanes such as isobutyl halides [23] or 1-chloro-2-methylbutane [12c] do not yield products resulting from methyl migration as illustrated in Scheme 5.

Scheme 5

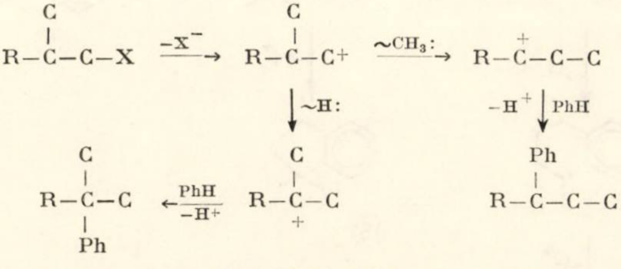

R = CH_3 or C_2H_5

As to the formation of 1,1-dimethylindan from chloride 13, it is evident from Table 2 that this product was usually produced in a percent ratio somewhat greater than that of 2-methyltetralin. It can be inferred from this finding that tertiary closure to a five-membered ring is somewhat favoured over primary closure to a six-membered ring.

EXPERIMENTAL

ANALYTICAL PROCEDURES

The infrared spectra (ir) were done using either a Pye Unicam Sp 200G Grating IR Spectrophotometer or a Beckman IR–5A Spectrophotometer. A varian A 60 spectrometer was used for nuclear magnetic resonance analysis (nmr). Vapour-phase chromatographic analysis (vpc) were carried out using either a Pye Series 104 Chromatograph or a Becman GC–2A instrument. The columns used were: a) 12-ft., 30% silicone gum rubber SE-30; b) 12 ft., 15% Bentone-34, c) 12-ft., 20% DEGA, d) 5-ft., 3% PEGA; e) 5-ft., 3% DNP.

SYNTHESIS OF STARTING MATERIALS AND FINAL PRODUCTS

Of the required materials, the following compounds were either available from previous work or were synthesized according to the procedures described in the references indicated: 1,2-dibromo-2-methylpropane (8; X = Br) [16]; 1-chloro-2-methyl-2-phenylpropane (9; X = = Cl)[16]; 1,2-diphenyl-2-methylpropane (10)[16]; 1,1-diphenyl-2-methylpropane (11)[16]; tetralin [11a]; 1,1-dimethylindan (15),[11a] 1-methyltetralin (16) [11a]; isopentylbenzene (17),[11a] 2-methyltetralin (18).[11a] The rest of the required materials were prepared as described below.

---

[23] R. M. Roberts and D. Shiengthong, *J. Amer. Chem. Soc.*, **82**, 732 (1960).

Synthesis of 1-chloro-4-phenylbutane (12):

Preparation of γ-chlorobutyrophenone: In a 250-ml roundbottomed flask equipped with a magnetic stirrer, a pressure-equalizing dropping funnel, and an efficient reflux condenser were placed 14.9 g (0.11 mole) of anhydrous $AlCl_3$, 18.3 g (0.3 mole) of nitromethane and 78 g (1 mole) of dry benzene, respectively.

A solution of 14.1 g (0.1 mole) of 4-chlorobutyryl chloride in 40 ml of dry benzene was placed in the dropping funnel and added over a period of one hour to the stirred solution in the flask. After addition was complete, the reaction mixture was stirred at room temperature for 2 hr and then decomposed by pouring over a 100 ml of cold 10% solution of hydrochloric acid. The organic layer was separated, washed with 10% sodium bicarbonate solution followed by water and finally dried for overnight over anhydrous sodium sulfate. Removal of the solvent under atmospheric pressure gave 14.5 g (75% yield) of γ-chlorobutyrophenone: b.p. 131–132° (4 mm); n_D^{25} 1.5528 lit.[24] b.p. 120–121° (3 mm); n_D^{20} 1.55433.

Reduction of γ-chlorobutyrophenone to 1-chloro-4-phenylbutane (12): This was accomplished catalytically using 9.1 g (0.05 mol) of γ-chlorobutyrophenone, 30 ml of glacial acetic acid, 0.5 ml of perchloric acid and 2 g of 5% palladium on carbon with an initial pressure of 65 psi.[25] When the required amount of hydrogen was consumed, the reaction mixture was removed from the apparatus. The catalyst was filtered off with a sintered glass crucible and discarded. The filtrate was diluted with water and extracted with petroleum ether (b.p. 60–80°) which was then washed with water followed by dilute sodium bicarbonate solution and finally dried over anhydrous sodium sulfate. Removal of the solvent and purification of the residue by distillation under vacuum gave 7.2 g (90% yield) of a colourless liquid whose physical and spectroscopic properties were identical with those published previously [11a] for 1-chloro-4-phenylbutane (12).

Synthesis of 1-chloro-2-methyl-4-phenylbutane (13):

Preparation of 2-Methyl-3-benzolylpropionic acid: 2-Methyl-3-benzoylpropionic acid was prepared by a modification of the procedure described previously.[11a] In a dry, one-liter, three-necked, round-bottomed flask fitted with a mechanical stirrer, a reflux condenser carrying a calcium chloride tube and a pressure-equalizing dropping funnel were placed 34.2 g (0.3 mol) of methylsuccinic anhydride (pyrotartaric anhydride) and 500 ml of dry thiophene--free benzene. A solution of 95 g (0.7 mol) of $AlCl_3$ in 183 g (3.0 mol) of nitromethane was added to the stirred contents of the flask. When addition was completed in 1.5 h, stirring was allowed to continue for two additional hours at room temperature and for half an hour at 60°. The reaction mixture was then decomposed with dilute hydrochloric acid and the organic layer was separated, washed with water and dried over anhydrous sodium sulfate. Evaporation of the organic solvent with gentle heating under suction left a solid residue which on crystallization from carbon tetrachloride gave 46 g (80% yield) of 2-methyl-3-benzoylpropionic acid: m.p. 141–142°. Reported m.p.: 140.5° by Oppenheim [26], 139–140° by Alexander and Mudrak [27] and 139 by Khalaf and Roberts.[11a]

Reduction of 2-Methyl-3-benzoylpropionic Acid to 2-Methyl-4-phenylbutyric Acid: This reduction was accomplished catalytically following essentially the procedure previously described [25] for the reduction of γ-chlorobutyrophenone to 1-chloro-4-phenylbutane with the exception that only water was used to wash the petroleum ether extract. Starting with 38.4 g (0.2 mol) of 2-methyl-3-benzoylpropionic acid, 100 ml of glacial acetic acid, 0.5 ml of 70% perchloric acid and 3 g of 5% palladium on charcoal gave 32 g (90% yield) of 2-methyl-4-phenylbutyric acid: b.p. 178–180° (18 mm) [lit. b.p. 176–178° (17 mm) [28] and 175–178° (16 mm) [11a]].

Conversion of 2-Methyl-4-phenylbutyric acid to 1-Chloro-2-methyl-4-phenylbutane (13): This conversion followed essentially the reported method.[11a] Accordingly, 2-methyl-4-phenylbutyric acid was reduced by lithium aluminum hydride [29] to 1-hydroxy-2-methyl-4-phenylbutane which upon treatment with thionyl chloride in pyridine [30] gave the desired 1-chloro-2-methyl-4-phenylbutane: b.p.: 136–138° (20 mm); n_D^{24} 1.5126 [lit.[11a] b.p. 134–135° (19 mm) and 100–101° (5 mm); n_D^{25} 1.5123]. The overall yield of the chloride was 68% based on the starting acid.

---

[24] J. B. Cloke, *J. Amer. Chem. Soc.*, **51**, 1174 (1929).

[25] R. M. Roberts, G. A. Ropp and O. K. Neville, *J. Amer. Chem. Soc.*, **77**, 1764 (1955).

[26] A. Oppenheim, *Ber.*, **34**, 4227 (1901).

[27] E. R. Alexander and A. Mudrak, *J. Amer. Chem. Soc.*, **72**, 3194 (1950).

[28] H. Adkins and J. W. Davis, *J. Amer. Chem. Soc.*, **71**, 2955 (1949).

[29] J. H. Hunta and J. A. Hogg, *J. Amer. Chem. Soc.*, **71**, 1924 (1949).

[30] L. Bateman, J. I. Cunneen and J. A. Lyons, *J. Chem. Soc.*, **1941**, 2290.

Synthesis of 1-Chloro-3-methyl-3-p-tolylbutane (14):

This was carried out as previously described by this author.[31]

ALKYLATION PROCEDURES

In all alkylations the apparatus used was a 50-ml, two-necked, round-bottomed flask fitted with a reflux condenser, a pressure-equalizing dropping funnel and a stirring magnet. A calcium chloride tube was also attached to the top of the condenser.

(a) *Intermolecular Alkylation of Benzene with 1,2-Dibromo-2-methylpropane (Isobutylene Dibromide) and 1-Chloro-2-methyl-2-phenylpropane (Neophyl Chloride), Using $AlCl_3/CH_3NO_2$ as Catalyst*: A solution of 0.66 g (0.05 mole) of $AlCl_3$ in 1.5 ml of CH_3NO_2 was introduced into the flask followed by 50 ml of CS_2. To the stirred contents of the flask was added rapidly through the dropping funnel a solution of 0.025 mole of the halide (1.2 g of neophyl chloride and 1.4 g of isobutylene dibromide) in 20.4 g (0.256 mole) of dry benzene. After one hour, the reaction mixture was decomposed by the addition of dilute hydrochloric acid and the organic layer was separated, washed, dried and analysed by vpc. The products from both chlorides were found to be mixtures of 63–67% 1,2-diphenyl-2-methylpropane and 37–33% 1,1,-diphenyl-2-methylpropane with none of the starting halides present.

(b) *Intramolecular Alkylation (Cyclialkylation) of 1-Chloro-4-phenylbutane (12), 1-Chloro-2-methyl-4-phenylbutane (13) and 1-Chloro-3-methyl-3-p-tolylbutane Using $AlCl_3/CH_3NO_2$ as Catalyst*: To a solution of 1.6 g of $AlCl_3$ in 3 ml of CH_3NO_2 was added at once a solution of 2.2 g of the chloride in 10 ml of CS_2 and the resulting reaction mixture was stirred while 0.1 ml samples were taken after varying time intervals and decomposed by rapid introduction into marked small vials containing dilute HCl. The organic layers resulting after decomposition were dried and analysed by vpc. The results obtained for chlorides 12 and 13 are embedded in Tables 1 and 2, respectively. Chloride 14 showed no appreciable reaction under the employed conditions, however.

---

[31] A. A. **Khalaf**, *Indian J. Chem.*, in press.

Revue Roumaine de Chimie, **19**, *8*, 1373–1380 (1974)

MODERN FRIEDEL-CRAFTS CHEMISTRY. VIII*

CYCLIALKYLATIONS OF SOME ARYL- AND DIARYLALKANOLS IN THE PRESENCE OF THE MILD $AlCl_3/CH_3NO_2$ CATALYST**

ALI ALI KHALAF

Department of Chemistry, Assiut University, Assiut, Arab Republic of Egypt

Received November 13, 1973

Alcohols 1 through 18 were obtained and their cyclidehydrations were investigated in the presence of the mild $AlCl_3/CH_3NO_2$ catalyst at ambient temperature. Under these conditions, both secondary and tertiary alcohols underwent facile cyclialkylation to tetralins but only tertiary alcohols could be closed to indans. The products obtained from these reactions were exactly similar to those obtained before from cyclialkylations of the same alcohols with H_2SO_4 or of the corresponding chlorides with $AlCl_3/CH_3NO_2$. However, the yields of the cyclialkylation products obtained under present conditions were, in most cases, better than those reported from other cyclization procedures starting with either the alcohols or the corresponding chlorides. This, in addition to the fact that undesirable side reactions are often minimized under the employed conditions, make the $AlCl_3/CH_3NO_2$ catalyzed cyclidehydrations of secondary and tertiary alcohols a very convenient and efficient pathway for the synthesis of both indan and tetralin derivatives.

INTRODUCTION

For some time, this author has been engaged in a number of research studies relating to the mechanistic aspects and synthetic potentialities of Friedel-Crafts cyclialkylation reaction.[1-7] These studies together with the work of others[8] have shown that direct formation of indan and tetralin derivatives can be achieved through two main routes: First, intermolecular alkylation of aromatics with bifunctional alkylating agents including diols, dienes and dihaloalkanes as exemplified by the reactions of equations 1[9,10] and 2.[8d] Second, intramolecular alkylations of arylhaloalkanes as exemplified by the reactions of equations 3[1,2] and 4.[5] In most instants, the catalysts employed to bring about cyclization were

---

* For preceding papers of this series see A. A. Khalaf, *Rev. Roumaine Chim.*, **18**, 297, 479, 1929, 1937 (1973); *ibid*, in press.

** Presented at the 7th Scientific Arab Congress, Cairo, Egypt, Sept. 22–26, 1973.

[1] A. A. Khalaf and R. M. Roberts, *J. Org. Chem.*, **31**, 89 (1966).

[2] A. A. Khalaf and R. M. Roberts, *J. Org. Chem.*, **34**, 3571 (1969).

[3] A. A. Khalaf and R. M. Roberts, *J. Org. Chem.*, **36**, 1040 (1971).

[4] R. M. Roberts, G. P. Anderson, Jr., A. A. Khalaf and Chow-Eng Low, *J. Org. Chem.*, **36**, 3342 (1971).

[5] A. A. Khalaf and R. M. Roberts, *J. Org. Chem.*, **37**, 4227 (1972).

[6] A. A. Khalaf and R. M. Roberts, *J. Org. Chem.*, **38**, 1388 (1973).

[7] A. A. Khalaf, *Rev. Roumaine Chim.*, **18**, 299 (1973).

[8] (a) This area has been reviewed by L. R. C. Barclay in "Friedel-Crafts and Related Reactions", vol. II, G. A. Olah, Ed., Interscience Publishers, Inc., New York, 1964, pp. 785–977. Other recent papers on this subject are: (b) L. R. C. Barclay, B. A. Ginn and C. E. Milligan, *Canad. J. Chem.*, **42**, 579 (1964); (c) L. R. C. Barclay, and E. C. Sanford, *Canad. J. Chem.*, **46**, 3325 (1968); (a) J. M. Balquist and E. R. Degginer, *J. Org. Chem.*, **36**, 3345 (1971).

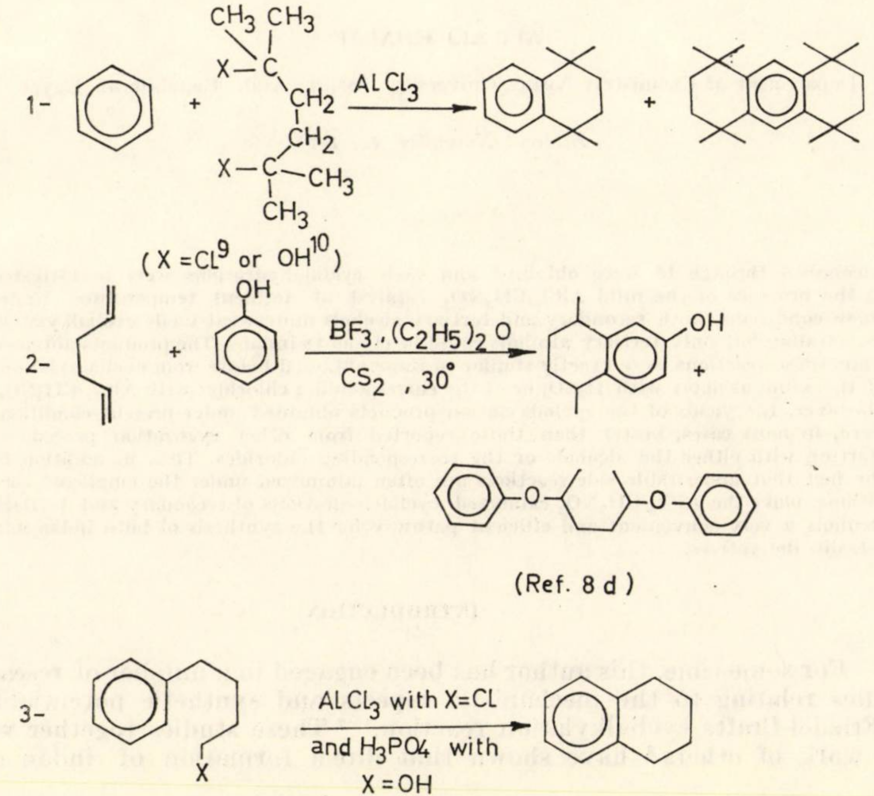

protonic-acids in reactions involving alcohols and alkenes but Lewis-acids in reactions involving halides. Very recently, the mild $FeCl_3$ and $AlCl_3$/ /CH_3NO_2 catalysts have been used extensively to effect cyclialkylations of secondary and tertiary arylhaloalkanes.[5,7] The application of such mild catalysts have been found to be superior to the strong $AlCl_3$ not only because they inhibit side carbonium ion processes but also because they give better yields of purer products.[7] A similar finding was also observed when some secondary and tertiary mono- and diphenylalkanols were cyclized in the presence of the mild $AlCl_3/CH_3NO_2$ catalyst.[5] Since the yields from these $AlCl_3/CH_3/NO_2$-catalyzed cyclialkylations of arylalkanols were as good as those obtained from similar reactions of the corresponding arylhaloalkanes, it seemed attractive to investigate more of these reactions in order to evaluate their usefulness and applicability in the synthesis of indan and tetralin derivatives. Understandably, the use of alcohols instead of the chlorides is preferable not only because it saves both the time and the effort needed to convert the alcohols to the chlorides, but also because it is more economical as it avoids the material loss which the conversion step necessitates. In the present work, a number of different mono- and diphenylalkanols were obtained and their cyclialkylations in the presence of $AlCl_3/CH_3NO_2$ were investigated.

RESULTS AND DISCUSSION

The primary : phenylalkanols 1 to 4 tolylalkanol 5 and diphenylalkanols 6 and 7, the secondary : phenylalkanols 8 to 11 and the tertiary : phenylalkanols 12 to 14, tolylalkanols 15 to 17 and diphenylalkanol 18 were subjected at room temperature to the action of $AlCl_3/$ $/CH_3NO_2$ catalyst in petroleum ether solvent. The results obtained are summarized in Table 1 and in equations 5 to 15.

5-

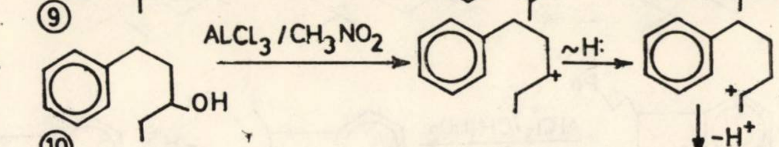

6-

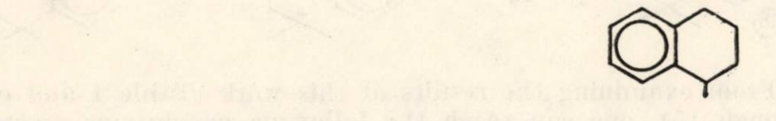

7-

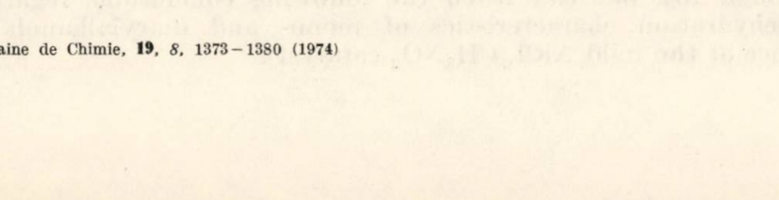

8-

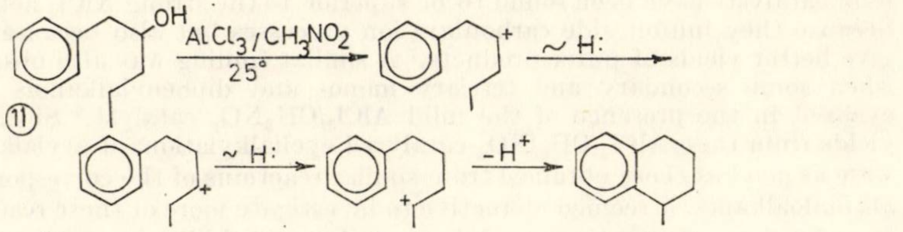
OH
AlCl3/CH3NO2
25°
~H:
⑪
~H:
+
-H+

9-

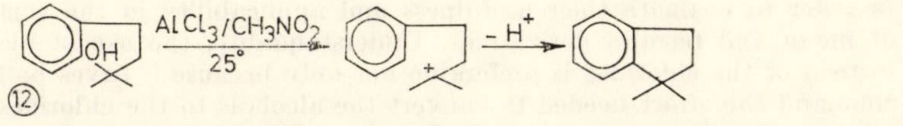
OH
AlCl3/CH3NO2
25°
+
- H+
⑫

10-

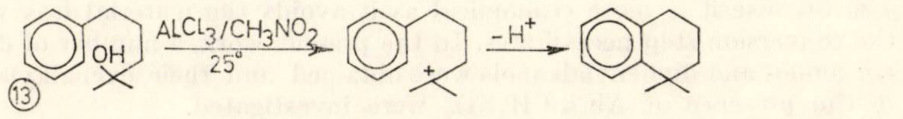
OH
AlCl3/CH3NO2
25°
+
-H+
⑬

11-

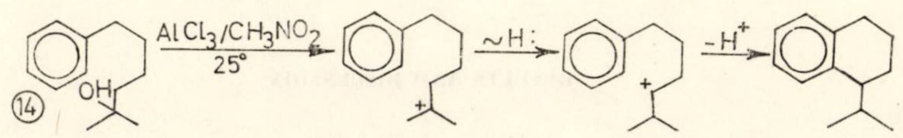
OH
⑭
AlCl3/CH3NO2
25°
+
~H:
+
-H+

12-

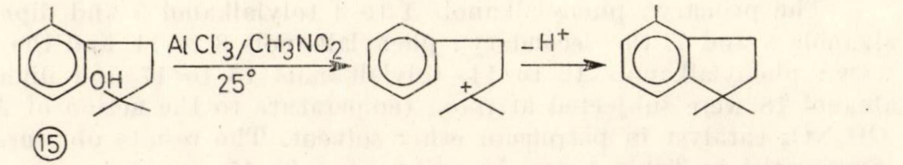
OH
⑮
AlCl3/CH3NO2
25°
+
-H+

13-

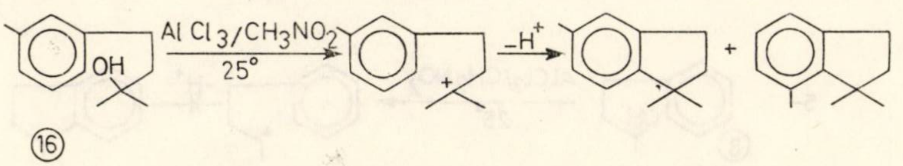
OH
⑯
AlCl3/CH3NO2
25°
+
-H+
+

14-

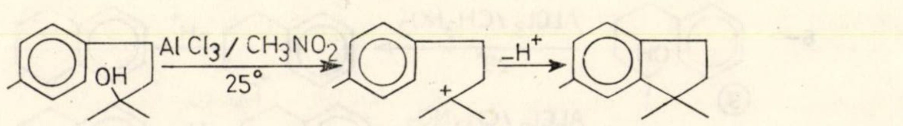
OH
AlCl3/ CH3NO2
25°
+
-H+

15-

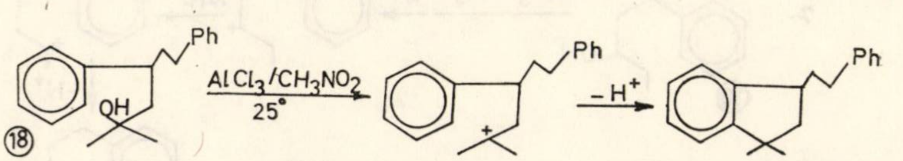
Ph
OH
⑱
AlCl3/CH3NO2
25°
Ph
+
-H+
Ph

From examining the results of this work (Table 1 and equations 5 through 15), one can reach the following conclusions regarding the cyclidehydration characteristics of mono- and diarylalkanols in the presence of the mild $AlCl_3/CH_3NO_2$ catalyst :

(1) The cyclidehydration of primary mono- and diarylalkanols cannot be effected with $AlCl_3/CH_3NO_2$ at ambient temperatures; the starting alcohols are recovered unchanged after hydrolysis.

(2) In contrast to primary mono- and diarylalkanols, secondary and tertiary mono- and diarylalkanols undergo facile cyclidehydration to tetralins either directly as in the cases of alcohols 9 and 13 (equations 6 and 10) or via rearrangement as in the cases of alcohols 10, 11 and 14 (equations 7, 8 and 11).

(3) With facilities comparable to those observed in cyclidehydrations of secondary and tertiary alcohols to tetralins, tertiary mono- and diarylalkanols undergo ring closures to indans (e.g. alcohols 12, 15, 16 and 17, equations 9, 12 ,13 and 14).

(4) In accordance with former findings,[1,2] secondary arylalkanols failed to cyclize to indans (e.g. alcohol 8; equation 5). As secondary arylalkanols have been shown to cyclize readily to tetralins, this noted failure cannot be attributed to a difficulty in ionizing the alcohol to the intermediate secondary carbonium ion (equation 5) but rather to a difficulty in closing this ion to an indan.[1,2,5,7]

(5) Similar to the previously reported cyclialkylations of secondary and tertiary alcohols with H_2SO_4[2,3] and of the corresponding secondary and tertiary chlorides with $AlCl_3/CH_3NO_2$ or $FeCl_3$[7] the cyclidehydration of secondary and tertiary alcohols with $AlCl_3/CH_3NO_2$ catalyst proceeds with none of the complicating side reactions which are known to accompany $AlCl_3$-catalyzed cyclialkylations.[1,5]

(6) The yields from the $AlCl_3/CH_3/NO_2$-catalyzed cyclidehydrations of alcohols 6 to 15 are, in most cases, better than those from the H_2SO_4-catalyzed cyclidehydration and, at least, as good as the yields from the $AlCl_3/CH_3NO_2$-catalyzed cyclialkylation of the corresponding chlorides.

Evaluation of the above findings, in terms of the motives that inspired this work, demonstrates clearly that the mild $AlCl_3/CH_3NO_2$ complex can be used to effect cyclidehydrations of both secondary and tertiary mono- and diarylalkanols. As this catalyst invariably produces good yields of clean cyclic products regardless of whether the starting material is the alcohol or the chloride, it is advantageous to start with the alcohol for reasons stated before in the introduction part.

Concerning the mechanism of interaction of the alcohols with the catalyst, it appears from the results that two distinct modes can be recognized. First, the interaction between primary alcohols and the catalyst which seems to involve the formation of aluminium trialkoxide as shown in equation 16. This proposed interaction

$$3\ RCH_2OH + AlCl_3 \rightarrow (RCH_2O)_3\,Al + 3\ HCl \qquad 16$$

is justified by two experimental observations: (a) the evolution of HCl gas upon the addition of alcohols to the catalyst, and (b) the recovery of the starting alcohols upon hydrolysis with water and that may occur as shown in equation 17.

$$(RCH_2O)_3Al + 3\,H_2O \rightarrow 3\,RCH_2OH + Al(OH)_3 \qquad 17$$

Second, the interaction between secondary and tertiary alcohols and the catalyst and that should be different from the case with primary alcohols. Accordingly, it is proposed that the initial step in the reaction with a

Table 1

Cyclidehydration of mono- and diphenylalkanols with AlCl$_3$/CH$_3$NO$_2$ in petroleum ether at room temperature

N°	Starting alcohol	Yield of cyclization product %	Composition of cyclization products (%)
	A. *Primary Alcohols*		
1	$PhCH_2CH_2CH_2OH$	0	Recovered starting material
2	$PhCH_2CH_2CH_2CH_2OH$	0	” ” ”
3	$PhCH_2CH_2CH_2CH_2CH_2OH$	0	” ” ”
4	$PhC(CH_3)_2CH_2CH_2OH$	0	” ” ”
5	$p-CH_3-C_6H_4C(CH_3)_2CH_2CH_2OH$	0	” ” ”
6	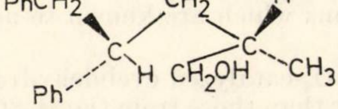	0	” ” ”
7	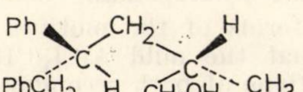	0	” ” ”
	B. *Secondary Alcohols*		
8	$PhCH_2CH_2CH(OH)CH_3$	0	Only high boiling materials
9	$PhCH_2CH_2CH_2CH(OH)CH_3$	80	1-Methyltetralin (100)
10	$PhCH_2CH_2CH(OH)CH_2CH_3$	76	1-Methyltetralin (100)
11	$PhCH_2CH(OH)CH_2CH_2CH_3$	50	1-Methyltetralin (100)
	C. *Tertiary Alcohols*		
12	$PhCH_2CH_2C(OH)(CH_3)_2$	82	1,1-Dimethylindan (100)
13	$PhCH_2CH_2CH_2C(OH)(CH_3)_2$	85	1,1-Dimethyltetralin (100)
14	$PhCH_2CH_2CH_2CH_2C(OH)(CH_3)_2$	65	1-Isopropyltetralin (100)
15	$o-CH_3C_6H_4CH_2CH_2C(OH)(CH_3)_2$	76	1,1,4-Trimethylindan (100)
16	$m-CH_3C_6H_4CH_2CH_2C(OH)(CH_3)_2$	74	1,1,5- (57) and 1,1,7- trimethylindan (43)
17	$p-CH_3C_6H_4CH_2CH_2C(OH)(CH_3)_2$	69	1,1,6-Trimethylindan (100)
18	$PhCH_2CH_2CH(Ph)CH_2C(OH)(CH_3)_2$	82	1,1-Dimethyl-3-(B-phenylethyl) indan (100).

secondary or a tertiary alcohol is the combination of alcohol and aluminium chloride by a dative bond in which the unshared electrons of the alcohol complete the electron octet of the aluminum atom and that is followed by the formation of an alkyl cation as shown in equation 18. A similar proposition was placed before by Huston and Awuapara.[11]

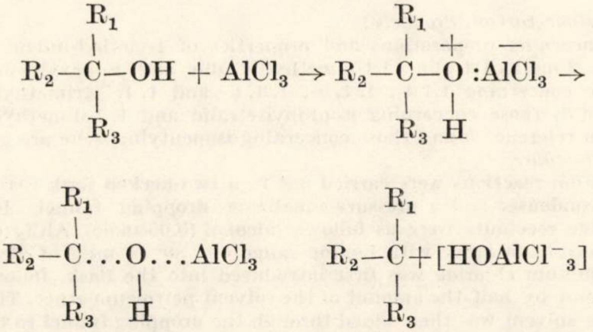

$$R_2-\overset{R_1}{\underset{R_3}{C}}-OH + AlCl_3 \rightarrow R_2-\overset{R_1}{\underset{R_3}{C}}-\overset{+}{\underset{H}{O}}:\overset{-}{AlCl_3} \rightarrow \qquad 18$$

$$R_2-\overset{R_1}{\underset{R_3}{C}}\ldots\underset{H}{O}\ldots AlCl_3 \quad R_2-\overset{R_1}{\underset{R_3}{C}}{}^{+}[HOAlCl_3^-]$$

It can be seen from the above general equation that the function of the catalyst is to loosen or break the carbon-oxygen bond in the alcohol, thus making the resulting species more electrophilic and hence a more effective attacking reagent for the aromatic ring.[12] In the light of the above mechanistic proposals, the difference in behaviour between primary alcohols on the one side and secondary and tertiary alcohols on the other side is primarily due to differences expected in the stabilities of the carbonium ions that may result from the cleavage of the carbon-oxygen bond. As it is known that, in general, the secondary and tertiary carbonium ions are much more stable than the primary ones, one need not be surprised that the formation of the latter is rendered more difficult.

EXPERIMENTAL

Analytical Procedures:

These were the same as those described in the preceding paper.[13]

Syntheses of Starting Materials and Final Products:

As all of the starting materials and final products needed for this study were either available from previous work or prepared according to formerly detailed procedures, it appeared sufficient here to refer to papers in which the original synthetic procedures are given.

Starting Mono- and Diarylalkanols: For synthetic procedures and physical properties of these alcohols see the references given in the following: 3-Phenyl-1-propanol (1) [11]; 4-phenyl-1-butanol (2) [1]; 5-phenyl-1-pentanol (3)[8b]; 3-methyl-3-phenyl-1-butanol (4) [2]; 3-methyl-3-p-tolyl-1-butanol (5) [3]; the two diastereomers of 2-methyl-4,5-diphenyl-1-pentanol

---

[9] L. R. C. Barclay, A. H. Gray and C. E. Milligan, *Canad. J. Chem.*, **39**, 870 (1961).

[10] I. P. Labunskii and I. P. Tsukerwenik, *Doklady Akad. Nauk.* SSSR, **80**, 369 (1951); *Chem. Abstr.*, **46**, 5022 (1952).

[11] R. C. Huston and J. Awuapara, *J. Org. Chem.*, **9**, 401 (1944).

[12] E. S. Gould, "Mechanisms and Structure in Organic Chemistry", Holt, Rinehart and Winston, New York, N. Y., 1960, p. 448.

[13] A. A. Khalaf, Part VII of this series, *Rev. Roumaine Chim.*, **19**, (1974).

[14] M. T. Bogert and D. Davidson, *J. Amer. Chem. Soc.*, **56**, 185 (1934).

(6 and 7)[6]; 4-phenyl-2-butanol (8)[1]; 5-phenyl-2-pentanol (9)[7,15]; 5-phenyl-3-pentanol (10)[7,15]; 1-phenyl-2-pentanol (11)[7,15]; 2-methyl-4-phenyl-2-butanol (12)[1]; 2-methyl-5-phenyl-2-pentanol (13)[1]; 2-methyl-6-phenyl-2-hexanol (14)[5,15]; 2-methyl-4-*o*-tolyl-2-butanol (15)[3]; 2-methyl-4-*m*-tolyl-2-butanol (16)[3]; 2-methyl-4-p-tolyl-2-butanol (17)[3]; 2-methyl-4,6-diphenyl-2-hexanol (18).[3]

Final Authentic Hydrocarbon Products:

Details concerning preparations and properties of 1-methyl-indan, 1,1-dimethylindan, 1-methyltetralin, 2-methyltetralin, 1,1-dimethyltetralin and isohexylbenzene are given in reference 1, those concerning 1,1,4-, 1, 1, 5-, 1, 1, 6- and 1, 1, 7-trimethylindan isomers are given in reference 3, those concerning isopropyltetralin and 1, 1-dimethyl-3-(β-phenylethyl)-indan are given in reference 5 and those concerning isopentylbenzene are given in reference.[16]

Cyclialkylation Procedure:

Cyclialkylation reactions were carried out in a two-necked flask fitted with a magnetic stirrer, a reflux condenser and a pressure-equalizing dropping funnel. In all experiments the amounts of the reactants were as follows: alcohol (0.05 mole), $AlCl_3$ (0.06 mole)/CH_3NO_2 (0.6 mole) and petroleum ether with boiling range 60—80° (4 ml/g of alcohol). In a typical reaction, the aluminum chloride was first introduced into the flask, followed first by nitromethane and second by half the amount of the solvent petroleum ether. The alcohol dissolved in the rest of the solvent was then added through the dropping funnel to the stirred contents of the flask over a period of 15 to 20 min. at ambient temperature. After this, the reaction mixture was stirred for two hours at the same temperature then it was decomposed by pouring into icecold dilute hydrochloric acid and the organic layer was taken into ether. The ether layer was washed with 10% sodium bicarbonate solution and water followed by drying over anhydrous sodium sulfate. The solvent was distilled at atmospheric pressure and, with the exception of the product from alcohol 18 which was a solid, the residue was distilled under vacuum. The distillate was analyzed by vapour phase chromatography to determine its composition by comparison with authentic samples.

Data concerning yields and composition of products are given in Table 1 in the results and discussion section.

---

[15] R. O. Roblin, Jr., D. Davidson and M. T. Bogert, *J. Amer. Chem. Soc.*, **57**, 151 (1935).

[16] R. M. Roberts, E. K. Baylis and G. J. Fonken, *J. Amer. Chem. Soc.*, **85**, 3454 (1963).

Revue Roumaine de Chimie, 19, 8, 1381–1391 (1974)

ELIMINATION REACTIONS IN THE 8-SUBSTITUTED TRICYCLO[7.3.1.$0^{2,7}$]TRIDECANE SERIES. V [1]

CONFIGURATION OF 8-SUBSTITUTED TRICYCLO-[7.3.1.$0^{2,7}$] TRIDECEN-13-OLS

N. S. BĂRBULESCU * and MINODORA LECA **

* University of Bucharest, Chemistry Department, Organic Chemistry Laboratory,
Splaiul Independenţei 89

** University of Bucharest, Chemistry Department, Macromolecular Chemistry Laboratory,
Bulevardul Republicii no. 13

Received October 31, 1973

The configuration of 8-substituted tricyclo [7.3.1.0 ^{2,7}]tridecen-13-ols obtained by various methods was established, by correlating the IR data with the retention time on carbowax 20M chromatographic column and the NMR signals given by the hydrogen atom geminal to hydroxyl group.

INTRODUCTION

The two hydroxyl groups of the 8-substituted tricyclo[7.3.1.$0_{2,7}$] tridecane-2,13-diols (I), substituents : H, CH_3, C_2H_5, C_3H_7, C_6H_5, are both axial,[2,3] this configuration being stabilized by the intramolecular hydrogen bonding between these two groups.

The hydroxyl group of the 8-substituted tricyclo[7.3.1.$0_{2,7}$] tridecen-13-ols (V–VIII) can be *endo* or *exo* with respect to the fused six-membered ring.

The study of the 8-substituted tricyclo[7.3.1.$0_{2,7}$]tridecen-13-acetates (IX–X) substituents H and CH_3[4] obtained by acetylation and dehydration of the diols Ia and Ib using acetic anhydride and zinc chloride led to the conclusion that, for CH_3, the acetate with the double bond C_2–C_7 (IXb) could exist as well as its isomer with the double bond C_7–C_8 (Xb). The gas-liquid chromatographic analysis on carbowax 20M, showd two peaks : the first very well resolved and the second one larger; their area ratio is about 5.5 : 1. The acetate having the double bond C_7-C_8 was the major product, as the NMR spectrum of the mixture shows.

---

[1] N. Bărbulescu and M. Leca, *Rev. Roumaine Chim.*, in press.

[2] S. Julia, D. Varech, Th. Bürer and Hs. H. Günthard, *Helv. Chim. Acta*, **43**, 1632 (1960).

[3] L. Ivan and N. Bărbulescu, *Anal. Univ. Bucureşti*, **41**, 155 (1963).

[4] N. Bărbulescu and M. Leca, *Rev. Roumaine Chim.*, in press.

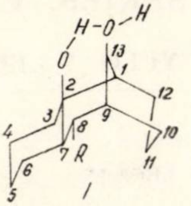

I

a : $R = H$
b : $R = CH_3$

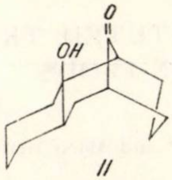

II

a : $R = H$
b : $R = CH_3$

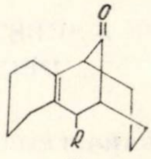

III

a : $R = H$
b : $R = CH_3$

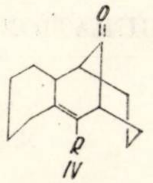

IV

a : $R = H$
b : $R = CH_3$

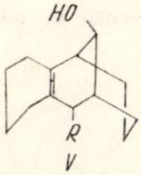

V

a : $R = H$
b : $R = CH_3$

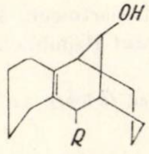

VI

a : $R = H$
b : $R = CH_3$

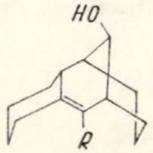

VII

a : $R = H$
b : $R = CH_3$

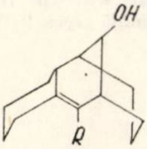

VIII

a : $R = H$
b : $R = CH_3$

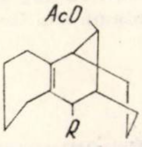

IX

a : $R = H$
b : $R = CH_3$

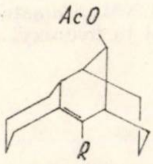

X

b : $R = CH_3$

The examination of the IXa, b and Xb acetates NMR spectra by Hassner's method[5] does not allow to establish their configuration, due to the conformational modifications generated by the double bond introduction: a 13-acetate group in this system, which is axial or equatorial in the cyclohexane ring, is pseudo-equatorial or pseudo-axial to the cyclohexene ring respectively.

If the acidic medium, causing epimerization at the C_{13} carbon atom, is avoided during the acetylation and dehydration processes of diols Ia, b, the acetate group is pseudo-equatorial to the cyclohexene ring, and the resulted acetates are *endo*. Therefore after distilling continuonsly the acetic acid arised from the reaction, one expects to obtain the *endo*-acetates.

---

[5] A. Hassner and C. Heathcock, *J. Org. Chem.*, **29**, 1350 (1964).

RESULTS AND DISCUSSION

The 8-substituted tricyclo[7.3.1.$0^{2,7}$]tridecen-13-ols (V—VIII), substituents H and CH_3 were obtained using three methods: the alkaline hydrolysis of unsaturated acetates IXa, b and Xb, the dehydration of the diols Ia, b with sulphuric acid, and the reduction of unsaturated ketones IIIa, b and IVa, b — resulted by dehydration of ketols IIa, b — with lithium aluminium hydride.

The hydrolysis of the acetate IXa leads to a crystalline product, melting point 68.4—69.3° after recrystallization from pentane. The gas-liquid chromatographic analysis on carbowax 20M shows one peak for the recrystallized alcohol as well as for the rough one. Its NMR spectrum (Figure 1) presents one complex absorption from $\delta = 1.00$ to 2.30 ppm, with an area corresponding to 19 protons, and one triplet at $\delta = 3.53$ ppm — $J = 3$ Hz — for the hydrogen atom attached to C_{13}.

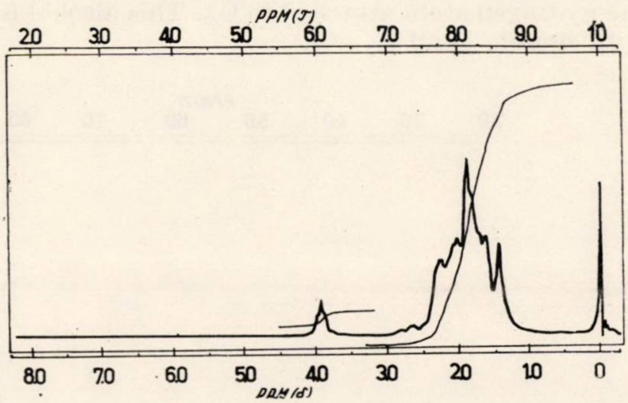

Fig. 1. — NMR spectrum of the tricyclo[7.3.1.$0^{2,7}$] trideca-2(7)-en-*endo*- 13-ol (Va).

The alcohol configuration assignment only on the basis of the coupling constant magnitude [6,7] is not sure, because the dihedral angles are almost equal, as Dreiding models show (57° for *endo* and 52°30′ for *exo*). The IR spectrum must, however, present distinct bands for the two isomers: the free hydroxyl group band for *exo*-isomer, and a band which shows intramolecular π-hydrogen bonding involving the hydroxyl group and the double bond for *endo*-isomer.[8,9]

The difference between the absortion bands of *anti*- and *syn*-1,5-dimethyl-bicyclo[3.3.1]non-2-en-9-ols is 56 cm^{-1}; *anti*- and *syn*-bicyclo[3.3.1]non-2-en-9-ols give for this difference the value 39 cm^{-1} [11];

---

[6] M. Karplus, *J. Chem. Phys.*, **30**, 11 (1958).

[7] M. Karplus, *J. Amer. Chem. Soc.*, **85**, 2870 (1963).

[8] P. von R. Schleyer, D. S. Trifan and R. Backsai, *J. Amer. Chem. Soc.*, **80**, 6691 (1958).

[9] F. Dalton, G. D. Meakins, J. H. Robinson and W. Zaharia, *J. Chem. Soc.*, **1962**, 1566.

[10] J. Martin, W. Parker and R. A. Raphael, *J. Chem. Soc.*, **1964**, 289.

[11] C. S. Dean, J. R. Dixon, S. H. Graham and D. O. Lewis, *J. Chem. Soc.*, **1968**, 1491.

syn-bicyclo[3.2.1]oct-2-en-8-01 presents a weak band at 3617 cm^{-1} and a stronger one at 3578 cm,$^{-1}$[12] the difference being 39 cm^{-1}; the association of hydroxyl group with benzene nucleus in *endo*-benzo-bicyclo[4.3.1] nonen-9-ol generates a shift of 30 cm.$^{-1}$ [13]

The IR spectrum of the unsaturated alcohol obtained by the acetate IXa hydrolysis exhibits a main band at 3588 cm^{-1}, with a shoulder at 3624 cm^{-1} (carbon tetrachloride solution, 2×10^{-2} mol/l). The difference of 36 cm^{-1} corresponds to the intramolecular association between the hydroxyl group and the double bond in the *endo*-epimer Va.

The gas-liquid chromatographic analysis of the IXb and Xb acetates mixture hydrolysis products, on a carbowax 20M column, shows two peaks in the 5.3 : 1 ratio. The NMR spectrum of the first peak, separated by gas-liquid preparative chromatography, presents the following signals (Figure 2) : one complex absorption from $\delta = 1.00$ to 2.90 ppm, on which the singlet specific for the $-\underline{CH}_3-Ar$ system at $\delta = 1.64$ ppm is superposed — for 21 protons; one triplet at $\delta = 3.57$ ppm, J = 3 Hz, for the hydrogen atom attached to C_{13}. This alcohol is then one of the epimers with double bond C_7-C_8.

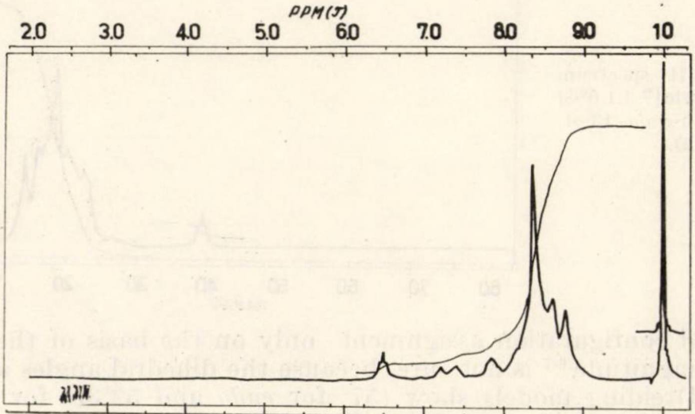

Fig. 2. — NMR spectrum of the 8-methyl-tricyclo[7.3.1.0 ^{2,7}] trideca-7(8)-en-*endo*-13-ol (VIIb).

Taking into account the ratio of the alcohols which, in the limits of the experimental errors, equalizes the ratio of the acetates, one can suppose that the second peak represents one of the epimeric alcohols with C_7-C_8 double bond. On the other hand, the NMR spectrum of the mixture of the alcohols presents also the methyl group doublet for the last alcohol at $\delta = 0.99$ ppm. The IR spectrum of this mixture (carbon tetrachloride solution, 4×10^{-2} mol/l) exhibits a main band at 3588 cm^{-1}, with a shoulder at 3624 cm^{-1}. It follows then that the first peak is the *endo*-alcohol VIIb and the second one the *endo*-alcohol Vb.

---

[12] N. A. LeBel and L. A. Spurlock, *Tetrahedron*, **20**, 215 (1964).

[13] H. Tanida and T. Irie, *J. Org. Chem.*, **36**, 2777 (1971).

The dehydration of the diol Ia with refluxing sulphuric acid 25% leads to two main components which are in the 1 : 1.58 ratio, as calculated from the chromatogram. The retention time of the second peak is identical with that of the alcohol Va. The two alcohols cannot be separated by chromatography on alumina and silicagel columns.

The NMR spectrum of the alcohol mixture (Figure 3) shows one multiplet from $\delta = 0.90$ to 2.90 ppm for 19 protons, one triplet at $\delta = 3.55$ ppm — $J = 3$ Hz — and one triplet centered at $\delta = 3.90$ ppm — — $J = 5$ Hz — for the hydrogen atom attached to C_{13}. The ratio of the two triplets area is 1.62 : 1.

There are a weak band at 3624 cm^{-1}, a main band at 3588 cm^{-1}, and a wide absorption from 3530 to 3425 cm^{-1}, the maximum being at 3480 cm^{-1},in the IR spectrum of the alcohol mixture (carbon tetrachloride solution, 4×10^{-2} mol/l). The wide band vanishes for 2.5×10^{-3} mol/l solution and the 3624 cm^{-1} band increases its intensity at the same time. Comparing the NMR spectrum (Figure 3) with that of the alcohol Va (Figure 1) one can reach the conclusion that the first peak, having the triplet at $\delta = 3.90$ ppm, represents the *exo*-alcohol VIa.

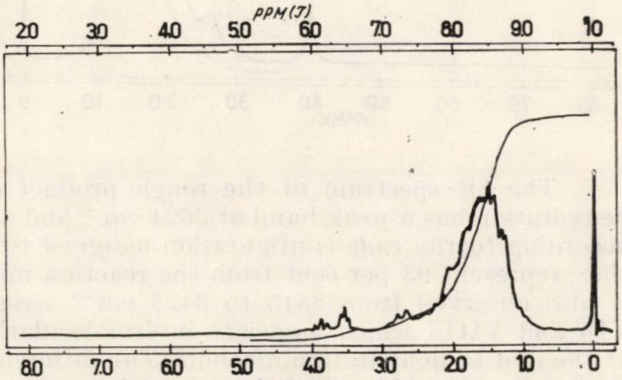

Fig. 3. — NMR spectrum of the mixture of *endo*- and *exo*-tricyclo [7.3.1.$0^{2,7}$]trideca-2(7)-en-13-ols (Va)and (VIa)respectively.

Some bicyclic [n.m.1] system epimers give also such shifts for the proton geminal to hydroxyl group : $\delta = 3.90$ ppm (triplet) for bicyclo-[3.2.1]oct-2-en-*syn*-8-ol and $\delta = 4.13$ ppm (singlet) for the *anti*-epimer [12], $\delta = 4.27$ ppm (singlet) for 7,8-benzo-bicyclo[4.2.1]nonen-endo-9-ol and $\delta = 4.72$ ppm (triplet) for the *anti*-epimer.[13] This can be explained by the more powerful screening, due to the double bond, of the hydrogen atom belonging to the *exo*- or *anti*-epimer, it being closer to the double bond and at a larger distance from its plane, as the Dreiding models show.

The wide absorption at 3480 cm^{-1} is produced by the alcohol VIa, which associates intramolecularly greater on steric grounds.

Dehydration of the diol Ib using sulphuric acid gives four peaks on chromatogram, with the following per cent concentrations : 5, 2, 50.8, and 42.2, respectively. The peak 3 has the same retention time as the alcohol VIIb, and the peak 4 the same as the alcohol Vb. The peaks 3 and 4 were separated by preparative gas-liquid chromatography on carbowax 20M and the NMR spectra were run, to verify the assignments. The peak 3 has the same spectrum as the alcohol VIIb (Figure 2), and the peak 4 (Figure 4) gives signals at : $\delta = 1.00$ ppm (doublet), $J = 7.5$ Hz, and $\delta = 3.65$ ppm (singlet) as the alcohol Vb does. A small quantity of a crystalline unsaturated alcohol, melting point 64—65°, was also obtained ; its NMR spectrum and retention time are identical with those of the alcohol Vb.

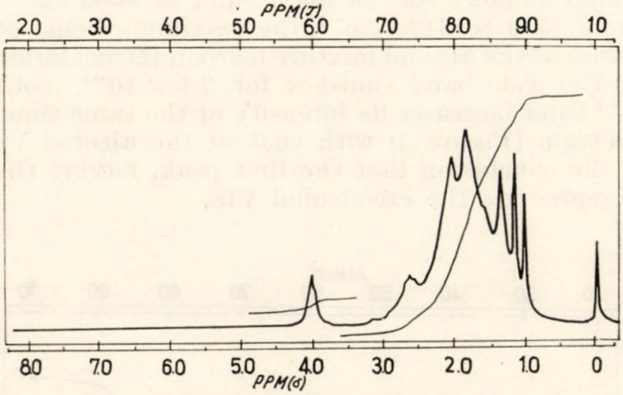

Fig. 4. — NMR spectrum of the 8-methyl-tricyclo-$[7.3.1.0^{2,7}]$trideca-2(7)-en-*endo*-13,-ol (Vb).

The IR spectrum of the rough product obtained by the diol Ib dehydration has a weak band at 3624 cm^{-1} and a strong one at 3588 cm^{-1}, according to the *endo* configuration assigned to the above two alcohols ; they represent 93 per cent from the reaction mixture. A very weak band is also observed from 3515 to 3425 cm^{-1}, assigned to the *exo* alcohols VIb and VIIIb which associate intermolecularly easier, on the analogy of the diol Ia dehydration alcohols. The difference of the retention times, similar to that of the alcohols Va and VIa, also support this assignment.

The stereochemistry of the carbonyl group reduction[14] does not allow to establish the configuration of the unsaturated alcohols, because of the conformational modification caused by the double bond introduction.

The dehydration of the ketol IIa leads to the mixture of unsaturated ketones IIIa and IVa. Their ratio is dependent on the dehydration agent.

The reduction of the mixture of unsaturated ketones with lithium aluminium hydride gives two alcohols : the first has the same retention time as the alcohol Va, and the second has a longer one. The NMR spectrum (Figure 5) presents the signals : one complex absorption from $\delta = 1.00$ to 2.60 ppm, one triplet at $\delta = 3.70$ ppm, $\delta = 3$ Hz, one singlet at $\delta = 3.93$ ppm and one doublet at $\delta = 5.27$ ppm, $J = 6.5$ Hz.

The IR spectrum exhibits a main band at 3630 cm^{-1} and a weak one at 3588 cm^{-1}. Repeated recrystallizations from ethyl alcohol give a crystalline alcohol, melting point 120.5—121.5°, having NMR signals at $\delta = 3.93$ and 5.27 ppm, a 3630 cm^{-1} IR band with a shoulder at 3588 cm^{-1}, and the same retention time as the second peak. On the basis of these data the structure Va was assigned to the first peak and the structure VIIIa to the second one.

---

[14] S. Patai, "The Chemistry of Carbonyl Group", Intescience Publishers, New York, 1966, p. 507.

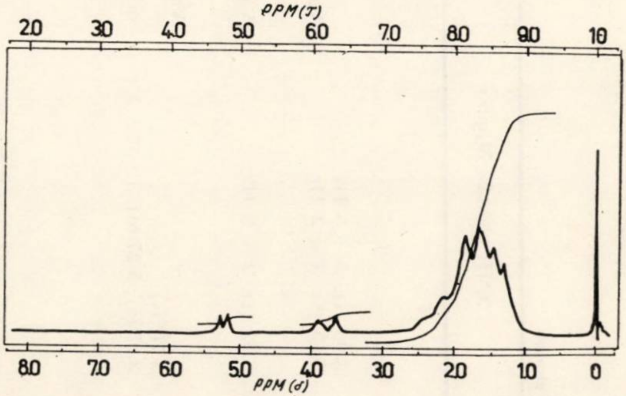

Fig. 5.—NMR spectrum of the alcohols obtained by the mixture of ketones IIIa and IVa reduction.

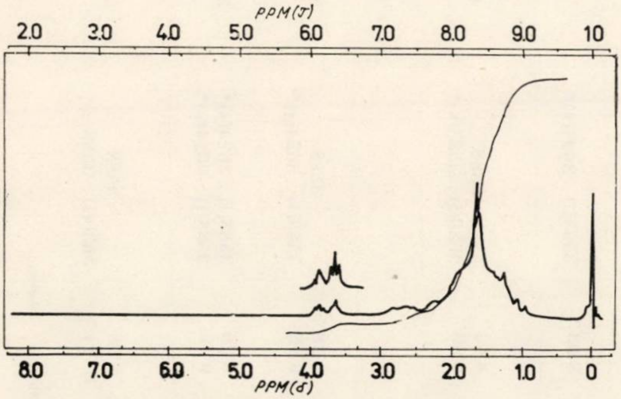

Fig. 6.—NMR spectrum of the alcohols obtained by the mixture of ketones IIIb and IVb reduction.

The dehydration of the ketol IIb gave also two ketones : IIIb and IVb. The reduction products of this mixture of ketones, analysed by gas-liquid chromatography, contain two peaks : the first with the same retention time as the alcohol VIIb and the second with a longer one. The following signals are superposed on the complex absorption of the NMR spectrum (Figure 6) : one doublet centered at $\delta = 1.01$ ppm specific for the $\underline{CH_3}—CH$ system, and the singlet of the $\underline{CH_3}—C =$ system at $\delta = 1.67$ ppm ; there are also : one triplet at $\delta = 3.67$ ppm, $J = 3$ Hz, and one triplet at $\delta = 3.89$ ppm, $J = 4$ Hz.

The IR spectrum shows two almost equal intense bands at 3630 and 3588 cm^{-1}. The crystalline alcohol, melting point 80—81°, separated

Table 1

The main characteristics of isomeric unsaturated alcohols

Alcohol preparation method	Peak number	Retention time	Hydroxyl group frequency, cm^{-1}	$\Delta\nu$, cm^{-1}	NMR signals, δ(ppm)	Configuration
				R=H		
Dehydration of diol Ia with H_2SO_4	1 2	5′01″ 8′03″	3624 3588(i) ; 3624(s)*	36	3.90 (t), J = 5 Hz 3.55 (t), J = 3 Hz	VIa Va, m.t. 68.4–69.3°
Acetate IXa hydrolysis	1	8′03″	3588(i) ; 3624(s)*		3.53 (t), J = 3 Hz	Va, m.t. 68.4–69.3°
Unsaturated ketones reduction with $LiAlH_4$	1 2	8′03″ 9′43″	3588 3630(i) ; 3588(s)*	42	3.70 (s) 3.93 (s) ; 5.27 (d), J = 6.5 Hz	Va, m.t. 68.4–69.3° VIIIa, m.t. 120.5–121.5 °
				R = CH_3		
Dehydration of diol Ib with H_2SO_4	3 4	8′28″ 9′48″	3588 3588(i) ; 3624(s)*	36	1.65 (s) ; 3.55 (t), J = 3 Hz 0.99 (d), J = 7.5 Hz ; 3.62 (s)	VIIb Vb, m.t. 64–65°
Acetates IXb and Xb hydrolysis	1 2	8′28″ 9′48″	3588(i) ; 3624(s)* 3588(i) ; 3624(s)*	36	1.56 (s) ; 3.55 (t), J = 3 Hz 0.99(d), J = 7.5 Hz ; 3.65 (s)	VIIb Vb, m.t. 64–65°
Unsaturated ketones reduction with $LiAlH_4$	1 2	8′28″ 10′24″	3588 3630(i) ; 3588(s)*	42	1.65 (s) ; 3.67 (t), J = 3 Hz 1.01 (d), J = 7.5 Hz 3.89 (t), J = 4 Hz	VIIb VIb, m.t. 80–81°

i – intense ; s* – shoulder ; d – doublet ; t – triple ; s – singlet.

from the mixture, presents the doublet at $\delta = 1.01$ and the triplet at $\delta = 3.89$ ppm in the NMR spectrum, and the band at 3630 cm^{-1} with a shoulder at 3588 cm^{-1} in the IR spectrum ; the retention time is identical with that of the second peak. Therefore, the first peak is the *endo*-alcohol VIIb, and the second one the *exo*-alcohol VIb.

The main characteristics of the unsaturated alcohols obtained by the above methods are summarized in Table 1.

CONCLUSIONS

The alkaline hydrolysis of the acetate IXa leads only to the tricyclo[$7.3.1.0^{2,7}$]trideca-2(7)-en-*endo*-13-ol Va. The hydrolysis of the mixture of acetates IXb and Xb gives the coresponding *endo*-alcohols : 8-methyl-tricyclo[$7.3.1.0^{2,7}$]trideca-2(7)-en-*endo*-13-ol Vb and 8-methyl-tricyclo[$7.3.1.0^{2,7}$]trideca-7(8)-en-*endo*-13-ol VIIb, in the 1 : 5.35 ratio.

The dehydration of the diol Ia using sulphuric acid 25% affords the mixture of *endo*- and *exo*-tricyclo[$7.3.1.0^{2,7}$]trideca-2(7)-13-ols Va and VIa, respectively. 50.8% 8-methyl-tricyclo[$7.3.1.0^{2,7}$]trideca-7(8)-en-*endo*-13-ol-VIIb, 42.2% 8-methyl-tricyclo [$7.3.1.0\lambda^{2,7}$]trideca-2(7)-en-*endo*-13-ol Vb and 7% mixture of *exo*-alcohols VIb and VIIIb were obtained by sulphuric acid dehydration of the diol Ib.

The reduction of unsaturated ketone IIIa using lithium aluminium hydride gives the *endo*-alcohol Va and that of ketone IVa the *exo*-alcohol VIIIa. The *exo*-alcohol VIb was obtained by lithium aluminium hydride reduction of ketone IIIb and the *endo*-alcohol VIIb by isomeric ketone IVb reduction.

EXPERIMENTAL PART

The preparation of the acetates IXa, b and Xb has been described in an earlier paper.[4]

Hydrolysis of the acetate IXa. a) 5.25 g acetate IXa were added to a stirred solution of natrium hydroxide (5 g) in methyl alcohol (50 ml) and water (20 ml); the stirring was continuated for 4 hours. The mixture was set aside overnight, then was diluted with water and extracted with ether (2 × 50 ml). The combined ethereal extracts were washed with water and dried on natrium sulphat. Removal of solvent gave 3.80 g (88.8% yield) white needles of unsaturated alcohol Va, m.p. 67–69°; recrystallization from pentane gives m.p. 68.4–69.3°.

b) 10.5 g acetate IXa and 100 ml solution of natrium hydroxyde in methyl alcohol (10%) were refluxed for 1 hour. 7.9 g (91.8% yield) white crystals, m.p. 66–69°, were obtained after cooling and dilution with water. Recrystallization from methyl alcohol-water gave 7.5 g unsaturated alcohol Va, m.p. 68–69°. Analytical gas-liquid chromatography on carbowax 20M gave one peak. NMR spectrum (CCl_4), δ : 3.53 ppm (t), $J = 3$ Hz ; IR spectrum CCl_4, 4×10^{-2} mol/l) : 3588 cm^{-1} (i), 3624 cm^{-1} (shoulder).

Hydrolysis of the isomeric acetates IXb and Xb. 10.2 g mixture of acetates IXb and Xb were worked as above, giving a semi-solid epimeric mixture (8.1 g, 96.4% yield) of the alcohols (VIIb and Vb). Analytical gas-liquid chromatography gave two peaks, which were separated by preparative chromatography. NMR spectrum of the mixture (CCl_4), δ : 0.99 ppm (d) $J = 7.5$ Hz, 1.65 ppm (s), 3.57 ppm (s) ; IR spectrum (CCl_4, 4×10^{-2} mol/l) : 3588 cm^{-1} (i), 3624 cm^{-1} (shoulder).

Dehydration of the diol Ia with sulphuric acid 25%. 20 g diol Ia was heated under reflux with 50 ml sulphuric acid 25%. The mixture was cooled and extracted with ether (3 ×

× 100 ml). The ethereal solution was washed with 10% sodium carbonate solution and dried on sodium carbonate. Removal of the ether gave 18.6 g (94% yield) row product which, by vacuum distillation, gave a semi-solid epimeric mixture. Analytical gas-liquid chromatography shows four peaks, two of them being of higher concentration. NMR spectrum (CCl_4), δ : 3.55 (t) J = 3 Hz, 3.90 ppm (t) J = 5Hz; IR spectrum (CCl_4) : 3624 cm^{-1} (weak), 3588 cm^{-1} (i).

Dehydration of the diol Ib with sulphuric acid 25%. 37 g diol Ib and 72 ml 25% sulphuric acid solution were heated under reflux as above. The mixture was worked up as above, giving 33 g (97% yield) row product which, by vacuum distillation, conducted to 24.8 g product, $n_D^{20} = 1.5350$. A semi-solid product was obtained by cooling and sitting aside. The chromatogram contains 4 peaks, two having higher concentration. Repeated recrystallization from pentane afforded a small quantity of crystalline alcohol, m.p. 64—65°, retention time the same as the last peak. NMR spectrum (CCl_4), δ : 0.99 ppm (d) J = 7.5 Hz, 3.62 ppm (s); IR spectrum (CCl_4) : 3588 cm^{-1} (i), 3624 cm^{-1} (shoulder).

Reduction of the mixture of ketones IIIa and IVa with lithium aluminium hydride. A solution of mixture of unsaturated ketones (5.04 g) in anhydrous ether (70 ml) was added within 1 hour to 30 ml anhydrous ether containing 1 g lithium aluminium hydride. The mixture was refluxed for 12 hours, then the aluminium alcoholate was decomposed by methyl alcohol (4 ml) and water (2 ml), and extracted with ether. Removal of the ether gave 4.77 g (94% yield) unsaturated alcohols. Reduction of unsaturated ketones obtained by dehydration of ketol IIa using sulphuric acid led to a semi-solid product. Gas-liquid chromatography, on carbowax 20M, showed the existence of 2 peaks, their ratio being 1 : 2.2. NMR spectrum of the mixture (CCl_4), δ : 0.85—2.90 ppm (m), 3.62 ppm (s), 3.82 ppm (s), 5.22 ppm (d) J = 6.5 Hz; IR spectrum (CCl_4) : 3630 cm^{-1}(i), 3588 cm^{-1} (weak). A solid product was obtained, m. p. 103—107°, when the ketones were obtained using the acetic anhydride-zinc chloride mixture as dehydration agent. Repeated recrystallization from ethyl alcohol gave white needle crystals, m. p. 120.5—121.5°. The chromatogram presented two compounds, 1.3 : 1 ratio, having the same retention times as above. NMR spectrum of the mixture is identical with the above one, but the doublet intensity increases; IR spectrum (CCl_4) : 3630 cm^{-1} (i), 3588 cm^{-1} (i).

Reduction of the mixture of ketones IIIb and IV b with lithium aluminium hydride. 6.71 g unsaturated ketones, obtained by sulphuric acid dehydration of the ketol IIb, gave at the reduction 6.50 g (94% yield) liquid product, in which needle crystals appeared in time. The chromatogram presented 2 peaks, 1 : 1 ratio. NMR spectrum (CCl_4), δ : 1.01 ppm (d) J = 7.5 Hz, 1.67 ppm (s), 3.60 ppm (t) J = 3 Hz, 3.80 ppm (s). By extracting the liquid portion on porous plate and recrystallizing from pentane, a crystalline compound, m. p. 80—81°, was obtained. IR spectrum (CCl_4) : 3630 cm^{-1}(i), 3588 cm^{-1}(shoulder). 3.5 g unsaturated ketones, obtained by acetic anhydride-zinc chloride dehydration of the ketol IIb, led to 3.35 g (94.2% yield) liquid product. The chromatogram shows 2 peaks, 2 : 1 ratio, the same retention time as above. NMR spectrum is identical with the above one; IR spectrum (CCl_4) : 3630 cm^{-1} (i), 3588 cm^{-1} (i).

Analytical chromatography has been performed on a Carlo Erba GT type gas-liquid chromatograph, using a 4 mm o. d. stainless steel column, 2 m in length. Packing material was 20% carbowax 20M on 60—80 mesh chromosorb W. The flame ionisation detector was used, with nitrogen as gas carrier. The conditions were as follows:

injection temperature	280°
column temperature	115—170°, 4°/min programing
detector temperature	280°
nitrogen flow rate	25 ml/min
injected quantity	0.6 µl

Preparative chromatography was carried out on a Carlo Erba GT type preparative chromatograph, equiped with peak discriminator, by employing a 10 mm o. d. stainless steel column, 2 m in length, and 20% carbowax 20M on 30—60 mesh chromosorb W was packing material. The thermal conductivity detector was used, with hydrogen as carrier gas. The conditions were:

injection temperature	280°
column temperature	195°
detector temperature	300°

hydrogen flow rate	650 ml/min
auxiliary gas flow rate	60 ml/min
injected quantity	100 μl

The purity verification of the collected samples was made using the above analytical column in the conditions :

injection temperature	240°
column temperature	120–180°, 6°/min programing
detector temperature	260°
nitrogen flow rate	30 ml/min
injected quantity	0.4 μl

using the flame ionisation detector.

Revue Roumaine de Chimie, **19**, *8*, 1393–1405 (1974)

ALTERNATING TENDENCY IN COPOLYMERIZATION. I

COPOLYMERIZATION OF BUTYL VINYL ETHERS WITH ACRYLIC MONOMERS

DAN SORIN VASILESCU
Laboratory of Macromolecular Chemistry, Polytechnical Institute,
Calea Victoriei 149, Bucharest, Romania

Received November 14, 1973

The copolymerization of *n*-butyl vinyl ether, *s*-butyl vinyl ether and *t*-butyl vinyl ether with methacrylonitrile, acrylonitrile and acrylamide was carried out. The reactivity ratios and the copolymerization rates for all binary systems, except those containing acrylamide, were determined. Also, the "Q" and "e" values for *s*-butyl vinyl ether were established. The calculated reactivity ratios are strongly dependent on the chemical structure of the monomer pair; some pairs show an alternating tendency. The structure of copolymers was evidenced by performed analyses.

1. INTRODUCTION

Vinyl ethers are known as monomers with strong electron donor substituents; they cannot polymerize by radicalic way. Polyvinyl ethers are usually produced working with Lewis acids as catalysts. However, vinyl ethers may be copolymerized, by radicalic way, with vinyl monomers containing electron attractive substituents. Several copolymers with maleic anhydride [1] or acrylate esters are better known; copolymers of ethyl acrylate with 2-chloroethylvinyl ether have been used as rubbers.[2] In such copolymerization vinyl ethers show a tendency towards an alternating structure; for instance, for the pair acrylonitrile-*t*-butyl vinyl ether, the values $r_1 = 0.14$ and $r_2 = 0.0032$, were reported.[3] The alternating copolymer results due to the formation of a molecular complex between the electron donor monomer and the electron acceptor monomer; this complex is assumed to have an important contribution in the free radicalic alternating copolymerization of many monomer pairs.[4]

Iwatsuki and Yamashita [5] have provided evidence for the participation of a charge transfer complex in the formation of alternating copolymers from the free radical copolymerization of *p*-dioxene or vinyl ethers with maleic anhydride. Terpolymerization of the monomer pairs which form alternating copolymers with a third monomer which had little interaction with either monomer of the pair, indicated that the polymerization was actually a copolymerization of the third monomer with the complex.[5] Similar results have been noted in terpolymerizations involving vinyl ether-fumaronitrile [6] monomer pair.

---

[1] R. B. Seymour, *Ind. Eng. Chem.*, **41**, 1509 (1949).

[2] W. Mast and C. H. Fischer, *Ind. Eng. Chem.*, **41**, 703, 790 (1949).

[3] L. J. Young, *J. Polymer Sci.*, **54**, 411 (1961).

[4] G. E. Ham, "Copolymerization", J. Wiley and Sons, New York, 1964.

[5] S. Iwatsuki and Y. Yamashita, *Makromol. Chem.*, **89**, 205 (1965).

When a charge transfer complex does not form, the r_1 and r_2 values are very different (e.g. for the N-vinyl succinimide — *n*-butyl vinyl ether system, Furukawa and co-workers [7] found $r_1 = 15$ and $r_2 = 0$).

H. Gilbert [8] reported some data about the behaviour of vinylidene cyanide-vinyl ethers systems; no copolymerization occurred, but two homopolymers, polyvinylidene cyanide and polyvinyl ether were produced by cross initiation.

Although several copolymers with vinyl ethers are prepared on a large scale, our theoretical knowledge about the behaviour of vinyl ethers in copolymerization processes is still poor.

In this paper we present the data concerning the copolymerization of *n*-butyl vinyl ether (nBVE), *s*-butyl vinyl ether (sBVE) and *t*-butyl vinyl ether (tBVE) with acrylic monomers; also we carried out tests upon obtained polymers in order to elucidate their structure.

2. EXPERIMENTAL

2.1. MATERIALS

Butyl vinyl ethers (BVE) were obtained by vinylation of butyl alcohols with acetylene in the presence of potassium alkoxide according to the methods described by Shostakovskii [9] and other authors [10]; crude products were washed with water to remove the unreacted alcohol. The monomers were dried and distilled on metallic sodium; the purity was tested by refractive index and chromatographic methods.

Acrylonitrile (AN) and methacrylonitrile (MAN) — provenience Schuchard — were purified according to the usual methods.

Acrylamide (AA) — provenience BDH — was twice recrystallized from ethyl acetate [11] and dried in vacuum.

Toluene (T), acetone (Ac), N, N-dimethyl formamide (DMF) and chloroform (CL) were purified by conventional ways; methanol and petroleum ether — reagents grade — were used without purifications.

Azobisisobutyronitrile (AIBN) as radicalic initiator was recrystallized from ethanol.

2.2. COPOLYMERIZATION PROCEDURE

The copolymerization reactions were carried out in the absence of air in glass ampoules with two charging arms[12]; after filling, one arm was closed and the ampoules were connected to a short vacuum assembly. The ampoules were frozen in liquid nitrogen, air-removed at

---

[6] S. Iwatsuki and Y. Yamashita, *J. Polymer Sci.*, A—1, **5**, 1753 (1967).

[7] J. Furukawa, T. Tsuruta, N. Yamamoto and H. Fukutami, *J. Polymer Sci.*, **37** 215 (1959).

[8] H. Gilbert, *J. Amer. Chem. Soc.*, **78**, 1669 (1956).

[9] M. F. Shostakovskii, "Prostyie vinilovyie efiry", Izd. Akad. Nauk S.S.S.R. Moscow, 1952.

[10] Kirk-Othmer "Encyclopedia of Chemical Technology", vol. **21**, J. Wiley and Sons, New York, Second Edition, 1970, p. 94.

[11] E. C. Leonard, "Vinyl and Diene Monomers", vol. **1**, J. Wiley and Sons, New York, 1970, p. 94.

[12] T. Otsu and H. Inoue, *Makromol. Chem.*, **128**, 31 (1969).

10^{-2} mm.Hg, filled with purified argon and warmed at 30°; this cycle was accomplished three times.

Finally, the ampoules were sealed; the tubes were put at the desired temperature in a thermostated bath and rapidly mixed. The copolymerizations were carried out in such a manner, in order to obtain small conversions. The copolymerization process was stopped by abrupt freezing; the ampoules were opened and the polymer was precipitated by pouring the solution into a large amount of nonsolvent (methanol or petroleum ether). After filtration, polymers were dried and weighted; some copolymers were reprecipitated.

2.3. Analyses of polymers

The composition of copolymers was determined by their nitrogen content (Dumas classical micromethod); copolymers with high content in AN, generally infusible, were reprecipitated to obtain fine powdered products.

Intrinsic viscosities of copolymers were calculated using the data obtained on diluted solutions (copolymer concentration less than 0.2 g/dl) with an Ubbelohde viscometer at 25° As solvents we used CL and DMF.

I.R. absorption spectra were recorded on a PYE-Unicam, SP-200 spectrophotometer; the NMR spectra were performed using a VARIAN apparatus (60 MHz), solvent $CDCl_3$, internal reference TMS.

3. RESULTS AND DISCUSSION

The copolymerization tests of methacrylonitrile with nBVE, sBVE and tBVE were carried out at 60°, in homogeneous solution, using AIBN as initiator; the molar ratio monomer mixture/AIBN = 300, was kept constant. For a more precise and rapid dosage of the initiator, toluene solution of AIBN (1 ml in each ampoule) was used. Because the molecular weights and densities of each monomer are different, the total molar concentration of both monomers varies in the range 6.3–8.2 mole/l. (Table 1)

Table 1

Copolymerization of MAN (M_1) at 60°; solvent toluene; molar ratio $\frac{/M_1/ + /M_2/}{/AIBN/} = 300$

$/M_1/$ in monomers (mole %)	M_2	$/M_1/ + /M_2/$ (mole/l)	Reaction time (min.)	Conversion (%)	N% Dumas	$/m_1/$ in copolymer (mole fraction)
90	nBVE	8.2	200	4.05	18.76	0.935
80	nBVE	7.9	240	3.62	17.73	0.896
70	nBVE	7.6	300	3.82	16.84	0.862
60	nBVE	7.4	360	4.61	16.13	0.835
50	nBVE	7.1	450	5.39	15.04	0.794
40	nBVE	6.9	450	4.32	13.59	0.736
30	nBVE	6.7	600	4.40	12.09	0.673
20	nBVE	6.5	720	3.22	10.78	0.609
90	sBVE	8.2	180	3.96	18.50	0.925
80	sBVE	7.9	210	4.68	17.04	0.870
60	sBVE	7.4	300	5.68	14.82	0.786
40	sBVE	6.9	240	3.24	12.76	0.701
30	sBVE	6.7	270	2.79	11.62	0.652
20	sBVE	6.5	660	5.95	10.49	0.601
10	sBVE	6.3	810	4.58	9.17	0.541
80	tBVE	7.9	150	5.63	14.78	0.784
70	tBVE	7.6	210	7.45	14.25	0.765
40	tBVE	6.9	240	5.40	11.91	0.666
30	tBVE	6.7	300	5.18	10.40	0.596
20	tBVE	6.5	270	3.83	9.48	0.553
10	tBVE	6.3	360	3.36	8.47	0.504

AIBN was used as initiator, as in the literature it is assumed that the scission rate of this substance is not influenced by the nature of the reaction medium.[13] As the process was carried out to obtain small conversions (max. 5.6%) these tests could be used to establish initial copolymerization rates (Fig. 1).

Some kinetic data regarding the dependence of the initial rate on the feed composition are given in figure 1. It is evident that the rates increase when the initial molar fraction of MAN in monomer mixture increases; the more reactive monomer is MAN. The BVE act as retarders of the polymerization process; the copolymerization of the tBVE—MAN pair develops fastest.

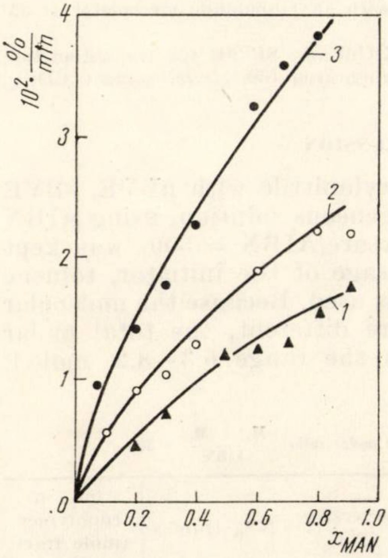

Fig. 1.—Dependence of the copolymerization rate upon the composition feed for the MAN — BVE systems; $M_1 + M_2 = 3.10^{-2}$ moles; AIBN $= 10^{-4}$ moles; solvent toluene (1 ml); temperature = 60° *1.* M_2=*n*BVE. *2.* M_2 = *s*BVE. *3.* M_2 = *t*BVE.

The precise computing of the copolymerization reactivity ratios has been tackled by several methods; but it is possible that a particular set of data lead to appreciably different values of the reactivity ratios.

To determine accurately r_1 and r_2 reactivity ratios the Fineman-Ross method [14] was chosen (linearization of the differential composition equation:)

$$Z = r_1 + Wr_2 \tag{1}$$

where: $Z = (Y - 1)/X$; $W = -Y/X^2$; $X = [M_1]/[M_2]$; $Y = [dm_1]/[dm_2]$.

Because of the possible errors of the method used to establish the copolymer composition (nitrogen content by the micro-Dumas method) it was utilized an analytic calculation — the least square method [15]:

$$r_1 = \frac{\Sigma W^2 \Sigma Z - \Sigma W \Sigma ZW}{n \Sigma W^2 - (\Sigma W)^2} \tag{2}$$

$$r_2 = \frac{n \Sigma WZ - \Sigma W \Sigma Z}{n \Sigma W^2 - (\Sigma W)^2} \tag{3}$$

where n is the number of accomplished tests.

The necessary data for the determination of the reactivity ratios at the MAN—BVE systems are given in Table 2.

---

[13] H. Boiley and G. Godin, *Trans. Faraday Soc.*, **52**, 68 (1956).

[14] M. Fineman and S. D. Ross, *J. Polymer Sci.*, **5**, 269 (1950).

[15] P. W. Tidwell and G. A. Mortimer, *J. Polymer Sci.*, A, **3**, 369 (1965).

Table 2

Data for the determination of the reactivity ratios in copolymerization; M_1 = MAN; M_2 = BVE

Experimental data				Calculated data				
X_1	Y_1	$X = X_1/X_2$	X^2	$Y = Y_1/Y_2$	$Z = (Y - 1)/X$	$-W =$ $= Y/X^2$	W^2	$-ZW$
$M_2 = n$BVE								
0.8	0.896	4.0000	16.0000	8.3077	1.8269	0.5191	0.2705	0.9463
0.7	0.862	2.3333	5.4444	6.2425	2.2467	1.1465	1.3449	2.5756
0.6	0.835	1.5000	2.2500	5.0606	2.7070	2.2499	5.0623	6.0907
0.5	0.794	1.0000	1.0000	3.8543	2.8543	3.8543	14.8540	11.0010
0.4	0.736	0.6666	0.4444	2.7807	2.6711	6.2565	39.1450	15.5955
0.3	0.673	0.4286	0.1836	2.0581	2.4689	11.2053	125.5600	27.6640
0.2	0.609	0.2500	0.0625	1.5575	2.2300	24.9200	621.0100	55.5716
					Σ 17.0049	50.1516	817.2467	119.4447
					$(\Sigma W)^2 = 2515.0$			
$M_2 = s$BVE								
0.9	0.925	9.0000	81.0000	12.3333	1.2592	0.1522	0.0232	0.1916
0.8	0.870	4.0000	16.0000	6.6923	1.4231	0.4183	0.1750	0.5953
0.6	0.786	1.5000	2.2500	3.6729	1.7819	1.6328	2.6660	2.9095
0.4	0.701	0.6666	0.4444	2.3467	2.0201	5.2801	27.8790	10.6660
0.3	0.652	0.4286	0.1836	1.8695	2.0291	10.1820	103.6800	20.6550
0.2	0.601	0.2500	0.0625	1.5062	2.0248	24.0992	580.7600	48.7870
0.1	0.541	0.1111	0.0123	1.1786	1.6074	95.4666	9113.9500	153.4500
					Σ 12.1456	137.2312	9829.1332	237.2544
					$(\Sigma W)^2 = 18832.0$			
$M_2 = t$BVE								
0.8	0.784	4.0000	16.0000	3.6297	0.6574	0.2269	0.0515	0.1491
0.7	0.765	2.3333	5.4444	3.2553	0.9666	0.5979	0.3575	0.5779
0.4	0.666	0.6666	0.4444	1.9940	1.4910	4.4865	20.1390	6.6894
0.3	0.596	0.4286	0.1836	1.4753	1.1090	8.0322	64.5150	8.9070
0.2	0.553	0.2500	0.0625	1.2372	0.9488	19.7952	365.7000	18.7810
0.1	0.504	0.1111	0.0123	1.0162	0.1453	82.3081	6774.5000	11.9630
					Σ 52.3181	115.4468	7225.2630	47.06825
					$(\Sigma W)^2 = 13327.5$			

X_1 – initial mole fraction of MAN in monomer mixture

Y_1 – mole fraction of MAN in copolymer.

The results are summarized in Table 3; the r_1 and r_2 values are in accordance to those predicted from the "Q–e" scheme.[16] The literature mentions no reactivity ratios for MAN – BVE systems.

---

[16] T. Alfrey and C. C. Price, *J. Polymer Sci.*, **2**, 101 (1947).

It is of interest to enquire whether the two r_1 and r_2 constants are alike meaningful. Moreover, it should be noticed that the obtained values have very different magnitudes ($r_1/r_2 = 10^3$); obviously, they were got with the same error. Supposing that r_1 value was obtained with an absolute error 0.01, this means that for r_2 values relative errors more than 100% may appear.

Table 3

Values of the copolymerization constants for the monomer pairs MAN (M_1) – BVE (M_2)

Monomer M_2	Least-squares method		Calculated from the Alfrey and Price's scheme	
	r_1	r_2	r_1	r_2
*n*BVE	2.47	0.0052	2.52	0.0069
*s*BVE	1.73	0.0001	—	—
*t*BVE	1.09	0.011	1.074	0.0031

Since this situation is not reasonable, it ought to consider practically $r_2 = 0$; we did this simplification and drew the curves from figure 2.

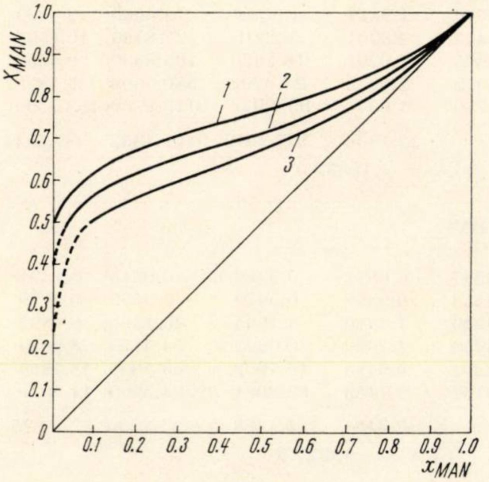

Fig. 2. — Monomer/copolymer composition curves for radical copolymerization of the MAN(M_1)—BVE (M_2) systems at 60°: *1.* M_2 = *n*BVE; *2.* M_2 = *s*BVE; *3.* M_2 = *t*BVE.

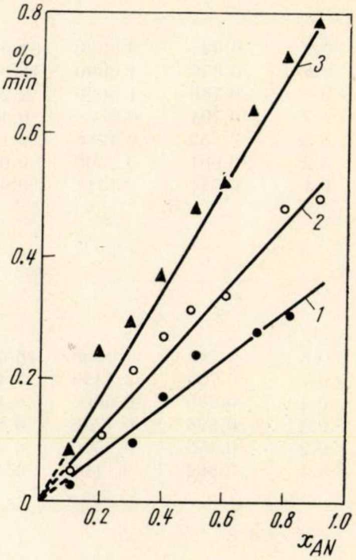

Fig. 3. — Copolymerization rate against composition feed for the AN-BVE systems; $M_1 + M_2 = 3.10^{-2}$ moles; AIBN = 10^{-4} moles; solvent toluene (1 ml); temperature = 60°. *1.* M_2 = *n*BVE. *2.* M_2 = *s*BVE. *3.* M_2 = *t*BVE.

As shown in figure 2, the molar fraction of MAN in copolymers has been always more than 50%; if MAN is M_1, as r_1 is smaller, the copolymerization process occurs faster (figure 1).

When instead of MAN was used AN in the same conditions, shorter polymerization times were necessary to obtain the same conversions (Table 4).

Table 4

Copolymerization of AN(M_1) with butyl vinyl ethers at 60°; solvent toluene; molar ratio $\frac{/M_1/ + /M_2/}{/AIBN/} = 300$

$/M_1/$ in monomers (mole %)	M_2	$/M_1/ + /M_2/$ (mole/l)	Reaction time (min)	Conversion (%)	N % Dumas	$/m_1/$ in copolymer (mole fraction)
70	nBVE	11.5	20	5.70	17.58	0.790
60	nBVE	11.1	—	—	15.43	0.726
50	nBVE	10.7	20	4.74	13.52	0.664
40	nBVE	10.3	40	6.48	12.61	0.633
30	nBVE	10.0	72	6.53	11.70	0.600
20	nBVE	9.6	120	2.79	10.71	0.562
90	sBVE	12.5	15	7.51	19.54	0.842
80	sBVE	12.0	10	4.80	16.38	0.755
70	sBVE	11.5	10	5.95	14.83	0.707
60	sBVE	11.1	20	6.82	12.77	0.640
50	sBVE	10.7	15	4.73	12.17	0.617
40	sBVE	10.3	25	6.90	11.07	0.576
30	sBVE	10.0	30	6.36	—	—
20	sBVE	9.6	90	9.95	9.89	0.530
10	sBVE	9.3	130	4.18	9.75	0.524
90	tBVE	12.5	7	5.61	16.64	0.763
80	tBVE	12.0	8	5.84	13.94	0.679
70	tBVE	11.5	9	5.85	11.88	0.607
60	tBVE	11.1	10	5.30	11.27	0.584
50	tBVE	10.7	10	4.79	11.02	0.570
40	tBVE	10.3	12	4.44	10.48	0.544
30	tBVE	10.0	30	8.60	10.07	0.537
20	tBVE	9.6	30	7.23	9.04	0.495
10	tBVE	9.3	60	6.62	—	—

AN is known as a monomer with a greater tendency towards alternation ("e" = + 1.20). The systems involving AN are more reactive than those containing MAN. This follows from figure 3 ; about the influence of the molar fraction of AN in initial monomer mixture, on the reaction rate, may be observed that when the AN content decreases, the rate drops sharply. This important shrinkage cannot be attributed to the reduction of total monomer concentration (from 11.5 to 9.3 mole/l), but to the great reactivity difference between monomers.

The same behaviour was observed by Tazuke [17] for the AN — isobutyl vinyl ether (iBVE) pair. Radicalic polymerization of AN is monotonously retarded by the addition of iBVE, when the system was initiated by AIBN in the dark. If the rate of initiation would be kept constant, therefore the change of the polymerization rate must be caused by a reduced rate of propagation or an enhanced rate of termination.[17]

---

[17] S. Tazuke, *Adv. Polymer Sci.*, **6**, 321 (1969).

Table 5

Experimental and calculated data for the determining of the AN(M_1) – BVE(M_2) systems reactivity ratios

Experimental data		Calculated data						
X_1	Y_1	$X = X_1/X_2$	X^2	$Y = Y_1/Y_2$	$Z = (Y - 1)/X$	$-W = Y/X^2$	W^2	$-ZW$
				$M^2 = n$BVE				
0.7	0.790	2.3333	5.4444	3.7619	1.1836	0.6909	0.4773	0.8178
0.6	0.726	1.5000	2.2500	2.6497	1.0998	1.1773	1.3861	1.2653
0.5	0.664	1.0000	1.0000	1.9762	0.9762	1.9762	3.9054	1.9292
0.4	0.633	0.6666	0.4444	1.7248	1.0872	3.8808	15.0610	4.2192
0.3	0.600	0.4286	0.1836	1.5000	1.1666	8.1699	66.6930	9.5270
0.2	0.562	0.2500	0.0625	1.2831	1.1324	20.5295	421.4450	23.2490
				Σ	6.6458	36.4246	508.9678	41.0075
				$(\Sigma W) = 1326.8$				
				$M_2 = s$BVE				
0.9	0.848	9.0000	81.0000	5.5789	0.5088	0.0689	0.0047	0.0350
0.9	0.842	9.0000	81.0000	5.3291	0.4810	0.0658	0.0043	0.0316
0.8	0.742	4.0000	16.0000	2.8759	0.4690	0.1797	0.0322	0.0843
0.8	0.755	4.0000	16.0000	3.0816	0.5204	0.1926	0.0371	0.1002
0.7	0.707	2.3333	5.4444	2.4130	0.6056	0.4432	0.1964	0.2684
0.6	0.640	1.5000	2.2500	1.7777	0.5185	0.7901	0.6243	0.4097
0.5	0.617	1.0000	1.0000	1.6109	0.6109	1.6109	2.5950	0.9841
0.4	0.576	0.6666	0.4444	1.3585	0.5377	3.0569	9.3446	1.6439
0.2	0.530	0.2500	0.0625	1.1277	0.5108	18.0432	325.5498	9.2165
				Σ	4.7627	24.4513	338.3885	12.7737
				$(\Sigma W^2) = 597.89$				
				$M_2 = t$BVE				
0.9	0.763	9.0000	81.0000	3.2194	0.2469	0.0397	0.0016	0.0098
0.8	0.679	4.0000	16.0000	2.1153	0.2788	0.1322	0.0175	0.0369
0.8	0.637	4.0000	16.0000	1.7548	0.1887	0.1072	0.0120	0.0207
0.7	0.607	2.3333	5.4444	1.5445	0.2334	0.2836	0.0804	0.0662
0.6	0.584	1.5000	2.2500	1.4039	0.2692	0.6239	0.3893	0.1680
0.5	0.570	1.0000	1.0000	1.3256	0.3256	1.3256	1.7572	0.4316
0.4	0.544	0.6666	0.4444	1.1933	0.2899	2.6852	7.2103	0.7785
0.3	0.537	0.4286	0.1836	1.1599	0.3731	6.3170	39.9049	2.3579
0.2	0.495	0.2500	0.0625	0.9802	−0.0792	15.6830	245.9600	− 1.2421
				Σ	2.1264	27.1974	295.3323	2.6275
				$(\Sigma W)^2 = 739.83$				

X_1 – initial mole fraction of AN in monomer mixture.
Y_1 – mole fraction of AN in copolymer.

The reckoning of r_1 and r_2 values was made by two different methods : the least square method (Table 5) and the intersection method of Mayo and Lewis [18] (Figure 4). The copolymers of acrylonitrile with *t*-butyl vinyl ether, made at feeds rich in *t*BVE, have compositions neighbouring to the equimolecular one.

---

[18] F. R. MAYO and F. M. LEWIS, *J. Amer. Chem. Soc.*, **66**, 1594 (1944).

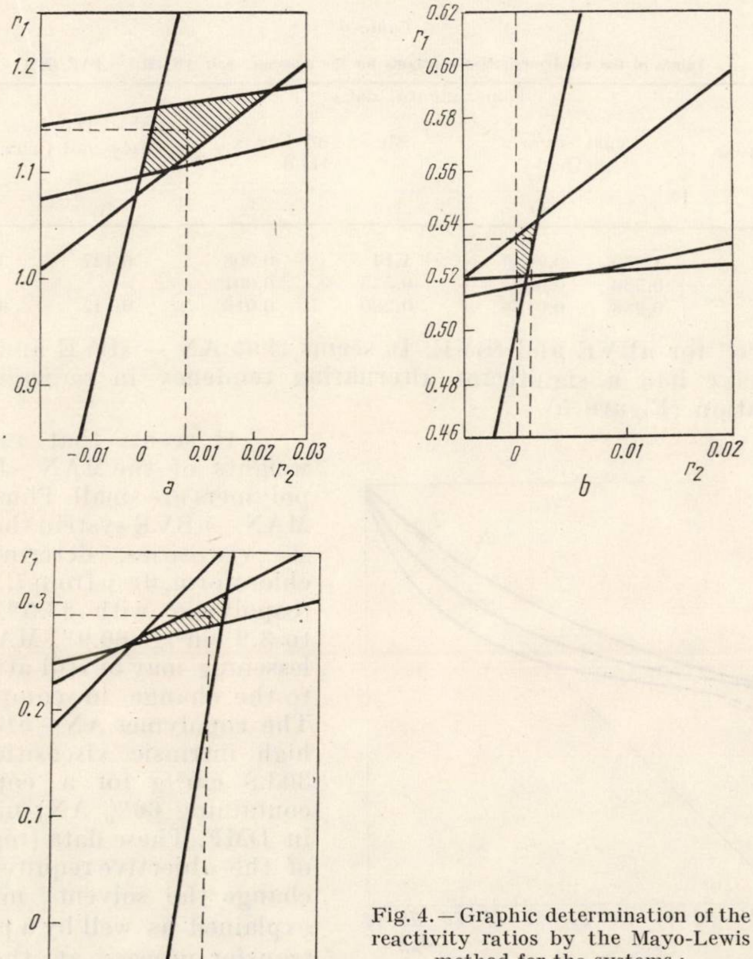

Fig. 4. — Graphic determination of the reactivity ratios by the Mayo-Lewis method for the systems :
*4*a) AN−*n*BVE ; $r_1 = 1.14$ $r_2=0.008$.
*4*b) AN−*s*BVE ; $r_1=0.535$ $r_2=0.001$.
*4*c) AN−*t*BVE ; $r_1 = 0.29$ $r_2=0.016$.

From the electronic point of view, the inductive effect decreases in the order *t*-butyl > *s*-butyl > *n*-butyl ; this appears obviously if we examine the r_1 and r_2 values. The experimental reactivity ratios are rather different from those calculated (by Alfrey and Price [16] scheme) and earlier reported data for the acrylonitrile *t*-butyl vinyl ether pair [3] ($r_1 = 0.14$ and $r_2 = 0.0032$). Therefore, the agreement with theoretical values is somewhat less satisfactory than that for the systems containing MAN.

The obtained data concerning the binary system involving *s*-butyl vinyl ether permitted us to calculate the values "Q" = 0.0417 and "e" = = − 1.54 for this monomer; the value "e" is placed between the known values "e" for *n*BVE and *t*BVE. It seems that AN − *s*BVE and AN − *t*BVE have had a significant alternating tendency in radicalic copolymerization (Figure 5).

Table 6

Values of the copolymerization constants for the monomer pair AN (M_1) − BVE (M_2)

Monomer M_2	Experimental data				Calculated data from the Alfrey and Price's scheme	
	Least-squares method		Mayo and Lewis method			
	r_1	r_2	r_1	r_2	r_1	r_2
nBVE	1.100	−0.0020	1.14	0.008	0.427	0.00897
sBVE	0.530	0.0007	0.535	0.001	—	—
tBVE	0.288	0.0178	0.290	0.016	0.142	0.00310

It seems that molecular weights of the MAN−BVE copolymers are small. Thus, at the MAN−*n*BVE system the intrinsic viscosities, determined in chloroform, drop from 7.12 cm³/g (copolymer with 83.5% MAN) to 3.9 cm³/g (60.9% MAN); this lessening may be still attributed to the change in composition. The copolymer AN−*n*BVE has high intrinsic viscosities (e.g. 303.8 cm³/g for a copolymer containing 66% AN) measured in DMF. These data (regardless of the objective requirement to change the solvent) might be explained as well by a powerful transfer process at the MAN BVE systems, as the participation of the charge transfer complexes of AN with BVE in copolymerization.

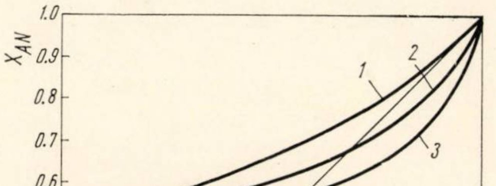

Fig. 5. — AN molar fraction in copolymer as a function of the AN molar fraction in initial monomer mixture at 60°. *1.* AN − *n*BVE pair; *2.* AN−*s*BVE pair; *3.* AN−*t*BVE pair.

To point out the presence of the vinyl ethers in the copolymer chain, IR absorption spectra were accomplished for the following copolymers: A = MAN (73.6%)−*n*BVE; B = MAN(60.1%)−*s*BVE; C = = MAN (55.3%)−*t*BVE; % represents the molar percentage, previous established by the nitrogen content. Characteristic vibration frequencies ν [cm^{-1}] are:

Compound A: 1085 s; 1190 m; 1385 m; 1460 s; 1755 m; 2240 m; 2960 vs.

Compound B : 1060 s ; 1380 s ; 1465 s ; 1730 m ; 2240 m ; 2910 vs.

Compound C : 1065 s ; 1195 s ; 1240 w ; 1365 s ; 1385 s ; 1460 s ; 1750 m ; 2235 m ; 2980 vs.

where : w-weak ; m-medium ; s-strong and vs-very strong.

A strong peak in the range 1060–1085 cm^{-1} (characteristic of the aliphatic ethers) and a medium absorption band at 2240 cm^{-1} may be attributed to the nitrile group.[19] Thus, the former analytical data regarding the copolymer composition, are confirmed.

Nuclear magnetic resonance spectroscopy (NMR) has lately become one of the polymer researcher's most important tools ; the use of NMR to study molecular composition and sequence distribution in copolymer has been more and more developed.[20] The NMR spectra of several copo-

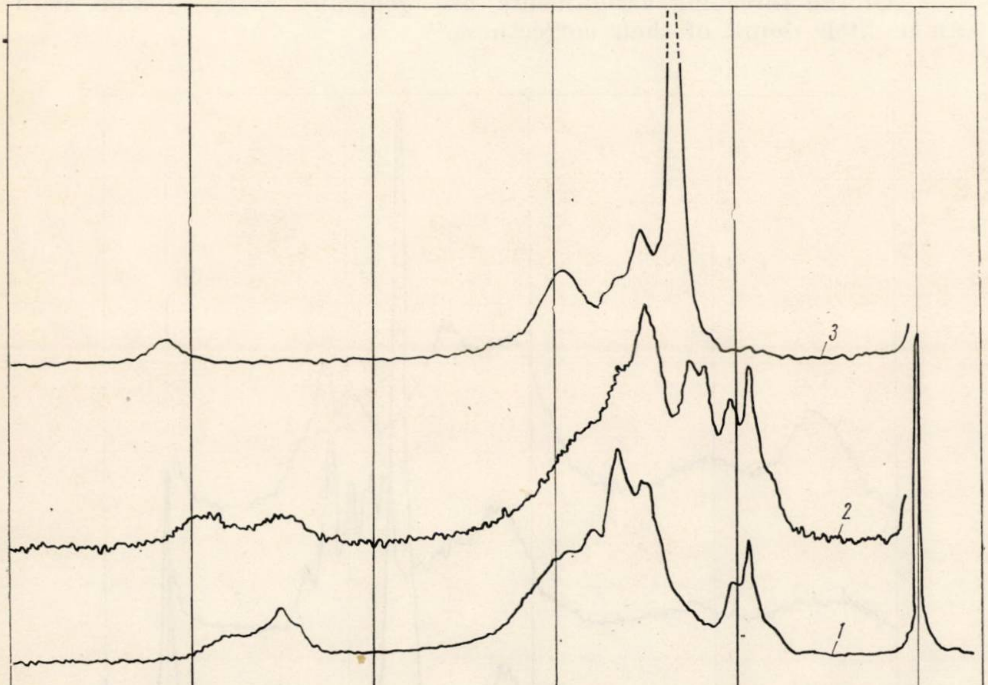

Fig. 6. — NMR spectra of the MAN-BVE copolymers.
1. MAN–*n*BVE (60.9 %). *2.* MAN–*s*BVE (54.1 %). *3.* MAN–*t*BVE (55.3 %).

---

[19] R. M. Silverstein and G. C. Bassler, "Spectrometric Identification of Organic Compounds", J. Wiley and Sons, New York–London, 1963, p. 49.

[20] A. Pidcok, Nuclear Magnetic Resonance ; in : "Polymer Science — a Materials, Science Handbook", Editor A. D. Jenkins, vol. **2**, North-Holland Publishing Company, Amsterdam–London, 1972, p. 1383.

lymers of MAN and AN with BVE, having compositions nearby to equimolecular one, were carried out.

Figure 6 shows a comparison of spectra for three copolymers of MAN with various BVE ; the three spectra were recorded under the same conditions.

Thus, the chain methylene resonance are centered at 8.31 τ and the α-methyl (from MAN) resonance occurs in the neighbourhood of 9 τ. The large area at 8.67 τ (copolymer MAN−*t*BVE) is ascribed to the CH_3 protons, present in great number [20,21] and the intensity of this resonance is proportional to the *t*BVE fraction.

In figure 7, we present the NMR spectra for the AN−*n*BVE, AN−*s*BVE and AN−*t*BVE copolymers with nearly equimolecular compositions. Especially there is observed the strong peak at 8.78 τ corresponding to the methyl groups from *t*BVE.

All the foregoing assignments are generally accepted and there can be little doubt of their correctness.[21]

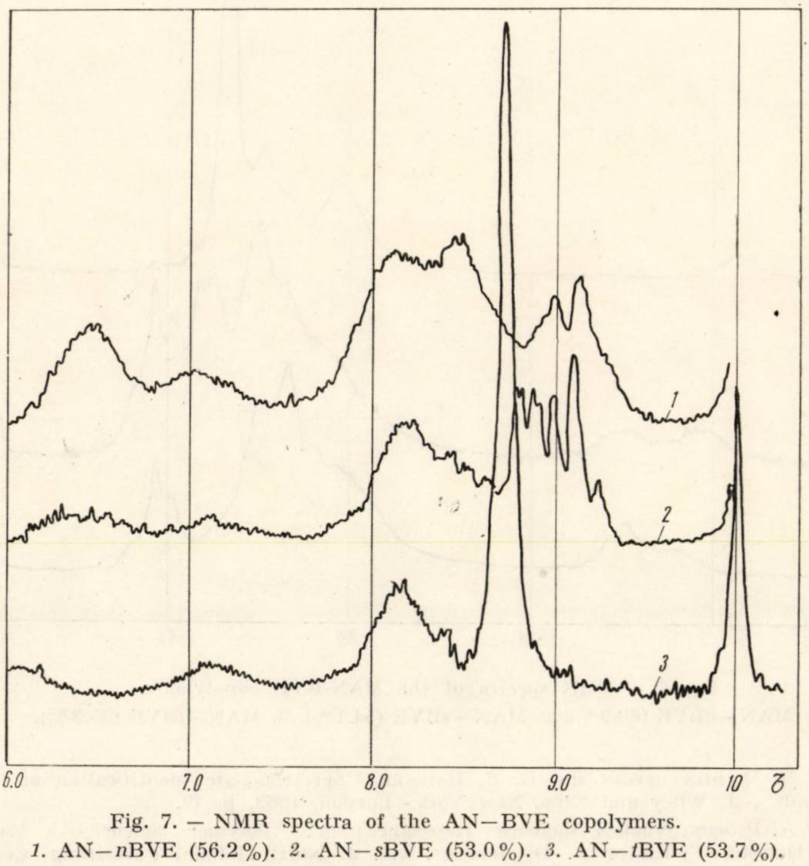

Fig. 7. — NMR spectra of the AN−BVE copolymers.
1. AN−*n*BVE (56.2%). *2.* AN−*s*BVE (53.0%). *3.* AN−*t*BVE (53.7%).

---

[21] B. Ke, "Newer Methods of Polymer Characterization", J. Wiley and sons, New York, 1964, p. 33.

In a copolymer of an acrylic monomer (A) with a vinyl ether (E) only the AE and AA diads and AAA, AEA and EAA triads are possible. The AE diad and AEA triad would be favoured at an equimolecular copolymer. Unfortunately, the lack of suitable standards did not permit us a complete interpretation of the NMR spectra, in order to establish the weight of each structure. Further study, with special emphasis on the sequence distribution, is needed.

AA acts in copolymerization processes with BVE in a different manner than MAN or AN. As the "e" value of acrylamide is +1.30,[4] then it would be expected that AA—BVE systems would show an increased alternating tendency.

The copolymerization tests were carried out in the same conditions as those described above, but acrylamide was poured in the ampoule with two arms, as a solution in acetone. Accordingly the concentration of both monomers (AA and BVE) varied in the range 2.0—4.2 mole/l.

The noticed polymerization rates were higher ($\simeq 0.6\%$/min.) than those observed at the MAN—BVE and AN—BVE systems; practically these rates do not depend on the feed composition.

The precipitated products are rather sticky and cause some difficulties in their analysis. Nevertheless, the nitrogen analyses showed that there was produced poly-AA. The polymer was dissolved in water and the solution evaporated to obtain pellicules. The IR absorption spectra were carried out on them and we acquired spectra alike to that reported by Hümmel[22] for polyacrylamide : 790 cm^{-1}(s) ; 1130 cm^{1} (w) ; 1420 cm^{-1} (m) ; 1660 cm^{-1} (vs) ; 2950 cm^{-1} (m) and 3340 cm^{-1} (s).

The lack of a strong peak at 1060—1080 cm^{-1} allows us to consider that BVE does not enter the chain.

On the other hand, the melting range of these products is high (200—220°) ; this fact may point a branched polymer due to the transfer reaction with the "dead" polymer.

The behaviour of AA—BVE systems might be explained in a similar manner to that of the styrene-vinyl acetate classical system.[4]

Further work is in progress.

The author wishes to thank to B. Mărculescu for the nitrogen analyses and expresses his gratitude to C. Drăghici for the NMR measurements.

---

[22] HÜMMEL/SCHOLL "Infrared Analysis of Polymers, Resins and Additives. An Atlas", vol. **1**, part 2, Wiley-Intersience, New York—London, 1969, p. 1239.

Revue Roumaine de Chimie, **19**, *8*, 1407 – 1411 (1975)

THE EFFECT OF S-CHAMBER SHAPE ON THE SEPARATION OF ETHANOLAMINES BY THIN LAYER CHROMATOGRAPHY

H. NAȘCU and C. LITEANU

University of Cluj, Department of Analytical Chemistry

Received June 29, 1973

The effect of S-Chamber shape (profile) in the thin layer chromatographic separation of a test dyes mixture and some ethanolamines was studied. The "A" type chambers (wedge shaped) are more advantageous leading to a better separation. These are a new type of unsaturated chambers which give the same reproducibility as the S-Chambers. When the R_f values do not exceed 0.5, an optimum dimension of chamber for a given separation was found.

Recently, the influence of the shape of chromatographic chamber on the quality of thin layer chromatographic (TLC) separation was a problem of great interest in the field of thin layer chromatography (TLC). Thus, besides the usual chromatographic chamber (chromatographic tank) 21 × 21 × 9 cm known as "N-Chamber", Stahl[1] and Davies[2] introduced the "S-Chambers" which subsequently were improved.[3–7] The S-Chamber was used for both descending[8] and horizontal[9] chromatography. In addition, the KS-[10] and BN-[11] Chambers are special chromatographic chambers which permit the selection of optimum humidity conditions and assure highly reproducible results respectively. The S-Chambers for continuous chromatography have also been proposed.[12–14]

---

[1] E. Stahl (ed.), "Thin Layer Chromatography", 2nd Ed., Springer Verlag, Berlin, 1969, 69.

[2] B. H. Davies, *J. Chromatog.*, **10**, 518 (1963).

[3] C. G. Honegger, *Helv. Chim. Acta*, **46**, 1730 (1963).

[4] D. Jänchen, *J. Chromatog.*, **14**, 261 (1964).

[5] D. Jänchen, *J. Chromatog.*, **33**, 195 (1968).

[6] F. Geiss and A. Schlitt, *Chromatographia*, **1**, 387 (1968).

[7] Toyo Roshi Kisha, Ltd., Pat. Fr. 2 067 796, 24 Sept. 1971, *Chem. Abstr.*, **76**, 128316f (1972).

[8] A. V. De Thomas, M. Zdankiewicz and D. Witkowic, *Microchem. J.*, **15**, 71 (1970).

[9] M. Brenner and A. Niederwieser, *Experientia*, **17**, 237 (1961).

[10] F. Geiss and A. Schlitt, *Chromatographia*, **1**, 392 (1968).

[11] G. Geiss and A. Schlitt, *J. Chromatog.*, **33**, 208 (1968).

[12] E. V. Truter, *J. Chromatog.*, **14**, 57 (1964).

[13] A. E. Sherwood, *Lab. Practice*, **21**, 184 (1972).

[14] S. Hara and K. Mibe, *J. Chromatog.*, **66**, 75 (1972).

A recent work has shown that a chamber similar to the S-Chamber, but wedge shaped with 10 cm at its bottom may be also useful in some TLC separations.[15]

The purpose of the present paper is to study the influence of the shape (profile) of such chambers on certain TLC separations e.g. a test dyes mixture and some ethanolamines by using a single solvent in the first case and a mixture of polar solvents in the second.

MATERIALS

The chambers were constructed according to the procedure of Sherwood[13] i.e. by glueing by means of an epoxi adhesive two pieces (wedge shaped) and a strip of glass on the three sides of a 10 × 14 cm glass plates in such a manner as to get chambers of different shapes but with one constant dimension after grinding (Figure 1.). The opposite side dimension, L, is variable. In this way two types of chambers called "A" and "V" have been obtained. The L dimension varies from 2.5 to 18 mm for the A type chambers and from 2.5 to 14 mm for the V type chambers, respectively. This dimension permits to handle the chambers with the same easiness as the usual S-Chambers.

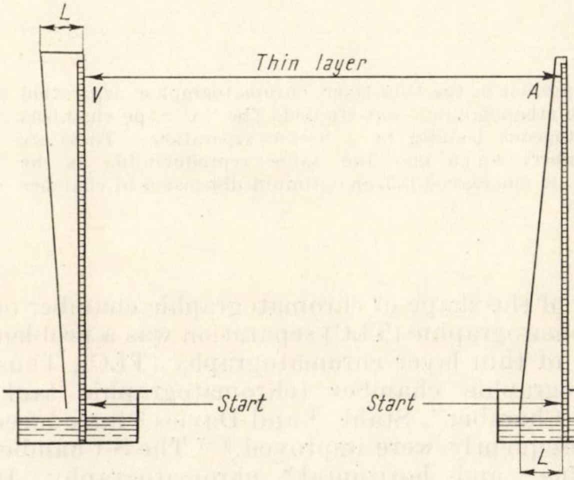

Fig. 1. — Schematic representation of the chambers :

A type chambers,
V type chambers

The L is the bottom and top width, respectively

Kieselgel H (Merck, Darmstadt, Germany) with 5% starch as binder was used to prepare 250 μ thick layers according to the procedure of Lees and De Muria.[16] The layers were air dried and kept above a saturated solution of potassium carbonate (45% relative humidity).

The solvents used were analytical grade reagents. Methil-ethilketone was purified by a distilling with potassium permanganate after a previousd rying with anhydrous potassium carbonate. Mono-(MEA), di-(DEA), and triethanolamines (TEA) (Merck, Darmstadt, Germany) were used as 2% aqueous solution. The test dyes mixture (Butter yellow, Sudan Red, and Indophenol) was used in the form supplied by Desaga (Heidelberg, Germany). A 0.2% ninhidrine in n-butanol (containing 2% acetic acid) was used as spray reagents for ethanolamines. Before and after spraying, the plate was kept for 10 minutes at 120°C in an oven.

---

[15] Eastman Kodak Co. (P. Clement, J. M. Gombert and R. Seve), British. Pat. 1 196 287, 14.11.1967, *Analyt. Abstr.*, **20**, 1377 (1971).

[16] T. Lees and De Muria, *J. Chromatog.*, **8**, 108 (1962).

RESULTS AND DISCUSSIONS

In order to check the effect of the chamber shape on the kinetics of the front and spot migration, the Desaga test dyes mixture as components and benzene as solvent were used. No essential modification in the equation of migration ($z^2 = \chi t$) as comparing with a S-Chamber ($10 \times 8 \times 0.25$ cm) was observed.

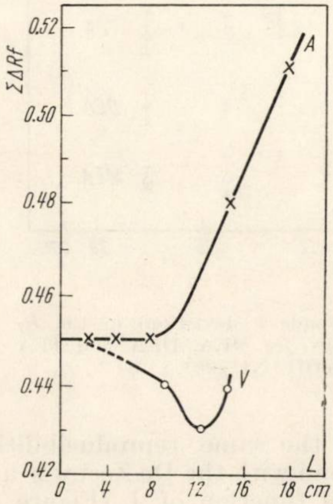

Fig. 2. — The plot of $\Sigma\Delta R_f$ vs. L for the test dyes mixture (Butter yellow, Sudan red and Indophenol). The length of migration at 10 cm.

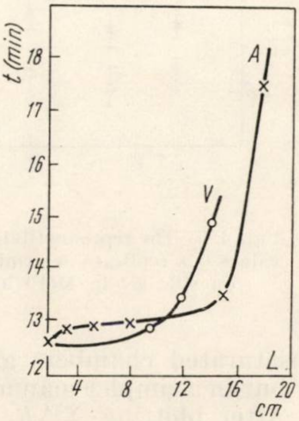

Fig. 3. — The plot of time of migration for benzene vs. chamber (shape A and V). Length of migration at 10 cm.

Taking into account the sum of differences between the R_f values ($\Sigma\Delta R_f$) at the same migration distance as a separation index, in the case of test dyes mixture and benzene, the graph in Figure 2 was obtained.

The plot of $\Sigma\Delta R_f$ vs. L shows an exponential increasing of the "separation" partly due to exponential increasing of the chamber volume. As for the V type chambers a better separation is noticed as compared to the S-Chamber.

The time required for the solvent to migrate 10 cm, was increasing with the L increase in both chambers, as shown in Figure 3.

Since the volume of these new studied chambers increases as compared to the S-Chambers and by increasing the volume, the reproducibility generally diminishes,[17] the effect of the A type chamber shape on reproducibility was tested. A solvent system in which MEA, DEA, and TEA are completely separated e.g. Me Et CO : MeOH : NH_3 (25%) 8 : 3 : 9 was used. As it can be seen from Figure 4, six replicate determinations of the R_f values give for the A type chambers reproducibilities (standard deviations) close and/or sometimes even better than those obtained in S-Chamber.

---

[17] F. Geiss, A. Schlitt and A. Klose, *Z. analyt. Chem.*, **213**, 331 (1965).

The F test proved that no signifiant differences exist between reproducibilities in the S-Chamber and the A type chamber. Thus, this new kind of unsaturated chambers gives the same reproducibilities as the S-Chamber but in a simpler manner than with the De Zeeuw's unsaturated chamber.[18] After plotting $\Sigma \Delta R_f$ as a function of L (Figure 5) only a correlation can be seen. The correlation coefficient $r = 0.57$ and the square of this, $r^2 = 0.33$ proves that 33% is the contribution of L to the distribution of these experimental points.

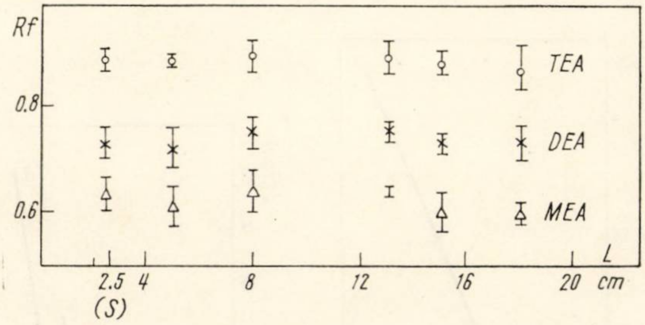

Fig. 4. — The reproductibility (standard deviation) of the R_f values (six replicate determinations) for MEA, DEA and TEA on silicagel in MeEtCO : MeOH : NH_3(25%), 8 : 3 : 9.

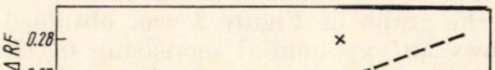

Fig. 5. — The plot of $\Sigma\Delta R_f$ vs. L for the separation of MEA, DEA and TEA on silicagel in MeEtCO : MeOH : NH_3(25%) 8 : 3 : 9. The correlation $r = 0.57$ ($r^2 = 0.33$).

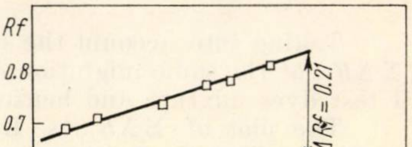

Fig. 6. — The plot of $\Sigma\Delta R_f$ vs. L for separation of MEA, DEA and TEA on silicagel with MeEtCO : MeOH : NH_3 (10%), 12 : 3 : 8. Time 30 min.

---

[18] R. A. DE ZEEUW and M. T. FEITSEMA, *Pharm. Weekblad*, **101**, 957 (1966).

Another solvent system used for quantitative determinations of TEA in DEA or MEA[19] was tested for its behaviour in the A type chambers (Figure 6.) In this case the new chambers are not more efficient than the S-Chamber, due to the fact that the real distance between these zones being smaller, the danger of contamination at elution from the plate increases.

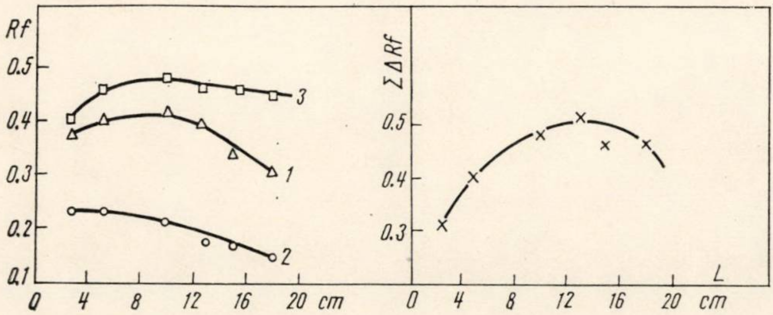

Fig. 7. — The plot of $\Sigma\Delta R_f$ vs. L for the separation of MEA, DEA and TEA on silicagel in MeEtCO : MeOH : NH_3(25%) 7 : 2 : 1. The length of migration at 10 cm.

In a solvent system which gives lower R_f values, a better separation can be obtained (Figure 7); thus there is an optimum chamber for a given separation.

CONCLUSIONS

The A type chambers may give better separations which are dependent upon the chromatographic system used. The reproducibility in these chambers does not differ significantly from the classical S-Chamber. They are unsaturated chambers easy to built and use. In the case of the TLC separations of ethanolamines when a solvent system gives low R_f values (<0.5) the "A" type chambers give better separations. The equation of front and zone migration is similar to that in the S-Chamber ($z^2 = \chi t$).

---

[19] C. Liteanu and H. Naşcu, Unpublished data.

Revue Roumaine de Chimie, **19**, *8*, 1407–1411 (1974)

Structure and bonding. 15. Springer Verlag, Berlin, Heidelberg, New York, 1973, 188 p.

The volume is devoted to various topics concerning the coordination interactions.

In the first chapter dealing with the complexes of chelating olefin-group V ligands, D. I. Hall, J. H. Ling and R. S. Nyholm describe the results of their studies aimed at stabilizing the complexes of a wide range of metals, investigating the effect of the metal on the reactions of the olefinic group. The stabilization is achieved, using the olefinic group as a part of a molecule containing a "b" class donor atom, usually P or As, occasionally O^- or S^-. The strongest effect results when two or three carbon atoms are present between the heavy atom and the vinyl group. Besides valuable information on the properties of olefin complexes produced, new synthetic routes have been achieved. The structures of the complexes mentioned above are often of interest themselves. Some mechanistic and structural considerations concerning the ability of the ligand to chelate, the possibility of isomerization of terminal olefins and the formation of metal-carbon σ bonds are also suggested.

In the following chapter, E. C. Baughan discusses a new system of ionic radii obtained from diamagnetism : the root-mean-square electron-cloud radii. Their comparison with the structural radii, shows that for ionic and van der Waals bonds, the structural radii are about twice the root-mean-square electron-cloud radius, but for localized covalent bonds they are only nearly equal. This distinction between electron-cloud radii and structural radii is further used to refine the system of ionic radii due to Pauling and Goldschmidt. A short discussion of solvation energies pleads that here also the electron-cloud radii are the less suitable.

Another chapter concerns the Lewis acid-base interactions. The author, R. S. Drago begins by showing that in almost any chemical reaction Lewis acid-base interactions are involved, in at least a certain step of the process. A discussion of the data to be obtained follows in order to account for the strength of the bonding. Next, a quantitative model is presented with the view to predict and correlate the enthalpies of the adduct formation. The interpretation of the resulting parameters, the exceptions to the above correlation, as well as their valid transformations are considered in the light of hard-soft acid-base and donor strength models of acid-base chemistry. Both concepts are shown to be incomplete models of coordination. The relationship between the new parameters and the $\sigma-\rho$ Hammett ones is quantitatively demonstrated. Potential uses and extension of this approach to acid-base chemistry are presented. Some indications are given concerning the attempts to deduce the magnitude of interaction from changes in the spectroscopic properties of donors and acceptors on coordination.

In the fourth chapter of the compendium, V. Gutman, based on a functional approach to chemical interactions aimed to account for the relations between redox-properties and coordination, considers that the redox potential is decisively influenced by differences in the actual net charges at the redox active centers of the oxidized and reduced species. In agreement with this concept, the author relates the oxidizing properties and the complex stability for cations, anions and by back-donation.

The volume closes with S. Ahrtand's article concerning the thermodynamics of stepwise formation of metal-ion complexes in aqueous solution. The hard acceptors and donors are postulated to be electrovalent ; the soft ones, to be covalent. The thermodynamic functions found for the stepwise formation of complexes in aqueous solution, are in very good agreement with the models proposed for complexes of different character. The models applied are based on evidence from several fields, both thermodynamic and non-thermodynamic. The fact that many characteristics related to the consecutive steps agree with the models, is a supplementary support for this plausibility.

Florica Popea

NOTE POUR LES AUTEURS

La *Revue Roumaine de Chimie* publie des articles en anglais, français, russe, allemand ou espagnol. Les auteurs sont priés d'envoyer des articles, notes, communications et comptes rendus inédits.

Les manuscrits seront dactylographiés à deux intervalles. Les tableaux seront dactylographiés sur des feuilles séparées, de même que la légende des figures. Les diagrammes seront tracés à l'encre de Chine sur papier calque. Les tableaux et les figures seront numérotés par des chiffres arabes, en nombre strictement nécessaire. Prière de ne pas inscrire les mêmes données dans les tableaux et les figures. Les formules chimiques seront incluses dans le texte ; en outre, elles seront transcrites sur des feuilles séparées. Les auteurs sont priés d'indiquer les caractères italiques (en soulignant les lettres au crayon), ainsi que tout autre caractère spécial. L'ordre des références bibliographiques sera celui de leur mention dans le texte ; le nom de l'auteur sera précédé de l'initiale du prénom ; les publications périodiques seront présentées suivant les prescriptions internationales. Les références seront ajoutées à la fin de l'article ; elles paraîtront comme des notes, au bas de la page. Le texte sera précédé d'un résumé comprenant 15 lignes au maximum.

L'entière responsabilité du contenu des articles appartient aux auteurs. On publie des articles dus aux collaborateurs roumains ou étrangers.

PRINTED IN ROMANIA

1974 DEC 17

TRAVAUX PARUS AUX ÉDITIONS DE L'ACADÉMIE DE LA RÉPUBLIQUE SOCIALISTE DE ROUMANIE

CRISTOFOR SIMIONESCU, MARGARETA GRIGORAŞ, AGATA CERNĂTESCU-ASANDEI et GHEORGHE ROZMARIN, **Chimia lemnului din România — plopul şi salcia** (La chimie du bois en Roumanie — le peuplier et le saule), 1973, 228 p., 28 lei.

ŢIBERIU NĂSCUŢIU, **Metode radiochimice de analiză** (Méthodes radiochimiques d'analyse), 1973, 384 p., 23 lei.

MARIA FITI, **Dozimetria chimică a radiaţiilor ionizante** (La dosimétrie chimique des radiations ionisantes), 1973, 240 p., 13,60 lei.

MIHAI FLORESCU, **Eficienţa economică a cercetării ştiinţifice** (L'efficience économique de la recherche scientifique), 1972, 115 p., 15 lei.

GEORGETA LĂZĂRESCU, **Sistematizarea informaţiilor în Chimia organică** (La systématisation des informations dans la Chimie organique), 1972, 252 p., 10,15 lei.

P. BALTĂ şi E. BALTĂ, **Introducere în chimia fizică a stării vitroase** (Introduction à la chimie physique de l'état vitreux), 1971, 240 p., 15,50 lei.

LYDIA-MARIA VAICUM, **Biodegrabilitatea detergenţilor** (La biodégrabilité des détergents), 1971, 254 p., 16 lei.

I. ZUGRĂVESCU et L. STOICESCU-CRIVETZ, **Polimeri heterociclici** (Polymères hétérocycliques), 1971, 190 p., 9,50 lei.

CRISTOFOR SIMIONESCU et C. V. UGLEA, **Fracţionarea compuşilor macromoleculari** (Fractionnement des composés macromoléculaires) 1962, 292 p., 18,50 lei.

I. MAXIM, **Materiale nucleare** (Matériaux nucléaires), 1969, 444 p., 30 lei.

CRISTOFOR SIMIONESCU et CLEOPATRA VASILIU-OPREA, **Mecanochimia compuşilor macromoleculari** (La mécanochimie des composés macromoléculaires), 1967, 344 p., 23,50 lei.

CORNEL BODEA et collab., **Tratat de biochimie vegetală, partea I, Fitochimie** (Traité de biochimie végétale, Ire partie, Phytochimie), Ier vol., 1964, 747 p. + 4 annexes + 2 pl., 41 lei; IIe vol., 1965, 1262 p., 1 pl., 56 lei; IIIe vol., 1967, 773 p., 35 lei.

V. GHEŢIE et V. MICUŞAN, **Analiza imunochimică. Teorie şi practică** (Analyse immunochimique. Théorie et pratique), 1966, 369 p., 28 lei.

R. PORTOCALĂ et L. POPA, **Acizii ribonucleici celulari şi virali** (Les acides ribonucléiques cellulaires et viraux), 1966, 375 p., 8 pl., 26 lei.

D. PURDELEA et R. VÎLCEANU, **Chimia compuşilor organici ai fosforului şi ai acizilor lui** (La chimie des composés organiques du phosphore et de ses acides) 1965, 540 p., 37 lei.

I.P.I. — c. 1492

43 426

Lei 25.—

F1103

ACADÉMIE DE LA RÉPUBLIQUE SOCIALISTE DE ROUMANIE

REVUE ROUMAINE DE CHIMIE

TOME 19
N° 9
Septembre 1974

RRCHAX, 19, *9*, 1415–1556 (1974)

ÉDITIONS DE L'ACADÉMIE DE LA RÉPUBLIQUE SOCIALISTE DE ROUMANIE

Rev. Roumaine Chim. 19, *9*, p. 1415–1556 (1974), Bucarest

ACADÉMIE DE LA RÉPUBLIQUE SOCIALISTE DE ROUMANIE

COMITÉ DE RÉDACTION

Rédacteur en chef :

I. G. MURGULESCU, membre de l'Académie de la République Socialiste de Roumanie

Rédacteurs en chef adjoints :

A. T. BALABAN et V. EM. SAHINI, membres correspondants de l'Académie de la République Socialiste de Roumanie

Collège de rédaction :

EM. BRATU, ELENA CEAUŞESCU, ECATERINA CIORĂNESCU-NENITZESCU, C. DRĂGULESCU, RALUCA RIPAN, CR. SIMIONESCU, membres de l'Académie de la République Socialiste de Roumanie; P. SPACU, membre correspondant de l'Académie de la République Socialiste de Roumanie; MARGARETA AVRAM, D. I. MARCHIDAN, I. MOLDOVAN, G. NIAC et D. SĂNDULESCU

Toute commande de l'étranger (fascicules ou abonnements) sera adressée à Întreprinderea Rompresfilatelia, Boîte Postale 2001, telex 011631, Bucarest, Roumanie

Les manuscrits, les livres et les revues proposés en échange, ainsi que toute correspondance seront envoyés à la rédaction :

REVUE ROUMAINE DE CHIMIE

23, str. Dumbrava Roşie, Bucarest, Roumanie, téléphone 12 41 60

ÉDITIONS DE L'ACADÉMIE DE LA RÉPUBLIQUE SOCIALISTE DE ROUMANIE

3 bis, str. Gutenberg, Bucarest, téléphone 16 40 79

REVUE ROUMAINE
DE
CHIMIE

ORSZÁGOS MŰSZAKI KÖNYVTÁR ÉS DOKUMENTÁCIÓS KÖZPONT 883

Tome 19, N° 9 **Septembre 1974**

I.G. MURGULESCU and MARILENA ŞERBAN, On the viscosity of molten metals. II. 1417–1427

ORTANSA LANDAUER, G. COSTEANU et CORNELIA MATEESCU, Sur la viscosité des systèmes mixtes : eau-monoéthylène-glycol, eau-monoéthanolamine et eau-diméthylesulfoxyde. L'influence de la température et des sels sur la viscosité de ces systèmes 1429–1433

D.I. MARCHIDAN and SPERANŢA TĂNĂSESCU, High-temperature thermodynamic data for some uranium oxides within the range $UO_{2.25} - UO_{2.60}$. 1435–1439

N.S. BIRADAR and T.R. GOUDAR, Spectral study of dioxouranium (VI) complexes with aromatic Schiff bases 1441–1445

I. ATANASIU and TEODORA BADEA, Electrochemical behaviour of 18Cr — 10Ni stainless steel in organic acid solutions. I. Formic acid . 1447–1453 R

C. DRĂGULESCU, ANA NIMARĂ and I. JULEAN, Contributions to the bismuth hydrolysis study. III. Electrometric investigations on bismuthyl perchlorate hydrolysis 1455–1459

MARIA MAVRODIN-TĂRĂBÎC, Contribution à l'étude de l'hydrolyse de l'uranium (VI) en milieu azotique 1461–1470

P. CASSOUX, F. GALLAIS, J.F. LABARRE and J.M. SAVARIAULT, Bonding and magnetic properties in tetrakis phosphine complexes of nickel 1471–1481

I. TEOREANU and MARCELA MUNTEAN, Calcium aluminosulphate formation and hardening properties 1483–1489

MARIA ENCULESCU, Influence of oxides of transitional elements on the properties of mineralogical components of clinkers of cements 1491–1502

M. VLASSA, Proton magnetic resonance spectra of some 1,2,3-trimethoxyacridines 1503–1506

EUGENIA CARP, MARIA DORNEANU and I. ZUGRĂVESCU, *o*-Diazabicyclic derivatives of benzo [*c*] cinnoline. IV. Addition reactions of 3,8-dimethylbenzo [*c*] cinnoline, via ylidic intermediates, leading to new *o*-diazabicyclic systems 1507–1512

I.V. NICOLESCU and I. SUCIU, Chromatographic study of acetylene and ethylene adsorption and of palladium dispersion from Pd/Al_2O_3 catalysts . . . 1513–1519 R

F. CUIBAN, STELIANA CILIANU and VERONICA BADEA, The synthesis of some *C*-terminal analogues of the peptides : eledoisin and physalaemin 1521–1533

Rev. Roumaine de Chimie **19**, *9*, p. 1415 – 1556 (1974), Bucureşti

C. ANDREI and I. NANU, Copolymers of conjugated dienes with maleic acid monoesters. VIII. Bulk copolymerization of isoprene with monobutyl maleate 1535–1544 A

J. VODNÁR and R. DEUTSCH, Hydroperoxidation of organic compounds at the liquid/ gas interface. VII. Contributions to the physico-mathematical characterization of the apparatus 1545–1549

A. CONSTANTINESCU and C. LITEANU, Separation of small amounts of aminoacids and their identification in complex mixtures with urea in excess 1551–1553

COMPTES RENDUS 1555–1556

Revue Roumaine de Chimie, **19**, *9*, 1417–1427 (1974)

ON THE VISCOSITY OF MOLTEN METALS. II[1]

I. G. MURGULESCU and MARILENA ŞERBAN
Physical Chemistry Department, Bucharest University,
Bd. Republicii 13, Bucharest, Romania

Received April 10, 1974

It is proposed a calculation relation for viscosity, starting from one of Eyring's equations. According to the cell pattern, it is supposed that all the molecules perform harmonic vibratory motion with constant frequencies. The lattice parameters are function of atomic volume and packing coefficient. Mott's relation for the evaluation of the vibration frequency of the liquid particles is proposed; the vibration frequency of the solid particles is evaluated with Lindemann's relation. In the result equation there are two parameters, one being a function of atomic mass, melting temperature and atomic volume and the other — the activation energy — remaining an adjustable parameter. The equation is satisfied by a series of normal metals.

INTRODUCTION

In a previous work[1] we studied the applicability of Batschinski's relation for the viscosity of molten metals and liquified rare gases, both of which having constituent particles with spheric symmetry. At the same time, it was established the molecular significance of the limiting molecular volume in this equation and the possibility of its estimation from the corresponding atomic radii. Thus, in Batschinski's relation remained only one parameter adjustable by the variation of experimental values of viscosity.

In the present paper we try to derive another expression for metal viscosity, with one adjustable parameter too. Thus, we shall start from the equation:

$$\eta = h \frac{\lambda_1}{\lambda_2 \lambda_3 \lambda^2} \frac{F}{\overset{*}{F}} \mathrm{e}^{E/RT}, \qquad (1)$$

which was deduced by Eyring[2], using the transition state theory at the viscous flow of liquids; we shall develop now this theory in a different way. In this equation, λ_1, λ_2, λ_3, are lattice parameters, λ is the equilibrium separation while F and $\overset{*}{F}$ are partition functions, per cm^3, of the normal and activated particles; E is activation energy of viscous flow. The other magnitudes in the equation have known significances.

---

[1] I.G. Murgulescu and M. Şerban, *Rev. Roumaine Chim.*, **17**, 431 (1972).

[2] S. Glasstone, K.J. Laidler and H. Eyring, "The Theory of Rate Processes", New York, London 1941, p. 483.

If we accept the valability of cell pattern for the metallic liquids, we can write the equation :

$$\lambda^2 \ \lambda_2 \ \lambda_3 \ / \ \lambda_1 = a^3 = \gamma \ V/N,$$

in which a represents the nearest neighbours separation while V is the atomic volume. The factor γ can be 1, $\frac{3}{4}\sqrt{3}$ or $\sqrt{2}$ as the structures are : cubic, cubic with centred body or cubic with centred faces and hexagonal close packed respectively. In conformity with the X-ray diffraction studies, the last value is in better agreement with experimental data, and is the very one we used in the sequel. Taking into account the last equation, the viscosity coefficient equation becomes :

$$\eta = \frac{Nh}{\gamma V} \frac{F}{\overset{*}{F}} e^{E/RT} . \tag{2}$$

According to the same cell pattern, we supposed that liquid monoatomic particles have only harmonic vibratory motion round their lattice points, which may be considered equilibrium positions. The transition state partition function $\overset{*}{F}$ has one freedom degree less than F ; therefore, the ratio of the two partition function becomes equal to the partition function of an harmonic oscillator :

$$\frac{F}{\overset{*}{F}} = \left(1 - e^{-h\nu/KT}\right)^{-1},$$

where ν is the vibration frequency of the oscillator. The viscosity coefficient equation becomes thus:

$$\eta = \frac{Nh}{\gamma M} \frac{\rho e^{h\nu/KT}}{e^{h\nu/KT} - 1} e^{E/RT} , \tag{3}$$

where V was substituted by the ratio between the atomic mass M and the density ρ.

At high temperatures, which are characteristic for the metallic liquid, the harmonic oscillator partition function may be well approximated by the well-known relation :

$$kT/h\nu.$$

With this simplification, equation (3) takes the form of :

$$\eta = \frac{R}{\gamma M} \frac{\rho T}{\nu} e^{E/RT} . \tag{4}$$

The difference between the results of equations (3) and (4) remains much under the limit of experimental errors of the viscosity measurements. Therefore, we would prefer, in the sequel, the equation (4). Besides, the frequency ν is supposed constant in the temperature ranges for which we found experimental viscosity coefficients.

The determination of the vibration frequency is very accessible for the solid state of metals. By melting, the vibration frequency ν_s of the solid decreases. The vibration frequency of the corresponding liquid particles is connected with ν_s by Mott's relation[3] :

$$\frac{\nu_s}{\nu} = e^{L/3RT_m},$$

where T_m and L are the melting temperature and heat. Due to this relation, the solid state vibration frequencies may be successfully turned to account in equations (3) and (4).

In table 1, the $e^{L/3RT_m}$ values are given for the elements with normal metallic character. We used the averages of the temperature T_m and the heat L values, found in references. [4–6] The results (4th column) are near enough to justify the use of their average for the frequency correction.

Table 1

The ν_s/ν ratio for the normal metals

Element	T_m, °K	L, cal/gatom	$e^{L/3RT_m}$
Li	453.7	720	1.305
Na	371	659	1.347
K	336.6	581	1.336
Rb	312.0	537	1.335
Cs	301.8	505	1.324
Cu	1356.2	3157	1.478
Ag	1234	2726	1.449
Au	1336.2	3105	1.477
Mg	924.2	2170	1.483
Zn	692.7	1660	1.495
Cd	594.2	1394	1.482
Hg	234.3	557	1.490
Al	933.3	2449	1.553
Pb	600.6	1143	1.376
Fe	1809	3720	1.412
Co	1765	3736	1.426
Ni	1726	4032	1.480
			Av :1.427

The average —1.427 — is near the value of $\sqrt{2}$ in the above equations of viscosity coefficient, with which it is thus simplified. The equation (4) becomes :

$$\eta = \frac{R}{M}\frac{\rho T}{\nu_s} e^{E/RT} \tag{5}$$

---

[3] N.F. Mott , *Proc. Roy. Soc.*, **146**, 465 (1934).

[4] K. Jellinek, "Lehrbuch der physikalischen Chemie", II, Stuttgart, 1928, p. 232.

[5] "American Institute of Physics Handbook", New York, Toronto, London, 1957, p. 131.

[6] Landolt-Börnstein, "Physikalisch-Chemische Tabellen", IV Band, Technik, 2 Teil, Bandte 1 a (1963), b (1964), c (1965).

In the table 2 there are the $e^{L/3RT_m}$ values for some elements without normal metallic character. As we expected, the results have considerable deviations from the average in table 1.

Table 2

The ν_s/ν ratio for the abnormal metals

Element	T_m, °K	L, cal/g atom	$e^{L/3RT_m}$
Ga	303.0	1338	2.098
Sn	505.1	1676	1.745
Sb	903.7	4797	2.437
Bi	544.2	2510	2.168

The viscosity coefficients of these elements cannot be expressed by the equation (5) but only in the more elaborate equation :

$$\eta = \frac{R}{\gamma M}\,\frac{\rho T e^{L/3RT_m}}{\nu_s}\,e^{E/RT}, \tag{6}$$

where for each element is introduced the correction given by the peculiar exponential value.

The frequency ν_s for the corresponding solid metal is to be deduced with sufficient accuracy according to the well-known Lindemann's relation[7] :

$$\nu_s = 2.8 \times 10^{12}\sqrt{\frac{T_m}{M V_m^{2/3}}}, \tag{7}$$

where T_m is, as above, the melting temperature while V_m is the atomic volume of the solid substance at this temperature.

Substituting ν_s in equations (5) and (6), we obtained successively :

$$\eta = 3.57 \times 10^{-13}\,\frac{R V_m^{1/3}}{M^{1/2} T_m^{1/2}}\,\rho\, T e^{E/RT} \tag{8}$$

for meltings of the normal metals, and

$$\eta = 3.57 \times 10^{-13}\,\frac{R V_m^{1/3}}{\gamma\, M^{1/2}\, T_m^{1/2}}\,e^{L/3RT_m}\,\rho T e^{E/RT} \tag{9}$$

for meltings of the abnormal metals.

---

[7] F.A. Lindemann, *Phys. Ztschr.*, **11**, 609 (1910).

RESULTS AND DISCUSSIONS

In order to verify equations (8) and (9), it is necessary to know the density ρ function of temperature and the activation energy E.

In most cases, the densities are specified in the same papers in which are given the viscosity measurement results, and which are indicated in tables 3 and 4.

Table 3

Preexponential constants of the normal metals

Element	T_m, °K	V_m^*, cm³/gatom	$A \times 10^7$, cm²s⁻¹grad⁻¹		E, cal/gatom	Valability range, °K	Ref.
			Calcd.	Experim.			
Li	453.7	13.368	12.55	20.61	2286	456–559	8
Na	371	24.12	9.285	9.346	2280	376–644 ; 959	9
				8.841	2322	371–628	10
K	336.6	45.97	9.267	8.976	2046	342–441 ; 623	9
				13.13	1793	337–449 ; 626	10
Rb	312	56.50	6.974	7.146	1871	311–493	8
Cs	301.8	71.15	6.141	6.209	1798	301–484	8
Cu	1356.2	7.527	1.981	2.697	6744	1356–1573	11
				0.779	10,440		12
Ag	1234	10.90	1.804	1.893	7303	1273–1523	13,14
				1.946	7001	1233–1573	15
				1.975	6959		12
Au	1336.2	10.694	1.274	1.766	6846	1336–1573	16
Mg	924.2	14.716	4.852	1.683	7253	923–1173	17
				1.955	6923	925–998	13
				0.496	9415		18

---

[8] E.N. DA C. ANDRADE and E.R. DOBBS, *Proc. Roy. Soc.*, **211 A**, 12 (1952).

[9] C.T. EWING., J.A. GRAND and R.R. MILLER, *J. Amer. Chem. Soc.*, **73**, 1168 (1951); *J. Phys. Chem.*, **58**, 1086 (1954).

[10] Y.S. CHIONG, *Proc. Roy. Soc.*, **157 A**, 264 (1936).

[11] E. GEBHARDT, M. BECKER and S. SCHÄFER, *Z. Metallkde.*, **43**, 292 (1952).

[12] E. GEBHARDT and G. WÖRWAG, *Z. Metallkde.*, **42**, 358 (1951).

[13] K. GERING and F. SAUERWALD, *Z. anorg. Chem.*, **223**, 204 (1935).

[14] C.J. SMITHELLS, "Metals Reference Book", vol. II. ed 2, London, 1955, p. 639.

[15] E. GEBHARDT, M. BECKER and E. TRÄGNER, *Z. Metallkde.*, **44**, 379 (1953).

[16] E. GEBHARDT and G. WÖRWAG, *Z. Metallkde.*, **43**, 106 (1952).

[17] E. GEBHARDT, M. BECKER and E. TRÄGNER, *Z. Metallkde.*, **46**, 90 (1955).

[18] M.F. CULPIN, *Proc. Phys. Soc.*, **70B**, 1079 (1957).

Table 3 (continued)

Element	T_m, °K	V_m^*, cm^3/gatom	$A\times10^7$, cm^{2}s^{-1}grad^{-1}		E, cal/gatom	Valability range, °K	Ref.
			Calcd.	Experim.			
Zn	692.7	9.538	2.958	3.026	4442	723−973	13,14
				4.400	3811	692−973	19
Cd	594.2	13.367	2.725	4.022	3118	623−873	13,14
Hg	234.3	14.134	3.310	5.039	1192	253−353 ; 573	20
Al	933.3	10.502	4.096	4.209	4768	931−1173	19
				5.630	4175		21
Pb	600.6	18.758	2.235	2.061	3695	623−873	13,14
				2.819	3172	600−1173	17
				2.905	3240	600−873	22
Fe	1809	7.75	1.848	2.515	9787	1809−2023	23
				0.958	13,639	1823−1923	24
				0.897	13,959	1805−1973	25
Co	1765	7.071	1.766	1.155	11,517	1768−2023	23
				0.972	13,318	1773−1973	25
Ni	1726	7.048	1.788	1.521	11,017	1728−1973	23
				1.348	11,329	1773−1923	24
				1.382	11,296	1728−1923	25

The activation energy E can be obtained from the experimental data, plotting log $\eta/\rho\ T$ against $1/T$. For the temperature range which exceeds only with some hundred degrees the melting point, straight lines are to be obtained, as we can see in figures 1 and 2, whose slopes lead to the activation energies. In more expanded temperature range, like in the case of Na and K, abnormal metallic elements and Hg, a slight departure from the linearity takes place. In these cases, we take the temperature ranges closer to the melting temperature, where the applicability of the cell pattern, on which our equations are based, is justified; beyond this range, the activation energy increases.

---

[19] E. Gebhardt and K. Detering, *Z. Metallkde.*, **50**, 379 (1959).

[20] "Handbook of Chemistry and Physics", ed. 41, 1959−1960.

[21] E. Gebhardt, M. Becker and S. Dorner, *Z. Metallkde.*, **44**, 510 (1953).

[22] E. Gebhardt and K. Köstlin, *Z. Metallkde.*, **48**, 636 (1957).

[23] G. Cavalier, *Compt. rend.*, **256**, 1308 (1963).

[24] H. Schenck, M.G. Frohberg and K. Hoffmann, *Arch. Eisenhuettenw.*, **34**, 93 (1963).

[25] H. Hiebler and H. Trenkler, *Berg- u. Hüttenmännische Monatshefte*, **112**, 150 (1967).

In order to verify the valability of equations (8) and (9), we calculated out of the corresponding physical magnitudes the preexponential

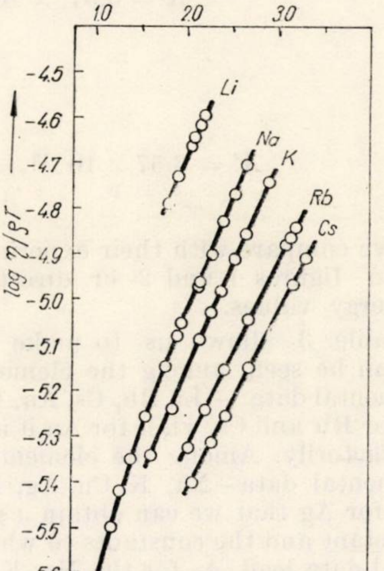

Fig. 1. — Dependence of log $\eta/\rho\, T$ on $1/T$ for the alkali metals.

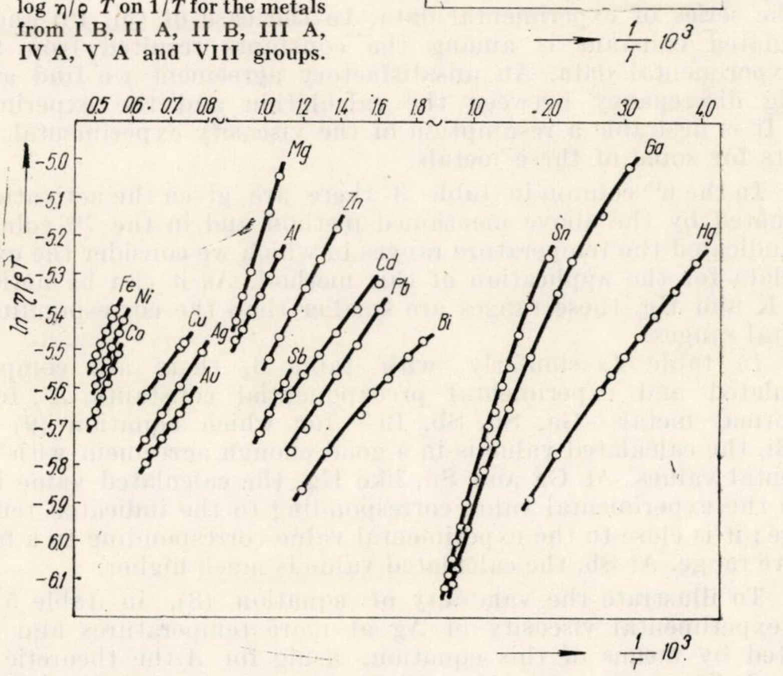

Fig. 2. — Dependence of log $\eta/\rho\, T$ on $1/T$ for the metals from I B, II A, II B, III A, IV A, V A and VIII groups.

constants :

$$A = 3.57 \times 10^{-13} \frac{RV_m^{1/3}}{M^{1/2}\, T_m^{1/2}} \tag{8'}$$

and

$$A' = 3.57 \times 10^{-13} \frac{RV_m^{1/3}}{\gamma M^{1/2}\, T_m^{1/2}} e^{L/3RT_m} , \tag{9'}$$

which we compare with their experimental values, that can be obtained either in figures 1 and 2 or directly, from the viscosity and activation energy values.

Table 3 allows us to make this comparison for normal metals. As it can be seen, among the elements for which we have one series of experimental data — Li, Rb, Cs, Au, Cd, Hg — there is a very good agreement for Rb and Cs, while for Au it is acceptable and for Li, Cd and Hg — unsatisfactorily. Among the elements for which we have more series of experimental data—Na, K, Cu, Ag, Mg, Zn, Al, Pb, Fe, Co, Ni — there is only for Ag that we can obtain a good agreement between the calculated constant and the constants to which the three series of available experimental data lead. As for the Na, K, Zn, Al, Ni, the calculated constant is in good or in satisfactory agreement only with that obtained from one of the series of experimental data. In the case of Cu, Pb and Fe, the calculated constant is among the constants resulted from the series of experimental data. An unsatisfactory agreement we find at Co and a big discrepancy between the calculation and the experiment — at Mg. It is desirable a resumption of the viscosity experimental measurements for some of these metals.

In the 6th column in table 3 there are given the activation energy evaluated by the above mentioned method and in the 7th column there are indicated the temperature ranges in which we consider the experimental data for the application of this method. As it can be noticed, with Na, K and Hg, these ranges are smaller than the corresponding experimental ranges.

In table 4, similarly with table 3, there are compared the calculated and experimental preexponential constants A', for several abnormal metals—Ga, Sn, Sb, Bi — for which equation (9) is valid. At Bi, the calculated value is in a good enough agreement with the experimental values. At Ga and Sn, like Hg, the calculated value is smaller than the experimental value corresponding to the indicated temperature range; it is close to the experimental value corresponding to a far temperature range. At Sb, the calculated value is much higher.

To illustrate the valability of equation (8), in table 5 we give the experimental viscosity of Ag at more temperatures and that calculated by means of this equation, using for A the theoretic value in table 3. The agreement between the two sets of values in the last two columns is good.

There is to be mentioned at least, that for the normal metals, the melting atomic volume V_m being nearly equal to the limiting atomic volume in the Bathschinski's equation, may be deduced from the atomic radii too :

$$V_m = 6.02\ \mathrm{N}r^3,$$

as it was established in the previous work.[1]

Table 4

Preexponential constants for abnormal metals

Element	T_m, °K	V^*_m, cm³/g atom	$\frac{\nu_s}{\nu}$	$A \times 10^7$, cm²s⁻¹ grad⁻¹ Calcd.	$A \times 10^7$, cm²s⁻¹ grad⁻¹ Experim.	E, cal/g atom	Valability range, °K	Ref.
Ga	303.0	11.77	2.098	6.891	9.427	1497	325 – 432 ; 1373	[26]
Sn	505.1	17.53	1.745	3.886	4.588	2508	505 – 623 ; 1573	[11,15,22,27,28]
Sb	903.7	18.75	2.437	4.096	2.143 1.612	4457 4932	903 – 1023 975 – 1275	[22] [29,11]
Bi	544.2	21.58	2.168	3.756	3.483 3.039	2453 2573	544 – 633 ; 833 577 – 673 ; 873	[30] [31,11]

The V_m values in tables 3 and 4 are those we used in ref. [1] (tab. 4)

Table 5

The viscosity coefficients of silver

$A = 1.804 \times 10^{-7}$ (cm²s⁻¹ grad⁻¹) ; $E = 7{,}303$ (cal/gatom)

T, °K	ρ, g/cm³	$\eta \times 10^2$ Poise Experim.	$\eta \times 10^2$ Poise Calcd.
1273.1	9.26	3.89	3.82
1323.1	9.22	3.62	3.54
1373.1	9.18	3.39	3.31
1423.1	9.135	3.18	3.11
1473.1	9.09	2.99	2.93
1523.1	9.05	2.83	2.78

Starting with the equation (1), Eyring[2] obtained in another way his well-known viscosity coefficient expression :

$$\eta = 1.09 \times 10^{-3} \frac{M^{1/2}\ T^{3/2}}{\Delta E_{\mathrm{vap}}\ V^{2/3}}\ \mathrm{e}^{E/RT}\ , \tag{10}$$

---

[26] K.E. Spells, *Proc. Phys. Soc.*, **48**, 299 (1936).

[27] E. Gebhardt, M. Becker and H. Sebastian, *Z. Metallkde.*, **46**, 669 (1955).

[28] E. Gebhardt, M. Becker and K. Köstlin, *Z. Metallkde.*, **47**, 684 (1956).

[29] A. Bienias and F. Sauerwald, *Z. anorg. Chem.*, **161**, 51 (1927).

[30] E. Gebhardt and K. Köstlin, *Z. Metallkde.*, **48**, 601 (1957).

[31] F. Sauerwald and K. Töpler, *Z. anorg. Chem.*, **157**, 117 (1926).

where ΔEvap is the vaporization heat. The other magnitudes have known significance. The equation (10), as the equations (8) and (9), has only one adjustable parameter : the activation energy E. The preexponential constant A has now the expression :

$$A = 1.09 \times 10^{-3} \frac{M^{1/2}}{\Delta E\text{vap}},$$

which obviously differs from the A and A' in equations (8) and (9). The activation energy may be evaluated by plotting log $\eta V^{2/3} \; / T^{3/2}$ against $1/T$, as the usual method. The calculated activation energy is also different from that evaluated by means of the equations (8) and (9).

To illustrate the applicability of Eyring's equation, we give in the table 6 the results for several metals. Comparing them with the corresponding data in the tables 3 and 4, we can see that the equation (10) expresses the preexponential constant satisfactorily, but less correct than the equations (8) and (9). The last ones have one advantage more : the fusion temperatures, which are in preexponential constant expressions, are much more available and more correctly known than the vaporization heats. As far as the melting atomic volume is concerned, it can be evaluated from the atomic radii too, as we mentioned above.

Table 6

The preexponential constants and activation energies calculated by means of Eyring's equation

Element	ΔE_{vap}, cal/gatom	A × 10^8, $g^{1/3}$ cm s^{-1} grad$^{-3/2}$		E, cal/gatom
		Calcd.	Experim.	
Rb	17,330[6]	2.997	2.340	2294
Ag[13,14]	60,000[6]	0.833	0.589	8849
Mg[17]	32,000[6]	2.001	0.292	8766
Hg	13,981[6]	3.222	4.167	1495
Pb[13,14]	41,914[6]	1.069	0.973	4472
Bi[31,14]	43,747[6]	1.023	0.801	4104
Co[23]	91,400[6]	0.605	0.281	13,842

Da C. Andrade[32] was the first who introduced in the viscous flow treatment the vibration of the liquid particles with constant frequencies, comparable with those of solid particles. He suggests the following relation for the viscosity calculation of simple liquids, at the melting point :

$$\eta_M = 5.7 \times 10^{-4}(A T_M)^{1/2} \, V_M{}^{-2/3} \tag{11}$$

A is atomic weight, while T_M and V_M are melting temperature and volume. In the numerical part there is contained the Lindemann's constant, taken by Andrade as 3.1×10^{12}. The equation (11) is obeyed by six normal metals and Ar; the abnormal metals — Sb, Bi and Ga — have deviations too.

---

[32] E.N. da C. Andrade, *Phyl. Mag.* **17**, 497 (1934) ; *Proc. Roy. Soc.*, **215 A**, 36(1952) ; ***Endeavour***, **13**, 117 (1954).

Starting from the Eyring's significant structures theory[33] and ascribing the vibratory motion to a fraction of the whole number of liquid particles and the translation motion for the rest, Misra[34] obtained a new equation for the liquid viscosity coefficient:

$$\eta = \eta_1 \left(\frac{T}{T_1} \right)^{1/2} \frac{1 - e^{-2\theta\left(T_1^{1/2} - T_m^{1/2}\right)}}{1 - e^{-2\theta\left(T^{1/2} - T_m^{1/2}\right)}}, \tag{12}$$

in which T_m and θ are two adjustable constants; T_m represents the temperature at which all the molecules have only vibratory motion and is slightly less than the ordinary melting point.

The equation (12) may be reduced to a simpler one, with only one adjustable parameter, T_m. The results for Na, Hg, Sn and Sb prove that the Misra's equation leads to values which are in good agreement with experimental ones.

Nachtrieb[35] also used the particle vibration in the treatment of the diffusion in liquid metals, to obtain a relation for calculating the melting selfdiffusion coefficient. More details are to be seen in the original work.

---

[33] H. Eyring, *Proc. Nat. Acad. Sci., Washington*, **44**, 683 (1958).

[34] S.C. Misra, *Indian J. Pure Appl. Phys.*, **7**, 289 (1969).

[35] N.H. Nachtrieb, *Adv. Phys.*, **16**, 309 (1967).

Revue Roumaine de Chimie, **19**, *9*, 1417 – 1427 (1974)

Revue Roumaine de Chimie, 19, 9, 1429–1433 (1974)

SUR LA VISCOSITÉ DES SYSTÈMES MIXTES : EAU-MONOÉTHYLÈNEGLYCOL, EAU-MONOÉTHANOLAMINE ET EAU-DIMÉTHYLESULFOXYDE

L'INFLUENCE DE LA TEMPÉRATURE ET DES SELS SUR LA VISCOSITÉ DE CES SYSTÈMES

ORTANSA LANDAUER, G. COSTEANU et CORNELIA MATEESCU
Chaire de Chimie Physique, Institut Polytechnique, Bucarest, 132, Calea Griviţei

Reçu le 1er novembre

Les auteurs ont étudié la viscosité des systèmes mixtes : eau-monoétylèneglycol, eau-monoéthanolamine et eau-diméthylesulfoxyde à différentes concentrations et à des températures de 20° à 50°. On a tiré des conclusions sur la variation de la viscosité avec la température, ainsi que sur l'influence des sels dissous.

Les solvants mixtes sont souvent utilisés comme milieu de réaction pour l'étude de l'influence de la constante diélectrique et de la viscosité du solvant sur la vitesse de réaction. Ils sont également utilisés comme agents de réfrigération.

La viscosité étant une des propriétés les plus importantes des liquides, parce qu'elle permet de tirer des conclusions sur leur structure, il nous a semblé intéressant d'étudier les systèmes mixtes mentionnés plus haut.

Les substances étudiées par nous, bien purifiées par distillation fractionnée, ont les caractéristiques suivantes :

	P. ébull°C	n_{20}^{D}
Monoéthylèneglycol-MEG	197,4	1,4318
Monoéthanolamine -MEA	171,0	1,4539
Diméthylesulfoxyde-DMSO	189,0	1,4785

Les mesures des viscosités ont été réalisées avec un viscosimètre Ubbelohde pour différentes concentrations des systèmes eau-constituant organique, aux températures de 20°, 30°, 40° et 50°.

Pour le calcul des viscosités en valeurs absolues, évaluées en cP, nous avons déterminé aussi les densités des différents mélanges aux températures déjà mentionnées.

Les énergies d'activation de l'écoulement visqueux ont été calculées par la méthode des moindres carrés.

Les viscosités des mélanges des systèmes étudiés par nous, ainsi que les énergies d'activation sont réunies dans les tableaux 1, 2 et 3.

Tableau 1

Valeurs des viscosités, en cP, et des énergies d'activation du système eau-MEG

% moles MEG	η_{20°	η_{30°	η_{40°	η_{50°	$E_{\text{cal/mole}}$
0	1,0050	0,8178	0,6852	0,5829	3522
3,76	1,3430	1,0560	0,8523	0,7163	3873
7,44	1,7245	1,3153	1,0675	0,8672	4207
12,09	2,2577	1,6932	1,3435	1,0896	4519
17,55	2,9523	2,1911	1,7037	1,3668	4842
32,20	5,1782	3,7290	2,1982	2,1747	5453
55,63	9,5731	6,6367	4,8381	3,6624	6312
100	19,7877	13,2715	9,1299	6,6663	6858

Tableau 2

Valeurs des viscosités, en cP, et des énergies d'activation du système eau-MEA

% moles MEA	η_{20°	η_{30°	η_{40°	η_{50°	$E_{\text{cal/mole}}$
0	1,0050	0,8178	0,6852	0,5829	3522
6,99	1,9529	1,4770	1,1766	0,9730	4355
16.54	4,2432	3,0586	2,2868	1,7605	5388
30,43	9,8933	6,6078	4,6543	3,4012	6698
62,04	23,1135	13,6476	9,3262	6,5925	7801
80,30	35,8537	15,7240	10,5436	7,2190	7959
100	24,0692	14,7613	9,9719	7,0105	7715

Tableau 3

Valeurs des viscosités, en cP, et des énergies d'activation du système eau-DMSO

% moles DMSO	η_{20°	η_{30°	η_{40°	η_{50°	$E_{\text{cal/mole}}$
0	1,0050	0,8178	0,6852	0,5829	3522
2,75	1,2907	1,0194	0,8362	0,7037	3830
5,94	1,6303	1,2689	1,0277	0,8485	4084
9,65	2,0928	1,5976	1,2401	1,0380	4432
14,08	2,6734	2,0035	1,5578	1,2616	4691
26,28	4,1166	3,0141	2,2831	1,8038	5183
35,26	4,3892	3,2413	2,4560	1,8835	5154
47,82	3,9017	2,9239	2,3344	1,9335	4543
100	2,2255	1,8180	1,5553	1,3110	3319

Dans les tableaux 4 et 5 sont rassemblées les viscosités du système eau-MEG en présence de 0,5 M de chlorure et d'iodure de sodium.

Tableau 4

Valeurs des viscosités, en cP, et des énergies d'activation du système eau-MEG en présence de 0,5 M NaCl

% moles MEG	η_{30°	η_{40°	η_{50°	$E_{\text{cal/mole}}$
0	0,8628	0,7215	0,6183	3143
3,76	1,0289	0,9009	0,7600	2953
7,44	1,4102	1,1307	0,9268	4086
12,09	1,8052	1,4368	1.1663	4240
32,20	4,1059	3,0759	2,3775	5322
55,63	7,0545	5,5114	4,1263	6244

Tableau 5

Valeurs des viscosités, en cP, et des énergies d'activation du système eau-MEG en présence de 0,5 M NaI.

% moles MEG	η_{30°	η_{40°	η_{50°	$E_{\text{cal/mol}}$
0	0,8336	0,7032	0,6041	3129
3,76	1,0013	0,9036	0,7508	3253
7,44	1,3423	1,0857	0,8974	3898
12,03	1,8002	1,3959	1,1317	4635
17,55	2,2098	1,7860	1,4060	4393
32,20	3,8373	3,1409	2,2649	5111
55,63	7,0626	5,2034	3,9401	6093
100	14,5806	11,6554	7,8113	6054

La variation de la viscosité des mélanges liquides est en rapport principalement avec le changement de volume au moment du mélange. C'est pourquoi il nous a semblé intéressant de calculer les volumes molaires des systèmes eau-MEG et eau-MEA à 20°, dont les valeurs sont réunies dans les tableaux 6 et 7.

Tableau 6

Valeurs des densités et des volumes molaires du système eau-MEG à 20°

X_{MEG}	$d_{20^\circ \text{g/ml}}$	V cm^3
0,035	1,0124	19,416
0,074	1,0266	20,727
0,120	1,0402	22,431
0,176	1,0551	24,390
0,322	1,0776	29,868
0,556	1,0976	38,725

Tableau 7

Valeurs des densités et des volumes molaires du système eau-MEA à 20°

X_{MEA}	$d_{20^\circ \text{g/ml}}$	V cm^3
0,070	1,0070	20,863
0,165	1,0179	24,666
0,304	1,262	30,302
0,620	1,0255	42,975
0,803	1,0403	50,556

Nous avons calculé aussi les volumes partiels molaires d'excès des systèmes eau-MEG et eau-MEA en fonction de la fraction molaire, dont les valeurs sont portées sur les figures 1 et 2.

On voit que $\overline{V}^E_{\mathrm{MEA}} > \overline{V}^E_{\mathrm{MEG}}$.

L'influence de la composition des solvants mixtes sur l'énergie d'activation de l'écoulement visqueux est représentée graphiquement dans les fig. 3, 4 et 5.

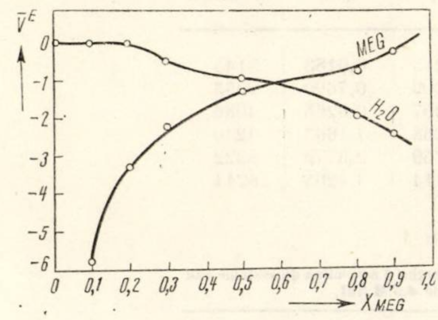

Fig. 1. — Volumes partiels molaires d'excès des mélanges eau-MEG en fonction de X_{MEG}.

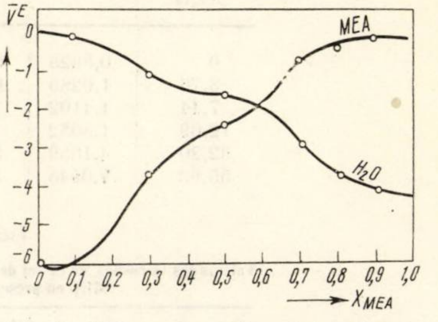

Fig. 2. — Volumes partiels molaires d'excès des mélanges eau — MEA en fonction de X_{MEA}.

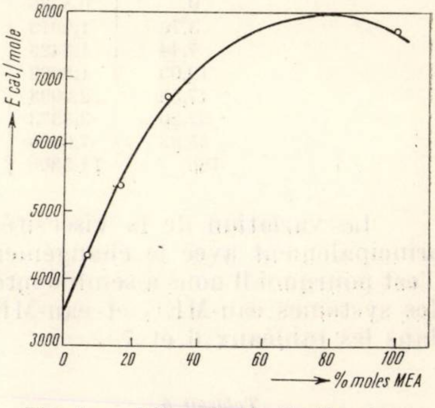

Fig. 4. — L'énergie d'activation du système eau-MEA en fonction de X_{MEA}.

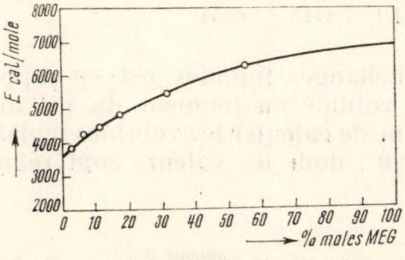

Fig. 3. — L'énergie d'activation du système eau-MEG en fonction de X_{MEG}.

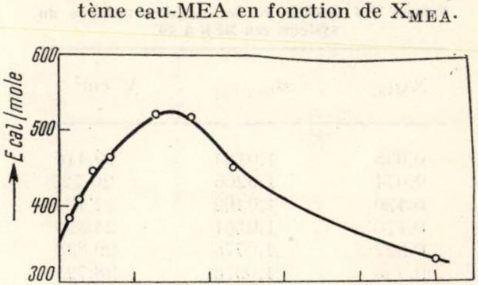

Fig. 5. — L'énergie d'activation du système eau-DMSO en fonction de X_{DMSO}.

On voit sur les tableaux 1, 2 et 3 que la viscosité du système eau-MEG croît régulièrement avec la concentration du constituant organique du solvant mixte, alors que pour les systèmes eau-MEA et eau-

DMSO elle passe par un maximum, d'autant plus marqué que la température est plus basse. Ce maximum est attribué à des interactions assez fortes entre les molécules de l'eau et les molécules du constituant organique du système. Une élévation de température, qui favorise l'agitation thermique, diminue dans tous les cas ces interactions.

L'existence de ces interactions dans le système eau-DMSO a été mise en évidence aussi par d'autres méthodes, à savoir la densité d'excès, l'indice de réfraction [1,2] et la cinétique chimique.[3]

Nous pouvons donc admettre que le système eau-MEA doit présenter également, au maximum de la viscosité, une structure privilégiée à laquelle on attribue le maximum de la courbe $E=f\ (X_{\mathrm{MEA}})$.

La variation toujours croissante de la courbe $E=f\ (X_{\mathrm{MEG}})$, du système eau-MEG, ne justifie pas l'existence d'une structure spécifique des molécules, comme on l'admet pour le système eau-MEA.

On voit, d'autre part, d'après l'allure des courbes $\bar{V}^E=f(X)$ qu'il y a une différence assez nette entre les deux systèmes.

On constate aussi, d'après les valeurs des énergies d'activation, que les interactions eau-MEA sont bien plus fortes que les interactions eau-MEG ; on a donc $E_{\mathrm{MEA}} > E_{\mathrm{MEG}}$.

En admettant que seules les molécules libres rendent compte de l'écoulement visqueux, et que d'après Miller[4,5] ces molécules représentent «le volume libre», on peut supposer qu'au maximum de la viscosité il y a un très petit nombre de molécules libres dans le système.

La viscosité toujours croissante du système eau-MEG pourrait être attribuée à une augmentation des molécules liées.

La présence des sels-NaCl et NaI — dans le système eau-MEG ne modifie pas sensiblement la viscosité du système.

---

[1] J. M. G. Cowie et P. M. Toporowski, *Canad. J. Chem.*, **39**, 2240 (1961).
[2] M. R. Reynaud, *Compt. rend.*, **266** C, 489 (1968).
[3] G. Costeanu et O. Landauer, *Rev. Roumaine de Chim.*, **17**, 1347 (1972).
[4] A. A. Miller, *J. Chem. Phys.*, **38**, 1568 (1963).
[5] A. A. Rizk, *Z. Phys. Chem. (Leipzig)*, **246**, 396 (1971).

Revue Roumaine de Chimie, **19**, **9**, 1435–1439 (1974)

HIGH-TEMPERATURE THERMODYNAMIC DATA FOR SOME URANIUM OXIDES WITHIN THE RANGE $UO_{2.25}-UO_{2.60}$

D.I. MARCHIDAN and SPERANȚA TĂNĂSESCU
Institute of Physical Chemistry
str. Galati 31, Bucharest

Received April 22, 1974

The two-phase region $U_4O_9 + U_3O_{8-y}$ is investigated. The electromotive force measurements on solid electrolyte galvanic cells have been carried out in order to obtain thermodynamic data for $UO_{2.46}$ and $UO_{2.50}$ uranium oxides. The partial molar free energies, enthalpies and entropies of solution of oxygen in uranium oxides and the corresponding integral quantities as a function of temperature, as well as the equilibrium pressures of oxygen over the oxides have been calculated.

INTRODUCTION

The phase relationships in the uranium-oxygen system have been studied by many scientists. But, owing to the complexity of this system the numerical information is still incomplete.

A consistent set of thermodynamic values for nonstoichiometric uranium oxides and more data on the limits of the UO_{2+x}, U_4O_9, U_3O_{8-y} phases are required.

In previous papers[1-3] we have related the values of the thermodynamic properties of some uranium oxides with nonstoichiometric compositions which are found disproportioned in two phases within certain temperature ranges. The method used was that of electromotive force measurements on high temperature galvanic cells with solid electrolyte.

The present paper extends the study on some nonstoichiometric uranium oxides that are part of the two-phase region $U_4O_9 + U_3O_{8-y}$. Thus, the oxides $UO_{2.46}$ and $UO_{2.50}$ were studied within a 1123–1373 K temperature range. The determinations were made with a high-temperature galvanic cell of the type :

Fe, wüstite/(0.85 ZrO_2 + 0.15 CaO) / uranium oxide.

---

[1] D.I. Marchidan and S. Matei, *Rev. Roumanie Chim.*, **17**, 195 (1972).

[2] D.I. Marchidan and S. Matei, *Rev. Roumaine Chim.*, **17**, 9 (1972).

[3] D.I. Marchidan and S. Matei-Tănăsescu, *Rev. Roumaine Chim.*, **18**, 1681 (1973).

EXPERIMENTAL

The cell assembly consisting of the electrolyte tablet between the two electrode tablets was inserted into a quartz cell, the form and construction of which have been previously shown[4,5].

The electromotive force measurements were carried out in a vacuum installation at the residual gas pressure of about 133.322×10^{-6}N.m^{-2}. The apparatus, the experimental procedure and the techniques of preparing the tablets were also minutely described in the above mentioned papers[4,5].

RESULTS AND DISCUSSIONS

The nonstoichiometric oxides $UO_{2.46}$ and $UO_{2.50}$ were studied in the temperature range of 1123–1373 K. The electromotive force values for these compositions were practically identical indicating the presence of a two-phase region.

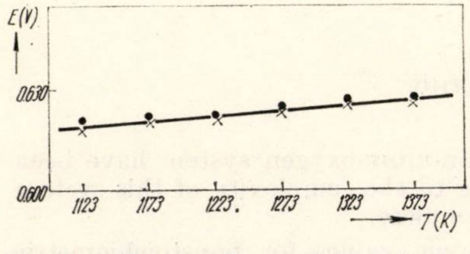

Fig. 1. — The variation of EMF with the temperature for $UO_{2.46}$ and $UO_{2.50}$

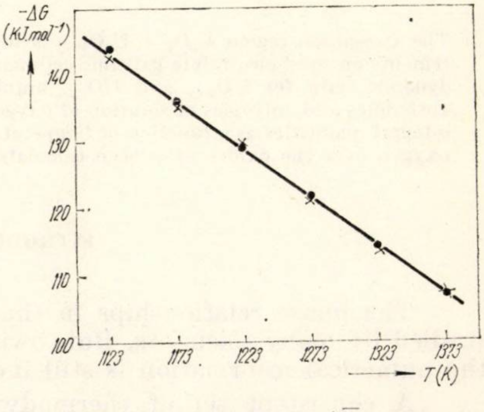

Fig. 2. — The variation of $\Delta\overline{G}_{O_2}$ with the temperature for $UO_{2.46}$ and $UO_{2.50}$

The partial molar free energy of oxygen in equilibrium with the uranium oxide $\Delta\overline{G}_{O_2}$ may be calculated by combining equations (1) and (2):

$$\Delta G_{cell} = -4\mathscr{F}E \tag{1}$$

$$\Delta G_{cell} = 2\,\Delta G^\circ \text{ wüstite } - \Delta\overline{G}_{O_2} \tag{2}$$

where ΔG° wüstite is the standard Gibbs free energy of formation of wüstite in equilibrium with iron and ΔG_{cell} is the measured free energy change of the cell.

---

[4] D.I. Marchidan and S. Matei, *Rev. Roumaine Chim.*, **15**, 1491 (1970).

[5] D.I. Marchidan and S. Matei, *Studii şi Cercetări Chim. Acad. R.S.R.*, **18**, 617 (1970).

Figure 2 illustrates that the shape of the curve obtained when $\Delta\overline{G}_{O_2}$ is plotted against T for the two-phase region is the same for these oxides. As the phase diagram of uranium-oxygen system[6,7] shows, this is the two-phase region $U_4O_9 + U_3O_{8-y}$. Considering the components in uranium oxide of any composition as UO_2 and O_2, the composition of the oxide is determined by the mole faction N_{UO_2} or N_{O_2}. The evaluation of the relative integral molar free energy ΔG and of the relative integral molar free energy per gram atom of uranium was made numerically from equation :

$$\Delta G = (1-N_{O_2})\int_{O}^{N_{O_2}} \frac{\Delta\overline{G}_{O_2}}{(1-N_{O_2})^2}\, dN_{O_2} \tag{3}$$

Table 1

The thermodynamic data for $UO_{2.46}$

Temp. K	$-\Delta\overline{G}_{O_2}$ (KJ.mol.$^{-1}$)	$-\Delta G$ (KJ.mol^{-1})	$-\Delta G/N_{UO_2}$ (KJ/g. atom uranium)	log P_{O_2} (N. m^{-2})
1123	142.825	26.893	33.079	1.624
1173	136.113	25.452	31.306	0.996
1123	129.097	24.140	29.692	0.448
1273	121.925	22.799	28.042	−0.063
1323	114.369	21.386	26.304	−0.550
1373	107.968	20.189	24.832	−0.958

$-\Delta\overline{H}_{O_2}$(KJ.mol^{-1})=305.038 $-\Delta S_{O_2}$(KJ.K^{-1}mol^{-1})=0.1435

$-\Delta H$(KJ.mol^{-1})=57.011 $-\Delta S$(KJ.K^{-1}mol^{-1})=0.02682

$-\Delta H/N_{UO_2}$(KJ.mol^{-1})=70.124 $-\Delta S/N_{UO_2}$(KJ.K^{-1}mol^{-1})=0.144

Table 2

The thermodynamic data for $UO_{2.50}$

Temp. K	$-\Delta\overline{G}_{O_2}$ (KJ.mol^{-1})	$-\Delta G$ (KJ.mol^{-1})	$-\Delta G/N_{UO_2}$ (KJ/g.atom uranium)	log P_{O_2} (N.m^{-2})
1123	142.670	28.534	35.667	1.570
1173	135.687	27.137	33.521	0.977
1223	128.904	25.781	32.226	0.440
1273	121.344	24.268	30.336	−0.087
1323	113.984	22.796	28.496	−0.566
1373	107.390	21.478	26.847	−0.980

$-\Delta H_{O_2}$(KJ.mol^{-1})=302.612 $-\Delta S_{O_2}$(KJ.K^{-1}mol^{-1})=0.1422

$-\Delta H$(KJ.mol^{-1})=60.522 $-\Delta S$(KJ.K^{-1}mol^{-1})=0.0284

$-\Delta H/N_{UO_2}$(KJ/g atom uranium) = 75.665 $-\Delta S/N_{UO_2}$(KJ.K^{-1} mol^{-1})=0.0355

---

[6] L.E.J. ROBERTS and A. WALTER, *J. Inorg. Nuclear Chem.*, **22**, 213 (1961).

[7] M.H. RAND and O. KUBASCHEWSKI, "The Thermochemical Properties of Uranium Compounds" Oliver and Boyd, Edinburgh, 1963, p. 26.

In tables 1 and 2 the thermodynamic data for $UO_{2.46}$ and $UO_{2.50}$ uranium oxides are presented. One observes that similar to the two-phase region $UO_{2+x}+U_4O_9$, the values of partial molar free energies practically do not change with composition.

The data on the thermodynamic properties of $UO_{2.28}$, $UO_{2.30}$, $UO_{2.371}$, $UO_{2.53}$ uranium oxides were reported in previous papers[1,3]. The values obtained for $UO_{2.46}$ and $UO_{2.50}$ are practically identical with those obtained for the above mentioned oxides indicating that the six oxides are part of the same two-phase region.

To ilustrate this, the values of relative partial molar free energy and of equilibrium oxygen partial pressure as a function of composition at 1073 K are plotted in fig. 3.

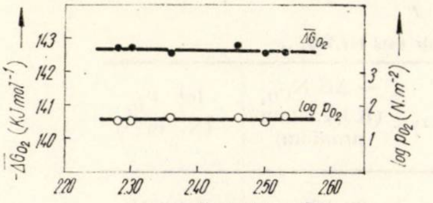

Fig. 3. — The variation with uranium oxide composition of relative partial molar free energy $\Delta\overline{G}_{O_2}$ and equilibrium oxygen partial pressure at 1073 K.

A considerable number of experimental measurements have been made by different methods on the two-phase regions and on their phase limits.

A concluding discussion on the $U_4O_9 - U_3O_8$ two-phase region may characterize this region. Although the upper and lower limits are not yet precisely known, the results for the two-phase regions tend to be in better agreement than those for single-phase regions because very small composition differences do not influence the thermodynamic properties.

Rand and Kubaschewski[7] studied the $U_4O_9-U_3O_8$ region from 298—1395 K. They accepted the results of Roberts and Walter [6] who had showen that the U_4O_9 phase decomposes peritectically at 1396 ± 5 K into U_3O_8 and UO_{2+x}.

Later results by Markin[8] and by Kiukkola[9] are in excellent agreement up to 1373 K. The region close to U_4O_9 has been studied by Kiukkola, who interprets his results as showing the U_4O_9 phase persisting up to 1488 K.

Kiukkola places the upper limit of the U_4O_9 phase at $O/U = 2.250$ because the results regarding this composition and $O/U = 2.300$ were identical, and in excellent agreement with Roberts and Walter's, who measured the identical pressures for the compositions $O/U = 2.250$, 2.257, 2.279 and 2.303. Blackburn's rather scattered results[10] for this phase limit determined by the interpolation of the effusion-cell measurements give higher values.

---

[8] T.L. Markin, L.E.J. Roberts and A. Walter, "Thermodynamics of Nuclear Materials", Ed. IAEA, Vienna, 1962, p. 693.

[9] K. Kiukkola, *Acta Chem. Scand.*, **16**, 327 (1962).

[10] P.E. Blackburn, *J. Phys. Chem.*, **62**, 897 (1958).

The lower limit of the U_3O_{8-y} phase is not much affected by the changes in temperature from 870 to 2000 K and it was reported by Biltz and Müller[11] as $UO_{2.607}$ at 1273 K and by Blackburn[10] as $UO_{2.607}$ to $UO_{2.616}$ at 1125 K to 1399 K, as suggested by the equilibrium measurements.

The results of Markin and Roberts indicate that the limiting composition is constant from 1396 to 873 K and probably nearly so from 1723 to 873. We have accepted the limit as $UO_{2,61}$ from 873 to 1473K[8].

The thermodynamic values given by Rand and Kubaschewski for this region are : At 298–1395 K ($U_4O_9-UO_{2.6}$) :
$\Delta\bar{H}_{O_2} = -304.595$ KJ. mol.$^{-1}$; $\Delta\bar{S}_{O_2} = -0.147$ KJ. mol^{-1} grad^{-1} and at 1395 – 1750 K ($UO_{2+x}-UO_{2.6}$) :
$\Delta\bar{H}_{O_2} = -313.381$ KJ.mol^{-1}; $\Delta\bar{S}_{O_2} = -0.153$ KJ. mol.$^{-1}$ grad^{-1}

Markin's values were combined with earlier values to give (from 873 to 1395 K) :
$\Delta\bar{H}_{O_2} = -328.862$ KJ mol.$^{-1}$; $\Delta\bar{S}_{O_2} = -0.164$ KJ. mol.$^{-1}$ grad^{-1} which are in excellent agreement with Kiukkola's[9] values who finds(from 1073 to 1473 K) :
$\Delta\bar{H}_{O_2} = -322.586$ KJ mol.$^{-1}$; $\Delta\bar{S}_{O_2} = 0.161$ KJ. mol.$^{-1}$ grad^{-1}

Acomparison of these data to our values over $U_4O_9-UO_{2.6}$ region, shows that our results are close to Rand and Kubaschewski's data.

Anyway more data are required on partial molar quantities in the region close to U_4O_9 up to 1473 K and in U_3O_{8-y} region at all temperatures.

We wish to express our deep gratitude to Professor I.G. Murgulescu for his interest in our work and to C. Volcovici, for his help in the construction of equipment.

---

[11] W. BILTZ and H. MÜLLER, *Z. anorg. Chem.*, **163**, 257 (1927).

Revue Roumaine de Chimie, **19**, *9*, 1441–1445 (1974)

SPECTRAL STUDY OF DIOXOURANIUM (VI) COMPLEXES WITH AROMATIC SCHIFF BASES

N.S. BIRADAR and T.R. GOUDAR,
Department of Chemistry, Karnatak University, Dharwar-3, India

Received June 26, 1973

A few complexes of dioxouranium (VI) have been prepared with aromatic Schiff bases and characterised by the elemental analysis. With the aid of infrared spectra it has been shown that O—U—O bonds of UO$_2^2$ ion are linear. These complexes are non-electrolytes in DMF and appear to have coordination number six.

INTRODUCTION

In the previous paper on dioxouranium (VI) Schiff base adducts[1] it has been shown that the O-U-O bonds are almost linear. In this paper, we have extended the study to the other aromatic Schiff bases shown below (I—X). While this work was in progress a few papers appeared on the same subject.[2-8] Yamada and Takeuchi[2] have shown that dioxouranium (VI) forms adducts in which the *o*-hydroxy group is the donor.

The present paper deals with the synthesis and spectral studies of dioxouranium (VI) Schiff base adducts.

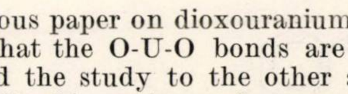

	R
I	H
II	CH_3
III	OCH_3
IV	Cl

---

[1] N.S. Biradar, T.R. Goudar, V.B. Mahale, V.H. Kulkarni and M.A. Pujar, *Proc. D.A.E. Chem. Symp.*, **1**, 321 (1970).

[2] S. Yamada and A Takeuchi, *Bull. Chem. Soc., Japan*, **42**, 2549 (1969) ; *Chem. Abstr.*, **72**, 27929 (1970).

[3] S.N. Poddar and N. Saha, *Indian J. Appl. Chem.*, **33**, 242 (1970).

[4] R.K. Mehta and R.K. Gupta, *Indian J. Chem.*, **9**, 1150 (1971).

[5] V.V. Zelentsov, I.A. Savich, and V.I. Spitsyn, *Chem. Abstr.*, **54**, 9593d (1960).

[6] A. Vanden Bergen, K.S. Murray and B.O. West, *Austral. J. Chem.*, **25**, 705 (1972).

[7] L. Cattalini, S. Degetto, M. Vidali and P.A. Vigato, *Inorg. Chim. Acta*, **6**, 173 (1972).

[8] V.G. Kulkarni, S.N. Ashtaputre and N.N. Sirmokadam, *J. Indian Chem. Soc.*, **49**, 111 (1972).

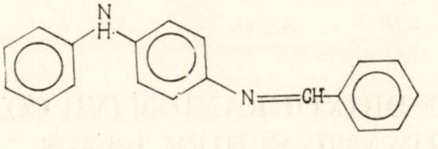

V

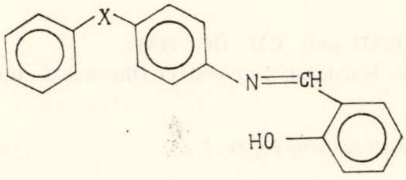

	X
VI	NH
VII	N=H

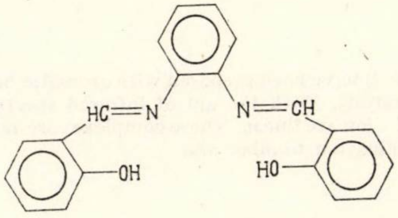

VIII

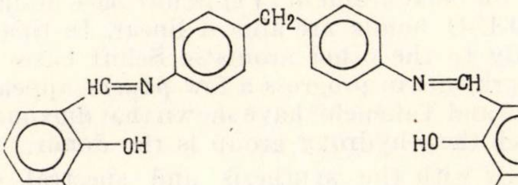

	R′
IX	H
X	$-OCH_3$

EXPERIMENTAL

The Schiff bases (I–X) were prepared according to the methods reported elsewhere.[9] Uranyl chloride in ethyl acetate was treated with a slight excess of Schiff base in the same solvent with vigorous shaking. Sufficient time was allowed for the complex to settle. The complex was filtered, washed free from the reagent and dried in vacuum over fused calcium chloride. The dry mass was powdered and extracted in a soxhlet apparatus with ethyl acetate and dried in vacuum over fused calcium chloride.

The complexes were analysed for their uranium, nitrogen and chloride contents.

PHYSICAL MEASUREMENTS

Conductance measurements were made using an ELICO, CM-82, conductivity bridge with a cell having cell constant 0.829 cm^{-1}, manufactured by Electronic and Industrial Instruments Co., Hyderabad. The solutions were prepared in DMF and diluted to the required strength (10^{-3}M).

The i.r. spectra of the ligands and the complexes were obtained on a Perkin Elmer infracord.

---

[9] N.S. BIRADAR and V.H. KULKARNI, *J. Inorg. Nucl. Chem.*, **33**, 2451; 3781 (1971).

RESULTS AND DISCUSSION

The elemental analyses (table 1) show that the Schiff base I—VII form the complexes of 1 : 2 stoichiometry whereas VIII—X form complexes of 1 : 1 stoichiometry.

Table 1

Elemental analysis of the complexes

Lig.N°	Comp.	N° Complex	% U	% N	% Cl
I	XI	$(C_{13}H_{11}NO)_2UO_2Cl_2$	32.70 (32.40)	3.71 (3.81)	9.79 (9.52)
II	XII	$(C_{14}H_{13}NO)_2UO_2Cl_2$	30.40 (30.80)	3.59 (3.67)	9.33 (9.17)
III	XIII	$(C_{14}H_{13}NO_2)_2UO_2Cl_2$	30.00 (29.60)	3.69 (3.44)	9.00 (8.79)
IV	XIV	$(C_{13}H_{10}ClNO)_2UO_2Cl_2$	30.10 (29.60)	3.37 (3.47)	8.94 (8.70)
V	XV	$(C_{19}H_{16}N_2)_2HO_2Cl_2$	26.12 (26.73)	2.98 (3.17)	8.10 (8.04)
VI	XVI	$(C_{19}H_{16}N_2O)_2UO_2Cl_2$	25.97 (25.79)	5.99 (6.12)	7.20 (7.26)
VII	XVII	$(C_{19}H_{15}N_3O)_2UO_2Cl_2$	25.32 (25.07)	9.11 (8.92)	7.71 (7.55)
VIII	XVIII	$(C_{20}H_{16}N_2O_2)UO_2Cl_2$	31.00 (31.37)	3.80 (3.70)	9.50 (9.38)
IX	XIX	$(C_{27}H_{22}N_2O_2)UO_2Cl_2$	30.92 (32.51)	3.74 (3.74)	10.15 (9.96)
X	XX	$(C_{29}H_{26}N_2O_2)UO_2Cl_2$	29.90 (30.20)	3.94 (3.59)	8.10 (8.29)

The values given in the parenthesis are calculated values.

All the complexes are intense coloured amorphous substances, insoluble in most of the organic solvents. These are soluble to a limited extent in DMF and DMSO. This limited solubility of the complexes in organic solvents did not permit the determination of the molecular weight. The molar conductance values determined in DMF at the concentration 10^{-3}M indicate that these are non-electrolytes in DMF.

The infrared frequencies along with their assignments are listed in table 2.

In the Schiff bases, the C=N stretch is reported[9] to occur in the region 1630—1600 cm^{-1}. We have assigned a strong band in the region 1620—1600 cm^{-1} to the C=N stretch in the case of Schiff bases I—VI and VIII—X. In the Schiff base VII one can expect to find the stretching frequencies due to C=N, N=N, and C=C. LeFevre and coworkers[10]

---

[10] a. C.N.R. Rao "Chemical Applications of Infrared Spectroscopy" Academic Press, London, 1963.
b. R.J.W. Le Fevre, M.F.O' Dwyer and R.L. Werner, *Austral. J. Chem.*, **6**, 341 (1953).

Table 2

Infrared frequencies (in cm^{-1}) of the dioxouranium (VI) complexes and their assignments

S. N°.	Assignments	XI	XII	XIII	XIV	XV	XVI	XVII	XVIII	XIX	XX
1.	CH	2940	2940	2940	2940	2940	2920	2920	2910	2910	2925
2.	C=N	1650 1600	1650 1600	1639 1608	1655 1610	1640 1600	1640 1600	1650 1570	1640 1600	1635 1600	1645 1600
3.	C=C	1550 1450	1550 1640	1548 —	1550 1525 1460	1525 1460	1520 1450	1525 1460	1525 1460	1545 1450	— 1460
4.	C–O	1280	1281	1279	1282 1260	1280	1270	1280	1280	1270	1300
5.	ν3	920 m	921m	925m	926m	920m	915m	920m	920 br	915br	910 br
6.	ν1	875 w	865w	877m	875m	—	—	—	860 w	—	—
7.	NH	—	—	—	—	3330	3320	—	—	—	—

m = Medium ; br = Broad ; w = Weak

have found that aromatic azocompounds show an absorption band around 1570 cm^{-1} and 1406 cm^{-1}. It may be pointed out that the specific assignment of the band to the N=N stretch in aromatic azocompounds is rather cumbersome and it is more difficult in the Schiff base containing N=N group such as VII. It is possible for one to expect bands for N=N, C=N, and C=C stretching vibrations. They may be found as a mixture of C=N + N=N or N=N + C=C. Taking into consideration the assignments done for the Schiff bases, we have assigned the band at 1610 cm^{-1} to ν(C=N) vibration and the band at 1565 cm^{-1} to the mixture of ν (N=N)+ ν(C=C) vibrations. In the complex, the first band appears at 1650 cm^{-1}, while the second is little affected.

In the complexes XI–XX, the band due to the stretch is found around 1645 cm^{-1}. The shift towards the higher frequency observed in all these complexes may be interpreted as a consequence of coordination of azomethine nitrogen to the metal ion. This results in an increase in the bond-order of carbon-nitrogen link.

The broad weak band due to the H-bonded –OH in the region 2700–2600 cm^{-1} of the Schiff bases is retained in the complexes, XI–XIV and XVI–XX. The absence of this band in the ligand V and its complex XV supports our assignments. The phenolic C–O vibration of the bases is not affected even after the complex formation. These observations show that the orthohydroxy group of the Schiff bases has not taken part in the complex formation.

It is known from the literature that uranyl ion possesses three characteristic vibrations,[11] viz., ν_1 sym. 860 cm^{-1}, ν_3 asy. 930 cm^{-1} and ν_2 bend. 210 cm^{-1}.

If UO_2 is not linear, all the three frequencies become active in Raman as well as infrared regions. And if, the UO_2 is linear, ν_2 and ν_3 are infrared active and ν_1 is Raman active. Sacconi *et al.*[12] have studied a number

---

[1] J. Selbin, *Angew, Chem. Internat. Edn.*, **5**, 712 (1966).

[2] L. Sacconi, G. Caroti and P. Paoletti, *J. Chem. Soc.*, 4257 (1958).

of uranyl salts and complexes. They observed a band in the region 830–828 cm^{-1} and they have assigned it to ν_1 vibration.

Invariably we observe a strong band in all the complexes in the region 925–900 cm^{-1} and it has been assigned to ν_3 vibration. Along with ν_3 band, another band of variable intensity is also found in the region 877–854 cm^{-1}. This band is weak in the complexes XI–XIV, XVIII and is not at all observed in the remaining complexes. This band is assigned to ν_1 vibration. It is in close agreement with the theoretical prediction that the intensity of the ν_3 band should be more than the intensity of ν_1 band.[12]

These observations agree well with the concept of almost linear uranyl group disturbed by strong local field.

The Schiff bases V and VI contain two coordinating centres, NH and C=N. It is of interest to know which of the coordination sites takes part in the coordinate bond formation. The infrared spectra of these Schiff bases show a band due to secondary NH vibration around 3330 cm^{-1}. This band in the complexes XV and XVI does not show any splitting indicating that the –NH– of the Schiff bases has not taken part in the complex formation. Similar observations have been made by previous workers in the transition metal complexes.[13,14] By analogy with these observations, it may be concluded that the N=N has not formed the coordinate bond in the case of base VII.

The complexes (XI–XVII) have 1 : 2 stoichiometry and the remaining complexes (XVIII–XX) have 1 :1 stoichiometry. All the complexes are non-electrolytes in DMF. All these observations taken together with spectral data lead to the conclusion that in all the complexes uranium has coordination number six. The complexes may, therefore, be represented in the following way.

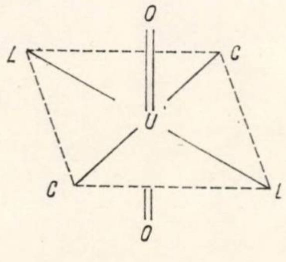

L=I–VII

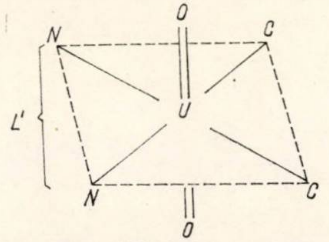

L=VIII–X

One of the authors (T.R.G.) is grateful to the Karnatak University, Dharwar, for the award of University Studentship.

---

[13] B. Das Sarma and J.C. Bailar, Jr., *J. Amer. Chem. Soc.*, **77**, 5476 (1955).

[14] N.S. Biradar and V.H. Kulkarni, *J. Inorg. Nucl. Chem.*, **33**, 3847 (1971).

Revue Roumaine de Chimie, **19**, 9, 1447–1453 (1974)

ELECTROCHEMICAL BEHAVIOUR OF 18Cr–10Ni STAINLESS STEEL IN ORGANIC ACID SOLUTIONS. I

FORMIC ACID

I. ATANASIU and TEODORA BADEA

Laboratory of Electrochemistry and Corrosion, Polytechnic Institute, str. Polizu 1,
Bucharest, Romania

Received October 26, 1973

Anodic, cathodic and potential/time studies for 18Cr – 10Ni stainless steel in formic acid of 10–80% concentration in aerated and deaerated solutions have been made by the potentiostatic method. The corrosion stability of 18Cr–10Ni stainless steel decreases with increasing formic acid concentration to a minimum value at 40% and then increases again. At 40% formic acid the characteristic currents – i_{corr}, i_{crit}, i_p – have shown maximum values.

The organic acids are used today in the chemical industry both in synthesis and for acid pickling of metal surfaces.

However, experimental data on the corrosion resistance of metals and alloys to organic acids as well as on the corrosion mechanism in their solutions are rather scarce.

The corrosion problems associated with the production and use of organic acids have been investigated by Bourrat,[1] Dillon [2] and Teeple.[3] The use of organic acid solutions for the pickling of ferrous materials and for the chemical cleaning of plants has been discussed by several authors.[4,5,6]

The corrosion behaviour of stainless steels in aqueous solutions is characterized by the marked tendency of the alloys to exhibit passivity. The anodic polarization measurements under potentiostatic conditions, including the primary passive potential, E_p, the critical anodic current density, i_{crit}, and the passive current density, i_p, are very important for the evaluation of the corrosion resistance of metallic materials.

Although the anodic behaviour of stainless steel has been studied in a wide variety of electrolyte solutions, there appears to be little evidence of studies using organic acids.[7,8]

---

[1] J. Bourrat, *Corrosion et Anticorrosion*, **11**, 140 (1963).
[2] C. P. Dillon, *Corrosion*, **13**, 124 (1957).
[3] H. O. Teeple, *Corrosion*, **8**, 14 (1952).
[4] M. A. Streicher, *Corrosion*, **14**, 59t (1958).
[5] L. G. Mac Laughlin, *Mater. Prot.*, **2**, 52 (1963).
[6] A. Callegaro, *Metallurgia Ital.*, **55**, 482 (1963).
[7] G. Trabanelli, F. Zucchi and A. Betti, *Corrosion Sci.*, **7**, 423 (1967).
[8] O. Radovici and E. Roman, *Revista de Coroziune*, **2**, 20 (1972).

The anodic polarization curve supplies information on the rate of anodic dissolution on the active-passive transitions, on the stability of the passive state and the behaviour of the materials in oxidizing medium. However, this information alone is insufficient to determine the active corrosion of the materials. In such a case, the cathodic polarization curve becomes indispensable, since the effect of the hydrogen overvoltage may become the decisive factor in determining the rate of active corrosion.

The present study has been confined to the effect of formic acid solutions of various concentrations on anodic and cathodic behaviour of 18Cr – 10Ni stainless steel under potentiostatic conditions.

EXPERIMENTAL

The stainless steel electrodes (18 %Cr ; 10 %Ni ; 0.04 % C ; 0.33 % Si), having the form and size indicated in fig. 1, were prepared from a band which was homogenized at 1050° for one hour and water-quenched. Specimens were wet polished with 3/0 emery paper, washed with carbon tetrachloride, followed by pickling for 5 minutes in a solution containing 15 % HNO_3, 2 % HF by volume at 60°. [9]

The solutions were prepared using chemically pure reagents and doubly-distilled water. The concentration of solutions of formic acid are expressed as % vol. For polarization studies in the absence of oxygen, the solutions were deaerated for 3 hours using prepurified nitrogen.

An all-glass cell was used for polarization studies (fig. 1).

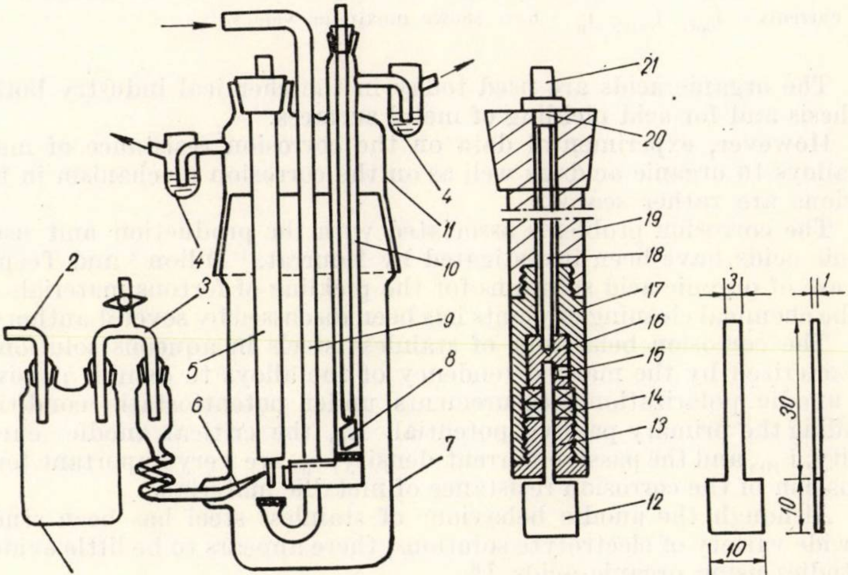

Fig. 1. – Schematic diagram of polarization cell (*a*) and electrode assembly (*b*) : *1*, intermediate vase with working solution ; *2*, electrolytic bridge with a saturated solution of KCl and agar-agar ; *3*, electrolytic bridge with working solution ; *4*, hydraulic close ; *5*, working electrode assembly ; *6*, Luggin probe ; *7*, cell ; *8*, Pt electrode ; *9*, gas bubbler ; *10*, counter-electrode space ; *11*, cover of the cell ; *12*, working electrode ; *13*, *17*, Teflon cap and rod ; *14*, rubber seal ; *15*, screen ; *16*, copper part ; *18*, copper rod ; *19*, polymethylmethacrylate cone to fit ; *20*, nut ; *21*, contact part.

---

[9] H. P. Leckie and H. H. Uhlig, *J. Electrochem. Soc.*, **113**, 1262 (1966).

The working electrode assembly was eccentrically mounted in the cover of the cell. Thus, the distance between electrode and Luggin capillary probe can be easily adjusted within rather wide limits. The tip of the Luggin probe was positioned about 1 mm from the electrode face. This distance was selected as a compromise designed to avoid shielding of the electrode surface (resulting in potential error) while minimizing the potential drop (IR) between the reference electrode and specimen during testing.

The electrode assembly was made of Teflon (fig. 1*b*) so that the solution studied was in contact only with glass, Teflon and electrode under investigation; this avoided eventual error sources associated with the mounting technique.[10]

For polarization measurements a PS 2 potentiostat was employed using stepwise technique of 40 mV/3 minutes. A standard activation was adopted for all specimens; this consisted of cathodic polarization at −0.8 V for five minutes.

Potential/time measurements have been made with a potentiometer Feussner using as zero instrument a Multiflex Galvanometer with a sensibility of 10^{-9} A/mm. The potentials were determined with reference to a saturated calomel electrode (SCE). All measurements were made at room temperature (23 ± 1°).

EXPERIMENTAL RESULTS

1. *Anodic polarization curves.* The effect of acid concentration on the anodic behaviour of 18Cr − 10Ni stainless steel is shown in fig. 2.

The anodic potentiostatic curves indicate the existence of the three characteristic regions : active, passive and transpassive, for 18Cr − 10Ni stainless steel in all tested solutions. In diluted solutions, 10 and 20% (curves *1* and *2*), one ascertains even the appearance of the secondary passivity at potentials nobler than + 0.850 V/SCE.

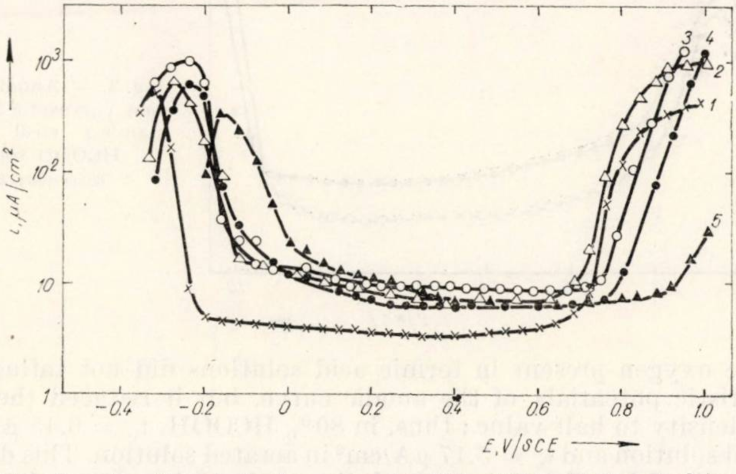

Fig. 2. − Anodic polarization curves for 18Cr—10Ni stainless steel in deaerated formic acid solutions :
1, 10% ; *2*, 20% ; *3*, 40% ; *4*, 60% ; *5*, 80%.

The passivation potential, E_p, showed a pronounced dependence on formic acid concentration, increasing with acid concentration. A similar shift of potential in positive direction was observed also in the transpassive region. Thus, the width of the stable passive region of 18Cr–10Ni stainless steel had the same absolute value in all formic acid solutions, but shifted in the noble potential direction at higher concentrations.

---

[10] N. D. Greene, W. D. France Jr. and B. E. Wilde, *Corrosion*, **21**, 275 (1965).

The critical current density, i_{crit}, increased with increasing acid concentration only over 10% – 40% HCOOH. A decrease in i_{crit} occurred as the acid concentration was increasing from 40 to 80% formic acid.

The passive current density, i_p, registered the minimum value of 3.65 μA/cm² in 10% HCOOH and the maximum value of 8.90 μA/cm² in 40% HCOOH (at the potential of + 0.400 V/SCE).

Thus, in 40% HCOOH solution, 18Cr–10Ni stainless steel showed the maximum current density both in active and in passive state; that is, the solution of 40% HCOOH was found to be the most aggressive. The i_{crit} value of 960 μA/cm² obtained in 40% HCOOH is comparable to the i_{crit} value of 1090 μA/cm² obtained for 18Cr–10Ni stainless steel in 1 N H_2SO_4,[11] while the i_p value in formic acid solution is four times grater than i_p in 1 N H_2SO_4. Accordingly, the passive state of 18Cr–10Ni stainless steel is less stable in formic acid solutions than in sulphuric acid solutions.

In order to evidence the role of oxygen in the corrosion of 18Cr–10Ni stainless steel, potentiostatic anodic curves in aerated formic acid solutions were determined. The general aspect of these curves was similar to the one presented in fig. 3.

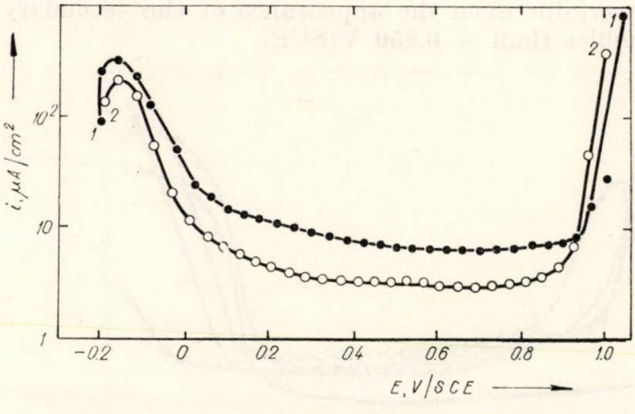

Fig. 3. — Anodic polarization curves for 18Cr–10Ni stainless steel in 80% HCOOH solution: *1*, deaerated; *2*, aerated.

The oxygen present in formic acid solutions did not influence the characteristic potentials of the anodic curve, but it reduced the passive current density to half value; thus, in 80% HCOOH, $i_p = 6.45$ μA/cm² in deaerated solution and $i_p = 3.17$ μA/cm² in aerated solution. This difference was maintained for all formic acid solutions, which shows that the presence of oxygen leads to an increased stability of the passive state of 18Cr–10Ni stainless steel.

2. *Cathodic polarization curves*. Fig. 4 presents the cathodic polarization curves obtained under potentiostatic conditions, in deaerated formic solutions of various concentrations.

---

[11] I. Atanasiu and T. Badea, *Revista de Coroziune*, **2**, 14 (1972).

The cathodic polarization curves have permitted the estimation of active corrosion rate expressed in current units, after Stern's method [12] — the extrapolation of the cathodic polarization curve in the Tafel region by the corrosion potential.

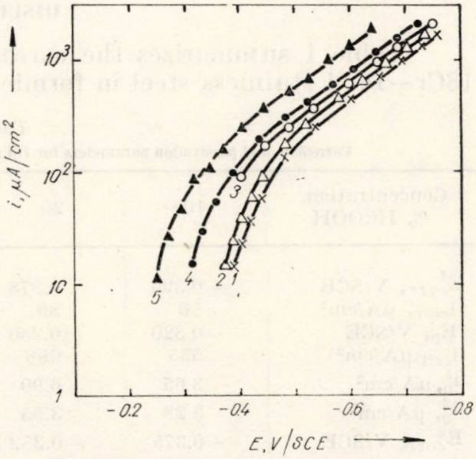

Fig. 4. — Cathodic polarization curves for 18Cr—10Ni stainless steel in deaerated HCOOH solutions :

1, 10% ; *2*, 20% ; *3*, 40% *4*, 60% ; *5*, 80%.

The current corrosion values thus obtained are high (table 1), indicating an appreciable active corrosion of 18Cr—10Ni stainless steel in formic acid solutions. The dependence of the active corrosion rate on formic acid concentration shows a maximum at 40%.

3. *Potential/time curves.* In order to characterize the behaviour of 18Cr—10Ni stainless steel at long immersion there was determined the corrosion potential dependence on time. The results are shown in fig. 5.

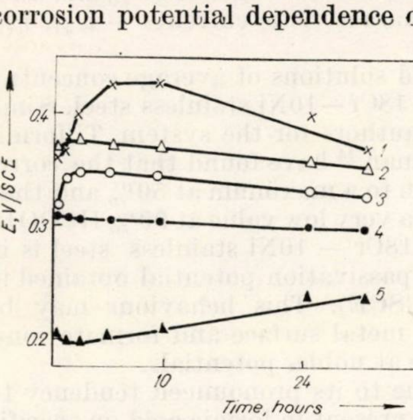

Fig. 5. — Potential/time relationships for 18Cr—10Ni stainless steel in aerated formic acid solutions :

1, 10% ; *2*, 20% ; *3*, 40% ; *4*, 60% ; *5*, 80%.

In the first hours after immersion, the electrode potential shifts to more negative values, indicating a supplementary activation of the 18Cr—10Ni stainless steel surface. After ten hours the potential reaches a minimum value and then it increases slightly, stabilizing itself after approximately 24 hours of immersion.

---

[12] M. Stern, *J. Electrochem. Soc.*, **102**, 363 (1965).

The corrosion potentials for 18Cr–10Ni stainless steel after 72 hours of immersion in 10–80% HCOOH have shown active values lower than the passivation potentials in solutions of the same concentration.

DISCUSSION

Table 1 summarizes the corrosion and passivation parameters for 18Cr–10Ni stainless steel in formic acid solutions.

Table 1

Corrosion and passivation parameters for 18Cr–10Ni stainless steel in formic acid solutions

Concentration, % HCOOH	10	20	40	60	80
E^1_{corr}, V/SCE	−0.390	−0.378	−0.365	−0.300	−0.240
i_{corr}, μA/cm²	56	89	112	75	45
E_p, V/SCE	−0.320	−0.280	−0.240	−0.240	−0.160
i_{crit}, μA/cm²	535	668	960	600	336
i^1_p, μA/cm²	3.65	6.90	8.90	6.50	6.45
i^2_p, μA/cm²	3.28	3.55	4.50	3.24	3.17
E^2_{corr}, V/SCE	−0.375	−0.352	−0.335	−0.305	−0.265

E^1_{corr} – corrosion potential in deaerated solutions; i_{corr} – corrosion current density; E_p – passivation potential; i_{crit} – critical current density; i^1_p – passive current density at E = +0.400 V/SCE in deaerated solutions; i^2_p – passive current density at E = + 0.400 V/SCE in aerated solutions; E^2_{corr} – corrosion potential after 72 hours of immersion in aerated solution.

The corrosion stability of 18Cr–10Ni stainless steel decreases with increasing formic acid concentration to a minimum value at 40% and then increases again. At 40% HCOOH the characteristic currents – i_{corr}, i_{crit}, i_p – have shown maximum values.

The high aggressivity of formic acid solutions of average concentration is not exceptional in the case of the 18Cr–10Ni stainless steel. Similar results were also obtained by other authors for the system Ti/formic acid. [13,14] Thus, Lane, Golden and Acherman [14] have found that the corrosion rate of Ti increases with concentration to a maximum at 50% and then falls rapidly with concentration, reaching a very low value at 90% HCOOH.

In the formic acid solutions the 18Cr – 10Ni stainless steel is in active state at potentials nobler than the passivation potential obtained in sulphuric acid solutions[9] ($E_p = 0.360$ V/SCE). This behaviour may be caused by a certain interaction between metal surface and formate ions, which maintains the metal in active state at nobler potentials.

The stability of stainless steel is due to its pronounced tendency to become passive and adsorption of species present in formic acid on specific metal sites may be important in inhibiting adsorption of species which react to give a passive film. There are considerable evidences for adsorption of formic acid and formates on metal surfaces. [15,16,17]

---

[13] A. R. Piggott, H. Leckie and L. L. Shreir, *Corrosion Sci.*, **5**, 185 (1965).

[14] I. R. Lane, L. B. Golden and W. T. Acherman, *Ind. Eng. Chem.*, **45**, 1067 (1957).

[15] E. Muller, *Z. Elektrochem.* **29**, 264 (1923); **33**, 561 (1927).

[16] K. Schwabe, *Z. Elektrochem.*, **61**, 743 (1957).

[17] M. W. Breiter, *Electrochim. Acta*, **8**, 447, 457 (1963).

The nature of formic acid is complex; Martin and Rossotti [18] have obtained equilibrium constants for various species (HA, HA_2^-, H_2A_2, A^-) which exist in solution. For $H^+ + HCOO^- = HCOOH$, $K = 10^{3.9}$ so that undissociated molecules will predominate at low concentration. Increase in concentration of formic acid will increase the concentration of A^-, HA_2^- and H_2A_2 (hydrogen bounded dimers).

It is possible that the specific electrochemical behaviour of 18Cr—10Ni stainless steel is due to the action of different species present in formic acid. It is apparent, therefore, that $HCOO^-$ must be active in the corrosion process and it is significant that the maximum aggressivity was obtained at 40% HCOOH — the concentration which has the highest conductivity.

Although the role of the other species in formic acid solutions is not clear, it is possible that they play an active part in the film-forming process in both the active and passive region. In particular, specific adsorption of formic acid dimers, which becomes more significant with increase in concentration of formic acid, may be important in preventing adsorption of $HCOO^-$.

These considerations might explain why the 40% HCOOH solution has shown the most aggressive character on 18Cr — 10Ni stainless steel.

---

[18] D. L. Martin and F. J. Rossotti, *Proc. Chem. Soc.*, **1959**, 60.

Revue Roumaine de Chimie, **19**, *9*, 1455–1459 (1974)

CONTRIBUTIONS TO THE BISMUTH HYDROLYSIS STUDY. III[1]. ELECTROMETRIC INVESTIGATIONS ON BISMUTHYL PERCHLORATE HYDROLYSIS

C. DRĂGULESCU, ANA NIMARĂ and I. JULEAN
Chemical Research Centre, Bd. Mihai Viteazul, No. 24, Timişoara, Romania

Received February 4, 1974

The equilibria between $Bi_6\ (OH)_{12}^{6+}$ – NaOH, in the pH range 3–10, were studied. The obtained data were rationalized by the direct analysis of the titration curves and by the method of the formation function. On these conditions the presence of the following compounds with the stability constants was identified :

$$9[Bi(OH)_2^+ + 0.44\ OH^-] \rightleftharpoons [Bi_9(OH)_{22}]^{5+} \quad \log K_1 = -2{,}765$$

$$9[Bi(OH)_2^+ + 0.54\ OH^-] \rightleftharpoons [Bi_9(OH)_{23}]^{4+} \quad \log K_2 = -5{,}928$$

$$9[Bi(OH)_2^+ + 0.76\ OH^-] \rightleftharpoons [Bi_9(OH)_{25}]^{2+} \quad \log K_3 = -6{,}701$$

In a previous note[1] we had in view the hydrolysis process which was the result of the pH modification by the simple replacement of the hydrogen ions with sodium in sodium perchlorate medium only till pH 3.

In order to study further the hydrolysis at a greater pH, we followed the effect of the addition of OH^- ions on the bismuthyl perchlorate solutions in the range of pH 3–10.

EXPERIMENTAL

REAGENTS AND APPARATUS

The used reagents were bismuthyl perchlorate, which was obtained by means of the described procedure[2], and sodium hydroxide, Merck *p.a.*

The experimental investigations were carried out with several bismuth concentrations (0.5 –1 M Bi^{3+}) in 0.1 M sodium perchlorate medium.

The determinations consisted in a series of pH-metric and conductometric titrations between bismuthyl perchlorate and sodium hydroxide.

The measurements were carried out on a " Radiometer" pH-meter PHM-25 with a G–202 C glass electrode and on a "Methrom" conductoscop E 369.

---

[1] Part II : C. DRĂGULESCU, A. NIMARĂ and I. JULEAN., *Rev. Roumaine de Chim.*, **17**, 1181 (1972).

[2] Part I : C. DRĂGULESCU, A. NIMARĂ and I. JULEAN, *Chem. Analit.*, **17**, 631 (1972).

DISCUSSION AND RESULTS

a) The direct analysis of the titration curves.

The results of the pH-metric and conductometric titrations are shown in figs 1 and 2.

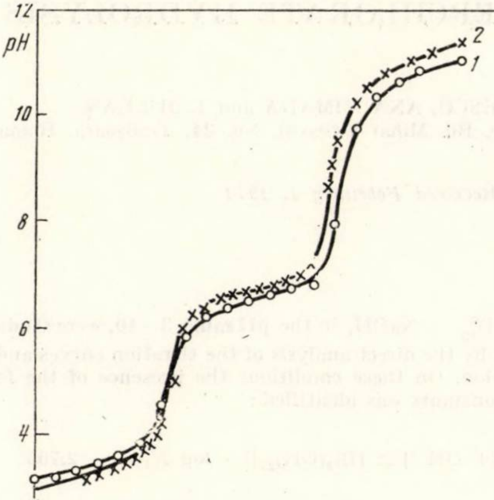

Fig. 1. — pH-titration curves of $BiOClO_4$ with 0.1 M NaOH, $NaClO_4$ 0.1M : 1 — 1M $BiOClO_4$; 2 — 5.10^{-1} M $BiOClO_4$.

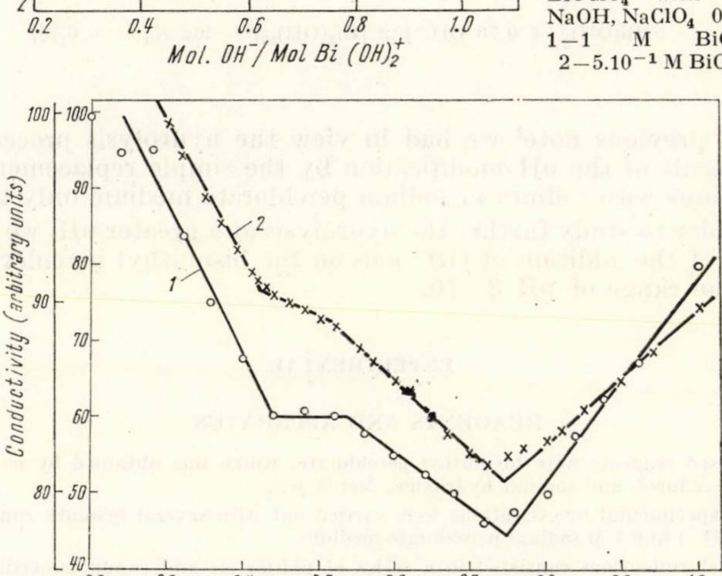

Fig. 2. — Conductometric titration curves of $BiOClO_4$ with 0.1 M NaOH, $NaClO_4$ 0.1 M : 1—1 M $BiOClO_4$; 2—5.10^{-1} M $BiOClO_4$.

It can be seen in fig. 1. the appearance of two inflexions in the ratio $OH^-/Bi(OH)_2^+ = 0.46$ and 0.76 showing the existence of at least two compounds in equilibrium.

The conductometric titration curves (fig. 2) give further information. Until a ratio of 0.42 $OH^-/Bi(OH)_2^+$ is reached, the solution remains clear, the conductibility decreases much enough, perhaps due to the neutralization of the hydrogen ions, which results from the bismuthyl hydrolysis.

Starting with a ratio of 0.44 $OH^-/Bi(OH)_2^+$ one can notice the appearance of an opalescence that increases with the addition of NaOH, the conductibility remaining either constant or decreasing a little to a ratio of 0.54 $OH^-/Bi(OH)_2^+$. In this interval, there is probably an equilibrium between two compounds, one turning into the other. A net precipitation follows, the conductibility decreases to a ratio of 0.76 $OH^-/Bi\ (OH)_2^+$, and it begins to increase thereafter due to the reagent excess.

From the direct analysis of the titration curves we may notice the following facts :

— the general aspect of the titration curves is the same, irrespective of the bismuthyl concentration, this showing that the reactions which take place in the system are also the same ;

— a characteristic feature of the curves of conductometric titration is the fact they have three inflexion points which correspond to the existence of three equilibrium compounds. The pH-metric curves have only two inflexion points, that could be explained by admitting that two of these compounds have close stability constants.

For simplification, considering the bismuthyl in a simple uncondensed form, we may write the following formation reactions :

$$Bi(OH)_2^+ + 0.44\ OH^- \rightleftharpoons [Bi(OH)_{2.44}]^{+0.56} \qquad (1)$$

$$Bi(OH)_2^+ + 0.54\ OH^- \rightleftharpoons [Bi(OH)_{2.54}]^{+0.46} \qquad (2)$$

$$Bi(OH)_2^+ + 0.76\ OH^- \rightleftharpoons [Bi(OH)_{2.76}]^{+0.24} \qquad (3)$$

These compounds correspond to the series[3] :

$$Bi_9(OH)_{22}^{5+} \rightleftharpoons Bi_9(OH)_{23}^{4+} \rightleftharpoons Bi_9(OH)_{25}^{2+}$$

b) The method of the formation curve.

In the case of the polynuclear compounds formation, it is known that the average number of ligands is both $[H^+]$ and $[M]$ dependent.

In the case of hydroxocomplexes, the method of the formation curve developed by Bjerrum[4] and adapted by Ahrland[5] for the special case of the hydrolysis reactions, allows a mathematical treatment of the experimental data.

---

[3] A. Olin, *Acta Chem. Scand.* , **13**, 1791 (1959).

[4] J. Bjerrum, "Metal Ammine Formation", P. Hase and Son, Copenhaga, 1957.

[5] S. Ahrland, *Acta Chem. Scand.*, **3**, 374 (1949).

The average number of ligands, $\bar{n}$, will be determined with the help of relation :

$$\bar{n} = \frac{C_{OH}}{C_M}$$

C_{OH} = the OH ion concentration which is consumed by the formation of the complexes. At a given moment of the titration C_{OH} is given by the relation :

$$C_{OH} = B - C_H + [H^+]$$

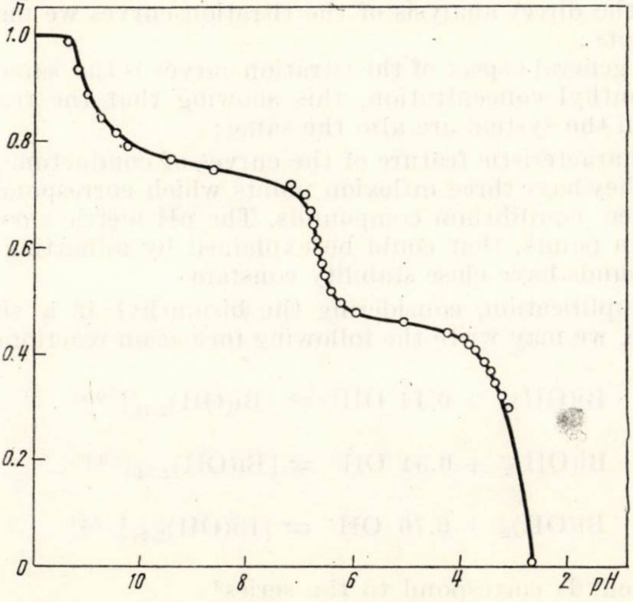

Fig. 3 — The formation curve for the bysmuthyl — OH^- ions in 0.1 M $NaClO_4$.

B = the total amount of the added base,

C_H = initial acid concentration of the solution which can be determined knowing the pH value,

$[H^+]$ = the concentration of the hydrogen ion resulting from the hydrolysis = the concentration of the free OH ions. Taking into consideration that the studied hydrolysis reaction occurs in the pH range 3—10, the concentration of the OH^- ions may be neglected as compared with the amount of the base added.

The experimental data allowed the calculation of $\bar{n}$, by means of which the formation curve $\bar{n} = f$ (pH) was built, as shown in fig. 3.

The approximate values of the stability constants may be read out directly from the diagram at half of the inflexion point.

These approximate constants were then refined with the help of the convergency formula deduced for N = 3[6]:

$$K_1 = [\mathrm{H}^+]\,\frac{\bar{n}}{0.44 - \bar{n}}, \tag{I}$$

$$K_2 = [\mathrm{H}^+]\,\frac{(\bar{n} - 0.44) + \dfrac{\bar{n}[\mathrm{H}^+]}{K_1}}{(0.54 - \bar{n})}, \tag{II}$$

$$K_3 = [\mathrm{H}^+]\,\frac{(n - 0{,}54) + \dfrac{(n - 0.54)\,[\mathrm{H}^+]}{\mathrm{K}_2} + \dfrac{\bar{n}[\mathrm{H}^+]}{\mathrm{K}_1\mathrm{K}_2}}{(0.76 - \bar{n})}. \tag{III}$$

The values of the successive stability constants are shown in table 1.

Table 1

The values of the stability constants as read out of the formation curve compared with the calculated values

Log. Stability constants	Values read out of the formation curve	Calculated value
K_1	− 2.90	− 2.765
K_2	− 5.90	− 5.928
K_3	− 6.70	− 6.701

In conclusion three compounds were identified in solution by pH-metric and conductometric method.

The first compound $Bi_9(OH)_{22}^{5+}$ is already known, the value of the stability constant established in the present paper, being identical with the one given in the literature.

---

[6] C. Luca and O. Enea, "Determinarea constantelor analitice", Editura didactică şi pedagogică, 1971, p. 45.

Revue Roumaine de Chimie, **19**, *9*, 1461–1470 (1974)

CONTRIBUTION À L'ÉTUDE DE L'HYDROLYSE DE L'URANIUM (VI) EN MILIEU AZOTIQUE

MARIA MAVRODIN-TĂRĂBÎC
Centre de Chimie Physique, 31, str. Galaţi, Bucarest

Reçu le 30 juillet 1973

On étudie, par voie pH-métrique (la méthode de l'analyse mathématique des courbes pH-métriques différentielles, la méthode de la fonction de formation et la méthode « core and links »), la nature et la stabilité des espèces ioniques formées par l'hydrolyse de l'uranium (VI) en milieu azotique. On tire la conclusion que l'hydrolyse de l'uranium en milieu azotique a lieu par une série de réactions dépendantes du pH qui conduisent à la formation des complexes polynucléaires du type « core and links », les espèces ioniques formées étant moins stables dans le milieu azotique que dans le milieu inerte d'acide perchlorique.

Dans des publications antérieures[1,2] on a exposé les résultats obtenus dans l'étude de l'hydrolyse de l'ion UO_2^{2+} en milieu inerte d'acide perchlorique.

Tenant compte de l'importance du milieu azotique, dans ce travail nous nous proposons de déterminer, par voie pH-métrique, la nature et la stabilité des espèces ioniques qui se forment par l'hydrolyse de l'uranium (VI) en milieu complexant d'acide azotique. Il faut mentionner que, dans la littérature de spécialité il n'y a que peu de travaux qui s'occupent de ce domaine. Parmi les plus importants on cite les études sur l'hydrolyse de l'uranium (VI) en milieu de sulfate[3] et d'azotate de magnésium[4].

PARTIE EXPÉRIMENTALE

1. RÉACTIFS ET APPAREILS

— Azotate d'uranyle $UO_2(NO_3)_2 \cdot 6\,H_2O$ (*p.a.* Merck). On a préparé une solution « stock » approximativement 0,1 M, dont on a obtenu, en diluant avec de l'eau bidistillée, les solutions d'azotate d'uranyle de différentes concentrations : 0,05 M ; 0,02 M ; 0,01 M ; 0,001 M. Les concentrations de ces solutions ont été vérifiées par voie gravimétrique (évaporation et calcination à l'état d'oxyde U_3O_8).

— Hydroxide de sodium (*p.a.* Merck). Les solutions utilisées ont été préparées en diluant une solution « stock » approximativement 0,1 M. La concentration des solutions d'hydroxyde de sodium a été établie avec du phtalate acide de kalium.

---

[1] M. Mavrodin-Tărăbîc, *Rev. Roumaine Chim.*, **18**, 73 (1973).
[2] M. Mavrodin-Tărăbîc, *Rev. Roumaine Chim.*, **18**, 609 (1973).
[3] H.S. Dunsmore, S. Hietanen et L.G. Sillen, *Acta Chem. Scand.*, **22**, 2644 (1963).
[4] U. Schedin et M. Frydman, *Acta Chem. Scand.*, **22**, 115 (1968).

Pour les titrages pH-métriques on a utilisé un pH-mètre Radiometer-Copenhagen (électrodes de verre et de calomel). Les déterminations ont été faites dans une installation fermée spécialement construite.

2. MODE DE TRAVAIL

Les déterminations pH-métriques ont été effectuées en titrant les solutions d'azotate d'uranyle avec de l'hydroxyde de sodium. Pour tirer des conclusions sur l'influence de la concentration sur la nature des espèces ioniques qui se forment par l'hydrolyse, on a travaillé avec des solutions d'azotate d'uranyle de différentes concentrations, comprises entre 0,1 — 0,001 M. L'influence de la force ionique a été évaluée en effectuant des déterminations, pour chaque concentration, à quatre forces ioniques : $I = 0{,}5$; 1 ; 1,5 et 2.

Les déterminations ont été faites par le titrage direct de la solution d'azotate d'uranyle avec de l'hydroxyde de sodium. On a travaillé dans un large domaine de pH, les titrages pH-métriques étant considérés terminés à l'apparition d'un précipité stable, de couleur orange, de polyuranate. Les titrages ont été répétés trois fois, les valeurs du pH représentées graphiquement et utilisées dans les calculs étant des valeurs moyennes.

RÉSULTATS ET DISCUSSIONS

L'étude de la nature des espèces ioniques formées par l'hydrolyse de l'ion UO_2^{2+} en milieu azotique a été faite par trois méthodes :

— l'analyse mathématique des courbes pH-métriques différentielles[5] ;

— la méthode de la fonction de formation[6] et

— la méthode « core and links » (ion central — ponts de liaison), caractéristique des complexes polynucléaires [7,8].

1. L'ANALYSE MATHÉMATIQUE DES COURBES pH-MÉTRIQUES DIFFÉRENTIELLES

Tenant compte que les courbes pH-métriques obtenues par le titrage des solutions d'azotate d'uranyle caractérisées par des concentrations variant entre 0,001 — 0,05 M et par les forces ioniques $I = 0{,}5$; 1 ; 1,5 et 2 ont la même allure, on présentera seulement les courbes caractéristiques des solutions 0,02 M (fig. 1).

Ainsi qu'on observe de la figure 1, les courbes de titrage présentent, à toutes les concentrations et forces ioniques, deux points d'inflexion (situés au pH=4,5 — 5 et au pH 6) qui correspondent aux rapports mol. UO_2^{2+} : équivalents de NaOH = 1 : 1,68 (pour la première inflexion) et 1 : 2,36 (pour la deuxième inflexion).

Les rapports $UO_2^{2+} : OH^- = 3 : 5 : 7$ indiquent que les réactions d'hydrolyse en milieu azotique impliquent trois ions UO_2^{2+} et cinq ions OH^- (pour la première inflexion) et trois ions UO_2^{2+} et sept ions OH^- (pour la deuxième) et plaident pour un mécanisme d'hydrolyse qui conduit, à des pH 4,5 — 5, à la formation des ions polynucléaires : $U_2O_5^{2+}$; $U_3O_8^{2+}$; $U_3O_8(OH)^+$; $U_3O_8(OH)$; $U_3O_8(OH)^-$; $U_3O_8(OH)_2^-$ etc. (On mentionne qu'un mécanisme de réaction analogue a été mis en évidence en milieu inerte d'acide perchlorique[1].)

---

[5] J. Sutton, *J. Chem. Soc.*, **1949**, 275.

[6] S. Ahrland, *Acta Chem. Scand.*, **3**, 374 (1949).

[7] S. Hietanen, *Acta Chem. Scand.*, **8**, 1607 (1954).

[8] S. Hietanen et L.G. Sillen, *Acta Chem. Scand.*, **13**, 1828 (1959).

La stabilité des ions $U_2O_5^{2+}$ et $U_3O_8^{2+}$ en milieu azotique a été déterminée en utilisant les relations qui expriment le bilan de l'uranium et l'électroneutralité de la solution[1].

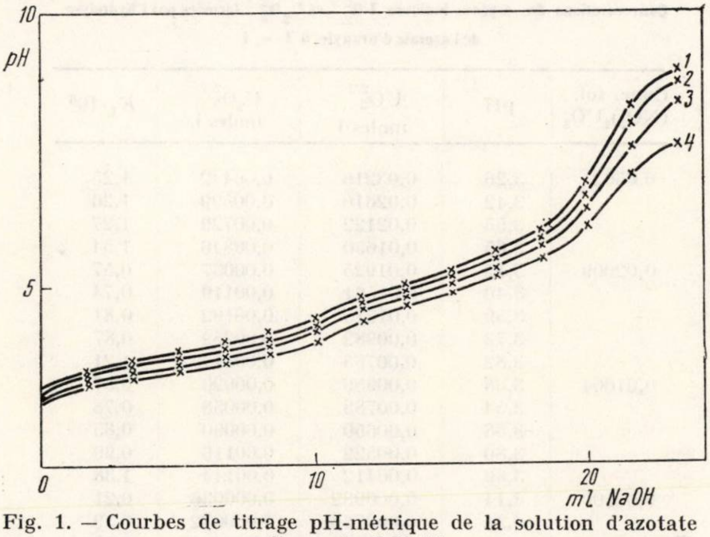

Fig. 1. — Courbes de titrage pH-métrique de la solution d'azotate d'uranyle 0,02 M
1 — I = 0,5 ; *2* — I = 1 ; *3* — I = 1,5 ; *4* — I = 2.

Les résultats obtenus pour différentes concentrations et forces ioniques sont présentés dans les tableaux 1—4.

Tableau 1

Concentrations des espèces ioniques UO_2^{2+} et $U_2O_5^{2+}$ formées par l'hydrolyse de l'azotate d'uranyle, à I = 0,5

Conc. sol. $(NO_3)_2UO_2$	pH	UO_2^{2+} moles/l	$U_2O_5^{2+}$ moles/l	$K_1 \cdot 10^6$
0,0502	2,85	0,04880	0,00070	0,58
	3,12	0,04028	0,00266	0,94
	3,30	0,03220	0,00440	1,06
	3,45	0,02610	0,00597	1,09
	3,57	0,02124	0,00728	1,17
	3,68	0,01650	0,00845	1,34
0,02009	3,12	0,01925	0,00037	0,57
	3,40	0,01561	0,00119	0,74
	3,59	0,01215	0,00192	0,81
	3,72	0,00981	0,00259	0,97
	3,85	0,00766	0,00317	1,05
0,01004	3,37	0,00962	0,00021	0,40
	3,56	0,00785	0,00057	0,67
	3,83	0,00523	0,00118	0,94
	4,04	0,00330	0,00165	1,25
0,00100	4,14	0,000932	0,000036	0,21
	4,28	0,000771	0,000069	0,31
	4,39	0,000628	0,000101	0,42
	4,50	0,000516	0,000127	0,45

Tableau 2

Concentrations des espèces ioniques UO_2^{2+} et $U_2O_5^{2+}$ formées par l'hydrolyse de l'azotate d'uranyle, à I = 1

Conc. sol. $(NO_3)_2UO_2$	pH	UO_2^{2+} moles/l	$U_2O_5^{2+}$ moles/l	$K_1 \cdot 10^6$
0,0502	3,26	0,03216	0,00442	1,25
	3,42	0,02610	0,00599	1,26
	3,55	0,02122	0,00729	1,27
	3,65	0,01650	0,00846	1,54
0,02009	3,12	0,01925	0,00037	0,57
	3,40	0,01561	0,00119	0,74
	3,59	0,01215	0,00192	0,81
	3,73	0,00982	0,00259	0,87
	3,82	0,00765	0,00317	1,21
0,01004	3,38	0,00959	0,00020	0,37
	3,54	0,00783	0,00058	0,78
	3,68	0,00650	0,00090	0,85
	3,80	0,00522	0,00119	0,99
	3,89	0,00412	0,00144	1,38
0,00100	4,14	0,000932	0,000036	0,21
	4,24	0,000766	0,000072	0,39
	4,35	0,000625	0,000102	0,50
	4,40	0,000508	0,000131	0,67
	4,47	0,000401	0,000154	1,04

Tableau 3

Concentrations des espèces ioniques UO_2^{2+} et $U_2O_5^{2+}$ formées par l'hydrolyse de l'azotate d'uranyle, à I = 1,5

Conc. sol. $(NO_3)_2UO_2$	pH	UO_2^{2+} moles/l	$U_2O_5^{2+}$ moles/l	$K_1 . 10^6$
0,0502	2,80	0,04870	0,00075	0,71
	3,22	0,03210	0,00440	1,53
	3,37	0,02600	0,00601	1,53
	3,50	0,02140	0,00730	1,56
	3,60	0,01650	0,00847	1,94
0,02009	3,10	0,01929	0,00035	0,47
	3,36	0,01557	0,00121	0,92
	3,55	0,01212	0,00194	1,03
	3,70	0,00980	0,00559	1,07
	3,82	0,00765	0,00317	1,21
0,01004	3,28	0,00948	0,00026	0,78
	3,61	0,00645	0,00092	1,28
	3,75	0,00520	0,00120	1,30
	3,98	0,00327	0,00166	1,81
0,001004	4,10	0,000925	0,000039	0,28
	4,19	0,000760	0,000075	0,53
	4,28	0,000617	0,000106	0,75
	4,40	0,000405	0,000157	1,52

Tableau 4

Concentrations des espèces ioniques UO_2^{2+} et $U_2O_5^{2+}$ formées par l'hydrolyse de l'azotate d'uranyle, à I = 2

Conc. sol. $(NO_3)_2UO_2$	PH	UO_2^{2+} moles/l	$U_2O_5^{2+}$ moles/l	$K_1 . 10^6$
0,0502	2,74	0,04840	0,00090	1,24
	3,00	0,04003	0,00278	1,70
	3,20	0,03210	0,00446	1,71
	3,32	0,02600	0,00603	1,97
	3,52	0,01640	0,00850	2,84
0,02009	3,06	0,01913	0,00043	0,89
	3,29	0,01549	0,00125	1,35
	3,46	0,01206	0,00197	1,56
	3,60	0,00975	0,00262	1,72
	3,70	0,00761	0,00319	1,98
	3,80	0,00555	0,00387	2,50
0,01004	3,29	0,00950	0,00025	0,73
	3,90	0,00325	0,00167	2,46
	4,02	0,00238	0,00185	2,93
0,001004	4,02	0,000730	0,000091	1,54
	4,12	0,000594	0,000118	1,88
	4,22	0,000487	0,000141	2,14
	4,50	0,000227	0,000196	3,87

Tel qu'on voit dans les tableaux 1—4, la stabilité de l'ion $U_2O_5^+$ est plus grande dans les solutions plus concentrées; la constante K_1 présente, dans le domaine de pH dans lequel on peut considérer que dans la solution coexistent seulement les ions UO_2^{2+} et $U_2O_5^{2+}$, une valeur moyenne d'environ 1.10^{-6}. A un certain pH (3,6—4) on constate une brusque augmentation de la valeur de K_1, ce qui démontre que dans ce domaine de pH il se forme aussi d'autres espèces ioniques qui ne peuvent être négligées.

Dans les figures 2 — 4 on présente quelques-unes des données qui caractérisent la stabilité des ions polynucléaires $U_2O_5^{2+}$ et $U_3O_8^{2+}$ en milieu azotique, en comparaison de la stabilité des mêmes espèces ioniques en milieu inerte[2].

De l'analyse comparative des courbes qui présentent les constantes K_1 et K_2, à différentes concentrations et forces ioniques, on tire la conclusion que la stabilité des polyions $U_2O_5^{2+}$ et $U_3O_8^{2+}$ est plus grande en milieu inerte.

2. L'ÉTUDE DU SYSTÈME AZOTATE D'URANYLE — EAU PAR LA MÉTHODE DE LA FONCTION DE FORMATION

Conformément à cette méthode, la détermination de la nature des espèces ioniques qui se forment par l'hydrolyse en milieu azotique a été faite en calculant $\bar{n}$, le nombre moyen de ligands OH^- liés à l'ion central d'uranyle et en analysant les courbes de la fonction de formation $\bar{n} = f(pH)$, pour les différentes concentrations de l'ion UO_2^{2+}.

La relation fondamentale utilisée dans le calcul a été la suivante :

$$\bar{n} = \frac{C_A - (A)}{C_M} \text{ dans laquelle}$$

C_A = la concentration totale du ligand OH^-, connue dès les données initiales du travail ; C_M=la concentration de l'ion central UO_2^{2+}, également connue dès les données initiales et A = la concentration du ligand « libre » déterminée par la méthode pH-métrique. On mentionne que les données déterminées expérimentalement se rapportent au ligand « libre » $(A) = (OH^-)$ d'une manière indirecte, la quantité mesurée directement étant la concentration des ions H^+ liée à OH^- par la relation : $(OH^-) = K_w(H^+)$.

Ainsi qu'on a démontré dans un travail antérieur[2], $\bar{n}$ dépend seulement de (H^+) si dans le système il ne se forme que des complexes mononucléaires ; $\bar{n}$ dépend tant de (H^+) que de (M) lorsque dans le système il se forme aussi des complexes polynucléaires.

Les données expérimentales et les résultats obtenus par le calcul pour les solutions d'azotate d'uranyle de différentes concentrations et forces ioniques sont présentés dans les tableaux 5 — 8.

Tableau 5

Concentrations de l'ion central et du ligand en fonction du pH (I = 0,5)

Conc sol. $(NO_3)_2UO_2$ moles/l	pH	$C_{OH}\cdot10^3$ moles/l	$C_M\cdot10^3$ moles/l	$\bar{n}$
0,1067	3,15	1,20	53,8	0,022
	3,20	2,16	53,3	0,040
	3,30	3,90	52,3	0,074
	3,40	6,99	50,8	0,130
	3,52	10,60	48,5	0,210
	3,65	14,32	46,3	0,300
	3,77	17,97	44,4	0,400
	4,01	23,89	41,0	0,580
	4,40	31,63	36,7	0,860
0,03556	3,20	1,15	17,9	0,064
	3,38	1,87	17,7	0,100
	3,67	4,51	17,2	0,262
	3,94	7,91	16,6	0,470
	4,16	10,37	16,1	0,640
	4,41	14,14	15,4	0,910
0,02134	3,64	1,68	10,6	0,150
	3,90	3,52	10,4	0,330
	4,07	5,28	10,2	0,510
	4,23	7,06	10,0	0,700
	4,44	8,63	9,8	0,880
0,01067	3,92	0,62	5,38	0,110
	4,12	1,53	5,33	0,280
	4,29	2,45	5,28	0,460
	4,60	4,32	5,17	0,830
	4,75	5,21	5,12	1,010

Tableau 6

Concentrations de l'ion central et du ligand en fonction du pH (I = 1)

Conc. sol. $(NO_3)_2UO_2$ moles/l	pH	$C_{OH}\cdot10^3$ moles/l	$C_M\cdot10^3$ moles/l	$\bar{n}$
0,1067	3,16	2,15	53,3	0,040
	3,25	3,96	52,3	0,075
	3,40	5,59	51,2	0,100
	3,52	8,90	49,3	0,170
	3,65	12,92	48,0	0,260
	3,85	17,94	44,4	0,400
	4,00	21,00	42,6	0,490
	4,41	29,23	38,1	0,760
0,03556	3,02	1,45	17,9	0,080
	3,50	2,71	17,6	0,150
	3,68	4,50	17,2	0,260
	3,92	6,72	16,9	0,390
	4,00	7,90	16,6	0,470
	4,25	12,75	15,7	0,810
0,02134	3,60	1,71	10,6	0,160
	3,74	2,58	10,5	0,240
	3,86	3,53	10,4	0,330
	3,94	4,41	10,3	0,420
	4,14	6,67	10,1	0,660
	4,30	7,85	9,9	0,790
0,01067	3,98	1,56	5,33	0,290
	4,20	2,46	5,28	0,460
	4,35	3,44	5,23	0,650
	4,50	4,33	5,17	0,830
	4,75	6,61	5,08	1,300

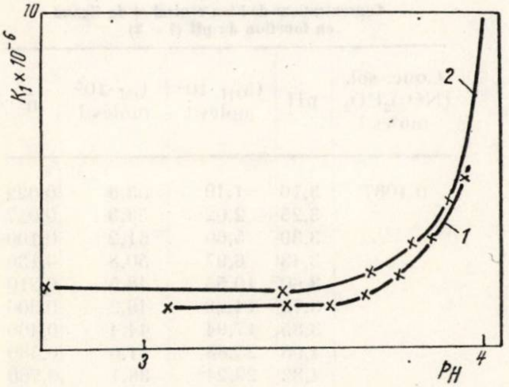

Fig. 2. — Courbes de comparaison concernant la stabilité de l'ion $U_2O_5^{2+}$ en milieu azotique 1) et en milieu inerte d'acide perchlorique (2). (Conc. = 0,05 M, I = 1).

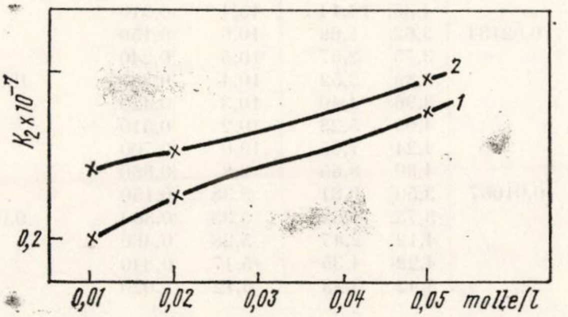

Fig. 3. — Courbes de comparaison concernant la stabilité de l'ion $U_3O_8^{2+}$ en milieu azotique (1) et en milieu inerte d'acide perchlorique (2).

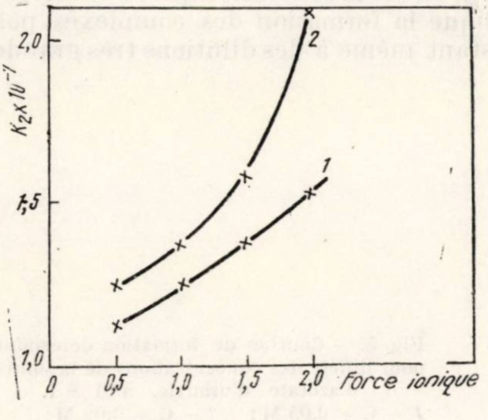

Fig. 4. — Courbes de comparaison concernant la stabilité de l'ion $U_3O_8^{2+}$ en fonction de la force ionique. *1*, en milieu azotique ; *2*, en milieu inerte d'acide perchlorique.

Tableau 7

Concentrations de l'ion central et du ligand en fonction du pH (I = 1,5)

Conc. sol. $(NO_3)_2UO_2$ moles/l	pH	$C_{OH} \cdot 10^3$ moles/l	$C_M \cdot 10^3$ moles/l	$\bar{n}$
0,1067	3,12	1,25	53,8	0,023
	3,24	2,03	53,3	0,038
	3,28	3,92	52,3	0,074
	3,38	7,01	50,8	0,130
	3,50	10,61	48,5	0,210
	3,65	14,32	46,3	0,300
	3,90	21,02	42,6	0,490
	4,10	26,67	39,5	0,670
0,03556	3,17	1,17	17,9	0,059
	3,35	1,90	17,7	0,100
	3,46	2,74	17,6	0,150
	3,62	4,53	17,2	0,260
	3,75	6,77	16,9	0,400
	4,07	10,38	16,1	0,640
	4,35	14,14	15,4	0,910
0,02134	3,62	1,69	10,6	0,150
	3,75	2,57	10,5	0,240
	3,89	3,52	10,4	0,330
	3,96	4,40	10,3	0,420
	4,05	5,28	10,2	0,510
	4,24	7,05	10,0	0,700
	4,30	8,65	9,8	0,880
0,01067	3,50	0,81	5,38	0,150
	3,75	1,63	5,33	0,300
	4,12	2,47	5,28	0,460
	4,29	4,35	5,17	0,840
	4,42	5,23	5,12	1,020

Tableau 8

Concentrations de l'ion central et du ligand en fonction du pH (I = 2)

Conc. sol. $(NO_3)_2UO_2$ moles/l	pH	$C_{OH} \cdot 10^3$ moles/l	$C_M \cdot 10^3$ moles/l	$\bar{n}$
0,1067	3,16	1,19	53,8	0,022
	3,25	2,02	53,3	0,037
	3,39	5,60	51,2	0,100
	3,43	6,97	50,8	0,130
	3,60	10,55	48,5	0,210
	3,72	14,29	46,3	0,300
	3,85	17,94	44,4	0,400
	4,08	23,88	41,0	0,580
	4,33	29,24	38,1	0,760
0,03556	2,96	1,59	17,9	0,080
	3,10	2,25	17,7	0,120
	3,25	2,96	17,6	0,160
	3,37	4,72	17,2	0,270
	3,50	6,91	16,9	0,400
	3,90	10,42	16,1	0,640
	4,05	12,78	15,7	0,810
	4,18	14,16	15,4	0,910
0,02134	3,45	1,81	10,6	0,170
	3,58	2,66	10,5	0,250
	3,76	4,47	10,3	0,430
	3,91	6,72	10,1	0,660
	4,17	7,86	9,9	0,790
	4,38	10,34	9,7	1,060
0,01067	3,69	1,66	5,33	0,310
	3,94	3,51	5,23	0,670
	4,22	5,26	5,12	1,020
	4,60	7,02	5,03	1,390

De l'analyse des courbes de formation (fig. 5) qui ne coïncident ni même pour les moindres valeurs de C_M, on tire la conclusion que l'hydrolyse de l'uranium en milieu azotique implique la formation des complexes polynucléaires, ce processus se manifestant même à des dilutions très grandes.

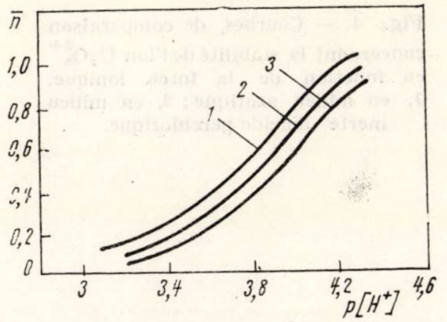

Fig. 5. — Courbes de formation déterminées pour différentes concentrations de la solution d'azotate d'uranyle, à I = 1.
1 — C = 0,05 M ; 2 — C = 0,02 M ; 3 — C = 0,01 M.

3. L'ÉTUDE DU SYSTÈME AZOTATE D'URANYLE – EAU PAR LA MÉTHODE « CORE AND LINKS »

Conformément à cette méthode [7,8], la nature des espèces ioniques formées par l'hydrolyse de l'uranium en milieu azotique a été déterminée en analysant les courbes $Z = f(\log h)_M$, analogues aux courbes $\bar{n} = f(\log h)_M$ (Z représente le nombre moyen d'ions OH^- liés à l'ion central d'uranyle ; h = la concentration des ions d'hydrogène « libres » ; M = la concentration totale des ions UO_2^{2+} libres ou liés dans les complexes).

Du fait que les courbes $Z = f(\log h)_M$ obtenues pour les solutions aqueuses d'azotate d'uranyle sont parallèles on tire la conclusion que l'ion UO_2^{2+} hydrolyse avec la formation des ions complexes polynucléaires du type « core and links » caractérisés par la formule générale $UO_2\,[(OH)_t\,UO_2]_n^{2+}$. La valeur de t ($t = -R = \log M/\log h$) a été établie à l'aide du diagramme $\log M = f(\log h)_Z$ (fig. 6).

Tel qu'on le voit dans la fig. 6, les droites sont parallèles et se caractérisent par une pente $\log M/\log h = 2$, ce qui mène à la conclusion que $t = -R = 2$, Z étant fonction de $X = \log M - 2 \log h$.

La valeur de t a été confirmée en représentant les données expérimentales dans le système de coordonnées $Y = Z/2 = f(X)$ (fig. 7).

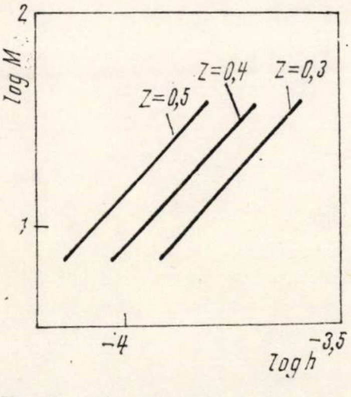

Fig. 6. — La détermination de la valeur de t caractéristique des complexes polynucléaires formés par l'hydrolyse de l'uranium en milieu azotique.

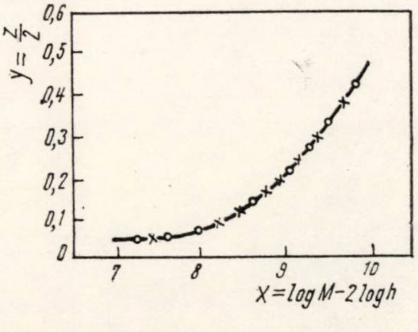

Fig. 7. — Diagramme $Y = f(X)$ caractéristique des complexes polynucléaires formés par l'hydrolyse de l'uranium en milieu azotique.
x – 0,05 M ; o – 0,025 M.

Du fait que les courbes $Y = f(X)$, obtenues pour les solutions d'azotate d'uranyle 0,05 et 0,025 M, se superposent, on tire la conclusion que la valeur de t est correcte et que la formule générale des complexes formés par l'hydrolyse de l'azotate d'uranyle est : $UO_2[(OH)_2UO_2]_n^{2+}$. (Ce processus est analogue à celui que nous avons mis en évidence, dans un travail antérieur, en milieu inerte.)

CONCLUSIONS

1. L'étude de l'hydrolyse de l'ion UO_2^{2+} en milieu azotique a démontré que cette réaction conduit à la formation d'une série de complexes polynucléaires caractérisés par la formule $UO_2[(OH)_2UO_2]_n^{2+}$.

2. Les premiers termes de cette série, les polyions $U_2O_5^{2+}$ et $U_3O_8^{2+}$, se caractérisent par les constantes de stabilité (valeurs moyennes) $K_1 = 1.10^{-6}$ et $K_2 = 1.10^{-7}$.

3. Les espèces ioniques $U_2O_5^{2+}$ et $U_3O_8^{2+}$ sont moins stables dans le milieu azotique que dans le milieu inerte d'acide perchlorique.

Revue Roumaine de Chimie, **19**, *9*, 1471–1481 (1974)

BONDING AND MAGNETIC PROPERTIES IN TETRAKIS PHOSPHINE COMPLEXES OF NICKEL

PATRICK CASSOUX, FERNAND GALLAIS, JEAN-FRANÇOIS LABARRE and
JEAN-MICHEL SAVARIAULT,
Laboratoire de Chimie de Coordination du CNRS, BP 4142, 31030 TOULOUSE CEDEX, France

Received March 8, 1974

The results of the studies on magnetic properties (^{31}P NMR, Faraday effect and Diamagnetism) of some 30 tetrakis phosphine complexes of nickel (0), NiL_4 (L = PXYZ; X, Y, Z = R, OR, F, Cl, Br, Ph, OPh; R = Me, Et, Pr, Bu, Am), are summarized and tentatively related with the bonding in such molecules. A semi quantitative analysis of the NMR data, based on LETCHER's and VAN WAZER's formalism alows approximate Ni-P bond orders to be estimated. The change in the coordination shift, $\Delta_P = \delta(NiL_4) - \delta(L)$, is discussed in terms of electronegativity and steric effect. The magnetooptical data place the complexes studied in the same qualitative order as the ^{31}P NMR studies — and as the magnetic susceptibilities measurements. The observed unexpected decrease of the Ni—P bond rotation may be explained by the following factors: a contribution of the free d-electrons of nickel and the magnetic rotary dispersion related with changes in the energy level on complexation.

For the last twenty years, a considerable number of studies have been devoted to evaluate the electron content of the dative nickel-phosphorus bond in nickel (0) phosphine complexes.

The studies on stability should be quoted first: the observed decreasing stability in the series $Ni(PF_3)_4 > Ni(PCl_3)_4 > Ni(PBr_3)_4$ made Wilkinson[1] suggest that the highly electronegative fluorine is more effective than the chlorine in freeing stable orbitals on phosphorus for use in forming π-bonds with the d-electrons of nickel. In contrast, although the alkoxy group OR is less electronegative than the fluorine, $Ni[P(OEt)_3]_4$ appears to be considerably more stable than $Ni(PF_3)_4$. Additionally to that, Basolo[2] demonstrated from the enthalpies of activation of Ni $[P(OMe)_3]_4$ and $Ni(CO)_4$ that these empirical stability considerations are not always consistent. Finally, Tolman[3] suggested on the basis of phosphorus ligand exchange equilibria studies the important rôle of the steric effects in determining the relative stability of such complexes. Numerous studies using infrared spectroscopy were carried out to throw light on the above problem: the substitution of CO in nickel carbonyl by a weaker π-bonding ligand increases the electron density on nickel which in turn induces a diminution of the CO force constant and frequency.[4] Such a correlation permits a quite consistent description of the π-acceptor character of many ligands, which can be arranged in the following order[5-11]: $PF_3 > PCl_3 > P(OR)Cl_2 > PR_2Cl > P(OPh)_3 > PPh_2Cl > P(OR)_3 > PPh_3 > PR_3$ (R = alkyl). This order rests on the assumption that the $\sigma(P \rightarrow Ni)$ charge transfer remains constant while the $\pi(Ni \rightarrow P)$ one varies. Bigorgne[12] and Angelici[13] adopt the reverse assumption : they obtain the same order as above, except that PF_3 is not the best π-acceptor ligand but the least basic one. Additionally, the anomalous place of the chlorine containing ligands in this series with respect to the electronegativity of chlorine may be noticed.

---

[1] G. Wilkinson, *J. Amer. Chem. Soc.*, **73**, 5501 (1951).

[2] M. Meier, F. Basolo and R.G. Pearson, *Inorg. Chem.*, **8**, 795 (1969).

[3] C.A. Tolman, *J. Amer. Chem. Soc.*, **92**, 2956 (1970).

Some inconsistencies in all these results caused us to prepare and study some 30 nickel (0) phosphine compounds in order to discover whether their magnetic rotation could be related to the extent of the corresponding π-back coordination, i.e. to the multiplicity of the Ni-P bonds. For this purpose we carried out Faraday effect and ^{31}P NMR measurements, as well as magnetic susceptibilities determinations.

The preparation of the NiL_4 complexes ($L = PXYZ$; $X,Y,Z = R, OR, F, Cl, Br, Ph, OPh$; $R = Me, Et, Pr, Bu, Am$) was previously described[14-20] and most of the experimental data are published[14-24] (the data obtained by the various experimental methods for R = Me, Et, Pr, Bu, Am, vary so little to make a separate discussion not justifiable). The purpose of this paper is to summarize and extend the empirical explanations which have been put forward in the hope that they will bring a step nearer a really quantitative approach.

---

[4] S.F.A. Kettle, *Spectrochim. Acta*, **22**, 1388 (1966).

[5] E.W. Abel, M.A. Bennet and G. Wilkinson, J. *Chem. Soc.*, **1959**, 2323.

[6] L.S. Meriwether and M.L. Fiene, *J. Amer. Chem. Soc.*, **81**, 4200 (1959).

[7] F.A. Cotton and C.S. Kraihanzel, *J. Amer. Chem. Soc.*, **84**, 4432 (1962) ; F.A. Cotton, *Inorg. Chem.*, **3**, 702 (1964).

[8] L.E. Orgel, *Inorg. Chem.*, **1**, 25 (1962).

[9] W.D. Horrocks and R.C. Taylor, *Inorg. Chem.*, **2**, 723 (1963) ; W.D. Horrocks and R.H. Mann, *Spectrochim. Acta*, **21**, 399 (1965).

[10] W. Strohmeier and F.J. Müller, *Z. Naturforsch.*, **22**, 451 (1967) ; *Chem. Ber.*, **100**, 2812 (1967).

[11] C.A. Tolman, *J. Amer. Chem. Soc.*, **92**, 2953 (1970).

[12] M. Bigorgne, *Bull. Soc. Chim. France.*, **1960**, 1986 ; M. Bigorgne and J. Benard, *Rev. Chim. Min.*, **3**, 831 (1966) ; A. Loutellier and M. Bigorgne, *J. chim. Phys.*, **67**, **78**, **99**, **107** (1970).

[13] R.J. Angelici and M.D. Malone, *Inorg. Chem.*, **6**, 1731 (1967).

[14] P. Cassoux and J.F. Labarre, *Compt. rend.*, **264**C, 496 (1967).

[15] P. Cassoux and J.F. Labarre, *idem*, **265**, 773 (1967).

[16] P. Cassoux, J.M. Savariault and J.F. Labarre, *Bulll. Soc. chim. France*, **1969**, 741.

[17] J.M. Savariault, P. Cassoux and J.F. Labarre, *Compt. rend.* **2690**, 496 (1969).

[18] J.M. Savariault, P. Cassoux and J.F. Labarre, *J. chim. Phys.*, 1970 ; **67**, 229 (1970).

[19] J.M. Savariault, P. Cassoux and F. Gallais, *idem*, **271**, 477 (1970).

[20] J.M. Savariault, M.H. Micoud, P. Cassoux and J.F. Labarre, *Bull. Soc. chim. France*, **1971**, 2413.

[21] M.H. Micoud, J.M. Savariault and P. Cassoux, *idem*, **1972**, 3774.

[21a] J.G. Verkade, *Coord. Chem. Rev.*, **9**, 1 (1972).

[22] P. Cassoux, J.F. Labarre and J.P. Laurent, *J. chim. Phys.*, **64**, 1813 (1967).

[23] P. Cassoux, J.M. Savariault and J.P. Laurent, *idem*, **67**, 258 (1970).

[24] P. Cassoux, J.M. Savariault, J.F. Labarre and F. Gallais, *idem*, **65**, 1185 (1968).

^{31}P NMR SPECTROSCOPY

The ^{31}P chemical shifts of the free ligands, δ(L), and of the complexes, δ(NiL_4), were determinated on a Perkin-Elmer R—10 spectrometer at 24.29 MHz, P_4O_6 being used as external reference. [20–23]

It might be expected on first consideration that the "coordination shift", $\Delta_p = \delta(NiL_4) - \delta(L)$ – which changes drastically throughout the series (Table 1) – should parallel the magnitude of the electronic shielding introduced by the coordination, which in turn should increase with the extent of the back-coordination. It is clear however that such an elementary interpretation is not valid for the following reasons :

Table 1

^{31}P coordination shift, $\Delta_p = \delta(NiL_4) - \delta(L)$, of NiL_4complexes

N°	COMPOUND	Δ_p	Ref.
1	$Ni(PMe_3)_4$	−41.1	3
2	$Ni(PBr_3)_4$	+98.0	*
3	$Ni(PMeCl_2)_4$	+15.0	*
4	$Ni(PCl_3)_4$	+47.0	20
5	$Ni[P(OR)Cl_2]_4$	+16.5	22
6	$Ni[P(OR)_2Cl]_4$	− 1.0	22
7	$Ni[P(OR)_3]_4$	−20.5	23
8	$Ni[P(OR)_2F]_4$	−28.1	23
9	$Ni[P(OR)F_2]_4$	−36.1	23
10	$Ni(PF_3)_4$	−42.8	23
11	$Ni(PPh_3)_4$	a	
12	$Ni(PPh_2Cl)_4$	a	
13	$Ni(PPhCl_2)_4$	+ 9.0	20
14	$Ni[P(OPh)Cl_2]_4$	+20.0	20
15	$Ni[P(OPh)_2Cl]_4$	+ 8.0	20
16	$Ni[P(OPh)_3]_4$	− 3.0	20
17	$Ni[P(OPh)_2F]_4$	−17.0	21
18	$Ni[P(OPh)F_2]_4$	−31.0	21
19	$Ni(PPhF_2)_4$	−10.0	21

* present work

a Δ_p not determined, because of extensive dissociation in solution.

(i) because Δ_p decreases steadily in the series $Ni(PBr_3)_4$, $Ni(PCl_3)_4$, $Ni[P(OR)_3]_4$, $Ni(PF_3)_4$* (figure 1) when the electronegativity of the atoms or groups linked to phosphorus increases, i.e. when the order of the Ni-P bond is also liable to increase ;

(ii) because even the Δ_p values of $Ni(PMeCl_2)_4$ and $Ni(PMe_3)_4$ do not fit the correlation (figure 1).

---

* The Δ_p values of the aromatic complexes were not plotted on figure 1 because the electronegativity of the aromatic group is not so well defined in the literature and is difficult to estimate ([21] and references quoted therein).

In fact, Δ_p is not only determined by the $d_\pi - d_\pi$ back-coordination (Ni→P) but also by the direct σ-coordination (P→Ni), by anisotropy, hybridization factors, etc ....[25-26]

Moreover, in the chemical shift itself, the screening constant, σ, appears to be the sum of three terms which may be called the diamagnetic, the paramagnetic and the anisotropy terms :

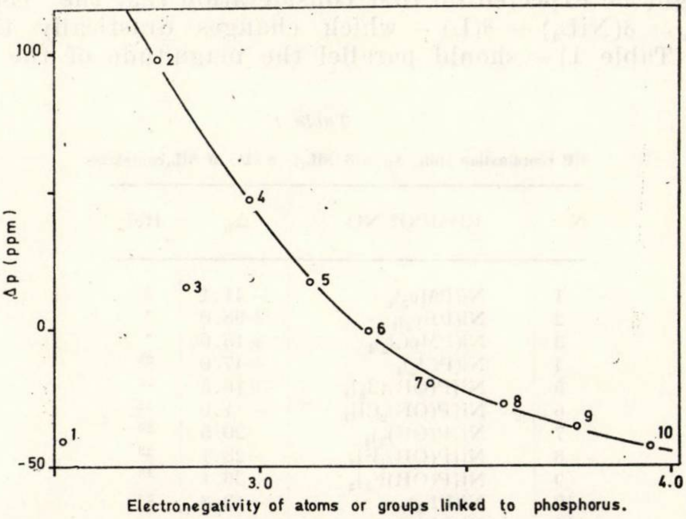

Fig. 1. — Plot of Δ_p, coordination shift of NiL_4 complexes vs. electronegativity of atoms or groups linked to phosphorus.

$$\sigma = \sigma_{dia} + \sigma_{para} + \sigma_{anisotropy}$$

According to Letcher and Van Wazer,[27] the diamagnetic term which accounts for the electronic shielding of the ^{31}P nucleus is by far less important than the paramagnetic one, the latter being due to the mixing of low lying excited states with the ground state; the third term (anisotropy) is negligible.

The formalism of Letcher and Van Wazer of the paramagnetic term leads to the following expression for the total number, n_π, of electrons in the phosphorus d orbitals :

$$n_\pi = \frac{-\delta + 11941.5 - 7940\,\zeta_1}{149.8};$$

δ is the chemical shift of a quadruply connected phosphorus nucleus (table 2) and 11941.5, 7940, 149.8 are semi-empirical coefficients.

---

[25] L.S. Meriwether and J.R. Leto, *J. Amer. Chem. Soc.*, **83**, 3192 (1961).

[26] G.S. Reddy and R. Schmutzler, *Inorg. Chem.*, **6**, 823 (1967).

[27] J.R. Van Wazer and J.H. Letcher "Topics in Phosphorus Chemistry", vol. 5, J. Wiley, New York, 1967, p 75—167.

The ζ_1 term is a function of two factors :

(i) the electronegativities of the atoms or groups linked to phosphorus,

(ii) the bond angles $\theta = ZPZ$ and they may be calculated or estimated from graphs.[27]

Table 2

Chemical shift, δ, of some Ni $(PZ_3)_4$ complexes

N°	COMPOUND	δ	Ref
1	$Ni(PMe_3)_4$	+134.7	3
2	$Ni(PBr_3)_4$	− 23.0	*
3	$Ni(PCl_3)_4$	− 60.0	20
7	$Ni[P(OR)_3]_4$	− 49.0	23
10	$Ni(PF_3)_4$	− 26.8	23

* present work.

The ζ_1 term cannot however be very accurately estimated, as the ZPZ angles are not accurately known, and hence, the n_π values we have calculated for five standard symmetrical NiL_4 molecules are only approximate. However, even when the values of θ vary somewhat from one complex to another (figure 2), the NMR results nevertheless permit a definite order of classification with regard to the n_π values and therefore to the multiplicity of the Ni-P bond, the PF_3 derivatives having the highest bond order and the PMe_3 derivatives the lowest. The total bond order approximately from 2 to 1.

Obviously, the negative n_π value for $Ni(PMe_3)_4$ is not significant and it results, as stated by Letcher and Van Wazer themselves[27] (p. 191), from the approximation of the method.

The overall picture is that which would be expected : the tendency of phosphorus to attract the d-electrons of nickel increases with the former's formal positive charge which is at its maximum when the electronegativity of the ligands is the highest ; i.e. in $Ni(PF_3)_4$.

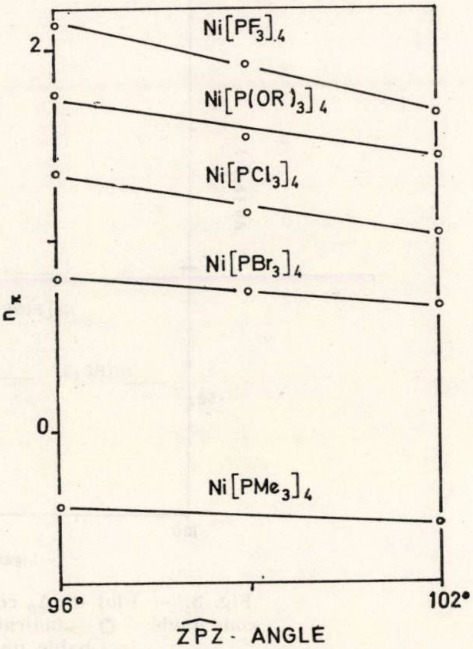

Fig. 2. — Plot of n_π values calculated for some $Ni(PZ_3)_4$ complexes vs. ZPZ angle.

It nevertheless remains true that the variations of the Δ_p values are not consistent with the results of the above semi-quantitative analysis. Reddy and Schmutzler suggested earlier that the surprising Δ_p value of $Ni(PCl_3)_4$ could be due to large changes in hybridization and bond angles on complexation[26]. This explanation was further extended by Tolman who emphasized (on the basis of ^{31}P NMR studies) the important role of steric effects in determining the ligand exchange equilibria in such complexes, and proposed a quantitative measure of these effects based on the determination of "ligand cone angles".[3] Similar ligand exchange equilibria studies, based on the ^{31}P NMR studies carried out by us,[21] led to the following classification of the aromatic complexes:

$$Ni[P(OPh)F_2]_4 > Ni(PPhF_2)_4$$

$$Ni[P(OPh)Cl_2]_4 > Ni(PCl_3)_4 > Ni(PPhCl_2)_4.$$

This confirms that the stability of these complexes decreases, with the increasing size of the ligand.

Moreover, UV spectroscopic[28] and NMR studies[3,20] show that $Ni(PPh_3)_4$ and $Ni(PPh_2Cl)_4$ (where its ligands are very large) are extensively dissociated in solution.

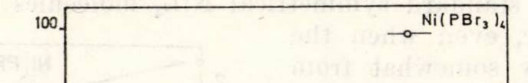

Fig. 3. — Plot of Δ_p coordination shift vs. ligand cone angle —O— indicates the magnitude of probable uncertainty.

We have attempted to correlate the Δ_p values with the ligand cone angles reported by Tolman[3] (figure 3). For many complexes, the greater the ligand cone angle is, the greater the corresponding value of Δ_p. However the surprisingly low Δ_p values for complexes, e.g. $Ni[P(OPh)_3]_4$ ($\Delta_p = -3$) and especially $Ni(PMe_3)_4$ ($\Delta_p = -41$), do not fit in this eventual correlation : Tolman has suggested that these ligands are bulky.[3] This anomalous behaviour of $Ni(PMe_3)_4$ may be due, as noticed by Verkade,[21a] to a possible metal-phosphorus bond shortening of trialkylphosphines complexes ; a shortening of a similar magnitude as for the more electronegative ligands.

---

[28] P. Heimbach, *Angew. Chem.*, **76**, 586 (1964).

FARADAY EFFECT MEASUREMENTS

The magnetic molecular rotations of the ligands, $[\rho]_M$ (L), and of the complexes, $[\rho]_M$ (NiL_4), have been measured, using a previously described apparatus,[29] at 20°C for the yellow wavelength ($\lambda = 578$ nm), either heat if the complexes are liquid, or in solution if they are solid.[14-21] Obviously, the coordination increment $\Delta\rho = \frac{1}{4}\{[\rho]_M(NiL_4) - 4[\rho]_M(L)\}$ is the result of all the electronic and geometric changes occurring on coordination and a classical magnetooptical analysis of these factors [30] leads to the following expansion of the "true" rotation of the Ni-P bond, ρ(Ni—P):

$$\rho(\mathrm{Ni.P}) = \Delta\rho + 2\,\rho(e)_p \pm \rho G \pm \delta\pi.$$

(i) $2\,\rho(e)$ is the contribution of the lone pair of electrons of the P(III) atom before σ-coordination has occurred. The values of $2\,\rho(e)_p$ were previously estimated.[31]

(ii) δG measures the changes of hybridization and ionic character : in fact, in contrast with the NMR results, the magnitude of the $\Delta\rho$ and $2\,\rho(e)_p$ values (table 3) allows this factor — the magnitude of which is far smaller [30] — to be neglected in this case.

(iii) $\delta\pi$ symbolizes the change in the π-character (where present) between the free and complexed ligand ; in particular the π-character of the P-F bond in the fluorophosphines has been repeatedly discussed.[32] The results of Faraday effect studies allowed us to suggest that this bond is a pure σ one.[31] This is confirmed by an *ab initio* calculation on PF_3[33], but is in contradiction with other calculations by Hillier and Saunders on the same molecule.[34]

[29] J.F. Labarre and F. Gallais, *Russian Chem. Rev.*, **40**, 346 (1971).
[30] F. Gallais, J.F. Labarre, J.P. Laurent and P. de Loth, *J. chim. Phys.*, **67**, 375 (1970).
[31] P. Cassoux, P. Castan, P. Swysen, M.C. Labarre and J.F. Labarre, *idem*, **66**, 1770 (1969).
[32] M.L. Huggins, *J. Amer. Chem. Soc.*, **75**, 4123 (1953).
H.S. Gutowsky and D.W. Mc Call, *J. Chem. Phys.*, **22**, 162 (1954).
J.R. Van Wazer, *J. Amer. Chem. Soc.*, **78**, 5709 (1956).
J.H. Letcher and J.R. Van Wazer, *J. Chem. Phys.*, **44**, 815 (1966).
T. Kruck, *Angew. Chem. Internat. Ed.*, **6**, 53 (1967).
[33] A. Serafini, J.F. Labarre, A. Veillard and G. Vinot, *Chem. Comm.*, **1971**, 997.
[34] I.H. Hillier and V.R. Saunders, *Chem. Phys. Lett.*, **6**, 253 (1970).

Even if some δ-character is present in the P-F bonds it can be neglected for our present discussion, as its magnitude is so small : the electron diffraction studies on PF_3 and $Ni(PF_3)_4$ show indeed that the length of the P-F bond is unchanged[35] and the photoelectron spectroscopy studies state that the bonding in PF_3 is unaltered on coordination to nickel[36] It might be expected however that this $\delta\pi$ factor would be very important in the case of the aromatic complexes : the magnetooptical contribution of a phenyl group is rather variable[37] and may vary on the coordination of the aromatic ligands to nickel. Fortunately it has been shown[21] that these variations may be considered as second order perturbations.

Under these conditions, approximate values of the bond rotation $\rho(Ni.P)$ may thus be deduced from the experimental data (Table 3). These values, which range from $\simeq 500$ to $\simeq 2200$ μr are all extremely high : such high values have never been found in other branches of chemistry.[29] Moreover, these two characteristics, and especially the second one, provide good experimental proof of the multiplicity of the Ni-P bond and its variation with structure as only $(\sigma + \pi)$ bonds are liable to vary so widely with the molecular environment.[29] The Faraday effect results arrange the complexes in an order which is quite consistent with that obtained by the previous semi-quantitative analysis of the NMR data. The Faraday effect is again demonstrated as a property which may be

Table 3

Faraday effect data and magnetic Ni-P bond susceptibilities of NiL_4 complexes

N°	COMPOUND	$\Delta\rho$	Ref	$2\rho(e)p^a$	$\rho(Ni.P)$	$\chi(Ni.P)$	Ref
2	$Ni(PBr_3)_4$	1834	19	300	2134	—	—
3	$Ni(PMeCl_2)_4$	966	*	300	1266	− 5.0	24
4	$Ni(PCl_3)_4$	966	19	300	1266	+ 2.7	24
5	$Ni[P(OR)Cl_2]_4$	857	14	300	1157	− 3.3	24
6	$Ni[P(OR)_2Cl]_4$	719	15	300	1019	−10.3	24
7	$Ni[P(OR)_3]_4$	571	18	300	871	−14.5	24
8	$Ni[P(OR)_2F]_4$	474	18	260	734	−15.0	18
9	$Ni[P(OR)F_2]_4$	432	18	215	647	−14.0	18
10	$Ni(PF_3)_4$	326	19	192	518	—	—
13	$Ni(PPhCl_2)_4$	1664	20	300	1964	− 8.8	20
14	$Ni[P(OPh)Cl_2]_4$	1010	20	300	1310	− 0.1	29
15	$Ni[P(OPh)_2Cl]_4$	958	20	300	1258	—	—
16	$Ni[P(OPh)_3]_4$	887	21	300	1178	—	—
17	$Ni[P(OPh)_2F]_4$	656	21	260	916	−12.8	21
18	$Ni[P(OPh)F_2]_4$	467	21	215	682	−11.1	21
19	$Ni(PPhF_2)_4$	669	21	215	884	− 9.0	21

a cf[31]

* present work

---

[35] Y. Morino, K. Kutchisu and T. Moritani, *Inorg. Chem.*, **8**, 867 (1969).
J.C. Mariott, J.A. Salthouse, M.J. Ware and J.M. Freeman, *Chem. Comm.*, **1970**, 595 ; A. Almenningen, B. Andersen and E.E. Astrup, *Acta Chem. Scand.*, **24**, 1579 (1970).

[36] J.C. Green, D.I. King and J.H.D. Eland, *Chem. Comm.*, **1970**, 1121 ;
I.H. Hillier, V.R. Saunders, J. Ware, P.J. Basset, D. R. Lloyd and N. Lynaugh, *idem*, **1970**, 1316.

[37] J.F. Labarre and F. Crasnier, *Topics in Current Chemistry*, **24**, 33 (1971).

extremely useful to follow the changes in the bonding throughout a series of related chemical compounds. Additionally, the third specific bond modulus, $\varkappa$(Ni.P) we obtained by an analysis of the diamagnetic susceptibility of some NiL_4 complexes gives (Table 3) nearly the same order as the other two experimental methods [except for Ni $(PPhCl_2)_4$]. We note that as expected,[38] the highest diamagnetic contribution parallels the highest Ni-P bond order in the fluorine containing complexes.

The magnetooptical behaviour of these molecules containing a transition element offers a striking contrast to compounds containing no transition elements. In the latter the π-bonding gives rise to very large increments in the magnetic rotation, these increments rising sharply when the bond order increases.[29] This striking difference may be accounted for by the following:

The influence of the electronegativity is illustrated by the fairly good correlation in figure 4 between ρ(Ni.P) and the electronegativity of atoms of groups linked to phosphorus. Moreover, this correlation leads to predicted electronegativity values for the OPh group ($\simeq 3.0$) and for the Ph group ($\simeq 2.35$) which are in good agreement with the more recent values proposed in the literature ([21] and references therein reported) and allows all the studied aromatic complexes to fit into this correlation. (+ points in figure 4); $Ni(PMeCl_2)_4$ is however anomalous.

In figure 5, we have attempted to correlate the ρ(Ni.P) values with ligand cone angle[3] : the greater cone angles are associated with the greater ρ(Ni.P) values.

The unusual magnetooptical behaviour of the complexes studied can be directly related to the specific nature of the central atom i.e. a transition metal involving free d-electrons. The decrease of ρ(Ni.P), when the order of this bond increases, may indeed be interpreted in terms of a resulting decrease of the electron population in the nickel d-orbitals.

Finally, attention is drawn to the fact that the considerable changes of ρ (Ni.P) experimentally observed parallel the occurrence of an "anomalous" and variable rotary dispersion, i.e. that the ratios ρ^g/ρ^y and ρ^i/ρ^y of the values we obtain by measurements using the yellow ($\lambda^y = 578$ nm), green ($\lambda^g = 546$ nm) and indigo ($\lambda^i = 436$ nm) wavelengths are not equal to the normal values (1.13 and 1.86) and furthermore are variable. Table 4 summarizes these results and we notice that the order of the complexes considered is not by the value of the wavelength seem to be related with the position of the first UV absorption band (λ_0). It may be thus objected that these rotations must be analysed in terms of molecular energy levels, as for example Briat *dt la.* did in the case of $TiCl_4$.[39] However, because of the size of the molecules studied, such calculations, in as much as they are possible in the current state-of-art, would involve computations of such magnitude to put them outside the scope of the present study.

---

[38] P. Pascal, F. Gallais and J.F. Labarre, *Compt. rend.* **1961**, 252.

[39] B. Briat, J.C. Rivoal and R.H. Petit, *J. chim. Phys.*, **67**, 463 (1970).

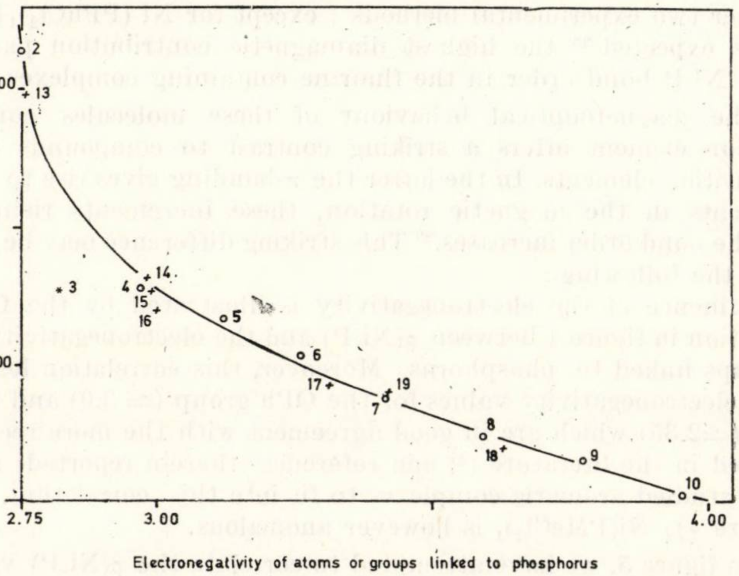

Fig. 4.—Plot of Ni—P bond rotation, ρ(Ni.P), vs. electronegativity of atoms or groups linked to phosphorus.

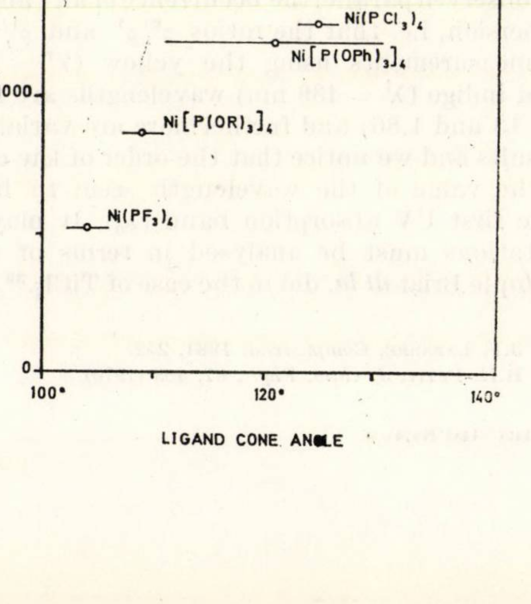

Fig. 5. — Plot of Ni-P bond rotation, ρ(Ni.P), vs. ligand cone angle —O— indicates the magnitude of probable uncertainty.

Table 4

Magnetic rotatory dispersion of some NiL_4 complexes

N°	COMPOUND	ρ^y(Ni.P)	ρ^g(Ni.P)	ρ^i(Ni.P)	$\frac{\rho^g}{\rho^y}$ (Ni.P)	$\frac{\rho^i}{\rho^y}$ (Ni.P)	λ_0 (nm)
4	$Ni(PCl_3)_4$	1266	1553	—	1.227	—	315
5	$Ni[P(OR)Cl_2]_4$	1157	1383	3203	1.195	2.77	284
6	$Ni[P(OR)_2Cl]_4$	1019	1206	2608	1.184	2.56	265
7	$Ni[P(OR)_3]_4$	871	1016	2023	1.166	2.32	237
8	$Ni[P(OR)_2F]_4$	734	852	1630	1.161	2.22	225
9	$Ni[P(OR)F_2]_4$	647	749	1418	1.158	2.19	224
10	$Ni(PF_3)_4$	518	598	1120	1.154	2.16	224

CONCLUSION

We attempted, by means of a critical discussion of the magnetic behaviour of some tetrakis phosphine complexes of nickel (0) to open a new view of bonding in such molecules. ^{31}P NMR and Faraday effect data — as well as the magnetic susceptibilities, permit a placing of these complexes in nearly the same order for all three methods, and this consistency is discussed in terms of the varying geometric or electronic factors.

The NMR results show that steric effects may be as important as electronic ones in determining the experimental coordination shifts; on the other hand, the semi-quantitative analysis of the chemical shifts themselves — based on Letcher's and Van Wazer's formalism — leads to approximate values of the total bond order of the nickel-phosphorus bond which are more dependent on the electronegativity of the atoms or groups linked to phosphorus than on the steric effects.

The Faraday effect results may be likewise discussed in terms of steric and electronegativity factors, but further complications may also result from the specific contribution of the free d-electrons of nickel, from “anomalous and variable rotary dispersion, from changes in energy levels on changing ligands — as shown by the changes in the first UV absorption band. All the above factors may contribute to why in such cases bond rotations do not fit into the general pattern which has proved to be so extremely useful in other branches of chemistry.

The authors are indebted to Professor R.A. SHAW, Birkbeck College, London, for his interest in this work, for stimulating the discussions and for the suggestions about the manuscript.

Revue Roumaine de Chimie, **19**, *9*, 1483–1489 (1974)

CALCIUM ALUMINOSULPHATE FORMATION AND HARDENING PROPERTIES

I. TEOREANU and MARCELA MUNTEAN
Polytechnic Institute
Str. Polizu, no. 1 — Bucharest — Romania

Received February 6, 1974

The present paper studies both the stability range and the properties of $3(CaO.Al_2O_3)CaSO_4$ and the changes induced by this compound in the mechanical strength value of the tricalcium silicate and of the dicalcium silicate. Calcium aluminosulphate starts being formed even et temperatures below 1000°, reaching a maximum formation rate around 1300°. Beyond 1300° its decomposition rate is higher than its formation rate. The calcium aluminosulphate shows a high interaction rate with water, developing slightly better mechanical strength than $3CaO.Al_2O_3$. The calcium aluminosulphate influences in a differentiated manner the hardening process of calcium silicates and their mechanical strength.

1. The formation of calcium aluminosulphate $3(CaO.Al_2O_3).CaSO_4$ in the systems $CaO-Al_2O_3$, $CaO-Al_2O_3-Fe_2O_3$, $CaO-Al_2O_3-SiO_2$ and $CaO-Al_2O_3-Fe_2O_3-SiO_2$ with additions of calcium sulphate and also in clinkers mineralized with gypsum or phosphogypsum has been previously reported.[1–16]

The hardening properties of clinkers containing calcium aluminosulphate are influenced by the latter which also influences the hardening

---

[1] J.A. ROGOZINA, *Zhur. priklad. Khim.*, **30**, 1742 (1957).

[2] J.A. ROGOZINA and M.A. AHMEDOV, *Epitöanyag*, **22**, 259 (1968).

[3] S.D. OKOROKOV, S.L. GOLYANKO - VOL'FSON, T.N. YARKINA and R.A. CHEPIK, *Zhur. priklad. Khim.*, **35**, 263 (1962).

[4] S.D. OKOROKOV, S.L. GOLYNKO-VOL'FSON, T.N. YARKINA and R.A. CHEPIK, *Zhur. priklad. Khim.*, **35**, 2448 (1962).

[5] W. GUTT and M.A. SMITH, *Trans. Brit. Ceram. Soc.*, **67**, 487 (1968).

[6] N. FUKADA, *Semento Gijusta Nengo*, **15**, 26 (1961).

[7] N. FUKADA, *Bull. Chem. Soc. Japan*, **34**, 138 (1961).

[8] P.P. BUDNIKOV, I. KUZNETSOVA and V.G. SAVELIEV, *Silikattechnik*, **16**, 414 (1965).

[9] P.P. BUDNIKOV, *Cement-Wapno-Gips*, **22/34**, 281 (1967).

[10] P.P. BUDNIKOV , I.P. KUZNETSOVA and V.G. SAVELIEV, *Cement-Wapno-Gips*, **20/32**, 153 (1965).

[11] P.P. BUDNIKOV, R. D. AZELITSKAIA, and A.A. LOKOTI, *Zhur. priklad. Khim.*, **41**, 953 (1968).

[12] R. TURRIZIANI and F. MASSAZZA, *Ann. Chim. (Ital.)*, **56**, 1172 (1966).

[13] P.P. BUDNIKOV, *Cement-Wapno-Gips*, **17/29**, 39 (1962).

[14] B. KOSTOV, *Compt. rend. Acad. Bulg. Sci.*, **18**, 335 (1965).

[15] O. HENNIG and H.D. NABHAN, *Wiss. Zeitschrift Hochschule Archit. Bauwesen Weimar*, **19**, 47 (1972).

[16] H. SCHOLZE and U. HILDEBRANDT, *Zement-Kalk-Gips*, **23**, 573 (1970).

of the other mineralogical compounds of clinker, particularly the silicate compounds.

2. The present paper studied both the stability range and the properties of $3(CaO.Al_2O_3).CaSO_4$ and the changes induced by this compound in the mechanical strength of the hardened tricalcium silicate and β-dicalcium silicate. Chemically pure, finely ground $CaCO_3$, Al_2O_3 and $CaSO_4.2H_2O$ were used in order to obtain $3(CaO.Al_2O_3).CaSO_4$. Based on the data from the literature,[8,10] the synthesis temperature chosen was 1300°. The calcination processes are achieved with the maintenance for 4 hours at a maximum temperature followed by 2 hours of cooling in the furnace and then in the air. The roentgenogram of the resulted product is exhibited in figure 1. Figure 2 presents the microscopic image of the compound in transparent light.

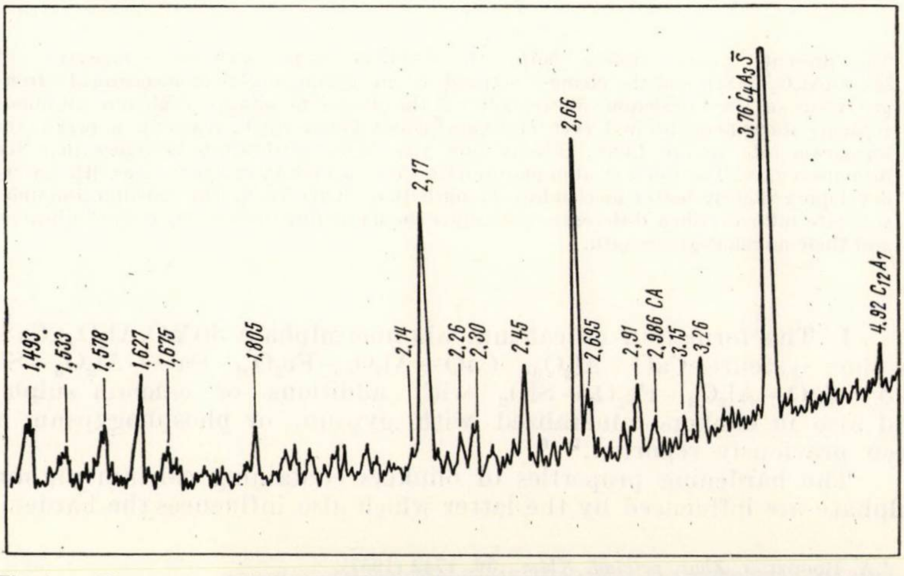

Fig. 1. — The roentgenogram of the calcium aluminosulphate synthesized at 1300°.

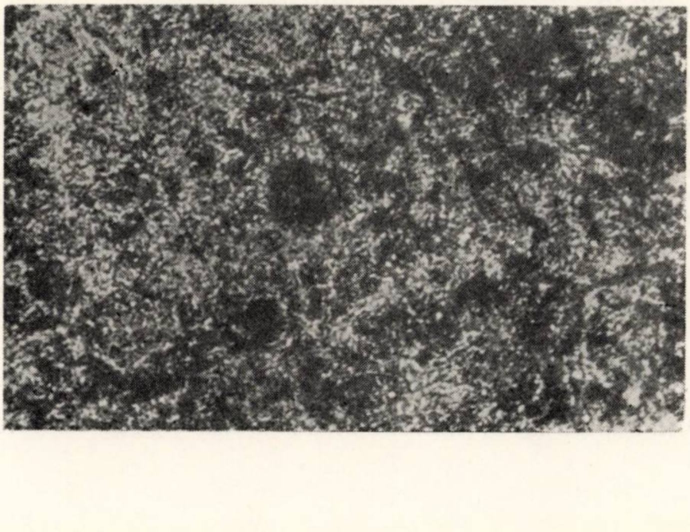

Fig. 2. — Microphotograph of calcium aluminosulphate synthesized at 1300° (× 300).

In order to follow the formation of calcium aluminosulphate at various synthesis temperatures and also its stability with the increase in the calcination temperature, the stoichiometric mixtures were also burnt at 800°, 900°, 1000°, 1100°, 1250°, 1380°, 1420° and 1500° allowing them to cool in the furnace up to roughly 800° and then in the air.

Since the roentgenogram presented in fig. 1 reveals the presence of $CaO.Al_2O_3$ and of $12CaO.7Al_2O_3$ together with $3(CaO.Al_2O_3).CaSO_4$ impulse measurements were made on the synthesized samples at various temperatures, by means of a X diffractometer corresponding to the diffraction lines $d = 2.97 Å$ – $CaO.Al_2O_3$, $d = 3.76$ Å – $3(CaO.Al_2O_3).CaSO_4$ and $d = 4.93$ Å – $12CaO.7Al_2O_3$. Similar measurements were also performed for $CaO.2Al_2O_3$ ($d = 3.51$ Å). The results obtained were plotted in figs. 3 and 4*. At the same time, determinations were made on the free CaO and SO_3 content of the synthesized samples (table 1 and table 2).

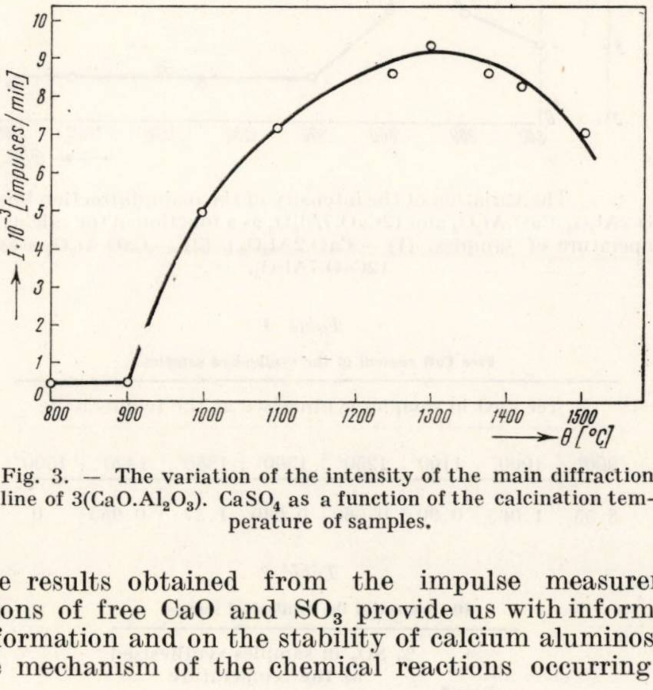

Fig. 3. – The variation of the intensity of the main diffraction line of $3(CaO.Al_2O_3).CaSO_4$ as a function of the calcination temperature of samples.

3. The results obtained from the impulse measurements and determinations of free CaO and SO_3 provide us with information on the kinetics of formation and on the stability of calcium aluminosulphate and also on the mechanism of the chemical reactions occurring during the calcination.

The positive existence of $CaO.2Al_2O_3$ and of $12CaO.7Al_2O_3$ is revealed at 800°. Beyond 900° the amount of $CaO.Al_2O_3$ and $3(CaO.Al_2O_3).CaSO_4$ from the mixture increases simultaneously, whereas the amount of $12CaO.7Al_2O_3$ and $CaO.2Al_2O_3$ decreases; beyond 1100°, the latter is practically absent from the synthesized samples. Since the formation of calcium aluminosulphate reaches a maximum at 1300°, the significant decrease of the $CaO.Al_2O_3$ proportion in samples calcined between 1000° and 1300° may be explained :

---

* The background impulse recording corresponds to approx. 350...400 impulses/min.

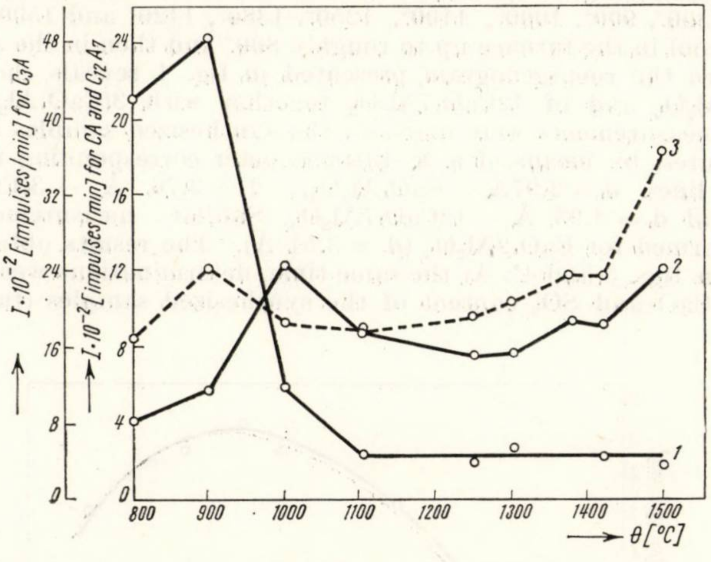

Fig. 4. — The variation of the intensity of the main diffraction lines of $CaO.2Al_2O_3$, $CaO.Al_2O_3$ and $12CaO.7Al_2O_3$ as a function of the calcination temperature of samples. (1) — $CaO.2Al_2O_3$; (2) — $CaO.Al_2O_3$; (3) — $12CaO.7Al_2O_3$.

Table 1

Free CaO content of the synthesized samples

% free CaO in samples synthesized at the temperature							
900°	1000°	1100°	1250°	1300°	1380°	1420°	1500°
8.55	1.065	0.90	0.060	0.040	1.37	0.955	0

Table 2

SO_3 content of the synthesized samples

% introduced SO_3	% SO_3 in samples synthesized at the temperature		
	1380°	1420°	1500°
13.11	10.63	10.76	6.32

$$3(Ca.O.Al_2O_3) + CaSO_4 \rightleftarrows 3(CaO.Al_2O_3).CaSO_4 \qquad (1)$$

The proportion of $CaO.Al_2O_3$ and also of $12CaO.7Al_2O_3$ is maintained within the mentioned temperature range at a relatively reduced level.

Beyond 1300°, the counter reaction rate illustrated by equation (1) becomes more important than the direct reaction rate : the calcium aluminosulphate becomes instable ; as a result of this instability in samples synthesized at 1500° the proportion of $CaO.Al_2O_3$ and $12CaO.7Al_2O_3$ obviously increases as compared to its value in the samples calcined at 1300°. The increase in the $12CaO.7Al_2O_3$ content when calcination takes place at very high temperatures may be explained by the saturation of $CaO.Al_2O_3$ resulted from the $3(CaO.Al_2O_3).CaSO_4$ decomposition. Indeed, the data reporting the SO_3 content of the synthesized samples attest an intense $CaSO_4$ decomposition at high temperatures (particularly in samples calcined at 1500°). An equilibrium of the process may be achieved at temperatures over 1500°, the equilibrium products being $CaO.Al_2O_3$ and $12CaO.7Al_2O_3$. The presence of the latter can be explained only if considering the relatively intense decomposition of $CaSO_4$ under these conditions, in addition to the high instability of the calcium sulphataluminate.

4. The hydration properties of $3(CaO.Al_2O_3).CaSO_4$ (a binder synthesized at 1300°) were investigated by mechanical strength tests on Kühl microprobes prepared of 1 : 3 mortar (binder : sand) with 13% water. Table 3 lists the data obtained as compared to those determined for $3CaO.Al_2O_3$. A comparison with the resistances of $3CaO.Al_2O_3$ is justified by the fact that the formation of $3(CaO.Al_2O_3) . CaSO_4$ in clinkers mineralized with gypsum blocks the formation of tricalcium aluminate. The results obtained show that the calcium aluminosulphate has somewhat better binding properties than $3CaO.Al_2O_3$.

Table 3

Relative mechanical strength of hardened $3CaO.Al_2O_3$ and $3(CaO.Al_2O_3) . CaSO_4$.

Binder	Relative strength of compression, after :			
	1 day	7 days	28 days	90 days
$3CaO . Al_2O_3$	100	187	209	194
$3(CaO.Al_2O_3).CaSO_4$	163	238	231	231

The roentgenographic study of hydrated calcium aluminosulphate showed that $3CaO.Al_2O_3.CaSO_4.12H_2O$ is formed after a day of hardening ; an increase in the hardening duration causes the occurrence of $3CaO.Al_2O_3.3CaSO_4.32H_2O$, its proportion increasing in the sample ; the only calcium aluminate sulphate hydrate existing in the binder hydrated for 28 days is ettringite.

5. Studies were also carried out on the mechanical properties of some mixture containing $3CaO.SiO_2$ with $3(CaO.Al_2O_3).CaSO_4$ and β-$2CaO.SiO_2$ with $3(CaO.Al_2O_3).CaSO_4$ (synthesized at 1300°). The mixtures were achieved in a proportion of 1 : 1, 2 : 1,3 : 1 and 10 : 1 calcium silicate/cal-

cium aluminosulphate. The determinations were again made on same Kühl microprobes using 1 : 3 mortar (binder : sand) with 13% water. The results of the tests are listed in table 4 (the obtained values were reported to the strength of compression of a $3CaO.Al_2O_3$ sample hardened for 1 day; the strength value of the latter sample was considered 100).

Table 4

Relative strength of mixtures containing calcium silicates and $3(CaO.Al_2O_3).CaSO_4$

Binder	Mixing ratio	Relative strength of compression, after: 1 day	7 days	28days	3 months
$3CaO.SiO_2$	—	318	650	1050	1470
β-$2CaO.SiO_2$	—	62.5	137	455	—
$3CaO.SiO_2$ / $3(CaO.Al_2O_3).CaSO_4$	1/1	209	635	975	1430
	2/1	244	672	1050	1460
	3/1	290	766	1290	1500
	10/1	351	1130	1760	1840
β-$2CaO.SiO_2$ / $3(CaO.Al_2O_3).CaSO_4$	1/1	395	830	1070	1230
	2/1	364	577	853	995
	3/1	216	520	680	905
	10/1	81.5	133	483	920

The calcium aluminosulphate is found to have an activating action on the hardening of β-$2CaO.SiO_2$ and this action becomes more intense as the aluminosulphate proportion in the mixture is higher. Conversely, the presence of the calcium aluminosulphate in a mixture with tricalcic silicate determines the decreases in the strength of the latter for short hardening periods; the reason must be sought in the internal tensions appearing in the hardening structure, due to high interaction rates of both compounds of the mixture with water. In the case of the longer hardening periods (7 days) this negative influence is attenuated and at 28 days and 3 months, the mechanical strength of hardened mixtures of tricalcic silicate and calcium aluminosulphate are significantly higher than those of the pure tricalcium silicate hardened for the corresponding periods of time; there seems to exist an optimum proportion of $3(CaO.Al_2O_3).CaSO_4$ in the mixture (shifted towards the low values).

For all the hardening periods of β-$2CaO.SiO_2$—$3(CaO.Al_2O_3).CaSO_4$ mixtures we can speak about an optimum ratio between the two components, which is however shifted towards large calcium aluminosulphate proportions.

It results from the data presented that the composition must be judiciously selected in clinkers mineralized with gypsum (phosphogypsum) calcined at low temperatures, so that to have an optimum $3CaO.SiO_2$/β-$2CaO.SiO_2$/$3(CaO.Al_2O_3).CaSO_4$ proportion from the point of view of the physical-mechanical properties of the hardened binder. To do this, the fact must be kept in mind that under the mentioned conditions, the formation of calcium aluminosulphate blocks the formation of tricalcium aluminate with the occurrence of an excess of CaO. The excess of calcium oxide may determine the formation of an increased amount of tricalcium silicate and the decrease of the β - $2CaO.SiO_2$ content in the final product compared to their potential value corresponding to the dosage used.

6. In conclusion, the investigations into the formation and the properties of calcium aluminosulphate result in the following findings :

a. The calcium aluminosulphate starts being formed even at temperatures below 1000°, its maximum formation rate being established at approx. 1300°.

b. At temperatures beyond 1300° the decomposition rate of calcium aluminosulphate is higher than its formation rate.

c. The formation of the calcium aluminosulphate in Portland cement clinkers calcined at lower temperatures may block the formation of tricalcium aluminate and favour the saturation of the dicalcium silicate in tricalcium silicate.

d. The calcium aluminosulphate shows a high interaction rate with water, developing somewhat better mechanical strength than those of tricalcium aluminate.

e. The calcium aluminosulphate has an intense activating action of β-$2CaO.SO_2$, which, accordingly, develops some relatively high initial strength. From the standpoint of the initial strength, the calcium aluminosulphate has a negative influence on the hardening of the tricalcium silicate. The above facts illustrate the need for a judicious choice of the composition of clinkers mineralized with gypsum or phosphogypsum, calcined at lower temperatures so that to obtain an optimum $3CaO.SiO_2/$ β-$2CaO.SiO_2$ / $(CaO.Al_2O_3).CaSO_4$ proportion from the point of view of the physical-mechanical properties of the hardened binder.

Revue Roumaine de Chimie, **19**, *9*, 1491–1502 (1974)

INFLUENCE OF OXIDES OF TRANSITIONAL ELEMENTS ON THE PROPERTIES OF MINERALOGICAL COMPONENTS OF CLINKERS OF CEMENTS

MARIA ENCULESCU

Institute for Research, Designing and Documentation in Binders and Asbestos Cement Industry,
Calea Victoriei No. 111, Bucharest, Romania

Received November 21, 1973

By carrying out our own investigations it was possible to establish the approximate values for the solubilization limits of some colouring oxides in calcium silicates and calcium aluminates. The solubilization degree of the chromophore ions, the manner in which they are included in the basic lattice, the binding energy with oxygen, the coordination explain the correlation with the basicity of calcium silicates and aluminates and their colour. By means of the ligand field theory we revealed the correlations between the colour characteristics and the basicity of calcium silicates and aluminates. Approaches were thus established for obtaining cements, mortars and concretes reinforced by high mechanical resistances and by a great colour stability. Cements of coloured Portland and aluminous clinkers were obtained in the laboratory and in factories, coloured on the base of raw materials for white cement and raw materials for ordinary cement, contributing thus to the production on scientific bases of cements falling in this category. Important results were obtained in achieving Portland cements with a high degree of whiteness.

1. INTRODUCTION

The utilization of finishing materials based on white and coloured cements has been largely extended in recent times. Considering some more limited investigations into coloured cements with superior characteristics obtained from coloured clinkers, our own studies[1–10] mainly focused on the influence of oxides of Fe, Mn, Cr, Co, Ni and Cu on the formation, stabilization and colouring of the principal mineralogical compounds of Portland and aluminous clinkers and also on their binding properties.

---

[1] M. Enculescu, Thesis, Polytechnic Institute, Bucharest, 1972.

[2] M. Enculescu, *Studii şi Cercetări de Chim.*, *Acad. R.S.R.*, **27**, 12, (1973).

[3] M. Enculescu, *Studii şi Cercetări de Chim. Acad. R.S.R.*, (under press).

[4] M. Enculescu, *Rev. Roumaine Chim. Acad. R.S.R.* (under press).

[5] M. Enculescu, *Revista de Materiale de Construcţii* (under press).

[6] M. Enculescu and E. Marton, *Rev. Construcţii şi Materiale de Construcţii*, **1967**, 321 (1968); **1968**, 145.

[7] M. Enculescu, *BIDT pt. Materiale de construcţii*, **1972**, 3; **1972**, 9.

[8] I. Teoreanu, M. Enculescu and E. Marton, ,,Cimenturi albe şi colorate'', Bucureşti, Ed. tehnică, 1969.

[9] I. Teoreanu, M. Enculescu and I. Roşescu, *Rev. des Mat. Construction*, **655**, 103 (1971).

[10] I. Teoreanu, M. Enculescu and T. Roşescu, *Rev. Roumaine Chim.*, **16**, 1091 (1971).

2. THE INFLUENCE OF THE OXIDES OF TRANSITIONAL ELEMENTS ON THE FORMATION OF CALCIUM SILICATES AND ALUMINATES

Using the results obtained from our personal studies,[1-10] and also the available information found in the speciality literature, we established with sufficient accuracy the solubilization limits of the oxides of transitional elements in clinker mineralogical compounds.

2.1. The main phase, highly important in clinkers of white and coloured cement, 3 $CaO.SiO_2$, has been the subject of a number of studies.[1,11-16] The isomorphism relations of tricalcium silicate with the oxides of transitional metals are of a great interest.

The *ferric oxides* are isomorphically added to the structure of tricalcium silicate. The tricalcium silicate samples with over 2% Fe_2O_3 revealed, in our own investigations,[1] the characteristic lines of C_2F (d = 2.71 Å and 2.81Å) and even of Fe_2O_3 (d = 2.68 Å and 2.79 Å), pointing to the fact that the solubilization limit is obviously exceeded, as illustrated in fig. 1.

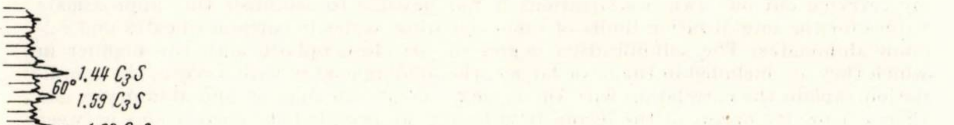

Fig. 1. — Diffractograms of pure anhydrous $3CaO.SiO_2$ and $3CaO.SiO_2$ with 0.5 – 2.0 – 4.0 – 8.0 % Fe_2O_3.

---

[11] H. Hornain, Service Physique du CERILH-L-P-T-(HH) j.L.D.—30701 Paris (1971).

[12] E.N. Maslîi, Politehn. Instit. im. S.M. Kirova, Tomsk, 1971.

[13] M. Regourd, "Symposium International de la Chimie du Ciment", Tokyo, 6—11 oct. 1968., *Rev. des Mat. Construction*, **1969**, 643 ; **1969**, 644.

[14] A. Dietzel and L. Tscheischwili, *Ber. dtsch. Keram,. Ges.*, **30** (1953).

[15] L. Revay, *Epitoanyag*, **1968**, 3.

[16] E. Woermann, W. Eysel and Th. Hahn, *Zement, Kalk, Gips*, **1968**, 6.

The examinations based on electron microprobe,[1] indicate with an increased precision that this solubilization limit is 0.68–0.79%, very close to that indicated by Woermann[16]. The solid solutions of tricalcium silicate with Fe_2O_3 are described by the formula :

$$(Ca_{3-x}\,.\,Fe_x)\;(Si_{1-y}\,.\,Fe_y)O_{5-z} \qquad (1)$$

in which $z = x + 2y - \frac{u}{2}(x + y)$, u being the valence of the cation.

The *manganese dioxide* is included in the lattice of tricalcium silicate leading to the occurrence of a monoclinic polymorphic form[11,12]. The diffractometric analysis shows for $3CaO.SiO_2$ samples with 2%, 4% and 8% MnO_2 characteristic lines of MnO_2 at d = 2.1994 Å and at d = 2.3422 Å, as seen in figure 2. The MnO_2 solubility limit in tricalcium silicate is about 1 %. The solid solutions of $3CaO.SiO_2$ with MnO_2 may be described by formula :

$$(Ca_{3-x}\,.\,Mn_x)\;(Si_{1-y}\,.\,Mn_y)\;O_{5-z} \qquad (2)$$

in which $z = x + 2y - \frac{u}{2}(x + y)$, u being the valence of the metallic cation.

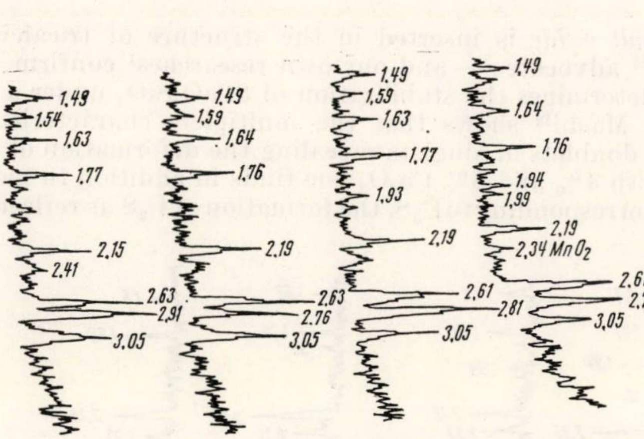

C_3S+0.5% MnO_2 C_3S+2.0% MnO_2 C_3S+4.0% MnO_2 C_3S+8.0% MnO_2

Fig. 2. — Diffractogram of tricalcium silicate with MnO_2.

The *chromium oxide* is included in the lattice of tricalcium silicate. Hornain[11] claims that it confers to the latter a hexagonal and monoclinic polymorphic form (MI_a), a fact confirmed by our own investigations in samples with 0.5 and 2% Cr_2O_3. In samples with 4% and 8% Cr_2O_3, the diffractograms in fig. 3 also reveal high intensity lines corresponding to $2CaO.SiO_2$, Cr_2O_3 (d = 2.2739 A) and calcium chromites (d = 3.65–3.90 Å).

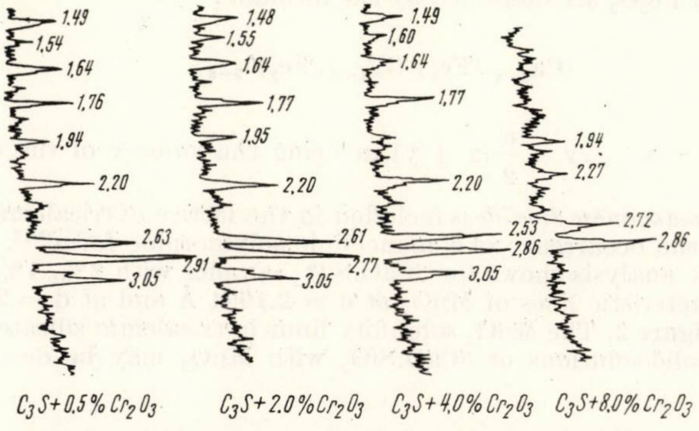

Fig. 3. — Diffractograms of tricalcium silicate with Cr_2O_3.

The solid solutions of $3CaO.SiO_2$ with Cr_2O_3 may be described by the formula:

$$(Ca_{3x} . Cr_x) (Si_{1-y} . Cr_y)O_{5-z} \quad (3)$$

The *cobalt oxide* is inserted in the structure of tricalcium silicate and Hornain[11] advocates — and our own researches[1] confirm — that the cobalt oxide determines the stabilization of $3CaO.SiO_2$ under a monoclinic form (M II). Maslîi[12] shows that the multiplets characteristic of pure C_3S pass into doublets or singlets revealing the deformation of C_3S lattice. In samples with 4% and 8% Co_2O_3 one finds in addition to maximum intensity lines corresponding to C_3S, the formation of C_2S as reflected in fig. 4.

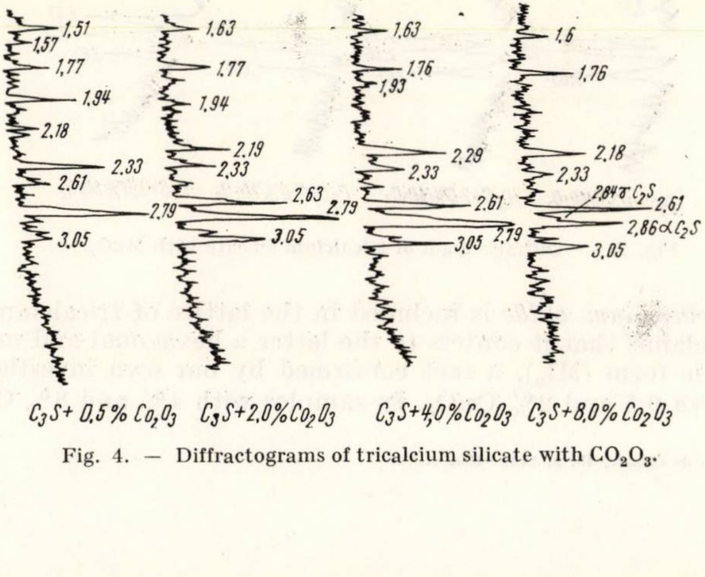

Fig. 4. — Diffractograms of tricalcium silicate with CO_2O_3.

The solid solutions of $3CaO.SiO_2$ with Co_2O_3 may be described by the formula :

$$(Ca_{3-x}.\ Co_x)\ (Si_{1-y}.\ Co_y)O_{5-z} \tag{4}$$

The *nickel oxide* confers to tricalcium silicate a monoclinic polymorphic form (M Ib) or hexagonal,[11] fact which was also confirmed by our own studies.[1] The solid solutions of tricalcium silicate with NiO may be described by the formula :

$$(Ca_{3-x}.Ni_x)SiO_5 \text{ in which } 0 \leqslant x \leqslant 0.04 \tag{5}$$

The *copper oxide* stabilizes the tricalcium silicate under a monoclinic form (M Ib), fact which was confirmed by Hornain's studies[11] and by our own investigations. For the systems with CuO additions, the solid solutions may be described by the formula :

$$(Ca_{3-x}.Cu_x)SiO_5 \text{ where } 0 \leqslant x \leqslant 0.04 \tag{6}$$

2.2. The *dicalcium silicate* represents one of the important crystalline phases in white and coloured Portland cement clinkers. They largely possess the property of forming solid solutions with the oxides of transitional elements.

The *ferric oxide* introduced in a proportion of 4% and 8% produces the probably physical stabilization of β $2CaO.SiO_2$. As a matter of fact, according to Dietzel and Tscheischwili[14] Fe^{3+} fails to stabilize crystallochemically β $2CaO.SiO_2$. The diffractograms in fig. 5 reveal the high intensity lines characteristic of β $2CaO.SiO_2$. However the line at d = 2.969 Å also appears, which is characteristic of Fe_2O_3. This fact proves that the solubilization limit of Fe_2O_3 has been exceeded by far in the dicalcium silicate.

The solid solutions of dicalcium silicate with ferric oxide may be described by the formula :

$$Ca_2[Fe_x.Si_{1-x}]O_4 - \frac{x}{2} \text{ where } 0 \leqslant x \leqslant 0.05 \tag{7}$$

The *manganese dioxide*, introduced up to 2% fails to stabilize the β $2CaO.SiO_2$ form ; diffractograms reflect the lines at d = 3.03 Å, 2.76 Å and 1.92 Å, characteristic of γ $2CaO.SiO_2$. By increasing the MnO_2 amount (from 2% to 4%) one observes an intensity of the main lines characteristic of β $2CaO.SiO_2$. The solid solutions of $2CaO.SiO_2$ may be described by the general formula :

$$(Ca_{2-x}.Mn_x)(Si_{1-x}\cdot Mn_x)O_{4-z} \text{ in which } z = x(3-n) \tag{8}$$

The *chromium oxide* introduced (like Cr^{6+} and Cr^{3+}) into the raw mixture of $2CaO.SiO_2$ and burnt at 1500° fails to lead to the stabilization of β $2CaO.SiO_2$. Chemical and electron spin resonance analyses[1] emphasized the fact that only Cr^{3+} exists at the working temperature involved and

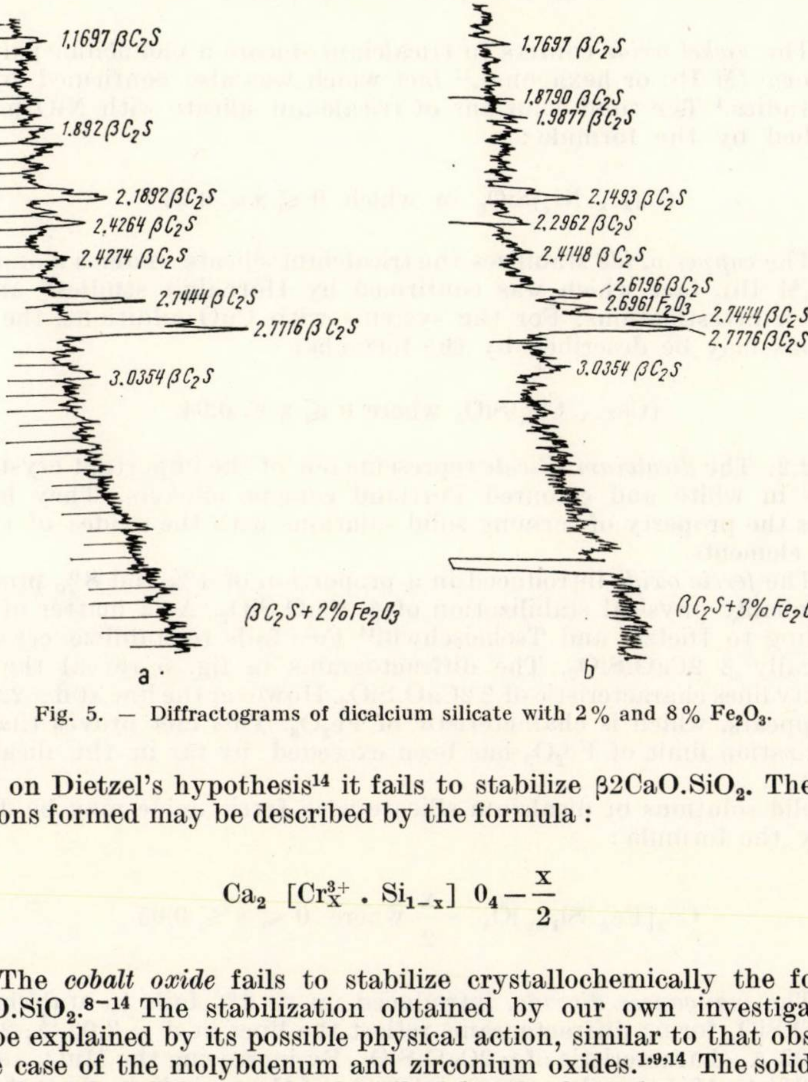

Fig. 5. — Diffractograms of dicalcium silicate with 2% and 8% Fe_2O_3.

based on Dietzel's hypothesis[14] it fails to stabilize $\beta 2CaO.SiO_2$. The solid solutions formed may be described by the formula :

$$Ca_2\ [Cr^{3+}_X\ .\ Si_{1-x}]\ 0_4 - \frac{x}{2} \qquad (9)$$

The *cobalt oxide* fails to stabilize crystallochemically the form β $\beta 2CaO.SiO_2$.[8-14] The stabilization obtained by our own investigations[1] may be explained by its possible physical action, similar to that observed in the case of the molybdenum and zirconium oxides.[1,9,14] The solid solutions of β $2CaO.SiO_2$ may be described by the formula :

$$(Ca_{2-x}.\ Co_x)\ (Si_{1-x}.\ Co_x)O_{4-z} \text{ in which } 0 \leqslant x \leqslant 0.06 \qquad (10)$$

The solid solutions of $\beta 2CaO.SiO_2$ with nickel oxide may be described by the formula :

$$(Ca_{2-x}.Ni_x)\ SiO_4 \qquad (11)$$

The formula of the solid solution of β $2CaO.SiO_2$ with copper oxide may be written down as follows:

$$(Ca_{2-x}.Cu_x)\ SiO_4 \qquad (12)$$

2.3. The *tricalcium aluminate* represents one of the crystalline phases which is always present in a proportion of at most 15% in white and coloured Portland cement clinkers. The penetration of the extraneous ions in the C_3A lattice leads to the modification of the parameters of the lattice.

The *ferric oxides* solubilize in the $3CaO.Al_2O_3$ lattice and for the corresponding solid solutions we may write the formula:

$$Ca_3\ [Al_{1-(0.02...0.03)} \cdot Fe_{(0.02...0.03)_2}]O_6 \qquad (13)$$

The *manganese dioxide* is included in a proportion below 2% in the $3CaO.Al_2O_3$ lattice; the formula of the solid solutions is:

$$Ca_3\ (Al_{1-x}.Mn_x)O_6 \text{ in which } 0 \geqslant x \geqslant 0.01 \ldots 0.02. \qquad (14)$$

The *chromium oxide and nickel oxide* are included as solid solutions in the lattice $3CaO.Al_2O_3$ producing modifications in the intensity of its characteristic lines.

2.4. The *monocalcium aluminate* is the basic constituent of white and coloured aluminous cement clinkers,[1,4,8,10,15] $CaO.Al_2O_3$ forms solid solutions with the oxides of the transitional elements.

The *ferric oxides* are included as solid solutions up to 2% in the $CaO.Al_2O_3$ lattice producing an intensification of characteristic lines; over 2 %, we find the obvious presence of C_4AF through line 2.6345 Å (2.6496 Å). Both in slowly cooled samples and in studdenly cooled ones there appear doublets or multiplets revealing the disturbance of the $CaO.Al_2O_3$ lattice. Considering that Fe^{3+} replaces Al^{3+}, the description of the formed solid solution may be made by the formula:

$$CaO\ (Al_2O_3)_{1-x}\ (Fe_2O_3)_x \text{ where } 0 \leqslant x \leqslant 0.015\ (0.02). \qquad (15)$$

The solubilization of the *manganese dioxide* in $CaO.\ Al_2O_3$ may be analyzed similarly to the solubilization of Fe_2O_3. The solubilization limit of MnO_2 in $CaO.Al_2O_3$ is far below 4% since new lines appear in the interval 2.5334 Å ... 2.8642 Å which may be assigned to some ternary compounds.

The *chromium oxide* forms solid solutions with $CaO.Al_2O_3$. The investigations carried out so far[1-15] show the existence in the $CaO.Al_2O_3$ system of some complex isomorphism relations. The solid solutions of $CaO.Al_2O_3$ with Cr_2O_3 may be expressed by the formula:

$$CaO.Al_2O_{3\ 1-x}.Cr_2O_3, \text{ in which: } 0 \leqslant x \geqslant 0.01\ (0.02). \qquad (16)$$

The studies made and the results obtained[1,4,7,10,15] indicate the possibility of including as a solid solution the cobalt oxide and the nickel oxide in the $CaO.Al_2O_3$ lattice under certain limits (1 – 2 %).

3. THE INFLUENCE OF THE OXIDES OF TRANSITIONAL ELEMENTS ON THE COLOURING OF CALCIUM SILICATES AND ALUMINATES

The ions of transitional metals which have free energetic levels allowing the passage of optically activated electrons present a large colouring capability. The colour of the calcium silicates depends on the nature of the chromophore ions, on the solubilization degree, on the manner in which they are included in the lattice, on the binding energy of the chromophore ions with oxygen, on their coordination. For this reason the colour saturation increases with the approach of the solubilization limit and is modified after exceeding it, as seen in figs. 6 and 7.

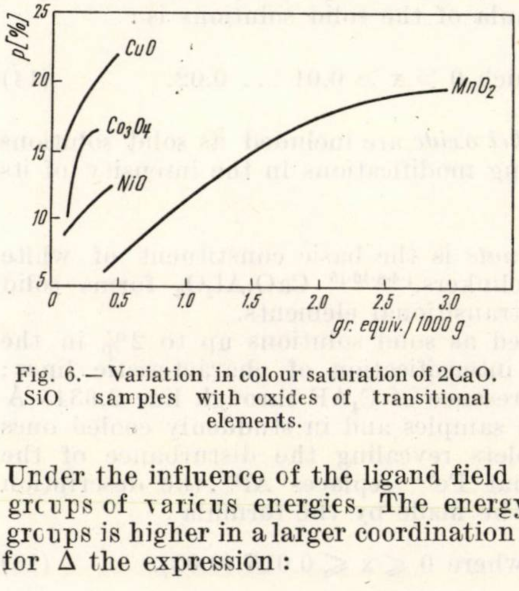

Fig. 6. — Variation in colour saturation of 2CaO. SiO samples with oxides of transitional elements.

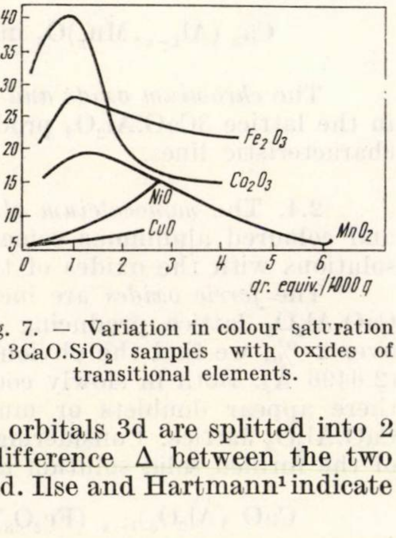

Fig. 7. — Variation in colour saturation of $3CaO.SiO_2$ samples with oxides of transitional elements.

Under the influence of the ligand field the orbitals 3d are splitted into 2 groups of various energies. The energy difference Δ between the two groups is higher in a larger coordination field. Ilse and Hartmann[1] indicate for Δ the expression :

$$\Delta = \frac{5.e.r.^{-4}}{3} \cdot \frac{q}{R} \text{ in which :} \qquad (17)$$

r = the average distance from the nucleus to the electrons 3d ;
e = the electron charge ;
q = the charge or the electric moment of the ligand ;
R = the ion-ligand distance.

The proportion of unbridged oxygen with high polarizability increases with the rise in the CaO concentration (q becomes higher and R becomes smaller) ; thus, in the case of $3CaO.SiO_2$ the absorption shifts towards the range of shorter wavelengths relative to β $2CaO.SiO_2$.[1] An inspection of the samples of $3CaO.SiO_2$ with Fe_2O_3, MnO_2, Cr_2O_3, Co_2O_3, NiO and

CuO by means of the ESR method (electron spin resonance) showed that the ion Fe^{3+} is also found as Fe^{2+}, Mn^{4+} is found as Mn^{2+}, Cr^{6+} is found as Cr^{3+}, Co^{3+} is found as Co^{2+} and the copper and nickel ions are divalent. Thus the plot of a function $\lambda = f(z/a^2)$ is a decreasing curve both in the case β $2CaO.SiO_2$ and in the case of $3CaO.SiO_2$ (fig. 8 and fig. 9). The dependences established between the colour saturation and the increase of the addition of colouring oxide, fig. 10 and fig. 11, and also between the wavelength and the intensity of the electrostatical field, fig. 12 and fig. 13, both for $CaO.Al_2O_3$ and for $3CaO.Al_2O_3$ are similar to those found with calcium silicates.[1]

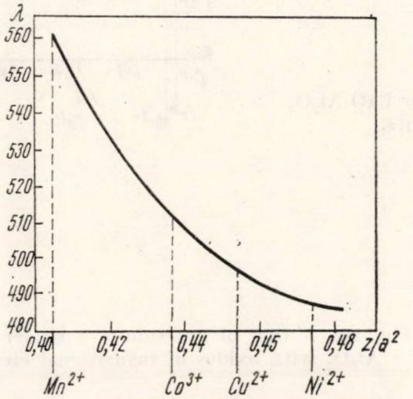

Fig. 8. — Plot of function $\lambda = f(z/a^2)$ for 2 $CaO.SiO_2$ with oxides of transitional elements.

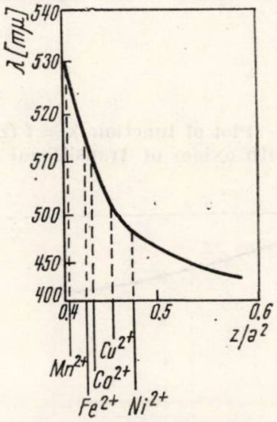

Fig. 9. — Plot of function $\lambda = f(z/a^2)$ for $3CaO.SiO_2$ with oxides of transitional elements.

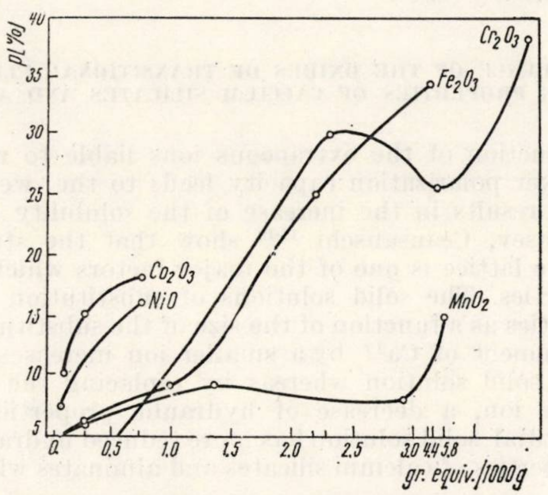

Fig. 10. — Variation in colour saturation of CaO. Al_2O_3 samples with oxides of transitional elements.

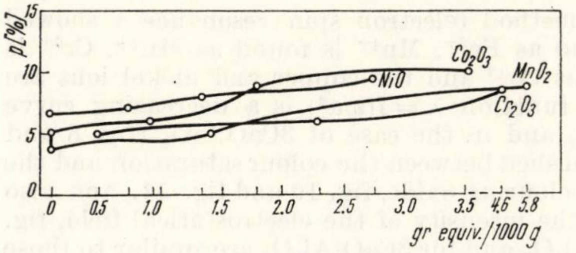

Fig. 11. — Variation in colour saturation of $3CaO.Al_2O_3$ samples with oxides of transitional elements.

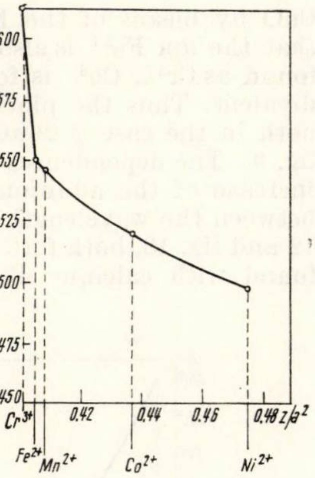

Fig. 12. — Plot of function $\lambda = f(z/a^2)$ for $CaO.Al_2O_3$ with oxides of transitional elements.

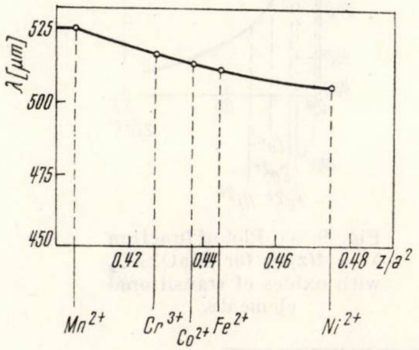

Fig. 13. — Plot of function $\lambda = f(z/a^2)$ for $3CaO.Al_2O_3$ with oxides of transitional elements.

4. THE INFLUENCE OF THE OXIDES OF TRANSITIONAL ELEMENTS ON THE BINDING PROPERTIES OF CALCIUM SILICATES AND ALUMINATES

The introduction of the extraneous ions liable to replace silicium and with a weaker polarization capacity leads to the weakening of the Si-O bond which results in the increase of the solubility of silicate.[1,11,13]

Butt, Timasev, Ceausanschi [14,18] show that the structure of the tricalcium silicate lattice is one of the major factors which determine its hydraulic properties. The solid solutions of substitution have different hydraulic properties as a function of the size of the substitute ion.

The replacement of Ca^{2+} by a smaller ion increases the hydraulic property of the solid solution whereas by replacing the Ca^{22} ion by a bigger substitute ion, a decrease of hydraulic properties takes place.

The interstitial solid solution has more reduced hydraulic properties. The binding properties of calcium silicates and alminates with and without

---

[17] I.M. Butt, and V.V. Timasev, *Epitoanyag*, **5**, 179 (1966).

[18] I.M. Butt, V.V. Timasev and V.E. Ceausauschi, „Proc. 9th Conf.Silicate Ind.", Budapest, 1968.

additions of oxides of transitional metals were examined by mechanical resistance determinations (on Kühl microprobes) and by roentgen and electromicroscopic analyses, in a more detailed work.

It has been found that in the samples synthesized with Fe_2O_3, MnO_2 and $Co_2\%O_3$ up to a certain value of their proportion, the mechanical resistances are higher having in general a maximum at the limit of the solid solution and starting to decrease thereafter. Even if the solubility limit of the ion of the transitional metal in C_3S, β C_2S, C_3A and CA is exceeded, compounds are formed including the oxide of the transitional metal with superior hydraulic properties compared to pure mineralogic compounds.

5. WHITE AND COLOURED CEMENTS

Our own investigations[1-10] are centered around the study of white Portland clinkers with high modules (with a content high in tricalcium silicate) in view of obtaining white cements with high initial resistances (300 – 400 daN/cm²) and high final resistances (500–600 daN/cm²) and also a high-grade white, over 80 %. Studies were carried out in parallel on the properties of white aluminous cements, proceeding thereafter to the study of the properties of coloured cements obtained from coloured clinkers.

The composition of the green, yellow and black Portland clinkers will include only tricalcium silicate, dicalcium silicate and tricalcium aluminate, compounds which from solid solutions with the added colouring oxides and whose structural particularities and quantitative ratio in the clinker will determine its colour. The quality of the coloured clinkers depends on the mineralogical composition, on the clinkerization conditions and on the cooling approach and to a large extent, on the percentage of the added colouring oxide. It was experimentally confirmed that the colour saturation increases with the approach of the solubility limit of the colouring oxide. Our own investigations[1] have indicated that some oxides have a more intense colouring action on alitic clinkers. By grinding the alitic Portland clinkers (green, yellow and black) we obtained cements with high initial resistances 300 – 400 daN/cm² and high final resistances 500 – 600 daN/cm², as well as a good colour stability at 80 hours UV radiation 30 gelinity cycles, artificial rain.

Based on the laboratory research it was possible to achieve green yellow and black cements at a semiindustrial level with a good reproducibility of the characteristics of the chemical-mineralogical composition, mechanical resistance and colour. Some results formed the subject of some invention patents[19,22].

---

[19] M. ENCULESCU and E. MARTON, Romanian patent No. 51751 – 1967.

[20] M. ENCULESCU, I. IONESCU and E. MARTON, Romanian patent No. 51805 – 1967.

[21] E. MARTON and M. ENCULESCU, Romanian patent No. 51468 – 1966.

[22] I. TEOREANU and M. ENCULESCU, Romanian patent No. 64952 – 1971.

6. CONCLUSIONS

The performed investigations led to the conclusion that the used transitional metal oxides form with calcium silicates interstitial solid solutions as well as substitution solid solutions, the probability on the last mentioned being greater.

By means of the performed investigations it was possible to determine the approximate values of the solubilisation limits of some colouring oxides in calcium silicates and in calcium aluminates. The solubilisation degree of the chromophore ions, the manner after which these are included in the base lattice, their bonding energy with oxygen, their coordination, clear up, in correlation with the silicates and calcium aluminates basicity, the colouring of these last mentioned.

Thus were established the ways by which hard cements, mortars and concretes with high mechanical resistance and high colour stability are obtained. In laboratory as well as in factory, Portland clinker cement and coloured aluminous cements were obtained starting from selected raw materials as well as from usual raw materials, clinkers with superior characteristics, thus contributing to the substantiation of the producing of this cement class. Very important results were obtained towards the direction of producing Portland cement with a high degree of white.

Revue Roumaine de Chimie, **19**, 9, 1503–1506 (1974)

PROTON MAGNETIC RESONANCE SPECTRA OF SOME 1,2,3-TRIMETHOXYACRIDINES

M. VLASSA
Institute of Chemistry, str. Donath 65–103, Cluj, Romania

Received October 8, 1973

The proton magnetic resonance spectra of some 1, 2, 3-trimethoxyacridines and 1, 2, 3-trimethoxyacridine-N-oxides are analysed. The influence of various substituents on the chemical shift of the acridine ring protons is discussed.

MO-calculations of physico-chemical properties of the 1,2,3-trimethoxyacridine (I) molecule[1] showed that the presence of the electron-releasing methoxy groups on the acridine ring increases the π-electronic density, especially in rings C and B, the + E effect being transmitted weakly to the ring A (see I). These calculations pointed out also that π-electronic densities at the methoxy groups are not equal.

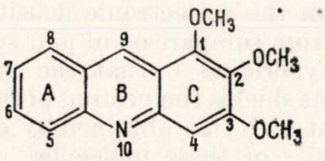

I

Although the π-electronic density gives only a rough approximation of the chemical shift, the above results suggest that in the proton magnetic resonance spectrum of 1, 2, 3-trimethoxycridine I, the resonance signals of the methoxy groups will be distinct, the most shielded among heteroaromatic protons will be H_4, the most deshielded H_9, and the ABCD type multiplet of $H_5 - H_8$ protons will appear between them. Because the + E effect is weakly transmitted in ring A, the position and shape of the $H_5 - H_8$ multiplet in acridine and in 1, 2, 3-trimethoxyacridine (I) pmr spectra are nearly the same. This fact allowed to analyse this multiplet by comparison with the acridine pmr spectrum recorded and analysed by Kokko and Goldstein.[2]

---

[1] M. Vlassa, M. Ionescu and J. Fabian, *Rev. Roumaine Chim.*, **18**, 99 (1973).

[2] J. P. Kokko and J. H. Goldstein, *Spectrochim. Acta*, **19**, 1119 (1963).

Comparison of experimental values of the chemical shifts of the 1,2,3,-trimethoxyacridine (I) protons with the previously calculated π-electronic density values[1] and with the chemical shift of acridine protons shows that the above assumption is correct (see table 1).

Table 1

The chemical shifts of acridine and of 1, 2, 3-trimethoxyacridine protons δ_H

Proton	$\pi-$electronic density of I[1]	δ_H of I	δ^+_H of acridine recorded by us	δ^{++}_H lit.[2]	$\Delta\delta_H = \delta^+_H - \delta_H$
H_4	1.095	7.33	8.22	8.25	0.89
H_5	1.008	8.18	8.22	8.25	0.04
H_6	0.986	7.76	7.81	7.80	0.05
H_7	1.015	7.42	7.55	7.55	0.13
H_8	0.996	8.00	8.06	8.06	0.06
H_9	0.928	8.91	8.71	8.71	−0.20
OCH_3	1.927	4.16	—	—	—
OCH_3	1.939	4.03	—	—	—
OCH_3	1.929	4.06	—	—	—

In spite of the rough correlation between chemical shifts and π-electronic densities, the two parameters show a parallel evolution, with the only exception of $H_5 - H_8$ protons (see table 1).

However, it is difficult to make an assignment of chemical shifts of the methoxy groups from the π-electronic densities values only.

We may conclude from comparison of pmr spectra of the acridine and of the 1, 2, 3-trimethoxyacridine I, that the presence of the methoxy groups in vicinal positions shields the protons of the acridine molecule. This conclusion is in agreement with that obtained by comparison of the calculated π-electronic densities of these molecules.

Studying the influence of various groups from position 9 of the 1, 2, 3-trimethoxyacridine I on the chemical shift of the protons, we note :

a) A deshielding effect for chlorine atom and a shielding one for SCH_3, OCH_3 and OC_6H_5 groups on $H_5 - H_7$ multiplet (see table 2), in good agreement with the order of magnitude of the Hammett substituent constants of the above groups (the shielding effect increases in the order $Cl < SCH_3 < OCH_3 < OC_6H_5$ and the values of the Hammett constants are $\sigma_{Cl} = +0.277$; $\sigma_{SCH_3} = -0.01$; $\sigma_{OCH_3} = -0.286$; $\sigma_{OC_6H_5} = -0.280$).[3,4] This shows that the shielding effect is mostly due to the electron-releasing strength of these groups.

b) A deshielding effect on the H_8 proton for all these groups (see table 2). This effect, well known in organic magnetic resonance as *peri* effect, is produced by various substituents[5] and was explained by Dudek[6]

---

[3] F. H. Westheimer, in "Steric Effects in Organic Chemistry", edited by M. S. Newman, John Wiley and Sons, Inc., Publishers, New York, 1956, p. 571.

[4] Ch. C. Price and S. Oae, "Sulfur Bonding", The Ronald Press Company, New York, 1962, p. 14.

[5] L. M. Jackman and S. Sternhell, "Applications of Nuclear Magnetic Resonance Spectroscopy in Organic Chemistry", 2nd edition, Pergamon Press, Oxford, 1969, p. 206, 208.

[6] J. O. Dudek, *Spectrochim. Acta*, **19**, 691 (1963).

Table 2

The chemical shifts of 9-R-substituted 1, 2, 3-trimethoxyacridine δ_H^*

Compound	H_4	H_5	H_6	H_7	H_8	OCH_3	OCH_3	OCH_3	R_9
-9-chloro-	s** 7.37	m*** centre at $\longleftarrow$ 7.82 $\longrightarrow$			m 8.54	s 4.08	s 4.06	s 4.08	—
-9-thiomethyl-	s 7.29	m centre at $\longleftarrow$ 7.76 $\longrightarrow$			m 8.60	s 4.05	s 3.81	s 3.81	s 2.50
-9-methoxy-	s 7.39	m centre at $\longleftarrow$ 7.69 $\longrightarrow$			m 8.37	s 4.11	s 4.07	s 4.08	s 4.20
-9-phenoxy-	s 7.32	m centre at $\longleftarrow$ 7.54 $\longrightarrow$			m 8.05	s 4.07	s 3.76	s 4.94	m 6.89

* $\delta_{H_5-H_8}$ centre of multiplet of 1,2,3- trimethoxyacridine = 7.77.

**s = singlet

*** m = multiplet

as a space interaction. The distance between the *peri* hydrogen and the substituent, e.g. the oxygen atom from the methoxy group, is 2.4 Å, that is smaller than the one encountered in a strong hydrogen bonding (2.7 Å).

This fact explains why the deshielding effect is greater for SCH_3 and chlorine than for the methoxy and phenoxy groups, through space the overlapping of the substituent and hydrogen orbitals being greater in the first two cases. The deshielding effect is greater for the SCH_3 group than for the chlorine atom because the sulfur atom is more basic due to the inductive effect of the methyl group.

Courtauld atomic model of the 1,2,3-trimethoxy-9-phenoxyacridine shows that, due to the steric hindrance of the benzene nucleus by the methoxy group from C_1 position, the H_8 proton lies above the benzene ring plane. It explains why methoxy group from C_9 has a stronger deshielding effect than the phenoxy group (see table 2).

The *peri* effect is exerted also by the methoxy group from C_1 position on the H_9 proton (see tables 1 and 3).

This explanation is also supported by the fact that in the case when a space interaction becomes impossible, the *peri* effect does not appear. For instance, the methyl group from C_4 position of the benzanthracene II produces on the H_{10} proton a shielding effect and not a deshielding one ($8.45\delta_{4-\text{methyl}-1,2\text{ benzanthracene}} - 8.29\ \delta_{1,2-\text{benzanthracene}} = 0.16$ ppm).[7]

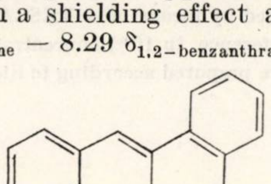

II

---

[7] P. DURAND, J. PARELLO and N. P. BUN-HOI, *Bull. Soc. chim. France*, **1963**, 2438.

Due to the interaction of these groups with the methoxy groups from 1, 2 and 3 positions, the influence of these substituents on the chemical shifts of the H_4 proton and of the vicinal methoxy groups has a rather complex character.

The effect of the N-oxide group on the chemical shifts of the 1, 2, 3-trimethoxyacridine protons consists in a deshielding effect on the H_4 and H_5 protons (see table 3).

Table 3

Chemical shifts of acridine-N-oxide derivatives δ_H

Compound	H_4	H_5	H_6	H_7	H_8	H_9	OCH_3	OCH_3	OCH_3
acridine-N-oxide	8.84	8.84	7.71	7.50	7.88	8.13	—	—	—
1,2,3-trimethoxyacridine-N-oxide	s 8.05	m 8.84	m. centre at ←7.75→			s 8.55	s 4.15	s 4.03	s 4.16
1,2,3-trimethoxy-9-chloro-acridine-N-oxide	s 8.07	m 8.69	m. centre at ←7.66→		m 8.05	—	s 4.05	s 3.96	s 3.96

The comparison of the chemical shifts of the acridine-N-oxide with those of the 1,2,3-trimethoxyacridine-N-oxide shows that the methoxy groups have the same effect as in the acridine case. The presence of the chlorine atom in position 9 is reflected in pmr spectrum by the deshielding effect on the H_8 proton (*peri* effect) and on the $H_5 - H_7$ multiplet (see table 3).

From comparison of δ_H values of the H_9 proton from 1,2,3-trimethoxy-acridine-N-oxide and from 1, 2,3-trimethoxyacridine, one can see that the electronic density is increased in the case of the N-oxide derivative (0.36 ppm). This suggests that it is at the C_9 position of the 1,2,3-trimethoxyacridine-N-oxide, as in the case of the acridine-N-oxide[8], that electrophilic substitution reaction may take place.

EXPERIMENTAL

The pmr spectra were recorded by means of a TESLA BS 487 C instrument, in $CDCl_3$ solutions, with TMS as internal reference, in 10% concentration.

The substances recorded were prepared according to literature data. [9,10]

---

[8] H. H. Mantsch, W. Seiffert and V. Zanker, *Rev. Roumaine Chim.*, **12**, 1137 (1967).

[9] M. Ionescu and M. Vlassa, *Rev. Roumaine Chim.*, **16**, 743 (1971).

[10] M. Ionescu, M. Vlassa and I. Goia, *J. prakt. Chem.*, **314**, 441 (1972).

Revue Roumaine de Chimie, **19**, *9*, 1507–1512 (1974)

o-DIAZABICYCLIC DERIVATIVES OF BENZO [*c*] CINNOLINE. IV

ADDITION REACTIONS OF 3,8-DIMETHYLBENZO [*c*] CINNOLINE, VIA YLIDIC INTERMEDIATES, LEADING TO NEW *o*-DIAZABICYCLIC SYSTEMS

EUGENIA CARP, MARIA DORNEANU and ION ZUGRĂVESCU
Department of Organic Chemistry "Al.I. Cuza" University, Iassy

Received February 16, 1974

The reaction of 3,8-dimethylbenzo [*c*] cinnoline with dimethyl acetylenedicarboxylate in dimethylformamide affords a stable cycloadduct. The synthesis and structure of the stable benzocinnolinium dicyano-methylides is discussed. Possible synthetic routes to obtain the dimethylbenzo [*c*] pyrazolo- and tetrazolo [1.2a] cinnolines, *via* unstable ylidic intermediate from N-phenacyl-benzocinnolinium salt, have also been investigated.

In the previous papers[1–3] an attempt was made to verify the possible dienophilic activity of the "azo" system of benzo [*c*] cinnoline. It was also shown that the ylids, derived from benzocinnolinium salts, can undergo 1,3-dipolar cycloaddition reactions towards some dipolarophiles to give new *o*-diazabicyclic systems.

Our interest in the chemistry of benzo [*c*] cinnoline led us to investigate the behaviour of this weak heterocyclic base and their substituted derivatives in the reaction with dimethyl acetylenedicarboxylate and the formation, starting from benzocinnolinium salts, of azomethine ylids which, acting as 1,3-dipoles, react with various dipolarophiles to give the corresponding *o*-diazabicyclic heterocyclic systems.

In order to achieve these we have studied the reaction of 3,8-dimethylbenzocinnoline with dimethyl acetylenedicarboxylate (DMAD) in several solvents and we have established that the reaction occurs in the best yield in dimethylformamide (DMFA) at 0°C, to give 1 : 2 molar

---

[1] E. Carp, M. Dorneanu și I. Zugrăvescu, *Anal. Sti. Univ. "Al.I. Cuza" Iași, Sect I*, **14**, 169 (1968); *Chem. Abstr.* **71**, 61320 (1969).

[2] M. Dorneanu, E. Carp și I. Zugrăvescu, *Anal. Sti. Univ. "Al. I. Cuza" Iași, Sect I*, **19**, 221 (1973).

[3] M. Dorneanu, E. Carp și I. Zugrăvescu, *Anal. Sti. Univ. "Al. I. Cuza" Iași, Sect I*, **20**, 35 (1974).

cycloadduct (I):

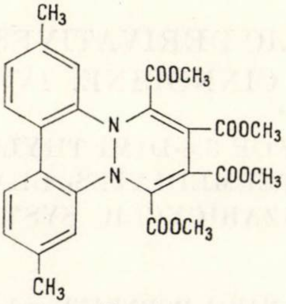

I

The cyclic structure assigned to this product is compatible with its elemental analysis and spectral data, as well as with its stability relative to other electrophilic reagents. In our experiments it is clear that the polarity of the solvent (DMFA) plays an important role and determines readily the cycloadduct formation, by (2 + 4) addition reaction. In this unusual type of Diels-Alder reaction, a possible open adduct system with charge separation is eluded because such a zwitterionic structure could allow the establishment of a new covalent bond between the carbanion and the neighbouring ring nitrogen, ultimately resulting the stable nonpolar cycloadduct. This zwitterionic structure probably appears rather as an intermediate in a stepwise mechanism for the addition reaction (2 + 4). The formation of the cycloadduct (I) by adding two molecules of DMAD across the "azo" system of dimethylbenzocinnoline can be accounted for on the assumption that an initial Michael-type reaction leads to the (1 : 1) molar zwitterionic intermediate, which attacks another molecule of the DMAD to afford the (1 : 2) zwitterion and this can then cyclise to the stable cycloadduct, as illustrated below:

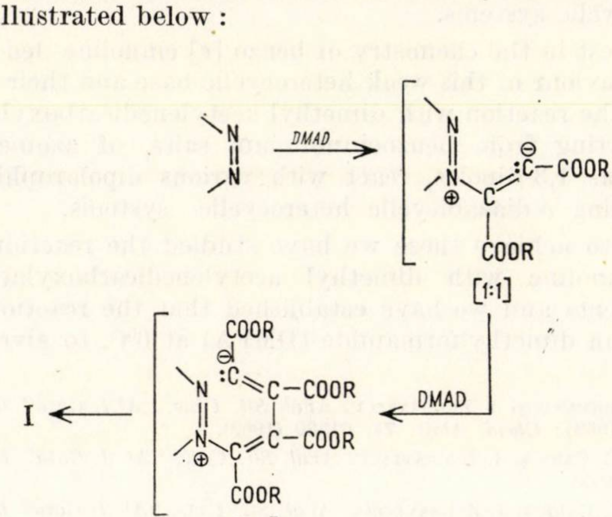

A similar mechanism has been postulated by other workers[4,5] in connection with the reaction of acetylenecarboxylate with conjugated systems containing heteroatomic bases. In the same manner we have already reported[1] the yielding of the 1 : 2 cycloadduct from benzocinnoline and DMAD in a better yield than it was described by another way in the literature.[6]

Further we have prepared the azomethine ylids, derived from the corresponding benzocinnolinium salts, such as benzocinnolinium and 3,8-dimethylbenzocinnolinium dicyano-methylides (II_a and II_b) and 3,8-dimethylbenzocinnolinium-N-phenacylide (II_c) :

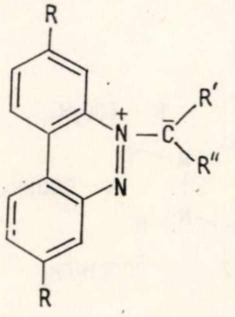

II

a. $R = H$; $R' = R'' = CN$
b. $R = CH_3$; $R' = R'' = CN$
c. $R = CH_3$; $R' = H$; $R'' = COC_6H_5$

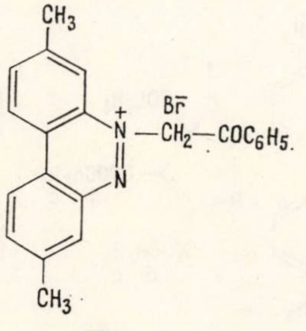

III

The dicyanomethylides, II_a and II_b, have been obtained by three different ways : a) by salt method from the corresponding heterocyclic bases and bromomalononitrile in acetonitrile solution, followed by the treatment with aqueous potassium carbonate ; b) by the reaction of benzocinnoline with tetracyanoethylene oxide, according to the Linn method[7] ; c) from benzocinnoline-N-oxide and malonodinitrile in the presence of thionyl chloride, an application of the Middleton procedure[8] for obtaining the analogous S-ylids. All these methods afford the corresponding stable nicely red-violet coloured ylids. The most interesting feature of these ylids is their stability relative to other benzocinnolinium ylids which possess only one electronwithdrawing substituent on the carbanion. They do not undergo 1,3-dipolar cycloaddition reactions and are unaffected by weak acids or bases. This chemical stability is due to the stabilizing effect of the two cyano groups on the carbanion charge, which would cause a pronounced decrease in the nucleophilic activity of the ylids.

---

[4] S.B. Needleman and M.C. Chang Kuo, *Chem. Rev.*, **62**, 416 (1962).
[5] R.M. Acheson and A.O. Plunkett, *J. Chem. Soc.*, **1962**, 3763.
[6] A.N. Hughes and T. Monkoltananont, *Chem. and Ind.*, **1967**, 662.
[7] W.J. Linn, O.W. Webster and R.E. Benson, *J. Amer. Chem. Soc.*, **87**, 3651 (1965).
[8] W.J. Middleton, E.L. Buhle, J.G. Mc Nally and M. Zanger, *J. Org. Chem.*, **30**, 2384 (1965).

3,8-Dimethylbenzocinnoline by the reaction with ω-bromoacetophenone has been converted in N-(phenacyl)-3,8-dimethylbenzocinnolinium bromide (III). On treatment with triethylamine of the N-phenacyl salt an unstable ylid (II_c) is produced, which can be trapped *in situ* by 1,3-dipolarophiles; otherwise it gives formal dimers. The formation of the ylid can be easily intercepted by the change of the colour in aprotic solvents from yellow to deep red.

The 1,3-dipolar contributory structure to the resonance hybrid is responsible for the 1,3-dipolar cycloaddition reactions of the ylid. We have thus obtained the expected cycloadducts (IV), (V) and (VI):

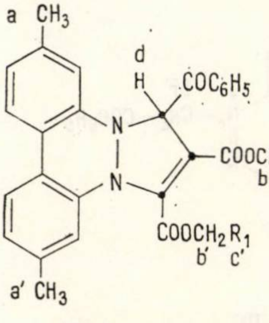

IV $R_1 = H$ (b,b')
V $R_1 = CH_3$ (c,c')

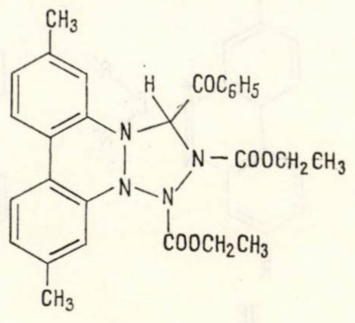

VI

by reaction of the ylid, generated *in situ* from the salt, with dimethyl and diethyl acetylenedicarboxylate and also with diethyl azodicarboxylate.

Thus, the application of the 1,3-dipolar additions is a successful route for the synthesis of some new *o*-diazabicyclic systems. Only few members belonging to this group are known in the literature.[9,10]

The i.r. and n.m.r. spectral data are in satisfactory agreement with the attributed structures for the cycloadducts.

EXPERIMENTAL

3,8-Dimethylbenzo[*c*]*cinnoline*. This compound was prepared by a similar procedure to that described by Badger[11] from 4,4'-dimethyl-2,2'-dinitrobiphenyl which was reduced with lithium aluminium hydride in refluxing anhydrous ether; needles from methanol, m.p. 187^0.

6,7,8,9-Tetracarbomethoxy-3,12,-dimethylbenzo [*c*] *pyridazino* [*1.2a*] *cinnoline* (*I*). A solution of 3,8-dimethylbenzocinnoline (1.04 g, 0.005 mole) and DMAD (1.42 g, 0.01 mole) in 35 ml DMFA was allowed to stand at 0°C for 5 days, and then at room temperature for 24 hrs. A red colour appeared and a precipitate was formed. The solvent was removed *in vacuo* and the red-dark residue was dissolved in methylene chloride and precipitated with petroleum ether. After recrystallization from benzene (by chromatography over alumina) and petroleum ether the crude product gave 1.2 g of a crystalline light-red adduct, m.p. 169°.

---

[9] D.G. Farnum, R.J. Alaimo and J.M. Dunston, *J. Org. Chem.*, **32** 1130 (1967).

[10] P.J. Abbott, R.M. Acheson, M.W. Foxton, N.R. Raulins and G.E. Robinson, *J. Chem. Soc., Perkin I*, **1972**, 2182.

[11] G.M. Badger, J.H. Seidler and B. Thompson, *J. Chem. Soc.*, **1951**, 3211.

Analysis : $C_{26}H_{24}N_2O_8$ Calcd : C% 63.40 ; H% 4.91 ; N% 5.68

Found : C 63.57 ; H 5.13 ; N 6.01

IR : $\nu_{C=O} = 1750, 1720\ cm^{-1}$; $\nu_{C-O-C} = 1250, 1120\ cm^{-1}$.

Benzo [c] cinnolinium dicyanomethylide (*II*$_a$). To a solution of benzocinnoline (0.9 g, 0.005 mole) in 20 ml acetonitrile, bromomalononitrile (0.72 g, 0.005 mole) was added dropwise with stirring and the resulting solution was allowed to stand at room temperature for two days. After the removal of the solvent under reduced pressure, the residue was taken up in aqueous potassium carbonate solution and the mixture was extracted with methylene chloride. The extract was dried over Na_2SO_4, concentrated and chromatographed over alumina. The ylid was precipitated from the eluate with petroleum ether, as red-violet crystals, m.p. 127–130°. The compound is very soluble in CH_2Cl_2, $CHCl_3$, CH_3COCH_3 with an intense violet colour.
Analysis : $C_{15}H_8N_4$

Calcd. : C% 73.76 ; H% 3.38 ; N% 22.95 Found : C 73.18 ; H 3.55 ; N 22.71
IR : $\nu_{CN} = 2208, 2205\ cm^{-1}$.

3,8-Dimethylbenzo [c] cinnolinium dicyanomethylide (*II*$_b$). To a solution of 3,8-dimethylbenzocinnoline (2.08g, 0.01 mole) in 70 ml acetonitrile a solution of bromomalononitrile (1.44 g, 0.01 mole in 70ml acetonitrile) was added with stirring and the reaction mixture was allowed to stand at room temperature for 3 days, when a violet dark colour appears. After it was refluxed for ½ hr the solvent was removed *in vacuo*, and the residual product was triturated with aqueous potassium carbonate solution and then extracted with methylene chloride. The extract, washed with water and dried, was evaporated to 20 ml and precipitated with petroleum ether. Violet-dark needles, m.p. 170°.
Analysis : $C_{17}H_{12}N_4$ Calcd. : C% 74.97 ; H% 4.44 ; N% 20.57

Found : C 74.31 ; H 4.37 ; N 19.90

IR : $\nu_{CN} = 2170, 2190\ cm^{-1}$.

N-(phenacyl) - 3,8 - dimethylbenzo[c]cinnolinium bromide (*III*). A solution of 3,8-dimethylbenzo cinnoline (2.08 g, 0.01 mole) and ω-bromoacetophenone (1.90 g, 0.01 mole) in methylene chloride was heated for 3 hrs on a steam bath and then was allowed to stand at room temperature for 3 days. The mixture was precipitated with petroleum ether and the crystalline mass was collected by filtration ; yellow-orange crystals, m.p. 85°.
Analysis : $C_{22}H_{19}N_2OBr$

Calcd. : C% 64.87 ; H% 4.70 ; N% 6.87 Found : C 64.58 ; H 4.43 ; N 6.59

IR : $\nu_{C=O} = 1705\ cm^{-1}$.

6-Benzoyl-6H-7,8-dicarbomethoxy-3,11-dimethylbenzo[c]pyrazolo [1.2a] cinnoline (*IV*). The DMAD (0.72 g, 0.005 mole) was added to a suspension of salt (2 g, 0.005 mole) in 50 ml methylene chloride and the mixture was treated dropwise with 0.8 ml triethylamine. The reaction mixture was allowed to stand at room temperature for 4 days and boiled under reflux for ½ hr. After cooling, the solution was washed with water and dried over anh. potassium carbonate and the solvent was removed *in vacuo*. Recrystallization from methanol or methylene chloride-petroleum ether gave red crystals ; m.p. 194°.
Analysis : $C_{28}H_{24}N_2O_5$

Calcd. : C% 71.78 ; H% 5.16 ; N% 5.95 Found : C 71.24 H 5.31 ; N 5.84

NMR ($CDCl_3$) : $\delta_{Me}a = \delta_{Me}a' = 2.30$ ppm ; $\delta_{Me}b = 3.61$ ppm ; $\delta_{Me}b' = 3.97$;

$\delta_{CH}d = 5.93$; $\delta = 6.70-8.20$ ppm (11 H aromatic)

IR : $\nu_{C=O} = 1743, 1697\ cm^{-1}$.

6-Benzoyl-6H-7,8-dicarbethoxy-3,11-dimethylbenzo [c] pyrazolo [1.2a] cinnoline (V). The 1,3-dipolar addition reaction was carried out in the same way as for compound (IV) from 1 g salt, 0.42 g diethyl acetylenedicarboxylate and 0.4 ml triethylamine. The crude product was recrystallized from ethanol to give yellow crystals ; m.p. 152–153°.
Analysis : $C_{30}H_{28}N_2O_5$

Calcd. : C% 72.56 ; H% 5.68 ; N% 5.64 Found : C 72.47 ; H 5.81 ; N 5.93

NMR ($CDCl_3$) : $\delta_{Me}a,a' = 2.31$ ppm ; $\delta_{Me}c = 1.15$; $\delta_{Me}c' = 1.41$;

$\delta_{CH_2}b = 4.10$; $\delta_{CH_2}b' = 4.48$; $\delta = 6.70-8.20$ (11H aromatic) ;

$\delta_{CH}d = 5.96$ ppm.

IR : $\nu_{C=O} = 1735, 1683\ cm^{-1}$.

6-Benzoyl-6H-7,8-dicarbethoxy-3,11-dimethylbenzo [*c*] *tetrazolo* [*1.2a*] *cinnoline* (*VI*). The adduct with diethyl azodicarboxylate was prepared from 1 g salt, 0.43 g diethyl azodicarboxylate and 0.5 ml triethylamine in the same manner as for compound (IV). Recrystallization from ethanol gives yellow crystals, m.p. 133°.

Analysis : $C_{28}H_{28}N_4O_5$ Calcd. : C % 67.18 ; H % 5.63 ; N % 11.19

Found : C 67.54 ; H 5.78 ; N 11.08

IR : $\nu_{C=O} = 1730, 1690, 1670\ cm^{-1}$.

We express our thanks to dr. I. Gabe and dr. V. Bărboi for determinations and interpretations of n.m.r. and i.r. spectra.

Revue Roumaine de Chimie, **19**, *9*, 1513–1519 (1974)

CHROMATOGRAPHIC STUDY OF ACETYLENE AND ETHYLENE ADSORPTION AND OF PALLADIUM DISPERSION FROM Pd/Al_2O_3 CATALYSTS

I.V. NICOLESCU* and I. SUCIU**
***Faculty of Chemistry. Department of Chemical Technology and Catalysis, Splaiul Independenţei nr. 89, Bucharest**
****Industrial Central for Refineries and Petrochemistry, Brazi.**

Received October 13, 1973

By using the pulse microreactor technique, acetylene and ethylene adsorption on Pd/Al_2O_3 catalysts at the temperature of 150° was studied in relation with the properties of the support, which resulted after applying various thermal treatments (600°–900°). It was found that the thermal treatment to which the support was subject, influences the adsorption properties of the catalysts. The studied catalysts : PdA_6, PdA_7, PdA_8 and PdA_9 (1 % palladium content) show different adsorbing capacities, both at first injection and at equilibrium. Palladium dispersion on the alumina support was calculated by using chemisorption data of acetylene. The size of the Pd particles is dependent on the textural properties of the support, treated thermally at 600°, 700°, 800° and 900°. The size of the Pd particles varies from 32.2 Å to 60.7 Å.

INTRODUCTION

Important progress in the study of the phenomena taking place at the interface reactant-catalyst was made by investigating the chemisorption of some gaseous components, with the help of various working techniques : infrared spectroscopy,[1,2] pulse microreactor combined with gaschromatography[3] or radiochromatography[4]. Our research work had the purpose to evidence the influence of the thermal treatment of alumina on the chemisorbing properties of C_2H_2 and C_2H_4 on Pd/Al_2O_3 catalysts. Also, considering that the chemisorption of acetylene on Pd is achieved on two active centres, the chemisorption data were used to determine palladium dispersion on the support. For this purpose, the pulse microreactor method was used.

Research work concerning the correlation of the chemisorbing capacity of a metal laid down on a support with its dispersion was carried out

---

[1] L.H. Little, "Infrared Spectra of Adsorbed Species", Academic Press, London and New York, 1966.

[2] L.H. Little, N. Sheppard and D.J.C. Yates, *Proc. Roy. Soc.*, **A–259**, 242 (1960).

[3] D. Cormack, S.J. Thomson and G. Webb, *J. Catalysis*, **5**, 224 (1966).

[4] G.F. Taylor, S.J. Thomson and G. Webb, *J. Catalysis*, **12**, 150 (1948).

by Boreskov and Karnaukhov.[5] In subsequent studies,[6-10] research work was carried out concerning chemisorption of hydrogen on platinum laid down on a support and the dispersion degree of platinum. Palladium catalysts were less studied from this point of view.[11-16]

EXPERIMENTAL

The apparatus (fig. 1) used in the present study included : a chromatograph, a device directing the gas-flow to the microreactor and to the chromatographic column, a pipette dosing the injection of the reactant, a microreactor and a chromatographic column.

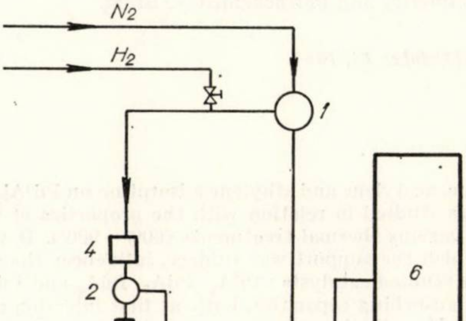

Fig. 1. — Scheme of the apparatus used in the study of acetylene and ethylene adsorption.
(N_2); *2.3* switch valve for bypassing the microreactor; *4*, device for sample injection; *5*, microreactor; *6*, chromatograph.

The catalysts were prepared by impregnating η-Al_2O_3 with palladium nitrate solution, for the concentration of 1 % Pd/support. After impregnation and drying, the catalysts were calcined under a dry air current. The general textural properties of the support are shown in table 1. The four catalysts, differing only by the calcinating temperature of the alumina-support, which is respectively 600°, 700°, 800° and 900° were marked with the indexes : PdA_6, PdA_7, PdA_8 and PdA_9.

---

[5] C.K. Boreskov and A.P. Karnaukhov, *Zhur. fiz. Khim.*, **26**, 1814 (1952).

[6] S.F. Adler and I. Keavnev, *J. Phys. Chem.*, **64**, 208 (1960).

[7] H.S. Gruber, *J. Phys. Chem.*, **66**, 68 (1961).

[8] J. Benson and M. Boudart, *J. Catalysis*, **4**, 704 (1965).

[9] S.F. Adler, R.A. Hermann, M.S. Goldstein and R.M. De Baum, *J. Phys. Chem.*, **66**, 2189 (1961).

[10] N.N. Zaidman, .V.A. Dzisko, A.P. Karnaukhov, N.P. Krasilenko, N.G. Koroleva and G.P. Vishnarkova, *Kinetika i Kataliz*, **9**, 863 (1968).

[11] I.S.F. Scholten and Van Monfort, *J. Catalysis*, **1**, 85 (1962).

[12] H. Kral, *Z. Phys. Chem. (Frankfurt)*, **48**, 129 (1960).

[13] V.A. Bolovnev, *Zhur. ·fiz Khim.*, **43**, 2461 (1970).

[14] L. Spendel and M. Boudart, *J. Phys. Chem.*, **64**, 204 (1960).

[15] D. Cismaru and Al. Fruma, *Rev. Roumaine Chim.*, **13**, 139 (1968).

[16] I.V. Nicolescu, Al. Fruma and I. Suciu, *Rev. Roumaine Chim.*, **16**, 1 (1971).

A quantity of 1 g of catalyst was introduced into the microreactor and activated with hydrogen at the temperature of 300° with a flow-rate of 50 ml/minute, for 30 minutes. After having activated the catalyst, the microreactor was switched on nitrogen circuit and the catalyst was flushed for 30 minutes with the same flow-rate of 50 ml/minute.

Table 1

Some general properties of the support-aluminas used for the preparation of the PdA_6-PdA_9 catalysts

Alumina	Calcination temperature of the alumina °C	Specific area (A)m^2/g	Total volume of pores (V_t) cm^3/g	Volume of micropores <75Å %	Volume of macropores > 75 Å %
$Al_2O_3-T_6$	600	220	0.546	55.0	45.0
$Al_2O_3-T_7$	700	200	0.486	54.0	45.8
$Al_2O_3-T_8$	800	186	0.543	53.7	46.3
$Al_2O_3-T_9$	900	160	0.452	42.1	57.9

After carrying out this work, the microreactor was cooled down to the working temperature (150°). To the catalyst treated in this way, successive samples of acetylene or ethylene of 0.3 ml content were introduced at equal time intervals, under nitrogen stream (which was at the same time the carrier gas for the chromatographic analysis of the injected C_2H_2 and C_2H_4 samples) via the capillary pipette, set up on a 8 way-valve.

The calibration of the acetylene and ethylene injection was carried out by introducing the sample directly into the chromatographic column and by bypassing the microreactor. The amount of adsorption, respectively the quantity of retained substance was determined by introducing into the microreactor containing the catalyst, which is connected with the chromatographic column (25% squalan on chromosorb W, 60–80 mesh, 1 = 10 m, Øi = 4 mm) the same volume of substance as for calibration, i.e. 0.3 ml.

From the difference of the chromatographic peak areas determined for the two cases related to the volume of the introduced sample, the quantity of substance retained by the catalyst results, according to the following equation :

$$V_r = V_i \ (S_1 - S_2)/S_1, \tag{1}$$

where :

V_r = volume of retained gas (cm^3).

V_i = volume of gas introduced into the microreactor by one injection (cm^3).

S_1 = area of the chromatographic peak, corresponding to V_1 at the calibration (cm^2).

S_2 = area of the chromatographic peak, corresponding to the substance introduced into the microreactor by one injection and not retained by the catalyst (cm^2).

The sample injections were carried out until the complete saturation of the catalyst was reached. The saturation moment was marked by the equality of areas S_1 and S_2.

RESULTS AND DISCUSSION

In order to have a more complete picture of the phenomenon studied, the retention at each newly added substance injection was measured, i.e. from the first injection to the equilibrium. The results obtained are shown in figures 2–5.

Adsorption at first injection. It was found that the retention capacity of the four catalysts studied was different. At first injection, only a higher or a smaller fraction of the sample was retained on the catalyst, depending on the thermal treatment of the support. In each case, the adsorption at first injection was smaller than its value at equilibrium (fig. 2). The thermal treatment temperature of the support is shown on the abscissa and the adsorbed quantity of C_2H_2 and C_2H_4, on the ordinate.

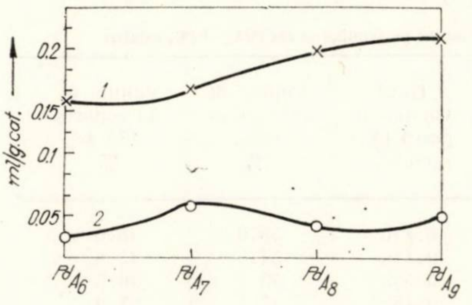

Fig. 2. — Acetylene and ethylene adsorption at first injection on PdA_6 — PdA_9 catalysts. 1 — C_2H_2; 2 — C_2H_4.

For acetylene, the maximum adsorption capacity at first injection is shown by catalyst PdA_9 and the minimum adsorption capacity by PdA_6, whereas catalysts, PdA_7 and PdA_8 are placed in intermediate positions.

Under identical conditions, the retained quantity of ethylene is by far smaller than the quantity of acetylene. But it was noticed that the two curves representing adsorption of acetylene and ethylene at first injection on the four catalysts have not the same aspect. For ethylene, maximum adsorption capacity is shown by catalyst PdA_7. Catalyst PdA_9 which for acetylene shows maximum adsorption capacity, shows for ethylene an intermediate value.

The decreasing order of acetylene and ethylene adsorption at first injection, depending on the thermal treatment of the support shows the following sequence :

— C_2H_2 adsorption : $PdA_9 > PdA_8 > PdA_7 > PdA_6$

— C_2H_4 adsorption : $PdA_7 > PdA_9 > PdA_8 > PdA_6$

Retention at equilibrium. Several injections (between 3 and 7) of reactant were necessary to reach an equilibrium.

Examining the evolution of the adsorption (figures 3, 4 and 5), it has been observed that if for acetylene the sequence of adsorption capacities at first injection is similar to that at equilibrium, for ethylene there are inversions (PdA_8 and PdA_9) and the catalysts which at first injection showed a maximum adsorption capacity for ethylene, at equilibrium have an intermediary position.

The curves representing the amount of acetylene and ethylene adsorbed at equilibrium (fig. 5) on the four catalysts depending on the calcinating temperature of the support show higher values, but in general, they keep the same aspect as in the case of retention at first injection, particularly for acetylene.

The decreasing sequence of acetylene adsorption at equilibrium is identical with that at first injection and varies in the same sense with the calcinating temperature of the support.

The ethylene adsorption at equilibrium is little influenced by the characteristics of the support. A minimum can be observed for the PdA_8 catalyst.

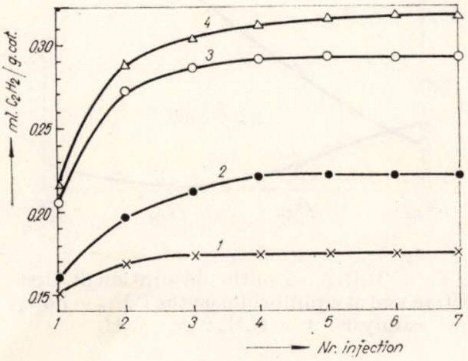

Fig. 3. — Acetylene adsorption on PdA_6—PdA_9 catalysts.

1 – PdA_6; *2* – ; PdA_7; *3* – PdA_8; 4 – PdA_9.

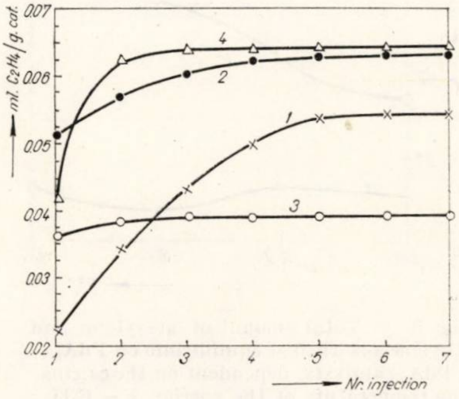

Fig. 4. — Ethylene adsorption on PdA_6—PdA_9 catalysts.

1 – PdA_6; *2* – PdA_7; *3*;PdA_8 – *4* – PdA_9.

By plotting the difference between the quantity of adsorbed gas at first injection and at equilibrium, diagrams shown in figure 6 were obtained. Catalyst PdA_8 (support calcinated at 800°) showing a minimum of ethylene adsorption and a value near to that of saturation for C_2H_2 is revealed. This fact could possibly be correlated with the selectivity of the catalyst in the selective hydrogenation reaction of acetylene to ethylene.

The differentiated adsorption which was noticed, could probably be interpreted in the sense of the strength of the π bond, which takes place at the interaction reactant-catalyst.

Determination of palladium particle size. In the present work, the relation between acetylene chemisorption and palladium dispersion on the support in connection with the thermal treatment of the support, respectively its capacity to disperse palladium was also studied.

For this purpose, the dispersion of the palladium granules on the support was determined from the gaschromatographic data, obtained according to the previously described method, taking into consideration acetylene adsorption.

Considering that palladium covers various zones of the support area with a bidimensional layer[16,17] and taking into account that the radius of the palladium is 1.37Å, the area of one gram of palladium is 424 m^2.

This result assumes that palladium laid down on the support has the shape of a continuous monoatomic film, without any interference with the support alumina.

The following relation was used[16,17] to determine the diameter of palladium particles :

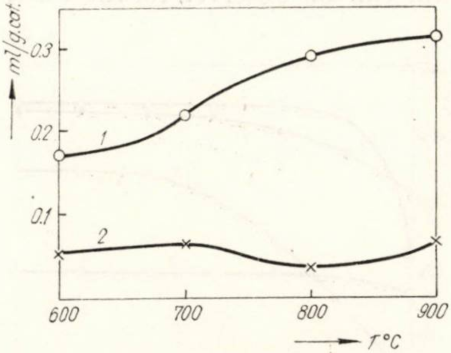

Fig. 5. — Total amount of acetylene and ethylene adsorbed at equilibrium on PdA_6—PdA_9 catalysts, dependent on the calcinating temperature of the carrier. 1 — C_2H_2 ; 2 — C_2H_4.

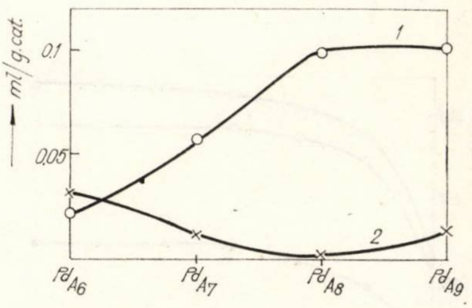

Fig. 6. — Difference of the adsorption at first injection and at equilibrium on the PdA_6 — PdA_9 catalysis. 1 — C_2H_2 ; 2 — C_2H_4

$$d_A = \frac{5 \times 10^4}{A \rho \theta}, \qquad (2)$$

where :

A = specific area of palladium (424 m^2/g).

ρ = specific gravity of palladium (g/cm^3).

θ = coverage degree of palladium with acetylene molecules.

In the present calculations concerning the size of palladium particles, it was assumed that acetylene adsorption on palladium takes place through π electrons, on two centres[18]. The size of palladium particles laid down on alumina by impregnation, differs from one catalyst to another.

The maximum particle size is shown by the PdA_6 catalyst (fig. 7).

In the case of C_2H_2 adsorption, the coverage degree θ, varies inversely with the particle size of palladium. Palladium dispersion in the catalysts prepared with an Al_2O_3 support, treated thermally at high temperatures of 600°—900°, increases with the rise of this temperature. It is an interesting conclusion for the manufacturing technology of this catalyst at industrial level.

---

[17] P.C. ABEN, *J. Catalysis*, **10**, 224 (1968).
[18] G.C. BOND and P.B. WEISZ, *J. Catalysis*, **4**, 211 (1965).

In order to find out if there is any connection between palladium dispersion and activity, respectively between chemisorption and activity in the selective hydrogenation reaction of acetylene, this reaction was carried out and the results will be reported in another paper.

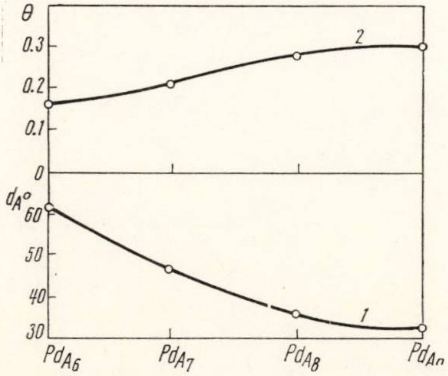

Fig. 7. — 1) Diameter of the palladium particles. 2) Coverage degree.

CONCLUSIONS

The results obtained show that the character of the support determines a specific structure of the palladium catalyst with different behaviour in acetylene and ethylene adsorption. The fact that the adsorption value for C_2H_2 and C_2H_4 both at first injection and at equilibrium differs according to the calcinating temperature of the influence of the support alumina, points to the influence of the support on the adsorption properties of the catalyst, particularly in the case of acetylene. In other words, the textural and structural characteristics of the support, resulting as a consequence of differential thermal treatment it has undergone, confer different adsorbing characteristics to the Pd/Al_2O_3 catalysts, probably as a consequence of the different distribution of palladium crystals on the support and of the orientation in various proportion, of the surfaces (100) and (110), towards the exterior or as a consequence of the differentiated dispersion of the palladium.

The particle size determined by us ranges within the values given by other authors in literature [19,20] and determined by other methods.

---

[19] D. Pope, W.L. Smith, M.J. Eastlake and R.L. Moss, *J. Catalysis*, **22**, 72 (1971).

[20] T.A. Dorling and R.L. Moss, *J. Catalysis*, **7**, 378 (1967).

Revue Roumaine de Chimie, **19**, 9, 1521–1533 (1974)

THE SYNTHESIS OF SOME *C*-TERMINAL ANALOGUES OF THE PEPTIDES : ELEDOISIN AND PHYSALAEMIN

F. CUIBAN*, STELIANA CILIANU and VERONICA BADEA
Institute for Chemical-Pharmaceutical Researches, Bucharest, Sos. Vitan 112

Received February 25, 1974

Several hexapeptides, *C*-terminal analogues of eledoisin and physalaemin were synthesized, in which modifications of the peptide chain could influence enzymatic hydrolysis. Some peptides are highly biologically active but of short duration.

Among the numerous peptides intensely studied with regard to amino acid composition-biological activity relationships, eledoisin and physalaemin are listed. They produce a strong vasodilator, hypotensive effect, stimulating also the smooth muscles, but the effect is of short duration. Being constituted of amino acids proper to animal and human organisms, the products are exposed to usual enzymatic degradation within the framework of proteic metabolism. Although they have related structures, physalaemin is several times more active than eledoisin, but the duration of activity is much shorter. Both peptides are inactivated by the enzymatic equipment of blood serum. Their cleavage may be undertaken also with purified enzymes as shown in scheme 1.

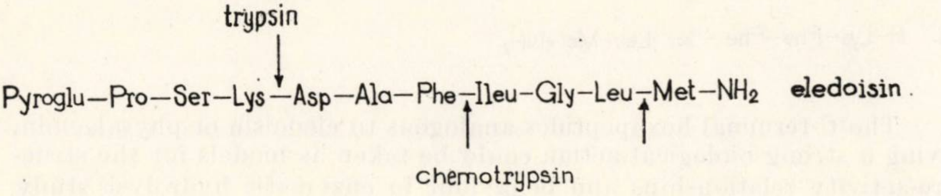
trypsin
Pyroglu–Pro–Ser–Lys–Asp–Ala–Phe–Ileu–Gly–Leu–Met–NH2
eledoisin
chemotrypsin
Pyroglu–Ala–Asp–Pro–Asp–Lys–Phe–Tyr–Gly–Leu–Met–NH2
NH2
physalaemin
trypsin

Scheme 1. Enzymatic cleavage of eledoisin and physalaemin.

A great number of analogous peptides were synthesized and especially fragments with *C*-terminal approached amino acid sequences and it was found that they produce even a stronger biological effect than the natural products. Among the biologically active fragments, there are also hexapeptides with related structure to the *C*-terminal part of eledoisin and physalaemin, but their action is also of short duration[1].

---

* Present address : Polytechnic Institute Timişoara, POB 103, Romania

In order to prolong the duration of the peptide activity, conditioning techniques were used, e.g. administration of the peptide suspensions in solvents[2] but which did not provide satisfactory results. One tried also to prepare some aliphatic or aromatic acyl-derivatives but in most cases the biological effect diminished[3] while the prolongation of the activity was unsignificant[4]. Starting from the observation that the loss of activity of oxytocin is due to the cleavage of the *N*-terminal residue by the action of oxytocinase, the substitution of the implied amino acids in the peptide bond (cysteine and tyrosine) by their N-methylated correspondents[5] was checked. An important decrease in biological action was observed with these products. The substitution of glycine by sarcosine in biologically active peptides resulted generally either in a variable or in the total loss of activity[1]. Investigating the hydrolysis of simple peptides, it was found that the enzymatic action was much more reduced than in the case of usual peptides. Some peptides with N-methylated amino acids can display a protease inhibitory function[6].

I. H–Lys–Phe–Phe–Gly–Leu–Met–NH_2

II. H–Lys–Phe–Phe–Gly–Leu–Met–$NHCH_3$

III. H–Ala–Phe–Val–Gly–Leu–Met–NH_2

IV. H–Lys–Phe–Val–Gly–Leu–Met–NH_2

V. H–Lys–Phe–Val–Gly–Leu–Met–$NHCH_3$

VI. H–Lys–Phe–Phe–Sar–Leu–Met–NH_2

Scheme 2. The structure of the *C*-terminal sequence of eledoisin hexapeptide analogues.

The *C*-terminal hexapeptides analogous to eledoisin or physalaemin, having a strong biological action could be taken as models for the structure-activity relationships and behaviour in enzymatic hydrolysis study by the methylation of *N*- and *C* -terminal fragments or by the substitution of natural amino acids with N-methyl-amino acids. For this purpose, we synthesized some analogous hexapeptides to the *C*-terminal residue of eledoisin with modifications in the chain which could influence the enzymatic hydrolysis[7]. The structure of these peptides is presented in scheme 2*.

---

[1] E. Schröder and K. Lübke, "The Peptides", vol. II, Academic. Press, New York, 1966, and literature herein cited.

[2] E. Stürmer and A. Fanchamps, *Dtsch. Med. Wschr.*, **90**, 1012 (1965).

[3] K. Lübke and E. Schröder, *Liebigs Ann. Chem.*, **692**, 237 (1966).

[4] L. Bernardi, R. De Castiglione, G.B. Fregnan and A. H. Glässer, *J. Pharm. Pharmacol.*, **19**,95 (1967).

[5] K. Jost, J. Rudinger and F. Sorm, *Coll. Czech. Chem. Comm.*, **28**, 1706, 2021 (1963).

[6] J. Greenstein and M. Winitz, "Chemistry of the Amino Acids", Vol. 3, John Wiley, New York, 1961.

The general synthesis scheme was approached experimentally by the condensation of peptide fragments. In most cases the *C*-terminal dipeptide was condensed with the tetrapeptide, obtained *via* stepwise synthesis or by the condensation of fragments. We adopted a slightly different way of synthesis for the dipeptide BOC-Leu-Met-NH_2 from that described in literature[8] in order to avoid the difficulties connected with the separation of H-Met-NH_2[9] and the use of the *o*-nitrophenylsulphenyl group in the protection of leucine[10]. By coupling BOC-leucine[11] with methionine methyl ester hydrochloride in the presence of DCC we obtained the methyl ester of the dipeptide in good yield. The ammonolysis of the ester by ammonia or by methylamine allowed to obtain the corresponding amines of high optical purity in practically quantitative yield.

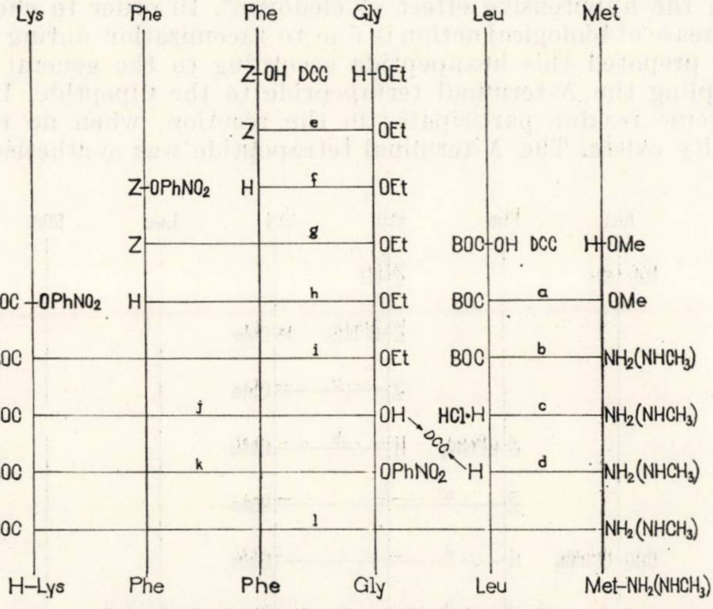
Lys
Phe
Phe
Gly
Leu
Met
Z-OH DCC H-OEt
Z e OEt
Z-OPhNO2 H f OEt
Z g OEt
BOC-OH DCC H-OMe
di-BOC-OPhNO2 H h OEt
BOC a OMe
di-BOC i OEt
BOC b NH2(NHCH3)
di-BOC j OH
DCC
HCl·H c NH2(NHCH3)
di-BOC k OPhNO2 H d NH2(NHCH3)
di-BOC l NH2(NHCH3)
H-Lys Phe Phe Gly Leu Met-NH2(NHCH3)

Scheme 3. Synthesis of peptides I and II.

The synthesis of hexapeptides (I) and (II) was realized for both compounds after the same scheme (scheme 3) which differs from that described in the literature.[12–15] Tetrapeptide (I_c) was synthesized by stepwise increasing the *C*-terminal end growth. For the preparation of dipeptide (I_e) the use of DCC proved to be more advantageous than activating the carboxyl function *via* its reactive ester$_8$. The use of DCC in the tetrapeptide (I_j) condensation with dipeptide (I_d) led to a strongly impurified compound by dicyclohexylurea derivatives from which the hexapeptide can be isolated with great losses. The use of activated ester (I_k) proved much more convenient for the same synthesis. Although some part of the ester remains unreacted, the isolation and purification of the end-product can be accomplished easily. If an excess of dipeptide (I_d) is employed with the purpose of a more complete conversion of the tetrapeptide ester (I_k), the purification losses will be much greater.

---

* The abbreviations according to the recommandations of I.U.P.A.C. – I.U.B. Commission on Biochemical Nomenclature (I.U.P.A.C. Information Bulletin Nrs. 26 and 27). All amino acids were L-amino acids. In addition: DCC = N,N′–dicyclohexylcarbodiimide; DCCU = = N,N′ -dicyclohexylurea; DMF = dimethylformamide.

[7] F. Cuiban, V. Badea and St. Cilianu, "Peptides 1968", North-Holland Publ. Comp., Amsterdam, 1968.

[8] L. Bernardi and O. Goffredo, *Gazz. chim. Ital.*, **94**, 853 (1964); **95**, 172 (1965).

[9] Fr. Chillemi, *Gazz. chim. Ital.*, **93**, 1079 (1963).

[10] P.H. Bentley and H. Gregory *J. Chem. Soc.*, **1964**, 6130, 6138.

[11] G. Anderson and A. Mc Gregor, *J. Amer. Chem. Soc.*, **79**, 5696, 6180 (1957).

The hexapeptide III was previously synthesized *via* coupling the *N*- and *C*-terminal tripeptides, and it was found it possessed only 15% of the hypotensive effect of eledoisin[9]. In order to check whether the decrease of biological action is due to racemization during the synthesis, we prepared this hexapeptide according to the general scheme i.e. by coupling the *N*-terminal tetrapeptide to the dipeptide. In this case, the glycine residue participates in the reaction, when no racemization possibility exists. The *N*-terminal tetrapeptide was synthesized stepwise,

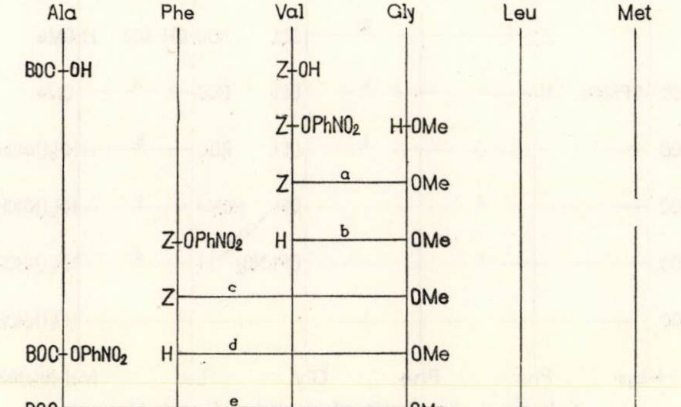

Scheme 4. Synthesis of peptide III.

---

[12] E. Stürmer, E. Sandrin and R.A. Boissonnas, *Experientia*, **20**, 303 (1964).

[13] L. Bernardi, G. Bosisio, F. Chillemi, G. De Carlo, R. De Castiglione, V. Erspamer, A. Glaesser and O. Goffredo, *Experientia*, **20**, 306 (1964).

[14] B. Camerino, G. De Carlo, R.A. Boissonnas, E. Sandrin and E. Stürmer, *Experientia*, **19**, 339 (1963).

[15] E. Schröder, *Experientia*, **20**, 19 (1964).

comparing the activation by DCC, mixed anhydride and *p*-nitrophenyl-ester. Almost in every case, better yields were obtained in the condensation by the *p*-nitrophenyl-esters. The details are given in the experimental part.

By preparing peptides (IV) and (V) the general synthesis route was followed using the common *C*-terminal dipeptides for compounds (I) and (II). The *N*-terminal protected tetrapeptide (IV_a) was synthesized by coupling the common tripeptide (III_c) of compound (III) to the *p*-nitrophenyl ester of di-BOC-N,N′-lysine. After the ester was hydrolysed, the tetrapeptide-COOH (IV_f) was coupled to the *C*-terminal dipeptide and the protecting groups were removed from the peptide (IV_c) *via* routine procedure. The synthesis of product (V) was effected similarly to the hexapeptide (IV).

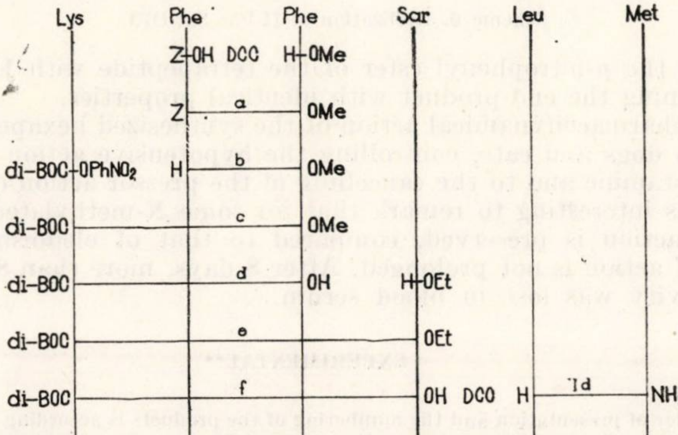

Scheme 5. Synthesis of peptide VI.

For the synthesis of peptide (VI) the adopted scheme was in principle the same, mentioning special difficulties encountered in the stepwise synthesis of the *C*-terminal tetrapeptide. Difficulties occurred even in the preparation of H-Phe-Sar-OEt. The *p*-nitrophenyl ester of carbobenzoxyphenylalanine does not react with ethyl sarcosinate. If carbobenzoxyphenylalanine is coupled with ethyl sarcosinate in the presence of DCC, the compound cannot be obtained in crystalline form. On removal of the amine protecting group, only the corresponding 2,5-diketopiperazine was isolated and characterized instead of the dipeptide ester, according to the reaction shown in scheme 6.

The obtaining of diketopiperazines in the case of dipeptide esters of glycine was evidenced earlier[16] but it appears that this cyclization tendency is much greater for sarcosine ester dipeptides. Following several experiments, the synthesis of peptide (VI) was achieved after a modified scheme (Scheme 5), when the tripeptide di-BOC-Lys-Phe-Phe-OH was first obtained then condensed with sarcosine and thereafter with the *C*-terminal dipeptide. The hexapeptide (VI) could also be prepared by condensing the *p*-nitrophenyl ester of the tetrapeptide with H-Leu-Met-NH_2, obtaining the end-product with identical properties.

---

[16] G. ÄGREN, *Arkiv Kemi. Mineral. Geol.*, **148**, (21) (1940); in *Chem. Abstr.*, **35**, 3968 (1941).

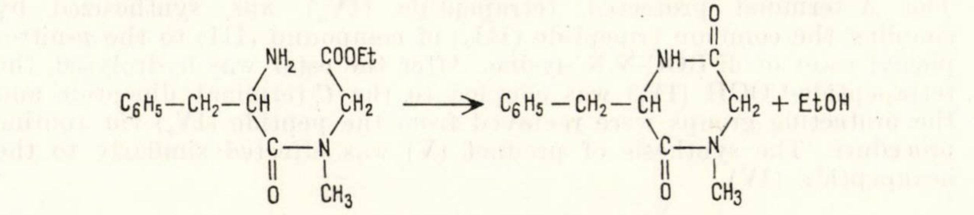

Scheme 6. Cyclization of H-Phe-Sar-OEt.

The pharmacodynamical action of the synthesized hexapeptides was checked on dogs and cats, controlling the hypotensive action in comparison to histamine and to the cancelling of the pressor action of noradrenaline. It is interesting to remark that for some N-methylated peptides, biological action is preserved, compared to that of eledoisin[*] but the duration of action is not prolonged. After 8 days, more than 80% of the initial activity was lost in blood serum.

EXPERIMENTAL[**]

The order of presentation and the numbering of the products is according to the indications in schemes 2—5. All melting points are uncorrected. Vacuum evaporation was effected by a rotatory evaporator. The purity of the compounds was checked by TLC on silica G plates or on Whatman paper nr. 1, colouring with iodine vapours and/or with ninhydrine. The R_f values are referring to the following solvent systems, in V/V : $R_f^0 = CHCl_3 - MeOH$ (20 :1) ; $R_f^a = CHCl_3 - MeOH$ (10 :1) ; $R_f^b = CHCl_3 - MeOH$(5 :1) ; $R_f^c = CHCl_3 - MeOH$ (2 :1) ; $R_f^d = CH_3COC_2H_5 : CH_3CH_2COOH : H_2O$ (6 :2 :3,5) ; $R_f^e = nBuOH - CH_3COOH - H_2O$ (4 :1 :5) ; R_f^j = nPrOH-ammonia 25% sol. (7 :1) ; R_f^k = nPrOH-ammonia 25% sol. (7 :3).

BOC-Leu-Met-OMe (I_a)

To the solution of 2.49 g (10mM) BOC-Leu-OH and 2.59 g (13mM) HMet-OMe.HCl, in 70 ml chloroform, cooled to 0°, 1.8 ml (13 mM) triethylamine was added under stirring. After some min a solution of 2.26 g (11mM) DCC in 10 ml chloroform was added dropwise stirring at 0° for further 5 hours. The mixture was allowed to stand at room temperature for 2 days. After cooling to $-10°$, the resulting DCCU was filtered, while the filtrate washed successively in a separatory funnel with 2 × 35 ml 2N HCl, 2 × 35 ml Na_2CO_3 10% solution and water. The solution was dried over anhydrous Na_2SO_4 and the solvent removed in vacuum. The oil-like residue solved in 30 ml methanol, ice-cooled, 30 ml water was added dropwise. The precipitate was dried at 60° after filtering, recrystallized from 120 ml n-heptane, yielding 2.9g (78%) BOC-Leu-Met-OMe, m.p. 103—104° ; $(\alpha)_D^{25} = -43.4$ (c = 1, MeOH) ; $R_f^0 = 0.5$. Calcd. : $C_{17}H_{32}N_2O_5S$, C : 54.2 ; H : 8.52 ; N : 7.44 ; S : 8.51 ; Found : C : 54.5 ; H :8.70 ; N : 7.50 ; S : 8.30%.

---

[*] Acknowledgement : The authors express their gratitude to Dr. L. Bernardi (Farmitalia) for the kind disposal of eledoisin and to Dr.N. Sterescu (Institute of Normal and Patological Physiology-Bucharest) for the pharmacodynamical tests.

[**] Acknowledgement. The authors express their gratitude to pharm. Cornelia Ioan, for the elemental analyses.

BOC-Leu-Met-NH$_2$ (I_b)

The solution of 2.2 g (5.8 mM) ester (I_a) in 40 anh. methanol, saturated with ammonia at −5° was allowed to stand for 2 days at 0−5°. After the solvent removal in vacuum, BOC-Leu-Met-NH$_2$ resulted in a quantitative yield, presenting a TLC a single spot. $R_f^c = 0.15$; m.p. 158−160°; $(\alpha)_D^{25} = -42.6$ (c=1, MeOH). Lit.[8] m.p. 158−159°; $(\alpha)_D^{25} = -42$.

H-Leu-Met-NH$_2$ (I_d) was prepared *via* literature[8] by removing the amino-protecting group with saturated solution of HCl in acetic acid, then neutralized with K_2CO_3 50 % solution, in 63 % yield; m.p. 124−126°.

Z-Phe-Gly-OEt (I_e)

To the solution of 8.97 g (30 mM) Z-Phe-OH and 5.2 g (37.5 mM) glycine methyl ester chlorohydrate in 60 ml DMF, cooled to 0°, 4.6 ml (37.5 mM) triethylamine was added dropwise, under stirring. After 10 min, a solution of 6.77 g (33 mM) DCC in 10 ml DMF was added drop-. wise. The mixture stirred for 5 hours at 0° was allowed to stand over night in the refrigerator. To the cooled solution 150 ml ethyl acetate was added and the resulting DCCU filtered. The filtrate was washed twice with 2N HCl (100 ml and 50 ml), then successively washed with 2 × 50 ml Na_2CO_3 10 % solution and water to neutral reaction. The solution was dried over anh. Na_2SO_4 and the solvent removed in vacuum. The crystalline residue was several times triturated with anh. ether, dried, achieving 7.2 g (I_e) (Yield- 62 %), m.p. 110−112°, identical to the product described in literature[8], chromatographically pure; $R_f^b = 0.77$.

Z-Phe-Phe-Gly-OEt (I_g), *di-BOC-Lys-Phe-Phe-Gly-OEt* (I_i) and *di-BOC-Lys-Phe-Phe-Gly-OH* (I_j) were prepared according to the procedure described in the literature [8], obtaining products with identical properties.

di-BOC-Lys-Phe-Phe-Gly-OPhNO$_2$ (I_k)

In a mixture of 100 ml dioxane and 66 ml ethyl acetate, 2.3 g (3 mM) tetrapeptide-COOH (I_j) and 0.66 g (4.9 mM) *p*-nitrophenol were solved. To the solution, 0.68 g (3.3 mM) DCC dissolved in 5 ml ethyl acetate was added dropwise under stirring and was kept for 2 days at room temperature. The mixture was cooled to −10° and the resulting DCCU from the reaction, filtered. After the solvent removal in vacuum the residue mixed with Et_2O and solved with 110 ml ethanol, under reflux. After cooling to 20° water was added until a slight opalescence, then cooled to −15°. After filtering and drying, 2 g of product (I_k) were obtained, m.p. 136−140° (yield−74 %). Calcd.: $C_{42}H_{54}N_6O_{11}$, C :61.58 ; H :6.64 ; N :10.26 ; Found : C :61.70 ; H :6.60 ; N :10.37 %.

di-BOC-Lys-Phe-Phe-Gly-Leu-Met-NH$_2$ (I_l)

1.42 g (1.68 mM) *p*-nitrophenyl ester of tetrapeptide (I_k) and 0.44 g (1.68 mM) leucylmethionine-amide (I_d) were solved in 32 ml DMF and stirred for 10 days at room temperature. After advanced solvent removal in vacuum, the oil-like residue was triturated with 20 ml water, filtered and washed with Et_2O, dried, achieving 1.4 g crude product (I_l). For purification, the crude product was solved in 6 ml DMF, ice-cooled and precipitated in 60 ml Et_2O, under stirring. After filtering, it was washed with 10 ml cooled Et_2O, dried, obtaining 0.5 g hexapeptide, m.p. 234−235° (yield −31 %) with identical properties to the product described in literature[8], chromatographically unitary, $R_f^b = 0.65$.

H-Lys-Phe-Gly-Leu-Met-NH$_2$*.2HCl* (I)

To 0.33 g (0.35 mM) of protected peptide (I_l), 27 ml glacial acetic acid with HCl 2 % were added. After 5 min, [88 ml anhydrous Et_2O was added to the filtered solution, cooling to −15°. After filtering and washing with absolute Et_2O, dried over P_2O_5 and NaOH, 0.255 g peptide (I) (yield-86 %) were achieved, m.p. 160−165°. The product is chromatographically unitary on silica G plates, $R_f^d = 0.66$, and on paper $R_f^e = 0.59$; Calcd. : $C_{37}H_{56}O_6N_8S.2HCl.2H_2O$, C :52.20 ; H :7,37 ; N :13.18 ; Found : C :52.10 ; H :7.40 ; N :13.00 %.

BOC-Leu-Met-NHCH$_3$ (II$_b$)

To the solution of 0.75 g (2 mM) ester (I_a) in 4 ml absolute ethanol, 5 ml methylamine 33 % alcoholic solution were added and allowed to stand for 3 days at room temperature. Adding 16 ml water the product was precipitated and filtered. For purification, it was dissolved in 10 ml EtOH by heating and 10 ml water was added, achieving 0.5 g BOC-Leu-Met-$NHCH_3$ (yield-66 %), m.p. 133−135° ; $(\alpha)_D^{25} = -45$ (c = 1, MeOH) ; $R_f^a = 0.37$; Calcd. : $C_{17}H_{33}O_4N_3S$, C : 57.37 ; H :8.80 ; N :11.32 ; S :8.53 ; Found : C :54.70 ; H : 9.00 ; N :11.27 ; S :8.30 %.

H-Leu-Met-NHCH$_3$*.HCl* (II$_c$)

1 g (2.66 mM) amide (II_b) was treated at room temperature with a solution of HCl 7 % in glacial acetic acid and allowed to stand for 1 hour. After adding 100 ml absolute Et_2O and cooling, it was filtered, avoiding the contact with atmospheric humidity, because the compound is hygroscopic. Dried in vacuum over P_2O_5 0.7 g H-Leu-Met-$NHCH_3$.HCl was obtained (yield-−87 %), displaying a single chromatographical spot, $R_f^c = 0.45$; Calcd. : $C_{12}H_{26}SO_2Cl$, Cl :11.38 ; S : 10.31 ; Found : Cl :11.60 ; S :10.00 %.

di-BOC-Lys-Phe-Phe-Gly-Leu-Met-NHCH$_3$ (II$_1$)

To the solution of 0.32 g (1 mM) leucyl-methionine-methyl amide chlorohydrate (II_c) in 10 ml DMF, cooled to 0° 0.1 g (1 mM) triethylamine was added and after 10 min, the triethylamine chlorohydrate was filtered. To the filtrate, 0.82 g (1 mM) *p*-nitrophenyl ester peptide (I_k) was added, stirring for 6 days at room temperature. After DMF removal in vacuum, the *sicc* residue was solved in 25 ml Et_2O, cooled to −10°, filtered, achieving 0.8 g impure peptide (II_1). For purification the product was dissolved under reflux in 15 ml methanol, hot filtered, ice-cooled and filtered after adding 4 ml water. When purification was repeated, 0.34 g pure hexapeptide (II_1) was obtained (yield-35 %), m.p. 235−237°, chromatographically pure, $R_f^a = 0.25$; Calcd. : $C_{40}H_{74}O_{10}N_8S$, C :60.35 ; H :7.80 ; N :11.73 ; Found : C :60.40 ; H :8.00 ;N :11.78 %.

H-Lys-Phe-Phe-Gly-Leu-Met-NHCH$_3$*.2HCl* (II)

0.25 g protected peptide (II_1) was treated at room temperature with 19 ml of HCl 9 % solution in glacial acetic acid and after 7 min vacuum filtered, through a porous crucible. The solution diluted with 200 ml absolute Et_2O was let to crystallize in the cold. The filtered product was dried over NaOH in an exicator, thereafter in a drying pistol over P_2O_5 at 35°, yielding 0.19 g (II) as dichlorohydrate, m.p. 152−153° ; $(\alpha)_D^{22} = -16.7$ (c = 0.43, MeOH :H_2O, 1 : 1). The product is chromatographically pure, $R_f^d = 0.7$ on silica G plates and $R_f^e = 0.76$ on paper. Calcd. : $C_{38}H_{58}O_6N_8S.2HCl.1\ 1/2\ H_2O$, C :53 :38 ; H :7.44 ; N :13.10 ; Found : C :53.30 ; H : 7.30 ; N :13.00 %.

Z-Val-OPhNO$_2$

In a magnetically stirred Erlenmeyer flask, 2.8 g (11 mM) carbobenzoxy-valine[11] and 1.56 g (11 mM) *p*-nitrophenol were dissolved in 10 ml ethyl acetate. Cooled to 0°, 2.3 g (11 mM) DCC dissolved in 3 ml ethyl acetate under stirring was added and kept at room temperature for 3 hours. Washed successively with $NaHCO_3$ saturated solution, 1N HCl and water. Thereafter dried over anhydrous Na_2SO_4, it was concentrated to *sicc* in vacuum. The residue was treated with 10 ml. absolute EtOH, and after filtering, precipitated with 5 ml petroleum ether. After filtering and washing with a solution consisting of equal volume absolute EtOH and petroleum ether, dried in vacuum, 2.54 g Z-Val-OPhNO$_2$ was obtained (yield-60 %), m.p. 63–65°, chromatographically pure, $R_f^a = 0.7$. Calcd. : N :7.32 ; Found : N :7.70 %.

BOC-Ala-OPhNO$_2$. To a solution of 3 g (16 mM) BOC-Ala-OH[11] and 2.24 g (16 mM) *p*-nitrophenol in 17 ml DMF, 3.3 g (16 mM) DCC dissolved in the same solvent, was added at 0°. After 2 hours stirring at 0° and 4 hours at room temperature, it was allowed to stand over night. After diluting the reaction media in 50 ml water and 5 ml ethanol, the yellow oil-like product crystallized in time. After filtering and washing with petroleum ether, 4.4 g BOC-Ala-OPhNO$_2$ were achieved (yield –90%), m. p. 225–227°, chromatographically unitary on silica G plates, $R_f^c=0.6$. Dioxane may be used also condensation solvent achieving very good yields. The removal of DCCU in this case is accomplished by filtering.

Z-Val-Gly-OMe (III$_a$)

(i) *Via p*-nitrophenyl ester : To a solution of 2.7 g (7 mM) Z-Val-OPhNO$_2$ and 0.9 g (7 mM) glycine methyl ester chlorohydrate in 15 ml DMF, an equivalent of triethylamine was added under stirring ; after stirring for 5 hours at room temperature, it was allowed to stand over night, then diluted in 30 ml water and filtered. The precipitate, dissolved in 3 ml EtOH, was again precipitated with 20 ml water. After filtering and drying in vacuum over P_2O_5, 2 g of product (III$_a$) were achieved (yield-86 %), m.p. 160–162°, chromatographically pure, $R^a{}_f=$ $=0.68$. Calcd. : $C_{16}H_{22}N_2O_5$, C :59.62 ; H :6.88 ; N :8.69 ; Found : C :59.50 ; H :6.54 ; N :8.80 % ·

(*ii*) Synthesis *via* DCC method. To a suspension of 1.2 g (9mM) methyl-glycinate chlorohydrate in 15 ml $CHCl_3$, 1.35 ml (9 mM) triethylamine then 2 g (8 mM) Z-Val-OH dissolved in $CHCl_3$ were added. After cooling to 0–5°, a solution of 1.64 g (8 mM) DCC in 2 ml $CHCl_3$ was added dropwise, the reaction media stirred for 2 hours at the same temperature, was let to stand thereafter, over night at room temperature. DCCU was filtered, the chloroformic solution successively washed with 3 × 15 ml 1N HCl, 3 × 15 ml $NaHCO_3$ saturated solution and 2 × 20 ml NaCl saturated solution. The organic solvent layer was dried over anh. $MgSO_4$ and evaporated to *sicc*. After solving the residue in 80 ml ethyl acetate and precipitation with petroleum ether, 0.9 g (III$_a$) were obtained (yield-35 %) with identical characteristics to the product resulted *via p*-nitrophenyl ester method (*i*).

Z-Phe-Val-Gly-OMe (III$_c$)

The equimolal mixtures (7 mM) of carbobenzoxyphenyl-alanine *p*-nitrophenyl ester[17] with dipeptide bromohydrate (III$_b$) obtained by deprotecting peptide (III$_a$) *via* routine techniques and triethylamine were dissolved in 17 ml DMF. After keeping for 5 days at room temperature, the mixture was diluted in 30 ml water and the precipitate washed with Et_2O, then dried in vacuum, achieving 2.94 g (III$_c$), m.p. 195–197°, (yield-88 %), chromatographically pure, $R_f^a=0.62$. Calcd. : N :8.94 ; Found : N :9.20 %. If condensation is made *via* mixed anhydride of Z-Phe-OH with isovaleric acid, the reaction yield diminishes to 20 %, while performing with DCC it is only 10 %, on account of the difficulties encountered at purification ; m.p. in the last scheme was somehow lower, 192–193°.

BOC-Ala-Phe-Phe-Val-Gly-OMe (III$_e$)

After deprotecting tripeptide (III$_c$) under usual conditions with HBr 33 % solution in glacial acetic acid and obtaining bromohydrate (VI$_d$), (7 mM) thereof was solved in 30 ml mixture of equal volume DMF : ethyl acetate (or the necessary amount of dioxane), equimolal amounts of triethylamine and BOC-Ala-OPhNO$_2$ were added. Kept at room temperature for 4 days the solvents were eliminated in vacuum. The *sicc* residue was purified by repeated precipitations with petroleum ether from ethyl acetate, chloroform or absolute ethanol and was used for the next operation. Reaction yield, 75.5% versus the tripeptide (III$_c$).

---

[17] V. Du Vigneaud and M. Bodanszki, *J. Amer. Chem. Soc.*, **81**, 6072 (1959).

BOC-Ala-Phe-Val-Gly-OH (III$_f$)

To the solution of 0.3 g (0.6 mM) tetrapeptide ester (III$_e$) in 36 ml absolute ethanol, prepared at 55–60°, 3 ml water was added. After cooling to room temperature, 1.5 ml 1N NaOH was added, stirring for 1 hour. The alcoholic solution was diluted with 70 ml water and acidulated to pH=2 with 2N HCl solution. After extraction with 100 ml Et_2O and drying over $MgSO_4$, the ether was removed in vacuum, achieving 0.3 g (in quantitative yield) product (III$_f$) chromatographically pure, m.p. 180–182°.

BOC-Ala-Phe-Val-Gly-Leu-Met-NH$_2$ (III$_g$)

To the solution of 0.24 g (0.485mM) tetrapeptide–COOH (III$_f$) and 0.15 g (0.575 mM) H-Leu-Met-NH$_2$ (I$_d$) in 12 ml anh. pyridine, cooled to 0°, 0.12 g (0.585 mM) DCC was added, maintaining the same temperature for 2 hours. After stirring for 2 days at room temperature, the solvent was removed in vacuum and the residue washed successively with 6 × 5 ml 1N HCl, 5 × 5 ml $NaHCO_3$ 5% solution and Et_2O. The precipitate was dissolved in 6 ml DMF, DCCU removed by filtering and the solution diluted with 28 ml ethyl acetate. After filtering and washing at 40–50° with ethyl acetate and chloroform, 0.043 g product (III$_g$) (yield–17.2%) were obtained, chromatographically pure, m.p. 248–249°.

H-Ala-Phe-Val-Gly-Leu-Met-NH$_2$.HCl (III)

To 2 ml HCl 7% solution in glacial acetic acid, 0.043 g (0.084 mM) protected hexapeptide (III$_g$) was added, allowed to stand for 25 min at room temperature, then filtering over a G$_3$ crucible in order to remove the very small amounts of insoluble products. To the filtrate, 10 ml anh. Et_2O was added, cooled to 0°, kept for 1–2 hours at this temperature, the precipitate was filtered and washed with anh. Et_2O avoiding contact with atmospheric humidity. After drying in vacuum over P_2O_5, 0.036 g hexapeptide chlorohydrate (yield-96%) were achieved, m.p. 288–290°, chromatograpphically pure, $R_f^d=0.68$ on silica plates and $R_f^e=0.65$ on paper. Calcd. : Cl^- :5.27 ; Found : 5.20%.

di-BOC-Lys-Phe-Val-Gly-OMe (IV$_a$)

3.5 g (7.4 mM) Z-Phe-Val-Gly-OMe (III$_c$) was treated at room temperature with 35 ml HBr 25% solution in anh acetic acid. After standing for 1 hour, 200 ml anh. EtOH were added and then cooled to –10° for 2 hours. The filtered product was dried in vacuum over P_2O_5 and NaOH. The achieved crystals were dissolved in 200 ml DMF, the solution cooled to –5° and treated with 0.85 g (7.4 mM) triethylamine. After filtering, 3.5 g (7.4 mM) N,N′-di-BOC-lysine *p*-nitrophenyl ester[13] were added to the solution, stirring for 6 days at room temperature. The reaction mixture was diluted with 100 ml water, ice-cooled, and after filtering, the precipitate was washed with Et_2O ; 3.5 g tetrapeptide (IV$_a$) were obtained (yield-70%), m.p. 190–192°, chromatographically pure on silica plates ; R_f^a =0.6. Calcd. : N :10.56 ; Found : 10.70%.

di-BOC-Lys-Phe-Val-Gly-OH (IV$_b$)

Into a mixture of 120 ml EtOH and 3 ml 1N NaOH solution, 2.4 g (3.6 mM) ester (IV$_a$) were solved and allowed to stand over night. The alcohol was removed in vacuum, 25 ml water

---

[18] E. Sandrin and R.A. Boissonnas, *Helv. Chim. Acta*, **46**, 1637 (1963).

was added after ice-cooled, it was acidulated to pH=3 with HCl 10 % solution. After filtering and drying in vacuum, 2 g peptide (IV_b) was obtained in 85 % yield, chromatographically pure on silica plates ; $R_f^o=0.1$, m. p, 154–156°. Calcd. : $C_{32}H_{51}N_5O_9$, C : 59.15 ; H : 7.91 ; N : 10.78 ; Found : C :59.00 ; H :7.90 ; N :10.80 %.

di-BOC-Lys-Phe-Val-Gly-Leu-Met-NH_2 (IV_c)

In a solution of 10 ml DMF and 5 ml acetonitrile, 0.85 g (1.3 mM) tetrapeptide (IV_b) and 0.33 g (1.5 ml) leucyl-methionine amide (I_d) were dissolved ; after cooling to −5°, 0.27 g (1.3 mM) DCC was added. It was kept over night at 0°, thereafter for 3 days at room temperature. The reaction mixture was slowly poured into 50 ml water and ice-cooled. The gel-like precipitate was filtered, dried in vacuum and 1.2 g crude product (IV_b) was achieved. The product was solved in 50 ml $CHCl_3$, filtered and the solution successively washed with 2 × 20 ml 1N HCl, 2×20 ml $NaHCO_3$ saturated solution and water. The solution was dried over anh. Na_2SO_4, the solvent removed in vacuum, the residue solved in 15ml DMF and diluted with 50ml water. After filtering and drying in vacuum over P_2O_5, the chromatographically pure product was obtained ; $R_f^a=0.7$ on silica plates, m. p. 220–225° (decomposition).

H-Lys-Phe-Val-Gly-Leu-Met-NH_2*.2HCl* (IV)

The protecting groups of the hexapeptide (IV_c) were removed *via* procedure described for the other peptides i.e. by means of the HCl 5 % solution in glacial acetic acid. Purification was effected by solving in DMF and allowing to precipitate in anh. Et_2O. The product was chromatographically pure, $R_f^d=0.7$ on silica plates. Calcd. : Cl^- :9.28 ; Found : 9.50 %.

di-BOC-Lys-Phe-Val-Gly-Leu-Met-$NHCH_3$ (V_a)

The synthesis was approached in a similar way to that applied in the synthesis of protected hexapeptide (IV_c), using for coupling dipeptide (II_d). At purification, identical techniques were performed, yielding a product (V_a), m.p. 235–240° (decomposition), $R_f^a=0.7$.

H-Lys-Phe-Val-Gly-Leu-Met-$NHCH_3$*.2HCl* (V)

Removal of the protecting groups was effected similarly to that for peptide (IV). $R_f^d=0.7$ on silica plates. Calcd. : Cl^- :9.12 ; Found : 9.40 %.

Z-Phe-Phe-OMe (VI_a)

To 2.15 g (10 mM) phenyl-alanine methyl ester chlorohydrate, prepared *via* literature references[19], solved in 15 ml DMF, cooled to −10°, 1.01 g (10 mM) triethylamine was added. After 15 min the triethylamine chlorohydrate was filtered, 2.29 g (10 mM) carbobenzoxy-phenylalanine added, allowing the temperature to increase to 0–2°. The same temperature was maintained while a solution of 2.20 g (11 mM) DCC in 10 ml ethyl acetate was dropwise added to the mixture, stirring for 2 hours. The solution was allowed to stand over night at 5°, then cooled to

---

[19] R.A. BOISSONNAS, *Helv. Chim. Acta*, **39**, 1421 (1956).

$-10°$ for 30 min for the complete precipitation of DCCU. After filtering, 100 ml ethyl acetate were added to the filtrate. The solution was washed successively with 2 × 20 ml 2 N HCl, 2 × × 20 ml Na_2CO_3 10 % and with water to neutral reaction. After drying over anhydrous Na_2SO_4, the solvent was removed in vacuum and residue recrystallized from 40 ml methanol, 3.5 g of (VI_a) (yield-76 %) were obtained, m.p. 148–150° ; $(\alpha)_D^{22} = -21.8$ (c=0.5, MeOH), chromatographically pure on silica plates, $R_f^o = 0.67$; Calcd. : $C_{27}H_{28}O_5N_2$, C : 70.41 ; H : 6.12 ; N : 6.08 ; Found : C :70.60 ; H :5.80 ; N :6.18 %.

di-BOC-Lys-Phe-Phe-OMe (VI_c)

4,6 g (10 mM) dipeptide ester (VI_a) was treated with a solution of 14 ml HBr 25 % in anh. acetic acid and allowed to stand for 1 hour ; 200 ml anh. Et_2O were added to the solution, cooled to $-10°$ for 1.5 hours, separating after filtering and drying in vacuum over NaOH and P_2O_5, the peptide ester bromohydrate (VI_b). This was dissolved in 30 ml DMF, cooled to $-10°$ and reacted with 1.01 g (10 mM) triethylamine when triethylaminebromohydrate precipitated. After filtering and washing with DMF, 4.67 g (10 mM) di-BOC-lysine *p*-nitrophenyl ester[3] was added to the solution of peptide (VI_b), keeping the mixture stirred at room temperature for 4 days. After cooling to $-10°$, 40 ml water were added and the precipitated product, separated by filtering, was dried at ambiant temperature. After careful washing by trituration with Et_2O, 4.7 g ester (VI_c) were achieved, m.p. 150–152°, $(\alpha)_D^{22} = -31.2$ (c = 0.5, MeOH), chromatographically pure on silica plates, $R_f^a = 0.53$. Calcd. : $C_{35}H_{50}N_4O_8$, C :64.20 ; H :7.70 ; N :8.56 ; Found : C :64.00 ; H :7.50 ; N :8.66 %.

di-BOC-Lys-Phe-Phe-OH (VI_d)

To 3 g (4.58 mM) peptide ester (VI_c) solved by refluxing 450 ml EtOH, 120 ml water was added and after cooling to 40°, 12 ml 1N NaOH solution was added dropwise, keeping at room temperature over night. The solution acidulated to pH=3–4 with HCl 10 % when EtOH was removed in vacuum. After cooling and filtering 2.8 g peptide (VI_d) were separated in 95 % yield, m.p. 186–189°, chromatographically pure on silica plates ; $R_f^i = 0.7$.

di-BOC-Lys-Phe-Phe-Sar-OEt (VI_e)

In 60 ml pyridine, 4.5 g (7 mM) peptide (VI_d) and 1.35 g (8.8 mM) sarcosine ethyl ester chlorohydrate were dissolved. After cooling to 2°, 1.65 g (8 mM) DCC was added and allowed to stand at room temperature for 2 days. Pyridine was removed in vacuum, the oil-like residue was washed several times with water after decanting and thereafter treated with 50 ml dioxane. Cooled to 10°, DCCU was separated by filtering and the filtrate concentrated in vacuum to *sicc.* The residue solved in 150 ml ethyl acetate and the solution washed successively with 3 × 35 ml 2N HCl, 35 ml Na_2CO_3 10 % solution, 2 × 35 ml $NaHCO_3$ 5 % solution and water. After drying the organic layer over anydrous Na_2SO_4, the solvent was removed in vacuum and the crystalline residue purified by triturating with 15 ml Et_2O cooled to $-10°$. After filtering and washing with Et_2O, 2.8 g ester (VI_e) were obtained (yield-55 %), m.p. 85–89°, $(\alpha)_D^{22} = -18.2$ (c=0.5, MeOH), chromatographically pure on silica plates ; $R_f^a = 0.47$. Calcd. : $C_{39}H_{57}N_5O_9$, C :63.30 ; H :7.77 ; N :9.46 ; Found : C :63.50 ; H :7.80 ; N :9.30 %.

di-BOC-Lys-Phe-Phe-Sar-Leu-Met-NH$_2$ (VI_g)

(*i*) Synthesis of acid tetrapeptide (VI_f). To the solution of 1 g (1.3 mM) ester (VI_e) in 50 ml ethanol and 10 ml water, 3 ml 1N NaOH were added, keeping under stirring at room temperature for 30 min. After acidulating with HCl 10 % to pH=3–4, the alcohol was removed in vacuum, the solution ice-cooled and filtered, achieving 0.9g tetrapeptide acid (VI_f) (yield–90 %), m.p. 122°, chromatographically pure on silica plates, $R_f^k = 0.77$.

(*ii*) Synthesis *via* *p*-nitrophenyl ester of tetrapeptide (VI_f). To the solution of 0.5 g (0.7 mM) peptide (VI_f) and 0.13 g (1 mM) *p*-nitrophenol in 30 ml anhydrous ethyl acetate cooled to 0°, 0.16 g (0.7 mM) DCC solved in 4 ml ethyl acetate were added. After stirring for 6 hours at room temperature and cooling to $-10°$, DCCU was filtered. After solvent elimination in vacuum, the residue consisting of peptide *p*-nitrophenyl ester (VI_f) was dissolved in 10 ml DMF together with 0.2 g (0.74 mM) leucyl-methionine amide (I_d) and stirred at room temperature for a week. After removing DMF in vacuum, the resulted oil-like residue was treated with 5 ml water, ice-cooled in order to promote crystallization and after filtering, was dried in vacuum over P_2O_5. The precipitate was solved in 100ml ethyl acetate and the solution successively washed with 5 × 20 ml 2N HCl, 8 × 20 ml Na_2CO_3 10% and water to neutral reaction. After drying the estereal solution over anhydrous Na_2SO_4, the residue was triturated in the cold with 8 ml Et_2O, then filtered and dried, the protected hexapeptide (VI_g) was obtained, chromatographically unitary on silica plates, $R_f^a=0.5$, m.p. 161–164°. Calcd. : $C_{48}H_{74}O_{10}N_8S$, C :60.35 ; H :7.81 ; N :11.73 ; Found : C :60.00 ; H :7.50 ; N :11.77%.

(*iii*) Synthesis *via* DCC method. To a solution of 0.5 g (0.7 mM) peptide (VI_f) and 0.36 g (1.4 mM) leucyl-methionine amide (I_d) in 7.5 ml pyridine cooled to 0°, 0.43 g (2.1 mM) DCC was added. After stirring for 1 week at ambiant temperature, pyridine was removed in vacuum, the *sicc* residue dissolved in 10 ml dioxane, thereafter cooled to 5–10° and DCCU removed by filtering. After concentrating to *sicc*, the precipitate was dissolved in 50 ml ethyl acetate and successively washed with 4 × 20 ml 2 N HCl, 4 × 20 ml Na_2CO_3 10% solution, then with water and dried over anh. Na_2SO_4. The residue achieved after solvent removal was solved in 4 ml methanol, the solution cooled to $-5°$ and small amounts of DCCU eliminated by filtering. After the solvent removal, the residue was triturated with Et_2O ; hexapeptide (VI_g) was yielded with identical properties to that described at (*ii*).

H-Lys-Phe-Phe-Sar-Leu-Met-NH$_2$.2HCl (VI)

The protected amide (VI_g) — 0.35 g — was treated at room temperature with 27 ml HCl 9% solution in glacial acetic acid. Filtered after 5 min, it was precipitated with 120 ml anh. Et_2O, obtaining after separation and drying over NaOH and P_2O_5 at 35°, 0.26 g (VI), m.p. 142–146° ; $(\alpha)_D^{22} = -13.8$ (c=0.62, MeOH :H_2O, 1 :1). The product was chromatographically unitary on silica plates and paper ; $R_f^d=0.75$, respectively $R_f^e=0.76$. Calcd. : $C_{38}H_{58}O_6N_8S.2HCl.2H_2O$, C :52.82 ; H :7.46 ; N :12.96 ; Found : C : 52.50 ; H :7.30 ; N :13.00%.

Revue Roumaine de Chimie, **19**, *9*, 1535 – 1544 (1974)

COPOLYMERS OF CONJUGATED DIENES WITH MALEIC ACID MONOESTERS. VIII[1]

BULK COPOLYMERIZATION OF ISOPRENE WITH MONOBUTYL MALEATE

C. ANDREI* and I. NANU**

* Research Laboratory, Ploieşti Petrochemical Industrial Group Brazi, Romania
** Chair of Macromolecular Chemistry, Polytechnic Institute, str. Karl Marx 3, Timişoara, Romania.

Received October 22, 1973

A study is carried out on bulk copolymerization of isoprene with monobutyl maleate in presence of free radicals (A.I.B.N.), in comparison with the concurrent Diels-Alder reaction between the two monomers. The appearance of the "Trommsdorf" effect is remarked in the bulk copolymerization reaction. On the basis of the studied kinetic aspects of the structure and microstructure of the coopolymers, a mechanism is admitted for the copolymerization reaction involving the participation of a *cisoid* donor-acceptor complex and which, at the same time, can be common to the Diels-Alder reaction. Some considerations are also presented on the donor-acceptor complex.

INTRODUCTION

The main kinetic aspects of the solution copolymerization reaction (homogeneous medium) of isoprene with different monoesters of maleic acid were presented in previous works.[2-5]

The values of the copolymerization constants, as well as the Q and e values showed a marked alternating tendency in copolymerization.

The study on bulk copolymerization of isoprene with monobutylmaleate is intended to provide additional information on the kinetics and mechanism of the copolymerization reaction in presence of free radicals and at the same time to give answers to the questions raised before.

This reaction takes place in a heterogeneous medium as the copolymers formed are insoluble in unreacted monomers (copolymerization with precipitation).

EXPERIMENTAL

MATERIALS

The isoprene used (Schuchardt) of $> 99\,\%$ mol. concentration was separated from the polymerization inhibitor by simple distillation.

Monobutyl maleate was prepared in the laboratory by esterification of maleic anhydride with butyl alcohol in molar ratio of 1 : 1 at 80° temperature. The monoester thus obtained had the following characteristics : colourless liquid, $d_{20}^{20} = 1.4570$ and acidity index (A.I.) = 326.7 – – 327.2.

The polymerization initiator, α,α'-azobisisobutyronitrile, was recrystallized twice from acetone or ethyl ether.

---

[1] Part VII, I. Nanu and C. Andrei, *Rev. Roumaine Chim.*, **19**, 115 (1974).
[2] I. Nanu and C. Andrei, *Rev. Roumaine Chim.*, **15**, 1883 (1970).
[3] I. Nanu and C. Andrei, *Rev. Roumaine Chim.*, **16**, 75 (1971).
[4] I. Nanu and C. Andrei, *Rev. Roumaine Chim.*, **17**, 741 (1972).
[5] I. Nanu and C. Andrei, *Rev. Roumaine Chim.*, **17**, 1043 (1972).

METHOD OF WORK

The process of mass copolymerization of isoprene with monobutyl maleate was carried out in closed Pyrex-phials blown beforehand with nitrogen.

The stirring of the reaction mixture was achieved by rotating of the phials in an oil bath maintained at an established working temperature.

After the reaction was carried out, the phials were cooled suddenly under 0° temperature, in order to break off the reaction.

In order to separate the copolymer from the reaction mixture, the latter was dissolved in ethyl ether and precipitated with petroleum ether.

Quantitative purification was achieved by repeated dissolution and precipitation of the copolymer, whereas drying was carried out at a temperature of 40°.

The composition of the copolymer was analyzed by elementary microanalysis.

RESULTS AND DISCUSSIONS

THE GEL EFFECT OR THE "TROMMSDORF EFFECT" IN BULK COPOLYMERIZATION

Unlike the solution copolymerization,[1] where it was established that the gel effect can be eliminated by dilution of monomers, in the case of bulk copolymerization the appearance of this effect is evident.

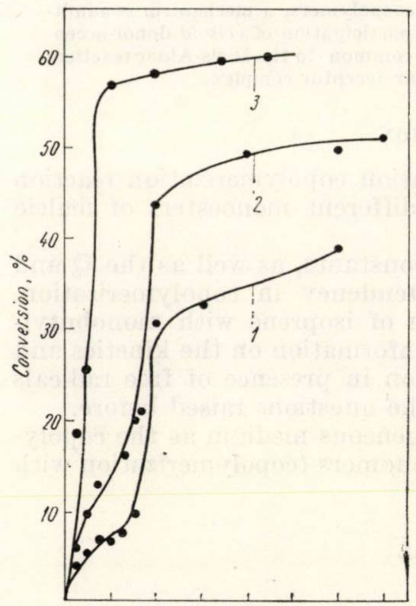

Fig. 1. — Conversion variation depending on bulk copolymerization time of isoprene with monobutylmaleate (1 :1 molar ratio). Reaction temperature :
1) 50°, 2) 60° and 3) 80° ; Initiator: (AIBN) × 10^2 = 4.30 moles/l.

In fig. 1 the conversion variation in time is represented for the bulk copolymerization of isoprene with monobutyl maleate (1 :1) (molar ratio) at different temperatures.

From this plotting it results that at a certain conversion the copolymerization process undergoes autoacceleration. This autoacceleration, found in the case of polymerization of other monomers too, was called the "gel effect" or the "Trommsdorf effect"[6-9] and is due to the increase of the medium's viscosity.

In these conditions the interruption reaction is controlled to a much greater extent by the diffusion process in comparison with the process carried out at small conversions.

Thus, due to the increase of the viscosity, a decrease in the diffusion rate of macroradicals takes place, the probability of interruption reaction (collision of macroradicals and their disappearance) becomes less and, as a result, an increase in the concentration of macroradicals takes place. The appearance

---

[6] E. Trommsdorf, *Makromol. Chem.*, **1**, 169 (1948).

[7] S. Fujii, *Bull. Chem. Soc. Japan*, **27**, 216 (1954).

[8] G. M. Burnett and G.L. Duncan, *Makromol. Chem.*, **51**, 154 (1962).

[9] G.P. Gladişev "Polimerizatsia vinilnykh monomerov", Izdatelstvo Akademii Nauk Kazahskoi SSR, Alma-Ata, 1964, p. 47

of "occluded" macroradicals in the reaction mass of the medium promotes the increase at high rate (autoacceleration).

The autoacceleration of the copolymerization process at temperature of 80°, from the very moment of initiation (fig. 1), is due to a higher concentration of free radicals, the period of halving the (A.I.B.N.) initiator being much shorter at this temperature.

FORMATION REACTION OF DIELS-ALDER ADDUCT CONCURRENT WITH COPOLYMERIZATION REACTION

From fig. 1 it also results that the value of conversion becomes constant after a period of time, but does not reach the maximum value (total copolymerization reaction). Supplementary addition of initiator to the copolymerization medium in this stage of reaction (constant conversion) did not lead to an increase of conversion. Naturally it was presumed that under these conditions a part of the reactants transform themselves into another product by other means and namely the formation of a Diels-Alder adduct.

Surprisingly no literature data were found on the Diels-Alder reaction of isoprene with maleic acid monoesters. Thus it was also necessary to investigate the evolution of this reaction.

In order to obtain a Diels-Alder adduct of isoprene with monobutylmaleate of high purity with the wiev of establishing its characteristics, we started with the Diels-Alder adduct of isoprene with maleic anhydride, well known in literature.[10,11]

The isoprene-maleic anhydride adduct (crystalline substance with melting point = 62−64°) was esterrified with *n*-butyl alcohol in equimolecular ratio at a temperature of 90° for 150 minutes, the method used also to obtain monoesters of maleic acid.[12] Thus isoprene-monobutyl maleate adduct was obtained, a very viscous liquid at room temperature, with acidity index (A.I.) = 232.9.

On the basis of the great difference between the acidity indexes of monobutyl maleate and isoprene-monobutyl maleate adduct, it was possible to establish a simple method of analysis of these from a mixture by simple or potentiometric titration.[12]

In order to observe the formation reaction of the Diels-Alder adduct, concurrent with the copolymerization reaction, the above indicated method of separation of the copolymers was used.

On termination of the bulk reaction of the two monomers (1 : 1 ratio) in presence or absence of free radicals and separation of the copolymer, the mixture between the unreacted monobutyl maleate and the Diels-Alder adduct (distinguished by I.R. spectrophotometry) was separated from isoprene, petroleum ether and ethyl ether by vacuum distillation and analysed by titration.

---

[10] M.C. Kloetzel "Organic Reactions" vol. 4, John Wiley, New York, 1948, p. 1−59.

[11] N.G. Gaylord, Pat. U.S.A. 3.491.068, 1970.

[12] I. Nanu and C. Andrei, *Bul. St. Tehnic I.P.T.* **17** (31), Fasc. 1,7 (1972)

In fig. 2 the variation of the conversion is shown in Diels-Alder adduct and in copolymer of the isoprene-butyl maleate system depending on the duration of the reaction at a temperature of 70° and in the absence of free radicals.

From this plotting the ease is remarked with which the Diels-Alder reaction of isoprene with monoesters of maleic acid takes place, as well as the fact that in the absence of free radicals the conversion in copolymer is very reduced.

The same variation of conversion in adduct and in copolymer of isoprene-monobutyl maleate system, but in the presence of (A.I.B.N.) free radicals is shown in fig. 3.

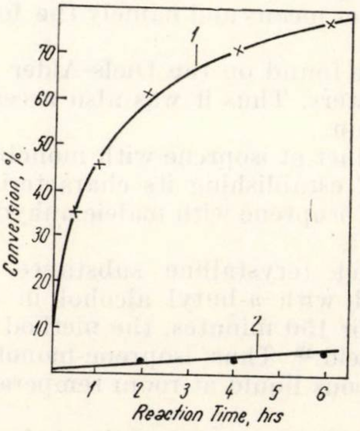

Fig. 2. — Conversion variation in Diels-Alder adduct and copolymer depending on reaction time of isoprene with monobutyl maleate (1 : 1 molar ratio) at a temperature of 70° and in absence of radicalic initiators.
1) conversion in Diels-Alder adduct, 2) conversion in copolymer.

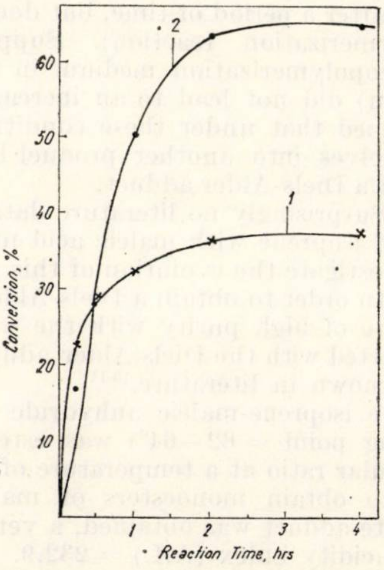

Fig. 3. — Conversion in Diels-Alder adduct and copolymer depending on reaction time of isoprene with monobutyl maleate (1 : 1 molar ratio) at a temperature of 70° and in presence of free radicals (AIBN).
1) conversion in Diels-Alder adduct, 2) conversion in copolymer; Initiator: (AIBN) × 10^2 = = 4.30 moles/l.

From this figure the competition between the two reactions reveals itself. After two hours of reaction, the conversion in copolymer reaches 63.5% and the conversion in adduct 36.5 %. Now it can be explained why the conversion did not increase further on, even by addition of supplementary initiator. A part of the monomers were reacting with the formation of copolymer and a part with the formation of Diels-Alder adduct, the consumption of monomers being total after a period of time.

It is also remarked that in the case of running the reaction at a temperature of 70°, the acceleration of the process takes place at the very moment of initiating.

In the period of over forty years since the discovery of the Diels-Alder reaction a great volume of experimental results was accumulated, however the interpretation of the mechanism of this reaction has remained somewhat behind the accumulation of these results. It is unlikely whether the formation of the two new bonds in the adduct is formed simultaneously by a one step mechanism (A = multicentres) or by a mechanism in two successive steps (B and C).[13]

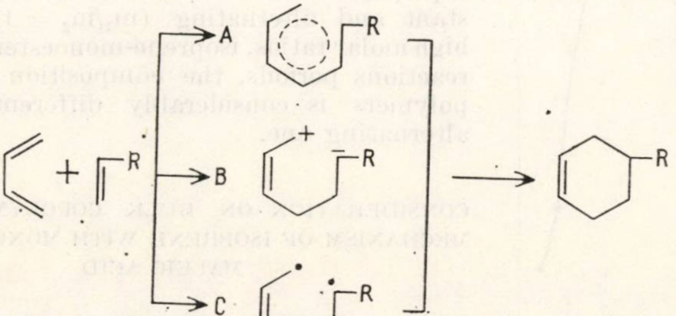

In an earlier work Woodward[14] suggested the fact that the Diels-Alder reaction is preceded by the formation of a complex with charge-transfer (transfer of electron form diene to dienophile), whereas later on to affirm that this reaction should take place through a two step mechanism, in which the bonds between the components are formed successively but without involving the transition states of the B and C type.[15]

Although the mechanism by which the Diels-Alder reaction takes place has not yet been accepted definitely, stereochemical considerations as well as the latest research work on transition state,[16–18] admit that the reaction takes place through a transition complex whose nature will require further investigations and in continuation new facts are being accumulated both in favour of one step and two step mechanism.

We consider that a parallel study of the Diels-Alder reaction and of the copolymerization reaction of the diene-dienophile systems will bring new elements on the mechanisms of both reactions.

THE INFLUENCE OF THE RATIO BETWEEN MONOMERS ON THE CONVERSION AND COMPOSITION OF COPOLYMERS

The variation of conversion depending on the ratio of the two monomers in the feed composition is shown in fig. 4 for copolymerization of isoprene with monobutyl maleate.

---

[13] J. SAUER, *Angew. Chem. internat. Edit.*, **5**, 211 (1966); **6**, 16 (1967)

[14] R.B. WOODWARD, *J. Amer. Chem. Soc.*, **64**, 3058 (1942).

[15] R.B. WOODWARD and T.J. KATZ, *Tetrahedron*, **5**, 70 (1959).

[16] R.A. GRIEGER and C.A. ECKERT, *J. Amer. Chem. Soc.*, **92**, 2918 (1970).

[17] R.A. GRIEGER and C.A. ECKERT, *Trans. Faraday Soc.*, **66**, 2579 (1970)

[18] M.J.S. DEWAR and R.S. PYRON, *J. Amer. Chem. Soc.*, **92**, 3098 (1970)

The highest value of conversion is obtained in case of molar ratio of 1 : 1 between isoprene and monobutyl maleate.

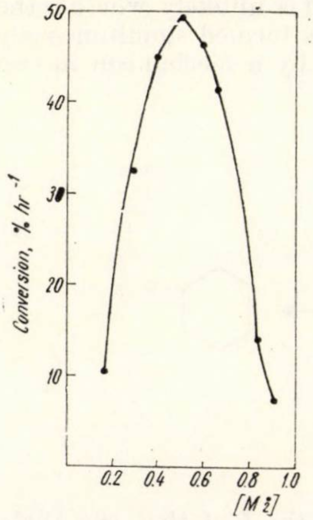

Fig. 4. — Ratio influence between monomers on conversion in bulk copolymerization reaction of isoprene with monobutylmaleate. Reaction temperature 70°, reaction time, 1 hour; Initiator : (AIBN) × 10^2 = 4.30 moles/l.

In table 1 is shown the composition of the copolymers obtained at different ratios of monomers in the feed composition.

It can be observed that the variation between monomers in the feed composition of the copolymers, the latter remaining relatively constant and alternating ($m_1/m_2 = 1$). Only at high molar ratios, isoprene-monoester and longer reactions periods, the composition of the copolymers is considerably different from the alternating one.

CONSIDERATION ON BULK COPOLYMERIZATION MECHANISM OF ISOPRENE WITH MONOESTERS OF MALEIC ACID

In a former work [5] it was shown that the strongly alternating tendency in solution copolymerization of isoprene with monoesters of maleic acid can be explained by the polarity difference of comonomers, as a result of a coulomb attraction between two dipoles, according to Alfrey and Price's theory of polar factors,[19] as well as by adopting Walling and Mayo's point of view,[20] consisting of an explanation of transition stability by dipolar structures of resonance, the transition state being the result of electron transfer between the radical and the monomer.

Table 1

Composition of isoprene-monobutyl maleate copolymers depending on monomer ratio of feed composition

Test n°	Feed composition (moles)			Copolymer composition		
	$[M_1^0]$	$[M_2^0]$	$[M_1^0]/[M_2^0]$	C, %	H, %	m_1/m_2
1	0.030	0.030	1.00	65.00	8.40	1.00
2	0.035	0.025	1.40	65.03	8.35	1.00
3	0.040	0.020	2.00	65.15	8.50	1.02
4	0.025	0.035	0.71	64.98	8.37	1.00
5	0.020	0.040	0.50	64.90	8.35	0.99
6	0.010	0.050	0.20	64.90	8.45	0.99
7	0.050	0.010	5.00	66.00	8.53	1.18
8	0.050	0.005	10.00	66.01	8.53	1.18
9	0.050*	0.0025*	20.00	71.60	9.37	2.41

— Reaction temperature, 70°.
— Reaction time, 1 hour. *) reaction time, 4 hours
— Theoretical value of C and H for an isoprene monobutyl maleate alternating copolymer : % C, 64.95 and % H, 8.38.

---

[19] T. Alfrey and C.C. Price, *J. Polymer Sci.*, **2**, 101 (1947).
[20] C. Walling and F.R. Mayo, *J. Polymer Sci.*, **3**, 895 (1948).

These points of view do not exclude however the participation in copolymerization reaction of a donor-acceptor complex, formed between the monomers.

The results of the kinetic study on bulk copolymerization reaction of isoprene with monobutyl maleate (copolymers with high alternation, indifferent of the ratio between the monomers of the feed composition and the maximum reaction rate at equivalent concentrations of monomers) can be explained convincingly on the basis of the mechanism involving the formation of a donor-acceptor complex between monomers of the type :

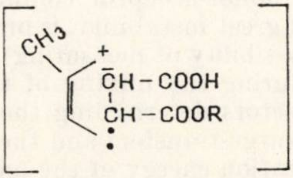

and its participation in the reaction in presence of free radicals :

$$D + A \rightarrow C$$

$$R^{\cdot} + C \rightarrow R - C^{\bullet}$$

$$R - C^{\cdot} + C \rightarrow R - (C)_x^{\cdot}$$

$$2R - (C)_x^{\cdot} \rightarrow \text{copolymer}$$

in which :

D — donor monomer (isoprene)

A — acceptor monomer (monoester) and

C — donor-acceptor complex

The enrichment of the copolymer in isoprene at high donor-acceptor ratios and at long reaction periods is due to the conventional addition of this monomer to the increasing chain,

$$R - (C)_x^{\cdot} + D \rightarrow R(C)_x D.$$

As an argument for the support of the proposed mechanism, the dilution effect on the conversion and composition of copolymers can be considered, as well as the influence of the solvent's nature on the copolymerization reaction presented in a former work.[1]

A similar mechanism but which implies homopolymerization only of the donor-acceptor complex, was proposed by Gaylord[21,22] for copolymerization of conjugated dienes with maleic anhydride. It is appreciated that the Diels-Alder reaction which develops easily in conditions of copolymerization, recognized as one of the most characteristic examples of donor-acceptor interaction, cannot proceed through a transition complex different to the one participating in the copolymerization reaction.

Gaylord[21] postulated that the Diels-Alder adduct, diene maleic anhydride, results from a complex in ground state and the copolymer from a complex in excited state.

The formation of a donor-acceptor complex between isoprene and monobutyl maleate, but of great instability, is proved by the instantaneous disappearance (without possibility of measuring) of the faint yellow-brown colour which is formed during the mixing of the two components. The fact is known that the factors determining the formation of the donor-acceptor complex (with charge-transfer) and the strength of its bond are, on the one hand, the ionization energy of the molecule which gave up the electron and, on the other hand, the affinity for the electron of the acceptor molecule, the complete transition of the electron taking place between very strong donors and acceptors only.

In the systems studied, isoprene is not a very strog donor. If stronger donors are added to monobutyl maleate, such as conjugated diene 1,4-diphenyl-1,3-butadiene or naphthalene, a yellow colouring appears whose intensity reaches a maximum at 1 :1 molar ratio. This colouring whose disappearance was not observed even after a long time is characteristic for the complex with stable charge transfer.

Taking the above into consideration, it can be admitted that associations of the "weak complexes" type are formed between isoprene and maleic acid monoesters, which are also called charge-transfer "contacts" by Mulliken and coworkers.[23,24] In case of formation of these weak complexes, the spectrum of the donor or acceptor is more or less modified by association and can or cannot contribute to the absorption of the charge-transfer.[25,26] For these weak complexes, which have not got independent bands of component molecules, the U.V. measurements are difficult and especially the determination of the equilibrium constant.

Dewar and Thompson,[25] as well as Matsuo and Higuchi,[27] referring to the concept of "weak complexes" showed that the interaction charge-transfer is not always the main force in formation of these complexes. In this sense they emphasized the essential part of the van der Waals forces in the ground state of these associations whose effects are stabilized in addition by the charge-transfer forces.

---

[21] N.G. Gaylord, *J. Polymer Sci. Part B*, **9**, 359 (1971).

[22] N.G. Gaylord, M. Stolka, A. Takahasi and S. Maiti, *J. Macromol. Sci. Chem.*, **A**$_5$, 867 (1971).

[23] R.S. Mulliken, *J. Amer. Chem. Soc.*, **74**, 811 (1952) .

[24] L.E. Orgel and R.S. Mulliken, *J. Amer. Chem. Soc.*, **75**, 4839 (1957).

[25] M.J.S. Dewar and C.C. Thompson, *Tetrahedron Suppl.*, **7**, 97 (1966).

[26] A.I. Scott and A.D. Wrixton, *Tetrahedron*, **28**, 933 (1972).

[27] T. Matsuo and O. Higuchi, *Bull. Chem. Soc. Japan*, **41**, 518 (1968).

The formation of a weak complex with charge-transfer between isoprene and butyl maleate is also in agreement with the rule established by Nimoura and Suruki.[28,29]

On the basis of copolymerization results of several α,β-disubstituted olefines, the latter established a relation between the "e" values of monomers (obtained according to Alfrey and Price[19]) and the reaction mechanism followed. As "Δ e" increases, the preferred mechanism is the following : mechanism according to Alfrey and Price ($\Delta e > 2.5$) → mechanism according to Mayo and Walling ($2.5 < \Delta e < 3$) → mechanism with participation of donor-acceptor complexes ($\Delta e > 3$).

The value of $\Delta e = 3.04$ for isoprene-monobutyl maleate,[5] although it is situated in the range of complex formation, is nevertheless near the demarcation limit of the last two mechanisms and therefore the idea of a Mayo and Walling mechanism is not eliminated entirely.

From what was presented, it clearly results that the determination of the reaction mechanism or the choosing of the most correct explanation for alternating copolymerization cannot be done by kinetic measurements only.

On analysing Mayo and Walling's point of view according to which the transition states are the result of the transfer of electron between the increasing macroradical and monomer,

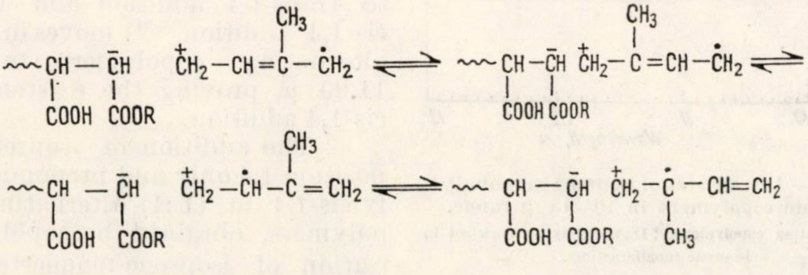

It can be noticed that according to this mechanism in the radicalic reaction of copolymerization, isoprene can be added in all positions, trans-1,4, addition —1,2, addition —3,4 and less cis —1,4 (as it is known from radicalic polymerization of isoprene), whereas the copolymers resulting from the reaction involving the participation of a cisoid complex should have a structure enriched in cis—1,4 addition of isoprene and at the same time the 1,2 and 3,4 addition is excluded.

Thus the study of the structure and microstructure of copolymers of different compositions will contribute to a great extent in eliminating the dualism of these reaction mechanisms.

---

[28] Y. Nimoura and Y. Suruki, Preprints, 15th Symposium on Macromolecular Chem. Japa n, Osaka, 1966.

[29] M. Rätzsch, *Plaste u Kautschuk*, **18**, 402 (1971).

In fig. 5 the I.R. spectra in 10–13μ range are shown, for two isoprene-monobutyl maleate copolymers with different ratios between the monomers in the chain.

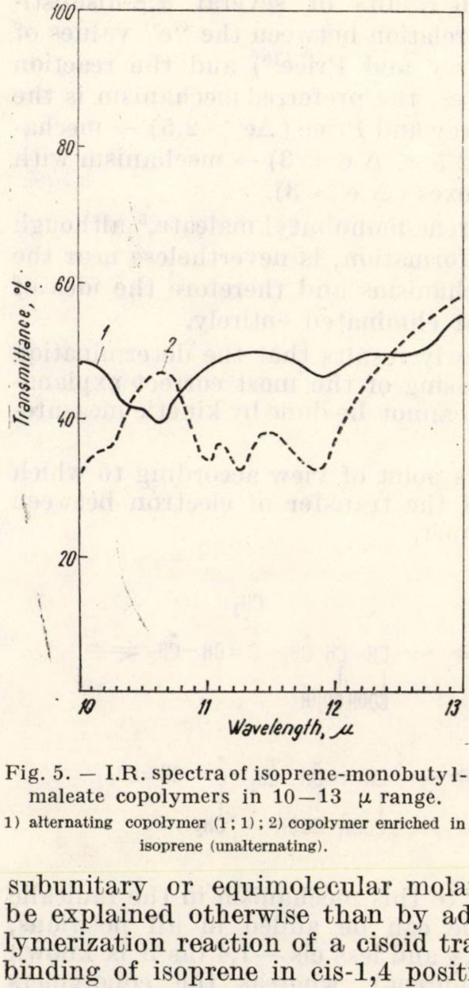

Fig. 5. — I.R. spectra of isoprene-monobutyl-maleate copolymers in 10–13 μ range.
1) alternating copolymer (1 ; 1) ; 2) copolymer enriched in isoprene (unalternating).

From investigation of the spectra of two copolymers differences are observed in the 10.5–12μ range owing to the manner of addition of isoprene.

In the copolymers spectrum enriched in isoprene (unalternating), bands characteristic to 1,2 addition (11μ) and 3,4 addition (11.28μ) of isoprene in the copolymer chain are distinguished. These bands are absent in the copolymer whose molar ratio between monomers is 1 :1, the addition of isoprene taking place in 1,4 (cis or trans) position only characterized by band from 11.87μ. At the same time the band from 11.87 μ specific to both cis-1,4 and trans-1,4 addition in unalternating copolymers (resulting from superpositioning of two bands : 11.83 μ attributed to trans-1,4 addition and 11.90μ cis-1,4 addition [30,31]) moves in (1 : 1) alternating copolymers towards 11.90 μ, proving the existence of cis-1,4 addition.

The addition of isoprene in position 1,4 only and preponderently cis-1,4 in (1 :1) alternating copolymers, obtained by copolymerization of isoprene-monoester at subunitary or equimolecular molar ratios in feed composition, cannot be explained otherwise than by admitting the participation in the copolymerization reaction of a cisoid transition complex which constrains the binding of isoprene in cis-1,4 position (stereodirected reaction through the cisoid donor-acceptor complex).

In unalternating copolymers obtained at superunitary isoprene-monoester molar ratios in feed composition and at lengthy periods of reaction, the uncomplexed isoprene is added by the conventional mechanism, the whole range of structures (cis-1,4, trans-1,4, addition -1,2 and 3,4) being obtained as in polymerization of isoprene in presence of free radicals.

Thus in this last case the structure of the copolymer is the result of the competition between the copolymerization reaction by the complex and the conventional addition.

---

[30] W.E. Richardson and A. Sacher, *J. Polymer Sci.*, **10**, 353 (1953).

[31] J.L. Binder, *J. Polymer Sci. Part A*, **1**, 37 (1963).

Revue Roumaine de Chimie, **19**, *9*, 1545–1549 (1974)

HYDROPEROXIDATION OF ORGANIC COMPOUNDS AT THE LIQUID/GAS INTERFACE. VII[1]

CONTRIBUTIONS TO THE PHYSICO-MATHEMATICAL CHARACTERIZATION OF THE APPARATUS

J. VODNÁR and R. DEUTSCH

"Babeş-Bolyai" University, Department of Organization and Technology
Piaţa Ştefan cel Mare 4, Cluj, Romania

Received October 31, 1973

The paper presents some contributions to the physico-mathematical characterization of the apparatus equipped with an outside spiral curved tube, used for the hydroperoxidation of organic compounds at the liquid/gas interface, patented by the author. The contributions are referring to the cases when the reaction rate between liquid and gas in tube II is so high, that more than 1 % (1 – 10 %) of the amount of gas passing through tube II reacts and the gas is not completely carrying off the liquid from tube II.

In a previous paper [1] some relations were described for the characterization of the apparatus equipped with an outside spiral curved tube, used for the hydroperoxidation of organic compounds at the liquid/gas interface, invented by the author. [2] In order to obtain mathematical relations which could underlie the design of such apparatus, we made use of a model with all the characteristics of the experimental installation (fig. 1).

The gas current (gaseous reactant), after penetration through a porous layer, moves upwards through tube II, carrying off the liquid of this tube, too. After the liquid in tube II has reached the upper part of the partition wall between tube I and II, the liquid passes into tube I and flows downwards. A permanent convection is thus occurring. The liquid with gas bubbles climbs in tube II and descends in tube I, without carrying off the bubbles.

We assumed that in tube II the liquid and the gas are mixing to such an extent that the mixture which is formed may be characterized by a mean density, $\bar{\rho}$, while the reaction rate between liquid and gas in tube II is so slow as not to react with more than 1% of the amount of gas passing through tube II. Under such conditions the mixture in the recycling tube I may be characterized by the approximately constant density ρ.

---

[1] J. Vodnár and R. Deutsch, "The IInd Conference on the Applied Physical Chemistry", vol. 2/2 1971, p. 601, Veszprem, Hungary.

[2] J. Vodnár, Patent of the Socialist Republic of Romania N⁰ 51928 (1969).

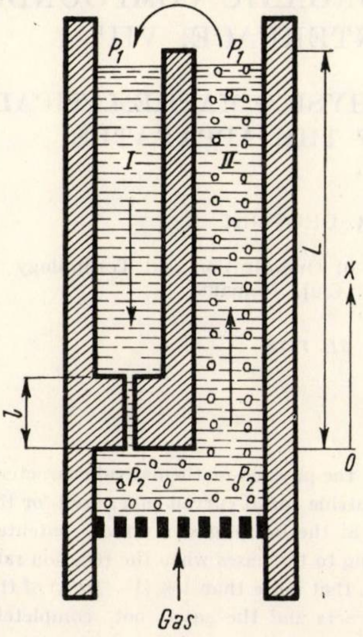

Fig. 1. — The model of the apparatus.

Using the Bernoulli equation:

$$p + \rho \cdot g \cdot h + 1/2 \rho \, v^2 = p_0 \text{ const.} \tag{1}$$

and considering that the expression $1/2 \rho \, v^2$ is negligible both in the rising current in tube II and in the descending current in the recycling tube, the following relation holds:

$$p + \rho \cdot g \cdot x = \text{const.} \tag{2}$$

and the difference in pressure at both ends of the capillary will be:

$$p_1 - p_2 = \rho \cdot g \cdot L \left[1 - \frac{l}{L} - K \right] \tag{3}$$

where K is a constant value, characterizing the apparatus used.

If we denote by Q_l the volumetric flow of the liquid, then, according to Poiseuille equation, we may write:

$$p_1 - p_2 = \frac{8 \mu \cdot l}{r^4 \cdot \pi} \cdot Q_l \tag{4}$$

If the gas is completely carrying off the liquid, then the rate of the liquid becomes equal in tube II with the gas rate; the volumetric flows of the liquid and gas are directly proportional to the partial volumes of the liquid and of the gas:

$$\frac{Q_l}{Q_g} = \frac{V_l}{V_g} \tag{5}$$

Using the definition:

$$K = \frac{V_l}{V_l + V_g} \tag{6}$$

one may write:

$$\frac{Q_l}{Q_g} = \frac{K}{1 - K} \tag{7}$$

By replacing this mathematical expression in (4) we get:

$$Q_g = \frac{r^4 \cdot \pi \cdot \rho \cdot g}{8\mu \cdot l \cdot K} (1 - K) \left[(1 - K)\, L - l\right] \tag{8}$$

In the cases when the reaction rate between liquid and gas in tube II is so high, that more than 1% (1 − 10%) of the amount of gas passing through tube II reacts, the mixture in tube II may be characterized by the mean density $\overline{\rho}(x)$, dependent on the x values. By approximation, for $\overline{\rho}(x)$ we can write:

$$\overline{\rho}(x) = \overline{\rho}(0) + \alpha \cdot x \tag{9}$$

The difference in pressure at height x will be:

$$p(0) - p(x) = \int_0^x \overline{\rho}(x) \cdot g \cdot dx = \overline{\rho}(0) \cdot g \cdot x + 1/2\, \alpha \cdot g \cdot x^2 \tag{10}$$

At height $x = 0$

$$p(0) = p(x) + \overline{\rho}(0) \cdot g \cdot x \cdot + 1/2\alpha \cdot g \cdot x^2 = p(L) + \overline{\rho}(0) \cdot g \cdot L + 1/2\alpha \cdot g \cdot L^2 \tag{11}$$

If we divide this expression with $\rho \cdot g \cdot L$, we obtain:

$$\frac{p(0)}{\rho \cdot g \cdot L} = \frac{p(L)}{\rho \cdot g \cdot L} + \frac{\overline{\rho}(0)}{\rho(0)} + \frac{1}{2}\, \frac{\alpha \cdot L}{\overline{\rho} \cdot (0)} \cdot \frac{\overline{\rho}(0)}{\rho(0)} \tag{12}$$

Because $\bar{\rho}/\rho = K$ and $\alpha \cdot L$ can be expressed as:

$$\frac{\alpha \cdot L}{\bar{\rho}(0)} = \frac{\Delta \rho}{\bar{\rho}(0)} = \gamma \tag{13}$$

where γ is the part of the bubble reacted in the process, we can write:

$$\frac{p(0)}{\rho \cdot g \cdot L} = \frac{p(L)}{\rho\, g \cdot L} + K + 1/2\ \gamma K \tag{14}$$

In the case when $K = 1/2$ and about 10% of the bubbles react, $\gamma = 0.1$ and the pressure variation caused by the chemical reaction will be about 0.025 (2.5%).

By introducing relation (14) into (4), we get:

$$Q_g = \frac{\mathrm{r}^4 \cdot \pi \cdot \rho \cdot g}{8\,\mu \cdot l \cdot x}(1 - K)\left[\left(1 - K - \frac{\gamma K}{2}\right)L - l\right] \tag{15}$$

This relation stands for the dependence between the gas flow (Q_g), the geometrical characteristics of the apparatus and the physical characteristics of the liquid in the case when more than 1% of the amount of gas passing through tube II reacts.

When the gas is not completely carrying off the liquid from tube II, one must make a correction.

Let us denote the liquid passing through the capillary tube under the above-mentioned conditions with:

$$Q_l - \Delta Q_l \tag{16}$$

and the part of the liquid not being carried off from tube II, with:

$$\beta = \frac{\Delta Q_l}{Q_l} \tag{17}$$

Thus,

$$Q_l - \Delta Q_l = Q_l(1 - \beta) \tag{18}$$

and instead of relation (4) one must introduce another one:

$$p_1 - p_2 = \frac{8 \cdot \mu \cdot l}{r^4 \cdot \pi}\, Q_l(1 - \beta) \tag{19}$$

By replacing Q_l from (7) in (19) and the difference of pressure corresponding to (19) in (15), we will get the final mathematical expression for Q_g :

$$Q_g = \frac{r^4 \cdot \pi \cdot \rho \cdot g}{8\mu \cdot l \cdot K} : \frac{1 - K}{1 - \beta} \left[\left(1 - K - \frac{\gamma K}{2} \right) L - l \right] \tag{20}$$

This final relation stands for the dependence between the gas flow, the geometrical characteristics of the apparatus and the physical properties of the liquid, in the case when more than 1%(1 – 10%) of the amount of gas passing through tube II reacts, and the gas is not completely carrying off the liquid from tube II.

Revue Roumaine de Chimie, 19, 9, 1551–1553 (1974)

SEPARATION OF SMALL AMOUNTS OF AMINO ACIDS AND THEIR IDENTIFICATION IN COMPLEX MIXTURES WITH UREA IN EXCESS

A. CONSTANTINESCU and C. LITEANU
Babeş-Bolyai University, Cluj, Str. Arany Janos, 11

Received November 9, 1973

By associating the electrophoretical method with the zonal melting technique it has become possible to reveal the presence of histidine and of arginine in a complex mixture of amino acids with urea in excess, obtained by a plasmochemical approach.

Chromatographic separation, effective in general, is hindered in the case of amino acids by the presence of urea in the solution under analysis. When urea is in excess, chromatography is no longer applied as a method for the separation and identification of amino acids, since by dislocation, amino acids identification according to R_f values becomes impossible.[1]

For this reason we have undertaken to develop a method which would enable the separation and identification of amino acids which are not revealed by chromatographic approach due to the presence of urea in excess.

WORKING PROCEDURE

The analysed solutions were supplied by the Laboratory of Physical Chemistry of the Faculty of Pharmacy in Bucharest where they had been obtained under plasmochemical conditions through high frequency electrical discharges over three gaseous mixtures each of them containing ammonia, water and one of the following hydrocarbonate components : methane, butane, petroleum ether, in an installation fitted with exterior electrodes, designed and achieved by Prof. D. Ştefănescu.

These solutions contain, among numerous compounds[2,3] small concentrations of various amino acids in addition to urea.[4]

0.02 ml of these solutions were chromatographed according to Mathias' technique, using the *n*-butanol + acetic acid + water (4 :1 :5 v/v) solvent system. After repeated irrigations, the chromatograms were dried. In order to reveal the plasmochemically formed amino acids, a few chromatograms were sprayed with a 0.2 % ninhydrin solution in acetone.

---

[1] M. Rizl, Dissertation, Karlova Universita, Praha, 1952.

[2] D. Ştefănescu, D. Moraru, I. Predescu, P. Bîrză, T. Stanciu and Fl. Coman, *Farmacia*, **1969**, 117.

[3] D. Ştefănescu, D. Moraru, L. Necula, I. Predescu and T. Stanciu, Communication presented at the Symposium of Biophysics, Iaşi, September, 1965.

[4] A. Constantinescu, Dissertation, Faculty of Chemistry, Cluj, 1971.

The identification of the separated amino acids was made by using Aji-No-Moto—Tokio pure reference amino acids which were chromatographed under similar conditions.

In order to identify the urea, a few other chromatograms were sprayed, this time with a 3.3 % *p*-dimethylaminobenzaldehyde acidic solution in ethanol. One single very large spot was obtained which we have attributed to urea, as it had the same R_f as the reference urea.

Further on, urea was separated from amino acids by using paper electrophoresis, the vertical technique. A 2 n formic acid solution was used as an electrolyte, the intensity of the electric current was 6 mA, the voltage was 420 V, the migration time was 6 h, and the paper bands were 24 cm long and 3 cm broad. Urea remains close to the starting line and turns yellow as the electrophoregram is sprayed with *p*-dimethylaminobenzaldehyde in ethanol.

By cutting out the zones corresponding to amino acids in a number of at least 50 electrophoregrams, after their fragmentation into small portions, the amino acids were extracted in aqueous solution. This solution was then evaporated and the residue was dissolved into one ml water, and this urea-free solution was then chromatographed according Mathias technique.

Arginine and histidine were absent, though their presence might have been possible since the UV absorption spectrum of these solutions indicated some absorption maxima seen in the UV spectra of arginine and histidine aqueous solutions and also in aqueous solutions of the mixture of these two amino acids.[5]

This shows that arginine and histidine could have been included during the separation of the urea macrocomponent. To verify this assumption, the electrophoretic zones corresponding to urea, resulting froma number of 50 electrophoregrams, were subjected to an aqueous extraction. After evaporation of the solution, the melting point of the resulted crystalline product was checked by means of a Boëtius apparatus.

A rather large range of melting temperature was obtained, between 111° – 125° which proved that the electrophoretically separated urea was not pure. The method of zonal melting was applied to investigate the impurities contained by urea. The device used reaches zonal melting with the simultaneous run of several zones, impressing an ascending motion to the substance bar. After a number of 17 runs, each taking two hours, the glass capillary tube was sectioned into 1 cm portions, the melting point of the substance being recorded for each of them on a Boëtius apparatus.

In order to reveal possible impurities, — amino acids, UV absorption spectra were taken for the portions of the zonal melting bar.

The first portion obtained by sectioning the zonal melting bar with the melting point at 132.7° contains high purity urea, in agreement with the data obtained from the literature.[6]

The UV absorption spectrum of the solution obtained when dissolving this first portion of the substance bar in water presents the same absorption maxima as pure urea.

The UV absorption spectrum of the aqueous solution obtained on dissolving the last portion indicates the additional presence of some absorption maxima characteristic of arginine and histidine amino acids in aqueous solution (fig. 1), which proves that these two amino acids, too, are plasmochemically obtained.

---

[5] D. Ştefănescu, A. Constantinescu and Fl. Coman, Communication Sci. Session Military Academy, 1970.

[6] J.H. Bexnon and R.A. Saunders, *J. Appl. Phys.*, **11**, *120* (1960).

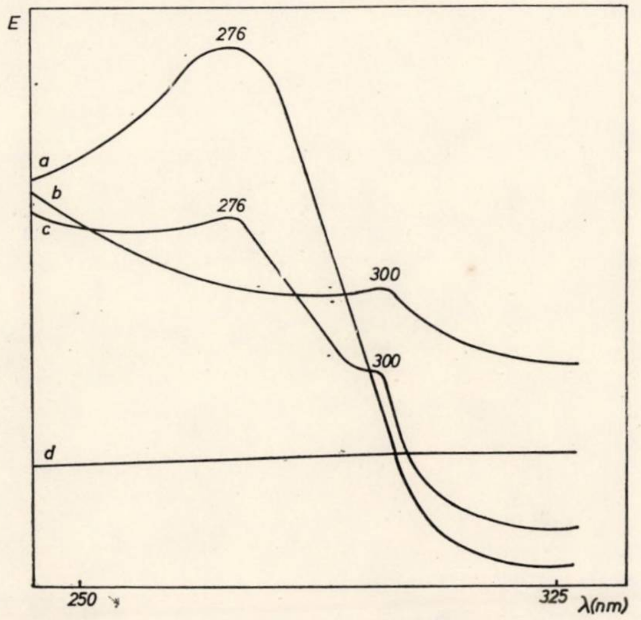

Fig. 1. — UV absorption spectra (250—325 mm):
a) UV absorption spectrum of histidine in H_2O; *b*) Idem, arginine; *c*) UV absorption spectrum of the solution in water of the last portion in the zonal melting bar; *d*) UV absorption spectrum of urea in water.

Revue Roumaine de Chimie, **19**, 9, 1555–1556 (1974)

COMPTES RENDUS

DIETER ZIESSOW, "On-line Rechner in der Chemie" W. de Gruyter, Berlin, New York, 1973, 376p.

The use of modern computers in chemistry, is developing in two main directions, namely : the use of big computers in processing numerical data regarding different chemical subjects and the use of "on-line" computers in which analogic data (physical, usually electrical signals) are processed.

The literature is sufficiently rich in papers regarding the first type of utilizations and a book has been already published on the subject in Romanian.

As far as the second type ot utilisation is concerned, in spite of the fact that it is more and more widely used, bibliographical materials are not so abundent. They are limited to manufacturer's literature and to a few papers published in scientific journals.

Dieter Ziessow's book fills on important gap regarding the problem of utilization of "on-line" computers. Although the book is not a synthesis of all the materials published in the domaine, (dealing especially with problems of Fourier spectroscopy) it presents the main problems regarding the use of "on-line" computers.

Thus, after a general introduction, the principal methods of analogic data transformation, the conversion of analogic data in numerical data, the problem of signal to noise ratio, the problem of mean values, etć, are presented in the book.

Also, the most used procedure of data processing such as differentiating or integrating, etc., are described.

After these general problems, some methods regarding the curve adjustment, simulation or line identification are presented.

The last part of the book deals with the general problems of Fourier spectroscopy and of Optical Fourier spectroscopy.

The whole book contains a great number of examples for the utilisation of " on-line" computers in chemistry and gives a number of programs in ASSEMBLER or in FORTRAN language.

An extensive bibliography is also given.

Şerban Moldoveanu

KARL HAUFFE und S. ROY MORRISON, Adsorption "Eine Einführung in die Probleme der Adsorption. Walter de Gruyter, Berlin, New York, 1974, 19p.

The basic problem in understanding the solid-fluid boundary processes is to find out the dependence of the process parameters on the solid surface properties. The adsorption studies aim at solving this problem.

A large number of very different fields like : heterogeneous catalysis, corrosion, flotation, substances'purification, chromatographic analysis, electronic tube engineering, profit from the results of adsorption studies. It seems that adsorption is also playing an important part in some biological processes like membrane equilibria, enzime action and even in the smell and taste sensations.

The book issued by Prof. Karl Hauffe and Dr. S. Roy Morrison is not that much of a monography as it is an introduction to the problematics of this phenomenon. The book is the result of a long and remarkable activity of the authors in this field. It is divided in 6 chapters.

The first chapter presents the general features of adsorption emphasizing the energetics of the process. Then the main isotherms are deduced and their principal uses shown ; e.g. the specific area measurements (chap. 2).

Chapter 3 refers to the adsorption involving the electron exchange both on metallic and semiconductor surfaces. Electrochemical thermodynamics is given a special attention in explaining chemisorption on semiconductors in contrast with physical adsorption on the same surface in which chemical thermodynamics is used. Plenty of space is assigned to photosorption and photodesorption as well as to the role of surface states in adsorption.

The metal-support catalytic systems are described in chapter 4 and the methods of evaluating the dispersion of the active component are indicated.

The fifth chapter is devoted to the impact of adsorption on the surface reactions, heterogeneous catalysis, chromatography, flotation, corrosion and oxidation of metals.

The last chapter is a critical review of some experimental techniques used in adsorption studies. The information one can get by this methods are also reviewed.

The references are given on chapters and the book concludes with subjects and authors indexes.

Some of the problems presented — such as the kinetics of the gas adsorption on oxide type semiconductors—are exhaustively presented and form an up-to-date critical synthesis of the results in the field.

Published in excellent graphical conditions, the book is intended by the authors for the use of large number of specialists from industry, research and universities as well as of students in related fields.

Dr. M.I. Vass
Dr. N.I. Ionescu
Centre of Physical Chemistry
31 Galaţi str., Bucharest 13

D. COSTACHE, "*Analiza chimică prin metoda cinetică*" (Chemical analysis through the kinetic method), Editura Academiei, Bucharest, 1974, 270 p.

The progress recorded by the chemical industry and other related branches has raised the necessity to determine some elements or substances in very small amounts. In addition to the microanalytical methods which use the same arsenal of substances for identification and dozing, the recent years have witnessed the appearance of new methods of analysis based on new principles. One of the procedures used for this purpose is that to determine the concentration of some substances which may influence the reaction rate (catalytic method of analysis). The kinetic methods used in analytical chemestry have won the unanimous recognition of specialists due to their sensitivity, selectivity, simplicity in execution as well as to the automation prospects.

The book has 14 chapters, based on a comprehensive bibliography which also includes author's works. It presents two large types of reactions used in the kinetic analysis, namely the oxido-reduction reactions and the enzyme reactions. There are also presented theoretical problems pertaining to the kinetic analysis as well as applicative problems. Thus, the first two chapters explain the general notions used in the kinetic analysis and the action of catalysts on which the kinetic methods are based, and Chapter 3 reviews the catalytic reactions. The following chapters discuss the obtaining and processing of the experimental data and the equipment employed for this purpose. Particular stress is laid on the application of the kinetic method to the determination of the concentration of inorganic compounds, some particularities being shown. Special chapters are devoted to the determination of pollutants (in which the characteristics of such types of analyses are shown) and to other determinations. It is found that the kinetic methods led not only to the determinations of concentrations, but can be also used for the examination of some complex combinations or for the calculation of some constants of importance in the analytical chemistry. An important place is given to the enzyme analysis and to the automation of the kinetic methods of analysis. The precautions to be taken in the kinetic analysis are shown, each factor contributing to the alteration of the results estimated. All reactions used are given in tables. The practical aspects are exemplified by several significant methods.

The book emphasizes the possibility of applying the kinetic methods in industry, control of water and air pollution, elucidation of some problems of the reaction mechanism, characterization of the solubility of some hardly soluble compounds, investigation of some complex equilibria on which new analysis methods or even procedures are based.

The book is intended to chemists working in universitary research, or plant laboratories, to biochemists, candidates for a doctor's degree and analytic chemists who wish to improve their post-graduation training.

Dr. doc. D. I. Marchidan
Centre of Physical Chemistry,
Bucharest

NOTE POUR LES AUTEURS

La *Revue Roumaine de Chimie* publie des articles en anglais, français, russe, allemand ou espagnol. Les auteurs sont priés d'envoyer des articles, notes, communications et comptes rendus inédits.

Les manuscrits seront dactylographiés à deux intervalles. Les tableaux seront dactylographiés sur feuilles séparées, de même que la légende des figures. Les diagrammes seront tracés à l'encre de Chine sur papier calque. Les tableaux et les figures seront numérotés par des chiffres arabes, en nombre strictement nécessaire. Prière de ne pas inscrire les mêmes données dans les tableaux et les figures. Les formules chimiques seront incluses dans le texte ; en outre, elles seront transcrites sur des feuilles séparées. Les auteurs sont priés d'indiquer les caractères italiques (en soulignant les lettres au crayon), ainsi que tout autre caractère spécial. L'ordre des références bibliographiques sera celui de leur mention dans le texte ; le nom de l'auteur sera précédé de l'initiale du prénom ; les publications périodiques seront présentées suivant les prescriptions internationales. Les références seront ajoutées à la fin de l'article ; elles paraîtront comme des notes, au bas de la page. Le texte sera précédé d'un résumé comprenant 15 lignes au maximum.

L'entière responsabilité du contenu des articles appartient aux auteurs. On publie des articles dus aux collaborateurs roumains ou étrangers.

PRINTED IN ROMANIA

NOTE POUR LES AUTEURS

Le texte [illegible] des articles [illegible] anglais. Toutefois, [illegible] les auteurs [illegible] des [illegible] notes, communications et [illegible].

Les manuscrits seront [illegible] dactylographiés à double interligne [illegible] les [illegible] figures [illegible] dans le texte [illegible] crayon, [illegible] les [illegible] texte [illegible] page [illegible] notes [illegible].

[illegible] responsabilité [illegible] contenu des articles [illegible] aux auteurs [illegible].

TRAVAUX PARUS AUX ÉDITIONS DE L'ACADÉMIE DE LA RÉPUBLIQUE SOCIALISTE DE ROUMANIE

TIBERIU NĂŞCUŢIU, **Metode radiochimice de analiză** (Méthodes radiochimiques d'analyse), 1973, 384 p., 23 lei.

MARIA FITI, **Dozimetria chimică a radiaţiilor ionizante** (La dosimétrie chimique des radiations ionisantes), 1973, 240 p., 13,50 lei.

MIHAI FLORESCU, **Eficienţa economică a cercetării ştiinţifice** (L'efficience économique de la recherche scientifique), 1972, 115 p., 15 lei.

GEORGETA LĂZĂRESCU, **Sistematizarea informaţiilor în Chimia organică** (La systématisation des informations dans la chimie organique), 1972, 252 p., 10,50 lei.

P. BALTĂ et E. BALTĂ, **Introducere în chimia fizică a stării vitroase** (Introduction à la chimie physique de l'état vitreux), 1971, 240, 15,50 lei.

LYDIA-MARIA VAICUM, **Biodegrabilitatea detergenţilor** (La biodégrabilité des détergents), 1971, 254 p., 16 lei.

TIBERIU NĂŞCUŢIU, **Metode radiometrice de analiză** (Méthodes radiométriques d'analyse), 1971, 346 p., 19,50 lei.

I. ZUGRĂVESCU et L. STOICESCU-CRIVETZ, **Polimeri heterociclici** (Polymères hétérocycliques), 1971, 190 p., 9,50 lei.

CRISTOFOR SIMIONESCU et C. V. UGLEA, **Fracţionarea compuşilor macromoleculari** (Fractionnement des composés macromoléculaires), 1962, 292 p., 18,50 lei.

I. MAXIM, **Materiale nucleare** (Matériaux nucléaires), 1969, 444 p., 30 lei.

CRISTOFOR SIMIONESCU et CLEOPATRA VASILIU-OPREA, **Mecanochimia compuşilor macromoleculari** (La mécanochimie des composés macromoléculaires), 1967, 344 p., 23,50 lei.

CORNEL BODEA et collab., **Tratat de biochimie vegetală**, partea I, **Fitochimie** (Traité de biochimie végétale, Ire partie, Phytochimie), Ier vol., 1964, 747 p. + 4 annexes + 2 pl., 31 lei; IIe vol., 1965, 1262 p., 1 pl., 56 lei; IIIe vol., 1967, 773 p., 35 lei.

V. GHEŢIE et V. MICUŞAN, **Analiza imunochimică. Teorie şi practică** (Analyse immunochimique. Théorie et pratique), 1966, 369 p., 28 lei.

R. PORTOCALĂ et L. POPA, **Acizii ribonucleici celulari şi virali** (Les acides ribonucléiques cellulaires et viraux), 1966, 375 p., 8 pl., 26 lei.

I.P.I. – c. 1583

43 426

Lei 25.—

F 1103

ACADÉMIE DE LA RÉPUBLIQUE SOCIALISTE DE ROUMANIE

R

REVUE ROUMAINE DE CHIMIE

TOME 19

N° 10

Octobre 1974

RRCHAX, **19**, *10*, 1557–1682 (1974)

ÉDITIONS DE L'ACADÉMIE DE LA RÉPUBLIQUE SOCIALISTE DE ROUMANIE

Rev. Roumaine Chim.

19, *10*, **p. 1557–1682 (1974), Bucarest**

ACADÉMIE DE LA RÉPUBLIQUE SOCIALISTE DE ROUMANIE

COMITÉ DE RÉDACTION

Rédacteurs en chef:

I. G. MURGULESCU, membre de l'Académie de la République Socialiste de Roumanie

Rédacteurs en chef adjoints:

A. T. BALABAN et V. EM. SAHINI, membres correspondants de l'Académie de la République Socialiste de Roumanie

Collège de rédaction:

EM. BRATU, ELENA CEAUŞESCU, ECATERINA CIORĂNESCU-NENITZESCU, C. DRĂGULESCU, RALUCA RIPAN, CR. SIMIONESCU, membres de l'Académie de la République Socialiste de Roumanie; P. SPACU, membres correspondants de l'Académie de la République Socialiste de Roumanie; MARGARETA AVRAM, D. I. MARCHIDAN, I. MOLDOVAN, G. NIAC et D. SĂNDULESCU

Toute commande de l'étranger (fascicules ou abonnements) sera adressée à Întreprinderea Rompresfilatelia, Boîte Postale 2001, telex 011631, Bucarest, Roumanie

Les manuscrits, les livres et les revues proposés en échange, ainsi que toute correspondance seront envoyés à la rédaction

REVUE ROUMAINE DE CHIMIE

23, str. Dumbrava Roşie, Bucarest, Roumanie, téléphone 12 41 60

ÉDITIONS DE L'ACADÉMIE DE LA RÉPUBLIQUE SOCIALISTE DE ROUMANIE
3 bis, str. Gutenberg, Bucarest, Roumanie, téléphone 16 40 79

XVIII. COLLOQUIUM SPECTROSCOPICUM INTERNATIONAL

Entre les 15–19 septembre 1975 aura lieu à Grenoble, France, le XVIIIe Colloquium Spectroscopicum International, organisé par le Groupement pour l'Avancement des méthodes spectroscopiques et physico-chimiques d'analyse — G.A.M.S.

Le Colloque comportera des conférences invités, des tables rondes et des communications.

Le domaine couvert par le programme scientifique comprend toutes les branches de la spectroscopie :

— la spectroscopie des rayonnements électromagnétiques,
— la spectroscopie des radiations corpusculaires,
— la spectroscopie γ, la spectroscopie Mösbauer,
— la spectroscopie moléculaire,
— la résonance magnétique nucléaire, la résonance paramagnétique électronique.

Les demandes de renseignements seront adressées à :

M. le Directeur du G.A.M.S.
XVIII. C.S.I.
10, rue du Delta
75009 PARIS

XVIII COLLOQUIUM SPECTROSCOPICUM INTERNATIONALE

Entre les 15—19 septembre 1975 aura lieu à Grenoble, France, le XVIIIe Colloquium Spectroscopicum Internationale, organisé par le Groupement pour l'Avancement des Méthodes Spectroscopiques et physico-chimiques d'Analyse — G.A.M.S.

Le Colloque comportera des conférences invitées, des table rondes et des communications.

Le domaine couvert par le programme scientifique comprend toutes les branches de la spectroscopie:

— la spectroscopie des rayonnements électromagnétiques,
— la spectroscopie des radiations corpusculaires,
— la spectroscopie γ et la spectroscopie Mössbauer,
— la spectroscopie moléculaire,
— la résonance magnétique nucléaire, la résonance paramagnétique électronique.

Les demandes de renseignements seront adressées à:

M. le Directeur du G.A.M.S.
XVIII C.S.I.
16, rue du [illegible]
75009 PARIS

REPORTS PUBLISHED BY IUPAC IN 1978

The following Reports were published by the International Union of Pure and Applied Chemistry during 1978 in its journal *Pure and Applied Chemistry*:

1. Recommended Methods for the Analysis of Alkyd Resins
2. Abbreviated Nomenclature of Synthetic Polypeptides
3. Definitive Nomenclature for Vitamin B-6 and Related Compounds.
4. Tables of Wavenumbers for the Calibration of Infrared Spectrometers — Parts III and IV: 600 cm^{-1},
5. A Collaborative Study of Dynamic Mechanical and Impact Properties of PVC—II.
6. Recommendations for Presentation of Raman Spectra for Cataloging and Documentation in Permanent Data Collections.

REPORTS PUBLISHED BY IUPAC IN 1973

The following Reports were published by the International Union of Pure and Applied Chemistry during 1973 in its journal *Pure and Applied Chemistry* :

1. Recommended Methods for the Analysis of Alkyd Resins
2. Abbreviated Nomenclature of Synthetic Polypeptides
3. Definitive Nomenclature for Vitamin B—6 and Related Compounds,
4. Tables of Wavenumbers for the Calibration of Infrared Spectrometers — Parts III and IV : 600 cm^{-1},
5. A Collaborative Study of Dynamic, Mechanical and Impact Properties of PVC—II,
6. Recommendations for Presentation of Raman Spectra for Cataloging and Documentation in Permanent Data Collections.

REVUE ROUMAINE DE CHIMIE

ORSZÁGOS MŰSZAKI KÖNYVTÁR ÉS DOKUMENTÁCIÓS KÖZPONT 18933

Tome 19, N° 10 Octobre 1974

TATIANA ONCESCU and M. CONTINEANU, Kinetics and mechanism of azibenzyl radiolysis in benzene solution. . . . . 1559—1567

LETIŢIA TOPOR, Thermodynamic data on vaporization of fused rubidium and cesium fluorides . . . . 1569—1572

Z. MOSER and K. FITZNER, Thermodynamic treatment of binary and ternary salt systems with single charge ions . . . . 1573—1586

C. I. LEPĂDATU and S. MOLDOVEANU, An improvement of Hoffmann's LCAO-MO method . . . . 1587—1591

R RALUCA RIPAN, GH. POP et ILEANA POP, L'acide ascorbique comme agent réducteur. IV. La cinétique de la réduction des ions Pt(II) par acide ascorbique en présence des ions Pb(II) . . . . 1593—1601

D.. NEGOIU and ALEXANDRA SCHIOPESCU, Ferrate (VI) ion salts with Ni(II) and Co(II) tetrapyridine-tetrapicoline complex combinations . . . 1693—1609

ALEXANDRU T. BALABAN, Chemical Graphs. XXIII. General cubic graphs with one loop, and homovalenes or their derivatives. . . . . 1611—1619

M. SAFTA and G. OSTROGOVICH, Studies in the *s*-triazine field (new series). XV. The protonation equilibria and indicator behaviour of E-1,3-dimethyl-6-(*p*-X-β-styryl)-2,4-dioxo-1H, 3H-1,3,5-triazines in 50 vol % aqueous-ethanolic solutions in the presence of sulphuric acid. . . . . 1621—1629

R L. CORMOŞ, A. POP and V. SBERA, Decomposition of organic hydroperoxides in the heterogeneous catalysis. II. Decomposition of cumene hydroperoxide on strongly acidic cationites . . . . 1631—1636

R D. S. VASILESCU, Alternating tendency in copolymerization. II. Copolymerization of 1,1—diphenyl ethylene with acrylic monomers. . . . . 1637—1644

GR. TEODORESCU, Méthodes de détermination de l'azotate de pilocarpine. Spectre en visible et infrarouge du composé résulté entre l'azotate de pilocarpine et le reineckate d'ammonium. . . . . 1645—1650

ELENA HOPÎRTEAN, C. LITEANU and EUGENIA ŞTEFĂNIGĂ, Membrane-electrodes of a metallic wire— plastic membrane type. I. K^+-selective membrane electrode . . . . 1651—1660

SOFIA MARCHIDAN, Application of niobium polarographic reduction in hydrochloric acid-thiocyanate medium to the analysis of ferroniobium alloys. . 1661—1667

SHAMSHAD ÅHMAD KHÅN and MAURICE STONE, Determination of lithium in silicate rocks and minerals using a simple flame photometer . . . . 1669—1676

COMPTES RENDUS . . . . 1677—1682

Revue Roumaine de Chimie, **19**, *10*, 1557—1682 (1974), Bucarest

Revue Roumaine de Chimie, **19**, *10*, 1559–1567 (1974)

KINETICS AND MECHANISM OF AZIBENZYL RADIOLYSIS IN BENZENE SOLUTION

TATIANA ONCESCU and M. CONTINEANU

Department of Physical Chemistry, University of Bucharest, Bd. Republicii 13

Received December 12, 1973

The radiolysis of benzene solutions of azibenzyl was studied in the concentration range $3 \times 10^{-1} - 3 \times 10^{3}$ mole/l and a first-order kinetics was found. A reaction mechanism was suggested which involves the energy transfer processes from irradiated-excited benzene molecules to dissolved azibenzyl molecules.

INTRODUCTION

The kinetics of diazocompounds radiolysis is not described in the literature. The only reference is our previous paper regarding the radiolysis of diphenyldiazomethane.[1] The present paper deals with the azibenzyl radiolysis in benzene solution performed as in the case of diphenyldiazomethane to confirm the decomposition mechanism proposed; it involves the excited benzene molecules as energy carriers.

At the same conclusion lead also the results obtained on irradiation of polycrystalline azibenzyl.[2]

EXPERIMENTAL

The benzene solutions of azibenzyl were irradiated with Cs^{137} radiations. The installation is a "Gammator" type fitted with three total activity sources 1600 Ci. Irradiations were simultaneously performed on four samples included in phials of identical geometry, symmetrically placed on a rack which was continually revolving in the irradiation chamber so that all the samples received the same dose. The absorbance of irradiated solution was measured on a Pye Unicam SP 1800 spectrophotometer.

The azibenzyl was prepared by oxidizing the benzylmonohydrazone with HgO according to the indications from literature.[3,4]

The E.P.R. measurements were carried out on an ART 5 apparatus which operates in an X band having a high frequency field modulation.

Benzene solutions of azibenzyl of a 3×10^{-3}; 1.65×10^{-3}; 3×10^{-2} and 3×10^{-1} moles/l concentration were irradiated as described above.

---

[1] T. Oncescu and M. Contineanu, *Rev. Roumaine Chim.*, in press, **19**, 931 (1974).

[2] M. Contineanu, O. Constantinescu and T. Oncescu, *Rev. Roumaine Chim.*, **18**, 2005 (1973).

[3] Th. Curtius, *Ber. dtsch. Chem. Ges.*, **22**, 2162 (1889).

[4] Th. Curtius and H. Lang, *J. prakt. Chem.*, **44**, 544 (1891).

The dosimetry was performed through chemical approach using a Fricke [5] dosimeter. The radiochemical decomposition of azibenzyl G was calculated from the relation :

$$G = \frac{n}{D} x\, 100,$$

where

n – number of decomposed azibenzyl molecules

D – absorbed dose, expressed in eV/cm^3, necessary for the decomposition of n molecules of azibenzyl.

The absorbed dose D in the dosimeter was calculated according to the formula below[6]

$$D = 1.75\text{c}10^{18} \frac{\varepsilon_i - \varepsilon_0}{l} \text{ eV/cm}^3,$$

where

ε_i – absorbance of the irradiated dosimetric solutions

ε_0 – absorbance of the non-irradiated dosimetric solution

l – thickness of absorbant solution in the spectrophotometric cell.

The energies obtained as a function of concentration are given in table 1.

Table 1

The dose calculation by the Fricke dosimeter method

Initial concentration of the solution in mole/l	3×10^{-3}	1.65×10^{-2}	3×10^{-2}	3×10^{-1}
Dose 10^{16} eV/cm^3.min.	8.52	8.4	9.3	8.92

Since the thermal decomposition of azibenzyl in a benzene solution occurred also at room temperature at which irradiations took place, a correction was necessary for this decomposition. To this purpose the sample was irradiated keeping at the same time another sample of the same solution at room temperature to serve as reference.

The absorbance of both irradiated and reference samples was measured at $\lambda = 320$ nm and $\lambda = 425$ nm where azibenzyl presents absorption maxima.

RESULTS AND DISCUSSION

The values for the absorbance of solution (ε_i) at various irradiated times (t) permitted the calculation of rate constants which verify the equation of the first-order reactions :

$$k = \frac{2{,}303}{t} \lg \frac{\varepsilon_0}{\varepsilon_i},$$

where ε_0 is the absorbance of the non-irradiated (reference) solution.

---

[5] H. Fricke and E. J. Hart, *J. Chem. Phys.*, **3**, 60 (1935).

[6] J. W. Spinks and R. J. Woods, "An Introduction to Radiation Chemistry", Wiley, New York, 1964, p. 108.

For illustration, Table 2 lists the values of rate constants for one of the studied concentrations.

Table 2

The rate constants and radiochemical yield determined by the radiolysis of a solution having an azibenzyl concentration of 1.62 × 10^{-2} mole/l

	λ = 320 nm			λ = 425 nm		
t (hours)	$\frac{\varepsilon_0}{\varepsilon}$	k × 10^6 s^{-1}	*G*	$\frac{\varepsilon_0}{\varepsilon}$	k × 10^6 s^{-1}	*G*
8	1.201	6.36	3.12	1.286	8.70	2.38
10	1.234	5.20	2.26	1.2859	7.21	1.42
13	1.369	6.71	2.83	1.414	7.34	1.64
16	1.481	6.80	2.90	1.516	6.81	1.71
18.5	1.494	6.01	2.82	1.571	6.76	1.80
23	1.667	6.13	2.74	1.79	7.02	1.75
27	1.818	6.10	2.64	1.973	6.89	1.63
32	2.118	6.48	2.45	2.36	7.42	1.54
41	2.500	6.20	2.00	2.795	6.95	1.14
52	2.941	5.76	1.51	3.857	7.21	0.91
55	3.030	5.62	1.44	4.153	7.22	0.88

k_m = 6.13 ± 0.14 k_m = 7.23 ± 0.16

Table 3 shows the average values of the rate constants determined for the four concentrations involved in this study.

Table 3

The rate constants for the radiolysis of azibenzyl solutions

Concentration	3 × 10^{-3}		1.65 × 10^{-2}		3 × 10^{-2}		3×10^{-1}	
λ (nm)	320	425	320	425	320	425	320	425
k × 10^6 s^{-1}	8.54	9.4	6.13	7.23	5.54	6.22	4	4.2

The following aspects have been observed from the above data :

1. The values of rate constants at the two wavelengths are close, slightly higher at λ = 425 nm, because in this region there is an overlapping of azibenzyl and diphenylketene absorption. The last one disappears more quickly from the system due to the reaction with the atmospheric oxygen, as our experimental data show.

2. The rate constant has been observed to decrease only twice with a concentration increase of hundred times (from $3 \cdot 10^{-3}$ to $3 \cdot 10^{-1}$) ; this can be explained by the radiolysis mechanism suggested below.

3. The radiochemical yield increases with the rise in the concentration of the irradiated solution, as it was expected.

It is of interest to compare the results from this radiolysis with those obtained in the thermal decomposition of azibenzyl.

It has been observed that in the case of radiochemical decomposition both absorption maxima decrease (λ = 425 nm and λ = 320 nm) whereas at the thermal[7] decomposition the absorption at λ = 425 nm increases and shifts towards 406 nm due to the absorption of diphenylketene occurring in the system.

Finally, a comparison between the radiochemical decomposition of diphenyldiazomethane and that of azibenzyl shows the azibenzyl to be more stable. This can be observed both from the values of the rate constants and from the value of the radiochemical yield which are lower in the case of azibenzyl.

In order to define the nature of radiolysis products, the following experiment was carried out.

An azibenzyl benzene solution having a 3×10^{-3} mole/l concentration, was irradiated after previously bubbling oxygen therein and its absorption spectrum was compared to that of a sample through which argon had been bubbled, irradiating under identical conditions. The UV absorbance values of the two samples (oxygen and argon) were practically similar. On the contrary, the visible absorbance decreases in samples through which oxygen had been bubbled (fig. 1) and this has been observed with all samples irradiated without degasing precautions.

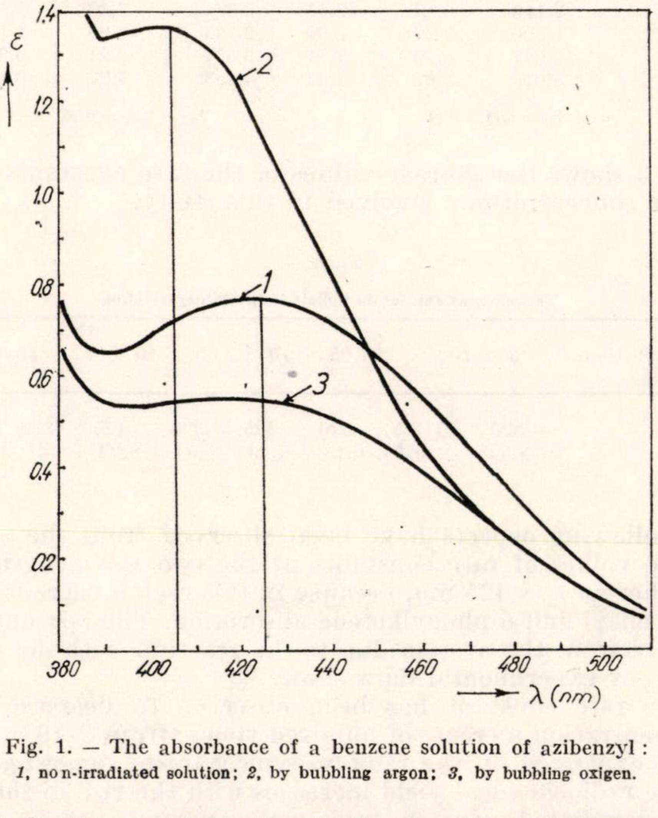

Fig. 1. — The absorbance of a benzene solution of azibenzyl : *1*, non-irradiated solution; *2*, by bubbling argon; *3*, by bubbling oxigen.

---

[7] M. Contineanu, T. Oncescu and R. N. Schindler, *Rev. Roumaine Chim.*, **18**, 549 (1973).

In contrast, an absorption increase in visible was found in the sample irradiated in an argon atmosphere, with a maximum at 406 nm, characteristic of diphenylketene. The oxygen was subsequently bubbled through this latter sample which was then kept in cold for a few hours, and the absorption spectrum was thereafter recorded as shows figure 1. The sudden absorbance decrease in the visible which is due to the reaction on diphenylketene with oxygen,[8] provides another evidence of its existence in the system as assumed by the mechanism proposed by us.

Considering these results, it is possible to explain the reason for the absorption decrease to 320 nm and to 425 nm. Observed in the air-irradiated samples, the diphenylketene occurring by irradiation of azybenzyl, reacts with oxygen[8] from the air dissolved into the solution forming an unstable peroxide under irradiation which is then converted into benzophenone and CO_2. The formation of benzophenone as a final reaction product was revealed by irradiating a concentrated azybenzyl solution in benzene for a long time, by filtering and recording the UV absorption spectrum.

In the case in which the irradiations take place *in vacuo* or in an inert atmosphere, the diphenylketene accumulates in the system and it may be revealed by its characteristic absorption at $\lambda = 406$ nm. Yet, diphenylketene is not stable at γ irradiation, either. An indirect experiment performed by us may be taken as an argument in support of this statement. In a previous study[9] we found that the diphenylketene obtained by thermal decomposition *in vacuo* of an azibenzyl benzene solution, regardless of the working temperature, presents an EPR signal due to a species which we ascribed to be :

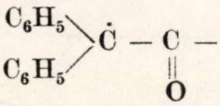

dentically with those found for the first time by Singer and Lewis.[10] Watching the kinetics of this radical species, it disappears through irradiation according to a first-order kinetics.

Figure 2 presents the plot of lg *I* as function of the irradiation time, where *I* represents the intensity of the EPR signal.

A rate constant of 4.1×10^{-4} s^{-1} was calculated from the slope of the straight line.

The solid azibenzyl samples irradiates[2] with the same dose as benzene solution do not reveal a significant change. This proves that the solvent molecules (benzene) play an important role in the radiolysis process, i.e. the decomposition occurs through the means of benzene-excited molecules[11] which disappear through a monomolecular process.

---

[8] E. F. Jenny, H. Droescher and A. Melzer, *Angew. Chem.*, **76**, 58 (1964).

[9] T. Oncescu, O. Constantinescu and M. Contineanu, to be published.

[10] L. S. Singer and I. C. Lewis, *J. Amer. Chem. Soc.*, **90**, 4212 (1968).

[11] R. Cooper and K. J. Thomas, *J. Chem. Phys.*, **48**, 5097 (1962).

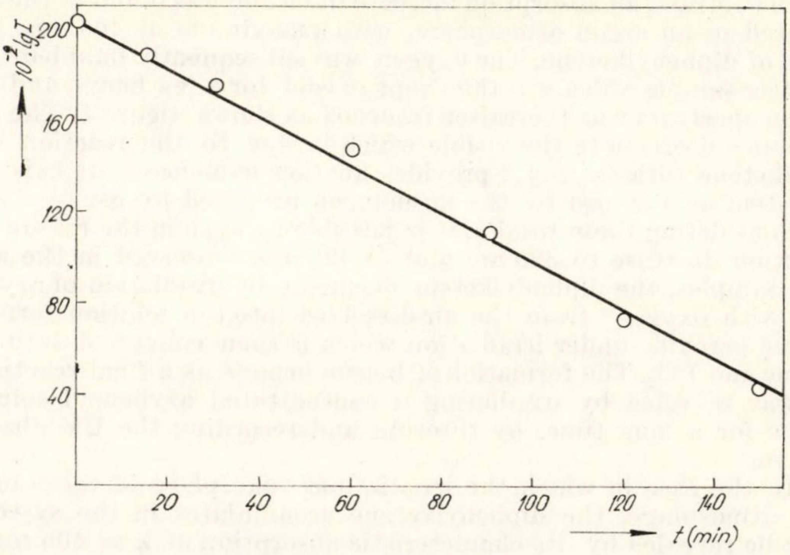

Fig. 2. — The plotting of lg *I* as a function of time for an irradiated diphenylketene benzene solution.

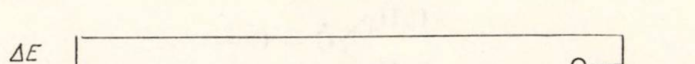

Fig. 3. — The absorption variation ($\Delta\varepsilon$) of an irradiated azibenzyl benzene solution with anthracene concentration.

In view of establishing the radiolysis mechanism we proceeded to the iradiation of azibenzyl benzene solutions in the presence of anthracene which is known from pulse radiolysis studies [12-14] to be a good energy trapping factor for benzene-excited molecules.

The results obtained are presented in figure 3 where $\Delta\varepsilon$ represents the difference between the absorption of the irradiated solution in the presence of anthracene and that of the anthracene-free irradiated one, as a function of anthracene concentration.

The plotting shows that the reaction rate decreases with the increase in the anthracene concentration, reaching a constant value.

Considering this behaviour, the following processes are highly probable:

$$4B \xrightarrow{k_0 I} 4B^* \tag{a}$$

$$B^* \xrightarrow{k_1} B \tag{b}$$

$$B^* + B \xrightarrow{k_2} 2B \tag{c}$$

$$2B^* + 2A \xrightarrow{k_3} 2B + 2A^* \tag{d}$$

$$A^* + B \xrightarrow{k_4} A + B \tag{e}$$

$$A^* \xrightarrow{k_5} Dc + N_2 \tag{f}$$

$$Dc + O_2 \xrightarrow{k_6} DcO_2 \tag{g}$$

$$DcO_2 \xrightarrow{k_7} Bz \tag{h}$$

where B, A, Dc, Bz represent benzene, azibenzyl, diphenylketene and benzophenine molecules and DcO_2 is the diphenylketene peroxide respectively.

The reaction rate for the azibenzyl molecules is:

$$\frac{dC_A}{dt} = -4k_3\, C_{B*}\, C_A + k_4\, C_{A*}\, C_B \tag{1}$$

---

[12] J. M. Nosworthy and J. P. Keene, *Proc. Chem. Soc.*, **5**, 114 (1964).
[13] J. W. Hunt and J. K. Thomas, *J. Chem. Phys.*, **46**, 2954 (1967).
[14] F. S. Dainton, *Pure Appl. Chem.*, **10**, 395 (1965).

By applying the principle of stationarity to intermediates A*, B*, DcO_2 one obtains:

$$\frac{dC_{A^*}}{dt} = 4k_3 C_{B^*} C_A - k_4 C_{A^*} C_B - k_5 C_{A^*} = 0 \tag{2}$$

$$\frac{dC_{B^*}}{dt} = 4k_0 I C_B - k_1 C_{B^*} C_B - 4k_3 C_{B^*} C_A = 0 \tag{3}$$

$$\frac{dC_{DcO_2}}{dt} = k_6 C_{DcO_2} C_{O_2} - k_7 C_{DcO_2} = 0 \tag{4}$$

From (2) and (3) one obtains:

$$C_{B^*} = \frac{4k_0 I C_B}{k_1 + k_2 C_B + 4k_3 C_A} \tag{5}$$

$$C_{A^*} = \frac{16\, k_0\, k_3 I C_B C_A}{(k_1 + k_2 C_B + 4k_3 C_A)(k_4 C_B + k_5)} \tag{6}$$

which introduced into (1), give:

$$\begin{aligned} \frac{dC_A}{dt} = &- 4\, k_3\, C_A \frac{4k_0 I C_B}{k_1 + k_2 C_B + 4k_3 C_A} + \\ &+ k_4 C_B \frac{16 k_0 k_3 I C_B C_A}{(k_4 C_B + k_5)(k_1 + k_2 C_B + 4k_3 C_A)} \end{aligned} \tag{7}$$

Since the irradiated solutions are relatively diluted, one may assume that:

$$4k_3 C_A << k_1 + k_2 C_B.$$

Under such conditions:

$$\frac{dC_A}{dt} = \left(- \frac{16k_0\, k_3\, I C_B}{k_1 + k_2 C_B} + \frac{16 k_0\, k_3\, k_4\, C_B^2}{(k_1 + k_2 C_B)\,(k_4 C_B + k_5)} \right) C_A = kC_A, \tag{8}$$

that is, the differential equation of a first-order reaction as it is verified by our experimental data.

This equation also accounts for the variation of the rate constant, with the solution concentration (see table 3).

The experimentally determined total rate constant k actually contains the rate constant k_1, k_2, k_3 and k_4 which characterize the proposed processes. The number of azibenzyl-excited molecules (process d) would be expected to increase with the increase of the concentration of azibenzyl irradiated solution. At the same time, the deactivation of the excited molecules (process e) clustered along the trajectory of secondary electrons is favoured and it competes with the process (f) since the solvent molecules are always in excess even for the most concentrated solution.

As has been seen in the case of the irradiations performed in the presence of anthracene (A_n), the reaction rate decreases significantly due to the process (i) with energy transfer.

$$B^* + An \xrightarrow{k_8} B + An \qquad \text{(i)}$$

which competes with the process (d) reducing the number of benzene-excited molecules in the system.

In conclusion, the radiolysis of benzene solutions of azibenzyl and also that of diphenyldiazomethane occurs by an indirect mechanism mediated by γ irradiation-excited benzene molecules.

This conclusion is in good agreement with our results obtained at the radiolysis of policrystalline azibenzyl,[2] which shows a much higher stability on γ irradiation in comparison to the benzene solution of azibenzyl.

Revue Roumaine de Chimie, **19**, *10*, 1569–1572 (1974)

THERMODYNAMIC DATA ON VAPORIZATION OF FUSED RUBIDIUM AND CESIUM FLUORIDES

LETIȚIA TOPOR

Institute of Physical Chemistry, str. Galați 31, Bucharest 13, Romania

Received February 6, 1974

The vapour pressures of molten RbF and CsF have been measured by the Rodebush-Dixon method on the temperature range 1189 K–1387 K and 1108 K–1288 K, respectively. The heats and entropies of vaporization, the heats of sublimation at 298 K and the boiling points have been calculated. The ΔH_{298} values allowing for the presence of dimers in the vapour phase are not essentially different from those calculated without any corrections.

The thermodynamic data on fused alkali fluoride vaporization as measured by the vapour pressure experiments have made the subject of publications to a much smaller extent than the data on other alkali halides. This can be explained by the experimental difficulty due to their great reactivity and higher melting point.

The vapour pressures of the molten RbF and CsF have been determined long ago by the boiling point method.[1,2] More recent measurements have been carried out on solid RbF and CsF by the torsion-effusion[3] and the molecular-beam velocity-selector[4] methods. The vapour pressure of the solid CsF has also been determined by the Knudsen effusion method in which case the beam intensities were measured by the method of surface ionization.[5] The alkali fluoride vapours in equilibrium with the condensed phase have been analysed by the mass spectrometric method.[6]

The purpose of the present work is to determine the thermodynamic data of vaporization in molten RbF and CsF from vapour pressure measurements.

EXPERIMENTAL

The vapour pressures of molten RbF and CsF have been determined by the quasi-static Rodebush-Dixon method. Tha apparatus and the required procedures have been previously described.[7] Because of the great reactivity of the molten fluorides we have used a platinum cell similar

---

[1] H. von WARTENBERG and H. SCHULZ, *Z. Elektrochem.*, **27**, 568 (1921).

[2] O. RUFF, G. SCHMIDT and S. MUGDAN, *Z. anorg. allgem. Chem.*, **123**, 83 (1922).

[3] A.C.P. PUGH and R. F. BARROW, *Trans. Faraday Soc.*, **54**, 671 (1958).

[4] M. EISENSTADT, G. M. ROTHBERG and P. KUSCH, *J. Chem. Phys.*, **29**, 797 (1958).

[5] M. D. SCHEER and J. FINE, *J. Chem. Phys.*, **36**, 1647 (1962).

[6] R. C. SCHOONMAKER and R. F. PORTER, *J. Chem. Phys.*, **30**, 283 (1959).

to the quartz ones previously utilized.[7-9] The body of the cell (30 mm outer diameter, 25 mm height) has attached to it two arms of 4 mm inner diameter. The values of the vapour pressure were measured with a mercury manometer using a cathetometer to within ±0.1 mm. The temperature was measured with a Pt—PtRh thermocouple and regulated to ±1° by a thermosetting device.

RbF and CsF Merck superpure grade were dried directly in the cell as follows: RbF was dried for 10 hours at 500 K and for 7 hours at 600 K under vacuum; CsF was dried for 16 hours at 450 K and for 5 hours at 600 K under vacuum. Tha salts were melted in dry argon.

RESULTS AND DISCUSSION

A number of 46 measurements of vapour pressures were carried out on RbF within the temperature range 1189K—1387K and 50 on CsF between 1108K and 1288K.

If the difference between the heat capacities of the gas and the liquid ΔC_p is assumed[10] -7 cal. mol^{-1} deg^{-1}, the variation of the vapour pressure *versus* temperature is expressed by the equation:

$$\log\ p = -\ \Delta H_0/4.576\ \mathrm{T} + \Delta C_p \log\ T/1.986 + I \qquad (1)$$

or if ΔC_p is zero or negligible eq. (1) becomes:

$$\log\ p = -\ \Delta H/4.576\ \mathrm{T} + C \qquad (2)$$

where ΔH_0 is the heat of vapcrization at OK, ΔH the heat of vaporization at the midtemperature of the experimental range, I and C are two constants. To obtain (1) type equation the experimental pressures were fitted by the Σ -plot method.[10] The calculations have been made by the least-square method on an IBM computer. The heat of vaporization ΔH_T and the constants I for RbF and CsF obtained from eq. (1) are given in table 1 together with those reported by Kelley [10] and determined by Wartenberg and Schulz [1] and Ruff, Schmidt and Mugdan.[2]

The following (2) type equations have been obtained: RbF (1189K —1387K)

$$\log p\,(\mathrm{mm}) = -\,(9589.5 \pm 68.5)/T + (8.625 \pm 0.053) \qquad (3)$$

CsF (1108 K — 1288 K)

$$\log p\,(\mathrm{mm}) = -\,(7725.6 \pm 25.8)/T + (7.907 \pm 0.021) \qquad (4)$$

The standard per cent deviations of the vapour pressure values for RbF and CsF are 3.55 and 1.33, respectively.

From equations (3) and (4) the heats of vaporization at the midtemperature are for RbF $\Delta H_{1300} = 43.88 \pm 0.3$ kcal. mol^{-1} and for CsF $\Delta H_{1200} =$

---

[7] I. G. Murgulescu and L. Topor, *Rev. Roumaine Chim.*, **11**, 1353 (1966).

[8] L. Topor and J. Wypartowicz, *Rev. Roumaine Chim.*, **17**, 831 (1972).

[9] L. Topor, *Rev. Roumaine Chim.*, **17**, 1503 (1972).

[10] K. K. Kelley, Bulletin 601, Bureau of Mines, 1962.

$= 35.35$ kcal.mol^{-1}. From the boiling point method the heats of vaporization are 40.0 kcal. mol^{-1} and 40.4 kcal. mol^{-1} for RbF[1,2] and 34.7 kcal.mol^{-1} and 33.6 kcal.mol^{-1} for CsF.[1,2]

Table 1

Heats of vaporization at temperature T and the constants I for RbF and CsF

Substance	ΔH_T kcal.mol^{-1}	I	References
RbF	$(52.84 - 7 \times 10^{-3}\ T) \pm 0.3$	21.109 ± 0.057	present data
	$51.280 - 7 \times 10^{-3}\ T$	—	10
CsF	$(43.65 - 7 \times 10^{-3}\ T) \pm 0.1$	20.275 ± 0.025	present data
	$54.00 - 7 \times 10^{-3}\ T$	—	10

The second-law values of ΔH_{298} for RbF and CsF have been deduced from the heats of vaporization at the melting point $\Delta H_{v,T_m}$ (calculated from table 1), the heats of sublimation at the melting point $\Delta H_{s,T_m}$ and the heat capacities of the solid and gas. The following values have been used for RbF : the melting point[11] $T_m = 1068$ K, the heat of fusion $\Delta H_m = 5.82$ kcal.mol^{-1}, the heat capacity for the solid and gas [3] $C_p(s) = 11.94 + + 2.37 \times 10^{-3}$ T and $C_p(g) = 8.88 - 4.42 \times 10^4 T^{-2}$, and for CsF : the melting point [11] $T_m = 976$ K, the heat of fusion [11] $\Delta H_m = 5.19$ kcal.mol^{-1}, the heat capacity for the solid [3] $C_p(s) = 11.315 + 2.71 \times 10^{-3}\ T$ and the heat capacity for the gas [10] $C_p(g) = 8.94 - 0.23 \times 10^5\ T^{-2}$.

For third-law values of ΔH_{298}, the differences between the free energy functions of rubidium fluoride [11] and cesium fluoride [12] in liquid and gaseous phase and the vapour pressures from the equations (3) and (4) have been used. These values of ΔH_{298} are shown in table 2. All the values have been obtained from vapour pressure measurements of molten fluorides except those of Pugh and Barrow[3] which are for the solid phase.

The agreement between our ΔH_{298} values calculated by the two methods is satisfactory. The discrepancies may be due to the heat capacity values; since the heat capacity of molten fluorides are not known we have assumed the difference between the heat capacities of the gas and liquid phase [10] to be -7 cal.mol^{-1} deg^{-1}.

Table 2

ΔH_{298} values for RbF and CsF from the second and third-law methods

Substance	ΔH_{298}, kcal.mol^{-1}		References
	II-law	III-law	
RbF	54.89	53.43	present data
	55.64	54.83	3
	52.1	54.6	2
	54.08	54.55	1
CsF	44.85	47.83	present data
	48.73	47.38	3
	42.9	50.3	2
	45.7	48.3	1

Mass spectrometric [6] and molecular-beam velocity-selector[4] studies have shown that the vapour in equilibrium with condensed alkali fluoride is complex and contains monomeric, dimeric and in some cases trimeric molecules. To calculate the thermodynamic data of gaseous alkali halides, Brewer and Brackett[11] take into account the molecular composition of these vapours. They have used the ratio of partial pressures of dimer to the monomer equal to 0.14 for RbF and 0.12 for CsF. Chao[12] has also calculated the thermodynamic data of alkali fluorides vaporization considering the presence of the associated species in gaseous phase. Scheer and Fine[5] have measured the vapour pressure of solid cesium halides. To obtain the CsF monomer vapour pressures they have corrected the experimental results for the presence of 7 per cent dimers in the gaseous phase. In table 3 ΔH_{298} are presented when associated species are considered. These values are in good agreement with those calculated from a third-law method without corrections for the associated species (table 2).

---

[11] L. Brewer and E. Brackett, *Chem. Rev.*, **61**, 425 (1961).

[12] J. Chao, *Thermochimica Acta*, **1**, 71 (1970).

Table 3

ΔH_{298} obtained if one takes into account the existence of associated species in vapours

Substance	ΔH_{298}, kcal.mol^{-1}	References
RbF	54.1	11
CsF	48.3	11
	49.0	5
	47.4	12

We have calculated ΔH_{298} using for the ratio of dimer to monomer partial pressures the values 0.14 for RbF and 0.12 CsF ; the values obtained in this way do not differ significantly from those in table 2.

From equations (3) and (4) we have calculated the entropies of vaporization and the boiling points : they are 26.29 ± 0.24 u.e. and 1669 K for RbF and 23.0 ± 0.09 u.e. and 1537 K for CsF, respectively.

Revue Roumaine de Chimie, **19**, *10*, 1573 – 1586 (1974)

THERMODYNAMIC TREATMENT OF BINARY AND TERNARY SALT SYSTEMS WITH SINGLE CHARGE IONS

Z. MOSER and K. FITZNER

Institute for Metal Research, Polish Academy of Sciences, Kraków, Reymonta 25, Poland

Received December 10, 1973

Krupkowski's formalism applied so far to solutions of metals was used for binary and ternary salt systems of single charge ions. Using chiefly experimental emf data of reversible formation cells of binaries : AgCl–RbCl, AgCl–KCl, NaCl–RbCl, NaCl–KCl, AgCl–NaCl and AgCl–LiCl the Eqs. for activity coefficients of both components were determined. Next, based on those relations, the values of molar enthalpy were calculated and compared with the calorimetric data. With the exception of the KCl–LiCl system which has been accepted as regular, the other binaries were classified as semiregular solutions when the $\omega(T)$ function in Krupkowski's formalism takes the form $\frac{\alpha}{T} - \beta$ or $-\frac{\alpha}{T} + \beta$, and the asymmetry coefficient m is close to 2. In the case of $m = 2$ the thermodynamic functions are symmetrical.

Next, the thermodynamic analysis of the ternary AgCl–RbCl–NaCl, AgCl – NaCl – – KCl and AgCl – KCl – LiCl systems was carried out in which the activity coefficients and the integral molar function, namely, the enthalpy and the excess free energy, were considered. Those functions calculated on the basis of binaries are in good agreement with the experimental data. In the case of the AgCl – LiCl – KCl system, the analysis of ln γ_{AgCl} when $X_{AgCl} = 0$ was performed and it was shown that as in the case of the solutions of metals, the deviation from linear dependence at the plot $(\ln\gamma_{AgCl})_{X_{AgCl}} \rightarrow 0$ *vs.* X_{KCl} is determined by the term

$$- \omega_{(Li,KCl)} (1 - XKCl)^{m(Li,K)Cl-2} X_{KCl} X_{LiCl}$$

connected with the KCl–LiCl system.

INTRODUCTION

Krupkowski's method,[1] which together with Darken's [2] and Wagner's [3] procedures is one of the possible solutions of the Gibbs-Duhem equation, is applied to the interpretation of the experimental results of binary and multicomponent systems. In a previous paper Krupkowski's formalism was used for liquid solutions of metals including also quaternary zinc systems. [4,5] This method was also applied to dilute solutions where the activity coefficients equations obtained over the entire range of concentrations[6,7] were used.

---

[1] A. Krupkowski, *Bull. Acad. Polon. Sci., Ser. A.*, **1**, 15(1950).

[2] L. S. Darken, *J. Amer. Chem. Soc.*, **2**, 2909 (1950).

[3] C. Wagner, "Thermodynamics of Alloys", Cambridge, Mass., 1952.

[4] W. Ptak and Z. Moser, *Trans. TMS–AIME,* **242**, 558 (1968).

[5] W. Ptak and Z. Moser, *J. Electrochem. Soc.*, **119**, 843 (1972).

It was shown that Krupkowski's and Darken's methods consisting in graphical integration when applied to ternary systems[8] result in very similar data of partial and integral thermodynamic functions. The fact that Krupkowski's method is frequently used in binary and multicomponent solutions of metals leads us to attempt its application to liquid salt solutions. First some simple binary and ternary systems with single charge ions were considered. In the previous attempts to interpret the experimental data in liquid salts for instance of the AgCl—RbCl—NaCl system, use was made of an analytical solution of the Gibbs-Duhem equation.[9] The application of this procedure requires the experimental data for the ternary system.

Markov[10] was also concerned with the calculation of the integral thermodynamic functions in ternary salt systems assuming them to be regular. Those considerations enabled the presentation of 5 models of integral excess free energy in ternary systems. On the one hand, the application of Krupkowski's formalism through the $\omega(T)$ function and exponent m takes into consideration the type of solution (not only regular) and its asymmetry, and on the other hand, makes it possible to base the results only on the thermodynamic properties of the binary systems. The further application of this method to the salt systems would enable the calculation of thermodynamic data even in the multicomponent systems in which the experiments are very difficult and sometimes even impossible.

APPLICATION OF KRUPKOWSKI'S FORMALISM TO BINARY SALT SYSTEMS

For the interpretation of the experimental data by means of Krupkowski's method, its application first to binary systems will be discussed, as those equations for the activity coefficients of both components are the starting point for calculating the integral molar function and for further analysis of the multicomponent system.

According to Krupkowski's concept[1] the activity coefficient of component i in a multicomponent system takes the following form:

$$\ln \gamma_i = \sum_{\substack{j,k=1 \\ j \neq k}}^{n} [\ln \gamma_i]_{j,k} \tag{1}$$

where: $[\ln \gamma_i]_{jk}$ is the partial contribution of the binary solutions.

---

[6] Z. Moser, *Met. Trans.*, **2**, 2175 (1971).

[7] Z. Moser, *Arch. Hutn.*, **14**, 371 (1969).

[8] Z. Moser and K. Fitzner, *Met. Trans.*, **3**, 3109 (1972).

[9] A. D. Pelton and S. N. Flengas, *J. Electrochem. Soc.*, **118**, 1307 (1971).

[10] B. F. Markov, *Rev. Roumaine Chim.*, **17**, 203 (1972).

[11] Z. Moser, *Rev. Roumaine Chim.*, **16**, 327 (1971).

The general form of Krupkowski's Eqs. for binary solutions[11] is as follows:

$$\ln \gamma_j = \omega_{jk}(T)\left[(1 - X_k)^{m_{jk}} - \frac{m_{jk}}{m_{jk} - 1} (1 - X_k)^{m_{jk}-1} + \frac{1}{m_{jk} - 1}\right] \quad (2)$$

$$\ln \gamma_k = \omega_{jk}(T)\ (1 - X_k)^{m_{jk}} \quad (3)$$

where: γ_j, γ_k are the activity coefficients of the substance j and k, ω_{jk} is the function dependent on temperature, m_{jk} is the experimental coefficient independent of temperature. The exponent m, for the majority of solutions, takes the values $1 < m \leqslant 2$, and the closer m to unity the higher the asymmetry of such thermodynamic functions as integral molar enthalpy and excess free energy. When $m = 2$, Eqs. (2) and (3) take the symmetrical form of Margules[12] relations:

$$\ln \gamma_j = \omega_{jk}(T)\ (1 - \mathrm{X}_j)^2 \quad (4)$$

$$\ln \gamma_k = \omega_{jk}(T)\ (1 - \mathrm{X}_k)^2 \quad (5)$$

The value of $m > 2$ suggests the appearance of some additional components. This is the case for instance in metal solutions when intermetallic compounds exist.[13] In the salt systems it is probably connected with the tendency to complex formation.

For the determination of Eqs. (2), (3) or (4), (5) of respective binary salt solutions use was made chiefly of experimental emf values of reversible formation cells, then, on the basis of those relations, the values of integral molar enthalpy were calculated. They were next compared with $\Delta H'$ data from calorimetric measurements.

It may generally be assumed that in the salt systems, contrary to metal solutions, less precise $\Delta H'$ from calorimetric data are obtained in comparison with analogical values based on emf measurements interpreted by Krupkowski's or Darken's method.

The resulting values of $\omega(T)$ function and m for the binary systems are summarized in table 1. Making use of those data and Eqs. (2)—(5) it is a simple procedure to verify the respective relations for the activity of both components. For the determination of $\omega(T)$ and m we assume that Eq. (3) will be applied to the component for which the partial thermodynamic functions may be obtained. The values of m were next obtained from the plot $\log \ln \gamma_k$ *vs.* $\log (1 - \mathrm{X}_k)$. The calorimetric data were only included in analysis when these data were available for only one temperature. Next, having m and γ_k, the values of $\omega(T)$ and the relation of this function *versus* temperature were calculated. In the case of the LiCl—KCl system the phase diagram [18] was used instead of the emf data, and for this system a $\omega(T)$ function is characteristic of regular solutions. The

---

[12] H. MARGULES, *Sitzber. Akad. Wiss. Wien*, **104**, 1243 (1895).
[13] Z. MOSER, *Met. Trans.*, **5**, 1445 (1974)

Table 1

The values of the functions ω (*T*) and *m* in binary systems

System Eq. (3) Eq. (4)	$\omega(T)$	m	References
AgCl — RbCl	$-\frac{1850}{T}+0.55$	1.95	[14]
AgCl — KCl	$-\frac{806}{T}+0.054$	1.80	[14]
NaCl — RbCl	$-\frac{390.1}{T}+0.147$	1.87	[15,16]
NaCl — KCl	$-\frac{245.1}{T}+0.104$	1.83	[15,16]
AgCl — NaCl	$\frac{839}{T}-0.333$	2.00	[14]
AgCl — LiCl	$\frac{1471}{T}-0.368$	2.40	[17]
KCl — LiCl	$-\frac{1097}{T}$	1.76	[18]

remaining systems from table 1 are classified as semiregular and, with the exception of the AgCl—LiCl system, m takes values lower than 2 as in metal solutions. From Eqs. (2)—(5) the relation for integral molar enthalpy takes the following form :

$$\Delta H' = \frac{R\alpha_{jk}}{m_{jk}-1}\left[X_j - X_j^m\right] \tag{6}$$

Eq. (6) is independent of temperature and is characteristic of regular and semiregular solutions. From Eq. (6) the integral molar enthalpies for binary salt systems were calculated and were found to be in good agreement with the calorimetric data (References as in table 1). Figure 1 gives the plots of the $\Delta H'$ values of binaries which are nearly symmetrical, this being connected with m oscillating slightly round 2.

---

[14] A. D. Pelton and S. N. Flengas, *J. Electrochem. Soc.*, **117**, 1130 (1970).

[15] L. S. Hersh and O. J. Kleppa, *J. Chem. Phys.*, **42**, 1309 (1965).

[16] L. U. Thulin, „Theoretical Treatment and Practical Applications of Galvanic Cells with Membranes", NTH Trondheim, 1970.

[17] M. B. Panish, T. F. Newton, W. R. Grimes and F. F. Blankenship, *J. Phys. Chem.*, **63**, 668 (1959).

[18] J. Lumsden, "Thermodynamics of Molten Salt Mixtures", Academic Press, London, 1966.

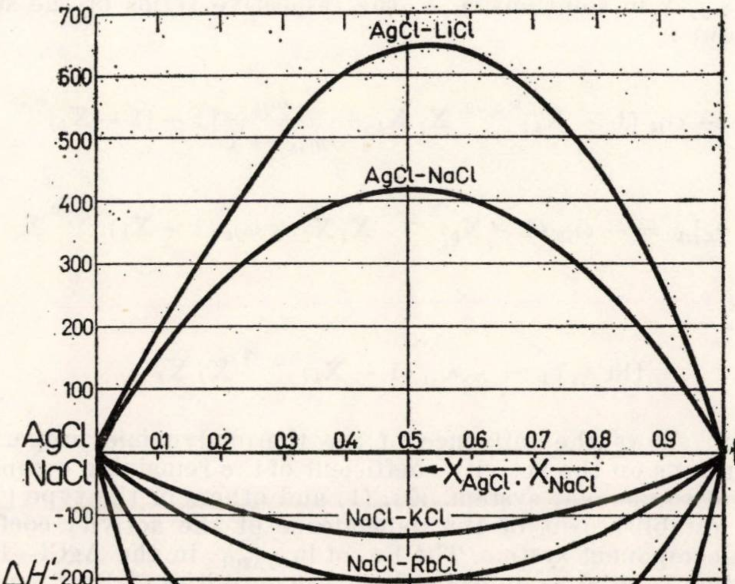

Fig. 1 — Integral molar enthalpies of mixing in binary systems calculated from Eq. (6) and table 1.

TERNARY SYSTEMS

From Eq. (1) relations in ternary solutions can be determined on the basis of the additivity of thermodynamic functions in the multicomponent system and the properties of binaries.

When the activity coefficients are given by Eqs. (2) and (3) for the components j, k in solutions, j, k, the respective terms of the sum (1), are as follows:

for $i = j$

$$[\ln \gamma_j]_{jk} = -\omega_{jk}(1 - X_k)^{m_{jk}-2} X_j X_k + \frac{\omega_{jk}}{m_{jk} - 1}\left[1 - (1 - X_k)^{m_{jk}-1}\right] \tag{7}$$

for $i = k$

$$[\ln \gamma_k]_{jk} = -\omega_{jk}(1 - X_k)^{m_{jk}-2} X_j X_k + \omega_{jk}(1 - X_k)^{m_{jk}-2} X_j \tag{8}$$

for $i \neq k$
$i \neq j$

$$[\ln \gamma_i]_{jk} = -\omega_{jk}(1 - X_k)^{m_{jk}-2} X_j X_k \tag{9}$$

Eq. (9) shows the influence of the thermodynamic properties of the j, k solutions on the activity coefficient of the remaining components i in the multicomponent system. Eq. (1) and others of the type (7)–(9) enable the establishment of the dependence of the activity coefficient in the multicomponent system. The Eq. of $\ln \gamma_{AgCl}$ in the AgCl–RbCl–NaCl system is cited as an example as the activities of RbCl and NaCl for this system were calculated, in the following part of this paper, and were used for isoactivity plots:

$$\begin{aligned}
\ln \gamma_{AgCl_{(Ag,Rb,Na)Cl}} &= -\omega_{(Ag,Na)Cl}(1 - X_{AgCl})^{m_{(Ag,Na)Cl}-2} X_{AgCl} \cdot X_{NaCl} + \\
&+ \omega_{(Ag,Na)Cl}(1 - X_{AgCl})^{m_{(Ag,Na)Cl}-2} X_{NaCl} - \omega_{(Ag,Rb)Cl} \\
&\cdot (1 - X_{AgCl})^{m_{(Ag,Rb)Cl}-2} X_{AgCl} X_{RbCl} + \omega_{(Ag,Rb)Cl}(1 - X_{AgCl})^{m_{(Ag,Rb)Cl}-2} X_{RbCl} - \\
&- \omega_{(Na,Rb)Cl}(1 - X_{NaCl})^{m_{(Na,Rb)Cl}-2} X_{NaCl} X_{RbCl} = \omega_{(Ag,Na)Cl} \cdot \\
&\cdot (1 - X_{AgCl})^{m_{(Ag,Na)Cl}-1} X_{NaCl} + \omega_{(Ag,Rb)Cl}(1 - X_{AgCl})^{m_{(Ag,Rb)}-1} X_{RbCl} - \\
&- \omega_{(Na,Rb)Cl}(1 - X_{NaCl})^{m_{(Na,Rb)Cl}-2} X_{NaCl} X_{RbCl}
\end{aligned} \tag{10}$$

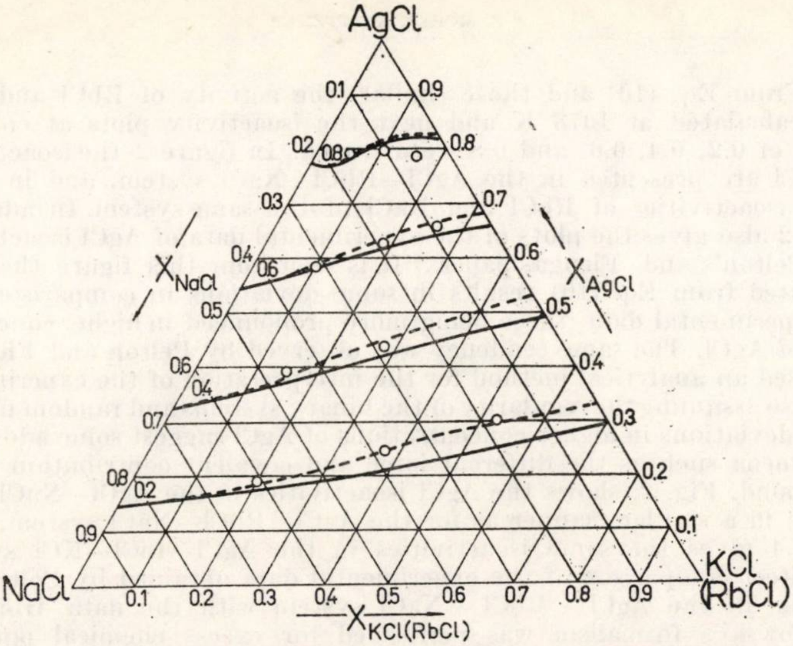

Fig. 2 — Isoactivities of AgCl in the AgCl—RbCl—NaCl system calculated from Eq. (10) (— — —), O — Ref.[9], (———) isoactivities of AgCl calculated in the AgCl—NaCl—KCl system.

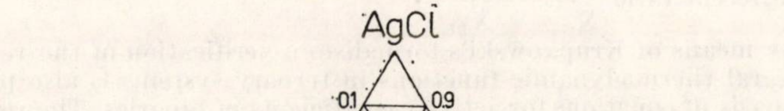

Fig. 3 — Isoactivities of RbCl (— — —) and NaCl (———) in the AgCl—RbCl—NaCl system.

From Eq. (10) and those similar, the activity of RbCl and NaCl were calculated at 1073 K and next the isoactivity plots at constant values of 0.2, 0.4, 0.6, and 0.8 were traced. In figure 2 the isoactivities of AgCl are presented in the AgCl—RbCl—NaCl system, and in figure 3 the isoactivities of RbCl and NaCl of the same system. In addition, figure 2 also gives the plots of the experimental data of AgCl isoactivities from Pelton's and Flengas'paper .[9] It is seen from this figure that a_{AgCl} calculated from Eq. (10) results in some deviations in comparison with the experimental data, these being more pronounced in higher concentrations of AgCl. The same tendency was observed by Pelton and Flengas [9] who used an analytical method for the interpretation of the experimental data also assuming the regularity of the binary systems and random mixing. Those deviations in higher concentrations of AgCl suggest some additional phenomena such as the different ionic and covalent contribution in the AgCl bond. Fig. 2. shows the AgCl isoactivities in the AgCl—NaCl—KCl system in a similar manner as for the AgCl—RbCl—NaCl system, while figure 4 gives the same isoactivities in the AgCl—LiCl—KCl system. The direct comparison of the experimental data obtained by Pelton and Flengas in the AgCl — RbCl — NaCl system with the data from the Krupkowski's formalism was performed for excess chemical potential of AgCl. For this purpose in fig. 5, $\Delta\bar{G}^{*}_{\mathrm{AgCl}}$ *vs.* X_{AgCl} at $T = 1073$ K was plotted. It is seen from this figure that a good agreement was obtained for a different ratio $\dfrac{X_{\mathrm{NaCl}}}{X_{\mathrm{NaCl}} + X_{\mathrm{RbCl}}}$.

By means of Krupkowski's formalism a verification of the relations for integral thermodynamic functions in ternary systems is also possible on the basis of equations for activity coefficients of binaries. The relations for integral excess free energy and molar enthalpy in the AgCl—RbCl—NaCl system will be discussed in this paper the more so that such thermodynamic functions are available for comparison with the results of Pelton and Flengas .[9] In the AgCl—RbCl—NaCl system, the equations for integral excess free energy and molar enthalpy are as follows :

$$\Delta G'^{*}_{(\mathrm{Ag,Rb,Na})\mathrm{Cl}} = \frac{R\,(\alpha + \beta T)_{(\mathrm{Ag,Na})\mathrm{Cl}}}{m_{(\mathrm{Ag,Na})\mathrm{Cl}}^{-1}} \left[1 - (1 - X_{\mathrm{AgCl}})^{m_{(\mathrm{Ag,Na})\mathrm{Cl}}^{-1}}\right] X_{\mathrm{NaCl}} +$$

$$+ \frac{R\,(\alpha + \beta T)_{(\mathrm{Ag,Rb})\mathrm{Cl}}}{m_{(\mathrm{Ag,Rb})\mathrm{Cl}}^{-1}} \left[1 - (1 - X_{\mathrm{AgCl}})^{m_{(\mathrm{Ag,Rb})\mathrm{Cl}}^{-1}}\right] X_{\mathrm{RbCl}} +$$

$$+ \frac{R\,(\alpha + \beta T)_{(\mathrm{Na,Rb})\mathrm{Cl}}}{m_{(\mathrm{Na,Rb})\mathrm{Cl}}^{-1}} \left[1 - (1 - X_{\mathrm{NaCl}})^{m_{(\mathrm{Na,Rb})\mathrm{Cl}}^{-1}}\right] X_{\mathrm{RbCl}} =$$

$$= (1667.1 - 0.622\ \mathrm{T})\, X_{\mathrm{AgCl}} X_{\mathrm{NaCl}} + (-3869.5 + 1.15\ T)\ [1 - (1 - X_{\mathrm{AgCl}})^{0.95}] \cdot$$

$$\cdot X_{\mathrm{RbCl}} + (-\ 890.9 + 0.336\ \mathrm{T})\ [1 - (1 - X_{\mathrm{NaCl}})^{0.87}] X_{\mathrm{RbCl}} \qquad (11)$$

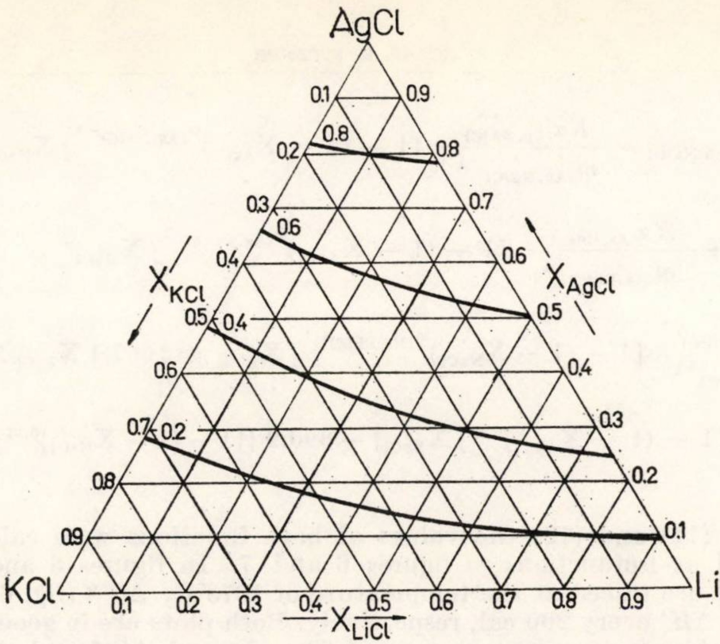
AgCl
KCl
LiCl
X_{KCl}
X_{AgCl}
X_{LiCl}
0.1
0.2
0.3
0.4
0.5
0.6
0.7
0.8
0.9
0.8
0.6
0.4
0.2

Fig. 4 — Isoactivites of AgCl in the AgCl–KCl – LiCl system.

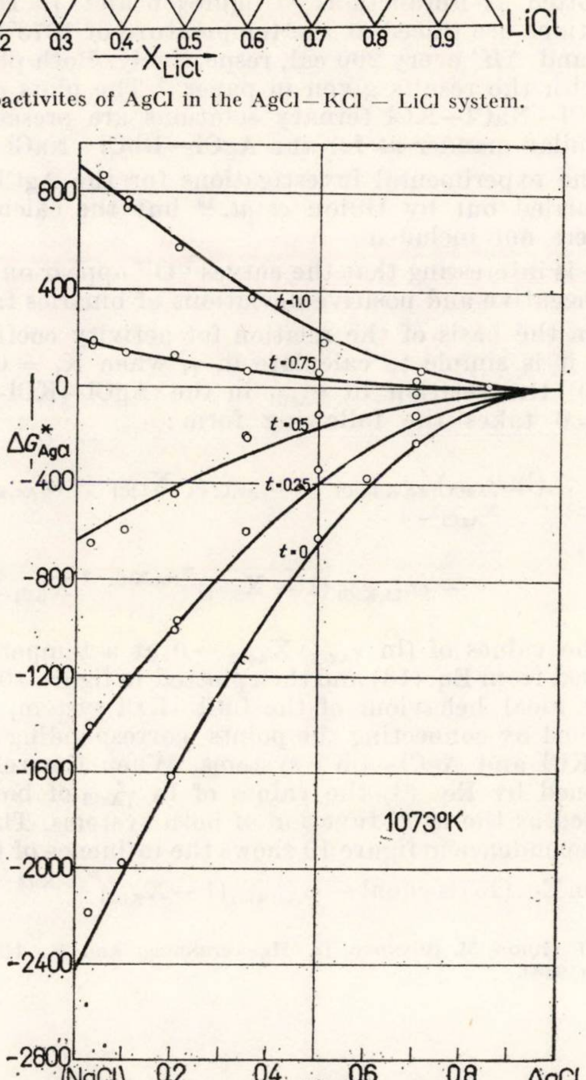

Fig. 5 — $\Delta\overline{G}^*_{AgCl}$ at 1073 K in the AgCl–RbCl–NaCl system. Lines are from relation $\Delta\overline{G}^*_{AgCl} = RT \ln \gamma_{AgCl}$ when $\ln \gamma_{AgCl}$ was calculated from Eq. (10). The points correspond to the experimental data of Pelton and Flengas[9]; $t = \frac{X_{NaCl}}{X_{NaCl} + X_{RbCl}}$

$$\Delta H'_{(\mathrm{Ag,Rb,Na})\mathrm{Cl}} = \frac{R\alpha_{(\mathrm{Ag,Na})\mathrm{Cl}}}{m_{(\mathrm{Ag,Na})\mathrm{Cl}}^{-1}} \left[1 - (1 - \mathrm{X}_{\mathrm{AgCl}})^{m_{(\mathrm{Ag,Na})\mathrm{Cl}}^{-1}}\right] \mathrm{X}_{\mathrm{NaCl}} +$$

$$+ \frac{R\alpha_{(\mathrm{Ag,Rb})\mathrm{Cl}}}{m_{(\mathrm{Ag,Rb})\mathrm{Cl}}^{-1}} \left[1 - (1 - \mathrm{X}_{\mathrm{AgCl}})^{m_{(\mathrm{Ag,Rb})\mathrm{Cl}}^{-1}}\right] \mathrm{X}_{\mathrm{RbCl}} +$$

$$+ \frac{R\alpha_{(\mathrm{Na,Rb})\mathrm{Cl}}}{m_{(\mathrm{Na,Rb})\mathrm{Cl}}^{-1}} \left[1 - (1 - \mathrm{X}_{\mathrm{NaCl}})^{m_{(\mathrm{Na,Rb})\mathrm{Cl}}^{-1}}\right] \mathrm{X}_{\mathrm{RbCl}} = 1667.1\, \mathrm{X}_{\mathrm{AgCl}}\, \mathrm{X}_{\mathrm{NaCl}} +$$

$$- 3869.5 \left\{\left[1 - (1 - \mathrm{X}_{\mathrm{AgCl}})^{0.95}\right] \mathrm{X}_{\mathrm{RbCl}}\right\} - 890.9 \left\{\left[1 - (1 - \mathrm{X}_{\mathrm{NaCl}})^{0.87}\right] \mathrm{X}_{\mathrm{RbCl}}\right\} \qquad (12)$$

From Eqs. (11) and (12) the values of both functions were calculated and plotted as isofunctions in figures 6 and 7. In figures 6 and 7 the isofunctions are traced at the temperature of 1073°K, $\Delta G'^*$ (fig. 6) every 50 cal, and $\Delta H'$ every 200 cal, respectively. Both plots are in good agreement with the results given in paper .[9] The plots of $\Delta G'^*$ and $\Delta H'$ for the AgCl—NaCl—KCl ternary solutions are presented in figs. 8 and 9 in a similar manner as for the AgCl—RbCl—NaCl system.

The experimental investigations for the AgCl—NaCl—KCl system were carried out by Guion *et al.* [19] but the calculations of $\Delta G'^*$ and $\Delta H'$ were not included.

It is interesting that the curves "O" appear on the plots as a result of the negative and positive deviations of binaries from the Raoult's law.

On the basis of the relation for activity coefficient in the ternary system it is simple to calculate ln γ_i when $\mathrm{X}_i = 0$. For example from Eq. (10) the relation ln γ_{AgCl} in the AgCl—KCl—LiCl system when $\mathrm{X}_{\mathrm{AgCl}} = 0$ takes the following form:

$$(\ln \gamma_{\mathrm{AgCl}})_{\substack{(\mathrm{Ag,K,Li})\mathrm{Cl} \\ \mathrm{X}_{\mathrm{AgCl}} \to 0}} = \omega_{(\mathrm{Ag,Li})\mathrm{Cl}}\, \mathrm{X}_{\mathrm{LiCl}} + \omega_{(\mathrm{Ag,K})\mathrm{Cl}}\, \mathrm{X}_{\mathrm{KCl}} -$$

$$- \omega_{(\mathrm{Li,K})\mathrm{Cl}} (1 - \mathrm{X}_{\mathrm{KCl}})^{m_{(\mathrm{Li,K})\mathrm{Cl}} - 2}\, \mathrm{X}_{\mathrm{KCl}}\, \mathrm{X}_{\mathrm{LiCl}}. \qquad (13)$$

The values of (ln γ_{AgCl}) $\mathrm{X}_{\mathrm{AgCl}} \to 0$ at a temperature of 823°K were calculated from Eq. (13) and then plotted in figure 10. On this plot, assuming the ideal behaviour of the LiCl—KCl system, a linear dependence is obtained by connecting the points corresponding to ln $\gamma^{\circ}_{\mathrm{AgCl}}$ in binary AgCl—KCl and AgCl—LiCl systems. When the relation for ln γ_{AgCl} is determined by Eq. (3) the values of ln $\gamma^{\circ}_{\mathrm{AgCl}}$ of both binaries may be calculated as the $\omega(T)$ function of both systems. The deviation from the linear dependence in figure 10 shows the influence of the LiCl—KCl system and from Eq. (13) is equal $- \omega_{(\mathrm{Li,K})\mathrm{Cl}} (1 - \mathrm{X}_{\mathrm{KCl}})^{m_{(\mathrm{Li,K})\mathrm{Cl}} - 2} \mathrm{X}_{\mathrm{KCl}} \mathrm{X}_{\mathrm{LiCl}}$. According

---

[19] J. Guion, M. Blander, D. Hengstenberg and K. Hagemark, *J. Phys. Chem.*, **72**, 2086 (1968).

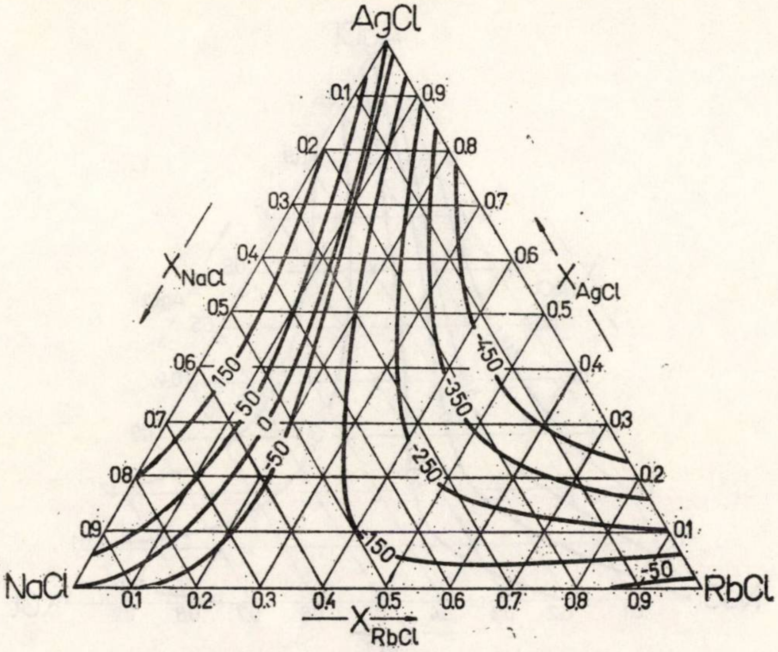

Fig. 6 — Iso- $\Delta G'^*$ plots at 1073°K in the AgCl—RbCl—NaCl system.

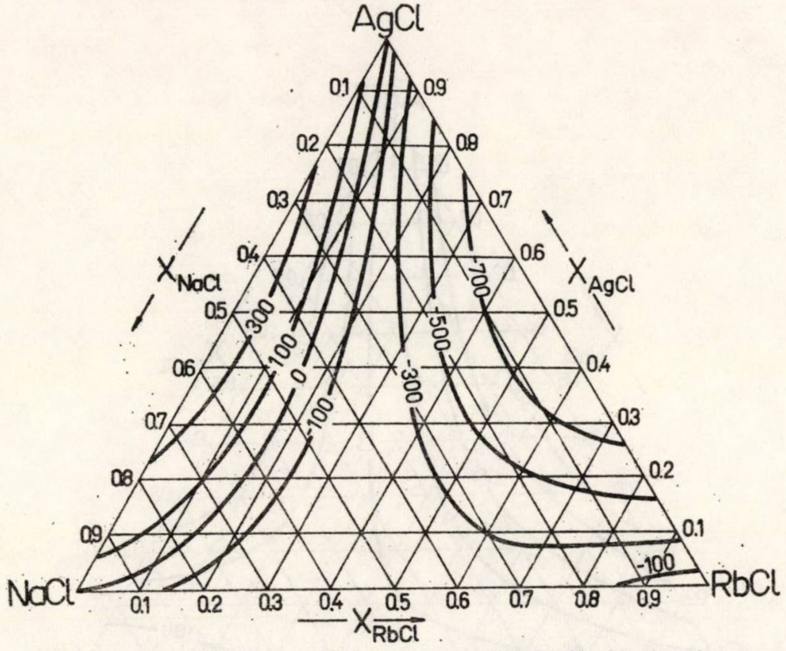

Fig. 7 — Iso- $\Delta H'$ plots at 1073°K in the AgCl—RbCl—NaCl system.

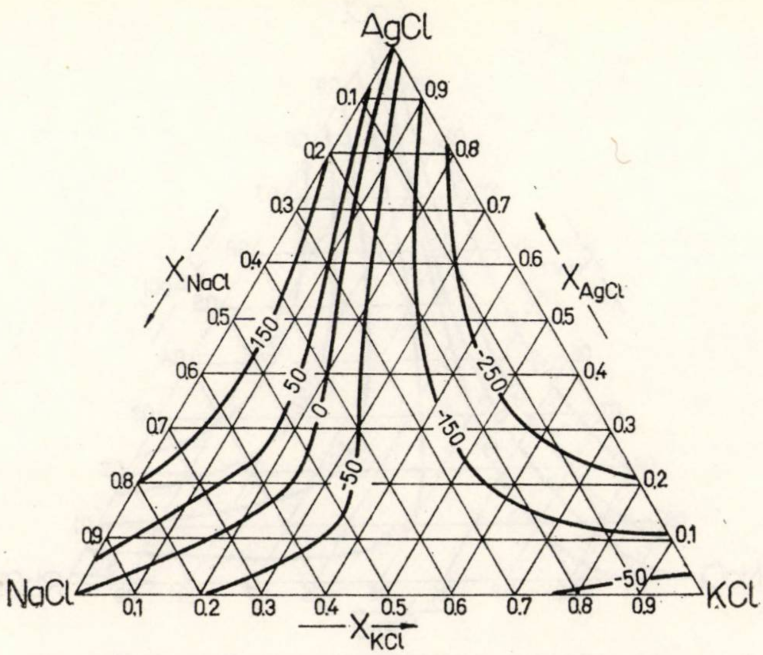

Fig. 8 — Iso - $\Delta G'^{*}$ plots at 1073°K in the AgCl—KCl—NaCl system.

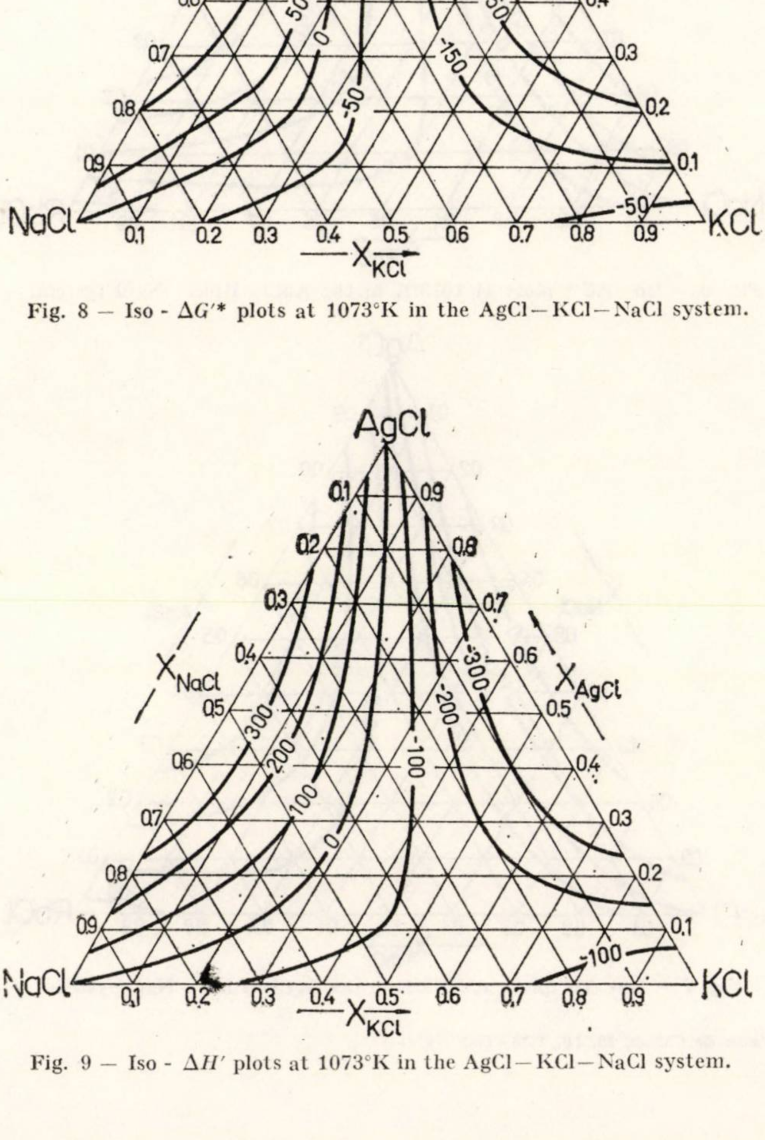

Fig. 9 — Iso - $\Delta H'$ plots at 1073°K in the AgCl—KCl—NaCl system.

to Eq. (13) in the case when the components 2—3 of the LiCl—KCl system show the negative deviations from the Raoult's law, a positive departure from the linear dependence is obtained. The opposite case is also valid when the negative deviations from the straight line appear.

Figure 10 also includes the value ln γ°_{AgCl} from the Yang and Hudson's paper[20] obtained by means of extrapolation of the experimental ln γ_{AgCl} values in eutectic LiCl—KCl to $X_{AgCl} = 0$. It is seen that the value of ln $\gamma^{\circ}_{AgCl_{(Ag,Li,K)Cl}}$ obtained from the data of Yang and Hudson correspond to some slighter deviations of the LiCl—KCl solutions from the Raoult's law than those suggested by the last term of Eq. (13).

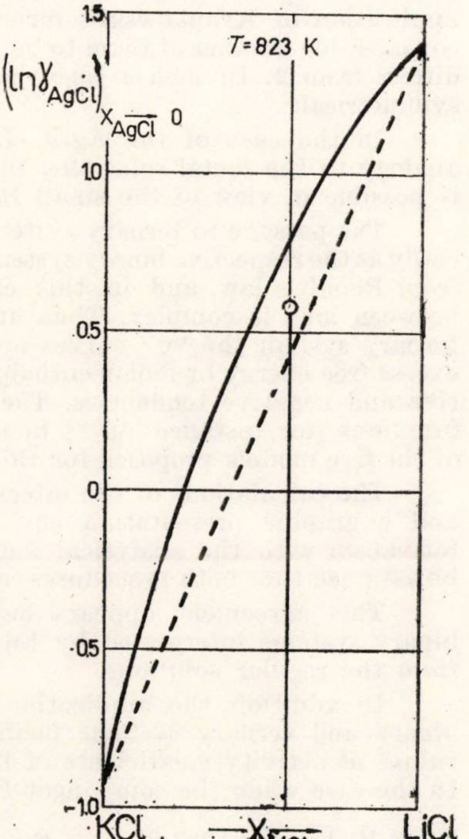

Fig. 10 — $(\ln \gamma_{AgCl})_{X_{AgCl}\to 0}$ *vs.* X_{LiCl} at 823 K in the AgCl—KCl—LiCl system.

DISCUSSION

Applying Krupkowski's formalism to the experimental data from literature the relations for activity coefficients of both components in liquid AgCl—RbCl, AgCl-KCl, AgCl-LiCl, NaCl-RbCl, AgCl—NaCl, NaCl—KCl and KCl—LiCl systems were determined. The resulting equations were used for the establishment of the relation of integral molar enthalpy of the given binaries. The value of $\Delta H'$ calculated from Eq. (6) is accurate to ± 100 cal when $X_1 = X_2 = 0.5$ molar fraction compared with calorimetric data.

This fact suggests that Eqs. (2)—(5) correspond well to the experimental data. On the basis of this fact and the relations (2)—(5) for respective binaries, equations for activity coefficients in ternary system were determined. Such a procedure enabled the calculations of activity and the tracing of isoactivity plots which show a good agreement with the experimental results corresponding to the AgCl—RbCl—NaCl system which were the subject of Pelton and Flengas's experiments .[9] Greater deviations between the experimental data and those from Eq. (10) were obtained at higher concentrations of AgCl as also shown in this paper. In a previous paper on the binary system AgCl$-$ACl (where A $=$ Na, K, Rb or Cs) Pelton and Flengas[14] drew attention to the mixed character of the bonding, namely the ionic – covalent one, which is also influenced by the magnitude of the ionic radius of component *A*. The application of Krupkowski's formalism to the binary systems shows a considerable number of them to be semi-regular solutions, when *m* slightly differs from 2. In such a case the thermodynamic functions are nearly symmetrical.

---

[20] L. Yang and R. Hudson, *Trans. TMS—AIME*, **215**, 589 (1959).

In the case of the AgCl$-$LiCl system $m > 2$ may suggest, by analogy to the metal solutions, the tendency to form complexes, which is possible in view of the small Li^+ion.

The passage to ternary systems seems to be more complicated especially as the respective binary systems show negative and positive departure from Raoult's law, and in this case the problem of the interactions between ions is complex. Then at a certain ratio of concentrations in ternary system the "0" curves appear on plots of isofunctions such as excess free energy or molar enthalpy as a result of the cancelling of positive and negative tendencies. The obtained plots of the integral molar functions (for instance $\Delta G'^*$) in the ternary system correspond to one of the five models proposed for this function by Markov.[10]

The calculations of the integral molar functions in ternary systems and a graphic presentation enabled the comparison of Krupkowski's formalism with the analytical Pelton and Flengas method.[9, 14] It may be assumed that both procedures result in similar values of $\Delta H'$ and $\Delta G'^*$.

This agreement appears because the experimental data of the binary systems interpreted by Eqs. (2)–(5) show only slight departure from the regular solutions.

In addition, the application of Krupkowski's formalism to both binary and ternary systems facilitates the calculation of the limiting values of activity coefficients of binary systems from Eqs. (2) and (3). In the case when the component *k* was applied to Eq. (3); $\ln \overset{\circ}{\gamma}_k = \omega_{jk}$, when to Eq. (2) then $\ln \overset{\circ}{\gamma}_j = \omega_{jk}\dfrac{1}{m_{jk} - 1}$. For symmetrical solutions when $m = 2$, $\ln \gamma = \ln \overset{\circ}{\gamma}_k = \omega_{jk}$.

Calculations of $(\ln \gamma_{AgCl})\, X_{AgCl} \to 0$ in the AgCl$-$LiCl$-$KCl system compared with the experimental results of Yang and Hudson[20] confirm the fact, that the departure from the linear dependence is produced by the term connected with the binary system 2$-$3, namely LiCl$-$KCl, which is also the case in metal solutions. The interpretation of the experimental data by the Krupkowski's method suggests the possibility of its successful application to the liquid salts systems with single charge ions. The good agreement of thermodynamic functions in binary and ternary systems with available experimental data indicates the applicability of the Krupkowski's method to the salt systems for the calculation of thermodynamic functions in multicomponent systems from binary systems, even when, as a result of the experimental difficulties, the experiments in multicomponent systems are impossible.

Revue Roumaine de Chimie, **19**, *10*, 1587–1591 (1974)

AN IMPROVEMENT OF HOFFMANN'S LCAO–MO METHOD

C. I. LEPĂDATU* and S. MOLDOVEANU**

* Center of Chemical Physics, Dumbrava Roşie, 23, Bucharest, Romania
** Faculty of Chemistry, University of Bucharest, Romania

Received May 31, 1973

The present paper describes a new method for MO calculations which may be considered as an improved Hoffmann method. The improvement consists in the introduction of the electrostatic interactions, screening constants, as well as the introduction of iterations of the VSIP's upon the charges as a result of the electron population analysis. Calculations performed for ethane in the staggered form are in good agreement with the results of the photoelectron spectroscopy.

One of the extended Hückel-type LCAO–MO methods which gives good results in the study of the hydrocarbons is the method proposed by Hoffmann.[1] This method is mainly used to obtain MO energies and wavefunctions for molecules with 1*s*, 2*s* and 2*p* AO's, taking into account all the overlap integrals.

The minimization of the energy of a molecule with n orbitals leads to :

$$\sum_{\nu=1}^{n} [H_{\mu\nu} - \varepsilon^{i} S_{\mu\nu}] c_{\nu i} = 0 \qquad (1)$$

$$\mu = 1,\dots n, \quad i = 1,\dots n$$

where $c_{\nu i}$ are the coefficients in the expression :

$$\psi_i = \sum_{\nu} c_{\nu i} \chi_\nu, \qquad (2)$$

ψ_i being the molecular orbitals, χ_ν the atomic orbitals in the given molecule, and

$$S_{\mu\nu} = \int \chi_\mu^* \chi_\nu \, \mathrm{dv} \qquad (3)$$

$$H_{\mu\nu} = \int \chi_\mu^* \hat{H} \chi_\nu \, \mathrm{dv} \qquad (4)$$

---

[1] R. Hoffmann, *J. Chem. Phys.*, **39**, 1397 (1963).

the overlap integral and the energy integral, $\widehat{H}$ being the hamilton operator of the system.

In the Hoffmann method $S_{\mu\nu}$ are exactly calculated but $H_{\mu\nu}$'s remain constant and independent of the charge density in the molecule.

The aim of the present paper is to find another way to estimate the $H_{\mu\nu}$'s, different of the recipe recommended by Hoffmann in his mentioned approach.

For this purpose, the one-electron hamiltonian has been approximated to:

$$\hat{H}^{\mu} = -1/2\,(\nabla^{\mu})^2 + V_A^{\mu} + \sum_{B\neq A} V_B^{\mu} \tag{5}$$

where the electron in the μ—AO belongs to the A-core, and B runs over all the other cores in the molecule.

Expression (5) is usually known under the name of Coulomb screened potential approximation, where:

$$V_B^{\mu} = -\,k\,(\mu,\ \mu)\ (Z_B/r_{AB}) \tag{6}$$

where Z_B is the effective charge on the B-core, r_{AB} the distance between the A and B cores.

What is new in our treatment is the introduction of the screening constant $k(\mu,\ \mu)$ determined by the electron densities in the outer shells enveloping the orbital "μ" which may reduce the interaction with the external Z_B charges on the other B cores in the molecule. This constant will be discussed later. In the one-electron approximation:

$$\hat{H}_{\text{mol}} = \sum_{\mu=1}^{n} \hat{H}^{\mu} \tag{7}$$

$$E_{\text{mol}} = \sum_{i=1}^{n} n^i\ \varepsilon^i \tag{8}$$

where n^i — is the electron number in the monoelectronic molecular orbital "i" given by (2), ε^i — the corresponding MO energy satisfying the equation:

$$\hat{\mathscr{H}}^{\mu}\ \psi_i = \varepsilon^i\ \psi_i. \tag{9}$$

Striking out the index μ in $\hat{\mathscr{H}}^{\mu}$ because of the identity of $\mathscr{H}^{\mu}$ for each of the μ orbitals, the equation (9) is reduced to:

$$\hat{\mathscr{H}}\ \psi_i = \varepsilon^i \psi_i, \tag{10}$$

which is solved in the LCAO—MO approximation according to (1).

The problem is now to have $S_{\mu\nu}$ and $H_{\mu\nu}$ values. According to (5) and (6), we have:

$$H_{\mu\mu} = \int \chi_\mu^* \left(-\frac{1}{2} \nabla^2 + V_A \right) \chi_\mu \, \mathrm{dv} - k(\mu, \mu) \sum_{B \neq A} \int \chi_\mu^* \frac{Z_B}{r_{AB}} \chi_\mu \, \mathrm{dv} \qquad (11)$$

where μ belongs to the A core.

If we take the first term in (11) as the valence state ionization potential (VSIP) with a changed sign, and putting down:

$$\int \chi_\mu^* \frac{1}{r_{AB}} \chi_\mu \, \mathrm{dv} = BI_{B\mu}, \qquad (12)$$

we obtain:

$$H_{\mu\mu} = - \mathrm{VSIP}\,(\mu) - k\,(\mu, \mu) \cdot \sum_{B \neq A} Z_B \cdot BI_{B\mu}, \qquad (13)$$

where Z_B is the effective charge on the B centres.

The VISP (μ) values are taken as a parabolic function of Z_A,

$$\mathrm{VSIP}\,(\mu) = \alpha Z_A^2 + \beta Z_A + \gamma \qquad (14)$$

where α, β, γ, are the coefficients found for each μ and element in the related literature.

To evaluate the $H_{\mu\nu}$ integrals we use the formula:

$$H_{\mu\nu} = - k\,(\mu, \nu) \cdot 0.5\ S_{\mu\nu}\ [(2 - |S_{\mu\nu}|)\ \ (\mathrm{VSIP}\,(\mu) + \mathrm{VSIP}\,(\nu)) +$$

$$+ (\sum_{B \neq A} Z_B BI_{B\mu} + \sum_{A \neq B} Z_A\, BI_{A\nu})], \qquad (15)$$

which comes from Cusach's approximation [2] if the electrostatic interactions and the screening constant $k(\mu, \nu)$ should be taken into account.

The expressions (13) and (15) show that the $H_{\mu\mu}$ and $H_{\mu\nu}$ values can be obtained if $S_{\mu\nu}$, $BI_{B\mu}$ and $k(\mu, \nu)$ as well as the effective charges on the cores in the molecule are known.

The overlap integrals $S_{\mu\nu}$ can be calculated using the master formulas given by Kruglyak *et al.*, [3] and the $BI_{B\mu}$ integrals using formulas given by Roothaan, [4] up to the orbital quantum number $l = 2$.

---

[2] L. Chopin-Cusach, *J. Chem. Phys.*, **43**, 1575(1965).

[3] Yu. Kruglyak, "Metody rascheta elektronnoi struktur i spektrov molecu l", Moscow, Dumca, Kiev, 1969.

[4] C. C. J. Roothaan, *J. Chem. Phys.*, **19**, 1445(1 951).

The effective charge on the cores in the molecule may be found from the electron population analysis:

$$Z_A = Z_A^0 - \sum_{\mu} q^{\mu} \tag{16}$$

where q^{μ} is the charge on the μ—AO, given by:

$$q^{\mu} = \frac{\sum\limits_{i=1}^{n} n^i - 0.5 \sum\limits_{\mu=1}^{n} \sum\limits_{i=1}^{n} n^i c_{\mu i} \sum\limits_{\mu \neq \nu} c_{\nu i} S_{\mu\nu}}{\sum\limits_{\mu=1}^{n} \sum\limits_{i=1}^{n} n^i c_{\mu i}^2} \sum_{i=1}^{n} n^i c_{\mu i}^2, \tag{17}$$

and the screening constant by:

$$k(\mu, \nu) = k'(\mu)\, k'(\nu), \tag{18}$$

where

$$k'(\mu) = [1 - (\sum_{i} n^i c_{\mu i}{}^2/m)]^{1/2}, \tag{19}$$

where $m = 2, 6, 10\ldots$ for the s-, p-, d-, ... — type AO's respectively.

ITERATION PROCEDURE

The iteration procedure is the following:

— We compute the $S_{\mu\nu}$ integrals, make an initial estimation of $k(\mu, \nu)$, Z_A, Z_B, etc. One computes the $BI_{B\mu}$ integrals and after that $H_{\mu\mu}$ and $H_{\mu\nu}$.

— We solve the equation system (1) and obtain ε^i and $c_{\nu i}$ values which are used to compute $k^{\text{new}}(\mu, \nu)$, Z_A^{new}, etc. using (16)—(19).

— then we put:

$$Z_A = 0.9\, Z_A^{\text{old}} + 0.1\, Z_A^{\text{new}}$$

. . . .

$$k(\mu, \nu) = 0.9\, k^{\text{old}}(\mu, \nu) + 0.1\, k^{\text{new}}(\mu, \nu),$$

and after that one computes new values for $H_{\mu\mu}$ and $H_{\mu\nu}$ which introduced in (1) give ε^i and $c_{\nu i}$. The procedure should be repeated until self-consistency.

The mixture of the output and input data during the iteration process has been made in order to speed up the convergence. [5]

The present method has been written by one of us (S.M.) in FORTRAN for an IBM 360/30 system digital computer for orbitals up to the orbital quantum number $l = 3$.

CALCULATION EXPERIMENT

The outlined method has been applied to ethane in the staggered form (symmetry group D_{3d}), using four iterations, after which the total energy remains constant.

---

[5] D. G. CAROLL, A. T. ARMSTRONG and S. P. MCGLYNN, *J. Chem. Phys.*, **44**, 1865 (1966).

For this purpose, the following interatomic distances were used; $r_{C-C} = 1.54$ Å; $r_{C-H} = 1.1$ Å. The AO set contains $1s_H$, $2s_C$ and $2p_C$ taken as Slater type orbitals. The corresponding VSIP's were taken as $A + BZ$ where Z is the effective charge, A and B constants being reported in the related literature.[6]

The bonding MO energies are collected in table 1 and compared with those obtained by different authors.[7-9]

Table 1

MO levels for ethane D_{3d} (energy in *eV*)

Level	Present method	Ref.[6]	Ref.[7]	Ref.[8]
$2a_{1g}$	−11.323	−14.11	−14.59	−13.32
e_g	−11.323	−13.76	−14.01	−13.93
e_u	−15.680	−15.86	−17.07	−15.60
a_{2u}	−18.734	−21.82	−23.37	−20.89
$1a_{1g}$	−25.053	−26.67	−28.30	−24.21

Table 2

Ionization potentials for ethane (*eV*)

Observed	Calculated	Ref.[8]
11.78	11.323	13.32
14.74	15.680	15.60
19.18	18.734	20.89

Table 2 shows the ionization potentials for ethane as they result from the photoelectron spectroscopy.[10] Assuming that during the ionization no molecular changes take place, i.e the Koopmans theorem holds, the observed ionization potentials should be equal to the MO energies with changed sign.

As may be seen from the tables 1–2, the MO levels obtained by the present method are comparable with those calculated by different authors. It must, however, be mentioned that the Hoffmann approach [7] leads to the inverted order $2a_{1g} < e_g$ which disagrees with the order obtained by other MO approximations or by the present method.

The atomization energy calculated for ethane (the total energy for the ethane in its ground state minus the total energy of the atoms) is found to be:

– 595.2 kcal/mol comparable with
– 671.6 kcal/mol, as experimentally evaluated.[11]

The authors express their thanks to Mrs. Agneta Caragheorghiopol, to Mr. Horia Căldăraru and to Mr. Andrei Savin for their help in the preparation of the present paper, and to the staff of the Computation Centre of University of Bucharest for the assistance in the use of IBM 360/30 system digital computer.

---

[6] A. Pullman, E. Kochanski, M. Gilbert and A. Denis, *Theor. Chim. Acta*, **10**, 231 (1968).

[7] R. Hoffmann, *J. Chem. Phys.*, **40**, 2047 (1964).

[8] R. M. Pitzer and W. N. Lipscomb, *J. Chem. Phys.*, **39**, 1995 (1963).

[9] T. Yonezawa, K. Yamaguchi and H. Kato, *Bull. Chem. Soc. Japan*, **40**, 536 (1967).

[10] G. Klopman and B. O'Leary, "All-Valence Electrons SCF Calculations", Springer Verlag, Berlin, 1970, p. 493.

[11] E. A. Moelwyn-Hughes, "Physical Chemistry", chap. X, Pergamon Press, London, 1961.

Revue Roumaine de Chimie, 19, 10, 1593–1601 (1974)

L'ACIDE ASCORBIQUE COMME AGENT RÉDUCTEUR. IV[1]

LA CINÉTIQUE DE LA RÉDUCTION DES IONS Pt(II) PAR ACIDE ASCORBIQUE EN PRÉSENCE DES IONS Pb(II)

RALUCA RIPAN, GH. POP et ILEANA POP

Institut de Chimie de Cluj, 65–103, str. Donath, Roumanie

Reçu le 14 mai 1973

On a étudié la cinétique de la réaction de réduction des ions Pt(II) par acide ascorbique, à 40°, dans un milieu d'acide chlorhydrique en présence des ions Pb(II) comme catalyseur. On a établi expérimentalement l'expression de la vitesse de réaction en fonction des facteurs qui l'influencent, selon la formule :

$$v = k[\mathrm{Pb}^{2+}]^2 \frac{[\mathrm{Pt}^{2+}][\mathrm{Asc}]}{[\mathrm{H}^+][\mathrm{Cl}^-]^2} \cdot e^{-\frac{E}{RT}} \qquad \text{(I)}$$

Nous avons abordé l'étude des systèmes redox dans le domaine des métaux précieux pour l'amélioration des méthodes d'analyse et de leur technologie de séparation. Ainsi l'étude de la cinétique de la réaction de réduction du Pd(II) par acide ascorbique [2] à été appliquée à la séparation de l'or, du palladium et du platine des solutions épuisées de l'électrolyse de l'or.[1,3]

Le réduction des ions Pt(II) à l'état de Pt métallique par acide ascorbique a lieu quantitativement conformément à la réaction :

$$\mathrm{Pt}^{2+} + \mathrm{C_6H_8O_6} \xrightarrow{\mathrm{HCl}} \mathrm{Pt} + \mathrm{C_6H_6O_6} + 2\mathrm{H}^+ \qquad \text{(II)}$$

à des concentrations d'acide chlorhydrique plus faibles que 0,07 N.

On a prouvé expérimentalement que la réaction redox (II) a lieu même à des concentrations plus fortes que 0,07 N HCl, en présence des ions Pb(II).

PARTIE EXPÉRIMENTALE

Réactifs nécessaires

1. Solution de $\mathrm{PtCl_2}$ *p.a.* $1{,}46.10^{-1}$ N
2. Solution d'acide ascorbique pur 3.10^{-1} N

---

[1] R. Ripan et Gh. Pop, *Rev. Roumaine Chim.*, **12**, 13 (1967).

[2] R. Ripan et Gh. Pop, *Rev. Roumaine Chim.*, **12**, 7 (1967).

[3] R. Ripan et Gh. Pop, Roum. Pat. 52249, 29.08.1966.

3. Solution d'acétate de plomb ch. p. 2,5 %
4. Solution de chlorure stanneux ch. p. 3,5 M
5. Acide chlorhydrique concentré *p.a.*

La vitesse de la réaction a été suivie en déterminant photocolorimétriquement la concentration du Pt(II), en présence du chlorure stanneux.[4] La température optimale de travail a été de 40° ou plus, étant donné qu'à plus basses températures la vitesse de réaction est trop faible. L'arrêt de la réaction a lieu dans un milieu de HCl 1,5 M à la température ambiante.

RÉSULTATS ET DISCUSSIONS

L'aspect général d'une courbe représentant la variation de la concentration du Pt(II) dans le mélange de réaction en fonction du temps est indiqué par la figure 1.

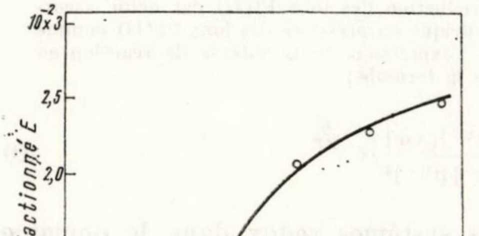

Fig. 1. — Réduction des ions Pt (II) par acide ascorbique dans un milieu de HCl 6.10^{-2} N, à 40°. /Pt^{2+} /= $2,92.10^{-2}$ N ; /Asc/ = 6.10^{-2} N.

On remarque la présence d'une période d'induction, comme dans le cas de la réaction de réduction des ions Pd(II) par l'acide ascorbique.[2] La vitesse de réaction (V) est mesurée par la méthode de tangentes au point où la concentration de ions Pt(II) est arrivée à la moitié de la concentration initiale.

INFLUENCE DE LA CONCENTRATION DES RÉACTANTS SUR LA VITESSE DE RÉACTION

La figure 2 rend l'influence de la concentration des ions Pt(II) sur la vitesse de réaction, à 40°, dans un milieu de HCl 6.10^{-2} N. On a représenté sur l'ordonnée la quantité de Pt(II) qui réagit et sur l'abscisse le temps. On remarque une croissance de la vitesse de réaction, proportionnelle à la croissance de la concentration de Pt(II), un phénomène également illustré par la figure 3.

L'influence de la concentration de l'acide ascorbique sur la vitesse de réaction est indiquée dans les figures 4 et 5. Les données expérimentales attestent une dépendance directement proportionnelle de la vitesse de réaction en fonction de la concentration de l'acide ascorbique.

---

[4] F. E. Beamish, « The Analytical Chemistry of the Noble Metals », vol. 24, Pergamon Press, Oxford, 1966, p. 458.

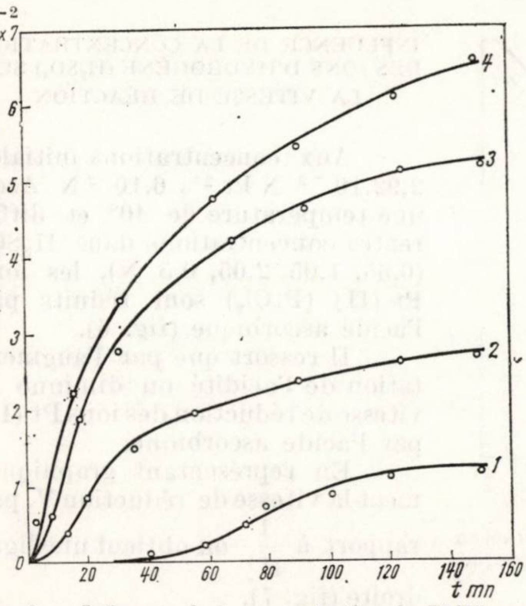

Fig. 2. — Influence de la concentration du Pt(II) sur la vitesse de réaction : dans un milieu de HCl 6.10^{-2} N et /Asc/ = $1,6.10^{-1}$ N ; t = 40°. 1 – 1,46 . 10^{-2}N Pt(II) ; 2 – 2,92.10^{-2} N Pt(II) ; 3 – 5,84.10^{-2} N Pt(II) ; 4 – 7,30.10^{-2} N Pt(II).

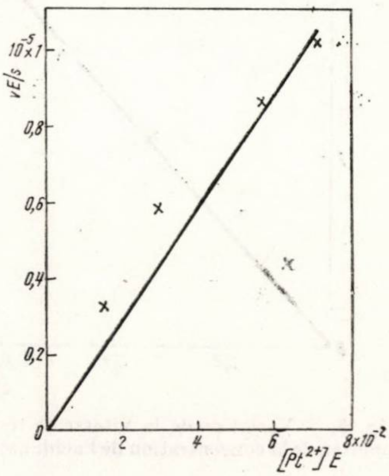

Fig. 3. — Dépendance de la vitesse de réaction de la concentration du Pt (II).

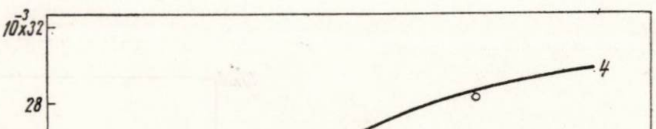

Fig. 4. — Influence de la concentration de l'acide ascorbique (Asc) sur la vitesse de réaction à 40°, dans un milieu de HCl 6.10^{-2} N (Pt^{2+} = 2,92. 10^{-2} N) ; 1 – 0,8.10^{-1} N Asc ; 2 – 1,6.10^{-1} N Asc ; 3 – 3,2.10^{-1} N Asc ; 4 – 6,4.10^{-1} N Asc.

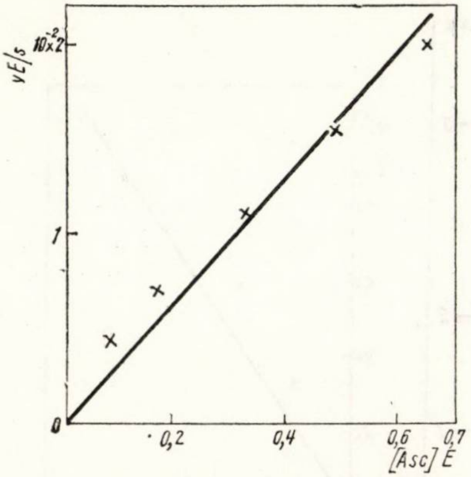

Fig. 5. — Variation de la vitesse de réaction en fonction de la concentration de l'acide ascorbique.

INFLUENCE DE LA CONCENTRATION DES IONS D'HYDROGÈNE (H_2SO_4) SUR LA VITESSE DE RÉACTION

Aux concentrations initiales $2{,}92.10^{-2}$ N Pt^{2+}, 6.10^{-2} N Asc., une température de 40° et différentes concentrations dans H_2SO_4 (0,55, 1,05, 2,05, 0,5 N), les ions Pt (II) ($PtCl_2$) sont réduits par l'acide ascorbique (fig. 6).

Il ressort que par l'augmentation de l'acidité on diminue la vitesse de réduction des ions Pt (II) par l'acide ascorbique.

En représentant graphiquement la vitesse de réduction V, par rapport à $\frac{1}{H^+_-}$ on obtient une ligne droite (fig. 7).

En examinant la figure 7, on peut déduire que la vitesse de réaction est inversement proportionnelle à la concentration des ions d'hydrogène.

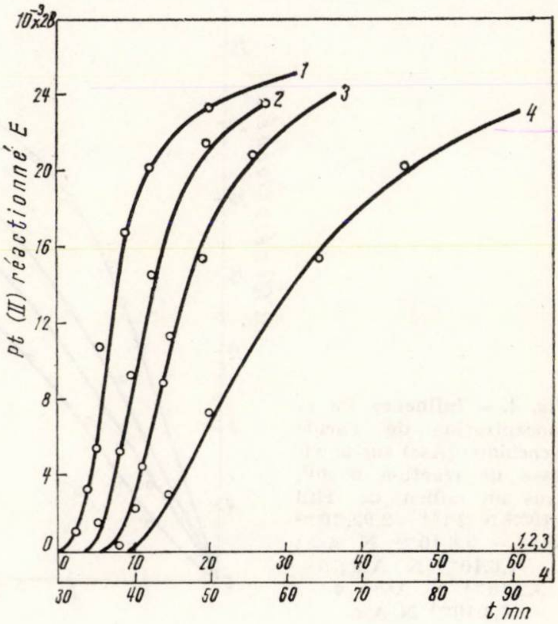

Fig. 6. — Influence de la concentration des ions $H^+(H_2SO_4)$ sur la vitesse de réduction des ions Pt (II) par l'acide ascorbique à 40° ($Pt^{2+} = 2{,}92.10^{-2}$ N ; Asc $= 6.10^{-2}$ N).1 — 0,55 N (H^+) ; 2 — 1,05 N (H^+) ; 3 — 2,05 N (H^+) ; 4 — 5 N (H^+).

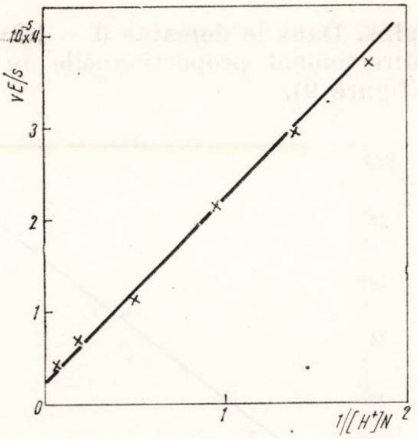

Fig. 7. — Dépendance de la vitesse de réaction, en fonction de l'inverse de la concentration des ions H^+.

INFLUENCE DE LA CONCENTRATION DE L'ACÉTATE DE PLOMB SUR LA VITESSE DE RÉACTION

La figure 8 donne la croissance de la vitesse de réaction d'une manière concomittante à la croissance de la concentration des ions Pb(II) présents dans le mélange de réaction. Mais la croissance a lieu seulement jusqu'à une certaine limite de la concentration de Pb(II), notamment $-6{,}4.10^{-3}$ N. Au-dessus de cette valeur la vitesse de réduction ne croît

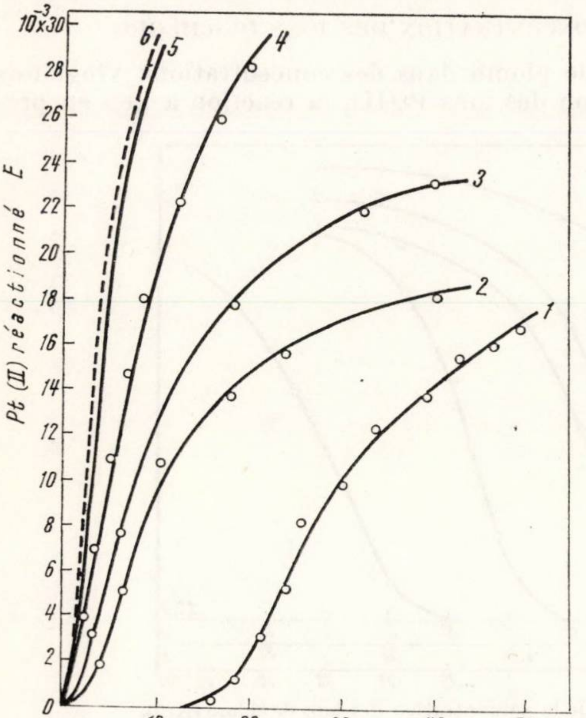

Fig. 8. — Influence de la concentration des ions Pb(II) sur la vitesse de réduction des ions Pt(II) par acide ascorbique à 40°, dans un milieu de HCl 6.10^{-2} N ($Pt^{2+} = 2{,}92.10^{-2}$ N, Asc $= 6.10^{-2}$ N). 1–0 N Pb(II) 2 – $0{,}32.10^{-3}$ N Pb(II) ; 3–$0{,}65.10^{-3}$ N Pb(II) ; 4–$1{,}30.10^{-3}$ N Pb(II) ; 5–$3{,}20.10^{-3}$ N Pb(II) ; 6–$6{,}40.10^{-3}$ N Pb (II).

plus. Dans le domaine 0 — $1{,}3.10^{-3}$ N Pb(II), la vitesse de réaction est directement proportionnelle au carré de la concentration des ions Pb (figure 9).

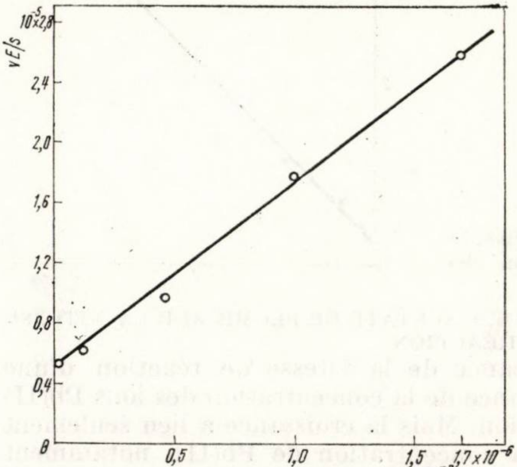

Fig. 9. — Variation de la vitesse de réaction en fonction de la concentration des ions Pb(II).

INFLUENCE DE LA CONCENTRATION DES IONS DE CHLORE

En présence des ions de plomb dans des concentrations vingt fois moindres que la concentration des ions Pt(II), la réaction a lieu en pré-

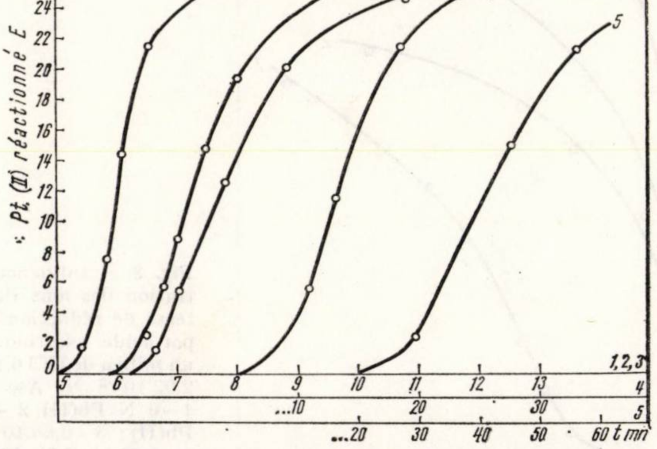

Fig. 10. — Influence de la concentration des ions de chlore (KCl) sur la vitesse de réaction, à 40°. $Pt^{2+} = (2{,}92.10^{-2}$ N ; Asc = $= 6.10^{-2}$ N ; $Pb^{2+} = 1{,}3.10^{-3}$ N ; $H^{+} = 0{,}1$ N). 1—$1{,}2.10^{-1}$ N Cl(I) ; 2—$1{,}7.10^{-1}$ N Cl(I) ; 3—$2{,}4.10^{-1}$ N Cl(I) ; 4 — $3{,}6.10^{-1}$ N Cl(I) ; 5—5.10^{-1} N Cl(I).

sence du chlorure de potassium de dilutions moindres que 0,5 N. La vitesse de la réaction de réduction des ions Pt(II) par l'acide ascorbique est inversement proportionnelle au carré de la concentration des ions de chlore (fig. 10 et 11).

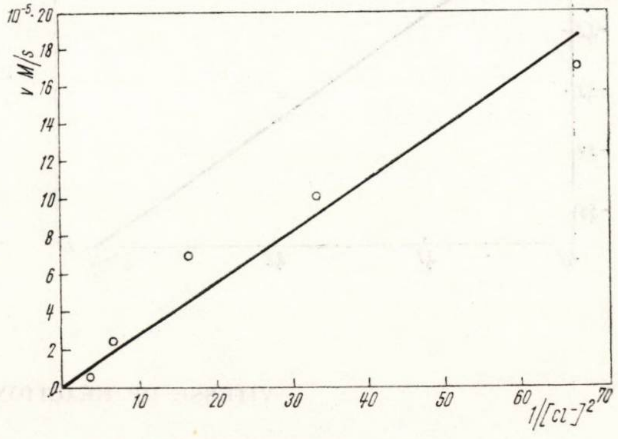

Fig. 11. — Variation de la vitesse de réaction en fonction de $1/Cl^{-2}$.

INFLUENCE DE LA TEMPÉRATURE

En étudiant l'influence de la température sur la vitesse de réaction dans un milieu de Cl^- 0,5 N et H^+ 0,1 N, en présence des ions Pb(II) ($1{,}3.10^{-3}$ N), on observe une croissance de la vitesse (figures 12 et 13) avec la croissance de la température.

La valeur obtenue pour l'énergie d'activation est : $E = 8$ *k*cal/mole.

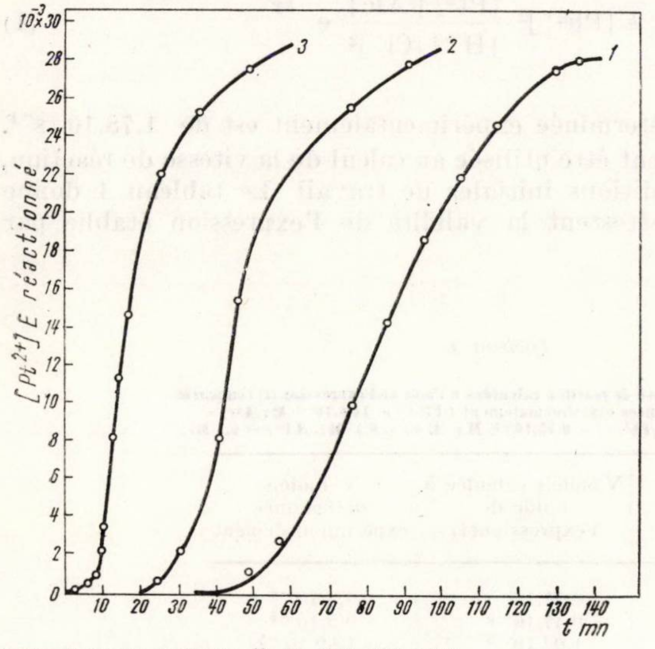

Fig. 12. — Influence de la température sur la vitesse de réaction dans un milieu de Cl^- 0,5 N et H^+ 0,1 N (Pt (II) $= 2{,}92.10^{-2}$ N Asc $=$ 6.10^{-2} N ; Pb (II) $=$ $1{,}3.10^{-3}$ N) ; 1 — 30° ; 2 — 40° ; 3 — 60°.

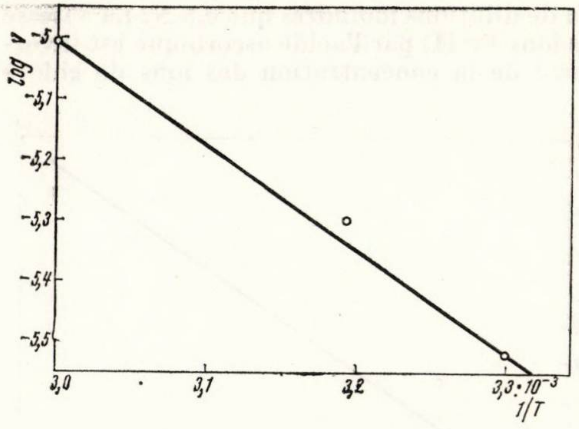

Fig. 13. — Variation de log V en fonction de 1/T.

VITESSE DE RÉACTION

Par l'interprétation des données expérimentales obtenues en étudiant l'influence des différents facteurs sur la vitesse de réduction des ions Pt(II) à l'état de Pt métallique à l'aide de l'acide ascorbique on est arrivé à l'expression suivante, caractérisant quantitativement la valeur v :

$$v = k\,[\mathrm{Pb}^{2+}]^2\,\frac{[\mathrm{Pt}^{2+}][\mathrm{Asc}]}{[\mathrm{H}^+]\,[\mathrm{Cl}^-]^2}\,e^{-\frac{E}{RT}} \qquad \text{(I)}$$

La valeur de k déterminée expérimentalement est de $1{,}78.10^{8}\,s^{-1}$.

L'expression (I) peut être utilisée au calcul de la vitesse de réaction, en connaissant les conditions initiales de travail. Le tableau 1 donne quelques données qui attestent la validité de l'expression établie par nous.

Tableau 1

Valeurs de la vitesse de réaction calculées à l'aide de l'expression (I) comparées à celles déterminées expérimentalement ($/Pt^{2+}/ = 14{,}6.10^{-3}$ M ; $/Asc/ = 29{,}2.10^{-3}$ M; $/Pb^{2+}/ = 0{,}75.10^{-3}$ M; $/H^+/ = 0{,}1$ M; $/Cl^-/ = 0{,}5$ M)

T °K	V mole/s calculée à l'aide de l'expression(I)	V mole/s déterminée expérimentalement
303	$0{,}31.10^{-5}$	$0{,}3.10^{-5}$
313	$0{,}47.10^{-5}$	$0{,}5.10^{-5}$
333	$1{,}02.10^{-5}$	$1{,}02.10^{-5}$

CONCLUSIONS

Les ions Pb(II) accélèrent la réaction de réduction des ions Pt(II) par acide ascorbique dans les limites de concentration $0-6{,}4.10^{-3}$ N.

Le mécanisme de la réaction n'a pas encore été élucidé, et continue à retenir notre attention.

L'étude effectuée par nous est applicable à la séparation du platine d'autres métaux précieux et à la détermination quantitative de celui-ci.

Revue Roumaine de Chimie, **19**, *10*, 1603–1609 (1974)

FERRATE (VI) ION SALTS WITH Ni(II) AND Co(II) TETRAPYRIDINE-TETRAPICOLINE COMPLEX COMBINATIONS

D. NEGOIU* and ALEXANDRA SCHIOPESCU**
* Department of Chemistry University of Bucharest, Spl. Independenței 87, Romania.
** Department of Chemistry and Physics, Institute of Petroleum and Geology, Bucharest, Str. Traian Vuia 6, Romania

Received October 6, 1973

Potassium ferrate (VI) has been prepared by using the corresponding hypochlorite as an oxidizing agent and the corresponding hydroxide as a precipitation medium. By reprecipitations from alkaline solutions of KOH of various concentrations, the potassium ferrate (VI) may be purified. We have prepared the following salts containing ferrate (VI) ion and Ni(II) and Co(II) tetrapyridine — tetrapicoline complex combinations:

$NiPy_4[FeO_4]$; $CoPy_4[FeO_4]$; $Ni(\alpha\text{-pic})_4[FeO_4]$;

$Co(\alpha\text{-pic})_4[FeO_4]$; $Ni(\beta\text{-pic})_4[FeO_4]$; $Co(\beta\text{-pic})_4[FeO_4]$;

$Ni(\gamma\text{-pic})_4[FeO_4]$; $Co(\gamma\text{-pic})_4[FeO_4]$; $Ni(2,6L)_4[FeO_4]$

$Co(2,6L)_4[FeO_4]$ (L-Lutidine)

The infrared spectra of these compounds have been measured and reported.

INTRODUCTION

The preparation of potassium ferrate (VI) is well known.[1-4] The basis of all methods for its preparing is the oxidation of $Fe(OH)_3$ in a strong alkaline medium, the difference between methods consisting in the oxidizing agent utilized and in connection with this, the possibility of obtaining it with a high purity and a good yield.

Among the oxidizing agents, we mention: sodium hypochlorite[1], potassium hypochlorite[2], chlorine bubbled through a suspension of $Fe(OH)_3$ in alkaline medium[3], H_2O_2 in the presence of E.D.T.A. in an alkaline medium. Most of metal ferrates (VI) have been prepared by applying double exchange reactions between potassium ferrate (VI) and salts of different metals.

We prepared the ferrate (VI) ion salts with complex cations. Infrared spectra have been obtained both in potassium ferrate (VI) and complex ammines.

[1] H. J. Hrostowschi and A. B. Scott, *J. Chem. Phys.*, **18**, 105 (1950).
[2] R. Scholder and K. Kraus, *Z. anorg. Chem.*, **268**, 279 (1952).
[3] B. Helferich and V. Lang, *Z. anorg. Chem.*, **263**, 169 (1950).
[4] F. R. Duke and T. W. Haas, *J. Phys. Chem.*, **65**, 304 (1961).

The data obtained are correlated with the existing ones given by Griffith[5], who studying the infrared spectra of the tetrahedral transition metal oxianions reports on the vibrational frequencies corresponding to $[FeO_4]^{2-}$ ion.

EXPERIMENTAL PROCEDURES

The method used for preparing potassium ferrate (VI) consists in the adaptation of the combined method of purifying and preparing the K_2FeO_4.[6]

This method reduces the losses and takes a short time for drying and washing off the compounds.

To obtain the ferrate (VI) ion salts with complex ammines of Ni(II) and Co(II) the corresponding Ni(II) and Co(II) tetrapyridine and tetrapicoline complexes have been prepared using the data from literature. The corresponding salts have been obtained by coupling these compounds with the ferrate (VI) ion.

The reagents used in this procedure were of high purity.

THE GENERAL PROCEDURE FOR PREPARING K_2FeO_4

0.3 mol Carbonate-free sodium hydroxide was added to 30 cm^3 distilled water. The resulting solution was cooled to 273 K with the help of a mixture of ice-sodium chloride.

By continuous stirring chlorine was slowly bubbled through this chilled solution. The chlorine was prepared in an auxiliary installation from $KMnO_4$ and concentrated HCl.

It is necessary to regulate the bubbling speed to a very small one, because an excess of chlorine would lead to a marked decomposition of the potassium ferrate obtained (VI). It is also necessary to regulate the temperature; a sharp rise is not permitted. This is maintained in the range 275 K — 279 K. The operation of chlorination lasts for about 40—45 min. The solution obtained was then made strongly basic by adding 0.9—1.0 mol of solid natrium hydroxide.

While the solution was constantly stirred, the temperature was allowed to rise up to 290 K when the hydroxide was added. The whole mixture was cooled in an ice-sodium chloride bath. After cooling, the precipitated alkali metal chloride was removed by filtration. The solution obtained was again introduced in the ice bath where it was kept for a period of 1/2 h.

After this, 13.5 mmol of pulverized nonahydrated ferric nitrate were added very slowly with continuous stirring. This operation must be performed very slowly, the necessary time was a period of 30—45 min. The temperature must be maintained at about 298 K ± 2 K.

The mixture obtained is rapidly filtered through a filter crucible (G_3 type) with the aid of a vacuum oil pump. In the resulting solutions, some solid potassium hydroxide was added by continuous stirring and maintaining the temperature below 300 K. The potassium ferrate (VI) was precipitated in the solution and recovered by rapid filtration through a filter crucible. The filtration was made with the aid of the same vacuum oil pump. The precipitated potassium ferrate (VI) was purified by dissolving and reprecipitating it in several solutions of potassium hydroxide. The dissolution took place in solutions of KOH 3M, and the reprecipitations in KOH 5M, KOH 6M solutions and saturated solution.

---

[5] W. P. GRIFFITH, *J. Chem. Soc.*, **1966**, 1467.

[6] G. W. THOMPSON, L. T. OCKERMAN and J. M. SCHREYER, *J. Amer. Chem. Soc.*, **73**, 1379 (1951).

The precipitation that has remained was washed on the filter with three 10 cm^3 portions of dry benzene in order to remove the water in excess and then washed with four 15 cm^3 portions of anhydrous ether. The ferrate (VI) sample was stored in a vacuum dessiccator to prevent a slow decomposition due to the traces of water. The results of the analyses using the method of total iron [7] gave good yield of K_2FeO_4.

With view to obtaining the salts containing the ferrate (VI) ion with complex ammines of nickel (II) and cobalt (II) the corresponding Ni(II) and Co(II) tetrapyridine and tetrapicoline compounds [8-10] have been prepared.

To prevent the loss of pyridine, picoline and lutidine, the compounds were maintained in a special container under pyridine α,-β-, γ-picoline and α-lutidine.

The following complex combinations have been prepared in this way :

$NiPy_4(SCH)_2$; $CoPy_4(SCN)_2$; $Ni(\alpha\text{-pic})_4Cl_2$;

$Co(\alpha\text{-pic})_4Cl_2$; $Ni(\beta\text{-pic})_4Cl_2$; $Co(\beta\text{-pic})_4Cl_2$;

$Ni(\gamma\text{-pic})_4Cl_2$; $Co(\gamma\text{-pic})_4(SCN)_2$; $Ni(\alpha\text{-lut})_4Cl_2$; $Co(\alpha\text{-lut})_4Cl_2$

These compounds have been analyzed : metal, halide and nitrogen have been determined. The results obtained correspond to the calculated data.

The procedure to obtain salts of ferrate (VI) ion with Ni(II) and Co(II) tetrapyridine and tetrapicoline complex compounds is explained below.

The tests containing 0.02 freshly prepared K_2FeO_4 which was previously dissolved in 5 cm^3 distilled water have been put in contact with the tests containing 0.03 mol tetrapyridine and tetrapicoline compounds. The potassium ferrate (VI) solution was previously kept in an ice-sodium chloride bath.

The ferrate (VI) ion salts containing Ni(II) and Co(II) complex ammines have been precipitated.
(The tetrapyridine compounds are dissolved in $CHCl_3$ and the tetrapicoline and tetralutidine compounds in dimethylformamide). All the operations were rapidly performed to prevent a possible decomposition of potassium ferrate (VI) with the formation of $Fe(OH)_3$. The resulting

---

[7] J. M. Schreyer, G. W. Thompson and L. T. Ockerman, *Analyt. Chem.*, **22**, 691 (1950).

[8] P. Moore and R. G. Vilkins, *J. Chem. Soc.*, **1964**, 3454.

[9] A. Logan and V. Carle, *J. Amer. Chem. Soc.*, **74**, 5224 (1952).

[10] A. Sinha, *J. Indian Chem. Soc.*, **32**, 414 (1952).

compound was rapidly filtered and dried by washing it with two 10 cm^3 portions of dry benzene in order to remove the excess water and then washed with three 10 cm^3 portions of anhydrous ether.

The same procedure was applied in all the cases. The following salts have been prepared:

$NiPy_4[FeO_4]$; $CoPy_4[FeO_4]$; $Ni(\alpha\text{-pic})_4[FeO_4]$;

$Co(\alpha\text{-pic})_4[FeO_4]$; $Ni(\beta\text{-pic})_4[FeO_4]$; $Co(\beta\text{-pic})_4[FeO_4]$

$Ni(\gamma\text{-pic})_4[FeO_4]$; $Co(\gamma\text{-pic})_4[FeO_4]$; $Ni(\alpha\text{-L})_4[FeO_4]$;

$Co(\alpha\text{-L})_4[FeO_4]$;

These compounds have been analyzed; iron, cobalt, nickel, nitrogen, carbon and hydrogen have been determined. The results obtained are shown in table 1.

For the determination of both cobalt and iron a complexonometric method was applied, using complexon III as complexing agent and salicilic acid as indicator [11].

The infrared spectra of the ferrate (VI) ion salts with Ni(II) and Co(II) complex ammines have been taken using a U.R − 10 Zeiss−Yena spectrometer with the method of diluted samples in KBr disks.

RESULTS AND DISCUSSION

We were able to obtain potassium ferrate (VI) of a purity range from 80−85%, by adapting the combined method of preparing and purifying K_2FeO_4 indicated by Thompson. [2]

We must mention some modifications brought to the procedure already existing in literature.

Thus, the decrease of chlorine bubbling speed through the alkaline solutions, combined with an extension of a chlorination time, led to a decomposition speed decrease of potassium ferrate (VI) which was formed in a previous stage.

All the operations were rapidly conducted and all the filtrations were made by means of a vacuum oil pump. In this way the necessary time for filtration decreased and in conclusion the decompositions existing on the walls of the filtration funnel were diminished. By treating the solution containing the ferrate (VI) ion with solid potassium hydroxide, K_2FeO_4 precipitated immediately. Using for the dissolving and reprecipitating procedure, KOH solutions of rising basicity, the losses in K_2FeO_4 were very much reduced.

Using only benzene and anhydrous ether for drying K_2FeO_4 the decomposition possibilities of the potassium ferrate (VI) are reduced.

---

[11] A. Schiopescu, unpublished.

Table 1

Chemical analysis results

Compd.		Fe %	Ni %	Co %	C %	H %	N %	O %	P.m.	Sum.
$NiPy_4[FeO_4]$	C	11.28	11.86	—	48.53	4.073	11.32	12.93	494.925	99.99
	F	11.31	11.99		46.05	4.10	11.14	—		—
$CoPy_4[FeO_4]$	C	11.27	—	11.902	48.51	4.071	11.31	12.92	495.148	99.98
	F	11.40		12.05	46.00	4.03	11.40	—		—
$Ni(\alpha\text{-pic})_4[FeO_4]$	C	10.13	10.65	—	52.31	5.12	10.16	11.61	551.033	99.98
	F	10.30	10.83		50.30	5.05	10.00	—		—
$Co(\alpha\text{-pic})_4[FeO_4]$	C	10.13	—	10.69	52.29	5.11	10.16	11.60	551.256	99.98
	F	10.28		11.00	51.30	5.03	10.30	—		—
$Ni(\beta\text{-pic})_4[FeO_4]$	C	10.13	10.65	—	52.31	5.12	10.16	11.61	551.033	99.98
	F	10.43	11.00		54.25	5.00	10.40	—		—
$Co(\beta\text{-pic})_4[FeO_4]$	C	10.13	—	10.69	52.29	5.11	10.16	11.60	551.256	99.98
	F	10.35			50.00	5.05	10.55	—		
$Ni(\gamma\text{-pic})_4[FeO_4]$	C	10.13	10.65	—	52.31	5.12	10.16	11.61	551.033	99.98
	F	10.43	10.85		50.05	5.10	10.30	—		—
$Co(\gamma\text{-pic})_4[FeO]_4$	C	10.13	—	10.69	52.29	5.11	10.16	11.60	551.256	99.98
	F	10.40		11.00	50.03	5.05	10.08	—		—
$Ni(\alpha\text{-lut})_4[FeO_4]$	C	9.19	9.66	—	55.39	5.97	9.22	10.54	607.141	99.97
	F	9.40	9.31		53.00	5.80	9.51	—		
$Co(\alpha\text{-lut})_4[FeO_4]$	C	9.19	—	9.70	55.37	5.97	10.53	9.22	607.364	99.88
	F	9.32		9.43	53.21	5.77	10.71	—		—

Those elements would appear when the drying with different alcohols is used (as an effect of oxidizing reactions due to the high oxidation power of K_2FeO_4).

Although the tetrahedral oxianions belonging to nonmetals as ligands in complex combinations have been studied, the oxianions of transitional metals have not been sufficiently studied yet.

This fact is partly due to the possible existence of some oxidizing reactions or of those of precipitate formation in such cases.

Our results regarding the production of some ferrate (VI) ion salts with complex ammines of Ni(II) and Co(II) must be noted.These resulting salts are the first of this class; no other data have been previously reported in literature.

For these salts containing ferrate (VI) ion and complex ammines of Ni(II) and Co(II) studies of infrared spectra have been made. For comparison the infrared spectrum of potassium ferrate (VI) and the infrared spectra of tetrapyridine, tetrapicoline and tetralutidine compounds of Ni(II) and Co(II) have been recorded.

In the case of ferrate (VI) ion [5] the positions of ν_1, ν_3, ν_4, frequencies are 778 cm^{-1}, 800 cm^{-1}, 320 cm^{-1}, and the ratio $\nu_1/\nu_3 = 0.98$.

The frequency ν_2 is not observed and can often coincide with ν_4, or it is not recorded if having a too small intensity. It has to be remarked for the ferrate (VI) ion and transitional metal oxianions too, that the site symmetry is lower than T_d and is closer to C_s[12], as a result, ν_3 would appear in infrared as a triplet ($2A' + A''$) and ν_1 as a singlet (A'). Concerning the ferrate (VI) ion, ν_3 does not appear as a triplet but reported as a singlet at 810 cm^{-1} with a small shoulder at 835 cm^{-1} in good agreement with the recent studies made by Audette. [13]

These characteristic bands corresponding to ferrate (VI) ion have also been found among the bands corresponding to the salts containing ferrate (VI) ion. It has been established that it is possible to record the displacements from the characteristic bands in the case of ferrate (VI) ion when this ion is coupled with complex ammines of Ni(II) and Co(II). The results obtained are shown in table 2.

Table 2

Vibrational frequencies of ferrate (VI) compounds (cm^{-1})

Compound	ν_1	ν_3
K_2FeO_4	790	810 835 (sh)
$[NiPy_4](FeO_4)$	740	800 830 (sh)
$[CoPy_4](FeO_4)$	745	800 840 (sh)
$[Ni(\alpha\text{-pic})_4]$ (FeO_4)	720	860
$[Co(\alpha\text{-pic})_4]$ (FeO_4)	780	870 880
$[Ni(\beta\text{-pic})_4]$ (FeO_4)	780	880
$[Co(\beta\text{-pic})_4]$ (FeO_4)	760	870 880
$[Ni(\gamma\text{-pic})_4]$ (FeO_4)	725	850 860
$[Co(\gamma\text{-pic})_4]$ (FeO_4)	790	860 865 (sh)
$[Ni(\alpha\text{-lut})_4]$ (FeO_4)	720	870
$[Co(\alpha\text{-lut})_4]$ (FeO_4)	770	860 870 (sh)

(sh) — shoulder.

---

[12] P. Tarte and G. Nizet, *Spectrochim. Acta*, **20**, 503 (1964).

[13] R. J. Audette and J. W. Quail, *Inorg. Chem.*, **11**, 1904 (1972).

The contribution made by the Ni(II) and Co(II) tetrapyridine and tetrapicoline complex combinations to the infrared spectra aspect must be discussed.

It is also remarked that in the case of the salts containing ferrate (VI) ion coupled with complex combinations, of Ni(II) and Co(II) the characteristic bands for these complexes have been found.

On the basis of the resulting data, in good agreement with the studies made by Allan[14] for the coordination compounds of pyridine and picoline with transitional metals, it is concluded that the vibrational frequencies of substituted pyridine and picoline do not change significantly when these are coordinated with the metals, so that, the infrared spectra of pyridine and substituted pyridine show a great similarity with the free ligand. Due to the lattice effects or because of the departures from the ideal symmetry, some shifts are split in the complex combination spectrum. The characteristic bands of the pyridine spectrum have been found with small deviations in the complex compound spectra.

The same aspect of the spectrum, common to pyridine, substituted pyridine and tetrapiridine, tetrapicoline and tetralutidine compounds of Ni(II) and Co(II) have been found in the infrared spectra corresponding to the salts of ferrate (VI) ion with the same complex compounds.

The fact that the characteristic frequencies for the $[FeO_4]^{2-}$ ion and for the complex compounds too, are found in the spectrum corresponding to the salts containing ferrate (VI) ion and complex combinations of Ni(II) and Co(II) (the salt's spectrum being a sum of these two spectra) gave us the possibility to characterize the band $[FeO_4]^{2-} - M(Ln)_4$ as a band of a preponderant ionic character.

CONCLUSIONS

Potassium ferrate (VI) has been prepared with good yield by adapting a method previously existing in literature, which underwent some modifications. With the help of the resulting potassium ferrate (VI), ten new salts containing ferrate (VI) ion with tetrapyridine and tetrapicoline complex compounds of Ni(II) and Co(II) have been prepared. The literature has not reported the data referring to the obtention of the salts of ferrate (VI) ion. The salts prepared by us are the first of this kind.

The infrared spectra have been taken and reported.

---

[14] J. R. Allan; *J. Inorg. Nuclear Chem.*, **27**, 1305 (1965).

Revue Roumaine de Chimie, **19**, *10*, 1611–1619 (1974)

CHEMICAL GRAPHS. XXIII[1]

GENERAL CUBIC GRAPHS WITH ONE LOOP, AND HOMOVALENES OR THEIR DERIVATIVES

ALEXANDRU T. BALABAN

Institute of Atomic Physics, P.O.B. 35, Bucharest, Romania

(*Received May 28 1974*)

A table of planar general cubic graphs with one loop and 4, 6, 8, or 10 points is presented. It contains all possible classical constitutional isomers of homovalenes, homovalenones and their ions, or of π-excessive heterocycles with one heteroatom, the total number of points in their reduced structural graphs being 3, 5, 7 or 9 (one point of degree two, the remaining ones of degree three). The table for 11 points is available on request. Examples of such chemical systems are given.

1. INTRODUCTION

The structural theory of organic chemistry can be applied simply to acyclic structures. Therefore, it is taught without the mathematical counterpart of graph theory. The numbers of constitutional isomers of acyclic structures can be found by algorithms which are so simple that any undergraduate is supposed to be able to cope with them. Recently they have been formalized and translated into computer programs.[2]

On the other hand, cyclic structures are much less prone to simple intuitive approaches, as can be observed by trying to find all isomers of quite simple systems such as C_4H_4O or C_5H_8.[3] The general problem is rather difficult [3] and only recently was an analogous computer program devised for this scope.[4]

We tried to apply graph theory to some problems of cyclic structures. In particular, we defined valence-isomerism on graph-theoretical bases,[1,5] and enumerated [*n*]valenes (valence isomers of [*n*]annulenes).*

---

* For short, valence isomers of [*n*]annulenes will be henceforth called [*n*]valenes. The definitions of valence isomerism and reduced structural graphs may be found in ref.[1]. Homovalenes have an extra CH_2 group.

[1] Preceding part, A. T. Balaban, *Rev. Roumaine Chim.*, **19**, 1323 (1974).

[2] J. Lederberg, G. L. Sutherland, B. G. Buchanan, E. A. Feigenbaum, A. V. Robertson, A. M. Duffield and C. Djerassi, *J. Amer. Chem. Soc.*, **91**, 2973 (1969).

[3] A. T. Balaban, *Rev. Roumaine Chim.*, **18**, 635 (1973); erratum, *ibid.*, **19**, 338 (1974).

[4] L. Masinter, N. S. Sridharan, J. Lederberg and D. H. Smith, Stanford Artificial Intelligence Laboratory Memo AIM–216.

[5] A. T. Balaban (ed.), "Chemical Applications of Graph Theory", Academic Press, London, 1975.

Cubic (trivalent) multigraphs are regular graphs where every point (vertex) has degree three. They represent reduced structural graphs of [*n*]valenes.

General graphs can have not only multiple bonds (i.e. circuits with two points) but also loops (i.e. circuits with one point). In a previous paper,[6] an algorithm for the stepwise construction of general cubic graphs was devised, and drawings of the general cubic graphs with $p = 2, 4, 6, 8,$ and 10 points were provided. It was pointed out that by replacing a point joined to one loop by a point of degree two, the general cubic graph of order p is converted into a graph with $p-2$ points of degree three and one point of degree two which may represent a structural reduced graph for valence isomers of heterocycles like oxepine or furan, of carbenium ions $(CH)_{p-1}^{\oplus}$ like tropylium or cyclopentadienylium, of homovalenes like tropylidene or cyclopentadiene, of homovalenones like tropone or cyclopentadienone, etc. In the previous paper, formulas for such systems with 5 and 7 points (carbon atoms or heteroatoms) were presented,[6] including both planar and non-planar graphs (here, planarity is a topological, not geometrical, concept).

The tremendous developments of the last years in this field prompted us to expand in the present paper these tables to include systems with 3—11 points. Throughout this paper we will deal only with connected general cubic graphs with one loop. In order to restrict the number of graphs only to those which may have chemical counterparts, non-planar graphs will be omitted.

2. GENERAL CUBIC GRAPHS WITH ONE LOOP

There are at least four procedures for obtaining all possible general cubic graphs with one loop and p points.

1) The first consists in the algorithm mentioned above, which consists in taking general cubic graphs of order $p-2$ and in applying for each of these the following procedure : on each line or pair of lines mark two new points and join these points by a new line.

2) The second procedure relies on the preceding one, which gives the possibility of obtaining by recurrence the table of cubic multigraphs. If the table of cubic multigraphs with p points is available, then the table of general cubic graphs may be obtained by the following correspondences[6] :

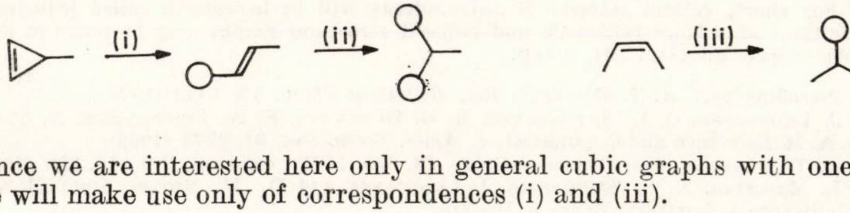

Since we are interested here only in general cubic graphs with one loop, we will make use only of correspondences (i) and (iii).

---

[6] A. T. Balaban, *Rev. Roumaine Chim.*, **15**, 463 (1970).

Expressed in words, these correspondences consist in replacing a double bond by a point joined to a loop. In this process, the number of double bonds is reduced by one (excepting the case of cyclopropenyl rings), and if the double bond is endocyclic the ring size is reduced by one.

The numbers of planar cubic multigraphs are presented in table 1.[6-8] By the above correspondences, those graphs with $\beta \geqslant 1$ will be converted into general cubic graphs with one loop. However, because of correspondence (i), the numbers of general cubic graphs with one loop and $\beta = 0$ will not be equal to those of planar cubic mutigraphs with $\beta = 1$. The numbers of planar general cubic graphs with one loop may be seen in table 2.

Table 1

Planar cubic multigraphs with n points and β double bonds

n \ β	0	1	2	3	4	5	6	Total
4	1	0	1	—	—	—	—	2
6	1	1	2	1	—	—	—	5
8	3	4	5	4	1	—	—	17
10	9	16	22	16	7	1	—	71
12	32	75	112	86	41	10	1	357

Table 2

Planar general cubic graphs with one loop [a]

$p-1$ \ β	0	1	2	3	4	5	Total
3	0	1	—	—	—	—	1
5	1	1	2	—	—	—	4
7	3	6	6	3	—	—	18
9	13	29	32	18	4	—	96
11	62	164	201	126	44	5	502

[a] Table 3 presents the graphs with $p-1 = 3, 5, 7$, and 9 from the present table.

13) Also relying on the table of cubic multigraphs, but with $p-2$ points, there is the following procedure for obtaining the general cubic graphs with p points and one loop : mark on each non-equivalent line a new point and join it to a loop.

4) There is a one-to-one correspondence between general cubic graphs with p points and one loop, and irregular graphs with $p-2$ points of degree three and one point of degree two. In fact, this is how the table of the latter graphs was compiled for $p = 2$ and 4.[3] If the table of the latter graphs is available, this constitutes a fourth approach to the solution of the problem.

For our purpose all four approaches may be useful. For $n = 4-10$, all-approaches give consistent results.

The tables of ref. [6] obtained by the first procedure can be applied directly for $p = 2$, 4, 6, 8, and 10. We will check the results by the fourth procedure [3] for $p = 2$ and 4, and by the second procedure[7] for all p values given above. In addition, the second procedure enables us to compile the table for $p = 12$.[8]

In table 3 the results are presented as a table of irregular graphs with $p-2$ points of degree three and one point of degree two as in the

---

[7] A. T. Balaban, *Rev. Roumaine Chim.*, **11**, 1097 (1966); erratum, *ibid.*, **12**, N⁰ 1, 103 (1967).

[8] A. T. Balaban, *Rev. Roumaine Chim.*, **17**, 865 (1972).

Table 3. **General cubic graphs with one loop (to be imagined attached to the black point) with $p=4,6,8$, and 10 points (including the missing loop-point).**

β p-1	0	1	2	3	4
3		4-1-1-1-0-1			
5	6-1-0-2-3-1	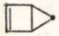 6-1-1-1-1-1	6-1-2-0-0-1 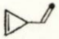 6-1-2-1-0-1		
7	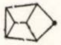 8-1-0-1-3-1 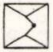 8-1-0-2-1-1 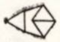 8-1-0-3-1-1	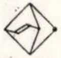 8-1-1-0-3-1 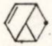 8-1-1-1-1-1 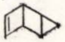 8-1-1-1-2-1 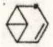 8-1-1-2-1-1 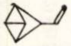 8-1-1-2-3-1 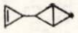 8-1-1-3-1-1	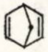 8-1-2-0-0-1 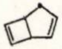 8-1-2-0-1-1 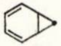 8-1-2-1-0-1 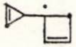 8-1-2-1-1-1 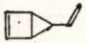 8-1-2-1-1-2 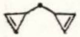 8-1-2-2-0-1	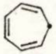 8-1-3-0-0-1 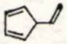 8-1-3-0-0-2 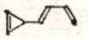 8-1-3-1-0-1	
9	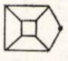 10-1-0-0-4-1 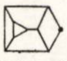 10-1-0-1-2-1 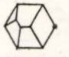 10-1-0-1-3-1 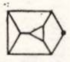 10-1-0-2-0-1 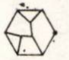 10-1-0-2-1-1 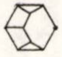 10-1-0-2-2-1 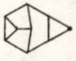 10-1-0-2-2-2 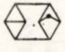 10-1-0-2-4-1 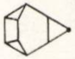 10-1-0-3-1-1 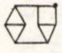 10-1-0-3-2-1 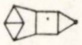 10-1-0-3-2-2 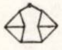 10-1-0-4-2-1 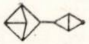 10-1-0-4-4-1	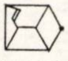 10-1-1-0-2-1 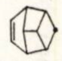 10-1-1-0-3-1 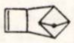 10-1-1-0-3-2 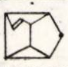 10-1-1-1-0-1 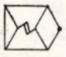 10-1-1-1-1-1 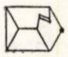 10-1-1-1-1-2 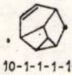 10-1-1-1-1-3 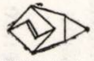 10-1-1-1-1-4 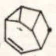 10-1-1-1-2-1 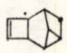 10-1-1-1-2-2 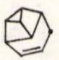 10-1-1-1-2-3 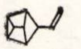 10-1-1-1-2-4 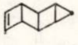 10-1-1-1-3-1 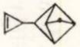 10-1-1-1-5-1 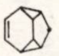 10-1-1-2-0-1 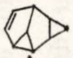 10-1-1-2-0-2 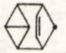 10-1-1-2-1-1 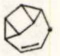 10-1-1-2-1-2 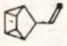 10-1-1-2-1-3 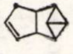 10-1-1-2-1-4 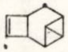 10-1-1-2-2-1 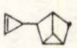 10-1-1-2-2-2 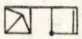 10-1-1-2-4-1 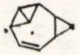 10-1-1-3-1-1 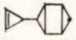 10-1-1-3-1-2 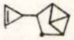 10-1-1-3-1-3 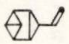 10-1-1-3-1-4 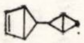 10-1-1-3-2-1 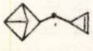 10-1-1-3-3-1	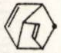 10-1-2-0-0-1 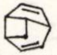 10-1-2-0-1-1 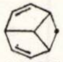 10-1-2-0-1-2 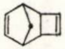 10-1-2-0-1-3 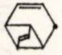 10-1-2-0-1-4 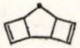 10-1-2-0-2-1 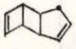 10-1-2-0-2-2 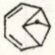 10-1-2-0-3-1 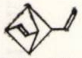 10-1-2-0-3-2 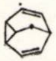 10-1-2-1-0-1 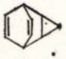 10-1-2-1-0-2 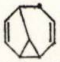 10-1-2-1-0-3 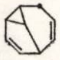 10-1-2-1-0-4 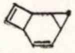 10-1-2-1-1-1 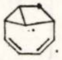 10-1-2-1-1-2 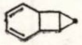 10-1-2-1-1-3 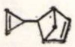 10-1-2-1-1-4 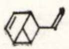 10-1-2-1-1-5 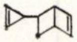 10-1-2-1-2-1 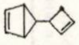 10-1-2-1-2-2 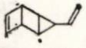 10-1-2-1-2-3 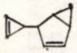 10-1-2-2-0-1 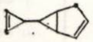 10-1-2-2-0-2 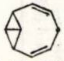 10-1-2-2-1-1 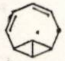 10-1-2-2-1-2 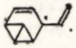 10-1-2-2-1-3 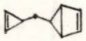 10-1-2-2-1-4 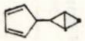 10-1-2-2-1-5 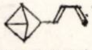 10-1-2-2-3-1 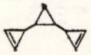 10-1-2-3-0-1 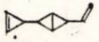 10-1-2-3-1-1 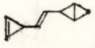 10-1-2-3-1-2	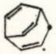 10-1-3-0-0-1 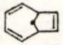 10-1-3-0-0-2 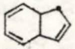 10-1-3-0-0-3 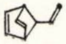 10-1-3-0-0-4 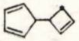 10-1-3-0-1-1 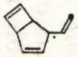 10-1-3-0-1-2 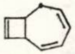 10-1-3-0-1-3 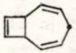 10-1-3-0-1-4 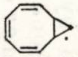 10-1-3-1-0-1 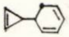 10-1-3-1-0-2 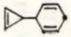 10-1-3-1-0-3 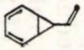 10-1-3-1-0-4 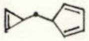 10-1-3-1-0-5 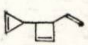 10-1-3-1-1-1 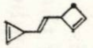 10-1-3-1-1-2 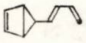 10-1-3-1-1-3 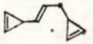 10-1-3-2-0-1 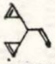 10-1-3-2-0-2	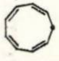 10-1-4-0-0-1 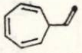 10-1-4-0-0-2 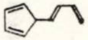 10-1-4-0-0-3 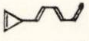 10-1-4-1-0-1

fourth procedure, but it will be understood that this is a simplification of the drawing and that we use the convention that the point of degree two should be imagined as joined to a loop. Accordingly, we will use the notation of the corresponding general cubic graphs.

The notation consists in a string of numbers, giving in order :

— p, the number of points in the general cubic graph with one loop : according to the convention of the preceding paragraph all graphs have in fact $p-1$ points.

— λ, the number of loops (circuits with one point) : in the present paper, this number will be always 1.

— β, the number of double bonds (circuits with two points).

— t, the number of triangles (circuits with three points).

— q, the number of quadrilaterals (circuits with four points).

— s, a serial number, which is 1 unless two or more graphs have the same values for all preceding numbers, when s discriminates among them. In order to make the assignment of s values non-arbitrary, a set of precedence rules * were recently devised :[5,9]

1) The discrimination is to made on the basis of increasing numbers of 5-, 6-, 7-circuits, etc.

There exist algorithms for finding out the number of r-membered rings in a graphs.[10-18] Visually this is easy for $r = 3$ and 4, and increasingly more difficult for $r = 5$, 6, 7 etc. Since, however, in the present paper the determination of the number of larger rings ($r \geqslant 6$) was necessary only occasionally, this was possible without using these algorithms. One can, however, concede that for $p > 12$ their use will be mandatory for this notation system.

2) When the preceding criterion fails, (i.e. for graphs which have the same set of rings) those graphs have precedence when they have the loops attached to :

— exocyclic points over those attached to rings (e.g. I—II, III—IV).

— smaller rings, over those attached to large rings (e.g. V and VI).

---

* In earlier papers,[3 6,8] these rules were not applied.

[9] A. T. Balaban, *Rev. Roumaine Chim.*, **19**, 1185 (1974).

[10] J. T. Welch Jr., *J. Assn. Comp. Mach.*, **13**, 205 (1966).

[11] R. Fugmann, U. Dolling and H. Nickelsen, *Angew. Chem.*, **79**, 802 (1967) ; *Angew. Chem. Internat. Ed.*, **6**, 732 (1967).

[12] G. C. Gottlieb and D. G. Corneil, *Comm. Assn. Comp. Mach.*, **10**, 780 (1967).

[13] N. E. Gibbs, *J. Assn. Comp. Mach.*, **16**, 564 (1969).

[14] K. Paton, *Comm. Assn. Comp. Mach.*, **12**, 514 (1969).

[15] E. J. Corey and W. T. Wipke, *Science*, **166**, 178 (1969) ; E. J. Corey and G. A. Peterson, *J. Amer. Chem. Soc.*, **94**, 460 (1972).

[16] M. Plotkin, *J. Chem. Docum.*, **11**, 60 (1971).

[17] M. Bersohn, *J. C. S. Perkin I*, **1973**, 1239.

[18] G. W. Adamson, J. Cowell, M. F. Lynch, W. G. Town and A. M. Japp, *J.C.S. Perkin, I*, **1973**, 863.

— a point adjacent to a larger number of double bonds or rings, rather than to a smaller number (e.g. VII–VIII, IX–X, XI–XII).

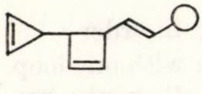

10-1-3-1-1-1
I

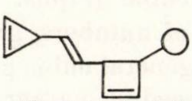

10-1-3-1-1-2
II

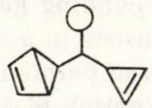

10-1-2-2-1-4
III

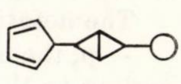

10-1-2-2-1-5
IV

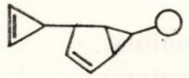

10-1-2-2-0-1
V

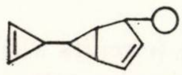

10-1-2-2-0-2
VI

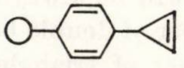

10-1-3-1-0-1
VII

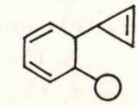

10-1-3-1-0-2
VIII

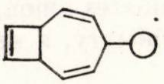

10-1-3-0-1-1
IX

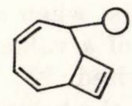

10-1-3-0-1-2
X

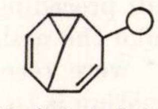

10-1-2-1-0-3
XI

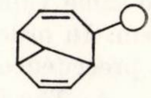

10-1-2-1-0-4
XII

Table 3 contains graphs with $p - 1 = 3$, 5, 7 and 9 points (one of which has degree two since it is imagined to be joined to a loop, and the remaining ones have degree three) with their notations. They are presented as function of p and β, and are arranged in the alphanumerical order of their notations. The table with the 502 graphs with $p-1 = 11$ points is available on request.

3. CHEMICAL COUNTERPARTS

The point of degree two can be a CH_2, CO, $CR^{\oplus}$, $CR^{\ominus}$ group or a heteroatom. A fascinating chemistry is presented by the carbenium ions [19] $(CH)_n^{\oplus}$ with odd n, owing to the readiness with which they rearrange (some of them presenting degenerate rearrangements), and to the unusual structures of some of these ions. The chemistry of these ions was reviewed.[19-21]

Three-membered systems. Only one valence isomer is possible and is illustrated by cyclopropene as a homovalene, cyclopropenone as a homovalenone, or cyclopropenylium as a homovalenium ion. Corresponding heterocycles (acetylene-oxide) are expected to be unstable because of their antiaromaticity.

Five-membered systems. In addition to the examples presented in the previous paper,[6] the photochemical valence isomerization of five-membered heterocycles 6–1–2–0–0–1 involving cyclopropene derivatives 6–1–2–1–0–1 was reviewed, [22] e.g. 2,5-disubstituted furans rearrange photochemically to 2,4-disubstituted furans.[23] A di-π-methane rearrangement[24] would convert 6–1–2–0–0–1 into 6–1–1–1–1–1.

---

[19] G. A. Olah, *Angew. Chem.*, **85**, 183 (1973); *Angew. Chem. Internat. Ed.*, **12**, 173 (1973).

[20] G. Maier, "Valenzisomerisierungen", Verlag Chemie, Weinheim, 1972.

[21] R. E. Leone and P. von R. Schleyer, *Angew. Chem.*, **82**, 889 (1970); *Angew. Chem. Internat. Ed.*, **9**, 860 (1970).

It should be emphasized that table 3 presents only "classical" structures. The structure of the $(CH)_5^{\oplus}$ cation was predicted theoretically by Stohrer and Hoffmann [25] to be, however, reminiscent of pentaborane (tetragonal pyramid XIII) rather than any of the classical structures XIV–XVII. This unusual structure XIII for electron-deficient compounds is calculated to have lower energy than "classical" structures XIV–XVI. This prediction was confirmed both experimentally[26] and theoretically using different methods for the calculation of energies[27,28] (no calculation has, however, estimated the energy of the vinylic cation XVII, which was also omitted in other reviews[21]).

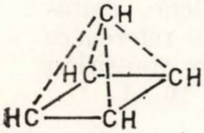

XIII·

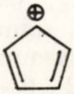

6-1-2-0-0-1

XIV

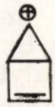

6-1-1-1-1-1

XV

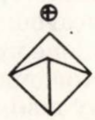

6-1-0-2-3-1

XVI.

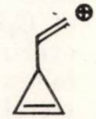

6-1-2-1-0-1

XVII.

Seven-membered systems. Leone and Schleyer[21] discussed the following $C_7H_7^{\oplus}$ cations : 8–1–0–1–3–1, 8–1–0–2–1–1, 8–1–2–0–0–1, 8–1–2–0–1–1, and 8–1–3–0–0–1.

The thermal valence isomerization of cycloheptatriene–norcaradiene was discussed at length in Maier's monograph,[20] which also includes heterocyclic analogues such as azepine–benzenimine,[29] or diazepine–diazanorcaradiene.[30]

Graphs from table 3 may also be useful in rationalizing the carbon scrambling on electron impact in C_7H_8, C_5H_6, or their heterocyclic congeners.[31] Meyerson's original observation on the appearance of tropylium in mass spectra of benzyl derivatives [32] was subsequently substantiated

[22] A. Lablache-Combier and M. A. Rémy, *Bull Soc. chim. France*, **1971**, 679.

[23] E. E. van Tamelen and T. H. Whitesides, *J. Amer. Chem. Soc.*, **93**, 6129 (1971).

[24] S. H. Hixson, P. S. Mariano and H. E. Zimmerman, *Chem. Rev.*, **73**, 531 (1973).

[25] W. D. Stohrer and R. Hoffmann, *J. Amer. Chem. Soc.*, **94**, 1661 (1972).

[26] S. Masamune, M. Sakai, U. Ona and A. H. Jones, *J. Amer. Chem. Soc.*, **94**, 8956 (1972).

[27] M. J. S. Dewar and R. C. Hadson, *J. Amer. Chem. Soc.*, **95**, 5836 (1973).

[28] H. Kollwar, H. O. Smith and P. von R. Schleyer, *J. Amer. Chem. Soc.*, **95**, 5834 (1973);
W. J. Hehre and P. von R. Schleyer, *ibid.*, **95**, 5837 (1973).

[29] W. D. Stohrer, *Chem. Ber.*, **106**, 970, 984 (1973).

[30] M. Nastasi and J. Streith, *Bull. Soc. chim. France* (2), **1973**, 635.

[31] R. A. Davidson and P. S. Skell, *J. Amer. Chem. Soc.*, **95**, 6843 (1973).

[32] S. Meyerson, *Appl. Spectrosc.* **9**, 120 (1955); *Record Chem. Progr.*, **26**, 257 (1965); H. M. Grubb and S. Meyerson, in "Mass Spectromety of Organic Ions" (F.W. Mc. Lafferty ed.), Academic Press, New York, 1973, chapter 10; P. N. Rylander and S. Meyerson, *J. Amer. Chem. Soc.*, **78**, 5799 (1956); S. Meyerson, P. N. Rylander, E. L. Eliel and J. D. Mc. Collum, *ibid.*, **81**, 2606 (1959); P. N. Rylander, S. Meyerson and H. M. Grubb, *ibid.*, **79**, 842 (1957); S. Meyerson, H. Hart and L. C. Leitch, *ibid.*, **90**, 3419 (1968).

by many additional data,[33] but the mechanism of the scrambling is not yet clear.[34]

Photochemical rearrangements of various C_7H_8 derivatives[35] were investigated.

The valence isomers of the unusually stable carbene resulted by loss of a proton from tropylium are not to be found in table 3 because some of these valence isomers have quaternary carbons corresponding to points of degree four.[36]

Nine-membered systems. In Leone and Schleyer's review[21] the following $C_9H_9^{\oplus}$ cations were discussed: 10−1−0−0−4−1, 10−1−0−2−5−1, 10−1−2−0−0−1, 10−1−2−1−0−1, 10−1−3−0−0−1, 10−1−3−0−0−2, 10−1−3−0−0−3, and 10−1−4−0−0−1. Some newer data on these cations exist.[37−39] Heterocyclic analogues (heteronins and their valence isomers) were reviewed by Anastassiou.[40] Valence isomers of C_9H_{10} hydrocarbons or their derivatives (e.g. barbaralene, deltacyclane, barbaralone were reviewed by Maier,[20] and some newer references follow.[41−43] Photochemical and catalytical interconversions (by transition metal ions, or by acids) between systems 10−1−2−0−2−1, 10−1−1−2−2−1 and 10−1−0−0−4−1 are known.[44]

Goldstein and Hoffmann's predicted bicycloaromaticity[45] in bicyclic delocalized systems caused by frontal overlap of π-orbitals was experimentally confirmed by the stabilization of an anion[46] corresponding to graph 10−1−3−0−0−1.

Eleven-membered systems. The same incentive, experimental proof for bicycloaromaticity, led **Goldstein** to prepare and protonate several ketones $C_{11}H_{10}O$ (XVIII–XX).[47]

---

[33] M. K. Hoffmann and J. C. Wallace, *J. Amer. Chem. Soc.*, **95**, 5064 (1973); A. Siegel, *ibid.*, **96**, 1251 (1974).

[34] M. Levsen, F. W. Mc. Lafferty and D. M. Jerina, *J. Amer. Chem. Soc.*, **95** 6532 (1973).

[35] L. A. Paquette and L. M. Leichter, *J. Amer. Chem. Soc.*, **92**, 1765 (1965).

[36] R. C. Joines, A. B. Turner and W. M. Jones, *J. Amer. Chem. Soc.*, **91**, 7754 (1969); W. M. Jones and C. L. Ennis, *ibid.*, **91**, 6391 (1969); J. A. Myers, R. C. Joines and W. M. Jones, *ibid.*, **92**, 4740 (1970); T. Mitsubashi and W. M. Jones, *ibid.*, **94**, 677 (1972); G. G. Vander Stouw, A. R. Kraska and H. Schechter, *ibid.*, **94**, 1655 (1972).

[37] A. G. Anastassiou and R. C. Griffith, *J. Amer. Chem. Soc.*, **93**, 3083 (1971); A. G. Anastassiou and E. Yakali, *Chem. Commun.*, **1972**, 92.

[38] P. Ahlberg, *Chem. Scripta*, **2**, 231 (1972).

[39] D. S. Sanders and H. Schechter, *J. Amer. Chem. Soc.*, **95**, 6858 (1973).

[40] A. G. Anastassiou, *Accounts Chem. Res.*, **5**, 281 (1972).

[41] M. J. S. Dewar and W. W. Schoeller, *ibid.*, **93**, 1481 (1971); R. Hoffmann and W. D. Stohrer, *J. Amer. Chem. Soc.*, **93**, 6941 (1971).

[42] P. K. Frerman, D. M. Balls and J. N. Blazevich, *J. Amer. Chem., Soc.*, **93**, 2051 (1971).

[43] J. E. Baldwin, A. H. Andrist and R. K. Prinschmidt Jr., *J. Amer. Chem. Soc.*, **94**, 5845 (1972); H. Tsuruta, T. Kumagai and T. Mukai, *Chem. Letters* (*Japan*), **1973**, 933.

[44] R. L. Cargill, T. Y. King and A. B. Sears, *J. Org. Chem.*, **36**, 1423 (1971); K. Yano, *Tetrahedron Letters*, **1974**, 1861.

[45] M. J. Goldstein, *J. Amer. Chem. Soc.*, **89**, 6357 (1967); M. J. Goldstein and R. Hoffmann, *ibid.*, **93**, 6193 (1971).

[46] M. J. Goldstein and S. Natowsky, *J. Amer. Chem. Soc.*, **95**, 6451 (1973); M. V. Moncur and J. B. Grutzner, *ibid.*, **95**, 6449 (1973).

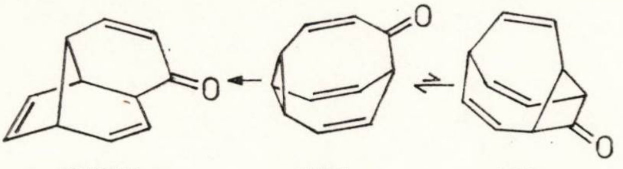
XVIII XIX XX

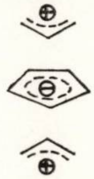
XXI

The stability of several cations $C_{11}H_{11}^{\oplus}$ is in agreement with theoretical predictions.[48] However, one isomer of $C_{11}H_{11}$ was found to present an unexpected NMR spectrum which could be interpreted [48] as an "organic sandwich complex" XXI. Hydrocarbons $C_{11}H_{12}$ are also known.[49]

Larger systems. Annulenones with 13,[50] or more, carbon atoms were prepared.[51] Little is yet known, however, about their valence isomers or the corresponding hydrocarbons.

---

[47] M. J. Goldstein and S.–H. Dai, *J. Amer. Chem. Soc.*, **95**, 933 (1973); M. J. Goldstein, R. C. Krauss and S.–H. Dai, *ibid.*, **94**, 680 (1972).

[48] M. J. Goldstein and S. A. Kline, *J. Amer. Chem. Soc.*, **95**, 935 (1973).

[49] J. F. Monthory, *Diss. Abstr.*, **33** B, 639 (1972).

[50] G. M. Pilling and F. Sondheimer, *J. Amer. Chem. Soc.*, **93**, 1970, 1977(1971).

[51] F. Sondheimer, *Pure Appl. Chem.*, **28**, 331 (1971); *Accounts Chem. Res.*, **5**, 81 (1972).

Revue Roumaine de Chimie, 19, 10. 1621–1629 (1974)

STUDIES IN THE *s*-TRIAZINE FIELD (NEW SERIES). XV*.

THE PROTONATION EQUILIBRIA AND INDICATOR BEHAVIOUR OF E-1,3-DIMETHYL-6-(*p*-X-β-STYRYL)-2,4-DIOXO-1H, 3H-1,3,5-TRIAZINES IN 50 VOL% AQUEOUS-ETHANOLIC SOLUTIONS IN THE PRESENCE OF SULPHURIC ACID

M. SAFTA and G. OSTROGOVICH

Laboratory of Organic Chemistry, Polytechnic Institute, Timişoara,
str. Bocşa 6, Romania

Received December 21, 1973

The pK_a values and the H'_0 acidity function scale were determined by the UV- and Vis.-spectrophotometric method, for the compounds and the solvent-system, specified in the title. The determinations were performed with a satisfactory accuracy due to the fact that at a H_2SO_4 concentration higher than the minimum value necessary for the complete protonation of the indicators, there exists a linear relationship with a finite slope between $C_{H_2SO_4}$ and the medium effect. This fact allows the determination of the log $C_{BH^{\oplus}}/C_B$ value by the complete protonation. It is to be observed that the scale of the function H'_0 of these systems is practically identical with that of the azo-compounds, in the same media containing $HClO_4$, and therefore coincident with the scale of the function H_0 of the nitroaniline standards. This fact proves that the β-styryl-s-triazine compounds have a typical Hammett base behaviour.

In a previous paper [2] we studied qualitatively by the spectrophotometric method in the ultraviolet and visible region the protonation of the fundamental unmethylated compounds. These precursor compounds were insufficiently soluble even in neutral or acidic 50% vol. aqueous-ethanol medium, a feature which made impossible the exact determination of their basicity and also the quantitative characterization of their behaviour as indicators.

For this purpose (as well as for a study concerning the activity of the methyl group from the mother compound, 6-methyl-2,4-dioxo-1H,

---

*) Part XIV[1]. A lack of attention caused several older papers from this series not to be numbered in their order of publication. This fact determined an error of numbering which affects three of the published notes, even those by the present authors. Thus, the paper published by us as the IVth in *Rev. Roumaine Chim.*, **15**, 799 (1970), is actually the Vth since number IV belongs in fact, to the work which appears in *Tetrahedron* **24**, 2701 (1968) (authors G. Ostrogovich, R. Bacaloglu and Elwine Fliegl). Similarly, the order numbers of the papers published by us in *Rev. Roumaine Chim.*, **17**, 2043 and 2055 (1972) as the Vth and the VIth are, in fact, the XIth and the XIIth.

[1] Part XIV., M. Safta and G. Ostrogovich, *Bul. St. Tehn. Inst. Politeh. Timişoara, Ser. chim.*, (1974), under press.

[2] G. Ostrogovich and M. Safta, *Rev. Roumaine Chim.*, **15**, 799 (1970).

3H-1, 3, 5-triazine and their N-mono-, di- and trimethylated compounds[3]) we have synthetized the 1,3-dimethylated analogous,[4] which are the subject of this paper and which, of course, are more soluble in 50% vol. aqueous ethanol.

The present paper gives the basicity measurements which were performed on these compounds, as entirely analogous substances with the initial ones, from which they differ only by the aprotic character of the *s*-triazinic part of the molecule. Since the basicity of these substances is relatively weak, the characterization of their indicator behaviour imposed an extension of the spectrophotometric studies on some more acidic solutions and, therefore, the determination of the H_0 function after the method of Hammett-Deyrup,[5] in medium conditions, which are also revealed by the title.

Although the actual literature data offer many examples for the determination of some H_0 functions in alcoholic or aqueous-alcoholic solutions,[6,7] we have found only a single case in which the authors used as a solvent a 50% volume aqueous-ethanol. We refer to the works of Vetesnik *et al.*,[8] who studied from this point of view a series of 2-hydroxy-azobenzenic indicators (besides the 2- and 4-nitroaniline) but towards perchloric acid. They found, in accordance with the literature data of Jaffé *et al.*[9,10] concerning some aromatic azo-derivatives in aqueous-ethanol 20% vol. as compared to H_2SO_4, that all the studied compounds, and all the primary nitranilinic standards in the same solvent present a satisfactory parallelism of the dependence log $C_{BH\oplus}/C_B$ *versus* $C_{H_2SO_4}$.

It is known that the verification of this parallelism represents the primordial condition for the construction of any function of acidity H_0, that is for the anchorage of the determined function in the case of a given organic substratum to the $pK_{BH^\oplus}$ value of the primary nitranilinic standard (which was determined at well defined values of pH in the same solvent).

For underlining the character of the Hammett bases (H_0 indicators) of the azoic compounds and at the same time the fact that the determinations were performed in aqueous-alcoholic solvents, the above mentioned authors have denoted the functions thus obtained with the symbol H_0', a notation which, as will be seen in the following, is justified in the case of our compounds too.

The protolytic equilibrium, for which we have determined the $pK'_{BH^\oplus}$ values and the acidity function H_0' in ~50% vol. aqueous ethanolic media with H_2SO_4, is the following :

---

[3] M. Safta, F. Chiraleu, A. T. Balaban and G. Ostrogovich, *Rev. Roumaine Chim.* **17**, 2055 (1972).

[4] G. Ostrogovich and M. Safta, *Rev. Roumaine Chim.*, **17**, 2043 (1972).

[5] L. P. Hammett and A. L. Deyrup, *J. Amer. Chem. Soc.*, **54**, 2721 (1932).

[6] M. A. Paul and A. F. Long, *Chem. Rev.*, **57**, 1 (1957).

[7] C. H. Rochester, "Acidity Functions", Academic Press, London, New York, 1970, pp. 217.

[8] P. Vetesnik, K. Rotschein, J. Socha and M. Vecera, *Coll. Czech. Chem. Comm.*, **34**, 1087 (1969); **35**, 3128 (1970).

[9] H. H. Jaffé and R. W. Gardner, *J. Amer. Chem. Soc.*, **80**, 319 (1958).

[10] Si-Jung Yeh and H. H. Jaffé, *J. Amer. Chem. Soc.*, **81**, 3274 (1959).

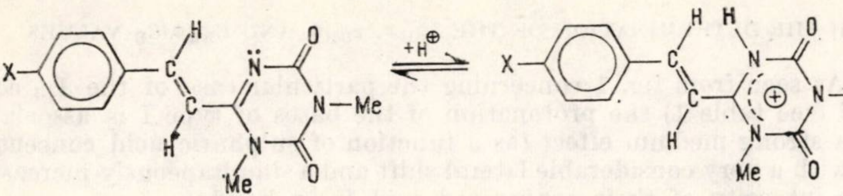

I_B $I_{BH^\oplus}$

The applicability of the Hammett equation (1) concerning the determination of pK values by the spectrophotometric method

$$\mathrm{pK} = H_0 + \log \frac{C_{BH^\oplus}}{C_B} = H_0 + \log \frac{\varepsilon - \varepsilon_B}{\varepsilon_{BH^\oplus} - \varepsilon} \qquad (1)$$

was connected to the properties of the indicator substratum, that is by the following conditions :

1) It must be a suitable region of the spectrum in which the absorbances of the B and $BH^\oplus$ species are different enough.

2) Their absorbance curves must be independent of the concentration of the mineral acid in the medium.

As the first of these requirements is satisfactorily achieved in most cases, it is known that the latter condition is seldom completely achieved, especially when the $BH^\oplus$ species exhibits a high intensity band.[11-12]

In several cases, for a small lateral displacement of this band, it was proved the possibility to perform some corrections.[13,14] Several methods for the determination of the $\lambda_{BH^\oplus}$ and $\varepsilon_{BH^\oplus}$ values[12-22] were proposed, but a few number of these ones solved the problem of the medium effects which implied not only a lateral displacement of the main band $BH^\oplus$, but also a more or less pronounced shift in the intensity of the $\varepsilon_{max.BH^\oplus}$ values parallel with the increasing of the mineral acid concentrations.[20-22]

---

[11] L. A. Flexser, L. P. Hammett and A. Dingwall, *J. Amer. Chem. Soc.*, **57**, 2103 (1935).

[12] D. S. Noyce and M. J. Jorgenson, *J. Amer. Chem. Soc.*, **82**, 4312 (1962).

[13] E. A. Braude and E. S. Stern, *J. Chem. Soc.*, **1948**, 1976.

[14] V. Gold and B. W. Hawes, *J. Chem. Soc.*, **1951**, 2102.

[15] J. C. D. Brand, *J. Chem. Soc.*, **1950**, 996.

[16] J. C. D. Brand, W. C. Borning and M. B. Thornley, *J. Chem. Soc.*, **1952**, 1374.

[17] W. M. Schubert and H. K. Latourette, *J. Amer. Chem. Soc.*, **74**, 1829 (1952).

[18] W. M. Schubert, J. Donohue and J. D. Gardner, *J. Amer. Chem. Soc.*, **76**, 9 (1954).

[19] C. T. Davis and T. A. Geissman, *J. Amer. Chem. Soc.*, **76**, 3507 (1954).

[20] Yu. L. Haldna, *Reaktsionnaya Sposobnost Organicheskikh Soedinenii*, **1** (2), 180 (1964).

[21] R. L. Reeves, *J. Amer. Chem. Soc.*, **88**, 2240 (1966).

[22] A. R. Katritzky, A. J. Waring and K. Yates, *Tetrahedron*, **19**, 4651 (1953).

RESULTS AND DISCUSSIONS

a) THE DETERMINATION OF THE $\lambda_{BH^{\oplus}}$, $\varepsilon_{BH^{\oplus}}$ AND $C_{BH^{\oplus}}/C_B$ VALUES

As seen from fig. 1 concerning the particular case of the I_{4B} compound (see table 1) the protonation of the bases of type I is associated with a strong medium effect (as a function of sulphuric acid concentration) with a very considerable lateral shift and a simultaneously increasing of the intensity of their conjugated acid $I_{4BH^{\oplus}}$ band.

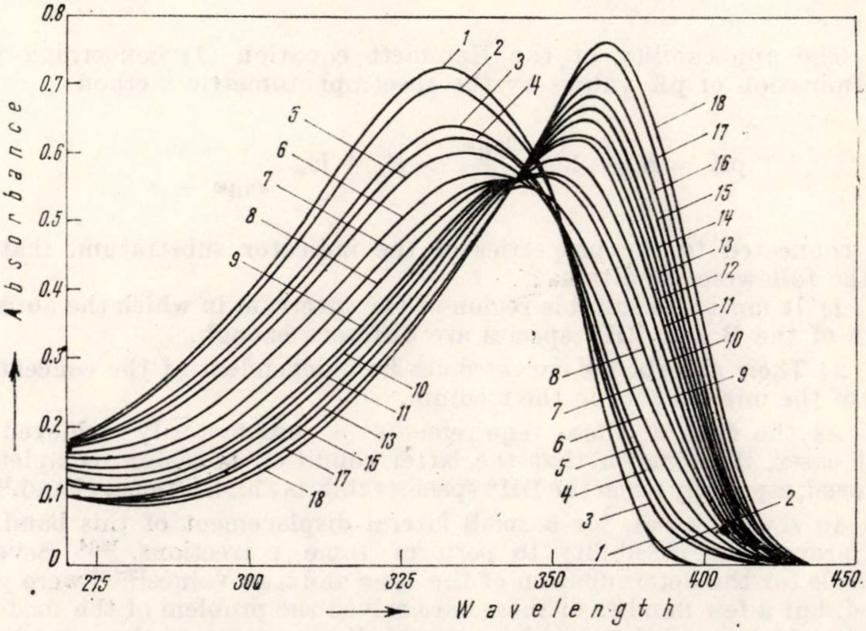

Fig. 1. – The changes of the spectra for compound $I_{4B}{}^{\oplus}$ and $I_{4BH}{}^{\oplus}$(see table 1) as a function of $C_{H_2SO_4}$ in a 50 % vol. aqueous-ethanol ($C_{I_{4B}} = 2.5.10^{-5}$ molar, cell width 1 cm) :

Curve N°	1	2	3	4	5	6	7	8	9	10	11	12	13	14	15	16	17	18
$C_{H_2SO_4}$ (val/l)	0	0.1	0.5	0.8	1.0	1.5	2.0	2.5	3.0	3.5	4.0	5.0	6.0	7.0	8.0	9.0	10	12.0 N

Consequently, for achieving the correct values of the $\lambda_{BH^{\oplus}}$ and $\varepsilon_{BH^{\oplus}}$ we used the Haldna method[20] which involves the plotting of the dependence $\varepsilon_{max.BH^{\oplus}} = f(C_{acid})$ not only in the limit of the titration curve but also in the range of the concentrations higher than the minimum value for the complete protonation. This makes possible the determination of the last one due to the fact that at this value the sinusoidal titration curve becomes linear with a finite slope. This fact allows to find the point indicating the beginning of the linear dependence and consequently to choose – from the extinction curves which were successively recorded at much higher concentration – the curve, which characterizes the $BH^{\oplus}$ species at the moment at which the B species disappear.

From the equation (1) it is evident that the most exact determination of the $C_{BH^{\oplus}}/C_B$ ratio can be achieved in the wavelength region in which the difference between $\varepsilon_{BH^{\oplus}}$ and ε_B is maximum. From fig. 1 results that in the respective particular case, this region is centered around $\lambda = 380$ nm, even bigger than $\lambda_{max.}$ of the most intensive band which we have recorded for the conjugated acid $I_{4BH^{\oplus}}$ at a value $C_{H_2SO_4} = 12$ N.

Fig. 2 presents, for the same particular case as fig. 1, the graphic aspect of the above mentioned procedure after Haldna (l.c.) that is the variation of the absorbance as a function of $C_{H_2SO_4}$ at 380 nm.

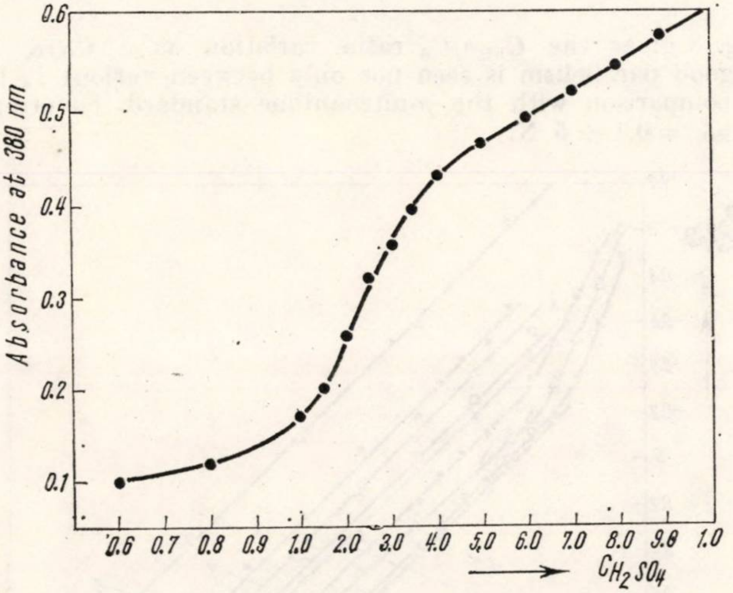

Fig. 2. – The titration curve of the base I_{4B} at 380 nm in a 50% vol. aqueous-ethanol ($C_{I_{4B}} = 2.5 \cdot 10^{-5}$ molar, cell width 1 cm).

It may be observed that the linearization of the curve begins at the moment when the H_2SO_4 concentration becomes 4N, that is, beginning with curve N° 11 from fig. 1. The accurate analysis of the phenomena and the relations performed by Haldna outline that the linearization is not other than the expression of a monotonous variation in the hydrated state of the $BH^{\oplus}$ species.

b) THE DETERMINATION OF THE pKa VALUES AND OF THE H_0' SCALE

The previous determinations with informative purposes have shown that the indicator with the most close basicity to our compounds is *p*-nitroaniline (*p*—NA) which therefore we choose as a reference indicator. The pKa value of their conjugated acid in a 50% vol. aqueous-ethanol was determined by Vetesnik [23] which found $pK_{(p-NA)} = +0.239$ at 20°C.

The estimation of the $(pK_{BH^+})_{I_n}$ values is based on the equation :

$$(pK_{BH^+})_{p-NA} - (pK_{BH^+})_{I_n} = \log\left(\frac{C_{BH^+}}{C_B}\right)_{p-NA} - \log\left(\frac{C_{BH^+}}{C_B}\right)_{I_n} + \log\left(\frac{f_B}{f_{BH^+}}\right)_{I_n}\left(\frac{f_{BH^+}}{f_B}\right)_{p-NA} \quad (2)$$

Fig. 3 gives the $C_{BH^\oplus}/C_B$ ratio variation as a $C_{H_2SO_4}$ function. A very good parallelism is seen not only between various I_n bases but also in comparison with the *p*-nitroaniline standard, covering all the field $C_{H_2SO_4} = 0.1 \div 5$ N.

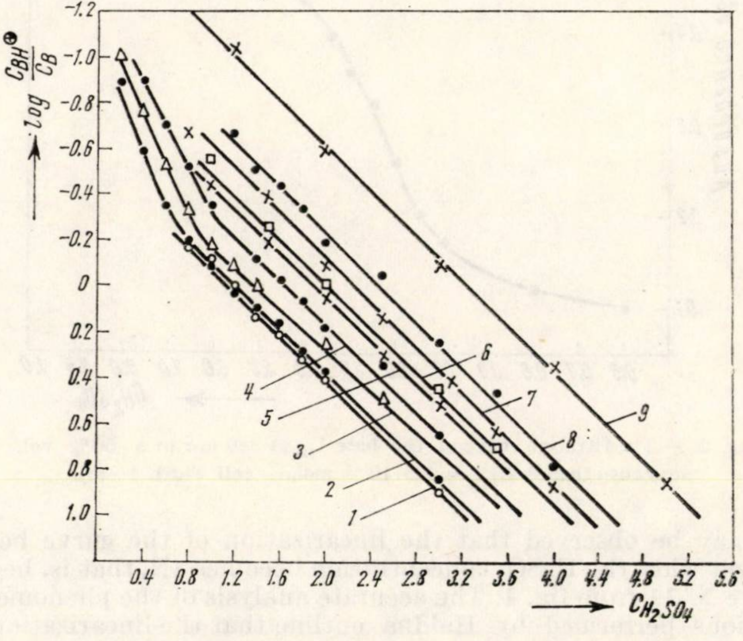

Fig. 3.— The functions log $(C_{BH^\oplus})/C_B$ *versus* $C_{H_2SO_4}$ for variously indicators I_n and for the *p*-NA standard :

Straight	1	2	3	4	5	6	7	8	9
X	*p*-OH	Standard	*p*-OCH_3	*m,p*-O-CH_2-O-	*p*-CH_3	*p*-$CH(CH_3)_2$	*p*-H	*p*-Cl	*p*$\overset{\oplus}{N}Me_3$

---

[23] P. Vetesnik, private communication.

Because this aspect denotes that both species B and $BH^{\oplus}$ possess the same activity coefficients it is right to consider that the latter term of the second member of the equation (2) is zero. Therefore the equation which can be used for the calculation is:

$$(pK_{BH^+})_{p-NA} - (pK_{BH^+})_{I_n} = \log\left(\frac{C_{BH^+}}{C_B}\right)_{p-NA} - \log\left(\frac{C_{BH^+}}{C_B}\right)_{I_n} \cdot \quad (3)$$

The $(pK_{BH^+})_{I_n}$ values calculated in this way are presented in table 1. Introducing these values in equation (1) the $(H'_0)_{I_n}$ values are obtained (see table 2).

Table 1

pk_a values for some E-1, 3-dimethyl-6-(p-X-β-styryl)-2,4-dioxo-lH, 3H-1,3,5-triazine indicators in a 50 % vol. aqueous-ethanol at 25 ± 1°C

N°	Indicator X	$pK_a \pm 0.02$	λ anal. (nm)
I_{1B}	$p-OH$	+ 0.25	410
I_{2B}	$p-OCH_3$	+ 0.12	410
I_{3B}	$m, p-O-CH_2-O-$	− 0.01	430
I_{4B}	$p-CH_3$	− 0.10	380
I_{5B}	$p-CH(CH_3)_2$	− 0.15	370
I_{6B}	H	− 0.26	360
I_{7B}	$p-Cl$	− 0.38	360
I_{8B}	$p-\overset{\oplus}{N}(CH_3)_3$	−0.77	330

Table 2

Dependence of $(H'_0)\,I_n$ on the concentration of sulphuric acid in a 50 % vol. aqueous-ethanol

Echiv./l H_2SO_4	H'_0	Indicators* I_n n
0.2	+1.40	2
0.4	+1.010	2, 3
0.6	+0.735	2, 3, 5
0.8	+0.475	2, 3, 5, 6
1.0	+0.325	1 − 6
1.2	+0.238	1 − 7
1.4	+0.140	1 − 7
1.6	+0.051	1 − 7
1.8	−0.050	1 − 7
2.0	−0.150	1 − 8
2.5	−0.385	3 − 8
3.0	−0.623	3 − 8
3.5	−0.86	4 − 8
4.0	−1.09	6 − 8
4.5	−1.29	7,8
5.0	−1.45	8

* Numbers correspond to those given in table 1.

c) COMPARISON OF THE $(H'_0)_{I_n}$ SCALE WITH OTHER H'_0 SCALES IN AQUEOUS-ETHANOLIC SOLUTIONS AND WITH $(H_0)_{NA}$ SCALES

Fig. 4 presents this comparison for the indicators type and for the media noticed in the same plotting.

As can be observed, the $(H'_0)_{I_n}$ scale of our compounds in the 50% vol. aqueous-ethanolic with H_2SO_4 media coincides practically excellently with Vetesnik's *et al.* scale [8] for the azocompounds, which is performed in the same solvent but with $HClO_4$. It is well known that up to a high limit of the acidity, the sulphuric- and perchloric acid power is practically identical. [6] On the other hand, this coincidence denotes that

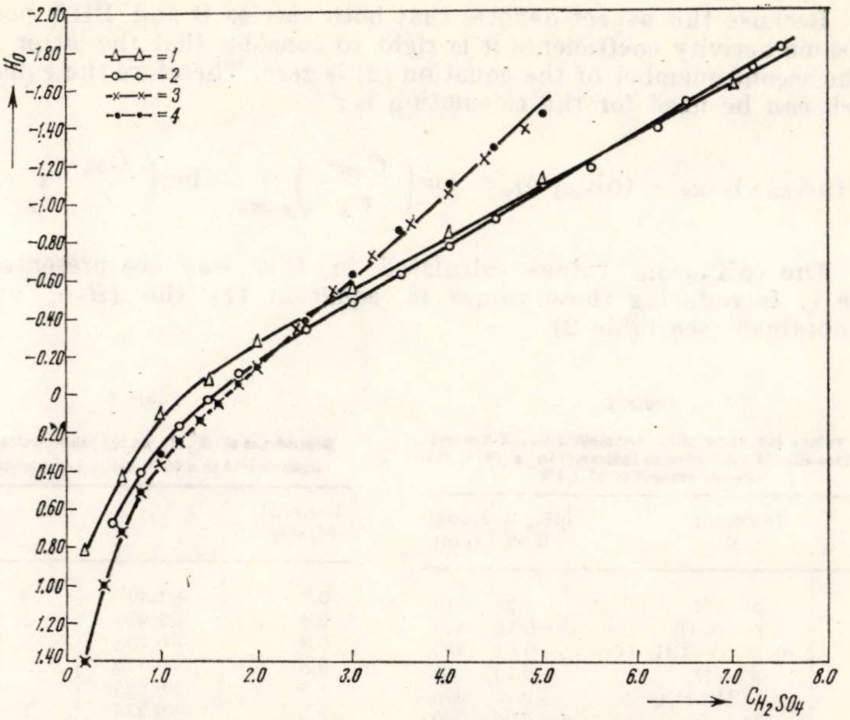

Fig 4. — H_0' (and H_0) scales for various types of indicators in various media

Curve	Indicator	Solvent system	Mineral acid
1	*p*-Nitroaniline	H_2O	H_2SO_4
2	Azo-compounds	$EtOH/H_2O$ 20/80 v	,,
3	,,	$EtOH/H_2O$ 50/50 v	$HClO_4$
4	$I_n$compounds	,,	H_2SO_4

both our type I bases and those from the azo-compounds series behave as Hammett bases (the corresponding H_0' scale was practically identical with that of the nitroaniline indicators in the same medium and in all our region).

From Fig. 4 it results similarly that in the range of low sulphuric acid concentrations the H_0' values for the aqueous-ethanolic sulphuric acid are more positive than H_0 for the aqueous sulphuric acid. This is in accordance with the generally known effect that the addition of dilute water-acid mixtures to organic solvents and to ethanol[24-31] decreases the

---

[24] P. Salomaa, *Acta Chem. Scand.*, **11**, 125 (1957).
[25] van Looy and L. P. Hammett, *J. Amer. Chem. Soc.*, **81**, 3872 (1959).
[26] I. T. Oiwa, *Sci. Repts., Tohoku Univ. I. Ser.*, **41**, 129 (1957).
[27] E. Nachbaur, *Monatsh.*, **91**, 749 (1960).
[28] Ch. Kalidas, R. P. Santi, *J. Chem. Soc.*, **1961**, 3398.
[29] E. M. Arnett, Ch. F. Douthy, *J. Amer. Chem. Soc.*, **86**, 409 (1964).
[30] F. Hauptschein-Brychmann and B. Tremillon, *Bull. Soc. chim. France*, **1965**, 1937.
[31] F. Strafelda and Z. Voznakova, *Chem. Listy*, **61**, 451 (1967).

activity of the hydrogen ion.[31] At acid concentrations $C_{H_2SO_4} > 3N$ in the case of 50% vol. aqueous-ethanol, the H_0' function increases linearly with the normality of the acid and namely more rapidly than in an aqueous solution. The H_0 slope increases proportionally with the ethanol percentage (0% EtOH < 20% EtOH < 50% EtOH).

This phenomenon is due to the fact that in the ethanol-water system the proton is preferentially solvated by water i.e., water is a stronger base than ethanol [13,24,32–34] and the equilibrium

$$\mathrm{Et\overset{\oplus}{O}H_2 + H_2O \rightleftharpoons H_3O^{\oplus} + EtOH}$$

is displaced to the right.

EXPERIMENTAL

THE PREPARATION OF THE COMPOUNDS

The *E-1,3-dimethyl-6-(p-X-β-styryl)-2,4-dioxo-1H, 3H-1,3,5-triazine* bases were prepared according to ref. 1 (for the compound I_{8B}) and 4 (for all the others).

MEASUREMENT OF LOG $C_{BH^{\oplus}}/C_B$ VALUES

6,25 ml of a solution containing the styryl-dioxo-s-triazine (1.0×10^{-4} M) in 96% ethanol a.r. was dropped into a 25 ml graded flask which then was filled near to the mark with aqueous sulphuric acid of the appropriate strength and with twofold distilled water. Solutions of exactly 0.1, 1.0, 10 and 30 N aqueous sulphuric acid were used. After cooling at room temperature (25 ± 1°C) it was filled to the mark by pipetting with twofold distilled water. The solution was than transferred in an 1 cm silica cell and the spectrum of the solution was recorded in the range 200–600 nm, using an UNICAM SP–8000 instrument. A blank solution prepared in the same manner with the same acid stock solution (using a U.C.B., a.r., sulphuric acid) was used in the reference beam.

The solutions were freshly prepared and kept in the dark before the determinations in order to avoid *trans-cis* photoisomerization. The use of the solution was made in a dark room using a red light.

---

[32] P. D. Barlett and J. D. Mc Collum, *J. Amer. Chem. Soc.*, **78**, 1441 (1956).

[33] R. W. Gurney, "Ionic Processes in Solution", McGraw Hill Inc., New York, 1953, pp. 36 and 115.

[34] H. Goldschmidt, *Z. pys. Chem.*, **89**, 129 (1914).

Revue Roumaine de Chimie, **19**, *10*, 1631–1636 (1974)

DECOMPOSITION OF ORGANIC HYDROPEROXIDES IN THE HETEROGENEOUS CATALYSIS. II*

DECOMPOSITION OF CUMENE HYDROPEROXIDE ON STRONGLY ACIDIC CATIONITES

L. CORMOŞ, A. POP and V. SBERA

Department of Organic and Technological Chemistry of the Faculty of Chemistry, Cluj,
Str. Arany Ianoş, 11, Romania

Received July 1, 1973

The present paper studies the macrokinetics of the decomposition reaction of cumene hydroperoxide in dilute solutions, on some strongly acidic cationites. The following cationites were used: amberlite I.R.-200, ostion KSP, zerolite-225 and lewatite S-200. The reaction rate constants were determined at three different temperatures for each separate cationite and the activation energies were calculated. A static working condition was used, the reactants being vigorously stirred. The cumene hydroperoxide solutions in cumene were about 10%.

In recent years, a series of solid catalysts were used in view of eliminating the drawbacks presented by the cumene procedure for obtaining phenol, by which the decomposition of cumene hydroperoxide occurs in a homogeneous catalysis.

Thus the decomposition of cumene hydroperoxide took place on silicagel,[1,2] on natural[3–5] or synthetic[6–9] silica-alumina and on various salts of metals with a variable valence.[10]

---

* The first part will appear in *Stud. Univ. Babeş-Bolyai, Chem.* **19** (1) 1974.

[1] P. V. Kucher and V. A. Soroka, *Zhur. priklad. Khim.*, **34**, 1573 (1961).

[2] A. Pop, L. Cormoş and L. Dulămiţă, *Rev. Roumaine Chim.*, **17** (11), 1917 (1972).

[3] Société des usines chimiques Rhone-Poulenc., Pat. Brit., 724.009, 16 febr. 1955 ; *Chem. Abstr.*, **50**, 4214 b (1956).

[4] H. Sodomann, B. Hanschultz and M. Hanke, Pat. Germ., 1.136.713, 20 sept. 1962 ; *Chem. Abstr.*, **58**, 4471 c (1963).

[5] S. Carra, *Chimica e Industria*, **45**, 1087 (1963).

[6] A. Pop, P. Kröbl, L. Cormoş and G. Lengyel, *Stud. Univ. Babeş-Bolyai. Chem.*, **12** (2), 89 (1967).

[7] A. Pop and L. Cormoş, *Stud. Univ. Babeş-Bolyai Chem.*, **16** (1), 61 (1971).

[8] A. Pop and L. Cormoş, *Stud. Univ. Babeş-Bolyai Chem.*, **16** (2), 101 (1971).

[9] L. Cormoş and S. Popica, *Stud. Univ. Babeş-Bolyai Chem.* **19** (1), 19 (1974).

[10] A. Pop and L. Cormoş, *St. cerc. Chim.*, **18** (10), 1009 (1970).

A number of research-workers[11-14] used for this purpose some strongly acidic cationites among which we mention Wofatite-P, Wofatite-F, KU-1, KU-2, Vionite CS-2, Vionite CS-3, Vionite CS-3A and Vionite CS-4A.

The present paper attempts to extend the investigations made so far to other cationites which have not yet been tested in this reaction.

EXPERIMENTAL

The following cationites were used in the model reaction: Amberlite IR-200, Ostion KSP, Zerolite-225 and Lewatite-S-100. Some of these cationites are found in H form, others, in Na form. For this reason the Na-Type ion-exchangers were introduced into a column and converted into H form, by treating with 10% sulphuric acid prior to the beginning of the experiments. The cationites were washed with deionized water, to remove the excess of acid.

Some determinations were made on the characteristics of the cationites used in this reaction.

The data obtained are listed in table 1.

Table 1

Characteristics of the utilized cationites

Cationite	Active groups	Exchange capacity in mval/ml		Structure	Maximum working temperature	Producing country
		Total	Useful			
Amberlite IR-100	$-SO_3Na$	1.75	0.7−0.9	micro-porous	120°	U.S.A.
Ostion KSP	$-SO_3H$	1.4−1.7	—	micro-porous	120°	Czechoslovakia
Zerolite-225	$-SO_3Na$	2.0	0.5−1.44	gel	120°	England
Lewatite S−100	$-SO_3Na$	2.2	1.8	gel	120°	W. Germany

The experiments were conducted in a thermostated glass device fitted with an inner cooling coil for a quantitative overtake of the heat released during the decomposition reaction. In this way, the local overheatings of the catalyst are avoided and a constant temperature is maintained during decomposition.

During our experiments we monitored the macrokinetics of the cumene hydroperoxide decomposition reaction at three different temperatures for each separate cationite; 25 ml solution 10% cumene hydroperoxide in cumene and about 2 grams of cationite were used for each determination.

---

[11] A. Teichert, Z. Leszczynski and H. Radoniewicz, Pat. Pol., 42.393, 30 sept. 1959; *Chem. Abstr.*, **55**, 7357 f (1961).

[12] A. O. Kolmakov, I. A. Miasnikova, A. M. Barembaum, N. A. Golitina and I. S. Izmailova, *Trudy po Khim. i Khim. Tehnol.*, **1**, 43 (1958).

[13] G. A. Razuvaev, V. A. Susunov and V. A. Iablokov, *Doklady Akad. Nauk S.S.S.R.*, **139**, 1128 (1961).

[14] I. Vodnar, *Rev. Chim.* (*Bucureşti*), **21**, 549 (1970).

The reaction was monitored by taking samples of 0.5 ml each, from time to time for the iodometric titration[15] of the non-decomposed hydroperoxide.

Table 2 presents the experimental data obtained from the decomposition on Amberlite IR-200 at temperatures of 20, 29.5 and 39.6°. The table contains:

n —number of determinations

X—time span from the start of the experiment until the samples were taken for the titration of the nondecomposed hydroperoxide, in minutes

α— conversion in %

Using the relation for the calculation of the most probable straight line, where : Y-which is lg $100/(100-\alpha)$ and n-number of determinations;

$$k = \frac{n\,\Sigma XY - \Sigma X \Sigma Y}{n\,\Sigma X^2 - (\Sigma X)^2}$$

the reactions rate constants were calculated for each temperature and listed in table 3.

Table 2

Data obtained from the decomposition of cumene hydroperoxide on Amberlite IR-200

Time in minutes	Conversion %		
	t=20°C	t=29,5°C	t=39,6°C
2	—	—	27,53
4	—	—	44,92
5	20,29	34,78	—
6	—	—	59,42
8	—	—	68,11
10	40.57	57,97	76,36
15	—	73,18	—
20	60,86	81,88	94,20
25	—	88,40	—
30	76,81	92,75	97,10
40	82,60	—	—
50	89,85	—	—
60	94,20	—	—

Table 3

Reaction rate constants and working temperatures

Cationite	k_1	k_2	k_3	t_1	t_2	t_3
Amberlite IR-200	$1.99.10^{-2}$	$3.80.10^{-2}$	$5.33.10^{-2}$	20.0	29.5	39.6
Ostion KSP	$3.83.10^{-3}$	$8.23.10^{-3}$	$13.90.10^{-3}$	56.4	71.7	83.0
Zerolite-225	$2.72.10^{-3}$	$5.45.10^{-3}$	$9.89.10^{-3}$	62.0	71.7	88.8
Lewatite S-100	$0.73.10^{-4}$	$3.52.10^{-4}$	$35.70.10^{-4}$	51.0	70.0	88.8

---

[15] H. Hook and H. Kropf, *Angew. Chem.*, **69**, 313 (1957).

A similar procedure was applied in the case of the other cationites. Table 4 presents the data on the decomposition on Ostion-KSP and table 5 refers to the decomposition on Zerolite-225. In the case of Lewatite the reaction rate has been found to be extremely low, the conversions of cumene hydroperoxide being below 15% even at 90° and after a delay of 10 hours after the onset of the experiment. That is why we consider that these data present no practical interest.

Table 4

Data obtained from the decomposition of cumene hydroperoxide on Ostion KSP

Time in minutes	Conversion %		
	t = 56,4°C	t = 71,7°C	t = 83°C
5	2,29	5,34	7.02
15	3,81	8,37	9,92
30	5,34	16,78	36,64
60	13,74	45,03	74,04
90	28,24	70,22	87,78
120	40,45	83.20	98,93
150	52,67	90,83	—
180	63,26	96,94	—
210	71,75	—	—
240	80,15	—	—
270	86,25	—	—
300	89,31	—	—
330	93,11	—	—
360	96,18	—	—

Table 5

Data obtained from the decomposition of cumene hydroperoxide on Zerolite-225

Time in minutes	Conversion %		
	t = 50°C	t = 71.8°C	t = 88.8°C
5	—	9,95	16,03
15	—	12,97	25,19
30	—	22,13	42,74
60	0,72	—	68,70
90	—	56,48	84,73
120	1,44	—	93,89
150	—	75,57	—
180	2,89	—	—
210	—	87,77	—
240	4,34	—	—
300	5,79	—	—
360	10,14	—	—

INTERPRETATION OF RESULTS

By plotting lg 100/(100-α) as a function of time, figs. 1, 2 and 3 illustrate that the straight lines are obtained for Amberlite IR-200, Ostion KSP and Zerolite-225 for conversions between 10–95%. This

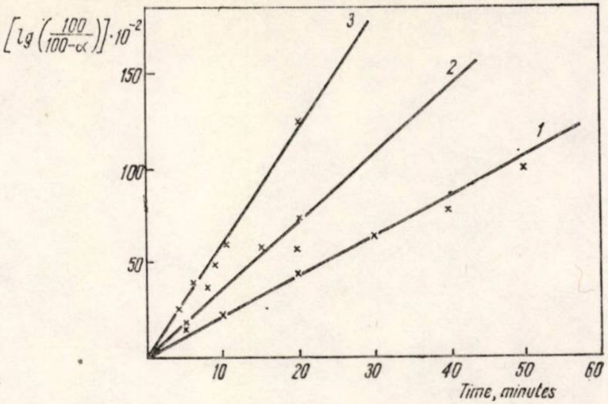

Fig. 1. — Linearization of first-order kinetic curves for the decomposition of cumene hydroperoxide on Amberlite IR-200.
1, at a temperature of 20° ; *2*, at a temperature of 29.5° ; *3* at a temperature of 39.6°.

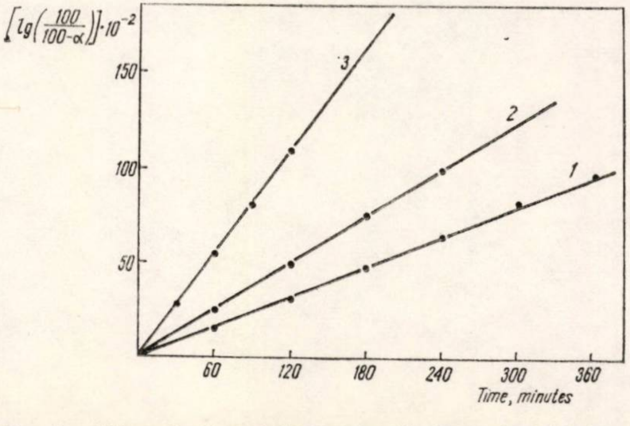

Fig. 3. — Linearization of first-order kinetic curves for the decomposition of cumene hydroperoxide on Zerolite-225.
1, at a temperature of 62° ; *2*. at a temperature of 71.7° ; *3*. at a temperature of 88.8°

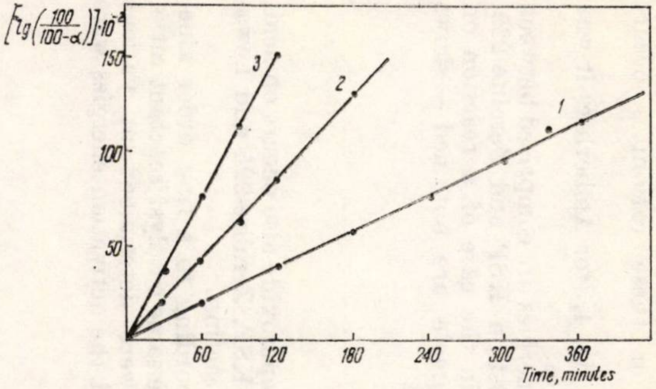

Fig. 2. — Linearization of first-order kinetic curves for the decomposition of cumene hydroperoxide on Ostion KSP.
at a temperature of 56.4° ; *2*, at a temperature of 71. 7° *3*, at a temperature of 83°.

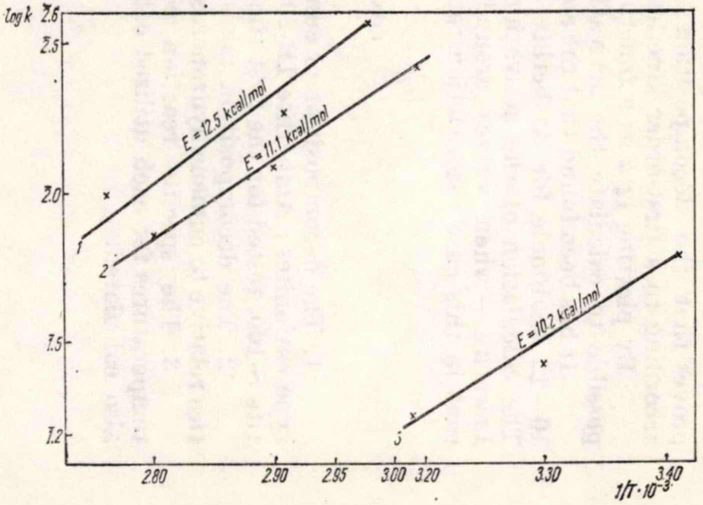

Fig. 4. — Graphic determination of the activation energy according to Arrhenius' equation.
1, for Zerolite-225 ; *2*, for Ostion KSP ; *3*, for Amberlite IR-200.

proves that the decomposition reaction on these cationites occurs according to a first-order kinetics.

By plotting lg *k* as a function of $1/T$, fig. 4, (for Amberlite) it was possible to calculate the activation energies.

It has been found that the activation energies are comprised between 10–12 kcal/mole for Amberlite IR-200, Ostion KSP and Zerolite-225. The calculation of the activation energy in the case of a reaction on Lewatite – when values around 25 kcal/mole are obtained – shows that in this case the reaction rate is small.

CONCLUSIONS

1. The decomposition of cumene hydroperoxide also occurs on acid-type cationites : Amberlite IR-200, Ostion KSP, Zerolite-225 and Lewatite S-100, tested for the first time in this reaction.

2. The decomposition takes place according to a first order kinetics relative to cumene hydroperoxide for the same catalyst/reactant ratio.

3. The specific reaction constants were determined at various temperatures for each utilized cationite and the activation energies were also calculated.

Revue Roumaine de Chimie, **19**, *10*, 1637 – 1644 (1974)

ALTERNATING TENDENCY IN COPOLYMERIZATION. II[1]

COPOLYMERIZATION OF 1,1–DIPHENYL ETHYLENE WITH ACRYLIC MONOMERS

DAN SORIN VASILESCU

Laboratory of Macromolecular Chemistry, Polytechnical Institute, Calea Victoriei 149, Bucharest, Romania

Received November 14, 1973

The copolymerization of methacrylonitrile and acrylonitrile with 1,1 diphenyl ethylene at 80° was studied. The reactivity ratios r_i of these pairs of monomers as well as the copolymerization rates were calculated. This paper deals also with the alternating tendency in these systems.

INTRODUCTION

1,1–diphenyl ethylene (DPE) is a well-known monomer for its inability to homopolymerize. The impossibility to produce by a radicalic way a homopolymer of DPE, was proved long time ago.[2]

The radicalic affinity of phenyl ethylenes may be considered from the viewpoint of the steric hindrance in the addition reaction of the radical to olefin, or in terms of the resonance stabilization of the newly formed radical; it seems that the former effect might be a factor of less importance than the latter.[3] Nevertheless, DPE can copolymerize with various vinyl monomers. Thus, the copolymers of DPE with acrylonitrile (AN)[4] are known; the reactivity ratios ($r_1 = 0$ and $r_2 = 0.028$) show a tendency towards an alternating structure for this system. In such copolymerizations, the DPE content in copolymer cannot exceed 50% (molar percentage); consequently, in a copolymer two successive units of DPE are not possible. This fact was proved by Ito and Yamashita,[5] who investigated the triad distribution in the DPE (1)–methyl acrylate (2) copolymer, determined from the NMR studies; only 222, 221 and 121 triads were found. The above specified authors reported the $r_1 = 0$ and $r_2 = 0.092$ values.

---

[1] Part. I. D. S. Vasilescu, *Rev. Roumaine Chim.*, **19**, (1974).
[2] T. Alfrey and W. H. Ebelke, *J. Amer. Chem. Soc.*, **71**, 3235 (1949).
[3] T. Fueno, T. Tsuruta and J. Furukawa, *J. Polymer Sci.*, **40**, 487 (1959).
[4] K. W. Doak and D. L. Dineen, *J. Amer. Chem. Soc.*, **73**, 1084 (1951).
[5] K. Ito and Y. Yamashita, *J. Polymer Sci.*, A–1, **4**, 631 (1966).

Also, DPE cannot homopolymerize by ionic way; dimers of DPE could be obtained in the presence of several typical cationic catalysts as $SnCl_4(H_2O)$ or $Sb_2Cl_2(HCl)$.[6] The DPE anion is very stable and does not produce poly-DPE, but may initiate the anionic polymerization of other monomers. As the olefin is prevented from polymerizing by its steric hindrance, it provides a useful tool for the study of initiation processes.[7] Yuki and co-workers[8] described the anionic copolymerization of styrene and DPE; an alternating copolymer is obtained in the presence of a large excess of DPE. Szwarc *et al.*[9] reported more elaborated data about the behaviour of this system. The rate constant of DPE addition to the "living" polystyrene was found to be 250 l/mole sec for a $\text{-S}^-\text{Na}^+$ ion pair; the addition of styrene to $\text{-D}^-\text{Na}^+$ was proved to be reversible.[9] The alternating character in the anionic copolymerization of DPE and 2,3 dimethyl butadiene (DMB), was attributed to the high reactivity of DPE toward an anion, owing to the high resonance stabilization of its anion, in spite of the lack of homopolymerizability, and by the lower reactivity of DMB.[10]

In the present work, we report some data regarding the radicalic copolymerization of DPE with acrylic monomers. The reactivity ratios and other kinetic features were determined; the obtained polymers were also investigated in order to elucidate their structure.

EXPERIMENTAL

MATERIALS

1,1—diphenyl ethylene was prepared according to the method described by Allen.[11] The phenyl magnesium bromide reacts with an aliphatic acetate and $CH_3C(C_6H_5)_2O$ Mg Br results; after hydrolysis, the dehydration of diphenyl methyl carbinol follows, getting DPE. DPE was distilled in vacuum (b.p. 107—109°/1 mm. Hg) over sodium and found to be practically pure on the basis of the gas-chromatography measurements.

The methacrylonitrile (MAN), acrylonitrile (AN), acrylamide (AA), azobisisobutyronitril (AIBN) and the solvents were purified by usual methods, as we reported in detail in an earlier work.[1]

COPOLYMERIZATION PROCEDURE

The operation way, chosen to avoid any contact with air during the copolymerization process, was also widely described.[1] The precipitation of the reaction mass was made with petroleum ether.

ANALYSES OF POLYMERS

The reprecipitated and dried products were submitted to the micro-Dumas nitrogen analysis, to establish their compositions.

Intrinsic viscosities of the copolymers were reckoned from the data obtained on dilute solutions (less than 0.2 g/dl) in chloroform at 25°; the viscosity measurements were carried out with an Ubbelohde viscometer.

[6] A. G. Evans, E. A. James and E. D. Oven, *J. Chem. Soc.*, **1961**, 3532.

[7] S. Penczek, J. Jagur—Grodzinski and M. Szwarc, *J. Amer. Chem. Soc.*, **90**, 2174 (1968).

[8] H. Yuki, K. Kosai, S. Murahashi and J. Hotta, *J. Pol mer Sci.*, B, **2**, 1121 (1964).

[9] E. Ureta, J. Smid and M. Szwarc, *J. Polymer Sci.*, A—1, **4**, 2219 (1966).

[10] H. Yuki, K. Hatada and T. Inoue, *J. Polymer Sci.*, A—1, **6**, 333 (1968).

[11] C. F. H. Allen and S. Converse, "Organic Syntheses ", Coll. **1**, H. Gilman and A. H. Blatt Eds., J. Wiley and sons, New York, 1956, p. 226.

In order to obtain further positive data regarding the DPE presence in the copolymer chain, IR absorption spectra of the copolymers were recorded; the tests were accomplished on a PYE-Unicam, SP—200 spectrophotometer in potassium bromide pellets.

The MAN—DPE copolymers were tested by means of differential thermal analysis (DTA). The measurements were carried out on a CNRS-type apparatus endowed with a "Sefram"—"Graphispot" recorder; we led the warming in purified and dried nitrogen atmosphere at the rate 6.5°/min.

RESULTS AND DISCUSSION

As we reported above, the DPE radical is stabilized; this fact acts on the rate of the copolymerization process. The preliminary tests showed the requirement to work at a higher temperature and with an increased initiator amount ($[M_1] + [M_2]/[\mathrm{AIBN}] = 100$).

Table 1

Copolymerization of acrylic monomers with DPE (M_2) at 80°; molar ratio ($[M_1]+[M_2])/([\mathrm{AIBN}]) = 100$

$[M_1]$ in monomers (mole %)	M_1	$[M_1]+[M_2]$ (mole/l)	Reaction time (hours)	Conversion (%)	*N* % Dumas	$[m_1]$ in copolymer (mole fraction)
95	MAN	7.81	20	4.90	15.05	0.951
90	MAN	7.55	25	5.12	14.55	0.860
80	MAN	7.04	35	4.84	12.44	0.798
70	MAN	6.64	47	5.04	11.12	0.754
60	MAN	6.28	48	3.19	9.66	0.698
50	MAN	5.90	54	2.79	8.24	0.636
40	MAN	5.64	60	2.41	7.81	0.614
30	MAN	5.37	70	1.19	6.76	0.571
90	AN	5.68	5	5.03	7.78	0.587
80	AN	5.35	10	5.90	7.77	0.586
70	AN	5.05	15	6.04	6.78	0.539
50	AN	4.62	25	3.52	6.12	0.506
30	AN	4.10	40	2.61	5.96	0.497
20	AN	3.97	50	1.95	5.50	0.471
10	AN	3.82	55	1.09	5.25	0.457
90	AA	1.76	3	26.22	—	—
80	AA	1.87	3	10.50	18.86	—
70	AA	1.99	4	6.84	19.01	—
50	AA	2.29	8	6.02	19.37	—
30	AA	2.69	15	3.08	19.03	—
20	AA	2.96	48	4.96	20.12	—
10	AA	3.28	59	2.46	19.68	—

Even in the specified conditions, the reaction times are rather long. Accordingly, it would arise the danger of some secondary reactions (e.g. oxidation); on the other hand, the more volatile monomer evaporation may occur. It might result a change into the monomer feed composition and, obviously, errors in the reactivity ratios calculation. Thus, the chosen operation way (in argon medium, in sealed off ampoules) appears as single reasonable; in this way the above described troubles were prevented and the reproducibility of the results was assured.

As is shown in table 1, the initial molar concentration of both monomers was not kept constant, but it varied in fairly good limits. This fact is due to the different molecular weights and densities of monomers, in the conditions where the total mole number was kept constant.

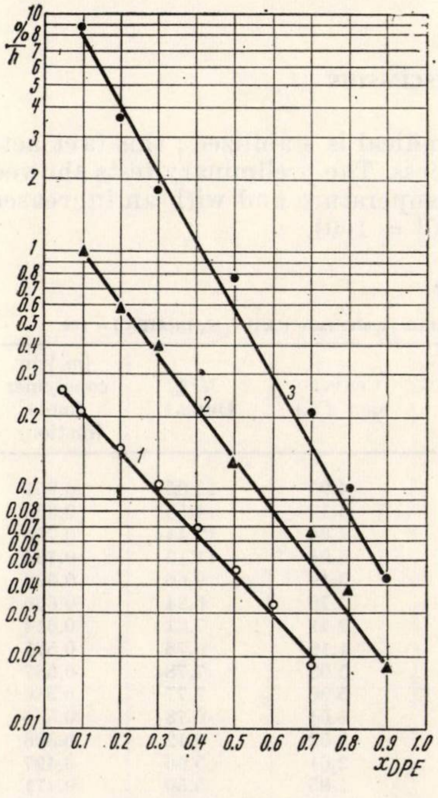

Fig. 1. — The effect of DPE (M_2) molar fraction on the copolymerization rate at 80°.

M_1 = MAN (1); AN(2); AA(3). ($[M_1] + [M_2])/[AIBN] = 100$.

In the tests involving AA, acetone was used as a solvent, because of the limited solubility of the monomer and, consequently, the total molar concentrations were correspondingly dropped.

As, generally, small conversions were obtained, the initial copolymerization rates could be determined, assuming a linear dependence of the conversion on time, in the first step.

The influence of the monomer composition feed on the reaction rate is evident — even in the conditions when differences in the molar concentration exist.

In all cases, DPE acts as a retarder of the copolymerization process.

On the other hand, as a function of the structure of the acrylic monomer, important differences in reactivity may occur; for instance, the higher the "e" value of the monomer, the higher the rate of the process. This effect is so significant, that it was necessary a logarithmicc scaale to represent the rates of all copolymerization processes in the same figure (fig. 1).

As the syntheses required a higher temperature and a rather large initiator amount, the molecular weights of the resulted products are of course reduced.

Thus, the intrinsic viscosities of the AN—DPE copolymers determined in chloroform vary between 8.72 cm³/g (58% AN) and 6.25 cm³/g (47% AN); this change is too small to be attributed to the molecular weight variation.

Values of more than 50% of the DPE content were observed at several copolymers with AN (e.g. tests 13, 14 and 15 — table 1); we consider that the differences from the equimolecular composition are negligibly small.

The nitrogen analyses results were used to establish the copolymer composition. These data were afterwards analysed by the least-square

Table 2

Calculated data for the determination of the reactivity ratios in copolymerization of DPE with acrylic monomers at 80°

$X = X_1/X_2$	$Y = Y_1/Y_2$	$Z = (Y - 1)/X$	$W = - Y/X^2$	W^2	ZW
		M_1 = MAN	M_2=DFE		
19.0000	19.3666	0.9666	−0.0536	0.0029	−0.0519
4.0000	3.9456	0.7363	−0.2466	0.0608	−0.1816
2.3333	3.0535	0.8801	−0.5608	0.3142	−0.4935
1.5000	2.3080	0.8720	−1.0258	1.0516	−0.8946
1.0000	1.7450	0 7450	−1 7450	3.0449	−1.3020
0.6666	1.5907	0.8860	−3.5794	12.8120	−3.1713
0.4285	1.3310	0.7725	−7.2499	52.5554	−5.6000
		Σ 5.8585	−14.4611	76.8418	−11.6949
		$(\Sigma W)^2 = 209.12$			
		M_1 = AN	M_2 = DFE		
9.0000	1.4195	0.0466	−0.0176	0.0008	−0.0003
4.0000	1.4155	0.1039	−0.0885	0.0078	−0.0092
2.3333	1.1692	0.0725	−0.2147	0.0473	−0.0158
1.0000	1.0245	0.0245	−1.0245	1.0495	−0.0251
0.4285	0.9901	−0.0231	−5.3905	29.0570	0.0989
0.2500	0.8903	−0.4388	−14.2448	202.9190	6.2507
0.1111	0.8416	−1.4256	−68.1696	4647.1000	97.1825
		Σ −1.6400	− 89.1502	4880.1814	103.4817
		$(\Sigma W)^2 = 7948$			

X_1 = molar fraction of M_1 in initial monomer mixture.
Y_1 = molar fraction of M_1 in copolymer (at small conversions).

method[12] (table 2). The use of this method to reckon the reactivity ratios eliminates some subjective interpretations, which are characteristic of the graphic methods; this calculation way was chosen in a previous paper [1] too.

The r_1 and r_2 reactivity ratios for these systems are small; little errors in the nitrogen content estimation lead to some difficulties in the reactivity ratios assessment by the Mayo and Lewis's intersection method.[13]

Some typical results are plotted in figures 2a and 2b.

One may remark that only for the MAN−DPE and AN−DPE pairs, analytical data could be used in order to obtain the copolymerization ratios. In the AA containing systems the great scatter of the N concentrations obtained makes any definite conclusion impossible. For these systems the intrinsic viscosities also had rather low values: 13.7 cm³/g (Test 16-table 1) and 5.3 cm³/g (Test 22-table 1).

---

[12] P. W. Tidwell and G. A. Mortimer, *J. Polymer Sci.*, A, **3**, 369 (1965).
[13] F. R. Mayo and F. M. Lewis, *J. Amer. Chem. Soc.*, **66**, 1594 (1944).

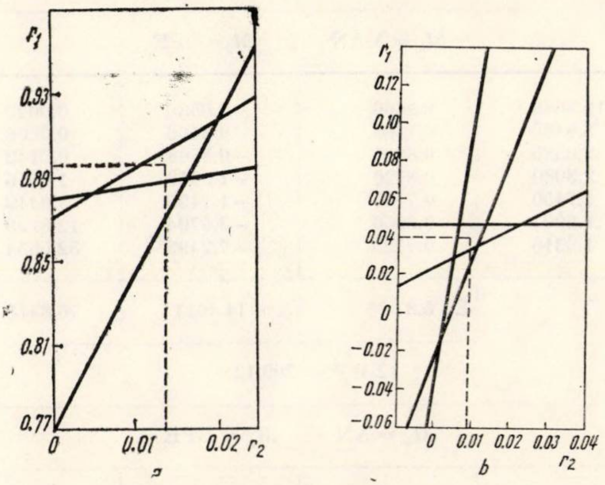

Fig. 2. — The reactivity ratio determination by the intersection method.
a) M_1 = MAN M_2 = DPE
b) M_1 = AN M_2 = DPE

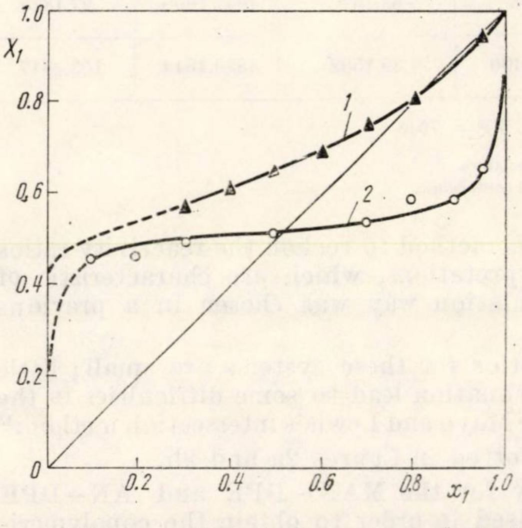

Fig. 3. — Copolymer/monomer feed composition curves for binary copolymerization of:
1. MAN(M_1) — DPE(M_2).
2. AN(M_1) — DPE(M_2).

The results of the accomplished reckonings are summarized in table 3. The r_1 and r_2 values obtained for the MAN—DPE pair are different from those predicted by the "Q-e" scheme [14]; the corresponding values for the AN–DPE pair are also distinct from those theoretically foreseen[14] and, moreover, from those reported many years ago. [4]

---

[14] T. ALFREY and C. C. PRICE, *J. Polymer Sci.*, 2, 101 (1947).

The values obtained permitted us to mark the composition curves for these systems.

Table 3

Reactivity ratios in copolymerization of acrylic monomers (M_1) with 1,1 diphenyl ethylene (DPE – M_2) at 80°

Monomer M_1	Experimental data				Calculated data from the Alfrey and Price's scheme	
	Least-squares method		Mayo and Lewis method			
	r_1	r_2	r_1	r_2	r_1	r_2
MAN	0.850	0.0087	0.896	0.014	0.129	0.072
AN	0.045	0.022	0.04	0.01	0.0187	0.079
AA*	—	—	—	—	0.025	0.035

The values r_1=0.028 and r_2=0 were earlier reported.[4]

It is notable a great alternating tendency for the AN–DPE system as the resulting copolymer composition tends to 50% in a wide range of the monomer feed composition.

Even for the MAND–PE pair, 1,1–diphenyl ethylene is present in copolymer in an appreciable proportion. This fact was evidenced by spectral analysis.

In table 4 the characteristic vibration frequencies of the MAN–DPE copolymers at various compositions are given; the same copolymer amount (2 mg) was submitted to the spectral analysis. The three spectra shown differ only by the intensity of the various absorption bands. Proportionally as the DPE content increases, the absorption bands at 710 cm^{-1} and 765 cm^{-1} (characteristic of the phenyl group) increase too; at the same time the bands from 2235 cm^{-1} (nitrile) and 1470 cm^{-1} (mehyl) [15] decrease. The peaks for methylene (2990 cm^{-1}; 2945 cm^{-1}) remain practically constant. These complementary data are in good agreement with the nitrogen analysis results.

Table 4

The absorbance noticed in the IR spectra of some MAN-DPE copolymers

Characteristic vibration frequencies ν cm^{-1}	Absorbance		
	Copolymer with 57.1 % MAN	Copolymer with 79.8 % MAN	Copolymer with 95.1 % MAN
2990	0.23	0.25	0.27
2945	0.21	0.21	0.23
2235	0.17	0.21	0.24
1470	0.27	0.31	0.34
1455	0.41	0.34	0.34
1395	0.14	0.16	0.17
1375	0.11	0.12	0.12
1220	0.14	0.16	0.19
765	0.32	0.25	0.12
710	0.78	0.52	0.28

The IR absorption spectra for the products obtained from AA and DPE are more complex than those of poly-AA described by Hümmel[16] (720 s, 820 s, 840 s, 890 w, 960 s, 990 s, 1050 w, 1135 s,

---

[15] R. M. Silverstein and G. C. Bassler, "Spectrometric Identification of Organic Compounds". J. Wiley and sons, New York, 1963, p. 56.

[16] Hümmel/Scholl "Infrared Analysis of Polymers, Resins and Additives — An Atlas", 1, part 2, Wiley-Interscience, New York–London, 1969, p. 1239.

1280 s, 1355 vs, 1425 vs, 1610 vs, 1670 vs, 1950 w, 2810 m, 3180 vs, 3360 vs, —where w-weak, m-medium, s-strong, vs-very strong and the values are in cm^{-1}) and do not permit us to draw certain conclusions.

The literature [17] indicates the glass-transition temperature (T_g) for poly-MAN at 120°. For the copolymers studied, the T_g values vary between 62° and 89° as a function of composition. This fact might show, that poly-MAN long sequences do not appear in the copolymer chain and that the volume effects brought about by the DPE substituents are important. Indeed, for a MAN—DPE copolymer (57%MAN) one may reckon the run number (according to Harwood[18]) $R = 62.4$, thus being pointed out the alternating tendency for this system too.

All the samples present endothermal processes in the range 320° to 390°.

The author is indebted to Mrs. Florina Mărculescu for the IR spectra achievement and expresses his sincere gratitude to Mrs. Elena Maftei for thermal measurements.

---

[17] B. Ke, "Newer Methods of Polymer Characterization", J. Wiley and sons, New York, 1964, p. 349.

[18] H. J. Harwood, *Angew. Chem.*, **77**, 1124 (1965).

Revue Roumaine de Chimie, **19**, *10*, 1645 – 1650 (1974)

MÉTHODES DE DÉTERMINATION DE L'AZOTATE DE PILOCARPINE. SPECTRE EN VISIBLE ET INFRAROUGE DU COMPOSÉ RÉSULTÉ ENTRE L'AZOTATE DE PILOCARPINE ET LE REINECKATE D'AMMONIUM

GRIGORE TEODORESCU

Institut Polytechnique de Bucarest, Chaire de Chimie inorganique et analytique,
Bucarest, 1, str. Polizu

Reçu le 17 décembre 1973

On présente des méthodes de détermination de l'azotate de pilocarpine, réalisées par la combinaison avec le reineckate d'ammonium, la dissolution du composé obtenu dans l'acétone, suivie de la précipitation de l'anion reineckate comme reineckate d'argent et titrage de l'excès d'azotate d'argent avec du thiocyanate d'ammonium. Vu que le composé formé est soluble en acétone, résultant une solution colorée, le composé a été déterminé aussi colorimétriquement. La structure du complexe obtenu a été vérifiée par la détermination de la masse moléculaire, à l'aide des spectres en visible, pour le reineckate d'ammonium et le reineckate de pilocarpine. La structure du reineckate de pilocarpine a été caractérisée aussi par le spectre en IR de l'azotate de pilocarpine et de son composé.

La pilocarpine est un alcaloïde (le stéréoisomère dextrogire) de la classe des alcaloïdes avec le composant N-méthyl-imidazolique.[1] La principale action physiologique de la pilocarpine réside dans excitation de la sécrétion des glandes salivaires, sudoripares, lacrymales (effet antagoniste de l'atropine). Elle est employée pour la constriction de la pupille sous forme de chlorhydrate ou d'azotate de pilocarpine.

La méthode classique de détermination utilisée est basée sur le titrage alcalimétrique du chlorhydrate ou de l'azotate.

Pour avoir le minimum d'erreur dans cette méthode, il faut employer des substances de pureté avancée ($> 99{,}5\%$).

Pour pouvoir faire aussi des déterminations sur des substances moins pures, on a établi une méthode de détermination basée sur la réaction de combinaison de l'azotate de pilocarpine avec le reineckate d'ammonium $[NH_4Cr(NCS)_4(NH_3)_2]$, abrégé $NH_4^+Rc^-$, réactif utilisé par l'auteur aussi à la détermination d'autres produits.[2-6]

---

[1] Preobrajenski, *Ber. dtsch. chem. Ges.*, **66**, 1536 (1933) ; *ibid.*, **68**, 850 (1935).
[2] Gr. Teodorescu, *Bul. Inst. Politeh. București*, **32**(2), 39 (1970).
[3] Gr. Teodorescu, *Bul. Inst. Politeh. București*, **32** (4), 79 (1970).
[4] Gr. Teodorescu, *Bul. Inst. Politeh. București*, **32** (1). 67 (1971).
[5] Gr. Teodorescu., *Rev. Roumaine Chim.*, **17**, 1481 (1972).
[6] Gr. Teodorescu, *Rev. Roumaine Chim.*, **17**, 1621 (1972).

L'azotate de pilocarpine (abrégé PCP) utilisé est soluble dans l'eau (1 partie de substance à 8 parties d'eau) avec une faible réaction acide. La réaction de combinaison est due à l'existence dans la molécule du PCP d'une position N-méthyl-imidazolique qui confère un caractère d'*oniu* et a lieu selon le schéma suivant :

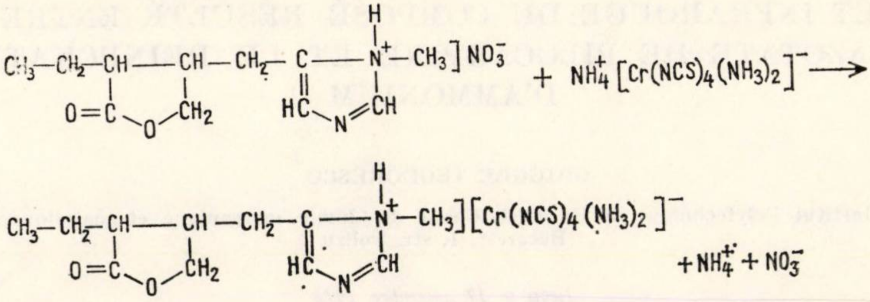

La réaction de combinaison avec le NH_4^+ Rc^- a été utilisée à la détermination du PCP, par les méthodes : volumétrique, colorimétrique et spectrale.

1. MÉTHODE VOLUMÉTRIQUE

La combinaison du PCP a lieu dans une solution aqueuse d'acide azotique avec le NH_4^+ Rc^-. Le précipité cristallin obtenu, de couleur rose, est filtré, lavé et ensuite dissous en acétone. La solution résultée est traitée par un excès de solution d'azotate d'argent 0,1 N, quand précipite le reineckate d'argent conformément à la réaction :

$$[Cr(NCS)_4(NH_3)_2]^- + Ag^+ \rightarrow Ag[Cr(NCS)_4(NH3)_2]$$

Après filtrage et lavage on titre l'excès d'azotate d'argent par thiocyanate d'ammonium en présence de l'alun de fer(III) et d'ammonium.

MODE OPÉRATOIRE

Du produit pharmaceutique dissous dans l'eau, de concentration 0,00534 g/ml, on prend des épreuves entre 0,0320–0,0800 g, on ajoute 0,5–1 ml d'acide azotique, 20 ml d'eau distillée et après, goutte à goutte, sous agitation continue, la solution fraîchement préparée de 3% NH_4^+ Rc^-. Il précipite le composé cristallin nâcré-rose-violet.

Le composé formé est filtré sur un creuset à filtre G_3, entraîné par une solution de $NH_4^+Rc^-$ 0,1 %, lavé ensuite à l'eau distillée (4°C), jusqu'au moment où la solution passe incolore et, finalement, 2–5 fois avec 5–10 ml d'éther.

On dissout le composé directement sur le creuset à filtre avec 10–20 ml d'acétone, jusqu'à dissolution totale. On lave finalement le creuset à 20 ml d'eau distillée et on prend la solution et les eaux de lavage dans un verre de 250 ml. On ajoute 100 ml d'eau distillée, 10 ml d'azotate d'argent 0,1 N et 3–4 gouttes d'acide azotique 2 N.

Le précipité de reineckate d'argent formé est filtré, lavé par décantage à l'eau distillée. Le filtrat et les eaux de lavage sont mis dans un flacon de 750 ml. On ajoute 3–4 ml de solution saturée d'alun de fer(III) et d'ammonium (environ 40 %), 3–4 gouttes d'acide azotique 2 N et on titre l'excès d'azotate d'argent par thiocyanate d'ammonium 0,1 N au facteur connu (F 0,1 N = 1,0526).

Un ml d'azotate d'argent 0,1 N correspond à 0,02713 g d'azotate de pilocarpine. Les résultats obtenus sont rapportés au tableau 1.

Tableau 1

Détermination volumétrique de l'azotate de pilocarpine

PCP dans l'épreuve g	PCP déterminé avec $NH_4^+Rc^-$		PCP déterminé alcalimétriquement %	Données statistiques
	g	%		
0,0320	0,0318	99,37	99–100	$N = 10$
0,0374	0,0371	99,20	99–100	$\overline{X} = 99,32$
0,0427	0,0425	99,53	99–100	$S = 0,2648$
0,0480	0,0477	98,38	99–100	$S_m = 0,08$
0,0534	0,0530	99,25	99–100	t^* variable student
0,0587	0,0586	99,82	99–100	$(P = 99\,\%,\ \nu = 9) = 3,25$
0,0640	0,0637	99,53	99–100	du tableau
0,0694	0,0690	99,42	99–100	Résulté = 99,32 ± 0,26 %
0,0747	0,0740	99,06	99–100	
0,0800	0,0794	99,02	99–100	

2. MÉTHODE COLORIMÉTRIQUE

Principe de la méthode colorimétrique. On précipite le PCP avec du NH_4^+ Rc^-, selon le même procédé, dans le rapport molaire 1 : 1. Vu que le composé formé est soluble en acétone, résultant une solution colorée en rouge, le PCP peut être déterminée aussi colorimétriquement.

MODE OPÉRATOIRE

On applique la méthode des courbes étalon. A cette fin on a employé une solution de NH_4^+ Rc^- avec $T = 0,0560$ g/ml dont on a pris des volumes correspondants, dans des ballons jaugés de 100 ml, dilués avec 50 ml d'acétone et complétés avec de l'eau distillée, afin d'obtenir des solutions avec des concentrations $T = 0,00028$; 0,000560 ; 0,000840 ; 0,00112 ; 0,001680 g. Les déterminations ont été faites à l'aide du photocolorimètre de type B. Lange, en utilisant des filtres verts (λ = 533 nm) et on a tracé la courbe étalon.

De la solution de PCP avec $T = 0,00534$ g/ml on a prélevé des épreuves entre 0,000320 et 0,000534 g et l'on a précipité avec du NH_4^+ Rc^- selon la méthode volumétrique.

Après précipitation, filtrage et lavage, les épreuves ont été quantitativement dissoutes avec de l'acétone, en prenant la solution dans des ballons jaugés à 100 ml. Après l'homogénéisation, les épreuves ont été colorimétrées, les résultats obtenus étant indiqués au tableau 2.

Tableau 2

Résultats du colorimétrage du reineckate de PCP

PCP dans l'épreuve g	PCP déterminée		Données statistiques
	g	%	
0,000320	0,000316	98,75	$N = 5$
0,000374	0,000368	98,39	$\overline{X} = 99{,}27$
0,000427	0,000425	99,53	$S = 0{,}3044$
0,000480	0,000484	100,41	$S_m = 0{,}13$
0,000534	0,000528	98,87	variabvle student $t^*(P = 99\,\%, \nu = 4) = 4{,}60$ du tableau Résultats $\% = 99{,}27 \pm 0{,}59$

3. ÉTUDE SPECTRALE

3.1. CARACTÉRISATION DU SPECTRE EN VISIBLE DU REINECKATE DE PCP

Dans le cas de la pilocarpine, comme dans le cas d'autres composés qui contiennent plusieurs atomes d'azote cationisable, il est utile de vérifier si la structure du complexe inclut un ou deux anions de reineckate.[7] La structure peut être vérifiée par la détermination de sa masse moléculaire, à l'aide de l'absorbance (A) et de l'absorptivité (K).

Les déterminations ont été faites avec le spectrophotomètre Zeiss de type VSU —1, avec une cuve de grosseur $l = 0{,}5$ cm et une concentration $g_1 = 0{,}1\,\%$.

Les chiffres trouvés ont été pour NH_4^+ Rc^- :

nm	Absorbance
394	0,138
420	0,102
452	0,030
482	0,093
520	0,155
560	0,105

et pour le reineckate de PCP :

nm	Absorbance
390	0,086
420	0,060
450	0,031
490	0,064
520	0,098
558	0,075

---

[7] KUM-TATT-LEE, *J. Pharm. Pharmacol*, **12**, 666 (1960).

Une caractéristique commune des spectres en visible du NH_4^+ Rc^- réside dans le fait que le maximum d'absorption (λ_{max}) est approximativement le même, $\lambda_{max} = 520$ nm pour NH_4^+ Rc^- (dans l'éthanol 95%) et $\lambda_{max} = 520$ nm pour le reineckate de PCP (aussi dans l'éthanol 95%).

L'absorptivité a été déterminée conformément à la relation :

$$K = (A/c)l$$

sur le $NH_4^+Rc^-$, dans l'éthanol 95% à la concentration $c = 0{,}00297$ mole gramme $NH_4^+Rc^-$, à une grosseur de la cuve $l = 0{,}5$ cm et pour l'absorbance $A = 0{,}155$ et correspondant à la valeur maximale $\lambda_{max} = 520$ nm.

La valeur K déterminée pour le $NH_4^+Rc^-$ peut être considérée dans les limites des erreurs acceptables, comme étant valable aussi pour le reineckate de PCP, étant donné que λ_{max} pour le reineckate de PCP est égal (ou presque égal) à λ_{max} pour le $NH_4^+Rc^-$.

La masse moléculaire (*Md*) est déterminée selon la relation :

$$Md = g_1/100.\ (K/\mathrm{A})\ l.1000 \tag{1}$$

Pour le cas $g_1 = 0{,}1$ g de reineckate de PCP pour 100 ml solution, la relation (1) devient :

$$Md = (K/\mathrm{A}).l \tag{2}$$

Pratiquement la détermination de l'absorption en visible du reineckate de PCP est faite dans l'éthanol 95%. L'absorbance pour $\lambda_{max} = 520$ nm à la concentration de 0,1% et à une cuve avec $l = 0{,}5$ cm (dans les mêmes conditions de travail) est de 0,098. En remplaçant dans la relation (2) on obtient :

$$Md = (103{,}70/0{,}098).0{,}5 = 529$$

Bien que la pilocarpine ait les deux atomes d'azote du noyau imidazolique quaternisables, la masse moléculaire du reineckate de PCP établie expérimentalement comparée à celle résultée du calcul pour le monoreineckate de PCP (Mc = 527,48) indique que la structure du composé obtenu est du type monoreineckate et non pas direineckate.

Caractéristique en infrarouge du reineckate de PCP. Le reineckate de PCP a été structuralement caractérisé aussi par spectre en infrarouge, que l'on a interprété par comparaison avec le spectre du $NH_4^+Rc^-$ (tabl. 3) et le spectre de l'azotate de PCP[8-12] (tabl. 4).

[8] Junosuke Fujita, Kazuo Nakamoto, Moshehisa Kabayashi, *J. Amer. Chem. Soc.*, **78**, 3295 (1956).

[9] B. Herzberg et C. Reid, *Discuss. Faraday Soc.*, **9**, 92 (1950).

[10] P. C. H. Mitchell et R.T.P. Williams, *J. Chem. Soc.*, **1961**, 4590.

[11] M. M. Chamberlain et I. C. Bailar, *J. Amer. Chem. Soc.*, **81**, 6412 (1959).

[12] M. E. Baldwin, *J. Chem. Soc.*, **1960**, 4369 ; **1961**, 471.

Tableau 3

Le spectre en IR du reineckate d'ammonium

$\bar{\nu}$(cm^{-1})			*T* %
472	(f)	δNCS	62
509	(f)		57
718	(i)	NH_3	39
833	(f)	ν_{C-S}	76
965			76
1265	(i)	$\delta^{Sym}_{NH_3}$	34
1405	(i)	δNH_4^+	32
1605		(H_2O)	50
2059		ν_{C-N}	14
2125	(i)		1
3015	(t.f)		38
3160	(f)		30
3195	(t.f)	ν_{NH_3}	32
3238	(f)		28
3315	(f)		27

f = faible
i = intense
t.f = très faible

Le spectre en IR du composé présente des bandes pouvant être attribuées aux groupements NH_3 et NCS de l'anion reineckate du complexe retrouvées aussi dans le spectre en IR du reineckate d'ammonium. Les bandes apparaissent à 499 cm^{-1} (δ_{NCS}), 1265 m^{-1} ($\delta\,\overset{\text{sym}}{\underset{\text{N-H}}{\text{NH}_3}}$) 2085 cm^{-1} ($\nu_{C-N}$), 3165—3330 cm^{-1} ($\nu\overset{\text{sym}}{\underset{\text{N-H}}{\text{NH}_3}}$). Le spectre présente aussi des bandes correspondant à la base organique (tabl. 4). Ces bandes existant à 617 cm^{-1}, 1190 cm^{-1}, 1620 cm^{-1}, 1725 cm^{-1}, 1762 cm^{-1}, 3130 cm^{-1} sont très peu modifiées comme position et intensité dans le spectre en IR du composé étudié, étant une nouvelle preuve pour le schéma donné.

Les spectres ont été déterminés avec un spectrophotomètre enregistreur en infrarouge type UR—20 Zeiss Jéna, utilisant la technique des pastilles de bromure de potassium. On a utilisé des prismes de KBr (400—700 cm^{-1}) NaCl (700—1800 cm^{-1}) et LiF (1800—4000 cm $^{-1}$).

Tableau 4

Spectre en IR de l'azotate de pilocarpine et du reineckate de pilocarpine

Spectre du PCP $\bar{\nu}$ (cm^{-1})	*T*%	Spectre du reineckate de PCP		Spectre du PCP $\bar{\nu}$ (cm^{-1})	*T*%	Spectre du reineckate de PCP	
		$\bar{\nu}$ (cm^{-1})	*T*%			$\bar{\nu}$ (cm^{-1})	*T*%
426 (t.f)	86						
470 (f)	74	499 (i)	60	1465 (f)	50	1389 (f)	75
540 (f)	78	557 (t.f)	90	1501 (m)	50	1470 (m)	72
635 (i)	46	592 (t.f)	88	1567 (m)	60	1565 (f)	80
650 (f)	76	617 (i)	60	1622 (i)	52	1620 (i)	61
682 (m)	74	700 (i)	54	1780 (t.i)	12	1762 (t.i)	31
720 (i)	63	725 (i)	58	1901 (t.f)	75		
765 (t.f)	78					2085 (t.i)	1
776 (f)	76	792 (t.f)	84			2300 (t.f)	91
830 (f)	68			2435 (t.f)	72		
880 (i)	34	852 (t.f)	84	2570 (t.f)	60		
920 (f)	66			2642 (f)	52		
950 (i)	52	952 (f)	84	2760 (t.f)	48		
1030 (i)	20	990 (m)	67	2815 (t.f)	46		
1049 (f)	53	1040 (m)	78	2890 (t.f)	39	2898 (t.f)	80
1080 (i)	36	1065 (f)	80	2940 (t.f)	40	2945 (t.f)	86
1100 (f)	59			2980 (t.f)	44	2960 (t.f)	84
1185 (i)	21	1110 (t.f)	76	3075 (i)	24		
1225 (f)	43	1130 (m)	72	3135 (i)	24	3130 (f)	62
1240 (f)	49	1190 (i)	50			3165 (f)	55
1330 (i)	5	1265 (i)	42			3252 (f)	46
1402 (i)	10	1335 (f)	79			3330 (f)	42

f = faible ; i = intense ; t.f. = très faible ; t.i = très intense ; m = moyenne.

Revue Roumaine de Chimie, **19**, *10*, 1651–1660 (1974)

MEMBRANE-ELECTRODES OF A METALLIC WIRE–PLASTIC MEMBRANE TYPE. I

K^+-SELECTIVE MEMBRANE ELECTRODE

ELENA HOPÎRTEAN, C. LITEANU and EUGENIA ŞTEFĂNIGĂ
"Babeş-Bolyai" University, Cluj, Department of Analytical Chemistry,
str. Arany János 11, Cluj

Received: January, 7, 1974

The paper discusses the manner of obtaining a K^+-selective electrode of a Pt wire type covered by a plastic membrane formed of PVC, plasticizer and potassium tetraphenylborate. Comparative studies are made on electrodes obtained with plasticizers : 3-nitro-*o*-xylene, dibutylphthalate and diisooctylphthalate. The basic characteristics of the resulted electrodes are established to this end, *viz.* : electrodic function, selectivity, electric resistance and response rate. Electrodes are used in the determination of potassium with sodium or calcium tetraphenylborate by potentiometric titration.

1. INTRODUCTION

One of the ion-selective membrane-electrode categories is that which involves a polymer as a support. A number of authors[1–10] successfully used PVC as a support, obtaining selective membrane-electrodes at H^+, K^+, Ca^{2+} ions, organic cations, etc. An important role in the operation of polymer matrix-based electrodes is played by the plasticizer used which may provide both a high degree of semipermeability to certain ions and some suitable physico-chemical properties (elasticity, resistance to tearing, etc.).

---

[1] A. Shatkay, *Analyt. Chem.*, **39**, 1056 (1967).

[2] C. Liteanu and E. Hopîrtean, *Rev. Roumaine Chim.*, **15**, 749 (1970).

[3] T. Higuchi, C. R. Illian and J. L. Tossoumian, *Analyt. Chem.*, **42**, 1674 (1970).

[4] G. J. Moody, R. B. Oke and J.D.R. Thomas, *Analyst*, **95**, 911 (1970).

[5] J. E. W. Davies, G. J. Moody and J.D.R. Thomas, *Analyst*, **97**, 87 (1972).

[6] S. Lal and G. D. Christian, *Analyt. Chem.*, **43**, 410 (1971).

[7] G. Baum and M. W. Wise, *Patent german*, 2.024.636, 10 Dec. 1970–3 June 1962 ; *Chem. Abstr.*, **74**, 71426 (1971).

[8] R. Scholer and W. Simon, *Helv. Chim. Acta*, **55**, 1801 (1972).

[9] G. Baum, M. Lynn and F. B. Ward, *Analyt. Chim. Acta*, **65**, 385 (1973).

[10] G. Baum and M. Lynn, *Analyt. Chim. Acta*, **65**, 393 (1973).

A recent trend in achieving membrane-electrodes consists in directly covering a platinum wire by an ion-selective membrane[11–16] thus eliminating the internal solution. The electric conductance of this type of electrodes is based on the combination of the electronic type conduction mechanism with the ionic one.[17,18]

As to K^+-selective electrodes with polymer support (PVC) the active electronic component used is observed to be the tetraphenylborate or the *p*-chlortetraphenylborate ion.[7,8,10,14]

In a previous work[19] we used $Na[B(C^6H_5)_4]$ to obtain a K^+-selective liquid electrode, employing cyclohexanone as a solvent and glass frit as a support.

This paper introduces a new manner of obtaining K^+-selective electrode by coating the Pt wire with a membrane formed of PVC, plasticizer and $K[B(C_6H_5)_4]$. The characteristics of the resulting membrane-electrode are studied: electrodic function, selectivity, electric resistance and response rate. The electrode is used in the determination of potassium found in solution in the absence or in the presence of other ions (Na^+, Ca^{2+}, Mg^{2+}), by potentiometric titration with sodium or calcium tetraphenylborate.

2. EXPERIMENTAL

2.1. MANNER OF OBTAINING THE ELECTRODE

Dosage of appropriate amounts of potassium tetraphenylborate, PVC and plasticizer resulted in a paste having the following composition: 3% $K[B(C_6H_5)_4]$, 35% PVC, 62% plastifier. An as homogeneous as possible paste is obtained by finally dispersing potassium tetraphenylborate into the plasticizer and by adding finely-ground PVC thereafter. Potassium tetraphenylborate was vacuum-dried at 120° prior to use. After becoming homogeneous, the paste is heated at about 200° and an approx. 5 mm long Pt wire (1) fixed at the end of a glass tube is introduced therein (2). The Pt wire is coated by a 0.2–0.3 mm thick membrane (3) over a span of about 5 mm of the glass tube. A thin paraffin layer is then applied over

[11] J. R. Settzo and M. W. Wise, *French Patent*, 1.530.500, 28 June 1968–3 May 1966; *Chem. Abstr.*, **71**, 56407 (1969).

[12] R. W. Cattral and H. Freiser, *Analyt. Chem.*, **43**, 1905 (1971).

[13] H. James, G. Carmack and H. Freiser, *Analyt. Chem.*, **44**, 856 (1972).

[14] J.E.W. Davies, G. J. Moody, W. M. Price and J.D.R. Thomas, *Lab. Pract.*, **22**, 20 (1973).

[15] T. Stworzewicz, J. Czapkiewicz and M. Seszko, communication presented at the symposium "Ion-Selective Electrodes", Mátrafüred, Hungary, Oct. 1972, E. Pungor (ed.), Akad. Kiadó, Budapest, Hungary, 1973, p. 245.

[16] M. B. Kneebone and H. Freiser, *Analyt. Chem.*, **45**, 449 (1973).

[17] H. Freiser and G. Carmack, *U.S. Nat. Tech. Inform. Serv. A. D. Rep.* 1973, N° 759073; *Chem. Abstr.*, **79**, 67227 (1973).

[18] P. Parrini, *Polymer*, **14**, 445 (1973).

[19] E. Hopîrtean and E. Ştefănigă, *Rev. Roumaine Chim.*, **19**, (1974).

the membrane on the glass tube and over approx. 2 cm of the tube, to provide optimum operating conditions for the electrode by avoiding an incidental Pt-solution contact. The diagram of the electrode achieved is presented in fig. 1.

2.2. CHARACTERISTICS OF THE ELECTRODE

2.2.1. *E-pK electrodic function.* The e.m.f. of the following electrolytic chain was measured to this end:

Pt | membrane | test solution | salt bridge | reference electrode Ag/AgCl

Potential measurements were performed at room temperature under non-stirring conditions, using a MV—11 pH-meter. The accuracy of measurements is ±1 mV. In order to avoid the contamination of the sample with K^+ ions of the reference electrode, a salt bridge $NaNO_3$ 10^{-1} M containing 1% agar-agar was used. *E-pK* electronic functions were established both in KCl pure solutions and in the presence of some interfering ions: Na^+, Ca^{2+}, Mg^{2+}.

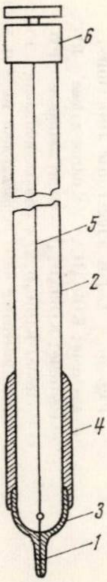

Fig. 1. — Membrane-electrode.

1, Pt wire; *2*, glass tube; *3*, membrane; *4*, paraffin layer; *5*, copper wire; *6*, contact terminal.

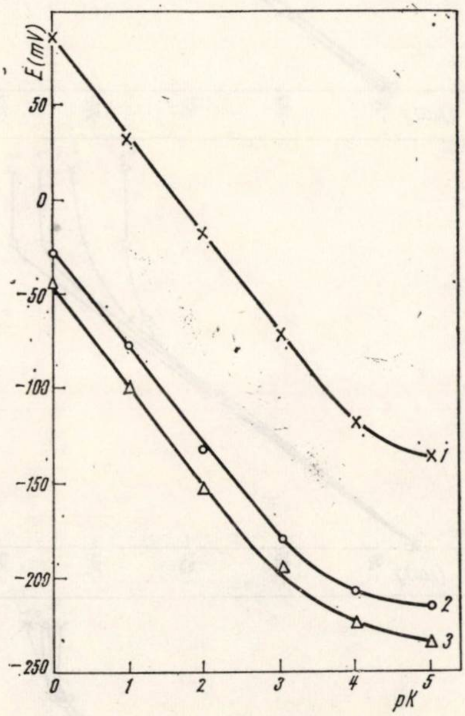

Fig. 2. — *F-pK* electrodic functions.

1, electrode: $K[B(C_6H_5)_4]$ + 3-nitro-*o*-xylene + PVC;
2, electrode: $K[B(C_6H_5)_4]$ + dibutylphthalate + PVC;
3, electrode: $K[B(C_6H_5)_4]$ + diisooctylphthalate + PVC.

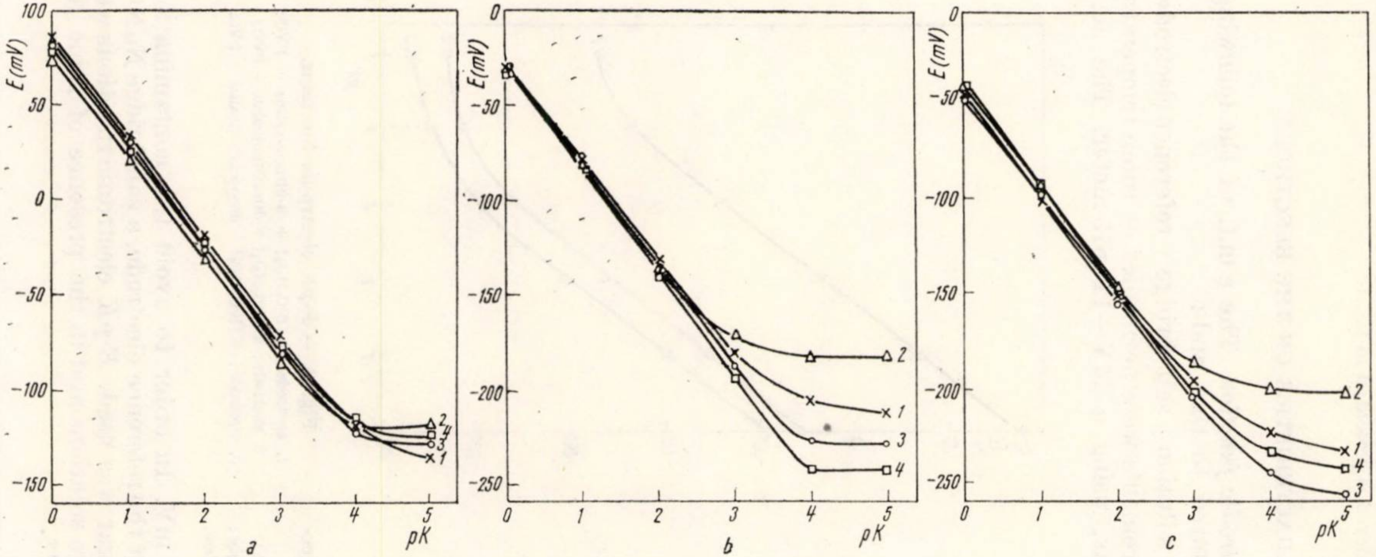

Fig. 3. — E-pK electrodic functions.

a) electrode ; $K[B(C_6H_5)_4]$ + 3-nitro-*o*-xylene + PVC ;
b) electrode ; $K[B(C_6H_5)_4]$ + dibutylphthalate + PVC ;
c) electrode ; $K[B(C_6H_5)_4]$ + diisooctylphthalate + PVC.
1, without interfering ions ; *2*, background 10^{-2} M NaCl ;
3, background 10^{-2} M $CaCl_2$; *4*, background 10^{-2} $MgMCl_2$.

In view of deciding on the optimum plasticizer, electrodes were prepared using the following plasticizers: 3-nitro-*o*-xylene[9,10] dibutylphthalate[9,10] and diisooctylphthalate. The electrodic functions obtained for K^+ ion in the absence of interfering ions, using the electrodes formed of the mentioned plasticizers, are presented in fig. 2.

Fig. 3 illustrates the electrodic functions obtained for K^+ with the same electrodes in the presence of interfering ions Na^+, Ca^{2+}, Mg^{2+} at a 10^{-2} M concentration.

In the case of the electrode with 3-nitro-*o*-xylene, electrodic functions were established for K^+ ion in the presence of NaCl at various concentrations (fig. 4).

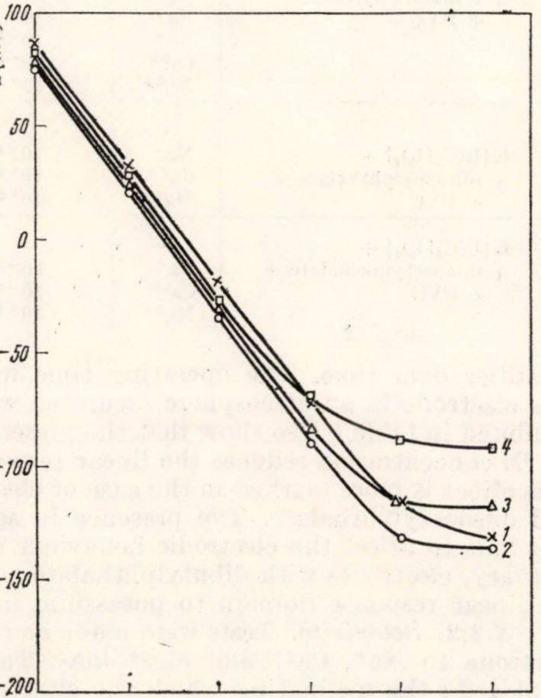

Fig. 4. — *E-pK* electrodic functions. Electrode: $K[B(C_6H_5)_4$ + 3-nitro-*o*-xylene + PVC.
1, without NaCl; *2*, background 10^{-3}M NaCl; *3*, background 10^{-2}M NaCl; *4*, background 10^{-1}M NaCl.

In order to have a good reproducibility of the electrode behaviour, their conditioning is indicated prior to use, by immersion in a 10^{-2} M KCl solution for roughly 30 min.

Values of the slopes of electrodic functions presented in figs. 2, 3 and 4 and also the linearity domain are shown in table 1.

Data supplied by table 1 with regard to the electrodic behaviour in the absence of interferences illustrate a better behaviour of the electrode with 3-nitro-*o*-xylene, particularly in relation to the concentration range of the linear response. In contrast, the operating time of electrodes with dibutylphthalate and diisooctylphthalate is longer (over 3 weeks) than of that with 3-nitro-*o*-xylene (2–3 days) which loses its electrodic capabilities within a shorter while due to a more pronounced loss of the plastifier over time. The operating time may be extended by keeping this electrode in an atmosphere saturated with plasticizer vapours. Data exhibited in table 1 also show that the presence of Na^+ ion a higher than 10^{-2}M concentration reduces the linear response domain of the electrode. This effect is more marked in the case of electrodes with dibutylphthalate and diisooctylphthalate. The presence in solution of Ca^{2+} and of Mg^{2+} ions fails to affect the electrodic behaviour to K^+ in either case. On the contrary, electrodes with dibutylphthalate and diisooctylphthalate extend the linear response domain to potassium in the presence of these ions.

Table 1

Electrodic behaviour

Electrode	Interfering ion	Concentration of interfering ion	Slope (mV/*pK*)	Concentration range (*pK*)
$K[B(C_6H_5)_4]$ + + 3-nitro-*o*-xylene + + PVC	—	—	53	0–3.7
	Na^+	10^{-3}M	55	0–3.7
	Na^+	10^{-2}M	53.5	0–3.2
	Na^+	10^{-1}M	53	0–2.5
	Ca^{2+}	10^{-2}M	54	0–3.7
	Mg^{2+}	10^{-2}M	54	0–3.7
$K[B(C_6H_5)_4]$ + + dibuthylphthalate + + PVC	—	—	52	0–3.0
	Na^+	10^{-2}M	52.5	0–2.5
	Ca^{2+}	10^{-2}M	53.5	0–3.7
	Mg^{2+}	10^{-2}M	54	0–3.7
$K[B(C_6H_5)_4]$ + + diisooctylphthalate + + PVC	—	—	51	0–2.8
	Na^+	10^{-2}M	52.5	0–2.5
	Ca^{2+}	10^{-2}M	53	0–3.7
	Mg^{2+}	10^{-2}M	53	0–3.3

2.2.2. *Selectivity.* Tests were made on the selectivity of the obtained electrode to Na^+, Ca^{2+} and Mg^{2+} ions. To do this, two methods were employed : the method by which the electrode potential has been determined in separate solutions of the two ions (K^+ ion and interfering ion), and the method using the electrode potentials determined in solutions containing the mixture of the two ions.[20]

In the case of the second method used, the alternative was selected in which the primary ion, K^+, has a constant concentration, the concentration of the interfering ion being modified by known additions of a concentrated solution (1 M) of the latter or even of the solid salt of the interfering ion for the 1 M concentration.

Selectivity constants exhibited in table 2 were calculated by the method suggested by Srinivasan and Rechnitz,[20] according to which this magnitude is given by the activity ratio of the two ions, primary and interfering, respectively, which determine the same electrode potential.

---

[20] K. Srinivasan and G. A. Rechnitz, *Analyt. Chem.*, **41**, 1203 (1969).

Table 2

Selectivity constants

Electrode	Selectivity constant		
	K_{KNa}	K_{KCa}	K_{KMg}
$K[B(C_6H_5)_4]$ + 3-nitro-*o*-xylene + PVC	2.8×10^{-2}	$\sim 10^{-4}$	5×10^{-3}
$K[B(C_6H_5)_4]$ + dibutylphthalate + PVC	7.0×10^{-2}	10^{-3}	$\sim 10^{-4}$
$K[B(C_6H_5)_4]$ + diisooctylphthalate + PVC	8.0×10^{-2}	10^{-3}	10^{-3}

Selectivity constants in table 2 are really supported both by the electrodic functions obtained for K^+ in the presence of interfering ions (fig. 3) and by the results presented in fig. 5.

Inspection of the data included in table 2 shows that the electrode with 3-nitro-*o*-xylene plasticizer provides a better potassium-sodium selectivity, which is an evidence of the role of the plasticizer in the behaviour of such types of electrodes, concerning the different permselectivity manifested to various ions. As to the selectivity of electrodes to Ca^{2+} and Mg^{2+}, respectively, a practically similar behaviour of electrodes formed of the three plasticizers has been found. The high electrode selectivity to Ca^{2+} and Mg^{2+} suggests the extension of the linear response domain in the case of electrodes with dibutylphthalate (fig. 3b) and diisooctylphthalate (fig. 3c). The presence of these practically indifferent electrolytes favours the electrode response to low potassium concentrat ions.

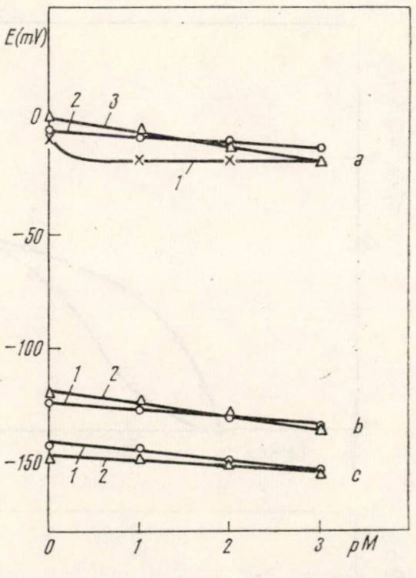

Fig. 5. — Response of the electrode in 10^{-2} M KCl solution depending on the concentration of the interfering ion.

a) electrode; $K[B(C_6H_5)_4]$ + 3-nitro-*o*-xylene + PVC; *1*, Na^+; *2*, Ca^{2+}; *3*, Mg^{2+}.

b) electrode; $K[B(C_6H_5)_4]$ + dibutylphthalate + PVC; *1*, Ca^{2+}; *2*, Mg^{2+}.

c) electrode; $K[B(C_6H_5)_4]$ + diisooctylphthalate + PVC; *1*, Ca^{2+}; *2*, Mg^{2+}.

2.2.3. *Electrical resistance and response rate*. The electric resistance was measured in a saturated KCl solution using a RLC type 221 bridge and a platinum counterelectrode.

The response rate was determined by recording the electrode potential on a Radelkis OH102 polarograph. Recordings were made both in the absence and in the presence of interfering ions of a 10^{-2} M concentration in solutions in which the concentratio- of K^+ ion was higher than 10^{-3} M. Results regarding the electric resist. ance and the response time of the electrodes studied are listed in table 3u

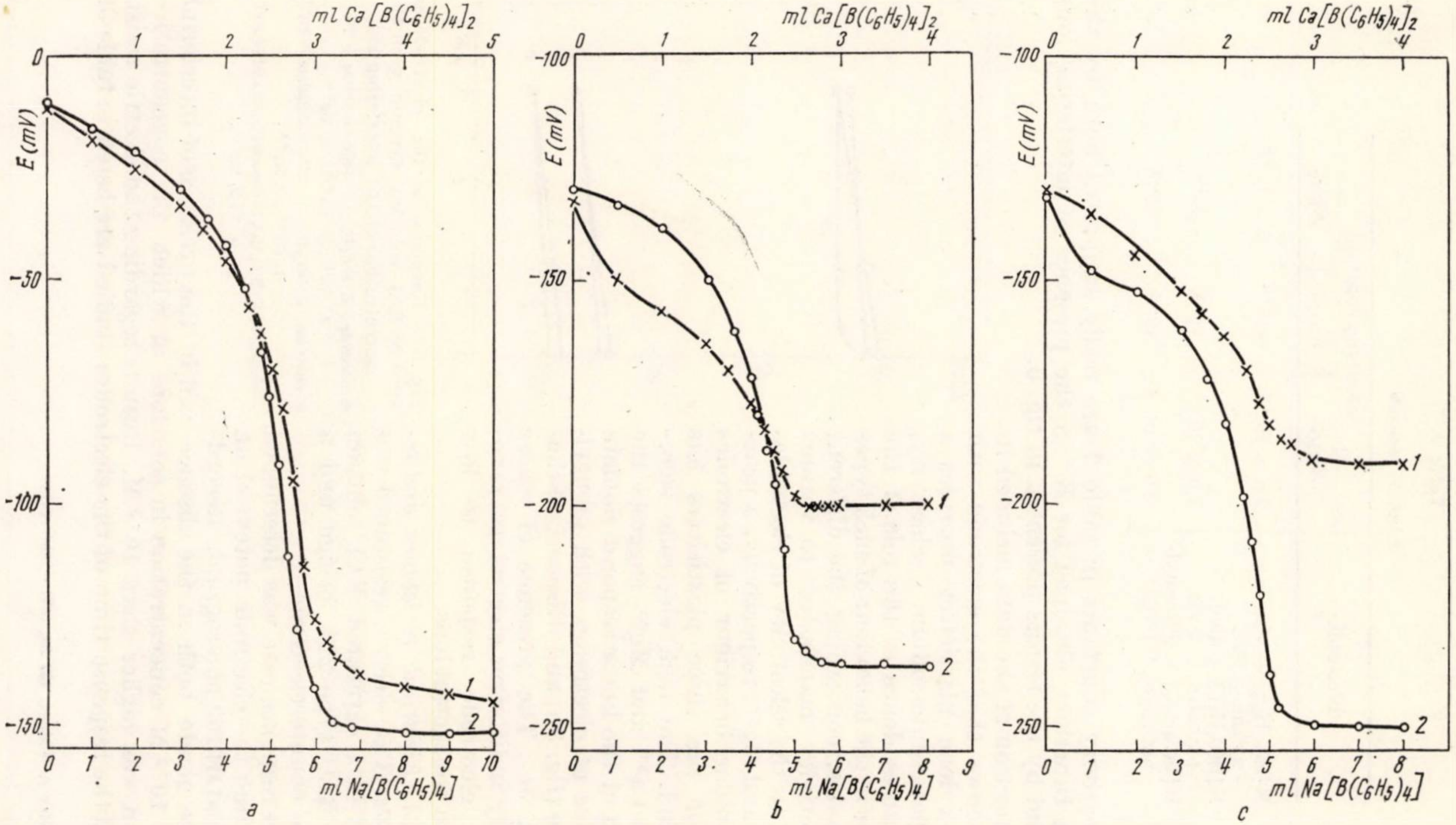

Fig. 6. — Titration of 10^{-2}M KCl with $\sim 5 \times 10^{-2}$M $Na[B(C_6H_5)_4]$ (*1*) and with $\sim 10^{-1}$M $Ca[B(C_6H_5)_4]$ 2 respectively (*2*).

a) electrode: $K[B(C_6H_5)_4]$ + 3 nitro-*o*-xylene + PVC;

b) electrode: $K[B(C_6H_5)_4]$ + dibutylphthalate + PVC;

c) electrode: $K[B(C_6H_5)_4]$ + diishooctylpthalate + PVC.

Table 3

Electric resistance and response time

Electrode	Electric resistance (ohms)	Response time (sec)
$K[B(C_6H_5)_4]$ + 3-nitro-*o*-xylene + PVC	1.1×10^7	60
$K[B(C_6H_5)_4]$ + dibutylphthalate + PVC	5.8×10^6	70–80
$K[B(C_6H_5)_4]$ + diisooctylphthalate + + PVC	6.5×10^7	30–40

In solutions in which the concentration of K^+ ions is below 10^{-3} M, the electrode response time is a few minutes (3–4 min).

2.3. ANALYTICAL USE

The electrodes developed were analytically used in the potentiometric titration of potassium with sodium or calcium tetraphenylborate. The resulted titration curves are plotted in fig. 6.

As a result of a good potassium-sodium selectivity of the electrode formed 3-nitro-*o*-xylene plastifier, the titration curve obtained with sodium tetraphenylborate as a titrant shows a distinct potential jump at the equivalence point ($\Delta E_{\pm 1\%} = 20$ mV) which is close to that obtained when using calcium tetraphenylborate as a titrant ($\Delta E_{\pm 1\%} = 25$ mV) (fig. 6a). Due to a lower potassium-sodium selectivity of electrodes with dibutylphthalate and diisooctylphthalate, respectively, titration curves obtained by using sodium tetraphenylborate as titrant have a small potential variation at the equivalence point (figs 6b and 6c). In the case of these electrodes, calcium tetraphenylborate is recommended as a titrant, obtaining in the case of both electrodes a potential variation around the equivalence point, $\Delta E_{\pm 1\%}$, of about 20 mV.

Titrations of K^+ were also performed together with Na^+, respectively, with Ca^{2+} or Mg^{2+} using the electrode with 3-nitro-*o*-xylene plasticizer and sodium tetraphenylborate as titrant. Titration curves obtained are presented in fig. 7.

Since, as seen in fig. 7, potassium determination can be successfully performed in the presence of any of the three tested ions (Na^+, Ca^{2+}, Mg^{2+}), the electrode may find various concrete practical applications.

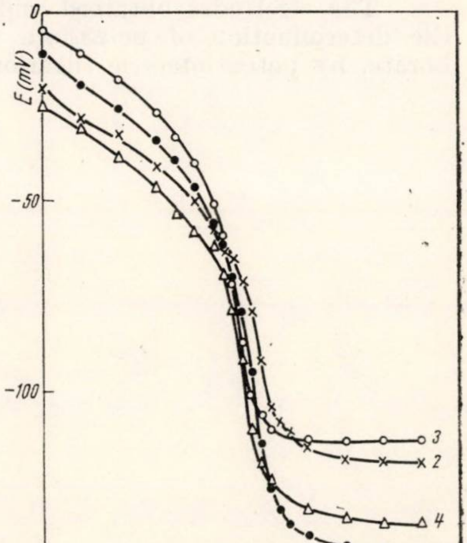

Fig. 7. — Titration of 10^{-2}M KCl with ~5×10^{-2} M $Na[B(C_6H_5)_4]$.

1, without background; *2*, background NaCl 10^{-2} M; *3*, background 10^{-2}M $CaCl_2$; *4*, background 10^{-2}M $MgCl_2$. Electrode: $K[B(C_6H_5)_4]$ + 3-nitro-*o*-xylene + PVC.

CONCLUSIONS

The paper presents an original manner of achieving a K-selective electrode of a platinum wire type coated by a plastic membrane formed of $K[B(C_6H_5)_4]$, plasticizer and PVC.

An analysis of the behaviour of electrodes with plasticizers : 3-nitro-*o*-xylene, dibutylphthalate and diisooctylphthalate results in the following :

— the electrode containing 3-nitro-*o*-xylene as a plastifier provides the advantage of a larger concentration range of the linear response yet it offers a short operating time.

— electrodes with dibutylphthalate and diisooctylphthalate, respectively, provide linear response in a somewhat more restricted concentration range offering, however, the advantage of a much longer operating time than the electrode with 3-nitro-*o*-xylene.

— potassium-sodium selectivity of all three types of developed electrodes is good. Particular mention is made of the fact that Ca^{2+} and Mg^{2+} ions do not practically disturb the electrode functioning. Therefore, the electrodes have a high potassium-calcium, and potassium-magnesium selectivity, respectively.

The electrodes obtained and studied may be successfully used in the determination of potassium with sodium or calcium tetraphenylborate, by potentiometric titration.

Revue Roumaine de Chimie, **19**, *10*, 1661–1667 (1974)

APPLICATION OF NIOBIUM POLAROGRAPHIC REDUCTION IN HYDROCHLORIC ACID-THIOCYANATE MEDIUM TO THE ANALYSIS OF FERRONIOBIUM ALLOYS

SOFIA MARCHIDAN
Centre of Physical Chemistry, Str. Galaţi 31, Bucharest, Romania

Received January 31, 1974

A polarographic method for the determination of niobium concentration in the presence of iron is described. The average value polarographically obtained for niobium content differs by + 0.59 % from the given value by chemical analysis. The developed method is fairly rapid, accurate and very suitable, since it may be applied directly, in the presence of the other alloy constituents (Fe, Ti, Si, Al, Cr, Ta etc.) without preliminary separations.

In the production of alloyed steels with niobium addition, ferroniobium alloys containing also other elements (Ti, Si, Cr, Al, Ta, etc.) in lower concentration are used rather than pure niobium. The polarographic reduction of niobium in HCl-thiocyanate-acetone medium has been applied to the determination of niobium concentration from the above mentioned alloy, without preliminary separations.

1. GENERAL CONSIDERATIONS

In a previous paper,[1] iron interference in the polarographic determination of niobium with thiocyanate has been described.

Experiments performed for the same niobium concentration ($2 \cdot 10^{-3}$ M), but variable iron concentrations, have shown that the height of niobium reduction wave decreases with the increase in iron concentration (figure 1, curve *1*), and the results are not quite reproducible.

Similar effects have also been met with other niobium concentrations. All these results suggested that it is not possible to obtain a suitable and quite precise method for niobium determination in the presence of iron, because of the following :

— the iron concentration in the sample should be determined beforehand ;

— the height of niobium wave strongly and nonlinearly decreases with the increase in iron concentration ;

— a two-dimensional regression analysis is needed which complicates the calculations.

---

[1] S. Marchidan, C. Drăgulescu and Gh. Facsko, *Rev. Roumaine Chim.*, **16**, 399 (1971).

When a large amount of titanium trichloride is added[2] the wave height, at the same niobium concentration, is much less sensitive to iron concentration and, beginning with the ratio Fe : Nb = 1 : 1 up to the maximum studied ratio of 5 : 1, it remains practically constant (figure 1, curves *2–4*).

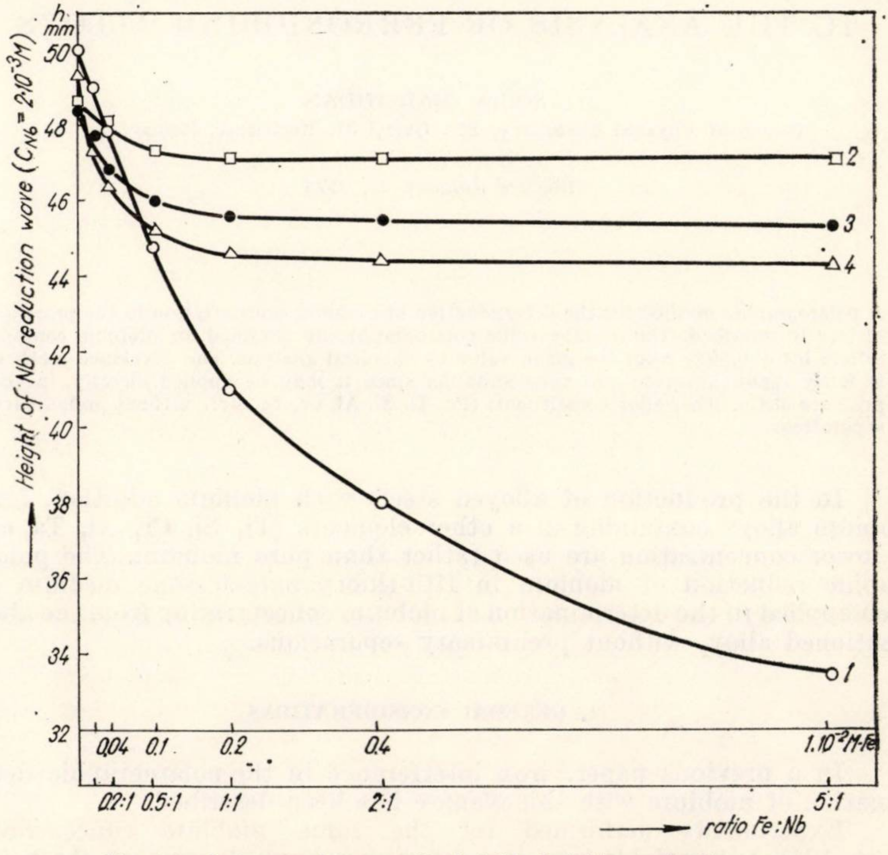

Fig. 1. — Influence of iron on the height of niobium reduction wave.

1 ; without $TiCl_3$ addition ; *2–4*, with $TiCl_3$ addition ; *2*, hydrochloric acid solutions without tartaric acid addition ; *3*, tartaric acid solutions 0.05 M ; *4*, tartaric acid solutions 0.2 M.

Although this effect of titanium trichloride addition does not completely remove iron interference, it shows that the previous determination of iron concentration is no longer needed, provided that, an iron excess is ensured (Fe : Nb ratio ⩾ 1 : 1) in Nb + Fe solution.

In tartaric acid solution (obtained from a niobium standard solution in tartaric acid, which is stable and very easy to prepare), the polarographic wave height of niobium, within the Fe : Nb = 1 : 1 ÷ 5 : 1 range, is smaller than the wave height of pure niobium standard. Obviously this fact has a slight influence upon the sensibility.

---

[2] S. Marchidan, C. Drăgulescu and Gh. Facsko, *Rev. Roumaine Chim.*, **16**, 813 (1971).

Additional experiments have been carried out in order to find out the conditions under which this decrease of the wave height is minimum. Thus, the influence of tartaric acid concentration was studied. Although the presence of tartatic acid does not affect the wave height of pure niobium standard solution,[3] it was found that in the solution containing both niobium and iron, the diminution percent of niobium wave height *versus* pure niobium standard, decreases with the decrease of tartaric acid concentration (figure 1, curves *3* and *4*), reaching a minimum value of about 3% in its absence (curve *2*).

When tartaric solutions are used, in order to increase the sensibility, it is recommended that the tartaric acid concentration should be as low as possible while for reproducibility reasons this concentration should be the same in both standard and sample.

The height of niobium reduction wave, in the presence of titanium trichloride and of a suitable iron excess at the same tartaric acid concentration, does not depend on iron concentration and allows niobium determination from ferroniobium alloys.

This problem can be solved in two different ways.

a) The influence of iron in the presence of titanium trichloride (and several tartaric acid concentrations) at different niobium concentrations should be studied by experiments similar to those described above, in order to find out whether or not a range of common values exists for the Fe : Nb ratio in which the wave height does not depend on iron concentration. Further on, if such a range exists, it must be verified by regression analysis whether these heights follow or not a linear dependence on the niobium concentration. If a linear dependence is found, a method may be advanced for niobium determination in the presence of iron, using the calibration graph and a statistic calculation of experimental data which will give the equations for the concentration estimation, standard deviation and confidence interval. If the dependence is not linear, the precision of such a method would be considerably lower.

b) A method can be advanced based only on the experimental results obtained in the studies of iron influence on the reduction wave of niobium in the presence of titanium trichloride at one niobium concentration ($2 \cdot 10^{-3}$ M). This concentration is in the middle of the linearity range found for the pure niobium standard[4,5] and for which all the interference studies were carried out.[1,2] This method only implies finding that aliquot from the stock solution which in the same volume, medium and conditions as standard Nb + Fe solution ($C_{\mathrm{Nb}} = 2 \cdot 10^{-3}$ M and Fe : Nb$\geqslant$1) will give a wave height whose difference *versus* standard should not be statistically significant. Thus, in the analysed solution the niobium concentration may be estimated as equal to that of standard and, the aliquot being known, the niobium percent in the sample is obtained by a simple calculation.

---

[3] C. Drăgulescu, S. Marchidan and Gh. Facsko, *Rev. Roumaine Chim.*, **14**, 737 (1969).

[4] S. Marchidan, Gh. Facsko and C. Drăgulescu, *Rev. Roumaine Chim.*, **12**, 635 (1967).

[5] C. Drăgulescu, S. Marchidan and Gh. Facsko, *Rev. Roumaine Chim.*, **14**, 1501 (1969).

In order to determine niobium concentration in a ferroniobium alloy, we have chosen this second procedure which is much simpler.

2. DETERMINATION OF NIOBIUM CONCENTRATION IN A FERRONIOBIUM ALLOY

Table 1 presents the heights of niobium reduction wave, *h*, (for hydrochloric or tartaric acid standard niobium solutions) in HCl-thiocyanate-acetone medium for values of Fe : Nb ratios ranging between 0 : 1 and 5 : 1 at the same niobium concentration of $2\cdot10^{-3}$ M. Curves 2 and 3 in figure 1 represent the averages of these values.

Table 1

Influence of iron on the height of niobium reduction wave ($C_{\mathrm{Nb}} = 2\cdot10^{-3}$ M)

Ratio Fe :Nb	Niobium hydrochloric standard solution		Niobium tartaric standard solution	
	h (mm)	$\bar{h}$ (mm)	h (mm)	$\bar{h}$ (mm)
0 :1	49.0	48.7	49.1	48.7
	48.8		48.3	
	48.4		48.6	
0.2 :1	48.3	48.1	46.8	46.8
	48.1		47.0	
	47.8		46.7	
0.5 :1	47.6	47.5	46.1	46.1
	47.3		45.9	
	47.7		46.2	
1 :1	46.8	47.2	46.0	45.7
	47.3		45.4	
	47.4		45.8	
2 :1	46.8	47.1	46.0	45.5
	47.4		45.3	
	47.0		45.2	
5 :1	47.4	47.1	45.4	45.5
	46.8		46.0	
	47.0		45.2	

The data listed in table 1 were obtained with a pure niobium hydrochloric or tartaric standard solution to which iron was added. It can be seen that for both, hydrochloric or tartaric solutions (concentration of tartaric acid in the final solution for polarographic measurements being the same, that is 0.05 M), the last nine values, corresponding to the ratios Fe : Nb = 1 : 1, 2 : 1 and 5 : 1, do not depend on iron concentration and may be considered as estimations of polarographic wave height of niobium for the interval Fe : Nb = 1 : 1 ÷ 5 : 1 and niobium concentration of $2\cdot10^{-3}$ M.

These values lie around the average of 47.1mm (standard deviation $s_1 = 0.091$) when a hydrochloric standard was used and around the average of 45.6 mm (standard deviation $s_2 = 0.119$) when a tartaric standard was used. The standard deviations were calculated by the equation :

$$s = \sqrt{\frac{\Sigma d^2}{n(n-1)}} \tag{1}$$

where $n = 9$ and d represents the deviation of an individual value from the average value, $\bar{h}$.

In conclusion, at a significance level of 99%, when the Student's variable for $n - 1 = 8$ degrees of freedom is $t = 3.36$, the two confidence intervals are:

$47.1 \pm 0.091\ t = 47.1 \pm 0.3$ for the hydrochloric standard solution

$45.6 \pm 0.119\ t = 45.6 \pm 0.4$ for the tartaric standard solution.

The experiments with mixtures of Nb + Fe standard led to the conclusion that, at a significance level of 99%, a solution of $C_{Nb} = 2 \cdot 10^{-3}$ M and Fe : Nb $\geqslant 1$, will give a polarographic wave height between 46.8 and 47.4 mm when hidrochloric niobium solution was used and of 45.2—46.0 mm with tartaric niobium solution. The very close confidence intervals, within which all the measured waves heights lie, prove a good reproducibility and ensure a good precision.

Once these confidence intervals are known, the following simple procedure for niobium determination in a ferroniobium alloy is advanced. A sample of m grams is weighed and a stock solution is obtained. Then, iron is added so that Fe : Nb $\geqslant 1$. Let V-ml be the volume of solution obtained this way. By some attempts the aliquot part, n-ml, is found which, in the volume, v-ml, used for polarographic analysis, in the same medium and conditions as standard solution, will give a height of polarographic wave placed within the confidence interval of the standard. It results that at a significance level of 99%, niobium concentration in v-ml sample solution may be estimated as being the same, that is $2 \cdot 10^{-3}$ M Nb. Consequently, in the n-ml aliquot there are:

$$\frac{2 \cdot 10^{-3} \times 92.906}{1000} v = 1.858 \cdot 10^{-4}\ v \text{ grams niobium} \tag{2}$$

where 92.906 is the molecular weight of niobium. The percentage of niobium in the alloy was calculated by the equation:

$$\% \text{ Nb} = 1.858 \cdot 10^{-2} \frac{vV}{nm} \tag{3}$$

and for $v = 10$ ml and $V = 100$ ml

$$\% \text{ Nb} = \frac{18.58}{nm} \tag{3'}$$

3. PROCEDURE

The polarographic behaviour of niobium in HCl-thiocyanate-acetone medium has been studied using hydrochloric or tartaric standard niobium solutions; these were prepared by fusing niobium pentoxide with potassium pyrosulfate.[4,5] The interference studies of different cations with the niobium reduction wave were also carried out and checked on synthetic samples containing mixtures of oxides which were made soluble by fusion with $K_2S_2O_7$ and dissolving the melt in tartaric acid.[1,2]

For ferroniobium alloys, as well as for metallic niobium, the method described in the literature consists of dissolution in hydrofluoric acid with or without nitric acid addition, depending on the composition of samples.

A sample of $m = 0.4015$ grams ferroniobium finely ground was weighed in a platinum crucible; then 4–5 ml hydrofluoric acid (40%) and 1–2 ml concentrated nitric acid was added. The crucible was carefully heated until complete dissolution has been reached and then its walls and lid were washed with 1–2 ml hydrofluoric acid. Further heating, close to complete evaporation, was followed by addition of a few drops of concentrated sulfuric acid to ensure the complete removal of silica. Then, 2–3 ml concentrated sulfuric acid was added and heated for a long time up to the formation of SO_3 fumes for complete removal of hydrofluoric acid and nitrogen oxides. After cooling, the sample was dissolved and transferred into a $V = 100$ ml volumetric flask with concentrated hydrochloric acid. At the same time a proper amount of ferric chloride was added to ensure an iron excess in the stock solution. Besides the niobium tartaric standard solution, a hydrochloric one was prepared from metallic niobium of spectral purity (Johnson Matthey) following exactly the same solubilization procedure as for the sample.

The solutions for polarographic measurements were obtained from n-ml aliquot (hydrochloric stock solution, hydrochloric acid, thiocyanate and titanium trichloride solution, acetone) which were pipetted and made up to $v = 10$ ml in volumetric flasks so that the final composition of the medium be optimum [2,4,5] and identical to that used for the standard, that is: $C_{HCl} = 6.0$ M; $C_{NH_4SCN} = 0.60$ M; $C_{TiCl_3} \cong 1.10^{-2}$ M; $C_{acetone} = 20\%$ for comparison with the hydrochloric standard and the same composition plus 0.05 M tartaric acid when

Table 2

Analysis of ferroniobium %

Element	Spectral analysis	Chemical analysis	Polarographic analysis		Difference ±
Nb	tens of percents	52.75	Sample 1 a	53.19	+0.83
			2 a	53.31	+1.06
			3 a	53.20	+0.85
			4 a	53.20	+0.85
			Sample 1 b	52.60	−0.28
			2 b	53.31	+1.06
			3 b	52.50	−0.47
			4 b	53.20	+0.85
			Average value :	53.06	
Fe	,,	15.3			
Si	,,	17.0			
Ti	percents	6.72	Samples 1–4a, *versus* hydrochloric niobium, standard solution.		
Al	,,	7.66	Samples 1–4b, *versus* tartaric niobium, standard solution.		
Cr	$10^{-1} - 5\cdot10^{-1}$	0.21			
Mn	$10^{-2} - 5\cdot10^{-2}$				
Ni	$5\cdot10^{-2} - 5\cdot10^{-3}$				
Co	$\sim 5\cdot10^{-3}$				
Mg	$10^{-2} - 5\cdot10^{-3}$				
Ta	$<5\cdot10^{-2}$				
Zr	$10^{-2} - 5\cdot10^{-3}$				
		99.64			

a tartaric standard was used. The working conditions were as previously established, that is $t = 25 \pm 0.1°C$ and the time elapsed from thiocyanate addition to the recording of the polarogram, between 40 and 50 minutes.

By a few preliminary attempts it was found for $n = 0.87$ and 0.88 ml aliqout which gave a height of the reduction wave within the confidence interval (47.1 ± 0.3 in the absence and 45.6 ± 0.4 in the presence of 0.05 M tartaric acid). Equation (3′) was applied and the following niobium percents in the sample were found :

1 a/ *versus* hydrochloric standard : 1 b/ *versus* tartaric standard :

$$\% \text{ Nb} = \frac{18.58}{0.87 \times 0.4015} = 53.19 \qquad \% \text{ Nb} = \frac{18.58}{0.88 \times 0.4015} = 52.60$$

i.e. very close results. This shows that the result of the determination does not depend on the kind of standard (hydrochloric or tartaric) which was used for comparison.

In order to verify these results, three more stock solutions were prepared with different quantities of alloy and following the same procedure as that described above.

Table 2 exhibits the polarographic results in comparison with the data from chemical and spectral analysis of the alloy.

As shown in table 2, the average value obtained for niobium percent, determined by the polarographic method differs by +0.59% from the value certified by chemical analysis, while the individual values differ from + 1.06 to − 0.47%.

It might be concluded that the polarographic method is fairly precise leading to results which are not significantly different from those obtained by chemical analysis. The proposed polarographic method is much more suitable since it may be applied directly in the presence of other alloy constituents, such as Si, Fe, Ti, Al, Cr, Ta etc., without preliminary separations.

Revue Roumaine de Chimie, **19**, *10*, 1669–1676 (1974)

DETERMINATION OF LITHIUM IN SILICATE ROCKS AND MINERALS USING A SIMPLE FLAME PHOTOMETER

SHAMSHAD AHMAD KHAN *
Pakistan Council of Scientific and Industrial Research Laboratories, Karachi, Pakistan
and
MAURICE STONE
Department of Geology, University of Exeter, England

Received October 22, 1973

A method is proposed for the determination of lithium in silicate rocks and minerals in the presence of other ions on the solution 'B', obtained after digestion in HF and H_2SO_4 or HF and perchloric acid [1,2] by a simple flame photometer. Interference due to potassium was overcome by the addition of 2000 p.p.m. K_2O (as K_2SO_4) "buffer". The precision and accuracy of this method has been tested by replicate analyses of rocks and standard, by adding known amounts of standards to the sample and by comparing the results with the atomic absorption method. The method is suitable for the rocks containing 95 p.p.m. to 3000 p.p.m. lithium corresponding to 200 p.p.m. to 6000 p.p.m. lithium oxide. This method could easily be incorporated into the analytical scheme of Shapiro and Brannock [1] and Riley[2].

INTRODUCTION

The rapid method described by Shapiro and Brannock [1] and Riley[2] for analysing major and minor elements present in silicate rocks do not provide a method for analysing lithium and as this element also occurs in significant quantities in many of the silicate rocks and minerals, so it was deemed desirable to develop a suitable analytical method for this element. This work was carried out in the Department of Geology, University of Exeter, England.

Lithium in rocks can be determined by gravimetric, [3,4] colorimetric, [5–8] spectrographic,[9] atomic absorption[10] and flame photometric methods.[11-17] « The gravimetric methods are rather slow and time consuming and are less accurate.[5] Both direct and indirect colorimetric methods for the determination of lithium require the separation of lithium from other metals, which makes the method more difficult.[5-8] Although spectrographic[9] and atomic absorption methods[10] are more accurate and sensitive but are very expensive.

---

* To whom correspondence should be addressed.

[1] L. Shapiro, and W. W. Brannock, *U.S.Geol. Survey Bull. No. 1036c,* (1956).

[2] J. P. Riley, *Analyt. Chim. Acta,* **19**, 413 (1958).

[3] A.W. Groves, "Silicate Analysis". Georgen Allen and Unwin Ltd., London (1951).

[4] A. Vogel, "A Textbook of Quantitative Inorganic Analysis". Third edition, Longmans, Green and Co. Ltd., London, 564 (1961).

[5] M.H. Brown, and J. H. Reedy, *Ind. Eng. Chem. Analyt. Ed.*, **2**, 304 (1930).

[6] E. B. Sandel, "Colorimetric Determination of Traces of Metals", Interscience Publishers, Inc., New York, 584c (1959).

[7] C. E. White, M. H. Fletcher and J. Parks, *Analyt. Chem.*, **23**, 478, (1951).

[8] F. Nelson, (reference in Sandel, 1959), *J. Amer. Chem. Soc.*, **77**, 813 (1955).

[9] J. J. Gurney and A. J. Erland, *Analyt. Chem.*, **38**, 1839 (1966).

[10] S. Abbey, *Can. Dep. Energ., Mines, Resour., Geol. Surg. Can. Pap. No. 67,* 35(1967).

Flamephotometric determination of lithium can be carried out in two ways: (i) Flame spectrophotometric and (ii) Flame photometric. Numerous references for flame spectrophotometric methods are cited in literature.[11-17] These are more sensitive owing to the variable slit-width control and monochromatic light source than those using a filter photometer.

As far as the authors are aware a simple filter flame photometer has not been used for the determination of lithium in rocks and minerals.

In this note a method has been designed to determine lithium in the presence of other ions. The method can be applied safely to a concentration range from 200 p.p.m. to 6000 p.p.m. Li_2O corresponding to 95 and 3000 p.p.m. lithium, covering the concentration range given for Diorite, Granite, Nepheline, Aegirine, Lipidomelane[18], Biotite[19] Tourmaline,[20-28] Tregonning-Godolphin Granite complex[24-26] and data given by other workers.[27-28]

EXPERIMENTAL

In all the analytical work on lithium, an E.E.L. flame photometer supplied with a lithium interference filter was used.

[11] P. Bruce, Adams, "Rapid Flame Photometric Determination of Alkalies in Glasses and Silicates", *Analyt. Chem.*, **73**, 1602 (1961).

[12] J. H. Gibson, and W. E. L. Grossman, "Excitation Process in Flame Spectrophotometry", *Analyt. Chem.*, **35**, 266 (1963).

[13] R.B. Ellestad, "Flame Photometric Determination of Lithium in Silicate Rocks", *Analyt. Chem.*, **27**, 299 (1955).

[14] K. Konopicky, and W. Schmidt, *Ber. deutsch, Keram, Ges.*, **37**, 368 (1960).

[15] P. E. Pilgrim, and F. R. Ford, *Analyt. Chem.*, **35**, 1735 (1963).

[16] H. L. Howling, and P. E. Landolt, *Analyt. Chem.*, **31**, 1818 (1959).

[17] J. P. Williams, and P. B. Adams, *J. Amer. Ceram. Soc.*, **37**, 306 (1954).

[18] Y. M. Goldschmidt, "Geochemistry", Oxford Univ. Press, 1958, 132 p.

[19] C. S. Exley, and M. Stone, "The Granitic Rocks of South-West England. Present Views on some Aspects of the Geology of Cornwall and Devon", 1964.

[20] Deer, Howie and Zussman, *Shorl, Yuzhakora, Urals* (Slivko, 1955). **1**, Analysis 7, Table 51 (1962).

[21] Deer, Howie and Zussman, "Black Tourmaline. Contact in Altered Dolerite, with Axinite and Actinolite, Carrick Dhu, St. Ives. Cornwall". **1**, Analysis 7, Table 51 (1962).

[22] Deer, Howie and Zussman, "Light Green Verdelite, Varutrask, Pegmatite, Sweden (Quensel and Gabrielson, 1939) **1**, Analysis 6, Table 52 (1962).

[23] Deer, Howie and Zussman, "Light Green Tourmaline, Meldon aplite, Okehampton, Devon", **1**, Analysis 6, Table 52 (1962).

[24] M. Stone, "The Tregonning-Godolphin Granite", Abstract Proc. 3rd, Conf. Geol. Geomorph, S.W. England, Royal Geol. Soc. of Cornwall, **13** (1960).

[25] M. Stone, "Lithium in Tregonning-Godolphin Granite Complex". Proceeding of the USSHER Soc. **1**, 51 (1963).

[26] M. Stone, Ph. D. Thesis, University of Birmingham (1965).

[27] E. L. Horstman, *Geochim. Cosmochim. Acta.*, **12**, 1, (1956).

[28] S.R. Taylor, *Geochim. Cosmochim. Acta.*, **28**, 1273 (1964).

EMISSION–CONCENTRATION CURVE

In order to determine the relation between flame emission and concentration of lithium, a series of solutions containing known amounts of lithium was used. These were prepared from a stock solution containing Li_2CO_3 dissolved in dilute hydrochloric acid and diluted to one litre. A graph of the scale reading against concentration of lithium (from 0 p.p.m. — 10 p.p.m. Li_2O) is shown in fig. 1. The relationship is clearly linear and the line passes through the origin.

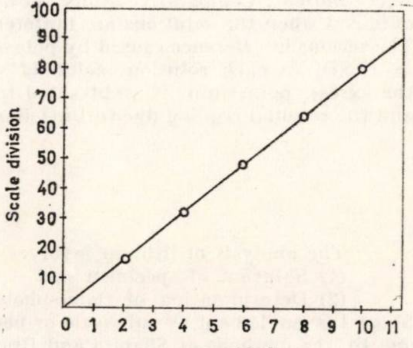

Fig. 1. — A graph of flame emission and concentration of lithium.

INTERFERENCE

A study of the literature shows that calcium, magnesium, sodium and potassium interfere in the determination of lithium by flame-photometry. The extent of such interference was determined by adding known concentrations of cations and anions like, calcium, magnesium, sodium, potassium, iron, aluminium, sulphate, nitrate and chlorate to the standard solution of Li_2O. It was found that some of these are negligible while others cancel out the effect of one another (for reference see tables 5,6,7,8)[29] except that a serious interference is caused by potassium [25] which was investigated by adding 10,25,50,100,150 and 200 p.p.m. K_2O, corresponding with 1.0, 1.25, 2.5, 5.0 and 10.0 percent K_2O in the rock, to standard solution of Li_2O. The measurements are made with and without 2000 p.p.m. K_2O "buffer". The comparative results are given in table 1. These gave differences of 5,10,15,25,30 and 35 scale division corresponding with 0.66, 1.33, 2.0, 3.3, 4.0 and 4.6 p.p.m.Li_2O, respectively, equivalent to 0.033, 0.066, 0.1, 0.16, 0.2 and 0.23 per cent Li_2O in the rock, as indicated in table 1. It is quite clear from table 1 that interference by potassium is very serious when the solutions are not "buffered" by 2000 p.p.m. K_2O.

10 p.p.m.K_2O without buffer (i.e. without 2000 p.p.m. K_2O) gave a reading of 5 scale divisions, corresponding to 0.66 p.p.m. Li_2O and 100 p.p.m. K_2O gave a reading of 25 scale divisions, equivalent to 3.3. p.p.m. Li_2O, while the same 100 p.p.m. K_2O in the presence of 2000 p.p.m. K_2O "buffer" gave a reading of only 1.5 scale divisions. This is quite small, and virtually linear, so that it can readily be corrected graphically.

Table 1

The interference due to potassium with and without 2000 p.p.m. K_2O "buffer"

Without 2,000 p.p.m. K_2O					With 2,000 p.p.m. K_2O	
p.p.m. K_2O	% K_2O	Scale division	p.p.m. Li_2O	% Li_2O	p.p.m. K_2O	Scale divisions
10	1.0	5	0.66	0.033		
25	1.25	10	1.33	0.066		
50	2.5	15	2.0	0.10		
100	5.0	25	3.3	0.16	100	1.5
150	7.5	30	4.0	0.20	100	2.0
200	10.0	35	4.6	0.23		

---

[29] S. A. KHAN, Ph. D. Thesis. University of Exeter (1966).

REMOVAL OF INTERFERENCE DUE TO POTASSIUM

Attempts were, therefore, made to remove interference from potassium by precipitation and solubility methods.[5] These were proved not satisfactory and time consuming. Some organic reagents like picric acid and tartaric acid were tried; these also proved failure as lithium was also coprecipitated. Attempt was also made to overcome the interference due to potassium, an amount of K_2O equivalent to that present in a suit of rock was added to the standard and blank, the rocks were analysed for lithium and the same rocks were analysed using 2000 p.p.m. K_2O "buffer". Comparative study shows that higher and probably more accurate results are obtained when the solutions are buffered with 2000 p.p.m. K_2O (for reference see table 12).[29] The serious interference caused by potassium was finally overcome by adding 2000 p.p.m. K_2O as K_2SO_4 to each solution including sample, standard and blank. The reading caused by the excess potassium is subtracted from the total reading due to potassium and lithium, and the residual reading due to Li_2O alone, are plotted graphically,

METHOD

The analysis of lithium involves two stages :

(1) Solution of specimen and

(2) Determination of flame-photometry.

Stage I is carried out by sulphuric or perchloric acid digestion with hydrofluoric acid according to the methods of Shapiro and Brannock [1] and Riley. [2] Analysis of lithium, therefore, is performed on "Solution B" of these authors.

1. *Apparatus*.E.E.L. Flame-photometer and lithium filter supplied by E.E.L. Ltd.
2. *Reagents*. All reagents are of analytical grade.

Sulphuric acid Analar. Concentrated 98 percent, sp. gr. 1.84. Stock sulphuric acid 5 N. Dilute about 140 ml of concentrated sulphuric acid to one litre.

Hydrofluoric acid Analar. 40 per cent w/v

Hydrochloric acid Analar. Concentrated, sp. gr. 1.18 and diluted : dilute 1 part of concentrated hydrochloric acid with 5 parts of water.

Nitric acid Analar. Concentrated, sp. gr. 1.42.

Potassium sulphate. Solution containing 10,000 p.p.m. K_2O. Weight accurately 18.5 g potassium sulphate and dilute to 1 litre.

Standard lithium solution. Weigh accurately 0.24 g lithium carbonate (Matthey "specpure"), dried at 110° for 2 hours, add 12.5 ml of 1 :5 hydrochloric acid, and dilute to 1 litre. 1 ml of this solution contains 100 μg Li_2O/ml.

PROCEDURE

Weigh accurately about 0.4 g (0.2g/100 ml when only lithium is to be determined) of powedered rock sample which has been crushed to pass through a 120 mesh sieve, and dried at 100°, into a platinum crucible. Add 15 ml of concentrated sulphuric acid. Cover the crucible with a lid and place it on a water bath. Allow the sample to digest until solution is complete. Remove the lid and reduce the volume to about 3 ml. Add 1 ml concentrated nitric acid. Remove the crucible from the water bath and heat gently on an electric hot plate, until fumes of sulphur trioxide are evolved. Cool, nearly fill the crucible with distilled water, transfer the solution to a beaker, add about 50 ml distilled water, and boil until the residue dissolves. Cool, transfer the solution to a 200 ml measuring flask and make up to the volume with distilled water. Transfer the solution immediately to a polyethylene container.

Pipette 15 ml of the solution into a 25 ml measuring flask, add 5 ml of 10,000 p.p.m. K_2O solution, and make up to the mark with distilled water; prepare zero setting solution by pipetting 20 ml of 10,000 p.p.m. K_2O and 10 ml of 5 $N.H_2SO_4$ into a 100 ml measuring flask and make up to the mark with distilled water.

Pipette 10 ml of 100 p.p.m. Li_2O standard solution into a 100 ml measuring flask, add 20 ml of 10,000 p.p.m. K_2O solution, and 10 ml of 5 $N.H_2SO_4$ and make up to the mark with distilled water.

Turn the sensitivity control of the flame-photometer clockwise to its fullest extent or until the 10 p.p.m. Li_2O standard gives a scale reading of *ca.* 80.

Determine the Li_2O content of the sample by comparing the scale readings with 10 p.p.m. Li_2O standard. Measure the zero and standard before and after taking each reading. Also run a blank solution.

The concentration of the sample solution is adjusted by diluting until it lies within the range of measurement.

Calculations

$$\% \, Li_2O \text{ rock} = \frac{\text{Scale reading of unknown}}{\text{Scale reading of standard}} \times 5/3X0.5/10$$

(On the basis of 0.4 g. rock sample, dissolved in 200 ml of distilled water and 15 ml of this sample solution diluted to 25 ml)

RESULTS AND DISCUSSIONS

The proposed method has been tested thoroughly for its precision and accuracy. Precision is obtained by replicate analyses and accuracy by analysing the standard firebrick N° 315, but much of the test of accuracy is dependent upon the "addition method", because in the author's opinion the addition method is superior or equal to that method which uses standard as a means of testing accuracy. Besides the analysis of standard firebrick, (B.C.S. N° 315) the results have also been compared with the atomic absorption method.

A variety of silicate materials has been analysed. These range from tourmaline, pelite and firebrick, on the one hand, and more acid members, including elvans and granite on the other hand. The granite includes both biotite-bearing and "lithionite"-bearing types.

PRECISION

Replicate analyses of Pelite and Granite

Analyses of a variety of rocks have been carried out. Each rock (including two "lithionite" granites, a pelitic state and pelitic hornfels) was analysed at six different times, i.e. the whole batch was determined on six separate occasions (for reference, see tables 13, 13A, B, C, D, and E)[29]. A summary of all the data is given in table 2. The data are also compared to the data reported by earlier workers and to those provided by the atomic absorption method, shown in table 2A. Close results have been obtained, which shows that the method has good precision.

Table 2

The replicate analyses of pelites and granites
Li_2O, wt. p.c.

Specimen N°	1 st	2nd	3rd	4th	5th	6th	Mean value	Standard deviation
E_1	0.58	0.56	0.56	0.55	0.57	0.57	0.57	0.01
D_1	0.22	0.22	0.22	0.22	0.22	0.22	0.22	0.00
WA_3	0.04	0.045	0.05	0.05	0.05	0.05	0.05	0.00
025a	0.65	0.65	0.60	0.62	0.65	0.65	0.64	0.02

Table 2A

Comparative results of pelites and granites obtained by other workers and by the atomic absorption method

Li_2O, wt. p.c.

Specimen N°	Simple Flame Photometric Method		Atomic Absorption Method
	Analyst S.A. Khan	Analyst M. Stone	Analyst S.A. Khan
	$\%Li_2O$	$\%Li_2O$	$\%Li_2O$
E_1	0.57	0.53	n.d.
D_1	0.22	0.19	n.d.
WA_3	0.05	0.05	0.04
025 a	0.64	0.62	0.58

E_1. Amblyganite-bearing leucogranite, roof zone, carn clodgy. D_1. Tregonning granite, trewaves head beneath roof zone. WA_3. Darkgrey slate bands, Porthleven. 025a. Hornfels in contact with roof of domelike mass of tregonning-granite, sea stocks, legreath zawn. n.d. Not determined.

ACCURACY

Accuracy of this method has been tested by the following three methods.

a) ANALYSIS OF STANDARD
(B.C.S. N° 315, Firebrick)

The results of eight analyses (consisting of 22 determinations) of B.C.S. N° 315, Firebrick are shown in table 3, and the results are compared with the data obtained by eight different analysts listed in the certificate supplied by the Bureau of Analysed Samples, Ltd.

The two sets of data agree reasonably well, and standard deviations and errors are similar, which confirms the accuracy of the method.

Table 3

The analysis of B.C.S. N° 315, Firebrick

Li_2O, wt. p.c.

Specimen N°	Results % Li_2O		Mean value		Standard deviation		Standard error	
	S.A. Khan	B.C.S. analysts	S.A. Khan	B.C.S. analysts	S.A. Khan	B.C.S. analysts	S.A. Khan	B.C.S analysts
B.C.S. N° 315 Firebrick	0.07	0.09	0.09	0.09	0.01	0.01	±0.004	±0.004
	0.08	0.09						
	0.10	0.08						
	0.09	0.08						
	0.09	0.08						
	0.09	0.08						
	0.08	0.07						
	0.09	0.09						

Result : 0.09 % Li_2O

B.C.S. – Bureau of Chemical Standards

b) ADDITION METHOD

The accuracy of the method has been further tested by the addition of known amounts of lithium (i.e. 4 p.p.m. Li_2O) to standard firebrick. The results have been calculated on the average scale division of sample and standard. A 0.312 scale division has been substracted from the scale division of firebrick due to K_2O present in firebrick. The data are given in table 4. This shows a satisfactory recovery of lithium which further confirms the accuracy of the method.

Table 4

The analysis of B.C.S. N° 315, Firebrick by the addition method (i.e.4.p.p.m. Li_2O. standard was added to firebrick and recovered)

Li_2O wt. p.c.

Specimen N°	Average standard	Scale division due to $K_2O + Li_2O$	Scale division due to K_2O	Scale division due to Li_2O	p.p.m. Li_2O from graph	Result % Li_2O	% 4 p.p.m. Li_2O
4 p.p.m. Li_2O	—	—	—	34.75	4.1	0.34(1)	0.34(1)
4 p.p.m. Li_2O	84.0	—	—	—	—	—	—
+							
Firebrick	—	44.75	0.312	44.45	5.2	0.4334	—
Firebrick	—	9.9	0.312	9.59	1.1	0.091	—

Result : 0.09 % Li_2O

c) COMPARISON OF THE RESULTS WITH THE ATOMIC ABSORPTION METHOD

Two rocks, namely slate (WA_3) and hornfels (025a) have been analysed by this method as well as by atomic absorption spectra (Hilger and Watts AA2 atomic absorption spectrophotometer) method. The comparative results given in table 2A, which are fairly close to one another, show that the method is accurate.

SUMMARY AND CONCLUSIONS

60 determinations have been made in all for 24 different silicate rocks and minerals which include granites, tourmaline, slate, firebrick and other rocks containing 95 p.p.m. – 3000 p.p.m. lithium.

This method has been tested for its precision and accuracy by replicate analyses, by comparing the results with the results obtained by earlier workers and by the atomic absorption method, by analysing standard firebrick N° 315 and by adding known amounts of Li_2O standard to firebrick as well as to rocks. The results, standard deviations and standard errors are similar to the earlier results and data obtained with the firebrick and atomic absorption method. The recovery of the known added standard is satisfactory and the results are within the expected range and are reproducible.

The main advantage of this method is that lithium can be determined satisfactorily and rapidly in the presence of other ions and the serious interference caused by potassium can be overcome by adding 2000 p.p.m. K_2O "buffer" to the sample, blank and standard.

The method is sensitive, cheap, simple and rapid and can be applied to the determination of lithium in silicate rocks and minerals.

The method can be fitted in the scheme for analysing rocks and minerals provided by Shapiro and Brannock[1] and Riley.[2]

The authors wish to thank technical staff, Mr. J. Sanders, Mr. Raymond Ellis and Mr. Willmington in the Department of Geology, University of Exeter, England. In particular, thanks go to Professor Scott Simpson for providing facilities and for help at many stages.

Revue Roumaine de Chimie, **19**, *10*, 1677–1682 (1974)

COMPTES RENDUS

J. JORTNER, N. R. KESTNER. *Electrons in fluids.* Springer Verlag, Berlin, Heidelberg, New York, 1973, 485 p.

This volume provides a record of the lectures, communications and discussions that took place at colloque Weyl III. The original aim of this colloque was to contribute to the understanding of metal-ammonia solutions. Colloque Weyl III extended the scope to include related works on electrons in polar and non-polar liquids and in dense fluids, the electronic states of disordered systems and the metal-insulator transition, thus the chemical and physical properties of electrons in fluids from a general point of view.

In the first article recent model calculations of an electron in a polar fluid are reviewed with primary emphasis on electrons in ammonia and water. These static calculations are compared with each other and with experimental data. These models are capable of explaining qualitatively and in most cases, quantitatively, the effects of variables such as temperature, pressure, molecular structure and density of the solvent. On this theoretical basis, brief qualitative statements about electrons in polar vapours, in solutions of higher metal (and electron) concentrations and in a wide variety of fluids, are made.

The articles concerning the dilute region of metal-ammonia solutions discuss their physical properties, the effect of electrolytes on the hydrogen-bonded structures of liquid ammonia, the nuclear spin relaxation phenomenon, the cases of the proton and nitrogen in these solutions, the chemical equilibria between anions and the ammoniated electron. It is well known that the decomposition of solutions of metals in ammonia is limited by the reverse reaction between the amide ion and hydrogen gas leading to the formation of solvated electrons. In the title paper is shown that such an equilibrium may exist between other anions and the solvated electrons in the presence of hydrogen.

A following paper reviews the most recent studies of metal solutions in amines and ethers, rich in information about distinguishable species. By studying the behaviour of these species as a function of temperature, solvent and metal, it has become possible to identify their stoichiometry and to measure some of their properties.

Some articles are devoted to ultrafast optical processes. Those of the order of 10^{-12} sec can be studied experimentally with picosecond pulses generated by lasers. Informations on solvated and quasi-free electrons obtained from photoelectron emission spectroscopy are also discussed. In the determination of the near infrared spectrum of the solvated electron in liquid ammonia, an anomaly, evidenced by a large transparence of the solutions, has been observed at wavelengths corresponding to the bands of ammonia in the 1500–2300 nm region. This anomaly appears in the presence of relatively high concentrations of KNH_2 and large hydrogen pressures. The increase of the anomaly with the concentration of the solvated electron suggests the formation of a complex between $\bar{e}$, KNH_2 and a certain number of ammonia molecules strongly linked so that they do not participate in the vibrational modes corresponding to the quoted wavelengths.

Studies of Raman spectroscopy of metal-ammonia solutions using a laser Raman spectrometer and infrared spectroscopy of the solvent are also reported.

A brief review is made of current understanding of the electronic structures of disordered materials. The basic band model for disordered materials is introduced and used to explain the basic experimental facts about amorphous semiconductors. The history of localization theory, which gives the formal justification of the basic band model is then reviewed and its present status assessed. Remarks are made on the relevance of these considerations for the theory of metal-ammonia solutions.

Some papers concern concentrated metal-ammonia solutions. A review is made of the properties of concentrated solutions. Comparison of transport and magnetic effects suggests that the temperature dependence results from density-of-state effects. Interpretation of these phenomena is given in terms of a model based on the assumption that solutions were composed of solvated ions, nonsolvating NH_3 molecules and free electrons.

Nuclear magnetic resonance studies of cesium-ammonia solutions as well a :conductivity measurements in the frequency range 0–70 GHz are also presented. Another article relates the strange magnetic behaviour and phase relations of metal — ammonia compounds of lithium, calcium, strontium and barium. The magnetic susceptibility has been measured down to 1.5 K; phase structure and ESR studies under pressure are indicated.

In another note the system $M'-NH_3$ (M' = metallic chalcogenide) has been studied. Based on the theory of electron donor-acceptor complexes it is assumed that the intermolecular forces between the crystalline layer material and small intercalate molecules are due to dispersion and charge transfer interactions.

An interesting discussion concerns the existing data and thermoelectric power of potassium, cesium and mercury, as a function of the density at supercritical temperatures, as well as a relation between the thermodynamic phase transition from a dense liquid to a low density vapour and the metal-nonmetal transition.

The volume includes interesting large reviews of the studies devoted to mobility of excess electrons in nonpolar hydrocarbons and to optical absorption spectrum of the solvated electron in ethers and in the binary liquid system.

On the whole, the different topics of the volume concern inorganic chemistry, theoretical chemistry, physical chemistry of fluids, theoretical physics, physics of fluids, radiation chemistry, solid state physics. This full and up-to-date account reveals the interrelationships between the chemistry and physics of electrons in disordered media in a variety way that appears to physicists as well as to chemists. The interdisciplinary nature of this field and related areas is clear from the range of contributors, which includes both theoretical and experimental chemists and physicists.

Florica Popea

M. FLORESCU, *Twenty Years of Progress in Socialist Romania's Chemical Industry*, Meridiane Publishing House, Bucharest, 1973, 300 p., 97 tables

The development of the Romanian chemical industry and the outstanding progress recorded particularly in the last 20 years have been thoroughly and comparatively presented in this book. The book is perfectly documented and contains over 90 tables providing significant data on the present and long-range development of the Romanian chemical industry, and also 8 figures illustrating the trends and use to great advantage of some raw materials. The book is also of a particular value owing to the fact that its author, engineer M. Florescu (corresponding member of the Academy of the Socialist Republic of Romania) is the Minister of the Chemical Industry.

The book includes a number of 11 chapters which review the Romanian chemical industry since its beginnings up to the future development plans. The book also reviews the related activities which make a direct and decisive contribution to its successful development (education, research, etc.)

Thus the first three chapters review stringent aspects of Romania's economic conditions between the two World Wars, the early stages of the chemical industry and the more important results obtained before World War II. The author makes an in-depth analysis of the situation considering that the formation of the chemical industry cannot be separated from the economic problems, the social aspects and primarily the political aspects of Romania.

After the end of the war and the take-over of the industry by the State, the Romanian people, determined to turn to account natural resources for its own benefit, has started the country's industrialization. These aspects are presented in Chapter 4 which shows that industrialization is the main objective of a modern economy.

From the 5-th chapter on, the author presents the modern Romanian chemical industry, the main technical-economic indices and the ways of reducing the production cost price. Figures illustrate the investments made in the chemical industry, the foreign trade of chemical products and the targets for the years 1971–1975. The main sub-branches of the Romanian chemical industry (Chapter 6) hold a major place in the book and refer to: inorganic chemical industry (chlorosoda products, sulphuric acid, etc.), chemical products for agriculture (fertilizers, pesticides and biostimulators), the plastic and synthetic resin industry, the synthetic fibre and yarn industry (Relon, Melana, Terom, etc.), the rubber industry, the varnish, paint and printing ink industry, the dye and organic pigment industry, the drug industry and last but not least, the building industry of equipment, fitting, pumps and measure- and control apparatus necessary for the chemical industry.

As shown above, the author places a special emphasis, in chapters 7 and 8, on the training of the labour force necessary for this industry and on the fact that scientific research is the main factor in the development of the chemical industry. Data are provided on the secondary and higher education in this field and on the manner in which the higher education will secure the specialized staff required.

The book presents the traditions of the Romanian school of chemistry, it recalls the names and activities of brilliant pioneers of the Romanian chemistry and also the early research activity. Similarly, the book presents technological or applied research units and basic research units pointing to their close cooperation relations. Chapter 8 ends by a review of the long-range development of research in the field of Romanian chemistry.

Chapter 9 deals with the organization of technological design while Chapter 10 elaborates on the use of electronic computers in the chemical industry (automation, modelling, data processing and systems, etc.).

The last chapter points to the ways and means for the future development of the Romanian chemical industry. Figures indicate the production values and the types of new materials for each separate sub-branch. The book concludes with some final thoughts of the author's.

D. I. Marchidan

D. A. ARMITAGE, "*Inorganic rings and cages*", Edward Arnold. (Publishers), Ltd., London, 1972, X+ 388 p.

This book deals with some very important aspects of modern inorganic chemistry, one of those interdisciplinary fields, which border apparently unrelated topics, in this case metal-organic chemistry, coordination chemistry, non-metal and non-transition metal chemistry. The formation of cyclic compounds, thought before as characteristic only of organic chemistry, appears now as an important feature of inorganic chemistry as well. The formation of polycyclic systems, known as "cage structures" is more typical of inorganic chemistry.

The book reviewed is a very readable presentation of the subject. It is intended to serve as a source for final year courses, but it is more than that and it is a very useful guide to the literature of inorganic rings and cages, giving the interested reader carefully selected examples and references to illustrate the ability of elements other than carbon to form ring systems, and sufficient details to suggest the full scope of the field.

The introduction clearly defines the aims and the scope of the book. Rings containing carbon (e.g. chelates) or non-metal heteroatom organic systems, transition-metal clusters and bridged complexes, were not treated. These topics do not realy pertain to the subject and in many cases are already treated in other monographs. Including such topics would have produced not only a much larger book, but a very unhomogeneous one. The careful selection of the material allows a clear delimitation of the field, which, however, borders various branches of organic and inorganic chemistry.

The book has an Introduction and seven chapters, plus Formula Index, Specific Index of Compounds and General Index. Chapter 1 (p. 1—7) deals with rings containing alkali-metals (e.g. in alkoxides, amides, etc.). Chapter 2 (pp. 8—40) discusses rings of beryllium and magnesium (including inorganic salts; hydrides; amides, alkoxides and organo-derivatives). Chapter 3 (pp. 41—151) is necessarily very comprehensive and deals with derivatives of the Group III elements (among which boron hydrides; carboranes; borazines and other boron-nitrogen compounds; phosphino and arsino-borines; borates and boroxines; cyclic sulphur and halogen derivatives). Another extensive chapter is Chapter 4 (pp. 152—265), discussing the ring systems of Group IV elements (cyclopolysilanes, -germanes, -stannanes; cyclosilazanes, cyclosiloxanes and related germanium and tin derivatives; sulphur-containing rings of the same elements). Chapter V (pp. 266—337) presents the rings made up of Group V elements (important topics covered are cyclopentazoles; cyclopolyphosphines and -arsines; cyclophosphazanes and cyclophosphazenes; cyclic oxygen and sulphur derivatives). Chapter 6 (pp. 338—360) is devoted to sulphur, selenium and tellurium rings (the main topics being element allotropes and sulphur-nitrogen compounds). A shorter Chapter 7 (pp. 361—363) mentions some cyclic interhalogen compounds.

A total of some 1400 references (published up to December 1970), some of them included in Appendixes to each Chapter, give the interested reader the key to more detailed information. Apparently, all important reviews are quoted; therefore, the reader can either be satisfied with the selection of the literature given by the author, or go further to the full literature, which can be recovered through these reviews.

The book is warmly recommended to anyone interested in getting a picture of a modern branch of inorganic chemistry, which did not receive the deserved attention until rather recently. This is a very useful, well-balanced, interesting presentation of the subject, and it does a good service to the field.

Ionel Haiduc

K. DIMROTH, "Phosphorus—Carbon Double Bonds" Fortschr. Chem. Forsch., **38**, 1973, Springer—Verlag, Berlin, 1973, 147 p.

This well-written book is intended to a large community of chemists familiar with those topics as well as to the general scientist who has no adequate background of phosphorus chemistry. The book is divided into three main sections, flanked by an Introduction and Outlook.

The first section is devoted to Phosphamethine-cyanines (13 pages), the second section deals with λ^3—Phosphorins (50 pages) while the third discusses λ^5—Phosphorins (70 pages). In each section the pattern of discussion is the following: Synthesis, Physical Properties, Bonding, Chemical Properties. In addition, an X-ray analysis of Phosphamethine-cyanines is presented and for λ^5 — Phosphorin an Introduction and a Review is given.

This volume gives an exhausted literature coverage of a topic traced back as early as 1964 up to early 1973. The reader will find in this book a model of clarity and conciseness; many spectroscopical discussions are richly illustrated with graphs and tables.

This is a useful reference book for anyone willing to keep abreast with advances in chemistry in general and phosphorus-carbon chemistry, in particular.

M. Gheorghiu

"Absorption Spectra in the Infrared Region", L. Lang Ed., S. Holly and P. Sohár, collaborators, Akadémiai Kiadó, Budapest, 1974, vol. 1, 320 p.

This is a collection of 300 spectra of familiar compounds and of other compounds recently synthesised by Hungarian workers, published between 1962—1970. The compounds were selected in keeping with research problems and developments in the chemical industry e.g. pharmaceutical, petrochemical, plastics and dyes.

Spectra are given in the range of 4000—400 cm^{-1}, mostly in KBr, few in CCl_4 or pure. Each spectrum is accompanied by structural and empirical formulae, molecular weight, melting point, n_D, sample, concentration, cell length, solvent and the equipment used, in this case a UR—10 spectrophotometer.

A subject index, formula and author indexes and bibliographic references are appended.

Excellent graphic presentation.

Prof. Lang was the Editor of the very successful "Absorption spectra in the ultraviolet and visible region". This new series dedicated to the IR spectra is welcomed by the community of chemists, therefore we recommend this book as a useful tool in any laboratory of organic chemistry.

We are looking foreward to the next volumes.

M. Gheorghiu

G. VARSÁNYI, "Assignments for Vibrational Spectra of 700 Benzene Derivatives", Vol. 1 and Vol. 2, Akadémiai Kiadó, Budapest, 1973, 668 p.

The present book is the result of a systematic study on vibrational spectra of benzene derivatives carried out by the author, professor of physical chemistry at the Technical University, Budapest. It has facilitated assignement of the vibrational spectra of several hundred benzene derivatives, eliminating the frequent errors occurring from analogies with aliphatic compounds spectra for aromatics.

The book is of great value to the practical analyses of vibrational spectra of aromatic compounds.

The principles of the general treatise are based on an earlier book of the author's "Vibrational Spectra of Benzene Derivatives", published by Akadémiai Kiadó, Budapest, and Academic Press, New York and London in 1969. Volume 1 begins with a brief theoretical discussion of the subject (25 pp), followed by vibrational assignment tables for all of the 700 compiled compounds. Volume 2 consists of a collection of infrared spectra of a great number of benzene derivatives.

In analysing normal vibrations of benzene derivatives, the author refers to tangential vibrations (C—C stretching, C—X and C—H in-plane bending), radial vibrations (radial skeletal, C—X and C—H stretching) for both light and heavy substituents, as well as out-of-plane vibrations (skeletal, C—X and C—H out-of-plane). The discussion is based on normal coordinate calculations performed by different authors for various benzene derivatives. A table listing the characteristic frequencies of the internal vibrations of substituents and the types of vibrations in chemical sequence (hydrogen, carbon, halogens, oxygen, nitrogen, sulfur, other heteroatoms) concludes the volume.

Tables containing the assigned vibrational spectra of various benzene derivatives make up the bulk of vol. 1 (approx. 400 pages). Seven hundred benzene derivatives are listed according to the increasing number of substituents. For derivatives having the same number of substituents, the order is defined by structural isomerism. These tables systematize unavailable information on the vibrational spectra of this large group of compounds, grouping them not only by the type of substitution but also by electron structure and mass of substituents.

The tables for each group of derivatives, designated by the same group number, are preceded by a Summarizing Table giving both possible frequency regions of the vibrations corresponding to the thirty normal modes of benzene and approximate vector diagrams of characteristic normal vibrations. The group number, defined on p. 33, is very useful for the reader to rapidly locate the spectrum of a compound. The specific designation of group numbers for all investigated compounds is listed on pp. 41—42.

Each table provides information on : *a*) vibrational frequencies (infrared bands and Raman lines), measured or calculated theoretically, in cm^{-1}, together with their serial numbers according to Wilson, *b*) characterization of infrared bands or Raman lines intensity as "strong", "medium", "weak", etc. *c*) polarization properties of Raman lines, if available, *d*) corresponding literature references and *e*) references to the spectra presented in vol. 2.

However, as the author himself remarks, "the assignments in the Tables are in many cases only tentative, [...] the main purpose of the present compilation being to help further research in this field."

Volume 2 consists of a collection of infrared spectra of benzene derivatives (transmission in % *vs.* cm^{-1}), recorded in Hungary on Perkin-Elmer 457, and Zeiss-Jena UR 10 and UR 20 spectrometers. The group number accompanying each spectrum establishes the connection with the detailed assignment tables in vol. 1.

An Index of substituents in which the compounds are arranged in the order established in vol. 1, concludes vol. 2, thus helping the reader in efficiently locating the spectra and vibrational assignments for a given compound.

The book may is a valuable tool for organic chemists and other workers investigating the structure of organic compounds or attempting to identify a certain benzene derivative when vibrational spectra are known.

Rodica Beldie

"Origins of Life Chemistry and Radioastronomy", Dr. Lynn Margulis Ed., Springer-Verlag Berlin, Heidelberg, New York, 1973

The book "Origins of Life-Chemistry and Radioastronomy" edited by Dr. L. Margulis, presents the dialogue between eminent scien tists in various research fields, on several aspects of the origin of life on Earth or in the Univers. It is, at the same time, the latest record of the series of conferences devoted to the "Origin of Life".

It is a record of the proceedings of the round table held on the occasion of the 1971 Conference organized by the "Interdisciplinary Communications Program", a NASA-sponsored foundation. Experimental results and the latest discoveries in the field of chemistry, biology, geology, genetics, astronomy, etc., are discussed and new hypotheses on the origins of life on Earth are postulated.

The first part dwells on some aspects regarding identification of amino acids, porphyrines as contamination products, and uptake of carbon oxide or dioxide into reduced organic matter under Martian conditions of high uv fluxes. Such contamination was experimentally attested by Hubbard's works.

Particular emphasis is placed on the energy sources that could largely contribute to the synthesis of organic combinations, starting from the early atmosphere. : the rôle of uv radiations, thunderstorms, shock waves, heat and the geothermal activity. The uv radiations are essential to the synthesis of formaldehyde from hydrogen and carbon oxide as well as to cyanide formation, both as precursors of the prebiotic synthesis. These reactions occurred in the aqueous medium of the seas and oceans or, more likely, in rain drops.

Although cyanide is presumably formed by electrical discharges, it could be synthesized with uv radiations using the hydrogen from H_2S photolysis. Another aspect of the efficiency of u.v. rays is their capacity for releasing almost completely their energy on a surface level, whether that of the ocean, or a solid-liquid or air-solid interface.

The intensity of electrical discharges depends on the evaporated water and quantity of water vapors transferred to the upper atmosphere liable to create appropriate conditions for a thunderstorm. Such conditions were created by the warmth of the early earth which could generate enough water vapors and moisture. An important contribution was made by solar energy and the geothermal activity.

These interdisciplinary confrontations afforded some conclusions on the apparition of organic macromolecular precursors (monomers). Yet, it is still difficult to ascert how these polymers or more complex combinations are being formed in prebiotic conditions. Unfortunately this problem was but little approached so far. An important question is the formation of L-amino acids i.e. of the optical activity of the matter have appeared.

Today's knowledge of the earth crust, applicability of "plate tectonic" discussed in the concluding part of this work enable the understanding of sedimentation processes of outgassing that have determined the particular evolution of the early atmosphere. The presence of ammonia in the early atmosphere, its capacity for absorbing infrared radiations at 10 microns, could prevent the ocean from freezing at the time when the sun radiation was reduced.

It is premature to say if the organic matter has an interstellar origin ; discussions revealed some evidence yielded by radioastronomical investigations whereby over 20 organic molecules have been identified in the interstellar space. The abiotical synthesis or the identification of precursors in meteorites is supported by experimental data, as summarized in 13 tables and 26 figures.

As the editor himself shows "those who are seeking in this book a sure, unequivocal and complete answer about the origin of life will be somewhat disappointed". However, this book remains a stimulus for new investigations in such an extremely complex field with so many unknowns.

The work edited by Dr. L. Margulis is addresed to all those engaged in elucidating the problem of the origins of life on earth : chemists, biologists, geochemists, astronomers etc. That is why we warmly recommend it to the readers.

Victor Bulacovschi

NOTE POUR LES AUTEURS

La *Revue Roumaine de Chimie* publie des articles en anglais, français, russe, allemand ou espagnol. Les auteurs sont priés d'envoyer des articles, notes, communications et comptes rendus inédits.

Les manuscrits seront dactylographiés à deux intervalles. Les tableaux seront dactylographiés sur feuilles séparées, de même que la légende des figures. Les diagrammes seront tracés à l'encre de Chine sur papier calque. Les tableaux et les figures seront numérotés par des chiffres arabes, en nombre strictement nécessaire. Prière de ne pas inscrire les mêmes données dans les tableaux et les figures. Les formules chimiques seront incluses dans le texte ; en outre, elles seront transcrites sur des feuilles séparés. Les auteurs sont priés d'indiquer les caractères italiques (en soulignant les lettres au crayon), ainsi que tout autre caractère spécial. L'ordre des références bibliographiques sera celui de leur mention dans le texte ; le nom de l'auteur sera précédé de l'initiale du prénom ; les publications périodiques seront présentées suivant les prescriptions internationales. Les références seront ajoutées à la fin de l'article ; elles paraîtront comme des notes, au bas de la page. Le texte sera précédé d'un résumé comprenant 15 lignes au maximum.

L'entière responsabilité du contenu des articles appartient aux auteurs. On publie des articles dus aux collaborateurs roumains ou étrangers.

PRINTED IN ROMANIA

1975 APR 23

TRAVAUX PARUS AUX ÉDITIONS DE L'ACADÉMIE DE LA RÉPUBLIQUE SOCIALISTE DE ROUMANIE

CRISTOFOR SIMIONESCU, MARGARETA GRIGORAŞ, AGATA CERNĂTESCU-ASANDEI et GHEORGHE ROZMARIN, **Chimia lemnului din România — plopul şi salcia** (La chimie du bois en Roumanie — le peuplier et le saule), 1973, 228 p., 28 lei.

TIBERIU NĂŞCUŢIU, **Metode radiochimice de analiză** (Méthodes radiochimiques d'analyse), 1973, 384 p., 23 lei.

MARIA FITI, **Dozimetria chimică a radiaţiilor ionizante** (La dosimétrie chimique des radiations ionisantes), 1973, 240 p., 13,50 lei.

MIHAI FLORESCU, **Eficienţa economică a cercetării ştiinţifice** (L'efficience économique de la recherche scientifique), 1972, 115 p., 15 lei.

GEORGETA LĂZĂRESCU, **Sistematizarea informaţiilor în cîmpia organică** (La systématisation des informations dans la chimie organique), 1972, 242 p., 10,50 lei.

P. BALTĂ şi E. BALTĂ, **Introducere în chimia fizică a stării vitroase** (Introduction à la chimie physique de l'état vitreux), 1971, 240 p., 15,50 lei.

LYDIA-MARIA VAICUM, **Biodegrabilitatea detergenţilor** (La biodégrabilité des détergents), 1971, 346 p., 19,50 lei.

I. ZUGRĂVESCU et L. STOICESCU-CRIVETZ, **Polimeri heterociclici** (Polymères hétérocycliques), 1971, 190 p., 9,50 lei.

I. V. MAXIM, **Materiale nucleare** (Matériaux nucléaires), 1969, 444 p., 30 lei.

CORNEL BODEA et collab., **Tratat de biochimie vegetală**, partea I, **Fitochimie** (Traité de biochimie végétale, Ire partie, Phytochimie), Ire vol., 1964, 747 p. + 4 annexes + 2 pl., 41 lei ; IIe vol., 1965, 1962 p., 1 pl., 56 lei ; IIIe vol., 1967, 773 p., 35 lei.

CRISTOFOR SIMIONESCU et CLEOPATRA VASILIU-OPREA, **Mecanochimia compuşilor macromoleculari** (La méchanochimie des composés macromoléculaires), 1967, 344 p., 23,50 lei.

V. GHEŢIE et V. MICUŞAN, **Analiza imunochimică. Teorie şi practică** (Analyse immunochimique. Théorie et pratique), 1966, 369 p., 28 lei.

R. PORTOCALĂ et L. POPA, **Acizii ribonucleici celulari şi virali** (Les acides ribonucléiques cellulaires et viraux), 1966, 375 p., 8 pl., 26 lei.

I.P.I. — c. 1604

43 426

Lei 25.—

F 1103

ACADÉMIE DE LA RÉPUBLIQUE SOCIALISTE DE ROUMANIE

REVUE ROUMAINE DE CHIMIE

DEPOZITIA

TOME 19

N° 11

Novembre 1974

RECHAX, **19**, *11*, 1683–1836 (1974)

ÉDITIONS DE L'ACADÉMIE DE LA RÉPUBLIQUE SOCIALISTE DE ROUMANIE

Rev. Roumaine Chim. **19**, *11*, **p. 1683–1836 (1974), Bucarest**

ACADÉMIE DE LA RÉPUBLIQUE SOCIALISTE DE ROUMANIE

COMITÉ DE RÉDACTION

Rédacteur en chef :

I. D. MURGULESCU, membre de l'Académie de la République Socialiste de Roumanie

Rédacteurs en chef adjoints :

A. T. BALABAN et V. EM. SAHINI, membres correspondants de l'Académie de la République Socialiste de Roumanie

Collège de rédaction :

EM. BRATU, ELENA CEAUȘESCU, ECATERINA CIORĂNESCU-NENITZESCU, C. DRĂGULESCU, RALUCA RIPAN, CR. SIMIONESCU, membres de l'Académie de la République Socialiste de Roumanie; P. SPACU, membre correspondant de l'Académie de la République Socialiste de Roumanie; MARGARETA AVRAM, D. I. MARCHIDAN, I. MOLDOVAN, D. NIAC et D. SĂNDULESCU

Toute commande de l'étranger fascicules ou abonnements) sera adressée à Întreprinderea Rompresfilatelia, Botte Postale 2001, telex 011631, Bucarest, Roumanie

Les manuscrits, les livres et les revues proposés en échange, ainsi que toute correspondance seront envoyés à la rédaction :

REVUE ROUMAINE DE CHIMIE

23, str. Dumbrava Roşie, Bucarest, Roumanie, téléphone 12 41 60

EDITIONS DE L'ACADÉMIE DE LA RÉPUBLIQUE SOCIALISTE DE ROUMANIE

3 bis, str. Gutenberg, Bucarest, téléphone 16 40 79

ORSZÁGOS MŰSZAKI KÖNYVTÁR ÉS DOKUMENTÁCIÓS KÖZPONT

REVUE ROUMAINE
DE
CHIMIE

Tome 19, No 11 Novembre 1974

V. E. SAHINI, JOSETTE WEINBERG, C. BENDIC and MARILENA MILESCU, Xylidine isomers III. Acid-basic properties of xylidines in their excited states 1685–1688

R TATIANA MEMETEA and J. PĂUN, Radiolysis of the complex oxalates in aqueous solutions. IV. The influence of some reducing free radicals scavengers on the potassium trisoxalatocobaltate radiolysis in aqueous solutions 1689–1694

D. R. ARMSTRONG, P. G. PERKINS and J. J. P. STEWART, A theoretical investigation of Ziegler-type catalysis. II. Species related to solid titanium trichloride. 1695–1707

IONEL HAIDUC, R. BRUCE KING and HENRY GILMAN, Reactions of some pentafluorophenyl-silicon derivatives with the π-cyclopentadienyliron dicarbonyl anion 1709–1715

D. NEGOIU and ALEXANDRA ŞCHIOPESCU, Thermal analysis of ferrate (VI) ion salts with Ni(II) and Co(II) complex ammines 1717–1725

R I. GABE, ANICA TOLEA and A. AIRINEI, Chelates and polychelates of amino acids. II. Complexes in copper solution (II) with N(R)-anthranilic acids 1727–1730

A. T. BALABAN and MARIA PARASCHIV, Molecular complexes with aromatic cations as electron acceptors. II. Charge-transfer spectrum of 2,4,6-triphenylpyrylium thiocyanate 1731–1734

M. SAFTA and G. OSTROGOVICH, Studies in the *s*-triazine field (new series). XVI. Acidic and tautomeric equilibrium constants of the conjugated acids of some E-1,3-dimethyl-6-(*p*-dialkylamino-β-styryl)2,4-dioxo-1H,3H-1,3,5-triazines 1735–1749

C F. URSEANU, C. DRĂGHICI and V. OLTEANU, Syntheses of naphth[2,3-c] acridan-5,8,14 trionic dyes 1751–1758

DIANA M. MONDESHKA and I. G. ANGELOVA, New direction of substituted β-hydroxy acids dehydration leading to 2,3-disubstituted 1-acetoxy-naphthalenes 1759–1766

Rev. Roumaine Chim. **19**, *11*, 1683–1836 (1974)

S. H. DOSS, SHOICHI KONDO, KATSUMI TANAKA and YOJIRO TSUZUKI, NMR studies on the effect of nitrogen atom on the anomeric proton of β-D-glucopyranosides 1767–1772

MARIA FRANGOPOL, P. T. FRANGOPOL and N. NEGOIŢĂ, Formation of new nitrogen free radicals from dinitro-sulpho-phenyl-N-alkoxyamines . . 1773–1781

R GH. MANDRIC, A. I. PAVLOV, V. V. KORSHAK and I. ZUGRĂVESCU, Thermostable polymers. III. Polybenzimidazole-imides 1783–1790

R. Z. TUDOSE, Heat transfer with chemical reaction modelling of thermal decomposition reactions 1791–1810

R S. K. JAIN, Silver-silver halide electrodes in molten sodium nitrate-barium nitrate eutectic 1811–1815

R **FLORICA BĂRBULESCU, AURORA GREF and MARGARETA CRAIU, The conductance of some alcaline alkoxides in ethanol-benzene and ethanol-dimethylformamide mixtures at 25°** 1817–1823

LUCIA BEU and JANA RUSSU, Synthesis and spectrophotometric studies in the trisubstituted carbetoxyphenylhydrazones series 1825–1834

COMPTE RENDU 1835

Revue Roumaine de Chimie, **19**, *11*, 1685–1688 (1974)

XYLIDINE ISOMERS III[1]

ACID-BASIC PROPERTIES OF XYLIDINES IN THEIR EXCITED STATES

V. E. SAHINI, JOSETTE WEINBERG, C. BENDIC* and MARILENA MILESCU

Centre of Physical Chemistry, Str. Galaţi 31, Bucarest, Romania

*Laboratory of Physical Chemistry, University of Bucharest, Bd. Republicii 13, Bucharest, Romania

Received March 11, 1974

The pK_a values of xylidine isomers in the first excited singlet state are determined using Förster's cycle, the experimental values being compared with the theoretical ones obtained by a SCF – MO calculation. Basic properties of xylidines are also discussed in terms of π-electron densities, frontier electron densities and steric effects.

Acid-basic properties of the molecules in their excited states were the subject of many experimental and theoretical papers.

In connection with this topic, the influence of factors such as electronic structure, effects of donor and acceptor substituents, steric effects and others on pK_a values were investigated.[2-6]

These studies show an increase of the donor or acceptor character of the substituents in the first excited singlet state of the molecules and in this way the decrease or the increase of their basic properties, respectively.[7-9]

The aim of the present paper is to study, in comparison with the fundamental state, the change of the basic properties of xylidines in their first excited singlet state and to correlate it with different structural quantities such as π-electron densities on the nitrogen atom, frontier electron densities and steric effects of the methyl group.

---

[1] Previous paper : V. E. Sahini and J. Weinberg, *Rev. Roumaine Chim*. **18**, 1493 (1973).

[2] C. A. Parker "Photoluminiscence of Solutions", Elsevier Publishing Co., Amsterdam 1968.

[3] E. Vander Donckt "Progress in Reaction Kinetics" vol. 5, Ed. G. Porter, Pergamon Press, Oxford, 1970 p. 274.

[4] J. Bertran, J. J. Dannenberg, R. Leute, C. Ponce, O. Chalvet and R. Daudel, *Theor. Chim. Acta.*, **17**, 249 (1970).

[5] E. Vander Donckt, *Bull. Soc. chim. belges*, **78**, 69 (1969).

[6] E. Vander Donckt, D. Lietaer and J. Nasielski, *Bull. Soc. chim. belges*, **79**, 289 (1970).

[7] R. Cetina, D. V. S. Jain, F. Peradejordi, O. Chalvet and R. Daudel, *Compt. rend.*, **264**, 874 (1967).

[8] J. Bertran, O. Chalvet and R. Daudel, *Theor. Chim, Acta*, **14**, 1 (1969).

[9] A. Streitwieser, *Tetrahedron Letters*, **6**, 23 (1960).

1. EXPERIMENTAL

Xylidine isomers (Schuchardt) were purified by fractional distillation under low pressure.

The acid and basic forms were obtained according to Beale [10] using the aqueous solutions over the concentration range $10^{-3}-10^{-4}$M.

In order to determine the pKa values in the first excited singlet state ($pK_a(s_1)$), we used Förster's cycle [11] for the following reversible reactions

$$R - NH_3^+ \overset{Ka}{\rightleftharpoons} R - NH_2 + H^+ \qquad (1)$$

$$(R - NH_3^+)^* \overset{K_a^*}{\rightleftharpoons} (R - NH_2)^* + H^+ \qquad (2)$$

where R is xylil radical and reaction (2) refers to the lowest excited singlet state of xylidines.

The O–O transition was taken by averaging the frequencies of the first absorption and the respective fluorescence maxima, for both acid and basic forms.

Ultraviolet and fluorescence spectra were recorded by means of a UNICAM SP-800 spectrophotometer and a PERKIN-ELMER 204 spectrofluorimeter.

The results of the absorption and fluorescence measurements are given in table 1.

Table 1

Absorption and fluorescence maxima for xylidine isomers

Species		ν_{max} (cm^{-1})				
		2.3–	2.5–	2.6–	3.4–	3.5–
		xylidine				
Absorption Spectra	$R-NH_3^+$	38.168	37.583	37.951	37.951	38.400
	$R-NH_2$	35.524	35.250	35.778	34.904	35.148
Fluorescence Spectra	$R-NH_3^+$	34.843	34.483	34.821	35.142	34.602
	$R-NH_2$	29.658	29.554	30.120	28.736	29.325

2. THEORETICAL

The models generally used for the theoretical treatment of the protonated form, consider either the existence of a charge transfer from the nitrogen atom towards the proton, performed by the formation of a covalent bond

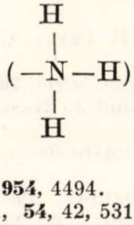

$$(-\overset{\displaystyle H}{\underset{\displaystyle H}{N}}-H)^+$$

---

[10] R. N. Beale, *J. Chem. Soc.*, **1954**, 4494.

[11] Th. Förster, *Z. Elektrochem.*, **54**, 42, 531 (1950).

or the localization of the proton near the nitrogen atom of the neutral molecule

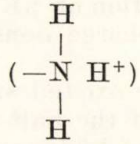

$$(-\underset{\underset{H}{|}}{\overset{\overset{H}{|}}{N}}\ H^+)$$

The latter model gives the best agreement of the experimental data with the theoretical ones.[12]

This model in the SCF–MO method consists in the modification of the Hamiltonian operator due to the effective charge of the proton by a change of the nitrogen ionization potential only.

In order to calculate the O–O transition, for both acid and basic forms, necessary for evaluating the $pK_a(S_1)$ using Förster's cycle, the SCF–MO–PPP method has been used, considering for the protonated form an increase in the absolute magnitude of the nitrogen ionization potential from $W_{2p} = -27.53$ eV to $W_{2p} = -41.55$ eV.[8]

The SCF results were used to calculate the $pK_a(S_1)$ values, π-electron densities and frontier electron densities.

3. RESULTS AND DISCUSSION

The experimental and theoretical values of $pK_a(S_1)$, the π-electron densities on the nitrogen atom, in both the ground q_N and first excited singlet q_N^* states, the frontier electron densities in S_1 state f_N^*, as well as the experimental values of $pK_a(S_0)$[10,13] are presented in table 2.

Table 2

pK_a (S_1) values, π-electron densities and frontier electron densities for xylidine isomers

Isomer	pK_a (S_0) (exper.)	pK_a (S_1) (exper.)	pK_a (S_1) (theoret.)	q_N	q_N^*	f_N^*
2,3-xylidine	4.72	−3.46	−2.68	1.8570	1.6698	0.1910
2,4-xylidine	4.84	—	−7.73	1.8667	1.6824	0.1896
2,5-xylidine	4·53	−3.06	−2.54	1.8570	1.7002	0.2024
2,6-xylidine	3.95	−3.27	−4.50	1.8712	1.6728	0.1984
3,4-xylidine	5.17	−4.75	−6.21	1.8528	1.6786	0.1792
3,5-xylidine	4.91	−4.04	−4.55	1.8433	1.6642	0.1792

The decrease of the basic properties of all xylidine isomers in the excited (S_1) state, is evident for both the experimental and theoretical values of $pK_a(S_1)$ in a quite similar sequences.

---

[12] S. Mataga and N. Mataga, *Bull. Chem. Soc. Japan*, **32**, 511 (1959).

[13] B. M. Wepster, *Rec. Trav. chim.*, **76**, 357 (1957).

This fact was expected since the donor character of the $-NH_2$ group increases in the excited state, leading to a decrease in the value of q_N^*. However, no direct correlation of $pK_a(S_1)$ with q_N^* in xylidine series, is obtained, as not only the charge density accounts for a protonation reaction.

In such a reaction in the excited state, an important contribution arises from the perturbation of the half-occupied levels of the molecule by the unoccupied level of the hydrogen ion.

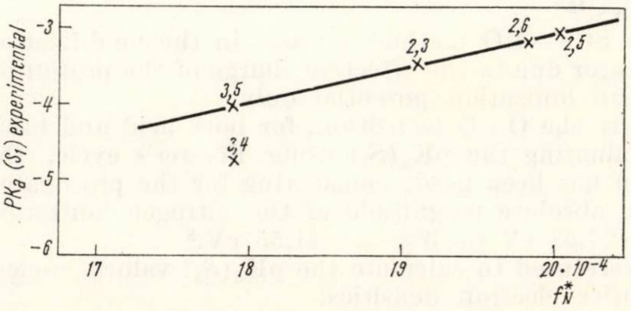

Fig. 1. — $pK_a(S_1)$ values of some xylidine isomers vs. the frontier electron densities f_N^* on the nitrogen atom.

This will be very important when the hydrogen ion level energy will be higher or nearly degenerate in comparison with the energy of the higher half-occupied level of the molecules. In this case the reaction will be a frontier electron density controlled one.[14,15]

In fig. 1 the $pK_a(S_1)$ values of xylidines were plotted against the corresponding frontier electron densities f_N^* on the nitrogen atom in the excited state S_1.

One may notice that for 3.5— ; 2.3— ; 2.6— and 2.5— xylidine, the decrease of $pK_a(S_1)$ is linear vs. f_N^*.

In the ground state, it was possible to divide xylidine isomers into classes according to the steric hindrance due to the methyl groups.

In the S_1 state, the higher frontier electron densities, the higher the π-stabilization energies due to the perturbation of the molecule by the proton.

As the isomers with the methyl group in the ortho and meta positions present the largest f_N^* values, the largest values for $pK_a(S_1)$ are found.

In the case of methyl group in the para position (3,4— and 2,4— xylidine), an appreciable decrease of the basicity in the S_1 state is observed according to the smallest frontier electron densities, as shown in table 2.

---

[14] K. Fukui, T. Yonezawa and H. Shingu, *J. Chem. Phys.*, **20**, 722 (1952).

[15] K. Fukui, T. Yonezawa, C. Nagata and H. Shingu, *J. Chem. Phys.*, **22**, 1433 (1954).

Revue Roumaine de Chimie, **19**, *11*, 1689–1694 (1974)

RADIOLYSIS OF THE COMPLEX OXALATES IN AQUEOUS SOLUTIONS. IV[1].

THE INFLUENCE OF SOME REDUCING FREE RADICALS SCAVENGERS ON THE POTASSIUM TRISOXALATOCOBALTATE RADIOLYSIS IN AQUEOUS SOLUTIONS

TATIANA MEMETEA and J. PĂUN

University of Bucharest, Radiation Chemistry Laboratory, Bd. Republicii 13, Bucharest Romania

Received December 6, 1973

The radiolysis of $[Co(C_2O_4)_3]^{3-}$ complex ion in aqueous solution in various conditions, the presence and the absence of air, neutral and acid medium and the presence of some reducing species scavengers such as NO_2^-, NO_3^-, N_3^- ions and acetone has been studied. At 2×10^{-3}M concentration the radiochemical yield $G(-[Co(C_2O_4)_3]^{3-}) = 4.96 \pm 0.05$ in the absence of air, and 3.19 ± 0.05 in the presence of air. At the same complex concentration, $G(-[Co(C_2O_4)_3]^{3-})_{pH=1} \doteq 5.62$. In the absence of air the reduction takes place by the reactions with hydrated electron and hydrogen atom. In the presence of air the complex ion is reduced by O_2^- ion.

In previous papers[1-3] we established that in various conditions of irradiation such as dose rate, L.E.T., pH, the concentration of the solution, the radiolysis of potasium trisoxalatocobaltate in aqueous solution obeys a zero order kinetic law. From the interpretation of the experimental data we proposed a general mechanism of the radiolysis.

For a better understanding of the radiolytic process we are reporting in the present paper some results concerning the influence of some reducing species scavengers on the kinetics of the radiation-chemical decomposition of $[Co(C_2O_4)_3]^{3-}$ ion.

EXPERIMENTAL

Potassium trisoxalatocobaltate was synthesized as described in literature.[4] In all the runs we used a constant complex concentration of 2×10^{-3}M. The solutions were prepared with triply distilled water. The substances used as scavengers were of analytical purity.

---

[1] Part III. J. Păun and T. Memetea, *Rev. Roumaine Chim.*, **19**, 971 (1974)

[2] I. G. Murgulescu, T. Oncescu, J. Păun and I. Mihalcea, *Rev. Roumaine Chim*, **12**, 573 (1967).

[3] I. G. Murgulescu and J. Păun, *Rev. Roumaine Chim.*, **19**, 9 (1974)

[4] S. P. L. Sörensen, *Z. anorg. Chem.*, **11**, 1 (1896).

The irradiations have been performed in a Co^{60} equipment of the mobile source type with telemanipulation having the initial activity of 500 Ci and specific activity of 20 Ci/g. The dosimetry was carried out by the chemical method using Fricke dosimeter. The dose rate was in the range from 6.73×10^{18} to 9.12×10^{19} eV/h/g.

The decomposition of the complex in aqueous solution during the irradiation was followed by spectrophotometrical method recording the diminution of the optical density at 420 nm.

The hydrogen peroxide produced during the irradiation was determined spectrophotometrically using the pertitanic acid method reagent and recording the optical density of the solution at $\lambda = 420$ nm ($k = 910\ M^{-1}\ cm^{-1}$).

RESULTS

a) The radiolysis of potassium trisoxalatocobaltate in neutral aqueous solution (natural pH) follows a zero order kinetic law in the presence as well as in the absence of air. In figure 1 is shown the decrease of the optical density of the 2×10^{-3}M complex in aqueous solution during the irradiation, in the presence and the absence of air. The rate of decomposition in the presence of air is lower than in its absence. The decomposition yields at this concentration are: $G(-[Co(C_2O_4)_3]^{3-})_{air} = 3.19 \pm 0.05$; $G(-[Co(C_2O_4)_3]^{3-})_{Ar} = 4.95 \pm 0.05$.

b) In the presence of 0.1N perchloric acid (pH = 1), the radiochemical decomposition of the complex also follows a zero order kinetic law, but the decomposition rate is lower, as shows in figure 1.

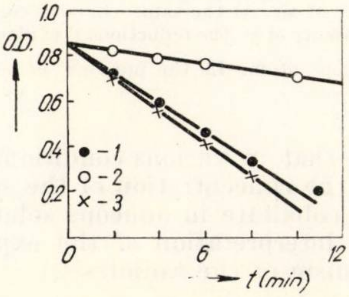

Fig. 1. — The influence of air and pH on the radiochemical decomposition of $K_3[Co(C_2O_4)_3]$ in aqueous solution. Dose rate: 9.12×10^{19} eV/h/g: *1*, absence of air; *2*, presence of air; *3*, absence of air, $HClO_4$ 0.1N.

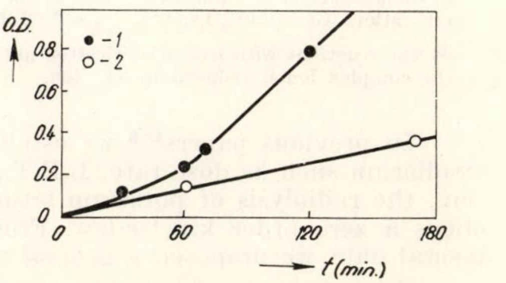

Fig. 2. — The accumulation of H_2O_2 in irradiated solution of 2×10^{-3}M $K_3[Co(C_2O_4)_3]$: *1*, presence of air; *2*, absence of air.

c) The hydrogen peroxide is building up continuously during the irradiation as shown in figure 2 where the optical density of the irradiated solution to which pertitanic acid reagent was added, is ploted against the irradiation time. The radiochemical yields of hydrogen peroxide, $G(H_2O_2)$, in the presence and in the absence of air are identical to those reported for the irradiation of pure water: 3.7 and 0.78 respectively.[5]

---

[5] Z. Draganič, I. Draganič and M. Kosanic, *J. Phys. Chem.*, **68**, 2085 (1964).

d) By adding some reducing species scavengers an appreciable decrease of the decomposition rate of the complex ion appears. We used acetone and NO_3^- ion as selective scavengers of hydrated electron, N_3^- as selective scavengers of H atoms and NO_2^- as scavenger of both reducing species. As the utility of the maleic and ithaconic acid in the radiochemical polymerisation is known some experiments were made in the presence of these acids.

The acetone has an effect of lowering to a great extent the rate of complex decomposition. Figure 3 shows the decrease of the optical density of the irradiated solution as a function of the irradiation time, in the presence of air, the acetone concentration ranging from 10^{-1} to 2M.

The NO_2^- and NO_3^- ions are strongly decreasing the decomposition rate of the complex in the presence as well as in the absence of air. Figure 4 shows the decrease of the decomposition yield of the complex ion as a function of scavenger concentration from 2×10^{-5} to 2×10^{-3}M, in the absence of air. It is noticeable that NO_2^- ions have a higher ability of reducing the rate of decomposition than NO_3^- ions; even at 10^{-4}M NO_2^- ions concentration, the radiochemical yield decreases with 42%, while in the presence of NO_3^- the decrease is 6% only.

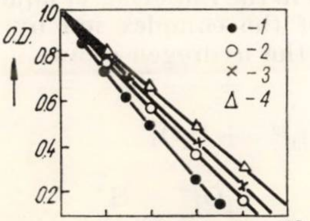

Fig. 3. — The influence of acetone on the radiochemical decomposition of aerated aqueous solution of $K_3[Co(C_2O_4)_3]$: *1*, without scavenger; *2*, acetone 10^{-1} M; *3*, acetone 1M; *4*, acetone 2M.

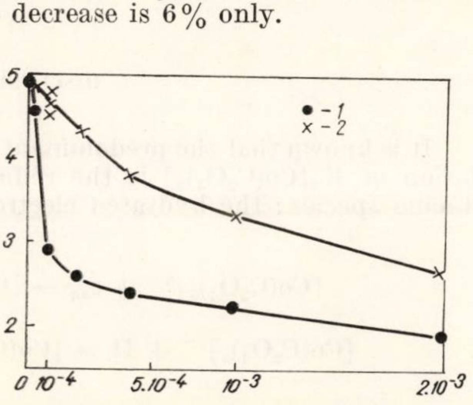

Fig. 4. — The decrease of $G(-[Co(C_2O_4)_3]^{-3})$ with the increasing concentration of (*1*), NO_2^-; *2*, NO_3^- ions

In the presence of N_3^- ions the decomposition rate of the complex diminishes by 40%. Figure 5 shows the optical density of the irradiated 2×10^{-3}M complex solution against time, to which 2×10^{-3} NaN_3, was added.

The effect of maleic and ithaconic acid results in a lowering of the decomposition rate of the complex (figure 6) indicating that these acids scavenge the reducing species.

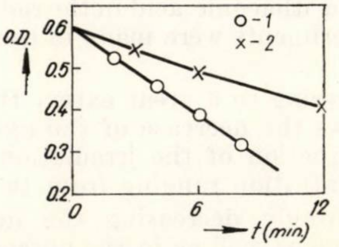

Fig. 5. – The influence of N_3^- ion on the radiochemical decomposition of the complex : *1*, without scavenger ; *2*, N_3^-.

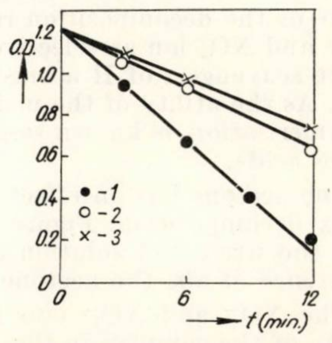

Fig. 6. – The influence of ithaconic and maleic acid on the radiochemical decomposition of $K_3[Co(C_2O_4)_3]$ aqueous solution : *1*, without scavenger ; *2*, maleic acid 10^{-1} M ; *3*, ithaconic acid 10^{-1}M.

DISCUSSION

It is known that the predominant process in the radiolysis of aqueous solution of $K_3[Co(C_2O_4)_3]$ is the reduction of the complex ion by the reducing species : the hydrated electron and the hydrogen atom

$$[Co(C_2O_4)_3]^{3-} + e_{aq}^- \rightarrow [Co(C_2O_4)_2]^{2-} + C_2O_4^{2-} \tag{1}$$

$$[Co(C_2O_4)_3]^{3-} + H \rightarrow [Co(C_2O_4)_2]^{2-} + C_2O_4^{2-} + H^+ \tag{2}$$

In the presence of air, these species are captured by O_2 as reactions (3) and (4) indicate

$$O_2 + e_{aq}^- \rightarrow O_2^- \tag{3}$$

$$O_2 + H \rightarrow HO_2 \rightleftharpoons H^+ + O_2^- \tag{4}$$

As is known, in neutral solution HO_2 radicals dissociate, the product of reaction (4) being the O_2^- ion too. The O_2^- concentration achieved corresponding to the solubility of air in water at room temperature ensures the reduction of the complex ion especially via reaction (5)

$$[Co(C_2O_4)_3]^{3-} + O_2^- \rightarrow [Co(C_2O_4)_2]^{2-} + C_2O_4^{2-} + O_2 \tag{5}$$

The lower value of $G(-[Co(C_2O_4)_3]^{3-})$ in the presence of air suggests that the rate constant of reaction (5) is lower than that of reaction (1).

The continuous building up of H_2O_2 during irradiation demonstrates that hydrogen peroxide does not take place in the radiolytic process. The reason for this is that the H_2O_2 concentration is lower than that of $[Co(C_2O_4)_3]^{3-}$ ion, so that the former cannot compete for the reducing species. According to Wormser[6] H_2O_2 does not oxidize the $[Co(C_2O_4)_2]^{2-}$ ion in our conditions.

By irradiation at pH $= 1$ the hydrated electrons are quantitatively converted to hydrogen atoms.

$$e_{aq} + H^+ \rightarrow H \tag{6}$$

so that the complex ion reduction occurs via reaction (2) only. Since the Co^{3+} ion as well as the $C_2O_4^{2-}$ ion are feeble H atom scavengers, it is also expected that $[Co(C_2O_4)_3]^{3-}$ ion reacts with the H atom with a rate constant less than $10^7 M^{-1}s^{-1}$. Recently, Shagisultanova[7] reported for k_2 a value of $4.6 \times 10^6 M^{-1}s^{-1}$, which means that the $[Co(C_2O_4)_3]^{3-}$ ion is a feeble H scavenger. If the complex ions would scavenge quantitatively the hydrogen atoms it should be expected that $G(-[Co(C_2O_4)_3]^{3-}) \cong G_H \cong \cong 3.6$. The value of 5.62 obtained by us indicates that apart from reaction (2) at the reduction of the complex ion some other processes are also taking part from which the most probable seems to be excitation processes involving $[Co(C_2O_4)_3]^{3-*}$ or $[Co(C_2O_4)_2]^{2-*}$. The evidence for the formation of $(M^{II} L_2)^{2-*}$, where M $=$ Co, Ru and L $=$ bipyridyl, in the radiolysis of complex ions $(M^{III} L_3)^{3-}$, has already been given by Pearson[8] and Hart.[9]

In the presence of hydrated electron selective scavengers, besides reaction (1), reactions (7) and (8) are taking place

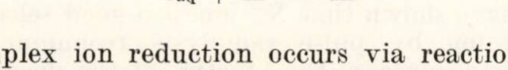

$$e_{aq}^- + H_3C\,COCH_3 \rightarrow H_3C-\underset{\displaystyle O^-}{\overset{\bullet}{C}}-CH_3 \tag{7}$$

respectively

$$e_{aq}^- + NO_3^- \rightarrow NO_3^{2-} \xrightarrow{H_2O} 2\,OH^- + NO_2 \tag{8}$$

where $k_7 = 5.9 \times 10^9 M^{-1} s^{-1}$ [10] $k_8 = 1.1 \times 10^{10} M^{-1} s^{-1}$.[10]

If the scavenger is the NO_2^- ion, reactions (9) and (10) occur in addition to reactions (1) and (2)

$$NO_2^- + e_{aq}^- \rightarrow NO_2^{2-} \xrightarrow{H_2O} NO + 2\,OH^- \tag{9}$$

---

[6] Y. Wormser and G. Herve, *Compt. rend.*, **256**, 1534 (1963).

[7] G. Shagisultanova, *Khim. Vysokii Energhii*, **5**, 2, 187 (1971).

[8] L. W. Waltz and R. G. Pearson, *J. Phys. Chem.*, **73**, 1941 (1969).

[9] J. Halpern and E. Hart, *J. Amer. Chem. Soc.*, **94**, 9238 (1972).

[10] M. Anbar and P. Neta, *Int. J. Appl. Radiation Isotopes*, **18**, 493, (1967).

$$\mathrm{NO_2^-} + \mathrm{H} \rightarrow \mathrm{NO_2^{2-}\cdot} + \mathrm{H^+} \qquad (10)$$

where $k_9 = 8.1 \times 10^{10}\ \mathrm{M^{-1}\,s^{-1}}$[10], $k_{10} = 1 \times 10^{9}\ \mathrm{M^{-1}\,s^{-1}}$[10].

The inhibition of the complex decomposition rate in the presence of the $\mathrm{N_3^-}$ ion is due to the competing action of this ion with the $[\mathrm{Co(C_2O_4)_3}]^{3-}$ ion for H atoms by reactions (2) and (11)

$$\mathrm{N_3^-} + \mathrm{H} \rightarrow \text{Products } (\neq \mathrm{H_2}) \qquad (11)$$

Czapski *et al.*,[11] have shown that $\mathrm{N_3^-}$ ion is a good selective H atom scavenger, determining by pulse radiolysis technique a k_1 value of $2.7 \times 10^{9}\ \mathrm{M^{-1}\,s^{-1}}$. In our case the kinetics of the decomposition process does not follow a zero order kinetic law, suggesting a more complicated process.

The attempt to make kinetic calculations using our results has been proved difficult, so new experimental data are in progress.

---

[11] E. Peled, N. Mirski and G. Czapski, *J. Phys. Chem.*, **75**, 31 (1971).

Revue Roumaine de Chimie, **19**, *11*, 1695 – 1707 (1974)

A THEORETICAL INVESTIGATION OF ZIEGLER-TYPE CATALYSIS. II.[1]

SPECIES RELATED TO SOLID TITANIUM TRICHLORIDE

D. R. ARMSTRONG, P. G. PERKINS and J. J. P. STEWART

Department of Pure and Applied Chemistry University of Strathclyde, Glasgow, C. 1

Received December 17, 1973

All-valence-electron self-consistent field calculations are presented for the $TiCl_3$ monomer and the $Ti_2Cl_{10}^{4-}$ anion. The ground-state geometry of the former species is planar and trigonal but the corresponding electronic state is ill-defined and may be either of $^2A_1'$ or $^2E''$ symmetry. The energy levels of $Ti_2Cl_{10}^{4-}$ form groups within which the levels are quite closely spaced. Those adjacent to the bonding-antibonding gap have predominantly 3*d* character and are formed from the "t_{2g}" sets of the individual titanium atoms. A multi-configuration interaction treatment shows the lowest state to be a triplet ($^3B_{3u}$) although a number of low-lying singly- and doubly-excited states do exist which involve the metal-metal interaction. The implications of the electronic structure of $Ti_2Cl_{10}^{4-}$ for that of the solid α $TiCl_3$ catalyst are discussed.

In Part 1[1] we presented a theoretical rationale of the Ziegler catalytic process, augmenting Cossee's scheme[2] and involving molecular catalysts. We now focus on the situation where a solid substance forms the basis of the catalyst system and here investigate theoretically two related species.

In the commercial production of stereoregular high polymers one catalyst in particular, titanium trichloride, together with the co-catalysts triethylaluminium and diethylaluminium chloride, has proved to be very efficient. This and related systems have been the subject of many previous papers.[3]

Single-crystal studies on titanium trichloride have shown that polymer growth occurs at the edges, cracks, and crushed areas of the medium,[4] and these are precisely those areas where exposed titanium atoms are expected to exist. Now the $TiCl_3$ monomer, which also has an "exposed" titanium atom, should be related electronically to isolated points on the catalyst surface. Hence we have carried out a series of calculations on this species to illuminate its electronic structure and formulate a more accurate description of the system.

---

[1] D. R. Armstrong, P. G. Perkins, and J. J. P. Stewart, *J. Chem. Soc.*, Dalton, **1972**, 1972.

[2] P. Cossee, "Advances in the Chemistry of the Coordination Compounds", Macmillan, N. Y., 1961, p. 241.

[3] J. Boor, *Macromol. Revs.*, **2**, 115, (1967).

[4] W. R. Carradine and H. F. Rase, *J. Applied Polymer Sci.*, **15**, 889 (1971).

Titanium trichloride can be obtained by reduction of $TiCl_4$ with $EtAlCl_2$. It exists in three distinct crystalline forms which are well characterised by colour : the α and γ modifications are violet whilst the β is brown.

The α-form is used commercially as a Ziegler catalyst and X-ray structural analysis[5] indicates that in the crystal each titanium is surrounded by an octahedron of chlorine atoms. It would be helpful to be able to calculate directly the bulk solid and surface band structure of the material but its complexity precludes a detailed calculation of this at the present time. Hence as a model for solid α $TiCl_3$, we replaced the lattice by a block of the type $Ti_2Cl_{10}^{4-}$. We believe that the ground-state properties would only be slightly modified by using larger blocks and although the full Brillouin zone between point Γ and other symmetry points cannot be mapped, a reasonable estimate of the electronic band widths should be obtained.

Titanium (III) is a d^1 system and, on crystal field theory, the absorption band of the α form which appears in the visible region should be due to transitions involving the "d" orbitals on titanium. Dijkgraaf and Rousseau[6] have assigned the shoulder in the spectrum at 14,300 cm^{-1} to the Laporto-forbidden $^2T_{2g} \rightarrow {}^2E_g$ transition, whilst the absorption at 18,900 cm^{-1} was attributed to charge-transfer; the latter assignment was based solely on the observed high intensity of absorption. In the context of octahedral titanium, the electronic structure of the chromophoric group $TiCl_6^{3-}$ has also been described in terms of crystal-field theory.[7]

A set of unpaired d electrons, one on each Ti of $TiCl_3$, should show an e.s.r. signal. Solid $TiCl_3$ prepared by reduction of $TiCl_4$ with $EtAlCl_2$ is said to have no unpaired electrons[8], whereas the precipitate and supernatant liquor resulting from the reaction of $TiCl_4$ with $EtAlCl_2$ does show an e.s.r. signal. These results possibly indicate that, as the reaction proceeds, isolated molecules of $TiCl_3$ are formed which rapidly crystallise out as a α $TiCl_3$ and in the latter the "odd" electrons are in some way paired between the titanium atoms.

METHOD

Whereas in Part 1[1] all the molecules studied were of closed-shell type, in the present work we must deal with open-shell systems. Two systems, $TiCl_3$ and $Ti_2Cl_{10}^{4-}$, were examined in detail. The structure of molecular $TiCl_3$ is unknown but it can be assumed that the symmetry is either C_{3v} or D_{3h} and that the Ti—Cl bond length lies between 0.218 and 0.245 nm[5,9]. The structure of $Ti_2Cl_{10}^{4-}$ was related directly to that of the α $TiCl_3$ lattice, where representative bond lengths are Ti—Cl=0.246 nm and Ti—Ti=0.354 nm.[5] For the latter calculation, each Ti was assumed to be octahedrally surrounded by six chlorine atoms, the octahedra sharing an edge and giving an overall molecular symmetry of D_{2h}. From pilot calculations on $TiCl_3$ and from previous work [10] the effect of *d* orbitals on chlorine turned out to be negligible (the occupation of the chlorine 3*d* orbital was ∼ 0.2e), hence these orbitals were neglected in subsequent calculations : those included for titanium were the 4*s*, 4*p*, and 3*d* orbitals. The input parameters for Ti and Cl were identical to those of the previous paper.[1] A difference occurs since $TiCl_3$ has an odd number of electrons and we therefore studied it by the open-shell SCF methods of Pople and Nesbet [11] and of Dewar.[12] Similarly, although $Ti_2C_{10}^{4-}$ contains an even number of electrons and, in addition, its symmetry is that of an abelian point group, we investigated the possibility of a non-spin-paired ground state. For this a multi-electron configuration-interaction treatment [13] involving all singly and doubly excited states formed from a specified set of orbitals was used.

---

[5] G. NATTA, P. CARRADINI, and G. ALLEGRA, *J. Polymer Sci.*, **51**, 399 (1961).

[6] C. DIJKGRAAF and J.P.G. ROUSSEAU, *Spectrochim. Acta*, **24**, 1212 (1968).

[7] C. K. JORGENSEN, "Absorption Spectra and Chemical Bonding in Complexes", Pergamon Press, London, 1961, p. 61.

[8] E. H. ADEMA, "International Symposium on Macromoleculare Chemistry", Prague, August, 1965; E. H. ADEMA, H.J.M. BARTELINK, and J. SMIDT, *Rec. Trav. chim.*, **80**, 173 (1961); **81**, 73 (1962).

Since the results obtained in the present work here apply equally to both α and γ $TiCl_3$, no discussion of the relative merits of α and γ $TiCl_3$ as catalysts is possible and further illumination of this point must await a detailed SCF solid-state calculation.

RESULTS AND DISCUSSION

1. GEOMETRY

The geometry of $TiCl_3$ was elucidated by minimising the total energy for various conformations, all with constant Ti—Cl bond length. We do not detail the results here but the calculations unambiguously assign the geometry as D_{3h}, all other geometries, *e.g.*, C_{2v} and C_{3v}, affording higher energies. The calculational method does not predict bond lengths accurately, hence no attempt was made to determine the equilibrium Ti—Cl distance.

2. MOLECULAR ORBITALS AND GROUND STATE OF TITANIUM TRICHLORIDE MONOMER

Before proceeding to consideration of the model for the catalyst, we first present and assess the theoretical results on the ground-state and excited-state properties of the monomer. The calculated energy levels and composition of the molecular orbitals are given in tables 1 and 2. Viewed over all the calculations a change in Ti—Cl bond length of 0.027 nm produces only limited variation in the majority of the bonding energy levels the overall picture remaining essentially unaltered.

It is in the set of energy levels which border the bonding-antibonding gap where the most significant changes occur. The two M.O.'s of lowest

[9] "Tables of Interatomic Distances in Molecules and Ions, *Chem. Soc., Special Publ.* N° 11, 1958.

[10] D. R. Armstrong, P. G. Perkins, and J.J.P. Stewart, *J. Chem. Soc.*, 3654 1971.

[11] J. A. Pople and R. K. Nesbet, *J. Chem. Phys.*, **22**, 5711 (1954).

[12] M. J. S. Dewar and N. Trinajstic, *Chem. Comm.*, **1970**, 646.

[13] D. R. Armstrong, R. Fortune, P. G. Perkins, and J.J.P. Stewart, *J. Chem. Soc., Faraday II*, **68**, 1839 (1972).

Table 1

Energy levels for titanium trichloride (eV)

Symmetry	Ti—Cl = 0.245 nm			Ti—Cl = 0.218 nm		
	Pople-Nesbet		Dewar	Pople-Nesbet		Dewar
	α	β		α	β	
$5e'$	3.25	3.25	3.24	4.17	4.17	4.18
$4a_1'$	2.08	2.08	2.07	3.51	3.51	3.51
$2a_2''$	1.52	1.52	1.51	2.65	2.65	2.65
$4e'$	−1.07	−1.07	−1.08	0.19	0.19	0.20
$2e''$	−1.18	−5.64	−1.19	−0.21	−0.21	−0.20
$3a_1'$	−1.17	−1.17	−5.66	−0.28	−9.26	−4.75
$3e'$	−11.06	−11.06	−11.06	−12.53	−11.51	−11.51
$1a_2'$	−11.23	−11.23	−11.23	−11.31	−11.31	−11.31
$1e''$	−11.34	−11.36	−11.33	−11.77	−11.77	−11.77
$2e'$	−11.98	−11.98	−11.97	−12.62	−12.62	−12.62
$1a_2''$	−12.52	−12.48	−12.51	−13.00	−13.00	−13.00
$2a_1'$	−12.67	−12.67	−12.68	−13.11	−13.17	−13.13
$1e'$	−24.83	−24.83	−24.83	−25.15	−25.15	−25.15
$1a_1'$	−25.94	−25.94	−25.94	−27.22	−27.22	−27.23
Ground state symmetry	$^2E''$		$^2A_1'$	$^2\mathrm{A}_1'$		$^2A_1'$

energy are mainly of chlorine $3s$ character and these are separated by *ca.* 2 eV from six sets of M.O.'s containing eighteen electrons and derived mainly from the $3p$ orbitals on chlorine. The M.O. of highest energy is partially occupied by the odd electron and has always chiefly titanium $3d$ character.

Table 2

Nature of the molecular orbitals for titanium trichloride monomer

Symmetry	Main character of orbital
$5e'$	p_x and p_y on Ti
$4a_1'$	s on Ti
$2a_2''$	p_z on Ti
$4e'$	$d_{x^2-y^2}$ and d_{xy} on Ti
$2e''$	$d_{(xz)}$ and $d_{(yz)}$ on Ti
$3a_1'$	$d_{(z^2)}$ on Ti
$3e'$	p_x on p_y on Cl, and $d_{x^2-y^2}$ and d_{xy} on Ti
$1a_2'$	p_x and p_y on Cl
$1e''$	p_z on Cl
$2e'$	p_x and p_y on Cl
$1a_2''$	p_z on Cl
$2a_1'$	p_x and p_y on Cl
$1e'$	s on Cl
$1a_1'$	s on Cl

Using Pople-Nesbet theory and a Ti-Cl bond length of 0.245 nm, the symmetry of this M.O. (with β spin) is e'' in contrast to the calculation by Dewar's method, which assigns it as a_1'. It is also assigned as a_1' by both calculations with a Ti-Cl bond length equal to 0.218 nm. In order to follow up this point, the relative energies of the derived electronic states $^2E''$ and $^2A_1'$; were next calculated, including excited states and a multi-electron configuration interaction technique. In both cases (Ti—Cl = 0.245 nm and Ti—Cl = = 0.218 nm), the state of lower energy was $^2A_1'$. This is as expected, since a ground-state symmetry of $^2E''$ would violate the Jahn-Teller theorem. Since distortion to a pyramidal shape does not lower the degeneracy and C_{2v} systems are less stable, then we must conclude that the Pople Nesbet calculation at 0.245 nm is incorrect. However, the $^2A_1' - {}^2E''$ interstate energy gap in both cases was small (*e.g.* where Ti—Cl $= 0.245$ nm, it was only *ca.* 0.05 eV).

Of the virtual orbitals, the four of lowest energy are principally composed of $3d$ on titanium, followed at progressively higher energies by titanium $4p_z$, $4s$, and $4p_x + 4p_y$. Simple electrostatic crystal-field arguments assign energy level ordering of the titanium d orbitals in a D_{3h} field as $d_{z^2} < d_{xz} = d_{yz} < d_{x^2-y^2} = d_{xy}$. However, because of the form of the electron repulsion integrals, a CNDO-based theory cannot admit of any angular dependence of electrostatic repulsion for d orbitals, hence both splitting and ordering must be rationalised on the basis of covalent bonding. The bonding M.O.'s involving titanium are not easily recognisable, due to the swamping contributions from the s and p on chlorine but it is seen that titanium-to-chlorine bond orders are arranged in the order $d_{x^2-y^2} - \mathrm{Cl} > d_{xz} - \mathrm{Cl} > d_{z^2} - \mathrm{Cl}$. Thus, $d_{x^2-y^2}$ and d_{xy} are stabilised by bonding to chlorine more than d_{xz} and d_{yz}, and both pairs more than d_{z^2}. Hence, we would expect the opposite order for the corresponding anti-bonding orbital set. These latter M.O.'s, because they are almost pure $3d$ on titanium, are easily recognisable and are in the order $a_1' < e'' < e'$, as would be expected.

The effect of the symmetrical bond length increase is to expand the orbital energy scale. Only the a_2' orbital contains no contribution from titanium and, hence, is expected to be relatively insensitive to changes in the Ti—Cl bond length. This is indeed what is found: whereas the orbitals immediately higher and lower than it in energy change by *ca.* 0.4 eV, the a_2' orbital changes by only 0.08 eV.

3. GENERAL PROPERTIES OF TITANIUM TRICHLORIDE

Table 3 lists the charges and valencies calculated for $TiCl_3$. The overall charges on titanium and chlorine are in general agreement with those expected for a transition-metal complex. The charge separation increases with increasing interatomic distance and this is rationalised by the fact that the extent of covalent bonding must decrease to zero as the interatomic distance increases indefinitely and as the bond length increases, the molecular orbitals will become increasingly localised on either the titanium or the chlorine.

The concept of valency[14] is poorly defined when applied to open-shell systems such as the one under consideration. Thus, the calculated valency for Ti is *ca.* 1.0 and 1.5 more than the sum of all bond indices to Ti for the $^2A_1'$ and $^2E'$ states, respectively. Nevertheless, the results indicate a covalency of titanium in $TiCl_3$ as 3.1 ± 0.1 and a free valency, due to the unpaired electron, as 0.99 ± 0.01 for the $^2A_1'$ states and 1.47 for the $^2E'$ state. (In a simple model of $TiCl_3$ the covalency of Ti is exactly

---

[14] D. R. Armstrong, P. G. Perkins, and J. J. P. Stewart, *J. Chem. Soc., Dalton*, **1973**, 838.

3.0 and the free valencies are exactly 1.0 and 1.5 for the $^2A_1'$ and $^2E'$ states respectively).

Table 3

Properties calculated for $TiCl_3$ (D_{3h})

	Ti–Cl = 0.245 nm		Ti–Cl = 0.218 nm	
	Pople-Nesbet	Dewar	Pople-Nesbet	Dewar
		Valency*		
Ti	4.43(2.96)	3.98 (2.99)	4.18 (3.19)	4.17 (3.19)
Cl	1.09	1.09	1.11	1.11
		Charge		
Ti	+1.22	+1.22	+1.13	+1.13
Cl	−0.41	−0.41	−0.38	−0.38
		Configuration		
Ti 4*s*	0.50	0.54	0.48	0.48
4*p*	0.75	0.76	0.72	0.72
3*d*	1.52	1.48	1.66	1.67
Cl 3*s*	1.78	1.78	1.77	1.77
3*p*	5.62	5.62	5.61	5.51
3*d*	0.00	0.01	0.00	0.10
		Bond indices		
Ti–Cl	0.99	1.00	1.06	1.06

Unpaired Electron Density in $TiCl_3$ (Pople-Nesbet only)

Ti–Cl = 0.245 nm	s	p_x	p_y		p_z	
Ti	0.000	0.000	0.000		0.001	
Cl	0.000	0.000	0.000		−0.004	
	$d_{x^2-y^2}$	d_{xz}	d_{z^2}		d_{yz}	d_{xy}
Ti	0.000	0.504	0.000		0.504	0.000
Cl	0.000	0.000	0.000		0.001	0.000
Ti–Cl = 0.218 nm	s	p_x	p_y		p_z	
Ti	0.061	−0.000	−0.000		0.000	
Cl	0.001	−0.000	0.003		0.000	
	$d_{x^2-y^2}$	d_{xz}	d_{z^2}	d_{yz}	d_{xy}	
Ti	−0.001	0.000	0.930	0.000	−0.001	
Cl	0.000	0.000	0.000	0.000	0.000	

* Quantities in parenthesis are the sums of all bond indices to titanium.

4. OPEN-SHELL RESULTS

A comparison of the results of Pople-Nesbet and Dewar's "half-electron" methods is valid because both methods use a common set of parameters. Both methods yield very similar results, for example, the majority of the orbital energies resulting from Dewar's method are within 0.01 eV of the average of α and β orbital energies resulting from using the Pople-Nesbet method.

The expectation value of $<S^2>$, calculated using programme MECI,[13] is 0.75. Most of the unpaired spin density is, as expected from energy considerations, in the *d* orbitals of titanium. Some negative spin density exists but is nowhere greater than 0.004. The positive spin density is greater than unity and, when positive and negative spin densities are summed, the total spin density is precisely unity.

5. ENERGY LEVELS IN $Ti_2C_{10}^{4-}$.

The formal symmetry of $Ti_2Cl_{10}^{4-}$ is D_{2h} and we first assumed a simple closed-shell ground-state. For the initial purposes of the work this is quite adequate. The energy levels of the anion are presented in figure 1, where, for brevity, only the limiting levels at the top and bottom of each group are given. The four "extra" electrons in this anion exert a repulsive effect which raises all the orbitals linearly in the energy scale. This "reverse-crystal-field effect" has been discussed previously[15] and could be removed by the superimposition of the appropriate number of cations situated around the ion if the basic geometry were known. It does not affect any conclusions drawn from the relative positions of orbitals in the scale.

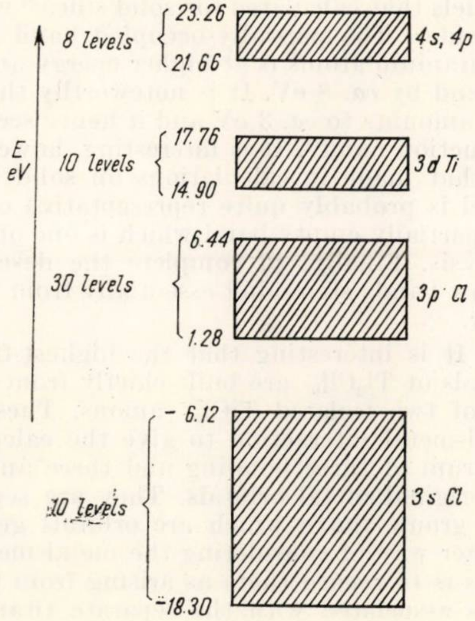

Fig. 1. — Energy levels for $Ti_2Cl_{10}^{4-}$.

---

[15] P. G. Perkins, *Rev. Roumaine Chim.*, **17**, 773 (1972).

In crystalline α $TiCl_3$ the energy levels will form a banded structure in which there will be a different energy band shape in different symmetry directions in the Brillouin Zone. The present calculation, which is essentially a cluster model, unfortunately cannot reproduce the band curvature or yield a density-of-states plot which would typify the crystal better. However, effective band widths are obtained from the cluster model and from the orbital energies we can obtain a relevant description which should carry over to the band structure.

We assume that the core orbitals on chlorine and titanium are completely occupied and, due to weak delocalisation, form very narrow bands at low energies : these can, therefore, be ignored in our description of crystalline $TiCl_3$. The atomic orbitals on chlorine give rise to two bands, namely, a band *ca.* 12 eV wide due to 3*s* and a band *ca.* 5 eV wide stemming from the 3*p* orbitals. The widths of these bands qualitatively reflects the degree of lateral interaction, the 3*s* chlorine orbitals bonding to Ti more strongly than the 3*p*. It is noteworthy that this behaviour parallels that calculated for solid silica[16] where also bands with *s* character are wider. The partially-occupied band formed from the 3*d* orbitals on the titanium atoms is at higher energy and is separated from the chlorine 3*p* band by *ca.* 8 eV. It is noteworthy that the total span of this *d* band only amounts to *ca.* 3 eV and it hence seems rather narrow for a "metalic conduction band". It is interesting, however, that this observation parallels that made in calculations on solid TiO and TiN[17] and, hence, our model is probably quite representative of the solid in this respect. It is this partially empty band which is one of the important factors in Ziegler catalysis. Finally, to complete the description, at still higher energies narrow bands stemming essentially from the 4*s* and 4*p* levels on titanium occur.

It is interesting that the highest-filled and lowest-five-unoccupied orbitals of $Ti_2Cl_{10}^{4-}$ are built chiefly from the two triply-degenerate "t_{2g}" sets of two isolated $TiCl_6^{3-}$ anions. These six orbitals are split by the metal-metal interaction to give the calculated closely-spaced eigenvalue spectrum of three bonding and three antibonding levels with respect to the original metal orbitals. They are separated by *ca.* 1.5 eV from the next group above which are orbitals generated by the e_g sets. Hence, another way of considering the metal-metal interaction and the resulting states is to regard them as arising from the interaction of a pair of $^2T_{2g}$ terms associated with the separate titanium atoms.

6. GROUND AND EXCITED STATES OF $Ti_2Cl_{10}^{2-}$

The closed-shell calculation pairs the highest energy electrons in the lowest of the above six levels. Clearly, however, electronic states will exist which may well be lower in energy than the singlet since the levels are closely spaced. Hence a multi-electron configuration-interaction calculation including all singlet and triplet states arising [from electronic configurations involving the three highest occupied M.O.'s and the two lowest unfilled M.O.'s was undertaken.

---

[16] A. Breeze and P. G. Perkins, *J. Chem. Soc., Faraday II*, **69**, 1237 (1973).

[17] A. Breeze and P. G. Perkins, to be published.

This involved a considerable number of doubly-excited states. The outcome of this calculation is that a triplet state exists which is slightly more stable than the simple closed-shell system. Table 4 lists the energies of the singly-excited states generated from the possible configurations.

The lowest two states have symmetries $^3B_{3u}$ and ^1A_g respectively. The first involves a configuration where the highest and lowest orbitals of the group are singly occupied by electrons with the same spin whilst the second is the lowest closed-shell configuration. These lowest two states are very similar in energy and this situation, together with the other singlets and triplets lying close to the ground-state will give rise to temperature-dependent magnetic effects as heavy thermal population of the states will occur. Because some of the thermally accessible states are singlets then a reduction in paramagnetism on increasing temperature is predicted.

Table 4

Singly excited states of $Ti_2Cl_{10}^{4-}$ arising from the pseudo-configurations t_{2g}^2 and t_{2g}^1 t_{2g}^1

Energy *	1Γ	3Γ
(kK)	0.03	0.16
	0.18	0.19
	0.19	16.90
	19.10	19.11
	23.69	33.90
	38.07	38.26
	38.26	
	47.42	
	55.80	

* the energies are relative to the ground state arbitrarily set to zero energy.

The nature of the configurations giving rise to these states means that even if experiment indicated that the electronic state is a singlet, effective bonding between the two titanium atoms does not necessarily exist since several of the sigglets involve pairing of electrons in which one resides in each set of three orbitals.

Because of the uncertainty of the lowest electronic state at ordinary temperatures it is not particularly meaningful to analyse the selection rules for the electronic spectra. However, the true symmetry (D_{2h}) is sufficiently low that certain transitions will be formally allowed and will appear in the visible region *e.g.* the two triplet-triplet transitions $^3B_{2g} \leftarrow \leftarrow {}^3A_u$ which involve promotions from the state lying at 0.2 kK to those at 16.9 and 19.1 kK. These transitions could account for the observed bands in α $TiCl_3$. Most of the doubly-excited states are fairly high in energy and so are of little importance to the magnetic properties. Moreover, optical transitions to them are two-photon processes and hence very weak. For these reasons we do not include them in table 4.

With regard to solid α $TiCl_3$ we expect that the "t_{2g}— t_{2g}" interaction between all pairs of titanium atoms, each in octahedral site symmetry, will result in a basically similar situation to that described above for $Ti_2Cl_{10}^{4-}$ the main difference being that the "bonding t_{2g}" and "antibonding t_{2g}" levels of the anion will form narrow bands in the solid. These are not expected to be much wider than the energy the levels span in the $Ti_2Cl_{10}^{4-}$ ion itself. With regard to the excited states of the solid these should only be modified in a minor way by the extension of the Ti-Ti interaction and should essentially form a set of weakly-delocalised excition states. This means that we would expect the predicted experimental optical spectrum to be closely similar to that for $Ti_2Cl_{10}^{4-}$.

7. CALCULATED GROUND STATE PROPERTIES OF $Ti_2Cl_{10}^{4-}$

These are presented in table 5. The properties in this table refer, of course, to the ^1A_g state which will be heavily thermally populated at ordinary temperatures. In this state both electrons reside in the lowest orbital of the "t_{2g}" set. Only the Ti-Ti bond is of particular interest, the other results being essentially similar to those obtained for the $TiCl_3$ monomer. There is a Ti-Ti bonding component which assumes some importance in this anion and the Ti-Ti bond interaction stems almost entirely from the contribution of the highest filled M.O. From the multi-electron C.I. results we know that the "true" ground state is built from configurations with one bonding and one antibonding electron. This antibonding component renders the overall Ti-Ti bond weak.

Table 5

Properties calculated for $Ti_2Cl_{10}^{4-}$

	Formal charge	Configuration	Valencies	Bond indices
Ti	+1.06	$4s^{0.40}\ 4p^{0.80}\ 3d^{1.74}$	4.89	Ti–Ti 0.43
Cl(br.)	−0.53	$3s^{1.75}\ 3p^{5.77}$	0.85	$Ti-Cl_{br}$ 0.36
Cl (ax.)	−0.63	$3s^{1.82}\ 3p^{5.81}$	0.69	$Ti-Cl_{ax.}$ 0.60
Cl (eq.)	−0.64	$3s^{1.83}\ 3p^{5.81}$	0.67	$Ti-Cl_{eq.}$ 0.57

8. ACTIVATION OF THE CATALYST SURFACE

Since we now know the general structure of the ground and excited states of a system related to α $TiCl_3$ we now attempt to say how our calculations apply to the catalytic activity of the crystal. We first consider therefore the activation of the catalyst surface. At the surfaces of α $TiCl_3$ there must be some chlorine vacancies in order that electroneutrality can be preserved. We would also expect that there are also labile chlorine atoms which can readily be alkylated by co-catalyst to form active sites for polymerisation. Arlman[18] has shown that the energy required to abstract one of these or to form a chlorine vacancy is far less when the atom is at an edge rather than in the middle of an α $TiCl_3$ sheet *i.e.* the (0001 face). We would expect these labile chlorine atoms to project somewhat out of the catalyst surface and so predispose them to replacement to give alkylated catalyst. The alkyl group attached to the catalyst would then be available for insertion of ethylene molecules to give the incipient polymer. Cossee[19] has presented a convincing rationalisation of the tacticity and reaction mechanism problems for simple polymerisations on $TiCl_3$ using geometrical arguments. We now consider how our results can add to his picture of the process. We also consider what is the function of the co-catalyst $AlCl_3$.

---

[18] E. H. Arlman, *J. Catalysis*, **3**, 89 (1964).

The level scheme of figure 1 is derived from the $Ti_2Cl_{10}^{4-}$ anion and is expected to apply to the volume band structure of α $TiCl_3$. At the surface of the crystal there will clearly exist surface states and, of these the most important will be dominated by the *3d* levels of titanium. Because of the weak Ti-Ti interactions in the crystal these surface bands will also be narrow and we would expect them to fall in the same energy region as the volume states. A difference here is that because of the discontinuity of potential and C_{4v} point symmetry at the surface titanium sites the "t_{2g}" levels would be split into e and b_2 at the Γ point of the Brillouin zone. This splitting will however not be large and we estimate it to be *ca.* 0.1 eV from comparison with data given for the molecular complex with a vacant site studied in ref.[1]. Overall we believe that the surface states will probably be submerged in the volume states of the crystal and hence figure 1 is a reasonable overall energy band picture.

Alkylation of the catalyst surface by removal of chlorine in the way suggested by Cossee[19] seems reasonable and we must next consider the modification this will bring about in the energy level diagram. From previous work on the methyltitanium chlorides[20] we know that the electrons in a Ti-C bond are strongly localised in one highly energetic bonding orbital. We may reasonably assume that this situation will obtain when Ti$-$C bands are formed on the surface of α $TiCl_3$.

With respect to the band structure of the solid these bonds constitute localised impurities and we must consider where they lie with respect to the main band structure : (the chlorine atoms which they replace are, of course, also impurities but are expected to yield levels lying submerged within the main bands). The Ti$-$C bonds should be localised because the separation of neighbouring Ti atoms, to which the alkyl is bound at the surface, is large enough to bring about localisation. Again the calculations on the series Me_xTiCl_{4-x} throw light on the situation. Taking the cases of $TiCl_4$ and $MeTiCl_3$, the Ti C σ bond is localised in the highest bonding orbital of $MeTiCl_3$ and this is *ca.* 2 eV less stable than the highest bonding orbital of $TiCl_4$. We conclude from this that, in the case of alkylated α $TiCl_3$ the Ti$-$C σ bonds on the surface will form accidentally-degenerate isolated energy levels lying above the Ti$-$Cl valence bands. Figure 1 shows that there is a substantial gap (*ca.* 8 eV) between the *3p* Cl valence bands and the bottom of the Ti *3d* band. The Ti$-$C σ levels are expected to be situated in this gap leaving the d band to be still only partly occupied by the "t_{2g}" electrons. Moreover, the Ti$-$C σ levels should lie rather close to the d band since it is the latter which are strongly involved in Ti—C bonds.[1,20] By analogy with $MeTiCl_3$ we expect the Ti—C σ^* orbitals also to be localised and to lie either in or slightly above the *d* band of Ti.

---

[19] P. Cossee, in "The Stereochemistry of Macromolecules", Vol. 1, (Ed. A. D. Ketley), Marcel Dekker, N. Y., 1967, Chapter 3. p. 145.

[20] D. R. Armstrong, P. G. Perkins, and J. J. P. Stewart, *Theor. chim. Acta*, submitted for publication.

We expect, overall, that the spectral properties of the system will still be dominated by the two "t_{2g}" electrons and the excited states generated by the *d* band, just as in $Ti_2Cl_{10}^{4-}$. However, the Ti—C σ bond will be energetically labile since electrons will be readily thermally excited to the *d* band and the Ti—C σ^* orbital; in fact rather more so than they are in the soluble catalyst where the orbital gap between bonding and antibonding sets is much larger[1]. For the rest, the electronic situation is closely analogous to that of the "soluble" catalyst and hence we expect that the mechanism shown to be operative for the *cis* insertion of ethylene in the latter case will be equally applicable to the present instance.

9. ROLE OF ALUMINIUM TRICHLORIDE IN THE CATALYST

Aluminium trichloride, in combination with α $TiCl_3$, is a more effective catalyst for the polymerisation of olefins than is $TiCl_3$ alone. It is believed to react with solid $TiCl_3$ to form a solid solution in which there are layers of $AlCl_3$ and $TiCl_3$.[21]

The best catalysts appear to be those which contain octahedrally-coordinated titanium, and clearly the ease of attaining this geometry together with steric control are important factors in the process. In α $TiCl_3$ the titanium atoms are maintained in octahedral site symmetry by chlorine bridging to other acceptor atoms and hence certain of the halogens are removed from the site of polymerisation. Because of its smaller radius, aluminium can remove the chlorine atoms from the region of the reaction site more effectively than can another titanium in the crystal and we postulate that this is one of the properties of aluminium which makes it so effective as a co-catalyst. This implies that any group or atom which is more effective than Ti in "tying-back" the chlorine atoms and producing octahedral site symmetry around titanium should enhance the activity of the catalyst.

In the uniform site theory of Ziegler catalysis,[21] $AlCl_3$ is assumed to be in solid solution in the $TiCl_3$ lattice so that Ti_8Cl_{24} clusters are isolated by layers of $AlCl_3$; it is this solid phase which is the catalyst. Accepting this, and the results of Carradine and Rase,[4] then some aspects of the catalysis can now be explained.

The activity of $TiCl_3$—$AlCl_3$ catalyst is greater than that expected for simple surface catalysis, based on the surface area of the crystals in the reaction. As the polymerisation proceeds, the growing polymer chain causes mechanical damage to occur,[22] with consequent fragmentation of the crystal. The $AlCl_3$ in solid solution presumably induces planes of weakness which can aid fragmentation of the catalyst crystal, at the

[21] V. W. Buls and T. L. Higgins, *J. Polymer Sci.*, A—1, **8**, 1025 (1970).

[22] L. A. M. Rodriguez and J. A. Gabant, *J. Polymer Sci. C.*, 125 (1963).

same time exposing active sites with Ti in a favourable steric environment, *i.e.*, assuming that, at the $AlCl_3-TiCl_3$ crystal interfaces, the bonding of Al to Ti *via* chlorine bridges occurs. Ultimately the particles of catalyst would become so small that isolated $AlCl_3-Ti_8Cl_{24}$ units would exist and the catalyst would become virtually homogeneous. Before this stage was reached a considerable degree of inhomogeneity in the solid phase would be manifest because of the quasi-random nature of the mechanical breakdown of the crystal : such inhomogeneity would be expected to produce different catalyst sites having modified activities. This latter suggestion helps to rationalise, to some extent, the wide range of molecular weights of the high polymer found when using aluminium-doped $TiCl_3$.

We thank the SRC for a Maintenance Grant (to J.J.P.S.).

Revue Roumaine de Chimie, **19**, *11*, 1709–1715 (1974)

REACTIONS OF SOME PENTAFLUOROPHENYL-SILICON DERIVATIVES WITH THE π-CYCLOPENTADIENYLIRON DICARBONYL ANION

IONEL HAIDUC[a], R. BRUCE KING[b] and HENRY GILMAN[c]

[a]Babeş-Bolyai University, Cluj (Romania),
[b]University of Georgia, Athens, Ga. (U.S.A.) and
[c]Iowa State University, Ames, Ia. (U.S.A.)

Received March 2, 1974

The π-cyclopentadienyliron dicarbonyl anion, π-$C_5H_5Fe(CO)_2^-$ reacts with some pentafluorophenyl-silicon derivatives, including $C_6F_5SiMe_3$, $(C_6F_5)_2SiPh_2$, $(C_6F_5SiMe_2)_2O$ and $C_6F_5SiMe_2(CH_2)_3SiMe_3$ by replacing a fluorine atom in the *para*- position to silicon, to give σ-organoiron derivatives of the general type π-$C_5H_5Fe(CO)_2-\sigma-C_6F_4-SiRR'_2$-*p*.

INTRODUCTION

The π-cyclopentadienyliron dicarbonyl anion, π-$C_5H_5Fe(Co)_2^-$ which can be readily generated by treating the π-cyclopentadienyliron dicarbonyl dimer [π-$C_5H_5Fe(CO)_2]_2$ with sodium amalgam in tetrahydrofuran,[1] reacts with hexafluorobenzene to give π-cyclopentadienyl-σ-pentafluorophenyliron dicarbonyl*

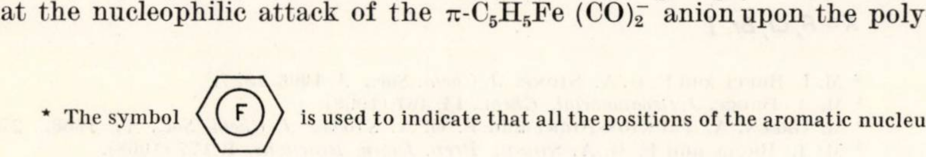

When substituents other than fluorine were also present on the aromatic nucleus, e.g. hydrogen, trifluoromethyl and other groups, it was found that the nucleophilic attack of the π-$C_5H_5Fe(CO)_2^-$ anion upon the poly-

---

* The symbol is used to indicate that all the positions of the aromatic nucleus which are not occupied by other groups are substituted with fluorine atoms.

[1] R. B. KING and M. B. BISNETTE, *J. Organometal. Chem.*, **2**, 38 (1964).

fluoroaromatic ring occurs in the *para*-position in respect with the substituent[1].

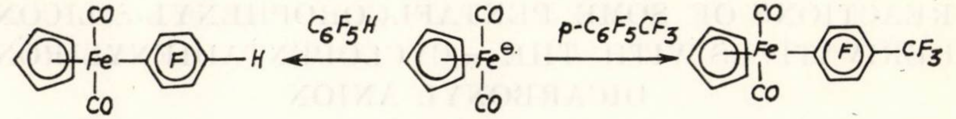

When the π-cyclopentadienyliron dicarbonyl anion reacted with halogenopentafluorobenzenes, $C_6F_5X (X = Cl, Br, I)$ two different reactions occurred. The major one was the replacement of a halogen atom, other than fluorine, to give the same product as the reaction with hexafluorobenzene $(X = F)$, namely π-$C_5H_5Fe(CO)_2C_6F_5$[2]; a secondary reaction was the formation of products like π-$C_5H_5Fe(CO)_2C_6F_4H$-p.[2,3]

Similar reactions were found with other polyfluorinated aromatic derivatives,[4,5] e.g. pentafluoropyridine,[4] and even with perfluoroolefins and perfluoroacetylenes; these reactions were reviewed.[5,6,7]

The mechanism of the reaction between metal carbonyl anions and polyfluorinated hydrocarbons was discussed in the literature[6,8] in terms of a nucleophilic attack of the anion upon the fluorocarbon, with the formation of an intermediate fluorinated carbanion, which further eliminates an F^- anion or (if present) a halide ion (X^-) or (in some instances) adds a proton. The possible pathways explaining all the product isolated from the reactions of metal carbonyl anions with polyfluoroaromatics are summarized in the following scheme[2,6] Since the reaction of the π-cyclo-

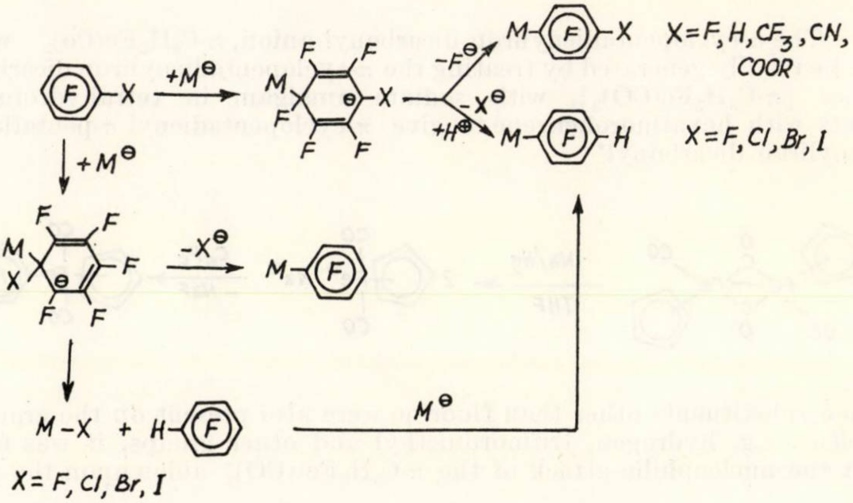

---

[2] M. I. Bruce and F. G. A. Stone, *J. Chem. Soc.*, *A*, **1966**, 1837.

[3] M. I. Bruce, *J. Organometal. Chem.*, **14**, 461 (1968).

[4] M. Green, A. Taunton-Rigby and F. G. A. Stone, *J. Chem. Soc.*, *A*, 1968, 2762.

[5] M. I. Bruce and F. G. A. Stone, *Prep. Inorg. Reactions*, **4**, 177 (1968).

[6] M. I. Bruce and F. G. A. Stone, *Angew. Chem.*, **80**, 835 (1968); *Angew. Chem., Internat. Ed. Engl.*, **7**, 747 (1968).

[7] S. C. Cohen and A. G. Massey, *Advan. Fluorine Chem.*, **6**, 83 (1970).

[8] R. D. Chambers and R. H. Robbs, *Advan. Fluorine Chem.*, **4**, 50 (1965).

pentadienyliron dicarbonyl anion with substituted pentafluoroaromatics can take various courses, we have investigated such reactions with pentafluorophenyl-silicon derivatives. The reactions considered as possible were : nucleophilic substitution of fluorine (in *para* or other position to silicon) or cleavage of the Si—C_6F_5 bond. It was found that the substitution of fluorine *para* to silicon occurs in all cases.

RESULTS AND DISCUSSION

We have investigated the reactions of π-cyclopentadienyliron dicarbonyl anion with the following four pentafluorophenyl-substituted organosilicon derivatives : pentafluorophenyltrimethyl-silane (I) ; bis (pentafluorophenyl) diphenylsilane (II) ; 1,3-bis (pentafluorophenyl) tetramethyldisiloxane (III) and pentafluorophenl-γ-trimethylsilylpropyldimethylsilane (IV).

The reactions were carried out in tetrahydrofuran, by adding the pentafluorophenyl-silicon compound to the solution containing the anion π-$C_5H_5Fe\ (CO)_2^-$, generated *in situ*, as described in the experimental part. Infrared and ^{19}F NMR spectroscopy were used to establish the structure of the compounds isolated.

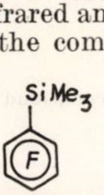

I

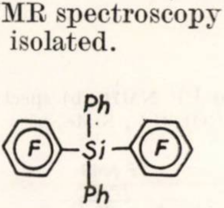

II

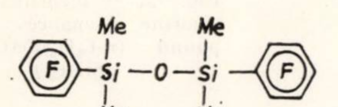

III

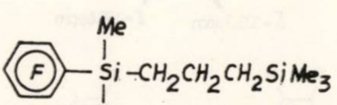

IV

The reaction of pentafluorophenyltrimethylsilane (I) with the π-cyclopentadienyliron dicarbonyl anion gave a pale yellow crystalline compound, m.p. 141°, identified as π-cyclopentadienyl-σ-(*p*-trimethylsilyltetrafluorophenyl)iron dicarbonyl (V) :

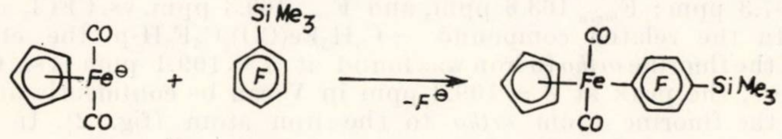

I V

The infrared spectrum of V contains in the carbonyl stretching (ν_{CO}) region two intense, sharp bands, at 2050 and 2001 cm^{-1}, showing a pattern characteristic of compounds of the π-$C_5H_5Fe(CO)_2R$ type (fig. 1a). The ^{19}F NMR spectrum shows and A_2X_2-type pattern and consists of only two pairs of doublets (fig. 1b), centered at $\delta = 109.3$ ppm and $\delta = 130.6$ ppm. vs. $CFCl_3$ as internal standard, thus indicating the presence of only two types of structurally non-equivalent fluorine atoms.

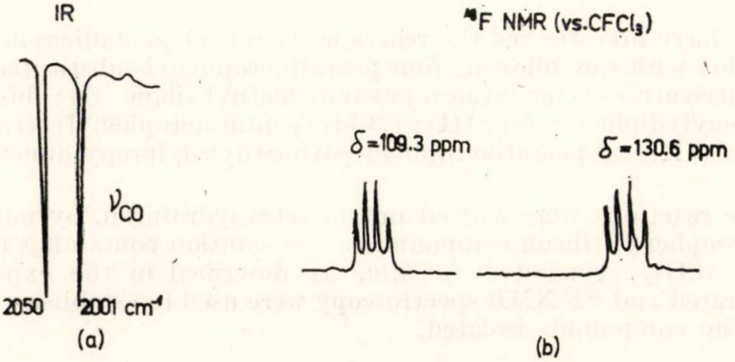

Fig. 1. — IR spectrum (a) and ^{19}F NMR (b) spectrum of compound $(\pi\text{-}C_5H_5)Fe(CO)_2\text{-}C_6F_4\text{-}SiMe_3\text{-}p$.

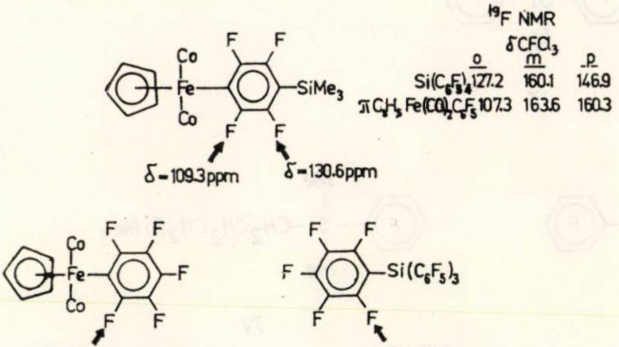

Fig. 2. — Identification of fluorine resonances in compound $(\pi\text{-}C_5H_5)Fe(CO)_2C_6F_4\text{-}SiMe_3\text{-}p$

A comparison of the ^{19}F NMR spectrum of V with the ^{19}F NMR spectra of π-$C_5H_5Fe(CO)_2C_6F_5$ [1] and Si $(C_6F_5)_4$ [9] allows an unequivocal assignment. Thus, in π-$C_5H_5Fe(CO)_2C_6F_5$ the ^{19}F chemical shifts are as follows: F_{ortho} 107.3 ppm; F_{meta} 163.6 ppm, and F_{para} 160.3 ppm. vs. $CFCl_3$ as standard. In the related compound π-$C_5H_5Fe(CO)_2C_6F_5H$-p the chemical shift of the fluorine *ortho* to iron was found at $\delta = 109.1$ ppm vs. $CFCl_3$.[2] Therefore, the peak at $\delta = 109.3$ ppm in V can be confidently attributed to the fluorine atom *ortho* to the iron atom (fig. 2). In the ^{19}F NMR spectrum of Si $(C_6F_5)_4$ the chemical shifts are : F_{ortho} 127.2 ppm ; F_{meta} 160.1 ppm, and F_{para} 146.9 ppm, vs. $CFCl_3$ as standard.[9]. Therefore, the peak at $\delta = 130.6$ ppm in the spectrum of V can be assigned to the fluorine atom *ortho to the silicon* atom (fig. 2). Since there are only two kinds of fluorine atoms in the molecule of V, with 1 : 1 ratio (from integrated peak area ratio), in *ortho* positions to either fluorine or silicon, it follows that compound V is the *para*-substituted compound. Other isomers (*ortho* or *meta*) would have an entirely different ^{19}F NMR spectrum.

The reaction of π-$C_5H_5Fe(CO)_2^-$ with bis (pentafluorophenyl (diphenylsilane) (II) in 1 : 1 molar ratio gave a yellow solid, m.p. 2°5−10° (dec.), identified as π-cyclopentadienyl-σ-[(*p*-pentafluorophenyldiphenylsilyl) tetrafluorophenyl] iron dicarbonyl (VI).

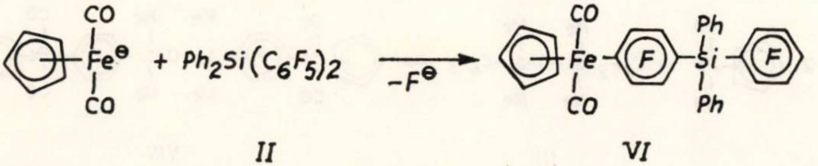

The infrared spectrum of VI contained two sharp, intense absorption bands in the ν_{CO} region, at 2050 and 2004 cm^{-1}, as expected for structure VI.

A 2 : 1 ratio of the same reagents, gave a yellow solid, m.p. 237°C, identified as the product of nucleophilic attack on both C_6F_5 groups in II, with the structure VII

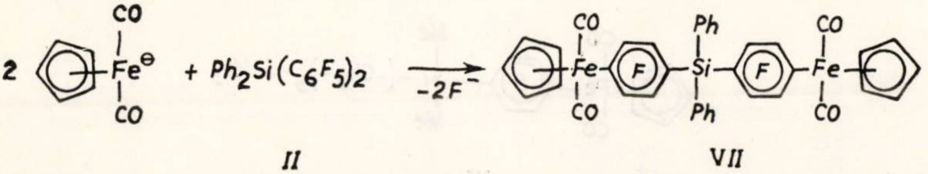

The structure VII, which contains only two kinds of fluorine atoms, in positions *ortho* to either silicon or iron, is confirmed by the ^{19}F NMR spectrum (fig. 3), which is of A_2X_2 type and contains only two pairs of

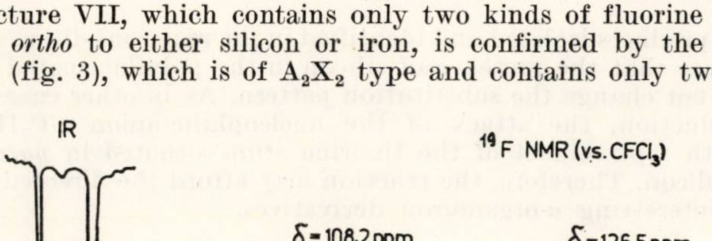

Fig. 3. — IR spectrum (a) and ^{19}F NMR spectrum (b) of compound $Ph_2Si[C_6F_4$-$Fe(CO)_2(\pi$-$C_5H_5)]_2$.

---

[9] K. W. Jolly and L. H. Sutcliffe, *Spectrochim. Acta*, A, **24**, 1191 (1968).

doublets, centered at $\delta = 108.2$ ppm and $\delta = 126.5$ ppm. The infrared spectrum of VII exhibits two sharp, intense absorption bands in the ν_{CO} region, at 2050 and 2004 cm^{-1}. The ^1H NMR spectrum exhibits peaks at $\tau = 4.98$ ppm (π-C_5H_5) and $\tau = 2.7-2.8$ ppm (C_6H_5), with the integrated area ratio, expected for structure VII.

From $[\pi\text{-}C_5H_5Fe(CO)_2]^{\theta}$ and the pentafluorophenyl-substituted disiloxane (III) a waxy yellow solid was obtained showing strong IR absorption bands at 2048 and 2001 cm^{-1}, characteristic of the carbonyl ligands of the π-$C_5H_5Fe(CO)_2$ groups, in accordance with structure VIII

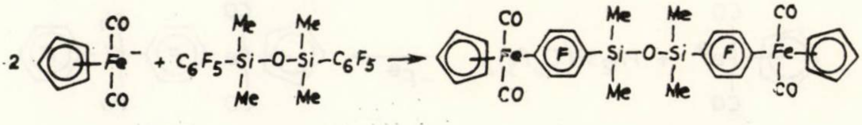

III VIII

The reaction of $\pi\text{-}C_5H_5Fe(CO)_2^-$ with IV, gave a yellow-orange oil, with strong absorption bands in the ν_{CO} region at 2051 and 2002 cm^{-1}, which was not investigated further. The infrared spectrum indicates the presence of π-$C_5H_5Fe(CO)_2$ groups in the molecule, thus suggesting structure IX, but the compound could not be purified satisfactorily for analysis.

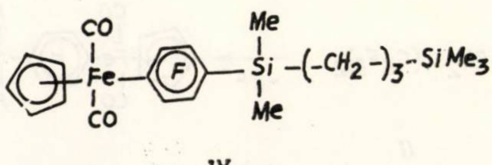

IX

The products isolated and identified in the reactions discussed above, demonstrate that the presence of silicon in the polyfluorinated aromatic ring does not change the substitution pattern. As in other cases, cited in the introduction, the attack of the nucleophilic anion $\pi\text{-}C_5H_5Fe(CO)_2^-$ occurs with replacement of the fluorine atom situated in *para* position towards silicon. Therefore, the reaction may afford the directed synthesis of some interesting σ-organoiron derivatives.

EXPERIMENTAL PART

The reaction described here were routinely conducted in an atmosphere of oxygen-free dry nitrogen. Anhydrous solvents were used throughout. Tetrahydrofuran was distilled over sodium-benzophenone ketyl, prior to use. The ^{19}F NMR spectra were recorded on a Varian HA—100 instrument in benzene solution and the IR spectra on a Perkin Elmer 621 A instrument, in n-hexane, at the University of Georgia.

Reaction of $\pi\text{-}C_5H_5Fe(CO)_2^-$ with I

The sodium salt of the $\pi\text{-}C_5H_5Fe(CO)_2^-$ anion was prepared by stirring 0.88 g (2.5 mmole) of $[\pi\text{-}C_5H_5Fe(CO)_2]_2$ with excess sodium amalgam (1%) in 100 ml. tetrahydrofuran, during 3—4 hrs. After removing the excess of sodium amalgam the orange yellow solution obtained was treated with 1.2 g (5 mmole) pentafluorophenyltrimethylsilane, introduced with a syringe through a rubber serum cap adapted to the neck of the three-neck reaction flask, and the mixture was stirred overnight at room temperature. The solution was evaporated, extracted with hexane, concentrated, chromatographed on Florisil ^{R} (a mixture of MgO and SiO_2) and the yellow band eluted with hexane and evaporated to give 0.95 g (47.7% yield) of a pale-yellow solid, m.p. 141°C, identified as π-cyclopentadienyl-σ-(*p*-trimethylsilyltetrafluorophenyl)iron dicarbonyl (V).

$C_{16}H_{14}F_4FeO_2Si$	*Calcd.* :	C 48.24%	H 3.52%	Fe 14.02%
	Found :	C 48.53%	H 3.34%	Fe 14.37%

Reaction of π-$C_5H_5Fe(CO)_2^-$ with II (1 : 1 ratio)

A sodium salt of π-$C_5H_5Fe(CO)_2^-$ prepared as above from 0.354 g (1 mmole) $[\pi\text{-}C_5H_5Fe(CO)_2]_2$ and excess sodium amalgam in 75 ml tetrahydrofuran, was treated with a solution containing 1.03 g (2 mmole) $Ph_2Si(C_6F_5)_2$ in 10 ml THF and stirred overnight. The reaction mixture was worked up as above and chromatography on Florisil on elution with acetone, gave after evaporation 0.59 g (59% yield) of a yellow solid, m.p. 205—210°C (dec.), identified as π-cyclopentadienyl-σ-[*p*-(pentafluorophenyldiphenylsilyl)tetrafluorophenyl]iron dicarbonyl (VI).

$C_{31}H_{15}F_9FeO_2Si$	*Calcd.* :	C 73.96%	H 3.00%
	Found :	C 73.45%	H 3.18%

Reaction of π-$C_5H_5Fe(CO)_2^-$ with II (2 : 1 ratio)

A sodium salt of π-$C_5H_5Fe(CO)_2^-$ anion prepared as above from 0.354 g (1 mmole) of $[\pi\text{-}C_5H_5Fe(CO)_2]_2$ and excess sodium amalgam in 100 ml THF was treated with a solution containing 0.516 g (1 mmole) $Ph_2Si(C_6F_5)_2$ dissolved in 10 ml. THF and stirred overnight. The mixture was worked up as above and chromatographed over Florisil ; elution with acetone gave a solution which on concentration deposited 0.45 g (51.6%) of a yellow solid, m.p. 237°, identified as bis [*p*-(π-cyclopentadienylirondicarbonyl)tetrafluorophenyl]diphenylsilane (VII).

$C_{38}H_{20}F_8Fe_2O_4Si$	*Calcd.* :	C 54.81%	H 2.42%	Fe 13.42%
	Found :	C 55.13%	H 2.74%	Fe 13.85%

Reaction of π-$C_5H_5Fe(CO)_2^-$ with III

The reaction was carried out as above, with 1.55 g (3.3 mmole) of $C_6F_5SiMe_2OSiMe_2C_6F_5$, to give after chromatography on Florisil and elution with hexane, a waxy yellow solid. A hexane solution of this material shows only two strong bands in the ν region, which can be assigned to compound VIII.

Reaction of π-$C_5H_5Fe(CO)_2^-$ with IV

The reaction was carried out as above, with 1.70 g (5 mmole) of $C_6F_5SiMe_2(CH_2)_3SiMe_3$, to give after chromatography on Florisil and elution with hexane and evaporation, a yellow orange oil. The infrared spectrum of this oil in hexane, showed peaks at 2051 and 2002 cm^{-1}, consistent with compound IX.

One of us (I.H.) is grateful to the Babeş-Bolyai University of Cluj (Romania) for two leaves of absence spent at Iowa State University and University of Georgia (U.S.A.) and expresses his appreciation for the hospitality enjoyed there.

Revue Roumaine de Chimie, **19**, *11*, 1717–1725 (1974)

THERMAL ANALYSIS OF FERRATE (VI) ION SALTS WITH Ni(II) AND Co(II) COMPLEX AMMINES

D. NEGOIU * and ALEXANDRA ŞCHIOPESCU **
*Department of Chemistry,
University of Bucharest, Spl. Independenţei 89, Romania.
**Department of Chemistry and Physics,
Institute of Petroleum and Geology, Str. Traian Vuia 6,
Bucharest, Romania

Received October 17, 1973

In order to elucidate some problems related to the thermal stabilities of complex combinations we provide in this paper data obtained from the thermal analysis applied to ferrate (VI) ion salts with Ni(II) and Co(II) tetrapyridine and tetrapicoline complex compounds.

1. INTRODUCTION

In recent decades, in the area of solid reaction, thermal analysis methods have gained increased acceptance as research methods of great practical importance. [1-2]

In a previous work [3] the synthesis of ferrate (VI) ion salts with Ni(II) and Co(II) complex ammines, has been presented.

This paper is concerned with the study of salts prepared by means of thermal analysis.

In the literature, referring to the thermal behaviour of ferrates (VI), only the study made by Scholder and his coworkers [4] on thermal behaviour of potassium ferrate (VI) in oxygen stream may be cited. Comparing the thermal behaviour of potassium ferrate (VI) and potassium permanganate in oxygen stream, it was possible to draw conclusion on the intermediate stages that may appear at decomposition.

2. EXPERIMENTAL METHODS

Two series of compounds belonging to Ni(II) and Co(II) complex compounds with pyridine and picoline, containing ferrate (VI) ion, have been prepared.

---

[1] W. W. WENDTLAND, "Thermal Methods of Analysis", Interscience – Wiley, New York, 1964, p. 120.

[2] P. GARN, "Thermal Methods of Chemical Investigation", Academic Press, New York, 1965, p. 300.

[3] D. NEGOIU and A. ŞCHIOPESCU, *Rev. Roumaine Chim.*, forthconing.

[4] R. SCHOLDER, H. V. BUNSEN and F. KINDERVATER, *Z. anorg. Chem.*, **282**, 268 (1955).

These salts are the following:

$NiPy_4[FeO_4]$; $Ni(\alpha\text{-pic})_4[FeO_4]$; $Ni(\beta\text{-pic})_4[FeO_4]$;
$Ni(\gamma\text{-pic})_4[FeO_4]$; respectively $CoPy_4$ $[FeO_4]$;
$Co(\alpha\text{-pic})_4[FeO_4]$; $Co(\beta\text{-pic})_4$ $[FeO_4]$; $Co(\gamma\text{-pic})_4$ $[FeO_4]$.

These substances have been studied by means of thermogravimetric analysis (A.T.G.) using a M.O.M. Budapest Paulik Paulik, Erdey apparatus.[5]

Tests were heated in the furnace atmosphere at a heating rate of 8 deg./min.

$NiPy_4[FeO_4]$. The test was heated in the presence of furnace air to 800°. An endothermal process at 120°, an exothermal process at 250° and another endothermal process at 620°, have been recorded.

$CoPy_4[FeO_4]$. The test is heated in the furnace atmosphere to 800°. Decomposition of the compound begins at 140°.

This fact corresponds to an endothermal process.

An endothermal process is recorded at 245°. Two exothermal processes are observed at 220° and 310°.

The same endothermal process found for Ni(II) compound previously presented was reproduced at 620°.

$Ni(\alpha\text{-pic})_4[FeO_4]$. An endothermal process at 90°, an exothermal process at 225° and another endothermal process at 620° have been recorded.

$Co(\alpha\text{-pic})_4$ $[FeO_4]$. An endothermal process at 125°, an exothermal process at 230° and another endothermal process at 620° have been recorded.

$Ni(\beta\text{-pic})_4$ $[FeO_4]$. An endothermal process at 105°, an exothermal at 235° and another endothermal process have been recorded.

$Co(\beta\text{-pic})_4[FeO_4]$. In this case an endothermal process at 130°, an exothermal at 250° and another endothermal process at 620° have been recorded.

$Ni(\gamma\text{-pic})_4[FeO_4]$. An endothermal process at 110°, an exothermal process at 240° and another endothermal process at 620° have been observed.

$Co(\gamma\text{-pic})_4$ $[FeO_4]$. An endothermal process at 150°, an exothermal process at 265° and another endothermal process at 645° have been observed.

3. DISCUSSION

Drawing a comparison between thermal behaviour of ferrate (VI) ion salts and thiocyanates of Ni(II) and Co(II) pyridine and picoline complexes, it is possible to conclude that for the compounds containing ferrate (VI) ion, the ligand elimination during heating time takes place in a single stage evidenced by an endothermal process.

For thiocyanates of Ni(II) and Co(II) complex ammines, ligand elimination takes place in two stages corresponding to the two endothermal peaks of A.T.D. curves as well as to losses in weight recorded by the A.T.S. curves.[6]

Thus, in the case of $NiPy_4$ $[FeO_4]$ at 120°, en endothermal process characterized by a 36.6% loss of weight is recorded. This corresponds to a loss of two pyridine molecules.

It is possible to suppose that $NiPy_4$ $[FeO_4]$ compound looses two pyridine molecules at room temperature, in fact, $NiPy_2$ $[FeO_4]$ is considered as initial compound.

An endothermal peak due to a phase transformation of resulting oxide is recorded at 620° on A.T.D. curve.

Following the thermal behaviour of $NiPy_4\,(SCN)_2$[6] a two-stage ligand elimination is observed.

---

[5] F. Paulik, J. Paulik and L. Erdey, *Talanta*, **13**, 1405 (1966).

[6] I. G. Murgulescu, E. Segal and D. Fătu, *J. Inorg. Nuclear Chem.*, **1965**, 27.

Two thermal effects at 188° and 275° connected with two endothermal peaks of A.T.D. are recorded.

These two effects correspond to those stages of ligand elimination.

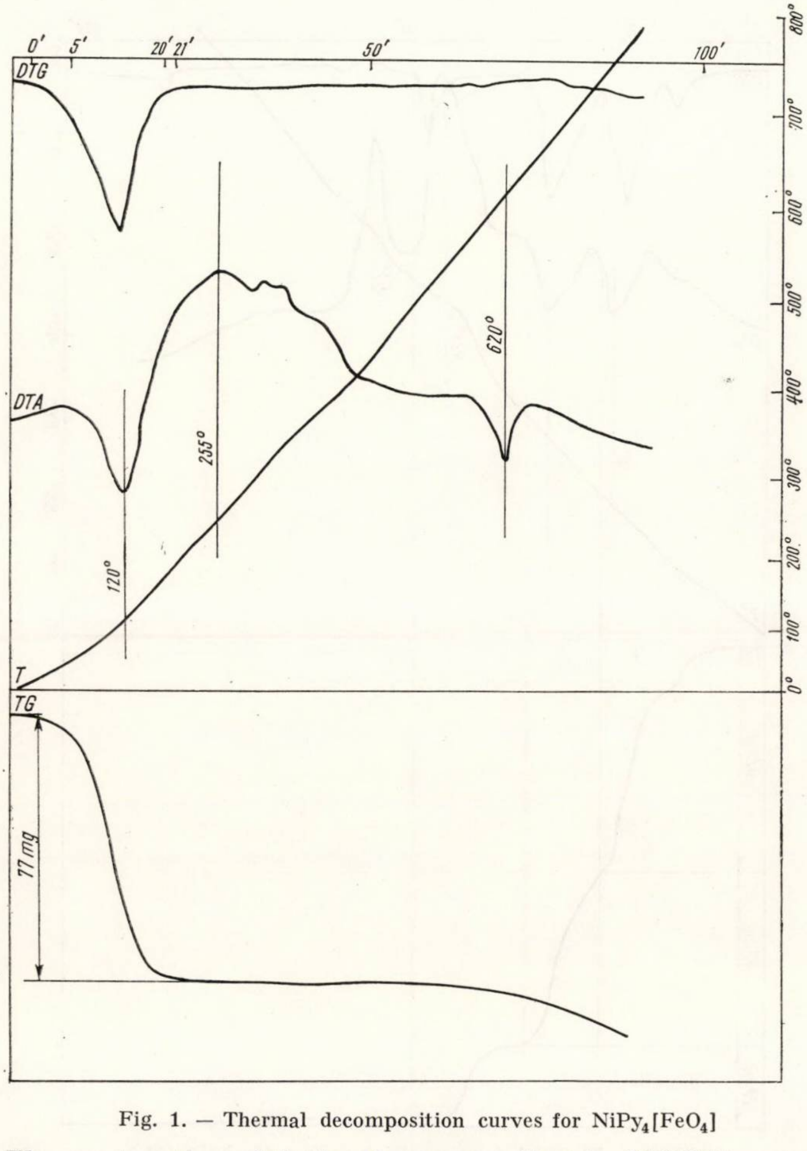

Fig. 1. — Thermal decomposition curves for $NiPy_4[FeO_4]$

The next section of the level corresponding to $Ni(SCN)_2$ compound is followed by decomposition associated with an oxidizing process of $Ni(SCN)_2$, decomposition of the resulting NiO and by recrystallization.

An analogous behaviour of the other thiocyanates of Co(II) and Ni(II) complex ammines has been established.

In the case of $CoPy_4$ $[FeO_4]$ the exothermal peak at 310° is connected with a crystallization process of the resulting compound. This corresponds to an exothermal process.

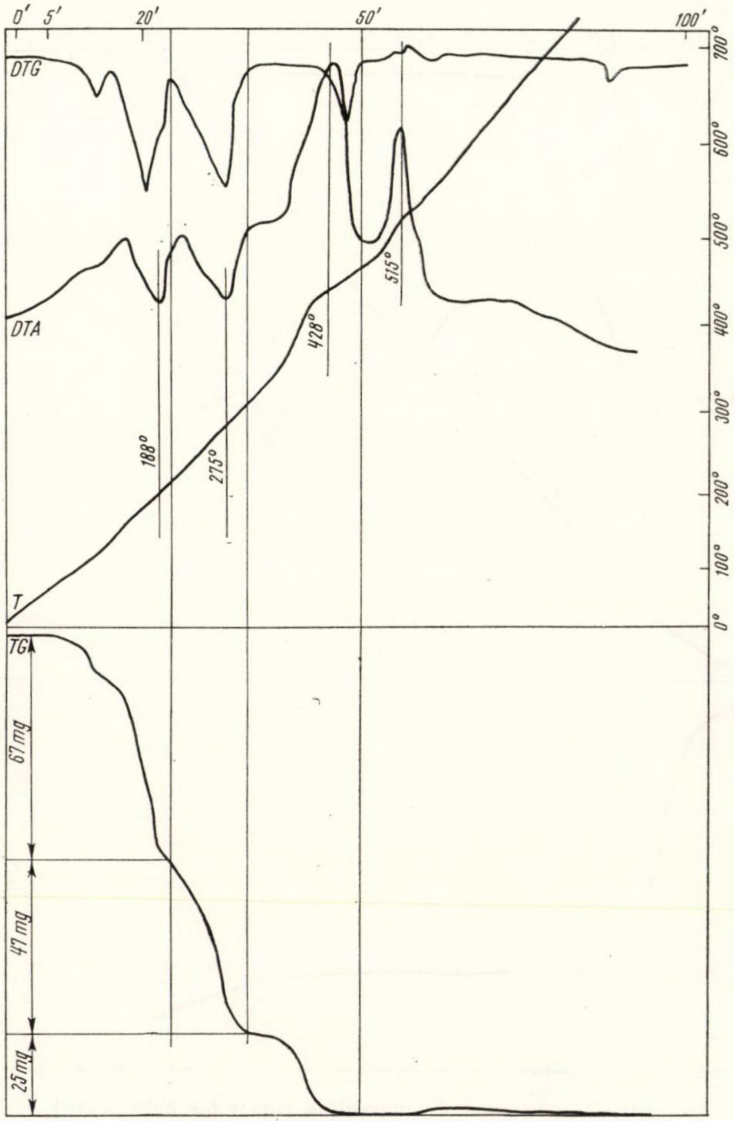

Fig. 2. — Thermal decomposition curves for $NiPy_4(SCN)_2$

An endothermal process connected with phase transformations of the compound is recorded at 620°.

Analysing the thermal behaviour of $Co(\gamma\text{-pic})_4[FeO_4]$, the existence of an endothermal process at 150° corresponding to ligand elimination and formation of metal oxides is established.

The temperature of 265°C, characterized by the existence of an exothermal peak of A.T.D. – corresponds to a recrystallization process of resulting oxides.

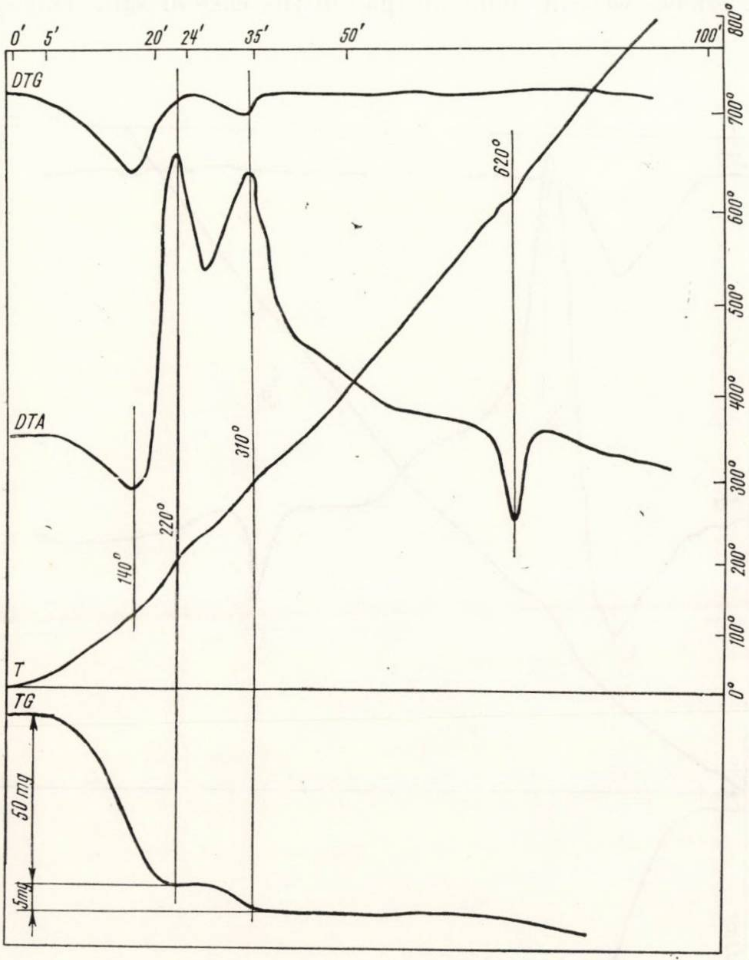

Fig. 3. – Thermal decomposition curves for $CoPy_4[FeO_4]$

An edothermal effect due to a crystalline transition or to a reaction between the resulting oxides is recorded at 645°.

Examining the aspect of the A.T.D. curve corresponding to $Ni(\gamma\text{-pic})_4[FeO_4]$ compound, an endothermal process is established at 110° marking the beginning of decomposition by ligand elimination and oxides formation. The exothermal process at 245° may be assigned to the recrystallisation of resulting oxides. An endothermal effect assigned to phase transformation or to reaction of resulting oxides is recorded at 620°.

We have focused here on γ-picoline compounds (the most stable ones), the behaviour of corresponding α and β compounds being analogous).

Examining the characteristic temperatures of endothermal and exothermal effects we can conclude that in the case of salts containing the

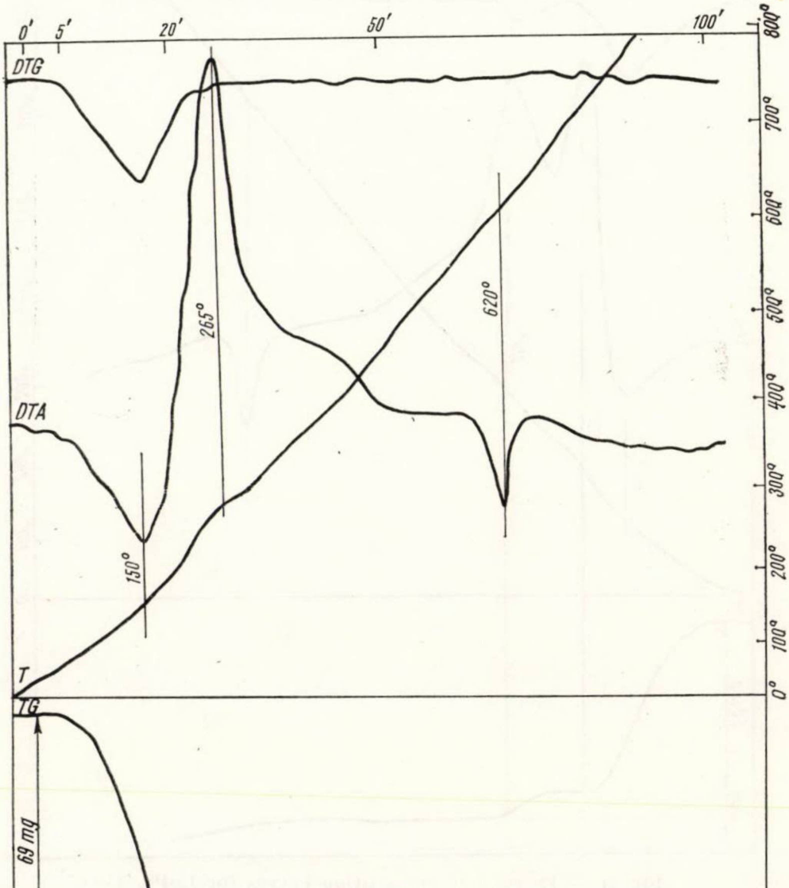

Fig. 4. — Thermal decomposition curves for $Co(\gamma pic)_4[FeO_4]$

ferrate (VI) ion the temperature of decomposition "tm" (and thermal stabilities of these compounds, too) are diminished when ferrate (VI) ion is introduced in their molecule.

The problem of the thermal behaviour of Ni(II) and Co(II) tetrapyridine and tetrapicoline complex compounds is well known in the literature.[6-9]

Table 1

Temperatures corresponding to endothermal and exothermal processes

Compound	Characteristic temperature "tm" (°)	Exothermal process temperature (°)	Endothermal process temperature (°)
$NiPy_4[FeO_4]$	120	255	620
$CoPy_4[FeO_4]$	140	220	620
$Ni(\alpha\text{-pic})_4[FeO_4]$	90	225	620
$Co(\alpha\text{-pic})_4[FeO_4]$	125	230	620
$Ni(\beta\text{-pic})_4[FeO_4]$	105	235	620
$Co(\beta\text{-pic})_4[FeO_4]$	130	250	620
$Ni(\gamma\text{-pic})_4[FeO_4]$	110	245	620
$Co(\gamma\text{-pic})_4[FeO_4]$	150	265	645

Obtaining some compounds that are thermally less stable while the ferrate (VI) ion is introduced, can be explained in terms of a π strong bond (metal-oxygen) that appears in the presence of $[FeO_4]^{2-}$ion.[10]

This leads to its great polarizability and to a strong field formation (in the case of salts containing it), greatly diminishing the positive charge of the central metal ion Ni(II), Co(II).

Thus, the sphere of action of the central metal ion decreases; having a diminished effective charge, this ion presents a smaller attraction power for polar ligand molecules.

In conclusion, a destabilization of compounds containing $[FeO_4]^{2-}$ with Ni(II) and Co(II) complex ammines is produced. This fact is also observed by ligand elimination in a single stage, corresponding to a single endothermal process.

In the case of thiocyanates of complex ammines the following intermediate complexes are formed[11]:

$$NiPy_4\ (SCN)_2(s) \longrightarrow NiPy_2(SCN)_2\ (s) + 2Py\ (g)$$

$$NiPy_2\ (SCN)_2\ (s) \longrightarrow Ni(SCN)_{2(s)} + 2\ Py(g)$$

The chemical analysis of compounds containing ferate (VI) ion after previous heating at various temperatures (200°, 400°, 600°) leads to the conclusion that in these stages, intermediate compounds do not form. We suppose only the formation of metal oxides. Among ferrate (VI) ion salts with picoline a greater stability of γ picoline compounds

---

[7] D. FĂTU and E. SEGAL, *Anal. Univ. Bucureşti, Sect. Chim.*, **2**, 49 (1968).

[8] D. FĂTU, S. FĂTU and E. SEGAL, *Rev. Roumaine Chim.*, **14**, 1107 (1969).

[9] D. FĂTU, S. FĂTU, A. TEODORESCU and E. SEGAL, *Rev. Roumaine Chim.*, **15**, 855 (1970).

[10] C. J. BALLHAUSEN and A. D. LIEHR, *J. Mol. Spectroscopy*, **2**, 342 (1958).

[11] I. G. MURGULESCU, E. SEGAL and D. FĂTU, *Rev. Roumaine Chim.*, **11**, 291 (1966).

is observed. A lower stability of α and β picoline compounds is evident due to a metal ligand bond weakening.

This is explained with the help of a steric hindrance existing in these cases. The endothermal process that appears and is reproduced for all compounds containing ferrate (VI) ion at about 620° reveals the existence of a common phenomenon for these compounds. (This temperature is not characteristic of Ni(II) and Co(II) tetrapyridine—tetrapicoline thiocyanates).

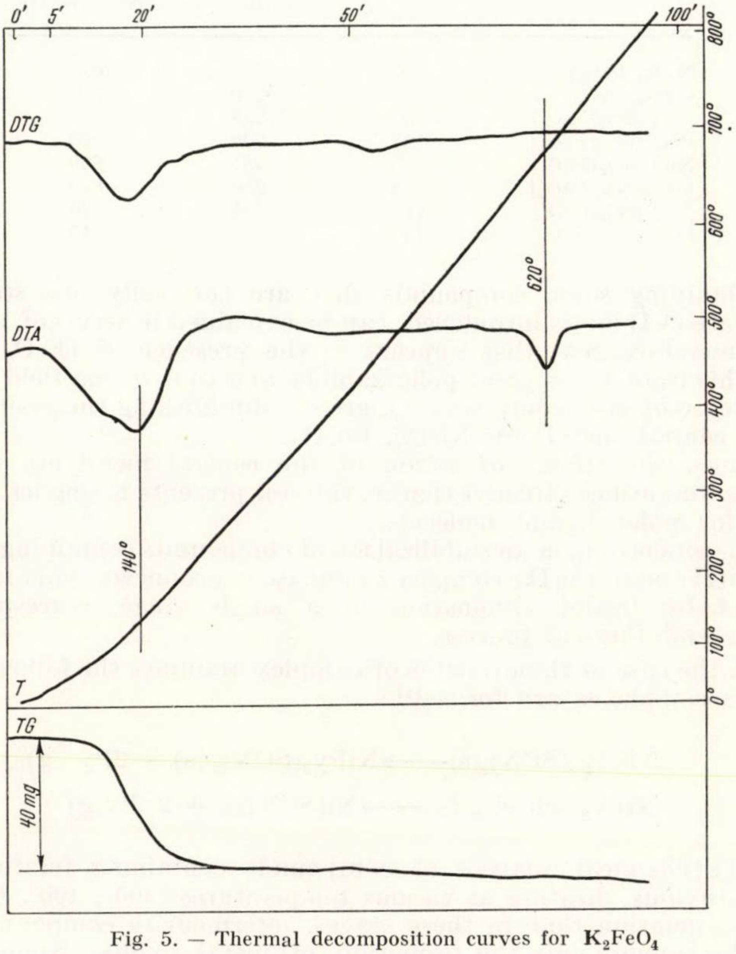

Fig. 5. — Thermal decomposition curves for K_2FeO_4

This phenomenon may be correlated with a phase modification of Fe_2O_3 formed in a previous stage.

The equilibrium between the two existing forms of Fe_2O_3 is known.[12] Thus $\gamma Fe_2O_3 \rightarrow \alpha Fe_2O_3$ (at about 600°).

---

[12] A. F. Wells, "Structural Inorganic Chemistry", 2nd ed. Oxford, University Press, 1962, p. 545.

Another explanation of the endothermal effect at 620° consists in the possible formation of some ferrites with the general formula $Fe_2O_3 . MO$ (M represents Co(II) or Ni (II)). These ferrites[13] belong to spinels groups. Examining the thermal behaviour of K_2FeO_4 (a study made in a separate note) an endothermal peak appears at 620° on A.T.D. curve).

The reproducibility of this phenomenon in the case of potassium ferrate (VI) leads to the conclusion of the existence of a phase transformation. The possibility for a spinel compound formation is not admitted.

This explanation is valid for all the studied compounds containing $(FeO_4)^{2-}$; the same endothermal process at 620° exists in all these cases.[7]

Correlating this endothermal process at 620° with changes in the magnetic properties of Fe_2O_3, the results were found to agree with the experimental data.[14]

Changes in the magnetic properties of Fe_2O_3 are produced by a single endothermal process (found in all the cases studied during phase transformation $\gamma Fe_2O_3 \rightarrow \alpha Fe_2O_3$ corresponding to an exothermal process).

4. CONCLUSIONS

The thermal behaviour of two series of salts containing ferrate (VI) ion with Ni(II) and Co(II) tetrapyridine and tetrapicoline compounds has been studied.

The influence of $[FeO_4]^{2-}$ ion is evidenced by the formation of compounds with relative lower thermal stabilities.

For compounds containing ferrate (VI) ion, ligand elimination takes place in a single stage due to a lower stability.

In all the cases studied, reproducibility of the same endothermal process at 620° (common for K_2FeO_4, too) suggests the existence of a change in Fe_2O_3 magnetic properties.

---

[13] A. Forestier and M. Chaudron, *Rev. Roumaine Chim.*, **1926**, 777.

[14] R. C. Mackenzie, "Differential Thermal Analysis", vol. I, Academic Press, New York, 1970, p. 274.

Revue Roumaine de chimie, **19**, *11*, 1727–1730 (1974)

CHELATES AND POLYCHELATES OF AMINO ACIDS. II[1]

COMPLEXES IN COPPER SOLUTION (II) WITH N(R)-ANTHRANILIC ACIDS

I. GABE, ANICA TOLEA and A. AIRINEI
"P. Poni" Institute of Macromolecular Chemistry
Aleea Grigore Ghica Vodă, 41A, Jassy

Received May 25, 1973

The complexes in solution of N-substituted anthranilic acids with copper (II) have been studied. Their formation constants have been calculated using the McConnell and Davidson's graphical method and some conclusions concerning the substituent influence of nitrogen atom of amino group on the formation ability of chelates have been drawn.

It is well known that many compounds appear in the formation reactions of complexes of some metal ions with α- and *o*-amino acids. The great attention paid to such complexes is caused by the fact that amino acids occupy an important place in the organic structure of the organisms of the animal kingdom. Connected with this, it is interesting to point out the studies underlain by the idea of blocking the viral carcinogenic functions by introducing some chelates into the affected cell, which may link the active amino- and carboxyl groups of the virus structure during metabolism.[2-19]

---

[1] I. Gabe and D. Leonte, *Rev. Roumaine Chim.*, **14**, 1535 (1969).

[2] A. Albert, *Austral. J. Sci.*, **30**, 1 (1967).

[3] S. E. Livingstone, J. D. Nolan and A. E. Mihkelson, *Inorg. Chem.*, **7**, 1447 (1968); **9**, 2545 (1970).

[4] J. D. Broome, *Nature*, **191**, 1114 (1961).

[5] A. A. Khan and W. V. Malik, *J. Indian Chem. Soc.*, **40**, 565 (1963).

[6] G. N. Rao and N. C. Li, *Canad. J. Chem.*, **44**, 1637 (1966).

[7] J. H. Ritsman, G. A. Wiegers and F. Jellinek, *Rev. Trav. chim.*, **84**, 1577 (1965).

[8] G. N. Rao and R. S. Subrahmanya, *Proc. Indian Acad. Sci.*, *Sect. A*, **60**, 165 (1964).

[9] G. N. Rao and R. S. Subrahmanya, *J. Electroanalyt. Chem.*, **9**, 364 (1965).

[10] P. Spacu and P. Ungureanu-Vicol, *Anal. Sti. Univ. Bucureşti, Ser. St. Nat., Chim.*, **15**, 109 (1966).

[11] G. G. Nenci and E. Lechler, *Boll. Soc. ital. Biol. sper.*, **43**, 1346, 1350 (1967).

[12] Y. M. Azizov, A. K. Miftakhora and V. F. Toropora, *Zhur. neorg. Khim.*, **12**, 661 (1967).

[13] D. S. Barnes and L. D. Pettit, *J. Inorg. Nuclear Chem.*, **33**, 2177 (1971).

[14] N. C. Li, E. Doody and J. M. White, *J. Amer. Chem. Soc.*, **80**, 5901 (1958).

[15] W. E. Bennett, *J. Amer. Chem. Soc.*, **81**, 246 (1959).

[16] K. M. Wellman, T. G. Mecca, W. Mungall and C. R. Hare, *J. Amer. Chem. Soc.*, **90**, 805 (1968); K. M. Wellman, S. Bogdanski, W. Mungall, T. G. Mecca and C. R. Hare, *Tetrahedron Letters*, 3607 (1967).

[17] E. A. Zakharova and V. N. Kumok, *Zhur. obshchei Khim.*, **38**, 1922 (1968).

[18] J. M. Tsangaris, J. W. Chang and R. B. Martin, *J. Amer. Chem. Soc.*, **91**, 726 (1969).

[19] L. I. Katzin and E. Gulyas, *Inorg. Chem.*, **7**, 2442 (1968).

In a previous paper,[1] we showed that bis-difunctional amino acids can react with transitional metal salts giving chelate polymers, insoluble in water and in usual organic solvents. This fact proves that the metal ion substitutes hydrogen in the carboxylic group and is linked through a donor-acceptor bond to the nitrogen atom of the amino group through the agency of the lone-pair electrons of this atom.

Experimental data[1] enabled the calculation of force constants and valence angles relative to the metal ion radius. Other series of our determinations refer to the copper complexes in solution. Our measurements show that the complexes in solution may have a molar ratio 2 : 1 and 1 : 1, the latter will not precipitate at room temperature, if sufficiently diluted solutions are used.

The complexes having a molar ratio 2 : 1 formed the object of many studies,[20] chelates being precipitated from water solutions and analysed in solid state (by infrared spectra and elemental analysis).

The complexes having a molar ratio 1 : 1 were less studied. In the case of anthranilic acid, for instance, there are such complexes used in the spectrophotometrical determinations of some cations.[21]

We studied the N(R)-anthranilic acids (R = methyl, ethyl, allyl, phenyl) prepared according to the literature.[22-25]

The complexes in solution were studied by McConnell and Davidson's method[26] and by Job's continuous variation method. [27,28] Concentrations between 6.25×10^{-4} M and 1.25×10^{-2} M for N-substituted acid and concentration of 1.25×10^{-2} M for copper perchlorate were used in both series of determinations.

The ionic strength of the solution was kept constant at 0.4, using sodium perchlorate.

We studied spectrophotometrically the variation of molar absorptivity at wavelengths of 664 nm and 650—680 nm, using the position of the absorption maxima of copper complexes with N-methyl and N-ethyl anthranilic acid, respectively.

The experimental data are shown in figures 1 and 2. We calculated from the curves of figure 1 the formation constants of complexes and obtained the values given in table 1.

The results of the studies of the systems discussed by Job's method are shown in figure 2. The shape of these curves reveals that the 2 : 1 complex forms first, and the 1 : 1 complex thereafter and that the two complexes coexist in different amounts at a given moment depending on the mixing ratios. The characteristic absorption maxima and their intensities do not change with time, as results from kinetic determinations. Substituting the amino nitrogen by a radical influences but very little the

---

[20] J. S. Decker and H. Frye, *Z. Naturforsch.*, **21b**, 522, 527 (1966).

[21] T. N. Bondareva, V. S. Shvarev and V. P. Perkins, *Zavodskaya Lab.*, **32**, 910 (1966).

[22] J. Houben and W. Brassert, *Ber. dtsch. chem. Ges.*, **39**, 3233 (1906).

[23] R. Willstatter and W. Kahn, *Ber. dtsch. chem. Ges.*, **37**, 401 (1904).

[24] H. Meyer, *Monatsh.*, **21**, 913 (1900).

[25] I. Goldberg, *Ber. dtsch. chem. Ges.*, **39**, 1691 (1906).

[26] H. McConnell and N. Davidson, *J. Amer. Chem. Soc.*, **72**, 3164 (1950).

[27] P. Job, *Ann. Chim. (France)*, **9**, 113 (1928); **6**, 97 (1936).

[28] W. C. Vosburgh and G. R. Cooper, *J. Amer. Chem. Soc.*, **63**, 437 (1941).

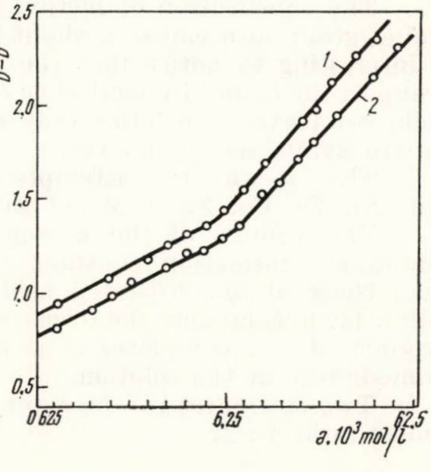

Fig 1. — Variation of molar extinction coefficients by the molar ratio method.
1, N-methylanthranilic acid copper complex; 2, N-ethylanthranilic acid copper complex.

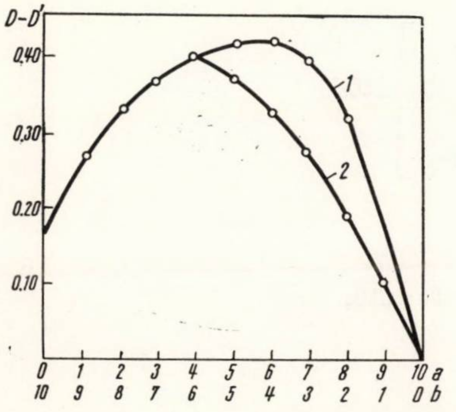

Fig. 2. — Variation of molar extinction coefficients by Job's method.
1, N-methylanthranilic acid copper complex; 2, N-ethylanthranilic acid copper complex.

Table 1

Formation constant values for copper complexes

Ligand	$K_1 \times 10^4$ Complex 2 : 1	$K_2 \times 10^4$ Complex 1 : 1
N-methylanthranilic acid	0.85	0.26
N-ethylanthranilic acid	0.78	0.18

ionization constant values of the 1 : 1 water-dioxane solutions; thus pK_a is 6.53 for the anthranilic acid and 6.58 for N-methylanthranilic acid.[29]

The substituent has a greater influence on formation constant values of the metal complexes of the respective acids, because the formation constant for the copper complex of N-methylanthranilic acid is 3.7×10^{-4} compared to 1.4×10^{-3} for anthranilic acid.[29]

---

[29] W. F. Harris and T. R. Sweet, *J. Phys. Chem.*, **60**, 509 (1956).

The substitution of methyl by ethyl in the nitrogen atom of the amino group also causes a slight decrease in the formation constant. It is interesting to notice that the substitution of hydrogen in the amino group of the ligand by methyl or ethyl causes some steric hindrances that yield complexes in solution only for those metals which can give plane-square symmetry complexes.

That is why our attempts to obtain complexes in solution with Mn, Ni, Fe, Co, Zn were not satisfactory.

The volume of the nitrogen substituent produces greater steric hindrance; formation constant values of substituted acids are lower than those of unsubstituted acids. The increase in the radical volume (allyl, phenyl) hinders the formation of 1 : 1 complexes and the solubility product of 2 : 1 complexes is so small, that these complexes precipitate immediately in the solution.

Two structures can be supposed for the complexes in solution at a molar ratio 1 : 1.

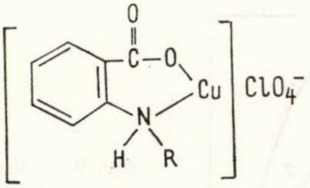

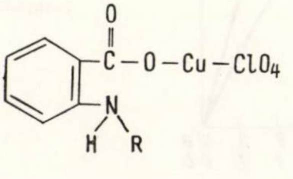

We take into account the first structure, i.e. the complex structure, because the IR absorption maximum of the amino group which is placed at about 3400 cm^{-1}, in sodium N-methylanthranilate,[20] is shifted to lower frequencies at about 3320 cm^{-1} due to complexation with copper ions. In this way, Decker's results,[20] concluded from the elemental analysis, that copper N-methylanthranilate would be a salt are invalidated.

IR spectral analysis proves the existence of a complex.

When discussing amino nitrogen donor ability we must have in view the influence of the substitution of hydrogen by electron repelling groups and strength modifications in the hydrogen bridge between the amino nitrogen and the carbonylic group of the acid function.

Revue Roumaine de Chimie, **19**, *11*, 1731–1734 (1974)

MOLECULAR COMPLEXES WITH AROMATIC CATIONS AS ELECTRON ACCEPTORS. II*

CHARGE-TRANSFER SPECTRUM OF 2,4,6-TRIPHENYLPYRYLIUM THIOCYANATE

ALEXANDRU T. BALABAN and MARIA PARASCHIV
Institute of Atomic Physics, P.O.B. 35, Bucharest

Received June 7, 1974

The orange-red colour of 2,4,6-triphenylpyrylium thiocyanate is due to a charge-transfer band at 488 nm (in dichloromethane).

The deeper colours of iodides of organic aromatic cations as compared to the corresponding perchlorates or tetrafluoroborates are due to charge transfer bands [1,2] involving transitions to less polar electronically excited states. In a crude approximation the ground and excited states can be represented by structures I and II, respectively

$$\underset{\text{I}}{R^{\oplus}\,X^{\ominus}} \overset{h\nu}{\rightleftharpoons} \underset{\text{II}}{R\cdot\ X\cdot} \rightleftharpoons \underset{\text{III}}{R - X}$$

Thus tropylium [3], pyrylium [4,5], and pyridinium iodides [6–8] present absorption bands in the visible range at frequencies decreasing in this order. In a previous paper,[5] we investigated in detail various pyrylium iodides. Nothing is known about charge transfer involving pseudohalide anions and the same cations. In the present paper we report a study of 2,4,6-triphenylpyrylium thiocyanate.

---

* Ref. 5 is to be considered as part I in this series.

[1] G. Briegleb, "Elektronen Donator-Acceptor Komplexe", Springer Verlag, Berlin, 1961 ; J. Rose, "Molecular Complexes", Pergamon Press, Oxford, 1967 ; R. S. Mulliken and W. B. Person, "Molecular Complexes", Wiley-Interscience, New York, 1969.

[2] R. Foster, "Organic Charge-Transfer Complexes" Academic Press, London, 1969, p. 292 ; A. Lablache-Combier, *Bull. Soc. Chim, France,* **1972**, 4791.

[3] W. E. Doering and H. Krauch, *Angew. Chem.*, **68**, 661 (1956) ; K. M. Harmon, F. E. Cummings, D. A. Davis and D. J. Diestler, *J. Amer. Chem. Soc.*, **84**, 120, 3349 (1962) ; E. M. Kosower, *J. Org. Chem.*, **29**, 956 (1964).

[4] M. Feldman and S. Winstein, *Tetrahedron Letters*, 853 (1962).

[5] A. T. Balaban, M. Mocanu and Z. Simon, *Tetrahedron*, **20**, 119 (1964).

[6] E. M. Kosower, *J. Amer. Chem. Soc.*, **77**, 3883 (1955) ; **80**, 3253 (1958) ; "Molecular Biochemistry", McGraw-Hill, New York, 1962, p. 180 ; in "Progress in Physical Organic Chemistry" editors S. G. Cohen, A. Streitwiser Jr. and R. W. Taft, Interscience-Wiley, New York, 1965, vol. 3, p. 85.

[7] E. M. Kosower and P. E. Klinedinst Jr., *J. Amer. Chem. Soc.*, **78**, 3493 (1956) ; E. M. Kosower, D. Hofmann and K. Wallenfels, *ibid.*, **84**, 2755 (1962) ; E. M. Kosower and J. A. Skorcz, in "Advances in Molecular Spectroscopy", ed. A. Mangini, Pergamon Press, Oxford, 1962, vol. 1, p. 413.

[8] R. A. Mackay, J. R. Landolph and E. J. Poziomek, *J. Amer. Chem. Soc.*, **93**, 5026 (1971) ; R. A. Mackay and E. J. Poziomek, *Ibid.*, **94**, 4167 (1972).

EXPERIMENTAL PART

PREPARATION OF 2,4,6-TRIPHENYLPYRYLIUM THIOCYANATE

2,4,6-Triphenylpyrylium perchlorate was converted into its pseudobase (1,3,5-triphenyl-2-penten-1-one) with sodium acetate in aqueous-ethanolic solution.[9] The pseudobase, m.p. 120°, was dissolved in ethanol and treated with excess 1 N sulphuric acid and a concentrated aqueous solution of ammonium thiocyanate. The brick-red precipitate was filtered off and recrystallized from acetic acid.

An alternative method, involving the treatment of a diluted acetic acid solution of triphenylpyrylium perchlorate with a concentrated aqueous solution of ammonium thiocyanate, must be repeated three to four times in order to afford a perchlorate-free product (as evidenced by the absence of IR absorption at 625 and 1100 cm^{-1}). Better results are obtained by preparing 2,4,6-triphenylpyrylium chloride (introducing gaseous hydrogen chloride into a benzene solution of the pseudobase), dissolving it in dil. ethanol, and treating the solution with aqueous ammonium or potassium thiocyanate.

A third method, which is rather cumbersome, involves the preparation of anhydrous thiocyanic acid from potassium thiocyanate and phosphoric acid at −70° in vacuum,[10] then treating it with the triphenylpyrylium pseudobase in benzene solution.

M.p. 192°. *Found*: N,3.81 ; $C_{23}H_{17}O^{\oplus}SCN^{\ominus}$ requires N, 3.82%.

Electronic absorption spectra were recorded with a CF−4 Optica (Milan) spectrophotometer.

RESULTS AND DISCUSSION

The structure of the brick-red product is ionic, as evidenced by the infrared absorption spectrum (KBr pellet) which contains all bands of the 2,4,6-triphenylpyrylium cation[11] and, in addition, the intense band at 2052 cm^{-1} of the thiocyanate anion.

The ultraviolet absorption spectrum of 2,4,6-triphenylpyrylium thiocyanate in ethanol is closely similar to that of the fluoroborate, chloride, or perchlorate, presenting bands at 264(sh), 280, 325(sh), 360, and 410 nm.[3] However, a dichloromethane solution of the thiocyanate has a deeper colour than the ethanolic solution, and its spectrum (fig. 1) presents the bands displayed in table 1.

For the bands designated as *x*-, *y*- and *x*-band [12,13] the agreement with the absorption spectrum of the 2,4,6-triphenylpyrylium iodide [5] is very good.

---

[9] A. T. Balaban, C. N. Rențea and M. Băcescu-Roman, *Rev. Roumaine Chim.*, **10**, 865 (1965).

[10] C. Reid, *J. Chem. Phys.*, **18**, 1512 (1950); C. I. Beard and B. P. Dailay, *ibid.*, **15**, 762 (1947).

[11] A. T. Balaban, G. D. Mateescu and M. Elian, *Tetrahedron*, **18**, 1083 (1962).

[12] A. T. Balaban, V. E. Sahini and E. Keplinger, *Tetrahedron*, **9**, 163 (1960).

[13] G. N. Lewis and M. Calvin, *Chem. Rev.*, **25**, 273 (1939); G. N. Lewis and J. Bigeleisen, *J. Amer. Chem. Soc.*, **65**, 2102, 2107 (1943); M. Simalty, J. Carretto and S. Sib, *Bull. Soc. chim. France*, **1970**, 2316; H. Khedija, H. Strzelecka and M. Simalty, *ibid,*. **1972**, 3173; M. Simalty, H. Strzelecka and H. Khedija, *Tetrahedron*, **27**, 3503 (1971).

The transition at 488 nm in CH_2Cl_2, which is absent in 2,4,6-triphenylpyrylium salts with non-intereacting anions such as ClO_4 or BF_4, must be ascribed to a charge-transfer similar to that of the iodide. 2,4,6-Triphenylpyrylium iodide has the charge transfer band at 551 nm in methylene chloride. The difference is to be ascribed to the smaller donor ability of the thiocyanate anion as compared to the iodide anion. A comparison between the acceptor abilities of thiocyanogen and iodine in charge-transfer spectra with aromatic donors was made by Vântu and coworkers.[14]

Table 1

Electronic absorption spectrum of 2,4,6-triphenylpyrylium thiocyanate in methylene dichloride : wavelength in nm, and ε in brackets

x'-Band	y-Band	x-Band	CT-Band
282 (16800)	369 (35300)	416 (25500)	488sh (230)

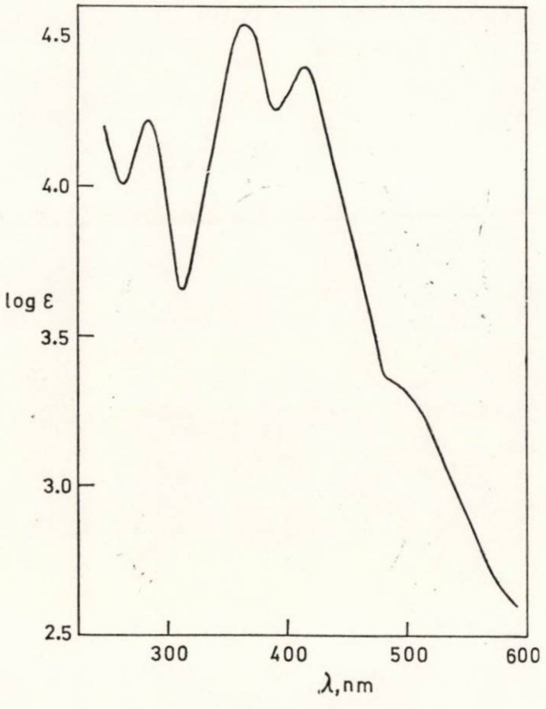

Fig. 1. — Absorption spectrum of 2,4,6-triphenylpyrylium thiocyanate in methylene dichloride.

---

[14] W. Scholz, A. Truţia and V. Vântu, *Tetrahedron Letters*, **1965**, 57.

A direct equilibrium in solution between ionic and covalent tropylium isocyanate was evidenced by NMR,[15] and this will necessitate a revision of earlier data.[16] However, on the time-scale of the electronic excitation, process II—III is too slow to affect the charge transfer I—II.

The NMR spectrum of triphenylpyrylium thiocyanate (I) in deuterochloroform containing 10% acetonitrile presents at —40° a broadening of signals, but fails to reveal the appearance of new bands due to a covalent form (III).

The elemental analysis was performed by Mrs. C. Popescu, and the NMR spectrum was recorded by Mrs. A. Vasilescu.

---

[15] H. Kessler and A. Walter, *Angew. Chem.*, **85**, 821 (1973); *Angew. Chem. Internat. Ed.*, **12**, 773 (1973).

[16] M. J. S. Dewar and R. Pettit, *J. Chem. Soc.*, **1956**, 2021, 2026; W. v. E. Doering and L. E. Helgen, *ibid.*, **1961**, 482.

Revue Roumaine de Chimie, **19**, *11*, 1735–1749 (1974)

STUDIES IN THE *s*-TRIAZINE FIELD (NEW SERIES). XVI.[1]

ACIDIC AND TAUTOMERIC EQUILIBRIUM CONSTANTS OF THE CONJUGATED ACIDS OF SOME E-1,3-DIMETHYL-6-(*p*-DIALKYLAMINO-β-STYRYL)-2,4-DIOXO-1H, 3H-1,3,5-TRIAZINES

M. SAFTA and G. OSTROGOVICH

Laboratory of Organic Chemistry, Polytechnic Institute "Traian Vuia"
Timişoara, str. Bocşa 6, Romania

Received December 21, 1973

The tautomerism constant K_T = [Ammonium ion] / [Triazinium ion] = K''_{a_1} (triaz.)/K'_{a_1} of first step conjugated acids of the title compounds, as well as the apparent acidity constant $Ka_1 = (K'_{a_1} . K''_{a_1})/(K'_{a_1} + K''_{a_1})$, have been determined by the spectrophotometric method. The Si Jung Yeh's [12b] and the Gerson's[14] modes of applying this method were discussed. It is presented another way to use the spectrophotometric data for the same purpose. The effective acidity constants K'_{a_1} and K''_{a_2} have been calculated. The substitution of Me by Et in the dialkylamino-compound determines an increase of both constants but much more of the K'_{a_1} one. This is fully analogous to the observations of the Japanese authors [22] by *p*-dialkylaminoazo-derivatives. It corresponds to the known anomalous high basicity of diethyl- in comparison with dimethylaniline.[24b] It has obviously the same explanation through the intervention of a solvation inhibiting steric effect in the base molecule, which surpasses the spectral manifested increase of the +M-effect.

A previous paper including a spectrophotometric study which led to semiquantitative results [2] allowed us to prove that the protonation in the first step of the 6-(*p*-dimethylamino-β-styryl)-2,4-dioxo-1H,3H-1,3,5-triazine, a yellow coloured base, is giving rise to an ammonium-triazinium tautomery entirely similar to the ammonium-azonium tautomery exhibited by the salts of *p*-amino-azo-derivatives with an acid equivalent.

Discovered by J. Thiele on the *p*-amino-azobenzenes hydrochlorides [3] and categorically elucidated for the first time, as is known, by Hantzsch *et al.*,[4] this particular type (which, besides others, belongs to the large enough and multiform genus of "benzoido-chinoido" tautomery) has become, from the beginning till nowadays, including some controversies,[5-10] the subject of extensive studies concerning a series of various amino-azoderivatives.

---

[1] Part XV, M. Safta and G. Ostrogovich, Rev. Roumaine Chim., 14, *10* (1974).

[2] G. Ostrogovich and M. Safta, *Rev. Roumaine Chim.*, **15**, 799 (1970).

[3] J. Thiele, *Chem. Ber.*, **36**, 3965 (1903).

[4] A. Hantzsch and F. Hilscher, *Chem. Ber.*, **41**, 1171 (1908) ; A. Hantzsch, *Chem. Ber.*, **52**, 509 (1919) ; A. Hantzsch and A. Burawoy, *Chem. Ber.*, **63** , 1760 (1930).

Especially in the last time these studies have been carefully performed, leading to the determination of the acidity constants of the conjugated acid pairs, respectively constants of the tautomeric equilibria established between those species in solution.[11-20]

For our compounds the tautomeric equilibrium (and the protolytic equilibrium involved) has been determined in 50 % vol. aqueous-ethanolic solution in the presence of sulphuric acid.

The tautomeric equilibrium for the 1,3-dimethylated compounds, which constitutes the object of this study, is described in the following scheme (1).

In contrast to many cases in which it was possible to isolate in crystalline form, as "chromoisomeric" species, both monoprotonated tautomeric compounds of some aminoazo-derivatives,[4] the product which crystallized from the aqueous or aqueous-ethanolic solutions employed is in our cases only the coloured tautomer of II″ type (obtained as the bisulphate $BH^{\oplus}HSO_4^{\ominus}$).[2,21]

Besides — as it was not seldom achieved with aminoazo-derivatives — we could also obtain the type III product, which arises by double protonation of the base I and which is, as expected, colourless.

In our first paper on this matter,[2] a preconceived opinion concerning the doubtless —M effect of the dioxo-*s*-triazinic nucleus, which causes the yellow colour of the type I base and the halochromism of the monoprotonated species II″ — i.e. this effect should be very strong — as

---

[5] C. R. Bury, *J. Amer. Chem. Soc.*, **57**, 2115 (1935).

[6] M. T. Rogers, T. W. Campbell and R. W. Maatman, *J. Amer. Chem. Soc.*, **73**, 5122 (1951).

[7] H. H. Jaffé, *J. Chem. Phys.*, **23**, 415 (1953).

[8] I. M. Klotz, H. A. Fies, I. Y. Chen-Ho and M. Mellody, *J. Amer. Chem. Soc.*, **76**, 5316 (1954).

[9] G. M. Badger, R. G. Buttery and G. E. Lewis, *J. Chem. Soc.*, **1954**, 1888.

[10] G. Cilento, E. C. Miler and J. A. Miler, *J. Amer. Chem. Soc.*, **78**, 1718 (1956).

[11] E. Sawicky, *J. Org. Chem.*, **21**, 605 (1956) ; **22**, 365, 621, 743, 1084 (1957).

[12a] H. H. Jaffé and Si-Jung Yeh, *J. Org. Chem.*, **22**, 1281 (1957) ; [b] Si-Jung Yeh and H. H. Jaffé, *J. Amer. Chem. Soc.*, **81**, 3283 (1959) ; M. Isaks, and H. H. Jaffé, *ibid.*, **86**, 2209 (1964) ; M. Isaks, *Diss. Abstr.*, **24**, 4998 (1964) ; H. H. Jaffé and A. L. Miller, *Reacț. Sposobn. Org. Soedin.*, **2**, vîp. **4** (6), 177 (1965) ; H. H. Jaffé and A. L. Miller, *Tetrahedron Letters*, **14**, 1489 (1966).

[13] J. Gränacher, H. Sühr and A. Zenhäusern, *Helv. Chim. Acta*, **44**, 313 (1961).

[14] F. Gerson and A. Heilbronner, *Helv. Chim. Acta*, **45**, 42 (1962).

[15] A. Zenhäusern and H. Zollinger, *Helv. Chim. Acta*, **45**, 188 (1962).

[16] R. Țițeica, G. Palade, G. Bănățeanu and A. Strugaru, *Bull. Inst. petrol gaze și geolog.* (*București*), **9**, 189 (1963).

[17] R. L. Reeves, *J. Amer. Chem. Soc.*, **88**, 2240 (1966).

[18] a). Yu L. Kaminskii, I. Ya, Berstein and O. F. Ghinzburg, *Doklady Akad Nauk S.S.S.R.* **45**, 330 (1962) ; b). I. Ya. Berstein, Yu L. Kaminskii, *Optica i spectroscopia*, **15**, 705 (1963) ; c). I. Ya Berstein and O. F. Ghinzburg, *Zhur. org. Kim.*, **3**, 2032 (1967) ; **4**, 1260 (1968) ; ibid., *Doklady Akad. Nauk S.S.S.R.* **180**, 98 (1968) ; ibid, *Uspekhi Khim.*, **2**, 5 (1972).

[19] Y. Tanizaki, T. Kobayashi and T. Hoshi, *Bull. Chem. Soc., Japan*, **39**, 558 (1966).

[20] B. A. Korolev and S. P. Tipova, *Zhur. org. Khim.*, **6**, 1188 (1971).

[21] G. Ostrogovich and M. Safta, *Rev. Roumaine Chim.*, **17** 2043 (1972).

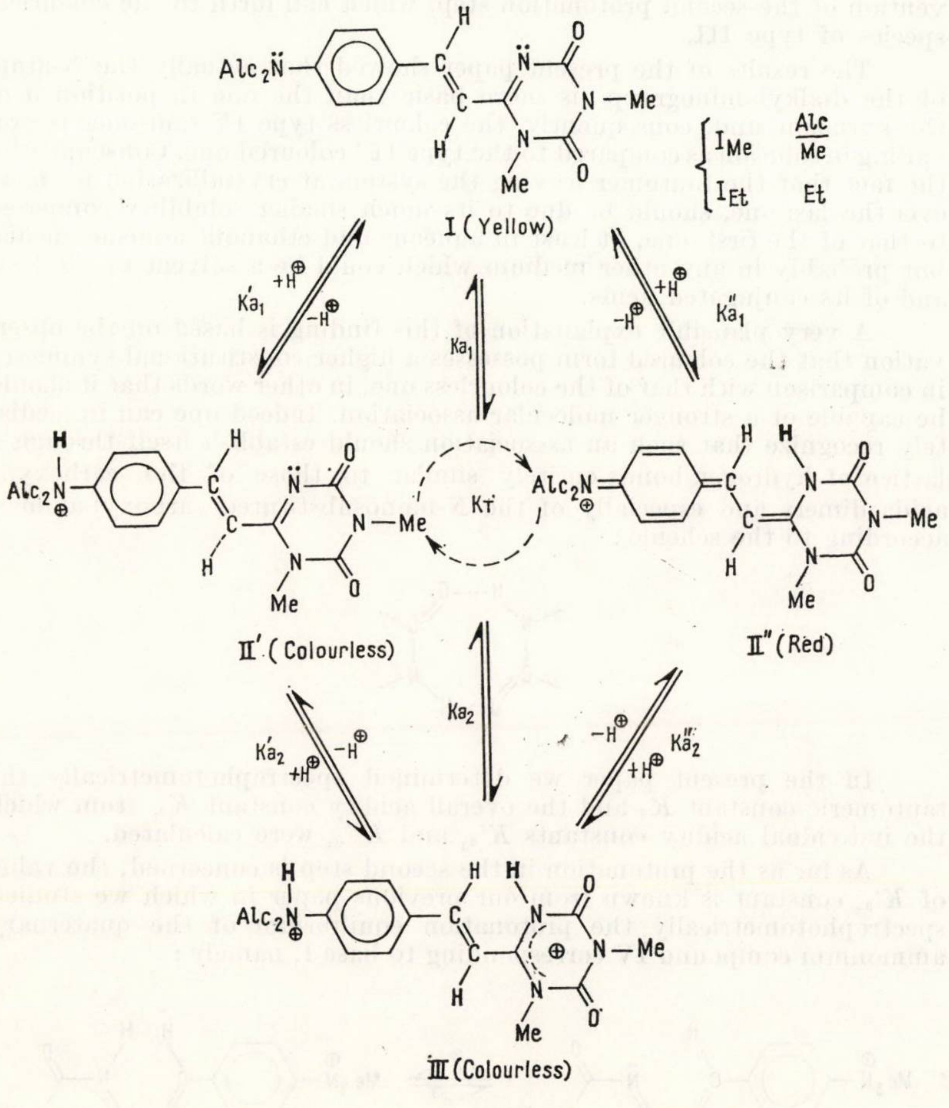
Alc₂N̈
H
O
N̈
N—Me
N
Me
I_Me Alc Me
I_Et Et
I (Yellow)
Ka'₁
+H⊕
−H⊕
Ka₁
Ka''₁
Alc₂N⊕
K_T
N—Me
II' (Colourless)
II'' (Red)
Ka₂
Ka'₂
Ka''₂
III (Colourless)

well as the fact that the coloured tautomer is the one which separates from the solution at crystallization, have induced us to assume in advance as very probable that in the equilibrium between the two monoprotonated species II′ and II″, the latter is the prevailing one, in other words that from the two basic centres of the molecule — the N atom at the 5 position of the triazine nucleus and that belonging to the dialkylamino group, the first one exhibits a higher basicity than the second. This misleaded us in interpreting the modifications of the solution spectrum as function of the medium acidity, of course complicated by the subsequent intervention of the second protonation step, which call forth to the colourless species of type III.

The results of the present paper showed that actually the N-atom of the dialkylaminogroup is more basic than the one in position 5 of the *s*-triazine and, consequently, the colourless type II′ tautomer is prevailing in solution as compared to the type II″ coloured one. Consequently, the fact that the tautomer leaving the system at crystallization is however the last one, should be due to its much smaller solubility compared to that of the first one, at least in aqueous and ethanolic-aqueous media, but probably in any other medium which could be a solvent of the base and of its conjugated acids.

A very plausible explanation of this finding is based on the observation that the coloured form possesses a higher constitutional symmetry in comparison with that of the colourless one, in other words that it should be capable of a stronger molecular association. Indeed one can immediately recognize that such an asssociation should establish itself through a lattice of hydrogen bonds entirely similar to those of the carboxylic acids dimers and especially of the N-monosubstituted carboxyl-amides, according to the scheme :

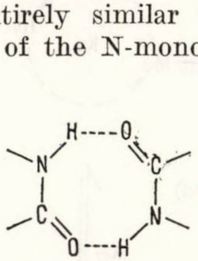

In the present paper we determined spectrophotometrically the tautomeric constant K_T and the overall acidity constant K_{a_1} from which the individual acidity constants K'_{a_1} and K''_{a_1} were calculated.

As far as the protonation in the second step is concerned, the value of K'_{a_2} constant is known from our previous paper in which we studied spectrophotometrically the protonation equilibrium of the quaternary ammonium compound IV corresponding to base I, namely :

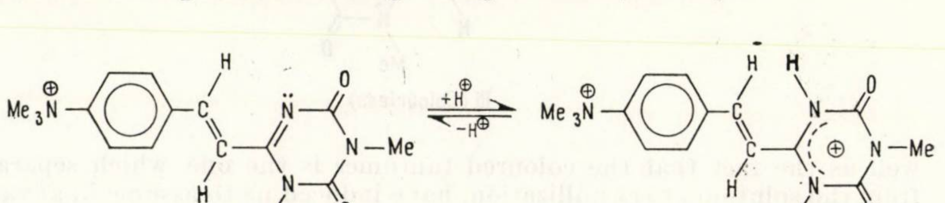

IV

V

The evaluation of the equilibrium constants of the monoprotonation process becomes possible from the moment at which we recorded the spectra of the *p*-dimethylamino-β-styryl-hemicyanine cation VI. The latter is metamer with IV — as II′ is tautomer with II″ — and has been synthetized by condensation of *p*-dimethylaminobenzaldehyde with the

1,3,5,6-tetramethyl-2,4-dioxo-1H,3H-1,3,5-triazinium iodide :

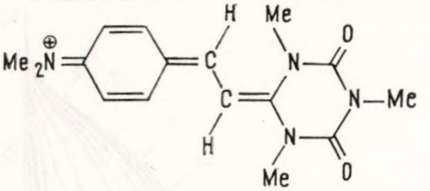

VI

The key of the problem was given by comparing this spectrum with that of the I + H_2SO_4 system, in the same medium.

Before the presentation of the results, it is necessary to refer to a very recent study performed by the Japanese authors Yamamoto *et al.*[22] which found that the K_T value belonging to the conjugated acids of *p*-dialkylaminoazobenzenes is considerably influenced by the volume of the alkyl group. They revealed that this influence is due to the abnormally basicity increase of the Et_2N-group compared to the Me_2N- one. In agreement with former studies concerning a N,N-dialkyl-aniline series,[23-25] this is due to the fact that in the molecule of the N,N-diethylamino base, besides the general conjugation effect, a steric effect is also present. The solvation of this base by proton bonds with the solvent molecules (a still very important solvation of the Me_2N-group) undergoes a practically complete inhibition by the steric effect, so that the free energy of the protonation process is adequately decreasing in this case compared to the Me_2N-group, determining thus a much higher basicity than that of the first one (i.e. a very important lowering of the conjugated acidity constant, K_a). These observations determined us to extend the present study from compound I, in which Alc = Me, to the one with Alc = Et.

RESULTS AND DISCUSSION

a) THE SPECTROSCOPIC BEHAVIOUR OF THE PROTONATION PROCESS

Figs 1 and 2 clearly show that in 50% vol aqueous-ethanolic solution and in the presence of H_2SO_4 up to a concentration $C_{H_2SO_4} \approx 0.4N$, the E-1,3-dimethyl-6-(*p*-dimethylamino-β-styryl)-2,4-dioxo-1H,3H-*s*-triazine (I, Alc = Me) exists in equilibrium with the two protonated tautomeric species II′ and II″ (Alc = Me). The species II'_{Me} exhibits a band in the ultraviolet range ($\lambda = 300$ nm, see fig. 1, curves *6* ÷ *11* and fig. 2, curve *1*) while II''_{Me} has a less intense band in the visible region ($\lambda = 523$ nm, see fig. 1, curve *10*).

---

[22] S. Yamamoto, N. Nishimura and S. Hasegawa, *Bull. Chem. Soc., Japan,* **46,** 194 (1973).

[23] H. C. Brown and A. Chan, *J.Amer. Chem. Soc.,* **72,** 2939 (1958).

[24] A. T. Botini and C. P. Nash, *J. Amer. Chem. Soc.,* **84,** 734 (1962); C.P. Nash and G. E. Maciel, *J. Phys. Chem.,* **68,** 832 (1964).

[25] J. W. Eates and M. H. Aldridge, *J. Chem. Soc.,* **1969,** 922.

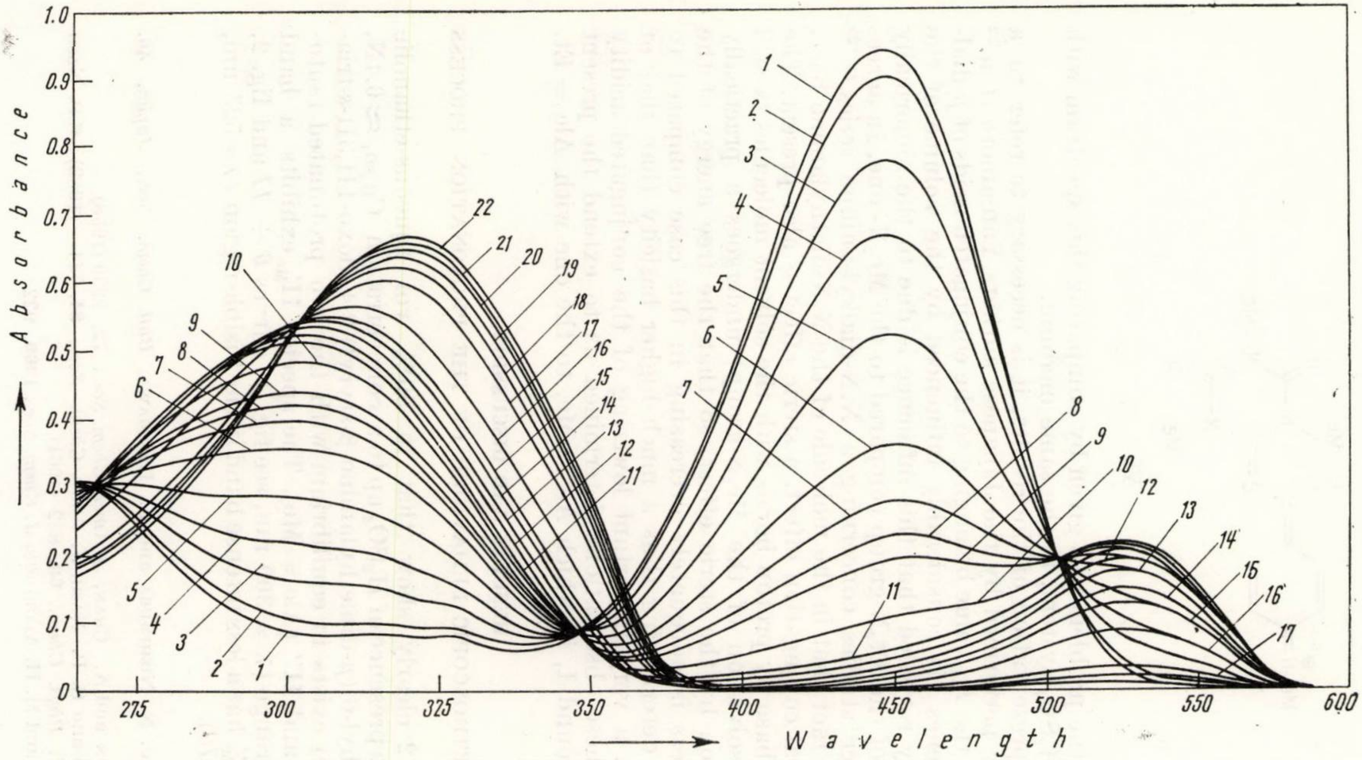

Fig. 1. — Influence of medium acidity (expressed as $C_{H_2SO_4}$ normality) on the absorption of the system initially formed from base I ($C = 2.5 \cdot 10^{-5}$ mol·l^{-1}; Alc = Me) and H_2SO_4 in 50 vol. % aqueous-ethanolic solution :

Curve Nº	1	2	3	4	5	6	7	8	9	10	11
$C_{H_2SO_4}$ (val/1)	0	10^{-3}	$5 \cdot 10^{-3}$	10^{-2}	$2 \cdot 10^{-2}$	$4 \cdot 10^{-2}$	$6 \cdot 10^{-2}$	$8 \cdot 10^{-2}$	10^{-1}	$2 \cdot 10^{-1}$	$4 \cdot 10^{-1}$

Curve Nº	12	13	14	15	16	17	18	19	20	21	22
$C_{H_2SO_4}$ (val/1)	$6 \cdot 10^{-1}$	$8 \cdot 10^{-1}$	1	1.5	3.0	5.0	6.0	7.0	8.0	9.0	10

The gradual acidity increase up to the above mentioned limit is expressed by the appearance and intensity increase of these two bands, together with the intensity decrease of the characteristic band of base I_{Me}, at 447 nm (fig. 1, curve *1*). The concentration of the last becomes negligible just when $C_{H_2SO_4}$ reaches the 0.4 N value (fig. 1, curve *11*). In the acidity range 0.4 N $\leqslant C_{H_2SO^4} \leqslant$ 1.5 N (fig. 1, curves *12—15*) only the monoprotonated species II′ and II″ are practically present in the system, afterwhich the second protonation is continuing in a rate increasing with acidity, the following equilibrium $(II' + II'') \rightleftharpoons III$ being established (fig. 1, curves *16 ÷ 22* and fig. 2). It is thus seen that the

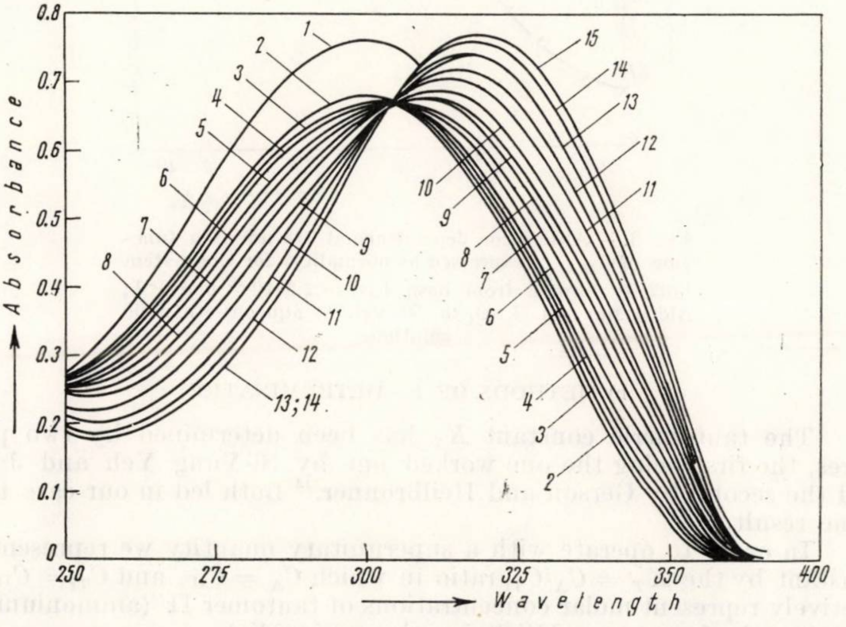

Fig. 2. — Spectral manifestation of the shifting of protolytic equilibrium system IV $\rightleftharpoons$ V with the H_2SO_4—normality increase, in 50 vol % aqueous-ethanolic solution ($C_{IV} = 2.5 \cdot 10^{-5}$ mol $\cdot l^{-1}$):

Curve N°	1	2	3	4	5	6	7	8	9	10	11	12	13	14	15
$C_{H_2SO_4}$ (val/1)	0	0.05	0.1	1.0	1.5	2.0	2.5	3.0	3.5	4.0	5.0	6.0	8.0	10.0	12.0

colourless, diprotonated species (III_{Me}) is characterized by a band with maximum at about 320 nm (321 nm fig. 1, curve *22*, respectively 318, fig. 2, curve *15*). The two successive protonation steps clearly appear as individual stages in fig. 3.

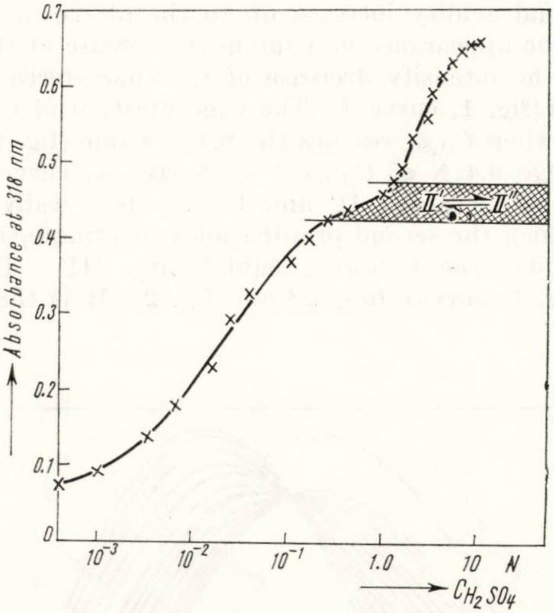

Fig. 3. — Absorption dependence at 318 nm as a function of $C_{H_2SO_4}$ (expressed as normality) for the system initially formed from base I ($C = 2.5 \cdot 10^{-5}$ mol $\cdot$ l^{-1}; Alc = Me) and H_2SO_4 in 50 vol. % aqueous-ethanolic solution.

b) METHODS OF K_T DETERMINATION

The tautomeric constant K_T has been determined by two procedures, the first being the one worked out by Si-Yung Yeh and Jaffe[12b] and the second by Gerson and Heilbronner.[14] Both led in our case to the same result.

In order to operate with a superunitary quantity we represent this constant by the $K_T = C_A/C_{Tr}$ ratio in which $C_A = C_{II'}$, and $C_{Tr} = C_{II''}$ respectively represent molar concentrations of tautomer II′ (ammonium-benzoido) and of tautomer II″ (triazinium-chinoidic).

1. — In agreement with the above mentioned authors [7b] it is reasonable to consider that the longest wavelength band at 300 nm is characterized by the same molar extinction coefficient value for both the pure compound II′ and for compound IV, which differs from the first one only by the substitution of one hydrogen atom by a methyl group in the ammonium group which is attached to the β-styryl system in the *para* position. In fact this premise is theoretically justified by the fact that the two groups $Me_2\overset{\oplus}{N}H$- and $Me_3\overset{\oplus}{N}$- must exhibit practically the same electronic effect, as it is also shown by the identical values of the substituent constants which were determined for the MeHN- and Me_2N-groups ($\sigma_{p-NHMe} = -0.83$ and $\sigma_{p-NMe_2} = -0.84$).[26]

---

[26] D. H. McDaniel and H. C. Brown, *J. Org. Chem.*, **23**, 420 (1958).

It is thus possible to determine, for each acidity value $C_{H_2SO_4}$, the concentrations C_A and C_{Tr} of species II′ and II″ by measuring the difference between the two molar extinction coefficients $\varepsilon_{IV}^{\lambda_A}$ and $\varepsilon_{VI}^{\lambda_A}$ of compounds IV and VI (at the same acidity value for the species IV) at the analytical wavelength ($\lambda_A = 300$ nm in our case) as compared with the apparent molar extinction ε^{λ_A} observed for the equilibrium mixture II′ ⇌ II″. This leads to :

$$K_T = \frac{C_A}{C_{Tr}} = \frac{\varepsilon^{\lambda_A} - \varepsilon_{Tr}^{\lambda_A}}{\varepsilon_A^{\lambda_A} - \varepsilon^{\lambda_A}} \tag{3}$$

Due to the fact that species VI (corresponding to tautomer II″) exhibits no absorbance at this wavelength ($\varepsilon_{VI}^{\lambda_A} = 0$), it results that in the entire acidity range, in which the system practically contains only the two tautomers, we have $\varepsilon_{Tr}^{\lambda_A} = 0$, so that equation (3) simplifies and becomes :

$$K_T = \frac{\varepsilon^{\lambda_A}}{\varepsilon_A^{\lambda_A} - \varepsilon^{\lambda_A}} \tag{4}$$

2. — The second procedure [14] is based on the extinction additivity both at the wavelength of the frontal band maximum of one tautomer and of that of the frontal band maximum of the other one. The additivity is expressed by the following equations :

$$\varepsilon^{\lambda_A} = \varepsilon_A^{\lambda_A} \cdot C'_A + \varepsilon_{Tr}^{\lambda_A} \cdot C'_{Tr} \tag{5}$$

$$\varepsilon^{\lambda_{Tr}} = \varepsilon_{Tr}^{\lambda_{Tr}} \cdot C'_{Tr} + \varepsilon_A^{\lambda_{Tr}} \cdot C'_A \tag{6}$$

in which C'_A and C'_{Tr} represent the molar fractions of each tautomer so that instead of relation $C_A + C_{Tr} = C_I$ (where C_I is the initial molar concentration of base I) the following equation may be written :

$$C'_A + C'_{Tr} = 1 \tag{7}$$

Deducing from eq (6) the expression for C'_{Tr} and substituting it in (5) one reaches the following equation :

$$K_T = \frac{C'_A}{C'_{Tr}} = \frac{(\varepsilon_{Tr}^{\lambda_A} \cdot \varepsilon^{\lambda_{Tr}} - \varepsilon_{Tr}^{\lambda_{Tr}} \cdot \varepsilon^{\lambda_A}) \cdot \varepsilon_{Tr}^{\lambda_{Tr}}}{(\varepsilon_A^{\lambda_{Tr}} \cdot \varepsilon_{Tr}^{\lambda_A} - \varepsilon_A^{\lambda_A} \cdot \varepsilon_{Tr}^{\lambda_{Tr}})(\varepsilon^{\lambda_{Tr}} - \varepsilon_A^{\lambda_{Tr}} \cdot C'_A)} \tag{8}$$

Due to the fact that none of the tautomer species II′ = A and II″ = Tr is not absorbing in the frontal band maximum range of the other one (just as the conjugated acids of the *p*-amino-azoderivatives),

($\varepsilon_{\mathrm{Tr}}^{\lambda_{\mathrm{A}}} = 0$ and $\varepsilon_{\mathrm{A}}^{\lambda_{\mathrm{Tr}}} = 0$), the second member of equation (8) is very much simplified. The expression of the K_T constant is thus given by the equation :

$$K_T = \frac{\varepsilon_{\mathrm{Tr}}^{\lambda_{\mathrm{Tr}}} \cdot \varepsilon^{\lambda_{\mathrm{A}}}}{\varepsilon^{\lambda_{\mathrm{Tr}}} \cdot \varepsilon_{\mathrm{A}}^{\lambda_{\mathrm{A}}}} \tag{9}$$

Besides the $\varepsilon^{\lambda_{\mathrm{A}}}$ and $\varepsilon^{\lambda_{\mathrm{Tr}}}$ values which can be directly obtained from the extinction curves of the tautomeric mixtures solutions, only $\varepsilon_{\mathrm{A}}^{\lambda_{\mathrm{A}}}$ is known from the spectrum of species IV. The value of the $\varepsilon_{\mathrm{Tr}}^{\lambda_{\mathrm{Tr}}}/\varepsilon^{\lambda_{\mathrm{Tr}}}$ ratio can be determined indirectly by means of equation (7′) which is equivalent to (7) :

$$\frac{\varepsilon^{\lambda_{\mathrm{Tr}}}}{\varepsilon_{\mathrm{Tr}}^{\lambda_{\mathrm{Tr}}}} = 1 - \frac{\varepsilon^{\lambda_{\mathrm{A}}}}{\varepsilon_{\mathrm{A}}^{\lambda_{\mathrm{A}}}} \tag{7′}$$

It may be clearly seen that when the above simplifications are justified, this procedure must lead to a K_{T} value practically identical to the one determined by Jaffé's *et al.* procedure, because by substituting the reverse value of the expression from the second member of eq. (7′) in equation (9) we reach exactly equation (4).

It has to be pointed out that the graphical method proposed by Kaminski *et al.* [18a,b,c] for the molar extinction coefficient determination of the two tautomers, based on the experimentally obtained straight line extrapolation up to the intersection with the coordinate axes – a method which was also successfully applied by the Japanese authors, for the *p*-amino-azoderivatives[22] – cannot be applied in our case because the acidity range in which the straight line, $\varepsilon^{\lambda_{\mathrm{Tr}}} = a \cdot \varepsilon^{\lambda_{\mathrm{A}}}$, can be obtained is too small, so that the extrapolation becomes inaccurate.

3. – We found that in the present case the spectrophotometric measurements can be also extended over the lower acidity range in which the protolytic equilibrium I ⇌ (II′ + II″) is established (and thus the system contains also base I, besides the two conjugated acids). This can be done, as we have $\varepsilon_{\mathrm{I}}^{\lambda_{\mathrm{A}}} \ll \varepsilon_{\mathrm{A}}^{\lambda_{\mathrm{A}}}$ and $\varepsilon_{\mathrm{I}}^{\lambda_{\mathrm{Tr}}} \ll \varepsilon_{\mathrm{Tr}}^{\lambda_{\mathrm{Tr}}}$ (practically $\varepsilon_{\mathrm{I}}^{\lambda_{\mathrm{Tr}}} = 0$).

Writing relation (10) which applies in these conditions

$$C'_{\mathrm{A}} + C'_{\mathrm{Tr}} + C'_{\mathrm{I}} = 1 \tag{10}$$

in which $C'_{\mathrm{I}} = \dfrac{\varepsilon^{\lambda_{\mathrm{I}}}}{\varepsilon_{\mathrm{I}}^{\lambda_{\mathrm{I}}}}$ and $C'_{\mathrm{A}} = \dfrac{\varepsilon^{\lambda_{\mathrm{A}}}}{\varepsilon_{\mathrm{A}}^{\lambda_{\mathrm{A}}}}$

follows that

$$C'_{\mathrm{Tr}} = \frac{\varepsilon^{\lambda_{\mathrm{Tr}}}}{\varepsilon_{\mathrm{Tr}}^{\lambda_{\mathrm{Tr}}}} = 1 - \left(\frac{\varepsilon^{\lambda_{\mathrm{I}}}}{\varepsilon_{\mathrm{I}}^{\lambda_{\mathrm{I}}}} + \frac{\varepsilon^{\lambda_{\mathrm{A}}}}{\varepsilon_{\mathrm{A}}^{\lambda_{\mathrm{A}}}} \right)$$

from which

$$K_T = \frac{C'_{\mathrm{A}}}{C'_{\mathrm{Tr}}} = \frac{\varepsilon^{\lambda_{\mathrm{A}}} \cdot \varepsilon_{\mathrm{I}}^{\lambda_{\mathrm{I}}}}{\varepsilon_{\mathrm{I}}^{\lambda_{\mathrm{I}}} (\varepsilon_{\mathrm{A}}^{\lambda_{\mathrm{A}}} - \varepsilon^{\lambda_{\mathrm{A}}}) - \varepsilon_{\mathrm{A}}^{\lambda_{\mathrm{A}}} \cdot \varepsilon^{\lambda_{\mathrm{I}}}} \tag{11}$$

As is seen, in the K_T expression there are four values which can be directly recorded, namely : ε^{λ_A}, $\varepsilon_A^{\lambda_A}$, ε^{λ_I} and $\varepsilon_I^{\lambda_I}$. As $\varepsilon_I^{\lambda_A} \neq 0$ (see fig. 1) the ε^{λ_A} values for various acidities have been corrected. Therefore, it was taken into account that $\varepsilon_I^{\lambda_A}$ is decreasing proportionally with the increase of sulphuric acid concentration, thus with the increase of the protonated II′ species concentration. The corrections thus calculated and the $\varepsilon_{cor}^{\lambda_A}$ values which allowed the computation of C'_A and C'_B values, and also of C' values, are given in table 2.

c) THE DETERMINATION OF THE TAUTOMERIC EQUILIBRIUM CONSTANTS AND THE INFLUENCE OF THE ALKYL GROUPS NATURE

As the tautomeric equilibrium constant K_T is a measure of the difference between the basicity of the amino nitrogen (pK'_{a_1}) and that of the *s*-triazine nitrogen (pK''_{a_1}) (eq. (12)) the examination of the effects of the N-alkyl groups on the pK'_{a_1} and pK'_{a_2} values is needed for the interpretation of these effects on the K_T values, because :

$$K_T = \frac{K''_{a_1}}{K'_{a_1}} \tag{12}$$

On the other hand, from the tautomeric equilibrium relations for the first protonation step, it can be shown that[27] :

$$\frac{1}{K_{a_1}} = \frac{1}{K'_{a_1}} + \frac{1}{K''_{a_1}} \tag{13}$$

and

$$K'_{a_1} = K_{a_1}(1 + K_T) \tag{14}$$

in which K_{a_1} is the apparent dissociation constant of the first protonation step.

From eqs. (14) and (12) it follows that if K_T and K_{a_1} are known values, the first dissociation constants K'_{a_1} and K''_{a_1} can be computed.

The K_{a_1} value for the two compounds (Alc $= -CH_3$ and $-C_2H_5$) has been determined directly by the graphical method [28,29] by means of fig. 4, in which $pK_{a_1} = \text{tg}\alpha$.

Concerning K_T, it was determined by means of equation (4) or (7′) and of equation (11) and the results obtained are given in tables 1 and 2 for Alc $= CH_3$, and in table 3 for Alc $= C_2H_5$.

---

[27] H. H. Jaffé and M. Orchin, "Theory and Applications of Ultraviolet Spectroscopy", John Wiley and Sons, Inc., New York, London, 1964, p. 572.

[28] S. Jerumanis and A. Bruylants, *Bull. Soc. chim. belges*, **72**, 69 (1963).

[29] E. Feytmans de Medicis and A. Bruylants, *Bull. Soc. chim. belges*, **72**, 603 (1963).

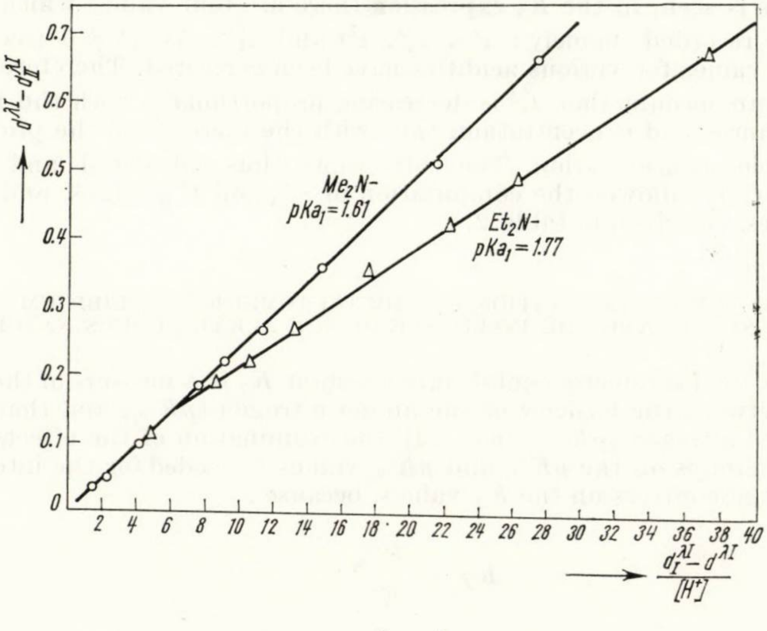

Fig. 4. — Plot of $d^{\lambda}I - d_{II}^{\lambda}I$ *versus* $\frac{d_I^{\lambda}I - d^{\lambda}I}{[H+]}$ for the determination of the $pKa_1 = \text{tg}\ \alpha$ values.

According to the data in table 2 the mean K_T value ($=3.66$) obtained by us, (eq. 11) is in very good agreement with the one based on equation (4) or (7′) ($K_T = 3.59$, table 1).

Knowing the value of pK_{a_2} (from the previous paper [1]) and of K_T, we calculated (for Alc $= CH_3$) the second ionization constants, K'_{a_2} and K''_{a_2}, by means of the following equations [27]:

$$K_{a_2} = K''_{a_2}\,(K_T + 1)$$

Table 1

Tautomeric equilibrium constant of E-1,3-dimethyl-6-(p-dimethylamino-β-styryl)-2,4-dioxo-1H,3H-1,3,5-triazine

Curve	$C_{H_2SO_4}$ val/1	$\varepsilon^{\lambda}A$	$\varepsilon_A^{\lambda}A$	K_T (C_A/C_{Tr})
11	0.4	20,500	26,800	3.26
12	0.6	20,800	26,800	3.47
13	0.8	21,000	26,800	3.62
14	1.0	21,200	26,800	3.79
15	1.5	21,200	26,800	3.79

Mean = 3.59

Table 2

Tautomeric equilibrium constant of E-1,3-dimethyl-6-(*p*-dimethylamino-β-styryl)-2,4-dioxo-1H,3H-1,3,5-triazine

Curve	$C_{H_2SO_4}$ (val/1)	$\varepsilon^{\lambda A}$	Cor.	$\varepsilon^{\lambda A}_{cor.}$	$C_A = \frac{\varepsilon^{\lambda A}_{cor.}}{\varepsilon^{\lambda A}_A}$	$\varepsilon^{\lambda I}$	$C_I = \frac{\varepsilon^{\lambda I}}{\varepsilon^{\lambda I}_I}$	$C_A + C_I$	C_{Tr}	K_T (C_A/C_{Tr})
3	5.10^{-3}	6,680	2,920	3,760	0.140	30,800	0.820	0.960	0.040	3.50
4	10^{-2}	8,400	2,520	5,880	0.220	26,680	0.717	0.937	0.063	3.50
5	2.10^{-2}	11,400	1,960	9,440	0.352	20,650	0.550	0.902	0.098	3.60
6	4.10^{-2}	14,400	1,360	13,040	0.487	14,300	0.380	0.867	0.133	3.66
7	6.10^{-2}	16,000	1,040	14,960	0,559	10,800	0.288	0.847	0.153	3.66
8	8.10^{-2}	17,000	800	16,200	0.605	8,800	0.234	0.839	0.161	3.76
9	10^{-1}	17,720	720	17,000	0.635	7,400	0.197	0.832	0.168	3.78
10	2.10^{-1}	19,370	360	19,010	0.710	4,000	0.106	0.816	0.184	3.86

Mean = 3.66

Table 3

Tautomeric equilibrium constant of E-1,3-dimethyl-6-(*p*-diethylamino-β-styryl)-2,4-dioxo-1H,3H-1,3,5-triazine

$C_{H_2SO_4}$ (val/l)	$\varepsilon^{\lambda A}$	$\varepsilon^{\lambda A}_A$	K_T (C_A/C_T)
0.4	21,800	21,800	(4.36)
0.6	22,720	26,800	5.57
0.8	22,720	26,800	5.57
1.0	22,720	26,800	5.57
1.5	22,720	26,800	5.57

Mean = 5.57

and

$$K_T = \frac{K'_{a_2}}{K''_{a_2}}$$

All the mentioned dissociation constants are given in table 4 as pK_a values.

Table 4

Various equilibrium constants of E-1,3-dimethyl-6-(*p*-dialkylamino-β-styryl)-2,4-dioxo-1H,3H-1,3,5-triazines

p-N(Alc)$_2$	pK_{a_1}	K_I	pK'_{a_1}	pK''_{a_2}	pK_{a_2}	pK'_{a_2}	pK''_{a_2}
$p-N(CH_3)_2$	1.61	3.60	1.50	0.94	−0.88	−0.77	−0.22
$p-N(C_2H_5)_2$	1.77	5.60	1.70	0.95	—	—	—

In order to find out the reason for which K_T has a greater value for Alc $= C_2H_5$ than for Alc $= CH_3$ we considered the electronic effects exhibited by the two bases belonging to type I (B band). The maximum of the bands most shifted towards greater wavelength of the mentioned species, together with those of their type II″ and II′ conjugated acids and of the metamer species IV and VI (Alc $= CH_3$), are given in table 5.

Table 5

The longest wavelength band of E-1,3-dimethyl-6-(*p*-dialkylamino-β-styryl)-2,4-dioxo-1H, 3H-1,3,5-triazines I, their conjugates acids II′, II″ and their metamer methyl-derivatives IV and VI.

Species	I B band		II′ A band		II″ Tr band	
	$\lambda_{max.}$	$\varepsilon_{max.}$	$\lambda_{max.}$	$\varepsilon_{max.}$	$\lambda_{max.}$	$\varepsilon_{max.}$
I (Alc = Me)	447	37,700	300	21,200	523	8,130
I (Alc = Et)	458	42,200	302	22,700	530	1,520
IV	—	—	300	26 ,800	—	—
VI*	—	—	—	—	520	16,800

* in H_2SO_4 0.1 N

It is seen that the N,N-diethylamino base absorbs at longer wavelength than its N,N-dimethylamino analogue. This fact is proving that the degree of resonance interaction between the lone pair electrons of the amin nitrogen and the π-electrons is greater for the former compound. In other words the contribution of the mesomeric form VII to the real state of the molecule is greater when Alc $= -C_2H_5$.

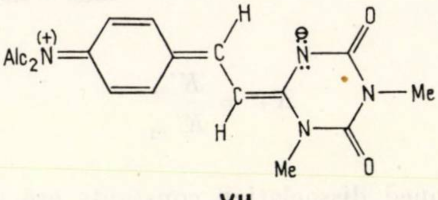

VII

For the same reason the pK''_{a_1} values increase in the order : dimethylamino < diethylamino (see table 4). The pK'_{a_1} values should therefore increase in the opposite order, namely diethylamino < dimethylamino, but actually they increase in the same order : diethylamino > dimethylamino as that for the N,N-dialkyl-aniline derivatives [23-25] and dialkylaminoazobenzenes.[22] This is due to the inhibition of the hydrogen bonding between the hydroxylic solvent and the aminonitrogen atom for base I, where Alc $= C_2H_5$. The decrease of solvation energy increases the free energy of this base and, consequently, reduces the energy gap between I (Alc $= -C_2H_5$) and its corresponding conjugated acid II′, thus increasing the basicity of this compound compared to its dimethylamino analogue. Obviously, this also finds its expression in the higher K_T value of the diethylamino-compound than that of the dimethyl-analogous ones.

EXPERIMENTAL

PREPARATION OF THE COMPOUNDS

The E-1,3-dimethyl-6-(p-*dimethylamino-β-styryl*)*-2,4-dioxo-1H,3H-1,3,5-triazine* and the corresponding *hemicyanine VI* were prepared following ref.[21] The compound IV was prepared following ref.[30]

The E-1,3-dimethyl-6-(p-*diethylamino-β-styryl*)*-2,4-dioxo-1H,3H-1,3,5-triazine* was prepared using piperidine catalysis as in the case of their *p*-dimethylamino-analogues. The same solvents for purification were used.

PREPARATION OF THE SOLUTIONS

The solutions were prepared as it was described in the previous paper (Part XV).[1] The spectra of these having the initial concentration of the base I equal to $2.5 \cdot 10^{-5}$ mol$\cdot$l^{-1} were recorded using an UNICAM SP-8000 instrument and a 1 cm cell.

---

[30] M. Safta and G. Ostrogovic, *Bul. St. Tehn., Inst. Politeh. Timişoara, Ser. chim.*, (1974), under press.

Revue Roumaine de Chimie, **19**, *11*, 1751–1758 (1974)

SYNTHESES OF NAPHTH[2,3-c]ACRIDAN-5,8,14-TRIONIC DYES

F. URSEANU, C. DRĂGHICI and V. OLTEANU
Laboratory of Chemistry and Technology of Aromatic Intermediates and Dyes, Polytechnic Institute, Bucharest, Calea Victoriei, 149

Received December 12, 1973

New syntheses for the preparation of dyes with 6-methyl-aminonapht[2,3-c]acridan-5,8,14-trione structure are described.

1. INTRODUCTION

The use of sythetic fibres on a large scale is conditioned by the output of various typical dyes. Thus, a special importance acquire disperse dyes, which can dye all categories of synthetic fibres (polyester, polyamide, polyacrylonitrile fibres) and cationic dyes used only for dyeing polyacrylonitrile fibres.

Numerous syntheses of these dyes showing various structures have been performed in recent years; among them are those with naphth[2,3-c]-acridan-5,8,14-trione structure,[1-9] which have remarkable tinctorial properties.

---

[1] D. C. Eaton and F. Irving, Brit. Pat. 944 513, Nov. 1, 1960; *Chem. Abstr.*, **60**, 10 846 a (1964).

[2] D. C. Raton, Brit. Pat. 944 722, Dec. 6, 1960; *Chem. Abstr.*, **60**, 10 846e (1964).

[3] Thoms River Chemical Corp., Brit. Pat. 1 027 576., Sept. 27, 1963; *Chem. Abstr.*, **65**, 2 392d (1966).

[4] Farbenfabriken Bayer, Brit. Pat, 775 802, May 29, 1957; *Chem. Abstr.*, **51**, 15 142 a (1957).

[5] F. Urseanu and M. Preoteasa, *Rev. Chim. (București)*, **22**, 583 (1971).

[6] F. Urseanu, M. Gheorghiu and L. Indrei, *Rev. Chim. (București)*, **24**, 165 (1973).

[7] F. Urseau, R. Vintilă and G. Nazarie, *Rev. Chim. (București)*, **24**, 517 (1973).

[8] F. Urseanu, C. Drăghici, R. Vintilă and E. Sliam, *Rev. Roum. Chim.*, **18**, 1019 (1973).

[9] J. Haase and A. Boehmova, Ceh. Pat. 97 989, Ian. 15, 1961; *Chem. Abstr.*, **58**, 6809 (1963).

In the present work we discuss the synthesis of three 6-methylaminonaphth[2,3-c]acridan-5,8,14-trione derivatives with the following general formula :

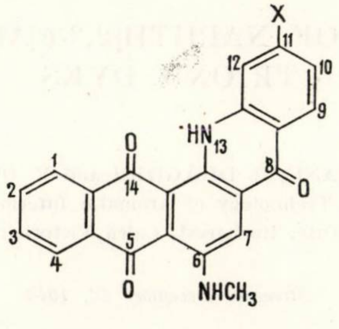

in which $X = NO_2,\ NH_2,\ NHCOCH_2\overset{+}{N}C_5H_5]Cl^-$

2. SYNTHESIS OF 6-METHYLAMINONAPTH[2,3-C]ACRIDAN-5,8,14-TRIONE DERIVATIVES

From the starting material 1-methylamino-4-bromoanthraquinone I, 6-methylaminonaphth [2,3-c]acridan-5,8,14-trione derivatives were obtained based on the reaction schemes given below.

2.1. CONDENSATION OF 1-METHYLAMINO-4-BROMOANTHRAQUINONE WITH 4-NITROANTHRANILIC ACID

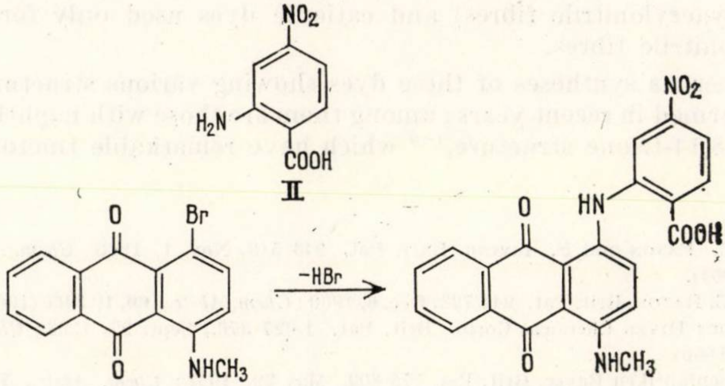

Condensation was performed by the Ullmann reaction,[10-12] by heating the reagents I and II in nitrobenzene at 180° for 10 hours, in the

---

[10] F. Ullmann, *Ber. dtsch. chem. Ges.*, **43**, 536 (1910).

[11] F. Ullmann and M. Sonne, *Liebigs Ann. Chem.*, **380**, 336 (1911).

[12] F. Ullmann and P. Ochsner, *Liebigs Ann. Chm.*, **381**, 1 (1911).

presence of copper powder and copper sulphate as catalysts and anhydrous sodium acetate, necessary to neutralize the hydrobromic acid formed during the reaction; 4-methylamino-1-anilinoanthraquinone-5′-nitro-2′-carboxylic acid III are thus obtained.

2.2. ACRIDONIC RING CLOSURE IN 4-METHYLAMINO-1-ANILINOANTHRAQUINONE-5′-NITRO-2′-CARBOXYLIC ACID

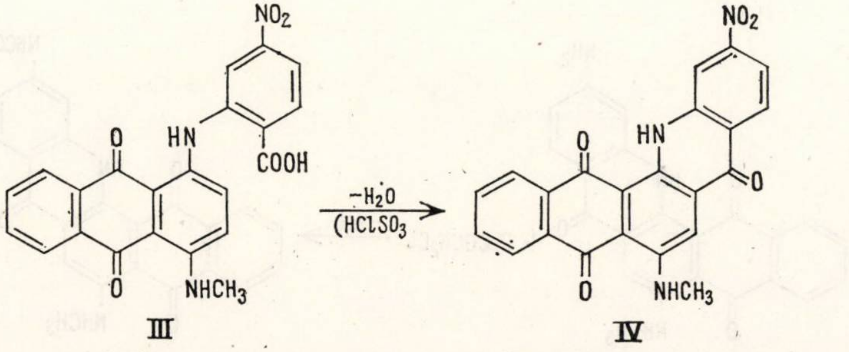

Acridonic ring closure was achieved in $HClSO_3$, at a temperature between 65—70°, at a relative short reaction time (15 minutes), according to literature procedures.[5,6,8,13] At the end the mixture was poured on ice in order to decompose the excess of chlorosulphonic acid and to precipitate the acridonic dye formed: 6-methylamino-11-nitronaphth[2,3-c]acridan-5,8,14-trione (III).

2.3. SYNTHESIS OF 11-AMINO-6-METHYLAMINONAPHTH[2,3-c]ACRIDAN-5,8,14-TRIONE

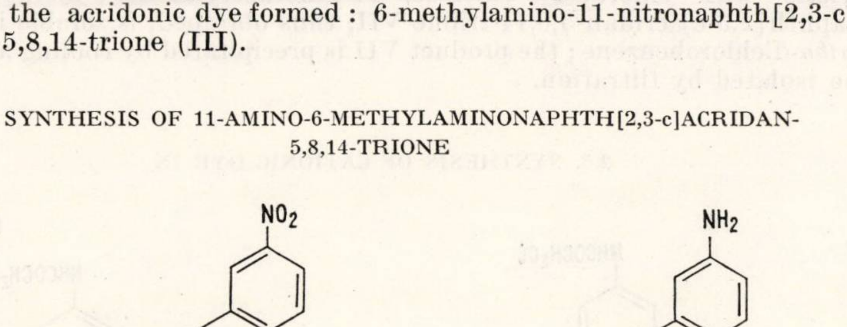

---

[13] B. S. Ioshi, B. D. Tilak and K. Venkataraman, *Proc. Indian Acad. Sci.*, **32A**, 201 (1950).

11-Amino-6-methylaminonaphth [2,3-c]acridan-5,8,14-trione dye V has been obtained by reduction with aqueous solution of natrium sulphide in N.N-dimethylformamide of the corresponding 6-methylamino-11-nitronaphth[2,3-c]acridan-5,8,14-trione derivative IV; reduction was performed by a three hours at 90°.

2.4. SYNTHESIS OF 11-CHLORACETYLAMINO-6-METHYLAMINONAPHTH[2,3-c] ACRIDAN-5,8,14-TRIONE (VII)

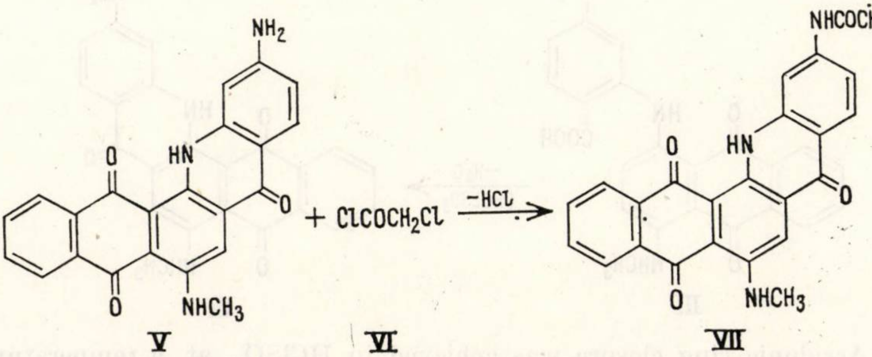
NH$_2$
O
HN
O
O
NHCH$_3$
+ ClCOCH$_2$Cl
−HCl
NHCOCH$_2$Cl
O
HN
O
O
NHCH$_3$
V
VI
VII

Acylation was carried out by heating at 160° for 2 hours in *ortho*-dichlorobenzene of 11-amino-6-methylaminonaphth[2,3-c] acridan-5,8,14-trione with chloracetyl chloride. 11-Chloracetylamino-6-methylaminonaphth[2,3-c]acridan-5,8,14-trione VII, thus obtained, is soluble in warm *ortho*-dichlorobenzene; the product VII is precipitated by cooling and may be isolated by filtration.

2.5. SYNTHESIS OF CATIONIC DYE IX

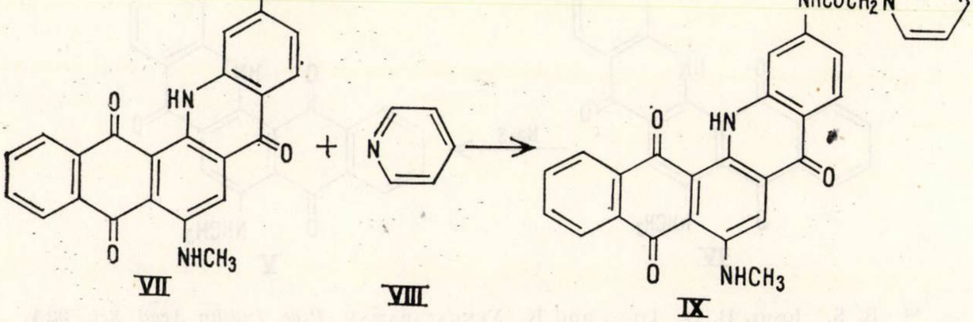
NHCOCH$_2$Cl
O
HN
O
O
NHCH$_3$
+
N
Cl
NHCOCH$_2$N$^+$
O
HN
O
O
NHCH$_3$
VII
VIII
IX

The solution of 11-chloracetylamino-6-methylaminonaphth [2,3-c] acridan-5,8,14-trione in *ortho*-dichlorobenzene was treated with calculated quantities of pyridine, at 130–140° for 15–20 minutes; cationic dye IX, thus formed by quaternization, is insoluble in *ortho*-dichlorobenzene.

3. EXPERIMENTAL

3.1. A mixture of 3.16 g (10 mmol) 1-methylamino-4-bromo-anthraquinone (I), 9.1 g (50 mmol) 4-nitroanthranilic acid (II), 1 g CH_3COONa, 0.1 g copper powder and 0.06 g $CuSO_4$ in 4 0 ml nitrobenzene is heated at 180° for 10 hours; the colour of the reaction mixture turns gradually from reddish-violet to bluish-violet. The conversion of 1-methylamino-4-bromoanthraquinone to product III is followed by means of paper-chromatography (eluent CH_3COOH 80%).

Finally, when the reaction is over, the mixture is cooled to 20°, filtered and the precipitate washed with benzene until the filtrate is colourless, dried at 80–85°, affording 10 g product (III + excess of II).

3.2. The 10 g of previously obtained mixture from the compounds III and II are dissolved in 80 ml $HClSO_3$ and the resulted solution is heated at 65–70° for 15 minutes. (A drop from the mixture, decomposed with water, forms a blue-green precipitate). The mixture is cooled at 20°, poured over 250 g crushed ice and the precipitate washed with water until the filtrate is neutral and colourless and dried at 75–80°. 3.5 g dye IV are obtained (87.7 yield from I).

Note: Since a quantity of the excess of compound II is dissolved in the aqueous acid filtrate, it may be recovered by precipitation with 25% ammonia solution at pH =4–4.5, filtered and dried 4.6 g compound II is thus recovered.

3.3. 1.999 g (5 mmol) compound IV are dissolved in 50 ml N.N-dimethylformamide at 80°; in the solution thus resulted a warm solutions of 0.45 g Na_2S in 10 ml water is droped for 15 min. The reaction is completed by heating at 90° for 3 hours; the mass colour turns from light green to dark green. The formation of the amino group by reducing the nitro group is determined by a characteristic colour reaction with the help of the Erlich reagent. Then, 50 ml water is added, the mixture cooled at 5–10°, neutralized with concentrated HCl at pH = = 7, the precipitate formed is filtered, washed with 50 ml water and dried at 70–80°, yielding 1.51 g dye V (81.9% yield).

3.4. 1.476 g(4 mmol) compound V are dissolved in 20 ml *ortho*-dichlorobenzene at 150–160°, then 0.37 ml (0.551 g; 4.88 mmol) chloracetyl chloride VI is added. The reaction is completed by heating at 160° for 2 hours; the mass colour turns from green to violet.

3.5. The warm solution of compound VII in *ortho*-dichlorobenzene is treated with 0.4ml (0.386 g; 4.88 mmol) pyridine VIII, at 130–140° for 15–20 minutes, the precipitate formed is filtered, washed with 10 ml benzene and dried at 30–40° and p = 10 mm Hg; 1.46 g dye IX are obtained (86% yield from V).

4. ANALYSES

The analyzed compounds * were previously purified by recrystallization from an appropriate solvent: ethanol, nitro-benzene (see table 1). The purified compounds were subjected to elemental, chromatographic, spectral and tinctorial analyses.

---

* Analyses were also made for the I and II compounds used as starting materials in this work and synthesized in laboratory according to literature procedures.[14–17]

[14] H. Sanielevici and L. Floru, "Sinteza intermediarilor aromatici și a coloranților", ed. 2, Ed. didactică și pedagogică, Bucharest, 1971, p. 63.

[15] BIOS Final Rep., 1484, p. 19.

[16] R. Justoni, M. Terruzzi and C. Pirola, *Farm. Sci. e tec.* (*Pavia*), 3059 (1948); *Chem. Abstr.*, **42**, 7 273e (1948).

[17] BIOS Final Rep., 1 153, p. 156.

4.1. ELEMENTAL ANALYSIS

Microcombustions were carried out, determining the nitrogen after the micro-Dumas method, while carbon, hydrogen and bromine were analyzed according to the modified Pregl method. The results are presented in table 1.

Table 1

Elemental analysis

Compound	Empirical formula	Solvent for recrystallization	M P °C	C % *Calcd.* *Found*	H % *Calcd.* *Found*	N % *Calcd.* *Found*	Br % *Calcd.* *Found*
I	$C_7H_6O_4N_2$	ethanol	179	46.16 46.35	3.32 3.48	15.38 15.12	—
II	$C_{15}H_{10}O_2NBr$	ethanol	269	56.98 57.17	3.19 3.38	4.43 4.16	25.27 24.98
IV	$C_{22}H_{13}O_5N_3$	nitrobenzene	>300	66.41 66.70	3.28 3.51	10.52 10.70	—
V	$C_{22}H_{15}O_3N_3$	nitrobenzene	>300	71.53 71.80	4.09 4.24	11.37 11.56	—

4.2. CHROMATOGRAPHY

Chromatographic analyses were carried out on Whatman paper No. 3 in ascendent system, at 25°, in order to follow the reactions and to check the purity of recrystallized compounds. The results are presented in table 2.

Table 2

Paper chromatography

Compound	I	II	III	IV	V	IX
Solvent	CH_3COOH	CH_3COOH	CH_3COOH	DMF	DMF	water
Eluent	CH_3COOH 80 %	CH_3COOH 80 %	CH_3COOH 80 %	HCOOH	HCOOH	CH_3COOH 80 %
Elution time (min)	40	40	40	15	15	20
R_f	0.117	0.686	0.357	0.250	0.715	0.890

DMF = N.N-dimethylformamide

In the case of eluents CH_3 COOH 80% and HCOOH, the chromatographic paper was impregnated with a 10% solution of 1-bromonaphthalene in ethanol.

4.3. SPECTRAL ANALYSIS

Infrared, ultraviolet and visible absorption spectra of the products were recorded.

IR spectra were recorded using a UR–10 spectrophotometer, in pellet KBr.

Characteristic vibration frequencies ν [cm^{-1}] :

Compound I : 720 v.s. ; 731 s. ; 998 s ; 1118 v.s. ; 1270 v.s. ; 1515 v.s. ; 1597 v.s. ; 1630 v.s. ; 1667 v.s. ; 2955 w. ; 3075 w. ; 3276 m.

Compound II : 731 v.s. ; 821 v.s. ; 1258 v.s. ; 1358 v.s. ; 1430 v.s. ; 1531 v.s. ; 1571 v.s. ; 1681 v.s. ; 2200–3300 ; 3395 v.s. ; 3512 v.s.

Compound IV : 731 s. ; 745 s. ; 1019 s. ; 1245 v.s. ; 1270 v.s. ; 1290 v.s. ; 1349 v.s. ; 1530 v.s. ; 1581 v.s. ; 1607 v.s. ; 1640 v.s. ; 3320 s. ; 3439 s.

Compound V : 731 m. ; 785 m ; 1021 s ; 1275 v.s. ; 1496 s. ; 1578 v.s. ; 1611 s. ; 3310 w. ; 3430 w.

Compound VII : 741 w. ; 789 w. ; 1026 m. ; 1050 m. ; 1247 m. ; 1270 s. ; 1590 s. ; 1620 m. ; 1699 m.

(w = weak ; m = medium ; s = strong ; v.s. = very strong).

Ultraviolet and visible spectra were determined with a Specord apparatus. Determinations were made in N.N.-dimethylformamide (for compounds IV and V) and water (for compound IX), also the extinction coefficients ε_{max} were calculated.

The characteristic absorption maxima λ_{max} and $\lg \varepsilon_{max}$ are presented in table 3.

Table 3

Maxima absorption in ultraviolet and visible

Compound	DMF $\lambda_{max.}$ [nm]	$\lg \varepsilon_{max}$	Compound	DMF $\lambda_{max.}$ [nm]	$\lg \varepsilon_{max}$	Compound	H_2O $\lambda_{max.}$ [nm]	$\lg \varepsilon_{max}$
IV	357 657.8	4.042 4.305	V	330 389 481 627 660	4.341 4.052 3.702 4.223 4.222	IX	261.1 566.5	4.450 3.464

DMF = N.N-dimethylformamide.

5. UTILIZATION OF THE PRODUCTS

The IV and V compounds synthesized were used as disperse dyes for "Terom" polyester fibres, while IX compound was used as cationic dye for polyacrylonitrile fibres.

Results of determinations are presented in table 4. The colours were defined according to C.I. Hue Chart.[18] A good agreement is observed between the colours seen on the dyed fibres and the values of absorption maxima.[19]

Table 4

Determinations with dyed fibres

Compound	Dyed fibres	Colour	Fastness					
			Light	Cold water	Washing at 40°	Perspiration		Rubbing
						acid pH = 5.5	alkaline pH = 8.4	
IV	PE	bluish green 40	5−6	5/5/5	5/5/5	4−5/5/4−5	4−5/5/4−5	5
V	PE	green (bright) 17	5	5/5/5	5/5/5	4−5/5/4−5	4−5/5/4−5	5
IX	PNA	bluish violet 37−13	4−5	5/5/5	5/5/5	5/5/5	5/5/5	4−5

PE = polyester fibres
PNA = polyacrylonitrile fibres

---

[18] C. I. Hue Indication Chart, American Association of Textile Chemists and Colourists, Lowell Institute, Lowell Massachusetts, USA.

[19] C. D. Nenițescu, "Chimia Organică", vol. 2, ed. 6, Ed. didactică și pedagogică, Bucharest, 1968, p. 520.

Revue Roumaine de Chimie, **19**, *11*, 1759–1766 (1974)

NEW DIRECTION OF SUBSTITUTED 4-HYDROXY ACIDS DEHYDRATION LEADING TO 2,3-DISUBSTITUTED 1-ACETOXY-NAPHTHALENES

DIANA M. MONDESHKA and I. G. ANGELOVA
Department of Organic Chemistry, Higher Institute of Chemical Technology
Sofia 56, Bulgaria

Received November 23, 1973

The dehydration reaction of several substituted 4-phenyl-3-hydroxy acids under the action of different agents has been investigated. It has been shown that the reaction discovered with 2,4-diphenyl-3-methyl-3-hydroxybutanoic acid, namely, its conversion on dehydration in acetic anhydride in the presence of anhydrous zinc chloride into 2-phenyl-3-methyl-1-acetoxy-naphthalene has a general validity and the dehydration of the above mentioned hydroxy acids leads also to the corresponding 1-acetoxy-naphthalenes. It has been found that in the presence of $AlCl_3$ a retro-aldol type decomposition of the hydroxy acids took place first, instead of cyclization to acetoxy-naphthalenes. It has been established that under the action of concentrated sulphuric acid mainly γ-lactones or indene-1-ones are formed. The structures of the obtained compounds are proved by UV, IR and NMR spectra.

Previous papers reported that in the attempts to obtain α, β-unsaturated methyl ketones from 2,4-diphenyl-3-methyl-3-hydroxybutanoic acid **(1a)** according to a previously proposed method (dehydration in acetic anhydride in the presence of anhydrous zinc chloride),[1,2] only trace amounts of unsaturated ketones were formed whereas, instead, the main product was a 2,3-disubstituted 1-naphthol which was acetylated under reaction conditions.[3]

Pertinent literature data, though comparatively scarce, offer some information as to the 2,4- and 3,4-diaryl- or alkyl-aryl-substituted 1-naphthols (or acetoxy naphthalenes). Several compounds were obtained but in relatively low yields and in a rather complicated manner.[4-6] Contrary to this there are almost no data concerning the preparation of the more difficult to be obtained 2,3-disubstituted isomers. Only one of the latter compounds has been quite recently reported.[7] On the other hand,

---

[1] CH. P. IVANOV and D. M. MONDESHKA, *Compt. rend. Acad. bulg. Sci.*, **20**, 1287 (1967).

[2] CH. P. IVANOV and D. M. MONDESCHKA, *J. prakt. Chem.*, **315**, 993 (1973).

[3] CH. P. IVANOV and D. M. MONDESHKA, *Tetrahedron*, **29**, 1745 (1973).

[4] R. T. ARNOLD and Y. S. BUCKLEY, *J. Amer. Chem. Soc.*, **71**, 1781 (1949).

[5] B. EISTERT and W. MENNICKE, *Chem. Ber.*, **100**, 3495 (1967).

[6] R. HUISDEN, L. A. FELLER and P. OTTO, *Chem. Ber.*, **102**, 3405 (1969).

[7] G. HENSEKE, H. SCHIEFER, C. KIPPING and K. SCHOENFELDER, Ger. (East), 71, 770, 20 March 1970 ; *Chem. Abstr.*, **74**, P 22605 f.

when trying to cyclize some 1,3-diaryl-2-arylmethyl-2-hydroxyglutaric acids to substituted benz- and dibenzanthrols by means of concentrared sulphuric acid it has been observed that on attempting to isolate from the reaction mixture the above compounds, they easily tautomerized to corresponding anthrones and, therefore, were not obtained in pure form.[8]

The purpose of the present investigations was to study the dehydration reaction of the substituted 4-phenyl-3-hydroxy acids **(1b—d)**, some of which may cyclize to indene-1-ones as well **(1d)** and to check whether under the above conditions the main direction of the reaction would lead to the formation of 2,3-disubstituted 1-acetoxy-naphthalenes. We also aimed to see whether a cyclization reaction would take place in a higher degree under the action of stronger cyclizing agents such as $AlCl_3$. Finally, we set ourselves the task to check if the dehydration of **1a-d** by means of concentrated sulphuric acid would bring about the formation of the corresponding 1-naphthols and whether the latter, if formed, would tautomerize during their isolation similarly to polynuclear phenols.

The present paper reports the result of a study on the dehydration of 2,4-diphenyl-3-methyl-3-hydroxybutanoic acid **1a**, 2,4-diphenyl-3-ethyl-3-hydroxybutanoic acid **1b**, 2,4-diphenyl-3-benzyl-3-hydroxybutanoic acid **1c** and 2,3,4-triphenyl-3-hydroxybutanoic acid **1d**.

The acids **1a-d** were prepared from magnesosodium phenylacetate and benzyl ketones.[9] The main isomer was purified by recrystallization. As the dehydration reaction of substituted β-hydroxy acids does not proceed stereospecifically,[2,10-14] some of the experiments were carried out with a treo-eritro acids mixture.

The dehydration of **1b-d** was carried out after[15] as well as after modified,[2] the latter leading mainly to the formation of α,β-unsaturated methyl ketones **3a-e** or **3'a-f**, on dehydration

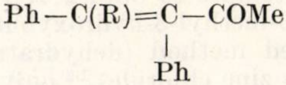

$$Ph-C(R)=\underset{Ph}{\underset{|}{C}}-COMe$$

3a-e

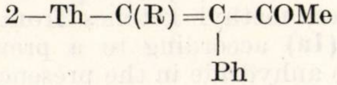

$$2-Th-C(R)=\underset{Ph}{\underset{|}{C}}-COMe$$

3'a-f

3a	R = Me	3d	R = Ph		3'a,B	R = Me
3b	R = Et	3e	R = Naphth		3'c,d	R = Et
3c	R = CH_2Ph				3'e	R = Ph
					3'f	R = 2 — Th

of 3-arylsubstituted-3-hydroxy acids.[1-3] The reaction mixture was treated as described,[1-3] i.e. hydrolysis with water, extraction of the organic products with ether and isolation of the neutral compounds. The composition of the neutral products was measured by TLC and IR-spectroscopy, the presence of absorption bands at about 1770, 1370 and 1200 cm^{-1} being an indication of the formation of acetylated 1-naphthols. It was observed that the yields of the acetoxy-naphthalenes formed, arose with the increase of the quantity of zinc chloride, optimal results being 0.6 — 0.7 g $ZnCl_2$ for 1 g hydroxy acid. At the same time a retroaldol type decomposition of **1b-d** into the initial ketones and phenyl-acetic acid took place as well,[2,3,16] though in a small degree. On dehydration after both methods[2,15] only traces of unsaturated ketones of type **3** were formed, as revealed by TLC and IR-spectra.

---

[8] Ch. P. Ivanov and L. Mladenova-Orlinova, "Yearbook of the Higher Institute of Chemical Technology-Sofia", **11**, 201 (1964).

[9] D. Ivanov and Al. Spassov, *Bull. Soc. chim. France*, **1931**, 377.

[10] E. Zimmerman and L. Ahramjian, *J. Amer. Chem. Soc.*, **81**, 2086 (1959).

[11] Ch. Kratchanov and B. Kurtev, *Tetrahedron Letters*, **1965**, 3085.

[12] B. Kurtev and Ch. Kratchanov, *J. Chem. Soc. (B)*, **1969**, 649.

[13] D. Noyce and W. Reed, *J. Amer. Chem. Soc.*, **80**, 5539 (1958); D. Noyce and L. Snyder, *ibid.*, **81**, 620 (1959).

[14] D. Noyce and Ch. Lane, *J. Amer. Chem. Soc.*, **88**, 1635 (1962).

[15] W. Johnson and J. Goldman, *J. Amer. Chem. Soc.*, **67**, 430 (1945).

[16] Ch. P. Ivanov and D. M. Mondeshka (to be published).

As we could not succeed to isolate pure compounds by recrystallization, the mixture of neutral products (72%—78% of the initial hydroxy acid) were subjected to preparative TLC. From the neutral products obtained by dehydration of **1b**, respectively **1c**, we isolated colourless crystalline compounds, stilbenes and complex mixture of other substances, the latter containing the initial ketone and α, β-unsaturated ketone (IR : bands at about 1715 cm^{-1} and 1690 cm^{-1}). In the IR spectra of the crystalline compounds appeared two intensive absorption bands at about 1770 cm^{-1} and 1200 cm^{-1} (the latter being split and of higher intensity) as well as a medium intensive band at about 1370 cm^{-1}. The UV spectra showed the multiplet structure, characteristic of naphthalene derivatives, the longest-wave maxima being positioned at about 322 nm. The NMR spectra of the above compounds confirmed their structures of 2-phenyl-3-ethyl-1-acetoxy-naphthalene **(2b)** and 2-phenyl-3-benzyl-1-acetoxy-naphthalene **(2c)**.

The dehydration of **(1d)** was carried out in the same way. The isolated mixture of neutral products, unlike to the above-mentioned experiments, was orange in colour. Its IR-spectrum revealed 3 bands in the region of carbonyl absorption, the most intensive one being positioned at 1776 cm^{-1}. The second one, of smaller intensity, was at 1721 cm^{-1}, i.e. in the range of carbonyl absorption of the five-membered conjugated ketones. From the mixture of neutral compounds besides stilbenes and small quantity of phenyl-benzyl ketone, an orange crystalline compound and a colourless one were isolated by preparative TLC. The orange compound was identified, by its m.p., IR spectrum and specific staining with concentrated sulphuric acid as the already known 2-phenyl-3-benzyl-indene-1-one, formed by intramolecular cyclization of the carboxyl group with the phenyl substituent at β-position in the hydroxy acid. On the basis of IR, UV and NMR spectra the colourless crystalline compound was assigned the structure of 2,3-diphenyl-1-acetoxy-naphthalene **(2d)**, obtained by intramolecular cyclization of the carboxyl group with the phenyl substituent at γ-position, followed by acetylation of the phenolic hydroxyl group. These results show that the formation of a naphthalene system from 4-phenyl-substituted-3-hydroxy acids has general validity and represents the main direction of the dehydration reaction of these acids under the above-stated conditions. Due to the comparatively good yields in which the described compounds were obtained, this new route of dehydration could be successfully used as a method of preparation of different 2,3-disubstituted 1-naphthols. From the above results it follows also that the formation of the naphthalene system is preferred here in comparison with the indene-1-one system, as shown by experiments with **1d**.

Formation of naphthalene derivatives could be explained by the following scheme:

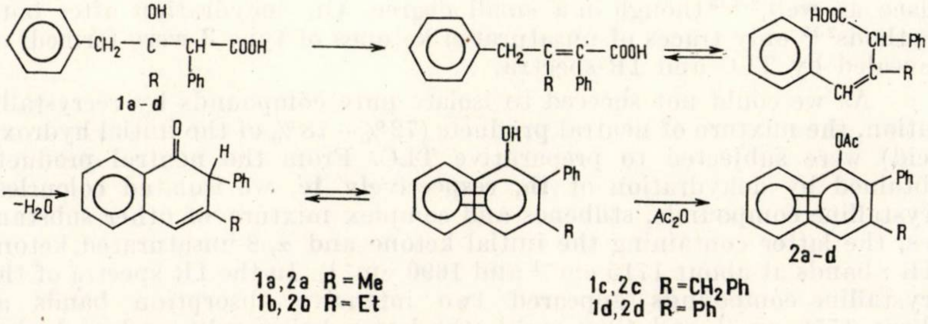

Whether the α, β-unsaturated acid is isomerized previously to the corresponding β, γ-unsaturated acid or first a cyclization to dihydro-ketonaphthalene takes place with the subsequent isomerization of the C=C bond, could not be affirmed with certainty. We assume, as more probable, a previous isomerization to β, γ-unsaturated acid having in view that the formation of α, β-unsaturated methyl ketones is evidently impeded. According to the proposed mechanism these ketones are formed through decarboxylation of the mixed anhydride of the corresponding α, β-unsaturated acid with the acetic acid.[1,2]

Further experiments for cyclization of **1a-d** were carried out in acetic anhydride in the presence of $AlCl_3$. Because of its greater catalyst ability, a higher degree of cyclization could be expected. Nevertheless all experiments proved that $AlCl_3$ favoured mainly the retro-aldol-type decomposition of **1a-d**; the cyclization reaction to substituted acetoxynaphthalenes proceeded at a much smaller rate. Such type of decomposition took place especially in the case of acids containing an aryl-substituent at the carbon atom connected with the tertiary hydroxyl group. These results are in agreement with the preliminary data obtained on dehydrating 3-aryl-substituted-3-hydroxy acids to indene-1-ones,[17] and show that $AlCl_3$ is not a very suitable cyclizing agent for substituted hydroxy acids.

Dehydration of **1a-d** by concentrated sulphuric acid was studied in order to check the possibility for their cyclization to free 1-naphthols as well as to establish the conditions under which they could be isolated having in view their tautomerism. Dehydration was carried out with 97% sulphuric acid within 5–15 min. The reaction mixtures were treated after the already known method [18] including consecutively isolation of sulphonic acids (extraction with water), of carboxylic acids (with Na_2CO_3 aq), of phenols (extraction with 2% NaOH aq) and of neutral compounds. Under the action of sulphuric acid, diarylsubstituted acids **1a, b**, especially **1a**, gave a high yield of substituted γ-lactones **4a, b**. The corresponding substituted 1-naphthols were formed in small quantities and mainly as the tautomeric dihydro-keto-naphthalenes as shown by the IR spectra (medium to intensive bands at about 1668 cm^{-1} and a very weak absorption at about 3550 cm^{-1}). From **1b** a mixture of two isomeric γ-lactones was obtained, one of which, **4b**, could be isolated. The second one, formed in small quantity, has probably structure **5**, on the basis of its IR and NMR spectra (the latter taken as a mixture with **4b**). The formation of **4a, b** could be explained by the rapid isomerization of α, β-unsaturated acids to the corresponding β, γ-ones with subsequent cyclization of the latter according to the scheme:

---

[17] D. M. Mondeshka (unpublished results).

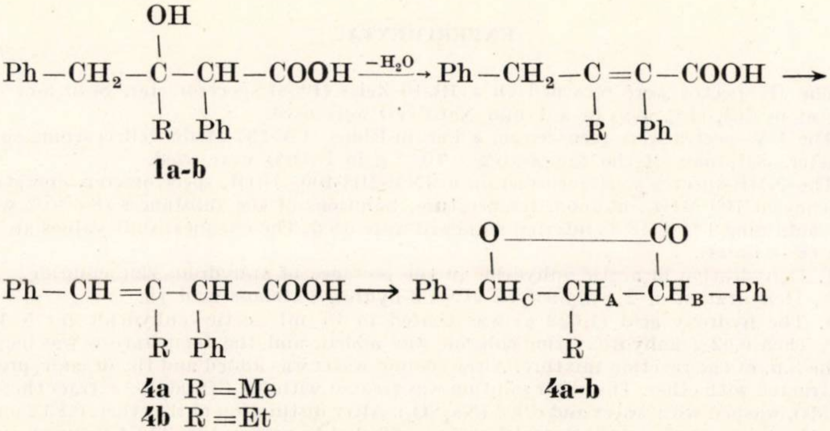

$$\mathrm{Ph{-}CH_2{-}\underset{R}{\overset{OH}{C}}{-}\underset{Ph}{CH}{-}COOH \xrightarrow{-H_2O} Ph{-}CH_2{-}\underset{R}{C}{=}\underset{Ph}{C}{-}COOH \longrightarrow}$$

1a-b

$$\mathrm{Ph{-}CH{=}\underset{R}{C}{-}\underset{Ph}{CH}{-}COOH \longrightarrow Ph{-}\overset{O}{CH_C}{-}\underset{R}{CH_A}{-}\overset{CO}{CH_B}{-}Ph}$$

4a R = Me
4b R = Et

4a-b

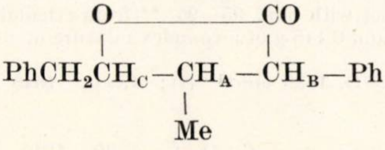

$$\mathrm{PhCH_2\overset{O}{CH_C}{-}\underset{Me}{CH_A}{-}\overset{CO}{CH_B}{-}Ph}$$

5.

Dehydration of **1d** led to a complex mixture of products: stilbenes, phenyl-benzyl ketone, 2-phenyl-3-benzyl-indene-1-one as well as to small quantities of γ-lactone and of the corresponding 1-naphthol, as seen from TLC and the IR-spectrum.

We did not succeed to isolate 1-naphthol, as in the experiments with **1a, b** evidently because of its fully conversion during isolation into the corresponding tautomeric dihydro-ketonaphthalene, as evidenced by the IR-spectrum : the absorption band at 3550 cm^{-1} disappeared and only an intensive one at 1665 cm^{-1} was observed. Dehydration of **1c**, contrary to that of **1a, b, d** proceeded at a lower rate with lactonization. Instead, the quantity of 1-naphthol, 2-phenyl-3-benzyl-1-hydroxy-naphthalene(**6**), increased and we succeeded in isolating part of it. The primary formation of a naphthol, in this case only, is difficult to be explained at the present stage.

---

[18] Ch. P. Ivanov and L. Mladenova-Orlinova, "Yearbook of the Higher Institute of Chemical Technology-Sofia", **10**, 257 (1963).

Nevertheless, the above results show that the products obtained under the action of sulphuric acid are strongly dependent on the initial hydroxy acid. The main directions of the dehydration reaction lead here to the formation of either substituted γ-lactones or indene-1-ones. A cyclization to the naphthalene system proceeds at an insignificant rate (with the exception of **1c**) and this method can be used for the preparation of substituted 1-naphthols only in limited cases.

EXPERIMENTAL

The IR-spectra were recorded on a IR-10 Zeiss (1958) spectrometer. Solutions of the substances in CCl_4 (1 % w/v) in a 1 mm NaCl cell were used.

The UV-spectra were recorded on a Perkin-Elmer, UV-137 Model selfrecording spectrophotometer. Solutions of the samples (2×10^{-5} g in EtOH) were used.

The NMR-spectra were recorded on a JNM-MH-100, JEOL spectrometer, operating at a frequency of 100 MHz., at room temperature. Solutions of the substances (8—10 % w/v) in $CDCl_3$, containing 1 % TMS as internal standard were used. The chemical shift values are given in ppm (δ — units).

1. Dehydration in acetic anhydride in the presence of anhydrous zinc chloride.

A. Dehydration of 2,4-diphenyl-3-ethyl-3-hydroxybutanoic acid 1b.

a. The hydroxy acid (1.022 g) was heated in 15 ml acetic anhydride for 5 hrs at 60—65°. Then 0.62 g anhydrous zinc chloride was added, and the temperature was increased up to the b.p. of the reaction mixture. After cooling water was added and the organic products were extracted with ether. The ether solution was treated with Na_2CO_3 aq (to extract the carboxylic acids), washed with water and dried (Na_2SO_4). After distillation of the ether, 0.83 g mixture of neutral products was obtained, which when subjected to preparative TLC* (solvent system, light petroleum : benzene : acetone = 45 : 15 : 1) yielded : 0.186 g stilbenes, 0.297 g (28.5 % of the initial acid) of a colourless crystalline product with m.p. 95—96° **(from ethanole) 2b, 0.035 g of light yellow noncrystalline substance 3b and 0.145 g of a complex mixture of neutral products.

Non-crystalline substance. IR-spectrum : $\nu C{=}O$, 1689 cm^{-1} (s) ; $\nu C{=}C$, 1640 cm^{-1} (vw) and $\delta_s CH_3CO$, 1363 cm^{-1} (m).

Substance with m.p. 95—96°.

IR-spectrum : —O.Ac : $\nu C{=}O$, 1771 cm^{-1} (vs) ; ν_s, $\nu_{as}{=}C{-}O{-}C$, 1190, 1215 cm^{-1} (vs. split) and 1040 cm^{-1} (m) ; δ_s CH_3CO, 1370 cm^{-1} (s).

UV-spectrum : λ_{max} at 252,287 and 325 nm.

NMR-spectrum: C_2H_5: 1.10 ppm (tr, 3H; $J=7.4$c/s) and 2.54 ppm (q,2H; $J=7.4$ c/s) ; O.Ac : 1.94 ppm (s,3H) ;
aromatic protons : 7.08—7.80 ppm(m, 10 H)

Found : C, 82.87 ; H, 6.40

Calcd. for $C_{20}H_{18}O_2$: C, 82.75 ; H, 6.25

b. The hydroxy acid (0.514 g) was heated in 10 ml 1 : 1 mixture of Ac_2O and glacial AcOH and 0.3g anhydrous zinc chloride for 40—45 min at the b.p. of the reaction mixture. The mixture was hydrolysed and treated as described in 1A. The mixture (0.370 g) of neutral products was subjected to preparative TLC under above conditions. The isolated products were

---

* For TLC Silica Gel Merck (type 60) has been used.

** All melting points (incorrected) were taken on a Koffler apparatus.

0.105 g stilbenes 0.123 g (23.7%) crystals with m.p. 95–96°, 2b, and a complex mixture of other substances.

B. Dehydration of 2,4-diphenyl-3-benzyl-3-hydroxybutanoic acid 1c.

a. According to 1Aa, 1.051 g hydroxy acid gave 0.792 g mixture of neutral products which when subjected to preparative TLC (light petroleum : chloroform : acetone=50 : 5 : 1.5) yielded 0.210 g stilbenes, 0.345 g (32.2%) colourless crystals with m.p. 98–99° (from ethanol) 2c, 0.031 g light yellow non-crystalline compound 3c and 0.150 g mixture of other products.

Non-crystalline substance. IR-spectrum : νC=O, 1690 cm^{-1} (s) ; νC=C, 1638 cm^{-1} (vw) ; δ_sCH$_3$CO, 1360 cm^{-1}(m).

Substance with m.p. 98–99°.

IR-spectrum : –O.Ac : νC=0,1775 cm^{-1}(vs) ; ν_s,ν_{as}=C–O–C, 1208,1180 cm^{-1} (vs, split) and 1035 cm^{-1}(m) ; δ_sCH$_3$CO, 1370 cm^{-1}(s).

UV-spectrum : λ_{max} at 251,287 and 321 nm.

NMR-spectrum : O.Ac : 1.96 ppm(s,3H) ; CH$_2$Ph : 3.88 ppm (s,2H) ; Ph : 7.08 ppm(s,5H) and 7.12 ppm(s,5H) ; Naphth : 6.98–7.78 ppm (m,5H).

Found : C, 85.10 ; H, 5.90
Calcd. for $C_{25}H_{20}O_2$: C, 85.22 ; H, 5.72

b. According to procedure 1Ab, from 0.531 g hydroxy acid, a mixture of 0.40 g neutral products was subjected to preparative TLC at the above conditions. The isolated products were : 0.108 g stilbenes, 0.194 g (36.5%) crystals with m.p. 98–99° 2c and a complex mixture of other products.

C. Dehydration of 2,3,4-triphenyl-3-hydroxybutanoic acid 1d.

a. According to procedure 1Aa, 0.998 g hydroxy acid gave 0.830 g mixture of neutral products. Preparative TLC (light petroleum : benzene : acetone=45 : 5 : 1) yielded 0.310 g stilbenes, 0.105 g phenyl-benzyl ketone, 0.080 g orange coloured crystals, 0.220 g almost colourless crystals and 0.090 g mixture of other products. After rechromatography (light petroleum : benzene : acetone=50 : 15 : 0.5) the crystalline fractions gave 0.057 g(7%) orange crystals with m.p. 135° (ethanol) (2-phenyl-3-benzyl-indene-1-one) and 0.239 g (24%) colourless needlelike crystals with m.p. 161–162° (from ethanol), 2d.

IR-spectrum : –O.Ac : νC=O, 1776 cm^{-1} (vs) ; ν_s,ν_{as}=C–O–C, 1205, 1178 cm^{-1}(vs, split) and 1035 cm^{-1} (m) ; δ_sCH$_3$CO, 1370 cm^{-1} (s).

UV-spectrum : λ_{max} 265,286 and 337 nm.

NMR-spectrum : O.Ac : 2.01 ppm(s,3H) ; Ph : 6.98 ppm(s,5H) and 7.02 ppm (s,3H) ; Naphth: 7.28–7.82 ppm(m, 5H).

Found : C, 85.32 ; H, 5.48
Calcd. for $C_{24}H_{18}O_2$: C, 85.35 ; H, 5.36

b. According to 1Ab, from 0.501 g hydroxy acid, the reaction yielded 0.36 g neutral products. Preparative TLC at above conditions gave stilbenes, phenyl-benzyl ketone, 0.061 g (15%) 2-phenyl-3-benzyl-indene-1-one and 0.105 g (21%) of 2d.

2. Dehydration by means of concentrated sulphuric acid.

A. Dehydration of 2,4-diphenyl-3-methyl-3-hydroxybutanoic acid 1a.

10 ml of concentrated sulphuric acid (97%) were added to 1.03 g of hydroxy acid, the mixture was vigourously shaken for 10 min, poured into 150 ml water and extracted with ether. The ether solution was washed with water (to extract monosulphonic acids, if formed) with Na$_2$CO$_3$ aq (to complete extraction of carboxylic acids), with 2.5% NaOH aq (to extract naphthols), with water to neutral reaction and dried (Na$_2$SO$_4$). After ether distillation a mixture of 0.62 g neutral products was obtained from which by recrystallization (ethanol) 0.515 g (56.8% of the initial acid) colourless crystals with m.p. 80–81°, soluble in warm alkali, 4a, were isolated.

IR-spectrum : νC=O, 1786cm^{-1}(vs) ; ν_s, ν_{as}=C–O–C, 1158cm^{-1} (s) and 1018 cm^{-1}(m).

NMR-spectrum : CH$_3$: 1.08 ppm(d,3H ; J = 6.5c/s) ; H$_A$: 2.44 ppm(m, 1H) ; H$_B$: 3.44 ppm(d,1H ; J = 6.3 c/s) ; H$_C$: 4.88 ppm (d,1H ; J = 5.0 c/s) ; Ph : 7.04 – 7.34 ppm (m, 10 H).

Found : C, 80.79 ; H, 6.43
Calcd. for $C_{17}H_{16}O_2$: C, 80.92 ; H, 6.31

The alkaline solution was acidified to pH 1, extracted with ether and the ether solution dried (Na$_2$SO$_4$). After distillation of ether a mixture of 0.045 g benzyl-methyl ketone (IR : ν C=O, 1717 cm^{-1}) and a carbonyl compound (IR : νC=O, 1667 cm^{-1}) was obtained.

B. Dehydration of 2,4-diphenyl-3-ethyl-3-hydroxybutanoic acid 1b.

According to 2A, 1.002 g hydroxy acid gave 0.42 g mixture of neutral products and 0.053 g products isolated from the alkaline solution.

From the neutral products was isolated after several recrystallizations (ethanol) 0.208 g (21 %) of colourless compound with m.p. 92–93°, soluble in warm alkali, 4b and 0.090 g mixture of this compound and another colourless one, 5.

Compound with m.p. 92–93°.

IR-spectrum : $\nu C = O$, 1782 cm^{-1}(vs) ; ν_s, $\nu_{as} = C-O-C$, 1160 cm^{-1} (s) and 1020 cm^{-1} (m).

NMR-spectrum : CH_3 : 0.99 ppm (tr, 3H ; J = 7.2 c/s) ; CH_2 : 2.30 ppm (qd, 2H ; J = 7.2 c/s and 6.3 c/s) ; H_A : 2.52 ppm(m,1H) ; H_B : 3.40 ppm(d,1H ; J = 6.1 c/s) ; H_C : 4.76 ppm(d,1H ; J = 4.9c/s) ; Ph : 7.01 – 7.22(m,1OH)

Found : C, 81.30 ; H, 6.25
Calcd. for $C_{18}H_{18}O_2$: C, 81.13 ; H, 6.11

Mixture of colourless compounds :

IR-spectrum : $\nu C=O$, 1782 cm^{-1} (m) and 1776 cm^{-1} (s) ;
$\nu_s = C-O-C$, 1160 cm^{-1} (m) and 1152 cm^{-1}(s).

NMR-spectrum : CH_3 : 1.10 ppm(d,3H ; J = 6.5 c/s) ; CH_2 Ph : 2.98 ppm (d,2H ;J = 5.2c/s) ; 2.50 ppm(m, H_A, **5**, and H_A**4b**) ; H_B : 3.46 ppm(d, 1H ; J=6.0c/s) ; 4.80 ppm(m,H_C, **5**, and H_C, **4b**) ; Ph : 7.00–7.30 ppm(m).

C. Dehydration of 2,3,4-triphenyl-3-hydroxybutanoic acid 1d.

According to procedure 2A, from 1.00g hydroxy acid were obtained 0.734 g neutral products and from the alkaline solution, a 0.040 g mixture of products. The mixture of neutral products consisted of stilbenes, 2-phenyl-3-benzyl-indene-1-one, γ-lactone, phenyl-benzyl ketone and small quantities of other products.

D. Dehydration of 2,4-diphenyl-3-benzyl-3-hydroxybutanoic acid 1c.

According to 2A, 1.02 g hydroxy acid gave 0.210 g mixture of neutral products, and the alkaline solution 0.070 g mixture of products. From the latter was isolated, through recrystallization (ethanol) 0.021 g colourless substance with m.p. 102–103° **6**.

IR-spectrum: ν_{OH}, 3550 cm^{-1}(m) and 1210 cm^{-1}(m).

Found : C, 88.82 ; H, 6.03
Calcd. for $C_{23}H_{18}O$: C, 89.00 ; H, 5.84

Revue Roumaine de Chimie, **19**, *11*, 1767–1772 (1974)

NMR STUDIES ON THE EFFECT OF NITROGEN ATOM ON THE ANOMERIC PROTON OF β-D-GLUCOPYRANOSIDES *

SENOT H. DOSS **, SHOICHI KONDO, KATSUMI TANAKA
and YOJIRO TSUZUKI***

** National Research Center, Cairo – Egypt, A.R.E.

*** Science University of Tokyo, Kagurazaka, Shinjuku-ku, Tokyo

Received June 8, 1973

The validity of the effect of the aryl group on the anomeric proton at C_1 is discussed with various model substances especially as to the effect of nitrogen bridge on the anomeric carbon in the case of β-D-glucopyranoside; the magnetic field of the aromatic ring is cancelled by the lone pair electrons of the nitrogen atom, enabling the signals of H_1 to appear as a doublet at $\tau = 3.05 - 4.84$, which depends on the nature of the substituents attached to the nitrogen atom.

It has been reported [1] that the signal of H_1 in β-aryl glucopyranosides was not assigned, because the signal is overlapped with those of the protons H_2, H_3 and H_4.

In this study we extended these observations with different, nitrogenous model substances with or without the aryl group to find the degree of shielding or deshielding on the anomeric proton at C_1, and also to reveal the effect of aryl substituent at C_6 on the anomeric proton.

RESULTS AND DISCUSSION

Table 1 and fig. 1 show the degree of shielding on the anomeric protons found with various glucopyranosylamines. The nitrogen atom with β-configuration at the anomeric carbon atom exhibits no effect on the chemical shift of the anomeric proton as in the case of β-aryl glucopyranosides. When the nitrogen atom forms a bridge with other aryl substituents, the chemical shifts of anomeric proton appeared in the range of $\tau = 3.05$ to 4.84 having a spacing of $J = ca.$ 4 to 9 Hz.

It may, therefore, be regarded, that the effect of the lone pair electrons is compensated by the effect of the magnetic field of the aromatic

---

* Dedicated to Professor Dr. Burckhardt Helferich in honour of his 87th birthday.

[1] Y. Tsuzuki and K. Tanaka, *Bull. Chem. Soc. Jap.*, **40**, 1208 (1967).

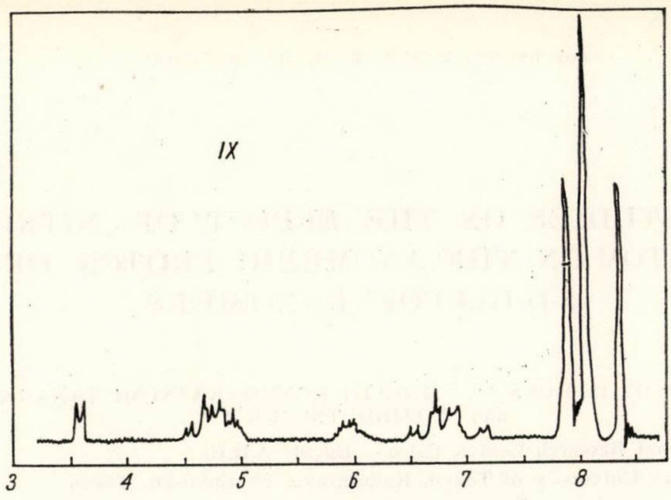

Fig. 1*a*

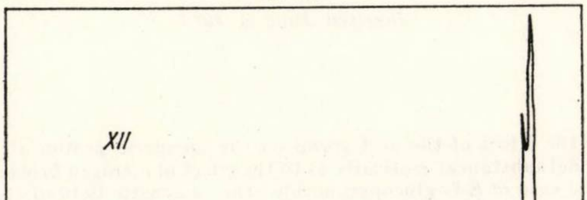

Fig. 1*b*

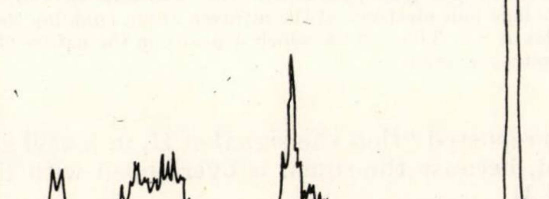

Fig. 1*c*

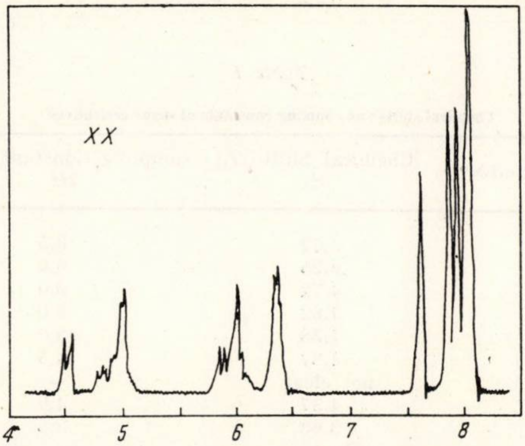

Fig. 1*d*

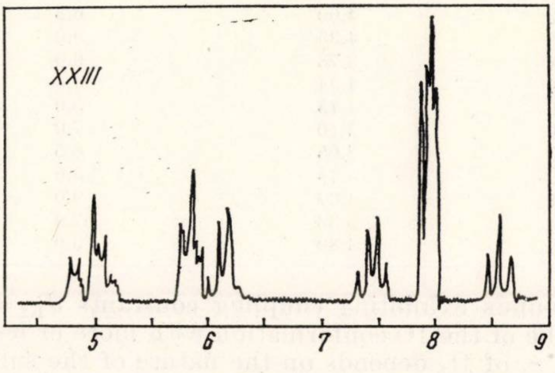

Fig. 1*e*

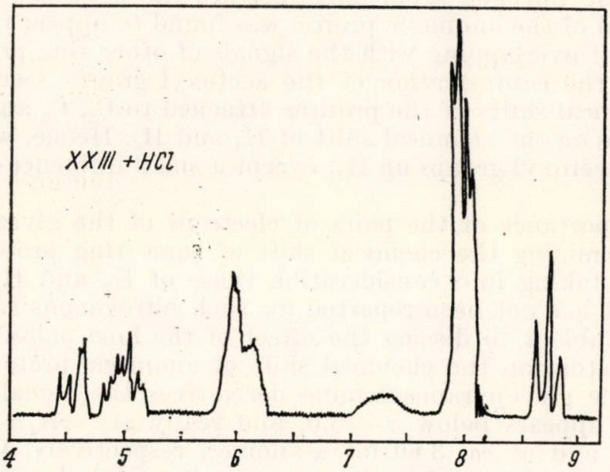

Fig. 1*f*

Fig. 1. *a*, *b*, *c*, *d*, *e*, *f*. — NMR spectra of IX, XII, XVI, XX, XXIII, and XXIII + HCl in $CDCl_3$ at 35°.

Table 1

Chemical shifts and coupling constants of sugar derivatives

Compound N°	Chemical Shift (H_1) τ	Coupling Constant ($J_{1,2}$) *Hz*
I	3.72	3.5
II	4.25	6.5
III	4.72	9.0
IV	4.62	7.0
V	4.38	5.0
VI	4.37	4.5
VII	not clear	—
VIII	4.37	4.0
IX	3.63	3.5
X	not clear	—
XI	4.84	4.0
XII	4.20	7.0
XIII	4.00	6.5
XIV	4.35	9.0
XV	3.78	9.0
XVI	4.34	4.0
XVII	4.15	5.0
XVIII	3.10	7.0
XIX	3.05	8.5
XX	4.78	3.0
XXI	4.67	9.0
XXII	3.33	2.0
XXIII	4.80	5.0

ring. The compounds exhibiting coupling constants $J_{1,2} = 2.0$ to 4.0 Hz are regarded to be of the 1C conformation with more or less deformation.

The value, τ, of H_1 depends on the nature of the substituents attached to the nitrogen atom as shown in table 1. Decrease of the lone paired electron on the nitrogen atom may increase the polarizability of H_1 so that the signal of the anomeric proton was found to appear in a relatively lower field, not overlapping with the signals of other ring protons. It was shown,[2] that the conformation of the acetoxyl groups seemed to affect only the chemical shifts of the protons attached to C_2, C_3 and C_6, but has little influence on the chemical shift of H_1 and H_4. Hence, we neglect the effect of the acetoxyl groups on H_1, except a small influence on the protonation effect.

This importance of the pairs of electrons of the glycosidic oxygen atom in determining the chemical shift of some ring protons has been pointed out [2] taking into consideration those of H_3 and H_5 of α-D-glucopyranose. It has not been reported for such nitrogenous sugar derivatives listed in table 2 to discuss the effect of the lone paired electrons of the nitrogen atom on the chemical shift of anomeric proton.

For some glucopyranosylamine derivatives the signal of the anomeric proton appears below $\tau = 5.0$, and really at $\tau H_1 = 4.30 - 4.15$ for β-anomer and at *ca.* 3.60 for α-anomer, respectively. On the other hand, for N-(tetra-O-acetyl-D-glucopyranosyl)-4-methyl pyridinium bro-

---

[2] B. Casu, M. Regginani, G. G. Gallo and A. Vigevani, *Carbohyd. Res.*, **12**, 157 (1970).

Table 2

Characteristic constants of sugar derivatives

Compound N°	Compound	m.p.(°C)	[α]*D*	Ref.
I	1,2,3,4,6-penta-O-acetyl-α-D-glucopyranose	114	101.2	a
II	1,2,3,4,6-penta-O-acetyl-β-D-glucopyranose	132	3.9	b
III	tert-butyl-2,3,4,6-tetra-O-acetyl-β-D-glucopyranoside	144	−11.6	c
IV	tert-butyl-2,3,4,6-tetra-O-acetyl-α-D-glucopyranoside	70	129	d
V	*o*-tolyl-2,3,4,6-tetra-O-acetyl-α-D-glucopyranoside	158	100	e
VI	*p*-tolyl-2,3,4,6-tetra-O-acetyl-α-D-glucopyranoside	172	86	f
VII	2-methoxy-phenyl 2,3,4,6-tetra-O-acetyl-β-D-glucopyranoside	156	29	g
VIII	6-*o*-trityl-1,2,3,4-tetra-O-acetyl-α-D-glucopyranose	131	98	h
IX	6-*o*-trityl-1,2,3,4-tetra-O-acetyl-β-D-glucopyranose	166	45	i
X	trityl-2,3,4,6-tetra-O-acetyl-β-D-glucopyranoside	149	22	—
XI	2,3,4,6-tetra-O-acetyl-β-D-glucopyranosyl azide	129	33	j
XII	N-picryl-2,3,4,6-tetra-O-acetyl-β-D-glucopyranoside	172	−127	k
XIII	N-methyl-N-picryl-2,3,4,6-tetra-O-acetyl-β-D-glucopyranoside	189	−75	k
XIV	2,3,4,6-tetra-O-acetyl-β-D-glucopyranosyl-phenylurea	104	11	l
XV	2,3,4,6-tetra-O-acetyl-α-D-glucopyranosyl-phenylurea	110	−22	j
XVI	N-acetyl-N-p-nitrophenyl-sulfoxide-2,3,4,6-tetra-O-acetyl-β-D-glucopyranosylamine	184	—	j
XVII	N-ditosyl-2,3,4,6-tetra-O-acetyl-β-D-glucopyranosalamine	130	−25	j
XVIII	(4-hydroxy-1-benzylidene)-2,3,4,6-tetra-O-acetyl-β-D-glucopyranosylamine	225	—	j
XIX	(5-nitro-2-hydroxy-benzylidene)-2,3,4,6-tetra-O-acetyl-β-D-glucopyranosylamine	180	—	j
XX	N-benzyl-N-methyl-2,3,4,6-tetra-O-acetyl-β-D-glucopyranosylamine	125	−5	m
XXI	(3-nitro-1-benzylidene)-2,3,4,6-tetra-O-acetyl-β-D-glucopyranosylamine	135	−4	j
XXII	(2-hydroxy-1-benzylidene)-2,3,4,6-tetra-O-acetyl-β-D-glucopyranosylamine	147	—	j
XXIII	N-benzyl-N-ethyl-2,3,4,6-tetra-O-acetyl-β-D-glucopyranosylamine	124	14	l

[a] M. L. Wolfrom and A. Thompson, "Methods in Carbohydrate Chemistry", vol. 2, 1963, p. 212.

[b] C. H. Hudson and J. K. Dole, *J. Amer. Chem. Soc.*, **37**, 1264 (1915).

[c] B. Lindberg, *Acta. Chem. Scand.*, **3**, 153 (1949).

[d] B. Helferich, V. Lampert and G. Sparmberg, *Ber.*, **67**, 1808 (1934).

[e] K. Nishizawa, *Bull. Chem. Soc. Japan.*, **16**, 155 (1941).

[f] B. Helferich and E. Schmitz-Hillebrecht, *Ber.*, **66**, 378 (1933).

[g] B. Helferich, L. Moog and A. Junger, *Ber.*, **58**, 872 (1925).

[h] E. A. Talley, "Methods in Carbohydrate Chemistry", vol. 2, 1963, p. 337.

[i] H. Bredereck, A. Wagner, W. Lück, H. Kleeberg and J. Renner, *Chem. Ber.*, **92**, 2405 (1959).

[j] B. Helferich and A. Mitrowsky, *Chem. Ber.*, **85**, 1 (1952).

[k] B. Helferich and D. Nachtsheim, *Monats.*, **88**, 460 (1957).

[l] B. Helferich and W. Portz, *Chem. Ber.*, **86**, 604 (1953).

[m] J. W. Baker *J. Chem. Soc.*, **1929**, 1205.

mide the signal appears at $\tau_{H_1} = 3.76$ for β-anomer and at $\tau_{H_1} = 3.20$ for α-anomer.[3] The signal of anomeric proton appeared below $\tau = 5.0$ as shown in table 1 is quite in accord with the results of Lemieux *et al.*[4]

For proof the validity of the idea of the nitrogen bridge, which is attributed to the lone pair of electrons on the nitrogen atom, the lone paired electrons of nitrogen atom can be blocked even with a drop of hydrochloric acid i.e. by protonating (XXIII) with HCl into its hydrochloride. The doublet signal of H_1 was shifted from $\tau = 4.80$ to 4.48, when (XXIII) was converted into its hydrochloride. It is interesting to note, that the signals of the acetoxyl protons attached to C_2 in the glucopyranosylamine derivatives show $\tau = 8.0 \pm 0.07$, since the acetoxyl group is not influenced by the anisotropic effect of benzene ring due to the effect of nitrogen bridge. By the way it may be mentioned, that the presence of the grouping $-O-CO-CH_2-Ar$ at C_1 places the aromatic ring in a position, which allows an easy and simultaneous approach of all of the protons of the C_2-acetoxyl group to the plane of the ring, so that the effect of an aromatic ring caused the signal of C_2-acetoxyl group to upfield shift.[5]

EXPERIMENTAL

The compounds examined were prepared by published procedures. Each substance was crystallized from a suitable solvent until further crystallization caused no change in either melting point or specific rotation. Thin layer chromatography was carried out on silicagel G (Merck) with the suitable solvent system and detection was made with 10% sulfuric acid. The characteristic constants of the materials are listed in table 2. The NMR spectra were measured at 35° with a Varian A–60 spectrometer. Tetramethylsilane was used as internal standard. All the measurements were carried out in 15% (W/V) deuteriochloroform solution.

---

[3] K. Kato, T. Komori, A. Yamamoto, T. Kawasaki and H. Tsukamoto, *Carbohyd. Res.*, **14**, 355 (1970).

[4] R. U. Lemieux and A. R. Morgan, *Canad. J. Chem.*, **43**, 2205 (1965).

[5] V. Pravdic andD. Keglevic, *Carbohyd. Res.*, **12**, 193 (1970).

Revue Roumaine de Chimie, **19**, *11*, 1773–1781 (1974)

FORMATION OF NEW NITROGEN FREE RADICALS FROM DINITRO-SULPHO-PHENYL-N-ALKOXYAMINES

MARIA FRANGOPOL, P. T. FRANGOPOL and N. NEGOIȚĂ
Institute of Atomic Physics, P.O.B. 35, Bucharest, Romania

Received December 15, 1973

Oxidation with lead tetraacetate of 2,6-dinitro-4-sulpho- (IV) and 2,4-dinitro-6-sulpho-phenyl-N-alkoxyamines (V) led to the corresponding stable dinitro-sulpho-phenyl-N-alkoxyaminyl free radicals, whose ESR spectra are presented and discussed. Watersoluble, new stable free radicals were also obtained by treatment of IV and V with alkali. Infrared and ultraviolet-visible spectra of the new secondary amines IV and V are reported.

We have previously reported [1] the formation of long-lived diarylamino free radicals I possessing one of the phenyl rings substituted with donor groups R = *o*-, *m*-, *p*- Me; *o*-, *m*-, *p*-OMe; *p*-NMe_2, *p*-NPh_2; 3,4-$(OMe)_2$ and the other with acceptors such as NO_2 and SO_3K.

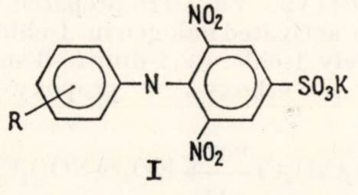

I

Interest in the nitrogen-free radicals with a sulphonic group in the molecule stems from their water-solubility. Since such radicals remain of high research interest because of their relevancy to the radiolysis of water [2] and biological reactions[3] — we extended our study to a new series of stable nitrogen free radicals.

In this paper we report the preparation and spectral properties of the stable dinitro-sulpho-phenyl-N-alkoxyaminyls II and III, obtained by oxidation of 2,6-dinitro-4-sulpho- and 2,4-dinitro-6-sulpho-phenyl-N-alkoxyamines IV and V. New stable free radicals were also obtained by treatment of IV and V with alkali, and details on them will be published later

---

[1] P. T. Frangopol, M. Frangopol, N. Negoiță and Elena Romaș, *Rev. Roumaine Chim.*, **14**, 527 (1969).

[2] L. Matus and G. V. Putirszkaja, *Magyar Kém Folyóirat*, **78**, 420 (1972); G. V. Putirszkaja and L. Matus, *Acta Chim. Acad. Sci. Hung.*, **38**, 249 (1963).

[3] M. Frangopol, P. T. Frangopol, C. L. Trichilo, F. E. Geiger and N. Filipescu, *J. Org. Chem.*, **38**, 2355 (1973), and the references cited therein.

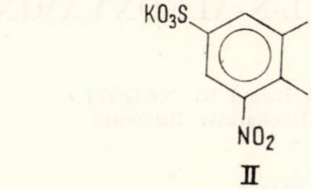

II

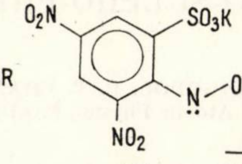

III

R
a. CH_3
b. C_2H_5
c. C_3H_7
d. C_4H_9

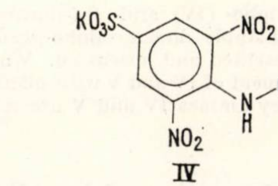

IV

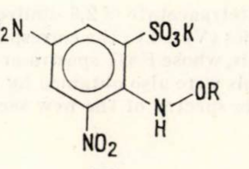

V

RESULTS AND DISCUSSION

2,6-Dinitro-4-sulpho-N-alkoxyamines (IVa—IVd) and 2,4-dinitro-6-sulpho-N-alkoxyamines (Va—Vd) were prepared by aromatic nucleophilic substitution [4] of the activated halogen in 1-chloro-2,6-dinitro-4-sulpho-benzene [5] and respectively 1-chloro-2,4-dinitro-6-sulpho-benzene [6] through alkoxyamines (methoxy-,[7–9] ethoxy-,[10,11,9] propoxy-,[11] and butoxy-amine[11])

$$KO_3S(NO_2)_2C_6H_2Cl \xrightarrow[-HCl]{H_2NOR} KO_3S(NO_2)_2C_6H_2NHOR$$

Actually, the alkoxyamines hydrochlorides and not the free bases were used, in a ratio of two moles to a mole of chloro-dinitro-sulpho-ben-

---

[4] A. T. Balaban, P. T. Frangopol, M. Frangopol and N. Negoiţă, *Tetrahedron*, **23**, 4661 (1967); A. T. Balaban , P. T. Frangopol, M. Mărculescu-Frangopol and I. Bally, *Tetrahedron*, **13**, 258 (1961).

[5] H. P. Schultz, *Org. Synth.*, **31**, 45 (1951).

[6] F. Ulmann and E. Herre, *Liebigs Ann. Chem.*, **366**, 111 (1909).

[7] R. M. Khomutov, *Zhur. Obshchei Khim.*, **31**, 1992 (1961).

[8] B. V. Joffe and K. N. Zelenin, *Izv. Vysshikh Uchebn. Zavedenii Khim. i Khim. Tekhnol.*, **6**, 78 (1963); cf. *Chem. Abstr.*, **59**, 6244 (1965); O. Scherer, G. Hoerlein, R. Hübner and G. Schneider (Farbverke Hoechst A–G), Ger. Pat. 1, 112, 082 (Oct. 21, 1959); cf. *Chem. Abstr.*, 58, 8561b (1962).

[9] A. T. Balaban, M. Frangopol, N. Negoiţă, P. T. Frangopol and M. Paraschiv, *Rev. Roumaine Chim.*, **14**, 941 (1969).

[10] Masahiro Torigore, *Chem. Pharm. Bull.* (*Japan*), **9**, 613 (1961).

[11] W. Teilacker and K. Ebke, *Angew. Chem.*, **68**, 303 (1956).

Table 1

Elementary analyses, M.Ps., Colour and yields of dinitro-sulpho-phenyl-N-alkoxyamines

Amine	*R* (Alkyl)	KSO_3 (position)	NO_2 (position)	Elementary analyses								M.p. °C	Colour	Yield %
				C		H		N		S				
				Calcd.	Found	Calcd.	Found	Calcd.	Found	Calcd.	Found			
IVa	CH_3	4	2,6	25,38	25.75	1.82	2.13	12.68	12.88	9.67	8.97	270 dec	orange yellow	62
IVb	C_2H_5	4	2,6	27.82	27.52	2.33	2.72	12.17	12.27	9.28	9.127	260 dec	orange yellow	70
IVc	C_3H_7	4	2,6	30.08	30.21	2.80	2.78	11.69	11.69	8.92	8.45	266dec	orange	42
IVd	C_4H_9	4	2,6	32.16	32.00	3.24	3.49	11.25	11.36	8.58	8.65	255 dec	yellow	45
Va	CH_3	6	2,4	25.38	25.72	1.82	1.95	12.68	12.43	9.67	8.77	210	yellow	70
Vb	C_2H_5	6	2,4	27.82	27.45	2.33	2.68	12.17	12.35	9.28	8.67	196	yellow	65
Vc	C_3H_7	6	2,4	30.08	30.17	2.80	2.88	11.69	11.95	8.92	8.68	182	yellow	50
Vd	C_4H_9	6	2,4	32.16	32.02	3.24	3.45	11.25	11.17	8.58	8.70	182	yellow	49

zene, carrying out the reaction in boiling ethanol in the presence of sodium bicarbonate.

The resulting dinitro-sulpho-phenyl-N-alkoxyamines IV and V are stable crystallized compounds. It is worth saying that the dinitro-sulpho-phenyl-N-propoxy- and dinitro-sulpho-phenyl-N-butoxyamines (IVc, IVd, Vc and Vd) are as stable as their lower homologues (IVa, IVb, Va and Vb), whereas in the polynitrophenyl-N-alkoxyamines series [9] the higher homologues (2,4,6-trinitro-phenyl-, 2,6- and 2,4-dinitro-phenyl-propoxy- and butoxyamines) were unstable.

The dinitro-sulpho-phenyl-N-alkoxyamines IVa—IVd and Va—Vd were characterised by melting point, analysis (Table 1), infrared spectra (Table 2) and UV-visible absorption spectra (Table 3).

Infrared absorption spectra. The structure of 2,6-dinitro-4-sulpho- and 2,4-dinitro-6-sulpho-phenyl-N-alkoxyamines was confirmed by the infrared absorption spectra determined in potassium bromide pellets. The ν NH values presented in Table 2 are in good agreement with the literature data [12] concerning the NH stretching band, usually placed at frequencies between 3300—3400 cm^{-1}. The correct assignment of the bands corresponding to the sulphonic group was also made by comparison with the literature data (1180—1200 and 1040 — 1070 cm^{-1}).[13]

Table 2

Infrared NH and KSO_3 bands ($cm-^1$) of dinitro-sulpho-phenyl-N-alkoxyamines (IV and V) in potassium bromide pellets

Amine	*R* (Alkyl)	NH	SO_3K[13]		
			1180—1220	1040—1070	
IVa	CH_3	3295	1195	1045	1055
IVb	C_2H_5	3305	1195	1054	1055
IVc	C_3H_7	3300	1195	1045	1055
IVd	C_4H_9	3300	1195	1045	1055
Va	CH_3	3295	1180	1050	1070
Vb	C_2H_5	3295	1185	1050	
Vc	C_3H_7	3295	1185	1040	1070
Vd	C_4H_9	3310	1180	1050	

Other significant IR absorption band in the spectra of the secondary amines IV and V were the asymmetric and symmetric nitro group vibration frequencies [14] at 1540 and 1340—1360 cm^{-1}, the NH deformation vibration at 1430—1435 cm^{-1} and the strong benzene ring vibrations at 1620 cm^{-1}.

Ultraviolet and visible absorption spectra. Electronic absorption maxima of dinitro-sulpho-phenyl-N-alkoxyamines in ethanol are presented in Table 3. The electronic absorption bands are denoted by letters (A, B, C) in the order of decreasing wavelengths. Band C, present in all the eight compounds, appears in the compounds V as shoulders rising toward low wavelengths. The exact localization of these shoulders was difficult and the corresponding ε-values have not been calculated. Band B is present in compounds V. Band A is present in compounds IV and has a low extinction coefficient (except the compound IVd). The absence of the band A in compounds V and of the band B in compounds IV is in agreement with our previous discussions of electronic absorption spectra of polynitrophenyl derivatives.[4,9,15]

---

[12] D. Hadzi, J. Jan and A. Ocvirk, *Spectrochim. Acta*, **25A**, 97 (1969).

[13] L. Ganguly, C. I. Jose and A. A. Biswas, *Spectrochim. Acta*, **24A**, 215 (1968); J. L. Bellamy, "The Infrared Spectra of Complex Molecules", Mathuen, 1959, pg. 350.

[14] A. R. Katritzky and P. Simmons, *Quart. Rev.*, **13**, 353 (1959); idem, *Rec. Trav. Chim.*, **79**, 361 (1960); G. Varsanyi, S. Holly and L. Imre, *Spectrochim. Acta*, **23A**, 1205 (1967).

Table 3

Electronic absorption maxima of dinitro-sulpho-phenyl-N-alkoxyamines (IV and V) in ethnaol (nm)

Amine	*R* (Alkyl)	Electronic absorption bands					
		A		B		C	
		λ	ε	λ	ε	λ	ε
IVa	CH_3	392	3300	—	—	241	20000
IVb	C_2H_5	394	2500	—	—	240	16500
IVc	C_3H_7	418	3800	—	—	238	18600
IVd	C_4H_9	410	20400	—	—	240	20400
Va	CH_3	—	—	337	7000	235 sh*	
Vb	C_2H_5	—	—	341	6900	237 sh	
Vc	C_3H_7	—	—	341	6500	237 sh	
Vd	C_4H_9	—	—	340	7500	232 sh	

* A shoulder or an inflection of the band envelope are indicated by "sh".

Electron spin resonance spectra. The oxidation of the secondary amines IV and V to the corresponding aminyl free radicals II and III was made by lead tetraacetate. The insolubility of the secondary amines IV and V in solvents currently used in the ESR techniques raised difficulties in the measurements. Capillaries or flat cells were used, but only high concentration of free radicals has been detected when solvents with high dielectric constant were utilized. Though sparingly soluble in dioxane we managed to oxidize in it the dinitro-sulpho-phenyl-N-alkoxyamines (IV and V) to paramagnetic species. Oxidation with lead tetraacetate in deaerated vials in the presence of helium gas, of the 2,6-dinitro-4-sulpho- and 2,4-dinitro-6-sulpho-phenyl-N-alkoxyamines (IVa — IVd and Va — Vd) afforded paramagnetic solutions whose ESR spectra were assigned to the corresponding dinitro-sulpho-phenyl-N-alkoxyaminyl free radicals (IIa — IId, IIIa — IIId). Since the 2,4-dinitro-6-sulpho-phenyl-N-alkoxyamines (V) are less soluble in dioxane than their 2,6-dinitro-4-sulpho-analogues, only weak and poorly resolved ESR signals were obtained. The ESR spectra of 2,6-dinitro-4-sulpho-phenyl-N-alkoxyaminyls (IIa — IId), obtained by oxidation of IVa — IVd with $Pb(OAc)_4$ in dioxane, in sealed vials under helium atmosphere are presented in figs 1, 2, 3 and 4.

---

[15] A. T. Balaban, P. T. Frangopol and E. Keplinger, *Spectrochim. Acta*, **19**, 367 (1963).

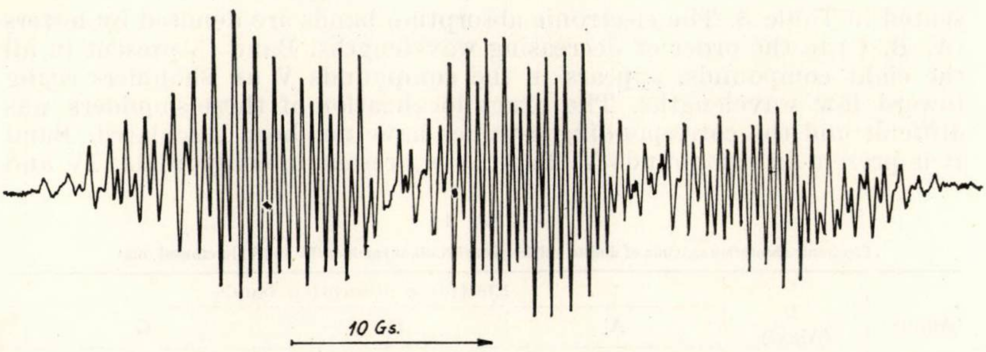

Fig. 1. — ESR spectrum of 2,6-dinitro-4-sulpho-phenyl-N-methoxyaminyl (IIa) in dioxane.

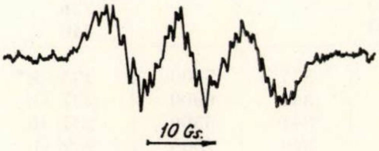

Fig. 2. — ESR spectrum of 2,6-dinitro-4-sulpho-phenyl-N-ethoxyaminyl (IIb) in dioxane.

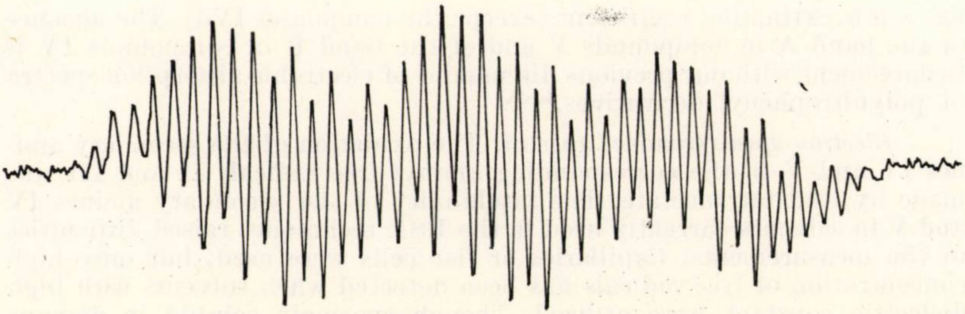

Fig. 3. — ESR spectrum of 2,6-dinitro-4-sulpho-phenyl-N-propoxyaminyl (IIc) in dioxane.

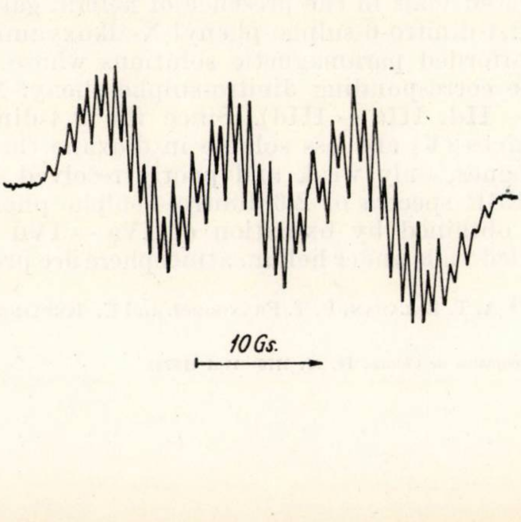

Fig. 4. — ESR spectrum of 2,6-dinitro-4-sulpho-phenyl-N-butoxyaminyl (IId) in dioxane.

The ESR spectra of the dinitro-sulpho-phenyl-N-alkoxyaminyls (II and III) have a total span of ~ 35 gauss and consist in a major triplet due to the interaction of the odd electron with the central nitrogen atom; the main triplet is split further into many lines revealing the interaction with other nitrogen or hydrogen atoms.

The *g*-values and the a_N coupling constants presented in Table 4 were determined by comparison with potassium peroxylamine disulphonate (Fremy salt, characterized by $g = 2.0055 \pm 0.00005$ and $a_N = 13.091$ gauss).[16] The isotropic *g*-values ranging from 2.0041 to 2.0047 are in agreement with the aminyl structure. It seems that the oxidation of the dinitro-sulpho-phenyl-N-alkoxyamines with lead tetraacetate did not lead to the corresponding nitroxides whose g-factor should have been higher than 2.0055.[17,18] The half-life of the dinitro-sulpho-phenyl-N-alkoxyaminyls is about two hours at room temperature in deaerated solutions in sealed vials.

Table 4

ESR spectral data for 2,6-dinitro-4-sulpho-phenyl-N-alkoxyaminyls

Radical	*R* (Alkyl)	*g*-value	a_N (gauss)	Total span (gauss)
IIa	CH_3	2.0046	11.7	36.9
IIb	C_2H_5	2.0041	10.0	36.1
IIc	C_3H_7	2.0043	10.1	32.3
IId	C_4H_9	2.0047	10.05	38.6

By analogy with the hydrazyls[19-21] and with the previously reported sulphonic diaryl-amino radicals [1] we assumed that the stability of sulpho-dinitro-phenyl-N-alkoxy-aminyls is due to the steric shielding exerted by the *ortho*-substituents and to the push-pull electronic effect introduced by the presence of both, the donor (alkoxy group) and the acceptor (nitro and sulpho substituents of the phenyl ring).

Treatment of dinitro-sulpho-phenyl-N-alkoxyamines [22] with alkaline solutions under N_2 atmosphere gave coloured paramagnetic solutions whose ESR signals paralleled the intensity of the colour.

---

[16] E. Fremy, *Ann. Chim. Phys.*, **15**, 459 (1845); G. E. Pake, J. Townsend and S. I. Weismann, *Phys. Rev.*, **85**, 682 (1952); J. P. Lloyd and G. E. Pake, *ibid.*, **84**, 579 (1954); J. Q. Adams and J. R. Thomas, *J. Chem. Phys.*, **39**, 1964 (1963); R. J. Faber and G. K. Fraenkel, *J. Amer. Chem. Soc.*, **92**, 5582 (1971).

[17] F. A. Neugebauer and P. H. H. Fischer, *Z. Naturforsch*, **21b**, 1036 (1966). P. H. H. Fischer and F. A. Neugebauer, *ibid.*, **19a**, 1514 (1964); E. T. Storm, A. L. Blum and J. Weinstein, *J. Org. Chem.*, **32**, 3853 (1967).

[18] E. G. Rozantsev, *Usp. Khim.*, **35**, 1549 (1966); R. M. Dupeyre and A. Rassat, *J. Amer. Chem. Soc.*, **88**, 3180 (1966).

[19] D. Braun, G. Peschk and E. Hechler, *Chem. Ztg.*, **94**, 703 (1970).

[20] D. Braun and G. Peschk, *Angew. Chem.*, **80**, 1002 (1968).

[21] D. Braun, G. Peschk and E. Hechler, *Chimia* (*Aarau*), **21**, 536 (1967).

[22] P. T. Frangopol and M. Frangopol, unpublished results.

The 2,6,dinitro-4-sulpho-phenyl-N-alkoxyamines (IV) generated in N NaOH under N_2 atmosphere blue solutions, while the 2,4,-dinitro-6-sulpho-analogues (V) gave red solutions. After evaporation of the blue and red solutions in an inert atmosphere, green and respectively red-brownish par amagnetic solide resulted, whose ESR spectra (simple line with g-value 2.0040 ± 0.0004) are exemplified by fig. 5.

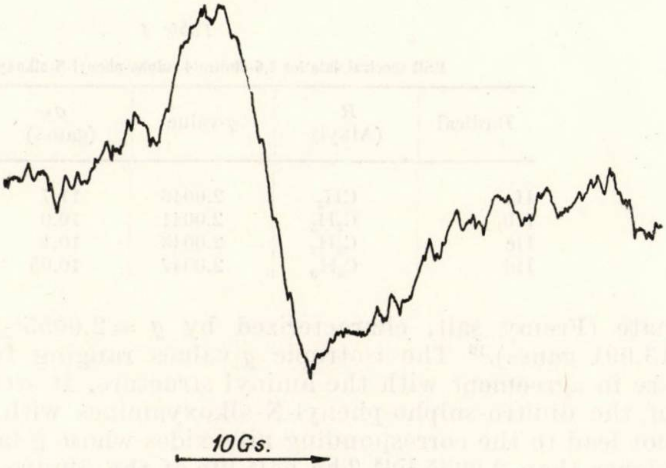

Fig. 5. — ESR spectrum of the solid free radical resulted from 2,6-dinitro-4-sulpho-phenyl-N-ethoxyamine (IVb) with N NaOH.

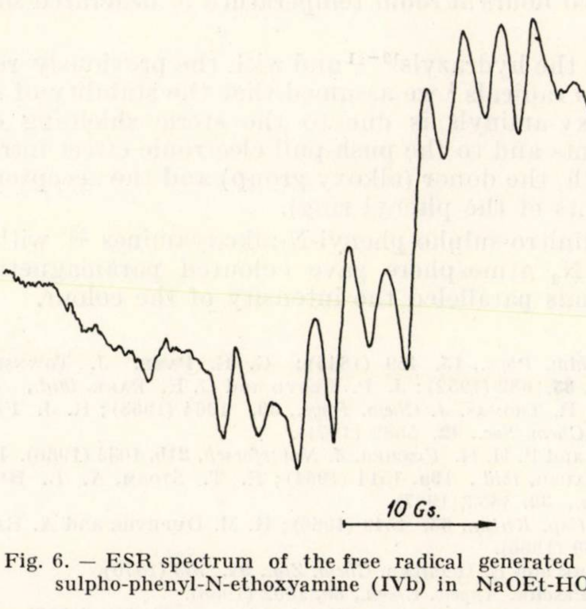

Fig. 6. — ESR spectrum of the free radical generated by 2,6-dinitro-4-sulpho-phenyl-N-ethoxyamine (IVb) in NaOEt-HOET-pyridine.

Attempts to transform into free radicals the dinitro-sulphophenyl-N-alkoxyamines were also carried out by treatment with a mixture of molar sodium ethoxide solution in ethanol — pyridine (1 — 1) under N_2 atmosphere. The paramagnetic species generated by the dinitro-sulpho-phenyl-

N-alkoxyamines in NaOEt-HOET-pyridine were violet for the 2,6-dinitro-4-sulpho- and purple for the 2,4-dinitro-6-sulpho-derivatives and displayed ESRspectra with *g*-values of 2.0033. The ESR spectrum of the free radical generated by the 2,6-dinitro-4-sulpha-phenyl-N-ethoxyamine (IVb) in NaOEt-HOEt-pyridine is represented in fig. 6.

EXPERIMENTAL

Apparatus. Infrared spectra were recorded on the Jena UR-10 double beam instrument in KBr pellets.

Ultraviolet-visible absorption spectra were recorded on the CF-4 Optica Milano spectrophotometer.

Electron spin resonance spectra were recorded on an instrument operating in the *X* band with a frequency of 9060MHz[23] and a Varian-E 12 instrument.

COMPOUNDS

Methoxyamine hydrochloride,[7-9] m.p.150°, was obtained by methylation with dimethylsulphate of potassium nitrosulphonate and acid hydrolysis of the resulted $MeON(SO_3K)_2$.

Ethoxyamine hydrochloride,[10] m.p.128°, was synthesized by ethylating acetoxime with 1-bromoethane and hydrolyzing the resulted O-ethyl-acetoxime, ($EtO-N=CMe_2$).

Propoxy-[10] and *butoxy-amine*[11] *hydrochlorides* were prepared by a procedure similar to that utilized for ethoxyamine hydrochloride, using 1-bromo-propane and 1-bromo-butane, respectively. After recrystallization from ethanol-ether, the melting point of propoxyamine hydrochloride was 155–157°, and the butoxyamine hydrochloride melted at 158° (as compared to 152–153° reported in the literature [24]).

Dinitro-sulpho-phenyl-N-alkoxyamines (IVa — IVd and Va — Vd). The reaction between two moles of alkoxyamine hydrochlorides and one mole of 1-chloro-2,6-dinitro-4-sulphobenzene [5] or 1-chloro-2,4-dinitro-6-sulphobenzene[6] in the presence of two moles of sodium bicarbonate was carried out in boiling ethanol by refluxing the mixture for 36 hours. The resulted secondary amines were purified by recrystallization from 95% ethanol.

The authors express their sincere thanks to Drs. I. Pascaru and R. Baican for the ESR spectra, to Mrs. M. Roman and C. Popescu for elementary analyses, to Mrs. E. Romaş and M. Paraschiv for IR and UV spectra and to Mr. D. Papae fof experimental assistance.

---

[23] I. Pascaru, *Nuclear Instruments and Methods*, **26**, 333 (1964).

[24] G. Palazzo, E. Rogers and G. Marini-Betollo, *Gazz. chim. Ital.*, **84**, 915 (1954).

Revue Roumaine de Chimie, **19**, *11*, 1783–1790 (1974)

THERMOSTABLE POLYMERS. III[1]

POLYBENZIMIDAZOLE-IMIDES

GH. MANDRIC*, A. I. PAVLOV,** V. V. KORSHAK ** and I. ZUGRĂVESCU*
* "P. Poni", Institute of Macromolecular Chemistry
Aleea Gr. Ghica Vodă 41 A, Jassy, Romania
** "D. I. Mendeleev" Institute of Technological Chemistry, Moscow, USSR

Received December 6, 1973

Two aminophenylbenzimidazoles were prepared by reacting 3,4,3′,4′-tetraaminodiphenylmethane and *m*- or *p*-aminobenzoic acids. Polyamic acid prepolymers were obtained by condensing benzimidazole containing diamines with pyromellitic anhydride. The prepolymers were cast onto glass plate and the films were obtained by heating at 80–100°. After a thermal treatment at 300° for 1 hr., the prepolymer films were converted to polybenzimidazole-imide films, with high thermal stability.

INTRODUCTION

Aromatic heterocyclic compounds have been used to prepare a wide variety of heat-resistant polymers. Among the more stable ring systems that have been used to prepare high polymers[1–5] are benzimidazoles and imides. These polymers are of considerable interest in preparing thermostable films, [6–8] fibers, [9,10], adhesives [11,12] and coatings. [13–15] An increasing interest in preparing and studying ordered copolymers [16–22] is apparent.

---

[1] Part II. Gh. Mandric and I. Zugrăvescu, *Rev. Roumaine Chim.*, **16**, 1419 (1971).

[2] H. Vogel and C. S. Marvel, *J. Polymer Sci.*, **50**, 511 (1961).

[3] A. A. Izyneev, V. V. Korshak, T. M. Frunze and V. V. Kurashev, *Izvest. Akad. Nauk. S.S.S.R., Otdel. khim. Nauk*, **10**, 1828 (1963).

[4] Idris Jones, F. W. Ochynski and F. H. Rackley, *Chem. and Ind.*, **81**, 1686 (1962).

[5] G. M. Bower and L. W. Frost, *J. Polymer Sci. A*, **1**, 5135 (1963).

[6] L. E. Amborski, *Ind. Eng. Chem. Prod. Res. Dev.*, **2**, 189 (1963).

[7] I. F. Heacock and E. C. Berr, *SPE Trans.*, **5**, 105 (1965).

[8] A. P. Rudakov, I. M. Bessonov, M. M. Koton and S. F. Florinskii, *Elektricestvo*, **11**, 84 (1966).

[9] A. P. Rudakov, I. M. Bessonov, M. M. Koton and S. F. Florinskii, *Khim. Volokna*, **5**, 20 (1966).

[10] R. W. Singleton, H. D. Noether and J. F. Tracy, *J. Polymer Sci. C*, **19**, 65 (1967).

[11] S. Litvak, *Appl. Polymer Symp.*, **3**, 279 (1966).

[12] R. Leppla and R. Carryer, *Insulation*, **9**, 35 (1963).

[13] K. Schmidt, G. Naubert and H. Rombrecht, *Electrotechn. Zt.*, **B 15**, 603 (1963).

[14] N. Todd, F. Wolff, R. Mallouk and F. Schwetzzer, *Maschine Design*, **36**, 228 (1964).

[15] A. P. Vasilieva and S. F. Shakai, *Aviatsionaia prom.*, **8**, 81 (1965).

[16] L. W. Frost, G. M. Bower, I. H. Freeman, H. A. Burgman, E. J. Traynor and C. R. Ruffing, *J. Polymer Sci. A 1*, **6**, 215 (1968).

[17] Gh. Mandric and I. Zugrăvescu, *Rev. Roumaine Chim.*, **16**, 1419 (1971).

[18] J. Preston and H. C. Bach, Belg. Patent, 660.339 (1966) ; *Chem. Abstr.*, **64**, 892 (1966).

[19] J. Preston and F. Dobinson, *J. Polymer Sci. B*, **2**, 1171 (1964).

[20] J. Preston and W. B. Black, *J. Polymer Sci. B*, **3**, 845 (1965).

[21] J. Preston and W. B. Black, *J. Polymer Sci. B*, **4**, 267 (1966).

[22] M. Strul, G. Neamțu, E. Măntăluță and I. Zugrăvescu, *Rev. Roumaine Chim.*, **16**, 941 (1971).

This paper deals with the synthesis and the properties of two new polybenzimidazole-imides.

RESULTS AND DISCUSSION

Two new benzimidazole containing diamines were prepared by reaction of 3,4,3′,4′-tetraaminodiphenylmethane and *m*- or *p*-aminobenzoic acids, as follows :

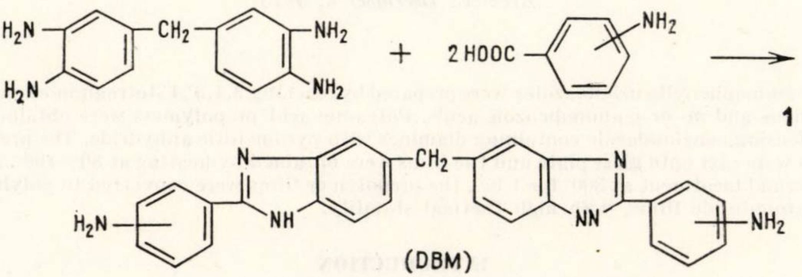
H₂N
CH₂
NH₂
H₂N
NH₂
+
2 HOOC
NH₂
N
NH
NN
(DBM)

1

2,2′-*p*-aminophenyl-5,5′-dibenzimidazolyl-methane (DBM-*p*) and 2,2′-*m*-aminophenyl-5,5′-dibenzimidazolyl-methane (DBM-*m*).

By condensing the diamines with pyromellitic anhydride, polyamic acid prepolymers (PAA) were obtained, and converted to polybenzimidazole-imides (PBI) by thermal treatment, as shown in eq. (2) :

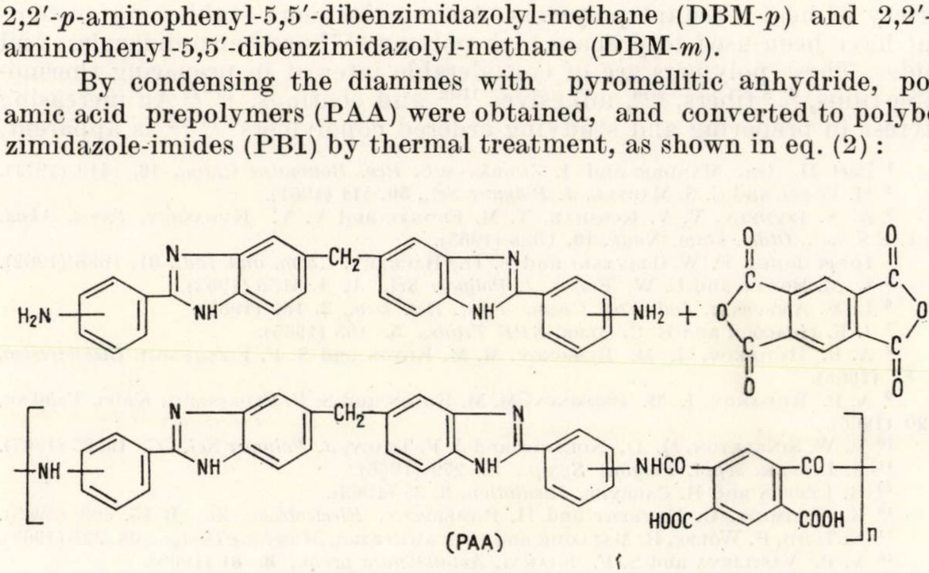
H₂N
N
CH₂
NH
NH₂
+
O
C
O
NH
NHCO
CO
HOOC
COOH
(PAA)
n
(PAA)
heat
-H₂O
N
CO
(PBI)
n

2

MONOMERS AND MODELS

Diamines were synthesized by condensing 3,4,3′,4′- tetraaminodiphenylmethane with *p*- or *m*-aminobenzoic acids, using polyphosphoric acid as solvent and condensing agent, by heating at 150°, under nitrogen flow for 10 hrs. Diamines were purified by methanol extraction, charcoal treatment, and water precipitation.

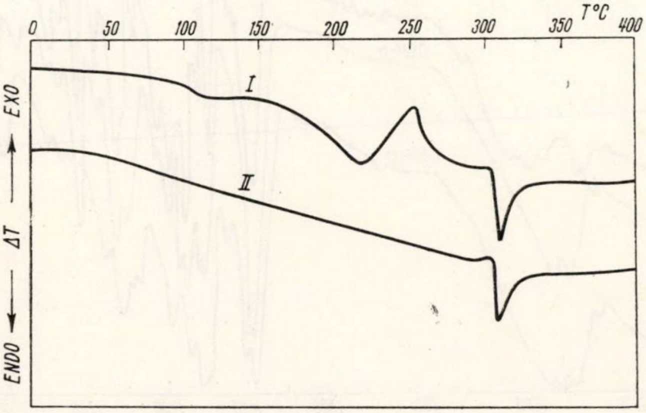

Fig. 1. — I. DTA thermogram of undried DBM-*p*, showing desolvation and melting point near 320°; II. DTA thermogram of dried DBM-*p*, showing only melting point.(Sample size : 20mg., heating rate: 12°/1 min., atmosphere : air).

The differential thermal analysis of undried DBM-*p* (fig. 1) shows diamine solvent complexing with loss of solvent near 230°.

Elemental analysis of undried and dried diamines are summarized in table 1.

Table 1

Elemental analysis of monomers

Compound	Condition	Carbon, %		Hydrogen, %		Nitrogen, %	
		Calcd.	*Found*	*Calcd.*	*Found*	*Calcd.*	*Found*
DBM-*p*	Undried	75.33	70.89	5.15	5.33	19.52	18.56
	Dried	75.33	75.31	5.15	5.17	19.52	19.83
DBM-*m*	Undried	75.33	70.80	5.15	5.78	19.52	18.45
	Dried	75.33	74.96	5.15	5.26	19.52	19.23

These results are in agreement with the proposed structure.

As model compounds for the study of infrared spectral changes we prepared 2-(*p*-aminophenyl) benzimidazole (M_1), phthalomonoanilide (M_2), N-phenylphtalimide (M_3), 2,2′ — di-(*p*-phthalaminodiphenyl)-5,5′-dibenzimidazolyl-methane (M_4) and 2,2′-diphthaliminophenyl)-5,5′ dibenzimidazolyl-methane (M_5).

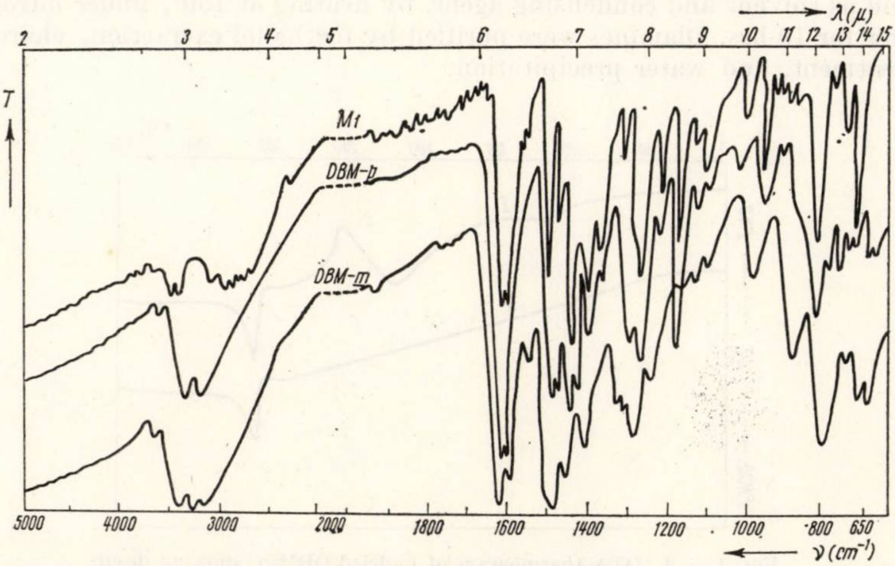

Fig. 2. — Infrared spectra of di-aminophenylbenzimidazoles (DBM) and the respective model compound M_1 (KBr pellet).

The infrared spectra of model compounds, monomers and polymers, shown in figs. 2—4, were recorded on a SP—200 Infrared Spectrometer.

POLYMERS

Polybenzimidazole-imides were prepared by the condensing reaction of benzimidazole containing diamines and pyromellitic anhydride by using dimethylsulfoxide as solvent. Other solvents as N-methylpyrrolidone, N-dimethylacetamide provide lower molecular weight polyamic acid prepolymers.

It was observed that the order of adding the reagents plays a proeminent part in obtaining high molecular weight polymers. High molecular weight polymers were obtained by adding theoretical amounts of solid dianhydride into a solution of diamine.

The condensation reaction takes place at 0° for 1 hr and for 8 hrs at room temperature. When the reaction takes place at room temperature only, a rapid growth of viscosity is observed, and the apparent "gel" yielded could be broken down by heating at 70° and vigorous stirring.

Absorption peaks of carboxyl groups were clearly observed in the infrared spectrum of model phthalomonoanilide (M_2) at 2450—2650, 1730 and 1240cm^{-1}. These absorption peaks of carboxyl groups in the polyamic acid and model compound (M_4) which contain benzimidazole rings, appear attenuated or replaced by absorption due to carboxylate ion near 1560 cm^{-1} (figs. 3 and 4).

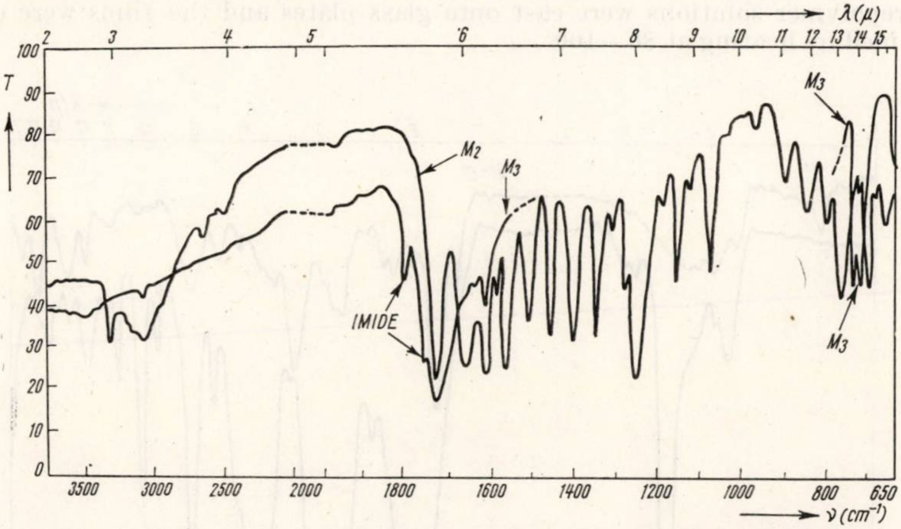

Fig. 3. — Infrared spectra of phthalomonoanilide (M_2) and N-phenylphthalimide (M_3) (KBr pellet).

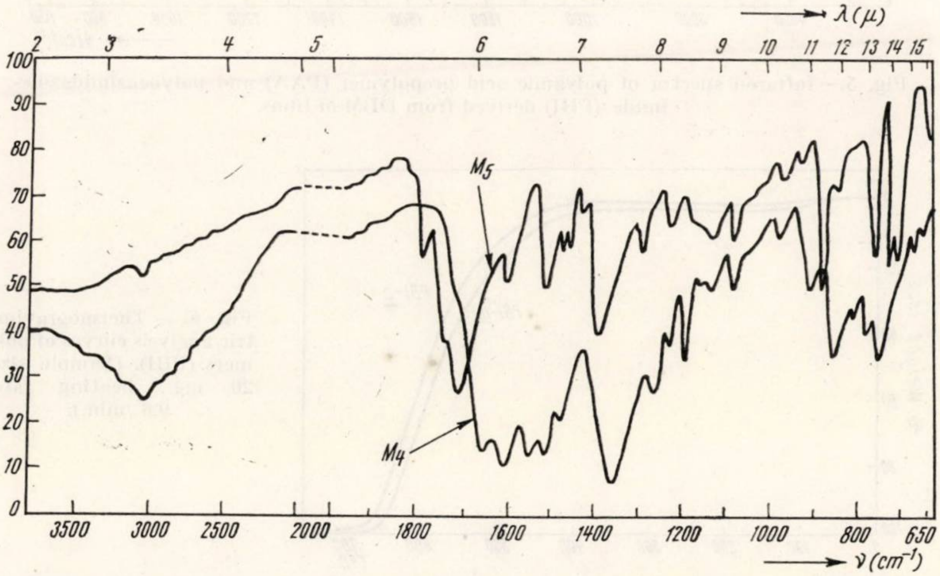

Fig. 4. — Infrared spectra of 2,2′-bis-(*p*-phthalamidophenyl)-5,5′-dibenzimidazolyl-methane (M_4) and 2,2′-bis-(*p*-phthaliminophenyl)-5,5′-dibenzimidazolyl-methane (M_5). (KBr pellet).

The broadening of the absorption peaks in the region of 1620 — —1720 cm^{-1} in the case of polyamic acid prepolymers, could be explained by the combined effects of carboxylate ions, nonionized acid and the amide groups, as supposed by Kurosaki and co-workers.[23] (fig. 5).

From polyamic acid prepolymer solutions good films could be cast. Prepolymer solutions were cast onto glass plates and the films were obtained by heating at 80–100°.

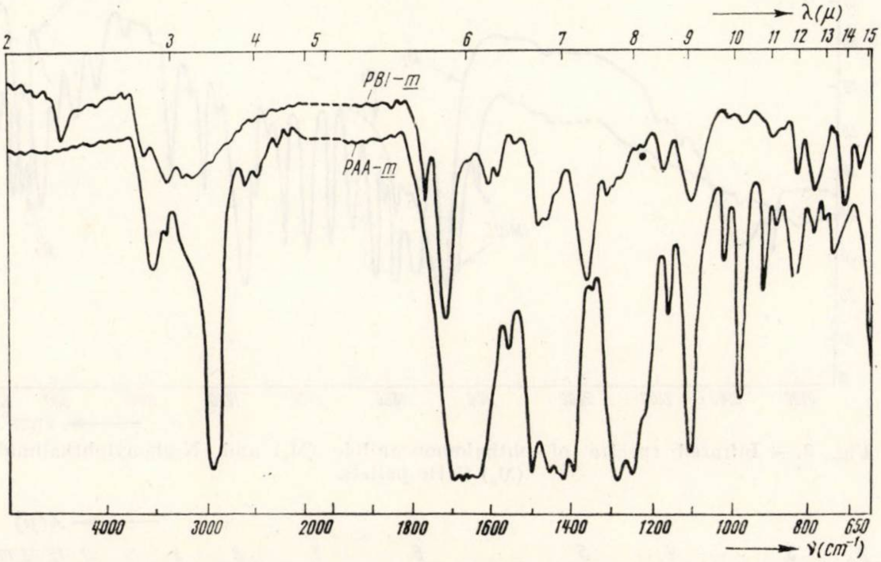

Fig. 5.—Infrared spectra of polyamic acid prepolymer (PAA) and polybenzimidazole-imide (PBI) derived from DBM-*m* films.

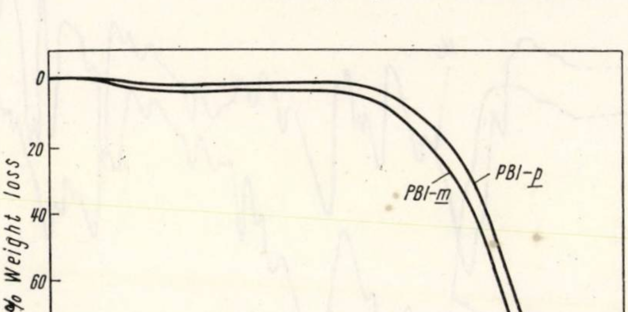

Fig. 6. — Thermogravimetric analysis curves of polymers (PBI). (Sample size: 20 mg., heating rate: 9.8°/min.).

Polyamic acid films were cured by 15′ heating at 150°, 180°, 230°, 260° and for 1 hr heating at 300° and converted in this way into transparent, flexible polybenzimidazole-imide films with great thermal stability. Disappearance of infrared absorption peaks of carboxyl and amide groups after thermal treatment at 300°, indicates that imidization took place (fig. 5).

---

[23] T. Kurosaki and P. R. Joung, *J. Polymer Sci., C*, **23**, 57 (1968).

Imide-absorption peaks appeared in the infrared spectra of polymers (PBI) around 720, 1710 and 1790 cm^{-1} (Fig. 5).

The inherent viscosities of polyamic acid prepolymers and the thermal stability of polymers (PBI) are summarized in table 2.

Table 2

Viscosity of polyamic acid prepolymers and thermal degradation of polymers (PBI)

Polymers	η inh[1]	Thermal degradation of polymers[2] (PBI) %				
		400°C	450°C	500°C	550°	600°C
PBI-*p*	1.68	0	3	9	21	53
PBI-*m*	0.74	0	6	14	35	62

[1] Inherent viscosity (η inh.) measurements were determined on a solution of 0.5 g. polymer dissolved in 100 ml dimethylsulfoxide.

[2] Samples were heated in air, temperature being increased at a rate of 9.8° C/min.

Thermal stabilities of polymers as depicted by TGA curves (fig. 6.) Initial weight losses occurred in the range 420–450°, in air.

EXPERIMENTAL

3,4,3′,4′-tetraaminodiphenylmethane was obtained, according to Meyer's method, [24–26] by the condensation of *o*-nitroaniline with formaldehide and reduction with tin and hydrochloric acid. It was recrystallized from benzene. m.p. 137–138° Lit. [26] m.p. 137–138°).

Aminobenzoic acids were purchased from Serva, Heidelberg. The commercial products were recrystallized from water, to yield colourless crystals, with m. p. 187–188° for *p*-aminobenzoic acid and m.p. 173–174°, for *m*-aminobenzoic acid.

Diaminophenylbenzimidazoles were prepared by Iwakura's method [27] of condensation of aminobenzoic acids and 3,4,3′,4′-tetraaminodiphenylmethane in polyphosphoric acid at 150° for 10 hrs. After purification and thermal treatment in vacuum, m.p. 322–323° was obtained (by DTA thermogram) for DBM-*p* and 206–209° for DBM-*m* (by the capillary method).

2-(p -aminophenylbenzimidazole (M_1) was prepared by the reaction of *o*-phenylenediamine and *p*-aminobenzoic acid. A 3.24 g (0.03 mole) amount of *o*-phenylenediamine was added with stirring to 80 ml of polyphosphoric acid (116 % P_2O_5) under a nitrogen atmosphere at 120°. *p*-Aminobenzoic acid (4.11g 0.03 mole) was added in small portions and heating was maintained at 150°, with stirring for 10 hrs, under nitrogen. The reaction mixture was precipitated with water. After filtration, the product was neutralized with aqueous ammonium hydroxide solution, filtered and dried. The product was purified by dissolution in methanol, treatment with charcoal, filtration and reprecipitation with water. Product yield was 48 %, m.p. 250–252° Lit. [23] m.p. 252°).

Anal. *Calc* . for $C_{13}H_{11}N_3$: C, 74.60 ; H, 5.31 ; N, 20.08 ;
Found : C, 74.13 ; H, 5.38 ; N, 20.42 %

---

[24] J. Meyer and M. Rohmer, *Ber. dtsch. chem. Ges.*, **33**, 252 (1900).

[25] J. Meyer and M. Rohmer, *Ber. dtsch. chem. Ges.*, **33** , 255 (1900).

[26] J. Meyer and M. Rohmer, *Ber. dtsch. chem. Ges.*, **30**, 257 (1897).

[27] Y. Iwakura, K. Uno, Y. Imai and M. Fukui, *Makromol. Chem.*, **77**, 41 (1964)

Phthalomonoanilide (M_2) was prepared by the reaction of phthalic anhydride (5.0 g., 0.0338 mole) and aniline (3.0 g, 0.0323 mole) in 30 ml. of benzene with stirring at 50°. The reaction product was recrystallized from ethanol. The yield of colourless crystals, m.p. 183—184°, was 85 %.

N-Phenylphthalimide (M_3)[23], was prepared from phthalomonoanilide by heating at 240° in a nitrogen atmosphere for 3 hrs. The product was recrystallized from tetrahydrofuran. m.p. 208—210°.

2,2′-bis-(p-Phthalamidophenyl)-5,5′-dibenzimidazolylmethane (M_4). 0.6 g of phthalic anhydride was added to a mixture of 0.86 g, 2,2′-di-(*p*-aminophenyl)-5,5′-dibenzimidazolyl-methane in 15 ml. of dimethylacetamide with stirring for 0.5 hr. The solid obtained was collected by filtration and washed with ethanol to give a yellow, infusible powder.

Anal. *Calcd.* for $C_{43}H_{30}N_6O_6$: C, 71.04 ; H, 4.02 ; N, 11.57 ;
Found : C, 69.48 ; H, 4.56 ; N, 11.88. (The product was complexed with solvent).

2,2′-bis-(p-Phtaliminophenyl)-5,5′-dibenzimidazolyl-methane (M_5). A 0.5 g amount of 2,2′-bis-(*p*-phthalamidophenyl)-5,5′-dibenzimidazolyl-methane was heated at 300° in a nitrogen atmosphere for 3 hrs. A yellow , infusible product was obtained.

Anal. *Calcd.* for $C_{43}H_{26}N_6O_4$: C, 74.76 ; H, 3.79 ; N, 12.17 ;
Found : C, 74.29 ; H, 3.86 ; N, 11.85.

Pyromellitic dianhydride. The dianhydride was purchased from Fluka AG, Buchs SG. The product was recrystallized from acetic anhydride and then sublimed at 260° at 1 mm, before use. m.p. 284—286°.

Polymerization. 2.15 g. of DBM-*p* or DBM-*m* was introduced into 29.2 ml dimethylsulfoxide with stirring, under nitrogen atmosphere, the solution being cooled to 0°. Solid dianhydride powder (1.10 g) was added slowly with stirring. The mixture was stirred at 0° for 1 hr and then at room temperature for 8 hrs. Sometimes, a "gel" was obtained. By heating at 70° or adding of solvent and rapid stirring the apparent "gel" was converted to a polymer solution.

The viscous polymer solution (from DBM-*p*) was cast by spreading polyamic acid solution onto glass plates, the solvent being evaporated at 80—100°, for 2—3 hrs. Polyamic acid films were cured by heating for 15′ in an oven at 150°, 180°, 230°, 260° and for 1 hr. at 300° in a nitrogen atmosphere. The films were brown, transparent, with great thermal stability.

Revue Roumaine de Chimie, **19**, *11*, 1791–1810 (1974)

HEAT TRANSFER WITH CHEMICAL REACTION MODELLING OF THERMAL DECOMPOSITION REACTIONS

RADU Z. TUDOSE
Polytechnic Institute of Jassy, Str. 23 August, 11, Jassy, Romania

Received September 17, 1973

The modelling of thermal decomposition reaction is derived for which heat transfer and chemical reaction may be limiting elementary processes. The unreacted-core shrinking model theory is extensively developed. Temperature distribution within the ash layer, as well as temperature at the grain surface and in the reaction zone are calculated. Conversion and conversion time are also estimated.

The study of heterogeneous catalytic reactions has attained a stage of development in which the theoretical basis of reactor design and operation have been laid. Engineering of the heterogeneous non-catalytic reaction is now in the stage of modelling and developing process mechanisms. Numerous attempts have been noticed in recent years for elucidating and systematizing the principal phenomenological aspects of these problems. Although these non-catalytic heterogeneous reactions are very complex, current knowledge of moment, heat and mass transfer processes on the one hand, and of kinetic data, on the other hand enable a comprehensive approach to these reactions.

Non-catalytic solid-gas reactions may often be influenced by a series of physical processes. In many practical cases mass and heat transfer are rate-controlling steps, influencing the chemical reaction to a greater extent.

A heterogeneous chemical reaction may develop by diffusing the gaseous reagent within the grain, where it reacts with the solid reagent, the heat effect being more or less important. However, in other cases, the gaseous phase does not contain the reagent, it acting only as heat carrier and as medium for gaseous reaction products. Consequently, the non-catalytic solid-gas reaction may be influenced, not only by the internal or external diffusion of reagents or reaction products, but also by the internal or external heat transfer, or by both.

According to the general model, developed in a previous paper, [1] the process takes place in three stages, the reaction developing within a reaction zone of δ_r thickness. By particularizing this model [2] one obtains the two models known in the literature as the "unreacted-core shrinking model"[3] and the "homogeneous model".[4,5] Mixed models[6] were also proposed which take into account the change of the process mechanism during reaction, as a consequence of the elementary process rate ratio variations. Wen and co-workers have extended the concept of "effectiveness factor,"[5] introduced for the catalytic reactions and developed the theory of non-catalytic heterogeneous reactions with thermal effects.[7]

---

[1] R. Z. Tudose, *Bul. Inst. Politeh. Iași,* **16**, 241, (1970).

The study of decomposition reactions, for which heat transfer is one of the determining elementary processes, is now at the stage of mathematical modelling trials, but all reported trials were devoted to particular cases.[8-10]

In the present paper an attempt is made to model these thermal decomposition reactions, for which either the external or internal heat transfer, or chemical reaction may be rate-controlling steps, some models being proposed whereby such a process can take place.

MODELLING OF THERMAL DECOMPOSITION REACTIONS

Decomposition reactions of carbonates and bicarbonates are endothermal. The gaseous phase is the heat carrier serving, at the same time, for entraining the reaction products. The overall process is based on the following elementary processes: heat transfer through the external limiting film, ash layer and reaction zone, chemical reaction and reaction products diffusion through the reaction zone, ash layer and external limiting film.

We shall discuss the case for which only the internal and external heat transfer as well as the reaction rate may be rate-controlling steps. This is the case of reactions developed at temperatures much higher than those corresponding to the equilibrium with reaction products.

Let us consider a reaction of the type given below:

$$B_{(s)} \rightarrow S_{(s)} + P_{(g)} + \Delta H \qquad (1)$$

where B is the solid reagent, S and P are the solid and gaseous reaction products, respectively and ΔH is the thermal effect of the reaction. Under certain reaction conditions the chemical reaction rate may be considered to be of zero order:

$$r_B = -k_s \qquad (2)$$

---

[2] R. Z. Tudose, *Génie Chim.*, **104**, 236 (1971).

[3] S. Yagi and D. Kunii, "Fifth Symposium (international) on Combustion", Reinhold, New York, 1955, p. 231.

[4] J. M. Ausman and C. C. Watson, *Chem. Eng. Sci.*, **17**, 323, (1962).

[5] M. Ishida and C. Y. Wen, *Amer. Inst. Chem. Engineers*, **14**, 311, (1968).

[6] R. Z. Tudose and E. Merică, *Bul. Inst. Politeh. Iași*, **18**, 42, (1972).

[7] C. Y. Wen and S. C. Wang, *Ind. Eng. Chem.*, **62**, 31, (1970).

[8] A. W. D. Hills, *Chem. Eng. Sci.*, **23**, 297, (1968).

[9] C. Calistru and L. Ifrim, *Bul. Inst. Politeh. Iași*, **14**, 209, (1968).

[10] C. Calistru and L. Ifrim, *Bul. Inst. Politeh. Iași*, **15**, 25, (1969).

where k_s denotes the reaction rate constant related to the surface. The physical model, accounting for the mechanism of such a reaction, depends on the ratio between the external, internal heat transfer resistance and chemical reaction resistance.

When the intensity of the thermal flux required for the reaction to develop is of the same order of magnitude as the intensity of the heat flux transferred by thermal conductivity within the grain, the reaction takes place within a zone of δ_r thickness. Its value will satisfy the condition $0 < \delta_r < R$. In this case the reaction develops in three stages, according to the general model with reaction zone, as shown in fig.1.

In the first stage, that of the formation of the reaction zone, two zones are to be found inside the grain : the reaction zone and the unreacted-core zone, fig. 1a.

At the very moment when the solid reagent is completely exhausted on the outer surface of the grain, the second stage, that of the shifting of the reaction zone, begins. One can distinguish now the outer ash layer, the reaction zone and the inner unreacted-core (fig. 1b). The third stage, the disappearance of the reaction zone, begins when the reaction zone reaches the centre of the grain, the unreacted-core disappearing completely. Thus, only the ash layer and the reaction zone remain inside the grain.

For cases in which resistance to chemical reaction is much greater than resistance to internal transfer, the reaction is considered to take place according to the two-stage homogeneous model, fig. 2., the thickness of the reaction zone being equal to the granule radius (($\delta_r = R$). In the first stage — forming of the reaction zone — only one zone exists inside the grain (fig. 2 a). The second stage — disappearence of the reaction zone — begins when the solid reagent concentration is equal to zero at the outer surface of the grain. Therefore only the reaction zone and the ash layer will coexist in the grain. fig. 2 b.

Thermal decomposition heterogeneous non-catalytic reactions in which resistance to chemical reaction is much smaller than resistance to internal heat transfer, take place according to the "one-stage unreacted-core shrinking model" of shifting of the reaction zone, fig. 3. Reaction zone thickness is zero, the reaction develops on a surface, and in the grain an ash layer and an unreacted-core zone separated by reaction interface is detected. The models presented in this paper lead to the conclusion that the mechanism of a thermal decomposition reaction depends significantly upon elementary process rate ratios. Depending on this ratio, for a R radius grain, a reaction zone is formed with a thickness comprised between zero and R, $0 \leqslant \delta_r \leqslant R$.

It is obvious that a perfect analogy exists between the models established for non-catalytic solid-gas reactions and for thermal decomposition reactions ; in both cases the reaction mechanism depends upon the ratio of elementary process rates. From the previously reported experimental studies on the decomposition of calcium carbonate[8] and sodium bicarbonate [9,10] one may conclude that the reaction takes place according to the "unreacted-core shrinking model". But the conclusions drawn on theoretical and practical grounds, by investigators of heterogeneous thermal descomposition reactions are sometimes rather contradictory.

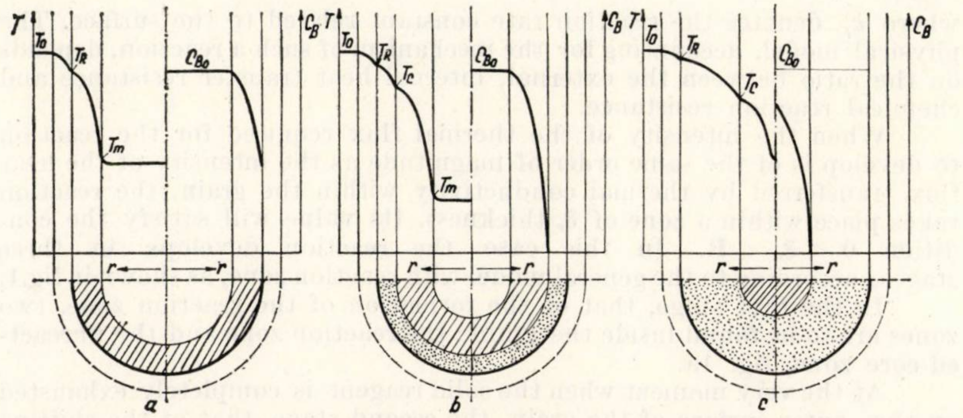

Fig. 1. — General model.

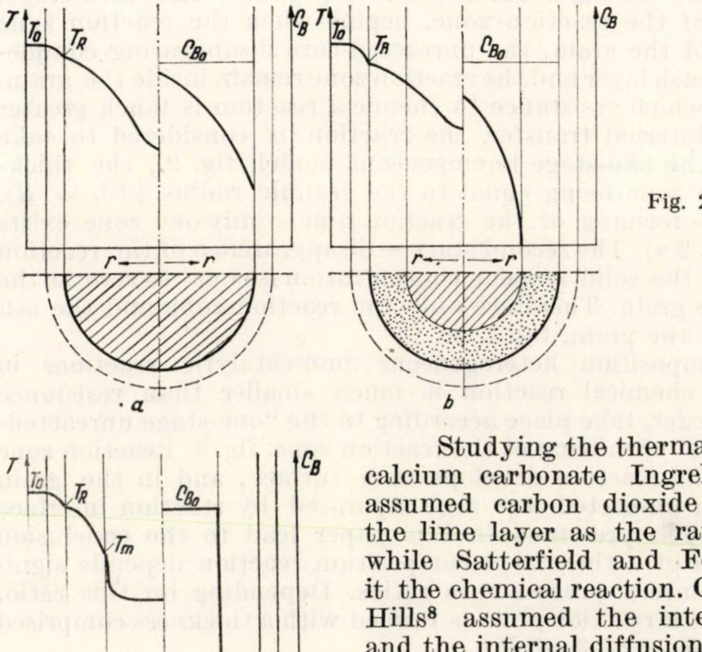

Fig. 2. — Homogeneous model.

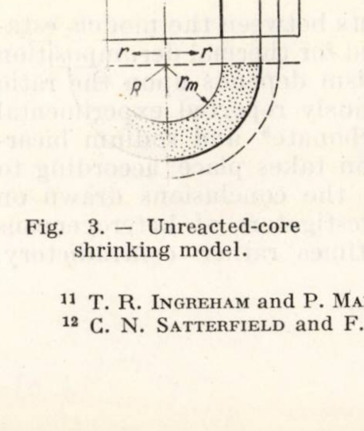

Fig. 3. — Unreacted-core shrinking model.

Studying the thermal decomposition of calcium carbonate Ingreham and Marier[11] assumed carbon dioxide diffusion through the lime layer as the rate-controlling step, while Satterfield and Feakes[12] considered it the chemical reaction. On the other hand, Hills[8] assumed the internal heat transfer and the internal diffusion of carbon dioxide as rate-controlling steps.

For the case of thermal decomposition of carbonates and bicarbonates the equilibrium relationship between the partial pressure of carbon dioxide and temperature has the shape shown in fig. 4 (curve 1).

If the process develops at atmospheric pressure and the temperature corresponds to equilibrium T_e, the reaction is influenced by the partial pressure of carbon dioxide in the entraining gas; the reaction order may be above zero. When $P_{CO_2}=1$, the reaction stops. Under the same pressure conditions there is a limiting temperature T_1, above which the reaction is not influenced by the carbon dioxide concentration in the entraining gas.

---

[11] T. R. Ingreham and P. Marier, *Canad. J. Chem. Eng.*, **41**, 170, (1963).

[12] C. N. Satterfield and F. Feakes, *Amer. Inst. Chem. Engineers J.*, **5**, 115 (1959).

At temperatures higher than the limiting temperature T_1, the reaction is of zero order. Thus, curve II separates a region (hatched) where the reaction is not influenced by the partial pressure of carbon dioxide in the entraining gas, its order being zero. Under these temperature conditions one may consider the reaction controlled either by external or internal heat transfer, or by heat consumption required for the chemical reaction to develop or only by one of these elementary processes.

The thermal effect of most thermal decomposition reactions is substantial and the reaction zone is an important heat consumer. As the thermal resistance of the ash layer is great, due to small thermal conductivity, it is obvious that most thermal decomposition reactions take place according to the unreacted-core shrinking model.

In the present paper the decomposition reactions of zero order taking place within the high temperature region (hatched region, fig. 4.) are modelled.

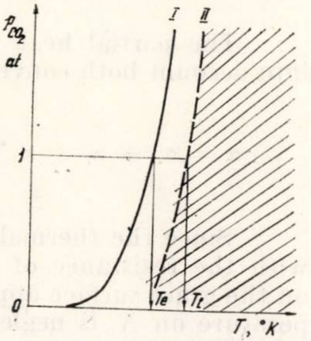

Fig. 4.—The equilibrium curve for the thermal decomposition of carbonates and bicarbonates.

THEORETICAL PART

Let us consider a spherical grain of homogeneous composition. At high temperatures a decomposition reaction takes place within the grain according to eq. 1. The grain diameter remains unchanged during the process. Based on the heat balance, for an unsteady-state regime, and taking the thermal effect into account one may write the following differential equation:

$$\frac{\partial T}{\partial t}=\frac{a}{r^2}\frac{\partial}{\partial r}\left(r^2\frac{\partial T}{\partial r}\right)-\frac{q'}{c_p\rho}$$

By differentiating the above equation and assuming a quasi-stationary regime one obtains:

$$\frac{\mathrm{d}^2 T}{\mathrm{d}r^2}+\frac{2}{r}\frac{\mathrm{d}T}{\mathrm{d}r}-\frac{q'}{\Lambda}=0 \tag{3}$$

where q' denotes the amount of heat expended per unit volume of the reaction zone and unit time. When the reaction takes place according to the unreacted-core shrinking model, hence on a surface, there is no heat-consuming within the ash layer and equation (3) is reduced to :

$$\frac{\mathrm{d}^2T}{\mathrm{d}r^2}+\frac{2}{r}\frac{\mathrm{d}T}{\mathrm{d}r}=0 \tag{4}$$

The boundary conditions at the two faces of the ash layer, according to fig. 3 will be :

$$\Lambda_c\frac{\mathrm{d}T}{\mathrm{d}r}=\alpha\,(T_0-T)\quad \text{at } r=R \tag{5}$$

$$T=T_m\qquad \text{at } r=r_m$$

The partial heat transfer coefficient, in the first condition, takes into account both convection and radiation heat transfer.

$$\alpha=\alpha_c+\alpha_r=\alpha_c+\alpha_r'\frac{T_0^4-T^4}{T_0-T}=\alpha_c+\alpha_r'\,(T_0+T)\,(T_0^2+T^2)$$

Since the thermal resistance of the gas film is small in comparison with the resistance of the other elementary processes, the temperature on the grain surface approaches T_0 and $\alpha_r\approx 4\alpha_r'\,T_0^3$. The effect of temperature on Λ_c is neglected.

By solving the equation (4) for the boundary conditions (5), the temperature distribution within the ash layer is obtained :

$$\frac{T-T_m}{T_0-T_m}=\frac{1-\dfrac{\lambda_m}{\lambda}}{1-\lambda_m+\dfrac{\lambda_m}{K_{\mathrm{Nu}}}} \tag{6}$$

The temperature at different points of the ash layer depends both on the reaction zone position and the value of Nusselt comparison number. This relationship is clearly depicted by the plots shown in fig. 5.

The reaction zone temperature may be determined by equating the heat amount transferred by thermal conductivity through the ash layer in the vicinity of the reaction zone, to the heat consumed during the chemical process.

The heat required for the grain to reach the reaction temperature is either neglected or included in the thermal effect of the reaction, under the assumption that heating of the solid to reaction temperature takes place as the reaction develops.

The heat transferred by thermal conductivity will be given by the Fourier laws :

$$q=-\Lambda_c\frac{\mathrm{d}T}{\mathrm{d}r}$$

The heat consumed during an endothermal reaction, of zero order, will be:

$$q = k_0 \, \Delta H \, \exp\left(- \frac{E}{R_g T_m} \right)$$

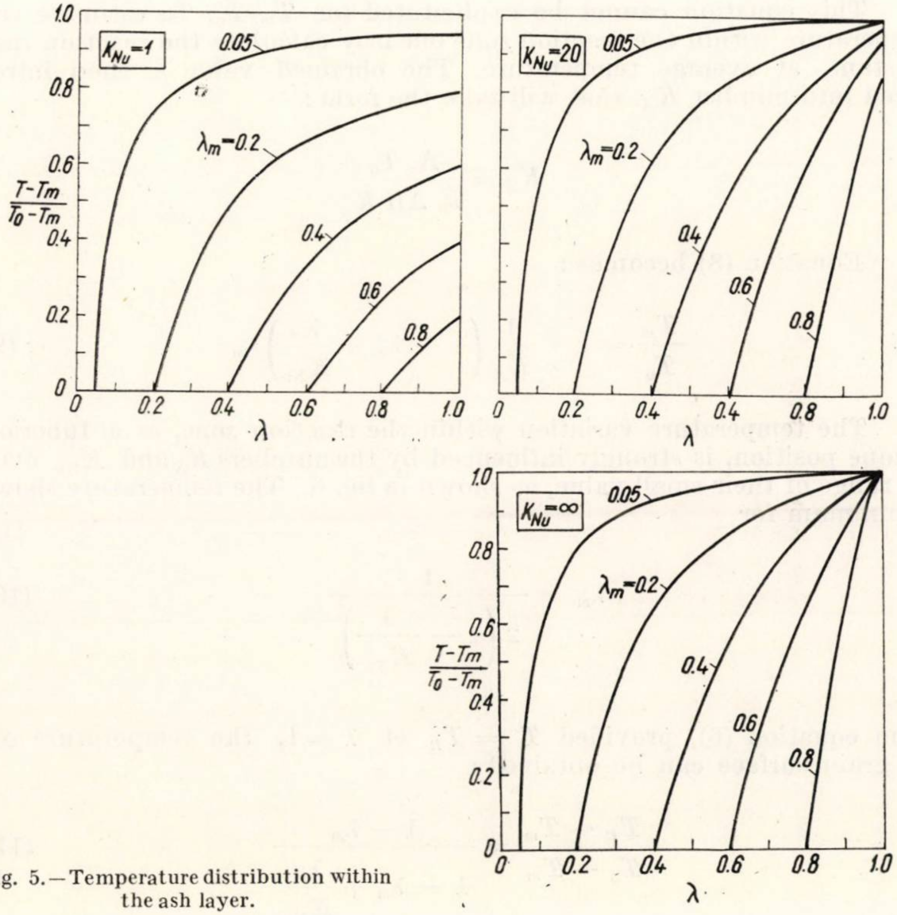

Fig. 5. — Temperature distribution within the ash layer.

For the case of quasi steady-state regime the two above heats may be equated, resulting the following equation:

$$\Lambda_c \frac{\mathrm{d}T}{\mathrm{d}r} = k_0 \, \Delta H \, \exp\left(- \frac{E}{R_g T_m} \right) \tag{7}$$

From eq. (7) and eq. (6) derivative, for $r = r_m$, the temperature of the reaction zone is obtained :

$$\frac{T_m}{T_0} = 1 - \frac{1}{K_A}\left(1 - \lambda_m + \frac{\lambda_m}{K_{\mathrm{Nu}}}\right)\lambda_m \exp\left(-\frac{K_{\mathrm{Ah}}}{T_m/T_0}\right) \tag{8}$$

This equation cannot be explicitated for T_m/T_0. To estimate the temperature within the reaction zone one may calculate the reaction rate constant, at average temperature. The obtained value is then introduced into number K_A, that will take the form :

$$\bar{K}_A = \frac{\Lambda_c\, T_0}{\bar{k}_s\, \Delta H\, R}$$

Equation (8) becomes :

$$\frac{T_m}{T_0} = 1 - \frac{1}{\bar{K}_A}\left(1 - \lambda_m + \frac{\lambda_m}{K_{\mathrm{Nu}}}\right)\lambda_m \tag{9}$$

The temperature variation within the reaction zone, as a function of zone position, is strongly influenced by the numbers K_{A} and K_{Nu} over the range of their small value, as shown in fig. 6. The temperature shows a minimum for

$$\lambda_m = \frac{1}{2\left(1 - \dfrac{1}{K_{\mathrm{Nu}}}\right)} \tag{10}$$

From equation (6), provided $T = T_R$ et $\lambda = 1$, the temperature on the grain surface can be obtained :

$$\frac{T_R - T_m}{T_0 - T_m} = \frac{1 - \lambda_m}{1 - \lambda_m + \dfrac{\lambda_m}{K_{\mathrm{Nu}}}} \tag{11}$$

Elimination of temperature T_m from eqs. (9) and (10) gives :

$$\frac{T_R}{T_0} = 1 - \frac{\lambda_m^2}{\bar{K}_B} \tag{12}$$

where number $\bar{K}_A = \bar{K}_A\, K_{\mathrm{Nu}} = \dfrac{\alpha\, T_0}{\bar{k}_s \Delta H}$

The temperature at the grain surface depends on the comparison numbers K_{Nu} or $\overline{K}_B$, as shown in fig. 7. At the onset of the conversion, for values $\overline{K}_R > 100$, the temperature at the grain surface is less than 1 % smaller compared to heat carrier temperature. This difference decreases as the conversion progresses.

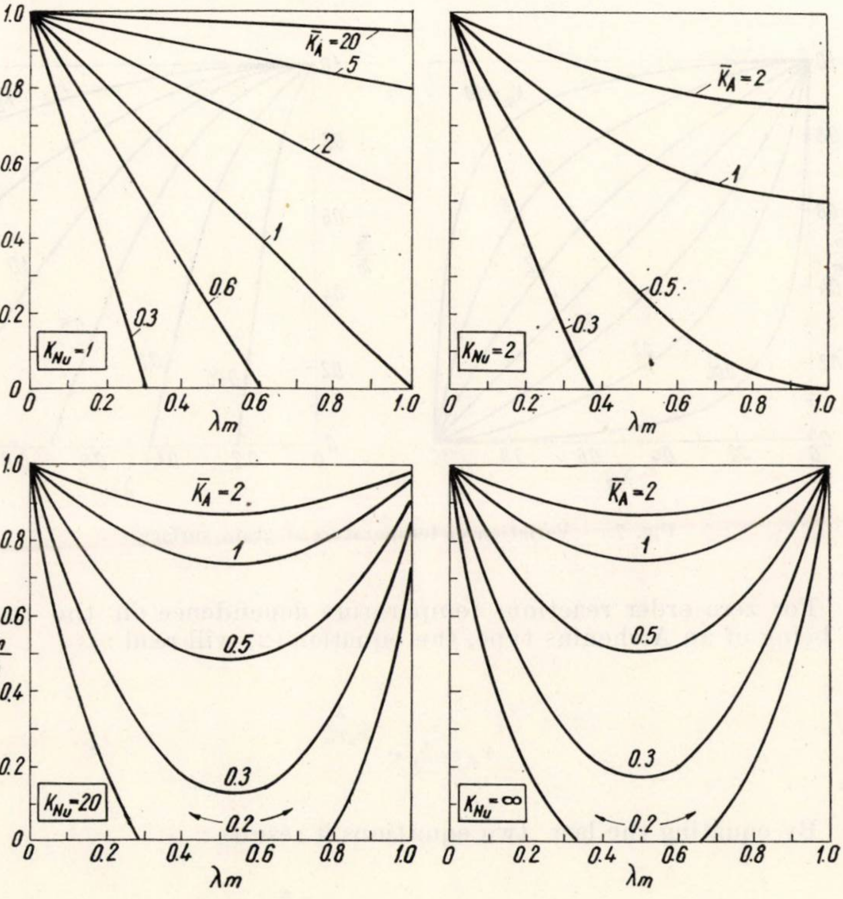

Fig. 6. — Variation of the reaction zone temperature, calculated by means of eq. (9)

The thermal decomposition reaction developing according to the "unreacted-core shrinking model" involves only one stage. The unreacted core of a homogeneous spherical grain keeps its size invariant, and the conversion is given by :

$$x = 1 - \left(\frac{r_m}{R}\right)^3 = 1 - \lambda_m^3 \tag{13}$$

During reaction the radius of the unreacted core is varying from R to zero. The reaction rate will have the form :

$$r_B = -\frac{1}{S}\frac{\mathrm{d}N_B}{\mathrm{d}t} = -\frac{1}{4\pi r_m^2} = \frac{\mathrm{d}\,(4/3\ \pi r_m^2\ C_{B_0})}{\mathrm{d}t} = -C_{B_0}\frac{\mathrm{d}\,r_m}{\mathrm{d}\,t} \qquad (14)$$

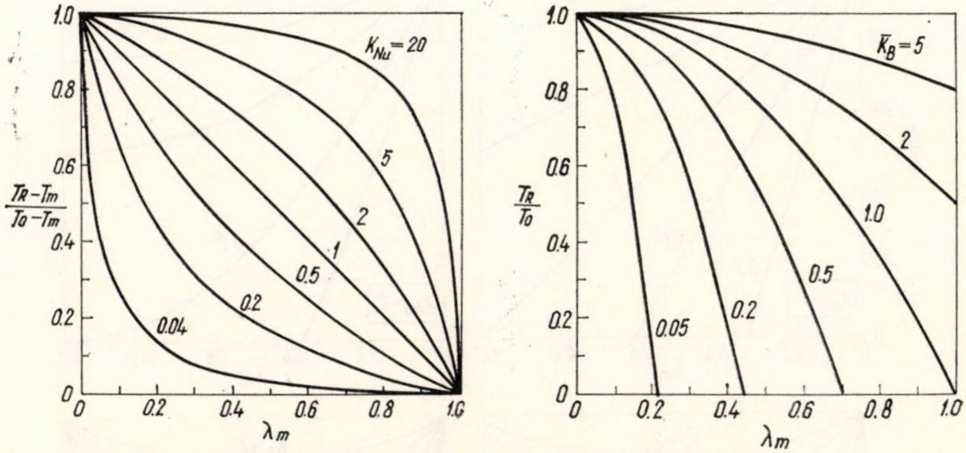

Fig. 7. — Variation of temperature at grain surface.

For zero order reactions temperature dependence on the reaction rate being of an Arrhenius type, the equation (2) will read :

$$r_B = k_0\,\mathrm{e}^{-\frac{E}{R_g T_m}} \qquad (15)$$

By equating the last two equations it results :

$$-\ C_{B_0}\frac{\mathrm{d}\,r_m}{\mathrm{d}\,t} = k_0\ \ \mathrm{e}^{-\frac{E}{R_g T_m}} \qquad (16)$$

After substituting the temperature of the reaction zone from equation (9) to equation (16) and separating the variables, the conversion time is obtained :

$$t_{1r} = -\frac{C_{B_0}}{k_0}\int_R^{r_m} \exp\left[\frac{E}{R_g\,T_0}\,\frac{1}{\frac{1}{\overline{K}_A R^2}\left(1 - \frac{1}{K_{\mathrm{Nu}}}\right) r_m^2 - \frac{1}{\overline{K}_A\,R}\ r_m + 1}\right]\mathrm{d}r_m \qquad (17)$$

The denominator has to fulfil the following condition :

$$\frac{1}{\overline{K}_A R^2}\left(1-\frac{1}{K_{\mathrm{Nu}}}\right) r_m^2-\frac{1}{\overline{K}_A R}\, r_m+1 \neq 0$$

The integral in equation (17) is of a transcedental type and may be solved only by expending it in series. If the first two terms of the series are considered it results :

$$t_{1r}=-\frac{C_{B_0}}{k_0}\left[\int_R^{r_m} \mathrm{d} r_m+K_{\mathrm{Ah}} \int_R^{r_m} \frac{\mathrm{d} r_m}{\frac{1}{\overline{K}_A R^2}\left(1-\frac{1}{K_{\mathrm{Nu}}}\right) r_m^2-\frac{1}{\overline{K}_A R}\, r_m+1}\right] \tag{18}$$

The second integral may admit three solutions, depending on the following conditions :

$$\begin{gathered}
\frac{1}{4 \overline{K}_A}+\frac{1}{K_{\mathrm{Nu}}}<1 \\
\frac{1}{4 \overline{K}_A}+\frac{1}{K_{\mathrm{Nu}}}=1 \\
\frac{1}{4 \overline{K}_A}+\frac{1}{K_{\mathrm{Nu}}}>1
\end{gathered} \tag{19}$$

By analysing the order of magnitude of the $\overline{K}_A$ and K_{Nu} comparators, one may conclude that only the solution corresponding to the first condition is of interest. After solving the two integrals and rearranging the terms the conversion time is obtained :

$$\begin{aligned}
t_{1r}=\frac{C_{B_0} R}{k_0}&\left\{1-\lambda_m+K_{\mathrm{Ah}} \frac{2 \overline{K}_A}{\sqrt{4 \overline{K}_A\left(1-\frac{1}{K_{\mathrm{Nu}}}\right)-1}}\,\cdot\right. \\
&\left.\cdot \tan^{-1}\left[\frac{(1-\lambda_m) \sqrt{4 \overline{K}_A\left(1-\frac{1}{K_{\mathrm{Nu}}}\right)-1}}{\left[2\left(1-\frac{2}{K_{\mathrm{Nu}}}\right)-1\right] \lambda_m+2 \overline{K}_A-1}\right]\right\}
\end{aligned} \tag{20}$$

For $\lambda_m=0$ the overall conversion time is given by :

$$\begin{aligned}
t_1=\frac{C_{B_0} R}{k_0}&\left\{1+K_{\mathrm{Ah}} \frac{2 \overline{K}_A}{\sqrt{4 \overline{K}_A\left(1-\frac{1}{K_{\mathrm{Nu}}}\right)-1}}\,\cdot\right. \\
&\left.\cdot \tan^{-1}\left[\frac{\sqrt{4 \overline{K}_A\left(1-\frac{1}{K_{\mathrm{Nu}}}\right)-1}}{2 \overline{K}_A-1}\right]\right\}
\end{aligned} \tag{21}$$

When the heat transfer through the external limiting film is not determining, $K_{\mathrm{Nu}} = \infty$ and the last two equations reduce to the form :

$$t_{1r} = \frac{C_{B_0}R}{k_0}\left\{1 - \lambda_m + K_{\mathrm{Ah}}\frac{2\overline{K}_A}{\sqrt{4\overline{K}_A - 1}}\tan^{-1}\left[\frac{(1-\lambda_m)\sqrt{4\overline{K}_{\mathrm{A}} - 1}}{\lambda_m + 2\,\overline{K}_{\mathrm{A}} - 1}\right]\right\} \tag{22}$$

$$t_1 = \frac{C_{B_0}R}{k_0}\left\{1 + K_{\mathrm{Ah}}\frac{2\overline{K}_A}{\sqrt{4\overline{K}_A - 1}}\tan^{-1}\left[\frac{\sqrt{4\overline{K}_A - 1}}{2\overline{K}_A - 1}\right]\right\} \tag{23}$$

In the equation set (20—23) the term $(C_{B_0}R/k_0) = b_0$ has a time dimension, so that it is possible to write them in the form of a dimensionless time. For instance, the last two equations become :

$$\tau_{1r} = 1 - \lambda_m + K_{\mathrm{Ah}}\frac{2\overline{K}_A}{\sqrt{4\overline{K}_A - 1}}\tan^{-1}\left[\frac{(1-\lambda_m)\sqrt{4\overline{K}_A - 1}}{\lambda_m + 2\overline{K}_A - 1}\right] \tag{24}$$

$$\tau_1 = 1 + K_{\mathrm{Ah}}\frac{2\overline{K}_A}{\sqrt{4\overline{K}_A - 1}}\tan^{-1}\left[\frac{\sqrt{4\overline{K}_A - 1}}{2\overline{K}_A - 1}\right] \tag{25}$$

By means of equations (13), (24) and (25) the plots shown in fig. 8 were depicted.

It can be seen that the conversion time is influenced by comparators $\overline{K}_A$ and $\overline{K}_{\mathrm{Nu}}$, but the influence of Arrhenius comparator is more significant. For low values of $\overline{K}_A$ the conversion time increases notably during the last stage of the reaction.

By integrating equation (18) for the third condition given in (19) one obtains the following equations for the current and overall conversion time, respectively :

$$t_{1r} = \frac{C_{B_0}R}{k_0}\left\{1 - \lambda_m + K_{\mathrm{Ah}}\frac{\overline{K}_A}{\sqrt{1 - 4\overline{K}_A\left(1 - \frac{1}{K_{\mathrm{Nu}}}\right)}}\ln \times\right.$$

$$\left.\times\frac{\left[2\left(1-\frac{1}{K_{\mathrm{Nu}}}\right)\lambda_m + \sqrt{1-4\overline{K}_A\left(1-\frac{1}{K_{\mathrm{Nu}}}\right)} - 1\right]\left[2\left(1-\frac{1}{K_{\mathrm{Nu}}}\right) - \sqrt{1-4\overline{K}_A\left(1-\frac{1}{K_{\mathrm{Nu}}}\right)} - 1\right]}{\left[2\left(1-\frac{1}{K_{\mathrm{Nu}}}\right)\lambda_m - \sqrt{1-4\overline{K}_A\left(1-\frac{1}{K_{\mathrm{Nu}}}\right)} - 1\right]\left[2\left(1-\frac{1}{K_{\mathrm{Nu}}}\right) + \sqrt{1-4\overline{K}_A\left(1-\frac{1}{K_{\mathrm{Nu}}}\right)} - 1\right]}\right\} \tag{26}$$

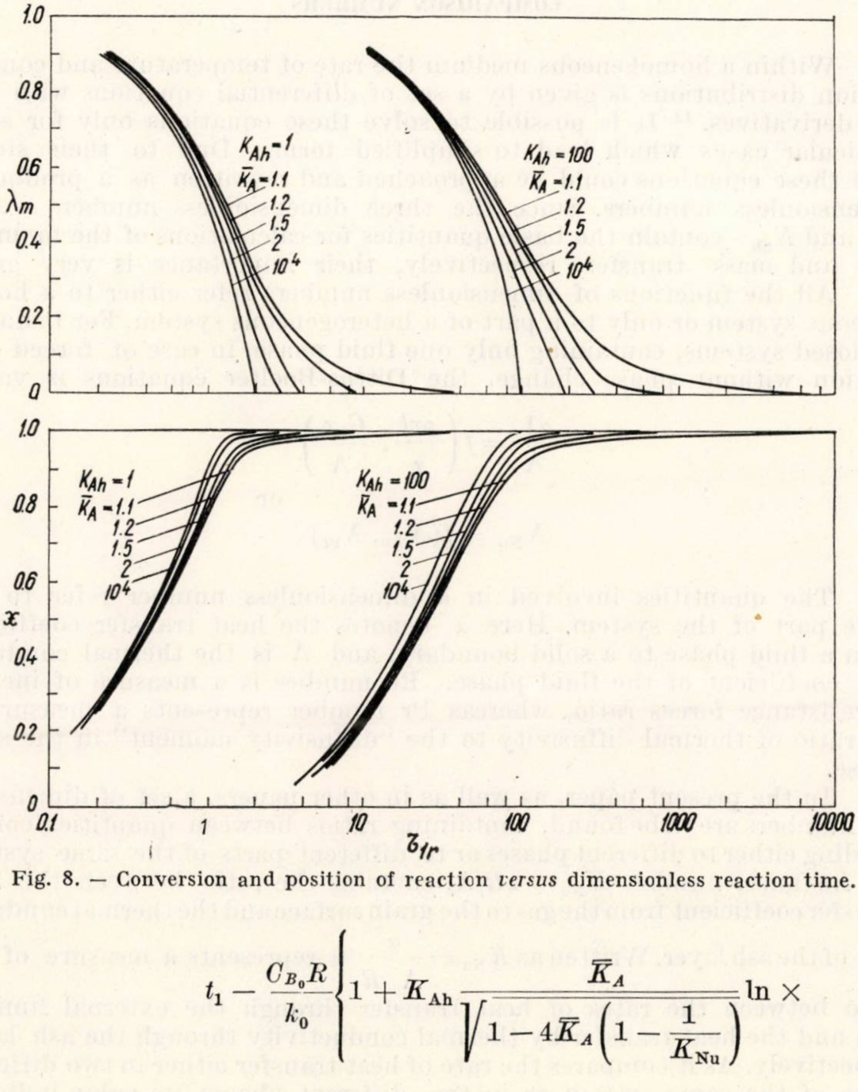

Fig. 8. — Conversion and position of reaction *versus* dimensionless reaction time.

$$t_1 = \frac{C_{B_0}R}{k_0}\left\{1 + K_{\mathrm{Ah}}\frac{\overline{K}_A}{\sqrt{1-4\overline{K}_A\left(1-\dfrac{1}{K_{\mathrm{Nu}}}\right)}}\ln \times\right.$$

$$\left.\times \frac{\left[1-\sqrt{1-4\overline{K}_A\left(1-\dfrac{1}{K_{\mathrm{Nu}}}\right)}\right]\left[2\left(1-\dfrac{1}{K_{\mathrm{Nu}}}\right)-\sqrt{1-4\overline{K}_A\left(1-\dfrac{1}{K_{\mathrm{Nu}}}\right)}-1\right]}{\left[1+\sqrt{1-4\overline{K}_A\left(1-\dfrac{1}{K_{\mathrm{Nu}}}\right)}\right]\left[2\left(1-\dfrac{1}{K_{\mathrm{Nu}}}\right)+\sqrt{1-4\overline{K}_A\left(1-\dfrac{1}{K_{\mathrm{Nu}}}\right)}-1\right]}\right\} \tag{27}$$

For $K_{\mathrm{Nu}} = \infty$ both equations get a simplified form. Nevertheless, their usefulness is rather limited.

COMPARISON NUMBERS

Within a homogeneous medium the rate of temperature and concentration distributions is given by a set of differential equations with partial derivatives.[13] It is possible to solve these equations only for some particular cases which lead to simplified forms. Due to their similitude these equations could be approached and rewritten as a product of dimensionless numbers. Since the three dimensionless numbers — N_{Eu}, N_{Nu} and N_{Sh} — contain the basic quantities for calculations of the moment, heat and mass transfer, respectively, their importance is very great.

All the functions of dimensionless numbers refer either to a homogeneous system or only to a part of a heterogeneous system. For instance, in closed systems, containing only one fluid phase, in case of forced convection without phase change, the Dittus-Boelter equations is valid:

$$\frac{\alpha 1}{\Lambda}=f\left(\frac{\rho v l}{\eta}, \frac{C_p \eta}{\Lambda}\right)$$

or

$$N_{\mathrm{Nu}}=f(N_{\mathrm{Re}}, N_{\mathrm{Pr}})$$

The quantities involved in a dimensionless number refer to the same part of the system. Here α denotes the heat transfer coefficient from a fluid phase to a solid boundary, and Λ is the thermal conductivity coefficient of the fluid phase. Re number is a measure of inertial to resistance forces ratio, whereas Pr number represents a measure of the ratio of thermal diffusivity to the "diffusivity moment" in the same phase.

In the present paper, as well as in other papers, a set of dimensionless numbers are to be found, containing ratios between quantities corresponding either to different phases or to different parts of the same system. For instance, number $K_{\mathrm{Nu}}=\alpha R/\Lambda_c$ contains the ratio between the heat transfer coefficient from the gas to the grain surface and the thermal conductivity of the ash layer. Written as $K_{\mathrm{Nu}}=\dfrac{\alpha}{\Lambda_c/R}$ it represents a measure of the ratio between the rates of heat transfer through the external limiting film and the heat transfer by thermal conductivity through the ash layer, respectively. As it compares the rate of heat transfer either in two different parts of the same system or in two different phases, its value indicates which of the processes is the determining one. Owing to their significance these numbers will be referred to as comparison numbers or comparators.

In equation (8) number K_A, given below, represents a measure of the ratio between the rate of heat transfer by thermal conductivity through the ash layer and the rate of heat consumption in the reaction zone.

The comparison number $K_{\mathrm{Ah}}=K_{\mathrm{Ah}}=E/\mathrm{R}gT$, known as exponent in the Arrhenius equation, has a similar meaning. The Arrhenius comparator is a measure of the reaction activation energy to the molecular kinetic energy ratio.

---

[13] R. B. Bird, W. E. Stewart and E. L. Lightfoot, "Transport Phenomena", John Wiley and Sons, New York, 1960, p. 71, 310, 554.

For the thermal decomposition reactions K_A and K_{Ah} comparators are particularly important, their value giving indications on the rate determined processes.

Temperature variation on the grain surface, given by equation (12), is a function of $\bar{K}_A$ and K_{Nu} comparators product. This product, written as $K_B = \alpha T_0/k_0 \; \Delta H$, is a measure of the ratio between the heat amount transferred through the external limiting film and that consumed in the reaction zone. Its value specifies which of the two processes above is the determining one.

In a previous paper[1,2] on the modelling of non-catalytic solid-gas reactions, the Sherwood comparators were introduced :

$$K_{Sh_r} = \frac{k_t R}{D_r} \qquad K_{Sh_c} = \frac{k_t R}{D_c}$$

Both numbers give a measure of the ratio of the mass transfer rate through the external limiting film to that through the reaction zone or ash layer, respectively. Two denominations are encountered in the reported papers : "fictitious Sherwood number"[1] and "modified Sherwood number"[7]. For the non-catalytic heterogeneous reactions the Thiele comparator, known in literature as the Thiele modulus, has a particular significance.

$$K_{Ti,r} = R \sqrt{\frac{a' k_v C_{B_0}}{D_r}} \qquad K_{Ti,c} = R \sqrt{\frac{a' k_v C_{B_0}}{D_c}}$$

The above Thiele moduli compare the rate of reactant consumption to that of reactant diffusion through the reaction zone or ash layer, respectively.

DISCUSSION

The models developed in this paper refer to those grains which do not change their size in the course of the process. To establish the mechanism (model), according to which a thermal decomposition reaction takes place, the dimensionless thickness of the reaction zone λ_r was taken as a principal criterion. In the case of endothermal reactions, with significant thermal effect, the thickness of the reaction zone is zero, the reaction taking place according to the unreacted-core shrinking model.

The mathematical analysis of endothermal heterogeneous non-catalytic chemical reactions, for which the internal and external heat transfer and the rate of heat consumption can be rate-determined processes, allows to calculate the temperature on the grain surface and in the reaction zone, as well as temperature distribution within the ash layer. The equations derived contain four dimensionless numbers which were termed comparison numbers or comparators. Each comparator gives a measure of a two elementary-processes rate ratio, its value providing information on the rate determined process. For thermal decomposition reactions comparators K_A and K_{Ah} are particularly important.

The temperature variation in the reaction zone, as a function of conversion, is given by eq. (8). However, its usefulness is rather limited because it cannot be explicited for estimating the T_m/T_0 ratio. By replacing the unexponential factor in the Arrhenius type equation of the reaction rate constant with the reaction rate constant itself, calculated at average temperature, equation (9) was obtained.

The reaction rate constant is significantly influenced by temperature. The admission of an average value $\bar{k}_s$ to simplify equation (8), seems to introduce great errors. However, calculating the temperature of the reaction zone relative to its position, based on eq. (8), by means of a computer, it was found that for numbers $K_A > 5$, the temperature in the reaction zone varies over a rather narrow range. The use of comparator K_A, calculated by means of the reaction rate constant average value, will introduce errors which do not affect significantly chemical engineering calculations.

As shown in figs. 6,9 the temperature passes through a minimum during conversion. The minimum, according to eq. (9) will correspond to the reaction zone position predicted by eq. (10). When the thermal resistance of the external limiting film is small enough to be completely neglected, the temperature on the grain surface is equal to T_0, and the minimum of the reaction zone temperature corresponds to $r_m = R/2$, when the external limiting film has a thermal resistance, $T_R < T_0$ and the minimum shifts to the grain centre.

The reaction zone temperature passes through a minimum, its position being strongly influenced by K_{Nu} comparator and, to a lesser extent, by K_{Ah}. This minimum may be assigned to the variation of the ratio

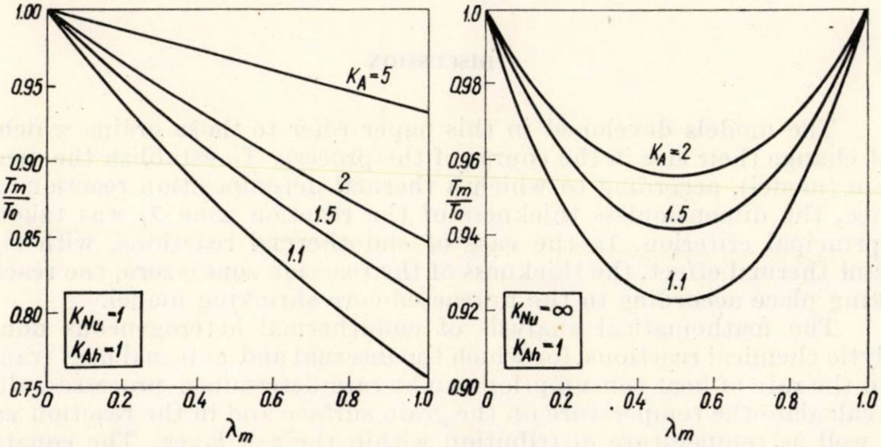

Fig. 9. — Variation of the reaction zone temperature estimated by means of eq. (8).

between the heat amount required for the reaction to develop and that transferred by thermal conductivity through the ash layer, during conversion course. The heat amount consumed during reaction is directly proportional to r_m^2, while the thermal resistance of the ash layer is directly proportional to the difference $(1/r_m) - (1/R)$.

These relationships account for the existence of a temperature minimum.

The time of conversion may be calculated by means of equations (20) and (21), as well as by means of the simplified equations (22, 23, 24 or 25). For numbers $K_A > 10$ variation of the reaction zone temperature is quite insignificant. Calculations may be made by using an average value $T_m = \overline{T}_m$ or, in cases in which the Nusselt comparator has great values, by letting $T_m = T_0$. Thus, equations (16) may be rewritten as follows :

$$- C_{B_0} \frac{\mathrm{d}r_m}{\mathrm{d}t} = \bar{k}_s \tag{28}$$

where $\bar{k}_s$ denotes the reaction rate constant, calculated by means of the average reaction zone temperature. Therefore, $\bar{k}_s$ is independent of r_m.

After separating the variables equation (28) becomes :

$$t_{1r} = - \frac{C_{B_0}}{k_0} \exp\left(\frac{E}{R_g \overline{T}_m}\right) \int_R^{r_m} \mathrm{d}r_m$$

and then:

$$t_{1r} = - \frac{C_{B_0}}{k_0} (1 - \lambda_m) \exp. \overline{K}_{\mathrm{Ah}} \tag{29}$$

For $\lambda_m = 0$, the overall conversion time is :

$$t_1 = \frac{C_{B_0} R}{k_0} \exp. \overline{K}_{\mathrm{Ah}} \tag{30}$$

Equations (29) and (30) may be rewritten under a dimensionless form, as given below :

$$\tau_{1r} = (1 - \lambda_m) \exp. \overline{K}_{\mathrm{Ah}} \tag{31}$$

$$\tau_1 = \exp. \overline{K}_{\mathrm{Ah}} \tag{32}$$

By comparing eq. (31) and (32) to eq. (24) and (25) it has been ascertained that they are approximately identical. For $K_{\mathrm{Ah}} > 10$ eq. (24) and (25) get the simplified forms :

$$\tau_{1r} = (1 - \lambda_m)(1 + K_{\mathrm{Ah}}) \tag{33}$$

$$\tau_1 = 1 + K_{\mathrm{Ah}} \tag{34}$$

where $1 + K_{\mathrm{Ah}}$ denotes the first two terms of the exponential series. The graphical representation of equation (31) in logarithmic coordinates results in a family of straight lines with slope equal to unity, as shown in fig. 10. The intersection of these lines with the line of abscissa of unity gives the overall conversion time.

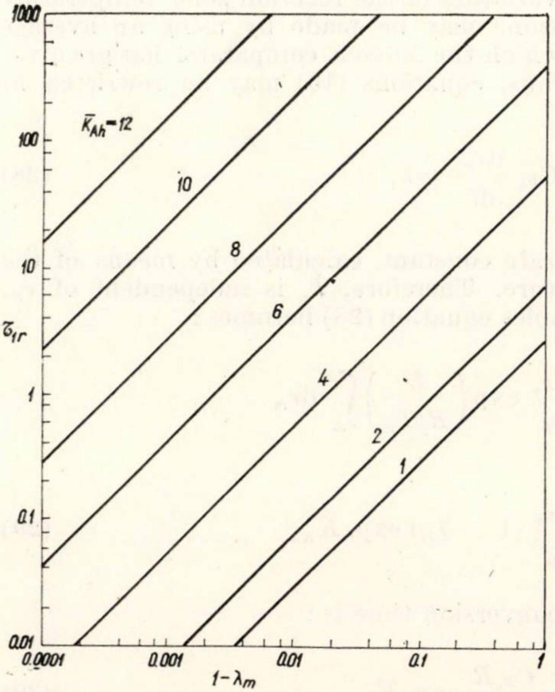

Fig. 10. — Conversion time *versus* position of the reaction zone for different values of K_{Ah} comparator.

Some studies concerning the kinetics of thermal decomposition reactions provide data for the activation energy and the rate constant of the reaction. These quantities depend upon the nature of the material i.e. on temperature, but also upon granulosity, which means that the apparent activation energy and the apparent reaction rate were determined, as the chemical process was masked by the physical one.

The modelling of these reactions points out the possibilities for determining the exact values of the two quantities. First, it is recomended to perform a kinetic study of the decomposition reactions on materials of different granulosities. Then, the relationship between the apparent reaction rate constant and the grain diameter is represented graphically. Extrapolation of the curve, for granulosity values of zero, will give the real reaction rate constant. The activation energy may be obtained in the same way, as well as by means of the real reaction rate constants determined at different temperatures.

The models developed in the present paper account for the mechanism whereby a thermal decomposition reaction takes place. Development of the unreacted-core shrinking model theory permits to calculate the temperature distribution in the ash layer, as well as the dependence of the reaction zone temperature and that of the grain surface upon the position of the reaction zone.

By means of the equations derived in the last part of the paper the conversion time may also be calculated.

NOMENCLATURE

a — thermal diffusivity coefficient, m^2/h

a' — stoichiometric coefficient, dimensionless

C_{B_0} — initial concentration of the solid reactant in the grain, mol/m^3

C_p — specific heat, $J/Kg°C$

D — effective diffusion coefficient, m^2/h

D_c — effective diffusion coefficient through the ash layer, m^2/h

D_r — effective diffusion coefficient through the reaction zone, m^2/h

E — activation energy of the reaction, J/mole

ΔH — thermal effect of the reaction, J/mole

k_s — reaction rate constant referred to area, $mole/m^2h$

$\bar{k}_s$ — ibid., calculated at the average temperature of the reaction zone, mol/m^2h

k_v — reaction rate constant referred to volume, $mole/\,/m^3h$

k_t — mass transfer coefficient through the external limiting film, m/h

$K_A = \dfrac{\Lambda_c T_0}{R k_0 \Delta H}$, comparison number A, dimensionless

$\bar{K}_A = \dfrac{\Lambda_c T_0}{R \bar{k}_s \Delta H}$, comparison number A, calculated by means of the average value of the reaction zone temperature, dimensionless

$K_{Ah} = \dfrac{E}{R_g T_0}$, Arrhenius comparison number, dimensionless

$K_B = \dfrac{\alpha T_0}{k_0 \Delta H}$, comparison number B, dimensionless

$\bar{K}_B = \dfrac{\alpha T_0}{\bar{k}_s \Delta H}$, comparison number B, calculated by means of the average value of the reaction rate constant, dimensionless

$K_{Nu} = \dfrac{\alpha_R}{\Lambda_c}$, Nusselt comparison number, dimensionless

$K_{Sh} = \dfrac{k_t R}{D}$, Sherwood comparison number, dimensionless

K_{Sh_c} — Sherwood comparison number referred to the ash layer, dimensionless
K_{Sh_r} — Sherwood comparison number referred to the reaction zone, dimensionless
$K_{\mathrm{Ti}} = R\sqrt{\frac{a' k_v C_{B_0}}{D}}$, Thiele comparison number, dimensionless
K_{Ti_c} — Thiele comparison number referred to the ash layer, dimensionless
K_{Ti_r} — Thiele comparison number referred to the reaction zone, dimensionless
l — current length, m
$N_{\mathrm{Eu}} = \Delta p/v^2\rho$, Euler number, dimensionless
$N_{\mathrm{Nu}} = \alpha l/\Lambda$, Nusselt number, dimensionless
$N_{\mathrm{Pr}} = C_p\eta/\Lambda$, Prandtl number, dimensionless
$N_{\mathrm{Re}} = \rho v l/\eta$, Reynolds number, dimensionless
p — partial pressure of a gaseous component, N/m^2
q — intensity of thermal flux, J/m^2h
q' — heat consumed during reaction, J/m^3h
r — distance from the grain centre m
r_B — chemical transformation rate of the solid reagent, B, mole/m²h
r_m — unreacted core radius, m
R — grain radius, m
R_g — gas constant, J/mole°C
S — area, m²
t — time, h
t_0 $= C_{B_0}R/k_0$, h
t_{1r} — current conversion time, h
t_1 — overall conversion time, h
T — temperature, K
T_0 — gaseous phase temperature, K
T_m — reaction zone temperature, K
T_R — temperature at the grain surface, K
v — velocity, m/s
x — conversion, dimensionless
α — partial heat transfer coefficient, w/m² °C
α_c — partial convective heat transfer coefficient, w/m² °C
α_r — partial radiation heat transfer coefficient, w/m² °C
α_r' — partial radiation heat transfer coefficient, w/m² $(\mathrm{C}^\circ)^4$
δ_r — reaction zone thickness, m
η — dynamic viscosity, N s/m²
λ $= r/R$, dimensionless
λ_m $= r_m/R$, dimensionless
Λ — thermal conductivity, w/m °C
Λ_c — thermal conductivity of the ash layer, w/m °C
ρ — density, kg/m³
τ — time, dimensionless
τ_{1r} $= t_{1r}/t_0$, conversion time, dimensionless
τ_1 $= t_1/t_0$, overall conversion time, dimensionless

Revue Roumaine de Chimie, **19**, *11*, 1811–1815 (1974)

SILVER-SILVER HALIDE ELECTRODES IN MOLTEN SODIUM NITRATE-BARIUM NITRATE EUTECTIC

SURENDER K. JAIN
Hindu College, University of Delhi, Delhi-110007, India.

Received January 17, 1974

Considering Ag/Ag^+ (1 mole kg^{-1}), as standard reference, the thermodynamic parameters for the electrode process have been evaluated from the temperature dependence of emf of the concentration cell (A). The reversibility of silver-silver halide electrodes in molten eutectic mixture of sodium nitrate-barium nitrate has been examined at 623 K.

INTRODUCTION

For the study of association equilibria in molten salts *emf* methods are among the most accurate and convenient, when suitable reversible electrodes are available. In molten nitrates, Ag/Ag^+ electrode has been the only suitable electrode of first kind and has been extensively used for the study of the association of silver ions with halide ion.[1–6] In similar studies for the metal cations e.g. Cd^{2+}, Pb^{2+} and TI^+, for which the electrode of first kind is not available, silver-silver halide electrodes, are successfully employed.[7] The only restricting factor is solubility of silver halides at working temperature in desired solvent. Solubilities of silver halides in this solvent, measured[8] over the range 620–695 K, are found reasonably low to facilitate the functioning of such electrode systems. As a preliminary step towards the studies for the association of Cd^{2+} and TI^+ with halide ions in this solvent it was necessary to establish the reversibility of the silver-silver halide electrode system in this solvent. The results obtained are presented in the paper.

---

[1] M. Blander, F. F. Blankenship and R. F. Newton, *J. Phys. Chem.*, **63**, 1259 (1959).

[2] D. G. Hill, J. Braunstein and M. Blander, *ibid.* **64**, 1038 (1960).

[3] J. Braunstein and M. Blander, *J. Phy. Chem.*, **64**, 10 (1960).

[4] J. Braunstein and J. D. Brill, *J. Phy. Chem.*, **70**, 1261 (1966).

[5] H. C. Gaur and R. S. Sethi, *Trans. Faraday. Soc.*, **64**, 445 (1968).

[6] H. C. Gaur and N. P. Bansal, *J. Chem. Soc.*, *Faraday* Transactions I, **68**, 1368 (1972).

[7] Peter C. Lammers and Jerry Braunstein, *J. Phy. Chem.*, **71**, 2626 (1967).

[8] H. C. Gaur, S. K. Jain and N. P. Bansal *J. Electronal. Chem.*, **30**, 225 (1971).

EXPERIMENTAL

A concentration cell (A) was set up. Experimental details were similar to those reported earlier.[8]

$$\begin{array}{c|c||c|c} \begin{array}{c}\mathrm{Ag}\\(-)\end{array} & \begin{array}{c}\mathrm{AgNO_3}(m')\text{ in}\\\text{molten solvent}\end{array} & \begin{array}{c}\mathrm{AgNO_3}(m)\\ \overset{+}{\mathrm{Na_X}}\text{ in molten solvent}\end{array} & \begin{array}{c}(\mathrm{Ag})\\(+)\end{array} \end{array} \qquad (A)$$

Reference half-cell Indicator half-cell.

In the absence of NaX (X =Cl, Br, I) the cell emf. exhibited Nernst behaviour. For measurements of cell (A) containing about 10^{-2} mole $\mathrm{Kg^{-1}}$ $\mathrm{AgNO_3}$ an equivalent amount of NaX was added to the indicator half-cell to ensure saturation of the solution *w.r.t.* silver halides. Thereafter solid Nax was added in small quantities and the corresponding emf (at 623 K) of the cell was measured (reproducible to ±0.0002 volts), the temperature dependence of the emf. was investigated in the presence of excess of AgX in the melt.

RESULTS AND DISCUSSION

In the presence of excess of halide ions (in a solution saturated w.r.t. AgX), the electrode system of right hand half-cell could be regarded as a silver-silver halide (second-kind) electrode, and the standard electrode potential of it would be expressed as,

$$E^\circ_{\mathrm{Ag\,|\,AgX(s)\,|\,X^-}} = E^\circ_{\mathrm{Ag\,|\,Ag^+}} + \frac{RT}{F}\ln K^\circ_{\mathrm{sp}} \qquad (1)$$

Taking Ag/Ag$^+$ (1 mole kg^{-1}) electrode as reference, eq. (1) becomes:

$$E^\circ_{\mathrm{Ag\,|\,AgX\,|\,X^-}} = \frac{RT}{F}\ln K^\circ_{\mathrm{sp}} \qquad (2)$$

and as a result of this assumption regarding standard reference, all thermodynamic quantities for the silver-silver halide electrode reaction are equal to the corresponding quantities for the dissolution process. If the enthalpy and entropy change over the entire range of temperature are assumed to be constant, the free energy for the dissolution reactions can be expressed as:

$$\Delta G^\circ = \Delta G^\circ_{623} - \Delta S^\circ\,(T - 623) \qquad (3)$$

The parameters ΔG°_{623} and ΔS°_{623} have been determined for AgCl, AgBr and AgI, by the least-square method. A non-random systematic distribution of the residuals when plotted *vs* temperature reflect that the linear relation is unsatisfactory for expressing these data, hence ΔH°, and ΔS° may not be temperature independent (Cf. ref.[9]) (equivalent to assuming $\Delta C_p \neq 0$). Now, assuming that $\Delta C_p^\circ \neq 0$, but remains constant over the temperature range, the expression for the various thermodynamic parameters are :

---

[9] G. A. Sacchetto, G. A. Mazzocchin and G. G. Bombi, *J. Electronalyt. Chem.*, **20**, 435 (1969).

$$\Delta H^{\circ} = \Delta H^{\circ}_{623} + \Delta C^{\circ}_{p}(T-623) \qquad (4)$$

$$\Delta S^{\circ} = \Delta S^{\circ}_{623} + \Delta C^{\circ}_{p} \ln\ (T/623) \qquad (5)$$

$$\Delta G^{\circ} = \Delta G^{\circ}_{623} + \Delta C^{\circ}_{p}\,(T-623-T\ln\,(T/623)) - \Delta S^{\circ}_{623}\,(T-623) \qquad (6)$$

Parameters ΔG°_{623} ΔC°_{p} and ΔS°_{623}, computed by least square method, are tabulated in table 1. Although eq. (16) did not completely eliminate nonrandomness of residuals it significantly reduced the standard deviations of the fit [0.064 to 0.029 for AgCl (32 points); from 0.042 to 0.028 for AgBr (24 points); and from 0.215 to 0.100 for AgI (58 points)]. It may be pointed out that ΔC°_{p} values, however, show a regular increasing trend from chloride to iodide but their magnitude should be taken with some cautions since a small error in the temperature dependence of the measured function could introduce significant error in ΔC°_{p}. The temperature dependence of various parameters for the electrode process is given by the following equations:

Table 1

Standard Thermodynamic Quantities (at 623 K) for the electrode reaction

$AgX(s) + \bar{e} \rightleftarrows Ag(s) + X^{-}$

X	ΔG°_{623} Kcal/mole	ΔH°_{623} Kcal/mole	ΔS°_{623} Cal/mole	ΔC°_{p}	$-E^{\circ}$ (mV)
Cl	11.441	17.042	8.99	8.94	489.26
Br	16.201	24.225	12.88	13.45	674.24
I	23.608	30.293	10.73	45.99	1018.5

AgCl

ΔG° (cal/mole) $= 11.441 - 8.99\ (T-623) + 8.94\ (T-623-T\ \ln\ (T/623))$

ΔH° (cal/mole) $= 17.042 + 8.94\ (T-623)$

ΔS° (cal/mole) $= 8.99 + 8.94\ \ln\ (T/623)$

ΔE° (mV) $= -489.3 + 0.022\ (T-623) - 6.287\ (T-623-T\ \ln\ (T/623))$

AgBr

ΔG° (cal/mole) $= 16.201 - 12.88\ (T-623) + 13.45\ (T-623-T\ \ln\ (T/623))$

ΔH° (cal/mole) $= 24.225 + 13.45\ (T-623)$

ΔS° (cal/mole) $= 12.88 + 13.45 \ln\ (T/623)$

ΔE° (mV) $= -674.2 + 2.33\ (T-623) - 55.97\ (T-623-T \ln\ (T/623))$

AgI

ΔG° (cal/mole) $= 23.608 - 10.73\ (T-623) + 45.99\ (T-623-T \ln\ (T/623))$

ΔH° (cal/mole) $= 30.293 + 45.99\ (T-623)$

ΔS° (cal/mole) $= 10.73 + 45.99 \ln\ (T/623)$

ΔE° (mV) $= -1018.5 - 0.107\ (T-623) - 7.74\ (T-623-T \ln\ (T/623))$

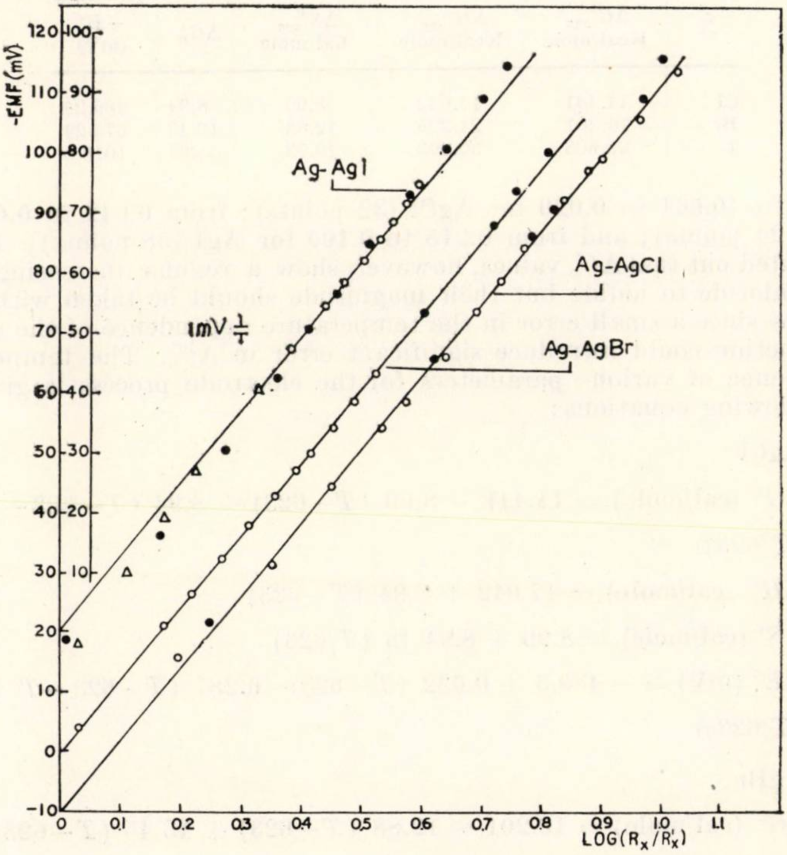

Fig. 1. — Plots of emf (mV) *vs* log R_{X^0}/R'_X–($R_{X'} = \dfrac{n_{X'}}{n_{X'} + n_{NO_3'}}$.

The reversibility of the silver-silver halide electrode systems (at 623 K) was investigated by measuring the *emf* of the cell (B):

$$\begin{array}{c|c|c|c} \text{Ag} & \text{X}^-\ (R')\ \text{in molten} & \text{X}^-\ (R)\ \text{in molten} & \text{Ag} \\ (-) & \text{solvent (sat. with} & \text{solvent (sat. with} & (+) \\ & \text{AgX)} & \text{AgX).} & \end{array} \quad \text{(B)}$$

Reference half-cell Indicator half-cell

as a function of halide ion concentration in indicator half-cell, the concentration of the reference half-cell being fixed. Plots of *emf vs*

$$\log\ (R_{X^-}/R'_{X^-})$$

where:

$$R_{X^-} = \frac{n_{X^-}}{n_{\text{NO}_3^-} + n_{X^-}}$$

over a considerable concentration range of halide ion are given in fig. 1. For Ag/AgCl and Ag/AgBr electrode system the Nernst slope in the plots ranged within ±1 mV to the theoretical value of 123.6 mV for one electron process at 623 K. The higher slope noted in the case of Ag/AgI system might be attributed to the partial oxidation of iodide to iodate in this solvent at higher temperatures.

ACKNOWLEDGEMENTS. The author wishes to express his sincere thanks to Prof. H.C. Gaur, University of Delhi, for providing research facilities.

Revue Roumaine de Chimie, **19**, *11*, 1817 – 1823 (1974)

THE CONDUCTANCE OF SOME ALKALINE ALKOXIDES IN ETHANOL-BENZENE AND ETHANOL-DIMETHYLFORMAMIDE MIXTURE AT 25°

FLORICA BĂRBULESCU*, AURORA GREF* and MARGARETA CRAIU**
*University of Bucharest, Bd. Republicii, 13, Romania
**Centre of Physical Chemistry, str. Galaţi, 31, Romania

Received January 31, 1974

Unlike methoxides, the Li, Na, and K ethoxides present interionic associations even in pure alcohol. The association constant varies appreciably with the variation of the dielectric constant of the solvent. The inadequacy of the significance assigned to the interionic parameter in the electrostatic theory of interionic association is pointed out. Conductance data are discussed comparatively with the results from the Raman spectra.

INTRODUCTION

The Alkoxides have both a theoretical and a practical interest; theoretically, they are interesting owing to their complex reaction mechanism in solutions, whereas practically, methoxides and ethoxides can be used as catalysts in many solution-phase reactions. The problems raised by such uses have revealed the insufficient knowledge of the properties of this class of compounds.

Conductometric and spectral (infrared and Raman) studies carried out upon solutions of alkoxides in pure alcohol or solvent mixtures containing alcohol have proved to be very useful for demonstrating the main interactions occurring among the particles of these systems: the ion-ion and ion-solvent interactions.

In this paper, some results are reported of conductometric and Raman-spectrometric studies carried out upon solutions of Li, Na, and K ethoxides in pure ethanol and in mixtures of ethanol with non-polar solvents (benzene) and with strongly polar solvents (dimethylformamide).

EXPERIMENTAL

Ethanol was anhidrised on iodine-activated magnesium, which had been refluxed in distillation flask for 10 – 15 hours and then fractionated in an inert atmosphere. The purity criterion was the specific conductance (in all determinations $\chi < 10^{-6} \Omega^{-1} cm^{-1}$). Traces of water were determined by the K. Fischer method, the higest admitted content being 0,01 %.

Benzene, kept on Na wire was freshly distilled before each utilization; benzene utilized in dielectric constant determinations was initially crystallized fractionary, retaining only the 5.50° fraction.

Dimethylformamide was dried on 4Å molecular sieves and then distilled at reduced pressure. ($\chi < 10^{-6}\Omega^{-1}\text{cm}^{-1}$).

Ethoxides were prepared by the direct reaction of the high purity metal with desaerated alcohol, in a vessel as in fig. 1. All manipulations were carried out under inert gas, in a chamber, to protect the reaction.

The determination of the ethoxide solution was made by conductometric titration with 0.1 N hydrochloric acid, as in the case of methoxides.[1]

Conductance determinations were carried out with an accuracy of 0.05% using a Wynne-Kerr bridge and a cell with a constant of $0.7790\ \text{cm}^{-1}$, estimated with KCl solutions in a range of $(1-6).10^3$N, according to the Fuoss-Zwolenik method.[2]

The experimental device used for the determination of conductance changes vs. concentration was described earlier.[3]

Determinations of the dielectric constant were performed with a DM01–WTW-type bridge with a dial extension of 4500 units; a self-made cell was used, that allowed to estimate the dielectric constant in a range of 1–35 DK units with an accuracy of 0.05%. (Fig. 2). The apparatus calibration was made with benzene, methanol, n-propanol and nitrobenzene, purified according to Bunger and Reddicks indications.[4]

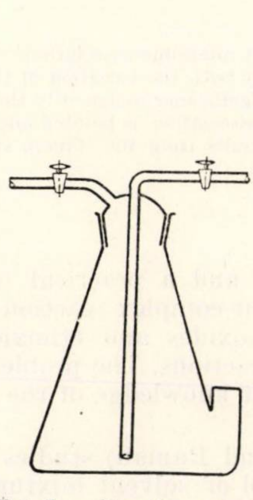

Fig. 1. — Reaction vessel.

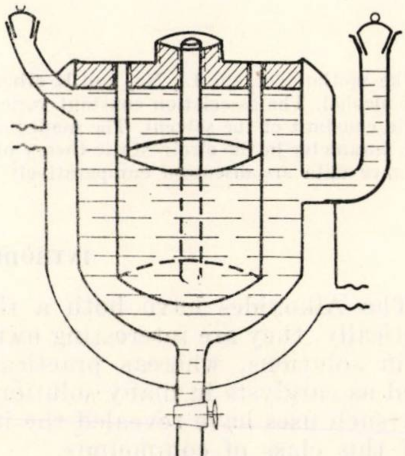

Fig. 2. — Cell for dielectric constant determination.

Viscosity determinations were made with a Höppler BH-2-type viscosimeter, the accuracy being 1%.

Densities were measured with a picnometer.

The Raman spectra were photoelectrically recorded with a Steinheil GH spectrograph, with a Toronto-type mercury lamp as excitation sourse. The accuracy in frequency measurement was ±1 cm^{-1} for narrow lines and $\pm 2-3\ \text{cm}^{-1}$ for broad lines.

RESULTS AND DISCUSSIONS

In table 1 the values of determined conductances in terms of ethoxide concentration in various solvents, at 25°, are given.

---

[1] Fl. Bărbulescu, A. Gref şi A. Botea, *Anale Univ. Buc.*, **21** (1), 19 (1972).

[2] J. E. Lind, I. J. Zwolenik and R. M. Fuoss, *J. Amer. Chem. Soc.*, **81**, 1557 (1959).

[3] Fl. Bărbulescu şi A. Gref, *Anale Univ. Buc.*, **20** (2), 6 (1971).

[4] J. A. Reddick and W. B. Bunger, "Organic Solvents, Physical Properties and Methods of Purification", Third Ed., 1970, p. 833.

Table 1

The Λ(*c*) values for Li, Na, and K ethoxides in mixtures of $C_2H_5OH-C_6H_6$ and $C_2H_5OH-DMF$ at 25°, for various molar fractions (x) of the added component

$LiOC_2H_5$

$x_{C_6H_6} = 0.068$		$x_{C_6H_6} = 0.141$		$x_{DMF} = 0.1663$	
$c.10^3$ [N]	$\Lambda(\Omega^{-1}cm^2)$	$c.10^3$ [N]	$\Lambda(\Omega^{-1}cm^2)$	$c.10^3$ [N]	$\Lambda(\Omega^{-1}cm^2)$
3.889	23.28	3.522	20.41	2.986	33.38
4.525	22.38	4.098	19.53	3.574	32.53
5.158	21.69	4.671	18.80	4.159	31.80
		5.809	17.59	4.740	31.30
5.788	21.60	6.934	10.65	5.319	30.47
6.414	20.50	8.048	15.88	5.895	29.90

$NaOC_2H_5$

$x_{DMF} = 0.0403$		$x_{DMF} = 0.0814$		$x_{DMF} = 0.166$	
2.599	35.73	2.172	37.46	1.951	40.54
3.240	34.90	2.707	36.64	2.433	39.92
3.879	34.09	3.240	35.87	2.912	39.22
4.512	33.33	3.770	35.18	3.388	38.64
5.145	32.68	4.297	34.54	3.862	37.85
5.773	32.08	4.822	33.95	4.333	37.18

KOC_2H_5

$x_{C_6H_6} = 0.0679$		$x_{C_6H_6} = 0.141$		$x_{DMF} = 0.0814$	
2.136	38.11	1.969	35.84	2.229	40.36
2.367	37.67	2.359	34.77	2.668	39.55
2.597	37.22	2.742	33.93	3.103	38.98
2.826	36.83	3.126	33.16	3.538	38.45
3.054	36.42	3.507	32.48	3.970	37.97
3.281	36.07	3.887	31.83	4.399	37.54

$x_{DMF} = 0.1663$	
1.973	42.86
2.362	42.44
2.748	41.72
3.133	41.18
3.515	40.64
3.895	40.15

Processing of conductance data was made using the Fuoss-Onsager[5] equation for the associate electrolytes:

$$\Lambda = \Lambda_0 - Sc^{1/2} r^{1/2} + Ecr \log cr + Jcr - K_A \Lambda cr f_\pm^2 \qquad (1)$$

using an IBM computer and a Fortran IV program. The constants necessary for the estimation of the coefficients in equation (1) (densities, viscosities, dielectric constants) had been previously determined, the corresponding values being given in table 2.

---

[5] R. M. Fuoss and F. Accascina, "Electrolytic Conductance", Int. Publ. New York, 1959, p. 127–207.

Table 2

Properties of the solvent mixtures at 25°

Solvent	γ added fraction	d [(g/cm³)]	η (Poisse)	χ (Ω^{-1}cm^{-1})	ε dielectric const.
C_2H_5OH*	0	0.7851	0.01084	5.10^{-7}	24.30
$C_2H_5OH+5\%C_6H_6$	0.03340	0.7903	0.01052	3.10^{-7}	23.41
$C_2H_5OH+10\%C_6H_6$	0.06796	0.7944	0.01030	3.10^{-7}	22.18
$C_2H_5OH+20\%C_6H_6$	0.1409	0.8036	0.00953	4.10^{-7}	19.72
$C_2H_5OH+5\%$DMF	0.03836	0.7932	0.01047	5.10^{-7}	25.16
$C_2H_5OH+10\%$DMF	0.07764	0.8024	0.01020	5.10^{-7}	25.75
$C_2H_5OH+20\%$DMF	0.1592	0.8182	0.00946	7.10^{-7}	26.88

* Landolt Börnstein, "Electrische Eigenschaften" I, Teil *6*, 1959, 677

In table 3 the values for the Λ_0, K_A and a parameters resulting from the optimisation of equation (1) are given, as well as the values of the limiting slopes, those calculated, $S_{calcd.}$, and those obtained from the experimental data, $S_{expl.}$, from the slope of the straight line $\Lambda(\sqrt{c})$. According to table 3, the difference between the experimental and the theoretical slope is positive for all ethoxides in pure alcohol, increasing with the decrease of the dielectric constant which accompanies the increase of the benzene content in solvent mixture. In DMF mixtures the difference decreases gradually, becoming insignificant at a molar fraction of 0.166 DMF.

Table 3

Conductance parameters for ethoxides in mixtures of $C_2H_5OH-C_6H_6$ and $C_2H_5OH-DMF$, at 25°

	$x_{ad.}$	$S_{expld.}$	$S_{calcd.}$	Eq.(1)			$\frac{\Lambda_0\eta_0}{D}$	$1/D$
				[Ω^{-1} cm^2] Λ_0 ($\pm$0.05)	K_A[1/mol] ($\pm$10%)	a(Å) ($\pm$0.1)		
$LiOC_2H_5(C_2H_5OH)$	0	178	141	39.50	79	3.30	0.0179	0.0412
$LiOC_2H_5(C_2H_5OH+C_6H_6)$	0.0679	180	145	37.67	132	3.50	0.0174	0.0451
,,	0.1409	199	170	36.27	317	3.85	0.0174	0.0507
$LiOC_2H_5(C_2H_5OH+DMF)$	0.1663	156	146	43.02	56	3.15	0.0151	0.0372
$NaOC_2H_5(C_2H_5OH)$	0	170	145	41.25	50	3.50	0.0188	0.0412
$NaOC_2H_5(C_2H_5OH+DMF$	0.0403	158	145	43.73	45	3.60	0.0183	0.0397
,,	0.0814	155	146	44.71	38	3.35	0.0177	0.0388
,,	0.1663	156	149	46.30	31	3.20	0.0162	0.0372
$KOC_2H_5(C_2H_5OH)$	0	165	147	44.67	36	3.70	0.0203	0.0412
$KOC_2H_5(C_2H_5OH+C_6H_6)$	0.0679	185	170	42.90	51	4.00	0.0199	0.0451
$KOC_2H_5(C_2H_5OH+DMF)$	0.0814	162	149	47.14	29	3.60	0.0187	0.0388
,,	0.1663	155	154	49.92	25	3.45	0.0175	0.0372

The variation of the limiting slope is in agreement with the variation of the association constant, explaining satisfactorily the variation of the limiting equivalent conductance with the fraction of added solvent.

The study of the total Walden product, $\Lambda_0\eta_0/D_0$[6], determined in these mixtures, shows that this product is constant in the case of $C_2H_5OH-C_6H_6$ and presents small variations, within 0.1%, in the case of C_2H_5OH-

---

[6] J. Lind and R. M. Fuoss, *J. Phys. Chem.*, **65**, 1413 (1961).

DMF. However, we could hardly conclude that in passing from one mixture of solvents to another, any change would occur in ion solvation.

Determiation of the interionic parameter from the $J(a)$ coefficient of the conductance equation has resulted in values that vary appreciably with the composition of the solvent. An increase of the interionic parameter with the decrease of dielectric constant was noticed, in disagreement with the requirements of the electrostatic theory of the interionic association, reminding the dependence of the critical parameter of association (R) on the dielectric constant, $R = e^2/2DkT$.

Starting from this remark, the plotting $\log \cdot K_A = f(1/D)$ must be a curve like that of fig. 3 and not a straight line, as it follows from the electrostatic theory of association, where a is a specific parameter for the electrolyte and is independent of the nature of the solvent. The logarithms of the association constants determined for the Li, Na, and K ethoxides present a linear variation in terms of $1/D$ (Fig. 4). This fact is due to the relative restricted range, of 19—27 D.K. units, on which the determinations were made.

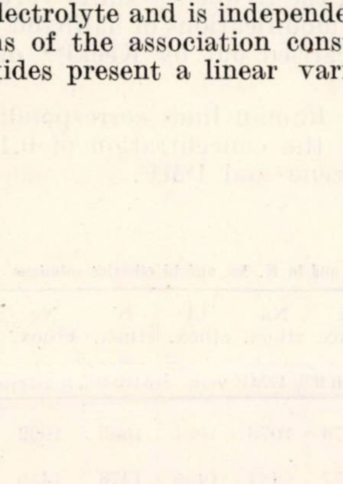

Fig. 3. — Variation of the association constant *vs.* reciprocical dielectric constant, provided that $a = f(1/D)$.

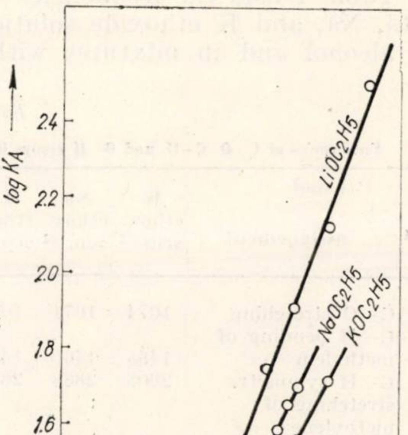

Fig. 4. — Variation of the association constant in the series of ethoxides *vs.* dielectric constant.

Other authors[7] effecting for association constants determinations on wider dielectric constant ranges have pointed out concavities like those in fig. 3. This fact was considered to result from systematic errors of determinations and not from discrepancies in the significance of the interionic parameter itself, as emphasized by our data.

At the same time we recorded the Raman spectra of ethoxides in pure ethanol and of ethoxides in ethanol with addition of benzene and DMF.

The modification of the frequencies corresponding to the vibration modes of the C—O, C—H, and O—H bonds was followed, as a consequence of the ion-ion or ion-solvent interactions that appear in the presence of the ethoxide. Also, together with the frequency shifts variations appear in the molar integral intensity and modifications of halfband width of the Raman lines. Such studies were carried out by Keçki[8,9] only in the case of methoxides.

Table 4 lists the frequencies of the Raman lines corresponding to the Li, Na, and K ethoxide solutions at the concentration of 0.1N, in pure alcohol and in mixtures with benzene and DMF.

Table 4

Frequencies of C—O, C—H, and O—H groups in ethanol and in K, Na, and Li ethoxide solutions

Ethanol		K ethox. νcm^{-1}	Na ethox. νcm^{-1}	Li ethox. νcm^{-1}	K ethox.	Na ethox.	Li ethox.	K ethox.	Na ethox.	Li ethox.
νcm^{-1}	assignement				with 9 % DMF νcm^{-1}			with 9% benzene νcm^{-1}		
1075	C—O stretching	1074	1071	1060	1076	1073	1054	1065	1039	1038
1457	C—H bending of methylene	1465	1460	1482	1477	1464	1455	1478	1435	1470
2893	C—H symmetr. stretching of methylene	2908	2888	2896	2907	2898	2891	2895	2866	2860
2930	C—H unsymmetrical stretching of methylene	2948	2934	2935	2945	2936	2935	2937	2907	2906
2960	C—H unsymmetrical stretching of methylene	2968	2958	2974	2962	2960	2960	2965	2945	2944
3001	—	3010	3000	3001 strong	3008	3001	3007 strong	3010	2989	2990 strong
3245	O—H	3244	3242	3248 strong	3264	3263	3256 strong	3243	3234	3230 strong

The presence of ethoxide in alcohol leads to a shift towards lower values of the frequency associated with C—O vibration and to the corresponding modifications of the frequencies associated with methyl and methylene C—H vibrations. It is observed that the frequency shift corresponding to the C—O vibration depends on the nature of the cation, being larger when the cation radius is smaller. This shift was assigned to an interaction with a positive charge on the bond direction, that is, to the formation of ion pairs. This fact is in agreement with the variation of the association constant obtained from the conductance data in the series of the studied ethoxides. The modification of the vibrations associated with the C—O bond leads to changes in the vibration modes of the other bonds e.g. of the C—H bond of methyl and methylene (table 4). At the same time the Raman spectra show modifications of the 3245 cm^{-1} band corresponding to the O—H bond in pure alcohol. In the case of ethoxides in pure alcohol this band does not present any great modifications in the frequency value, as an indication of the conservation and also of the intensification of interactions through hydrogen bonds in these systems. This band splits in the presence of benzene and DMF, showing a trend for O—H group frequency shift towards values corresponding to the O—H free vibration. Also, in the 3000 cm^{-1} region a strong line was observed, which is very weak in pure alcohol and increases with the increase of the ethoxide concentration. The assignment of this line to a vibration mode and the explanation of the problem will make the object of a future paper.

---

[7] H. Sadek and R. M. Fuoss, *J. Amer. Chem. Soc.*, **81**, 4507 (1959).

[8] Z. Keçki, *Spectrochim. Acta*, **18**, 1155 (1962).

[9] Z. Keçki and J. Witanovschi, *Roczniki Chem.*, **37**, 881 (1963).

Revue Roumaine de Chimie, **19**, *11*, 1825 1834 (1974)

SYNTHESIS AND SPECTROPHOTOMETRIC STUDIES IN THE TRISUBSTITUTED CARBETOXYPHENYLHYDRAZONES SERIES

LUCIA BEU and JANA RUSSU
Institute of Chemical and Pharmaceutical Research
Str. Fabricii 126, Cluj, Romania

Received February, 26, 1974

Twelve trisubstituted arylhydrazones containing a nitrile group have been prepared. Their I.R. and U.V. spectra, dissociation and rate constants related to the substituent and its position in the molecule have been studied.

This report is a sequel to the studies concerning the relations between the structure and properties of the trisubstituted phenylhydrazones having the general formula :

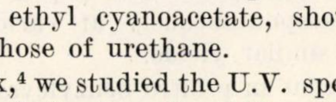

$$\underset{\displaystyle CN}{R-C}=N-NH-C_6H_4-Z \qquad (I)$$

In the last few years it has been established that azo-, respectively hydrazo groups,[1-3] confer antineoplastic, bactericidal and antiviral properties to these derivatives and the tests performed with the substances prepared by coupling ethyl cyanoacetate, showed their antileukemic properties, similar to those of urethane.

In a previous work,[4] we studied the U.V. spectra of some compounds having the general formula I, where $R = C_6H_5$ and $Z = H$, *o*, *m*, $p-COCH_3$. We are continuing these studies in the series of derivatives having $R = C_6H_5$, $p-NO_2-C_6H_5$ or $COOC_2H_5$ and $Z = H$, *o*, *m*, $p-COOC_2H_5$.

The synthesis of these phenylhydrazones has been performed either through direct coupling of diazonium salt with a compound possessing an active methylene group (equation 1 *a*) or an active methine

---

[1] H. Garg and R. Sharma, *J. Med. Chem.*, **12**, 1122 (1968).

[2] A. Harharn, *J. prakt. Chem.*, **315**, 23 (1973).

[3] E. Schrötter and E. Högel, *Die Pharmacie*, **2**, 93 (1972).

[4] L. Beu and J. Russu, *Rev. Roumaine Chim.*, **18**, 723 (1973).

group (equation 1 *b*) :

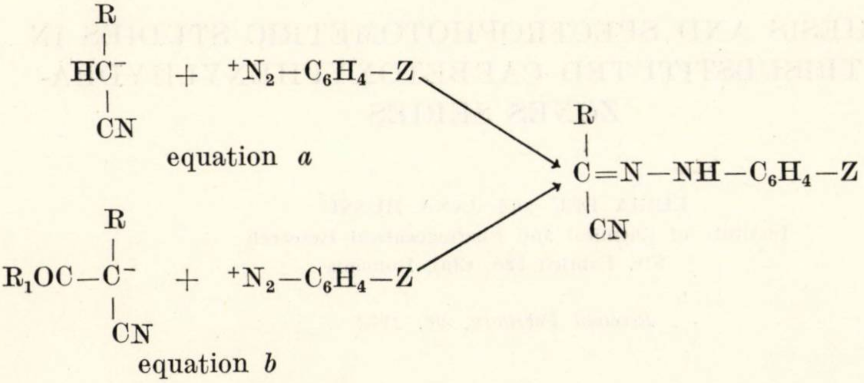

(1)

where $R_1 = H, CH_3, C_6H_5, OC_2H_5$

R	Z	R	Z	
C_6H_5	H (I)	$C_6H_4-NO_2(p)$	$m-COOC_2H_5$	(VII)
C_6H_5	$o-COOC_2H_5$(II	$C_6H_4-NO_2(p)$	$p-COOC_2H_5$	(VIII)
C_6H_5	$m-COOC_2H_5$(III)	$COOC_2H_5$	H	(IX)
C_6H_5	$p-COOC_2H_5$(IV)	$COOC_2H_5$	$o-COOC_2H_5$	(X)
$C_6H_4-NO_2(p)$	H (V)	$COOC_2H_5$	$m-COOC_2H_5$	(XI)
$C_6H_4-NO_2(p)$	$o-COOC_2H_5$(VI)	$COOC_2H_5$	$p-COOC_2H_5$	(XII)

The results of the coupling reaction are listed in table 1.

As the reactivity of methylene in benzylcyanide is much reduced, the product cannot react directly with diazonium salts, so we have synthesized the phenylhydrazones of benzoylcyanide (I–IV) by coupling α-acyl-benzylcyanide with diazonium salts (eq. 1 *b*). Acyl splitting, i.e. decarboxylation took place spontaneously at various temperatures and pH values, giving quite similar yields.

The nitro group present in p-nitro-benzylcyanide, enhances methylene reactivity and permits a direct reaction with the diazonium salts (eq. 1 *a*) (V–VIII). The phenylhydrazones IX–XII resulted from coupling ethylcyanoacetate with diazonium salts (vide 1*a*). The need for the presence of sodium or potassium acetate, or for other basic reagents such as : pyridine, triethylamine, dicyclohexylamine, N-methyl- and N-benzyldicyclohexylamine, in these reactions, should be emphasized.

The infrared spectra of these phenylhydrazones show the following stretching vibration ν_{NH}, $\nu_{C\equiv N}$, $\nu_{C=O}$, $\nu_{C=C/arom}$ and ν_{NO_2} in the case of substances having a NO_2 substituent (table 2).

The spectra show a strong band at 3200–3280 cm^{-1}, characteristic of the NH group, confirming the hydrazo structure of these derivatives

Table 1

Phenylhydrazones of general formula $R-\overset{\overset{\displaystyle CN}{|}}{C}=N-NH-C_6H_4-Z$

N°	Synthesis method	Yield %	m.p. °C (solvent)	Formula	Analysis calc C% H% N% found	lit.
I	A	99	148−149 (EtOH)*	$C_{14}H_{11}N_3$		5.6
II	B,D	98	154−158 (EtOH)	$C_{17}H_{15}N_3O_2$	69.62 5.16 14.32 69.67 5.39 14.74	—
III	F	95	164−165 (Tl)	”	69.62 5.16 14.32 69.45 4.95 14.00	—
IV	A,C,H,	95	154−156 (EtOH)	”	69.62 5.16 14.32 69.90 5.29 13.96	—
V	A	90	198−200 (AcOH)	$C_{14}H_{10}N_4O_2$		7
VI	G	75	175−180 (AcOH)	$C_{17}H_{14}N_4O_4$	60.32 4.17 16.56 60.00 4.22 16.74	—
VII	G	88	194−195 (AcOH)	”	60.32 4.17 16.56 60.48 4.33 16.45	—
VIII	A	98	233−235 (AcOH)	”	60.32 4.17 16.56 60.56 4.46 16.15	—
IX	lit.[8]		127−130 (MeOH)	$C_{11}H_{11}N_3O_4$		8,9,10
X	A,H	95	124−125 (EtOH)	$C_{14}H_{15}N_3O_4$	58.12 5.23 14.53 58.28 5.33 14.38	—
XI	E,H	90	114−116 (Tl+PE)	”	58.12 5.23 14.53 58.28 5.33 14.38	—
XII	E,H	96	132−134 (MeOH)	”	58.12 5.23 14.53 58.42 5.29 14.64	— —

* **EtOH = ethanol, MeOH = methanol, AcOH = acetic ac., Tl = toluen, PE = petroleum ether.**

Table 2

The I.R. spectra of the phenylhydrazones $R-\overset{\overset{\displaystyle CN}{|}}{C}=N-NH-C_6H_4-Z$ **(cm⁻¹, KBr pellets)**

N°	ν_{HN}	$\nu_{C\equiv N}$	$\nu_{C=O}$	$\nu_{C=N}$	$\nu_{C=C/arom}$	ν_{NO_2}
I	3240 vs	2220 m	—	1640 w	1600 s	—
II	3140 m	2215 m	1690 s	1650 w	1600 vs	—
III	3255 m	2220 m	1720 vs	1645 w	1600 s	—
IV	3245 vs	2210 s	1720 vs	—	1600 vs	—
V	3240 vs	2210 s	—	1635 w	1600 vs	1545 vs 1340 vs
VI	3150 m	2210 m	1680 vs	1650 w	1590 vs	1520 vs 1340 vs
VII	3240 vs	2205 s	1720 vs	1620 w	1600 s	1550 vs 1340 vs
VIII	3285 s	2210 s	1715 vs	—	1610 vs	1540 vs 1345 vs
IX*	3160	2210 s	1690 vs	1660 w	1600 s	—
X	—	2210 s	1720 vs 1690 s	1615 s	1600 vs	—
XI	3240 vs	2210 vs	1730 vs 1710 vs	1625 m	1600 s	—
XII	3220 vs	2210 s	1730 vs 1700 vs	1645 w	1615 vs	—

* Izom. m.p. 127−130 °C (Lit.[8]).

---

[5] K. Valker, *J. Chem. Soc.*, **125**, 1622 (1924).

[6] J. Thesing and D. Witzel, *Chem. Ber.*, **88**, 119 (1955).

[7] E. Perkin, *J. Chem. Soc.*, **43**, 111 (1883).

[8] A. Balog, L. Beu and E. Hamburg, *Rev. Chim.* (*București*), **21**, 523 (1970).

[9] S. Parmenter, "Organic Synthesis" **X**. cap. 1, Ed. John Wiley and Sons., New York 1959.

[10] D. Curtin and Ch. Russell, *J. Amer. Chem. Soc.*, **73**, 4975 (1951).

in solid state.[11-15] The shift of this band to 3140 cm^{-1} in the case of two *ortho* derivatives, II and VI, and its disappearance in the case of substance X is being explained by the marked tendency of the *ortho* derivative to give hydrogen bonds of the following type:

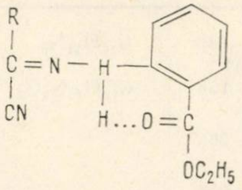

This fact is illustrated by the comparative I.R. spectra of *ortho*-respectively *para*-carbethoxyphenylhydrazones of benzylcyanide, shown in table 2.

The *ortho* derivative II ($Z = o-COOC_2H_5$) has, at 3140 cm^{-1}, a ν_{NH} vibration with lower intensity and wavelength and the *para* derivative IV ($Z = p - COOC_2H_5$) has a high maximum at 3200 cm^{-1}. In the case of carbethoxy derivatives II—IV and VI—VIII, R and $C \equiv N$ groups do not form hydrogen bondings. *Ortho*-derivatives having $R = COOC_2H_5$ may possibly form two kinds of internal hydrogen bondings (equation 2):

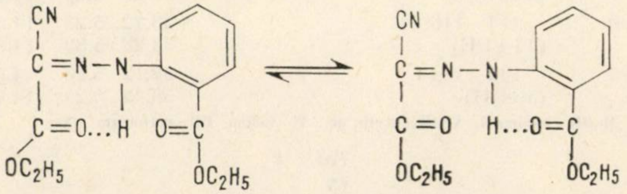

(eq. 2)

In the I.R. spectra of the *ortho* derivative X, the stretching vibration ν_{NH} is absent. The shift of the C=O band is obvious due to the presence of the hydrogen bonding, in the case when $Z = o-COOC_2H_5$, from 1720 to 1680 cm^{-1}.

The exact assignment of the C=N vibration, close to the C=O and C=C/arom., was made by synthesizing the I and V derivatives in which the C=O group is absent. These derivatives show a fairly strong stretching vibration due to the conjugated double bond of the aromatic nucleus at 1590—1600 cm^{-1}. We may, thus, consider the mean intensity band at 1615 cm^{-1} as due to the C=N stretching vibration.

This was also confirmed by studying spectra of tetrasubstituted phenylhydrazones.[16]

---

[11] C. Reichart and V. Grahn, *Chem. Ber.*, **103**, 1065 (1970).

[12] C. Reichart and V. Grahn, *Tetrahedron*, **27**, 3745 (1971).

[13] H. Yao and P. Resnik, *J. Org., Chem.*, **30**, 2832 (1965).

[14] L. Beu and A. Balog, *Rev. Chim. Analitică*, **2**, 154 (1972).

[15] J. Russu and L. Beu, The Third Republican Physico-Chemical Conference Bucureşti, Sept. 1972.

[16] L. Beu and A. Balog, *Rev. Chim.* (*Bucureşti*), **24**, 163 (1973).

The ultraviolet spectra serve to confirm the hydrazone structure of these substances. The literature[8,13,14,18] attributes the band of about 350 nm to a $>C=N-NH-$ structure and that of about 450 nm to a $>CH-N=N-$ structure.

In our case the spectra in hexane, methanol and carbon-tetrachloride show two maxima at 240 nm and 360 nm which may be attributed to a $>C=N-NH-$ structure.

Table 3

The U.V. spectra of the phenylhydrazones $R-\overset{\displaystyle CN}{\overset{|}{C}}=N-NH-C_6H_4-Z$ in methanolic solution

R	$\lambda_{max}/(E_1^1)$			
	$Z=H$	$Z=o-COOC_2H_5$	$Z=m-COOC_2H_5$	$Z=p-COOC_2H_5$
$COOC_2H_5$	240 360 (424) (1035)	250 360 (332) (862)	245 350 (384) (822)	240 350 (300) (1080)
C_6H_5	240 370 (910) (1150)	220 380 (698) (950)	230 370 (832) (790)	240 380 (587) (1300)
$C_6H_4-NO_2(p)$	245 400 (490) (1175)	230 400 (431) (838)	— 400 (960)	265 410 (492) (1160)

In these spectra the R substitution influences the 360 nm maximum. The Z substitution is being evidenced on the 240 nm maximum especially in the case of the *ortho* derivatives. The bathochromic shift in the case of the substances where $R=C_6H_5$, $Z=o-COOC_2H_5$ confirms the existence of intramolecular hydrogen bonding (eq. 2).

In the case of $Z=o-COOC_2H_5$ the derivatives having $R=C_6H_5$, or $p-NO_2-C_6H_4$, show a strong steric effect which produces a shift of the maximum from 240 nm to shorter wavelengths (220 resp. 230 nm).

The spectra in hexane, carbontetrachloride, aqueous methanol (1 :1), HCl 1 N in aqueous methanol and $HClO_4$ 1N in methanol do not show differences if compared to spectra in pure methanol. In sodium methoxide solution or in KOH in methanol-water (1 : 1) the 350–400 nm band has a bathochromic shift up to 420–520 nm corresponding to the following equilibrium :

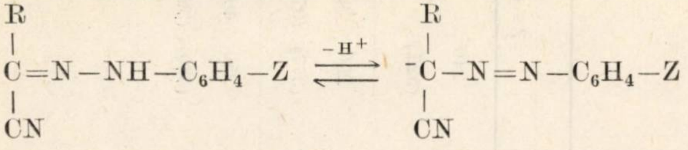

$$\begin{array}{c} R \\ | \\ C=N-NH-C_6H_4-Z \\ | \\ CN \end{array} \underset{}{\overset{-H^+}{\rightleftharpoons}} \begin{array}{c} R \\ | \\ {}^-C-N=N-C_6H_4-Z \\ | \\ CN \end{array} \qquad \text{(eq.3)}$$

The equilibrium established very quickly and could not be studied spectrophotometrically.

---

[17] D. Iffland, M. Mc. Aneny and D. Veber, *J. Chem. Soc.*, (*C*), **1969**, 1703.

[18] R. Wiley and C. Jarboe, *J. Amer. Chem. Soc.*, **77**, 403 (1955).

Table 4

The U.V. spectra of phenylhydrazones in alkaline (KOH 1 N) methanol-water solution (1;1)

R	λ_{max} nm$(E^{1\%}_{1cm})$											
	Z=H			$Z=o-COOC_2H_5$			$Z=m-COOC_2H_5$			$Z=p-COOC_2H_5$		
$COOC_2H_5$	240		380	240		380	240		385	240		400
	(527)		(1160)	(445)		(795)	(406)		(885)	(402)		(1150)
C_6H_5	250	320	440	250		380	255	320	440	260	330	460
	(377)	(376)	(1265)	(486)		(852)	(440)	(274)	(997)	(420)	(281)	(1755)
$p-NO_2-C_6H_4$	250	400	530	250	400	530	240	400	530	260	400	530
	(380)	(380)	(1325)	(266)	(284)	(907)	(440)	(309)	(1130)	(301)	(354)	(1190)

The $C_6H_5-\overset{\overset{\textstyle CN}{|}}{C}=N-NH-C_6H_4-NO_2(p)$ derivative has been synthesized to prove the azo structure in alkaline media. Its spectrum in alkaline medium was compared with that of the $R=p-NO_2-C_6H_4$, $Z=H$ derivative (fig. 1). It may be seen that the intensity of the 540 nm band shows higher increases when $Z=p-NO_2$ than when $R=p-NO_2-$ $-C_6H_4$, thus confirming the $\rangle CH-N=N-$ structure in this case.

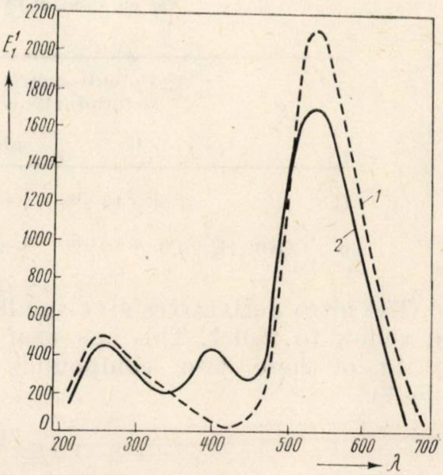

Fig. 1. — The U.V. spectra of phenylhydrazones in aqueous methanolic solution (1 :1) 1 N.

1 $C_6H_5-\overset{\overset{\textstyle CN}{|}}{C^-}-N=N-C_6H_4-NO_2(p)$;

2 $(p)NO_2-C_6H_4-\underset{\underset{\textstyle CN}{|}}{C^-}-N=N-C_6H_5$

The dissociation constants of the studied derivatives depend upon the **R** substitution (table 5). The acidity of these substances descreases in the order $R=COOC_2H_5$, $p-NO_2-C_6H_4$, C_6H_5.

Table 5

pK values of the phenylhydrazones $\overset{\overset{\textstyle R}{|}}{\underset{\underset{\textstyle CN}{|}}{C}}=N-NH-C_6H_4\,Z$ spectrophotometric determinations

R	*Z=H*		$Z=o-COOC_2H_5$		$Z=m-COOC_2H_5$		$Z=p-COOC_2H_5$	
	K	pH	K	pK	K	pK	K	pK
$-COOC_2H_5$	$1.94.10^{-10}$	9.71	$5.44.10^{-11}$	10.26	$8.95.10^{-10}$	9.04	$5.08.10^{-10}$	9.25
$C_6H_4NO_2$ (p)	$2.00.10^{-11}$	10.70	$1.34.10^{-12}$	11.87	$3.40.10^{-11}$	10.47	$3.55.10^{-11}$	10.26
$-C_6H_5$	$1.50.10^{-13}$	12.72	$5.90.10^{-14}$	13.23	$4.65.10^{-13}$	12.34	$3.10.10^{-12}$	11.51

As regards the substitution, the *ortho* derivatives are the weakest acids in each series, the unsubstituted and *p*-substituted derivatives having very similar acidities in each series. The values of the dissociation constants, vary in the same order for the *Z* = *ortho*, *metha*, and *para* substitution, irrespective of the *R* substitution.

The spectrophotometrically obtained dissociation constants were verified in the case of the two derivatives which have $R=COOC_2H_5$. The data obtained by means of a potentiometric titration are very similar to spectroscopic ones.

Table 6

The pK values of

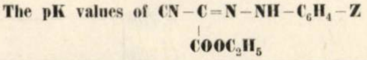

$$\begin{array}{c}CN-C=N-NH-C_6H_4-Z\\ | \\ COOC_2H_5\end{array}$$

Z	Potentiometric determinations		Spectrophotometric determinations	
	K	pK	K	pK
H	1.58×10^{-10}	9.80	1.94×10^{-10}	9.71
$p-COOC_2H_5$	4.36×10^{-10}	9.36	5.08×10^{-10}	9.29

The nitro derivatives give in alkaline solution a sharp colour change from yellow to violet. This has enabled us to determine the dissociation constant of these two compounds by spectrophotometric titration (table 7).

Table 7

The pK values of

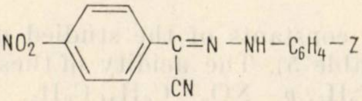

Z	Colorimetric determinations		Spectrophotometric determinations	
H	K	pK	K	pK
H	1.5×10^{-11}	10.59	2.00×10^{-11}	10.70
$COOC_2H_5$	3.46×10^{-11}	10.46	3.40×10^{-11}	10.47

The phenylhydrazones studied show, as in the previously studied cases, a decrease of the 400–530 nm maximum in alkaline media. The reaction is independent of the KOH concentration and takes place also in the absence of oxygen. Simultaneously, an increase of the 350–400 nm maximum has been observed (eq. 4), suggesting a monomolecular transition of the chromophore :

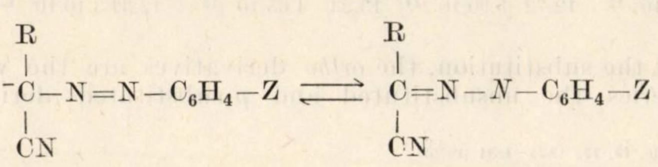

$$\begin{array}{l}R\\ |\\ {}^{-}C-N=N-C_6H_4-Z\\ |\\ CN\end{array} \rightleftarrows \begin{array}{l}R\\ |\\ C=N-\mathit{N}-C_6H_4-Z\\ |\\ CN\end{array} \qquad \text{(eq. 4)}$$

The rate constants are given in table 8. The transition is reversible, acid treating of the solution restores the initial spectra in acid solution.

Table 8

Variation of phenylhydrazones rate constants relative to R and Z substitution

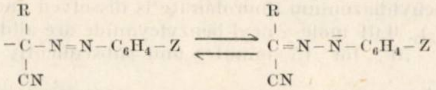

$$-\overset{R}{\underset{CN}{C}}-N=N-C_6H_4-Z \rightleftarrows \overset{R}{\underset{CN}{C}}=N-\bar{N}-C_6H_4-Z$$

R	Z=H	Z=o−COOC$_2$H$_5$	Z=m−COOC$_2$H$_5$	Z=p−COOC$_2$H$_5$
	k sec.$^{-1}$			
COOC$_2$H$_5$	7.20×10^{-7}	4.86×10^{-6}	6.96×10^{-7}	2.06×10^{-6}
C$_6$H$_5$	3.63×10^{-5}	5.25×10^{-5}	7.94×10^{-5}	4.57×10^{-6}
C$_6$H$_4$ NO$_2$(p)	1.37×10^{-6}	2.00×10^{-4}	6.80×10^{-6}	1.88×10^{-6}

In conclusion, the new phenylhydrazones prepared by us have a hydrazonic structure in solid form and in organic solvents or aqueous-organic solvents, as confirmed by I.R. and U.V. spectra. The anionic form which exists in alkaline solution undergoes reversible isomerization. These reactions largely depend upon R substitution as against Z substitution.

EXPERIMENTAL

Melting points are uncorrected.

Infrared spectra were recorded in KBr pellets with a Carl Zeiss UR−10 spectrophotometer. The U.V. spectra were determined with a Carl Zeiss VSU−1 spectrophotometer, with 1 cm quartz cells. The concentration of phenylhydrazones was $0.5-2\times10^{-1}$ M/1. The solutions were prepared in methanol, hexane, carbontetrachloride, methanol-H$_2$O 1 :1, 0.1 N sodium-methoxide, 0.1 N methanolic HClO$_4$ and methanolic aqueous solution (1 :1) of KOH or HCl 0.05 1 N. The dissociation constants were determined at 25° and the rate constants at 20°. The extinctions were determined at every 2 nm. The ionic strength reached 0.1 with KCl. The values of the dissociation constants were corrected to 0 time, when necessary.

The potentiometric pK values were determined with a MV 11 type pH-meter, with a glass electrode and a SKE, titrated with a methanolic water solution (1 :1) of KOH 0.1 N. The end point was sufficiently clear to permit pK determination. The temperature was maintained at 25±1°.

Colorimetric pK determinations were made by first establishing the end point approximately; subsequently more accurate determinations were made at constant ionic strength and temperature.

SYNTHESIS OF PHENYLHYDRAZONES

Method A. 0.01 mole of derivative possessing an active methine or methylene group are suspended in 10 ml AcOH and 5 ml B (OCH$_3$)$_3$ are added. The solution is cooled to 0° and 0.01 mole of Z-phenyldiazonium fluoroborate is added under stirring. After 10 minutes 5 g AcONa dissolved in 10 ml AcOH are added. The reaction mixture is kept under stirring for 3 hours, then poured over 300 ml water. The precipitate formed is filtered off, washed with water and dried at room temperature.

Method B. 0.01 mole of Z-phenyldiazonium fluoroborate is suspended in the cold in 20 ml methanol and 3 ml $B(OCH_3)_3$. To this mixture, 0.01 mole derivative possessing an active methine is added under stirring. After 2 hours the reaction mixture is diluted with 200 ml water, and subsequently the precipitate formed is filtered off.

Method C. 0.01 mole Z-phenyldiazonium fluoroborate is dissolved under gentle heating in 20ml AcOH and 10 ml $N(OCH_3)_3$. 0.01 mole α-acyl-benzylcyanide are added, and the reaction mixture is maintained at 60–70°, for 15 minutes and subsequently the precipitate formed is filtered off.

Method D. 0.01 mole Z-phenyldiazonium fluoroborate and 0.01 mole of derivative possessing an active methine group, are dissolved in 20 ml AcOH at 50–60°. A spontaneous precipitation occurs. An hour later the mixture is diluted with 500 ml water and filtered off.

Method E. 0.01 mole Z-phenylamine are dissolved in 25 ml AcOH and 2.5 ml HCl and are diazoted at 0° with 1.2 ml butylnitrite. This solution is poured into a solution containing 0.01 mole derivative possessing an active methine or methylene group dissolved in 20 ml AcOH and 5 ml $B(OCH_3)_3$. 3 g AcOK dissolved in 15 ml AcOH are added under continuous stirring. After an interval of 24 hours the mixture is diluted with 400 ml water and the precipitate filtered off.

Method F. 0.01 mole Z-phenylamine are dissolved in a mixture of 25 ml AcOH and 2.5 ml HCl and diazotized at 0° with 2 ml solution containing 0.9 g $NaNO_2$. After 20 minutes the mixture is treated with 5 ml $B(OCH_3)_3$. 0.01 mole derivative possessing an active methine or methylene group and 2.5 g AcONa are dissolved in 10 ml AcOH. After 3 hours the mixture is poured into water and the precipitate formed is filtered off.

Method G. 0.01 mole Z-phenylamine. HCl is dissolved in 20 ml AcOH and 2 ml $HClO_4$ 70% and diazotized in the cold with 1.2 ml butylnitrite. To this solution, 0.01 moles p-nitrobenzylcyanide is being added under stirring. After 30 minutes 2.5 g AcONa dissolved in 10 ml of water are added. Two hours later the reaction mixture is diluted with 300 ml water and the precipitate formed is filtered off after another 3 hours.

Method H. To 2 ml phenylcyanoacetate 7.6 ml ethanolic KOH 8% are added. The mixture is cooled at 0° and 0.01 mole Z-phenyldiazoniumfluoroborate are added. After 2 hours the mixture is poured into 400 ml water and the precipitate formed is filtered off.

The products are recrystallized from the solvents indicated in table 1.

Revue Roumaine de Chimie, 19, *11*, 1835–1836

COMPTE RENDU

C. LITEANU and S. GOCAN, "Gradient Liquid Chromatography" Ellis Horwood Ltd., Chichester, 1974, 338 p.

This book was issued in the analytical chemistry series published by Dr. R. A. Chalmers and is intended for the chemists who work in research laboratories and in industry and also for the students in the upper classes. It has many fields of application, as it refers not only to chemistry, but also to biology, metallurgy, agriculture, mining, pharmacy, food industry, environmental control, sanitary control etc.

Its contents are divided into two main parts: the fundamental problems of chromatography (Part I) and the use of gradients (Part II).

Chapter 1, under the title: "Kinetics of Eluent Migration", has a theoretical character and includes open-column kinetics (ascending, descending and horizontal chromatography) and closed-column kinetics. It also discusses the non-uniform distribution of single-component and multicomponent eluents.

The kinetics of zone migration are described in Chapter 2. The problems debated are: migration rate in open chromatographic columns (isothermal chromatography and temperature-gradient chromatography) as well as relative migration rate of the zone.

The factors which influence the reproducibility of R_f values are discussed in Chapter 3. Thus, the factors determined by the composition of the stationary phase, by the composition of the mobile phase and by the medium are taken into consideration. Thence ensue the working conditions for achieving a reproducibility of R_f values both with paper and thin-layer chromatography.

The highly important problem of the estimation of separation efficiency is described in Chapter 4. Both the closed and the open chromatographic columns were taken into account in this case, too. A clear definition of the basic parameters (HEPT — the height equivalent to a theoretical plate, N — the number of theoretical plates of a chromatographic column etc.) is followed by a description of the possibilities of determining experimentally the separation efficiency.

This chapter also includes a discussion on chromatographic selectivity. After defining the fundamentel constants, the selectivity coefficient and the separation factor, they are correlated to the R_f values and examined from the viewpoint of practical results.

Resolution and the parameters of resolution both closed-column and open-column ones, are then defined.

In Chapter 5 the authors discuss the optimization of the chromatographic process, taking into account all the factors which influence separation. The chapter is divided in terms of the nature of the process. Thus, in the case of adsorption and partition chromatography in closed columns the following factors are taken into consideration: the dimensions of the column, the nature of the adsorption agent, the flow rate and viscosity of the eluent, the structure of the bed, as well as temperature, pressure and time. The next to be discussed are the ion-exchange chromatography and the partition and adsorption chromatography in open columns (choice of the mobile and stationary phase, pH, humidity, temperature).

Part II refers to the use of gradients and opens with an introduction (Chapter 6) offering a short history of gradient chromatography, the classification of gradients and their nomenclature.

Chapter 7 deals with the mobile-phase gradients. The appliances for obtaining such gradients are described first. Thus, as far as the closed columns are concerned, the information offered involves the discontinuous elution gradients, the concave and convex exponential gradients, the linear gradient, the concave and convex parabolic gradients, the composite gradients. A description of the methods for obtaining gradients with paper and thin-layer chromatography is also included.

The next section of this chapter (7.2) is of particular importance as it goes deeply into the theory of mobile-phase gradient chromatography. Following the same sequence, the closed columns are discussed first, as regards the calculation of the position of the peak and resolution and open columns next.

The last part of Chapter 7 refers to the use of mobile-phase gradients in the separation of substances (organic acids, carbohydrates, aromatic hydrocarbons, amino acids, proteins, lipids, nucleic acids, steroids, antibiotics, inorganic ions).

The stationary-phase gradients are comprised in Chapter 8, which offers a description of appliances (for discontinuous and continuous gradient), resolution and the applications of composition, impregnation, activity and pH gradients.

The environmental gradients (temperature, vapour, section and flow velocity) are discussed in Chapter 9, which describes the appliances for various cases (parallel, antiparallel and orthogonal gradient), the variation in R_f, resolution and a comparison between the parallel temperature gradient technique and other chromatographic techniques.

The last chapter (10) includes a description of combined gradients : mobile-phase and temperature, combined mobile-phase.

Three annexes are appended.

Each chapter is provided with figures and auxiliary graphs, which illustrate with the utmost clarity both the practical and the theoretical part. Moreover, each chapter comprises exhaustive references, judiciously selected according to the theoretical and practical value of the works.

The clear, concise and consistent style is to a great extent a help in assimilating the content and in rendering it profitable. The excellent graphic conditions deserve special mention.

This book, written by two remarkable researchers in the field of gradient chromatography is of the highest topical interest. It distinguishes itself by its high theoretical level and by its practical utility. The readers have the possibility of going thorougly into the theory, modelling and use of the calculations for the forectasting and optimization of separations. At the same time, they are offered an efficient means for assimilating and completing various gradient chromatography techniques. By its investigating and selecting a great number of works published up to the present, this book is, at the same time, a complete monograph of the field.

Simon Fişel

NOTE POUR LES AUTEURS

La *Revue Roumaine de Chimie* publie des articles en anglais, français, russe, allemand ou espagnol. Les auteurs sont priés d'envoyer des articles, notes, communications et comptes rendus inédits.

Les manuscrits seront dactylographiés à deux intervalles. Les tableaux seront dactylographiés sur feuilles séparées, de même que la légende des figures. Les diagrammes seront tracés à l'encre de Chine sur papier calque. Les tableaux et les figures seront numérotés par des chiffres arabes, en nombre strictement nécessaire. Prière de ne pas inscrire les mêmes données dans les tableaux et les figures. Les formules chimiques seront incluses dans le texte ; en outre, elles seront transcrites sur des feuilles séparées. Les auteurs sont priés d'indiquer les caractères italiques (en soulignant les lettres au crayon), ainsi que tout autre caractère spécial. L'ordre des références bibliographiques sera celui de leur mention dans le texte ; le nom de l'auteur sera précédé de l'initiale du prénom ; les publications périodiques seront présentées suivant les prescriptions internationales. Les références seront ajoutées à la fin de l'article ; elles paraîtront comme des notes, au bas de la page. Le texte sera précédé d'un résumé comprenant 15 lignes au maximum.

L'entière responsabilité du contenu des articles appartient aux auteurs. On publie des articles dus aux collaborateurs roumains ou étrangers.

PRINTED IN ROMANIA

1975 APR 23

TRAVAUX PARUS AUX ÉDITIONS DE L'ACADÉMIE DE LA RÉPUBLIQUE SOCIALISTE DE ROUMANIE

I. ZUGRĂVESCU et MAGDA PETROVANU, **Chimia N- Ilidelor** (La chimie des N Ylures), 1974, 347 p., 19 lei.

MARGARETA AVRAM, **ANTIDĂUNĂTORI** (Pesticides), 1974, 494 p., 41 lei.

CR. SIMIONESCU, VIORICA RUSAN et N. POPA., **Chimia algelor marine** (La chimie des algues merines), 1974, 211 p., 18 lei.

CRISTOFOR SIMIONESCU, MARGARETA GRIGORAŞ, AGATA CERNĂTESCU-ASANDEI et GHEORGHE ROZMARIN, **Chimia lemnului din România — plopul şi salcia** (La chimie du bois en Roumanie — le peuplier et le saule), 1973, 228 p., 28 lei.

TIBERIU NĂŞCUŢIU, **Metode radiochimice de analiză** (Méthodes radiochimiques d'analyse), 1973, 384 p., 23 lei.

MARIA FITI, **Dozimetria chimică a radiaţiilor ionizante** (La dosimétrie chimique des radiations ionisantes), 1973, 240 p., 13,60 lei.

MIHAI FLORESCU, **Eficienţa economică a cercetării ştiinţifice** (L'efficience économique de la recherche scientifique), 1972, 115 p., 15 lei.

GEORGETA LĂZĂRESCU, **Sistematizarea informaţiilor în Chimia organică** (La systématisation des informations dans la Chimie organique), 1972, 252 p., 10,15 lei.

P. BALTĂ şi E. BALTĂ, **Introducere în chimia fizică a stării vitroase** (Introduction à la chimie physique de l'état vitreux), 1971, 240 p., 15,50 lei.

LYDIA-MARIA VAICUM, **Biodegrabilitatea detergenţilor** (La biodégrabilité des détergents), 1971, 254 p., 16 lei.

I. ZUGRĂVESCU et L. STOICESCU-CRIVETZ, **Polimeri heterociclici** (Polymères hétérocycliques), 1971, 190 p., 9,50 lei.

I. MAXIM, **Materiale nucleare** (Matériaux nucléaires), 1969, 444 p., 30 lei.

CRISTOFOR SIMIONESCU et CLEOPATRA VASILIU-OPREA, **Mecanochimia compuşilor macromoleculari** (La mécanochimie des composés macromoléculaires), 1967, 344 p., 23,50 lei.

CORNEL BODEA et collab., **Tratat de biochimie vegetală**, partea I, **Fitochimie** (Traité de biochimie végétale, Ier partie, Phytochimie), Ier vol., 1964, 747 p. + 4 annexes + 2 pl., 41 lei ; IIe vol., 1965, 1262 p., 1 pl., 56 lei ; IIIe vol., 1967, 773 p., 35 lei.

I. P. I. — c. 1646

43 426

Lei 25.—

F 1103

04-001 Dé

ACADÉMIE DE LA RÉPUBLIQUE SOCIALISTE DE ROUMANIE

REFERÁLVA

REVUE ROUMAINE DE CHIMIE

Hommage à
RALUCA RIPAN
pour son 80e anniversaire

TOME 19

N° 12

Décembre 1974

RECHAX, 19, *12*, 1837–1990 (1974)

ÉDITIONS DE L'ACADÉMIE DE LA RÉPUBLIQUE SOCIALISTE DE ROUMANIE

Rev. Roumaine Chim. 19, *12*, p. 1837–1990 (1974), Bucarest

ACADÉMIE DE LA RÉPUBLIQUE SOCIALISTE DE ROUMANIE

COMITÉ DE RÉDACTION

Rédacteurs en chef:

I. G. MURGULESCU, membre de l'Académie de la République Socialiste de Roumanie

Rédacteurs en chef adjoints:

A. T. BALABAN et V. EM. SAHINI, membres correspondants de l'Académie de la République Socialiste de Roumanie

Collège de rédaction:

EM. BRATU, ELENA CEAUŞESCU, ECATERINA CIORĂNESCU-NENITZESCU, C. DRĂGULESCU, RALUCA RIPAN, CR. SIMIONESCU, membres de l'Académie de la République Socialiste de Roumanie; P. SPACU, membre correspondant de l'Académie de la République Socialiste de Roumanie; MARGARETA AVRAM, D. I. MARCHIDAN, I. MOLDOVAN, G. NIAC et D. SĂNDULESCU

Toute commande de l'étranger (fascicules ou abonnements) sera adressée à Întreprinderea Rompresfilatelia, Boîte Postale 2001, télex 011631, Bucarest, Roumanie

Les manuscrits, les livres et les revues proposés en échange, ainsi que toute correspondance seront envoyés à la rédaction

REVUE ROUMAINE DE CHIMIE

23, str. Dumbrava Roşie, Bucarest, Roumanie, téléphone: 12 41 60

EDITURA ACADEMIEI REPUBLICII SOCIALISTE ROMÂNIA
3 bis, str. Gutenberg, Bucarest, Roumanie, téléphone: 16 40 79

REVUE ROUMAINE
DE
CHIMIE

ORSZÁGOS MŰSZAKI KÖNYVTÁR ÉS DOKUMENTÁCIÓS KÖZPONT

Tome 19, N° 12 Décembre 1974

Hommage à Raluca Ripan 1839–1840

I. G. MURGULESCU and I. BICĂ, Pyrolysis and oxidative pyrolysis of isobutene. I 1841–1853

CONST. GH. MACAROVICI et E. CHIŞ, Un nouveau réactif du type EDTA 1855–1860

P. SPACU, FLORICA POPEA, C. I. LEPĂDATU, C. A. BANCIU, EUGENIA IVAN, SILVIA PLOŞTINARU, ZAMFIRA TOMA and CRISTINA RUSU, Palladium (II) and platinum (II) square-planar complexes with tris (*p*-methoxyphenyl) arsine and halide ions 1861–1876

A. SWINARSKI et ANNA ZYTKOWICZ, Mécanisme de l'activité catalytique des métaux de transition déposés sur un support actif 1877–1881

MARIA BREZEANU and IOANA JITARU, Coordination compounds with choline perchlorate 1883–1888

N. CALU, ADINA POPA-RANG et MARIA CALENCIUC, Combinaisons complexes du Mn(III) et du Mn(IV). I. Le système Mn(III, IV) – acide aniline-4 sulphonique 1889–1897

EUGENIA GAVRILĂ und I. CĂDARIU, Über Triazine. L. Mitteilung potentiometrische Bestimmung der Aciditätskonstanten von 4-Hydroxy-6-Oximintetrahydrotriazinyl-2-Formaldoxim 1899–1908

CONSTANŢA GHEORGHIU, MARIA CONSTANTINESCU, O. CONSTANTINESCU and VALERICA POCOL, Study of some Cu(II) selenocyanate complexes with biguanide derivatives 1909–1919

D. NEGOIU, ANGELA KRIZA et MARTHA NASTA, Sur les composés du trichlorure de l'éthoxytitane avec des bases Schiff. 1921–1926

A. BARABÁS and A. T. BALABAN, Chemical Graphs. XXIV. Isomerizations and isographic transformations 1927–1940

C. LITEANU and H. NAŞCU, Studies concerning the optimisation of separations by thin layer chromatography on silicagel. I. Separation of some ethanolamines in several polycomponent solvent systems 1941–1947

D. C. CÖRMÖS, IOVANCA HAIDUC and P. STEŢIU, Synthetic single crystal PbSe electrode. Potentiometric titration of Cu(II) with Na_2EDTA 1949–1955

S. GOCAN und CHRISTINE KYRI, Trennung einiger Aminosäuren durch Dünnschichtchromatographie mit orthogonalem Temperaturgradient 1957–1961

M. STRĂJESCU, and C. DRĂGULESCU, Formation and structure of cobalt and titanium mixed oxides obtained from mixed complexes 1963–1967

COMPTE RENDU 1969

INDEX DES AUTEURS 1971–1981

INDEX DES SUJETS 1981–1989

Rev. Roumaine de Chimie **19**, *12*, p. 1837–1990 (1974), Bucarest

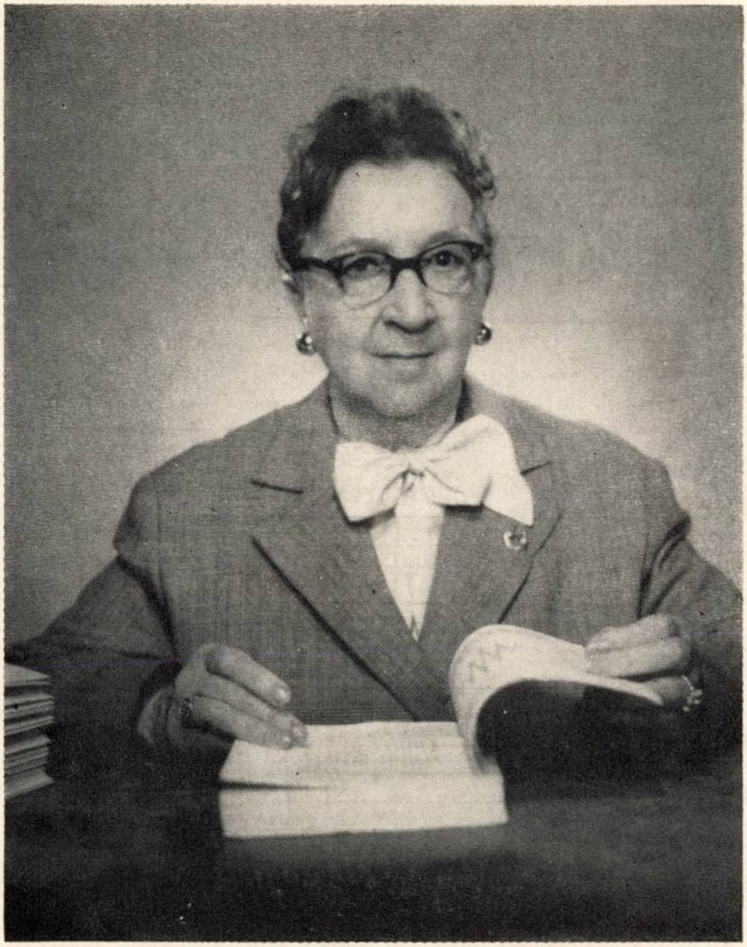

Raluca Ripan

Academician professor dr. doc. Raluca Ripan, a prominent personality of Romanian science, celebrates 55 years of highly reputed activity developed in the field of scientific research, of education and of social-cultural life.

On this occasion, the journal Revue Roumaine de Chimie pays tribute to the personality of the eminent scientist, of the dedicated teacher and of the active militant for progress.

Acad. Raluca Ripan was born in Iaşi on June 27, 1894.

She graduated from the Faculty of chemistry in the year 1919 and was appointed assistant professor at the chair of physical chemistry of the Iassy University.

In 1920 she was transferred to the University of Cluj, the chair of inorganic chemistry headed by professor Gh. Spacu. While carrying out a dedicated and untiring activity, she passed through all the hierarchical levels of higher education, holding the position of professor of inorganic chemistry in 1941.

Her rich and many-sided activity has assumed a new meaning after the country's liberation from the fascist yoke when comrade Academician Raluca Ripan became a member of the Romanian Communist Party.

The scientific activity of Acad. Raluca Ripan is comprised in a number of approximately 300 works published in Romanian and foreign journals in her field of interest. Most studies are concerned with the elucidation, the constitution and the application of complex compounds to analytical chemistry and their use in industry.

Special mention should be made of studies on iso- and heteropolycompounds. Acad. Raluca Ripan and her coworkers have made valuable contributions to this field by applying some modern techniques such as chromatography, electrochromatography, radiochromatography, spectrography, polarography and the use of radioactive isotopes.

One of Acad. Raluca Ripan's basic concerns was to link research to production, to the needs of our national economy. An example in this sense, are the studies concerning the development of some technological methods for using to great advantage some indigenous raw materials (kaolin from Arghireş, colloidal gold, etc).

For the valuable results obtained in the sphere of research she was elected member of the Academy of the Socialist Republic of Romania.

Part of the results of scientific research were presented at international chemistry congresses in Budapest, Moscow, Lisbon, Geneva, Paris, Detroit, Munich, London, Wroclaw, etc and aroused a great interest, being unanimously appreciated by participants.

An expression for the wide international recognition given to her scientific activity was the title of doctor honoris causa awarded to her by the Copernicus University from Poland.

In her capacity of professor and head of the chair of inorganic chemistry she developed an untiring activity devoted to training and guiding the young members of the staff.

By published textbooks, by well-equipped laboratories and particularly by her personal example she has trained a number of highly-qualified researchers who carry out a notable activity in the universities and laboratories of our country.

In parallel with the didactic and scientific activity, Acad. Raluca Ripan has also developed a rich managing and political-public activity.

As a Dean of the Faculty of Chemistry, Rector of the University, Director of the Institute of Chemistry and then President of the Cluj Branch of the Academy of the Socialist Republic of Romania, her main concern was to assure to students, teaching staff and researchers the best possible conditions for study and for work.

As a deputy in the People's Council of the Cluj-Napoca town, chairman of the Committee for Culture and Art of the Cluj district, deputy in the Great National Assembly, member of the Presidium of the Great National Assembly, she has fully manifested all her potentialities as a real revolutionary scientific worker in the political life of our country, making an active contribution to the building of socialism in our country.

Acad. Raluca Ripan's remarkable scientific and political-public activity was honoured by orders, titles and medals. She is a State Prize laureate and has been awarded the following titles: hero of socialist work and emeritus scientist; she has also been granted the orders Star of the Socialist Republic of Romania, Ist class, and 23 August, Ist class. In 1959, the World Peace Council conferred on her a diploma of honour.

The whole activity developed by Acad. Raluca Ripan is an example of commitment to the noble mission of a teacher and of a scientist who has devoted all her efforts to the advancement of education and of science in our country.

Revue Roumaine de Chimie, **19**, *12*, 1841–1853 (1974)

Dedicated to
RALUCA RIPAN
on the occasion of her 80th anniversary

PYROLYSIS AND OXIDATIVE PYROLYSIS OF ISOBUTENE. I

I. G. MURGULESCU and I. BICĂ
Institute of Physical Chemistry
Str. Galaţi, 31 – Bucharest, Romania

Received October 10, 1974

A comparative kinetic study of the pyrolysis and the oxidative pyrolysis of isobutene has been performed at an atmospheric pressure and over a 500–600° temperature range. The primary products have been determined as well as the influence of the reaction time and of the isobutene/oxygen ratio on the distribution of products. The addition of small oxygen amounts to the pyrolysis reaction does not modify the isobutene order yet it causes a marked decrease of the activation energy.

INTRODUCTION

Pyrolysis of isobutene has formed the subject of a number of studies, [1-3] which have focused on the mechanism of this reaction.

By introducing various substances in the reactant medium it was possible to draw valuable conclusions concerning the role of additives and of various radicals in the pyrolysis reaction.[4,5]

Letort [6] has shown that a part of the oxygen at 100,000 doubles the initial decomposition rate of acetaldehyde at 477°.

Neiman *et al* [7] have found that the decomposition of n-butene is sensitized by addition of small amounts of oxygen. Subsequently, other researchers have also confirmed that oxygen traces accelerate the initial pyrolysis rate of n-butane and of other hydrocarbons.[8-12]

---

[1] H. P. LEFTIN and A. CORTES, *Ind. and Eng. Chem, (Process Design.)*, **11**, 613 (1972).

[2] Iu. I. LEADOVA, V. I. VEDENEEV and V.V. VOEVODSKII, *Doklady Akad. Nauk S.S.S.R.*, **114**, 1269 (1957).

[3] V. D. MOISEEV, Iu. O. LEADOVA, V. I. VEDENEEV, M. B. NEIMAN and V. V. VOEVODSKII, *Doklady Akad. Nauk S.S.S.R.*, **123**, 292 (1958).

[4] S. I. KOROCIUK, R. A. KALINENKO and K. P. LAVROVSKI, *Doklady Akad. Nauk S.S.S.R.*, **197**, 593 (1971).

[5] Iu. P. CIJOV, F. K. VELICIKO and S. A. KARAPETIAN, *Zhur. prikld. Khim.* **44**, 2692 (1971).

[6] M. LETORT, *Chim. Ind.*, **76**, 430 (1956).

[7] Z. K. MAIZUS, V. G. MARCOVICI and M. B. NEIMAN, *Doklady Akad. Nauk. S.S.S.R.*, **66**, 1121 (1949).

[8] J. ENGEL, A. COMBE, N. LETORT and M. NICLAUSE, *Rev. Inst. franc. Pétrole.*, **12**, 627 (1957).

[9] W. D. APPLEBY, W. H. AVERY, W. K. MEERBOT and A. F. SARTOR, *J. Amer. Chem. Soc.*, **75**, 1809 (1953).

[10] V. K. SKARCENKO and C. P. KUZMICEV, *Kinetica i Kataliz.*, **11**, 845 (1970).

[11] J. FUSY, R. MARTIN, M. DZIERZYNSKI and M. NICLAUSE, *Bull. Soc. chim. France*, **1966**, 3783.

[12] G. SCACCHI, Thèse de doctorat in sciences physique, Nancy, 1969.

However, little attention was paid to the role played by O_2 in the pyrolysis of olefines. Mention must be made of the work of Bradley *et al.*[13] which has been concerned with the pyrolysis of propene in the presence of O_2 in a strongly argon-diluted medium.

The present paper is an attempt to find out whether oxygen traces manifest a similar action in the case of olefines as well. To do this, we made a comparative study of the pyrolysis and of the oxidative pyrolysis of isobutene.

EXPERIMENTAL

INSTALLATION

The installation used is schematically illustrated in Fig. 1. The cylindrical-shaped reactor (Fig. 2) with an inner diameter of 1 cm and a volume of 5.1 cm^3 was made up of quartz.

The reduction of the exit pressure of feeding gases and the adjustment and measuring of their flows were made by means of pressure reducers, gas taps and flowmeters (Fig. 1).

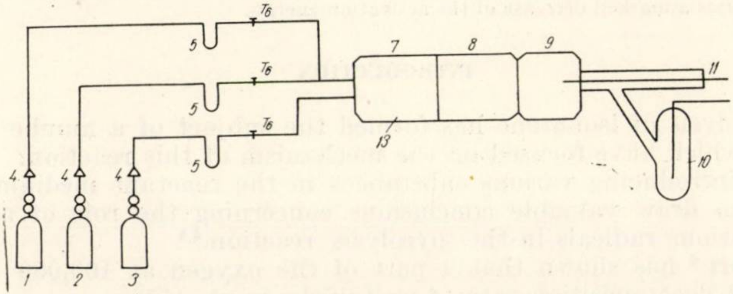

Fig. 1. — Schematic representation of the installation.

1, isobutene ; *2*, oxygen ; *3*, argon ; *4*, control valves for gas discharge ; *5*, flowmeter ; *6*, *3*-way tap ; *7*, preheater ; *8*, reactor ; *9*, refrigerator ; *10*, trapping vessel for liquid products ; *11*, Cr-Al thermocouple.

The temperature of the furnace was kept constant by using a voltage stabilizer, a transformer and a thermoregulator connected to the furnace by means of a Pt-Rh-Pt thermocouple. It was thus possible to maintain the desired temperature in the reactor.

SUBSTANCES

Oxygen and isobutene of 99.9% and 99.7% purity, respectively, were used without further processing. The impurities in isobutene were methane (0.03%) propene (0.02%) 1-butene (0.2%) and 2-butene (0.09%).

The purification of argon used in the simple pyrolysis reaction was achieved by removing the oxygen content on a column with B.T.S. catalyst.

The moisture from isobutene was removed by passing the gas through a tube containing anhydrous calcium sulphate while a column of indicator silicagel was used in the case of the other gases.

Impurities from the argon used as a carrier gas in the chromatographic analysis were retained on a molecular sieve column which was periodically regenerated.

---

[13] J. N. Bradley and D. A. Durden, *Combustion and Flame*, **19**, 452 (1972).

EXPERIMENTAL PROCEDURE

Reactant gases were preheated in separate tubes and their rapid mixing in the reactor was accomplished by the axial introduction of oxygen in the isobutene current through small orifices situated on the surface of a tube whose plane was perpendicular to the axis of the reactor (Fig. 2).

To avoid subsequent reactions, when leaving the reaction zone, the mixture of products and nontransformed gases was suddenly cooled in a refrigerator fixed at the end of the reactor. This helped to eliminate complications usually resulting when large volumes of inert cooling diluent are introduced. From the refrigerator, the gases were passed into a vessel cooled to 0° for the condensation of products with higher boiling points and were then led to the chromatograph.

Two Pye chromatographs, series 104, were used for the analysis; one was equipped with a thermal conductivity cell and the other was fitted with a flame ionization detector.

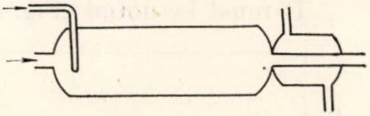

Fig. 2. — Schematic representation of the reactor.

The following columns were used :

— one formed of polyethylene glycol for the determination of carbon dioxide and of the unreacted isobutene;

— another with 5A molecular sieves for the determination of permanent gases.

A Squalan column was used for the other gases.

Tests were also made on a silicagel column and also on a dimethylsulpholan column.

The qualitative identification was made by comparing the retention times of the products under analysis with the retention times of pure compounds supposed to be present. The quantitative determination was made by using calibration curves corrected for each component in terms of certain variations recorded on the chromatograph, using iC_4H_8 as a standard.

The reaction was studied in a dynamic regime at atmospheric pressure and at temperatures ranging between 500 and 600° and the reaction time varied between 0.3 and 1.8 sec, small conversions being thus obtained.

RESULTS AND DISCUSSIONS

The main reaction products both in the case of simple pyrolysis and of oxidative pyrolysis were : methane, propene, ethylene and alene.

Apart from these products, the oxidative pyrolysis provided carbon dioxide in a proportion similar to propene and also significant amounts of water and liquid products.[14] The water was also found in the pyrolysis of butane in the presence of small amounts of oxygen.[9-11]

Carbon oxide could not be identified at the conversion obtained and with the sensitivity of the catarometer used, regardless of the working conditions. Although Bradley[13] and Blakemore[15] support the existence of carbon oxide in the pyrolysis in the presence of O_2 of propylene and of n-butane, respectively, they have failed to determine it.

On the other hand, Dechaux[16] and Knox[17] observe an increase in the CO_2 content to the detriment of CO with the increase in the hydrocarbon/oxygen ratio during the combustion of butane and of propylene, respectively.

---

[14] I. G. Murgulescu and I. Bică, *Rev. Roumaine Chim.*, in press.

[15] J. E. Blakemore, J. R. Barker and W. H. Corcoran, *Ind. and Eng. Chem. (Fundamentals)*, **12**, 147 (1973).

[16] J. N. C. Dechaux, J. L. Flament and N. Lucquin, *Combustion and Flame*, **17**, 205 (1971).

[17] W. Falconer and J. H. Knox, *Proc. Roy. Soc. A.*, **250**, 493 (1950).

Similarly, neither propane nor ethane were found among the products in accordance to Leftin's results.[1]

Molera and Stubbs[18] also note the absence of propane in the pyrolysis of isobutene and Rice[19, 20] obtains alene over a large domain of conversions.

By extrapolating the concentration of products to zero conversions of isobutene we find which are the primary products in the pure pyrolysis (Fig. 3) and in the oxidative pyrolysis (Fig. 4).

It must be noted (Fig. 3) that whereas methane presents a constant growth, propylene has a sensible initial growth and it becomes almost constant thereafter. It is clear that while methane is both a primary and a secondary product, propene is certainly a primary product.

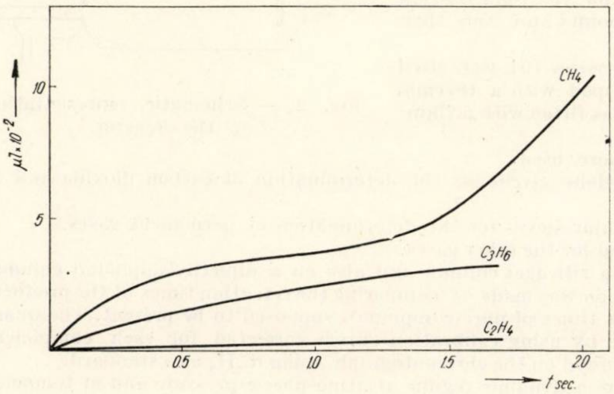

Fig. 3. — Variation of products with time in isobutene pyrolysis. $T = 500°$.

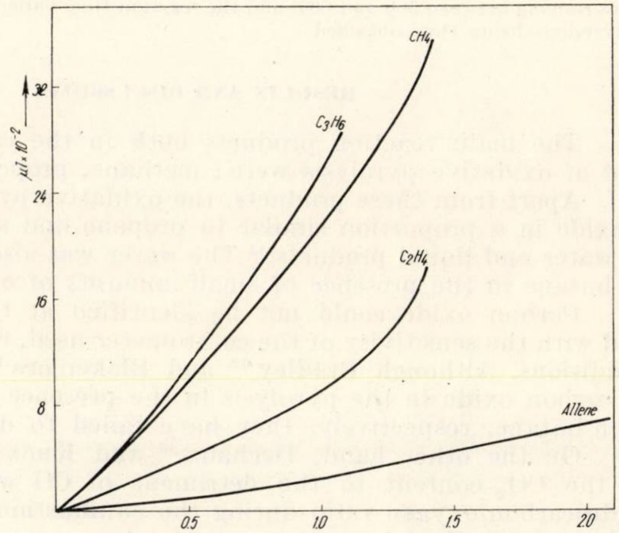

Fig. 4. — Variation of products with time in the oxidative pyrolysis of isobutene. $T = 500°$; $iC_4H_8/O_2 = 20$.

---

[18] M. J. Molera and F. J. Stubbs, *J. Chem. Soc.*, **1952**, 38.

[19] F. O. Rice and W. S. Haynes, *J. Amer. Chem. Soc.*, **70**, 964 (1948).

[20] F. O. Rice and L. A. Wall, *J. Amer. Chem. Soc.*, **72**, 3967 (1950).

At the same time, although the shape of the curves in Fig. 4 is less evident, it permits however to conclude that propene and alene are only primary products whereas methane and ethylene are also secondary products.

INFLUENCE OF THE iC_4H_8/O_2 RATIO

The concentration of oxygen in the initial mixture varied between 5 and 10%. At all isobutene/oxygen ratios used during the working procedure, oxygen consumed at 500° represents merely a small part of the total oxygen present in the reactant mixture.

We observe from Figs. 5 and 6 that the distribution of cracking products in the presence or the absence of oxygen is approximately similar. For a given concentration of isobutene, the increase in the O_2 amount in the reactant mixture resulted in the increase of the amount of products (points 1′, 2′, 3′). A comparison between these data and those obtained in the simple pyrolysis, shows that oxygen has a marked increasing effect on the reaction products. At 550° the formation of methane and of ethylene

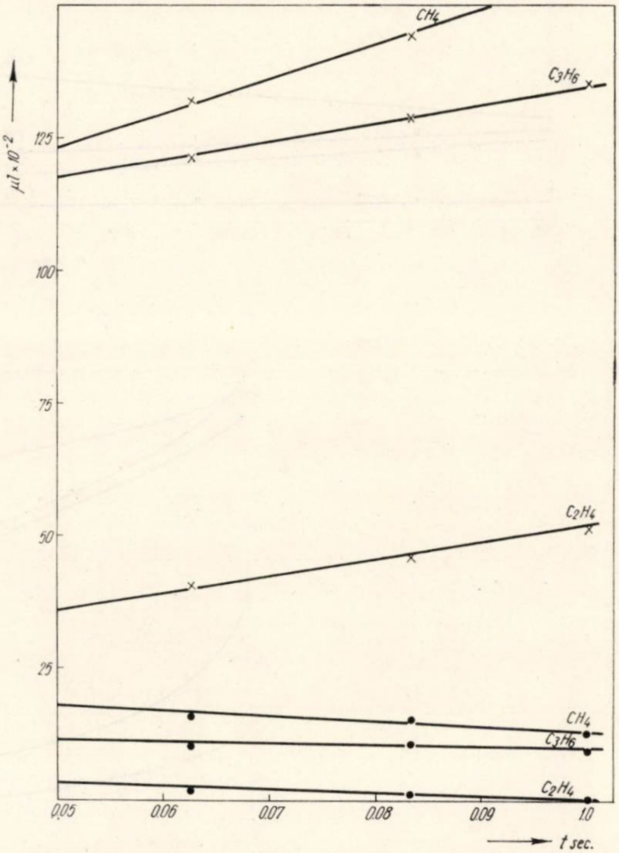

Fig. 5. — Influence of the oxygen/isobutene (X) and Ar/isobutene (.) ratio on the products. $T = 550$; $t = 1.4$ sec.

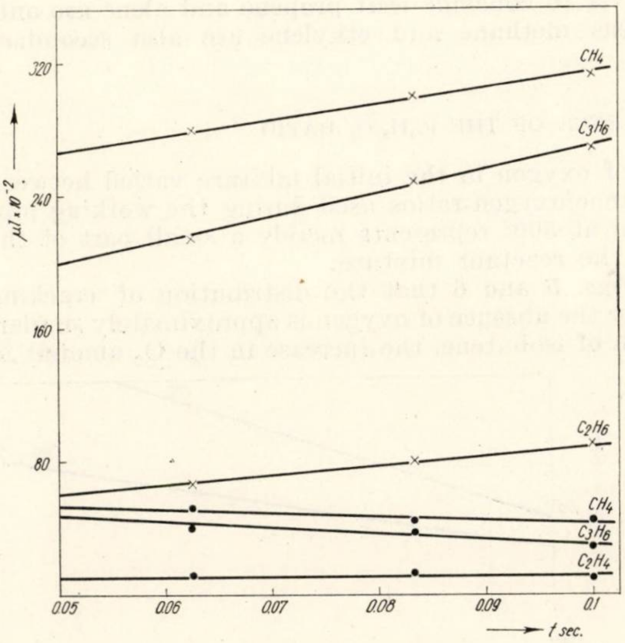

Fig. 6. — Influence of the oxygen/isobutene (x) and Ar/isobutene (.) ratio on the products. $T = 600°$; $t = 1.0$ sec.

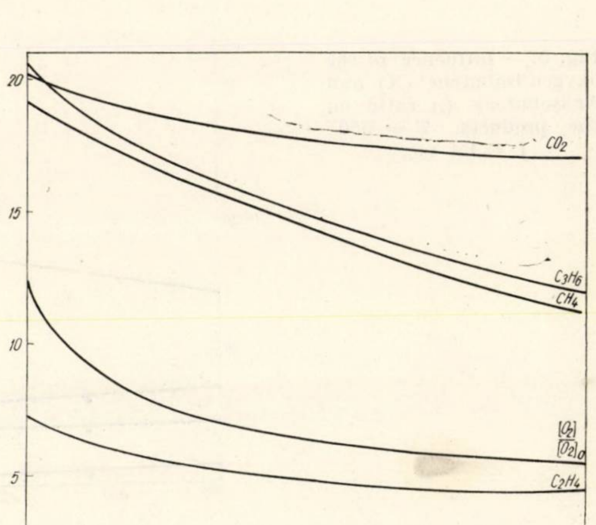

Fig. 7. — Variation of oxygen conversion and of the selectivity of the main products with the oxygen/isobutene ratio. $T = 500°$; $t_r = 0.3$ sec.

is the most strongly influenced whereas at 600° propylene is the product with the most marked increase. The substitution of O_2 by equivalent argon amounts, the other conditions remaining unchanged, leads to a slight decrease in the amount of products (points 1, 2, 3, Figs. 5 and 6).

It must be observed that the largest oxygen fraction is consumed at lower concentrations of the latter (Fig. 7). At all iC_4H_8/O_2 ratios, the propene selectivity was maintained higher than that of methane and the low O_2 concentrations favour the formation of C_3H_6 more than that of CO_2.

By increasing the oxygen concentration one observes a sensible decrease in the selectivity of all products, the strongest variation being found with C_3H_6 and CH_4. This proves that since oxygen participates in the reaction with various radicals, it largely hinders those leading to the formation of methane and of propylene. The carbon dioxide presents a more pronounced decrease at low oxygen concentrations, tending to become independent of it thereafter.

INFLUENCE OF TEMPERATURE AND OF THE REACTIONN TIME

Fig. 8 illustrates the variation with temperature of the main products resulting from the simple pyrolysis (1, 2, 3, 4) and from the oxidative pyrolysis (1, 2, 3, 4). One observes a strong effect of the temperature increase on the products and in particular on those resulting from the oxidative pyrolysis. It can be noted that the reaction products are more sensitive to temperature variations than to the change in the hydrocarbon/oxygen ratio, at the used oxygen concentrations. The ethylene behaviour is worth noticing, as it presents in both cases less sensible growths.

Nevertheless we think that the influence of the reaction time on the amount of the main reaction products is edifying (Figs. 9—11). In the oxidative pyrolysis, methane, propene and ethylene (dotted curves) have a pronounced growth tendency with the increase in the reaction time. Yet in the case of pure pyrolysis, while methane and propylene present monotonous growths with the increase of the reaction time, ethylene tends rather to decrease.

A plot of the variation in the selectivity of products with the reaction time (Fig. 12) in the oxidative pyrolysis shows that short reaction times are more favourable to the formation of such products.

KINETICS OF THE PROCESS

Two sets of experiments were carried out for the determination of reaction orders. The procedure applied in the first set involved various iC_4H_8/O_2 ratios and the initial rates were measured from plots of oxygen concentration at various reaction times (Fig. 13). The total order was determined from plots of the slopes of lines log V versus log O_2 (Fig. 14).

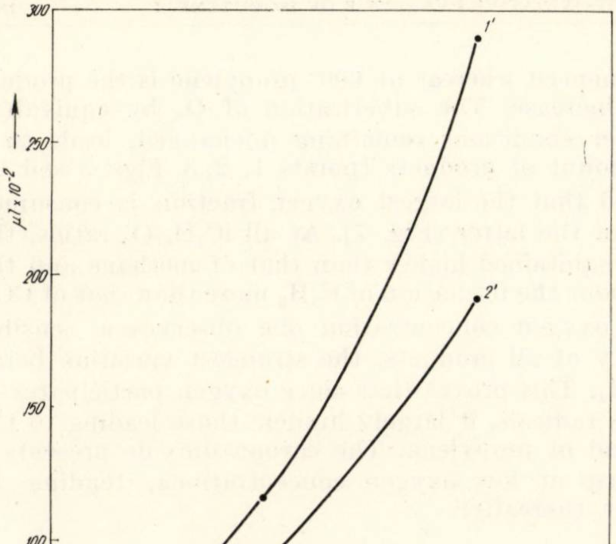

Fig. 8. — Distribution of products as a function of temperature. *1—1'*, CH_4 ; *2—2'*, C_3H_6 ; *3—3'*, C_2H_4 ; $iC_4H_8/O_2 = 20$; $t_r = 1.0$ sec.

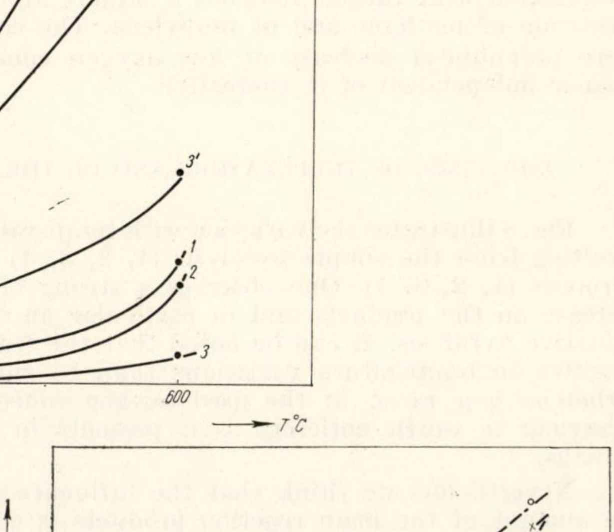

Fig. 9. — Methane distribution as a function of time. $T = 550°$; $iC_4H_8/O_2 = 20$ ($\times = 16$; ○ $= 12$) ; iC_4H_8/Ar (● $= 20$; $\times = 16$; ○ $= 12$).

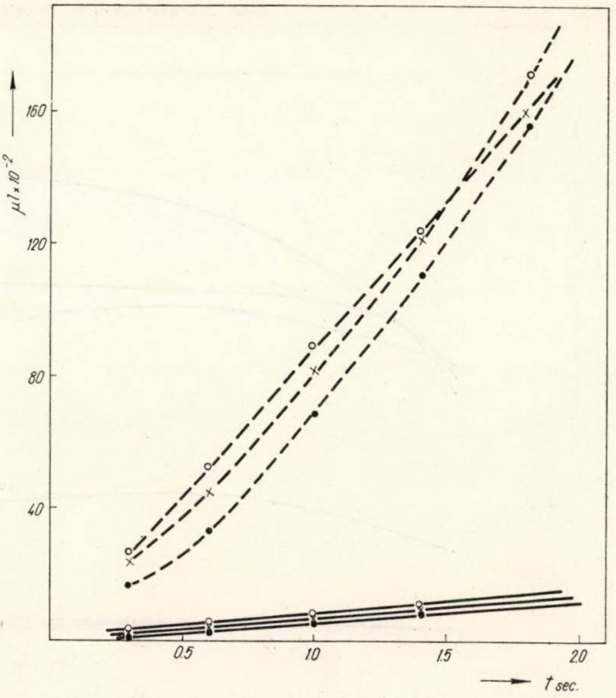

Fig. 10. — Propylene distribution as a function of time. $T = 550°$; iC_4H_8/O_2 (◉ =20 ; × =16 ; ○=12) ; iC_4H_3/Ar (● = 20 ; × =16 ; ○ = 12).

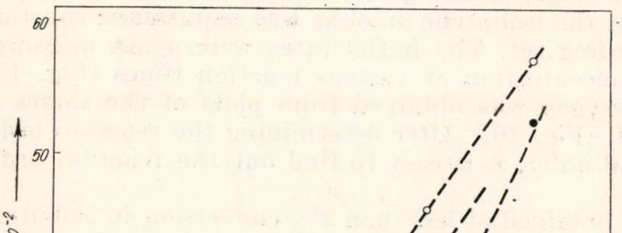

Fig. 11. — Ethylene distribution as a function of time. $T = 550°$; iC_4H_8/O_2 (● =20 ; × =16 ; ○=12) ; iC_4H_8/Ar (● =20 ; × = 16 ; ○ = 12).

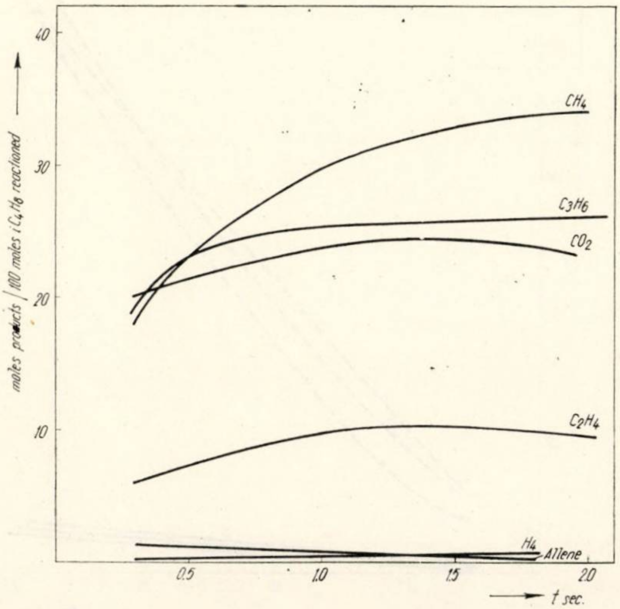

Fig. 12. — Variation of products selectivity with time in the oxidative pyrolysis. $T = 500°$; $iC_4H_4/O_2 = 20$.

The second set of experiments also involved various $i\text{-}C_4H_2/O_2$ ratios in which, however, the isobutene amount was maintained constant in contrast to the preceding set. The initial rates were again measured from plots of oxygen concentration at various reaction times (Fig. 15). The reaction order in oxygen was obtained from plots of the slopes of lines log V versus log O_2 (Fig. 16). After determining the reaction order of O_2 as well as the total order, it is easy to find out the reaction order in isobutene.

All the values were obtained at less than 2% conversion in isobutene and were therefore real measurements of reaction rates.

Experimental data indicate the value 1 of the reaction order both for oxygen and for isobutene and the rate differential equation assumes the form

$$\frac{d\,[O_2]}{dt} = K\,[iC_4H_8]\,[O_2].$$

A number of researchers [1, 2, 19] have also obtained a reaction order 1 in isobutene in the case of a simple pyrolysis of this hydrocarbon.

On the other hand, as in the case of the reaction studied by us, Appleby [9] and Scacchi [12] have found that the reaction order in butane and ethane remains the same regardless whether the pyrolysis of the respective hydrocarbons takes place in the presence or in the absence of oxygen.

The integrated form of equation (1) in our case, i.e. for an isobutene concentration much higher than that of oxygen [21] is the following :

$$\ln \frac{1}{\alpha} = K\,[iC_4H_8]_0\,(t - t_0)$$

---

[21] D. MARGERISON in G. H. BANFORD and C. F. H. TIPPER, "Comprehensive Chemical Kinetics", Elsevier Publishing Company, Amsterdam, 1969, p. 387.

Fig. 13. – Variation of oxygen concentration with time. $T = 500°C$.

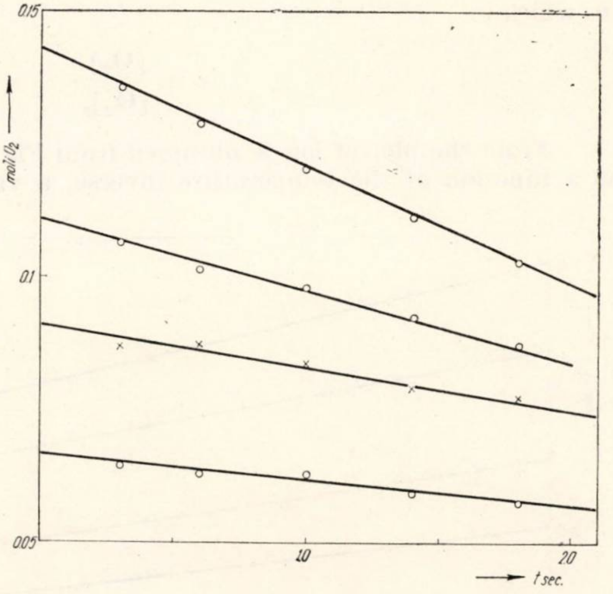

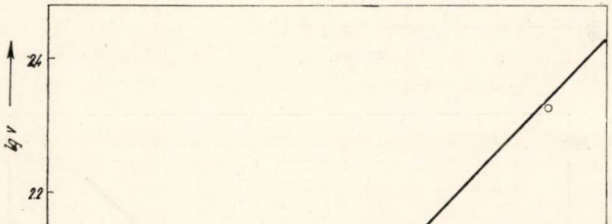

Fig. 14. – Plot of log V versus log $[O_2]_0$.

in which

$$\alpha = \frac{[O_2]}{[O_2]_0}.$$

From the plot of log K obtained from Fig. 16 and from formula (2) as a function of the temperature inverse, a value of 24.9 kcal/mol was determined for the activation energy (Fig. 17) of the oxidative pyrolysis reaction. This value is much smaller compared to the value of the activation energy for the simple pyrolysis reaction, [2,18] of 48 kcal/mol in

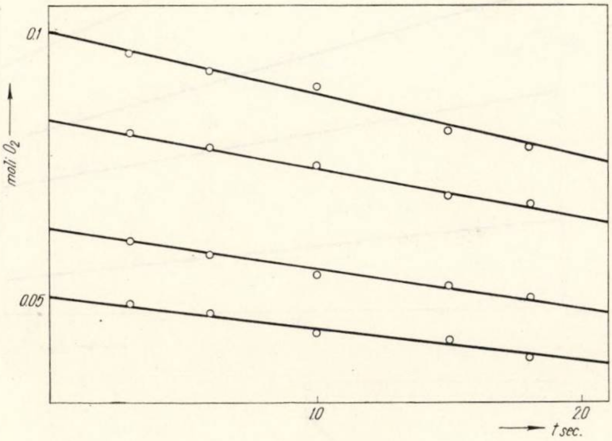

Fig. 15. — Variation of oxygen concentration with time.

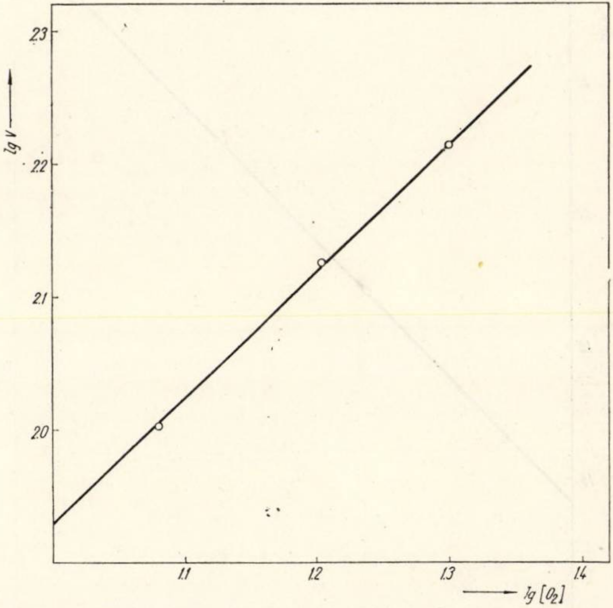

Fig. 16. -- Plot of log V versus log $[O_2]_0$.

the range 542—600° and 53.3 in the range 580° and is in agreement with the existence of an initiation stage in addition to that produced by pyrolysis in the absence of oxygen, with a lower activation energy.

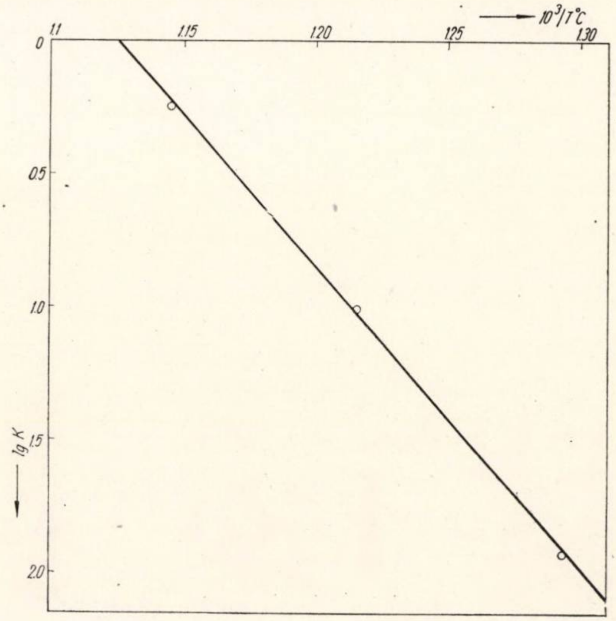

Fig. 17. — Arrhenius plot

It results that oxygen addition causes a lowering of the activation energy of the pyrolysis reaction, a fact also observed by Hausmann [22] in the pyrolysis of ethylbenzene in the presence of oxygen, where he obtains a value of 70 kcal/mol for the activation energy of the simple pyrolysis and 48.5 kcal/mol for that of pyrolysis in the presence of oxygen.

Similarly, in the pyrolysis of n-butane in the presence of oxygen, Appleby [9] obtains a very low value of the activation energy (21 kcal/mol) compared to the values necessary for the activation of the simple pyrolysis reaction of this hydrocarbon, values that vary between 61.4 and 73.9 kcal/mol.

---

[22] E. D. Hausmann and C. J. King, *Ind. and Eng. Chem.* (*Fundamentals*), **5**, 295 (1966).

Revue Roumaine de Chimie, **19**, *12*, 1855–1860 (1974)

Hommage à
Raluca Ripan
pour son 80e anniversaire

UN NOUVEAU RÉACTIF DU TYPE EDTA

CONST. GH. MACAROVICI et EUGEN CHIŞ
Faculté de Chimie, Université « Babeş-Bolyai », Cluj,
Faculté de Physique et Chimie, Université de Braşov

Reçu le 16 mars 1974

On a synthétisé l'acide 4,4'-diaminodiphénylméthane-N,N'-diacétique et son sel de sodium. On en a établi la composition et la structure par analyse chimique, titrage potentiométrique, conductométrique, analyse thermogravimétrique et le spectre en infrarouge (formule II). Le sel de sodium respectif se comporte tout comme un ligand tétradenté à possibilités d'utilisation en chimie analytique.

Depuis l'apparition du réactif complexométrique EDTA proposé par Schwarzenbach et Ackermann [1] on a manifesté un intérêt particulier pour obtenir des substances aminopolycarboxyliques comme réactifs plus sensibles, plus sélectifs ou plus spécifiques pour différents ions métalliques. Actuellement on connaît tout une série de ce type de substances ayant à la base différentes amines aliphatiques ou aromatiques.

Dans le présent ouvrage nous nous sommes proposé d'obtenir un réactif similaire à partir du 4,4'-diaminodiphénylméthane, d'en étudier la structure, les propriétés et les éventuelles applications en chimie analytique.

PARTIE EXPÉRIMENTALE

On a synthétisé la substance de base, c'est-à-dire le 4,4'-diaminodiphénylméthane à partir des données de la littérature[2], au point de fusion 92–93°.

Pour la synthèse de l'acide 4,4'-diaminodiphénylméthane-N, N'-diacétique, non signalé encore dans la littérature de spécialité, plusieurs variantes ont été essayées.

Selon l'une des variantes (a), une solution formée de 48 g (0,5 moles) d'acide monochloracétique en 200 ml eau distillée se neutralise le plus exactement possible, à froid (au-dessous de 10°) par NaOH *n* en présence de phénolphtaléine. Cette solution est ajoutée progressivement et sous agitation continue à une suspension en 200 ml eau distillée de 49 g (0,25 moles) de 4,4' diaminodiphénylméthane ; on réchauffe progressivement de 30 à 70° au bain-marie. Par la suite de cette réaction qui a lieu au niveau des groupes $-NH_2$ et de l'abaissement du pH, grâce aux ions H^+ libérés, à commencer aux environs du pH = 5, l'acide libre, 4,4'-diaminodiphénylméthane-N,N'-diacétique se sépare. Au bout d'environ une heure on ajoute encore, sous agitation continue, un excès (environ 20%) de solution chaude (30—40°) d'acide monochloracétique neutralisé. On continue de réchauffer tout le mélange, sous agitation continue, à 70—80°, pendant encore 1—2 heures, après quoi on le laisse refroidir. On filtre et on lave à l'eau distillée (30—40°) jusqu'à l'élimination de l'ion Cl—. On continue le lavage à l'eau et alcool éthylique (de préférence) mélangés en proportions égales, afin d'éliminer les petites quantités de base qui éventuellement n'ont pas entièrement réagi.

---

[1] G. Schwarzenbach et A. Ackermann, *Helv. Chim. Acta*, **30**, 1798 (1948).

[2] H. Rivier et A. Marne, *Helv. Chim. Acta*, **12**, 865 (1947).

Selon une autre variante (b) les réactants pris dans les proportions mentionnées ci-dessus sont réchauffés progressivement et sous agitation continue à une température modérée de 55—60° jusqu'à ce que l'acide libre commence à se séparer. On refroidit jusqu'à 30° et on ajoute goutte à goutte et sous agitation continue NaOH *n* jusqu'à la dissolution de l'acide, respectivement jusqu'à la réalisation du pH 8—9. On continue de réchauffer à 45—50° en ajoutant goutte à goutte du NaOH, lorsqu'on remarque l'abaissement du pH au-dessous de 8. La réaction est considérée finie approximativement après l'addition d'une quantité de NaOH équivalente à celle de l'acide chlorhydrique mis en liberté par la réaction, respectivement alors que pendant 1—2 heures on ne remarque plus de baisse du pH au-dessous de 8. La solution contient le sel de sodium de l'acide 4,4'-diaminodiphénylméthane-N,N'-diacétique. Après filtrage, pour écarter les impuretés résineuses habituellement formées en petite quantité, la solution du sel de sodium est diluée d'une volume approximativement double d'eau distillée et on y ajoute goutte à goutte, sous agitation lente du HCl *n*. A mesure que le pH de la solution baisse, à environ 4,5—5 commence la séparation de l'acide libre, de couleur blanc-jaune. Lorsqu'on parvient au pH 3—3,5 on laisse le tout en repos pendant quelques heures. On filtre et on procède par la suite tout comme au cas de la variante (a) ci-dessus. Des données analytiques (tableau 1) on déduit la formule brute $C_{17}H_{18}O_4N_2$ à masse moléculaire 314,35, confirmée par la méthode Rast (en camphre).

Tableau 1

Données de l'analyse élémentaire

Substance		C %	H %	N %	Na %
$C_{17}H_{18}O_4N_2$	calculé :	64,95	5,73	8,91	—
$C_{17}H_{18}O_4N_2$ variante a	trouvé :	65,00	5,96	9,19	—
$C_{17}H_{18}O_4N_2$ variante b	trouvé :	64,61	5,88	8,50	—
$C_{17}H_{16}O_4N_2Na_2$	calculé :	56,98	4,50	7,82	12,83
$C_{17}H_{16}O_4N_2Na_2$	trouvé :	57,15	5,06	8,09	12,62

La synthèse de l'acide 4,4'-diaminodiphénylméthane-N,N'-diacétique peut également être réalisée en utilisant à la place de l'acide monochloracétique, l'acide monobromacétique ou monoiodacétique. Avec ces réactifs la vitesse de réaction est visiblement plus grande même à 45—50°. Les réactions qui ont lieu peuvent être représentées schématiquement de la manière suivante :

$$\underset{\text{I}}{H_2N-C_6H_4-CH_2-C_6H_4-NH_2} + 2ClCH_2-COOH \longrightarrow$$

$$\longrightarrow \underset{\text{II}}{HOOC-CH_2-NH-C_6H_4-CH_2-C_6H_4-NH-CH_2-COOH} + 2HCl$$

Le point de fusion de l'acide libre est compris entre 180—185°. Il est pratiquement insoluble dans l'eau froide, éther éthylique, benzène, toluène, tétrachlorure de carbone, chloréthane, sulfure de carbone, acétone, dioxanne. Il est peu soluble dans l'eau bouillante (2% à 80°) dont on peut facilement le recristalliser. Il est moins soluble dans le méthanol (0,5%) et l'éthanol (0,2%) ; facilement soluble dans l'acide acétique glacial et les acides minéraux.

Le sel de sodium ($C_{17}H_{16}O_4N_2Na_2$, M = 358,31) s'obtient par évaporation à sec, à vide, de la solution d'acide 4,4'-diamino-diphénylméthane-N,N'-diacétique neutralisée par NaOH,

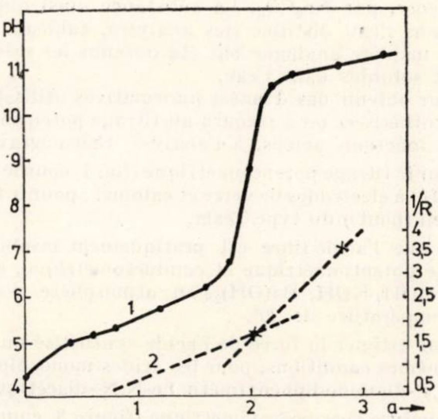

Fig. 1. — Courbe de titrage potentiométrique de l'acide 4,4'-diaminodiphénylméthane-N,N'-diacétique n/100 avec NaOH n/10.

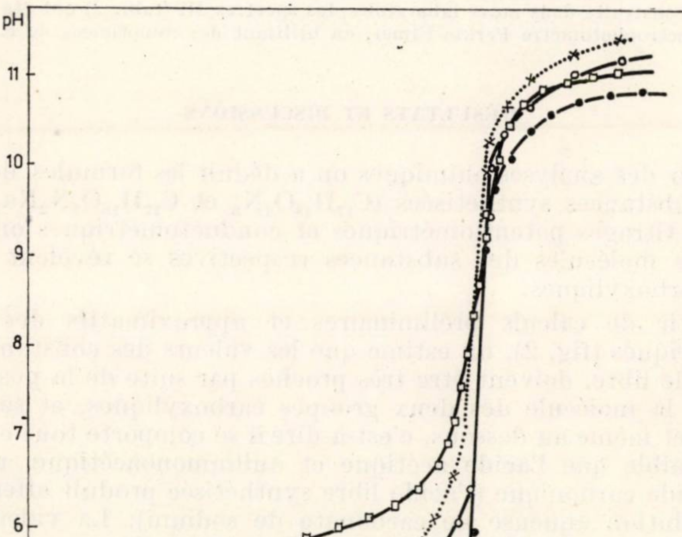

Fig. 2. — Courbes de titrage potentiométriques des : *1*, L'acide monochloracétique n/100 avec NaOH n/10 ; *2*, L'acide acétique n/100 avec NaOH n/10 ; *3*, L'acide anilinmonoacétique n/100 avec NaOH n/10 ; *4*, L'acide 4,4'-diaminodiphénylméthane-N,N'-diacétique n/100 avec NaOH n/10.

mieux encore, par Na_2CO_3. La substance ainsi obtenue est de couleur jaune et facilement soluble dans l'eau distillée (les analyses, tableau 1).

De manière analogue ont été obtenus les sels de lithium, potassium, calcium, baryum, également solubles dans l'eau.

Pour obtenir des données informatives utilisables en vue d'établir la structure des substances synthétisées on a recouru au titrage potentiométrique et conductométrique pour déterminer les fonctions acides, à l'analyse thermogravimétrique et les spectres en infrarouge.

Pour le titrage potentiométrique (fig. 1, courbe *1*) on a utilisé le pH-mètre du type Radelkis OP 401/2 à électrodes de verre et calomel ; pour le titrage conductométrique (fig. 1, courbe *2*), un appareil (pont) du type Tesla.

Vu que l'acide libre est pratiquement insoluble dans l'eau (à froid on a eu recours à son titrage potentiométrique et conductométrique, en suspension aqueuse, avec des solutions n/10 de NaOH, KOH, $Ba(OH)_2$, en atmosphère d'azote, à la puissance ionique de 0,1 mole KCl et température de 20°.

Pour estimer la force de l'acide synthétisé on a effectué des titrages potentiométriques dans les mêmes conditions, pour les acides monochloracétique, acétique, anilinmonoacétique et l'acide 4,4'-diaminodiphénylméthane-N,N'-diacétique (fig. 2).

L'analyse thermogravimétrique (figure 3, courbes *1*, et *2*) a été réalisée au moyen d'une thermobalance construite dans notre laboratoire, les spectres IR (tabl. 2) ont été obtenus au moyen d'un spectrophotomètre Perkin-Elmer, en utilisant des comprimées de KBr.

RÉSULTATS ET DISCUSSIONS

À partir des analyses chimiques on a déduit les formules de composition des substances synthétisées ($C_{17}H_{18}O_4N_2$ et $C_{17}H_{16}O_4N_2Na_2$), tandis que par des titrages potentiométriques et conductométriques on a établi que dans les molécules des substances respectives se révèlent les deux fonctions carboxyliques.

À partir de calculs préliminaires et approximatifs des données potentiométriques (fig. 2), on estime que les valeurs des constantes d'acidité de l'acide libre, doivent être très proches par suite de la position distancée dans la molécule des deux groupes carboxyliques, et seraient de l'ordre 10^{-7} et même au-dessous, c'est-à-dire il se comporte tout comme un acide plus faible que l'acide acétique et anilinmonoacétique, mais plus fort que l'acide carbonique (l'acide libre synthétisée produit effervescence avec une solution aqueuse de carbonate de sodium). La valeur exacte des constantes sera vérifiée aussi par d'autres moyens.

L'analyse thermogravimétrique révèle que l'acide libre (fig. 3, courbe *1*) commence à se décomposer à environ 100° et après quelques points d'inflexion à 250, 350 et 450° il se décompose complètement à 700°.

De la courbe thermogravimétrique du sel de sodium (fig. 3, courbe *2*) il s'ensuit que la décomposition de celui-ci commence à environ 200° et après une baisse brusque jusqu'à 430°, correspondant à une perte de poids de 42,75%, la succession des transformations, marquées par les points d'inflexion à 700 et 800° se finalise par un palier très peu incliné depuis environ 800° jusqu'à 1000°. Il est à remarquer le fait qu'à 750° le résidu est de 29,56% par rapport à la masse de l'échantillon mis en œuvre, une valeur pratiquement égale à celle calculée (29,58) correspondant à Na_2CO_3 qui devrait se former par la décomposition du sel de sodium de l'acide synthétisé. Nous estimons que cette concordance peut servir en tant que preuve de la composition du sel de sodium synthétisé. En continuant le chauffage, à 1000° environ, la masse de résidu arrive à 23,6% de la masse de l'échantillon analysé et correspond à un mélange de Na_2CO_3 et Na_2O. Le début de la décomposition du Na_2CO_3 à 750°, donc à une température de 100° inférieure à celle de décomposition qui lui correspond (850°) et la formation de Na_2O, s'expliquent par la réaction qui a lieu, à haute température, entre Na_2CO_3 et les restes de carbone qui proviennent par la combustion incomplète de la substance organique.

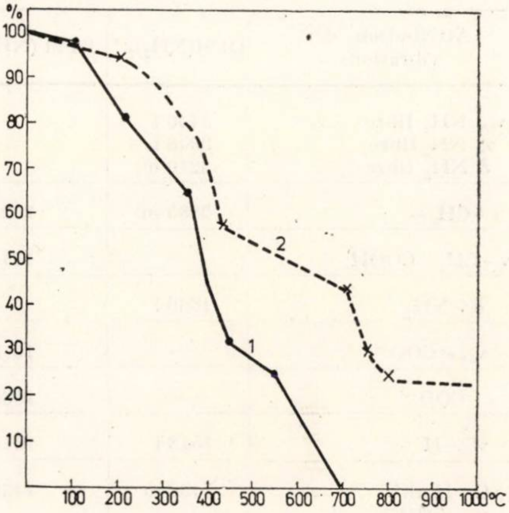

Fig. 3. —Courbes thermogravimétriques des : *1*, l'acide 4,4'-diaminodiphénylméthane-N,N'-diacétique ; *2*, le sel de sodium de l'acide 4,4'-diaminodiphénylméthane-N,N'-diacétique.

L'analyse des spectres en IR. Si l'on compare le spectre de la base (4,4'-diaminodiphénylméthane) au spectre de l'acide libre et à celui du sel de sodium respectif, on constate que dans les spectres de ces derniers les vibrations correspondant au groupement $-NH_2$ libre n'apparaissent plus ; cependant dans le spectre de l'acide libre apparaissent les vibrations caractéristiques au groupement acétique ($-CH_2-COOH$) à 1715, 1320, 1232 cm^{-1}, valeurs qui sont en bonne concordance avec celles signalées dans la littérature [3-6] ; ces vibrations n'apparaissent plus dans le spectre du sel de sodium. En plus, apparaissent aussi les vibrations du groupement $-COO^-$, tant au cas de l'acide libre (1580, 1430 cm^{-1}) qu'au cas du sel de sodium (1590 , 1425 cm^{-1}) [7].

Puisque dans le spectre IR de l'acide et du sel de sodium on ne remarque plus les vibrations qui correspondent aux groupements $-NH_2$ libres, on peut déduire que les groupements acétiques sont greffés symétriquement sur les deux fonctions amino des extrémités de la molécule.

---

[3] Const. Gh. Macarovici et A. Doruţiu, *Stud. Univ. Babeş Bolyai. Chem.*, **1966**, 135.

[4] Const. Gh. Macarovici et G. Schmidt, *Studii şi cercet. Chim. Acad. RPR.* **13**, 733 (1964).

[5] Y. Moriguki, M. Miyazaki et K. Ueno, *Bull. Chem. Soc. Japan,* **14**, 1344 (1968).

[6] M. Miyazaki, Y. Moriguki et K. Ueno, *Bull. Chem. Soc. Japan,* **14**, 838 (1968).

[7] E. Uhling et D. Hermann, *Z. anorg. Chem.*, **359**, 135 (1968).

Cette supposition est également confirmée par l'aspect de la courbe de titrage potentiométrique de l'acide libre synthétisé.

Par conséquent, compte tenu des résultats de l'analyse chimique, des titrages potentiométriques et conductométriques, thermogravimétriques et de spectres en IR, on peut estimer que la formule de constitution de l'acide libre synthétisé est celle qu'on s'est proposée de réaliser (formule II).

Tableau 2

Spectres en IR des substances synthétisées

Attribution des vibrations	$DFM(NH_2)_2$*	DFM $(NHAc\ H)_2$*	$DFM(NHAc\ Na_2)$*
ν_{as} NH_2 libre	3446 i	—	—
ν_s NH_2 libre	3348 i	—	—
δ NH_2 libre	3210 m	—	—
$\nu-CH_2-$	2885 m	2920 m	2890 m
$\nu-CH_2-COOH$	—	1715 m	—
$\delta-NH_2$	1630 i	—	—
$\nu_{as}-COO^-$	—	1615 i	1610 m
$\nu-COO^-$	—	1580 m	1590 m
$\nu C-H$	1515 i	1515 i	1514 m
$\nu C-H$ alif. ν_s-COO^-	1436 m	1430 i	1425 m
$\nu-CH_2-COOH$	—	1320 m	—
$\nu C-N$ libre	1288 m 1275 m	—	—
$\nu-CH_2-COOH$	—	1232 m	—
$\nu C-N$ liée $CH-NH-CH$	—	1190 m	1190 m

* $DFM(NH_2)_2$ = 4,4'-diaminodiphénylméthane ; $DFM(NHAcH)_2$ = l'acide 4,4'-diaminodiphénylméthane-N,N'-diacétique ; $DFM(NHAcNa)_2$ = sel de sodium de l'acide 4,4'-diaminodiphénylméthane-N,N'-diacétique.

Le sel de sodium correspond à la même structure où les ions H^+ sont substitués par des ions de sodium. Il réagit comme ligand tétradenté avec les différents métaux en formant des combinaisons du type des complexes internes, sur lesquelles nous allons revenir dans nos communications futures.

Revue Roumaine de Chimie, **19**, *12*, 1861–1876 (1974)

Dedicated to
RALUCA RIPAN
on the occasion of her 80th anniversary

PALLADIUM (II) AND PLATINUM (II) SQUARE-PLANAR COMPLEXES WITH TRIS (*p*-METHOXYPHENYL) ARSINE AND HALIDE IONS

P. SPACU, FLORICA POPEA, C. I. LEPĂDATU, A. C. BANCIU, EUGENIA IVAN,
SILVIA PLOŞTINARU, ZAMFIRA TOMA and CRISTINA RUSU
Centre of Physical Chemistry, Str. Dumbrava Roşie 23, Bucharest

Received March 11, 1974

In the present paper, 5 new *tris* (*p*-methoxyphenyl) arsine compounds of the general formula ML_2X_2 are reported ($M = Pd(II)$, $Pt(II)$; $L = As(p\text{-}CH_3OC_6H_4)_3$; $X = Cl^-$, Br^- or I^- for $M = Pd$ (II), and $X = Br^-$ or I^- for $M = Pt$ (II)). Chemical analyses and physical determinations (X-ray diffraction data, i.r. vibration spectra, electronic spectra, melting points) as well as a quantitative quantum study of the metal-ligand bonds in these square-planar complexes were performed. Some hints concerning the catalytic activity of these compounds are also given.

INTRODUCTION

In recent years, extensive studies concerning the coordination chemistry of the transition metals, are devoted to their applications to homogeneous catalysed processes.

Previous work reports [1-3] that among the coordination compounds of the transition metals, the d^8 square-planar of the VIIIth group (Pd > Pt) displays a remarkable catalytic activity enhanced by the presence of a halide ion in the coordination sphere, in the sequence $Cl < Br < I$.

Based on these considerations, the goal of the present work was to obtain some new complexes in view of their possible applications to homogeneous catalysed hydrogenation reactions. For this purpose Pd (II) and Pt(II) complexes formed by tris-(*p*-methoxy-phenylarsine) and halogen ions were synthetized. The last mentioned were Cl^-, Br^- and I^- for the Pd(II) complexes and Br^- and I^- for the Pt(II) complexes.

Indeed, the methoxy substituent in the para position on the benzene ring, displays besides the inductive effect a strong conjugation effect. This later effect enhances significantly the electronic density on the As atom bound to the aryl group and on the metal atom bound with As in the arsine complexes. These facts produce an increase in the cova-

---

[1]. G. N. SCHRAUZER, "Transition Metals in Homogeneous Catalysis", chap. 2, Marcel Dekker, Inc. New York, 1971.

[2]. M. L. H. GREEN, "Organometallic Compounds. The Transition Metals", chap. 9, Methuen, London, 1968.

[3]. H. KELM, *Ber. Bunsenges. phys. Chem.*, **76**, 1038 (1972).

lency degree of the metal-organic ligand bond and subsequently some increase in the stability of the complexes (compared with that of the triphenylarsine, the unsubstituted ligand).

In the last twenty years, the theoretical treatments concerning the transition metal complexes were confined mostly to the octahedral and tetrahedral ones.[4] Those regarding the square-planar compounds were only qualitative and sometimes conflicting.[5-11] One of the reasons is the more complicated effect of the ligands on the atomic orbitals of the central metal atom.

These facts substantiated the opportunity of a quantitative quantum treatment of the metal-ligand bonds in these compounds, possibly useful as homogeneous catalysts.

QUANTUM MOLECULAR STATES IN THE SQUARE-PLANAR COMPLEXES

For the reasons discussed above we shall present, in the following pages, the quantum treatment of the molecular states in the complex *trans*- [Pd (II) Ars_2Cl_2], where Ars = tris (*p*-methoxyphenyl) arsine, to which a *trans* coordination geometry which minimizes the repulsions between ligands has been ascribed (Fig. 1).

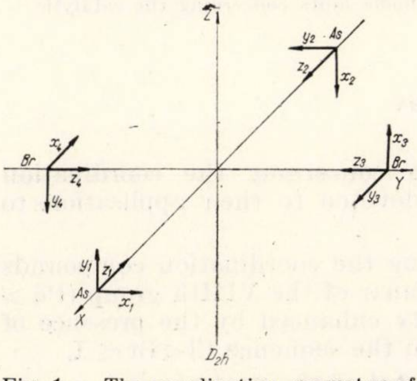

Fig. 1. — The coordination geometry of trans- [Pd (II)Ars_2Br_2] complex (D_{2h}).

For this purpose, the following minimal set of orbitals has been used :

Palladium (9 orbitals) : $4d_{xy}$, $4d_{xz}$, $4d_{yz}$, $4d_{z^2}$, $4d_{x^2-y^2}$; 5s ; $5p_x$, $5p_y$, $5p_z$

Chlorine (3 orbitals) : $h = 0.900 |3p_z> + 0.435 | 3s >$ (see the Appendix) $3p_x$,$3p_y$

Arsenic (1 orbital) : sp^3 (tetrahedral hybridization)

All the orbitals used are Slater type orbitals (STO), the effective principal quantum numbers and exponents being chosen according to Slater's rules[12], as follows

$$Pd^{2+} : \alpha_{4d} = 2.69 ; \quad n^* = 3.7$$

$$\alpha_{5s5p} = 1.525 ; n^* = 4$$

---

[4] M. Wolfsberg and L. Helmholz, *J. Chem. Phys.*, **20**, 837 (1952).

[5] R. L. Belford, M. Calvin and G. Belford, *J. Chem. Phys.*, **26**, 1165 (1957).

[6] J. Chatt, G. A. Gamlon and L. E. Orgel, *J. Chem. Soc.*, **1958**, 486.

[7] H. B. Gray and C. J. Ballhausen, *J. Amer. Chem. Soc.*, **85**, 260 (1963).

[8] H. Basch and H. B. Gray, *Inorg. Chem.*, **6**, 365 (1967).

[9] C. K. Jørgensen, *Progr. Inorg. Chem.*, **12**, 101 (1970).

[10] C. K. Jørgensen, "Modern Aspects of Ligand Field Theory", North-Holland Publ. Comp. Amsterdam, 1971.

[11] A. B. P. Lever, "Inorganic Electronic Spectroscopy", Elsevier Publ. Comp., Amsterdam, 1968.

[12] S. S. Batsanov and R. A. Zvyagina, "Integraly perekryvaniya", Tom. 1, Izd. Nauka, 1966.

$$Cl^- : \ \alpha_{3s,3p} = 1.858 ; \ n^* = 3$$

$$As : \ \alpha_{4s\ 4p} = 1.78 ; \ n^* = 3.7$$

STO's instead of other analytical Hartree-Fock orbitals available in the related literature [13-14] have been preferred, since a preliminary analysis of the overlap integrals obtained with the last type of AO's, has led to numerical values incompatible with the radial extent assumed for the 4d-metal orbitals.

To solve the secular equation and to facilitate the interpretation of the results (especially the selection rules for transitions), the minimal orbital set of the interacting atoms has been classified according to the symmetry classes of the D_{2h} group to which the complex, as represented in Fig. 1, belongs. The group-theoretical analysis made according to the well known methods [15-16], leads to the results given in Table 1.

Table 1

The interacting orbitals set classified upon the symmetry classes of D_{2h} group

D_{2h}	Central metal AO's	Symmetry adapted ligand orbitals
A_g	$4d_{z^2}, 4d_{x^2-y^2}, 5s$	$\frac{1}{\sqrt{2}}(sp_1^3 + sp_2^3) ; \frac{1}{\sqrt{2}}(h_3 + h_4)$
B_{1g}	$4d_{xy}$	$\frac{1}{\sqrt{2}}(x_4 + y_3)$
B_{2g}	$4d_{xz}$	
B_{3g}	$4d_{yz}$	$\frac{1}{\sqrt{2}}(x_3 + y_4)$
B_{1u}	$5p_z$	$\frac{1}{\sqrt{2}}(x_3 - y_4)$
B_{2u}	$5p_y$	$\frac{1}{\sqrt{2}}(h_3 - h_4)$
B_{3u}	$5p_x$	$\frac{1}{\sqrt{2}}(sp_1^3 - sp_2^3) ; \frac{1}{\sqrt{2}}(x_4 - y_3)$

Since the symmetry classes have orthogonal representations, the total secular equation splits into A_g (5×5) ; B_{1g} (2×2) $B_{2g}(1)$; B_{3g} (2×2) ; B_{1u} (2×2) ; B_{2u} (2×2) ; B_{3u} (3×3), each factorized secular equation being of the form

$$C_{ij}\,[H_{ij} - G_{ij}E] = 0$$

---

[13] J. W. Richardson, M. J. Blackman and J. E. Ranochak, *J. Chem. Phys.*, **58**, 3010 (1973).

[14] H. Basch and H. B. Gray, *Theor. Chim. Acta*, **4**, 367 (1966).

[15] F. A. Cotton, "Chemical Applications of Group Theory", Interscience, New York, 1963.

[16] J. A. McMillan, "Introduction to Group Theory and Applications to Physics and Chemistry of Atoms and Molecules", 1973 (Book preprint).

where C_{ij} are the mixing coefficients of the molecular wavefunctions (Eigenfunctions),

G_{ij} — the group overlap integrals, i.e. the overlap integrals between the central metal orbitals and the symmetry adapted orbitals of the ligands,

H_{ij} — the energy matrix elements, and

E — the molecular energies (Eigenvalues).

The group overlap integrals have been expressed in terms of diatomic integrals, which have been estimated for the interatomic distances [17–18] $R_{Pd-Cl} = 2.37$ Å and $R_{Pd-As} = 2.38$Å.

The diagonal energy matrix elements have been approximated, in the usual way, to valence state ionization potentials, and the off-diagonal elements according to Cusach's approximation [19]

$$\underset{i>j}{H_{ij}} = G_{ij}(2 - |G_{ij}|)\frac{H_{ii} + H_{jj}}{2}$$

The ionization potentials used in the MO calculations are as folows

Palladium $H_{4d} = -8.5$ eV
$H_{5s} = -6.4$ eV
$H_{5p} = -3.2$ eV
Arsenic $H_{sp^3} = -11.2$ eV from $H_{4s} = -17.6$ eV
$H_{4p} = -9.05$ eV
Chlorine $H_h = -16.0$ eV (see the Appendix)
$H_{3p} = -13.7$ eV

The ionization potentials for chlorine and arsenic have been taken from references [20–21], H_{4d} for the palladium ion from reference, [13] and H_{5s}, H_{5p} using the ratios $H_{nd}/H_{(n+1)s}/H_{(n+1)p}$ for Ni^{2+} ($3d^8$) ion. [20]

The molecular energies (Eigenvalues) obtained by solving the secular equations by means of a double diagonalization subroutine in FORTRAN-IV for an IBM/360 computer, are as follows : Molecular energies (eV)

$$\Gamma_{Ag}\ \sigma_1 A_g(h) = -16.364$$
$$\sigma_2 A_g(sp^3) = -12.095$$
$$\sigma_3^* A_g(4d_{z^2}) = -8.040$$
$$\sigma_4^* A_g(4d_{x^2-y^2}) = -4.470$$
$$\sigma_5^* A_g(5s) = +35.070$$

---

[17] P. SPACU and M. BREZEANU, "Chimia Combinaţiilor Complexe", Ed. didactică și pedagogică, Bucharest, 1969.

[18] J. R. MILLER, "Advances in Inorganic Chemistry and Radiochemistry", vol. 4, Academic Press, Inc., New York, 1962, p. 174.

[19] L. CHOPIN-CUSACH, *J. Chem. Phys.*, **43**, 1575 (1966).

[20] C. J. BALLHAUSEN and H. B. GRAY, "Molecular orbital Theory", W. A. Benjamin, Inc., New York, 1964.

[21] H. B. GRAY, "Electrons and Chemical Bonding", W. A. Benjamin, Inc., New York, 1965.

$$\Gamma_{B_{1g}}\ \pi_1 B_{1g}(3p_{Cl}) = -13.732$$

$$\pi_2\, B_{1g}(d_{xy}) = -8.482$$

$$\Gamma_{B_{2g}}\ n_1 B_{2g}(d_{xz}) = -8.500$$

$$\Gamma_{B_{3g}}\ \pi_1 B_{3g}(3p_{Cl}) = -13.732$$

$$\pi_2^* B_{3g}(d_{yz}) = -8.482$$

$$\Gamma_{B_{1u}}\ \pi_1 B_{1u}(3p_{Cl}) = -13.708$$

$$\pi_2\, B_{1u}(5p_z) = -2.706$$

$$\Gamma_{B_{2u}}\ \sigma_1 B_{2u}(h) = -16.451$$

$$\sigma_2^*\, B_{2u}(5p_y) = +2.365$$

$$\Gamma_{B_{3u}}\ (\pi + \sigma)_1\, B_{3u}\, (3p_{Cl}) = -13.720$$

$$(\sigma + \pi)_2\, B_{3u}(sp^3) = -11.815$$

$$(\sigma^* + \pi^*)_3 B_{3u}(5p_x) = +4.319,$$

where σ, π show the bond type, the asterisk the antibonding state and "n" the nonbonding state.

By means of the molecular wave functions obtained by solving the secular equations, the 24 electrons, i.e. Pd^{2+} (8) ; 2 × As (2) ; 2 × Cl (6), have been redistributed on the molecular centres according to Mulliken's electron population analysis [22-23] and for the ground molecular state of the complex $\psi^2\,(\sigma_1 B_{2u})$

$$\psi^2\,(\sigma_1 A_g)\,\psi^4\,(\pi_1\,(B_{1g} + B_{3g}))\,\psi^2\,((\pi + \sigma)_1\, B_{3u}\psi^2\,(\pi_1\, B_{1u})\,\psi^2\,(\sigma_2\, A_g)$$

$$\psi^2\,((\sigma + \pi)_2.\, B_{3u})\,\psi^2\ (nB_{2g})\ \psi^4\,(\pi_2^*(B_{1g} + B_{3g}))\,\psi^2\,(\sigma_3^*\, A_g).$$

As may be later seen, the two uncoupled electrons of the free Pd^{2+} ($4d^8$) ion will be paired in the antibonding molecular state $\psi^2(\sigma_3^*\, A_g)$, in other words the complex behaves as a low spin complex.

The electron population analysis leads to the following distribution of electronic densities and net charges on the atoms

$$Pd^{+1.004}\,[(4d)^{8.206}\ (5s)^{0.388}\,(5p)^{0.401}]$$

$$As\ [(sp^3)^2]$$

$$Cl^{-0.499}\ [(3p)^{3.982}\ h^{1.519}]$$

---

[22] R. S. Mulliken, *J. Chem. Phys.*, **23**, 1833, 1841 (1955).
[23] R. S. Mulliken, *J. Chem. Phys.*, **36**, 3428 (1962).

As may be observed, the net charge on the palladium ion is reduced to $+1$ as a consequence of the σ (π) chemical bond formation. The chloride ions become more positive (from -1 to ~ -0.5) and the arsenic atoms have no formal charges mainly due to the neighbouring chloride ions, via the molecular quantum state described by the wave function ψ ($\sigma_1 A_g$), which compensates the transfer of electron densities in "σ" As $\rightarrow$ Pd bonds. The upper 5s and 5p orbitals of the central metal ion are involved in chemical bonding to a considerable extent, in spite of the assertion reported in literature[13] about the chemical inadequacy of these orbitals. The $5p_z$ palladium orbital which forms "π" bonds with 3p chlorine orbitals ($\Gamma_{B_{1u}}$), does not substantially participate in chemical bonding (electronic density $(5p_z)^{0.014}$).

Nevertheless, this metal orbital could play an essential role in the SN_2 attack of the reagents which may, from sterical reasons, come along the "z" axis. The approach of the reagents will primarily weaken the "π" Pd—Cl bonds, and will favour the removal of the chloride ion from the complex. This conclusion is very important in explaining the formation mechanism of active coordination centres in the homogeneous catalysis, where square-planar complexes are frequently used as catalysts. Another surprising fact is the mixing of $4d_{z^2}$ and 5s palladium orbitals in the molecular state described by ψ ($\sigma_3^* A_g$), which has been previously suggested by Jørgensen.[9] It may be stated, in this context, that a d_{z^2} — s hybridization would take place. Since the 5s orbital has a very great radial extension, its mixing with $4d_{z^2}$ will enlarge the radial extension of the last orbital, thus leading to a decreased repulsion between the donor electron pair of the incoming reagent along the "z" axis, and that of the molecular level $\sigma_3^* A_g(4d_{z^2})$. The approach of the reagent will therefore labilize to an almost equal extent the "σ" Pd—Cl and Pd—As bonds and facilitates the ligand rearrangement in the coordination sphere of the intermediate 5-coordinate complex with the most probable coordination geometry, trigonal bipyramid (D_{3h}) (the molecular orbital stabilization energy of each coordination point in D_{3h} geometry in a square-planar complex[24]). The decrease of the repulsion between the electron pair in the $\sigma_3^* A_g(4d_{z^2})$ level and that of the reagent may be also achieved if electronic densities from $\sigma^*{}_3 A_g(4d_{z^2})$ are transferred in the upper 5d levels of the arsenic atoms involved in the "π" back-donation bonds metal $\rightarrow$ ligand.

From these considerations it follows that the catalytic properties of the square-planar complexes depend on the existence of a direction suitable for the attack of the reagents ("z" axis), as well as on the presence of "π" metal-halide bonds which favour the formation of active coordination centres, and, finally, on the "π" back-donation metal-arsenic bonds which facilitate the incoming of the reagent.

EXPERIMENTAL

Materials. Palladium (II) and platinum (II) chlorides were purchased from Reanal (Budapest). All other chemicals were reagent grade or equivalent.

Analyses were carried out by micromethods : C, H, N were determined by microcombustion, Pd metal gravimetrically by ignition.

---

[24] C. I. Lepădatu, *J. Cryst. Mol. Structure (London)*, **1**, 397 (1971).

Measurements. The uncorrected melting points were measured in sealed tube immersed in silicon oil.

The X-ray diffraction data were obtained by Debye-Scherrer powder technique, using the X-ray source TuR_M -60 (GDR). The procedure involved the Cu $K_\alpha(\lambda = 1.5418$ Å) radiation filtered on nickel (at 30 kV and 19 mA) and a 57.3 mm diameter camera.

The electronic absorbiton spectra were run at room temperature on a VSU-2 C. Zeiss Jena spectrophotometer. In the u.v. range (220 − 360 mμ) $0.25\ 10^{-4}$ M and $0.5.10^{-4}$ M absolute ethanol solutions for the compounds and for the ligand respectively, were employed. In the visible range (350 − 8007 m μ) acetone solutions were used. The low solubility of the compounds in most of the usual solvents, did not allow to obtain solutions of proper concentration in order to cover the whole range.

The i.r. spectra of the ligand and of all the complexes were recorded on potassium bromide pellets, by means of a UR 10 C. Zeiss Jena spectrophotometer in the 400 − 4000 cm^{-1} range.

The ligand tris(p-methoxyphenyl)arsine. The title compound was obtained in a Wurtz-Fittig type reaction, allowing the *p*-chloroanisole to react with arsenic trichloride in absolute diethyl ether and in the presence of sodium metal.[25]

p-chloro-anisole was prepared via *p*-anisidine diazotization, strongly acidifying with hydrochloric acid. The resulted diazonium salt yielded the *p*-chloro-anisole in a Sandmeyer type reaction[25]

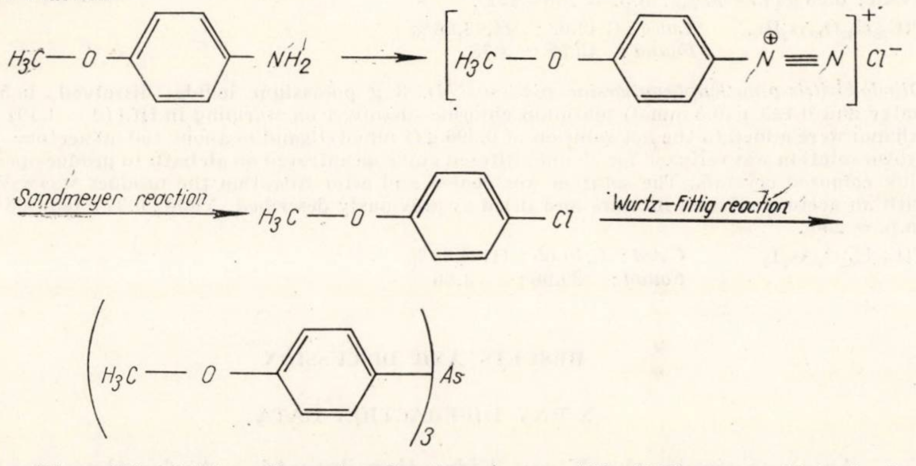

The white tris(*p*-methoxyphenyl)arsine (m.p. = 156 − 157°) was obtained from *p*-chloro-anisole, the yield being about 15%.

The coordination compounds were prepared in acetone, in the molar ratio M/L = 1/2 (M = Pd (II), Pt(II) ; L = tris(*p*-methoxyphenyl)arsine) and were formulated on the basis of the elemental analysis. In order to obtain some further data concerning the nature of the complexes investigated and to assign their most probable structure, their X-ray, vibration and electronic spectra (in u.v. and visible range) have been recorded.

Dichloro-bis(tris-p-methoxyphenyl) arsine palladium (II). A solution obtained by dissolving 0.0886 g (0.5 mmol) $PdCl_2$ in 25 ml hot water in the presence of 1 ml HCl (d = 1.19), was added to 150 ml warm solution of 0.3960 g (1 m mol) ligand. The resulting yellow solution was refluxed about 1 hour on a steam bath, until orange crystals appeared. After stirring for 5 min the orange microcrystals were filtered and washed with warm acetone. The product recrystallized from acetone was dried in vacuo over P_4O_{10}. Yield 0.35 g (75 − 80%) ; m.p. = 215 − 218°

		Pd	C	H
$PdC_{42}H_{42}O_6As_2Cl_2$	*Calcd* :	10.97 ;	52.03 ;	4.33 %
	Found :	11.43 ;	51.63 ;	4.34

Dibromo-bis(tris-p-methoxyphenyl)arsine palladium(II). To a hot solution of 0.600 g (1.6 mmol) ligand in about 130 ml acetone, 20 ml aqueous solution of 0.134 g (0.75 mmol) $PdCl_2$ and 1.6 g KBr previously dissolved in 5 ml water was added. An orange fluffy compound separated immediately. The mixture was warmed on a steam bath and stirred continuously for 10 min. The orange crystalline powder was then filtered off and washed with acetone. The product recrystallized from acetone was dried in vacuo over P_4O_{10}. Yield : 1.2 g (35–40 %) ; m.p. = 217–219°

---

[25] W. Brydowna, *Roczniki Chem.*, **7**, 436 (1927) ; C. A. **22**, 2372 (1928).

$PdC_{42}H_{42}O_6As_2Br_2$ *Calcd* : Pd 10.05 : C, 47.67 ; H, 3.97 %
Found : 10.11 ; 47.70 ; 4.22

Diiodo-bis(tris-p-methoxyphenyl)arsine palladium(II). To the hot solution of 0.396 g (1 mmol) ligand in about 150 ml acetone, a brown suspension of potassium iodide and palladium iodide (1.0 g KI in 5 ml water and 0.088 g, 0.5 mmol $PdCl_2$) was added gradually. The mixture was refluxed about 1 hr 45 min on a steam bath. After cooling, brown crystals separated which were filtered and washed with acetone. The recrystallization and drying were as described above. Yield : 0.226 g (40–45 %) ; m.p. = 228–230°.

$PdC_{42}H_{42}O_6As_2I_2$ *Calcd* : Pd, 9.22 ; C, 43.79 ; H, 3.64 %
Found : 9.22 ; 43.28 ; 3.89

Dibromo-bis(tris-p-methoxyphenyl)arsine platinum(II). A solution of 3.0 g sodium bromide in 5 ml water and 0.133 g (0.5 mmol) $PtCl_2$ dissolved on warming in a mixture of hydrochloric acid and ethanol were added to the hot solution of 0.396 g (1 mmol) ligand in about 150 ml acetone. The mixture was refluxed 15–20 min and then cooled. The lemon-yellow coloured crystals were filtered, washed with an acetone-ethanol mixture and dried in vacuo over P_4O_{10}. Yield : 0.25 g (45–50 %) ; m.p. = 230–232°.

$PtC_{42}H_{42}O_6As_2Br_2$ *Calcd* : C,43.98 ; H, 3.66 %
Found : 43.58 ; 3.75

Diiodo-bis(tris-p-methylphenyl)arsine platinum(II). 3 g potassium iodide dissolved in 5 ml water and 0.133 g (0.5 mmol) platinum chloride dissolved on warming in HCl (d = 1.19) and ethanol were added to the hot solution of 0.396 g (1 mmol) ligand in about 150 ml acetone. The brown solution was refluxed for 45 min, filtered and concentrated on air bath to produce peach-pink coloured crystals. The solution was cooled and after filtration the product was washed with an acetone-ethanol mixture and dried as previously described. Yield : 0.37 g (60–65 %) ; m.p. = 250°.

$PtC_{42}H_{42}O_6As_2I_2$ *Calcd* : C,40.65 ; H, 3.38 %
Found : 39.96 ; 3.66

RESULTS AND DISCUSSION

X-RAY DIFFRACTION DATA

As an example, the X-ray diffraction data (d = Å) for the complex $[PdBr_2\,(As\,(p-CH_3O-C_6H_4)_3)]$ and the starting materials ($PdCl_2$ and Ars) are comparatively summarized in Table 2.

It can be seen, that the values of the diffraction lines of the complex differ from those of the starting reagents. This may indicate a new unitary compound with characteristic diffraction lines. The mean intensity of these values, along the whole range of the angles measured, suggests an ordered structure of low symmetry.

VIBRATIONAL SPECTRA

The i.r. spectra of the ligand and of the 5 new compounds exhibit an unusual similarity in the whole measured range (400–4000 cm $^{-1}$). This fact is not surprising, because the expected dissimilar vibrations ν_{M-L}(L = Cl, Br, I) and ν_{M-As} (M = Pd (II), Pt (II)) appear only below 400 cm^{-1}, which is out of our measurement possibilities. The remarkable similarity of the spectra mentioned above, indicates the presence of the

Table 2

X-ray diffraction data for [Pd(II)Ars$_2$Br$_2$], arsine and PdCl$_2$

[Pd (II) Ars$_2$Br$_2$] d Å	Ars d Å	PdCl$_2$ ASTM 1−228(dÅ)
7.23	3.5337	5.30
6.188	3.2108	3.29
4.756	3.0113	3.11
3.9973	2.7961	2.39
3.6186	2.5306	2.25
3.2429	2.4099	2.02
3.0721	2.2424	1.93
2.8132	2.1434	1.87
2.6106	2.0350	1.82
2.3598	1.9512	1.77
2.1720	1.8645	1.64
2.0798	1.7446	1.61
1.9810	1.6709	1.57
1.8440	1.6247	1.54
1.7366	1.5503	1.50
1.5508	1.4422	1.43
1.4253	1.3520	1.33
1.3944	1.3079	1.31
1.1835	1.2772	1.21
1.1237	1.2273	1.13
1.1030	1.2112	1.02
1.0814	1.1624	
1.0533	1.0718	
1.0123	1.0474	
1.0063	1.0144	
0.99324	0.96920	
0.98312	0.96421	
0.97389	0.95981	
0.96307	0.94647	
0.90386	0.93496	
0.88727	0.86332	
0.88307		
0.87990		
0.84905		
0.84243		

arsine ligand in all the complexes investigated. The most probable assignments [26−27] of the i.r. spectral bands of the free ligand and of the two representative complexes are shown in Table 3.

ELECTRONIC SPECTRA

In Figs. 2−6 the electronic spectra of the complexes and of the ligand are shown. In the u.v. range, they exhibit the characteristic bands for the $\pi-\pi^*$ transitions in the phenyl groups of the arsine. The additional band, characteristic of the compounds will be thoroughly discussed bellow.

The molecular energy levels calculated for *trans*-[Pd (II) Ars$_2$Cl$_2$], are schematically shown in Fig. 7.

As may be observed in Fig. 7, the antibonding effects are stronger than the bonding ones, which is to be expected in the case of heteropolar chemical bonds. In spite of all this, the complex is stable. The molecular orbital stabilization energy of each coordination point (Bonds Stabilization Energy) [24, 28] calculated for the electronic configuration, as represented in Fig. 7, assumes a value of −0.96 eV (−22.16 kcal/mol).

---

[26] L. J. Bellamy, "The Infrared Spectra of Complex Molecules", Methuen, London, 1962.

[27] M. Avram and G. D. Mateescu, "Spectroscopia în infraroşu. Aplicaţii în Chimia Organică", Ed. tehnică, Bucharest, 1966.

[28] C. I. Lepădatu, *Rev. Roumaine Chim.*, **17**, 863 (1972).

Table 3

IR Spectra of $[Pd(II)Ars_2Br_2]$, $[Pt(II)Ars_2Br_2]$ and the free arsine ligand

Ars	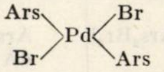	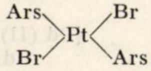	Assignments
485 ω	470 ω	485 ω	γ_2 As-Aryl vibration
530 m	525 m	525 m	
595 ω	605 ω	605 ω	
635 ω	640 ω	—	
720 ω	—	—	
800 m	800 m	800 m	γ C–H bending vibrations of 1 : 4 – disubstituted benzene ring
830 s	815 m	—	
840 s	820 m 835 s	820 s 835 s	
1015 ω	—	—	
1040 s	1035 s	1035 s	ν C–O–C sym. vibr. of etheric group
1060 ω	—	—	
1080 s	1090 s	1090 s	
1115 ω	1115 ω	1115 ω	vibration of O–CH_3 group
1185 s	1190 s	1190 s	
1255 s	1265 s	1260 s	ν C–O–C asym. vibr. of etheric group
1295 s	1300 s	1300 s	
1315 m	—	—	
1410 m	1415 ω	1415 ω	
1450 m	1450 m	1450 ω	ν C–C stretching vibration of 1 : 4 disubstituted benzene ring
1470 m	1475 m	1470 m	
1505 s	1510 s	1510 s	ν C–C stretching vibration of 1 : 4 – disubstituted benzene ring
1580 m	1580 m	1580 m	
1600 s	1600 s	1605 s	
1650 ω	—		
2845 ω	2850 ω	2840 ω	ν CH_3 stretching vibration
2940 ω	2960 ω	2960 ω	
2970 ω	—		
3500 ω	—	3450 ω	ν C–H stretching vibration of 1 : 4 – disubstituted benzene ring

w – weak, m – medium, s – strong

According to the energy diagram (Fig. 7), the following electric dipole allowed transitions are to be expected :

$$\nu_1 = \sigma_1 B_{2u}(h_{Cl}) \rightarrow \sigma_4^* A_g(4d_{x^2-y^2})$$

$$\nu_2 = \pi_1 B_{1u}(3p_{Cl}) \rightarrow \sigma_4^* A_g(4d_{x^2-y^2})$$

$$\nu_3 = (\pi + \sigma)_1 B_{3u}(3p_{Cl}) \rightarrow \sigma_4^* A_g(4d_{x^2-y^2})$$

$$\nu_4 = (\sigma + \pi)_2 B_{3u}(sp^3_{As}) \rightarrow \sigma_4^* A_g(4d_{x^2-y^2})$$

where ν_2, ν_3 are quasi-degenerate. Since the electric dipole projections M_x, M_y, M_z belong to B_{3u}, B_{2u}, B_{1u} symmetry classes of the group D_{2h}, it is not difficult to see that ν_3 and ν_4 are *x* — ν_2 "z" — and ν_1 "y" —

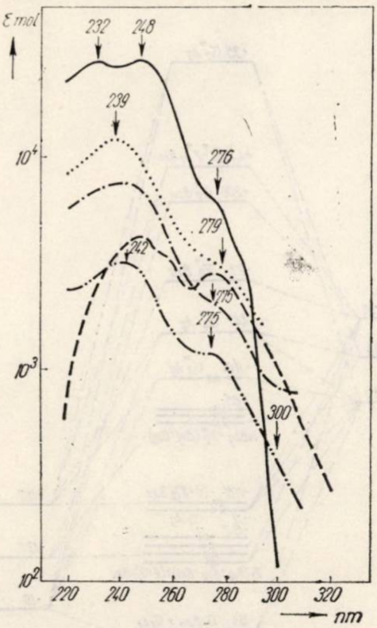

Fig. 2. — The electronic spectra of [M(II) Ars_2X_2] in UV range :
Arsine —— ;
[Pd (II) Ars_2Cl_2] —·—·— ;
[Pd(II) Ars_2Br_2] ······· ;
[Pd (II) Ars_2I_2] — — — ;
[Pt(II)Ars_2Br_2] —··—··— ;

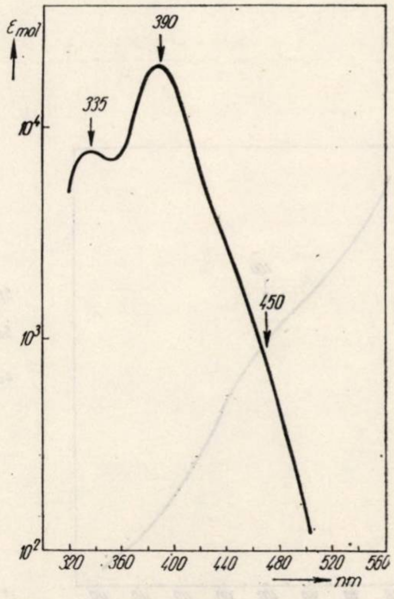

Fig. 3. — The electronic spectrum of [Pd(II)Ars_2Cl_2] in visible range.

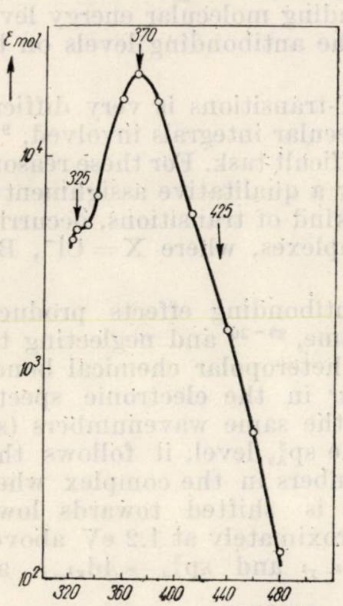

Fig. 4. — The electronic spectrum of [Pd(II)Ars_2Br_2] in visible range.

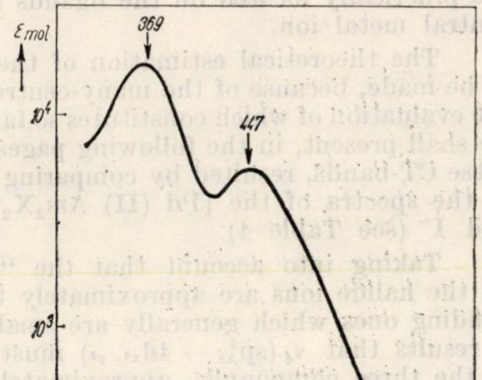

Fig. 5. — The electronic spectrum of [Pd(II) Ars_2I_2] in visible range.

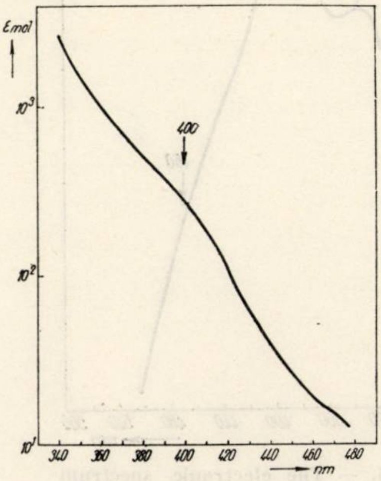

Fig. 6. — The electronic spectrum of $[Pt(II)Ars_2Br_2]$ in visible range.

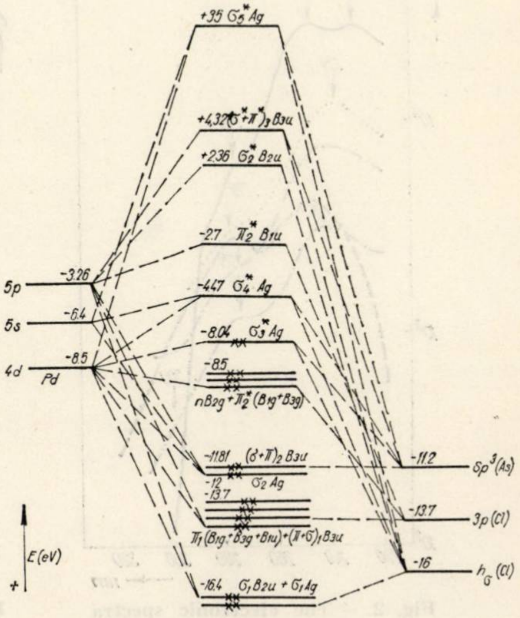

Fig. 7. — The MO energy diagram for trans-$[Pd(II)Ars_2Br_2]$.

allowed transitions. These transitions might occur in the electronic spectrum as very intense absorption maxima ; they may be regarded as charge-transfer ligand → metal bands, since the bonding molecular energy levels are practically located on the ligands and the antibonding levels on the central metal ion.

The theoretical estimation of these CT-transitions is very difficult to be made, because of the many-centre molecular integrals involved, [9–10] the evaluation of which constitutes so far a difficult task. For these reasons, we shall present, in the following pages, only a qualitative assignment of these CT-bands, resulted by comparing this kind of transitions, occurring in the spectra of the $[Pd\ (II)\ Ars_2X_2]$ complexes, where $X = Cl^-$, Br^- and I^- (see Table 4).

Taking into account that the "σ" antibonding effects produced by the halide ions are approximately the same, [29–30] and neglecting the bonding ones which generally are small for heteropolar chemical bonds, it results that $\nu_4\ (sp^3_{As} \rightarrow 4d_{x^2-y^2})$ must occur in the electronic spectra of the three compounds, approximately at the same wavenumbers (see Table 4). Since $3p_{Cl}$ level is placed below the sp^3_{As} level, it follows that $3p_{Cl} \rightarrow 4d_{x^2-y^2}$ must occur at higher wavenumbers in the complex where $X = Cl^-$, but the transition $^4p_{Br} \rightarrow 4d_{x^2-y^2}$ is shifted towards lower wavenumbers, because the $4p_{Br}$ level lies approximately at 1.2 eV above[21] the $3p_{Cl}$ level. The transitions $5p_y \rightarrow 4d_{x^2-y^2}$ and $sp^3_{As} \rightarrow 4d_{x^2-y^2}$ are

---

[29] C. I. Lepădatu, *Z. Physik. Chemie (Frankfurt)*, **60**, 202 (1968).

[30] C. I. Lepădatu, Ph. D. Thesis, University of Bucharest, 1969.

inverted in the complex [Pd (II) Ars_2I_2], because the $5p_y$ shell has an energy of about [31] 10.5 eV and therefore placed above the sp^3_{As} level in the energy diagram, as shown in Fig. 7.

Table 4

Assignments of electronic transitions in [Pd(II) Ars_2 X_2]

X	Absorption maxima (cm^{-1}) (intensity ε_{mol})	Assignment
Cl^-	I 30,700 (4500)	$3p_{Cl} \rightarrow 4d_{x^2-y^2}$
	II 27,000 (25000)	$sp^3_{As} \rightarrow 4d_{x^2-y^2}$
	III 23,530 (~2000)	d–d
Br^-	I 29,850 (7800)	$4p_{Br} \rightarrow 4d_{x^2-y^2}$
	II 25,650 (19500)	$sp^3_{As} \rightarrow 4d_{x^2-y^2}$
	III 22,220 (1400)	d–d
I^-	I 27,100 (17100)	$sp^3_{As} \rightarrow 4d_{x^2-y^2}$
	II 22,370 (15500)	$5p_I \rightarrow 4d_{x^2-y^2}$
	III 17,540 (~200)	d–d

Besides the electric dipole allowed CT-transitions, in the electronic spectra of the palladium (II) complexes a further absorption band of lower intensity ($\varepsilon_{mol} \approx 200-2000$) is observed at higher wavelengths (Table 4). This absorption band could be assigned to an electron transition between the antibonding molecular levels $\sigma_3^*A_g(4d_{z^2}) \rightarrow \sigma_4^*A_g(4d_{x^2-y^2})$. Since these molecular states belong to a total symmetric class A_g, and the projections of the electric dipole belong to *"u"* (ungerade) classes of the D_{2h} point group, this transition must take place only through a vibronic coupling. This kind of transition may be considered as being of d–d type, the antibonding molecular levels $\sigma_3^*A_g$ and $\sigma_4^*A_g$ being practically localized on the central metal ion.

To facilitate the discussion, we adopt the following notations for the metal orbitals, familiar in the ligand field theory [32]

$$\psi\,(nB_{2g}\,;\,d_{xz}) = \eta$$

$$\psi\,(\pi_2^*B_{3g}\,;\,d_{yz}) = \xi$$

$$\psi\,(\pi_2^*B_{1g}\,;\,d_{xy}) = \varphi$$

$$\psi\,(\sigma_3^*A_g\,;\,d_{z^2}) = u$$

$$\psi\,(\sigma_4^*A_g\,;\,d_{x^2-y^2}) = v$$

---

[31] * * * "Energhii razryva khimiheskikh sviazei", Izd. Akad. Nauk SSSR, M oskva 1962.

[32] N. WATANABE, "Operator Methods in Ligand Field Theory", Prentice Hall, Inc., Englewood Cliffs, New Jersey, 1966.

Considering all the bonding levels as being included in the molecular core, the eigenfunctions of the spectral terms between which the u → v transition can take place, are

Singlet states

$$ {}^1A_g(I) \qquad \eta^2\ \xi^2\ \varphi^2\ u^2 $$

$$ {}^1A_g(II) \qquad \frac{1}{\sqrt{2}}(\eta^2\ \xi^2\ \varphi^2\ u^+\ v^- - \eta^2 \xi^2\ \varphi^2\ u^- v^+) $$

$$ {}^1A_g\ (III) \qquad \eta^2\ \xi^2\ \varphi^2\ v^2 $$

Triplet state

$$ {}^3A_g : \eta^2\ \xi^2\ \varphi^2\ u^+ v^+\ (\text{or}\ \eta^2\ \xi^2\ \varphi^2\ u^- v^-) $$

If the relativistic effects (spin-orbit coupling) were neglected, using MO's truncated to orbitals having the highest mixing coefficients, the spectral term energies are

$$ \begin{array}{c|c|c|c|} & {}^1A_g(I) & {}^1A_g(II) & {}^1A_g(III) \\ {}^1A_g(I) & W + 2\varepsilon(u) - E & 0 & 4B + C \\ {}^1A_g(II) & 0 & W + \varepsilon(u) + \varepsilon(v) - 4B - C - E & 0 \\ {}^1A_g(III) & 4B + C & 0 & W + 2\varepsilon(v) - E \end{array} = 0 $$

$$ E\ ({}^3A_g) = W + \varepsilon(u) + \varepsilon(v) + 12B + 3C $$

where

$$ W = E^{core} + 2\ \varepsilon(\eta) + 2\varepsilon(\xi) + 2\varepsilon(\varphi) + 28A - 22B + 24C $$

E^{core} being the core energy, ε-one-electron energies (levels in figure 7), A, B, and C – The Racah parameters for the interelectronic repulsion energies.

From these equations, one obtains

$$ E\ [{}^1A_g\ (I)] = W + \varepsilon(u) + \varepsilon(v) - \sqrt{[\varepsilon(u) - \varepsilon(v)]^2 + (4B+C)^2} $$

$$ E\ [{}^3A_g] = W + \varepsilon(u) + \varepsilon(v) + 12B + 3C $$

$$ E\ ({}^1A_g(II)] = W + \varepsilon(u) + \varepsilon(v) - 4B - C $$

$$ E\ ({}^1A_g(III)] = W + \varepsilon(u) + \varepsilon(v) + \sqrt{[\varepsilon(u) - \varepsilon(v)]^2 + (4B+C)^2} $$

where the singlet $^1A_g(I)$ corresponds to the low spin electron distribution and the triplet ^3A_g to the high spin one, the other spectral terms corresponding to a single electron jump $u \rightarrow v(^1A_g(II))$ or to a double electron jump $u^2 \rightarrow v^2\ (^1A_g(III))$. In order to establish which of the electronic configurations becomes ground state in our complexes, we must compare the energy expressions of the $^1A_g(I)$ and ^3A_g terms. Assuming that the low spin state is fundamental, and neglecting the configuration interaction one obtains

$$E[^1A_g(I)] < E\,(^3A_g), \text{ or}$$

$$\varepsilon\,(u) - \varepsilon\,(v) < 12B + 3C$$

where the left-hand of the inequality represents the difference between orbital energies, i.e. $\varepsilon\,(\sigma_4^* A_g) - \varepsilon\,(\sigma_3^* A_g)$ in Fig. 7, and the right-hand the spin-pairing energy.[33] With $B = 826\ cm^{-1}$ and $C = 2620\ cm^{-1}$ for the palladium ion,[34] the condition is fulfilled, the complex *trans*- [Pd(II) Ars_2Cl_2] being therefore in the low spin state, as has been earlier assumed in the electron population analysis.

The spin-allowed d-d transitions between singlet terms, will be

$$\nu_1\,[^1A_g(I) \rightarrow {}^1A_g(II)] = \sqrt{[\varepsilon\,(u) - \varepsilon(v)]^2 + [4B + C]^2} - 4B - C$$

$$\nu_2\,[^1A_g(I) \rightarrow {}^1A_g\,(II)] = 2\sqrt{[\varepsilon(u) - \varepsilon(v)]^2 + (4B + C)^2}$$

or numerically

$$\nu_1 = 23{,}474\ cm^{-1}\ (\text{exp. } 23530\ cm^{-1})$$

$$\nu_2 = 58{,}796\ cm^{-1}\ (\text{out of measurement})$$

As may be seen from Table 4, the *d—d* transition is shifed towards smaller wavenumbers going from Cl^- to Br^- and I^-, the "σ" antibonding effects of the halide ions being progressively diminished [29-30] in the series Cl^-, Br^-, I^-.

In the electronic spectrum of the complex [Pt (II) $Ars_2\,Br_2$] (see experimental) besides the absorption bands due to the $\pi - \pi^*$ transitions of the arsine phenyls, two absorption bands occur at 3000 Å ($33{,}300\ cm^{-1}$) and 4000 Å ($25{,}000\ cm^{-1}$). Since the ionization potential value of 5d platinum shell is approximately [31] 9 eV and therefore close to that of 4d palladium shell (8.5 eV), by analogy with the similar palladium complex, these last bands can be described as being due to CT-transitions, $4p_{Br} \rightarrow 5d_{x^2-y^2}$ and $sp^3_{As} \rightarrow 5d_{x^2-y^2}$, respectively.

---

[33]. C. J. Ballhausen and A. D. Liehr, *J. Amer. Chem. Soc.*, **81**, 538 (1959).

[34]. J. S. Griffith, "The Theory of Transition-Metal Ions", Univ. Press, Cambridge, 1964.

APPENDIX

The participation of 3s chlorine orbital to "σ" bonding has been estimated from the minimization condition [35]

$$\theta = \frac{\lambda^2 E(3p) + (1-\lambda^2)E(3s)}{\lambda S_\sigma(3p_{Cl}, \varphi_{Pd}) + \sqrt{1-\lambda^2}\, S_\sigma(3s_{Cl}, \varphi_{Pd})}$$

where φ_{Pd} represents the metal orbital, S_σ the diatomic overlap integral, λ — the mixing coefficient from the linear combination

$$h_{Cl} = \lambda | 3p > + \sqrt{1-\lambda^2}\, | 3s >$$

With [21] E (3p) = 13.7 eV and E (3s) = 25.3 eV, for the 4d, 5s and 5p Palladium orbitals, one finds $\lambda \simeq 0.9$.

---

[35]. C. J. Ballhausen and H. B. Gray, *Inorg. Chem.*, **1**, 111 (1962).

Revue Roumaine de Chimie, **19**, *12*, 1877–1881 (1974)

Hommage à
Raluca Ripan
pour son 80e anniversaire

MÉCANISME DE L'ACTIVITÉ CATALYTIQUE DES MÉTAUX DE TRANSITION DÉPOSÉS SUR UN SUPPORT ACTIF

ANTONI SWINARSKI et ANNA ZYTKOWICZ
Institut de Chimie de l'Université Nicolas Copernic
Toruń, Pologne

Reçu le 28 octobre 1974

On a déposé d'une solution diluée de nitrates les cations des métaux de structure d^3 à d^{10} sur du charbon activé. Sur la surface du charbon on a formé préalablement une concentration élevée d'oxydes superficiels de caractère acide. Les cations des métaux de transition ont été fixés sur la surface du charbon par chémosorption sous forme d'aquo-complexes. On a appliqué trois températures différentes de séchage des échantillons du charbon ainsi dopé. La température de 60° n'a pas détruit l'aquo-complexe déposé. La température de 100° a partiellement changée l'aquo-complexe en oxyde, cette opération étant nettement plus avancée à 150°. Par la réaction d'oxydation de l'hydrogène sulfuré on a pu constater une différence très nette entre l'activité catalytique des échantillons dopés séchés aux températures de 60°—100°—150°. On a pu observer que l'activité catalytique du cation déposé dépendait directement de l'énergie d'activation dans la réaction S_N2 de l'aquo-complexe formé dans le cas du séchage à 60°. Cette activité catalytique change nettement avec la destruction thermique de l'aquo-complexe formé. Plus la température de séchage est haute, plus l'activité catalytique de l'échantillon tend à devenir proportionnelle au pouvoir oxydant de l'oxyde formé sur la surface du charbon.

Sur la surface du charbon activé on peut faire développer une concentration élevée des oxydes superficiels de caractère acide par une activation appropriée[1]. On a préparé plusieurs échantillons de ce charbon qui ont eu la même surface spécifique et la même répartition des pores. Par l'immersion prolongée du charbon dans des solutions diluées de nitrates de Cr^{3+}, Mn^{2+}, Fe^{3+}, Co^{2+}, Ni^{2+}, Zn^{2+}, Hg^{2+}, Ag^{+}, on arrive à déposer sur la surface du charbon par chémosorption des quantités définies de cations. Le cation étant lié à la surface du carbon, l'anion qui l'accompagne —le nitrate — se laisse facilement éliminer par simple lavage avec de l'eau distillée.

Les échantillons ont été séchés à 60° pendant 84 heures. En mesurant l'acidité initiale du charbon et celle qui a subsistée après l'adsorption du cation déposé on a pu évaluer le nombre des protons qui ont été remplacés par le cation appliqué. Les résultats sont présentés sur le tableau 1.

Les cations liés à la surface du charbon par chémosorption y remplacent le nombre de protons équivalents à la valence du cation. Ce n'est

---

[1] A. Swinarski et J. Siedlewski, *Roczniki. Chem.*, **35**, 999 (1961).

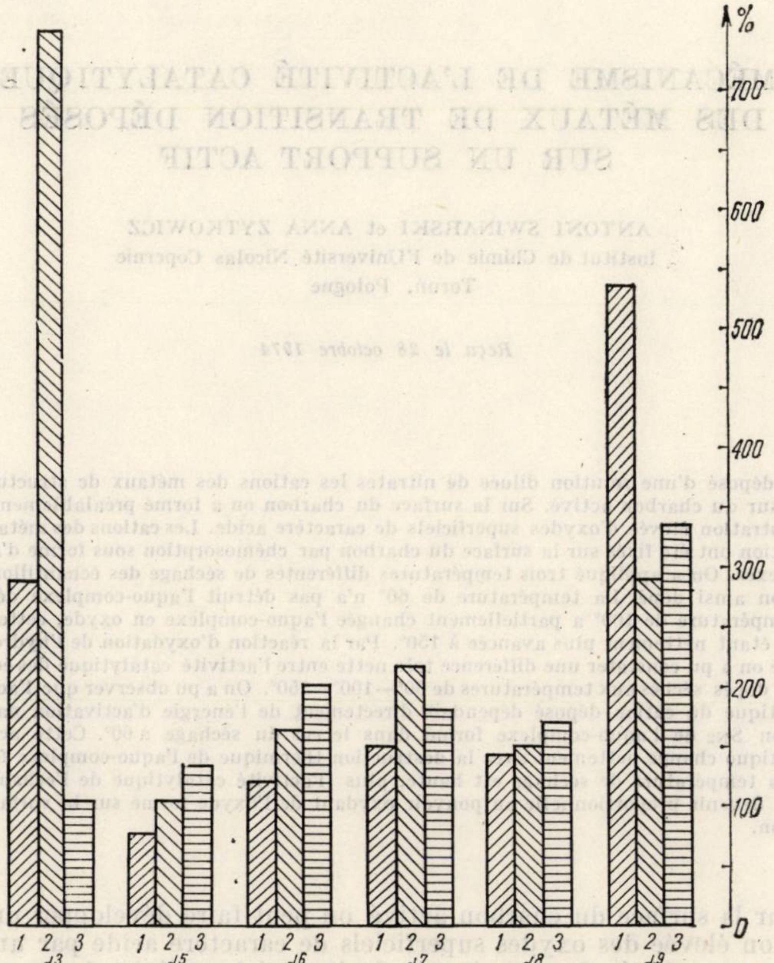

Fig. 1. — L'activité catalytique des échantillons de charbon dopé par les cations de métaux de transition.

1, température de séchage 60° ; *2*, température de séchage 100° ; *3*, température de séchage 150°.

que l'ion Fe^{3+}, et l'ion Hg^{2+} qui au cours de l'adsorption sont réduits à l'état de Fe^{2+} et Hg_2^{2+}.

L'activité catalytique des échantillons dopés et séchés à la température de $60^{\circ 1}$, de $100^{\circ 2}$ et $150^{\circ}C^{3}$ est présentée par rapport à l'activité de l'échantillon non dopé mis comme 100% sur la figure 1.

Les résultats laissent voir un changement considérable de l'activité catalytique suivant la température de séchage appliquée à l'échantillon.

En comparant l'activité catalytique des échantillons dopés par différents métaux et séchés à la même température de 100 et 150° on trouve une dépendance régulière entre l'activité catalytique et la chaleur de formation des oxydes correspondants.

Tableau 1

L'échange des ions sur la surface du charbon activé sous l'influence des cations de métaux de transition

Cation déposé	Nombre de protons sur un m^2 de la surface du charbon	Nombre de cations sur un m^2 de la surface du charbon	Nombre de protons remplacés par un cation
Cr^{3+}	$4{,}99.10^{17}$	$0{,}97.10^{17}$	3
Mn^{2+}	5,72	1,17	2
Fe^{3+}	6,10	0,85	2
Co^{2+}	5,44	1,05	2
Ni^{2+}	5,79	0,51	3
Cu^{2+}	5,99	0,86	2
Zn^{2+}	6,55	0,63	2
Hg^{2+}	6,23	1,61	1
charbon non dopé	7,70		

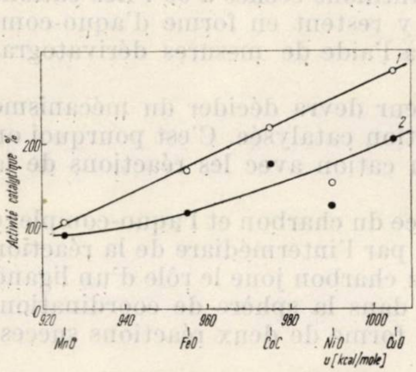

Fig. 2. — L'activité catalytique des échantillons de charbon dopé par les cations de métaux de transition en fonction de la chaleur de formation de leurs oxydes correspondants.

1, température de séchage 100° ; *2*, température de séchage 150°.

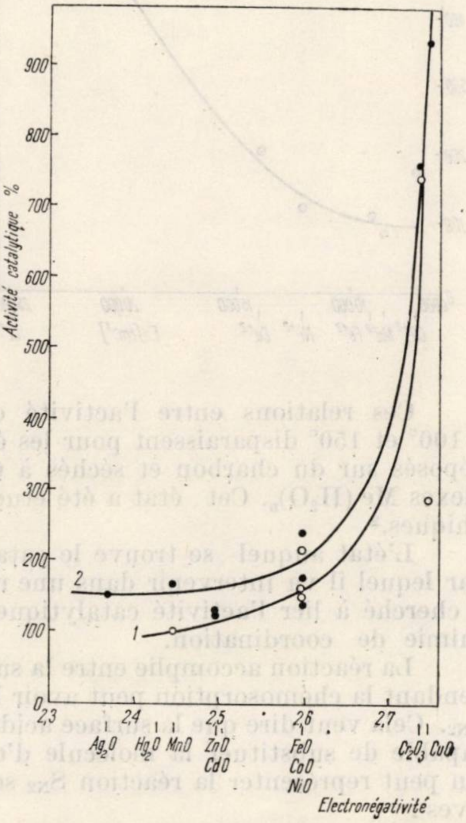

Fig. 3. — L'activité catalytique des échantillons de charbon dopé par les cations de métaux de transition en fonction de l'électronégativité moyenne de leurs oxydes correspondants.

1, température de séchage 150° ; *2*, température de séchage 100°.

Une autre dépendance régulière est à signaler entre l'activité catalytique des échantillons séchés à 100 et 150° et l'électronégativité moyenne des oxydes correspondants. L'électronégativité moyenne d'après Pauling peut être considérée comme une valeur représentative de la capacité du cation considéré à lier l'oxygène. Cette dépendance est présentée sur la figure 3.

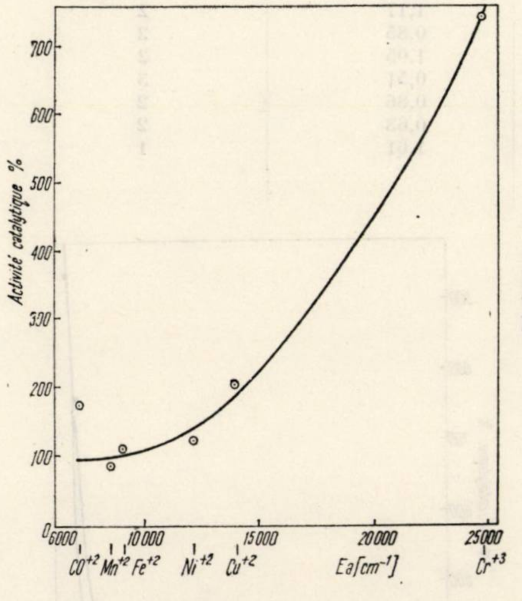

Fig. 4.—L'activité catalytique des échantillons de charbon dopé par les cations de métaux de transition d^3-d^9 en fonction de l'énergie d'activation de la réaction S_{N2}. Température de séchage 60°.

Ces relations entre l'activité catalytique des échantillons séchés à 100° et 150° disparaissent pour les échantillons séchés à 60°. Les cations déposés sur du charbon et séchés à 60° y restent en forme d'aquo-complexes $Me(H_2O)_n$. Cet état a été étudié à l'aide de mesures dérivatographiques.[2]

L'état auquel se trouve le catalyseur devra décider du mécanisme par lequel il va intervenir dans une réaction catalysée. C'est pourquoi on a cherché à lier l'activité catalytique du cation avec les réactions de la chimie de coordination.

La réaction accomplie entre la surface du charbon et l'aquo-complexe pendant la chémosorption peut avoir lieu par l'intermédiare de la réaction S_{N2}. Cela veut dire que la surface acide du charbon joue le rôle d'un ligand capable de substituer la molécule d'eau dans la sphère de coordination. On peut représenter la réaction S_{N2} sous forme de deux réactions successives :

$$Me(H_2O)_6 + C_xO_y = Me(H_2O)_6 \cdot C_xO_y$$

$$Me(H_2O)_6 \cdot C_xO_y = Me(H_2O)_5 \cdot C_xO_y + H_2O$$

[2] A. Swinarski et A. Zytkowicz, *Chemia Stosow.*, sous presse 1974.

La première réaction fait apparaître un complexe à sept ligands. Ce complexe étant instable se décompose en libérant l'eau.

A l'aide des valeurs de l'énergie d'activation, nécessaire pour accomplir le passage indiqué par la réaction S_{N2} [3], on trouve que l'activité catalytique reste en dépendance régulière de cette énergie pour chacun des cations mis en jeu (fig. 4).

Les résultats obtenus nous permettent de tirer quelques conclusions générales :

1. Le charbon activé se comporte comme un support actif pour les cations des métaux de transition utilisés comme catalyseurs d'oxydation.
2. La chémosorption sur la surface du charbon augmente sensiblement l'activité catalytique du cation déposé.
3. La température de séchage de l'échantillon dopé par les métaux permet d'obtenir le cation déposé soit sous forme d'aquo-complexe (temp. 60°), soit sous forme d'oxyde, au moins partiellement (100 et 150°).
4. L'activité catalytique du cation sous forme d'aquo-complexe est définie par la valeur de l'énergie de stabilisation.
5. Cette activité dans le cas des oxydes est proportionnelle à la facilité de l'oxyde à libérer l'oxygène. Cette faculté peut être quantitativement mise en évidence en présentant l'activité catalytique en fonction de la chaleur de formation des oxydes correspondants soit en fonction de l'électronégativité moyenne de l'oxyde.

---

[3] F. Basolo, « Chemia Koordynacyjna », PWN, Warszawa, 1968; A. D. Dowden et D. Wells, « Actes du 2me Congrès International sur la Catalyse », Paris, 1961, p. 1499.

Revue Roumaine de Chimie, **19**, *12*, 1883–1888 (1974)

Dedicated to
Raluca Ripan
on the occasion of her 80th anniversary

COORDINATION COMPOUNDS WITH CHOLINE PERCHLORATE

MARIA BREZEANU and IOANA JITARU

University of Bucharest, Inorganic Chemistry Laboratory, Splaiul Independenţei, 87,
Bucharest, Romania

Received April 29, 1974

This paper reports the preparation of a series of perchlorate complexes of some 3d metals with choline perchlorate, which belong to two general types: $[ML_4^+(ClO_4)_2](ClO_4)_4$ (M^{II}=Ni, Co) and $[ML_4^+](ClO_4)_6$ (M^{II} = Mn, Cu, Zn), in which $L^+ = (CH_3)_3^+N-C_2H_4-OH$, behaves as a cationic ligand. The compounds obtained were characterized by elemental chemical analysis, molecular weight determinations, molecular electrical conductivity, electronic and vibrational spectra. The data obtained were used in establishing the probable structure of these compounds and also the coordination of choline and of perchlorate anion.

The literature has recently reported several papers concerned with the synthesis and characterization of some complex compounds with cationic ligands. The largest number of papers in this field report the coordination capacity of cationic ligands derived from diamines (primary, secondary or tertiary), tertiary diphosphines, aminophosphines and tertiary diarsines.[1–14]

---

[1] J. V. Quagliano, J. T. Summers, S. Kida and L. M. Vallarino, *Inorg. Chem.*, **3**, 1557 (1964).

[2] V. L. Goedken, L. M. Vallarino and J. V. Quagliano, *Inorg. Chem.*, **10**, 2682 (1971).

[3] A. S. Murthy, J. V. Quagliano and L. M. Vallarino, *Inorg. Chim. Acta*, **6**, 49 (1972).

[4] A. K. Banerjee, L. M. Vallarino and J. V. Quagliano, *Coord. Chem. Reviews*, **1**, 239 (1966).

[5] D. J. Bryson and R. H. Nuttall, *Inorg. Nuclear Chem.*, **32**, 2569 (1970).

[6] V. L. Goedken, J. V. Quagliano and L. M. Vallarino, *Inorg. Chem.*, **8**, 2331 (1969).

[7] L. M. Vallarino, V. L. Goedken and J. V. Quagliano, *Inorg. Chem.*, **12**, 102 (1973).

[8] J. V. Quagliano, A. K. Banerjee, V. L. Goedken and L. M. Vallarino, *J. Amer. Chem Soc.*, **92**, 482 (1970).

[9] L. M. Vallarino, V. L. Goedken and J. V. Quagliano, *Inorg. Chem.*, **11**, 1466 (1972).

[10] C. Ercolani and J. V. Quagliano, *Inorg. Chim. Acta*, **3**, 421 (1969).

[11] D. Berglund and D. W. Meek, *J. Amer. Chem. Soc.*, **92**, 518 (1968).

[12] D. Berglund and D. W. Meek, *Inorg. Chem.*, **8**, 2602 (1969).

[13] C. R. Taylor, *J. Chem. Soc. (D).*, **1970**, 813.

[14] C. Ercolani and J. V. Quagliano, *J. Chem. Soc.(D).*, **1969**, 1094.

The study of the coordination capacity of cationic ligands is of particular interest for several reasons. In the first place, new aspects may be revealed in such systems with regard to electronic interaction in the coordination sphere of a complex compound, which may affect the stoichiometry and the stereochemistry of the respective compound. On the other hand, compounds containing cationic ligands whose complex ion is characterized by a high positive charge, i.e. water-soluble compounds, play an important role in biochemical reactions.

In the frame of a more general research concerning the coordination capacity of aminoalcohols, we have considered of interest to study the donor properties of some quaternary ammonia ions of aminoalcohols, for which the donor atom is the oxygen of the hydroxyl group. Consequently, we undertook a study on the coordination ability of choline, the quaternary ammonium ion derived from monoethanolamine.

Depending on the nature of the anion, a different behaviour of choline is expected, i.e. as a cationic ligand or as an uncoordinated ion, stabilizing a series of complex anions.

In the presence of anions with a relatively high coordination capability (halogens, pseudohalogens, etc.), choline behaves as a free uncoordinated ion, in the ionization sphere of some complex compounds of the $L_2^+[MX_4]$ type.

In the presence of anions with a reduced coordination ability (acetate, perchlorate, etc.) complex compounds in which choline behaves as a cationic ligand could be obtained.

Owing to this fact, we first used choline perchlorate and acetate in our study.

The present paper reports the results obtained in the synthesis and characterization of complex compounds of some 3d metal perchlorates with choline perchlorate. These compounds belong to the following general types: $[ML_4^+(ClO_4)_2](ClO_4)_4$ ($M^{II} = Ni$, Co; $L^+ = (CH_3)_3^+N-C_2H_4-OH$) and $[ML_4^+](ClO_4)_6$ ($M^{II} = Mn$, Cu, Zn).

Attempts to obtain complex compounds of other 3d elements (Cr^{III}, Fe^{III}) with choline perchlorate under similar experimental conditions failed.

RESULTS AND DISCUSSION

Mn(II), Co(II), Ni(II), Cu(II) and Zn(II) perchlorates react in alcoholic solution (see the Experimental section) with choline perchlorate, leading to complex compounds of the $ML_4^+(ClO_4)_6$ type.

Molecular weight determinations have established the monomer nature of the latter.

Based on electronic and vibrational spectra, it could be established that these compounds, with the same empirical formula, belong to two structurally different types, i.e. octahedral $[ML_4^+(ClO_4)_2](ClO_4)_4$ ($M^{II} = Co$, Ni) and tetrahedral $[ML_4^+](ClO_4)_6$ ($M^{II} = Mn$, Cu, Zn).

As it can be seen, in the case of compounds of the first type, hexacoordination is achieved by the coordination of two perchlorate ions.

These compounds are air-stable, practically insoluble in most organic solvents (ethyl alcohol, methyl alcohol, isopropyl alcohol, ethyl ether, petroleum ether, acetone, carbon tetrachloride, chloroform); they decompose in water or undergo solvation (with colour change) by dissolution in solvents with good donor properties (dimethyl formamide, dimethylsulphoxide). In acetonitrile, the obtained compounds are rather easily dissolved without colour change.

Electronic spectra. Two absorption bands of a relatively low intensity appear in the spectrum of compound $CoL_4^+(ClO_4)_6$, the first in the visible range (530 mm) assigned to $^4T_{1g}(P) \leftarrow {}^4T_{1g}$ transition, and the second in the near infrared range (1100 nm) assigned to $^4T_{2g} \leftarrow {}^4T_{1g}$ transition.

The spectrum of this compound may be thus satisfactorily interpreted in terms of an octahedral configuration, which leads to the following formulation $[CoL_4^+(ClO_4)_2](ClO_4)_4$.[15]

In the spectrum of compound $NiL_4^+(ClO_4)_6$, there appear also two absorption bands, one in the visible range (740 nm) assigned to $^3T_{1g}(F) \leftarrow {}^3A_{2g}$ transition for d^8 ion in octahedral symmetry field, the second in the near infrared range (1240 nm) assigned to $^3T_{2g} \leftarrow {}^3A_{2g}$ transition. The shoulder in the range of higher frequencies may be assigned to $^3T_{1g}(P) \rightarrow {}^3A_{2g}$ transition. Based on these data and on molecular electrical conductivity determinations, the compound was formulated as $[NiL_4^+(ClO_4)_2](ClO_4)_4$.[16]

An extremely broad band, of a relatively low intensity, present in the spectrum of compound $CuL_4^+(ClO_4)_6$ indicates a tetrahedral configuration, compatible with formulation $[CuL_4^+](ClO_4)_6$ (fig. 1).[17]

Vibrational spectra. In order to establish the function of the perchlorate anion (ionic, mono, or bidentate ligand) and also of choline, vibrational spectra of compounds obtained within the 400–3600 cm^{-1} range were obtained.

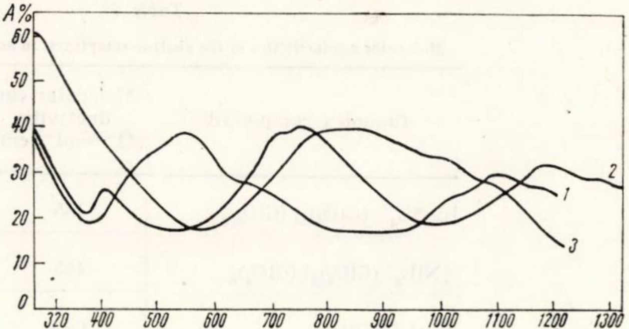

Fig. 1. — Electronic spectra of compounds: *1.* $[CoL_4^+(ClO_4)_2](ClO_4)_4$; *2.* $[NiL_4^+(ClO_4)_2](ClO_4)_4$; *3.* $[CuL_4^+](ClO_4)_6$

Spectra of compounds $[ML_4^+](ClO_4)_6$ and $[ML_4^+(ClO_4)_2](ClO_4)_4$ reveal small differences in the domain of vibration modes of ClO_4^- ion. In this respect, mention could be made of the greater width and additional splitting of the band at 1100 $cm^{-1}(\nu_3)$ and also of intensification and band splitting at 900 $cm^{-1}(\nu_1)$ in the spectra of compounds $[ML_4^+(ClO_4)_2](ClO_4)_4$ compared to those of compounds $[ML_4^+](ClO_4)_6$.

---

[15] A. B. P. Lever, *"Inorganic Electronic Spectroscopy"*, New York, 1968, p. 318.

[16] A. B. P. Lever, *"Inorganic Electronic Spectroscopy"*, New York, 1968, p. 333.

[17] L. Sacconi and M. Ciampolini, *J. Chem. Soc.*, **1964**, 276.

These results suggest that in the first type of compounds, at least part of perchlorate ions is coordinated.

It is difficult to make a definite assignment of the absorption bands of the perchlorate ion, since some bands characteristic of choline itself, also appear in this region.[18]

Choline coordination as a positive ligand does not induce basic changes in its vibration spectrum (the symmetry of cation $(CH_3)_3^+N-$$-C_2H_4-OH$ does not seem to be significantly affected by the formation of the M$-$O bond) except for the OH stretching vibration frequency (ν_{OH}), which shifts towards smaller values.[19,20]

In free choline, the ν_{OH} frequency appears at $\sim$3450 cm^{-1} as a result of some inter—or intramolecular hydrogen bonds. In the spectra of compounds $ML_4^+(ClO_4)_6$ this frequency appears at lower values (3300 cm^{-1} or 3265 cm^{-1}), this shift indicating choline coordination by oxygen.

Molecular conductivity determinations. The formulation suggested for the studied compounds was confirmed by molecular electrical conductivity determinations performed in acetonitrile solution.

Data referring to the conductivity of acetonitrile solutions are unfortunately extremely scarce in the literature.

Assignments made according to the existing data, lead, however, to the conclusion that while Ni(II) and Co (II) complex perchlorates are 1 : 4 electrolytes, the complex perchlorates of the other metals (Mn(II), Cu(II), Zn(II)) are 1 : 6 electrolytes (see table 1).

Table 1

Molecular conductivities of the choline complexes, in acetonitrile solution

Complex compound	Molecular conductivity ($\Omega^{-1}mol^{-1}cm^2$)	Type of electrolyte
$[Co^*L_4^+ (ClO_4)_2](ClO_4)_4$	485	1 : 4
$[NiL_4^+ (ClO_4)_2](ClO_4)_6$	465	1 : 4
$[CuL_4^+[(ClO_4)_6$	690	1 : 6
$[ZnL_4^+](ClO_4)_6$	710	1 : 6
$[MnL_4^+][(ClO_4)_6$	690	1 : 6

* $L+ = (CH_3)_3+N-C_2H_4-OH$ solution 10^{-3} M, t = 25°, solvent-acetonitrile.

---

[18] B. J. Hathaway and A. E. Underhilll, *J. Chem. Soc.*, **1961**, 3091.

[19] L. J. Bellamy, *"The Infrared Spectra of Complex Molecules"*, London, 1958, p. 108.

[20] K. Nakamoto *"Infrared Spectra of Inorganic Coordination Compounds"*, London, 1963, p. 159.

Molecular weight determinations. Molecular weight determinations performed for compounds of $ML_4^+(ClO_4)_6$ type have established their monomeric nature (see table 2).

Table 2

Mocular weights of choline complexes

Complex compound	Melting point	Molecular weight	
		calcd.	found
$[CoL_4^+ (ClO_4)_2] (ClO_4)_4$	210 (d)	1072.32	1085.10
$[NiL_4^+ (ClO_4)_2] (ClO_4)_4$	230 (d)	1072.08	1090.20
$[CuL_4^+] (ClO_4)_6$	205	1076.92	1092.00
$[MnL_4^+] (ClO_4)_6$	245	1068.32	1080.15
$[ZnL_4^+)] (ClO_4)_6$	240	1078.76	1095.00

EXPERIMENTAL

I. *Synthesis of complexes.* Mn(II), Co(II), Ni(II), Cu (II) and Zn(II) complex choline perchlorates were obtained by mixing hot ethanol solutions of metal perchlorates with a hot ethanol solution of choline perchlorate, in a M(II) : choline = 1 : 5 molar ratio.

Crystalline compounds are separated from ethanol solutions by concentration on a water bath at 70–80° ; their colour is light-pink for Mn(II), violet-pink for Co(II), light-blue for Ni(II), blue-green for Cu (II), and white for Zn(II).

Compounds are filtered, washed with hot ethyl alcohol and then with cold ethyl alcohol.

A similar type of compounds is also obtained at higher values of the M(II) : choline ratio (example 1 : 7).

Elemental analysis data are listed in table 3.

II. Molecular Conductivities. Molecular conductivity measurements were made at 25° on freshly prepared acetonitrile solutions with a Conductometer II (Czechoslovakia) with a unit cell $K = 0.52$.

III. Molecular Weights. Molecular weights of the compounds studied were determined by means of the Rast micromethod, using camphor as solvent.

IV. Electronic Spectra. The electronic spectra in the range 320–1300 nm were recorded at room temperature, on a VSU_1 spectrophotometer, C. Zeiss, Jena using magnesium oxide as reference.

V. *Vibrational Spectra.* The IR spectra in the range 400–3600 cm^{-1} were measured on a UR-20 spectrophotometer C. Zeiss, Jena using the KBr disks technique.

Table 3

Analytical data

Complex compound	M %		ClO_4 %		N %		C %	
	calcd.	found	calcd.	found	calcd.	found.	calcd.	found
$[CoL_4^+ (ClO_4)_2] (ClO_4)_4$	5.49	5.56	55.65	55.90	5.22	5.40	22.40	22.80
$[NiL_4^+ (ClO_4)_2] (ClO_4)_4$	5.47	5.50	55.66	55.93	5.22	5.47	22.40	22.60
$[CuL_4^+)] (ClO_4)_6$	5.90	6.24	55.41	55.81	5.20	5.45	22.30	22.50
$[ZnL_4^+) (ClO_4)_6$	6.05	6.25	55.31	55.75	5.19	5.50	22.26	22.70
$[MnL_4^+](ClO_4)_6$	5.14	5.30	55.85	56.00	5.25	5.55	22.48	22.70

Revue Roumaine de Chimie, 19, 12, 1889–1897 (1974)

Hommage à
RALUCA RIPAN
pour son 80e anniversaire

COMBINAISONS COMPLEXES DU Mn(III) ET DU Mn(IV).I

LE SYSTÈME Mn(III, IV)–ACIDE ANILINE-4 SULPHONIQUE

NICOLAE CALU, ADINA POPA-RANG et MARIA CALENCIUC
Faculté de Chimie, Université « Al.I. Cuza », Jassy, 11 str. 23 august

Reçu le 24 juin 1974

On a étudié par spectrophotométrie, polarographie et chromatographie sur papier les complexes formés en solution pour les rapports 1 Mn (IV) : 2 L et 1 Mn (IV) : 4 L, où L est l'acide aniline-4 sulphonique. Les complexes du Mn (IV) sont obtenus aussi par la disproportion du Mn(III) de l'ion $[Mn(H_2P_2O_7)_3]^{3-}$ en présence de l'acide aniline-4 sulphonique, d'après une réaction du premier ordre avec $k = 2,13.10^{-2}$ sec^{-1} pour 21° et $E_a = 19,84$ kcal/mole. Le spectre champ cristallin du complexe $Mn\,L_4$ du système MnO_2–L a le paramètre $D_q = 1130$ cm^{-1} et celui néphélauxétique $\beta_{35} = 0.63$.

Les sels de Mn(III) et de Mn(IV) sont caractérisés par une petite stabilité et dans des solutions aqueuses celle-ci est influencée par le p_H, la nature des anions, la présence des ligands et par d'autres facteurs.

Dans la figure 1 on voit le domaine d'existence de certains composés du manganèse dans différents états d'oxydation, en fonction du p_H. On constate que, dans un milieu acide, l'ion Mn^{3+} peut subir un processus de disproportion et d'hydrolyse, avec la formation de MnO_2 et de Mn^{2+}.

Souvent, les cations Mn(III) et Mn(IV) sont stabilisés par le processus de coordinence. On connaît, ainsi, des complexes du Mn(III) et du Mn(IV)

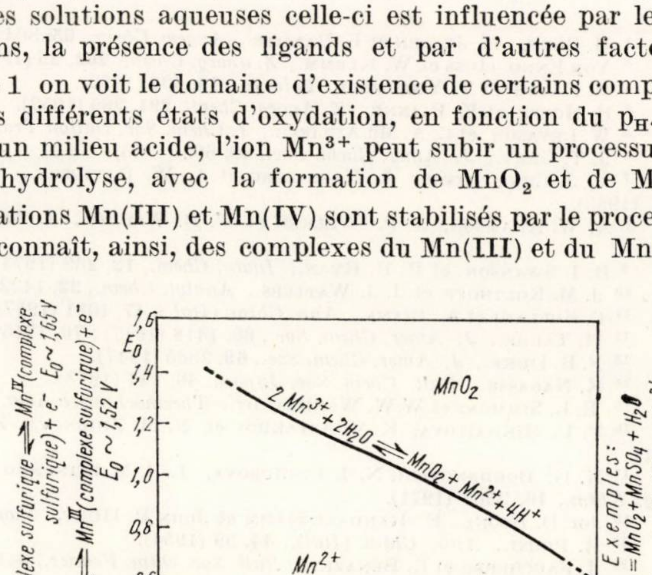

Fig. 1. — Données concernant les propriétés de certains composés du Mn(III, IV).

avec différents ligands, comme : les anions halogènes [1-6] et pseudo-halogènes, [7-9] les anions de certains acides polybasiques, [10-15] les ligands à fonctions mixtes comme des amines tertiaires avec des fonctions alcool ou acide,[16-22] l'acétylacétone,[23] les bases Schiff [24-25] et d'autres. [26,27]

Nos recherches ont comme but les combinaisons complexes du Mn(III) et du Mn(IV) avec des ligands à fonctions mixtes de la classe des acides aminosulphoniques aromatiques, etc. Ces ligands dissolvent (grâce à leur fonction SO_3H) des oxydes de manganèse, comme le MnO_2 et le Mn_2O_3, avec la formation de complexes ; ils provoquent parfois la disproportion du Mn(III) dans le Mn(IV) et le Mn(II) ou ils réduisent le Mn(IV) dans le Mn(III) et le Mn(II).

Ces recherches ont un intérêt pratique dans l'étude des minerais contenant des oxydes supérieurs de manganèse.

Dans ce travail, on présente les résultats obtenus dans l'étude du système Mn(III, IV)-acide aniline-4 sulphonique dans lequel les complexes avec Mn(IV) sont stables.

RÉSULTATS ET DISCUSSION

A) RÉACTIFS

Le Mn(III) a été utilisé sous forme de Mn_2O_3 et du complexe $[Mn^{III}(H_2P_2O_7)_3]^{3-}$ en solution aqueuse de concentration autour de 2.10^{-2} moles/l. Cet ion complexe a été obtenu en solution à partir de Mn_2O_3, $K_4P_2O_7$ et H_2SO_4 au pH$\sim$2,5. Il est suffisamment stable en solution aqueuse au pH de l'obtention.

[1] H. Bode, H. Jensen et F. Bandte., *Angew. Chem.*, **65**, 304 (1953).

[2] Von Enno Huss et W. Klemm., *Z. anorg. Chem.*, **262**, 25 (1950).

[3] M. Katoh et T. Yoshimori, *Talanta.*, **19**, 407 (1972).

[4] R. Hoppe et K. Blinne., *Z. Anorg. Chem.*, **291**, 269 (1957).

[5] W. Levason et C. A. Mc.Auliffe., *J. Chem. Soc. Dalton Trans.*, *1973*, 455.

[6] J. T. Grey., *J. Amer. Chem. Soc.*, **68**, 605 (1946).

[7] V. J. Christensen, J. Kleinberg et A. W. Davidson., *J. Amer. Chem. Soc.*, **75**, 2495 (1953).

[8] A. W. Adamson, J. P. Welker et W. B. Wright., *J. Amer. Chem. Soc.*, **73**, 4786 (1951).

[9] B. I. Swanson et R. R. Ryan., *Inorg. Chem.*, **12**, 283 (1973).

[10] J. M. Kolthoff et J. J. Watters., *Analyt. Chem.*, **22**, 1422 (1950).

[11] C. Furlani et A. Ciana., *Ann. Chim. (Ital.)*, **47**, 1081 (1957).

[12] H. Taube., *J. Amer. Chem. Soc.*, **69**, 1418 (1947) ; **70**, 1216 (1948).

[13] F. R. Duke., *J. Amer. Chem. Soc.*, **69**, 2885 (1947).

[14] K. Nagasse., *Bull. Chem. Soc. Japan.*, **46**, 144 (1973).

[15] E. L. Simmons et W.W. Wendlandt., *Thermochimica Acta.*, **2**, 217 (1971).

[16] T. U. Mikhailova, K. V. Astakhov et N. M. Zhirnova., *Zhur. fiz. Khim.*, **45**, 2345 (1971).

[17] N. G. Bogdanovich, N. I. Pechurova, L. I. Martinenko et V. V. Piunova., *Zhur. neorg. Khim.*, **16**, 2507 (1971).

[18] Joe D. Boone, E. Randall Hamm et John P. Hunt, *Inorg. Chem.*, **11**, 1060 (1972).

[19] R. Pirisi., *Ann. Chim. (Ital).*, **44**, 59 (1954).

[20] J. Faucherre et C. Benazet., *Bull. Soc. chim. France.*, 841 (1955).

[21] E. Jaffé., *Ann. Chim. (Ital)*, **41**, 397 (1951).

[22] M. Gibaud., *Compt. rend.*, **236**, 814 (1953).

[23] W. S. Fyve., *Analyt. Chem.* **23**, 174 (1951).

[24] V. V. Zentzov et I. K. Somova., *Doklady Akad. Nauk. S.S.S.R.*, **208**, 385 (1973).

[25] K. Dey et K. C. Ray., *J. Indian Chem. Soc.*, **50**, 66 (1973).

[26] G. Waterbury., *J. Amer. Chem. Soc.*, **75**, 4162 (1953).

[27] N. Goldenberg., *Trans. Faraday Soc.*, **36**, 847 (1940).

Le Mn(IV) a été employé comme le MnO_2.

Le ligand : l'acide aniline-4 sulphonique (L) a été utilisé comme des solutions aqueuses de concentration environ 2.10^{-2} moles/l.

En solution, ce ligand existe comme amphion selon l'équilibre :

$$H_2N - C_6H_4 - SO_3^{\ominus} + H^{\oplus} \rightleftharpoons H_3N^{\oplus} - C_6H_4 - SO_3^{\ominus}$$

ainsi que pour la concentration 2.10^{-2} moles/l le pH est 2,5.

B) RÉACTION ENTRE LES COMPOSÉS DU Mn(III, IV) ET L'ACIDE ANILINE-4 SULPHONIQUE

Les composés Mn_2O_3 et $[Mn(H_2P_2O_7)_3]^{3-}$ réagissent avec l'acide aniline-4 sulphonique et les équilibres sont déplacés vers les complexes du Mn(IV) et l'ion Mn^{2+}.

Le bioxyde de manganèse forme avec le ligand utilisé des complexes de Mn(IV).

Ces réactions et les produits obtenus ont été étudiés par plusieurs voies.

Par les études spectrophotométriques, on a suivi l'identification des complexes du Mn(III) et du Mn(IV) et on a déterminé la composition et la stabilité des ions complexes du Mn(IV). On a obtenu, en même temps, des épreuves sur le processus de disproportion du Mn(III) en Mn(IV) et l'ion Mn^{2+}, à l'aide de la polarographie et de la chromatographie sur papier.

C) COMPOSITION ET STABILITÉ DES IONS COMPLEXES DU SYSTÈME Mn(III, IV)—ACIDE ANILINE-4 SULPHONIQUE

1) Déterminations spectrophotométriques

Dans les figures 2 et 3, on représente les spectres d'absorption, dans le domaine visible, de quelques solutions contenant le système Mn(III, IV)$-L$.

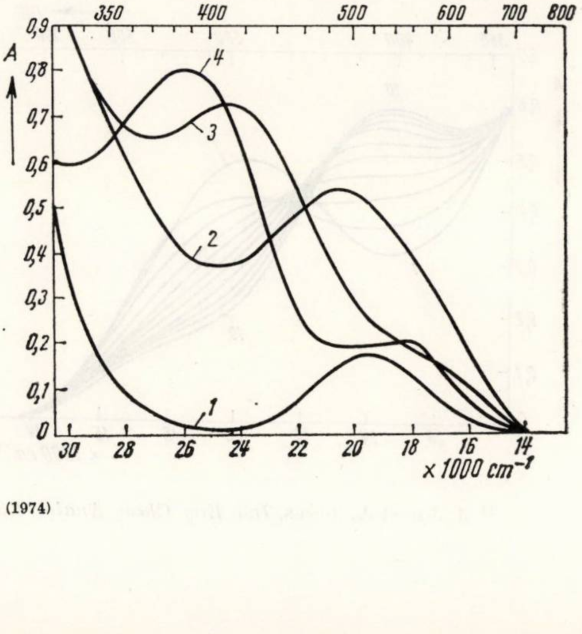

Fig. 2. — Spectres d'absorption dans le domaine visible des solutions du système Mn (III, IV) — L. *1*, Ion $[Mn(H_2P_2O_7)_3]^{3-}$; conc. 2.10^{-2} moles/l ; cuve 0.1 cm. *2*, Système $[Mn(H_2P_2O_7)_3]^{3-}-L$; $t = 0$; conc. Mn (III) ; $6,6.10^{-3}$ moles/l ; cuve 0,1 cm. *3*, Système (2) pour $t = 80'$. *4*, Système MnO_2-L ; conc. Mn(IV) :$3,3.10^{-4}$ moles/l ; cuve 1 cm. Dans les mélanges 2,3 et 4, le ligand est en excès.

L'ion $[Mn(H_2P_2O_7)_3]^{3-}$, contenant le Mn(III), un cas d^4, présente une seule bande champ cristallin (fig. 2, courbe *1*,), bande qui correspond à la transition spin permis ${}^5T_{2g} \leftarrow E_g$, dans le champ faible O_h. Cette bande est fortement affectée dans la réaction de l'ion $[Mn(H_2P_2O_7)_3]^{3-}$ avec l'acide aniline-4 sulphonique. Ainsi, au début de la réaction, la bande devient plus grande et elle est déplacée vers des longueurs d'onde plus petites (fig. 2, courbe 2). A la longue, à sa place apparaissent 3 bandes : deux en visible et une au-dessus de 800 nm (fig. 2, courbe 3), modification qui peut être due à plusieurs causes. Celle qui se vérifie cependant, expérimentalement, est la disproportion du Mn(III) et la formation du Mn(IV), auquel on peut attribuer ces bandes.

En effet, théoriquement, ces complexes du Mn(IV), un cas d^3, dans la symétrie O_h présentent 3 bandes d'absorption champ cristallin, correspondant aux transitions ${}^4T_{2g} \leftarrow {}^4A_{2g}$, ${}^4T_{1g}(F) \leftarrow {}^4A_{2g}$ et ${}^4T_{1g}(P) \leftarrow$ $\leftarrow {}^4A_{2g}$.

Le Mn_2O_3 est dissous dans la solution de l'acide aniline-4 sulphonique et présente un spectre ressemblant à celui des complexes du Mn(IV), preuve de la disproportion du Mn(III) dans ces conditions.

Le Mn O_2, dissous dans la solution de l'acide aniline-4 sulphonique, présente le spectre caractéristique des complexes du Mn(IV) — fig. 2, courbe *4* — preuve que, dans cette réaction, le manganèse ne change pas d'état d'oxydation.

Pour les spectres enregistrés, à la longue, sur une solution avec le système $[Mn(H_2O_2O_7)_3]^{3-}—L$, on observe un point isosbestique qui marque la disproportion du Mn(III) en Mn(IV) et l'ion Mn^{2+} (fig. 3).

Dans le cas d'éventuels complexes du Mn(II), dans la symétrie O_h, les transitions sont Laporte et spin interdites et, selon les tests effectués, leurs spectres ne sont pas perceptibles dans les systèmes étudiés.

La composition des complexes du Mn(IV) des systèmes Mn(III, IV)—L a été établie par spectrophotométrie et les résultats obtenus par la méthode des rapports molaires [28] sont présentés sur les figures 4 et 5.

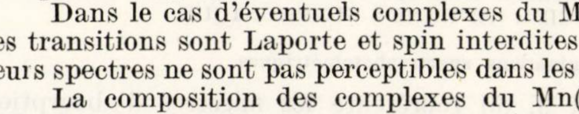

Fig. 3. — Spectres enregistrés à la longue sur le système 1 $[Mn(H_2P_2O_7)_3]^{3-}$ — 2L, conc. Mn(III) : $6{,}76.10^{-3}$ moles/l. *1*, $t = 2'$; 10 — t = 66' ; cuve 0,1 cm ; temp. = 21°.

---

[28] J. Joe et A. Jones, *Ind. Eng. Chem. Analyt. Ed.*, **16**, 11 (1944).

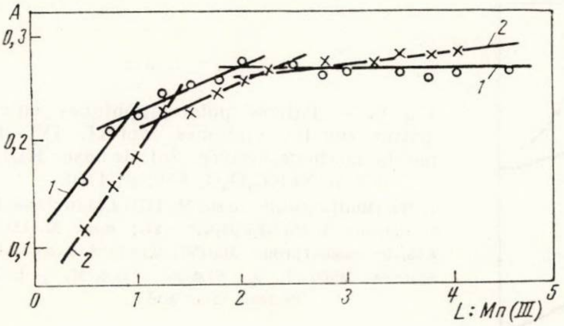

Fig. 4. — Composition des ions complexes du système $[Mn(H_2P_2O_7)_3]^{3-}$ — — L par la méthode des rapports molaires; conc. Mn(III) : 1,6.10^{-3} moles/l ; conc. Mn(IV) : 0,80.10^{-3} moles/l ; cuve 0,2 cm.
1, t = 5' ; λ = 490nm ; 2, t = 120' ; λ=411 nm.

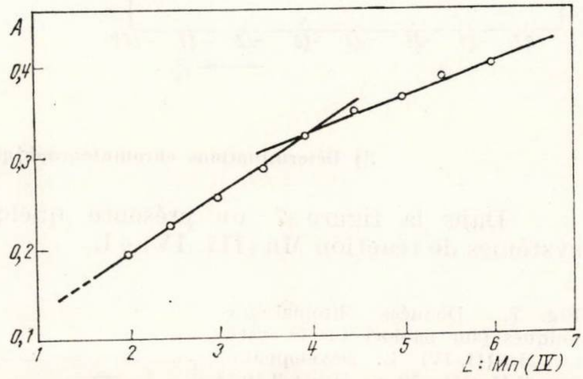

Fig. 5. — Composition de l'ion complexe du système MnO_2—L par la méthode des rapports molaires; conc. Mn (IV) : 8,33.10^{-4} moles/l ; cuve 0,5 cm ; λ=396 nm ; t=72 h.

Dans le cas des réactifs avec le Mn(III), la concentration des complexes avec le Mn(IV)- obtenus par disproportio—nest la moitié de celle totale en manganèse. On a fait abstraction de l'ion Mn^{2+}.

Ainsi, dans le premier système (fig. 4), on admet les complexes pour les rapports : 1 Mn(IV) : 2L et 1 Mn (IV) : 4L.

Dans le système avec MnO_2 comme réactif, (fig. 5), le complexe pour le rapport 1 Mn(IV) : 4L, noté MnL_4, est évident.

La stabilité de ce dernier complexe a été déterminée par la méthode Edmonds-Birnbaum [29] et on a obtenu $\beta_4 = 2{,}80.10^{16} 1/mole^{-1}$.

2) Déterminations polarographiques

Dans la figure 6, on représente quelques polarogrammes enregistrés par la méthode dérivée, sur des solutions de l'ion $[Mn(H_2P_2O_7)_3]^{3-}$, de même que sur des solutions des systèmes de réaction Mn(III, IV)—L.

On constate que, à l'addition du ligand, le palier caractéristique de l'ion $[Mn(H_2P_2O_7)_3]^{3-}$ avec $E_{1/2} = -1{,}08$ v subit des modifications. À sa place, apparaîssent 2 paliers : l'un pour —0,27 v, commun avec celui du complexe obtenu dans le système MnO_2—L et l'autre pour —1,24 v, commun avec l'ion Mn^{2+}.

Ces résultats confirment le processus de disproportion susmentionné.

---

[29] S. Edmonds et N. Birnbaum, *J. Amer. Chem. Soc.*, **63**, 1471 (1941).

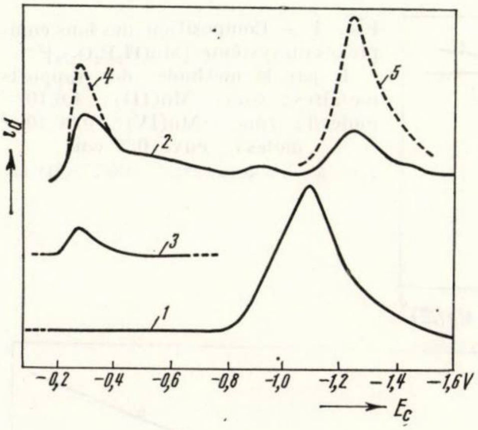

Fig. 6. — Paliers polarographiques enregistrés sur les systèmes Mn(III, IV)—*L* par la méthode dérivée. Sol. de base : KOH 6M et $NaKC_4H_4O_6$ 6M ; s : 1/10.

1, Ion $[Mn(H_2P_2O_7)_3]^{3-}$; conc. Mn(III) : $4,35.10^{-3}$ mole/l. *2*, Système 1 $[Mn(H_2P_2O_7)_3]^{3-}-2L$; conc. Mn(III) : $4,35.10^{-3}$ moles/l ; conc. Mn(IV) : $2,18.10^{-3}$ moles/l. *3*, Système MnO_2-L. *4*, Système (2) + MnO_2-L. *5* Système (2) + Mn^{2+}

3) Déterminations chromatographiques (sur papier)

Dans la figure 7 on présente quelques chromatogrammes des systèmes de réaction Mn (III, IV)—L.

Fig. 7. — Données chromatographiques (sur papier) sur le système Mn(III, IV)—L. Développant : 50p. C_2H_5OH+50 p. H_2SO_4 2.10^{-2} moles/l. Papier Whatman n° 1.

1, Mn^{2+} ; $R_F \sim 0,80$; KOH + H_2O_2 ; brun ; *2*, Mn^{2+} + $[Mn^{III}(H_2P_2O_7)_3]^{3-}$; Mn^{2+} : $R_F \sim 0,75$; KOH + H_2O_2 ; brun ; Mn(III) : $R_F \sim 0,20$ rouge ; KI (H+) et amidon : bleu. *3*, 1 $[Mn(H_2P_2O_7)_3]^{3-} -2L$ (2h) ; Mn^{2+} = R_F 0,83 ; KOH + H_2O_2 : brun ; Mn(IV) : $R_F \sim 0,90$ rouge. *4*, $1MnO_2-4L$; Mn^{2+} ; $R_F \sim 0,85$; KOH + H_2O_2 : brun (traces) ; Mn (IV) : $R_F \sim 0,90$; rouge-orange.

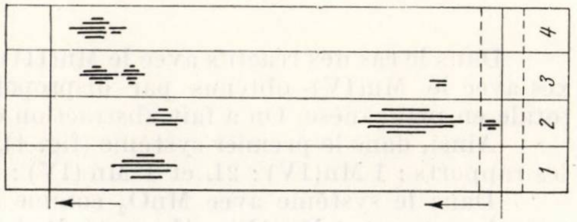

On constate que le spot caractéristique de l'ion $[Mn(H_2P_2O_7)_3]^{3-}$ avec $R_F \sim 0,20$ est presque effacé dans le système de réaction $[Mn(H_2P_2O_7)_3]^{3-}$ — L. À sa place apparaissent deux spots : l'un avec $R_F \sim 0,90$, commun avec celui du complexe obtenu dans le système MnO_2—L et l'autre avec $R_F \sim 0,83$, commun avec l'ion Mn^{2+}.

Les spots sont en grande mesure superposables, mais différenciés à l'aide d'une réaction de couleur. Les identifications des composés du Mn(IV) et du Mn(II) constituent, de même, des arguments en faveur du processus de disproportion.

D) LA CINÉTIQUE DU PROCESSUS DE DISPROPORTION DU Mn(III)

Dans le tableau 1 on présente les données cinétiques, obtenues dans l'étude du processus de disproportion du Mn(III) dans le système $[Mn(H_2P_2O_7)_3]^{3-}$ — L.

La variation, à la longue, de la concentration des composés du Mn(IV) et du Mn(III) a été déterminée sur la base des relations [30]:

$$A_1 = x\varepsilon_{\mathrm{Mn(III)}}\lambda_1 + y\varepsilon_{\mathrm{Mn(IV)}}\lambda_1$$

$$A_2 = x\varepsilon_{\mathrm{Mn(III)}}\lambda_2 + y\varepsilon_{\mathrm{Mn(IV)}}\lambda_2$$

où A_1 et A_2 = les absorbances du système pour λ_1 et respectivement λ_2; ε Mn(III) λ_1 et ε Mn(IV) λ_1 = les coefficients molaires d'absorption pour λ_1 et pour λ_2; x=la molarité en Mn(III) et y=la molarité en Mn(IV).

Le processus de transfert électronique suit donc une loi de vitesse du premier ordre et la voie de la réaction passe par un complexe activé qui contient les réactifs.

E) LE SPECTRE ÉLECTRONIQUE DU COMPLEXE $[MnL_4]$

Dans les complexes du Mn(IV), se réalise une configuration octaédrique, configuration qu'on admet aussi pour le complexe $[MnL_4]$, obtenu par la dissolution du MnO_2 dans l'acide aniline-4-sulphonique. Dans ce cas, le ligand est coordiné par des groupements $-NH_2$ et $-SO_3H$, et la microsymétrie de l'ion complexe est inférieure à celle O_h. Elle peut être D_{4h}, C_{2v}, etc.

Malgré cela, le complexe a un spectre champ cristallin caractéristique de la microsymétrie O_h, ce qui prouve que, dans la symétrie plus basse, la scission des niveaux dégénérés est petite et n'apparaît pas dans le spectre.

Dans les tableaux 2 et 3, on présente les données caractéristiques des bandes d'absorption du spectre électronique du complexe MnL_4, obtenu dans le système MnO_2-L.

Dans la région étudiée en UV, l'acide aniline-4 sulphonique présente 3 bandes d'absorption, notées ν_1, ν_2, et ν_3. Les bandes ν_1 et ν_2 sont dues à des transitions $\pi^* \leftarrow \pi$ et celle ν_3 est due à une transition $\pi^* \leftarrow n$. Les mêmes bandes d'absorption sont retrouvées dans le complexe $[MnL_4]$, avec de très petits déplacements hypsochromiques ou batochromiques. Pour $\lambda \sim 283$ nm, il se précise un point isosbestique.

Tableau 1

Données cinétiques concernant le processus de disproportion du Mn(III) dans le système $[Mn(H_2P_2O_7)_3]^{3-}-L$

Temp. °C	Ordre de réaction	Constante de vitesse K.sec^{-1}	Énergie d'activation kcal/mole
2	1	$0{,}21.10^{-2}$	19,84
14		$0{,}86.10^{-2}$	
21		$2{,}13.10^{-2}$	

---

[30] R. S. Drago, « Physical Methods in Inorganic Chemistry », New York Corporation Reinhold Publishing, 1965, p. 128.

Tableau 2

Données concernant les bandes d'absorption du spectre UV du système MnO_2-L

Composé	ν_1		ν_2		ν_3	
	λ_{max} nm	ε_{max} 1 mole^{-1} cm^{-1}	λ_{max} nm	ε_{max} 1-mole^{-1} cm^{-1}	λ_{max} nm	ε_{max} 1.mole^{-1} cm^{-1}
L	204	$1{,}65.10^4$	249	$1{,}16.10^4$	282	$1{,}7.10^3$
MnL_4	203	$5{,}55.10^4$	249	$3{,}65.10^4$	283	$7{,}00.10^3$

Tableau 3

Caractéristiques des bandes champ cristallin du complexe $[MnL_4]$ du système MnO_2-L (fig. 2, courbe 4)

$^4T_{2g} \xleftarrow{\nu_1'} {}^4A_{2g}$		$^4T_{1g} \xleftarrow{\nu_2'} {}^4A_{2g}$		$^4T_{1g}(P) \xleftarrow{\nu_3} {}^4A_{2g}$		D_q cm^{-1}	β_{35}
λ_{max} cm^{-1}	ε_{max} 1 mol^{-1} cm^{-1}	λ_{max} cm^{-1}	ε_{max} 1 mol^{-1} cm^{-1}	λ_{max} cm^{-1}	ε_{max} 1 mol^{-1} cm^{-1}		
11300 (885nm)	267	18400 (543 nm)	340	25600 (391 nm)	950	1130	0,63

Donc, dans le spectre UV du complexe $[MnL_4]$, les bandes d'absorption caractéristiques du ligand sont dominantes.

Dans le domaine visible, apparaissent les bandes de type cristallin du complexe $[MnL_4]$. Elles sont interprétées sur la base du diagramme des niveaux énergétiques propres au cas d^3 dans la symétrie O_h.[31]

Les valeurs des coefficients molaires d'absorption pour les bandes champ cristallin du complexe $[MnL_4]$ sont plus élevées que celles communes à des spectres champ cristallin. Cela est dû, entre autres, à l'état élevé d'oxydation du générateur de complexe.

Le paramètre champ cristallin 10 D_q et celui néphélauxétique β_{35} ont été calculés par une méthode graphique,[31] à la base des représentations :

$$\nu_m/\nu_n = f(Dq/B) \quad \text{et}$$

$$\nu_3/\nu_n = f(E\nu_3/B)$$

où $m = 2,3$; $n = 1,2$; $E\nu_3$ = l'énergie de la bande avec $\lambda_{max} = 25600$ cm^{-1}; B = le paramètre Racah.

CONCLUSIONS

— Les composés $[Mn(H_2P_2O_7)_3]^{3-}$, Mn_2O_3 et MnO_2 réagissent avec la solution de l'acide aniline-4-sulphonique et forment certains composés du Mn(IV). Dans le cas des réactifs avec le Mn(III), les complexes sont obtenus à la suite d'un processus de disproportion du Mn(III) en Mn(IV) et l'ion Mn^{2+}.

---

[31] A. B. P. LEVER, « Inorganic Electronic Spectroscopy », Elsevier Publishing Company, Amsterdam, 1968, p. 216, 392–400.

— Par spectrophotométrie, polarographie et chromatographie sur papier, on a mis en évidence les complexes pour les rapports 1 Mn(IV) : 2L et 1 Mn(IV) : 4L. La constante globale de formation du complexe $[MnL_4]$ est $\beta_4 = 2{,}80 . 10^{16} 1/\text{mole}^{-1}$.

— La disproportion du Mn(III) dans le système $[Mn(H_2P_2O_7)_3]^{3-}$—L a été étudiée du point de vue cinétique ; la réaction est du premier ordre avec $K = 2{,}13 . 10^{-2}$ sec^{-1} pour 21° et $E_a = 19{,}84$ kcal/mole.

— Le spectre champ cristallin du complexe MnL_4 du système MnO_2—L a été interprété à l'aide du diagramme des niveaux énergétiques propres au cas d^3, la symétrie *Oh*. Le paramètre D_q est 1130 cm^{-1} et celui néphélauxétique $\beta_{35} = 0{,}63$.

Revue Roumaine de Chimie, **19**, *12*, 1899–1908 (1974)

Gewidmet Akod.
RALUCA RIPAN
gelegentlich ihrer 80jährigen Geburtstagsfeier

ÜBER TRIAZINE*

L. MITTEILUNG.

POTENTIOMETRISCHE BESTIMMUNG DER ACIDITÄTSKONSTANTEN VON 4-HYDROXY-6-OXIMINTETRAHYDROTRIAZINYL-2-FORMALDOXIM

EUGENIA GAVRILĂ und ION CĂDARIU
Lehrstuhl für physikalische Chemie der Babeş-Bolyai Universität
Cluj-Napoca, str. Arany János 11

Eingegangen 13. Mai 1974

Die potentiometrische Titration von 4-Hydroxy-6-oximintetrahydrotriazinyl-2-formaldoxim zeigt, daß eine tribasische Säure vorliegt, deren Ionisierungsstufen sich überlappen. Aus der Titrationskurve wurden durch nacheinanderfolgende Näherungen unter Verwendung zweier Rechenmethoden (nach Ong und nach Bjerrum) die thermodynamischen Aciditätskonstanten erhalten, deren Werte bei Zimmertemperatur $pK_{a2} = 7{,}7$, $pK_{a3} = 9{,}9$ und $pK_{a4} = 10{,}9$ betragen. Mit Hilfe dieser Konstanten konnten die Extinktionskoeffizienten der entsprechenden Ionen berechnet werden; es wurden auch – unter Verwendung der Daten aus einer früheren Mitteilung – die Punkte der spektrophotometrischen Titrationskurve neu berechnet.

ALLGEMEINES

Für die spektrophotometrische Untersuchung des Eisen(III)-Komplexes von 4-Hydroxy-6-oximintetrahydrotriazinyl-2-formaldoxim (Kurzbezeichnung: Dioxim) war die Kenntnis der Aciditätskonstanten notwendig. Da die Substanz schwer löslich ist, hofften wir, daß die spektrophotometrische Methode zu genügend genauen Ergebnissen für die Werte dieser Konstanten führen wird.

Das UV-Spektrum des Dioxims ändert sich in Abhängigkeit von der Art des Mediums [1]; die graphische Darstellung der Abhängigkeit der Extinktion vom pH-Wert ergibt eine Kurve mit 3 Stufen bzw. Bereichen, in denen die Extinktion pH-unabhängig ist. In diesen Bereichen existiert die Substanz in einer einzigen Form:

$$\begin{array}{lll} \text{protoniertes Dioxim} & \text{bei pH} \cong 0 & \\ & & pK_{a1} = 1{,}6 \\ \text{neutrales Dioxim} & \text{bei pH} = 3 \text{ bis } 7{,}5 & \\ & & pK_{a2} = 9{,}2 \\ \text{Dioximanion} & \text{bei pH} > 11 & \end{array}$$

---

[*] Teil XLIX. E. GAVRILĂ, G. NIAC und I. CĂDARIU, *Z. phys. Chem.* (*Leipzig*), **251**, 383 (1972).

[1] I. CĂDARIU, E. GAVRILĂ und G. NIAC, *Z. phys. Chem.* (*Leipzig*), **242**, 391 (1969).

Es hat uns überrascht, daß eine zweite Säurefunktion des Oxims nicht in Erscheinung trat, um so mehr als A. Ostrogovich und I. Cădariu das Dinatriumsalz des Oxims isolieren konnten.[2]

Wir kamen zu der Vermutung, daß die zwei anionischen Formen wahrscheinlich bei derselben Wellenlänge absorbieren, oder aber die zwei verschiedenen Wellenlängen sehr dicht beieinander liegen, und dementsprechend auch die Werte der Aciditätskonstanten sich nur minimal unterscheiden.

Allerdings, das Einsetzen der Spektraldaten in die lineare Gleichung des Ausdruckes $\log \frac{\alpha}{1-\alpha}$ in Abhängigkeit von pH, wobei die erhaltene Steigung die Zahl der aus der Dissoziation entstandenen H^+-Ionenen ergibt, führt zu einem Wert von 0,8, und die einzelnen Punkte zeigen eine relativ große Streuung. Diese Tatsachen berechtigen die Annahme, daß der spektrophotometrisch bestimmte Wert für pK_{a2} eine zusammengesetzte Größe ist.

Für den Fall, in dem mittels Spektrum die molekularen Spezies nicht einzeln identifizierbar sind, ist es üblich, elektrometrische Methoden zu benutzen. Wir haben in unserem Fall potentiometrische Messungen durchgeführt.

EXPERIMENTELLER TEIL

Die Dioximlösung—mit einer Konzentration von $1{,}8436.10^{-3}$ M—wurde durch Lösen der Festsubstanz (auf Mikrowaage gewogen) in bidestilliertem, CO_2-freiem Wasser, hergestellt. Um die protonierte Form zu erhalten, wurde die Dioximlösung mit einer 0,103 M $HClO_4$-Lösung titriert; dann wurde diese mit einer 0,1037 M NaOH-Lösung und zum Schluß wieder mit $HClO_4$-Lösung zurück titriert.

Die $HClO_4$- bzw. NaOH-Lösungen wurden durch Verdünnen der 70%-igen $HClO_4$-Lösung p.a. bzw. einer — aus NaOH p.a. hergestellten gesättigten NaOH-Lösung mit bidestilliertem, CO_2-freiem Wasser erhalten.

Die EMK-Kette bestand aus einer gesättigten Kalomel-Bezugselektrode und einer Wasserstoff-Meßelektrode. Die EMK wurde mit einem Potentiometer QLK-Metra gemessen. Die Messungen wurden bei 24—24,5°C durchgeführt.

Zur Titration wurden 10 ml Dioximlösung vorgelegt. Es wurde eine Mikrobürette verwendet, die gegen CO_2- Eintritt aus der Luft geschützt wurde.

Die Messungen wurden auch mit einer Glaselektrode durchgeführt, und die Ergebnisse waren identisch mit denen, die mit der Wasserstoffelektrode erhalten wurden. Für die Diskussion der Ergebnisse wurden die mit der Wasserstoffelektrode durchgeführten Messungen vorgezogen, weil für die spektrophotometrischen Bestimmungen auch die Wasserstoffelektrode verwendet wurde, und außerdem sind mit der H_2-Elektrode größere pH-Werte zugänglich.

DISKUSSION UND ERGEBNISSE

Aus der Tirationskurve —Abb. 1 — ist ersichtlich, daß das protonierte Dioxim vier Ionisierungsstufen aufweist. Die Ionisierung des ersten Protons ist vollständig, und die erste Stufe ist deutlich ausgebildet, so wie auch aus den spektrophotometrischen Messungen hervorgeht[1]. Die anderen Ionisierungsstufen überlappen sich, da die folgenden Ionisierungskonstanten sich wenig unterscheiden.

Wenn man die umgekehrte Titration durchführt (Titration des dreiwertigen Dioximanions mit $HClO_4$), stellt man fest, daß die erhaltene

---

[2] A. Ostrogovich und I. Cădariu, *Gazz. chim. Ital.*, **71**, 505 (1941).

Kurve sich nicht mit der Kurve der Direkttitration deckt; es besteht also eine Hysteresis, die wahrscheinlich den tautomeren Umwandlungen im alkalischen Medium zuzuschreiben ist. Infolgedessen sind die Konstanten K_{a2}, K_{a3} und K_{a4} mit einem Bestimmungsfehler von etwa 0,4 pK_a-Einheiten behaftet.

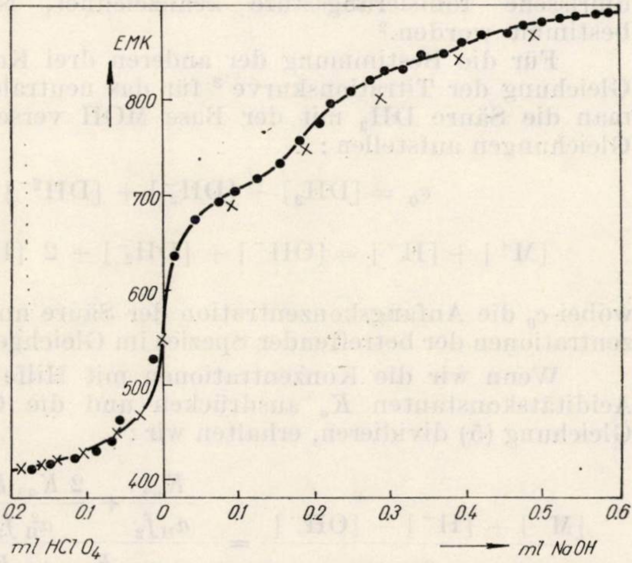

Abb. 1. — Änderung der EMK in Abhängigkeit von dem Titrierlösungsvolumen. $c_0 = 1{,}84 \cdot 10^{-3}$ M, (●) — 0,1 N NaOH-Lösung, (×) — 0,1 N HClO$_4$-Lösung.

Wenn man annimmt, daß die Oxo-Gruppe des Dioxims im alkalischen Medium enolisiert (I), existieren drei ionisierbare H-Atome, und wir werden dementsprechend das Dioxim kurz DH_3 bezeichnen (und nicht DH_2 wie in der Mitteilung[1]).

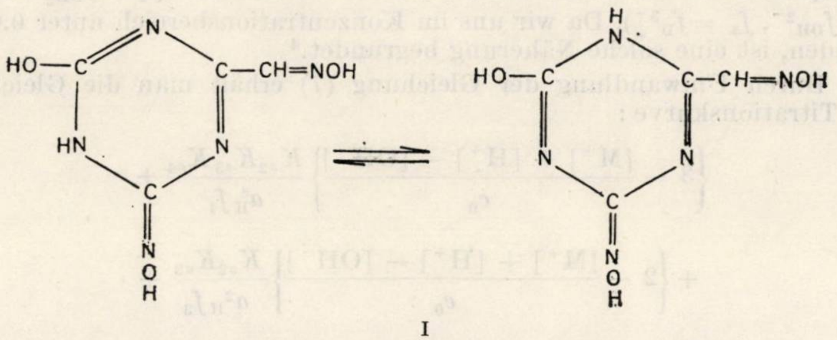

I

Das Dioxim ist also eine poliprotische Säure, die folgende Gleichgewichte aufweisen kann:

$$DH_4^+ \xrightleftharpoons{K_{a1}} DH_3 + H^+ \tag{1}$$

$$DH_3 \xrightleftharpoons{K_{a2}} DH_2^- + H^+ \tag{2}$$

$$DH_2^- \xrightleftharpoons{K_{a3}} DH^{2-} + H^+ \tag{3}$$

$$DH^{2-} \xrightleftharpoons{K_{a4}} D^{3-} + H^+ \tag{4}$$

Die thermodynamische Konstante K_{a1}, die die erste, deutlich umrissene Ionisierungsstufe kennzeichnet, ist spektrophotometrisch bestimmt worden.[2]

Für die Bestimmung der anderen drei Konstanten werden wir die Gleichung der Titrationskurve [3] für das neutrale Dioxim ableiten. Wenn man die Säure DH_3 mit der Base MOH versetzt, lassen sich folgende Gleichungen aufstellen :

$$c_0 = [DH_3] + [DH_2^-] + [DH^{2-}] + [D^{3-}] \tag{5}$$

$$[M^+] + [H^+] = [OH^-] + [DH_2^-] + 2\ [DH^{2-}] + 3\ [D^{3-}] \tag{6}$$

wobei c_0 die Anfangskonzentration der Säure und die Klammer die Konzentrationen der betreffender Spezies im Gleichgewicht bedeuten.

Wenn wir die Konzentrationen mit Hilfe der thermodynamischen Aciditätskonstanten K_a ausdrücken und die Gleichung (6) durch die Gleichung (5) dividieren, erhalten wir :

$$\frac{[M^+] + [H^+] - [OH^-]}{c_0} = \frac{\dfrac{K_{a2}}{a_H f_2} + \dfrac{2\ K_{a2} K_{a3}}{a_H^2 f_3} + \dfrac{3\ K_{a2} K_{a3} K_{a4}}{a_H^3 f_4}}{1 + \dfrac{K_{a2}}{a_H f_2} + \dfrac{K_{a2} K_{a3}}{a^2_H f_3} + \dfrac{K_{a2} K_{a3} K_{a4}}{a_H^3 f_4}} \tag{7}$$

wobei a_H die Protonenaktivität und f der für die Ionenstärke am Halbstufenpotential berechnete Aktivitätsfaktor bedeutet ($f_2 \equiv f_{DH_2^-} \equiv f_{H^+}$, $f_3 \equiv f_{DH^{2-}}$, $f_4 = f_{D^{3-}}$). Da wir uns im Konzentrationsbereich unter 0,01 M befinden, ist eine solche Näherung begründet.[4]

Durch Umwandlung der Gleichung (7) erhält man die Gleichung der Titrationskurve :

$$\left\{3 - \frac{[M^+] + [H^+] - [OH^-]}{c_0}\right\} \frac{K_{a2} K_{a3} K_{a4}}{a_H^3 f_4} +$$

$$+ \left\{2 - \frac{[M^+] + [H^+] - [OH^-]}{c_0}\right\} \frac{K_{a2} K_{a3}}{a^2_H f_3} +$$

$$+ \left\{1 - \frac{[M^+] + [H^+] - [OH^-]}{c_0}\right\} \frac{K_{a2}}{a_H f_2} = \frac{[M^+] + [H^+] - [OH^-]}{c_0} \tag{8}$$

---

[3] „The International Encyclopedia of Physical Chemistry and Chemical Physics", Topic 15, vol. 4, Ed. E. A. Guggenheim, J. E. Mayer and F. C. Tompkins.
— E. J. King, "Acid-Base Equilibria", Pergamon Press, Oxford, 1965, p. 227.

[4] "Physical Methods in Heterocyclic Chemistry", vol. I, cap. I, Ed. A. R. Katritzky, Academic Press, New York, 1963.

wobei der Ausdruck $\frac{[M^+] + [H^+] - [OH^-]}{c_0} = h^*$ die Anzahl der von der mehrbasischen Säure in Freiheit gesetzten Protonen und das Verhältnis $\frac{[M^+]}{c_0} = \bar{h}$ die mittlere theoretische Anzahl der von der zugesetzten Base verbrauchten Protonen bedeutet.

Die Titrationskurve des unprotonierten Dioxims, die aus der Gleichung : $h^* = f(-\log[H^+])$ hervorgeht, ist im Abb. 2 wiedergegeben.

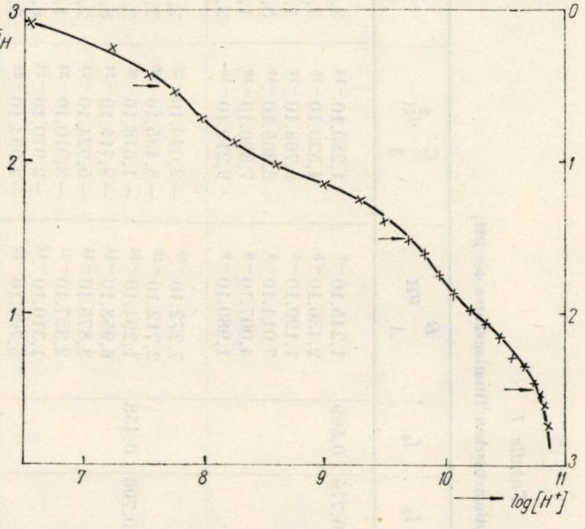

Abb. 2. — Titrationskurve des DH_3 in h^*, $\bar{n}_H$-Koordinaten, in Abhängigkeit vom $-\log$ $[H^+]$.

Gekürzt kann die Gleichung (8) in folgender Form geschrieben werden :

$$A\, K_{a2}K_{a3}K_{a4} + B\, K_{a2}K_{a3}\, a_H + C\, K_{a2}\, a_H^2 = D\, a_H^3 \tag{9}$$

wobei :

$$A = \{(3 - \bar{h})\, c_0 - [H^+] + [OH^-]\}\, \frac{1}{f_4} = \frac{(3 - h^*)}{f_4} \tag{10}$$

$$B = \{(2 - \bar{h})\, c_0 - [H^+] + [OH^-]\}\, \frac{1}{f_3} = \frac{(2 - h^*)}{f_3} \tag{11}$$

$$C = \{(1 - \bar{h})\, c_0 - [H^+] + [OH^-]\}\, \frac{1}{f_2} = \frac{(1 - h^*)}{f_2} \tag{12}$$

$$D = \bar{h}\, c_0 + [H^+] - [OH^-] = h^* \tag{13}$$

Tabelle 1

Daten der potentiometrischen Titrationskurve des DH_3

Nr.	ml NaOH	EMK mV	$\bar{h}$	pH	J	f_2	f_3	f_4	$\frac{B}{A} a_H$	$\frac{C}{A} a_H^2$	$\frac{D}{A} a_H^3$	$\bar{n}_H$	$-\log[H^+]$
1	0,016	636	0,090	6,585	$2,9.20^{-3}$	0,939	0,779	0,569	$1,245.10^{-7}$	$1,280.10^{-14}$	$3,093.10^{-22}$	2,910	6,557
2	0,046	675	0,259	7,282					$2,436.10^{-8}$	$4,520.10^{-16}$	$7,770.10^{-24}$	2,741	7,252
3	0,076	692	0,427	7,570					$1,199.10^{-8}$	$9,768.10^{-17}$	$1,837.10^{-24}$	2,573	7,543
4	0,096	705	0,540	7,791					$7,014.10^{-9}$	$2,965.10^{-17}$	$5,310.10^{-25}$	2,460	7,763
5	0,126	718	0,709	8,012					$4,007.10^{-9}$	$7,320.10^{-18}$	$1,631.10^{-25}$	2,291	7,918
6	0,156	734	0,877	8,292					$1,980.10^{-9}$	$9,210.10^{-19}$	$3,172.10^{-26}$	2,124	8,263
7	0,181	756	1,018	8,646	$5,6.10^{-3}$	0,917	0,706	0,458	$7,272.10^{-10}$	$-2,040.10^{-20}$	$2,704.10^{-27}$	1,984	8,908
8	0,206	778	1,159	9,039					$2,712.10^{-10}$	$-3,435.10^{-20}$	$2,291.10^{-28}$	1,847	9,002
9	0,226	795	1,271	9,331					$1,294.10^{-10}$	$-1,618.10^{-20}$	$3,391.10^{-29}$	1,742	9,292
10	0,251	808	1,412	9,548					$6,953.10^{-11}$	$-9,715.10^{-21}$	$8,973.10^{-30}$	1,609	9,510
11	0,276	819	1,552	9,735					$3,875.10^{-11}$	$-5,924.10^{-21}$	$2,927.10^{-30}$	1,480	9,697
12	0,296	828	1,665	9,880					$2,357.10^{-11}$	$-3,910.10^{-21}$	$1,236.10^{-30}$	1,380	9,842
13	0,321	835	1,806	9,998					$1,310.10^{-11}$	$-2,970.10^{-21}$	$6,370.10^{-31}$	1,254	9,958
14	0,346	843	1,946	10,13					$5,700.10^{-12}$	$-2,094.10^{-21}$	$3,064.10^{-31}$	1,134	10,092
15	0,371	851	2,087	10,27	$8,7.10^{-3}$	0,897	0,648	0,377	$8,260.10^{-13}$	$-1,150.10^{-21}$	$1,121.10^{-31}$	1,027	10,223
16	0,396	859	2,227	10,40					$-1,768.10^{-12}$	$-7,491.10^{-22}$	$5,107.10^{-32}$	0,928	10,358
17	0,421	866	2,368	10,58					$-3,295.10^{-12}$	$-5,065.10^{-22}$	$2,494.10^{-32}$	0,839	10,483
18	0,456	872	2,565	10,63					$-5,955.10^{-12}$	$-4,315.10^{-22}$	$1,599.10^{-32}$	0,717	10,583
19	0,476	878	2,677	10,73					$-5,859.10^{-12}$	$-3,016.10^{-22}$	$8,802.10^{-33}$	0,651	10,684
20	0,501	882	2,818	10,80					$-8,000.10^{-12}$	$-2,855.10^{-22}$	$6,799.10^{-33}$	0,530	10,754
21	0,526	885	2,958	10,85					$-9,220.10^{-12}$	$-2,714.10^{-22}$	$5,676.10^{-33}$	0,471	10,804
22	0,546	888	3,071	10,88								0,391	10,833
23	0,576	890	3,240	10,91								0,256	10,863
24	0,591	892	3,324	10,95								0,221	10,903

Für Säuren mit mehr als zwei ionisierbaren H-Atomen—und besonders für solche, deren Ionisierungsstufen sich überlappen—ist die Gleichung sehr schwer aufzulösen.

Ong (^{3} s 227) berechnet unter Anwendung nacheinanderfolgender Näherungen aus der Titrationskurve die Konstanten der Pyridin-pentacarboxylsäure. Wir verwendeten ein analoges Verfahren.

Die einzelnen Daten (auch die berechneten) für die Titrationskurve sind in der Tabelle 1 enthalten.

Aus dem Endabschnitt der Titrationskurve ermittelt man einen ungefähren Wert für die Konstante K_{a4}. Für diesen Abschnitt (die Bestimmungen 21 — 18) ist die H^+ - Ionenaktivität klein, und die Größen a_H^2 und a_H^3 können vernachlässigt werden; die Gleichung (9) nimmt dann die Form an:

$$K_{a3} K_{a4} + \frac{B}{A} K_{a3}\, a_H \approx 0 \qquad (14)$$

Es ergibt sich:

$$K_{a4} \approx -\frac{B}{A} a_H \qquad (15)$$

Den so erhaltenen Wert K_{a4} führen wir in die Gleichung (14) ein, die diesmal für den nächstfolgenden Abschnitt der Titrationskurve (Bestimmungen 17 — 15) angewandt wird; wir erhalten somit einen ersten Wert für K_{a3}. Diesen K_{a3} - Wert führen wir in die Gleichung (14) ein, die wieder für den Endabschnitt der Titrationskurve geschrieben wird, und wir erhalten einen K_{a4} - Wert in der zweiten Näherung.

Mit den so erhaltenen Werten für K_{a3} und K_{a4} bestimmen wir einen ersten Wert für K_{a2} (Bestimmungen 6—4). Die Näherungen für die Berechnung der Konstanten werden—vom Endabschnitt zum Aufangsabschnitt der Titrationskurve ausgehend — weiter fortgesetzt, bis die erhaltenen Werte konvergieren. Wir haben festgestellt, daß die Streuung der berechneten Werte in folgenden $\bar{h}$-Bereichen am kleinsten sind: 0,5 — 1 für K_{a2}, 1,5 — 2 für K_{a3} und 2,5 — 3 für K_{a4}.

Die erhaltenen Daten sind in Tabelle 2 zusammengefaßt; die stark abweichenden Werte wurden zur Ermittlung des Mittelwertes nicht berücksichtigt.

Tabelle 2

Werte der Säurekonstanten des DH_3

	K_{a2}	K_{a3}	K_{a4}
Ong Methode	$1{,}9.10^{-8}$	$1{,}3.10^{-10}$	$1{,}0.10^{-11}$
Bjerrum Methode	$1{,}7.10^{-8}$	$1{,}1.10^{-10}$	$1{,}2.10^{-11}$
Mittelwerte	$1{,}8.10^{-8}$	$1{,}2.10^{-10}$	$1{,}1.10^{-11}$

Einen anderen Rechnungsweg bietet die Methode nach Bjerrum; die Bezugssubstanz ist in diesem Falle die total unprotonierte Form D^{3-}.

Man rechnet mit der Bildungsfunktion $\bar{n}_H$, deren Wert die mittlere Anzahl der durch die mehrbasische Säure gebundenen Protonen ausdrückt:

$$\bar{n}_H = \frac{3\,c_0 - [H^+] + [OH^-] - [M^+]}{c_0} \tag{16}$$

Durch die Darstellung von $\bar{n}_H$ in Abhängigkeit von $(-\log[H^+])$ erhält man dieselbe Titrationskurve — Abb. 2 — wie im Falle der Darstellung von h^* in Abhängigkeit von $(-\log[H^+])$, lediglich der Nullpunkt ist verschoben, da die Beziehung $\bar{n}_H = 3 + h^*$ gilt.

Die Halbstufenpotentiale liefern die ersten ungefähren Werte für die Aciditätskonstanten, die—mittels Konzentrationen bei der entsprechenden Ionenstärke ausgedrückt—folgendes ergeben:

$$(K_2)_{\bar{n}=0,5} = 2.10^{-8} \quad (K_3)_{\bar{n}=1,5} = 2.10^{-10} \quad (K_4)_{\bar{n}=2,5} = 1,7.10^{-11}$$

Wenn wir diese ersten Werte in die Konstantenausdrücke [5]:

$$K_2 = \left(\frac{1}{[H^+]}\right)_{\bar{n}=0,5} \frac{1}{1 + 3\,K_3\,[H^+]_{\bar{n}=0,5} + 5\,K_2 K_3 [H^+]^2_{\bar{n}=0,5}} \tag{17}$$

$$K_3 = \left(\frac{1}{[H^+]}\right)_{\bar{n}=0,5} \frac{1 + \dfrac{3}{K_2\,[H^+]_{\bar{n}=0,5}}}{1 + 3\,K_4\,[H^+]_{\bar{n}=1,5}} \tag{18}$$

$$K_4 = \left(\frac{1}{[H^+]}\right)_{\bar{n}=2,5} \left(1 + \frac{3}{K_3[H^+]_{\bar{n}=2,5}} + \frac{5}{K_2 K_3\,[H^+]_{\bar{n}=2,5}}\right) \tag{19}$$

einführen, erhalten wir die ungefähren Konstantenwerte, die wieder in die obigen Ausdrücke eingeführt werden. Das Verfahren wird wiederholt, bis die erhaltenen Werte konvergieren; in unserem Fall ist die Konvergenz bei folgenden Werten erreicht:

$$K_2 = 1,9.10^{-8} \; K_3 = 1,5.10^{-10} \; K_4 = 2,2.10^{-11}$$

Unter Verwendung folgender Beziehungen:

$$K_{a2} = K_2 f_2^2 \; K_{a3} = K_3 f_3 \text{ und } K_{a4} = K_4 \frac{f_4 f_2}{f_3} \tag{20}$$

können dann die thermodynamischen Aciditätskonstanten berechnet werden; die erhaltenen Werte sind in Tabelle 2 zusammengefaßt, und sie sind in befriedigender Übereinstimmung mit den nach der Methode von Ong berechneten Werten.

---

[5] C. Luca und O. Enea, "Determinarea constantelor analitice", Ed. didactică şi pedagogică, Bukarest, 1971, S. 46.

Um die Ergebnisse zu überprüfen, haben wir die Extinktionskoeffizienten (ε) aller Dioximspezien und daraus die spektrophotometrische Titrationskurve im alkalischen Medium berechnet.

Da die Extinktion (E) additiv ist, kann man folgende Gleichung aufstellen :

$$\frac{E}{\mathrm{d}} = [\mathrm{DH_3}]\ \varepsilon_1 + [\mathrm{DH_2^-}]\ \varepsilon_2 + [\mathrm{DH^{2-}}]\ \varepsilon_3 + [D^{3-}]\ \varepsilon_4 \qquad (21)$$

Wenn man die Konzentrationen durch die Konstanten K_2, K_3 und K_4 bei der gegebenen Ionenstärke ausdrückt und die Beziehungen (20) berücksichtigt, wandelt sich die Gleichung (21) zu :

$$\frac{E}{\mathrm{d}} = [\mathrm{DH_3}]\left[\varepsilon_1 + \frac{K_2}{[\mathrm{H^+}]}\varepsilon_2 + \frac{K_2K_3}{[\mathrm{H^+}]^2}\varepsilon_3 + \frac{K_2K_3K_4}{[\mathrm{H^+}]^3}\varepsilon_4\right] \qquad (22)$$

Gleichung (22) dividiert durch die Gleichung (5) und zweckmäßig umgeordnet führt zu der Gleichung :

$$\frac{E}{\mathrm{d}\,c_0}\left([\mathrm{H^+}]^2 + K_2[\mathrm{H^+}] + K_2K_3 + \frac{K_2K_3K_4}{[\mathrm{H^+}]}\right) - \varepsilon_1\ [\mathrm{H^+}]^2 - \frac{K_2K_3K_4\,\varepsilon_4}{[\mathrm{H^+}]} = \qquad (23)$$

$$= K_2\varepsilon_2\ [\mathrm{H^+}) + K_2K_3\ \varepsilon_3$$

wobei d die Küvettendicke darstellt.

Die Werte der Extinktionskoeffizienten für das neutrale Dioxim — ε_1 und für das völlig unprotonierte Dioxim — ε_4 können aus der Extinktion der waagerechten Abschnitte der Kurve $E = f(\mathrm{pH})$ [1] berechnet werden ; mit d $= 2{,}003$ cm und $c_0 = 4 . 10^{-5}$ Mol/1 erhält man folgende Werte :

$\lambda = 280$ nm $\quad \varepsilon_1 = 3250 \quad \varepsilon_4 = 18750$ l.mol^{-1}. cm^{-1}
$\lambda = 350$ nm $\quad \varepsilon_1 = 3150 \quad \varepsilon_4 = \quad 1337$ ”

Mit Hilfe dieser Werte und denen der Aciditätskonstanten bei der Ionenstärke $J = 0{,}3$:

$$K_2 = 3{,}57 . 10^{-8} \quad K_3 = 4{,}72 . 10^{-10} \quad K_4 = 8{,}57 . 10^{-11}$$

kann man das erste Glied der Gleichung (22) berechnen.

Diese Funktion, die von $[\mathrm{H^+}]$ linear abhängig ist, werden wir mit F bezeichnen. Die den zwei Wellenlängen entsprechenden Daten sind in der Tabelle 3 zusammengefaßt.

Tabelle 3

Ergebnisse bezüglich der berechneten spektrophotometrischen Titrationskurve

pH	$[H^+]$	$\lambda = 280$ nm F.10^{13}	 E_{exp}	 E_{ber}	$\lambda = 350$ nm F.10^{13}	 E_{exp}	 E_{ber}
8,32	$6{,}75.10^{-9}$	22,4	(0,630)	0,666	6,9	0,220	0,206
9,00	$1{,}41.10^{-9}$	7,2	0,860	0,847	1,6	(0,192)	0,192
9,08	$1{,}17.10^{-9}$	6,9	0,945	0,879	—	—	—
9,10	$1{,}12.10^{-9}$	—	—	—	1,3	0,188	0,189
9,55	$3{,}97.10^{-10}$	4,0	1,07	1,08	—	—	—
9,64	$3{,}23.10^{-10}$	4,3	1,16	1,13	—	—	—
10,25	$5{,}62.10^{-11}$	3,0	1,36	1,37	0,4	0,145	0,140
(11,00)	$1{,}41.10^{-11}$	—	—	—	—	(0,118)	0,137
11,07	$1{,}20.10^{-11}$	2,9	1,48	1,48	—	—	—
(12,00)	$1{,}41.10^{-12}$	—	(1,40)	1,50	—	(0,107)	0,110
(13,00)	$1{,}41.10^{-13}$	—	(1,50)	1,50	—	(0,107)	0,110

Die in Klammern angegebenen Werte wurden aus der spektrophotometrischen Titrationskurve abgelesen.[1]

Die durch die graphische Darstellung von $F = f([H^+])$ erhaltenen Geraden — Abb. 3 — haben die in der Tabelle 4 aufgeführten Steigungen und Nullpunktsordinaten.

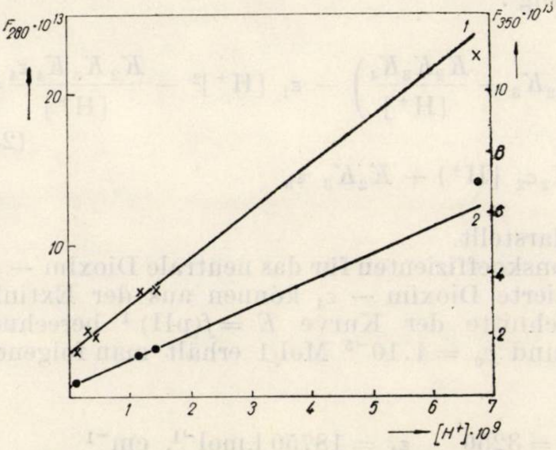

Abb. 3. — Graphische Darstellung von $F = f([H^+])$. *1*, $\lambda = 280$ nm, *2*, $\lambda = 350$ nm.

Mit den nun bekannten Aciditätskonstanten und Extinktionskoeffizienten haben wir unter Verwendung der Gleichung (23) die Extinktionen berechnet (Tabelle 3).

Tabelle 4

Extinktionskoeffizienten des Mono bzw. Dianions des DH_3

λ_{nm}	$K_2K_3\varepsilon_3$	$K_2\varepsilon_2$	ε_2	ε_3
280	$2{,}8.10^{-13}$	$3{,}1.10^{-4}$	$8{,}7.10^{3}$	$1{,}7.10^{4}$
350	$0{,}3.10^{-13}$	$0{,}9.10^{-4}$	$2{,}5.10^{3}$	$2{,}0.10^{3}$

Die experimentellen Werte stimmen zufriedenstellend mit den berechneten überein. Die Existenz des waagerechten Kurvenabschnitts bei pH-Werten über 11 ist gleichfalls bestätigt.

Revue Roumaine de Chimie, **19**, *12*, 1909–1919 (1974)

Dedicated to
Raluca Ripan
on the occasion of her 80th anniversary

STUDY OF SOME Cu(II) SELENOCYANATE COMPLEXES WITH BIGUANIDE DERIVATIVES

CONSTANŢA GHEORGHIU *, MARIA CONSTANTINESCU, **
O. CONSTANTINESCU ** and VALERICA POCOL *
* Department of Inorganic Chemistry, University of Bucharest, Romania
** Institute for Atomic Physics, Bucharest, Romania

Received April 16, 1974

A new series of Cu(II) coordination compounds with biguanide derivatives of the type: [Cu $(RBig)_2$] $(SeCN)_2$ and $CuRBig(SeCN)_2$ where RBig = N^1-dimethylbiguanide, N^1-morpholinbiguanide, N^1-phenylbiguanide, N^1-*p*-chlorophenylbiguanide, N^1-*p*-tolylbiguanide, N^1-*p*-chlorophenyl-N^5-isopropylbiguanide, have been studied. The compounds were characterized by chemical elementary analysis, IR and electronic spectra, electric conductivity measurements, magnetic susceptibility and EPR spectra. From these data and by correlating the electronic spectral parameters with those of the EPR spectra, information on the structure and the chemical bonding was obtained.

I. INTRODUCTION

The study of Cu(II) selenocyanate complexes is of a special interest due to the fact that the SeCN group can function as a monodentate bifunctional ligand. The literature mentions rather few papers on the Cu(II) selenocyanate complexes. The first indications signal out [Cu en_2] $(SeCN)_2$ formations.[1,2] In 1964, $[Cu(NH_3)_4]$ $(SeCN)_2 . H_2O$ was obtained.[3] Subsequently [4–6] other compounds of the type: $[CuA_2](SeCN)_2$ and CuA_2SeCNX where A = substituted diamines, and X = NO_3^-, ClO_4^-, were also studied. With the $CuMBen_2(SeCN)$ (NO_3) it was signalled out that the SeCN group will be in a bridge. There are also indications about the existence of $CuHg(SeCN)_4$ [7].

We considered interesting to extend the study on the Cu(II) selenocyanate complexes, using as ligands, biguanide derivatives π donors, which can stabilize transition metals in the high valence states.

---

[1] G. Morgan and I. H. Burstall, *J. Chem. Soc. part. I*, **1927**, 1259.
[2] G. Spacu and C. Macarovici, *Bul. Soc. de Ştiine-Cluj*, **6**, 95 (1931).
[3] V. V. Skopenko and T. V. Tinţadze, *Zhur. neorg. Khim.*, **9**, 2675 (1964).
[4] M. E. Farago and J. M. James, *Inorg. Chem.*, **4**, 1706 (1965).
[5] K. Patel and D. E. Goldberg, *Inorg. Chem.*, **11**, 759 (1972).
[6] K. Patel and D. E. Goldberg, *J. Inorg. Nuclear Chem.*, **34**, 637 (1972).
[7] Iu. Haritonov and V. V. Skopenko, *Zhur. neorg. Khim.*, **10**, 1803 (1965).

In the present paper we continue our study concerning Cu(II) coordination compounds with substituted biguanides [8-10] presenting the synthesis and the study by electronic, IR, and EPR spectra, magnetic and conductometric measurements on some new Cu(II) selenocyanate complexes of the type: $[Cu(RBig)_2](SeCN)_2$ and $Cu(RBig)(SeCN)_2$.

II. EXPERIMENTAL

a. Chemical procedures. We used $CuCl_2 \cdot 2H_2O$ Merck *p.a.*,KSeCN prepared by the method indicated by literature [11] and the following biguanide derivatives (RBig):
N^1-dimethylbiguanide ($C_4H_{11}N_5$), Me_2Big;
N^1-morpholinbiguanide ($C_6H_{13}N_5O$), MorBig;
N^1-phenylbiguanide ($C_8H_{11}N_5$), PhBig;
N^1-*p*-chlorophenylbiguanide ($C_8H_{10}N_5Cl$), ClPhBig;
N^1-tolylbiguanide ($C_9H_{13}N_5$), TolBig;
N^1-*p*-chlorophenyl-N^5-isopropylbiguanide ($C_{11}H_{16}N_5Cl$), Pald.

$[Cu(RBig)_2](SeCN)_2$ compounds could be obtained by 3 methods: either by a direct method in aqueous medium, at pH = 8, from $CuCl_2 \cdot 2H_2O$, RBig and KSeCN in a molar ratio 1 : 2 : 2, or by the exchange reaction between $[Cu(RBig)_2]Cl_2$ and KSeCN in aqueous or alcoholic medium, or by mixing $Cu(RBig)Cl_2$ with KSeCN molar ratio 1 : 2, 1 in acetone or DMF medium, at pH = 8. By these 3 methods, the same pink products noted with 1—6 in table 1, hardly soluble in water, ethanol, and partly soluble in acetone and DMF, were obtained.

Table

	Compound	Analy			
		Cu %		N %	
		calc.	found.	calc.	found.
1	$[Cu(Me_2Big)_2](SeCN)_2$	11.95	12.07	31.60	31.53
2	$[Cu MorBig)_2](SeCN)_2$	10.32	10.19	27.29	27.08
3	$[Cu(PhBig)_2](SeCN)_2$	10.12	9.98	26.27	26.86
4	$[Cu(ClPhBig)_2](SeCN)_2$	9.12	9.20	24.13	24.02
5	$[Cu(TolBig)_2](SeCN)_2$	9.69	9.51	25.63	25.48
6	$[Cu Pald_2](SeCN)_2$	8.14	8.02	21.53	21.46
7	$Cu(Me_2Big)(SeCN)_2$	15.78	15.60	24.35	24.56
8	$Cu(PhBig)(SeCN)_2$	14.10	14.35	21.76	21.72
9	$Cu(ClPhBig)(SeCN)_2$	13.10	13.40	20.21	20.02
10	$Cu(Tol Big)(SeCN)_2$	13.68	13.51	21.10	20.69
11	$CuPald(SeCN)_2$	12.06	11.88	18.60	18.45

---

[8] P. Spacu, C. Gheorghiu, O. Constantinescu and I. Pascaru, *Z. phys. Chem.* (*Frankfurt*), **65**, 248 (1969).

[9] P. Spacu, C. Gheorghiu, O. Constantinescu and I. Pascaru, *Rev. Roumanie Chimie*, **16**, 667 (1971).

[10] P. Spacu, C. Gheorghiu, M. Constantinescu, I. Pascaru and O. Constantinescu, *Z. anorg. Chem.*, **384**, 184 (1971).

[11] G. R. Watkins and R. Schutt, *Inorg. Synth.*, **2**, 186 (1946).

$CuRBig(SeCN)_2$ compounds were obtained by the action of KSeCN on $Cu(RBig)Cl_2$, molar ratio 2,1 : 1, in ethanol or DMF medium. Filtered solutions were immediately treated with alkalinized water (pH = 7.5) when brown precipitates were separated. They were filtered, washed with water after which they were dried in vacuum. The brown selenocyanates noted with 7—11 in table 1 are hardly soluble in water, ethanol, ether, and very slightly soluble in DMF and DMSO.

b. Instrumentation.

IR spectra were recorded in the range 3400—400 cm^{-1} with a spectrophotometer UR—10 Zeiss Jena, using the pelleted powder method.

Electronic spectra of DMF solutions in visible and UV were recorded with a VSU_1 Universal spectrophotometer (Zeiss Jena).

Reflectance spectra were recorded with the same apparatus either on pure compounds or on dilutions with MgO.

EPR spectra were obtained by using an X band spectrograph with high frequency field modulation (100 kHz).

Polycrystalline powder, samples magnetically diluted with $[Zn(RBig)_2](SeCN)_2$ and $PdRBig(SeCN)_2$ as well as DMF solution were used. In order to determine the g values, DPPH and Mn^{2+} were used as standard.

Conductance measurements were effected in DMF solutions with a conductometer type OK 102/1 Radelkis with the measure range 0.1μs—0.5s, the apparatus constant being calculated by using NaCl solutions of different normalities. The results are given in table 1.

1

ses Se %		I.R. Spectra $[cm^{-1}]$ $(\nu_{C\equiv N})$	Electronic diffuse reflectance spectra. Reflectance minima		Elecronic absorption spectra of DMF solution (cm^{-1})	Molar conductivity $\left[\frac{ohm^{-1}\,cm^2}{mol^{-1}}\right]$
calc.	found.		Δ_{xy} (cm^{-1})	Δ_{xz} (cm^{-1})		
29.69	29.77	2070	19608	—	19608	126.2
25.64	25.39	2075	19802	—	19608	126.6
25.15	25.00	2070	19608	—	19608	143
22.66	22.69	2075	19230	—	19608	132.5
24.08	23.88	2070	19230	—	19230	129.6
20.22	20.04	2100	18868	—	20000	117.7
39.22	39.30	2135	11110	27777	—	—
35.04	34.69	2145	11110	27472	—	—
32.55	32.64	2115	11110	27777	—	—
33.98	33.70	2145	11110	27472	—	—
29.95	29.69	2145	10638	27472	—	—

III. RESULTS

1. IR SPECTRA (400—3400 cm^{-1})

In table 1 are given the values of vibration frequency $\nu_{C\equiv N}$ for the considered selenocyanate complexes. The pink dibiguanide compounds, noted from 1 to 6, present for $\nu_{C\equiv N}$ values of about 2070 cm^{-1} very close to the recorded value in KSeCN ($\nu_{C\equiv N} = 2072$ cm^{-1}). This would indicate that in these complexes, the SeCN group would be ionically bound. With the brown monobiguanide compounds, noted 7—11, values higher than 2120 cm^{-1} were recorded for $\nu_{C\equiv N}$. Inasmuch as $\nu_{C\equiv N}$ shifts usually by coordination towards higher values of the wavenumbers, this behaviour indicates the fact that in this compounds we meet Cu-SeCN bonding. It is known that if the SeCN group is bound by selenium an increase of $\nu_{C\equiv N}$ takes place and a diminution of ν_{C-Se} by comparison to vibration modes proper to the non-coordinated ion. If the coordination takes place by nitrogen then ν_{C-Se} increases and $\nu_{C\equiv N}$ diminishes slightly.

In Cu(RBig) (SeCN)$_2$ both SeCN groups are equivalent, because in the spectrum only a single band corresponding to the $\nu_{C\equiv N}$ vibration mode appears without any splittings.

2. ELECTRONIC SPECTRA

In table 1 are given the values of absorption maxima from the reflectance spectra of the considered compounds and, for dibiguanide complexes, from the absorption spectra of DMF solutions as well. In fig. 1., typical spectra of these compounds are given as examples.

In the reflectance spectra of pink dibiguanide compounds only a maximum observable at values above 19000 cm^{-1} was pointed out. The absorption spectra of the same complexes in DMF present maxima at values close enough to those from the reflectance spectra except for the compound noted with 6, indicating that, by solving, important changes do not occur. These bands are similar to those observed at a series of Cu(II) planar complexes as for example the complexes with aldimine,[12] with the pyrrole derivatives with succinimide [13] with *o*-alkyl-1-amidinourea, [14] and so on.

The reflectance spectra of monobiguanide complexes present two bands, the one with the maximum at about 11 000 cm^{-1} and the other, at about 27 500 cm^{-1}. It should be mentioned that the former is large, flattened, rendering difficult the accurate determination of the values corresponding to the maxima. The band from 27 500 cm^{-1} originates in the electronic transitions proper to coordinated SeCN (in the free ion it appears at 42500 cm^{-1}) as well as in Δ_{xz} transition. A band proper to the ligand (the aryl derivative of biguanide) situated at about 39000cm^{-1}

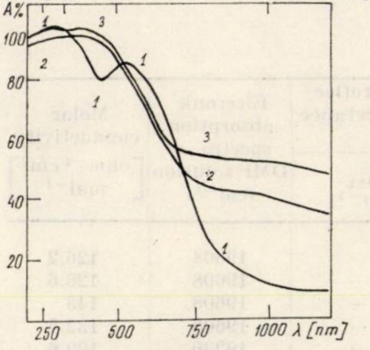

Fig. 1. Reflectance spectra of complexes :
1) [Cu (ClPhBig)$_2$] (SeCN)$_2$
2) CuMe$_2$Big (SeCN)$_2$
3) CuClPhBig(SeCN)$_2$

---

[12] R. E. Clarke and J. H. Weber, *J. Inorg. Nuclear Chem.*, **30**, 1837 (1968).

[13] S. Yamada and S. Miki, *Bull. Chem. Soc. Japan*, **36**, 680 (1963).

[14] J. R. Wasson and C. Trapp, *J. Phys. Chem.*, **73**, 3763 (1969).

appears also in the spectra of the compounds noted with 3–6 and 8–11. The other band proper to the non-coordinated ligands ranging between 41000–43000 cm^{-1} is shifted in far UV due to the conjugated system characteristics of the cycles formed after complexation.

3. EPR SPECTRA ANALYSIS

With dibiguanide complexes, EPR spectra of DMF solutions are recorded. Under these conditions, at room temperature, isotropic spectra which present a hyperfine structure with 4 components corresponding to the interaction of the unpaired electron with the nuclear spins of ^{63}Cu and ^{65}Cu $\left(\text{both equal with } I = \frac{3}{2}\right)$, were obtained (fig. 2).

In this case, a resolving of the splittings from ^{63}Cu and ^{65}Cu was not observed, perhaps due to the line broadening. On the hyperfine components of the spectra located at higher fields, a supplementary superhyperfine structure was observed resulting from the interaction of Cu unpaired electron with the nuclear spins of ligand atoms forming the bond. In fig. 3, the superhyperfine structure recorded on the hyperfine components located at high field of $[Cu(PhBig)_2](SeCN)_2$ are given as an example.

Fig. 2. EPR spectrum of $[Cu(PhBig)_2](SeCN)_2$ solution in DMF recorded at room temperature.

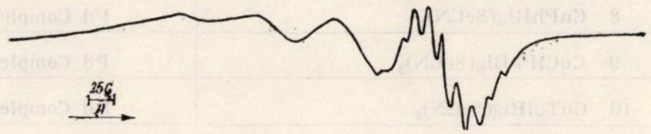

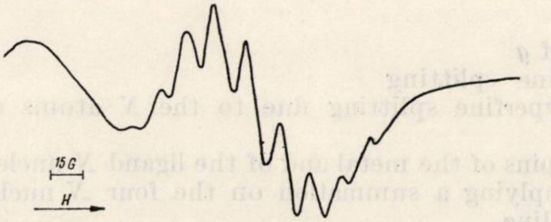

Fig. 3. Superhyperfine structure of $[Cu(PhBig)_2](SeCN)_2$ in DMF at room temperature.

The analysis of the superhyperfine structure pattern in these complexes showed it to present 9 components with a splitting of 14–15 G and the intensities ratio very close to 1 : 4 : 10 : 16 : 19 : 16 : 10 : 4 : 1. This pattern was assigned to the Cu unpaired electron interaction with 4 equivalent N nuclei ($I = 1$). The EPR spectra of these solutions can be well interpreted by means of a spin Hamiltonian of the type :

$$H_{Sp} = g_0 \beta H + A_0 SI + \sum_n A_0^N SI^N \qquad (1)$$

Table

Values and Hyperfine Structure Constants

	Compound	Medium	g_0	a_{0G}
1	$[Cu(Me_2Big)_2](SeCN)_2$	DMF	2.0913	88.0
2	$[Cu(MorBig)_2](SeCN)_2$	DMF Zn Complex	2.0911 2.0957	89.8 86.9
3	$[Cu(PhBig)_2](SeCN)_2$	DMF Zn Complex	2.1033 2.0954	91.6 92.6
4	$[Cu(ClPhBig)_2](SeCN)_2$	DMF Zn Complex	2.0995 2.0974	89.5 91.5
5	$[Cu(TolBig)_2](SeCN)_2$	DMF Zn Complex	2.1009 2.0930	87.2 84.4
6	$[CuPald_2](SeCN)_2$	DMF Zn Complex	2.0998 2.1001	96.9 95.3
7	$CuMe_2Big(SeCN)_2$	Pd Complex	2.1009	92.2
8	$CuPhBig(SeCN)_2$	Pd Complex	2.1015	85.0
9	$CuClPhBig(SeCN)_2$	Pd Complex	2.1011	86.1
10	$CuTolBig(SeCN)_2$	Pd Complex	2.1007	85.6
11	$CuPald(SeCN)_2$	Pd Complex	2.1024	84.1

where

g_0 — isotropic value of g
A_0 — isotropic hyperfine splitting
A_0^N — isotropic superhyperfine splitting due to the N atoms of the ligand.

I and I^N refer to the nuclear spins of the metal and of the ligand N nuclei, respectively, the last term implying a summation on the four N nuclei which participate in the bonding.

From these spectra we could determine the isotropic values of the spectroscopical splitting factors g_0, of the hyperfine structure constant A_0 and of the superhyperfine structure constants A_0^{λ} (table 2).

We recorded also the EPR spectra of DMF solutions of these complexes, frozen at 77 K. These spectra consist of two sets of hyperfine lines corresponding to $g_{||}$ and $g_{\perp}$ tensors (fig. 4).

The hyperfine structure with 4 components corresponding to $g_{||}$ is well resolved but the one corresponding to $g_{\perp}$ is not, the latter overlapping the components of $g_{||}$ located at high field. Moreover, these spectra also present a superhyperfine structure which is observed on the high field components rendering the spectrum analysis difficult in this range.

We recorded also the EPR spectra of these complexes in powders magnetically diluted with $[Zn(RBig)_2](SeCN)_2$ (ratio 1 : 100) at room temperature as well as 77 K. The obtained spectra are similar to those of the frozen DMF solutions (at 77 K).

2

for Copper (II) Complexes

$g_{\parallel}$	$A_{\parallel G}$	$g_{\perp}$	$A_{\perp G}$	$g_{\perp}$ calc.	$A_{\perp}$ calc.	$A^N_{0_G}$
2.1614	203.5	2.0553	32.0	2.0549	30.3	14.4
2.1628	214.4	2.0581	29.4	2.0552	27.5	15.1
2.1721	204	2.0575	28.4			
2.1892	203	2.0605	37.8	2.0603	35.9	14.3
2.1721	202.7	2.0571	37.5			
2.1753	206.9	2.0577	31.5	2.0616	30.8	14.8
2.1746	200.3	2.0589	37.1			
2.1806	208	2.0577	31.0	2.0610	26.8	14.5
2.1658	203.9	2.0566	24.7			
2.1867	206	2.0607	39.4	2.0563	42.3	
2.1791	195.4	2.0607	45.3			
2.1850	207.8	2.05589	35.2			
2.1882	197.5	2.0582	28.7			
2.1858	199.7	2.0588	29.3			
2.1831	195.9	2.0595	30.4			
2.1890	193.8	2.0591	29.2			

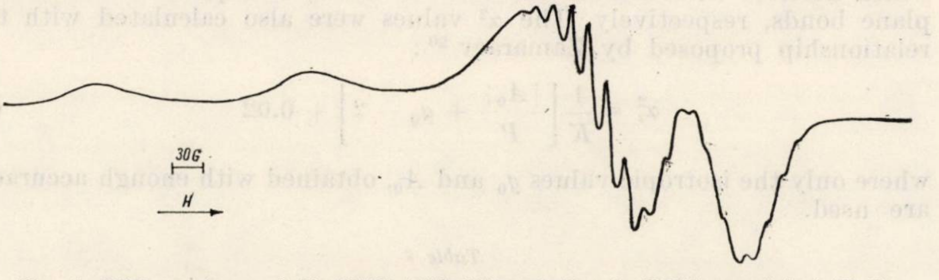

Fig. 4. EPR spectrum of $[Cu(PhBig)_2](SeCN)_2$ solution in DMF recorded at 77 K.

From these spectra we could determine with accuracy $g_{\parallel}$ and $A_{\parallel}$ values which are summarized in table 2. In the same table are given also the $g_{\perp}$ and $A_{\perp}$ values determined with a lower accuracy from the spectra of diluted powders or of DMF frozen solutions, as well as the values of these parameters, obtained by using Kivelson [15] and McConnell's [16] relationships:

---

[15] D. Kivelson, *J. Chem. Phys.*, **33**, 1094 (1960).

[16] H. M. McConnell, *J. Chem. Phys.*, **25**, 709 (1956).

$$3g_0 = g_{\|} + 2g_{\perp} \tag{2}$$

$$3A_0 = A_{\|} + 2A_{\perp} \tag{3}$$

From this table, some differences between the parameter values obtained in DMF solutions and those from the magnetically diluted powders can be observed. They can be assigned to the used solvent effect.

Concerning the monobiguanide complexes, inasmuch as they are not soluble in usual solvents, we recorded the spectra of the powders magnetically diluted with $PbRBig(SeCN)_2$ [17] (ratio 1 : 100). From these spectra, $g_{\|}$, $A_{\|}$, $g_{\perp}$ and $A_{\perp}$ values were determined and then the g_0 and A_0 values were obtained by means of these values using Kivelson and McConnell's relationships (table 2). Inasmuch as $g_{\perp}$ and $A_{\perp}$ cannot be obtained with a great accuracy, due to the overlapping with the hyperfine components corresponding to $g_{\|}$, the g_0 and A_0 values will also be affected by this lack of precision. With these complexes one also observes a superhyperfine structure on the high field components but due to the superpositions, it is difficult to precisely state the ligand nuclei with which the unpaired Cu electron interacts.

In order to calculate the molecular orbital parameters of the dibiguanide complexes on the basis of EPR and electronic spectra characteristics the approximate M.O. theory of Kivelson and Neiman [18] and Gersman and Swallen [19] was used. We preserved the same notations as in our previous works.[1,9,10] Thus, by using the wavefunctions defined in,[8] making the same approximations and considering Δ_{xy} from table 1 as ΔE_{xy} we calculated the values of α^2 coefficients and with these ones the α'^2 and β^2 values for the considered complexes. α, β and δ are coefficients which describe the covalent character of the σ, π in-plane and π out-of-plane bonds, respectively. The α^2 values were also calculated with the relationship proposed by Zamaraev [20]:

$$\alpha_z^2 = \frac{1}{K}\left[\frac{|A_0|}{P} + g_0 - 2\right] + 0.02 \tag{4}$$

where only the isotropic values g_0 and A_0, obtained with enough accuracy, are used.

Table 3

LCAO – MO parameters

Compound	α^2	α'^2	α_z^2	β^2
1 $[Cu(Me_2Big)_2](SeCN)_2$	0.79_6	0.294	0.78_8	0.68_7
2 $[Cu(MorBig)_2](SeCN)_2$	0.82_6	0.260	0.79_8	0.65_4
3 $[Cu(PhBig)_2](SeCN)_2$	0.82_6	0.258	0.84_2	0.74_7
4 $[Cu(ClPhBig)_2](SeCN)_2$	0.82_2	0.256	0.79_8	0.70_2
5 $[Cu(Tol\ Big)_2](SeCN)_2$	0.83_0	0.255	0.80_6	0.70_2
6 $[CuPald_2](SeCN)_2$	0.83_3	0.251	0.86_8	0.70_8

---

[17] P. Spacu, E. Cristureanu and C. Gheorghiu, *Anal. Univ. Buc.*, **18**, 115 (1968).

[18] D. Kivelson and N. R. Neiman, *J. Chem. Phys.*, **35**, 149 (1961).

[19] H. R. Gersman and I. D. Swalen, *J. Chem. Phys.*, **36**, 3221 (1962).

[20] K. I. Zamaraev, *Zhur. strukt. Khim.*, **1**, 33 (1969).

The obtained values for the considered complexes are very near to those calculated with the Kivelson [18] and Gersman [19] relationships, the differences being comprised between 0.01 and 0.03. The obtained results are summarized in table 3.

As regards δ^2 values, we could not calculate them since ΔE_{xz} values from the electronic spectra could not be accurately determined.

With the monobiguanide complexes, we did not calculate these coefficients since, being insoluble, we could not obtain the isotropic EPR spectra which would have indicated us the manner in which the Cu atom is bound with the ligands.

III. DISCUSSION

A number of 11 new Cu(II) selenocyanate complexes belonging to two types : $[Cu(RBig)_2](SeCN)_2$ dibiguanide complexes and $Cu(RBig)(SeCN)_2$ monobiguanide complexes, were synthetized.

The stable, pink-coloured dibiguanide complexes were prepared either by a substitution reaction between the respective chlorocompounds $[Cu(RBig)_2]Cl_2$ and KSeCN, using ethanol as a solvent, either by a direct method, or by using the monobiguanide compound in acetone or DMF medium. In the last method, the following reaction is considered to take place :

$$2\ Cu(RBig)Cl_2 + 2\ KSeCN \rightarrow [Cu(RBig)_2](SeCN)_2 + K_2[CuCl_4]$$

If the development of the reaction by this mechanism was not admitted, a formation of hardly soluble products, $Cu(SeCN)_2$ brown and CuSeCN white, respectively, which would impurify the synthetized compounds should be supposed. The chemical and physicochemical deteminations are arguments attesting the formation of only pink-coloured, hardly soluble dibiguanide selenocyanates; as for the $CuCl_4^{-2}$ ion, it passes into solution (table 1).

The physico-chemical methods used provide valuable information on the Cu valence state and the bonding manner of the SeCN and biguanide groups, in these complexes. Thus, the molar conductance determinations effected on the DMF solutions of these complexes present values in the range of 117–143 $ohm^{-1}\ cm^2\ mol^{-1}$ (table 1) which shows that they are electrolytes of 1:2 type.

Magnetic susceptibility measurements led to values of $\mu_{ef} = 1.6 - - 1.68$ MB showing that these complexes are paramagnetic, copper being divalent (d^9). It results that in the formation reactions of these selenocyanate complexes, in the above mentioned conditions, redox reactions between Cu(II) and $SeCN^-$ did not take place.

IR spectra showed that, with these complexes, the vibration frequency $\nu_{C\equiv N}$ (table 1) does not practically shift towards the corresponding value from KSeCN which pleads for an ionic bonding of selenocyanate group, supporting the conclusions obtained from conductance determinations.

The results obtained from electronic spectra fall into the same category. Thus it was pointed out that the substitution of halogen ions from $[Cu(RBig)_2]X_2$ with $SeCN^-$ does not lead to a sensible shift of the adsorption band located at about 19800 cm^{-1}, band which is encountered in all the pink dibiguanide complexes studied,[1,9,10] suggesting a structure similar to these.

On the basis of the above mentioned facts, these complexes can be formulated $[Cu(RBig)_2](SeCN)_2$.

EPR spectra supplied information concerning the Cu(II) bonding with the biguanide ligand, showing that the bonding is performed by 4 equivalent or almost equivalent N atoms coming from the two biguanide molecules. The calculus of parameters using the EPR spectral data, also showed that with the dibiguanide complexes, the α^2 values ranging between 0.80—0.83 (table 3), σ bondings present a moderate covalency degree. It should also be mentioned that there are no marked differences between these values for compounds with different derivatives of substituted biguanide, values somewhat higher being, however, recorded for the compounds with N^1-*p*-chlorophenyl-N^5-izopropylbiguanide and with tolylbiguanide.

The β constant describes the covalent character of the in-plane π bonds. From table 3 it results that with the dibiguanide compounds, β^2 has values in the range 0.65—0.75 indicating a more accentuated covalent character for the π in-plane bands. This is especially found in the $[Cu(MorBig)_2](SeCN)_2$ and $[Cu(Me_2Big)_2]$ $(SeCN)_2$, the β^2 values of which are sensibly smaller than for the other compounds considered.

Generally, as in the case of other dibiguanide compounds studied,[1,9,10] the β^2 values for these complexes are more differentiated than the α^2 values, which allows us to consider them as being a more sensible indication of the covalent bonding character.

The brown monobiguanide compounds $Cu(RBig)$ $(SeCN)_2$ were prepared by the reaction between the chlorocompounds $Cu(RBig)Cl_2$ and KSeCN, molar ratio 1 : 2, using ethyl alcohol or DMF as solvent. The separation in the solid state of these compounds was made by direct treatment with cold water lightly alkalinized ($pH = 7.5$). The syntheses of all these selenocyanates obtained present a certain degree of difficulty in that they are sensitive to pH-variations below 7, decomposing with red selenium separation.

The monobiguanide selenocyanates present a light brown colour, more intensive than that of the analogous thiocyanates. They are stable in solid state, hardly soluble in water and in other usual solvents. The aryl-radical from the biguanide derivative confers to these compounds a greater stability than the alkyl-radical.

Similar to the dibiguanide compounds, in this case, too, susceptibility measurements showed that these compounds are paramagnetic, the paramagnetism coming from an unpaired electron (d^9) which of course is due to the Cu(II) existing in the complex.

IR spectra of these complexes showed a strong shift of the vibration frequency $\nu_{C\equiv N}$ towards higher values, over 2120 cm^{-1} (table 1). This would indicate, on the one hand, that the selenocyanate group is coordinated at Cu and, on the other hand, it would suggest that coordination would take place through Se, inasmuch as it is known from literature [21-22] that coordination through Se leads to a sensible increase of $\nu_{C\equiv N}$ towards the value of 2072 cm^{-1} from KSeCN.

An attempt was made to determine the corresponding ν_{C-Se}, ν_{Cu-Se}, and δ_{SeCN} from the spectra which would provide supplementary information on the manner in which the selenocyanate group is bonding, but the overlapping with the biguanide ligand bands did not allow their determination.

Important shifts are also recorded in the band positions of the electronic spectra. Thus, with these complexes we do not observe the band from 19000 cm^{-1} as we signalled out for the corresponding pink complexes, but a large band with a maximum at about 11000 cm^{-1} and another at 27500 cm^{-1} were observed.

If we consider that in monobiguanide compounds of the type $Cu(RBig)X_2$, where $X = NO_3$, NCS, NCO, N_3 previously studied [1,9,10] (in which the coordination was supposed to occur through N), absorption bands at values about 15000—17000 cm^{-1} were recorded, the lower value recorded in the case of Cu(RBig) $(SeCN)_2$ would suggest a coordination through Se, this fact being due to the strong, distorting character of the SeCN group, leading to a planar structure.

The EPR spectral parameters of these compounds are different from those corresponding to the dibiguanide complexes. Thus, isotropic g_0 factors have greater values while the A_0 values are somewhat smaller than those recorded in the pink compounds. Similarly, higher $g_{||}$ values and lower $A_\perp$ values were recorded for the brown compounds. The $g_\perp$ and $A_\perp$ values which do not differ sensibly proved to be less sensitve to the transition from one category of complexes to the other.

Unfortunately, the EPR spectra of these compounds could not supply additional information as these compounds were not soluble in usual solvents so that it was not possible to obtain the isotropic spectra from which we could have observed how the selenocyanate group is coordinated. From anisotropic spectra obtained on magnetic dilution with Pd(RBig) $SeCN)_2$ it is difficult to state if the coordination takes place through N or through Se because the superhyperfine structure corresponding to $g_\perp$, which is obserwed, results from the overlapping of a relatively great number of lines and, in addition, there is an overlapping with the lines from the hyperfine structure corresponding to $g_{||}$ as well. Due also to the fact that the monobiguanide compounds are not soluble, the molar conductivity and the molecular mass could not be determined.

Nevertheless, on the basis of the synthesis of the data of chemical analysis as well as from those obtained by I.R., electronic and EPR spectra these compounds can be formulated as Cu(RBig) $(SeCN)_2$ the biguanide ligand being coordinated by 2 nitrogen atoms and the selenocyanate group being, presumably linked with copper by selenium.

---

[21] H. W. Morgan, *J. Inorg. Nuclear Chem.*, **16**, 367 (1961).

[22] C. Pecile, *Inorg. Chem.*, **5**, 210 (1966).

would take place through Se, inasmuch as it is known from literature [21–22] that coordination through Se leads to a sensible increase of ν_{CN} towards the value of 2072 cm^{-1} from KSeCN.

An attempt was made to determine the corresponding ν_{C-Se}, ν_{Cu-Se}, and δ_{SeCN} from the spectra which would provide supplementary information on the manner in which the selenocyanate group is bonding, but the overlapping with the biguanide ligand bands did not allow their determination.

Important shifts are also recorded in the band positions of the electronic spectra. Thus, with these complexes we do not observe the band from 19000 cm^{-1} as we signalled out for the corresponding pink complexes, but a large band with a maximum at about 11000 cm^{-1} and another at 27500 cm^{-1} were observed.

If we consider that in monobiguanide compounds of the type Cu(RBig)X_2, where X = NO_3, NCS, NCO, N_3 previously studied [14–16] (in which the coordination was supposed to occur through N), absorption bands at values about 15000–17000 cm^{-1} were recorded, the lower value recorded in the case of Cu(RBig) $(SeCN)_2$ would suggest a coordination through Se, this fact being due to the strong, distorting character of the SeCN group, leading to a planar structure.

The EPR spectral parameters of these compounds are different from those corresponding to the dibiguanide complexes. Thus, isotropic g_0 factors have greater values while the A_0 values are somewhat smaller than those recorded in the pink compounds. Similarly, higher $g_\parallel$ values and lower $A_\parallel$ values were recorded for the brown compounds. The $g_\perp$ and $A_\perp$ values which do not differ sensibly proved to be less sensitive to the transition from one category of complexes to the other.

Unfortunately, the EPR spectra of these compounds could not supply additional information as these compounds were not soluble in usual solvents so that it was not possible to obtain the isotropic spectra from which we could have observed how the selenocyanate group is coordinated. From anisotropic spectra obtained on magnetic dilution with Pd(RBig) $(SeCN)_2$ it is difficult to state if the coordination takes place through N or through Se because the superhyperfine structure corresponding to $g_\perp$, which is observed, results from the overlapping of a relatively great number of lines and, in addition, there is an overlapping with the lines from the hyperfine structure corresponding to $g_\parallel$ as well. Due also to the fact that the monobiguanide compounds are not soluble, the molar conductivity and the molecular mass could not be determined.

Nevertheless, on the basis of the synthesis of the data of chemical analysis as well as from those obtained by I.R., electronic and EPR spectra these compounds can be formulated as Cu(RBig) $(SeCN)_2$ the biguanide ligand being coordinated by 2 nitrogen atoms and the selenocyanate group being presumably linked with copper by selenium.

---

[21] H. W. Morgan, J. Inorg. Nuclear Chem., 16, 367 (1961).

[22] C. Pecile, Inorg. Chem., 5, 210 (1966).

Revue Roumaine de Chimie, **19**, *12*, 1921–1926 (1974)

Hommage à
Raluca Ripan
pour son 80e anniversaire

SUR LES COMPOSÉS DU TRICHLORURE DE L'ÉTHOXYTITANE AVEC DES BASES SCHIFF

D. NEGOIU, ANGELA KRIZA et MARTHA NASTA
Université de Bucarest, Faculté de Chimie, chaire de Chimie inorganique, 89, Splaiul Independenței

Reçu le 9 mars 1974

On a obtenu et étudié cinq nouveaux composés du titane (IV) avec des bases Schiff aromatiques, à partir du trichlorure d'éthoxytitane. La structure des composés obtenus a été établie à l'aide des spectres IR et électroniques.

INTRODUCTION

Les recherches actuelles sur la chimie du titane sont dirigées vers les composés de ce métal avec des ligands dont la molécule comprend des atomes d'oxygène et d'azote. Parmi ceux-ci les salicylaldimines occupent une place importante. Lorsque les bases Schiff contiennent le groupement hydroxyle dans une position proche à la condensation, par réaction avec des ions métalliques elles peuvent former des cycles chélates, à nombre variable de membres.

Le nombre des composés du titane avec des salicylaldimines est très petit par rapport à d'autres métaux transitionnels. Ceci n'est pas surprenant si l'on tient compte des conditions extrêmement difficiles que réclament la synthèse et, d'autant plus, l'étude de tels composés du titane.

Les premiers composés du titane (IV) avec des salicylaldimines ont été obtenus en 1960.[1]

En 1967, pendant des recherches entreprises au Laboratoire de Chimie inorganique à la Faculté de Chimie de Bucarest on a abordé le problème de la synthèse des complexes du titane avec des bases Schiff dérivées du salicyl- et benzaldéhyde et des amines aliphatiques et aromatiques.

Pendant ces recherches on a remarqué que les bases Schiff dérivées d'orto-oxyaldéhydes peuvent former avec le tétrachlorure de titane, en certaines conditions, des complexes moléculaires du type $TiCl_4(SB)_2$.[2] Des complexes internes, du type « chélate », n'ont pas été obtenus par réaction directe du tétrachlorure de titane avec les bases Schiff mais seulement via alcoxydes de titane. Les composés obtenus de cette manière ont les formules suivantes : $Ti(OR)_2SB$ et $Ti(SB)_2$.[3,4]

---

[1] Chijuan-Ya, Ui, I. A. Savichi, A. V. Lapitzkii, V. P. Samorukov et L. G. Titov, *Vestnik. Mosk. Univ.*, **3**, 40 (1960).

[2] D. Negoiu et A. Kriza, *Anal. Univ. Buc.*, **20**, 39 (1971).

Nous précisons qu'en 1969, Bradley et ses collaborateurs[5] ont obtenu et étudié quelques chélates du titane (IV) : $Ti(SB)_4$, composés obtenus à partir du tétra(diméthylamino)titane: $Ti(NMe_2)_4$. Mais les substances nécessaires à la synthèse, c'est-à-dire le tétra(diméthylamino)titane, tout comme les alcoxydes du titane, ont été obtenues en conditions très difficiles.

Pendant nos recherches nous avons essayé d'obtenir des complexes du type $TiCl_2(SB)_2$. Nous n'avons pas réussi d'obtenir de tels composés unitaires par réaction directe du tétrachlorure de titane et des azométhynes dérivées d'amines aromatiques et aliphatiques, moins volumineuses.

Conformément à des remarques ultérieures, à savoir que les atomes de chlore tout comme les groupements alcoxydes chloroalcoxydes du titane peuvent être remplacés par réaction avec des ligands bidentés, nous avons essayé à obtenir de cette manière des chélates du titane avec des salicylaldimines.

C'est ainsi que, par réaction du trichlorure de l'éthoxytitane avec des salicylaldimines aromatiques, nous avons obtenu cinq nouveaux composés (tabl. 1).

Tableau 1

Composés du titane (IV) avec des bases Schiff

Composé	Couleur	Ti%		Cl%		N%	
		calc.	exp.	calc.	exp.	calc.	exp.
$TiCl_2(SA)_2$	rouge	9,33	9,45	13,83	13,88	5,46	5,40
$TiCl_2(SPT)_2$	brun	8,89	8,70	13,16	13,70	5,19	5,07
$TiCl_2(SOT)_2$	brun	8,89	8,68	13,16	13,81	5,19	5,17
$TiCl_2(SPA)_2$	rouge	8,38	8,02	12,41	13,20	4,90	4,94
$TiCl_2(SOA)_2$	brun	8,38	8,06	12,41	12,81	4,90	5,00

(SA) = salicylal-aniline ; SPT = salicylal-*p*-toluidine ; SOT = salicylal-*o*-toluidine ; SPA = salicylal-*p*-anisidine ; SOA = salicylal-*o*-anisidine.

RÉSULTATS ET DISCUSSIONS

Par réaction par rapport molaire 1 : 2 on remplace le groupement alcoxy ainsi qu'un atome de chlore du chlorure d'éthoxytitane par deux molécules de base Schiff. La structure de ligand bidenté des bases Schiff indique la possibilité de la formation d'une liaison Ti-O. Pour vérifier cette hypothèse on a étudié les déplacements des fréquences caractéristiques des groupements azométhyne et phénoxy dans les spectres IR des composés par rapport aux spectres IR des ligands. Dans le tableau 2 on remarque les maxima d'absorption du spectre IR, déterminé dans les domaines 1100 et 1700 cm^{-1} et 2800 et 3600 cm^{-1}, pour les composés et les salicylaldimines correspondantes.

---

[3] D. Negoiu et A. Kriza, *Anal. Univ. Buc.*, **18**, 113 (1969).

[4] D. Negoiu et A. Kriza, *Anal. Univ. Buc.*, **19**, 31 (1970).

[5] D. C. Bradley, M. B. Hurthouse et J. F. Rendall, *Chem. Comm.*, **12**, 672 (1969).

Si des chélates s'étaient formés, on aurait dû remarquer un déplacement de la fréquence de vibration $\nu_{C=N}$ vers des valeurs plus petites et, à la fois, un déplacement de la bande caractéristique du groupement phénoxy vers des fréquences plus élevées.

Tableau 2

Spectres IR des composés $TiCl_2(SB)_2$

Composé	ν_{Ph-O} (cm^{-1})		$\nu_{C=N}$ (cm^{-1})	
	ligand	composé	ligand	composé
$TiCl_2(SA)_2$	1278	1285	1625	1645
$TiCl_2(SPT)_2$	1280	1290	1625	1645
$TiCl_2(SOT)_2$	1280	1290	1630	1645
$TiCl_2(SPA)_2$	1278	1290	1630	1647
$TiCl_2(SOA)_2$	1280	1287	1625	1647

Parmi les données du tableau 2 on remarque vraiment une augmentation de la fréquence du groupement phénoxy. Cette remarque tout comme l'absence de la fréquence caractéristique du groupement hydroxyle chélaté par liaisons hydrogène dans les spectres des composés par rapport aux spectres des ligands atteste la présence des liaisons Ti—O.

On remarque aussi une augmentation du $\nu_{C=N}$ ce qui ne concorde pas avec la formation d'un cycle quasi aromatique comprenant l'atome de titane ainsi qu'il est représenté par la formule :

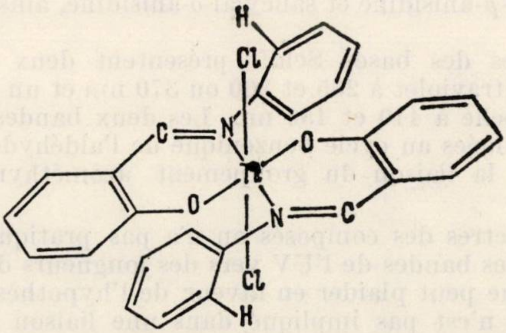

La liaison hydrogène qui apparaît entre l'hydrogène de l'hydroxyle et l'azote de l'azométhyne ferme un cycle conjugué de six membres. Dans ce type de systèmes conjugués l'énergie de la liaison hydrogène est due 90% à la conjugaison $\pi - \pi$. La contribution des électrons *p* de l'azote à la formation de la liaison hydrogène est assez insignifiante. Par formation des composés, la liaison hydrogène est détruite. La libération du groupement azométhyne de cette conjugaison mène à l'augmentation de la fréquence de ce groupement dans le spectre IR des composés.

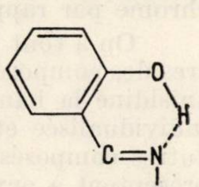

La remarque que $\nu_{C=N}$ n'est pas déplacée vers de valeurs plus petites nous permet donc de supposer que le cycle comprenant l'atome de titane ne se ferme pas, à cause des empêchements stériques, et la liaison donneur-accepteur ne se forme pas.

Les composés obtenus pourraient être formulés de cette manière :

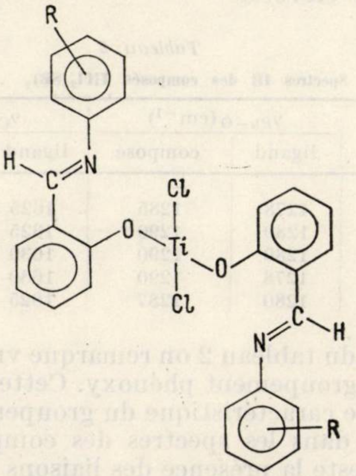

On a déterminé aussi les spectres électroniques des salicylaldimines et des composés dans le domaine 250—600 nm. La figure 1 représente les spectres électroniques des composés obtenus à partir de : salicylal-*p*-toluidine, salicylal-*p*-anisidine et salicylal-*o*-anisidine, ainsi que les spectres de ces ligands.

Les spectres des bases Schiff présentent deux bandes intenses dans le domaine ultraviolet à 265 et 360 ou 370 nm et un point d'inflexion dans le visible proche à 440 et 450 nm. Les deux bandes de l'ultraviolet peuvent être attribuées au cycle benzénique de l'aldéhyde aromatique et, respectivement, à la liaison du groupement azométhyne conjuguée au cycle benzénique.

Dans les spectres des composés on n'a pas pratiquement remarqué de déplacements des bandes de l'UV vers des longueurs d'onde plus grandes. Cette remarque peut plaider en faveur de l'hypothèse que le groupement azométhyne n'est pas impliqué dans une liaison avec l'atome de titane (l'apparition d'une liaison donneur-accepteur par l'intermédiaire du doublet électronique libre de l'azote aurait déterminé un effet bathochrome par rapport aux bandes de 360 ou 370 nm).

On a tout de même remarqué que dans le domaine visible des spectres des composés obtenus à partir de la salicylal-*p*-toluidine et salicylal-*p*-anisidine la bande de 440 ou 450 nm est déplacée à 460 nm, très bien individualisée et un peu élargie. Dans le même domaine du spectre, les autres composés et surtout celui obtenu à partir de la salicylal-*o*-anisidine présentent à environ 520 nm une bande moins précisée. On ne peut pas faire de précisions sur les déplacements des bandes dues, probablement, à des transitions internes des ligands. La littérature ne présente pas de spectres électroniques des composés analogues à ceux préparés par nous ; on ne peut donc faire aucune corrélation. Quand même on ne peut pas totalement exclure une transition de transfert de charge.

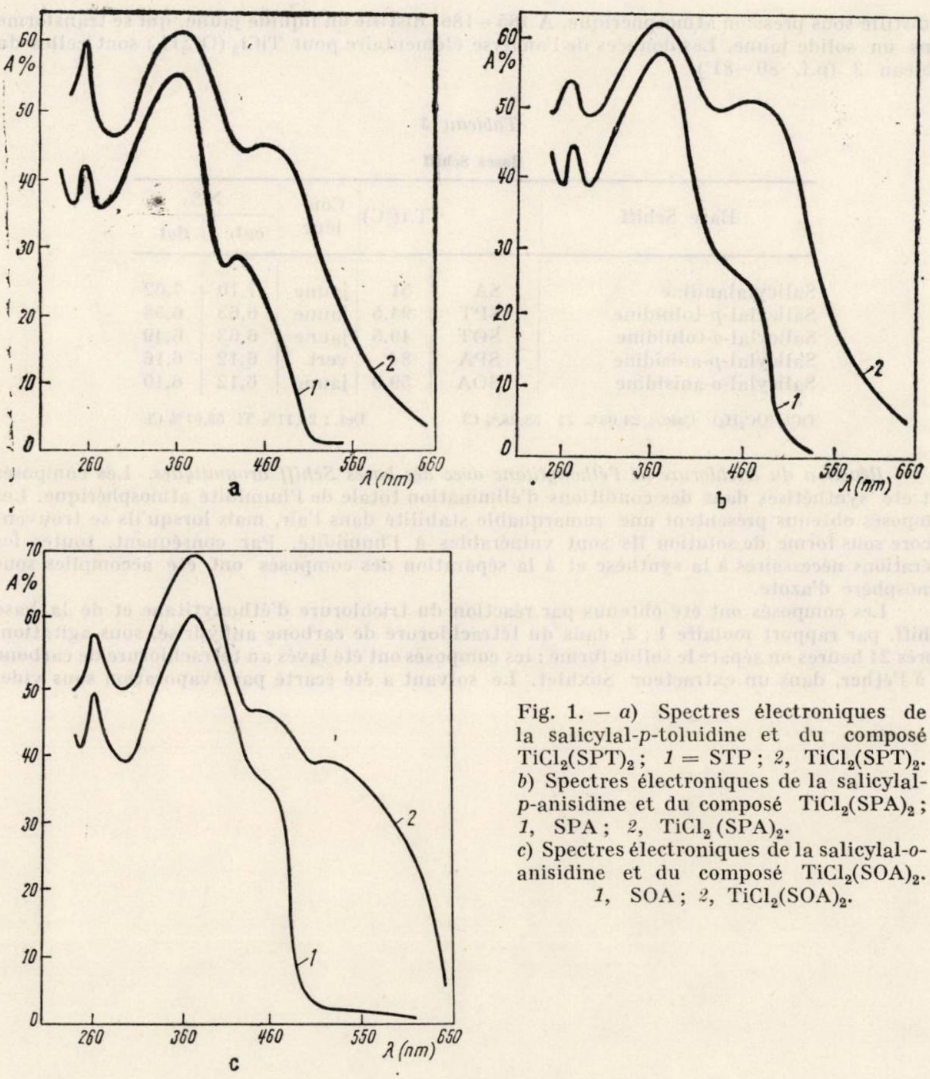

Fig. 1. — *a*) Spectres électroniques de la salicylal-*p*-toluidine et du composé $TiCl_2(SPT)_2$; *1* = STP ; *2*, $TiCl_2(SPT)_2$. *b*) Spectres électroniques de la salicylal-*p*-anisidine et du composé $TiCl_2(SPA)_2$; *1*, SPA ; *2*, $TiCl_2(SPA)_2$. *c*) Spectres électroniques de la salicylal-*o*-anisidine et du composé $TiCl_2(SOA)_2$. *1*, SOA ; *2*, $TiCl_2(SOA)_2$.

PARTIE EXPÉRIMENTALE

Bases Schiff. Les salicylaldimines ont été obtenues par des méthodes indiquées dans la littérature, par réaction directe du salicylaldéhyde et de l'amine aromatique (rapport molaire 1 : 1) dans de l'acool éthylique anhydrisé. Après l'ébullition on sépare les bases Schiff du tableau 3. Toutes les bases Schiff ont été purifiées par cristallisation.

Le trichlorure d'éthoxytitane a été obtenu dans une installation pourvue de tous les accessoires nécessaires aux synthèses dans l'atmosphère inerte. On ajoute de l'alcool éthylique dissous dans du chloroforme à un excès de tétrachlorure de titane, dans du chloroforme anhydrisé, sous agitation et à 0°. On porte à l'ébullition pendant huit heures, jusqu'au complet écartement de l'acide chlorhydrique. Après 24 heures, le composé solide formé a été séparé et distillé sous pression atmosphérique. A 185—186° distille un liquide jaune, qui se transforme dans un solide jaune. Les données de l'analyse élémentaire pour $TiCl_3(OC_2H_5)$ sont celles du tableau 3 (p.f. 80—81°).

Tableau 3

Bases Schiff

Base Schiff		T.t(°C)	Couleur	N%	
				calc.	det.
Salicylalaniline	SA	51	jaune	7,10	7,02
Salicylal-*p*-toluidine	SPT	94,5	jaune	6,63	6,58
Salicylal-*o*-toluidine	SOT	49,5	jaune	6,63	6,49
Salicylal-*p*-anisidine	SPA	84	vert	6,12	6,16
Salicylal-*o*-anisidine	SOA	59,5	jaune	6,12	6,10

$TiCl_3(OC_2H_5)$ Calc. : 24,03% Ti 53,25% Cl Det. : 24,11% Ti 53,97% Cl.

Réaction du trichlorure de l'éthoxytitane avec des bases Schiff aromatiques. Les composés ont été synthétisés dans des conditions d'élimination totale de l'humidité atmosphérique. Les composés obtenus présentent une remarquable stabilité dans l'air, mais lorsqu'ils se trouvent encore sous forme de solution ils sont vulnérables à l'humidité. Par conséquent, toutes les opérations nécessaires à la synthèse et à la séparation des composés ont été accomplies sous atmosphère d'azote.

Les composés ont été obtenus par réaction du trichlorure d'éthoxytitane et de la base Schiff, par rapport molaire 1 : 2, dans du tétrachlorure de carbone anhydrisé, sous agitation. Après 24 heures on sépare le solide formé : les composés ont été lavés au tétrachlorure de carbone et à l'éther, dans un extracteur Soxhlet. Le solvant a été écarté par évaporation sous vide.

Revue Roumaine de Chimie, 19, 12, 1927–1940 (1974)

Dedicated to
RALUCA RIPAN
on the occasion of her 80th anniversary

CHEMICAL GRAPHS. XXIV.[1]

ISOMERIZATIONS AND ISOGRAPHIC TRANSFORMATIONS

A. BARABÁS * and A. T. BALABAN**
* Institute of Chemistry, Str. Donath 65, Cluj-Napoca, Romania
** Chair of Organic Chemistry, The Polytechnic Institute, Bucharest, Romania

Received November 13, 1974

Isographs and isographic transformations are defined as graph-theoretical correspondents to topological (constitutional) isomers, and to topological isomerizations, respectively. In graph theoretical language, isographs are labelled graphs with the same partition of their vertex degrees. The nonvariant graph of a family of isographs is defined as the common spanning subgraph of the constitutional graphs of two (or more) topological isomers. Topological isomerizations can be rigorously and conveniently classified by relating them to the connectivity of the nonvariant graph.

INTRODUCTION

In a previous paper,[2] the definition of rearrangements and isomerizations was discussed. The present paper is concerned with isomerizations. Isomerization processes are usually classified as shown in table 1. In degenerate processes (automerizations or topomerizations), enantiomerizations and diastereomerizations, the constitutional formula, or constitutional graph, remains unchanged. Therefore topological (constitutional) isomerizations, or for short isomerizations, are those chemical processes which conserve the molecular formula of the reagent but modify its constitutional formula, which indicates the connectivities between atoms.

Table 1

Classification of various types of isomerizations by noting modified or conserved properties (conformational changes involving rotations around single bonds are ignored)

Name of the molecular transformation	Constitutional formula	Stereochemical formula	
	Topology of atoms	Distances between non-bonded atoms	Tridimensional orientation of atoms
Automerization[2, 3] (topomerization[4])	Conserved	Conserved	Conserved
Enantiomerization	Conserved	Conserved	Modified
Diastereomerization	Conserved	Modified	Modified
Constitutional (topological) isomerization	Modified	Modified	Modified

---

[1] Part XXIII, A. T. BALABAN, *Rev. Roumaine Chim.*, **19**, 1611 (1974).

[2] A. T. BALABAN and D. FĂRCAȘIU, in ,,*Proceedings of the Second International Meeting on Preparing and Storing Labelled Compounds*'', Euratom, Brussels, 1968, p. 611.

The authors' impression that there is, as yet, no systematic classification of isomerizations, and that the graph theory may be useful as a basis for such a classification, is expressed in the present paper.

ISOGRAPHS

For an adequate graph-theoretical treatment of topological isomerizations the concept of *isographs* has to be introduced. In the following, we shall deal with general graphs (where loops and multiple bonds are allowed) which need not be connected. Isolated points, i.e. with degree equal to zero, shall not be discussed.

A family of isographs is defined as a set of p labelled points, the degree of each point remaining the same in all the graphs of the family; this means that the number q of lines connecting these points is the same for all the members of the family. Consequently, all members of a family of isographs have the same partition of their vertex degrees. Thus, as seen in figure 1, there exist three isographs with three points and partition $2q = 3 + 2 + 1$. Owing to labelling, a family of isographs is usually more numerous than the family of non-labelled graphs with the same partition. In non-labelled graphs, no distinction is made between points of the same degree: the permutation of two such points will always result in an isomorphic graph. In labelled graphs, however, only permutations between two equivalent points will result in an isomorphic graph. Equivalence of two points in a labelled graph means that they (i) have the same degree and (ii) are either isolated (possibly having loops) or are connected only to one and the same point, and/or to each other, by single or multiple bonds. In a labelled graph, any permutation between two non-equivalent points of the same degree will result in a non-isomorphic graph from the same family of isographs. Let us take as example the isographs with four points and partition $2q = 3 + 1 + 1 + 1$.

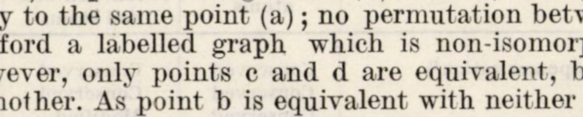

In graph I, all points of degree one (b, c and d) are equivalent, being connected only to the same point (a); no permutation between points b, c and d can afford a labelled graph which is non-isomorphic with I. In graph II, however, only points c and d are equivalent, being connected only to one another. As point b is equivalent with neither c, nor d, it will afford graphs III and IV, non-isomorphic with II, on permutation with c

---

[3] A. T. Balaban and D. Fărcaşiu, *J. Amer. Chem. Soc.*, **89**, 1958 (1967).

[4] G. Binsch, E. L. Eliel and H. Kessler, *Angew. Chem.*, **83**, 618 (1971); *Angew. Chem. Internat. Edit.*, **10**, 570 (1971).

q	p	Partition of 2q	Multigraphs[b]	General graphs[c]
1	2	1+1	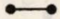	
2	2	3+1		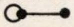
		2+2	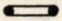	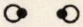
	3	2+1+1	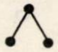	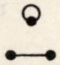
	4	1+1+1+1	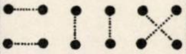	
3	2	5+1		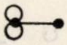
		4+2		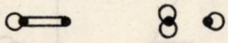
		3+3	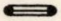	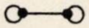
	3	2+2+2	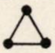	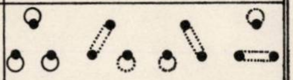
		3+2+1	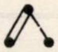	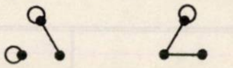
		4+1+1		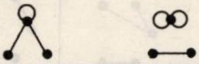
	4	3+1+1+1	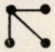	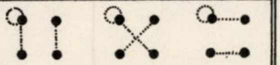
		2+2+1+1	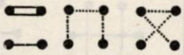	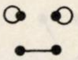

Fig. 1. — The simplest families of possible isographs resulted from permutation of $q = 1$, 2 or 3 lines between $p=2$, 3 or 4 points.[a]

[a] Graphs which would be isomorphic in the absence of labelling are indicated by dotted lines.

[b] Multigraphs are defined as connected or disconnected graphs with single or multiple bonds, but without loops.

[c] General graphs are defined as under *b* but with loops allowed.

and d, respectively. All graphs I — IV are of course isographs from the same family, but II, III and IV would be isomorphic in the absence of labelling.

A family of isographs, thus, consists of all non-isomorphic labelled graphs having the same partition, with the degree of each vertex (point) being constant. As examples, some of the simplest families of isographs are enumerated in figures 1 — 4.

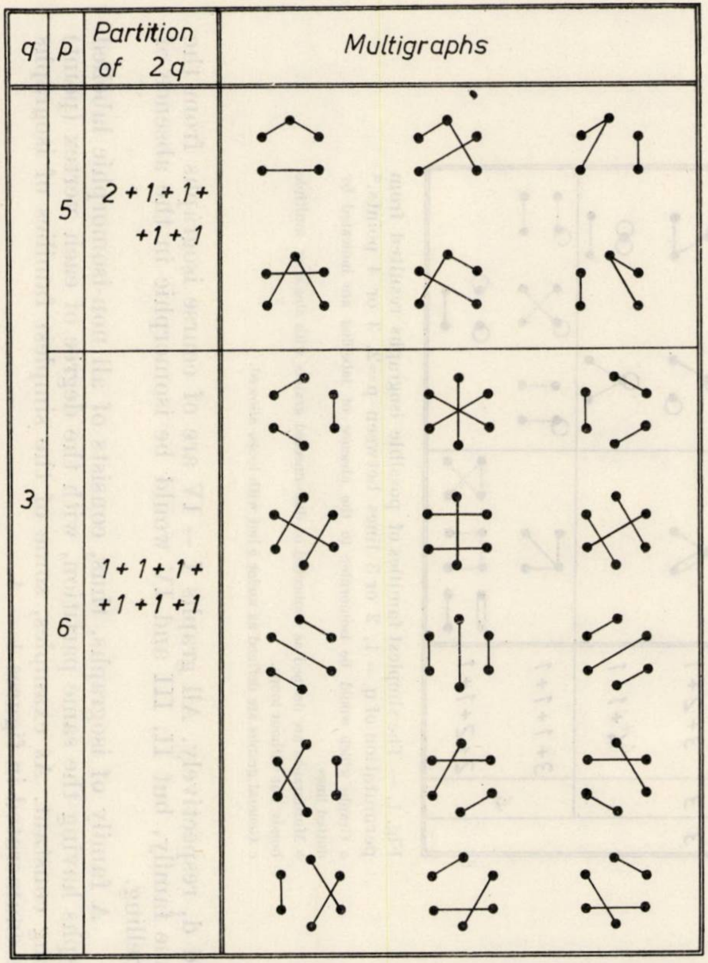
q
p
Partition of 2q
Multigraphs
3
5
2 + 1 + 1 + +1 + 1
6
1 + 1 + 1 + +1 + 1 + 1

Fig. 2. – Continuation of fig. 1 for q = 3 and p = 5 or 6, omitting general graphs.

a All graphs with the same partition in this table would be isomorphic in the absence of labelling.

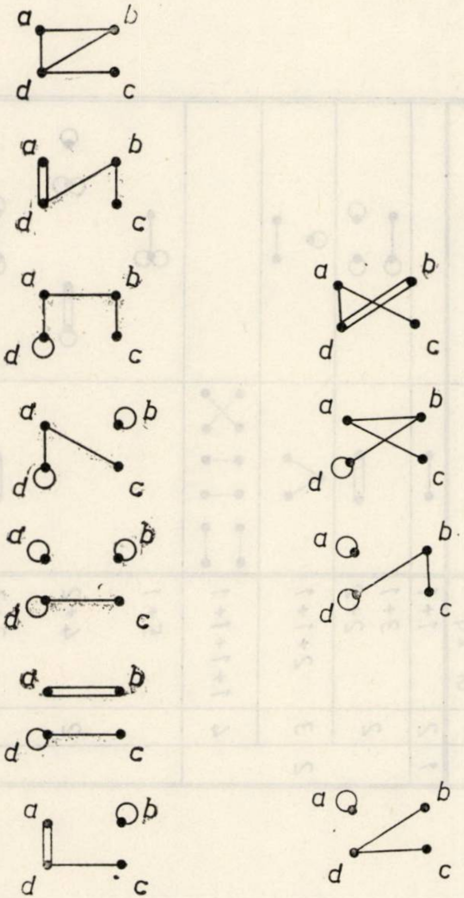

Fig. 3. – All isographs with the partition 2q = 3 + 2 + 2 + 1. Graphs which would be isomorphic without labelling are placed on the same line.

The enumeration of all n members of a family of isographs is interesting for finding out all topological isomers with the same molecular formula: these isomers correspond to the connected isographs of the given family. The labelled points correspond to atoms; points with the same degree may have the same, or different, chemical or isotopic [5] identities.

Such enumerations remain the main application of graph theory in chemistry. An appreciable amount of work has been done in this field,[6–10]

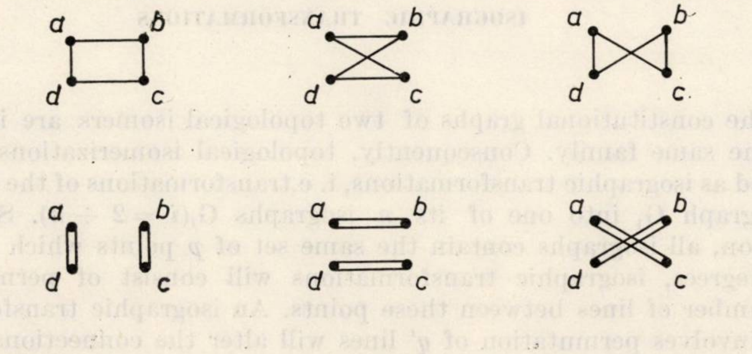

Fig. 4. — All isographs with the partition 2q = 2 + 2 + 2 + 2. Graphs which would be isomorphic without labelling are placed on the same line.

---

[5] A. T. BALABAN, D. FĂRCAŞIU and F. HARARY, *J. Labelled Comp.*, **6**, 211 (1970).

[6] A. CAYLEY, *Philos. Mag.*, **67**, 444 (1874); *Ber. dtsch. chem. Ges.*, **8**, 1056 (1875); *Amer. J. Math.*, **4**, 266 (1875).

[7] H. R. HENZE and C. M. BLAIR, *J. Amer. Chem. Soc.*, **53**, 3042, 3077 (1931); **55**, 680 (1933); **56**, 157 (1934).

[8] A. T. BALABAN, *Rev. Roumaine Chim.*, **18**, 635 (1973) and further references therein.

[9] A. T. BALABAN (ed.), *"Chemical Applications of Graph Theory"*, Academic Press, London, 1975.

[10] G. SCHROLL, A. M. DUFFIELD, C. DJERASSI, B. G. BUCHANAN, G. L. SUTHERLAND and J. LEDERBERG, *J. Amer. Chem. Soc.*, **91**, 7440 (1969) and further papers in the series.

starting with Cayley's algorithm for the number of alkanes. In this paper, however, the concept of isographs will be used for a different purpose: classification of topological isomerizations on the basis of changes in the constitutional formula (graph) during that process.

ISOGRAPHIC TRANSFORMATIONS

The constitutional graphs of two topological isomers are isographs from the same family. Consequently, topological isomerizations may be regarded as isographic transformations, i. e.transformations of the constitutional graph G_1 into one of its n isographs $G_i(i = 2 \div n)$. Since, by definition, all isographs contain the same set of p points which conserve their degrees, isographic transformations will consist of permutations of a number of lines between these points. An isographic transformation which involves permutation of q' lines will alter the connections of only those p' points which were connected by the above q' lines in the original graph ($p \geqslant p' \leqslant 2q'$). The highest possible number of topological isomers obtainable from the molecule corresponding to G_1 by modifying only the connections of the p' atoms symbolized by the above subset of p' points will be equal to the number of possible isographs in the family g_i (subgraphs of G_i) consisting of the p' points and q' lines involved in the transformation.

Let us discuss the simplest examples, which are the only ones interesting for the chemist, consisting of the loop-free graphs from figures 1 and 2. Isographic transformations involving less than four lines are thus possible only in those cases from figures 1 and 2 which contain more than one multigraph for a given partition, namely $q = 2$, $p = 4$; $q = 3$, $p = 4$, 5 or 6. Commonly encountered isomerizations have $p = 2q$, and such cases can be described by the following two rules:

a) Permuting q lines between $p = 2q$ points, n isographs are formed, where $n = (p-1)\ (p-3)\ (p-5) \ldots 5.3.1$.

b) Between the n isographs described above, w isographic transformations implying permutation of 2, 3, ..., q lines are possible, w being the number of pairwise combinations of the n isographs. This second rule will apply, of course, also for cases where $p < 2q$.

Detection of the p points and q lines taking part in the isographic transformation which describes a given topological isomerization may be useful in two respects:

(i) The enumeration of all possible n isomeric products and w isomerization processes will set the chemical problem in clearer terms.

(ii) Parameters q and p are closely related to the mechanism of the soimerization process under investigation. According to the Woodward —

Hoffmann rules,[11] an isomerization characterized by $q = 2$, $p = 4$, will have a four-centre mechanism, generally allowed photochemically. On the other hand, an isomerization corresponding to an isographic transformation with $q = 3$, $p = 6$, will have a thermally allowed six-centre mechanism with an aromatic transition state.[12,13]

The usefulness of the graph-theoretical approach to topological isomerizations may be illustrated by the following example:[14] cycloöctatetraene (V) was observed to undergo valence isomerization photochemically [15] as well as thermally,[16] yielding in both cases bicyclo[4.2.0]octa-2,4,7-triene (VI). This is possible, without contradicting the Woodward — Hoffmann rules, if different atoms and bonds are involved in the two processes:

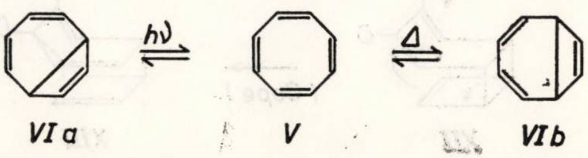

Only two bonds ($q = 2$) and four atoms ($p = 4$) are involved in the photochemical isomerization, whereas three bonds and six atoms ($q = 3$, $p = 6$) take part in the thermal isomerization. The two processes afford the same product only due to molecular symmetry.

Other similar cases of photochemical *versus* thermal valence isomerizations may be imagined, where the products of the two processes may (VI) or may not (VIII, X) be identical.

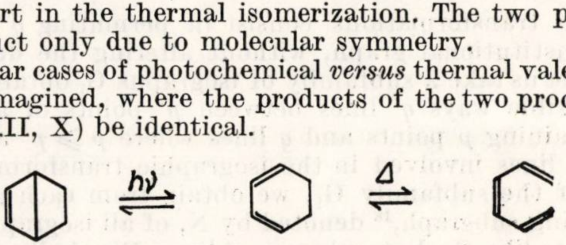

The formation of Nenitzescu's hydrocarbon (XIII) thermally from basketene (XI), which apparently could proceed by a retro 2 + 2 cycloreversion in disagreement with the Woodward – Hoffmann rules was shown by deuterium labelling to involve only thermally allowed steps, namely a retro-Diels-Alder reaction followed by a Cope rearrangement.[17]

---

[11] R. B. Woodward and R. Hoffmann, "*The Conservation of Orbital Symmetry*", Academic Press — Verlag Chemie, New York, 1969; P. Wieland and H. Kaufmann, "*Die Woodward-Hoffmann-Regeln. Einführung und Handhabung*", Birkhäuser Verlag, Basel, 1972; N. T. Anh, „*Les règles de Woodward-Hoffmann*", Ediscience, Paris, 1970.

[12] A. T. Balaban, *Rev. Roumaine Chim.*, **12**, 875 (1967), reprinted in „*Recherches sur la philosophie des sciences*", Ed. Academiei, Bucharest, 1969, p. 207.

[13] M. J. S. Dewar, *Angew. Chem.*, **83**, 859 (1971); *Angew. Chem. Internat. Edit.*, **10**, 761 (1971);

J. B. Hendrickson, *Angew. Chem.*, **86**, 71 (1974); *Angew. Chem. Internat. Edit.*, **13**, 47 (1974);

J. Mathieu and A. Rassat, *Tetrahedron*, **30**, 1753 (1974).

[14] F. Badea, „*Organic Reaction Mechanisms*", Editura Ştiinţifică — Abacus Kent, Bucharest — London, 1975, chapter 12.

[15] G. J. Fonken, *Chem. and Ind.*, **1963**, 1625.

[16] R. Huisgen and M. Mietzsch, *Angew. Chem.*, **76**, 36 (1964).

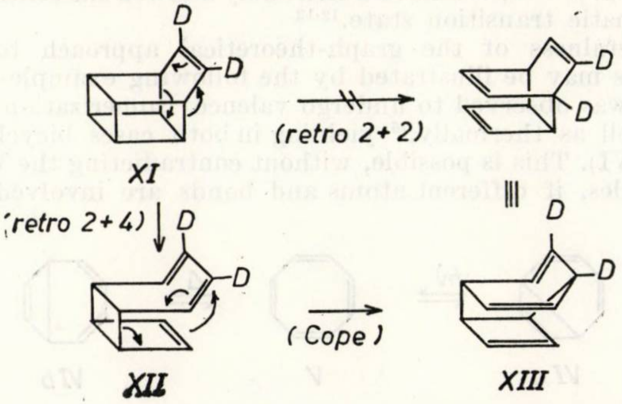

NONVARIANT GRAPH OF A FAMILY OF ISOGRAPHS

Isographic transformations consist in permuting q lines between p points of a constitutional graph, without altering the degree of any of these points. Let us take a subfamily of isographs G_i obtained by permuting in all possible ways q' lines between p' points of a constitutional graph G_1 (containing p points and q lines where $p \geqslant p'$ and $q \geqslant q'$). By deleting the q' lines involved in the isographic transformations between the members of the subfamily G_i, we obtain from each graph the same common spanning subgraph,[18] denoted by N, of all isographs G_i. Graph N contains p points like G_1, but only $q - q'$ lines. We shall call this common spanning subgraph N of a family of isographs G_i, the *isographic nonvariant graph*, or briefly, the *nonvariant*. The nonvariant may be thought as the graph with those lines which are common to both reagent and product of reaction. On this basis, the reactions with six-membered cyclic transition state were discussed earlier.[12]

An example is given in figure 5 which illustrates the di-π-methane rearrangement [19] and the valence isomerizations between cyclopentene, vinylcyclopropane and bicyclo[2.1.0]pentane. In fig. 5, the same capital letters, plain or primed, designate graphs which would be identical in the absence of labelling. Figure 5 includes four (A – D) of the five possible[8] valence isomers of cyclopentene; the fifth one is bicyclo[1.1.1]pentane.

We will show in the following that the nature of an isographic transformation is a function of the connectedness of the nonvariant, and that topological isomerizations and cognate processes may be classified according to this criterion. Since we only relate initial to final products without regard to kinetics or mechanism, it is irrelevant if the process is concerted or not, rapid or slow.

---

[17] L. T. Scott and M. Jones Jr., *Chem. Revs.*, **72**, 181 (1972);
G. Maier, „*Valenzisomerisierungen*", Verlag Chemie, Weinheim, 1972, p. 133;
S. Masamune and N. Darby, *Accounts Chem. Res.*, **5**, 272 (1972);
E. E. van Tamelen, *ibid.*, **5**, 186 (1972).

[18] F. Harary, „*Graph Theory*", Addison-Wesley, Reading, Mass., 1969.

[19] S. S. Hixson, P. S. Mariano and H. P. Zimmermann, *Chem. Revs.* **73**, 531 (1973)

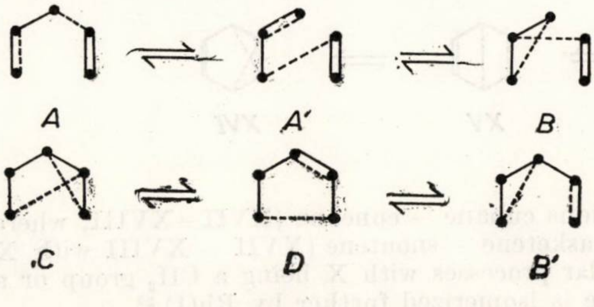

Fig. 5. — Isographic nonvariants (full line) in the di-π-methane rearrangement (above), and in valence isomerizations of cyclopentene (below). In both cases there are $q' = 2$ broken lines connecting $p' = 4$ points involved in the isographic transformation. In both cases the partition is the same $2q = 3 + 3 + 2 + 2 + 2$.

In the following discussion, for each category of nonvariant, two cases will be examined : A, $q' = 2$, $p' = 4$; B, $q' = 3$, $p' = 6$. For the sake of simplicity, only the p′ points in question will be shown explicitly ; the subgraphs connecting them, which together with the above p' points constitute the nonvariant, are drawn as curved full lines to differentiate them from covalent bonds which are drawn as straight lines. In other words, a straight line denotes a covalent bond, whereas a curved line denotes one or more covalent bonds.

TYPES OF NONVARIANT GRAPHS

The following three possibilities may be differentiated.

1. THE NONVARIANT IS A CONNECTED GRAPH

This is equivalent to say that none of the q' lines involved in the isographic transformations (drawn in fig. 5 and in the following formulae as broken lines) is a bridge [18] in any member of the subfamily G_i of isographs in question. Any two points of the constitutional graph may be linked by some path in all isographs of such a family, *via* the nonvariant.

1A. $q' = 2, p' = 4$

The known or possible examples involve either photochemical reactions, or catalyses by transition metal ions.

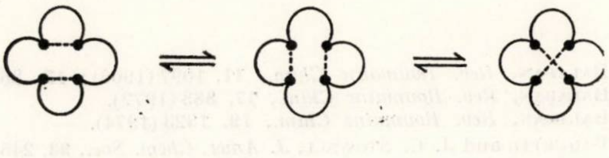

To this type of nonvariant belong the valence isomerizations of benzene (XIV), Dewar-benzene (XV) and benzvalene (XVI);

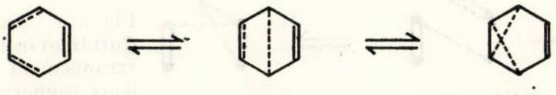

XIV XV XVI

also the valence isomerizations cubane – cuneane (XVII–XVIII, where X is a covalent bond), basketene – snoutene (XVII – XVIII with X being CH=CH), and similar processes with X being a CH_2 group or a heteroatom.[17,20–23] Snoutene is isomerized further by Rh(I).[24]

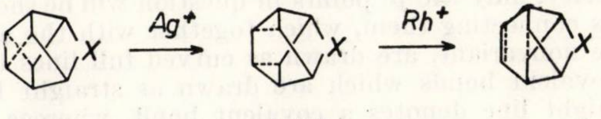

XVII XVIII

Another nonvariant of the same type is the following:

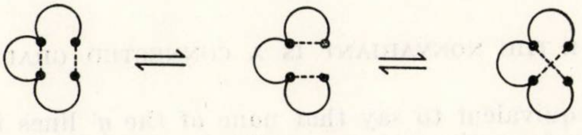

As examples for this nonvariant, are the interconversions C – D – B′ in fig. 5, and the valence isomerizations between cyclobutene (XIX), butadiene (XX) and bicyclobutane (XXI).

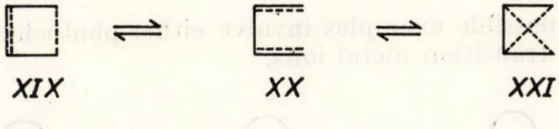

XIX XX XXI

---

[20] A. T. Balaban, *Rev. Roumaine Chim.*, **11**, 1097 (1966); **17**, 865 (1972).

[21] A. T. Balaban, *Rev. Roumaine Chim.*, **17**, 883 (1972).

[22] A. T. Balaban, *Rev. Roumaine Chim.*, **19**, 1323 (1974).

[23] L. A. Paquette and J. C. Stowell, *J. Amer. Chem. Soc.*, **93**, 2459 (1970).

[24] A. de Meijere and L.-U. Meyer, *Tetrahedron Letters*, **1974**, 1849.

1B. $q' = 3,\ p' = 6$

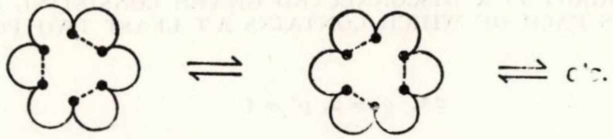

We shall illustrate this case of thermally allowed intramolecular reactions by degenerate rearrangements (automerizations or topomerizations): homotropylidene (XXII), semibullvalene (XXIII), bullvalene (XXIV), hypostrophene (XXV), snoutene (XXVI), lumibullvalene (XXVII) and 9,10-dihydronaphthalene (XXVIII).[17,20,21]

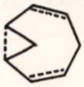
XXII

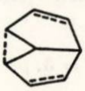
XXIII

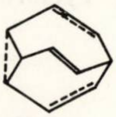
XXIV

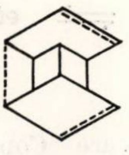
XXV

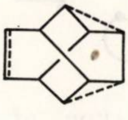
XXVI

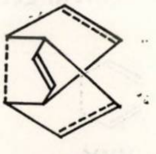
XXVII

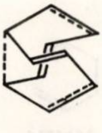
XXVIII

Another type of nonvariant belonging to this case is the following:

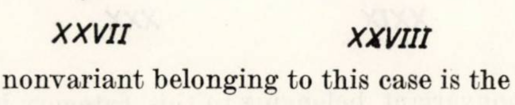

Examples for this nonvariant are the valence isomerizations of 1,3,5-hexatrienes and 1,3-cyclohexadienes, or of 2,4-pentadien-1-ones (e. g. pyrylium pseudobases in the enolic form) and $2H$-pyrans. Such processes are illustrated by formulae IX and X.

All isographic transformations characterized by a connected nonvariant correspond to topological isomerizations known in chemistry as valence isomerizations. The reverse is not true, however, since some valence isomerizations may have disconnected nonvariants, e. g. the degenerate Cope rearrangement of 1,5-hexadiene as will be shown in the next paragraph.

2. THE NONVARIANT IS A DISCONNECTED GRAPH CONSISTING OF TWO COMPONENTS EACH OF WHICH CONTAINS AT LEAST TWO POINTS

2A. $q' = 2$, $p' = 4$

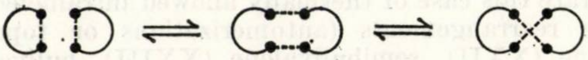

Examples for this type of nonvariant are photochemical 2 + 2 cycloadditions and cycloreversions, and interconversions A – A′ – B in figure 5.

2B. $q' = 3$, $p' = 6$

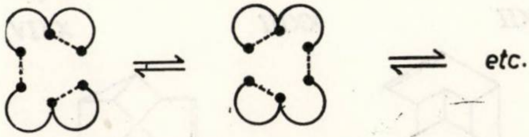

Examples for this type of nonvariant are Cope rearrangements XXIX – XXX, which according to substituents may be degenerate or non-degenerate. With heteroatoms, related rearrangements are possible (Claisen, oxy-Cope, etc.).

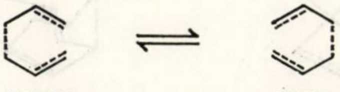

XXIX XXX

Another type of nonvariant belonging to this category is the following :

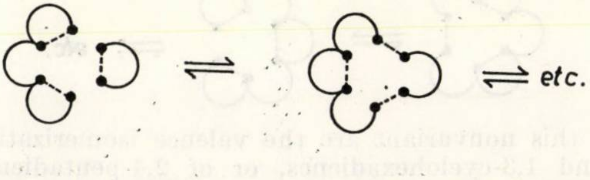

Examples for this nonvariant are the large class of thermal 4 + 2 cycloadditions (Diels-Alder reactions) and their reversions XXXI – XXXII with cyclic six-membered transition state.[12]

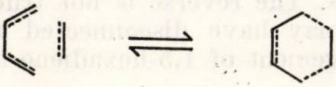

XXXI XXXII

Also in this category is the following nonvariant :

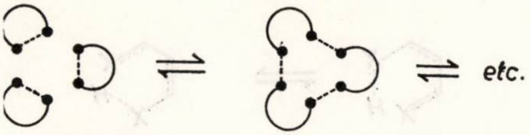

Examples are the thermal 2 + 2 + 2 cycloadditions and cycloreversions XXXIII — XXXIV.[12,13]

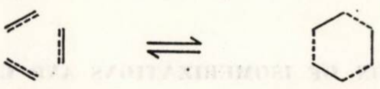

XXXIII XXXIV

3. THE NONVARIANT IS A DISCONNECTED GRAPH CONSISTING OF TWO OR MORE COMPONENTS, SOME OF WHICH CONTAIN ONE POINT

3A. $q' = 2, p' = 4$

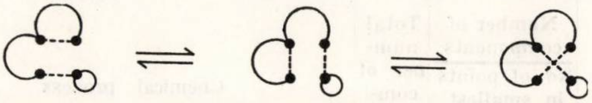

Examples for this type of nonvariant are the enolization of carbonyl derivatives (very rapid tautomeric equilibration) or the slower interconversions between allene (1,2-propadiene) and methylacetylene (propyne), which are both prototropic reactions. Also to this case belong 1,2-rearrangements such as the isomerizations butane — isobutane, or cyclohexane — methylcyclopentane ; or ring-chain isomerizations such as the formation of dichlorophthalide from phthaloyl chloride. All these processes are not concerted ; therefore their occurrence in thermal reactions under the influence of appropriate catalysts does not violate the Woodward — Hoffmann rules.

3B. $q' = 3, p' = 6.$

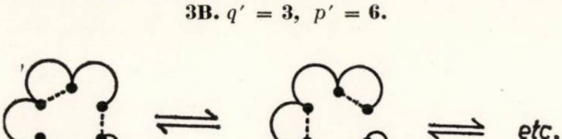

Examples for this case are the numerous thermal 1,5-hydrogen migrations, or the rapid interconversions between the two enolic forms of 1,3-diketones involving one or the other carbonyl group, XXXV — XXXVI, where X may be CR_2, NR, or O.

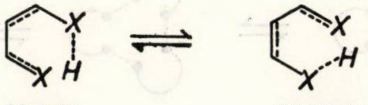

XXXV XXXVI

Similar processes are known where the migrating or reacting group is not a hydrogen atom : sigmatropic and cheletropic reactions.

CLASSIFICATION OF ISOMERIZATIONS AND COGNATE REACTIONS

According to the connectedness of the nonvariant and to the number of points in its components, isomerizations and cognate reactions may be classified as presented in table 2.

Table 2

Classification of isomerizations and related reactions according to the connectedness of the nonvariant and to the number of points in its components

Case	Number of components — No. of points in smallest component		Total number of components	Chemical process
	1	>1		
1	0	1	1	Valence isomerism
2	0	>1	$\geqslant 2$	Valence isomerism, cycloaddition, fragmentation
3	$\geqslant 1$	$\geqslant 1$	$\geqslant 2$	Prototropism, sigmatropism, cheletropism, isomerism

In conclusion, consideration of the nonvariant (i. e. of the graph containing those bonds which are common to the initial and final molecules) helps the systematization of chemical reactions, particularly of isomerizations.

Revue Roumaine de Chimie, **19**, *12*, 1941–1947 (1975)

Dedicated to
RALUCA RIPAN
on the occasion of her 80th anniversary

STUDIES CONCERNING THE OPTIMISATION OF SEPARATIONS BY THIN LAYER CHROMATOGRAPHY ON SILICAGEL. I

SEPARATION OF SOME ETHANOLAMINES IN SEVERAL POLYCOMPONENT SOLVENT SYSTEMS

C. LITEANU and H. NAŞCU

Chair of Analytical Chemistry, "Babeş-Bolyai" University, Cluj-Napoca, Romania

Received August 19, 1974

The paper presents the thin layer chromatographic behaviour of some ethanolamines mixtures vs. solvent composition in three ternary solvent systems of the following type: proton donor or acceptor solvent: methanol: ammonia (d = 0.905). The optimum composition of the solvents is presented on Gibbs ternary diagrams while the R_f values are illustrated in graphs. The results may be qualitatively explained if we assume that the retention of these amines takes place through a donor-acceptor (Lewis) interaction.

A rather unusual method for the selection of solvent systems expected to perform a certain separation (besides that making use of solvent-solute interactions [1–4] or that of eluotropic series [5–9]) is the "universal solvent system" method adopted by some laboratories [10–12] on the basis of a long-term experience. Recently, Snyder [13] has introduced a new system for solvent classification which permits a logical selection of solvents both in terms of polarity and selectivity, proving theoretically the validity of such universal solvent systems. These systems permit the separation of a large number of components, on condition that the optimum ratio between the individual components of the mixture [10] be determined.

---

[1] V. PELLONI-TAMAŞ and F. IOHAN, "*Cromatografia în strat subţire*", Ed. tehnică, Bucureşti, 1971, p. 65.

[2] L. S. BARK and R. J. T. GRAHAM, *J. Chromatog.*, **27**, 109 (1967).

[3] L. S. BARK and R. J. T. GRAHAM, *J. Chromatog.*, **27**, 131 (1967).

[4] M. BIEGONOWSKA, E. SOCZEWINSKI and ST. BIEGONOWSKA, *J. Chromatog.*, **45**, 121 (1969).

[5] E. SOCZEWINSKI, W. GOLKIEWICZ and H. SZUMILO, *J. Chromatog.*, **45**, 1 (1969).

[6] L. R. SNYDER and R. J. FETT, *J. Chromatog.*, **18**, 461 (1965).

[7] L. R. SNYDER, *J. Chromatog.*, **44**, 1 (1969).

[8] T. J. BULENKOV, *Zhur. analyt. Khim.*, **23**, 348 (1968).

[9] L. R. SNYDER, "*Principles of Adsorption Chromatography*", Marcel Dekker, New York, 1968, p. 186.

[10] G. ROUSER, *J. Chromatog. Sci.*, **11**, 60 (1973).

[11] R. A. EGLI, *Deut. Apoth. Zeitung*, **27**, 987 (1970).

[12] Thin-Layer Chromatography with Eastman Chromatogram Sheet and Developing Apparatus, Kodak Publication No. JJ–6.

[13] L. R. SNYDER, *J. Chromatog.*, **92**, 223 (1974).

The simplest way for determining the optimum ratio in the case of polycomponent systems is that of using Gibbs diagrams and the graphical presentation of the results.[14-16]

The solvents so far proposed in literature for the separation of ethanolamines by paper and thin layer (TLC) chromatography,[17-26] generally contain an alcohol, and an aqueous solution of concentrated ammonia or acetic acid, when silicagel and cellulose (adsorbents with $-OH$ superficial groups) are used. Besides these solvents ammonia and methanol systems contain a secondary solvent too : ethanol,[17] ethyl acetate,[24] acetone,[25] or chloroform.[23] There are no references in the literature to the mechanism of retention in such solvents. The aim of the present paper is to fill in this gap and to find some guidelines for the selection of optimum solvent systems in the case of ethanolamines separation by TLC on silicagel.

MATERIALS AND METHODS

Glass plates 9 × 4.5 cm were used, on which thin layers of Silicagel H (Merck, Darmstadt, Germany) with 1 % starch as binder were spread with a manual device. After preparation the plates were air-dried for 24 hours. Developments were run at 5–6 cm distance from the starting point, immediately after solvent introduction in the tank (6 × 10 × 2 cm) After application of the spot (3–4 µl standard solution) at 1 cm distance from the inferior edge of the plate and after drying, the plate was introduced in the tank without any presaturation.

The solvents and concentrated ammonia (d = 0.905) were analytical grade reagents. The 1 % aqueous solutions of ethanolamines : monoethanolamine (MEA), diethanolamine (DEA), triethanolamine (TEA), and 2-N-dimethylaminoethanol (NDEA) were prepared by weighing, starting from analytical grade reagents (Merck, Darmstadt, Germany). The preparation of solvent mixtures and developments was carried out at 23 ± 1°C. In all cases 20 ml eluent were prepared with a measuring precision of 0.5 %. Two determinations were made for each solvent mixture.

The visualisation reagent used was 0.2 % ninhydrin in n-butanol containing 2 % acetic acid. The plates, dried and heated for 10 minutes at 120°C in an oven, were sprayed with the above reagent and again introduced for 10 minutes in the oven.

After a series of preliminary investigations the following solvent systems were selected :

1. MeEtCO : MeOH : NH_3 (d = 0.905)
2. $CH_3COOC_2H_5$: MeOH : NH_3 (d = 0.905).
3. $CHCl_3$: MeOH : NH_3 (d = 0.905)

These three systems differ only by their first component. In the first and second solvent system it is a proton acceptor while in the last case it is a proton donor. Acetone proved to be

---

[14] G. Parissakis and D. Vrandi-Piscou, ,,Journées Hellènes des séparation immédiate et de chromatographie'' (III-ème J.I.S.I.C.) 1965, p. 43.

[15] A. Waksmundzky and J. K. Rozylo, *J. Chromatog.*, **49**, 313 (1970).

[16] J. K. Rozylo, *J. Chromatog.*, **85**, 136 (1973).

[17] M. Frank and M. Hajkova, *Coll. Czech. Chem. Comm.*, **24**, 4403 (1959).

[18] J. Gasparic, J. Boreczky, K. Obruba and J. Hanzlik, *Coll. Czech. chem. Comm.*, **26**, 2950 (1961).

[19] J. Dewry, *Analyst*, **89**, 75 (1964).

[20] H. K. Zimmerman and A. Cosmatos, *J. Chromatog.*, **7**, 77 (1962).

[21] E. A. Mistryukov, *J. Chromatog.*, **9**, 314 (1962).

[22] G. Szasz and M. Szasz, *Acta Pharm. Hung.*, **32**, 260 (1962).

[23] I. A. Chekulaeva, I. B. Bystrova, G. V. Talypina and S. A. Ostrovskii, *Zhur. analit. Khim.*, **28**, 1026 (1966).

[24] L. Levinţa, personal communication.

[25] C. Liteanu and M. Lungu, Unpublished data.

[26] E. R. Reichel in ''*Some General Problems of Paper Chromatography*'', Liblice, 1961, p. 117 ; *Chem. Abstr.*, **60**, 6h (1964).

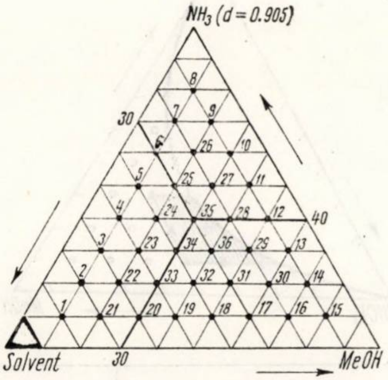

Fig. 1. – Diagram of the number of solvent mixtures of the type: solvent : MeOH : NH_3 (d = 0.905) used in the present paper.

less efficient than methyl-ethyl-ketone as component of the solvent mixture in the case of the studied ethanolamines. The tests were made within the region of total miscibility of the Gibbs triangle by taking equal size increments. In this respect, 36 equidistant points were set, as shown in fig. 1. The selected mixture tested had the same volume percent composition as these points.

RESULTS

The tested solvent systems are presented in figs. 2, 3 and 4. The hatched zones represent solvents which permit clear separations to be obtained i.e., compact, round and completely separated zones, at least for two of them, in the case of MEA, DEA and TEA mixtures. The separation of NDEA from TEA is not always complete but compact zones were also obtained in this case.

The R_f values obtained in these cases are graphically presented in figs. 5, 6 and 7.

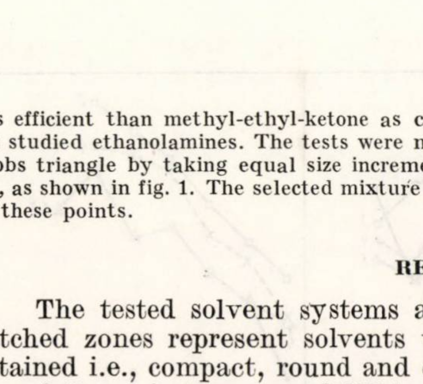

Fig. 2. – Diagram of solvent systems of the type: MeEtCo : MeOH : NH_3 (d= 0.905) studied and the region where high selectivity was obtained; ○ – poor resolution, tails or elongated spots; ● – incomplete separation: ▲ – efficient separation; ▨ – solvents of practical use.

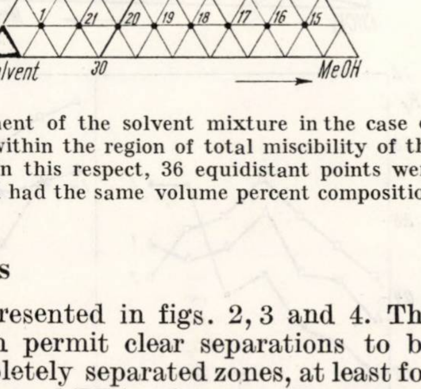

Fig. 3. – Diagram of solvent systems of the type: $CH_3COOC_2H_5$: MeOH : NH_3 (d=0.905) studied and the region in which high selectivity was obtained. ○ – poor resolution, tails or elongated spots; ● – incomplete separation; ▲ – efficient separation; ▨ – solvents of practical use.

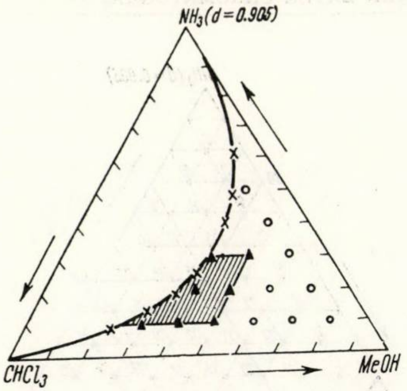

Fig. 4. — Diagram of solvent systems of the type : $CHCl_3 : MeOH : NH_3$ (d = 0.905) studied and the region in which high selectivity was obtained. ○ — poor resolution, tails or elongated spots ; ● — incomplete separation ; ▲ — efficient separation ; ▨ — solvents of practical use.

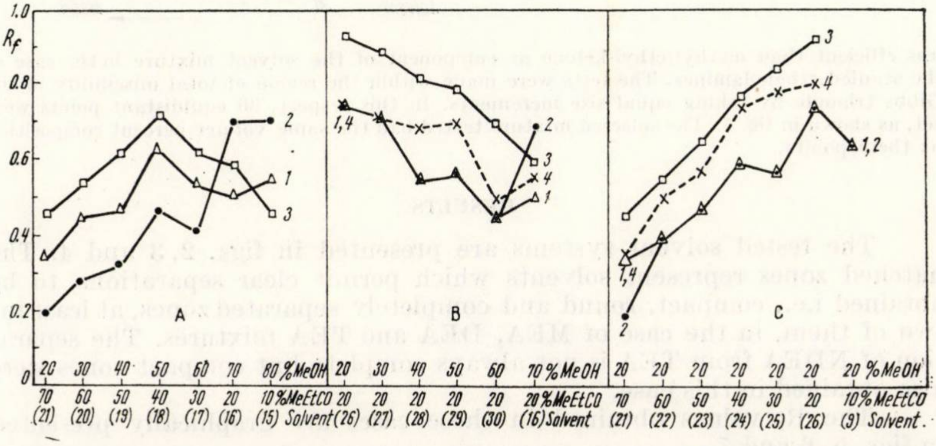

Fig. 5. — The R_f values obtained in some solvent systems : MeEtCo : MeOH : NH_3 (d=0.905), which allowed the complete separation of MEA, DEA and TEA. (1) MEA ; (2) DEA ; (3) TEA ; (4) NDEA.

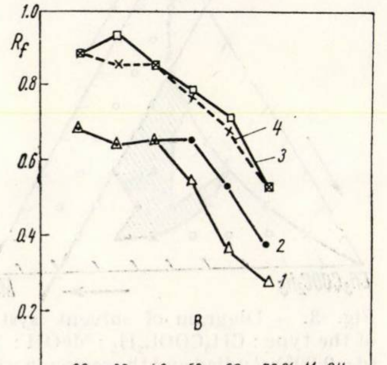

Fig. 6. — The R_f values obtained in some solvent systems : $CH_3COOC_2H_5 : MeOH : NH_3$ (d = 0.905) which allowed the complete separation of TEA from MEA and DEA. (1) MEA ; (2) DEA ; (3) TEA ; (4) NDEA.

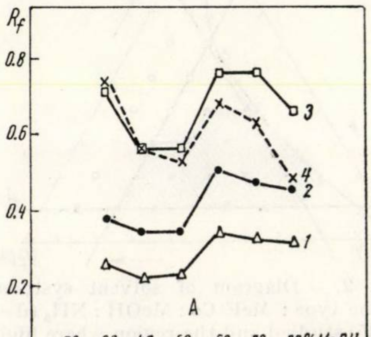

Fig. 7. The R_f values obtained in some solvent systems : $CHCl_3 : MeOH : NH_3$ (d = 0.905) which allowed the complete separation of MEA, DEA and TEA. (1) MEA ; (2) DEA ; (3) TEA ; (4) NDEA.

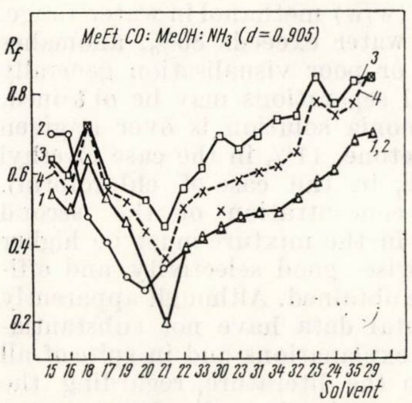

Fig. 8. — Variation of R$_f$ values vs. solvent composition (sections A, B and C in fig. 2). (1) MEA ; (2) DEA ; (3) TEA ; (4) NDEA.

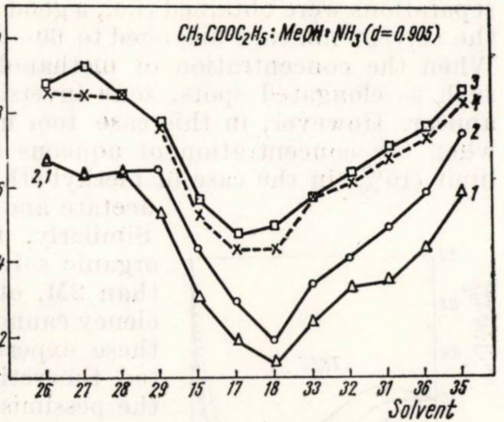

Fig. 9. — Variation of R$_f$ values vs. solvent composition (section B in fig. 3). (1) MEA ; (2) DEA ; (3) TEA ; (4) NDEA.

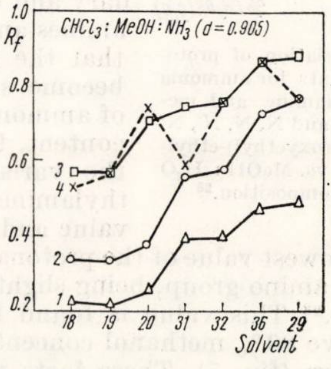

Fig. 10. — Variation of R$_f$ values vs. solvent composition (section A in fig. 4). (1) MEA ; (2) DEA ; (3) TEA ; (4) NDEA.

By drawing a parallel line to one side of the triangle passing through the area containing the tested points, the effect of solvent composition on migration of solutes can be observed (figs. 8, 9 and 10).

DISCUSSION

By comparing the diagrams presented in figs. 8a, 8b and 8c it can be seen that in the case of a constant composition of methyl-ethyl-ketone the increase in water-ammonia content, detrimental to the methanol content leads to higher R$_f$ values. This proves that the main contributing factor to the eluent "strength" is the content of the first mixture.

Looking at the data and the chromatograms obtained with the tested solvent, one can see that in the great majority of cases, when good separations were obtained (i.e., a good resolution of MEA, DEA and TEA), the solvent mixture belonged to 60—80% (w/w) methanol in water range. When the concentration of methanol in water exceeds 80%, anomalies such as elongated spots, zone inversions or poor visualisation generally appear. However, in this case too, useful separations may be obtained, when the concentration of aqueous ammonia solution is over a given limit (10% in the case of methyl-ethyl-ketone, 11% in the case of ethyl acetate and 10% in the case of chloroform). Similarly, the concentration of the second organic solvent in the mixture must be higher than 2M, otherwise good selectivity and efficiency cannot be obtained. Although apparently these experimental data have not substantiated theoretical explanations and in spite of all the pessimism in the literature, regarding the mechanism of separation in such solvents, some qualitative theoretical proofs can be formulated. Thus, the studies of solvent effect on protonation constants in methanol-water mixtures [27,28] in the case of ammonia and some primary, secondary and tertiary amines and also of some polyamines and polyaminoalcohols evidence the fact that the protonation constants of these amines become smaller than the protonation constant of ammonia at 65% (w/w) methanol in water content. In addition, as can be seen from fig. 11, the variation of protonation constants for methylamine and ethylamine are identical both in value and aspect.[28]

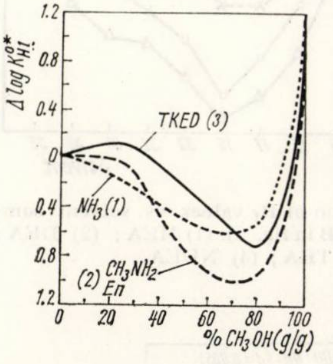

Fig. 11. —Variation of protonation constants for ammonia (1), ethylendiamine and methylamine (2) and N, N, N′, N′ tetrakis (2-hidroxyethyl)-ethylendiamine (3) vs. MeOH : H_2O mixture composition.[28]

The lowest value of the protonation constant differs from the primary to tertiary amino group, being slightly affected by the radical attached to this group.[28] This value is found for the tertiary amino group in the region above 80% methanol concentration as compared with the primary amino group (fig. 7). These facts partly explain the statement that in most cases the resolution is optimum when the concentration of methanol in water exceeds 60% (w/w). Since in our experiments the second organic solvent acts, with regard to the amino groups, as an inert diluent for methanol and the concentration of the first is generally low, as a first approximation, its action on the protonation constant of amines and ammonia can be neglected. When methanol concentration falls below 60% useful separations can be obtained only with high concentrations of ammonia (over 7 m), probably, due to a compensatory effect of higher ammonia concentration which adversely affects the stability of the adduct with the stationary phase. At higher concentrations of methanol in water (over 80%) the sudden rise of protonation constants leads, probably, to a low rate exchange kinetics and to an excessive zone broadening. The inversion in zone succession on the chromatograms may be explained by the fact that the minimum

---

[27] C. L. de Ligny, *Rec. Trav. chim.*, **79**, 731 (1960).

[28] D. B. Rorabacher, W. J. Mac Kellar, F. R. Shu and S. M. Bonavita, *Analyt. Chem.*, **43**, 561 (1971).

values of the protonation constant appear at different concentrations of ammonia in water. As regards the second organic solvent it can be ascertained that when this is a proton donor only (group VIII after Snyder's classification [13]) solvent selectivity is higher.

CONCLUSIONS

The solvent composition regions in which efficient separations take place, greatly facilitate the selection of a solvent system for separating substances with primary, secondary and tertiary amino groups.

All these groups are probably retained by the stationary phase formed on silicagel through a mechanism of protonation via —OH superficial groups. Solvent selectivity is based, in this case, on the existing difference between protonation constants of solutes and ammonia.

Since with the solvent mixture used in the present study an efficient separation may be obtained, the solvent composition should be adjusted in such a way that the protonation constants of amines be lower then the corresponding value for ammonia and, at the same time, low enough for ensuring a quick mobile phase-stationary phase transfer kinetics. This leads to a minimum value for the mass transfer resistance.

The selection of a solvent from the hatched area in Gibbs triangles presented in figs. 2, 3 and 4 assures, in the majority of cases, the best conditions for efficient separations.

Taking into acount the fact that the "universal" solvents proposed [11,12] have a similar composition with those presented in this paper, the separation mechanism suggested here may be valid in other similar cases whenever the retention mechanism is based on an acid-base (Lewis) interaction.

Revue Roumaine de Chimie, **19**, *12*, 1949–1955 (1974)

Dedicated to
Raluca Ripan
of the occasion of her 80th anniversary

SYNTHETIC SINGLE CRYSTAL PbSe ELECTRODE POTENTIOMETRIC TITRATION OF Cu(II) WITH Na_2EDTA

D. C. CÖRMÖŞ *, IOVANCA HAIDUC * and P. STEȚIU **
* Babeş-Bolyai University, Cluj, Chemistry Department, Chair of Analytical Chemistry, str. Arany J., 11, Cluj-Napoca, Romania
** Babeş-Bolyai University, Cluj, Physics Department, Isotopes and Solid State Laboratory, Cluj-Napoca, Romania

Received April 2, 1974

The characteristics of the synthetic single crystal PbSe electrode against Cu(II) ions were determined. The electrode function is 29 mV per pCu unit in the range of pCu = 1 to 6 at pH = 4. The reaction rate depends upon concentration and is 10 sec at pCu = 6 and 40 sec at pCu = 1. The electrode was used as indicating electrode in the titration of Cu(II) with Na_2EDTA. The influence of temperature, NH_3 concentration, amount of NH_4OH-NH_4Cl buffer and the NaCl concentration were investigated.

INTRODUCTION

Copper (II) ions are frequently determined potentiometrically. For titrations, several ion-selective electrodes have been proposed.[1–24]

---

[1] W. M. Latimer, "*The Oxidation States of the Elements and their Potential in Aqueous Solutions*", 2nd ed. Prentice Hall, Englewood Clifs, New York, 1969, p. 150.

[2] M. Sato, *Electrochim. Acta*, **11**, 361 (1966).

[3] J. Ruzicka and C. G. Lamm, *Analyt. Chim. Acta*, **53**, 206 (1971).

[4] N. I. Savin, V. S. Shterman, A. V. Gordievskii and A. Ya Syrchenkov, *Zavodskaya Lab.*, **37**, 1025 (1971).

[5] H. Hiroshi and I. Masano, British Patent 1249288, 20.4.69, 1972; *Analyt. Abstr.*, **23**, 3634 (1972).

[6] H. Hirata, J. Higashiyama and K. Date, *Analyt. Chim. Acta*, **51**, 209 (1970).

[7] A. Torbjoern and J. Daniel, *Analyt. Chim. Acta*, **56**, 477 (1971).

[8] H. Hirata and K. Date, *Talanta*, **17**, 883 (1970).

[9] J. Vesely, *Coll. Czech. Chem. Comm.*, **36**, 3364 (1971).

[10] "*Preliminary Instruction Manual for Cupric Selenide Electrode F 1112 Cu*", Radiometer A/S, Copenhagen, 1971.

[11] H. Adametzova and J. Gregr, *Chem. průmysl.*, **21**, 506 (1971).

[12] H. Hirata and K. Higashiyama, *Talanta*, **19**, 391 (1972).

[13] "*Instruction Manual Cupric Ion Electrode 94–29*", Orion Inc. Mass 1968.

[14] J. W. Ross, "*Solid-state and Liquid Membrane Ion Selective Electrodes*", NBS Publ. 314 (R. A. Durst Ed), Washington, 1969.

[15] "*Beckman Instruction 8i8 U, Select Ion Cupric Electrode*", Fullerton California, 1969.

[16] E. H. Hansen, C. G. Lamm and J. Ruzicka, *Analyt. Chim. Acta*, **59**, 403 (1972),

[17] M. Mascini and A. Liberti, *Analyt. Chim. Acta*, **53**, 202 (1971).

[18] T. Nomura and G. Nakagawa, *Bunseki Kagaky*, **20**, 1570 (1971); *Chem. Abstr.*, **76**, 94090 (1972).

[19] M. Sharp and G. Iohansson, *Analyt. Chim. Acta*, **54**, 13 (1971).

[20] M. Sharp, *Analyt. Chim. Acta*, **59**, 137 (1972).

[21] A. Burdin, J. Mesplede and M. Porthault, *Compt. rend.*, **276**, 65 (1973).

[22] J. Ruzicka and J. C. Tjell, *Analyt. Chim. Acta*, **49**, 346 (1970); **51**, 1 (1970).

[23] J. B. Harrell, A. D. Jones and C. R. Choppin, *Analyt. Chem.*, **41**, 1459 (1969).

[24] L. Sudarshan and G. D. Gary, *Indian. J. Chem.*, **10**, 123 (1972).

In table 1 the electrodes used for this purpose are presented, as is the material they have been made of, the concentration range in which a Nernst response takes place and the pH at which the electrode function was determined.

Table 1

Selective Copper (II) electrodes

Electrode		Nernst response		References
Type	Material	pCu	pH	
Solid state	Cu	4–1*	9	1
	CuS	12–1*	9	2
	CuS/graphite rod	6–3	—	3
	Cu_2S	5–1	—	4
	Cu_2S/CuS	8–2	—	5
	Cu_2S/Ag	6–1, 5–7	—	6,7
	Cu_2S/silicone rubber	6–1	—	8
	$Cu_{1.8}Se$	6–3	6	9
	Cu_2Se/CuSe	10–1	9	10, 11
	Cu_2Te	6–1	—	12
	CuS/Ag_2S	11–1*	9	13, 14
		6–1	9	15
		12–1*	9	15
		13–1*	9	16
	CuS/Ag_2S/polyethylene	6–1	—	17
	CuS/HgS	11–1*	9	16
	CuS/CdS	6–1*	9	16
	CuI/vinylchloride polymer	5–2	—	18
	organic radical ion salt	5–1	—	19, 20
Liquid membrane electrode	Cu dithizonate in xylene/graphite rod	5–1	—	21
	Cu dithizonate/porous carbon	5–1	—	22
	Dinonylnaphthylene sulphonic acid	5–1	—	23

* electrode response in metal buffers.

Table 1 shows that the range of Nernst response of some selective copper electrodes extends up to pCu = 12–13 when metal buffers are used.[16,25] Copper selective electrodes have also been used in the complexonometric potentiometric titration of Cu(II).[26–31]

---

[25] R. Blum and A. G. Fog, *J. Electroanalyt. Chem.*, **34**, 385 (1972).

[26] E. W. Baumann and R. M. Wallace, *Analyt. Chem.*, **41**, 2072 (1969).

[27] J. W. Ross and M. S. Frant, *Analyt. Chem.*, **41**, 1900 (1969).

[28] L. Sucha and M. Suchanek, *Analyt. Lett.*, **3**, 613 (1970).

[29] G. A. Rechnitz and N. C. Kenny, *Analyt. Lett.*, **3**, 509 (1970) ; **2**, 395 (1969).

[30] E. Hakoila, *Analyt. Lett.*, **3**, 273 (1970).

[31] T. Anfalt and G. Jagner, *Analyt. Chim. Acta*, **56**, 477 (1971).

In the present paper we describe the behaviour of the synthetic single crystal PbSe electrode in the potentiometric titration of Cu(II) with Na_2EDTA, with good results.

EXPERIMENTAL

The electrode. The PbSe single crystal was obtained from spectral pure selenium and lead. The single crystal was mounted without internal solution.

The solutions. All the solutions used were made from reagent grade substances and doubly distilled water. The constant ionic strength was achieved with a KNO_3 solution.

The apparatus. The PbSe electrode potentials were measured with a MV-11S potentiometer with a precision of ±2 mV and are referred to SCE.

RESULTS AND DISCUSSION

The electrode response for Cu(II). For the determination of the electrode response to Cu(II) ions, the potentials of the synthetic single crystal PbSe electrode were measured in solutions prepared by successive dilution of $Cu(NO_3)_2$ 10^{-1}M, at ionic strength J = 0.1. All the solutions were brought to pH = 4 with HNO_3 10^{-2}M. Measurements were made at pH = 4 since the electrode potential in 10^{-1} Cu(II) solution is constant for the pH range from 2.5 to 6.0. In fig. 1 the electrode response is depicted:

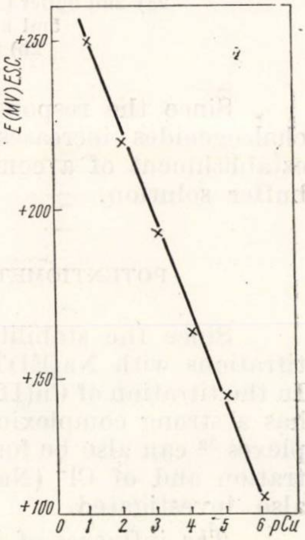

Fig. 1. – The PbSe single crystal electrode response to Cu(II).

The synthetic single crystal PbSe electrode has a nernstian response to Cu(II) in the range of pCu = 1–6. The reproducibility of potential values is very good and the electrode can be used both for the potentiometric titration of Cu(II) and for direct potentiometry.

Response rate. The response rate of the electrode investigated was determined for Cu(II) ions under the conditions of potentiometric titration with Na_2EDTA. For this purpose potential-time curves were plotted at pH = 10, on $2 \cdot 10^{-3}$ M Cu(II) solutions, at various concentrations of the buffer. These curves are given in fig. 2a:

The potential-time curves show changes which decrease with the increase of the buffer concentration used. To determine the buffer concentration at which the electrode potential is constant at t = 0, the PbSe electrode potential values in Cu(II) solutions were plotted at various buffer concentrations at t = 0 and t = 30 sec (the time at which the potential becomes constant). The straight lines obtained are shown in fig. 2b. Their intersection shows the buffer concentration for which the electrode response is constant with time.

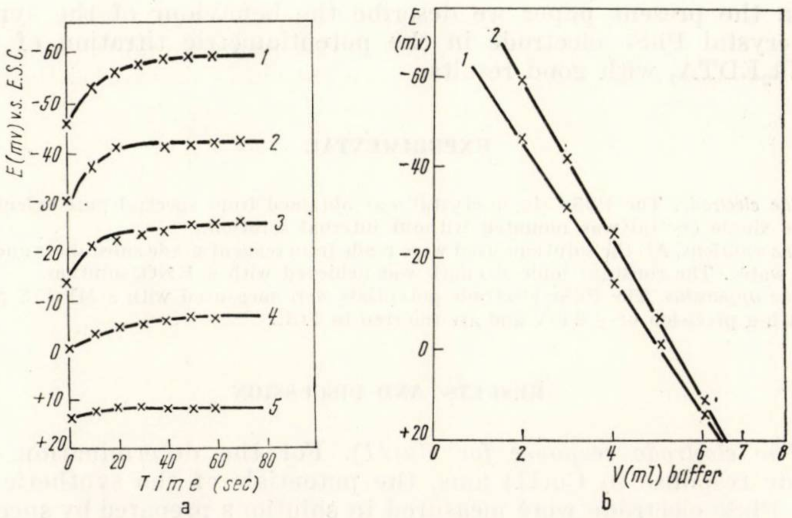

Fig. 2. — Response rate of PbSe single crystal electrode in $2 \cdot 10^{-3}$ M Cu(II) buffered solution (pH = 10 with $NH_4OH + NH_4Cl$) : 2a) 2ml buffer (curve *1*), 3ml buffer (curve *2*), 4ml buffer (curve *3*), 5ml buffer (curve *4*), 6 ml buffer (curve *5*). 2b) *t* = 0 (curve 1), t = 30 sec (curve *2*).

Since the response rate of the electrodes based on heavy metal chalcogenides increases with decreasing ion concentration, the rapid establishment of a constant potential is favoured by the addition of a buffer solution.

POTENTIOMETRIC TITRATION OF Cu(II) WITH Na_2EDTA

Since the stability of metal complexonates is a function of pH, titrations with Na_2EDTA are made in the presence of buffer solutions. In the titration of Cu(II) the NH_4OH/NH_4Cl buffer is used. Since ammonia has a strong complexing action upon Cu(II) and copper (II)-chlorocomplexes [32] can also be formed, the influence of ammonia, of buffer concentration and of Cl^- (NaCl) concentration upon the titration curve were also investigated.

The influence of NH_3 concentration. In order to determine the optimal concentration of ammonia several titrations of Cu(II) with Na_2EDTA were made at the following molar ratios between NH_3 and Cu(II) : 1, 2, 4, 6, 8 and 10.

In all solutions the molar concentration of Cu(II) was $2 \cdot 10^{-3}$ and the initial volume of the solution was 50 ml. The results of titrations are shown in fig. 3.

The increasingly negative value of the electrode potential with increasing $[NH_3]/[Cu]$ ratio is due to the complexation of Cu(II) by

---

[32] W. E. Hatfield and R. Whyman, *Transition Metal Chem.*, **5**, 123 (1969).

NH_3. The equivalence volume remains constant with ratios, but the shape of the titration curve and the potential jump around the equivalence vary. The titration curve 1 is very asymmetrical due to the instability of the Cu-EDTA complexes in the presence of the hydrogen ions resulted from the reaction, which are incompletely neutralized at the ratio $[NH_3]/[Cu] = 1$. After the equivalence (curves *3–6*) the potentials are not negativated according to the ammonia : copper ratio, because of the excess of ammonia, which destabilizes the Cu-EDTA complex. The titration curve *2* (corresponding to the ratio $[NH_3]/[Cu] = 2$) is the most symmetrical, and has a potential jump around the equivalence $\Delta E \pm 1\% = 110$ mV. For the $[NH_3]/[Cu] = 2$ ratio the two hydrogen equivalents released during the reaction are entirely neutralized by ammonia.

The titration of Cu(II) with Na_2 EDTA can also be performed in the following way : the Na_2EDTA solution is chosen so as to contain the ammonia concentration required to neutralize the H^+ ions resulted from the reaction. In this case the initial potentials will be determined by the Cu(II) concentration and the potential jump will be higher than in the case of Cu(II) – NH_3 solutions. In the titration of a Cu(II) M/50 solution with a Na_2EDTA M/50 solution in NH_4OH M/25 the potential jump observed is $\Delta E_{\pm 1\%} = 160$ mV.

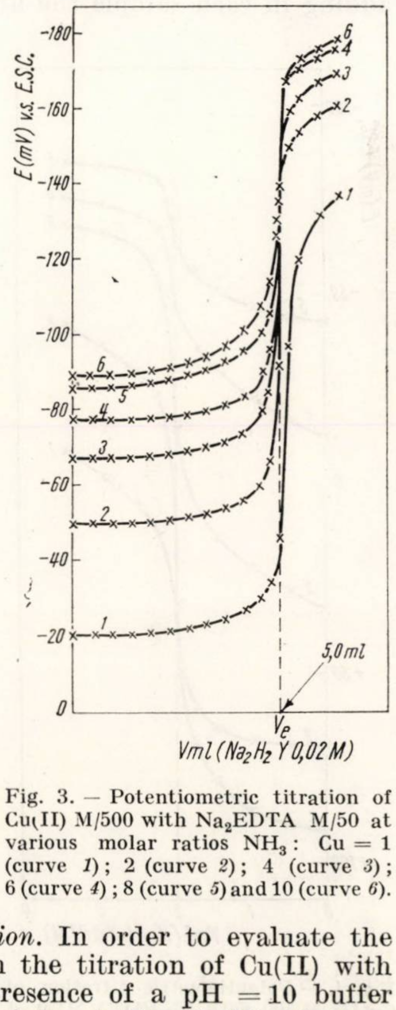

Fig. 3. – Potentiometric titration of Cu(II) M/500 with Na_2EDTA M/50 at various molar ratios NH_3 : Cu = 1 (curve *1*) ; 2 (curve *2*) ; 4 (curve *3*) ; 6 (curve *4*) ; 8 (curve *5*) and 10 (curve *6*).

The influence of the buffer concentration. In order to evaluate the influence of the buffer concentration upon the titration of Cu(II) with Na_2EDTA, a series of titrations in the presence of a pH = 10 buffer (with a ratio $[NH_3]/[NH_4^+] = 6.5$) were carried out. The Cu(II) solutions had a concentration of $4 \cdot 10^{-5}$ moles in 50 ml solution, and the buffer was added from 0.25 to 10.0 ml. The titration data are shown in Fig. 4

The figure shows that all the titration curves exhibit the same variation around the equivalence and the shape of the titration curve varies. The highest potential jump (70 mV) corresponds to curve *2*, fig. 4. By comparing the titration curves in fig. 3 with those in fig. 4 the influence of the presence of NH_4Cl is quite obvious. The concentration of NH_4Cl in the buffer solution should be 3 times lower than the concentration of copper.

The influence of NaCl concentration. In order to determine the influence of Cl^- ions upon the titration of Cu(II) with Na_2EDTA with PbSe electrodes, the titrations illustrated in fig. 3 were repeated by adding in each sample the amount of sodium chloride required to keep the molar ratio $[NH_3]/[NaCl]$ constant. For this purpose 50 ml samples of Cu(II) M/500 were titrated. The molar concentrations of these samples in NH_3 respectively in NaCl were: $2\cdot 10^{-2}$, $4\cdot 10^{-2}$, $8\cdot 10^{-2}$, 1.2×10^{-1}, 1.6×10^{-1} and 2.0×10^{-1}. The titrating reagent was a Na_2EDTA M/50 solution.

The titration data thus obtained are given in table 2.

By comparing the potential variation around the equivalence, we can notice wide variations in the titrations made in the presence of NaCl, up to ammonia concentration of $8\cdot 10^{-2}$ M, after which this variation remains constant. Therefore, the Cl^- ions (introduced in solution as NaCl) do not have a depressing effect upon the potential jump and in the case the NH_4OH-NH_4Cl buffer is used, the ammonia ions are the ones exhibiting a strong depressing effect. At high NaCl concentrations the potential jump around the equivalence is much decreased ($\Delta E_{\pm 1\%} = 20$ mV in the titration in the presence of NaCl compared to $\Delta E_{\pm 1\%} = 70$ mV in the absence of NaCl). The titration curves are shown in fig 5. In this case 50 ml of a M/500 Cu(II) solution, containing $2\cdot 7 \times 10^{-2}$ moles of ammonia and $1\cdot 76 \times 10^{-1}$ moles of NaCl.

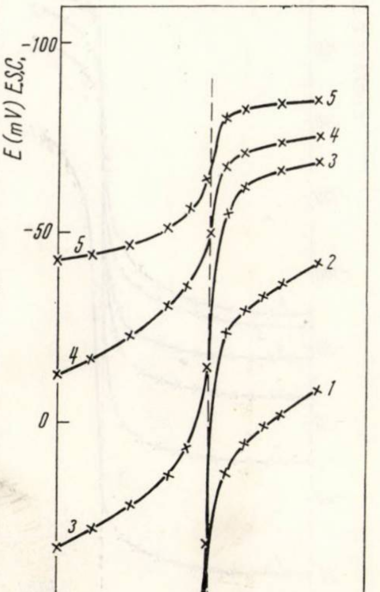

Fig. 4. — Potentiometric titration of Cu(II) M/500 with Na_2EDTA M/50 at pH = 10 ($NH_4OH + NH_4Cl$ buffer). 0.25 ml buffer (curve *1*); 0.5ml buffer (curve *2*); 3 ml buffer (curve *3*); 5 ml buffer (curve *4*); 10 ml buffer (curve *5*).

The influence of temperature. The temperature is a factor which can influence both the titration reactions and the electrode processes In fig. 6 are shown the titration curves obtained by titrating 50 ml of Cu(II) M/500 in the presence of 2ml of 2M NH_4OH at 22° and 55°.

It is noticed that potentials are shifted towards more positive values, without a significant change of the equivalence volume. The smaller potential jump ($\Delta E_{\pm 1\%} = 60$ mV at 55°, compared to $\Delta E_{\pm 1\%} = 90$ mV at 22°) recommends the titration of Cu(II) with Na_2EDTA be performed at room temperature.

Table 2

Potentiometric data titration of Cu(II) M/500 with Na_2EDTA M/50 in NH_4OH and $NH_4OH + NaCl$

NH_4OH ml	NaCl ml	$E_{0\%}$ mV	$E_{100\%}$ mV	$E_{150\%}$ mV	$E_{\pm 1\%}$ mV
0.5	—	−20	−60	−138	40
0.5	0.5	0	−70	−134	80
1.0	—	−50	−100	−160	70
1.0	1.0	−12	−100	−133	85
2.0	—	−67	−130	−170	60
2.0	2.0	−40	−130	−150	55
3.0	—	−78	−140	−176	65
3.0	3.0	−55	−138	−156	55
4.0	—	−86	−140	−176	45
4.0	4.0	−66	−140	−162	45
5.0	—	−91	−140	−179	35
5.0	5.0	−86	−145	−169	35

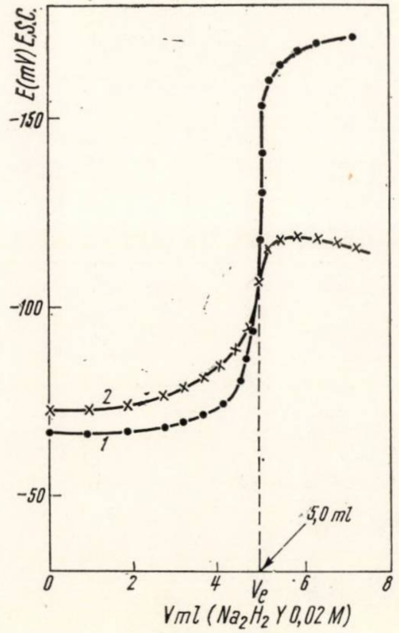

Fig. 5. — Potentiometric titration of Cu(II) M/500 with Na_2EDTA M/50 in the presence of NaCl: curve *1* without addition of NaCl; curve *2* in the presence of 1.76×10^{-1} M NaCl.

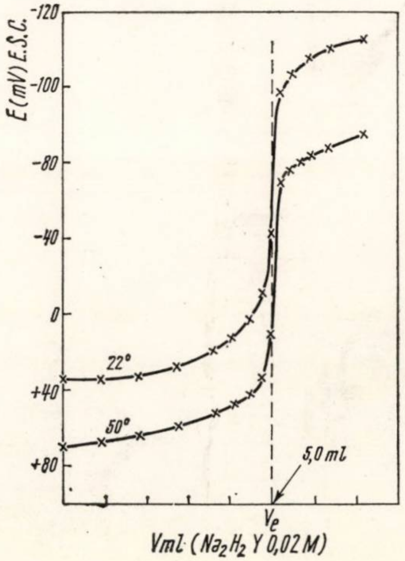

Fig. 6. — Potentiometric titration of Cu(II) M/500 with Na_2EDTA M/50 at various temperatures: curve *1*. 22°; curve *2*.55°.

In titration of Cu(II) with Na_2EDTA and PbSe single crystal electrode, Pb^{2+}, Cd^{2+}, Hg^{2+}, Ag^{+} and SO_4^{2-} are interfering ions. The relative error is about $\pm 0.2\%$ for Cu(II) $5 \cdot 10^{-3}$ M.

Revue Roumaine de Chimie, **19**, *12*, 1949–1955 (1974).

Revue Roumaine de Chimie, **19**, *12*, 1957–1961 (1974)

Gewidmet Akad.
Raluca Ripan,
gelegentlich Ihrer 80jährigen Geburtstagsfeier

TRENNUNG EINIGER AMINOSÄUREN DURCH DÜNNSCHICHTCHROMATOGRAPHIE MIT ORTHOGONALEM TEMPERATURGRADIENT

S. GOCAN und CHRISTINE KYRI

Lehrstuhl für Analytische Chemie der Universität ,,Babeş-Bolyai",
Cluj-Napoca, str. Arany János, nr. 11

Eingegangen am 20. Feb. 1974

Es wird die Möglichkeit der Anwendung des orthogonalen Temperaturgradienten bei der Trennung einiger Aminosäuren durch Dünnschichtchromatographie (in der S-Kammer) gezeigt. Der orthogonale Temperaturgradient begünstigt die Trennung der Komponenten. Man erhält eine viel bessere Auflösung als bei Entwicklung in isothermen Bedingungen.

Auf die Möglichkeit der Anwendung eines orthogonalen Temperaturgradienten in der S-Kammer wies Niederwieser hin.[1]

Um die Vorteile der Dünnschichtchromatographie mit orthogonalem Temperaturgradient zu überprüfen, wählten wir ein System von sechs Aminosäuren: 1. Histidin, 2. Glycin, 3. Glutaminsäure, 4. Alanin, 5. Valin, 6. Leucin.

Die Trennung dieses Gemisches erfolgte auf mikrokristalliner Cellulose (Merck), die Schichtdicke betrug 0,2 mm. Als Fließmittel wurde ein Gemisch[2] von *n*-Butanol-Aceton-Eisessig-Wasser (35–35–10–20, v/v) verwendet. Zur Sichtbarmachung der Aminosäuren wurden die Platten mit einer 0,2% Ninhydrinlösung (0,2% Ninhydrin in 2% Essigsäure in *n*-Butanol) besprüht, anschließend 5 Minuten im Trockenschrank bei 110° getrocknet. Die Aminosäuren erscheinen als blaue Zonen.

Apparatur: Auf die beiden Platten einer S-Kammer wurden zwei Heizplatten angebracht,[1] die einen Temperaturunterschied zwischen den beiden gegenüberliegenden Platten der S-Kammer gewährleisteten, und zwar derart, daß die DC-Platte eine Temperatur t_2 besitzt, die größer ist als die Temperatur t_1 der Gegenplatte. Die Distanz d zwischen DC-Platte und Gegenplatte betrug 3 mm.

Der orthogonale Temperaturgradient (senkrecht auf die Schicht und Fließrichtung) wurde nach folgender Gleichung berechnet:

$$\text{Grad. } t = (t_2 - t_1)/\text{d} \quad (^\circ\text{C/mm})$$

Bevor die Platten in den Fließmitteltrog eingeführt wurden, wartete man in allen Fällen etwa 20 Minuten bis zum Einstellen des orthogonalen Temperaturgradienten. Die weitere Ausführung erfolgte wie bei normaler Dünnschichtchromatographie.

---

[1] A. Niederwieser, *Chromatographia*, **2**, 362 (1969).

[2] F. Kraffczyk, R. Helger und H. Lang, *Z. klin. Chemie u. klin. Biochem.*, **7**, 521 (1969).

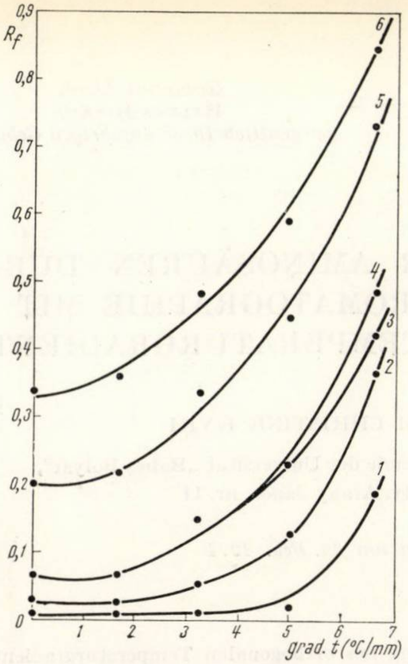

Abb. 1. — Abhängigkeit der R_f-Werte vom orthogonalen Temperaturgradient. Entwicklungsdauer :

1, Stunde, $t_1 = 20°$. Aminosäuren ; 1, Histidin, 2, Glycin, 3, Glutaminsäure, 4, Alanin, 5, Valin und 6, Leucin.

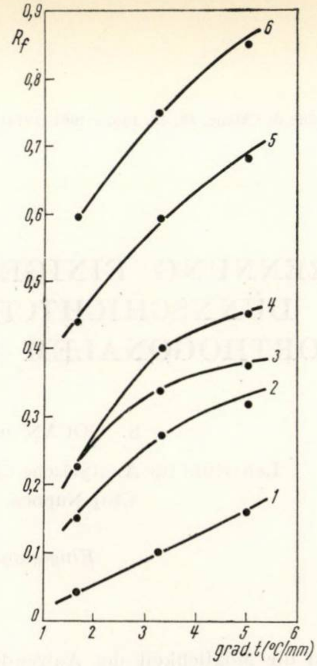

Abb. 2. — Abhängigkeit der R_f-Werte vom orthogonalen Temperaturgradient. Entwicklungsdauer :

2, Stunden, $t_1 = 20°$. Aminosäuren ; 1, Histidin, 2, Glycin, 3, Glutaminsäure, 4, Alanin, 5, Valin und 6, Leucin

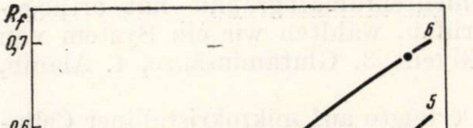

Abb. 3. R_f-Werte als Funktion der mittleren Temperatur t des Intervalls das den Gradienten schuf. (Grad. $t = \Delta t/d = 5/3 = 1{,}66°/\text{mm}$). Entwicklungsdauer :

1 Stunde. Aminosäuren ; 1, Histidin, 2, Glycin, 3, Glutaminsäure, 4, Alanin, 5, Valin und 6, Leucin.

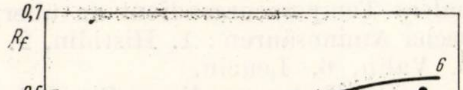

Abb. 4 — Abhängigkeit der R_f-Werte von der Entwicklungsdauer. Grad. t = konstant $= (25-20)/3 = 1{,}66°/\text{mm}$. Aminosäuren :

1, Histidin, 2, Glycin, 3, Glutaminsäure, 4, Alanin, 5, Valin und 6, Leucin.

Ergebnisse : Wir untersuchten in erster Linie die Abhängigkeit der R_f-Werte vom orthogonalen Temperaturgradienten. Die Entwicklungsdauer blieb konstant und zwar betrug sie eine Stunde (Abb. 1), beziehungsweise zwei Stunden (Abb. 2)

Anschließend wurden die Platten bei konstantem orthogonalen Temperaturgradient entwickelt, der aber verschiedenen Bereichen der Temperaturskala angehörte. In Abb. 3 sind die erhaltenen R_f-Werte in Funktion der mittleren Temperatur t des Intervalls, das den Gradienten schuf, dargestellt.

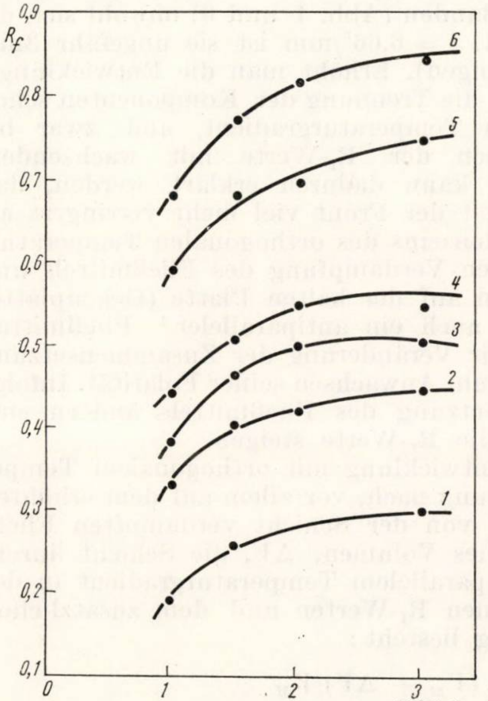

Abb. 5. — Abhängigkeit der R_f-Werte von der Entwicklungsdauer. Grad. t = konstant = (40−35)/3 = 1,66°/mm. Aminosäuren : *1*, Histidin, *2*, Glycin, *3*, Glutaminsäure, *4*, Alanin, *5*, Valin und *6*, Leucin.

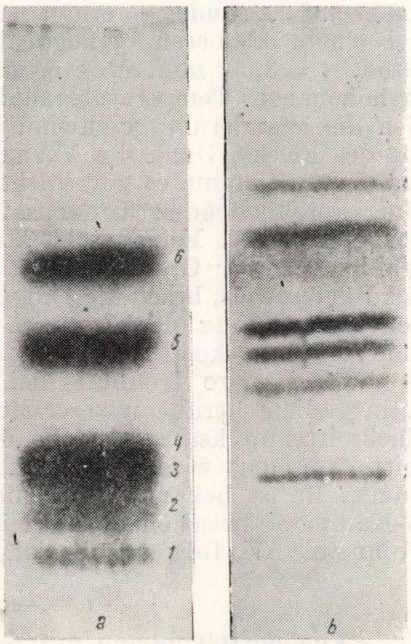

Isotherm 0= Temperaturgradient

t = 20° $\frac{40-35}{3} = 1{,}66°/\text{mm}$

Abb. 6. — Dünnschichtchromatogramme : a) erhalten durch Entwicklung in isothermen Bedingungen. b) erhalten durch Entwicklung im orthogonalen Temperaturgradient. Aminosäuren : *1*, Histidin, *2*, Glycin, *3*, Glutaminsäure, *4*, Alanin, *5*, Valin und *6*, Leucin.

Arbeitet man bei konstantem orthogonalen Temperaturgradient und ändert die Entwicklungsdauer, so erhält man die in Abb. 4 und 5 wiedergegebenen Ergebnisse.

Vergleicht man die in Abb. 6 wiedergegebenen Chromatogramme, bemerkt man die viel besseren Trennergebnisse, die man bei Entwicklung mit orthogonalem Temperaturgradient erhält.

Der positive Einfluß des orthogonalen Temperaturgradienten ist übrigens auch aus den Abbildungen 1—5 ersichtlich.

Diskussion: Arbeitet man in isothermen Bedingungen bei 20° so erhält man eine schwache Trennung der Komponenten 1—4, Glycin und Alanin bleiben ungetrennt, weil die entsprechenden Bande breit sind und sich überlagern (Abb. 1 und 6). Arbeitet man dagegen mit orthogonalem Temperaturgradient so erhält man eine zufriedenstellende Trennung der 6 Aminosäuren bei sehr scharfen Banden (Abb. 1 und 6) obwohl sich die Laufstrecke verringert: (für Grad. $t = 6{,}66°/\mathrm{mm}$ ist sie ungefähr 3mal kleiner als in isothermen Bedingungen). Erhöht man die Entwicklungsdauer auf 2 Stunden so erhält man die Trennung der Komponenten schon bei einem kleineren orthogonalen Temperaturgradient, und zwar bei Grad. $t = 3{,}33°/\mathrm{mm}$. Das Wachsen der R_f-Werte mit wachsendem orthogonalem Temperaturgradient kann dadurch erklärt werden, daß sich die Wanderungsgeschwindigkeit der Front viel mehr verringert als die des Flecks. Dank des Vorhandenseins des orthogonalen Temperaturgradienten kommt es zur selektiven Verdampfung des Fließmittels und einer anschließenden Kondensation auf der kalten Platte (Gegenplatte) der S-Kammer. Es entsteht also auch ein antiparalleler [1] Fließmittelgradient. Dieser Gradient führt zur Veränderung der Zusammensetzung des Fließmittels, beziehungsweise zum Anwachsen seiner Polarität. Infolge der Veränderung der Zusammensetzung des Fließmittels ändern sich die Verteilungskoeffizienten und die R_f-Werte steigen.

Die bessere Trennung bei Entwicklung mit orthogonalem Temperaturgradient beruht, unserer Meinung nach, vor allem auf dem erhöhten Fließmitteldurchsatz. Anstelle des von der Schicht verdampften Fließmittelvolumens wird ein zusätzliches Volumen, ΔV, die Schicht durchsetzen. Es ist bekannt [3], daß bei parallelem Temperaturgradient in der N-Kammer zwischen den erhaltenen R_f-Werten und dem zusätzlichen Volumen, ΔV, folgende Beziehung besteht:

$$R_f = R_{f(\mathrm{iso})}\,(V_M + \Delta V)/V_M$$

V_M = Fließmittelvolumen auf der Schicht und ΔV = von der Schicht verdampftes Fließmittelvolumen.

Es besteht also eine gewisse Analogie zwischen der Wirkung des orthogonalen Temperaturgradienten in einer S-Kammer und der des parallelen Temperaturgradienten in einer N-Kammer.[4–7] Selbst der Verlauf der in beiden Fällen erhaltenen Schaubildern ist ähnlich.[4,6]

Die Trennergebnisse ändern sich, wenn man denselben orthogonalen Temperaturgradient in andere Bereiche der Temperaturskala lagert. So z.B. erhält man schon nach einer Stunde eine sehr gute Trennung aller

[3] C. Liteanu und S. Gocan, *Bull. Soc. chim. France*, **1967**, 3836.

[4] S. Gocan, T. Hodişan, M. Liteanu und C. Liteanu, *Stud. Univ. Babeş-Bolyai, Chem.*, **16**, 37 (1971).

[5] S. Gocan, C. Ciupală-Costea, T. Hodişan und C. Liteanu, *Rev. Roumaine Chim.*, **16**, 1069 (1971).

[6] C. Liteanu und S. Gocan, *Bull. Soc. chim. France*, **1970**, 4527.

[7] S. Gocan und C. Liteanu, *Rev. Roumaine Chim.*, **17**, 661 (1972).

6 Komponenten wenn der Grad. $t = 1{,}66°/\mathrm{mm}$ zwischen 40—35° gelagert wird (Abb. 3), während man bei demselben Gradient, aber zwischen 25—20° gelagert erst nach 3 Stunden eine zufriedenstellende Trennung erhält (Abb. 4).

Gute Ergebnisse erhält man auch wenn man den Gradienten $(40-20)/3 = 6{,}66°/\mathrm{mm}$ verwendet, (Entwicklungsdauer 1 Stunde; Abb. 1), nur ist die Laufstrecke kürzer als beim Gradienten $(40-35)/3 = 1{,}66°/\mathrm{mm}$, was zu einer schwächeren Auflösung führt.

Das Verlängern der Entwicklungsdauer hat einen positiven Einfluß auf die Trennergebnisse (Abb. 5). Eine zu lange Entwicklungsdauer führt auch hier, ähnlich wie in anderen Entwicklungstechniken, zur Verschlechterung der Auflösung.

Revue Roumaine de Chimie, **20**, *12*, 1963–1967 (1974)

Dedicated to
RALUCA RIPAN
on the occasion of her 80th anniversary

FORMATION AND STRUCTURE OF COBALT AND TITANIUM MIXED OXIDES OBTAINED FROM MIXED COMPLEXES

M. STRĂJESCU * and C. DRĂGULESCU **

* Institute of Chemistry, Cluj, str. Donath 65–103, Romania
** Department of Industrial Chemistry, Polytechnic Institute of Timişoara,
Bd. 30 Decembrie 2, Timişoara, Romania

Received September 6, 1974

On the basis of the X-ray diffraction patterns, the formation of cobalt and titanium mixed oxides by thermolysis of mixed complexes is proved. Inside the limits of the investigated oxidic compounds, only an ilmenite type structure was found.

By the thermal decomposition of the cobalt and titanium mixed complexes, at temperatures of 300°–400°, mixed oxides are directly obtained, whose oxygen content decreases with rising the temperature.[1,2] Thus, during the thermolysis of cobalt (III) hexammine-titanyl oxalate, the mixed oxides given in table 1 were obtained.

Table 1

Composition of mixed oxides obtained by thermolysis of cobalt (III) hexammine titanyl-oxalate

N° *	Temperature, °C	Composition of oxides
1 a	330	$2/3Co_3O_4.3TiO_2.0.9O_2$
1 b	420	$2/3Co_3O_4.3TiO_2.1/3O_2$
1 c	490	$2/3Co_3O_4.3TiO_2$
1 d	505	$2CoO.3TiO_2.1/4O_2$
1 e	540	$2CoO.3TiO_2.0.2O_2$
1 f	575	$2CoO.3TiO_2.0.1O_2$
1 g	750	$2CoO.3TiO_2.0.04O_2$
1	1000	$2CoO.3TiO_2$

*) The numbers correspond to those given in fig. 1. The composition of the complex from which the oxides were obtained is given in Ref. 1 and 2.

Table 2

Composition of mixed oxides obtained by thermolysis of several mixed complexes, at 1000°

N° *	Composition of mixed oxides
1	$2CoO.3TiO_2$
2	$3CoO.4TiO_2$
3	$3CoO.2TiO_2$
4	$CoO.2TiO_2$
5	$CoO.TiO_2$

*) The numbers correspond to those given in fig. 1. The composition of the complexes from which the oxides were obtained are given in Ref. 2.

The mixed oxides obtained at 1000°, by the thermal decomposition of all mixed complexes which were synthesized, are given in table 2.

---

[1] C. GH. MACAROVICI and M. STRĂJESCU, *Rev. Roumaine Chim.*, **13**, 1601 (1968).
[2] M. STRĂJESCU, *Anal. Univ. Timişoara, Seria Sti. Fiz.-Chim.*, **X**, 73 (1972).

The X-ray photographs of the oxides, which are shown in tables 1 and 2, were produced with a T.U.R.M. 60 Dresden apparatus by the Debye-Scherrer powder method. A Cu anti-cathode (λ_{Cu}, $K\alpha_1 = 1.54050$ Å) and a Ni filter were employed at 50 Kw and 10 mA. The diameter of the camera was of 57.5 cm. The exposure time was 3–4 hours.

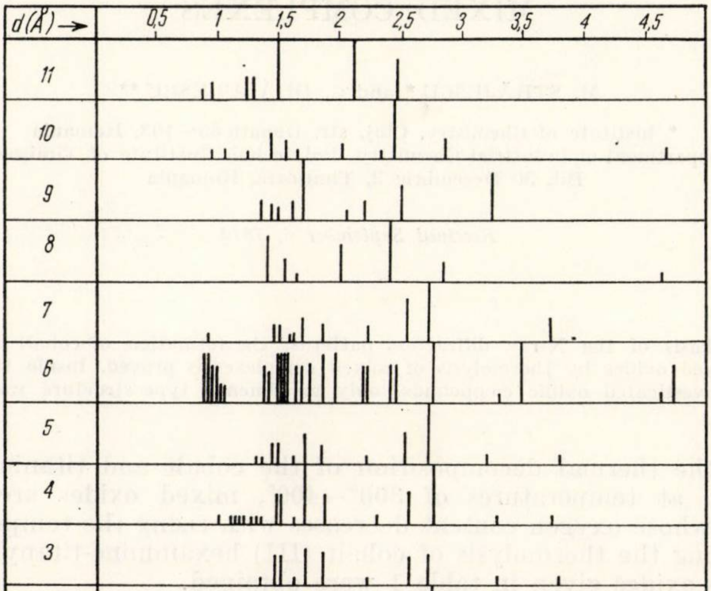

Fig. 1. — X-ray diffraction patterns of mixed oxides of cobalt and titanium. (The composition of the mixed oxides is given in tables 1 and 2. The diffraction patterns *6–11* were reproduced from literature [3,4]: *6* = $CoO.2TiO_2$; *7* = $CoO.TiO_2$; *8* = $2CoO.3TiO_2$; *9* = TiO_2 — rutile; *10* = Co_3O_4 and *11* = CoO).

Figure 1 shows the X-ray powder diffraction patterns. The numbering of the diagrams given in figure 1 is identical with that of the oxides listed in tables 1 and 2. In addition, the d/n values for the simple oxides of cobalt and of titanium, as well as for the cobalt ortho-, meta- and dititanate [3,4] are given.

By comparing the diffraction patterns it has been ascertained for absolutely all cases of mixed oxides which we have obtained that the diffraction lines correspond to those of the metatitanate, $CoTiO_3$, with an ilmenite structure. This structure shows up immediately after decomposition of the initial mixed complex has ended, i.e. above 330° (table 1) and is maintained up to 1000°. By rising the temperature, the diffraction lines become more intense and lines that could not be discerned at lower temperatures, are visible.

The fact that only an ilmenite structure is obtained by the thermal decomposition of the mixed complexes of cobalt and titanium up to 1000°, irrespective of the Ti : Co ratio in the initial complex in the investigated range (Table 2), respectively in the mixed oxides, is in good agreement with the reports of other authors. [5] In the case of the solid state reaction between CoO and TiO_2, at temperatures higher than 1000°, the metatitanate always forms first and, depending on the initial ratio of these two oxides, it remains as such or is converted into cobalt ortho- or dititanate, at temperatures above 1200°.

The formation of the spinel Co_2TiO_4 first [6,7] is categorically contradicted. [8]

The only titanate that has an ilmenite structure is the metatitanate whose CoO : TiO_2 ratio is one. In the oxides obtained by us, this ratio differs from one, being 2 : 3, 3 : 4 and 1 : 2. As there is an excess of TiO_2 in comparison with the composition of metatitanate, we would expect the diffraction lines of rutile to be present in the spectra, too. However, these lines were either not observed or, at best, of the three strong lines of the rutile at 3.24, 2.49 and 1.69 Å, the first is very weak and the last two are shifted and superposed over the $CoTiO_3$ lines. The following would account for this fact.

The titanate with formula $2CoO \cdot 3\,TiO_2$ is not present in the phase diagram of the $CoO-TiO_2$ system.[9,10] Joubert and Durif [11] prepared it by reacting cobalt sulphate with cobalt and lithium titanate. It follows that, in particular conditions, they may also form other types of titanates.

---

[3] A. I. Kitaigorodskii, "Rentgenostrukturnyi analiz melkokristalliceskikh i amorfnykh tel", Gosudarstennoe izdatelstvo tekhnico-teoreticheskoi literatury, Moskva, 1952, 422–578.

[4] A.S.T.M. index 9–238, 9–418 and 15–866.

[5] T. Kubo, M. Kato, K. Nakazato and K. Fujita, *Kogyo Kagaku Zasshi*, **67**, 1502 (1964).

[6] H. Schmaizried, *Z. phys. Chem. (Frankfurt)*, **33**, 111 (1962).

[7] H. Schmalzried, *Angew. Chem.*, **75**, 353 (1963).

[8] G. Fink, *Z. phys. Chem. (Frankfurt)*, **44**, 122 (1964).

[9] H. J. Strimple, Doctor's thesis, Rutgers University, Mai 1957.

[10] B. Brezny and A. Muan, *J. Inorg. Nuclear Chem.*, **31**, 649 (1969).

[11] J. C. Joubert and A. Durif, *Bull. Soc. Franc. Mineral. Crist.*, **87**, 517 (1964).

An ordinary isomorphism of $CoTiO_3$ and TiO_2 is excluded [12] because they belong to different spatial groups and even to crystallographic systems, trigonal and tetragonal, respectively. Therefore they cannot form solid solutions.

The absence of the diffraction lines of rutile in the X-ray spectra of the mixed oxides containing an excess of TiO_2 in comparison with the metatitanate, might be explained by assuming the syncrystallization of the excess of titanium dioxide in an identical system with that of $CoTiO_3$.

The uncommon reaction conditions proceed precisely from the way in which the mixed oxides were obtained, i.e. by thermal decomposition of the mixed complexes, which leads to a perfect homogeneous distribution between CoO and TiO_2, at molecular scale. Since $CoTiO_3$ is formed in the system, the problem of a reaction between this compound and the exceeding TiO_2 appears.

Dietzel's theory [13] of the cationic fields intensity asserts that, in order that two oxides form stable combinations, the difference between the cationic fields intensities must exceed a certain minimum value which, expressed in Z/a^2 units is $\Delta(Z/a^2) > 0.3$ (Z = cation charge; a = anion-cation distance). However, we mention that, since Dietzel's empiric rule implies a spherical symmetry of the cationic field, it has a much more limited value for the transition metal ions, which have not such a symmetry, because of the suppresion through coordination of the "d" orbitals degeneration. [14–17]

Since Dietzel's rule is given for a pair of binary oxides, we make an approximation, considering $CoTiO_3$ as a binary oxide. The approximation is possible due to the fact that, in the ilmenite structure of $CoTiO_3$, the two cations are found only in octahedral sites, the Ti–O distances being of 1.92 or 2.06 Å, and the Co–O distances, of 2.08 or 2.16 Å, the mean distances being of 1.99 and 2.12 Å, respectively. [18]

By presuming, instead of the Ti^{4+} and Co^{2+} cations, one cation (M) with a mean charge $(4 + 2)/2 = 3$, that is M^{3+} and by using the average of the mean interatomic distances, i.e. the value 2.055, a Z/a^2 ratio of $3/2.055^2 = 0.71$ was found.

Since in TiO_2,[19] $Z/a^2 = 1.25$, for the fictitious oxidic system $M_2^{3+}O_3-Ti^{4+}O_2$, $\Delta(Z/a^2) = 1.25 - 0.71 = 0.54$. From this value it results that the formation of a stable combination between $CoTiO_3$ and TiO_2 has a considerable probability ($0.54 > 0.3$).

If we admit the reaction as being likely, on the basis of the above mentioned reasons, and considering the fact that cationic radii of Ti^{4+} and Co^{2+} are not too different (0.64 respectively 0.82 Å), it would result that a mixed lattice of ilmenite type is formed. In this lattice, the exceeding titanium cations, likely under the form of Ti^{2+} or Ti^{3+} cations, occupy also the sites of Co^{2+} which is absent from the system in comparison with the stoichiometric ratio of these two metals in the metatitanate. The radius of $Ti^{2+} = 0.76$ Å. The possibility of reducting Ti^{4+} to Ti^{2+} would be offered by the electrons of additional chemically bound oxygen, which evolves out of the system with rising temperature. The absence of the diffraction lines of rutile in the spectra of cobalt and titanium mixed oxides obtained from complexes, might thus be explained.

---

[12] I. Imreh, "Cristalografie", Ed. didactică și pedagogică, Bucharest, 1966, 211–220.

[13] A. Dietzel, *Z. Elektrochem.*, **48**, 9 (1942).

[14] J. D. Dunitz and L. E. Orgel, *J. Phys. and Chem. Solids*, **3**, 20 (1957).

[15] D. S. McClure, *J. Phys. and Chem. Solids*, **3**, 311 (1957)

[16] E. W. Gorter, *Philips Res. Repts.*, **9**, 295 (1954).

[17] G. Blasse, *Philips Res. Repts. Suppl.*, **3**, 1 (1964).

[18] R. E. Newnham, J. H. Fang and R. P. Santoro, *Acta Cryst.*, **17**, 240 (1964).

[19] M. Zaharescu, Doctor's thesis, Institute of Chemistry Cluj, 1971.

CONCLUSIONS

By the thermolysis of certain mixed complexes of the cobalt (III) ammine titanyl-oxalate type, up to 1000°, mixed oxides of cobalt and titanium were obtained, whose composition differs from that of known cobalt titanates,[10,11] namely cobalt ortho-, meta-, di- and trititanate. The latter have the following oxidic compositions : $2\,CoO.TiO_2$, $CoO.TiO_2$, $CoO.2TiO_2$ and $2CoO.3TiO_2$.

Even in the case when a mixed oxide with $2CoO.3TiO_2$ composition was obtained, the crystalline structure of the latter was not of a spinel type, of the form $Co_2(Ti_3\,\square)\,O_8$ ($\square$=gap), but of an ilmenite type, similar to that of $CoO \cdot TiO_2$. The same structure was obtained in all cases.

Nevertheless, from the thermal decomposition processes of the mixed complexes of cobalt and titanium, mixed oxides are directly obtained, at temperatures of 300°–600° and by no means physical mixtures of TiO_2 and Co_3O_4 with an appreciable quantity of physically retained oxygen and an ilmenite structure, irrespective of the ratio between these two constituent oxides. This structure which appears simultaneously with the first oxide system at 300°–600°, is consolidated up to 1000°, although the oxygen content of the mixed oxides decreases to values corresponding stoichiometrically to the TiO_2 and CoO of the given oxidic system. The loss of oxygen is monotonous since it does not significantly modify the shape of the thermal analysis curves. [1,2]

The X-ray photographs of the mixed oxides which we obtained were similar to those of the non-equilibrium solid solutions. These are essentially systems with disordered and distorted crystalline structures having many deficiencies and deviations from the stoichiometry of equilibrium systems. These facts, besides the above mentioned ones, are revealed by the X-ray photographs which, especially for the large angles of reflection, show weak and broadened diffraction lines against a dark background. [20]

The size of the particles in the mixed oxides was approximately 1000 Å, a fact certified by the width of the diffraction lines. The same fact ascertains the non-homogeneity of the structural microdeformation in the synthesized mixed oxides.

---

[20] I. I. Ioffe and L. M. Pismen, "Cataliza eterogenă în ingineria chimică", Ed. tehnică, Bucharest, 1967, 349.

"Molecular Motions in Liquids" Proceedings of the 24-th Annual Meeting of the Société de Chimie Physique, Paris–Orsay, 2–6 July 1972, edited by Jean Lascombe. D. Reidel Publishing Company, Doddrecht, Holland/Boston – U.S.A.

In the past forty years remarkable progress has been obtained in the development of new concepts, autocorrelations and molecular dynamics as well as in the perfection of some established methods such as dielectric dispersion, infrared and Raman spectroscopy and Rayleigh scattering and the elaboration of new methods of investigation such as inelastic neutron scattering and ultrasonic sound propagation.

The purpose of the "Molecular motions in liquids" Conference in Orsay was, as Jean Lascombe said, to update the results obtained in the study of fluctuation states.

The introductory report to the meeting was Jaques Yvon's paper on phenomena ascribable to classical mechanics and quantum theory, intermolecular forces, impenetrability of molecules, free surfaces, gravity and the role of applied fields, the theory of grand ensembles, chemical potential, metastable states, negative pressures, fluctuations, neutron and light scattering in transparent liquids.

After a survey of the conference programme, the book highlights on other theoretical and experimental papers dealing with: transport phenomena, viscoelastic and ultrasonic relaxation, autocorrelation functions, isotope effects, permittivity and dipole correlations, the influence of FIR absorption on the dielectric behaviour, dielectric relaxation, molecular vibrations in liquids, Raman and infrared spectroscopic studies, hydrogen-bonded systems, nuclear magnetic resonance studies of association and reorientation in liquids, electron spin and nuclear magnetic resonance relaxation studies, self-diffusion, investigation of molecular liquids by neutron spectroscopy, computer "experiments" on simple liquids, study of the relaxation and mechanism by Brillouin spectra, molecular motions in liquids from low-frequency depolarized light scattering, molecular theory of non-linear electro-optical effects in isotropic media, Rayleigh scattering of light from supercooled liquids, Brillouin scattering in the inert-gas liquids, interpretation of far infrared spectra in terms of collision distribution, dielectric absorption of non-polar liquids in the microwave and far infrared region, etc.

The high theoretical and experimental level of the papers presented to the Proceedings of the 24-th Annual Meeting of the Société de Chimie Physique has proved that this field is still subject to active research, owing to the refinement of spectroscopic methods, high speed calculations and the development of applications of the statistical mechanics to the study of the liquid state.

The book gives physical chemists a general view of the state-of-the-art in fluctuation states and stimulates the interest for further work in this field.

D. I. Marchidan

INDEX DU TOME 19, 1974

INDEX DES AUTEURS

A

Ababi V., voir Bourceanu G. 207
— , voir Onu P. 1279
Airinei A., voir Gabe I. 1727
— , voir Voiculescu N. 399
Aleem M. A., voir Ismail S. M. . . 847
Ali A., voir Ismail S. M. 847
Angelova I. G., voir Mondeshka D. . 1759
Amălinei I., voir Cobianu N. 1251
Andrei C., voir Nanu I. 115
— and I. Nanu, Copolymers of conjugated dienes with maleic acid monoesters. VIII. Bulk copolymerization of isoprene with monobutylmaleate 1535
Andrei G. and Gh. Şerban, C. Floriţa, Catalytic dehydrogenation kinetics of n-butenes to butadienes 727
Angelescu A., voir Iovu M. 1061
Anghelache I. and D. Săndulescu, V. Vântu, Hydrogen transfer reactions between hydrocarbons and free radicals. II. The study of molecular combinations between aromatic hydrocarbons and the 1,1-diphenyl-2-picrylhydrazyl free radicals (DPPH) 1045
Armstrong D. R. and P. G. Perkins, K. S. Sorbie, The electronic structures of BH_3 and BH_4^- 747
—and P. G. Perkins, J. J. P. Stewart, A theoretical investigation of Ziegler-type catalysis. II. Species related to solid titanium trichloride 1695
Atanasiu I. and T. Badea, Electrochemical behaviour of 18 Cr—10 Ni stainless steel in organic acid solutions. I. Formic acid. 1447
Attia M. E., voir Bishara S. W. . . 1099
Avram M., voir Dinulescu I. G. . . . 1197
Avramovici S. and I. Ciocoiu, G. I. Rusu, Electrical conductivity of some salicylidenanils 1053

B

Badea F., voir Glatz A. M. 87
Badea V., voir Cuiban F. 1521
Badea T., voir Atanasiu I. 1447
Bădilescu S., Molecular interaction in solutions. Calculations of the interaction potential energy in the carbon disulphide-chloroform system . . . 991
— , Simultaneous vibrational transitions. III. Collision complexes of chloroform in nonpolar solvents . . 1139
— , Simultaneous vibrational transitions. IV. Shape of some bands of carbon disulphide and chloroform, and relaxation mechanisms in solutions 1145
Balaban A. T., Chemical graphs. XXI. Valence isomers of benzoannulenes 1185
— , Chemical graphs. XXII. Valence isomers of heteroannulenes or of substituted annulenes. Coisomeric cubic multigraphs 1323
— , Chemical graphs. XXIII. General cubic graphs with one loop, and homovalenes or their derivatives 1611
— , voir Barabas A. 1927
— and F. Kerek, Chemical graphs. XX. Graphs of parallel and/or subsequent substitution reactions . . . 631
— and M. Paraschiv, Molecular complexes with aromatic cations as electron acceptors. II. Charge-transfer spectrum of 2, 4, 6-triphenylpyrilium thiocyanate 1731
— and C. Pomponiu, Computer program for determining all possible ESR spectra with equidistant lines 581
Balog A. and E. Vargha, D. Breazu, F. Gőnczy, C. Daicoviciu, L. Beu, Peptides. XV. The use of β-dicarbonyl N-protected asparagine and glutamine in peptide synthesis 689
Banciu A. and M. Elian, A. Bucur, D. Georgescu, E. Ciorănescu, C. D. Nenitzescu, Carbonium ion reactions. IX. Synthesis and acetolysis of 2 : 3.5 : 6-dibenzobicyclo-[5.1.0] octa-2.5-dien-4-yl-methyl tosylate and 2 : 3.5 : 6-dibenzobicyclo [5.1.0] octa-2.5-dien-4-yl-ethyl-β-tosylate . . . 213
Banciu A. C., voir Spacu P. 1861
— and P. Spacu, Co (II) chelates with 1-methyl-2-carbethoxy-glyoxa-

lanil-(1)-methoxy-phenylhydrazones-(2) 1169
— and P. Spacu, Co (II) chelates with 1-methyl-2-carbethoxy-glyoxalanil-(1)-tolylhydrazones-(2) 1019
— and P. Spacu, Ni(II) chelates synthetized with 1-methyl-2-carbethoxy-glyoxalanil-(1)-methoxy-phenylhydrazones-(2) 1307
— and P. Spacu, Ni (II) chelates synthetized with 1-methyl-2-carbethoxy-glyoxalanil-(1)-tolylhydrazones-(2) 817
Banciu M. and E. Dragu, D. Georgescu, E. Cioränescu, Carbonium ion reactions. X. Nitrous acid deamination of 5-aminomethyl-5H-6,7-dihydrodibenzo[*a*, *c*]cycloheptene . . 1343
— and M. Elian, C. Drăghici, E. Cioränescu, The PdCl$_2$-induced rearrangement of dibenzobullvalene into dibenzo[*g*, *h*] bicyclo [4.2.2] deca-2, 4, 7, 9-tetraene 1179
Bansal N. P., Interdiffusion coefficients of silver (I) in molten sodium nitrate-alkaline earth nitrates mixtures . . 1287
Barabas A. and A. T. Balaban, Chemical graphs. XXIV. Isomerizations and isographic transformations . . 1927
Bărboiu V., Magnitudes and signs of ^{13}C coupling constants in several organic molecules by double resonance 363
Bărbulescu A., Synthesis and thermal analysis of titanium oxyhidrate ultrafine powders 833
Bărbulescu N., Les tensions superficielles des fluides 169
Bărbulescu F. and A. Gref, M. Craiu, The conductance of some alcaline alkoxides in ethanol-benzene and ethanol-dimethylformamide mixtures at 25° 1817
Bărbulescu N. and M. Leca, Elimination reactions in the 8-R-tricyclo-[7, 3, 1, $0^{2,7}$]-tridecane series. III. Dehydration of 8-R-tricyclo [7, 3, 1, $0^{2,7}$] tridecane-2,13-diols 233
— and M. Leca, Elimination reactions in the 8-R-tricyclo [7.3.1.$0^{2,7}$] tridecane series. IV. Pyrolytic elimination of tricyclo[7.3.1.$0^{2,7}$]trideca-2-en-13-acetate 443
— and M. Leca, Elimination reactions in the 8-substituted-tricyclo-[7.3.1.$0^{2,7}$] tridecane series. V. Configuration of 8-substituted-tricyclo-[7.3.1.$0^{2,7}$] tridecen-13-ols 1381
— et A. Nicolae, Recherches dans la série des tricyclo [7.3.1.$0^{2,7}$] tridécanes. III. Hydrazones de la 2-hydroxy-8-R-tricyclo [7.3.1.$0^{2,7}$] tridécan-one-13 869
Bendic C., voir Sahini V. E. 1685
Benedikt G. M., voir Moraru M. . . 877
Beu L., voir Balog A. 689
Beu L. and J. Russu, Synthesis and spectrophotometric studies in the trisubstituted carbetoxyphenylhydrazones series 1825
Bhatia R. L. and H. C. Gaur, Chronopotentiometric study of Ag(I) in molten mixtures of alkali-alkaline earth metal nitrates 779
Bică I. and M. Căldăraru, γ-radiolysis of gaseous isobutylene. The influence of experimental conditions on the radiochemical yields of the main radiolysis products 17
— , voir Murgulescu I. G. . . . 1841
Biradar N. S. and T. R. Goudar, Spectral study of dioxouranium (VI) complexes with aromatic Schiff bases 1441
— and A. L. Locker, V. H. Kulkarni, Addition compounds of zirconyl chloride with aromatic Schiff bases 45
Birou M., voir Macarovici Const. Gh. 49,805
Bishara S. W. and M. E. Attia, H. N. A. Hassan, Microdetermination of organic sulphur or inorganic sulphate . 1099
Bodea C., voir Oşianu D. 1203
— , voir Tămaş V. 701
Boghină C., voir Cobianu N. 1251
БОЙЕШАН В. и Д. ФЕЛЬДМАН, Влияние условий распылительной сушки на свойства пастообразующего поливинилхлорида. Сообщение. I. Экспериментальная часть 283
БОЙЕШАН В. и Д. ФЕЛЬДМАН, Влияние условий распылительной сушки на свойства пастообразующего поливинилхлорида. II. Морфологические исследования . . . 493
Borcan R., voir Zuca Şt. 553
Bossanyi M., voir Micu-Semeniuc R. 1157
Botar A. V., voir Marcu Gh. 577
— , voir Marcu Gh. 827
Bourceanu G. and Gh. Popa, M. Sanduloviciu, V. Ababi, Transformation of the toluene-water mixture in the high frequency discharge plasma 207
Breazu D., voir Balog A. 689
Brezeanu M. and I. Jitaru, Coordination compounds with choline perchlorate 1883
Buchwald P. and F. Domnariu, The synthesis of 2,2-dichloro-benzoaldoxime from 4-nitro-toluene 1221
Bucur A., voir Banciu A. 213
Budrugeac P. and M. I. Vass, Some considerations concerning Gibbs free energy of gas-solid interface . . . 1153
Burnea I. und M. Pleniceanu, L. Burnea, Spektrophotometrische Untersuchung des Systhems Vanadium (V) Solochromviolett R.S. Die spektrophotometrische Bestimmung des Vanadiums 501

Burnea L., voir Burnea I. 501

C

Cădariu I., voir Gavrilă E. 1899

Căldăraru M., voir Bică I. 17

Calenciuc M., voir Calu N. 1889

Calu N. et A. Popa-Rang, M. Calenciuc, Combinaisons complexes du Mn (III) et du Mn (IV). I. Le système Mn (III, IV) — acide aniline — 4 sulphonique 1889

Carp E. and M. Dorneanu, I. Zugrăvescu, *o*-Diazobicyclic derivatives of benzo [*c*] cinnoline. IV. Addition reactions of 3,8-dimethylbenzo [*c*] cinnoline, via ylidic intermediates, leading to new *o*-diazabicyclic systems . . 1507

Cassoux P. and J. F. Labarre, J. M. Savariault, Bonding and magnetic properties in tetrakis phosphine complexes of nickel 1471

Chiraleu F., voir Dinulescu I. G. . 1197

Chiş E., voir Macarovici Const. Gh. 1855

Chorbadjiev S., voir Markov P. . . . 1317

Cilianu S., voir Cuiban F. 1521

Cîmpeanu G., voir Iovu M. 881

Cincu C., voir Cobianu N. 1251

Ciocăzanu I., voir Vîlcu R. 785

Ciocea N., voir Teoreanu I. 561

Ciocoiu I., voir Avramovici S. 1053

Ciolac S. and O. Radovici, The corrosion of carbon steel and some austenitic stainless steels in synthetic river waters 543

Ciomârtan D., voir Pârlog C. 1303

Ciorănescu E., voir Banciu M. 213, 1179, 1343

— , voir Drăguţan I. 67

Cîrje M., Über 1, 2, 3, 4-tetrahydroacridin-9-carboxyl-säure derivate. II. Ester und Thioester 249

Cobianu N. and C. Boghină, B. Mărculescu, C. Cincu, I. Amălinei, Copolymerization of N-vinylcaprolactam with vinylpyridines 1251

Comptes Rendus, 337, 517, 518, 735, 1113, 1113, 1115, 1117, 1118, 1283, 1418, 1555, 1555, 1556, 1677, 1678, 1679, 1680, 1680, 1681, 1682, 1835, 1969

Constatinescu A. and C. Liteanu, Separation of creatinine from leucine in a proteic hydrolysate by paper chromatography with a combined temperature and stationary phase section gradient 1107

— and C. Liteanu, Separation of small amounts of amino acids and their identification in complex mixtures with urea in excess 1551

Constantinescu C. und S. Fişel, Spektrophotometrische Bestimmung des Thaliums mit Meta-Nitralgrün . . 329

— und S. Fişel, Spektrophotometrische Bestimmung des Tl (III) mit Ortho-Nitral und Para-Nitralgrün . 509

Constantinescu M., voir Gheorghiu C. 1909

Constantinescu O., voir Gheorghiu C. 1909

Contineanu M., voir Oncescu T. 931, 1559

Coriciuc C., voir Mocearov V. 1271

Cőrmős D. C. and I. Haiduc, P. Steţiu, Synthetic single crystal PbSe electrode. Potentiometric titration of Cu(II) with Na_2EDTA 1949

Cormoş L. and A. Pop, V. Sbera, Decomposition of organic hydroperoxides in the heterogeneous catalysis. II. Decomposition of cumene hydroperoxide on strongly acidic cationites 1631

Cornea F. et C. Fulea, S. Moldoveanu, Complexes moléculaires des thioamides. II. Complexes de transfert de charge du phénylthioacetamide et phénylthioacétopiperidide avec l'iode 429

Costeanu C., voir Landauer O. . . . 1429

Costin R., voir Zuca Şt. 181

Craiu M., voir Bărbulescu F. . . . 1817

Craiu M., voir Sahini V. E. 165

Csomontanyi G., voir Mocearov V. . 1271

Cuiban F. and S. Cilianu, V. Badea, The synthesis of some C-terminal analogues of the peptides : eledoisin and physalaemin 1521

D

Deutsch R., voir Vodnár J. 1545

Dimonie V., voir Donescu D. 1243

— and D. Donescu, I. Gavăt, Copolymerization of epichlorhydrin and propylene oxide with the $AlEt_3$—H_2O catalytic system 125

— and D. Donescu, M. Munteanu, C. Hagiopol, I. Gavăt, Kinetics of emulsion polymerization of vinyl acetate in the presence of polyvinyl alcohol 903

Dinulescu I. G. and M. Pop, F. Chiraleu, M. Avram, C. D. Nenitzescu, Investigations in the cyclobutane series. XXXIII. Synthesis of *syn*-dibenzo [*c*, *g*] tricyclo $[4.2.2.0^{2,5}]$ deca-3, 7, 9-triene. A new dibenzo $(CH)_{10}$ hydrocarbon 1197

Donescu D., voir Dimonie V. 125

— , voir Dimonie V. 903

— and C. Hagiopol, M. Munteanu, V. Dimonie, I. Gavăt, Chain transfer in emulsion polymerization of vinyl acetate 1243

Domnariu F., voir Buchwald P. . . . 1221

Dorneanu M., voir Carp E. 1507

Doss S. H. and S. Kondo, K. Tanaka, Y. Tsuzuki, NMR studies of the effect of nitrogen atom on the anomeric proton of β-D-glucopyranosides 1767
Drăghici C., voir Banciu M. 1179
— , voir Drăguţan I. 67
Drăghici C., voir Urseanu F. 1751
Dragu E., voir Banciu M. 1343
Drăgulescu C. and A. Nimară, I. Julean, Contributions to the bismuth hydrolysis study. III. Electrometric investigations on bismuthyl perchlorate hydrolysis 1455
— and S. Policec, T. Simonescu, Complexes of anthranil-N,N-diacetic acid with trivalent metals. II. Entropy change calculation 801
— , voir Solacolu I. 415
— , voir Străjescu M. 1963
Drăguţan I. and C. Drăghici, A. Haneş, A. Dumitriu, E. Ciorănescu, C. D. Nenitzescu, Carbonium ion reactions. VIII. Benzobicyclooctene derivatives through π-route 67
Druţă I., voir Zugrăvescu I. . . . 647,659
Dumitrescu P., voir Pop A. 1073
Dumitriu A., voir Drăguţan I. . . . 67

E

El-Abbady A. M. and M. A. Omara, Kandil N. G., Condensation of β-aroylpropionic acids with isatin under Perkin conditions 79
Elian M., voir Banciu A. 213
— , voir Banciu M. 1179
Enculescu M., Influence of oxides of transitional elements on the properties of mineralogical components of clinkers of cements 1491

F

Fabian J., voir Vlassa M. 665
Facsko Gh. und M. Nemeş, Die amperometrische Titrierung des Quecksilbers (II) in stark alkalischem Medium mit Thioacetamid 141
— and M. Poraicu, Kinetic study of oxido-reduction reactions by means of the vibrated electrode technique 341
Fătu D. and A. Schiopescu, Thermal decomposition of potassium ferrate (VI) 1297
Feldman D., voir Boişan V. . . 283,493
Filip P., voir Gheorghiu M. D. 859
Finta Z., voir Ripan R. 37
Fişel S., voir Constantinescu C. . 329,509
Fiti M., Some aspects of radiolytic oxidation of phenol in aqueous solution 1083
Fitzner K., voir Moser Z. 1573
Florea I., Spektrophotometrische Dosierung des Benzidins und o-Tolidins mit Natriumhypochlorit 157
Florescu M., Romanian research, a message of Romania's peaceful policy. 3
Floriţa C., voir Andrei G. 727
Frangopol M. and P. T. Frangopol, N. Negoiţă, Formation of new nitrogen-free radicals from dinitro-sulphophenyl-N-alkoxyamines 1773
Frangopol P. T., voir M. Frangopol. 1733
Fulea C., voir Cornea F. 429

G

Gabe I. and A. Tolea, A. Airinei, Chelates and polychelates of amino acids. II. Complexes in solution of copper-(II) with N(R)-anthranilic acid . . 1727
Găinar I., voir Vîlcu R. 1123
Galasiu I., voir Sternberg S. . . 523,967
Ganovici L., voir Petrescu N. 187
Gaur H. C., voir Bhatia R. L. 779
Gavăt I., voir Dimonie V. 125,903
— , voir Donescu D. 1243
Gavrilă E. und I. Cădariu, Über Triazine. L. Mitteilung. Potentiometrische Bestimmung der Aciditätskonstanten von 4-Hydroxy-6-Oximintetrahydrotriazinyl-2-formaldoxim 1899
Georgescu D., voir Banciu A. . 213,1343
Gheorghiu C. and M. Constantinescu, O. Constantinescu, V. Pocol, Study of some Cu(II)selenocyanate complexes with biguanide derivatives . 1909
Gheorghiu M. D. and P. Filip, Electronic structure of cyclobutadiene fused with heterocyclic ring. I. Heterobenzocyclobutadienes. 859
Ghiran D., voir Simiti I. 1067
Gilman H., voir Haiduc I. 1709
Glatz A. M., Aluminium chloride catalyzed condensations of unsaturated acids with benzene 455
— and V. Wertheimer, F. Badea, Aluminium chloride catalyzed reactions of unsaturated acids with benzene. VI. Reaction of cyclopentylacrylic acid 87
Gocan S. und C. Kyri, Trennung einiger Aminosäuren durch Dünnschichtchromatographie mit orthogonalem Temperaturgradient 1957
Gőnczy F., voir Balog A. 689
Goudar T. R., voir Biradar N. S. . . 1441

Gref A., voir Bărbulescu F. . . . 1817

Grigorescu-Sabău C., voir Spiridon Şt. 131

Győrfi Z., voir Suciu D. 671

H

Hagiopol C., voir Dimonie V. 903

— , voir Donescu D. 1243

Haiduc I., voir Cőrmős D. C. 1949

Haiduc I. and R. B. King, H. Gilman, Reactions of some pentafluorophenylsilicon derivatives with the π-cyclopentadienyliron dicarbonyl anion. . 1709

Haneş A., voir Drăguţan I. 67

Hassan H. N. A., voir Bishara S. W. . . 1099

Herdan J., voir Zugrăvescu I. . . 647,659

Herdlicka C., voir Sternberg S. . . 197,763

Hillebrand M. and M. Răileanu, Radical ions. II. Nitrophenothiazine radical-ions 1227

Hőlszky C. und C. Suciu, D. Săndulescu, Über den Einfluss der Elektrolyten auf die Zähigkeit der Polyvinylalkohol-Lösungen 887

Hopîrtean E. and C. Liteanu, Studies on the electroanalytical behaviour of membrane-electrodes under current. V. The E-pH electrode function and the use of the PVC + tricresylphosphate membrane in the acid-base potentiometric titration at constant direct current 157

— and C. Liteanu, A. Maşa, Studies on the polymer + plasticizer membrane-electrode. XI. Influence of the plasticizer of the PVC on its electrode behaviour 921

— and C. Liteanu, E. Ştefănigă, Membrane-electrodes of a metallic wire-plastic membrane type. I. K^+-selective membrane electrode . . . 1651

— and E. Ştefănigă, Liquid membrane-electrodes. V. Electrodic behaviour of sodium tetraphenylborate in cyclohexanone to certain monovalent cations 1265

Hubin R., Etude du spectre vibrationnel, infrarouge et Raman, du pyrophosphate de plombIV—PbP_2O_7 . . 947

I

Ionescu I., Quelques remarques sur les propriétés des bétons aux résines synthétiques sans liants minéraux. I. 99

— , Quelques remarques sur les propriétés des bétons aux résines synthétiques sans liants minéraux. II. . . . 293

Ionescu M., voir Vlassa M. 665

Iovu M. and A. Angelescu, Bis-thioethers. I. Condensation alkali thiophenolates with dichloromethylated derivatives 1061

— et G. Cîmpeanu, N. Miclovici, Tris-éthers. II. Condensation du bis (chlorométhyle) éther avec des cyclohexylphénoxides, methylcyclohexylphénoxides et chlorocyclohexylphénoxides de sodium 881

— et E. Tudor, Formation d'isomères dans les réactions de cyclohexylation catalytique de benzène . . 1207

Ismail S. M. and M. A. Aleem, A. Ali, The activation of palladium catalysts by rare earth and other oxides for the hydrogenation of cyclohexene . . . 847

Ivan E., voir Spacu P. 1861

Ivana E., voir Sahini V. E. 165

J

Jain S.K., Silver-silver halide electrodes in molten sodium nitrate-barium nitrate eutectic 1811

Jitaru I., voir Brezeanu M.. 1883

Julean I., voir Drăgulescu C.. . . . 1455

K

Kandil N. G., voir El-Abbady A. M. 79

Kerek F., voir Balaban A. T. . . . 631

Khalaf A. A., Modern Friedel-Crafts chemistry. VII. On the question of group participation in the rate-determining ionization step during inter- and intramolecular Friedel-Crafts alkylations and the mechanism of formation of 1-methyltetralin during the $AlCl_3$-catalysed reaction of 1-chloro-2-methyl-4-phenylbutane 1361

— , Modern Friedel-Crafts chemistry. VIII. Cyclialkylations of some aryl- and diarylalkanols in the presence of the mild $AlCl_3/CH_3N_2$ catalyst 1373

— and R. M. Roberts, Modern Friedel-Crafts chemistry. V. The fragmentation and dealkylation of straight-chained diphenylbutanes under the influence of water-activated aluminium chloride at 100°. 1351

Khan S. A. and M. Stone, Determination of lithium in silicate rocks and minerals using a simple flame photometer 1669

King R. B., voir Haiduc I. 1709

Kondo S., voir Doss S. H. 1767

Korshak V. V., voir Mandric Gh. . . 1783

Kraus H., voir Răileanu M. 709

Krehm H. and G. F. Wright, The hydroxymercuration of nor-bornene . . . 839

Kriza A., voir Negoiu D. 1039,1921

Kulkarni V. H., voir Biradar N. S. 45

Kyri C., voir Gocan S. 1957

L

Labarre J. F., voire Cassoux 1471

Landauer O. et C. Costeanu, C. Mateescu, Sur la viscosité des systèmes mixtes : eau-monoéthylèneglycol, eau-monoéthanolamine et eau-diméthylesulfoxyde. L'influence de la température et des sels, sur la viscosité de ces systèmes 1429

Leca M., voir Bărbulescu N. . . 233,1381

— , voir Bărbulescu N. 443

Leibovici A., voir Murgulescu I. G. 739

Lepădatu C. and S. Moldoveanu, An improvement of Hoffmann's Lcaomo method 1587

— and C. Rusu, On the redox potentials in the transition-metal complexes 811

— , voir Spacu P. 1861

— and V. Tufoi, On the equivalence between the crystal field and M.O. parametric approaches 533

Liga A. and I. Negulescu, Cr. Simionescu, Researches in the terpolymerization field. IV. Preliminary theoretical structural studies of some binary copolymers 911

Liteanu C., voir Constantinescu A. . . 1551

— , voir Constantinescu A., Separation of creatinine from leucine in a proteic hydrolysate by paper chromatography with a combined temperature and stationary phase section gradient 1107,157,921,1651

— , voir Nașcu H.. 1407

— and H. Nașcu, Studies concerning the optimisation of separations by thin layer chromatography on silicagel. I. Separation of some ethanolamines in several polycomponent solvent systems. 1941

Locker A. L., voir Biradar N. S. . . 45

Lucinescu E., voir Vîlcu R. 791

M

Macarovici Const. Gh. and M. Birou, E. Perțe, M. Străjescu, Cobalt and germanium double oxides 805

— et E. Chiș, Un nouveau réactif du type EDTA 1855

— , voir Micu-Semeniuc R. 1157

— and E. Perțe, M. Străjescu, M. Birou, Contribution to the study of the binary system $In_2O_3-TiO_2$ . . 49

— and M. Zaharescu, Contributions to the study of the $NiO-SiO_2-TiO_2$ ternary system 1009

Maior O., voir Rășanu N. 255

Mandric Gh. and A. I. Pavlov, V. V. Korshak, I. Zugrăvescu, Thermostable polymers. III. Polybenzimidazole-imides 1783

Mánok F. und C. S. Várhelyi, R. Oprean, Kinetik unde Mechanismus der Oxydation des Urans(IV) mit Natriumpersulfat 407

Marchidan D. I. and S. Tănăsescu, High-temperature thermodynamic data for some uranium oxides within the range $UO_{2.25}-UO_{2.60}$ 1435

Marchidan S., Application of niobium polarographic reduction in hydrochloric acid-thiocyanate medium to the analysis of ferroniobium alloys . 1661

Marcu Gh. and M. Rusu, A. V. Botar, Heteropolytungstates with U(IV) as central atom. Synthesis and physical-chemical study of the UL_2 complex where $L = P_2W_{17}O_{61}^{10-}$ 827

— und M. Suciu, A. V. Botar, Papierelektrophoretische Untersuchung der Bildung von Verbindungen des Indiums mit R-Weinsäure 577

Mărculescu B., voir Cobianu N. . . . 1251

Markov P. and S. Chorbadjiev, V. Tarpanov, On the reactivity of some metal-sulfur combinations in liquid ammonia 1317

Mașa A., voir Hopîrtean E. 921

Mateescu O., voir Landauer O. . . 1429

Mavrodin-Tărăbîc M., Contributions à l'étude de l'hydrolyse de l'uranium (VI) en milieu azotique 1461

Memetea T., voir Păun J. 941

— and J. Păun, Radiolysis of the complex oxalates in aqueous solutions. IV. The influence of some reducing free radicals scavengers on the potassium trisoxalatocobaltate radiolysis in aqueous solutions 1689

Miclovici N., voir Iovu M. 881

Micu-Semeniuc R. and C. Gh. Macarovici, M. Bossanyi, Investigation of complex compounds with diaminobiphenyl derivatives. XXVIII. Cobalt(II) complex pseudohalides . . 1157

Milescu M., voir Sahini V. F. . . . 1685

Mocearov V. and G. Csomontanyi, C. Coriciuc, A. Panovici, Correlation of the porous structure to the activity and selectivity of some dehydrogenation catalysts 1271

Moldoveanu I., voir Topor I. 985

Moldoveanu S., voir Cornea F. . . . 429

— , voir Lepădatu C. 1587

Mondeshka D. and I. G. Angelova, New direction of substituted β-hydroxy acids dehydration leading to 2,3-disubstituted 1-acetoxy-naphthalenes 1759

Moraru M. and G. M. Benedikt, On the conformational mobility of bicyclo [3.3.1] nonane-2-ones and bicyclo [3.2.1] octane-2-ones 877

Moser Z. and K. Fitzner, Thermodynamic treatment of binary and ternary salt systems with single charge ions 1573

Moţoc I., Matematische Darstellung der Homologie und der homologen Serien. I. Über die Beschreibung der chemischen Systeme mit-Hilfe der be-Matrizen. 1233

— , Mathematische Darstellung der Homologie und der homologen Serien. II. Behandlung in Kategorien . . . 1239

Munteanu M., voir Teoreanu I. . . 371

— , voir Teoreanu I. . 561,1483

Munteanu M., voir Dimonie V. . . . 903

— , voir Donescu D. . . . 1243

Mureşan I., voir Zador L. 353

Mureşan V., voir Negoiu D. 1031

Murgulescu I. G. and I. Bică, Pyrolysis and oxidative pyrolysis of isobutene. I. 1841

— and A. Leibovici, An equation of state for metallic liquids . . . 739

— and J. Păun, The radiolysis of the complex oxalates in aqueous solutions. II. Kinetics and mechanism of the radiolysis of cobalt-trisoxalato-complex in neutral aqueous solutions with α-Po^{210} irradiations 9

— and M. Şerban, On the viscosity of molten metals. II. 1417

N

Nanu I., voir Andrei C. 1535

— und C. Andrei, Copolymere konjugierter Diene mit Monoestern der Maleinsäure. VII. Andere Aspekte der Reaktionskinetik der radikalischen Copolymerisation von Isopren mit Monoestern der Maleinsäure . . 115

Naşcu H., voir Liteanu C. 1941

— and C. Liteanu, The effect of S-chamber shape on the separation of ethanolamines by thin-layer chromatography 1407

Nasta M., voir Negoiu D. . . . 1039,1921

Negoiţă N., voir M. Frangopol . . . 1773

Negoiu D. et A. Kriza, M. Nasta, Sur les composés d'addition du tétrachlorure de thorium avec des azométhynes 1039

— et A. Kriza, M. Nasta, Sur les composés du trichlorure de l'ethoxytitane avec des bases Schiff. . .

— and V. Mureşan, Contributions to the chemistry of thiocomplexex. V. Complex compounds of Pt(II) with thioamides 1031

— , voir Pârlog C. 1303

— and C. Pârlog, D. Săndulescu, New coordinate compounds with molecular nitrogen. I. Synthesis and characteristic properties of some dinitrogen compounds of cobalt, nikel, iron with triaryl-phosphines, triaryl-arsines and triaryl-stibines . . 387

— and L. Paruta, Complex combinations of the transition metals with tertiary stibines. II. Spectral studies Pd(II) complex combinations with tritolylstibines 57

— and A. Şchiopescu, Thermal analysis of ferrate (VI) ion salts with Ni(II) and Co(II) complex ammines 1717

— and A. Şchiopescu, Ferrate (VI) ion salts with Ni(II) and Co(II) tetrapyridine-tetrapicoline complex combinations 1693

Negulescu I., voir Liga A. 911

Negulianu C., voir Simionescu Cr. . 259

Nemeş M., voir Facsko Gh. 141

Nenitzescu C. D., voir Banciu A. . . 213

— , voir Dinulescu I. G. 1197

— , voir Drăguţan I. 67

Nicoară E., voir Oşianu D. 1203

Nicolae A., voir Bărbulescu N. . . . 869

Nicolescu I. V. and I. Suciu, Chromatographic study of acetylene and ethylene adsorption and of palladium dispersion from Pd/Al_2O_3 catalysts 1513

Nimară A., voir Drăgulescu C. . . . 1455

Nuţiu M., voir Nuţiu R. 679

Nuţiu R. and I. Sebe, M. Nuţiu, 2-Thio-5-nitrobarbituric acid . . . 679

Olteanu M., voir Zuca Şt. 181
Olteanu V., voir Urseanu F. 1751
Omara M. A., voir El-Abbady A. M. 79
Oncescu T. and M. Contineanu, Kinetics and mechanism of azibenzyl radiolysis in benzene solution . . . 1559
— and M. Contineanu, Kinetics and mechanism of diphenyldiazomethane radiolysis in benzene solution . . . 931
Onu P. and V. Ababi, Rare earth ion exchange of synthetic faujasite substituted isomorphously by boron . . 1279
Oprean R., voir Mánok F. 407
Oşianu D. and E. Nicoară, C. Bodea, Inchain-epoxides of carotenoids. IV. Metal-chlorides complexes of canthaxanthin inchain-epoxides 1203
Ostrogovich G., voir Safta M. . 1621,1735

P

Panovici A., voir Mocearov V. . . . 1271
Paraschiv M., voir Balaban A. T. . . 1731
Pârlog C. and D. Ciomârtan, D. Săndulescu, D. Negoiu, The crystal structure of ammonium hexahalogenoosmiate and its dinitrogen compounds 1303
— , voir Negoiu D. 387
Paruta L., voir Negoiu D. 57
Păun J., voir Memetea T. 1689
— and T. Memetea, Radiolysis of the complex oxalates in aqueous solutions. III. The influence of some OH scavengers on the radiol ysis of potassium trisoxalatocobaltate in neutral aqueous solution 941
— , voir Murgulescu I. G. . . . 9
Pavlov A. I., voir Mandric Gh. . . . 1783
Perkins P. G., voir Armstrong D. R. 747,1695
Perţe E., voir Macarovici Const. Gh.49,805
— and M. Străjescu, Gallium metatitanate 395
Petrescu N. and L. Ganovici, Diffusive atomic transport in molten antimony 187
Petrescu S., voir Sternberg S. . . . 955
Petrescu V., voir Sternberg S. . . 25,955
Petrovanu M. and A. Sauciuc, I. Zugrăvescu, Phthalazinium ylids. VI. Action of dimethylacetylene-dicarboxylate on disubstituted at the exocyclic carbon phthalazinium-ylids . . 437
Pleniceanu M., voir Burnea I. . . . 501
Ploştinaru S., voir Spacu P. 1861

— and P. Spacu, Mixed ligand compounds of lanthanides with neutral ligands containing donor oxygen atoms. Chlorosalicylates of lanthanides with triphenylarsine oxide 567
Pocol V., voir Gheorghiu C. 1909
Policec S., voir Drăgulescu C. . . . 801
Pomponiu C., voir Balaban A. T. . . 581
Pop A., voir Cormoş L. 1631
— and P. Dumitrescu, Study of cyclohexane dehydrogenation equilibrium and kinetics in pulsed reactor 1073
Pop Gh., voir Ripan R. 1593
Pop I., voir Ripan R. 1593
Pop M., voir Dinulescu I. G. 1197
Pop R. D., voir Simiti I. 1067
Popa Gh., voir Bourceanu G. . . . 207
Popa-Rang A., voir Calu N. 1889
Popea F., voir Spacu P. 1861
Popescu I., voir Voiculescu N. . . . 399
Poraicu M., voir Facsko Gh. 341

R

Radovici O., voir Ciolac S. 543
Radulian I., voir Răileanu M. . . . 709
Răileanu M., voir Hillebrand M. . . 1227
— und I. Radulian, H. Kraus, Säure-Basen-Indikatoren vom Phenothiazin Typ. I. Die Anwendung von 3-H-Phenothiazin - 3 - [4-Anil-Sulfonsäures Kalium] 3H-Phenothiazin-3-[2-Anilsulfonsaüres Kalium] als Säure-Basen Indikatoren 709
Rao N. U. M., voir Taneja A. D. . . 1093
Răşanu N. and O. Maior, Synthesis based on formyl furo-(2,3-b) benzothiachromone 255
Rimer D., Generalisations du triangle de Gibbs pour les systèmes quaternaires et quinaires 997
Ripan R. and Z. Finta, Cs. Várhelyi, On α-dioximine complexes of the transition metals. XXXVIII. The $[Co(DH)_2(NO_2)(CN)]^-$ion and its basic hydrolysis kinetics 37
— et Gh. Pop, I. Pop, L'acide ascorbique comme agent reducteur. IV. La cinétique de la réduction des ions de Pt(II) par acide ascorbique en presence des ions de Pb(II) . . 1593
Roberts R. M., voir Khalaf A. A. 1351
Rusu C., voir Lepădatu C. I. . . . 811
Rusu C., voir Spacu P. 1861
Rusu E., voir Solacolu Ş. 381
Rusu G. I., voir Avramovici S. . . . 1053
Russu J., voir Beu L. 1825
Rusu M., voir Marcu Gh. 827

S

Safta M. and G. Ostrogovich, Studies in the s-triazine field (new series). XV. The protonation equilibria and indicator behaviour of E-1,3-dimethyl-6-(*p*-X-β-styryl)-2,4-dioxo-1H, 3H-1, 3, 5-triazines in 50 vol % aqueous-ethanolic solutions in the presence of sulphuric acid 1621

— and G. Ostrogovici, Studies in the s-triazine field (new series). XVI. Acidic and tautomeric equilibrium constants of the conjugated acids of some E-1,3-dimethyl-6-(*p*-dialkylamino-β-styryl) 2,4-dioxo-1H, 3H-1,3,5-triazines 1735

Sahini V. E. and M. Craiu, E. Ivana, Spectrographic determination of traces of copper, lead, chromium, nickel, molibdenum and cobalt in natural waters 165

— and J. Weinberg, C. Bendic, M. Milescu, Xylidine isomers. III. Acid-basic properties of xylidines in their excited state 1685

Şancu O., voir Teoreanu I. 561

Săndulescu D., voir Anghelache I. . 1045

— , voir Hölszky C. 887

— , voir Negoiu D. 387

— , voir Pârlog C. 1303

— , voir Solacolu I. 415

Sanduloviciu M., voir Bourceanu G. 207

Sauciuc A., voir Petrovanu M. . . . 437

Savariault J. M., voir Cassoux P. . 1471

Sbera V., voir Cormoş L. 1631

Şchiopescu A., voir Fătu D. 1297

— , voir Negoiu D. 1693,1717

Schwartz I., voir Simiti I. 1067

Sebe I., voir Nuţiu R. 679

Şerban Gh., voir Andrei G. 727

Şerban M., voir Murgulescu I. G. . . 1417

Simion A., voir Vîlcu R. 977

Simionescu Cr., voir Liga A. 911

— and C. Vasiliu Oprea, C. Negulianu, Syntheses of new polymers by destructive methods. II. Mechanochemical complexation and complexation by irradiation using ^{60}Co γ-rays in the system : poly(ethyleneterephtalate), ethylene-diamine and metallic salts 259

Simiti I. and D. Ghiran, I. Schwartz, R. D. Pop, Study of some heterocycles. XXVI. Nitration of 2-anilino-5-phenyl-1, 3, 4-oxadiazole 1067

Simonescu T., voir Drăgulescu C. . . 801

Solacolu I. et D. Săndulescu, C. Drăgulescu, La structure cristalline et l'interaction avec la molecule de l'hydrocarbure incluse dans les clathrates du type $M(SCN)_2(4-MePy)_4$. *p*-xylène 415

Solacolu Ş. and E. Rusu, Aspects of the vitreous phase separation process in the $Fe_2O_3-BaO-B_2O_3$ system 381

Sorbie K. S., voir Armstrong D. R. 747

Spacu P., voir Banciu A.C. 817,1019,1169,1307

— , voir Ploştinaru S. 567

— and F. Popea, C. I. Lepădatu, A. C. Banciu, E. Ivan, S. Ploştinaru, Z. Toma, C. Rusu, Palladium (II) and platinum (II) square-planar complexes with tris (*p*-methoxyphenyl) arsine and halide ions . . . 1861

Spiridon Şt. and C. Grigorescu-Sabău, The influence of cross-linkage of anion exchangers on the distribution coefficient of samarium in mixed systems of organic solvent and mineral acid 131

Ştefănigă E., voir Hopîrtean E. 1265,1651

Sternberg S. et I. Galasiu, L'étude galvanostatique du processus de l'adsorption électrochimique sur l'électrode d'iode-charbon actif dans les sels fondus. II. Influence de la température 967

— and I. Galasiu, The galvanostatic study of the electrochemical adsorption process on the iodine-active carbon electrode in molten salts. I. The current intensity effect 523

— and C. Herdlicka, Chronopotentiometric method at high temperatures 197

— and C. Herdlicka, Interdiffusion and selfdiffusion of monovalent cations in fused alkali nitrates and chlorides 779

— and V. Petrescu, The galvanostatic study of the electrochemical adsorption process on the chlorine-active carbon electrode in molten salts. I. Anodic and cathodic polarization curves 25

— and S. Petrescu, V. Petrescu, The galvanostatic study of the electrochemical adsorption process on the chlorine-active carbon electrode in molten salts. III. Anodic polarization (charging) equation 955

Steţiu P., voir Cőrmős D. C. 1949

Stewart J. J. P., voir Armstrong D. R. 1695

Stone M., voir Khan S. A. 1669

Străjescu M. and C. Drăgulescu, Formation and structure of cobalt and titanium mixed oxides obtained from mixed complexes 1963

— , voir Macarovici Const. Gh. 49,805

— , voir Perţe E. 395

Suciu C., voir Hőlszky C. 887

Suciu D. and Z. Győrfi, Electronic spectra and acid-base equilibrium of some α-acylamino-N-heterocycles . 671

Suciu I., voir Nicolescu I. V., Chromatographic study of acetylene and ethylene adsorption and of palladium dispersion from Pd/Al_2O_3 catalysts 1513

Suciu M., voir Marcu Gh. 577

Swinarski A. et A. Zytkowicz, Mécanisme de l'activité catalytique des métaux de transition déposés sur un support actif 1877

T

Taneja A. D. and N. U. M. Rao, Potentiometric determination of dissociation constants of some aromatic acetoamides 1093

Tămaş V. and C. Bodea, Azlactones of carotinoids. II. Retinal azlactone and transformation products . . . 701

Tanaka K., voir Doss S. H. 1767

Tănăsescu S., voir Marchidan D. I. 1435

Tarpanov V., voir Markov P. 1317

Tătaru S. A., An ion-exchange process for gold recovery 717

Teodorescu Gr., Méthodes de détermination de β, β'-dichloro-diéthyl-amine. Spectre en visible et infrarouge du composé résulté entre le β, β'-dichloro-diethyl-amine et le reineckate d'ammonium 321

— , Méthodes de détermination de l'azotate de pilocarpine. Spectre en visible et infrarouge du composé résulté entre l'azotate de pilocarpine et le reineckate d'ammonium . . . 1645

— , Methods for the determination of 2-aminopyridine. Visible and infrared spectra of the combination with ammonium Reineckate . . . 485

Teoreanu I. and M. Muntean, Calcium aluminosulphate formation and hardening properties 1483

— and M. Muntean, The study of the hardening processes in tricalcium silicate-water-electrolyte system . . 371

— and M. Muntean, N. Ciocea, O. Şancu, Mechanism and kinetics of the dissolution in water of some hydrated binders 561

Tolea A., voir Gabe I. 1727

Toma Z., voir Spacu P. 1861

Topor L., Thermodynamic data on vaporization of fused rubidium and cesium fluorides 1569

— and I. Moldoveanu, Vapor pressures of molten $CdBr_2$, CdI_2, $MgBr_2$ and molecular association in gaseous phase 985

Tsuzuki Y., voir Doss S. H. 1767

Tudor E., voir Iovu M. 1207

Tudose R. Z., Heat transfer with chemical reaction modelling of thermal decomposition reactions . . . .

Tufoi V., voir Lepădatu C. 533

U

Urseanu F. and C. Drăghici, V. Olteanu, Syntheses of naphth [2,3-c] acridan-5,8-14, trionic dyes 1751

V

Vântu V., voir Anghelache I. 1045

Vargha E., voir Balog A. 689

Várhelyi Cs., voir Mánok F. 407

— , voir Ripan R. 375

Vasilescu D. S., Alternating tendency in copolymerization. I. Copolymerization of butyl vinyl ethers with acrylic monomers 1393

— , Alternating tendency in copolymerization. II. Copolymerization of 1,1-diphenyl ethylene with acrylic monomers 1637

Vasiliu Oprea C., voir Simionescu Cr. 259

Vass M. I., voir Budrugeac P. . . . 1153

Vîlcu R. and I. Ciocăzanu, Calorimetric kinetics. IV. The reaction of benzoyl chloride with sodium methoxide and ethoxide 785

— and I. Găinar, The interaction second virial coefficient of gas mixtures. I. The nitrogen + hydrogen mixture 1123

— and E. Lucinescu, Enthalpies of mixing of the carboxylic acid-water systems 791

— and A. Simion, Thermodynamic excess magnitudes of binary systems of organic liquids 977

Vlădescu C., voir Volanschi E. . . . 755

Vlassa M., Proton magnetic resonance spectra of some 1, 2, 3-trimethoxyacridines 1503
— and M. Ionescu, J. Fabian, The electronic spectrum of 1, 2, 3-trimethoxyacridine-N-oxide 665

Vodnár J. and R. Deutsch, Hydroperoxidation of organic compounds at the liquid/gas interface. VII. Contributions to the physico-mathematical characterizing of the apparatus . . 1545

Voiculescu N. et A. Airinei, I. Popescu, Les réactions des ligands coordinés. IV. L'étude spectroscopique et thermogravimetrique des combinaisons aluminium-organiques des diméthylglioximes coordinées 399

Volanschi C., voir Volanschi E. . . . 755

Volanschi E. and C. Vlădescu, C. Volanschi, E. S. R. spectra of some anion-radicals from dibenzo-[*b, e*]-thiepinone and related compounds 755

W

Weinberg J., voir Sahini V. E. . . . 1685

Wertheimer V., voir Glatz A. M. . . 87

Wright G. F., voir Krehm H. . . . 839

Z

Zador L. and I. Mureşan, Viscosimetric study of polyarylic acid in water-ethanol mixtures 353

Zaharescu M., voir Macarovici Const. Gh. 1009

Zuca Şt. and R. Borcan, Viscosity of binary molten alkali chloride systems 553
— and R. Costin, M. Olteanu, Influence of NaCl and LiF on the density and viscosity of molten $Na_3AlF_6BaCl_2$ system 181

Zugrăvescu I., voir Carp E. 1507
— et J. Herdan, I. Druţă, Benzimidazoliumylures. I. L'action des acétylènes activés sur quelques benzimidazoliumylures 647
— et J. Herdan, I. Druţă, Benzimidazoliumylures. II. Sur les réactions de quelques benzimidazoliumylures avec des philodiènes 659
— , voir Mandric Gh. 1783
— , voir Petrovanu M. 437

Zytkowicz A., voir Swinarski A. . . 1877

INDEX DES SUJETS

A

1-Acetoxy-naphthalenes, New direction of substituted β-hydroxy acids dehydration leading to 2,3-disubstituted-, D. M. Mondeshka and I. G. Angelova . . . .

Acetylenes with transition metals. VI. Reaction of the -allyl complex of 6-chloro-1, 3, 6-tri-t-butyl-1, 2-dihydrofulvene with carbon monoxides, Reactions of —, E. Avram and M. Avram . . . .

Acide ascorbique comme agent reducteur. IV. La cinetique de la reduction des ions de Pt(II) par acide ascorbique en presence des ions de Pb (II), L'—, R. Ripan, Gh. Pop and I. Pop 1593

α-Acylamino-N-heterocycles, Electronic spectra and acid-base equilibrium of some —, D. Suciu and Z. Győrfi 671

Addition compounds of zirconyl chloride with aromatic Schiff bases, N. S. Biradar, A. L. Locker and V. H. Kulkarni 45

Aluminium chloride catalyzed reactions of unsaturated acids with benzene. VI. Reaction of cyclopentylacrylic acid, A. M. Glatz, V. Wertheimer and F. Badea 87

Amino acids and their identification in complex mixtures with urea in excess, Separation of small amounts of —, A. Constantinescu and C. Liteanu 1551

Aminoacids. II. Complexes in solution of copper (II) with N(R)-anthranilic acid, Chelates and polychelates of —, 1727
I. Gabe, Anica Tolea and A. Airinei

2-Aminopyridine. Visible and infrared spectra of the combination with ammonium Reineckate, Methods for the determination of —, Gr. Teodorescu 485

Ammonium hexahalogenoosmiate and its dinitrogen compounds, The crystal structure of —, C. Pârlog, D. Ciomârtan, D. Săndulescu and D. Negoiu 1303

Azibenzyl radiolysis in benzene solution, Kinetics and mechanism of —, T. Oncescu and M. Contineanu . . . 1559

Azlactones of carotenoids. II. Retinal azlactone and transformation products, V. Tămaș and C. Bodea 701

B

Benzidins und *o*-Tolidins mit Natriumhypochlorit, Spektrophotometrische Dosierung des —, I. Florea . . . 157

Benzimidazolium-ylures. I. L'action des acétylènes activés sur quelques benzimidazolium-ylures, I. Zugrăvescu, J. Herdan et I. Druță 649

Benzimidazolium-ylures. II. Sur les réactions de quelques benzimidazolium-ylures avec des philodiènes, I. Zugrăvescu, J. Herdan et I. Druță 659

Benzo [*c*] cinnoline. IV. Addition reactions of 3,8-dimethylbenzo [*c*] cinnoline, via ylidic intermediates, leading to new *o*-diazobicyclic systems, *o*-Diazobicyclic derivatives of —, E. Carp, M. Dorneanu and I. Zugrăvescu 1507

Bétons aux résines synthétiques sans liants minéraux. I. Quelques remarques sur les propriétés des —, I. Ionescu 99

Bétons aux résines synthétiques sans liants minéraux. II. Quelques remarques sur les propriétés des —, I. Ionescu 293

Bicyclo [3.3.1] nonane-2-ones and bicyclo [3.2.1] octane-2-ones, On the conformational mobility of —, M. Moraru and G. M. Benedikt 877

Binary system $In_2O_3-TiO_2$, Contribution to the study of the —, Const. Gh. Macarovici, E. Perțe, M. Străjescu and M. Birou 49

Bis-thioethers. I. Condensation of sodium thiophenolates with dichloromethylated derivatives, M. Iovu and A. Angelescu 1061

Bismuth hydrolysis study. III. Electrometric investigations on bismuthyl perchlorate hydrolysis, Contributions to the —, C. Drăgulescu, A. Nimară and I. Julean 1455

C

Calcium aluminosulphate formation and hardening properties, I. Teoreanu and M. Muntean. 1483

Calorimetric kinetics. IV. The reaction of benzoyl chloride with sodium methoxide and ethoxide, R. Vîlcu and I. Ciocăzanu 785

Carbethoxy-phenylhydrazones series, Synthesis and spectrophotometric studies in the trisubstituted —, L. Beu and J. Russu . . . .

Carbonium ion reactions. VIII. Benzobicyclooctene derivatives through π-route, I. Drăguțan, C. Drăghici, A. Haneș, A. Dumitriu, E. Ciorănescu and C. D. Nenitzescu. . . . 67

Carbonium ion reactions. IX. Synthesis and acetolysis of 2 :3.5 :6-dibenzobicyclo[5.10] octa-2.5-dien-4-yl-methyl tosylate and 2 :3.5 :6-dibenzobicyclo [5.1.0] octa-2.5-dien-4-yl-ethyl-β-tosylate, A. Banciu, M. Elian, A. Bucur, D. Georgescu, E. Ciorănescu and C. D. Nenitzescu 213

Carbonium ion reactions. X. Nitrous acid deamination of 5-aminomethyl-5H-6,7-dihydro-dibenzo [*a*, *c*] cycloheptene, M. Banciu, E. Dragu, D. Georgescu and E. Ciorănescu. . . 1343

Carotenoids. IV. Metal-chlorides complexes of cantaxanthin inchain-epoxides, Inchain-epoxides of —, D. Oșianu, E. Nicoară and C. Bodea 1203

Catalythic dehydrogenation kinetics of *n*-butenes to butadiene, G. Andrei, Gh. Șerban and C. Florița. . . . 727

Chemical graphs. XX. Graphs of parallel and/or subsequent substitution reactions, A. T. Balaban and F. Kerek 631

Chemical graphs. XXI. Valence isomers of benzoannulenes, A. T. Balaban 1185

Chemical graphs. XXII. Valence isomers of heteroannulenes or of substituted annulenes. Coisomeric cubic multigraphs, A. T. Balaban 1323

Chemical graphs. XXIII. General cubic graphs with one loop, and homovalenes or their derivatives, A. T. Balaban 1611

Chemical graphs. XXIV .Isomerizations and isographic transformations, A. Barabas and A. T. Balaban . . . 1927

Chromatographic study of acetylene and ethylene adsorption and of palladium dispersion from Pd/Al_2O_3 catalysts, I. V. Nicolescu and I. Suciu. . . 1513

Chronopotentiometric method at high temperatures, S. Sternberg and C. Herdlicka. 197

Clathrates du type $M(SCN)_2(4\text{-}MePy)_4$. *p*-xylène. La structure cristaline et l'interaction avec la molécule de l'hydrocarbure incluse dans les —, I. Solacolu, D. Săndulescu et C. Drăgulescu 415

Clinkers of cements, Influence of oxides of transitional elements on the properties of mineralogical components of —, M. Enculescu 1491

Co(II) chelates with 1-methyl-2-carbethoxy-glyoxalanil-(1)-methoxy-phenylhydrazones-(2), A. C. Banciu and P. Spacu 1169

Co(II) chelates with 1-methyl-2-carbethoxy-glyoxalanil-(1)-tolylhydrazones-(2), A. C. Banciu and P. Spacu . . 1019

Cobalt and germanium double oxides, C. Gh. Macarovici, M. Birou, E. Perțe and M. Străjescu 805

Cobalt and titanium mixed oxides obtained from mixed complexes, Formation and structure of —, M. Străjescu, and C. Drăgulescu 1963

Combinaisons complexes du Mn(III) et du Mn(IV). I. Le système Mn(III, IV)-acide aniline-4 sulphonique, N. Calu, A. Popa-Rang et M. Calenciuc . . 1889

Complex combinations of the transition metals with tertiary stibines. II. Spectral studies Pd(II) complex combinations with tritolylstibines, D. Negoiu and L. Paruta 57

Complex compounds with diaminobiphenyl derivatives. XXVIII. Cobalt (II) complex pseudohalides, Investigation of —, R. Micu-Semeniuc, C. Gh. Macarovici and M. Bossanyi 1157

Complexes moléculaires des thioamides. II. Complexes de transfert de charge du phénylthioacétamide et de la phénylthioacétopipéridide avec l'iode, F. Cornea, C. Fulea et S. Moldoveanu 429

Complex of anthranil-N,N-diacetic acid with trivalent metals. III. Entropy change calculation. C. Drăgulescu, S. Policec and T. Simonescu . . . 801

Composés d'addition du tétrachlorure de thorium avec des azométhynes, Sur les —, D. Negoiu, A. Kriza et M. Nasta 1039

Composés du trichlorure de l'ethoxytitane avec des bases Schiff, Sur les —, D. Negoiu, A. Kriza et M. Nasta 1921

Comptes Rendus 337, 517, 518, 735, 1113, 1113, 1115, 1117, 1118, 1283, 1413, 1555, 1555, 1556, 1677, 1678, 1679,1680, 1680, 1681,1682, 1835,1969

Computer program for determining all possible E.S.R. spectra with equidistant lines, A. T. Balaban, and C. Pomponiu 581

Condensation of β-aroylpropionic acids with isatin under Perkin conditions, A. M. El-Abbady, M. A. Omara and N. G. Kandil 97

Condensations of unsaturated acids with benzene, Aluminium chloride catalysed —, A. M. Glatz 455

Conductance of some alcaline alkoxides in ethanol-benzene and ethanol-dimethylformamide mixtures at 25°, The — , F. Bărbulescu, A. Bref and M. Craiu 1817

Coordinate compounds with molecular nitrogen. Synthesis and characteristic properties of some dinitrogen compounds of cobalt, nickel, iron with triaryl-phosphines, triaryl-arsines and triaryl-stibines, New —, D. Negoiu, C. Pîrlog and D. Săndulescu 387

Coordination compounds with choline perchlorate, M. Brezeanu and I. Jitaru 1883

Copolymere konjugierter Diene mit Monoestern der Maleinsäure. VII. Andere Aspekte der Reaktionskinetik der radikalischen Copolymerisation von Isopren mit Monoestern der Maleinsäure, I. Nanu und C. Andrei 115

Copolymerization. I. Copolymerization of butyl vinyl ethers with acrylic monomers, Alternating tendency in —, D. S. Vasilescu 1393

Copolymerization. II. Copolymerization of 1,1-diphenyl ethylene with acrylic monomers, Alternating tendency in —, D. S. Vasilescu 1637

Copolymerization of epichlorhydrin and propylene oxide with the $AlEt_3-H_2O$ catalytic system, V. Dimonie, D. Donescu and I. Gavăt 125

Copolymerization of N-vinylcaprolactam with vinylpyridines, N. Cobianu, C. Boghină, B. Mărculescu, C. Cincu and I. Amălinei 1251

Copolymers of conjugated dienes with maleic acid monoesters. VIII. Bulk copolymerization of isoprene with monobutylmaleate, C. Andrei and I. Nanu 1535

Copper, lead, chromium, nickel, molybdenum and cobalt in natural waters, Spectrographic determination of traces of —, V. Em. Sahini, M. Craiu and E. Ivana 165

Corrosion of carbon steel and some austenitic stainless steels in synthetic river waters, The —, S. Ciolac and O. Radovici 543

Creatinine from leucine in a proteic hydrolysate by paper chromatography with a combined temperature and stationary phase section gradient, Separation of —, A. Constantinescu and C. Liteanu 1107

Crystal field and MO parametric approaches. On the equivalence between the —, C. Lepădatu and V. Tufoi 533

Cu(II) selenocyanate complexes with biguanide derivatives, Study of some —, C. Gheorghiu, M. Constantinescu, O. Constantinescu and V. Pocol 1909

Cyclobutadiene fused with heterocyclic ring. I. Heterobenzocyclobutadienes, Electronic structure of —, M. D. Gheorghiu and P. Filip 859

Cyclobutane series. XXXIII. Synthesis of *syn*-dibenzo [*c*, *g*] tricyclo-$[4.2.2.0^{2,5}]$ deca-3, 7, 9-triene. A new dibenzo $(CH)_{10}$ hydrocarbon, Investigations in the —, I. G. Dinulescu, M. Pop, F. Chiraleu, M. Avram and C. D. Nenitzescu. . . 1197

Cyclohexane dehydrogenation equilibrium and kinetics in pulsed reactor, Study of —, A. Pop and P. Dumitrescu 1073

Cyclohexylation catalitique de benzène, Formation d'isomères dans les réactions de —, M. Iovu et E. Tudor 1207

D

Dehydrogenation catalysts, Correlation of the porous structure to the activity and selectivity of some —, V. Mocearov, G. Csomontanyi, C. Coriciuc and A. Panovici. 1271

Dibenzo-[*b*, *e*]-thiepinone and related compounds, ESR spectra of some anion-radicals from —, E. Volanschi, C. Vlădescu and C. Volanschi. . 755

Dibenzo [*g*, *h*] bicyclo [4.2.2] deca-2, 4, 7, 9-tetraene, The $PdCl_2$-induced rearrangement of dibenzobullvalene into —, M. Banciu, M. Elian, C. Drăghici and E. Ciorănescu 1179

β,β′-Dichloro-diéthyl-amine. Spectre en visible et infrarouge du composé resulté entre le β,β′-dichloro-diéthylamine et le reineckate d'ammonium, Méthodes de détermination de —, Gr. Teodorescu 321

2,2-Dichlorobenzaldoxime from 4-nitrotoluene, The synthesis of—, P. Buchwald and F. Domnariu 1221

Dinitro-sulphophenyl-N-alkoxyamines, Formation of new nitrogen-free radicals from —, M. Frangopol, P. T. Frangopol and N. Negoiță. . . . 1773

α-Dioximine complexes of the transition metals. XXXVIII. The $[Co(DH)_2(NO_2)(CN)]^-$ion and its basic hydrolysis kinetics, On —, R. Ripan, Z. Finta and CS. Várhelyi. 37

Dioxouranium (VI) complexes with aromatic Schiff bases, Spectral study of —, N. S. Biradar and T. R. Goudar 1441

Diphenyldiazomethane radiolysis in benzene solution, Kinetics and mechanism of —, T. Oncescu and M. Contineanu 931

Distribution coefficient of samarium in mixed systems of organic solvent and mineral acid, Șt. Spiridon and C. Grigorescu-Sabău 131

Dünnschichtchromatographie mit orthogonalem Temperaturgradient, Trennung einiger Aminosäuren durch —, S. Gocan und C. Kyri 1957

E

Electrochemical behaviour of 18Cr—10Ni stainless steel in organic acid solutions. I. Formic acid, I. Atanasiu and T. Badea 1447

Electronic structures of BH_3 and BH_4, The —, D. R. Armstrong, P. G. Perkins and K. S. Sorbie 747

Elimination reactions in the 8-R-tricyclo-$[7.3.1.0^{2,7}]$-tridecane series. III. Dehydration of 8-R-tricyclo$[7.3.1.0^{2,7}]$ tridecane-2,13-diols, N. Bărbulescu, and M. Leca 233

Elimination reactions in the 8-R-tricyclo-$[7.3.1.0^{2,7}]$ tridecane series. IV. Pyrolytic elimination of tricyclo-$[7.3.1.0^{2,7}]$ trideca-2-en-13-acetate, N. Bărbulescu and M. Leca . . . 443

Elimination reactions in the 8-substituted-tricyclo $[7.3.1.0^{2,7}]$ tridecane series. V. Configuration of 8-substituted-tricyclo-$[7.3.1.0^{2,7}]$ tridecen-13-ols, N. Bărbulescu and M. Leca 1381

Emulsion polymerization of vinyl acetate, Chain transfer in —, D. Donescu, C. Hagiopol, M. Munteanu, V. Dimonie and I. Gavăt. 1243

Enthalpies of mixing of the carboxylic acid-water systems, R. Vîlcu and E. Lucinescu 791

F

Ferrate (VI) ion salts with Ni(II) and Co(II) complex, Thermal analysis of —, D. Negoiu and A. Șchiopescu. . . 1717

Ferrate (VI) ion salts with Ni(II) and Co(II) tetrapyridine-tetrapicoline complex combinations, D. Negoiu and A. Schiopescu 1693

Ferroniobium alloys, Application of niobium polarographic reduction in hydrochloric acid-thiocyanate medium to the analysis of —, S. Marchidan 1661

Fluides, Les tensions superficielles des —, N. Bărbulescu 169

Formyl furo(2,3-b)benzothiachromone, Synthesis based on —, N. Rășanu and O. Maior 255

Fused alkali nitrates and chlorides, Interdiffusion and selfdiffusion of monovalent cations in —, S. Sternberg and C. Herdlicka 763

Fused rubidium and cesium fluorides, Thermodynamic data on vaporization of —, L. Topor. 1569

G

Gallium metatitanate, E. Perțe and M. Străjescu 395

Galvanostatic study of the electrochemical adsorption process on the chlorine-active carbon electrode in molten salts. I. Anodic and cathodic polarization curves, The —, S. Sternberg and V. Petrescu 25

Galvanostatic study of the electrochemical adsorption process on the chlorine-active carbon electrode in molten salts. III. Anodic polarization (charging) equation, The —, S. Sternberg, S. Petrescu and V. Petrescu 955

Gas mixtures. I. The nitrogen + hydrogen mixture, The interaction second virial coefficient of —, R. Vîlcu and I. Găinar 1123

Gas-solid interface, Some considerations concerning Gibbs free energy of —, P. Budrugeac and M. I. Vass. . . 1153

β-D-Glucopyranosides, NMR studies on the effect of nitrogen atom on the anomeric proton of —, S. H. Doss S. Kondo, K. Tanaka and Y. Tsuzuki 1767

Gold recovery, An ion-exchange process for —, S. A. Tătaru. 717

H

Hardening process in tricalcium silicate-water-electrolyte system, The study of the —, I. Teoreanu and M. Muntean 371

Heat transfer with chemical reaction modelling of thermal decomposition reactions, R. Z. Tudose. 1791

Heterocycles. XXVI. Nitration of 2-anilino-5-phenyl-1, 3, 4-oxadiazole, Study of some —, I. Simiti, D. Ghiran, I. Schwartz and R. D. Pop. . . . 1067

Heteropolytungstates with U(IV) as central atom. Synthesis and physico-chemical study of the UL_2 complex where $L = P_2W_{17}O_{61}^{10-}$, Gh. Marcu, M. Rusu and A. V. Botar. . . . 827

High frequency discharge plasma. I., Transformation of the toluene — water mixtures in the —, G. Bourceanu, Gh. Popa, M. Sanduloviciu and V. Ababi 207

High-temperature thermodynamic data for some uranium oxides within the range $UO_{2.25}-UO_{2.60}$, D. I. Marchidan and S. Tănăsescu 1435

Hoffmann's LCAOMO method, An improvement of —, C. I. Lepădatu and S. Moldoveanu 1587

Homologie und der homologen Serien. I. Über die Beschreibung der chemischen Systeme mit Hilfe der be-Matrizen, Darstellung der —, I. Moțoc 1233

Homologie und der homologen Serien. II. Behandlung in Kategorien, Mathematische Darstellung der —, I. Moțoc 1239

Hydrated binders, Mechanism and kinetics of the dissolution in water of some —, I. Teoreanu, M. Muntean, N. Ciocea and O. Șancu. . . 561

Hydrogen transfer reactions between hydrocarbons and free radicals. II. The study of molecular combinations between aromatic hydrocarbons and the 1,1-diphenyl-2-picrylhydrazyl free radical (DPPH), I. Anghelache, D. Săndulescu and V. Vântu 1045

Hydroperoxidation of organic compounds at the liquid/gas interface. VII. Contributions to the physico-mathematical characterizing of the apparatus, J. Vodnár and R. Deutsch 1545

Hydroxymercuration of nor-bornene, The —, H. Krehm and G. F. Wright 839

I

Indikatoren vom Phenothiazin Typ. I. Die Anwendung von 3H-Phenothiazin-3-[4-anilsulfonsäures Kalium], 3H-Phenothiazin-3-[3-Anilsulfonsäures

Kalium] und 3H-Phenothiazin-3-[2-anilsulfonsäures Kalium] als Säure-Basen-Indikatoren, Säure-Basen —, M. Răileanu, I. Radulian und H. Kraus 709

Indiums mit R-Weinsäure, Papierelektrophoretische Untersuchung der Bildung von Verbindungen des —, Gh. Marcu, M. Suciu und A. V. Botar 577

L

Lanthanides with neutral ligands containing donor oxygen atoms. II. Chlorosalicylates of lanthanides with triphenylarsine oxide, Mixed ligand compounds of —, S. Ploștinaru and P. Spacu 567

Ligands coordinés. IV. L'étude spectroscopique et thermogravimétrique des combinaisons aluminium-organiques de diméthylglyoxime coordinée, Les réactions des —, V. Voiculescu, A. Airinei et I. Popescu 399

Liquid membrane-electrodes. V. Electrodic behaviour of sodium tetraphenylborate in cyclohexanone to certain monovalent cations, E. Hopîrtean and E. Ștefanigă 1265

Lithium in silicate rocks and minerals using a simple flame photometer, Determination of —, S. A. Khan and M. Stone 1669

M

Magnitudes and signs of ^{13}C coupling constants in several organic molecules by double resonance, V. Bărboiu . 363

Membrane-electrode. XI. Influence of the plasticizer of the PVC on its electrode behaviour, Studies on the polymer+plasticizer —, E. Hopîrtean, C. Liteanu and A. Mașa 921

Membrane-electrodes of a metallic wire-plastic membrane type. I. K^+-selective membrane electrode, E. Hopîrtean, C. Liteanu and E. Ștefănigă 1651

Membrane-electrodes under current. V. The E-pH electrode function and the use of the PVC + tricresylphosphate membrane in the acid-base potentiometric titration at constant direct current, Studies on the electroanalytical behaviour of —, E. Hopîrtean and C. Liteanu 145

Metal-sulfur combinations in liquid ammonia, On the reactivity of some —, P. Markov, S. Chorbadjiev and V. Tarpanov 1317

Metallic liquids, An equation of state for —, I. G. Murgulescu and A. Leibovici 739

Métaux de transition déposés sur un support activ, Mécanisme de l'activité catalytique des —, A. Swinarski et A. Zytkowicz 1877

Microdetermination of organic sulphur or inorganic sulphate S. W. Bishara, M. E. Attia and H. N. A. Hassan 1099

Modern Friedel-Crafts chemistry. V. The fragmentation and dealkylation of straight-chained diphenylbutanes under the influence of water-activated aluminium chloride at 100°C, A. A. Khalaf and R. M. Roberts 1351

Modern Friedel-Crafts chemistry. VII. On the question of group participation in the rate-determining ionization step during inter- and intramolecular Friedel-Crafts alkylations and the mechanism of formation of 1-methyltetralin during the $AlCl_3$-catalysed reaction of 1-chloro-2-methyl-4-phenylbutane, A. A. Khalaf . . . 1361

Modern Friedel-Crafts chemistry. VIII. Cyclialkylations of some aryl- and diarylalkanols in the presence of the mild $AlCl_3/CH_3NO_2$ catalyst, A. A. Khalaf 1373

Molecular complexes with aromatic cations as electron acceptors. II. Charge-transfer spectrum of 2, 4, 6-triphenylpyrylium thiocyanate, A. T. Balaban and M. Paraschiv . . . 1731

Molecular interactions in solutions. Calculations of the interaction potential energy in the carbon disulphide-chloroform system, S. Bădilescu 991

Molten alkali chloride systems, Viscosity of binary —, Șt. Zuca and R. Borcan 553

Molten antimony, Diffusive atomic transport in —, N. Petrescu and L. Ganovici 187

Molten metals. II. On the viscosity of —, I. G. Murgulescu and M. Șerban 1417

Molten mixtures of alkali-alkaline earth metal nitrates, Chronopotentiometric study of Ag(I) in —, R. L. Bhatia and H. C. Gaur 779

Molten $Na_3AlF_6-BaCl_2$ system, Influence of NaCl and LiF on the density and viscosity of —, Șt. Zuca, R. Costin and M. Olteanu 181

Molten salts. I. The current intensity effect, The galvanostatic study of the electrochemical adsorption process on the iodine-active carbon electrode in —, S. Sternberg and I. Galasiu 523

Molten sodium nitrate-alkaline earth nitrates mixtures, Interdiffusion coefficients of silver (I) in —, N. P. Bansal 1287

N

Naphth [2,3—c] acridan-5,8—14, trionic dyes, Syntheses of —, F. Urseanu, C. Drăghici and V. Olteanu 1751

Ni(II) chelates synthetized with 1-methyl-2-carbethoxyglyoxalanil-(1)-methoxy-phenyl-hydrazones-(2), A. C. Banciu and P. Spacu 1307

Ni(II) chelates synthetized with 1-methyl-2-carbethoxyglyoxalanil-(1)-tolyl-hidrazones-(2), A. C. Banciu and P. Spacu 817

O

Optimisation of separations by thin-layer chromatography on silicagel. I. Separation of some ethanolamines in several polycomponent solvent systems, Studies concerning the —, C. Liteanu and H. Nașcu 1941

Organic hydroperoxides in the heterogeneous catalysis. II. Decomposition of cumene hydroperoxide on strongly acidic cationites, Decomposition of —, L. Cormoș, A. Pop and V. Sbera 1631

Oxido-reduction reactions by means of the vibrated electrode technique, Kinetic study of —, Gh. Facsko and M. Poraicu 341

Oxydation des Urans(IV) mit Natriumpersulfat, Kinetik und Mechanismus der —, F. Mánok, Cs. Várhelyi und R. Oprean 407

P

Palladium catalysts by rare earth and other oxides for the hydrogenation of cyclohexene, The activation of —, S. M. Ismail, M. A. Aleem and A. Ali 847

Palladium (II) and platinum (II) square-planar complexes with tris(*p*-methoxyphenyl) arsine and halide ions, P. Spacu, F. Popea, C. I. Lepădatu, A. C. Banciu, E. Ivan, S. Ploștinaru, Z. Toma and C. Rusu 1861

Pentafluorophenyl-silicon derivatives with the π-cyclopentadienyliron dicarbonyl anion, Reactions of some —, I. Haiduc, R. Bruce King and H. Gilman 1709

Peptides: eledoisin and physalaemin, The synthesis of some C-terminal analogues of the —, F. Cuiban, S. Cilianu and V. Badea 1521

Peptides. XV. The use of β-dicarbonyl N-protected asparagine and glutamine in peptide synthesis, A. Balog, E. Vargha, D. Breazu, F. Gönczy and L. Beu 689

Phtalazinium ylids. VI. Action of dimethylacetylenedicarboxylate on disubstituted at the exocyclic carbon phatalizinium-ylids, M. Petrovanu, A. Sauciuc and I. Zugrăvescu 437

Pilocarpine. Spectre en visible et infrarouge du composé résulté entre l'azotate de pilocarpine et le reineckate d'ammonium, Méthodes de détermination de l'azotate de —, Gr. Teodorescu 1645

Поливинилхлорида II. Морфологические исследования. Влияние условий распылительной сушки на свойства пастообразующего —, В. Бойешан и Д. Фельдман 493

Поливинилхлорида. Сообщение. I. Экспериментальная часть. Влияние условий распылительной сушки на свойства пастообразующего—, В. Бойешан и Д. Фельдман. 283

Polybenzimidazole-imides, Thermostable polymers. III. —, Gh. Mandric, A. I. Pavlov, V. V. Korshak and I. Zugrăvescu 1783

Polymerization of vinyl acetate in the presence of polyvinyl alcohol, Kinetics of emulsion —, V. Dimonie, D. Donescu, M. Munteanu, C. Hagiopol and I. Gavăt 903

Polymers by destructive methods. II. Mechano-chemical complexation and complexation by irradiation using ^{60}Co γ-rays in the system: poly(ethylenete-rephthalate), ethylenediamine and metallic salts, Syntheses of new —, Cr. Simionescu, C. Vasiliu Oprea and C. Negulianu 259

Polyvinyl-Alkohol-Lösungen, Über den Einfluss der Elektrolyten auf die Zähigkeit der —, C. Hölszky, C. Suciu und D. Săndulescu 887

Potassium ferrate (VI), Thermal decomposition of —, D. Fătu and A. Șchiopescu 1297

Potentiometric determination of dissociation constants of some aromatic acetoacetamides, A. D. Taneja and N. U. M. Rao 1093

Potentiometric titration of Cu(II) with Na_2EDTA, Synthetic single crystal PbSe electrode, D. C. Cörmös, I. Haiduc and P. Stețiu 1949

Pyrolysis and oxidative pyrolysis of isobutene. I. I. G. Murgulescu and I. Bică 1841

Pyrophosphate de plomb (IV) — PbP_2O_7, Etude du spectre vibrationnel, infrarouge et Raman, du —, R. Hubin 947

Q

Quecksilbers (II) in stark alkalischem Medium mit Thioacetamid, Die amperometrische Titrierung des —, Gh. Facsko und M. Nemeș 141

R

Radical ions. II. Nitrophenothiazine radical-ions, M. Hillebrand and M. Răileanu 1227

γ-Radiolysis of gaseous isobutylene. The influence of experimental conditions on the radiochemical yields of the main radiolysis products, I. Bică and M. Căldăraru 17

Radiolysis of the complex oxalates in aqueous solutions. II. Kinetics and mechanism of the radiolysis of cobalt-trisoxalato-complex in neutral aqueous solution with α-Po^{210} irradiations, The —, I. G. Murgulescu, and J. Păun 9

Radiolysis of the complex oxalates in aqueous solutions. III. The influence of some OH scavangers on the radiolysis of potassium trisoxalatocobaltate in neutral aqueous solution, J. Păun and T. Memetea . . . 941

Radiolysis of the complex oxalates in aqueous solutions. IV. The influence of some reducing free radicals scavengers on the potassium trisoxalatocobaltate radiolysis in aqueous solutions, T. Memetea and J. Păun . . . .

Radiolytic oxidation of phenol in aqueous solution, Some aspects of —, M. Fiti 1083

Rare earth ion exchange of synthetic faujasite substituted isomorphously by boron, P. Onu and V. Ababi 1279

Réactif du type EDTA, Un nouveau —, Const. Gh. Macarovici et E. Chiș

Romanian research, a message of Romania's peaceful policy, M. Florescu 3

S

Salicylidenanils, Electrical conductivity of some —, S. Avramovici, I. Ciocoiu and G. I. Rusu 1053

Salt systems with single charge ions, Thermodynamic treatment of binary and ternary —, Z. Moser and K. Fitzner 1573

Sels fondus. II. Influence de la température, L'etude galvanostatique du processus de l'adsorption électrochimique sur l'électrode d'iode-charbon actif dans les —, S. Sternberg et I. Galasiu 967

Silver—silver electrodes in malten sodium nitrate-barium nitrate eutectic, S. K. Jain . . . .

Systèmes quaternaires et quinaires, Généralisations du triangle de Gibbs pour les —, D. Rimer 997

T

Ternary system, Contributions to the study of the $NiO-SiO_2-TiO_2$ —, C. Gh. Macarovici and M. Zaharescu 1009

Terpolymerization field. IV. Preliminary theoretical structural studies of some binary copolymers, Researches in the —, A. Liga, I. Negulescu and Cr. Simionescu 911

1, 2, 3, 4-Tetrahydroacridin-9-carboxyl-Säure Derivate. II. Ester und Thioester, Über —, M. Cîrje 249

Tetrakis phosphine complexes of nickel (O), Bonding and magnetic properties in —, P. Cassoux, J. F. Labarre and J. M. Savariault 1471

Thalliums mit Meta-Nitralgrün, Spektrophotometrische Bestimmung des —, C. Constantinescu und S. Fișel 329

Thermodynamic excess magnitudes of binary systems of organic liquids, R. Vîlcu and A. Simion 977

Thin-layer chromatography, The effect of S-chamber shape on the separation of ethanolamines by thin-layer chromatography, H. Nașcu and C. Liteanu 1407

2-Thio-5-nitrobarbituric acid, R. Nuțiu, I. Sebe and M. Nuțiu 679

Thiocomplexes. V. Complex compounds of Pt(II) with thioamides, Contributions to the chemistry of —, D. Negoiu and V. Mureșan . . . 1031

Titanium oxyhydrate ultrafine powders, Synthesis and thermal analysis of —, A. Bărbulescu 833

Titanium trichloride, A theoretical investigation of Zigler-type catalysis. II. Species related to solid —, D. R.

Armstrong, P. G. Perkins and J. J. P. Stewart 1695

Tl(III) mit Ortho-Nitral und Para-Nitrolgrün, Spektrophotometrische Bestimmung des —, C. Constantinescu und S. Fişel 509

Transition-metal complexes, On the redox potentials in the —, C. I. Lepădatu and C. Rusu 811

Triazine. L. Mitteilung potentiometrische Bestimmung der Aciditätskonstanten von 4-Hydroxy-6-Oximintetrahydrotriazinyl-2-Formaldoxim, Über —, E. Gavrilă und I. Cădariu . . .

s-Triazine field (new series). XV. The protonation equilibria and indicator behaviour of E-1,3-dimethyl-6-(*p*-X-β-styryl)-2,4-dioxo-1H, 3H-1, 3, 5-triazines in 50 vol % aqueous-ethanolic solutions in the presence of sulphuric acid, M. Safta and G. Ostrogovich 1621

s-Triazine field (new series). XVI. Acidic und tautomeric equilibrium constants of the conjugated acids of some E-1,3-dimethyl-6-(*p*-dialkylamino-β-styryl) 2,4-dioxo-1H, 3H-1, 3, 5-triazines, Studies in the —, M. Safta and G. Ostrogovich . . . .

Tricylo [7.3.1.$0^{2,7}$] tridécanes. III. Hydrazones de la 2-hydroxy-8-R-tricyclo [7.3.1.$0^{2,7}$] tridécan-one-13, Recherches dans la série des —, N. Bărbulescu et A. Nicolae 869

1, 2, 3-Trimethoxyacridine-N-oxide, The electronic spectrum of —, M. Vlassa, M. Ionescu and J. Fabian 665

1, 2, 3-Trimethoxyacridines, Proton magnetic resonance spectra of some —, M. Vlassa 1503

Tris-éthers. II. Condensation du bis (chlorométhyl)ether avec des cyclohexylphenoxydes, methylcyclohexylphenoxydes et chlorocyclohexylphenoxydes de sodium M. Iovu, G. Cîmpeanu et N. Miclovici 881

U

Uranium (VI) en milieu azotique, Contributions à l'etude de l'hydrolyse de l' —, M. Mavrodin-Tărăbîc . . 1146

V

Vanadium (V)-Solochrom-violett R. S. Die spektrophotometrische Bestimmung des Vanadiums, Spektrophotometrische Untersuchung des Systems —, I. Burnea, M. Pleniceanu und L. Burnea 501

Vapor pressures of molten $CdBr_2$, CdI_2, $MgBr_2$ and molecular association in gaseous phase, L. Topor and I. Moldoveanu 985

Vibrational transitions. III. Collision complexes of chloroform in nonpolar solvents, Simultaneous —, S. Bădilescu 1139

Vibrational transitions. IV. Shape of some bands of carbon disulphide and chloroform, and relaxation mechanisms in solutions, Simultaneous, S. Bădilescu 1145

Viscosimetric study of polyacrylic acid in water-ethanol mixtures, L. Zador and I. Mureşan 353

Viscosité des systèmes mixtes : eau-monoéthylèneglycol, eau-monoethanolamine et eau-diméthylesulfoxyde. L'influence de la température et des sels sur la viscosité de ces systèmes, Sur la —, O. Landauer, G. Costeanu et C. Mateescu 1429

Vitreous phase separation process in the $Fe_2O_3-BaO-B_2O_3$ system, Aspects of the —, S. Şolacolu and E. Rusu 381

X

Xylidine isomers. III. Acid-basic properties of xylidines in their excited state, V. E. Sahini, J. Weinberg, C. Bendic and M. Milescu 1685

CORRIGENDA

The following corrections are to be made in **Nos** 8, 9, **1974** **of this** journal :

In table 9, column 4, top, the following was omitted : b.p. 85—184°.

On page 1361, footnote 1, replace in press (1974) by **19**, 1351 (1974).

On page 1364, line 12, replace diphenyl by diphenylated products.

On page 1371, line 21, replace *3-benzolylpropionic* by *3-benzoyl-propionic*.

On page 1373, footnote *, replace in press by **19**, 1351, 1361 (1974).

The name of Fernand Gallais has appeared among the authors, by mistake.

On pages 1471, 1479 and 1481 the word "rotary" should be replaced by "rotatory"

On page 1472 : — line 3 — read C1 instead of CI ;
— in reference 18 erase, "1970" ;
— in reference 19, replace idem by Compt. rend.

On pages 1473, 1476, 1477 read Δ p instead of Δ_p

On page 1475 — line 1 and 6 ζ (zeta) should be replaced by ξ (csi).
— line 16 and the following 4 lines should be read: bond, the PF_3 derivative having the highest bond order and the PMe_3 derivative the lowest. The total bond order varies approximately from 2 to 1.

On page 1477 — line 16, replace ρ (Ni—P) : by ρ (Ni.P)
— the formula should be written as follows : $\rho(Ni.P) = \Delta\rho + 2\rho(e)_P \pm \delta G \pm \delta\pi$
— and in the first and the second lines after the formula $2\rho(e)$ should be replaced by $2\ \rho(e)_P$

On page 1478 — line 1, δ should be replaced by π
— in table 3, column 8, No. 14, replace 29 by 20 column 6, No. 16 replace 1178 by 1187
— in reference 35, read KUCHITSU instead of KUTCHISU
— in reference 36, read BASSETT instead of BASSET

On page 1479 — line 3 $\varkappa$ (kappa) should be replaced by χ (hi)
— line 16 read "or groups" instead of "of groups"
— line 37 should be read : considered is not affected by the value of the wavelength and seems to be related
— in reference 38, "1961, 252" should be replaced by **252**, 1644 (1961).

CORRIGENDA

The following corrections are to be made in Nos 8 & 9, 1974 of this journal:

In table 6, column 4, for the following was omitted: [illegible] 154°.

On page 1361, footnote 4, replace in press (1974) by 19, 1351 (1974).

On page 1363, line 13, replace diphenyl by diphenylated products.

On page 1371, line 21, replace [illegible] by [illegible].

On page 1372, footnote 7, replace in press by 19, 1351, 1361 (1974).

The name of Fernand [illegible] has appeared among the authors by mistake.

On pages 1371, 1375 and 1381 the word "rotary" should be replaced by "rotatory".

On page 1472 — line 3 — read C1 instead of C4;
— in reference 15 [illegible] "1975";
— reference 18, replace [illegible] by Compt. rend.

On pages 1423, 1470, 1477 read Δ p instead of Δ.

On page 1473. — line 1 and 2 [illegible] should be replaced by [illegible].
— line 10 and the following 4 lines should be read: bond, the PF$_3$ derivative having the highest bond order and the [illegible] derivative the lowest. The total bond orders varies approximately from 2 to 1.

On page 1477 — line 16: replace (Ni—P) by [illegible]
— the formula should be written as follows: [illegible]
— and in the first and the second lines after the formula [illegible] should be replaced by [illegible]

On page 1478 — line 1, 8 should be replaced by π
— in table 3, column 3, No. 14, replace 20 by 30; column 4, No. 14 replace 1158 by 1187
— in reference 36, read [illegible] instead of [illegible]
— in reference 37, read [illegible] instead of [illegible]

On page 1480 — line 5 [illegible] should be replaced by [illegible]
— line 16 read "of groups" instead of "of groups"
— line 27 should be read: [illegible] is not affected by the value of the wavelength, and seems to be related
— in reference 38 "1961, 855" should be replaced by "272, 1953 [illegible]".

NOTE POUR LES AUTEURS

La *Revue Roumaine de* **Chimie** publie des articles en anglais, français, russe, allemand ou espagnol. Les auteurs sont priés d'envoyer des articles, notes, communications et comptes rendus inédits.

Les manuscrits seront dactylographiés à deux intervalles. Les tableaux seront dactylographiés sur des feuilles séparées, de même que la légende des figures. Les diagrammes seront tracés à l'encre de Chine sur papier calque. Les tableaux et les figures seront numérotés par des chiffres arabes, en nombre strictement nécessaire. Prière de ne pas inscrire les mêmes données dans les tableaux et les figures. Les formules chimiques seront incluses dans le texte ; en outre, elles seront transcrites sur des feuilles séparées. Les auteurs sont priés d'indiquer les caractères italiques (en soulignant les lettres au crayon), ainsi que tout autre caractère spécial. L'ordre des références bibliographiques sera celui de leur mention dans le texte ; le nom de l'auteur sera précédé de l'initiale du prénom ; les publications périodiques seront présentées suivant les prescriptions internationales. Les références seront ajoutées à la fin de l'article ; elles paraîtront comme des notes, au bas de la page. Le texte sera précédé d'un résumé comprenant 15 lignes au maximum.

L'entière responsabilité du contenu des articles appartient aux auteurs. On publie des articles dus aux collaborateurs roumains ou étrangers.

PRINTED IN ROMANIA

1975 MAR 21

1975 JUN 11

TRAVAUX PARUS AUX ÉDITIONS DE L'ACADÉMIE DE LA RÉPUBLIQUE SOCIALISTE DE ROUMANIE

I. ZUGRĂVESCU, MAGDA PETROVANU, **Chimia N-Ilidelor** (La Chimie des N-Ylures), 1974, 347 p., 19 lei.

MARGARETA AVRAM, **Antidăunători** (Pesticides), 1974, 494 p., 41 lei.

CR. SIMIONESCU, VIORICA RUSAN, N. POPA, **Chimia algelor marine** (La Chimie des algues marines), 1974, 211 p., 18 lei.

MARIA FITI, **Dozimetria chimică a radiaţiilor ionizante** (La dosimétrie chimique des radiations ionisantes), 1973, 240 p., 13,60 lei.

MIHAI FLORESCU, **Eficienţa economică a cercetării ştiinţifice** (L'efficience économique de la recherche scientifique), 1972, 115 p., 15 lei.

GEORGETA LĂZĂRESCU, **Sistematizarea informaţiilor în chimia organică** (La systématisation des informations dans la Chimie organique), 1972, 252 p., 10,50 lei.

P. BALTĂ şi E. BALTĂ, **Introducere în chimia fizică a stării vitroase** (Introduction à la chimie physique de l'état vitreux), 1971, 15,50 lei.

LYDIA-MARIA VAICUM, **Biodegrabilitatea detergenţilor** (La biodégrabilité des détergents), 1971, 254 p., 16 lei.

TIBERIU NĂŞCUŢIU, **Metode radiometrice de analiză** (Méthodes radiométriques d'analyse), 1971, 346 p., 19,50 lei.

I. ZUGRĂVESCU et L. STOICESCU-CRIVETZ, **Polimeri heterociclici** (Polymères hétérocycliques), 1971, 190 p., 9,50 lei.

CRISTOFOR SIMIONESCU et C. V. UGLEA, **Fracţionarea compuşilor macromoleculari** (Fractionnement des composés macromoléculaires), 1962, 292 p., 18,50 lei.

I. V. MAXIM, **Materiale nucleare** (Matériaux nucléaires), 1969, 444 p., 30 lei.

CRISTOFOR SIMIONESCU et CLEOPATRA VASILIU-OPREA, **Mecanochimia compuşilor macromoleculari** (La mécanochimie des composés macromoléculaires), 1967, 344 p., 23,50 lei.

CORNEL BODEA et collab., **Tratat de biochimie vegetală**, partea I, **Fitochimie** (Traité de biochimie végetale, Ire partie, Phytochimie), Ire vol., 1964, 747 p. + 4 annexes + 2 pl., 41 lei; IIe vol., 1965, 1262 p., 1 pl., 56 lei; IIIe vol., 1967, 773 p., 35 lei.

I.P.I. — c. 1725

43 426

Lei 25.—